

1001

Mice Lacking Tuberous Sclerosis 2 in Osteoblasts Develop Insulin Resistance with Increased Bone and Fat Mass. Ryan Riddle^{*1}, Julie Leslie², Douglas Digirolamo², Thomas Clemens². ¹Johns Hopkins University School of Medicine, USA, ²Johns Hopkins University, USA

Recent studies demonstrate that insulin receptor (IR) signaling in osteoblasts is required for osteoblast differentiation and for the regulation of global glucose metabolism in mice. To interrogate insulin-responsive pathways in osteoblasts responsible for these metabolic actions, we examined the role of *Tsc2*, which encodes a component of the tuberous sclerosis complex that regulates mTOR activity. Insulin stimulates mTOR activity by inactivating the Tsc1/Tsc2 complex, and thereby enhances protein synthesis, glucose utilization, and cell growth. Mice selectively lacking *Tsc2* in osteoblasts (Δ Tsc2) exhibited striking increases in trabecular bone (122% vs. controls at 12 wks). With age, the Δ Tsc2 mice developed metabolic abnormalities similar to those observed previously in mice lacking the IR in osteoblasts. Body weights of Δ Tsc2 mice were significantly higher than controls by 5 weeks of age and were accompanied by the development of hyperglycemia and low levels of serum insulin. Formal glucose and insulin tolerance tests confirmed that Δ Tsc2 mice were severely glucose intolerant and mildly insulin resistant. In vitro, calvarial osteoblasts rendered deficient for *Tsc2* had increased levels of phospho-S6 kinase, an indicator of mTOR activation, and differentiated poorly with reduced expression of *runx2* and *osterix* mRNA when compared to controls. Notably, Δ Tsc2 osteoblasts expressed 3-fold higher levels of osteoprotegerin mRNA, suggesting that defective osteoclastogenesis contributed to the dramatic increase in bone volume in the mutant mice. Δ Tsc2 osteoblasts expressed normal levels of IR but were refractory to insulin as evidenced by impaired insulin-stimulated Akt phosphorylation. The blunted insulin responsiveness was associated with decreased levels of IRS-1, elevated levels of markers of ER stress (Chop and Grp78) and increased phospho-JNK levels, changes compatible with known mechanisms for accelerating turnover of IRS-1. Together, our data suggest a model in which IR generated signals converge on *Tsc2* to ensure proper mTOR signaling, which in turn is required for normal osteoblast development and function. We speculate that this same pathway enables negative feedback regulation of insulin signaling in the osteoblast through *Tsc2*/mTOR mediated alterations in ER stress response pathways, which dampen insulin receptor signaling by triggering accelerated IRS-1 turnover.

Disclosures: Ryan Riddle, None.

1002

Neuropeptide Y Receptor Signaling in Osteoblasts is Required for Normal Glucose Homeostasis in Mice. Nicola Lee¹, Daniela Sousa², Ronaldo Enriquez³, Amanda Sainsbury³, Herbert Herzog³, Paul Baldock^{*1}. ¹Garvan Institute of Medical Research, Australia, ²INEB - Instituto de Engenharia Biomedica, Portugal, ³Garvan Institute, Australia

The skeleton has recently emerged as a potential player in the control of whole-body glucose metabolism; however, the mechanism behind this regulatory axis has not been fully elucidated. Here we demonstrate that neuropeptide Y (NPY) receptor signalling in osteoblasts is required for normal glucose metabolism, in addition to bone formation. The osteoblastic NPY receptor (Y1R) was deleted from the osteoblast lineage by crossing Y1R floxed mice with collagen 1 α 1 3.6 Cre mice (Y1R KO_{OB}). In addition, the circulating Y1R ligand, peptide YY (PYY), was over expressed in osteoblasts by crossing collagen 1 α 1 3.6 Cre mice with Cre-inducible PYY transgenic mice, which drives PYY expression through a CMV promoter (PYY TG_{OB}). Mice were examined for glucose homeostasis at 13-14 weeks and culled at 18 weeks of age.

Mice lacking Y1 receptors solely in cells of the osteoblastic lineage displayed a high bone mass phenotype. Cancellous bone volume of the distal femoral metaphysis was greater in Y1R KO_{OB} due to significantly increased mineral apposition rate and bone formation rate. This was an uncoupled response, as the bone resorption marker, osteoclast surface, was reduced. Y1R KO_{OB} mice also displayed altered whole-body glucose metabolism. This was due to significantly decreased pancreatic insulin content, pancreas weight, and decreased insulin secretion leading to elevated glucose levels and reduced glucose tolerance, but with no effect on insulin induced glucose clearance.

Furthermore, increased activity of Y1R signalling induced by over-expression of its ligand, PYY in osteoblastic cells, in PYY TG_{OB} mice also led to impaired glucose tolerance. However, insulin secretion was elevated and insulin sensitivity was impaired. Expression of osteocalcin, ATF4, Esp and Foxo1 in whole bone extracts were unaltered in either model compared to respective wild type.

Together these data reveal a novel mechanism by which NPY receptor signalling in bone tissue is involved in the control of glucose and energy homeostasis. Maintenance of Y1R signalling activity in osteoblasts appears crucial to preservation of optimal glucose homeostasis.

Disclosures: Paul Baldock, None.

1003

Altering AP-1 Transcription via Δ FosB in the Hypothalamus Regulates Bone and Energy Homeostasis through the ARC and VMH Nuclei, Respectively. Kazusa Sato^{*1}, Glenn C Rowe², Min Yin¹, Hiroaki Saito¹, Sutada Lotinun¹, William Horne¹, Roland Baron³. ¹Harvard School of Dental Medicine, USA, ²Beth Israel Deaconess Medical Center, USA, ³Harvard Medical School, Endocrine Unit, Massachusetts General Hospital, & Harvard School of Dental Medicine, USA

Bone homeostasis and energy balance are regulated by endocrine and neural pathways that originate from the hypothalamus. Two nuclei in the mediobasal hypothalamus, the arcuate nucleus (ARC) and ventromedial hypothalamic nucleus (VMH), play a pivotal role in mediating these pathways.

Δ FosB is a naturally truncated form of the AP-1 transcription factor FosB. Overexpression of Δ FosB under the control of the enolase 2 promoter (ENO2), which drives expression in several tissues including bone, white and brown fat, and the brain including hypothalamus, results in increased bone mass and energy expenditure, this latter leading to decreased fat mass. We also have shown that targeted injections of adeno-associated virus (AAV) encoding Δ FosB and DNJunD, an artificial antagonist of AP-1 activity, to the mediobasal hypothalamus in mice phenocopied the observations in ENO2- Δ FosB mice.

To examine the role of ARC and VMH nuclei neurons in Δ FosB-mediated regulations of bone mass and energy balance, we performed chemical lesion of these two nuclei in ENO2- Δ FosB mice and control littermates by monosodium glutamate (MSG) treatment for ARC lesion or gold thioglucose (GTG) for VMH lesion.

MSG treatment induced an osteopenic phenotype in both Δ FosB and control mice. In addition, the increased bone mass in Δ FosB mice was cancelled by MSG treatment. On the other hand, GTG treatment had no effect on bone homeostasis in both Δ FosB and control mice.

Both MSG and GTG treatments progressively promoted obesity as expected. However, MSG-treated Δ FosB mice showed partial but significant suppression in weight and fat gain compared to MSG-treated control mice while GTG-treated Δ FosB mice gained weight and developed adiposity to the same extent as GTG-treated controls.

Consistent with this, increased energy expenditure and improved insulin sensitivity and glucose tolerance in Δ FosB mice were cancelled by GTG-treatment, not by MSG-treatment. GTG-treated Δ FosB mice had exacerbated hyperinsulinemia along with hypertrophic pancreatic islets while these deleterious changes were significantly suppressed in MSG-treated Δ FosB mice.

Overall, these results suggest that hypothalamic signaling downstream of Δ FosB affects bone and energy through two different neuronal circuits: it regulates bone remodeling through MSG-sensitive neurons in ARC nucleus, while mediating energy balance and glucose homeostasis through GTG-sensitive neurons in VMH nucleus.

Disclosures: Kazusa Sato, None.

1004

Reduced Peripheral Leptin Signaling Drastically Decreases Bone Formation. Urszula Iwaniec^{*}, Carmen P. Wong, L. Bailey Lindenmaier, Kenneth Philbrick, Dawn Olson, Russell Turner. Oregon State University, USA

The skeletal abnormalities observed in leptin-deficient ob/ob mice are corrected by long duration central (hypothalamic) leptin gene therapy. However, this finding does not preclude an important role for peripheral leptin in regulation of bone metabolism. To determine the effects of loss of peripheral leptin signaling on bone formation and energy metabolism, we performed bone marrow transplantations where the bone marrow (BM) from wild type (WT) or leptin receptor-deficient db/db donor mice was used to reconstitute the hematopoietic and mesenchymal stem cell compartments in 8-week-old WT recipient mice. Four groups of mice (n=8/group) were studied: 1) untreated leptin receptor-deficient db/db, 2) untreated WT, 3) WT mice that received WT BM (WT to WT), and 4) WT mice that received db/db BM (db/db to WT). Four additional WT mice received BM from GFP donor mice (GFP to WT) to track the reconstitution and differentiation of donor-derived cells. Compared to WT (100%), db/db mice consumed significantly more food (215%), weighed more (226%), had higher blood glucose (325%), and higher white adipose tissue mass (1.762%). WT mice engrafted with db/db BM did not differ in energy homeostasis from untreated WT mice or WT mice engrafted with WT BM. The GFP tracking studies revealed that BM engraftment resulted in quantitative replacement of hematopoietic and mesenchymal lineage cells in spleen and bone marrow, respectively. In contrast, the gene for GFP was not detected in brain tissue. Compared to WT, db/db mice had significantly lower bone formation at the femoral endocortical diaphysis (20%) and cancellous sites in the femur (metaphysis, 31% and epiphysis, 30%) and lumbar vertebra (LV, 37%). This finding indicates that leptin signaling is required for normal bone formation. Bone formation rates in WT mice engrafted with WT BM did not differ from untreated WT mice (diaphysis, 75%; metaphysis, 107%; epiphysis, 103%; and LV5, 100%). In contrast, engraftment of WT mice with cells from db/db donor mice resulted in significantly lower bone formation rates compared to untreated WT mice at all sites examined (diaphysis, 14%; metaphysis, 25%; epiphysis, 25%; and LV, 33%). Bone formation rates in WT mice engrafted with db/db cells did not differ from the low rates observed in untreated db/db mice. In summary, these surprising findings indicate that peripheral leptin is predominantly responsible for the ability of the hormone to maintain bone formation in normal mice.

Disclosures: Urszula Iwaniec, None.

1005

In vivo Fate Mapping identifies Mesenchymal Progenitor Cells. Danka Grcevic¹, SLAVICA PEJDA², DARIO REPIC³, Liping Wang³, Haitao Li³, Mark Kronenberg³, Peter Maye³, Douglas Adams³, David Rowe³, Hector Aguila³, Ivo Kalajzic³. ¹University of Zagreb, Croatia, ²University of Connecticut, USA, ³University of Connecticut Health Center, USA

Adult mesenchymal progenitor cells have enormous potential for use in regenerative medicine. However, the true identity of the progenitors in vivo and its progeny has not been precisely defined. We hypothesize that cells expressing smooth muscle α -actin promoter (α SMA) directed transgene represent mesenchymal progenitors of adult bone tissue. By combining complementary colors in combination with transgenes activating at mature stages of the lineage we confirmed the ability of isolated α SMA⁺ cells to progress from a progenitor to mature osteoblasts and adipocytes. In order to determine whether α SMA promoter can identify cells with progenitor activity in vivo, we generated α SMACreERT2 transgenic mice and we characterized its expression by crossing it with the Ai9 reporter transgenic line to generate α SMACreERT2/Ai9 (SMA9) mice. In vivo lineage tracing experiments using new bone formation model confirmed the osteogenic phenotype of α SMA⁺ cells. The labeling pattern of SMA9 cells defined a small population of cells present in primary spongiosa or within the periosteum two days after tamoxifen induction. No cells expressing SMA9 reporter were detected within the bone matrix. Interestingly, 17 days after the tamoxifen activation we found numerous osteoblast and osteocytes labeled by the transgene. Similarly, in fracture healing model α SMA⁺ cells served as a pool of fibrocartilage and skeletal progenitors. One week following injury we could observe the expansion of SMA9⁺ cells within bone marrow and periosteum. Interestingly, we detected also the presence of SMA9⁺ expressing cells in newly formed chondrogenic areas of the fracture callus, and a numerous areas of osteoblasts. We observed that the osteoblasts derived from SMA9 progenitor cells showed intense deposition of new bone, indicated by the tight correlation between calcein label (green) and tdTomato (red) positive cells. To track more specifically the population of SMA9⁺ cells into mature osteoblast we bred a bone specific transgene into the SMA9 mice. The expression of SMA9⁺ cells co-localized to Col2.3emd expressing mature osteoblasts and osteocytes. This finding was a direct evidence for terminal differentiation of SMA9⁺ cells into mature osteoblast lineage cells. Our findings provide a novel in vivo identification of defined population of mesenchymal progenitor cells with active role in bone remodeling and regeneration.

Disclosures: Ivo Kalajzic, None.

1006

Nestin as a Marker for Bone Marrow Mesenchymal Stem Cells. Xiaoli Zhao^{*1}, Bing Yu¹, Lingling Xian², William Lu³, Mei Wan⁴, Xu Cao¹. ¹Johns Hopkins University, USA, ²Johns Hopkins university school of Medicine, USA, ³The University of Hong Kong, Hong Kong, ⁴Johns Hopkins University School of Medicine, USA

Markers are critical in study of stem cells. Lack of a unique marker has been the challenge in the characterization of bone marrow mesenchymal stem cells (MSCs). Murine bone marrow Sca-1+CD29+CD45-CD11b- cells are recognized MSCs and recruited during bone remodeling. Recent study reveals that nestin+ bone marrow cells contain all the bone-marrow CFU-F activity of MSCs and can self-renew and differentiate into osteoblasts. In this study, we demonstrate that bone marrow nestin+ cells are self-renewal and multi-potential MSCs. We first characterized the nature of nestin+ cells in comparison with Sca-1+CD29+CD45-CD11b- MSCs. GFP-labeled MSCs were isolated from GFP transgenic mice and Sca-1+CD29+CD45-CD11b- or nestin+ MSCs were sorted by fluorescence activated cell sorting (FACS). Further flow cytometry analysis revealed that Sca-1+CD29+CD45-CD11b- cells were 91 percent nestin-positive, and the sorted nestin+ cells were 97 percent Sca-1-positive, indicating that nestin is a marker of MSCs and represent the same population of Sca-1+CD29+CD45-CD11b- cells.

To assess the multilineage differentiation capacity, nestin+ MSCs were cultured in single cell suspensions for single colony forming. Individual and well-separated colonies were selected and individually expanded. Each clonal strain derived from a single CFU-F underwent osteogenic, adipogenic, and chondrogenic induction by different culture media. These clones were capable of osteogenesis, adipogenesis and chondrogenesis. To examine self-renewal of nestin+ MSCs in vivo, GFP+ clonal strains were injected individually into the femur cavity of 8-week-old Rag2^{-/-} mice. GFP+ cells from the injected bone were collected by FACS 8 weeks after injection and plated in culture. This procedure resulted in the generation of secondary CFU-Fs. Importantly, the colonies generated were positive for nestin. The clonal strains were then pelleted, resuspended in matrigel, and injected underneath the renal capsule of Rag2^{-/-} mice to generate heterotopic ossicles for assessing their osteogenic differentiation capacity in vivo. Complete ossicles, including bone, sinusoids, and hematopoietic components, were generated from individual clones. The lining cells on the bone surface and osteocytes in the bone matrix were GFP+, indicating that the donor cells induced osteogenesis. Collectively, our results demonstrate that nestin is a unique marker for Sca-1+CD29+CD45-CD11b- MSCs.

Disclosures: Xiaoli Zhao, None.

1007

A Y Chromosome Gene, Uty, Defines Sexual Dimorphism in Skeletal Phenotype. KAZUKI INOUE^{*1}, Yuuki Imai¹, Shigeki Kato². ¹The University of Tokyo, Japan, ²University of Tokyo, Japan

Males have higher bone mass and larger skeletal size than females. Such gender-specific bone phenotype has considered to be generated by the actions of sex steroid hormones. However, an uncharacterized Y chromosome gene is assumed as a significant factor to form gender-specific bone phenotype from clinical observations of patients mutated in the GCY (Growth Controlling region on the Y chromosome).

To reveal the biological functions of Y chromosome gene in skeletal systems, we ablated mouse *Uty* (Ubiquitously transcribed tetratricopeptide repeat gene, Y chromosome) gene, whose human ortholog is located in the GCY. Using a Cre/loxP system and two step ES gene-targeting methods that are potent to low efficiency of homologous recombination in Y chromosome, successfully, *Uty* gene was genetically disrupted for the first time among the Y chromosome genes. *Uty* knockout mice (*Uty*^{XIL/-}) exhibited short stature with shortened trunk and long bones like wild-type (WT) female littermates, while no endocrine disturbance was detected. In *Uty*^{XIL/-}, the thickness of growth plates, especially at proliferative zone, was significantly reduced when compared with that of WT male littermates. As expected, primary cultured chondrocytes from *Uty*^{XIL/-} showed decreased proliferative ability with increased expression of *Col10a1*, a marker of hypertrophic chondrocytes. These results suggest that *Uty* regulates male skeletal length by controlling cartilage development. Since *Uty* bears a JmjC domain, we assumed *Uty* function as an epigenetic regulator. In a co-immunoprecipitation assay, *Uty* was found to associate with Runx2 and Hdac4, the key factors in chondrocytes differentiation. Consistently, *Uty* was potent to repress transcriptional activity of Runx2 in an OSE-luc assay. A ChIP assay showed that these factors were recruited to the Runx2 target gene (*Col10a1*) promoter. Moreover, recruitment of Hdac4 was reduced and several histone modifications of *Col10a1* promoter were altered in *Uty*^{XIL/-} chondrocytes.

Thus, these findings suggest that *Uty* is a negative regulator for Runx2 by recruiting a transcriptional co-repressor HDAC4, expressed at hypertrophic chondrocytes, and thereby facilitates cartilage development. Taken together, the present study has uncovered a molecular basis of gender-specific cartilage development.

Disclosures: KAZUKI INOUE, None.

1008

Transcriptional Coregulator Jab1 Is Essential for Chondrocyte Differentiation in vivo. Dongxing Chen¹, Bojian Liang¹, Martina Panattoni², Keiko Tamai¹, Ruggero Pard², Brendan Lee³, Guang Zhou^{*1}. ¹Case Western Reserve University, USA, ²Scientific Institute San Raffaele, Italy, ³Baylor College of Medicine & Howard Hughes Medical Institute, USA

Evolutionarily conserved factor Jab1 plays critical roles in cell differentiation, proliferation, and apoptosis by modulating the activity of diverse transcription factors and regulating the output of various signaling pathways. However, Jab1 function in skeletogenesis is largely unknown. In this study, we utilized loxP/Cre system with *Col2a1*-Cre transgene and *Jab1*^{lox} allele to delineate the specific role of Jab1 in cartilage formation. *Col2a1-Cre;Jab1*^{lox/lox} mutants exhibited neonatal lethal chondrodysplasia with severe dwarfism. In E18.5 mutant embryos, all the skeletal elements developed via endochondral ossification were extremely small with severely disorganized chondrocyte columns. *Jab1*-null chondrocytes exhibited increased apoptosis and cell cycle defect. Interestingly, the chondrocytes immediate adjacent to hypertrophic chondrocytes, the presumptive pre-hypertrophic zone, were of abnormally large size and ectopically expressed Runx2, a positive regulator of chondrocyte maturation. Real-time RT-PCR analysis confirmed the increased expression of hypertrophic chondrocyte markers *Col10a1* and *Runx2* in *Jab1* mutants. Jab1 has been shown to directly interact with Runx3 and negatively regulate Runx3 function. Interestingly, in our preliminary study, Jab1 can also inhibit Runx2 transcriptional activity in a dose-dependent manner. Thus, in *Jab1* mutants, chondrocyte maturation is dysregulated likely in part due to up-regulated Runx2 expression. Additionally, our study showed that Jab1 is a novel inhibitor of BMP signaling in chondrocytes. BMP signaling regulates the critical Ihh-Pthrp feedback loop to control chondrocyte differentiation. In *Jab1*-null primary chondrocytes, gene expression profiling analysis revealed heightened expression of BMP targets, including *Ihh* and *Noggin*. The expression of BMP downstream effector, phospho-Smad1/5/8, was also upregulated in *Jab1*-null cartilage. Furthermore, *Jab1*-null primary chondrocytes exhibited an enhanced response to exogenous BMP treatment. Together, our novel study demonstrates that Jab1 is essential for proper cartilage formation in vivo, likely in part by repressing BMP signaling and Runx2 activity. Loss of Jab1 in chondrocytes leads to accelerated chondrocyte hypertrophy and enhanced BMP signaling. We are currently further analyzing the *Jab1* mutant mice to dissect the detailed mechanisms underlining the intricate interaction between Jab1, Runx2, and BMP signaling during chondrocyte differentiation.

Disclosures: Guang Zhou, None.

1009

Notch/Rbpj/Hes1 Signal in Chondrocytes Modulates the Terminal Stage of Endochondral Ossification during Skeletal Growth and Osteoarthritis Development. Yoko Hosaka^{*1}, Taku Saito¹, Shurei Sugita¹, Atsushi Fukai¹, Tomohiro Hikata², Haruhiko Akiyama³, Takashi Nakamura³, Kozo Nakamura⁴, Ung-Il Chung⁵, Hiroshi Kawaguchi⁶. ¹University of Tokyo, Graduate School of Medicine, Japan, ²Keio University School of Medicine, Japan, ³Kyoto University, Japan, ⁴The University of Tokyo, Japan, ⁵University of Tokyo Graduate Schools of Engineering & Medicine, Japan, ⁶University of Tokyo, Faculty of Medicine, Japan

Here we have examined the role of the Notch signaling pathway in chondrocytes during the endochondral ossification process that is essential for skeletal growth and osteoarthritis (OA) development. In cultures of mouse primary costal chondrocytes and chondrogenic ATDC5 cells, Notch1, 2, the transcriptional effector Rbpj, and the target transcription factor Hes1 were strongly expressed in their terminal differentiation stages during Mmp13 and Vegf expression, while Notch3, 4 and other target Hes/Hey members were little expressed throughout the differentiation stages. In the limb cartilage of mouse embryos and in the knee joint cartilage of a mouse experimental OA model with surgical induction of instability, intracellular domains (ICD) of Notch1, 2 were localized in the nucleus of highly differentiated chondrocytes in the hypertrophic zone and in the degraded cartilage, respectively, while they remained in the cytoplasm of less differentiated chondrocytes of the proliferative zone and undegraded cartilage. Rbpj and Hes1 were also co-expressed in the nucleus of highly differentiated chondrocytes, while other Notch ICDs and Hes/Hey members were not detected in either cartilage. We then created conditional knockout mice of Rbpj in chondroprogenitor cells (*Sox9-Cre;Rbpj^{fl/fl}*) and chondrocytes (*Col2a1-Cre;Rbpj^{fl/fl}*). Although the *Sox9-Cre;Rbpj^{fl/fl}* mice died shortly after birth, the embryos exhibited dwarfism with impaired matrix degradation and vascular invasion into the cartilage primordia due to decreases of Mmp13 and Vegf expression. When we created the experimental OA model in a *Col2a1-Cre;Rbpj^{fl/fl}* mouse line with partial Rbpj inactivation causing normal skeletal growth, the knee OA development was suppressed as compared to the *Rbpj^{fl/fl}* littermates, with prevention of the terminal stage of endochondral ossification, similar to the *Sox9-Cre;Rbpj^{fl/fl}* limb cartilage. Retroviral overexpression of Notch1-ICD or Notch2-ICD in ATDC5 cells caused enhancement of Alizarin red S and ALP stainings, as well as Mmp13, Vegf, and Hes1 expression. These effects were inhibited by a Notch inhibitor DAPT. Luciferase analyses revealed that the Hes1 transfection enhanced the *Mmp13* and *Vegf* promoter activity most potently among the Hes/Hey members. In conclusion, the Notch/Rbpj/Hes1 signal in chondrocytes modulates the terminal stage of endochondral ossification during skeletal growth and OA development, indicating it to be a possible therapeutic target of OA.

Disclosures: Yoko Hosaka, None.

1010

Notch Inhibits Nuclear Factor of Activated T-Cells (NFAT) Transactivation in Primary Epiphyseal Chondrocytes In Vitro. Stefano Zanotti^{*}, Maria Monarca, Ernesto Canalis. St. Francis Hospital & Medical Center, USA

Notch proteins are transmembrane receptors that determine lineage specification between neighboring cells. In the canonical signaling pathway, activation of Notch receptors results in the cleavage, release and nuclear translocation of the Notch intracellular domain (NICD). In the nucleus, NICD interacts with C Promoter Binding Factor 1, Suppressor of Hairless and Lag-1 (CSL) to activate the transcription of target genes, such as *Hairy enhancer of split (Hes)* or *Hes related with YRPW motif (Hey)*. Conditional overexpression of NICD in cartilage impairs endochondral bone formation. However, the mechanisms involved have not been defined. Nuclear Factor of Activated T-Cells (NFAT)c1 to c4 are transcription factors that determine cell differentiation and function, and NFAT signaling is required for chondrogenic differentiation *in vitro*. *Nfatc2* null mice display lesions reminiscent of osteoarthritis, although this may be the consequence of B- and T-cell proliferation and dysregulated cytokine synthesis. We postulated that Notch could act in cartilage through the regulation of NFAT signaling. The mechanisms of Notch action were studied in primary epiphyseal chondrocytes harvested from the fore and hind limbs of 3 to 5 day old *Rosa^{Notch}* mice. In this model, delivery of Cre recombinase induces the excision of a STOP cassette flanked by *loxP* sequences, allowing expression of NICD under the control of the *Rosa26* promoter. Adenoviral vectors where the cytomegalovirus promoter directs the expression of Cre recombinase were used to induce Notch. Notch transactivated a reporter construct where 12 copies of a CSL consensus sequence control *Luciferase* expression. Accordingly, Notch induced the activity of fragments of the *Hes1*, *Hey1* and *Hey2* promoters and increased Hes1, Hey1 and Hey2 transcript levels, confirming the validity of the *Rosa^{Notch}* model to investigate the role of Notch signaling in cartilage. In agreement with the impaired chondrogenesis observed in Notch transgenic mice, overexpression of Notch in chondrocytes suppressed collagen type II $\alpha 1$ transcripts. Furthermore, Notch inhibited NFAT transactivation. Since NFAT is required for chondrogenesis, these results suggest that the effects of Notch on this process could be mediated by a downregulation of NFAT activity. In conclusion, Notch impairs chondrogenesis and suppresses NFAT transactivation in chondrocytes.

Disclosures: Stefano Zanotti, None.

1011

C/EBP- β and RUNX2 Cooperatively Control Cartilage Degradation with MMP-13 as the Target and HIF-2 α as the Inducer in Chondrocytes. Makoto Hirata^{*1}, Fumitaka Kugimiyama², Atsushi Fukai¹, Taku Saito³, Akihiko Mabuchi¹, Bishwa Raj Sapkota¹, Toru Akune¹, Fumiko Yano⁴, Toshivuki Ikeda¹, Nao Nishida¹, Noriko Yoshimura⁵, Takumi Nakagawa¹, Kozo Nakamura⁴, Katsushi Tokunaga⁶, Ung-Il Chung⁷, Hiroshi Kawaguchi⁶. ¹University of Tokyo, Japan, ²Sensory & Motor System Medicine, University of Tokyo, Japan, ³University of Tokyo, Graduate School of Medicine, Japan, ⁴The University of Tokyo, Japan, ⁵22nd Century Medical & Research Center, University of Tokyo, Japan, ⁶University of Tokyo, Faculty of Medicine, Japan, ⁷University of Tokyo Graduate Schools of Engineering & Medicine, Japan

The endochondral ossification is a crucial process in normal skeletal growth and osteoarthritis (OA) development. Aiming at elucidation of the molecular mechanism underlying this process and identification of therapeutic targets for OA, we examined the signal network around CCAAT/enhancer-binding protein- β (C/EBP- β), a regulator of chondrocyte functions. Computational predictions and a C/EBP motif-reporter assay identified RUNX2 as the most potent transcriptional partner of C/EBP- β in chondrocytes. Both C/EBP- β and RUNX2 were co-expressed in the terminal differentiation stage of chondrocytes in several cell culture systems, in the mouse limb cartilage, and in the OA joint cartilage of mice and humans. To determine the involvement of C/EBP- β and RUNX2 in the endochondral ossification process, we generated their compound knockout mice: *Cebpb^{-/-};Runx2^{+/-}* and *Cebpb^{+/-};Runx2^{-/-}*, because *Runx2^{-/-}* mice died just after birth. The *Cebpb^{-/-};Runx2^{+/-}* mice showed more severe dwarfism than the *Cebpb^{-/-}* and *Runx2^{+/-}* littermates with impaired cartilage degradation but unaffected chondrocyte differentiation. Although *Cebpb^{+/-};Runx2^{+/-}* mice showed normal skeletal growth, they exhibited greater suppression of knee OA development in surgical and age-related OA models than their *Cebpb^{+/-}* and *Runx2^{+/-}* littermates. Histological analyses in the limb cartilage and the OA joint cartilage showed that the compound knockout caused a considerable decrease of matrix metalloproteinase-13 (MMP-13) among various factors related to endochondral ossification. In cultured chondrocytes, C/EBP- β and RUNX2 cooperatively enhanced endogenous expression and promoter activity of *MMP13* shown by real-time RT-PCR and luciferase assay. The specific and direct binding of C/EBP- β and RUNX2 as a protein complex to a C/EBP-binding motif and an OSE2 motif in the *MMP13* promoter was shown by EMSA and ChIP-reIP assay. Lastly, to identify the upstream mechanism, we performed a screening of transcription factors using a human *CEBPB* promoter fragment among putative factors regulating chondrocyte differentiation, and identified hypoxia-inducible factor-2 α (HIF-2 α) as the most potent and functional inducer of C/EBP- β expression in chondrocytes through specific binding to a hypoxia-responsive element. In conclusion, C/EBP- β and RUNX2, with MMP-13 as the target and HIF-2 α as the inducer, cooperatively control cartilage degradation. This molecular network in chondrocytes may represent a therapeutic target for OA.

Disclosures: Makoto Hirata, None.

1012

Two Major microRNA Species in Chondrocytes, miR-140 and let-7 miRNAs, Regulate Endochondral Bone Growth through Distinct Mechanisms. Jennifer Inloes^{*}, Tatsuya Kobayashi. Massachusetts General Hospital, USA

microRNAs (miRNAs) regulate gene expression at the post-transcriptional level. In chondrocytes, a few hundred miRNAs are present at detectable levels. Global miRNA deficiency in mouse chondrocytes causes skeletal dysplasia with reduced chondrocyte proliferation and accelerated post-mitotic hypertrophic differentiation; however, the physiological roles of individual miRNAs in endochondral bone development remain largely unknown. The chondrocyte-specific miRNA, miR-140 (encoded by *Mir140*), and the let-7 miRNAs are some of the most abundantly expressed miRNAs in chondrocytes. To investigate the roles of these miRNAs, we generated *Mir140*-null mice and mice expressing *Lin28*, a protein that suppresses let-7 miRNA expression. *Mir140*-null mice exhibit mild longitudinal skeletal growth defects and shortened naso-occipital length due to impaired endochondral bone growth. *Mir140*-null chondrocytes show normal proliferation but also show a reduction in size of the columnar proliferating zone and an increase in size of the resting zone, suggesting that *Mir140* negatively regulates resting chondrocyte differentiation. *Lin28* overexpression in chondrocytes reduces most let-7 miRNAs with the exception of let-7c. Known let-7 target genes, including *Hmga2* and *Igf2bp2*, were upregulated. Mice overexpressing *Lin28* in chondrocytes show few gross growth defects, but their growth plate chondrocytes show significantly reduced proliferation, increased cell death, altered cell morphology, and disorganized extracellular matrix. *Mir140*-null and *Lin28* transgenic compound mutants show growth defects that are significantly more severe than those of single mutant mice, suggesting a synergistic regulation of endochondral bone growth by *Mir140* and let-7 miRNAs. The growth plate of compound mutants shows an increase in size of the resting zone, decreased cell proliferation, and shortening of the columnar zone, a phenotype containing features of both *Mir140*-null and *Lin28* transgenic mice. These results demonstrate that miR-140 and let-7 miRNAs cooperatively regulate endochondral bone growth through distinct pathways; miR-140 regulates cell differentiation, while let-7 miRNAs regulate cell proliferation and survival.

Disclosures: Jennifer Inloes, None.

1013

Targeting the TGF- β /Smad Pathway in Neurofibromatosis Type 1 Skeletal Defects. Steven Rhodes^{*1}, Yongzheng He¹, Xiaohua Wu¹, Lisa Hong Chen¹, Ping Zhang², Shi Chen¹, Chang Jiang³, Hiroki Yokota³, Xianghong Peng¹, Khalid Mohammad¹, Theresa Guise¹, Feng-Chun Yang¹. ¹Indiana University, USA, ²Indiana University School of Medicine, USA, ³Indiana University Purdue University Indianapolis, USA

Neurofibromatosis type 1 (NF1) is a common genetic disorder that arises from mutations in the NF1 gene that encodes Neurofibromin, a negative regulator of Ras. In addition to the hallmark soft tissue tumors, NF1 patients experience skeletal pathologies including osteoporosis and pseudarthrosis of the tibia – non-union fractures that have no medical therapy and often require amputation. Here, we establish that transforming growth factor-beta1 (TGF- β 1), a critical cytokine for skeletal development and homeostasis, is overexpressed by *Nf1*^{+/+} osteoprogenitors resulting in pathological bone remodeling.

We found that TGF- β 1 was overexpressed by 2-3 fold in *Nf1*^{+/+} osteoprogenitors vs. WT controls, quantified at both the mRNA and protein level by RT-PCR and ELISA. Differentiation assays were also performed to assess the effects of TGF- β 1 on osteoclast and osteoblast development. We found that TGF- β 1 promoted osteoclast formation *in vitro* while inhibiting terminal osteoblast differentiation. Moreover, *Nf1*^{+/+} osteoprogenitors and osteoclasts were hyperresponsive to limiting doses of TGF- β 1, correlating with increased phosphorylation of Smad2 by western blot. Importantly, a pharmacologic TGF- β inhibitor, SD-208, blocked Smad phosphorylation and enhanced osteoblast differentiation in TGF- β treated osteoprogenitors *in vitro*.

As an *in vivo* proof of concept, SD-208 (60 mg/kg/day) was administered by gavage in an ovariectomy (OVX) model of NF1 associated osteoporosis to determine whether blocking TGF- β dependent Smad phosphorylation could restore bone mass in *Nf1*^{+/+} mice. BMD and trabecular microarchitecture were assessed by pDEXA and micro-CT. Static and dynamic bone histomorphometry were also performed. We found that *Nf1*^{+/+} OVX mice lost significantly more bone than both WT OVX mice and sham operated controls. SD-208 treatment restored bone mass and trabecular architecture in both WT and *Nf1*^{+/+} OVX mice as compared to vehicle treated controls. Intriguingly, the *Nf1*^{+/+} OVX mice exhibited a greater response to the SD-208 treatment as compared to WT OVX controls, suggesting that the TGF- β /Smad pathway may be a critical effector in the NF1 pathological bone remodeling process. Further study is warranted to investigate the potential clinical application of TGF- β inhibitors as a novel therapy for NF1 osseous defects such as osteoporosis, and particularly pseudarthrosis, where current treatments are lacking.

Disclosures: Steven Rhodes, None.

1014

Plekhl1 is Essential for Bone Resorption in Mice and Regulates Cathepsin K Secretion through Linking Lysosomes to Microtubules in Osteoclasts. Shiqiao Ye^{*1}, Kai Liang², Yi-Ping Li³, Stavros Manolagas¹, Haibo Zhao¹. ¹University of Arkansas for Medical Sciences, USA, ²Department of Dermatology, University of Arkansas for Medical Sciences, USA, ³University of Alabama at Birmingham, USA

PLEKHM1 is the causative gene of osteopetrosis in *ia/ia* rats as well as a subset of patients with intermediate osteopetrosis. However, whether Plekhl1 is essential for bone homeostasis and resorption in mice and the molecular mechanisms of its action in osteoclasts (OCs) remain unknown. To address these issues and to facilitate further mechanistic studies, we have generated a Plekhl1 floxed mouse line in which exon 3 of the murine PLEKHM1 gene was flanked by two LoxP sites. To obtain Plekhl1 OC conditional knockout (cKO) mice we crossed floxed Plekhl1 and Cathepsin K-Cre (CTSK-Cre) transgenic mice, thereby deleting the Plekhl1 gene only in OCs. The progeny of Plekhl1^{+/+};CTSK-Cre and Plekhl1^{Flox/Flox};CTSK-Cre were designated Plekhl1 wild type (WT) and Plekhl1 OC cKO mice, respectively. Ablation of Plekhl1 protein expression in cKO OCs was confirmed by western blots. The development and tooth eruption of Plekhl1 cKO mice were normal, but the animals had increased bone mass at 1 and 2 months of age as assessed by longitudinal measurements of BMD by DEXA, as compared to WT mice. Impaired bone resorption in Plekhl1 cKO mice was reflected by a decreased serum Ctx-I level. While OC differentiation was indistinguishable between Plekhl1 WT and cKO bone marrow macrophage cultures, the resorptive capacity of OCs lacking Plekhl1 was compromised as revealed by a significant decrease in resorption pits formation and a diminished medium Ctx-I level. Moreover, double staining of CTSK and F-actin by immunofluorescence showed an inhibition of CTSK secretion into the resorption lacuna in Plekhl1-depleted OCs. Consistent with cell autonomous functions of Plekhl1 in OCs, the impaired bone resorption and CTSK secretion in Plekhl1-null OCs were normalized by retroviral expression of WT full-length but not the N-terminal half and the C-terminal half fragments of the protein. Furthermore, we have uncovered that the N-terminal localized RUN and PH1 domains of Plekhl1 mediate its interaction with LIS1, a critical molecule regulating microtubule dynamics and the function of cytoplasmic dynein, a microtubule-based motor complex. The extreme C-terminal region of Plekhl1 is responsible for lysosomal and the ruffled border targeting and the binding of Plekhl1 to Rab 7, a small GTPase regulating lysosome biogenesis and trafficking. Thus, Plekhl1 is a lysosomal adaptor protein linking

lysosomes to microtubules in OCs and is essential for OC bone resorption *in vivo* and *in vitro*.

Disclosures: Shiqiao Ye, None.

1015

Increased Osteoclast Formation and Bone Resorption in the Brtl Osteogenesis Imperfecta Mouse Occur through Marrow Mesenchymal Stromal Cell and Abnormal Matrix Dependent Mechanisms. Patricia Collin-Osdoby^{*1}, Linda Rothe¹, Matthew Kwong¹, Wayne Cabral², Rajeev Aurora³, Joan C. Marini⁴, Philip Osdoby¹. ¹Washington University in St. Louis, USA, ²NIH, NICHD, USA, ³St Louis University, USA, ⁴NIH NICHD, USA

Brtl mice, which contain a glycine substitution (G349C) in half of their type I collagen α 1(I) chains, provide a valuable model for investigation of the pathogenesis and treatment of moderately severe osteogenesis imperfecta. In addition to a smaller body size, reduced cortical and trabecular bone volumes, and matrix insufficiency, Brtl mice exhibit abundant osteoclasts (OCs), brittle bones, and an increased propensity to fracture. Bone sections from Brtl vs. WT mice have increased OC numbers, sizes, TRAP stain intensities, and associated *in vivo* bone resorption. The mechanisms responsible for stimulating OC formation and bone resorption in Brtl OI mice are not yet clear. Although RANKL and OPG mRNA and protein levels are increased in Brtl vs. WT bones and in mesenchymal stromal cells (MSCs) cultured from such bones, RANKL/OPG ratios are equivalent and therefore not a simple explanation for the increased OC formation and activity in Brtl mice. Moreover, RANKL-induced OC formation *in vitro* from pre-OC marrow cells is higher in Brtl vs. WT cultures. This suggests a greater RANKL sensitivity and/or an expanded OC precursor pool exists in Brtl marrow, in keeping with our finding of higher RANK mRNA levels in Brtl bones and greater numbers of CD11b⁺ myeloid precursors in Brtl marrow by FACS analysis. In mixed co-cultures of Brtl or WT marrow pre-OCs with Brtl or WT MSCs, OC formation was 2-fold greater only when Brtl MSCs were present and was independent of the pre-OC origin (Brtl or WT). Therefore, Brtl MSCs are both necessary and sufficient for driving enhanced osteoclastogenesis in co-cultures with marrow pre-OCs. RT-PCR microarray profiling revealed key cytokines and other signals that are altered in Brtl vs. WT MSCs and may mediate these actions. Furthermore, the abnormal collagenous OI bone matrix in Brtl mice appears particularly prone to OC degradation. The seeding of pre-OCs onto Brtl vs. WT isolated calvarial bone did not influence RANKL-induced OC formation, whereas Brtl bone markedly stimulated the activity of individual OCs and overall bone turnover. Overall, we conclude that increased formation and function of bone-resorbing OCs in Brtl OI mice is multifaceted and involves an expanded OC precursor pool, crucial MSC-derived regulatory signals that drive elevated osteoclastogenesis, and increased activation of OCs to resorb the abnormal collagenous OI matrix. Further elucidation of these pathways may lead to novel therapeutic approaches for OI.

Disclosures: Patricia Collin-Osdoby, None.

1016

The V-ATPase a3 Subunit Mutation R740S Results in Osteoclast Apoptosis Due to Uncoupled ATP Hydrolysis in Homozygous Mice. Noelle Ochotny^{*1}, Ann Flenniken², Celeste Owen³, Irina Voronov¹, Morris Manolson⁴, Jane Aubin⁵. ¹University of Toronto, Canada, ²Centre for Modeling Human Disease, Samuel Lunenfeld Research Institute, Mount Sinai Hospital, Canada, ³Centre for Modeling Human Disease, Samuel Lunenfeld Research Institute, Mt Sinai Hospital, Canada, ⁴University of Toronto, Canada, ⁵University of Toronto Faculty of Medicine, Canada

Osteoclast-mediated acidification via a vacuolar-type H⁺-ATPase (V-ATPase) is necessary for bone resorption. V-ATPases are proton pumps composed of 14 subunits, including the 'a' subunit. Of the 4 'a' isoforms in mammals, a3 is enriched in osteoclasts where it is essential for bone resorption. Humans with mutations to both a3 alleles are severely osteopetrotic and die within 6 years without treatment. The two mouse models for osteopetrosis that lack a3, *Tcirl*^{-/-} and *ocloc*, survive for 4-6 weeks. During a mouse genome-wide mutagenesis screen for dominant mutations affecting bone mineral density, we identified a mouse with an osteopetrotic phenotype carrying the dominant V-ATPase a3 missense mutation, R740S. While all osteoblast parameters appear normal, *Tcirl*^{R740S/R740S} pups have osteopetrotic features like increased trabecular bone, no marrow spaces and widening of growth plates. Despite normal size and weight at birth, whole mount staining of *Tcirl*^{R740S/R740S} pups reveal a poorly mineralized mandibular chondyle. By day 10, *Tcirl*^{R740S/R740S} pups can be distinguished from their WT littermates by a lack of incisor eruption, smaller size and weight. Transmission electron microscopy analysis of newborn *Tcirl*^{R740S/R740S} bones reveals abnormal looking osteoclasts with poorly developed ruffled borders, while 14 day old *Tcirl*^{R740S/R740S} pup long bones contain numerous osteoclasts with an abnormal apoptotic-like morphology. TUNEL staining confirms that most of the osteoclasts from 14 day old *Tcirl*^{R740S/R740S} pups undergo apoptosis. In contrast, osteoclasts from *Tcirl*^{-/-} and *ocloc* mice are normal in appearance and number, but fail to resorb. We attempted but failed to isolate primary osteoclasts from long bones of 4 day old *Tcirl*^{R740S/R740S} mice. We therefore generated osteoclasts *in vitro* from RANKL-MCSF treated spleen cells of 4 day old

Tcirl^{R740S/R740S} and WT pups. Osteoclasts from *Tcirl^{R740S/R740S}* pups express the $\alpha 3$ subunit as revealed by western blotting. Preliminary studies demonstrate that the *Tcirl^{R740S/R740S}* osteoclast membranes have similar rates of concanamycin-sensitive ATP hydrolysis to WT. Our data leads us to hypothesize that *Tcirl^{R740S/R740S}* osteoclasts undergo apoptosis due to depletion of cellular ATP levels caused by the uncoupling of V-ATPase-dependent ATP hydrolysis from proton translocation. We are measuring cellular ATP levels and proton pumping of osteoclast membranes to test this hypothesis.

Disclosures: Noelle Ochotny, None.

1017

Embryonic Loss of Cytochrome P450 Reductase in Mice Results in Antley-Bixler Syndrome-Like Craniofacial and Bone Mass Defects. Satya Panda¹, Anyonya Guntur², Rekha Kar³, Kejian Tang¹, Bettie Sue Masters¹. ¹UTHSCSA, USA, ²Maine medical center research institute, USA, ³The University of Texas Health Science Center, USA

Craniosynostosis and midface hypoplasia are among the most common dysmorphic features of patients harboring mutations in NADPH-cytochrome P450 oxidoreductase (CYPOR) and are similar to the phenotypes of Antley-Bixler syndrome patients. Patients with CYPOR deficiency, caused by mutations in the reductase (of which >40 have been reported), also present with ambiguous genitalia and abnormal steroidogenic profiles. CYPOR is the obligate electron donor for cytochromes P450, dehydrocholesterol reductase, heme oxygenase, squalene monooxygenase, and cytochrome b₅. These enzymes play various physiological roles, including endo- and xeno-biotic metabolism, cholesterol biosynthesis, and heme degradation. The complete knockout of CYPOR in mice leads to embryonic lethality. In order to probe the possible roles played by CYPOR during bone development, we have generated conditional knockout mice by cross breeding *Cyp^{lox/lox}* and Dermo 1 (Twist 2) Cre mice. Dermo 1 Cre recombinase is active from embryonic day of 9.5 and will delete the gene of interest in both chondrocytes and osteoblasts. Here we report the first mouse model showing craniofacial abnormalities upon deletion of CYPOR. Differential staining of CKO mice skulls using Alizarin red and Alcian blue show premature fusion of spheno-occipital synchondrosis (SOS) and anterior intraoccipital synchondrosis (AIS). Malocclusion was also noticed in a few adult knockout mice, leading to unusual growth of the lower incisors. Micro CT analysis of the tibia samples showed the deletion of CYPOR also caused a reduction in the bone mineral density compared to its age- and sex-matched littermate control sample without affecting the cortical bone thickness. Shorter long bones were also observed in these mice using hematoxylin and eosin staining of paraffin-embedded tissue sections. These results recapitulate the human CYPOR deficiency phenotype and offer an approach to study the sequelae of mutations in NADPH-cytochrome P450 reductase.

Disclosures: Satya Panda, None.

1018

BMN 111, a CNP Analogue, Promotes Skeletal Growth and Rescues Dwarfism In Two Transgenic Mouse Models of Fgfr3-related Chondrodysplasia. Florence Lorget¹, Nabil Kaci², Jeff Peng¹, Catherine Benoist², Federico Di Rocco², Emilie Mugniery², Sherry Bullens¹, Stuart Bunting¹, Laurie Tsuruda¹, Charles O'Neill¹, Arnold Munnich², Laurence Legeai-Mallet². ¹BioMarin Pharmaceutical Inc, USA, ²INSERM U781 - Universite Paris Descartes, Hopital Necker, France

Although Fgfr3-related chondrodysplasia were identified more than 20 years ago, no corrective treatments are available and therapeutic interventions are limited to surgical procedures. Achondroplastic patients display a short stature with disproportionate shorter proximal bones, narrow trunk and macrocephaly. The severity of the phenotype ranges from mild (hypochondroplasia) to severe (achondroplasia) and lethal (thanatophoric dysplasia) depending on the point mutation. C-type natriuretic peptide (CNP) is considered to be a potential therapeutic agent because of its inhibition of Fgfr3 downstream signaling. Targeted in vivo overexpression of a CNP transgene or continuous infusion of native CNP were shown to rescue the impaired bone growth in a mouse model of achondroplasia. To overcome the short half-life of native CNP, BioMarin developed a CNP analogue, BMN111, with an increased half-life allowing daily subcutaneous administration. BMN111 pharmacological activity was characterized in two transgenic mouse models of Fgfr3-related chondrodysplasia. In the Fgfr3G380R mouse model(1), the transgene expression is restricted to the chondrocytes while it is ubiquitously expressed in the Fgfr3Y367C/+ mouse model(2). A more severe phenotype is observed with the Fgfr3Y367C/+ (shorter bones, pronounced prognathism and reduced lifespan). The mice received daily subcutaneous administrations of BMN111 from 6 days of age in the Fgfr3Y367C/+ mice and three weeks of age in the Fgfr3G380R mice, supporting both achondroplastic and hypochondroplastic pediatric populations. The Fgfr3Y367C/+ mice were treated for 10 days at dose levels up to 800 ug/kg. The Fgfr3G380R mice were treated for 5 weeks at dose levels up to 280 ug/kg. Overall, the treatment was well tolerated. A dose related increase in the axial and appendicular skeletons was measured in both models (~5-10% increase in the high dose groups). Normalization of bone age and growth plate architecture was observed in the Fgfr3Y367C/+ mice. Based on these data, BMN111 may be a potential therapeutic agent for achondroplasia and hypochondroplasia.

References:

- 1) Naski MC et al. Repression of hedgehog signaling and BMP4 expression in growth plate cartilage by fibroblast growth factor receptor 3. Development. 1998 Dec;125(24):4977-88
- 2) Pannier S et al. Activating Fgfr3 Y367C mutation causes hearing loss and inner ear defect in a mouse model of chondrodysplasia. Biochim Biophys Acta. 2009 Feb;1792(2):140-7.

Disclosures: Florence Lorget, BioMarin, 3

This study received funding from: BioMarin Pharmaceutical Inc

1019

Inflammatory Markers and the Risk of Hip and Spine Fractures in Older Men: MrOS. Jane Cauley¹, Yona Keich Cloonan², Michelle Danielson², Kristine Ensrud³, Howard Fink⁴, Eric Orwoll⁵, Robert Boudreau². ¹University of Pittsburgh Graduate School of Public Health, USA, ²University of Pittsburgh, USA, ³Minneapolis VA Medical Center / University of Minnesota, USA, ⁴GRECC, Minneapolis VA Medical Center, USA, ⁵Oregon Health & Science University, USA

Cytokines play major roles in regulating bone remodeling in the bone microenvironment but their relationship to incident fractures in older men is uncertain. Using data from the Osteoporotic Fracture in Men Study (MrOS), we tested the hypothesis that men with higher levels of circulating cytokines at baseline will have a higher risk of fracture. We used a case-cohort design and measured cytokines in a random sample of 980 men and in 538 men with incident fractures including 98 clinical spine fractures and 97 hip fractures. Average follow up was 6.96 years. Levels of pro-inflammatory cytokines including interleukin (IL)-6, high sensitivity C-reactive protein (CRP), tumor necrosis factor (TNF- α), soluble receptors (SR) of IL-6 (IL-6SR) and TNF (TNF-SR1 and TNF-SR2); IL-10, an anti-inflammatory cytokine, was also measured. Cytokines and SR were measured in fasting frozen serum using ELISA. CRP assay was standardized according to the WHO International Reference Standard. Average inter-assay coefficients of variations ranged from 1.5 to 10.7%. Total hip BMD was measured by DXA. The risk of non-spine, hip and clinical spine fracture was compared across quartiles of cytokines (quartile 1=referent) using Cox proportional hazard models. Quartile cutoffs were determined based on the distributions in the random cohort. Tests for linear trend were performed. The average age of men was 73.8y (random cohort) and 75.3y (fracture cases); 92% were Caucasian. In multivariable adjusted models, the risk of hip and clinical spine fracture increased with increasing TNF- α , TNF-SR1, TNF-SR2 and IL-6. Men with the highest cytokines (Q4) had a 1.9-4.35 fold higher risk of hip and clinical spine fracture than men with the lowest cytokine (Q1), Table. Similar results were observed for all non-spine fractures but the magnitude of the association was lower (data not shown). There was no association between CRP and IL-6SR. Men with the highest IL-10 (Q4) had a 41% lower risk of hip fracture and a 64% lower risk of spine fracture compared to men with the lowest IL-10. We conclude that inflammation plays an important role in the etiology of fractures in older men.

Table: Multivariable* adjusted hazard ratio (95% CI) for hip and clinical spine fractures across quartiles (Q) of cytokine

Hip Fractures					
	Quartiles				
	Q1	Q2	Q3	Q4	P trend
TNF- α	Ref	3.33 (1.4, 8.0)	2.41 (1.0, 6.0)	2.60 (1.1, 5.9)	0.022
TNF-SR1	Ref	0.92 (0.3, 2.9)	3.5 (1.3, 9.9)	3.3 (1.1, 9.6)	<0.0001
TNF-SR2	Ref	1.86 (0.7, 5.3)	1.7 (0.6, 4.8)	2.83 (1.0, 7.1)	0.014
CRP	Ref	1.33 (0.6, 3.2)	0.79 (0.3, 2.0)	1.17 (0.5, 2.8)	0.94
IL-6	Ref	1.28 (0.5, 3.2)	1.63 (0.7, 4.0)	2.22 (0.9, 5.6)	0.019
IL-6SR	Ref	0.62 (0.3, 1.5)	1.19 (0.6, 2.6)	0.77 (0.4, 1.7)	0.95
IL-10	Ref	1.24 (0.6, 2.8)	0.68 (0.3, 1.6)	0.59 (0.2, 1.5)	0.026
Clinical Spine Fractures					
	Quartiles				
	Q1	Q2	Q3	Q4	P trend
TNF- α	Ref	1.52 (0.7, 3.6)	2.25 (1.0, 5.1)	2.33 (1.1, 5.1)	0.004
TNF-SR1	Ref	0.87 (0.3, 2.3)	3.66 (1.6, 8.6)	4.35 (1.7, 11.2)	<0.0001
TNF-SR2	Ref	0.76 (0.3, 1.9)	2.46 (1.1, 5.44)	4.02 (1.8, 9.1)	<0.0001
CRP	Ref	0.69 (0.3, 1.5)	0.69 (0.3, 1.5)	1.15 (0.6, 2.4)	0.63
IL-6	Ref	1.37 (0.7, 2.9)	1.52 (0.7, 3.2)	1.94 (0.9, 4.1)	0.037
IL-6SR	Ref	0.70 (0.3, 1.5)	1.01 (0.5, 2.1)	1.00 (0.5, 2.0)	0.60
IL-10	Ref	0.50 (0.3, 1.0)	0.33 (0.2, 0.7)	0.26 (0.1, 0.5)	<0.001

*Ref=referent; adjusted for age, race, site, height, weight, smoking, alcohol intake, physical activity, calcium intake, diabetes, osteoarthritis, stroke, COPD, CHD, NSAIDs, statins, corticosteroids, fracture history, total hip BMD.

Disclosures: Jane Cauley, None.

1020

Serum OPG and sRANKL Levels and Incident Hip Fracture in the Women's Health Initiative. Andrea LaCroix¹, Rebecca Jackson², Aaron Aragaki¹, Charles Kooperberg¹, David Duggan³. ¹Fred Hutchinson Cancer Research Center, USA, ²The Ohio State University, USA, ³Translational Genomics Research Institute, USA

The discovery of osteoprotegerin (OPG) in 1997 led quickly to the understanding that the OPG/RANKL/RANK System is central to the coupling of osteoclasts and osteoblasts in bone biology. However, large epidemiologic studies relating new generation, high sensitivity serum biomarkers in this pathway to future risk of hip fractures have not yet been reported. We conducted a nested case-control study within the Women's Health Initiative Observational Study. 400 incident hip fracture cases that occurred between baseline (1993-1998) and September 2005 were randomly selected and individually matched to randomly selected controls who reported no postmenopausal fractures at baseline and were free of hip fracture during follow-up. Case-control pairs were Caucasian and matched on age (+/-1yr), enrollment date (+/-365 days) and current hormone therapy use at baseline (exact). OPG and soluble RANKL (sRANKL) were measured by ELISA (Osteoprotegerin EIA, and ampli-sRANKL EIA, Biomedica distributed by American Laboratory Products Company, LTD; Salem, NH) at Ohio State University. Odds ratios for quartiles of each serum biomarker (defined by the control distribution) were computed from conditional logistic regression models adjusting for the matching variables, plate, and WHO FRAX score. No association was observed between sRANKL and hip fracture (p-trend=0.25) or the ratio of OPG/sRANKL (p-trend=0.27). OPG levels in the highest quartile were associated with a two-fold increased risk of hip fracture as shown in the table below. These results are consistent with a recent study showing an association of higher OPG levels (but not RANKL or OPG/RANKL levels) with height loss in men and postmenopausal women not using hormone therapy. We conclude that high serum OPG levels are associated with an increased risk of hip fracture in postmenopausal women.

Quartile (range)	OddsRatio (95% CI)	p-value for trend (1 df)
1 (< 4.0 pmol/L)		0.005
2 (4.0-5.0 pmol/L)	1.40 (0.89-2.19)	
3 (5.0-6.0 pmol/L)	1.24 (0.78-1.96)	
4 (> 6.0 pmol/L)	2.11 (1.32-3.37)	

WHI OPG and Fracture Table

Disclosures: Andrea LaCroix, None.

1021

High Sensitive CRP Is an Independent Risk Factor for Fractures in Elderly Men: The MrOS Sweden Study. Sofia Moverare Skrtic¹, Anna-Lena Eriksson², Osten Ljunggren³, Magnus Karlsson⁴, Dan Mellstrom⁵, Claes Ohlsson⁶. ¹Center for Bone & Arthritis Research at the Sahlgrenska Academy, Sweden, ²University of Gothenburg, Sweden, ³Uppsala University Hospital, Sweden, ⁴Skane University Hospital Malmo, Lund University, Sweden, ⁵Sahlgrenska University Hospital, Sweden, ⁶Center for Bone Research At the Sahlgrenska Academy, Sweden

Background: Osteoporosis-related fractures constitute a major health concern not only in women but also in men. Chronic inflammatory diseases are associated with an enhanced fracture risk. However, it is still unclear whether low-grade inflammation as estimated by high sensitivity C-reactive protein (hs-CRP) is associated with an increased fracture risk in men.

Methods: To investigate the predictive role of hs-CRP, serum levels of hs-CRP were measured in elderly men (n = 2910, mean 75 years of age) included in the prospective population-based MrOS Sweden cohort, using ultrasensitive immunoturbidimetry. Fractures occurring after the baseline visit were validated (average follow-up at analyses 5.4 years). The incidence for having at least one validated fracture after baseline was 23.7/1000 person-years.

Results: In hazard regression analyses adjusted for age, weight and height, hs-CRP was related to fracture risk. Study participants were divided into tertile groups based on their serum levels of hs-CRP. Serum levels of hs-CRP were [<1.812], [≥ 1.812 , <2.760] and [≥ 2.760] mg/L in the lowest, medium and highest tertiles, respectively. The HR of fracture for the highest tertile of hs-CRP, compared with the lowest and the medium tertiles combined, was 1.54 (95% CI, 1.25-1.89). Femoral neck BMD was not associated with hs-CRP, and the predictive role of hs-CRP for fracture risk was essentially unchanged after adjustment for femoral neck BMD (HR 1.45, 95% CI 1.17-1.79). Exploratory sub-analyses of fracture type demonstrated that hs-CRP was clearly associated with clinical vertebral fractures (HR 1.73, 95% CI 1.20-2.48). The association with non-vertebral fractures was of borderline significance (HR 1.36, 95% CI 0.98-1.89).

Conclusions: We demonstrate, using a large prospective population-based study, that elderly men with high hs-CRP have increased risk of fractures. This was true also when vertebral fractures were studied separately. The association between hs-CRP and fractures was independent of BMD.

Disclosures: Sofia Moverare Skrtic, None.

1022

The Effects of Adiponectin and Leptin on Changes in Bone Mineral Density of the Hip. Kamil E. Barbour¹, Joseph M. Zmuda¹, Robert Boudreau¹, Elsa S. Strotmeyer¹, Mara J Horwitz², Rhobert W. Evans³, Alka M. Kanaya³, Tamara B. Harris⁴, and Jane A. Cauley¹ for the Health ABC study. ¹Department of Epidemiology, Graduate School of Public Health, University of Pittsburgh, Pittsburgh, Pennsylvania, USA. ²Division of Endocrinology and Metabolism at the University of Pittsburgh School of Medicine, Pittsburgh, Pennsylvania, USA. ³Division of General Internal Medicine, University of California, San Francisco, California. ⁴Laboratory of Epidemiology, Demography, and Biometry, National Institute of Aging, Bethesda, Maryland

Leptin and adiponectin are hormones secreted by adipose cells that may impact bone mineral density (BMD) and modulate bone formation. Few studies have evaluated the longitudinal association of leptin and adiponectin with rates of BMD loss. To test the hypothesis that low leptin and high adiponectin levels are associated with a higher rate of BMD loss we studied 3,075 men and women, aged 70-79, from the Health Aging and Body Composition (Health ABC) study. Areal BMD (aBMD) of the hip was measured 5 times using dual energy x-ray absorptiometry (DXA) over a 10 year period. Random slope and intercept models accounted for within person correlation and multivariate models adjusted for age, race, BMI, weight change, diabetes, and baseline hip aBMD. Among women, the annualized rate of hip BMD loss in the highest tertile of adiponectin was -0.67% compared to -0.43% in the lowest tertile, p trend=0.019. In men, BMD loss was greatest in the high adiponectin group (tertile 3), however this association was not significant, p trend=0.148. After adjusting for weight change in women, the association between leptin and BMD loss was attenuated and no longer significant, p trend=0.134. Among men, leptin did not predict BMD loss in crude or adjusted models. Results suggest that adiponectin, but not leptin is a risk factor for bone loss in women. Future studies are needed to evaluate and explain the physiological basis underlying these associations. Identification of potential mediators in the causal pathway may better explain these findings.

Disclosures: Kamil Barbour, None.

1023

Serum Cystatin C and Risk of Hip Fractures in Older Women. Kristine Ensrud¹, Neeta Parimi², Yelena Slinin³, Teresa Hillier⁴, Jane Cauley⁵, Michael Steffes⁶, Steven Cummings⁷. ¹Minneapolis VA Medical Center / University of Minnesota, USA, ²California Pacific Medical Center Research Institute, USA, ³University of Minnesota / VA Medical Center, USA, ⁴Kaiser Center for Health Research, USA, ⁵University of Pittsburgh Graduate School of Public Health, USA, ⁶University of Minnesota, USA, ⁷San Francisco Coordinating Center, USA

Serum cystatin C is a biomarker of renal function; higher levels indicate worse function. Previous studies have reported an increased risk of hip fracture among postmenopausal and older women with higher cystatin C, but it is uncertain whether the association persists after adjustment for BMD. To test the hypothesis that older women with higher cystatin C are at increased risk of hip fracture, we conducted a case-cohort analysis in the cohort of 7008 white women attending a Year 10 SOF examination that included 300 women with incident hip fracture and a random sample of 1170 women from the cohort. Cystatin C was measured using a particle-enhanced immunonephelometric assay (inter- and intra-assay CV 3.1% and 2.8%, respectively). Hip fractures (identified during an average follow-up 5.4 years) were confirmed with x-ray reports. Modified proportional hazards models were used to estimate the relative hazards (RH) of fracture across quartiles of cystatin C (cutpoints 0.84, 0.96, 1.11 mg/L). In models adjusted for age, site and body mass index, higher cystatin C was associated with an increased risk of hip fracture (p for trend 0.009) with women in Q4 having a 1.8-fold (95% CI 1.2-2.8) higher risk of hip fracture compared with those in Q1 (ref group) (Table). Additional adjustment for several potential confounders including health status, fall history, prior fracture, prevalent CVD, frailty status, and total hip BMD only slightly attenuated the association (p for trend 0.06); the risk of hip fracture was 1.6-fold higher (95% CI 1.1-2.6) in women in Q4 compared with those in Q1. In conclusion, older women with renal dysfunction as manifested by higher serum cystatin C have an increased risk of hip fracture independent of traditional risk factors including age, prior fracture, frailty status, body weight, and hip BMD.

Table. Association between Cystatin C and Risk of Hip Fracture

Hip Fracture	RH of Fracture (95% CI) by Quartile of Cystatin C				p for trend
	Q1	Q2	Q3	Q4	
Base model*	1.0 (ref)	1.5 (1.0-2.2)	1.4 (1.0-2.1)	1.8 (1.2-2.8)	0.009
Base + BMD	1.0 (ref)	1.5 (1.0-2.2)	1.4 (0.9-2.1)	1.8 (1.2-2.8)	0.01
Base + frailty status	1.0 (ref)	1.5 (1.0-2.2)	1.4 (0.9-2.0)	1.7 (1.1-2.5)	0.04
Final MV model†	1.0 (ref)	1.4 (0.9-2.1)	1.3 (0.9-2.0)	1.6 (1.1-2.6)	0.06

*model adjusted for age, site, and body mass index

†base model further adjusted for health status, fall history, prior fracture, prevalent CVD, frailty status, and total hip BMD

Association between Cystatin C and Risk of Hip Fracture

Disclosures: Kristine Ensrud, None.

1024

Clinical Characteristics of Women Who Fracture Despite Anti-Osteoporosis Medication. The Global Longitudinal Study of Osteoporosis in Women. Adolfo Diez-Perez^{*1}, Philip Sambrook², Juliet Compston³, Jonathan Adachi⁴, Frederick Hooven⁵, Nelson Watts⁶, Stuart Silverman⁷, Susan Greenspan⁸, Cyrus Cooper⁹, Steven Boonen¹⁰, Allison Wyman¹¹, Stephen Gehlbach¹². ¹Autonomous University of Barcelona, Spain, ²Royal North Shore Hospital, Australia, ³University of Cambridge School of Clinical Medicine, United Kingdom, ⁴St. Joseph's Hospital, Canada, ⁵University of Massachusetts Medical School, USA, ⁶University of Cincinnati Bone Health & Osteoporosis Center, USA, ⁷Cedars-Sinai/UCLA, USA, ⁸University of Pittsburgh, USA, ⁹University of Southampton, United Kingdom, ¹⁰Center for Metabolic Bone Disease & Division of Geriatric Medicine, Belgium, ¹¹UMass Medical School, USA, ¹²University of Massachusetts, USA

Background: Little is known about the characteristics of women who fracture while on anti-osteoporosis medication (AOM). Using data from the Global Longitudinal Study of Osteoporosis in Women (GLOW), we analyzed the clinical characteristics of women who had an incident fracture after ≥ 1 year on AOM.

Methods: Among the 46,443 participants in GLOW at the end of year 2, we identified 6584 women on AOM at baseline, year 1, and year 2, with known fracture status at the end of year 2. We performed multivariable logistic regression to predict fracture at year 2, beginning with all of the variables significant on univariate analysis.

Results: 338 women (340 fractures) fractured while on AOM. Compared with women who did not fracture, women who fractured were older (median age 72 vs. 70), sicker (higher rates of chronic bronchitis or emphysema, osteoarthritis, stroke, Parkinson's disease, and diabetes), and at baseline had higher rates of previous fracture (after age 45), current cortisone use, and greater alcohol consumption. Rib (19%), wrist (18%), spine (18%), ankle (8.7%), hip (7.5%) and upper arm (7.2%) were the most common fractures. In multivariable analysis, age, prior stroke, Parkinson's disease, diabetes, prior fracture (wrist, spine, rib), current corticosteroid use and high alcohol intake were independent predictors of fracture on treatment (Table).

Conclusions: Comorbidities, prior fracture, corticosteroid use, and high alcohol consumption were associated with higher rates of fracture despite AOM. Women with these risk factors remain at high risk despite being on therapy.

Baseline characteristic	Odds ratio	95% CI	P-value
Age (per 10-year increase)	1.18	1.03-1.36	0.018
History of stroke	1.67	1.05-2.66	0.031
History of Parkinson's disease	2.86	1.06-7.74	0.038
History of diabetes	2.74	1.61-4.68	<0.001
Prior fracture			
Wrist	1.46	1.09-1.95	0.011
Spine	2.00	1.38-2.88	<0.001
Rib	2.08	1.49-2.90	<0.0001
Cortisone use (vs. never use)			0.006
Current	1.94	1.29-2.92	0.002
Past	1.15	0.87-1.51	0.32
Alcohol intake (>20 vs <20 drinks/week)	8.02	2.81-22.85	<0.0001

Table

Disclosures: Adolfo Diez-Perez, None.

This study received funding from: Warner Chilcott Company, LLC and sanofi-aventis

1025

LLP2A-Alendronate, a Novel Compound That Directs Mesenchymal Stem Cells to Bone, Prevents Bone Losses Induced By Aging or Ovariectomy. Min Guan^{*1}, Nancy Lane², Ruiwu Liu³, Kit Lam³, Liping Meng³, Junjing Jia², Brian Panganiban⁴, Robert Ritchie⁴, Wei Yao². ¹Department of Internal Medicine, University of California at Davis Medical Center, USA, ²University of California, Davis Medical Center, USA, ³Department of Biochemistry & Molecular Medicine, University of California at Davis Medical Center, USA, ⁴Department of Materials Science & Engineering, University of California at Berkeley, USA

Aging reduces the number of mesenchymal stem cells (MSCs) in the bone marrow which leads to impairment of osteogenesis. However, if MSCs could be directed toward osteogenic differentiation, they could be a viable therapeutic option for bone regeneration. We have developed a method to direct the MSCs to the bone surface by attaching a synthetic high affinity and highly specific peptidomimetic ligand (LLP2A) against integrin $\alpha 4 \beta 1$ that expressed on the MSC surface, to a bisphosphonate (alendronate, Ale), that has high affinity for bone. We have previously reported that LLP2A-Ale increased MSCs migration and osteogenic differentiation *in vitro*. One single intravenous injection (i.v.) of LLP2A-Ale increased bone formation and trabecular bone mass in both xenotransplantation and immune competent mice. In

this report, we evaluated the efficacy of LLP2A-Ale on disease states, i.e., in preventing bone losses associated with age or estrogen deficiency (ovariectomized, OVX). Eight-week old C57/BL6 mice were sham-operated or OVX for two weeks. The mice were treated with one single i.v. injection of LLP2A-Ale (0.9nmol/mouse). PTH (1-34) (25 μ g/kg/d, 5x/week) was used as positive control. The mice were sacrificed at four or eight weeks after the treatments.

In sham-operated mice, the femoral trabecular bone volume (BV/TV) decreased by approximately 30% after 4-weeks and 45% after 8-weeks in PBS-treated mice. In contrast, BV/TV increased by approximately 10% after 4-weeks and 50% after 8-weeks in LLP2A-Ale treated mice. LLP2A-Ale treatment induced significantly higher mineral deposition and bone formation rate as compared to PBS-treated animals. After 6 weeks of estrogen deficiency, OVX mice treated with PBS experienced a 30% decrease in their vertebral trabecular bone mass. However, treatment with LLP2A-Ale partially prevented the trabecular bone loss that the BV/TV was 34% higher than the OVX but 14% lower than the Sham-treated group. LLP2A-Ale treatment increased osteoblast surface, and their activities (osteocalcin levels and mineral apposition rate).

The bone formation rate/bone surface was increased above the sham-treated mice with LLP2A-Ale treatment. The activation of bone formation by LLP2A-Ale was comparable to that of PTH-treated OVX mice in preventing trabecular bone loss in this acute estrogen deficiency model.

Our findings demonstrate that LLP2A-Ale augments bone formation and prevents bone losses associated with aging or estrogen deficiency.

Disclosures: Min Guan, None.

This study received funding from: NIAMS- 5R21AR057515 (to WY)

1026

Therapeutic RNAi targeting CKIP-1 for Promoting Bone Formation in an Aged Rat Model of Postmenopausal Osteoporosis. Baosheng GUO^{*1}, Baoting Zhang², Heng WU¹, Tao Tang³, Yixin HE⁴, Gang Li³, Leungkim HUNG¹, Fuchu HE⁵, Lingqiang ZHANG⁵, Ling QIN¹, Ge ZHANG¹. ¹Musculoskeletal Research Laboratory, Department of Orthopaedics & Traumatology, The Chinese University of Hong Kong, Hong Kong, ²Prince of Wales Hospital, The Chinese University of Hong Kong, Hong Kong, ³The Chinese University of Hong Kong, Hong Kong, ⁴The Chinese University of Hong Kong, Hong Kong, ⁵State Key Laboratory of Proteomics, Beijing Proteome Research Center, Beijing Institute of Radiation Medicine, Beijing, China, China

Introduction: Currently, the only FDA-approved anabolic agent is PTH. However, dominant bone resorption after long-term using with PTH is a great concern. Casein kinase-2 interacting protein-1 (CKIP-1) gene is a newly discovered negative regulator gene of bone formation without activating bone resorption. Recently, we have identified a specific cross-species CKIP-1 siRNA sequence with high knock down efficiency. Further, a bone targeting siRNA delivery system i.e. (DSS)6-liposome) was successfully developed.

Hypothesis & objectives: Our hypothesis was that therapeutic RNAi targeting CKIP-1 might promote bone formation for reversing postmenopausal bone loss.

Methodology: Six-month-old female SD rats were either ovariectomized (OVX) or sham-operated (SHAM). At 9 months post surgery, the OVX and SHAM rats were injected intravenously with (DSS)6-liposome-CKIP-1 siRNA (siRNA group) or (DSS)6-liposome (OVX group) or vehicle (SHAM group) via tail vein every two weeks for 6 weeks. Before and during treatment, left proximal tibia was in vivo monitored by microCT every two weeks and registration analysis was also performed between week 0 and week 2, 4, 6. The rats were injected intraperitoneally with xylanol (25mg/kg) and calcein green (30mg/kg) at 10 and 3 days before sacrifice and left femur was subjected to histomorphometric analysis.

Results: In vivo microCT analysis demonstrated that the siRNA group showed a significantly increase in BMD, BV/TV and Tb.Th, at week 6 in relation to week 0, respectively. Further, the siRNA group showed higher in BMD, BV/TV and Tb.Th, respectively, when compared to that in OVX group at week 6 after treatment. Furthermore, the Tb.Th in the siRNA group reached the level in the SHAM group after 6-week treatment. Registration analysis between week 0 and other time point demonstrated that more newly formed was found in the siRNA group, compared to either OVX or SHAM groups (Fig. 1, 2). Histomorphometric analysis showed that MAR, BFR and Ob.S/BS in either distal or mid-shaft femur and Ps.Pm at mid-shaft femur in the siRNA group were all significantly higher than those in the OVX group at week 6, whereas no difference was found in Oc.S/BS between the OVX and siRNA groups (Fig. 3).

Conclusion: Therapeutic RNAi targeting CKIP-1 could exert anabolic action on bone in aged rat model of postmenopausal osteoporosis, without activating bone resorption, which indicated its translational potential for reversing established osteoporosis.

Disclosures: Baosheng GUO, None.

This study received funding from: The Direct Grant in Chinese University of Hong Kong (2041478 & 2041525)

1027

A Delivery System Specifically Approaching Bone Formation Surfaces To Facilitate Translating RNAi-based Anabolic Therapy. Ge Zhang^{*1}, Baosheng GUO², Heng Wu³, Tao Tang⁴, Baoting Zhang⁵, Leungkim Hung³, Fuchu He⁶, Lingqiang Zhang⁶, Ling Qin³. ¹Prince of Wales Hospital, Hong Kong, ²Prince of Wales Hospital, Hong Kong, ³Musculoskeletal Research Laboratory, Department of Orthopaedics & Traumatology, The Chinese University of Hong Kong, Hong Kong SAR, China, Hong Kong, ⁴The Chinese University of Hong Kong, Hong Kong, ⁵Prince of Wales Hospital, The Chinese University of Hong Kong, Hong Kong, ⁶State Key Laboratory of Proteomics, Beijing Proteome Research Center, Beijing Institute of Radiation Medicine, Beijing, China, China

Impaired bone formation during bone disease is a great clinical challenge. One approach to treat this defect would be to silence bone formation-inhibitory genes by small interference RNAs (siRNAs) in osteogenic lineage cells that occupy the niche surrounding the bone formation surfaces. However, a bone-targeting delivery system for RNAi-based bone anabolic therapy is still lacking. Here, we developed a targeting system involving DOTAP-based cationic liposomes attached to six repetitive sequences of aspartate-serine-serine (DSS)6 for delivering siRNAs to specifically approach bone formation surfaces (Figure 1 and Figure 2). Using the system, we encapsulated an osteogenic siRNA targeting casein kinase-2 interacting protein-1 (CKIP-1), a protein that interacts with and augments the osteoblast-suppressing activity of the ubiquitin ligase Smurf1, which was identified by our joint group (Lu K, et al. Nature Cell Biology 2008). In vivo systemic delivery of CKIP-1 siRNA in rats using the (DSS)6-liposome system resulted in the siRNA's selective enrichment in osteogenic lineage cells (Figure 3-1 and Figure 3-2) and subsequent efficient depletion of CKIP-1. Histomorphometry and microCT analysis further demonstrated that this approach significantly promoted bone formation, enhanced the micro-architecture and increased bone mass in healthy rats. We also used the same approach in an osteoporotic rat model, and found it consistent with the effects seen in healthy rats, as evidenced by marked improvement in microarchitecture and bone mass (Figure 4). Collectively, these results demonstrate (DSS)6-liposome as a promising targeted delivery system, thus providing a potential solution to the bottleneck in translating RNAi-based bone anabolic therapies.

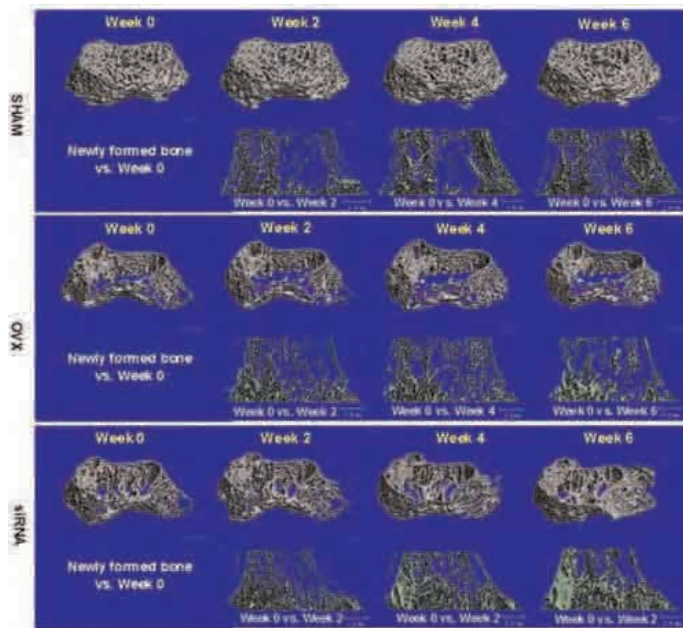
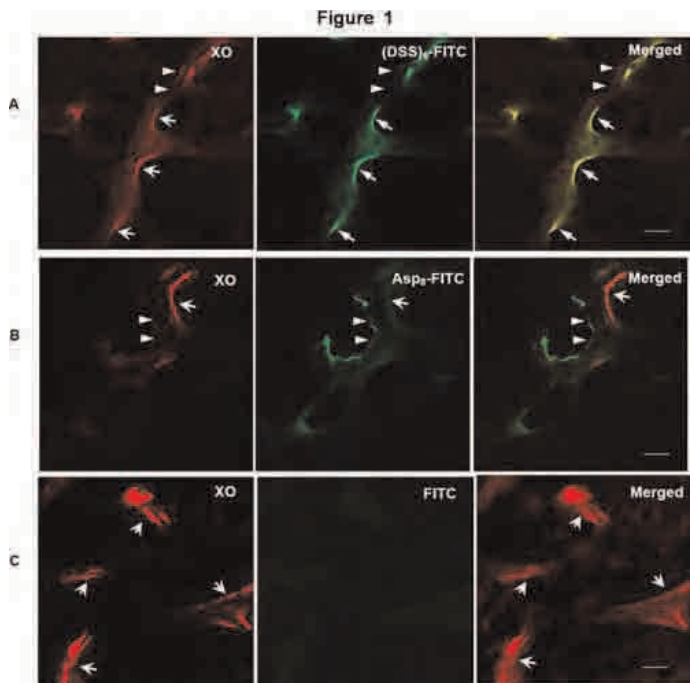


Figure 1 Representative 3-D reconstruction images of in vivo micro-CT measurement followed by regist

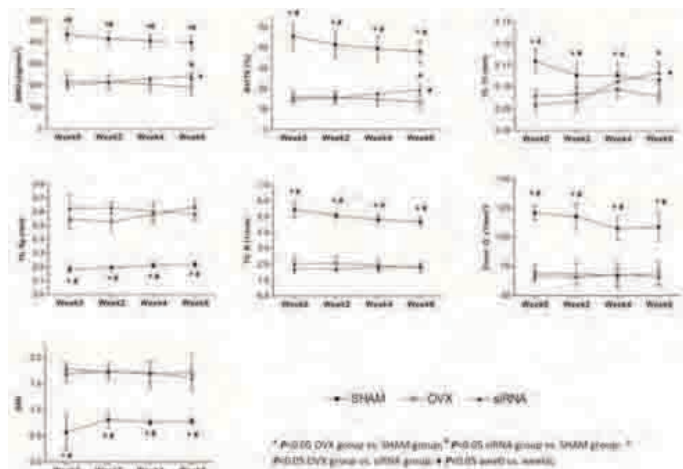


Figure 2 BMD and micro-architecture parameters of in vivo micro-CT measurement at proximal tibia 0

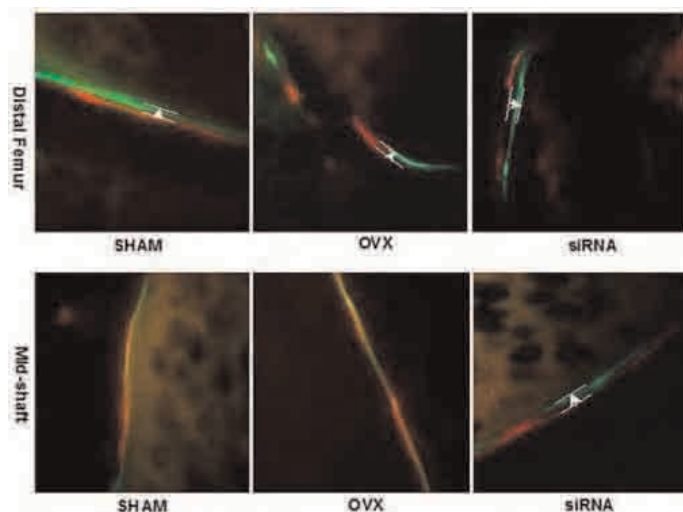


Figure 3 Histomorphometric analyses at distal and mid-shaft femur after 6 weeks treatment

Figure 2

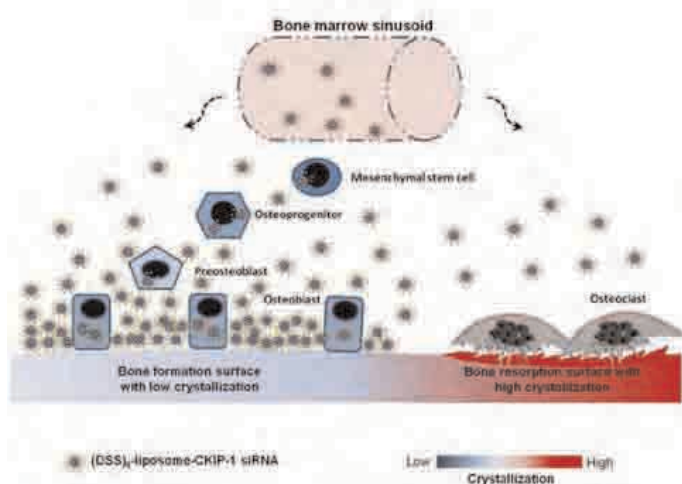


Figure 3-1

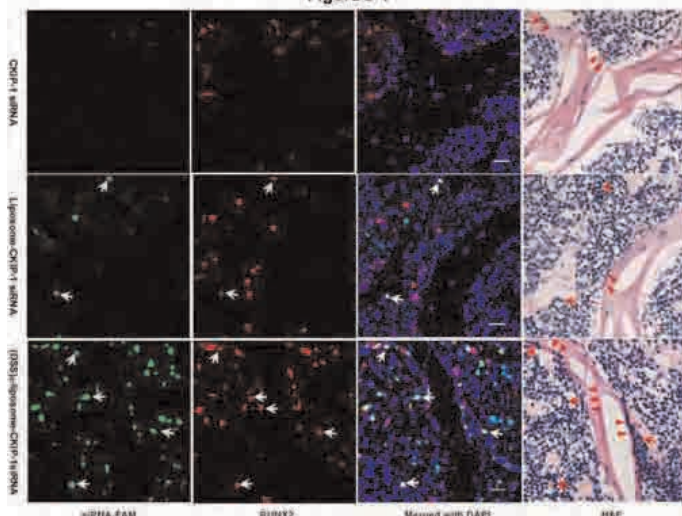


Figure 3-2

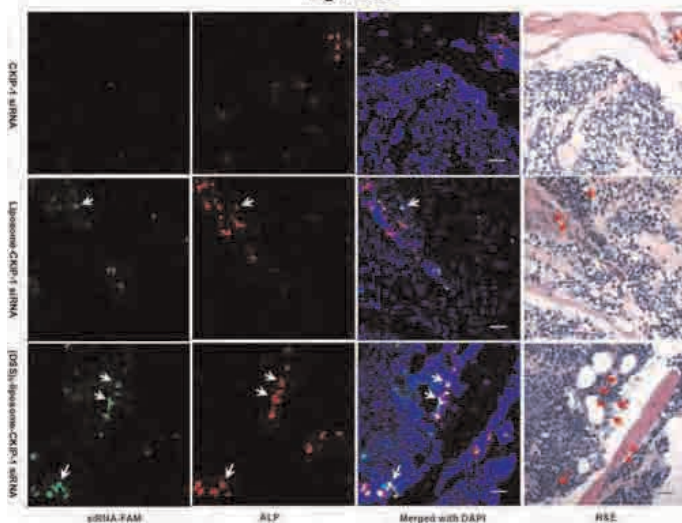
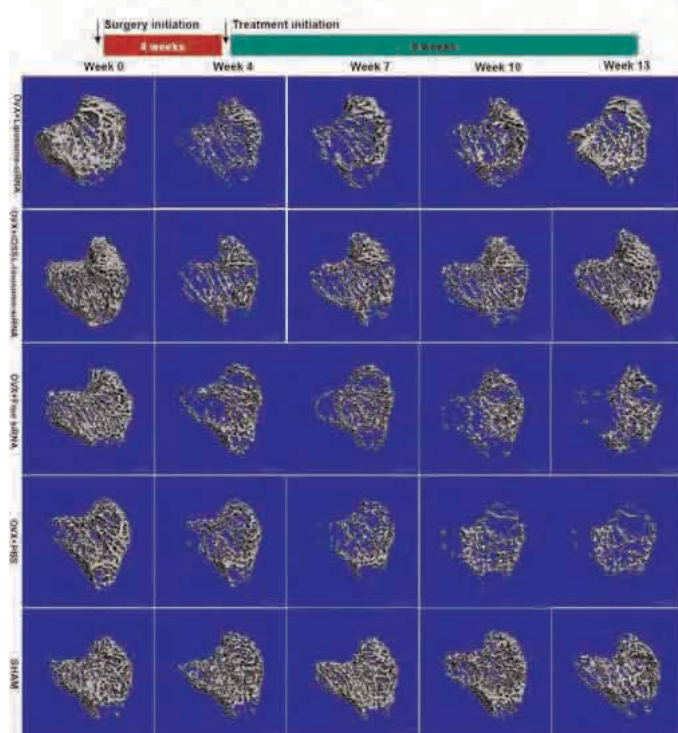


Figure 4



Disclosures: Ge Zhang, None.

1028

A Combined Fc-OPG/hPTH(1-34) Therapy to Restore Impaired Skeletal Growth and Bone Loss in a Mouse Model of IL-6 Dependent Juvenile Inflammatory Diseases. Andrea Del Fattore^{*1}, Marta Capannolo², Barbara Peruzzi², Alfredo Cappariello¹, Nadia Rucci², Fabrizio De Benedetti¹, Anna Teti². ¹Children Hospital Bambino Gesù, Italy, ²University of L'Aquila, Italy

Premature osteoporosis and stunted growth are common complications of juvenile chronic inflammatory diseases and have a significant impact on patients' quality of life. Presently no treatment regimens are available for these defects in childhood. To test a new therapeutic approach, growing mice overexpressing the pro-inflammatory cytokine IL-6 (TG) showing a generalized bone loss and stunted growth were used. Since TG mice present increased bone resorption and impaired bone formation, we hypothesized that a combined therapy with the antiresorptive modified osteoprotegerin, Fc-OPG, and the anabolic PTH could counteract their skeletal failure and improve growth. We therefore treated TG mice with Fc-OPG 0.25 mg/Kg once at the 4th day of life and with 80 µg/Kg hPTH(1-34) everyday from the 16th to the 30th day of age. Treated mice presented a complete rescue of growth, as showed by a body weight of 93% and a tibia length of 92% of WT ($p < 0.05$ vs TG vehicle), and of bone phenotype (BV/TV %; WT vehicle 6.38±2.46; TG vehicle 3.12±0.82; TG Fc-OPG/hPTH 5.24±0.66[#]; $p < 0.02$ vs TG vehicle), due to a normalization of osteoclast and osteoblast parameters. Restoring of normal bone turnover was confirmed by RT-PCR on femurs of Fc-OPG/hPTH-treated mice that showed normalization of TRAcP, ALP and RUNX2 expression compared to vehicle-treated TG mice, rescuing levels similar to WT mice. In vitro cultures from Fc-OPG/hPTH-treated mice confirmed the full rescue of osteoclast and osteoblast activity, reaching levels similar to those observed in cultures from WT mice. The phenotypic rescue of TG mice was due to the combined treatment, because TG mice treated once at the 4th day of life with Fc-OPG 0.25 mg/Kg alone showed an increase of body weight (WT vehicle 14.61±1.72 g; TG vehicle 7.64±0.7 g^{*}; TG Fc-OPG 10.4±1.12 g^{*}; $p < 0.05$ vs WT vehicle), tibia length and bone volume to intermediate levels between those observed in WT and in vehicle-treated TG mice. Similar partial improvement was observed treating TG mice with hPTH alone since the 16th day of life. In contrast, intermittent injections of hPTH since the 4th day of age caused distress of the mice with no effects on the somatic growth. In conclusion, our results identified the sequential treatment with Fc-OPG/hPTH as a treatment regimen to rescue the somatic growth and bone disorder in TG mice, thus providing the proof of principle for a new therapeutic approach to correct these defects in juvenile inflammatory diseases

Disclosures: Andrea Del Fattore, None.

1029

The Impaired Anabolic Effect of PTH In the Absence of Endogenous FGF2 Is Partially Due to Reduced ATF4 Expression. Yurong Fei^{*1}, Liping Xiao¹, Thomas Doetschman², Douglas Coffin³, Marja Marie Hurley⁴. ¹University of Connecticut Health Center, USA, ²University of Arizona, USA, ³The University of Montana, USA, ⁴University of Connecticut Health Center School of Medicine, USA

Parathyroid hormone (PTH) is currently the only approved anabolic agent for osteoporosis pharmacotherapy in the USA. PTH increases FGF2 and FGF receptor expression in osteoblasts. Further, PTH treatment upregulates serum FGF2 associated with increased bone formation in osteoporotic patients. However, the ability of PTH to stimulate bone formation is impaired in *Fgf2*^{-/-} mice. These studies indicate that the anabolic action of PTH in bone formation requires FGF2.

Studies showed that intermittent FGF2 treatment positively regulates osteoblast differentiation and bone formation. However, its downstream targets are not fully defined. Activating transcription factor 4 (ATF4) was recently identified to be a downstream target of PTH signaling in osteoblasts and FGF2 is able to rapidly increase ATF4 mRNA and protein expression in osteoblasts. Furthermore, ATF4 expression is markedly reduced in *Fgf2*^{-/-} osteoblasts. Therefore, we hypothesize that the impaired anabolic effect of PTH in *Fgf2*^{-/-} mice is partially due to reduced ATF4 expression. To test this hypothesis, we examined the ability of PTH to increase ATF4 expression in vitro and in vivo. In vitro data showed that PTH induced a significant increase in ATF4 mRNA expression as early as 15min in *Fgf2*^{+/+} primary bone marrow stromal cells (BMSCs) but not in *Fgf2*^{-/-} BMSCs. In vivo data showed that treatment with hPTH (1-34) (40ug/kg/d) for 2 weeks increased lumbar vertebrae bone mineral density in *Fgf2*^{+/+} female mice (16.9% in 17-19ms, 13.8% in 21-23ms). In contrast there was a 4.7% increase in 17-19ms and a 2.1% decrease in 21-23ms *Fgf2*^{-/-} female mice. Interestingly, basal ATF4 mRNA expression was significantly lower in tibiae of *Fgf2*^{-/-} female mice (46% decrease) compared to *Fgf2*^{+/+} mice. hPTH treatment increased ATF4 mRNA by 15% (p=0.08) and 97% (p<0.05), respectively, in 17-19ms and in 21-23ms *Fgf2*^{+/+} compared to 51% (p<0.05) and 8% (p=0.57), respectively, in 17-19ms and in 21-23ms *Fgf2*^{-/-} mice. Immunohistochemistry of vertebrae showed less ATF4 staining in *Fgf2*^{-/-} tissue, and treatment with hPTH increased ATF4 staining in *Fgf2*^{+/+} but the increase was attenuated in *Fgf2*^{-/-} tissue.

The impaired anabolic response of PTH in *Fgf2*^{-/-} mice is consistent with our previous report. Reduced ATF4 expression may result in decreased osteoblast differentiation, and possibly contribute to the impaired stimulation of PTH on bone formation in *Fgf2*^{-/-} mice.

Disclosures: Yurong Fei, None.

1030

Efficacy of the Combination of Parathyroid Hormone plus Odanacatib or Alendronate, as compared to the Monotherapies in Estrogen-Deficient Rabbits. Brenda Pennypacker^{*1}, Guoxin Wu², Rachel Korn², Rana Samadfam³, Susan Y. Smith³, Le Thi Duong¹. ¹Merck Research Laboratories, USA, ²Merck & Co., Inc., USA, ³Charles River Laboratories, Canada

The cathepsin K inhibitor odanacatib (ODN) and alendronate (ALN) have been shown to effectively prevent bone loss in ovariectomized (OVX) rabbits. While ALN reduces bone remodeling, ODN preserves trabecular and cortical bone formation (BF) in this model. Intermittent administration of human parathyroid hormone 1-34 (PTH) is an approved anabolic agent for the treatment of osteoporosis. Here, we compare the potential additive effects on bone mass and remodeling in rabbits treated with ODN or ALN combined with PTH, or to the respective monotherapy. Adult (7 mo.) rabbits were Sham (N=20) or OVX'd (N=120) for 6-mo. prior to study start. OVX-rabbits were randomized by lumbar vertebrae 5-6 (LV) BMD into the following treatment groups: OVX-vehicle (Veh), PTH (15µg/kg, 5x/wk), ALN (100µg/kg, 2x/wk), ODN (~7µM·24hr, in food), PTH+ALN, and PTH+ODN. After 6 months of treatment, the combined regimens were switched to the respective antiresorptive for the 10 mo. study duration. In-life DXA LV5-6, urinary helical peptide (uHP) and serum bone specific alkaline phosphatase (sBSAP), were determined at 0, 6 and 10 mo. LV4 dynamic histomorphometry was performed based on dual tetracycline labeling at mo. 6, and calcein labeling prior to necropsy at 10 mo. Baseline LV BMD in OVX decreased by 9% (p<0.05) vs. Sham. After 6 mo. of treatment, Veh lost BMD/body weight (BW) by 16% (p<0.001) vs. Sham. PTH, ODN, and ALN increased LV BMD/BW (p<0.01) by 20%, 16%, 18%, respectively. Both PTH+ALN and PTH+ODN groups gained BMD/BW by 32% (p<0.001). uHP and BSAP were elevated in response to OVX. uHP was reduced in ODN (85%, p<0.05), PTH + ODN (69%, p=0.06), ALN (65%, p=0.07) and PTH+ALN (13%, NS) vs. Veh at 6 mo, but was increased 3-fold by PTH (p<0.001). BSAP was reduced by ALN (26%, p<0.05) at 3 mo. and remained elevated in OVX-rabbits treated with PTH at 6 mo (48%, p<0.001), ODN (14%, NS) or PTH+ODN (66%, p<0.001) vs. Veh. ALN alone or in combination with PTH significantly reduced LV mineralizing surface or bone formation rate in OVX-rabbits. Unlike ALN, the BF parameters in ODN and PTH+ODN were comparable to those in PTH and Veh. Taken together, this study demonstrates that ALN and ODN are additive to PTH in providing BMD gains, but ALN blunts BF in the trabecular LV of OVX-rabbits, whereas ODN does not. By preserving BF in this model, ODN in combination with PTH may provide better

long-term BMD gains compared to the PTH+ALN combo, or to the respective monotherapy.

Disclosures: Brenda Pennypacker, None.

1031

Heart Failure is a Clinically and Densitometrically Independent and Novel Risk Factor for Major Osteoporotic Fractures: Population-Based Cohort Study of 45,509 Subjects. Sumit Majumdar^{*1}, Justin A. Ezekowitz¹, Lisa M. Lix², William Leslie³. ¹University of Alberta, Canada, ²University of Saskatchewan, Canada, ³University of Manitoba, Canada

OBJECTIVES: To determine if heart failure is associated with an increased risk of major osteoporotic fractures and whether this risk is independent of low bone mineral density (BMD).

METHODS: We conducted a population-based cohort study in Manitoba, Canada. We linked a clinical registry of all adults age 50 years and older who underwent initial BMD testing from 1998-2007 with provincial databases and followed them until 2009. We collected traditional osteoporosis risk factors, comorbidities, medications, and BMD results. Using validated diagnostic coding algorithms we identified heart failure during the 2-years before BMD test and major non-traumatic osteoporotic fractures (i.e., vertebrae, distal radius, humerus, hip) diagnosed after BMD test. Multivariable Cox proportional hazards models were used to determine if heart failure was independently associated with incidence of major fractures.

RESULTS: The cohort consisted of 45,509 adults of whom 1,841 (4%) had diagnosed heart failure. Subjects with heart failure were significantly (p<0.001) older (mean 74 vs 66 years), more likely to be men (17% vs 7%), had more previous major osteoporotic fractures (21% vs 13%) and had lower total hip BMD than those without heart failure (T-score -1.3[SD1.3] vs -0.9[SD1.2], p<0.001). There were 2,703 incident fractures over a median 5-years observation. Overall, 10% of heart failure subjects had incident major fractures compared with 5% of those without (FIGURE; age-sex adjusted hazard ratio[aHR] 1.64, 95%CI 1.45-1.86). Adjustment for osteoporosis risk factors, comorbidities, and medications attenuated but did not eliminate this association (aHR 1.33, 95%CI 1.11-1.60) as did further adjustment for total hip BMD (aHR 1.28, 95%CI 1.06-1.53).

CONCLUSIONS: Heart failure is associated with an almost 30% increase in major osteoporotic fractures and this is independent of traditional clinical risk factors and BMD. Subjects with heart failure represent a previously unrecognized but easily identified high-risk population that would benefit from increased screening and treatment for osteoporosis.

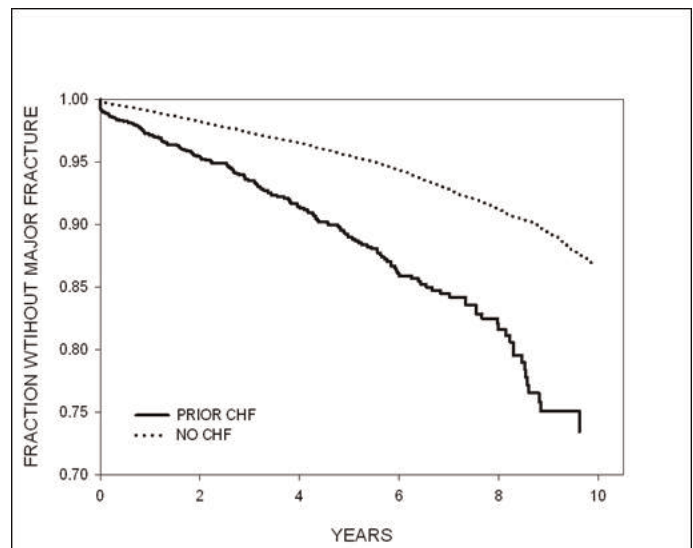


FIGURE: Kaplan-Meier Curves for Major Fractures According to Heart Failure Status (log-rank p<0.001)

Disclosures: Sumit Majumdar, None.

1032

A Screening Programme for Identification of Vertebral Fractures Increases Bisphosphonate Prescribing and Reduces Fractures: Results of a Large RCT. Emma Clark*, Leigh Morrison, Miranda Cuming, Virginia Gould, Jon Tobias. University of Bristol, United Kingdom

Background: Osteoporotic vertebral fractures (VF) are common in the elderly and are associated with morbidity and mortality, but in particular an increased risk of further osteoporotic fractures. Medications are available to reduce this future fracture risk by approximately 50%. Yet despite this there are no national screening programmes to identify individuals with osteoporotic VFs in the community.

Aim: To investigate whether a primary care-based screening tool to identify postmenopausal women with osteoporotic VFs can appropriately increase prescription of medications for osteoporosis, leading to a reduction in fracture risk.

Methods: We performed a pragmatic individual patient-based randomised controlled trial (RCT) of 3200 women aged 65-80. Women were enrolled from 15 General Practices within the Bristol area of the UK with no exclusion criteria. In those randomised to the active group, a simple screening tool was carried out by a nurse in primary care to identify women at high risk of prevalent osteoporotic VFs. All women identified as high-risk on the basis of a pre-defined algorithm, developed from a previous cross sectional study performed in a similar population, were offered a diagnostic thoraco-lumbar radiograph at their local hospital. Radiographs were reported using standard NHS reporting with results sent back to each participant's General Practitioner. Those randomised to the control arm did not receive the screening tool or radiographs. Analysis was by intention-to-treat for the main outcome measure, which was self-reported prescription of medication for osteoporosis at 6 months (a random 5% sub-sample was verified against electronic GP records). Secondary outcome was self-reported incidence of new fractures.

Results: In the screening group prescription of osteoporosis medications was increased by 124% compared to the control arm (OR for prescription 2.24 at 6 months (95%CI 1.16 to 4.33). 64.3% of women prescribed bisphosphonates within 6 months of starting the study had been identified with definite or probable osteoporotic VF. Fracture incidence was also reduced in the screening versus control arm by 72% between 6 and 12-months follow-up (OR for new fracture 0.28, 95%CI 0.12 to 0.67).

Conclusion: Adoption of a simple screening tool for prevalent VF in older postmenopausal women in primary care not only increased bisphosphonate prescribing, but also reduced fracture incidence, suggesting such an approach is likely to be highly cost effective

Disclosures: Emma Clark, None.

1033

Persistent Skeletal Exposure to Bone Morphogenetic Proteins is Detrimental and Causes Osteopenia. Ernesto Canalis*, Lisa Brunet², Kristen Parker³, Stefano Zanotti¹. ¹St. Francis Hospital & Medical Center, USA, ²University of California, USA, ³Saint Francis Hospital & Medical Center, USA

Bone morphogenetic proteins (BMPs) induce endochondral bone formation, but the role of BMPs in osteoblastogenesis has been challenged since they decrease Wnt signaling and activity. BMP activity is controlled by BMP antagonists. Noggin is a secreted specific BMP antagonist and its only function is to bind BMPs and prevent signaling. Therefore, *Noggin* inactivation results in persistent tissue exposure to BMPs. Studies from transgenics overexpressing noggin in the skeletal environment reveal that BMPs are required to maintain skeletal homeostasis; however, unregulated tissue exposure to BMPs may have detrimental effects on bone. Models of *Noggin* inactivation are ideal to test this possibility, but the global inactivation of *Noggin* results in serious developmental abnormalities and prenatal lethality. To study the consequences of *Noggin* inactivation in the postnatal skeleton and consequently the persistent skeletal exposure to BMPs, mice, where the *Noggin* allele was flanked by *loxP* sequences, were mated with mice expressing the Cre recombinase under the control of the osteocalcin promoter, and compared to littermate control mice. Calvarial *noggin* mRNA was decreased by 50 to 70% in *Noggin* conditional null mice. Bone mineral density, microcomputed tomography and histomorphometry revealed marked osteopenia in male and female *Noggin* conditional null mice. Trabecular bone volume was decreased by 40 to 50% due to a decrease in trabecular number, and connectivity density was decreased by 60 to 70%. The osteopenic phenotype was observed at 1 and 3 months of age, but subsided partially at 6 months possibly due to a decline in osteocalcin promoter activity. The osteopenia following *Noggin* inactivation was generalized and observed in femoral and vertebral trabecular bone, and was not compartment-specific since cortical thickness was decreased by nearly 30%. Histomorphometry revealed no changes in osteoblast number, but osteoclast number and eroded surface were increased in male *Noggin* conditional null mice. Although bone formation also increased, it was not sufficient to maintain trabecular structure and reverse the osteopenic phenotype. In conclusion, the conditional inactivation of *Noggin* in the skeleton causes marked osteopenia due to an increase in bone remodeling, indicating that persistent exposure of the skeleton to BMPs is detrimental. Consequently, therapies targeting BMP antagonists may not prove successful in the management of osteoporosis.

Disclosures: Ernesto Canalis, None.

1034

Brown Fat Regulates Bone Mass Through Modulation of Sympathetic Tone. Katherine Motyl*, Masanobu Kawai², Sheila Bornstein², Victoria Demambro¹, Leeann Louis³, Sutada Lotun⁴, Mark Horowitz⁵, Roland Baron⁶, Mary Boussein³, Clifford Rosen². ¹Maine Medical Center Research Institute, USA, ²Maine Medical Center, USA, ³Beth Israel Deaconess Medical Center, USA, ⁴Harvard School of Dental Medicine, USA, ⁵Yale University School of Medicine, USA, ⁶Harvard School of Medicine & of Dental Medicine, USA

Brown adipose tissue (BAT) is critical for energy homeostasis in rodents. Loss of BAT leads to lower body temperature but activates an alternative thermogenic program through the sympathetic nervous system (SNS) to white adipose tissue (WAT). Skeletal metabolism is under the control of the SNS, although it is uncertain whether BAT dysfunction affects bone mass through the SNS. In this study, we examined skeletal and metabolic changes in two mouse models: 1) the *Misty* mouse, a spontaneous mutant with altered BAT function and 2) *Ucp1*^{-/-} mice that have no functional BAT. At 12 wks, *Misty* have low body temperature and greater sympathetic tone. White adipocytes were more 'brown-like' in their appearance and several BAT lineage determination and fatty acid oxidation genes were up-regulated in WAT. Skeletal phenotyping revealed that 8 wk female *Misty* mice had significantly lower total areal bone mineral density (aBMD) ($p < 0.01$) and distal femoral trabecular bone volume (BV/TV) fraction ($p < 0.001$) compared to controls. By 16 wks *Misty* lost significantly more bone mass than controls ($p < 0.0001$) and this difference (64%) was associated with a reduced BFR/BV, increased osteoclast number and a greater eroded surface by histomorphometry compared to controls. Importantly, the low aBMD and the trabecular thickness, but not trabecular number, of *Misty* were rescued by treatment with a beta-blocker. Similarly, trabecular BV/TV in the distal femur was enhanced although not totally restored by the 8-wk beta-blocker treatment. To confirm the indirect effects of BAT dysfunction on bone were non-cell autonomous, we studied uncoupling protein 1 null (*Ucp1*^{-/-}) mice that require elevated temperatures to maintain thermoneutrality. These mice have increased energy expenditure, are lean and have 'brown-like' adipocytes in inguinal WAT. We found that *Ucp1*^{-/-} mice had very low aBMD of the femur and low BV/TV of the distal femur at 6 wks ($p < 0.001$). These differences were significantly accentuated at 16 wks such that trabecular BV/TV was reduced by 80% ($p < 0.0001$) compared to controls. This is the first report demonstrating that alterations in BAT function affect the rate of bone loss in mice. Further studies are required to define whether age-associated bone loss is linked with BAT dysfunction in humans and to determine whether responders to beta-blocker therapy, with respect to BMD and/or fracture risk, are those with the greatest resting sympathetic tone.

Disclosures: Katherine Motyl, None.

1035

Unexpected Enhanced Response to Mechanical Loading of Mice Lacking Cx43 Exclusively in Osteocytes. Nicoletta Bivi*, Nathan Farlow², Lucas Brun³, Jeffrey Benson², Keith Condon², Alexander Robling¹, Teresita Bellido², Lilian Plotkin². ¹Indiana University, USA, ²Indiana University School of Medicine, USA, ³University of Rosario, Argentina

The osteocyte network is crucial for the response of bone to mechanical force. Within this network, connexin 43 (Cx43) mediates the communication of osteocytes and osteoblasts among themselves and with the extracellular milieu. Although Cx43 appears to be important for the response of osteocytic cells to mechanical stimulation *in vitro*, the contribution of Cx43 expression in osteocytes to mechanotransduction *in vivo* is not known. To this end, we examined the anabolic response to loading of mice lacking Cx43 in osteocytes (Cx43^{ΔOT}) generated by crossing Cx43^{fl/fl} mice with DMP1-8kb-Cre mice. Unlike the 10kb fragment that directs gene expression to osteocytes and some osteoblasts, the 8kb fragment of the DMP1 promoter targets gene expression only to osteocytes. Indeed, Cre recombinase mRNA was detected only in green fluorescent protein (GFP) positive cells (osteocytes) and not in GFP negative cells (osteoblasts) isolated from calvaria of DMP1-8kb-Cre mice crossed with DMP1-8kb-GFP mice. Immunohistochemistry confirmed lack of Cx43 expression only in osteocytes in Cx43^{ΔOT} bone sections. Moreover, Cx43 mRNA was reduced by 88% in osteocyte-enriched cortical bone of Cx43^{ΔOT} mice compared to control Cx43^{fl/fl} littermates. Right ulnae of control and Cx43^{ΔOT} mice were subjected to axial loading at equivalent low, medium, and high strain magnitudes during 1min/d for 3 consecutive days; left ulnae were used as non-loaded controls. Bone formation rate (BFR/BS) was quantified 14d later. Loading induced strain-dependent increases in periosteal BFR/BS of 1.4-, 1.8-, and 2.2-fold in control animals. To our surprise, loading induced a greater response in Cx43^{ΔOT} mice (2.5-, 4.3- and 4.9-fold), due to a combination of higher mineralizing surface covered by osteoblasts (MS/BS) and higher rate of mineral apposition by individual osteoblasts (MAR). These results suggest that the absence of Cx43 in osteocytes unleashes bone formation by periosteal osteoblasts and are consistent with previously reported higher basal periosteal bone formation in femora from Cx43^{ΔOT} mice. The apparent discrepancy with earlier evidence showing decreased endosteal BFR/BS induced by tibia loading in mice lacking Cx43 in both osteocytes and osteoblasts (col1-2.3kb) can be explained by the fact that, in the latter model, osteoblasts are unable to function optimally. We conclude that the intrinsic function of Cx43 in osteocytes is to restrain the response of osteoblasts to mechanical loading.

Disclosures: Nicoletta Bivi, None.

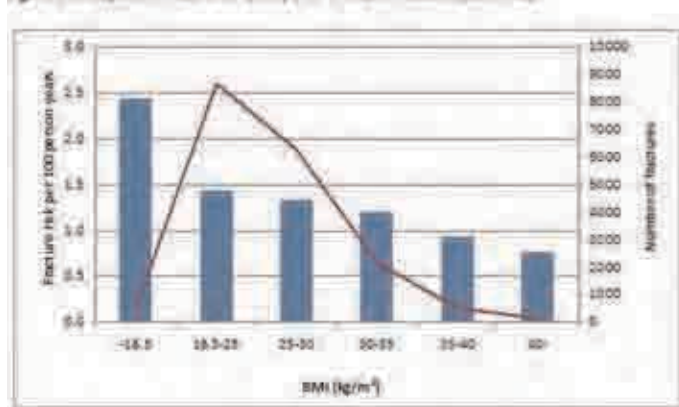
High Body Mass Index, Adjusted for BMD, Is a Risk Factor for Fracture in Women. Helena Johansson^{*1}, John Kanis², Anders Oden¹, Eugene McCloskey³, R. Chapurlat⁴, C. Christiansen⁵, S. Cummings⁶, Adolfo Diez-Perez⁷, John Eisman⁸, Saeko Fujiwara⁹, Claus-C Gluer¹⁰, Didier Hans¹¹, K-T Khaw¹², Marc-Antoine Kriegel¹³, Heikki Kroger¹⁴, Andrea La Croix¹⁵, Edith Lau¹⁶, William Leslie¹⁷, Dan Mellstrom¹⁸, L. Joseph Melton¹⁹, Terry O'Neill²⁰, Julie Pasco²¹, J. Prior²², David Reid²³, Fernando Rivadeneira²⁴, David Torgerson²⁵, Tjeerd vanStaa²⁶, Noriko Yoshimura²⁷, M. Zillikens²⁸.
¹University of Gothenburg, Sweden, ²University of Sheffield, Belgium, ³University of Sheffield, United Kingdom, ⁴Lyon Hospital, France, ⁵Nordic Bioscience, Denmark, ⁶University of San Francisco, USA, ⁷Autonomous University of Barcelona, Spain, ⁸Garvan Institute of Medical Research, Australia, ⁹Radiation Effects Research Foundation, Japan, ¹⁰Christian Albrechts Universitaet zu Kiel, Germany, ¹¹Lausanne University Hospital, Switzerland, ¹²Cambridge University, United Kingdom, ¹³University Hospital, Switzerland, ¹⁴Kuopio University Hospital, Finland, ¹⁵Women's Health Initiative, United Kingdom, ¹⁶Hong Kong Orthopaedic & Osteoporosis Center for Treatment & Research, Hong Kong, ¹⁷University of Manitoba, Canada, ¹⁸Sahlgrenska University Hospital, Sweden, ¹⁹Mayo Clinic, USA, ²⁰University of Manchester, United Kingdom, ²¹Deakin University, Australia, ²²Hospital, Canada, ²³University of Aberdeen, United Kingdom, ²⁴Erasmus University Medical Center, The Netherlands, ²⁵University of York, United Kingdom, ²⁶MHRA, United Kingdom, ²⁷22nd Century Medical & Research Center, University of Tokyo, Japan, ²⁸Erasmus MC Rotterdam, The Netherlands

We studied 27 prospective population-based cohorts from more than 25 countries. Height and weight were measured at baseline and body mass index (BMI) was calculated as kg/m². Bone mineral density (BMD) was measured at the femoral neck by DXA. Fractures during follow up were collected by self-report and, in some cohorts, confirmed by radiography. An extension of Poisson regression was used to examine the relationship between BMI and fracture risk adjusted for age, BMD and time since baseline within each cohort. The results were merged and weighted according to the variance.

Baseline data on BMI were available in 296 736 women aged 20-105 years with an average of 62.7 years. Femoral neck BMD was measured in 74 394 women aged 67.0 years, who were followed for 368 000 person-years. The prevalence of obesity (BMI ≥ 30 kg/m²) was 18%. During overall follow-up of 1.4 million person-years, 18,336 osteoporotic fractures (4,509 hip fractures) occurred. A majority of fractures (85%) arose in non-obese women (Figure 1). The risk of osteoporotic and hip fracture decreased progressively with increasing BMI. Compared to a BMI of 26, the hazard ratios (HR, 95%CI) for osteoporotic fracture at a BMI of 35 or 40 were 0.89 (0.84-0.93) and 0.83 (0.77-0.90), respectively. Interestingly, when adjusted for BMD, the corresponding HRs were 1.14 (1.06-1.23) and 1.23 (1.10-1.39), respectively. The HR for hip fracture was also reduced at higher BMIs (0.75 [0.67-0.85] and 0.64 [0.53-0.78] at 35 and 40 vs. 26 kg/m²). When adjusted for BMD, the corresponding HRs were 1.09 (0.91-1.30) and 1.14 (0.86-1.50), respectively.

Our results demonstrate that at a population level, obesity is protective for fracture in women and this protection is mediated by effects on BMD. At a given BMD, obesity appears to be a weak risk factor for fracture.

Figure 1 Osteoporotic fracture risk (bars) and number of fractures (solid line).



figure

Disclosures: Helena Johansson, None.

Osteocytes Regulate Bone Microenvironment Through Gsa Signaling to Support Normal Hematopoiesis. Keertik Fulzele^{*1}, Daniela Krause², Kevin Barry³, Sutada Lotinun⁴, Roland Baron⁵, Lynda Bonewald⁶, Jian Feng⁷, Min Chen⁸, Lee Weinstein⁹, David Scadden¹⁰, Paola Divieti Pajevic¹¹.
¹Massachusetts General Hospital; Harvard Medical School, USA, ²Center of Regenerative Medicine, Massachusetts General Hospital & Harvard Medical School, USA, ³Massachusetts General Hospital & Harvard Medical School, USA, ⁴Harvard School of Dental Medicine, USA, ⁵Harvard School of Medicine & of Dental Medicine, USA, ⁶University of Missouri - Kansas City, USA, ⁷Texas A&M Health Science Center, USA, ⁸Metabolic Diseases Branch, NIDDK, NIH, USA, ⁹National Institute of Diabetes & Digestive & Kidney Diseases, USA, ¹⁰Center for Regenerative Medicine Massachusetts Gen, USA, ¹¹Massachusetts General Hospital Harvard Medical School, USA

Osteocytes, the most abundant and long living cells of bone, coordinate bone remodeling by regulating osteoblast and osteoclast activity, in part, via G-protein coupled receptor signaling. Osteoblasts and osteoclasts also control hematopoiesis primarily by influencing self-renewal, differentiation, and mobilization of hematopoietic stem cells in their endosteal bone niche. Here, we hypothesized that osteocytes may directly or indirectly regulate hematopoiesis through the stimulatory subunit of G-protein, Gsα, signaling. To test this, we engineered mice lacking Gsα in osteocytes (DMP1-GsαKO) using the Cre-loxP recombination technique. Consistent with the previously established role of osteocytes in regulation of bone remodeling, DMP1-GsαKO mice showed severe osteopenia with an 86% decrease in trabecular bone volume and a 40% decrease in cortical thickness (p<0.01, N=5) as revealed by micro-CT analysis of femurs from 21-week old mice. Histomorphometric analysis of femurs from 7-week old mice showed that the osteopenia in the KO mice was due to a dramatic 95% decrease in osteoblast numbers (p<0.001, N=6) whereas the number and activity of osteoclasts was unaffected. To determine if the Gsα-deficient osteocytes may influence hematopoiesis, we examined the hematopoietic profile. DMP1-GsαKO mice displayed hematopoietic abnormalities that resembled myelodysplastic disease (MPD) characterized by a dramatic and significant increase in leukocytes, neutrophils, and platelets in the peripheral blood (p < 0.001, N=8) and increased myeloid cells in bone marrow (BM) and spleen (p<0.01, N=6). Surprisingly, the number of hematopoietic colonies formed in-vitro from BM cells were not changed indicating the requirement of the bone microenvironment to induce MPD. Indeed, transplantation of BM from control to DMP1-GsαKO mice rapidly recapitulated the MPD whereas converse transplantation completely normalized the hematopoietic abnormality. Co-culture of osteocyte-enriched bone explants from DMP1-GsαKO mice with control BM cells significantly increased the number of hematopoietic colonies compared to control explants. Furthermore, considering that mice lacking Gsα in osteoblasts or in hematopoietic cells do not display MPD, MPD in DMP1-GsαKO mice is most likely a direct effect of Gsα-null osteocytes. In summary, our results present the first evidence for osteocyte-mediated regulation of hematopoiesis via Gsα-signaling-induced alteration of the BM microenvironment.

Disclosures: Keertik Fulzele, None.

Conditional Knockout of IGF-I in Osteocytes Surprisingly Accelerates Fracture Repair. Matilda Sheng^{*1}, Xiaodong Zhou¹, Kin-Hing William Lau², Lynda Bonewald³, David Baylink¹.
¹Loma Linda University, USA, ²Jerry L. Pettis Memorial VA Medical Center, USA, ³University of Missouri - Kansas City, USA

Past studies indicate that the osteocyte is an important regulator of bone formation (BF) and that bone-derived IGF-I is essential for BF and regeneration. IGF-I is expressed in osteocytes as well as osteoblasts. The goal of this study was to determine the effect of osteocyte-derived IGF-I on the enhanced BF required for fracture repair. For this work, we generated mice with conditional knockout (KO) of IGF-I gene in osteocytes by crossing DMP1-Cre mice with the IGF-I loxp mice. Fractures were created on the tibia of 10 weeks-old males by 3 point bending. At 21 and 28 days post-fracture, the % increases in total bone density (P=.01 and .04), cortical mineral contents (P=.03 for each), sub-cortical mineral contents (P=.04 and P=.02), cortical bone area (P=.04 and P=.06), and cortical thickness (P=.01 for each) were greater each by 13-26% in the healing calluses of KO mice than wild-type (WT) calluses. The basal periosteal BF per bone surface was not different between the KO mice and WT mice (1.57.09 vs. 1.44.12, P>.05), indicating that this increased BF during fracture repair was not due to a different basal BF. There was a 85% decrease in % cartilage (P=.06) and >2 fold increase in the number of TRAP+ osteoclasts within the KO callus, suggesting that the endochondral bone in the KO callus had been remodeled more rapidly, resulting in accelerated bony bridging of the fracture gap, which was confirmed by x-ray and histology. The mRNA levels of the BF genes [cbfa1, BMP2, and osteocalcin] in the KO callus were also increased by 149% (P=.04), 73% (P=.04), and 150% (P=.09), respectively, than those in WT calluses. These results, together, support the conclusion that targeted deletion of IGF-I in osteocytes would result in an increase in bone callus remodeling with a balance shifted toward BF; the end result being an accelerated fracture healing including bridging. Importantly, because IGF-I is a potent BF stimulator in osteoblasts, our findings that the KO of

osteocyte-derived IGF-I not only did not impede, but actually accelerated, BF during the fracture healing process, suggest a novel inhibitory function of osteocyte-derived IGF-I in fracture repair. More importantly, in a separate study these KO mice exhibited an obliterated BF response to the mechanical loading challenge in vivo. Thus, the enhanced fracture repair in the absence of loading BF response challenges the generally accepted dogma that loading is essential for an optimal fracture healing.

Disclosures: Matilda Sheng, None.

This study received funding from: Department of Defense

1039

Osteocyte Autophagy Declines with Age in Mice and Suppression of Autophagy Decreases Bone Mass. Haibo Zhao, Jinhu Xiong, Melda Onal, Priscilla Cazer, Robert Weinstein, Stavros Manolagas, Charles O'Brien*, Center for Osteoporosis & Metabolic Bone Diseases, Central Arkansas Veterans Healthcare System, University of Arkansas for Medical Sciences, USA

Osteocyte viability is reduced in aged bone, but the mechanisms responsible are unclear. The viability of other long-lived cells is sustained by autophagy, an intracellular process in which organelles and proteins are delivered to lysosomes for degradation and reuse of their components. Specifically, genetic suppression of autophagy in long-lived cells leads to increased numbers of damaged mitochondria, oxidative stress, and cell death. Based on this, the accumulation of damaged cellular components that occurs with age has been attributed to decreased autophagy. To determine whether autophagy in osteocytes declines with age, we quantified the expression of several genes involved in autophagy in femoral cortical bone after digestion with collagenase to remove surface cells. In two different mouse strains (DBA/2 and C57BL/6), BNIP3 and LC3 mRNA levels were reduced in cortical bone from 20 month old mice compared with 6 month old mice. Based on this finding and evidence in other tissues that reduced autophagy leads to increased mitochondrial DNA, we compared mitochondrial mass by quantifying mitochondrial DNA, normalized to nuclear DNA, in cortical bone of young and old mice. We found that mitochondrial DNA was significantly higher in cortical bone from aged mice, consistent with the contention that autophagy in osteocytes declines with age. To directly address whether autophagy is functionally important in osteocytes, we deleted a conditional allele for ATG7, a gene that is essential for autophagy, from osteocytes using the DMP1-Cre transgene. Suppression of autophagy in osteocytes was confirmed by demonstrating that conversion of LC3 protein from form I (unlipidated) to form II (lipidated) was significantly reduced in cortical bone of conditional knockout (KO) mice. Similar to the results we obtained from aged mice, the reduction in autophagy in the conditional KO mice was associated with an increase in the levels of mitochondrial DNA isolated from cortical bone. Moreover, bone mineral density was significantly lower, compared to littermate controls, in the spines and femurs of both male and female conditional KO mice beginning at 4 months of age and continuing to at least 6 months of age without differences in body weight between genotypes. These results demonstrate that loss of autophagy in osteocytes leads to low bone mass and suggest that a decline in osteocyte autophagy with age contributes to the low bone mass associated with aging.

Disclosures: Charles O'Brien, None.

1040

Sclerostin Deficiency does not Induce Bone Gain in Mice Lacking Osteocyte \hat{O} -catenin. Ming-Kang Chang*, Ina Kramer, Michaela Kneissel, Novartis Institutes for Biomedical Research, Switzerland

Wnt/ \hat{O} -catenin signaling controls bone homeostasis by impacting on the entire osteoblastic cell lineage and osteoclastic bone resorption. In consequence, mice lacking osteocyte \hat{O} -catenin (*Ctnnb1^{loxP/loxP};Dmp1-cre*) develop severe osteoporosis. Osteocytes secrete the bone formation inhibitor sclerostin encoded by *Sost*. Sclerostin is thought to act as a paracrine inhibitor of osteoblast Wnt/ \hat{O} -catenin signaling. However the final proof that sclerostin indeed targets this pathway in bone is lacking. Furthermore the possibility that sclerostin targets osteocytes in an autocrine manner cannot be excluded. To address these questions, we generated mice lacking both osteocyte \hat{O} -catenin and sclerostin (*Ctnnb1^{loxP/loxP};Dmp1-cre;Sost^{-/-}*). We previously reported that sclerostin deficiency did not prevent bone loss induced by the lack of osteocyte \hat{O} -catenin. To elucidate bone turnover in these mutant mice, we performed histomorphometry on the femur of 10-week-old male mice (wildtype, *Sost^{-/-}*, *Ctnnb1^{loxP/loxP};Dmp1-cre* = single KO, *Ctnnb1^{loxP/loxP};Dmp1-cre;Sost^{-/-}* = double KO). Endocortical bone forming surfaces were increased in *Sost^{-/-}* mice compared to wildtype controls (e.g. +40% mineralizing surface). However this was abolished in the osteocyte \hat{O} -catenin deficient background and double KO mice when compared to single KO mice. Endocortical bone resorption was non-significantly reduced in *Sost^{-/-}* animals (-64% osteoclast surface; -19% eroded surface), while single KO mice displayed increases (+72% and +189% respectively) as observed before. Bone resorption perimeters were comparable in single and double KO mice. Cancellous bone volume was increased in *Sost^{-/-}* mice (+56%), while it was decreased in single and double KO mice (-67% and -88% respectively). Bone formation parameters were increased in *Sost^{-/-}* mice (e.g. +175% osteoblast surface). As previously reported osteoblast parameters were non-significantly elevated on the few trabeculae of single KO mice. Double KO mice displayed a similar phenotype. Bone resorption was

elevated in double KO mice compared to other genotypes, however without reaching significance due to variability based on paucity of the bone template. The results demonstrate that bone turnover was overall comparable between *Ctnnb1^{loxP/loxP};Dmp1-cre* single and *Ctnnb1^{loxP/loxP};Dmp1-cre;Sost^{-/-}* double KO mice. The data indicate that sclerostin indeed targets \hat{O} -catenin dependant signaling in bone possibly in an autocrine fashion.

Disclosures: Ming-Kang Chang, Novartis, 3

This study received funding from: Novartis

1041

Increased RANKL Production by Osteocytes is a Major Mechanism Underlying the Bone Loss Induced by Unloading. Jinhu Xiong*, Melda Onal, Priscilla Cazer, Stavros Manolagas, Charles O'Brien, Center for Osteoporosis & Metabolic Bone Diseases, Central Arkansas Veterans Healthcare System, University of Arkansas for Medical Sciences, USA

Osteocytes are thought to control the response of bone to changes in mechanical forces; and bone loss due to mechanical unloading has been attributed to both increased bone resorption and decreased bone formation. However, the mechanisms by which osteocytes may mediate these responses remains unclear. To determine whether osteocytes control bone resorption via production of RANKL, we crossed mice with a conditional allele for RANKL with DMP1-Cre mice, which express the Cre recombinase predominately in osteocytes. Mice lacking RANKL in osteocytes, hereafter referred to as RANKL conditional knock out (CKO) mice, displayed normal tooth eruption and were not grossly osteopetrotic. However, at 5 weeks of age RANKL CKO mice had a small but significant elevation of bone mass, compared with control littermates, and this difference increased with time so that at 6 months of age there was a 30% increase in bone mineral density (BMD). At this age, both RANKL mRNA in bone and osteoclast number were significantly reduced in RANKL CKO mice. These results demonstrate that osteocytes produce a significant amount of the RANKL present in bone and that they are an essential source of the RANKL that controls basal bone remodeling. Next, we examined whether RANKL produced by osteocytes contributes to the bone resorption induced by mechanical unloading. Six-month-old RANKL CKO mice and control littermates were either tail-suspended or left grounded for 3 weeks. Tail-suspension of control mice reduced femoral BMD by 12% ($p < 0.05$), while the grounded mice did not show any change in bone mass. In contrast, tail-suspension of the RANKL CKO mice reduced BMD by only 4%, which was significantly less than the effect of tail-suspension on control littermates ($p < 0.05$ by ANOVA). Moreover, unloaded control mice exhibited a significant decrease in femoral cortical thickness, compared to their grounded controls, as measured by microCT. In contrast, unloading had no effect on cortical thickness in the RANKL CKO mice. Consistent with this, unloading significantly elevated RANKL mRNA in the cortical bone of control, but not RANKL CKO, mice. Taken together, these results demonstrate that osteocytes produce RANKL, and that this production increases in response to mechanical unloading. Moreover, the increased RANKL production by osteocytes is a major contributor to the bone resorption and bone loss associated with mechanical unloading.

Disclosures: Jinhu Xiong, None.

1042

Sclerostin Stimulates Osteocyte Support of Osteoclast Activity by a RANKL-Dependent Pathway. Asiri Wijenayaka, Masakazu Kogawa, David Findlay, Gerald Atkins*, University of Adelaide, Australia

Sclerostin is a product of mature osteocytes embedded in mineralised bone and is a negative regulator of bone mass and osteoblast differentiation. Both animal (1) and human (2) studies employing a neutralising anti-sclerostin antibody have reported decreases in bone resorption parameters. Thus, while it is clear that sclerostin has an anti-anabolic role, it is also possible that sclerostin has direct catabolic activity. To test this we examined the effect of recombinant human sclerostin (rhSCL) on pro-osteoclastic gene expression in cultures of human primary immature osteoblasts and differentiated late-osteoblast/pre-osteocyte cultures. Sclerostin dose-dependently up-regulated expression of RANKL mRNA and down-regulated that of OPG mRNA, causing an increase in the RANKL:OPG mRNA ratio in late osteoblast/pre-osteocyte-like cultures, a phenotype we showed previously to be exquisitely sensitive to rhSCL(3). We also found that the RANKL:OPG mRNA ratio was increased in mouse osteocyte-like MLO-Y4 cells in response to rhSCL. To examine the functional effects of rhSCL on resulting pro-osteoclastic activity, MLO-Y4 cells plated onto a bone-like substrate were primed with rhSCL for 3 days and then either mouse splenocytes or human peripheral blood-derived mononuclear cells (PBMC) were added. Analysis of resorptive activity after 14 days revealed that rhSCL elevated osteoclast resorptive activity approximately 7-fold. The increased resorption was abolished by co-addition of recombinant OPG. SCL increased to a small extent the number of TRAP-positive multinucleated cells formed, and significantly increased the size of the cells formed. rhSCL had no effect on TRAP-positive cell formation from monocultures of either splenocytes or PBMC. rhSCL did not induce apoptosis of MLO-Y4 cells, as determined by caspase activity assays and nuclear morphology. Together, our findings suggest that sclerostin may have a catabolic action through promotion of osteoclast formation and activity by viable osteocytes, in a RANKL-dependent manner.

References:

1. Li et al. 2009 J Bone Miner Res 24:578.
2. Padhi et al. 2011 J Bone Miner Res 26:19.
3. Atkins et al. 2011 Sclerostin is a locally acting regulator of late-osteoblast/pre-osteocyte differentiation and regulates mineralization through a MEPE-ASARM dependent mechanism. J Bone Miner Res DOI:10.1002/jbmr.1345.

Disclosures: Gerald Atkins, None.

1043

Deletion of the Rho-GEF Kalirin Leads to Bone Loss Due to Defects in the Function of Osteoblasts and Osteoclasts. Su Huang¹, Pierre Eleniste¹, Cameron Carter¹, Melissa Kacena², Matthew Allen², Angela Bruzzaniti¹.
¹Indiana University School of Dentistry, USA, ²Indiana University School of Medicine, USA

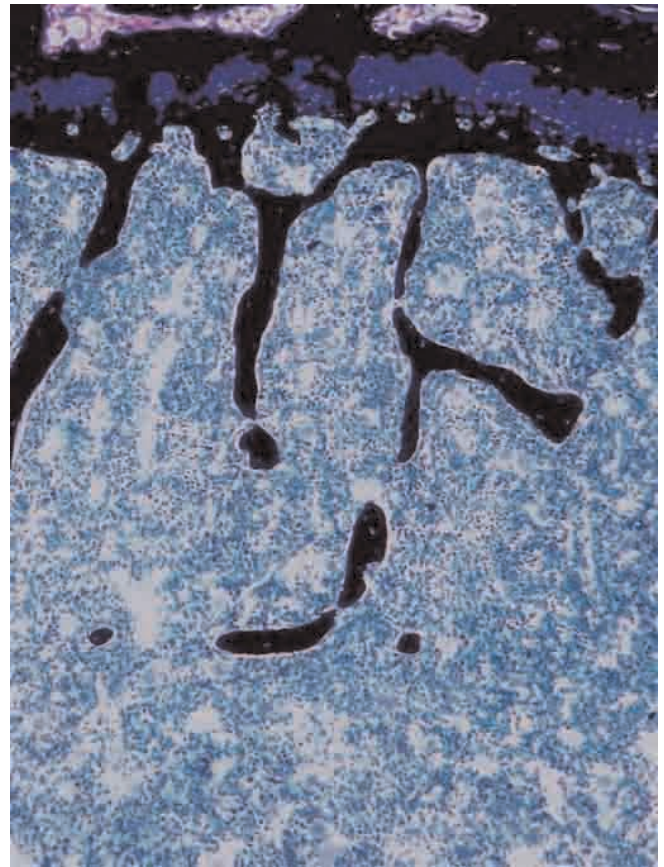
The guanine nucleotide exchange factors (GEFs) control to the activation of the Rho-GTPases and are known to play a critical role in cellular motility and cytoskeletal reorganization. Kalirin, a recently identified Rho-GEF belonging to the family of Dbl-homology proteins, has been shown to play a role in cytoskeletal remodeling and dendritic spine formation in neuronal cells, but its function in non-neuronal cells is largely unknown. We confirmed by Western blotting and real time PCR that Kalirin is expressed in human and mouse osteoclasts (OCs) and mouse osteoblasts (OBs). Given that cytoskeletal remodeling is critical for the function of bone cells, we examined the role of Kalirin in regulating OC and OB activity *in vitro*, and bone mass *in vivo*. Micro-CT analysis of the distal femurs of 14 week old female mice revealed a dramatic 45% decrease in bone volume/trabecular volume (BV/TV) in Kalirin KO mice, compared to littermate controls. Moreover, trabecular number and trabecular thickness was decreased by 38% and 26%, respectively. Histomorphometric analysis of bone sections stained for tartrate-resistant acid phosphatase (TRAP) also revealed an increase in OC surface/bone surface and OC number/bone surface, respectively, in Kalirin KO mice, suggesting that OC differentiation was accelerated *in vivo*. In support of this, increased levels of RANKL and decreased levels of OPG were detected in the serum of Kalirin KO mice. Next, OCs were generated from the bone marrow of WT and Kalirin KO mice by treatment with RANKL and M-CSF. We detected an increase in the number of TRAP-positive multinucleated OCs in cultures from Kalirin KO mice, compared with WT mice. Importantly, OCs lacking Kalirin also exhibited a 30% increase in bone resorbing activity on dentin. Next, we examined the role of Kalirin in OBs. Consistent with an increase in the ratio of RANKL/OPG in serum, we detected increased RANKL and decreased OPG levels in conditioned media from Kalirin KO calvarial OBs. Furthermore, ectopic expression of Kalirin in OBs led to an increase in the secretion of OPG. Taken together, our studies demonstrate that Kalirin is a novel regulator of bone mass. Moreover, Kalirin's effects on bone are due cell-autonomous defects in both OCs and OBs, which leads to an increase in OC number and activity and to dysregulation of the bone remodeling process.

Disclosures: Angela Bruzzaniti, None.

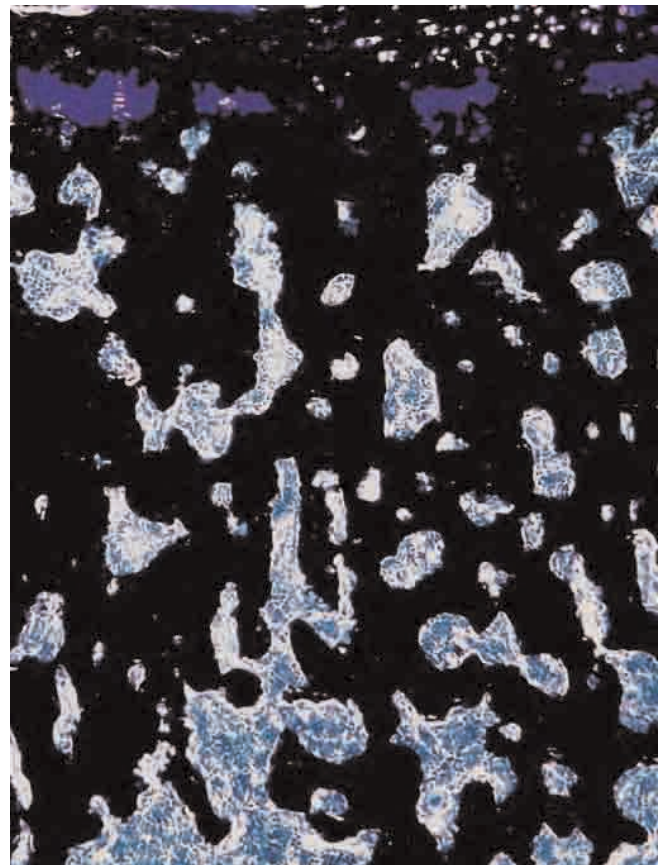
1044

Osteopetrosis in Mice with Knockout of Leucine-Rich Repeat Kinase 1 (Lrrk1) Gene. Robert Brommage¹, Jeff Liu¹, Peter Vogel¹, Thomas Wronski². ¹Lexicon Pharmaceuticals, USA, ²University of Florida, USA

As part of Lexicon Pharmaceuticals' Genome5000™ program, high-throughput DEXA scans were performed on 2995 knockout (KO) mouse lines. KO of Lrrk1 had the highest body vBMD value (T score = 7.0). LRRK1 is a serine/threonine kinase with GTPase activity and related to LRRK2, which has been implicated in Parkinson's disease. KO mice appear healthy through 79 weeks of age. Bone shape is normal with ~10% reductions in femur and tibia lengths. Bones contain extensive cancellous trabeculae with numerous osteoclasts. At 10 weeks of age, serum TRAP5b levels are elevated (6.2 ± 0.3 versus 3.8 ± 0.2 U/liter, P < 0.001). Retention of mineralized cartilage and primary spongiosa occur below the growth plates. At 70 weeks of age DEXA BMD values in male KO mice were elevated 65% for total body, 85% for femur and 2.9-fold for spine. KO mice had reduced serum levels of PINP, suggesting lower bone remodeling. KO mice respond normally to the anabolic actions of teriparatide, as 8 days of daily teriparatide treatment increased serum PINP levels greater than 4-fold in both WT and KO mice. By microCT, tibial cortical bone in male KO mice at 79 weeks of age has a normal diameter, but reduced marrow cavity area, resulting in elevated cortical thickness (P < 0.001) at both the midshaft (Δ = 22%) and tibia-fibula junction (Δ = 35%). Material BMD is increased by 3% (P = 0.002) in KO cortical bone, suggesting slight hypermineralization or reduced porosity. Analyses of trabecular bone in a 1.2 mm thick region of the mid vertebral body (away from the extensive primary spongiosa near the growth plates) showed severe osteopetrosis, as BV/TV increased from 8.5 ± 1.1 to 53.1 ± 3.9 percent. Female mice underwent sham or ovariectomy (OVX) surgery at 16 weeks of age, with DEXA BMD measurements at baseline and 12 weeks. At baseline, BMD values in KO mice were elevated by 40% in whole body, 64% in spine, and 65% in femur. OVX induced loss of BMD in sham controls but was without effect in KO mice (P < 0.01 for effect of genotype by two-factor ANOVA) at all three bone sites. Tibia cortical bone thickness was elevated 14% in KO mice. OVX decreased cortical thickness in WT mice (Δ = 7%, P = 0.04), but not in KO mice (Δ = 1%, P = 0.83). Disruption of the mouse Lrrk1 gene results in severe osteopetrosis from osteoclast dysfunction and protects against OVX-induced bone loss.



WT Mouse LV4 Section



KO Mouse LV4 Section

Disclosures: Robert Brommage, Lexicon Pharmaceuticals, 3
This study received funding from: Lexicon Pharmaceuticals

1045

Estrogen Indirectly Suppresses Mesenchymal Cell Migration and Mineralization by Stimulating Sclerostin and Sostdc1 Expression in Osteoclasts. Kuniaki Ota^{*1}, Patrick Quint², Moustapha Kassem³, Jennifer Westendorp¹, Sundeep Khosla⁴, Merry Jo Oursler¹. ¹Mayo Clinic, USA, ²Mayo Clinic Rochester, USA, ³Odense University Hospital, Denmark, ⁴College of Medicine, Mayo Clinic, USA

Estrogen is a critical regulator of osteoblast differentiation and bone turnover. Reduced estrogen levels lead to postmenopausal osteoporosis. Osteoclast-mediated resorption and osteoblast-mediated bone formation are tightly coupled processes and the involvement and influences of estrogen on this coupling are unclear. In vitro studies have reported direct, but often contradictory, effects of estrogen on coupling of osteoclasts to osteoblasts during mesenchymal stem/stromal cell (MSC) recruitment and differentiation. We examined the influences of estrogen on coupling of osteoclasts to osteoblast lineage recruitment and differentiation using bone marrow-derived osteoclasts and hMSC-TERT cells. Estrogen had no direct effects on hMSC-TERT cell migration or mineralization. Conditioned media from mature osteoclasts enhanced hMSC-TERT cell migration and mineralization. Surprisingly, estrogen reduced osteoclast-driven hMSC migration and mineralization. We have published that osteoclasts secrete Wnt10b and BMP6 to promote mesenchymal cell mineralization. Estrogen did not alter expression of either coupling factor. We next determined if estrogen affects expression of Sclerostin, which suppresses Wnt signaling, and Sostdc1, which suppresses BMP signaling. Western blot analysis of osteoclast conditioned media revealed that estrogen stimulated Sclerostin secretion. Because no functional antibodies could be identified for Sostdc1, we employed QPCR analysis to examine gene expression. Estrogen treatment increased Sostdc1 gene expression in osteoclasts.

Next, osteoclasts were differentiated from bone marrow of Estrogen Receptor knock-in (NERKI) mice. NERKI osteoclasts have elevated levels of ER-beta and are unable to activate classical ER-alpha signaling. NERKI osteoclasts exhibited enhanced estrogen induction of Sclerostin and Sostdc1 compared to wildtype controls. These data indicate that either non-classical ER-alpha signaling and/or ER-beta signaling in osteoclasts regulates Sclerostin and Sostdc1 production to inhibit Wnt and BMP support of mesenchymal cells.

Disclosures: Kuniaki Ota, None.

1046

Critical Role of ATF4 in Regulating Osteoclast Differentiation and Bone Resorption. Huiling Cao^{*1}, Shibing Yu², Zhi Yao³, Deborah Galson¹, Yu Jiang⁴, Xiaoyan Zhang⁵, Jie Fan⁴, Binfeng Lu⁴, Youfei Guan⁵, Min Luo⁴, Yumei Lai⁴, Noriyoshi Kurihara⁶, Kenneth Patrene⁴, G. David Roodman⁷, Guozhi Xiao¹. ¹University of Pittsburgh School of Medicine, USA, ²University of Pittsburgh Medical Center, USA, ³Tianjin Medical University, China, ⁴University of Pittsburgh, USA, ⁵Peking University, China, ⁶Center for Bone Biology, University of Pittsburgh, USA, ⁷VA Pittsburgh Healthcare System (646), USA

Activating Transcription Factor 4 (ATF4) has a critical role in regulating osteoblast differentiation and bone formation. However, its direct role in osteoclasts differentiation has not been addressed yet. In order to define the role of ATF4 in osteoclasts, we deleted ATF4 expression in mice or targeted expression of ATF4 to the osteoclast lineage using the tartrate-resistant acid phosphatase (TRAP) promoter. Osteoclast differentiation was severely impaired in primary bone marrow monocyte (BMM) cultures and bones from *Atf4*^{-/-} mice. Coculture with wt osteoblasts or a high concentration of receptor activator of NF-kappaB ligand (RANKL) failed to restore the osteoclast differentiation defect in *Atf4*^{-/-} BMM cultures. Conversely, *Trap*-ATF4-tg mice display a severe osteopenia with dramatically increased osteoclastogenesis and bone resorption. We further demonstrated that ATF4 is a novel upstream activator of the critical transcription factor nuclear factor of activated T cells c1 (NFATc1) gene and is critical for RANKL activation of multiple MAPK pathways in osteoclast precursors. Further more, ATF4 is crucial for M-CSF induction of receptor activator of NF-kappaB (RANK) expression on BMMs, and lack of ATF4 caused a shift in osteoclast precursors to macrophages, thereby increasing macrophages. Finally, ATF4 is largely modulated by M-CSF signaling and the PI3K/AKT pathways in BMMs. These results for the first time demonstrate that ATF4 plays a critical direct osteoclast-intrinsic role in regulating osteoclast differentiation and suggest that it may be a therapeutic target for treating bone diseases associated with increased osteoclast activity.

Disclosures: Huiling Cao, None.

1047

Deletion of Dynamin-1 and Dynamin-2 in Osteoclasts Shows that Dynamins are Required for the Fusion of Osteoclast Precursors and for Bone Resorption in vivo. Shawn Ferguson¹, William Horne², Pietro De Camilli¹, Lynn Neff², Hiroaki Saito², Nah-Young Shin^{*3}, Roland Baron⁴. ¹Yale University School of Medicine, USA, ²Harvard School of Dental Medicine, USA, ³Harvard University, USA, ⁴Harvard School of Medicine & of Dental Medicine, USA

We have previously shown that the large GTPase dynamin (Dyn), which is best known for playing a critical role in endocytic membrane fission, also contributes to the regulation of podosomes and bone resorption. Here we found that all three classical Dyn isoforms, Dyn-1, -2 and -3, are expressed in osteoclasts (OCs). Interestingly, we observed that the expression of Dyn-2, the predominant isoform in OCs, is highly increased at the stage when OC precursors (OCPs) are fusing to form multinucleated cells (MNCs). To determine the role of dynamin in OC differentiation, we analyzed Dyn-deficient OCs derived from Dyn-1/Dyn-2 double floxed mice crossed with 4-hydroxy-tamoxifen-inducible Cre mice. The number of MNCs formed in vitro from M-CSF and RANKL-treated Dyn-1/Dyn-2-null bone marrow macrophages (BMMs) and the number of nuclei incorporated into MNCs were both decreased by ~65%, while the number of TRAP+ mononuclear OCPs in these cultures was increased by about 3-fold, suggesting that the fusion of OCPs was impaired in the absence of Dyn-1 and Dyn-2. To test this hypothesis, we developed a fusion assay mixing DiI (red)- and DiO (green)-labeled live BMMs in the presence of M-CSF and RANKL and determined the percentage of fused (yellow-orange) MNCs. The results confirmed that deletion of Dyn-1 and Dyn-2 reduced the fusion activity of OCPs by about half. The expression of OC differentiation markers, including cathepsin K, calcitonin receptor, integrin beta3 and TRAP, were all decreased in the Dyn-1/Dyn-2-null cells, as was the expression of the fusion-mediating membrane proteins DC-STAMP and E-cadherin, which are important for the generation of fusogenic OCPs. Dyn-1/Dyn-2-null OCs also showed significantly reduced in vitro bone resorption activity. In Dyn-deficient OCPs and OCs, a pronounced accumulation of endocytic clathrin coated pits labeled with F-actin and the Dyn-binding BAR domain protein endophilin, which was associated with a decreased internalization of DC-STAMP, a process required for the fusion of OCPs, were observed by confocal microscopy. These results suggest that dynamins are required for the fusion of OCPs, possibly through their role in endocytosis. Finally, we generated Dyn-1;Dyn-2;Cathepsin K-Cre mice and found a significant increase in bone density. Thus, Dyn-1 and Dyn-2, and possibly endocytosis, are critical for OCP fusion, in addition to dynamin's role in podosomes and bone resorption.

Disclosures: Nah-Young Shin, None.

1048

Contrasting Roles of Leukemia Inhibitory Factor (LIF) in Neonatal Bone Development and Adult Bone Remodeling Involve Region-Specific Regulation of Vascular Endothelial Growth Factor (VEGF). Ingrid J Poulton¹, Narelle E McGregor¹, Sueli Pompolo¹, Emma C Walker¹, Natalie Sims^{*2}. ¹St. Vincent's Institute of Medical Research, Australia, ²St. Vincent's Institute for Medical Research, Australia

Leukemia inhibitory factor (LIF) is expressed in pre-hypertrophic chondrocytes and osteoblasts, suggesting roles in bone development and remodeling. In this study, age- and region-specific analyses of LIF deficient (KO) mice reveal independent roles for LIF in osteoclast and osteoblast activity in these processes.

LIF KO neonates demonstrated many "giant" osteoclasts, as previously described. In 12 week old LIF KOs, osteoclast number was doubled, and osteoclast size increased by 30%. Surprisingly, this was only observed in those osteoclasts destroying mineralized growth plate cartilage (chondroclasts). Osteoclast number and size in the secondary spongiosa were not modified in LIF KO. Although osteoclast formation was normal in LIF KO remodeling bone, osteoblast surface, mineral appositional rate and bone formation rate were all significantly reduced (by 75%, 50% and 60% respectively) and marrow adipocyte volume was increased 3-fold. Consistent with this, LIF delayed adipocyte formation and stimulated mineralization by murine stromal cells and inhibited sclerostin expression.

To understand the region-specific role of LIF in osteoclast formation, we examined neonatal bone development. Chondrocyte proliferation and hypertrophy, vascularization and osteoclast invasion were timed identically in LIF KO and WT phalanges and metatarsals. However, once vascular invasion commenced, the vessels of LIF KO metatarsals were larger and more numerous than WT. Furthermore, in adult LIF KO bones, blood vessel area was significantly increased (3-fold) compared to WT littermates, but only immediately below the growth plate. To explore the control of vascularisation and osteoclast formation at the growth plate, LIF receptor (LIFR) was assessed by immunohistochemistry and was detected at very high levels in hypertrophic chondrocytes. Furthermore, in LIF KO bones, consistent with early reports of LIF inhibiting VEGF expression in retina and placenta, VEGF mRNA levels were significantly elevated (3-fold), and VEGF immunohistochemical staining was greater in LIF KO chondrocytes compared to WT littermates. In conclusion, LIF influences the skeleton in a region-specific manner. Chondrocytic LIF acts as a brake on VEGF production; in its absence, vascularization and osteoclast formation is enhanced in bone development and growth. LIF is not required for normal osteoclast

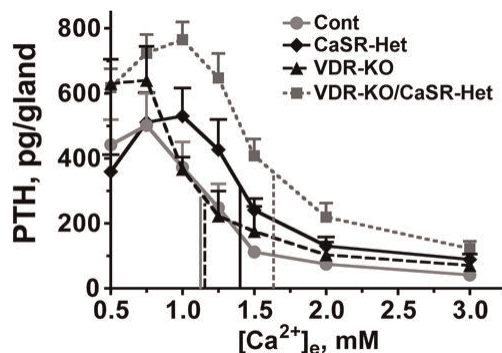
formation in bone remodeling however, but stimulates osteoblast formation at the expense of adipogenesis.

Disclosures: Natalie Sims, None.

1049

Autocrine/Paracrine Actions of Cyp27b1, VDR, and CaSR Signaling in the Regulation of Parathyroid Function: Studies of Parathyroid-Specific Knock-out Mice. Zhiqiang Cheng, Chialing Tu, Alfred Li, Michael You, Dolores Shoback, Daniel Bikle, Wenhan Chang*. University of California, San Francisco, USA

The Ca^{2+} -sensing receptor (CaSR) and vitamin D receptor (VDR) mediate critical suppression of PTH secretion by parathyroid cells (PTCs). The 1,25 (OH)₂ vitamin D (1,25D) produced by renal Cyp27B1 is thought to be the major source of ligand that achieves these suppressive actions in PTCs. The demonstration of CYP27B1 activity in PTCs, however, raises the question whether these cells also produce 1,25D to regulate PTH secretion directly. To address the source of 1,25D and the role of the VDR and CaSR in the control of PTC function, we generated mice with homozygous Cyp27B1 (Cyp-KO) or VDR (VDR-KO) gene KO targeted specifically to PTCs. We performed similar gene KO in the background of CaSR-Het mice (which lack one allele of the CaSR gene) to produce VDR-KO/CaSR-Het or Cyp-KO/CaSR-Het double KO mice. Serum Ca^{2+} , phosphate (Pi), and PTH levels in these mice and their control littermates (Cont), which carry floxed alleles (but no Cre), were compared. PTC glands (PTGs) were also isolated for PTH secretion assays to determine the Ca^{2+} -set-point ($[\text{Ca}^{2+}]$) inhibiting 50% of PTH secretion) and maximal PTH secretory response on a per-gland basis (PTH-Max) in an organ culture system. As shown (see Table), serum PTH levels were increased by $\approx 25\%$ in both VDR-KO and CaSR-Het mice and much more robustly ($\approx 100\%$) in the VDR-KO/CaSR-Het double KO (d-KO) mice, compared to Cont mice. PTH secretion from PTGs from CaSR-Het mice (but not VDR-KO mice) displayed a right-shift in the Ca^{2+} -set-point vs Cont (see Figure; Cont: 1.2 mM; CaSR-Het: 1.4 mM; and VDR-KO: 1.2 mM). However, mice with VDR KO (and intact CaSR alleles) showed a 30% increase in the PTH-Max vs Cont or CaSR-Het mice. In PTGs from VDR-KO/CaSR-Het mice, the Ca^{2+} -set-point was further right shifted to ≈ 1.6 mM along with a more profound increase in PTH-Max by $\approx 60\%$, indicating a synergistic effect of CaSR and VDR KO in expanding PTH pools and decreasing Ca^{2+} -sensitivity. Hypercalcemia and hypophosphatemia developed only in the CaSR-Het mice and not in VDR-KO mice, suggesting that VDR and CaSR signaling may have different effects on the patterns of PTH secretion (pulsatility, amplitude, duration) that have different effects on mineral metabolism. Importantly, Cyp-KO mice also showed increased PTH and serum $[\text{Ca}^{2+}]$ equivalent to VDR-KO (see Table), with similar increases in PTH-Max in vitro, supporting the idea that locally produced 1,25-D plays a critical role in regulating PTH function via the VDR in the PTC.



Figure

Genotype (N)	Cont (40)	CaSR-Het (15)	VDR-KO (10)	d-KO (16)
PTH, pg/ml	123±8	157±12*	166±22*	246±43**
Ca^{2+} , mg/dL	10.2±0.1	11.0±0.2*	9.9±0.2	11.3±0.3**
Pi, mg/dL	8.1±0.2	7.5±0.2*	8.3±0.4	8.0±0.4
Genotype (N)	Cont (30)	CaSR-Het (6)	Cyp-KO (5)	d-KO (9)
PTH, pg/ml	134±10	194±11**	317±46**	465±58**
Ca^{2+} , mg/dL	9.9±0.3	11.1±0.3*	9.6±0.2	10.6±0.1*
Pi, mg/dL	7.4±0.4	6.5±0.3*	7.2±0.2	6.9±0.4

* p<0.05, **p<0.01 compared to Cont

Table

Disclosures: Wenhan Chang, None.

1050

Conditional Deletion of the Parathyroid Hormone (PTH) Receptor 1 from Osteocytes Results in Decreased Bone Resorption and a Progressive Increase in Cancellous Bone Mass. Xiaolin Tu*, Rachel Edwards¹, Naomie Olivis¹, Jeffrey Benson¹, Carlo Galli², Gretel Pellegrini³, Nicoletta Bivi⁴, Lilian Plotkin¹, Teresita Bellido¹. ¹Indiana University School of Medicine, USA, ²Università Degli Studi Di Parma, Italy, ³seccion osteopatias medicas, Hospital de Clínicas Jose de San Martín, Argentina, ⁴Indiana University, USA

Some skeletal actions of PTH might be mediated by direct effects of the hormone on osteocytes. To explore the physiological role of the PTH receptor (PTHr1) in these cells, we generated conditional knockout mice (cKO) by mating PTHr1^{flx/flx} mice with DMP1-8kb-Cre mice. Cre mRNA was detected in green fluorescent protein (GFP) positive cells (osteocytes) but not in GFP negative cells (osteoblasts) isolated from DMP1-8kb-Cre mice crossed with DMP1-8kb-GFP mice. PTHr1 mRNA was reduced by 54% in lumbar vertebra and 73% in tibial diaphysis of cKO mice compared to control PTHr1^{flx/flx} littermates. cKO mice exhibited no gross skeletal abnormalities. BMD (DEXA) progressively increased in lumbar spine (5.3% to 14.8%), but not in the femur, in 2 to 8 month-old female cKO mice. Cancellous bone volume (BV/TV) and trabecular number and thickness (micro-CT) were increased in spine and distal femur, without changes in femoral cortical bone, at 4 months. At this age, the resorption marker CTX was 22% lower in plasma from cKO mice, whereas osteocalcin was similar to controls. The discrepancy with the reported reduced BMD without changes in BV/TV or CTX in PTHr1^{flx/flx};DMP1-10kb-CreERT2 mice might be due to the fact that the 10kb fragment directs gene expression to osteocytes and some osteoblasts, whereas the 8kb fragment only targets osteocytes. In tibial diaphysis (composed of cortical bone and enriched in osteocytes) the expression of RANKL and the Wnt target genes OPG, naked2, Cx43, Smad6 and BMP4 was lower in cKO mice. In contrast, in lumbar vertebra (mostly composed of cancellous bone), only RANKL was decreased resulting in a reduction in the RANKL/OPG ratio. This suggests that osteocytes are the main source of RANKL whereas OPG is also contributed by other osteoblastic cells relatively more abundant in cancellous versus cortical bone. Thus, removal of the PTHr1 only from osteocytes leads to a site specific reduction in the RANKL/OPG ratio resulting in increased cancellous but not cortical bone mass in the cKO mice. Reduced bone resorption induced by deletion of PTHr1 in osteocytes is consistent with earlier evidence that, conversely, osteocyte-specific activation of PTHr1 increases osteoclasts and bone resorption. We conclude that actions of the PTHr1 in osteocytes are required to maintain basal levels of Wnt signaling and RANKL, and that the primary effect of absence of the receptor in osteocytes is a reduction in osteoclast activity in cancellous bone.

Disclosures: Xiaolin Tu, None.

1051

PTH/PTHrP (PPR) Receptor Signaling in Osteocytes Regulate Bone Development in Temporal Manner. Vaibhav Saini*, Kevin Barry², Keertik Fulzele³, Jian Feng⁴, Paola Pajevic Divieti⁵. ¹Research Fellow, MGH, Harvard Medical School, USA, ²Massachusetts General Hospital, USA, ³Massachusetts General Hospital; Harvard Medical School, USA, ⁴Texas A&M Health Science Center, USA, ⁵MGH- Harvard Medical School, USA

Osteocytes, the terminally differentiated cells of the osteoblastic lineage, regulate bone remodeling by influencing osteoblast and osteoclast activities. Osteoblasts are targets for numerous systemic hormones, including parathyroid hormone (PTH), which acts through the PTH/PTHrP receptor (PPR). Clinically, PTH is the only available anabolic agent to treat osteoporosis. Recent evidence suggests that osteocytes may partially mediate the anabolic effects of PTH via PTH mediated suppression of the osteocyte-specific protein sclerostin, a potent Wnt signaling inhibitor. To understand the role of PPR signaling in osteocytes and to determine if osteocytes directly mediate the effects of PTH on bone, we generated mice with osteocyte-specific ablation of PPR (DMP1-PPRKO) using Cre-loxP recombination technique. Mice with floxed PPR alleles were mated with mice expressing Cre-recombinase driven by a 10Kb-DMP1 promoter which has been shown to be active in osteocytes. Littermates lacking Cre expression were used as controls for all experiments. Real-time PCR analysis of mRNA from osteocyte-enriched long bones showed a 70% reduction in PPR expression in the DMP1-PPRKO mice compared to controls, indicating successful PPR deletion. Alizarin-red/alcalin-blue staining of newborn pups' skeletal preparations showed no obvious patterning defects in the KO mice compared with controls. To assess PPR ablation in osteocytes in the context of aging, we performed dual-energy X-ray absorptiometry (DXA) at 8, 10, 12, and 24 weeks on KO and controls. Total body BMD (g/cm²) was comparable at 8 weeks of age. However, at 10, 12, and 24 weeks, DMP1-PPRKO mice showed a significantly higher BMD compared to controls. Moreover, microCT analysis at 14 weeks, revealed a significant increase in trabecular BV/TV%, trabecular number, cortical thickness and bone area (BA) in DMP1-PPRKO compared with controls. While osteoblasts are important for bone formation during growth (until 8-weeks of age), osteocytes are critical for remodeling in later life. Our results suggest an important role of PPR on osteocytes in bone homeostasis and bone remodeling and support a key role of PTH signaling via PPRs in osteocytes for proper bone modeling and remodeling. Taken

together, these data suggest that PPR signaling may regulate bone development in temporal and spatial manner.

Disclosures: Vaibhav Saini, None.

1052

The Calcium Sensing Receptor Synergizes with PTH in Modulating Bone Turnover. Yingben Xue¹, Yongjun Xiao², Jingning Liu³, Andrew Karaplis⁴, Martin Pollak⁵, Edward Brown⁶, Dengshun Miao⁷, David Goltzman⁸. ¹Calcium Research Lab, McGill University, Canada, ²the Centre for Bone & Periodontal Research, McGill University, Canada, ³Calcium Research Laboratory, McGill University Health Centre & Department of Medicine, Canada, ⁴McGill University, Can, ⁵Renal Division, Department of Medicine, Brigham & Women's Hospital, USA, ⁶Brigham & Women's Hospital, USA, ⁷Nanjing Medical University, Peoples Republic of China, ⁸McGill University Health Centre, Canada

Both parathyroid hormone (PTH) and the calcium sensing receptor (CaSR) may influence skeletal function, however the interaction of the two *in vivo* requires clarification. We infused human PTH (1-34) for 2 weeks into wild-type (WT) mice; into mice with genetic deletion of the gene encoding PTH (PTH^{-/-} mice); and into mice with genetic deletion of the genes encoding both PTH and the CaSR (PTH^{-/-}CaSR^{-/-} mice). We examined the effects biochemically, histologically and by skeletal imaging. The results showed that continuous PTH administration increased alkaline phosphatase positive area, osteoblast numbers and osteoclast numbers in cortical bone in all three genotypes. This increased turnover was associated with increased cortical porosity and loss of cortical bone volume and by a decrease in femoral bone mineral density (BMD). Relative to effects in PTH^{-/-} mice, however, PTH^{-/-}CaSR^{-/-} mice displayed reduced PTH-stimulated bone turnover in cortical bone, less marked PTH-induced reductions of cortical bone volume, decreased PTH-induced increases in cortical porosity and reduced PTH-induced reductions in femoral BMD. *Ex vivo* and *in vitro* studies demonstrated reductions of PTH-stimulated receptor activator of nuclear factor kappa B ligand (RANKL) and tartrate resistant acid phosphatase (TRACP) expression, and *in vitro* studies demonstrated reductions in PTH-stimulated osteoclastogenesis. In trabecular bone, continuous PTH also induced increased bone turnover, but this was associated with increases in trabecular bone volume and trabecular number. In PTH^{-/-}CaSR^{-/-} mice, PTH-stimulated bone turnover in trabecular bone was significantly lower and PTH-induced increases in genetic markers of osteoblast activity i.e., expression of the transcription factor Runx2 and of Nkx2, a marker of Wnt activity, were lower than in PTH^{-/-} mice. These studies show that following PTH infusion, genetic deletion of CaSR substantially impaired PTH-induced bone turnover, and bone loss in cortical bone, while also modestly impeding PTH-induced bone turnover and osteoblastic stimulation in trabecular bone. These results are consistent with a role for CaSR in differentially modulating both PTH-induced resorption and PTH-induced formation in discrete skeletal compartments.

Disclosures: Yingben Xue, None.

1053

Mammary-Specific Ablation of the Calcium-Sensing Receptor Gene Results in Alterations in Systemic Calcium Metabolism and Breast Calcium Transport During Lactation. Ramanaiah Mamillapalli¹, Joshua VanHouten², Pamela Dann², Laleh Ardeshirpour¹, Wenhan Chang³, Dolores Shoback⁴, Daniel Bikle⁵, John Wysolmerski². ¹Yale University, USA, ²Yale University School of Medicine, USA, ³University of California, San Francisco, USA, ⁴VA Medical Center, USA, ⁵Endocrine Research Unit, Division of Endocrinology UCSF, USA

The calcium-sensing receptor (CaSR) is expressed on mammary epithelial cells (MECs) during lactation. Pharmacological data suggested that activation of the CaSR on MECs inhibits the secretion of PTHrP into milk and the circulation, but stimulates the transport of calcium into milk. Global deletion of the CaSR results in severe hypercalcemia and early death. Therefore, in order to provide genetic support for the functions of the mammary gland CaSR, we ablated the CaSR gene specifically in MECs. Mice bearing a floxed CaSR gene (CaSR^{lox/lox}) were bred to mice expressing Cre recombinase driven by a milk protein gene (beta-lactoglobulin) promoter (BLG-Cre). In BLG-Cre/CaSR^{lox/lox} mice, the CaSR gene is disrupted only in MECs and only at the end of pregnancy. Deletion of the CaSR did not affect mammary alveolar development and BLG-Cre/CaSR^{lox/lox} mice lactated normally. Mammary CaSR mRNA levels were reduced from 60 to 95 percent in lactating BLG-Cre/CaSR^{lox/lox} mice. As expected, loss of the CaSR resulted in elevated levels of mammary gland PTHrP mRNA and milk PTHrP concentrations. Loss of the mammary CaSR also led to a reduction in milk calcium concentrations. Lactational bone loss by PIXImus was not accelerated in BLG-Cre/CaSR^{lox/lox} mice, but on microCT measurements, mineral density was decreased although bone volume was not. Loss of the mammary CaSR led to transient hypercalcemia. On day 2 of lactation, mean calcium levels in BLG-Cre/CaSR^{lox/lox} mice were 13.80.6 as compared to 10.70.3 in controls. However, on day 9 of lactation, circulating calcium concentrations were the same in each group. In contrast on day 9, urinary calcium excretion was 5 times higher in BLG-Cre/CaSR^{lox/lox} mice as compared to controls.

Since other sites of CaSR expression remain intact in these mice, the transient nature of the hypercalcemia is likely due to stimulation of the renal CaSR and compensatory hypercalciuria. These data demonstrate that the mammary CaSR regulates systemic calcium metabolism and calcium transport in MECs during lactation.

Disclosures: Ramanaiah Mamillapalli, None.

1054

Skeletal Mineralization Defect of FGF23 Deficient Mice Is Mediated by Increased Osteopontin. Quan Yuan¹, Yan Jiang², Tadatoshi Sato¹, Reinhold Erben³, Beate Lanske¹. ¹Harvard School of Dental Medicine, USA, ²Peoples Republic of China, ³University of Veterinary Medicine, Austria

Excessive FGF23 has been identified as the pivotal phosphaturic factor leading to renal phosphate wasting, and the subsequent development of rickets and osteomalacia through impaired osteoblastic mineralization. Interestingly, Fgf23-ablated (Fgf23^{-/-}) mice also exhibit a skeletal phenotype characterized by a severe mineralization defect. The reason for this abnormality is largely unknown. Through *in situ* hybridization and immunohistochemical staining, we found that expression of osteopontin (Opn), an inhibitor of bone mineralization, was markedly increased in Fgf23^{-/-} bones. These results were confirmed by qPCR analyses of the cortical bone and ELISA measurement of serum Opn. To investigate whether the elevated levels of Opn are contributing to the bone mineralization defect of Fgf23^{-/-} mice, we generated Fgf23^{-/-}Opn^{-/-} double knockout mice (DKO), and compared their phenotype to the one of wild-type (WT), Fgf23^{-/-} and Opn^{-/-} single knockout mice. Biochemical analyses showed that the hypercalcemia and hyperphosphatemia observed in Fgf23^{-/-} mice remained unchanged in the DKO mice. However, additional ablation of Opn in Fgf23^{-/-} mice resulted in larger, heavier, and more active DKO mice when compared to Fgf23^{-/-} littermates. The length and radiopacity of the femora in the DKO mice were significantly increased. MicroCT analyses of femurs showed that cancellous bone volume in Fgf23^{-/-} mice was reduced compared with WT and Opn^{-/-} mice, but restored to the values found in Opn^{-/-} mice in DKO mice. Deletion of Opn also improved femoral trabecular number, trabecular thickness, and cortical thickness in Fgf23^{-/-} mice. In addition, the elevated serum CTX levels found in Fgf23^{-/-} mice were normalized in compound mutants. Opn^{-/-} mice showed lower CTX levels compared to those of WT. In summary, our results suggest that increased osteoblastic Opn expression is an important pathogenetic factor mediating the mineralization defect and the alterations in bone metabolism observed in Fgf23^{-/-} bones.

Disclosures: Quan Yuan, None.

1055

Age, Bone Mineral Density, and Spine Fracture Status for Predicting Fracture Risk. John Krege¹, Xiaohai Wan¹, Brian Lentle², Claudie Berger³, Lisa Langsetmo⁴, Jonathan Adachi⁵, Jerilynn Prior², Alan Tenenhouse³, Jacques Brown⁶, Nancy Kreiger⁷, Wojciech P. Olszynski⁸, Robert Josse⁹, David Goltzman¹⁰, CaMos Research Group¹⁰. ¹Eli Lilly & Company, USA, ²University of British Columbia, Canada, ³McGill University, Canada, ⁴Canadian Multicenter Osteoporosis Study, Canada, ⁵St. Joseph's Hospital, Canada, ⁶Laval University, Canada, ⁷University of Toronto, Canada, ⁸University of Saskatchewan, Canada, ⁹St. Michael's Hospital, University of Toronto, Canada, ¹⁰McGill University Health Centre, Canada

Using data from 2761 subjects from the Canadian Multicentre Osteoporosis Study (CaMos), we previously reported that the most predictive risk factors for incident fracture were age, BMD, and spine fracture status. A model considering these risk factors captured almost all of the predictive information provided by other models that included additional risk factors. The objective was to validate the previous analysis using data from subjects (1447 women, 517 men) whose spine radiograph assessments were not complete and were excluded from the previous analyses. CaMos is a prospective study following a randomly selected, population-based community cohort of non-institutionalized men and women. Prevalent and incident spine fractures were assessed by quantitative morphometry of lateral spine radiographs at baseline and 5 years. Incident nonvertebral fractures were determined by an annual, mailed questionnaire with validation; fragility fracture was defined as a fracture with minimal trauma, i.e. fall from a standing height or without trauma. The endpoint was 5-year risk of an osteoporotic fracture defined as morphometric vertebral fracture and/or a nonvertebral fragility fracture. The results in these 1964 subjects were similar to the published results for the 2761 subjects. A logistic regression model including age, femoral neck BMD, and spine fracture status (yes/no) revealed a gradient of risk/SD (GR/SD) of 1.88. This model captured almost all of the predictive information provided by a model with spine fracture status plus the WHO risk factors (GR/SD 1.92) and provided greater predictive information than a model considering the WHO risk factors alone (GR/SD 1.74). The five-year risk of incident fragility fracture in the women based on age, femoral neck T-score, and spine fracture status is shown (Table). Fracture risk was markedly impacted by spine fracture status at all ages and BMD, including those with younger age and higher BMD. We repeated all analyses for the overall population (N = 4725) and the results were very similar. The data confirm that morphometric spine fracture status along with age and BMD predicted

future fracture risk with greater simplicity and higher prognostic accuracy than consideration of more complex models including the WHO risk factors. Spine fracture status provides useful prognostic information regarding future fracture risk and an assessment of spine fracture status should be performed in patients at risk.

Femoral Neck T-Score	Spine Fracture	Age (Yr)							
		50	55	60	65	70	75	80	85
-1	No	12	12	13	14	14	15	16	16
	Yes	23	24	25	26	27	28	29	31
-1.5	No	15	15	16	17	18	18	19	20
	Yes	28	29	30	31	32	34	35	36
-2	No	18	19	20	21	22	23	24	25
	Yes	33	34	35	37	38	39	41	42
-2.5	No	22	23	24	25	26	27	28	29
	Yes	39	40	41	43	44	46	47	48
-3	No	27	28	29	30	31	32	34	35
	Yes	45	46	48	49	50	52	53	55
-3.5	No	32	33	34	36	37	38	39	41
	Yes	51	52	54	55	57	58	59	61
-4	No	38	39	40	42	43	44	46	47
	Yes	57	59	60	61	63	64	65	66

Table. Five-year Risk of Incident Fragility Fracture in the Women

Disclosures: John Krege, Eli Lilly & Co, 3; Eli Lilly & Co, 1
This study received funding from: Eli Lilly and Company

1056

Recency and Duration of Glucocorticoid Use and Fracture Prediction: The Manitoba BMD Cohort. William Leslie^{*1}, Sumit Majumdar², Suzanne Morin³, Colleen Metge¹, Lisa Lix⁴. ¹University of Manitoba, Canada, ²University of Alberta, Canada, ³McGill University Health Centre, Canada, ⁴University of Saskatchewan, Canada

BACKGROUND: Glucocorticoid (GC) use, conventionally defined as any history of exposure to supra-physiologic doses for 90-days or more, is a major risk factor for osteoporosis and fracture and is included in the WHO fracture risk assessment (FRAX) algorithm. FRAX does not, however, distinguish between recent (versus remote) exposure or short-duration (versus prolonged) GC use, and such distinctions may be clinically important. **METHODS:** We identified all adults over age 40-years with baseline femoral neck (FN) DXA testing between April 1998 and March 2007 within a comprehensive clinical BMD database for Manitoba, Canada. Using linkages to a province-wide pharmacy network, we identified total dose (based on GC dispensed before BMD testing in the last 12-months and cumulatively since 1995) and stratified this by timing ("recent" if last 12-months versus "remote" if earlier) and duration (short [<90 days] versus prolonged [≥ 90 days]). Other relevant covariates, osteoporosis medications, and major fractures to March 2010 were obtained from a population-based administrative health data repository. Multivariable adjusted least squares mean (LSM) FN T-score was estimated according to patterns of GC use with ANCOVA. Time to fracture was estimated according to patterns of GC use after multivariable (including FN T-score) adjustment using Cox proportional hazards models. **RESULTS:** Among 52,070 subjects included in the analysis, prior GC was identified in 12,818 (see Table). GC users were slightly younger than nonusers (mean age 63 vs 64, $p < .001$) and more likely to be men (14% vs 6%, $p < .001$). Only recent GC use for ≥ 90 days was associated with a significant reduction in FN T-score (LSM -0.07 versus non-use, $p < .001$). Major osteoporotic fractures occurred in N=2,842 (566 hip fractures) subjects. Recent (but not remote) GC users were more likely to sustain major osteoporotic fracture than non-users (6.5% vs 5.3%, $p < .001$) or hip fractures (1.5% vs 1.0%, $p = .001$). Recent GC use ≥ 90 days showed a significant BMD-independent increase in major osteoporotic fracture risk (adjusted HR 1.25, $p = 0.003$) and hip fracture risk (adjusted HR 1.61, $p = 0.003$). Non-significant trends were seen for remote exposure and short duration GC use. **CONCLUSIONS:** We confirmed that prior GC use is a risk factor for reduced FN BMD and osteoporotic fractures. The largest and most consistent effect, however, was seen with recent and prolonged GC use. These findings may inform risk-prediction and permit physicians to take a more precise and useful GC history.

GC Use	N	LSM (95% CI)	HR (95% CI)	HR (95% CI)
		FN T-score	Major #	Hip #
Recent use <90 days	2644	+0.01 (-0.01 to +0.03)	1.16 (0.97-1.38)	1.26 (0.87-1.83)
Recent use ≥ 90 days	2896	-0.07 (-0.09 to -0.05)	1.25 (1.07-1.45)	1.61 (1.18-2.2.0)
Remote use <90 days	6453	+0.06 (+0.05 to +0.08)	1.14 (1.00-1.29)	0.98 (0.72-1.32)
Remote use ≥ 90 days	825	-0.01 (-0.04 to +0.01)	1.29 (0.99-1.69)	1.05 (0.54-2.03)

Bolded results are statistically significant. LSM=least squares mean (ANCOVA), HR=hazard ratio (Cox survival model). All results adjusted for sex, age, BMI, prior fracture, RA, COPD, substance abuse diagnosis, osteoporosis treatment. HRs also adjusted for FN T-score.

Table: Effect of prior GC use versus non-use on FN T-score and fracture outcomes.

Disclosures: William Leslie, None.

1057

Low Bone Turnover and Abnormal Collagen Crosslinking in Women with Atraumatic Fractures and Near- Normal BMD: A Disease Entity Different from Post-Menopausal Osteoporosis. Hartmut Malluche^{*1}, Daniel Porter², Marie-Claude Faugere¹, Hanna Mawad³, David Pienkowski². ¹University of Kentucky Medical Center, USA, ²University of Kentucky, USA, ³University of Kentucky, Division of Nephrology Bone & Mineral Metabolism, USA

Osteoporotic fractures normally occur with minimal or no-trauma and are associated with low bone mineral density (BMD); however, atraumatic fractures may also occur with near-normal BMD. This study addresses potential abnormalities in bone quality associated with atraumatic fractures in women who are non-osteoporotic by BMD criteria. Anterior iliac crest bone samples were obtained from 19 pre- or perimenopausal untreated Caucasian women with nonosteoporotic t-scores in this IRB approved study. Ten of these women sustained one or more low-trauma bone fractures. The other nine women were normal volunteers (no fractures, normal BMD). BMD was measured by DEXA. Fourier transform infrared (FTIR) spectroscopy and histomorphometry (static and dynamic bone parameters) were employed to quantify the material, microstructural, and turnover characteristics. Cancellous bone volume was in the normal range and not different between the groups. Lumbar t-scores were not different between the groups, while hip t-scores were greater in the fracture group vs. normal controls (Table). Bone turnover in the fracture group was lower, as shown by 66% lower activation frequency and 85% lower osteoblast numbers/bone perimeter. Additionally, women in the atraumatic fracture group had 10% more enzymatic collagen crosslinking. No differences were detected in the other measured parameters. The greater hip t-scores in the fracture group, compared to the non-fracture controls, demonstrate the limitations of BMD as a general metric of fracture resistance. The obvious explanation for this limitation is that neither bone turnover nor collagen crosslinking can be evaluated by BMD. Prior studies linked crosslinking abnormalities to decreased bone strength (1) and low bone turnover to increased fracture risk (2). The present findings agree with prior studies that showed either matrix (3) or turnover (4) abnormalities in women with atraumatic fractures. This study is novel in reporting both abnormalities concurrently. The data indicate that occurrence of atraumatic fractures in women with normal or near-normal BMD might be a different disease entity than what is conventionally considered "post-menopausal osteoporosis". 1. Saito, M. et al., Osteoporos Int, 2010. 21(2): p. 195-214. 2. Coco, M., et al., Am J Kidney Dis, 2000. 36(6): p. 1115-21 3. Gourion-Arsiquaud, S., et al, J Bone Miner Res, 2009. 24(9): p. 1565-71 4. Donovan, M.A., et al, J Clin Endocrinol Metab, 2005. 90(6): p. 3331-6

BMD, Histomorphometric & FTIR Results

	Fracture (n=10)	Control (n=9)
BMD Hip (t-score)	0.17 ± 1.13**	-1.01 ± 0.77
BMD Spine (t-score)	0.12 ± 1.04	-0.48 ± 0.82
BV/TV (%)	18.3 ± 2.54	20.1 ± 3.92
NOB/BPm (#/100 mm)	12.9 ± 9.58*	119 ± 86.1
Ac.f (yr ⁻¹)	0.17 ± 0.16*	0.49 ± 0.24
Crosslinking	3.87 ± 0.26**	3.53 ± 0.31

*p < 0.01; **p < 0.05; (Mean ± SD)

FTIR= Fourier transform infrared

BMD= Bone Mineral Density Measured by DXA

BV/TV= Cancellous Bone Volume

NOB/BPm= osteoblast numbers/bone perimeter

Ac.f= Activation Frequency

BMD, Histomorphometric and FTIR Results

Disclosures: Hartmut Malluche, None.

1058

Is the Ability of FRAX to Predict Fractures Comparable in Obese and Non-obese Postmenopausal Women? Melissa Premaor^{*1}, Richard Parker², Li-Yung Lui³, Teresa Hillier⁴, Kristine Ensrud⁵, Jane Cauley⁶, Juliet Compston⁷. ¹Federal University of Santa Maria, Brazil, ²Department of Public Health & Primary Care, Institute of Public Health, University of Cambridge, United Kingdom, ³California Pacific Medical Center Research Institute, USA, ⁴Center for Health Research, Kaiser Permanente Northwest/Hawaii, USA, ⁵Minneapolis VA Medical Center / University of Minnesota, USA, ⁶University of Pittsburgh Graduate School of Public Health, USA, ⁷University of Cambridge School of Clinical Medicine, United Kingdom

There is increasing evidence that low trauma fractures in obese postmenopausal women contribute significantly to the overall fracture burden. FRAX-generated fracture probabilities in obese women are likely to be lower than in non-obese women because of higher bone mineral density (BMD) and body mass index (BMI); in addition, clinical risk factors for fracture in obese women may differ from those in the non-obese population. We compared the ability of FRAX to predict fractures in obese (BMI ≥ 30 kg/m²) and non-obese (BMI < 30 kg/m²) women in the Study of Osteoporotic Fractures (SOF) cohort. SOF is a prospective population-based study of 9704 Caucasian older postmenopausal women followed up for a mean(SD) of 12.8 (5.4) years. As FRAX generates 10-year probabilities, the follow-up was truncated to ten years. Data for FRAX clinical risk factors and femoral neck BMD were available in 6252 women. Incident fracture outcomes included hip fracture, major osteoporotic fracture (hip, clinical vertebral, wrist, or humerus), and any clinical fracture. Fracture probability was estimated using FRAX. Receiver operating characteristic (ROC) curve analysis was used to compare fracture prediction in obese and non-obese women.

18.5% women in the cohort were obese. Incident clinical fractures occurred during the follow-up period in 26.9% and 32.7% of obese and non-obese women respectively. FRAX-derived probabilities in women with incident hip and major osteoporotic fractures were significantly lower in obese than in non-obese women (without BMD; 5.8 vs 11.4% for hip and 17.6 vs 23.6% for major osteoporotic fracture $p < 0.0001$); with BMD: 7.1 vs 10.9% for hip and 18.2 vs 23.3% for major osteoporotic fracture $p < 0.0001$). ROC analysis showed no significant differences in the ability of FRAX models without or with BMD to predict fractures in obese and non-obese women (Table 1). In conclusion, FRAX-derived probabilities for both hip and major osteoporotic fractures are significantly lower in obese women than in non-obese women. The ability of FRAX to predict fracture in obese postmenopausal women is similar to that in non-obese women, although its relatively poor performance for non-vertebral fractures indicates that addition of unmeasured risk factors may improve prediction. Addition of BMD to FRAX risk factors enhanced hip fracture prediction more in obese than non-obese women, probably reflecting the differing effect on fracture probability of BMI in the model with and without BMD.

Table 1 Comparison of the area under the curve [AUC (95% CI)] from receiver operating characteristic curve (ROC) for the FRAX algorithm between obese and non-obese women

	Body mass index < 30 kg/m ²	Body mass index ≥ 30 kg/m ²	p
FRAX algorithm not including BMD			
Women with hip fractures	0.689 (0.665, 0.714)	0.656 (0.587, 0.725)	0.19
Women with major osteoporotic fracture (hip, clinical vertebral, wrist, and humerus)	0.630 (0.610, 0.650)	0.633 (0.587, 0.679)	0.13
Women with any clinical fracture (non-vertebral and clinical vertebral)	0.603 (0.586, 0.620)	0.586 (0.547, 0.624)	0.21
FRAX algorithm including BMD			
Women with hip fractures	0.734 (0.711, 0.757)	0.755 (0.698, 0.812)	0.48
Women with major osteoporotic fracture (hip, clinical vertebral, wrist, and humerus)	0.675 (0.656, 0.695)	0.696 (0.655, 0.737)	0.18
Women with any clinical fracture (non-vertebral and clinical vertebral)	0.628 (0.611, 0.645)	0.637 (0.600, 0.674)	0.34

Disclosures: Melissa Premaor, None.

1059

Baseline BMD T-score and Time to Fracture in Older Women: the Study of Osteoporotic Fractures. Margaret Gourlay^{*1}, Jason P. Fine¹, Chenxi Li¹, John S. Preisser¹, Ryan C. May¹, Li-Yung Lui², Kristine Ensrud³. ¹University of North Carolina, USA, ²California Pacific Medical Center Research Institute, USA, ³Minneapolis VA Medical Center / University of Minnesota, USA

Lower BMD predicts increased fracture risk, but the time to fracture has not been determined for different BMD T-score ranges. To estimate the time to hip or clinical vertebral fracture accounting for the competing risk of incident osteoporosis using WHO diagnostic criteria, we conducted competing risks analyses of 4914 women aged 67 years and older without osteoporosis or hip or clinical vertebral fracture at the Year 2 SOF Exam (baseline). Participants had DXA BMD measurements at the femoral neck and total hip at 2 to 5 visits in up to 15 years of follow-up. We estimated the time during which 2% of women suffered a hip or clinical vertebral fracture for

four baseline T-score ranges: normal BMD (T-score ≥ -1.00); mild (T-score -1.01 to -1.49), moderate (T-score -1.50 to -1.99) or advanced (T-score ≤ -2.00 to ≤ -2.49) osteopenia. Parametric cumulative incidence curves for the time to hip or clinical vertebral fracture were estimated from log logistic cumulative incidence models for interval censored data adjusting for age, BMI, estrogen use, any fracture after age 50, current smoking, oral glucocorticoid use and self-reported rheumatoid arthritis. Participants were censored for use of bisphosphonates, calcitonin or raloxifene, death or termination of study participation. Transitions from normal BMD (n=1252 women) and osteopenia (n=4163 women) were analyzed separately; 501 women who transitioned from normal BMD to osteopenia prior to incident osteoporosis, treatment, or hip or clinical vertebral fracture contributed to both analyses. Adjusting for covariates, estimated times for 2% of women to transition to hip or clinical vertebral fracture were: normal BMD, 22.21 years; mild osteopenia, 14.26 years; moderate osteopenia, 5.24 years; advanced osteopenia, 5.21 years (table). For women with baseline osteopenia, T-score group, age, BMI, any fracture after age 50, rheumatoid arthritis, and the interaction of age by rheumatoid arthritis were significant predictors of time to incident hip or clinical vertebral fracture (all $P < 0.04$). These results suggest that older women with normal BMD or mild osteopenia are unlikely to sustain hip or clinical vertebral fractures in the subsequent 10 years. However, for older women with moderate or advanced osteopenia at baseline, findings suggest that repeat BMD testing should be deferred no longer than 5 years to identify potential candidates for antifracture therapy before a hip or clinical vertebral fracture occurs.

Baseline T-score range	N	N(%) with incident hip or clinical vertebral fracture	Time between DXA exams for 2% of participants to transition to fracture	
			Unadjusted years (95% CI)	Adjusted* years (95% CI)
Normal BMD (T-score ≥ -1.00)	1252	9 (0.72%)	22.44 (5.60, 89.96)	22.21 (5.67, 87.00)
Mild osteopenia (T-score -1.01 to -1.49)	1369	17 (1.24%)	13.41 (8.05, 22.37)	14.26 (8.65, 23.50)
Moderate osteopenia (T-score -1.50 to -1.99)	1464	53 (3.62%)	4.39 (3.16, 6.08)	5.24 (3.82, 7.19)
Advanced osteopenia (T-score ≤ -2.00 to ≤ -2.49)	1330	46 (3.46%)	4.60 (3.27, 6.47)	5.21 (3.74, 7.26)

* adjusted for age, BMI, current estrogen use, any fracture after age 50 years, current smoking, oral glucocorticoid use, rheumatoid arthritis (N=4047 complete cases). For normal BMD group, time was conservatively estimated for lowest BMD in the normal range, results adjusted for continuous BMD and age only (N=1252 complete cases).

Disclosures: Margaret Gourlay, None.

This study received funding from: National Center for Research Resources, National Institute on Aging, National Institute of Arthritis and Musculoskeletal and Skin Diseases

1060

Height Loss Starting in Middle Age Predicts Increased Mortality in Elderly Men and Women. Saeko Fujiwara^{*1}, Naomi Masunari², Fumiyoshi Kasagi³, Toshitaka Nakamura⁴. ¹Radiation Effects Research Foundation, Japan, ²Faculty of Pharmacy, Iwaki Meisei University, Japan, ³Department of Epidemiology, Radiation Effects Research Foundation, Japan, ⁴University of Occupational & Environmental Health, Japan

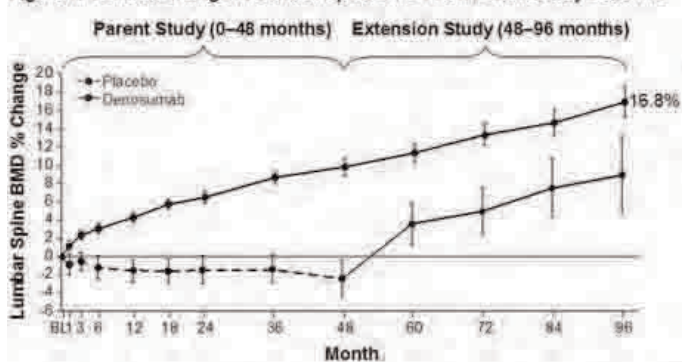
Objective: Our previous report demonstrated that height loss and vertebral deformity significantly and independently affected quality of life (QOL) in the elderly (Osteoporos Int. 2007;18:1493). The objective of this study was to determine mortality risk among Japanese elderly men and women with height loss starting in middle age, taking into account lifestyle and physical factors. **Methods:** From among a population-based community cohort, the Adult Health Study, 2,498 subjects (755 men and 1,743 women) aged 47 to 91 years old were enrolled in a prospective and longitudinal cohort study in Hiroshima, Japan. These individuals underwent physical examinations including BMD measurement as well as a questionnaire during the period 1994-95, and were followed for mortality status through 2003. Mortality risk was estimated using an age-stratified Cox proportional hazards model. In addition to sex, radiation dose, lifestyle and physical factors such as smoking status, alcohol intake, total cholesterol, blood pressure, and diagnosed diseases were included as adjustment factors for analysis of total mortality and mortality from each cause of death. **Results:** There were a total of 302 all-cause deaths, 46 coronary heart disease and stroke deaths, 58 respiratory deaths including 45 pneumonia deaths, and 132 cancer deaths during the follow-up period. Participants were followed for 20,787 person-years after baseline. Prevalent vertebral deformity and hip fracture were not associated with mortality risk. However, at least 2 cm of height loss starting in middle age showed significant association with all-cause mortality among the study participants (HR=1.76, 95% CI 1.31-2.38, $p=0.0002$), after adjustment was made for sex, atomic-bomb radiation exposure, and lifestyle and physical factors. Such a level of height loss was also significantly associated with coronary heart disease- and stroke-caused death (HR=3.35, 95% CI 1.63-6.86, $p=0.0010$) as well as respiratory-disease death (HR=2.52, 95% CI 1.25-5.22, $p=0.0130$), but not cancer death. **Conclusions:** Height loss starting in middle age predicted coronary heart disease- and stroke-caused death as well as respiratory-disease death although prevalent vertebral deformity was not associated with mortality risk.

Disclosures: Saeko Fujiwara, None.

Effects of Denosumab on Bone Mineral Density and Biochemical Markers of Bone Turnover: 8-Year Results of a Phase 2 Clinical Trial. Michael McClung¹, E. Michael Lewiecki², Michael A. Bolognese³, Munro Peacock⁴, Richard Weinstein⁵, Beiyang Ding⁶, Michelle L. Geller⁷, Andreas Grauer⁶, Rachel B. Wagman⁶, Paul Miller⁸. ¹Oregon Osteoporosis Center, USA, ²New Mexico Clinical Research & Osteoporosis Center, USA, ³Bethesda Health Research Center, USA, ⁴Indiana University Medical Center, USA, ⁵Diablo Clinical Research, Inc., USA, ⁶Amgen Inc., USA, ⁷Amgen Inc. & University of California Los Angeles, USA, ⁸Colorado Center for Bone Research, USA

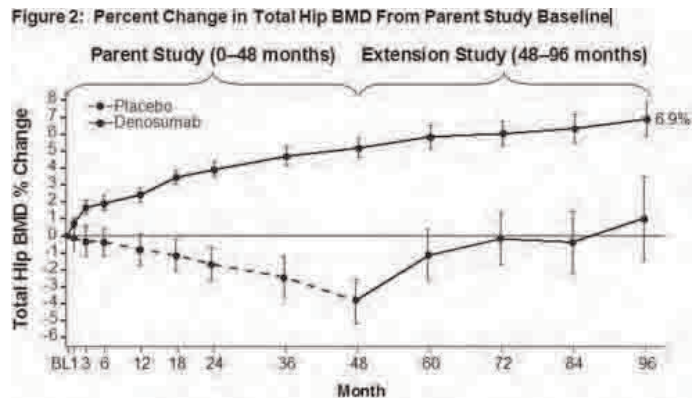
Denosumab (DmAb) is a fully human monoclonal antibody that inhibits RANKL, reduces bone resorption by osteoclasts, and reduces the risk of new vertebral, hip, and nonvertebral fractures at 3 years compared with placebo (Cummings *NEJM* 2009). With its unique mechanism of action, long-term experience with DmAb therapy is of clinical interest. Here we present the effects of 8 years of DmAb treatment on bone mineral density (BMD) and bone turnover markers (BTM) in a phase 2 study. In the phase 2 parent study, postmenopausal women with a BMD T-score between -1.8 and -4.0 (lumbar spine) and/or -1.8 and -3.5 (total hip or femoral neck) were randomized to receive placebo, alendronate (ALN), or 1 of 7 different doses of DmAb. After 2 years on study, subjects were reallocated to maintain, discontinue, or discontinue and reinitiate DmAb; discontinue ALN; or maintain placebo for an additional 2 years (Miller *Bone* 2008). In the extension phase of this study, all subjects received open-label DmAb 60 mg every 6 months (Q6M). Here our results focus on subjects who received DmAb treatment for 8 years and those who received placebo for 4 years followed by DmAb for 4 years. Of the 262 subjects who completed the parent study, 200 enrolled in the extension study and of these, 116 (58%) had completed the 4-year extension study at the time of the submission. For the 80 subjects who received 8 years of DmAb treatment, BMD at the lumbar spine and total hip increased on average by 16.8% and 6.9%, respectively, compared with their parent study baseline (Figures 1 and 2). For the 11 subjects in the previous placebo cohort, 4 years of DmAb treatment resulted in gains in BMD comparable with those observed during the first 4 years of 60 mg Q6M in the parent study. Reductions in CTX and BSAP were sustained over the course of continuous DmAb treatment. Reductions in these BTMs also were observed when the placebo group transitioned to DmAb treatment. The adverse event profile was overall similar to what has been reported previously. These data demonstrated that DmAb treatment for up to 8 years was associated with continued gains in BMD and persistent reduction in markers of bone turnover, and was well tolerated.

Figure 1: Percent Change in Lumbar Spine BMD From Parent Study Baseline



Results are based on available data at time of submission. Data are least squares mean (95% CI). N = number of subjects with parent study baseline (BL) and ≥ 1 post-BL measurement.

Figure 1



Results are based on available data at time of submission. Data are least squares mean (95% CI). N = number of subjects with parent study baseline (BL) and ≥ 1 post-BL measurement.

Figure 2

Disclosures: Michael McClung, Amgen, Merck, Warner Chilcott, 2; Amgen, Lilly, Merck, Novartis, Warner Chilcott, 5; Amgen, Lilly, Novartis, Warner Chilcott, 8. This study received funding from: Amgen Inc.

1062

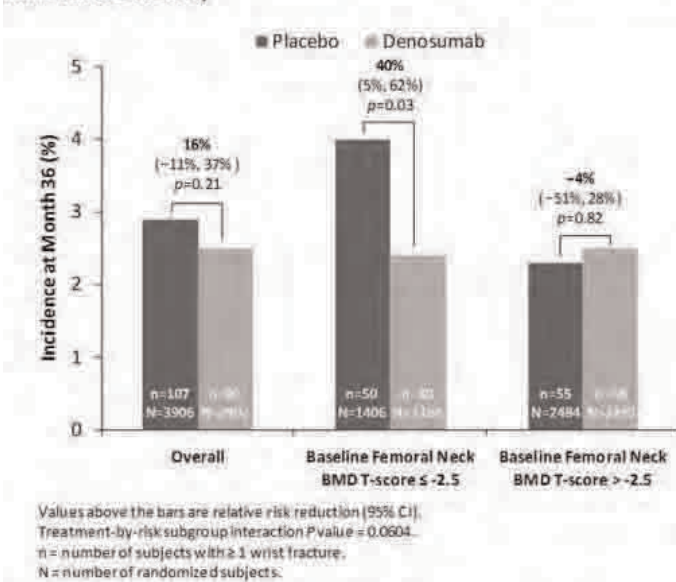
Effects of Denosumab on Radius BMD, Strength, and Wrist Fractures: Results From the Fracture Reduction Evaluation of Denosumab in Osteoporosis Every 6 Months (FREEDOM) Study. J Simon¹, C Recknor², A Moffet³, J Adachi⁴, E Franek⁵, EM Lewiecki⁶, CA Mautalen⁷, S Ragi⁸, GC Nicholson⁹, C Muschitz¹⁰, R Nuti¹¹, O T'Jerring¹², A Wang¹³, C Libanati¹³. ¹George Washington University, USA, ²United Osteoporosis Centers, USA, ³OB-GYN Associates of Mid Florida, USA, ⁴St. Joseph's Hospital, McMaster University, Canada, ⁵Central Clinical Hospital MSWiA, Poland, ⁶New Mexico Clinical Research & Osteoporosis Center & University of New Mexico School of Medicine, USA, ⁷Centro de Osteopatias Medicas, Argentina, ⁸CEDOES Centro de Diagnostico e Pesquisa, Brazil, ⁹Barwon Health, The Geelong Hospital, Australia, ¹⁰St. Vincent Hospital, Austria, ¹¹University of Siena, Italy, ¹²Karolinska Institutet Sodersjukhuset, Sweden, ¹³Amgen Inc., USA

Purpose: Denosumab (DmAb) is an approved therapy for postmenopausal women with osteoporosis at increased risk of fracture. DmAb increases cortical bone mineral density (BMD) and thickness, and reduces cortical porosity, contributing to improved bone strength. Here, we report the effects of DmAb in cortical and trabecular bone at the radius using DXA and QCT scans, and the wrist fracture reduction observed in the FREEDOM study.

Methods: Women received placebo (Pbo) or 60 mg DmAb every 6 months for 3 years. BMD, bone mineral content (BMC), and polar moment of inertia (PMI, a measure of bone strength) at the radius were assessed in a DXA substudy (N=209 Pbo, N=232 DmAb) or QCT substudy (N=79 Pbo, N=103 DmAb) at baseline and months 12, 24, and 36. The incidence of wrist fractures was evaluated for all FREEDOM subjects (N=3906 Pbo, N=3902 DmAb) and in a higher-risk subgroup for nonvertebral fractures (baseline femoral neck BMD T-score ≤ -2.5 ; N=1406 Pbo, N=1384 DmAb).

Results: DmAb significantly increased DXA BMD at all radius regions of interest (1/3, ultradistal, and total radius; Table) at 12, 24, and 36 months compared with Pbo and baseline (all $p < 0.05$). QCT BMD changes were consistent with DXA results. DmAb also significantly improved BMC and PMI compared with Pbo and baseline (proximal, distal, and ultradistal; all $p < 0.05$). At 36 months, all measurements decreased significantly from baseline in Pbo subjects (all $p < 0.05$). For the entire study population, the incidence of wrist fractures was 2.9% and 2.5% for the Pbo and DmAb subjects, respectively (hazard ratio: 0.84, $p = 0.21$). In the higher-risk subgroup, DmAb significantly reduced the relative risk by 40% (absolute risk reduction 1.6%; $p = 0.03$; Figure). The wrist fracture reduction could not be explained by fewer subjects reporting falls (7.4% Pbo, 7.2% DmAb; $p = 0.73$). Wrist fracture incidence in DmAb subjects at higher risk for fracture (baseline femoral neck BMD T-score ≤ -2.5) was similar to Pbo subjects with lower risk (baseline BMD femoral neck T-score > -2.5).

Conclusion: DmAb significantly improved DXA BMD and QCT BMD, BMC, and calculated strength compared with baseline and Pbo along the radius. In higher risk women, DmAb treatment significantly reduced the incidence of wrist fractures to the level observed in women with lower risk. The positive effects of DmAb on the cortical compartment may explain the beneficial wrist fracture outcomes in women at higher risk for nonvertebral fractures.

Figure. Cumulative Subject Incidence of Wrist Fracture Through Month 36 in the FREEDOM study

Figure

Table. Percent Change From Baseline at Month 36 in Radius Parameters

	DXA Substudy		QCT Substudy			
	BMD		BMD		BMC	
	Pbo N=209	DMAB N=232	Pbo N=79	DMAB N=103	Pbo N=79	DMAB N=103
1/3 (DXA) or Proximal (QCT)	-1.2 [†]	2.2 ^{†*}	-2.2 [†]	1.9 ^{†*}	-2.0 [†]	1.7 ^{†*}
Distal	N/A	N/A	-2.5 [†]	3.2 ^{†*}	-2.5 [†]	2.7 ^{†*}
Ultradistal	-2.3 [†]	3.4 ^{†*}	-2.5 [†]	5.9 ^{†*}	-2.4 [†]	5.5 ^{†*}
Total	-2.0 [†]	2.3 ^{†*}	N/A	N/A	N/A	N/A

Values shown are LS mean.

N = number of randomized subjects enrolled in the substudy.

[†]P value < 0.05 compared with baseline.^{*}P value < 0.05 compared with placebo.

Table

Disclosures: EM Lewiecki, Abbott Laboratories, Agile Therapeutics, Inc., Amgen Inc., Ascend Therapeutics, Azur Pharma, Inc., BioSante, Boehringer Ingelheim, Depomed, Inc., 5; Fabre-Kramer, Laboratoire HRA Pharma, Mediterra Pharmaceuticals, Merck, Merriam Pharmaceuticals, NDA Partners, Inc., Novo Nordisk, Novogyne, Pfizer, Inc., Shionogi, Inc., 5; Amgen, Ascend, Bayer, Boehringer Ingelheim, KV, Merck, Novartis, Novo Nordisk, Novogyne, Teva, Warner Chilcott, 8; BioSante, Boehringer Ingelheim, Endoceutics, Inc., Novo Nordisk, Novogyne, Teva, 2; Slate Pharmaceuticals, Teva, Warner Chilcott, Trovis Pharmaceuticals LLC, Watson Pharmaceuticals, 5
This study received funding from: Amgen Inc.

1063

Efficacy of Five Years of Denosumab: A Novel "Virtual Twins" Method for Minimizing Bias in Extensions of Trials. Steven Cummings¹, Nadia Daizadeh², Eric Vittinghoff³, Cesar Libanati², Jacques P Brown⁴, Christian Roux⁵, Matthew Austin², Andreas Grauer², Socrates Papapoulos⁶, Henry G Bone⁷. ¹San Francisco Coordinating Center, USA, ²Amgen Inc., USA, ³University of California, San Francisco, USA, ⁴CHUC-CHUL Research Centre, Laval University, Canada, ⁵Paris Descartes University, France, ⁶Leiden University Medical Center, Netherlands, ⁷Michigan Bone & Mineral Clinic, USA

Purpose: In the 3 year FREEDOM trial, denosumab reduced the risk of new vertebral, hip, and nonvertebral fractures by 68%, 40%, and 20%, respectively (Cummings, NEJM, 2009). FREEDOM was extended to continue the evaluation of fracture rates with long-term denosumab treatment. However, only a self-selected portion of participants in FREEDOM continued into the extension and there is no equivalent placebo control group. To provide a reference group for the observed fracture rates during the extension, we used a novel "virtual twin" simulation method (Vittinghoff, Stat Med, 2010) to estimate expected fracture rates in a cohort of placebo controls with baseline characteristics that are identical to subjects who continued denosumab treatment into the extension.

Methods: During the first 2 years of the extension, all women in the long-term group received 60 mg denosumab every 6 months, reflecting 5 years of continuous denosumab exposure (N=2343). Linear, Poisson, and logistic prediction models were developed using actual FREEDOM data on bone mineral density, fracture history, body mass index, and age for subjects who received placebo during the 3 years of FREEDOM. These models were then used to calculate fracture outcomes for virtual twins of the denosumab-treated women during the extension. Inferences on the differences in fracture rates between long-term denosumab subjects and their virtual twins used bootstrapping.

Results: During FREEDOM, denosumab reduced the risk of new vertebral and nonvertebral fractures during each year of the trial compared with placebo (Figures 1 and 2). In the first 2 years of the extension, the observed fracture rates remained below the estimated fracture rates had the denosumab subjects who enrolled in the extension received placebo ("twins"). During years 4 and 5 of treatment, denosumab significantly reduced the estimated risk of new vertebral fractures by 36% (RR: 0.64; 95% CI: 0.43 to 0.93) and nonvertebral fractures by 51% (RR: 0.49; 95% CI: 0.35 to 0.65) compared with their placebo "twins."

Conclusion: Using a novel method that minimizes bias, the risk of new vertebral and nonvertebral fractures during the 4th and 5th years of continuous denosumab treatment in postmenopausal women with osteoporosis was significantly reduced compared with the estimated placebo rate over the same period.

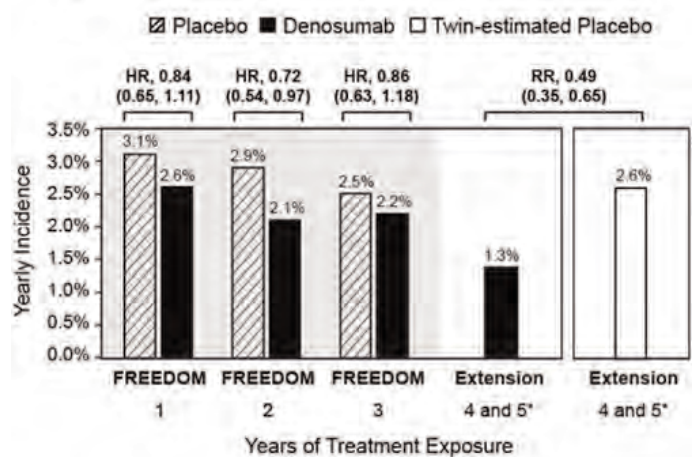
Figure 2. Subject Incidence of Nonvertebral Fractures

Figure 2

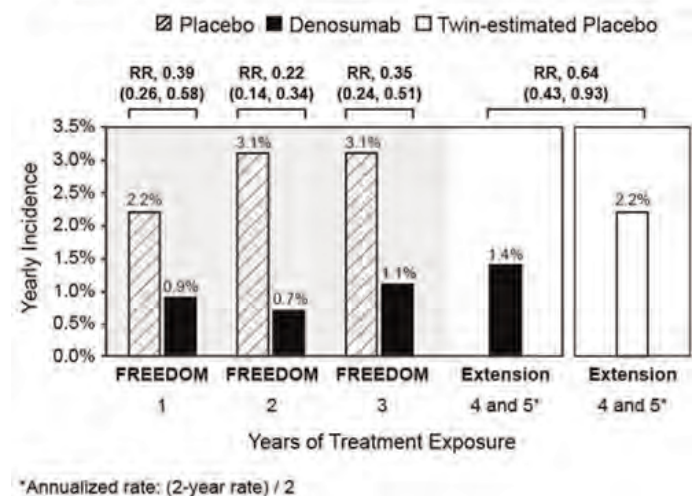
Figure 1. Subject Incidence of New Vertebral Fractures

Figure 1

Disclosures: Steven Cummings, Amgen Inc., 5
This study received funding from: Amgen Inc.

The Transitory Increase in PTH Following Denosumab Administration is Associated With Reduced Intracortical Porosity: a Distinctive Attribute of Denosumab Therapy. Ego Seeman^{*1}, Cesar Libanati², Matt Austin², Roland Chapurlat³, Steven Boyd⁴, Roger Zebaze¹, David A. Hanley⁴, Jose R. Zanchetta⁵, Andreas Grauer², John P. Bilezikian⁶. ¹Austin Health, University of Melbourne, Australia, ²Amgen Inc., USA, ³INSERM UMR 1033, Université de Lyon, France, ⁴University of Calgary, Canada, ⁵Instituto de Investigaciones Metabolicas, Argentina, ⁶College of Physicians & Surgeons, Columbia University, USA

The benefit of an antiresorptive upon the material composition and structure of bone is largely determined by its direct and indirect effects on the volumes of bone resorbed and deposited by each bone remodeling unit (BMU), and by the number of BMUs inhibited in both the trabecular and cortical compartments. Denosumab (DMAb) rapidly reduces bone resorption by existing BMUs and markedly inhibits the birth rate of new BMUs during the initial months following administration. This acute remodeling reduction is accompanied by a transitory increase in circulating PTH which could increase osteoblast longevity and/or activity. We hypothesized that the direct effect of DMAb on resorption inhibition, and the possible indirect effect on bone formation mediated by an increase in PTH in the face of inhibited osteoclastic activity by the BMU, would reduce cortical porosity in women at risk for fracture.

Postmenopausal women (N=247) with a mean (SD) age of 60.6 (5.4) yrs and low BMD were randomly assigned in a double-blind, double-dummy trial to DMAb 60mg Q6M (N=83), alendronate (ALN) 70mg QW (N=82), or placebo (Pbo; N=82). PTH was measured at baseline (BL), wk 1, and mos 1, 3, 6, 6.25, 7, 9, and 12. An area under the curve (AUC) for PTH was derived from the change from BL for each subject. Porosity was evaluated in the compact-appearing cortex of the distal radius at BL and mo 12 by HR-pQCT. Associations between PTH AUC and change in porosity were evaluated.

Transitory increases in PTH were seen in the DMAb and ALN groups, but not Pbo (Fig 1). The increase in PTH was larger following DMAb than ALN ($P<0.05$) and was observed after each DMAb dose. At the radius by 12 mos, porosity increased in the Pbo group, increased less in the ALN group, and was reduced by DMAb (+5.2%, +2.9%, and -3.0%, respectively). In the Pbo and ALN groups, porosity increased with increasing PTH (Fig 2). With DMAb, porosity decreased as PTH increased. These relationships were maintained after adjusting for BL remodeling.

In conclusion, DMAb partly reverses microarchitectural deterioration; predominantly by directly reducing bone remodeling intensity, but perhaps also indirectly, by transiently increasing PTH, and so positively influencing BMU balance. The results describe a unique mechanism of DMAb action due to its direct effect to fully and rapidly inhibit osteoclastic activity at cortical and trabecular bone, and its indirect effect to increase PTH when osteoclastic resorption is fully inhibited.

Fig 1: Median and Interquartile Range of Percent Change From Baseline in PTH by Visit

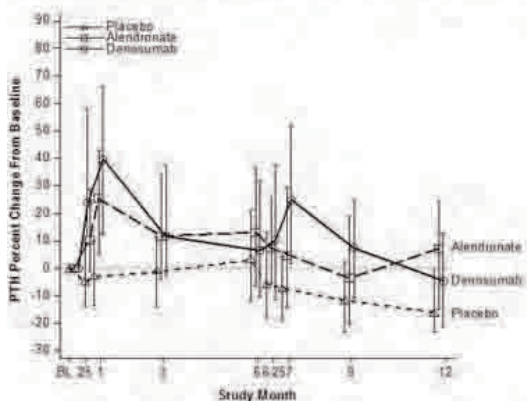
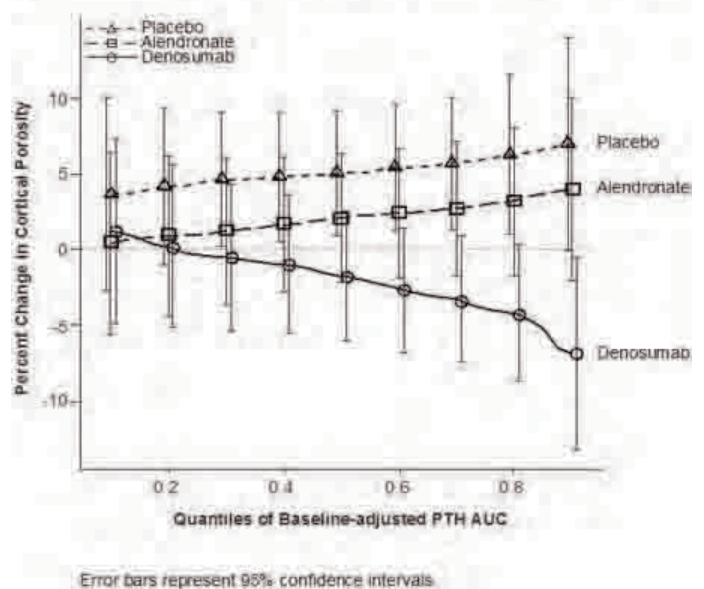


Fig 2: Relationship Between PTH and Cortical Porosity at 12 Months



Disclosures: Ego Seeman, Amgen Inc., MSD, Servier, 2; Amgen Inc., Novartis, Eli Lilly, Warner Chilcott, 8; Amgen Inc., Novartis, Warner Chilcott, Servier, 5. This study received funding from: Amgen Inc.

1065

Safety Observations From Denosumab Long-term Extension and Cross-over Studies in Postmenopausal Women With Osteoporosis. Henry G Bone^{*1}, Roland Chapurlat², Cesar Libanati³, Maria L Brandi⁴, Jacques P Brown⁵, Edward Czerwinski⁶, Marc-Antoine Kriegel⁷, Zulema Man⁸, Dan Mellstrom⁹, Sebastiao C Radominski¹⁰, Jean-Yves Reginster¹¹, Heinrich Resch¹², Jose A. Roman Ivorra¹³, Christian Roux¹⁴, Nadia S Daizadeh³, Andreas Grauer³, Steve R Cummings¹⁵, Socrates Papapoulos¹⁶. ¹Michigan Bone & Mineral Clinic, USA, ²Hopital Edouard Herriot, France, ³Amgen Inc., USA, ⁴University of Florence, Italy, ⁵CHUQ-CHUL Research Centre, Laval University, Canada, ⁶Krakow Medical Centre, Poland, ⁷University Hospital of Lausanne, Switzerland, ⁸Centro Medico TIEMPO, Argentina, ⁹University of Gothenburg, Sweden, ¹⁰Universidade Federal do Parana, Brazil, ¹¹University of Liege, Belgium, ¹²St. Vincent's Hospital, Austria, ¹³Hospital Universitario La Fe, Spain, ¹⁴Paris Descartes University, France, ¹⁵San Francisco Coordinating Center, CPMC Research Institute, USA, ¹⁶Leiden University Medical Center, Netherlands

Purpose: Denosumab (DMAb) is an approved therapy for the treatment of postmenopausal women with osteoporosis at increased risk for fracture. A favorable DMAb risk/benefit profile was demonstrated in the pivotal, 3-year FREEDOM trial. All women who completed FREEDOM were eligible to participate in an extension to investigate the safety and efficacy of DMAb treatment for up to 10 years. We previously reported that 5 years of DMAb treatment maintained bone turnover reduction, increased BMD, and was associated with low fracture rates. Here, we provide details on the yearly incidence of serious adverse events (SAEs) of infection and adverse events (AEs) of malignancy in FREEDOM and the extension.

Methods: Of the 6478 women who completed FREEDOM, 4550 (70%) enrolled in the extension, during which, all women receive 60 mg DMAb every 6 months and supplemental calcium and vitamin D daily. For the analyses reported here, women from the FREEDOM DMAb group received 2 more years of DMAb for a total of 5 years of exposure (long-term group; N=2343) and women from the FREEDOM placebo group received 2 years of DMAb exposure (cross-over group; N=2207). The analyses of AEs were descriptive and are reported as exposure-adjusted subject incidence rates.

Results: The year-to-year observed subject incidence rates of SAEs of infection (Table 1) and AEs of malignancy (Table 2) in the placebo group exhibited some variation during the 3 years of the FREEDOM trial. The yearly subject incidence rates in the first 2 years of the extension for the long-term and cross-over groups were similar to or lower than the observed yearly rates in the FREEDOM placebo group. This was also the case for individual SAEs of infection (by preferred term) including cellulitis or erysipelas (Table 1) and individual malignancies (by preferred term; Table 2). One case of oral osteomyelitis and one case of bone necrosis in the cross-over group were adjudicated as consistent with ONJ.

Conclusions: The year-to-year observed AE rates in placebo subjects provide a valuable indicator of the expected variation in untreated subjects and assist in the interpretation of safety results associated with therapy. Yearly incidences of SAEs of infection and AEs of malignancies did not increase over 5 years of continuous DMAB treatment of postmenopausal women with osteoporosis. The imbalances in SAEs of skin infections reported in the original FREEDOM study were not observed with DMAB treatment in the extension study.

Table 1. Yearly Incidence of Serious Adverse Events of Infections

		FREEDOM			Extension	
		Year 1 r (n)	Year 2 r (n)	Year 3 r (n)	Year 1 r (n)	Year 2 r (n)
All SAEs of Infections	Cross-over (Pbo/DMAB)	1.1 (42)	1.4 (50)	1.4 (48)	1.5 (33)	1.6 (32)
	Long-term (DMAB/DMAB)	1.5 (56)	1.6 (58)	1.6 (54)	1.3 (30)	1.2 (26)
Pneumonia	Cross-over	0.3 (12)	0.4 (13)	0.4 (12)	0.4 (9)	0.4 (8)
	Long-term	0.3 (12)	0.3 (9)	0.4 (13)	0.3 (7)	0.3 (7)
Urinary tract infection	Cross-over	0.1 (4)	0.1 (5)	<0.1 (1)	<0.1 (1)	0.2 (4)
	Long-term	<0.1 (3)	0.2 (8)	0.1 (5)	<0.1 (1)	<0.1 (1)
Diverticulitis	Cross-over	0	0.1 (5)	<0.1 (1)	0.1 (3)	<0.1 (1)
	Long-term	0.1 (4)	<0.1 (2)	<0.1 (3)	<0.1 (2)	<0.1 (2)
Gastroenteritis	Cross-over	<0.1 (3)	<0.1 (2)	<0.1 (2)	0	<0.1 (2)
	Long-term	<0.1 (3)	0.1 (4)	<0.1 (2)	0	<0.1 (1)
Appendicitis	Cross-over	0.1 (4)	<0.1 (1)	<0.1 (2)	0	<0.1 (1)
	Long-term	0.1 (4)	<0.1 (3)	0	<0.1 (2)	<0.1 (1)
Cellulitis or erysipelas	Cross-over	0	0	<0.1 (1)	0	<0.1 (1)
	Long-term	0.1 (4)	<0.1 (1)	0.2 (8)	<0.1 (2)	<0.1 (1)
Bronchopneumonia	Cross-over	<0.1 (2)	0	0.1 (5)	<0.1 (1)	0
	Long-term	<0.1 (1)	<0.1 (3)	<0.1 (2)	0	<0.1 (2)
Lower respiratory tract	Cross-over	<0.1 (1)	<0.1 (2)	0	0	<0.1 (1)
	Long-term	<0.1 (2)	0.1 (4)	<0.1 (2)	<0.1 (1)	0

Treatment groups are the original randomized assignments in the FREEDOM study. All subjects in the extension study are receiving denosumab. Denosumab treatment is shown in grey. Events are listed if ≥ 4 subjects reported an adverse event in any group in any year.
r = exposure-adjusted subject incidence per 100 subject-years.
n = total number of subjects with ≥ 1 adverse event.

Table 1

Table 2. Yearly Incidence of Adverse Events of Malignancies

		FREEDOM			Extension	
		Year 1 r (n)	Year 2 r (n)	Year 3 r (n)	Year 1 r (n)	Year 2 r (n)
All AEs of Malignancies	Cross-over (Pbo/DMAB)	1.8 (69)	1.6 (57)	1.5 (50)	1.8 (39)	1.4 (29)
	Long-term (DMAB/DMAB)	1.8 (69)	1.5 (53)	2.2 (74)	1.8 (42)	2.2 (47)
Skin	Cross-over	0.6 (24)	0.3 (10)	0.5 (17)	0.5 (11)	0.6 (12)
	Long-term	0.6 (22)	0.3 (10)	0.5 (17)	0.6 (13)	0.6 (17)
Gastrointestinal	Cross-over	0.2 (9)	0.3 (11)	0.1 (4)	0.4 (9)	0.1 (3)
	Long-term	0.3 (11)	0.3 (11)	0.4 (13)	0.3 (7)	0.4 (9)
Breast (including nipple)	Cross-over	0.2 (9)	0.3 (11)	0.2 (8)	0.1 (3)	0.2 (5)
	Long-term	0.3 (10)	0.3 (10)	0.4 (14)	0.3 (6)	0.2 (5)
Respiratory	Cross-over	0.3 (11)	0.3 (10)	0.1 (4)	<0.1 (2)	<0.1 (2)
	Long-term	<0.1 (3)	0.1 (4)	0.2 (7)	0.2 (4)	0.1 (3)
Reproductive	Cross-over	0.2 (8)	<0.1 (2)	<0.1 (2)	<0.1 (1)	0.1 (3)
	Long-term	0.2 (7)	0.2 (6)	0.2 (6)	<0.1 (1)	<0.1 (2)
Metastases	Cross-over	0.1 (5)	0.1 (4)	<0.1 (1)	<0.1 (1)	<0.1 (1)
	Long-term	0.1 (4)	0.1 (4)	<0.1 (1)	<0.1 (1)	<0.1 (2)
Renal and urinary tract	Cross-over	0.1 (4)	<0.1 (2)	<0.1 (3)	0.2 (4)	0
	Long-term	<0.1 (1)	0.1 (4)	<0.1 (1)	0.1 (3)	0
Plasma cell	Cross-over	0	<0.1 (2)	<0.1 (2)	<0.1 (2)	<0.1 (1)
	Long-term	<0.1 (1)	0	0.1 (5)	<0.1 (1)	<0.1 (2)
Endocrine	Cross-over	0	0	<0.1 (2)	<0.1 (1)	<0.1 (1)
	Long-term	0.1 (5)	<0.1 (1)	<0.1 (1)	0.1 (3)	0
Nervous system	Cross-over	<0.1 (1)	0	0.2 (6)	<0.1 (1)	0
	Long-term	<0.1 (2)	<0.1 (1)	<0.1 (2)	0	0

Treatment groups are the original randomized assignments in the FREEDOM study. All subjects in the extension study are receiving denosumab. Denosumab treatment is shown in grey. Events are listed if ≥ 4 subjects reported an adverse event in any group in any year.
r = exposure-adjusted subject incidence per 100 subject-years.
n = total number of subjects with ≥ 1 adverse event.

Table 2

Disclosures: Henry G Bone, Novartis, Tarsa, Amgen, and Merck, 5; Nordic Bioscience, Amgen, and Merck, 2; Amgen, 8
This study received funding from: Amgen Inc.

1066

Reduction in Incidence of Vertebral Fractures with Once Yearly Zoledronic Acid in Men with Osteoporosis. Steven Boonen¹, Jean-Marc Kaufman², Jean-Yves Reginster³, Rene Rizzoli⁴, Kurt Lippuner⁵, Dirk Vanderschueren⁶, Josef Hruska⁷, Oscar Antunez⁸, Philemon Papanastasiou⁷, Guoqin Su⁸, Eric Orwoll⁹. ¹Katholieke Universiteit Leuven, Belgium, ²University Hospital of Ghent, Belgium, ³University of Liege, Belgium, ⁴University Hospitals & Faculty of Medicine of Geneva, Switzerland, ⁵Osteoporosis Policlinic, University of Bern, Switzerland, ⁶Leuven University Hospital, Belgium, ⁷Novartis Pharma AG, Switzerland, ⁸Novartis Pharmaceuticals, USA, ⁹Oregon Health & Science University, USA

Introduction

Male osteoporosis and associated fracture risk have not been adequately studied and, to date, therapeutic trials in osteoporotic men have not included fracture endpoints. This 24-month multicentre, randomized, controlled trial investigated the efficacy and safety of annual intravenous zoledronic acid 5 mg (ZOL) in men with osteoporosis.

Methods

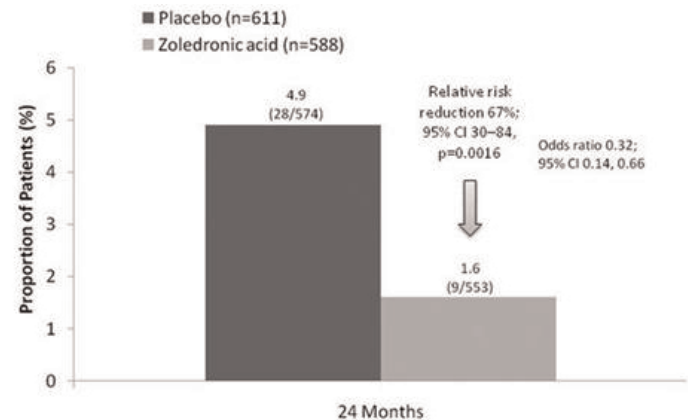
In total, 1199 men (range 50–85 years) with primary osteoporosis, or secondary osteoporosis due to hypogonadism, were randomized to receive once-yearly ZOL as a 15-min intravenous infusion or placebo (PBO). Patients also received daily calcium 1000–1500 mg and vitamin D 800–1200 IU. The primary endpoint was the proportion of patients with ≥ 1 new morphometric vertebral fracture over 24 months. Secondary endpoints included changes in biochemical markers of bone resorption and formation including β-CTX and PINP, change in height, and overall safety.

Results

At baseline, 32.1% of patients had ≥ 1 vertebral fractures. The proportion of patients with ≥ 1 new morphometric vertebral fracture over 24 months was significantly lower in the ZOL group (1.6%), compared with the PBO group (4.9%; odds ratio 0.32; 95% CI 0.14, 0.66 [relative risk reduction 67%; 95% CI 30–84, p=0.0016]) [Graph]. ZOL also reduced moderate–severe fractures by 63% compared with placebo. Over 24 months, ZOL showed significantly lower serum β-CTX and PINP levels relative to PBO (p<0.0001) at all post-baseline timepoints. With these markers, a significant between-treatment difference was achieved at Month 3 and maintained over the 24-month period. Men treated with ZOL for 24 months experienced less height loss than those treated with PBO (LSM –2.34 mm vs –4.49 mm, respectively; p=0.0020). ZOL was generally well-tolerated, with a similar incidence of serious adverse events between groups (ZOL, 25.2%; PBO, 25.3%).

Conclusion

Treatment with ZOL for a period of 24 months reduces the risk of new vertebral fractures in men with osteoporosis. This is the first clear demonstration of the efficacy and safety of bisphosphonate treatment for fracture risk reduction in men with osteoporosis.



Proportion of Patients with New Morphometric Vertebral Fractures at 24 months

Disclosures: Steven Boonen, Novartis, 2; Novartis, 5

This study received funding from: The study was funded by Novartis Pharma AG

1067

PTH Receptor 1 Expression in Osteocytes Is Indispensable for the Anabolic Effect of Mechanical Loading in Mice. Xiaolin Tu^{*1}, Gretel Pellegrini², Carlo Galli³, Jeffrey Benson¹, Keith Condon¹, Nicoletta Bivi⁴, Lilian Plotkin¹, Alexander Robling⁴, Teresita Bellido¹. ¹Indiana University School of Medicine, USA, ²seccion osteopatias medicas, Hospital de Clínicas Jose de San Marti, Argentina, ³Universita Degli Studi Di Parma, Italy, ⁴Indiana University, USA

Osteocytes play an essential role in skeletal homeostasis by integrating the responses of bone to mechanical and hormonal stimuli. Both mechanical loading and activation of the PTH receptor 1 (PTH1R) in osteocytes promote new bone formation by downregulating the expression of sclerostin, the inhibitor of bone formation secreted by osteocytes, and thereby activating the Wnt pathway. To explore a potential crosstalk between PTH1R signaling and mechanotransduction, we examined the osteogenic response to loading of mice lacking the PTH1R specifically in osteocytes (cKO). Mice were generated by crossing PTH1R^{fl/fl} mice, in which the E1 exon of the PTH1R is flanked by loxP sites, with DMP1-8kb-Cre mice, which express Cre recombinase in osteocytes but not in osteoblasts. PTH1R mRNA was reduced in all bones examined, in particular by 73% in long bones of cKO mice compared to control PTH1R^{fl/fl} littermates. Female, 4 month-old cKO mice exhibited no significant changes in ulnae geometry or in material density. However, ex vivo loading induced 20% higher strains in cKO mice (1541.7µε/N) compared to controls (1229.1µε/N), indicating less resistance of cKO bones to mechanical force. Right ulnae from control and cKO mice were loaded at equal strains of low, medium, and high magnitude during 1min/day for 3 consecutive days and sacrificed 14 days later; left ulnae were non-loaded controls. Dynamic histomorphometric analysis revealed that basal periosteal bone formation rate (BFR) was similar in control and cKO mice. Loading caused a strain-dependent increase in BFR in controls (0.130.06; 0.180.13; and 0.380.15 µm³/µm²/day), resulting from an increase in both mineralizing surface covered by osteoblasts (MS/BS) as well as activity of individual osteoblasts (MAR). In contrast, loading-induced BFR was dramatically reduced in cKO mice by 23%, 44%, and 71% (0.100.05, 0.100.05, and 0.110.08 µm³/µm²/day) with minimal but significant changes induced only by medium and high strains. This effect resulted mainly from the lack of stimulation of MAR by loading at any strain magnitude. Loading-induced MS/BS was also reduced in the cKO mice, with significant increases induced only by medium and high strains. We conclude that signaling downstream of the PTH1R in osteocytes is required for the osteogenic response induced by mechanical force.

Disclosures: Xiaolin Tu, None.

1068

β-catenin Haploinsufficiency in Osteocytes Abolishes the Osteogenic Effect of Mechanical Loading In Vivo. Behzad Javaheri^{*1}, Mark Dallas¹, Hong Zhao¹, Lynda Bonewald¹, Mark Johnson². ¹University of Missouri - Kansas City, USA, ²University of Missouri, Kansas City Dental School, USA

Targeted deletion of β-catenin in osteoblasts and osteocytes results in a severely compromised and fragile skeleton. We have also shown that β-catenin signaling is activated by mechanical loading. To determine whether β-catenin signaling is required for the anabolic bone formation response to mechanical loading we used an osteocyte conditional knockout approach. As loading of the osteocyte β-catenin homozygous knockout was not possible due to the fragile skeleton and premature death of these mice, our approach was to conditionally delete a single allele of β-catenin in osteocytes by crossing β-catenin fl/fl mice with Dmp1-Cre mice. The haploinsufficient heterozygous mice have a modest reduction in bone mass and are perfectly viable. We examined load-induced new bone formation in these heterozygous mice compared to fl/fl littermates.

The right ulnae of 15 week-old female β-catenin osteocyte heterozygous knockout mice (n=3) (HET cKO) or β-catenin fl/fl controls (WT) (n=3) were subjected to in vivo loading on 3 days per week for 3 weeks (100 cycles, 2N, 2500µε). The left ulnae of these mice served as the non-loaded controls. Bone responses to loading were determined by dynamic histomorphometry, following calcein (5mg/kg) and alizarin complexone dihydrate (20mg/kg) injections on 10 and 3d prior to sacrifice, respectively. Right and left ulnae were analyzed by µCT and histomorphometry. The loaded right ulnae of the fl/fl control mice showed a 7.4% increase in cortical thickness compared to the unloaded left ulnae (p<0.05). In contrast, no increase in thickness was detected in the HET cKO mice. Histomorphometric analysis of the comparable region is shown in Table 1. There was a significant increase in endocortical (Ec) and periosteum (Ps) MAR and BFR/BS, BFR/BV and BFR/TV in WT mice (p<0.05). In contrast no significant increase was detected in HET cKO mice.

These data indicate that deleting a single copy of β-catenin in osteocytes is sufficient to inhibit new bone formation in response to anabolic levels of mechanical loading. This provides compelling evidence for a requirement for β-catenin signaling in regulating new bone formation in response to loading and suggests that a critical threshold level of β-catenin is needed for this response.

	WT		HET cKO	
	Left	Right	Left	Right
EcMAR (µm/d)	0.11 ± 0.21	2.65 ± 1.04*	0.06 ± 0.21	0.14 ± 0.32
EcBFR/BS (µm ³ /µm ² /d)	0.01 ± 0.01	1.82 ± 0.75*	0.01 ± 0.03	0.01 ± 0.03
EcBFR/BV (%/y)	0.00 ± 0.00	0.67 ± 0.30*	0.00 ± 0.01	0.00 ± 0.01
EcBFR/TV (%/y)	0.00 ± 0.00	0.57 ± 0.24*	0.00 ± 0.01	0.00 ± 0.01
PsMAR (µm/d)	0.00 ± 0.00	5.25 ± 1.80*	0.35 ± 0.54	0.81 ± 0.61
PsBFR/BS (µm ³ /µm ² /d)	0.00 ± 0.00	1.67 ± 0.44*	0.02 ± 0.03	0.09 ± 0.07
PsBFR/BV (%/y)	0.00 ± 0.00	1.66 ± 0.40*	0.02 ± 0.03	0.09 ± 0.07
PsBFR/TV (%/y)	0.00 ± 0.00	1.42 ± 0.36*	0.02 ± 0.03	0.08 ± 0.07

*Compared to right HET cKO and non-loaded controls

Histomorphometric analysis of loaded and non-loaded ulnar sections of WT and HET cKO mice

Disclosures: Behzad Javaheri, None.

1069

Treatment with Sclerostin Antibody Increases Bone Mass and Strength During Hindlimb Unloading. Jordan Spatz^{*1}, R Ellman¹, AM Cloutier², D Dwyer³, Marina Stolina⁴, HZ. Ke³, Mary Boussein⁵. ¹Harvard-MIT Division of Health Sciences & Technology (HST), USA, ²Center for Advanced Orthopedic Studies, Beth Israel Deaconess Medical Center, USA, ³Amgen Inc., USA, ⁴Amgen Inc, USA, ⁵Beth Israel Deaconess Medical Center, USA

Sclerostin, a protein made by osteocytes, inhibits bone formation and plays a key role in mechanotransduction. We tested the ability of an anti-sclerostin antibody (Scl-AbIII) to prevent bone loss in adult female mice (C57Bl/6J, 12 wks of age) subjected to hindlimb unloading (HLU) for 21 days. Mice were assigned to one of four groups (n=8/group): 1) control, fully loaded + vehicle (CON-VEH), 2) control + Scl-AbIII (CON-SclAbIII), 3) HLU + vehicle (HLU-VEH), and 4) HLU + Scl-AbIII (HLU-SclAbIII). Mice were injected subcutaneously with either Scl-AbIII (25 mg/kg) or vehicle twice weekly. Scl-AbIII completely inhibited the trabecular and cortical bone deterioration due to disuse, with bone properties in HLU-SclAbIII being at or above values of fully loaded, VEH mice. Total body BMD decreased -5.3 2.8% in HLU-VEH, whereas it increased 4.4 2.8%, 16.3 4.8% and 30.7 4.6% in CON-VEH, HLU-SclAbIII and CON-SclAbIII, respectively, vs. baseline (p<0.0001). Trabecular bone volume (Tb.BV/TV %), assessed by µCT imaging of the distal femur, was lower in HLU-VEH vs CON-VEH (p<0.05), and was 2-3 fold higher in Scl-AbIII-groups vs VEH (p<0.001)(see Table). Midshaft femoral strength assessed by 3-pt bending and distal femoral trabecular strength assessed by micro-finite element analysis (µFEA) was significantly higher in Scl-AbIII vs VEH-groups in both loading conditions. Serum sclerostin was higher in HLU-VEH (134 16 pg/ml) compared to CON-VEH (116 22 pg/ml, p<0.05) at sacrifice. Serum osteocalcin was decreased by hindlimb suspension (98 22 ng/ml vs 149 54 ng/ml in HLU-VEH vs CON-VEH), and increased by SclAbIII treatment (133 22 ng/ml and 203 44 ng/ml in HLU-SCLAbIII, and CON-SCLAbIII), respectively. SclAbIII did not influence the muscle loss seen in HLU. Altogether, these results indicate increased serum sclerostin levels with unloading, and via its anabolic activity, demonstrated the ability of Scl-AbIII to abrogate disuse-induced bone deterioration. These data suggest that sclerostin antibody can increase bone mass by increasing bone formation in normal loaded or under-load bones, though it seems that sclerostin antibody is more effective in increasing bone mass in normally loaded bone than in under-loaded bones.

Table 1: µCT Parameters and Mechanical Strength Results

	CON-SclAbIII	CON-VEH	HLU-SclAbIII	HLU-VEH
Distal Femur				
Tb.BV/TV (%)	32.0 ± 4.9 ^{a,b}	10.3 ± 1.4 ^b	21.7 ± 4.0 ^a	8.0 ± 1.9
Tb.N (mm ⁻³)	4.32 ± 0.16 ^{a,b}	3.86 ± 0.14 ^b	4.05 ± 0.17 ^a	3.72 ± 0.23
Tb.Th (mm)	0.097 ± 0.008 ^{a,b}	0.053 ± 0.002 ^b	0.075 ± 0.006 ^a	0.047 ± 0.003
Femur Midshaft				
Ct.Thickness (mm)	0.21 ± 0.01 ^{a,b}	0.16 ± 0.01 ^b	0.17 ± 0.01 ^a	0.13 ± 0.01
3-point Bending Max Force (N)	18.6 ± 1.1 ^b	12.4 ± 0.9 ^b	15 ± 1.2 ^a	10 ± 0.8

a: p<0.05 SclAbIII vs VEH treatment within the CON or HLU;
b: p<0.05 HLU vs CON within the SclAbIII and VEH treatment groups.

Table 1: µCT Parameters and Mechanical Strength Results

Disclosures: Jordan Spatz, None.

This study received funding from: Amgen

1070

Sclerostin Antibody Increased Bone Mass and Reduced Fractures in Osteogenesis Imperfecta Mice. Jean-Pierre Devogelaer¹, Catherine Behets², Patrick Ammann³, Michael Ominsky⁴, Christine Coppin², Daniel H Manicourt². ¹St. Luc University Hospital, Belgium, ²Université catholique de Louvain, Belgium, ³Division of Bone Diseases, Switzerland, ⁴Amgen, Incorporated, USA

Osteogenesis imperfecta (OI) type III is a severe genetic condition that results in poor bone quality and a high rate of fractures in children. Treatments to prevent these fractures are limited; therefore we tested the effects of a potential therapeutic agent, sclerostin neutralizing monoclonal antibody (Scl-Ab) on bone mass, bone strength and fracture reduction in oim/oim mice, a model of OI type III.

Twenty four 7-week-old OI and 24 wild/wild (WT) control mice were treated with either vehicle (PBS) or Scl-Ab at 25 mg/kg twice per week for 10 weeks. Skeletal fractures excluding rib fractures were detected using mammography X-ray. Bone biomechanical properties were assessed using a three points-bending test and axial compression of the tibia, respectively; ultimate load, elastic energy and plastic energy were determined. Peripheral quantitative computerized tomography (pQCT) was used to measure bone geometry and mineral density (BMD). Statistical analysis included parametric analysis of variance (ANOVA) followed by post hoc tests.

Scl-Ab reduced the number of fractures in OI mice by 56% (mean SD = 2.8 0.6 versus 6.3 1.5 in PBS; $p < 0.001$). In OI mouse tibia, Scl-Ab increased ultimate strength (midshaft: +30%, proximal: +98% versus PBS; all $p < 0.001$), stiffness (midshaft: +132%, proximal: +88% versus PBS; all $p < 0.01$) and plastic energy (midshaft: +125%, proximal: +260% versus PBS; all $p < 0.01$). These strength increases corresponded to significant increases in tibia BMD (midshaft: +30%, proximal: +50% versus PBS; $p = 0.02$ and 0.001 , respectively) and in tibia cortical thickness (midshaft: +40%, proximal: +75% versus PBS; all $p < 0.001$). Scl-Ab-therapy was also associated with significant increases in BMD and cortical thickness in both the humerus and lumbar vertebra, so that at the end of therapy, the strength, BMD and cortical thickness of bones of the OI skeleton were similar to those found in corresponding bones of PBS-treated WT control mice (Table). Scl-Ab-therapy also increased the strength, BMD and cortical thickness in tibia, humerus and vertebra of WT normal mice.

By increasing cancellous and cortical bone mass throughout the skeleton, Scl-Ab improved bone biomechanical properties and reduced the prevalence of bone fractures in OI mice. These results suggest that Scl-Ab might be a promising therapy for human type III OI.

Parameter	Site	OI mice		WT mice	
		Scl-Ab	PBS	Scl-Ab	PBS
Ultimate load (N)	Tibia midshaft	7.6 ± 0.6*	5.7 ± 0.3	19.7 ± 0.9*	10.7 ± 2.7
	Proximal tibia	23.6 ± 6.6*	11.9 ± 0.6	87.2 ± 14.1*	30.4 ± 7.8
Stiffness (N/mm)	Tibia midshaft	24.2 ± 2.3*	10.4 ± 1.5	48.7 ± 2.3*	33.1 ± 9.1
	Proximal tibia	179 ± 49*	95 ± 50	402 ± 23*	252 ± 38
Plastic energy (N*mm)	Tibia midshaft	0.9 ± 0.4*	0.4 ± 0.4	1.0 ± 0.3	1.1 ± 0.4
	Proximal tibia	1.8 ± 0.4*	0.5 ± 0.3	5.5 ± 1.3	4.7 ± 0.6
BMD (mg/cm ³)	Tibia midshaft	951 ± 88	740 ± 65	1045 ± 73	845 ± 35
	Proximal tibia	677 ± 76*	448 ± 91	872 ± 54*	643 ± 78
Cortical thickness (mm)	Tibia midshaft	0.25 ± 0.02	0.18 ± 0.03	0.39 ± 0.05	0.26 ± 0.01
	Proximal tibia	0.14 ± 0.03*	0.08 ± 0.01	0.21 ± 0.03*	0.15 ± 0.01

* $p < 0.02$ versus PBS control

Table

Disclosures: Jean-Pierre Devogelaer, None.

1071

Osteocyte-derived IGF-I Functions as a Portion of the Circuitry For Normal Loading Activation Response in Osteoblasts: Data From the Osteocyte IGF-I Conditional Knockout Mouse. Matilda Sheng¹, Kin-Hing William Lau², Xiaodong Zhou¹, Lynda Bonewald³, David Baylink¹. ¹Loma Linda University, USA, ²Jerry L. Pettis Memorial VA Medical Center, USA, ³University of Missouri - Kansas City, USA

Earlier studies have demonstrated that the IGF-I and its signaling in osteoblasts are essential for the bone formation (BF) response to mechanical loading, and that osteocytes are the primary mechanoresponsive cells in the bone. This study sought to test the hypothesis that osteocyte-derived IGF-I plays a key role in mechanical stimulation of osteoblastic BF by determining the osteoblastic BF response to loading of a mutant mouse with a conditional knockout (KO) of the IGF-I gene in osteocytes, which was generated by crossing the DMP1-Cre transgenic mice with the IGF-I LoxP mice in which the IGF-I exon 4 is flanked by the LoxP site. Analyses by q-PCR and immunohistochemical staining for IGF-I confirmed that the deficient IGF-I expression was restricted to osteocytes. The tibia of the KO mice and wild-type (WT) littermates were subjected to 2 weeks of 4-point bending exercise. The loading force was 9.70.2 and 11.10.1 N for the KO and WT mice, respectively, at a frequency of 2 Hz

for 36 cycles to adjust for the ~11% difference in the bone size. This loading force is equivalent to a loading strain of 4153235 $\mu\epsilon$ in KO mice and 4671265 $\mu\epsilon$ in WT mice ($p > 0.05$). A number of pQCT parameters (total, cortical, subcortical, and trabecular bone mineral contents (BMCs) and bone area) of the loaded tibia were each increased by 35-66% in WT mice; whereas only 9-10% increase was detected in each of these parameters in the KO mice ($P < .001$ for each parameter). Bone histomorphometry revealed that increased BF surface and mineral apposition rate both contributed to the osteoblastic BF response to loading in WT mice. The changes in these parameters in KO mice were too small to be determined with confidence. A loading strain dosage study (Fig. 1) indicates that at each equivalent loading strain, the osteoblastic BF response in KO mice was significantly much less than that in WT controls, confirming that deletion of IGF-I in osteocytes drastically reduced the BF response to loading. In conclusion: 1) this study shows for the first time that osteocyte-derived IGF-I is an important positive regulator of osteoblastic BF to mechanical loading; 2) the 11% smaller cross section area and periosteal circumference in tibia of KO mice than WT mice could be explained by the impaired sensitivity of the KO mouse to mechanical loading, and 3) because osteocyte IGF-I is an important determinant of bone size, it follows that it is also important to determine the bone strength.

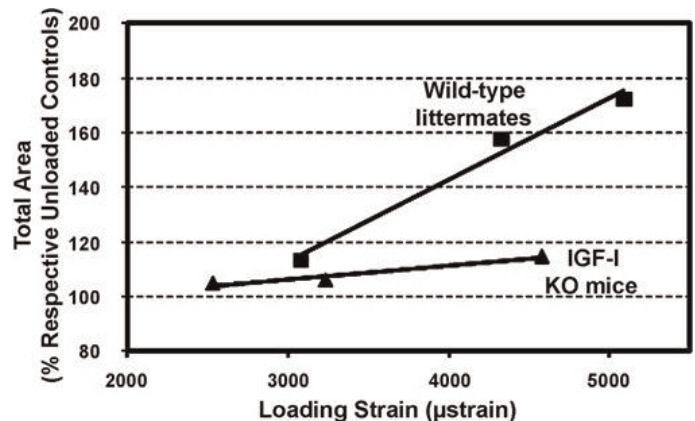


Figure 1. Loading strain dose response curves of osteocyte IGF-I conditional KO mice and WT mice.

Disclosures: Matilda Sheng, None.

1072

Low Trabecular Bone Volume in α_2 C-Adrenoceptor Knockout Mice. Marilia Teixeira¹, Gisele Martins², Cristiane Costa³, Patrícia Brum⁴, Cecília Gouveia². ¹University of Sao Paulo, Brazil, ²Institute of Biomedical Science, Brazil, ³Institute of Biomedical Science, Brazil, ⁴School of Physical Education and Sport, Brazil

Evidence demonstrates that sympathetic nervous system (SNS) activation causes osteopenia via β_2 -adrenoceptor (β_2 -AR) signaling. In a recent study, we showed that female mice with chronic sympathetic hyperactivity due to double knockout of adrenoceptors that negatively regulate norepinephrine release, α_2 a-AR and α_2 c-AR (α_2 a/ α_2 c-AR KO), present an unexpected and generalized phenotype of high bone mass with decreased bone resorption and increased bone formation. These findings suggest that β_2 -AR is not the single adrenoceptor involved in bone turnover regulation and show that α_2 -AR signaling may also mediate the SNS actions in the skeleton. To further investigate the participation of the SNS and α_2 ARs in the regulation of bone mass, we are evaluating the bone phenotype of α_2 c-AR knockout mice (α_2 c-AR^{-/-}). A cohort of 120 day-old female congenic α_2 c-AR^{-/-} mice in a C57BL/6J background and their wild-type (WT) controls (n=7/group) were studied. Single knockout mice presented decreased retroperitoneal fat pad (40%, $p < 0.01$), decreased body length (4%, $p < 0.001$) and decreased femur length (4%, $p < 0.001$). Surprisingly, microtomography analysis of the distal metaphysis of the femur showed that α_2 c-AR^{-/-} mice present a 15% decrease in trabecular bone volume (BV/TV; $p < 0.01$). These findings suggest that α_2 a-AR, but not α_2 c-AR, may have a role in mediating the deleterious effects of the sympathetic activation in trabecular bone.

Disclosures: Marilia Teixeira, None.

1073

Bmp2 Gene in Osteoblasts Controls Bone Quantity and Quality by Regulating the Vascular Niche for Skeletal Stem Cells (SCCs) in both Periosteum and Trabeculae. Wuchen Yang^{*1}, Valentin David², Jeffry Nyman³, Marie Harris¹, Yong Cui¹, Jelica Gluhak-Heinrich¹, Ivo Kalajzic⁴, Barbara Kream⁴, David Rowe⁴, Alexander Lichtler⁴, Xiao-Dong Chen¹, Yuji Mishina⁵, Stephen Harris¹. ¹University of Texas Health Science Center At San Antonio, USA, ²UTHSC, USA, ³Vanderbilt University Medical Center, USA, ⁴University of Connecticut Health Center, USA, ⁵University of Michigan, USA

In vivo studies indicate that *BMP2* action in osteoblasts is much more complex and plays fundamental roles in both periosteal and trabecular function. The *Bmp2* gene now appears to control both quantity and quality of bone. We generated *BMP2* conditional floxed allele and removed the *Bmp2* gene from early osteoblasts postnatally (*Bmp2*-cKO^{ob} mouse model) using 3.6Col-Cre transgenic mice and from earlier preosteoblasts using the OsterixBAC-Tet-off-Cre model (*Bmp2*-cKO^{Sp7Cre}). The *Bmp2*-cKO^{ob} mice display progressive osteopenia that mimics bone ageing, including loss of bone (smaller bones and smaller cross-sectional diameter) and increased brittleness (post yield toughness in a mechanical test), and reduced vascular system (3D vascular profusion). The microvascular 3D mapping demonstrates a 50 to 70% reduction in blood vessels associated with the periosteum and trabeculae. By dynamic bone formation rate, *Bmp2*-cKO^{ob} and *Bmp2*-cKO^{Sp7Cre} mice show severely deteriorated capacity to appose mineral to the outside (periosteum) and inside (trabeculae) of the bone. We established that there was a 70% decrease in SSCs in a CFU-F bone marrow assay, and confirmed these results *in vivo* by showing reduced CD146+ and Sma-Cherry+ cells on the small blood vessels associated within the periosteal and the trabecular region. There is even fewer SSCs per length of microvessel (<12um). By histomorphometric analysis and *in situ* hybridization (Col1a1, Osterix, Osteocalcin and VegfA), we demonstrated that the osteoblasts of the *Bmp2*-cKO^{ob} do not mature to cuboidal matrix producing osteoblasts and cannot produce high level of the *Bmp2* induced gene VegfA, which is required for this *Bmp2* induced vascularization. We now demonstrate this late osteoblast differentiation defect is linked to the vascular niche and SSCs in both the periosteum and trabecular bone. This establishes a cycle between late osteoblast function and regulation of the SSCs through regulation of the vascular niche. With more limited studies with the *Bmp2*-cKO^{Sp7Cre} model, we have determined that the bones are all smaller or thinner, more brittle by mechanical loading tests, and have reduced blood vessels in both the periosteum and trabecular region. However, to our surprise, a dramatic increase in CD146+ cells on the fewer blood vessels was observed, suggesting that the SSCs may not be able to egress from their vascular niche when the *Bmp2* gene is deleted in this earlier stage in the osteoblast lineage.

Disclosures: Wuchen Yang, None.

1074

Absence of NFATc2 Results In High Bone Mass and Impaired Hematopoiesis. Martina Rauner^{*1}, Wolfgang Bauer², Ivonne Habermann², Michael Haase³, Gerhard Ehninger², Lorenz Hofbauer⁴, Alexander Kiani². ¹Medical Faculty of the TU Dresden, Germany, ²Technical University Dresden, Department of Medicine I, Germany, ³Technical University of Dresden, Institute of Pathology, Germany, ⁴Dresden University Medical Center, Germany

Nuclear factor of activated T cells (NFAT) constitutes a family of transcription factors which are critically involved in T cell activation and modulation of bone remodeling. NFATc1 has been identified as the master transcription factor for osteoclasts and also suppresses osteoblast function. By contrast, the role of other NFAT members such as NFATc2 is poorly understood. Based on our observation that NFATc2 is highly expressed in hematopoietic stem cells and regulated during myeloid commitment in a lineage-specific manner, we hypothesized that NFATc2 is an essential regulator of both hematopoiesis and bone mass. To test this hypothesis, we characterized the haematological and skeletal phenotype of NFATc2^{-/-} mice. Besides a reduced number of blood platelets and total bone marrow cells, young NFATc2^{-/-} mice of less than 3 months did not show any hematologic abnormalities compared to wild-type (WT) mice. However, detailed assessment of old NFATc2^{-/-} mice older than 12 months revealed mild microcytic, hypochromic anemia, lymphocytosis (20%) and severe thrombocytopenia. The femora of old NFATc2^{-/-} mice showed a 46% reduction of bone marrow cells, wherein the megakaryocytic/erythroid lineage was most affected. Of note, the differentiation of myeloid progenitor cells as assessed by colony formation was intact. Strikingly, all NFATc2^{-/-} mice displayed an ossified bone marrow space with subsequent extramedullary hematopoiesis in the spleen. Bone histology revealed numerous osteoblasts and osteoclasts at the bone surface of the trabeculae in NFATc2^{-/-} mice, indicating a high bone turnover underlying osteosclerosis. *Ex vivo*, NFATc2^{-/-} osteoblasts displayed a 2.3-fold increased ALP activity (WT: 23.6 10.3 relative units; NFATc2^{-/-}: 54.3 14.2 relative units, *p* < 0.01) and produced twice as much mineralized matrix as WT cells (*p* < 0.05). Moreover, osteoclast differentiation, as determined by counting TRAP-positive, multinucleated cells, was diminished by 30% in NFATc2^{-/-} mice (*p* < 0.05). In conclusion, our data demonstrate that prolonged absence of NFATc2 enhances bone mass by stimulating osteoblastic functions and concurrently suppressing osteoclast

formation. Moreover, NFATc2 is critical in the maintenance of steady-state hematopoiesis in adult organisms. This indicates that NFATc2 is a central player in the intimate relationship of hematopoiesis and bone homeostasis within the bone/bone marrow microenvironment.

Disclosures: Martina Rauner, None.

1075

Interleukin-6 Receptor Signaling Links Hematopoietic and Anabolic Actions of PTH in Bone. Sun Wook Cho^{*1}, Flavia Pirihi¹, Megan Michalski¹, Matt Eber¹, Seo jin Oh¹, Thomas Wronski², Laurie McCauley³. ¹University of Michigan School of Dentistry, USA, ²University of Florida, USA, ³University of Michigan, School of Dentistry, USA

Intermittent administration of parathyroid hormone (PTH) increases bone mass by stimulating bone formation. Interleukin (IL)-6 is upregulated by PTH and is a critical mediator of PTH effects on hematopoietic cells. The purpose of this study was to determine the role of IL-6 signaling on hematopoietic and skeletal action of PTH. Intermittent PTH (PTH 1-34, 50 µg/kg/day) was administered to wildtype (WT) and IL-6 deficient (IL-6 KO) mice at two different ages (young 3~24day and adult 16~22week). There was a similar PTH mediated increase in bone area via histomorphometry (tibia and vertebrae), bone volume via microCT (femurs), and bone formation rates via dynamic histomorphometry in young and adult WT and KO mice. To investigate IL-6 compensatory mechanisms, protein levels of soluble IL-6 receptor (sIL-6r) were evaluated in 16-week-old WT and IL-6 KO mice after PTH administration (2 weeks). Under basal conditions, serum sIL-6r was significantly reduced in IL-6 KO vs. WT mice, however bone marrow sIL-6r was similar. Interestingly, treatment with PTH significantly increased bone marrow sIL-6r in both WT and IL-6 KO mice suggesting potential compensation. Hence, the sIL-6r transsignaling pathway was investigated *in vivo* using soluble glycoprotein 130 receptor (sgp130r) blocking. Young IL-6 KO mice were treated with vehicle, PTH, sgp130r or PTH plus sgp130r for 2weeks. PTH increased bone volume and trabecular number in IL-6 KO mice which was significantly attenuated when sgp130r was combined with PTH. Consistently, PTH increased serum PINP and sgp130 prevented the PINP increase. Since PTH in concert with fms-like tyrosine kinase-3 ligand (Flt-3L), expands hematopoietic cells in an IL-6 dependent manner, whether sIL-6r could replace these IL-6 actions was evaluated. In an *ex vivo* bone marrow expansion study, sgp130r inhibited the cell expansion response to PTH with Flt-3L. Additionally sIL-6r treatment resulted in earlier cell amplification, and in combination with PTH, sIL-6r expanded cells independently of Flt-3L. Collectively, PTH depends on IL-6 for its hematopoietic cell expansion, whereas IL-6 appears to be compensated for by sIL-6r in both hematopoietic cell expansion and the anabolic actions of PTH in bone. These findings link together IL-6 targeted signaling in the bone and marrow microenvironments toward a better mechanistic understanding of PTH anabolic actions.

Disclosures: Sun Wook Cho, None.

1076

Circulating Human Lineage Negative/Osteoblast Progenitor Cells Support Hematopoiesis in Tk-Rag Mice. Pilar Peris^{*1}, Robert Jilka², Sundeep Khosla³, Ulrike Moedder³. ¹Hospital Clinic of Barcelona, Spain, ²University of Arkansas for Medical Sciences, USA, ³College of Medicine, Mayo Clinic, USA

Hematopoietic stem cells (HSC) are multi-potent cells that generate a lifelong supply of all blood cell types. HSC self-renewal is regulated, in part, by cells of the osteoblast lineage within the hematopoietic niche. We have previously identified osteoblast-like (lineage negative/alkaline phosphatase positive [lin-/AP+] cells) in peripheral blood in humans. Here, we tested for the ability of these lin-/AP+ cells to support hematopoiesis *in vivo*. To do so, we first bred mice expressing thymidine kinase (tk) under the control of the Col3.6 promoter into an immuno-compromised (Rag) background, designated tk-Rag mice. Daily treatment of 4-week-old male tk-Rag mice (*n* = 32) with ganciclovir (300µg/d) resulted in the ablation of osteoblast progenitors from cancellous bone and subsequent loss of hematopoiesis, as measured by the number of bone marrow erythroid precursors (Ter119+) using flow cytometry. Human bone marrow-derived mesenchymal stem cells (Clonetic) or *ex vivo* expanded peripheral blood lin-/AP+ cells (~10⁵ cells each) were infused locally into both femoral bone marrow cavities of tk-Rag mice; control tk-Rag mice received saline infusions (*N* = 6-11 per group). The infusion of the cells was performed after an initial treatment period with ganciclovir of 18 days to insure that a complete depletion of osteoblasts and hematopoietic cells had occurred. The ganciclovir treatment was continued throughout the entire experiment and all the mice were euthanized 12 days following cell (or saline) infusion. Ganciclovir caused a significant (7.4-fold, *P* < 0.001) reduction of Ter119+ cells in the bone marrow of ganciclovir-treated tk-Rag mice compared to tk-Rag control mice given saline injections. Infusion of MSCs into ganciclovir-treated mice resulted in an (3.3-fold, *P* = 0.08) increase in Ter119+ cells compared to mice treated with ganciclovir but not receiving any cells. Similarly, infusion of lin-/AP+ cells into ganciclovir-treated mice resulted in a significant (2.7-fold, *P* < 0.001) increase in Ter119+ cells compared to mice not receiving any cell infusion. This study thus demonstrates that human peripheral blood lin-/AP+ cells have the capacity to support and maintain hematopoiesis in mice and are as potent as bone marrow MSCs in this experimental model. Further studies are aiming to

determine whether the infused cells home to the hematopoietic niche itself and how long they reside there.

Disclosures: Pilar Peris, None.

1077

Hematopoietic Stem Cells Give Rise to Osteo-chondrogenic Cells During Fracture Repair. Meenal Mehrotra*, Jonathan D McGuirt, Christopher R Williams, Makio Ogawa, Amanda C LaRue. Research Services, Ralph H Johnson VAMC & Medical University of South Carolina, USA

There are approximately 6.5 million fractures in the United States per year which represents a substantial cause of morbidity, missed work and medical cost. About 5-10% of these fractures result in delayed union or non-union, meaning that the bone does not heal in a timely manner or does not heal at all. Bone healing is unique in that, once a fracture is sustained, the injured bone has the capacity to remodel and regenerate its original structure and integrity. Remodeling of skeletal bone requires the recruitment and proliferation of stem cells with the capacity to differentiate to functional osteoblasts that deposit and mineralize extracellular bone matrix. Given the close association of bone and bone marrow, it has been suggested that bone marrow may serve as a source of these progenitors. Bone marrow is thought to contain two types of stem cells, mesenchymal stem cells (MSCs) and hematopoietic stem cells (HSCs). To test the ability of HSCs to give rise to osteo-chondrogenic cells, we used a single HSC transplantation paradigm in conjunction with a tibial fracture model. For transplantation, mice were lethally irradiated and transplanted with a clonal population of cells derived from a single enhanced green fluorescent protein positive (EGFP+) HSC. After confirming multilineage engraftment, non-stabilized fracture was created through tibial mid-diaphysis. To confirm fracture remodeling, micro-computed tomography images of tibia were taken two months post non-stabilized fracture. These images and morphometric analysis show the presence of a large fracture callus and bone remodeling. Longitudinal paraffin sections were then examined at 7 days, 2 weeks and 2 months after fracture. A large number of EGFP+ hypertrophic chondrocytes, osteoblasts and osteocytes were identified in and around the fracture callus. The morphology of the callus was confirmed by staining serial sections with Massons Trichrome stain. The cells in the callus were further characterized by co-localization of EGFP expression and Runx-2 or osteocalcin expression. A majority of the cells stained positive for Runx-2 or osteocalcin and were also EGFP+ demonstrating their origin from the HSC. These data demonstrate that HSCs can differentiate into hypertrophic chondrocytes, osteoblasts and osteocytes and contribute to fracture healing. Together, these findings strongly support the concept that HSCs can generate bone cells and suggest therapeutic potentials of HSCs in fracture repair.

Disclosures: Meenal Mehrotra, None.

1078

Transdifferentiation of Hematopoietic Stem Cells into Mesenchymal Stem Cells for Use in Bone Regeneration. Xianmei Meng*, Amanda Neises¹, Kin-Hing William Lau², David Baylink¹, Xiaobing Zhang¹. ¹Loma Linda University, USA, ²Jerry L. Pettis Memorial VA Medical Center, USA

Mesenchymal stem cells (MSCs) from marrow or adipose tissues have been demonstrated in animal and preclinical studies to have important potential in regenerative medicine applications such as bone fracture healing and critical-sized bone formation. However, the procedures to harvest MSCs are invasive and often do not produce enough MSCs for use in clinical treatment. Thus, we have sought for alternative approaches for transdifferentiation of readily available cells, such as blood cells, into MSCs. Recently, reprogramming factors used in generating induced pluripotent stem cells have also found to be able to convert one cell type to another. We hypothesized that some of these reprogramming factors may also promote transdifferentiation of CD34⁺ hematopoietic stem cells into MSCs. To test this hypothesis, we cloned OCT4, SOX2, MYC and KLF4 into a lentiviral vector and transduced human cord blood CD34⁺ cells with these reprogramming factors in various combinations. One day after transduction, CD34⁺ cells were seeded into 6-well plates that were pre-coated with MEF feeder cells and cultured in DMEM/10% FBS. After several attempts, we have identified the combination of OCT4+MYC as the best condition to transdifferentiate CD34⁺ cells into MSC-like cells in 1 week, with an efficiency of up to 5%. Cells were further cultured in well plates without feeder support and passaged every 2-3 days. Flow cytometry analysis at 2-3 weeks after transduction showed that 80-95% cells expressed MSC markers CD29, CD44, CD73, CD90, CD105 and CD166. 20-30% cells also expressed CD271, a marker used for purification of MSCs from marrow and adipose tissue. Expression of hematopoietic markers like CD14, CD34 and CD45 was not detectable. Our data suggest that the blood-turned cells manifest MSC phenotype. These cells expanded robustly for more than 1 month, with generation time of 30-40 hours. Functional test of these cells in preliminary in vitro studies showed that these MSCs can be induced to differentiate into osteoblasts, adipocytes and chondrocytes when cultured in corresponding differentiation media for 3 weeks. In conclusion, we have, for the first time, developed an effective and convenient approach to transdifferentiate hematopoietic stem cells into MSCs. This new development is exciting because it may facilitate and expand the therapeutic applications of MSCs for the regeneration of bone as well as other tissues.

Disclosures: Xianmei Meng, None.

1079

A Novel Syndrome Characterized By Intermittent Hypercalcemia, Hypercalciuria, Elevated Serum Calcitriol And Undetectable 24,25-Dihydroxyvitamin D Concentrations, Nephrolithiasis, Osteoporosis, And Mutations In The CYP24A1 (25-Hydroxyvitamin D/1, 25-Dihydroxyvitamin D 24-Hydroxylase) Gene. Peter Tebben¹, Dawn Milliner², Ronald Horst³, Rajiv Kumar⁴. ¹Mercy Health, USA, ²Mayo Clinic, USA, ³Heartland Assays, Inc., USA, ⁴Mayo Clinic College of Medicine, USA

We describe a novel syndrome in a 44-year-old Caucasian male characterized by intermittent hypercalcemia, hypercalciuria, elevated serum 1,25-dihydroxyvitamin D, undetectable serum 24, 25-dihydroxyvitamin D, nephrolithiasis, and reduced bone mineral density. In 2005, the patient developed left renal colic and a stone was removed with laser lithotripsy. Analysis of stone fragments revealed calcium oxalate. A new calculus was noted in the left kidney in 2008. This increased in size over a period of two years from 4 mm to 6 mm. Bone densitometry of the lumbar spine revealed low BMD (Z score lumbar spine of -3.1). Laboratory investigations performed on several occasions over 12 months are shown in table 1.

Angiotensin converting enzyme concentrations were normal. Monoclonal proteins in the serum and urine were negative. Fungal serologies were nonreactive. A CT of the chest showed a 2X6 millimeter calcified nodule in the right major fissure. CT of the abdomen showed multiple small bilateral renal cysts suggestive of an early or mild form of polycystic kidney disease. A 6 mm stone was noted in the mid left kidney. We obtained DNA for sequencing of the 25-hydroxyvitamin D 1 α -hydroxylase (Cyp27b1) and 25-hydroxyvitamin D or 1, 25-dihydroxyvitamin D 24-hydroxylase (Cyp24a1) genes. The sequence of the Cyp27b1 gene was normal without evidence of duplication. The sequence of the Cyp24a1 gene showed 2 intron-exon splice junction abnormalities that would result in altered 25-hydroxyvitamin D/1, 25-dihydroxyvitamin D 24-hydroxylase expression.

Family history revealed an unaffected mother (father was deceased) and three children (two daughters and one son) among whom a 3-1/2-year-old daughter exhibited similar phenotypic features with elevated serum 1, 25-dihydroxyvitamin D concentrations, hypercalciuria, nephrocalcinosis and renal cysts.

Conclusions: Elevated 1, 25-dihydroxyvitamin D and undetectable 24,25-dihydroxyvitamin D concentrations in a patient with intermittent hypercalcemia, hypercalciuria, nephrolithiasis and renal cysts were associated with splice-junction abnormalities of the 25-hydroxyvitamin D/1, 25-dihydroxyvitamin D 24-hydroxylase (Cyp24a1) gene. The data suggests that in humans, 25-hydroxyvitamin D/1, 25-dihydroxyvitamin D 24-hydroxylase activity regulates 1, 25-dihydroxyvitamin D concentrations, and abnormalities in the Cyp24a1 gene can result in a clinically important phenotype.

TABLE 1											
Serum Analyte Concentration (normal values within parentheses)											
T Ca mg/dL (8.9-10.1)	Ca** mg/dL (4.8-5.7)	Pi mg/dL (2.5-4.5)	25(OH)D ng/mL (25-66)	1,25(OH) ₂ D pg/mL (15-66)	24,25(OH) ₂ D pg/mL (1.2-2.8)	PTH pg/mL (15-65)	PTH- RP pM (0-9)	Ak # U/L (45- 115)	B ak # µg/L (0-20)	β2-MG pg/mL (50-600)	β2-MG pg/mL (50-600)
10.4, 10.0, 10.1, 11.1	5.29, 5.29, 5.17	3.6, 4.4, 3.7, 4.8	50, 36, 48, 60	123, 62, 44, 90	<0.2	8.1, 9.6, 6.3, 6.0	0.3, 0.4	91	24, 20, 14	860, 146, 423	
Urine Analyte mg/24h (normal values within parentheses)											
Ca (25-300)	Pi (<100)	Oxalate (2.7-40.5)	Citrate (321- 1191)	Uric acid (<750)	Mg (75-150)	Creatinine (15-25 mg/kg)					
374, 367, 505	1250, 750, 1500	24.7, 26.4, 46.7	478, 565, 683	700, 600, 600	168, 109, 151	1725, 1200, 1650					

Table 1

Disclosures: Rajiv Kumar, None.

1080

Hajdu-Cheney Syndrome: Serum Biomarker Profiling, Bone Radiography and Histopathology, and Germline Mutation Analysis Indicate Complex Dysregulation of Skeletal Cells from Gain-of-Function Truncation of NOTCH2. Michael P. Whyte*, Marina Stolina², William H. McAlister³, Deborah Wenkert⁴, Deborah V. Novack⁵, Xiafang Zhang⁶, Angela R. Nenner⁴, Denise C. Dwyer⁷, Vivienne T. Lim⁴, Nelson Watts⁸, David L. Lacey⁷, Steven Mumm¹. ¹Shriners Hospital for Children & Washington University School of Medicine, St. Louis, USA, ²Amgen Inc, USA, ³Department of Pediatric Radiology at the Mallinckrodt Institute of Radiology, St. Louis Childrens Hospital at the Washington University School of Medicine, St. Louis, USA, ⁴Shriners Hospital for Children, St. Louis, USA, ⁵Washington University in St. Louis School of Medicine, USA, ⁶Washington University in St. Louis School of Medicine, St. Louis, USA, ⁷Amgen Inc., USA, ⁸University of Cincinnati Bone Health & Osteoporosis Center, USA

Hajdu-Cheney syndrome (HCS) is the rare, autosomal dominant disorder that features acroosteolysis together with generalized osteoporosis presenting in childhood. The skeletal abnormalities advance with aging (Figure). Notch refers in humans to four, single-pass, transmembrane receptors that share multiple ligands and function

ubiquitously in cell differentiation and apoptosis. This year, two research groups discovered that heterozygous, truncating mutation within the final coding exon of *NOTCH2* causes HCS (Nat. Genet. 43:303,306 2011). The mutant mRNA would evade nonsense mediated decay, disrupt a carboxy-terminal proteolytic recognition sequence thereby preventing ubiquitination, and consequently activate Notch signaling.

Here, we confirm in six sporadic instances of HCS and in five affected individuals from two HCS families that heterozygous truncating mutation in exon 34 of *NOTCH2* causes HCS. Mutations for our patient cohort include one unique nonsense mutation, five unique small (one or two base pairs) deletions or insertions, and two small (one or two base pairs) deletions shared with previous reported cases. Our patients' radiographs demonstrated a complex skeletal disease including compromise of fracture repair. Bone histopathology of one child and two adults with HCS showed increased cortical porosity and decreased trabecular bone mass and connectivity, but without obvious changes in osteoclasts or osteoblasts. In a distal phalanx, there was absence of bone without inflammation, necrosis, or fibrovascular changes. Biomarker profiling of four HCS patients suggested multifactorial dysregulation of bone cells with markedly diminished serum levels of sclerostin, serotonin, and vegf (and usually dickkopf1 and TGF β), and significantly increased levels of prostaglandin E₂.

Heterozygous truncating mutation in the carboxy-terminal exon of *NOTCH2* causes HCS by Notch activation and seems to disrupt the skeleton by a complex pathogenesis involving the LRP5/WNT, TGF β , and other signaling pathways.



This 46-year-old woman with HCS has remarkable acro-osteolysis of the distal and middle phalanges (arrows).

Figure

Disclosures: Michael P. Whyte, Amgen, Inc., 5
This study received funding from: Amgen Inc

1081

Paget's Disease-causing Mutations in Sequestosome-1 Impair Autophagic Protein Degradation. Eman Azzam, Miep Helfrich, Lynne Hocking*. University of Aberdeen, United Kingdom

Paget's disease of bone (PDB) is characterised by focal lesions of increased bone turnover, driven by overactive osteoclasts. Mutations affecting Sequestosome-1 (SQSTM1/p62) ubiquitin-associated domain have been identified in individuals with PDB, which impair binding to ubiquitylated proteins targeted for degradation. We have previously shown elevated abundance of p62, ubiquitin, proteasomal subunits and LC3 (marker of autophagic protein degradation) in osteoclasts from Pagetic biopsies, suggesting generalised defects in protein degradation occur. The aim of this study was to examine the effect of PDB-causing mutations on p62 degradation.

HEK293 cell lines stably expressing exogenous p62 (wildtype or mutant P392L, E396X or G425R) were generated using the FlpIn System (Invitrogen). Exogenous p62 is under the control of a CMV promoter such that differences in protein abundance cannot be due to transcriptional upregulation. These cell lines also express endogenous p62, thereby approximating heterozygous mutations. Cells were examined under normal growth conditions, and following amino acid starvation to induce autophagy, or bafilomycin treatment to inhibit autophagy. Lysates were western blotted for exogenous p62 and GAPDH. Protein abundance was measured using LiCOR Odyssey and results expressed relative to GAPDH, normalised to the wildtype p62 cell line.

Exogenous p62 abundance was increased for all mutants compared with wildtype under normal growth conditions, suggesting p62 degradation is impaired by PDB mutations. Upon amino acid starvation, mutant exogenous p62 still exhibited increased abundance compared with wildtype. When autophagy was inhibited, the difference between wildtype and mutant exogenous p62 was lost, suggesting that pharmacological inhibition of autophagy prevents degradation of wildtype p62 to a similar extent as the presence of PDB-causing mutations.

We have shown that autophagic protein degradation is impaired by PDB-causing SQSTM1 mutations. Dissection of protein degradation dynamics (autophagic and proteasomal) will provide important insights into the regulation of osteoclast function by protein degradation pathways, and into the influence of SQSTM1 mutations on these.

Disclosures: Lynne Hocking, None.

1082

Mutations of SQSTM1 Cause Dysregulation of the Autophagy Pathway in Osteoclast Precursors and Are Responsible for Development of Intranuclear Inclusions in Paget's Disease. Anna Daroszevska¹, Robert Van't Hof¹, Lorraine Rose¹, Ken Rose¹, Rob Layfield², Stuart Ralston^{*1}. ¹University of Edinburgh, United Kingdom, ²University of Nottingham, United Kingdom

Osteoclasts in patients with Paget's disease of bone (PDB) characteristically contain nuclear inclusion bodies. These were originally thought to be paramyxovirus nucleocapsids, but their true identity is unknown and previous investigators have noted that the Pagetic inclusions differ morphologically from those found in subacute sclerosing panencephalitis the archetypal slow virus disease caused by measles virus infection. On the other hand, intracellular inclusions have long been recognized to be a feature of human neurodegenerative disorders such as Alzheimer's disease and Parkinson's disease which are thought to be caused in part by defects in degradation of abnormal protein aggregates by the proteasome and autophagy. In order to clarify the nature of the intranuclear inclusions in PDB we generated a mouse model of the disease in which the P392L mutation of SQSTM1 (P394L in the mouse) was created by gene targeting. The P394L mutant mice developed a bone disorder with remarkable similarity to PDB characterized by the development of focal osteolytic and osteosclerotic bone lesions characterised by high bone turnover and woven bone. Osteoclasts within the lesions were larger than normal and contained intranuclear inclusion bodies almost identical to those observed in human PDB. The inclusions consisted of multiple microcylindrical structures approximately 12 nm in diameter arranged in a paracrystalline array as in human PDB. To determine if this might be associated with abnormalities in the autophagy pathway we measured expression of marker genes for this process including SQSTM1, the microtubule associated protein 1 light chain 3 gene (LC3) and the autophagy related gene 5 (ATG5) using real-time PCR. There was a significant increase in SQSTM1, LC3 and ATG5 expression in osteoclast precursors from P394L mutant mice when compared with wild type littermates ($p < 0.02$). Interestingly, no difference in expression of these genes was observed in macrophages indicating that the abnormalities observed were specific to osteoclasts. We went onto perform Western blotting for LC3-II (a marker of autophagosome formation) and found that levels were significantly higher in P394L mutant osteoclasts as compared to wild type controls ($p < 0.001$), consistent with dysregulation of the autophagy pathway. We conclude that the nuclear inclusions observed in human PDB and in the model described here most probably represent abnormal protein aggregates related to dysregulation of autophagy system, rather than viral particles, confirming the importance of genetics as opposed to persistent viral infection as the cause of this disorder.

Disclosures: Stuart Ralston, None.

1083

Mutations in *SERPINF1* cause Osteogenesis Imperfecta Type VI. Erica Homan^{*1}, Ingo Grafe², Frank Rauch³, Caressa Lietman¹, Jennifer Doll⁴, Brian Dawson¹, Terry Bertin¹, Dobrawa Napierala⁵, Roy Morello⁶, Richard Gibbs¹, Lisa White¹, Rika Miki⁷, Daniel Cohn⁷, Susan Crawford⁴, Rose Travers⁸, Francis Glorieux⁹, Brendan Lee¹⁰. ¹Baylor College of Medicine, USA, ²Department of Molecular & Human Genetics, Baylor College of Medicine, USA, ³Shriners Hospital for Children, St. Louis, Canada, ⁴NorthShore University Health System Research Institute, USA, ⁵University of Alabama at Birmingham School of Dentistry, USA, ⁶University of Arkansas for Medical Sciences, USA, ⁷University of California, Los Angeles, USA, ⁸Shriners Hospital for Children, Canada, ⁹Shriners Hospital for Children & McGill University, Canada, ¹⁰Baylor College of Medicine & Howard Hughes Medical Institute, USA

Osteogenesis Imperfecta (OI) is a spectrum of genetic disorders characterized by low bone mass and fragility. It is caused by dominant mutations affecting the synthesis and/or structure of type I procollagen or by recessively inherited mutations in genes responsible for the post-translational processing/trafficking of type I procollagen. In all but one class of OI, the histopathological and clinical features cannot predict the causative gene or functional defect among affected individuals. However, recessive OI type VI is characterized by a pathognomonic increase in the amount of unmineralized osteoid, thereby suggesting a distinct disease mechanism. OI type VI is of unknown etiology and identifying the disease gene will add to our understanding of matrix mineralization and identify potential therapies.

To identify the gene region, homozygosity mapping was carried out using the genomic DNA of 3 members of a consanguineous French Canadian family. A single region of homozygosity was shared by all three of these related OI VI patients defined by the markers rs8074026 and rs1362761. Next generation sequencing of one patient from this family identified homozygosity for a stop mutation in exon 4 (g.4130C>T, p.R99X) of serpin peptidase inhibitor, clade F, member 1 (*SERPINF1*) which was confirmed by Sanger sequencing in all affected family members. The stop codon mutation was predicted to result in nonsense mediated decay (NMD) of the *SERPINF1* transcript and realtime RT-PCR of patient fibroblasts confirmed that this is the case. Sanger sequencing the 8 exons of *SERPINF1* in 10 unrelated patients identified additional mutations. Interestingly, the g.4130C>T mutation was identified in additional patients of French Canadian origin, suggesting the presence of a founder allele in the population. *SERPINF1* encodes the 50kDa secreted protein, Pigment Epithelium-derived Factor (PEDF). Serum PEDF levels were undetectable in OI type VI patients in contrast to classical OI patients (caused by mutations affecting type I collagen) in whom PEDF serum levels were comparable to normal controls.

These data suggest that mutations in *SERPINF1* resulting in loss of PEDF cause OI type VI. This provides an avenue for proper OI diagnosis of patients, where PEDF could be measured in serum for confirmation. In addition, PEDF is a secreted protein, suggesting therapy with recombinant PEDF could be used as a potential therapy for OI type VI patients.

Disclosures: Erica Homan, None.

1084

Large-scale meta-analyses of Genome-Wide Association Studies for Fracture Risk: The GEFOS Consortium. Ling Oei^{*1}, Houfeng Zheng², Evangelia Ntzani³, Karol Estrada¹, Paul Ridker⁴, Melissa Garcia⁵, Yi-Hsiang Hsu⁶, Terho Lehtimäki⁷, Stella Trompet⁸, Stephen Kaptoge⁹, Scott Wilson¹⁰, Yongmei Liu¹¹, Joel Eriksson¹², Najaf Amin¹³, Annie Kung¹⁴, Konstantinos Tsilidis³, Carolina Medina-Gomez¹⁵, Lynda Rose⁴, Albert Vernon-Smith¹⁶, Ching-Ti Liu¹⁷, Jorma Viikari¹⁸, Alireza Moayyeri¹⁹, Ryan Minster²⁰, Mattias Lorentzon²¹, Su-Mei Xiao²², Nicholas Wareham²³, Ville Aalto²⁴, Thor Aspelund²⁵, William Leslie²⁶, David Goltzman²⁷, Steven Cummings²⁸, L Cupples¹⁷, Evangelos Evangelou³, Kay-Tee Khaw¹⁹, Robert Luben¹⁹, Olli Raitakari²⁴, Kristin Siggeirsdottir²⁹, Cornelia van Duijn¹³, Jane Cauley³⁰, David Karasik³¹, Pak Sham²², M Zillikens³², Claes Ohlsson²¹, Tamara Harris³³, Tim Spector³⁴, Jonathan Reeve³⁵, J Kukema⁸, John Ioannidis³, Mika Kahonen³⁶, Douglas Kiel³¹, Vilmundur Gudnason²⁹, Andre Uitterlinden³⁷, Daniel Chasman⁴, Brent Richards², Fernando Rivadeneira¹.

¹Erasmus University Medical Center, The Netherlands, ²McGill University, Canada, ³University of Ioannina Medical School, Greece, ⁴Brigham & Women's Hospital, USA, ⁵NIA, NIH, USA, ⁶Hebrew SeniorLife Institute for Aging Research & Harvard Medical School, USA, ⁷Department of Clinical Chemistry, University of Tampere & Tampere University Hospital, Finland, ⁸Leiden University Medical Center, Netherlands, ⁹University of Cambridge Bone Research Group, United Kingdom, ¹⁰Sir Charles Gardner Hospital, Australia, ¹¹Wake Forest University School of Medicine, USA, ¹²Center for Bone & Arthritis Research, Institute of Medicine, Sahlgrenska Academy, University of Gothenburg, Sweden, ¹³Erasmus MC, Netherlands, ¹⁴Dr. Kung-Wai Chee Clinic, Hong Kong, ¹⁵Erasmus Medical Center, The Netherlands, ¹⁶Icelandic Heart Association & University of Iceland, Iceland, ¹⁷Boston University School of Public Health, USA, ¹⁸University of Turku & Turku University Hospital, Finland, ¹⁹University of Cambridge, United Kingdom, ²⁰University of Pittsburgh, USA, ²¹Center for Bone Research at the Sahlgrenska Academy, Sweden, ²²The University of Hong Kong, China, ²³Medical Research Council (MRC), Epidemiology Unit, United Kingdom, ²⁴Research Centre of Applied & Preventive Cardiovascular Medicine, University of Turku & the Department of Clinical Physiology, Finland, ²⁵Icelandic Heart Association, Iceland, ²⁶University of Manitoba, Canada, ²⁷McGill University Health Centre, Canada, ²⁸San Francisco Coordinating Center, USA, ²⁹Icelandic Heart Association Research Institute, Iceland, ³⁰University of Pittsburgh Graduate School of Public Health, USA, ³¹Hebrew SeniorLife, USA, ³²Erasmus MC Rotterdam, The Netherlands, ³³Intramural Research Program, National Institute on Aging, USA, ³⁴King's College London, United Kingdom, ³⁵Addenbrookes Hospital, United Kingdom, ³⁶Department of Clinical Physiology, University of Tampere & Tampere University Hospital, Finland, ³⁷Rm Ee 575, Genetic Laboratory, The Netherlands

Aim: While genetic factors appear to confer susceptibility to the risk of fracture, no large-scale GWAS meta-analysis consortia have been undertaken to identify the common variants associated with fracture within the framework of the Genetic Factors of Osteoporosis (GEFOS) consortium. We therefore sought the largest GWAS meta-analysis to date to identify the common genetic variants associated with fracture. **Methods:** We broadly defined fracture, as fracture of any bone occurring in individuals 18 years and older, confirmed through medical, radiological and/or questionnaire reports regardless of trauma type. This definition maximizes the case sample size, since common variants generally confer small risks for common disease. The GWAS discovery meta-analysis comprised 13 GWAS cohorts (n=53,016, of which, 9,185 were fracture cases). Additive association with fracture risk was tested for ~2.5 million imputed SNPs (HapMap CEU release 22, build 36) employing logistic regression models adjusted for gender, age, height, weight and population stratification when applicable. Results were meta-analyzed using inverse variance fixed-effects using METAL. Genome-wide significance (GWS) was set at $P < 5 \times 10^{-8}$ while suggestive significance at $P < 5 \times 10^{-6}$. Results: The strongest signal included six SNPs associated at GWS (lowest $P = 1.7 \times 10^{-10}$, odds ratio = 1.13, 95% CI: 1.09 - 1.17) and maps to the novel 18p11 locus recently identified as a BMD locus by our parallel GEFOS BMD effort. This locus contains a gene coding for a protein of unknown function (C18orf19) with no other clear candidate gene on the vicinity. Other suggestive signals included a known variant in *LRP5* ($P = 3.1 \times 10^{-6}$) and novel signals mapping in or near *MDH2* ($P = 4.8 \times 10^{-6}$), *RGS9* ($P = 4.8 \times 10^{-6}$), *FAM20C* ($P = 2.3 \times 10^{-6}$) and *MYO3B* ($P = 9.0 \times 10^{-7}$). Interestingly, mutations in *FAM20C* cause Rayne syndrome which presents with intracranial calcification, generalized osteosclerosis and enhanced periosteal bone formation. These variants will undergo further replication through GWAS and de-novo genotyping in > 80,000 individuals (~30,000 cases). **Conclusion:** In this first large-scale GWAS meta-analysis assessing fracture risk we confirmed the BMD locus on chromosome 18p11 as associated with fracture, albeit with modest effect size, and highlighted other loci in or near genes,

some known to cause skeletal monogenetic disorders. These findings help to understand the genetic basis of fracture susceptibility.

Disclosures: Ling Oei, None.

1085

Activation of Notch Signaling in Bone Cells Causes Osteoma and Osteosarcoma. Janning Tao¹*, Shan Chen¹, Ming-ming Jiang¹, Yangjin Bae¹, Terry Bertin¹, Francis Gannon¹, Lisa Wang¹, Lawrence Donehower¹, Brendan Lee². ¹Baylor College of Medicine, USA, ²Baylor College of Medicine & Howard Hughes Medical Institute, USA

Human osteosarcoma (OS) is the most common primary bone cancer, comprising approximately 20% of all bone tumors and about 5% of pediatric tumors overall. Most OS occurs sporadically and our understanding of its molecular basis is still limited. Recently, we found that human and p53^{-/-} mouse osteosarcoma tumor samples show evidence of upregulated Notch signaling. Moreover, chemical or genetic inhibition of Notch signaling decreased tumor growth in a xenograft mouse model of human osteosarcoma. Notch signaling plays an important role in the developmental processes and tissue homeostasis. Altered Notch signaling has been associated with several cancers in which the data suggest that Notch can act both as an oncogene and tumor suppressor depending on its expression level and timing. To generate a mouse osteosarcoma model and examine the role of Notch signaling in bone tumorigenesis, we utilized a bitransgenic mouse model that constitutively expressed a single copy of Notch NICD in osteoblasts. The resulting bitransgenic Notch gain-of-function (GOF) mice developed osteosclerosis at age of two months. Histomorphometric and molecular analysis of cavarial and long bones indicated that Notch could stimulate proliferation of immature osteoblasts while inhibiting their differentiation into mature osteoblasts. This gain of function phenotype was reminiscent of osteoblastic tumors. Indeed, aging studies of these GOF mice showed that they spontaneously developed osteoma/OS lesions with 100% penetrance at a mean of 9.5 months. To explore a genetic interaction of Notch and p53 pathways in the pathogenesis of OS, the GOF mice were bred with p53-conditional mice. We found that p53-null GOF mice have increased significantly tumorigenic potential, as mice develop osteosarcomas at a mean of 5 months. This result suggests that the genetic interaction of Notch and p53 plays a critical role in OS development. Together, our data support that p53-Notch interaction may be a dominant mechanism in OS pathogenesis.

Disclosures: Janning Tao, None.

1086

Hedgehog Signaling Modulates Osteoclast Formation and Bone Metastasis. Michelle Hurchla¹*, Emanuela Heller², Kyu-Sang Jeong², Marcos Vidal³, Jochen Schneider⁴, Leah Goldberg², Hongju Deng², Mary C. Hornick², Julie Prior², David Piwnica-Worms², Fanxin Long², Ross Cagen³, Katherine Weilbaecher². ¹Washington University in St. Louis, USA, ²Washington University in St. Louis School of Medicine, USA, ³Mount Sinai School of Medicine, USA, ⁴Washu, USA, ⁵Washington University School of Medicine, USA

Using a novel whole animal drosophila-based cancer metastasis drug screen, we identified inhibitors of the Hedgehog (Hh) regulator Smoothened (SMO), as powerful anti-metastatic compounds. The Hh pathway plays a critical role in tumor development and cancer progression in addition to being necessary for proper embryonic bone development and osteoblast differentiation. We hypothesized that Hh antagonism could inhibit bone metastasis through direct effects on both tumors and host cells within the bone microenvironment. Evaluation of the SMO antagonist cyclopamine in adult non-tumor bearing mice resulted in increased trabecular bone volume and decreased osteoclastic bone resorption. In vitro, both cyclopamine and Cre-mediated deletion of Smoothened inhibited osteoclastogenesis, suggesting direct regulation of osteoclast (OC) activity by Hh. Furthermore, mice with enhanced Hh signaling due to heterozygous loss of the Hh inhibitory receptor Patched (Ptc^{+/+}) showed increased cell autonomous OC function in vivo and in vitro. OC activation is critical to tumor-associated bone loss and tumor growth in bone. Pharmacologic inhibition of Hh with cyclopamine decreased bone and lung metastases and decreased bone tumor burden following intra-arterial or intra-tibial inoculation of 4T1 murine breast cancer cells. 4T1 breast cancer cells have an intact Hh signaling pathway and cyclopamine was directly toxic to 4T1 in vitro. To evaluate the contribution of Hh signaling in tumor-associated stromal cells, we examined Ptc^{+/+} mice, with enhanced Hh signaling in host cells. Ptc^{+/+} mice had increased tumor burden in the bone following intra-arterial inoculation with osteolytic B16 melanoma cells, suggesting that increased Hh activation in host cells promotes tumor growth. Bone marrow transplantation experiments demonstrated that Hh activation in both hematopoietic and non-hematopoietic cells contribute to tumor growth. Together these data suggest a novel role for Hh signaling in the regulation of OC activity and that inhibition of the Hh pathway can reduce tumor burden in bone through direct effects on tumor cells, osteoclasts and stromal cells within the bone microenvironment, making Hh a promising therapeutic target for bone metastases.

Disclosures: Michelle Hurchla, None.

1087

New Players in the Tumor Bone Vicious Cycle: Myeloid Derived Suppressor Cells Enhance Bone Tumor Growth in Osteopetrotic PLCγ2^{-/-} Mice. Aude-Helene CAPIETTO¹*, SEOKHO KIM², Roberta Faccio². ¹Washington University School of Medicine, USA, ²Washington University in St Louis School of Medicine, USA

We have recently shown that PLCγ2^{-/-} mice are more susceptible to tumor growth in bone compared to WT immunocompetent mice, despite a decrease in osteoclast (OC) number and function. PLCγ2 expression is confined to cells of hematopoietic origin, including all myeloid-derived cells but not T-cells. Surprisingly, we find that increased bone tumor growth in PLCγ2^{-/-} mice is accompanied by reduced anti-tumor CD8⁺ T cell responses. Since one of immune-evasion mechanism of tumor development is to recruit CD11b+Gr-1⁺ myeloid derived suppressor cells (MDSC), we then hypothesized that this immature myeloid population could be responsible for inhibiting CD8⁺ T cells, thus promoting the tumor outgrowth in bone of OC-deficient PLCγ2^{-/-} mice. Supporting this hypothesis, increased tumor size following B16 melanoma and Lewis Lung Carcinoma tumor inoculation in PLCγ2^{-/-} mice is associated with a 2-fold increase in the percentage of MDSC compared to WT mice both in spleen and at the tumor site (p<0.01). In addition to their higher number, MDSC isolated from tumor-bearing PLCγ2^{-/-} mice present a more immature phenotype with a lower expression of F4/80, CD11c and B7.2 markers. Importantly, PLCγ2^{-/-} MDSC are more efficient than WT in suppressing antigen-specific CD8⁺ T cell proliferation, via increased ROS and NO production. To further confirm the relevance of MDSC in tumor growth, MDSC isolated from tumor-bearing PLCγ2^{-/-} or WT mice were injected into subcutaneous tumor bearing WT mice. Animals receiving PLCγ2^{-/-} MDSC displayed an increased tumor burden compared to mice receiving WT-MDSC. This increase in tumor growth was accompanied by a greater expansion of MDSC in the spleen (WT mice+WT-MDSC: 8.20.8%, WT mice +PLCγ2^{-/-} MDSC: 16.71.4%, p<0.001). As downregulation of β-catenin is associated with MDSC development and mobilization, we analyzed its expression in PLCγ2^{-/-} MDSC and found reduced β-catenin levels both in vitro and in vivo. Thus, PLCγ2 regulates MDSC expansion and migration from bone marrow to spleen and at tumor sites, possibly via the Wnt pathway, and modulates their capacity to suppress CD8⁺ T cell activation. In conclusion, suppression of anti-tumor T cell responses by MDSC can lead to increased tumor growth in bone, even in mice with defective OC. Thus, the vicious cycle of tumor growth in bone, in which tumor cells and OC stimulate each other, should be expanded to include MDSC as important positive regulators of tumor growth, independent of OC.

Disclosures: Aude-Helene CAPIETTO, None.

1088

Parathyroid Hormone-related Peptide (PTHrP) Up-regulates Myeloid-Derived Suppressor Cells (MDSC) in the Bone Marrow, Contributing to Prostate Cancer Growth and Angiogenesis. Serk In Park¹*, William Sadler¹, Amy Koh¹, Fabiana Soki¹, Laurie McCauley². ¹University of Michigan, USA, ²University of Michigan, School of Dentistry, USA

The tumor microenvironment consists of primary tumor cells mixed with multiple types of stroma, in which a significant fraction originates from the bone marrow. Among those bone marrow-derived cells, CD11b⁺Gr1⁺ cells (MDSCs) correlate with tumor progression. MDSCs compromise the T cell-mediated host immune response, and serve as a predominant source of pro-tumorigenic factors such as matrix metalloproteinases (MMP). However, regulation of MDSCs in their organ of origin (i. e. bone marrow) by distant solid tumors remains unclear. PTHrP is functionally homologous with PTH, and is expressed by solid tumors including prostate cancer (PCa) that has a strong affinity for bone. This study addressed the hypothesis that PCa-derived PTHrP regulates MDSCs in the bone marrow, contributing to tumor growth and angiogenesis. Two PCa cell lines, PC-3 (expressing high basal PTHrP) and Ace-1 (expressing undetectable PTHrP), were used. PTHrP gene expression was targeted via shRNA in PC-3 cells (resulting in PTHrP^{hi} and PTHrP^{Lo} PC-3 clones), whereas PTHrP was overexpressed in Ace-1 cells (resulting in Ace-1^{PTHrP} and Ace-1^{pcDNA}). Stable clones were selected and grown subcutaneously in male athymic mice. As PTHrP is a known mitogen, low-PTHrP expressing tumors were grown for a longer period, resulting in tumors of similar size between groups. Tumor tissues were then analyzed by flow cytometry, immunostaining and quantitative PCR. PCa-derived PTHrP levels correlated with MDSC recruitment in the tumor tissue and also with tumor microvessel density, potentially mediated by MDSC-derived MMP-9 expression, but not by tumor-derived VEGF. In addition, administration of recombinant PTHrP (1-34) to mice carrying Ace-1^{pcDNA} tumors expanded MDSCs both in both the tumor tissue and in bone marrow, with increased angiogenesis. Furthermore, MDSCs were sorted out by flow cytometry from the bone marrow of Ace-1^{PTHrP} or Ace-1^{pcDNA} tumor-bearing mice, followed by co-injection with tumor cells. Interestingly, tumors co-injected with MDSCs from mice bearing PTHrP-expressing tumors were significantly larger than the tumors co-injected with MDSCs from non-PTHrP tumor mice. In summary, PCa-derived PTHrP circulates to expand and potentiate MDSCs in the bone marrow, which then return to the tumor tissue contributing to tumor angiogenesis and growth. These data suggest that tumors positively regulate the bone marrow microenvironment via PTHrP expression to promote tumor angiogenesis and immune suppression.

Disclosures: Serk In Park, None.

1089

The Heparin Binding Domain of PRELP: a New Therapeutic Approach for the Treatment of Breast Cancer Induced Bone Metastases. Nadia Rucci¹, Mattia Capulli², Barbara Peruzzi², Anna Rufo², Marta Capannolo³, Barbara Peruzzi¹, Dick Heinegard⁴, Anna Teti¹. ¹University of L'Aquila, Italy, ²Department of Experimental Medicine, University of L'Aquila, Italy, ³Department of Experimental Medicine University of L'Aquila, Italy, ⁴Lund University, Sweden

hbdPRELP, a peptide corresponding to the heparin binding domain of the matrix protein PRELP, inhibits osteoclastogenesis by impairing NF- κ B transcriptional activity. Hence, we hypothesized a potential application of hbdPRELP for the management of bone loss diseases. We observed that hbdPRELP counteracted bone loss in ovariectomized (OVX) mice treated with daily injections of 10 mg/kg starting both three days or 5 weeks after OVX. Potency was similar to that of alendronate and the effect specifically impaired osteoclast number and activity. hbdPRELP treatment was well tolerated also at high doses and in prolonged treatments. Balb/c nu/nu mice were then intracardially injected with the human breast cancer cell line MDA-MB-231, stably transfected with the firefly luciferase (MDA-LUC) to monitor tumor progression by bioluminescence. In a preventive protocol, mice were treated with 3.7 and 15 mg/kg hbdPRELP, 5 days/week, starting the day after tumor cell injection. Compared to controls, in hbdPRELP treated mice we found a dose dependent decrease of mortality (85% vehicle vs 36% hbdPRELP, $P=0.03$) and incidence of bone metastases (55% vehicle vs 18% hbdPRELP, $P=0.04$), together with a decrease of the bone resorption marker CTX (vehicle 31.55.1 vs hbdPRELP 18.81.7 ng/ml, $P=0.005$). Of note, in these experiments hbdPRELP also reduced visceral metastasis size. We next applied a curative protocol treating animals after the appearance of metastases and observed a 40% reduction of bone metastasis size. When MDA-LUC cells were directly injected into the tibia, hbdPRELP did not alter tumor take and osteolytic lesion incidence, while it decreased osteolytic area (vehicle 6.60.14, hbdPRELP 2.70.05, arbitrary units, $P=0.03$), osteoclast surface (vehicle 163.9 vs hbdPRELP 3.30.4, $P=0.049$) and osteoclast number per bone surface (vehicle 10.42.1 vs hbdPRELP 3.0.9, $P=0.05$), suggesting that the decreased incidence was determined by the reduced homing ability of circulating tumor cells induced by hbdPRELP. MDA-LUC cells were also orthotopically injected into the mammary fat pad. Treatment with hbdPRELP reduced tumor volume, evaluated up to 23 days after cell injection (vehicle 2.10.1 vs hbdPRELP 1.30.3 cm³, $P=0.04$). Taken together, these pre-clinical data indicate a translational application of hbdPRELP in the treatment of osteoporosis and metastatic disease of breast cancer, with the expectation that its endogenous nature could minimize drug therapy side effects.

Disclosures: Nadia Rucci, None.

1090

ER stress Signaling Molecule XBP1s Regulates Bone Marrow Stromal Cells in Multiple Myeloma Bone Disease. Guoshuang Xu¹, Kai Liu¹, Judy Anderson¹, Suzanne Lentzsch¹, G. David Roodman², Hong-Jiao Ouyang¹. ¹University of Pittsburgh, USA, ²VA Pittsburgh Healthcare System (646), USA

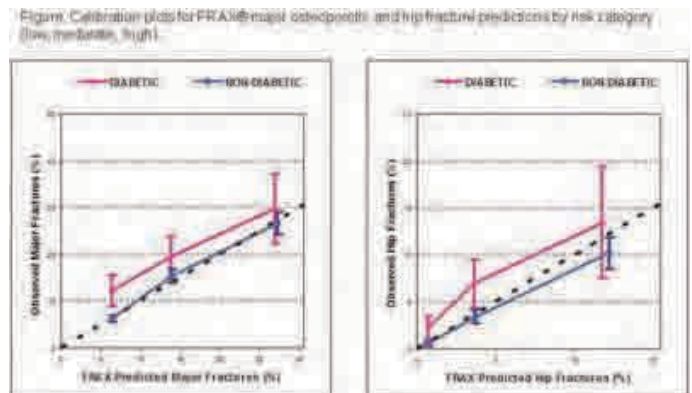
Multiple myeloma (MM) is one of the most frequent cancers that affect skeleton and induces osteolytic lesions. Complex cell-cell interactions among MM tumor cells and their microenvironment are essential for tumor growth, survival and MM-induced osteolytic lesions. Bone marrow stromal cells (BMSCs) are considered a key player in the microenvironmental support of MM cell growth and bone destruction. In order to disrupt the protective effects of BMSCs on MM cell growth and osteoclast (OCL) formation, it is essential to achieve a thorough understanding of the molecular changes in BMSCs induced by MM cells in MMBD. Spliced form of x-box binding protein-1 (XBP1s) is a major proximal effector of the ER stress/unfolded protein response (UPR) signaling. It is highly expressed in MM cells and plays an indispensable role in survival and growth of MM cells. However, it remains completely unknown if XBP1s plays a role in regulating MM microenvironment support to MM cell growth and OCL formation. Our results demonstrated that XBP1s was induced in BMSCs from MM patients compared with the healthy donors. TNF α , a major inflammatory cytokine secreted by MM cells, also induced XBP1s mRNA splicing and protein expression in normal donors' BMSCs. Overexpression of XBP1s in normal BMSCs enhanced both baseline and TNF α -induced the protein levels of adhesion molecule VCAM-1 as well as secretion of osteoclastogenic cytokines IL-6 and RANKL. Consequently, overexpression of XBP1s in BMSCs increased their support of MM cell growth and OCL formation. Conversely, deficiency of XBP1 in normal donors' BMSCs displayed a range of effects on BMSCs opposite to that of overexpression of XBP1s. Further, knockdown of XBP1 in MM patients' BMSCs greatly compromised their hypersensitivity to TNF α as to VCAM-1 protein expression and IL-6 and RANKL secretion. Consequently, knockdown of XBP1 in MM patients' BMSCs reversed their enhanced capacity to support MM cell growth to a level that was comparable to that of normal donors. Further, knockdown of XBP1 in murine BMSCs significantly reduced their support of OCL formation. Taken together, our results, for the first time, demonstrate that XBP1s is a pathogenic factor underlying BMSCs supports of MM cell growth and OCL formation. These results imply a great therapeutic potential of targeting the XBP1 signaling to disrupt the BMSCs support of MM cell growth and bone resorption as a means to treat MM bone disease.

Disclosures: Guoshuang Xu, None.

1091

FRAX® Underestimates Fracture Risk in Patients with Diabetes. Lora Giangregorio¹, William Leslie², Lisa Lix³, Helena Johansson⁴, Anders Oden⁵, Eugene McCloskey⁶, John Kanis⁷. ¹University of Waterloo, Canada, ²University of Manitoba, Canada, ³University of Saskatchewan, Canada, ⁴Swedish University of Agricultural Sciences, The Biomedical Center, Sweden, ⁵Chalmers University of Technology, Sweden, ⁶University of Sheffield, United Kingdom, ⁷University of Sheffield, Belgium

OBJECTIVE: To determine whether diabetes is a risk factor for incident hip or major osteoporotic fractures independent of FRAX®. **METHODS:** Men and women with diabetes (N=3,518) and non-diabetics (N=36,085) age ≥ 50 y at the time of BMD testing (1987-2008) were identified in a large clinical database from Manitoba, Canada. FRAX probabilities were calculated and fracture outcomes to 2008 were established via linkage with a population-based data repository. Diagnosed diabetes prior to BMD testing was from a validated algorithm. Multivariable Cox proportional hazards models were used to determine if diabetes was associated with incident hip fractures or major osteoporotic fractures after controlling for FRAX risk factors, and after controlling for derived FRAX probabilities. Fracture probabilities from FRAX were categorized as low (<10%), moderate (10-20%), or high (>20%), and observed 10 y fracture risk was estimated using the Kaplan-Meier method. **RESULTS:** Mean probabilities were similar between groups for major fractures (diabetic 11.17.2 vs. non-diabetic 10.97.3, $p=0.116$) and hip fractures (diabetic 2.94.4 vs. non-diabetic 2.84.4, $p=0.400$). After controlling for age, sex, medication use, BMD and FRAX risk factors, diabetes was a significant predictor of subsequent major osteoporotic fracture (HR 1.61 [95% CI: 1.42-1.83]). Similar results were seen after adjusting for FRAX probability directly (HR 1.59 [95% CI: 1.40-1.79]). No diabetes interactions were observed with age, sex or femoral neck WHO category. Age (but not sex or femoral neck WHO category) modified the effect of diabetes on hip fracture risk (p -interaction $p=0.002$) with diabetes a stronger predictor of hip fracture in those age <65 y after adjustment for hip fracture probability (HR 5.34 [95% CI: 3.14-9.08], $p<0.001$) than in those ≥ 65 (HR 2.06 [HR 1.59-2.6], $p<0.001$). Higher mortality from diabetes attenuated but did not eliminate the excess fracture risk. FRAX underestimated observed major osteoporotic and hip fracture outcomes in diabetics (adjusted for competing mortality), but was well calibrated for non-diabetics (Figure). **CONCLUSIONS:** Diabetes confers an increased risk of fracture that is independent of FRAX derived with BMD. The current study suggests that diabetes might be considered for inclusion in future iterations of FRAX.



Figure

Disclosures: Lora Giangregorio, None.

1092

Reduced Fracture Risk After Kidney Transplant With Early Corticosteroid Withdrawal Regimens: An Analysis of the United States Renal Data System. Lucas Nikkel¹, Sumit Mohan¹, Chiyuan Zhang², Donald McMahon³, David Cohen¹, Lloyd Ratner¹, Geoffrey Dube¹, Bekir Tanriover¹, Christopher Hollenbeak⁴, Stephanie Boutroy¹, Mary Leonard⁵, Elizabeth Shane³, Thomas Nickolas¹. ¹Columbia University Medical Center, USA, ²Columbia University, USA, ³Columbia University College of Physicians & Surgeons, USA, ⁴Penn State Hershey College of Medicine, USA, ⁵Children's Hospital of Philadelphia, USA

Corticosteroid (CS) based immunosuppression (CSBI) after kidney transplant (KTx) is associated with rapid bone loss and fractures (Fx). Early CS withdrawal (ECSW) protocols are being implemented at KTx centers across the United States, and more than 30% of KTx recipients are now managed with ECSW. In contrast to CSBI, ECSW does not cause rapid spine or hip bone loss. However, the impact of ECSW on Fx risk has not been assessed. We hypothesized that ECSW would be associated with fewer Fx than CSBI.

Using the United States Renal Data System, 92,699 adults who had a KTx between January 1, 2000 and December 31, 2006 were identified. CS use was determined from UNOS immunosuppression forms completed at time of KTx in an intent-to-treat analysis. First Fx events requiring hospitalization were identified from discharge ICD-9 codes after KTx. Continuous covariates (age, BMI, HLA mismatches) were compared with Students t tests and categorical covariates were compared with χ^2 analysis. Time to first Fx after KTx was modeled by the Kaplan-Meier method and Cox proportional hazards.

Patients on ECSW differed slightly but significantly from CSBI patients in age (50 vs 48 years; $p<0.001$), gender (62% vs 60% male, $p<0.001$), race/ethnicity (69% vs 67% white; $p<0.001$), BMI (27.1 vs 26.6 kg/m², $p<0.001$), donor (48% vs 39% live donor; $p<0.001$), and prior transplant (4% vs 16%; $p<0.001$). Fx rates were similar pre-KTx. Median (IQR) follow-up was 1428 (784-2042) days. Fx associated with hospital admissions post-KTx were more common among patients initiating CSBI than ECSW (total incidence 3.3% vs 1.8%, $p<0.001$). After KTx, 2890 Fx hospitalizations were observed during follow-up (362620 person-yr). There were 6.3 Fx per 1000 patients/year for ECSW and 8.2 Fx per 1000 patients/year with CSBI. On multivariate analysis, ECSW reduced Fx risk by 28% (HR 0.72; $p<0.001$). Fx risk increased with older age, pre-transplant Fx, female gender, low BMI, pre-transplant diabetes, prior transplant, and pre-transplant dialysis. ECSW and Asian or Black race were associated with reduced Fx risk. Lower Fx incidence with ECSW versus CSBI was significant by 29 months post-KTx (Figure 1).

After KTx, ECSW is associated with a 28% lower Fx rate associated with hospitalization compared to CSBI. As most Fx are treated as outpatients, these results likely underestimate the fracture burden. Prospective studies are needed to quantify the effects of ECSW on all-fracture incidence after KTx.

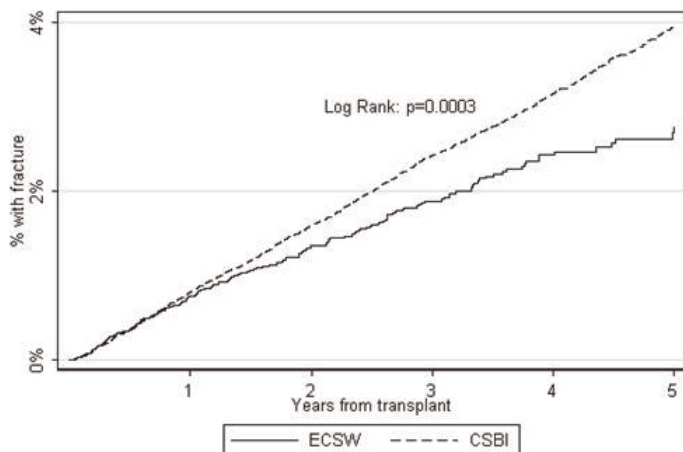


Figure 1: Time to fracture after kidney transplantation by immunosuppression regimen.

Disclosures: Lucas Nikkel, Doris Duke Charitable Foundation, 2

1093

Bone Resorption and Bone Mineral Density Across the Menopausal Transition in the Study of Women Across the Nation (SWAN). Beth Prairie*¹, Leslie Mevn², Kristine Ruppert², Yinjuan Lian³, Carolyn Crandall⁴, Gail Greendale⁴, Joel Finkelstein⁵, Mary Fran Sowers⁶, Jane Cauley⁷. ¹University of Pittsburgh, Magee-Womens Hospital, USA, ²University of Pittsburgh, USA, ³University of Pittsburgh, USA, ⁴University of California, Los Angeles, USA, ⁵Massachusetts General Hospital, USA, ⁶University of Michigan, USA, ⁷University of Pittsburgh Graduate School of Public Health, USA

Evidence suggests that N-telopeptide of Type I collagen (NTx) is a sensitive marker of bone resorption in women, and that NTx is very sensitive to changes in the hormonal milieu. To evaluate the association and diagnostic value of NTx for changes in bone mineral density (BMD) in women across the menopausal transition, we studied 2,359 multi-ethnic women, aged 42-53 years, enrolled in SWAN. Women were pre- or peri-menopausal at enrollment and attended up to 8 annual follow-up clinical visits. At each visit, BMD of the total hip and total spine were measured by dual-energy x-ray absorptiometry (DXA) and urinary cross-linked NTx/creatinine ratio was assayed. Generalized linear mixed models were used to evaluate the longitudinal relationship of baseline and time-varying NTx with annual BMD measurements. The correlation between annual NTx measurements with BMD and percent change in BMD was assessed using Spearman's correlation coefficient (r). The area under receiver operating characteristic curves (AUC) and likelihood ratios (LR) were calculated to assess the utility of NTx for detecting an annual BMD loss of 5% or more. Data were censored when a participant had a hysterectomy, bilateral oophorectomy, started hormone or other antiresorptive therapy. The mean baseline age was 45.8 \pm 2.7 years. Half of the women were White, 28% African American, 11% Chinese, and 11% Japanese. Both NTx and BMD measurements were available for 11,273 visits. Higher NTx values (baseline and time-varying) were associated with

lower total hip and total spine BMD ($P<0.0001$), even after adjustment for time, study site, race, menopausal status, body mass index, follicle-stimulating hormone, and baseline age, activity, and osteocalcin. There was a significant negative correlation between NTx and both BMD measures: total hip ($r = -0.158$), and total spine ($r = -0.236$), as well as percent annual change in BMD: total hip ($r = -0.165$), and total spine ($r = -0.237$). The AUCs for a 5% loss of total hip and total spine BMD were 0.698 and 0.708 (Figure 1). Table 1 shows the LR for ranges of NTx values in detecting a 5% total spine and hip BMD loss. The overall negative predictive value of NTx for a 5% loss of BMD at total hip and total spine is 97.4% and 94.9%, respectively. With an NTx >60 (90% percentile of NTx), a woman is twice as likely to have lost 5% BMD in the past year as not. Urinary NTx may be a useful clinical tool in the future for predicting women at higher risk for decreased BMD.

Table 1. Likelihood ratios for NTx predicting a 5% loss in total hip or total spine

NTx Value	No. (Proportion) of Women with 5% Total Hip BMD loss (N=221)	No. (Proportion) of Women with <5% Total Hip BMD loss (N=8175)	Likelihood Ratio	No. (Proportion) of Women with 5% Total Spine BMD loss (N=433)	No. (Proportion) of Women with <5% Total Spine BMD loss (N=7925)	Likelihood Ratio
70+	36 (0.158)	440 (0.054)	2.93	80 (0.185)	390 (0.048)	3.78
60-69.99	25 (0.118)	409 (0.050)	2.35	57 (0.132)	374 (0.047)	2.79
50-59.99	40 (0.181)	701 (0.086)	2.11	64 (0.148)	671 (0.085)	1.75
40-49.99	42 (0.190)	1456 (0.178)	1.07	90 (0.208)	1401 (0.177)	1.18
<40	78 (0.353)	5167 (0.632)	0.56	142 (0.328)	5069 (0.642)	0.51

Table 1.

Figure 1. Receiver operating characteristic curves (AUC) for 5% loss of total hip and total spine BMD.

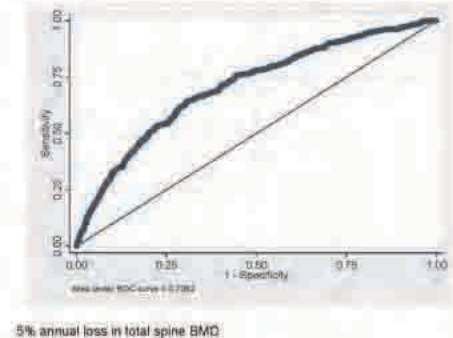
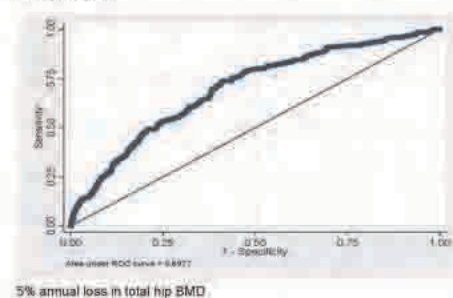


Figure 1.

ACKNOWLEDGMENT: The Study of Women's Health Across the Nation (SWAN) has grant support from the National Institutes of Health (NIH), DHHS, through the National Institute on Aging (NIA), the National Institute of Nursing Research (NINR) and the NIH Office of Research on Women's Health (ORWH) (Grants NR004061; AG012505, AG012535, AG012531, AG012539, AG012546, AG012553, AG012554, AG012495). The content of this abstract is solely the responsibility of the authors and does not necessarily represent the official views of the NIA, NINR, ORWH or the NIH.

Disclosures: Beth Prairie, None.

Trajectories of Femoral Neck Strength Over the Menopause Transition. Shinya Ishii¹, Jane Cauley², Carolyn Crandall¹, Mei-Hua Huang³, Michelle Danielson⁴, Gail Greendale¹, Arun Karlamangla¹. ¹University of California, Los Angeles, USA, ²University of Pittsburgh Graduate School of Public Health, USA, ³UCLA, USA, ⁴University of Pittsburgh, USA

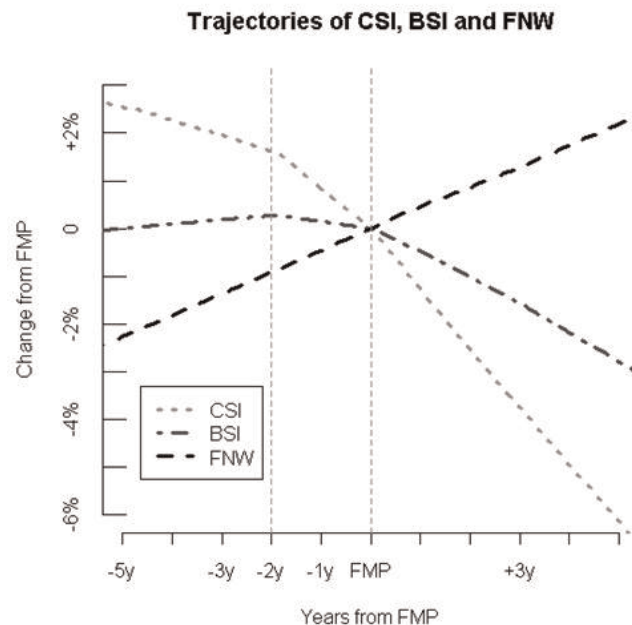
Composite indices of femoral neck strength, which integrate dual energy x-ray absorptiometry (DXA) derived areal bone mineral density (aBMD) and bone size with body size, have been shown to be inversely associated with hip fracture risk. Our objective was to describe longitudinal trajectories of the strength indices across the menopausal transition and determine major influences on trans-menopausal declines in strength.

We analyzed data from 921 women (Caucasian 406, African American 254, Chinese 126 and Japanese 135) in the Study of Women's Health across the Nation (SWAN) who had ≥ 3 hip DXA scans and had reliable final menstrual period (FMP) dates. Participants were pre- or early peri-menopausal, ages 42-53 at baseline, and were followed for 9.11.8 years. Composite indices of femoral neck strength in different failure modes were created from repeated DXA-based observations of aBMD, femoral neck width (FNW), and femoral neck axis length (FNAL), as $aBMD \cdot FNW / \text{weight}$ for compression strength index (CSI), $aBMD \cdot FNW^2 / (FNAL \cdot \text{weight})$ for bending strength index (BSI) and $aBMD \cdot FNW \cdot FNAL / (\text{height} \cdot \text{weight})$ for impact strength index (ISI). Based on examination of LOESS plots as a function of time from FMP, we fit piecewise linear mixed effects models to the repeated measurements, with two knots at FMP -2 years and FMP for all three indices. We adjusted for age at FMP, body mass index (BMI), race/ethnicity, smoking status, physical activity, and medication use.

FNW increased linearly at 0.1 mm/year throughout the study period. CSI and ISI declined slightly prior to FMP -2 year but decline accelerated thereafter. BSI increased slightly prior to FMP -2 years, plateaued, then began to decline after the FMP (Figure). Mean decline over the 10 years (5 preceding and 5 following FMP) was 7.7% in both CSI and ISI, and 3.4% in BSI. Women with higher BMI had slower declines in CSI and ISI, but not in BSI. Japanese women had slower increase in FNW and faster declines in CSI and BSI.

Despite increases in bone size to compensate for declines in bone density, femoral neck strength declines significantly during the menopausal transition, with rapid declines commencing two years before the FMP. The rates of decline are modified by BMI and race/ethnicity.

Research supported by NIH/DHHS (NR004061, AG012505, AG012535, AG012531, AG012539, AG012546, AG012553, AG012554, and AG012495). The content of this abstract is solely the responsibility of the authors and does not necessarily represent the official views of the NIA, NINR, ORWH or the NIH.

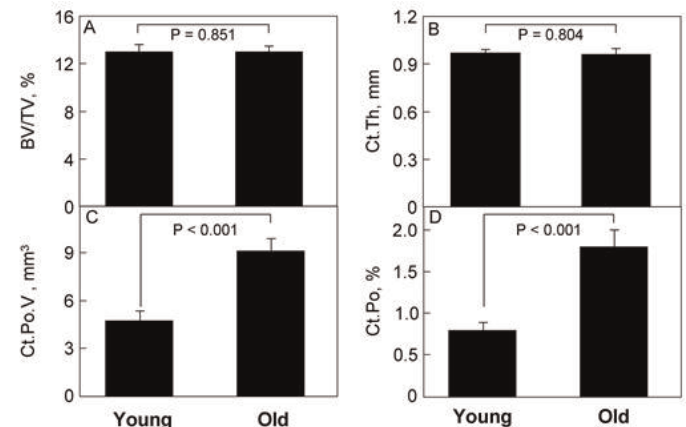


Trajectories of femoral neck width and strength indices

Disclosures: Shinya Ishii, None.

Young and Elderly Women Matched for Areal BMD by DXA at the Radius Have Profound Differences in Cortical Porosity, but Not Trabecular Microstructure. Kristy Nicks¹, Shreyasee Amin¹, Elizabeth Atkinson¹, Byron Riggs¹, L. Joseph Melton¹, Sundeep Khosla². ¹Mayo Clinic, USA, ²College of Medicine, Mayo Clinic, USA

Previous studies using DXA have demonstrated that age is a major predictor of bone fragility and fracture risk independent of areal BMD (aBMD). Thus, for the same aBMD, a 70-yr-old woman has >10-fold the risk of fragility fracture as a 30-yr-old (Hui et al, JCI 1988). While this BMD-independent effect of age has been attributed to poorer bone "quality" in elders, the structural basis for this effect remains unclear. Since high resolution peripheral quantitative computed tomography (HRpQCT) can assess trabecular and cortical microarchitecture, we matched young and elderly women for aBMD at the radius and then evaluated for differences in trabecular or cortical microstructural parameters by HRpQCT. From an age-stratified, random sample of community adults, we selected from women not currently on osteoporosis treatment who had DXA and HRpQCT scans at the radius (n = 155), to match 44 women <50 yrs (mean age, 41 yrs) with 44 women ≥ 50 yrs or over (mean, 62 yrs) by radius aBMD from DXA (mean SEM, young, 0.69 0.01 g/cm²; elderly, 0.69 0.01 g/cm²; p = 0.71). HR-pQCT (Xtreme CT, Scanco; voxel size, 82 μ m) provided trabecular (bone volume/tissue volume [BV/TV], trabecular number [TbN], thickness [TbTh], and separation [TbSp]) and cortical microstructure (cortical thickness [CtTh], cortical pore volume [CtPoV], and percent cortical porosity [CtPo]). In young and elderly women matched for DXA aBMD, trabecular BV/TV and was not statistically different (Figure panel A), with similar findings for TbN, TbTh and TbSp (data not shown). Interestingly, while CtTh was similar in young and elderly women (panel B), both CtPoV and CtPo were significantly higher (by 125%) in older as compared with younger women (panels C and D). Since both groups were matched on DXA aBMD, these differences in CtPoV and CtPo clearly were not captured by aBMD. Collectively, our findings indicate that young and elderly women matched for DXA aBMD, at least at an appendicular site represented by the radius, have identical trabecular microarchitecture but clearly different cortical microstructure, with a marked increase in CtPoV and CtPo. Further studies are needed to define the extent to which this deterioration in cortical microstructure contributes to the BMD-independent effect of age on bone fragility and fracture risk at the radius as well as other sites of osteoporotic fractures, such as the spine and hip.



Disclosures: Kristy Nicks, None.

Differences in Hip Geometry Between Older Men With and Without Hip Fracture. Laura Yerges-Armstrong¹, Marc Hochberg², William Hawkes¹, Lisa Reider³, Thomas Beck⁴, Denise Orwig⁵, Jay Magaziner¹. ¹University of Maryland, USA, ²University of Maryland School of Medicine, USA, ³School of Public Health At Johns Hopkins, USA, ⁴Quantum Medical Metrics, LLC, USA, ⁵University of Maryland, Baltimore, USA

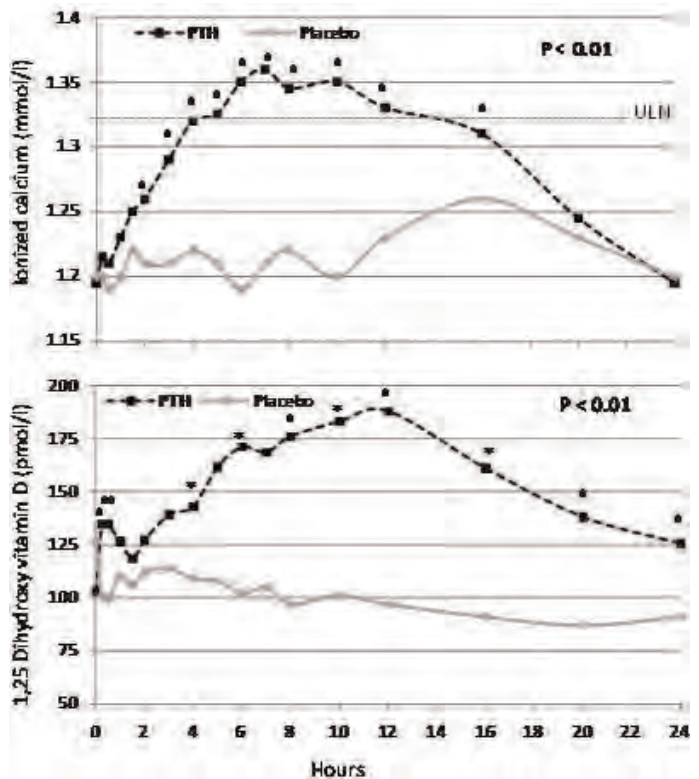
While bone mineral density (BMD) is an important risk factor for hip fracture, measures of proximal femur shape and structure have also been associated with hip fracture risk. However, most prior studies have been performed in women. This analysis was conducted to compare hip structural geometry parameters from the contralateral proximal femur in male hip fracture cases to male controls. Cases were older men (age ≥ 65 years) who were enrolled in the Baltimore Hip Study (BHS)-7, a prospective cohort study of hip fracture outcomes in community dwelling elders, and underwent dual energy x-ray absorptiometry (DXA) of the contralateral femoral head within 2 weeks of hospitalization for repair of hip fracture. Controls were men enrolled in the Baltimore Male Osteoporosis Study (MOST), a prospective cohort study of men age 65 and older from the Baltimore metropolitan area recruited without regard to their skeletal health. DXA scans were analyzed using the hip structural

PTH(1-84) Replacement Therapy in Hypoparathyroidism (HypoPT): a Randomized Controlled Trial on Pharmacokinetics and Dynamic effects Following 24 Weeks of treatment. Tanja Sikjaer*, Lars Reinmark, Lars Rolighed, Leif Mosekilde, Aarhus University Hospital, Denmark

In HypoPT, lack of PTH necessitates treatment with calcium and vitamin D analogues in order to avoid hypocalcemia. To study if replacement with the missing hormone possesses advantages, we randomized 62 patients with HypoPT to 24-wks with a daily SC injection in the thigh of PTH(1-84) 100 µg or similar placebo, as add to conventional therapy. At end of study, we performed a 24h biochemical monitoring on 39 patients (22 on PTH) in order to assess effects on diurnal variations in calcium-phosphate homeostasis. Following injection, blood samples were obtained at 0.25, 0.5, 1.0, 1.5, 2, 3, 4, 5, 6, 7, 8, 10, 12, 16, 20, 24h and urine was collected for the time intervals: 0-2, 2-4, 4-8, 8-16, and 16-24h.

Overall, during the 24-wks of therapy patients on PTH reduced their daily dose of calcium and active vitamin D significantly by 75% and 73%, respectively. Plasma PTH levels rose immediately, reaching a peak level of median 246 (interquartile range (IQR): 181–396) pg/ml at the first time point of measurement (15 min after injection). Thereafter, PTH levels decreased gradually reaching pre-dosing levels after app. 16h, with a plasma $t_{1/2}$ of 4.7 (IQR 4.0–5.8)h. PTH caused significant changes in the diurnal rhythms of plasma ionized calcium and 1,25(OH)₂D levels (Figure), with rising levels reaching a peak app. 8h following the injection. 4 to 12h following injection, asymptomatic hypercalcemia (>1.32 mmol/l) was present in 41% of PTH treated patients. Despite hypercalcemia, renal excretion of calcium was significantly lower 4-8h following injection in the PTH- compared with the placebo-group, and 24h urinary calcium did not differ between groups. Renal excretion rates of magnesium was significantly lower in the PTH- compared with the placebo-group throughout the 24h of study causing a decreased total (24h) magnesium loss in the PTH- (4.7, IQR: 4.1–6.7 mmol/d) compared with the placebo- (5.7; IQR: 4.0–7.7 mmol/d, $p < 0.05$) group. PTH caused lower phosphate levels, although treatment did not affect diurnal rhythms of plasma phosphate- or magnesium- levels, or the calcium-phosphate product.

In conclusion, a fixed dose of 100 µg/d PTH(1-84) may be too high, as transient hypercalcemia developed in some patients. However, PTH decreased urinary calcium losses in the hour following injection and magnesium losses throughout the study period. Accordingly, PTH may possess advantages compared with conventional treatment if administered in doses adapted to the patient's needs.



Figure

Disclosures: Tanja Sikjaer, None.

This study received funding from: NPS pharmaceuticals, Nycomed Denmark

analysis (HSA) program (Beck et. al; Inv. Radiol 1990) to compute geometry parameters at the narrow neck and intertrochanteric regions. Statistical analyses testing for differences between men with and without fracture were adjusted for participant's age. HSA data were available for 41 cases and 688 controls. Unadjusted values for selected HSA parameters are presented in Table 1. Compared to controls, men with hip fracture had a 24.4% higher buckling ratio ($p < 0.0001$) at the narrow neck region and a 24.3% higher buckling ratio at the intertrochanteric region ($p < 0.0001$) compared to controls. In addition, there was a 9.9% smaller narrow neck cross-sectional area ($p = 0.001$) and 7.7% smaller intertrochanteric cross-sectional area ($p = 0.02$) observed in men with hip fracture compared to controls. These results demonstrate that hip geometry parameters in the contralateral proximal femur that are markers for decreased bone strength (higher buckling ratio and smaller cross sectional area) are associated with hip fracture in older men.

		BHS-7 N=41 Mean (Std. Dev)	MOST N=688 Mean (Std. Dev)
Narrow Neck Region			
	Cross-Sectional Area (cm ²)	2.17 (0.52)	2.48 (0.47)
	Subperiosteal Width (cm)	3.59 (0.25)	3.47 (0.25)
	Section Modulus (cm ³)	1.21 (0.33)	1.31 (0.28)
	Buckling Ratio	17.50 (4.79)	13.65 (3.32)
Intertrochanteric Region			
	Cross-Sectional Area (cm ²)	3.94 (1.23)	4.35 (0.84)
	Subperiosteal Width (cm)	6.00 (0.58)	5.82 (0.40)
	Section Modulus (cm ³)	4.17 (1.54)	4.17 (0.90)
	Buckling Ratio	12.75 (3.69)	10.11 (2.21)

Table 1

Disclosures: Laura Yerges-Armstrong, None.

1097

Treatment of Hypoparathyroidism with PTH(1-84) is Safe and Effective For Up to 4 Years. Natalie Cusano*¹, Mishaela Rubin², Donald McMahon¹, Rebecca Ives³, Jim Sliney Jr³, John Bilezikian¹. ¹Columbia University College of Physicians & Surgeons, USA, ²Columbia University, USA, ³Columbia University Medical Center, USA

Hypoparathyroidism (HypoPT) is a rare disorder characterized by low serum calcium and PTH levels. Standard treatment is oral calcium and vitamin D but maintaining normal serum calcium levels can be a therapeutic challenge. We previously described our 2-yr experience with PTH(1-84) in 30 HypoPT subjects. Calcium (Ca) and calcitriol supplementation requirements fell, while BMD of the lumbar spine (LS) increased and of the distal one third distal radius (DR) decreased. In view of the chronic nature of HypoPT, information about longer term effects of PTH(1-84) treatment on calciotropic parameters and BMD is needed. This report, for the first time, provides information on the use of PTH(1-84) in HypoPT for 48 months.

18 HypoPT subjects [age 49 ± 13 yr, 4 men and 14 women (6 postmenopausal), serum Ca 8.3 ± 0.8 mg/dl, PTH 3.0 ± 5.4 pg/ml, T-scores at LS, +1.2 ± 2.2, femoral neck (FN), +0.28 ± 1.4, total hip (TH), +0.55 ± 1.4, and distal radius (DR), -0.14 ± 0.97] were treated with PTH(1-84) 100 µg qod for 4 years (3 switched to 100 µg q3d and 3 to 100 µg qd after 1 yr). Biochemistries and BMD were measured q 6 months. Treatment with PTH(1-84) reduced supplemental Ca requirements by 36% (3011 ± 2275 to 1929 ± 1193 mg/d from baseline to 48 months; $p < 0.01$). Calcitriol requirements fell (0.6 ± 0.7 to 0.4 ± 0.5 µg/d; $p = NS$), with 3 subjects able to stop all calcitriol. Serum Ca remained stable (8.3 ± 0.2 to 8.5 ± 0.2 mg/dl; $p = NS$). Urinary Ca fell from 277 ± 26 mg/d to 181 ± 28 at 12 months ($p = 0.007$), remaining lower throughout the remaining years (at 48 months, 222 ± 27 mg/d). Phosphorus levels fell from 4.4 ± 0.2 to 4.0 ± 0.2 mg/dl ($p < 0.0001$). BMD increased at the LS by 2.4 ± 1.2% at 12 months ($p = 0.05$); by 4.1 ± 1.2% at 24 months ($p = 0.002$); and by 6.0 ± 1.2% at 48 months ($p < 0.0001$). FN and TH BMD remained unchanged throughout while DR BMD fell slightly (-1.8 ± 0.8%) over the first 24 months ($p = 0.03$), not changing further at 48 months (-2.1 ± 0.9%; $p = NS$ from 24 months). There were only 3 transient episodes of mild hypercalcemia in 3 subjects over 4 years.

The data show that PTH(1-84) treatment of HypoPT for up to 4 years maintains serum Ca while reducing supplemental Ca and calcitriol requirements and urinary Ca excretion. LS BMD continued to increase while the initial small decline in DR did not progress. These data provide support for the safety and efficacy of PTH in HypoPT for up to 4 years.

Disclosures: Natalie Cusano, None.

This study received funding from: NPS Pharmaceuticals

1099

Parathyroidectomy Improves Abnormal Cardiovascular Indices in Mild Primary Hyperparathyroidism. Marcella Walker^{*1}, Tatjana Rundek², Shunichi Homma¹, Marco DiTullio¹, James A. Lee¹, Chiu-Yuan Zhang¹, Donald J. McMahon¹, Ralph L. Sacco¹, Shonni J. Silverberg¹. ¹Columbia University, USA, ²University of Miami, USA

We have reported that mild primary hyperparathyroidism (PHPT) is associated with subclinical cardiovascular (CV) abnormalities, including increased carotid intima-media thickness (IMT), maximal carotid plaque thickness (MCPT) and carotid stiffness. To assess whether CV abnormalities are reversible with parathyroidectomy (PTX), patients (n=44, 80% female, 627 yrs, calcium 10.5 ± 0.1 mg/dl, PTH 977 pg/ml) had carotid ultrasound and echocardiograms at baseline, 1 and 2 yrs post-PTX (mixed model analysis; Table data mean ± SE). Blood pressure was normal at baseline (123/74/1) and did not change after PTX. BMI did not decline and only 1 patient initiated BP or cholesterol lowering medication. In the 2nd post-PTX yr, elevated carotid IMT declined from 12 mo values (p<0.05) and increased carotid stiffness decreased into the normal range (p=0.056 vs. baseline). Neither MCPT nor carotid plaque number regressed. Cardiac structure and function were normal at baseline. After PTX, left ventricular mass index (LVMI) and cardiac calcifications (myocardial and mitral annular) did not change. Measures of diastolic function either worsened within the normal range (intraventricular relaxation time [IVRT], tissue Doppler e' [e']), or were unchanged (deceleration time (DT), early to late mitral annular velocity [E/A]). In patients who were abnormal at baseline, certain CV indices improved significantly by 2 years after PTX. Elevated IMT, present in 73% at baseline, declined although it did not normalize (0.9970.096 to 0.9700.068 mm; p<0.03). Increased carotid stiffness, present in 40% at baseline, tended to decrease (9.03.4 to 6.41.9; p=0.058), and became normal in 8 of 17 patients. Diastolic dysfunction normalized in those with abnormal E/A (25% of patients; 0.670.06 to 0.830.15; p<0.005) and elevated IVRT (18% of patients; 11411 to 9912 msec; p<0.05). LVMI did not improve. In summary, in a cohort of PHPT patients with subclinical CV disease, the CV response to PTX was modest. However, those with abnormal carotid indices or diastolic dysfunction before PTX had clear improvement in, and in many cases normalization of those abnormalities after surgery. While the effect of these changes on CV events is unknown, the documented improvement in CV indices after PTX, particularly in those with baseline abnormalities, suggests that CV evaluation should be included in the assessment of patients with PHPT who otherwise do not meet criteria for PTX.

	Baseline	12 months	24 months	NI Range
	Baseline	12 months	24 months	Normal
BP	123±2.3/74±1	122±2.4/76±1	125±2.6/78±2	<140/90
IMT mm	0.961±0.007	0.971±0.008	0.946±0.008*	0.7-0.9
Stiffness	6.3±0.4	6.4±0.4	5.2±0.5 ^{ab}	<6
MCPT mm	0.89±0.07	1.08±0.07 ^c	0.924±0.16	<1.9
Plaque #	0.95±0.24	1.19±0.24	1.14±0.24	
LVMI g/m ²	96±2	99±2	100±2	F ≤108 M ≤131
IVRT msec	85.5±2.3	92.3±2.4 ^c	99.9±2.5 ^{ac}	50-102
E/A	1.07±0.04	1.13±0.04	1.09±0.04	0.75-1.5
e' mm	11.4±0.3	10.3±0.3 ^c	10.0±0.3 ^c	≥7
DT msec	162±5	168±4	164±5	140-220

CV Table

Disclosures: Marcella Walker, None.

1100

Administration of Oral Bisphosphonates Prior to the Diagnosis of Breast Cancer is Associated with a Reduction in the Development of Skeletal Metastases Independent of Stage of Disease at Diagnosis. Richard Kremer^{*1}, Ari N. Meguerditchian², Bruno Gagnon², Lyne Nadeau², Nancy Mayo². ¹McGill University, Royal Victoria Hospital, Canada, ²McGill University Health Center, Canada

Bisphosphonates are widely used for the treatment of osteoporosis. Their strong anti-bone resorbing effect has triggered their use in osteolytic bone disease and in particular for osteolytic lesions of metastatic breast cancer.

An earlier study indicates that intravenous administration of Pamidronate, an amino-bisphosphonate highly effective in the treatment of malignancy-associated hypercalcemia, significantly delays the progression of adverse skeletal events in breast cancer patients with established bone metastases. Pamidronate is approved for the treatment of metastatic breast cancer to bone since 1996. In another study the bisphosphonate Clodronate, given immediately after tumour removal, was found to be effective in preventing skeletal metastasis in a group of high risk breast cancer patients.

The effect of bisphosphonates is not restricted to inhibition of osteolysis but seems to reduce the tumour burden in bone in animal models of metastatic breast cancer. As the efficacy of bisphosphonates in skeletal metastasis is now established, it remains to be determined if these agents can be used widely in the prevention of skeletal metastasis, even before the breast cancer occurs.

The aim of this study was therefore to determine whether bisphosphonate use prior to a diagnosis of breast cancer could prevent development of bone metastases.

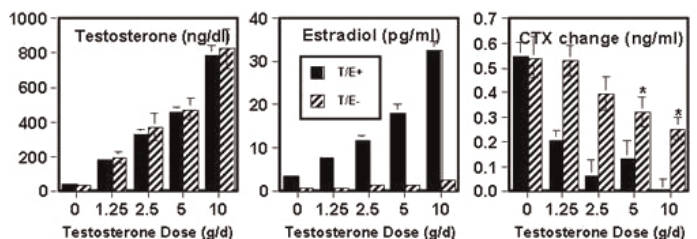
A cohort study comprising 21,664 women with breast cancer was carried out using health administrative data. Of these women, 77% were Stage 0 or 1 and 10.2% (n=2221) used a bisphosphonate in the 2 year period prior to diagnosis. The most common bisphosphonate was alendronate (66%), followed by risedronate (23%) and etidronate (11%). The modal age was 50 to 64 years; the median (maximum) follow-up time was 5 (10) years. Of the women with no pre-breast cancer bisphosphonate use (n=19,443), 6.5% developed bone metastases compared with 4% of women with pre-breast cancer bisphosphonate use (n=2,221). The unadjusted hazard ratio (HR) was 0.70 (95% CI: 0.57-0.87); adjusted for age, socioeconomic status, comorbidities, and stage, the HR was 0.78 (95% CI: 0.63-0.98). These results indicate the strong potential for bisphosphonates to be protective for the development of bone metastases when administered prior to the diagnosis of breast cancer independent of stage of disease at diagnosis. The study supports the Paget's seed and soil hypothesis that reducing bone turnover deters the establishment of cancer cells in bones.

Disclosures: Richard Kremer, Merck Frosst Canada, 8; Sanofi-Aventis, 8

1101

Hypogonadism in Men (HIM) and Hypogonadism with Estrogen Removal (HER): Effects of Androgens and Estrogens on Bone Resorption in Young Adult Men. Joel Finkelstein^{*1}, Hang Lee¹, Elaine Yu¹, Sherri-Ann Burnett-Bowie¹, J. Carl Pallais¹, Benjamin Leder². ¹Massachusetts General Hospital, USA, ²Massachusetts General Hospital/Harvard Medical School, USA

Both androgen and estrogen deficiency contribute to the increase in bone resorption in severely hypogonadal men. Methods: To determine the roles of androgens and estrogens on bone resorption across the physiologic range of testosterone (T) levels, we recruited 2 cohorts of healthy men aged 20-50. All men received goserelin acetate (Zoladex[®], AstraZeneca LP, 3.6 mg q4wk) to suppress endogenous T and estradiol (E). In addition, men in Cohort 1 (T/E+, n=198) were randomized to treatment with 1 of 5 doses of a T gel (AndroGel[®], Abbott) daily for 16 weeks (G1-placebo; G2-1.25g; G3-2.5g; G4-5g; G5-10g). Men in Cohort 2 (T/E-, n=200) were randomized to the same T doses plus all men received anastrozole (Arimidex[®], AstraZeneca LP, 1 mg/d) to block conversion of T to E. Serum T, E, and CTX levels were measured every 4 weeks. Changes in CTX within the T/E- cohort were determined to assess T effects (i.e. G1 of T/E- cohort vs G2, G3, G4, and G5). If T has an independent effect on bone resorption, CTX should increase more as the T dose is reduced in the T/E- cohort because T levels will differ while all groups have similar (and low) E levels. Changes in CTX between groups receiving the same T dose in the T/E+ and T/E- cohorts were determined to assess E effects (i.e. G1 of T/E+ vs G1 of T/E-, G2 of T/E+ vs G2 of T/E-, etc). If E has an independent effect on bone resorption, changes in CTX should differ at each dose between the T/E+ and T/E- cohorts because T levels are matched while E levels are discordant (except in G1 where T and E are low in both cohorts). Results: Mean serum T and E levels and the change in CTX are shown in the Figure. Mean T levels in G1-G5 were 44, 185, 327, 458, and 790 ng/dL with T/E+ and 40, 198, 374, 478, and 827 ng/dL with T/E-. Within the T/E- cohort, CTX increased more in G1 than in G4 or G5 (P=0.03 and P=0.004) whereas changes in CTX were similar in G1, G2, and G3 indicating that a substantial decline in T is needed to increase CTX when E production is blocked. CTX increased more in G2, G3, G4, and G5 (P<0.05) in men treated with T plus an aromatase blocker than in men treated with T alone, indicating that even a modest fall in E levels (e.g. from 8 to 1 pg/ml in G2) is sufficient to increase bone resorption when T levels are matched. Conclusions: Both androgens and estrogens regulate bone resorption in adult men. However, the skeleton in adult men appears to be more sensitive to a decline in estrogens than to a fall in androgens.



Figure

Disclosures: Joel Finkelstein, Abbott, 9; AstraZeneca, 9

This study received funding from: Supported by NIH Grants R01 AG030545, K24 DK02759, and RR-1066 and an investigator-initiated grant from Abbott. AndroGel® was provided as a gift from Abbott. Zoladex® and Arimidex® were provided as gifts from AstraZeneca Pharmaceuticals LP.

1102

Serum Sclerostin Levels Across a Wide Range of Bone Turnover. Maria Yavropoulou*¹, Antoon Van Lierop², Neveen Hamdy², Socrates Papapoulos². ¹Aristotle University of Thessaloniki, Greece, ²Leiden University Medical Center, The Netherlands

Background: Evidence has been accumulating on the role of osteocytes, as players in the regulation of bone remodeling. One of the main products of these ubiquitous cells, sclerostin, regulates bone formation through inhibition of the Wnt signaling pathway. Circulating sclerostin levels have been evaluated in healthy individuals, but data are scarce regarding different ranges of bone turnover. To address this issue we evaluated serum sclerostin levels in patients with Paget's disease of bone (PD) with predominantly increased bone resorption at different stages of disease activity, and in patients with prostate cancer (PC) metastatic to the skeleton with predominantly increased bone formation at different levels of skeletal involvement. **Patients and Methods:** Sclerostin levels were measured in 94 patients with PD, 28 patients with PC and 77 healthy individuals. Patients with PD and PC had bone scintigraphy to establish the extent of skeletal involvement. Bone turnover was evaluated by measuring serum levels of procollagen type I amino-terminal propeptide (PINP) in all individuals studied and β -carboxy-terminal cross-linking telopeptide of type I collagen (β -CTX) only in patients. None of the patients had renal or liver dysfunction, vitamin D deficiency, or other diseases known to affect bone metabolism. **Results:** The population studied had a wide age range (20 -88 years) and a wide range of bone turnover with serum PINP ranging from 8.4 to 1872 ng/ml and β -CTX ranging from 50 to 3120 pg/ml. Patients with PD and with PC had significantly higher serum sclerostin levels (53.58 \pm 22.4 pg/ml and 57.55 \pm 24.7 pg/ml, respectively) compared to healthy controls (40 \pm 12.8 pg/ml) ($p < 0.001$). Serum sclerostin levels significantly correlated with age ($r = 0.238$, $p < 0.001$) and with PINP ($r = 0.295$, $p < 0.001$), but not with β -CTX ($r = 0.094$, $p = 0.303$) across the wide range of bone turnover. **Discussion:** Circulating sclerostin levels are significantly increased in patients with increased bone turnover, regardless of underlying disease pathology, whether predominantly increased bone resorption as in Paget's disease or predominantly increased bone formation as in metastatic prostate cancer. Sclerostin levels also significantly correlate with bone formation but not resorption markers across a wide range of bone turnover.

Disclosures: Maria Yavropoulou, None.

1103

Non-collagenous Proteins Influence Bone Mineral Size, Shape and Orientation: A SAXS Study. Atharva Poundarik*¹, Caren Gundberg², Deepak Vashishth³. ¹Rensselaer Polytechnic University, USA, ²Yale University School of Medicine, USA, ³Rensselaer Polytechnic Institute, USA

Bone is a complex hierarchical composite. The organization of bone contributes significantly to toughening its matrix. Recently, non-collagenous proteins (NCPs) have come to light as structural elements in bone's extracellular matrix. Besides, it has been studied that NCPs including osteocalcin (OC) and osteopontin (OPN) regulate the process of mineralization and crystal growth [1, 2]. We hypothesize that their deletion from the matrix is likely to alter crystal formation and growth, and hence modify mineral organization at the ultra-structural level. To this end, we investigate using small angle x-ray scattering (SAXS), the mineral characteristics of knock-out (KO) mice which are deficient in either OC, OPN or both OC and OPN.

SAXS spectra of cortical bone samples of WT, OC-/-, OPN-/- and OC-OPN-/- (double KO) (n=3 each) were acquired (Bruker Nanostar) at a specimen-detector distance of 65.5cm. For each acquisition point, intensity (I), scattering vector (q) and polar angle (θ) data was extracted. Crystal thickness and shape were determined by the computation of two invariants - Porod's constant and the area under the q^{-1} vs. q plot. I vs. q plots were used to analyze orientation of crystals within the plane of the sample.

Crystal thickness of WT group (1.8960.110nm) was greater than OC-/- (1.7770.152nm) and OC-OPN-/- (1.7700.118nm) groups ($p < 0.05$). There was no significant difference observed between the WT and OPN-/- (1.8400.102nm) groups. Shape analyses revealed that crystals of OC-/- and OC-OPN-/- mice were more plate-like as compared to WT mice, whereas OPN-/- mice crystals were more rod-like. Finally, crystals of the OC-OPN-/- mice were less aligned along the collagen fibrils than those of WT ($p < 0.001$), OC-/- ($p = 0.01$) and OPN-/- ($p = 0.002$).

We conclude that OC is a stronger regulator of mineral crystal size and shape, and OPN behaves as a compensatory molecule in the absence of OC. This is evident from OC-OPN-/- mice, where characteristics seen in OC-/- mice are heavily accentuated. NCPs also appear to facilitate orientation of crystals along the long axis of collagen and their absence results in poor crystal alignment. Thus the absence of NCPs may alter the organizational hierarchy of bone at higher scales reducing toughness [4].

References:

[1]: Boskey et al. Bone, Vol 23, 1998

[2]: Boskey et al. Calcif Tissue Int, Vol 71, 2002

[3]: Fratzl et al. Connect Tissue Res, Vol 34, 1996

[4]: Poundarik et al. Presentation No. A09003207, ASBMR 2009

Disclosures: Atharva Poundarik, None.

1104

Exercise When Young Provides Lifelong Benefit to Cortical Bone Structure and Strength in Men. Sara Mantila Roosa*, Andrea Hurd, Robyn Fuchs, Stuart Warden. Indiana University, USA

Exercise induces the greatest bone gains during growth; however, the persistence of these effects is unknown in the aged skeleton. Previous work suggests exercise-induced gains in bone mass are lost with age; however, exercise during growth primarily influences bone structure rather than mass to increase bone strength. The current study explored whether exercise-induced gains in bone structure and strength accrued when young persist lifelong in men. Former Major League Baseball (MLB) pitchers and catchers (n=81, age 31-85 yrs) were recruited as former exercisers/throwers and compared to control subjects (n=44, age 30-86 yrs). Former MLB players are unique as: 1) unilateral upper extremity loading associated with throwing enables the contralateral side to serve as an internal control; 2) throwing athletes have large dominant-to-nondominant (D-to-ND) differences in midshaft humeral properties, and; 3) former MLB pitchers and catchers were consistently exposed to extreme loading, reducing variations in exercise levels between generations. Peripheral quantitative computed tomography (pQCT) was used to assess the D and ND midshaft humeri, and D-to-ND percent differences were plotted against age. Regression lines for former throwers and controls were assessed for convergence, which represented the age when exercise benefits were predicted to be lost. Exercise when young induced significant skeletal benefits, with recently retired (30-yr-old) throwers having 30% D-to-ND difference in cortical BMC (Ct.BMC), cortical area (Ct.Ar) and total area (Tt.Ar), and 61% D-to-ND difference in estimated ability to resist torsion (polar moment of inertia, I_p). However, the Ct.BMC and Ct.Ar benefits of exercise were lost with age as former thrower and control regression lines converged by 83 yrs. In contrast, D-to-ND differences in Tt.Ar and periosteal perimeter (Ps.Pm) were maintained, with regression lines not converging until 168 yrs. The maintenance of exercise benefits on bone structure, despite loss of mass benefits, contributed to regression lines for D-to-ND difference in I_p not converging until 112 yrs. On average, 80-yr-old former throwers maintained a D-to-ND difference for I_p of >2.5 times that observed due to habitual loading associated with arm dominance in controls. These data indicate that exercise when young has lifelong benefits on cortical bone structure and strength, independent of benefits on bone mass.

Disclosures: Sara Mantila Roosa, None.

1105

Osteocyte Apoptosis is Required for Production of Pro-Osteoclastogenic Signals Following Bone Fatigue in vivo. Oran Kennedy*¹, Daniel Leong², Herb Sun³, Robert Majeska⁴, Mitchell Schaffler⁵. ¹The City College of New York, USA, ²City College New York, USA, ³Mount Sinai School of Medicine, USA, ⁴City College of New York, USA, ⁵City College of New York, USA

Introduction: Osteocyte apoptosis is spatially, temporally and functionally linked to replacement of microdamaged bone via remodeling. The precise molecular mechanisms linking osteocyte death to osteoclastogenesis are unknown. Osteocytes have two potential pathways to recruit osteoclasts to damage sites, one is via apoptotic debris transport or alternatively by production of osteoclastogenic signaling molecules. Transport of debris through the canalicular system is physically problematic. In contrast, cells near microdamage have been shown to upregulate osteoclastogenic signaling molecules. We tested the hypothesis that inhibition of apoptosis blocks expression of pro-osteoclastogenic signaling by cells near microdamage in bone.

Methods: A pan-caspase inhibitor, Q-VD-OPh (QVD) was used to inhibit apoptosis in rats. Two groups were subject to ulnar fatigue loading, and two groups were non-loaded. One fatigued group received 20 mg/kg/day QVD (FAT/QVD) and the other received a corresponding dose of vehicle (FAT/VEH). Two remaining non-loaded groups received identical dosing (CON/QVD and CON/VEH) serving as independent controls. Outcomes were evaluated at 3 and 7 days post-fatigue. These represent pre-resorptive phases in the remodeling response to microdamage. Tissue was harvested at the mid-ulna, a unique site which has a negligible marrow cavity. This combined with removal of the periosteum results in an osteocyte enriched system. RNA was isolated and extracted from this segment and cDNA synthesized. Transcripts were evaluated by qPCR and gene expression analyzed in the main regulatory pathways associated with control of bone resorption: RANKL/OPG/M-CSF. Immunohistochemistry (IHC) assays were also used to confirm gene expression data and to provide spatial information on the origin of these signals relative to damage sites in situ.

Results and Discussion: RANKL/OPG ratio, a primary indicator of osteoclastogenesis, was increased in FAT/VEH group 6-fold at 3d and 18-fold at 7d, M-CSF was unchanged in all groups. In contrast, when osteocyte apoptosis was prevented, despite the presence of the similar damage levels expression of pro-osteoclastogenic signals was absent. IHC data confirmed these findings with apoptosis inhibition preventing expression of signaling factors.

Conclusion: Following fatigue loading, the robust expression of pro-resorptive signaling molecules by resident osteocytes is completely abrogated when apoptosis is inhibited.

Disclosures: **Oran Kennedy**, None.

1106

The Adaptive Response of Cancellous Bone to In Vivo Loading Is Diminished in Adulthood: A Longitudinal Study. Bettina Willie^{*1}, Annette Birkhold¹, Marta Aido², Tobias Thiele¹, Alexander Schill¹, Russell Main³, Georg Duda¹. ¹Charite- Universitätsmedizin Berlin, Germany, ²Charite- Universitätsmedizin Berlin, Deu, ³Purdue University, USA

Bone can adapt to mechanical stimuli to attain an optimized structure. With aging there may be a reduced adaptive response of cancellous bone to normal mechanical loading, resulting in low bone mass and microarchitectural deterioration. It is unclear how early this reduction in mechanosensitivity manifests. We hypothesize that a reduced adaptive response to mechanical loading may already be present in adulthood. We performed in vivo cyclic compressive loading of the left tibia in female postpubescent adolescent (10wk old) and adult (26wk old) C57Bl/6 mice, with the right limb as an internal control. A peak load of -11N was applied at 4Hz for 216 cycles/day, 5days/week for 2 weeks. This load magnitude engendered peak strains of 1200 µε on the medial tibial midshaft for both ages. Longitudinal microcomputed tomography at 10.5µm voxel resolution was performed at Day 0, 5, 10, and 15 (n=6/age) of the experiment. Additional mice were also loaded and only imaged at Day 15 (n=4/age). Sham loaded control mice were also only imaged at Day 15 (n= 3/age). Cancellous bone volume fraction (BV/TV), tissue mineral density (TMD, mg HA/cm³), trabecular thickness (TbTh, µm) and separation (TbSp, µm) were assessed in the proximal tibial metaphysis. An ANOVA of the inter-limb difference was used to assess within-subject (scan day) and between-subject (age) effects, and interactions. BV/TV, TbTh, and TMD were greater in the loaded relative to control limbs in both age groups. The inter-limb difference in BV/TV, TbTh, and TMD were significantly influenced by scan day (Table 1). Age significantly affected the response to loading. In adolescent mice, the inter-limb difference in BV/TV and TMD were due to load-induced increases in the loaded limb. In contrast, in adult mice the inter-limb difference was due to decreased BV/TV and TMD in the non-loaded control limbs, which were similar to sham loaded limbs at day 15, while applied load maintained bone mass in the loaded limb during the study. In conclusion, in vivo loading enhanced bone mass, density and architecture in adolescent mice and maintained bone mass in adult mice. These data suggest that the adaptive response of cancellous bone to mechanical loading is reduced in adulthood, but that loading may still be beneficial to maintain bone mass in individuals of advanced age.

Table 1: Mean SD, %Δ: (Loaded - Control)/Control × 100; *age effects, §scan day effects, and #interaction effects; p < 0.05 for all significant effects

	Day 0, (n=6/age)			Day 5, (n=6/age)			Day 10, (n=6/age)		
	Loaded	Control	%Δ	Loaded	Control	%Δ	Loaded	Control	%Δ
10 wk old									
BV/TV [%]#§	2.0 ± 0.2	1.9 ± 0.3	5	4.0 ± 1.6	2.4 ± 0.2	67	4.9 ± 1.0	2.5 ± 0.6	96
TMD [mg HA/cm ³]#§	200 ± 7	173 ± 4	16	220 ± 21	176 ± 4	25	226 ± 14	169 ± 17	34
TbTh [µm]§	29.5 ± 1.3	30.2 ± 1.6	-2	35.0 ± 1.4	32.8 ± 1.9	7	43.5 ± 2.9	34.0 ± 4.3	28
TbSp [µm]	407.3 ± 55.8	447.8 ± 21.7	-9	418.5 ± 95.6	420.6 ± 49.6	0	391.0 ± 70.1	444.3 ± 47.8	-12
26 wk old									
BV/TV [%]#§	3.6 ± 0.9	3.4 ± 0.7	6	3.4 ± 0.7	2.7 ± 0.7	26	3.7 ± 0.9	2.5 ± 0.9	48
TMD [mg HA/cm ³]#§	212 ± 14	188 ± 19	13	201 ± 7	179 ± 11	12	203 ± 13	178 ± 24	14
TbTh [µm]§	50.2 ± 2.9	53.4 ± 6.1	-6	50.4 ± 2.7	52.3 ± 7.4	-4	55.0 ± 5.8	53.6 ± 6.1	3
TbSp [µm]	472.1 ± 24.7	479.1 ± 35.3	-1	505.3 ± 54.9	526.6 ± 62.8	-4	485.5 ± 36.0	547.6 ± 74.9	-11
	Day 15, (n=6/age)			Day 15, (n=10/age)			Day 15 Sham, (n=3/age)		
	Loaded	Control	%Δ	Loaded	Control	%Δ	Left	Right	%Δ
10 wk old									
BV/TV [%]#§	7.3 ± 1.1	2.0 ± 0.6	265	8.0 ± 1.4	2.7 ± 1.0	196	2.9 ± 0.5	2.8 ± 0.6	4
TMD [mg HA/cm ³]#§	254 ± 13	167 ± 9	52	264 ± 18	182 ± 22	45	205 ± 9	181 ± 25	13
TbTh [µm]§	53.8 ± 4.9	34.3 ± 2.2	57	53.4 ± 4.7	34.5 ± 2.0	55	33.3 ± 2.0	33.4 ± 3.5	0
TbSp [µm]	421.4 ± 37.3	483.0 ± 61.3	-13	388.4 ± 56.4	437.2 ± 78.5	-11	386.0 ± 65.7	434.6 ± 45.6	-11
26 wk old									
BV/TV [%]#§	3.5 ± 0.9	1.9 ± 1.0	84	3.8 ± 0.8	2.2 ± 0.9	73	2.6 ± 0.4	2.2 ± 0.4	18
TMD [mg HA/cm ³]#§	199 ± 13	153 ± 18	30	205 ± 16	160 ± 21	28	191 ± 12	158 ± 18	21
TbTh [µm]§	61.6 ± 3.9	48.4 ± 4.7	27	61.5 ± 5.1	48.8 ± 5.1	26	46.0 ± 4.4	44.0 ± 3.4	5
TbSp [µm]	520.2 ± 29.6	565.8 ± 76.0	-8	514.4 ± 35.8	541.9 ± 70.7	-5	472.2 ± 51.9	502.0 ± 16.7	-6

Table 1

Disclosures: **Bettina Willie**, None.

1107

Bone Mineral Density (BMD) of Individual Trabeculae in Human Trabecular Bone. Ji Wang^{*1}, Bin Zhou¹, X.Tony Shi¹, Xiaowei Liu², X. Guo¹. ¹Columbia University, USA, ²Columbia University College of Physicians & Surgeons, USA

Recently developed individual trabeculae segmentation (ITS)-based morphological analyses have demonstrated the importance of trabecular type (plate vs. rod) in determining the mechanical properties of trabecular (Tb) bone. However, tissue mineralization in individual trabeculae of different types and orientations has not yet been investigated. In this study, we developed a novel technique which measures tissue mineral density of each individual trabecula (Tb.TMD). We first hypothesized that distribution of Tb.TMD varies between different Tb types and orientations; second, volumetric BMD (vBMD) categorized by Tb types and orientations has implications in apparent mechanical properties of human Tb bone.

22 Tb bone cylinders from human proximal tibiae were imaged by µCT at 15 µm resolution (Scanco VivaCT40). A calibration phantom was used to convert

attenuation data to hydroxyapatite (HA) densities. Tb microstructure was first segmented into individual plates and rods with their orientations determined, and the Tb.TMD was calculated for each trabecula (Fig. 1A). Mean Tb.TMD of all trabecular plates (pTb.TMD) and rods (rTb.TMD) were examined, as well as those of different orientations. The axial vBMD (axBMD) was defined as the vBMD of both trabecular plates and rods along the axial direction. Elastic moduli and yield strengths were determined from (1) direct mechanical testing and (2) µCT image-based finite element analysis using heterogeneous tissue modulus.

Results suggested that Tb plates were 0.7% more mineralized than rods (p<0.001, Fig.1B). Furthermore, Tb.TMD varied significantly in Tb plates with different orientations (p<0.001): transverse>oblique>longitudinal (Fig.1C). In contrast, Tb.TMD was uniform in rods with different orientations (Fig.1D). aXBMD showed stronger correlation with experimental yield strength (r²>0.90) and elastic modulus (r²>0.86) than the overall vBMD (r²>0.79). The ITS-based vBMD categorized by Tb types and orientations correlated equally as well as the ITS-based morphological parameters with the measured or calculated yield strength and elastic modulus.

The ITS-based Tb.TMD assessment reveals the type and orientation-associated heterogeneous mineralization distribution in Tb bone. Interestingly, Tb plates, particularly transverse plates, are most highly mineralized. Furthermore, this novel technique provides unique measures for both tissue mineralization and Tb microstructure that are critical determinants of bone strength.

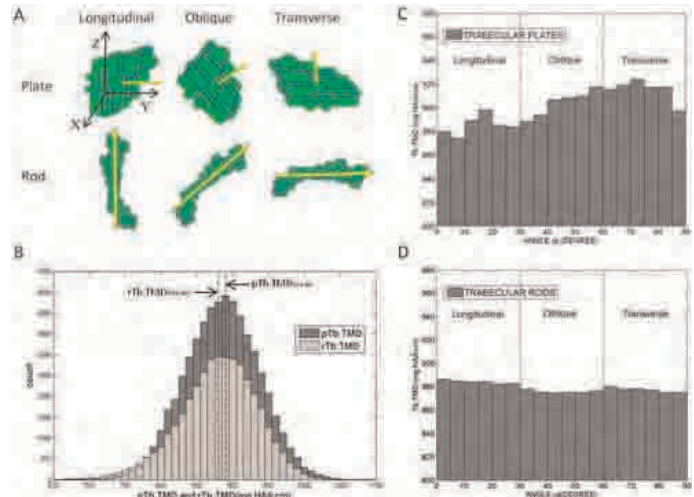


Figure 1

(A) Illustration of longitudinal, oblique and transverse trabecular plates/rods. (B) Histogram of pTb.TMD and rTb.TMD. (C) Tb.TMD distribution of plates oriented at different angles. (D) Tb.TMD distribution of rods oriented at different angles.

Figure 1

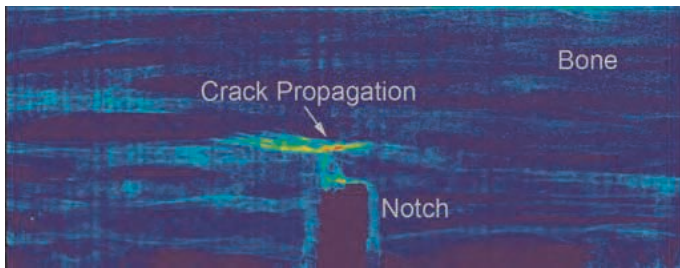
Disclosures: **Ji Wang**, None.

1108

How Vitamin D Deficiency Affects the Nature of Fracture Propagation in Human Bone. Bioern Busse^{*1}, Hrishikesh Bale², Elizabeth Zimmermann¹, Brian Panganiban², Holly Barth², Alessandra Carriero², Michael Hahn³, Joel Ager², Michael Amling³, Robert Ritchie². ¹University of California, Berkeley, USA, ²University of California - Berkeley, Lawrence Berkeley National Laboratory, USA, ³University Medical Center Hamburg-Eppendorf, Germany

Vitamin D deficiency unquestionably increases fracture risk in human bone. However, osseous changes in structure, collagen and/or mineralization with hypovitaminosis D and their corresponding effect on fracture risk are complex to interpret. Because cracks in human bone grow diversified, bone fracture can be described as a combination of intrinsic mechanisms acting on small length scales (mineral and collagen characteristics) resisting initiation of cracks and extrinsic mechanisms resisting the growth of cracks acting on coarser length scales (crack propagation). To address this issue, we carried out a study focusing on 2-D *in situ* fracture tests in an environmental scanning electron microscope to evaluate crack initiation and growth toughness. 3-D *ex situ* examination of crack paths and bone structure using synchrotron x-ray computed tomography was used to determine how changes in microarchitectural features with disease correlated with the extrinsic crack-growth toughness; changes to the mineral and collagen were evaluated using UV Raman spectroscopy and Fourier Transform Infrared Spectroscopy and correlated to changes in the intrinsic initiation toughness. Cortical iliac crest bone samples with a 25 (OH)D concentration below 10 µg/l were compared to 15 normal cases with a 25(OH)D level above 25 µg/l. Histomorphometric assessment of osteoid indices confirmed osteomalacia in cases with low 25(OH)D concentration; being absent in cases with levels above 25 µg/l. Cortical structure indices in vitamin D deficient bone demonstrated significantly increased cortical porosity, mean osteon diameter and osteocyte lacunar volume accompanied by significantly decreased cortical thickness. The osteon density remained unchanged in osteomalacic bone in comparison to the

normal cases. These structural features correlated with significantly decreased crack growth toughness, while alterations to the collagenous environment in osteomalacic bone correlated with significantly decreased crack initiation values. In conclusion, this study demonstrated that Vitamin D deficiency is not solely a matter of decreased mineralized bone volume due to hyperostoidosis but that changed characteristics on the bone tissue level may lead to losses in bone toughening mechanisms as well. These findings strongly support that well-balanced 25(OH)D is essential to avoid detrimental crack propagation as in osteomalacia, which compromises the bone's structural integrity and its resistance to fracture.



Back projected transmission image demonstrating the path of a crack due to in situ 3 point bending

Disclosures: Bjoern Busse, None.

1109

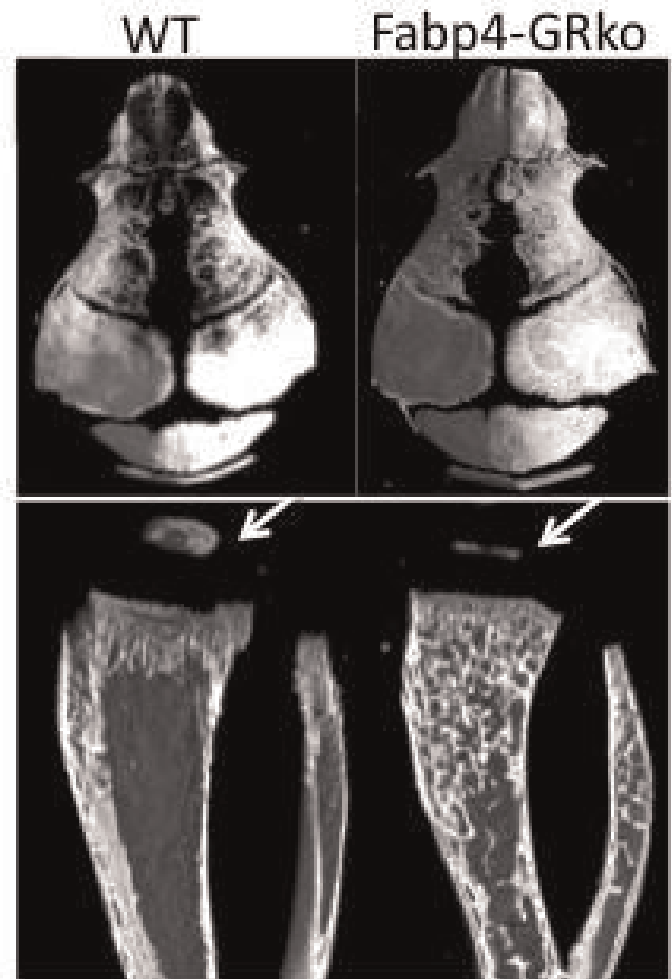
Targeted Disruption of the Glucocorticoid Receptor in Adipocytes Results in, an Osteosclerotic Phenotype, Increased Fat Mass and Growth Retardation in Mice. Yaqing Zhang¹, Jinwen Tu¹, Julian Kelly¹, Tara Brennan-Speranza¹, Alexander Rauch², Colin Dunstan³, Jan Tuckermann², Markus Seibel⁴, Dr. Hong Zhou^{*4}. ¹Bone Research Program, ANZAC Research Institute, University of Sydney, Australia, ²Tissue specific Hormone Action, Leibniz Institute for Age Research, Fritz Lipmann Institute, Germany, ³University of Sydney, Australia, ⁴Bone Research Program, ANZAC Research Institute, The University of Sydney, Australia

Background: The mechanisms by which glucocorticoids (GCs) exert their receptor-mediated effects on bone and fat cells are poorly understood. In the present study we aimed to elucidate the role of the glucocorticoid receptor (GR) in adipocytes, and its interaction with bone, through characterisation of an adipocyte GR-deficient mouse line.

Methods: GR^{flox/flox} mice were crossed with Fabp4-Cre mice to generate GR^{Fabp4Cre} mice, in which the cre recombinase is under the control of the mouse fatty acid binding protein 4 (Fabp4) promoter. Cre-negative GR^{flox/flox} mice served as denote wild type (WT) controls. Mice were analysed for post-natal skeletal changes (by whole body bone and cartilage staining), body composition (by DEXA; Piximus) and bone volume (by micro-CT).

Results: GR^{Fabp4Cre} and their WT littermates had a similar phenotype at birth, with normal skeletal size and regular bone and cartilage staining. Both groups developed normally until day 6, when GR^{Fabp4Cre} mice started to display a pleiotropic phenotype with significant growth retardation, pronounced alopecia followed by premature death within 2 weeks after birth. On day 10, skeletal size and body weight were significantly reduced in GR^{Fabp4Cre} mice when compared to WT littermates ($p < 0.05$). Analysis of body composition revealed a significant increase in total body fat mass and a significant decrease in total body lean mass in GR^{Fabp4Cre} mice compared to WT littermates ($p < 0.05$ for both). In contrast, trabecular bone volume was significantly increased in Fabp4-GRko mice ($p < 0.05$). Despite delayed secondary calcification (Figure, arrows), GR knock-out in adipocytes significantly increased tibial BV/TV, compared to WT mice ($p < 0.05$ compared to WT littermates). In addition, calvaria bone density was increased in GR^{Fabp4Cre} mice (Figure), indicating that both endochondral and intramembranous bone formation are altered by adipocyte specific GR knock-out mice.

In summary, our results suggest that adipocytic glucocorticoid signalling through the GR plays an important role in the post-natal development and growth of mice with profound skeletal effect.



Figure

Disclosures: Dr. Hong Zhou, None.

1110

ER α -deletion from Osteoblast Progenitors Abolishes the Protective Effect of Estrogens on Cortical Bone Mass in Both Female and Male Mice. Srividhya Iyer^{*}, Shoshana Bartell, Aaron Warren, Li Han, Marta Martin-Millan, Elena Ambrogini, Jinhu Xiong, Robert Weinstein, Robert Jilka, Charles O'Brien, Maria Almeida, Stavros Manolagas. Center for Osteoporosis & Metabolic Bone Diseases, Central Arkansas Veterans Healthcare System, University of Arkansas for Medical Sciences, USA

The accelerated cancellous bone loss caused by menopause results predominantly from trabecular perforation and loss of connectivity. This phase is followed a few years later by a phase of slower bone loss that primarily affects cortical sites; this later stage occurs in both women and men and is associated with a decrease in osteoblast number and bone formation rate. Deletion of the estrogen receptor (ER) α in cells of the osteoclast lineage increases osteoclastogenesis, abrogates the effects of estrogens on osteoclast apoptosis, and causes loss of cancellous bone; but it does not affect cortical bone in females and has no effect in either cancellous or cortical bone in males. Here, we have tested the hypothesis that actions of estrogens on osteoblasts must be responsible for their protective effects on the cortical compartment in either sex. To this end, we deleted a conditional ER α allele in early precursors of the mesenchymal lineage of the appendicular skeleton, using a Prx1-Cre transgene. Cortical thickness in the femurs of 2 month old ER α -flox;Prx1-Cre was decreased in both females and males; while cancellous bone volume was unaffected. In contrast to ER α -flox littermate control mice, ER α -flox;Prx1-Cre mice did not lose bone following ovariectomy at 7 weeks of age. Further, we sought to elucidate the contribution of the effects of estrogens on mature osteoblasts, as opposed to progenitors, by deleting the conditional ER α allele in osteoblasts expressing collagen1 (ER α -flox;2.3kbCol1a1-Cre mice). In difference to the ER α -flox;Prx1-Cre mice, the ER α -flox; 2.3kbCol1a1-Cre mice had no changes of BMD up to 6 months of age as compared to controls, but they did exhibit a 2-fold increase in osteoblast apoptosis. These results demonstrate that ER α expressed in osteoblast progenitors is indispensable for the protective effects of estrogens on cortical bone in both male and female mice. Moreover, they strongly suggest that shortening the lifespan of mature osteoblasts in and of itself may not lead

to discernable loss of bone mass unless it is accompanied by decreased osteoblastogenesis (as in the setting of aging) and/or increased osteoclastic bone resorption (as in the acute phase of estrogen deficiency). Albeit, loss of estrogen action in osteoclasts is sufficient for loss of bone in the cancellous compartment because complete perforation of trabeculae by osteoclastic resorption precludes subsequent refilling of the cavities by the bone-forming osteoblasts.

Disclosures: *Srividhya Iyer, None.*

1111

MKP-1 in Canonical 1,25(OH)₂D₃-signaling and Skeletal Homeostasis. Alfred Griffin*, Keith Kirkwood. Medical University of South Carolina, USA

Vitamin D₃ and its most active form 1,25(OH)₂D₃ are well known to stimulate osteoclastogenesis through stromal cell induction of the receptor activator of nuclear factor kappaB (NF-kappaB) ligand (RANKL). Mitogen activating protein kinase phosphatase-1 (MKP-1) is a phosphatase classically known to negatively regulate the innate immune response through dephosphorylation of p38, ERK, and JNK activity. Here we describe a new, novel function of MKP-1 in permitting genomic 1,25(OH)₂D₃ signaling and downstream osteoclastogenesis through RANKL and an altered skeletal phenotype in developing MKP-1^{-/-} mice. Initially, qRT-PCR and immunoblot analysis comparing BMSCs revealed that 1,25(OH)₂D₃-induced VDR, CYP24a1 and RANKL mRNA expression and protein were significantly attenuated or absent in MKP-1^{-/-} BMSCs. When stable RANKL-BAC reporter UAMS-32 stromal cells containing the entire RANKL gene with 120kb of 5' flanking region including 5 validated VDREs were treated with MKP-1 siRNA or control siRNA, we found MKP-1 siRNA treated UAMS-32 stromal cells had a 4.79-fold decrease in RANKL reporter activation and a 3.22-fold decrease in VDR mRNA induction in the same cell line. BMSCs from tibias and femurs of MKP-1^{-/-} mice treated with 1,25(OH)₂D₃ and co-cultured with RAW 264.7 cells had a 91% decrease in osteoclastogenesis (TRAP+, ≥3 nuclei) compared with WT co-cultures (p<.0001). Immunoblot analysis from cellular fractions of WT and MKP-1^{-/-} BMSCs stimulated with 10⁻⁷M 1,25(OH)₂D₃ for 1 hr revealed that RXRα nuclear import was impaired in MKP-1^{-/-} BMSCs, while VDR import was not affected. To address skeletal changes due to loss of MKP-1, DXA and plasma analysis were performed on 4- and 12-week old mice. DXA analysis revealed that the 4- and 12-week MKP-1^{-/-} skeleton had a significant decrease (8.6% reduction) in BMD, and a 22.6% decrease in BMC. Plasma results from age and sex matched mice showed significant decreases in bsALP and TRAcP enzyme activity along with a concurrent 3-fold elevation in PTH serum levels in both male and female 4-week old MKP-1^{-/-} mice (p<.05). These results reveal an unexpected and highly novel role for MKP-1 in permitting canonical 1,25(OH)₂D₃ signaling via RXRα nuclear import and downstream osteoclastogenesis through stromal cell RANKL expression. While the skeletal and plasma phenotype of MKP-1^{-/-} mice may be partly due to a defect in vitamin D signaling, it also clear that MKP-1's role in skeletal biology is not limited to these findings.

Disclosures: *Alfred Griffin, None.*

1112

The VDR Interacts Directly with Mediators of Hedgehog Signaling: Implications for the Development of Alopecia in VDR Null Mice. Francesca Gori*¹, Hilary Luderer¹, Eric Zhu², Marie Demay². ¹Massachusetts General Hospital, USA, ²Massachusetts General Hospital & Harvard Medical School, USA

Vitamin D receptor (VDR) knockout mice develop alopecia due to impaired regeneration of hair follicles after the morphogenic period. Postnatally, the hair follicle goes through cycles of proliferation (anagen), apoptosis (catagen) and quiescence (telogen). Initiation of anagen, which leads to follicle regeneration, is dependent upon activation of the canonical Wnt and hedgehog signaling pathways. In vitro investigations demonstrate that VDR ablation impairs canonical Wnt signaling in primary keratinocytes. Activation of hedgehog signaling in vivo induces hair growth in VDR null mice. Studies were undertaken to determine the effect of VDR ablation on the hedgehog signaling pathway in keratinocytes. Primary keratinocytes were cultured under proliferative conditions. RNA was isolated to evaluate the expression of genes involved in hedgehog and Wnt signaling. Gli1 expression was found to be repressed 3.9±0.6 fold in keratinocytes of VDR null mice relative to wildtype mice and the expression of the classic Wnt target gene, c-Myc was repressed 2.7±0.1 fold. Shh mRNA was not detected in proliferating primary keratinocyte cultures. To determine whether the VDR was required for activation of hedgehog signaling at the onset of anagen, 18 day old mice were subjected to depilation to initiate a new hair cycle. In contrast to wildtype mice, where a 70±18 fold increase in Shh, a 5.8±1.5 fold induction of Gli1 and a 3.7±0.3 fold induction in Patched mRNA was observed after 3 days, no induction of these genes was observed in the skin of VDR null mice. Consistent with these findings ISH demonstrated induction of Shh and Gli1 expression in the region of the hair follicle below the sebaceous gland by 3 days post depilation in wildtype, but not VDR null mice. To determine if the unliganded VDR was able to interact directly with regulatory regions of the Shh and Gli1 genes, chromatin immunoprecipitation analyses were performed. These studies demonstrated interactions of the VDR with DNA sequences in both these genes. Furthermore, transient transfection of the VDR into keratinocytes of VDR null mice resulted in a 2.0±0.3 fold increase in Gli1 expression. Thus, these

studies demonstrate that the VDR is required for induction of hedgehog signaling at the onset of the anagen phase of the hair cycle and implicate absence of VDR-mediated hedgehog signaling in the development of alopecia in the VDR null mice.

Disclosures: *Francesca Gori, None.*

1113

Bone Formation in Mice Deficient for the Vitamin D-24-hydroxylase Gene, Cyp24a1. Abdallah Hussein^{*1}, Alice Arabian², Rene St-Arnaud³. ¹Shriners Hospital & McGill University, Canada, ²Shriners Hospital for Children, Canada, ³Shriners Hospital for Children & McGill University, Canada

Vitamin D is a key regulator of bone homeostasis. The enzyme CYP24A1 initiates the C24-oxidation pathway that leads to degradation of the hormonal form of vitamin D, but is also responsible for the synthesis of 24,25-(OH)₂D. The putative biological activity of 24,25-(OH)₂D remains unclear. Previous studies showed an increase in the circulating levels of this metabolite following a fracture in chicks. Our laboratory has engineered a mouse model deficient for the Cyp24a1 gene in order to study any putative role of 24,25-(OH)₂D. We set out to study the role of 24,25-(OH)₂D in endochondral and intramembranous bone formation in fracture repair using this mouse model. Methods: wild-type and mutant Cyp24a1-deficient mice were subjected to two different surgical procedures. To mimic endochondral ossification, we performed intramedullary nailing of the tibia followed by an induced fracture. To evaluate intramembranous ossification, we applied distraction osteogenesis to mouse tibia using a mini Ilizarov external fixator apparatus. Histomorphometric parameters and gene expression differences in fracture repair and bone formation between the mutant mice and the wild-type controls were measured using micro computed tomography, histology and reverse-transcription quantitative PCR (RT-qPCR), respectively. Results: quantitative histomorphometric results showed a delay in endochondral fracture repair in the mutant mice calluses as compared to the wild-type mice calluses. In this model, gene expression of type X collagen in the callus was reduced in the Cyp24a1 mutant mice. These significant differences were fully rescued by treating the mutant mice with exogenous 24,25-(OH)₂D. In the intramembranous bone formation model, we found a trend towards reduced bone formation in the gap created by the distraction process in the Cyp24a1 mutant mice as compared to wild-type littermates, but the differences did not reach statistical significance. Conclusion: our results support a role for 24,25-(OH)₂D in fracture repair which is more dominant in endochondral ossification. Although our results did not reach statistical significance in the predominantly intramembranous ossification model, the observed trend suggests a role in this bone formation process as well. Further study of the role of 24,25-(OH)₂D in bone healing has the potential to support novel approaches in accelerating bone formation and fracture repair.

Disclosures: *Abdallah Hussein, None.*

1114

The Role of Vitamin D Receptor in Motor Function. Sadaoki Sakai^{*1}, KOICHI ENDO², Keisuke Tanaka³, Masahiko Mihara³. ¹Chugai Pharmaceutical Co., Ltd., Japan, ²Chugai Pharmaceutical Co., Ltd., Japan, ³CHUGAI PHARMACEUTICAL CO., LTD, Japan

The purpose of osteoporosis treatment is to reduce bone fracture. In achieving this purpose, an anti-osteoporotic medicine should ideally not only improve bone mineral density (BMD) and bone strength but also aid in preventing falls and maintaining locomotive ability. Active vitamin D₃ improves BMD and bone strength. Moreover, some studies have found that vitamin D₃ decreases the risk of falls. However, we have very little knowledge about the relationship between active vitamin D₃ and peripheral nerve function, which is known to decline with age. In this study we used vitamin D receptor knockout (VDR KO) mice to investigate the effect of VDR signaling on motor function. Wild type (WT) and VDR KO mice were trained on a rotarod five times a week (15 rpm, 5 min, 3 times/day) for 4 weeks, and locomotive performance was then measured by an accelerating rotarod test. Four-week training led to an increased duration on the rotarod in the WT mice but not in the VDR KO mice, suggesting that VDR signaling is essential for the improvement of motor function. Histological observations of sciatic nerve cross sections revealed that the axon diameter was smaller in VDR KO mice than in WT mice. Additionally, the distribution of acetylcholine receptor on the extensor digitorum longus was not as broad and the pattern of distribution was simpler in the VDR KO mice. Furthermore, active vitamin D dose-dependently upregulated mRNA expression of insulin-like growth factor-I (IGF-I) and myelin basic protein (MBP) in Schwann cells isolated from neonatal rats. In conclusion, VDR signaling plays a critical role in upregulating motor function in the rotarod training model. Stimulation with active vitamin D increased mRNA expression of IGF-I and MBP in Schwann cells in vitro. IGF-I broadens acetylcholine receptor distribution and increases the production of lipids that are included in the myelin sheaths, and the amounts of serum IGF-I and amounts of MBP in the sciatic nerve decrease with age. These results suggest that active vitamin D may improve motor function via the induction of IGF-I and MBP from peripheral Schwann cells.

Disclosures: *Sadaoki Sakai, CHUGAI PHARMACEUTICAL CO., LTD, 3*

1115

NLRP3 Inflammasome is a Major Regulator of Bone Resorption. Sheri Bonar¹, Matthew McGeough², Marcus Watkins¹, Susan Grimston¹, Susannah Brydges², James Mueller², Carla Pena², Roberto Civitelli¹, Hal Hoffman², Gabriel Mbalaviele¹. ¹Washington University in St. Louis School of Medicine, USA, ²University of California, San Diego, USA

The Nod Leucine rich Repeat with a Pyrin domain 3 (NLRP3) inflammasome is an intracellular protein complex responsible for the maturation of IL-1 β family members into their active forms, and for proteolytic inactivation of poly(ADP-ribose) polymerase 1 (PARP1), a negative regulator of osteoclast (OC) development. Recent studies indicate NLRP3 is involved in low grade aseptic inflammation in metabolic diseases. NLRP3 senses cues triggered by crystalline particulates or degradation products of endogenous extracellular matrix as danger associated molecular patterns (DAMPs). Since mineral and organic bone degradation products can traffic through bone resorbing OC, we first tested whether hydroxyapatite crystals (HA) activate NLRP3 in OC lineage in vitro. Exposure of LPS-stimulated bone marrow macrophages to HA increased the processing of pro-IL-1 β to IL-1 β by 10-fold (ELISA) and PARP1 inactivation (immunoblot analysis) in NLRP3-, time-, concentration- and particle size- dependent manner. Since NLRP3 activating mutations cause skeletal malformations and low bone mass in patients with neonatal onset multisystemic inflammatory disease, we studied knock-in mice globally expressing a constitutively active NLRP3 allele. At age P14 (maximal lifespan), mutant mice were significantly smaller and osteopenic (whole body DXA) relative to WT mice. Accordingly, μ CT analysis of mutant femurs revealed rarefied and fragmented trabeculae, significantly decreased cortical bone volume and thickness, and larger bone marrow cavity relative to WT bones. Reduced hypertrophic zone in the growth plate and increased TRAP⁺ OC on the endosteal surfaces were observed on histology of mutant mice, associated with >10-fold higher serum CTX-1 levels, a marker of bone resorption. At the cellular level, the number of OC developing from unfractionated bone marrow cells in the presence of M-CSF and RANKL was 3-4-fold higher in mutants compared to WT cells; and FACS analysis revealed 3-fold higher number of CD11b⁺ OC precursors in marrow of mutant mice relative to WT mice. In summary, NLRP3 activation by bone relevant DAMPs stimulates cytokine maturation, and in mice constitutive NLRP3 activation dramatically increases bone resorption resulting in very low bone mass. Thus, NLRP3 is a major regulator of bone resorption, perhaps mediating pro-inflammatory signals originating from the bone matrix during normal bone remodeling.

Disclosures: Gabriel Mbalaviele, None.

1116

PTH Induces Hemopoietic Stem Cell Expansion Through T Cell Produced Wnt10b. Jau-Yi Li¹, Brahmachetna Bedi¹, Hesham Tawfeek¹, Jonathan Adams¹, Timothy F. Lane², Tatsuya Kobayashi³, M. Neale Weitzmann¹, Henry Kronenberg³, Roberto Pacifici¹. ¹Emory University School of Medicine, USA, ²University of California, Los Angeles, USA, ³Massachusetts General Hospital, USA

Activation of Wnt signaling in stromal cells (SCs) is required for PTH to expand hemopoietic stem cells (HSCs). Since PTH induces T cell production of Wnt10b, a Wnt ligand critical for PTH action in bone, we investigated the role of T cell produced Wnt10b in PTH induced HSC expansion. PTH treatment (PTH 1-34, 80 μ g/kg SQ daily for 4 weeks) increased by 2 fold the number of HSCs (Lin-Sca-1+c-Kit⁺ cells) in WT mice but not in Wnt10b^{-/-}, T cell deficient TCR α ^{-/-}, or PPRT cells ^{-/-} mice, a strain lacking PTH receptor 1 (PPR) signaling in T cells. PTH increased Wnt10b production by T cells from control but not PPRT cells ^{-/-} mice by 4 fold. PTH also increased SC expression of Jagged1 (a Notch ligand critical for HSC expansion) in WT but not TCR α ^{-/-}, PPRT cells ^{-/-}, and Wnt10b^{-/-} mice. Adoptive transfer of WT but not Wnt10b^{-/-} or PPRT cells ^{-/-} T cells into TCR α ^{-/-} mice restored PTH mediated expansion of HSCs and SC Jagged1 expression. Thus, PPR mediated T cell produced Wnt10b is required for PTH to expand HSCs through upregulation of Jagged1 in SCs. Next, we measured survival rates in lethally irradiated WT mice transplanted with sub-optimal numbers of bone marrow (BM) cells. PTH treatment of recipient mice in the first 4 weeks after transplantation of WT BM increased survival from ~20 % to ~80%. PTH however did not increase survival of mice transplanted with BM from TCR α ^{-/-}, PPRT cells ^{-/-}, and Wnt10b^{-/-} mice. Confirming the relevance of T cell produced Wnt10b in vivo, PTH treatment of donor WT mice, but not TCR α ^{-/-}, PPRT cells ^{-/-}, and Wnt10b^{-/-} mice, increased survival of untreated WT recipients by 4 fold. Finally, to assess if T cells enhance HSC engraftment a competitive transplant experiment was conducted in which CD45.2⁺ WT mice, TCR α ^{-/-} mice and TCR α ^{-/-} mice previously reconstituted with WT T cells were treated with PTH for 4 weeks. Their BM was then mixed with BM from untreated CD45.1⁺ WT mice (1:2 ratio), and transplanted into lethally irradiated untreated WT CD45.1⁺ recipients. Analysis of CD45.2⁺ cells at 4 weeks demonstrated that PTH treatment improved by 2 fold the expansion of CD45.2 monocytes, granulocytes and B cells in WT and reconstituted TCR α ^{-/-} recipient mice, but not T cell deficient TCR α ^{-/-} mice. In summary, activation of PTHR1 in T cells and the resulting production of Wnt10b and stimulation of Notch signaling are required for PTH to stimulate HSC expansion and engraftment and improve survival after BM transplantation.

Disclosures: Jau-Yi Li, None.

1117

The Novel Osteoinductive Wnt Regulator NELL-1 Potently Antagonizes BMP2-induced Adipogenesis and Augments BMP2-induced Osteogenesis. Jia Shen¹, Ronald Siu², Sheng Pang³, Janette Zara⁴, Jinny Kwak⁵, Xinli Zhang², Aaron James², Michael Chiang⁵, Richard Ngo⁵, Weiming Li⁶, Min Lee⁷, Kang Ting², Chia Soo³. ¹University of California, Los Angeles, California, USA, ²University of California, Los Angeles, USA, ³Department of Orthopaedic Surgery, University of California, Los Angeles, USA, ⁴UCLA, USA, ⁵School of Dentistry/Section of Orthodontics, University of California, Los Angeles, USA, ⁶First Clinical Hospital, Harbin Medical University Department of Orthopaedics, China, ⁷Division of Advanced Prosthodontics, Biomaterials & Hospital Dentistry, University of California, Los Angeles, USA

NELL-1, a novel Runx2-regulated growth factor with critical roles in osteogenesis, demonstrated synergy with bone morphogenetic protein-2 (BMP2) in repair of calvarial and femoral defects. BMP2 is a major osteoinducer used clinically in spinal fusion and treatment of skeletal defects; unfortunately the supraphysiological dosages required clinically has resulted in numerous adverse effects. In previous work, we found that high doses (>300 μ g/ml) of BMP2 induced adipogenesis and cyst-like bone void formation. In this study, we asked whether NELL-1 could ameliorate these side effects and significantly improve BMP2-based skeletal repair.

To accomplish this goal, we applied BMP2 in a rat femoral segmental defect (FSD) model with and without co-treatment of NELL-1 and evaluated healing at 2 and 8 weeks post operation. Furthermore, we treated murine M2-10B4 cells with BMP2 or in combination with NELL-1 in vitro to gain mechanistic insight in support of our *in vivo* findings.

With BMP2 monotherapy, massive expansion of PPAR γ -positive cells was observed at 2 weeks, which progressed to terminally differentiated adipocytes and adipose-filled cyst-like bone voids by 8 weeks. Interestingly, the combination of NELL-1 with BMP2 preferentially accelerated the osteogenic differentiation of these cells at the expense of proliferation and adipogenesis, completely abolishing heterotopic, cyst-like bone formation and resulting in more organized and mature bone (Fig.1,2). Canonical Wnt signaling is known to enhance osteogenesis and conversely suppress adipogenesis. Interestingly, NELL-1 stimulated canonical Wnt pathway activity *in vivo* and *in vitro*, as supported by increased nuclear localization of β -catenin with NELL-1 treated FSDs and M2-10B4 cells (Fig.3). Importantly, the ability of NELL-1 to bias cells induced toward osteogenic differentiation by BMP2 was Wnt-dependent, as treatment with two different canonical Wnt inhibitors eliminated the anti-adipogenic and pro-osteogenic effects of NELL-1 (Fig.4).

To our knowledge, this was the first demonstration of an adjunctive treatment that could both improve BMP2-mediated bone healing and simultaneously alleviate its associated adverse effects, which could potentially increase the clinical safety and efficacy of current BMP2 orthopedic applications. Furthermore, understanding the role of NELL-1 and Wnt in the balance between bone and adipose tissue formation will be valuable for osteoporosis and other disorders of bone homeostasis.

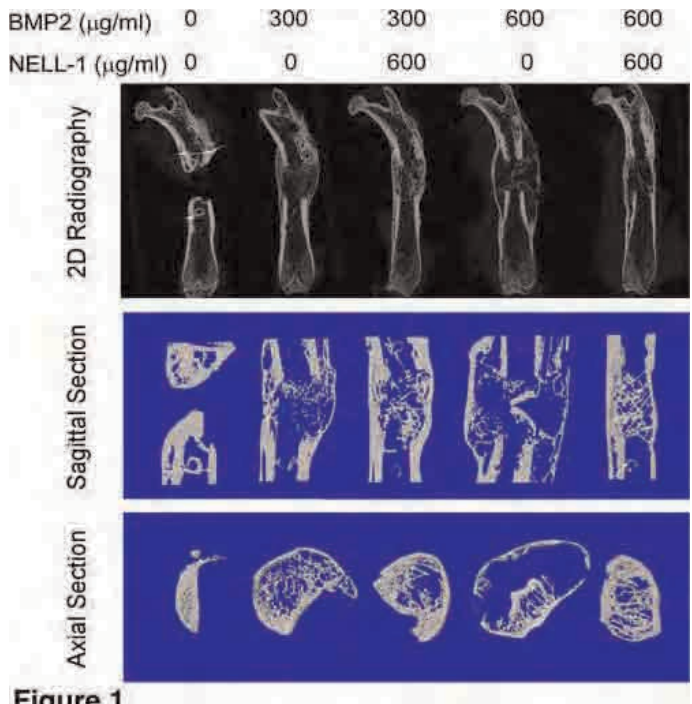


Figure 1

1118

Mx2-Wnt Signaling Inhibits and Dkk1 Promotes The Endothelial-Mesenchymal Transition In Primary Aortic Endothelial Cells. Su-Li Cheng^{*1}, Dwight Towler². ¹Washington University in St. Louis School of Medicine, USA, ²Washington University in St. Louis, USA

Endothelial cells (ECs) can undergo an endothelial-mesenchymal transition (EnMT) during cardiovascular development. Canonical Wnt/beta-catenin activity helps drive EnMT necessary for heart valve morphogenesis. EnMT also occurs in pathological conditions that contribute to cardiac fibrosis and ectopic ossification. We've previously demonstrated that Wnt/beta-catenin signals play an important role in the arteriosclerotic calcification and fibrosis that arises with diabetes. Increasing Wnt activity in vascular mesenchymal cells with Wnt7b or Mx2 increases osteogenic differentiation and matrix fibrosis via paracrine signals that are inhibited by the LRP receptor antagonist, Dkk1. We wish to test if canonical Wnt signaling exerted similar actions on aortic ECs, potentially contributing to calcification and fibrosis via EnMT. Thus, we transduced primary bovine aortic ECs (BAECs) with retroviruses expressing Mx2, Wnt7b, Dkk1, or LacZ (control). To our surprise, expression of either Mx2 or Wnt7b promoted the "cobblestone pavement" cell shape of well-differentiated ECs, with upregulation of EC phenotypic markers such as claudin 5. These effects were phenocopied by 20 ng/ml Wnt3a treatment. Moreover, when cultured under conditions that promote mineralization of mesenchymal cells, Mx2 and Wnt7b suppressed calcium deposition and collagenous matrix production. Conversely, transduction of ECs with the SFG-Dkk1 suppressed claudin 5, PECAM, VE-cadherin, Tie1 and Tie2. Myofibroblast and osteoblastic markers such as SM22, Osx, Runx2, type I collagen and alkaline phosphatase were upregulated. Dkk1 expression induces cell shape change, converting the cuboidal monolayer into a spindle shaped cell multilayer, and inhibited endothelial tube formation in matrigel. Moreover, Dkk1 enhanced matrix mineralization of BAECs cultured under osteogenic conditions– the inverse of the Dkk1 response elicited in cultured mesenchymal cells. Pulse-chase experiments of DiI-Ac-LDL tagged BAECs confirmed that Dkk1 enhanced EnMT, viz. the trans-differentiation of cuboidal ECs into spindle shaped mesenchymal cells. Thus, EC Mx2-Wnt signaling stabilizes the endothelial phenotype, while Dkk1 enhances the EnMT in differentiated BAECs. Endothelial response to Mx2, Wnt7b, and Dkk1 are the inverse of those responses elaborated by mesenchymal cells, potentially providing a mechanism that finely couples angiogenic with osteo/fibrogenic requirements during tissue injury and repair.

Disclosures: Su-Li Cheng, None.

1119

Vascular Tissues Are a Primary Source of BMP2 Expression during Bone Formation Induced by Distraction Osteogenesis. Hidehiko Matsubara¹, Daniel Hogan², Douglas Mortlock³, Elise Morgan⁴, Thomas Einhorn⁵, Louis Gerstenfeld^{*1}. ¹Boston University School of Medicine, USA, ²Boston University College of Engineering, USA, ³Vanderbilt University School of Medicine, USA, ⁴Boston University, USA, ⁵Boston Medical Center, USA

Skeletal development after injury or surgery is co-dependent on vascularization. While this co-dependency is often thought of in terms of the skeletal tissue's need for appropriate nutrition and oxygen, vascular morphogenesis provides the structural template around which Haversian and trabecular units of bone are formed, suggesting therefore that there are molecular mechanism that tightly coordinate skeletal and vascular tissue morphogenesis. Prior studies showed that bone regeneration during distraction osteogenesis (DO) was dependent on vascular tissue formation and that inhibition of vessel formation inhibited the expression of BMP2. A combination of micro-computed tomography analysis of vascular and skeletal tissues, histological analysis using transgenic mice containing ~239 kilobase BAC transgene in which beta-galactosidase has been inserted into the coding region of BMP2, and qRT-PCR analysis were used to determine the cellular origins of BMP2 during DO. The results showed within both the surrounding musculature and regenerating bone that BMP2 expression was induced in both smooth muscle and vascular endothelial cells lining arteries and veins but not in lymphatic vessels. Within the region of developing bone, BMP2 was expressed by hypertrophic chondrocytes and osteocytes. Separate peaks of BMP2 mRNA expression were induced in muscular tissues and the distraction gap, and each peak corresponded with a peak of expression of endothelial cell marker genes and vessel formation and remodeling. Earlier peaks of expression of these genes were always seen in the musculature preceding those in the bone. Interestingly peaks of DKK and Sost expression were also observed in both tissue compartments and these occurred slightly later than the BMP2 peaks suggesting that these morphogens are also produced during vascular tissue formation. These results suggest that during post natal bone regeneration vascular tissues in surrounding musculature and within the developing bone are the predominant source of BMP2 in the developmental environment and suggest that BMP2 carries out functional roles in both vascular and skeletal regeneration.

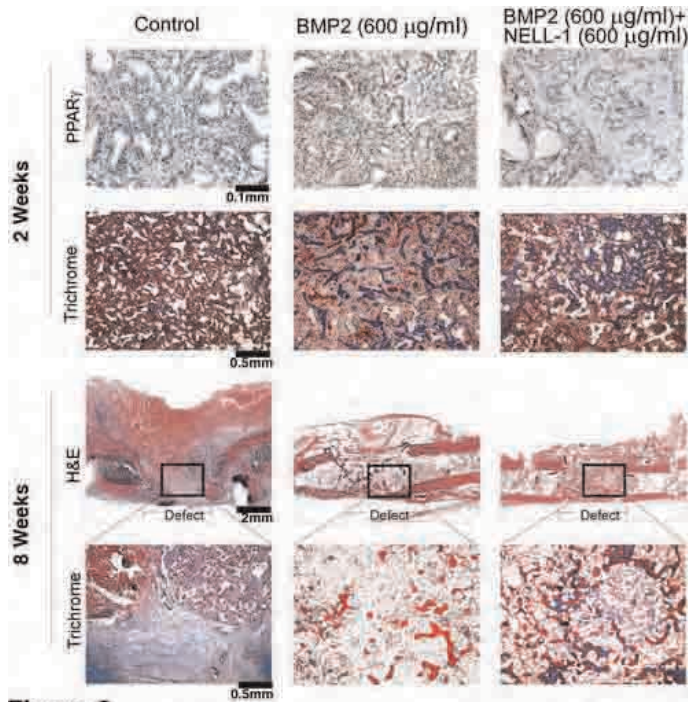


Figure 2

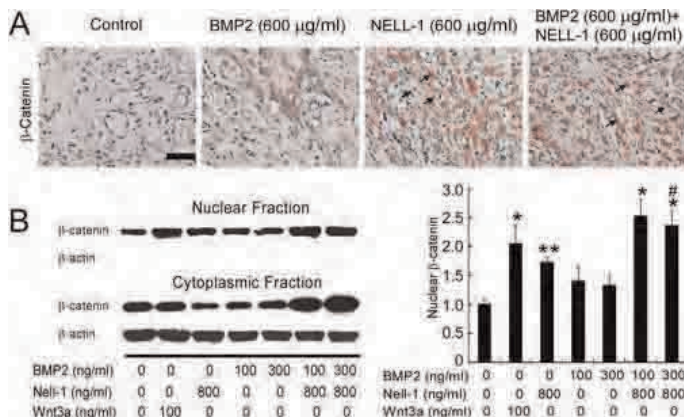


Figure 3

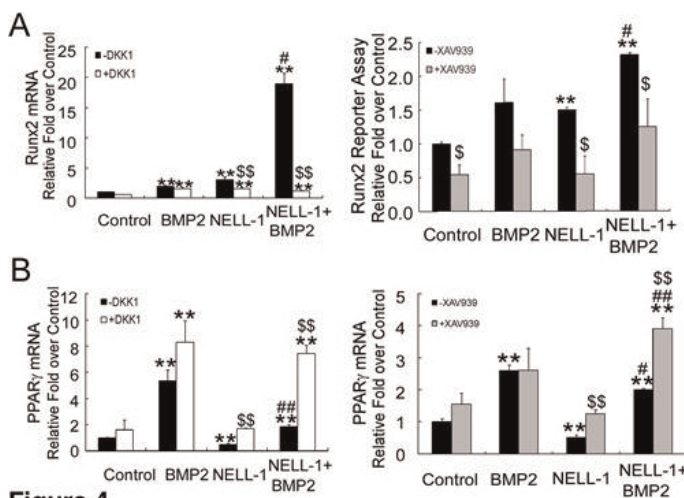


Figure 4

Disclosures: Jia Shen, None.

1121

TGF β Inducible Early Gene-1 Plays a Critical Role in Mediating Estrogen and Canonical Wnt Signaling in the Growing Mouse Skeleton. John Hawse^{*1}, Muzaffer Cicek², Kevin Pite³, Sarah Grygo⁴, Kenneth Peters⁴, Nalini Rajamannan⁵, Urszula Iwaniec⁶, Russell Turner⁶, Merry Jo Oursler², Thomas Spelsberg², Malayannan Subramaniam². ¹Mayo Clinic College of Medicine, USA, ²Mayo Clinic, USA, ³University of Minnesota, USA, ⁴Mayo Clinic College of Medicine, USA, ⁵Northwestern University Medical School, USA, ⁶Oregon State University, USA

TGF β Inducible Early Gene-1 (TIEG) knockout (KO) mice display a gender specific osteopenic phenotype characterized by low bone mineral density, bone mineral content and overall loss of bone strength in female mice. We therefore speculated that loss of TIEG expression may impair the actions of estrogen on bone balance in female mice. In order to test this hypothesis, we performed sham or ovariectomy (OVX) surgeries on one month old WT and KO mice supplemented with placebo or 17-beta estradiol (E2) pellets at a dose of 0.063 ug/day. DXA, pQCT and μ CT analyses were conducted on all mice at 2 months of age. Analysis of whole body skeleton, tibias, femurs and L5 vertebrae revealed that WT mice lost significantly more bone following OVX than TIEG KO mice. Furthermore, the bone anabolic actions of E2 were approximately halved in the KO animals suggesting an important role for TIEG in mediating E2 signaling in the mouse skeleton. In order to begin to understand the molecular mechanisms responsible for these observations, we performed gene expression studies on the cortical shells of long bones isolated from these mice. A dramatic increase in the expression levels of bone marker genes such as Runx2, osterix, alkaline-phosphatase, osteocalcin and bone sialoprotein were observed following E2 administration in WT mice. In parallel with the bone phenotype, these increases in gene expression were significantly reduced in TIEG KO mice. Additionally, the expression levels of a number of Wnt pathway genes were also determined to be differentially regulated between these two genotypes. Of particular interest, the levels of sclerostin (SOST) were elevated by 12-fold in KO mice relative to WT controls suggesting that loss of TIEG expression alters canonical Wnt signaling. To determine if Wnt signaling is significantly affected in KO mice, we crossed these animals with the TOPGAL reporter mouse. Histochemical analysis of the L5 vertebrae revealed a 2-fold decrease in β -gal staining in KO animals compared to WT littermates. As an extension of these studies, we have also shown that TIEG mediates beta-catenin nuclear translocation and serves as a co-activator on TCF/Lef enhancer elements in osteoblasts. Taken together, these data clearly implicate a role for TIEG in mediating E2 and Wnt signaling in the mouse skeleton and suggest that defects in these pathways may be responsible for the gender specific osteopenic phenotype observed in TIEG KO mice.

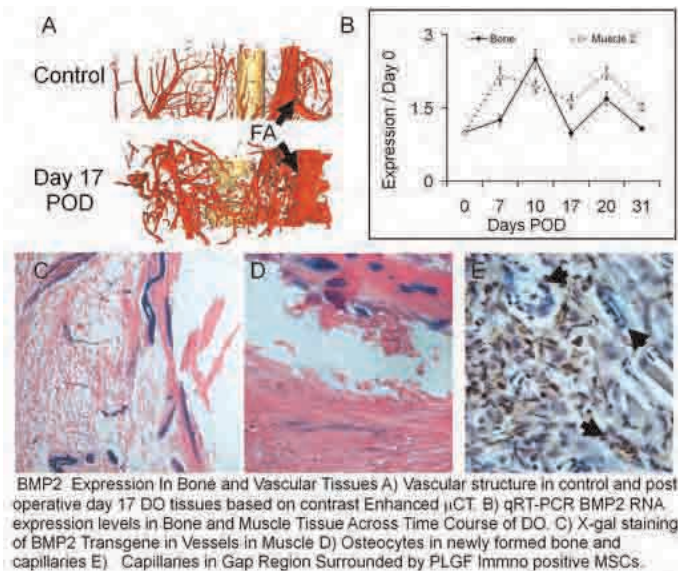
Disclosures: John Hawse, None.

1122

Targeted Disruption of TGFBI in Mice Reveals Novel Role for this Gene in Regulating Peak Bone Size. Hongrun Yu^{*1}, Heather Watts², Anil Kapoor², Yongliang Zhao³, Jon Wergedal², Subburaman Mohan². ¹JLP Memorial VA Med Ctr, USA, ²Jerry L. Pettis Memorial VA Medical Center, USA, ³Center for Radiological Research, USA

Transforming growth factor beta-induced (TGFBI) protein, also known as betaig-h3, is an extracellular matrix (ECM) protein strongly induced by TGF- β , and structurally unrelated to similar TGF- β Inducible Early Gene-1 (TIEG1). TGFBI contains domains and motifs that interact with integrins and other ECMs to mediate cell adhesion and migration. It is highly expressed in bone, cartilages, and skin. Based on previous findings that TGFBI inhibits osteoblast differentiation in vitro, we tested the hypothesis in this study that TGFBI is a negative regulator of bone formation. Heterozygous mice with targeted deletions of exons 4-6 of TGFBI were crossed to generate homozygous knockout (KO) mice and wild type (WT) littermates. Skeletal phenotypes were analyzed by PIXImus, micro-CT and histomorphometry. Bone mineral density (BMD) as measured by PIXImus in total body, femur, tibia and vertebra was decreased by 8%, 19%, 15% and 15% (all $P < 0.01$), respectively, in KO mice compared to WT mice at 4 weeks of age. Lack-of-TGFBI induced skeletal deficits were seen in both genders, and were sustained up to a study period of 12 weeks of age. Micro-CT measurements revealed 25% and 15% decreases in total volume at the tibial diaphyseal and metaphyseal regions, respectively, indicating a reduction in bone size. Because TGFBI KO mice exhibited reduced body weight, we also adjusted for body and bone size, and found that body weight adjusted tibia bone mineral content (BMC) as well as bone length adjusted tibial bone size were reduced by 10% and 19%, respectively, in the KO mice compared to WT mice at 12 weeks of age. Micro-CT measurements of tibial metaphysis revealed no significant differences in trabecular bone parameters between KO and WT mice at 12 weeks of age. Histomorphometric analysis revealed an 11% reduction in total area at the femoral midshaft of KO mice, consistent with a reduced bone size. Accordingly, periosteal bone formation rate adjusted for bone surface was reduced by 25% in KO mice compared to WT mice. In contrast, bone formation rate at the endosteum was not significantly affected. Based on these results, we conclude: 1) Lack-of-TGFBI reduces peak bone size by affecting periosteal bone formation. 2) On the contrary to the known inhibitory effects of TGFBI on osteoblast differentiation based on in vitro studies, our in vivo studies using targeted disruption of TGFBI demonstrate a positive regulatory effect of TGFBI on periosteal bone formation.

Disclosures: Hongrun Yu, None.



BMP2 Expression in Vascular Tissues

Disclosures: Louis Gerstenfeld, None.

1120

BMP3 Suppresses Osteoblast Differentiation of Bone Marrow Stromal Cells via Interaction with Acvr2b. Shoichiro Kokabu^{*1}, Laura Gamer¹, Karen Cox¹, Kunikazu Tsuji², Regina Raz³, Aris Economides³, Takenobu Katagiri⁴, Vicki Rosen¹. ¹Harvard School of Dental Medicine, USA, ²Tokyo Medical & Dental University, Japan, ³Regeneron Pharmaceuticals, Inc., USA, ⁴Saitama Medical University Research Center for Genomic Medicine, Japan

Bone morphogenetic proteins (BMPs) were identified as signals that induce ectopic bone formation through effects on skeletal progenitor cells present in adult animals. Enhancing BMP signaling increases bone formation in a variety of settings that target bone repair; however, a physiological role for BMP signaling in the maintenance of adult bone mass remains to be determined. Here we focus on BMP3 because targeted disruption of BMP3 in mice results in increased trabecular bone formation (Daluiski A et al., 2001) while transgenic over-expression of BMP3 in skeletal cells leads to delayed mineral deposition during endochondral ossification and spontaneous fracture (Gamer LW et al., 2009). These data are consistent with BMP3 having an inhibitory role in osteoblast function. To define the pathway by which BMP3 affects osteoblast function, we created mice carrying a lacZ knock-in allele to the Bmp3 locus and used them to examine the expression of BMP3 in the postnatal skeleton. We find that osteoblasts and osteocytes are the source of BMP3 present in adult bone, and show that periosteal osteoprogenitors and bone marrow stromal cells (BMSC) do not express BMP3. Based on the distribution of Acvr2b, the BMP3 receptor, we hypothesize that BMP3, produced by mature bone cells acts to reduce BMP signaling in bone marrow stromal osteoprogenitors. In support of this hypothesis we show that loss of BMP3 increases CFU-OB in BMSC cultures, while increased levels of BMP3 reduce CFU-OB. We also determine that knockdown of endogenous Acvr2b in BMSC diminishes the suppressive effect of BMP3 on osteoblast differentiation. The importance of Acvr2b as a mediator of BMP3 action is confirmed by data showing that mutations in either BMP3 or Acvr2b that prevent the BMP3/ Acvr2b interaction result in the loss of BMP3 mediated osteoblast inhibition. Taken together, these data confirm that BMP3 regulates trabecular bone formation by inhibiting the osteoblast differentiation of BMSC and support the idea that endogenous BMPs have a physiological role in regulating adult bone mass.

Disclosures: Shoichiro Kokabu, None.

1123

TGF- β Type II Receptor Signaling Plays An Essential Role in Knee Development. Tieshi Li¹, Lara Longobardi¹, Froilan Granero-Molto¹, Timothy Myers², Douglas Mortlock³, Anna Spagnoli¹. ¹University of North Carolina at Chapel Hill, USA, ²University of North Carolina, USA, ³Vanderbilt University Medical Center, USA

We have previously reported that TGF- β type II receptor (*Tgfr2*) signaling is essential for joint morphogenesis. *Tgfr2*^{PRX-1KO} mouse, in which the *Tgfr2* is conditionally inactivated in developing limbs, lacks interphalangeal joints (Spagnoli A et al, J Cell Biol, 2007). To further investigate the function of Tgfr2 signaling in knee development, we evaluated the knee phenotype of the *Tgfr2*^{PRX-1KO} mouse. At E14.5 the *Tgfr2*^{PRX-1KO} showed segmentation of the knee skeletal elements but joint space was narrower compared with the space found in the *Tgfr2*^{lox/lox} control mouse. At E16.5 the *Tgfr2*^{PRX-1KO} mouse lacked the formation of the menisci and the patella. At P0, the knee of the *Tgfr2*^{PRX-1KO} mouse showed a dramatic phenotype characterized by a lack of posterior/anterior cruciate ligaments, synovial capsule, menisci, patella and showed abnormal shapes of the tibial plateau and femoral condyles. The space between the segmented tibia and femur was filled with disorganized cellular elements. In our lab we have also generated a Tgfr2- β -Gal-GFP-BAC transgenic mouse containing β -galactosidase (β -Gal) as an imaginable reporter for Tgfr2 expression under the control of endogenous (within 195.8kb) Tgfr2 gene regulatory sequences including the promoter. Using the Tgfr2- β -Gal-GFP-BAC transgenic mouse, we found that within the knee, Tgfr2 expression started at E13.5. At E14.5, we found that Tgfr2 was highly and specifically expressed in both the knee dorsal and ventral sides and in some restricted cells in the center of the joint. At E16.5 expression became related to well identifiable components of the joint. Consistently, at P0, Tgfr2 expression was localized specifically at the superficial sides of the menisci, patella, the tendons, along with synoviocytes, the capsule, and in restricted areas of the articular cartilage. The expression pattern of Tgfr2 is consistent with TGF β 2 expression and detection of phosphorylated Smad2 by immunohistochemistry in E14.5, E16.5 and P1 knees. Within the developing knees, we found a co-localization of Tgfr2-Lac-Z activity with joint marker genes such as Jagged1, Noggin, GDF5 and Notch1. At E14.5, the lack of Tgfr2 signaling in the knee of the *Tgfr2*^{PRX-1KO} mouse was associated with a decrease of Jagged1, Noggin, GDF5, Notch1 and phosphorylated Smad2. Our findings indicate that Tgfr2 expressing cells in the knee provide a signaling niche for the developing of the critical joint elements.

Disclosures: Tieshi Li, None.

1124

Anti TGF- β Antibody Attenuates Increased Bone Turnover in Rodent Models of High Turnover Chronic Kidney Disease-Mineral Bone Disorder (CKD-MBD). Shiguang Liu^{*}, Wenping Song, Joseph Boulanger, Wen Tang, Christina Bracken, Sue Ryan, Robert Fogle, Yves Sabbagh, Susan Schiavi. Genzyme Corporation, USA

Altered bone turnover is a key pathologic feature of CKD-MBD. TGF- β 1 plays an important role in regulating bone turnover and has been shown to be an important mediator of the anabolic effect of PTH on bone. TGF- β 1 expression is increased in bone biopsies from individuals with high bone turnover raising the possibility that it may contribute to the pathogenesis of renal osteodystrophy. Our data also demonstrated that TGF- β 1 expression is increased in bones from a CKD-MBD mouse model. To assess the relevance of elevated TGF- β 1 on the pathogenesis of high-turnover disorder in CKD-MBD, we administered a neutralizing anti-TGF- β antibody (1D11) to three independent rodent models of CKD-MBD: Jck mice, adenine-treated, and 5/6 nephrectomized rats. 1D11 treatment significantly attenuated the increase in serum osteocalcin levels in all 3 models and was associated with trends toward decreased serum type I collagen C-telopeptides (CTX) levels. μ CT analysis confirmed improvements in bone morphology in both adenine-induced and 5/6 nephrectomized rat models. To explore the potential efficacy of 1D11, we expanded characterization of its effects in jck mice as this genetic model of CKD-MBD has been shown to exhibit progressive changes in serum biochemistry, bone and vasculature mimicking human CKD-MBD. 1D11 was injected IP (0.5, 2 or 5 mg/kg) 3 times a week for 7 weeks. Bone histomorphometric analysis indicated that 1D11 significantly suppressed the elevated bone turnover in a dose-dependent manner. Importantly, in this model, 1D11 treatment did not significantly improve kidney function or reduce serum PTH levels indicating that the effect of 1D11 on bone may be independent of changes in renal or parathyroid function. 1D11 had no significant effect on the increased expression of osteoclast gene markers (Trap5, Ctsk, and Rank) but resulted in a significant increase in Sost mRNA expression consistent with an effect on the osteoblast/osteocyte lineage. Taken together, our data demonstrate that a neutralizing anti-TGF- β antibody can attenuate high turnover bone disease, providing further support for a pathological role of TGF- β in CKD-MBD.

Disclosures: Shiguang Liu, Genzyme, 3

1125

TGF- β -dependent Regulation of Sclerostin during Mechanical Loading. Jacqueline Nguyen^{*}, Simon Tang, Dan Nguyen, Tamara Alliston. University of California, San Francisco, USA

The mechanical stimulation of exercise induces bone formation and maintains bone health. Though several molecules required for load-induced bone formation have recently been identified, many questions remain. Motivated in part by the observation that loading of rat tibiae increases TGF β 1 mRNA expression, we hypothesized that TGF β signaling participates in load-induced bone formation. Since TGF β can be regulated post-transcriptionally, we assessed the effect of *in vivo* loading on the activities of downstream TGF β effectors, called Smad2/3, using transgenic mice that express a Smad2/3 responsive promoter-luciferase reporter construct. We applied cyclic axial load of approximately 10 times the mouse body weight to the right tibia of Smad2/3-luciferase mice at 1 Hz for 600 cycles once a day and used the unloaded contralateral tibia as control. A 5-day loading regimen of *in vivo* mechanical stimulation induces a 14% increase in cortical thickness ($p < 0.05$). Within 5 hours of one load application, Smad2/3 activity was increased 20% ($p < 0.05$), showing that load increases a rapid activation of Smad2/3 activity. To determine if this correlation between load-induced bone formation and Smad2/3 activation is causal, we applied mechanical load to DNT β R11 mice, which express a dominant negative TGF β type II receptor under control of the osteocalcin promoter, and wild-type (WT) littermates. Unlike WT mice, DNT β R11 mice do not respond to mechanical load with increased bone deposition. Using immunohistochemistry, we next investigated whether this TGF β loss of function mutation is sufficient to impair the load-sensitive regulation of Sclerostin, a protein implicated in the control of load-induced bone formation. Consistent with previous reports, mechanical loading over 5 days caused a downregulation of Sclerostin expression in WT tibial cortical bone. However, mechanical load did not alter Sclerostin expression levels in DNT β R11 bone ($p < 0.05$). *In vitro* studies further document the regulation of SOST expression by TGF β . Together, these data reveal a novel pathway that participates in load-induced bone formation. Specifically, mechanical load activates TGF- β signaling in a Smad2/3 dependent manner to induce bone formation through a pathway that intersects with SOST. The molecular basis of this interaction remains under investigation.

Disclosures: Jacqueline Nguyen, None.

1126

A New Role for the TGF β R11-MCP-5 Axis as a Key Regulator in the Interplay between the Articular Cartilage and the Forming Bone during Limb Development. Lara Longobardi¹, Tieshi Li², Timothy Myers³, Froilan Granero-Molto¹, yun van³, ying li³, Anna Spagnoli¹. ¹University of North Carolina at Chapel Hill, USA, ²UNC, USA, ³UNC-CH, USA

In our previous studies we found that within the developing joint interzone a down-regulation of the cytokine MCP-5 is required for normal joint development (Longobardi L. et al. ASBMR 2010, OR#1116). The Tgfr2PRX-1KO mouse generated in our lab which lacks Tgfr2 in developing limbs, shows an aberrant up-regulation of MCP-5 in the interzone and fails joint development and chondrocyte hypertrophy. Genetically modified mice lacking joint development (noggin-KO, gdf5-KO) exhibit inappropriate skeletal morphogenesis, indicating that the developing joint is an essential regulator of skeletal element development. A derangement of the interplay between the articular cartilage and the subchondral bone is found in arthritic joints. Aberrant expressions of MCP-1 (MCP-5 human homologue) and its unique receptor CCR2 are found in arthritic joints. In the present studies we evaluated using *ex vivo* and *in vivo* approaches the effects of MCP-5 embryonic manipulations to the growth plate and ossification center development. In the *ex-vivo* approach, using a micro-injector unit and glycol-chitosan nanoparticles for sustained protein release, either MCP-5 protein or MC-21 antibody (against CCR2) were injected into the developing joints of dissected E13.5 WT or Tbr2PRX-1KO limbs respectively, that were cultured for 2 days. In the *in-vivo* approach, pregnant females potentially generating Tbr2PRX-1KO, were treated with RS504393 (CCR2 inhibitor) starting at E11.5 (4mg/Kg/day, PO). At E18.5 mice were sacrificed. Release of MCP-5 into developing WT joints abolished Ihh spatial distribution within the developing growth plate and decreased Col10 expression. Blockage of the CCR2 signaling in Tbr2PRX-1KO and WT mice either *ex-vivo* or *in-vivo*, led to a rescue of the Tbr2PRX-1KO growth plate phenotype restoring Ihh, Col10 and Col1 expression patterns; in the WT determined an increase in Col10 by hypertrophic chondrocytes and Col1 in the ossification center. Our data indicate that a correct spatial distribution of MCP-5 in the interzone and adjacent developing bone is crucial for the progression of growth plate chondrocytes to hypertrophy and the correct ossification of the mineralization center. Our findings, by providing evidence for a new role for MCP-5/TGF β R11 signaling as a key regulator in the interplay between articular cartilage and developing bone, open novel prospective for their function in adult joint-skeletal homeostasis and for the prevention and treatment of arthritis.

Disclosures: Lara Longobardi, None.

1127

Precise 3D Localisation of a Cortical Thinning Defect Associated With Femoral Neck Fracture in Life. Kenneth Poole^{*1}, Graham Treece¹, Paul Mayhew¹, Martin Horak², Jan Stepan³, Andrew H Gee¹. ¹University of Cambridge, United Kingdom, ²Bulovka Hospital, Czech Republic, ³Charles University, Czech Republic

Thinning of the proximal femoral cortex with ageing and osteoporosis is considered a cause of fracture and a modifiable target for bone active treatment. We applied a novel 3D cortical thickness mapping technique to ordinary clinical CT scans in order to discover whether femoral cortical bone in patients with an acute hip fracture was thinner than femoral cortical bone from community dwelling controls without fracture. The technique allowed us to pinpoint systematic differences and visualise the magnitude of the differences with a colour map displayed on an average femur model.

In a case-control study, we analysed Siemens CT scans from 75 women volunteers with acute fracture and 75 age-matched controls from the Prague Study of Hip Joint in Trauma. We classified the fracture location as femoral neck or trochanteric before creating cortical thickness maps of the unfractured contralateral hip. After non-rigid registration to an average femur shape and statistical parametric mapping, we were able to pinpoint statistically significant foci of cortical thinning associated with each fracture type.

The cortex was approximately 10% thinner in fracture cases than controls throughout the femur. More remarkably, there were several distinct foci of statistically significant ($p < 0.02$) thinning of up to 30% which coincided anatomically with stereotypical fracture sites (femoral neck or trochanteric, fig. 1). The focal thinning of the head-neck junction associated with femoral neck fracture (fig. 1a) also coincided with the focus of peak tensile stress in Cristofolini's cadaveric and FE models of spontaneous femoral neck fracture (J Biomech 2007). Taken alongside the 3D density analyses of the whole hip of Li et al (Bone 2009), our results suggest that the DXA 'femoral neck' box ROI could eventually be replaced by more specific, fracture-critical ROIs in risk estimation, diagnostic and treatment strategies.

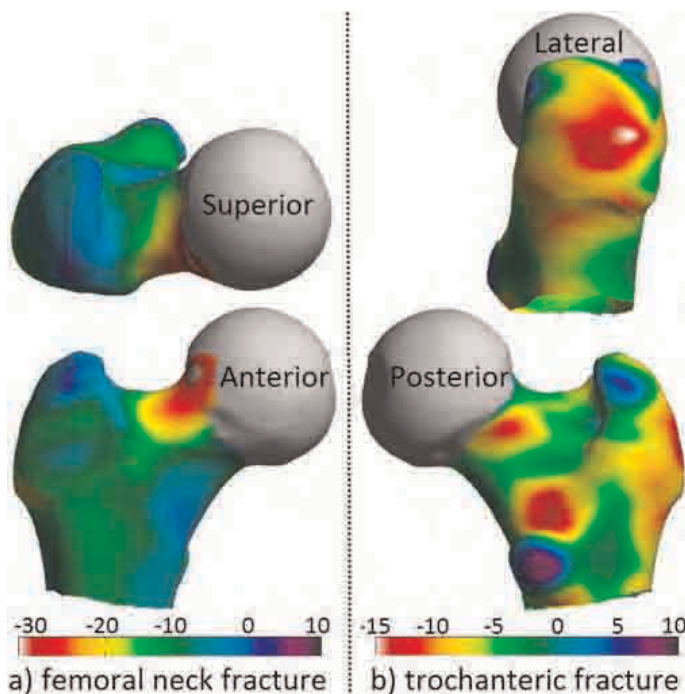


Fig.1. % difference in cortical thickness between controls & fractures (negative=fractures thinner)

Disclosures: Kenneth Poole, None.

1128

Patterns of Prevalent and Incident Vertebral Fracture in the Spine: Differentiating Prevalent Fracture from Deformity. Thomas Fuerst^{*1}, Gabriele von Ingersleben², Chun Wu², Souhila Ounadjela², Pierre Colombel², Jan Szechinski³, Karina Hufert³, Harry Genant⁴. ¹Synarc, Inc., USA, ²Synarc Inc, USA, ³Synarc Inc, Germany, ⁴UCSF/Synarc, USA

Vertebral fracture is a hallmark of osteoporosis signifying both presence of disease and increased risk of future fracture. As such, accurate assessment of prevalent vertebral fracture is critical to clinical practice as well as clinical research. Previous reports have documented the difficulty of differential diagnosis of vertebral fracture

versus deformities of other etiology. We investigated the spatial pattern of prevalent and incident vertebral fracture as a means to assess the validity of prevalent fracture assessment.

Postmenopausal women ($n=7,848$) >60 years old with osteoporosis (spine or hip T-score < -2.5) participating in a clinical trial had spine radiographs at screening and annual follow-up visits. Prevalent and incident vertebral fracture was assessed centrally using the Genant Semiquantitative method. The number of prevalent vertebral fractures at each vertebral level T4 to L4 was determined in total and by each fracture severity. The percentage of fractures at each level was calculated. In a similar fashion incident vertebral fractures over the 3 years of follow-up were counted and summarized.

In total 2,662 prevalent vertebral fractures were identified (80% mild, 17% moderate, 3% severe) compared with 509 incident fractures (42% mild, 38% moderate, 20% severe) found in 373 women. A similar distribution of fracture was seen throughout the spine for both prevalent and incident fracture except in the mid thoracic region (T7-T8) where the rate of prevalent fractures increased to double the rate of incident fractures. Broken down by fracture severity, the patterns were the same with most of the mid-thoracic disagreement explained by differences in the rate of mild fractures.

These data suggest a tendency to over call mild prevalent vertebral fracture in the mid-thoracic region of the spine. This is likely due to chronic stress-induced remodeling with subchondral microfractures or degenerative remodeling at this apex of thoracic curvature. These processes may cause gradual wedging of the vertebral body that mimics mild prevalent fractures. Accurate assessment of prevalent fractures requires careful assessment of these vertebrae for radiographic features indicative of fracture such as endplate bowing or buckling, distinguishing them from non-fracture deformities (Jiang et al, Osteoporosis Int 2004).

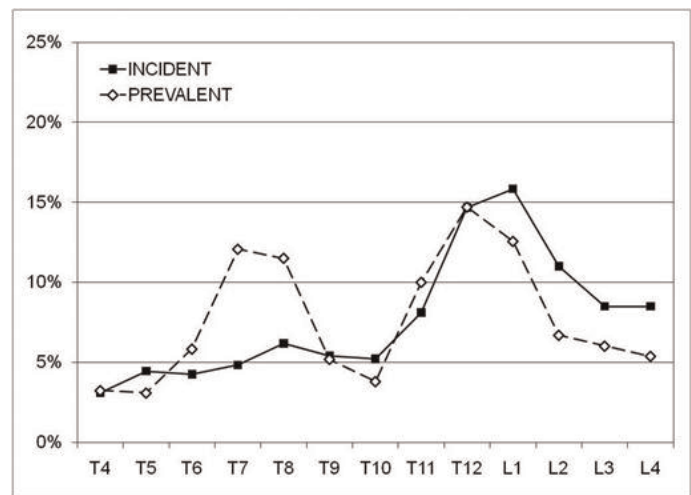


Fig. 1

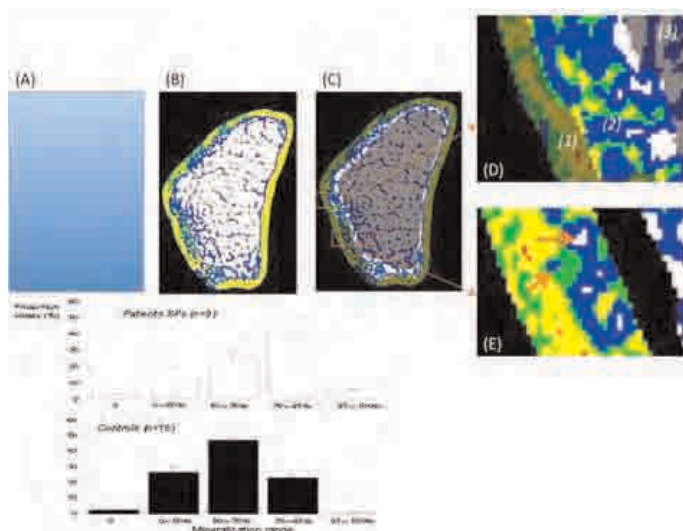
Disclosures: Thomas Fuerst, Synarc Inc, 3

1129

CT Methods That Use Thresholding Throw Out the Baby with the Bath Water. Ego Seeman^{*1}, Roger Zebaze¹, Ali Ghasem-Zadeh¹, Aloys Mbala². ¹Austin Health, University of Melbourne, Australia, ²Strax Corp, Australia

Methods using thresholding to separate cortical and trabecular bone binarize voxels into cortical or trabecular bone based on predefined density thresholds. This introduces errors in assessment of bone structure and its changes during ageing and therapy. Cortices that are thin and porous are discarded because they are below the threshold that nominally defines 'cortical' bone. Regions with high porosity are excluded so porosity is underestimated. At the cortical-trabecular interface, fragmentation of cortices (trabecularization) overestimates trabecular bone density in old age and so underestimates age-related decline in trabecular density. Thresholding also fails to 'see' and so quantify porosity due to small pores (i.e., < 82 microns). Most pores are <100 microns (haversian canals, blue areas in image). Only 10% are >100 microns (white areas). We report that the increase in porosity across age due pores >82 microns is only ~15%. When pores <82 microns are included, porosity increases across age by ~70%.

Segmentation without thresholding overcomes these limitations and allows measurement of tissue mineral density in vivo. Bisphosphonate treatment produces a right shift in the frequency distribution curve reflecting an increase in the proportion of voxels containing predominantly bone and a decrease in proportion of voxels occupied by void (figure). In patients receiving BPs, 55% of the bone is mineralized at 70-95% (yellow voxels), in age-matched untreated peers, mineralization is normally distributed, only 23% of the bone mineralized at 70-95% range. The higher cortical area is due to filling of intracortical pores as voxels within cortex adjacent to marrow fill with bone. The change at the voxel level precedes changes in other morphological parameters and is detected with this new method.



Disclosures: Ego Seeman, None.

1130

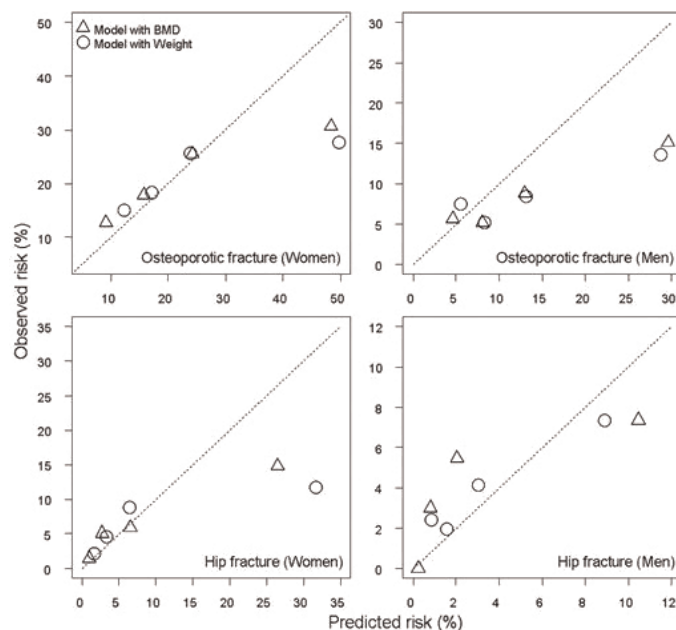
External Validation of the Garvan Nomograms For Predicting Absolute Fracture Risk: the Tromsø Study. Luai A. Ahmed¹, Nguyen Nguyen², Ashild Bjørnerem³, Ragnar M. Joakimsen³, Lone Jørgensen¹, Dana Bliuc², Jacqueline Center², John Eisman², Tuan Nguyen², Nina Emaus⁴. ¹Department of Health & Care Sciences, Faculty of Health Sciences, University of Tromsø, Norway, ²Garvan Institute of Medical Research, Australia, ³Department of Clinical Medicine, Faculty of Health Sciences, University of Tromsø, Norway, ⁴University of Tromsø, 9037 Tromsø, Norway

Absolute risk or individualized prognosis is considered a preferred approach for assessing fracture risk and making treatment decision for an individual. We have developed a prognostic model that uses age, bone mineral density, prior fracture, and fall for predicting absolute risk of fracture (Garvan nomograms). The present study was designed to validate and evaluate the performance of the Garvan nomograms for predicting 10-year risk of fragility fracture in a Norwegian cohort of men and women.

This prospective cohort study in Tromsø, Norway, included 1614 women and 1314 men (aged 60 years plus). Information on the clinical risk factors were collected in the fifth Tromsø survey in 2001. During 8 years follow-up from 2001 to 2009, the incidence of fragility fracture was ascertained by computerized search in the radiographic archives. Non-hip non-vertebral (NHNV) fractures occurred in 350 women and 114 men and 92 women and 49 men suffered a hip fracture. Predicted 10-year probabilities of NHNV and hip fractures were determined using Garvan's models with and without BMD. The concordance between observed and predicted incidence of fracture was used as a measure of fit. Reclassification analysis was used to compare the performance of models.

The overall incidence (per 1000 person-years) of NHNV and hip fracture during the follow-up was 34.6 and 9.1 in women, respectively; and 12.3 and 5.4 in men, respectively. In both sexes, the predicted 10-year probability of fractures in the fracture group was consistently higher than the non-fracture group for all models. For hip fracture, the predicted probabilities of fracture in the fracture group was 2.8 (women) to 3.1 times (men) higher than those in the non-fracture group. There was a close agreement between predicted and actual risk of fracture in both men and women. However, among those in the highest quartile of risk, the model over-estimated the risk of fracture (Figure). Models with BMD + clinical risk factors performed better than models with body weight + clinical risk factors in terms of correct classification of fracture and non-fracture cases in their risk.

In conclusion, the Garvan nomograms are valid and reasonably accurate in identifying individuals at high risk of fracture. Although the nomograms over-predicted the risk of fracture in high risk individuals, its predictive ability at the individual level can potentially be useful in clinical practice.



Concordance between the predicted and observed risk of non-hip non-vertebral (NHNV) fracture (upper panel) and hip fracture (lower panel) in the Tromsø Study cohort, according to the Garvan nomogram. Quartile cutoffs for the predicted 10-year risk (%) of NHNV fracture in women were: 12.8, 19.3 and 30.6 for model with BMD (M1), and 14.7, 20.0 and 29.8 for model with weight (M2). Corresponding features in men were 6.2, 10.1 and 16.9 for M1, and 6.8, 10.2, 16.5 for M2. Quartile cutoffs for the predicted 10-year risk of hip fracture in women were: 1.8, 4.0 and 10.3 for M1 and 2.4, 4.4 and 10.3 for M2. In men, 0.5, 1.3 and 3.2 for M1, and 1.2, 2.1 and 4.3 for M2.

Predicted and observed fracture risk in the Tromsø Study according to the Garvan nomogram.

Disclosures: Luai A. Ahmed, None.

1131

A Long Femur Scan Field does not Substantially Alter Proximal Femur BMD measurements by DXA. Neil Binkley³, Fergus McKiernan¹, Richard Berg², James Linneman², Jane Hocking¹, Susan Cournoyer¹. ¹Marshfield Clinic, USA, ²Biomedical Informatics, Marshfield Clinic Research Foundation, USA, ³University of Wisconsin, Madison, USA

We postulated that a longer DXA femur scan field might be useful for the detection of atypical, subtrochanteric femur fractures. Before implementing this strategy it is necessary to demonstrate that this would not alter BMD measurements made at important diagnostic and monitoring proximal femur sites. 30 adult subjects underwent triplicate measures of FN and TH BMD by DXA using a conventional (i.e., short) and a longer femur scan field after randomization to either a long-short-long or a short-long-short scan field measurement sequence. Simple estimates of the standard deviation between paired long-long and paired short-short scan field BMD studies were 0.011 G/cm² for mean FN and 0.007 G/cm² for mean TH. The difference in mean FN BMD measured from a conventional (i.e., short) versus a long femur scan field was 0.008 G/cm² 0.002 (p=.002). The difference in mean TH BMD measured from a conventional (i.e., short) versus a long femur scan field was 0.004 G/cm² 0.002 (p=.079). Differences in measured BMD between the two scan field lengths were small and less than the precision error inherent in DXA testing. A longer proximal femur scan field does not substantially alter BMD measurements made at the FN or the TH and might be useful in clinical practice as a means of surveillance for the detection of atypical, subtrochanteric femur fractures.

Disclosures: , None.

1132

Postmenopausal Women with Vertebral and Non-vertebral Fragility Fractures Have Marked Differences in Tibial Microarchitecture. Emily Stein¹, Thomas Nickolas², Adi Cohen², Donald McMahon¹, Xiaowei Liu¹, Mafo Kamanda-Kosseh³, Jeri Nieves⁴, Felicia Cosman⁴, X Guo³, Elizabeth Shane¹. ¹Columbia University College of Physicians & Surgeons, USA, ²Columbia University Medical Center, USA, ³Columbia University, USA, ⁴Helen Hayes Hospital, USA

Abnormal skeletal microarchitecture predisposes postmenopausal women to fragility fractures. Whether microarchitecture differs between women with vertebral (VFX) and non-vertebral fractures (NVFX) is unknown. We hypothesized that the

pattern of microarchitectural deterioration would be similar in women with VFX and NVFX, but more severe in VFX.

Women with a history of postmenopausal low trauma VFX (n=27), NVFX (n=70), and controls (C; n=120) with no fractures and normal spine x-rays had aBMD of the lumbar spine, total hip, femoral neck, 1/3 radius and ultradistal radius (UDR) measured by DXA. Trabecular (Tb) and cortical (Ct) volumetric BMD and microarchitecture were measured by high resolution peripheral computed tomography (HRpQCT, voxel size ~82 µm) of the distal radius (RAD) and tibia (TIB).

Mean age of subjects was 68.7yrs, 75% were Caucasian. The most common NVFX were wrist (39%) and ankle (26%). Groups were similar with respect to age, race, years since menopause and BMI. Mean T-scores were >-2.5 at all sites and aBMD did not differ from C at any site except the UDR (VFX 9% lower, p<0.02; NVFX 5% lower, p<0.04). In contrast, there were substantial microarchitectural differences among the groups (Table). Compared to C, VFX had smaller Ct and larger Tb area, lower total, Ct and Tb density, lower Ct thickness, lower Tb number and thickness at both radius and tibia. Tb separation and network heterogeneity were greater only at the tibia. NVFX had smaller Ct and larger Tb area, lower total and Tb density at both sites. Tb number was lower, and Tb separation and heterogeneity were substantially greater than C at the radius but did not differ from C at the tibia. Tb thickness was lower only at the tibia. There were no significant differences between VFX and NVFX at the radius. However, at the tibia, VFX had worse Ct and Tb microarchitecture than NVFX, specifically a trend toward lower Ct area, and significantly lower total and Tb density, Ct thickness, Tb number and greater Tb separation and heterogeneity.

In summary, Ct and Tb microarchitecture were substantially worse in women with VFX and NVFX compared to C. At the radius, microarchitectural differences between VFX and NVFX, albeit sizable, were not statistically significant. However, at the tibia, Ct and Tb abnormalities were significantly greater in VFX than NVFX. We conclude that women with VFX have more severe microarchitectural deterioration than those with NVFX, particularly at the tibia.

Microarchitecture in VFX and NVFX compared to C (% difference)

	RAD VFX	TIB VFX	RAD NVFX	TIB NVFX
Ct Area (mm ²)	-13 ¹	-20 ^{2,A}	-7 ¹	-10 ¹
Tb Area (mm ²)	+10	+10 ¹	+5 ¹	+4
Total Density (mgHA/cm ³)	-16 ²	-18 ^{3,B}	-10 ²	-9 ²
Ct Density (mgHA/cm ³)	-4 ¹	-4 ¹	-1	-2
Ct Thickness (mm)	-16 ²	-22 ^{3,B}	-8 ¹	-10 ¹
Tb Density (mgHA/cm ³)	-18 ²	-17 ^{3,B}	-16 ³	-8 ¹
Tb Number (1/mm)	-9 ¹	-17 ^{2,C}	-11 ³	-8
Tb Thickness (mm)	-10 ¹	-8 ²	-4	-7 ¹
Tb Separation (mm)	+12	+15 ^{2,B}	+25 ²	+2
Network heterogeneity (mm)	+15	+32 ^{2,C}	+44 ²	0

¹p<0.05, ²p<0.01, ³p<0.001 vs. C, ^Ap<0.10, ^Bp<0.05, ^Cp<0.01 vs. NVFX

Disclosures: Emily Stein, None.

1133

Effects of Bazedoxifene/Conjugated Estrogens on Bone Mineral Density and Bone Turnover Markers in Postmenopausal Women: A Double-Blind, Randomized, Placebo- and Active-controlled Phase 3 Study. J. Christopher Gallagher¹, Robert Lindsay², Kaijie Pan³, Sebastian Mirkin³, Arkadi Chines³. ¹Creighton University Medical Center, USA, ²Helen Hayes Hospital, USA, ³Pfizer Inc, USA

Bazedoxifene (BZA) combined with conjugated estrogens (CE) is a tissue selective estrogen complex (TSEC) that has been shown to be effective for the treatment of menopausal symptoms and prevention of osteoporosis while ensuring endometrial safety in women with a uterus. In this randomized, double-blind, placebo (PBO)-controlled phase 3 study (Selective Estrogens, Menopause, And Response to Therapy [SMART]-5) of nonhysterectomized postmenopausal women, the 2 primary endpoints were the mean percent change from baseline in lumbar spine bone mineral density (BMD) and the incidence of endometrial hyperplasia (results reported separately). Of 1,843 subjects who were randomized and received ≥1 dose of study drug, 590 (mean age standard deviation [SD], 52.9 y 3.4 y; mean years since last menstrual period SD, 2.5 y 1.5 y) participated in the osteoporosis study. Subjects were randomly assigned to daily oral doses of BZA 20 mg/CE 0.45 mg (n = 135), BZA 20 mg/CE 0.625 mg (n = 154), BZA 20 mg (n = 73), medroxyprogesterone acetate (MPA) 1.5 mg/CE 0.45 mg (n = 70), or PBO (n = 158); mean lumbar spine BMD T-scores at baseline were -0.91, -0.91, -0.82, -0.77, and -0.95, respectively. The mean percent changes from baseline in BMD at the lumbar spine at 12 months are shown below (Table). Significant improvements in BMD were also seen with BZA 20 mg/CE 0.45 mg, BZA 20 mg/CE 0.625 mg, BZA 20 mg, and MPA 1.5 mg/CE 0.45 mg at the total hip, femoral neck, and femoral trochanter versus PBO (Table; P < 0.01 for all). In addition, serum osteocalcin and C-telopeptide levels were significantly reduced with both BZA/CE doses compared with placebo (P < 0.001 for each) and BZA alone (P < 0.01 for each; Table). Both BZA/CE doses were associated with a favorable endometrial safety profile. In conclusion, BZA 20 mg/CE 0.45 or 0.625 mg showed significant improvements in BMD as well as significant reductions in bone turnover markers at 12 months while protecting the endometrium.

Table. Percent Change From Baseline at 12 Months (SMART-5)

	BZA 20 mg/ CE 0.45 mg (n = 135)	BZA 20 mg/ CE 0.625 mg (n = 154)	BZA 20 mg (n = 73)	MPA 1.5 mg/ CE 0.45 mg (n = 70)	Placebo (n = 158)
BMD					
Lumbar spine					
Mean, % (SE)	0.24 (0.29) [†]	0.60 (0.27) [†]	0.07 (0.60) [†]	1.30 (0.19) [†]	-1.28 (0.28)
Total hip					
Mean, % (SE)	0.50 (0.20) [†]	0.89 (0.18) [†]	0.47 (0.27) [†]	0.71 (0.26) [†]	-0.72 (0.18)
Femoral neck					
Mean, % (SE)	-0.07 (0.26) [†]	0.84 (0.24) [†]	0.13 (0.37) [†]	0.52 (0.34) [†]	-1.00 (0.23)
Femoral trochanter					
Mean, % (SE)	1.31 (0.34) [†]	1.57 (0.29) [†]	1.26 (0.44) [†]	1.35 (0.41) [†]	-0.29 (0.29)
Bone turnover markers					
Osteocalcin					
Median, % (I.Q., U.Q.)	-36.46 (-40.77, -31.70) [†]	-37.82 (-46.87, -21.30) [†]	-16.65 (-33.67, 2.17) [†]	-32.79 (-48.70, -13.07) [†]	-5.28 (-19.29, 11.16)
C-telopeptide					
Median, % (I.Q., U.Q.)	-40.86 (-55.71, -24.01) [†]	-40.86 (-63.47, -29.90) [†]	-27.39 (-49.55, 0.73) [†]	-42.84 (-69.17, -28.88) [†]	-5.52 (-30.17, 19.93)

[†]p < 0.001 vs placebo.

[†]p < 0.01 vs placebo.

[†]p < 0.001 vs BZA 20 mg.

[†]p < 0.01 vs BZA 20 mg.

Table

Disclosures: J. Christopher Gallagher, Wyeth Advisory Board, 5; Wyeth, 2
This study received funding from: Pfizer Inc

1134

Results of the ORACAL Trial: A Phase 3 Randomized Trial of the Safety and Efficacy of Orally Administered Recombinant Salmon Calcitonin Tablets in Postmenopausal Women with Osteoporosis. Neil Binkley¹, Michael Bolognese², James Gilligan³, David Krause³. ¹University of Wisconsin, USA, ²Bethesda Health Research, USA, ³Tarsa Therapeutics, USA

BACKGROUND: An oral preparation of recombinant salmon calcitonin (oral rsCT) has previously been shown to be orally bioavailable, safe, and to suppress CTx in short term use. **METHODS:** In this Phase 3, multinational, three-armed, double-blind, double-dummy study, women were randomized 4:3:2 to receive daily 200 µg oral rsCT tablets plus nasal placebo, oral placebo and 200 IU commercially available synthetic nasal salmon calcitonin (nasal ssCT), or placebo-placebo for 48 weeks. All doses were administered at bedtime. Calcium and vitamin D (1000mg/800IU) were provided to subjects for daily use. Major inclusion criteria included vitamin D replete postmenopausal women age ≥ 45 years, with a bone mineral density (BMD) T score ≤ -2.5 at the lumbar spine (LS), femoral neck or total hip, or ≤ 2.0 with a prior vertebral fracture. Replicate DXA scans were obtained at baseline, weeks 24 and 48, and read centrally. The primary efficacy variable was the % change in LS-BMD over 48 weeks in the modified intent-to-treat (mITT) population. Biomarkers of bone resorption (CTx, NTx) and formation (P1NP) were also assessed. **RESULTS:** 565 subjects were enrolled in 6 countries; 411 were in the mITT population and contributed efficacy data, 549 contributed safety data. The mean age was 66.5y and mean LS T score -2.84. The increase in LS BMD are shown in TABLE:

Although powered to show non-inferiority, oral rsCT was superior to nasal ssCT (delta 0.77% [95% CI: 0.09, 1.45], p=0.026). Conclusions for the per-protocol population were similar (delta 1.05% [95% CI: 0.32, 1.78], p=.005). Consistent with the change in BMD, fasting CTx at the exit visit decreased by 29.9%, 11.4% and 11.8% in the oral, nasal, and placebo arms (oral rsCT vs. nasal ssCT: p < 0.001). Tolerability was similar among the groups; the most common adverse events (AEs) in each group were GI; few serious AEs occurred. Most AEs were mild or moderate in severity. Few fractures occurred. **CONCLUSIONS:** After 48 weeks of treatment subjects receiving oral rsCT tablets had an improvement in LS-BMD which was superior to that of subjects receiving nasal ssCT. The efficacy data (i.e., bone turnover markers and BMD) were robust and internally consistent. The safety and tolerability profiles were similar. Oral rsCT has potential to provide an additional oral treatment option for postmenopausal women with osteoporosis.

	N	% Increase LS BMD (SD)	Change From Baseline
Oral rsCT	189	1.53 (3.17)	p < 0.001
Nasal ssCT	140	0.76 (2.91)	p = 0.014
Placebo	82	0.47 (3.21)	p = ns

TABLE

Disclosures: Neil Binkley, Tarsa Therapeutics, 2
This study received funding from: Tarsa Therapeutics

1135

Effects of the Cathepsin K Inhibitor, ONO-5334, on BMD as Measured by 3D QCT in the Hip and the Spine After 2 Years of Treatment. Klaus Engelke¹, Shinichi Nagase², Thomas Fuerst³, Richard Eastell⁴, Harry Genant⁵, Maria Small², Tomohiro Kuwayama², Steve Deacon². ¹Synarc Inc, Germany, ²Ono Pharma UK Ltd, United Kingdom, ³Synarc, Inc., USA, ⁴University of Sheffield, United Kingdom, ⁵UCSF/Synarc, USA

Purpose: To evaluate the efficacy of the Cathepsin K inhibitor, ONO-5334 in a randomized, double-blind, parallel-group study using quantitative computed tomography (QCT).

Methods: 285 post-menopausal female subjects (age: 55-75) with osteoporosis (with no fragility fractures) or osteopenia (with a fragility vertebral fracture) were equally randomized to five study arms: three doses of ONO-5334 (50mg bd, 100 or 300mg qd), placebo (PBO) or alendronate (ALN, 70mg qw). Calcium and vitamin D were given to all subjects. 3D QCT scans of the spine (L1 and L2) and of the proximal femur were taken at baseline after 1 (Y1) and after 2 years (Y2). QCT (exploratory endpoint) analysis was performed for those patients who provided informed consent for this assessment, with MIAF (Medical Image Analysis Framework) in various integral, cortical and trabecular volumes of interest. 120 subjects had baseline and 2 year follow-up femur scans, 118 subjects had baseline and follow-up spine scans.

Results: Percentage BMD changes in total vertebral body of L1 plus L2 and total femur after 12 and 24 months relative to baseline are shown in the table. Vertebral and total femur volume did not change in any treatment. BMD continued to increase in Y2. For 300mg qd ONO-5334 the additional BMD increase between Y1 and Y2 for total, trabecular and cortical BMD in the spine was 68%, 83% and 30%, of the BMD increase observed between BL and Y1. In the femur, results for the neck were very similar to those of the total femur but in the trochanter integral %BMD changes were slightly higher for the ONO-5334 and ALN groups. In all hip regions, trabecular % BMD changes were higher for ONO-5334 50mg, 300mg and ALN groups. Cortical thickness of the hip did not change significantly in any group. For 300mg qd ONO-5334 trabecular and cortical BMD in the femur linearly increased over the two years, total BMD also continued to increase in Y2 but at a slightly lower rate compared to Y1.

Conclusions: After two years of treatment ONO-5334 50 mg bd and 300 mg qd demonstrated similar increases from baseline that were consistently superior to 100 mg qd, mirroring the results seen after one year. Response to ONO-5334 was roughly equivalent to ALN at the spine and at least as great at all compartments in the hip. Moreover, ONO-5334 trended toward larger gains in year 2 compared to ALN. ONO-5334 showed persistent gains over two years in QCT BMD at two important fracture sites with minimal attenuation of effects in the second year of therapy.

Table: Percentage change from baseline in volumetric BMD \pm SD

VCM		Duration of Treatment	PBO	ONO-5334 50mg qd	ONO-5334 100mg qd	ONO-5334 300mg qd	ALN 70mg qd
Total vertebral body	Int BMD	1y	-1.3 \pm 4.2	7.0 \pm 5.1	5.4 \pm 4.6	7.0 \pm 4.8	7.6 \pm 3.3
		2y	-1.4 \pm 8.4	10.3 \pm 5.3	8.9 \pm 6.3	11.7 \pm 5.3	11.1 \pm 4.1
	Trab BMD	1y	-2.0 \pm 6.8	8.4 \pm 7.5	7.3 \pm 7.6	6.8 \pm 6.7	9.0 \pm 5.6
		2y	-0.5 \pm 10.4	12.8 \pm 7.4	13.7 \pm 11.2	12.5 \pm 7.6	12.8 \pm 6.2
	Cort BMD	1y	-1.1 \pm 4.3	5.1 \pm 5.4	3.6 \pm 4.2	5.9 \pm 5.1	6.2 \pm 5.1
		2y	0.7 \pm 3.3	8.9 \pm 5.9	5.6 \pm 4.0	7.7 \pm 6.5	9.5 \pm 5.2
Total femur	Int BMD	1y	-0.6 \pm 2.4	1.2 \pm 2.1	1.7 \pm 2.7	3.2 \pm 3.2	3.4 \pm 2.6
		2y	-0.7 \pm 3.3	4.8 \pm 3.2	3.3 \pm 2.1	5.6 \pm 4.6	4.8 \pm 3.4
	Trab BMD	1y	1.8 \pm 8.9	7.4 \pm 5.6	4.8 \pm 6.3	7.9 \pm 9.5	5.6 \pm 8.1
		2y	1.5 \pm 9.7	12.5 \pm 6.8	10.4 \pm 7.5	10.0 \pm 14.7	11.2 \pm 10.1
	Cort BMD	1y	-0.4 \pm 2.2	1.9 \pm 2.5	1.2 \pm 2.5	1.7 \pm 2.8	2.7 \pm 2.7
		2y	0.3 \pm 2.4	3.0 \pm 2.6	2.1 \pm 3.2	3.4 \pm 4.1	2.9 \pm 3.1

Mean \pm SD, Full Analysis Set was used

Table

Disclosures: Klaus Engelke, Synarc, 3

This study received funding from: Ono UK

1136

Controlled Trial of Two Interventions to Increase Osteoporosis Treatment in Patients with "Incidentally" Detected Vertebral Fractures on Chest Radiographs (NCT00388908). Sumit Majumdar^{*1}, Finlay A. McAlister¹, Jeffrey A. Johnson¹, Debbie Bellerose¹, Kerry Siminoski¹, David Hanley², Quazi Ibrahim¹, Douglas A. Lier¹, Robert G. Lambert¹, Anthony S. Russell¹, Brian H. Rowe¹. ¹University of Alberta, Canada, ²University of Calgary, Canada

BACKGROUND: Most vertebral compression fractures (VCF) are not clinically recognized, investigated, or treated. We conducted a controlled trial in older patients with VCF reported on chest radiographs taken for other reasons and compared usual care (control) with interventions directed at physicians (opinion-leader endorsed evidence summaries and reminders) or physicians+patients (activation with leaflets and telephone counseling).

METHODS: Patients 60 years of age and older discharged home from local Emergency Departments who had VCF reported and were not treated for osteoporosis were allocated to control or physician intervention using alternate-week time series. After 3-months, untreated controls were crossed-over to the physician+patient intervention. Allocation was concealed. Analyses were intent-to-treat. Primary outcome was starting prescription osteoporosis treatment within 3-months. Secondary outcomes were bone mineral density (BMD) testing and the composite endpoint of BMD testing or treatment.

RESULTS: 1315 consecutive patients were screened, 1075 were excluded, and 240 allocated to control (n=123) or physician intervention (n=117). Groups were similar at baseline (average 74 years, 45% female, 50% had previous fractures). Compared with controls, the physician intervention significantly increased osteoporosis treatment (20 [17%] vs 2 [2%], p<0.001), BMD testing (51 [44%] vs 5 [4%], p<0.001), and the composite of BMD testing or treatment (57 [49%] vs 7 [6%], p<0.001; FIGURE). 3-months after untreated controls (n=121) were crossed over to the physician+patient intervention, rates of new osteoporosis treatment, BMD testing,

and composite endpoints were 22%, 56%, and 65%. The physician+patient intervention significantly increased BMD testing or osteoporosis treatment another 16% compared with physician intervention alone (65% vs 49%, p=0.01).

CONCLUSIONS: Even when VCF are reported on chest radiographs, osteoporosis testing or treatment is rarely initiated. An opinion-leader based intervention targeting physicians substantially improved rates of BMD testing and osteoporosis treatment compared to usual care. Somewhat better management was achieved by adding patient activation to the physician intervention.

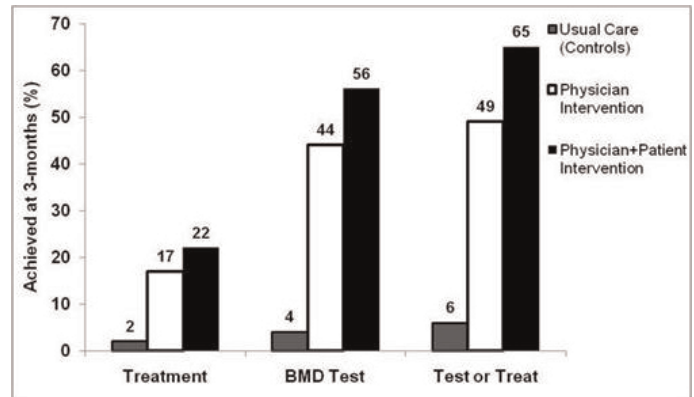


FIGURE: BMD Testing and Osteoporosis Treatment Within 3-Months of the Interventions vs Usual Care

Disclosures: Sumit Majumdar, None.

1137

The 25(OH)D Level Associated With A Favorable Bisphosphonate Response Is >33ng/ml. Amanda Carmel^{*1}, Albert Shieh¹, Richard Bockman². ¹Weill Cornell Medical College, USA, ²Hospital for Special Surgery, Weill Medical College, USA

Background: The results of clinical trials are not always reproduced in the real world setting. The Fracture Intervention Trial with alendronate reported significant increases in hip bone mineral density (BMD) in 97.5% of patients, and a 12% rate of incident fracture. BMD was subsequently shown to be maintained for 10 years. In nearly all drug trials in osteoporosis, supplement use is imposed. Several studies that estimated vitamin D intake suggested that clinical response to bisphosphonates could in part be dependent on circulating vitamin D. This study examined the association between serum 25 hydroxy vitamin D [25(OH)D] level and bisphosphonate response using a composite definition of response. **Methods:** Postmenopausal women with low BMD being treated with > 18 months of bisphosphonates who had at least two dual energy x-ray absorptiometry (DEXA) scans separated by 18-60 months were identified from two ambulatory practices in New York City. Patients were excluded if they had a history of chronic steroid use, metabolic bone disease, or were not compliant with bisphosphonate therapy. Patients were categorized as bisphosphonate non-responders if they had a T score < -3 that persisted between DEXA scans, a > 3% decrease in BMD, or an incident fracture on bisphosphonate therapy, criteria based on the Eurofors trial. Demographic and clinical data including mean 25(OH)D levels between scans were obtained. Mean 25(OH)D levels were compared between responders and non-responders and multiple logistic regression analysis was performed to identify factors associated with non-response. **Results:** A total of 210 patients (mean age 65) with low bone mass (mean femoral neck T-score = -2.0) were included. The mean Charlson comorbidity index was low. Mean duration of bisphosphonate treatment was 63 months. The majority of the patients were Caucasian (83%), approximately half were treated with alendronate, a quarter with risedronate, and ~18% received intravenous zoledronate. Only 99 of 210 patients (47%) had a favorable response to bisphosphonates. Patients with a mean 25(OH)D \geq 33 ng/ml had a 4.5 fold greater odds of bisphosphonate response (estimated OR 4.5, P<0.0001). 25(OH)D level (as a continuous variable) was significantly associated with response to bisphosphonates - 1ng/ml decrease in 25(OH)D was associated with ~ 5% decrease in odds of responding (OR=0.95, 95% CI=[0.92, 0.98], P=0.0007). **Conclusions:** The current study is the first to identify a threshold level of 25(OH)D that defines improved outcome to bisphosphonate therapy such that patients with a mean 25(OH)D \geq 33 ng/ml had a substantially greater likelihood of responding to bisphosphonates. This threshold value of \geq 33 ng/ml for 25(OH)D is higher than the level considered adequate by the Institute of Medicine report for the general population, arguing that higher levels may be required for specific therapeutic outcomes.

Disclosures: Amanda Carmel, None.

Early Detection of Lateral Cortical Lesions in Atypical Subtrochanteric Fracture Using Dual Energy X-ray Absorptiometry (DXA) Hip Images. Kyu Hyun Yang^{*1}, Sungjun Kim², Young-Kyun Lee³, HanKook Yoon⁴, Chang-Wug Oh⁵, Hyeung Keun Song¹. ¹Gangnam Severance Hospital, South Korea, ²Yonsei University College of Medicine Gangnam Severance Hospital, South Korea, ³Seoul National University Bundang Hospital, South Korea, ⁴National Health Insurance Corporation Ilsan Hospital, South Korea, ⁵Kyungpook National University Hospital, South Korea

Purpose: To assess whether DXA hip images, which have been used to measure and monitor the bone mineral density, can be used to depict changes on the lateral cortex of the proximal femur in the patients who take bisphosphonate before atypical subtrochanteric fracture occurs. **Methods:** We retrospectively reviewed the medical records of forty-seven women who sustained atypical subtrochanteric fractures and their latest 52 DXA hip images, which were taken before the fracture, were analyzed. Thirty-three ipsilateral DXA hip images and 19 contralateral ones were available. Mean time of bisphosphonate administration was 5.9 years. Forty one patients took alendronate for prevention or treatment of osteoporosis. **Results:** Among 33 ipsilateral DXA images, diffuse lateral cortical thickening was found in 10 cases and positive focal changes in the lateral cortices were identified in 20 cases. Positive focal changes were external periosteal callus (6 cases), internal medullary callus (11 cases) and combined external-internal lesions (3 cases). Three images were negative. Two of them didn't include the fracture level in DXA hip examination. Mean time gap between positive DXA and ipsilateral fracture was 14.3 months. Hip pain was complained in 14 cases (42%). Mean T score of the total hip BMD was -1.2. The lateral cortical changes of 19 contralateral DXA hip images were as follows: two positive focal changes, 9 diffuse cortical thickening, and 8 negative findings. Detection rate of the focal positive findings on the ipsilateral DXA is significantly higher than on the contra-lateral one ($P<0.001$). **Conclusion:** Vigilance for the aforementioned 4 lateral cortical changes during serial DXA monitoring could help identifying the cortical stress lesions in asymptomatic long-term bisphosphonate users to prevent progression to complete subtrochanteric fracture.

Figure 1. 4 types of lateral cortical change in subtrochanteric area

Figure 2. Cumulative positive rate of DXA hip images and ipsilateral hip pain

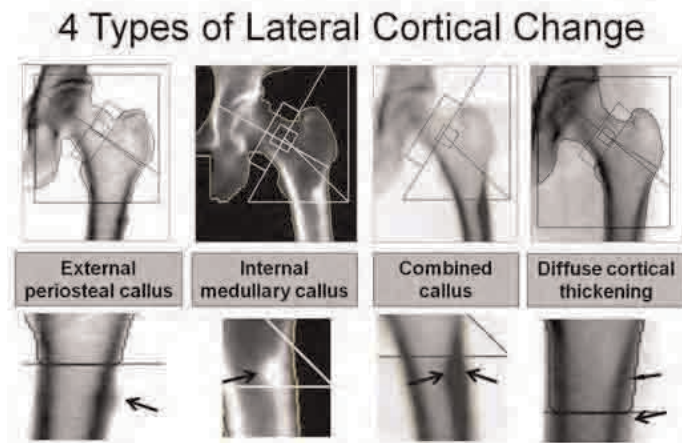


Figure 1. 4 types of lateral cortical change

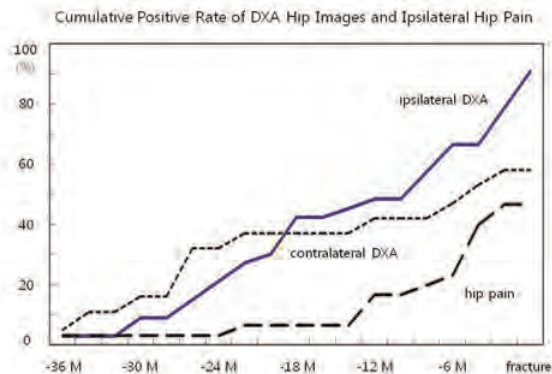


Figure 2. Cumulative positive rate of DXA

Disclosures: Kyu Hyun Yang, None.

Breastfeeding in Infancy and Bone Mass in British Children at 10 and 16 Years of Age. Alexa Gallagher^{*1}, Jihong Liu¹, Jon Tobias², Jim Hussey¹, Charlotte Atkinson², Susan Steck¹. ¹University of South Carolina, USA, ²University of Bristol, United Kingdom

Introduction: Little is known about the role that infant feeding plays on bone health in later childhood. We sought to examine this relationship using data from the Avon Longitudinal Study of Parents and Children (ALSPAC).

Methods: We assessed the relationship between bone measurements taken by total body DXA scans at age 10 [2356 boys, 2415 girls] and infant feeding practice [breastfeeding initiation and duration, as well as feeding type (breast milk only, breast milk and formula, formula only) at 5 months of age]. Analysis of covariance was used to adjust for age at the time of the scan, lean mass, fat mass, height, season of birth, gestational age, birth weight, maternal smoking during pregnancy, maternal education, age at introduction to solid foods, calcium intake at age 11, and physical activity at age 10. Due to significant interactions between sex and the breastfeeding variables at the 0.05 level, results were presented for boys and girls separately. To confirm our findings, the analysis was repeated using total body DXA scans [1425 boys, 1592 girls] taken at age 16.

Results: At age 10, ever breastfed boys had lower bone mineral density (BMD) [β -5.25, $p=0.02$] than never breastfed boys. A similar, but partially attenuated relationship was observed at age 16 [β -4.06, $p=0.40$]. At age 10, each additional month of breastfeeding in boys was associated with a 0.68 g/cm^2 [$p=0.02$] decrease in BMD [age 16: β -0.64, $p=0.31$]. Lastly, compared to boys fed only formula at 5 months, boys fed only breast milk [β -6.50, $p=0.01$] or breast milk and formula [β -4.81, $p=0.03$] had lower BMD at age 10. By age 16, similar, but partially attenuated results were again observed with boys fed only breast milk [β -6.28, $p=0.26$] or breast milk and formula [β -3.19, $p=0.52$] having lower BMD than those fed only formula. In girls, differences were observed only for type of feeding at 5 months. At ages 10 and 16, girls fed only breast milk at 5 months of age had lower BMD [age 10: β -3.83, $p=0.06$; age 16: β -10.07, $p<0.01$] than those who had been fed breast milk and formula.

Conclusion: In late childhood (age 10), boys who were breastfed had lower bone mass than their formula fed counterparts. Partial attenuation of these deficits was evident by late adolescence (age 16). Deficits seen in the bone mass of girls fed only breast milk for 5 months continued to be seen into late adolescence.

Disclosures: Alexa Gallagher, None.

Lumbar Spine Bone Mineral Density Is Enhanced in Breast Fed Infants Receiving 800 or 1200 IU of Vitamin D Daily from 4 to 20 Weeks of Age. Sina Gallo^{*1}, Celia Rodd¹, Catherine Vanstone¹, Sherry Agellon¹, Mary L'Abbe², Ali Khamessan³, Hope Weiler¹. ¹McGill University, Canada, ²University of Toronto, Canada, ³EURO-PHARM INERNAIONAL CANADA INC, Canada

In North America, it is recommended that all breastfed infants be supplemented with 400 IU of vitamin D daily beginning at birth. This recommendation is to prevent deficiency and bone diseases such as rickets. Whether higher doses than the current standard of care would result in optimal bone mineral accrual has not been explored. The primary objective of this study was to determine whether 800 or 1200 IU daily supplementation of vitamin D given to breastfed infants would support higher bone after 8 and 20 weeks compared to 400 IU/day. Healthy, term breastfed infants ($n=116$) from the Montreal area (NCT00381914 clinicaltrials.gov) were randomized to one of 3 study groups of vitamin D3 (400, 800 or 1200 IU) daily beginning between 4-6 weeks of age. This analysis includes all data up to 20 weeks of supplementation, ~6 months of age. At each time point, whole body and lumbar spine (L1-4) bone BMC were measured using dual-energy x-ray absorptiometry (QDR 4500A, Hologic Inc.). Areal BMD for lumbar spine was also examined. Differences were tested using repeated measures ANOVA (by ITT) accounting for within-subject serial correlations as well as baseline parameters. Age did not differ among groups at each time point ($p=0.995$). Treatment dosage interacted with time ($p<0.05$) without main effects. Targeted estimate statements identified differences in comparison to the 400 IU group at 8 and 20 weeks for spine BMD only. Mean values by time and treatment are given below. This data provides promising evidence to suggest that additional vitamin D may be superior for bone growth. Continued evaluation to one year of age will better establish treatment effects on bone development.

	Treatments		
	400 IU/day (n=38)	800 IU/day (n=39)	1200 IU/day (n=39)
Baseline	0.247 \pm 0.026	0.233 \pm 0.027	0.235 \pm 0.026
8 weeks	0.232 \pm 0.007	0.256 \pm 0.008*	0.246 \pm 0.008
20 weeks	0.256 \pm 0.035	0.266 \pm 0.035	0.279 \pm 0.035*

* $p<0.05$ vs. 400 IU/day treatment

Estimated mean lumbar spine (L1-4) BMD SE (g/cm²) at baseline, 8 and 20 weeks of supplementation

Disclosures: Sina Gallo, None.

1141

An Investigation Of Relationships Between Fracture Risk, Total Body DXA And Tibial pQCT Reveals Independent Influences Of Areal And Cortical BMD in Adolescence: Is There a Case For Combining DXA And pQCT In Assessing Fracture Risk?. Adrian Sayers*, Chau Jacky, Kate Tilling, Jon Tobias, University of Bristol, United Kingdom

Introduction: Areal bone mineral density (aBMD) as measured by total body DXA has previously been found to be related to fracture risk in children, particularly when adjusted for body size, possibly reflecting an influence of true volumetric bone density. Cortical BMD is likely to contribute to aBMD, and can be directly measured by pQCT. However, whether DXA and pQCT evaluate equivalent determinants of fracture risk is unknown. To address this question we examined whether, in the Avon Longitudinal Study of Parents and Children, areal and cortical BMD, as measured by total body DXA and pQCT respectively, are independently related with fracture risk.

Methods: Total body DXA and mid-tibial pQCT were linked to fracture history in the preceding three years in 2849 boys and girls mean 15.5 years of age. Fracture risk was investigated using multivariable logistic regression. Relative risk and absolute risk differences were calculated for minimally adjusted (age) and more fully adjusted models (height, fat and lean mass).

Results: In adjusted models aBMD and cortical BMD were both inversely associated with fracture risk: 25.3% reduction in odds of fracture per SD increase in aBMD ($b=0.747$ [95%CI: 0.636, 0.878], $p=0.0004$, $r^2=0.047$); 24.1% reduction in odds of fracture per SD increase in cortical BMD ($b=0.759$ [95%CI: 0.660, 0.874], $p=0.0001$, $r^2=0.048$). In a combined model, although individual associations were marginally attenuated, SD increases in aBMD and cortical BMD were still associated with 19.8% and 20% reductions in odds of fracture respectively ($b_{aBMD}=0.802$, [95%CI: 0.678, 0.949], $p=0.010$ / $b_{cBMD}=0.8$ [95%CI: 0.691, 0.926], $p=0.0029$, $r^2=0.051$). Finally, the absolute risk reduction between lower and upper quartiles of aBMD (-4.5%) and cortical BMD (-4.3%), was significantly improved when both were used in combination (-6.6%) $p<0.001$.

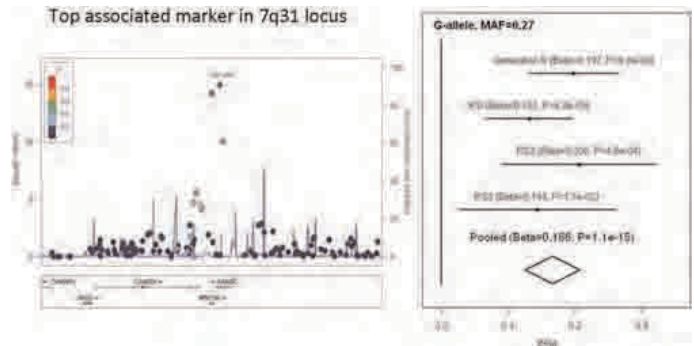
Conclusions: Whereas fracture risk in adolescence is related to both aBMD and cortical BMD, the inclusion of cortical BMD into a DXA based model of risk significantly improves fracture risk prediction, implying that these factors act in part independently. Further studies are justified to examine the utility of combined use of DXA and pQCT to evaluate fracture risk not only in adolescents, but also in older populations.

Disclosures: Adrian Sayers, None.

1142

Variants in *WNT16* are Strongly Associated with Total Body Mineralization in Children of Different Ethnic Background and with Total Body BMD of Elderly Adults. Carolina Medina-Gomez*¹, Karol Estrada², Denise Hepp³, Lizbeth Herrera², Rodinde Bloot², Mette Offerhaus², Ling Oei², Albert Hofman⁴, Vincent Jaddoe³, Paul Eilers⁵, Andre G Uitterlinden², Fernando Rivadeneira². ¹Erasmus Medical Center, The Netherlands, ²Department of Internal Medicine, Erasmus Medical Center, Netherlands, ³The Generation R Study Group, Erasmus Medical Center, Netherlands, ⁴Department of Epidemiology, Erasmus Medical Center, Netherlands, ⁵Department of Biostatistics, Erasmus Medical Center, Netherlands

Aim: Bone Mineral Density (BMD), the major parameter to assess skeletal health is a highly heritable trait. In children, the rapid skeletal changes with growth makes it difficult interpreting BMD. Area-adjusted BMC (aBMC) has been proposed as a measure of mineral content fully independent of skeletal size and so suitable for pediatric studies. We ran a genome-wide association study (GWAS) on aBMC to identify common genetic determinants of bone accrual in children of diverse ethnic background; and replicated findings in 3 studies of Northern European individuals age > 45 years. **Methods:** Subjects are part of the *Generation R* study, a multiethnic birth cohort in Rotterdam, The Netherlands; we included 2,196 children (mean age=6.2, SD=0.28 years) with total body DXA measurements (GE-Lunar iDXA) and GWAS data (Illumina 660K). aBMC was calculated from BMC regressed on total body region area. Replication was pursued in adults from the Rotterdam Study I (RS-I; n=2436), II (RS-II; n=749), and III (RS-III; n=668) with total body BMD and GWAS data (age range 45-95). Analyses were adjusted for age, sex, weight and 20 (children) or 4 (adults) genomic principal components, using PLINK and results meta-analyzed with METAL. A $P<5\times 10^{-8}$ was considered genome-wide significant (GWS). **Results:** Genomic inflation factors were close to unity indicating stratification was controlled. We identified in children a GWS signal ($\beta=0.19$, $P=1.1\times 10^{-8}$) for a SNP mapping to *7q31* near the *WNT16* gene. The association was replicated in all adult studies RS-I ($P=6.3\times 10^{-5}$), RS-II ($P=5.2\times 10^{-4}$) and RS-III ($P=0.02$). The summary effect in the meta-analysis was highly significant ($P=1.1\times 10^{-15}$). **Conclusion:** We robustly show that *WNT16* exerts an effect on bone mineralization in children of different ethnicities and influences total body BMD variation in adulthood. *WNT16* has been shown to be highly expressed in the perichondrium and periosteum of developing long bones, in line with our results suggesting a role of Wnt factors on bone formation throughout life. These early effects of *WNT16* are likely to be influencing the development of peak bone mass and impacting the risk of osteoporosis in later life.



GWS SNP in 7q31 locus

Disclosures: Carolina Medina-Gomez, None.

1143

Racial and Ethnic Disparity in Fracture Risk among Pediatric Populations in the United States. Tishya Wren*¹, John Shepherd², Heidi Kalkwarf³, Babette Zemel⁴, Joan Lappe⁵, Sharon Oberfield⁶, Karen Winer⁷, Vicente Gilsanz¹. ¹Children's Hospital Los Angeles, USA, ²University of California, San Francisco, USA, ³Cincinnati Children's Hospital Medical Center, USA, ⁴Children's Hospital of Philadelphia, USA, ⁵Creighton University Osteoporosis Research Center, USA, ⁶Columbia University Medical Center, USA, ⁷National Institutes of Health, NICHD, USA

Fracture risk is substantially higher in elderly subjects of European descent when compared to other racial/ethnic groups. However, few studies have examined whether similar discrepancies exist in younger subjects. The purpose of this prospective multi-center study was to examine risk factors for fracture in a diverse cohort of healthy, normally developing children in the United States. The study subjects were 1,470 healthy boys and girls of different population ancestry groups, ages 6 to 16 years, who were followed longitudinally for 6 years in the multi-center Bone Mineral Density in Childhood Study (BMDCS). Subjects underwent annual examinations in which height, weight, body mass index (BMI), Tanner stage of sexual development, calcium intake, physical activity levels, and DXA measures of the whole body, lumbar spine, hip, and forearm were obtained. Fracture information was also obtained at each annual visit, and risk factors for fracture were examined using the Cox proportional hazard model.

Overall, 14% of subjects (212/1470) reported a fracture during the 6-year follow-up period, with 2% (36/1470) reporting multiple fracture incidents. The overall fracture incidence was 3.4 fractures per person-year. Most fractures occurred in the upper extremity (166/257, 65%) and during sports or similar activities (185/257, 72%). As expected, the fracture rate was higher for males (131/726, 18%) than for females (81/744, 11%) ($P<0.001$), but unexpectedly fracture rates were also higher for white subjects compared with all other population ancestry groups ($P<0.001$) (Table 1). In multivariable analysis, being white ($HR=2.7$, $P<0.001$) and male ($HR=1.6$, 95% $P<0.001$) were the strongest risk factors for fracture (Table 2). Younger age, more advanced Tanner stage, lower body fat percentage, and greater sports participation were also significant risk factors for fracture. DXA Z-scores and calcium intake did not influence fracture risk.

These results provide compelling evidence that population ancestry is a major determinant of fracture risk in U.S. children. Healthy boys and girls of European descent had 270% greater fracture risk than healthy children of other backgrounds including Hispanics, African Americans, and Asians. In comparison, the difference in fracture risk between boys and girls was 160%. Additional research is needed to identify the phenotypes underlying the greater susceptibility to fractures of the developing skeleton in white children.

Table 2: Risk factors for fracture using the Cox proportional hazard model

	HR	95% CI	P
White	2.75	2.00, 3.77	<0.001
Male	1.57	1.08, 2.27	0.02
Age (yr)	0.88	0.80, 0.95	0.002
Tanner	1.23	1.04, 1.46	0.02
Body fat (%)	0.96	0.94, 0.99	0.005
Sports (days/wk)	1.08	1.00, 1.17	0.03
BMC Z-score, WBLH	0.94	0.81, 1.08	0.37
Calcium (mg/day)	1.00	1.00, 1.00	0.86

WBLH=whole body less head; HR=hazard ratio; CI=confidence interval

Table 2

Table 1: Fracture rates in different population ancestry groups

	N	Fractures	%
White	693	147	21.2
Black	342	24	7.0
Hispanic	247	19	7.7
Asian	104	12	11.5
Mixed/Other	84	10	11.9

Table 1

Disclosures: Tishya Wren, None.

1144

Changes in the Genetic Architecture of Bone Health during Childhood. Dana L. Duren^{*1}, Richard J. Sherwood², Miryoung Lee², Maja Seselj³, Thomas Dyer⁴, Shelley Cole⁴, Roger M. Siervogel³, Stefan A. Czerwinski³, John Blangero⁴, Bradford Towne². ¹Lifespan Health Research Center, Department of Community Health, Wright State University; Department of Orthopaedic Surgery, Wright State University, USA, ²Lifespan Health Research Center, Department of Community Health, Wright State University; Department of Pediatrics, Wright State University, USA, ³Lifespan Health Research Center, Department of Community Health, Wright State University, USA, ⁴Texas Biomedical Research Institute, USA

Skeletal growth and development are directed by both genetic and environmental influences. The environmental envelope surrounding the developing skeleton will change as a child is exposed to novel experiences (diet, exercise, etc.). Likewise, the genetic influences on the growth and development of the pediatric skeleton can change over the course of childhood. We examined the genetic underpinnings of measures of bone health (cortical thickness and biomechanical properties) in three cross-sectional samples of genotyped children participating in the Fels Longitudinal Study representing distinct stages of childhood development: ages 3, 12 and 18 years (n = 359, 442, and 279, respectively). All analyses were conducted using a maximum-likelihood variance decomposition approach in SOLAR with age, sex, and skeletal age as covariates. Quantitative genetic analysis revealed significant heritability of bone measures in each of the three age groups. Heritabilities ranged from 0.47 (section modulus in the 12 year olds) to 0.82 (total cortical bone thickness in the 18 year olds). Suggestive linkages were identified for QTL on chromosomes 6q, 17q and 22p in the 3 year olds; on chromosomes 2p, 6p, 11p and 22p in the 12 year olds; and on chromosomes 1p, 6q, 7q, and 14q in the 18 year olds. A number of these genomic regions contain previously identified candidate genes for bone-related phenotypes (e. g., BMD, osteoporosis), while others include plausible candidate genes that have not previously been identified by population-level linkage or association approaches. Our results demonstrate that pediatric bone health is influenced by genes throughout childhood, and although some genomic regions appear to consistently influence bone health across ages each developmental stage is also characterized by genetic factors that are unique to that time period.

Disclosures: Dana L. Duren, None.

This study received funding from: Supported by NIH grants R01HD056247, R01AR055927, R37MH059490, and R01HD012252.

1145

sFrp4 Differentially Regulates Trabecular and Cortical Bone Mass via Canonical Wnt and Ror2-BMP-Sclerostin Signaling, Respectively. Hiroaki Saito^{*1}, Eric Hesse², Kei Yamana³, Riku Kiviranta⁴, Lynn Neff⁵, Nicolas Solban⁶, William Horne¹, Roland Baron⁷. ¹Harvard School of Dental Medicine, USA, ²Harvard Schools of Medicine & Dental Medicine, USA, ³Teijin Pharma Limited, Japan, ⁴Medical Biochemistry & Genetics & Turku PET Centre, University of Turku, Finland, ⁵Harvard School of Dental Medicine, Oral Medicine, Infection & Immunity, USA, ⁶Accelaron Pharma, USA, ⁷Harvard School of Medicine & of Dental Medicine, USA

Osteoporosis often results from defective osteoblast (OB) function, with Wnt and BMP signaling playing central roles. Secreted Frizzled Related Protein 4 (sFrp4) is a Wnt decoy receptor that represses Wnt signaling. To determine the role of sFrp4 in bone, we established *Sfrp4*-deficient mice. Expectedly, *Sfrp4*^{-/-} and *Sfrp4*^{+/-} mice presented an increased trabecular bone mass (TBV) due to increased OB-dependent bone formation (MAR and BFR). To investigate whether this phenotype resulted from increased canonical Wnt-activity, *Sfrp4*^{+/-} mice were crossed with mice overexpressing the canonical Wnt inhibitor *Dkk1* targeted to OBs (*Dkk1*^{Tg}) and with *Dkk1*^{-/-} mice. *Dkk1*-overexpression in *Sfrp4*^{+/-} mice normalized the increased TBV and *Dkk1*-deficiency aggravated it. In vitro studies revealed an increase in activated

β -catenin in *Sfrp4*^{-/-} OBs and a dose-dependent repression of the Wnt3a-induced TopFlash reporter gene activation by exogenous sFrp4, demonstrating that *Sfrp4*-deletion causes a canonical Wnt-induced increase in TBV. Unexpectedly, cortical bone thickness (CBT) was reduced in *Sfrp4*^{+/-} mice due to a decrease in periosteal and endosteal MAR, which was not affected by gain or loss of *Dkk1* function. Thus, deletion of *Sfrp4* decreases CBT in a canonical Wnt-independent manner. Acting as a Wnt decoy receptor, sFrp4 also regulates the non-canonical Wnt pathway. Indeed, *Sfrp4*^{-/-} OBs demonstrated an increased level of total and phospho-JNK1/2/3. Furthermore, exogenous sFrp4 abolished the Wnt5a-induced activation of the non-canonical Wnt-specific Ror2-luc reporter gene assay, suggesting that in the absence of sFrp4, non-canonical Wnt activity is increased. Further in vitro analysis revealed a non-canonical Wnt-mediated activation of BMP signaling with an increase of p-Smads in *Sfrp4*^{-/-} OBs and an increased expression of the BMP target gene *Id2* in cortical but not in trabecular bone of *Sfrp4*^{+/-} mice. In turn, activation of BMP signaling increased the expression of the canonical Wnt inhibitor Sclerostin (Sost) specifically in the cortex of *Sfrp4*^{+/-} mice and injection of the BMP inhibitor RAP-661 fully reversed the thin cortical bone in *Sfrp4*^{+/-} mice. In conclusion, *Sfrp4*-deficiency 1/ activates canonical Wnt, causing an increase in TBV and 2/ activates non-canonical Wnt, resulting in increased BMP activity and Sost expression thereby reducing cortical bone formation. Thus, non-canonical Wnt signaling activates BMP signaling, exerting a negative effect on cortical bone in mice.

Disclosures: Hiroaki Saito, None.

1146

Conditional Ca²⁺-Sensing Receptor Knockouts in Mature Osteoblasts and Osteocytes Reveal Critical Roles for this Molecule in Maintenance of Bone Mass and Fracture Healing. Wenhan Chang¹, Zhiqiang Cheng¹, Tsui Hua Chen¹, Nathan Liang², Michael You², Alfred Li², Chialing Tu¹, Christian Santa Maria², Dolores Shoback^{*3}. ¹University of California, San Francisco, USA, ²VA Medical Center, San Francisco, USA, ³VA Medical Center, USA

Extracellular Ca²⁺ receptors (CaSRs), which detect changes in extracellular [Ca²⁺] in parathyroid cells, are also expressed in osteoblasts (OBs) and osteocytes (OCs). Conditional knockout of the CaSR in OBs early in differentiation produce severe growth retardation, underdeveloped bones, and early death of the mice (by 4-5 weeks of age). This prevents the assessment of the role of CaSRs at later stages of cell differentiation and in fracture healing in adult animals. To address these questions, we generated mice with homozygous CaSR KO targeted to mature OBs [osteocalcin (OCN)-CaSR-KO] or to OCs [dentin matrix protein (DMP)-CaSR-KO] by breeding floxed CaSR mice with mice expressing Cre recombinase (Cre) under the control of an OCN or DMP promoter, respectively. OCN-CaSR-KO and DMP-CaSR-KO mice developed normally to adulthood. Trabecular (Tb) bones in distal femurs from these mice and control mice (Cont) at 3 months of age were analyzed by micro-computed tomography (μ CT) for bone mineral content (BMC) and structural parameters. BMC as indicated by the Tb bone volume/tissue volume ratio (Tb.BV/TV) was decreased by $\approx 25\%$ in both OCN-CaSR-KO and DMP-CaSR-KO mice in both genders (Table 1), when compared to Cont mice. This was accompanied by decreased Tb connectivity density (CD), number (Tb.N), and thickness (Tb.Th) and increased Tb spacing (Tb.Sp) (Table 1). These data suggest that CaSRs in mature OBs and/or OCs play critical roles in maintaining bone mass in adult animals. To assess the role of CaSRs in fracture healing, we performed mid-shaft tibial fractures on 3-month-old male OCN-CaSR-KO and Cont mice and examined fracture calluses 4 weeks later by histomorphometry and gene expression profiling. In calluses from KO mice, we observed a decreased bone fraction (BV/TV) by $\approx 25\%$, accompanied by a decreased Tb.N and an increased Tb.SP without a change in Tb.Th (Table 2). Double fluorescence-labeled bone sections showed marked decreases in mineralizing surface (MS/BS) and bone formation rates (BFR/BS) in OCN-CaSR-KO vs Cont calluses. Quantitative PCR of RNA extracted from calluses showed decreased expression of early and late osteogenic markers (type I collagen, osteopontin, OCN, DMP, and sclerostin) by 50-75% in KO vs Cont mice, indicating delayed bone cell differentiation. Our data together support a critical role for the CaSR in maintaining bone mass and responding to challenges to skeletal homeostasis in both physiological and pathological states.

Table 1: Structural parameters of trabecular bones in distal femurs by μ CT

	OCN-CaSR	BV/TV (%)	CD (1/mm ³)	Tb. N. (1/mm)	Tb. Th (mm)	Tb. Sp (mm)
Male	Cont	14.6 \pm 1.3	211.1 \pm 28.3	5.28 \pm 0.19	0.045 \pm 0.002	0.19 \pm 0.01
	KO	11.0 \pm 0.9	154.8 \pm 19.4	4.76 \pm 0.23	0.040 \pm 0.001	0.21 \pm 0.01
	p-value*	0.02	0.05	0.05	0.09	0.04
	% Change**	-24	-27	-10	-7	13
Female	Cont	11.23 \pm 0.69	157.3 \pm 15.5	4.64 \pm 0.19	0.043 \pm 0.001	0.22 \pm 0.01
	KO	8.28 \pm 0.46	107.2 \pm 13.7	4.22 \pm 0.16	0.041 \pm 0.001	0.24 \pm 0.01
	p-value*	0.001	0.01	0.05	0.02	0.08
	% Change**	-26	-32	-9	-6	9
	DMP-CaSR	BV/TV (%)	CD (1/mm ³)	Tb. N. (1/mm)	Tb. Th (mm)	Tb. Sp (mm)
Male	Cont	12.6 \pm 1.0	195.8 \pm 21.6	5.38 \pm 0.16	0.042 \pm 0.001	0.19 \pm 0.01
	KO	9.3 \pm 1.4	113.5 \pm 30.8	4.80 \pm 0.22	0.04 \pm 0.002	0.21 \pm 0.01
	p-value*	0.04	0.02	0.02	0.27	0.02
	% Change**	-26	-42	-11	-4	13
Female	Cont	7.75 \pm 0.69	99.6 \pm 13.4	4.16 \pm 0.15	0.040 \pm 0.001	0.25 \pm 0.01
	KO	5.94 \pm 0.38	65.5 \pm 7.1	3.92 \pm 0.09	0.039 \pm 0.001	0.26 \pm 0.01
	p-value*	0.013	0.015	0.08	0.03	0.22
	% Change**	-23	-34	-6	-5	3

*t-test comparing KO to control mice; **% change comparing KO to control mice

Table 1

Table 2: Histomorphometric parameters of trabecular bone in calluses

OCN-CaSR	BV/TV (%)	Tb. N. (1/mm)	Tb. Th (µm)	Tb. Sp (µm)	BFR/BS (µm/day)
Cont	46.4 ± 6.9	7.5 ± 2.9	78.4 ± 30.1	100.7 ± 53.3	1.7 ± 0.3
KO	35.4 ± 4.4	4.4 ± 0.9	81.8 ± 13.0	152.7 ± 38.8	1.0 ± 0.1
p-value*	0.01	0.05	0.40	0.04	0.003
% Change**	-25	-41	-	+52	-41

*t-test KO vs control mice; **% change comparing KO to control mice

Table 2

*Disclosures: Dolores Shoback, None.***1147**

In vivo Multiphoton Imaging of Mesenchymal Stem Cell-Mediated Skeletal Repair. Chunlan Huang, Ming Xue, Xinping Zhang*. University of Rochester Medical Center, USA

Mesenchymal stem cells (MSCs) have demonstrated enormous potential in repair of skeletal defect. Understanding stem cell interactions with their microenvironment is critically important for development of material-based approaches to control stem cell behavior for enhanced repair and regeneration. Current studies to elucidate the mechanisms of interactions of MSCs in a complex in vivo bone healing environment are limited due to the lack of technology and an appropriate animal model that permits dynamic and high-resolution analysis. To overcome this, we have recently established a chronic cranial defect window chamber model in mouse, which permits in vivo real time analyses of cellular recruitment, cell-matrix interactions and vascular ingrowth during skeletal repair. Utilizing multiphoton-laser scanning microscopy (MPLSM) as the imaging platform, we are able to obtain high resolution images to simultaneously visualize extracellular/bone matrix via second harmonic generation (SHG), bone forming cells via fluorescence labeling, and vascular network via intravenously perfusion of dextran-conjugated fluorophore in a dynamic and real-time fashion. Skeletal defect can be further reconstructed in a three-dimensional format, enabling quantitative and qualitative characterization of extracellular matrix synthesis and neovascularization at the cellular level. Using this model, we examined the collagen matrix synthesis, remodeling and neovascularization over a time course of 1 month following implantation of a collagen gel plug encapsulated with bone marrow derived MSCs at the site of the cranial defect. Our data revealed a distinctive pattern of collagen compaction and remodeling by MSCs, which resulted in the formation of a porous matrix template that allows ingrowth of the newly formed blood vessels. In summary, establishment of a multiphoton based image modality in an in vivo cranial defect window chamber model enables high resolution assessment of the interactions of MSCs with fibrous matrix and neovascularization at cellular and subcellular level. With the possibility of using various transgenic animal models, this approach could open up research opportunities to study detailed molecular and cellular mechanisms underlying MSC-based bone repair and regeneration, further offering an experimental testing modality for therapeutic strategies.

*Disclosures: Xinping Zhang, None.***1148**

N-cadherin Interferes with LRP5/6-PTH Receptor Association. Leila Revollo*, Valerie Salazar, Jin Norris, Gabriel Mbalaviele, Roberto Civitelli. Washington University in St. Louis School of Medicine, USA

Recent data indicate that the anabolic effect of PTH is in part mediated by an interaction between PTH receptor (PTH1R) and low-density lipoprotein receptor-related protein 6 (LRP6). Others have shown that N-cadherin interacts with LRP5/6 via axin, resulting in negative regulation of canonical Wnt/ β -catenin signaling. Since we find that the bone anabolic effect resulting from Wnt signaling activation is also dependent on N-cadherin, we hypothesized that N-cadherin may modulate bone cell response to PTH through LRP5/6 signaling. We studied this interaction in vivo and in vitro, using mice with a selective deletion of the N-cadherin gene (Cdh2) in osteoblasts, driven by the 2.3kb Col1 α 1 promoter (Cdh2flox/flox; Col1 α 1-Cre: cKO). Mice were injected with a single dose of PTH1-34 [40ug/kg], and protein preparations were obtained from tibias of cKO and wild type (WT) mice at different time-points. We observed a progressive up-regulation of β -catenin abundance reaching maximal levels 120 min after PTH1-34 injection in WT, while full effect was obtained in cKO after only 60 min. However, abundance of GSK3 α/β and p-GSK3 β did not change in cKO and WT mice. By contrast, p-ERK1/2 was up-regulated in N-cadherin WT mice after a single dose of PTH1-34, and it remained elevated in cKO mice for a longer time. These data suggest non-canonical mechanisms of β -catenin up-regulation in response to PTH. We then used bone marrow stromal cells (BMSC) from cKO and WT mice to further test LRP5/6-PTH interactions. Intriguingly, LRP5 abundance was significantly higher in cKO relative to WT BMSC, corroborating increased LRP5 mRNA and protein in bone lysates from cKO mice. Furthermore, LRP5/6 co-immunoprecipitated with N-Cadherin and PTH1R in MC3T3-E1 mouse calvarial cells. Preliminary studies suggest that PTH increases LRP5/6-N-Cadherin and decreases LRP6-PTH1R association. Surface membrane biotinylation of MC3T3-E1 cells revealed increased levels of N-cadherin at the plasma membrane 30 and 60 min after exposure to PTH1-34. In summary our results provide evidence that the response to PTH may be modulated by N-Cadherin through interference with LRP5/6 abundance at the plasma membrane.

*Disclosures: Leila Revollo, None.***1149**

BMP Type II Receptors Further Stimulate Constitutively Activated Mutant ALK2 found in Fibrodysplasia Ossificans Progressiva. Satoshi Ohte*¹, Hiroki Sasanuma², Masashi Shin¹, Katsumi Yoneyama², Seiya Suzuki², Toru Fukuda³, Shoichiro Kokabu⁴, Takenobu Katagiri². ¹Saitama Medical University, Japan, ²Saitama Medical University Research Center for Genomic Medicine, Japan, ³Keio University School of Medicine, Japan, ⁴Harvard School of Dental Medicine, USA

Bone morphogenetic proteins (BMPs) induce heterotopic bone formation in skeletal muscle. Intracellular signaling of BMPs is activated by binding to type I and type II transmembrane serine/threonine kinase receptors. In the ternary complex, type II receptor phosphorylates an intracellular domain of the type I receptor, and then the activated type I receptor phosphorylates Smad1/5. Fibrodysplasia ossificans progressiva (FOP) is a rare autosomal dominant congenital disorder characterized by progressive heterotopic endochondral bone formation in skeletal muscle. Muscle injury induces acute heterotopic bone formation in FOP. Several mutations in the intracellular domain of ALK2, a BMP type I receptor, have been found in typical and atypical patients with FOP. We found that not only a typical mutation but also other atypical mutations moderately activated phosphorylation of Smad1/5 and a BMP specific Id1-luc reporter. We examined effects of BMP type II receptors on ALK2 because the expression level of BMPR-II was increased at the site induced muscle regeneration in vivo. In the absence of BMPs, co-transfection of Actr-IIB or BMPR-II with one of mutant ALK2 strongly induced phosphorylation of Smad1/5 and ALP activity in C2C12 cells. Wild-type BMPR-II, but not a kinase activity-deficient BMPR-II, phosphorylated ALK2. That was higher in wild-type ALK2 than that in a typical FOP mutant ALK2. Interestingly, the kinase activity-deficient BMPR-II still stimulated biological activities of some types of FOP mutant ALK2, suggesting that a novel mechanism in addition to phosphorylation is involved in the activation of ALK2 by BMPR-II. Taken together, these results suggest that moderately activated mutant ALK2 are further stimulated by BMP type II receptors in FOP. Inhibitors of BMP type II receptors as well as that of ALK2 may aid in the establishment of novel treatments to prevent heterotopic ossification in FOP.

*Disclosures: Satoshi Ohte, None.***1150**

In Vivo Effect of Bone-Specific EphB4 Overexpression in Mice on Subchondral Bone and Cartilage during Osteoarthritis. Gladys Valverde-Franco*¹, Mohit Kapoor¹, David Hum¹, Koichi Matsuo², Bertrand Lussier³, Jean-Pierre Pelletier¹, Johanne Martel-Pelletier¹. ¹Osteoarthritis Research Unit, University of Montreal Hospital Research Centre (CRCHUM), Canada, ²School of Medicine, Keio University, Japan, ³University of Montreal, Faculty of Veterinary Medicine, Clinical Sciences, Canada

Background: In humans, evidence suggests subchondral bone to be an active component of the osteoarthritis (OA) process. Some members of the ephrin system, including the receptor EphB4 and its specific ligand, ephrin-B2, were found to be involved in bone biology. Recently, our group¹ showed that in vitro ephrin-B2 activation of the EphB4 receptor inhibits the resorptive activity of human OA subchondral bone osteoblasts. We further investigated, in mice, the in vivo effect of bone-specific EphB4 overexpression on OA development.

Methods: Morphological evaluation of the mouse skeleton was performed at postnatal day 5 (P5) with alizarin red/alcan blue staining and, in adults, radiographically. On the OA induced knee, histology (OARSI grading), cartilage collagen meshwork disorganization grading (sirius red staining), and micro-computed tomography scans (microCT) were performed on the medial compartment.

Results: Homozygous conditional type I collagen EphB4 overexpressing mice and wild type (WT) were used. Morphometric analysis and skeletal staining at P5 showed no obvious phenotypic difference in bone development between EphB4 and WT mice. Although 10-week-old WT and EphB4 mice had similar body size and bone length, EphB4 mice demonstrated increased bone density. OA was induced, using the partial medial meniscectomy (DMM) model, in the 10-week-old mice. Eight and 12 weeks after surgery, histology revealed EphB4 mice had significantly less articular alterations than WT in both medial condyle and tibia at 8 (4.90.1 vs. 3.10.4, p<0.008; 3.40.3 vs. 2.10.3, p<0.0009, respectively) and 12 weeks (3.40.3 vs. 2.40.30, p<0.04; 4.50.3 vs. 3.30.4, p<0.04) post-surgery. Evaluation of collagen fibril revealed significantly higher levels of disorganization in WT mice compared with EphB4 mice in the tibia at 8 (2.40.4 vs. 1.10.2, p<0.0007) and 12 weeks (2.30.2 vs. 1.10.1, p<0.0003) post-surgery. In addition, microCT of the medial tibia performed 12 weeks after surgery demonstrated a decrease in sclerotic subchondral bone in EphB4 compared with WT mice.

Conclusion: This study is the first to provide in vivo evidence that bone-specific EphB4 receptor overexpression exerts a protective effect on structural changes that occur in OA articular cartilage and subchondral bone. These data also support the notion that this system could be targeted as a specific therapeutic approach for OA.

Reference: 1. Kwan Tat S, et al. Arthritis Rheum 2008;58:3820-30.

Disclosures: Gladys Valverde-Franco, None.

1151

Functional Redundancy of GSK-3 α and GSK-3 β to Control Chondrocyte Differentiation through Phosphorylation of RelA/NF- κ B p65. Shozo Itoh^{*1}, Taku Saito², Makoto Hirata³, Masahiro Ushita³, Toshiyuki Ikeda⁴, Kozo Nakamura¹, Ung-Il Chung⁵, Hiroshi Kawaguchi⁶. ¹The University of Tokyo, Japan, ²University of Tokyo, Graduate School of Medicine, Japan, ³University of Tokyo, Japan, ⁴Information Technology Services, Inc., Japan, ⁵University of Tokyo Graduate Schools of Engineering & Medicine, Japan, ⁶University of Tokyo, Faculty of Medicine, Japan

Several principal signals in chondrocytes are mediated by glycogen synthase kinase-3 (GSK-3). Here we examined individual roles of the two mammalian isoforms, GSK-3 α and GSK-3 β , in chondrocyte differentiation and skeletal development. Both isoforms were largely unphosphorylated and active in the early differentiation stages during SOX9, type II collagen (COL2A1), and aggrecan expression in cultured chondrogenic ATDC5 cells and in the mouse limb cartilage. Although *Gsk3a*^{-/-} mice and *Gsk3b*^{+/-} mice showed normal skeletal development, their compound *Gsk3a*^{-/-};*Gsk3b*^{+/-} mice exhibited dwarfism with impairment of early chondrocyte differentiation without affecting the later differentiation or proliferation. Gain- and loss-of-function analyses using cultures of ATDC5 cells and primary chondrocytes from the knockout mice with overexpression of GSK-3 isoforms and their siRNAs revealed that GSK-3 α and GSK-3 β induced early chondrocyte differentiation with functional redundancy in a cell-autonomous fashion. This was independent of the canonical Wnt signaling, since none of the transcriptional activity (TOPflash), protein level, nor subcellular localization of β -catenin was altered by the *Gsk3* genotypes. Instead, computational predictions followed by *SOX9* and *COL2A1* promoter assays identified RelA (NF- κ B p65) as a key phosphorylation target of GSK-3, and further analyses by mutagenesis in the 12 putative phosphorylation sites of RelA revealed that the Thr254-phosphorylation was essential for GSK-3 to induce chondrocyte differentiation. The gain- and loss-of-function analyses above showed that GSK-3 α and GSK-3 β caused the Thr254-phosphorylation in early differentiation stages without affecting the RelA protein level, subcellular localization, I κ B phosphorylation, or IKK level. The Cre-mediated deletion of RelA in the *Rela*tm chondrocyte culture caused suppression of the early differentiation markers, which was restored by the RelA overexpression, but not by the Thr254 mutant or the GSK-3 overexpression. Lastly, we created conditional knockout mice of *Rela* in undifferentiated limb mesenchyme (*Prx1*-Cre;*Rela*tm) and in cartilage (*Col2a1*-Cre;*Rela*tm), and confirmed that both mouse models exhibited dwarfism with impairment of early chondrocyte differentiation, similar to the *Gsk3a*^{-/-};*Gsk3b*^{+/-} mice. In conclusion, the redundant functions of GSK-3 α and GSK-3 β through phosphorylation of RelA at Thr254 play a crucial role in early stages of chondrocyte differentiation.

Disclosures: Shozo Itoh, None.

1152

Runx2 Regulates Axin2 Modulation of Mesenchymal Stem Cell Fate in Cranial Sutures. Meghan McGee-Lawrence^{*1}, Amel Dudakovic¹, David Razidlo¹, Wei Hsu², Jane Lian³, Jennifer Westendorf¹. ¹Mayo Clinic, USA, ²URMC, USA, ³University of Massachusetts Medical School, USA

Runx2 and Axin2 are key regulators of skeletal development. Deletion of either gene causes craniofacial phenotypes in mice: Runx2^{+/-} mice develop cleidocranial dysplasia (CCD), whereas Axin2^{-/-} mice develop craniosynostosis. We discovered that Axin2 and Runx2 molecularly interact in ChIP, EMSA, and transcription assays, suggesting a direct relationship between these two factors in vivo. To determine if Axin2 and Runx2 are components of the same molecular pathway, we crossed Runx2^{+/-} and Axin2^{-/-} mice to generate Axin2^{-/-};Runx2^{+/-} mice. Axin2 deficiency reduced skull length and increased skull width, whereas Runx2^{+/-} mice were normal. Axin2^{-/-};Runx2^{+/-} mice skull dimensions fell between those of the single mutants, suggesting Runx2 is essential for enhanced calvarial bone formation in Axin2^{-/-} mice. Consistent with this hypothesis, bone marrow stromal cells (BMSC) from Axin2^{-/-} mice expressed mature osteoblast markers (e.g., osteocalcin) at high levels, whereas BMSC from Axin2^{-/-};Runx2^{+/-} mice had expression levels similar to wildtypes when cultured under osteogenic conditions.

Surprisingly, Axin2 deficiency did not rescue, but rather exacerbated the CCD phenotype of the Runx2^{+/-} mice as fontanel size increased two-fold in Axin2^{-/-};Runx2^{+/-} as compared to Runx2^{+/-} mice. MicroCT revealed that the endocranial layer of the posterior frontal (PF) suture failed to ossify in the double mutants. We performed mRNA and miR microarrays with calvarial RNA and found genes related to cartilage development (e.g., Aggrecan, Sox9 and miR140) were upregulated in Axin2^{-/-};Runx2^{+/-} mice, whereas genes related to blood vessel morphogenesis (e.g., Slit2) were downregulated. Histomorphometry of the PF suture revealed cartilaginous and fibrous tissues but no calcified bone in the enlarged fontanel of the double mutants.

In conclusion, Axin2 expression modulates mesenchymal stem cell fate. In the endocranial layer of the PF suture, decreasing Axin2 expression triggers formation of cartilage that is subsequently vascularized and ossified. Axin2^{-/-} mice rapidly close the PF suture due to enhanced Wnt signaling that accelerates endochondral ossification. Our data suggest that Runx2 regulates this process, since Runx2 haploinsufficiency on

the Axin2^{-/-} background increased chondrogenesis but decreased ossification in the PF suture. Downregulation of blood vessel gene expression likely reflects impaired vascularization of this cartilage, leading to defective calvarial ossification.

Disclosures: Meghan McGee-Lawrence, None.

1153

PTHrP Regulates the Modeling of Cortical Bone and Ligament and Tendon Insertion Sites During Linear Growth. Joshua VanHouten^{*1}, Randy L. Johnson², Guoying Liang³, Arthur Broadus¹. ¹Yale University School of Medicine, USA, ²M.D. Anderson Cancer Center, USA, ³Yale University, USA

PTHrP is widely expressed in the fibrous periosteum (PO) and in tendon and ligament insertion sites (entheses). In most such sites, PTHrP is mechanically-induced and is temporally associated with subadjacent osteoclast (OC) and/or osteoblast (Ob) populations. We tested here the working hypothesis that PTHrP might regulate the modeling of cortical bone and/or entheses by conditionally deleting PTHrP using scleraxis sequences (Scx-Cre); Scx is a bHLH transcription factor that is expressed in the fascia and connective tissues that bind bone and muscle together and to each other. A PTHrP-lacZ null allele enabled lacZ to speak for PTHrP gene expression in both KO and CT mice.

The Scx-KO mice display two types of abnormalities, one involving entheses and the other cortical size and shape. Of the enthesis abnormalities, the medial collateral ligament (MCL) insertion is particularly informative. The MCL inserts into the proximal tibial metaphysis below the growth plate, so that it must migrate during linear growth. PTHrP is load-driven and highly expressed at this site, and the migration is mediated by OCs at the migrating edge and Obs at the trailing edge. In the Scx-KO mice, these bone cell populations do not form, migration fails, and the MCL site is converted into a massive traction tuberosity that distorts the entire proximal tibia. Similar traction abnormalities are seen at the origins or insertions of the lateral triceps, pronator teres, and tibialis posterior, all muscles that are heavily engaged in the mouse because it walks on pronated and flexed limbs. Each of these sites is concordant as regards lacZ expression in PTHrP-lacZ and Scx-Cre/R26R mice.

All adult Scx-KO long bones are foreshortened (e.g., KO vs CT humeri 11.7 0.3 vs 10.4 0.4 mm, n=7, M SD, p<0.001). The bones are also squat, with an increase in moment of inertia (KO vs CT humeri 0.29 0.02 vs 0.23 0.01 mm⁴, M SEM, n=3, <0.05) but normal cortical thickness (0.22 0.01 vs 0.21 0.01, pNS). The PO in the metaphyses of some of these bones are concordant as regards lacZ expression in PTHrP-lacZ and Scx-Cre/R26R mice, suggesting that PTHrP regulation of cortical modeling may be responsible for this phenotype.

These data provide the first genetic evidence that PTHrP regulates the formation and function of membranous bone cell populations at the surface of long bones. These functions reflect the use of PTHrP as a tool by which mechanical forces sculpt cortical bone.

Disclosures: Joshua VanHouten, None.

1154

Deficiency of EED, a Critical Component of the Polycomb Repressor Complex 2, Causes Cell Death Due to Competitive Inhibition of HIF1 α by aryl Hydrocarbon Receptor in Chondrocytes. Erinn Rankin¹, Jennifer Inloes², Huafeng Xie³, Stuart Orkin³, Ernestina Schipani⁴, Tatsuya Kobayashi^{*2}. ¹MGH, USA, ²Massachusetts General Hospital, USA, ³Children's Hospital Boston & Dana-Farber Cancer Institute, USA, ⁴Indiana University School of Medicine, USA

Chromatin structure, regulated largely through histone tail modifications, controls gene expression by changing accessibility of transcription factors. This mechanism ensures robustness of gene expression patterns and cells' phenotypes. Polycomb repressive complex 2 (PRC2), whose core components include EZH1/2, EED and SUZ12, catalyzes tri-methylation of lysine 27 of histone 3 (H3K27me3) and silences chromatin. PRC2 binds to and regulates genomic loci containing key differentiation-related genes in ES cells and plays an essential role in ES cell pluripotency. However, the physiological role of PRC2 in somatic cells, let alone skeletal cells, remains unclear. To investigate the role of PRC2 in mouse skeletal development, we ablated the EED gene in chondrocytes. EED conditional knockout (cKO) mice were born and survived postnatally, but developed growth retardation and kyphosis, and the mice usually died before weaning. EED cKO growth plates showed a dramatic decrease in cell proliferation and increase in cell death, reminiscent of growth plates missing hypoxia-inducible factor 1 alpha (HIF1A), but showed normal cell differentiation patterns. We found that HIF-inducible genes, including *Pgk1* and *Bnip3* were downregulated in EED cKO chondrocytes. We found that HIF-inducible genes, including *Pgk1* and *Bnip3*, were downregulated in EED cKO chondrocytes. Downregulation of HIF1 activity was confirmed in primary chondrocytes using a reporter assay. In addition to known PRC2 target-genes including *Bmp4* and *Left1*, we found upregulation of aryl hydrocarbon receptor (AHR) in EED cKO chondrocytes. We found increased expression in EED cKO chondrocytes of AHR target genes, including *Cyp1b1*. Upregulation of AHR activity in EED cKO chondrocytes was confirmed using an AHR reporter assay. The aryl hydrocarbon receptor nuclear translocator, ARNT, binds both HIF's and AHR. Chromatin immunoprecipitation revealed increased ARNT binding to the *Cyp1b1* promoter and decreased binding to

HIF target genes, suggesting that HIF activity was, at least in part, competitively inhibited in EED cKO chondrocytes by AHR. The AHR gene was not associated with H3K27me3, and therefore the upregulation of AHR is likely an indirect consequence of deregulated gene expression caused by the loss of PRC2 function. These results demonstrate the critical role of PRC2 function in chondrocyte proliferation and survival, and provide evidence for the reciprocal regulation of HIF's and AHR *in vivo*.

Disclosures: Tatsuya Kobayashi, None.

1155

The Transcription Factor Arid5B Is a Novel Partner of Sox9 in Endochondral Bone Formation. Rikako Takashima^{*1}, Kenji Hata¹, Makoto Wakabayashi¹, Masako Nakanishi¹, Koichiro Ono¹, Katsuhiko Amano¹, Robert Whitson², Yoshinobu Maeda¹, Riko Nishimura¹, Toshiyuki Yoneda¹. ¹Osaka University Graduate School of Dentistry, Japan, ²Beckman Research Institute of City of Hope, USA

The transcription factor Sox9 plays an essential role in chondrocyte differentiation. Mutations of Sox9 gene in human cause severe chondrodysplasia and chondrocyte specific Sox9-deficient mice exhibited profound skeletal malformations. Furthermore, Sox9 overexpression in the pluripotent mesenchymal C3H10T1/2 cells up-regulates chondrocyte phenotypic genes including Col2a1. However, introduction of Sox9 in some mesenchymal cells such as NIH3T3 cells failed to induce chondrogenesis, suggesting that C3H10T1/2 cells express a transcription factor (s) which is required for Sox9-dependent chondrogenesis. Based on this hypothesis, Solexa sequencing was performed to compare gene expression profiles between C3H10T1/2 and NIH3T3. As a result we found the transcription factor Arid5b (AT-rich interactive domain 5b) is highly expressed in C3H10T1/2 cells. Whole mount *in situ* hybridization demonstrated a discernible expression of Arid5b mRNA in the developing limbs where Col2a1 and Sox9 were specifically localized. More importantly, Arid5b deficient mice (Arid5b^{-/-}) showed pronounced growth retardation at birth and postnatal stage. Arid5b^{-/-} mice also exhibited shortened limbs with decreased width of proliferating chondrocytes. These data suggest that Arid5b is critical for chondrogenesis.

We next further verified the functional role of Arid5b in chondrocyte differentiation. Overexpression of Arid5b in C3H10T1/2 cells using adenovirus system enhanced Sox9-induced Col2a1 mRNA expression, although Arid5b had no effect on Sox9 expression. Of interest, transcriptional activity of Sox9 on Col2a1 gene promoter activity was markedly up-regulated by Arid5b. Pull-down and two-hybrid analyses showed that Arid5b physically associated with Sox9. Direct binding of Arid5b to the AT-rich motif (CATAT) present in the Col2a1 gene promoter was shown by DNAP and ChIP experiments and the mutation of this element caused the reduction of Sox9-induced Col2a1 promoter activity. Moreover, overexpression of dominant-negative mutant (DN) Arid5b inhibited BMP2-induced chondrocyte differentiation of mouse embryo limb bud cells. Consistently, DN-Arid5b transgenic mice driven by the Prx-1 gene promoter showed delayed endochondral ossification and reduced Col2a1 mRNA expression. In conclusion, our results suggest that Arid5b promotes chondrocyte differentiation as a transcriptional partner of Sox9 and provide further insights into the molecular mechanism by which Sox9 regulates chondrogenesis.

Disclosures: Rikako Takashima, None.

1156

Direct Role of Nkx3.2 to Promote the Primary Chondrocytic Differentiation. Yoshitaka Kawato^{*1}, Makoto Hirao², Kosuke Ebina¹, Hiroki Oze¹, Shoichi Kaneshiro¹, Kenrin Shi¹, Akira Myoui³, Hideki Yoshikawa¹, Jun Hashimoto⁴. ¹Osaka University Graduate School of Medicine, Japan, ²Department of Orthopaedics, National Hospital Organization Osaka Minami Medical Center, Japan, ³Osaka University Hospital, Japan, ⁴Center of Immune Diseases, National Hospital Organization Osaka Minami Medical Center, Japan

Nkx3.2 is known to be a novel transcriptional factor to repress Runx2 function, leading to down-regulation of hypertrophy of chondrocyte. Spondylo-megaepiphyseal-metaphyseal dysplasia (SMMD) is a skeletal dysplasia, which shows metaphyseal dysplasia, markedly defective ossification of vertebral body centres, and enlarged epiphyses. SMMD is caused by homozygous inactivating mutations in the NKX3.2. The phenotypes observed in SMMD patients are very similar to that of Nkx3.2 knockout mice. On the other hand, it is also pointed out that Nkx3.2 has a tight relationship with Sox9 in a positive regulatory system initiated by Shh. Then, we hypothesized that Nkx3.2 might have a direct and positive role for primary chondrocytic differentiation. C3H10T1/2 cells were cultured with 300ng/mL of BMP2 to induce endochondral ossification. Overexpression of WT-Nkx3.2 up-regulated the expression of chondrogenic marker genes, such as Col2a1, Aggrecan, Comp, Col11a2, Col10a1, and Sox9, furthermore glycosaminoglycan (GAG) production was also promoted. On the other hand, down-regulation of Nkx3.2 using RNAi system strongly inhibited these genes expression and GAG production. Interestingly, Nkx3.2 affected on such chondrogenic events before the effect on Sox9 gene expression was observed. This phenomenon led us to consider that Nkx3.2 might also have a direct role to promote early chondrocytic differentiation independently of Sox9. To elucidate this hypothesis, we checked whether Nkx3.2 binds to the enhancer

elements of chondrogenic marker genes, Col2a1, Aggrecan, and Col11a2, using luciferase reporter assay and ChIP assay. WT-Nkx3.2 up-regulated the activity of 48bp-Col2a1 enhancer element about 10 fold compared to MOCK both in C3H10T1/2 and N1511 cells. And the activity was clearly stimulated in a dose dependent manner. ChIP assay revealed that Nkx3.2 directly binds to Col2a1, Aggrecan, and Col11a2 enhancer elements. Taken together, it is suggested that Nkx3.2 also has a direct role to promote early chondrocytic differentiation.

Disclosures: Yoshitaka Kawato, None.

1157

OC-STAMP and DC-STAMP are both essential for cell-cell fusion in osteoclasts and foreign body giant cells. Kazuhiro Chiba¹, Hiroya Miyamoto^{*2}, Takeshi Miyamoto³, Yoshiaki Toyama¹, Hideo Morioka¹. ¹Department of Orthopedics, University of Keio, Japan, ²University of Keio, Japan, ³Keio University School of Medicine, Japan

Osteoclasts are unique cells to resorb bone and play a role in regulating bone homeostasis. Osteoclast multi-nucleation by cell-cell fusion plays a role in regulating osteoclast resorbing activity and physiological bone mass, and that we tried to clarify the molecular mechanism of osteoclast cell-cell fusion. We identified osteoclast stimulatory transmembrane protein (OC-STAMP) by a subtractive microarray screen between M-CSF induced mono-nuclear macrophages and M-CSF plus RANKL induced multi-nuclear osteoclasts. We generated OC-STAMP-deficient (KO) mice and found that osteoclasts cell-cell fusion was completely abrogated in OC-STAMP KO mice. OC-STAMP KO mono-nuclear osteoclasts demonstrated normal expression of TRAP, NFATc1 and CathepsinK, indicating that OC-STAMP is specifically required for cell-cell fusion rather than differentiation of osteoclasts. Foreign body giant cells (FBGCs) are also multi-nuclear macrophages induced by cell-cell fusion of mono-nuclear cells. FBGCs are formed in response to foreign body reaction at the site of implantation, and are reportedly cause a loosening of implanted materials. OC-STAMP KO mice also completely failed to form multi-nuclear FBGCs. Thus, OC-STAMP is also essential for cell-cell fusion in FBGCs. OC-STAMP expression in osteoclasts depended on NFATc1 in the presence of M-CSF plus RANKL. While, in FBGCs, OC-STAMP expression was regulated by STAT6 under IL4 signal. DC-STAMP is required for cell-cell fusion in osteoclasts and FBGCs, and DC-STAMP KO mice also exhibited complete abrogation of cell-cell fusion in both cells. The expression of DC-STAMP in OC-STAMP-KO cells, and OC-STAMP expression in DC-STAMP-KO cells were both comparable to WT osteoclasts and FBGCs, suggesting that OC-STAMP and DC-STAMP are both required for cell-cell fusion of macrophage lineage cells. We also generated OC-STAMP-Tg mouse, in which OC-STAMP expression is driven under an actin promoter, and crossed with OC-STAMP-KO mouse to generate OC-STAMP-KO/Tg mouse. OC-STAMP over-expression in OC-STAMP-KO mice restored the inhibited cell-cell fusion in osteoclasts and FBGCs. OC-STAMP KO mono-nuclear osteoclasts showed significant reduction of bone resorbing activity, and OC-STAMP KO mice exhibited increased bone mass. Thus our data inform a molecular understanding of cell-cell fusion in osteoclasts and FBGCs, and thus OC-STAMP can be a therapeutic target for osteoporosis and implant failure.

Disclosures: Hiroya Miyamoto, None.

1158

Notch-RBP-J Signaling Predominantly Suppresses TNF- α Induced Osteoclastogenesis and Inflammatory Bone Resorption. Baohong Zhao^{*1}, Shannon Grimes², Xiaoyu Hu¹, Lionel Ivashkin¹. ¹Hospital for Special Surgery, USA, ²Hospital for Special Surgery, USA

TNF- α plays a key role in the pathogenesis of inflammatory osteoclastogenesis and bone resorption. Mechanisms that regulate the direct osteoclastogenic properties of TNF- α to limit pathological inflammatory bone resorption are mostly unknown. In this study, we found that deletion of RBP-J, the master transcription factor in Notch signaling, in bone marrow macrophages resulted in dramatic induction of osteoclastogenesis by TNF- α in the absence of exogenous RANKL. TNF- α -induced mouse osteoclasts derived from RBP-J deficient cells formed actin rings and resorbed dentin slices *in vitro*. Similar results were obtained using TNF- α -treated human osteoclast precursors in which RBP-J expression was knocked down using RNA interference. RBP-J deficiency had a much milder augmenting effect on RANKL-induced osteoclastogenesis. Mechanistically, RBP-J deficiency resulted in dramatically increased TNF- α -induced NFATc1 expression and RNA Pol II occupancy at the NFATc1 gene locus. RBP-J suppressed NFATc1 induction by attenuating c-Fos activation and suppressing induction of Blimp1, thereby preventing downregulation of transcriptional repressor IRF-8 that blocks osteoclast differentiation. Mice with a myeloid-specific deletion of RBP-J (*Rbpj^{fl/fl}LysMcre*) did not exhibit a bone phenotype under physiological conditions. However, *Rbpj^{fl/fl}LysMcre* mice showed dramatically increased osteoclast formation, severe bone destruction and increased serum TRAP levels relative to littermate controls in a TNF- α -induced model of inflammatory bone resorption. Strikingly, further deletion of RBP-J in myeloid compartment in *Rank^{-/-}* mice (*Rank^{-/-};Rbpj^{fl/fl}LysMcre* mice) enabled TNF- α to effectively induce osteoclast formation and bone resorption *in vivo*, indicating that RBP-J deficiency allowed TNF- α -induced osteoclastogenesis and bone resorption to proceed independently of RANKL. Importantly, a gain of function approach to activate RBP-J in mice with

myeloid-specific constitutive expression of Notch intracellular domain NICD1 (*Rosa^{Notch1}+/+*; *LysMcre*) significantly prevented inflammatory arthritic bone resorption in an antibody-induced arthritis model. These findings identify a key role for Notch-RBP-J signaling in restraining inflammatory TNF- α -induced osteoclastogenesis and bone resorption and provide mechanisms by which RBP-J suppresses NFATc1 induction. Notch-RBP-J signaling plays a more prominent role in inhibiting osteoclastogenesis in inflammatory settings than under physiological conditions.

Disclosures: Baohong Zhao, None.

1159

Dual Specificity Phosphatase 1 Limits Inflammatory Osteolysis. Youridies Vattakuzhi^{*1}, Sonya Abraham², Adel Ersek², Dany P. B. Perocheau², Richard O. Williams², Andy R. Clark², Nicole Horwood². ¹Kennedy Institute of Rheumatology/Imperial College, GBR, ²Kennedy Institute of Rheumatology, United Kingdom

Dual specificity phosphatase 1 (DUSP1) dephosphorylates and inactivates p38 mitogen-activated protein kinase (MAPK). It is upregulated by various pro-inflammatory stimuli and is essential for constraining p38 MAPK signalling and expression of p38-dependent genes such as tumor necrosis factor α (TNF α). p38 MAPK plays a central role in both differentiation and activation of osteoclasts (OCL). TNF α , a potent activator of p38 MAPK, is known to activate OCL, causing bone resorption in inflammatory diseases like rheumatoid arthritis. The aim of this study was to investigate whether DUSP1 may function as a negative regulator of inflammatory osteolysis.

Bone marrow cells of *Dusp1*^{+/+} and *Dusp1*^{-/-} mice were harvested for *in vitro* OCL assays. OCL formation and activity were analysed by evaluating tartrate resistant acid phosphatase (TRAP) staining and by measuring the resorption area on dentine. Expression of DUSP1 was measured in mouse bone marrow derived OCL precursors after RANKL (receptor activator of nuclear factor κ B ligand) stimulation. RANKL induced DUSP1 gene expression, and *in vitro* differentiation and activation of OCL were enhanced in the absence of DUSP1. This enhanced activation was particularly striking in the presence of low concentrations of TNF α and RANKL.

Dusp1^{+/+} and *Dusp1*^{-/-} mice were immunized with type II chicken collagen to induce chronic arthritis. Development of disease and bone resorption of the affected paws were assessed by histological examination, TRAP staining and micro-CT analysis. Compared to *Dusp1*^{+/+} mice, *Dusp1*^{-/-} mice showed earlier development and more severe disease, characterised by increased numbers of OCL and bone loss in affected joints.

These observations demonstrate that DUSP1 plays an important role in limiting OCL differentiation and activation by regulating the p38 MAPK pathway in OCLs under inflammatory conditions both *in vitro* and in an *in vivo* model of chronic arthritis.

Further highlighting the role of DUSP1 in OCL activation we observed that a *Dusp1*^{-/-} mouse strain with mixed (129Sv and C57BL/6) genetic background developed spontaneous inflammation of their toes, with neutrophilic infiltration, fibrosis, and dramatic osteolytic destruction of distal phalanges.

We speculate that DUSP1 negatively regulates OCL activation in humans, and that variations in its expression or function may play a role in diseases characterised by inflammatory osteolysis.

Disclosures: Youridies Vattakuzhi, None.

1160

Deletion of β -catenin in Osteoclast Precursors and their Progeny Increases Osteoclastogenesis and Induces Cortical Bone Loss. Marta Martin Millan^{*1}, Maria Carmen Gonzalez-Martín², Shoshana Bartel³, Maria Jose Almeida³, Marian Ros⁴, Jesus Gonzalez MacUas⁵. ¹Instituto de Formacion e Investigacion Marques Valdecilla, Esp, ²Instituto de Biomedicina y Biotecnología de Cantabria, Spain, ³University of Arkansas for Medical Sciences, USA, ⁴Instituto de Biomedicina y Biotecnología de Cantabria, Spain, ⁵Instituto de Formacion e Investigacion Marques Valdecilla, University of Cantabria, Spain

It is well established that activation of Wnt/ β -catenin in cells of the osteoblast lineage leads to an increase in bone mass through a dual mechanism: Increased osteoblastogenesis and decreased osteoclastogenesis. It remains unclear, however, whether a cell autonomous effect of β -catenin on osteoclasts is involved in bone mass regulation. To this end, we first examined *in vitro* the effects of Wnt3a recombinant protein on bone marrow (BM)-derived osteoclasts. Wnt3a increased the protein levels of β -catenin and induced osteoclast apoptosis, as assayed by caspase 3 activity. Moreover, Wnt3a attenuated M-CSF and RANKL-induced osteoclast formation, as determined by enumeration of TRAP positive cells. The Wnt3a-induced increase in β -catenin levels, as well as the pro-apoptotic effect on osteoclasts was abrogated by DKK1, indicating that the canonical Wnt signaling is required for the pro-apoptotic effect of Wnt3a. To examine the role of β -catenin on osteoclasts *in vivo*, we generated mice in which β -catenin was selectively deleted from cells of the monocyte/macrophage lineage. To this end β -catenin-floxed mice (*Catnb*^{fl/fl}) were crossed with the *LysM*:Cre deleter line (hereafter Δ Catnb;*LysM*). Δ Catnb;*LysM* mice were born at the expected Mendelian ratios and had the same body weight than their littermate

controls. β -catenin mRNA level in macrophages and osteoclasts from Δ Catnb;*LysM* mice was 70% decreased as compared to the *Catnb*^{fl/fl} controls as measured by RT-PCR. To determine the effect of the deletion on osteoclastogenesis, triplicate BM cultures from each of 3 animals per genotype were established in the presence of RANKL and M-CSF. After 5 days TRAP positive cells with 3 or more nuclei were counted. The number of osteoclasts in cultures from the Δ Catnb;*LysM* mice was 2-fold higher than in control mice (426 \pm 18 per well versus 238 \pm 77, $p=0.015$). In line with these findings, both Δ Catnb;*LysM* female and male mice exhibited a significant decrease in femoral cortical thickness as determined by micro-CT at 28 weeks of age (0.20 \pm 0.003 versus 0.215 \pm 0.004, $p=0.03$; 0.19 \pm 0.004 versus 0.20 \pm 0.005, $p=0.01$, respectively), while vertebral trabecular bone was not affected. These results provide compelling evidence for a cell-autonomous effect of β -catenin in osteoclasts, and indicate that osteoclast β -catenin contributes to the protective effect of the canonical Wnt signaling in cortical, but not in trabecular bone.

Disclosures: Marta Martin Millan, None.

1161

Osteoclast-Dependent Canalicular Formation in Cortical Bone That Mediates Bone Remodeling. Nobuhito Nango^{*1}, Shogo Kubota¹, Wataru Yashiro², Atsushi Momose², Yasunari Takada³, Koichi Matsuo³. ¹Ratoc System Engineering Co., Ltd., Japan, ²Department of Advanced Materials Sciences, School of Frontier Sciences, The University of Tokyo, Japan, ³School of Medicine, Keio University, Japan

Bone remodeling occurs through osteoclastic bone resorption and osteoblastic bone formation. In addition, osteocytes presumably contribute to rapid increases and decreases in skeletal calcium levels. However, the detailed structural basis for cortical bone remodeling remains unclear. Last year, we presented the first model showing canalicular structure in cortical bone based on X-ray microscopic tomography using the Japanese synchrotron radiation facility SPring-8. We now examine a potential link between mineral metabolism and fine structures within cortical bone in relation to osteoclasts. Here, we compared cortical bones of wild-type versus Fos KO mice, which show impaired formation of the bone marrow cavity and lack osteoclasts. For comparisons, we cut 300 μ m-wide columnar cortical bone specimens bound by the endosteal and periosteal surfaces from the tibia of wild-type and mutant mice at postnatal weeks 4, 16, and 28. Using the synchrotron X-ray microscope, we scanned specimens with a spatial resolution of 0.2 μ m using a multi-scan method consisting of differential phase contrast and defocus contrast. From the former, we acquired gray-scale images revealing the degree of calcification, while defocus contrast analysis revealed fine structures inside cortical bone such as lacunae, canaliculi, and canal structures. The degree of calcification surrounding fine structures was measured under high resolution and sensitivity. In wild-type mice, a canalicular network was observed between lacunae as well as between lacunae and bone canals, and the degree of calcification was altered along canaliculi indicative of bone remodeling activity. Analysis of Fos KO mice revealed that the shell matrix of hypertrophic chondrocytes was highly calcified and trabecular bone did not form in the diaphysis. Interestingly, in Fos mutant mice, while a canal network passing through the cartilage shell was developed, canaliculi between lacunae in cortical bone formed at significantly lower levels compared to controls. From these observations, we postulate that canaliculi in cortical bone form the basis of mineral metabolism and that osteoclasts are essential for formation of canalicular structures in cortical bone.

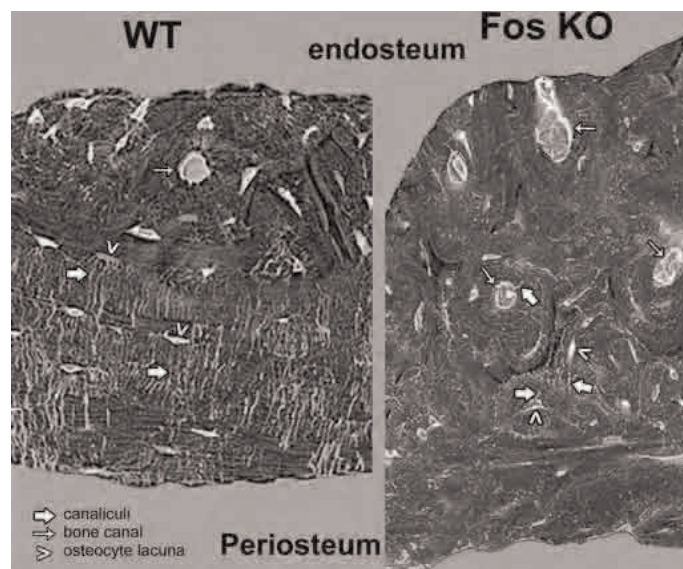


Fig.1

Disclosures: Nobuhito Nango, None.

1162

Selective Deletion of the Receptor for CSF1, c-fms, in Mature Osteoclasts Results in a High Bone Mass Phenotype In Vivo but a Normal Response to an Anabolic PTH Regimen. Meiling Zhu^{*1}, Ben-hua Sun¹, Karl Insogna².¹Yale University, USA, ²Yale University School of Medicine, USA

The receptor for Colony Stimulating Factor 1 (CSF1), c-fms, is highly expressed on mature osteoclasts. While CSF1 is known to be required for normal osteoclastogenesis, the expression of its receptor on mature cells suggests a role for this cytokine in regulating the function of these cells. Consistent with this idea, CSF1 stimulates cytoskeletal remodeling and motility, augments the activity of the electroneutral $\text{Na}^+/\text{HCO}_3^-$ co-transporter, NBCn1 and induces c-fos gene transcription in mature osteoclasts. To better define the role of CSF1 in mature osteoclasts, we conditionally deleted c-fms in these cells (c-fms-OC^{-/-}) by crossing c-fms^{lox/lox} mice with mice expressing Cre under the control of the cathepsin K promoter. The c-fms-OC^{-/-} mice were of normal weight and had normal tooth eruption. However, BMD was significantly higher as assessed by DXA: +15% in the spine, +18% in the femur and +10% for total body ($p < 0.001$ for each site). MicroCT analysis of femurs showed that the c-fms-OC^{-/-} mice had significantly increased trabecular bone mass, BV/TV + 80% ($p = 0.02$), Conn-Density + 76% ($p = 0.003$) and Tb.N + 48% ($p = 0.002$). There was a concomitant 30% reduction in Tb.Sp ($p = 0.003$). Histomorphometric analysis of the femoral trabecular bone compartment demonstrated a trend toward increased numbers of osteoclasts, +26% in Noc/BPm and +22% in OcS/BS in the k/o animals. There was a trend toward reduced numbers of osteoblasts, -25% in Obs/BS and -24% in Nob/BPm. None of these cellular changes were significant. Typically, mature osteoclasts show a marked spreading response when exposed to CSF1 in a non-gradient fashion. However, osteoclasts freshly isolated from c-fms-OC^{-/-} mice had a near complete abrogation of this response, with a mean increase in cell area of only 143% as compared to 569% in wild-type cells ($p < 0.0001$). Interestingly, co-culturing osteoblasts and bone marrow cells isolated from c-fms-OC^{-/-} in the presence of prostaglandin E2 and 1,25-dihydroxyvitamin D₃ failed to result in osteoclast-like cell (OCL) formation while abundant numbers of OCLs were generated when the experiment was repeated using wild type cells. C-fms-OC^{-/-} mice treated with (1-34) hPTH 80 ng/kg/d for 30 days showed similar increases in BMD as did wild type animals treated in the same way. Taken together, these data indicate an important non-redundant role for c-fms in regulating mature osteoclast function in vivo.

Disclosures: Meiling Zhu, None.

1163

Three Monthly, Oral 150,000 IU Cholecalciferol Supplementation Effects On Falls, Mobility and Muscle Strength in Older Postmenopausal Women. Paul Glendenning^{*1}, K Zhu², Peter Howat³, Charles Inderjeeth⁴, Joshua Lewis⁵, Richard Prince⁶. ¹Royal Perth Hospital, Australia, ²School of Medicine & Pharmacology, Australia, ³CBRCC, Curtin University, Australia, ⁴University of Western Australia, Australia, ⁵The University of Western Australia, Australia, ⁶Sir Charles Gairdner Hospital, Australia

Calcium and vitamin D supplementation has been shown to reduce falls and fractures in elderly women. Because of adherence problems we trialed the effects of supervised 3 monthly vitamin D administration.

686 women over 70 years of age were recruited at random from the ambulant population to receive either vitamin D3 150,000 IU po every 3 months (n=353) or an identical placebo (n=333) for nine months. All participants were advised to increase calcium intake by dietary means. Falls data were collected using a validated diary every 3 months, muscle strength was measured by hand held dynamometer and a subset of 40 (20 per group) patients had 25OHD measured at baseline and 3 monthly intervals after dosing.

Mean age was 76.7 ± 4.1 years. Calcium intake at baseline and 9 months was 864 ± 412 and 855 ± 357 mg/day, respectively. Hand held dynamometer strength at baseline was similar in the two groups (vitamin D 19.9 ± 4.9, placebo 19.9 ± 5.2 kg). The average serum 25(OH)D value at baseline in the 40 randomly selected subjects was 65.8 ± 22.7 nmol/L. With supplementation, the 25(OH)D levels of the vitamin D group were approximately 15 nmol/L higher than the placebo group after 3, 6 and 9 months.

Falls rates in the vitamin D group were 102/353 (31%/9mths) and in the placebo group were 89/333 (27%/9mths) OR 1.112 (95% CI 0.789, 1.567). There was no effect of vitamin D compared to placebo on muscle strength at 9 months. The study had a power of 0.8 to detect a 30% reduction in falls rate.

Oral cholecalciferol 150,000 IU every 3 months has neither beneficial nor adverse effects on falls or grip strength in elderly female subjects despite significant increases in 25OHD. Possible reasons include dosage chosen, frequency of vitamin D replacement or lack of calcium supplementation. Based on previous studies suggesting a benefit of daily calciferol therapy on falls risk reduction, daily supplementation may be desirable (despite adherence concerns) instead of less frequent, higher dose therapy as the latter does not demonstrate the same benefit on falls risk reduction.

Disclosures: Paul Glendenning, None.

1164

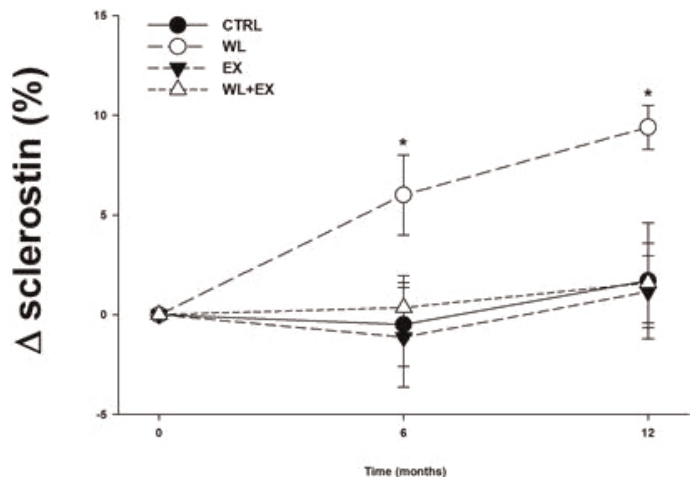
Sclerostin Mediates the Skeletal Effects of Weight Loss and Exercise Therapy In Obese Older Adults. Reina Armamento-Villareal^{*1}, Corinn Sadler¹, Suresh Chode², Nicola Napoli³, Clifford Qualls¹, Krupa Shah⁴, David Sinacore⁵, Dennis Villareal¹. ¹University of New Mexico School of Medicine, USA, ²St. Mary's Hospital, USA, ³University Campus Biomedico, Italy, ⁴University of Rochester School of Medicine, USA, ⁵Washington University in St. Louis, USA

Purpose: The loss of mechanical stress on the skeleton from unloading is believed to result in bone loss in patients undergoing weight loss (WL) therapy. However, the primary mediator for bone loss and the osteoprotective effect of exercise (EX) is unknown. Sclerostin (SCL), a protein produced by osteocytes that inhibits bone formation, is increased with skeletal unloading, while loading inhibits SCL production. We hypothesize that the effect of WL and EX on the skeleton is modulated by changes in SCL levels. We also hypothesize that bone loss leads to deterioration in hip geometry (i.e. femoral strength) which is prevented by EX. The objective of this study is to examine the changes in SCL levels and hip geometry parameters in obese older adults undergoing WL, EX and WL+EX.

Methods: 107 obese (BMI>30), older (age ≥ 65) adults were randomized into 4 treatment groups for 1 yr: control (CTRL) (n=27), WL (n=26), EX (n=26) and WL+EX (n=28). WL was achieved by dietary/behavioral intervention designed to induce a WL of 10% of body weight. EX intervention consisted of supervised resistance/aerobic exercise sessions 3x/wk. CTRL was instructed to continue usual dietary and activity habits. Measurements of SCL and bone turnover markers were performed by ELISA at baseline, 6 and 12 mos; BMD by DXA at baseline, 6 and 12 months; and hip geometry parameters were obtained from DXA imaging at baseline and 12 mos using hip structure analysis (HSA) software.

Results: BMD data were reported elsewhere (NEJM 2011). SCL levels significantly increased ($p < 0.05$) in WL at 6 (6.0%) and 12 mos (8.7%), while the CTRL, EX and WL+EX had no change in SCL levels (Fig. 1). Changes in SCL correlated with the changes in hip BMD and in bone turnover markers (C-telopeptide and osteocalcin) (all $p < 0.05$). HSA showed negative effects of WL on hip geometry, i.e. decreased cross-sectional area of the femoral narrow neck (NN) and femoral shaft (FS), decreased section modulus in the NN and increased buckling ratio in the FS. Aside from a significant increase in FS cortical thickness in EX, there were no significant changes in any of these parameters in the other treatment groups.

Conclusion: SCL may mediate bone loss in obese older adults undergoing voluntary WL. Furthermore, hip geometry appears to be adversely affected by WL. However, the addition of EX to WL program prevented the negative effects of WL on the increase in SCL and the deterioration in measures of femoral strength.



Changes in sclerostin with weight loss

Disclosures: Reina Armamento-Villareal, None.

1165

Multi-Phenotype Genome-Wide Association Meta-Analysis on both Lean Body Mass and BMD Identified Novel Pleiotropic Genes that Affected Skeletal Muscle and Bone Metabolism in European Descent Caucasian Populations. Yi-Hsiang Hsu¹, Xing Chen², Carola Zillikens³, Karol Estrada⁴, Serkalem Demissie⁵, Ching-Ti Liu⁶, Yanhua Zhou⁷, David Karasik⁸, Joanne Murabito⁹, Andre Uitterlinden¹⁰, L. Adrienne Cupples⁵, Fernando Rivadeneira⁴, Douglas Kiel⁸. ¹Hebrew SeniorLife Institute for Aging Research & Harvard Medical School, USA, ²Harvard University, USA, ³Erasmus University Medical Center, Netherlands, ⁴Erasmus University Medical Center, The Netherlands, ⁵Dept. Biostatistics, Boston University, School of Public Health, USA, ⁶Boston University School of Public Health, USA, ⁷Boston University, USA, ⁸Hebrew SeniorLife, USA, ⁹Boston University Medical School, USA, ¹⁰Rm Ee 575, Genetic Laboratory, The Netherlands

The positive relation between muscle mass and bone mass in adults has been well established and that may be due to the physical loading of muscle on bone as well as hormone, lifestyle, dietary and genetic factors. Previously, we have demonstrated significantly genetic correlations between lean mass (whole body and appendicular) and BMD in the Framingham Study, which indicates that shared genetic determinants may regulate both muscle and bone. To identify pleiotropic genes that associated with both lean mass and BMD traits, we performed a multiple-phenotypes genome-wide association analysis (GWAS) in the Framingham Study by modeling both lean mass and BMD phenotypes simultaneously using our newly developed multivariate analytical approach, directly linear-combined test statistics (DC). BMD (at the lumbar spine and femoral neck) and lean mass (whole body and appendicular) was measured by DXA. Multivariate GWAS analysis was performed on ~2.5 millions imputed SNPs (based on HapMap CEU phase II panel) in 4,524 Framingham participants (1,984 Men and 2,542 women with mean age of 62 years old). An additive genetic effect model was applied with adjustment for age, sex, height, fat mass, ancestral genetic background and pedigree structure. SNPs with multivariate p-values less than 10^{-3} and less than univariate p-values from both lean mass and BMD traits were selected for replication. The replication was performed using the DC multivariate analysis approach by combining test statistics from univariate GWAS meta-analysis on lean mass in CHARGE consortium (n=33,824 men and women) and on BMD in GEFOS (n=32,000 men and women) consortium. SNPs with multivariate p-values $\leq 5 \times 10^{-8}$ were considered as genome-wide significance. Only SNPs with multivariate p-values significantly less than univariate p-values were considered as potential pleiotropic genetic effects. Several potential pleiotropic loci were replicated and achieved genome-wide significance with multivariate association p-values $< 5 \times 10^{-8}$, i.e. SNPs in or near *SAPL*, *GAL* (near *LRP5* gene), *TNRC6B*, *WNT2B* and *GRB10* genes. Several suggestive loci ($p < 5 \times 10^{-6}$) were also found, i.e. *RSP03/C6orf173* region, *ST7L*, *MTHFSD*, *RUNX1*, *LEPR* and *ADAMTSL3* genes. These top associated SNPs are being further evaluated in gene expression analysis of human bone and muscle tissues. In conclusion, our results reveal novel pleiotropic genes to further elucidate the link between the skeletal muscle and bone metabolism.

Disclosures: Yi-Hsiang Hsu, None.

1166

Effects of High Velocity Power and Functional Training on BMD and Physical Function in High Risk Older Adults: A 12-month Randomised Controlled Trial. Jenny Gianoudis¹, Christine Bailey², Peter Ebeling², Caryl Nowson³, Kerrie Sanders⁴, Keith Hill⁵, Robin Daly^{3*}. ¹Department of Medicine, The University of Melbourne, Australia, ²The University of Melbourne, Australia, ³Centre for Physical Activity & Nutrition Research, Deakin University, Australia, ⁴University of Melbourne, Australia, ⁵School of Physiotherapy, La Trobe University, Australia

Multi-component exercise programs are recommended for preventing osteoporosis and falls, but few studies have evaluated their effectiveness in high risk older adults in a 'real world' community setting. In addition, most programs have used traditional slow speed progressive resistance training (PRT) coupled with weight-bearing and/or balance activities. However, emerging data suggests that muscle power (ability to produce force rapidly) is a more crucial variable to functional decline than strength. The aim of this community-based RCT was to investigate the effects of a multi-component high speed exercise program coupled with an osteoporosis education and behavioural change program, termed *Osteo-cise: Strong Bones for Life*, on BMD and body composition as well as functional muscle power and performance in older adults. 162 men and women (meanSD; 676 years) at increased risk for falls and fractures were randomised to the *Osteo-cise* program (n=81) or a usual-care control group (n=81). Exercise consisted of high-velocity PRT and weight-bearing activities (60-180 impacts/session) and balance training 3 d/wk for 12 months. All participants were given Ca-Vit D supplements. Total body FM, LM and BMC and regional BMD were assessed by DXA at baseline and 12 months. Maximal muscle strength and functional power (stair climbing test) and performance (4-square test, functional reach, TUG, sit-to-stand) were assessed at baseline, 6 and 12 months. In total 150 participants (93%) completed the study and the groups were well matched at baseline. Exercise attendance averaged 59%. After 6 months, there were significant exercise-induced net

gains in back (13%) and leg (12%) muscle strength ($P < 0.01$), which were maintained after 12 months. There was no effect of exercise on LM or FM, but significant net gains of 1.0% (95%, 0.2, 1.8) and 1.1% (0.2, 2.0) were observed in FN and L1-L4 BMD relative to controls (both $P < 0.05$). Exercise also improved stair climbing power [net gain 4.7% (1.0, 8.4), $P < 0.05$], sit-to-stand [12.7% (6.0, 19.3), $P < 0.001$] and the 4-square balance test [0.4 sec (-0.7, -0.1), $P < 0.05$] after 6 months. These benefits were maintained after 12 months, with a further 7% improvement observed in the sit-to-stand test. In conclusion, a community-based, multifaceted program incorporating high speed PRT and functional training is effective for improving BMD, muscle strength and functional power and performance in older adults at increased risk of fracture.

Disclosures: Robin Daly, None.

1167

Systemic Administration of Soluble Activin Receptors Produces Differential Anabolic Effects in Muscle and Bone in Mice. Douglas Digirolamo^{*}, Vandana Singhal, Thomas Clemens, Se-Jin Lee. Johns Hopkins University, USA

Myostatin and related activin ligands are powerful negative regulators of skeletal muscle growth. Recent studies demonstrate that administration of soluble ActRII (ACVR2) fusion proteins, which sequester these muscle inhibitory factors, increases both skeletal muscle and bone mass in rodents and primates. Whether the observed bone anabolism results from direct actions in osteoblasts or is secondary to the increased muscle mass is unclear. To begin to address this question, 8 week-old female C57BL/6 mice were administered 10 mg/kg of ACVR2/Fc, ACVR2B/Fc or vehicle by IP injection, once a week, for 4 weeks. Wet weights of pectoralis, triceps, quadriceps and gastrocnemius muscles were increased by ~15% over vehicle in mice receiving ACVR2/Fc and by 40% in mice treated with ACVR2B/Fc. Micro CT analysis of the distal femur revealed a striking 3-fold increase in trabecular BV/TV in the ACVR2B/Fc group, but no significant change in cortical thickness at the midshaft. By contrast, mice treated with ACVR2/Fc demonstrated a more modest increase in trabecular BV/TV (13.6% vs. 7.6% in controls), but also had significantly increased cortical thickness at the femoral midshaft (204.5µm vs. 162.1µm in controls). Interestingly, ACVR2/Fc increased calvarial bone volume to a greater extent than ACVR2B/Fc. The increase in calvarial bone (a non load-bearing bone) and rapid accrual of trabecular bone in mice administered ACVR2B/Fc suggested direct actions of activin receptor signaling in bone. Consistent with this notion, real-time PCR performed on mRNA from primary mouse osteoblasts revealed expression of activin receptors and ligands at levels comparable to those seen in skeletal muscle, with the exception of myostatin, which was not expressed by osteoblasts. Additionally, phosphorylation of Smad2, an immediate substrate of activin receptor activation, was decreased in a time- and dose-dependent manner following exposure of osteoblasts to ACVR2B/Fc. These changes in Smad phosphorylation were accompanied by a modest decrease in osteoblast proliferation as indexed by BrdU incorporation. To further explore the effects of blocking activin receptor signaling on osteoblast performance, osteoblasts were differentiated in the presence of ascorbic acid and β-glycerolphosphate, with or without increasing concentrations of ACVR2B/Fc. Alkaline phosphatase and alizarin red staining were increased in osteoblasts treated with ACVR2B/Fc versus control. Taken together, our results suggest that activin receptor signaling functions directly in osteoblasts to regulate bone mass. Further, ACVR2/Fc and ACVR2B/Fc exerted differential anabolic activity in bone and muscle, an attractive property for a potential therapy for osteopenia and/or sarcopenia.

Disclosures: Douglas Digirolamo, None.

1168

Combined Deletion of the Transcription Factors FoxO1, 3, and 4 from Osteoblast Progenitors Expressing Osterix Causes Bone Anabolism and Postpones the Adverse Effects of Aging on Bone. Srividhya Iyer^{*}, Elena Ambrogini, Li Han, Shoshana Bartell, Aaron Warren, Randall Shelton, Robert Weinstein, Charles O'Brien, Stavros Manolagas, Maria Almeida. Center for Osteoporosis & Metabolic Bone Diseases, Central Arkansas Veterans Healthcare System, University of Arkansas for Medical Sciences, USA

Wnt/β-catenin signaling increases bone mass, at least in part, by promoting the progression of Osterix (Ox)-expressing cells to bone producing osteoblasts. Based on this and evidence that FoxOs compete with Tcf for β-catenin, we have deleted FoxO1,3,4 from Ox-expressing cells, by crossing mice with conditional alleles (FoxO1,3,4-flox) with mice expressing the Cre recombinase under the control of the murine osterix promoter (Ox-Cre). Both female and male FoxO1,3,4-Flox;Ox-Cre mice exhibited a 20% increase in BMD by DEXA or micro-CT analysis at 3 months of age. This was associated with an increase in cancellous bone volume, trabecular number, and connectivity in both the vertebrae and the femur. Moreover, FoxO1,3,4-Flox;Ox-Cre mice had increased femoral cortical width caused by increased periosteal apposition, indicated by a larger external, but not internal, diameter of the diaphysis of the femur. Ox-GFP positive calvaria cells sorted by flow cytometry exhibited 90% decreased mRNA and protein levels of FoxO1, 3, and 4, as well as decreased expression of the FoxO-target genes Gadd45, nocturnin, Adm, and BMP4 as determined by microarray and qRT-PCR. Consistent with the contention that

FoxOs antagonize Wnt/Tcf signaling and osteoblastogenesis, the expression of the β -catenin/Tcf target genes cyclinD1, connexin43, col6a1, and mmp16 in *Osx-GFP* positive cells, as well as the mRNA expression of osteocalcin in bone, and the bone formation rate in vertebral sections, were all increased. Further, *Osx-GFP* positive cells exhibited increased proliferation rate as determined by BrdU incorporation. Resorption markers in the serum and OPG expression were unaffected by FoxO deletion. Induction of the FoxO1,3,4 deletion at 3 months of age, by activating a Tet-off system incorporated into the *Osx-Cre* transgene led to an increase in femoral and spinal BMD 18 weeks later, similar to that observed when the deletion occurred since conception, indicating that the increased bone mass was not due to changes imparted during development or growth. Most importantly, the high bone mass phenotype of the FoxO1,3,4-Flox;*Osx-Cre* mice was maintained up to 19 months of age. These findings strongly suggest that selective inactivation of FoxOs in *Osx*-positive cells causes bone anabolism by unleashing the restraining effects of FoxOs on Wnt signaling, and may counteract the effect of aging on bone.

Disclosures: *Srividhya Iyer, None.*

1169

Hyponatremia Causes Bone Loss and Sarcopenia. Nikhil Sharma¹, Joseph G Verbalis², Michael B Manigrasso¹, Helen Tam¹, Julia (Julianna) Barsony^{*2}, Qin Xu¹. ¹Georgetown University, USA, ²Georgetown University Hospital, USA

Chronic hyponatremia (CHN) is a frequent disorder of hospitalized and ambulatory elderly people due to the syndrome of inappropriate antidiuretic hormone secretion (SIADH) and other causes. The consequences of pronounced CHN (serum $[Na^+] < 130$ mmol/L) on fall and fracture risks and osteoporosis have been recognized by our studies, as well as others. We recently reported that pronounced CHN causes loss of bone mineral density (BMD) in a rat model of SIADH. Moreover, our studies on cultured cells have demonstrated that even moderate lowering of extracellular $[Na^+]$ increased osteoclastogenesis and osteoclastic resorption, and oxidative stress. Using the same rat model of SIADH, we explored the possibility that mild CHN would also cause bone loss over time. We generated hyponatremia for 3 months in female rats (8 per group) by either high dose (5 ng/h) or low dose (0.5 ng/h) desmopressin (DDAVP) infusion in conjunction with a liquid diet, whereas normonatremic controls (NN) were pair-fed with the same liquid diet without infusing DDAVP. We monitored bone mineral density (BMD) using serial *in vivo* measurements, and also measured BMD in excised femur and L4 by densitometry at the end of the study. Pronounced CHN (serum $[Na^+] = 114.58$ mmol/L) caused marked and progressive decrease of BMD both in the spine ($p < 0.01$) and femur ($p < 0.01$) compared to NN rats (serum $[Na^+] = 146.61.3$ mmol/L). Mild CHN (serum $[Na^+] = 130.92.7$ mmol/L) caused moderate decrease of BMD in the spine (*in vivo* 24.16.7% below baseline; excised L4 HN: 0.11790.0049, NN: 0.12710.007 g/cm²; $p < 0.01$) and femur (*in vivo* 7.31.8 % below baseline; CHN: 0.16000.0031, NN: 0.16860.0025 g/cm²; $p < 0.05$). In another study on aged rats, we found that pronounced CHN for 3 months induced progressive decline of thigh muscle mass with an initial 3.66 1.0 % decrease over the first two weeks of hyponatremia ($p < 0.01$), followed by a steady decline at a rate of 2.1% per month to a maximum of 17% decline by the end of the study. We also found that CHN induced cardiomyopathy, manifested as increased heart per body weight, histomorphometric evidence of reduced myocyte number, and marked perivascular and interstitial fibrosis. In summary, our studies demonstrated that even mild hyponatremia causes significant bone loss, sarcopenia and cardiomyopathy in a rat model of SIADH, and therefore likely represents a significant detrimental factor to health in the aging population by virtue of increased fall and fracture risks.

Disclosures: *Julia (Julianna) Barsony, None.*

This study received funding from: NIH/NIA R01-AG029477

1170

Arrest of the Reversal Phase in Postmenopausal and Glucocorticoid-Induced Osteoporosis. Pia Jensen^{*1}, Thomas Andersen², MOHAMED ABDELGAWAD³, Ellen Hauge⁴, Jens Bollerslev⁵, Jean-Marie Delaisse⁶. ¹Vejle Hospital, Denmark, ²Vejle Hospital, IRS-CSFU, University of Southern Denmark, Denmark, ³CLINICAL CELL BIOLOGY DEPARTMENT, VEJLE HOSPITAL, Denmark, ⁴Aarhus University Hospital, Denmark, ⁵National University Hospital, Norway, ⁶Vejle Hospital, CSFU-IRS, University of Southern Denmark, Denmark

Histomorphometric assessment of bone remodeling focuses generally on osteoclastic (OC) resorption and osteoblastic (OB) formation. Only little attention is given to the intermediate phase, known as the reversal phase, although it is by nature, the one coupling bone resorption to bone reconstruction. Actually, we do not even know the nature of the cells colonizing the ES after the departure of the OCs, or whether miss-function of these "reversal cells" (RvC) may contribute to bone loss in diseases such as glucocorticoid-induced (GIO) and postmenopausal osteoporosis (PMO). These two basic questions are therefore addressed in the present study.

Masson trichrome-stained plastic sections of cancellous bone from 15 GIO patients, 23 PMO patients and 10 sex- and age-matched controls were assessed for the extent of eroded (ES), osteoid (OS), osteoclast (Oc.S), and osteoblast surface (Ob.S) relative to total bone surface (BS). Reversal surfaces (Rv.S) were defined as ES without OCs. The Rv.S was subdivided into active (Ac.Rv.S) defined as Rv.S with

flanking OCs or OS and arrested (Ar.Rv.S) defined as Rv.S without neighboring OCs or OS. Immunohistochemical characterization of the RvC was conducted on paraffin sections.

RvCs stained for factors which are typically expressed by OBs, but not for markers expressed by macrophages and OCs, thereby indicating that RvCs are OB lineage cells. Arrested RvCs were flatter and about 2 times less dense than active RvCs, as assessed in PMO. While the extent of Ac.Rv.S/BS was at the same level in all groups, the extent of Ar.Rv.S/BS was increased in both GIO and PMO patients, compared to controls. Statistical significance was however only borderline in PMO. These observations show that GIO and PMO affect the bone remodeling cycle well upstream of the bone formation step. Interestingly, a close negative correlation was found between the proportion of Ar.Rv.S and the extent of OS (PMO, $r = -0.41$; GC, $r = -0.38$) and Ob.S (PMO, $r = -0.45$; GC, $r = -0.38$). These correlations and the fact that Ar.Rv.Ss are away from OCs and OS, suggest that arrest of RvCs might prevent the transition from resorption to formation thus resulting in accumulation of Ar.Rv.S and deficient bone formation.

In conclusion, the reversal phase is performed by OB lineage cells. Arrest of the reversal phase may contribute significantly to the bone loss in both PMO and GIO. Therefore, RvCs could be future targets for treating diseases characterized by deficient bone formation.

Disclosures: *Pia Jensen, None.*

1171

FSH is Associated with Lean Mass and Fat Mass but not with BMD in Younger Postmenopausal Women. Margaret Gourlay^{*1}, Chenxi Li¹, Catherine Hammett-Stabler¹, Jordan Renner¹, Janet Rubin². ¹University of North Carolina, USA, ²University of North Carolina, Chapel Hill, School of Medicine, USA

Higher concentrations of follicle stimulating hormone (FSH) have been associated with lower bone mineral density (BMD), but a causal relationship has not been confirmed. We found no association between FSH and low BMD in a previous multivariable analysis of younger postmenopausal women that adjusted for weight. To study relationships among FSH, lean mass, fat mass and BMD, we conducted a new cross-sectional analysis of 111 postmenopausal women aged 50 to 64 years of mixed ethnic background. Lean mass, fat mass, and areal BMD (g/cm²) at the lumbar spine, femoral neck and total hip were measured using dual-energy X-ray absorptiometry (DXA, Hologic Discovery). Trabecular and cortical BMD were measured at the 4% and 33% distal radius respectively (XCT2000 peripheral QCT scanner; Stratec/Orthometrix). Multiple linear regression models were constructed for the outcomes of lean mass and fat mass, with independent variables age, race, years since menopause, ever-use of hormone therapy, FSH, bioavailable estradiol, bioavailable testosterone, LH, PTH and SHBG. Separate linear regression models were constructed using areal BMD and pQCT measures as outcomes, with age, race, FSH, bioavailable estradiol, bioavailable testosterone, LH, TSH, SHBG, BSAP, lean mass and fat mass as independent variables. FSH (range 1.6-270 mIU/mL) was moderately and inversely correlated with lean mass ($r = -0.62$, $p < 0.001$) and fat mass ($r = -0.48$, $p < 0.001$). After adjusting for the covariates, FSH was independently associated with lean mass ($\beta = -0.079$, $p = 0.010$) and fat mass ($\beta = -0.13$, $p = 0.011$), but not with any areal BMD or pQCT outcomes. Similar associations were seen for SHBG, but not for bioavailable estradiol or testosterone. These results show consistent and independent relationships between higher concentrations of FSH and lower lean mass and lower fat mass, but no statistically significant association between FSH and BMD. Previously reported correlations between FSH and BMD might have been due to indirect effects via lean mass or fat mass.

Disclosures: *Margaret Gourlay, None.*

This study received funding from: National Institute of Arthritis and Musculoskeletal and Skin Diseases, National Center for Research Resources

1172

Calcium Deficiency-induced Bone Loss is Exacerbated by Disruption of Claudin-18 Gene in Mice. Gabriel R. Linares^{*1}, Catrina Alarcon², Robert Brommage³, David Powell⁴, Weirong Xing², Jon Wergedal², Subburaman Mohan². ¹Jerry L Pettis VA Med Ctr, USA, ²Jerry L. Pettis Memorial VA Medical Center, USA, ³Lexicon Pharmaceuticals, USA, ⁴Lexicon Pharmaceuticals, USA

Claudin-18 (Cldn-18) is a member of tight junction family of proteins and we recently showed that targeted disruption of Cldn-18 decreases endosteal bone volume (BV) by increasing bone resorption (BR). Since calcium (Ca) deficiency decreases endosteal BV by RANKL-mediated increase in BR and Cldn-18 negatively modulates RANKL-induced osteoclast differentiation, we evaluated if Ca-deficiency induced bone loss is further exacerbated by disruption of Cldn-18 in mice. Cldn-18 knockout (KO) and control mice (16-wks) were subjected to either normal Ca (0.6%) or low Ca (0.01%) diet for 2 wks. PIXImus revealed that total body, femur and lumbar BMD were reduced by 13, 14 and 31% respectively (all $P < 0.001$) after 2 wks of Ca deficiency in control mice. As expected, total body, femur and lumbar BMD were reduced 15, 13, and 27% (all $P < 0.001$) in Cldn-18 KO mice compared to control mice at normal Ca diet. Treatment of Cldn-18 KO mice with low Ca diet resulted in further skeletal deficits (total body, femur, and lumbar BMD were reduced by 22, 22, and 43% of

control mice). Gene-diet interaction was significant for lumbar BMD. To determine if combination of low Ca diet and loss of Cldn-18 compromises bone quality, we performed μ CT analysis of vertebra. BV/TV was reduced by 42% in the low Ca Cldn-18 KO group compared to 21% in the KO control group. Trabecular (Tb) number was decreased by 30% in the low Ca Cldn-18 KO group compared to 16% in the KO control group while Tb separation was increased 40% in the low Ca Cldn-18 KO group compared to 18% in the KO control group. Changes in Tb number and separation were significantly different in the low Ca Cldn-18 KO group compared to low Ca WT and normal Ca KO group. Histomorphometric analyses of vertebra revealed that %TRAP labeled surface/bone surface was significantly greater in the low Ca KO group compared to normal Ca KO and low Ca WT group. Accordingly, elevated serum PTH levels in the normal Ca KO mice were further increased (62%, $P < 0.01$) by Ca deficiency. Measurement of bone strength parameters in the femur by 3-point bending revealed that bone breaking strength and stiffness were severely compromised by combined deficiency of Cldn-18 and Ca compared to either deficiency alone. Conclusions: 1) Loss of Cldn-18 further exacerbates Ca deficiency-induced bone loss by influencing BR. 2) Loss of Cldn-18 function together with Ca deficiency results in mechanically weaker bone and thereby increases fracture risk.

Disclosures: Gabriel R. Linares, None.

1173

Increased Density of Capillaries and Dividing Cells at Remodeling Sites in Adult Human Bone. Helene Kristensen^{*1}, Thomas Andersen², Prof. Niels Marcussen³, Lars Rolighed⁴, Jean-Marie Delaisse⁵. ¹Vejle Hospital Kabbeltøft 257100 Vejle Denmark, Denmark, ²Vejle Hospital, IRS-CSFU, University of Southern Denmark, Denmark, ³Odense University Hospital, Denmark, ⁴Aarhus University Hospital, Denmark, ⁵Vejle Hospital, CSFU-IRS, University of Southern Denmark, Denmark

In bone development and fracture healing osteogenesis depends critically on vascularisation. It is unknown whether a similar relation exists between vascularisation and cancellous bone remodeling. Here, we investigated how capillaries and the cell division marker Ki67 distributed above eroded surface (ES), osteoid surface (OS), and quiescent surface (QS), and are related to the presence of the bone remodeling compartment (BRC) canopy. The study included 9 paraffin-embedded iliac crest biopsies from control patients. Adjacent sections were stained so that information from histomorphometry and immunohistochemistry could be combined. Capillary density was counted on the CD56/CD34 double stained section, while the density of proliferating cells was counted on the Ki67 stained section. The distance from the bone or canopy to the target of interest was measured orthogonal to the bone surface until 100 μ m into the bone marrow. Electron microscopy (EM) was performed on EPON-embedded biopsies from 3 patients with primary hyperparathyroidism. The capillary density within 0-50 μ m above ES and OS was respectively 1.85 and 1.32 times higher than above QS in the absence of the BRC canopy, while 2.78 and 1.99 times higher in the presence of the BRC canopy. The frequency of light microscope assessed contacts between capillaries and BRC canopies above ES and OS were 3.39 and 2.35 times higher than contacts between capillaries and QS. The capillary density within 51-100 μ m above ES and OS equalled the level above QS. EM showed that the capillaries line the BRC canopy at less than 1 μ m distance, and that cells performed diapedesis through the capillary wall and the BRC canopy. The density of Ki67-positive nuclei up to 50 μ m above ES was 1.45 times higher compared to QS, while the density above OS and QS was similar. The density of Ki67 positive nuclei within 51-100 μ m was similar above all surfaces, as for the capillary density. All the reported differences are statistically significant with at least $P < 0.01$. These data support that capillaries are an important component of the mechanism controlling adult human cancellous bone remodeling. The higher density of capillaries above ES compared to OS indicates that capillaries are present from the beginning of the remodeling process. Thus, capillaries appear to participate in the recruitment of osteoclast and osteoblast progenitors as also suggested by our observations of diapedesis and the distribution of dividing cells.

Disclosures: Helene Kristensen, None.

1174

Peripheral Blood Monocyte-Expressed Anxa2 Gene Is Involved in Pathogenesis of Osteoporosis in Humans. Fei Yan Deng^{*1}, Shu-Feng Lei², Yan Zhang³, Yu-Ling Zhang⁴, Yan-Peng Zheng⁵, Li-Shu Zhang⁵, Yunxia (Yesha) Lundberg⁶, Yao-Zhong Liu⁷, Christopher Papasian⁸, Hong-Wen Deng¹. ¹Tulane University, USA, ²College of Life Sciences, Hunan Normal University, China, ³Department of Genetics, Boys Town National Research Hospital, USA, ⁴Center of Systematic Biomedical Research, University of Shanghai for Science & Technology, China, ⁵College of Life Sciences & Bioengineering, Beijing Jiaotong University, China, ⁶Boys Town National Research Hospital, USA, ⁷Center of Bioinformatics & Genomics, Tulane University School of Public Health & Tropical Medicine, USA, ⁸School of Medicine, University of Missouri-Kansas City, USA

Low BMD is a risk factor of osteoporosis and has strong genetic determination. Genes influencing BMD and fundamental mechanisms leading to osteoporosis have

yet to be fully determined. Peripheral blood monocytes (PBM) could access to bone resorption surfaces and differentiate into osteoclasts to resorb bone. Herein, we attempted to identify osteoporosis susceptibility gene(s) and characterize their function(s), through initial proteome profiling of PBM *in vivo*, and using a strategy of multi-disciplinary and integrative studies.

We recruited 3 independent case-control samples ($N = 28, 80, 44$, respectively), including Caucasians with extremely low vs. high hip BMD from bottom 16% vs. top 10% of distribution in population, and one population sample including 1,000 unrelated Caucasians. We utilized quantitative proteomics methodology to profile PBM proteomes in the 1st case-control sample to discover proteins, thus gene(s), functionally relevant to low BMD. Differentially expressed protein(s) identified were verified by western blotting. Then, comparative analyses at mRNA expression level in PBM in the 2nd case-control sample were conducted. For gene(s) also differentially expressed at mRNA level, we further analyzed nucleotide sequences in the 3rd case-control sample to identify sequence variations associated with low BMD; we also tested association of gene SNPs with hip BMD in the population sample. Based on integrative evidence, gene(s) of interest were selected and subjected to functional validation *in vitro*.

Among 1,539 proteins identified in PBM, *Anxa2* was up-regulated 2.0-fold in subjects with low BMD. Up-regulation of *Anxa2* gene expression in low BMD subjects were verified, and further replicated at mRNA level. Three sequence variations in *Anxa2* were found associated with low BMD ($p < 0.05$). Three SNPs in *Anxa2* were associated with BMD variation ($p < 0.05$). The above integrative evidence strongly supports that *Anxa2* is involved in the pathogenesis of osteoporosis in humans. Furthermore, monocyte migration across endothelial barrier *in vitro* was elevated up to 4.9-fold by *Anxa2* stimulation, suggesting that *Anxa2* may stimulate more PBM to migrate from blood to bone resorption surfaces to differentiate into osteoclasts *in vivo*, hence leading to increased bone resorption and decreased BMD.

In conclusion, this study identified a novel osteoporosis susceptibility gene, and suggested a novel pathophysiological mechanism, mediated by *Anxa2*, for osteoporosis in humans.

Disclosures: Fei Yan Deng, None.

1175

Sex-specificity in femoral neck growth during adolescence and young adulthood: evidence from 15-years of longitudinal data. Saja Kontulainen^{*1}, Stefan Jackowski¹, Joel Lanovaz², James Johnston¹, Adam Baxter-Jones¹.

¹University of Saskatchewan, Canada, ²Assistant Professor, Canada

Introduction. About 70-80% of hip fractures occur in women. Sex-specific development during growth and later deterioration in hip structure and strength may partly explain the greater hip fracture incidence in females. However, there is limited longitudinal evidence of sex-specific hip structure growth during adolescence and young adulthood. The purpose of the present study was to investigate sex differences in femoral neck development over 15-years of growth.

Methods. Data were from 121 participants (64 females) of the Saskatchewan Pediatric Bone Mineral Accrual Study (PBMA). Proximal femur and total body lean mass were measured with dual energy x-ray absorptiometry (DXA) annually from 1991-97 and 2002-2006. We used Hip Structural Analysis to estimate peri- and endosteal diameters (cm) and bone cross-sectional area (CSA, cm²) (as an indicator of compressive strength) from femoral neck DXA scans. Peak height velocity (PHV) was determined for each participant and the age from PHV was calculated to define biological age (BA=age from PHV) at each measurement time. Random effects models were used to identify the interactions and independent effects of BA, sex, height and lean mass on femoral neck growth from adolescence to adulthood.

Results. There was a sex by BA interaction in periosteal (Beta coefficient -2.2, Standard Error of Estimate, SEE 0.4) and endosteal (-3.0, SEE 0.5) diameters indicating that females had greater periosteal and endosteal diameters prior to PHV, and lower periosteal and endosteal diameters after PHV than males with same height and lean mass. Another sex by BA interaction was observed in femoral neck CSA (2.2, SEE 0.5), indicating that females had smaller CSA prior PHV and larger CSA after PHV than males when height and lean mass were controlled.

Conclusion. After the growth spurt, periosteal growth at the femoral neck is greater in males while females gain larger bone area due to diminished endosteal resorption. These longitudinal results from adolescence to young adulthood support the theory that during pubertal growth females develop bone mineral reserve at the endosteal bone surface for reproductive needs. Loss of this reserve after menopause will reduce bone area at the femoral neck, leading to thin cortices susceptible to local buckling and hip fracture if the female hip is exposed to impact forces from a fall.

Disclosures: Saja Kontulainen, None.

1176

Serum Osteocalcin Levels Are Associated With Testosterone Levels In Boys During Maximal Skeletal Growth. Salman Kirmani^{*1}, Elizabeth Atkinson², L. Joseph Melton¹, Byron Riggs¹, Shreevasee Amin¹, Sundeep Khosla². ¹Mayo Clinic, USA, ²College of Medicine, Mayo Clinic, USA

Recent provocative studies in rodents have demonstrated that osteocalcin (OCN) regulates testosterone (T) production and fertility in males, but not in females. This effect is mediated by the active form of OCN, undercarboxylated (UC) OCN, which binds a G-protein coupled receptor (GPCR6a). We hypothesized that this novel bone-

testis axis may be most relevant during rapid skeletal growth in adolescent males to help maximize bone size. Thus, we measured serum T levels by mass spectroscopy and total and UC OCN as well as PINP levels by immunoassay in 56 boys with a bone age of 4-20 years, in whom we also measured periosteal circumference at the radius using Xtreme CT. In all boys combined, OCN was correlated with T levels (bone age-adjusted $r = 0.30$, $P = 0.024$), with a similar trend for UC OCN. However, serum T levels did not correlate with PINP levels (bone age-adjusted $r = 0.14$, $P = 0.307$). Serum T began to increase in the boys at bone age 11 years, and serum OCN reached maximal levels at bone age 14 years, representing peak skeletal growth. Thus, we divided the boys into 3 bone age groups: 4-10 years ($n = 16$, prior to increases in T levels), 11-14 years ($n = 18$, the phase of increasing bone formation), and 15-20 years ($n = 22$, the phase of declining bone formation). Serum OCN, but not PINP, was highly correlated with T levels in the boys of bone age 11-14 years ($r = 0.57$, $P = 0.013$), with a similar trend for UC OCN. No significant associations between serum T levels and OCN, UC OCN, or PINP were found in the younger or older boys. Bone size (periosteal circumference) was highly correlated with T levels in the boys of bone age 11-14 years ($r = 0.75$, $P < 0.001$). In these boys, serum OCN levels were also correlated with periosteal circumference ($r = 0.49$, $P = 0.037$); importantly, adjusting for T levels eliminated this correlation (T adjusted $r = 0.12$, $P = 0.660$), suggesting that T mediated the association of OCN with bone size. Collectively, these human data support the recent findings in rodents of a novel bone-testis axis. Moreover, our data suggest that this axis may be most relevant during rapid skeletal growth in males, when serum T levels are rising under the influence of the hypothalamic-pituitary axis and OCN levels are rising due to skeletal growth: during this phase, OCN may further stimulate testicular T production which, in turn, leads to an increase in bone size and ensures an evolutionarily conserved sexual dimorphism of the skeleton.

Disclosures: Salman Kirmani, None.

1177

Dose-Response Effect of Vigorous Aerobic Exercise on Bone Turnover, Insulin Sensitivity, and Adiposity in Obese Children: A Randomized Controlled Trial. Norman Pollock^{*1}, Paul Bernard², Barbara A. Gower³, Karl Wenger¹, Sudipta Misra¹, Jerry Allison¹, Alexis M. Stranahan¹, Catherine L. Davis¹. ¹Georgia Health Sciences University, USA, ²Medical College of Georgia, USA, ³University of Alabama-Birmingham, USA

Animal data have uncovered a unique "bone-fat-pancreas" axis that regulates energy homeostasis, coordinates energy partitioning between bone and adipose tissue, and impacts insulin sensitivity. The existence of the "bone-fat-pancreas" axis in humans is unknown. In this study, we determined the dose-response effect of vigorous aerobic exercise on bone turnover, insulin sensitivity and adiposity in obese children. We also investigated associations between the changes in bone turnover and the changes in insulin sensitivity and adiposity. Obese children ($N=222$, aged 7-11 years, 58% female, 58% black) were randomly assigned to three experimental conditions: no-exercise control condition ($n=78$), low dose (20 min/d, $n=71$), or high-dose (40 min/d, $n=73$) aerobic exercise program for 12-weeks (5 d/wk). The low- and high-dose exercise groups participated in various types of instructor-led activities that involved running, jumping, skipping, kicking, and throwing. At baseline and posttest, an oral glucose tolerance test was used for assessment of insulin sensitivity (Matsuda index), bone formation [total osteocalcin (OC) and procollagen type I amino propeptide (PINP)], and bone resorption [carboxyterminal telopeptide region of type I collagen (ICTP)]. Total fat mass (FM) and visceral adipose tissue (VAT) were measured by DXA and MRI, respectively, at baseline and posttest. A significant linear upward trend indicating dose-response to exercise was observed for OC, PINP, and insulin sensitivity (all $P < 0.04$). A dose-response benefit of exercise was also observed for FM and VAT as indicated by significant downward trends (both $P < 0.04$). There was no dose-response effect of exercise on ICTP. Multiple linear regression adjusting for age, sex and race revealed that changes in both OC and PINP were positively associated with changes in insulin sensitivity but negatively associated with changes in VAT (all $P < 0.04$). Changes in bone resorption were not associated with changes in VAT, nor were changes in bone formation or resorption associated with changes in FM. In obese children, 12-weeks of vigorous exercise increased bone formation and insulin sensitivity and decreased total and visceral adiposity in a dose-response manner. However, the relationship observed between bone formation and central, rather than total, adiposity suggests the need for further studies identifying the link between bone formation and visceral fat, which may be explained by glucose homeostasis.

Disclosures: Norman Pollock, None.

1178

Mutant Mouse Models Reveal Indispensable Role for Thyroid Hormone (TH) Acting Via Growth Hormone (GH)-dependent and -independent Mechanisms to Regulate Bone and Fat Phenotypes during the Pre-pubertal Growth Period. Weriong Xing^{*}, Heather Davidson, Sheila Pourteymoor, Anil Kapoor, Subburaman Mohan, Jerry L. Pettis Memorial VA Medical Center, USA

Mouse models with disruption of IGF-I and GH actions have shown that while GH is the major regulator of bone accretion during pubertal and post-pubertal periods, GH-independent mechanisms predominantly contribute to bone accretion during prepubertal growth. Accordingly, our recent studies with TH-deficient mutant mouse models ($Tshr^{hyt/hyt}$ and $Duox2^{-/-}$) reveal that TH is indispensable for

prepubertal bone accretion. To determine the relative contribution of GH and TH axis to prepubertal rise in bone accretion, we evaluated skeletal phenotypes in mice lacking TH ($Tshr^{hyt/hyt}$), GH ($Ghrh^{lit/lit}$) or both ($Tshr^{hyt/hyt};Ghrh^{lit/lit}$). We found TH deficiency-induced reductions in total body, femur and tibia BMD (12, 30 and 27%) were significantly greater than those (5, 13 and 10%) seen in GH-deficient mice at the end of prepubertal growth period. In contrast, % body fat was increased similarly (30%) in TH and GH-deficient mice. While mice that are deficient in both TH and GH did not exhibit significantly greater skeletal deficit than TH deficiency alone, % body fat increase (49%) was significantly greater in double mutant mice. Treatment of TH deficient $Tshr^{hyt/hyt};Ghrh^{lit/+}$ mice with administration of T3/T4 during day 5-14 rescued IGF-I, bone and fat phenotypes. Total body, femur and tibia BMD were increased by 24, 37 and 39% respectively while % body fat was decreased by 30% compared to vehicle treatment. While treatment of $Tshr^{hyt/hyt};Ghrh^{lit/lit}$ double mutant mice with both GH and T3/T4 increased total body, femur and tibia BMD by 14, 24 and 30%, respectively neither T3/T4 nor GH treatment alone rescued the skeletal phenotype in the double mutant mice. Micro-CT measurements of femur metaphysis revealed significant decreases in trabecular BV/TV (24%) and thickness (12%) in the double mutant mice that were rescued by combined GH/TH treatment but not by individual treatment. In contrast, T3/T4 or GH treatment alone significantly decreased % body fat in the double mutant mice. Conclusions: 1) TH deficiency produces greater skeletal deficit than GH deficiency during prepubertal growth period; 2) While T3/T4 treatment rescues skeletal deficit in TH deficient mice, administration of both GH and T3 are required during prepubertal growth period to rescue skeletal deficit in the double mutant mice; and 3) TH effects on fat phenotype is GH-independent, thus suggesting that mechanisms that mediate TH actions in target tissues are complex.

Disclosures: Weriong Xing, None.

1179

Catch Up in Bone Acquisition in Young Adult Men with Late Puberty. Anna Darelid^{*1}, Claes Ohlsson², Martin Nilsson³, Jenny Kindblom⁴, Dan Mellstrom², Mattias Lorentzon². ¹Gothenburg University, Sweden, ²Center for Bone Research At the Sahlgrenska Academy, Sweden, ³Centre for Bone & Arthritis Research At the Sahlgrenska Academy, Sweden, ⁴Sahlgrenska University Hospital, Sweden

Late menarche has been associated with lower bone mineral density (BMD) at the time of peak bone mass as well as lower adult BMD and elevated risk of osteoporosis in studies of women. The influence of pubertal timing on adult BMD in men is not clear. We have earlier reported, in the GOOD Study of 19-year old males in Sweden, that late puberty was associated with lower BMD in a cross-sectional study. The aim of the present study was to investigate whether late puberty was associated with remaining low BMD in early adulthood, or if a catch up effect occurs. In total, 501 men (18.90.5 yrs at baseline and 24.10.6 yrs at follow-up) were included in this five-year longitudinal study. Areal BMD (aBMD), volumetric BMD (vBMD) and cortical bone size were assessed using DXA and pQCT. Detailed growth and weight charts were used to estimate peak height velocity (PHV), an objective assessment of pubertal timing. PHV (mean 13.51.0 yrs) was found to be a positive predictor of the increase in total body, radius, and lumbar spine aBMD between 19 and 24 yrs ($p < 0.0001$). Late puberty was also associated with a lesser decrease in femoral neck aBMD ($p < 0.0001$). Subjects were divided into tertiles (early, average, late) according to PHV. At the total body, men in the late tertile gained markedly more in aBMD (0.060.04 vs 0.030.04 g/cm², $p < 0.0001$) and lost less in femoral neck aBMD (-0.020.07 vs -0.050.06, $p < 0.0001$) than men in the early tertile. A similar pattern was seen for the radius and the lumbar spine (Figure 1). At age 24, no significant differences between the tertiles in aBMD of the lumbar spine, femoral neck, or total body were observed, while a deficit of 4.2% in radius aBMD was seen for men in the late vs. the early tertile ($p < 0.0001$). However, this deficit was markedly lower than what was observed at the baseline exam (8.2%). Thus, a notable catch up in BMD occurred over the five-year study period. pQCT measurements of the radius at follow-up demonstrated no significant differences in bone size, whereas cortical and trabecular vBMD were 0.7% ($p < 0.001$) and 4.8% ($p < 0.05$) lower in the late compared to the early tertile, respectively. In conclusion, our results demonstrate that late puberty in males was associated with a substantial catch up in aBMD in young adulthood, leaving no deficits in aBMD of the lumbar spine, femoral neck or total body at age 24, whereas aBMD of the radius was still significantly lower in men with late pubertal onset.

CHANGE IN ABMD OVER FIVE YEARS ACCORDING TO PEAK HEIGHT VELOCITY

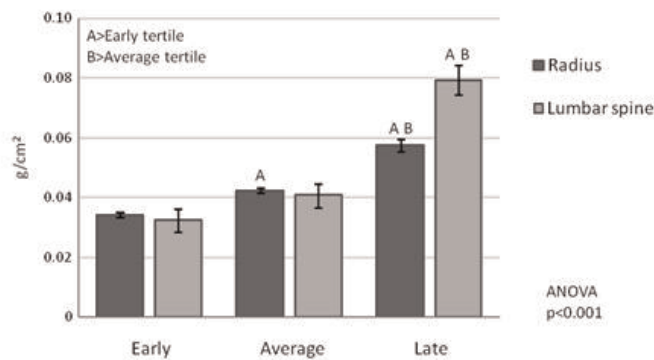


Figure 1 - Catch Up in Bone Acquisition in Young Adult Men with Late Puberty

Disclosures: Anna Darelid, None.

1180

Vitamin D Binding Protein Genotype Is Associated with Vitamin D Status and Bone Health in Finnish Children and Adolescents. Elisa Saarnio¹, Minna Pekkinen², Heli Viljakainen³, Outi Makitie⁴, Christel Lamberg-Allardt². ¹University of Helsinki, Finland, ²University of Helsinki, Finland, ³Helsinki University Central Hospital for Children & Adolescents, Fin, ⁴Hospital for Children & Adolescents, Helsinki University Hospital, Finland

Vitamin D and its metabolites in serum are transported by vitamin D binding proteins (DBP, or group-specific component, Gc) into target tissues. Studies have shown that DBP correlate positively with serum vitamin D metabolites and that DBP phenotype influences serum 25-hydroxyvitamin D (25-OHD) concentration. DBP also impacts bone cell metabolism by activating osteoclasts. Furthermore protein isoform has been associated with decreased bone mineral density (BMD) and increased fracture risk.

Our aim was to study the role DBP genotypes on vitamin D status and (BMD) in 231 healthy children and adolescents (160 girls, 71 boys) aged 7-19 years. Lumbar spine (LS), femoral head (Fem) and whole body (WB) BMD was measured with DXA (Hologic Discovery A), and for a subgroup of 174 subjects, volumetric BMD was measured from non-dominant radius with pQCT (XCT-2000; Stratec). Dietary intakes of vitamin D and calcium were calculated with a validated food frequency questionnaire. The concentrations of serum 25-OHD, PTH and Ca were determined. DNA was isolated from blood samples. Genotyping was performed with qPCR (MX3000P, Stratagene) based on single nucleotide polymorphism (rs4588=Thr420Lys) in the DBP gene (homozygote 1/1, heterozygote 1/2, homozygote 2/2). Statistical analyses were performed with PASW18.

The distribution of the SNP among the subjects was: Gc 1/1 68%, Gc 1/2 26% and Gc 2/2 6%. There was a significant difference in 25-OHD levels between the genotypes, the concentration being highest in Gc 1/1 (47.4 nmol/L), intermediate in Gc 1/2 (42.6 nmol/L) and lowest in Gc 2/2 (40.6 nmol/L) based on ANCOVA-analysis, adjusted for PTH, vitamin D and Ca intake ($p=0.018$). Gc genotype associated with BMD Z-scores in boys with mean WB BMD Z-scores of +0.23 vs -0.26 ($p=0.029$) and LS BMD Z-scores of +0.39 vs -0.20 ($p=0.017$) in genotypes 1/1 ($n=53$) 1/2 and 2/2 ($n=18$). In girls no difference in BMD values was observed between the genotype groups. In both genders, Gc genotype was independently associated with stress and strain index Z-scores (SSI) in multivariate regression models adjusted for height, Ca intake, 25-OHD, PTH, fat %, lean body mass, pubertal stage and exercise, ($p=0.001$).

These results suggest that 25-OHD differ among vitamin D binding protein genotypes and that there is variation in BMD and bone strength among them. Variation in 25-OHD among genotypes may suggest differences in vitamin D utilization. DBP may be one factor affecting bone mass accrual in adolescence.

Disclosures: Elisa Saarnio, None.

1181

Sc65 is a Novel Regulator of Bone Homeostasis. Brittany Hendrix¹, Katrin Gruenwald¹, Patrizio Castagnola², Dana Gaddy¹, Larry Suva¹, Roy Morello¹. ¹University of Arkansas for Medical Sciences, USA, ²National Institute for Cancer Research, Italy

We and others recently showed that mutations in the *CRTAP* (encoding cartilage-associated protein) and *LEPRE1* (encoding prolyl 3-hydroxylase 1 or P3H1) genes cause recessive osteogenesis imperfecta (OI). This represented a major step forward in understanding the molecular basis of this disease and has now led to the identification of additional genes (*PPIB*, *SERPINH1* and *FKBP10*) linked to recessive human OI.

Such findings have shifted current OI research from matrix components (i.e. type I collagens) to rough endoplasmic reticulum resident proteins, and highlighted the complex cellular task of synthesizing and folding a collagen trimeric molecule. Having previously characterized the prolyl 3-hydroxylation complex, containing *Crtap*, *P3h1* and *Cyclophilin B* (*CypB*), we now extended our studies to determine the role of *Sc65*, a poorly known member of the *Leprecan* gene family and coding for the most closely related protein to *Crtap* with >50% amino acid identity. While *Sc65* was originally described as a nuclear epitope and then more recently as a cytoplasmic 'adaptor protein', we show that it localizes to the rER similarly to the other *Leprecan* proteins and it is highly expressed during skeletal formation. We then identified a gene-trap ES cell clone containing a proviral insertion in exon 5 of the *Sc65* gene. We obtained chimeric, heterozygotic and then homozygotic mice for this insertional construct. Western blot from *Sc65* mutant and WT tissues reveal absence or markedly reduced *Sc65* protein in the former. Micro-CT analysis of the appendicular skeleton at 10 weeks of age ($n=6$ males) shows statistically significant reduction in BV/TV and other static parameters in both tibia and femur. Cortical scans of the femur also demonstrate significantly reduced cortical cross sectional area (CSA) and thickness, with increased total CSA and endosteal perimeter. Histomorphometric analysis suggests no difference in dynamic indices of bone formation or in osteoclast parameters in tibias of *Sc65* mutant mice compared to controls. Current efforts are aimed at elucidating the cellular and molecular mechanisms causing low bone mass. In conclusion, our data suggest that impaired *Sc65* function has an impact on bone homeostasis, similarly although not as dramatically to what we have observed with lack of *Crtap* function.

Disclosures: Roy Morello, None.

1182

Aberrant Osteoblast and Osteoclast Activity in Connexin43 G60S Missense Mutant Mice Leads to Age-related Bone Anomalies. Tanya Zappitelli¹, Frieda Chen¹, Marc Grynpas², Janet E. Henderson³, Luisa Moreno², Ralph Zirngibl¹, Jane Aubin⁴. ¹University of Toronto, Canada, ²Samuel Lunenfeld Research Institute, Canada, ³McGill University, Canada, ⁴University of Toronto Faculty of Medicine, Canada

Oculodentodigital dysplasia (ODDD) is a human disease caused by a mutation in the *GJA1* gene which encodes Connexin43 (Cx43). Using a genome-wide ENU-mutagenesis screen, we isolated a mutant mouse line, *Gja1*^{Jr/+}, with a dominant negative G60S missense mutation in Cx43 (Flenniken et al. 2005). In addition to having the classical symptoms of ODDD, such as craniofacial deformities and syndactyly, *Gja1*^{Jr/+} mice are osteopenic, but differences in BMD compared to wild type (WT) littermates become less pronounced with age. To elucidate the mechanisms underlying the bone anomalies, we performed histomorphometric and cell and molecular biology experiments. Histomorphometry confirmed that *Gja1*^{Jr/+} mouse bones exhibit significantly lower BV/TV and trabecular number and thickness than WT bones at 2 and 4 months, but differences diminished to non-significance by 12 months of age, concomitant with increases in cortical bone in *Gja1*^{Jr/+} but not WT mice. No differences were seen in osteoblast or osteocyte number in bones from *Gja1*^{Jr/+} versus WT mice, but expression of several mature osteoblast markers, most notably *Bsp* and *Ocn*, were significantly higher in RNA from trabecular bone and late differentiation time points in stromal cell cultures, suggesting that *Gja1*^{Jr/+} osteoblasts make an abnormal bone matrix. Osteoprogenitor numbers in the *Gja1*^{Jr/+} mutant were largely unchanged, however a non-significant increase in older mice was noted. Osteoclast surface per bone surface was significantly increased in *Gja1*^{Jr/+} versus WT bone, along with a significant increase in expression of *Cathpsink* mRNA. *In vitro* bone marrow or spleen cell cultures supplemented with M-CSF and RANKL showed no differences in osteoclast differentiation, fusion or resorption activity in *Gja1*^{Jr/+} versus WT. However, immunoblots showed a significant increase in *Rankl* protein expression from trabecular bone of *Gja1*^{Jr/+} mice versus WT. We conclude first that the G60S allele results in hyperactivity of osteoblasts, as reflected in overexpression of *Bsp* and *Ocn* matrix proteins, as well as osteoclast differentiation and activation cytokine *Rankl*. The latter results in more and hyperactive osteoclasts in *Gja1*^{Jr/+} mice, resulting in a high turnover state and ensuing osteopenia in young *Gja1*^{Jr/+} mice. Second, increased osteoblast activity and osteoprogenitor number leads to significant new bone accrual, protecting older *Gja1*^{Jr/+} mice from the age-related bone loss that occurs in WT.

Disclosures: Tanya Zappitelli, None.

1183

Modeling Skeletal Diseases in iPS Cells. Edward Hsiao¹, Yohei Hayashi², Trieu Nguyen², Sahar Tahari², Matthew Spindler², Christopher Schlieve², Salma Sami², Shinya Yamanaka², Bruce Conklin², Robert Nissenson³. ¹University of California, San Francisco, USA, ²Gladstone Institute of Cardiovascular Disease, USA, ³VA Medical Center & University of California, San Francisco, USA

Skeletal diseases are a growing medical concern worldwide. Human diseases affecting the skeleton are challenging to study because of the lack of human models. Skeletal tissues derived from induced pluripotent stem (iPS) cells are promising tools for studying human genetic diseases from patients with known phenotypes. However, our understanding of how pluripotent stem cells can be guided to form skeletal tissues

is rudimentary. We established a robust and simple in vitro model of osteoblast differentiation based on human iPS cell cultures. The osteogenic media contains FBS, ascorbic acid, dexamethasone, and beta glycerol phosphate. iPS cell-derived osteoblasts showed strong mineralization after day 15 as detected by von Kossa staining. We also found high expression of osterix at day 6 of differentiation and increasing levels of collagen I and osteocalcin at days 15 and 24, indicating formation of both immature and mature osteoblasts in our culture system. To test whether the iPS model could recapitulate aspects of human skeletal disease, we established human iPS cell lines from patients with Fibrodysplasia Ossificans Progressiva (FOP), a disease with dramatically increases skeletal tissue formation. Multiple iPS cell lines were successfully generated by viral transduction of four pluripotency-inducing factors (Oct4, Sox2, Klf4, and cMyc) into skin fibroblasts from two independent FOP patients carrying the classical R206H mutation in ACVR1. We confirmed that the FOP iPS cells carried the R206H mutation and expressed pluripotency markers. Embryoid bodies derived from FOP iPS cells expressed marker genes for all three germ layers, but teratomas formed by the FOP iPS cells had decreased neuronal elements by histology. Osteogenic differentiation of FOP iPS cells showed significantly more mineralization as compared to wildtype controls. Although further analysis of the gene expression profiles of these cells is underway, our current results indicate that the R206H mutation in FOP iPS cells may confer increased mineralization activity as compared to control iPS cells. These findings show that stem cell-based models could be valuable for studying genetic diseases of osteoblast formation and function. These models will also be useful for dissecting the molecular pathogenesis and identifying new therapeutic approaches for disorders affecting skeletal tissues.

Disclosures: Edward Hsiao, None.

1184

Increased Levels of TAF12 with IL-6 Can Substitute for MVNP to Induce Pagetic-Osteoclasts. Jumpei Teramachi¹, Jolene Windle², Noriyoshi Kurihara¹, G. David Roodman³. ¹University of Pittsburgh & The Center for Bone Biology at UPMC, USA, ²Virginia Commonwealth University, USA, ³University of Pittsburgh, The Center for Bone Biology at UPMC, & VA Pittsburgh Healthcare System, USA

We have shown that osteoclasts (OCL) from Paget's (PD) patients express measles virus nucleocapsid protein (MVNP), that anti-sense MVNP significantly blocked the increased OCL formation and nuclei per OCL, TATA box-binding protein associated factor 12 (TAF-12) expression, 1,25-(OH)₂D₃-stimulated IL-6 production, and bone resorption characteristic of OCL formed in PD patient marrow cultures. In contrast, PD patients not expressing MVNP and normals formed normal OCL. There was no effect of anti-sense MVNP on OCL formation or any other parameters of OCL activity in cultures from PD patients not expressing MVNP or normals. These results indicate that MVNP was responsible for the unique characteristics of OCL generated from PD patients. Mice expressing MVNP in cells of the OCL lineage formed pagetic OCL and bone lesions, which were lost when they were bred with IL-6^{-/-} mice. These results demonstrate an important role for IL-6 in the development of PD OCL and bone lesions. It is our hypothesis that both increased VDR responsiveness induced by TAF12 and high levels of IL-6 are sufficient to induce pagetic OCL. Therefore, we generated transgenic mice with TAF12, IL-6 or both TAF12/IL-6 targeted to the OCL lineage using the TRAP promoter and determined if pagetic OCL formed. OCL precursors from TAF12 and TAF12/IL-6 mice were hyper-responsive to 1,25-(OH)₂D₃ and formed OCL at low concentrations (10⁻¹⁰ M) of 1,25-(OH)₂D₃ compared to WT. Further, OCL that formed from TAF12/IL-6 mice were hyper-multinucleated compared to IL-6 or WT mice. 1,25-(OH)₂D₃ increased bone resorption in marrow cultures from the three transgenic mice compared to WT with the percent of area of bone resorption dramatically increased in TAF12/IL-6 (28.02.2) compare to WT (0.80.1), TAF12 (4.91.1) and IL-6 (6.92.1) mice. OCL precursors from these mice were then incubated with 1,25-(OH)₂D₃, and activation of MAPKs and STAT3 pathways determined. Increased levels of the phosphorylated forms of Erk and p38 were found in TAF12, IL-6 and TAF12/IL-6 lysates at 2-5 minutes after incubation with 1,25-(OH)₂D₃. OCL precursors from IL-6 and TAF12/IL-6 but not TAF12 mice showed increased p-STAT3 activation (up to 3-fold) as compared to WT OCL precursors treated with 1,25-(OH)₂D₃. These results suggest increased endogenous levels of IL-6 in combination with hyper-responsivity of OCL precursors to 1,25-(OH)₂D₃ may be sufficient to induce pagetic OCL in vivo via enhanced ERK, p38 and STAT3 signaling.

Disclosures: Jumpei Teramachi, None.

1185

Sclerostin Antibody Improves Bone Mass and Mechanical Properties in an Adult Brtl/+ Model of Osteogenesis Imperfecta. Benjamin Sinder¹, Logan White¹, Michelle Caird¹, Joan Marin², Kenneth Kozloff³. ¹University of Michigan, USA, ²National Institute of Child Health & Human Development, USA, ³University of Michigan Department of Orthopaedic Surgery, USA

Osteogenesis imperfecta (OI) is a genetic collagen disorder characterized by brittle bones. While OI fracture risk is generally greater in a pediatric population, it can remain a problem into adulthood. No anabolic therapy has yet been shown consistently effective in treating OI. Sclerostin is a negative regulator of the Wnt pathway, and a neutralizing sclerostin antibody (Scl-Ab) therapy has proven anabolic

in other fragility models. The purpose of this study was to evaluate Scl-Ab in an adult Brtl/+ mouse model of OI with G349C mutation on colla1. At 6 months, Brtl/+ has previously shown reduced trabecular MAR and BFR vs. WT, making this a good model for OI patients with diminished osteoblast activity to evaluate Scl-Ab. Male 6 month WT and Brtl/+ were treated with Scl-Ab or Vehicle twice per week, for five weeks, at 25mg/kg. All changes noted are p<0.05, n=7-9/group. Body weight was not changed by Scl-Ab therapy in either WT or Brtl/+ during the five weeks of treatment. Dynamic histomorphometry at femoral mid-diaphysis on a subset (n=5/group) showed that Scl-Ab increased periosteal BFR in both WT (159%) and Brtl/+ (205%). This was a result of increases in MAR (WT 98%; Brtl/+ 95%) and MS/BS (WT 35%; Brtl/+ 63%). MicroCT of the distal metaphyseal femur revealed Scl-Ab increased BV/TV in both WT (117%) and Brtl/+ (119%). BV/TV increases were a result of increased Tb.Th (WT 38%; Brtl/+ 29%) and Tb.N (55% WT; Brtl/+ 70%). Scl-Ab increased cortical thickness (WT 42%; Brtl/+ 22%) and cross sectional area (WT 36%; Brtl/+ 21%) at femoral mid-diaphysis with no effect on tissue mineralization (TMD). Functionally, Scl-Ab increased femoral diaphyseal Ultimate Force (WT 129%; Brtl/+ 127%) and Energy to Failure (WT 526%; Brtl/+ 509%) as measured by four-point bending. Scl-Ab did not change the estimated elastic modulus in WT or Brtl/+, in agreement with microCT TMD data. The mid span yield-displacement to failure-displacement ratio was reduced with Scl-Ab (WT 47%; Brtl/+ 36%), suggesting Scl-Ab reduced bone brittleness. In summary, Scl-Ab increased osteoblast activity, improved bone mass and whole bone mechanical properties, and reduced brittleness in an adult Brtl/+ model of OI characterized by low osteoblast activity. These initial data support that Scl-Ab may be beneficial for the treatment of OI patients by stimulating the deficient osteoblast population and reducing fracture risk.

Disclosures: Benjamin Sinder, None.

1186

Genetic Deletion of Osteopontin Restores Unloading Mediated Bone Loss in a NF1 Murine Model. Ping Zhang¹, Shi Chen², Yongzheng He², Xiaohua Wu², Steven D. Rhodes², Xianlin Yang², Jin Yuan², Li Jiang², Feng-Chun Yang². ¹Indiana University School of Medicine, USA, ²Indiana University School of Medicine, USA

Osteopontin (OPN), the spp1 gene product, plays an important role in bone biology. Neurofibromatosis type 1 (NF1) patients have a high incidence of osteoporosis/osteopenia. We previously reported that Nf1 haploinsufficient (^{+/-}) preosteoblasts hypersecrete OPN leading to a gain in osteoclast bone resorptive activity in vitro. The object of this study is to evaluate whether genetic deletion spp1 (OPN) prevents bone loss in hindlimb unloaded Nf1^{+/-} mice, a model of osteopenia.

Four genotypes of mice were used for this study: WT, Nf1^{+/-}, spp1^{-/-}, and Nf1^{+/-}; spp1^{-/-}. 12 age-matched mice per genotype were subjected to tail suspension for 2 weeks, and non-unloaded mice were used as controls. Changes in femoral BMD and BMC were measured by pDEXA. The impact of the osteoclast lineage on the bone loss following the unloading was also assessed by (1) scoring the osteoclast area in the femoral metaphyses following tartrate-resistant acid phosphatase (TRACP) staining and (2) scoring the frequency of osteoclast progenitors by the colony forming unit-macrophage assay (CFU-M). To assess osteoclast function in vitro, osteoclast formation and migration were examined by TRACP staining and transwell assays respectively.

Unloading induced a significantly greater loss of femoral BMD and BMC in Nf1^{+/-} mice compared to WT controls. Importantly, genetic deletion of spp1 restored BMD and BMC in Nf1^{+/-} mice to WT levels (p<0.01). In addition, the femoral metaphyses of Nf1^{+/-} unloaded mice displayed a dramatic increase in TRACP⁺ area compared to WT mice (p<0.001), and Nf1^{+/-};spp1^{-/-} mice showed significantly reduced TRACP⁺ area in the femoral metaphyses. While unloading induced a significant increase in total of CFU-M in Nf1^{+/-} mice, deletion of spp1 reduced the CFU-M in Nf1^{+/-} mice to basal levels. Furthermore, bone marrow derived osteoclastic migration and formation were dramatically reduced in Nf1^{+/-};spp1^{-/-} cultures following unloading compared to that in Nf1^{+/-} cultures as determined by the transwell assay, TRACP⁺ area, and nuclear numbers per osteoclast (p<0.05).

Taken together, this study shows that Nf1^{+/-} mice exhibit accelerated bone loss following hindlimb unloading, which is associated with increased osteoclast formation. Importantly, genetic deletion of spp1 is sufficient to prevent bone loss in unloaded Nf1^{+/-} mice. This study provides evidence that OPN may be a potential molecular target for preventing bone loss in NF1 patients.

Disclosures: Ping Zhang, None.

1187

Targeting of the DAP12-associated, Osteoclast-specific Receptor Siglec-15 by Antibody 25E9 Inhibits Differentiation and Resorption Activity. MATTHEW STUIBLE^{*}, Annie Fortin, Elisabeth Viau, Marc Sasseville, Aida Kalbakji, Anna Moraitis, Mario Filion, Gilles Tremblay. Alethia Biotherapeutics, Canada

With the objective of developing monoclonal antibodies for novel therapeutic approaches in cancer-associated bone loss, we used a sensitive discovery platform to compare the molecular signature of mature human osteoclasts with that of their

precursor cells. Expression profiling in human osteoclast samples led to the prioritization of several candidate osteoclast-specific genes. One of these encodes Siglec-15, an immunoglobulin-like sialic acid-binding receptor. Members of the Siglec family play various roles in immune signaling and have expression patterns that are characteristically restricted to specific hematopoietic lineages. We confirmed by RT-PCR that Siglec-15 mRNA is upregulated in mouse bone marrow cells, human peripheral blood mononuclear cells and RAW264.7 cells upon induction of osteoclast differentiation with RANKL. Conversely, Siglec-15 expression was not detected in other cell types with the exception of lung tissue, where very weak expression was observed. To establish its functional relevance, Siglec-15 expression was attenuated by vector-based shRNA resulting in reduced differentiation and function of osteoclasts derived from mouse and human cells. These initial results prompted us to pursue development of therapeutic antibodies against human Siglec-15. After screening a library of antibodies by various binding and functional criteria, clone 25E9 was selected as the lead candidate. 25E9 detects Siglec-15 on the cell surface, and most importantly, it impairs differentiation of osteoclast precursor cells and bone resorption similar to Siglec-15-targeted shRNA. Since little was known regarding the normal cellular function of Siglec-15, the antibodies were used to explore its role in osteoclast signaling. We found that a complex of Siglec-15 and the ITAM-bearing co-receptor DAP12 was readily detectable in lysates from osteoclasts but not their precursors. The importance of DAP12 in osteoclastogenesis is well established, but its principal partner in this context was believed to be another receptor, TREM2. Our results suggest that the Siglec-15/DAP12 complex may in fact be more specific to osteoclasts than TREM2/DAP12, and we are currently investigating the downstream signaling pathways that are modulated when Siglec-15 is bound by 25E9. In conclusion, we have identified Siglec-15 as a functionally important osteoclast receptor that could be targeted by therapeutic antibodies such as 25E9 to control bone resorption in a highly specific manner.

Disclosures: MATTHEW STUIBLE, Alethia Biotherapeutics, 3
This study received funding from: Alethia Biotherapeutics

1188

Knockin Mice Bearing an Inactivating Mutation in the RANK IVVY Motif Exhibit Increased Bone Mass Due to Impaired Osteoclastogenesis. Zhenqi Shi*, Joel Jules, Bob Kesterson, Xu Feng. University of Alabama at Birmingham, USA

The receptor activator of NF- κ B (RANK) ligand (RANKL) and its receptor RANK play a vital role in osteoclastogenesis. As a member of the tumor necrosis factor (TNF) receptor family, RANK has been shown to promote osteoclastogenesis by activating various signaling pathways including NF- κ B, JNK, ERK and p38 by recruiting TNF receptor-associated factors (TRAFs). Nonetheless, several lines of evidence suggested that RANK may also activate unidentified TRAF-independent signaling pathways that are essential for osteoclastogenesis. To elucidate the hypothesized novel RANK signaling pathways, we previously carried out a systematic structure/function study of the RANK cytoplasmic domain using a non-biased in vitro mutation analysis approach, leading to identification of a specific 4-AA RANK motif (IVVY⁵³⁵⁻⁵³⁸) which plays a critical role in osteoclastogenesis by mediating commitment of macrophages to the osteoclast lineage. To validate the role of this IVVY motif in osteoclastogenesis in vivo, we have developed knockin (KI) mice bearing an inactivating mutation in the IVVY motif with a replacement type targeting vector which converts the wild type RANK allele to a mutated allele encoding a 2-AA substitution in the IVVY motif (IVVY to IVAF). Homozygous KI (RANK^{AF/AF}) mice are viable, born at the expected Mendelian frequency, and have normal tooth eruption. However, X-ray and micro-computed tomography (μ CT) analysis of femurs of 8-week old wild type (WT), heterozygous (RANK^{+AF}) and RANK^{AF/AF} mice have revealed a dramatic increase in bone mass in RANK^{AF/AF} compared to age and sex matched WT counterparts. Moreover, RANK^{+AF} mice exhibit increased bone mass compared to WT mice, suggesting that the presence of a single mutant RANK in RANKL-induced RANK trimers is sufficient to impair the normal signaling from the IVVY motif. Bone marrow macrophages (BMMs) from RANK^{AF/AF} mice failed to form osteoclasts in vitro in response to M-CSF and RANKL treatment. Consistent with the in vivo data, BMMs from RANK^{+AF} demonstrated reduced capacity to form osteoclasts compared to WT BMMs. Importantly, flow cytometric analysis showed that BMMs from RANK^{AF/AF} and RANK^{+AF} have similar levels of RANK cell surface expression compared to WT cells, ruling out the possibility that the failure of RANK^{AF/AF} BMMs to form osteoclasts is caused by a decrease in RANK surface expression. Taken together, these data indicate that the RANK IVVY motif plays a crucial role in osteoclastogenesis in vivo.

Disclosures: Zhenqi Shi, None.

1189

Targeted FoxO3 Overexpression in Osteoclast Progenitors and Mature Osteoclasts Inhibits NF-Kb Signaling and Osteoclastogenesis and Increases Bone Mass. Shoshana M. Bartell*, Elena Ambrogini, Li Han, Aaron Warren, Randal S. Shelton, Haibo Zhao, Xiahua Qiu, Joseph Goellner, Charles A. O'Brien, Maria Jose S. Almeida, Stavros C. Manolagas. Center for Osteoporosis & Metabolic Bone Diseases, Central Arkansas Veterans Healthcare System, University of Arkansas for Medical Sciences, USA

An increase in the generation of reactive oxygen species (ROS) has been strongly implicated in the decreased bone formation associated with advancing age as well as the increased resorption associated with estrogen deficiency. In line with this evidence, increased ROS production in osteoblasts stimulates apoptosis and decreases bone formation. On the other hand, ROS are a critical requirement for RANKL-induced osteoclast generation, activation, and survival. Based on this and evidence that global combined deletion of FoxO1,3,4 - an important transcriptional defense mechanism against excessive ROS generation- leads to an increase in ROS and osteoclast progenitor number and that the age-associated progressive increase in ROS production is not accompanied by an increase in mature osteoclast numbers in bone, we have hypothesized that FoxO activation is responsible for the dampening of osteoclast generation in aged mice. To test this hypothesis, we generated transgenic mice overexpressing FoxO3 in cells of the monocyte/macrophage lineage by crossing FoxO3-flox stop (FS) mice with LysM-Cre mice (FoxO3-FS;LysM-Cre). These mice exhibited a significant increase in BMD, as well as an increase in cancellous bone volume at 3 months of age as determined by micro-CT, in both vertebrae and femora. FoxO3-FS;LysM-Cre mice also exhibited increased trabecular number and decreased trabecular separation. Consistent with the changes in bone mass, the serum levels of the resorption marker CTx, as well as the mRNA levels of the osteoclast markers TRAP and cathepsin K in vertebral bone, were decreased. The osteoblast marker osteocalcin was unaffected. In line with these changes, bone marrow cultures established in the presence of RANKL and M-CSF from FoxO3-FS;LysM-Cre mice exhibited a significant decrease in osteoclast progenitors and mature osteoclast formation, increased osteoclast apoptosis, but normal macrophage proliferation. In line with the decreased osteoclastogenesis, activation of NF- κ B by RANKL is attenuated in macrophages from FoxO3-FS;LysM-Cre, as determined by I κ B phosphorylation. The demonstration of a suppressive effect of the gain of FoxO function on osteoclast generation and survival suggests that FoxO activation in response to OS not only plays a major role in the adverse effects of aging on osteoblasts but may influence osteoclasts as well.

Disclosures: Shoshana M. Bartell, None.

1190

Comprehensive Epigenetic Analysis Reveals Nedd9 is a Key Downstream Molecule of TGF- β Involving in RANKL-Induced Osteoclastogenesis. Yasunori Omata*, Tetsuro Yasui¹, Takumi Matsumoto¹, Hironari Masuda¹, Jun Hirose¹, Naoto Tokuyama¹, Hisataka Yasuda², Shuichi Tsutsumi³, Aburatani Hiroyuki⁴, Kozo Nakamura¹, Sakae Tanaka¹. ¹The University of Tokyo, Japan, ²Oriental Yeast Company, Limited, Japan, ³Genome science Division, RCAST, Univ.Tokyo, Japan

Previous studies found that TGF- β promotes RANKL-induced osteoclastogenesis, however its key downstream molecules remain unclear. We employed recently-established chromatin immunoprecipitation sequencing (ChIP-seq) method and comprehensively analyzed genes regulated by TGF- β in bone marrow-derived macrophages (BMMs). Smad2/3 work as transcription factors in TGF- β signal transduction. After treating BMMs with 2 ng/ml TGF- β for 1.5 hrs, cells were collected and chromatin immunoprecipitation using anti-Smad2/3 antibody was performed. To identify Smad2/3 binding sites globally, the immunoprecipitates were subjected to massively parallel DNA sequencing and the obtained data were mapped to the genome. 2,786 Smad2/3 binding sites were detected, and 992 of them (903 genes) exist around promoter region of RefSeq genes. Microarray analysis demonstrated that the expression of these Smad2/3 target genes was significantly upregulated by TGF- β treatment. To specify the key regulatory genes of osteoclast differentiation, we analyzed histone modification profiles of BMMs. Recent studies have revealed that histone modifications such as trimethylation of histone H3 lysine 4 (H3K4me3) and lysine 27 (H3K27me3) regulate gene transcription. It is elucidated that histone modifications of key developmental genes tend to change from H3K4me3/H3K27me3 bivalent to H3K4me3 monovalent status and then active transcription is induced. Through ChIP-seq analysis using anti-H3K4me3 antibody and anti-H3K27me3 antibody, we identified 35 genes whose histone modification pattern was converted from K4/K27 bivalent to K4 monovalent by TGF- β . Seven of them were Smad2/3 target genes, and Nedd9 is one of these extracted genes. Nedd9 is known as a member of the Crk-associated substrate (CAS) family and is expressed in lymphocytes and epithelial cells, and also involved in cell migration, metastasis of cancer cell and integrin- β 1 signaling although its role in osteoclasts remains unknown. In vitro gene silencing of Nedd9 using small interfering RNA induced remarkable suppression of RANKL-induced osteoclastogenesis. Indeed, Nedd9 knockout mice exhibited increase of bone mass with decreased osteoclastogenesis. These results indicate that Nedd9 is a key downstream target of TGF- β which critically regulates osteoclast differentiation. In summary, we performed comprehensive analysis using a novel ChIP-seq method and identified Nedd9 as an important downstream molecule of TGF- β .

Disclosures: Yasunori Omata, None.

1191

Bone Marrow Adiposity Affects Osteoclastogenesis by Modulating the Bone Marrow Niche. He Fu^{*1}, Dominique Pierroz², Anne Wilson³, Serge Ferrari⁴, Beatrice Desvergne⁵. ¹CIG University of Lausanne, Switzerland, ²University Hospital of Geneva, Switzerland, ³LICR@UNIL, Switzerland, ⁴Geneva University Hospital & Faculty of Medicine, Switzerland, ⁵CIG UNIL, Switzerland

The nuclear receptor PPAR γ inhibits osteogenesis by favoring adipogenesis from common mesenchymal progenitors. The PPAR γ agonist (anti-diabetic drug TZD) could cause bone loss and accumulation of marrow adiposity in mice and in postmenopausal women, suggesting a link between PPAR γ and bone turnover. Until recently PPAR γ -/- mice were not available due to embryonic lethality. However, we recently succeeded in generating mice carrying a total deletion of PPAR γ . They exhibit a severe lipodystrophy in addition to further effects on bone homeostasis.

PPAR γ +/- mice have elevated bone mineral density (BMD), consistent with previous data reported. PPAR γ -/- mice also have elevated BMD in their vertebrae. Strikingly, the tibia and femur exhibited a lower BMD than heterozygous controls (77.9 \pm 3.9a vs. 87.5 \pm 2.1). Analyses of osteoblast differentiation from mesenchymal stem cells and calcium deposition from pre-osteoblast cultures did not provide an explanation for the paradoxical phenotype between long and short bones. We thus further investigated osteoclastogenesis from hematopoietic stem cells (HSC). PPAR γ -/- HSCs produce an increased number of TRAP+ osteoclasts in culture compared to WT and heterozygous controls (171 \pm 29ab vs. 125 \pm 23 vs. 69 \pm 12). Histological analyses confirmed larger resorption areas in PPAR γ -/- long bones.

While flow cytometry analyses showed a general decrease in HSCs and progenitors, an increased proportion of osteoclast progenitors (GMP) were observed in PPAR γ -/- bone marrow. In addition extramedullary hematopoiesis was found in peripheral organs and confirmed by histological analysis. Moreover, the lack of adipose tissue created a favorable niche for osteoclastogenesis since conditioned medium made from differentiated adipocytes, 3T3L1, inhibited osteoclastogenesis from both PPAR γ -/- and WT cells. Thus, adipokine deficiency in PPAR γ -/- mice contributes to de-repress osteoclastogenesis. Using a specific blocking antibody, we further identified adiponectin as the major player among dozens of adipokines.

These data suggest that PPAR γ regulates bone turnover by both a direct effect on cell differentiation and an indirect effect on cell fate determination through adipocyte and adipokine secretion. These specific characteristics provide support for a key role of PPAR γ at the cross roads of osteogenesis, adipogenesis and hematopoiesis/osteoclastogenesis.

a, p<0.05 vs. PPAR γ +/- ; b, p<0.05 vs. PPAR γ +/-

Disclosures: He Fu, None.

1192

Lis1 Plays an Important Role in Bone Resorption by Regulating Microtubule Organization and Dynein Function in Osteoclasts. Shiqiao Ye^{*1}, Tristan Fowler¹, Nathan Pavlos², Pei Ying Ng³, Yunfeng Feng⁴, Ming Hao Zheng², Richard Kurten⁵, Stavros Manolagas¹, Haibo Zhao¹. ¹University of Arkansas for Medical Sciences, USA, ²University of Western Australia, Australia, ³The University of Western Australia, Australia, ⁴Department of Internal Medicine, Washington University School of medicine, USA, ⁵Department of Physiology & Biophysics, University of Arkansas for medical Sciences, USA

Cytoskeleton reorganization is critical for osteoclast (OC) activation and function. Microfilaments are first organized into podosomes and then form an actin-ring at the sealing zone of active OCs. Microtubules (MTs), stabilized by tubulin acetylation, are required for podosome patterning and the sealing zone formation. In mammalian cells, MT organization is regulated by MT-associated proteins (MAPs) such as MT plus-end capping proteins, CLIP-170 and EB1. The transportation of these MAPs to the cell cortex is essential for MT distribution and the process is mediated by MT-based motor, cytoplasmic dynein, and LIS1, a critical molecule regulating MT dynamics and dynein function. To determine whether the LIS1/dynein pathway plays a role in OC MT organization and bone resorption, we have generated LIS1 macrophage conditional knockout (cKO) mice by crossing LIS1-floxed mice with LysM-Cre mice. LIS1 expression was abolished in macrophages and OCs isolated from LIS1 cKO mice but not in those from wild type (WT) mice, as shown by western blots. LIS1 cKO mice were normal in size and tooth-eruption. However, at 3 months of age, the mice had increased BMD and BV/TV measured by DEXA and micro-CT, as compared to their WT littermates. Reflecting an impaired OC bone resorption in LIS1 cKO mice, macrophages isolated from these mice had intrinsic defects in OC differentiation and function as revealed by a decreased number of TRAP+ mature OCs, aberrant MT organization, decreased resorption pits formation, and reduced levels of TRAP 5b and CTx-I in culture medium. The attenuated OC formation in LIS1-null macrophages was associated with a significant decrease in macrophage proliferation, osteoclast differentiation and survival, due to a reduced activation of ERK and AKT by M-CSF and a prolonged RANKL-induced JNK activation. Consistent with its critical role in MT organization and dynein function in other cell

types, we found that LIS1 binds to and colocalizes with dynein in OCs. Loss of LIS1 led to disorganized MTs and aberrant dynein function, as demonstrated by dispersed Golgi apparatus and abnormal distribution of CLIP-170 and EB1. More importantly, depletion of LIS1 in OCs inhibited Cathepsin K secretion into the resorption lacuna and OC motility as examined by confocal and time-lapse video microscopy. In conclusions, the LIS1/dynein pathway represents a previously unappreciated and novel mechanism regulating OC MTs and differentiation/function in vivo and in vitro.

Disclosures: Shiqiao Ye, None.

1193

IGF-1 Maintains Bone Mass by Inducing Osteoblast Differentiation of MSCs during Bone Remodeling. Lingling Xian^{*1}, Xiangwei Wu², LIJUAN PANG², Tao Qiu², Frank Frassica³, Clifford Rosen⁴, Shouhong Xuan⁵, Argiris Efstratiadis⁵, Mei Wan², Xu Cao⁶. ¹Johns hopkins university school of Medicine, USA, ²Johns Hopkins University School of Medicine, USA, ³Department of Orthopaedic Surgery, Johns Hopkins University School of Medicine, USA, ⁴Maine Medical Center, USA, ⁵Medical Center of Genetics & Development, Columbia University, USA, ⁶Johns Hopkins University, USA

Bone mass peaks in late adolescence, plateaus for several years, and then declines to a point in which osteoporosis is established. Maintenance of peak bone mass (PBM) is thought to prevent osteoporosis and reduce risk of fracture. IGF-1 is integral to the acquisition of PBM. However, it is unclear how IGF-1, abundantly deposited in the bone matrix, maintains bone mass in adults. Here we report that IGF-1 released from bone matrix stimulates osteoblast differentiation of MSCs for bone formation during bone remodeling. The bone resorption conditioned medium (CM) induces osteoblast differentiation of MSCs, and IGF-1 antibody inhibited the differentiation. Osteoclast CM with bone slices contains high level of IGF-1, but the control CMs including osteoclasts alone do not have detectable level of IGF-1. Moreover, phosphorylated IGF-1R is primarily found at the bone resorptive sites as defined by the presence of TRAP+ osteoclasts while the IGF-1R+ cells are evenly distributed in the bone marrow, indicating that IGF-1 is released during osteoclastic bone resorption.

To demonstrate that IGF-1 induces osteoblast differentiation of the recruited MSCs at bone resorptive sites, GFP-labeled Sca-1+ MSCs isolated from either Igf-1r-/- mice or their WT littermates were injected in the femoral cavity of immunodeficient Rag2-/- mice. The injected MSCs in the femur were co-immunostained for GFP and osteocalcin. IGF-1R WT-derived GFP-labeled MSCs were found to be osteocalcin+ at bone surfaces whereas Igf-1r-/- derived MSCs were rarely positive for osteocalcin two weeks after injection, indicating IGF-1 is essential for differentiation of the recruited MSCs. The Igf-1r-/- mice exhibited low bone mass and reduced mineral apposition rates. The CFUs of Igf-1r-/- mice was equivalent to their WT littermates, but the CFU-Obs decreased, indicating the osteogenic potential of the MSCs is reduced in Igf-1r-/- mice. We then crossed the floxed IGF-1R mice with Osteix-Cre:GFP mice to generate IGF-1R knockout mice in which IGF-1R was specifically deleted in the osteoblast-expressing cells and labeled with expression of GFP. The IGF-1R-deficient osteoprogenitors were GFP+ and primarily found at the bone surface, but not osteocalcin+, indicating release of IGF-1 from bone matrix is essential for osteoblast differentiation of MSCs. Collectively, IGF-1 released from the bone matrix stimulates osteoblast differentiation of MSCs for new bone formation in each remodeling cycle to maintain bone mass.

Disclosures: Lingling Xian, None.

1194

Parathyroid Hormone-related Peptide (PTHrP) Inhibits Chondrocyte Hypertrophy by Stimulating Actions of Histone Deacetylase (HDAC) 4. Shigeki Nishimori^{*1}, Forest Lai¹, Elena Kozhemyakina², Eric Olson³, Andrew B. Lassar², Henry Kronenberg¹. ¹Massachusetts General Hospital, USA, ²Department of Biological Chemistry & Molecular Pharmacology, Harvard Medical School, USA, ³UT Southwestern Medical Center At Dallas Department of Molecular Biology, USA

Both PTHrP and HDAC4 inhibit chondrocyte hypertrophy, but it has been unknown whether they work in a common pathway. A recent report from Lassar's group used chick primary chondrocytes and a chondrocyte cell line *in vitro* to show that PTHrP, through activation of protein phosphatase 2, leads to HDAC4 inhibition of myocyte enhancer factor 2C (MEF2C), the master transcriptional regulator of chondrocyte hypertrophy (MCB, 2009). Here we report *in vivo* studies that support this hypothesis.

The HDAC4 knockout (KO) mouse has a phenotype that resembles that of the PTHrP KO mouse, with shortening of the distance from the top of the growth plate to the start of the hypertrophic region. To demonstrate that PTHrP and HDAC4 share a common pathway that slows chondrocyte hypertrophy, the phenotype of double heterozygous (het) mice was determined in the tibial growth plate. Neither the HDAC4 het mouse nor the PTHrP het mouse differs from wild type (WT) in growth cartilage. If PTHrP and HDAC4 work independently, then the double het mice should also show no phenotype. In contrast, the PTHrP and HDAC4 double het mouse has growth plates with a phenotype similar to that of the individual knockout mice,

though considerably less severe. This phenotype demonstrates that PTHrP and HDAC4 must work through a common pathway.

To determine how much PTHrP's action is dependent on the HDAC4 pathway, we examined the effect of the HDAC4 knockout on the phenotype of mice overexpressing PTHrP in the growth plate through transgenic (Tg) expression of PTHrP driven by the collagen 2 (Col2) promoter. The Col2-PTHrP-Tg mice have short limbs caused by delayed chondrocyte maturation (Weir, et al, PNAS, 1996). Their long bones are 50% shorter than those of WT at birth, and the long bones are composed of only round chondrocytes until one week after birth. Interestingly, the Col2-PTHrP Tg phenotype is reversed in the HDAC4-KO;Col2-PTHrP-Tg mice. These mice have tibiae considerably longer than those of the Col2-PTHrP Tg mice and closely resemble the HDAC4 KO mice, except that they have a longer hypertrophic layer (about 3-times longer than the HDAC4 KO or WT at birth). Even heterozygosity for HDAC4 partially reverses the Col2-PTHrP Tg phenotype; these mice have longer bones than the Col2-PTHrP Tg, as well as flat and hypertrophic chondrocytes. These results are consistent with the idea that HDAC4 is a major effector in the PTHrP signaling pathway.

Disclosures: *Shigeki Nishimori, None.*

1195

Erg and PTHrP Genetically Cooperate to Maintain Articular Cartilage Long-term Function. Yoichi Ohta^{*1}, Takahiro Okabe², Shuji Asai³, Motomi Enomoto-Iwamoto³, Maurizio Pacifici⁴, Masahiro Iwamoto⁵.

¹Translational Research Program in Pediatric Orthopaedics, Division of Orthopaedic Surgery, Department of Surgery, The Children's Hospital of Philadelphia Research Institute, USA, ²Department of Orthopaedic Surgery, Osaka city University, Graduate school of Medicine, Japan, ³The Children's Hospital of Philadelphia Research Institute, USA, ⁴Children's Hospital of Philadelphia, USA, ⁵The Children's Hospital of Philadelphia, USA

During embryogenesis, chondrocytes located at the epiphyseal ends of long bone anlagen acquire a permanent articular phenotype, while those located in the shaft become organized in growth plates, undergo maturation and hypertrophy and are replaced by bone. The mechanisms regulating such critical developmental bifurcation remain unclear. Previously we showed that the ets transcription factor member Erg is preferentially expressed in developing articular cartilage and that transgenic over-expression of Erg in the embryonic skeleton suppresses chondrocyte maturation and ossification and maintains all the chondrocytes in an immature articular-like phenotype. To further analyze the roles of Erg in articular cartilage formation, we generated a floxed Erg mouse line and conditionally ablated the gene in developing joints by mating with Gdf5-Cre mice. The mutant mice did not exhibit major developmental abnormalities and appeared normal in size and general appearance postnatally. Interestingly, however, the mice exhibited signs of osteoarthritis (OA) with aging compared to age-matched controls. Developing joints are also known to express parathyroid hormone-related protein (PTHrP) that actually shares the ability with Erg to suppress chondrocyte maturation; in addition, Erg and PTHrP are often co-expressed as recent transcriptome analyses revealed. Thus, we asked whether Erg regulates PTHrP expression and whether the two factors functionally cooperate in articular chondrocytes. Adenovirus-driven over-expression of Erg in cultured chondrocytes up-regulated PTHrP expression, while siRNA inhibition of Erg strongly suppressed PTHrP expression in explant mouse limbs. In addition, Erg over-expression increased the activity of a PTHrP P2 promoter reporter, the main PTHrP promoter in cartilage and, interestingly, such increase was largely abolished when a conserved ets binding site in the promoter was mutated. Lastly, we subjected 2 month-old conditional Erg^{-/-} mice in PTHrP^{+/+} background to surgically-induced OA model and found that they exhibited OA-like defects sooner than conditional Erg^{-/-} littermates. In conclusion, the data indicate that Erg is required for long-term maintenance of permanent articular cartilage and genetically cooperates with PTHrP to exert such critical role.

Disclosures: *Yoichi Ohta, None.*

1196

The Heparin Binding Domain of IGFBP-2 is an Important Regulator of Murine Hematopoiesis and Human Stem Cell Proliferation. Anne Breggia^{*1}, Casey Doucette², Masanobu Kawai¹, David Clemmons³, Clifford Rosen¹.

¹Maine Medical Center, USA, ²Maine Medical Center Research Institute, USA, ³University of North Carolina, USA

IGFBP2 (BP2) is one of 6 IGF binding proteins that shuttles IGFs to their respective receptors. BP2 is expressed at high levels in marrow stromal cells as well as osteoblasts, and is regulated by PTH. Global deletion of BP2 results in small spleens, very low bone formation, impaired bone resorption and increased marrow adiposity. We have demonstrated BP2 null males also have a hematopoietic phenotype in which there are increased percentages of both lymphoid and myeloid subpopulations in the peripheral blood. Both the low bone phenotype and hematopoietic phenotype are rescued by non competitive bone marrow transplantation of WT donor cells. However, donor cells obtained from BP2^{-/-} male mice inefficiently engraft in the marrow of wild type (WT) recipients. We have synthesized a peptide that contains the

sequence of a unique heparin binding domain (HBD) within IGFBP-2 that increases bone density of metacarpal explants and rescues dysregulated hematopoiesis in vivo in BP2^{-/-} mice. In this study, we tested the ability of the peptide to 1) improve engraftment of BP2^{-/-} donor cells in vivo and 2) increase proliferation of human hematopoietic stem cells in vitro. Bone marrow donor cells from BP2^{-/-} male mice were transplanted into lethally irradiated LY5.1 WT recipients. Recipient mice received IP injections of HBD, scrambled control peptide (50ug of each) or PBS on the day of transplant and every other day for 2 weeks. At 8 weeks post transplant, the HBD caused a significant decrease in CD19+ B cells (p=0.005) and a significant increase in CD3+ T cells (0.05) compared to both scrambled peptide and PBS controls. In vitro, HBD significantly expanded human CD34+ hematopoietic stem cells as compared to scrambled peptide and no-treatment controls (p≤0.002). Flow cytometric analysis demonstrated the majority of HSC treated with the HBD remained undifferentiated after 7 days in culture as ≥72% of the cells were positive for the stem cell marker CD34. We have identified a putative receptor present on both osteoblasts and human HSC to which the HBD binds. Future investigations will determine if this receptor-ligand interaction is responsible for HBD-induced HSC expansion and increased bone density and identify signaling events downstream of receptor-HBD ligand binding. Taken together these data demonstrate that IGFBP2 is a potent regulator of hematopoiesis and may specifically control stem cell fate in an IGF binding independent manner within the marrow niche.

Disclosures: *Anne Breggia, None.*

1197

BMP4 Regulates the Hematopoietic Stem Cell Niche Size in Bone Marrow. Kunikazu Tsuji^{*}, Ichiro Sekiya, Takeshi Muneta. Tokyo Medical & Dental University, Japan

BMP4 (Bone morphogenetic protein 4) signal has critical roles in inducing hematopoietic tissues during embryogenesis. However, evaluating the importance of BMP4 in bone marrow hematopoiesis is complicated by early embryonic lethality in mice lacking BMP4, and by conservation of signaling pathways for osteogenic BMPs. To overcome these limitations and to define the roles of BMP4 in bone marrow hematopoiesis, we established BMP4 conditional knockout mice in which we inactivated BMP4 in adult bone marrow (Bmp4Mx1cre). Here we report that the loss of BMP4 in bone marrow cells significantly reduced the hematopoietic stem cell population. BMP4 gene was knocked-out by the intraperitoneal injection of poly I:C into Bmp4Mx1cre mice at 6 weeks of age. Six to 8 weeks after the injection (after inducing the genomic recombination), total bone marrow cells were isolated from femurs and tibiae, stained by hematopoietic cell surface markers, and analyzed by a flow-cytometry (BD FACS Calibur). We found that the populations of differentiated blood cells such as Erythrocytes (Ter119+), T-cells (CD3+), B-cells (CD19+), and Monocytes/Macrophages (CD11b+) were not significantly altered in the absence of BMP4. However, the hematopoietic stem cell fraction (Lin⁻, c-Kit⁺, Sca-1⁺) was significantly decreased in Bmp4Mx1cre mice. These results are specific for the loss of BMP4, because we did not observe any alteration in hematopoietic cell population in the absence of BMP7 (Bmp7Mx1cre). We also did not observe any synergistic effect in the regulation of hematopoietic stem cell population in the co-absence of BMP4 and BMP7 (Bmp4/7Mx1cre). These results suggest that the unique and important roles of BMP4 in the regulation of hematopoietic stem cell niche size in adult bone marrow.

Disclosures: *Kunikazu Tsuji, None.*

1198

Caspase-1 Activity is Required for Cleavage of Bone Morphogenetic Protein Receptor Type Ia and its Translocation into the Nucleus to Induce Adipogenesis. Oleksandra Moseychuk^{*}, Jeremy Bonor, Hemanth Akkiraju, Anja Nohe. University of Delaware, USA

Therapeutics that increase the number of osteoblasts and reduce the number of adipocytes in the bone marrow would be beneficial for the treatment of osteoporosis. Bone Morphogenetic Protein 2 (BMP2) is a key growth factor that drives both adipogenesis and osteogenesis. BMP2 is FDA approved for spinal fusions, complicated cases of open tibial shaft fractures, and tibial nonunions. One of the drawbacks of BMP2 is the varying responses seen with patients; this could be due to its ability to drive adipogenesis and osteogenesis. We recently identified Casein Kinase II (CK2) as a BMP receptor type Ia (BMPRIa) interacting protein at three potential sites. The release of CK2 induces mineralization in vitro, however its potential role in adipogenesis is unknown. Mutants of BMPRIa lacking the CK2 phosphorylation sites were created. The effect of overexpression of these mutants on osteoblast differentiation and adipogenesis was determined by von Kossa and Oil Red O staining. We also blocked this interaction between BMPRIa and CK2 using peptides or siRNA to downregulate CK2. Our data revealed that the different CK2 phosphorylation sites regulate either adipogenesis and/or osteogenesis. The mechanism of adipogenesis compared to osteogenesis is mediated by a Caspase-1 cleavage site between two of the CK2 binding sites. Our data indicate that CK2 release leads to Caspase-1 cleavage of the BMPRIa and translocation of a segment of BMPRIa together with peroxisome proliferator-activated receptor gamma (PPARγ) into the nucleus as measured by confocal microscopy. In conclusion our data reveal a new mechanism of BMP2 mediated adipogenesis in which a segment of BMPRIa translocates into the nucleus. Moreover, we demonstrated that Caspase-1 is a key

player in osteoblast and adipocyte differentiation and is regulated by CK2 as a key switch in stem cell differentiation.

Disclosures: Oleksandra Moseychuk, None.

1199

Parathyroid Hormone 1-84 Accelerates Fracture Healing in Pubic Bones of Elderly Osteoporotic Women. Gerold Holzer^{*1}, PETER PEICHL², Lukas Holzer¹, Richard maier³. ¹Medical University of Vienna, Austria, ²EVANGELISCHES KRANKENHAUS VIENNA, Austria, ³Thermenklinikum, Austria

Background: Parathyroid hormone (PTH) was shown to increase BMD and reduce the risk of fractures in patients with osteoporosis. A few studies also tested the ability of PTH to improve fracture healing. Pelvic fractures due to osteoporosis are less frequent, but require a longer healing period with immobilisation. The effect of PTH 1-84 on the course of fracture healing and functional outcome was tested prospectively in postmenopausal women receiving PTH 1-84 for the treatment of osteoporosis and conservatively treated pelvic fractures without requiring surgery.

Methods: Six-five patients (mean age: 82.8 years) had plain x-rays and a computer tomography (CT) scan to verify fractures and were scanned for osteoporosis. Twenty-one patients received a once daily injection of 100µg PTH 1-84 starting within two days after admission to the hospital. Forty-four patients without PTH treatment served as a control group. All patients received 1000 mg Calcium and 800 IU Vitamin D. CT scans were repeated every fourth week until radiographic evidence of cortical bridging was confirmed. Functional outcome was assessed using a pain Visual Analogue Scale (VAS) and a Timed Up and Go (TUG) test.

Results: In all 21 patients treated with PTH 1-84 pelvic fractures were healed at a mean of 7.8 weeks, whereas in patients with no PTH treatment fractures had healed after 12.6 weeks ($p < 0.001$). At week 8 all fractures in the treatment group were healed and four fractures in the control group (healing rate 100% versus 9.1%; ($p < 0.001$). Both the VAS and TUG improved statistically significant ($p < 0.001$) compared to control.

Conclusions: In elderly patients with osteoporosis, PTH 1-84 accelerates fracture healing in pelvic fractures and improves functional outcome.

Disclosures: Gerold Holzer, None.

1200

Increased Trabecular Tissue Mineral Density Partially Explains the Improvement in Trabecular Volumetric BMD in Premenopausal Women with Idiopathic Osteoporosis Treated with Teriparatide. Xiaowei Liu^{*1}, Adi Cohen², Emily Stein¹, David Dempster³, Hua Zhou⁴, Joan Lappe⁵, Robert Recker⁵, Polly Chen³, Donald McMahon¹, Elizabeth Shane¹. ¹Columbia University College of Physicians & Surgeons, USA, ²Columbia University Medical Center, USA, ³Columbia University, USA, ⁴Helen Hayes Hospital, USA, ⁵Creighton University Osteoporosis Research Center, USA

We have reported that premenopausal women (PreM) with idiopathic osteoporosis (IOP) have decreased volumetric BMD (vBMD), abnormal trabecular (Tb) microstructure and reduced bone stiffness. The degree of tissue mineralization, or tissue mineral density (TMD), is known to influence BMD and affect tissue-level mechanical properties. In this study, we investigated Tb TMD in PreM IOP and its response to Teriparatide (TPTD) treatment. We hypothesized that PreM IOP is associated with lower Tb TMD and that both Tb vBMD and Tb TMD would increase in response to TPTD.

High resolution peripheral quantitative CT (HRpQCT) of the distal radius (DR) and tibia (DT) was performed in 18 PreM with IOP (age 41.5 yrs) at baseline and after 12-18 months (M) of TPTD (20 mcg daily). By digital topological analysis, we classified Tb bone voxels as belonging to one of 3 envelopes: surface Tb bone, central Tb bone and intervening (middle) Tb bone occupying the envelope between surface and central Tb bone (Fig 1). TMD was calculated for surface (sTMD), central (cTMD), and middle (mTMD) envelopes. TMD increased from surface to center of trabeculae: cTMD was higher than mTMD (by 7.12.5% and 8.42.3% at DR and DT; $p < 0.001$), and mTMD was higher than sTMD (by 14.41.2% and 16.41.2% at DR and DT; $p < 0.001$). Compared to 18 PreM controls (396 yrs), PreM with IOP had 2.1% lower sTMD at DR ($p = 0.02$) and 1.4% lower sTMD at DT ($p = 0.06$).

After 12-18M of TPTD, lumbar spine (LS) BMD increased by 9.73.3% ($p < 0.05$). Tb vBMD increased by 5.28.3% at the DT and 2.32.7% at the DR (both $p < 0.05$). At the DR, sTMD increased by 0.740.99% ($p < 0.01$) while mTMD and cTMD did not change. At the DT, sTMD and mTMD increased by 0.770.75% ($p < 0.001$) and 0.631.03% ($p = 0.02$) and cTMD tended to increase by 0.541.1% ($p = 0.07$). At the DT, % change in TMD correlated with % change in vBMD: sTMD $r = 0.49$ and cTMD $r = 0.47$, $p < 0.05$; mTMD $r = 0.44$, $p = 0.08$. Moreover, % change in DT cTMD tended to correlate with % change in LS BMD ($r = 0.45$, $p = 0.07$). In addition, there was a direct, though non-significant association between cTMD and bone formation rate/bone surface on transiliac biopsy ($r = 0.40$, $p = 0.11$). In contrast, % change in DR TMD did not correlate with % change in LS BMD, vBMD or biopsy parameters.

In conclusion, PreM IOP is associated with lower Tb TMD. There were significant increases in Tb TMD measured on HRpQCT scans of the DT in PreM with IOP treated with TPTD that were associated with improved Tb vBMD.

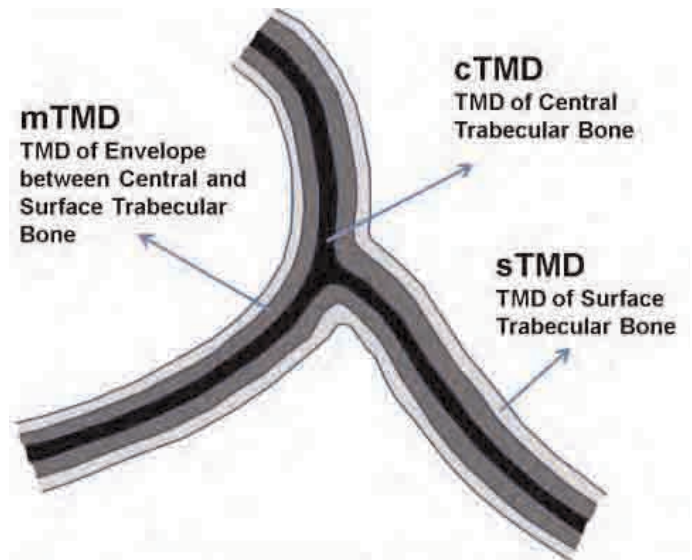


Figure 1. Classifications of surface Tb bone (sTMD), central Tb bone (cTMD) and intervening Tb bone (mTMD) occupying the envelope between surface and central Tb bone.

Figure 1

Disclosures: Xiaowei Liu, None.

1201

Effect of Weekly Teriparatide in Patients with Osteoporosis. Toshitaka Nakamura^{*1}, Toshitsugu Sugimoto², Tetsuo Nakano³, Hideaki Kishimoto⁴, Masako Ito⁵, Masao Fukunaga⁶, Hiroshi Hagino⁷, Teruki Sone⁶, Hideki Yoshikawa⁸, Yoshiki Nishizawa⁹, Masataka Shiraki¹⁰. ¹University of Occupational & Environmental Health, Japan, ²Shimane University School of Medicine, Japan, ³Tamana Central Hospital, Japan, ⁴San-in Rosai Hospital, Japan, ⁵Nagasaki University Hospital, Japan, ⁶Kawasaki Medical School, Japan, ⁷Tottori University, Japan, ⁸Osaka University Graduate School of Medicine, Japan, ⁹Osaka City University Medical School, Japan, ¹⁰Research Institute & Practice for Involuntal Diseases, Japan

Introduction: Daily teriparatide (human parathyroid hormone 1-34) injection is effective in reducing fracture risk and increasing BMD. However, the effect of weekly subcutaneous injection of teriparatide on fracture risk has not been tested.

Methods: To examine the anti-fracture efficacy and safety of weekly subcutaneous injection of 200 units of teriparatide (56.5 µg) in Japanese patients (65-95 years old) with primary osteoporosis, a randomized, double-blind, placebo-controlled trial was conducted in 578 patients with 1-5 prevalent vertebral fractures and low BMD (L2-4 BMD $< 80\%$ of young adult mean). Patients were randomly assigned to receive weekly teriparatide injection ($n = 290$; 13 men) or placebo ($n = 288$; 10 men) for 72 weeks, with daily supplements of calcium 610 mg and vitamin D 400 IU. The primary endpoint was new vertebral fractures.

Results: As compared with placebo, teriparatide reduced the risk of new vertebral fractures, with a cumulative incidence of 3.1% in the teriparatide group, versus 14.5% in the placebo group ($p < 0.0001$), and a relative risk reduction of 79.9% (95% confidence interval, 54.7-91.1%). BMD increases at 72 weeks were significant in the teriparatide group compared to the placebo group (L2-L4: 6.7% vs. 0.3%, $P < 0.0001$; total hip: 3.1% vs. 0.1%, $P < 0.000$). Serum osteocalcin increased and urinary NTX decreased in the teriparatide group. Transient headache, malaise and nausea after injection were more frequent in the teriparatide group than in the placebo group, but were generally mild and tolerable.

Conclusion: Weekly injection of teriparatide (56.5 µg) is safe and effective in reducing vertebral fracture in patients with primary osteoporosis with prevalent vertebral fracture.

Disclosures: Toshitaka Nakamura, Teijin Pharma, 5; Chugai Pharmaceutical Co., 5; Daiichi Sankyo Co., 5; Asahi-Kasei Pharma Co., 5
This study received funding from: Asahi-Kasei Pharma Corporation

1202

Teriparatide for Premenopausal Women with Idiopathic Osteoporosis: A Paired Transiliac Bone Biopsy Study. Adi Cohen^{*1}, Emily Stein², David Dempster³, Robert Recker⁴, Joan Lappe⁴, Hua Zhou⁵, Thomas Nickolas¹, Alexander Zwahlen⁶, Thomas Kohler⁶, Ralph Muller⁶, Polly Chen³, Kavita Pandit³, Elizabeth Shane². ¹Columbia University Medical Center, USA, ²Columbia University College of Physicians & Surgeons, USA, ³Columbia University, USA, ⁴Creighton University Osteoporosis Research Center, USA, ⁵Helen Hayes Hospital, USA, ⁶ETH Zurich, Switzerland

Idiopathic osteoporosis (IOP) in premenopausal women is an uncommon disorder of uncertain pathogenesis in which fragility fractures and/or low bone mineral density (BMD) occur in otherwise healthy women with intact gonadal function. Transiliac bone biopsies (BX) have revealed thinner cortices, fewer, thinner, more widely separated, and heterogeneously distributed trabeculae, and reduced stiffness in women with IOP compared to controls. Although dynamic histomorphometric remodeling parameters were heterogeneous and did not differ between subjects and controls, subsets of women with IOP had low or high bone turnover assessed by bone formation rate/bone surface (BFR/BS). We hypothesized that teriparatide (TPTD), an agent that directly increases osteoblast activity, would improve BMD by DXA, trabecular (Tb) bone volume fraction (BV/TV), and bone microarchitecture in women with IOP. In an open-label pilot study of 22 premenopausal women with IOP treated with TPTD 20 mcg SC daily, lumbar spine (LS) BMD increased from baseline by 9.73.3% (SD; p<0.05) by 18 months and also increased at the total hip and femoral neck (data not shown). Herein, we report interim paired transiliac BX results (baseline and 18 months) from the first 11 subjects. BXs were analyzed by 3D micro-computed tomography (μ CT) and 2D histomorphometry (2DH). By μ CT (Table), there was a 38% increase in BV/TV, a 19% increase in Tb number, a 9% decrease in Tb separation (all p<0.01), and no change in Tb thickness; comparable effects were observed with 2DH (data not shown). By 2DH, cortical (Ct) area increased by 57%, Ct porosity by 58%, and there was a non-significant 12% increase in Ct width. Wall width (W.Wi) of completed osteons, a static parameter that reflects the amount of bone synthesized by osteoblasts, increased significantly by 14%. However, dynamic remodeling parameters did not differ from baseline. In summary, after 18 months of TPTD, there were significant increases in Tb BV/TV and Tb number, decreased Tb separation, increased cortical area and porosity. There was an increase in W.Wi, but no differences in dynamic remodeling parameters. We conclude that TPTD improves both BMD and Tb microarchitecture at the iliac crest in premenopausal women with IOP. These changes likely reflect earlier increases in bone formation rate that have returned to baseline after 18 months of TPTD.

PARAMETER	BASLINE	18 MONTHS	p
BV/TV (%) by μ CT	21.1 \pm 6.8	29.2 \pm 8.1	0.004
Tb Number (#/mm) by μ CT	1.54 \pm 0.22	1.83 \pm 0.29	0.003
Tb Thickness (μ m) by μ CT	181 \pm 44	188 \pm 31	0.61
Tb Separation (μ m) by μ CT	726 \pm 69	663 \pm 57	0.0004
Cortical Width (μ m) by 2DH	642 \pm 225	718 \pm 289	0.18
Cortical Area (%) by 2DH	21 \pm 9	33 \pm 16	0.02
Cortical Pore Area (%) by 2DH	4.8 \pm 1.4	7.6 \pm 4.5	0.03
Osteoid Width (# lamellae)	3.6 \pm 1.2	2.8 \pm 0.9	0.15
Wall Width (μ m)	35 \pm 5	41 \pm 5	0.009
Mineralized Perimeter (%)	3.4 \pm 1.6	3.4 \pm 2.3	0.96
Mineral Apposition Rate (μ m/day)	0.62 \pm 0.08	0.61 \pm 0.10	0.68
BFR/BS (mm ³ /mm ² /year)	0.008 \pm 0.004	0.008 \pm 0.006	0.81

Table

Disclosures: Adi Cohen, None.

This study received funding from: Eli Lilly and Company

1203

Skeletal Histomorphometry in Patients On Teriparatide or Zoledronic Acid Therapy (SHOTZ) Study: 6-Month Results of a Randomized Clinical Trial. David W. Dempster^{*1}, Hua Zhou¹, Robert R. Recker², Jacques P. Brown³, Michael A. Bolognese⁴, Christopher Recknor⁵, David L. Kendler⁶, E. Michael Lewiecki⁷, David A. Hanley⁸, D. Sudhaker Rao⁹, Paul Miller¹⁰, Grattan C. Woodson, III¹¹, Robert Lindsay¹, Neil Binkley¹², Xiaohai Wan¹³, Valerie A. Ruff¹⁴, Boris Janos¹⁵, Kathleen A. Taylor¹⁴. ¹Regional Bone Center, Helen Hayes Hospital, USA, ²School of Medicine, Creighton University, USA, ³Groupe de recherche en maladies osseuses, Laval University, Canada, ⁴Bethesda Health Research, USA, ⁵United Osteoporosis Center, USA, ⁶Prohealth Clinical Research, Canada, ⁷New Mexico Clinical Research & Osteoporosis Center, USA, ⁸Heritage Medical Research Clinic, Canada, ⁹Henry Ford Hospital, USA, ¹⁰Colorado Center for Bone Research, USA, ¹¹Atlanta Research Center, USA, ¹²University of Wisconsin, USA, ¹³Eli Lilly & Company, USA, ¹⁴Lilly USA, LLC, USA, ¹⁵Eli Lilly Canada Inc., Canada

Purpose: Mechanisms of action (MOA) of bone active drugs are often investigated by histomorphometric analysis of bone biopsies. Standard conventions have been developed to assess a panel of tetracycline-based, dynamic parameters of bone formation to demonstrate whether a drug is anabolic or antiresorptive. Recent studies

on the MOA of osteoporosis drugs have rekindled interest in how to present and interpret dynamic histomorphometric parameters. This cross-sectional biopsy study compared the effects of an established anabolic agent, teriparatide (TPTD), with those of a prototypical antiresorptive agent, zoledronic acid (ZOL).

Methods: This randomized, double-blind, active comparator-controlled study compared histomorphometric parameters of bone remodeling in postmenopausal women with osteoporosis receiving ZOL (5 mg/y IV infusion) or TPTD (20 μ g/d SC injection). Transiliac crest bone biopsies were obtained after double tetracycline labeling from 58 subjects. The primary endpoint, cancellous mineralizing surface/bone surface (MS/BS), and a standard panel of cancellous histomorphometric indices were assessed at month 6.

Results: Dynamic indices of bone formation, including MS/BS and bone formation rate (BFR), were significantly higher in the TPTD group (Table). Mineral apposition rate (MAR) was significantly greater with TPTD than ZOL regardless of whether values for samples containing only single labels were imputed or treated as missing. However, when MAR was calculated using only double labels, fewer double labels were available for analysis in the ZOL group (53%) than in the TPTD group (100%). Also, 40% of the ZOL subjects had no detectable tetracycline labels compared to 0% in the TPTD arm. The lower BFR in the ZOL group was primarily due to the lower MS/BS rather than to the small differences in MAR, regardless of how MAR was calculated. ZOL decreased serum markers of bone formation and resorption (P1NP, OC and CTX), while TPTD increased these markers, further supporting mechanistic differences observed by histomorphometric analysis.

Conclusions: TPTD and ZOL possess fundamentally different MOAs with opposite effects on bone formation based on data that evaluated a full panel of histomorphometric indices. An important mechanistic difference between these 2 drugs was the substantially higher MS/BS in the TPTD group. These results define the dynamic histomorphometric characteristics of anabolic versus antiresorptive activity in these 2 drug classes.

Table. Dynamic Indices of Bone Formation in Postmenopausal Women

Cancellous	TPTD (n = 28)	ZOL (n = 30)	P Value
MS/BS, %	5.60 (3.00, 11.73)* (n=28)	0.16 (0.00, 0.58)* (n=30)	<0.001
MAR (1), μ m/d	0.50 (0.48, 0.62)* (n=28)	0.50 (0.48, 0.52)* (n=16)	0.03
MAR (2), μ m/d	0.56 (0.48, 0.62)* (n=28)	0.49 (0.37, 0.51)* (n=18)	0.009
BFR/BS (1), mm ³ /mm ² /y	0.0116 (0.0051, 0.0265)* (n=28)	0.0009 (0.0003, 0.0012)* (n=16)	<0.001
BFR/BS (2), mm ³ /mm ² /y	0.0116 (0.0051, 0.0265)* (n=28)	0.0008 (0.0003, 0.0011)* (n=18)	<0.001
Number of samples (%) with the following:			
Double Label			
With Single Label	28 (100%)	13 (43.33%)	NA
Without Single Label	0 (0%)	3 (10.00%)	NA
Single Label Only	0 (0%)	2 (6.67%)	NA
No Label	0 (0%)	12 (40.00%)	0.0001

*Values shown are medians (interquartile range).

BFR/BS=bone formation rate bone surface; MAR=mineral apposition rate; MS/BS=mineralizing surface/bone surface; NA=not applicable; TPTD=teriparatide 20 μ g/d subcutaneous injection; ZOL=zoledronic acid 5 mg/y intravenous infusion.

MAR and BFR calculated using: (1) double labels only; (2) double labels plus an imputed value of MAR=0.3 μ m/d in subjects with single labels only.

Statistical analyses were conducted at a 2-sided alpha level of 0.05 using Wilcoxon rank-sum test. Fisher's exact test was used to analyze the association between treatment groups and the presence or absence of label.

Table. Dynamic Indices of Bone Formation in Postmenopausal Women

Disclosures: David W. Dempster, Eli Lilly and Company, 2; Eli Lilly and Company, 5; Eli Lilly and Company, 8

This study received funding from: Eli Lilly and Company

1204

Increases in both Vertebral and Femoral Strength in Postmenopausal Osteoporotic Women after 18 months of Treatment with Teriparatide. Tony Keaveny^{*1}, David Kopperdahl², Valerie Ruff³, Xiaohai Wan⁴, Kelly Krohn⁵. ¹University of California, Berkeley, USA, ²O.N. Diagnostics, USA, ³LILLY USA, LLC, USA, ⁴Eli Lilly & Company, USA, ⁵Lilly USA, USA

Purpose: Finite element analysis of quantitative CT scans is one of the popular methods available in clinical studies for non-invasive assessment of vertebral and femoral bone strength. Since very few finite element data have been reported to date on changes in vertebral and femoral strength for patients treated with teriparatide [rhPTH (1-34)], the biomechanical effects of teriparatide treatment in postmenopausal women are not well understood. To address this issue, we used finite element analysis to analyze the effects of 18-month daily treatment of 20 μ g of teriparatide on both vertebral and proximal femoral strength in a new open-label study of 30 postmenopausal women with osteoporosis and related these changes in strength to changes in the underlying (volumetric) bone mineral density.

Methods: Quantitative CT of the lumbar spine and hip was obtained at baseline and 18 months (or early termination visit). All patients who had two evaluable CT scans at both time points were included in the analysis (n= 30 spine; n=26 hip). Density was measured for the trabecular, peripheral (outer 2–3 mm of bone that contained both cortical and some adjacent trabecular bone), and both (“integral”) compartments. Non-linear finite element analysis was performed for uniform compression for the spine and a sideways fall for the hip to provide measures of vertebral and femoral strength.

Results: We found statistically significant increases in both vertebral and femoral strength compared with baseline. For the spine this was accompanied by significant increases in both trabecular and peripheral densities and, for the hip, by a significant increase in the trabecular density and no change in the peripheral density (Table).

Conclusion: Both vertebral and femoral strength increased after 18 months of treatment with teriparatide compared to baseline.

Disclosures: Tony Keaveny, Eli Lilly and Company, 5
This study received funding from: Eli Lilly and Company

1205

FoxO1 is a Transcriptional Mediator of the Regulation of Bone Formation by Circulating Serotonin. Aruna Kode¹, Barbara Silva¹, Ioanna Mosialou¹, Charles Duncan¹, Tim M Townes², Rene Hen³, X.Edward Guo³, Stavroula Kousteni¹. ¹Columbia University Medical Center, USA, ²University of Alabama, USA, ³Columbia University, USA

Serotonin is a critical regulator of bone mass that fulfills different functions depending on its site of synthesis. Brain-derived serotonin acts as a neurotransmitter to promote osteoblast proliferation whereas duodenal-derived serotonin acts as a hormone suppressing osteoblast proliferation and bone formation. Hence, inhibiting duodenal-derived serotonin is a therapeutic target for the treatment of osteoporosis. To understand the molecular mechanisms of duodenal serotonin action on osteoblasts, we focused on the Forkhead transcription factor, FoxO1 for two reasons. First, in *C. elegans* the FoxO homolog mediates serotonin signaling in a wide spectrum of its physiological processes. Second, FoxO1 is a crucial regulator of several aspects of osteoblast biology. Using a combination of cell culture assays and mouse genetic experiments we observed that serotonin upregulates the activity of FoxO1 and the expression of FoxO1 transcriptional targets that control cell cycle. Moreover, serotonin failed to suppress osteoblast proliferation and *cyclin D1* and *D2* expression in FoxO1-deficient osteoblasts. Consistent with these results, removal of one allele of FoxO1 from *Lrp5*-deficient mice that harbor high circulating serotonin levels rescued their low bone mass phenotype by normalizing cell cycle gene expression and osteoblast proliferation. Further demonstrating that FoxO1 is a mediator of serotonin signaling, the high bone formation phenotype observed in mice lacking one allele of *Htr1b*, the predominantly expressed serotonin receptor in osteoblasts, was corrected by removing one allele of FoxO1 from osteoblasts in compound heterozygous (*Htr1b* +/-; FoxO1^{osb}/+) mice. Downstream of Htr1b, we identified CREB as the transcriptional partner that interacts with FoxO1 and regulates its activity in response to serotonin. CREB forms a functional complex with FoxO1 suppressing FoxO1 transcriptional activity. Upon treatment of cells with serotonin the FoxO1/CREB interaction is disrupted; this unleashes FoxO1 transcriptional activity resulting in suppression of *cyclin* gene expression and osteoblast proliferation. In agreement with these *in vitro* findings, removal of one allele of FoxO1 in mice haploinsufficient for FoxO1 and Creb (FoxO1^{osb}/+; Creb^{osb}/+) rescued the low bone mass phenotype of Creb knockout mice by increasing osteoblast proliferation. Collectively these findings identify FoxO1 as a crucial determinant of the anti-proliferative actions of gut-derived serotonin in osteoblasts.

Disclosures: Aruna Kode, None.

1206

Dkk1 Inhibition Promotes Bone Formation in Growing, but Not in Aged Osteopenic Rats. William G. Richards¹, Mario Grisanti², Denise Dwyer¹, Qing-Tian Niu¹, Franklin Asuncion², Marina Stolina³, Michael Ominsky², Xiaodong Li⁴. ¹Amgen Inc., USA, ²Amgen, Incorporated, USA, ³Amgen Inc, USA, ⁴Amgen, Inc., USA

Initial discoveries in individuals with osteoporosis-psuedoglioma syndrome and high bone mass that identified loss-of-function and gain-of-function mutations respectively in the Wnt co-receptor LRP5 led to the well appreciated role of the Wnt signaling pathway in bone. The contribution of various members of this complex signaling pathway to bone physiology continues to be elucidated. Towards that end we studied the role of Dickkopf-1 (Dkk1) during postnatal bone growth and in estrogen-deficient rats by utilizing an antibody to Dkk1 (Dkk1-Ab) that blocked the Wnt inhibitory activity of Dkk1.

Four-week old female Sprague Dawley rats were treated with Dkk1-Ab (30 mg/kg 2X/wk) or PTH 1-34 (100 µg/kg 5X/wk) for four weeks. Dkk1-Ab treatment resulted in a significant (P<0.001) increase in lumbar (L1-L5) BMD compared to vehicle treated young rats (0.144 vs. 0.126 g/cm²). Significant increases in trabecular BV/TV (30.21.5 vs. 21.72.3%), Tb.N (4.40.1 vs. 3.50.3); Ob.S/BS (6.21.0 vs 1.30.4%) and BFR/TV (113.411.3 vs. 70.610.4%/year) were observed at distal femur in Dkk1-Ab treated

compared to vehicle treated young rats. Cortical area (4.380.17 vs. 3.690.08mm²) and thickness (0.550.03 vs. 0.460.01mm) at the femur midshaft were both significantly increased by Dkk1-Ab treatment.

In contrast, treatment of adult ovariectomized Sprague Dawley rats (8-month old, 2-months post-OVX) with Dkk1-Ab (5 or 25 mg/kg 2X/wk) for four weeks did not appreciably impact BMD and histomorphometric parameters at either trabecular or cortical sites; the positive control PTH significantly impacted a number of these parameters. Additional studies in aged OVX rats confirmed these findings. Serum and bone tissue samples were collected from rats at various ages to determine whether changes in Dkk1 expression could account for differences in efficacy observed between young and adult rodents treated with Dkk1-Ab. Serum Dkk1 levels declined as rats age. Bone Dkk1 protein levels decreased significantly between 3 and 6 months of age, and remained low at 12 months.

The divergent effects of Dkk1-Ab on growing and adult bone were attributed to decreased Dkk1 expression in serum and bone of older rats. These data suggest that, while Dkk1 significantly regulates bone formation in younger animals, its role in older animals is limited to pathologies that lead to the induction of Dkk1 expression in bone and/or serum, such as multiple myeloma, inflammation and or traumatic injury.

Disclosures: William G. Richards, Amgen, Inc, 1; Amgen, Inc, 3
This study received funding from: Amgen

1207

Sclerostin Inhibition Prevents Low Bone Mass Associated with Type 2 Diabetes Mellitus in Rats. Christine Hamann¹, Yvonne Hoehna¹, Martina Rauner², Claudia Goettsch³, Klaus-Peter Guenther¹, Michael Ominsky⁴, Lorenz Hofbauer¹. ¹Dresden University Medical Center, Germany, ²Medical Faculty of the TU Dresden, Germany, ³Brigham & Women's Hospital/Cardiovascular Division, USA, ⁴Amgen, Incorporated, USA

The pathogenesis of low bone mass in diabetes mellitus is poorly defined and efficient therapies are limited. The Zucker Diabetic Fatty (ZDF) rats, an established rodent model of diet-induced type 2 diabetes mellitus, have low bone mass characterized by impaired osteoblastogenesis *in vitro*. We tested whether antibodies directed against sclerostin (Scl-Ab), a soluble inhibitor of Wnts and osteoblasts, could reverse diabetes-induced low bone mass in this rat model. Saline or 25 mg/kg Scl-Ab was administered S.C. twice weekly to 9-week old non-diabetic (+/+) and diabetic (fa/fa) ZDF rats for 12 weeks, and terminal BMD was assessed by pQCT. At 21-weeks of age, diabetic rats had significantly lower total BMD at the distal femur and the lumbar vertebra compared to non-diabetic rats (Table 1). At the distal femur, total, trabecular, and cortical/subcortical BMD were 22%, 63%, and 12% lower, respectively, in rats with diabetes. At the femoral shaft, cortical thickness was 15% lower in diabetic rats. At the fourth lumbar vertebra, total (-18%), trabecular (-44%), and cortical/subcortical BMD (-9%) were significantly lower in diabetic rats compared to non-diabetic rats. Scl-Ab treatment in diabetic rats resulted in increased BMD at the distal femur (total BMD +59%, trabecular BMD by 4-fold and cortical/subcortical BMD +27%), at the femoral shaft (cortical thickness +31%) and at the lumbar spine (total BMD +86%, trabecular BMD by 3-fold and cortical/subcortical BMD +39%) compared to saline controls (Table 1). The relative increase in BMD parameters with sclerostin inhibition was comparable in diabetic and non-diabetic animals. All BMD parameters of diabetic rats receiving sclerostin antibodies were significantly higher than those of non-diabetic rats treated with saline control. Treatment with sclerostin antibody was not associated with changes of renal function and serum levels of glucose, calcium, and phosphate in diabetic and non-diabetic animals after 21 weeks. In conclusion, sclerostin inhibition can fully reverse the adverse effects of type 2 diabetes mellitus on bone mass in rats.

Table 1

Parameter	Non-diabetic		Diabetic	
	Saline	Sclerostin Ab	Saline	Sclerostin Ab
L4 Vertebra Total BMD (mg/cm ³)	549 ± 10.8	852 ± 16.7*	449 ± 14.7	834 ± 22.5*
L4 Vertebra Trabecular BMD (mg/cm ³)	326 ± 24.4	800 ± 35.8*	183 ± 16.0	718 ± 42.6*
Distal Femur Total BMD (mg/cm ³)	571 ± 14.1	862 ± 7.30*	448 ± 10.9	712 ± 44.4*
Distal Femur Trabecular BMD (mg/cm ³)	244 ± 21.6	735 ± 28.4*	91.1 ± 14.2	434 ± 74.8*
Femur Shaft Cortical Thickness (mm)	0.61 ± 0.01	0.75 ± 0.01*	0.52 ± 0.01	0.68 ± 0.03*

Numbers indicate means ± SEM. For vertebra and femur n=4-6. *p < 0.0001 and *p < 0.005 for sclerostin antibody vs. saline in non-diabetic mice. †p < 0.0001, ‡p < 0.005, and §p < 0.01 for sclerostin antibody vs. saline in diabetic mice.

Table 1

Disclosures: Christine Hamann, None.

1208

Sclerostin Antibody Prevents Bone Loss and Increases Bone Formation in Female Rats with High Turnover due to Ovariectomy. Xiaodong Li^{1*}, Kelly S Warmington², Xue Chun Xia³, Aly A Williams³, Mario Grisanti², Qing-Tian Niu², Denise Dwyer², Marina Stolina⁴, Chris Paszty², Thomas Wronski³, Hua Zhu Ke². ¹Amgen, Inc., USA, ²Amgen Inc., USA, ³University of Florida, USA, ⁴Amgen Inc, USA

Purpose: Sclerostin inhibition by monoclonal antibody has been well studied in restoration studies in estrogen-deficient rodents with established osteopenia when bone turnover is relatively low (treatment). However, it has not been studied at the early stage of ovariectomy when bone turnover is relatively high (prevention). In this study, we examined the effects of sclerostin antibody (Scl-Ab) administration on bone in adult rats immediately following ovariectomy.

Methods: Six-month-old female SD rats were sham-operated or ovariectomized (OVX). Immediately after surgery, OVX rats were treated with vehicle or a ratized Scl-Ab (Scl-AbVI) at 25 mg/kg (2x/week, sc) for 6 weeks (12-13/group). Sham rats received vehicle (2x/week, sc) as controls.

Results: *In vivo* DXA measurements demonstrated progressive increases in areal BMD at the lumbar spine and femur-tibia regions in the Scl-Ab group. The percent increases from baseline in lumbar spine BMD in the Scl-Ab group were 11%, 21%, and 32% at weeks 2, 4, and 6, respectively, whereas OVX controls lost 6.5% in lumbar spine BMD at week 6. Histomorphometric analysis at the distal femoral metaphysis demonstrated that Scl-Ab increased trabecular bone volume (BV/TV) to a level that was significantly greater than Sham controls (Table 1). The increase in BV/TV was primarily due to increased trabecular thickness. There was a 3.7-fold increase in trabecular bone formation rate (BFR/BS) in the Scl-Ab group compared with OVX controls, but osteoclast surface was similar between the two groups. Histomorphometric analysis at the tibial shaft showed significant increases in cortical thickness (+13.4% vs OVX) in the Scl-Ab group. Dynamic histomorphometric analysis at the tibial shaft revealed a marked increase in endocortical BFR/BS (+84-fold vs OVX) in the Scl-Ab group. Periosteal BFR/BS was almost doubled in the Scl-Ab group compared with OVX controls. OVX controls had a 4-fold increase in Ps.BFR/BS compared with the Sham group.

Conclusions: Sclerostin antibody treatment increased trabecular and cortical bone formation, increased trabecular and cortical bone mass, and improved trabecular architecture in rats with high turnover due to ovariectomy. These results suggest that sclerostin inhibition may be a promising therapeutic approach for preventing bone loss in the early stage of disease progression in postmenopausal osteoporosis.

Site	Endpoints	Sham-Vehicle (n=13)	OVX	
			Vehicle (n=12)	Scl-Ab 25 mg/kg (n=13)
Distal Femur	Trabecular BV/TV (%)	20.0±1.5	10.0±1.6*	28.5±2.7 ^{ab}
	BFR/BS (µm ³ /µm ² /dx100)	15±1	30±2*	112±3 ^{ab}
	Oc.S/BS (%)	1.4±0.2	2.3±0.3*	2.1±0.3
Tibial Shaft	Cortical Thickness (µm)	790.7±13.6	736.4±14.6	834.7±15.6 ^{ab}
	Ps.BFR/BS (µm ³ /µm ² /dx100)	25.9±4.9	108.8±9.5*	209.0±17.7 ^{ab}
	Ec.BFR/BS (µm ³ /µm ² /dx100)	2.0±1.1	2.1±1.3	176.7±7.5 ^{ab}

Data are mean ± SEM. *p<0.05 vs Sham-Vehicle, ^ap<0.05 vs OVX-Vehicle

Table 1

Disclosures: Xiaodong Li, Amgen Inc., 3; Amgen Inc., 1
This study received funding from: Amgen Inc.

1209

Deletion of the Pro-Apoptotic Proteins Bax and Bak from Osteoblasts and Osteocytes Increases Bone Mass, and Retards the Loss of Cancellous Bone but Dramatically Accelerates Cortical Porosity in Aged Mice. Robert Jilka^{*}, Annick DeLoose, Leslie Climer, Stuart Berryhill, Charles O'Brien, Robert Weinstein, Stavros Manolagas, Center for Osteoporosis & Metabolic Bone Diseases, Central Arkansas Veterans Healthcare System, University of Arkansas for Medical Sciences, USA

Delay or hastening of osteoblast apoptosis has been associated with changes in bone formation and bone mass, but a cause and effect relationship has not been established. Based on evidence that both Bax and Bak, proapoptotic Bcl-2 family members, are required for activation of the mitochondrial apoptosis cascade, we sought to establish a causal link between osteoblast/osteocyte apoptosis and bone homeostasis by generating mice lacking both Bax and Bak in osteoblasts and osteocytes (Bax/BakΔOb/Ot mice). This was accomplished by crossing Bak null mice bearing a floxed Bax gene with mice expressing Cre recombinase under the control of an osteocalcin (OCN) promoter. Bax

deletion was confirmed by qPCR of DNA from the femur. Femoral but not vertebral BMD of Bax/BakΔOb/Ot mice progressively increased from 3 to 12 mo of age, whereas it reached a plateau at 6 mo of age in Bak null or OCN-Cre control mice. At 8 mo of age, Bax/BakΔOb/Ot mice exhibited cancellous bone throughout the femoral diaphysis, whereas cancellous bone was present only in the metaphyses of control mice as determined by micro-CT. Further, cancellous bone volume and connectivity density were increased, and apoptotic osteocytes were reduced, in Bax/BakΔOb/Ot mice. Moreover, the loss of femoral and vertebral cancellous bone that occurred between 12 and 22 mo of age in control mice was attenuated in Bax/BakΔOb/Ot mice. Most strikingly, Bax/BakΔOb/Ot mice exhibited an age-related increase in femoral cortical bone porosity, characterized by the presence of cortical voids containing osteoclasts. Practically identical changes in cancellous bone mass and cortical porosity were observed in a second mouse model in which Bax and Bak were deleted from osteoblast progenitors using the Osterix promoter to drive Cre expression. These findings demonstrate that the apoptosis of cells of the osteoblast lineage, perhaps at all stages of lineage progression, is a critical determinant of their genesis and function, and thereby the formation and maintenance of cancellous bone. Moreover, they indicate that lifelong prevention of apoptosis produces dysfunctional cortical osteocytes that cause an increase in intracortical resorption. This mechanism is independent of Haversian architecture, which is absent in mice, and could be informative for the increased intracortical porosity and fracture risk associated with old age in human long bones (Zebaze et al, Lancet, 375:1729, 2010).

Disclosures: Robert Jilka, None.

1210

Inhibition of BMP Signaling Using RAP-661, a Soluble Form of BMPRIA, Increases Bone Mass in Ovariectomized Mice. Aaron Mulivor^{*}, Yoshimi Kawamoto, Ravi Kumar, Jasbir Seehra, R. Scott Pearsall, Nicolas Solban, Acceleron Pharma, USA

Bone Morphogenetic Proteins (BMPs) induce endochondral bone formation and regulate osteoblastogenesis and osteoclastogenesis. Recently, it was shown that targeted inactivation of the BMP2 receptor BMPRIA (ALK3) in osteoblasts causes an increase in bone formation. To investigate new therapeutic strategies for skeletal fragility indications, a soluble BMPRIA receptor-Fc fusion protein (RAP-661) was generated to inhibit BMP signaling through the endogenous receptor.

Eight week old C57BL/6 mice underwent ovariectomy (OVX) or SHAM surgery and were aged 12 weeks post-surgery to establish an osteopenic phenotype. Mice received either twice weekly injections of RAP-661 (10 mg/kg, IP), five injections per week of parathyroid hormone (PTH: 0.08 mg/kg, SC), one injection of Zoledronate (ZOL: 0.02 mg/kg, IP) or vehicle (PBS) for six weeks. DEXA and microCT were used to evaluate the effect of RAP-661 on bone.

DEXA measurements at 6 weeks revealed increases in total BMD of 12% (RAP-661), 9% (PTH), 8% (ZOL) and 1% (PBS) compared to baseline values measured at week 0 in SHAM operated mice. In OVX mice total BMD increases of 14% (RAP-661), 14% (PTH), 7% (ZOL) and 2% (PBS) were observed after 6 weeks.

MicroCT measurements of the tibia exhibited increased cortical thickness in SHAM mice of 17% (RAP-661), 10% (PTH) and 2% (ZOL) compared to PBS treated animals. In OVX mice increases in cortical thickness of 19% (RAP-661), 16% (PTH) and 1% (ZOL) were observed after 6 weeks. Similar increases were observed in trabecular bone volume of the proximal tibia.

Serum biomarker and bone histomorphometry analysis demonstrated RAP-661 treatment was both antiresorptive and anabolic. RAP-661 treatment increased OPG 56% ($p < 0.05$), BSALP 37% ($p < 0.01$), mineralizing surface 115% ($p < 0.05$), bone formation rate 80% ($p < 0.05$) and decreased RANKL 52% ($p < 0.05$), TRAP5b levels 67% ($p < 0.01$), eroded surface 36% ($p < 0.05$), and osteoclast surface 44% ($p < 0.05$) after 2 weeks of treatment.

These preclinical results demonstrate RAP-661 increases bone mass in normal and osteopenic mice to an extent comparable to or greater than approved anabolic or antiresorptive agents. Bone biomarker analysis suggests that RAP-661 leads to new bone formation by both inhibiting osteoclast activity and increasing osteoblast activity. Therefore, inhibition of BMP signaling using a soluble form of BMPRIA represents a promising new therapeutic approach for the treatment of bone loss.

Disclosures: Aaron Mulivor, Acceleron Pharma, 3
This study received funding from: Acceleron Pharma

1211

Rosiglitazone Reduced BMD in Women with Type 2 Diabetes and the Effect was Attenuated After Switching to Metformin. John P. Bilezikian¹, Richard Eastell², Antonio J. Nino³, Allison R. Northcutt³, Barbara Kravitz³, Gitanjali Paul³, Alexander R. Cobitz³, Robert Josse⁴, Lorraine Fitzpatrick^{3*}. ¹Columbia University, College of Physicians & Surgeons, USA, ²University of Sheffield, United Kingdom, ³GlaxoSmithKline Pharmaceuticals, USA, ⁴University of Toronto, Canada

Postmenopausal women (PW) treated with rosiglitazone (RSG) are at increased risk of fracture. The aim of the study was to understand the mechanism of this risk. This was a double-blind, randomized study in PW with T2DM; BMD T-score >-2.5 at femoral neck (FN), lumbar spine (LS), total hip (TH). Subjects were randomized to RSG or metformin (MET) for 52 Weeks (Wk) followed by a 24Wk open-label MET phase. In RSG, BMD at FN decreased (-1.59%) from baseline (BL) to Wk52,

decreased less from Wk52 to Wk76 (RSG to MET; -0.27%), with an overall decrease (-2.05%) from BL to Wk76. Differences in percent change from BL between groups (RSG vs. MET) were significant at Wk52 ($p=0.0039$) and Wk76 ($p=0.0036$). In RSG, BMD at LS decreased (-1.60%) from BL to Wk52, increased (0.54%) from Wk52 to Wk76. Differences from BL at the LS between groups were significant at Wk52 ($p=0.0012$) and Wk76 ($p=0.0002$). In RSG, CTX and PINP increased (18.1% and (9.0%) respectively, and BSAP decreased (-12.3%) from BL to Wk52. Differences at Wk52 from baseline (RSG vs. MET) were statistically significant, CTX ($p=0.0123$), PINP and BSAP (both $p<0.0001$). CTX (-26.3%) and PINP (-12.1%) trended towards BL levels from Wk52 to Wk76. In RSG from BL to Wk52, there were decreases in integral (INT) and trabecular (TRB) vBMD at TH and TRB vBMD at LS. INT and TRB vBMD increased at TH and LS from Wk52 to Wk76 when subjects on RSG moved to open-label MET. The overall effect from BL to Wk76 was a loss in INT and TRB vBMD at TH and in TRB vBMD in LS. In RSG cortical (CRT) vBMD decreased at TH at Wk52 from BL and there was an increase in CRT vBMD from BL to Wk76. In MET from BL to Wk52, there were increases in INT and TRB vBMD at TH, and a decrease in TRB vBMD at LS. In MET INT vBMD decreased and TRB vBMD increased at TH, and TRB vBMD decreased at the LS from Wk52 to Wk76. CRT vBMD at TH increased modestly from BL to Wk76 in MET.

Adverse events were consistent with previous studies; 5 subjects in RSG and 1 in MET experienced a fracture.

Treatment for 52Wk with RSG resulted in bone loss at the FN and LS and increased bone turnover. Changes in aBMD were attenuated and vBMD trended towards BL levels upon switching RSG to MET, and bone markers reverted towards BL levels. These data suggest that an increase in bone turnover results in BMD loss and the effect is partially attenuated when RSG is switched to MET.

% Change in Hip and Spine vBMD-QCT				
QCT vBMD (g/cm ³)		Adjusted % Change, Mean±SE		RSG - METFORMIN
		RSG	METFORMIN	Mean % diff, [95% CI], p-value
Total Hip		32/31/30*	35/30/30*	
Integral:	BL - Week 52	-3.60±0.59	0.99±0.65	-4.59, [-6.17, -3.0], <0.001
	BL - Week 76	-1.70±0.66	0.85±0.79	-2.55, [-4.34, -0.76], 0.006
	Week 52 - 76	2.24±0.48	-0.20±0.57	2.44, [1.12, 3.77], <0.001
Trabecular:	BL - Week 52	-3.63±1.24	0.21±1.38	-3.85, [-7.24, -0.45], 0.027
	BL - Week 76	-2.66±1.21	0.70±1.45	-3.36, [-6.68, -0.05], 0.047
	Week 52 - 76	0.90±1.25	1.15±1.49	-0.25, [-3.71, 3.21], 0.88
Cortical:	BL - Week 52	-0.54±0.54	0.52±0.60	-1.07, [-2.53, 0.39], 0.15
	BL - Week 76	0.23±0.42	0.50±0.52	-0.27, [-1.43, 0.90], 0.65
	Week 52 - 76	0.94±0.45	-0.06±0.55	1.01, [-0.24, 2.26], 0.11
Vertebral trabecular		32/31/30	35/30/30	
BL - Week 52		-6.71±1.45	-1.72±1.60	-4.98, [-8.93, -1.04], 0.014
	BL - Week 76	-5.15±1.12	-3.91±1.34	-1.24, [-4.31, 1.84], 0.43
	Week 52 - 76	3.53±1.45	-2.11±1.73	5.64, [1.64, 9.64], 0.007

% Change in Hip and Spine vBMD-QCT

Disclosures: Lorraine Fitzpatrick, GlaxoSmithKline Pharmaceuticals, 5
This study received funding from: GlaxoSmithKline Pharmaceuticals

1212

Undercarboxylated Osteocalcin does not Predict Development of Diabetes In older Adults In the Health, Aging and Body Composition Study. Ann Schwartz^{*1}, Caren Gundberg², Douglas Bauer¹, Susan Ewing¹, Eric Vittinghoff¹, Elsa Strotmeyer³, Kenneth Feingold¹, Patrick Garner⁴, Tamara Harris⁵, Alka Kanaya¹, Annemarie Koster⁶, Suzanne Satterfield⁷, Steven Cummings⁸. ¹University of California, San Francisco, USA, ²Yale University School of Medicine, USA, ³University of Pittsburgh, USA, ⁴INSERM Research Unit 664 & Csbio Bioassays, France, ⁵Intramural Research Program, National Institute on Aging, USA, ⁶National Institutes of Health, USA, ⁷University of Tennessee, USA, ⁸San Francisco Coordinating Center, USA

Mouse models have identified the bone product, osteocalcin (OC), in particular the undercarboxylated form (ucOC), as a hormone affecting insulin production and sensitivity. OC^{-/-} mice are more likely to develop diabetes (DM) on a high fat diet. To assess whether this mechanism plays a role in human physiology, we used data from the Health, Aging and Body Composition longitudinal study of 3,075 older adults in a case-cohort design to determine if baseline levels of ucOC, %ucOC (ucOC/total OC) or total OC predict development of DM. Participants were asked about DM status and medication use at annual visits, and fasting glucose (FG) was measured at baseline, and 1, 3 and 5 years later. A 2-hr glucose tolerance test (OGTT) was obtained at baseline. Participants who reported use of oral steroids or warfarin at baseline were excluded. Among those without DM at baseline, a random sample was identified from those with impaired glucose metabolism (elevated FG or OGTT) (N=171) and those with normoglycemia (N=172). Incident DM cases (N=161) were identified based on self-report, initiation of DM medication, or an elevated FG (≥ 126 mg/dl) during an average follow-up of 6.0 2.5 years. OC, ucOC, N-propeptide of type I procollagen (PINP), and serum type I collagen C-telopeptides (S-CTX) were measured in baseline serum specimens. ucOC was measured with the hydroxyapatite (HAP) binding assay. The baseline sample was 52% women and 59% white with mean age 73.6 (SD 2.9) years. OC, but not ucOC or %ucOC, was lower in those with DM at baseline. However, in proportional hazards models, higher baseline levels of ucOC,

OC and PINP, but not %ucOC or sCTX, were associated with incident DM in models adjusted for age, gender, race, clinic site and baseline strata (impaired glucose metabolism or normoglycemia). After further adjustment for renal function, oral estrogen use and physical performance score, none of the baseline bone markers predicted DM. Additional adjustment for smoking status, physical activity, use of osteoporosis drugs, statins or thiazide diuretics did not substantially change the estimated associations. In contrast to mouse models that found increased DM risk in mice lacking OC, our findings do not support a role for ucOC levels in the development of type 2 diabetes in older adults.

Table. Hazard ratio (HR) and 95% confidence interval (95% CI) for incident diabetes for each 1 SD increase in baseline bone turnover marker

Marker	Minimally adjusted ^a		Multivariable adjusted ^b	
	HR	(95% CI)	HR	(95% CI)
ucOC	1.26	(1.01, 1.57)	1.17	(0.92, 1.48)
%ucOC	1.17	(0.91, 1.51)	1.19	(0.91, 1.57)
Total OC	1.32	(1.07, 1.64)	1.15	(0.89, 1.48)
PINP	1.32	(1.08, 1.62)	1.24	(0.96, 1.59)
sCTX	1.09	(0.88, 1.35)	1.01	(0.79, 1.30)

^a Adjusted for age, gender, race, clinic site, baseline strata (impaired glucose metabolism or normoglycemia).

^b Adjusted for above plus cystatin-c, oral estrogen use, physical performance score.

Table

Disclosures: Ann Schwartz, Merck, GlaxoSmithKline, 2; GlaxoSmithKline, Amgen, 5

1213

Deletion of *Nocturnin* Protects Against Rosiglitazone-Induced But Not Age-Related Bone Loss. Phuong Le^{*1}, Anyonya Guntur¹, Sheila Bornstein², Leeann Louis³, Masanobu Kawai², Mary Boussein³, Beata Lecka-Czernik⁴, Clifford Rosen². ¹Maine Medical Center Research Institute, USA, ²Maine Medical Center, USA, ³Beth Israel Deaconess Medical Center, USA, ⁴University of Toledo College of Medicine, USA

Nocturnin (*Noc*) is a circadian gene expressed in bone and fat which encodes a deadenylase that is a downstream target of PPAR γ and up-regulated by rosiglitazone (Rosi). *Noc* also binds to PPAR γ and enhances its transport to the nuclear membrane. Sixteen week *Noc*^{-/-} mice have high bone mass, are resistant to diet induced obesity, and have lower body temperature than ^{+/+} mice. But the importance of *Noc* in osteogenesis has not been well delineated. To test the functional importance of *Noc* relative to body composition and bone mass, we aged both *Noc*^{-/-} and *Noc*^{+/+} to 6 months. We also treated 12 wk *Noc*^{-/-} mice and their age- and gender matched ^{+/+} controls with 20 mg/kg/day Rosi for 8 wks. In the aging study, *Noc*^{-/-} total aBMD by DXA was slightly reduced compared to ^{+/+} mice ($p=0.10$). Trabecular tibial and lumbar BV/TV by μ CT were reduced by 50% in the *Noc*^{-/-} mice vs ^{+/+} ($p=0.03$ and 0.04 respectively). There were no differences in marrow fat between genotypes. Gene expression studies in femur revealed no significant differences in Wnt10b or β 3AR. However, FoxC2 expression in *Noc*^{-/-} mice was increased 1.7 fold vs ^{+/+} femurs ($p=0.04$). In the Rosi treatment study, both *Noc*^{-/-} and ^{+/+} mice gained total body weight ($p=0.002$ and 0.003 respectively vs control diet mice). The ^{+/+} mice had a 20% increase in total percent fat on Rosi ($p=0.021$) while the *Noc*^{-/-} showed no change in total percent fat on Rosi vs control feeding. Importantly, Rosi treated ^{+/+} female and ^{+/+} male mice lost total aBMD ($p=0.055$) and aBMC ($p=0.025$) compared to ^{+/+} control treated mice, while *Noc*^{-/-} male and female mice were resistant to Rosi induced bone loss. Trabecular BV/TV, Conn-Dens., and Tb.N were greater in Rosi treated ^{+/+} mice vs Rosi treated ^{+/+} ($p=0.016$, 0.010, 0.008). To explore the mechanisms responsible for the skeletal changes downstream of *Noc*, we over-expressed *Noc* in MC3T3 cells and found a marked decrease in osteocalcin ($p=0.008$) and ATF4 ($p=0.0002$) mRNA expression with a modest decrease in *FoxO1* mRNA ($p=0.06$) relative to GFP. In summary, *Nocturnin* is an important determinant of body composition through its actions on PPAR γ . Absence of *Noc* prevents rosiglitazone-induced fat mass gain and protects against skeletal bone loss. However, with age *Noc*^{-/-} lose significantly more bone than ^{+/+} mice. The effects of *Nocturnin* on bone are complex; it includes cell autonomous direct modulation of PPAR γ action and indirect actions on brown adipose tissue and the sympathetic nervous system.

Disclosures: Phuong Le, None.

1214

N-Cadherin/Wnt Signalling Interaction Controls The Switch Between Osteoblast and Adipocyte Mesenchymal Cell Differentiation In Aging Mice. Eric Hay^{*1}, Thibault Buczkowski², Pierre Marie³. ¹INSERM 4606, France, ²INSERM U606 & University Paris Diderot, France, ³INSERM Unit 606 & University Paris Diderot, France

The aging skeleton is characterized by decreased number of bone-forming cells and increased number of adipocytes in the bone marrow. The mechanisms controlling the switch between osteoblast and adipocyte differentiation of mesenchymal stromal cells (MSC) during aging are poorly understood. Here, we investigated the role of the N-cadherin/Wnt interaction in the control of MSC bifurcation into osteoblasts or adipocytes. Overexpression of N-cadherin in C3H10T1/2 cells increased adipocyte

gene expression (PPARGgamma, C/EBPalpha, LPL) and adipogenesis, indicating that N-cadherin controls adipocyte differentiation in MSC. We next analysed bone marrow adipogenesis in aging mice overexpressing N-cadherin in osteoblasts. RT-qPCR and histomorphometric analyses showed that in adolescent (1.5 month old) mice, N-cadherin overexpression increased adipocyte gene expression, adipocyte number (+300 %, $P < 0.05$) and volume in the bone marrow (+300 %, $P < 0.05$) compared to wild-type mice. This effect was associated with decreased expression of osteoblast markers (Runx2, ALP, COL1A1, OC), decreased bone formation rate and bone mass associated with decreased Wnt5 and Wnt10b mRNA levels in the bone marrow. At 6 months of age, however, this bone phenotype was corrected and bone mass was normalized in N-cadherin transgenic mice. Remarkably, at 18 months of age, N-cadherin transgenic mice exhibited increased osteoblast markers, increased bone formation rate (+80%), and decreased adipocyte number (-75 %) and volume (-80 %) in the bone marrow compared to wild-type mice. This reversal of the bone phenotype in aging mice was associated with reduced expression of N-cadherin and increased Wnt5a and Wnt10b expression in the bone marrow. The results show that N-cadherin/Wnt signalling interaction controls the age-related switch between osteoblast and adipocyte differentiation. In young mice, N-cadherin overexpression reduces Wnt signalling, resulting in increased adipocyte differentiation and decreased osteoblast differentiation, causing decreased bone formation and bone mass. With aging, N-cadherin expression declines and Wnt signalling increases concomitantly, resulting in reduced adipogenesis and increased bone formation and bone mass. This provides novel mechanisms by which modulation of Wnt signaling by N-cadherin governs the bifurcation between osteoblasts and adipocytes which in turn regulates bone formation and bone mass in aging mice (supported by the FP7 Program Talos).

Disclosures: Eric Hay, None.

1215

Mice Lacking AMP-activated Proteine Kinase (AMPK)-alpha1 Catalytic Subunit have Attenuated Bone Responses to Ovariectomy and Intermittent PTH Treatment. Jeshmi Jeyabalan^{*1}, Mittal Shah¹, Benoit Viollet², Marta Korbonits³, Chantal Chenu¹. ¹Royal Veterinary College, United Kingdom, ²Institut Cochin Inserm, France, ³Barts & the London Medical School, United Kingdom

AMPK is a key regulator of cellular and body energy homeostasis. We previously demonstrated that AMPK activation in osteoblasts increases bone formation in vitro while deletion of the AMPK α 1 subunit, the dominant catalytic subunit expressed in bone, leads to decreased bone mass in vivo. To determine whether bone turnover can be stimulated in the absence of AMPK α 1 subunit, we subjected wild-type (WT) and AMPK α 1^{-/-} mice to catabolic (ovariectomy: OVX) and anabolic (intermittent PTH administration: iPTH) hormonal challenges. 3 month-old female AMPK α 1^{-/-} (n=16) and WT (n=16) mice were ovariectomized. 4 weeks after OVX, mice were randomly divided into two groups, one receiving saline and the other PTH (1-34) treatment (80µg/kg/day) for 4 weeks. Tibiae were harvested from these mice, bone micro-architecture determined by micro-computed tomography and bone formation and resorption parameters measured by histomorphometric analysis. AMPK α 1^{-/-} mice displayed a decreased bone loss after OVX in the trabecular compartment compared to WT mice. This was demonstrated by higher trabecular bone volume (+38%; $p < 0.01$), trabecular number (+40%; $p < 0.001$) and decreased trabecular separation (-37%; $p < 0.001$) in AMPK α 1^{-/-} mice versus WT mice. The cortical indexes showed non-significant increases in bone area and cortical thickness in AMPK α 1^{-/-} mice versus WT mice after OVX. As expected, iPTH increased cortical and trabecular bone indexes in both WT and AMPK α 1^{-/-} mice. However, AMPK α 1^{-/-} mice showed lower trabecular bone volume (-17%; $p < 0.01$), trabecular number (-10.4%; $p < 0.05$), trabecular thickness (-10%; $p < 0.05$) and increased trabecular separation (+13%; $p < 0.05$) compared to WT mice in response to iPTH treatment. The cortical indexes, bone area (-15%; $p < 0.01$) and cortical thickness (-9.8%), were similarly lower in AMPK α 1^{-/-} mice compared to WT mice. Neither AMPK α 1^{-/-} nor WT mice bone length or body weight were altered. Surprisingly, parameters of bone formation and resorption were not significantly modified between WT and AMPK α 1^{-/-} mice, while we observed a massive decrease in the number of adipocytes in the AMPK α 1^{-/-} mice. Overall these results demonstrate that AMPK α 1^{-/-} mice are less affected by catabolic and anabolic changes in bone turnover induced by OVX and PTH respectively, suggesting that AMPK activation plays a role in the hormonal regulation of bone remodeling.

Disclosures: Jeshmi Jeyabalan, None.

1216

Altered Bone Fatty Acid Metabolism in Obesity and After Diet-Induced Weight Loss. Riku Kiviranta^{*1}, Jussi Raisanen², Tam Pham², Anna Karmi², Antti Viljanen², Riitta Parkkola², Jarna Hannukainen², Pirjo Nuutila². ¹Medical Biochemistry & Genetics & Turku PET Centre, University of Turku, Finland, ²Turku PET Centre, University of Turku, Finland

Obesity has complex effects on bone tissue. Overweight results in increased bone mass but is also associated with increased bone marrow adiposity, thus having putatively negative effects on bone metabolism. Free fatty acids (FFAs) serve as an energy source for several tissues. FFA tissue uptake and oxidation are increased in

obesity especially in myocardium, liver and adipose tissue while FFA uptake is reduced by weight loss in these tissues. However, there is no information on FFA utilization in bone tissue of normal or obese subjects.

To understand the crosstalk between energy metabolism and bone, we analyzed bone FFA utilization in controls and in obese subjects before and after very low calorie diet (VLCD) using positron-emission tomography (PET) imaging.

Nine control subjects (BMI=25.13.3) were imaged at baseline and seventeen obese subjects (BMI=33.94.0) before and after a six-week VLCD using [¹⁸F]-fluoro-6-thia-heptadecanoic acid ([¹⁸F]-FTHA) for the assessment of FFA uptake in tissue. FFA uptake was measured in the bone marrow area at mid-femoral diaphysis in both groups and in the trabecular bone of L3 and Th7-10 vertebral bodies in the obese subjects.

At baseline FFA uptake in the femoral diaphysis was significantly higher in obese subjects than in the nine lean ones (0.370.16 vs. 0.150.07 µmol/(min*dl), $p < 0.01$). In obese subjects the FTHA uptake was lower in femurs than in vertebrae (0.37 vs 1.41 µmol/(min*dl), $p < 0.001$), but did not differ between thoracic and lumbar vertebrae. After six weeks of VLCD, obese subjects had lost weight in average 12 kg (101 12 kgs to 89 11 kgs, $p = 0.008$). Subsequently, FFA uptake was reduced by 19% in femoral diaphysis ($p < 0.03$). The reduction in FTHA uptake was much greater in thoracic and lumbar vertebrae (-27% and -26%, respectively, $p < 0.01$), again not significantly differing between the vertebrae.

Our results indicate that FFA uptake in bone marrow is increased in obese patients and that weight loss reduces FFA utilization in bone, as we have previously observed in other tissues. Interestingly, the overall FFA uptake is significantly higher and the diet-induced reductions greater in vertebrae, where the amount of bone marrow fat is low compared to femurs. Thus FFAs are likely utilized by *bona fide* bone cells in addition to bone marrow adipocytes. In conclusion, bone FFA metabolism is altered by obesity and diet-induced weight loss further supporting the link between energy metabolism and bone.

Disclosures: Riku Kiviranta, None.

1217

Positive Feedback Regulation of microRNA-218 Linked to Wnt Signaling Promotes Osteoblast Differentiation. Mohammad Hassan^{*1}, Yukiko Maeda¹, Mohammad Jafferji¹, Jonathan Gordon¹, Zhaoyong Li¹, Carlo Croce², Andre Van Wijnen¹, Janet Stein¹, Gary Stein¹, Jane Lian¹. ¹University of Massachusetts Medical School, USA, ²The Ohio State University, USA

Gene expression during osteoblast differentiation is controlled at multiple transcriptional and post-transcriptional levels. MicroRNAs (miRNAs), non-coding ~22 nucleotide RNAs, regulate virtually every biological process by binding to the 3'-untranslated region (UTR) of mRNAs to attenuate protein synthesis. Using microarray and high-throughput miRNA profiling, we identified pre- and mature miRs that are up-regulated during differentiation of osteoprogenitors to mature osteoblasts. Bioinformatics revealed that several miRNAs target well established pathways for bone formation, including Wnt, BMP and MAPK pathways. Here we show that miR-218 suppresses inhibitors of Wnt signaling, Sclerostin (SOST), Dickkopf2 (DKK2) and Secreted Frizzled-Related Protein 2 (SFRP2), as well as the BMP signaling inhibitor TOB1. LUC/3'-UTR reporter assays validated that miR-218 controls each target. Endogenous expression of miR-218 increased during differentiation of calvarial osteoblasts to day 28, the mineralization stage. We tested biological activity of miR-218 by examining if its ability to suppress Wnt/BMP signaling inhibitors promotes osteoblast differentiation in MC3T3 cells. Exogenous expression of miR-218 up-regulated early markers Runx2 and Alk Phos on day 7 and late osteoblast markers at mature stages (days 21-28). Importantly, miR-218 suppressed expression of Wnt inhibitors, induced Wnt targets, and activated a canonical Wnt responsive promoter (TOP-Flash reporter assay). We also show mechanistically that miR-218 is upregulated in osteoblasts by activation of Wnt signaling, evident by elevation of LEF1, TCF1 and beta-catenin, presumably via a putative LEF1 binding site 5' to miR-218. Taken together, these results demonstrate that miR-218 is a key stimulator of osteogenic differentiation and functions in a positive Wnt/miR-218/Wnt inhibitor feedback loop that sustains Wnt signaling during osteoblast differentiation.

Disclosures: Mohammad Hassan, None.

1218

Wnt11 Is a Novel Inhibitor of Trabecular Bone Mass. Mariya Sweetwyne^{*}, Bernadette Hsu, Megan Hays, Kurt Hankenson. University of Pennsylvania, USA

Studies have established that Wnt signaling through beta-catenin stabilization increases bone formation. Wnts are classified as either canonical (beta-catenin dependent) or non-canonical. Previous work from our group demonstrated that over expression of Wnt11 in vitro in MC3T3E1 cells increased osteoblastogenesis through canonical signaling. Therefore, we hypothesized that loss of Wnt11 in vivo would decrease bone mass.

With the exception of female Wnt11^{-/-} mice, all genotypes and genders are fertile and produce viable offspring. However, Wnt11^{-/-} viability is low with only 20% of the offspring predicted by Mendelian inheritance surviving past postnatal day 2. Mice were harvested at 4, 8 and 12 months of age. MicroCT analysis of femurs at 4 and

8 months of age shows that total loss of Wnt11 increases trabecular, but not cortical, bone. At 8 months, Wnt11^{-/-} mice have a 2-fold increase in trabecular bone when compared to wild-type (WT). This difference is dependent on gene copy number as Wnt11^{+/-} mice have a trabecular phenotype intermediate to the null and WT mice. Regardless of genotype or gender, trabecular bone volume declines between 8 and 12 months of age.

Comparing cortical and trabecular bone volume independent of age, gender, and body weight demonstrates a positive correlation between the two sites in WT mice ($R^2 = 0.901$, $p = 0.013$) but not Wnt11^{-/-} mice ($R^2 = 0.028$, $p = 0.753$). Wnt11^{+/-} mice have an intermediate phenotype ($R^2 = 0.885$, $p = 0.057$). These results indicate that Wnt11 may play a more prominent role in trabecular bone or in coupling cortical and trabecular bone.

Western blot and immunofluorescence analysis of beta-catenin expression in primary, unstimulated mesenchymal stem cells (MSC) and dermal fibroblasts (harvested 4, 8 and 12 months of age) show that Wnt11^{-/-} cells have increased levels of active nuclear beta-catenin. In addition, Wnt11 deficient cells have reduced: actin stress fibers, rates of proliferation and cell-cell contact in proliferating colonies.

These studies are the first to demonstrate that Wnt11 regulates bone; unexpectedly, we conclude that Wnt11 is an inhibitor of trabecular bone mass. As a Wnt traditionally classified as non-canonical, Wnt11 has been shown to inhibit canonical Wnt signaling in other tissues. We hypothesize that physiological levels of Wnt11 inhibit trabecular bone formation by suppressing canonical beta-catenin signaling.

Disclosures: Mariya Sweetwyne, None.

1219

Implantation of Hedgehog-Activated Mscs Regenerates Periosteal Like Bone Formation in a Murine Bone Allograft Repair Model. Chunlan Huang¹, Ming Xue¹, Fanjie Zhang¹, Regis O'Keefe², Xinping Zhang¹. ¹University of Rochester Medical Center, USA, ²University of Rochester, USA

Periosteum plays an essential role in skeletal repair and reconstruction. To the end of understanding the molecular pathways underlying periosteum-mediated repair and reconstruction, we isolated a population of mesenchymal stem cells (MSCs) from the periosteum at the cortical bone healing site. These cells express typical MSC markers and are capable of differentiating into osteoblasts, adipocytes, and chondrocytes. Characterization of these cells demonstrates that activation of the hedgehog (Hh) pathway effectively promotes osteogenic differentiation of periosteum MSC in vitro. When implanted subcutaneously in athymic nude mice, these hedgehog-overexpressing cells induce robust bone formation in vivo. To further determine the effects of Hh-activated periosteum MSCs in repair and reconstruction, we implanted the periosteum MSCs overexpressing an N-terminal sonic hedgehog peptide around a devitalized bone allograft to repair a 4mm segmental femoral bone defect in mice. Our results demonstrated that implantation of the Hh-activated MSCs induced robust bone formation around bone allografts. MicroCT imaging analyses showed a 3-fold induction of new bone formation around bone allografts as compared to the controls ($n=6$). A contiguous periosteal collar bone was regenerated around bone allografts engrafted with Hh-activated periosteum MSCs. In comparison, the control allografts demonstrated a nearly complete absence of effective periosteal bone formation around allografts. These results strongly suggest that the engraftment of Hh activated periosteum MSCs is effective in enhancing skeletal repair and reconstruction. In an effort to further identify Hh-responsive MSCs from other available sources for repair and reconstruction, we examined the effects of Hh activation in cells isolated from murine neonatal dermis. We found that overexpression of Hh ligand or Gli1, a key activator of the Hh pathway, induced ALP staining and osteoblastic differentiation in isolated neonatal dermal cells. The induction further synergized with BMP-2. These data strongly indicate the potential utility of Hh-activated dermis MSCs as a periosteum replacement for skeletal repair and reconstruction. Taken together, our data support the role of Hedgehog pathway as a positive regulator for osteoblastic differentiation for early stage mesenchymal progenitors.

Disclosures: Chunlan Huang, None.

1220

Wnt Ligands from Osteoblasts are Critical for Bone Accrual. Zhendong Zhong¹, Cassandra Diegel¹, Bart Williams². ¹Van Andel Institute, USA, ²Van Andel Research Institute, USA

A great deal of work has shown that the gain-of-function or loss-of-function mutations in the components of Wnt pathway affect the bone homeostasis. But little is known about where the Wnt ligands originate in the bone tissue.

Several recent genome-wide association studies of European and Asian descendants found that GPR177 (1p31.3) is significantly related to bone mass density (Nat. Genet. 2009 and PlosOne 2010). Wntless/GPR177 is a newly identified chaperone protein that specifically escorts Wnt ligands for secretion, which potentially plays an important role in bone metabolism by regulating Wnt/ β -catenin signaling pathway.

To investigate the necessity of Wnt ligands from osteoblasts, we generated osteoblast-specific Wntless-deficient mice (Oc-cre; Wntless-flox). Homozygous mutant mice were born at a normal Mendelian frequency with no obvious skeletal abnormality in the early stage. Whole body Dual X-Ray Absorptiometry (DXA) scan revealed that the bone mass accrual was significantly inhibited in homozygotes from 20 days of age. MicroCT analysis and histomorphometric data showed a dramatic

reduction of both trabecular bone mass and cortical bone thickness in homozygous mutants. The bone formation in vivo was severely impaired while osteoclast activity was increased significantly. No obvious phenotype change was observed for heterozygotes. In vitro study showed that Wntless-deficient osteoblasts had a dramatic defect in differentiation and mineralization with significant decreased expressions of key osteoblast differentiation regulators.

Due to spontaneous fractures causing severe retardation, premature lethality happens in most of the homozygotes shortly after the weaning age. However, these homozygotes could have a robust fracture healing shortly after fracture, which might be due to the Wnt ligands coming from chondrocytes or other cell types at the fracture site. The Wntless-deficient osteoblasts were hypersensitive to Wnt3a, and showed a strong activation of Wnt/ β -catenin signaling after Wnt3a treatment in vitro.

Taken together, these results reveal a surprising and critical role of osteoblast-secreted Wnt ligands for bone accrual, and add more complexities to how Wnt regulates the bone formation/resorption locally in the bone.

Disclosures: Zhendong Zhong, None.

1221

ENU Chemical Mutagenesis Reveals That the Distal Region of Mouse Chromosome 11 Contains a Key Bone Size Mechanoresponsive Gene. Chandrasekhar Kesavan¹, Apurva Srivastava², David Baylink³, Tara Azizi⁴, Subburaman Mohan¹. ¹Jerry L. Pettis Memorial VA Medical Center, USA, ²NCI (National Cancer Institute), USA, ³Loma Linda University, USA, ⁴Musculoskeletal Disease Center, JLP VA Medical Center, USA

Bone size is a particularly important contributor of its overall strength and the hereditary component contributes 50-85% to the variation in bone size. Using a sensitized N-ethyl-N-nitrosourea (ENU) mutagenesis screen, we have identified a mutant C57BL/6J mouse strain (14104) that exhibits a 40% reduction in cross sectional area. Genome-wide linkage analysis revealed that the mutant locus is located in the 109-119 Mb region of mouse chr 11 with axin2, Map2K6, Rab37, Grb2, Sox9 and Socs3 as functional positional candidates. Because mechanical strain (MS) is a known contributor to periosteal expansion during postnatal growth and because a mechanical loading (ML) QTL has been identified in the same chromosomal region in the C57BL/6J X C3H/HeJ intercross, we predicted that 14104 gene is a mediator of the MS response in the skeleton. To test this prediction, we evaluated whether skeletal anabolic response to ML is impaired in mutant mice compared to wild type (WT) mice. Because the amount of MS the skeleton receives for a given load is largely dependent on its size, we measured MS by using a strain-gauge technique on tibia metaphyses of both genotypes to ensure a similar amount of strain is applied to mutant and WT mice. We found that a 6N (641 μ e) load in mutant female mice produced MS similar to that of 10N load (623 μ e) in WT mice. Adjusted loads were applied on right tibia of both sets of mice by performing axial loading for 3 alternative days for 2 weeks while the left tibia served as an internal control. Micro-CT measurements at 10.5 μ m revealed a 40% ($p < 0.01$) increase in trabecular (Tb) BV/TV which is caused by 12% and 15% increases in the Tb number and thickness, respectively, in WT mice. In contrast, none of the Tb parameters were significantly increased in the loaded bones of mutant mice. Similarly, axial loading caused a significant increase in cortical bone area (8%, $p < 0.05$) at the tibial mid-diaphysis of WT but not mutant mice. Consistent with Micro-CT measurements, gene expression profiling revealed that levels of ephrin signaling pathway genes (EFNB1, A2 and EphB2), that are known to be modulated by ML, are increased in response to loading in WT mice (2-fold, $p < 0.05$) but not in 14104 mutant mice. Based on these data, we conclude that the distal region of mouse chr 11 harbors a mechanoresponsive gene that is upstream of the ephrin signaling pathway and plays a critical role in regulating bone size during postnatal growth in mice.

Disclosures: Chandrasekhar Kesavan, None.

1222

Smad4 Antagonizes Osteoblast Proliferation via Competitive Recruitment of β -catenin. Valerie Salazar¹, Nicholas Zarkadis², Lisa Huang¹, Jin Norris¹, Gabriel Mbalaviele¹, Roberto Civitelli¹. ¹Washington University in St. Louis School of Medicine, USA, ²Kansas City University of Medicine, USA

We previously demonstrated Smad4 expression inversely correlates with the ability of Wnt3a or activated β -catenin to stimulate TCF/Lef-dependent transcription, *CCND1* expression, and proliferation in C3H10T1/2 cells. We examined the molecular mechanisms of this novel interaction between Smad4 and canonical Wnt signaling. Immunoblot analysis in MC3T3 cells indicates that the abundance and phosphorylation status of critical components of the canonical Wnt pathway are not changed by Smad4 over-expression, thus making autocrine or paracrine regulation unlikely. In contrast to subconfluent MC3T3 cells where BMP2 can stimulate nuclear accumulation of β -catenin in approximately 75% of cells, confluent MC3T3 cells exhibit primarily nuclear localization of β -catenin, along with Smad4, TCF3, and TCF4. However, BMP-2 does not activate, and in fact inhibits LiCl-stimulated TCF/Lef transcriptional activity. Pull-down assays reveal that BMP-2 triggers recruitment of β -catenin to a heteromeric transcription complex that binds DNA oligonucleotides encoding classic Smad-binding sequences. Importantly, this complex also contains

Smad4, phosphorylated R-Smads (1/5/8), and TCF4; whereas TCF3 is not recruited. Mutational analysis demonstrates that disruption of Smad4 DNA-binding activity greatly diminishes its ability to antagonize basal *CCND1* promoter activity, which is regulated by TCF/Lef promoter elements. The nuclear export signal, linker domain, and Smad4-dependent transcriptional activity are not required. Such antagonism by Smad4 on cell cycle is also operative *in vivo*. Tamoxifen-induced ablation of Smad4 in *Smad4^{fllox/flox}; Osx-CreERT2* mice results in a 4-fold increase in the number of BrdU+ cells in trabecular bone, an effect significantly greater than that obtained by activating LRP5/6 with a systemic anti-Dkk1 antibody treatment. Thus, Smad4 operates at the Osterix+ stage of osteoblast differentiation to dampen proliferation, a mechanism that is at least partially mediated by BMP-2-dependent recruitment of β -catenin/TCF4 to Smad4-containing transcription complexes. Our results are consistent with a competitive recruitment model whereby Smad4 can sequester the β -catenin/TCF transcriptional machinery away from canonical Wnt target genes to BMP response elements, thereby inhibiting osteoblast proliferation.

Disclosures: Valerie Salazar, None.

1223

MMP13 is A Critical Target Gene during the Development of Osteoarthritis.

Jie Shen^{*1}, Hongting Jin¹, Meina Wang¹, Bing Shu², Baoli Wang², Erik Sampson¹, Regis O'Keefe¹, Di Chen². ¹University of Rochester, USA, ²University of Rochester Medical Center, USA

Osteoarthritis (OA) is a common joint degenerative disease affecting more than 25% of people over the age of 18. The pathogenesis of OA is poorly understood and currently there is no effective disease-modifying treatment for OA. Recent human genetic studies have demonstrated that mutations in the *FrzB* and *Smad3* genes are associated with high incidence of hip and knee OA in patients. However, the downstream target gene(s) for these signaling pathways during OA development remains unknown. MMP13, also known as collagenase 3, is up-regulated in articular chondrocytes in OA patients. In this study, we investigated the role of *Mmp13* in OA development in TGF- β receptor conditional knockout [*Tgfb2(Col2ER)*] and β -catenin conditional activation [β -cat-ex3(*Col2ER*)] mice. Tamoxifen was administered to 2-week-old mice (1 mg/10g body weight, i.p., x5 days) and mice were sacrificed at 3 and 6 months of age. In 3-month-old *Tgfb2(Col2ER)* mice (n=11) and 6-month-old β -cat-ex3(*Col2ER*) mice (n=8), a severe OA-like phenotype was observed, including increased chondrocyte expression of *Col10a1* and *Mmp13* in the superficial zone of the articular cartilage, severe loss of articular cartilage tissue and osteophyte formation. To determine the role of *Mmp13* in OA development in these mice, we have crossed *Tgfb2(Col2ER)* and β -cat-ex3(*Col2ER*) mice with *Mmp13(fx/fx)* mice (n=6). Deletion of the *Mmp13* gene completely reversed most OA-like features observed in *Tgfb2(Col2ER)* and β -cat-ex3(*Col2ER*) mice. We then investigated the mechanism of *Mmp13* up-regulation and found that inhibition of TGF- β or activation of β -catenin signaling up-regulates *Mmp13* expression in a Runx2-dependent manner. Mutation of the Runx2 binding site in the proximal human *Mmp13* promoter (3.4 kb) completely blocked *Mmp13* promoter activity in the setting of TGF- β signaling inhibition (*Tgfb2* siRNA) or β -catenin activation (BIO, 1 μ M) in chondrogenic RCS cells. ChIP analysis further demonstrated binding of Runx2 to the *Mmp13* promoter. Additional studies demonstrated that deletion of the *Mmp13* gene in *Mmp13* conditional KO mice [*Mmp13(Col2ER)*], decelerated meniscal-ligamentous injury (MLI)-induced OA and treatment with an MMP13 inhibitor (CL82198, 1, 5 and 10mg/kg) also decelerated the progression of MLI-induced OA in wild-type mice. Our studies demonstrate that multiple signaling pathways involved in OA converge on MMP13 and identify MMP13 as a potential key target for therapeutic approaches.

Disclosures: Jie Shen, None.

1224

Human Embryonic Stem Cell Derived Therapy for Articular Cartilage Shows Strong Efficacy Outcomes Without Immune Suppression. David Pier¹, Jordi Tremoleda², Derek Dauphin¹, Val mann¹, Brendon Noble^{*3}. ¹UCS, United Kingdom, ²Imperial College, United Kingdom, ³University Campus Suffolk, United Kingdom

The combined clinical burden of traumatic cartilage injuries and osteoarthritic degeneration is high due both to its prevalence and strong influence on quality of life and loss of independence. Cartilage is notable for its low or non-existent regenerative capacity. Cell-based methods of assisting regeneration will contribute to the reduction of clinical burden, however challenges remain over the sourcing and efficient production of clinical cell therapies.

To overcome these limitations, a method has been developed in which highly scaleable human embryonic stem cells (hESCs) undergo directed differentiation along the chondrogenic lineage producing a cell population capable of improving regeneration while escaping deletion by the immune system *in vivo*. Prior to implantation the expression of SOX9, was found to increase 8-fold relative to parental hESCs (P = 0.0027). Collagen type II was largely undetectable by western blot analysis and immunohistochemistry. Gene expression analysis of COL2A1 IIA splice variants increased nearly 30-fold (P = 0.0005) while COL2A1 IIB remained unchanged. No protein or gene expression of pluripotency markers was found and implanted therapy failed to produce teratomas in immune compromised rodents

indicative of commitment to the chondrogenic lineage and an absence of undifferentiated cell contaminants.

Implantation into partial thickness articular cartilage defects enhanced tissue regeneration at 1, 4 and 9-months post-implantation in wild-type rats receiving no immune suppression. Regenerate tissue exhibited characteristics of hyaline articular cartilage and achieved full integration with adjacent native tissue. Using a histological grading system incorporating measures of surface regularity, regenerate tissue and cellular morphology, architecture, tidemark formation, chondrocyte cloning, subchondral bone integrity and Safranin O staining, treatment was found to result in a significant improvement in tissue regeneration over empty defects at 1- and 4-months post-operation (P < 0.001 *** for both). Human cells were detected at the defect site throughout the 9-month study indicating they play a role the observed tissue regeneration. These results suggest that hESC-derived therapies possess clinical utility in allogenic format and without necessitating an immune suppressive regime. Their intrinsic expandable nature makes them an ideal candidate for future cell therapy development.

Disclosures: Brendon Noble, None.

This study received funding from: geron Corporation

1225

Accelerating Fracture Healing Correlates with Enhancing Angiogenesis and Mesenchymal Stem Cells in Matrilin-1 Knockout Mice. Xin Li¹, Qian Chen^{*2}. ¹Brown University, USA, ²Brown University School of Medicine, USA

Matrilin-1 (MATN1) is a cartilage specific, non-collagenous extracellular matrix protein produced by pre-hypertrophic chondrocytes of the growth plate, which is critical for the transition from cartilage to bone during endochondral ossification. MATN1 knock-out (KO) mice present abnormal collagen fibrils in cartilage matrix, but are otherwise normal during skeletal development. Thus, its role *in vivo* was unknown. In this study, we determined whether MATN1 plays a role in fracture healing, which begins with hematoma formation and involves the vascular network in the whole process. A closed tibia fracture was created in the right leg of mice while the left leg served as sham control with pin fixation but no fracture. Both MATN1 KO and wildtype (WT) mice were analyzed by *in vivo* imaging, real-time RT-PCR, micro-CT, and mechanical testing. MATN1 KO mice have significantly more blood vessels and blood pool formed during the early stage of fracture healing (Day 4 post-fracture). In the mid-stage (Day 14), expression levels of the mesenchymal stem cell markers including STRO-1 and N-cadherin are significantly increased in the fracture callus of MATN1 KO mice. In the late stages (Day 21), MATN1 KO mice have significant more mineralization and bone formation but less cartilaginous tissues in the fracture callus. At the end stage of fracture healing (Day 28), total callus bone volume and mechanical torsion properties are increased in the KO mice. Our data suggest that MATN1 KO mice have increased angiogenesis, mesenchymal stem cell production, and bone formation during fracture healing process. As a result, the KO mice's bone fracture heals faster than the WT mice. The mechanism for MATN1 in regulating fracture healing is not understood. Recently, we have shown strong interactions of matrilin family members with various growth factors including the angiogenic growth factor VEGF. In addition, MATN1 has been identified as an anti-angiogenic molecule in cartilage, which is devoid of blood vessels. It is thus possible for MATN1 to regulate fracture healing process by affecting angiogenesis. In summary, this study has identified the first physiological role for MATN1 *in vivo*. It shows that MATN1, as a cartilage-specific matrix molecule, negatively regulates fracture healing process by inhibiting angiogenesis, mesenchymal stem cell levels, and bone formation.

Disclosures: Qian Chen, None.

1226

Adverse Effects of Hyperlipidemia on Bone Regeneration and Strength. Flavia Pirih^{*1}, Sotirios Tetradis², Maria-Grazia Ascenzi¹, Linda Demer³, Tara Aghaloo¹, Yin Tintut¹. ¹University of California, Los Angeles, USA, ²UCLA, USA, ³David Geffen School of Medicine At University of California Los Angeles, USA

Hyperlipidemia increases the risk for generation of lipid oxidation products, which accumulate in the subendothelial spaces of vasculature and bone. Atherogenic high-fat diets increase serum levels of oxidized lipids, which are known to attenuate osteogenesis in culture and to promote bone loss in mice. In this study, we investigated whether oxidized lipids affect bone regeneration and mechanical strength. Wild type and hyperlipidemic (*Ldlr*^{-/-}) mice were placed on a high-fat (HF) diet for 13 weeks. Bilateral cranial defects were introduced on each side of the sagittal suture, and 5 weeks post-surgery on the respective diets, the repair/regeneration of cranial bones and mechanical properties of femoral bones were assessed. MicroCT and histological analyses demonstrated that bone regeneration was significantly impaired by the HF diet in WT and *Ldlr*^{-/-} mice. In femoral bone, cortical bone volume fraction (BV/TV) was significantly reduced while cortical porosity was increased by the HF diet in *Ldlr*^{-/-} but not in WT mice. Femoral bone strength and stiffness, measured by three-point bending analysis, were significantly reduced by the HF diet in *Ldlr*^{-/-}, but not in WT mice. Serum analysis showed that the HF diet significantly increased levels of parathyroid hormone, TNF-alpha, and calcium, whereas it reduced procollagen type I

N-terminal propeptide, a serum marker of bone formation, in *Ldlr*^{-/-}, but not in WT mice. The serum level of carboxyl-terminal collagen crosslinks, a marker for bone resorption, was also 1.7-fold greater in *Ldlr*^{-/-} mice. These findings suggest that hyperlipidemia induces secondary hyperparathyroidism and impairs bone regeneration and mechanical strength.

Disclosures: Flavia Pirih, None.

1227

Adipocyte-specific Expression of FoxC2 Increases Bone Mass through Upregulation of Wnt10b Expression and Increase in Energy Production in Marrow Adipocytes. Sima Rahman^{*1}, Yalin Lu¹, Piotr Czernik¹, Clifford Rosen², Ormond MacDougald³, Sven Enerback⁴, Beata Lecka-Czernik⁵.

¹University of Toledo Health Sciences Campus, USA, ²Maine Medical Center, USA, ³University of Michigan Medical School, USA, ⁴University of Gothenburg, Sweden, ⁵University of Toledo College of Medicine, USA

A relationship between the status of energy metabolism and bone mass has been actively debated. FoxC2 transcription factor regulates the expression of genes which determine the function of metabolically active brown fat, and these include an adrenergic response, adaptive thermogenesis, mitochondrial biogenesis, and angiogenesis. Ectopic expression of FoxC2 in adipose tissues under the control of FABP4 promoter renders lean animals which are insulin sensitive, and protected from high fat diet-induced obesity and insulin resistance. Most importantly, these animals acquire significantly higher bone mass. In general, bones of Tg-FoxC2 mice are larger in diameter with the same cortical thickness as compared to control mice. This results in an increase of the polar moment of inertia (pMOI) by 25%, which is an indicator of stronger bone. Both males and females have significantly more trabecular bone in proximal tibia, distal femur, and vertebra. Trabecular bone volume of Tg-FoxC2 mice is increased by approximately 2-fold due to increase in the trabecular number, thickness, and connectivity. Remarkably, increased trabecular bone mass in tibia and femur is respectively associated with 4- and 65-fold increase in fat volume within corresponding regions, indicating a positive effect of fat on bone structure. To investigate a possibility that marrow adipocytes (ADs) regulate bone remodeling by modulating marrow environment, we have expressed FoxC2 in cell line representing committed marrow ADs. Ectopic expression of FoxC2 in AD2 cells resulted in up-regulation of gene markers of brown ADs energy-producing activity, and included UCP-1, β_3 -adrenergic receptor, Prdm16, and Dio2. Conditioned media from cultures of FoxC2-ADs increased alkaline phosphatase activity in osteoblasts indicating that these cells produce pro-osteoblastic paracrine factors. Further, we have shown that FoxC2 in ADs induces the expression of Wnt10b, a member of Wnt signaling, which has an anabolic effect on bone and positive effect on energy homeostasis. Taken together, we hypothesize that FoxC2 induces BAT-like metabolic and/or paracrine activities in marrow ADs. These activities, which may include increased energy production and Wnt10b production, have beneficial effect on bone. In conclusion, the Tg-FoxC2 model provides a proof of concept that energy metabolism is integral for the maintenance of bone metabolism and allows for consideration of bone fat as therapeutic target to improve bone mass.

Disclosures: Sima Rahman, None.

1228

A Dkk3 Reporter Identifies Progenitors of the Fibrocartilage and Periosteum of the Fracture Callus. Yu Mori^{*}, Xi Jiang, Douglas Adams, David Rowe. University of Connecticut Health Center, USA

Mesenchymal progenitor cells are capable of generating a wide variety of mature cells that constitute the connective tissue system. The SMAA-GFP reporter is proving to be an effective tool for identifying these cells prior to the expression of markers of differentiation characteristic of bone, fat, muscular blood vessels or fibrocartilage. Based on a microarray study of SMAA-GFP sorted cells derived from a 4-7 day BMSC culture, we observed high expression of Dkk3, a non-canonical member of the wnt pathway. Because its expression is not associated with osteogenesis, we obtained a Dkk3-GFP reporter mouse to determine what cell type was generating the RNA signal. In primary culture, clusters of Dkk3-GFP cells developed which were independent of Col3.6GFP cells that had formed bone nodules. A 3 color reporter mouse was generated by crossing SMAA-GFPcherry x Col3.6GFPcyan x Dkk3-eGFP and subjected to tibial fracture. Three days post fracture, the proliferating SMAA-red cells were also beginning to express either Dkk3 or Col3.6. By day 5 the two populations had diverged with the Dkk3 cells being on the outer surface of the developing callus while the Col3.6 cells were forming bone at the base of the callus. By day 7 when the callus is filled with cartilage, Dkk3 is active in cells that are in transition from elongated cells on the external surface of the callus to fibrocartilaginous cells that now express low levels of Col3.6. The zone of cells that express Dkk3 appear to block the passage of the surrounding vasculature into the underlying cartilage and does not deposit fibronectin. By day 14-21 when the cartilage core is resorbed, the only remaining Dkk3 is located in the newly formed periosteum external to the active endocortical bone forming activity associated with the inward remodeling of the outer cortical shell. We interpret these findings that Dkk3 marks a non-osteogenic limb of the SMAA progenitor population that within the fracture partitions the osteogenic signals away from the surrounding skeletal muscle and the underlying differentiating fibrocartilage. It is a progenitor to cells that form

fibrocartilage in the fracture zone as well as the tenascin C positive cells that populate the fibrous zone of the periosteum, and it resides in the cambial zone of the periosteum. Knowing the biological and molecular function of these cells should lead to a fuller appreciation of the pro- and anti-osteogenic factors that regulate skeletal repair.

Disclosures: Yu Mori, None.

1229

Prevention of Tumor Growth and Bone Destruction in Myeloma by Pim Kinase Inhibition. Masahiro Hiasa^{*1}, Ayako Nakano², Keiichi Watanabe³, Cui Qu², Takeshi Harada², Shirou Fujii², Hirokazu Miki², Shingen Nakamura², Kumiko Kagawa², Kyoko Takeuchi², Eiji Tanaka¹, Kenzo Asaoka¹, Shuji Ozaki², Toshio Matsumoto⁴, Masahiro Abe⁵.

¹University of Tokushima Graduate School, Japan, ²University of Tokushima Graduate School of Medicine, Japan, ³The University of Tokushima Graduate School of Oral Science, Japan, ⁴University of Tokushima Graduate School of Medical Sciences, Japan, ⁵University of Tokushima, Japan

Myeloma (MM) cells potentially enhance osteoclastic bone resorption and suppress osteoblastogenesis from bone marrow stromal cells (BMSCs) to cause devastating bone destruction. BMSCs and osteoclasts (OCs) create a "MM niche" to support MM cell growth and survival. We recently reported that MM-BMSC interaction potentially up-regulate in MM cells the serine/threonine kinase Pim-2 which plays as a critical survival factor in MM cells (Leukemia, 2011). We also found that the MM cells suppressed osteoblast (OB) differentiation from BMSCs along with up-regulation of Pim-2 expression in BMSCs. In the present study, we therefore explored the role of Pim-2 in osteoblastogenesis and the effects of Pim inhibition on tumor growth and bone destruction in MM. Treatment with Pim-2 siRNA or the Pim inhibitor SMI-16a facilitated mineralized nodule formation by BMP-2 in MC3T3-E1 cells. The Pim-2 siRNA also enhanced bone formation in calvaria organ cultures. However, enforced expression of Pim-2 in MC3T3-E1 cells abrogated the mineralized nodule formation, suggesting antagonism of bone formation by Pim-2. The Pim-2 knockdown further up-regulated smad1/5 and p38MAPK phosphorylation as well as osterix expression induced by BMP-2 in MC3T3-E1 cells. Importantly, the Pim-2 knockdown restored mineralized nodule formation in MC3T3-E1 cells suppressed by MM cell conditioned media. We next studied in vivo effects of Pim inhibition using SCID-rab mice in which a rabbit femur was subcutaneously implanted. INA6 MM cells were inoculated directly into the bone marrow cavity in the rabbit bones. After confirming MM cell growth, the mice were treated with the Pim inhibitor SMI-16a at 20 mg/kg every other day. Control mice exhibited extensive bone destruction along with tumor expansion in the bone marrow and outside the bone in microCT images and in bone sections. However, the treatment with SMI-16a markedly decreased MM tumor size and prevented the progression of bone destruction in the rabbit bones. Similar results were observed in MM mouse models by intratibial inoculation of murine 5TGM1 MM cells. Besides its anti-apoptotic role in MM cells in the bone marrow microenvironment, these results suggest that Pim-2 induced in BMSCs by MM cells plays as a negative regulator for bone formation, and that Pim inhibition is able to resume bone formation while reducing tumor burden in MM. Therefore, Pim inhibitors may become a candidate of novel therapeutic agents targeting the MM-BMSC interaction.

Disclosures: Masahiro Hiasa, None.

1230

The Role of S100A4/RAGE Signaling in Prostate Cancer Bone Metastasis.

Jennifer Paige-Robinson^{*1}, Leland Chung², Omar Hameed¹, John A. Petros³, Majd Zayzafoon⁴. ¹University of Alabama-Birmingham, USA, ²Cedars Sinai Medical center, USA, ³Emory University & Atlanta VA Medical Center, USA, ⁴University of Alabama at Birmingham, USA

Prostate carcinoma (PCa) is the most commonly diagnosed cancer, and is the second leading cause of cancer mortality for men in the United States. Metastasis, specifically to the bone, is a critical step in the progression of PCa. S100A4, a member of the S100 calcium-binding protein family, has been shown to bind to and activate the Receptor for Advanced Glycation End products (RAGE) signaling pathway. Here we show that in human clinical samples RAGE is not expressed in normal and benign prostatic hyperplasia (BPH) samples, but is highly expressed in metastatic PCa tissues. In vitro data demonstrates that benign prostatic epithelial cells (RWPE-1) do not express RAGE, while the bone metastatic prostate cancer cells (C4-2B) express high levels of RAGE. To further examine the role of S100A4 on the metastatic ability of PCa cells, we treated RAGE expressing C4-2B cells with human recombinant S100A4. We discovered that C4-2B cells treated with S100A4 showed a 66% increase in invasion and a 100% increase in the gene expression of Matrix metalloproteinase 13 (MMP-13), a protein which aids in metastasis. Increases in invasion and motility in C4-2B cells are mediated by activation of Calcium calmodulin-dependent kinase II (CaMKII α), Focal Adhesion Kinase (FAK), and Ras-related C3 botulinum toxin substrate 1 (Rac1). Pre-treatment with KN93 (the pharmacologic inhibitor of CAMKII), or with soluble RAGE (the decoy receptor of RAGE), abolished the S100A4 induced Ca²⁺ dependent signaling as well as invasion and motility of C4-2B cells in vitro. C4-2B cells were also sorted using flow cytometry into two populations:

a group that expresses high levels of RAGE (RAGE-high) or low levels of RAGE (RAGE-low). Extracellular S100A4 increased the motility as well as Ca²⁺ dependent signaling in PCa RAGE-high expressing cells but not in RAGE-low expressing cells. PCa cells were then injected intratibially into athymic nude mice. We discovered that mice which were injected with RAGE-high cells developed very large tumors, as shown by x-ray, uCT imaging, and histology. This increase was not seen in mice that were injected with RAGE-low expressing cells. Taken together, our data suggests that RAGE plays a significant role in the growth and local invasion of human prostate cancer.

Disclosures: Jennifer Paige-Robinson, None.

1231

Leukemia Progression Depends on the Presence of Osteoblasts. Barbara Silva^{*1}, Maria Krevvata², J. Sanil Manavalan², Chiyuan Zhang³, Linda Johnson⁴, Renier Brentjens⁵, Aris Economides⁶, Ellin Berman⁵, Stavroula Koustem¹. ¹Columbia University Medical Center, USA, ²Department of Medicine, Division of Endocrinology, College of Physicians & Surgeons, Columbia University, USA, ³Columbia University, USA, ⁴Comparative Pathology & Laboratory Medicine, Cornell University & Memorial Sloan-Kettering Cancer Center, USA, ⁵Memorial Sloan-Kettering Cancer Center, USA, ⁶Regeneron Pharmaceuticals, Inc., USA

The bone marrow niche has been implicated in the pathogenesis of leukemia, as a permissive microenvironment required for the emergence and/or progression of the disease. To examine whether malignant cells influence specific cell populations within the bone niche we injected two types of leukemia cells, murine myelomonocytic or lymphoma/lymphoblastic into immunocompetent, syngenic mice. In leukemic mice osteoblastogenesis was decreased, and osteoblast - osteoclast uncoupling was noted, leading to a marked decrease in osteoblast numbers and bone formation rate and eventually trabecular bone loss. The marked changes in osteoblast number and function suggested that these cells could influence leukemia progression. To examine this hypothesis we ablated osteoblasts by crossing mice in which an inactive form of the diphtheria toxin A chain (DTA) has been introduced into the ubiquitously expressed ROSA26 locus with transgenic mice expressing Cre under the control of the osteoblast-specific collagen type I $\alpha 1$ promoter. Compound progeny carries one allele of floxed DTA locus and one with active DTA (DTAosb/+). DTAosb/+ mice show 50% reduction in osteocalcin levels, osteoblast numbers and bone formation rate. EL4 lymphoma/lymphoblastic leukemia cells transduced with a GFP/Luciferase fusion gene were injected, intravenously, into DTAosb/+ mice, and their wild type littermates (DTA fl/+). Cell trafficking and tumor progression were assessed, noninvasively, by bioluminescence imaging. Bone marrow engraftment was observed by *in vivo* images, and confirmed at autopsy. Results were averaged from the peak light-emitting exposure from each group, and mice lacking osteoblasts showed a significant increase in total counts, indicating increased tumor burden. Additionally, over a 4-week period, mice lacking osteoblasts had a significantly shorter overall survival ($P = 0.04$ log-rank test), and a 50% increase in hind-limb paralysis, suggesting increased tumor burden in bone sites in mice lacking osteoblasts. These data demonstrate that osteoblasts play a fundamental role in propagating leukemia in the bone marrow. They suggest that identifying signals emanating from osteoblasts and affecting leukemia engraftment or progression could be therapeutic targets to interfere with tumor progression.

Disclosures: Barbara Silva, None.

1232

Inhibition of Discoidin Domain Receptor-1 (DDR1) Impairs Tumor-Induced Bone Metastatic Homing and Colonization. Karmele Valencia^{*1}, Cristina Ormazabal², Carolina Zanduet², Diego Luis-Ravelo², Iker Anton², Susana Martı́nez-Canarias², Fernando Lecanda¹. ¹Foundation for Applied Medical Research, Spain, ²Center for Applied Medical Research (CIMA), Spain

Cell-matrix and cell-cell interactions within the bone microenvironment are critical for the initiation and development of osseous metastasis. However, the mechanisms mediating bone homing and colonization remain poorly understood. The aim of this study was to investigate the role of collagen binding receptor DDR1 in these processes. High levels of DDR1 were found in human lung tumor cells lines by qPCR and western blot analysis as compared to normal cells. Lentiviral transduction of a lung tumor cell line with shRNA using two different targets led to more than 80-90% inhibition. Knock-down (shDDR1) cells displayed a stunted decrease invasiveness in collagen type I and type IV substrates as compared to control and scramble cells ($p < 0.001$), whereas growth kinetics was unaltered *in vitro* and *in vivo*. To delineate the functional contribution of DDR1 in metastatic activity, tumor burden and osteolytic lesions were evaluated by bioluminescence imaging (BLI), X-Ray and μ CT image analysis, after intracardiac inoculation (i.c.) in athymic nude mice. At day 7, BLI showed a dramatic decrease in skeletal tumor burden in shDDR1 injected mice. More importantly, a marked reduction in osteolytic lesions assessed by X-Ray imaging and μ CT scans was also detected in shDDR1 inoculated mice at day 14 ($p < 0.001$). To evaluate whether these effects were the result of impaired bone homing, we performed i.c. inoculation of shDDR1 cells and we assessed tumor burden at day

5. BLI was decreased in shDDR1 injected mice as compared to control mice. Quantification of metastatic cell number in hind limbs revealed a marked decrease in shDDR1 mice ($p < 0.01$) indicating that DDR1 was critical in early events of bone homing. To explore its possible contribution in bone colonization, we intratibially injected shDDR1 cells. Significant decrease in BLI was correlated with a decrease in osseous tumor burden, evaluated by histological image analysis of shDDR1 injected mice, suggesting an impaired colonization ability of shDDR1 cells. Interestingly, antiapoptotic effects mediated by collagen type I were inhibited in shDDR1 cells, measured by PARP cleavage. Thus, these data indicate that disruption of DDR1 hampers tumor cell survival leading to impaired early tumor-bone engagement during skeletal homing. Inhibition of DDR1 critically alters osseous colonization delaying the appearance of osteolytic lesions. We suggest that DDR1 represents a novel therapeutic target involved in bone metastasis.

Disclosures: Karmele Valencia, None.

1233

The Ubiquitin E3 Ligase WWP1 Negatively Regulates Breast Cancer Bone Metastasis by Promoting Lysosomal Degradation of CXCR4. Lei Shu^{*1}, Kristina Subik¹, Qianqian Liang¹, David Hicks¹, Brendan Boyce¹, Linda Schiffhauer¹, Di Chen¹, Ping Tang¹, Lianping Xing². ¹University of Rochester Medical Center, USA, ²University of Rochester, USA

Advanced breast cancers preferentially metastasize to bone where the bone microenvironment produces factors for cancer cell homing and growth. Expression of the ubiquitin E3 ligase WWP1 is increased in some breast cancers, but its role in bone metastasis is unknown. To examine this, we knocked down WWP1 in MDA-MB-231 breast cancer cells using shRNA and inoculated shWWP1 cells and control (Ctl) virus infected cells into the left ventricle of athymic nude mice. X-rays show that mice that given shWWP1 cells had more osteolytic lesions (4.3+0.8 vs 1.8+0.5 osteolytic lesions/mouse in Ctl cells). Histology confirmed increased tumor area in the bone marrow of the mice given shWWP1 cells (8+0.8 vs 4+0.6 mm²/leg in Ctl cells). WWP1 knockdown did not affect tumor cell growth, survival or osteoclast inducing potential *in vivo*, but significantly increased cell migration toward a CXCL12 (chemokine SDF-1) gradient (% migrated cells: 13+0.6 vs 5+0.4 in Ctl cells) *in vitro*. To examine the mechanisms whereby WWP1 affects cell migration, we treated Ctl cells with the CXCL12 and found that CXCL12 reduced the levels of its receptor CXCR4, an effect largely prevented by the lysosome inhibitor chloroquine, but only slightly by the proteasome inhibitor MG132 (% CXCR4 degradation: 75% in vehicle-, 20% in chloroquine-, 50% in MG132-treated cells). CXCL12-induced CXCR4 degradation was almost abolished in shWWP1 cells (15+1%). CXCL12 enhanced co-localization of CXCR4 with the lysosome protein, LAMP2, in Ctl cells (61% vs 39% in PBS), but not in shWWP1 cells (47% vs 41% in PBS). Stronger CXCR4 immuno-staining was detected in bone mets from mice given shWWP1 cells. To investigate the translational significance of our findings, we immuno-stained for WWP1 in a breast cancer tissue microarray containing cores of tumor samples from 118 patients and found that 80 cases were WWP1 negative or had weak staining. Among these 80 cases, 3-fold more cases were ER+/PR-, typical of breast cancers that metastasize to bone, compared to WWP1 positive tumors. In summary, WWP1 negatively regulates breast cancer cell migration to a CXCL12 gradient by promoting CXCR4 lysosomal degradation, thereby enhancing tumor cell metastasis to bone. We conclude that WWP1 is a potential prognostic indicator for breast cancer bone metastasis, and factors that increase WWP1 expression or activity in breast cancer cells may decrease their capacity to metastasize to bone.

Disclosures: Lei Shu, None.

1234

Dual Function of the Estrogen Receptor Related Receptor Alpha (ERR α) In Breast Cancer and Bone Metastasis Formation: Implication of VEGF and Osteoprotegerin. Anais Fradet¹, Helene Sorel¹, Lamia Bouazza¹, Delphine Goehrig¹, Baptiste Depalle¹, Akeila Bellahcene², Vincent Castronovo², Helene Follet¹, Francoise Descotes³, Jane Aubin⁴, Philippe A.R. Clezardin⁵, Edith Bonnelve^{*6}. ¹Inserm, UMR1033, France, ²GIGA-Cancer, University of Liege, Belgium, ³Service de Biochimie Biologie Molculaire Sud, Centre hospitalier Lyon Sud, France, ⁴University of Toronto Faculty of Medicine, Canada, ⁵INSERM & University of Lyon, Fra, ⁶Faculte de Medecine RTH Laennec, France

Bone metastases are a frequent complication of cancer, occurring in up to 70 percent of patients with advanced breast cancer. Estrogen receptor related receptor alpha (ERR α) is a nuclear receptor that belongs to the orphan receptors family, for which no ligand have yet been determined. ERR α that shares structural similarities with the estrogen nuclear receptors ER α and ER β can impinge on estrogen pathway and is involved in breast cancer and bone development. We then decide to address ERR α function in bone metastasis development. ERR α is highly expressed *in situ* in breast cancer cells that metastasized to bone in patients. Similar observation was made in bone metastases 30 days after intravenous inoculation in mice of the MDA-231 derived cells MDA-BO2 (BO2) breast cancer cells, known to be highly metastatic to bone. Then modulation of ERR α expression in BO2 cells shows that human BO2 cells over-expressing wild-type ERR α (ERR α WT) induced osteolytic bone metastasis

in BALB/c nude mice (n=10) that were reduced (150.9 for Bone volume (BV/TV)(%) and 214.8 for skeletal tumor burden (TB/STV)(%) compared to that observed with parental BO2-CT cells (111.1(BV/TV) and 364.2(TB/STV)), whereas osteolysis was enhanced (6.40,4(BV/TV) and 713.2(TB/TV)) in animals bearing BO2 tumors expressing a dominant negative form (ERRaΔAF2(coactivator domain deleted)) of ERRa. Osteoclasts were directly affected *in vivo* and *in vitro* in primary culture of bone marrow cells performed in presence of RANKL/MCSF and BO2 clones conditioned media. Moreover the osteoprotegerin (OPG), an osteoclastogenesis inhibitor was up and down-regulated in BO2-ERRaWT and ERRaΔAF2 cells respectively. Osteopontin and MMP1 were also regulated. On the other side, we reinforce ERRa as a bad prognostic factor in primary tumor as growth of BO2-ERRaWT cells in the mammary gland was increased. Tumors were highly vascularized compared to BO2 and BO2-ERRaΔAF2 cells and the vascular endothelial growth factor (VEGF), a known target gene for ERRa was up-regulated in BO2-ERRaWT cells. Finally we show that elevated expression of ERRa mRNA in breast carcinomas (cohort of 254 patients) is also associated with high level of VEGF and OPG. In conclusion, our data provide for the first time evidence that ERRa plays a dual role during breast cancer progression, promoting local tumor growth (via angiogenesis and VEGF), but decreasing osteolytic lesions in bone (via the direct impact on osteoclasts and OPG).

Disclosures: Edith Bonnellye, None.

1235

Variable Bone Formation Response to Skeletal Axial Load in Mice With a Conditional Deletion of the Connexin43 (Cx43) Gene (*Gja1*). Susan Grimston^{*1}, Marcus Watkins¹, Michael Brodt², Matthew Silva¹, Roberto Civitelli¹. ¹Washington University in St. Louis School of Medicine, USA, ²Washington University in St. Louis, USA

We have previously shown an attenuated endocortical bone formation response to 3-point bending mechanical loading in mice with a conditional deletion of *Gja1* driven by the *Col1A1* promoter. Consistent with a key role of Cx43 in skeletal responses to mechanical stimuli, we have also found reduced sensitivity of cortical bone to the effects of muscle paralysis in these mice. In this study, we assess the response to tibial compression, a more physiologic loading regime, in mice where *Gja1* ablation is driven by *Dermo1/ Twist2* promoter in the entire chondro-osteoprogenitor lineage (cKO). Since these cKO mice have significantly enlarged marrow cavity and thin cortices relative to wild type (WT) mice, strain gauge studies were performed, and these indicated that a load of 12 N was required to generate a periosteal strain of 1200µε in the cKO, whereas in WT mice a load of 8N was sufficient to generate the same strain. We then tested the response to load (5 days per week, 60 cycles/day) in cKO (12N, 1200µε) relative to WT mice subjected to either the same strain (8N, 1200µε) or the same load (12N, 1900µε). Using *in vivo* µCT, we detected a significant increase in cortical bone volume in all groups post-load. Surprisingly, dynamic histomorphometry revealed a significant reduction in endocortical mineralizing surfaces in the cKO (-23.51.95%; $p < 0.05$) and downward trends in the 1200µε (-9.973.8%) and 1900µε (-5.25.7%) WT groups. However, there was a significant increase in periosteal mineralizing surface (Ps.MS/BS) in the cKO with 1200µε load (83.626.9%; $p < 0.05$), while it required 1900µε load to increase Ps.MS/BS in the WT (68.117.8%; $p < 0.05$). Periosteal MS/BS did not increase significantly in WT 1200µε (7.49.91%). Thus, contrary to 3-point bending, axial tibial compression at these loads does not stimulate endocortical bone formation, but rather periosteal bone apposition. Also at variance with the 3-point bending method, Cx43 deficiency enhances the sensitivity of periosteal bone formation response to axial loading, while it negatively affects endocortical bone formation. Therefore, the role of Cx43 in mechanotransduction is complex, and depends upon the type of mechanical stimulus and anatomical skeletal site.

Disclosures: Susan Grimston, None.

1236

Periostin Deficiency Increases Cortical Microcracks and Reduces Woven Bone Formation in Mice Subjected to Fatigue Loading. Nicolas Bonnet^{*1}, Markus burkhart², Andres Laib³, Serge Ferrari⁴. ¹Division of Bone Diseases, Geneva University Hospital & Faculty of Medicine, S, Switzerland, ²SCANCO Medical AG, Switzerland, ³Scanco Medical, Switzerland, ⁴Geneva University Hospital & Faculty of Medicine, Switzerland

Susceptibility to microcracks depends on bone microstructure, turnover and material properties, however the role of distinct bone matrix constituents on fatigue damage and repair remains poorly understood. We previously reported that deficiency of the bone matrix protein periostin is associated with decreased collagen crosslinks. Here we analyzed the role of periostin in response to fatigue, including cortical porosity, microcracks and callus formation (repair).

Twelve week-old *Postn*^{-/-} and *Postn*^{+/+} male mice were subjected to a unique fatigue stimulus of the tibia by *in vivo* axial compression. Two weeks after the fatigue, we evaluated tibia bone microarchitecture by µCT40 *ex vivo*; the number of "pores" (>14µm) and osteocytic lacunae at the 1/3rd distal by µCT50 (1µm nominal resolution); cracks by fuschin staining on undecalcified bone; and cortical strength by 3 points bending. In *Postn*^{+/+}, fatigue significantly increased Ct.TV and Ct.BV (+14.8% and +12.7% vs contralateral tibia $p < 0.05$). A woven bone response was

present in 75% of the fatigued bone by both µCT and histology. The number of pores increased 8 fold in the fatigued tibia, whereas cracks number/BPm and surface/BS increased +172% and +375%, respectively, compared to the non-fatigued side ($p < 0.05$). In contrast, in *Postn*^{-/-}, fatigue did not change Ct.TV and Ct.BV, and only 16% of the fatigued bones presented a woven bone response. In the control tibias, *Postn*^{-/-} tended to have higher number of osteocyte lacunae compared to *Postn*^{+/+} with a significant lower SMI (Shape index) (-18.7%, $p < 0.05$); and significant higher cracks surface/BS than *Postn*^{+/+} (4.181.14% vs 0.850.17%, $p < 0.05$). Fatigue increased the number of pores in the same range than *Postn*^{+/+}. Fatigue increased cracks number/BPm and surface/BS (+78% and +83% vs non fatigued bone, $p < 0.05$). Despite *Postn*^{-/-} response similarly to fatigue on cracks than *Postn*^{+/+}, cracks number/BPm was higher in the fatigued tibia of *Postn*^{-/-} compared to *Postn*^{+/+} (2.220.17 1/mm vs 0.970.10 1/mm, $p < 0.05$). In accordance with a lower repair, fatigue decreased stiffness and plastic energy in *Postn*^{-/-} (-29.4% and -38.4% in fatigue vs non-fatigue tibia, $p < 0.05$) but not in *Postn*^{+/+}. In absence of periostin, cracks reached a high proportion in fatigued bone and woven bone repair at the periosteum surface is reduced. The possible link between more osteocyte lacunae and microcracks and lower woven bone formation are still under investigation.

Disclosures: Nicolas Bonnet, None.

1237

Osteocyte Level Strain Determination Using A Multiscale Mouse Forearm Model. Ganesh Thiagarajan¹, Yunkai Lu², Mark Dallas³, Mark Johnson^{*4}. ¹University of Missouri - Kansas City, USA, ²UMKC School of Computing & Engineering, USA, ³UMKC School of Dentistry, USA, ⁴University of Missouri, Kansas City Dental School, USA

Bone is a dynamic organ that is known to adjust its mass, material and architectural properties with respect to the load environment. We have previously developed a first generation combined ulna and radius (URM) mouse forearm finite element (FE) model that simulates *in vivo* loading and compared it with the traditional ulna only model (UM). There were significant differences in strain distributions within axial cross sections in the URM versus UM model. We observed that the URM predicts a peak strain in the bones which is twenty percent higher than the UM prediction.

The osteocyte is the mechanosensory cell in bone, and any reduction in its ability to respond to load would have significant consequences on bone mass. Whereas the magnitude of strain necessary to induce bone formation at the macro level is 1500-2000 µstrain, a major gap exists in our knowledge of what the actual magnitude of strain the individual osteocyte senses will elicit a biological response. We have developed a next generation micro FEA model at the osteocyte level of resolution (7-12 micrometers) to test the hypothesis that local (micro) strain fields around osteocytes determine osteocyte response to mechanical loading. A 3-D representation of osteocyte lacunae was obtained from histological serial sections and the lacunae locations were built into a thin (72 microns) slice of the macro model. Displacement boundary conditions obtained from a 2N level of load on the macro model were determined and applied to the micro FE model and strain fields were mapped. Peak strains around lacunae were observed as high as 20,000-30,000 microstrains and the homogenous strain fields observed in the macro FEA models were transformed into a spatially heterogeneous pattern. In addition, micro FEA modeling showed heterogeneity of strain pattern at the osteocyte lacunae from a temporal perspective.

Using the TOPGAL reporter mouse we are now determining the microstrain levels needed to activate β-catenin signaling in osteocytes using our models. By combining our micro FEA model with biological response data, we will for the first time begin to define how osteocyte level strains and the threshold for activation of a biological response are influenced by bone material properties and changes associated with aging. These findings could enable us to design skeletal anabolic strategies based on new drugs that enhance the effects of exercise and thereby reduce the risk of fracture.

Disclosures: Mark Johnson, None.

This study received funding from: NIH NIAMS RO1 AR053949; NIH NIAMS PO1 AR46798; NIH NIAMS RC2058962

1238

Previous Exposure to Microgravity Does not Adversely Affect Second Exposure in the Tibia of Hindlimb Unloaded Adult Male Rats. Yasaman Shirazi-Fard^{*1}, DERRICK MORGAN¹, Joshua Kupke¹, JOSHUA DAVIS¹, Florence Lima², Elizabeth Greene¹, Alyssa McCue¹, Joseph Marchetti¹, Joey Thompson¹, Susan Bloomfield¹, Harry Hogan¹. ¹Texas A&M University, USA, ²University of Maryland School of Medicine, USA

Bone response to extended microgravity remains a concern for astronaut health. A particular question is how prior missions affect subsequent missions. Animal experiments were conducted to test the hypothesis that previous exposure to unloading would exacerbate the effects of a 2nd exposure. This study focused on proximal tibia metaphysis (PTM) and tibia diaphysis (TD).

Adult male Sprague-Dawley rats (6 mo.) were assigned to 2 groups: aging cage control (CC), hindlimb unloaded (HU). HU animals were further divided into subgroups: 1HU and 2HU. The 2HU group had 28d of HU at 6 mo. (2HU6), followed by 56d of recovery, and another 28d of HU (2HU9) starting at 9 mo. (day 84). The 1HU group had one bout of HU (1HU9) starting on day 84 (to match

2HU9). Animals were scanned by pQCT *in vivo* every 28d at PTM and TD. A group (n=15) was euthanized every 28d (days 0, 28, 56, 84, 112 & 168) from each of CC, 1HU, and 2HU groups. Excised tibiae were scanned by pQCT and tested to failure in 3-point bending.

PTM total (integral) BMC and vBMD decreased (7%) significantly for 2HU6 but not for 2HU9 (2nd exposure). Both were lower for 2HU9 but only by 2-3% (n.s.). Total BMC and vBMD were also significantly lower (5-7%) for 1HU9. This indicates that the 1st HU for either group has significant negative effects (5-7% reductions) despite different ages. The milder losses of 2nd HU may be attributable to the fact that 2HU animals did not recover fully from 2HU6. Means of BMC, vBMD, and Ct.Ar returned to day 0 levels after 56d of reloading, but remained lower than age-matched CC animals (and 1HU). The cross-sectional area of the cortical shell (Ct.Ar) in PTM showed a similar response. For 2HU, Ct.Ar decreased 7% for 2HU6 (sig.) but only 3% for 2HU9 (n.s.). For 1HU, Ct.Ar decreased 7% due to HU (sig.). There was only mild decrease (1-2%, n.s.) in total area, which suggests thinning of the cortical shell. TD fracture force from 3-point bending showed no effect for 2HU6, but drastic reductions (sig.) for 2HU9 (28%) and 1HU9 (29%). Stiffness was similar (11-26% losses, but n.s.). In contrast, there was no change in TD Ct.Ar for 2HU9 or 1HU9.

Contrary to our hypothesis, PTM losses from 2nd HU were less than the 1st regardless of age. For TD, losses in fracture force were dramatic for the 2nd HU vs. no change for the 1st. Unexpectedly, the same dramatic losses occurred for age-matched single HU, indicating no effect of prior exposure, with the main effect being the age at HU (9 mo.).

Disclosures: Yasaman Shirazi-Fard, None.

1239

Increased Sensitivity to Skeletal Unloading in Connexin43-deficient Mice. Shane Lloyd*, Emmanuel Paul, Yue Zhang, Henry Donahue. The Pennsylvania State University College of Medicine, USA

Previous studies have elucidated a role of gap junctional intercellular communication in the process of bone mechanosensing. In particular, Connexin43 (Cx43) has been demonstrated as an integral component of the skeletal response to mechanical loading. However, very little work has focused on Cx43's role in mechanical unloading. Practical examples of skeletal unloading include extended periods of bed rest due to neurological injury or the microgravity environment of spaceflight. We sought to characterize the skeletal phenotype of Cx43-deficient mice in response to mechanical unloading via hindlimb suspension (HLS). We utilized 6-month-old male mice with an osteocalcin-driven deficiency of Cx43 specific to osteoblasts and osteocytes (KO) and their WT-equivalent littermates. Mice were subjected to HLS for just 7 days. At day 0 (baseline) and day 7 all mice were subjected to a microcomputed tomography scan of one hindlimb. Trabecular bone parameters were assessed at the proximal tibia and cortical bone at the femur midshaft. At baseline, KO mice demonstrated expanded cortices consistent with an osteopenic phenotype characteristic of this model: periosteal volume in KO was greater than WT (1.13 vs. 0.7 mm³; P<0.05) as was endocortical volume (0.74 vs. 0.45 mm³; P<0.05). No significant differences were seen in cortical thickness or cortical BMD at baseline, although there was a trend suggesting increased cortical porosity in KO mice vs. WT. KO mice had greater trabecular connectivity density (68 vs. 21 mm⁻³; P<0.05) and trabecular bone volume fraction (14.9 vs. 6.7%; P<0.01) than WT mice. Individual trabeculae in KO mice were also thicker than WT (0.061 vs. 0.048 mm; P<0.01). The difference between WT and KO mice on day 7 followed a similar pattern. Not surprisingly, the relatively short duration of HLS did not affect any measured bone parameters in WT mice between baseline and day 7; however, KO mice showed a significant 15% and 10% decrease in trabecular connectivity and volume fraction, respectively (P<0.05) over the period of HLS. These results confirm a phenotype of medullary expansion, but increased trabecular bone at the proximal tibia in Cx43-deficient mice. More importantly, KO mice displayed an increased sensitivity to unloading in that even short duration HLS (one week) resulted in trabecular bone loss in these skeletally mature mice. These results highlight a contrasting role for Cx43 in cortical and trabecular bone during unloading.

Disclosures: Shane Lloyd, None.

1240

Mechanical Regulation of GSK3 β in MSC is Dependent on Akt Activation via Rictor/mTORC2. Natasha Case^{*1}, Jacob Thomas², Buer Sen³, Zhihui Xie², Maya Styner¹, Janet Rubin¹. ¹University of North Carolina, Chapel Hill, School of Medicine, USA, ²UNC, USA, ³University of North Carolina At Chapel Hill, USA

GSK3 β is emerging as a critical signaling node of mechanical responses in mesenchymal stem cells (MSC). Mechanical signals inactivate GSK3 β via phosphorylation, resulting in stabilization of β -catenin, and when repeated daily, block adipogenesis induced by soluble factors in the local environment. The proximal pathways required for mechanical inhibition of GSK3 β activity are unknown. We considered whether Akt, which decreases GSK3 β activity in response to insulin, was critical for mechanical effects. Mechanical strain (2%, 0.17Hz) activated Akt via phosphorylation at both Thr 308 and Ser 473 by 15 minutes. Blocking strain activation of Akt using an AKT1/2 inhibitor or by Akt siRNA knockdown resulted in a complete loss of GSK3 β Ser9~P in response to mechanical strain. PI3K is known to mediate Akt phosphorylation by membrane recruitment via PIP3, and PI3K action is

necessary for Akt~P by insulin. The PI3K inhibitor LY294002 prevented strain-induced phosphorylation at T308~P, but, in contrast to insulin treatment, phosphorylation at S473 was unimpaired; importantly, mechanical inactivation of GSK3 β was not blocked by PI3K inhibition, indicating that S473~P alone was sufficient to initiate the downstream mechanoresponse. With this information, we concentrated on S473~P: we considered that Rictor/mTORC2 is known to specifically transduce insulin-induced phosphorylation at this serine. The mTOR inhibitor KU-0063794 completely prevented S473~P by both mechanical and insulin stimulation. Blocking S473~P had differential effects on GSK3 β ~P; mechanical inactivation of GSK3 β was blocked, but insulin inhibition of GSK3 β , presumably through predominant effects on T308 was unaffected. Interestingly, the PKC inhibitor Calphostin C resulted in a loss of Akt Ser473~P by both strain and insulin, suggesting PKC involvement in mTORC2 function. In sum, mechanical input initiates a signaling cascade that requires mTORC2 phosphorylation of Akt S473, which induces Akt phosphorylation of GSK3 β , even in the absence of T308~P. Our data indicate that the mechanical regulation of GSK3 β downstream of Akt is uniquely dependent on Akt S473~P in a manner distinct from that of growth factors. We speculate that mechanical Akt/GSK3 β coupling involves molecules which are already present at the membrane. These differences provide clues as to the unique processes by which mechanical input, conscripting common signaling pathways, regulates MSC function.

Disclosures: Natasha Case, None.

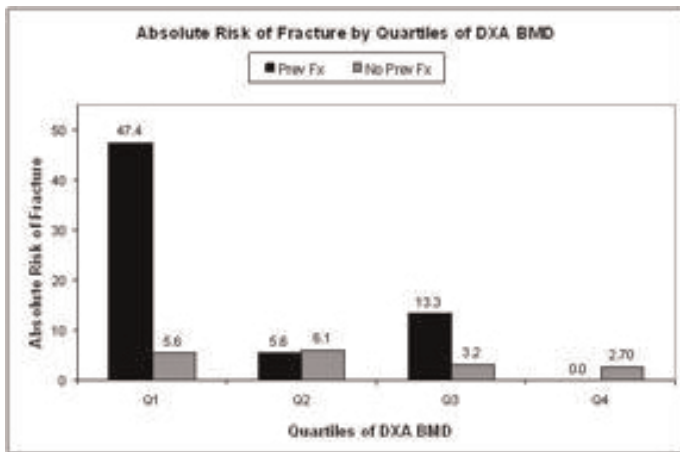
1241

A Prospective Study of Predictors of Radiographic Spine Fracture in Men: the MROS study. Dennis Black^{*1}, Katherine Wilt Peters², Kristine Ensrud³, Jane Cauley⁴, Eric Orwoll⁵, Steven Cummings⁶, John Schousboe⁷. ¹University of California, San Francisco, USA, ²California Pacific Medical Center, USA, ³Minneapolis VA Medical Center / University of Minnesota, USA, ⁴University of Pittsburgh Graduate School of Public Health, USA, ⁵Oregon Health & Science University, USA, ⁶San Francisco Coordinating Center, USA, ⁷Park Nicollet Clinic/University of Minnesota, USA

The main predictors of vertebral fracture have been well studied in women, including age, BMD and prevalent vertebral fractures. Predictors of vertebral fractures in men have been less well studied. We examined predictors of incident vertebral fracture in community dwelling older men (mean age 72.6 \pm 5.4 years) from the MROS study. For this analysis, we had baseline and follow-up lateral spine radiographs from a random sample of 841 men who also had with both DXA and QCT BMD measurements of the lumbar spine. Vertebral fracture status was evaluated by the semi-quantitative scale (SQ); incident vertebral fracture was defined by a vertebra which increased by ≥ 1 point on the SQ scale. The mean time between the baseline and follow up radiographs was 4.7 years. We examined multiple possible baseline predictors including age, weight, height, BMI, physical activity by PASE score, smoking, corticosteroid use, history of non vertebral fracture, prevalent vertebral fracture at baseline (SQ ≥ 2), and lumbar spine BMD by DXA and by QCT. Variables were included in multivariate logistic regression models if they were significant at p<0.1 in a univariate model. Age was also included in multivariate models. Odds ratios in both univariate and multivariate adjusted models are reported.

There were 44 new spine fractures among these 841 men for an incidence rate of 5.2% over the 4.7 year follow-up. In univariate analyses, a prevalent vertebral fracture was a strong predictor of incident vertebral fracture (OR=4.4, p<0.01). DXA BMD was significantly related (OR/SD = 1.9, p<0.01) as was trabecular BMD by QCT (OR/SD=1.8, p<0.01). Age was not related to risk of incident vertebral fracture nor was weight, height, BMI, physical activity, smoking, corticosteroid use, or history of non vertebral fracture. In the multivariate model including age, both prevalent fracture and DXA BMD remained predictive (OR=3.8, p<0.01, and OR/SD = 1.7, p<0.01 respectively). Remarkably similar results were observed in the multivariate QCT BMD (OR=3.5, p<0.01, and OR =1.7, p<0.01 respectively).

In conclusion, these findings suggest that older men with existing vertebral fractures and/or low BMD are at very high risk of new spine fracture within five years. Multiple other clinical risk factors, including age, had minimal value in predicting incident vertebral fracture.



MrOS graph

Disclosures: Dennis Black, None.

1242

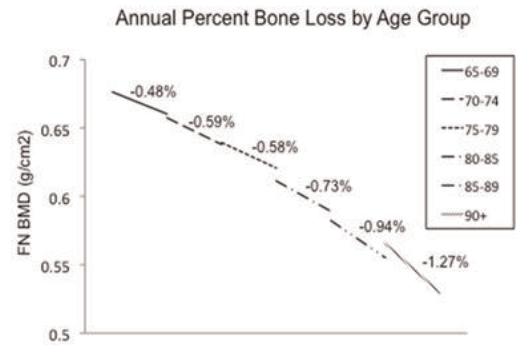
Bone Loss Accelerates After Age 75: A Prospective, Longitudinal Study. Steven Cummings^{*1}, Lily Lui¹, Jane Cauley², Kristine Ensrud³, Teresa Hillier⁴, Marc Hochberg⁵. ¹San Francisco Coordinating Center, USA, ²University of Pittsburgh Graduate School of Public Health, USA, ³Minneapolis VA Medical Center / University of Minnesota, USA, ⁴Kaiser Center for Health Research, USA, ⁵University of Maryland School of Medicine, USA

Background: Loss of BMD begins in midlife, increases around menopause then continues at a slower pace. Cross-sectional studies suggest that BMD is lost at a steady rate after age 60 years. However, the course of bone loss with advanced age is not known.

Methods: We measured femoral neck BMD every 2-4 years during 20 years of follow-up of the Study of Osteoporotic Fractures, a community-based cohort of women age 65 years or older at baseline. Hip BMD was measured with Hologic QDR-1000 scanners at all exams. We analyzed rates of change in BMD in 3741 women who had at least two BMD measurements and excluded women who took treatments that may affect bone. We compared the absolute and percentage mean BMD change for each of six age groups (65-69, 70-74, 75-79, 80-84, 85-89, 90+) and tested statistical significance using pair-wise t-tests. To determine whether loss could be due to decreased weight with advancing age, we also adjusted for baseline weight.

Results: Femoral neck BMD steadily decreased at approximately 0.5% per year from age 67 through age 74 years. Bone loss began to accelerate after age 75 and doubles to 1.3% per year by age 90 years (figure). The results were similar when analyzed as absolute change in mineral or by percentage loss and were also unchanged by adjustment for weight.

Conclusion: On average, in older white women, the loss of BMD in the femoral neck remains constant through from age 65 through 74 then accelerates, to more than 1% per year after 90 years. This accelerated loss contributes to the exponential increase in risk of hip fracture after age 75. Prevention of bone loss may particularly important after age 75.



Table

Disclosures: Steven Cummings, None.

1243

Prediction of Fracture Risk in Men: A Cohort Study. Liisa Byberg^{*1}, Rolf Gedeberg², Thomas Cars², Johan Sundstrom², Lars Berglund³, Lena Kilander², Hakan Melhus⁴, Karl Michaelsson³. ¹Uppsala Universitet, Sweden, ²Uppsala University, Sweden, ³Uppsala Clinical Research Center, Sweden, ⁴Uppsala University Hospital, Sweden

In order to target interventional efforts, accurate identification of men with a high future risk of osteoporotic fracture is of importance. Our aim was therefore to determine how much of the variation in fracture rate in men that can be explained by the WHO fracture risk assessment tool FRAX, comorbidity, medication, and behavioral factors, separately and in combination, and at different ages.

The Uppsala Longitudinal Study of Adult Men (ULSAM) is a population-based cohort study. All men born 1920-24 and resident in Uppsala in January 1970 were invited and 2322 (82%) participated. Reinvestigations among survivors were performed at ages 60 (n=1852), 71 (n=1221), and 82 (n=526) years. Follow-up was until 31 December 2009. Bone mass density (BMD) was measured using DXA at age 82. The prognostic value estimated by survival analysis R^2 representing the proportion of variation in time to any fracture and hip fracture was calculated for FRAX, comorbidity, medication, and behavioral factors, separately and in combination.

During follow-up, 897 fractures occurred in 585 individuals. The 10-year rates of any fracture were 5.7/1000 person-years at risk from age 50 and 25.9/1000 person-years at risk from age 82. Corresponding hip fractures rates were 2.9 and 11.7/1000 person-years at risk. The full model combining FRAX, comorbidity, medications, and behavioral factors had the highest R^2 values at all ages both for all fractures and for hip fracture, explaining 25-45% of all fractures and 80-92% of hip fractures, depending on age. The corresponding prognostic values of the FRAX model were 7-17% for all fractures and 41-60% for hip fractures. Within the highest quintile of predicted fracture risk with the full model, 1/3 of the men had a fracture within 10 years after the age of 71 years and 2/3 after the age of 82 years. Addition of BMD at age 82 to the full model improved discrimination further whereas number of previous falls did not.

The addition of comorbidity, medication and behavioral factors to FRAX can substantially improve the ability to identify men at high risk of fracture, especially hip fracture. Future studies need to assess whether additional measurement of BMD, vitamin status and other factors can guide the physician towards the appropriate treatment.

Variation in fracture rate explained by FRAX model and the full model, R^2 (95% confidence intervals)

	No. (%) fractures	FRAX model	Full model
Any fracture within 10 years, from age			
50 yrs	126 (5)	14.3 (6.5-24.9)	37.5 (25.8-51.3)
60 yrs	109 (6)	14.7 (5.2-28.8)	42.6 (27.6-59.6)
71 yrs	143 (12)	7.0 (2.4-15.1)	24.7 (15.1-38.5)
82 yrs	64 (12)	17.1 (6.7-33.9)	44.6 (28.5-63.3)
Hip fracture within 10 years, from age			
50 yrs	9 (0.4)	not analyzed	not analyzed
60 yrs	22 (1)	60.5 (27.8-87.6)	92.2 (71.5-99.3)
71 yrs	41 (3)	40.8 (17.6-68.2)	80.4 (64.9-92.3)
82 yrs	30 (6)	57.0 (29.8-81.9)	86.6 (67.1-97.1)

Table

Disclosures: Liisa Byberg, None.

1244

Fracture Prediction from Repeat BMD Measurements in Routine Clinical Practice for: The Manitoba BMD Cohort. William Leslie^{*1}, Suzanne Morin², Lisa Lix³. ¹University of Manitoba, Canada, ²McGill University Health Centre, Canada, ³University of Saskatchewan, Canada

BACKGROUND: In routine clinical practice, many patients receive repeat BMD measurements. Whether subsequent measurements are as useful for fracture risk assessment as the baseline measurement, and whether this is affected by recent osteoporosis therapy (OTX) or changing BMD are unclear. **METHODS:** We identified N=50,215 patients over age 50 at the time of baseline BMD testing between 1990 and 2009 in a large clinical BMD database for the Province of Manitoba, Canada. 2nd BMD tests were performed in N=14,619, 3rd BMD tests in N=4,722, and 4th BMD tests in N=1,500. Patient subgroups were identified with 2 scans (N=13,481) or 3 scans (N=4,087). Using linkage to a population-based administrative health data repository, we identified other relevant covariates, medication use, and fracture outcomes up to March 2010. Cox proportional hazards models were used to assess major osteoporotic fracture risk and hip fracture risk according to BMD (total hip [base model], lumbar spine, femoral) at baseline and follow up after adjustment for OTX and multiple covariates (sex, age, BMI, prior fracture, prolonged glucocorticoid use, rheumatoid arthritis, COPD [smoking proxy] and alcohol/substance abuse). **RESULTS:** Prevalence of recent OTX increased from 18% at baseline to 55% by scan #4. Total hip BMD was strongly predictive of major osteoporotic fractures at all time points (Figure). In the patient subgroup with 2 measurements, major fracture prediction with the 1st scan (HR per SD 1.45 [95% CI 1.34-1.56]) was similar to the 2nd scan (1.64 [1.48-1.81]). Similar results were seen in the patient subgroup with 3 scans. No significant differences were seen between when 2nd scan results were stratified by recent OTX using the medication possession ratio for the prior year (HRs 1.50 [1.28-1.76] for MPR=0, 1.46 [1.09-1.96] for MPR <0.5, 1.83 [1.30-2.58] for MPR 0.5-0.8, 2.08 [1.72-2.51] for MPR >0.8; p-interaction NS) or by BMD change (HR for 1.58 [1.37-1.82] no change, 1.50 [1.09-2.06] for significant increase, 1.66 [1.30-2.13] for significant decrease; p-interaction NS). Similar results were seen for hip fracture prediction, or when lumbar spine and femoral neck BMD were analyzed. **CONCLUSIONS:** BMD measurement is a robust predictor of fractures, and this does not diminish on repeat measurements or after prior OTX.

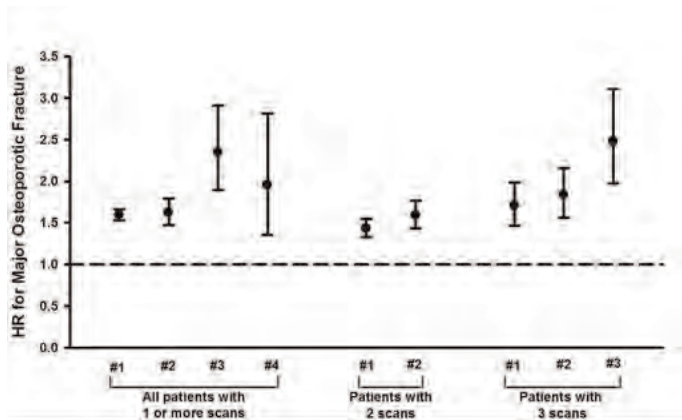


Figure: Adjusted hazard ratios per SD decrease in total hip BMD to predict major fracture.

Disclosures: William Leslie, None.

1245

Subtrochanteric/femoral Shaft versus Hip Fractures: Incidence and Identification of Risk Factors. Milka Maravic^{*1}, Agnes Ostertag², Martine Cohen-Solal³. ¹Département d'Information Médicale, Hôpital Leopold Bellan, France, ²U606 INSERM, France, ³Centre Viggo Petersen, France

Introduction: Subtrochanteric and femoral shaft (ST/FS) fractures are now considered as fragility fractures in osteoporotic patients. Although rare, there is growing evidence showing the burden of this type of fracture. The evolution of the incidence of ST/FS fractures is poorly known. The aim of this study was to assess the incidence of ST/FS fractures from 2002 to 2009 in France as well as the associated risk factors.

Methods: Data were obtained from the French National Database which includes all hospital discharge codes in public and private acute care settings from 2002 to 2009. All hospital stay for primary surgical management of neck/trochanteric (hip) and subtrochanteric/femoral shaft (ST/FS) fractures in patients aged 50 years and older was selected and described in different age-groups. Incidence per million were calculated using the estimate French population adjusted for each year and by age and gender. Evolution was assessed for each site of fractures throughout this period. The factors of co-morbidity in relation to these fractures were assessed in 2009 using multivariate logistic regression.

Results: From 2002 to 2009, the incidence of hip fractures decreased significantly from 4368 to 4044 per million in women ($p<0.001$) and increased significantly from

1476 to 1609 per million in men ($p<0.0001$). In contrast, the incidence per million of ST/FS increased significantly in both gender, i.e. from 353 to 481 per million in women and from 146 to 203 per million in men. The most significant variation was particularly observed in the elderly above the age of 70 y. The percentage of ST/FS fractures among fractures of the femur was about 7.5-10.6% in women and 8.9-11.2% in men. In 2009, the incidence of ST/FS in the general population remained low at the level of 0.05% and 0.02% in women and men respectively. However, this percentage reached 0.3% and 0.2% in women and men aged 90 years and over. The adjusted risk of having a ST/FS fracture compared to hip fracture was significantly higher with obesity (OR: 2.2; 1.77-2.74) and dementia (adjusted OR 1.22; 1.16-1.29) but slightly decrease with age >84 years (OR: 0.85 (0.81-0.89), cardiac arrhythmia (OR 0.92; 0.85-0.99) and hypertension: OR (0.93; 0.88-0.98).

Conclusion: In contrast to hip fractures, the incidence of ST/FS fractures increased significantly from 2002 to 2009 in France and affects mostly the elderly. Moreover, obesity and dementia are the major risk factors associated with this fracture site.

Disclosures: Milka Maravic, None.

1246

Recent Trends in Hip Fracture Rates by Race/Ethnicity in Older US Adults. Nicole Wright^{*1}, Wilson Smith¹, Kenneth Saag¹, Jeffrey Curtis¹, Michael Morrissey¹, Meredith Kilgore², Huifeng Yun¹, Jie Zhang¹, Elizabeth Delzell¹. ¹University of Alabama at Birmingham, USA, ²University of Alabama At Birmingham School of Public Health, USA

Purpose: Hip fracture incidence among Caucasians has declined in the US since 1995. Limited data are available on recent trends in racial and ethnic minorities. The goal of this study was to investigate hip fracture incidence trends in Medicare beneficiaries.

Methods: We used the Medicare national random 5% sample to determine annual hip fracture incidence rates during 2000-2009. Eligibility in each year was restricted to days when the beneficiary was in the 5% sample, was 65+ years of age, lived in the 50 states or Washington DC, and had full fee-for-service Medicare coverage. To ensure that only incident hip fractures were identified, each day of observation was preceded by 90 days of continuous fee-for-service coverage with no hip fracture claims. Race/ethnicity was self-reported by the beneficiary. We identified incident hip fractures using claims data consisting of inpatient hospital diagnosis codes and outpatient diagnosis codes paired with fracture repair procedure codes. We computed age-standardized rates using the 2009 Medicare population ≥65 years as the standard, and tested trends in the rates over time among each racial/ethnic group using linear regression.

Results: On average, 822,000 women and 585,000 men contributed person-time to the analysis each year. Beneficiaries were predominantly White (88%), with African, Hispanic, and Asian Americans making up 8%, 2%, and 1.5% of the population, respectively. In women, a decreasing significant trend ($p<0.05$) in hip fracture incidence from 2000 to 2009 was present in all racial/ethnic groups (Figure). This trend was most consistent across years in Whites and African Americans, with the hip fracture incidence rates declining by 17% in Whites and 20% in African Americans between 2000-2009. White men also had a significant decline in hip fracture rates ($p<0.001$); however, rates for other groups of men were based on relatively small numbers and did not display consistent trends.

Conclusion: Among Medicare beneficiaries, incidence rates of hip fracture decreased between 2000-2009 in women of all racial/ethnic groups and in White men. No significant decline was observed in men of other racial/ethnic groups. The results suggest that additional hip fracture prevention efforts are needed among the growing population of ethnic/racial minorities, particularly men, in the US.

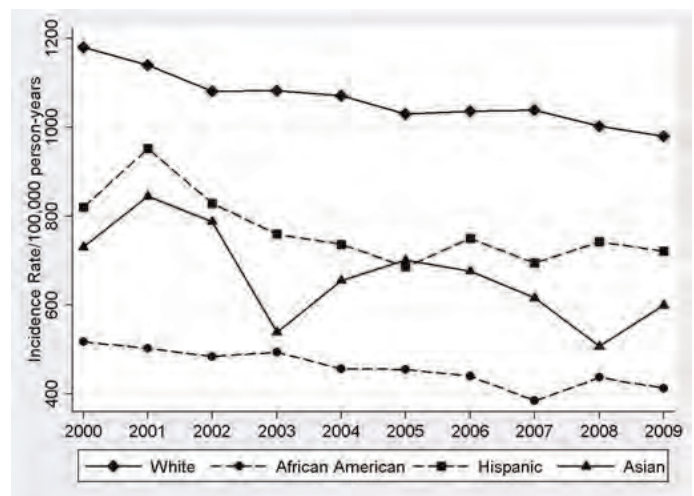


Figure: Age-standardized Trends in Hip Fracture Incidence Among Female Medicare Beneficiaries

Disclosures: Nicole Wright, Amgen, 2
This study received funding from: Amgen

1247

Fractures and Mortality in Relation to Different Osteoporosis Treatments. Huifeng Yun^{*1}, Elizabeth Delzell¹, Robert Matthews¹, Meredith Kilgore², Kenneth Saag¹, Cathleen Colon-Emeric³, Christopher O'Connor⁴, Kenneth Lyles³, Michael Morrissey¹, Jeffrey Curtis¹. ¹University of Alabama at Birmingham, USA, ²University of Alabama At Birmingham School of Public Health, USA, ³Duke University Medical Center, USA, ⁴Duke University, USA

BACKGROUND: Few studies have assessed the effectiveness of different drugs for postmenopausal osteoporosis (OP).

OBJECTIVES: We compared fracture incidence and mortality among Medicare beneficiaries initiating various OP medications.

METHODS: Using the Medicare national random 5% sample, we identified new users of oral bisphosphonates (BPs), intravenous (IV) ibandronate (IBN), IV zoledronic acid (ZOL), calcitonin (CAL), raloxifene (RAL) and parathyroid hormone (PTH). Eligible subjects were ≥ 65 years; continuously enrolled in fee for service and part D Medicare; and newly treated during 2006-2008. New treatment was defined as therapy initiated after 12 month baseline during which no prescription was filled for the drug. Subjects remained in their initial drug category regardless of any switching of medication during follow-up. Cox proportional hazards models evaluated associations between different OP drugs and mortality and also first hip, distal radius/ulna, clinical vertebral, or humerus fracture. Analyses used IV ZOL as the referent and adjusted for multiple confounders. Further confounder control was examined using propensity score (PS) quintile adjusted and PS matched analyses.

RESULTS: We identified 24537 new users for oral BPs, 750 for IV IBN, 1962 for IV ZOL, 7231 for CAL, 986 for PTH and 2222 for RAL. These cohorts experienced, respectively, 8.4%, 12.9%, 8.8%, 17.0%, 13.6%, 7.8% fractures and 8.8%, 7.6%, 6.1%, 21.2%, 12.9% and 6.4% deaths during follow-up. After multivariable adjustment (ZOL referent), hazard ratios for fracture were 1.41 (95% CI: 1.03-1.93) for IV IBN, 1.33 (1.06-1.66) for oral BPs; 1.47 (1.16-1.86) for CAL, 1.27 (0.97-1.67) for RAL and 1.05 (0.78-1.42) for PTH; and for mortality were 0.84 (0.60-1.22) for IBN, 0.94 (0.76-1.18) for oral BPs, 1.47 (1.17-1.85) for CAL, 0.99 (0.75-1.31) for RAL and 1.31 (0.98-1.75) for PTH.

CONCLUSIONS: Compared to IV ZOL, fracture rates among users of other BPs or CAL were 33-47% higher; mortality was 47% greater among users of CAL. While fracture benefit may be in part mediated through improved adherence to IV ZOL, the mechanism for a possible mortality benefit remains unclear.

Table: Compare the crude and adjusted hazard ratios between different osteoporosis drugs				
Treatment	Fractures		Death	
	Crude	Adjusted	Crude	Adjusted
IV Zoledronic acid	Ref	Ref	Ref	Ref
IV Ibandronate	2.30 (0.95-1.76)	1.41 (1.03-1.93)	0.86 (0.60-1.22)	0.84 (0.59-1.20)
Oral BP	0.82 (0.67-1.00)	1.33 (1.06-1.66)	1.04 (0.84-1.28)	0.94 (0.76-1.18)
Calcitonin	1.63 (1.30-2.04)	1.47 (1.16-1.86)	2.48 (1.99-3.09)	1.47 (1.17-1.85)
Raloxifene	0.73 (0.56-0.95)	1.27 (0.97-1.67)	0.75 (0.57-0.98)	0.99 (0.75-1.31)
Parathyroid Hormone	1.21 (0.90-1.62)	1.05 (0.78-1.42)	1.46 (1.10-1.93)	1.31 (0.98-1.75)

Note: We adjusted age, gender, race, geographic region, income, osteoporosis related conditions, other comorbidities and medications at baseline.

Compare the crude and adjusted hazard ratios between different osteoporosis drugs

Disclosures: Huifeng Yun, Amgen, 2

This study received funding from: Amgen

1248

Who Is at Highest Risk for New Vertebral Fractures After 3 Years of Annual Zoledronic Acid and Who Should Remain on Treatment? Felicia Cosman^{*1}, Jane Cauley², Richard Eastell³, Steven Boonen⁴, Lisa Palermo⁵, Ian Reid⁶, Steven Cummings⁷, Dennis Black⁵. ¹Helen Hayes Hospital, USA, ²University of Pittsburgh Graduate School of Public Health, USA, ³University of Sheffield, United Kingdom, ⁴Center for Metabolic Bone Disease & Division of Geriatric Medicine, Belgium, ⁵University of California, San Francisco, USA, ⁶University of Auckland, New Zealand, ⁷San Francisco Coordinating Center, USA

In the HORIZON-PFT Extension study (E1), 1223 women who had already received 3 annual zoledronic acid (ZOL) infusions in the original HORIZON-PFT trial (Core) were randomized to receive 3 more ZOL infusions (Z6, n=616) or 3 placebo infusions (Z3P3, n=617). We previously showed that there were modest, but statistically significant, reductions in hip BMD, and increments in bone turnover markers, as well as a significantly higher incidence in new morphometric vertebral fractures in Z3P3 vs Z6 during E1 (Black et al. ASBMR 2010). The goal of the current analysis was to identify the predictors of new vertebral fracture risk during E1 and to determine which subgroups of patients would be most likely to benefit from continuation of ZOL for 3 additional years. Predictor variables considered and analyzed in the Z3P3 group by logistic regression included age, persistent osteoporosis by total hip (TH) or femoral neck (FN) BMD, remote history of vertebral or nonvertebral fracture, recent incident morphometric vertebral or nonvertebral fracture (during Core), PINP level at E1 baseline, % change TH BMD during Core, BMI and weight loss. Individual logistic regression models were then

used to determine if continued treatment with ZOL during E1 affected fracture outcomes (using both Z6 and Z3P3 groups) in subgroups defined by the predictors identified in the Z3P3 group. The most important predictors of new Morphometric fracture risk in the Z3P3 group were FN or TH T-score at E1 Baseline < -2.5 [Odds Ratio (95%CI)= 3.3 (1.4,8.0), $p=0.008$; and 4.01 (1.8,8.9), $p=0.0007$, respectively], and incident morphometric vertebral fracture during Core [OR 4.74 (1.3,16.7), $p=0.0156$]. Significant treatment effects with continued ZOL in E1 were seen in these high risk subgroups (See Table). In women who appear to remain at elevated fracture risk after 3 years of ZOL (those with incident vertebral fracture during the first 3 years or persistent hip osteoporosis), absolute fracture risk reductions are greatest with continued ZOL and therefore Numbers Needed to Treat (NNT) for 3 additional years are lowest. In those women who do not appear to be at elevated risk for fracture, discontinuation of treatment should be considered.

Table. Incident Morphometric Vertebral Fracture in Z3P3 and Z6 groups by Subgroup

	Z3P3	Z6	OR (CI)	Rx Effect P	NNT/3 Yrs
FN\leq-2.5	23/250 (9.2%)	9/257 (3.5%)	0.36 (0.15, 0.77)	0.011	17.5
FN$>$-2.5	7/235 (3%)	5/210 (2.4%)	0.79 (0.23, 2.53)	0.698	167.3
Yes Core Vert	4/16 (25%)	0/11	0	n/a	4
No Core Vert	26/464 (5.6%)	12/451 (2.7%)	0.46 (0.22, 0.9)	0.029	34

Table

Disclosures: Felicia Cosman, Merck Eli Lilly, Amgen, Novartis, 5; Eli Lilly, Amgen, Novartis, 8; Eli Lilly, Novartis, Amgen, 2

This study received funding from: Novartis Pharmaceuticals

1249

Increase of Serum PINP Is Associated with Trabecular Microstructural Improvement in Patients on Teriparatide Pretreated with Alendronate. Astrid Fahrleitner-Pammer^{*1}, Harald Dobnig², Jan Stepan³, Helmut Petto⁴, Imre Pavo⁵. ¹Medical University Graz, Austria, ²Department of Internal Medicine, Division of Endocrinology & Metabolism, Medical University of Graz, Austria, ³Charles University, Czech Republic, ⁴Lilly Research Center, Austria, ⁵Eli Lilly & Company, Austria

Early increase in serum amino terminal propeptide of type I procollagen (PINP) after the initiation of teriparatide (TPTD) treatment has been demonstrated to positively correlate with increase of lumbar spine bone mineral density (BMD). Consequently, PINP response has been proposed to predict the efficacy of TPTD therapy. In the initial treatment phase with TPTD therapy, alendronate (ALN) pretreatment may blunt the PINP response. The aim of this exploratory, post-hoc analysis was to investigate the correlation between changes in PINP and bone microstructure, a component of bone quality, in patients receiving TPTD subsequent to ALN pretreatment.

Sixty-six postmenopausal women with osteoporosis (mean age of 68.0 [SD 7.0] years and mean BMD T-score of -1.7 [SD 0.9] at total hip and -2.8 [SD 0.8] at lumbar spine; 62% with prevalent fractures) have been treated with 20 µg/day subcutaneous TPTD for 24 months. Thirty-eight stopped previous ALN treatment (10 mg/day or 70 mg/week for a mean duration of 63.6 months), and switched to TPTD, while 28 were osteoporosis treatment naive (TN). Paired iliac crest biopsies were collected and analyzed by micro-CT at baseline and after 24-month TPTD administration. The serum levels of PINP, type I collagen cross-linked C-telopeptide (CTX) and bone-specific alkaline phosphatase (BSAP) were determined at baseline, 1, 3, 6, 12 and 24 months of treatment. The changes of biochemical markers from baseline to different treatment durations were correlated (Spearman rank correlation coefficient) with 24 months changes of bone microarchitectural variables.

ALN pretreatment did not delay the increase of PINP. One, 3 and 6 months changes of bone markers did not demonstrate consistently correlation with 24 months changes in microstructural variables. After 12 months, the change in PINP revealed significant positive correlations with three-dimensional indices of improved trabecular microarchitecture (Table).

The correlations were not different between TN and ALN pre-treated groups (Fisher z-test). Our results support the use of PINP as a surrogate marker of bone efficacy of teriparatide, including patients previously treated with a potent aminobisphosphonate like ALN.

3-D trabecular micro-architectural indices	Spearman Rank Correlation coefficients (95% CI)	
	All (n=45)	ALN pre-treated (n=29)
Bone tissue volume	0.49(0.23 to 0.68)**	0.55(0.22 to 0.76)**
Thickness (µm)	0.31(0.02 to 0.56)*	0.39(0.02 to 0.66)*
Number (mm ⁻³)	0.39(0.11 to 0.62)**	0.43(0.08 to 0.69)*
Separation (µm)	-0.46(-0.66 to -0.19)**	-0.48(-0.72 to -0.13)**

*p<0.05, **p<0.01

Table: Correlations between changes of trabecular micro-architectural indices and PINP

Disclosures: Astrid Fahrleitner-Pammer, None.

This study received funding from: Eli Lilly and Company

1250

Parathyroid Hormone (1-84) and Ibandronate Administered Concurrently Vs. Sequentially: The PTH and Ibandronate Combination Study (PICS) Randomized Trial. Anne Schafer¹, Lisa Palermo², Dolores Shoback³, Deborah Sellmeyer⁴, Dennis Black². ¹University of California, San Francisco & the San Francisco VA Medical Center, USA, ²University of California, San Francisco, USA, ³VA Medical Center, USA, ⁴The Johns Hopkins Bayview Medical Center, USA

Parathyroid hormone (PTH) therapy improves bone mineral density (BMD) and decreases fracture risk in postmenopausal osteoporosis, but its use has been limited by factors including cost and the burden of daily injections. There is great interest in exploring alternative dosing strategies, with the goals of increased flexibility for patients and improved understanding of optimal dosing schedules. The objective of this study was to evaluate 2 approaches to the use of 6 months of PTH therapy. We conducted a randomized, double-blind trial of the effects of 2 combinations of PTH(1-84) (100 µg daily) and ibandronate (150 mg monthly) in 44 postmenopausal women with low bone mass. Each participant had a T-score ≤ -1.5 at the spine, total hip, or femoral neck, or a T-score ≤ -1.0 with an additional risk factor for osteoporosis. Participants received either 6 months of concurrent PTH daily injections and ibandronate monthly tablets, followed by 18 months of ibandronate (Group A); or 2 sequential courses of 3 months of PTH daily injections followed by 9 months of monthly ibandronate (Group B), for a total of 2 years of medication for each participant. Placebo injections and tablets ensured appropriate blinding. Areal and volumetric BMD (aBMD and vBMD) were assessed by dual-energy X-ray absorptiometry and quantitative computed tomography, respectively. Markers of bone turnover were measured on fasting blood samples. BMD at the spine increased similarly in the 2 groups (Table). At the total hip, vBMD increased in both groups; there was a trend towards a greater increase in Group B (sequential PTH). At the femoral neck, vBMD increased in both groups, and cortical thickness increased. Femoral neck buckling ratio, a measure of cortical instability, decreased similarly in the 2 groups (a favorable change). In Group B, the second 3-month course of PTH led to increases in markers of bone formation (e.g., a 209% increase in PINP, $p < 0.001$), on par with the increases observed during the first course. We conclude that 6 months of PTH(1-84) produces similar increases in areal and volumetric BMD, as well as decreases in cortical instability, when administered with concurrent monthly ibandronate followed by a continuation of the ibandronate, or when administered as two 3-month courses, each followed by ibandronate. Multiple short courses of PTH may provide the benefits of anabolic therapy for osteoporosis with heightened flexibility for patients.

TABLE. Mean percentage changes over 2 years

Variable	Group A (PTH+ibandronate) then ibandronate		Group B PTH → ibandronate PTH → ibandronate		p-value (between groups)
		p-value		p-value	
Spine aBMD	7.5%	<0.01	8.2%	<0.01	0.65
Total hip aBMD	3.6%	<0.01	2.9%	<0.01	0.54
Femoral neck aBMD	2.9%	<0.01	1.7%	0.08	0.39
Spine vBMD	12.5%	<0.01	14.0%	<0.01	0.77
Total hip vBMD	5.7%	<0.01	11.3%	<0.01	0.06
Total hip cortical vBMD	2.1%	0.05	4.7%	<0.01	0.08
Total hip trabecular vBMD	1.8%	0.08	2.7%	0.02	0.57
Femoral neck vBMD	4.9%	0.01	7.7%	<0.01	0.27
Femoral neck cortical thickness	12.4%	<0.01	8.7%	0.06	0.56
Femoral neck buckling ratio	-6.3%	0.03	-9.4%	<0.01	0.44

Table

Disclosures: Anne Schafer, None.

This study received funding from: Genentech, Inc., a Member of the Roche Group

1251

Use of oral Bisphosphonates and the Risk of Subtrochanteric and Diaphyseal Fractures in Older Men and Women. Suzanne Morin¹, Behloul Hassan², William Leslie³, Jacques Brown⁴, David Goltzman¹, Louise Pilote⁵. ¹McGill University Health Centre, Canada, ²McGill University Research Institute, Canada, ³University of Manitoba, Canada, ⁴Laval University, Canada, ⁵McGill University, Canada

Purpose Bisphosphonates are recommended as first-line agents to reduce fracture risk in patients with osteoporosis. However, recent studies have reported that bisphosphonates may also be associated with rare, but serious adverse effects such as atypical subtrochanteric and diaphyseal fractures of the femur. If so, bisphosphonates may be associated with increased risk of fractures at the subtrochanteric and diaphyseal sites at the population level. Methods We conducted a population-based, nested case-control study to determine if exposure to alendronate and risendronate is associated with a higher risk of subtrochanteric and diaphyseal fractures compared to femoral neck and intertrochanteric fractures. Using the Province of Quebec, Canada, administrative databases, we identified as cases all men or women 65 years and older, who experienced a subtrochanteric or diaphyseal fracture from November 8th 2005 to March 31st 2008 and matched them with up to 4 controls who sustained femoral neck or intertrochanteric fractures. Adjusted odds ratios (aOR) and 95% confidence intervals (CI) were computed using conditional logistic regression models based on the

matched sets of cases and controls to estimate the effect of any and, cumulative bisphosphonates use on the risk of subtrochanteric and diaphyseal fractures (versus femoral neck and intertrochanteric fractures). Results There were 9650 hospitalizations for proximal femur fractures (7.9% subtrochanteric, 2.5% diaphyseal, 49.8% femoral neck, 39.7% intertrochanteric) during the study period. We identified 973 individuals with a subtrochanteric or diaphyseal fracture and 3892 controls (Mean age 83.1 [SD 7.6] years, 25.5% men). Among the cases, 37.9% had claimed at least one prescription for a bisphosphonate prior the index fracture as opposed to 24.0% among the controls; most were taking a weekly dose of medication. Mean cumulative duration of use of bisphosphonates in cases was 2.8 [SD 1.9] years and 2.1 [SD 1.8] years in controls. Any use of bisphosphonate was associated with an aOR of 2.0 (95% CI 1.7- 2.4) of sustaining a subtrochanteric or diaphyseal fracture compared to femur neck and intertrochanteric fractures. Cumulative duration of use was also found to be associated with increased risk of subtrochanteric and diaphyseal fractures, both in men (for each additional year of use, aOR 1.4; 95% CI 1.1- 1.7) and in women (aOR 1.3; 95% CI 1.2- 1.4). Compared with no use, treatment for ≥ 4 years duration (at a medication possession ratio of ≥ 80%) was associated with a three-fold increase in the risk (aOR 3.3; 95% CI 2.3- 4.6) of sustaining a subtrochanteric or diaphyseal fracture. Conclusion Among older men and women, treatment with alendronate and risendronate is associated with an increased risk of subtrochanteric and diaphyseal fractures of the femur.

Disclosures: Suzanne Morin, Amgen, Novartis, 8; Amgen, Novartis, Eli Lilly, Warner-Chilcott, 5; Amgen, 2

1252

The Effect of Glucocorticoid Therapy on Regulators of Bone Formation in Postmenopausal Women Treated with Teriparatide or Alendronate. Fatma Gossiel¹, Nancy Lane², Richard Eastell³. ¹The University of Sheffield, United Kingdom, ²University of California, Davis Medical Center, USA, ³University of Sheffield, United Kingdom

Glucocorticoid therapy induces bone loss primarily through inhibition of osteoblast function. The osteocyte produces regulators of bone formation (RBF) that inhibit the wnt signalling pathway. Treatment of mice with prednisolone increased SOST expression in tibiae, and this effect can be reversed by treatment with parathyroid hormone but not with bisphosphonate (Yao (2008) Arthritis Rheum 58:3485-3497).

The aims of this study were to examine the effects of: 1) glucocorticoids (GC) on RBF in postmenopausal women; 2) teriparatide or alendronate therapy on RBF in these women.

We studied 53 postmenopausal women (mean age 63 years) who were randomised to receive either teriparatide (20µg/day, subcutaneous injection) (N = 28) or alendronate (10mg/day orally) (N=25). Subjects have received glucocorticoid therapy at an average dose of at least 7.5 mg/day of prednisone or its equivalent for a minimum of 3 consecutive months prior to study entry. A fasting serum sample was obtained at baseline, 6 and 18 months. Dkk1 and sclerostin were measured by ELISA (Biomedica Gruppe, Austria). We compared them to a group of 50 healthy premenopausal women (mean age 38; range 35 to 40 years).

The median levels (95% confidence intervals) of sclerostin were significantly higher in the GC group 38.6 pmol/l (35.6-47.1), compared to the premenopausal group 14.9 pmol/l (12.7-16.6) ($p < 0.0001$, Mann-Whitney test). The mean increase in GC group was 4.8 standard deviations compared to the control group. The median levels of Dkk1 were significantly lower, 133 pmol/l (112.8- 161.3) compared to 475.3 pmol/l (436.0-512.8), ($p < 0.0001$, Mann-Whitney test). The mean decrease in GC group was 3.0 standard deviations compared to the control group. There was no effect of either treatment on levels of sclerostin or Dkk-1 (repeated measures analysis of variance).

Conclusions: Glucocorticoid therapy (or the underlying disease for which therapy was given) is associated with higher levels of sclerostin (as expected from the animal model) but lower levels of Dkk-1. These changes were not reversed by treatment with licenced doses of teriparatide or alendronate.

Disclosures: Fatma Gossiel, None.

1253

Nuclear Factor of Activated T-Cells (NFAT)c2 Inhibits Notch Canonical Signaling. Stefano Zanotti*, Anna Smerdel-Ramoya, Ernesto Canalis. St. Francis Hospital & Medical Center, USA

Nuclear Factor of Activated T-Cells (NFAT)c1 through c4 are transcription factors expressed by osteoblasts with critical effects on osteoclastogenesis and osteoblastogenesis. Notch are transmembrane receptors that suppress osteoblastogenesis. In the Notch canonical signaling pathway, nuclear translocation of the Notch intracellular domain (NICD) and its association with the DNA-binding protein C Promoter Binding Factor 1, Suppressor of Hairless and Lag-1 (CSL) induces gene expression. To identify intracellular signals interacting with Notch, we explored the actions of Notch on NFAT expression. Notch suppressed NFATc1 transcription, induced NFATc2 expression by post-transcriptional mechanisms and did not modify NFATc3 or c4 mRNA levels in osteoblasts. We postulated that induction of NFATc2 may mediate actions of Notch and serve as control mechanism to limit Notch activity. Therefore, we studied the consequences of Notch and NFATc2 activation on the differentiation of osteoblasts harvested from *Rosa^{Notch}* mice, where NICD expression under the control of the *Rosa26* promoter is induced following the excision of a STOP

cassette flanked by *loxP* sites. To test the effects of NFATc2, *Rosa^{Notch}* osteoblasts were infected with an adenoviral vector expressing a constitutively active NFATc2 mutant. Notch and NFATc2 suppressed early osteoblast gene markers, either when expressed individually or in combination. The inhibitory effect of Notch on alkaline phosphatase activity was reversed following downregulation of NFATc2 by RNA interference, suggesting that NFATc2 mediates selected actions of Notch in osteoblasts. In parallel experiments, NFATc2 opposed the activity of a Notch reporter construct, the transactivation of Notch target genes promoter fragments, and the expression of their respective transcripts. The mechanism of the inhibitory effects of NFATc2 on Notch signaling was investigated by electrophoretic mobility shift assay. Nuclear proteins from *Rosa^{Notch}* osteoblasts bound to a radiolabeled DNA probe containing a Csl consensus sequence, which was displaced by unlabeled *Nfat* oligonucleotides. Accordingly, unlabeled Csl oligonucleotides displaced a radiolabeled *Nfat* consensus sequence bound to nuclear proteins, indicating competition of Csl and NFATc2 for DNA binding. In conclusion, Notch and NFATc2 inhibit osteoblastogenesis, and NFATc2 suppresses Notch canonical signaling establishing a local negative feedback mechanism that regulates osteoblastogenesis.

Disclosures: Stefano Zanotti, None.

1254

NF- κ B RelB Negatively Regulates Osteoblast Function and Bone Formation. Zhenqiang Yao^{*1}, Yanyun Li², Lianping Xing¹, Brendan Boyce². ¹University of Rochester, USA, ²University of Rochester Medical Center, USA

RelB is a member of NF- κ B family which regulates osteoclast (OC) functions. RelB null (KO) mice have normal basal OC formation but they have impaired metastasis-mediated resorption. The role of RelB in osteoblast (OB) functions is unknown. We found that KO mice develop age-related cortical bone thinning and increased diaphyseal trabecular bone mass (TBM) both starting at 4 and persisting at 12-14 wks-old. To test if the increased TBM in KO mice is due to impaired OC or enhanced OB function, we injected 4 wk-old mice with calcein and sacrificed them 6 wks later when KO mice have high TBM. We found labeling in secondary ossification centers but not in KO or WT trabeculae, indicating that labeled bone had been fully resorbed and replaced by new trabeculae in KO mice. Consistently, TNF whose concentration is elevated in KO mice generated more and larger resorption pits from KO spleen cells than WT cells. The KO mice must have enhanced OB generation or function. Indeed, 4 wk-old KO mice have increased OB surface (305 vs 216% in WT mice) although bone formation rate (BFR) was reduced in 6-8 wk-old KO mice in the diaphysis where TBM had increased. Although RelB KO bone marrow (BM) CD45-CD105+ mesenchymal stem cell (MSC) numbers were normal, KO BM cells produced more MSCs in vitro (7.2% vs 3.4% WT). Accordingly, KO BM cells formed more ALP+ colonies (1037 vs 406) and mineralized nodules (653 vs 215/mm²) with 3- and 10-fold induction of Runx2 and osteocalcin mRNA. The increased TNF in KO mice would secondarily affect OB function. Indeed TNF dose dependently inhibited ALP+ OB differentiation in both mice. Of note, KO mice had 5-fold more macrophages, a major source of TNF, mainly distributed in the diaphysis where BFR is reduced. Interestingly, the cortical thickness and TBM phenotypes were rescued in RelB/TNF double knockout mice. Finally, we filled bilateral 3x6 mm tibial cortical bone defects in SCID mice with bovine decalcified bone matrix carrying 2x10⁵ bone-derived WT or KO MSCs. The new bony callus and woven bone formed from KO MSCs was higher than from WT MSCs after 2 wks (0.370.05 vs 0.060.01 mm²) and 4 wks (0.640.03 vs 0.250.1 mm²) evaluated by histology. Micro-CT confirmed that KO MSCs formed more new bone than WT cells at 4wks: 214 vs 70.6% of the defect. We conclude that RelB negatively regulates TNF expression by macrophages to limit TNF-induced bone resorption. It also negatively regulates MSC differentiation into osteoblasts to limit trabecular bone formation. Targeted inhibition of RelB in OBs should lead to increased bone formation.

Disclosures: Zhenqiang Yao, None.

This study received funding from: NIH

1255

Alteration of the Wnt/ β -Catenin Pathway by Runx2 Overexpression *In Vivo*. Coline Haxaire*, Eric Hay, Valerie Geoffroy. INSERM Unit 606, France

In vivo overexpression of Runx2 (Runx2 mice) in osteoblasts leads to severe osteoporosis. We have shown that bone loss induced by high level of Runx2 is associated with an alteration of the final steps of osteoblast maturation and with an increase of bone resorption.

The aim of our study was to determine whether the Wnt/ β -Catenin pathway could affect the Runx2-dependant osteoblast differentiation.

Ex vivo, β -Catenin expression and its translocation into the nucleus are lower in Runx2 compared to wild-type (WT) primary osteoblasts. Moreover, the expression of LEF-1 was lower and DKK2, an inhibitor of Wnt/ β -Catenin pathway, was higher in Runx2 than in WT osteoblastic cells. Using WT-TopGal and Runx2-TopGal primary osteoblasts, we evaluate β -Catenin activity (by assessing β -Gal activity) in presence or absence of LiCl or Wnt3a. Both treatments significantly increased the β -Gal activity in both WT-TopGal and Runx2-TopGal osteoblasts. Surprisingly, treatments were more efficient at increasing β -Gal activity in Runx2-TopGal than in WT-TopGal primary osteoblasts suggesting deficient Wnt/ β -Catenin pathway in Runx2 mice.

To confirm these results *in vivo*, Runx2 overexpressing mice were treated with lithium chloride (LiCl) that has been recently shown to increase nuclear β -Catenin through GSK-3 inhibition. Eight-week-old WT and transgenic female mice were treated orally by LiCl (200mg/kg/day, 5 days/week) or by vehicle (Veh) during 4 weeks. Femurs were used for histomorphometric analysis.

LiCl induced a significant increase in bone volume (BV/TV; 37% and 68% respectively), and a significant decrease in trabecular separation (Tr.Sp; -20% and -45% respectively) in both WT and Runx2 mice compared to Veh-treated mice. In addition, our results showed that *in vivo* LiCl therapy completely rescue the trabecular bone phenotype in Runx2 mice as BV/TV and Tr.Sp are not significantly different between LiCl-treated Runx2 mice and Veh WT mice. Interestingly, dynamic bone formation parameters, MAR (+ 31%) and bone formation rate (BFR, +32%), were significantly increased by LiCl in Runx2 but not in WT mice.

To conclude, our data demonstrate that overexpression of Runx2 affects the Wnt/ β -Catenin pathway. Our results also suggest that this interaction may also affect bone resorption in this context. Activation of the canonical Wnt/ β -Catenin pathway using LiCl is able to rescue the bone phenotype induced by Runx2 overexpression *in vivo*.

Disclosures: Coline Haxaire, None.

1256

Smad4 Coordinates BMP Signaling through p38 in Osteoblasts and is Required for Bone Anabolic Response to Canonical Wnt Signaling. Valerie Salazar*, Lisa Huang, Jin Norris, Sheri Bonar, Gabriel Mbalaviele, Roberto Civitelli. Washington University in St. Louis School of Medicine, USA

TGF β /BMP family members activate cytosolic kinase cascades and Smad transcription factors, including the common mediator, Smad4. Separately, we report that Smad4 inhibits osteoblast proliferation *in vivo*, in part via direct and competitive interference with canonical Wnt signaling. To further examine the role of Smad4 in bone formation, we generated *Smad4^{Flox/Flox}; Sp7-EGFP::Cre* mice (*Smad4^{Δ/Δ}*), where *Smad4* is ablated in Osx+ cells. Whole mount staining of *Smad4^{Δ/Δ}* neonates reveals hypomineralization of the skull, clavicle hypoplasia, and malformations of the rib cage. At day P28, *Smad4^{Δ/Δ}* mice are severely runted and μ CT indicates the cranial vault, scapulae, and sternal segment of the clavicles are still hypomineralized. Trabecular bone volume at the proximal tibia is normal relative to a smaller bone. However, *Smad4^{Δ/Δ}* mice exhibit delayed development of a medullary cavity in long bones. This correlates with diminished endocortical osteoclasts and a reduced ability of *Smad4^{Δ/Δ}* BMSCs to support osteoclastogenesis from bone marrow macrophages. *Smad4* ablation does not impede *Runx2*, *Col1 α 1*, *DMP1*, or *PheX* expression in bone, but sharply decreases expression of genes involved in collagen crosslinking including *Lox*, *Plod*, and *P4Ha*, which is consistent with abnormal Picrosirius Red staining. Importantly, *Smad4^{Δ/Δ}* mice fail to respond to the osteo-anabolic effect of anti-Dkk1 antibody, with sparse single calcein labels present on bone surfaces after 4 weeks of treatment as opposed to abundant wide double-labels in WT mice. Accordingly, *Smad4^{Δ/Δ}* BMSCs fail to mineralize in culture, and are not rescued by either BMP-2 or Wnt3a. Mechanistically, *Smad4* ablation disrupts p38 and Smad(1/5/8) phosphorylation in bone, instead enhancing Caspase-3 activity and the abundance of apoptotic TUNEL+ osteoblasts. Whereas BMP2-dependent expression of *Lox* is mediated by the p38 MAPK pathway, the resistance to anabolic Wnt signaling can be linked to loss of β -catenin transcriptional activity, a consequence of Caspase-3-mediated cleavage of the β -catenin C-terminal transcriptional activation domain. Thus, acute removal of *Smad4* directly favors canonical Wnt signaling and mitosis, while long-term deficiency of *Smad4* indirectly impairs Wnt signaling and osteoblast function. In summary, *Smad4* regulates osteoblast proliferation, survival, and function via coupling of canonical Smad with non-canonical MAPK pathways and via multifaceted regulation of canonical Wnt/ β -catenin signaling.

Disclosures: Valerie Salazar, None.

1257

Blockade of EphrinB2/EphB4 Interactions Disrupts Osteoblast and Osteoclast Differentiation *In Vivo*. Farzin Takyar^{*1}, Stephen Tonna¹, Patricia Ho¹, Blessin Criméen-Irwin¹, Holly Brennan¹, Valery Krasnoperov², T. John Martin¹, Natalie Sims³. ¹St. Vincent's Institute of Medical Research, Australia, ²Vasgene Therapeutics Inc., USA, ³St. Vincent's Institute for Medical Research, Australia

Parathyroid hormone (PTH) rapidly enhances ephrinB2 expression *in vivo* and in cultured osteoblasts, and blockade of the ephrinB2/EphB4 interaction inhibits osteoblast differentiation. Furthermore, osteoclast differentiation *in vitro* is inhibited by ephrinB2 reverse signaling.

We have used a specific antagonist of EphrinB2/EphB4 signaling to determine its role in the anabolic action of PTH. Soluble extracellular domain of the receptor EphB4 (sEphB4) blocked EphB4 (but not EphB2) tyrosine phosphorylation induced by clustered ephrinB2-Fc in primary calvarial osteoblasts. 8-week-old male C57Bl/6 mice were treated with sEphB4 (10mg/kg; 3/week), either alone or with PTH (30ug/kg/day; 5/week) for 4 weeks. Femora, vertebrae and tibiae were analyzed by micro-CT and histomorphometry.

No change in bone structure was observed in sEphB4 treated mice compared to controls but osteoblast number and surface were both increased by 50% (p=0.02 and

0.01 respectively) and osteoid volume and surface were increased by 45% ($p=0.04$ and $p=0.01$). Despite this increase in osteoblast number osteoid thickness, bone formation rate and mineral apposition rate were not changed by sEphB4 treatment vs. vehicle. This indicated that sEphB4 increased formation of osteoblasts that produce less osteoid and mineralized bone. This block in osteoblast differentiation is consistent with *in vitro* effects of ephrinB2/EphB4 blockade.

PTH treatment increased trabecular number (Tb.N) and thickness (Tb.Th), and dramatically increased all osteoblast and bone formation parameters without increasing osteoclast numbers. sEphB4 significantly impaired the effect of PTH on trabecular structure; tibial Tb.N and Tb.Th were reduced by 20 and 15%, respectively ($p=0.02$ and 0.03) in sEphB4/PTH treated mice compared to PTH alone. Similar results were observed in femora and vertebrae by microCT. sEphB4 augmented the effect of PTH on osteoblast numbers (a further 30% increase, $p<0.05$), but did not increase the PTH-elevated mineral apposition rate. This suggests that increased osteoblasts formed with sEphB4 treatment have impaired ability to mineralize bone. In addition, reduced trabecular bone volume in sEphB4/PTH mice was associated with a 50% increase in osteoclast number ($p=0.05$).

These results establish that signaling between ephrinB2 and EphB4 is required for both normal mineralization and normal osteoclastogenesis in bone remodeling and that its pharmacological blockade inhibits the anabolic action of PTH.

Disclosures: Farzin Takyar, None.

1258

Nck, Actin Cytoskeleton Protein, Supports Osteoblastic Bone Increment and Suppresses Osteoclastic Bone Loss. Smriti Aryal A.C.¹, Kentaro Miyai², Yoichi Ezura³, Tadayoshi Hayata⁴, Takuya Notomi⁵, Tetsuya Nakamoto², Tony pawson⁶, Masaki Noda². ¹Department of molecular pharmacology, Tokyo medical & dental university, Japan, ²Tokyo Medical & Dental University, Japan, ³Tokyo Medical & Dental University, Medical Research Institute, Japan, ⁴Medical Research Institute, Tokyo Medical & Dental University, Japan, ⁵GCOE, Tokyo Medical & Dental University, Japan, ⁶Mount Sinai hospital, Canada

Nck proteins are adaptor molecules and regulate actin organization. Mammals carry 2 Nck genes Nck1 and Nck2 (collectively termed Nck). However, the role of Nck and its mechanism of action in bone metabolism are not known. To define Nck actions in bone cells specifically in osteoblasts and osteoclasts, mice carrying floxed Nck2 allele (Nck2^{fl/fl}) in which exon I is flanked by the loxP sites and Nck1^{-/-} allele were crossed to transgenic mice expressing cre recombinase under the control of 2.3kb type I collagen promoter and also with cathepsin K promoter. Mice lacking cre expression were used as a control. Micro CT analysis of the distal femur of 10 weeks old osteoblast specific Nck-dKO (ob-Nck-dKO) showed significant reduction in trabecular bone volume (BV/TV) and trabecular number (Tb.N/BS) in comparison to the control. In contrast to the trabecular bone, the cortical bone mass was increased in the ob-Nck-dKO mice. Bodian staining of the cortical bone of ob-Nck-dKO showed reduced number of osteocytes per bone in comparison to the control. *In vitro* migration of ob-Nck-dKO derived primary osteoblasts was significantly reduced in comparison to the control. Furthermore, Nck1 over expressing stable MC3T3-E1 cells showed increased migration ability in transwell assay and motility in wound healing assay in comparison to the control. To examine the effects of Nck on bone formation in adult mice, bone marrow ablation experiments were conducted in ob-Nck-dKO (7 weeks old; $n=3$) this experiment showed reduction of BMD of newly formed bone in ob-Nck-dKO in comparison to the control. Moreover, micro CT analysis of the femur (8 weeks old; $n=3$) of osteoclast specific Nck-dKO (oc-Nck-dKO) mice showed significant reduction in BV/TV in comparison to the control. Taken together, our data shows that Nck supports osteoblastic bone increment and suppresses osteoclastic bone loss.

Disclosures: Smriti Aryal A.C. None.

This study received funding from: Global Center of Excellence (GCOE)

1259

High Cumulative Incidences of Poor Outcomes Following Osteoporotic Fractures in Elderly Women and Men: A Competing Risk Analysis. Dana Blümc*, Nguyen Nguyen, Tuan Nguyen, John Eisman, Jacqueline Center. Garvan Institute of Medical Research, Australia

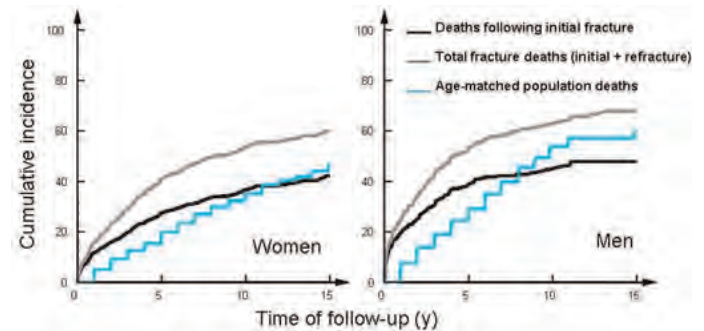
Increased risks of both subsequent fracture and mortality occur following an osteoporotic fracture in the elderly. However, the long term risks of these outcomes are less clear, partly due to their interdependency (ie risk of re-fracture depends upon survival). In this situation, Kaplan-Meier analysis can be unreliable. We thus examined cumulative incidences of re-fracture, mortality and sustaining both outcomes in men and women aged 60+ using competing risk analyses.

Subjects from the Dubbo Osteoporosis Epidemiology Study were followed from 1989-2007. Initial and subsequent fractures and mortality status were obtained. Competing risk models with 4 possible outcomes: death without re-fracture, death following re-fracture, re-fracture but alive, and event-free were considered.

There were 2245 women and 1760 men followed for 29,660 and 20,171 p-ys, respectively. 952 women and 342 men had an initial osteoporotic fracture, following which 23% of women and 21% of men re-fractured and 28% of women and 39% of

men died within the first 5 yrs. After 5yrs both mortality and re-fracture rates decreased significantly. The long term (>5-10yr) cumulative re-fracture incidence was reduced in both women and men by the competing risk of death, particularly in the older age groups with higher death rates. Following re-fracture 50% of women and 75% of men died within 5 yrs so total 5-yr mortality was 41% in women and 58% in men. By 10 years only 30% were alive and free of further fractures. The mortality following re-fracture occurred predominantly in the first 5 yrs post fracture, however, total mortality (post initial and re-fracture) was elevated above population mortality for ≥ 10 yrs following initial fracture with most of the 5-10yr excess mortality due to that following re-fracture. Re-fracture within 5 years was associated with a higher mortality than re-fracture after 5yrs [adjusted HR 2.44 (95%CI, 1.73-3.45)].

There is a high incidence of adverse outcomes following all osteoporotic fractures. Re-fracture and mortality were highest immediately post fracture, however, excess mortality was observed for up to 10yrs post fracture, primarily due to that following re-fracture. However, those who survived and were fracture-free 5-10 yrs post initial fracture had a very low risk of further adverse outcomes, suggesting a less aggressive approach may be appropriate for this population.



Cumulative incidence of adverse outcomes

Disclosures: Dana Blümc, None.

1260

Direct Medical Resources Utilization Associated with Osteoporosis-Related Fractures in Postmenopausal Women. Sonia Jean¹, Louis Bessette², Etienne Belzile³, Suzanne Morin⁴, K. Shawn Davison³, Louis-Georges Ste-Marie⁵, Bernard Candas³, Sylvie Dodin³, Jacques Brown³. ¹INSTITUT NATIONAL DE SANTE PUBLIQUE DU QUEBEC, Canada, ²Centre Hospitalier De L'Université Laval, Canada, ³Laval University, Canada, ⁴McGill University Health Centre, Canada, ⁵Hospital Saint-LucCHUM, Canada

Purpose: Although several osteoporotic fracture sites are an important and growing public health problem, research has primarily focused on hip fractures. The purpose of this study is to assess the direct medical resources utilization related to treatment of non-vertebral osteoporotic fractures within one year post-fracture.

Methods: Utilizing a previously developed and validated algorithm using physicians' claims databases, 15,327 women ≥ 50 years old with incident fractures at non vertebral osteoporotic sites were identified between January 1, 2004 and December 31, 2005 in three health regions of the province of Quebec, Canada. Fractures were grouped by sites as occurring at the hip/femur, pelvis, wrist, forearm/elbow, shoulder/humerus, tibia/fibula, or ankle/foot. Health administrative databases of the health services available to all residents in Quebec were used to establish fracture-related health resources utilization in the year following the fracture. Data were linked by a unique personal identifier, creating a longitudinal cohort of health resource utilization for all fracture cases. We assessed the proportion of fractures treated by an open reduction, closed reduction, cast or immobilization or conservative treatment (i.e. follow-up visit with an orthopaedic surgeon (OS) without casting or immobilization), the mean number of claims associated to a consultation with an OS or other clinicians, rate of hospitalization and length of stay (LOS).

Results: Table 1 and 2 provide the resources utilization related to fracture treatment, physician consultation and hospitalization. Hip/femur fractures represent the highest rate of resource utilization since the majority of these fractures require surgery (91%) and hospitalization (95%) with a mean LOS of 38.6 days. However, altogether other fracture sites require significant clinical care of surgery (27.8%), follow-up OS consultations (74.6%) and hospitalization (27.3% of total LOS). Even pelvic fractures that often not require surgical treatment, has a high rate of resource utilization due to the high rate of hospitalization (67%) with a mean LOS of 34.2 days.

Conclusions: Osteoporotic fractures account for substantial health care resource utilization. With an aging population and an increased prevalence of osteoporotic fracture, strategies for the management of osteoporotic condition need to be introduced to reduce the burden on health care resources.

Fracture site (N)	Proportion of fracture (%) ^a				Mean number of fracture related claims		
	Open Reduction	Closed Reduction	Immobilization	Principal Consultation with an OS	All claims ^b	Consultation with an OS ^c	Consultation with other clinicians ^d
Pelvis (291)	7.2	3.4	2.4	86.9	8.3	1.8	6.3
Hip/femur (4,536)	91.1	0.6	0.4	7.9	9.7	1.9	6.6
Shoulder/humerus (2,603)	16.9	9.6	24.8	48.7	5.5	2.4	2.5
Forearm/elbow (1,498)	13.0	28.8	25.9	32.2	4.4	2.2	1.4
Wrist (3,157)	7.9	58.0	18.0	16.2	5.2	2.4	1.5
Tibia/Fibula (638)	40.1	6.7	15.1	38.1	6.8	2.6	3.3
Foot (769)	2.6	9.0	25.1	63.3	3.4	1.7	1.3
Ankle (1,835)	32.9	7.2	19.2	40.7	5.7	2.6	2.4

^a Most important treatment is an open reduction of fracture, the second most important treatment is a closed reduction of fracture, the third most important treatment is an immobilization and finally the last most important treatment is a follow-up (principal visit or consultation) with an OS.

^b Open reduction, closed reduction, immobilization, principal visit, consultation or follow-up visit.

^c Principal visit, consultation or follow-up visit with OS.

^d Principal visit, consultation or follow-up visit with general practitioner and other specialist.

Table 1: Health resources use for treatment & medical consultation within 1 year post-fracture

Fracture site (N)	Number of fracture with at least one hospital stay related to the fracture		Total number of hospital stays related to the fracture	Length of stay (days) ^a	
	N	(%)	N	Mean (SD)	Median
Pelvis (291)	196	67.4	207	34.2 (30.0)	26
Hip/femur (4,536)	4,286	94.5	4,664	38.6 (35.8)	31
Shoulder/humerus (2,603)	799	30.7	894	22.4 (30.8)	8
Forearm/elbow (1,498)	281	18.8	305	12.4 (22.3)	3
Wrist (3,157)	1,050	33.3	1,122	7.5 (19.8)	1
Tibia/Fibula (638)	346	54.2	398	26.2 (32.8)	9
Foot (769)	63	8.2	77	15.8 (23.5)	4
Ankle (1,835)	766	41.7	855	16.4 (30.8)	3

^a A hospitalization stay includes an initial admission plus any admission within one day.

Table 2: Health resources use for hospitalization within 1 year post-fracture

Disclosures: *Sonia Jean, None.*

This study received funding from: Merck, Warner Chilcott, sanofi-aventis, Amgen, Eli Lilly, and Novartis

1261

Duration of Excess Mortality After Hip Fractures in Oslo, Norway: A Long Term Follow Up. Trine Elisabeth Finnes¹, Haakon E. Meyer², Tore Wentzell-Larsen³, Cathrine Marie Lofthus⁴. ¹Department of Internal Medicine, Innlandet Hospital Trust, Hamar, Norway, Norway, ²Department of Community Medicine, Faculty of Medicine, University of Oslo, Norway & Division of Epidemiology, Norwegian Institute of Public Health, Oslo, Norway, Norway, ³Biostatistics & Epidemiology Unit, Oslo University Hospital, Norway, ⁴Department Of Clinical Endocrinology, Oslo University Hospital, Aker, Norway, Norway

Aim The aims of the study were to estimate the duration of excess mortality following hip fractures, and to investigate if the duration has changed over the past decades in Oslo, Norway.

Methods Men and women with a hip fracture identified in previous published incidence studies from three different decades (1978/79, 1988/89, and 1996/97) in Oslo, were followed with respect to all causes of mortality until 31.12.2007. Age- and sex-specific mortality rates for the general population of Oslo from 1978-2007 were provided by Statistics Norway. Expected survival curves stratified for sex and predefined age groups were estimated for each of the three cohorts. Time framed Kaplan-Meier curves for 5 years intervals were compared with the corresponding expected survival curves. Were the observed curves started to parallel the expected curves, additional curves for five- and one year survival were made to judge when mortality in hip fracture patients became the same as in the background population. One sample log rank tests were used to test for differences between the observed and expected curves. Analyses were performed using SPSS 14.0 and R 2.10.1.

Results The results for the age-group 65-84.9 years, constituting around 2/3 of all hip fractures, are presented (Table 1). The excess mortality lasted for at least 10 years in all three cohorts. In the 1978/79- and 1988/89-cohort, men had a shorter duration of excess mortality than women. In the 1996/97-cohort, the mortality among male hip fracture patients was still higher than in the background population at end of follow up (10 years). The duration of excess mortality could therefore not be estimated in this group. In women, there was a trend towards a shorter duration of excess mortality from 1978/79 to 1996/97.

Conclusion Although a trend towards shorter duration of excess mortality during the decades was observed, the excess mortality after hip fracture still lasts for up to 10 years in both men and women aged 65-85. Further studies focusing on modifiable risk factors for death after hip fractures are warranted.

Table 1

Sex	Cohort	No.	Duration of excess mortality (years)
Men	78-79	281	15
	88-89	363	11
	96/97	170	*
Women	78-79	1041	22
	88-89	1243	14
	96/97	549	10

*Still excess mortality at end of follow up

Duration of excess mortality after hip fractures in men and women aged 65-84 years

Disclosures: *Trine Elisabeth Finnes, None.*

1262

Mortality and Fracture Rate before and after Introduction of a Fracture Liaison Service. Sandrine Bours¹, Tineke Van Geel², Piet Geusens³, Kirsten Huntjens², Geert-Jan Dinant⁴, Joop Van Den Bergh⁵. ¹Maastricht University Medical Centre, The Netherlands, ²Maastricht University, The Netherlands, ³University Hasselt, Belgium, ⁴Maastricht University, Netherlands, ⁵VieCuri MC Noord-Limburg & Maastricht UMC, USA

Purpose: To evaluate the effect of the Fracture Liaison Service (FLS) by comparing the mortality and incidence of non-vertebral fractures before and after introduction of the FLS during 2 year follow up.

Methods: In total, 1908 patients who sustained a fracture before (pre) initiation of the FLS and 666 patients after (post) initiation of the FLS were included in this study. All patients visited the emergency room of VieCuri Medical Centre, The Netherlands. Of these patients, age, fracture location(s) and date of fracture(s), whether they were deceased and date of death was known. Of the post-FLS group, patients completed a detailed questionnaire on clinical risk factors for fractures, medical history, medication, previous fractures, calcium intake and were evaluated by DXA and blood tests. Patients with osteoporosis and / or metabolic bone disease were treated. Cox proportional hazard regression models were used with pre vs. post FLS as covariate, with as dependent variables subsequent fracture or mortality. Time was calculated as initial fracture to event or end of study (24 months).

Results: Of the 1908 pre-FLS patients (mean age: 68 years, standard deviation (SD): 11.0, 70% were women) 134 (7.2%, 3.9 per 100 person-years) sustained a subsequent fracture and 237 (12.4%, 6.7 per 100 person-years) died. Of the post-FLS patients, 471 did (mean age: 66 years, SD: 10) and 195 did not (mean age: 73 years, SD: 12) show up at the FLS. In total, 498 of the post-FLS patients (75%) were women. Of the post-FLS patients, 51 (7.7%, 4.2 per 100 person-years) sustained a subsequent fracture and 52 (7.8%, 4.1 per 100 person-years) died.

After adjusting for gender, age at first fracture and fracture location, there was no significant difference between the pre- and post-FLS patients with regard to subsequent fracture risk (HR: 1.0, 95% confidence interval: 0.7-1.3). After the same adjustment, mortality was significantly lower in the post- versus pre-FLS patients (HR: 0.61, CI: 0.45-0.83).

Conclusion: After initiation of the FLS, the mortality rate decreased by nearly 40%, but fracture incidence remained unchanged. Further studies are needed to analyze which factors are predictors for the reduction in the post-FLS mortality.

Disclosures: Sandrine Bours, None.

1263

Falling Rates of Fractures in the United States from 1992-1997 to 2002-2007.

Steven Cummings^{*1}, Li-Yung Lui², Jane Cauley³, Teresa Hillier⁴, Marc Hochberg⁵. ¹San Francisco Coordinating Center, USA, ²California Pacific Medical Center Research Institute, USA, ³University of Pittsburgh Graduate School of Public Health, USA, ⁴Kaiser Center for Health Research, USA, ⁵University of Maryland School of Medicine, USA

Background: According to Medicare data, the rate of hip fracture in older women declined 24.5% from 1995-2005 (Brauer, JAMA 2009;302:1573). It is not known if the rates of other fractures have also decreased. If so, could the changes be explained by improvements in BMD or other risk factors for fracture?

Methods: The Study of Osteoporotic Fractures recruited 9,704 Caucasian women from community-based listings in 4 US urban areas in 1986-8 and measured hip BMD every 2 – 4 years using the same DXA scanners. Follow-up for x-ray confirmed fractures >90% complete during >20 years follow-up; a small proportion of fractures might not be self-reported. We analyzed cohorts of women in 5-year intervals. Specifically, compared the rates of fractures and mean femoral neck BMD values in women who were age 80-84, and 85+ in 1992 to women who were 80-84 or 85+ in 2002. Fracture rates were assessed from 1992 to 1997 and 2002 to 2007. We also compared the prevalence of vertebral fractures using identical morphometric methods on lateral spine x-rays taken between 1990-92 and 2002-4. We predicted change in fracture rate from change in BMD and association between FN BMD and type of fracture. Falls were assessed every 4 months and medications every 2-4 years.

Results: Rates of self-reported hip fracture in the 80-84 and 85+ year-old women declined approximately 23.3 and 18.6% between 1992-7 and 2002-7 (table), similar to the decline in US Medicare data. We observed similar decreases in all other types of fractures. Mean FN BMD also improved by 0.28 to 0.42 standard deviations during that period, which could explain most of the decline in hip fracture but less for other types (table). Increased use of treatments that reduce fracture risk (e.g. 15% increased use of bisphosphonates in 80-84 year olds) could not explain the decreases, and rates of falling increased over that interval (e.g. 14.5% to 21.2% for 2+ falls/year in 80-84 year olds).

Conclusion: From this community-based cohort, the rates of all types of fractures decreased substantially from 1992-7 to 2002-7, at least partly due to improvements in BMD, not explained by increased use of drug therapy.

Fracture rates (per 1,000 woman-years) and percent changes

Type	1992-1997	2002-2007	% Decrease	Predicted by change in BMD	95% CI
Age 80 to 84 years old					
Hip	15.4	11.8	23.3	17.3	10.3, 23.7
Wrist	9.9	6.9	30.2	12.3	-4.0, 19.9
Humerus	6.8	4.4	33.5	9.4	-0.4, 18.2
Nonvertebral	45.8	39.7	15.6	9.6	5.9, 13.2
Vertebral*	32.5%	24.4%	25.0	12.5	7.9, 16.9
Age 85+ years old					
Hip	31.8	25.9	18.6	22.5	13.8, 30.3
Wrist	11.3	8.1	28.4	12.3	-6.2, 27.6
Humerus	8.2	6.0	27.7	18.8	-2.0, 35.4
Nonvertebral	71.0	53.4	24.8	16.9	10.7, 22.7
Vertebral*	42.0%	34.0%	19.1	15.0	8.7, 22.5

* Percent of women with a vertebral fracture on a radiograph taken during that interval

Falling rates of fracture

Disclosures: Steven Cummings, None.

1264

Secular Trends in Incidence of Osteoporosis-related Fractures Differ Depending on Fracture Type. Bjorn Rosengren^{*1}, Ingemar Peterson², Magnus Karlsson¹, Martin Englund². ¹Skane University Hospital Malmö, Lund University, Sweden, ²Musculoskeletal Sciences, Department of Orthopedics, Clinical Sciences Lund, Lund University, Lund, Sweden, Sweden

Purpose: During the recent decade the incidence of hip fracture has been reported to decrease in most parts of the world. However, if a similar decrease has occurred for other types of osteoporosis-related fractures is unknown.

Methods: Through the Skane Health Care Register, a diagnosis-based register covering all in- and outpatient health care data of residents in the County of Skane, Sweden (1.2 million inhabitants), we registered typical osteoporosis-related fractures of the hip (n=26 952), os pubis (n=4 215), proximal humerus (n=12 445), wrist (n=23 068), proximal tibia (n=3 336) and ankle (n=9 459) sustained by individuals aged 50 years or older from year 1998 until 2009 (5.1 million person-years). We calculated gender-specific age-standardized incidence for each fracture type using one-year age- and sex-specific population figures from the population register, where the average population of the examined years was used as the standard population. Trends of incidence were evaluated by linear regression, and we present data as means with their 95% confidence interval (95% CI) with two-tailed α -level set to 0.05.

Results: During the evaluated years, the age-standardized hip fracture incidence decreased significantly in both women (-12 per 100 000 and year [95% CI -15, -9]) and men (-3 per 100 000 [95% CI -5, -1]). In contrast, during the same period the annual incidence of proximal humeral fractures increased significantly in women (4 per 100 000 [95% CI 0, 7]) and non-significantly in men (1 per 100 000 [95% CI -0, 3]). Furthermore, the incidence of pubic fractures increased significantly in men (1 per 100 000 [95% CI 0, 2]) but not in women (0 per 100 000 [95% CI -2, 1]). The incidence of ankle fractures was stable in both men and women as was the annual incidence of wrist fractures and proximal tibial fractures (data not shown).

Conclusion: In this study covering the recent decade, the different types of examined osteoporosis-related fractures showed different secular trends in incidence. Hence, the decrease in hip fracture incidence evident in this and other studies can not be extrapolated to all types of osteoporosis-related fractures when estimating the future total burden of fragility fractures in society.

Disclosures: Bjorn Rosengren, None.

FR0002

Deletion of the Redox Amplifier p66^{shc} Decreases ROS Production in Murine Bone and Increases Osteoblast Resistance to Oxidative Stress and Bone Mass. Shoshana M. Bartell*, Li Han, Srividhya Iyer, Aaron Warren, Robert W. Bradsher, Randal S. Shelton, Maria Jose S. Almeida, Stavros C. Manolagas. Center for Osteoporosis & Metabolic Bone Diseases, Central Arkansas Veterans Healthcare System, University of Arkansas for Medical Sciences, USA

P66Shc is a 66-Kd isoform of the growth factor adapter Shc with a pivotal role in oxidative stress, apoptosis, and aging, as demonstrated by evidence that deletion of p66Shc enhances resistance to oxidative stress and apoptosis, decreases mitochondrial metabolism, prolongs lifespan in mice by as much as 30%, and protects from a variety of age-associated diseases including atherosclerosis. p66Shc amplifies ROS production within mitochondria by catalyzing the reduction of O₂ to H₂O₂ through electron transfer from cytochrome c; H₂O₂ in turn causes opening of the permeability transition pore, swelling, and apoptosis. Increased ROS production and osteoblast/osteocyte apoptosis caused by aging or sex steroid deficiency in the murine skeleton is linked with an increase in the phosphorylation of p66Shc. Conversely, p66Shc phosphorylation and apoptosis decrease with antioxidant administration, estrogen, or androgen replacement. We have sought mechanistic evidence causally linking p66Shc to the adverse effects of oxidative stress and sex steroid deficiency on bone mass. For this purpose we used a p66shc knockout mouse (a model provided to us by Dr. T. Prolla, Univ. Wisconsin). We report that these mice were born at the expected Mendelian ratios and had normal body weight. The deletion of p66shc caused a decrease in ROS and an increase in the level of glutathione in the bone marrow. Moreover, calvaria-derived osteoblasts from these mice were resistant to H₂O₂-induced apoptosis as determined by caspase 3 activity. P66shc knockout mice also exhibited an increase in mesenchymal progenitor cells, as determined by the number of colony forming osteoblast progenitors (CFU-OB) present in bone marrow. Moreover, osteoblast mineralization was increased in primary cultures of bone marrow derived progenitors in the presence of ascorbic acid, as determined by alizarin red staining. In line with these findings, at six month of age, both female and male p66shc knockout mice exhibited increased bone mineral density at the spine and femur as determined by DEXA. These results strongly suggest that p66shc is an essential mediator of the deleterious effects of oxidative stress on apoptosis, osteoblastogenesis, and bone mass; hence, causally linked to the adverse effects of both aging and sex steroid deficiency on the skeleton.

Disclosures: Shoshana M. Bartell, None.

FR0003

Insulin Signaling in Bone Favors Male Fertility. Franck OURY*, Tatsuya YOSHIZAWA, Mathieu Ferron, Patricia Ducy, Gerard Karsenty. Columbia University, USA

Insulin is known to affect, through its signaling in a wide variety of cell types, many physiological functions. For instance, insulin signaling in osteoblasts was recently shown to affect physiological functions as diverse as bone remodeling and glucose metabolism. Since, it has also been shown previously that insulin signaling is needed for male and female fertility, we asked whether insulin favors male fertility by acting, at least in part, in osteoblasts. Consistent with this hypothesis we observed that at 3 months of age male mice lacking the insulin receptor selectively in osteoblasts (*InsR^{Ob}*^{fl/fl} mice) displayed smaller testicular and seminal vesicle size and weight, decreased sperm count and circulating testosterone levels. As a result there was a decrease in litter size and frequency when *InsR^{Ob}*^{fl/fl} male mice were crossed with WT females. Next, we asked whether this function of insulin signaling in osteoblasts occurs through its activation of osteocalcin. To test this hypothesis, we generated compound mutant male mice lacking one allele of osteocalcin and one allele of the insulin receptor selectively in osteoblasts (*Osteocalcin^{Ob}*^{fl/+}; *InsR^{Ob}*^{fl/+} male mice). These latter mutant mice demonstrated lower testicular and seminal vesicle weights, decreased sperm count and circulating testosterone levels and decreased fertility. That this reproduction phenotype is similar to the one of the *Osteocalcin*^{-/-} mice supports the notion that insulin signaling in osteoblasts favors male fertility through its documented activation of osteocalcin. To add further credence to this hypothesis we generated and analyzed mice lacking one allele of the insulin receptor in osteoblasts and one allele of Gprc6a, the receptor for osteocalcin in Leydig cells. The phenotypic analysis of these mice will be presenting at the meeting. Taken together these observations establish that insulin signaling in osteoblasts regulate male fertility. As such they highlight the growing importance of the skeleton as an integrator of multiple endocrine signals and as a global regulator of a growing number of physiological processes.

Disclosures: Franck OURY, None.

FR0004

Nicotinamide Phosphoribosyltransferase (Namt) Affects the Lineage Fate Determination of Mesenchymal Stem Cells: A Possible Cause for Reduced Osteogenesis and Increased Adipogenesis In Senile Osteoporosis. Yan Li*¹, Xu He², Urban Lindgren¹. ¹Karolinska Institute, Sweden, ²a Karolinska Institute; b Jilin University, Sweden

The accelerated marrow adipogenesis in aging might reflect an unbalanced mesenchymal stem cell (MSC) differentiation scheme. However, how aging makes the preferential shift from osteogenesis to adipogenesis is largely unknown. Sirt1 has been shown to regulate lifespan in lower organisms and affect age-related diseases in mammals. We previously showed that Sirt1 activity affected the lineage fate determination between osteogenesis and adipogenesis of MSCs (Backesjo CM, Li Y, et al, 2006, J Bone Miner Res 21: 993-1002). Since Sirt1 activity is largely dependent on the availability of NAD⁺ and influenced by the intracellular concentration of nicotinamide we supposed that MSC differentiation could be affected by enzymes involved in the NAD⁺ salvaging pathway.

The present study showed that the bone marrow stromal cells derived from 15-month-old C57BL/6 mice developed fewer bone nodules (as shown by von Kossa and alizarin red staining) and more adipocytes (as shown by oil red O staining) than cells derived from 4-week-old mice (Fig. 1 A). The cells derived from aged mice had significantly lower intracellular NAD⁺ concentration (Fig. 1 B) and lower Sirt1 activity (Fig. 1 C). However, the expression of Sirt1 protein was not reduced by aging (Fig. 1 D). We also found that the potent and specific Nampt inhibitor, FK866 (Sigma) significantly increased the adipocyte formation in mesenchymal stem cell line C3H10 cells (Fig. 2 A). In addition, adipocyte formation was significantly increased in cells transfected by Nampt shRNA Lentiviral transduction particles (Sigma) (Fig. 2 B). Q-PCR analysis showed that the expression of the adipocyte specific transcription factor PPAR γ was significantly higher in Nampt deficient cells while the osteoblast key transcription factor Runx2, as well as the osteoblast marker genes, osteocalcin and OPG, were significantly downregulated (Fig. 3 A). A significant reduction of Sirt1 activity was found in Nampt deficient cells (Fig. 3 B), which had significantly lower NAD⁺ and higher intracellular concentration of NAM (Fig. 3 C).

In conclusion, the present study showed that the lineage fate determination of MSCs could be affected by the activity of Nampt, the enzyme catalyzing NAD⁺ resynthesis from nicotinamide, possible through affecting Sirt1 function. Therefore, senile osteoporosis might occur with a deregulation of cell energy metabolism in mesenchymal stem cells.

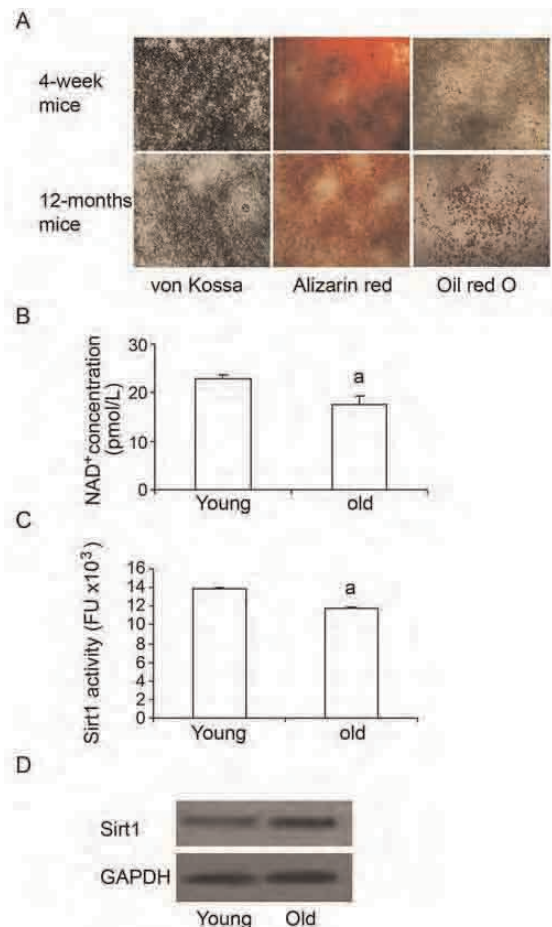


Fig. 1

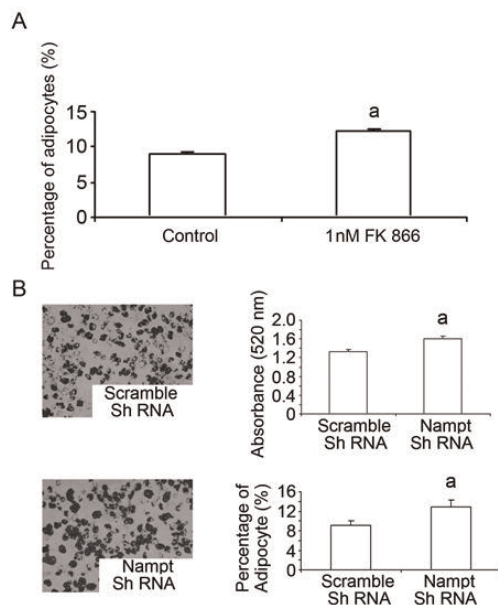


Fig. 2

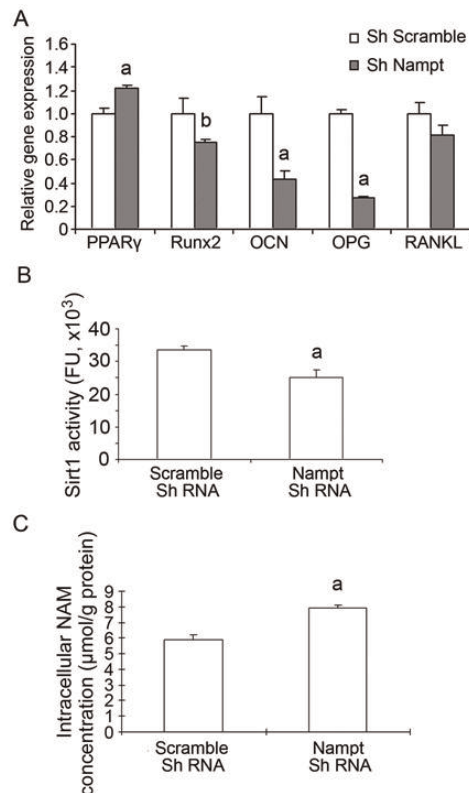


Fig. 3

Disclosures: Yan Li, None.

FR0005

The $\hat{\text{O}}$ -catenin Activating Factor, Wnt3a, stimulates Skeletal Muscle Myogenesis. Sandra Romero-Suarez^{*1}, ChengLin Mo², Nuria Lara³, Katharina Jaehn³, Mark Johnson⁴, Lynda Bonewald³, Marco Brotto³. ¹Muscle Biology Group-MUBIG, School of Nursing, University of Missouri-Kansas City, USA, ²Muscle Biology Group-MUBIG, School of Nursing & Pharmacy, University of Missouri-Kansas City, USA, ³University of Missouri - Kansas City, USA, ⁴University of Missouri, Kansas City Dental School, USA

We hypothesized that muscle and bone communicate at a molecular level via biochemical factors that are reciprocally important for optimal function. We recently showed that conditioned media from MLO-Y4 osteocytes accelerates the differentiation of C2C12 myotubes.

Wnt signaling is critical for bone function and is also thought to be important for muscle development and maturation, but less is known about its roles in mature skeletal muscles.

The expression of Wnts, particularly Wnt3a, is dramatically increased in MLO-Y4 osteocytes exposed to fluid flow shear stress.

To test the putative role of Wnt3a in skeletal muscle myogenesis, we treated C2C12 myoblasts with 10ng Wnt3a and found that it significantly enhanced myogenesis (>13 myotubes per random field of view in Wnt3a; vs. 3-5 myotubes in Control, $n=3$, $p < 0.01$). Furthermore, myotubes formed in the presence of Wnt3a were larger (4,319 $642 \mu\text{m}^2$ untreated, $n=22$; vs. 9,833 $1013 \mu\text{m}^2$ for Wnt3a treated myotubes, $n=19$, $p < 0.001$), suggesting that hypertrophic signaling was activated under these conditions. Intriguingly, Fura-2 calcium transients induced by caffeine were characterized by multiple and oscillatory peaks in Wnt3a treated myotubes, but not in control myotubes. A custom-developed qPCR array approach revealed that Wnt3a promoted the overexpression by at least 2-fold of myogenic related factors (MyoD, myogenin) as well as specific genes related to intracellular calcium signaling and calcium homeostasis that help explain the functional changes observed in C2C12 myotubes treated with Wnt3a.

Our studies provide new evidence that Wnt3a is a potent modulator of the function of C2C12 myotubes and identify it as a candidate factor that may mediate crosstalk between bone and muscle cells.

Detailed understanding of the molecular pathways that mediate crosstalk between bone cells and muscle cells could lead to new therapeutic targets to treat musculoskeletal diseases and reduce morbidity and mortality associated with these conditions.

Disclosures: Sandra Romero-Suarez, None.

FR0009

Genetic Variation in DHCR7/NADSYN1 (rs12785878) Predicts Skeletal Muscle Response to Resistance Training and Vitamin D Levels in Men. Sreya Talasila¹, Jordan Ruby¹, F Orkunoglu-Suer², H Gordish-Dressman², K Panchapakesan², BT Harmon², Eric Hoffman², Joe Devaney², Laura Tosi^{*2}. ¹George Washington University School of Medicine, USA, ²Children's National Medical Center, USA

Objective: The contribution of Vitamin D to the development of skeletal muscle strength has not been fully elucidated. Our goal was to determine whether genome wide association study-identified single nucleotide polymorphisms (SNPs) associated with circulating Vitamin D levels are also associated with skeletal muscle size, strength, and response to resistance training.

Methods: 753 college-aged subjects (449 female, 304 male) underwent 12 weeks of supervised resistance training of their non-dominant arm using five specific exercises. Pre- and post-training strength measurements included (one repetition max [1RM] and maximal voluntary contraction [MVC]). Upper arm skeletal muscle volume of the trained arm was measured via MRI before and after the 12-week program. The study participants were genotyped for four genetic variants (rs2282679, rs2060793, rs12785878, and rs3829251) recently demonstrated to be associated with circulating levels of Vitamin D in persons of European ancestry. Mean phenotypes were compared among genotypes using ANCOVA with age and baseline weight as covariates. For co-dominant associations showing a significant F-test, pair-wise post-hoc comparisons were performed and resulting p-values adjusted for multiple comparisons using the Sidak method.

Results: Males with two copies of the common allele (T allele) for rs12785878 demonstrated a significantly larger increase in skeletal muscle volume ($p=0.035$) with resistance training and a greater percent change in MVC ($p=0.026$). No associations with any of our measured phenotypes were demonstrated with the other three SNPs.

Conclusion: The role of genetic versus environmental influences on vitamin D status and subsequent health outcomes remains unclear. In this study, the presence of two copies of the common, T allele, at the rs12785878 SNP was associated with a greater increase in skeletal muscle size and strength following exercise training. Genetic variation in the rs12785878 SNP (DHCR7/NADSYN1) has recently been demonstrated to be correlated with vitamin D insufficiency. This SNP is located in the promoter of the DHCR7 gene that encodes the enzyme 7-dehydrocholesterol (7-DHC) reductase. This enzyme converts 7-DHC to cholesterol, thereby removing the substrate from the synthetic pathway of Vitamin D3, a precursor of 25-

hydroxyvitamin D3. The effect of this enzyme on Vitamin D levels and measures of health status requires further investigation.

Disclosures: Laura Tosi, None.

FR0010

High Serum Adiponectin Is Associated with Frailty and Predicts Mortality in Elderly Men. Mr OS Sweden. Dan Mellstrom¹, Helena Johansson², Carl-Johan Behre³, Hans Jutberger², John Kanis⁴, Anders Oden², Asa Tivesten³, Ulf Lerner², Magnus Karlsson⁵, Osten Ljunggren⁶, Claes Ohlsson⁷, Mattias Lorentzon⁷. ¹Sahlgrenska University Hospital, Sweden, ²Centre for Bone & Arthritis Research (CBAR), Sahlgrenska Academy University of Gothenburg Sweden, Sweden, ³Wallenberg Laboratory for Cardiovascular Research, Institute of Medicine, University of Gothenburg, Sweden, ⁴University of Sheffield, Belgium, ⁵Clinical & Molecular Osteoporosis Research Unit, Department of Clinical Sciences, Lund University & Department of Orthopaedics, Malmö University Hospital, Malmö, Sweden, Sweden, ⁶Department of Medical Sciences, University of Uppsala, Uppsala, Sweden, Sweden, ⁷Center for Bone Research At the Sahlgrenska Academy, Sweden

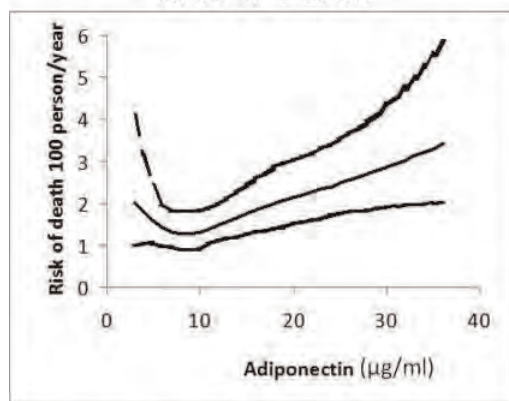
High serum concentrations of the adipokine, adiponectin, have been associated with low bone mineral density and increased risk for incident fractures in elderly men. This study examines whether serum adiponectin is related to other risk factors for frailty and mortality.

Elderly men (69-80 years) participated in the population based Mr OS Sweden, Gothenburg cohort (n=1010). All plasma and serum samples were collected at 8 am after at least 10 hours fasting and non-smoking. Serum adiponectin was analysed with an ELISA-kit (Linco Research, Missouri USA). Body composition and bone mineral density were measured with DXA (Hologic QDR 4500/A Delphi). History of falls during the last year was assessed using a questionnaire.

Serum adiponectin increased with age ($r=0.14$ $p<0.001$) and was inversely associated with BMI ($r=-0.24$ $p<0.001$) and total lean mass ($r=-0.16$ $p<0.001$). Men in the highest tertile of serum adiponectin tested against tertile 1 and 2 had an age adjusted increased risk of falls (OR=1.6; 95% CI=1.1-2.2). Poorer hand grip strength (OR=1.3; 95% CI=1.1-1.5 per SD decrease in grip strength), less total lean mass (OR=1.4; 95% CI=1.2-1.6 per SD decrease in lean mass) and longer time for rising 5 times (OR=1.2; 95% CI=1.0-1.3) was associated with increased risk of belonging to the highest tertile of adiponectin. Men in the highest tertile of adiponectin reported more often a decrease in BMI from the age of 25 years (OR=2.4; 95% CI=1.6-3.6). A linear age adjusted regression model showed that walking speed was inversely related to serum adiponectin ($p=0.015$). High serum adiponectin predicted mortality in a multivariate model (GR per SD increase=1.20; 95% CI 1.06-1.37; $p<0.01$). A large number of variables were tested as covariates including age, BMI, BMD and diabetes. A spline curve was estimated from a Poisson regression model describing the relation between serum adiponectin and risk of death (Figure).

High serum adiponectin was associated with increased risk of falls, muscle weakness, less lean mass and a decrease in BMI since the age of 25 years. High serum adiponectin predicted mortality in a multivariate model. Our data suggest that serum adiponectin is a proxy for falls, frailty and increased mortality beyond the increased risk for low bone mineral density and fractures.

SERUM ADIPONECTIN AND THE RISK OF DEATH



Variables in the model: age, time since baseline, BMD.

Figure

Disclosures: Dan Mellstrom, None.

FR0011

Lean Mass and the Longitudinal Probability of Mobility Disability in the Framingham Study: A Multinomial Approach for Studies of Aging. Robert McLean¹, Elizabeth Newton², Alyssa Dufour², Joanne Murabito³, Marian Hannan⁴, Douglas Kiel². ¹Hebrew SeniorLife, Harvard Medical School, USA, ²Hebrew SeniorLife, USA, ³Framingham Heart Study & Boston University, USA, ⁴HSL Institute for Aging Research & Harvard Medical School, USA

Sarcopenia (age-related loss of muscle mass and strength) is common in older adults and associated with mobility disability. While longitudinal studies with repeated measures over time have examined whether baseline sarcopenia predicts mobility disability, results may represent only the healthiest elders as analyses did not account for 2 sources of missing data common to studies of aging: 1) unobserved outcomes due to missed visits, 2) high death rates. Further, prior studies have examined time to incident disability, which does not account for individuals who recover. Our objective was to determine the association of baseline lean mass with mobility disability over time in an elderly cohort using a multinomial approach to include all possible outcomes. Participants included 243 men and 440 women from the Framingham Study Original Cohort. Lean mass (appendicular lean mass divided by height²) was measured via whole body DXA (Lunar DPX-L) at visit 1 (1992-93). At each of visits 1-7 (2 yrs apart) participants experienced 1 of 4 states of a multinomial outcome (STATUS): not disabled, disabled, dead or missing. Mobility disability was defined as self-reported inability to walk 0.5 mi, walk up and down stairs, or perform heavy work around the house. Separately by sex, we used generalized logit models to predict the probability of being in 1 of the 4 STATUS states at any time over follow-up. The model gave regression coefficients for the odds of being disabled, dead or missing, relative to not disabled, as a function of baseline lean mass, age (yrs), BMI (kg/m²) and visit. A random effect for subject accounted for within-subject correlation. At visit 1 mean age was 78.2 yrs (range 72-92), and 16% of men and 29% of women were disabled. Over 12 yrs of follow-up 58% of participants died and the percent of missing outcomes at visits 2-7 ranged from 10 to 14 (Figure 1). 20% of men and 25% of women experienced disability recovery. In men, higher lean mass was associated with lower odds of being disabled or dead vs. not disabled (Table 1). In women, higher lean mass was associated with lower odds of being disabled vs. not disabled, but not with being dead. Lean mass was not associated with the status missing. Our results suggest greater lean mass is protective against mobility disability over time in elders. Previous studies that did not account for the multiple states possible during follow-up of an elderly cohort are likely biased by including only healthy survivors.

Table 1. Regression coefficients ($\beta \pm SE$) from the general logit model* for the longitudinal association of ALM/ht² with the multinomial outcome STATUS (healthy, disabled, dead, missing) among elderly men and women of the Framingham Study.

STATUS category	Men		Women	
	$\beta \pm SE$	P-value	$\beta \pm SE$	P-value
Healthy (Ref)	-	-	-	-
Disabled	-0.486 \pm 0.143	<0.001	-0.259 \pm 0.129	<0.05
Dead	-0.307 \pm 0.141	<0.03	0.035 \pm 0.140	0.80
Missing	-0.297 \pm 0.173	0.09	-0.190 \pm 0.158	0.23

*Model includes lean mass, age, BMI, visit

$$\text{STATUS} \begin{cases} \text{No disability (ref)} \\ \text{Disabled} \\ \text{Dead} \\ \text{Missing} \end{cases} = \text{lean mass} + \text{age} + \text{BMI} + \text{visit}$$

table 1

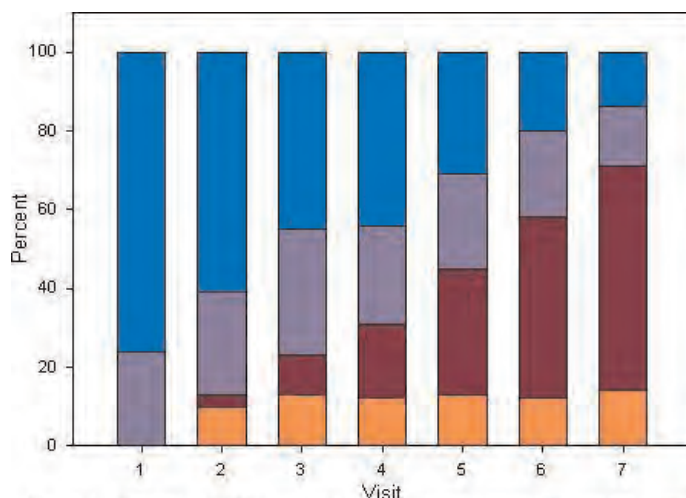


Figure 1. Percent of 683 Framingham participants seen at baseline, with STATUS at each biennial visit classified as not disabled (blue), disabled (purple), or missing (orange).

figure 1

Disclosures: Robert McLean, None.

FR0013

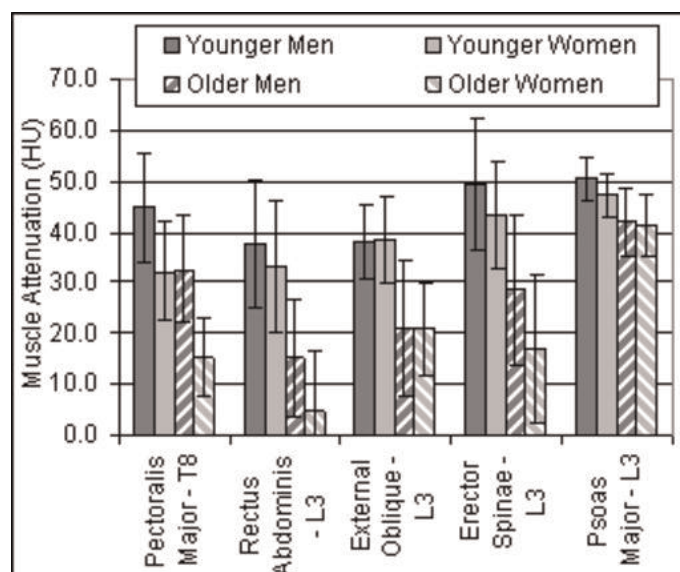
Trunk Muscle Fat Infiltration is Greater in Women than Men and Increases with Age. Dennis Anderson^{*1}, John D'Agostino¹, Alexander Bruno², Douglas Kiel³, Mary Bouxsein¹. ¹Beth Israel Deaconess Medical Center, USA, ²Stony Brook University, USA, ³Hebrew SeniorLife, USA

Age-related sarcopenia is a significant contributor to frailty and loss of function in older adults. Increased fat infiltration into muscle, as indicated by reduced x-ray attenuation of muscles in quantitative computed tomography (QCT) scans, is a marker of muscle quality and may contribute to reduced muscle function. Reduced muscle attenuation in the thigh has been associated with reduced knee extensor strength independent of muscle size and increased risk of hip fracture independent of BMD. However, sex- and age-related differences in muscle attenuation have not been examined in trunk muscles.

We randomly selected younger and older men and women (n = 25/group) from participants in the Framingham Heart Study Offspring and Third Generation Multidetector CT Study, in whom QCT scans of the trunk had been obtained. Ages of the younger and older subjects were 41.8 ± 4.1 and 78.3 ± 3.2 years, respectively. Muscle attenuation was determined for 11 muscle groups at the T8 and L3 vertebral levels. We performed a multiple regression analysis to examine age and sex differences in muscle attenuation, with and without adjustment for the self-reported physical activity index (PAI) score.

Muscle attenuation averaged 34.915.0 Hounsfield Units (HU) across all muscles, ages and sexes, and was on average 37% (15.9 HU) lower in older vs. younger adults ($p < 0.001$), and 20% (7.7 HU) lower in women than men ($p < 0.02$). Age effects were significant for all muscles, and sex effects for all muscles, except psoas major ($p = 0.05$) and external oblique ($p = 0.98$). Attenuation values as well as age and sex effects varied between muscles (Figure). Increased PAI was significantly associated with increased attenuation in pectoralis major, latissimus dorsi, and erector spinae ($p < 0.05$), but did not attenuate age and sex associations.

In summary, we found reduced muscle attenuation in women and older adults. This indicates that fat infiltration of all trunk muscles increases with age in both women and men, although intramuscular fat tends to be higher in women than men throughout adult life. In addition, while increased activity level may reduce fat infiltration of trunk muscles, it does not alter the age-related increase in intramuscular fat. Future studies should determine if increased fat infiltration of muscle contributes to reduced strength of trunk musculature in older adults, and examine effects on postural stability, spinal loading, and risk of vertebral fractures.



Mean (SD) attenuation for 5 muscles, illustrating variations with age, sex and between muscles.

Disclosures: Dennis Anderson, None.

FR0020

A Childhood Fracture is a Risk Factor for Both Low BMD at Growth and Low Peak Bone Mass - a Mean 28 Years Prospective Controlled Study. Magnus Karlsson¹, Christian Buttazzoni^{*2}, Lennart Landin³, Jan-Ake Nilsson³, Bjorn Rosengren¹, Magnus Tveit⁴. ¹Skane University Hospital Malmö, Lund University, Sweden, ²Department of Clinical Sciences & Orthopaedics, Lund University, Sweden, ³Department of Clinical Sciences & Orthopaedics, Lund University, Sweden, ⁴Clinical & Molecular Osteoporosis Research Unit, Sweden

Purpose: A fracture in childhood is associated with low bone mineral density (BMD). However, it is uncertain if low BMD "tracks" into adulthood with associated higher fracture risk. We therefore designed this prospective controlled study to answer if low BMD "tracks" during growth and if a fracture in childhood is a risk factor for low peak bone mass and higher fracture risk.

Methods: Distal forearm bone mineral density (BMD, g/cm²) was measured with single photon absorptiometry (SPA) in 48 boys and 26 girls with mean age 9.8 years (range 4-16), who recently had sustained a fracture, and in 41 boys and 43 girls with mean age 10.2 years (range 4-16) with no fracture. Incident fractures were then prospectively registered until peak bone mass was measured with the same SPA apparatus mean 28 years (range 26-29) later. At follow-up, BMD was also measured by dual energy absorptiometry (DXA, g/cm²) and by quantitative ultrasound (QUS, speed of sound (SOS)). BMD Z-scores at childhood and adulthood were calculated for each individual with a fracture based on our control population at childhood and adulthood, respectively. Data are presented as Z-scores with 95% confidence intervals (95% CI).

Results: There was a correlation between BMD at childhood and adulthood ($r = 0.54$, $p < 0.001$). Children with fracture had at the fracture event a mean distal forearm BMD Z-score of -0.32 (95% CI -0.54, -0.10) and at follow-up of -0.37 (95% CI -0.62, -0.12). Thus, the relative BMD deficit remained at peak bone mass since there was no changes in BMD Z score during the follow-up period (mean delta value 0.05 (95% CI -0.23, 0.33)). The BMD deficit was similar when estimated by DXA and QUS, with mean values for Z-score total hip -0.76 (95% CI -1.03, -0.49), lumbar spine -0.55 (95% CI -0.79, -0.31) and calcaneal SOS -0.44 (95% CI -0.73, -0.16). The mean BMD deficit in individuals with an index fracture was larger in boys than in girls and in those with a low than a moderate or high energy fracture. During the follow-up period, 21/73 (29%) of the children with an index fracture, and 18/84 (21%) of the children with no index fracture, sustained additional fractures.

Conclusions: BMD in childhood seems to "track" into adulthood and a childhood fracture is a risk factor for both low BMD at growth and low peak bone mass, in this study accompanied by a 38% higher fracture risk than expected.

Disclosures: Christian Buttazzoni, None.

FR0023

Feeding Blueberry Diets during Early Development Is Sufficient to Prevent Senescence of Osteoblasts and Bone Loss in Adulthood. Jin-Ran Chen^{*1}, Jian Zhang², Oxana P. Lazarenko², Michael L. Blackburn², Kartik Shankar², Thomas M. Badger², Martin J. Ronis². ¹University of Arkansas for Medical Science, Arkansas Children's Nutrition Center, USA, ²UAMS/ACNC, USA

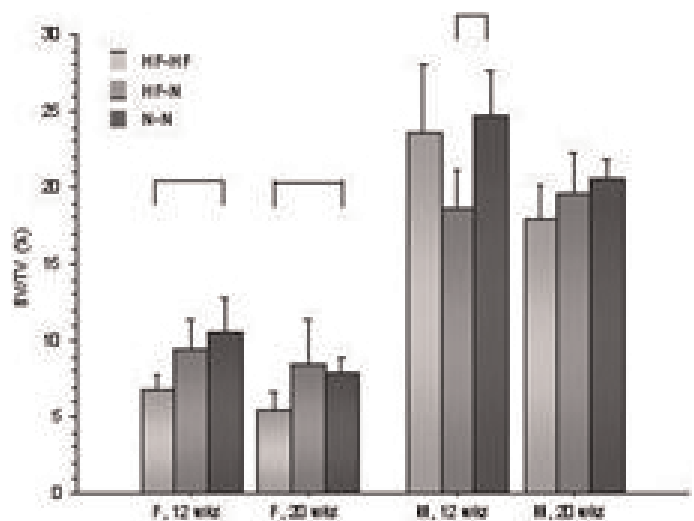
Appropriate nutrition during early development is essential for optimal bone mass accretion; however, linkage between early nutrition, childhood bone mass and prevention of bone loss later in life has not been extensively studied. In this report, we show that feeding a high quality diet supplemented with blueberries (BB) to pre-pubertal rats throughout development or only between postnatal day 20 (PND20) and PND34 prevented ovariectomy (OVX)-induced bone loss in adult life. This protective effect of BB is due to suppression of osteoblastic cell senescence which is associated with acute and profound loss of myosin expression after OVX. Early exposure of pre-osteoblasts to serum from BB-fed rats was found to consistently increase myosin expression. This led to maintenance osteoblastic cell development and differentiation and delay cell entrance into senescence by regulation of the Runx2 gene. High bone turnover after OVX results in insufficient collagenous matrix support for new osteoblasts and their precursors to express myosin and other cytoskeletal elements required for osteoblast activity and differentiation. Co-immuno-precipitation revealed an association between myosin and Runx2 in osteogenic cells and osteoblast precursors, and serum from OVX control rats decreased ($P<0.05$) this myosin and Runx2 complex. Knockdown of the non-muscular myosin II gene in ST2 cells resulted in reduced expression of Runx2 mRNA, and reduced the potential for cells to differentiate into osteoblasts even in the presence of BB serum. Following treatment with shRNA to myosin, ST2 cells expressed greater ($P<0.05$) senescence-associated beta-galactosidase activity, indicating increased stromal cell senescence. These results indicate: 1) a significant prevention of OVX-induced bone loss in adult rats can occur with only 14 days consumption of a BB-containing diet immediately prior to puberty; and 2) the molecular mechanisms underlying these effects involves increased myosin production which stimulates osteoblast differentiation and reduces mesenchymal stromal cell senescence. Supported in part by ARS CRIS #6251-51000-005-03S.

Disclosures: Jin-Ran Chen, None.

FR0025

Interactions of Maternal and Postnatal Diet Alter Skeletal Acquisition in Male and Female Mice: Evidence for Developmental Programming of Bone Acquisition. Maureen Devlin^{*}, Leeann Louis, Christine Conlon, Alison Cloutier, Mary Bouxsein, Beth Israel Deaconess Medical Center, USA

Early life nutrition substantially influences postnatal health, with both low and high birthweight linked with higher offspring metabolic disease risk, but little is known about potential skeletal effects. Here we test the hypothesis that interactions of maternal and postnatal nutrition affect offspring skeletal acquisition and maintenance. Methods: We compared postnatal skeletal acquisition in pups from C57Bl/6J mothers fed a high fat (HF, 45% kCal/fat) or normal (N, 10% kCal/fat) diet from 6 wks prior to breeding through gestation and lactation. At 3 wks of age we weaned male (M) and female (F) pups ($N=2-8/\text{grp}$) onto the same diets as their mothers (HF-HF or N-N) or onto the opposite diet (HF-N). Outcomes at 12 and 20 wks of age included body mass, body length, % body fat, whole body bone mineral content (BMC, g) via PIXImus, cortical and trabecular bone architecture at the midshaft and distal femur via μCT , glucose tolerance, and serum leptin and IGF-1 levels by ELISA. Results: M and F pups from HF diet mothers were longer and heavier vs. N-N at weaning, and remained so when raised on HF diet (HF-HF) ($p<0.05$ for all). HF-HF and HF-N had impaired glucose tolerance (F) and lower leptin levels (M) vs. N-N at 12 wks of age ($p<0.05$ for all). BMC was initially 5-10% higher in HF-HF and HF-N vs. N-N, but by 20 wks of age was 20% lower in HF-HF, along with 36-50% higher body fat ($p<0.05$ for all). Offspring of HF mothers had lower distal femur Tb.BV/TV: -32-36% in F HF-HF at 12 and 20 wks of age, and -25% in M HF-N at 12 wks of age, vs. N-N ($p<0.05$ for all, Figure). Midshaft femur cortical BA/TA (%) was lower in HF-N M at 12 wks of age, but M and F HF-HF and HF-N had greater bone area and polar moment of inertia vs. N-N ($p<0.05$). In conclusion, maternal HF diet impairs skeletal acquisition and maintenance, particularly when combined with postnatal HF. HF-N exhibit lower trabecular bone volume, but higher cortical bone strength, vs. N-N. HF-HF exhibit more severe changes, including markedly lower BMC and trabecular bone volume. The fact that exposure to maternal HF worsens the skeletal effects of postnatal HF demonstrates that maternal diet induces developmental programming of the skeleton that alters response to postnatal diet.



Figure

Disclosures: Maureen Devlin, None.

FR0026

Sport-Specific Association Between Exercise Loading and Density, Geometry, and Microstructure of Weight-Bearing Bone in Young Adult Men. Martin Nilsson^{*1}, Claes Ohlsson², Dan Mellstrom³, Mattias Lorentzon². ¹Centre for Bone & Arthritis Research At the Sahlgrenska Academy, Sweden, ²Center for Bone Research At the Sahlgrenska Academy, Sweden, ³Sahlgrenska University Hospital, Sweden

It is well known that bones adapt to the specific mechanical loading which they are habitually exposed to. Exercise by resistance training is common and increasingly popular in the younger population and can offer several health benefits. The aim of this cross-sectional study was to test the hypothesis that long-term sport-specific exercise loading determines areal and volumetric density, geometry, and microstructure of weight-bearing bone in young adult men.

A total of 186 male athletes, 24.00.6 years of age (meanSD), representing strength training and soccer, and their 177 nonathletic age matched controls, were measured with DXA, pQCT, and high resolution 3D pQCT devices. Grip strength was assessed using a Jamar hydraulic hand dynamometer.

One-way analysis of variance followed by Bonferroni post hoc test was used for evaluating differences between the groups. The mean amount of exercise exceeded three hours per week and the mean time of activity exceeded five years in all groups of athletes.

Men in the strength training group had significantly higher grip strength, 53.29.2 Nm (meanSD), and higher lean mass, 59.45.9 kg, than those in the nonathletic group (48.610.5 Nm, $p<0.01$; 56.36.1 kg, $p<0.001$, respectively). However, strength training men did not have higher bone density, or a more favourable bone microstructure or geometry than their nonathletic referents (Table 1). In contrast, men in the soccer playing group had denser bones at the femoral neck and lumbar spine, larger cortical bone size and higher trabecular number at the tibia than men in the nonathletic group (Table 1). There were no significant differences in age, height, weight, or calcium intake between the different groups.

The association between exercise loading and bone parameters was sport-specific. While, weight-bearing exercise, particularly by playing soccer, was associated with areal and volumetric density, bone geometry, as well as trabecular microstructure of weight-bearing bone, exercise by strength training was not a determinant of the corresponding bone traits in young adult men. These findings indicate that resistance exercise is not conducive to increase bone density and improve bone geometry in young men.

Table 1. Sport Specific Association Between Exercise Loading and Density, Geometry, and Microstructure of Weight-bearing Bone in Young Adult Men

	Nonathletic referents	Type of exercise		ANOVA <i>p</i>
		Strength training	Soccer	
Number of subjects	177	108	78	
Areal bone mineral density				
Lumbar spine (g/cm ³)*	1.21 ± 0.13	1.23 ± 0.14	1.36 ± 0.15 ^{A,B}	<0.001
Femoral neck (g/cm ³)*	1.06 ± 0.14	1.07 ± 0.15	1.26 ± 0.17 ^{A,B}	<0.001
Radius non-dominant (g/cm ²)	0.62 ± 0.06	0.63 ± 0.05	0.63 ± 0.05	0.116
Tibial diaphysis				
Cortical cross sectional area (mm ²) [†]	266 ± 34	274 ± 37	310 ± 34 ^{A,B}	<0.001
Cortical periosteal circumference (mm)*	73.1 ± 4.8	73.9 ± 4.8	76.7 ± 4.3 ^{A,B}	<0.001
Radial diaphysis				
Cortical periosteal circumference (mm)*	41.4 ± 3.1	42.2 ± 2.8	42.7 ± 2.8 ^A	0.002
Tibial metaphysis				
Trabecular bone density (mg/cm ³)*	212 ± 31	211 ± 31	243 ± 28 ^{A,B}	<0.001
Trabecular number (mm ⁻³)*	2.07 ± 0.28	2.04 ± 0.28	2.25 ± 0.27 ^{A,B}	<0.001
Trabecular thickness (μm)*	85.8 ± 11.1	86.8 ± 12.3	90.8 ± 11.0 ^A	0.006

Mean ± SD of bone parameters are presented. Differences between groups tested by ANOVA followed by Bonferroni post hoc test were performed. n=363, *n=360, n=362. *p* values for ^Avs. nonathletic and ^Bvs. strength training. Capital and capital bold type letters represent *p*<0.01 and *p*<0.001, respectively.

Table 1

Disclosures: Martin Nilsson, None.

FR0029

Determinants of Improvements in Bone Mineral Density (BMD) and Structure Following Initiation of Infliximab (IFX) Therapy for Childhood Crohn Disease (CD). Meena Thayu¹, Justine Shults², Robert Baldassano², Babette Zemel³, Mary Leonard³. ¹The Children's Hospital of Philadelphia, USA, ²University of Pennsylvania School of Medicine, USA, ³Children's Hospital of Philadelphia, USA

In addition to its role in the pathogenesis of intestinal inflammation in CD, TNF- α has direct, detrimental effects on osteoblast number and function. Objectives: To identify growth-related determinants of changes in BMD and structure following IFX (anti-TNF- α) therapy. Methods: 70 participants ages 5-21 yr with moderate to severe CD received IFX induction (5 mg/kg/dose) at weeks 0, 2, and 6 followed by maintenance therapy for 12 months. Tibia peripheral quantitative computed tomography (pQCT) scans were obtained at baseline and 12 months. Race-, sex-, age- and/or tibia length-specific Z-scores were generated for trabecular BMD, cortical BMD, cortical dimensions, and muscle area based on reference data in over 650 controls. Linear regression was used to identify determinants of changes in Z-scores, adjusted for baseline values. Results: Height, trabecular BMD, cortical BMD, and endosteal circumference Z-scores improved significantly over 12 months (Table). The average change in trabecular BMD Z-score, was greater in Tanner 1-4 vs. Tanner 5 participants (mean change: 0.53 0.74 vs. -0.14 0.42, *p*<0.005). Declines in cortical BMD Z-scores were independently associated with increases in endosteal apposition (*p*<0.001) and greater height velocity (*p*<0.01). Decreases in endosteal circumference Z-scores and increases in muscle Z-scores were associated with greater height velocity (*p*<0.0001 and *p*=0.001, respectively). Changes in cortical BMD and endosteal circumference were not associated with Tanner stage of maturation, independent of height velocity. Despite significant improvements in muscle Z-scores, periosteal circumference and section modulus Z-scores did not improve. Conclusions: These data suggest that the reversal of TNF- α effects on osteoblasts is greater in the growing vs. the mature skeleton in pediatric CD, but periosteal and section modulus deficits persist.

Z-Scores at Baseline and 12 months			
Z-Score	Baseline	12 month	p-value
Height	-0.57 ± 1.00	-0.36 ± 1.00	<0.0001
Trabecular BMD	-1.56 ± 1.13	-1.15 ± 1.07	<0.0001
Cortical BMD	0.15 ± 1.09	-0.71 ± 1.14	<0.0001
Endosteal Circumference*	0.29 ± 1.12	0.05 ± 1.01	<0.0001
Periosteal Circumference*	-0.53 ± 1.12	-0.51 ± 1.12	NS
Section Modulus*	-0.71 ± 1.28	-0.61 ± 1.24	NS
Muscle*	-0.74 ± 1.04	-0.37 ± 1.00	=0.0001

*adjusted for age and tibia length

Table

Disclosures: Meena Thayu, None.

FR0030

High Incidence of New Vertebral Fractures in Children with Leukemia after 12 months of Chemotherapy: Results of the Canadian Steroid-associated Osteoporosis in the Pediatric Population (STOPP) Research Program. N. Alos¹, R. Grant², J. Halton³, S. Atkinson⁴, D. Cabral⁵, R. Couch⁶, E. Cummings⁷, M. Matzinger³, P.M. Miettunen⁸, H. Nadel⁵, C. Rodd⁹, N. Shenouda³, D. Stephure⁸, R. Stein¹⁰, S. Taback¹¹, F. Rauch⁹, B. Lentle³, K. Siminoski⁶, L.M. Ward³, - and the Canadian STOPP Consortium¹². ¹Universite de Montreal, Canada, ²University of Toronto, Canada, ³University of Ottawa, Canada, ⁴McMaster University, Canada, ⁵University of British Columbia, Canada, ⁶University of Alberta, Canada, ⁷Dalhousie University, Canada, ⁸University of Calgary, Canada, ⁹McGill University, Canada, ¹⁰University of Western Ontario, Canada, ¹¹University of Manitoba, Canada, ¹²Canadian Pediatric Bone Health Working Group, Canada

Background: Vertebral fractures are an important complication of childhood acute lymphoblastic leukemia (ALL). The frequency of incident vertebral fractures (IVFs) at 12 months following initiation of chemotherapy, as well as their relationship to key clinical indices have not been systematically studied.

Methods: We evaluated spine health in children with ALL enrolled in a prospective, observational study through a national bone health research program during the first 12 months of chemotherapy. Vertebral morphometry was carried out by the Genant semi-quantitative method on lateral thoracolumbar spine radiographs around the time of diagnosis and at 12 months, with the sum of the Genant grades from T4 to L4 in each patient expressed as the Spinal Deformity Index at both timepoints. Clinical features including VF at diagnosis, lumbar spine areal BMD (LSaBMD) Z-score, back pain, and cumulative glucocorticoid/methotrexate doses were analyzed for association with IVFs.

Results: Of 155 children (median age 6.4 years, 91 boys) with natural history data to 12 months, 25 (16%) had a total of 61 IVFs (46 thoracic and 15 lumbar). Most fractures occurred in the midthoracic and thoracolumbar regions; 32/61 IVFs (52%) were moderate or severe. The clinical characteristics at diagnosis differed significantly for children with IVFs at 12 months compared to those without, as follows: 1. VFs were present at diagnosis in 52% of the children with IVFs at 12 months compared to 9 percent of children without IVFs (*p*<0.001). 2. The mean LSaBMD Z-score at diagnosis was one standard deviation lower in children with IVFs compared to those without (-2.01.5 versus -1.01.2; *p*<0.001). 3. A greater percentage of children with IVFs manifested back pain at diagnosis (52% versus 23%, *p*=0.006). There was no difference in glucocorticoid or methotrexate exposure during the 12 month period. Each unit increase in the Spinal Deformity Index at diagnosis was associated with a 35% increase in the odds for IVF at 12 months (95% CI: 9 to 68%, *p*=0.007).

Conclusions: This study shows a high incidence (16%) of IVFs at 12 months post-chemotherapy initiation in children with ALL. The Spinal Deformity Index at diagnosis was an important determinant of new VFs at 12 months

Disclosures: N. Alos, None.

FR0032

Mechanism of Hexa-D-Arginine Curative Effects on the HYP Phenotype. Baozhi Yuan¹, Stephen Bowman², Robert Blank², Iris Lindberg³, Marc Drezner². ¹University of Wisconsin, Madison, USA, ²University of Wisconsin, USA, ³University of Maryland, USA

The increased serum FGF-23 level in *hyp*-mice, a homologue of X-linked hypophosphatemia (XLH), results from impaired degradation and enhanced production of FGF-23. We have previously reported that decreased Phex-dependent 7B2 production in osteoblasts and an apparent diminished 7B2-SPC2 (subtilisin-like protein convertase 2) activity underlie the increased serum FGF-23 and biochemical phenotype in *hyp*-mice. We recently found that treatment of *hyp*-mice with Hexa-D-Arginine (D6R), a stable small peptide known to inhibit furin and stimulate SPC2, normalizes the biochemical phenotype in these mutants. In addition, we have documented that such treatment likewise normalizes the bone mineralization in *hyp*-mice and heals the rickets/osteomalacia. Despite these observations, it remains unknown if the positive effects of D6R are mediated by increasing 7B2-SPC2 activity. Therefore, in the present study, we examined the dose-dependent effects of D6R (0-200 μM) on SPC2 activity in hTert osteoblasts (MOB) and M3C3T3 osteoblasts in culture. D6R treatment of hTert osteoblasts (50 μM) for 48 hours significantly increased SPC2 activity to a maximum level (12118 vs 32917 fluorescent units/min; *p*<0.01). Treatment of MC3T3 cells for a similar period likewise increased enzyme activity to a maximum at 200 μM (12414 vs 1717 fluorescent units/min; *p*<0.05). Treatment of the MOB cell line with D6R, and the consequent increase in SPC2 enzyme activity, as anticipated, decreased FGF-23 mRNA expression (1.00.7 vs 0.20.1 fold; *p*<0.001). Further study revealed that the D6R-dependent enhancement of SPC2 enzyme activity in MOB cells occurred in association with an increase in 7B2 mRNA expression (1.00.2 vs 3.60.4 fold; *p*<0.001), but without change in SPC2 mRNA expression. In summary, our data indicate that the curative effects of D6R on the HYP phenotype likely result from enhanced osteoblast 7B2-SPC2 activity, which can normalize the decreased enzyme function present in the *hyp*-mouse osteoblast. Moreover, the associated D6R stimulation of 7B2 mRNA expression suggests that

increased enzyme activity may be secondary to enhanced 7B2 production, which overcomes the central PheX-dependent abnormality in the *hyp*-mouse osteoblast.

Disclosures: Baozhi Yuan, None.

FR0044

Increased Cortical Bone Mass Is Associated with Increased Bone Strength by Treatment with the Cathepsin K Inhibitor, ONO-5334, but not with Alendronate in Ovariectomized Monkeys. Yasuo Ochi^{*}, Hirovuki Yamada, Yasutomo Nakanishi, Akiko Kunishige, Satoshi Nishikawa, Yasuaki Hashimoto, Hiroshi Mori, Masafumi Sugitani, Kazuhito Kawabata. Ono Pharmaceutical Co., Ltd., Japan

We have previously reported that ONO-5334 increased bone mass and bone strength in the lumbar vertebra in an ovariectomized (OVX) monkey study where animals received either vehicle, ONO-5334 (1.2, 6 or 30 mg/kg p.o., once daily), or alendronate (ALN, 0.05 mg/kg i.v., once every 2 weeks) for 16 months (N=19-20 per group)¹. Also, it has been demonstrated that ONO-5334 has an efficacy on cortical bone in the lumbar vertebra in OVX monkeys¹.

In this post-hoc analysis, we investigated the relationship between bone mass (integral vBMC measured by pQCT) and bone strength (maximum load) in the lumbar vertebra within each treated group. Linear regression lines between bone mass and bone strength with 6 and 30 mg/kg ONO-5334 groups ($r^2=0.56$ and 0.57 , respectively) shifted toward increasing bone strength compared to those with the OVX control ($r^2=0.68$) and the ALN groups ($r^2=0.37$), i.e. higher bone strength for ONO-5334 was observed compared to OVX control and ALN assessed at the same bone mass level. To further investigate this effect, we focused on the different efficacy on trabecular and cortical bone mass between ONO-5334 and ALN. Subpopulations from the 30 mg/kg ONO-5334 and the ALN groups were selected in a way that their mean values for lumbar integral vBMC were comparable (ONO-5334 subgroup; integral vBMC range 46.2-55.1 mg/mm, mean 49.5 mg/mm, N=10, ALN subgroup; integral vBMC range 46.2-52.1 mg/mm, mean 49.7 mg/mm, N=10), and compared bone strength, trabecular and cortical vBMC between both subgroups. Bone strength was significantly higher in the ONO-5334 subgroup than in the ALN subgroup ($p<0.05$) with comparable integral vBMC. The mean value of trabecular vBMC in the ALN subgroup was higher than in the ONO-5334 subgroup. Conversely, the mean value of cortical vBMC in the ONO-5334 subgroup was higher than in the ALN subgroups. This outcome was also confirmed when analyzing subpopulations with higher and lower mean values of lumbar integral vBMC covering the entire vBMC range.

These results suggest that increased cortical bone mass by treatment with ONO-5334 is associated with an increase in bone strength in the lumbar vertebra in OVX monkeys. Thus ONO-5334 may increase bone strength not only in lumbar vertebra but also in non-vertebral bone where cortical bone predominates in osteoporosis patients.

¹ ASBMR 2010, FR0438

Disclosures: Yasuo Ochi, None.

FR0045

In-situ synchrotron SAXS Combined with Micromechanical Testing to Serve as an In-Vitro Nanomechanical Functional Imaging Technique to Measure the Bone Quality Degradation in Metabolic Bone Diseases. Angelo Karunaratne^{*1}, Himadri Gupta¹, Rajesh Thakker², Chris Esapa³, Jennifer Hiller⁴, Alan Boyde⁵, Nick J. Terrill⁴, Asa Barber⁶, J. H. D. Bassett⁷, Roger Cox⁸, S. Brown⁸, Matthew Brown⁹, R Head¹⁰, Peter Croucher¹¹, Graham Williams⁷. ¹School of Engineering & Material Sciences, Queen Mary University of London, United Kingdom, ²Academic Endocrine Unit, Nuffield Department of Clinical Medicine, Oxford Centre for Diabetes, Endocrinology & Metabolism, United Kingdom, ³Academic Endocrine Unit, Nuffield Department of Clinical Medicine, United Kingdom, ⁴122 Non-crystalline Diffraction Diamond Light Source Harwell Science & Innovation Campus, United Kingdom, ⁵Queen Mary University of London, Oral Growth & Development, Institute of Dentistry, Bart's & The London School of Medicine, United Kingdom, ⁶School of Engineering & Material Sciences, Queen Mary University of London, United Kingdom, ⁷Molecular Endocrinology Group, MRC Clinical Sciences Centre & Division of Investigative Sciences, Imperial College London, United Kingdom, ⁸MRC Mammalian Genetics Unit & Mary Lyon Centre, MRC Harwell, Harwell Science & Innovation Campus, United Kingdom, ⁹Diamantina Institute of Cancer, Immunology & Metabolic Medicine, Australia, ¹⁰Academic Endocrine Unit, Nuffield Department of Clinical Medicine, Oxford Centre for Diabetes, Endocrinology & Metabolism, University of Oxford, United Kingdom, ¹¹The Mellaby Centre for Bone Research, United Kingdom

Metabolic bone disorders like rickets and osteoporosis cause significant reduction in bone material quality, leading to dramatic reductions in mechanical parameters like fracture resistance. However, the ultrastructural mechanism by which altered mineralisation & bone quality affects mechanical properties is far from well understood. Here we determine the functional link between reduced mineralization and abnormal fibrillar-level deformation & fracture using a novel real-time X-ray nanoscale imaging method on a mouse model exhibiting reduced extrafibrillar mineralization. A murine model for hypophosphatemic rickets (Elvis) was induced via *N*-ethyl-*N*-nitrosourea (ENU) mutagenesis. The tissue and organ level phenotypic changes in Elvis mice included elevated plasma alkaline phosphatase, bowed tibia and a reduction in bone mineral density, consistent with features in X-linked Hypophosphatemic Rickets. We use high brilliance *in-situ* synchrotron small angle X-ray scattering to measure, in real-time, the changes in axial periodicity of the nanoscale mineralized fibrils (D-period) in bone during tensile loading. From these measurements, functional nanomechanical parameters like fibril elastic modulus and maximum fibril strain were determined for both Elvis and control mice femora as a function of development. The mineral content in the femora is estimated independently using backscattered electron imaging. We find a significant reduction of fibril modulus as well as an enhancement of maximum fibril strain in Elvis mice. Both modulus and maximum fibril strain increase consistently with age within both the Elvis and wild-type series. The mean mineral content is on average 21 % less for Elvis than for the wild-type mice, and is far more heterogeneous in its distribution. We show how our results are consistent with a simple nanostructural mechanism where incompletely mineralized fibrils show greater extensibility and lower stiffness, leading to known macroscopic outcomes like greater bone bending. Our results demonstrate the power of this novel *in-situ* X-ray nanomechanical imaging approach to directly link alterations in bone nanostructure to nano- and macroscale mechanical deterioration, and the technique can be applied to clinically relevant conditions like osteoporosis.

Figure 3

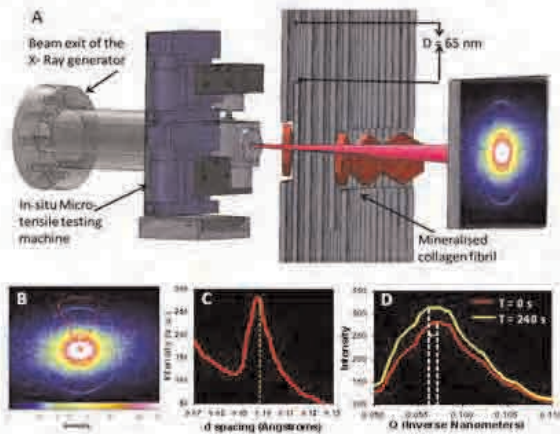


Figure 1: In-situ Tensile testing with Synchrotron small angle X-ray scattering and data reduction procedure (A) Schematic view of the micro tensile testing machine. The sample is immersed in Phosphate buffered saline. Tensile load is applied along the parallel collagen fibril axis as shown in the schematic of mineralised collagen fibril (inset) (B) 2D SAXS pattern from parallel fibril bone, showing the discrete reflections arising from the collagen D period, and the diffuse scattering intensity from the mineral nanocrystallites. (C) Integrated intensity profile in the radial directions in the angular region (red dash lines) shown in (b), showing the first order of the collagen reflections. (D) Shift of the 1st order collagen peak position with increasing tissue strain, for tissue strain = 0% (Time = 0) (red line) and tissue strain = 0.5% (Time = 240s) (yellow line).

Figure 4

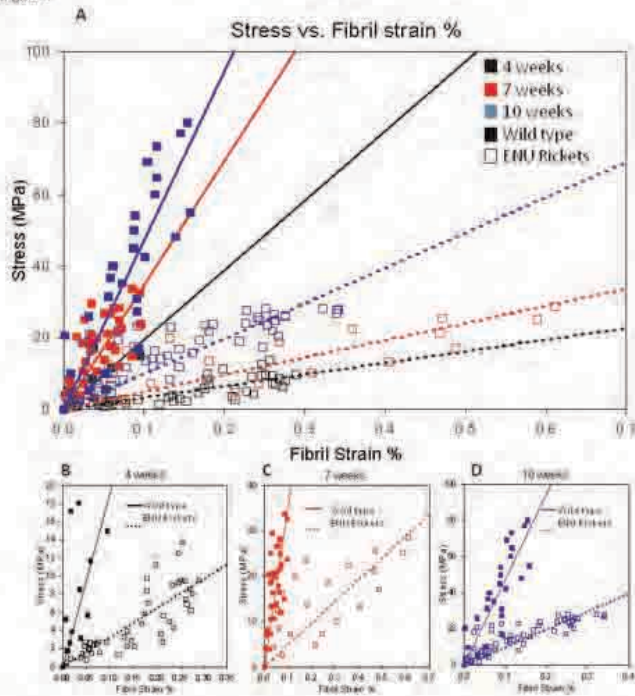


Figure 3: (A) Stress versus measured fibril strain as a function of disease state (open symbols: ENU rickets; closed symbols: wild type) and age (4 week: black; 7 week: blue; 10 week: red). For each age and disease state, the number of samples n is given in the Table 1. (B) - (D) show individual plots of stress versus fibril strain at each age group, to reduce data overlap.

Figure 6



Figure 5: Quantitative Backscattered Scanning Electron microscopy images collected from the mid shaft of the cortical bone from 1 week to 16 weeks (left to right) for wild type (top row) and ENU rickets mice (bottom row).

Figure 7

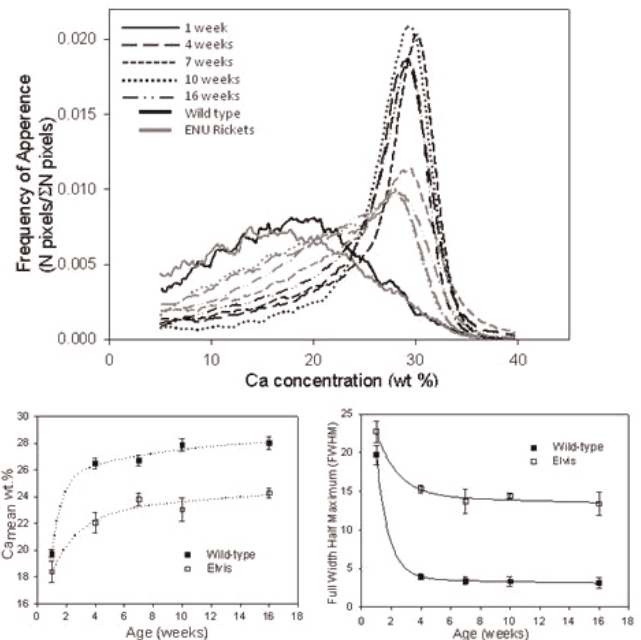


Figure 6: (A) Bone Mineral Density Distributions (BMDD) were produced for each genotype (solid lines: wild type and dotted lines: ENU rickets) and for each age (black: 1 week; green: 4 weeks; pink: 7 weeks; blue: 10 weeks and brown: 16 weeks). (B) Mean Ca% plotted as a function of development (1 week to 16 weeks) and genotype (wild type: closed symbols and ENU rickets, open symbols). Significant increment in Ca content can be only seen in wild type from 1 week 4 weeks and subsequently stabilises for later ages. Solid lines are regression lines. (C) Full Width at Half Maximum (FWHM) corresponds to the distribution in local variation of Calcium content plotted as a function of development (1 week to 16 weeks) and genotype (wild type: closed symbols and ENU rickets, open symbols). Significant reduction in FWHM can be only seen in wild type from 1 week 4 weeks and subsequently stabilises for later ages. Solid lines are regression lines.

Figure 2

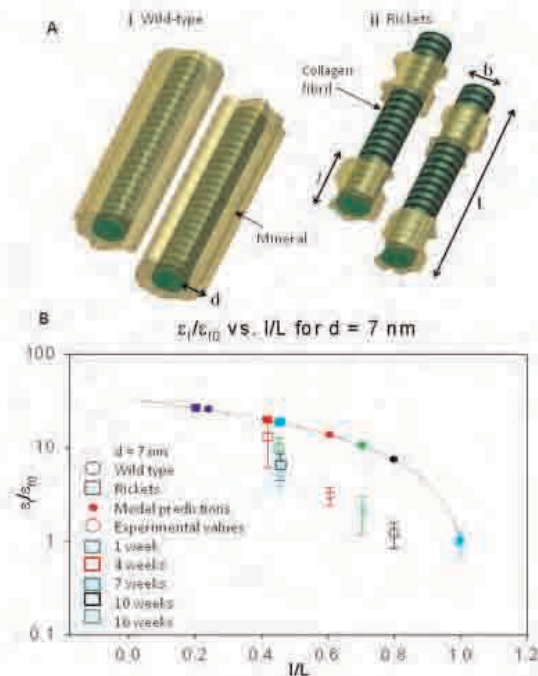


Figure 7: Proposed variation of mineralized collagen fibril structure between wild type and rickets mice and the variation of relative fibril strain as function of mineral coverage. **(A)** Light yellow zone (colour online) denotes mineral phase. (i) In wild type condition, the full length of fibril is covered with mineral. (ii) In contrast ENHJ rickets condition fibrils are only partly covered by mineral which is also discontinuous along the length. **(B)** The mineral thickness d as a constant. Wild type 16 weeks mice volume fraction has been considered to be fully mineralised. Circles and squares denote wild type mice and rickets mice respectively (Black - 1 week, red - 4 weeks, green - 7 weeks, yellow - 10 weeks and blue - 16 weeks). Filled symbols denote model predictions and open symbols denoted experimental data (the ratio of the effective fibril modulus E_f/E_0 (data calculated from results shown in figure 4) is the inverse of the relative fibril strain).

Disclosures: Angelo Karunaratne, None.

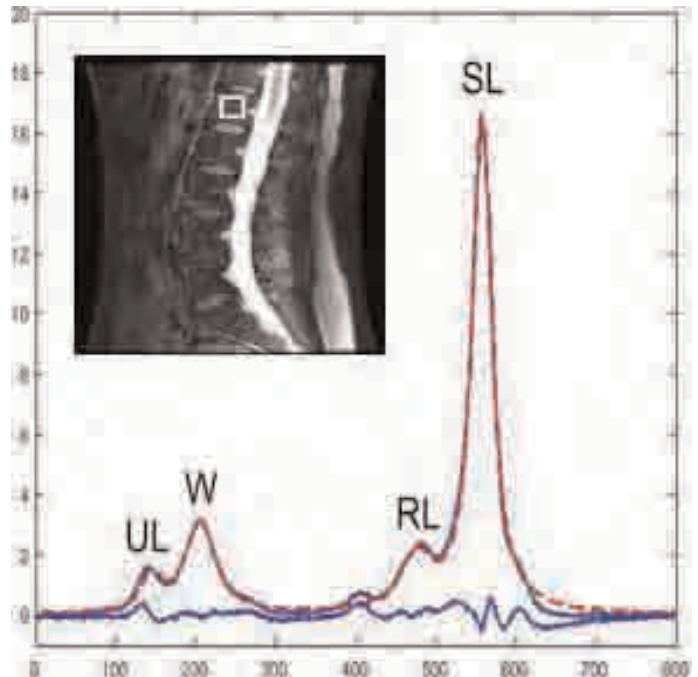
This study received funding from: Queen Mary University of London and Diamond Light Source, Harwell, United Kingdom

FR0049

Non-Invasive Assessment of Bone Marrow Lipids Captures Fracture Risk Profile of Postmenopausal Women Irrespective of Diabetes History. Janina Patsch¹, Thomas Baum², Paron S. Yap², Xiaojuan Li², Dimitrios Karampinos², Sharmila Majumdar², Ann Schwartz², Thomas M. Link². ¹UCSF, USA, ²University of California, San Francisco, USA

Type 2 diabetes is associated with higher fracture risk and, paradoxically, with higher bone density by DXA, suggesting a deficit in bone quality that is not captured by DXA. Clinical bone marrow Magnetic Resonance (MR) Spectroscopy has been introduced as a new tool to study bone quality and has been shown to discriminate subjects of varying BMD. The purpose of this study was to non-invasively assess bone marrow fat properties of diabetic patients with and without fractures in comparison with normal postmenopausal controls and non-diabetic patients with fragility fractures. All postmenopausal subjects (controls n=17; controls with fractures n=15; diabetics without fracture n=15; diabetics with fracture n=7) underwent single-voxel proton MR spectroscopy (1H-MRS) of the lumbar spine (3T, Signa, GE; 4-channel spine coil, GE). A Point Resolved Spectral Selection (PRESS) sequence was used to acquire vertebral body spectra from L1-L3 (TR/TE=3000/37ms, 64 averages without water suppression, sweep width = 5000Hz, data point = 4096, voxel size = 15x15x20mm³ = 4.5cm³ box size). In addition DXA scans of the lumbar spine and the hip were performed. We also measured fasting blood glucose, HbA1c, c-peptide, CRP, PTH and vitamin D levels. Using DXA we found normal bone density in fractured diabetic individuals and unfractured controls, which further underlines DXA's limitations in assessing fracture risk in diabetic patients. Average BMD in non-diabetic fracture patients and non-fractured diabetics was in the osteopenic range. Total marrow fat content using 1H-MRS was similar in all four patient groups. However, the amount of unsaturated lipids was significantly reduced in controls with fractures (L2 -25.8%, p=0.047; L3 -25.1%, p=0.026) and diabetics with fractures (L2 -50.3%, p=0.007; L3 -36%, p=0.045) when compared with non-diabetic controls. We found similar unsaturation changes when comparing diabetics with and without fractures (L2 -39.2%, p=0.04; L3 -23.9%, p=0.04). Lipid unsaturation did not differ between the two unfractured groups. There were no significant correlations between 1H-MRS results, BMD and blood parameters. We conclude that bone marrow

spectroscopy seems to be a promising tool for fracture risk assessment irrespective of diabetes history. This technique could serve as a novel biomarker to identify diabetic patients at risk for fracture. However, the pathophysiology leading to decreased marrow lipid unsaturation in fracture patients remains to be elucidated.



Representative MR Spectroscopy Setup

Disclosures: Janina Patsch, None.

FR0052

Pubertal Influences on Bone Strength: Results from the Fels Longitudinal Study. Maja Seselj¹, Ramzi W. Nahhas¹, Richard J. Sherwood², Wm. Cameron Chumlea¹, Roger M. Siervogel¹, Stefan A. Czerwinski¹, Bradford Towne², Dana L. Duren³. ¹Lifespan Health Research Center, Department of Community Health, Wright State University, USA, ²Lifespan Health Research Center, Department of Community Health, Wright State University; Department of Pediatrics, Wright State University, USA, ³Lifespan Health Research Center, Department of Community Health, Wright State University; Department of Orthopaedic Surgery, Wright State University, USA

Elucidating the pattern of bone accrual in children is crucial for a proper understanding of bone strength and quality in later stages of life, and has significant potential for predicting adult fracture and osteoporosis risks. For example, it has been suggested that girls who enter puberty at a younger age have a higher bone mineral content (BMC) and density (BMD). A bone's ability to resist bending and torsion, however, is also a function of its cross-sectional geometric properties and is negatively impacted by reducing external bone diameter, which itself is influenced by the timing of puberty. In pubescent girls, elevated levels of estrogen impede subperiosteal bone growth and increase endosteal bone deposition, resulting in bones averaging a smaller external and internal diameter relative to boys. In addition, a secular trend for younger age at menarche is well-documented world-wide, suggesting that the age at which the rate of subperiosteal bone deposition decreases is occurring earlier as well.

In this study we examined the relationship between pubertal timing and bone strength in girls. Specifically, we investigated the effects of age at menarche on bone strength indicators (polar moment of inertia, polar section modulus) determined from cross-sectional geometry of the second metacarpal (MC2) using data derived from serial hand-wrist radiographs of 203 female participants in the Fels Longitudinal Study with repeated measures of MC2 between the ages of 7 and 38 years. These strength indicators, representing torsional and bending strength and rigidity of bone, respectively, were evaluated in multivariate regression models predicting polar moment of inertia and polar section modulus in young adulthood from their pre-pubertal values and age at menarche. Results indicate that both measures of bone strength in adulthood are positively influenced by age at menarche, i.e. a later age at menarche is associated with higher bone strength scores (R² ranged between 0.49 and 0.69, p<0.001), when controlling for pre-pubertal bone strength. Thus, although an earlier age at menarche is reportedly beneficial for BMC and BMD, it is not beneficial for bending and torsional strength and rigidity of bone. In combination, these results suggest that bone strength is multifactorial, and that prevention or intervention measures should consider those variables with the greatest influence at a specific skeletal site given its susceptibility to certain mode of fractures.

Disclosures: Maja Seselj, None.

This study received funding from: Supported by NIH grants R01HD012252 and R01HD056247.

FR0058

The Effect of Denosumab on the Bone Matrix Mineralization in Mice.

Barbara Misof¹, Paul Roschger^{*1}, Michael Ominsky², Phaedra Messmer¹, Paul Kostenuik³, Klaus Klaushofer¹. ¹Ludwig Boltzmann Institute of Osteology at the Hanusch Hospital of WGKK & AUVA Trauma Centre Meidling, 1st Medical Department, Hanusch Hospital, Vienna, Austria, ²Amgen, Incorporated, USA, ³Amgen, Inc., USA

Introduction: Denosumab (DMAb), a potent inhibitor of bone turnover, was recently introduced for the treatment of postmenopausal osteoporotic women at increased risk of fracture. A 6-month study in mice with a humanized RANKL gene (huRANKL mice) showed that DMAb significantly increased bone mineral density (BMD) and bone volume (by microCT) of the leg and lumbar vertebrae. Compared to vehicle controls, DMAb-treated mice exhibited significantly greater femur and vertebral peak load, without changes in material parameters. We now report the first data on the effect of DMAb on bone matrix mineralization, which could enhance the understanding of treatment-related changes in BMD and bone strength.

Materials & Methods: Cancellous bone mineralization density distribution (BMDD) in the vertebra and cortical BMDD at the tibial midshaft were measured by quantitative backscattered electron imaging (qBEI) in huRANKL mice. Adult mice (6 to 8 months old) were dosed twice per week for a total of 6 months. Three groups were compared: vehicle (VEH, n=9), alendronate (ALN, 0.1mg/kg, sc; n=9), and denosumab (DMAb, 25mg/kg, iv; n=7) treated.

Results: Two-way repeated measures ANOVA revealed no interaction between treatment (VEH/ALN/DMAb) and site (trabecular/cortical) for the studied BMDD variables average and mode calcium concentration (CaMean and CaPeak, respectively) and heterogeneity of mineralization (CaWidth). Treatments did not cause a change in CaMean or CaPeak, however, CaWidth was significantly affected in both treatment groups. Both ALN and DMAb treated groups revealed lower CaWidth (-7.6%, p=0.005; -14.2%, p<0.001, respectively) compared to VEH, and CaWidth for the DMAb group was lower than the ALN group (p<0.05). Regression analyses indicated that reduced CaWidth was not associated with reduced material properties, including toughness.

Conclusion: The lack of significant changes in mean mineral content after DMAb treatment indicates that the observed increase in BMD is more likely related to an increase in bone volume than in mineral content. The reduction of the heterogeneity in mineralization is typical for a sudden reduction of bone turnover and confirms the antiresorptive action of DMAb. The data suggest that improvements in mechanical competence of whole bones in mice treated with DMAb are mainly due to an increase in bone volume, while the influence of a reduced heterogeneity in mineralization at material level remains unclear.

Disclosures: Paul Roschger, None.

This study received funding from: Amgen Inc.

FR0059

The Loss of ATF4 Reduces the Toughness of Bone. Jeffry Nyman^{*1}, Alexander Makowski², Sandra Wade², Matthew Murry², Xiangli Yang².

¹Vanderbilt University Medical Center, USA, ²Vanderbilt University, USA

The age-related increase in fracture risk is not solely due to a loss in bone mass, and by extension bone strength, leading to the idea that bone quality is an important attribute of fracture resistance. Despite the critical role of collagen as a determinant of bone toughness (or brittleness), there is an incomplete understanding of how genes important to its organization regulate material properties of bone. To test the hypothesis that transcriptional activity can affect bone properties related to fracture resistance, we characterized the compositional, architectural, and biomechanical properties of bones from wild-type mice and mice null for the activating transcription factor 4 (ATF4^{-/-}), a factor that influences osteoblast maturation and collagen synthesis.

Bones were harvested from ATF4^{+/+} (n=15 per age) and ATF4^{-/-} (n=9 per age) mice at 8 wk and 20 wk of age (male). μ CT analysis quantified structural differences in the femur diaphysis, architectural differences in the femur metaphysis and L6 vertebral body (VB), and tissue mineral density (TMD) of each compartment. Next, three point bending and compression testing of the femur and VB, respectively, assessed fracture resistance. The differences in each bone property among age and genotype were tested for significance using a two-way ANOVA.

Loss of ATF4 affected bone structure in that the null femurs were shorter with a thinner cortex and a ~30% lower moment of inertia, regardless of age. ATF4 deficiency also caused lower trabecular bone volume fraction and lower connectivity density in the metaphysis and VB. Not surprisingly then, the ATF4^{-/-} femur and VB were weaker in bending and compression, respectively, relative to ATF4^{+/+}. Factoring out the structural contribution, the estimated material strength of the mid-shaft was not different between ATF4^{+/+} and ATF4^{-/-} mice but increased from 8 wk to 20 wk. Interestingly, a higher TMD for the null diaphysis - a 2.2% increase from wild-type - did not impart higher material strength. Also, the ATF4^{-/-} bones were clearly more brittle with substantially lower post-yield displacement and work-to-fracture per

cross-sectional area (Fig 1). This is likely due to a defect in the ability of ATF4-deficient osteoblasts to synthesize collagen protein despite its mRNA expression being normal.

Ultimately, there could be novel targets beyond increasing bone mass for improving fracture resistance by elucidating the factors important to the organization of the organic matrix.

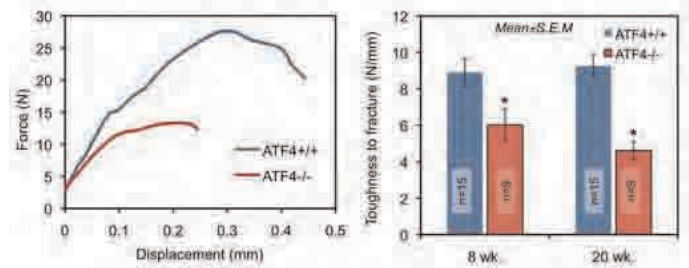


Fig 1: ATF4-deficient bone is brittle relative to wild-type bone.

Disclosures: Jeffry Nyman, V.A, 2

FR0061

Women with Type 2 Diabetes Have Increased Femoral Neck BMD but Not Increased Femoral Strength. Dana Carpenter^{*1}, Joyce Keyak², Janina Patsch², Paron Yap², Thomas Baum², Ann Schwartz¹, Thomas Lang², Thomas Link².

¹University of California, San Francisco, USA, ²University of California, USA

PURPOSE: Women with type 2 diabetes mellitus are at an increased risk of hip fracture. The purpose of this study was to determine whether diabetes affects the volumetric bone mineral density (BMD) and strength of the proximal femur measured with quantitative computed tomography (QCT) and finite element modeling (FEM).

METHODS: Sixty-two women aged 50-75 years were placed in four groups depending on diabetes and fracture status: 20 healthy women with no history of fracture, 18 healthy women with a history of fracture, 20 diabetic women with no history of fracture, and 7 diabetic women with a history of fracture. Subjects' hips were imaged using QCT with an in-plane pixel size of 0.94 mm and a slice thickness of 2.5 mm. Volumetric BMD of the trabecular (tBMD), cortical (cBMD), and integral (iBMD, including trabecular and cortical bone) compartments of the left femoral neck were measured using a solid calcium hydroxyapatite reference phantom. Three-dimensional FEA was used to compute the fracture load of the left proximal femur under stance and posterolateral fall loading conditions. Differences in BMD and fracture load among the four groups were detected using ANOVA and Tukey post-hoc comparisons.

RESULTS: Diabetics with no history of fracture had a higher iBMD than healthy controls with and without a history of fracture (Fig.1), and tBMD in diabetics with no history of fracture was higher than in both healthy controls with a history of fracture (p < 0.01) and diabetics with a history of fracture (p < 0.05). The cBMD of the femoral neck did not differ significantly among the four groups. Results of FEM in the fall loading configuration showed that the healthy controls had significantly higher fracture load than controls with a history of fracture and diabetics with a history of fracture, but fracture load did not differ significantly between healthy controls and diabetics with no history of fracture (Fig.1). Stance fracture load did not differ significantly among the four groups.

CONCLUSIONS: Type 2 diabetic women have increased BMD in the femoral neck, but the higher BMD does not translate to a stronger proximal femur. These results suggest that aspects of bone structure other than BMD, which are captured by QCT-based FEM, may be related to the higher risk of fracture in diabetics.

FR0063

Development and Validation of a Mouse Model of Adynamic Bone Disease (ABD). Adeline Ng^{*1}, Benjamin Alman², Marc Grynpas³. ¹University of Toronto Samuel Lunenfeld Research Institute, Canada, ²SICK CHILDREN'S HOSPITAL, Canada, ³Samuel Lunenfeld Research Institute, Canada

INTRODUCTION: The etiology of Adynamic Bone Disease (ABD) is poorly understood but the hallmark of ABD is a lack of bone turnover. ABD occurs in renal osteodystrophy (ROD) and is suspected to occur in elderly patients on long-term anti-resorptive therapy. A major clinical concern of ABD is diminished bone quality and increased fracture risk. To our knowledge, experimental animal models for ABD other than RO-ABD have not been developed or studied. The objectives of this study were to develop a mouse model of ABD without the complications of renal ablation, and to characterize changes in bone quality in ABD relative to controls.

METHODS: To create the adynamic bone condition, 4-month old female Col2.3^{Atk} mice were treated with ganciclovir to specifically ablate osteoblasts, and pamidronate to inhibit osteoclastic resorption. Four groups of animals were used to characterize bone quality in ABD: Normal bone controls, No Formation controls, No Resorption controls, and an Adynamic group. After a 6-week treatment period, animals were sacrificed and bones were harvested for analyses. Bone quality assessments were conducted using established techniques including bone histology, backscattered electron imaging, DXA and microcomputed tomography.

RESULTS: Histomorphometry confirmed osteoblast-related hallmarks of ABD in our mouse model. Bone formation was near complete suppression in the No Formation and Adynamic specimens. Inhibition of bone resorption in the Adynamic group was confirmed by tartrate-resistant acid phosphatase (TRAP) stain. Normal bone mineral density and architecture was maintained in the Adynamic group, whereas the No Formation group showed a reduction in bone mineral content and trabecular thickness relative to the Adynamic group. As expected, the No Formation group had a more hypomineralized profile and the Adynamic group had a higher mean mineralization profile that is similar to low bone turnover in human. This data confirm successful replication of the adynamic bone condition in a mouse.

DISCUSSION: Similarity of our mouse model to the human condition was confirmed using the same histological technique that is used to diagnose ABD in human ROD. Our proposed approach is the first model of ABD that uses pharmacological manipulation in a transgenic mouse to mimic the bone cellular dynamics observed in the human ABD condition. Our model will help understand changes to bone quality and fracture risk as a consequence of a lack of bone turnover.

Disclosures: Adeline Ng, None.

FR0066

Incidence Of Skeletal Fractures After Spinal Cord Injury. Laia Gifre^{*1}, Pilar Peris², Joan Vidal³, Jesus Benito³, Enric Portell³, Margarida Valles³, Ana Monegal¹, Nuria Guanabens¹. ¹Hospital CIUñic of Barcelona, Spain, ²Hospital Clinic of Barcelona, Spain, ³Spinal Cord Unit. Guttman Institute, Spain

Spinal cord injury (SCI), due to the absence of mechanical load, is associated with a marked increase in bone remodelling and bone loss, thus increasing the risk of fractures in this process. However, few studies have analysed the incidence and complications of skeletal fractures in these patients. Therefore, we analysed the incidence of skeletal fractures in patients with traumatic SCI, as well as the factors related to the development of fractures and their clinical complications. **Methods:** Retrospective study including all patients attended in the SCI Unit (from January to December 2000) of a specialized center for a recent traumatic SCI. The medical reports were reviewed with special attention to risk factors for osteoporosis and the type of SCI injury, analyzing the incidence of fractures during a 10-year period after SCI in all patients. In addition, we evaluated the severity of SCI, through the ASIA score (American Spinal Injury Association: A-E), weight bearing rehabilitation, the level of SCI (paraplegia/tetraplegia), the type of lesion (spastic/flaccid) as well as the cause, location and evolution of the fracture. **Results:** Of the 129 patients attended at the Unit during the study period, 75 had traumatic SCI (12 died and 9 had no posterior follow-up). Finally, 54 patients were included in the study (45M/9W) with a mean age of 3318 years (13-78); 36 had paraplegia and 18 tetraplegia. 72% had complete motor injury (ASIA A score) and 85% had spasticity. 35% of patients with complete motor injury developed fractures after SCI. The femur, was the most frequent location of the fractures, followed by the tibia, vertebra, pelvis and metatarsus. Fractures were observed 53 years after SCI (range 2-10 yrs) all being observed in males. Most fractures (75%) were related to low impact injuries (including transferences), or were overlooked (no known cause for the fracture). Most patients were treated with conservative approach (75% cases). No significant differences were observed in the clinical characteristics of patients with and without fractures (including age, type and level of lesion, weight bearing, clinical risk factors for osteoporosis). **Conclusion:** After complete motor SCI 35% of patients develop fractures, especially in the femur, after 10 years of follow-up. Most of these fractures are related to minor trauma or are even overlooked. Awareness of the factors related to this complication and its therapeutic approach are mandatory in these patients.

Disclosures: Laia Gifre, None.

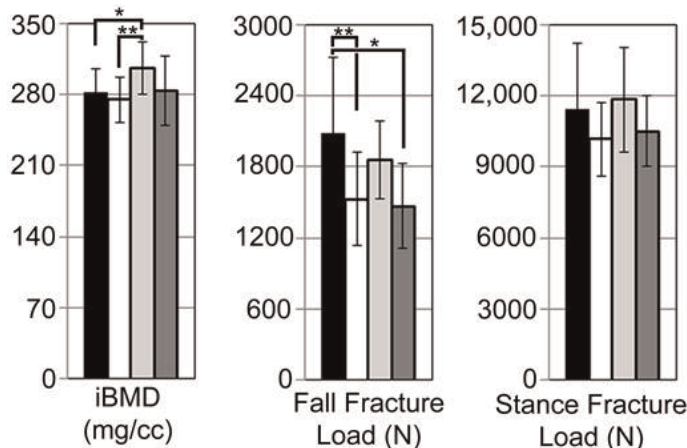


Fig.1. Femoral neck iBMD and FEM fracture load for controls (■), controls with a history of fracture (□), diabetics with no history of fracture (▤), and diabetics with a history of fracture (■). *p < 0.05 **p < 0.01

Fig.1

Disclosures: Dana Carpenter, None.

FR0062

Bone Tissue Micromechanical Properties are Altered Independently of Mineralization in Postmenopausal Osteoporotic Women Long-Term Treated with Alendronate. Yohann Bala^{*1}, Baptiste Depalle¹, Thierry Douillard², Sylvain Meille², Jerome Chevalier², Roland Chapurlat³, Georges Boivin¹. ¹INSERM, UMR 1033; Université de Lyon, France, ²INSA Lyon, MATEIS, CNRS 5510, France, ³E. Herriot Hospital, France

In the treatment of postmenopausal osteoporosis (PMOP), the bisphosphonate alendronate (ALN) decreases the risk of vertebral and non vertebral fractures over a 10 year treatment period¹. Given recent concern about long-term safety of ALN therapy, we have studied the variations of intrinsic properties on iliac bone structural unit (BSU) after a 82 yr ALN treatment (n=6, age:692 yrs, ALN_{LT}) compared to age-matched untreated PMOP women (n=5, PMOP). Quantitative microradiography² of 100 µm-thick sections from embedded bone samples allowed the measurement of the degree of mineralization of bone (DMB) in 150 cortical BSUs chosen to get the widest range of DMB (95 and 55 in ALN_{LT} and PMOP, respectively). Micromechanical properties of the same BSUs were measured on microradiographed sections. High load (>500 mN) nanoindentation tests were used to measure elastic modulus (E), contact hardness (H_c), and the elastic and plastic energies associated to an indentation loading-unloading cycle³. Mineral maturity, crystallinity index and collagen maturity were assessed in same BSUs using Fourier Transform InfraRed Microspectroscopy⁴. Mean DMB was similar between the 2 groups. Compared to PMOP, prolonged ALN treatment was associated with lower E (-12%, p<0.0001) and H_c (-6%, p<0.05) and higher collagen maturity (p<0.001). However, crystallinity index, inversely proportional to crystal size/perfection, was higher in ALN_{LT} than in PMOP (25.290.76 vs. 24.780.70, p<0.001), and was inversely correlated with E and H_c (r=-0.43 and r=-0.54, p<0.001, respectively). Collagen maturity was positively correlated to E and H_c in the two groups (r ranged from 0.40 to 0.70, p<0.0001). Stepwise forward multiple regression including partial correlations revealed that in ALN_{LT}, crystallinity index had a significant entry in the definition of both E and H_c, contrary to PMOP. Treated bone was also less able to plastically resist to deformation at constant strain. To conclude, long-term ALN treatment, while preserving the whole bone strength, may alter the mineral crystallinity and subsequently impair the mechanical behavior at BSU level. This provides rational to include multiscale analysis of material properties in the study of fragility associated with prolonged bisphosphonate therapies.

1.Black et al, Lancet 348:1535, 1996/ 2.Black et al, JAMA 296:2927, 2006/ 3.Boivin et al, Bone 43:532, 2008/ 4.Oliver & Pharr, J Mater Res 7:1564, 1992/ 5.Farlay et al, J Bone Miner Metab 28:433, 2010.

Disclosures: Yohann Bala, None.

FR0067

QTL that Define Trabecular Bone's Micro-mechanical Adaptations to Altered Mechanical Demand. Engin Ozcivici^{*1}, Weidong Zhang², Leah Rae Donahue³, Stefan Judex⁴. ¹Izmir Institute of Technology, Turkey, ²Jackson Laboratories, USA, ³Jackson Laboratory, USA, ⁴Stony Brook University, USA

Loss of functional weightbearing induces a catabolic response in trabecular bone while reambulation is anabolic. The magnitude of either response is modulated by an individual's genetic make-up. As changes in bone morphology are only surrogate measures for bone's risk to fail mechanically, here we identified quantitative trait loci (QTL) that define trabecular bone's micro-mechanical changes during disuse and reambulation. F2 female progeny of BALB and C3H (high and low mechanosensitivity) inbred strains (n=359) were hindlimb unloaded (disuse) for 3wks followed by 3wks of reambulation. At baseline and after the disuse and reambulation periods, the distal femoral metaphysis was scanned by in vivo microCT. Images were evaluated morphologically and micro-mechanically via finite element modeling. Losses in trabecular bone volume fraction amounted to 4317% during disuse, accompanied by a 2715% increase in peak trabecular stress and 10481% increase in skewness of the stress distribution (i.e., efficiency in load bearing with higher numbers indicating lower efficiency). Upon reambulation, trabecular bone volume showed a mean increase of 1022%, while average peak stresses decreased by 108% and the skewness of the stress distributions decreased by 2210%. Genome wide scans identified 5 major (p<0.01) QTL that accounted for 20% of the total variability in baseline peak stress while 3 major QTL accounted for 14% of the variability in the disuse induced increase in peak stress and 1 major QTL accounted for 5% of the variability in the reduction of peak stress during reambulation. The genomic locations identified here differed from previously reported QTL that may modulate morphological adaptations to altered mechanical demand, suggesting that they may harbor novel mechano-sensitive genes. Together, our data show a strong genetic role in the regulation of trabecular bone's micro-mechanical parameters during altered mechanical demand and will ultimately serve towards identifying the underlying genes.

Disclosures: Engin Ozcivici, None.

FR0068

The Role of Oxidative Stress and Antioxidant Enzymes In Bone Under Mechanical Unloading. Daichi Morikawa^{*1}, Yoshitomo Saita², Hidetoshi Nojiri², Keiji Kobayashi¹, Kenji Watanabe¹, Yoshinori Asou³, Kazuo Kaneko², Takahiko Shimizu¹. ¹Molecular Gerontology, Tokyo Metropolitan Institute of Gerontology, Japan, ²Department of Orthopaedics, Juntendo Univ., Japan, ³Tokyo Medical & Dental University, Japan

Mechanical loading is important for maintaining homeostasis both in skeletal muscle and bone. In skeletal muscles, reduced mechanical stimulation leads to increase the level of oxidative stress and change the expression level of antioxidant enzymes, resulting in imbalance of protein synthesis and degradation (i.e., muscle atrophy). However, in bone, relevance of mechanical stimulation and oxidative stress is unclear. The purpose of this study was to clarify whether skeletal unloading increases oxidative stress and changes antioxidant capacity in bone. We analyzed oxidative stress level and gene expression of antioxidant enzymes on skeletal unloading using tail suspension model in mouse.

Unloading significantly increased the level of reactive oxygen species in bone marrow cells collected from hindlimb. A serum marker of oxidative stress (derivatives of reactive oxygen metabolites: d-ROMs) was higher in unloading compared with control (p<0.05). With respect to antioxidant capacity, hindlimb unloading upregulated the expression of CuZn-SOD (*Sod1*), one of the major antioxidant enzymes in cytoplasm, while the expressions of other antioxidant enzymes did not change (Mn-SOD, catalase, glutathione peroxidase1). Therefore, we hypothesized that *Sod1* might have a role to protect from elevated oxidative stress by unloading, and we subjected skeletal unloading for 2 weeks in *Sod1*-deficient (*Sod1*^{-/-}) and wild-type mice (WT). In dual X-ray absorptiometry, *Sod1*^{-/-} showed approx 1.7-fold decrease in BMD of femur by unloading compared with WT (*Sod1*^{-/-}: -13.1%, WT: -7.7%, p<0.05). Similarly, the micro CT analysis showed that *Sod1* deficiency resulted in approx 2-fold decrease in BV/TV by unloading (*Sod1*^{-/-}: -48%, WT: -24%, p<0.01). In dynamic bone formation parameters, *Sod1* deficiency exacerbated in decrease of bone formation rate and mineralizing surface by unloading, while in bone resorption parameter, osteoclast surface, was not changed between WT and *Sod1*^{-/-}. These data indicated that *Sod1* deficiency exacerbated bone loss under reduced mechanical loading due to suppression of osteoblastic bone formation activity.

These results demonstrate that in bone reduced mechanical stimulation leads to increase oxidative stress and an antioxidant enzyme deficiency exacerbated bone loss by unloading.

Disclosures: Daichi Morikawa, None.

FR0069

A Physiome Map of Mechanical and Pharmaceutical Treatment in a Mouse Model of Postmenopausal Osteoporosis. Gisela Kuhn^{*1}, Claudia Weigt², Floor Lambers², Ralph Muller³. ¹ETH Zurich, Switzerland, ²Institute for Biomechanics, ETH Zurich, Switzerland, ³ETH Zurich, Switzerland

Comparisons of results of different studies are often difficult due to variation in design and evaluation techniques. Furthermore, in cross-sectional study designs differences between treatment groups can be alleviated by inter-individual differences at the start, which cannot be determined. Therefore, we investigated the effects of anabolic (parathyroid hormone; PTH), antiresorptive (bisphosphonate; BIS) treatment, and mechanical loading on caudal vertebrae in a mouse model for postmenopausal osteoporosis longitudinally. The ultimate goal of this project is to combine all of the results in a physiome map that allows direct comparison of all physiological effects on a standardized time axis.

Bone loss was induced in 15 week old female C57Bl/6 mice by ovariectomy (OVX). Four weeks of treatment was started either 5 or 11 weeks after OVX, and included a combination of mechanical loading (0N or 8N on the 6th tail vertebra at 3000 cycles and 10 Hz, 3x/week), and either injection of zoledronate (100 µg/kg once), PTH (80µg/kg daily), or corresponding vehicle. An additional group of sham operated animals was subjected to the mechanical loading regime. Bone microarchitectural parameters of the 6th tail vertebra were assessed by in vivo micro-CT before OVX, at treatment start and after 2 and 4 weeks of treatment.

To create the physiome map, the values at treatment start (2nd point) were normalized to the basal measurement for each mouse. The effect of the treatment was calculated regarding to treatment start and percent change was scaled according to the main scale of the first measurement. Here we show the map of trabecular bone volume fraction (Fig. 1) but corresponding maps were created for both cortical and trabecular morphometric parameters.

All OVX mice showed a significant bone loss of 24% and 30% at 5 and 11 weeks after surgery, respectively. Mechanical loading resulted in 16-28% of bone gain. While zoledronate stopped bone loss and slightly increased BV/TV, PTH treatment restored the values to the basal level. The combination of pharmaceutical treatment and mechanical loading was additive in the BIS groups while a slightly synergistic effect was found in the PTH early loading group.

The physiome map allows a fast overview on the relative efficacy of each intervention and presents a powerful tool to compare the different groups on a single time axis. By including results from future longitudinal animal studies the physiome map can be extended easily.

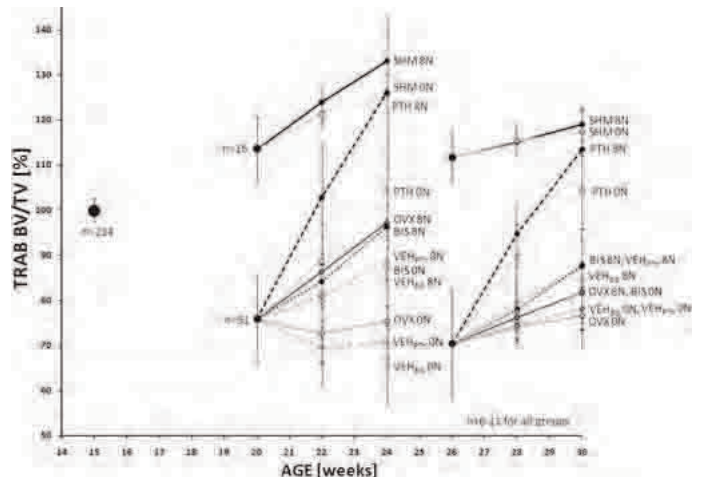


Fig. 1: Physiome map of BV/TV

Disclosures: Gisela Kuhn, None.

FR0070

Does Loading Direction Influence the Cell's Response to High Frequency, Low Magnitude Vibration? Sarah Manske^{*}, Gunes Uzer, Stefan Judex. Stony Brook University, USA

Evidence from human, animal and cell culture studies suggests that cells are responsive to high-frequency mechanical input even when the magnitude of the applied force is very small. The mechanism by which cells can sense such small vibratory oscillations is unknown. It is possible that the cytoskeleton and its attachments may directly respond to the vibratory stimulus to counteract the dynamic forces to which it is subjected. If so, then exposing cells in culture dishes to different loading directions should induce different structural responses in the cells. To test this hypothesis, we applied high-frequency (60 Hz), low-magnitude (0.2 g) vibration to MC3T3-E1 cells. To evaluate short-term structural changes, cells were seeded at 3000 cells/mL on Permanox chamber slides. Cells were exposed to one of the following vibration protocols for 30min: horizontal, vertical, horizontal (15min) + vertical (15min), or no vibration (control). Cells were then stained with alexa fluor 546

phalloidin for actin filaments, and mounted with medium containing DAPI. To evaluate mineralization with alizarin red, cells were seeded at 25,000 cells/mL and cultured until they reached sub-confluency. Next, cells were vibrated 30min/d for 10d during which osteogenesis was induced by α MEM supplemented with 10% FBS, 10% β -glycerolphosphate and 1% ascorbic acid. There was no apparent trend in short-term changes in either actin filament quantity or orientation for any of the vibration protocols. After 10 d, there was a trend towards greater mineralization with horizontally vibrated groups when compared with controls. Continuum-level finite element models of our set-up showed that fluid shear stress acting on the cells is negligible during vertical but not horizontal vibration. Thus, these results suggest that either fluid shear stress may play a role in enhancing mineralization during horizontal vibration or that the signal perceived by the cell depends on the direction of loading. Further, the absence of actin stress fiber formation typically induced by larger magnitudes of fluid shear stress could indicate that either cumulative small-magnitude stimulation may induce cytoskeletal changes or that cytoskeletal changes are not required for the low-level oscillatory signal to become effective. Ultimately, a better understanding of the role that the cytoskeleton plays in sensing and responding to the signal is critical for identifying and optimizing effective and safe loading regimes.

Disclosures: Sarah Manske, None.

FR0071

Inhibition of Angiogenesis during Loading Induced Osteogenesis using α v β 3-targeted Nanoparticle Delivery of Fumagillin. Ryan Tomlinson^{*1}, Anne Schmieder¹, Gregory Lanza¹, Matthew Silva². ¹Washington University in St. Louis, USA, ²Washington University in St. Louis School of Medicine, USA

Angiogenesis plays an important role in regulating osteogenesis. In fact, anti-angiogenic treatment has been shown to inhibit femoral fracture healing as well as mandibular distraction osteogenesis. However, little is known about the effects of vascularity on osteogenesis following mechanical loading. In this study, we inhibited blood vessel formation following osteogenic mechanical loading using perfluorocarbon nanoparticles targeted to integrin α v β 3 that contain the anti-angiogenic agent fumagillin.

Woven bone formation was induced using an established protocol of forelimb compression in adult rats. Nanoparticles or saline was administered daily for three or five days, followed by euthanasia three or seven days after loading, respectively. The vasculature of each animal was perfused using radiopaque plastic (Microfil). Vascular outcomes were quantified in 2D using histological sections stained with H&E and in 3D using μ CT. In addition, we considered vessel maturity by quantifying histological sections stained with antibodies against CD105 and α SMA.

We observed minimal vascular effects from treatment three days after loading; there were no significant differences between treated and non-treated animals in vessel count, area, or volume, but there was a significant decrease (50%) in the number of vessels with angiogenic endothelial cells (CD105 positive) in treated animals. However, seven days after loading, we observed significant vascular differences between treated animals and non-treated controls: 30% decrease in vessel count, 40% decrease in vessel area, and 33% decrease in vessel volume (Figure 1). In addition, treatment significantly decreased mature vessel count (α SMA positive) by 33%. Finally, treatment significantly decreased new bone volume by 25% compared to non-treated controls (Figure 1).

These results indicate that anti-angiogenic treatment by α v β 3-targeted fumagillin nanoparticles impairs new vessel formation between three and seven days after mechanical loading. This decrease in vascularity is preceded by a decrease in angiogenic vessels three days after loading, and ultimately diminishes the woven bone formation response seven days after loading.

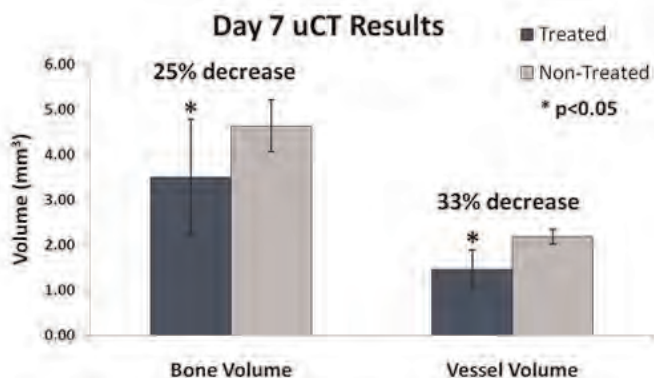


Figure 1 – Anti-angiogenic treatment results in decreases in Bone Volume and Vessel Volume on Day 7

Disclosures: Ryan Tomlinson, None.

FR0072

Mechanical Induction of Focal Adhesion Assembly in MSC Amplifies Anti-adipogenic Signaling Pathways. Buer Sen^{*1}, Christophe Guilluy², Zhihui Xie², Natasha Case³, Maya Styner³, Jacob Thomas², Ipek Oguz², Clinton Rubin⁴, Keith Burrige², Janet Rubin³. ¹University of North Carolina At Chapel Hill, USA, ²UNC, USA, ³University of North Carolina, Chapel Hill, School of Medicine, USA, ⁴State University of New York at Stony Brook, USA

The differentiation of mesenchymal stem cell (MSC) integrates chemical, spatial and physical signals. Mechanical stimuli suppress adipogenesis, preserving MSC potential for alternate pathways such as osteogenesis. The converse is also true as absence of mechanical signals permits increase in adiposity and decrease in bone. The anti-adipogenic effect of mechanical signals, which requires GSK3 β inhibition with β -catenin nuclear translocation, can be enhanced if the challenges are segregated into distinct bouts, enabling both the number of cycles and the magnitude of the load to be reduced. To elucidate mechanisms responsible for the amplification of MSC mechanoreponse, we cultured bone marrow derived MSC in adipogenic medium, and applied mechanical strain at 1 or 2% in bouts of 50, 100 or 200 cycles @10 cpm. We found that mechanical suppression of adipogenesis was significantly enhanced if the mechanical bout was repeated after a 3h rest period. Mechanical induction of Akt phosphorylation and its downstream phosphorylation/inactivation of GSK3 β was also enhanced by this regimen: 100 cycles of mechanical strain induced Akt and GSK3 β phosphorylation to levels 50% higher in cells exposed to mechanical input 3 h earlier compared to cells not exposed. A third mechanical application, reflecting a 2nd recovery period of 3h, further enhanced Akt activation. To understand how mechanical force primes this MSC mechanoreponse, we asked if focal adhesion (FA) assembly was associated with Akt signal augmentation. Vinculin staining showed that FA number increased from 284.6 to 905.2/cell after 50 strain cycles. RhoA activity, which accompanies FA formation, was similarly increased by mechanical treatment. FA disassembled w/in 24h. Preventing FA assembly (blebbistatin or ROCK inhibitor) blocked mechanical Akt~P, but did not inhibit insulin induced Akt~P, indicating that cytoskeletal FA are critical to the ability of the cell to respond to physical, but not necessarily hormonal, challenges. As such, mechanically activated signaling pathways that restrict MSC adipocyte differentiation are directly regulated by force altered, adaptable cytoskeletal events. The transient nature of the cytoskeletal adaptation to mechanical input should be considered as key to optimizing mechanical input; mechanical induction of FA may enhance exercise based strategies to maximize bone quality and prevent acquisition of fat.

Disclosures: Buer Sen, None.

FR0073

Mechanical Loading Activates Integrin α 5 β 1 Leading to the Opening of Connexin 43 Hemichannels in Osteocytes - a Mechanism for Extracellular Release of Small Bone Anabolic Factors. Nidhi Batra¹, Sirisha Burra², Sumin Gu², Xuechun Xia³, Lynda Bonewald⁴, Eugene Sprague², Martin Schwartz⁵, Jean Jiang^{*6}. ¹University of Texas Health Science Center at San Antonio (UTHSCSA), USA, ²University of Texas Health Science Center, USA, ³University of Florida, USA, ⁴University of Missouri - Kansas City, USA, ⁵University of Virginia, USA, ⁶University of Texas Health Science Center at San Antonio, USA

Connexin 43 (Cx43) hemichannel in osteocytes is a major portal for the release of factors important for the anabolic effects of mechanical loading on bone. Mechanical stimulation in the form of fluid flow shear stress has been shown to induce the opening of Cx43 hemichannels in MLO-Y4 osteocyte-like cells releasing prostaglandins, ATP and potentially other signaling molecules. Previously, we found that Cx43 consistently co-localizes and associates with the integrin α 5 β 1, but not with the focal adhesion proteins, vinculin or paxillin. Blocking antibody to integrin α 5 inhibits and integrin α 5 siRNA totally abolishes the opening of hemichannels. Here, by protein pull down and surface plasmon resonance (SPR) analyses, we demonstrated the direct interaction between Cx43 and integrin α 5 through their cytoplasmic C-termini. Overexpression of Cx43 C-terminal domain inhibited the hemichannel dye uptake and the interaction between endogenous Cx43 and integrin α 5, suggesting that integrin α 5 interaction with Cx43 through their cytoplasmic C-termini is critical for the opening of Cx43-hemichannel in response to mechanical stress. To examine if ligand engagement of integrin α 5 with the fibronectin substrate was required for its function upon mechanical stimulation, application of extracellular matrix substrate, fibronectin or integrin binding ligand RGD peptide, to MLO-Y4 cells had no effect on the opening of hemichannels by shear stress, indicating that integrin α 5, not fibronectin, is the target for opening hemichannels by shear stress. Furthermore, to establish a direct role for integrin α 5 β 1 in force-dependent regulation of Cx43-hemichannels, magnetic beads coated with either anti- α 5 integrin antibody or fibronectin were perturbed by a magnetic field after attachment to the cell surface which resulted in the opening of hemichannels. Moreover, incubation with an integrin β 1 activating antibody was sufficient for opening the hemichannels in the absence of any mechanical stimulation. This data suggest that activation of integrin possibly through conformational change is a likely mechanism opening the hemichannels in response to mechanical stimulation. Together, these results suggest a novel function of integrin α 5 β 1 that

acts as a mechanical tether to induce opening of hemichannels, a function independent of association with fibronectin substrate.

Disclosures: Jean Jiang, None.

FR0074

Runx2 S301,S319 phosphorylation Controls Mechanical Force-Induced Osteoblast Gene Expression *In Vitro* and *In Vivo*. Yan Li^{*1}, Chunxi Ge², Jason Long¹, Jose Rodriguez², Dana Begun¹, Steven Goldstein³, Renny Franceschi⁴. ¹University of Michigan, USA, ²University of Michigan School of Dentistry, USA, ³University of Michigan Orthopedic Research Labs, USA, ⁴Dept of Periodontics & Oral Medicine, University of Michigan School of Dentistry, USA

Mechanical force is a major anabolic signal in bone that enhances mass and strength. Little is known about how mechanical signals induce changes in gene expression necessary for increased bone formation. In the present study, we explore this mechanism *in vitro* and *in vivo* using fluid flow shear stress (FFSS) and ulnar loading models. The ERK/MAPK pathway is one of several signal transduction pathways induced by mechanical loading. We recently showed that activation of this pathway is required for extracellular matrix-induced osteoblast differentiation, gene expression and bone development. ERK functions in part by phosphorylating Runx2 on specific serine residues. Of these, S301 and S319 are critical for transcriptional activity (Ge et al. JBC 284:32533, 2009). To evaluate whether Runx2 phosphorylation is also important in the response to mechanical loading, we employed a recently developed antibody that specifically detects Runx2-S319-P. Exposure of MC3T3-E1 subclone 42 preosteoblast cells to cyclic FFSS (0.033 Hz, 2Pa for 60 minutes) dramatically induced osteopontin (SSP1), bone sialoprotein (Ibsp) and osteocalcin (Bglap2), but not Runx2 mRNAs. As little as 5 min. of FFSS increased P-ERK1/2 and Runx2-S319-P and this response persisted for several hours after stimulation was terminated. Immunofluorescence, co-IP and chromatin immunoprecipitation (ChIP) analysis showed that FFSS induced P-ERK translocation from cytoplasm to nucleus where it co-localized with and phosphorylated Runx2 on the chromatin of *Bglap2* and *Ibsp* target genes. Coincident with these events, increases in histone H3 and H4 acetylation and histone H3-S10 phosphorylation were also detected in promoter regions of *Ibsp* and *Bglap2*. Application of U0126, a MAP inhibitor, prior to FFSS abolished all FFSS-induced events including Runx2 phosphorylation, histone modification and gene expression. Similarly, prevention of phosphorylation by introduction of S301A,S319A mutations into Runx2 completely blocked the response to FFSS. To examine Runx2 phosphorylation *in vivo*, a murine ulnar loading model was employed. Three days of cyclical loading (2000 μ strain, 500 cycles at 2 Hz/day) on the left ulna dramatically induced gene expression of osteopontin (200 fold), *Ibsp* (500 fold), *Bglap2* (1200 fold) and *Runx2* (70 fold) compared to the unloaded right ulna. ERK and Runx2-S319-P both increased after as little as one loading cycle. These studies establish a novel mechanism to explain how mechanical loads induce changes in gene expression involving ERK/MAPK phosphorylation and activation of Runx2, histone modification and increased transcription.

Disclosures: Yan Li, None.

FR0078

Inhibition of the SDF-1/CXCR4 Signaling Axis Attenuates Load-Induced Bone Formation. Sara Temiyasathit¹, Philipp Leucht², Vasavi Ramachandran¹, Christopher Jacobs³, Jill Helms², Alesha Castillo^{*4}. ¹Veterans Affairs Palo Alto Medical Center, USA, ²Stanford University, USA, ³Columbia University, USA, ⁴Palo Alto Veterans Affairs Medical Center, USA

Introduction: Mechanical loading activates new bone formation through a complex chain of events that involves osteocyte signaling, osteoblastic differentiation, and mobilization of mesenchymal stromal cells (MSCs), but relatively little is known about signaling events controlling these processes. Stromal cell-derived factor-1 (SDF-1) is a potent attractive cue for progenitors expressing its receptor, CXCR4, which is expressed in many cell types including MSCs and osteoblasts [1]. The purpose of this study was to determine the role of SDF-1/CXCR4 signaling in load-induced bone formation.

Materials and Methods: Right ulnae in 18-wk-old C57BL/6 mice were subjected to axial loading (120 cyc, 2 Hz, 3N). SDF-1 levels in bone were detected by *in situ* hybridization [2]. MLO-Y4 osteocyte-like cells were exposed to oscillatory fluid flow (10 dyn/cm², 1 Hz), and SDF-1a concentrations in conditioned media were determined by ELISA. Eighteen-wk-old C57BL/6 mice were treated with AMD3100, a CXCR4 antagonist (5 mg/kg, IP, daily), or vehicle, and subjected to *in vivo* ulnar loading (120 cyc, 2 Hz, 2.8N). Relative periosteal bone formation rates were calculated [3, 4]. Differences in means were tested for significance using a Student's t-test. Data are presented as mean standard error.

Results: SDF-1 was expressed in osteocytes, periosteal cells and marrow cells. In *in vivo* ulnar loading resulted in enhanced expression of SDF-1 in both osteocytes, periosteal cells and bone marrow cells. MLO-Y4 cells exposed to oscillatory fluid flow exhibited greater SDF-1a release (3.71.6 pg/mg) at 2 hr post-flow compared to no flow

samples (9.84.7 pg/mg) although the difference was not significant ($p=0.23$). Blocking SDF-1/CXCR4 signaling with the CXCR4 antagonist, AMD3100, resulted in significantly attenuated relative mineralizing surface ($p<0.001$) and relative bone formation rates ($p=0.002$) (Fig. 1).

Conclusions: Taken together our data suggest that mechanical stimulation enhances expression of SDF-1 in osteocytes, periosteal cells and bone marrow cells. Blocking SDF-1/CXCR4 signaling significantly attenuates load-induced bone formation suggesting that the SDF-1 signaling plays a key role in mechanically-induced osteogenesis.

Acknowledgements: This work was funded by a Veterans Affairs Career Development Award and NIH grant.

References: [1] Nagasawa et al., PNAS 1996; [2] Albrecht et al., In: Datson GP (ed) 1997; [3] Parfitt et al., J Bone Miner Res 1987; [4] Castillo et al., Bone 2006.

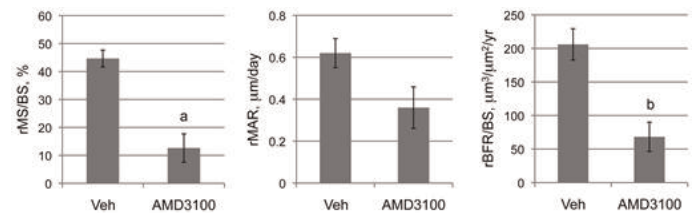


Figure 1. Load-induced relative (r) periosteal bone formation parameters

Disclosures: Alesha Castillo, None.

FR0079

Role of CKIP-1 in Normal Fracture Healing. Yixin HE^{*1}, Baosheng GUO², Zhong Liu³, Dahu Li⁴, Fuchu HE⁴, Lingqiang Zhang⁴, Ling Qin⁵, Ge Zhang⁶. ¹The Chinese University of Hong Kong, Hong Kong, ²Prince of Wales Hospital, Hong Kong, ³The Chinese University of Hong Kong, Hong Kong, ⁴State Key Laboratory of Proteomics, Beijing Proteomics Research Center, The Academy of Military Medical Sciences, China, ⁵Chinese University of Hong Kong, Hong Kong, ⁶Prince of Wales Hospital, Hong Kong

Introduction: Bone morphogenetic protein (BMP) signaling pathway is an important one responsible for fracture healing. Smad 1/5 have been shown to be the major molecules in BMP signaling. Smurf 1 was identified as an E3 ubiquitin ligase to degrade the Smad 1/5. Recently, we have found that Casein kinase-2 interacting protein-1 (CKIP-1) interacts with Smurf1 and enhances the ligase activity of Smurf1 to promote degradation of Smad1/5. Further, active osteogenesis and subsequent high peak bone mass were found in our established CKIP-1 gene knockout mice when compared to the wild type, indicating the potential role of CKIP-1 in fracture healing. This study aimed to examine the role of CKIP-1 in fracture healing

Methods: Twelve female 3-month-old CKIP-1knockout mouse (KO) and 12 female age-matched wild type C57BL/6 mice (WT) were used in the study. Transverse fracture creation at mid-shaft of right femur will be performed in both groups. 3 mice from each group will be sacrificed at 1, 2, 4 and 6 weeks post fracture. After sacrifice, the fractured specimens will be performed by microCT examination and biomechanical testing. To differentiate newly formed mineralized callus from old cortices, the low- and high-density mineralized tissues were reconstructed using different thresholds. Morphometric parameters used for evaluation were total tissue volume (TV, μm^3), volume of high-density bone (BVh), volume of low-density bone (BVL), total bone volume (BVT, mm^3 , equivalent to BVh+BVL) and normalized percentage of the tissue volumes including BVh/TV, BVL/TV, BVT/TV.

Results: At different time points, reconstructed mineralized calluses showed different morphologic characteristics between groups in the 3D micro-CT images (Fig.1). At 1 week post-fracture, TV and BVL showed higher values in the KO group, but the differences were not statistically significant. At 2 weeks post-fracture, TV, BVT, BVL, BVL/TV and BMC were significantly higher in the KO group than in the WT group. At 4 weeks post-fracture, the KO group presented higher BVL, BVL/TV and BMC than the WT group. At 6 weeks post-fracture, KO groups still have significant larger BVL, BVL/TV and BMC than WT group. Consistently, KO mice also showed significant higher ultimate load and energy to failure compared to the WT mice at 6 weeks post-surgery (Fig.2).

Conclusion: CKIP-1 plays an important role in fracture healing in adult mice.

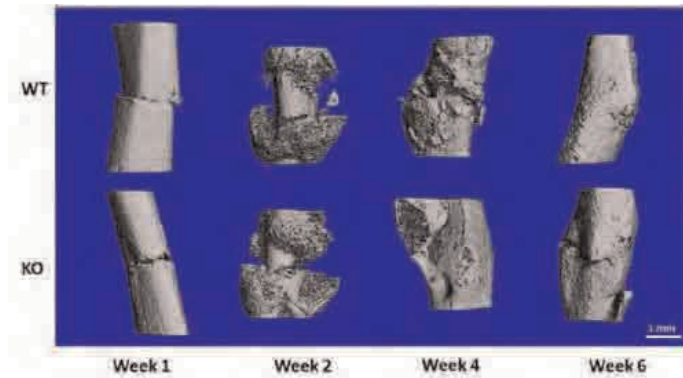


Figure 1 Micro-CT 3D images of fracture healing.

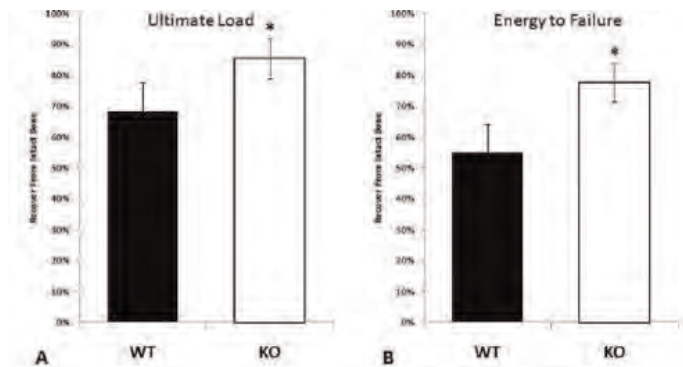


Figure 2 Biomechanical testing of callus at 6 weeks post-fracture. * $P < 0.05$ compared to WT mice by independent t test.

Disclosures: Yixin HE, None.

FR0086

Hdac3 Controls Growth Plate Matrix Secretion and Akt/mTOR Pathway Activation. Elizabeth Bradley*, David Razidlo, Bridget Stensgard, Jennifer Westendorf. Mayo Clinic, USA

The histone deacetylases (Hdacs) regulate tissue development and cellular differentiation because they modify chromatin structure and influence gene expression. Endochondral ossification is a highly organized and tightly controlled developmental process that relies on Hdacs, particularly Hdac4, for proper execution. We previously demonstrated that conditional deletion of *Hdac3* in osteo-chondro-progenitor cells with osterix-Cre causes a runted phenotype characterized by decreased growth plate width and reduced bone mass. The goal of this project was to further define the role of *Hdac3* in chondrocyte differentiation using these animals. Using immunohistochemistry, we found that Hdac3 is expressed at the articular surface and within the resting and pre-hypertrophic zones of the growth plate in a two-week old mouse, but not within the proliferating and hypertrophic zones. Conditional *Hdac3* deficiency accelerated chondrocyte hypertrophy but decreased hypertrophic cell size, and disrupted the columnar chondrocyte array. This change was accompanied by decreased alcian blue staining and lower expression of *aggrecan*, *osteopontin* and *mepe*, suggesting that matrix deposition may be altered with conditional *Hdac3* deficiency. To further explore the role of *Hdac3* during chondrocyte differentiation, we developed an *in vitro* model using immature mouse articular chondrocytes (iMACs) cultured in micromass to recapitulate chondrocyte differentiation. Similar to *in vivo* results, iMACs from *Hdac3* conditional knockout mice demonstrated accelerated chondrocyte hypertrophy, but decreased matrix deposition and lower expression of matrix genes including *aggrecan*, *osteopontin* and *mepe*. Activation of the Akt/mTOR pathway increases cell size and matrix deposition. *Hdac3* conditional deficiency decreased Akt/mTOR phosphorylation and activation of the downstream translational regulator S6 kinase and 4E-BP1 in iMAC cultures. Thus, Hdac3 may regulate growth plate matrix deposition by promoting the activation of the Akt/mTOR pathway during endochondral ossification.

Disclosures: Elizabeth Bradley, None.

FR0087

Disruption of Mitogen Inducible Gene 6 (MIG6) in the Mouse Genome Accelerates Surgical Induced Osteoarthritis and Down Regulates Wnt Signaling. Danese Joiner^{*1}, Michael Morris², Donald Scholten², Ben Staal³, George Vande Woude³, Clifford Jones⁴, Debra Sietsema⁴, Yu-Wen Zhang³, Jim Mason⁵. ¹Van Andel Research Institute, USA, ²Orthopaedic Cell & Tissue Mechanics Laboratory, Van Andel Research Institute, USA, ³Molecular Oncology Laboratory, Van Andel Research Institute, USA, ⁴Orthopaedic Associates of Michigan, USA, ⁵Van Andel Institute, USA

The interaction between pathological joint mechanics and osteoarthritis is recognized but not well understood. Here we examine the role of mitogen inducible gene 6 (MIG6) through its interaction with Wnt signaling in this process. Mig6 knock out (KO) mice were generated as described previously (Zhang, Y. PNAS 2005). Ligament and meniscus transections were performed on the right knee (RK) of 11 four-week-old wild type (WT) and 11 four-week-old Mig6 KO animals as described previously (Kamekura, S. OA and Cartilage 2005). The left knees (LK) of each of these animals were intact and served as a contralateral control. After 4 weeks, animals were euthanized for micro CT, histological, and RT-PCR analysis. Knees were harvested from WT (n=3) and KO (n=3) mice and scanned at a 10 micron voxel size with a Skyscan 1172 System (Skyscan, Belgium Germany). Images were reconstructed and bone and joint structure were observed. Knees were harvested from WT (n=5) and KO (n=5) mice, fixed for 48h in 10% Neutral Buffered Formalin, and then placed in Decal for 48h. Samples were embedded into a paraffin mold and sectioned at 5 um, stained with Weigerts Hematoxylin, fast green solution, Safranin O solution, dehydrated, and cleared. Mouse knees were aseptically harvested from WT (n=3) and KO (n=3) animals, homogenized in 1mL of TRIzol, chloroform-precipitated and RNA extracted with an RNeasy Mini Kit (Qiagen, Valencia, CA). Relative mRNA transcript levels were measured by RT-PCR utilizing a RT2 Profiler Wnt Signaling PCR Array (SABiosciences, Frederick, MD). Student t test statistics were applied. Joint degradation and osteophyte formation were more severe in the transected knee of Mig6 KO animals compared to the contralateral control Mig6 KO knee and Mig6 WT knees (Fig. 1A) Safranin O staining (red) suggests the formation of abnormal outgrowing nodules with abundant proteoglycans in the Mig6 KO RK (Fig. 1B). Wnt gene expression in the RK compared to the untouched LK was decreased in Mig6 KO animals compared to WT, significantly for Lrp6, Gsk3b, Kremen1, Axin1, and Dvl2 (Fig. 2). Data from this study demonstrates that OA is accelerated in Mig6 KO mice knees after ligament transection and meniscus removal. Mig6 is therefore an important regulator of mechanotransduction in the normal and pathological joint.

Figure 2: Wnt Gene Fold Changes (RK Relative to LK) * $p < 0.05$

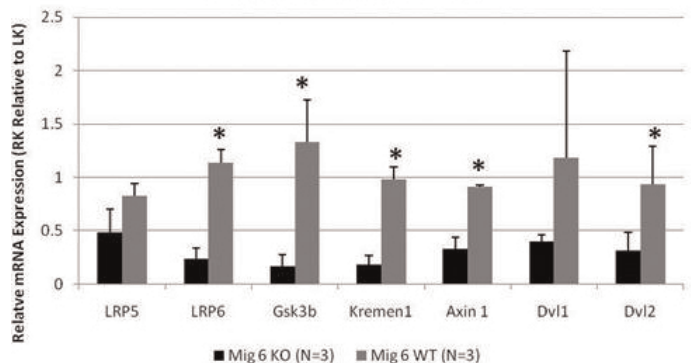


Figure 2

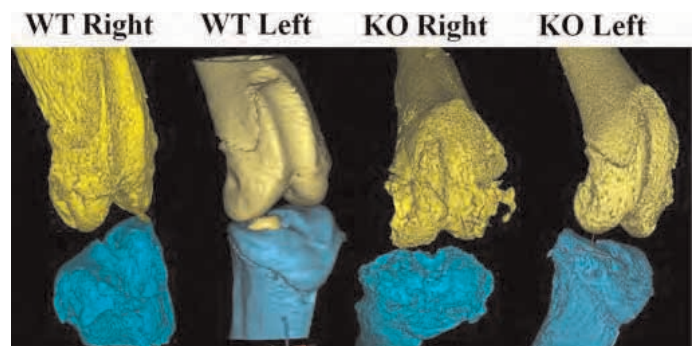


Figure 1A

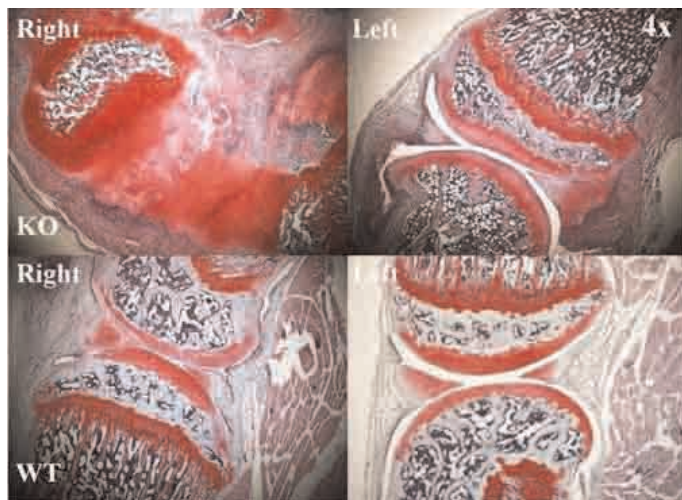


Figure 1B

Disclosures: Danese Joiner, None.

FR0088

NELL-1 Promotes Cartilage Regeneration in an *In Vivo* Rabbit Model.

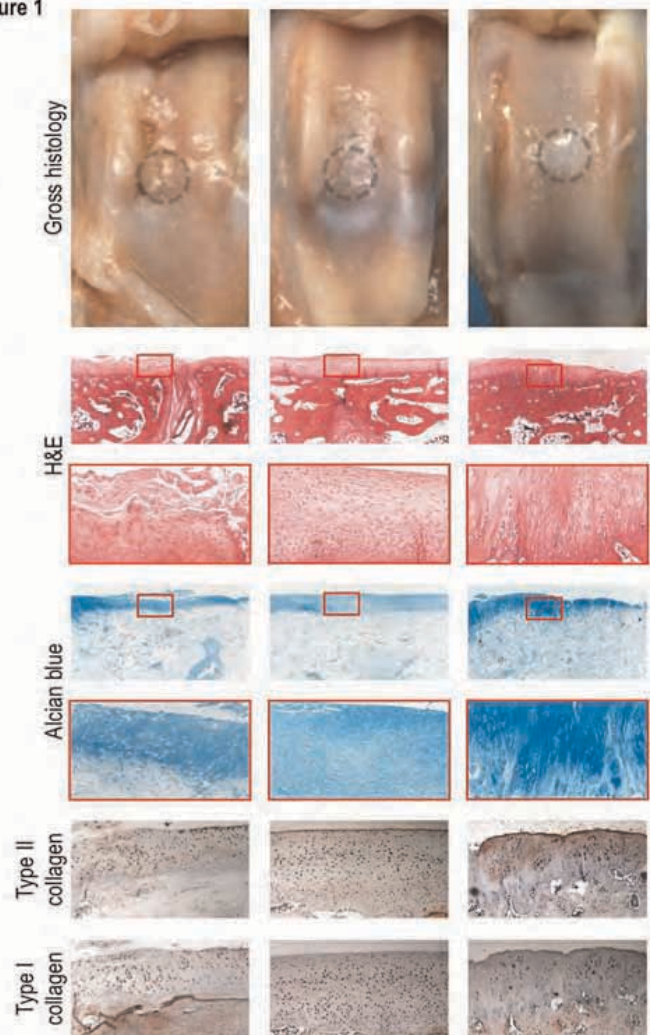
Ronald Siu^{*1}, Janette Zara², Yaping Hou¹, Jinny Kwak¹, Xinli Zhang¹, Aaron James¹, Karina Covarrubias¹, Benjamin Wu¹, Kang Ting¹, Chia Soo¹, Min Lee¹. ¹University of California, Los Angeles, USA, ²UCLA, USA

Repair of cartilage due to joint trauma remains challenging due to the poor healing capacity of cartilage, adverse effects related to current growth factor-based strategies, and the propensity of chondrocytes to dedifferentiate *in vitro*, which limits autologous chondrocyte transplantation approaches. Nell-1 (*Nel-like molecule-1*), a Runx2-regulated growth factor we first characterized in the context of premature cranial suture fusion, plays important roles in normal chondrogenesis and cartilage organization during development. Translational studies with purified Nell-1 protein support the hypothesis that Nell-1 accelerates differentiation along the osteochondral lineage.

We previously demonstrated the ability of Nell-1 protein to maintain the cartilaginous phenotype of explanted rabbit chondrocytes *in vitro*, as assessed by proteoglycan deposition and type II collagen expression. Our objective in the present study is to determine whether Nell-1 can affect endogenous chondrocytes in an *in vivo* cartilage defect model. To achieve controlled Nell-1 release and provide a biocompatible, biodegradable scaffold for tissue repair, Nell-1 was incorporated into chitosan nanoparticles and embedded into alginate hydrogels. These implants were press-fit into critical-sized, 3-mm circular osteochondral defects created in the femoral condylar cartilage of 3-month-old New Zealand White rabbits ($n=10$). Controls included unfilled defects ($n=8$) and defects filled with Nell-free alginate ($n=8$). Rabbits were sacrificed 3 months post implantation for histological analysis.

Defects filled with alginate containing Nell-1 demonstrated significantly improved cartilage regeneration. Remarkably, histology of Nell-1 treated defects closely resembled that of native cartilage, including stronger Alcian blue staining and increased deposition of type II collagen and absence of type I collagen, as demonstrated by immunohistochemistry (Figure 1). Our results suggest that Nell-1 may produce functional cartilage with properties similar to native cartilage and appropriate distributions of extracellular matrix molecules, and is an exciting candidate for novel tissue engineering-based approaches for treating osteoarthritis and other diverse pathologies of cartilage defects and degeneration.

Figure 1



Disclosures: Ronald Siu, None.

FR0089

PTHrP Blocks Thyroid Hormone Signaling Through PP2A/HDAC4/Mef2 Pathway in Growth Plate Chondrocytes. Lai Wang*, Yvonne Shao, R. Tracy Ballock. Cleveland Clinic, USA

Thyroid hormone is a critical modulator of skeletal maturation *in vivo*. Hypertrophic differentiation of growth plate chondrocytes is severely impaired in hypothyroid mice, correlated with a decrease in type X collagen expression and increased expression of PTHrP. PTHrP has been recently reported to repress chondrocyte hypertrophy through a PP2A/HDAC4/Mef2 pathway. The association of myocyte enhancer factor-2c (Mef2c) and its corepressor histone deacetylase 4 (HDAC4) controls chondrocyte hypertrophy and endochondral bone development. Our hypothesis is that PTHrP inhibits the effects of thyroid hormone on terminal differentiation of growth plate chondrocytes through the PP2A/HDAC4/Mef2c pathway.

Pellet cultures of newborn rat distal femoral growth plate chondrocytes were maintained in serum-free medium in the presence or absence of T3, PTHrP and the PP2A inhibitor okadaic acid (OA). T3 treatment significantly downregulated PTHrP mRNA expression and increased the expression of its receptor PTHR. T3 increased both Mef2c mRNA expression and Mef2 transcriptional activity, and these effects were inhibited by addition of PTHrP. PTHrP inhibited T3-dependent thyroid hormone receptor TR α 1-mediated transcriptional activation, and markedly decreased T3-increased Col10a1 mRNA expression and alkaline phosphatase (ALP) activity in a dose-dependent manner. Addition of OA reversed the inhibitory effects of PTHrP and synergistically enhanced T3 activity in growth plate chondrocytes. Overexpression of HDAC4 resulted in decreases in T3-induced Col10a1 mRNA expression and ALP activity. Immunoblot analysis showed that T3 increased phosphorylation of HDAC4 and promoted the translocation of HDAC4 from the nucleus to the cytoplasm, which prevented HDAC4 from binding to Mef2c and inhibiting its activity. PTHrP decreased T3-mediated HDAC4 phosphorylation and promoted nuclear translocation of HDAC4.

This study identifies that thyroid hormone decreases PTHrP expression and enhances Mef2c expression and activity in growth plate chondrocytes. PTHrP may suppress T3-induced hypertrophy by dephosphorylation of HDAC4, nuclear translocation of HDAC4, and consequent inhibition of Mef2c activity. In addition, PTHrP inhibits TR transcriptional activity, indicating that PTHrP is a potent negative regulator of thyroid hormone signaling in the growth plate chondrocyte terminal differentiation.

Disclosures: Lai Wang, None.

FR0090

Roles of the Heterotypic CCN2/CTGF-CCN3/NOV and Homotypic CCN2-CCN2 Interactions in Matrix Synthesis in Chondrocytes. Mitsuhiro Hoshijima^{*1}, Takako Hattori², Eriko Aoyama³, Takashi Nishida¹, Takashi Yamashiro⁴, Masaharu Takigawa⁵. ¹Okayama University, Japan, ²Department of Biochemistry & Molecular Dentistry Okayama University Graduate School of Medicine, Dentistry & Pharmaceutical Sciences, Japan, ³Biodental Research Center, Okayama University Dental School, Japan, ⁴Department of Orthodontics & Dentofacial Orthopedics Okayama University Graduate School of Medicine, Dentistry & Pharmaceutical Sciences, Japan, ⁵Okayama University Graduate School of Medicine, Dentistry & Pharmaceutical Sci., Japan

[Objective] CCN family member 2 / Connective tissue growth factor (CCN2) is strongly expressed in cartilage and modulates chondrocyte differentiation and proliferation. The aim of this study is to identify CCN2-interactive proteins and to investigate their influence on the matrix-stimulating activity of CCN2 in chondrocytes. [Methods] We carried out a yeast two-hybrid screening of a cDNA library derived from the human chondrocytic cell line HCS-2/8, using CCN2 as a bait, and specified the interaction sites in both CCN2 and its binding partners. CCN2 and interactive proteins were expressed ectopically in the COS7 cells to study their binding and their cellular localization. In addition, direct interactions between purified recombinant proteins of CCN2 and interactive proteins were investigated by immunoprecipitation and SPR (surface plasmon resonance) analysis *in vitro*. The influence that interaction of these proteins gave on cartilage matrix gene expression was monitored by real-time PCR. [Results] The yeast two-hybrid screening for CCN2 binding proteins revealed both CCN2 and CCN3/NOV as homotypic and heterotypic ligands, respectively. Among the four domains in CCN2, the IGFBP, VWC and CT domains exhibited direct homotypic interaction with CCN2, while only VWC and CT domains of CCN2 showed direct interaction with CCN3. These interactions were confirmed by immunoprecipitation and SPR analysis *in vitro* ($KD \approx 1 \times 10^{-9}$ M), using recombinant proteins of CCN2 and CCN3. Ectopically expressed CCN2 and CCN3 in COS7 cells showed good co-localization by indirect immunofluorescence staining, and binding by immunoprecipitation *in vivo*. Addition of CCN2 to chondrocytes enhanced expression of the extracellular matrix genes such as aggrecan mRNA, whereas addition of CCN3 impaired expression of these genes. The combination of CCN2 and CCN3 abolished the impaired expression of extracellular matrices by CCN3 in a dose-dependent manner of CCN2. [Conclusion] These results suggest that CCN2 may form a homodimer as well as heterodimer with CCN3. CCN2 promotes, while CCN3 inhibits expression of aggrecan mRNA in chondrocytes. Because the restraint by CCN3 was improved dose-dependently by CCN2, our data suggests that activity of CCN2 is regulated by the interaction with CCN3.

Disclosures: Mitsuhiro Hoshijima, None.

This study received funding from: Japan Society for the Promotion of Science

FR0092

TGF β and Substrate Stiffness Interact to Direct Chondrocyte Differentiation. Jessica Orr^{*}, Tamara Alliston. University of California, San Francisco, USA

Physical cues, like biochemical cues, can regulate cell differentiation. Specifically, the stiffness of the extracellular matrix (ECM) directs stem cell differentiation and plays a key role in cancer and other diseases. Though ECM stiffness is tightly defined throughout articular cartilage and is disrupted in osteoarthritis, the effect of ECM stiffness on chondrocyte differentiation is unclear. To test the hypothesis that chondrocyte differentiation is stiffness-sensitive, ATDC5 chondroprogenitor cells were grown for 7 days on polyacrylamide substrates with a range of stiffnesses (0.02 – 2MPa) spanning the stiffness of articular cartilage. To facilitate cell attachment, the gels are conjugated with collagen II. The substrate stiffness closest to articular cartilage (1MPa) potentially induced the expression of chondrocyte differentiation genes, Sox9, Col2a1, and aggrecan 5, 19, and 16-fold, respectively, relative to cells on plastic. Similar results are observed in mesenchymal stem cells. Like other mechanosensitive responses, the stiffness-dependent induction of chondrogenic differentiation was sensitive to inhibition of ROCK (Y27632).

Little is known about the mechanisms by which physical cues such as ECM stiffness interact with biochemical cues to direct cell differentiation. Since TGF β is a key regulator of chondrocyte differentiation, we sought to determine whether ECM stiffness and TGF β cooperate to control chondrocyte differentiation. Compared to a 5-10-fold induction of Col2a1 and aggrecan expression induced by TGF β in ATDC5

cells grown on plastic, TGF β stimulated 140 and 70-fold-induction of these genes in ATDC5 cells grown on 1MPa substrates. Cooperative induction of Col2a1 was also observed within 24 hrs of TGF β treatment. To determine if synergy utilized the Smad or non-Smad arms of the TGF β pathway, we performed loss of function studies using shRNA for Smad3 or chemical inhibitors of Erk/MAPK. Both Smad3 and p38 signaling are required for the cooperative induction of Col2a1 by TGF β and ECM stiffness. This is consistent with the increased Smad3 and p38 phosphorylation, detected by Western analysis, in ATDC5 cells grown on 1 MPa substrates relative to plastic, even in the absence of added TGF β . In summary, we found that TGF β and ECM stiffness synergize to enhance chondrocyte differentiation through Smad3 and p38 dependent pathways, revealing a novel molecular mechanism by which physical and biochemical cues interact to direct cell differentiation.

Disclosures: Jessica Orr, None.

FR0094

Vinculin-mediated Signaling from Extracellular Matrix Interacts with the Signaling Triggered by Humoral Factors and Regulates Chondrocyte Differentiation in a Sox9-independent Manner. Takao Koshimizu^{*1}, Masanobu Kawai¹, Kanako Tachikawa¹, Keiichi Ozono², Toshimi Michigami¹. ¹Osaka Medical Center & Research Institute for Maternal & Child Health, Japan, ²Osaka University Graduate School of Medicine, Japan

Vinculin is a cytoskeletal protein which functions in adhesion and/or signaling between the extracellular matrix (ECM) and the cell. Although a recent work demonstrated a tissue-specific function of vinculin in cardiomyocytes, its roles in skeletogenesis have not been elucidated. We applied a gene-trap mutagenesis in a chondrogenic cell line ATDC5, and isolated a clone where *vinculin* gene was trapped. Interestingly, the trapping of *vinculin* gene resulted in impaired differentiation to mature chondrocytes, which has brought us to hypothesize that vinculin might play a role in chondrocyte differentiation. In immunostaining using an anti-vinculin antibody, chondrocytes in mouse growth plates were positively stained, and the immunoreactivity was intense in prehypertrophic and hypertrophic chondrocytes. Moreover, the expression of vinculin was gradually elevated during the differentiation of primary chondrocytes isolated from mouse rib cages. Then, we further investigated the role of vinculin in chondrocytes by miRNA-mediated knock down in primary chondrocytes using adenoviral transfer. Adhesion-induced phosphorylation of FAK was markedly increased both in *vinculin* knocked-down chondrocytes and *vinculin*-trapped clone, indicating that signaling from ECM was altered in these cells. When cultured in differentiation medium, primary chondrocytes with *vinculin* knocked-down exhibited marked decrease in the expression of *Col2a1* and *aggrecan*, and so did *vinculin*-trapped clone. To our surprise, the expression of *Sox9* was retained in both *vinculin*-knocked down chondrocytes and *vinculin*-trapped clone, suggesting that vinculin might regulate chondrocyte differentiation in a Sox9-independent manner. The expression of *Sox5* was also retained, while that of *Sox6* was decreased. Consistently, knockdown of vinculin in organ culture system of mouse embryonic metatarsal bone resulted in impaired growth of cartilage. Finally, to clarify the mechanism for the regulation of chondrocyte differentiation by vinculin, we comprehensively investigated the alteration in signaling by knockdown or trapping of *vinculin* gene during chondrocyte differentiation, and found that phosphorylation of SHP-2 and Akt was markedly increased either by knockdown or trapping of *vinculin*. Our findings imply that vinculin-mediated signaling from ECM regulates chondrocyte differentiation in a Sox9-independent manner, through the interaction with the signals evoked by growth factors such as IGF and FGF.

Disclosures: Takao Koshimizu, None.

FR0095

Wnt5a Signaling Gradient Controls Directional Cartilage Growth by Establishing Planar Cell Polarity in Chondrocytes. Bo Gao^{*1}, Hai Song¹, Kevin Bishop¹, Gene Elliot¹, Lisa Garrett¹, Milton English¹, Philipp Andre¹, James Robinson¹, Raman Sood¹, Yasuhiro Minami², Aris Economides³, YINGZI YANG⁴. ¹National Human Genome Research Institute, USA, ²Kobe University, Japan, ³Regeneron Pharmaceuticals, Inc., USA, ⁴NIH, USA

The longitudinal growth of long bone requires proximal-distal elongation of the cartilaginous anlage. However, the mechanism underlying directional elongation of the long bone cartilage is unclear. Wnts are a large family of secreted signaling molecules that govern multiple essential morphogenetic processes and adult tissue homeostasis, including bone formation and remodeling. In addition to the well-characterized canonical Wnt/beta-catenin signaling pathway, we and others have shown that the beta-catenin-independent Wnt/Planar Cell Polarity (PCP) pathway is critically required in many developmental processes by conveying and transmitting positional information. PCP, which originally refers to the polarity of epithelial cells within a plane orthogonal to their apical-basal axis, is regulated by a group of evolutionarily conserved core PCP components including a four-pass transmembrane protein, Vangl2. PCP is established in response to a global positional cue. However, the identity and mechanism of such positional cue were unknown in vertebrate

morphogenesis prior to our work. Here we found that Wnt5a signaling gradient in the limb bud controls cartilage elongation by establishing PCP in chondrocytes along the proximal-distal axis. We provided both biochemical and genetic evidence that Ror2, a Wnt5a-binding receptor tyrosine kinase, and Vangl2 transduce Wnt5a signaling in multiple developmental processes in the mouse embryos. Importantly, we found that Wnt5a induced Vangl2 phosphorylation through Ror2 in a dose-dependent manner both *in vitro* and *in vivo*, and such Vangl2 phosphorylation was essential for its function in controlling PCP. Our data revealed that dose-dependent induction of Vangl2 phosphorylation is an essential mechanism by which chondrocytes in the long bone sense positional information and establish PCP by interpreting Wnt5a doses. This study has also provided significant new insight in the molecular mechanism underlying Robinow Syndrome and Brachydactyly type B1 (BDB1) that are caused by mutations in human WNT5A or ROR2 and characterized by shortened skeletal elements. Reference: *Dev Cell*. 2011 Feb 15;20(2):163-76.

Disclosures: Bo Gao, None.

FR0098

Histone Deacetylase-4 Plays a Role in Palatogenesis Through the Regulation of Neural Crest Cell Migration in Zebrafish. Yukio Nakamura^{*1}, April Delaurier², Shigeyuki Wakitani³, Hiroyuki Kato⁴, Charles Kimmel². ¹Shinshu University School of Medicine, Japan, ²Institute of Neuroscience, University of Oregon, USA, ³Department of Health & Sports Sciences, Mukogawa Women's University, Japan, ⁴Department of Orthopaedic Surgery, Shinshu University School of Medicine, Japan

Craniofacial malformations are associated with more than half of all human birth defects including cleft palate. Patients with cleft palate have impaired oral and/or auditory functions. Therefore, understanding the pathophysiology of cleft palate is important for developing effective treatments. Recently, aberrant expression of the transcriptional repressor histone deacetylase-4 (Hdac4) has been shown to underlie some cases of human cleft palate disorders. The anterior neurocranium in zebrafish is functionally equivalent to the human palate, therefore, we created the zebrafish as a model for understanding the *in vivo* role of Hdac4 in palatogenesis. Bioinformatics analyses of the zebrafish genome identified one copy of the Hdac4 gene. RNA *in situ* hybridization showed that Hdac4 was initially expressed in migrating neural crest cells (NCCs) at 15-17 hours post fertilization (hpf) and then the expression became restricted to regions in the mesenchyme surrounding the pharyngeal arch at 72hpf. Hdac4 was co-expressed with a NCC regulator platelet-derived growth factor receptor- α (pdgfra), suggesting the possible role of Hdac4 in regulation of NCC function. The functional *in vivo* assays creating Hdac4 and pdgfra double mutant zebrafish have been underway. We then knocked down Hdac4 using morpholinos (MOs). Reduced Hdac4 expression in MO-injected fish was confirmed by immunoblot and qRT-PCR analyses. MO-mediated Hdac4 knockdown resulted in failure of midline closure of the neurocranium. This defect was rescued by co-injection of Hdac4 mRNA, indicating the specificity of MO-mediated knockdown. To investigate when and how Hdac4 affects NCC migration, we used Sox10:egfp and foxp2-enhancerA:egfp zebrafish in which GFP-labeled NCCs. Sox10:egfp showed that at 14 hpf and 16 hpf, the absolute distance of cells behind the eye or dorsal to the eye was significantly reduced in the MO-injected embryos, and that the MO-injected embryos showed a substantial reduction of GFP-positive cells behind the eye. Foxp2-enhancerA:egfp revealed that trabeculae communis failed to form by 60 hpf, ethmoid plate failed to widen and a lack of cells filling the anterior-most midline of the ethmoid plate from 60 hpf onwards. These results demonstrate that Hdac4 regulates the migration of NCCs and palatal development in developing zebrafish. In contrast, overexpression of Hdac4 mRNA resulted in midline defects, including cyclopia and a "stick-like" neurocranium lacking both trabecular branching and the ethmoid plates, suggesting that the overexpressing the Hdac4 gene affects the same palatal structure as blocking the gene. Taken together, these results indicate that Hdac4 has a critical role in palatogenesis regulating NCC migration in zebrafish. Understanding the function of Hdac4 in zebrafish may lead to further understanding the mechanism of how loss of Hdac4 in humans results in midline craniofacial defects.

Disclosures: Yukio Nakamura, None.

FR0100

Long-Chain Saturated Fatty Acids Promote the Differentiation of Cells of the Marrow Stromal Line Kusa4b10 into Adipocytes. Dorit Naot^{*1}, Jessica Costa², David S Musson¹, Jian-Ming Lin¹, Jillian Cornish¹, Andrew Grey¹. ¹University of Auckland, New Zealand, ²University of Auckland, Nz

Body weight, and particularly fat mass, is positively correlated to bone mass. The relationships between fat and bone tissue are mediated directly through skeletal loading, and through hormonal and neuronal pathways. Feeding experiments, showing that fat ingestion acutely influences bone turnover, have raised the possibility that ingested nutrients have direct bone effects, and could function as an additional link between fat and bone. We have recently reported that the long-chain, saturated fatty acids palmitic acid (C18) and stearic acid (C16) inhibit osteoclastogenesis *in vitro*, and that the G-protein coupled receptors (GPR) for fatty acids are expressed in bone cells. In the current study, we investigated the effects of palmitic and stearic acids on adipogenic differentiation, using the murine marrow stromal cell line, Kusa4b10.

Kusa4b10 cells were grown to confluence and then cultured for 11 days in adipogenic medium containing dexamethasone, IBMX and insulin. BSA-conjugated palmitic and stearic acids were added at concentrations of 10-75 μ g/mL (30-225 μ M) and BSA alone served as a negative control. Adipogenesis was measured by Oil-Red-O staining and quantified by dye release and spectrophotometry. RNA extracted from the cultures on different days was used for analysis of gene expression by quantitative PCR, using TaqMan assays (ABI). We found that palmitic and stearic acids potentially induce adipogenesis in KUSA4b10 cells. Analysis of gene expression demonstrated significant induction of mRNA levels of the adipocytic genes adiponectin, AP2, adipin and PPAR γ . We found high levels of expression of the long chain fatty acid receptor GPR120 in KUSA4b10 cells, and low expression levels of GPR40/41. Treatment of the cells with the GPR40/41 GPR120 agonist GW9508 produced similar effects to the fatty acids treatment; increase in adipogenesis and in levels of mRNA of adipocyte genes.

Our results identify the marrow stromal cell as a novel target of fatty acids. Palmitic and stearic acids promote adipogenic differentiation of marrow stromal cells, possibly by signalling through GPR120 and GPR40/41.

Disclosures: Dorit Naot, None.

FR0106

Klf4 Regulates Osteoblast Differentiation. Ikumi Michikami^{*}, Makoto Abe. Osaka University Graduate School of Dentistry, Japan

Kruppel-Like Factor 4 (Klf4) is a Zinc finger type of transcription factor highly expressed in the skin, intestine, testis, lung and bone. It is also known as a growth inhibitor which functions through antagonizing canonical Wnt- or Notch-dependent pathways. The role played by Klf4 has been studied extensively in normal epithelial development; however its role in bone cell is completely unknown. To understand the possible role(s) played by Klf4 in bone cells, we examined the effect of over-expression and knockdown of Klf4 in mouse calvarial osteoblasts *in vitro*. Further, we examined the skeletal phenotype of the transgenic mice over-expressing Klf4 under 2.3 kb mouse *Colla1* regulatory sequence (*Colla1-Klf4 TG*).

Over-expressing Klf4 in mouse calvarial osteoblasts strongly repressed its differentiation and down-regulated most of the osteoblastic gene expressions. Unexpectedly, siRNA-mediated knockdown of Klf4 or over-expressing dominant-negative Klf4 also repressed osteoblast differentiation. Klf4 induced expressions of *Axin2* and *Left1*, which are both direct targets of canonical Wnt signaling, and Klf4 activated the canonical Wnt signaling reporter in calvarial osteoblasts. Consistent with this observation, GSK3 inhibition by LiCl strongly repressed calvarial osteoblast mineralization. *Colla1-Klf4 TG* embryos exhibited skeletal deformities including ill-formed calvarial bones and delayed formation of the primary ossification center in the long bones. These results indicate that 1) Klf4 regulates osteoblast differentiation both *in vitro* and *in vivo*, 2) precise regulation of the timing and level of Klf4 expression is crucial for normal osteoblast differentiation.

Disclosures: Ikumi Michikami, None.

FR0111

Characterization of Collagen-GFP Transgenic Mice and Evidence for Osteocyte Deposition of Perilacunar Collagen. Patricia Veno¹, Suzan Kamel¹, Yongbo Lu², Yixia Xie³, Karl Kadler⁴, Yinhui Lu⁵, Charlotte Phillips⁶, Vladimir Dusevich³, Sarah Dallas^{*3}. ¹University of Missouri, Kansas City, USA, ²Baylor College of Dentistry/Texas A&M Health Science Center, USA, ³University of Missouri - Kansas City, USA, ⁴Wellcome Trust Center for Cell Matrix Research/University of Manchester, United Kingdom, ⁵Wellcome Trust Center for Cell-Matrix Research/University of Manchester, United Kingdom, ⁶University of Missouri-Columbia, USA

Type I collagen is the major structural matrix protein in bone. It is a heterotrimer of two α 1(I) and one α 2(I) chains encoded by separate genes and mutations in either gene cause osteogenesis imperfecta. We have previously generated fluorescent collagen fusion proteins, in which GFP (green) or mCherry (red) were placed in the pro- α 2(I) N-terminus, and have reported their use in time lapse imaging studies of collagen assembly in living osteoblasts. We have also generated transgenic mice expressing α 2(I)-collagen-GFP driven by the 3.6kb *COL1A1* promoter. Here we report the further validation and characterization of these mice and using this model we show evidence for osteocyte deposition of perilacunar collagen.

Four collagen-GFP transgenic lines were obtained that showed varying levels of GFP-collagen expression in bone matrix, with line 35 giving the strongest GFP signal in bone. Intense GFP-collagen fluorescence was seen in the osteocyte perilacunar matrix in active bone forming areas. All lines also showed strong GFP-collagen expression in tendon, ligament and dentin, with moderate expression in skin. Small focal areas of GFP-collagen were present around blood vessels and in fibrous connective tissue in kidney and lung as well as in the heart valve leaflets. Low expression was seen in the intestinal submucosa. No overt abnormalities were observed in GFP-collagen mice, even though incorporation of 26kDa of GFP sequence in the α 2(I)-collagen N-terminus is analogous to mutations in patients with Ehlers Danlos type VIIb in which the N-propeptide cleavage site is lost and the propeptide is retained. These patients show skin and joint laxity. However, no significant difference in skin laxity was seen in GFP-collagen transgenic mice

compared to littermate controls and TEM analysis of skin and ligament collagen showed no Ehlers Danlos-like fibril abnormalities. No major skeletal abnormalities were observed by radiography and bone collagen fibrils appeared normal by TEM, with no significant difference in D-band periodicity. These data show the successful generation of GFP-collagen transgenic mice and suggest that the GFP insertion into pro- $\alpha 2(I)$ -collagen results in minimal disruption to collagen fibril structure in these mice. Expression of GFP-collagen in kidney, lung and skin suggests that this model will be useful for fibrosis research and the strong GFP expression in the perilacunar matrix provides new evidence for osteocyte deposition of perilacunar collagen.

Disclosures: Sarah Dallas, None.

FR0114

Sympathetic Control of Bone Mass Regulated By Osteopontin. Masashi Nagao^{*1}, Yoshitomo Saita², RYO HANYU³, Tadayoshi Hayata⁴, Tetsuya Nakamoto⁵, Yayoi Izu⁵, Takuya Notomi⁶, Shu Takeda⁷, Gerard Karsenty⁸, Susan Rittling⁹, Yoichi Ezura¹⁰, Jean-Pierre Vilardaga¹¹, Masaki Noda⁵. ¹Juntendo University Nerima Hospital, Japan, ²Department of Orthopaedics, Juntendo University School of Medicine, Japan, ³MEDICAL RESEARCH INSTITUTE, Japan, ⁴Medical Research Institute, Tokyo Medical & Dental University, Japan, ⁵Tokyo Medical & Dental University, Japan, ⁶GCOE, Tokyo Medical & Dental University, Japan, ⁷Keio University, Dept. of Nephrology, Endocrinology & Metabolism, Japan, ⁸Columbia University, USA, ⁹The Forsyth Institute, USA, ¹⁰Tokyo Medical & Dental University, Medical Research Institute, Japan, ¹¹University of Pittsburgh, School of Medicine, USA

Stimulation of the sympathetic nervous system suppresses bone mass by mechanisms that remain incompletely elucidated. One of the major causes of bone loss is disuse-induced event. Using mice genetics and cell-based approaches, we showed that this bone deterioration requires osteopontin (OPN), a cytokine and one of the major components of non-collagenous extracellular matrix proteins of bone. The stimulation of the sympathetic tone by isoproterenol (ISO) increased the level of OPN expression in the plasma and bone. While in wild type (WT), ISO treatment reduced the levels of bone volume, OPN-deficient mice were resistant to such ISO-induced bone loss. ISO treatment suppressed bone formation parameters in WT. However, OPN deficiency mitigated ISO-induced reductions these bone formation parameters. ISO-treatment also increased the levels of bone resorption parameters in wild type, while these parameters were unaffected by ISO in OPN deficient mice. At the cell level, OPN deficiency enhanced ISO-induced CRE-luciferase activity as well as forskolin and IBMX induced events. OPN-deficiency also enhanced phosphorylation of CRE-binding protein, CREB. We therefore examined the role of OPN at the signaling levels in osteoblasts. The time course of cAMP generation by ISO was much longer in cells depleted of OPN. Conversely OPN overexpression reduced cAMP generation in response to ISO. These data indicated that OPN modulates cAMP by acting at the level of the receptor and/or the stimulatory G protein (Gs). In fact, pull-down experiment revealed the existence of OPN-Gs complex. Our results indicate that OPN plays a critical role in sympathetic tone regulation of bone mass and this OPN regulation is taking place through modulation of the $\beta 2AR/GS$ signaling system.

Disclosures: Masashi Nagao, None.

FR0115

Temporal Analysis of mechanical force-induced bone formation Using Quantitative Proteomics based on 8 plex- iTRAQ. Wei-Bing Zhang^{*1}, Wei-Jie Zhong², Lin Wang². ¹Nanjing Medical University, Chn, ²Nanjing Medical University, China

Skeletal tissue has the capability to adapt its mass and structure in response to mechanical stress. However, the molecular mechanism of bone and cartilage to respond to mechanical stress are not fully understood. To obtain better insights into proteome analysis of bone and cartilage response to mechanical stress in vivo, we have conducted studies of midpalatal suture expansion. The midpalatal suture, located between the maxillary bones in the palate, contains secondary cartilage that is highly responsive to various mechanical forces. A total of 96 male C57BL/6 mice, 6-week-old and 19–20g in weight, were used. Half of animals were subjected to palatal suture expansion by opening loops (Fig1) for the periods of 1, 3, 7, 14 days. Specimens were harvested at a series of post load time points, and the cellular response to loading was evaluated by histomorphometric. Micro-CT was used for morphometric analysis. Fluorescence labeling by incorporation of alizarin/ calcein in newly formed bone minerals qualitatively demonstrated new bone formation (fig3). Quantitative proteomic profiling using a multiplexed approach (Fig2) capable of analyzing eight different samples simultaneously was carried out to monitor the temporal dynamics of protein abundance during the period of expansion. A catalog of ~726 proteins along with their relative quantitative expression patterns was generated. Differential expression analysis in the experimental groups and control group showed significant changes for 78 proteins. The differential expression of the large majority of these proteins has not previously been reported or studied in the context of mechanical signal transduction in mechanical force-induced bone formation. 54 proteins were upregulated in differentiating and proliferation, but 24 proteins were downregulated

related to apoptosis or catabolic. Our data suggest that 18 proteins were assigned a role in cell communication. 10 proteins were assigned a role in anabolic process. Comparisons of anabolic versus catabolic features of the proteomes show that 13 proteins were related to catabolic. 15 proteins were related to regulation of signal transduction. 7 proteins were related to regulation of angiogenesis. 26 proteins were related to apoptosis. (Fig4, Fig5) We validated some of the novel markers of the process of bone formation induced by force using immunoblotting and immunocytochemical labeling. To our knowledge, this is the first large-scale temporal proteomic profiling of bone formation induced by mechanical force highlighting proteins with limited or undefined roles.



Fig.1 Mid-palatal suture expansion in mice. Experimental/Expansion maxilla with the opening loop bon

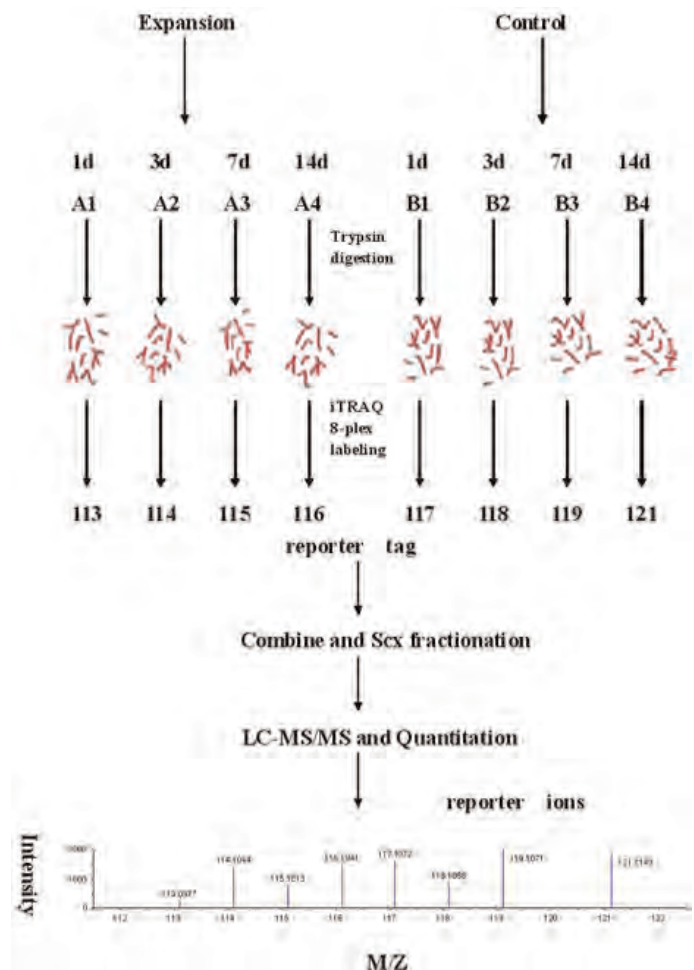


Fig2 Experiment design

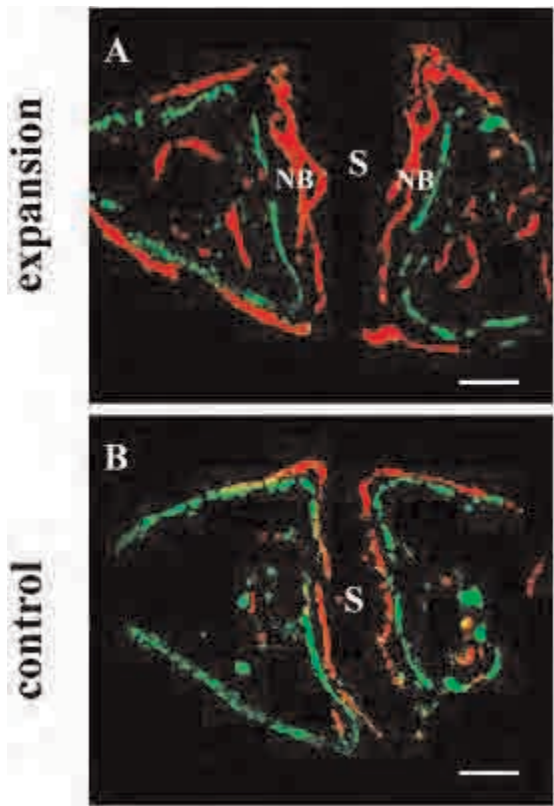


Fig.3 Representative photomicrographs of newly formed sutural bone double-labeled

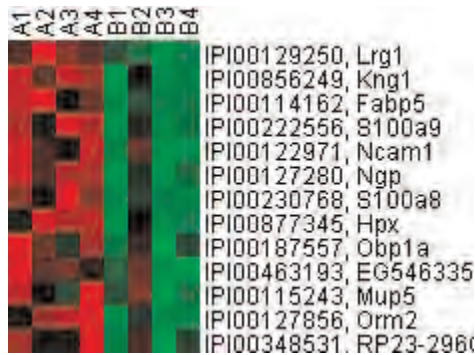


Fig.4 differentially expressed proteins Cluster analyse

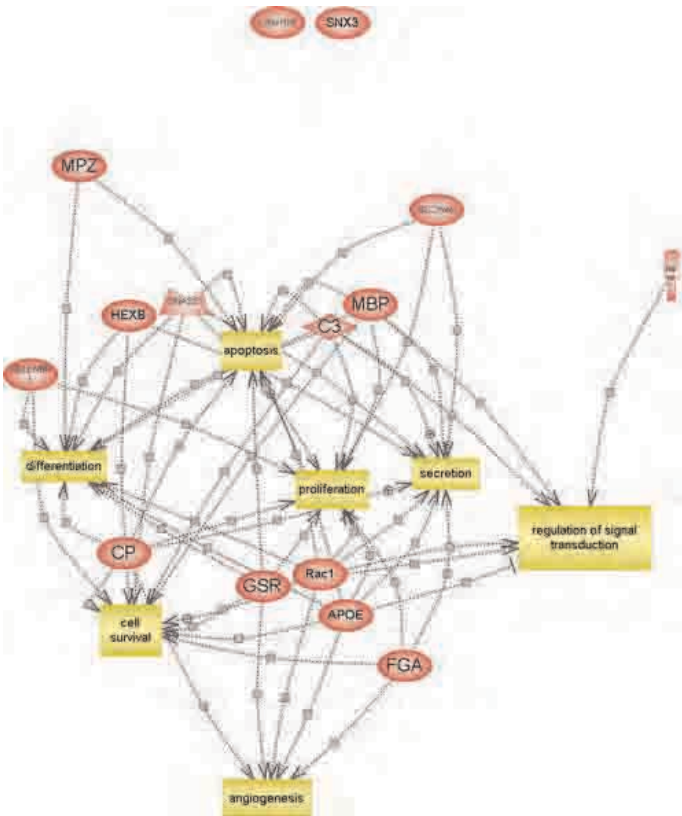


Fig.5 Regulated pathways involving differentially expressed proteins

Disclosures: Wei-Bing Zhang, None.

FR0116

Osteoblastic Cells Rely on MT1-MMP as a Regulator of Skeletal Homeostasis. Emily Purcell*, Joanne Shi, Susan Yamada, Pamela Robey, Kenn Holmbeck, National Institute of Dental & Craniofacial Research, USA

Purpose: Bone and cartilage formation require the ability of skeletal progenitors to remodel their resident matrix to enable proper cell function. This is achieved in part by pericellular proteolysis mediated by membrane-type matrix metalloproteinases (MT-MMPs). Accordingly, congenital or adult-onset MT-MMP deficiency results in severe disruption of skeletal development and homeostasis. Because MT-MMPs are expressed in a wide variety of skeletal-associated cells, the cell-specific contribution to the observed defects is difficult to assign. In an effort to characterize osteoblastic vs. chondrocytic dependence on MT-MMP activity, we initiated cell/tissue-specific deletion of MT-MMP in the skeleton.

Methods: We utilized a mouse strain modified with a floxed conditional knockout allele of MT1-MMP. By crossing this mouse line with an Osterix (Osx) Cre-expressing mouse, we have obtained specific ablation of MT1-MMP in Osx-expressing cells.

Results: We demonstrated that selective ablation of MT1-MMP in the Osx-expressing subset of cells leads to dwarfism, osteopenia, malocclusion of teeth, and apparent loss of bone. Computer-assisted tomography of long bones revealed a dramatic reduction of trabecular bone, thin cortices, and apparent bone loss at ligament insertion sites.

Conclusion: Based on these results, we hypothesize that cells of the osteoblastic lineage rely on MT1-MMP for proper regulation of bone development and homeostasis through pericellular proteolytic activity.

Disclosures: Emily Purcell, None.

FR0119

Control of Iron Status Alters Phosphate Metabolism in a Mouse Model of Autosomal Dominant Hypophosphatemic Rickets (ADHR). Emily Farrow^{*1}, Lelia Summers¹, Munro Peacock², Kenneth White¹. ¹Indiana University School of Medicine, USA, ²Indiana University Medical Center, USA

Autosomal dominant hypophosphatemic rickets (ADHR) is unique among the heritable disorders of renal phosphate wasting involving FGF23, as patients carrying the R176Q/W and R179Q/W mutations in the ¹⁷⁶RXXR₁₇₉ proteolytic cleavage motif can have early onset disease from birth, or have late onset following puberty or pregnancy, biological states prone to iron deficiency. We have shown that when placed on low-iron diet, wild type (WT) and novel R176Q-Fgf23 knock-in mice (ADHR mice) significantly increase bone Fgf23 mRNA. In the face of elevated Fgf23 production, WT mice maintained normal intact serum Fgf23 by cleaving excess Fgf23 into fragments as detected by increased C-terminal ELISA (3-6 fold; P<0.0001), whereas the low-iron ADHR mice had elevated intact and C-terminal Fgf23 with hypophosphatemia (P<0.0001) and osteomalacia after 8 weeks. To test whether control of systemic iron could rescue the ADHR phenotype, ADHR mice received low-iron diet for 6 weeks followed by iron repletion for 2 weeks. This treatment normalized serum Fgf23 (C-terminal Fgf23: 2580325 pg/mL for 8 week low-iron vs. 29520 pg/mL replete; P<0.001) and serum phosphate (7.50.2 low-iron diet vs. 100.3 replete). Anemia in pregnancy can be transferred to neonates, thus we also tested iron deficiency as a mechanism for early onset ADHR by providing female breeder mice low-iron diet on day 14 of pregnancy and during nursing. WT and ADHR pups receiving low-iron had markedly increased Fgf23 mRNA compared to control diet mice (>45 fold; P<0.01). WT mice regulated serum intact Fgf23 through proteolytic cleavage (WT intact: 17329 pg/mL; C-terminal: 14,136206 pg/mL). In contrast, the ADHR pups had >10-fold elevated intact Fgf23 (P<0.001), but C-terminal Fgf23 was not different from WT (ADHR intact: 1,911355 pg/mL; C-terminal: 14,4541338 pg/mL), as well as significant hypophosphatemia (8.0 mg/dL ADHR vs. 11.3 mg/dL WT; P<0.0001). Therefore, in ADHR mice, the increased serum Fgf23 and hypophosphatemia can be reversed by iron repletion, potentially providing novel therapeutic targets for controlling Fgf23. Further, early onset ADHR in some patients may be due to maternal-neonate transfer. The finding that Fgf23 is strongly up-regulated during iron deficiency provides insight into why ADHR patients, although hypophosphatemic are unable to suppress FGF23 production, and demonstrates that the ADHR phenotype can be dramatically influenced by gene-environment interactions.

Disclosures: Emily Farrow, None.

FR0120

Fgf23 Regulates Calcium and Sodium Reabsorption in Renal Distal Tubules through SGK1 Signaling. Olena Andrukhova^{*1}, Carmen Streicher², Ute Zeitze³, Beate Lanske³, Reinhold Erben². ¹Inst. of Physiology, Pathophysiology & Biophysics, Austria, ²University of Veterinary Medicine, Austria, ³Harvard School of Dental Medicine, USA

Fibroblast growth factor-23 (Fgf23) is an endocrine signal originating from osteocytes which downregulates renal tubular phosphate reabsorption and vitamin D hormone synthesis. Here, we examined the effects of long-term Fgf23 deficiency on mineral and bone homeostasis in 9-month-old wild-type (WT) mice, *vitamin D receptor (VDR)* mutant mice, and *Fgf23/VDR* compound mutant mice on both a standard rodent chow and a rescue diet (RD) enriched with calcium, phosphorus, and lactose. The RD largely corrected mineral and bone homeostasis in *VDR* mutant mice. However, compound mutants on RD showed hypocalcemia, hyperphosphatemia, and very high serum parathyroid hormone. Secondary hyperparathyroidism (sHPT) in compound mutants on RD was associated with renal calcium wasting and cortical bone thinning. Analysis of the expression of proteins involved in renal calcium transport revealed reduced membrane abundance of the fully glycosylated epithelial calcium channel TRPV5 and decreased levels of intracellular calbindin D28k in compound mutants. Similar changes in distal tubular protein expression were seen in 4-week-old *Fgf23^{-/-}*, *Klotho^{-/-}*, and *Fgf23/VDR* and *Klotho/VDR* compound mutants. Immunoprecipitation experiments revealed a physical interaction of TRPV5 and with-no-lysine kinase-4 (WNK4). Analysis of the upstream intracellular signaling mechanisms showed decreased phosphorylation of one of the main regulators of WNK4, serum- and glucocorticoid-inducible kinase-1 (SGK1), in kidneys of compound mutants. SGK1 is known to be activated by extracellular signal-regulated kinase-1/2 (ERK1/2), and to be involved in aldosterone signaling. In agreement with an Fgf23 deficiency-induced downregulation of signaling through the Fgf receptors, phosphorylated ERK1/2 was reduced in kidneys of compound mutants. Despite higher aldosterone in serum and urine, compound mutants showed increased urinary loss of sodium relative to WT and *VDR* mutants. Our data have uncovered that Fgf23 signaling regulates phosphorylation of SGK1 through ERK1/2 in renal distal tubules in a vitamin D independent fashion. Decreased SGK1 phosphorylation in *Fgf23* and *Klotho*-ablated mice leads to a downregulation in WNK4-mediated transport of glycosylated TRPV5 to the plasma membrane, and reduced sodium reabsorption despite elevated circulating aldosterone. In conclusion, our results suggest that Fgf23 has a previously unknown function in distal renal tubular calcium and sodium reabsorption.

Disclosures: Olena Andrukhova, None.

FR0121

MEPE-derived Phosphorylated ASARM Is Involved in FGF23/soluble Klotho-dependent Hypomineralization. Yukiko Konishi^{*1}, Yuji Yoshiko², Tomoko Minamizaki¹, Hirotaaka Yoshioka¹, Masahiro Maeda³, Atsushi Shimizu⁴, Jane Aubin⁵, Norihiko Maeda¹. ¹Hiroshima University Graduate School of Biomedical Sciences, Japan, ²Hiroshima University, Japan, ³Immuno-Biological Laboratories Co., Ltd, Japan, ⁴Raffinco International Co. Ltd., Japan, ⁵University of Toronto Faculty of Medicine, Canada

Members of the small integrin-binding ligand N-linked glycoprotein (SIBLING) family, includes matrix extracellular phosphoglycoprotein (MEPE), play roles in bone mineralization. A proteolytic fragment containing an acidic serine- and aspartate-rich motif (ASARM) of SIBLINGs binds to hydroxyapatite and inhibits bone mineralization *in vitro*. ASARM peptide is also a candidate substrate for phosphate regulating endopeptidase homolog X-linked (PheX), suggesting that accumulation of ASARM in bone may cause mineralization defects in X-linked hypophosphatemic rickets. Recently, we showed that fibroblast growth factor 23 (FGF23) and the truncated form of the extracellular domain of Klotho (soluble Klotho, sKL) cooperatively inhibit bone mineralization independently of serum phosphate levels. Amongst downstream events of FGF23/sKL binding, the expression of *PheX* was downregulated in mouse bone as well as in rat/mouse osteoblast/osteocyte (Obc cell) cultures. To clarify the interplay between ASARM peptide and FGF23/sKL, we developed an antibody against human MEPE-associated phosphorylated ASARM (pASARM). This antibody recognized pASARM (Ser518/520/522) and MEPE, but not partially phosphorylated (Ser520/522, Ser518, Ser520 or Ser522) and non-phosphorylated (npASARM) ASARM or other SIBLINGs. In the rat Obc cell culture model, anti-pASARM antibody inhibited not only pASARM- but also FGF23/sKL-dependent hypomineralization. By immunohistochemistry, pASARM was localized in osteoblasts/osteocytes, and staining intensity was significantly higher in Klotho mutant (*kll/kll*) versus wild type mice. Upregulation of *PheX* in *kll/kll* bone *ex vivo* was abrogated by treatment with sKL in parallel with ERK phosphorylation and increased *Egr-1* mRNA expression, markers for FGF23-specific signaling. pASARM immunoreactivity was high in Obc cell cultures treated with FGF23/sKL, and was decreased by U0126, an inhibitor of ERK phosphorylation. The inhibitory effect of pASARM on matrix mineralization was lost when the N-terminus amino acid residues including the PheX-cleavage site or phosphorylation of Ser518/520/522 was used. Treatment with an excess amount of npASARM that included the PheX-cleavage site shifted the effective concentrations of pASARM from higher to lower. Taken together, these results suggest that FGF23/sKL negatively regulate bone mineralization via their inhibitory effect on *PheX* expression, followed by accumulation of pASARM in bone.

Disclosures: Yukiko Konishi, None.

FR0124

Mice Expressing a Phosphorylation-Deficient PTH Receptor Have Blunted Calcemic and Phosphaturic Responses to Acute PTH Challenge. Akira Maeda^{*1}, Makoto Okazaki¹, Matthew Mahon¹, Hiroko Segawa¹, Abdul Abou-Samra², Harald Jueppner¹, John Potts¹, Thomas Gardella¹. ¹Massachusetts General Hospital, USA, ²Wayne State University, School of Medicine, USA

Phosphorylation of the PTHR1 C-terminal tail is thought to play a key role in receptor signal regulation and internalization. A phosphorylation-deficient mutant PTHR1 (PD) exhibits defective internalization in cells, and PD-knock-in mice exhibit prolonged blood cAMP increases after PTH(1-34) injection (Bounoutous, 2006, Endocrinology). We now compared the acute, PTH-induced blood ionized calcium (Ca⁺⁺) and plasma phosphate (Pi) responses of PD and WT mice.

Injection of PTH(1-34) into WT mice caused Ca⁺⁺ levels to increase from 1-4 h post injection, whereas injection into PD mice caused no change in Ca⁺⁺ levels. Injection of a longer-acting PTH analog, M-PTH(1-28), into WT mice increased Ca⁺⁺ levels for at least 6 hours, whereas injection into PD mice resulted in no change in Ca⁺⁺ for up to 2 h, and only a partial increase (50% vs. WT) at 4-6 h. In WT mice, PTH(1-34) suppressed Pi levels from 1 to 2 h post injection, and M-PTH(1-28) suppressed Pi levels for at least 4 h. In contrast, in PD mice, neither PTH(1-34) nor M-PTH(1-28) suppressed Pi levels. Injection of PTH(1-34) or M-PTH(1-28) in WT mice caused transient increases in blood cAMP levels (peak at 15 min), whereas injection in PD mice caused more robust and prolonged increases in blood cAMP, as compared to WT. Surprisingly, urine cAMP did not increase in ligand-injected PD mice, whereas it rose significantly in WT mice. A very long-acting hybrid analog, M-PTH(1-14)/PTHrP(15-36) (Shimizu ASBMR 2009), induced robust and prolonged (up to 20 h) hypercalcemic and hypophosphatemic responses in WT mice; surprisingly, however, it induced frank hypocalcemia and hyperphosphatemia in PD mice. Fluorescent confocal microscopy analysis of kidneys obtained from WT mice injected with TMR-M-PTH(1-28) revealed fluorescence localized to distinct, internalized punctae below the apical membrane of proximal tubule cells, whereas in PD mice fluorescence was localized to the apical cell surface.

The findings show that PTHR1 phosphorylation plays a critical role in mediating the acute Ca and Pi responses to PTH. They further suggest that in renal tubular cells, PTHR1 internalization, as mediated by C-terminal phosphorylation, contributes

importantly to the localization of cAMP signaling and down-stream effects on Ca and Pi transporters.

Disclosures: Akira Maeda, Chugai, 2

This study received funding from: Chugai Pharmaceutical Co. Ltd. Japan

FR0126

PTHrP Regulated BMP Signaling Plays A Role In The Specification Of The Mammary Mesenchyme. Minoti Hiremath^{*1}, Pamela Dann², John Wysolmerski³. ¹Boise State University, USA, ²Yale University, USA, ³Yale University School of Medicine, USA

PTHrP regulates mammary cell fate by specifying the mammary mesenchyme during embryonic mammary development. Loss of PTHrP (PTHrP^{-/-}) or its receptor (PTH1R^{-/-}) permits mammary bud cells to revert to an epidermal fate and disrupts mammary bud outgrowth. In contrast, overexpression of PTHrP in the epidermis (K14-PTHrP) induces inappropriate differentiation of the ventral epidermis into nipple-like skin. In previous studies, PTHrP-mediated upregulation of BMP1a was implicated in mammary bud outgrowth. Therefore, we hypothesized that PTHrP might regulate levels of BMP signaling in the mammary mesenchyme. We first examined BMP-signaling in the embryonic mammary mesenchyme expression using a transgenic Bre-lacZ reporter mouse. The reporter transgene consists of Smad binding elements of the Id1 gene promoter placed upstream of a lacZ reporter gene. X-gal staining of whole embryos detected Bre-lacZ expression in the mammary mesenchyme as early as day 12 and up to day 18 of embryogenesis. Reporter expression was first noted in mammary bud 2, followed by bud 3, 4, 1 and 5. Interestingly, the order of reporter expression in the mammary buds did not follow the order of mammary placode development suggesting that BMP signaling in the placodes is regulated independently of mammary epithelial specification. Expression of the reporter was restricted to the mammary mesenchyme, as demonstrated by co-localization with mammary mesenchyme markers such as androgen receptor, estrogen receptor and Lef1. Reporter expression was not detected in the mammary epithelium and did not co-localize with mammary epithelial markers such as gata3, p63 and keratin 14. These data demonstrate that BMP signaling occurs specifically in the mammary mesenchyme. To determine whether PTHrP regulates BMP signaling, we examined expression of the BMP reporter in PTHrP^{-/-} and K14-PTHrP mice. Our studies show that loss of PTHrP abolishes reporter expression and overexpression of PTHrP results in ectopic activation of BMP reporter along the flank of the embryo, demonstrating that PTHrP regulates BMP signaling. To determine the contribution of BMP signaling in mammary mesenchyme specification, we genetically deleted BMP1a using the Dermo1 promoter to drive cre recombinase expression in the mammary mesenchyme of BMP1a^{lox/lox} mice. A preliminary histological analysis of mammary buds from these mice indicated that there are fewer layers of cells in the condensed mammary mesenchyme and that expression of Tenascin-c in the mesenchyme is reduced. These preliminary analyses suggest that BMP signaling via BMP1a is required for functional differentiation of the mammary mesenchyme and for mammary bud outgrowth. Taken together, our studies suggest that PTHrP regulated BMP signaling in the mammary mesenchyme is critical for mesenchyme specification.

Disclosures: Minoti Hiremath, None.

FR0128

Silencing of PTH Receptor 1 in T Cells Blunts the Bone Anabolic Activity of Intermittent PTH Treatment. Brahmchetna Bedi¹, Jau-Yi Li^{*1}, Jonathan Adams¹, Ming-Kang Chang², Tatsuya Kobayashi³, M. Neale Weitzmann⁴, Michaela Kneissel², Henry Kronenberg³, Roberto Pacifici¹. ¹Emory University School of Medicine, USA, ²Novartis Institutes for Biomedical Research, Switzerland, ³Massachusetts General Hospital, USA, ⁴Emory University School of Medicine, Atlanta VA Medical Center, USA

T cells are required for intermittent PTH (iPTH) treatment to exert its full anabolic effect as iPTH stimulates their production of Wnt10b. This osteogenic Wnt ligand is critical for iPTH-induced activation of Wnt signaling in osteoblasts (OBs) and the resulting increase in bone formation and bone mass. However it is unknown whether direct activation of the PTH receptor PTH receptor 1 (PPR) in T cells is required for iPTH to induce Wnt10b production and bone growth. To investigate this matter we generated a strain with a silent PPR in T cells (PPRT cells -/- mice) by crossing PPR floxed (PPR fl/fl) mice with LCK-Cre mice, a strain that expresses Cre recombinase in all T cells. We found that in vivo iPTH treatment (80 µg/kg/day sub-Q) for 4 weeks increased production of Wnt10b by CD8+ T cells from control (PPRfl/fl and PPRfl/+/- Lck-Cre) but not PPRT cells -/- mice. Moreover, the effect of iPTH on stromal cell differentiation, OB proliferation, differentiation and apoptosis and expression of Wnt dependent genes in OBs was 2-3 fold lower in PPRT cells -/- mice than control mice. Prospective in vivo BMD measurements revealed that iPTH caused a smaller increase in BMD in PPRT cells -/- than in control mice (26 % in PPRfl/fl mice vs. 41 % in PPRT cells -/- mice; p<0.05). Histomorphometric analysis of femoral trabecular bone volume (BV/TV) revealed a less pronounced response to PTH in PPRT cells -/- mice than in control mice (33% in PPRT cells -/- mice vs. 234 % in PPRfl/fl mice; p<0.001). µCT measurements of BV/TV confirmed that iPTH induced a smaller increase in trabecular BV/TV in PPRT cells -/- than in control mice (69 % in PPRfl/fl mice vs. 160 % in PPRT cells -/- mice; p<0.01). Trabecular number, connectivity density, and volumetric density were more substantially improved in control mice than in PPRT

cells -/- mice. Measurements of histomorphometric (N.OB/BS and Ob.S/BS) and biochemical (serum osteocalcin) indices of bone formation demonstrated that iPTH induced bone formation was attenuated in PPRT cells -/- mice as compared to control mice. Conversely, histomorphometric and biochemical indices of bone resorption were equally increased by iPTH in all strains. Taken together, these findings demonstrate that PPR signaling in T cells plays an essential role in the anabolic activity of iPTH by promoting T cell production of Wnt10b, a factor required for iPTH to stimulate osteoblastogenesis, bone formation and bone accretion.

Disclosures: Jau-Yi Li, None.

FR0129

The Adjuvant Effects of Intermittent PTH Therapy on Massive Allograft Healing are Associated with Decreased Vasculogenesis via Differential Angiopoietin Expression and Increased Allograft Remodeling. Robinder Dhillon^{*1}, Chao Xie², Laura Calvi³, Regis O'Keefe¹, Edward Schwarz¹. ¹University of Rochester, USA, ²Center for Musculoskeletal Research, University of Rochester, USA, ³University of Rochester School of Medicine, USA

Purpose: Previous studies of PTH (teriparatide) therapy for femoral allografting in mice showed remarkable decreases in fibrosis and vascularity, with increased remodeling. Here we investigated the expression of angiogenic (VEGFs), and vasculogenic (angiopoietins) factors. We also tested if the PTH effects were initiated by osteoblasts proximal to the allograft by utilizing Col1-caPTHr transgenic mice as hosts and live isograft donors.

Methods: WT mice received a 4mm mid-diaphyseal femoral osteotomy that was replaced with an allograft, and were randomized to PTH(1-34) 40ug/kg/day) or placebo. PTH effects on gene expression (*vegfs*, *ang-1*, *ang-2*, *vegfrs*, and *tie-2*) were assessed at 7, 10, 14, 21, 28 days by QRT-PCR. PTH effects on vascularity and allograft remodeling were assessed by vascular microCT and histology. In a second study, Col1-caPTHr mice and their WT littermates received allografts or live isografts from Col1-caPTHr mice, and microCT and histology were done on days 21 and 28.

Results: Vascular microCT revealed that PTH significantly decreased allograft vascularity vs. placebo (vascular volume=0.580.10vs.1.060.19 mm³; mean vessel diameter=0.080.01vs.0.100.01 mm; p<0.05). Histomorphometry confirmed PTH-inhibition of vasculogenesis with a concomitant decrease of fibrosis. qRT-PCR results were unremarkable, except for a 8-fold increase in Ang-1, and a 70-fold decrease of Ang-2 expression on day 7. Vascular micro-CT analyses of allografts in Col1-caPTHr mice revealed a decreased vascularity vs. their WT littermates on day 21 (vascular volume 0.360.09 vs.1.010.31 mm³; vessel number 1.010.11 vs.1.260.06 mm; p<0.05). Similar significant differences were also seen at 28 days. Histomorphometry confirmed the dramatic differences in vascularity between WT and Col1-caPTHr mice. It also revealed significant PTH-induced allograft resorption, with a concomitant significant increase in osteoclasts number/graft area (9.095.49vs.5.533.08; p<0.05) and resorption surface vs. allografts in WT mice. Interestingly, allografts in Col1-caPTHr mice were completely resorbed by day 42.

Conclusions: In addition to its known anabolic effects, here we demonstrate that PTH therapy augments allograft healing by decreasing vasculogenesis via differential Ang-1 vs. Ang-2 expression. It also silences the host immune/fibrotic response that inhibits osseous integration, which allows for necrotic graft remodeling into live cortical bone with marrow.

Increased Angiopoietin 1 and suppressed Angiopoietin 2 expression observed on day 7 with PTH treatment

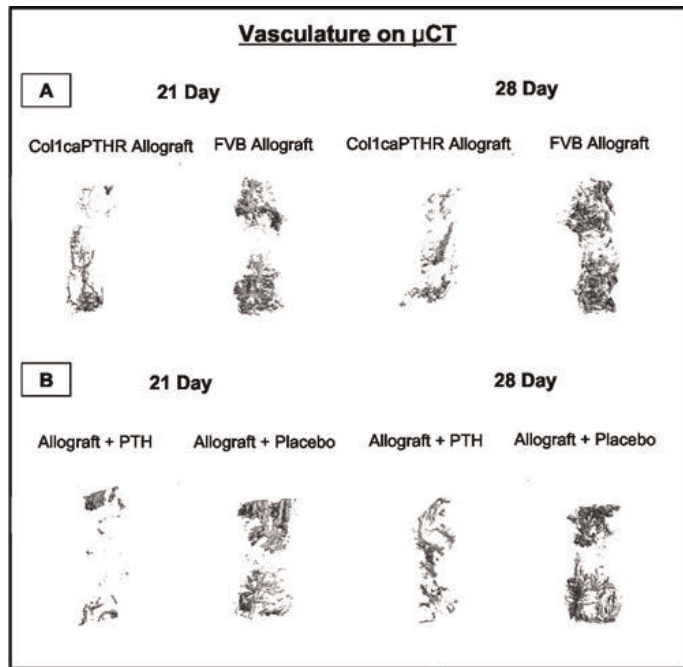


Figure 1: Decreased vasculogenesis in allografts from Col1-caPTHR mice and WT mice treated with PTH. Col1-caPTHR mice and WT littermates (A), or WT mice treated with PTH or placebo (B), received femoral allografts and were euthanized via vascular perfusion with Microfil on the indicated day (n=5). The grafted femurs were harvested for demineralized micro-CT, and representative 3D reconstructed images of the perfused vasculature are shown.

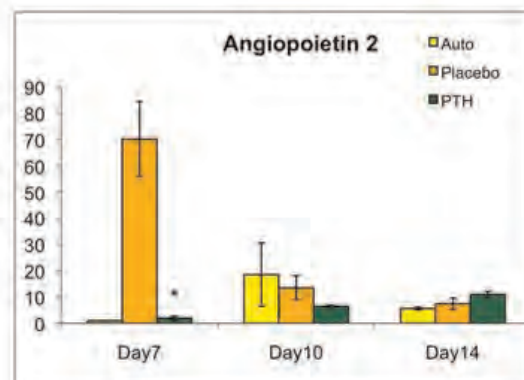
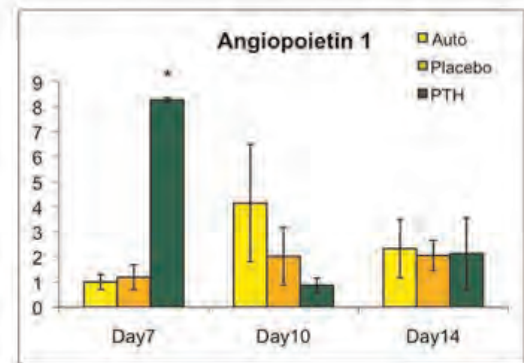
MicroCT Images

Table 1. Histomorphometry of allografts into a Col1CAPTHR and WT host mice at 21 days of healing

Parameters	Col1CaPTHR Allograft	WT Allograft
Total region of interest area (mm ²)	5.362±0.75	6.80±0.89
Host bone area (mm ²)	2.41±0.68	2.11±1.07
Graft bone area (mm ²)	0.53±0.20*	0.78±0.08
Osteoclast number/graft area (/mm ²)	9.09±5.49*	5.53±3.08
Osteoclast surface/graft surface (%)	36.37±21.97*	22.13±12.31

Values are Mean ± SD (n=5) for each group. *p<0.05 vs. WT Allograft.
ROI is 2mm of graft + 1mm of host at both proximal and distal graft host junctions.

Histomorphometry Data



Angiopoietin 1 and Angiopoietin 2 expression on RT-PCR with PTH treatment

Disclosures: Robinder Dhillon, None.

FR0131

The Transcriptional Co-Activator CITED1 is Required for Normal Bone Volume and for the Full Anabolic Response to PTH *In Vivo*. Hila Bahar¹, Jun Guo², Hiroaki Saito³, Rajaram Manoharan⁴, Dehong Yang², Toshi Shioda², Mary Boussein⁴, Roland Baron⁵, F. Richard Bringham². ¹MGH & HMS, USA, ²Massachusetts General Hospital, USA, ³Harvard School of Dental Medicine, USA, ⁴Beth Israel Deaconess Medical Center, USA, ⁵Harvard School of Medicine & of Dental Medicine, USA

CITED1, a transcriptional co-activator, interacts directly with CBP/p300 and is capable of enhancing TGF-beta and estrogen-dependent transcription and inhibiting beta-catenin-dependent transcription. CITED1 mRNA expression is rapidly and transiently upregulated by PTH in cultured osteoblasts (Obs) in a manner dependent on cAMP signaling. Also, the cAMP-mediated Obs-differentiating effect of intermittent PTH in vitro is selectively suppressed by CITED1. To define the role of CITED1 in bone and in the anabolic actions of PTH in vivo, bones of 8-week old CITED1 global knockout (KO) and wild type (WT) C57BL/6 mice were analyzed using microCT, DXA, and histomorphometry (n=6) before and after daily (5d/week) sc injections of vehicle (VEH) or 80 ug/kg hPTH(1-34) (PTH) for 4 weeks. Baseline DXA analysis at 8 weeks revealed mild osteopenia in KO mice, mainly in the trabecular (Tb) bone. MicroCT analysis showed a significantly lower (7%) Tb bone volume (BV) in KO vertebra and no difference in the distal femur and cortical bone compared to WT. Histomorphometric analysis of femurs showed a significant decrease in BV (30%), BFR (30%), Ob number (54%) and osteoclast (Oc) number (40%) but no change in MAR or O.Th, suggesting that deletion of CITED1 reduced BV by limiting the number of active Obs and decreasing bone formation in the context of a low bone-turnover state. Four weeks of PTH treatment significantly augmented Tb BV at the distal femur (100%-KO, 150%-WT) and cortical thickness (6%-KO, 17%-WT), as measured by microCT, but the overall effect was attenuated in KO. No differences were seen by microCT between WT and KO treated with VEH, and BMD of the total body and femur were similar in VEH-treated KO vs WT as well. PTH significantly increased BMD in both KO (8%-total body, 20%-distal femur) and WT (9%, 40% respectively) but the increase was significantly impaired in KO. Histomorphometry showed similar responses to PTH in KO and WT for all parameters apart from a significantly lower increase in BV in KO (210%) vs WT (315%) and higher Oc number in KO (143%) vs WT (34%), suggesting selective

enhancement of the osteoclastic component of the increased bone turnover in response to intermittent PTH. Serum Ca, Pi and creatinine were normal in all treated mice. These results suggest a possible role of CITED1 in regulating the number of active Ob, the extent of bone formation, and the balance of osteoclastic vs osteoblastic responses induced by intermittent PTH treatment.

Disclosures: Hila Bahar, None.

FR0132

Chronic Stress Increases Breast Cancer Metastasis to Bone via α 2AR on Osteoblasts. Florent Elefteriou¹, J. Campbell^{*2}, Julie Sterling³, Xiangli Yang¹. ¹Vanderbilt University, USA, ²Vanderbilt Center for Bone Biology, USA, ³Vanderbilt University Medical Center, USA

Increased sympathetic nervous (SNS) outflow, a hallmark of mental stress, controls multiple processes in the bone, such as hematopoietic stem cell trafficking, osteoblast proliferation, osteoclastogenesis, and inflammation via β 2-adrenergic receptors (β 2AR) and cytokines also involved in cancer metastasis, such as SDF-1, RANKL, and IL-6. These observations suggest the involvement of SNS activation in cancer osteotropism, tumor burden, and the formation of osteolytic lesions, which may underlie the increased mortality and recurrence observed clinically with prolonged psychosocial stress. To address this hypothesis, we used an established model of osteolytic metastasis in which MDA-MB-231 human breast cancer cells are injected via left cardiac ventricle into athymic nude. The effects of chronic stress, simulated with restraint stress, were compared to Isoproterenol (ISO), a β AR agonist acting independently of the hypothalamic-pituitary-adrenal axis (HPA). Osteolytic lesions, tumor burden and BV/TV were assessed with Faxitron, 3D-microtomography, and histology. Both chronic stress and ISO treatment before MDA-MB-231 inoculation increased the number of bone lytic lesions ($p < 0.05$), while treatment after bone metastasis increased the size of the lytic lesions ($p < 0.05$). Furthermore, the effects of restraint stress were rescued by treatment with a commonly prescribed β -blocker, propranolol, suggesting that chronic stress alters the bone microenvironment (BMM) through the β 2AR to make it favorable for cancer cell bone colonization and growth. *In vitro*, direct stimulation of the β 2AR in MDA-MB-231 cells produced no effect on migration, cell growth or PTHrP, Rank and CXCR4 expression. In contrast, stimulation of the β 2AR in bone marrow stromal cells, calvarial and MC3T3 osteoblasts increased Rankl but not Sdf1 expression ($p > 0.005$). The conditioned media of ISO-treated osteoblasts increased MDA-MB-231 migration ($p < 0.005$), which could be blocked by OPG but not by the CXCR4 antagonist AMD3100. These results suggest that the increase in osteolysis and metastasis observed following SNS activation *in vivo* are due predominantly to a bone stromal effect. These findings support the hypothesis that depression, via sympathetic activation, makes the BMM permissive to cancer metastasis, growth, or recurrence, and imply that β -blockers may reduce both bone tumor burden and relapse in breast cancer patients.

Disclosures: J. Campbell, None.

FR0133

Genome-Wide Reciprocal Modulation of Runx2 and Estrogen Signaling in Breast Cancer Cells: Identification of a Clinically Prognostic Cell Cycle-Related Gene Cluster. Nyam-Orsor Chimgé^{*1}, Sanjeev Baniwal¹, Jingqin Luo², Simon Coetzee¹, Ben Berman¹, Debu Tripathy¹, Ellis Matthew², Baruch Frenkel¹. ¹University of Southern California, USA, ²Washington University in St. Louis, USA

The mitogenic effect of estrogens in breast epithelial cells is one of the best examples of hormonal carcinogenesis. Both estradiol (E2) and Runx2 play paradoxical roles in cancer where they can function as either dominant oncogenes or tumor suppressors. The mechanisms underlying these contrasting manifestations in cancer are not fully understood. In this study we developed a novel experimental approach that allowed us to study the complex interaction between Runx2 and E2 signaling genome-wide. MCF7/Runx2dox breast cancer (BCa) cells engineered to express Runx2 in response to doxycycline (dox) were treated with dox, E2, or both. Soft agar growth assays confirmed the reciprocal effects of E2 and Runx2 on cell proliferation. Microarray analysis of cells under the four conditions revealed that E2 globally attenuated Runx2 activity and visa versa. A substantial portion of Runx2 regulated genes was independently regulated by E2. These "common" genes were comprised of four clusters; those downregulated by both Runx2 and E2 (Cluster I), those upregulated by both (Cluster III), and those with opposite responses to Runx2 and E2 (Clusters II and IV). Cluster IV upregulated by E2 and inhibited by Runx2, was significantly enriched in cell cycle regulated genes. Given the oncogenic and tumor suppressor properties of E2 and Runx2, we speculated that genes in Cluster IV may represent a critical hybrid growth regulatory circuit mediating the oncogenic property of E2 and the tumor suppressor function of Runx2 in BCa. We therefore investigated how the status of Runx2 and E2 interactions could inform BCa treatment strategies. Estrogen deprivation by letrozole treatment in BCa patients increased overall Runx2 activity. Four weeks of letrozole treatment led to a dramatic decrease of Cluster IV metagene, indicating that absence of E2 abolished not only its stimulating effect on expression of Cluster IV genes but also inhibitory effect of E2 on Runx2 activity that strongly suppressed these genes. Remarkably, higher expression change of the Cluster IV metagene in response to letrozole was significantly associated with higher Ki67 staining at surgery, and was much stronger than that for any of 1,000

randomly selected sets of E2 stimulated genes. In summary, genes co-regulated by E2 and Runx2 may provide a powerful prognostic tool and may guide the development of novel therapeutic approaches that take into consideration the interaction between E2 and Runx2 signaling in BCa.

Disclosures: Nyam-Orsor Chimgé, None.

FR0135

Identification of Runx2 Responsive Genes Counter-regulated by Estrogen: SNAI2 as a Mediator of Runx2-induced Invasiveness. Nyam-Orsor Chimgé^{*}, Sanjeev Baniwal, Yunfan Shi, Baruch Frenkel. University of Southern California, USA

Runx2 and estrogens play crucial roles in both bone metabolism and carcinogenesis. To decipher genes mediating the pro-metastatic properties of Runx2 we engineered the MCF7/Runx2^{dox} subline, which expresses Runx2 in response to doxycycline (dox). Runx2 expression in MCF7/Runx2^{dox} cells increased cell invasiveness and induced epithelial-mesenchymal transformation (EMT) evidenced by morphological changes as well as decrease of CDH1 and increase of VIM expressions. E2 attenuated the pro-invasive properties of Runx2. Genome-wide study of dox- and E2-responsive genes in MCF7 cells revealed a group of 530 genes independently regulated by both stimuli, and hierarchical clustering of these genes revealed four distinct clusters (I-IV). We speculated that Cluster II, upregulated by Runx2 and downregulated by E2, plays a role in the pro-cancerous properties of Runx2 and the favorable effect of E2 on BCa. Indeed, shRNA-mediated knockdown of SNAI2, the most responsive gene in Cluster II, abrogated Runx2-driven EMT and invasiveness. Bioinformatic analysis of a cohort of 557 BCa patients revealed that Cluster II metagene and SNAI2 were strongly associated with poor metastasis-free survival. Further analysis of the same dataset showed positive association between Runx2 activity and SNAI2, and negative correlation between estrogen receptor and SNAI2 expression. Kaplan-Meier curves of ER-positive patients showed increased metastasis-free survival by Cluster II and SNAI2 as compared to ER-negative patients; this beneficial effect of ER α was more prominent in the first 40 months. Survival probability of breast tumors that metastasized to different sites revealed that SNAI2 dramatically reduced metastasis-free survival of patients with bone, but to a lesser extent those with lung and brain metastases. These data support the view that SNAI2 is associated with more aggressive type of cancer and suggest that it may be responsible for priming breast tumors for metastasis to bone. Hierarchical clustering of 58 metastatic tissues revealed that SNAI2 was among the list of 11 genes upregulated only in bone metastasis. In summary we identified a cluster of genes, which likely contribute to the pro-metastatic property of Runx2 and its counteraction by E2 signaling. We show that SNAI2 plays a crucial role in mediating the pro-invasive and anti-tumorigenic properties of Runx2 and E2, respectively, in BCa, and provide evidence supporting a specific role for SNAI2 in bone metastasis.

Disclosures: Nyam-Orsor Chimgé, None.

FR0136

Interleukin 6 Modulates Tumor Behavior in Bone via a RANKL Dependent Pathway. Yu Zheng^{*1}, Katja Boerner², Anastasia Mikusheva³, Dennis Basel⁴, Robert L Sutherland⁵, Frank Buttgeriet³, Colin Dunstan⁶, Dr. Hong Zhou⁷, Markus Seibel⁷. ¹Bone Research Program, ANZAC Research Institute, The University of Sydney, Australia, ²Bone Research Program, ANZAC Research Institute, University of Sydney, Australia, ³Department of Rheumatology & Clinical Immunology, Charite University Medicine (CCM), Germany, ⁴ANZAC Research Institute, the University of Sydney, Australia, ⁵Cancer Research Program, Garvan Institute of Medical Research, Australia, ⁶University of Sydney, Australia, ⁷Bone Research Program, ANZAC Research Institute, The University of Sydney, Australia

High levels of circulating interleukin-6 (IL-6) in patients with metastatic breast cancer are associated with poor outcomes. In this study, we investigated the effect of tumor-derived IL-6 *in vitro*, and *in vivo* on MDA-MB-231 breast cancer cells using a xenograft model of skeletal metastasis.

In vitro studies with MDA-MB-231 cells demonstrated that RANKL up-regulates IL-6 expression by the cancer cells, while treatment with IL-6 significantly up-regulates their RANK expression. These results indicate that tumor-derived IL-6 may drive a positive forward-loop sensitizing the tumor cells to RANKL.

To further define the role of tumor-derived IL-6 on tumor growth in bone, we knocked down (by 80%) IL-6 expression in MDA-MB-231 cells via lentiviral-transduced stable shRNA expression (MDA-KD). Non-target (NT) cells served as controls. Silencing IL-6 expression significantly reduced tumor cell invasiveness but not proliferation *in vitro*. NT and MDA-KD cells were implanted intra-tibially into 4-week-old BALB/c nu/nu female mice kept on a low (0.1%) calcium diet to induce high bone turnover. Compared to NT cells, MDA-KD cells developed significantly smaller osteolytic lesions on day 10, 17 and 21 ($p < 0.05$, by X-ray analysis), and tumor area at endpoint (day 21; by histomorphometry) (3.20 0.76 vs. 5.57 0.98 mm², $p < 0.05$). When NT or MDA-KD cells were implanted into the mammary fat pad of nude mice, tumor growth was similar, indicating that the effects of tumor-derived IL-6 are mediated through the bone microenvironment.

In further experiments, IL-6 receptor (IL-6R) signalling was disrupted by treating mice implanted intra-tibially with MDA-MB-231 cells with the anti-human IL-6R antibody, Tocilizumab (Tmab). Compared to controls, Tmab at 50 mg/kg s.c every 3 days reduced the number and size of osteolytic lesions (1.530.24 vs. 1.980.23mm², $p<0.05$), and tumor area (2.170.27 vs. 5.620.67 mm², $p<0.01$). Mitotic activity decreased by 60% while apoptosis increased by 70%.

In conclusion, our results identify a new 'vicious cycle' in bone in which RANKL induces cancer cell IL-6 and subsequent RANK expression leading to enhanced tumor growth. Targeting IL-6 activity is a potential treatment strategy in breast cancer bone metastasis.

Disclosures: Yu Zheng, None.

FR0137

PMEPA1, a Negative Regulator of Transforming Growth Factor- β (TGF β) Signaling Pathway, Inhibits Bone Metastases from Prostate Cancer in Mice. Pierrick Fournier^{*1}, Gregory Clines², John Chirgwin¹, Theresa Guise¹. ¹Indiana University, USA, ²University of Alabama at Birmingham, USA

Most patients with advanced prostate cancer (>70%) develop metastases to bone, a rich source of TGF β that promotes bone metastases from breast cancer and melanoma. In this study, we investigated the role of TGF β signaling in prostate cancer bone metastases in mice.

A small molecule inhibitor of TGF β type 1 receptor, SD208, decreased osteolytic lesions (-56% vs vehicle, $P<0.05$) caused by PC-3 prostate cancer cells inoculated in the left cardiac ventricle of mice and increased their survival (57 vs 69 days median survival, $P<0.05$). To identify TGF β -regulated genes in prostate cancer, we analyzed PC3 cells TGF β (5ng/mL, 48h) by Affymetrix gene array and qRT-PCR. Upregulated genes included PTHrP, IL-11, CTGF and ADAM19, which increase bone resorption and MMP13 and TSP1, two TGF β activators. The most increased gene was PMEPA1 (23x, $P<0.03$). Alternate splicing gives rise to membrane-bound and cytosolic isoforms of PMEPA1 both increased by TGF β in prostate (PC3, DU145), breast (MDA-MB-231) and lung (A549) cancer cells.

Overexpression of membrane-bound PMEPA1 decreased TGF β signaling in dual-luciferase experiments. Mutation of the 2 PPxY domains that allow PMEPA1 to interact with Smurf ubiquitin ligases (regulators of Smad degradation) or the Smad Interaction Motif (SIM) that allows interaction with Smad2/3 prevented TGF β inhibition. In coimmunoprecipitation experiments, the interaction Smad2-Smurf2 was increased by PMEPA1, suggesting a role of scaffold protein. Interestingly, cytosolic PMEPA1 despite the presence of a SIM did not interact with Smad2/3 nor inhibit TGF β signaling. Knockdown of PMEPA1 (all isoforms) using siRNA increased Smad2 phosphorylation and the *IL-11*, *MMP13* and *ADAM19* mRNA induced by TGF β in PC3 cells.

The role of PMEPA1 in bone metastases was tested by stably transfecting PC3 cells to express shRNA control or anti-PMEPA1 (>90% decrease of mRNA or protein vs shRNA control) and two clones of each were inoculated in the left cardiac ventricle of mice to cause bone metastases. PMEPA1 knockdown in PC3 significantly increased osteolysis area on x-ray, compared to mice that received shCtrl cells consistent with an increased TGF β signaling.

Our results show that TGF β promotes the expression of pro-osteolytic genes in PC3 cells and of PMEPA1 that controls a negative feedback loop of TGF β signaling. Loss of PMEPA1 increases bone metastases in mice, consistent with reported decreases of PMEPA1 in prostate cancer with increasing tumor grade.

Disclosures: Pierrick Fournier, None.

FR0138

The Development of Bone Metastatic Lesions Is Modified By Circulating Fibronectin. Anja von Au, Matthaeus Vassel, Inaam Nakchbandi*. Max-Planck Institute for Biochemistry & University of Heidelberg, Germany

Fibronectin is required for new blood vessel formation. The tip cell of the newly forming blood vessel establishes a path that other endothelial cells will take and that is lined by fibronectin. The presence of fibronectin is one of the cues required by the endothelial cells to establish a blood vessel. The source of this local fibronectin and the role of circulating fibronectin during new blood vessel formation in tumors remain elusive however.

To examine this issue we used transgenic mice in which only circulating fibronectin was deleted. Using mice carrying the albumin promoter attached to cre that are at the same time homozygote for the floxed fibronectin gene we deleted fibronectin in the hepatocytes, the main source of circulating fibronectin and confirmed deletion of circulating fibronectin by almost 90% in conditional knockout mice (CT: 18526 vs. cKO: 195 mg/l, $n=8$ and 7; $p<0.001$). We then injected tumor cells (MDA-MB-231/luc+) in the tibia and followed their growth using bioluminescence. Deletion of fibronectin in the circulation resulted in a significant delay in tumor growth (Day 40: CT: 204 vs. cKO: 52 $\times 10^7$ RLU, $n=16$ and 10; $p<0.01$). This was associated with a significant decrease in osteolysis as determined by x-ray examination of the bones (Lytic surface: CT: 10.40.3 vs. cKO: 7.20.8 mm², $n=10$ and 5; $p<0.001$).

In order to determine whether this decrease in growth was due to decreased new blood vessel formation, tissue sections were stained for CD31 (PECAM-1) which stains blood vessels. There was a significant decrease in the number of blood vessels in

the tumors originating from mice lacking circulating fibronectin when compared to control mice (CT: 14811 vs. cKO: 795 blood vessels/mm², $n=8$ and 3; $p<0.01$). This was associated with a decrease in proliferation of tumor cells as detected by staining with anti-BrdU antibodies (CT: 65343 vs. cKO: 45213 cells/mm², $n=4$ and 3; $p<0.05$), without an increase in apoptosis examined by staining active caspase 3 (CT: 281 vs. cKO: 277 cells/mm², $n=7$ and 3; $p=ns$).

In summary, deletion of circulating fibronectin results in a significant decrease in tumor growth due to decreased blood vessel formation and decreased tumor cell proliferation. Thus, circulating fibronectin supports new blood vessel formation in tumors.

Disclosures: Inaam Nakchbandi, None.

FR0139

The Impact of Macrophage Depletion on Bone Homeostasis and Prostate Tumor Growth. Fabiana Soki^{*1}, Sun Wook Cho¹, Amy Koh², Serk In Park², Laurie McCauley³. ¹University of Michigan School of dentistry, USA, ²University of Michigan, USA, ³University of Michigan, School of Dentistry, USA

Bone contains a population of resident macrophages termed osteomacs, which play a role in bone remodeling, repair and hematopoietic stem cell niche maintenance. Macrophages are recruited to tumors where they contribute to growth, progression and metastasis in different types of cancer. The link between macrophages residing in different compartments and their functions under various environmental stimuli remain elusive. The role of macrophages in bone and tumor growth was investigated using the macrophage fas-induced apoptosis (MAFIA) mouse model. Administration of a synthetic dimerizer (AP20187) activates a suicide gene downstream of the c-fms promoter, leading to Fas-mediated apoptosis of myeloid cells. AP20187 (AP, 10mg/kg) or vehicle was administered to 16 week female MAFIA mice for 3 consecutive days for initial macrophage ablation and every third day (1mg/kg) for up to 4wks. Macrophage depletion treatment resulted in splenomegaly and a 20% reduction of total bodyweight. Bone marrow flow cytometric analysis (FACS) revealed a 22% reduction of macrophages (c-fms+CD11b+F4/80+) in AP-treated mice vs. vehicle. Serum TRAP was significantly decreased (50%) after 3d of AP injection and tended to remain suppressed for 4 weeks. Bone histomorphometric analysis revealed an osteopenic phenotype with loss of bone marrow adipocytes in macrophage depleted mice. To analyze the role of macrophages in prostate cancer tumor growth, 16wk male MAFIA mice were injected with AP or vehicle for 3d (10mg/kg) and every third day (5mg/kg) for 2wks. RM-1 (mouse prostate cancer) cells were seeded subcutaneously in MAFIA mice either by injection with Matrigel or co-implanted in single vertebral bodies dissected from 7 day old C57BL/6 mice (vossicles). Macrophage (CD11b+F4/80+) numbers in Matrigel RM-1 tumors were significantly decreased in AP treated mice. FACS confirmed an 80% macrophage suppression with an increase in CD11b+ Gr1+ myeloid derived suppressor cells (MDSCs) in the bone marrow of macrophage ablated mice. RM-1 cell tumors in matrigel or vossicles showed a trend of being smaller in macrophage depleted mice. In conclusion, macrophage depletion for 4wks altered the bone phenotype and bone marrow populations. Macrophage recruitment to tumors was reduced in macrophage ablated mice and tumors were marginally smaller. These findings demonstrate the importance of macrophages in normal bone remodeling and suggest a role for macrophages in the tumor microenvironment.

Disclosures: Fabiana Soki, None.

FR0147

Host-derived Prostaglandin E Regulates Bone Metastases of Malignant Melanoma through Angiogenesis. Morichika Takita, Satoshi Yokoyama, Masaki Inada*, Chisato Miyaura. Tokyo University of Agriculture & Technology, Japan

Metastasized tumor is frequently accompanied by neo-vascularization in various organs. In tumor metastasis, the growth is closely related to its surrounding angiogenesis. We reported that sequential pathway of osteoblastic prostaglandin E (PGE) biosynthesis in bone, which is mediated by an inducible PGE synthase, membrane-bound PGE synthase-1 (mPGES-1). In bone tumor of malignant melanoma (B16), host-osteoblasts induced PGE production and RANKL expression in autocrine and/or paracrine manner via PGE receptor subtype EP4. The treatment of EP4 antagonist clearly suppressed bone destruction by inhibiting osteoclastogenesis. In the present study, we investigated the roles of PGE on neo-vascularization which associated with tumor metastasis, using mPGES-1-null mice (mPGES-/-). When B16 cells were injected intravenously into wild-type mice (WT), numerous metastasized loci were found in various tissues including bone, lung, liver, and kidney. In mPGES-/-, however, the number of metastasized loci was markedly suppressed at all. In the laser imaging for *in vivo* detection of neo-vascularization, a red fluorescent labeled polyethyleneglycol particle was used to detect angiogenesis, since the particle was able to incorporate specifically into growing endothelial cells. In WT, the fluorescent signals of neo-vascularization were strongly detected in B16 metastasized foci, but not in mPGES-/- . In the experiments of subcutaneous injection of B16 cells to WT and mPGES-/-, the neo-vascularization was only found in WT. To further elucidate the roles of host-stromal cell derived PGE2 in neo-vascularization for tumor, skin stromal cells from WT and mPGES-/- were co-cultured with fixed-B16

cells. In the co-cultures, stromal cells from WT, but not from mPGES^{-/-}, markedly produced PGE after cell-to-cell interaction with B16 cells. WT derived stromal cells produced vascular endothelial cell growth factor (VEGF)-A and basic fibroblast growth factor (bFGF), and the production of both factors was increased by the treatment with PGE. On the other hand, VEGF-A and bFGF production was dramatically decreased in mPGES^{-/-} derived stromal cells. These results suggest that PGE produced by host-stromal cells including osteoblasts elicits the induction of angiogenic factors such as VEGF-A and bFGF. PGE may control the circumstance of tumor associated with angiogenesis, and modulate the growth of metastasized tumor cells.

Disclosures: Masaki Inada, None.

FR0148

IAP antagonist BV6 Increases Bone Metastasis via NIK-Mediated Osteoclast Activation. Chang Yang^{*1}, Jennifer Davis², Kathleen McCoy¹, Roberta Faccio¹, Deborah Novack³. ¹Washington University in St Louis School of Medicine, USA, ²Washington University in St. Louis, USA, ³Washington University in St. Louis School of Medicine, USA

IAPs (inhibitor of apoptosis proteins) have been associated with cancer and resistance to chemotherapies, and IAP antagonists are currently in development as anti-cancer agents. Additionally, IAP antagonists activate alternative NF- κ B by stabilizing NIK. We have previously shown that constitutive NIK activation increases osteoclast activity and causes osteoporosis. Thus, we proposed that IAP antagonists might also cause bone loss. In mice treated weekly with IAP antagonist BV6 for 4 weeks, beginning at 6 weeks of age, bone mass (BV/TV) was decreased by 35%. Indices of both osteoclast and osteoblast activity were significantly increased (serum CTX 49%, Oc.S/BS 43%, serum osteocalcin 47%, BFR 59%; all $p < 0.05$), indicating an osteoporosis associated with high bone turnover. To understand the mechanism of BV6 activity in bone, we treated NIK-deficient mice with BV6 and found them to be completely resistant to bone loss. In vitro, BV6 increased NIK and RelB activation alone and in combination with RANKL, and enhanced RANKL-mediated osteoclastogenesis in control, but not NIK^{-/-} cultures. Since high bone turnover can provide a favorable microenvironment for tumor growth, we examined whether BV6 can alter tumor growth in bone separate from its anti-tumor effects. We utilized the 4T1 mouse breast cancer line, which is resistant to BV6-induced apoptosis, and injected 4T1-Fluc directly into the tibia or left cardiac ventricle between the 3rd and 4th BV6 doses. Consistent with its pro-resorptive effects, BV6 increased tumor growth in bone by 5.5-fold (intratibial) and 3.2-fold (intracardiac) on day 10 after tumor inoculation (both $p < 0.01$). There was no significant difference in visceral tumors between BV6 and vehicle treated mice in the cardiac injection model, indicating that the tumor-enhancing effects of BV6 are specific to bone. To examine if bisphosphonates can block the tumor enhancing effect of BV6, we gave zoledronic acid (ZA) and BV6 in both intra-tibial and intra-cardiac injection tumor models. ZA decreased tumor mass in bone to the levels found in mice receiving only vehicle in both models. In summary, although BV6 may possess anti-tumor activity, its direct effects on osteoclasts cause osteoporosis and enhance growth of drug-resistant tumors in bone by activating NIK. Increased bone metastasis can be blocked by osteoclast-targeting therapies such as bisphosphonates, preserving BV6 as a potential therapeutic agent for tumors that may spread to bone.

Disclosures: Chang Yang, None.

FR0152

Oncologic Doses of Zoledronic Acid Induce ONJ-Like Lesions in Rice Rats (*Oryzomys palustris*) with Periodontitis. J. Aguirre^{*1}, Mohammed Akhter², Jennfer Pingel³, Xuechun Xia³, Aly Williams³, Marda Jorgensen⁴, Kent Edmonds⁵, Mercy Rivera⁶, Lakshmya Kesavalu⁶, Thomas Wronski¹. ¹University of Florida, USA, ²Creighton University Osteoporosis Research Center, USA, ³Department of Physiological Sciences, University of Florida, USA, ⁴Cell & Tissue Analysis Core, McKnight Brain Institute, University of Florida, USA, ⁵Department of Biology, Indiana University Southeast, USA, ⁶Department of Periodontology & Oral Biology, College of Dentistry, University of Florida, USA

Though osteonecrosis of the jaw (ONJ) is temporally associated with the use of nitrogen-containing bisphosphonates (BPs), no cause/effect relationship has been established. We hypothesize that ONJ is a two-stage process: a) risk factors initiate pathologic processes in the oral cavity that lead to a supranormal rate of hard tissue necrosis, and b) powerful anti-resorptives (e.g. N-BPs) reduce the rate of removal of necrotic bone sufficiently to allow its net accumulation in the jaw. To begin testing this hypothesis, we used the rice rat that appears to be an animal model of periodontitis. At age 28 days, rats (n=15/group; 10 males and 5 females) were placed on a pelleted high sucrose and casein diet to exacerbate the development of periodontitis. Animals were injected SC biweekly with alendronate (ALN, 0 or 15 μ g/kg), or IV once monthly with 0, 8 or 80 μ g/kg of zoledronic acid (ZOL) and sacrificed after 6, 12, and 18 wks. Mandibles and maxillae were analyzed to determine the effects on: a) progression of periodontitis, b) integrity of alveolar bone, and c) status of bone resorption and formation by using morphometric, histologic, histomorphometric, and microCT analyses. We found that rats treated with 80 μ g/kg of ZOL (oncogenic

dose) had higher incidence and severity of periodontal lesions after 18 wks of treatment than other groups, particularly in females. Histologic lesions included gingival epithelial hyperplasia, inflammatory cell infiltration, and areas of exposed alveolar bone with empty osteocyte lacunae and/or osteolysis. In males, ALN and ZOL had no effect on horizontal and vertical bone loss. In females, 80 μ g/kg of ZOL ameliorated vertical bone loss at 6 and 12 but not at 18 wks. Also, 80 μ g/kg of ZOL increased bone volume and BMD at the interdental alveolar bone at 6 and 12 but not at 18 wks. Remarkably, 80 μ g/kg of ZOL increased the area of interdental alveolar bone devoid of basic fuchsin stain (necrotic bone) only at 18 wks. All doses of ALN and ZOL decreased mineralizing surface and bone formation rate at 6, 12 and 18 wks, but reduced eroded surface and osteoclast number only at 6 and/or 12 wks. These data indicate that 80 μ g/kg of ZOL decreased bone remodeling before the appearance of increased amount of hyperdense interdental alveolar bone in the jaw. This is followed by exacerbation of the inflammatory response at the periodontium, exposed necrotic alveolar bone and/or osteolysis. These features resemble those observed in patients with ONJ.

Disclosures: J. Aguirre, None.

FR0157

A Novel Mouse Model of Tibial Pseudarthrosis Featuring Localized Double Inactivation of the *Nf1* Gene. Aaron Schindeler^{*1}, Jad El-Hoss², Kate Sullivan¹, Tegan Cheng¹, Kathy Mikulec¹, Lauren Peacock¹, Paul Baldock³, Ian Alexander⁴, David Little¹. ¹The Children's Hospital at Westmead, Australia, ²University of Sydney, Australia, ³Garvan Institute of Medical Research, Australia, ⁴Children's Medical Research Institute, Australia

Congenital tibial dysplasia (CTD) is a severe orthopaedic condition, recalcitrant to standard surgical intervention. A majority of clinical cases are observed in children with Neurofibromatosis type 1 (NF1) and it has been previously reported that osseous lesions in CTD exhibit local double-inactivation of NF1 (Stevenson et al. Am J Hum Genet. 79:143-8, 2006). We have developed a mouse model that recapitulates the localized double inactivation of NF1 in cultured osteoprogenitors and in open and closed tibial fractures. *Nf1*^{flx/flx}, *Nf1*^{flx/-}, and wild type control mice had either closed fractures or open osteotomies (with periosteal stripping) performed. *Nf1*^{flx} alleles were deleted via delivery of a Cre expressing adenovirus (AdCre) injected into the fracture site at day zero. Recombination was also confirmed in ZAP reporter mice. In closed fractures, bridging was 100% in control fractures and <40% in *Nf1*^{flx} fractures ($P < 0.05$). In open fractures, bridging was 75% in control fractures and <30% in *Nf1*^{flx} fractures ($P < 0.05$). In both open and closed fracture repair models the *Nf1*^{flx} state was associated with a significant increase of up to 15-fold more fibrotic tissue invading the callus by week 3. TRAP+ cells were observed histologically in the *Nf1*^{flx} fibrotic tissue. Closed *Nf1*^{flx} fractures also showed a significant increase in proliferating BRDU labelled cells in the callus. No statistically significant differences were seen with between *Nf1*^{flx/flx} and *Nf1*^{flx/-} mice suggesting that a heterozygous background is not critical for impaired healing in this model. *In vitro* experiments demonstrated that cultured *Nf1*^{flx} calvarial pre-osteoblasts were impaired in their capacity to differentiate into osteoblasts. However, when *Nf1* was deleted later in mature osteoblasts, their capacity for mineralization was unaffected. Similar findings were found in cultured *Nf1*^{flx} primary myoblasts from a novel transgenic mouse model. In summary, we report that knocking-out *Nf1* locally in a fracture callus is sufficient to induce poor rates of bridging and can lead fibrous non-unions. This fibrous tissue contains several characteristics of a NF1 pseudarthrosis, including osteoclast-like cells surrounded by proliferative fibrous tissue. This model provides valuable insight into the pathobiology of the disease, and will be helpful for trialling new therapeutic compounds.

Disclosures: Aaron Schindeler, Celgene Inc, 2

FR0158

Patients with Turner Syndrome and Isolated *SHOX* Deficiency Have Similar Bone Geometry At the Radius. ONDREJ SOUCEK^{*1}, Jan Lebl², Jirina Zapletalova³, Dana Novotna⁴, Ivana Plasilova⁵, Stanislava Kolouskova², Dana Zemkova², Miloslav Rocek⁶, Katerina Hirschfeldova⁷, Zdenek Sumnik². ¹2nd Faculty of Medicine, Charles University, Prague, Czech Republic, ²Department of Pediatrics, Charles University, 2nd Faculty of Medicine, University Hospital Motol, Czech Republic, ³Department of Pediatrics, Palacky University, Faculty of Medicine, University Hospital Olomouc, Czech Republic, ⁴Department of Pediatrics, Masaryk University, Faculty of Medicine, University Hospital Brno, Czech Republic, ⁵Department of Pediatrics, Charles University, Faculty of Medicine, University Hospital Hradec Kralove, Czech Republic, ⁶Department of Radiology, Charles University, 2nd Faculty of Medicine, University Hospital Motol, Czech Republic, ⁷Institute of Biology & Department of Medical Genetics, Charles University, 1st Faculty of Medicine, General University Hospital, Czech Republic

Purpose

Girls with Turner syndrome (TS) have altered bone density and geometry at the radius, which may pose an increased fracture risk in adulthood. The etiology of their low bone strength remains unknown, despite assumptions have been made on the influence of hypogonadism and the haploinsufficiency of the X chromosome. Since short stature homeobox (*SHOX*) gene plays a major role in long bone growth and patients with *SHOX* deficiency share some skeletal features with TS, *SHOX* gene has been suggested as a causal one. We aimed to assess bone geometry and volumetric bone density in patients with isolated *SHOX* deficiency and to compare their results to girls with TS.

Methods

Fourteen patients with *SHOX* deficiency (median age 11.8 yrs, range 6.0-36.8, 10 children and 4 adults) were examined by peripheral quantitative CT (pQCT) at the non-dominant forearm. Results were expressed as Z-scores using published reference data and then compared to the results of 67 girls with TS (median age 13.7 yrs, range 6.0-19.4). The differences from reference data were tested by one-sample T test and differences between TS and *SHOX* deficiency were tested by two-sample T test.

Results

Trabecular volumetric bone mineral density (vBMD) was decreased in TS (mean Z-score -0.71.3, $p < 0.001$) but normal in isolated *SHOX* deficiency (Z-score 0.31.3, n.s., group difference $p < 0.01$). Cortical vBMD was low in both groups (Z-score -1.61.5, $p < 0.001$ and -1.92.3, $p < 0.01$, respectively) without significant group difference. Both groups had increased total bone cross-sectional area (CSA) at the diaphysis (Z-score 0.71.7, $p < 0.01$ and 2.31.5, $p < 0.001$, respectively), but normal cortical bone CSA (Z-score 0.01.0, n.s. and -0.72.3, n.s., respectively). Consequently, cortical thickness was decreased in both groups (Z-score -0.80.6, $p < 0.001$ and -1.41.4, $p < 0.01$, respectively).

Conclusions

Patients with Turner syndrome and isolated *SHOX* deficiency have similar bone geometry at the radius. Our results support the hypothesis that skeletal abnormalities in patients with TS are caused by *SHOX* deficiency. Low trabecular vBMD in TS is probably a consequence of hypogonadism due to ovarian failure.

Disclosures: *ONDREJ SOUCEK, None.*

FR0160

Unique Contributions of Endothelial vs. Smooth Muscle *Msx* Gene Expression In Arteriosclerotic LDLR-Deficient Mice. Jian Su Shao¹, Su-Li Cheng², Abraham Behrmann¹, Kathryn Distelhorst¹, Linda Halstead¹, Robert Maxson³, Dwight Towler^{*1}. ¹Washington University in St. Louis, USA, ²Washington University in St. Louis School of Medicine, USA, ³University of Southern California, USA

When male LDLR-deficient mice are fed high fat diabetogenic diets (HFD), osteochondrogenic transcription factors such as Runx2 and members of the *Msx* and *Sox* gene families are upregulated in the aorta with progressive calcium deposition. In vivo and in vitro, *Msx2* expression enhances osteogenic mesenchymal cell mineralization via activation of paracrine Wnt7 signals and the inhibition of Dkk1, an LRP Wnt receptor antagonist. In the absence of diabetes, *Msx* genes are dynamically expressed in postnatal endothelial cells (ECs), smooth muscle cells (SMCs), and myofibroblasts. To better understand the roles of vascular *Msx* genes in arteriosclerosis, we've implemented Tagln-Cre and Cdh5-Cre mice to conditionally delete floxed alleles in SMCs and ECs, respectively. As compared to *Msx2(f/f);LDLR +/-* controls, Tagln-Cre;*Msx2(f/f);LDLR +/-* mice exhibit only 6% of basal aortic *Msx2* mRNA expression, with no impact upon *Msx1*. Aortic Col1A1 and Col10A1 are concomitantly reduced, along with *Sox2*, a *Sox* factor required for osteoprogenitor renewal. Additional reduction in SMC *Msx* "tone" in Tagln-Cre;*Msx2(f/f);Msx1(f/+);LDLR +/-* mice, decreased aortic *Msx1* (by 70%), and *Sox9* (by 40%), but did not further reduce Col1A1, Col10A1, or *Sox2*. Significant upregulation of Dkk1 was noted but Wnt7b was unaltered. Remarkably, while Cdh5-Cre;*Msx2(f/f);LDLR +/-* animals exhibited only minor changes in aortic *Msx2* and Dkk1, aortic Wnt7b, Wnt4, Wnt3a, & Wnt10a mRNA levels were dramatically reduced by >85%. In cultured bovine aortic endothelial cells (BaEC), augmenting *Msx2* and Wnt7b expression supports EC molecular phenotype and epithelial morphology, and suppresses the endothelial-mesenchymal transition (EnMT). Consistent with this, Cdh5-Cre;*Msx2(f/f);LDLR +/-* mice exhibit significantly reduced aortic expression of claudin 5, a marker & mediator of endothelial integrity, and increased Col1A1 mRNA. Furthermore, as compared to *Msx2(f/f);LDLR +/-* controls, Cdh5-Cre;*Msx2(f/f);LDLR +/-* mice exhibited increased arterial calcification when challenged with HFD for 12 weeks (3.8+/-0.1 vs 6.2+/-1.0 ug/mg, $p = 0.04$). Thus, *Msx* genes contribute unique activities in aortic ECs vs. SMCs. *Msx2* regulates aortic Col1A1, Col10A1, and Dkk1 expression primarily in SMCs, but supports vascular Wnt7b expression primarily in ECs. Differential endothelial vs. mesenchymal *Msx*-Wnt signals may couple EC phenotypic modulation with osteo/fibrogenic arteriosclerotic responses in part via regulation of EnMT.

Disclosures: *Dwight Towler, None.*

FR0163

Measles Virus Nucleocapsid Protein induces Autophagy in Osteoclasts: Implications for the Pathogenesis of Paget's Disease of Bone. Feng-Ming Wang^{*}, Deborah L. Galson. University of Pittsburgh, Medicine/Hematology-Oncology, The Center for Bone Biology of UPMC, & VA Pittsburgh Healthcare System, USA

Paget's disease of bone (PDB) is characterized by abnormal osteoclast (OCL) that express a pagetic phenotype, that includes increased OCL number and hypermultinuclearity, as well as increased IL-6 production. Measles virus nucleocapsid protein (MVNP) contributes to the pathogenesis of PDB as demonstrated by published studies from both patients and transgenic animals. However, it remains unclear how MVNP induces the abnormal features of pagetic OCL. Recently published data revealed that measles virus infection induces autophagy in HeLa cells. Another recent report revealed that autophagy plays a pivotal regulatory role in hypoxia-induced OCL formation. Therefore, we examined the impact of MVNP expression on autophagy in the OCL generated in vitro from the bone marrow monocytes of wild-type and TRAP-MVNP transgenic mice by treatment with M-CSF and RANKL. Immunoblot measurements of microtubule-associated protein light chain 3 (LC3) conversion to the LC3-II form and degradation of p62 indicated that autophagy was induced during osteoclast differentiation. On day 3, the OCL generated from TRAP-MVNP mice had a higher ratio of LC3-II/I and lower levels of p62 than the OCL generated from wild-type mice, paralleling the increased TRAP-positive multinucleated cells observed with MVNP+ cells. We examined the LC3-II/I ratio in NIH3T3 cells stably transduced with MVNP (NIH3T3-MVNP) and compared empty vector-transduced NIH3T3 cells (NIH3T3-EV). NIH3T3-MVNP cells exhibited a higher ratio of LC3-II/I than NIH3T3-EV cells. Further, transmission electron microscopy demonstrated that NIH3T3-MVNP cells were rich in autophagosomes. Given that cytosolic FoxO1 is essential for the induction of autophagy, we investigated the sub-cellular localization of FoxO1 in these cells. We observed that cytosolic FoxO1 was increased in the NIH3T3-MVNP cells. We also found that MVNP is cytosolic in NIH3T3-MVNP cells, suggesting that MVNP may directly interact with FoxO1. Interestingly, the accumulation of FoxO1 in the nucleus was inhibited by the presence of MVNP when the cells were treated with LY294002 and resveratrol, both of which trigger nuclear translocation of FoxOs. These results suggest that MVNP induces abnormal pagetic OCL through sequestering cytosolic FoxO1 and thereby promoting autophagy in PDB.

Disclosures: *Feng-Ming Wang, None.*

FR0164

Microarray Profile of p62^{P392L} and Measles Virus Nucleocapsid Protein (MVNP) Regulated Gene Expression During Osteoclast Differentiation. Kumaran Sundaram^{*1}, Srinivasan Shanmugarajan¹, Sudhaker Rao², Sakamuri Reddy¹. ¹Charles P. Darby Children's Research Institute, USA, ²Henry Ford Hospital, USA

Paget's disease of bone (PDB) is a chronic localized bone disorder affecting 2-3% of the population over 60 years of age. PDB is inherited as an autosomal dominant trait with genetic heterogeneity. SQSTM1/p62 UBA domain mutation (p62^{P392L}) is widely identified in PDB and has been shown to increase osteoclastogenesis. Further, environmental factors such as paramyxovirus are implicated in PDB and MVNP has been shown to induce Pagetic phenotype in osteoclasts. However, the molecular mechanisms underlying p62^{P392L} and MVNP stimulation of osteoclast differentiation in PDB are unclear. We therefore determined p62^{P392L} and MVNP regulated gene expression profiling during osteoclast differentiation. Total RNA isolated from normal human bone marrow mononuclear cells transduced with p62^{WT}, p62^{P392L}, MVNP retroviral expression vectors and stimulated with M-CSF and RANKL for 48 h were subjected to Agilent microarray (~26,000 genes) analysis. We identified 9.7% and 8.4% of genes were upregulated (> 4-fold) in p62^{P392L} and MVNP transduced cells respectively. p62^{P392L} mutant increased Integrin β 3 (185 fold), integrin β 5 (26 fold), IL-1 α (11 fold), IL-6R (8 fold), CXCL-2 (7.5 fold), CXCL-3 (5 fold) compared to p62^{WT} transduced cells. Similarly, MVNP increased integrin β 3 (63 fold), NFAT activating protein (6.5 fold), OSCAR (5.5 fold), TRAF5 (8.5 fold) mRNA expression compared to empty vector (EV) transduced cells. MVNP also elevated gene expression of cytokines/growth factors such as IL-17 (18 fold), IL-1F7 (10 fold), IL-17R (4.5 fold) and IL-11 (7 fold). Interestingly, MVNP transduced cells demonstrated a high level expression of signal regulatory protein beta 1 (SIRPB1) (353 fold). SIRPB1 has been shown to interact with DAP 12, an ITAM containing adaptor protein which plays an important role in osteoclast differentiation. Real-time PCR analysis of total RNA isolated from normal human peripheral blood monocytes transduced with MVNP confirmed upregulation of SIRPB1 mRNA expression in the absence of RANKL stimulation. In contrast, RANKL stimulation did not alter SIRPB1 expression in these cells. Furthermore, bone marrow mononuclear cells derived from patients with PDB showed high levels of SIRPB1 mRNA expression compared to normal subjects. Thus, p62^{P392L} mutant and MVNP regulated gene expression profiling during osteoclast differentiation provides new insights into the molecular mechanisms and therapeutic targets to control elevated osteoclast activity in PDB.

Disclosures: *Kumaran Sundaram, None.*

This study received funding from: Department of Defense

FR0165

TANK Binding Kinase 1 (TBK1) Mediates MVNP Effects in Pagetic Osteoclasts. Quanhong Sun^{*1}, Benedicte Sammut¹, Fengming Wang¹, Jolene J. Windle², Noriyoshi Kurihara¹, G. David Roodman¹, Deborah L. Galson¹. ¹University of Pittsburgh, Medicine/Hematology-Oncology, The Center for Bone Biology of UPMC, & VA Pittsburgh Healthcare System, USA, ²Virginia Commonwealth University, Department of Human & Molecular Genetics, USA

Paget's disease is characterized by abnormal osteoclasts (OCL) that express a phenotype which includes increased: sensitivity of OCL progenitors to 1,25(OH)₂D₃, RANKL and TNF- α , number of OCL, nuclei/OCL, and expression of the VDR coactivator TAF12 and the cytokine IL-6. Measles virus nucleocapsid protein (MVNP) contributes to the pathogenesis of pagetic osteoclasts as demonstrated by published studies from both patients and transgenic mice. However, the direct interactions of MVNP that generate pagetic OCL are unknown. TANK binding kinase 1 (TBK1) and I κ B kinase-epsilon (IKK ϵ) are IKK-related family members which have been reported to physically interact with MVNP and can activate both the IRF3 and the NF- κ B pathways. We have found in our studies that TBK1 protein, but not IKK ϵ protein, is increased in OCL precursors from TRAP-MVNP mice as compared to OCL precursors from wildtype mice. Interestingly, both TBK1 and IKK ϵ were increased early in OCL differentiation (at day 1), and then decreased at day 3, in cells from both TRAP-MVNP and wildtype mice, suggesting a possible role in normal osteoclastogenesis. However, only TBK1 was further enhanced in the presence of MVNP. Both TBK1 and IKK ϵ expression vectors co-transfected with a -1200 IL-6 promoter luciferase reporter into HEK293 cells stimulated IL-6 promoter activity. Strikingly, over-expression of both TBK1 and IKK ϵ as well as MVNP cDNA transfection induced the endogenous IL-6 gene in both NIH3T3 and pre-osteoclastogenic RAW264.7 cells. We investigated the role of TBK1 in MVNP induction of IL-6 using NIH3T3 cells stably transfected with MVNP or empty virus (EV) as a model system. The NIH3T3-MVNP cells produce much larger amounts of both IL-6 mRNA and secreted protein than NIH3T3-EV cells. We found that similar to the effects of MVNP on TBK1 levels in OCL, TBK1 protein levels were increased in NIH3T3-MVNP as compared to NIH3T3-EV cells. After overnight serum starvation (2% serum), TNF- α increased TBK1 phosphorylation in a similar biphasic pattern in both NIH3T3-EV and NIH3T3-MVNP cells, but there was significantly more phospho-TBK1:total TBK1 as well as total TBK1 in the NIH3T3-MVNP cells at each time point. Knockdown of TBK1 with a shRNA lentivirus impaired IL-6 secretion induced by MVNP as well as decreased TAF12. These results demonstrate that TBK1 plays a critical role in mediating the effects of MVNP on the expression of both TAF12 and IL-6, key contributors to the pagetic OCL phenotype.

Disclosures: Quanhong Sun, None.

FR0166

The Expression of Measles Virus Nucleocapsid Protein (MVNP) Gene in Osteoclasts (OCLs) Induces Expression of Coupling Factors that Stimulate Bone Formation. Yoko Uehata^{*1}, Jumpei Teramachi¹, Jolene Windle², Noriyoshi Kurihara¹, G. David Roodman³. ¹University of Pittsburgh & The Center for Bone Biology at UPMC, USA, ²Virginia Commonwealth University, USA, ³University of Pittsburgh, The Center for Bone Biology at UPMC, & VA Pittsburgh Healthcare System, USA

We reported that 70% of Paget's disease (PD) patients express MVNP and that transgenic mice with targeted expression of MVNP to cells in the OCL lineage formed pagetic-like bone lesion that display both increased bone resorption and rapid new bone formation (J Bone Miner Res 2006). In contrast, mice with targeted expression of the p62^{P392L} mutation linked to OCL (TRAP-p62^{P392L}) have increased bone resorption but do not have increased bone formation in vivo (J Clin Invest 2007). Further, loss of IL-6 in TRAP-MVNP mice prevents the development of pagetic OCLs and reduces bone formation parameters in these animals. These results suggested that IL-6 plays an important role in linking bone formation to bone resorption in PD (Cell Metab 2011). Ephrin-B2 and EphB4 were recently identified as key coupling factors for OCL and osteoblasts. Ephrin-B2 is produced by OCL and dramatically enhances osteoblast function and bone formation in vitro and in vivo through specific interactions with EphB4 on osteoblasts. To determine if Ephrin-B2 and EphB4 play a role in the effects of MVNP on bone formation, we collected bone marrow from 20-month-old wild type (WT), TRAP-MVNP, TRAP-MVNP/IL-6^{-/-} and TRAP-p62^{P392L} mice and examined the role of Ephrin-B2/EphB4. Bone marrow cells were cultured 3 days on non-tissue culture dishes with 50 ng/ml of BMP-2. The adherent cell population, containing the committed OCL-precursors (OCL-P) and pre-osteoblasts, was co-cultured with 1,25(OH)₂D₃, and the levels and ratio of Ephrin-B2/EphB4 were determined. Ephrin-B2/EphB4 was increased in MVNP expressing bone marrow cultures compared to WT and p62^{P392L} cultures. CD11b(+) cells (early OCL-P) from TRAP-MVNP mice expressed decreased levels of Ephrin-B2 when treated with 1,25(OH)₂D₃ compared to WT. More differentiated MVNP expressing OCL-P expressed enhanced Ephrin-B2 compared to OCL from WT and p62^{P392L} mice. Osteoblasts derived from bone marrow cultures of MVNP mice had increased expression of EphB4 and Runx2 when treated with 1,25(OH)₂D₃ compared to WT and p62^{P392L}. Further, MVNP/IL-6^{-/-} mice had decreased expression of Ephrin-B2, EphB4 and Runx2, consistent with the lack of increased bone formation in these mice. These results show that MVNP increases both OCL activity and bone formation

by promoting OCL and osteoblast interactions, suggesting that the mechanism responsible for the increased expression of Ephrin-B2/EphB4 induced by MVNP is dependent on IL-6.

Disclosures: Yoko Uehata, None.

FR0177

High Turnover Renal Osteodystrophy is Associated with β -Catenin Repression in Osteocytes. Yves Sabbagh^{*}, Wen Tang, Christina Bracken, Stephen O'Brien, Lucy Phillips, Sue Ryan, Shiguang Liu, Susan Schiavi. Genzyme Corporation, USA

Chronic kidney disease-mineral bone disorder (CKD-MBD) is defined by abnormalities in mineral and hormone metabolism, bone histomorphometric changes and/or the presence of vascular or soft tissue calcification. Emerging evidence suggests that features of CKD-MBD may occur early in disease progression and are associated with changes in osteocyte function. To identify early pathological changes in bone, we utilized the *Jck* mouse, a genetic model of polycystic kidney disease that exhibits progressive biochemical features of CKD-MBD, similar to what is observed in the human population. At 6 weeks of age these mice have normal renal function and no evidence of bone disease but exhibit progressive decline in renal function starting at 8 weeks and death by 18 weeks of age. We investigated temporal bone changes in *Jck* relative to wild-type (WT) mice from 6 through 18 weeks of age. The presence of high bone turnover was observed as early as 9 weeks of age based on increased BFR in *Jck* (0.570.04mm³/mm²/yr) relative to WT mice (0.360.02mm³/mm²/yr). To capture the early molecular and cellular events mediating the progression of CKD-MBD in *Jck* we examined specific molecular pathways associated with osteocyte function and bone remodeling at the protein and gene expression level. Immunohistochemistry staining for the osteocyte specific Wnt-antagonist, sclerostin (SOST) demonstrated that it was significantly elevated in *Jck* mice at 9 weeks of age. This alteration paralleled increased Phospho-Ser33/37- β -catenin protein expression in *Jck* osteocytes supporting inhibition of the Wnt/ β -catenin pathway. Although osteoprotegerin (OPG) gene expression was not altered in *Jck* bone, RANKL ligand was significantly elevated leading to a shift in the OPG/RANKL ratio favoring osteoclast activity. These results are consistent with published reports demonstrating that Wnt/ β -catenin pathway inhibition leads to enhanced osteoclast activity. As serum PTH was rising with disease progression, SOST expression was down-regulated both at the protein and mRNA level. Interestingly, sFRP4 mRNA, another Wnt antagonist, was also significantly elevated early in disease in the *Jck* but unlike SOST its elevated expression was sustained during the same time frame. These data provide evidence for early changes in osteocytes which may negatively influence bone remodeling. Overall repression of Wnt/ β -catenin pathway appears to be sustained during disease progression in CKD-MBD.

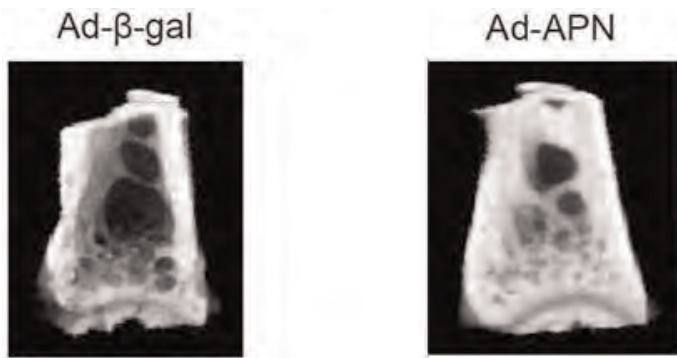
Disclosures: Yves Sabbagh, Genzyme Corporation, 3
This study received funding from: Genzyme Corporation

FR0178

Adenovirus-Mediated Gene Transfer of Adiponectin Reduces Osteoclasts Differentiation and Bone Erosion of Collagen-Induced Arthritis in Mice. Kosuke Ebina^{*}, Kazuya Oshima, Makoto Hirao, Jun Hashimoto, Kenrin Shi, Hideki Yoshikawa. Osaka University, Graduate School of Medicine, Department of Orthopedics, Japan

Adiponectin (APN) is a hormone released by adipose tissue with anti-diabetic and anti-atherogenic properties. In addition, APN inhibits osteoclasts differentiation and pro-inflammatory cytokines production from macrophages by inhibiting NF- κ B activity *in vitro*. However, APN also exhibits pro-inflammatory effects by promoting pro-inflammatory cytokines production from synovial fibroblasts. We have previously reported that serum APN levels are elevated and associated with disease severity in patients with rheumatoid arthritis (RA), but its effect remains unclear. The purpose of this study is to examine the effects of systemic delivery of APN in murine arthritis model. Collagen-induced arthritis (CIA) is an established murine arthritis model with many similarities to RA. CIA was induced in DBA1/J mice by injection of chicken type II collagen in complete Freund's adjuvant twice with a 21-day interval. 2 \times 10⁸ plaque-forming units of adenoviral vectors encoding human APN (Ad-APN) or beta-galactosidase (Ad-b-gal) as control were injected intravenously either before or after arthritis onset. Clinical severity of arthritis was assessed by all limb swelling, yielding a maximum score of 16 per mouse. Tissue samples were obtained on 35 days after CIA induction. Serum APN levels were elevated in Ad-APN infected mice about 5-fold on 2 days, and about 30-fold on 16 days after adenovirus injection compared to control group. Systemic APN delivery at both time points significantly decreased clinical disease activity scores of CIA (before onset treatment: Ad-APN infected mice 1.76 0.63, Ad-b-gal infected mice 8.68 1.06; P < 0.001 / after onset treatment: Ad-APN infected mice 5.17 1.25, Ad-b-gal infected mice 9.17 1.15; P < 0.05). APN treatment significantly decreased histological scores of inflammation, cartilage damage, and pannus formation and mRNA levels of pro-inflammatory cytokines in the joints. Interestingly, APN treatment significantly decreased the number of TRAP-positive cells in the joints (TRAP-positive cells per field: Ad-APN infected mice 8.15 3.31, Ad-b-gal infected mice 27.6 2.85; P < 0.001). In addition, APN treatment resulted in amelioration of bone erosion in the ankle joints of CIA mice evaluated by μ CT (BV/TV(%): Ad-APN infected mice 31.9 5.01, Ad-b-gal infected

mice 21.4 \pm 5.68; $P < 0.05$). These results provide novel evidence that systemic APN delivery inhibits bone erosion and inflammation of murine arthritis model joints.



Three-dimensional μ CT scan of the distal tibia of adenovirus-infected CIA mice

Disclosures: Kosuke Ebina, None.

FR0182

Bone Histomorphometry Findings in Pediatric Solid Organ Transplant Patients. Inari Tamminen¹, Helena Valta², Hanna Isaksson³, Sari Salminen⁴, Mervi K. Mayranpää⁵, Hannu Jalanko⁵, Heikki Kroger⁶, Outi Makitie⁷. ¹Bone & Cartilage research Unit (BCRU), University of Eastern Finland, Finland, ²Hospital for Children & Adolescents, University of Helsinki, Helsinki Finland, Finland, ³University of Eastern Finland, Finland, ⁴Children's Hospital, Helsinki University Central Hospital, Finland, ⁵Children's Hospital, Helsinki University Central Hospital & University of Helsinki, Finland, ⁶Kuopio University Hospital, Finland, ⁷Hospital for Children & Adolescents, Helsinki University Hospital, Finland

Solid organ transplantation may lead to secondary osteoporosis in children. Metabolic abnormalities related to the underlying disease, disturbances in pubertal development and medication affect bone metabolism leading to low bone mass and increased fracture risk. This study characterized bone histomorphometric findings in pediatric kidney, liver and heart transplant recipients who were assessed for suspected secondary osteoporosis.

Iliac crest biopsies were obtained from 19 children (aged 7.6-18.8 years, 11 males) who had undergone kidney ($n=6$), liver ($n=9$) or heart ($n=4$) transplantation 6.8 \pm 5.7 years (range 0.6-16.3 years) earlier. Secondary osteoporosis was suspected based on low bone mineral density (BMD) measured by DXA and/or fracture history. All children had received glucocorticoids (GCs) for several years. Results of histomorphometric analyses were compared with reference values and correlated with clinical characteristics.

Of the 19 patients, 21% had sustained peripheral fractures and vertebral compressions were found in 58%. Nine children (47%) had a lumbar spine BMD Z-score below -2.0. Histomorphometric analyses showed decreased trabecular thickness in 12 patients (63%), increased trabecular number in 14 patients (74%) and decreased trabecular separation in 8 patients (42%). Trabecular bone volume was low (<-1.0 SD) in 5 children (26%). Low turnover was observed in 37% and high turnover in 32% of the children. No significant differences in bone histomorphometry were found between children with mild vs. moderate kidney dysfunction ($p>0.05$). Children with compression fractures ($n=11$) had higher present and cumulative GC dose (mg) than children without compression fractures ($n=8$) ($p<0.05$), and their biopsies showed lower osteoblast surface (Ob.S/BS) Z-score and mineralizing surface (MS/BS) Z-score ($p<0.05$) than children without compression fractures. Turnover rate tended to be lower for children with than without vertebral fractures.

Abnormal bone biopsy findings were common in children after solid organ transplantation. The observed changes in bone quality (*i.e.* abnormal turnover rate and thin trabeculae) rather than the actual loss of trabecular bone, might explain the increased fracture risk in pediatric solid organ transplant recipients.

Disclosures: Inari Tamminen, None.

FR0186

PHOSPHO1: a Novel Therapeutic Target for Medial Vascular Calcification. Tina Kiffer-Moreira¹, Manisha C. Yadav¹, Dongxing Zhu², Yalda Bravo³, Russell Dahl³, Sonoko Narisawa¹, Boguslaw Stec¹, Vicky E. MacRae², Colin Farquharson⁴, Jose Luis Millan¹. ¹Sanford Children's Health Research Center, Sanford-Burnham Medical Research Institute, USA, ²The Roslin Institute, The University of Edinburgh, United Kingdom, ³Conrad Prebys Center for Chemical Genomics, Sanford-Burnham Medical Research Institute, USA, ⁴The Roslin Institute, The University of Edinburgh, USA

Calcification of the medial layer of arteries, also known as Monckeberg's sclerosis, is increasingly recognized as an important clinical problem in chronic kidney disease, diabetes, and aging. Children with idiopathic infantile arterial calcification (IIAC), due to deficiency of the enzyme that produces inorganic pyrophosphate (NPP1), die of heart failure. We have documented that medial vascular calcification is accompanied by an increase in the expression of tissue-nonspecific alkaline phosphatase (TNAP) both in the *Enpp1*^{-/-} mouse model of IIAC (Narisawa et al., 2007) as well as in uremic rats (a model of end-stage renal disease) (Lomashvili et al., 2008). We have recently documented that expression of PHOSPHO1, an enzyme crucial for initiation of skeletal mineralization (Yadav et al., 2011) and the prevention of greenstick fractures (Huesa et al., 2011), affects TNAP expression. Further, we observed that *Phospho1*^{-/-} vascular smooth muscle cells (VSMCs) have markedly reduced ability to calcify in vitro compared to WT cells. PHOSPHO1 shows high phosphohydrolase activity towards phosphoethanolamine (P-Etn) and phosphocholine (P-Cho). Using high throughput screening, we have identified potent and specific inhibitors of PHOSPHO1, without the cross-inhibition of TNAP and NPP1 activity observed with lansoprazole, ebelsens and SCH-202676 (Roberts et al., 2007). Here, we present a detailed kinetic analysis of the inhibition of PHOSPHO1 with nine new small molecule compounds using PHOSPHO1's natural substrates P-Etn and P-Cho. We observed that MLS-0390837, MLS-0390838 and MLS-0263839 showed stronger inhibition than all the other compounds tested, with IC50 values of 0.22, 0.14 and 0.09 μ M, respectively. Our kinetic, computer modeling and docking predictions of MLS-0263839 and MLS-0390837 indicate a competitive type of inhibition. The MLS-0263839 and MLS-0390838 compounds were then used to demonstrate that inhibition of PHOSPHO1 leads to a reduction in the degree of calcification in *Enpp1*^{-/-} VSMCs. Thus, PHOSPHO1 appears to be a novel target for the prevention of medial vascular calcification. Narisawa et al., J. Bone Miner. Res. 22: 1700-1710 (2007). Roberts et al., J. Bone Miner. Res. 22: 617-627 (2007). Lomashvili et al., Kidney Int. 73, 1024-1030 (2008). Yadav et al., J. Bone Miner. Res. 26: 286-297 (2011). Huesa et al., Bone, In Press (2011).

Disclosures: Tina Kiffer-Moreira, None.

FR0187

A 4-bp Deletion Mutation in DLX3 Enhances Anti-adipogenic Activity of DLX3. Hye-Lim Lee¹, Kyung Hwa Baek², Kyung Mi Woo³, Hyun-Mo Ryoo¹, Gwan-Shik Kim¹, Jeong-Hwa Baek³. ¹Seoul National University School of Dentistry, South Korea, ²Seoul National University School of Dentistry, South Korea, ³Seoul National University, School of Dentistry, South Korea

DLX3 is a homeodomain protein that is involved in osteoblast differentiation. Deletion of 4 bps in DLX3 is causally related to tricho-dento-osseous syndrome, a genetic disorder manifested by taurodontism, hair abnormalities and increased bone density. The molecular mechanisms explaining the increased bone density phenotype have not been clearly elucidated. Osteoblasts and adipocytes are derived from common bone marrow mesenchymal progenitors, and there is a reciprocal regulation in the differentiation of osteoblasts and adipocytes. In this study, we examined whether DLX3 negatively regulates adipocyte differentiation and whether there are any differences in anti-adipogenic effects between wild type DLX3 (wtDLX3) and 4-bp deletion mutant DLX3 (mtDLX3). Over-expression of wtDLX3 and mtDLX3 in human bone marrow mesenchymal stem cells or 3T3-L1 murine preadipocytes suppressed adipogenic differentiation. However, anti-adipogenic effect of mtDLX3 is much stronger than that of wtDLX3. Adipogenic induction of 3T3-L1 cells suppressed Dlx3 expression whereas knock-down of Dlx3 enhanced adipogenic differentiation of 3T3-L1 cells. The expression of PPAR γ , a master transcription factor for adipogenesis, was suppressed by wtDLX3 and mtDLX3 whereas over-expression of PPAR γ rescued adipogenic differentiation of 3T3-L1 cells that over-express wtDLX3 or mtDLX3. Although there was no putative DLX-binding element within 2 kb of the PPAR γ promoter sequence, C/EBP α -induced PPAR γ promoter activity was suppressed by both wtDLX3 and mtDLX3 and CREB-induced PPAR γ promoter activity was suppressed by mtDLX3. Co-immunoprecipitation assays demonstrated that mtDLX3 binds to CREB and C/EBP α whereas wtDLX3 binds only to C/EBP α . Furthermore, the chromatin immunoprecipitation and in vitro DNA binding assays demonstrated that mtDLX3 prevents both C/EBP α and CREB from binding the PPAR γ promoter whereas wtDLX3 inhibits the DNA binding of C/EBP α only. Binding of DLX3 to C/EBP α required only homeobox domain whereas that of CREB to mtDLX3 required both homeobox domain and frame-shifted C-terminal domain. These results indicate that DLX3 is a negative regulator for adipocyte differentiation and that a frameshift by 4-bp deletion provides enhanced anti-adipogenic activity to mtDLX3. Enhanced anti-adipogenic activity of mtDLX3 may

be involved in increased bone density phenotype of tricho-dento-osseous syndrome, at least in part.

Disclosures: Hye-Lim Lee, None.

FR0189

Differential Effect of ApoE Isoforms on Trabecular Bone Mass and Bone Turnover in Mice. Marco Dieckmann¹, F. Timo Beil², R. Percy Marshall², Alexander Bartelt², Wolfgang Ruether², Michael Amling², Joachim Herz³, Andreas Niemeier^{*2}. ¹UT Southwestern Medical Center, USA, ²University Medical Center Hamburg-Eppendorf, Germany, ³Center for Alzheimer's & Neurodegenerative Disease, USA

Purpose We have previously shown that apoE ^{-/-} mice display a high bone mass phenotype due to an increased bone formation rate, but the underlying mechanism remains incompletely understood. Mice have only one form of apoE and do not express isoforms, while in humans three common isoforms of apoE (E2, E3, E4) exist. The isoforms differentially affect lipoprotein metabolism and apoE4 is a well-established risk factor for Alzheimer's disease, whereas the expression of apoE2 is associated with the development of hyperlipidemia. A substantial body of literature has been published on the question whether the human apoE isoforms have a differential impact on BMD and fractures, but the issue remains highly controversial. Part of the reason for this controversy is the asymmetric allele frequency of the apoE gene (approx. $\epsilon_2 = 0.08$, $\epsilon_3 = 0.77$, $\epsilon_4 = 0.15$ in Caucasians) which renders human studies difficult to perform. We therefore addressed the question whether human apoE isoforms have an impact on bone in vivo using apoE "knock-in" (apoE ki) mice that have been genetically modified to express the human apoE2, E3 and E4 isoforms instead of the murine apoE.

Methods Biochemical serum and urinary bone turnover markers (osteocalcin, Alkaline phosphatase, OPG, RANKL and DPD crosslinks) were measured with standard procedures. 12-week old female animals (n=8 per group) were sacrificed and the skeletal status was assessed by conventional X-ray, μ CT, histomorphometry and biomechanical testing.

Results ApoE2 ki animals, as compared to apoE3 ki and apoE4 ki displayed a significantly increased concentration of serum RANKL with decreased OPG / RANKL ratio and increased resorption markers (urinary DPD). Correspondingly, there was a significantly reduced lumbar trabecular bone mass (BV/TV) and distal femur trabecular bone mass (μ CT analyses) due to a significantly reduced bone formation rate (BFR) in apoE2 mice. In contrast, apoE4 animals, as compared to apoE2 and E3, displayed a significantly lower concentration of serum osteocalcin and urinary DPD, indicating low bone turnover but no change in lumbar or femur trabecular bone mass as compared to apoE3 ki. Accordingly, testing of the biomechanical stability revealed significantly lower maximum force resistance in lumbar vertebrae of apoE2 animals as compared to E3 and E4.

Conclusions In conclusion, this study provides the first unequivocal genetic evidence that the human apoE isoforms E2, E3 and E4 differentially affect bone turnover and bone mass in vivo in mice. It remains to be determined by which mechanisms the isoform-specific differences can be explained, but the current data strongly underline the general importance of apoE as a gene that regulates bone metabolism. Based on the current results, the rare apoE2 isoform merits further study as a potential genetic risk factor for low bone mass in human clinical investigations.

Disclosures: Andreas Niemeier, None.

FR0190

Etanercept for the Treatment of Inflammation in Cherubism Mice. Teruhito Yoshitaka^{*1}, Tomoyuki Mukai², Ernst Reichenberger³, Yasuyoshi Ueki⁴. ¹University Missouri-Kansas City School of Dentistry, USA, ²University of Missouri - Kansas City, USA, ³University of Connecticut Health Center, USA, ⁴University of Missouri-Kansas City School of Dentistry, USA

Cherubism is a genetic disorder caused by a mutation of SH3BP2, which involves bone destruction especially of the jaw. We had previously created a mouse model for cherubism and demonstrated that homozygous mutant mice show TNF α -dependent systemic inflammation leading to bone erosion and joint destruction. The critical role of TNF α in this inflammatory bone destruction was confirmed by creating TNF α -deficient homozygous cherubism mutants, in which systemic inflammation and bone destruction was dramatically reduced. These results suggest a key role of TNF α in disease progression in cherubism. In the current study, homozygous cherubism mice were injected with the anti-TNF α drug, Etanercept, which is currently used for the treatment for inflammatory disorders such as rheumatoid arthritis. Etanercept was subcutaneously injected twice a week into homozygous mutant and wild-type control mice starting from 6-11 days of age for 6.5 weeks. Homozygous mice were separated into 3 groups: low (0.5mg/kg) and high (25mg/kg) dose Etanercept and a PBS vehicle control group for comparison with wild-type mice. Histological analysis by H&E staining was performed on liver, lung, and stomach tissues to evaluate the anti-inflammatory effect of treatment. Quantitative real-time PCR analysis for TNF α in the liver was performed. For the evaluation of inflammatory joint destruction, microCT was used. Homozygous mice treated with the high dose Etanercept showed greatly decreased systemic inflammation and joint destruction while no significant effect was observed with the low dose and vehicle treated groups. In liver, the high dose treatment group showed a significant decrease in inflammatory area (0.10.1%),

while the low dose (9.97.2%) was comparable to the vehicle control group (10.65.0%). The expression level of TNF α mRNA in liver tissue of homozygotes was significantly decreased in the high dose (7.31.1-fold increase to wild-type) compared with low dose (25.816.2) and vehicle treatment (28.512.4) groups. Bone and joint destruction in the high dose group was rescued to the level of the wild-type control group. Decreased inflammation was also observed in the other tissues from the high dose group. In summary, administration of high dose Etanercept significantly reduced the progression of inflammation and bone destruction in homozygous cherubism mice. These results provide evidence that human cherubism patients might benefit from treatment with anti-TNF α therapeutics.

Disclosures: Teruhito Yoshitaka, None.

This study received funding from: R01DE020835 (NIDCR)

FR0191

Mechanisms of Bone Loss in Cystic Fibrosis Bone Disease. Katrina Clines, Joon Chung, Gregory Clines^{*}. University of Alabama at Birmingham, USA

Purpose: Low bone mass and increased fracture risk occurs with cystic fibrosis (CF), a genetic disease caused by mutations in the cystic fibrosis transmembrane regulator (CFTR). Impaired osteoblast bone formation coupled with enhanced osteoclastic bone resorption is characteristic of CF bone disease in humans and in animal models. Intestinal malabsorption, vitamin D deficiency and inflammatory cytokines contribute to CF bone disease, but epidemiological investigations and animal models support a direct causal link between CFTR inactivation in bone and CF bone disease.

Methods: CFTR expression in bone was determined by mRNA analysis and immunostaining. *Ex vivo* calvarial and primary osteoblasts cultures derived from *Cfr* knock out and WT mice were examined for changes in bone formation, differentiation and gene expression.

Results: *Cfr* message was detected in murine primary osteoblasts but not RAW264.7-derived multinucleated cells. Protein expression by immunostaining paralleled mRNA expression with CFTR expressed in primary osteoblasts but not marrow-derived osteoclasts. Osteoblast CFTR was not localized to the cell membrane characteristic of epithelial cells but in the cytoplasmic compartment. In the calvarial organ culture assay, CFTR inactivation reduced bone formation and osteoblast numbers. However CFTRinh-172, a small-molecule inhibitor that blocks CFTR-specific Cl⁻ membrane conductance, did not alter osteoblast activity in this assay, a result that is consistent with CFTR absence from the cell membrane. Mechanisms for uncoupled bone turnover with CFTR inactivation were next investigated. *Cfr* null calvarial osteoblasts expressed significantly less *Osterix*, *Collagen 1a1* and *Osteocalcin* than WT osteoblasts indicating delayed osteoblast differentiation. The lack of osteoclast CFTR expression suggested dysfunction in osteoblast-derived RANKL/OPG as a cause for enhanced bone resorption of CF. *Cfr* null and WT calvarial osteoblasts expressed equivalent amounts of *Rankl* mRNA, but *Opg* mRNA was reduced by 65% in *Cfr* null osteoblasts. Overall, the *Rankl:Opg* ratio was 2.7X higher in *Cfr* null vs. WT osteoblasts translating into higher osteoclast activity and bone resorption.

Conclusion: We present a novel role for CFTR in bone and provide evidence that uncoupled bone turnover of CF bone disease is a direct consequence of osteoblast CFTR inactivation by delaying osteoblast differentiation and enhancing osteoclastogenesis via reduced osteoblast *Opg* expression.

Disclosures: Gregory Clines, None.

FR0192

Osteoanabolic Treatment of Adult Osteogenesis Imperfecta with Teriparatide: Preliminary Results of an 36-month prospective observational study. Parvis Farahmand^{*1}, Johann Ringe¹, Thomas Nickelsen². ¹West German Osteoporosis Center, Leverkusen Clinic, University of Cologne, Germany, ²Eli Lilly Deutschland GmbH, Germany

Introduction: Osteogenesis imperfecta (OI) is a genetic disorder of collagen synthesis. So far only antiresorptive therapies with bisphosphonates have shown beneficial effects on the clinical outcome of OI in children. The use of osteoanabolic drugs has not been described in this disorder except from interim results of this study.

Methods: The aim of the ongoing prospective, observational, single-center 36-month open-label "Teriparatide in Osteogenesis Imperfecta" trial (TOI-trial) is to study the efficacy of an anabolic treatment of teriparatide (rPTH-1-34) in adults with clinically symptomatic OI. Inclusion criteria are age >30 years, one or more prevalent vertebral and non-vertebral fracture during the last year, BMD at lumbar spine T-score <-3.0 and at total hip <-2.0. All patients received 1200mg calcium and 800 IU vitamin D per day (months 1-36). During the first 18 months all patients received subcutaneous injections of 20 μ g teriparatide. During the following 18 months all patients receive bisphosphonates.

Results: 12 patients (7 men, 5 women) were included: mean age 45.4 years, mean height 153cm, mean weight 67kg, average lumbar spine BMD -3.9 and total hip -3.0 T-score, and a mean number of 1.8 new vertebral and 0.7 non-vertebral fractures per patient during the last year before intervention. BMD measured at 6 months intervals showed highly significant increases at both sites and amounted to an average gain of 11.4% at the lumbar spine and 7.1% at the total hip after 18 months. During the 18 months we observed only one new vertebral and only two non-vertebral fractures.

This is remarkable in relation to the respective average fracture rates during the last year before intervention. There was no height loss during the first 18 months. There was a significant decrease in back pain and moderate non-persisting adverse events occurred in 6 out of 12 patients.

Conclusion: In the present cohort of adult patients with OI, treatment with teriparatide 20 µg/day over an 18-month period was associated with increases in spine and hip BMD, a numerical decrease in new fractures, and a statistically significant decline in back pain.

Teriparatide was well tolerated; adverse effects were mild and not associated with an early discontinuation of therapy. Based on these encouraging preliminary results we have included further patients. These results should encourage further, controlled trials of an anabolic therapy in osteogenesis imperfecta at a larger scale.

Disclosures: Parvis Farahmand, None.

FR0193

Over Expression of Tissue-nonspecific Alkaline Phosphatase in Osteoblasts Increases Bone Mineralization by Dephosphorylating Osteopontin. Sonoko Narisawa^{*1}, Manisha Yadav², Jose Luis Millan³. ¹Sanford Burnham Medical Research Institute, USA, ²Burnham Institute for Medical Research, USA, ³Sanford-Burnham Medical Research Institute, USA

Tissue nonspecific alkaline phosphatase (TNAP) is a marker of osteoblastic differentiation. We previously reported that inorganic pyrophosphate (PPi) is elevated in TNAP knockout mouse (*Akp2*^{-/-}), a well-characterized model of infantile hypophosphatasia (HPP) and that an important *in vivo* function of TNAP is to hydrolyze extracellular PPi to restrict the concentration of this mineralization inhibitor (Hessle et al., 2002). We also observed increased levels of osteopontin (OPN) in the plasma and bone tissue of *Akp2*^{-/-} mice and we surmised that they contribute to the HPP phenotype (Harmey et al., 2006). Phosphorylated OPN inhibits mineralization; however, the phosphorylation status of the increased OPN levels found in *Akp2*^{-/-} mice has not been studied. We have generated a transgenic mouse line expressing human TNAP under control of 2.3 kb *colla1* promoter (*colla1* TNAP Tg). The transgene is expressed in osteoblasts, periosteum, and cortical bones, and plasma levels of TNAP are 10 - 20 times higher than those in wild-type (WT) mice. The *colla1* TNAP Tg animals are healthy and exhibit increased bone mineralization, as µCT analysis reveals significantly increased bone volume fraction in the vertebrae bone. Crossbreeding *colla1* TNAP transgenic mice to *Akp2*^{-/-} mice rescues the lethal hypophosphatasia phenotype characteristic of this mouse model. Osteoblasts isolated from *colla1* TNAP Tg mice mineralize better than WT cells, and osteoblasts from [*colla1* TNAP Tg; *Akp2*^{-/-}] mice are able to mineralize to the level of *Akp2*^{+/+} osteoblasts, while *Akp2*^{-/-} osteoblasts show no mineralization. The increased levels of OPN in bone tissue of *Akp2*^{-/-} mice are comprised of only phosphorylated forms of OPN while WT and [*colla1* TNAP Tg; *Akp2*^{-/-}] mice had both phosphorylated and dephosphorylated forms of OPN, indicating that accumulated phosphorylated OPN contributes to the inhibition of mineralization in *Akp2*^{-/-} mice and that overexpression of human TNAP reduces the inhibitory effect of OPN via dephosphorylation. Our data suggest that OPN is an *in vivo* protein substrate of TNAP and that interaction between TNAP and OPN modulates mineralization of bone.

Hessle et al., Proc. Natl. Acad. Sci. USA. 99: 9445-9449 (2002).

Harmey et al., J. Bone Miner. Res. 21: 1377-1386 (2006).

Disclosures: Sonoko Narisawa, None.

FR0194

SH3BP2 Cherubism Mutation Enhances Lipopolysaccharide-induced Osteoclastogenesis. Tomoyuki Mukai^{*1}, Teruhito Yoshitaka², Yasuyoshi Ueki³. ¹University of Missouri - Kansas City, USA, ²University Missouri-Kansas City School of Dentistry, USA, ³University of Missouri-Kansas City School of Dentistry, USA

Cherubism is an autosomal dominant craniofacial disorder in children characterized by the extensive growth of fibrous lesions containing TRAP-positive multinucleated cells, resulting in facial swelling and extreme malformation of the jaw bones. We had previously reported that gain-of-function mutations in a signaling adaptor protein, SH3BP2 are responsible for cherubism and have shown that the heterozygous mouse model for cherubism (*KI/+*) exhibit trabecular bone loss and that homozygous mutant mice (*KI/KI*) develop TNF-α-dependent systemic macrophage inflammation leading to bone and joint destruction. However, it remains unclear why destructive bone resorption occurs mainly in the jaws of human cherubism patients. Given the fact that the human mouth is abundant with pathogenic microorganisms, we hypothesized the exacerbated jaw bone resorption and swelling is due to increased osteoclastogenesis in response to bacterial pathogens such as lipopolysaccharide (LPS). To test this hypothesis, we examined the effect of LPS on osteoclastogenesis in *KI/+* mice, which have trabecular bone loss but do not develop TNF-α-mediated inflammatory bone erosions. LPS (2.5mg/kg) was subcutaneously injected over the calvarial midline between eyes and ears of wild-type and *KI/+* mice and animals sacrificed after 5 days. Micro-CT analysis showed a more severely eroded bone surface in LPS-treated *KI/+* mice compared to LPS-treated wild-type mice. Bone histomorphometric analysis showed increased eroded surface per bone surface area (29.712.4%) and increased osteoclast number per bone perimeter (4.81.5) in calvarial

bone from LPS-treated *KI/+* mice compared to LPS-treated wild-type mice (11.34.2%, 2.30.6, respectively). Next we cultured bone marrow derived macrophages from *KI/+* and wild-type mice with M-CSF (25ng/ml) for 2 days followed by the LPS (100ng/ml) for 6 days. When *KI/+* bone marrow cells were cultured with M-CSF and LPS alone, TRAP-positive multinucleated cells formed (16.2021.9/well), while wild-type cells failed to form any TRAP-positive, multinucleated cells (0/well). These results suggest RANKL is not necessary and that LPS can replace RANKL in forming osteoclasts in *KI/+* cells and that SH3BP2 plays a role in LPS-induced osteoclastogenesis.

Disclosures: Tomoyuki Mukai, None.

FR0195

Teriparatide Increases Bone Mineral Density in a Man with Osteoporosis Pseudoglioma. John Bilezikian¹, Marise Lazaretti Castro², Elizabete Ribeiro Barros³, Henrique Arantes^{*4}, Ilda Kunii³. ¹Columbia University College of Physicians & Surgeons, USA, ²Federal University of Sao Paulo, Brazil, ³Sao Paulo Federal University, Brazil, ⁴Brazil

Osteoporosis-pseudoglioma (OPPG), a rare genetic disease characterized by severe juvenile-onset osteoporosis and ocular abnormalities, is caused by an inactivating mutation of the Lipoprotein receptor-related protein 5 (LRP5) gene. The purpose of this study was to evaluate, for the first time in an adult with OPPG, the efficacy of teriparatide. The 12-year old patient was blind, had multiple fractures, and a lumbar spine Z-score by DXA of -3.99 (0.512 g/cm²). A younger brother also had OPPG with congenital blindness and fracture. The parents were consanguineous and healthy. Molecular analysis showed a novel homozygotic missense mutation in the LRP5 gene. At age 20, 1 year after stopping pamidronate, a 2-year course of teriparatide (20 mcg/day) was initiated. He had received intravenous pamidronate for 6 years, the last 3 years of which were associated with minimal effects on BMD. Measurements in serum were made of C-terminal telopeptide of type I collagen (CTX), N-terminal propeptide of type I collagen (PINP), total and ionized calcium, phosphate, uric acid, complete blood count, renal and liver function tests. Urinary calcium/creatinine ratio was determined. BMD was measured by DXA yearly. BMD increased by 9.7% in lumbar spine and 10.2% in the hip. CTX rose early, peaking in month 3, followed by an increase in PINP, peaking in month 9. Both indices returned to baseline by month 24. There were no fractures nor any other adverse events during treatment. The gain in lumbar spine bone mass after 2 years was similar to the major densitometric gains experienced in the pivotal clinical trial that led to the approval of the drug. The time course of change in bone turnover markers – an increase in CTX before the increase in PINP – is opposite from what has traditionally been seen when teriparatide is used in subjects with osteoporosis. In other osteoblast deficiency states, such as the *Lrp5*^{-/-} knockout mouse and hypoparathyroidism, the same “reverse” pattern of bone marker changes is seen. The results indicate that in OPPG, teriparatide markedly increases BMD in the lumbar spine and hip, and that this anabolic effect does not require the LRP5 protein. Assuming that teriparatide interacts with the Wnt signaling pathway, the data suggest that teriparatide's effect occurs distal to this control point.

Disclosures: Henrique Arantes, None.

FR0197

Bone Mineral Density is Reduced in Subjects with Familial Defective Apolipoprotein B-100. Laura Yerges-Armstrong^{*1}, Haiqing Shen¹, Elizabeth Streeten², Alan Shuldiner¹, Braxton Mitchell¹. ¹University of Maryland, USA, ²University of Maryland School of Medicine, USA, ³University of Maryland, Baltimore, USA

Although numerous epidemiologic studies have documented associations of osteoporosis and bone loss with cardiovascular disease, the mechanisms underlying this association remain to be clarified. One hypothesis is that hyperlipidemia may be a common predisposing factor to both atherosclerotic heart disease and accelerated bone turnover, although past results have been equivocal. To evaluate this hypothesis more fully, we have compared bone mineral density (BMD) between subjects with and without the R3500Q mutation that is responsible for familial defective apolipoprotein B-100 (APOB). While this mutation is relatively uncommon in most populations (<0.5% minor allele frequency), it is present at a higher frequency (~6%) in the Old Order Amish population due to a founder effect. In the Amish, each copy of this mutation is associated with a ~59 mg/dl increase in LDL cholesterol (LDL-C) levels. The relatively high frequency of the R3500Q mutation in the Old Order Amish population affords us the opportunity to evaluate skeletal traits for their association with this variant. We conducted analysis on 1068 Amish individuals from a population survey with DXA-measured BMD and who were genotyped for the R3500Q mutation in APOB. On average the population was 53.2 years old (range 20-95) and 52% were female. After adjusting for age, sex, BMI and family structure, carriers for the APOBQ risk allele had significantly lower BMD than non-carriers at the femoral neck (p=0.04), total hip (p=0.04) and lumbar spine (p=0.013). Sex stratified analyses revealed that this mutation was not associated with BMD at any skeletal site in men (p>0.2) but was associated with lower BMD at the femoral neck (p=0.005), total hip (p=0.0007) and lumbar spine (p=0.006). In women, the risk allele was associated with a 0.26-0.31 standard deviation lower BMD value at the three skeletal sites. It is possible that skeletal growth and homeostatic effects of estrogen may be muted in the hyperlipidemic environment, but additional studies to clarify the mechanism for this gender specific association are needed. These results utilize the unique genetic architecture of the Old Order Amish

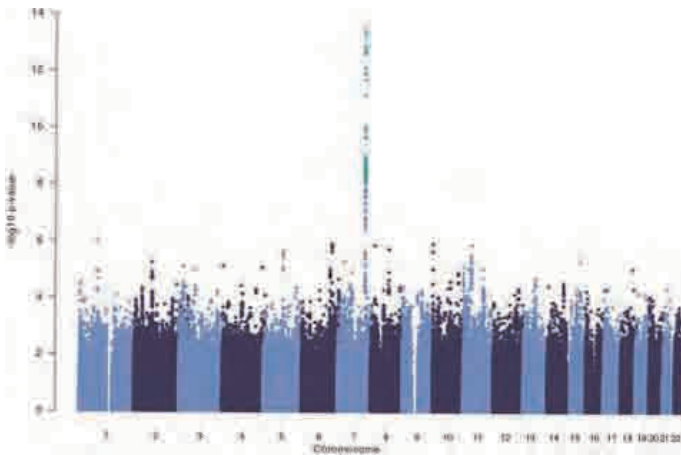
population to expand on previous studies suggesting a common genetic link between cardiovascular and skeletal traits.

Disclosures: Laura Yerges-Armstrong, None.

FR0199

Large-scale Meta-analysis of Genome-Wide Association Studies for Bone Mineral Density at Radius: the GEFOS Consortium. Hou-Feng Zheng^{*1}, Laura Yerges-Armstrong², Joel Eriksson³, Emma Duncan⁴, Braxton Mitchell⁵, Claes Ohlsson⁶, Elizabeth Streeten⁷, Mattias Lorentzon⁶, Brent Richards⁸. ¹Department of Human genetics & Epidemiology & Biostatistics, McGill University, Canada, ²University of Maryland, USA, ³Center for Bone & Arthritis Research, Institute of Medicine, Sahlgrenska Academy, University of Gothenburg, Sweden, ⁴Royal Brisbane & Women's Hospital, Australia, ⁵University of Maryland, Baltimore, USA, ⁶Center for Bone Research At the Sahlgrenska Academy, Sweden, ⁷University of Maryland School of Medicine, USA, ⁸McGill University, Canada

Backgrounds: Recent Genome-Wide Association Studies (GWASs) have identified multiple common variants associated with bone mineral density (BMD) at lumbar spine and femoral neck sites. However, while all BMD sites across the body are partially correlated, they separately provide additional information on risks of fracture, particularly, site-specific fractures. **Aim:** To identify common genetic variants associated with BMD at the forearm, we performed a GWAS meta-analysis within the Genetic Factors of Osteoporosis (GEFOS) consortium. **Methods:** This meta-analysis comprised 4 cohorts (n=4,777). Association with radius BMD was tested for ~2.5 million imputed SNPs (HapMap CEU release 22, build 36) using linear regression models adjusted for sex, age, height, weight, family-relatedness and population stratification when applicable. Genetic effect estimates across studies were combined using an inverse-variance fixed-effects meta-analysis. **Results:** 60 SNPs in 7q31 showed genome-wide significance ($P < 5 \times 10^{-8}$), the most significant SNP was rs2536189 ($P = 3.99 \times 10^{-14}$, effect -0.16 standard deviations per risk allele). This locus maps to wingless-type MMTV integration site family member 16 (WNT16). WNT16 is a member of the Wnt signaling pathway that is known to play an important role in the regulation of bone mass and bone turnover. To investigate the effect of BMD loci on the fracture, we tested the 60 genome-wide significant SNPs in an independent cohort containing 273 forearm fracture cases and 1613 controls, and found that rs2254595 in WNT16, which was strongly associated with BMD ($P = 8.04 \times 10^{-13}$, $BETA = -0.14$), was also moderately associated with forearm fracture ($P = 9.92 \times 10^{-3}$, $OR = 1.28$). In addition, 37 SNPs showed suggestive association signals ($P < 5 \times 10^{-6}$), including 6 variants in known locus 5q14.3 (MEF2C, $P = 2.34 \times 10^{-6}$) and novel signals in or near 6q23 (RPS12, $P = 1.29 \times 10^{-6}$), 10p15 (DIP2C, $P = 1.26 \times 10^{-6}$), and 11p13 (PDHX and CD44, $P = 1.39 \times 10^{-6}$). **Conclusion:** In this first large-scale GWAS meta-analysis for forearm BMD, we identified WNT16 as an important genetic determinant of forearm BMD and fracture and highlighted other novel loci. These variants will soon undergo further replication in upcoming GWAS and by de-novo genotyping for BMD and fracture. These findings increase our understanding of the genetic basis of osteoporosis.



Manhattan plots of the forearm BMD genome wide association meta analysis

Disclosures: Hou-Feng Zheng, None.

FR0201

Inflammation Induces Expression of BMP3, an Inhibitor of Bone Formation, in Inflammatory Arthritis. Melissa Matzelle^{*1}, Anita Shaw¹, Jun Li¹, Sougata Karmakar¹, Catherine Manning¹, Nicole Walsh², Vicki Rosen³, Ellen Gravalles¹. ¹University of Massachusetts Medical School, USA, ²St Vincent's Institute of Medical Research, Australia, ³Harvard School of Dental Medicine, USA

In rheumatoid arthritis (RA), synovial inflammation leads not only to osteoclast-mediated articular bone erosion, but also to an inhibition of osteoblast-mediated bone formation. We have previously shown that formation of mineralized bone is reduced at bone surfaces adjacent to inflammation (erosion sites) in the murine K/BxN serum transfer (STA) model of inflammatory arthritis. Furthermore, cells within the arthritic synovium produce factors, including antagonists of the Wnt/ β -catenin signaling pathway, that impact osteoblast function. In addition to the Wnt signaling pathway, osteogenic BMP signaling is also critical to osteoblast differentiation. Mice deficient in BMP3, one known inhibitor of BMP signaling, accrue trabecular bone with age, supporting a role for BMP3 in the inhibition of osteoblast-mediated bone formation. To determine the potential role of BMP3 during inflammation-induced bone loss, STA was generated in 12 week-old C57Bl/6J mice and expression of BMP3 in the hind paws was assessed by immunohistochemistry, in situ hybridization, and quantitative RT-PCR (qPCR). BMP3 protein was expressed late in the course of arthritis, most notably by osteoblasts lining inflammation-bone interfaces and, to a lesser degree, by lining cells within the synovium. BMP3 mRNA expression followed a similar pattern histologically and as assessed by qPCR, with a maximal induction at day 15 in tissue isolated from the midfoot bones and a minimal induction in isolated synovial tissues. Given these cellular sources of BMP3 mRNA and protein, synovial fibroblasts and bone marrow-derived osteoblasts were isolated from C57Bl/6J mice and treated with the pro-inflammatory cytokines TNF, IL-1 β , or IL-17; expression of BMP3 mRNA was determined by quantitative RT-PCR (qPCR). TNF (10 ng/ml), but not IL-1 β or IL-17, induced expression of BMP3 mRNA approximately 20-fold in cultured synovial fibroblasts over the course of 72 hours. In contrast, IL-17 (10 and 50 ng/ml), but not TNF or IL-1 β , induced BMP3 expression 6-fold in mature differentiated osteoblasts (day 28). Together, these data implicate BMP3, which is induced within the inflamed synovium and in osteoblasts at sites of articular bone erosion, as a candidate factor that may contribute to focal bone loss in RA through impairment of osteoblast function.

Disclosures: Melissa Matzelle, Abbott Bioresearch Center, 9

FR0202

Transplanted Mesenchymal Stem Cell-derived BMP2 Rescues Fracture Healing in BMP2-deficient Mouse Limbs. Timothy Myers^{*1}, Froilan Granero-Molto², Lara Longobardi², Yun Yan¹, Tieshi Li¹, Ying Li¹, Anna Spagnoli². ¹University of North Carolina, USA, ²University of North Carolina at Chapel Hill, USA

There is a compelling need to develop novel therapies to improve fracture healing and to treat fracture non-unions. Bone marrow mesenchymal stromal stem cells (MSC) are an attractive therapeutic approach due to their ability to differentiate into distinctive end stage mesenchymal cell types and secrete bioactive molecules that regulate the regenerative microenvironment. Previous results from our lab demonstrate that MSC transplant into a tibial fracture model improves healing through organization of the callus and bridge between gaps. Interestingly, only a small fraction of the transplanted MSC incorporate into new bone, suggesting the more substantial effect of MSC is due to the release of paracrine-acting factors. Bone morphogenetic protein-2 (BMP2) is a critical factor in fracture repair as evidenced by its early expression in fracture healing and the complete lack of initiation of repair in mice lacking BMP2 in mesenchyme limb progenitor cells. Our data reveals that MSC express BMP2 at the site of injury and uniquely along the endosteum. To determine the essential role of MSC-derived BMP2 in fracture healing, MSC were transplanted into mice haploinsufficient for BMP2 in early limb mesenchyme using Prx1Cre-mediated recombination (BMP2^{+/+}) with a stabilized tibia fracture. Fractured bones from BMP2^{+/+} and either BMP2^{+/+}/flox or BMP2^{flox/flox} control mice were dissected 14- and 21-days post-fracture and subjected to μ -CT, biomechanical and histological analyses. At both 14- and 21-days, BMP2^{+/+} mice had smaller calluses, less soft tissue and less new bone than control mice. Statistical significance was set at $p < 0.05$; $n \geq 5$ for each group. When MSC obtained from the bone marrow of control littermates were transplanted, formation of new bone was returned to wild type levels at day 14. Histological analyses revealed a decrease in the pre-osteoblast marker osterix at 7-days and the osteoblast marker osteocalcin at 14-days post-fracture in BMP2^{+/+} mice that was increased in MSC-BMP2^{+/+} mice. Biomechanical analyses supported the findings of rescued new bone levels. By 21-days, both MSC-BMP2^{+/+} and MSC-control mice exhibited the presence of increased highly mineralized bone that bridged the fracture gap from within the BM cavity and was mostly absent in untransplanted mice. These results demonstrate that MSC-derived BMP2 is sufficient to restore bone formation in BMP2-deficient mice through the paracrine regulation of intrinsic fracture healing cells.

Disclosures: Timothy Myers, None.

FR0205

Analysis of Wnt System Components in Cranial Defect Healing in CXC Receptor Knock-out (mCXCR^{-/-}) Mice by Microarray. David Bischoff^{*1}, Weibiao Huang¹, Erwin Kruger², Nalini Makhijani³, Dean Yamaguchi⁴.
¹VA Greater Los Angeles Healthcare System & David Geffen School of Medicine at UCLA, USA, ²UCLA, USA, ³VA GLAHS, USA, ⁴VA Greater Los Angeles Healthcare System, USA

The role of CXC chemokines bearing the glu-leu-arg (ELR⁺) motif in bone repair was studied using a mouse cranial defect (CD) model in mCXCR^{-/-} mice. During bone repair, ELR⁺ CXC chemokines, released by inflammatory cells, serve as angiogenic factors signaling through mouse CXC receptor (mCXCR) which is homologous to the human CXC receptor 2). Previously we showed that osteogenic differentiation of human mesenchymal stem cells increases expression of the ELR⁺ CXC chemokine, CXCL8, and that mice lacking mCXCR were osteopenic and had a defect in bone repair. In this study we explored the possibility of ELR⁺ chemokine signaling through the wnt system. We created 1.8 mm CDs in 6 week old male mCXCR^{-/-} and wild-type mice and allowed the CDs to heal for 7 days. RNA was isolated from the CD early callus and microarray analysis was used to determine >2-fold differences in wnt system gene expression with the Mouse Wnt Signaling Pathway RT² Profiler PCR Array from SABiosciences. Expression of several genes involved in degradation of β -catenin under non-wnt conditions was downregulated in mCXCR^{-/-} mice (APC, GSK3B, BtrC). Genes involved in canonical wnt signal activation (Dvl1, LRP5), β -catenin regulated transcription (TCF7, LEF1), lipidation of wnt proteins for secretion/activation (Porcn), and several genes involved in negative regulation of wnt signaling including NKD1 (inhibits Dvl1), DKK1 (inhibits LRP5), WIF1 (Frizzled [Fz] dummy receptor), Fz1B (soluble Fz1 receptor expressed in cartilage), and Sox17 (inhibits TCF transcription) were also downregulated. Expression of several wnt ligands and Fz1 receptors was also decreased in mCXCR^{-/-} mice including wnt4, wnt5a (non-canonical wnt signaling, inhibition of cell proliferation, chondrocyte differentiation), wnt5b, wnt6, wnt7a (CNS vascularity), Fz3 (wnt4 receptor), and Fz5 (yolk sac/placental angiogenesis, co-localization with wnt5a). There were only 5 genes up-regulated >2-fold and four have roles in cell proliferation including Fosl1, RhoU (induced by non-canonical wnt1), wnt2, and wnt11 (non-canonical signaling). The expression of cell proliferation co-repressors Tle1 and Tle2 was also decreased suggesting more cell proliferation in mCXCR^{-/-} mice, although due to lack of wnt signaling, less differentiation. Conclusion: mCXCR^{-/-} mice have decreased expression of genes involved in wnt activation/expression, inhibition of cell proliferation, and Fz1 receptors and wnt proteins involved in angiogenesis.

Disclosures: David Bischoff, None.

FR0206

Differential Impact of Dkk1 Neutralizing Antibodies on Wnt Signaling and Bone Mineral Density. Wei Fan^{*1}, Grisanti Mario¹, Jilin Sun¹, Hsieng S. Lu¹, Xiaodong Li², William G. Richards¹. ¹Amgen Inc., USA, ²Amgen, Inc., USA

Dickkopf-1 (Dkk1) inhibits canonical Wnt signaling through different mechanisms: by promoting the internalization of the wnt co-receptors LRP5 and LRP6 through interactions with kremen proteins, and by directly blocking the ability of wnt proteins to bind these receptors. To study the role of this wnt signaling inhibitor in bone formation we developed antibodies that blocked the activity of Dkk1.

The neutralizing antibodies identified recognized distinct epitopes on Dkk1. Antibodies from bin A (Dkk1-AbA) recognized a C-terminal epitope on Dkk1, whereas antibodies from bin B (Dkk1-AbB) recognized a more N-terminal epitope. Dkk1-AbA was capable of blocking wnt signaling, as assayed in a wnt dependent TCF-lef luciferase assay, to a greater extent than Dkk1-AbB. Additionally, in co-immunoprecipitation experiments Dkk1-AbA was capable of blocking the interaction of Dkk1 with both LRP6 and Kremen2. Dkk1-AbB did not prevent the interaction of Dkk1 with either LRP6 or Kremen2.

To determine whether the cell-based and biochemical differences between the epitope bins translated into different responses on bone mineral density, six-week old male mice were injected with either Dkk1-AbA or Dkk1-AbB (3, 10 and 30 mg/kg; 2 times per week). After two-weeks of dosing the lumbar vertebrae (L1-L5) and whole leg were analyzed by DXA. Mice injected with the 30 mg/kg dose of Dkk1-AbA had a significant (P<0.05) increase in BMD compared to vehicle-injected control mice at both the lumbar vertebrae (0.057 vs. 0.050 g/cm²) and whole leg (0.056 vs. 0.051 g/cm²). BMD was not significant altered in mice injected with Dkk1-AbB. BMD in mice injected with Dkk1-AbA trended to be greater at all doses when compared to Dkk1-AbB, and was significantly greater (P<0.05) at the lumbar spine with the 30 mg/kg dose (0.057 vs. 0.051 g/cm²).

These data confirm the ability of Dkk1 inhibition to increase bone mass in growing mice. Furthermore the data indicate that antibodies recognizing different epitopes are capable of inhibiting Dkk1 activity by different mechanisms that translate into differential responses in both cell-based assays and in vivo. We suggest that Dkk1-AbA prevents Dkk1 from both blocking wnt binding to and promoting internalization of LRP5/6, and that Dkk1-AbB bound Dkk1 may not impair LRP5/6 internalization and likely prevents Dkk1 from blocking a subset of Wnts from binding LRP5/6.

Disclosures: Wei Fan, Amgen, Inc, 1; Amgen, Inc, 3
 This study received funding from: Amgen, Inc

FR0208

Increased WNT Signaling in Sclerostin/Sostdc1 Double Knockouts Causes Preaxial Polydactyly. Richard Harland¹, Deepa Muruges², Gabriela Loots³, Cristal Yee⁴, Nicole Collette^{*2}. ¹University of California, Berkeley, USA, ²Lawrence Livermore National Laboratory, USA, ³LLNLUC Merced, USA, ⁴University of California, Merced, USA

Sclerostin (Sost) is negative regulator of bone formation; loss-of-function mutations associated with this gene cause sclerosteosis and van Buchem disease, two rare skeletal dysplasias characterized by increased bone density throughout the skeleton. Sostdc1 (aka Sostl, USAG-1, Wise, ectodin) is a paralog of Sost. Loss of Sostdc1 has been shown to cause supernumerary tooth development. Both proteins are secreted cysteine knot proteins that function as antagonists of both BMP and WNT signaling. We have recently shown that overexpression of human SOST causes dosage-dependent loss of distal posterior skeletal elements. This loss results from altered FGF, WNT, and SHH signaling during the patterning of the limb bud. Sostdc1 was shown by others to antagonize LRP receptor signaling and to similarly affect FGF and SHH signaling in the developing tooth bud, suggesting that Sostdc1 may antagonize similar pathways as Sost, in vivo. Sost knockout mice display a low penetrance (~5% of KOs) of limb defects consistent with the soft-tissue syndactyly, nail dysplasia, and radial deviation that occurs in some sclerosteosis patients; while Sostdc1 knockouts show no limb defects. Here we show that Sost; Sostdc1 double mutant mice exhibit preaxial polydactyly, a common limb-associated birth defect characterized by extra digit(s) in the anterior autopod, and is often caused by ectopic sonic hedgehog (Shh) expression in the anterior limb bud. Sost and Sostdc1 are expressed in complementary yet non-overlapping domains in the developing limb, where their combined domains cover most of the ectoderm and mesenchyme of the developing limb bud prior to cartilage condensation. Through a combination of skeletal stains and in situ hybridization we show here that Wnt signaling functions upstream of Shh to restrict Shh expression in the posterior limb. Through the release of Lrp5/6 receptor inhibition from Sost and Sostdc1 Wnt antagonists expressed in the ectoderm and mesenchyme, hyperactive Wnt signaling ectopically activates Shh in the anterior limb bud to transform autopod patterning and morphology.

This work performed under the auspices of the U.S. Department of Energy by Lawrence Livermore National Laboratory under Contract DE-AC52-07NA27344. LLNL-ABS-475371.

Disclosures: Nicole Collette, None.

FR0209

Intermittent Injections Of Osteocalcin Improve Glucose Metabolism and Prevent Type 2 Diabetes In Mice. Mathieu Ferron^{*1}, Marc McKee², Patricia Ducy¹, Gerard Karsenty¹. ¹Columbia University, USA, ²McGill University, Canada

We have shown previously that the uncarboxylated form of the osteoblast-specific secreted molecule osteocalcin functions as a hormone favoring glucose handling and increasing energy expenditure. As a result, the absence of osteocalcin leads to glucose intolerance in mice, and genetically modified mice with an increase in uncarboxylated osteocalcin are protected from type 2 diabetes and obesity.

To assess the therapeutic relevance of these observations we tested whether osteocalcin injected once daily could affect glucose metabolism in wildtype (WT) mice. We show here that injection of osteocalcin (3 or 30 ng/g/day) once a day significantly improved glucose tolerance, as assessed by glucose tolerance tests (GTT), in WT mice fed a normal chow. Moreover, insulin sensitivity was also improved after 4 weeks of this regimen as measured by insulin tolerance tests (ITT). Blood glucose after feeding was significantly reduced following osteocalcin daily injections. Remarkably, daily injections of osteocalcin increased β -cell proliferation, β -cell mass and insulin secretion. Thus, daily injection of osteocalcin has a beneficial effect on glucose metabolism in mice fed a normal chow.

We next asked whether daily injections of osteocalcin could have these beneficial effects on glucose tolerance and insulin sensitivity in a model of diet-induced type 2 diabetes. To that end WT mice were fed a high fat diet (HFD) for 8 weeks and then injected once a day with osteocalcin (30 ng/g/day) for 8 weeks. Osteocalcin daily injections increased the number of mitochondria in skeletal muscle and stimulated energy expenditure, thereby preventing body weight gain. Moreover, fasting blood glucose and serum insulin levels were markedly reduced when compared to placebo-treated mice, and insulin sensitivity, as measured by the Homeostasis Model Assessment (HOMA), was partially restored. As a result, glucose tolerance was significantly improved in animals maintained on HFD and injected once a day with osteocalcin. Finally, the hepatic steatosis induced by HFD was completely absent in mice fed a HFD and receiving osteocalcin daily. Overall these results provide evidence that, at least in mice, osteocalcin injected once a day does improve glucose handling and prevents the development of type 2 diabetes.

Disclosures: Mathieu Ferron, None.

FR0210

Modulation of SDF-1/CXCR4 Axis Enhances rhBMP-2-induced Ectopic Bone Formation. Joel Wise, D. Rick Sumner, Amarjit Viridi*. Rush University Medical Center, USA

Enhancement of in vivo mobilization and homing of endogenous mesenchymal stem cells (MSCs) to an injury site is an innovative strategy for improvement of bone tissue engineering and repair. The present study was designed to determine if the delivery of agents known to affect mobilization (AMD3100) and homing (stromal cell-derived factor-1; SDF-1) of MSCs enhance de novo bone formation induced by rhBMP-2 in absorbable collagen sponges (ACS) in vivo at the ectopic implant site in an established rat model. Sprague-Dawley rats (male; ~350g; 12 weeks old) received intraperitoneal injection of either saline or AMD3100 treatment 1 hour prior to harvesting of bone marrow for in vitro CFU-F assay or the in vivo subcutaneous implantation of absorbable collagen sponges loaded with saline (n=6), rhBMP-2 (10µg; n=6), SDF-1 (200ng; n=6), or the combination of SDF-1 and rhBMP-2 (n=6), for ectopic bone formation assay.

AMD3100 treatment (n=5) resulted in a significant decrease in CFU-F number in bone marrow cultures, compared to saline (n=3), which confirmed that a single systemic AMD3100 treatment rapidly mobilized MSCs from the bone marrow. At 28 and 56 days, bone formation in the explanted ACS was assessed by microcomputed tomography (µCT) and histology. At 28 days, AMD3100 and/or SDF-1 had no statistically significant effect on bone volume (BV) or bone mineral content (BMC), but histology revealed more active bone formation with treatment of AMD3100, loading of SDF-1, or the combination of both AMD3100 and SDF-1, compared to saline-treated rhBMP-2 loaded ACS. At 56 days, the addition of AMD3100 treatment, loading of SDF-1, or the combination of both, resulted in a statistically significant stimulatory effect on BV and BMC, compared to the saline-treated rhBMP-2 loaded ACS. Histology of the 56-day ACS were consistent with the µCT analysis, exhibiting more mature and mineralized bone formation with AMD3100 treatment, SDF-1 loading, or the combination of both, compared to saline-treated rhBMP-2 loaded ACS. The present study is the first to provide evidence of the efficacy of AMD3100 and SDF-1 treatment to stimulate trafficking of MSCs to an ectopic implant site, in order to ultimately enhance rhBMP-2-induced long-term bone formation.

Disclosures: Amarjit Viridi, None.

FR0211

New Function of Nell-1 Protein in Regulating Bone Maintenance. Aaron James*, Xinli Zhang¹, Janette Zara², Michael Chiang¹, Wei Yuan¹, Raghav Goyal¹, Cymbeline Culiati³, Kang Ting¹, Chia Soo¹. ¹University of California, Los Angeles, USA, ²UCLA, USA, ³Oak Ridge Laboratories, USA

Introduction: Osteoporosis is a multifactorial disease process involving genetic and environmental etiologies. Nell-1 is a potent, pro-osteogenic molecule first identified to have osteogenic properties by its isolation from prematurely fusing cranial sutures. A recent study of genome wide polymorphisms implicated the cytokine Nell-1 in the etiology of osteoporosis.

Methods: This study expands on this association between Nell-1 and bone maintenance, by examining the effects of loss of function in Nell-1. Deficiency in Nell-1 was achieved via ENU-mutagenesis in mice. Analysis of the axial and appendicular skeleton was performed in neonatal, young (1 month) and aged (18 months) mice by high-resolution micro computed tomography (CT), live combined CT / fluoride ion incorporation assays, serum studies (serum TRAP5b, PINP), and standard histologic analysis.

Results: Although Nell-1 haploinsufficient mice appeared normal at birth and 1 month of age by all examined markers (N=10 per group), Nell-1 loss resulted in significant and severe osteopenia in aged mice, including significant reductions in BV, BMD and BV/TV (N=30 per group). This was due to a defect in bone formation (reduction in fluoride ion uptake and serum PINP concentration) as well as inappropriate osteoclast activity (increased TRAP5b concentration when normalized to bone volume). Histological analysis confirmed these biochemical and radiologic findings.

Discussion: Results demonstrate a new and critical role of Nell-1 in bone maintenance and osteoblast:osteoclast crosstalk. Not only is Nell-1 of importance in developmental bone biology, but these studies highlight a critical role of Nell-1 in bone maintenance across an animal's lifetime. This new finding has significant ramifications for the genesis of osteoporosis and potential new osteoporotic therapies.

Disclosures: Aaron James, None.

FR0213

Transgenic Adult Murine Mesenchymal Stem Cells Conditionally Over-expressing SDF-1β Enhance New Bone Formation in Both *In Vitro* and *In Vivo* Model Systems. Samuel Herberg*, Sadanand Fulzele, Nianlan Yang, Galina Kondrikova, Khaled Hussein, Mohammed E. Elsalanty, Maribeth Johnson, Xingming Shi, Mark Hamrick, William D. Hill, Georgia Health Sciences University, USA

Purpose: BMSC differentiation is regulated through SDF-1. Interaction with its receptor CXCR4 directs the migration of stem cells in injury repair. In vitro preconditioning with SDF-1 prior to transplantation enhances cell engraftment and new tissue formation; however, it does not allow for direct modulation of SDF-1 in vivo. Tetracycline-dependent regulatory systems provide for tight control of transgene expression in vitro and in vivo. SDF-1α is the most abundant splice variant, however, SDF-1β is twice as potent. Recently, we described the development of a Tet-Off-SDF-1β transgenic stem cell line conditionally overexpressing SDF-1β. The current study evaluated the regenerative potential of this novel cell line using in vitro and in vivo analyses. **Methods:** In vitro osteogenic differentiation of Tet-Off-SDF-1β BMSCs was assessed using ELISA (osteocalcin; OCN), Alizarin red S (ARS) staining, and qRT-PCR analysis (e.g., OCN, Runx2, Col1) after culturing cells in differentiation medium BMP-2 for 21 d. Doxycycline (Dox) was added to suppress SDF-1β transgene expression in controls. For in vivo studies, lethally irradiated 6-month-old C57BL/6 male mice were given tibial transplants (left: 9.24x10⁵ cells/70 µl; right: saline for vehicle control). Control mice had access to Dox in drinking water +5% glucose. After 4 wks, animals were euthanized and tibias collected for BMD analysis and 3-D histomorphometry with µCT (e.g., BV/TV, Tb.N). **Results:** ELISA of Tet-Off-SDF-1β BMSCs (-Dox) revealed increased OCN production relative to controls. SDF-1β transgene expression accelerated and significantly enhanced osteogenic differentiation (BMP-2) compared to controls, detected by ARS staining (p<0.001). qRT-PCR confirmed that SDF-1β transgene expression enhanced BMP-2-induced upregulation of osteogenic markers (e.g., OCN: 17.2-fold/-Dox; 6.5-fold/+Dox; p<0.05). Tibial µCT analyses showed significant augmentation of new bone formation in experimental and control transplants relative to vehicle controls (p<0.0001). SDF-1β transgene expression resulted in even greater bone formation compared to controls (e.g., BV/TV: 46.0/-Dox; 28.5/+Dox; p<0.05). **Conclusion:** In vitro and in vivo analyses indicate a critical role of SDF-1β in BMP-2-induced osteogenic differentiation and high regenerative potential of our novel Tet-Off-SDF-1β transgenic stem cell line. Future studies will examine the use of these cells in acute and chronic bone injury models.

Disclosures: Samuel Herberg, None.

FR0214

Ephrin B2-EphB4 Bidirectional Signaling Mediates the Actions of IGF-I Signaling in Regulating Chondrocyte and Osteoclast Differentiation. Yongmei Wang*, Hashem Elalieh, Wenhan Chang, Daniel Bikle. Endocrine Unit, University of California, San Francisco/VA Medical Center, USA

It has been proposed that chondrocytes, osteoblasts (OB) and osteoclasts (OCL) interact to control skeletal development, but the mechanisms underlying these interactions remain unclear. We and others have shown that insulin-like growth factor-I (IGF-I) stimulates proliferation and differentiation of these cells and is required for the interactions between OBs and OCLs via RANK/RANKL signaling. Recent studies found that ephrin B2-EphB4 bidirectional signaling mediates OB and OCL differentiation and communication. To address whether such signaling is involved in IGF-I action, we used knockout mouse models and in vitro culture systems to investigate the role of IGF-I signaling in regulating the interaction between chondrocytes and OCLs with particular attention to the role of ephrin B2/EphB4. In wild-type (WT) bones, immunohistochemistry demonstrated that ephrin B2 is expressed in OBs and OCLs, while EphB4 is expressed only in OBs. In the growth plate (GP) cartilage, both ephrin B2 and EphB4 are expressed in late-stage proliferating and prehypertrophic chondrocytes. The mRNA levels of ephrin B2, EphB4 and RANKL were decreased 40%, 43% and 88%, respectively, in mice lacking the IGF-I receptor (IGF-IR) specifically in chondrocytes (cart.IGF-IR KO, floxed IGF-IR X type II collagen driven Cre recombinase) compared with their WT littermates. In mice with an IGF-IR null mutation in OCLs (OCLIGF-IRKO), (floxed IGF-IR X TRAP5b driven Cre recombinase), immunohistochemistry identified a reduction in ephrin B2 not only in OCLs, but also, to our surprise, in the late-stage proliferating and prehypertrophic chondrocytes in the GP. In vitro, blocking the interaction of EphB4 and ephrin B2 by TNYL-RAW in ATDC5 cell cultures (a chondrocyte cell line) significantly decreased mRNA levels of type II collagen (40%) and type X collagen (45%), and reduced the mineralization in the cultures. Compared with the vehicle treated co-cultures of ATDC5 cells and OCL, blocking the interaction of EphB4 and ephrin B2 by TNYL-RAW in these co-cultures decreased the formation of TRAP positive cells by 55%, with a 43% reduction in the mRNA levels of NFATc1. OPG was much less effective in preventing ATDC5 induction of OCL formation. Our data indicate that IGF-I/IGF-IR modulates OCL and chondrocyte differentiation in part through the ephrin B2/EphB4-mediated cell-cell interactions.

Disclosures: Yongmei Wang, None.

FR0215

Requirement of Shp2 in Chondrogenesis and Cartilage Homeostasis. Yingnan Yu^{*1}, Jianguo Wang², Kai Zhao², Douglas Moore², Zhengke Wang³, Qian Wu⁴, Di Chen⁵, Quesenberry Peter⁶, Wentian Yang⁷. ¹Brown University Alpert Medical School & Rhode Island Hospital, USA, ²Departments of Orthopedics, RI Hospital & Brown University Alpert Medical School, USA, ³Roger Williams Hospital, USA, ⁴Department of Pathology & Laboratory Medicine, University of Connecticut Health Center, USA, ⁵Center for Musculoskeletal Research, Department of Orthopaedics & Rehabilitation, University of Rochester, Rochester, NY, USA, ⁶Departments of Medicine, RI Hospital & Brown University Alpert Medical School, USA, ⁷Brown University Alpert Medical School, USA

The src homology 2 domain-containing protein tyrosine phosphatase (PTPase) Shp2 (Ptpn11) is required for most, if not all, receptor tyrosine kinases (RTK), cytokines and extracellular matrix protein signaling to regulate the proliferation and differentiation of various types of cells, but its role in chondrogenesis and cartilage homeostasis remains elusive due to the early embryonic lethality caused by global Shp2 deficiency. Understanding how cellular signal transduction governing chondrogenesis and cartilage homeostasis is regulated by PTPase Shp2 will provide insights for developing novel therapeutics to treat cartilage-related skeletal diseases. We hypothesize that Shp2 is essential for chondrocyte development and cartilage homeostasis by regulating RTK and cytokine signaling in chondrocytes. To test this hypothesis, we previously generated a Ptpn11 floxed allele; mice carrying Ptpn11 floxed allele were crossed to collagen 2 α 1-Cre(Col2 α 1-Cre) and tamoxifen inducible Col2 α 1-Cre (Col2 α 1-CreERTm) mice respectively to generate cartilage-specific Shp2 deficient animals. Surprisingly, mice lacking Shp2 in Col2 α 1-expressing cells were embryonic lethal (around E11.5). Inducible ablation of Shp2 in these cells leads to dwarfism and multiple joint deformations by impairing both the column organization of growth plate cartilage and the cellular structure of articular cartilage. Expression of chondrogenic genes Sox9, runx2, Col2 α 1 and Col10 α 1 were all compromised in the epiphyseal cartilage of Shp2 mutant mice. By focusing on IGF1 signaling in chondroprogenitor ATDC5 cells, we found that Shp2 is required, at least, for IGF1-evoked chondrogenesis by negatively regulating the tyrosyl phosphorylation of IGF1-Rbeta, IRS1 and subsequent Erk and Akt activation. Altered signaling in these pathways in Shp2 mutant chondrocytes may contribute to the defective chondrogenesis and cartilage homeostasis. Our study found that Shp2 is a key regulator for chondrogenesis and cartilage homeostasis. Manipulating Shp2 and Shp2-regulated signaling pathways in cartilage has the potential for developing novel means to prevent and treat cartilage developmental and degenerative diseases.

Disclosures: Yingnan Yu, None.

FR0223

Decreased Bone Formation and Bone Resorption Following Fracture in Osteoblast-Osteocyte Specific Connexin 43 Deficient Mice. Alayna Loiselle^{*1}, Emmanuel Paul², Gregory Lewis², Henry Donahue³. ¹Penn State Hershey, USA, ²Penn State College of Medicine, USA, ³The Pennsylvania State University College of Medicine, USA

Connexin 43 (Cx43), the most abundant gap junction protein in bone, is required for osteoblast differentiation. Mice with osteoblast/osteocyte specific loss of Cx43 display decreased gap junctional intercellular communication (GJIC), bone density and cortical thickness. To determine the role of Cx43 in fracture healing, a closed fracture was produced in femurs by three-point bending in Osteocalcin-Cre+; Cx43^{flx/flx} (Cx43cKO) and Cre- Cx43^{flx/flx} (WT) mice. We tested the hypothesis that loss of Cx43 results in decreased bone formation and impaired healing following fracture.

Abundant Cx43 expression was observed in the fracture callus in WT but not Cx43cKO mice, between 10 and 35 days. Alterations in bone formation were observed in Cx43cKO fractures with decreased areas of mineralized tissue, relative to WT, in the fracture callus. This observation was consistent with decreased Collagen I expression, and a significant decrease in total bone volume at day 28 (WT:2.7 0.7; KO:1.3 0.5, n=5, p=0.04). A dramatic reduction in the size of the callus, relative to WT fractures, occurred by 21 days in Cx43cKO fractures. Additionally, there was a significant decrease in TRAP+ osteoclast number in Cx43cKO fractures compared to WT at 14 and 28 days post-fracture (Day 14- WT:62.5 2.6, KO:31.6 1.9 p=0.021; Day 28- WT:33.9 2.8, KO:13.4 3.6, p=0.024, n=4). Furthermore, using a novel μ CT parameter to measure low-density bone volume (BVlow) as an indicator of remodeling, a significant decrease in BVlow was detected at 28 days in Cx43cKO fractures compared to WT (WT: 0.8 0.15; KO:0.38 0.02, p=0.038, n=5). RANKL was decreased, while Osteoprotegerin was increased in Cx43cKO compared to WT fractures by *in situ* hybridization. Taken together, these data suggest that Cx43cKO fractures, relative to WT fractures, heal with less mineralized callus formation, and subsequently decreased osteoclastic remodeling. Despite changes in both bone formation and osteoclastic remodeling, there was no significant difference in the ultimate torque at failure in WT and KO fractures at 21(WT: 18.3 3.2, KO:19.5 5.7) and 35 days post-fracture (WT:18.8 4.1, KO:21.2 4.1).

These studies identify a novel role for the gap junction protein Cx43 during fracture healing, suggesting that loss of Cx43 can result in both decreased bone

formation, and bone resorption. Therefore, enhancing Cx43 expression or GJIC may provide a novel means to enhance bone formation during fracture healing.

Disclosures: Alayna Loiselle, None.

FR0224

Disruption of the Runx2 Response to SMAD signaling Affects Bone Turnover in Adult Mice. Yang Lou^{*1}, Sadiq Hussain², Dana Frederick², Andre Van Wijnen², Garv Stein², Jane Lian², Janet Stein². ¹University of Massachusetts, USA, ²University of Massachusetts Medical School, USA

Bone morphogenetic protein (BMP) and transforming growth factor- β (TGF β) are required for bone formation and bone turnover *in vivo*. Previous studies have shown that three critical residues (HTY426-428) of the transcription factor RUNX2 are required for its interaction with Smad proteins. Mutation of HTY426-428 to AAA426-428 can abolish the activity of RUNX2 to execute and complete BMP2/TGF β signaling for osteoblastogenesis in culture. Here, we describe a mouse model with this triple amino acid mutation inserted into the endogenous Runx2 locus to test the consequences of disruption of a Runx2-Smad transcriptional complex *in vivo*. Although development of craniofacial intramembranous bone appeared normal immediately after birth, the RUNX2^{HTY426-428AAA} mice began to exhibit increased trabecular bone by 3 months of age. Compared to wild-type, the adult homozygous mice have similar bone length but have an extended length of trabecular area in tibia and femur (P<0.01) together with a decreased bone marrow cavity area, observed by histology and microCT imaging. Dynamic bone formation measurement of femurs in 5-month-old mice show no significant difference between wild type and mutants. Histological analysis reveals that the homozygous mice have fewer osteoclasts in the trabecular bone area and significantly decreased mRNA levels of TRAP (n=5 mice per group, P<0.01), as well as lower levels (about ~25% decrease) of RANKL in the metaphyses of the tibia. Because RANKL is regulated by Runx2-related BMP2 signaling, our results suggest that bone resorption is partly compromised by the Runx2HTY mutation, which caused increased trabecular bone in our RUNX2^{HTY426-428AAA} knock-in mice. Taken together, our findings suggest that a RUNX2-SMAD functional complex may be dispensable for normal skeletal development, but is required for the balance between bone formation and bone resorption *in vivo*.

Disclosures: Yang Lou, None.

FR0231

Osterix Deficiency Disrupts Ameloblast and Odontoblast Maturation but Not Tooth Morphogenesis. Ji-Myung Bae^{*1}, Harunur Rashid¹, Haiyan Chen², David Summerford¹, Mitra Adhami¹, Dobrawa Napierala³, Krishna Sinha⁴, Soraya Gutierrez⁵, Benoit DeCrombrughe⁴, Amjad Javed². ¹School of Dentistry, University of Alabama at Birmingham, USA, ²University of Alabama at Birmingham, USA, ³University of Alabama at Birmingham School of Dentistry, USA, ⁴UT MD Anderson Cancer Center, USA, ⁵Universidad De Concepcion, Chile

Runx2 and Osterix (Osx) are master genes essential for osteoblast differentiation and bone formation. In humans, mutations in Runx2 and Osx are associated with CCD and osteogenesis imperfecta, respectively. Tooth development in Runx2 null mice is arrested at late bud stage. Unlike Runx2, nothing is known about Osx role in tooth morphogenesis or differentiation of ameloblasts and odontoblasts. During skeletogenesis, Osx functions downstream of Runx2, but it is not clear if both act independently or are part of the same pathway that controls tooth morphogenesis. To investigate tooth development we established Osx null mouse and performed analysis at embryonic day 18 (E18), a stage by which basic morphogenesis is established. In sharp contrast to Runx2, tooth development in Osx null mice progressed till late bell stage. The incisor and multi-cusped 1st and 2nd molar were noted in wild type (WT) and homozygous mutants. During normal development, tooth epithelium differentiates into ameloblasts that synthesize enamel, and tooth mesenchyme gives rise to odontoblasts which produce dentin. Maturation of both cell types progressed simultaneously in WT embryos with elongated and well separated ameloblasts and odontoblasts. However, Osx null showed only cuboidal and aggregated cells in epithelial and mesenchyme portions of teeth. To better understand if the Osx null reflects a developmental arrest or a delayed differentiation, we compared tooth organs of new born littermates. WT mice clearly exhibited nuclear polarity with columnar shape of ameloblast and odontoblast. Osx null mutants on the other hand showed only cuboidal and disorganized cells as noted at E18. Together, these data demonstrate that during tooth development, Osx is required for maturation of both ameloblast and odontoblast. Since the Osx null died shortly after birth, we analyzed post-natal tooth development in surviving heterozygotes (Het). Although we observed normal and age appropriate dentition in both mice, ameloblasts and odontoblasts of WT were well differentiated from a morphological standpoint than those of Het mice. Moreover, the deposited enamel and dentin layers were 20-24% smaller in Het mice. Thus Osx haploinsufficiency affect the terminal phases of ameloblast and odontoblast differentiation. In conclusion, we report for the first time that Osx is obligatory for epithelial and mesenchymal cell signaling but not tooth development.

Disclosures: Ji-Myung Bae, None.

FR0232

Protection of Bone Loss by Targeting of Semaphorin 4D Expressed by Osteoclasts. Takako Koga*, Masahiro Shinohara, Hiroshi Takayanagi. Tokyo Medical & Dental University, Japan

Bone is continuously renewed by a process called bone remodeling, in which the resorption phase is followed by the formation phase. Each of these phases and also the transition between them requires a fine regulation by humoral factors or molecules mediating the communication among bone cells, which are either secreted by bone cells, expressed on the membrane of bone cells or released from the bone matrix.

Osteoporosis results from an ongoing imbalance between the processes of bone formation and resorption. While most of the currently available drugs inhibit the osteoclastic bone resorption, there are a few drugs which promote the osteoblastic bone formation. It is thus becoming increasingly important to identify the factors which regulate bone formation.

We found that osteoclasts express semaphorin 4D (Sema4D), known as an axon guidance molecule, which potentially inhibits bone formation. As expected, the mice lacking Sema4D exhibited the high bone mass phenotype due to an increase in bone formation activity by osteoblasts. We found that the binding of Sema4D to its receptor Plexin-B1 on osteoblasts led to the activation of the small GTPase RhoA, which inhibited osteoblast differentiation. Similar to Sema4D knockout mice, both Plexin-B1 knockout mice and the mice expressing dominant negative-RhoA specifically in osteoblasts had a high bone mass. Notably, anti-Sema4D antibody treatment significantly prevented bone loss in a model of postmenopausal osteoporosis.

Thus, this study identifies osteoclast-derived Sema4D as a crucial mediator of osteoclast-osteoblast communication in bone remodeling. Sema4D may function as an inhibitor of bone formation in the bone resorption phase, in which osteoblast differentiation and function are suppressed until osteoclastic bone resorption is accomplished. Now Sema4D has emerged as a new therapeutic target for the discovery and development of bone-increasing drugs.

Disclosures: Takako Koga, None.

FR0233

R-spondin 2 is a New Key Player in Human Osteoarthritis Osteoblasts to Orchestrate Their Abnormal Canonical Wnt Signaling. Elie Abed*, Thomas Chan¹, Aline Delalandre¹, Johanne Martel-Pelletier¹, Jean-Pierre Pelletier¹, Daniel Lajeunesse². ¹CHUM, Hopital Notre-Dame, Canada, ²CRCHUM, Hopital Notre-Dame, Canada

The canonical Wnt/ β -catenin (cWnt) signaling pathway plays a key role in osteogenesis by promoting the differentiation and mineralization of osteoblasts (Ob). R-spondin-1 (Rspo1) and 2, members of a family of secreted proteins, act as Wnt agonists and are present in bone tissues. Both clinical and in vitro studies suggest that subchondral bone sclerosis and altered bone remodeling, due to abnormal functions of Ob, are involved in the progression and/or onset of osteoarthritis (OA). Here, we questioned if an alteration of cWnt in OA Ob could be responsible for their abnormal osteogenesis and the potential role of Rspo1 and 2 in this process. We prepared primary human subchondral Ob using the sclerotic medial portion of the tibial plateaus of OA patients undergoing total knee arthroplasty, or from normal individuals at autopsy. The expression and production of Rspo1 and 2 were evaluated by qRT-PCR and by Western blot (WB) analysis. The regulation of Rspo1 and 2 was evaluated in response to transforming growth factor- β 1 (TGF- β 1) and the differentiation of Ob. The inhibition of Rspo2 was performed using siRNA and the effect of Rspo2 was evaluated using human recombinant Rspo2. cWnt signaling was evaluated by measuring target gene activity using the TOPflash TCF/lef luciferase reporter assay, and intracellular β -catenin levels by WB. Mineralization was evaluated by Alizarin red staining. TGF- β 1 expression and production were evaluated by qRT-PCR and ELISA. The expression and production of Rspo1 were similar in all Ob whereas they were reduced for Rspo2 in OA Ob compared to normal. TGF- β 1 expression and production were elevated in OA Ob, and TGF- β 1 reduced Rspo2 expression in all Ob. Wnt3a-dependent cWnt signaling and mineralization were reduced in OA Ob compared to normal. Recombinant human Rspo2 alone failed to trigger cWnt signaling in OA Ob, however, it stimulated about two-fold the Wnt3a-dependent cWnt signaling in these cells and increased their β -catenin levels. Rspo2 treatments also corrected the abnormal mineralization of OA Ob. Conversely, inhibition of Rspo2 by siRNA reduced cWnt signaling and the mineralization of normal Ob. These data demonstrate for the first time that Rspo2 is a new key player in abnormal OA Ob function. Reduced Rspo2 levels in OA Ob are responsible, at least in part, for their reduced cWnt signaling and abnormal mineralization. As Rspo2 is a secreted soluble protein, this could lead to potential new avenues of treatment of OA.

Disclosures: Elie Abed, None.

FR0235

Vitamin D Signaling in Osteoblasts/Osteocytes Is Required to Shift Calcium from Bone to Serum. Liesbet Lieben*, Karen Moermans¹, Lynda Bonewald², Jian Feng³, Geert Carmeliet¹. ¹Katholieke Universiteit Leuven, Belgium, ²University of Missouri - Kansas City, USA, ³Texas A&M Health Science Center, USA

The direct role of active vitamin D, 1,25(OH)₂D, on the skeleton is unclear. The beneficial effects of vitamin D receptor (VDR) signaling are mainly attributed to the stimulation of intestinal calcium transport and we recently observed that increased 1,25(OH)₂D levels reduce bone mass and mineralization to transfer calcium to serum in response to a negative calcium balance. We therefore hypothesized that VDR action in bone is redundant when sufficient calcium is absorbed, but is crucial to preserve normocalcemia when calcium supply is compromised. To validate this hypothesis, we genetically inactivated the VDR in the late stages of the osteoblastic lineage, by crossing *Vdr*^{fllox} mice with *Dmp1-Cre* mice (*Vdr*^{fllox}).

On a standard calcium diet, *Vdr*^{fllox} mice displayed no abnormalities in calcium and bone homeostasis. Serum calcium levels and bone mass (μ CT) were comparable to *Vdr*^{fllox} mice. Osteoblast differentiation and function was not changed as assessed by serum osteocalcin, gene expression of osteoblastic differentiation markers, histomorphometric analysis of osteoblast number and osteoid abundance, and dynamic bone formation parameters. Also bone resorption was unaltered, shown by normal serum CTx levels, *Rankl/Opg* mRNA ratio, and presence of TRAP⁺ cells. No manifest defects were observed in the osteocytes as histological and gene expression analysis revealed regular cell numbers and differentiation markers.

An inappropriate increase of 1,25(OH)₂D is known to cause hypercalcemia and bone defects. In *Vdr*^{fllox} mice, 1,25(OH)₂D treatment (0.5 μ g/kg BW/d for 1 wk) indeed resulted in hypercalcemia and mobilization of calcium from bone through an increase in bone resorption (serum CTx) and inhibition of bone mineralization (excess osteoid). In *Vdr*^{fllox} mice, the increase in serum calcium was less pronounced and bone mass was better preserved with normal CTx and osteoid levels. *In vitro* experiments confirmed that 1,25(OH)₂D inhibits the mineralization of osteoblastic (MC3T3-E1) cells and showed that this effect was accompanied by increased levels of the mineralization inhibitor PPI (pyrophosphate). Lowering PPI levels rescued the 1,25(OH)₂D-mediated inhibition of mineralization.

In conclusion, these findings demonstrate that VDR signaling in late osteoblasts/osteocytes is not essential for bone homeostasis in normal conditions, but that VDR is required to transfer calcium from bone to serum by increasing bone resorption and inhibiting mineralization via increased PPI levels.

Disclosures: Liesbet Lieben, None.

FR0241

Environment Contaminant Tributyltin-Induced Osteoporosis: Distinct Involvement of PPAR γ and RXR in Suppression of Osteogenesis. Amelia Baker*, Brett D Meeks¹, Faye V. Andrews², Danielle Salazar¹, Louis Gerstenfeld¹, Jennifer Schlezinger³. ¹Boston University School of Medicine, USA, ²Boston University School of Public Health, USA, ³Boston University School of Public Health, USA

Bone marrow performs multiple functions, from maintaining bone homeostasis to sustaining hematopoiesis. The balance of differentiation of multipotent mesenchymal stromal cells (MSC) between osteogenesis and adipogenesis is a central element of bone homeostasis. Peroxisome proliferator activated receptor γ (PPAR γ) sits at the crossroad, promoting adipogenesis and suppressing osteogenesis. Exposure to environmental PPAR γ agonists (phthalates, organotins) is ubiquitous. Tributyltin (TBT) is unique in that it is a highly potent ligand for both PPAR γ and retinoid X receptors (RXR). While PPAR γ forms a permissive heterodimer with RXR, it has recently been shown that the efficacy of heterodimer activation by RXR ligands is cell-type dependent. Here, we determined the mechanisms by which TBT alters MSC differentiation and, subsequently, impacts bone structure. We also explored the role of RXR and the permissivity of PPAR γ during the differentiation of primary MSCs. TBT's ability to bind PPAR γ and RXRs suggests that it would have similar yet distinct effects than either a PPAR γ (rosiglitazone; Rosi) or RXR (bexarotene; Bex) agonist. TBT, Rosi, and Bex increased adipocyte-specific proteins (PPAR γ 2, FABP4) with similar potency (EC50 ~10 nM) but differing efficacy (Rosi>TBT>Bex) in a PPAR γ -dependent manner in an MSC line (BMS2). Knockdown of PPAR γ reduced adipogenic response (Nile Red staining) to TBT to a lesser extent than to rosiglitazone. Gene expression studies support the idea that the TBT-induced transcriptional program is distinct from that induced by Rosi. While both induce FABP4, induction of TGM2 and ABCA1 only by TBT suggests recruitment of multiple nuclear receptor pathways (RXR homodimers and LXR/RXR, respectively). In primary bone marrow cultures, TBT induced adipogenesis and suppressed osteogenesis (alkaline phosphatase activity, nodule number, mineralization); Bex suppressed osteogenesis without stimulating adipogenesis; Rosi dramatically increased adipogenesis and also suppressed osteogenesis. *In vivo* exposure to TBT and Rosi altered serum markers of bone turnover (TRAP5b, PINP), decreased cortical thickness and increased marrow adiposity by histology. These data suggest TBT alters bone homeostasis and that RXR and PPAR γ may contribute independently to TBT-induced adipogenesis and reduction in osteogenesis. These studies show that exposure to TBT shifts MSC differentiation *in vitro* from osteoblasts to adipocytes and *in vivo* leads to bone loss.

defects in hair, teeth and bone development. Although clinical observations suggest that *Dlx3* plays a crucial role in craniofacial bone development, the function of *Dlx3* in these tissues has not been elucidated.

As *Dlx3* is expressed in several structures derived from the neural crest cell population, including craniofacial bones, we address the role of *Dlx3* in craniofacial bone development by deleting *Dlx3* in the neural crest using *Wnt1-cre* and *Dlx3*-floxed mice.

Our data show that mice lacking *Dlx3* (cKO) in the neural crest exhibit developmental defects in craniofacial bone structure. High-resolution X-ray and micro-CT analysis at 8 weeks reveal that cKO mice present higher alveolar bone porosity, a more rounded shape for the calvarial bones, suggesting an early developmental defect, and a significant reduction in parietal and frontal bone thickness ($p < 0.01$) compared to controls. These defects are associated with a significant decrease ($p < 0.0001$) in bone mineral density in alveolar, frontal and parietal bones of cKO mice. In addition to bone defects, cKO mice also exhibit teeth malformations such as dentin hypoplasia.

At the molecular level, microarray and qPCR analysis at P0 show that the neural crest deletion of *Dlx3* alters the mRNA expression of several markers of bone and tooth involved in mineralized tissue formation in cKO mice (e.g. Osteocalcin).

In this study, we establish that neural crest specific deletion of *Dlx3* results in alterations in bone structure, in bone mineral density, and in the expression of proteins associated with a mature mineralized tissue. Our findings demonstrate that the expression of *Dlx3* in neural crest-derived cells is essential for normal development of teeth, and mandible/ calvarial bones that are formed by intramembranous ossification.

Disclosures: *Juliane Isaac, None.*

FR0245

Identification of a Transcriptional Network Associated with Osteoblast Activity Using Systems Genetics. Charles Farber¹, Ana Lira¹, Brian Bennett², Luz Orozco², Hyun Kang², Calvin Pan², Eleazar Eskin², Aldons Lusis². ¹University of Virginia, USA, ²University of California, Los Angeles, USA

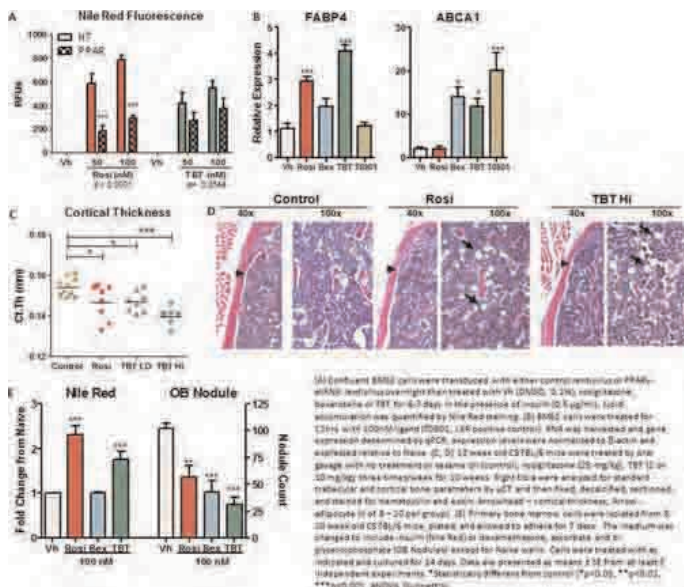
One of the main goals of systems genetics is to unravel the molecular mechanisms of disease by determining how genetic variation perturbs cellular networks. Here, we used systems genetics to identify and characterize an *in vivo* gene co-expression network for cells of the osteoblast lineage. A gene co-expression network was generated using bone microarray data from 96 different inbred mouse strains that are part of the Hybrid Mouse Diversity Panel. The resulting network consisted of 10 co-expression gene modules. Of the 10, one module (the purple module or PM) of 259 genes was significantly enriched for genes that were i) preferentially expressed in osteoblasts and ii) known to participate in osteoblast biology. These data suggested that PM genes and their interactions were important for osteoblast activity. To investigate the importance of the PM in an independent model, siRNAs were used to knockdown the expression of its most highly connected gene, *Maged1*, in primary calvarial osteoblasts. The reduction in *Maged1* preferentially altered the expression of PM genes (but not genes from other modules), and increased osteoblast proliferation and differentiation. We next identified specific genetic variants in the mouse genome that regulated the expression of PM genes. This analysis uncovered a single nucleotide polymorphism (SNP) on Chromosome 8 that was significantly associated with PM gene expression. This SNP was located ~20 Kbp downstream of *Sfrp1*, an antagonist of Wnt signaling and a known negative regulator of osteoblast proliferation and differentiation. This SNP was also found to regulate *Sfrp1* expression. Causality modeling predicted that 162 of the 259 PM genes were downstream targets of *Sfrp1*. Many of these genes have not been previously implicated in osteoblast function. This work identifies a novel network of genes involved in regulating osteoblast activity in mice.

Disclosures: *Charles Farber, None.*

FR0250

Overexpression of Transcription Factor Pitx1 Inhibits Osteoblast Differentiation and Bone Mineralization. Alain Moreau¹, Nancy Karam², Anita Franco³. ¹Sainte-Justine Hospital, Canada, ²Sainte-Justine University Hospital Research Center, Canada, ³Sainte-Justine-University Hospital Research Center, Canada

During mouse development, PITX1, a homeobox transcription factor, is highly expressed in articular joints and in the perichondrium of hind limb long bones suggesting its importance in skeletal development. Indeed, Pitx1-null mice displayed poorly developed joints with reduced length of adjacent skeletal elements exhibiting a marked expansion of the hypertrophic chondrocyte zone in the growth plate. Interestingly, ageing Pitx1^{+/+} heterozygous mice, which are normal at birth, progressively developed OA-like lesions in cartilage associated with a drastic increase in cortical and trabecular bone formation. Conversely, expression analysis of osteoblasts derived from monozygotic twins discordant for osteoporosis reported a 10-fold up-regulation of Pitx1 expression in osteoblasts from osteoporotic twins when compared to healthy ones. Collectively, these data prompted us to investigate the role of this transcription factor in osteoblast differentiation and bone mineralization. Transgenic mice (mCol1a1-Pitx1) over-expressing Pitx1 specifically in bone tissue



TBT-Induced Osteoporosis: Figure 1

Disclosures: *Amelia Baker, None.*

FR0242

Epigenetic Regulation of Mesenchymal Cell Commitment to the Osteoblast Lineage by *Dlx3*. Jonathan Gordon¹, Mohammad Hassan¹, Hai Wu¹, Maria Morasso², Andre Van Wijnen¹, Janet Stein¹, Gary Stein¹, Jane Lian¹. ¹University of Massachusetts Medical School, USA, ²Developmental Skin Biology Section, NIAMS/NIH, USA

Homeobox genes encode DNA-binding proteins well known for their ability to establish body axes during embryonic development and regulate lineage commitment in a wide variety of cells. Homeodomain proteins are primary targets for a wide variety of signaling molecules and are primary mediators involved in the initiation of chromatin remodeling during lineage commitment. One specific homeodomain-containing protein, *Dlx3*, is vital for craniofacial development and has been reported to activate several gene promoters in osteoprogenitors and early stage osteoblasts. In order to establish the role of *Dlx3* in mesenchymal cell commitment, a genome-wide screen of *Dlx3* targets in bone marrow stromal cells undergoing osteogenic differentiation was performed using chromatin immunoprecipitation followed by high-throughput sequencing (ChIP-seq). Analysis of *Dlx3* binding sites within the mouse genome revealed that *Dlx3* associates primarily with the conventional homeobox group A motif (TAAAT), which is mainly distributed within intergenic and promoter regions of genes encoding known osteogenic regulators. Thus we find *Dlx3* bound to osteoblast growth and differentiation markers (*Twist2*, *Spp1*, *Gli3*, *Smad2*, *Ibsp*, *Bglap2*), as well as several homeodomain-containing proteins involved in developmental regulation and tissue morphogenesis (*Pknox2*, *Pax8*, *Six2*, *Irx6*). *Dlx3* is bound to the proximal promoters (<2000 bp from transcriptional start site) of 356 genes. Analysis of H3K4 trimethylation (related to chromatin activation) demonstrated that *Dlx3* was associated with 232 active genes. Analysis of H3K9 trimethylation (linked to chromatin repression) revealed *Dlx3* association with 63 repressed genes. *Dlx3*-mediated gene expression was validated using cells isolated from mice with conditionally ablated *Dlx3* or BMSCs treated with *Dlx3*-shRNA. Gene ontology analysis of genes regulated by *Dlx3* in BMSC-derived osteoblastic cells suggests that *Dlx3* plays a central role in several regulatory loops involved in tissue morphogenesis, cell fate commitment and skeletal development. The present studies support an important role for homeodomain proteins in promoting adult bone development and provide mechanistic insight for increased bone density in *Dlx3*-conditional null mice. In addition, these results may provide insight into the bone mass phenotypes in patients with aberrant *Dlx3* protein (TDO).

Disclosures: *Jonathan Gordon, None.*

FR0243

Expression of *Dlx3* in Neural Crest-derived Cells Is Essential for Normal Formation of Craniofacial Bones. Olivier Duverger¹, Juliane Isaac¹, Anne K. Bartels¹, Angela Zah¹, Jane Lian², Ariane Berdal³, Joonsung Hwang¹, Maria I. Morasso¹. ¹Developmental Skin Biology Section, NIAMS/NIH, USA, ²University of Massachusetts Medical School, USA, ³INSERM, UMR872, Universites Paris 5 & 6, Team 5, France

Human mutations in the homeodomain transcription factor *DLX3* gene are etiologic to Tricho-dento-osseous (TDO), an ectodermal dysplasia characterized by

under the type-I collagen promoter (2.1kb fragment) were generated and phenotypically characterized. MicroCT analysis showed a 30% decrease in the cortical thickness of transgenic mice affecting both males (M) and females (F) at 2, 5 and 7.5 months ($p < 0.0025$), a decrease in the trabecular thickness by 15 to 30% and a 16% to 50% reduction in the trabecular separation and connectivity, with a shift of the trabecular micro-architecture from rod-like to plate-like forms when compared to the wild-type ones. Biomechanical assessment of transgenic bones (femurs) using the tribending test points revealed a reduction of 25% and 58% in bone strength for females and males respectively when compared to age- and sex-matched wild-type mice ($F p < 0.037$ and $M p < 0.042$). At the biochemical level, plasma OPG levels were increased by 50% ($p < 0.0046$) and RANKL levels decreased by 50% in transgenic mice when compared to wild-type ones suggesting a compensatory mechanism to alleviate the effects of PITX1 by reducing osteoclastogenesis. Differentiation assays *in vitro* showed that overexpression of PITX1 hardly abrogates the maturation of mColla1-Pitx1 osteoblasts when compared with wild-type ones. Collectively, these data define an unrecognized and crucial role for PITX1 in the regulation of osteoblast differentiation and bone mineralization.

Disclosures: Alain Moreau, None.

FR0252

Activation of Distinct Nucleotide Receptor Subtypes Determines the Duration of Calcium-NFATc1 Signaling in Osteoblasts over a Remarkably Wide Dynamic Range of ATP Concentrations: A Novel Mechanism for Dose-to-Duration Coupling. Matthew Grol¹*, Shu Xing², Alexey Pereverzev¹, Stephen M. Sims¹, Svetlana Komarova², S. Jeffrey Dixon¹. ¹The University of Western Ontario, Canada, ²McGill University, Canada

Nucleotides, released by mechanical stimuli, signal through two families of P2 receptors. P2Y are G protein-coupled receptors that often couple to release of calcium from intracellular stores; whereas P2X are ATP-gated channels that permit influx of calcium. Osteoblasts express a number of P2 receptors, including P2Y1,2,4,6 and P2X2,4-7; however, the significance of expression of multiple receptors with varying affinities for ATP is unexplored. Our purpose was to characterize signaling in osteoblasts by P2 receptors through calcium and its downstream target NFATc1. To monitor cytosolic free calcium, osteoblasts were loaded with fluo-4. A low concentration of ATP (10 μ M, activates some P2Y and all P2X receptors except P2X7, [low ATP]) induced transient elevation of cytosolic free calcium; whereas a high concentration of ATP (1 mM, activates some P2Y and all P2X receptors including P2X7, [high ATP]) elicited more sustained elevation. Further analyses revealed that graded increases in the calcium signal could be achieved over a remarkable million-fold range of ATP concentrations (1 nM to 1 mM). In this regard, mathematical modeling demonstrated that a wide dynamic range in ATP sensitivity can arise through coexpression of P2 receptors with varying affinities for ATP. To assess activation of NFATc1, we monitored subcellular localization of EGFP-tagged NFATc1. [Low ATP] caused transient nuclear localization of NFATc1; whereas [high ATP] elicited more sustained localization. Osteoblasts from P2X7 knockout mice stimulated with [high ATP] or the P2X7 agonist BzATP showed only transient calcium-NFATc1 signaling, in contrast to sustained signaling observed in wild type cells, establishing that prolonged calcium-NFATc1 signaling is mediated by the low affinity P2X7 receptor. [High ATP] and BzATP, but not [low ATP], elicited robust expression of the NFAT target gene *Ptgs2* (encoding COX2), consistent with a critical role for duration of calcium-NFAT signaling in regulating target gene expression. Taken together, this study provides the first evidence that P2 receptors couple to the calcium-NFATc1 pathway in osteoblasts and, for the first time in any system, that expression of multiple P2 subtypes increases the range over which differences in ATP concentration can be sensed by the cell. This phenomenon provides a novel mechanism by which osteoblasts may transduce differences in ATP concentration and intensity of mechanical stimuli over a remarkably wide dynamic range.

Disclosures: Matthew Grol, None.

FR0253

PTH differentially regulates PRG expression in Osteoblasts. Hyewon Choi¹*, Clara Magyar¹, Guillermo Arellano², Olga Bezouglia¹, Jeanne Nervina³, Sotirios Tetradis⁴. ¹University of California, Los Angeles, USA, ²University of Nevada, Las Vegas, USA, ³University of Michigan, USA, ⁴UCLA, USA

Intermittent PTH (iPTH) is anabolic, while continuous PTH (cPTH) is catabolic in bone homeostasis. Primary response genes (PRGs) are the first genes to be induced in PTH responsive cells. We explored the role of PTH exposure and signaling activation in PRG expression in primary osteoblasts and MC3T3-E1 cells. To mimic iPTH, cells were treated with 10 nM PTH, washed, and PTH-free media was added for the remaining treatment. For cPTH, cells were treated the same except that media containing 10 nM PTH was added after the washes. Interestingly, 30 min iPTH maximally induced *Nurr1*, *Nur77* and *cox2*, while cPTH was required for maximal *RANKL* and *IL-6* induction. This suggests two classes of PTH-induced PRGs: those requiring continuous PTH presence for maximal induction and those that do not. Intriguingly, *Nurr1* is associated with anabolic PTH effects, while *RANKL* mediates catabolic PTH effects. We then examined time-dependent pathway manipulation on PTH-induced *Nurr1* and *RANKL* expression. PKA inhibition before PTH attenuated

both *Nurr1* and *RANKL* expression. However, PKA inhibition 1 or 2 h after PTH increased *Nurr1*, but inhibited *RANKL* expression. Thus, initiating PKA activity appears sufficient for *Nurr1* induction, but continuous PKA activity is required for *RANKL* induction. Additionally, *Nurr1* expression was unaffected by pre- or post-PTH erk inhibition, while *RANKL* expression was attenuated in both cases. Importantly, PTH increased histone H4 acetylation at the transcription start site (TSS) of both *Nurr1* and *RANKL*. PKA, but not erk, inhibition decreased this effect. PTH alters actin organization. Inhibiting actin polymerization blocked PTH-induced *RANKL*, but not *Nurr1* expression. Furthermore, PTH-induced erk activity was required for Rho activation. Blocking the downstream Rho GTPase effector ROCK inhibited *RANKL*, but not *Nurr1*, induction. Interestingly, H4 acetylation on *Nurr1* and *RANKL* TSS was unaffected. This suggests that PTH-induced cytoskeletal rearrangement is involved in *RANKL* regulation through PTH-activated Rho GTPase. Together, our data reveal two classes of PTH-induced PRGs. Those for which PTH-initiated PKA signaling triggers maximal induction that proceeds independent of PTH or PKA vs those for which continuous PTH presence, continuous PKA and erk activation, and actin cytoskeleton rearrangement are required for maximal induction. These distinctions may contribute to the *in vivo* anabolic vs catabolic effects of iPTH vs cPTH.

Disclosures: Hyewon Choi, None.

FR0254

The p38 α MAPK Regulates Osteoblast Function and Postnatal Bone Acquisition. Cyril Thouverey¹, Joseph Caverzasio²*, ¹Division of Bone Diseases, Switzerland, ²Division Bone Diseases, Switzerland

Various osteogenic ligands that stimulate osteoblast differentiation and function act, in part, through the p38 mitogen-activated protein kinase (MAPK) pathway. A recent *in vivo* investigation has highlighted the physiological role of the TAK1 in osteoblastogenesis and bone formation (M.B. Greenblatt et al., J. Clin. Invest. 2010). Although TAK1 can activate different signaling cascades, the authors have suggested that the MKK3/6-p38 pathway may be an important regulator of osteoblast function. To elucidate the specific role of p38 α in regulating osteoblast function, we generated mice lacking p38 α in mature osteoblasts. Mice expressing Cre recombinase under the control of the *osteocalcin* promoter (*Ocn-Cre*) were crossed with mice harboring floxed p38 α -encoding gene (*p38 α ^{fl}*). The bone phenotype of control (*p38 α ^{fl}*) and mutant (*Ocn-Cre;p38 α ^{fl}*) female mice was assessed by dual energy X-ray absorptiometry, micro-computed tomography, histomorphometry and *ex vivo* gene expression analyses at 3 months of age (n=6 per group). Mutant mice exhibited lower bone mineral density compared to control mice (-8.2 %, $p=0.003$). *Ocn-Cre;p38 α ^{fl}* mice displayed an important reduction in trabecular bone volume at the distal femoral metaphysis (-37.1 %, $p=0.002$) associated with low trabecular thickness (-20.7 %, $p<0.001$). A similar pattern of low trabecular bone mass was observed at the fifth lumbar vertebral body. In addition, *Ocn-Cre;p38 α ^{fl}* mice also showed a decreased cortical thickness at the femoral midshaft (-20.2 %, $p<0.001$) that was associated with reduced endosteal mineral apposition rate (-22.7 %, $p=0.007$) and bone formation rate (-40.8 %, $p<0.001$). Consistent with this low bone mass phenotype, *Oss*, *Colla1*, *Alp* and *Ocn* expressions were respectively reduced by 34, 32, 10 and 40 % in long bones of mutant mice, indicating a defective function of osteoblasts lacking p38 α . These findings indicate that p38 α is an essential regulator of osteoblast function and bone formation *in vivo*.

Disclosures: Joseph Caverzasio, None.

FR0255

WNT5A Is a Novel Regulator of Cytokine and Chemokine Expression In Bone Marrow Stromal Cells. Martina Rauner¹*, Nicola Stein², Maria Winzer², Claudia Goettsch³, Lorenz Hofbauer⁴. ¹Medical Faculty of the TU Dresden, Germany, ²Technical University Dresden, Department of Medicine III, Germany, ³Brigham & Women's Hospital/Cardiometabolic Division, USA, ⁴Dresden University Medical Center, Germany

Rheumatoid arthritis (RA) is a chronic inflammatory disease that negatively affects bone mass by enhancing cytokine-driven osteoclastogenesis and suppressing osteoblast functions. Recently, Dickkopf-1, an inhibitor of WNT signaling, has been found to be induced by TNF- α and suppress bone formation in RA. Here, we aimed to identify other members of the WNT signaling pathway that are regulated by inflammatory stimuli and affect bone remodelling. Of several WNT ligands investigated, only WNT5A was consistently induced by 3-fold at the mRNA and protein level in human bone marrow stromal cells (BMSCs) after stimulation with 1 μ g/ml lipopolysaccharide (LPS). In addition, an increased expression of WNT5A was found in the synovial tissue of 10 weeks-old TNF-transgenic mice compared to wild-type controls as assessed by immunohistochemistry. The LPS-induced WNT5A expression in BMSCs was completely blocked when cells were pre-treated with an antibody against toll-like receptor 4 (10 μ g/ml) or with specific inhibitors of the NF- κ B (BAY-7082, 1 μ M) and MAPK (U0126, 10 μ M) pathways. Of note, the WNT5A receptor ROR2 was up-regulated 6-fold by LPS and the induction was also NF- κ B and MAPK-dependent. BMSCs respond to LPS stimulation by highly up-regulating the expression of several cytokines and chemokines including IL-1b, IL-6, TNF- α , CCL2, CCL5, and CXCL12. Knock-down of WNT5A using siRNA potently suppressed the basal and LPS-induced expression of IL-1b, IL-6, CCL2, and CCL5,

but not that of TNF- α or CXCL12. In line with these data, BMSCs treated with 500 ng/ml human recombinant WNT5A for 48 h induced the expression of IL-1b, IL-6, CCL2, and CCL5. To unravel the underlying signaling pathways, cells were pre-treated for 1 h with pathway blockers (NF- κ B: BAY-7082, 1 μ M; MAPK: UO126, 10 μ M; PI-3K: LY-294002, 50 μ M, NFAT: VIVIT, 1 μ M). While WNT5A-induced IL-1b expression was solely regulated by the MAPK pathway, the induction of IL-6 expression was dependent on the NF- κ B and MAPK pathways. The chemokines CCL2 and CCL5 were regulated by multiple pathways including NF- κ B, MAPK, and Ca2+/NFAT. Of note, WNT5A also induced its own expression, which was dependent on the Ca2+/NFAT pathway. Taken together, WNT5A is induced under inflammatory conditions in BMSCs and controls the expression of cytokines and chemokines. The relevance of this regulatory circuit for osteoimmunology needs to be further explored *in vivo*.

Disclosures: Martina Rauner, None.

FR0259

Connexin43 (Cx43) in Osteogenic Cells Regulates Osteoclastogenesis via Paracrine Osteoprotegerin (OPG) Production, without Direct Osteoblast-Osteoclast Gap Junctional Communication. Marcus Watkins*, Roberto Civitelli. Washington University in St. Louis School of Medicine, USA

We have previously reported that conditional ablation of the Cx43 gene (Gja1) in differentiated osteoblasts or osteoprogenitors results in increased cross-sectional bone area, expansion of the marrow cavity and thinning of cortical bone; the result of increased endocortical osteoclast number and bone resorption. Furthermore, bone marrow stromal cells (BMSC) isolated from conditionally Gja1 ablated mice using the Dermo-1 promoter (cKO) induce 4-fold higher number of osteoclasts when cultured with either wild type (WT) or cKO macrophages. Since Cx43 is expressed in both the osteoblast and osteoclast lineages, we studied the potential role of loss of gap junction communication in this phenotype. Undifferentiated WT BMSC express low levels of Cx43, but its abundance rapidly increases with progressing differentiation, whereas extremely low Cx43 abundance is seen in cKO BMSC. Conversely, both WT and cKO bone marrow macrophages and differentiated osteoclasts express Cx43, confirming specificity of Gja1 ablation. We tested gap junctional intercellular communication (GJIC) by monitoring the diffusion of calcein from pre-loaded cells grown in monolayer to lipophilic carbocyanine-labeled acceptor cells "parachuted" on top of the monolayer. As anticipated, differentiated BMSC osteoblasts exhibit a high degree of GJIC when parachuted onto other osteoblasts; whereas macrophages do not show GJIC when parachuted on other macrophages. Some dye diffusion occurs among multinucleated osteoclasts, although to a lesser extent than among BMSC. Importantly, undifferentiated BMSCs do not exhibit GJIC when in contact with other BMSCs, macrophages, osteoclasts or even osteoblasts, consistent with low Cx43 abundance. Furthermore, differentiated osteoblasts did not exchange dye with macrophages or differentiated osteoclasts. BMSC isolated from cKO mice rapidly up-regulate Rankl when cultured in osteoclastogenic media (containing vitamin D3 and dexamethasone), as do WT cells. However, cKO BMSC fail to upregulate Opg mRNA and protein, consistent with the reported decreased Opg, but unchanged Rankl mRNA expression in cKO bone extracts. In summary, despite Cx43 expression by both lineages, there is no evidence of direct GJIC between osteogenic and osteoclastic cells. Thus, the increased osteoclastogenesis in cKO mice cannot be related to loss of heterotypic gap junctional communication, but rather to altered Opg expression by osteoblastic cells.

Disclosures: Marcus Watkins, None.

FR0260

CXCR4 Signaling in Osteoblasts is Essential for Bone Homeostasis. Vivian Chu¹, Mohammad Shahnazari², Thomas Wronski³, Bernard Halloran^{*1}. ¹VA Medical Center (111N), USA, ²UCSF VA Medical Center, USA, ³University of Florida, USA

CXCR4 is the G-protein coupled receptor for CXCL12 (stromal derived factor-1). CXCL12/CXCR4 signaling plays an important role in hematopoiesis. CXCL12 is necessary to maintain the hematopoietic stem cell niche and is known to play a critical role in the formation and survival of osteoclasts (OC). The role of CXCL12/CXCR4 signaling in osteoblasts (OB), however, has yet to be adequately described. Using Cre-Lox technology to selectively ablate CXCR4 signaling in maturing OB we studied the role of signaling in OB function. We interbred CXCR4^{fllox/fllox} mice with collagen type 1a1 (Col2.3)-Cre mice to yield conditional knockouts (KO) in which CXCR4 was deleted from OB expressing Col2.3. We have characterized the bones of mice at 6 weeks of age by using microCT analysis, histomorphometry, cell culture, and gene expression analysis. CXCR4 KO mice were compared to wild-type, CXCR4^{fllox/fllox}, and Col2.3-Cre only littermates as controls. MicroCT analysis revealed significant differences at the distal femur. CXCR4 KO mice exhibited a 40% decrease in cancellous bone volume fraction (p=0.01), which was associated with decreased connectivity density, trabecular number and thickness, and increased trabecular spacing. Cancellous bone took on a more rod-like structure. Bone marrow stromal cell cultures (BMSC) showed 400% more colony forming units compared to controls. BMSC from KO mice also demonstrated 660% more alkaline phosphatase-positive colonies by Day 9 of culture. Induction of osteoclastogenesis in the non-adherent fraction of BMSC cultures yielded fewer osteoclasts (TRAP+, multinucleated cells) when compared to controls. Gene expression analysis of OB cultures on Day 14 indicated that CXCR4

ablated mice had decreased expression of CXCR4 and increased expression of CXCL12, Runx2, osterix, ALP, and Col2.3. Our data suggests that CXCL12/CXCR4 signaling in the maturing OB plays an important role in bone homeostasis. Signaling in OB appears to regulate cancellous bone volume, the mesenchymal stem cell and osteoprogenitor pool sizes, recruitment to the OB lineage and OB maturation. It also appears crucial for communication between OB and hematopoietic cells to regulate the osteoclast precursor pool size.

Disclosures: Bernard Halloran, None.

FR0262

Engineering Vascularized Bone: Osteogenic and Pro-Angiogenic Potential of Murine Periosteal Cells. Nick Van Gestel^{*1}, Scott Roberts², Sophie Torrekens¹, Jan Schrooten¹, Frank Luyten³, Geert Carmeliet¹. ¹Katholieke Universiteit Leuven, Belgium, ²KULEUVEN, Belgium, ³University Hospitals KU Leuven, Belgium

One of the key challenges in cell-based bone tissue engineering is the timely formation of blood vessels that promote the survival of the cells in the implant. The presence of cells with pro-angiogenic properties could thus be crucial for the successful outcome of a tissue engineered construct. Since fracture healing is enhanced when the periosteum is present, periosteum-derived cells (PDC) may prove to contribute not only to osteogenesis but also to angiogenesis. In this study, we therefore characterized the ability of murine PDC (mPDC) to support angiogenesis, in addition to their osteogenic potential.

We first established a protocol to specifically isolate periosteal cells from long bones of adult mice and characterized the obtained cell population. Mesenchymal stem cells (MSC) were abundantly present as more than 50% of the mPDC expressed the MSC markers CD105, CD90, CD73 and SCA-1, whereas hematopoietic and endothelial markers were not detected. The mPDC furthermore possessed trilineage differentiation potential *in vitro* (osteogenic, chondrogenic, adipogenic), confirming the presence of MSC in the mPDC population and their osteogenic capacity.

When seeded on a calcium phosphate-collagen carrier and implanted ectopically in mice for 8 weeks, mPDC formed mature bone, illustrated by the presence of osteocytes and osteocalcin-positive osteoblasts. When compared to carriers implanted without cells, mPDC-seeded scaffolds attracted numerous blood vessels which were closely associated with the sites of bone formation. Moreover, some of the blood vessels had developed into larger, sinusoid-like structures and the formation of a bone marrow compartment was observed.

To further elucidate the pro-angiogenic properties of mPDC, we used an *in vitro* culture system. Culturing mPDC under low oxygen tension increased HIF-1 α and VEGF protein levels and hypoxia-conditioned medium from mPDC enhanced the proliferation of human umbilical vein endothelial cells (HUVEC). In addition, co-culture of mPDC with HUVEC resulted in stabilization of the pseudo-vascular structures formed by the HUVEC, in which the mPDC were localized in a pericyte-like fashion. Consistent herewith, mPDC express pericyte markers such as α -SMA and PDGFR- β .

In conclusion, we demonstrate that periosteal cells can contribute to fracture repair, not only through their strong osteogenic potential, but also their pro-angiogenic features and thus may provide an ideal cell source for bone regeneration.

Disclosures: Nick Van Gestel, None.

FR0267

PPR-Dependent Signaling in the Osteoblast Lineage Regulates Bone Marrow B Cell Development. Cristina Panaroni^{*1}, Rhiannon Chubb¹, Joy Wu². ¹Endocrine Unit, Massachusetts General Hospital, USA, ²Massachusetts General Hospital, USA

It is now widely accepted that osteoblasts are a crucial component of the hematopoietic stem cell (HSC) niche. Signaling through the parathyroid hormone (PTH)/PTH-related peptide (PTHrP) receptor (PPR) in osteoblastic cells can increase HSC numbers, as demonstrated using mice expressing a constitutively active form of PPR targeted to osteoblasts. Recent findings demonstrate that, beyond support of HSCs, osteoblasts are also necessary to sustain B lymphopoiesis in bone marrow. The PPR is a G protein-coupled receptor (GPCR) that signals through multiple G proteins. One major downstream mediator of PPR signaling is Gs α , which stimulates cyclic-AMP-dependent signaling. We have previously demonstrated that deletion of Gs α early in the osteoblast lineage in Osterix-Cre:Gs α (fl/fl) mice results in reduced bone mass with fewer osteoblasts and impaired differentiation of bone marrow B cell precursors blocked at the pre-pro B to pro-B transition *in vivo*. The relevant GPCR upstream of Gs α is of great interest. Since PTH is known to regulate HSCs *in vivo* and enhances support of B lymphocytes differentiation by osteoblastic cells *in vitro*, signaling downstream of the PPR may be relevant to the regulation of B lymphopoiesis in addition to HSCs. We therefore hypothesized that ablation of PPR in osteoblasts would negatively affect bone marrow B lymphopoiesis. Osterix-Cre:PPR(fl/fl) conditional knockout (KO) mice were generated using the Cre recombinase under the control of the Osterix promoter to ablate PPR in osteoblast precursors. The resulting mutant mice develop postnatal growth retardation and a dramatic decrease in trabecular bone at 3 weeks of age. Compared to WT littermates,

3 week-old PPR KO mice were significantly smaller but bone marrow cellularity was not affected. Analysis of the bone marrow of PPR KO mice revealed, as previously shown in Gsz KO mice, a reduction in the B220+IgM-CD93+ B cell precursor population. More specifically, we found a statistically significant increase in pre-pro-B cells accompanied by a decrease in pro-B cells and pre-B cells. Our results demonstrate that PPR signaling upstream of Gsz in cells of the osteoblast lineage plays a direct role in bone marrow B cell differentiation.

Disclosures: Cristina Panaroni, None.

FR0268

The Host Immune Response to Allogeneic and Syngeneic Mesenchymal Stem Cells Modulates Osteogenesis. Scott Yang*, Vedavathi Madhu, Abhijit Dighe, Gary Balian, Quanjun Cui. University of Virginia, USA

Purpose: Evidence from major histocompatibility complex (MHC) mismatched allogeneic mesenchymal stem cell (MSC) implantation animal studies have shown controversial evidence for both bone formation and rejection. A systematic analysis of the whether MSCs are capable of evading MHC barriers in different immune models and ultimately produce a relevant bone forming response is imperative.

Methods: The MSC line (D1), isolated from bone marrow of Balb/c mice was injected subcutaneously in six each of syngeneic Balb/c, allogeneic immunocompetent C57BL/6, allogeneic immunocompromised NCR Nude/Nude and C57BL/6 Pfp/Rag2 KO mice. NCR Nude mice are athymic, and lack T-cell function. C57BL/6 Pfp/Rag2 KO mice lack mature T & B-cells and also lack perforin mediated cytolytic activities of NK & CD8+T-cells. D1 cells were labeled with PKH26 to track survival. Implants were analyzed at four time points post cell injection: 36 hrs, 1-, 3-, and 6 weeks by analysis with x-ray and micro-CT, histology for PKH26 labeled cell survival, flow cytometry of immune cell populations, and RT-PCR of osteogenic markers.

Results: Ectopic bone formed only in syngeneic or allogeneic immunocompromised mouse groups (Fig. 1). The survival of D1 cells was also evident through six weeks in these mouse groups. Although no ectopic bone formed in allogeneic immunocompetent hosts, the implanted cells partially survived for up to three weeks before rejection (Fig. 2). A significantly greater proportion of F4/80+ macrophages (at 36 hours) and CD4+ T-cells (at 1 week) was present in C57BL/6 implants as compared to Balb/c implants. Also, the proportion of CD4+CD25+ T reg cells in Balb/c mice increased compared to C57BL/6 mice. In addition, the immune response in all allogeneic hosts inhibited expression of the Wnt/ β -catenin pathway genes as well as the alkaline phosphatase and osteocalcin genes. However, expression of the runx2 and BSP genes was not inhibited in implants retrieved from allogeneic immunocompromised C57BL/6 Pfp/Rag2 KO mice.

Conclusions: The late rejection of D1 cells after the 3rd week in C57BL/6 mice suggests that a T-cell mediated adaptive host response is responsible. The host immune response modulated not only the survival of D1 cells but also osteogenic differentiation of D1 cells. Although allogeneic stem cell mediated bone repair is attractive, further investigation is required to design interventional strategies to reduce host immune response to stem cells.

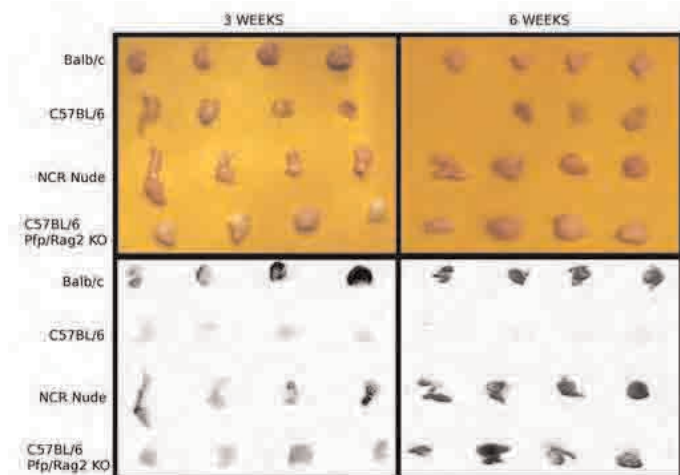


Fig.1 Morphology and corresponding radiographs of retrieved implants.

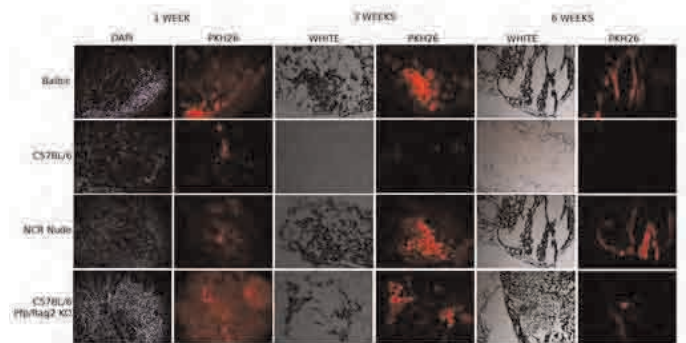


Fig. 2 PKH26 red staining to track presence of mesenchymal stem cells

Disclosures: Scott Yang, None.

FR0269

Transplantation of Human Umbilical Cord Blood-Derived Mesenchymal Stem Cells or Their Conditioned Medium Prevent Bone Loss in Ovariectomized Nude Mice. Jee Hyun An*, Jung Ah Song¹, Kyoung Ho Ki¹, Sol Ip Jung¹, Jae-Yeon Yang¹, Hyung Jin Choi¹, Sun Wook Cho², Sang Wan Kim³, Seong Yeon Kim¹, Soo Jin Choi⁴, Wonil Oh⁴, Chan Soo Shin¹.

¹Department of Internal Medicine, Seoul National University College of Medicine, South Korea, ²University of Michigan School of Dentistry, USA, ³Seoul National University Boramae Hospital, South Korea, ⁴Biomedical Research Institute, MEDIPOST, Co., Ltd., South Korea

Umbilical cord blood-derived mesenchymal stem cells (UCB-MSCs) have advantages over other source of MSCs, including the ease of harvesting and storage, the low immunogenic potential, and the high capacity of differentiation into osteoblasts. We studied the effects of systemic injection of human UCB-MSCs and their conditioned medium (CM) on ovariectomy (OVX)-induced bone loss in nude mice. Ten-week-old female nude mice were divided into 5 groups: Sham-operated mice treated with Vehicle (Sham-Vehicle); OVX mice treated with UCB-MSCs (OVX-MSC); CM of UCB-MSCs (OVX-CM); Zoledronate (OVX-Zol) or Vehicle (OVX-Vehicle). Whole body bone mineral density (BMD) measurement by PIXIMUS showed that OVX-MSC group exhibited significant attenuation of OVX-induced bone loss compared with OVX-Vehicle group (0.0479 ± 0.0008 vs. 0.0459 ± 0.0004 g/cm² at 4 weeks, $p < 0.01$; 0.0483 ± 0.0008 vs. 0.0465 ± 0.0004 g/cm² at 8 weeks, $p < 0.01$). Furthermore, microCT analysis of proximal tibia at 8 weeks after treatment demonstrated significant increase in trabecular bone volume (BV/TV, 49 %), trabecular number (TbN, 48 %) and trabecular thickness (TbTh, 15 %) in OVX-MSC group compared to OVX-Vehicle group (all $p < 0.01$). Notably, the effects on bone density and microstructures in OVX-CM group were comparable to that in OVX-MSC group (6.2 % higher BMD, 51 % higher BV/TV, 49 % higher TbN, 14 % higher TbTh, all $p < 0.01$). In addition, OVX-MSC and OVX-CM group showed higher bone formation rate (38 % and 41 %, respectively, all $p < 0.01$) and mineral apposition rate (29 % and 32 %, respectively, all $p < 0.01$) than OVX-Vehicle group in dynamic histomorphometric analysis of lumbar spine. Serum PINP levels were also significantly higher in OVX-MSC (1.42 ± 0.13 ng/ml) and OVX-CM (1.58 ± 0.31 ng/ml) group compared with OVX-Vehicle group (1.23 ± 0.11 ng/ml, $p < 0.01$). However, cell trafficking analysis with FACS for detecting CFDA-labeled MSCs in bone marrow of OVX mice was not able to demonstrate engraftment of MSCs in bone after 24hr of treatment. In vitro, when C3H10T1/2 cells were treated with CM of UCB-MSCs, alkaline phosphatase (ALP) activities and expression of Col type 1, Runx2, osterix measured by quantitative real-time PCR were significantly increased. Furthermore, treatment of CM of UCB-MSCs inhibited osteoclastic differentiation in bone marrow macrophage culture, and enhanced the osteocyte-like morphological changes of MLO-Y4 cells and their survival in apoptosis assay. Taken together, these results suggest transplantation of UCB-MSC is a promising option for treatment of osteoporosis and the effect seems to be mediated by paracrine factors rather than direct engraftment of the MSCs.

Disclosures: Jee Hyun An, None.

FR0274

The Association Between The Microtubule Plus End Protein EB1 And Cortactin Controls Podosomes And Bone Resorption. Martin Blosse Duplan^{*1}, Sebastien Stephens¹, Frank PL Lai², Margit Oelkers³, Daisuke Kitamura⁴, Klemens Rottner³, William Horne¹, Roland Baron⁵. ¹Harvard School of Dental Medicine, USA, ²Institute of Medical Biology, Immunology, Singapore, ³Institute of Genetics, University of Bonn, Germany, ⁴Research Institute for Biological Sciences, Tokyo University of Science, Japan, ⁵Harvard School of Medicine & of Dental Medicine, USA

We and others have established the importance of microtubules (MTs) for the formation and stability of the peripheral podosome belt (PB), a unique feature of osteoclasts (OCs) that is critical for bone resorption. Although roles for Pyk2 and c-Cbl have been suggested, the mechanism by which MTs interact with and control podosomes has yet to be identified.

We performed a genome-wide screen of genes expressed in OCs and identified several "plus end tracking proteins" (+TIPs), proteins that are present at the growing ends of MTs, including EB1, a master regulator of +TIP interaction complexes. Expression of EB1 increased significantly as OCs matured. Live cell imaging revealed that EB1-positive MT ends targeted podosomes and EB1 was enriched in the PB. Agents that disturb or stabilize the association of EB1 with MTs respectively decreased or increased podosome density at the OC periphery, and depleting EB1 or expressing a dominant-negative mutant of EB1 in OCs strongly antagonized PB formation. Looking for targets of EB1 in podosomes, we found that cortactin (CTTN), an actin regulatory protein enriched in podosomes, associated with EB1 and that this interaction was dependent on MT stability. OCs from CTTN knockout mice showed reduced PB formation and bone resorption, whereas deletion of its close homolog hematopoietic lineage cell-specific protein 1 (HS1) did not alter OC activity. The SH3 domain of CTTN was required both for the interaction with EB1 and for rescuing PB formation and bone resorption in the CTTN KO OCs, supporting our hypothesis that EB1 and CTTN interact in a pathway that connects MTs and podosomes. Also, in the absence of CTTN, MT targeting of podosomes was reduced. Mechanistically, disrupting MTs or depleting EB1 increased CTTN phosphorylation by Src whereas stabilizing MTs decreased it. In addition, CTTN phosphorylation was decreased by another post-translational modification of CTTN, acetylation, and both phosphorylation and acetylation had to be reversible for normal PB formation. Finally, to investigate *in vivo* the role of CTTN, we examined the bone phenotype of mice lacking HS1 or CTTN in mature OCs (HS1^{-/-} and Cathepsin K^{Cre/+}: CTTN^{fl/fl} mice) by μ CT and histomorphometry. Bone resorption was impaired in 6 week old CTTN-KO mice, resulting in increased bone mass, whereas HS1 deletion did not affect bone mass.

These data identify a novel pathway that links MTs to podosomes and is critical for OC podosome organization and bone resorption.

Disclosures: Martin Blosse Duplan, None.

FR0279

Unique RANKL Determinants Associated with RANK Versus OPG Engagement. Julia Warren^{*}, Christopher Nelson, Yik Yu, Steven Teitelbaum, Daved Fremont. Washington University in St. Louis School of Medicine, USA

The interaction between Receptor Activator of NF- κ B Ligand (RANKL) and its receptor RANK is key to the differentiation and function of the osteoclast, the sole bone resorbing cell. Osteoprotegerin (OPG), a soluble homodimer, acts as a decoy receptor for RANKL. RANK and OPG contain a similar four cysteine-rich repeat domain (CRD) region but OPG binds RANKL with markedly different kinetics. An imbalance in the RANK/RANKL/OPG axis with decreased OPG and/or increased RANKL is associated with diseases that favor bone loss, including osteoporosis. The co-crystal structures of RANK/RANKL and OPG/RANKL show that both receptors use primarily CRD-2 and CRD-3 to form the interface with RANKL; however, the details of these interfaces are distinct. To explore the structural basis of RANK versus OPG binding to RANKL, we designed more than thirty point and short insertional RANKL mutations. We focused on three critical RANKL loops (the AA' loop, the CD loop, and the GH loop) along with several residues that form salt bridges or hydrogen bonds to RANK and/or OPG. These mutant RANKL proteins were expressed in *E. Coli*, purified, and screened for osteoclast formation and function using TRAP staining, TRAP solution assay, qRT-PCR, and western blotting for proximal signaling events. We also determined the apparent K_D of RANKL binding to OPG or RANK using Bio-layer Interferometry (BLI) spectroscopy. Our initial screens have identified six candidate RANKL mutants, all of which contain CD loop insertions that retain variable levels of OPG binding (including normal) but no detectable binding to RANK. In keeping with absent RANK association, the same mutants are incapable of promoting osteoclastogenesis. These findings are also in accordance with the crystal structures which demonstrate a dramatic rearrangement of the RANKL CD loop when bound to RANK versus OPG and may explain the observed differences in kinetics despite the similar footprints of the interfaces. Importantly, our findings suggest an anti-bone resorption therapeutic strategy involving the targeting of specific components of RANKL.

Disclosures: Julia Warren, None.

FR0281

Apoptotic Osteocytes Promote In Vitro Osteoclastogenesis Directly through RANKL and Indirectly Through M-CSF and VEGF. Saja Al-Dujaili^{*1}, Esther Lau¹, Axel Guenther¹, Lidan You². ¹University of Toronto, Canada, ²Mechanical & Industrial Engineering, University of Toronto, Canada

Fatigue-induced bone microdamage has been implicated with increased osteocyte apoptosis that is co-localized with bone resorption spaces [1]. We hypothesize that apoptotic osteocytes may target bone resorption by regulating osteoclast precursor recruitment and osteoclast formation. We previously used *in vitro* serum-starvation to model reduced nutrient transport in microdamaged bone, thus inducing apoptosis in MLO-Y4 osteocyte-like cells [2]. We obtained conditioned media from: 1) serum-starved apoptotic osteocytes (aOCY), 2) osteocytes treated with aOCY conditioned media (i.e. healthy osteocytes in the presence of apoptosis cues; atOCY), and 3) osteocytes treated with non-apoptosis conditioned media (i.e. healthy osteocytes in the absence of apoptosis cues; natOCY). We found that aOCY and atOCY promoted osteoclast precursor migration and osteoclast formation, while natOCY had no effect.

Here, we aimed to determine the mechanism for aOCY and atOCY induced osteoclastogenesis. We measured RANKL, M-CSF and VEGF (known osteoclastogenic factors expressed by osteocytes) concentration in conditioned media. RANKL was upregulated in aOCY up to 426% relative to atOCY and natOCY conditioned media ($p < 0.001$). M-CSF was elevated up to 70% and VEGF up to 286% relative to aOCY and natOCY conditioned media ($p < 0.001$).

To determine if these factors are indeed responsible for increased osteoclastogenesis, we used antibodies to neutralize the effect of RANKL in aOCY, and VEGF and M-CSF in atOCY conditioned media. Conditioned media were then applied to RAW264.7 cells to induce migration through Boyden chambers, or osteoclast formation. RANKL blocking abolished the effect of aOCY on osteoclast precursor migration (up to 42% decrease; $p < 0.002$) and osteoclast formation (up to 66% decrease; $p < 0.03$).

Blocking either VEGF or M-CSF in atOCY conditioned media had similar effects with up to 63% reduction in osteoclast precursor migration ($p < 0.001$) and 50% reduction in osteoclast formation ($p < 0.003$), thus abolishing the effect of atOCY. Neutralizing both VEGF and M-CSF had the same response as blocking individual proteins, suggesting that VEGF and M-CSF act synergistically on osteoclast precursors. Findings from this study support our hypothesis that in the presence of microdamage apoptotic osteocytes directly and indirectly (through neighboring healthy osteocytes) regulate osteoclastogenesis.

[1] Cardoso et al. *JBM*, 2009.

[2] Al-Dujaili et al. *Proceed. ASBMR*, 2010.

Disclosures: Saja Al-Dujaili, None.

FR0283

Diacylglycerol Maintains Bone Homeostasis by Regulating Osteoclast Differentiation and Function. Corinne Decker^{*1}, Viviana Cremasco², Roberta Faccio³. ¹Washington University in St. Louis, USA, ²Washington University School of Medicine, USA, ³Washington University in St Louis School of Medicine, USA

Previous work from our lab identified PLC γ 2 as a central mediator of both osteoclast (OC) development and bone resorption. PLC γ 2 is activated downstream of RANK and α v β 3 integrin to generate IP3 and diacylglycerol (DAG). The relative contribution of these second messengers is not completely understood; in particular, the role of DAG in OC formation and function is unclear, in part due to the impossibility of direct genetic manipulation of DAG. To gain more insight into the role of DAG in the OC, we turned to the diacylglycerol kinase (DGK)- ζ $-/-$ mice, which accumulate DAG due to lack of DGK ζ -mediated DAG turnover. In contrast to osteopetrotic PLC γ 2 $-/-$ mice (decreased DAG), we find that DGK ζ $-/-$ mice (increased DAG) are osteopenic by 4 weeks of age (BV/TV: WT=14.4; KO=8.4 $p=0.003$). DGK ζ $-/-$ mice have fewer trabeculae and significant erosion of cortical bone owing to an increase in OC number. DGK ζ $-/-$ bone marrow macrophages (BMM) cultured with MCSF and RANKL form more OC than WT with enhanced mRNA expression of common OC markers. DGK ζ $-/-$ OC plated on bone in equal number as WT cells also display increased resorptive activity (pit area: WT=29.4; KO=66.2 $p=0.03$), indicating a critical role of DAG in both OC formation and function. To further characterize downstream signaling, we investigated DAG-dependent pathways in DGK ζ $-/-$ cells. We found that phosphorylation of protein kinase C (PKC)- δ , a DAG-dependent kinase, is enhanced in DGK ζ $-/-$ BMM compared to WT. PKC δ is also activated in OC plated on bone. Deletion of the DAG-dependent effector PKC δ leads to 397% increase in BV/TV compared to WT at 6 weeks of age, supporting the conclusion that DAG accumulation is responsible for the osteopenic phenotype of DGK ζ $-/-$ mice. PKC δ $-/-$ mice continue to maintain high bone mass with age and are protected from bone loss after ovariectomy (% loss: WT=29.53; KO=8.95 $p=0.002$). This phenotype is not due to a defect in OC formation, as PKC δ $-/-$ mice have similar numbers of OC as WT *in vivo* and *in vitro*. Instead, we found that PKC δ $-/-$ OC fail to resorb bone (pit area: WT=28.75; KO=6.82 $p=0.008$). Despite forming normal actin rings and ruffled borders, PKC δ $-/-$ OC cultured on bone fail to localize Cathepsin K vesicles within the resorptive lacunae. Altogether, our findings indicate that DAG initiates distinct pathways in the OC: a PKC δ -independent mechanism of OC formation and a PKC δ -dependent mechanism of bone resorption.

Disclosures: Corinne Decker, None.

FR0284

Dual Osteoclast Precursor and Suppressor Function of a Ly6C^{hi} Population Increased in Murine Inflammatory Arthritis. Julia Charles^{*1}, Lih-Yun Hsu², Erene C. Niemi², Arthur Weiss², Mary Nakamura². ¹University of California, San Francisco & VA Medical Center, USA, ²University of California, San Francisco, USA

We have identified a CD11b^{lo} Ly6C^{hi} bone marrow population with osteoclast precursor activity that is increased in murine autoimmune arthritis. CD11b^{lo} Ly6C^{hi} cells isolated from bone marrow by fluorescence activated cell sorting contain the majority of osteoclast precursor (OCP) activity present in bone marrow, and colonies expanded from single cells retain the ability to differentiate into osteoclasts. OCP are further defined by the markers CX3CR1⁺ CCR2⁺ CD135^{lo} CD115⁺ CD11c⁻ and are distinct from previously characterized myeloid precursors, suggesting that osteoclasts derive from a distinct precursor analogous to the common dendritic cell precursor. OCP have features of both M1 and M2 monocytes and are significantly increased in inflammatory arthritis. However, further increasing OCP number in inflammatory arthritis by adoptive transfer does not increase erosive disease, but instead decreases arthritis severity. Using the adoptive transfer model of SKG arthritis, we find that co-adoptive transfer of OCP with SKG CD4⁺ T-cells into RAG^{-/-} recipients ameliorated inflammatory arthritis compared to transfer of CD4⁺ T-cells alone, suggesting OCP might have suppressive function. Isolated OCP robustly suppress *in vitro* antibody-stimulated T-cell proliferation, and share characteristics with previously described monocytic myeloid derived suppressor cells (M-MDSC), including monocytic morphology, CD49d and CD124/IL4R α expression. Using antibody blockade, genetically deficient animals, and enzyme inhibitors, we show that suppression by OCP is dependent on IFN γ and NOS2, similar to the mechanism described for M-MDSC. Our findings suggest that a myeloid precursor population with both T-cell suppressive activity and the potential to become osteoclasts is expanded in inflammatory arthritis.

Disclosures: Julia Charles, None.

FR0285

Dynamic *in vivo* Imaging of Bone-Resorptive Functions of Mature Osteoclasts in Live Bones By Using Intravital Two-Photon Microscopy. Junichi Kikuta^{*1}, Yoh Wada², Masaru Ishii¹. ¹Immunology Frontier Research Center, Osaka University, Japan, ²Institute of Scientific & Industrial Research, Osaka University, Japan

Osteoclasts are bone-resorbing giant polykaryons that differentiate from mononuclear macrophage/monocyte-lineage hematopoietic precursors. Upon the stimulation of essential factors such as M-CSF and RANKL, monocytoïd cells isolated from bone marrow can successfully be differentiated into multinucleated cells *in vitro*, called 'osteoclast-like cells', which often contain more than one hundred nuclei. However it remains unclear whether such extraordinarily large polykaryons are formed *in vivo* and how the activity of osteoclasts is controlled *in vivo* once they form. To answer these questions, we utilized an advanced imaging system for visualizing live bone tissues with intravital two-photon microscopy that we have recently established.

Fully differentiated osteoclasts form an extracellular compartment ('resorption lacunae') between the plasma membrane ('ruffled border') and the bone surface. A large number of vacuolar type H⁺-ATPases (V-ATPase) are specifically expressed along the ruffled border membrane to keep highly acidic conditions in resorption pit. V-ATPase consists of multiple subunits and each subunit has several isoforms. Among them the $\alpha 3$ isoform of 'a subunit' is specifically expressed in osteoclasts. To label mature osteoclasts fluorescently, we generated mice in which $\alpha 3$ subunit-GFP fusion proteins are expressed under the original promoter of the $\alpha 3$ subunit ($\alpha 3$ -GFP knock-in mice).

By using intravital two-photon microscopy of calvaria bone tissues of $\alpha 3$ -GFP knock-in mice, we have succeeded in visualization of live mature osteoclasts on the bone surface. Because GFP is expressed as a fusion protein with $\alpha 3$ subunit, GFP fluorescence not only serves as a marker for mature osteoclasts, but it provides information on the subcellular distribution of V-ATPase in osteoclasts. We identified two different populations of live mature osteoclasts on the bone surface, such as 'static - bone resorptive' and 'moving - non resorptive' ones. Furthermore treatment with recombinant RANKL or bisphosphonate (risedronate) changed the composition of these two populations as well as total number of mature osteoclasts. These approaches would be quite beneficial for studying the osteoclast dynamics *in vivo* and thus useful also for evaluating novel anti-bone resorptive drugs currently developed in the world.

Disclosures: Junichi Kikuta, None.

FR0287

Identification and Characterization of OCAN, a Novel Osteoclastogenic Co-activator for NFATc1. Min-Young Youn^{*}, Sally Fujiyama-Nakamura, Yuuki Imai, Shigeaki Kato. The University of Tokyo, Japan

Osteoclastogenesis is the highly regulated process governed by diverse transcriptional factors. Among them, NFATc1 is a prime transcriptional factor throughout osteoclastogenesis. During differentiation stages, NFATc1 can interact with

epigenetic factors to regulate a particular set of target genes at each stage, indicating that distinct epigenetic complexes contribute to the spatiotemporal regulation of each gene expression by NFATc1 during osteoclastogenesis. However, epigenetic complexes assisting transcriptional activity of NFATc1 during osteoclastogenesis remain to be identified. To address this issue, we tried to biochemically purify epigenetic regulators associating with NFATc1. Nuclear extracts prepared from RANKL-induced Raw264 cells were applied into NFATc1-antibody column, and then candidate proteins were identified by MALDI-TOF/MS analysis. Among several identified factors, we focused on an uncharacterized protein 'osteoclastogenic co-activator for NFATc1 (designated as OCAN)', which has shown relatively high expression in osteoclasts. Simultaneously, Brg1 and Baf proteins involved in SWI/SNF-type chromatin remodeler complex were purified with OCAN. These physical interactions were also confirmed by co-immunoprecipitation experiment, suggesting that OCAN is a novel component of SWI/SNF-type chromatin remodeler complex in osteoclasts to support NFATc1 function. To uncover the function of OCAN, transcriptional activity of NFATc1 with OCAN over-expression was examined by luciferase assay. Interestingly, its transcriptional activity was enhanced by OCAN over-expression. Consistently, OCAN knockdown resulted in decreased expression of osteoclast-specific genes, such as Ctsk and TRAP, with inhibiting osteoclast formation. These results indicate that OCAN plays a role as a co-activator of NFATc1 during osteoclastogenesis. To define the molecular mechanism of OCAN, the recruitment of NFATc1 on promoters of its target genes was detected with ChIP assay. NFATc1 could not be recruited on its target genes without OCAN protein. Similarly, recruitment of Brg1 was reduced in OCAN-knockdown cells. Taken together, OCAN can be considered as a novel component of a SWI/SNF-type chromatin remodeler complex to reorganize the chromatin status for DNA-binding ability of NFATc1. Generation of the osteoclast-specific OCAN knockout mice must help to clarify the physiological function of OCAN in bone metabolism *in vivo*.

Disclosures: Min-Young Youn, None.

FR0289

Microtubule Contribution to Osteoclastogenesis – Stathmin Deficiency Induces Low Bone Mass In Mice by Increasing Osteoclastogenesis. Hongbin Liu^{*1}, Rongrong Zhang¹, Babatunde Oyajobi², Hong-Wen Deng¹, Ming Zhao¹. ¹Tulane University, USA, ²University of Texas Health Science Center at San Antonio, USA

The small cytosolic phosphoprotein, stathmin is a ubiquitous endogenous microtubule regulating protein that inhibits microtubule assembly and disrupts microtubule network within cells. In this study, we investigated the skeletal phenotype of mice engineered to be deficient in stathmin, particularly focusing on osteoclastogenesis. The global stathmin knockout mice, in which exons 2 and 3 of stathmin gene were removed, were maintained as heterozygotes on a C57BL/6 background and the bone phenotype of homozygous mutant mice and their wild-type littermates were examined at two months of age. μ CT and histological analyses revealed a substantial reduction in bone mass in stathmin-deficient mice compared with control age-matched littermates, as evidenced by decreased bone mineral density, trabecular bone volume, trabecular thickness, trabecular number and increased trabecular separation in long bones. Histomorphometry showed that deletion of the stathmin gene promoted osteoclast formation, as evidenced by increased number of TRAP positive multi-nucleated cells and increased bone resorptive surface in metaphysis. Real time PCR showed that the mRNA levels of osteoclast marker genes, including Rank, Rankl, Atp6, Ctsk, were all significantly increased in bone tissues from stathmin knockout mice, compared to their wild-type littermate controls. This was accompanied by a decrease in Opg level, which in turn resulted in an increase in Rankl/Opg ratio. The increase in expression of osteoclast markers RANKL and CTSK in stathmin-deficient bone tissues was further confirmed immunohistochemically. These results suggest that stathmin deficiency in bone induces osteoclastogenesis. To further confirm a role for stathmin in regulating osteoclast formation, stathmin was overexpressed in osteoclast progenitor RAW264.7 cells and normal primary bone marrow-derived cells and this resulted in significantly reduced formation of TRAP positive osteoclasts in culture. The reduction in osteoclast formation in RAW264.7 cells overexpressing stathmin was associated with marked disruption in the microtubule filament structure detected by immunofluorescence. Together, the findings from these loss- and gain-of-function studies demonstrate that the microtubule targeting protein stathmin is an endogenous inhibitor of osteoclastogenesis, and suggest that microtubules play an essential role in osteoclastogenesis and maintenance of postnatal bone mass.

Disclosures: Hongbin Liu, None.

FR0290

Molecular Basis of the Requirement of RANK Signaling for Interleukin-1 (IL-1)-Mediated Osteoclastogenesis. Joel Jules^{*}, Jason Ashley, Ping Zhang, Shi Wei, Zhenqi Shi, Jianzhong Liu, Suzanne Michalek, Xu Feng. University of Alabama at Birmingham, USA

Interleukin-1 (IL-1), a proinflammatory cytokine, plays a crucial role in immune and inflammatory responses. However, IL-1 production is markedly elevated in various pathological conditions and deregulation of IL-1 expression has been implicated in the pathogenesis of postmenopausal osteoporosis and inflammatory

bone loss associated with rheumatoid arthritis (RA) and periodontitis. IL-1 induces bone loss by stimulating the formation, survival, and function of osteoclasts. While IL-1 can directly target mature osteoclasts to prolong survival and activate function, this cytokine can only promote osteoclastogenesis in the presence of permissive levels of RANKL. However, the precise molecular mechanism underlying the requirement of RANKL for IL-1-mediated osteoclastogenesis has not been fully elucidated. In this study, we show that while IL-1 is unable to activate the expression of the genes encoding matrix metalloproteinase 9 (MMP9), cathepsin K (Ctsk), tartrate-resistant acid phosphatase (TRAP) and carbonic anhydrase II (Car2) in bone marrow macrophages (BMMs), RANKL renders these osteoclast genes responsive to IL-1. RANK, the receptor for RANKL, has an IVVY535-538 motif which commits BMMs to the osteoclast lineage in RANKL- and tumor necrosis factor- α (TNF)-mediated osteoclastogenesis. Here, we further demonstrate that the IVVY motif also controls the RANKL-induced osteoclast lineage commitment in IL-1-mediated osteoclastogenesis by changing osteoclast genes to an IL-1-inducible state. Mechanistically, while IL-1 alone fails to induce the BMM expression of NFATc1, a master transcriptional regulator of osteoclastogenesis, this cytokine can up-regulate NFATc1 expression in BMMs in the presence of permissive levels of RANKL or with RANKL pretreatment. Moreover, the IVVY motif is specifically involved in rendering the NFATc1 gene responsive to IL-1. Finally, we show that MyD88, a known critical component of the IL-1R signaling pathway, plays a crucial role in IL-1-mediated osteoclastogenesis from RANKL-primed BMMs by up-regulating the expression of NFATc1 and the four osteoclast genes (MMP9, Ctsk, TRAP and Car2). These findings provide important new insights into the molecular basis of the dependence of IL-1-mediated osteoclastogenesis on RANKL. Significantly, the IVVY motif, due to its critical role in IL-1- and TNF-mediated osteoclastogenesis, has the potential to serve as a therapeutic target for bone disorders such as osteoporosis, RA and periodontitis.

Disclosures: Joel Jules, None.

FR0291

NIBP: A Novel Regulator of Osteoclast Differentiation and Function. Kevin Crawford¹, Joyce Belcher², Roshanak Razmpour¹, Yonggang Zhang³, Wen-Hui Hu³, Steven Popoff¹, Fayez Safadi¹. ¹Temple University School of Medicine, USA, ²Temple University, School of Medicine, USA, ³Temple University School of Medicine Department of Neuroscience, USA

NF- κ B (Nuclear Factor of activated B cells) is a family of transcription factors involved in a number of different clinical pathologies. In bone, NF- κ B is involved in osteoclast differentiation upon stimulation with the RANKL. NIBP (NIK and IKK β Binding Protein) also known as TRAPPC9 (Trafficking Protein Particle Complex 9), is a novel upstream regulator of the NF- κ B pathway. NIBP enhances NF- κ B activity by binding to NIK (NF- κ B Inducing Kinase) and IKK β (a I κ B kinase subunit) in multiple cell types. Mutations in the NIBP gene in human have been associated with mental retardation and postnatal microcephaly. To date, NIBP expression has been identified in several cell types; however, its expression and function in bone is unknown. In this study, we identify the expression of NIBP in osteoclasts, and examine its regulatory role in osteoclast differentiation and function. Immunohistochemical staining of NIBP in mouse embryo (e 14.5) and mouse femur (12 week) identify protein expression in osteoclasts, osteoblasts, and chondrocytes. Cultured bone marrow osteoclasts from 8 week-old C57Black6 mice were differentiated in the presence of RANKL and M-CSF. Immunofluorescent staining shows NIBP is localized in the cytoplasm of osteoclasts, particularly in perinuclear regions suggesting its role as a trafficking protein.

Next, we examined the temporal expression pattern of NIBP during osteoclast differentiation. NIBP expression was highest during mature stages of osteoclast differentiation. Similar pattern of expression was also observed in the RAW264.7 cell line. To determine the functionality of NIBP in vitro, loss of function experiments using shRNA specific for NIBP in the RAW264.7 cells showed that knocking down NIBP inhibits osteoclast differentiation and function determined by TRAP positive multinucleated osteoclasts. In addition, we have utilized a Tamoxifen inducible Cre-Lox NIBP knockdown approach. Bone marrow osteoclast derived from the cre (control) and cre-lox mice and treated with Tamoxifen ex vivo, only the cre-lox (NIBP knockdown) osteoclast exhibited impaired differentiation and function. These results suggest NIBP plays a critical role in osteoclast differentiation and function. Taken together, further studies are warranted to elucidate the functional role of NIBP in osteoclast differentiation and function in vivo.

Disclosures: Kevin Crawford, None.

FR0292

Osteoclasts in Bone Modeling, As Revealed By In Vivo Imaging, Are Essential for Organogenesis in Fish. Masahiro Chatani¹, Yoshiro Takano², Akira Kudo¹. ¹Tokyo institute of technology, Japan, ²Tokyo Medical & Dental University, Japan

The organs, nerves, blood vessels, bones, etc. grow with an increase in body size from birth to adult. Bone modeling is the central system controlling the formation of bone including bone growth and shape in early development, in which bone is continuously resorbed by osteoclasts and formed by osteoblasts. However, this system has not been well documented, because it is difficult to trace osteoclasts and osteoblasts in vivo during development. Here we showed the important role of

osteoclasts in organogenesis by establishing osteoclast-specific transgenic medaka lines and by using a zebrafish osteoclast-deficient line. Using in vivo imaging of osteoclasts in the transgenic medaka carrying an enhanced GFP (EGFP) or DsRed reporter gene driven by the medaka TRAP (Tartrate-Resistant Acid Phosphatase) or Cathepsin K promoter, respectively, we examined the maturation and migration of osteoclasts. Our results showed that osteoclasts in the vertebral body were specifically localized at the inside of the neural and hemal arches, but not at the vertebral centrum, as flat-shaped multinucleated cells that had initially differentiated from TRAP- or cathepsin K-positive mononuclear cells residing around bone. These mononuclear cells became multinucleated and then later died by apoptosis on the bone surface. The zebrafish panther mutant lacks a functional c-fms (receptor for macrophage colony-stimulating factor) gene crucial for osteoclast proliferation and differentiation and thus has a low number of osteoclasts. Analysis of this mutant revealed deformities in both its neural and hemal vertebral arches, which resulted in abnormal development of the neural tube and blood vessels located inside these arches. Our results provide the first demonstration that bone resorption during bone modeling is essential for proper development of neural and vascular systems associated with fish vertebrae.

Disclosures: Masahiro Chatani, None.

FR0293

Runx-related transcription factor 1 (Runx1) Regulates Macrophage/Osteoclast Lineage Commitment and Osteoclast Differentiation. Wei Chen, Yi-Ping Li^{*}. University of Alabama at Birmingham, USA

Despite the recent insights gained from the effects of targeted deletion of the c-fos, PU.1, NF- κ B, and NFATc1 transcription factor genes, further study is needed to define the mechanism underlying why M-CSF alone induces precursors to differentiate into macrophage while both M-CSF and RANKL induce precursors to differentiate into osteoclasts.

The cathepsin K critical cis regulatory element (CCRE) that responds to M-CSF/RANKL stimulation was analyzed using the CAT assay. We used livers derived from E12.5 Runx1^{+/+}, Runx1^{-/-}, and PU.1^{-/-} embryos as a source of myeloid cells with M-CSF and RANKL stimulation for osteoclast differentiation analysis. Runx1 expression was knocked down by lentivirus-mediated shRNA in mouse bone marrow cells (MBM) induced by M-CSF/RANKL. In addition, we forced expression of Runx1 in WT MBM cells and RAW264.7 cells induced with varying doses of RANKL. Western blot, Northern blot, RT-PCR, and immunohistochemical staining were used to characterize the expression of Runx1, PU.1, and Nfatc1. We used nonspecific esterase staining and immunostaining of CD11b and F4/80 antibodies to determine monocyte/macrophage formation. Osteoclast formation, acid production, and resorption pits were evaluated by TRAP, acridine orange, and a scanning electronic microscope respectively.

Our results revealed that Runx1 is a trans-regulatory factor of the cathepsin K CCRE. Runx1 expression is only induced by the simultaneous application of M-CSF and RANKL. Knockout of Runx1 impaired commitment and differentiation of both the osteoclast and monocyte/macrophage lineages. However, Runx1 RNAi knock-down *in vitro* impaired osteoclast differentiation, activation, and function, but had no effect on monocyte/macrophage differentiation. Forced expression of Runx1 increased osteoclast differentiation. Neither Runx1 nor PU.1 was detected in Runx1^{-/-} cultured myeloid cells, but Runx1 expression was normal in PU.1^{-/-} cultured myeloid cells.

In conclusion, the presence of RANKL and M-CSF together cause higher levels of Runx1, which promotes osteoclast commitment and differentiation. Thus, Runx1 may be a key regulator for osteoclast differentiation, functioning downstream of RANKL. Runx1 potentially controls osteoclast cell lineage commitment and regulate osteoclast gene expression and differentiation through up-regulating PU.1 and NFATc1. These results may provide additional targets for therapeutic intervention in diseases of excessive bone resorption

Disclosures: Yi-Ping Li, None.

FR0299

IL-17 Mediates Estrogen-deficient Osteoporosis. Carl DeSelm¹, Yoshifumi Takahata², Jean Chappel², Taimur Khan², Xiaoxia Li³, Wei Zou⁴, Steven Teitelbaum⁴. ¹Washington University School of Medicine, USA, ²Washington University in St. Louis, USA, ³Cleveland Clinic, USA, ⁴Washington University in St. Louis School of Medicine, USA

Estrogen-deficient osteoporosis may be an inflammatory disorder and we therefore asked if IL-17 participates in its pathogenesis. Deletion of the principal IL-17 receptor, (IL-17RA) protects mice from ovariectomy (OVX)-induced bone loss. Further supporting a central role of IL-17 in its pathogenesis, OVX-induced osteoporosis is prevented by a blocking antibody targeting the cytokine. The source of IL-17 is likely IL-17-expressing NK1.1 cells as they increase 10 fold within the marrow following OVX. IL-17 promotes osteoclastogenesis by stimulating RANK ligand (RANKL) expression by osteoblastic cells, mediated by the IL-17RA SEFIR/TILL domain which recruits the adaptor protein and E3 ubiquitin ligase, Act1. Similar to IL-17RA^{-/-} mice, those lacking Act1 are protected from OVX-induced bone loss. Also mirroring IL-17RA-deficiency, absence of Act1 in osteoblasts, but not osteoclasts, impairs osteoclastogenesis via dampened RANKL expression. While transduction of WT Act1 into Act1^{-/-} osteoblasts substantially rescues their

osteoclastogenic capacity, the same construct, lacking its SEFIR domain or ubiquitinating U-box, fails to do so. These data suggest NK cell-produced IL-17 and its effector molecules are candidate therapeutic targets in post-menopausal osteoporosis.

Disclosures: Carl DeSelm, None.

FR0303

The ADP receptor P2Y₁₂ Regulates Osteoclast Function and Pathologic Bone Loss. Xinming Su^{*1}, Desiree Floyd², alun hughes³, Kaiming Wu², Ozge Uluckan², Sarah Townsley², Angela Hirbe², Jochen Schneider⁴, Emanuella Heller², Michelle Hurchla², Hongju Deng³, Mark Eagleton², Deborah Novack⁵, Pamela Conley², Michael Rogers³, Katherine Weilbaecher⁵. ¹Washington University in Saint Louis, USA, ²Washington University in St. Louis, USA, ³University of Aberdeen, United Kingdom, ⁴Washu, USA, ⁵Washington University in St. Louis School of Medicine, USA

The ADP receptor P2Y₁₂ plays a critical role in platelet aggregation and microglial migration, and P2Y₁₂ inhibitors are clinically used to prevent cardiac and cerebral thrombotic events. ADP has been shown to increase osteoclast (OC) activity, but the expression and function of P2Y₁₂ in OC biology has not been evaluated. Mice lacking P2ry12 had increased bone mass and decreased serum levels of osteoclast activity marker, CTX, and were partially protected from age associated bone loss compared to littermate controls. We found that P2Y₁₂ was expressed in developing OCs. Loss of P2ry12 resulted in delayed OC formation, Exogenous ADP enhanced WT OC formation but had little effect on P2ry12^{-/-} OCs. In the presence of ADP, P2ry12^{-/-} OCs had impaired adhesion and bone resorption pit formation compared to P2ry12^{+/+} OCs. Ligation of the P2Y₁₂ receptor results in the activation of the alpha IIb beta 3 platelet integrin through Rap1 phosphorylation. Likewise, P2ry12^{-/-} OCs had decreased Rap1 phosphorylation in response to ADP stimulation compared to WT OCs. Expression levels of Rap1 family genes and P2ry1 were not significantly different between P2ry12^{-/-} and WT OCs. Evaluation of OC mediated pathologic bone loss demonstrated that P2ry12^{-/-} mice were partially protected from osteolysis associated with serum transfer arthritis and tumor growth in bone. Wild-type mice administered the clinical therapeutic P2Y₁₂ inhibitor, clopidogrel, had modest increases in trabecular bone volume compared to vehicle-treated mice. These results demonstrate a role for exogenous ADP and the ADP receptor P2Y₁₂ in OC-mediated bone resorption and suggest that ADP and P2Y₁₂-targeted therapies may affect bone mass and prevent pathologic bone loss.

Disclosures: Xinming Su, None.

FR0305

P²¹Ras Mediated Activation of PI3K Results in Enhanced Survival of Osteoclasts in the Absence of Cbl-PI3K Interaction Independent of Cbl-b. Nagasuresh Adapala^{*1}, Alexander Tsygankov², Mary Barbe³, Archana Sanjay³. ¹University of connecticut health center, USA, ²Temple University, USA, ³Temple University School of Medicine, USA

Cbl and Cbl-b are E3 ubiquitin ligases and adaptor proteins required for normal osteoclast (OC) survival and function. Cbl interacts with PI3K upon phosphorylation of tyrosine-737 in YEAM motif, which is absent in Cbl-b. Loss of Cbl-PI3K interaction due to Y737F mutation in mice led to enhanced OC survival, but defective resorption, whereas loss of Cbl-b resulted in hyperresorptive OCs suggesting that Cbl and Cbl-b perform very distinct roles in OCs. To investigate if Cbl-b affects survival mediated by Cbl-PI3K interaction and whether defective function due to YF mutation can negate hyperresorption by Cbl-bKO OCs, we generated Y737F mice lacking Cbl-b (CYB mice). Following RANK stimulation, Cbl-PI3K interaction leads to PI3K activation which promotes OC survival. Paradoxically, loss of this interaction resulted in enhanced PI3K activity in both YF and CYB as reflected by increased AKT phosphorylation, along with enhanced RANK signaling leading to increased ERK phosphorylation, suggesting hyperactivation of Ras-Raf-1 pathway. PI3K is a major substrate of Ras and co-IP with p85 subunit of PI3K showed more Ras-PI3K binding in YF and CYB OCs, compared to WT and Cbl-bKO OCs. In addition, Ras GTPase activity in response to RANKL was also increased in both YF and CYB OCs. Ras inhibition by FPT III resulted in decreased ERK activation in both CYB and WT OCs but PI3K activity was inhibited only in CYB OCs suggesting that when unsequestered by Cbl, PI3K becomes available for activation by Ras independent of Cbl-b. Increased PI3K activity in CYB OCs resulted in increased survival and Ras inhibition abrogated enhanced survival of CYB OCs (%TUNEL+: 24.2 7.3; FPTIII: 76.2 5), but not in WT OCs (%TUNEL+: 42.6 5.4; FPTIII: 41.1 8.3). While Cbl-b did not influence OC survival, it negatively regulated bone resorption. In contrast to WT and YF OCs both CYB and Cbl-b KO OCs were hyperresorptive and their resorption ability was comparable (pit area/OC: WT 0.660.02; CYB 1.430.28; Cbl-bKO 1.630.01). The increased OC function resulted in decreased bone volume in CYB mice (BV/TV% 6.40.1) compared to WT (% 8.20.1) suggesting that defective OC function due to CblYF mutation does not rescue increased bone resorption caused by the loss of Cbl-b in CYB mice. Therefore, Cbl modulates PI3K availability preventing excessive activation by Ras thus controlling OC survival whereas Cbl-b negatively regulates bone resorption, which is not affected by loss of Cbl-PI3K interaction.

Disclosures: Nagasuresh Adapala, None.

FR0306

Selective Deletion of Rac1 and Rac2 in Mature Osteoclasts Results in Osteopetrosis, Failed Tooth Eruption and Defects in both Osteoclast and Osteoblast Function. Meiling Zhu^{*1}, Ben-hua Sun¹, Katarzyna Kolodziejczak¹, Karl Insogna². ¹Yale University, USA, ²Yale University School of Medicine, USA

Rac plays a central role in mediating cytoskeletal reorganization and bone resorption in osteoclasts. There are three Rac isoforms 1, 2 and 3. Rac1 and Rac2 are the two isoforms expressed by osteoclasts but their roles in regulating mature osteoclast function have not been well-defined. It has been reported that Rac2^{-/-} mice grow normally and have normal tooth eruption but have increased bone mass despite greater numbers of osteoclasts (OCs) in bone. Rac2^{-/-} OCs have an abnormal actin cytoskeleton and reduced resorptive activity in vitro. We have generated mice with selective deletion of Rac1 in mature OCs (Rac1-OC^{-/-}) by crossing Rac1^{fllox/fllox} mice with mice expressing Cre under the control of the cathepsin K promoter. These mice have normal BMD by DXA and normal tooth eruption when studied up to 2 months of age. Rac1-OC^{-/-} mice were crossed with Rac2^{-/-} animals to generate mice with selective deletion of both isoforms in mature OCs (DKO). DKO mice were small and either toothless or had markedly delayed tooth eruption. Compared to CTRL animals, DKO mice had significantly higher BMD by DXA at all measured sites: +33% at the spine (P<0.05), +21% at the femur, and +24% (P<0.001) for total body (p<0.001). DKO mice had a 15% lower mean body weight and when normalized to weight, the differences in BMD were magnified: +59% at the spine, +45% at the femur and +49% for total body BMD (p<0.0001 for each site). Bone histology revealed a marked increase in metaphyseal trabecular bone in the DKO mice extending well into the diaphysis of the femur. In contrast, the cortices were thin and porous in these animals. Consistent with this latter finding, μ CT analysis showed a marked reduction in cortical bone volume (-89%; p= 0.002). Histomorphometric analysis showed a significant reduction in OcS/BS (-35%) and Noc/BPm (-34%) in DKO animals but also in Obs/BS (-45%), Nob/Opm (-23%) and OS/BS (-32%); p \leq 0.05 for each. Serum CTX was 52% lower than CTRL mice (p<0.01). DKO OCs had markedly impaired actin ring formation with only 18% of DKO OCs able to form actin rings, while 87% of wild type cells had normal actin ring formation. In an initial experiment, osteoblasts isolated from DKO animals were able to mineralize normally in vitro suggesting that reduction on bone formation in vivo was secondary to an osteoclast-induced defect in bone modeling/remodeling. These data highlight the complementary and critical roles of Rac1 and Rac2 in skeletal metabolism.

Disclosures: Meiling Zhu, None.

FR0307

The Rho-GEF Kalirin Regulates Dynamin's GTPase Activity and Osteoclast Function. Pierre Eleniste^{*}, Su Huang, Heather Largura, Angela Bruzzaniti. Indiana University School of Dentistry, USA

Dysregulated osteoclast activity can lead to bone loss and osteoporosis. Kalirin, a Rho GDP-GTP exchange factor (GEF), plays a key role in cytoskeletal organization and dendritic synapse formation in hippocampal neurons. Three major kalirin isoforms have been reported (Kal7, Kal9 and Kal12) which potentially have unique cellular functions. We recently found that global deletion of kalirin in mice leads to a decrease in bone mass, in part due to increased osteoclast (OC) differentiation and bone resorbing activity. However the mechanism of action of Kalirin in OCs and the signaling pathways that regulate OC function are unknown. Dynamin is a GTP-hydrolyzing protein that functions in actin cytoskeletal remodeling and endocytosis. Previously, we reported that dynamin stimulates OC bone-resorbing activity in a GTPase-dependent manner. Dynamin exists as a monomer, dimer or tetramer in solution, and liposomes induce the tetrameric form of dynamin, which further increases its GTPase activity and is essential for its role in endocytosis. However, the function of the monomeric or dimeric forms of dynamin are unknown. In this study, we sought to further examine the role of dynamin and Kalirin in OCs and to determine if Kalirin regulates the GTPase activity of dynamin. We coexpressed wild-type dynamin or the assembly-defective mutant (dyn-I684K) in the presence or absence of different Kalirin isoforms in HEK293cells stably expressing the vitronectin receptor (293VnR). Dynamin was immunoprecipitated and its activity determined using a calorimetric GTPase assay in vitro. Our data revealed that the GTPase activity of wild-type dynamin was differentially regulated by the Kalirin isoforms. Moreover, a GEF-inactive Kal7 mutant stimulated dynamin's activity to a much greater extent than active Kal7, suggesting that kalirin GEF activity may also important for regulating dynamin function. We next examined the role of Kalirin in the assembly-stimulated increase in dynamin GTPase activity. As expected, the GTPase activity of assembly-defective dyn-I684K was significantly lower than WT dynamin. However, the activity of dynamin-I684K was increased close to wild-type levels by GEF-inactive Kal7. In contrast, Kal12 failed to stimulate dyn-I684K GTPase activity. Thus, our data indicate that Kalirin influences dynamin's basal GTPase activity and potentially its oligomerization which may control dynamin's effects on actin remodeling, endocytosis and OC bone resorbing activity.

Disclosures: Pierre Eleniste, None.

FR0309

Constitutive Protein Kinase A Activities in Osteocytes Leads to Increased Bone Formation without Increased Bone Resorption. Richard Kao^{*1}, Wei-Dar Lu², Dylan O'Carroll², Peter Mailhot², Robert Nissenson³. ¹UCSF/VAMC, USA, ²VA Medical Center, USA, ³VA Medical Center & University of California, San Francisco, USA

Osteocytes have been implicated in regulating the rate of bone formation. However, the signal transduction pathways that regulate the physiological function of osteocytes are poorly defined. Limited evidence suggests an important role for the cAMP/PKA pathway in osteocyte function. We explored the hypothesis that PKA activation in osteocytes plays a key role in controlling skeletal homeostasis. To test this hypothesis, we mated mice harboring a Cre-conditional, mutated PKA catalytic subunit allele that encodes a constitutively-active form of PKA (CA-PKA) with mice expressing Cre under the control of the osteocyte-specific promoter, DMP1. This allowed us to direct the expression of CA-PKA to osteocytes in double transgenic progeny. Expression of CA-PKA in osteocytes produced significant increases in periosteal (+8.5%, $p < 0.01$) and endosteal (+20.8%, $p < 0.01$) perimeters of the region proximal to the tibio-fibular junction (TFJ) in 3-month old female mice, as assessed by static histomorphometry. In the distal femur, trabecular bone volume over total volume (+146.8%, $p < 0.01$), trabecular thickness (+28.7%, $p < 0.05$), and trabecular number (+78.7%, $p < 0.01$) all significantly increased compared to sex-matched littermate controls. Dynamic histomorphometry demonstrated increased endocortical bone formation rate per bone surface (BFR/BS; +132.3%, $p < 0.001$) as well as increased periosteal mineral apposition rate (+68.2%, $p < 0.05$) in the cortical bone proximal to the TFJ. Trabecular BFR/BS (+30.6%, $p < 0.05$) in the distal femur also significantly increased. Elevated serum alkaline phosphatase (ALP) levels (+30.5%, $p < 0.05$) corroborated the dynamic histomorphometric results. Analysis of whole bone transcript levels of osteoblast and osteocyte marker genes detected significantly up-regulated expression of *runx2* and *collagen 1a1*. On the other hand, serum levels of pyridinoline were unchanged, and the ratio of the transcript levels of *RANKL:OPG* was not significantly altered. Indeed, the percent osteoclast surface/bone surface (-25.9%, $p < 0.01$) was reduced. In summary, constitutive PKA signaling in osteocytes increased cortical and trabecular bone formation. This was associated with up-regulation of serum ALP and genes associated with osteoblast differentiation. No evidence for changes in bone resorption was detected. We conclude that constitutive PKA signaling in osteocytes can increase bone formation without an accompanied increase in bone resorption.

Disclosures: Richard Kao, None.

FR0310

Estrogen Receptor α (ER α) Expression in Osteocytes is Necessary to Maintain Normal Bone Mineral Density (BMD) and Reduce Bone Loss due to Unloading. Yuuki Imai¹, Lynda Bonewald², Shino Kondoh^{*1}, Shigeaki Kato¹. ¹The University of Tokyo, Japan, ²University of Missouri - Kansas City, USA

Estrogen is thought to be a viability factor for cells of the osteoblast lineage and is also thought to increase bone mechanosensitivity so that bone responds more favorably to loading. Osteocytes make up more than 90-95% of cells in adult bone where they are thought to function as mechanosensors. To determine the role of estrogen in osteocytes, ER α was deleted in late osteoblasts/osteocytes by crossing ER α floxed mice with Cre recombinase expressing mice driven by the *Dmp1* promoter (cKO). BMD of 12-week-old female cKO mice was significantly decreased at the proximal tibia compared to control mice (-5.6%, $p < 0.05$ DXA, -10.1%, $p < 0.01$ μ CT). To further explore the cellular basis for the bone loss seen in the cKO, dynamic bone histomorphometry was performed showing that the number of osteoblasts (-46.5%, $p < 0.005$), osteoblast surface (-41.6%, $p < 0.001$) and bone formation rate (-11.3%, $p < 0.05$) in cKO were significantly decreased, as was the number of osteocytes/area (-16.0%, $p < 0.05$). Bone resorption parameters such as osteoclast numbers or surfaces were not altered which was consistent with the observation that TUNEL staining for osteoblast/osteocyte apoptosis was not significantly different between control and cKO. This was unexpected as estrogen is thought to be a viability factor for osteocytes and that apoptotic osteocytes send signals to initiate osteoclastic bone resorption. These data suggest other functions for estrogen during osteoblast to osteocyte differentiation and of an osteoprotective function by maintaining positive signals from osteocytes to osteoblasts.

Estrogen/ER α signaling is known to be involved in mechanosensing and increasing bone formation under loading conditions. Also, it is reported that tail suspension induced bone loss is significantly enhanced by ovariectomy. To determine if ER α in osteocytes plays a role in bone loss due to unloading, tail suspension experiments were performed starting at 8 weeks of age for 4 weeks. Tail suspension induced bone loss in the femoral diaphysis of cKO female mice greater than that of control mice (% reduction: -5.06.7% control, -12.74.8% cKO, $p < 0.05$) suggesting that estrogen reduces bone loss due to immobilization.

In summary, these findings indicate that ER α in osteocytes is not involved in prevention of osteocyte apoptosis and recruitment of osteoclasts, but is a pivotal factor to protect bone mass under normal loading and unloading conditions by regulating osteoblast activity.

Disclosures: Shino Kondoh, None.

FR0311

NFATc1 Expression in Osteocytes Regulates Bone Formation by Regulating Sclerostin Expression. Todd Spears^{*1}, Jennifer Paige-Robinson², Majd Zayzafoon¹. ¹University of Alabama at Birmingham, USA, ²University of Alabama-Birmingham, USA

We have previously reported that calcineurin/Nuclear Factor of Activated T Cells (Cn/NFAT) in osteoblasts negatively regulates osteoblast differentiation and bone formation. The role of Cn/NFAT in osteocytes is not known. To determine whether Cn/NFAT exerts direct actions in osteocytes, we generated mice lacking Cnbl (Cn regulatory subunit) in osteocytes (Δ CnblOCY) using Cre-mediated recombination methods. Transgenic mice expressing Cre recombinase, driven by the dentin matrix protein 1 (DMP1) promoter, were crossed with homozygous mice that express loxP-flanked Cnbl. Bone mineral density and bone mineral content increased 4% and 10%, respectively in Δ CnblOCY mice. Microcomputed tomography analysis of femora at 12 weeks revealed an increase in bone mass in Δ CnblOCY mice when compared with controls. In order to characterize NFATc1 during osteocyte differentiation, western blot analysis was performed and showed that during osteocyte differentiation the activation of NFAT is significantly increased 21% by 3 days and 15% by 7 days in MLO-Y4 osteocytes. This indicates that NFAT effects on bone are indirectly mediated by regulating secreted factors from osteocytes. To examine the direct role of NFATc1 during osteocyte differentiation, we used shRNA technology to knockdown NFATc1 in MLO-Y4 cells. We saw no effect on osteocytic markers, indicating NFATc1 does not directly affect osteocytes. However, we discovered a 6-fold reduction in sclerostin gene expression. Sclerostin is known to negatively regulate canonical Wnt signaling, which is important for osteoblast differentiation. Therefore, we treated MC3T3-E1 osteoblasts with conditioned media collected from NFATc1-deficient osteocytes, which resulted in an increase in differentiation and mineralization and was associated with an increase in TCF/LEF transactivation when compared with control. In order to demonstrate whether NFATc1 regulates sclerostin gene expression, we performed chromatin immunoprecipitation (ChIP) assay and noted that NFATc1 associates with SOST gene regulatory regions in MLO-Y4 cells. In shNFATc1 MLO-Y4 cells, this association was reduced preventing the transcription of the SOST gene. Our findings suggest that NFATc1 in osteocytes regulates bone formation by the regulation of sclerostin.

Disclosures: Todd Spears, None.

FR0312

Pharmacological Activation of Canonical Wnt Signaling Improves Bone Homeostasis and Regeneration by Directly Promoting MSC Osteoblast Differentiation. Tripti Gaur^{*1}, John Wixted¹, Sadiq Hussain¹, Jennifer Colby¹, Mary Clare McCorry¹, Stacey Russell¹, Ellen Gravallese¹, Andre Van Wijnen¹, Ivo Kalajic², David Rowe², Janet Stein¹, Gary Stein¹, Jane Lian¹. ¹University of Massachusetts Medical School, USA, ²University of Connecticut Health Center, USA

Genetic mouse models have firmly established that physiological activation of Wnt signaling has an anabolic effect on bone. Here we addressed the in vivo effects on bone homeostasis and fracture healing by inducing canonical Wnt signaling using the small molecule GSK3 β inhibitor TDZD8. We observed that TDZD8 does not affect bone marrow stromal cell (BMSC) proliferation. However, TDZD8 effectively enhances osteogenic differentiation of BMSCs, as reflected by a ~2-fold upregulation of the osteoblast-specific markers *Col1a1*, *Osx* and *OC*, 14 days after Wnt induction. Next, we generated mid-diaphyseal transverse fractures in femurs of WT mice, and treated them with either vehicle or TDZD8 (1mg/kg/day) beginning 24 hrs post-surgery for 2 weeks. MicroCT on day 14 indicated reduced total volume (TV) of the fracture callus, but increased bone volume (BV; expressed as %BV/TV) in TDZD8-treated mice compared to controls. Molecular mechanisms supporting bone repair in TDZD8-treated mice were identified. On day 7 post-fracture, decreased histone H4 transcript levels reflected a reduced number of proliferating cells, consistent with decreased callus size; on day 14, *Col2a1* and *Sox9* levels were significantly downregulated, indicating reduced chondrogenesis. Osteocalcin expression was upregulated in treated mice, reflecting increased bone and decreased cartilage. Furthermore, after 3-weeks of TDZD8 administration, μ CT identified increased bone mass in trabecular bone of the contralateral non-fractured limb. Based on these findings, we postulate that TDZD8 directs mesenchymal cells into the osteoblast lineage. Therefore, we performed lineage tracing in femoral fractures in double fluorescent reporter mice (expressing SMAA-Cherry, marking mesenchymal cells, and Col3.6-Cyan, marking early osteoblasts). The results show that TDZD8 does not increase Col3.6-Cyan positive osteoblasts, but increases SMAA-Cherry positive stem cells in areas of new bone formation. The latter indicates that an increased number of mesenchymal stem cells has directly entered the osteoblast lineage. Our findings indicate that pharmacological stimulation of canonical Wnt signaling by the GSK3 β inhibitor TDZD8 promotes fracture repair and increased bone mass through recruitment of MSCs directly into the osteoblast lineage.

Disclosures: Tripti Gaur, None.

FR0317

Association of the $\alpha_2\delta_1$ Subunit with $\text{Ca}_v3.2$ Enhances Membrane Expression and Regulates Mechanically-Induced ATP Release and ERK1/2 Signaling in Osteocytes. William Thompson^{*1}, Amber Majid², Kirk Czymmek², Albert Ruff³, Jesus Garc  a⁴, Randall Duncan¹, Mary Farach-Carson⁵.

¹University of Delaware, USA, ²University of Delaware, Department of Biological Sciences, USA, ³US Army Medical Research Institute of Chemical Defense, Cell & Molecular Biology Branch, Research Division, USA, ⁴University of Illinois at Chicago, Department of Physiology & Biophysics, USA, ⁵Rice University, USA

Voltage sensitive calcium channels (VSCCs) mediate signaling events in bone cells in response to mechanical loading. Osteoblasts predominantly express L-type VSCCs composed of the α_1 pore-forming subunit and several auxiliary subunits. Osteocytes, in contrast, express T-type VSCCs, but relatively few L-type α_1 subunits. Auxiliary VSCC subunits have several functions including modulating gating kinetics, trafficking of the channel and phosphorylation events. The influence of the $\alpha_2\delta$ auxiliary subunit on T-type VSCCs and the physiological consequences of that association are incompletely understood and have yet to be investigated in bone. In this study, we postulated that the auxiliary $\alpha_2\delta$ subunit of the VSCC complex modulates mechanically-regulated ATP release in osteocytes via its association with the T-type, $\text{Ca}_v3.2$ (α_{1H}) subunit. We demonstrated by RT-PCR, Western blotting, and immunostaining that both MLO-Y4 osteocyte-like cells and osteocytes in cortical bone express the T-type, $\text{Ca}_v3.2$ (α_{1H}) subunit more abundantly than the L-type, $\text{Ca}_v1.2$ (α_{1C}). We also demonstrated that the $\alpha_2\delta_1$ subunit, previously described as an L-type auxiliary subunit, complexes with the T-type $\text{Ca}_v3.2$ (α_{1H}) subunit in MLO-Y4 cells. Interestingly, siRNA mediated knockdown of $\alpha_2\delta_1$ completely abrogated ATP release in response to membrane stretch in MLO-Y4 cells. Additionally, knockdown of the $\alpha_2\delta_1$ subunit reduced ERK1/2 activation. Together these data demonstrate a functional VSCC complex that plays a critical role in osteocyte signaling. Immunocytochemistry following $\alpha_2\delta_1$ knockdown showed decreased membrane localization of $\text{Ca}_v3.2$ (α_{1H}) at the plasma membrane, suggesting that the diminished ATP release and ERK1/2 activation in response to membrane stretch resulted from a lack of $\text{Ca}_v3.2$ (α_{1H}) at the cell membrane. Together, these studies identify a new functional complex that plays a role in bone responses to mechanical signals.

Disclosures: William Thompson, None.

FR0319

Evidence that Osteocytes Elaborate Endocrine Regulation of Internal Organs Size: Data From the Osteocytes IGF-I Conditional Knockout Mice. Xiaodong Zhou^{*1}, Kin-Hing William Lau², Lynda Bonewald³, David Baylink¹, Matilda Sheng¹. ¹Loma Linda University, USA, ²Jerry L. Pettis Memorial VA Medical Center, USA, ³University of Missouri - Kansas City, USA

As in various cell types, cellular organs also need to communicate and coordinate with each other. Recent studies have shown that the bone is no exception. This is substantiated by our studies in mice with conditional IGF-I KO in osteocytes (generated from crossing DMP1-Cre with IGF-I Loxp mice). The IGF-I expression in the bone of these KO mice was decreased by 52% ($p < 0.01$) but IGF-I expression in osteoblasts isolated from these KO mice was not different from that in wild-type osteoblasts, indicating that the osteocyte is a major cell source of IGF-I in the bone. The KO mice had a 9-20% decrease in body weight ($p < 0.01$) in as early as 2 weeks of age and sustained throughout the entire growth period. This was not due to retarded endochondral ossification as their long bones were normal in length. The periosteal circumference was smaller by 8% ($P = .01$) in KO mice, suggesting that osteocytic IGF-I is essential for periosteal expansion but not endochondral bone growth. The marrow space ($P = .03$) and cortical bone area ($P = .05$) were each reduced by $>12\%$ in KO mice. We next evaluated the effect of the IGF-I KO in osteocytes on the development of key organs such as the kidney, liver and spleen. All of these organs in KO mice were smaller by 14-20% ($P < 0.05$ for each) compared to those of control mice. There was no difference in serum IGF-I level between KO mice and WT controls (373.624 vs. 379.8 vs. 21.6 ng/ml, $P > .05$), indicating that the reduced organ sizes in KO mice were not due to lower circulating IGF-I levels. The effect of osteocytic IGF-I on other key organs is exciting. First, it implies that osteocytes in the bone have a regulatory endocrine action on other organs in the body. This is analogous to the secretion by osteocytes of FGF23 to regulate phosphate metabolism and by osteoblasts of osteocalcin to regulate energy metabolism. Accordingly, our study provides a mechanism for the coordinated growth of the skeleton with other key organs. Second, this study differs from other IGF-I KO studies. Total or liver IGF-I KO mice showed a generalized retardation of growth. Conditional KO of IGF-I in osteoblasts or chondrocytes led to a coordinated decrease in longitudinal bone growth and bone size. In conclusion, our study solidifies the concepts that osteocytes are an endocrine organ and specifically that an important part of the action of the osteocyte to accomplish this coordinated growth is mediated in part by osteocytic IGF-I.

Disclosures: Xiaodong Zhou, None.

FR0325

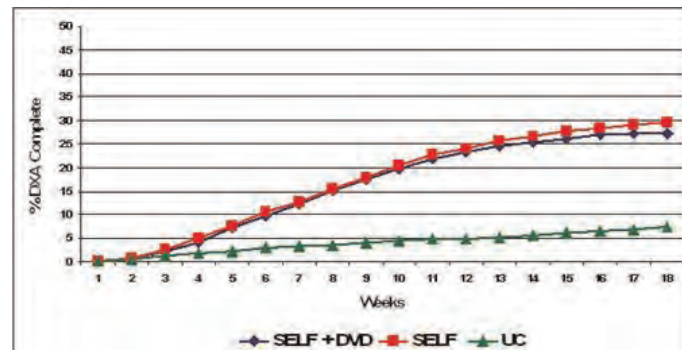
Allowing Patient Self-Referral of DXA Significantly Improves Osteoporosis Screening. Amy Warriner^{*1}, Ryan Outman², Jeffrey Curtis², Adrienne Feldstein³, David Redden², Mary Rix³, Brandi Robinson³, Douglas Roblin³, Ana Rosales³, Monika Safford², Kenneth Saag². ¹UAB, USA, ²University of Alabama at Birmingham, USA, ³Kaiser Permanente Center for Health Research, USA

Purpose: Current U.S. guidelines recommend bone density screening with central dual energy x-ray absorptiometry (DXA) in all women 65 years or older. However, less than one-third of eligible U.S. women undergo this testing. We evaluated whether a simple, low-cost intervention for patients to more easily schedule DXAs might improve osteoporosis screening rates compared to the current requirement of physician referral.

Methods: We conducted a group randomized controlled trial involving 14 primary care clinics within the Kaiser Permanente Northwest Region (KPNW). Women 65 years or older with no identifiable DXA scan in the past 5 years and no identifiable anti-osteoporosis treatment in the past 12 months were eligible for the study. Clinics were randomized into 1 of 3 groups: A self-referral intervention (SELF) (eligible patients invited by mail to get a DXA and provided opportunity to self-schedule a DXA); self referral + DVD (SELF+DVD) (consisting of SELF, plus an educational brochure and DVD promoting patient-provider communication about osteoporosis screening, enhanced through patient story-telling); and, Usual care (UC) (No DVD or self referral). Providers in all groups were directed to web-based CME training on osteoporosis screening and treatment.

Results: Of 8879 eligible women, 3218 women were randomized to SELF, 3752 to SELF+DVD, and 1909 to UC. A total of 29.6% of women in SELF and 28.4% in SELF+DVD completed a DXA scan, compared to 9.3% of women in UC; the risk difference for DXA receipt in SELF and DVD+SELF vs. UC was 19.6, (95% CI 17.9 – 21.3).

Conclusions: DXA scan scheduling and receipt was improved significantly by allowing patients to self-schedule their own scans. The addition of an educational DVD using patient story-telling to promote patient-provider communication did not significantly improve DXA screening over DXA self-scheduling alone. Allowing eligible women to self-schedule screening DXA scans (similar to mammography self-scheduling) may be an effective low cost strategy to increase rates of osteoporosis screening.



Receipt of DXA by Week

Disclosures: Amy Warriner, None.

FR0327

Degenerative Changes at the Lumbar Spine - Implications for Bone Mineral Density Measurement in Elderly Women. Kristina Akesson^{*1}, Max Tenne², Jack Besjakov³, Paul Gerdhem⁴, Fiona McGuigan⁵. ¹Skane University Hospital, Malmo, Sweden, ²Clinical & Molecular Osteoporosis Research Unit, Department of Clinical Science Malmo, Lund University, Sweden, ³Dept of Radiology Malmo, Skane University Hospital, Malmo, Sweden, ⁴Karolinska Institutet, Sweden, ⁵University of Lund, Malmo, Skane University Hospital, Malmo, Sweden

Purpose: In the elderly, degenerative manifestations in the lumbar spine may result in falsely elevated BMD values, consequently missing a large proportion of those with osteoporosis. Our aim is to determine the impact of degenerative changes on lumbar spine dual energy x-ray absorptiometry (DXA) measurements over time and the implications for the clinical diagnosis of osteoporosis.

Methods: The study participants were 1044 Swedish women from the population based Osteoporosis Prospective Risk Assessment study (OPRA) cohort. All the women were 75 years old at invitation and followed up after 5 years ($n = 698$) and at 10 years ($n = 380$). BMD was assessed using the Lunar DPX-L DXA. Degenerative changes (disc space narrowing, osteophytes, asymmetric subchondral sclerosis or facet joint sclerosis) were evaluated visually on the DXA image for each vertebra L1-L4

(intra observer precision kappa values 0.66-0.7). Evaluation of spinal X-rays was also made for comparison.

Results: At baseline, degenerative changes were more frequent in the distal part of the lumbar spine: 5% (L1), 15% (L2), 26% (L3), 36% (L3) and increased over time. At 10-year follow-up incidence was: 20% (L1), 39% (L2), 59% (L3), 72% (L3), manifesting as a significant increase in overall BMD. Re-analysis following exclusion of all cases with degenerative changes resulted in BMD remaining stable between 75-85 rather than the expected bone loss. Using the criteria (L2-L4 BMD <2.5SD), at baseline, 33% of women had osteoporosis. Excluding individuals with degenerative changes, this proportion increased to 42%. Using L1-L2, which are less prone to degenerative changes, as the diagnostic site, 46% of women were classified as osteoporotic. Use of bisphosphonates, calcium, D-vitamin or HRT did not significantly alter the results.

Conclusions: Our results confirm that degenerative changes are common in elderly women, accelerate disproportionately over time, are more frequent in vertebrae further distally, with a gradient from L1-L4 and have significant impact on DXA measurements. Interestingly, even in the absence of degenerative changes, BMD is maintained rather than lost over time in elderly women. We conclude that the DXA image offers sufficient precision to detect degenerative changes and used in conjunction with BMD measurements improves interpretation of osteoporosis status. Clinically, diagnosis of osteoporosis and evaluation of therapy would be improved by routinely assessing vertebrae L1-L2.

Disclosures: Kristina Akesson, None.

FR0328

Distal Forearm BMD combined with FRAX Probabilities for Fracture Prediction. Sreekanth Vasireddy¹, Helena Johansson², Anders Oden³, Diane Charlesworth¹, John Kanis⁴, Eugene McCloskey^{*1}. ¹University of Sheffield, United Kingdom, ²Swedish University of Agricultural Sciences, The Biomedical Center, Sweden, ³University of Gothenburg, Sweden, ⁴University of Sheffield, Belgium

The objective of this study was to evaluate the impact of combining distal forearm bone mineral density (BMD) with FRAX 10-years probabilities, calculated by clinical risk factors (CRFs) alone, on predicting future fractures in an elderly female population. Comparison was made with combining with femoral neck (FN) BMD.

5212 women, aged 75 years and older, randomly selected from the local population were studied regardless of the presence or absence of osteoporosis. The incidence of hip or any osteoporotic fractures was captured during a median of 4 years follow-up. The baseline 10-year probability of major osteoporotic or hip fracture in each woman was computed by the FRAX[®] tool using clinical risk factors including BMI, prior fracture, corticosteroid use, parental hip fracture, smoking, alcohol and secondary osteoporosis, but not femoral neck BMD. The combination of this probability with distal forearm BMD, FN BMD or both was examined by Poisson regression analysis and expressed as the gradient of risk (GR) per standard deviation decrease in BMD.

In analyses adjusted for age and time since baseline, distal forearm BMD was comparable to that of FN BMD for prediction of any fracture (GR 1.5, 95%CI 1.4-1.6 and 1.6, 1.5-1.8 respectively, both p<0.001) but the prediction of hip fracture was somewhat lower than FN BMD (1.7, 1.4-2.0 vs. 2.3, 2.2-2.5 respectively, both p<0.001). Further adjustment for FRAX probabilities of major osteoporotic fractures had little impact on the GRs of forearm and FN BMD for predicting any fracture (1.4, 1.3-1.6 vs. 1.5, 1.4-1.7 respectively, both p<0.001). Similarly, the GRs for hip fracture were little altered following adjustment for FRAX hip fracture probabilities (1.6, 1.3-1.9 vs. 2.2, 1.9-2.7 respectively, p<0.001). When forearm BMD and FN BMD were included in the same model, and adjusted for the appropriate FRAX probabilities, forearm BMD remained a weak but significant predictor of any fracture (Table) but was no longer associated with future hip fracture.

Distal forearm BMD is a significant predictor of osteoporotic fractures including hip fractures. Its predictive ability, alone or in combination with FRAX probabilities, is somewhat less than FN BMD and measurement of forearm BMD is of little additional value when Fn BMD is known. In the absence of access to FN BMD, it should be possible to develop algorithms which combine forearm BMD in a FRAX-like model.

Outcome	Any fracture		Hip fracture	
	p-value	GR (95% CI)	p-value	GR (95% CI)
Forearm BMD	0.0012	1.2 (1.1, 1.3)	>0.30	1.0 (0.8, 1.3)
FN BMD	<0.001	1.4 (1.3, 1.6)	<0.001	2.2 (1.8, 2.7)

GRs for combined FN and forearm BMD models

Disclosures: Eugene McCloskey, None.

FR0330

Forearm BMD Measurement Variability Using DXA. Diane Krueger^{*1}, Nellie Vallarta-Ast², Jessie Libber³, Mary Checovich¹, Neil Binkley³. ¹University of Wisconsin, Madison, USA, ²UW Osteoporosis Research, USA, ³University of Wisconsin, USA

Background: Radius BMD is a valuable cortical bone measurement in clinical trials, patients with hyperparathyroidism and older adults with spinal degenerative changes. However, we have observed substantial variability in serial forearm measurements. Here we report precision assessment, identify a confounder to radius BMD measurement and propose a technical approach to avoid this inaccuracy.

Methods: Three technologists performed forearm BMD precision assessment following ISCD recommendations using a Lunar iDXA. Briefly, each technologist scanned 30 men and 30 women (n = 180) twice with repositioning between scans. Mixed effects linear regression models were used to estimate precision error and least significant change (LSC), based on technologist and sex. Upon demonstration of a larger than expected LSC, and substantial between technologist differences, detailed examination of all images, including bone, soft tissue, neutral and air point-typing was conducted. An "ideal" LSC was calculated using 30 scan pairs with optimal point-typing. Potential causes of point-typing variability were explored.

Results: Substantial differences (p < 0.001) in BMD variability, e.g., an almost two-fold difference in LSC (0.038 to 0.073 g/cm²), was observed between technologists and with our "ideal" LSC (0.031 g/cm²). Much of this appears to result from differences in automated "soft tissue" identification in these scans. Investigation of potential confounders, e.g., sex, BMI, and positioner placement did not reveal an apparent explanation for these inconsistencies. Compared to the manufacturer's ideal depiction, suboptimal soft tissue point-typing was present in 25/190 individuals (14%). In these 25 individuals, 22 (88%) had a paired scan appropriately point typed; BMD variability between these scan pairs greater than our ideal LSC was found in 17/25. In the entire group of 180, 34 individuals had BMD differences greater than our ideal LSC, of these, 17 had suboptimal soft tissue identification.

Conclusions: In this older adult cohort, substantial variability in one-third radius BMD measurement was not rare. This appears to result from automated soft tissue detection inaccuracies. It seems probable that clinicians will not appreciate these occurrences, thus leading to incorrect interpretation. Technologists must evaluate soft tissue assessment as part of routine forearm DXA analysis and, if suboptimal, an immediate scan reacquisition to produce a valid scan is required.

Disclosures: Diane Krueger, None.

FR0331

Rate of BMD Change Does Not Enhance Fracture Prediction: The Manitoba BMD Cohort. William Leslie^{*1}, Suzanne Morin², Lisa Lix³. ¹University of Manitoba, Canada, ²McGill University Health Centre, Canada, ³University of Saskatchewan, Canada

BACKGROUND: BMD measurements are widely used in clinical practice to assess fracture risk and for monitoring. Decrease in BMD likely contributes to the age-related increase in fractures, but there are conflicting data on whether rate of BMD loss is independently predictive. METHODS: We identified all women over age 50 at the time of second (repeat) BMD testing between April 1996 and March 2007 in a large clinical BMD database for the Province of Manitoba, Canada. The median interval between tests was 3.7 years (IQR 2.9-5.1). Using linkage to a population-based administrative health data repository, we identified other relevant covariates, medication use, and fracture outcomes up to March 2010 (median observation 3.2 years, IQR 1.6-5.5). Among 12,457 women, 3,926 were designated as untreated (less than 90 days use of HRT or non-HRT osteoporosis therapies before and between BMD tests). Cox proportional hazards models were used to assess major osteoporotic fracture risk according to BMD change after adjustment for final BMD, baseline BMD, treatment and FRAX covariates. RESULTS: 562 women sustained a major osteoporotic fracture (147 among the untreated women). Annualized percent change in total hip BMD was similar for fracture versus non-fracture women in the overall group (+0.12.1% vs +0.12.3%, P=.928) and in the untreated subgroup (-0.31.8% vs -0.61.5%, P=.077). After adjustment for final total hip BMD, other covariates and medication use, rate of total hip BMD change did not predict major osteoporotic fractures in the overall cohort (HR 1.07 per SD decrease, 95% CI 0.99-1.16) or in the untreated subgroup (HR 0.96 per SD decrease, 95% CI 0.81-1.14). When baseline (rather than final) total hip BMD was used then hip BMD change was statistically significant in the overall cohort (HR 1.22 per SD decrease, 95% CI 1.13-1.32). Secondary analysis showed similar negative results for a categorical decrease in total hip BMD exceeding the 95% LSC for the overall cohort (HR 1.12, 95% CI 0.86-1.46) and the untreated subgroup (HR 0.95, 95% CI 0.58-1.53). There was no evidence of a significant age (decade) interaction. Parallel analyses based upon change in lumbar spine and femoral neck BMD gave similar results (see Table). CONCLUSIONS: Rate of BMD change does not enhance future fracture prediction in older women when adjusted for final BMD and other covariates. This would argue against inclusion of BMD change in future modifications to the FRAX algorithm.

	Adjusted for final BMD *		Adjusted for baseline BMD *	
	HR (95% CI)	p-value	HR (95% CI)	p-value
ΔTotal hip BMD per y	1.07 (0.99-1.16)	0.093	1.22 (1.13-1.32)	<.001
ΔL14 BMD per y	1.05 (0.96-1.15)	0.268	1.12 (1.02-1.23)	0.013
ΔFemoral neck BMD per y	1.02 (0.95-1.09)	0.667	1.14 (1.07-1.23)	<.001

Table: Adjusted hazard ratios for each SD decrease in BMD to predict major osteoporotic fracture.

Disclosures: William Leslie, None.

FR0332

The Discriminatory Capacity of Clinical Risk Factors and BMD Measurements at Different Skeletal Sites for Detecting Patients with Vertebral Fractures. Christian Muschitz^{*1}, Friederike Kuehne², Roland Kocijan³, Angela Trubrich², Christina Bittighofer², Reinhart Waneck⁴, Heinrich Resch⁵. ¹St. Vincent's Hospital, Austria, ²The VINFORCE Study Group - St. Vincent Hospital - Medical Department II, Austria, ³St. Vincent Hospital Vienna, Austria, ⁴St. Vincent Hospital - Department of Radiology, Austria, ⁵Medical University Vienna, Austria

Purpose: Since the clinical outcome of osteoporosis is bone fracture, attention is focused on the identification of patients at high risk for fractures rather than the identification of people with osteoporosis defined by BMD. We investigated measurements of BMD of the calcaneus by DXL as a possible alternative device for the assessment of BMD together with the implementation of clinical risk factors (CRF) compared to DXA at standard skeletal sites.

Methods: Baseline characteristics of 494 outpatient treatment naive postmenopausal women (67.915.0 ys) and 97 men (61.512.7 ys) were evaluated for a preplanned 5 year follow up period. All subjects had prior spine X-rays and evaluation of CRF according to FRAX guidelines. Each subject had DXA of spine/hip and DXL of the calcaneus on the same day. We calculated receiver operating curves (ROC) expressed as area under the curve (AUC) to describe the sensitivity and specificity of DXA of spine/hip and for DXL at calcaneus to discriminate between patients at risk for vertebral fracture. Furthermore we generated a univariate multiple logistic regression model for CRF alone and for CRF including BMD by DXA or DXL.

Results: Out of 591 subjects, 160 patients had prevalent vertebral fractures (72.612.1 vs 61.4 9.3ys; P<0.001). In the ROC analysis the AUC of BMD alone was 0.669 for DXA femoral neck, 0.665 for DXL calcaneus, 0.661 for DXA total hip and 0.598 for DXA lumbar spine (P=0.034). The AUC for CRF without BMD was 0.805. In this model significant CRF (P<0.05) were previous fragility fractures (OR 24.5; 95%CI 13.4, 44.6), age (OR 1.04; 95%CI 1.02; 1.06) and BMI (OR 1.05; 95%CI 1.00; 1.90). After combination of DXA femoral neck and CRF the AUC improved to 0.869. Significant ORs (P<0.05) were previous fractures (20.9; 95%CI 10.5; 41.6), alcohol use (3.9; 95%CI 1.05; 14.46) and BMD femoral neck (0.68; 95%CI 0.48; 0.94). The AUC for DXL calcaneus and CRF was 0.861 including significant factors (P<0.05) such as age (OR 1.03; 95%CI 1.00; 1.05), previous fracture (OR 23.9; 95%CI 12.5; 45.7) alcohol use (OR 2.94; 95%CI 0.86; 10.02) and BMD calcaneus (OR 0.77; 95%CI 0.57; 1.04; P=0.09).

Conclusions: Our data clearly demonstrate that the predictive value of specific CRFs and BMD measured by DXA or DXL is similar and improves the discriminatory capacity for detecting patients with vertebral fractures compared to BMD measurements or assessment of CRF alone

Disclosures: Christian Muschitz, None.

FR0335

Reproducibility of a Vertebral Deformity Tool (VDT) using an Statistical Shape Modeling Workflow Tool. Colin Miller^{*1}, Alan Brett², Eric Bogner³, Monique Tan⁴, Rebecca Cope⁵, Melanie Jenkins⁶, Jane Haslam⁷, Joes Staal⁸, Curtis Hayes⁹. ¹BioClinica, Inc. (formerly Bio-Imaging Technologies, Inc.), USA, ²Optasia Medical Ltd., United Kingdom, ³Hospital for Special Surgery, USA, ⁴Novartis Pharmaceutical, USA, ⁵BioClinica Inc, USA, ⁶Novartis Pharmaceuticals, USA, ⁷Optasia Medical Ltd, United Kingdom, ⁸Optasia Medical, United Kingdom, ⁹Virginia Commonwealth University School of Medicine, USA

Introduction: There is need for enhanced radiographic measurement techniques for the detection and diagnosis of vertebral deformities (VDs). This study assesses the inter and intra reader reproducibility of a novel clinical workflow tool that uses model-based shape recognition technology for the semi-automated annotation of T4 to L4 vertebrae using digitized plain-film radiography.

Methods: Lateral spine radiographs digitized at 150µm of 52 subjects with suspected VDs, obtained from the Canadian Multicenter Osteoporosis Study (CaMos) were independently assessed by two radiologists (EB & CH) using a semi-automated protocol based on a previously described 95 point vertebral annotation¹. This annotation captures the full lateral vertebral shape including endplate rims, endplate depression and osteophytes. This VD Tool (VDT) was applied using a read system developed by BioClinica and embedded software from Optasia Medical. For

each vertebra, the mean position of each of the 95 points was computed. Then, for each point, the squared distance between the mean position and each read was computed and summed to assess the variance of each point in the contour. Also we collated all variance measures and computed their mean value and 95% confidence interval (CI) using a bootstrap method at each vertebral level. After taking the square root of the mean value and the confidence interval we obtained the average reproducibility (RMSSD) for each vertebral level in millimeters displacement. Reproducibility in terms of percentage of average vertebral height was also calculated using a similar method.

Results: There were nine intra-reader labeling differences and 17 intra-reader labeling disagreements due to different choices being made of eg T12 annotation in either the thoracic or lumbar image of each subject pair. The mean reproducibility in mm (percent of vertebral height) for CH ranged between 0.53 (1.87%) - 0.94 (2.77%), and for EB between 0.87 (3.46%) to 1.53 (5.27%). The inter-reader variability ranged from 0.87 to 1.34 mm or 3.17% to 4.57%. See Table 1.

Conclusion: We report good reproducibility of 95 point placement using this tool. This software tool shows potential for full vertebral shape characterization which may be used as a diagnostic tool for vertebral deformity. This method minimizes the user time and variability seen in manual vertebral six-point morphometry placement.¹ Brett et al, *Spine* 34(22): 2437-2443, 2009.

Level	CH	EB	Inter-Reader
T4	0.64 (0.62-0.65)	0.87 (0.85-0.89)	1.06 (1.02-1.09)
T5	0.53 (0.52-0.54)	0.97 (0.95-1.01)	0.96 (0.95-1.02)
T6	0.54 (0.53-0.56)	0.99 (0.94-1.03)	0.81 (0.79-0.86)
T7	0.56 (0.55-0.59)	1.02 (0.98-1.06)	0.87 (0.85-0.90)
T8	0.61 (0.60-0.64)	1.13 (1.09-1.17)	1.06 (1.04-1.11)
T9	0.65 (0.63-0.69)	1.18 (1.13-1.22)	1.03 (1.01-1.08)
T10	0.58 (0.57-0.61)	1.25 (1.19-1.30)	1.08 (1.03-1.21)
T11	0.71 (0.68-0.75)	1.29 (1.23-1.33)	1.29 (1.25-1.35)
T12	0.90 (0.86-0.94)	1.34 (1.28-1.39)	0.97 (0.94-1.01)
L1	0.94 (0.89-0.98)	1.53 (1.44-1.65)	1.10 (1.06-1.16)
L2	0.65 (0.62-0.67)	1.36 (1.27-1.44)	1.13 (1.10-1.19)
L3	0.73 (0.70-0.75)	1.22 (1.16-1.27)	1.18 (1.15-1.24)
L4	0.82 (0.79-0.84)	1.49 (1.44-1.53)	1.34 (1.30-1.40)

Table 1: Inter- and Intra-Reader reproducibility in mm as RMSSD (95% CI).

Disclosures: Colin Miller, BioClinica, 3; Novartis Pharmaceuticals, 6
This study received funding from: Novartis Pharmaceuticals

FR0339

Quantitative Ultrasound Measurements Predict Fracture Risk in Non-osteoporotic Women. Tuan Nguyen¹, John Eisman¹, Jacqueline Center¹, Mei Chan^{*2}, Nguyen Nguyen¹. ¹Garvan Institute of Medical Research, Australia, ²Osteoporosis & Bone Biology, Australia

Fracture is a multi-factorial disorder, and bone mineral density (BMD) alone account for around 50% of fracture cases. Indeed, more than 50% of women who sustained a fracture have BMD above osteoporotic threshold (T-score > -2.5). Calcaneal quantitative ultrasound measurements (QUS) are significant predictors of fracture. This study was designed to test the hypothesis that in non-osteoporotic women, lower measured values of QUS are associated with increased fracture risk.

The study is part of the on-going Dubbo Osteoporosis Epidemiology Study, which is a prospective population-based study of risk factors for fracture and outcomes. The study included 340 women aged 62-89 with BMD T-score > -2.5 who had QUS measurements. QUS was measured in broadband ultrasound attenuation (BUA) at calcaneus using CUBA sonometer (McCue Ultrasonics, Winchester, UK). BMD was measured at the femoral neck (FNBMD) by dual energy X-ray absorptiometry (DXA) using GE Lunar DPX-L densitometer (Lunar Corporation, Madison, Wisconsin, USA). The individuals had been followed-up for a median of 13 years (from 1994 to 2009). The incidence of fragility fracture during the follow-up period was ascertained by X-ray report.

Of the 340 women without osteoporosis, 27% (n = 92) had experienced at least one fragility fracture during the follow up. Women with fracture had significantly lower baseline FNBMD and BUA than those without fracture (P< 0.001). In unadjusted analysis, increased fracture risk was associated with decrease in QUS (RR 1.68 per standard deviation [SD]; 95% CI: 1.25-2.29), and reduced BMD (1.51 per SD; 1.07-2.18). After adjusting for age, weight, and lifestyle factors, increased risk of fracture was significantly associated with decreased BUA (RR 1.37; 1.05-1.77), but not with FNBMD (RR 1.23; 0.97-1.55). The association between BUA and fracture was also observed for hip fracture (RR 2.93; 1.26-6.82), but not for vertebral fracture (RR 1.28; 0.83-1.97).

These results suggest that calcaneal QUS is an independent predictor of any and hip fracture in women without osteoporosis. The results further underscore the potential utility of QUS in the enhancement of fracture prediction at the individual level.

Disclosures: Mei Chan, M & D. Roche and Novartis, 9

FR0347

Peri-Aortic Fat Is Negatively Associated with Volumetric Bone Mineral Density, Cross-Sectional Area and Compressive Strength of Lumbar Vertebrae: the Framingham Osteoporosis Study. Yi-Hsiang Hsu¹, Caroline S. Fox², Mary Bouxsein³, Udo Hoffmann⁴, LA Cupples⁵, Douglas Kiel⁶. ¹Hebrew SeniorLife Institute for Aging Research & Harvard Medical School, USA, ²National Heart, Lung, & Blood's Framingham Heart Study, USA, ³Beth Israel Deaconess Medical Center, USA, ⁴Massachusetts General Hospital, Department of Cardiac MR PET CT & Harvard University, USA, ⁵Biostatistics Dept., School of Public Health, Boston University, USA, ⁶Hebrew SeniorLife, USA

Both obesity and osteoporosis are increasingly recognized as major health problems worldwide. The long prevailing view that BMI defined obesity is associated with beneficial effects on the skeleton has recently been challenged by contrasting studies demonstrating that visceral fat is associated with lower bone density. Peri-aortic adipose tissue volume (PAAT) is the adipose tissue surrounding the aorta, which is anatomically adjacent to the spine. Cellular studies have suggested that PAAT may have a paracrine effect on the adjacent aortic vessel walls leading to a higher risk of arterial disease. We hypothesized that PAAT is associated with bone measures and it may be due to its local paracrine effect on the adjacent lumbar vertebrae. Methods: To determine the association between PAAT and bone measures at the lumbar vertebrae, PAAT (cm³) and volumetric integral BMD (In.vBMD, cm³); volumetric trabecular BMD (Tb.vBMD, cm³); and cross-sectional area (CSA, cm²) of L3 were measured by QCT on 1,631 men and 1,507 women (mean age: 53.12.3 years old) from the Framingham Osteoporosis Study. The Compress Strength (CS, Newtons) of vertebrae body was calculated as ((In.vBMD x 3230) - 34.7) x CSA x 0.68. Subcutaneous abdominal tissue volume (SAT) and visceral abdominal tissue volume (VAT) were also estimated from the same QCT scans. Pearson partial correlation coefficients between PAAT and the QCT bone measures were estimated. Sex-specific mixed effects models were used to calculate least-squares means and to assess regression coefficients for the bone measures across PAAT quartiles. Results: PAAT was positively correlated with VAT, BMI and SAT with partial correlation coefficients (adjusted for age, sex and height) equal to 0.75, 0.52 and 0.41, respectively. Significantly negative correlations (-0.21 ~ -0.08) between PAAT and the bone measures were found in both men and women after adjusting for age, height, BMI and menopause status (women only). The magnitude of the correlations was stronger than that between BMI and the bone measures, and was in the opposite direction (Table). Adjusted for age, height and BMI, the multivariable-adjusted mean In.vBMD, Tb.vBMD, CSA and CS all significantly decreased from the lowest (Q1) to the highest (Q4) PAAT quartile (Figure: representative CS result) in both men and women. In conclusion, our study suggests that increased fat deposits adjacent to vertebrae may have a detrimental effect on bone density and strength of vertebrae.

Table. Pair-Wise Pearson Partial Correlation Coefficients

	Men (N=1,631)			Women (N=1,507)		
	In.vBMD (cm ³)	Tb.vBMD (cm ³)	CSA (cm ²)	In.vBMD (cm ³)	Tb.vBMD (cm ³)	CSA (cm ²)
BMI (kg/m ²)	0.10	0.10	0.11	0.18	0.16	0.09
Weight (lbs)	n.s. (0.07)	n.s. (0.08)	0.15	0.19	0.16	0.12
PAAT (cm ³)	-0.13	-0.14	-0.11	-0.21	-0.17	-0.08
SAT (cm ³)	-0.15	-0.13	-0.13	-0.04 (n.s.)	-0.02 (n.s.)	-0.11
VAT (cm ³)	-0.09	-0.11	-0.16	-0.11	-0.10	-0.10

BMI: Adjusted for age; Weight: Adjusted for age and height;

PAAT, SAT and VAT: Adjusted for age, height and weight

Except for n.s., all pair-wise correlation coefficients are significant at $p < 0.05$

Figure. Adjusted Mean Compressive Strength (Newtons, N) by PAAT Quartiles

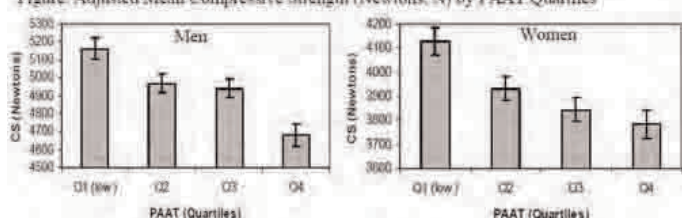


Table and Figure

Disclosures: Yi-Hsiang Hsu, None.

FR0353

Determination of Absolute Risk of Fracture Threshold for Intervention: A Decision Curve Analysis. Nguyen Nguyen¹, Dana Blünc¹, Steven Frost², Jacqueline Center¹, John Eisman¹, Tuan Nguyen¹. ¹Garvan Institute of Medical Research, Australia, ²University of Western Sydney, Australia

The assessment of fracture risk can now be individualized by existing absolute risk models based on an individual's risk profile. However, one of the most important questions in using these absolute risk models is: what is the appropriate threshold of

risk that is warranted an intervention. In this study, we used the decision curve analysis (DCA) method to determine the intervention threshold.

The present study was part of the ongoing Dubbo Osteoporosis Epidemiology Study which involved 1358 women and 858 men, whose bone health has continuously been monitored since 1989. All individuals aged 60 or older as at 1989. Baseline measurements included femoral neck BMD, prior fracture, a history of falls and body weight. During the follow-up period, 426 women and 149 men had sustained a low-trauma fracture. We considered 3 Cox's proportional hazards models for predicting fracture risk: model I included only prior fracture; model II included age and BMD; and model III included age, BMD, prior fracture and falls. From each model, we estimated 10-y predicted probability of any fracture and hip fracture for each individual. We then calculated the "net benefit" for each intervention threshold (T). The net benefit (NB) is a function of total sample size (n), true positives (TP) and false negatives (FN) as follows: $NB = TP/n - (FN/n) * (T/(1-T))$.

Decision curve analysis suggested that for any fracture, optimal net benefit was reached when the 10-year fracture risk is 10% regardless of models used; however, at this risk level, almost all individuals are subject to intervention. For risk threshold between 10% and 20%, optimal net benefit was achieved with model III. For risk threshold between 20% and 50%, the net benefit would be declined in women, but not in men (Figures A-B). For hip fracture, models II and III yielded similar optimal net benefit at threshold between 6% and 10%. Clinical decision based on prior fracture alone yielded suboptimal net benefit for hip fracture (Figures C-D). For all models and for a given threshold, the net benefit was greater in women than in men.

These results suggest that a 10-year risk of any fracture between 10-20% or hip fracture risk between 6-10% provides optimal net benefit.

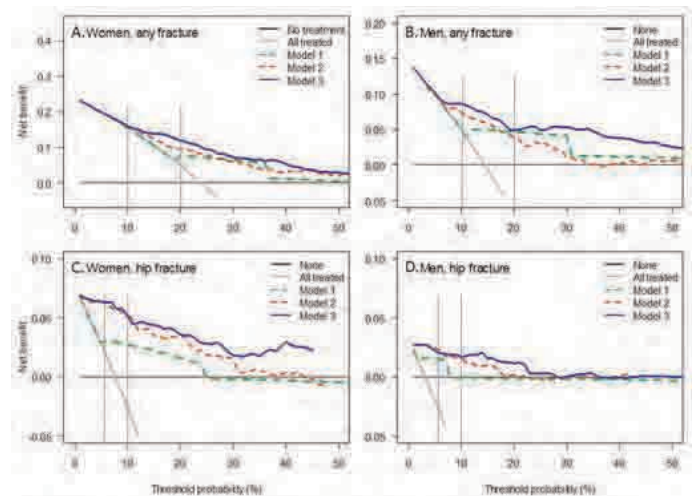


Figure. Decision curve for prognostic models predicting absolute risk for any fracture in women (A) and men (B), and for hip fracture in women (C) and men (D).

The gray line is the net benefit of treatment all population; the "zero" horizontal line is the net benefit of no treatment.

Model 1 included only prior fracture; model 2 included age and femoral neck BMD; and model 3 included age, BMD, prior fracture and falls.

Figure. Decision curve for prognostic models predicting absolute risk

Disclosures: Nguyen Nguyen, None.

FR0354

Epidemiologic Findings Shed Light Upon A Case Definition For Atypical Subtrochanteric and Femoral Shaft Femoral Fractures (STFSF). Adrianne Feldstein¹, Dennis Black², Nancy Perrin³, A. Gabriela Rosales³, Darin Friess⁴, David Boardman⁵, Richard Dell⁶, Arthur Santora⁷, Julie Chandler⁷, Anne De Papp⁸, Mary Rix³, Eric Orwoll⁴. ¹Kaiser Permanente Center for Health Research, USA, ²University of California, San Francisco, USA, ³Kaiser Permanente Northwest, Center for Health Research, USA, ⁴Oregon Health & Science University, USA, ⁵Kaiser Permanente NW, USA, ⁶Kaiser, USA, ⁷Merck Research Laboratories, USA, ⁸Merck & Co., Inc., USA

The case definition for atypical Subtrochanteric and Femoral Shaft Femoral Fractures (STFSF) is critical for evaluating their risk factors. The incidence and characteristics of subtrochanteric and femoral shaft fractures (STFSF) with and without atypia were determined from electronic medical record and radiograph review at Kaiser Permanente Northwest from January 1996 – June 2009. Of 197 STFSF observed over 13.5 years, 75 met ASBMR major criteria [AFM= shaft location, minimal trauma, transverse or short oblique, non-comminuted] (5.9/100,000 py (95% CI 4.6,7.4)). Of those, 22 also met ASBMR criteria for minor features (lateral beaking, increased cortical thickness, signs of stress fracture) (1.7/ 100,000 person-years (95% CI= 1.1-2.6)). Whereas the incidence of AFM appeared flat, the proportion of atypical fractures with major and minor features [AFMm] increased over time. AFM subjects were older, and had fewer dispensings of bisphosphonates and glucocorticoids compared to subjects with AFMm.

Conclusions: Patients with atypical subtrochanteric fractures with major features only appear to be different from patients with atypical subtrochanteric fractures with major and minor features and it may be that the former group constitutes a long-standing type of osteoporotic fracture and that only the latter group is atypical and increasing in frequency. There may be multiple associated risk factors for atypical fractures. Future epidemiologic studies of atypical STFSF should evaluate AFM and AFMm separately.

	AFM (major criteria ONLY)	AFMm
All Fractures	53	22
N, %	79 (51.4)	71 (51.2)
Age, mean (SD)	41 (7.4)	20 (9.9)
n, % female	47 (92.2)	19 (90.5)
Race - White, n (%)	N=51	N=21
BMI, mean (SD)*	27.9 (5.4)	28.0 (5.4)
Hx of Proximal pain	N=5	6 (27.3)
T score spine, mean (SD)*	-4.0 (0.7)	-1.0 (2.4)
BPs- Any dispense prior to fracture event, N, (%)	8 (16.3)	13 (61.9)
BPs- years of ≥ 1 dispensing*	N=8	N=13
Oral GCs- Any dispense prior to fracture event N, (%)	2 (5.1)	5 (33.3)
Oral GCs- years of ≥ 1 dispensing*	17 (34.7)	8 (38.1)
	2 (5.1)	4 (19.0)

*determined among those with ≥ 12 months of health plan membership

Table

Disclosures: *Adrianne Feldstein, Amgen, 2; Merck, 2*
This study received funding from: *Merck*

FR0355

Incidence of and Predictors of False Negative Self-Reports of Hip Fractures in Cohort Studies: the Study of Osteoporotic Fractures (SOF). *Beth Vinnig¹, Brent Taylor¹, Kristine Ensrud², Misti Paudel¹, Sara Durham¹, John Schousboe³*. ¹University of Minnesota, USA, ²Minneapolis VA Medical Center / University of Minnesota, USA, ³Park Nicollet Clinic/University of Minnesota, USA

Background: Cohort studies generally rely on patient self-report to identify incident fractures. While follow-up examination of clinical radiographs can identify false positive self-reports, few studies have examined the proportion of fracture self-reports that are false negatives. Medicare claims data has been shown to identify incident hip fractures with 98% accuracy. Our study aims were; a) using SOF data merged with Medicare claims, determine the proportion of incident hip fractures identified in claims that were NOT reported to SOF; and b) identify predictors of false negative self reports.

Methods: Successful matches of SOF participants from 3 of the 4 SOF study sites with their Medicare claims were confirmed for 92.1% (6,285 women) of the cohort still alive and enrolled in the SOF study as of 1/1/1992. Incident first hip fractures were identified for this subset in available claims between 1/1/1992 and 12/31/2007 by a primary or secondary discharge ICD-9 diagnosis of hip fracture (820.0x). Fracture self reports were solicited on post-cards mailed to participants every 4 months, with a 99% response rate. True positive self-reports were those confirmed by review of reports of x-rays taken within 31 days of the first hip fracture admission date in claims. False negative self reports were follow-up post-cards with no self-reported pelvis, proximal femur, or distal femur fractures in SOF within 31 days of the fracture date in claims. The multivariable adjusted associations of predictor variables with false negative hip fracture self reports were estimated with logistic regression.

Results: Of 770 women identified with an incident hip fracture in Medicare claims, 161 (20.9%) did not report their hip fracture to SOF. Living with others (compared to living alone), lower mini-mental status exam score (MMSE), and being unable to stand without use of arms were associated with false negative hip fracture self-reports (table).

Conclusions: A significant minority of hip fractures are likely to be missed in cohort studies that rely on self-report to be the first signal of a fracture event. This misclassification of hip fracture events may bias estimated associations of predictors with hip fractures toward the null, and reduces power to establish the statistical significance of these associations. Strategies to detect fracture events with higher accuracy in cohort studies are needed.

Predictor	Odds of False Negative vs. True Positive Hip Fracture Self Report (95% C.I.)
Age Category:	
<80 years	1.00 (Reference)
80-84 years	0.82 (0.40 – 1.69)
≥ 85 years	0.98 (0.75 – 1.28)
Unable to stand without use of arms	2.89 (1.04 – 8.03)
MMSE score (1 SD decrease)	1.25 (1.04 – 1.50)
Living With Others (vs. living alone)	1.59 (1.08 – 2.34)
Walk speed : Tertile 3	1.00 (Reference)
Tertile 2	1.03 (0.64 – 1.65)
Tertile 1	1.44 (0.86 – 2.43)

Table

Disclosures: *John Schousboe, None.*

FR0357

Muscle Density, a Surrogate of Intermuscular Adiposity Derived from pQCT, Is an Independent Correlate of Fractures in Women. *Andy Kin On Wong^{*1}, Aakash Bhargava¹, Karen Beattie¹, Christopher Gordon¹, Laura Pickard¹, Colin Webber², Alexandra Papaioannou², Jonathan Adachi³*. ¹McMaster University, Canada, ²Hamilton Health Sciences, Canada, ³St. Joseph's Hospital, Canada

Muscle loading contributes to stronger bones and lower fracture risk, but may be affected by adiposity. Objective: To determine the influence of pQCT-derived muscle measures on fragility fractures in women.

Methods: A single slice (2.30.5 mm) scan at the 66% site of the calf muscle was acquired in women ≥ 50 years of age from the Hamilton cohort of the Canadian Multicentre Osteoporosis Study (CaMos) using peripheral quantitative computed tomography (pQCT). Grip strength and timed 'up-and-go' (TUG) physical function tests were assessed at study visit. Participants also completed a questionnaire on duration of antiresorptive therapy, vitamin D and calcium supplements. Prevalence of fragility fractures over the past 15 years was determined from the CaMos database archive. Muscle was segmented from bone and subcutaneous fat using density thresholds. Muscle area and density were computed using manufacturer software. Binary logistic regression analyses determined the relationship between prevalence of fractures and muscle measures, adjusting for age, body mass index (BMI), duration of medication use, physical function, and total hip (TH) areal bone density (aBMD). Odds ratios were reported with 95% confidence intervals (CI). Receiver-operator characteristics (ROC) curve analyses for fractures was examined for the same variables, reporting areas under the curve (AUC). AUCs for muscle measures were compared with AUC for TH aBMD, and with a null AUC of 0.50 using a Wilcoxon signed ranks test.

Results: Of 38 women (mean age: 74.6 \pm 8.4 years; BMI: 26.5 \pm 4.2 kg/m²), 16 (42.1%) had sustained a fragility fracture. Higher muscle density, but not area, was significantly associated with reduced odds for fracture independent of anthropometrics and medication use (Table 1). Including muscle area or TH aBMD led to lower odds for fractures but not to significance. Higher physical function contributed to 36% reduction in fracture odds. Muscle density exhibited an AUC of 0.835 (95% CI: 0.705, 0.966) for discriminating those with fractures, significantly larger than 0.50 and AUC for TH aBMD of 0.638 (95% CI: 0.500, 0.756). 87.5% sensitivity and 68.2% specificity was observed.

Conclusions: pQCT-derived muscle density, reflective of intermuscular fat, is an independent risk factor for fractures able to discriminate women with fractures with over 80% accuracy. Women with greater physical function plus denser or leaner calf muscles have further reduction in odds for fracturing.

Table 1. Odds for fractures in women explained by pQCT muscle measures. Muscle volumetric density was examined as a correlate of fractures in conjunction with muscle area and total hip areal bone mineral density (TH aBMD) with adjustment for anthropometrics (age, BMI), medication use (duration of antiresorptive therapy, vitamin D and calcium), and physical function measures (maximum grip strength (GSMax), timed 'up-and-go' (TUG) time). Bold p-values indicate significance at the 95% confidence level.

Model	Covariates	OR	Lower CI	Upper CI	P-value
	Muscle volumetric density	0.531	0.342	0.823	0.005
	Muscle area	1.000	0.999	1.001	0.654
Model1	Age, BMI	0.533	0.333	0.855	0.009
Model2	Model1+Duration of Ca, Vitamin D, Antiresorptive therapy	0.507	0.298	0.864	0.013
Model3	Model1+GSMax,TUGTime	0.169	0.03	0.964	0.045
Model4	Model1+ Muscle area	0.472	0.282	0.788	0.004
Model5	Model1+TH aBMD	0.473	0.275	0.815	0.007
Model6	Model2+ Muscle area	0.497	0.288	0.859	0.012
Model7	Model2+TH aBMD	0.396 ^a	0.199	0.791	0.009
Model8	Model3+ Muscle area	0.162	0.027	0.954	0.044
Model9	Model3+TH aBMD	0.106	0.012	0.925	0.042

^a indicates poor fit of regression model based on Hosmer-Lemeshow test at 95% CI

Table 1.

Disclosures: Andy Kin On Wong, None.

FR0358

Novel Genetic Factors and Biological Pathways Influencing BMD and Risk of Fracture. Karol Estrada^{*1}, Evangelis Evangelou², Yi-Hsiang Hsu³, Unnur Styrkarsdottir⁴, Ching-Ti Liu⁵, Alireza Moayyeri⁶, Stephen Kaptoge⁷, Emma Duncan⁸, Dave Evans⁹, Najaf Amin¹⁰, Ling Oei¹, Ulrika Pettersson¹¹, Terence O'Neill¹², Jose Riancho¹³, Osten Ljunggren¹⁴, Francois Rousseau¹⁵, William Leslie¹⁶, David Goltzman¹⁷, Barbara Obermayer¹⁸, Bente Langdahl¹⁹, Xavier Nogues²⁰, Richard Prince²¹, Paul Lips²², Sulin Cheng²³, Janja Marc²⁴, George Dedoussis²⁵, Panagoula Kollia²⁵, Maria Luisa Brandi²⁶, Lynne Hocking²⁷, Rita Khushnava²⁸, Cyrus Cooper²⁹, Rebecca Jackson³⁰, Terho Lehtimäki³¹, Jung-Min Koh³², Claus Christiansen³³, John Eisman³⁴, Nelson Tang³⁵, Daniel Chasman³⁶, Vilmundur Gudnason³⁷, Stella Trompet³⁸, Paul M Ridker³⁶, Douglas Kiel³⁹, David Karasik³⁹, Omar Albagha⁴⁰, Matthew Brown⁴¹, Tim Spector⁴², M Zillikens⁴³, Claes Ohlsson⁴⁴, Gudmar Thorleifsson⁴, Jonathan Reeve⁴⁵, Liesbeth Vandenput⁴⁶, Ryan Minster⁴⁷, Candace Kammerer⁴⁸, Laura Yerges-Armstrong⁴⁹, Brent Richards⁵⁰, Jane Cauley⁴⁸, Annie Kung⁵¹, Daniel Koller⁵², John Ioannidis², Stuart Ralston⁴⁰, Andre Uitterlinden⁵³, Fernando Rivadeneira¹, for the AOGC, GENOMOS and GEFOS consortia⁵⁴. ¹Erasmus University Medical Center, The Netherlands, ²University of Ioannina School of Medicine, Greece, ³Hebrew SeniorLife Institute for Aging Research & Harvard Medical School, USA, ⁴Decode Genetics, Iceland, ⁵Boston University School of Public Health, USA, ⁶University of Cambridge, United Kingdom, ⁷University of Cambridge Bone Research Group, United Kingdom, ⁸Royal Brisbane & Women's Hospital, Australia, ⁹University of Bristol, United Kingdom, ¹⁰Erasmus University Medical Center, Netherlands, ¹¹Umea University, Sweden, ¹²Manchester University, United Kingdom, ¹³University of Cantabria, Spain, ¹⁴Uppsala University Hospital, Sweden, ¹⁵Universite Laval & CHUQ, Canada, ¹⁶University of Manitoba, Canada, ¹⁷McGill University Health Centre, Canada, ¹⁸Medical University, Austria, ¹⁹Aarhus Sygehus, Aarhus University Hospital, Denmark, ²⁰Autonomous University of Barcelona, Spain, ²¹Sir Charles Gairdner Hospital, Australia, ²²VU University Medical Center, The Netherlands, ²³University of Jyväskylä, Finland, ²⁴University of Ljubljana, Slovenia, ²⁵University of Athens, Greece, ²⁶University of Florence, Italy, ²⁷University of Aberdeen, United Kingdom, ²⁸Institute of Biochemistry & Genetics USC RAS, Russia, ²⁹University of Southampton, United Kingdom, ³⁰The Ohio State University, USA, ³¹Tampere University Hospital, Finland, ³²Asan Medical Center, South Korea, ³³CCBR, Center for Clinical & Basic Research, Denmark, ³⁴Garvan Institute of Medical Research, Australia, ³⁵The Chinese University of Hong Kong, China, ³⁶Brigham & Women's Hospital, USA, ³⁷Icelandic Heart Association Research Institute, Iceland, ³⁸Leiden University Medical Center, Netherlands, ³⁹Hebrew SeniorLife, USA, ⁴⁰University of Edinburgh, United Kingdom, ⁴¹Diamantina Institute of Cancer, Immunology & Metabolic Medicine, Australia, ⁴²King's College London, United Kingdom, ⁴³Erasmus MC Rotterdam, The Netherlands, ⁴⁴Center for Bone Research At the Sahlgrenska Academy, Sweden, ⁴⁵Addenbrookes Hospital, United Kingdom, ⁴⁶University of Gothenburg, Sweden, ⁴⁷University of Pittsburgh, USA, ⁴⁸University of Pittsburgh Graduate School of Public Health, USA, ⁴⁹University of Maryland, USA, ⁵⁰McGill University, Canada, ⁵¹Dr. Kung-Wai Chee Clinic, Hong Kong, ⁵²Indiana University School of Medicine, USA, ⁵³Rm Ee 575, Genetic Laboratory, The Netherlands, ⁵⁴ USA

Aim: Genome-Wide Association Studies (GWAS) have identified 22 BMD loci associated at genome-wide significant (GWS) level, none of which were GWS-associated with fracture (FX) risk. The aim of this study was to identify additional BMD loci and test for association with FX risk, using novel data from the largest meta-analyses conducted to date from the Genetic Factors of Osteoporosis (GEFOS) consortium. **Methods:** The discovery meta-analysis consisted of 17 GWAS (n=34,191) studying ~2.5 million SNPs in relation to lumbar spine (LS-) and femoral neck (FN-) BMD. The top-associated BMD SNPs (P<5x10⁻⁶) were assessed in 50,933 independent subjects for association with BMD, and for risk of (any type of) FX in 31,016 cases and 102,444 controls from 50 studies of the GENOMOS consortium including subjects of European (predominantly) and Asian ancestry. We applied pathway analysis (GRAIL) and modeled allelic risk scores for low BMD (n=36,917) and fracture risk (n= 45,359). **Results:** The meta-analysis of BMD GWAS identified 82 loci with P<5x10⁻⁶; after replication 54 reached GWS (44 FN-BMD, 40 LS-BMD, 30 both). GRAIL analysis identified relationships between 25/82 loci within RANK/RANKL/OPG, Wnt or MSC-differentiation signaling pathways. Of the GWS BMD loci, 15 were associated with FX risk (Bonferroni P<5x10⁻⁴; six were GWS). FX Odds ratios (OR) ranged from 1.04 to 1.09. The strongest FX risk locus (OR: 1.09, 95%CI

1.06-1.11; $P=2 \times 10^{-14}$) contains a gene coding for a protein of unknown function on 18p11 (C18orf19). Notably, no variants in the RANK/RANKL/OPG loci were associated with FX. Mean FN-BMD difference between subjects with high number of BMD-decreasing alleles ($>64\%$; $n=217$) and the population mean (50-52% of alleles; $n=6,434$) was 0.52 SDs. Subjects with a high number of FX risk alleles ($>70\%$; $n=178$ cases/252 controls) had 1.2 increased risk compared to subjects carrying 50-55% of FX risk alleles (4635 cases/8961 controls). Conclusion: We identified 33 novel and confirmed 22 loci underlying BMD variation, 15 of which are associated with FX risk highlighting potential clinical implications. Individuals carrying the highest number of BMD decreasing alleles have a difference in BMD analogous to the effect of being 16 years older. The joint effect of the FX risk alleles (e.g. OR:1.2 increased risk from subjects with highest number of FX alleles) is similar to those of some environmental risk factors for fracture (e.g. OR:1.3 for corticosteroids).

Disclosures: Karol Estrada, None.

FR0359

Objective Assessment of Physical Activity and Risk of Non-spine Fractures: Osteoporotic Fractures in Men Study: (MrOS). Jane Cauley^{*1}, Stephanie Harrison², Dawn Mackey³, Kristine Ensrud⁴, Eric Orwoll⁵, Peggy Cawthon⁶. ¹University of Pittsburgh Graduate School of Public Health, USA, ²San Francisco Coordinating Center, USA, ³CPMC Research Institute, USA, ⁴Minneapolis VA Medical Center / University of Minnesota, USA, ⁵Oregon Health & Science University, USA, ⁶California Pacific Medical Center Research Institute, USA

Few studies have examined the association between physical activity (PA) and non-spine fractures in older men and existing studies are inconclusive. Most previous studies relied on self-reported PA questionnaires which primarily focus on leisure time sports participation. Lower intensity PA is more difficult to quantify by self-report. As part of the third MrOS visit (2007-09), we measured energy expenditure and minutes of PA objectively in 3137 men, average age 79 years using the multi-sensor SenseWear Pro Armband (Innervue software version 5.1, Body Media, Pittsburgh, PA). Men wore the armband for an average of 5 days (range 1-10). Total daily energy expenditure (TEE) and minutes spent in sedentary (metabolic equivalent (MET) <3 e.g., computer usage, laundry), moderate (MET 3- <6 e.g., golf, dancing) and vigorous (MET >6 e.g., running) activities were quantified and divided into quintiles (Q). Non-spine fractures were identified through postcards/phone calls every 4 months. All fractures were confirmed by radiographic report. 150 men (4.8%) experienced an incident non-spine fracture over an average follow-up of 2.7 0.6 years. Cox proportional hazards models were used to assess the relative hazard (RH) (95% confidence interval (CI)) of non-spine fracture across quintiles of PA; quintile 5 (Q5) formed the referent group. Of the total minutes per day, average number of minutes of sedentary activity was 1286; moderate, 74.6 minutes and vigorous, 7.4 minutes. Median TEE (kcal/d) was lower in men who fractured (2127) vs no fracture (2287), $p=0.008$. Median minutes of moderate or greater (MET >3) PA per day was also lower in men who had a non-spine fracture (51.7) vs no fracture (67.6), $p=0.003$. In multiply adjusted models, men with the lowest (Q1) total TEE had a higher risk of non-spine fracture (HR=1.57; 95% CI, 1.07-2.31) compared to men with higher activity (Q2-Q5). However, separate examination of the average minutes of sedentary, moderate and vigorous activity revealed different results by activity intensity (Table). Sedentary activity was unrelated to the risk of non-spine fracture. Men with the lowest minutes of moderate and vigorous activity had a higher risk of fracture that was independent of age, BMD and other covariates (p trend, <0.05). Our results suggest that PA must be at least of moderate intensity to lower risk against non-spine fractures; 30-50 m/day of moderate activity or greater is needed.

Table: Multivariable adjusted* relative hazard (95% CI) of non-spine fracture across quintiles of minutes (m/day) of physical activity of various intensities

Sedentary		Moderate		Vigorous	
Quintile (m/day)	HR(95%CI)	Quintile (m/day)	HR(95%CI)	Quintile (m/day)	HR(95%CI)
1 (<1231)	0.88 (0.50, 1.5)	1 (0- <29)	1.50 (0.9, 2.6)	1 (0- <0.8)	1.65 (1.0, 2.9)
2 (1231- <1286)	0.82 (0.50, 1.4)	2 (29- <51)	1.46 (0.9, 2.5)	2 (0.8- <2.6)	1.23 (0.7, 2.1)
3 (1286- <1324)	0.86 (0.5, 1.5)	3 (51- <76)	0.81 (0.4, 1.5)	3 (2.6- <5.6)	0.96 (0.5, 1.7)
4 (1324- <1359)	1.06 (0.6, 1.7)	4 (76- <113)	0.91 (0.5, 1.6)	4 (5.6- <11.4)	1.04 (0.6, 1.8)
5 (≥ 1359)	Referent	5 (≥ 113)	Referent	5 (≥ 11.4)	Referent
P trend	0.40	P trend	0.03	P trend	0.05

* Adjusted for age, race, clinic, total hip BMD, weight, height, diabetes, health status, current smoking.

table

Disclosures: Jane Cauley, None.

FR0366

Interaction of Genome Wide Variants with Dietary Vitamin D Intake on Serum Vitamin D Concentration: The Framingham Osteoporosis Study. Yue Fang^{*1}, Ching-Ti Liu², Yi-Hsiang Hsu³, Adrienne Cupples⁴, David Karasik⁵, Douglas Kiel⁵. ¹Hebrew SeniorLife Center at Harvard Medical School, USA, ²Boston University School of Public Health, USA, ³Hebrew SeniorLife Institute for Aging Research & Harvard Medical School, USA, ⁴Department of Biostatistics, Boston University School of Public Health, USA, ⁵Hebrew SeniorLife, USA

Vitamin D is an important contributor to many diseases and health conditions, including osteoporosis. As is true for other complex genetic traits, vitamin D status is regulated by multiple genetic and environmental factors, as well as their interaction. Most Genome Wide Association Studies (GWAS) have focused on the independent main genetic effects on phenotypes, including a recent meta-analysis from the "SUNLIGHT Consortium". These studies ignore the observation that the serum response to vitamin D intake varies considerably between individuals, suggesting that genetic factors may interact with dietary of vitamin D on serum concentrations. We therefore investigated the interaction between whole genome single nucleotide polymorphisms (SNPs) and dietary vitamin D intake on serum vitamin D level in the Framingham Osteoporosis Study (2,315 men and 2,668 women, mean age = 65 yrs). Dietary vitamin D intake was estimated by food frequency questionnaire that included the use of vitamin D supplements. 25(OH)D concentration was measured by radioimmunoassay. Genotyping used the Affymetrix 500+50K Genechips, and >2.4 mil genome-wide SNPs imputed with the HapMap CEU phase II panel. The interaction between each genome-wide SNP and continuous vitamin D intake on ln25 (OH)D was assessed with the linear regression that included an interaction term between SNP and vitamin D intake, adjusted for age, sex, BMI, season of vitamin D measurement, total energy intake and principal components of ancestry. We observed 17 SNPs with an interaction p -value $<10^{-6}$. Eight common SNPs (allele frequencies 9-19%), six in the cadherin 11 (CDH11) and two in the tetratricopeptide repeat domain 27 (TTC27) gene, had interaction p -values of $2.6-4.4 \times 10^{-7}$, which indicated that genotypes of SNPs in CDH11 and TTC27 genes may modify the association between dietary vitamin D intake and serum vitamin D concentration. Though CDH11 gene was reported to modulate postnatal bone growth and osteoblast differentiation in vivo and in vitro, TTC27 gene was sensitive to damage by hypoxic condition in brain, we are unclear how they influence the association of vitamin D intake and serum level. Thus, our findings need to be replicated in other independent studies. In conclusion, we observed potential interaction between CDH11 and TTC27 genes with dietary vitamin D intake on serum vitamin D concentration in our cohort, it suggests that there may be genes that modify the serum response to vitamin D intake.

Disclosures: Yue Fang, None.

FR0367

Meta-analysis of Genome-wide Association Studies in Premenopausal White Women Identifies Variants in WNT16, ESR1, and Novel BMD Loci. Daniel Koller^{*1}, David Karasik², Hou-Feng Zheng³, Laura Yerges-Armstrong⁴, Ching-Ti Liu⁵, Dongbing Lai¹, Karol Estrada⁶, Fernando Rivadeneira⁶, Andre Uitterlinden⁷, Sylvie Giroux⁸, Francois Rousseau⁹, Stefan Czerwinski¹⁰, Bradford Towne¹⁰, Michael Econs¹, Braxton Mitchell¹¹, Brent Richards³, Douglas Kiel², Tatiana Foroud¹. ¹Indiana University School of Medicine, USA, ²Hebrew SeniorLife, USA, ³McGill University, Canada, ⁴University of Maryland, USA, ⁵Boston University School of Public Health, USA, ⁶Erasmus University Medical Center, The Netherlands, ⁷Rm Ee 575, Genetic Laboratory, The Netherlands, ⁸Centre de recherche CHUQ-SFA, Canada, ⁹University Laval, Canada, ¹⁰Wright State University Boonshoft School of Medicine, USA, ¹¹University of Maryland, Baltimore, USA

Several genome-wide association studies (GWAS) have identified gene variants associated with bone mineral density (BMD) variation, typically in combined samples of elderly women and men. Meta-analysis of these results (Rivadeneira et al, Nat Gen 2009) identified 20 genome-wide significant SNPs of modest effect in both novel genes as well as in genes previously shown to influence BMD variation. BMD in older adults is influenced by genes underlying bone accrual as well as bone loss processes. To identify genes influencing peak bone mass, we performed a GWAS meta-analysis restricted to premenopausal white women ($n=4,061$ women, ages 20 to 45) from 4 cohorts (Framingham Osteoporosis Study, Amish Family Osteoporosis Study, Indiana Sisters Study, and Twins UK). BMD was measured at the lumbar spine and femoral neck by DXA. GWAS genotypes in each cohort were imputed to HapMap II r22 and samples with call rates below 95% as well as SNPs with deviation from Hardy-Weinberg equilibrium ($p<0.0001$) were removed. Age- and weight-adjusted BMD values were tested for association with each SNP. Inverse variance fixed-effects meta-analysis using METAL was performed, applying double-genomic control correction.

22 SNPs (Table) provided suggestive evidence of association ($p<10^{-5}$) with either spine or femoral neck BMD after pruning by minor allele frequency ($<3\%$), LD ($r^2>0.2$) with a SNP already identified, and singleton associations in high LD ($r^2>0.5$)

with other non-associated SNPs. Several of these associations were previously reported in men and women across a broad age range (e.g. *WNT16*, *ESR1*, *C6orf97* and *SOX6*). In addition, we identified several SNPs in genes not previously associated with BMD that provided suggestive evidence of association in our sample of premenopausal women (bold in Table). We are currently performing replication genotyping in approximately 3,700 independent samples of premenopausal women. Our results confirm that some of the genes contributing to peak BMD in premenopausal women also influence BMD variation across sexes and ages. However, our approach also seems to identify novel BMD associations that may be more specific to premenopausal women.

SNP	Chr	MAF	BMD	P-value ^a	Gene ^b
rs3801387	7	0.28	Spine	1.69E-09	WNT16
rs4870044	6	0.29	Spine	1.32E-08	C6orf97
rs1566045	16	0.21	Neck	2.57E-07	SALL1(148kb)
rs10784173	12	0.28	Spine	2.80E-07	PGBD3P1(63kb)
rs1992965	3	0.15	Neck	5.22E-07	CABYRP(3kb)
rs17140337	16	0.12	Neck	6.04E-07	A2BP1
rs7258173	19	0.11	Spine	6.93E-07	RHPN2
rs2982575	6	0.47	Spine	8.27E-07	ESR1
rs6930633	6	0.33	Spine	1.03E-06	C6orf97(15kb)
rs6774742	3	0.35	Spine	1.95E-06	LOC391533(10kb)
rs11648832	16	0.33	Neck	2.19E-06	A2BP1(18kb)
rs11247864	1	0.33	Spine	3.11E-06	CATSPER4
rs12041939	1	0.04	Neck	3.63E-06	MIR3134(18kb)
rs818215	3	0.46	Neck	4.40E-06	CDM2
rs10258526	7	0.13	Spine	4.70E-06	PHF14(18kb)
rs8071899	17	0.06	Spine	5.12E-06	KCNJ16(140kb)
rs7386	11	0.45	Neck	6.12E-06	C11orf48
rs12996362	2	0.23	Spine	6.71E-06	LOC100287217(15kb)
rs7117858	11	0.21	Neck	7.59E-06	SOX6(293kb)
rs16912067	12	0.32	Spine	7.86E-06	LMO3(12kb)
rs760825	6	0.36	Neck	8.21E-06	MIR548A1(19kb)
rs10158553	1	0.29	Neck	8.77E-06	SRGAP2

^a novel associations are indicated in bold type

^b distance from nearest gene in parentheses if applicable

Disclosures: Daniel Koller, None.

FR0368

Women With Inadequately Controlled Type 2 Diabetes Are At Increased Risk Of Osteoporotic Fractures Despite Higher Bone Mineral Density: The Rotterdam Study. Ling Oei^{*1}, Martha Castano-Betancourt¹, Huibert Pols¹, Abbas Dehghan², Andre Uitterlinden³, Fernando Rivadeneira¹, M Zillikens⁴. ¹Erasmus University Medical Center, The Netherlands, ²Erasmus MC, Netherlands, ³Rm Ee 575, Genetic Laboratory, The Netherlands, ⁴Erasmus MC Rotterdam, The Netherlands

Aim: Patients with type 2 diabetes mellitus display an increased fracture risk found after controlling for higher BMD. The increased fracture risk is mainly attributable to the increased risk of falling. Our aim was to investigate if the relationship between diabetes, BMD and osteoporotic (OP) fractures is influenced by diabetes control across genders.

Methods: This is a large prospective population-based study including 4135 participants with baseline (1991-1993) information on diabetes status, BMD, and incident OP fracture events with follow-up (mean 8.2 years SD=2.95). HbA1c was computed at baseline from fructosamine levels:

HbA1c = 0.017 * Fructosamine [μmol/L] + 1.61. Inadequate glucose control in diabetes was defined as a serum HbA1c level ≥ 7.5%. Comparison groups included non-diabetics (ND;n=3715), adequately controlled diabetics (ACDM;n=203) and inadequately controlled diabetics (ICDM;n=217) stratified by gender. Femoral neck (FN) and lumbar spine (LS) BMD was measured by DXA. Mean differences in BMD levels were tested in linear regression models adjusted for age and BMI. OPfx were defined as those not caused by focal lesions, hand, skull or facial fracture and derived from physician records. Cox proportional hazard regression models were used to estimate the risk of fracture adjusted for age and weight.

Results: In both genders diabetics had higher BMD. ICDM women had significantly higher BMD (g/cm²) at both the LS (1.10;P=0.0001) and FN (0.86; P=0.005) as compared to ACDM women (LS:1.03;FN:0.83) and non-diabetics (LS:1.03;FN:0.82). No differences in BMD were seen between ACDM and ICDM men. No increased risk for incident non-vertebral fracture was observed in either type of diabetics in either gender after correction for age and BMI. After additional correction for FN-BMD ICDM women had 1.6 times (95%CI 1.07-2.25; P=0.02) increased risk of fracture as compared to non-diabetics. ACDM women had no increased risk of fracture (HR: 0.88 95%CI 0.57-1.36; P=0.57). In men no significant risk of fracture was observed in either group of diabetics.

Conclusion: Elderly subjects with Type 2 diabetes have higher BMD levels than non-diabetics. In women higher levels are mostly driven by inadequately controlled

diabetics. After correcting for femoral neck BMD, inadequately controlled diabetic women have increased risk of incident non-vertebral fracture. These findings suggest inadequate control of diabetes is a risk for fracture in elderly women.

Disclosures: Ling Oei, None.

FR0369

BMD and Breast Cancer Risk: A Positive Association in Women ≥50 Years and a Negative in Women <50 Years? The HUNT Study, Norway. Siri Forsmo^{*1}, Kathinka Slørdahl², Arnulf Langhammer³. ¹Norwegian University of Science & Technology, Norway, ²Faculty of Medicine, Norwegian University of Science & Technology, Norway, ³Dept. of Public Health & General Practice, Norwegian University of Science & Technology, Norway

Purpose: To explore the association between forearm bone mineral density (BMD) and incident breast cancer in a cohort of 13,072 Norwegian women aged 19-89 years, followed up to 14 years.

Methods: Distal and ultradistal forearm BMD was measured in the second Nord-Trøndelag Health Study (1995-97), a multipurpose health survey. Reproductive health and life-style data were collected by self-administered questionnaires. A total of 210 incident breast cancer cases were identified by record linkage with the Norwegian Cancer Registry. Limits of identification were set for breast cancer registered between two months after BMD assessment until the end of follow-up at Dec. 31, 2008. Follow-up time was calculated as the difference in time between BMD assessment until the event of incident breast cancer, death (N=2,598), emigration (N=25) or the end of follow-up, whichever occurred first. Due to missing or incomplete BMD, weight or height measurements, a total of 12,881 women were eligible for analyses. The association between BMD and incident breast cancer was analysed in Cox' proportional regression models with BMD in tertiles of Z-score, i.e. standard deviations from age-specific mean BMD. The analyses were performed in two age strata, under 50 years and 50 and above.

Results: Mean time of follow-up was 11.4 years (3 weeks-14.1 years) or 146,614 person-years. A total of 42 cases (0.8/1000 person-years) was observed among women <50 years and 168 (1.8/1000 person-years) among women aged 50 or above. The risk of incident breast cancer was positively associated with BMD in women 50+ with a hazard ratio (HR) of 0.65 (95% CI, 0.45-0.94) for women in the lowest tertile of Z-scores relative to women in the highest (HR=1) and with a statistically significant linear trend across the Z-score tertiles (p=0.02). The association between BMD and breast cancer risk in the younger women seemed to be negative, especially for BMD measured at the ultradistal radius where the HR of breast cancer was 1.9 (95% CI, 0.9-4.1) for women in the lowest tertile compared to those in the highest and with a linear trend across the tertiles (p=0.1). Adjusting for weight explained some of the association found in women 50+, but not among the younger.

Conclusion: High BMD in women aged 50+ is associated with increased risk of breast cancer whereas the inverse association is observed in younger women, indicating age-related differences in breast cancer etiology.

Disclosures: Siri Forsmo, None.

FR0375

Fat Mass and Fracture Risk in Elderly Men and Women: A Prospective Study. Shuman Yang^{*1}, Nguyen Nguyen², Jacqueline Center², John Eisman², Tuan Nguyen². ¹Garvan Institute, Australia, ²Garvan Institute of Medical Research, Australia

Background and aim: The relationship between body fat mass and fracture risk is controversial, due primarily to lack of prospective data. The present study sought to examine the association between whole body and abdominal fat mass and fracture risk in postmenopausal women and elderly men.

Materials and methods: The present study was part of the ongoing Dubbo Osteoporosis Epidemiology Study (DOES) recruited a cohort of 1129 participants (361 men and 768 women), whose total body bone mineral density (BMD) scans were available. BMD at the femoral neck and lumbar spine, total body fat mass and abdominal fat mass were measured by dual energy X-ray absorptiometry (GE-LUNAR Corp, Madison, WI). Baseline characteristics of participants including age, height, physical activity, history of falls, smoking and prior fracture were ascertained at the initial visit. The incidence of low-trauma and non-pathological fractures was ascertained from X-ray reports. The Cox's proportional hazards regression was used to evaluate the association between fat mass and fracture risk, with adjustment for baseline covariates.

Results: During the median 5 years of follow-up, 19 (5%) men and 107 (14%) women had sustained a fragility fracture. Women with fracture had lower BMD, lower body fat mass and body weight than those without a fracture. In women, increased risk of fracture was associated with lower abdominal fat mass (hazard ratio/standard deviation [HR/SD]: 1.33; 95% CI: 1.07-1.65), after adjusting for age (HR/SD: 1.32; 1.08-1.63), femoral neck BMD (HR/SD: 1.26; 1.03-1.56), and prior fracture (HR/SD: 1.41; 1.15-1.73). Compared with women in the highest tertile of abdominal fat, those in the lowest tertile had a 2.1-fold (95%CI: 1.25-3.55) increase in fracture risk. Further analyses revealed that lower body fat mass was also associated with increased fracture risk, but the association was not independent of BMD. The

magnitude of association between fat mass and fracture risk (HR/SD: 1.32; 1.08-1.63) was greater than that of body weight and fracture risk (HR/SD: 1.15; 0.94-1.41). Approximately 27% of population fracture liability was attributable to abdominal fat mass.

Conclusion: Lower total body fat mass, particular lower abdominal fat, was significantly associated with increased fracture risk in women, not in men. These results suggest that the incorporation of fat mass into existing fracture prognostic models may enhance their predictive accuracy.

Disclosures: Shuman Yang, None.

FR0377

Fracture Incidence in Obese Postmenopausal Women: The Global Longitudinal Study of Osteoporosis in Women. Juliet Compston^{*1}, Nelson Watts², Roland Chapurlat³, Cyrus Cooper⁴, Steven Boonen⁵, Susan Greenspan⁶, Johannes Pfeilschifter⁷, Stuart Silverman⁸, Adolfo Diez-Perez⁹, Robert Lindsay¹⁰, Kenneth Saag¹¹, Coen Netelenbos¹², Stephen Gelhbach¹³, Frederick Hooven¹⁴, Julie Flahive¹³, Jonathan Adachi¹⁵, Maurizio Rossini¹⁶, Andrea Lacroix¹⁷, Christian Roux¹⁸, Philip Sambrook¹⁹, Ethel Siris²⁰. ¹University of Cambridge School of Clinical Medicine, United Kingdom, ²University of Cincinnati Bone Health & Osteoporosis Center, USA, ³E. Herriot Hospital, France, ⁴University of Southampton, United Kingdom, ⁵Center for Metabolic Bone Disease & Division of Geriatric Medicine, Belgium, ⁶University of Pittsburgh, USA, ⁷Alfried Krupp Krankenhaus Steele, Germany, ⁸Cedars-Sinai/UCLA, USA, ⁹Autonomous University of Barcelona, Spain, ¹⁰Helen Hayes Hospital, USA, ¹¹University of Alabama at Birmingham, USA, ¹²VU Medical Center, The Netherlands, ¹³UMass Medical School, USA, ¹⁴University of Massachusetts Medical School, USA, ¹⁵St. Joseph's Hospital, Canada, ¹⁶University of Verona, Italy, ¹⁷Fred Hutchinson Cancer Research Center, USA, ¹⁸Hospital Cochin, France, ¹⁹Royal North Shore Hospital, Australia, ²⁰Columbia University College of Physicians & Surgeons, USA

Purpose: Low body mass is an important risk factor for fracture, while obesity is widely believed to be protective. However, two recent studies in postmenopausal women have challenged this view [1,2]. The aim of this study was to examine the incidence of clinical fractures in obese postmenopausal women in the Global Longitudinal study of Osteoporosis in Women (GLOW) study - a multinational, prospective, population-based observational study in 60,393 women - over a 2-year follow-up period.

Methods: Data were collected using self-administered questionnaires covering domains that included patient characteristics, fracture history, risk factors for fracture, and anti-osteoporosis therapy.

Results: Fracture history and body mass index (BMI) were available at baseline and at 2 years in 44,534 women. Of these, 23.4% were obese (BMI ≥ 30 kg/m²), 74.9% non-obese (BMI 18.5-29.9 kg/m²), and 1.7% underweight (BMI < 18.5 kg/m²). In obese women, the prevalence of fractures at baseline was 222 per 1,000 and incidence at 2 years was 61.7 per 1,000, similar to rates in non-obese women (227 and 66.0 per 1,000, respectively). Fractures in obese women accounted for 22% of all incident fractures. Higher BMI was associated with ankle ($p < 0.001$) and lower leg fractures ($p = 0.02$) and was inversely related to wrist ($p = 0.01$) and pelvis fractures ($p = 0.02$). Non-obese and obese women with incident fracture had similar rates of previous fracture (42% and 39%, respectively). Obese women with incident fracture were more likely to have experienced early menopause and to report two or more falls in the past year ($p < 0.001$). Self-reported asthma, osteoarthritis, and type 1 diabetes were all significantly associated with higher BMI ($p < 0.001$). At 2 years, only 27% of obese women with incident fracture were receiving bone-protective medication, compared with 41% of non-obese and 57% of underweight women.

Conclusions: Our results demonstrate that nearly one in four postmenopausal women with an incident clinical fracture is obese and that obesity is a risk factor for fractures of the lower leg and ankle. Our findings have major public health implications in view of the rapidly rising incidence of obesity. Further studies are required to establish the pathogenesis of fractures in the obese population and to develop effective strategies for their prevention.

1. Premaor MO et al. J Bone Miner Res. 2010;25:292-297.

2. Compston J et al. ASBMR Annual Meeting 2010 S460.

Table Fractures among obese, non-obese, and underweight women (n = 44,534; rates per 1000 Women)

	Obese (BMI ≥ 30 kg/m ²) (n = 10,441)	Non-obese (BMI 18.5- 29.9 kg/m ²) (n = 33,349)	Underweight BMI < 18.5 kg/m ²) (n = 744)
Previous fracture	222	227	300
Incident fracture (1- or 2-year follow-up)	62	66	72
With previous fracture	46	52	45
Without previous fracture	116	114	141

Table

Disclosures: Juliet Compston, None.

This study received funding from: Warner Chilcott Company, LLC and sanofi-aventis

FR0380

New Loop Diuretic Prescriptions Increase the Acute Risk of Hip Fracture.

Sarah Berry^{*1}, Yanyan Zhu², Hyon Choi², Douglas Kiel³, Yuqing Zhang².

¹Hebrew SeniorLife/Beth Israel Deaconess Medical Center, USA, ²Boston University School of Medicine, USA, ³Hebrew SeniorLife, USA

Purpose: Conflicting data exist on the association between diuretics and risk of hip fracture. We hypothesized that older adults would have a short term increased risk of hip fracture following a new prescription for a diuretic due to acute urinary symptoms that could result in a fall due to hurrying. We determined the effect of a new loop and other diuretic prescription on the acute risk of hip fracture using a case-crossover study design in The Health Improvement Network (THIN).

Methods: THIN is a primary care database from more than 400 practices and 7 million persons in the UK. Participants of the current study (1986-2010) included 28,707 members, aged ≥ 50 years, who experienced a hip fracture > 365 days from enrollment. Fractures were identified using diagnostic codes. A new diuretic prescription was defined as an oral diuretic prescription without a history of use within the past 180 days. We defined the case period as 1-7 days before the fracture and the control period as 31-37 days before the fracture in the same individual. Odds ratios of hip fracture were estimated by comparing the frequency of new loop and other diuretic prescriptions during the case and control periods using conditional logistic regression models. To address confounding by indication we repeated our analysis using a comparator class of medications that are not expected to be associated with falls or fractures: ACE-inhibitors.

Results: Mean age was 89 yrs (SD 10 yrs), and 77% were female. During the case periods, 64 subjects with hip fracture received a new prescription for a loop diuretic compared with 35 in the control periods. The odds ratio of experiencing a hip fracture within 7 days of a new loop diuretic prescription was 1.8 (95%CI 1.2, 2.8). There was no association between a new prescription of other diuretics (OR:1.1, 95% CI 0.7, 1.7) or ACE-inhibitors (OR:0.8, 95% CI 0.4, 1.5) and the acute risk of hip fracture.

Conclusions: Risk of hip fracture was elevated by 80% during the week following a new loop diuretic prescription, but not following other diuretic or ACE-inhibitor prescriptions. The acute risk may relate in part to urinary symptoms, which are more prominent with loop diuretic initiation. Although new loop diuretic prescriptions were associated with a small absolute number of excess hip fractures, increased awareness and toileting interventions might be effective in reducing hip fractures and other injurious falls in vulnerable older adults during this time.

Disclosures: Sarah Berry, None.

FR0383

QCT vBMD and Vascular and Valvular Calcification: The Framingham Study.

Elizabeth Samelson^{*1}, Christopher O'Donnell², Kerry Broe³, Udo Hoffmann⁴, Sekar Kathiresan², Serkalem Demissie⁵, L. Adrienne Cupples², Mary Boussein⁶, Douglas Kiel⁷.

¹Hebrew SeniorLife, Harvard Medical School, USA, ²National Heart, Lung & Blood Institute's Framingham Heart Study, USA, ³Hebrew Senior Life, USA, ⁴Massachusetts General Hospital, USA, ⁵Department of Biostatistics, Boston University School of Public Health, USA, ⁶Beth Israel Deaconess Medical Center, USA, ⁷Hebrew SeniorLife, USA

Previous studies provide evidence for a shared pathogenesis between osteoporosis and atherosclerosis, highly prevalent conditions with significant morbidity and mortality in older adults. Because DXA assessment of lumbar spine BMD can be confounded by the presence of abdominal aortic calcification and by bone size, 3-D technology is needed for precise measurement. Prior work focused on the association of coronary artery and aortic calcification to BMD in highly selected individuals.

Valve calcification and resulting stenosis are also clinically significant. Similar to vascular calcification, valve calcification is an active process sharing features of bone formation. We conducted a cross-sectional study to determine the association between volumetric bone density (vBMD) and severity of atherosclerotic and valvular calcification in the community-based Framingham Study.

Participants included 700 women and 630 men in the Framingham Offspring Study (mean age 60 years, range 36-83 years) who underwent imaging using an 8-slice MDCT scanner in 2002-05. Coronary artery, abdominal aortic, aortic valve, and mitral valve calcium were each scored using previously published, modified Agatston methods. ANCOVA was used to calculate mean log-transformed calcium scores across sex-specific quartiles (1=low) of integral vBMD at the lumbar spine (L3), adjusted for age, BMI, height, smoking, physical activity, and for women, menopause status and estrogen use.

Prevalence of any calcium (score > 0) was 57% for coronary artery, 77% for abdominal aorta, 20% for mitral valve, and 32% for aortic valve calcium. We found an inverse association between severity of vascular calcification (coronary artery and abdominal aorta) and vBMD in women (TABLE), although no association was observed in men. No association between aortic and mitral valve calcium and vBMD was seen in women or men.

We used MDCT technology to measure both vascular and valvular calcification as well as spine bone density in a community-based population of women and men. The sex-specific findings of an inverse association between vascular calcification and vBMD are consistent with previous studies suggesting differences between women and men in the underlying pathophysiology of bone mineralization, vascular calcification, or both. A lack of association between vBMD and valve calcification may be due to a low prevalence compared to vascular calcification or due to pathophysiological or other differences.

	Women	Men	Women	Men	Women	Men	Women	Men
Quantile 1 (Low)	1.00	0.42	1.15	0.00	1.21	1.01	1.14	0.42
Quantile 2	0.57	0.40	0.57	0.00	0.84	0.84	0.84	0.42
Quantile 3	0.57	0.40	0.57	0.00	0.84	0.84	0.84	0.42
Quantile 4 (High)	0.57	0.40	0.57	0.00	0.84	0.84	0.84	0.42
Mean	1.00	0.42	1.15	0.00	1.21	1.01	1.14	0.42

TABLE.

Disclosures: Elizabeth Samelson, None.

FR0384

Temporal Trends in 25-Hydroxyvitamin D levels and parathyroid hormone in a population-based study. Claudia Berger^{*1}, Linda Greene-Finestone², Lisa Langsetmo³, Lawrence Joseph¹, Nancy Kreiger⁴, Brent Richards¹, Christopher Kovacs⁵, Kurtis Sarafin⁶, K. Shawn Davison⁷, Jonathan Adachi⁸, Jacques Brown⁷, David Hanley⁹, David Goltzman¹⁰. ¹McGill University, Canada, ²Public Health Agency of Canada, Canada, ³Canadian Multicenter Osteoporosis Study, Canada, ⁴University of Toronto, Canada, ⁵Memorial University of Newfoundland, Canada, ⁶Health Canada, Canada, ⁷Laval University, Canada, ⁸St. Joseph's Hospital, Canada, ⁹University of Calgary, Canada, ¹⁰McGill University Health Centre, Canada

We examined vitamin D and calcium intake, sun-exposure, and body mass index (BMI) in relation to changes in serum 25-hydroxyvitamin D [25(OH)D] and parathyroid hormone (PTH) over a ten-year period among participants in the Canadian Multicenter Osteoporosis Study.

We studied 1896 women and 829 men aged 25+ years who had 3896 blood samples drawn in 1995-1997, 2000-2002 and/or 2005-2007. PTH and 25(OH)D were analyzed in the same laboratory using a Diasorin Liaison instrument. Hierarchical models using up to 10 years of longitudinal data were used to determine changes over time in vitamin D supplement intake and in serum 25(OH)D and PTH; the non-linear association between PTH and 25(OH)D (polynomials); and predictors of 25(OH)D and PTH. All models were adjusted for season.

Vitamin D supplement intake increased annually by 31.7 (27.2; 35.9) IU/day in women and 19.3 (13.5; 25.2) IU/day in men. 25(OH)D increased annually by 0.9 (0.7; 1.1) nmol/L in women and by 0.4 (0.1; 0.6) nmol/L in men. When adjusted for vitamin D supplement intake, 25(OH)D still increased annually by 0.5 (0.2; 0.7) nmol/L in women and by 0.3 (-0.1; 0.6) nmol/L in men. PTH decreased annually by 0.8 (95% CI: 0.6; 1.2) pg/ml in women and by 0.5 (0.0; 0.9) pg/ml in men. After adjustment for serum 25(OH)D levels, there was still an annual decline of 0.6 (0.3; 0.8) pg/ml and 0.3 (-0.1; 0.8) pg/ml in PTH in women and men. Further adjusting for total calcium intake did not change the decrease in PTH over time. Figure 1 shows the relation obtained from PTH and 25(OH)D. Serum 25(OH)D samples collected in summer were higher in both women [6.9 (4.9; 8.8) nmol/L] and men [8.4 (5.4; 11.5) nmol/L]. Higher 25(OH)D levels were also associated with younger age, lower BMI, participation in regular physical activity, sun exposure and higher total calcium intake. Lower PTH levels

were associated with younger age and higher 25(OH)D levels in both women and men. In women, it was further associated with lower BMI and participation in a regular physical activity. PTH levels were not associated with total calcium intake.

These results indicate a trend toward increasing 25(OH)D levels and decreasing PTH levels over 10 years. Secular increases in supplemental vitamin D have impacted both serum 25(OH)D and PTH, but do not explain all variation in these measures.

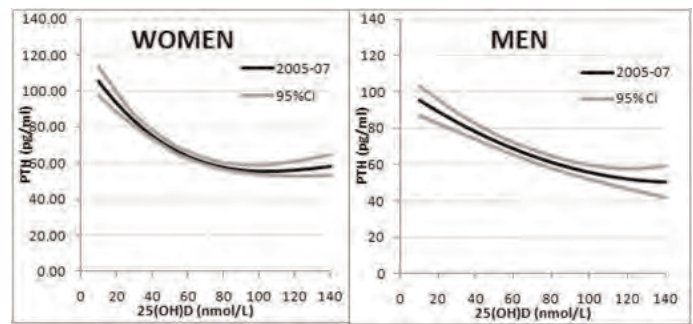


Figure 1: PTH by 25(OH)D in women and men

Disclosures: Claudia Berger, None.

FR0385

The Association Between Fracture and Obesity Is Site-Dependent: A Population-Based Study. Daniel Prieto-alhambra^{*1}, Francesc Fina Aviles², Eduard Hermosilla³, Daniel Martinez-Laguna⁴, Cristina Carbonell⁵, Robert Guerri⁶, Xavier Nogues⁶, Adolfo Diez-Perez⁶. ¹Institut Municipal D'Investigacio Medica, Spain, ²SIDIAP Database, IDIAP Jordi Gol i Gurina; Barcelona Primary Care Dept, Institut Catala de la Salut, Spain, ³SIDIAP Database, IDIAP Jordi Gol i Gurina, Spain, ⁴Barcelona Primary Health Care Department, Institut Catala de la Salut, Spain, ⁵Healthy Primary Care Via Roma Barcelona.Facultat de Medicina Universitat de Barcelona, Spain, ⁶Department of Internal Medicine, URFOA IMIM-Hospital del Mar, Parc de Salut Mar, Autonomous University of Barcelona, RETICEF (Red Tematica de Investigacion Cooperativa en Envejecimiento y Fragilidad), Instituto Carlos III, Barcelona, Spain, Spain

OBJECTIVE: The available evidence on the association between obesity and fracture is controversial. We aimed to study the existing relationship between body mass index (BMI) and fracture occurrence at different sites among women aged ≥ 50 .

METHODS: The Spanish public health system covers >98% of the population. The SIDIAP database (www.idiapigol.org/sidiap.php) contains the validated clinical information collected in the computerized medical records of >2,500 GPs in Catalonia (North-East Spain), with information on a representative sample which accounts for 80% of the population (>5 million people). In 2009, 1,039,878 women ≥ 50 were eligible in SIDIAP, and 832,775 (80.1%) of them had a BMI measurement available. These were categorized (according to WHO criteria) as underweight/normal (302,414 women), overweight (266,798 subjects) and obese (263,563 people). Fractures were ascertained using ICD-10 codes. We derived age-specific fracture incidence rates for diverse fracture sites (hip, clinical spine, wrist/forearm, tibia, pelvis and proximal humerus) for the 2 extreme BMI groups. Secondly, we estimated age-adjusted rate ratios (and p-values) to compare obese and normal/underweight women using Poisson Regression.

RESULTS: Age-specific fracture rates for extreme BMI groups (normal/underweight versus obese) are shown in Figure 1. Hip (RR 0.49 [95CI 0.44 to 0.55] $p<0.001$), clinical spine (RR 0.87 [95CI 0.77 to 0.98] $p=0.021$), wrist/forearm (RR 0.83 [95CI 0.75 to 0.91] $p<0.001$) and pelvis fracture rates (RR 0.43 [95CI 0.19 to 0.97] $p=0.028$) were higher in the normal/underweight than in the obese. Conversely, obese women were at significantly higher risk of proximal humerus fracture than the normal/underweight: RR 1.23 [95CI 1.07 to 1.41] $p=0.002$. Tibial fracture rates were not different between groups ($p=0.488$).

DISCUSSION: The association between obesity and fracture is site-dependent: while obesity protects from hip, clinical spine, wrist/forearm and pelvis fractures, it is also related to an almost 25% increase in risk for proximal humerus fractures. This should be considered for fracture prevention among obese patients.

FR0392

Chronic Central Administration of Ghrelin Increases Bone Mass Through Mechanisms Independent of Appetite Regulation. Hyung Jin Choi¹, Kyoung Ho Ki¹, Jae-Yeon Yang¹, Bo Young Jang¹, Jung Ah Song¹, Wook-Young Baek², Jung Hee Kim³, Jee Hyun An¹, Sang Wan Kim⁴, Seong Yeon Kim¹, Jung-Eun Kim⁵, Chan Soo Shin¹. ¹Department of Internal Medicine, Seoul National University College of Medicine, South Korea, ²Department of Molecular Medicine, Cell & Matrix Research Institute, Kyungpook National University School of Medicine, South Korea, ³Seoul National University College of Medicine, South Korea, ⁴Seoul National University Boramae Hospital, South Korea, ⁵Kyungpook National University School of Medicine, South Korea

Leptin has been shown to play a critical role in the central regulation of bone mass. Ghrelin is a gut-derived hormone that counteracts leptin in hypothalamus regarding appetite control. In the present study, we have investigated the effect of chronic intracerebroventricular (ICV) administration of ghrelin on bone mass changes. The effects of ghrelin on food intake, body weight, and bone metabolism were determined following ICV administration of ghrelin (1.5ug/day) for 21 days in Sprague-Dawley rats. Rats were divided into control, ad lib-fed, and pair-fed groups. Bone mineral density, bone microstructure, bone formation rate and daily body weight were determined by DXA, MicroCT, and calcein double labeling. ICV infusion of ghrelin for 21 days significantly increased body weight in ad lib-fed rats (331.4 g, $p < 0.05$) but not in pair-fed rats (311.9 g) compared with control rats (312.9 g). Ghrelin ad lib-fed rats had significantly higher spine BMD compared with control rats (0.161 vs. 0.148 g/cm²; $P < 0.05$). Ghrelin pair-fed rats tended to have a higher bone mass in femur (BV/TV) (26.6 vs. 22.4 %; $p = 0.07$) and had significantly higher trabecular thickness in femur (72.1 vs. 67.8 μ m; $p < 0.05$) compared with control rats. There was no significant change in trabecular number or trabecular spacing between ghrelin pair-fed and control group. In dynamic assessment of bone formation using calcein double labeling study, ghrelin pair-fed rats (5.2 \pm 1.0 μ m/d, $p < 0.05$) and ghrelin ad lib-fed rats (5.6 \pm 1.3 μ m/d) had significantly higher mineral apposition rate (MAR) compared with control (3.8 \pm 0.9 μ m/d). However, we were unable to demonstrate significant changes in serum PINP at 9 weeks of age. In conclusion, chronic central administration of ghrelin increased bone mass through mechanisms independent of body weight changes, suggesting that ghrelin antagonizes leptin in bone mass regulation as it does in appetite control.

Disclosures: Hyung Jin Choi, None.

FR0394

Circulating Sclerostin Levels and Bone Turnover in Type 1 and 2 Diabetes. Ranuccio Nuti¹, Roberto Valenti², Daniela Merlotti¹, Elena Ceccarelli³, Martina Ruvio³, Maria Giulia Pietrini³, Cosimo Capodacqua³, Maria Beatrice Franci³, Anna Calabro³, Konstantinos Stolkis³, Francesco Dotta³, Luigi Gennari¹. ¹University of Siena, Italy, ²S. Maria Alle Scotte Hospital, Italy, ³Dept. Internal Medicine Endocrine Metabolic Sciences & Biochemistry University of Siena, Italy

Evidence from experimental and clinical studies indicates that both type 1 (DM1) and 2 (DM2) diabetes can impact bone strength and increase fracture risk. However the pathogenetic mechanisms remain in great part unknown and are only in part reflected by variation in BMD. Previous experimental and histomorphometry observations often evidenced a condition of low bone turnover and decreased osteoblast activity in both DM1 and DM2. Sclerostin (SOST) is a secreted Wnt antagonist produced by osteocytes that regulate osteoblast activity and thus bone metabolism. Its levels increase with age and are regulated by both estrogens and PTH in both women and men. The aim of the present study was to evaluate SOST levels in patients with DM1 (n= 43) or DM2 (n=40) with normal renal function, compared with age and sex-matched control subjects (CT, n= 50), and to analyze its relationship with PTH, 25 OH-vitamin D and bone turnover markers (bone alkaline phosphatase, BALP; total osteocalcin, OC; and serum crosslaps, CTX). As expected BMD at the femoral neck was lower in DM1 and slightly higher in DM2 with respect to age-matched controls, while a reduction in bone turnover markers was observed in both DM1 and DM2. In the overall cohort of subjects, circulating SOST levels were higher in males than in females and significantly increased with age and BMI in both genders. The positive correlation between SOST and age was maintained in both DM1 and DM2 patients. In all study groups bone turnover markers were not significantly correlated with serum SOST, except that BALP that was negatively associated with SOST in control men ($r = -0.46$, $p = 0.02$). Moreover, SOST levels were higher in DM2 than in controls or DM1 patients, and this difference persisted when adjustments were made for age and BMI. Consistent with previous clinical and experimental observations, SOST levels were negatively correlated with serum PTH in nondiabetic patients ($r = -0.59$, $p < 0.001$), independently of age and gender. Conversely, an unexpected positive correlation between PTH and SOST was observed in both DM1 ($r = 0.26$, $p = 0.09$) and DM2 ($r = 0.32$, $p = 0.07$) groups. Taken together our findings suggest that the transcriptional suppression of SOST production by PTH (previously demonstrated in animal and human studies) is impaired in both DM1 and DM2.

Disclosures: Ranuccio Nuti, None.

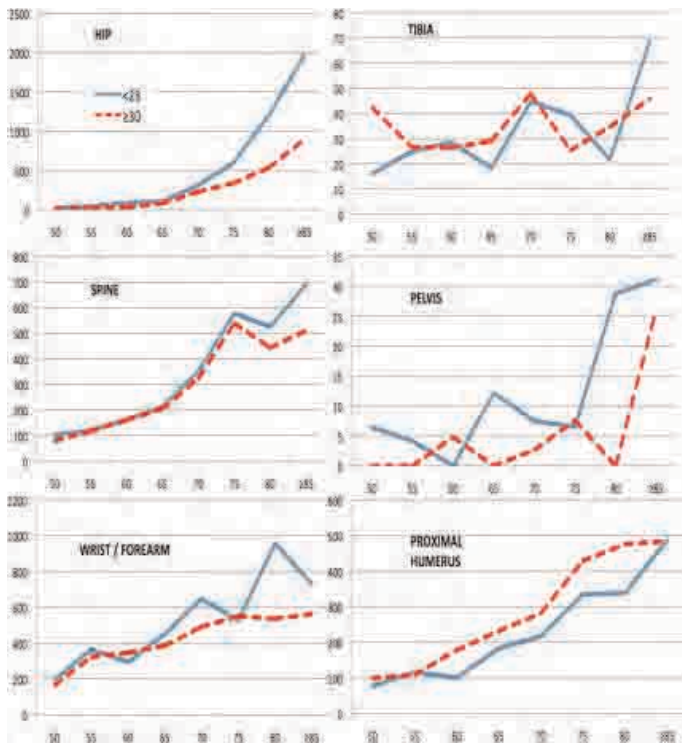


Fig 1. Age-specific fracture incidence rates (/100,000 pyar) in normal/underweight and obese women

Disclosures: Daniel Prieto-alhambra, None.

FR0391

Blockade of Endogenous Gi Signaling in Osteoblasts Stimulates Bone Formation and Prevents Age-Related Bone Loss. Liping Wang¹, Susan M. Millard², Dylan O'Carroll¹, Lalita Wattanachanya³, Richard Kao⁴, Wei-Dar Lu¹, Aaron J. Fields⁵, Jeffrey C. Lotz⁵, Robert Nissenson³. ¹VA Medical Center, San Francisco, USA, ²University of Queensland, Australia, ³VA Medical Center & University of California, San Francisco, USA, ⁴UCSF/VAMC, USA, ⁵Department of Orthopaedic Surgery, UCSF, USA

Loss of bone with aging is an important risk factor for fractures in the elderly. Signaling by G protein-coupled receptors (GPCRs) plays a crucial role in regulating osteoblast function. We previously demonstrated that endogenous Gi signaling in osteoblasts restricts bone formation in adult mice and hypothesized that blockade of Gi signaling in osteoblasts may prevent bone loss during aging. We used female transgenic mice in which expression of the pertussis toxin (PTX) gene, under the control of 2.3 kb Collagen I α promoter (Col1(2.3)), was regulated via a tetracycline responsive promoter. Expression of PTX was delayed until 8 weeks of age and the distal femurs were then studied by μ CT in vivo at 2.5, 6, 9, and 12 months of age. It was found that from 2.5 to 12 months of age, the cancellous BV/TV had progressively decreased by 64% ($p < 0.001$) in the littermate control mice while BV/TV had increased by 181.4% ($p < 0.001$) in the Col1(2.3).PTX mice. With histomorphometry, we found that at 12 months of age, the PTX transgenic mice had higher cancellous BV/TV (25.17.6 vs. 1.90.4%, $p < 0.001$), trabecular number (8.982.6 vs. 0.520.1mm⁻¹, $p < 0.001$), and bone formation rate (BFR) (1.590.4 vs. 0.470.3 μ m/day, $p < 0.001$) in the distal femur than the age-matched controls. Moreover, the Col1(2.3).PTX mice had increased cortical thickness (409108 vs. 27434 μ m, $p < 0.01$) and decreased bone marrow area (0.840.1 vs. 1.270.2mm², $p < 0.01$) at mid-femur, with a higher BFR seen only at the endocortical surface (0.590.28 vs. 0.040.04 μ m/day, $p < 0.001$). A 3 point bending test of femoral diaphyses revealed that bone strength was 29% higher in the transgenic than in the control mice (47.06.4 vs. 36.23.1N, $p < 0.05$). To test the effects of the blockade of Gi signaling on fracture healing, we fractured the tibiae of 3 month old female mice and found that, 4 weeks after fracture, the PTX transgenic mice had higher fractional BV/TV (43.03.6 vs. 30.52.8%, $p < 0.01$) and higher BFR (1.930.2 vs. 1.090.4 μ m/day, $p < 0.01$) within the callus as compared to the fractured control mice. Collectively, our results indicate that blockade of Gi signaling with PTX in osteoblasts stimulates bone formation, increases bone strength, and accelerates fracture healing in the adult female Col1(2.3). PTX mice. Therapies designed to inhibit GPCR-mediated Gi activation in osteoblasts could be useful in the treatment of age-related osteoporosis and in promoting fracture repair.

Disclosures: Liping Wang, None.

FR0396

Bone Microarchitecture Assessment in Postmenopausal Women with Atypical Fractures of the Femur and Long Term Bisphosphonate Therapy. Maria Belen Zanchetta¹, Ana Galich¹, mirena buttazzoni², maria diehl², Candela Fernandez³, fernando silveira², Fabio Massari¹, Cesar Bogado¹, Jose Ruben Zanchetta¹. ¹Instituto de Investigaciones Metabolicas (IDIM), Argentina, ²md, Argentina, ³Hospital De Clinicas - Universidad De Buenos Aires, Argentina

In recent years concern has been raised on a possible association between atypical fractures at the subtrochanteric region of the femur and long-term bisphosphonate use. The pathophysiology of these events remains unknown.

Our aim was to describe bone microarchitecture in patients with atypical fractures during long term bisphosphonate treatment using High Resolution peripheral computerized Tomography (HR-pQCT) scans of the distal radius and tibia. Additionally, to compare these results with two control groups with similar age and BMI selected from our database: one of postmenopausal women chronically treated with bisphosphonates and one of postmenopausal women who have never received treatment. We identified 10 postmenopausal women who suffered an atypical fracture of the femur during long term bisphosphonate treatment (mean treatment time 16.2 \pm 5.1 years). All major features defined by the ASBMR Task Force (location in the subtrochanteric region and femoral shaft, transverse or short oblique orientation, minimal or no associated trauma, a medial spike when the fracture is complete, and absence of comminution) were present to designate a femoral fracture as atypical. Minor features and clinical characteristics are described in table1. We compared bone volumetric density and architectural parameters measured by HR-pQCT of the radius and tibia in these patients with 30 postmenopausal women who have also received long term treatment with bisphosphonate (mean 8.63.5 years) and who have not suffered an atypical fracture and with 54 postmenopausal women who have never received treatment. All women had no conditions known to affect bone or mineral metabolism. Areal BMD at the lumbar spine and femoral neck was measured using DXA. Volumetric BMD and microarchitecture were measured at the distal radius and tibia using a HR-pQCT scanner (XtremeCT; Scanco Medical AG). Comparisons between groups was assessed by the two-sample T test. A p value <0.05 was considered statistically significant.

There were no statistically significant differences in age, years since menopause, BMI and BMD T-scores between the three groups. There were no statistically significant differences in almost any of the parameters measured by HR-pQCT between the groups. However, in atypically fractured patients cortical thickness was 9% lower in radius and 4% lower in tibia compared to the chronically treated women and 6% lower in radius and 5 % lower in tibia compared to the non treated group. These differences must be confirmed in larger studies.

Minor features	
	alendronate 60%, pamidronate IV 20%, combination of alendronate and ibandronate 20%
Bisphosphonate used (n 10)	
Comorbidities (n 9)	0%
Other drugs (n 9)	Proton pump inhibitors 20%
Bilaterality (10)	50%
Delayed healing (n 10)	10%
Cortical thickening (n 8)	100%
Prodromal pain (n 9)	70%
Biopsy results (n 4)	very low bone turn over 100%
Previous osteoporotic fracture (n 9)	20% (wrist)
Osteopenic by dxa at fracture time (n 7)	60%
Osteoporotic by dxa fracture time (n 7)	50%
Crosslaps suppressed (n 4)	100%

Table 1

	Atypical fractures	Control group 1 n 30	p	Control group 2 n 54	p
Age (years)	71 \pm 3.7	66.9 \pm 6.9	0.0636	70.3 \pm 3.1	0.2258
T-score L2-L4	-2.2 \pm 0.4	-3.1 \pm 0.5 (n=7)	0.0984	-2.5 \pm 0.5	0.7304
T-score C.F.	-1.8 \pm 0.6	-1.7 \pm 0.7	0.9413	-2.0 \pm 0.7	0.6725
Mean treatment time (years)	16.2 \pm 6.1	10.0 \pm 4.0	0.0041		
Distal radius					
Tb. Number (10mm)	1.52 \pm 0.44	1.42 \pm 0.40	0.54	1.49 \pm 0.40	0.56
Deomp (mg HA/ccm)	803.5 \pm 71.6	814.1 \pm 61.6	0.66	791.4 \pm 70.0	0.63
Ct. Th (mm)	0.514 \pm 0.139	0.565 \pm 0.169	0.42	0.546 \pm 0.157	0.58
Distab (mg HA/ccm)	117.0 \pm 36.1	106.8 \pm 33.0	0.43	99.9 \pm 36.1	0.19
Distal tibia					
Tb. Number (10mm)	1.49 \pm 0.31	1.43 \pm 0.31	0.61	1.47 \pm 0.30	0.81
Deomp (mg HA/ccm)	789.9 \pm 32.3	801.4 \pm 57.6	0.45*	784.9 \pm 52.0	0.70*
Ct. Th (mm)	0.774 \pm 0.170	0.804 \pm 0.252	0.69*	0.815 \pm 0.205	0.57
Distab (mg HA/ccm)	120.6 \pm 20.6	115.2 \pm 28.7	0.60	112.4 \pm 30.3	0.32*

Table 2.

Disclosures: Maria Belen Zanchetta, None.

FR0402

Bone Steatosis And Osteocyte Apoptosis In Alcohol-induced Bone Loss. Delphine Maurel¹, Stephane Pallu², Christelle Jaffre³, Nathalie Boisseau⁴, Nick Fazzalari⁵, Rustem Uzbekov⁶, Gael Rochefort⁷, Claude-Laurent Benhamou⁸. ¹Inserm Unit 658Hôpital Porte MadeleineOrleansFrance, France, ²INSERM U 658 / University of Orleans, France, ³INSERM Unit U658, France, ⁴Laboratory of Physical Activity Biology, Blaise Pascal University, France, ⁵Institute of Medical & Veterinary Science, Australia, ⁶Microscopy Department, Medical Faculty, Tours University, France, ⁷INSERM U658, France, ⁸INSERM Unit U658, CHR Orleans, France

Alcoholism is one of the world's major health problems and it has long been known that excessive alcohol consumption has catastrophic effects on many organs. In bone tissue, alcohol has been shown to decrease osteoblast number and proliferation and to increase osteoclast activity in vitro, thus modifying bone metabolism and causing bone loss. Alcohol consumption has been shown to induce osteocyte apoptosis and fat excess but the relationship between osteocyte apoptosis and fat excess in bone is not well understood. We thus designed an in vivo study to assess the relationship between increase of adiposity in the marrow and osteocyte apoptosis in the case of alcohol-induced bone loss.

12 male Wistar rats, 8 weeks old at baseline, were treated with 35% v/v ethanol in the drinking water during 17 weeks (A) and compared to 12 control animals (C). At the end of the study, we measured whole body weight, lean, fat mass and bone mineral density (BMD) by DXA. Osteocyte apoptosis was assessed through cleaved caspase-3 and toluidine blue staining while osteocyte morphology and organelles were analyzed with transmission electron microscopy on ultra-thin tibia sections. Fat content in bone marrow and cortical bone micro-vessels were evaluated on semi-thin sections stained with toluidine blue.

BMD confirmed that chronic alcohol consumption induces bone loss. After alcohol treatment, the number of apoptotic osteocytes was increased, as shown by the increased cleaved caspase-3 staining (186.2 \pm 42.7 vs 23.9 \pm 7.2 in A and C, p < 0.001) and the higher empty osteocyte lacunae in A versus C. We observed lipid droplet accumulation within the osteocytes (95.5 \pm 7.2 vs 11.2 \pm 13.1%, p < 0.001), the bone marrow (29.3 \pm 13.0 vs 4.1 \pm 4.9%, p < 0.001) and the cortical bone micro-vessels in A vs C (21.3 \pm 15.5 vs 0.2 \pm 0.5%, p < 0.003). At last, we found an inverse correlation between BMD and osteocyte apoptosis (r = -0.72, p = 0.002) and strong significant correlations between osteocyte apoptotic number and lipid droplet accumulation in osteocyte (r = 0.95, p < 0.001), bone marrow (r = 0.65, p < 0.02) and bone micro-vessels (r = 0.83, p < 0.005).

These data show that the alcohol-induced bone loss is associated with osteocyte apoptosis and lipid accumulation in the bone tissue. This bone "steatosis" is correlated to lipid accumulation in bone marrow and blood micro-vessels.

Disclosures: Delphine Maurel, None.

FR0405

Anti-Retroviral Therapy Drives Bone Loss in AIDS Patients as a Consequence of Immune Reconstitution. Ighovwerha Ofotokun¹, Tatvana Vikulina¹, Ashwini Vunnavu¹, Susanne Roser-Page¹, Masayoshi Yamaguchi¹, Francois Villinger¹, Kenneth Rogers¹, Majid Zayzafoon², Anandi Sheth¹, Jeffrey Lennox¹, M. Neale Weitzmann¹. ¹Emory University School of Medicine, USA, ²University of Alabama at Birmingham, USA

Skeletal renewal is strongly influenced by the immune system, a consequence of a deep integration and centralization of common cell types and cytokine mediators

comprising the “immuno-skeletal interface”. This includes T cells and B cells, a significant source of osteoclastogenic cytokines including RANKL and TNF and/or the RANKL decoy receptor OPG. Consequently, bone loss is common in conditions associated with immune activation but also in immunodeficiency, including infection by the human immunodeficiency virus (HIV) that leads to acquired immunodeficiency syndrome (AIDS). In fact, osteoporosis and bone fracture are recognized as serious complications of HIV/AIDS and 75% of AIDS patients are already osteopenic at first diagnosis. However, contrary to expectation, anti-retroviral therapy (ART) exacerbates rather than ameliorates bone loss. Recent studies show a reduction in BMD within the first 2 years of ART before tapering off suggesting that the majority of bone loss occurs early on during ART. As the majority of previous studies have focused on relatively late time points we examined C-terminal telopeptide of collagen (CTX), an index of in vivo bone resorption, at early time points following ART initiation. We found a spike in bone resorption within just 2 weeks, peaking around 12 weeks, and remaining significantly elevated for at least 24 weeks. Consistent with the surge in bone resorption serum concentrations of RANKL and TNF, but not OPG, climbed to significant levels by 24 weeks. Interestingly, T cell recovery with ART is established to reach a significant magnitude at 12 weeks, the same time point at which the surge in resorption peaked. As lymphocytes are known to mediate bone loss in inflammatory contexts by secreting RANKL and/or TNF this suggested a possible link between immune reconstitution and bone resorption. We hypothesized that bone resorption may be driven by a mechanism involving immune recovery and reconstitution, synonymous with T cell and/or B cell activation, as a consequence of ART-induced disease reversal. To investigate this hypothesis we mimicked ART-induced immune reconstitution in vivo by means of T cell adoptive transfer into T cell null TCR β knockout mice. T cell reconstitution likewise initiated a surge in bone resorption (CTX), concurrent with pronounced loss of bone mineral density (BMD) and bone volume within the same 12 week window. As in humans on ART, RANKL and TNF, but not OPG, were significantly elevated in T cell reconstituted mice. Taken together our data suggest that the majority of bone loss associated with ART may occur in the early period of therapy as a consequence of immune reconstitution. Importantly, our data suggest the possibility that short-term preemptive antiresorptive treatment may be effective in blocking ART-induced bone loss thus preserving BMD during the early phase of ART when bone resorption peaks.

Disclosures: M. Neale Weitzmann, None.

FR0407

Circulating Levels of Sclerostin Are Increased In Patients With Type 2 Diabetes Mellitus. Antonia Garc  a-Mart  n¹, Pedro Rozas-Moreno², Sonia Morales-Santana³, Beatriz Garc  a-Fontana³, Jose Antonio Garc  a-Salcedo⁴, Rebeca Reyes⁵, Manuel Munoz-Torres⁶. ¹Bone Metabolic Unit. Endocrinology Division., Spain, ²Endocrinology Division. Hospital General de Ciudad Real. Ciudad Real, Spain., Spain, ³Proteomic Research Service. Hospital Universitario San Cecilio., Spain, ⁴Bone Metabolic Unit (RETICEF). Endocrinology Division. Hospital Universitario San Cecilio., Spain, ⁵Bone Metabolic Unit., Spain, ⁶University Hospital, Spain

Sclerostin, produced by osteocytes, is a potent inhibitor of Wnt signaling and bone formation. Diabetes mellitus is a risk factor for osteoporotic fractures. However, there is currently no information on the circulating levels of sclerostin in type 2 diabetes mellitus (T2DM). We tested the hypothesis that sclerostin concentrations are elevated in patients with T2DM, which promotes the deterioration of osteoblastogenesis and increased bone fragility. Sclerostin was measured in serum from 76 patients with T2DM and 54 healthy controls using enzyme-linked-immunosorbent assays (ELISA). Sclerostin levels were significantly higher in T2DM than controls (53.9 29.9 vs 41.3 15.9 pmol/L, $p=0.007$). Sclerostin levels were significantly higher in men than women, both in T2DM (63.2 27.1 vs 43.1 17.1 pmol/L, $p=0.001$) and controls (46.8 18.3 vs 36.9 12.5 pmol/L, $p=0.03$). In T2DM males and controls, sclerostin levels were positively associated with age ($r=0.338$, $p=0.031$ and $r=0.251$, $p=0.04$, respectively) but no in T2DM women. In analysis age-adjusted, serum sclerostin concentration was positively correlated with glycated haemoglobin (A1c) in T2DM ($\beta=0.262$, $p=0.023$). In T2DM males, lumbar spine, femoral neck and total hip bone mineral density (BMD) by dual-energy X-ray absorptiometry (DXA) were positively correlated with serum sclerostin levels ($r=0.325$, $p=0.05$, $r=0.382$, $p=0.018$ and $r=0.470$, $p=0.003$, respectively) but in analysis age-adjusted no significant association. In T2DM patients, sclerostin levels were significantly lower in osteoporotic than non-osteoporotic (42.9 19.2 vs 56.9 25.9 pmol/L, $p=0.041$). There were no differences according to presence or absence of morphometric vertebral fractures. In conclusion, (1) patients with T2DM have higher serum sclerostin than healthy controls, (2) circulating sclerostin levels are related to A1c and (3) circulating sclerostin levels are lower in T2DM with osteoporosis. Further studies are needed to evaluate the role of sclerostin as a marker of bone metabolism in this population.

Disclosures: Antonia Garc  a-Mart  n, None.

FR0409

RANKL Production by B Lymphocytes Contributes to the Bone Loss Induced by Inflammation and Ovariectomy. Melda Onal^{*}, Jinhu Xiong, Priscilla Cazer, Stavros Manolagas, Charles O'Brien. Center for Osteoporosis & Metabolic Bone Diseases, Central Arkansas Veterans Healthcare System, University of Arkansas for Medical Sciences, USA

Increased production of RANKL by B cells is thought to contribute to the bone loss associated with inflammation or sex steroid deficiency. However, heretofore, there have been no studies that functionally link RANKL expression in B cells with bone loss in these conditions. Therefore, we deleted the RANKL gene specifically from B cells by crossing CD19-Cre mice, which express Cre recombinase in B cells beginning early in their differentiation, with mice harboring a RANKL conditional allele and examined the impact of this deletion on the loss of bone associated with inflammation or estrogen deficiency. Quantitative PCR confirmed deletion of the RANKL gene in B cells, but not in T cells or in cortical bone, demonstrating the specificity of the deletion. Bone mass, as measured by DEXA, was not altered in mice lacking RANKL in B cells compared to control littermates up to 7 months of age, suggesting that RANKL produced by B cells does not play a role in basal bone remodeling. However, consistent with the role of RANKL in B cell lymphopoiesis, deletion of RANKL led to a small decrease in the percentage of CD19-positive B cells in the bone marrow and spleen, while the percentage of T cells was not affected. To examine the role of B cell RANKL during inflammatory bone loss, 4-month-old conditional KO mice and control littermates were injected with LPS (10 mg/kg bw) every 4 days for 16 days. LPS caused a decrease in bone mineral density (BMD) at all sites examined in control mice. However, deletion of RANKL from B cells partially protected mice from inflammatory bone loss in the femur and total body as measured by DEXA. Moreover, microCT analysis of the L4 vertebra revealed that conditional KO mice were protected from cancellous bone loss. We next assessed the role of B cell RANKL in ovariectomy (OVX)-induced bone loss using 6-month-old conditional KO and control mice. Deletion of RANKL from B cells blunted the OVX-induced increase in B cells that occurred in control mice. Moreover, conditional KO mice were partially protected from OVX-induced bone loss in the spine but not in the femur as measured by DEXA. MicroCT analysis of L4 vertebra demonstrated that cancellous bone loss was blunted in the spines of the conditional KO mice. Taken together, these results demonstrate that RANKL produced by B lymphocytes contributes to inflammation- and OVX-induced bone loss.

Disclosures: Melda Onal, None.

FR0410

Rapid Loss of Bone Mass and Strength after Non-bone Focal X-ray Irradiation in Growing Mice. Peter Corry, Dan Jia^{*}. University of Arkansas for Medical Sciences, USA

Introduction: Partial abdominal irradiation (AI) is a common anti-tumor modality for malignancies residing in the pelvis-abdomen cavities. We have reported that AI elicits significant suppression of the un-irradiated bone marrow (BM) in mice. Since BM hosts the precursors of the osteoblastic and osteoclastic lineages and supports the survival and function of these cells, we reasoned that a depletion of the bone marrow cell pool by AI would have a profound impact on the skeleton. **Methods:** Male C57BL/6 mice, 10-12 weeks of age, were given either a single dose (0, 5, 10, 15, or 20 Gy) or fractionated (3 Gy per fraction, twice per day for 15 consecutive fractions) x-ray AI, resembling the total dose and dose schedule used in a pelvic-abdominal radiotherapy. Longitudinal assessment of bone mineral density (BMD) was done by DEXA. Blood and BM cells were collected for bone turnover marker and ex vivo bone cell differentiation assays. **Results:** Serum TRAP5b increased while osteocalcin decreased in irradiated mice measured 7 days after a single dose AI ($p < 0.05$ vs sham controls). Ex vivo BM osteoblast differentiation was greatly suppressed ($p < 0.01$) while osteoclast formation was slightly increased ($p > 0.05$) evaluated 7 days after a single dose AI. DEXA analysis revealed a dose- and time-dependent loss of whole body BMD detected 7-14 days after a single dose AI ($p < 0.001$ vs sham controls) and 14-28 days after fractionated AI. Under both irradiation schemes tibia and femurs showed the greatest susceptibility to AI-induced BMD loss (up to -7.5%/-3.5% in tibia, $p < 0.001$ vs sham controls), whereas the spine was the least affected ($p > 0.05$ vs sham controls). Furthermore, AI induced a 10-15% decrease in femoral peak load tested by 3-point bending 7-14 days after a single dose AI ($p < 0.01$ vs sham controls). **Summary and conclusions:** These results demonstrate that AI at dose schedules mimicking the clinical use could induce adverse effects on the non-exposed skeleton in growing mice. These effects are mediated by altered number and activity of the cells of both osteoblast and osteoclast lineages, and manifested by the deterioration of BMD and strength of the affected bones. These skeletal responses to AI are previously unknown side effects of radiotherapy. This phenomenon merits further investigations in basic research and additional cautions in treatment planning.

Disclosures: Dan Jia, None.

FR0411

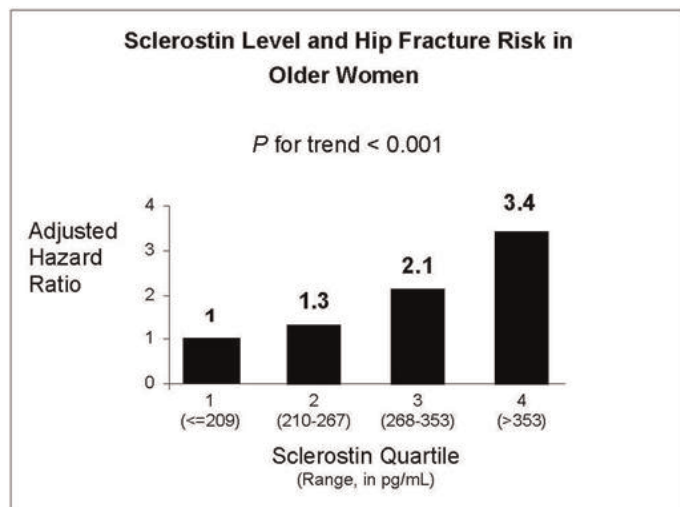
Sclerostin and Risk of Hip Fracture in Older Women. Aarthi Arasu¹, Peggy Cawthon², Thy Do³, Puneet Arora⁴, Li-Yung Lui², Jane Cauley⁵, Kristine Ensrud⁶, Steven Cummings⁷. ¹University of California, San Francisco, USA, ²California Pacific Medical Center Research Institute, USA, ³Amgen, Inc., USA, ⁴Amgen, USA, ⁵University of Pittsburgh Graduate School of Public Health, USA, ⁶Minneapolis VA Medical Center / University of Minnesota, USA, ⁷San Francisco Coordinating Center, USA

Context: Sclerostin, a protein secreted by osteocytes, antagonizes osteoblast differentiation and mineralization, and increases mature osteoblast apoptosis by inhibiting the Wnt pathway. Individuals with absent or reduced circulating levels of sclerostin due to genetic mutations have very high bone mass. Therefore, it is hypothesized that women with increased circulating sclerostin levels have a greater risk for hip fractures.

Design, Setting and Participants: This is a case-cohort study of community-dwelling women from the Study of Osteoporotic Fractures (SOF) database, a prospective cohort of 9516 women aged 65 years and greater. Hip fractures, including both intertrochanteric and femoral neck, were adjudicated centrally. Serum was collected at visit 2 in 1988-89 and stored at -190 C. In 2010, serum sclerostin levels were measured by an electrochemiluminescence sandwich assay in 228 women with incident hip fractures and 227 women in a randomly selected sample; average follow up time was 9.8 years.

Results: Sclerostin levels (mean 293.5 SD 122.4 pg/mL) were significantly associated with hip fracture risk, which was further strengthened after adjustment for total hip bone mineral density (BMD). Compared to women in the lowest quartile of sclerostin, the risk of hip fracture was significantly elevated among those in the third quartile (HR 2.1, 95% CI 1.1-3.8) and fourth quartile (HR 3.4, 95% CI 1.7-7.0), after adjusting for age, body mass index, total hip BMD, estrogen use, and history of fracture since age 50. The test for linear trend in hazard ratios across the quartiles was statistically significant ($P < 0.001$) suggesting a linear relationship between the quartile of sclerostin concentration and risk of hip fracture. The results were similar for both femoral neck and intertrochanteric hip fractures.

Conclusion: We conclude that higher sclerostin levels are associated with a greater risk of hip fractures in older women.



Risk of Hip Fracture Across Sclerostin Quartiles

Disclosures: Aarthi Arasu, Amgen, 5
This study received funding from: Amgen

FR0413

Comparative Effects of Teriparatide and Risedronate in Glucocorticoid-Induced Osteoporosis in Men: 18-Month Results of the EuroGIOPS Trial. Claus-C Gluer¹, Fernando Marin², Christian Graeff¹, Jaime Pena³, Andreas Reisinger⁴, Helmut Petto⁵, Philippe Zysset⁴. ¹Biomedical Imaging, Department of Diagnostic Radiology, UKSH, Germany, ²Lilly Research Center, United Kingdom, ³Biomedical Imaging, Department of Diagnostic Radiology, UKSH, Germany, ⁴Institute for Lightweight Design & Structural Biomechanics, Vienna University of Technology, Austria, ⁵Lilly Research Center, Austria

Bone loss and fractures secondary to glucocorticoid (GC) use is the most prevalent form of secondary osteoporosis. Data on the effects of osteoporosis drugs in men with GC-induced osteoporosis are scarce. We ran an 18-month randomized, open-label, controlled trial in men who had taken GCs for >3 months (prednisone equivalent >5

mg/d), and had an areal BMD T-score <-1.5 SD. Subjects received either 20 µg/d teriparatide (TPTD, n=45) or 35 mg/wk risedronate (RIS, n=47), and 1 g calcium and 1200 IU vitamin D daily. The primary objective was to compare the increase in lumbar spine (L1-L3) volumetric BMD between groups, as measured by quantitative computed tomography (QCT). Secondary outcomes were changes in 3D microstructure variables measured by high-resolution QCT (HRQCT) at T12, biomechanical effects evaluated by finite element (FE) analysis, areal BMD determined by dual-energy X-ray absorptiometry (DXA), biochemical markers and safety. Radiological evaluations were performed at 0, 6, and 18 months. The calibrated HRQCT images of T12 were converted into digital FE models and subjected to axial compression, anterior bending and axial torsion. Stiffness and strength were computed for each model and loading mode. A predefined mixed model repeated measures (MMRM) was used to analyze the changes from baseline and the between-group differences. Subjects had a mean [SD] age of 56. [14.2] years. Median GC daily dose and use duration was 8.8 mg and 6.4 years, respectively. A total of 36 (39.1%) randomized subjects had a prevalent fracture, and 30 subjects (32.6%) were prior bisphosphonate users. Both treatments significantly increased L1-L3 vBMD, with greater increases in the TPTD group in the fully-adjusted analysis at 18 months (median: 17.1% vs 5.3%; $p=0.004$ from MMRM model). Microstructure-derived HRQCT trabecular and cortical variables significantly increased from baseline in both groups, but they did not reach between-group significant differences. There was a trend for higher BV/TV in the TPTD group (median: 23.1% vs 7.3%; $p=0.074$). Vertebral stiffness and strength increased significantly in both groups, with statistically higher increases in the TPTD group for all tests. Adverse events were not different between groups. Fewer patients had a new clinical fracture with TPTD (0/45, 0%) than with RIS (5/47, 10.6%) ($p=0.056$). In this 18 month trial in men with GC-induced osteoporosis TPTD showed higher increases in spine vBMD and biomechanical properties than RIS

Disclosures: Claus-C Gluer, None.

This study received funding from: Lilly Research Center, Europe

FR0414

Effects of Teriparatide on Cortical Histomorphometric Variables in Patients Receiving Long-term Alendronate Therapy. Jan Stepan¹, Harald Dobnig², Astrid Fahrleitner-Pammer³, Yanfei Ma⁴, Qing Zeng⁴, Xiaohai Wan⁴, Fernando Marin⁵, Imre Pavo⁶. ¹Charles University, Czech Republic, ²Department of Internal Medicine, Division of Endocrinology & Metabolism, Medical University of Graz, Austria, ³Medical University Graz, Austria, ⁴Eli Lilly & Company, USA, ⁵Eli Lilly & Company, Spain, ⁶Eli Lilly & Company, Austria

Teriparatide (TPTD) treatment increases bone turnover and bone formation in patients previously treated with potent antiresorptives, such as alendronate (ALN, Stepan et al. 2010)⁴. However, no histological information exists on the effects of TPTD on cortical bone in the ALN pre-treated patients. In addition, there is limited information of osteoporosis medications on their effects on the periosteal surface of the bone. The aim of this post-hoc analysis was to investigate the changes in cortical microstructure and dynamic histomorphometric indices in patients with osteoporosis with or without prior therapy with ALN, who were treated with TPTD 20 µg/day subcutaneous for 24 months.

Sixty-six postmenopausal women with osteoporosis, mean age (SD) of 68.0 (7.0) years and mean BMD T-score of -1.7 (0.9) at total hip and -2.8 (0.8) at lumbar spine; 62% with prevalent fractures) were included in the study. Thirty-eight stopped previous ALN treatment (10 mg/day or 70 mg/week for a mean duration of 63.6 months), and switched to TPTD, while 28 were osteoporosis pre-treatment naive (TN). 45 paired iliac crest biopsies were collected and analyzed by micro-computer tomography for three dimensional structural and dynamic cortical histomorphometry indices at baseline and after 24-month (BFR/BS=bone formation rate/bone surface). Wilcoxon rank sum test and two-sample t-test were used to compare differences between groups. Nonparametric signed-rank test was used to compare the effect after TPTD treatment with baseline within each group or for the overall population. In the ALN pretreated group, mineralizing surface/bone surface (MS/BS, %) values were lower than in the TN, at both the periosteal (baseline: 0.611.29 vs 1.390.96; $p=0.04$; post-TPTD: 1.341.05 vs 3.942.7; $p=0.002$), and endocortical levels (baseline: 3.165.05 vs 6.195.07; $p=0.06$; post TPTD: 4.954.03 vs 119.57; $p=0.027$). In the pooled analysis, indices of periosteal and endocortical dynamic variables, cortical thickness and porosity increased significantly compared to baseline (Table).

Our results indicate the bone forming effects of TPTD in the cortical bone in patients previously treated with the ALN or treatment naive. The observed increase in cortical porosity in both groups may be the consequence of increased intracortical remodeling. ⁵Stepan et al. Osteoporos Int (2010), 21:2027-2036

% Change in indices Mean	Pre-treatment naïve (n=16)	ALN pre-treated (n=29)	Pooled (n=45)
3D Total cortical area	28	43 *	39 *
3D Cortical thickness	38	32 *	34 *
2D Cortical porosity	69	65*	67*
Periosteal MS/BS	184*	118*	164*
Periosteal BFR/BS	275*	312	282*
Endocortical MS/BS	78	57*	71*
Endocortical ; BFR/BS	143	47	107*

*p<0.05, compared to baseline

Table: Baseline-endpoint changes of structural and dynamic cortical histomorphometric indices

Disclosures: Jan Stepan, None.

This study received funding from: Eli Lilly and Company

FR0415

In Premenopausal Women with Idiopathic Osteoporosis, Baseline Bone Turnover Predicts Response to Teriparatide. Adi Cohen¹, Emily Stein², David Dempster³, Hua Zhou⁴, Robert Recker⁵, Joan Lappe⁵, Chiyuan Zhang³, Donald McMahon², Polly Chen³, Kavita Pandit³, Clifford Rosen⁶, Elizabeth Shane². ¹Columbia University Medical Center, USA, ²Columbia University College of Physicians & Surgeons, USA, ³Columbia University, USA, ⁴Helen Hayes Hospital, USA, ⁵Creighton University Osteoporosis Research Center, USA, ⁶Maine Medical Center, USA

Idiopathic osteoporosis (IOP) in premenopausal women is an uncommon disorder of uncertain pathogenesis in which fragility fractures and/or low bone mineral density (BMD) occur in otherwise healthy women with intact gonadal function. We have reported that women with IOP have thinner cortices, fewer, thinner, more widely separated, and heterogeneously distributed trabeculae, reduced stiffness, and lower osteoid width and mean wall width than controls. Dynamic histomorphometric remodeling parameters were heterogeneous and did not differ between subjects and controls. However, the IOP group included women with low and high bone turnover as assessed by bone formation rate/bone surface (BFR/BS). We hypothesized that teriparatide (TPTD), an agent that directly increases osteoblast activity, would improve BMD in IOP. Herein, we report interim results of an open-label pilot study of 22 premenopausal women with IOP (17 with fractures, age 39.6 yrs) treated with TPTD 20 mcg SC daily. At 12 months (12M) and 18M, lumbar spine (LS) BMD increased from baseline by 7.5 3.8% (SD) and 9.7 3.3% respectively (both p<0.05). Total hip and femoral neck (FN) BMD rose by 2.4 2.3 and 2.3 3.3%, respectively, at 12M (p<0.05) but did not increase further at 18M. There was no change at the radius (0.6 1.9%; p=0.3). Baseline serum bone turnover markers (BTMs) correlated with 12M percent change in BMD at the LS (osteocalcin: r=0.512, p=0.02) and FN (CTX: r=0.445, p=0.049; PINP: r=0.453, p=0.04). Five women did not have a significant increase in LSBMD at 12M; Non-responders resembled Responders in terms of age, BMI, baseline BMD, calciotropic and gonadal hormones, and bone volume fraction. However, baseline serum CTx, cancellous and endocortical BFR/BS were significantly lower and serum IGF1 was significantly higher in Non-responders (Table). In conclusion, TPTD resulted in significant increases in BMD in most premenopausal women with IOP. Those who did not respond were characterized by very low bone turnover and high IGF1 at baseline, suggesting that osteoblast dysfunction and IGF-1 resistance may limit responsiveness to TPTD in IOP.

	Responders (n=17)	Non-responders (n=5)	p
Mean 12M % Change in LS BMD	9.3 ± 4.1	1.0 ± 1.3	<0.0001
BASELINE:			
Cancellous BV/TV by µCT (%)	21.3 ± 7.1	20.9 ± 5.4	0.9
IGF-1 (age adjusted, ng/mL)	153 ± 38	209 ± 38	0.01
Osteocalcin (ng/mL)	18.5 ± 5.8	14.1 ± 9.9	0.2
PINP (µg/L)	51.0 ± 11.6	39.8 ± 21.7	0.1
CTX (ng/mL)	0.376 ± 0.096	0.246 ± 0.156	0.04
Cancellous BFR/BS	0.011 ± 0.006	0.004 ± 0.003	0.03
Endocortical BFR/BS	0.024 ± 0.016	0.007 ± 0.008	0.04

Table

Disclosures: Adi Cohen, None.

This study received funding from: Eli Lilly and Company

FR0418

Teriparatide and Antiresorptive Combination Treatment subsequent to 9 months of Teriparatide Monotherapy. Christian Muschitz^{*1}, Roland Kocjan², Astrid Fahrleitner-Pammer³, Friederike Kuhne⁴, Christina Bittighofer⁴, Angela Trubrich⁴, Reinhart Waneck⁵, Heinrich Resch⁶. ¹St. Vincent's Hospital, Austria, ²St. Vincent Hospital Vienna, Austria, ³Medical University Graz - division of Endocrinology & Metabolism, Department of Internal Medicine, Austria, ⁴The VINFORCE Study Group - St. Vincent Hospital - Medical Department II, Austria, ⁵St. Vincent Hospital - Department of Radiology, Austria, ⁶Medical University Vienna, Austria

Purpose: Increased bone formation without meaningful increase of resorption and a consequent marked anabolic response on teriparatide (TPTD) is evident shortly after treatment initiation. This anabolic window is supposed to be reflected also in the marked initial BMD increase on TPTD. Due to coupling mechanisms, the sustained increase of bone formation and ongoing anabolic effects are associated with significantly increased bone resorption as well. Antiresorptives are able to influence the balance of formation and resorption. We investigated effects of addition of antiresorptives to the second half of TPTD cycle when resorption is already also markedly elevated. Methods: We prospectively randomized 117 pmp women (mean age 71.7 8.5 years, T-score L1-L4 -2.45 1.38; 91.5% prevalent fractures) after 9 months of TPTD treatment into three different open-label groups for another 9 months: either alendronate (ALN, 70 mg/week, 41 patients), raloxifene (RAL, 60 mg/day, 34 patients) or no medication (TPTD mono, 42 patients) was added to the continued TPTD treatment. All subjects received daily supplementation of 1000mg calcium and 800 IU vitamin D. Serum level of intact amino terminal propeptide of type I procollagen (PINP) and type I collagen cross-linked C-telopeptide (CTX) as well as BMD measured by DXA at lumbar spine, total hip and femoral neck BMD was evaluated from the time of TPTD treatment initiation, at baseline of randomization, and after 3, 6 and 9 months during the combination treatment. Results: After 18 months TPTD treatment, the increase in lumbar spine BMD was significantly higher in the ALN (+0.08 g/cm², p=0.046) and RAL (+0.09 g/cm², p=0.026) group when compared with the TPTD mono group (+0.05 g/cm²). In the total hip region, addition of RAL (+0.03 g/cm²) did not alter the BMD effects of TPTD monotherapy (+0.03 g/cm²), but addition of ALN resulted in significantly more increase in total hip BMD (+0.05 g/cm²) than RAL (p=0.026) or TPTD alone (p=0.048). Elevation of PINP and CTX was significantly lower in the ALN and RAL group at the end of the 18 months treatment compared to TPTD treatment alone. Conclusions: Our data suggest that addition of ALN to the second 9 months of TPTD treatment cycle results in augmented BMD increase. This BMD increase may reflect either favorable balance of bone formation and resorption towards more formation or increased secondary mineralization of newly formed bone matrix.

Disclosures: Christian Muschitz, None.

FR0419

Teriparatide has Different Effects on Trabecular and Cortical Bone as Measured by ¹⁸F-Fluoride Positron Emission Tomography. Michelle Frost^{*1}, Musib Siddique¹, Glen M. Blake¹, Amelia EB. Moore¹, Paul J. Schleyer¹, Paul K. Marsden¹, Richard Eastell², Ignac Fogelman³. ¹King's College London, United Kingdom, ²University of Sheffield, United Kingdom, ³Guy's Hospital, United Kingdom

We used ¹⁸F-fluoride positron emission tomography (¹⁸F PET) to compare the changes in bone metabolism at trabecular and cortical sites in response to teriparatide. The subjects were 18 postmenopausal women with osteoporosis (mean age 65.3 years). Subjects had a 1-hour dynamic PET/CT scan of the spine (L1-L4) followed by a 10-minute static scan of the pelvis and femur at baseline and after 6 months treatment with teriparatide 20 µg/day. Blood samples were taken to find the arterial input function. We evaluated the ¹⁸F plasma clearance to trabecular bone (units mL min⁻¹ mL⁻¹) by placing an elliptical region of interest (ROI) in each vertebral body on the dynamic scan and analysing the bone time-activity curve using the Hawkins 3-compartment model. Spine plasma clearance was also estimated by the Patlak plot method using the 10-60 minute dynamic scan data, and also by a new two-point Patlak method that used a single bone uptake measurement at the end of the dynamic scan together with the population mean volume of distribution of ¹⁸F tracer in the bone ROI. CT scans were used to define ROIs in a 6 cm section of cortical bone in the femoral shaft, an area equivalent to the DXA total hip ROI, and the pelvis. After the CT defined ROIs were mapped onto the static PET scan, ¹⁸F plasma clearances at these sites were evaluated using the two-point Patlak method. Data for right and left were averaged. After 6 months treatment with teriparatide ¹⁸F plasma clearance in trabecular bone in the spine increased by 23.8% (P = 0.0003) when calculated using the Hawkins model, by 24.1% (P < 0.0001) when using the 10-60 minute Patlak plot, and by 26.4% (P < 0.0001) when using the two-point Patlak method. When data from the static scans were analysed ¹⁸F plasma clearance at the femoral shaft increased by 71% (P = 0.0001), at the total hip ROI by 47% (P = 0.0008), and at the pelvis by 34% (P = 0.0006). When compared with the changes in trabecular bone in the spine, the changes in the cortical bone at the femoral shaft were statistically significantly different (P = 0.006), while differences between the spine and total hip ROI approached but did not

quite attain significance ($P = 0.068$). Changes in bone turnover markers and BMD were consistent with previous trials of teriparatide. We conclude that the changes in bone metabolism during teriparatide treatment as measured by ^{18}F PET differ at different skeletal sites, with larger increases in cortical bone than in trabecular bone.

Disclosures: *Michelle Frost, Lilly, 2*
This study received funding from: Lilly

FR0421

A Single Dose of Zoledronic Acid Prevents Periprosthetic Bone Loss in Female Patients with Cementless Total Hip Arthroplasty. Hannu Aro^{*1}, Niko Moritz¹, Petteri Lankinen¹, Satu Timlin², Erkki Svedstrom².
¹University of Turku, Finland, ²Turku University Hospital, Finland

Periprosthetic bone loss is common during the first year after total hip arthroplasty (THA). The factors that lead to periprosthetic bone loss are not clearly understood but are thought to be associated with an increase in osteoclastic activity. The primary objective of this trial was to demonstrate that zoledronic acid, given as a single intravenous infusion after THA, reduces periprosthetic bone loss measured by DXA.

This randomized double-blind placebo-controlled trial included postmenopausal female patients with hip osteoarthritis. Excluding criteria included evidence of secondary osteoporosis, an ongoing bisphosphonate or corticosteroid therapy. Of the 49 eligible patients, 14 (29%) had normal preoperative systemic BMD, 24 (49%) osteopenia and 11 (22%) osteoporosis. All patients received a cementless total hip prosthesis with marked stem for RSA (radiostereometric analysis). Postoperatively, the patients received a single dose (5mg) of zoledronic acid or placebo intravenously. In cases of postoperative hypocalcaemia, the infusion was postponed until normocalcaemic state was achieved. All patients received calcium and D-vitamin supplementation. The response to zoledronic acid therapy was monitored by measurements of serum markers (CTX, TRAP, and PINP). Periprosthetic BMD was measured by DXA at 0, 3, 6, and 12 months. In order to measure 3D migration of the femoral stem, RSA imaging was performed at 0, 3, 6, and 12 months. Functional recovery was evaluated by means of gait analysis, balance master, and patient reported outcome measures.

At the baseline, the patients of zoledronic acid (n=25) and placebo (n=24) groups showed minor imbalances in the mean age (65 vs. 71 years), 25(OH)D-vitamin levels (65 vs. 52) and HSS scores (55 vs. 43). Periprosthetic total hip BMD did not change with time in patients with zoledronic acid treatment, while placebo-treated patients showed loss of periprosthetic bone. The intergroup difference was 6.3 % at 3 months ($p=0.0071$), 6.0% at 6 months ($p=0.0105$) and 6.8% at 12 months, $p=0.0039$, RMANCOVA). RSA imaging showed no significant difference in stem migration between the two patient groups. Based on WOMAC and HSS scores, the two groups showed no significant differences in the functional outcome at 12 months.

This trial demonstrates that zoledronic acid is efficient in prevention of early periprosthetic bone loss in female THA patients. Based on RSA, the treatment had no adverse effects on implant osseointegration.

Disclosures: *Hannu Aro, Novartis, 2; Stryker Inc, 2; Novartis, 8*
This study received funding from: Novartis, Stryker Inc.

FR0423

Bisphosphonates and acute kidney injury. Safety signal identification in the Food and Drug Administration Adverse events reporting system (FDA AERS): A Report from the Research on Adverse Drug events And Reports (RADAR) Project. Beatrice Edwards^{*1}, Sarah Usmani², Dennis Raisch³, June McKoy⁴, Steve Belknap⁵, Athena Samaras⁵, Dustin Liebling⁴, Jaimie Holbrook⁵, Craig Langman⁶, Ali Abu Alfa⁷, Dennis P. West⁵.
¹Northwestern University Medical School, USA, ²Northwestern University Hospital, USA, ³University of New Mexico College of Pharmacy, USA, ⁴Northwestern University, Division of Geriatrics, USA, ⁵Northwestern University, Department of Dermatology, USA, ⁶Children's Memorial Hospital, USA, ⁷Yale School of Medicine, Division of Nephrology, USA

Objective: The FDA placed on alert on Zoledronic acid for acute kidney injury (AKI) in 2009. We evaluated the existence of an association between bisphosphonate (BP) exposure and AKI in The FDA AERS. Methods: Searches of adverse event reports in FDA Adverse Event Reporting System (AERS) dataset, the peer-reviewed medical literature, and safety publications from FDA, websites and safety databases maintained by the FDA, European Medicines Agency (EMA), Canada Health, and Australia's Adverse Drug Reactions Advisory Committee (ADRAC) and Advisory Committee on the Safety of Medicines (ACSOM) were completed. The FDA AERS database was searched (period: January 1998-June 2009), using 76 terms relating to renal problems combined with all drug names for BPs. We identified signals of disproportional association by calculating the proportional reporting ratio (PRR) for zoledronic acid, alendronate, risendronate, and ibandronate. Results: The FDA reported 24 cases of AKI associated with use of zoledronic acid (Reclast) in 2009. Within the FDA AERS dataset from January 1987- December 2008, there were 633 cases associated with BP use in the setting of non-malignant disease, with 328, 147, 80,

43, and 22 cases associated with zoledronic acid ZOL (zometa), alendronate, zoledronic acid (reclast), risendronate and ibandronate. Co-morbidities: diabetes mellitus, heart failure, and hypertension. The PRR was 0.94 (95% C.I. 0.89-0.98), reflecting a non-significant safety signal. An additional 480 cases of AKI in cancer patients were reported. Malignancies: multiple myeloma (n=220, 46%), breast cancer (n=98, 20%), prostate cancer (n=24, 5%) and undefined (n=139, 29%). Agents: ZOL (n=411, 87.5%), pamidronate PAM (n=8, 17%), and alendronate (n=36, 2%). The PRR for ZOL was 1.22 (95% C.I. 1.13, 1.22) and for PAM 1.55 (95% C.I. 1.25, 1.65). BPs are highly effective agents in osteoporotic fractures, skeletal metastasis, and hypercalcemia. Conclusions: Although safety notifications by the FDA have focused on zoledronic acid, AKI with other BPs have also been reported. Our analysis of the FDA AERS did not identify an association with AKI in the setting of osteoporosis or cancer. Nonetheless, clinicians should be aware that creatinine clearance or glomerular filtration rate (GFR) are sensitive measures of renal function and BP use is best reserved for patients with GFR > 30 cc/min/m². AKI is not clearly identified within the FDA AERS as a manifestation of BP therapy.

Disclosures: *Beatrice Edwards, Dr. Edwards reports having served as a speaker for Eli Lilly and Company, Warner Chilcott, and Amgen. , 8*

FR0429

Long-Term Impact of Adherence to Oral Bisphosphonates on Osteoporotic Fracture Incidence. John S. Sampalis^{*1}, Jonathan Adachi², Emmanouil Rampakakis³, Julie Vaillancourt³, Angela Karellis³, Christian Kindundu⁴.
¹McGill University & Jewish General Hospital, Canada, ²St. Joseph's Hospital, Canada, ³JSS Medical Research, Canada, ⁴Novartis, Canada

Background

Adherence to osteoporosis treatments is a critical parameter resulting in suboptimal effectiveness in real-life practice. The long-term effect of adherence on fracture risk has not been assessed.

Methods

Retrospective study using provincial health insurance claims databases to assess the association between adherence to oral bisphosphonates (OBP) and incidence of osteoporotic fractures in all Ontario patients with osteoporosis between April 1996 and December 2009. Multivariate logistic regression models were used to assess the association between OBP adherence and fracture risk. Treatment duration was classified into two-year intervals. Compliance was estimated with the medication possession ratio (MPR) and persistence was defined as the length of continuous therapy without a gap in refills >30 days.

Results

A total of 636,114 patients comprised the study cohort with a mean age of 72 years and 84% being female. Overall, the mean compliance for the total cohort was 0.72 (0.30) with 53.5% of the patients having a compliance of >80% during the 14-year follow-up period. Among the patients with 0-2 years of follow-up only 49.9% were compliant. After this period, compliance declined steadily with time from 58.9% in patients with 2-4 years of follow-up to 49.9% in patients treated for 12-14 years. With regards to persistence, 24.6% of the total cohort was persistent during the 14-year period. Persistence decreased steadily from 41.0% in patients with 0-2 years of treatment to 3.3% in patients with 12-14 years of treatment. Significant associations between high compliance and persistence and reduced fracture risk over the entire 14-year period of the study were observed. The overall odds ratio for categorical compliance (MPR > 80% or MPR ≤ 80%), continuous compliance and persistence were 0.909 (95% C.I. 0.893-0.925), 0.918 (95% C.I. 0.893 and 0.944) and 0.804 (95% C.I. 0.787-0.821), respectively.

Conclusions

In a real-life setting, adherence to OBP in osteoporosis management is suboptimal. A significant positive association exists between poor adherence and increased risk of osteoporotic fractures which becomes augmented with longer treatment duration.

Disclosures: *John S. Sampalis, JSS Medical Research, 4*
This study received funding from: Novartis Pharma Canada Inc.

FR0433

Adherence with Intravenous Zoledronic Acid and Ibandronate for Osteoporosis among U.S. Medicare Beneficiaries. Jeffrey Curtis^{*}, Huifeng Yun, Robert Matthews, Kenneth Saag, Elizabeth Delzell, University of Alabama at Birmingham, USA

Background: Poor long-term adherence with oral bisphosphonates is widely recognized. The extent to which less frequently dosed intravenous (IV) bisphosphonates might yield better adherence is unknown.

Objectives: To evaluate adherence beyond 1 yr among new users of zoledronic acid (ZA) and IV ibandronate (IB) among Medicare enrollees.

Methods: We used 5% random sample Medicare data from 1/05-12/09 to evaluate new users of IV ZA and IB. Eligibility: Medicare part A+B+D, 18 months followup. A 1-yr baseline characterized covariates. ZA adherence defined as 2 ZA infusions or switching to IB; IB adherence defined as 5 IB infusions or switching to ZA. Hypothesized factors associated with ZA adherence > 1 yr were evaluated with logistic regression.

Results: Among 22,220 eligible patients, 15,100 were new users of ZA and 7,120 were new users of IV IB. The median (IQR) age was 78 (8) and 78 (9) yrs. A majority

received prescription(s) for oral glucocorticoids (62 and 73%, respectively). For both drugs, 43% of 1st infusions were in a facility setting; for infusions performed in physician offices, 26 (ZA) and 31% (IB) were rheumatologist/endocrinologists, 15 (ZA) and 6% (IB) oncologists, and 10 (ZA) and 13% (IB) internal medicine. The proportion of ZA users persistent >1 yr was 66% and was greater than with IV IB (35%, $p < 0.0001$). Factors associated with ZA adherence (referent to non-persistent with ZA) were male gender (odds ratio [OR]=0.35, 95% CI 0.11-1.11), age 85+ (referent to age 65-69) (OR=0.41, 0.21- 0.80), glucocorticoid use (OR=0.74, 0.53-1.03), prior non-adherence of osteoporosis drugs

(OR=0.66, 0.42-1.04) and prior fractures (OR=0.89, 0.51-1.56). Compared to infusions from oncologists, adherence was greater for those receiving infusions from internal medicine (OR=1.84, 0.92-3.70) and rheum/endocrinologists (OR=1.45, 0.86-2.45).

Conclusions: Adherence > 1 yr with IV ZA and IV IB was comparable or somewhat greater than adherence reports with oral bisphosphonates. However, > 1/3 of IV bisphosphonate users did not continue > 1 yr. Less frequently dosed medications may improve adherence but ongoing efforts are needed to maximize adherence with osteoporosis therapies.

Disclosures: Jeffrey Curtis, Amgen, 2; Proctor and Gamble, 2; Roche, 2; Novartis, 5; Novartis, 2; Amgen, 5; Roche, 5; Merck, 5; Merck, 2; Eli Lilly, 5; Eli Lilly, 2
This study received funding from: Amgen

FR0438

Population-Based Trends in BMD Testing and Osteoporosis Treatment for New Initiations of Long-Term Systemic Glucocorticoids (1998-2008). Sumit Majumdar¹, Lisa M. Lix², Colleen Metge³, Suzanne Morin⁴, Marina Yogendran³, William Leslie³. ¹University of Alberta, Canada, ²University of Saskatchewan, Canada, ³University of Manitoba, Canada, ⁴McGill University Health Centre, Canada

OBJECTIVES: To determine rates and correlates of bone mineral density (BMD) testing or osteoporosis treatment in new long-term glucocorticoid initiations and describe changes in glucocorticoid-induced osteoporosis (GIOP) care from 1998-2008.

METHODS: A population-based study of all adults 20-years and older in Manitoba, Canada, was conducted using comprehensive healthcare databases. We identified subjects each fiscal year with long-term systemic glucocorticoid use (defined as >90-days per year) and then restricted analyses to new initiations by excluding those with >90-days of use in the previous year. High quality GIOP care was defined by the composite of new BMD tests or new osteoporosis treatments dispensed within 6-months of starting glucocorticoids. We describe temporal trends and analyses of GIOP care stratified by age, sex, and dose based on daily prednisone-equivalents (low <5mg; medium 5-10mg; high>10mg).

RESULTS: We studied 17,736 new long-term glucocorticoid initiations (32% low-, 36% medium-, 32% high-dose). Among all new initiations, the overall 6-month rates of new BMD testing were 6%, osteoporosis treatment starts were 22%, and the composite of BMD testing or treatment was 25%. From 1998-2008 (FIGURE), there were statistically significant ($p < 0.001$ for each trend) but modest increases in BMD testing (from 2% to 6%), osteoporosis treatments dispensed (from 10% to 24%), and the composite of testing or treatment (from 11% to 27%). High quality GIOP care varied significantly ($p < 0.001$ for each comparison) according to age (12% for those <50-years vs 29% for those 50-years and older), sex (13% for men vs 34% for women), and glucocorticoid dose (23% low- vs 26% medium- vs 27% high-dose).

CONCLUSIONS: The quality of GIOP care has improved slowly over time but remains suboptimal with only one-quarter of those starting long-term systemic glucocorticoids receiving BMD testing or osteoporosis treatment within 6-months of initiation. Interventions to improve GIOP care, especially targeting younger patients and men, need to be developed.



Temporal Trends in Osteoporosis Management Among New Long-Term Glucocorticoid Users (1998-2008)

Disclosures: Sumit Majumdar, None.
This study received funding from: AMGEN

FR0439

Predicting Adherence among Women Participating in the Global Longitudinal Registry of Osteoporosis in Women. Jeffrey Curtis¹, Allison Wyman², Gordon FitzGerald², Adolfo Diez-Perez³, Stephen Gehlbach⁴, Christian Roux⁵, Kenneth Saag¹, Ethel Siris⁶, Stuart Silverman⁷. ¹University of Alabama at Birmingham, USA, ²University of Massachusetts Medical Center, USA, ³Autonomous University of Barcelona, Spain, ⁴University of Massachusetts, USA, ⁵Hospital Cochin, France, ⁶Columbia University College of Physicians & Surgeons, USA, ⁷Cedars-Sinai/UCLA, USA

Background

Numerous factors have been associated with adherence to osteoporosis medications, but only limited work has been focused on developing tools to predict future adherence.

Objective

To develop a predicted adherence score that validly identifies future 1-year persistence among women initiating osteoporosis medications.

Methods

Participants who were not current users of any osteoporosis medication at baseline were identified within the Global Longitudinal Registry of Osteoporosis in Women (GLOW). Women self-reporting new use of any oral or injected (but not intravenous) osteoporosis medication on the year 1 GLOW survey were eligible for analysis (n=1450). The outcome was 1-year persistence measured at the year 2 GLOW survey. Women who switched therapies and remained on any osteoporosis treatment at the date of the year 2 survey were considered persistent. All GLOW survey questions were assessed; factors associated with persistence with bivariate $p < 0.20$ were included in a backwards elimination multivariable logistic regression model; significant variables (adjusted $p < 0.10$) were retained in the final model. Model estimates from the logistic regression were converted to an integer-based clinical prediction rule. Calibration of the final prediction model was assessed using the Hosmer-Lemeshow goodness of fit (GoF) test and by evaluating observed persistence across deciles of predicted persistence categories.

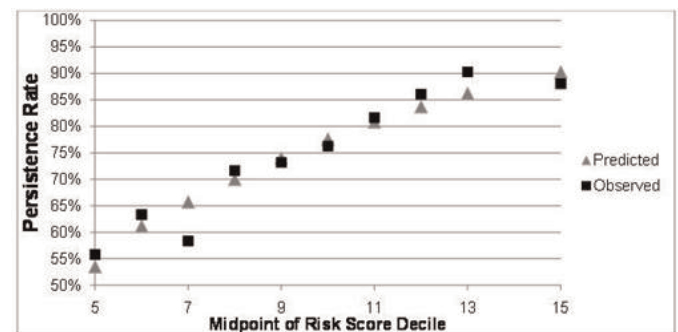
Results

Among eligible GLOW women initiating a new osteoporosis medication, 1077 (74%) were persistent 1 year later. Of the women who persisted on therapy, most continued their initial medication and approximately 11% switched therapies.

Numerous factors measured at baseline were significantly associated with future persistence; 12 were included in the final adherence risk score. Of the 12, 7 were demographic characteristics or comorbidities; 5 were from GLOW surveys. The strongest factors associated with persistence were paternal history of hip fracture, prior hip or vertebral fracture, BMI < 20 and being a non-smoker. Calibration of the adherence risk score was good: Hosmer-Lemeshow GoF $p = 0.24$; there was high agreement between predicted persistence categories and observed persistence (Figure).

Conclusion

One-year persistence could be predicted with high validity among new users of osteoporosis medications participating in GLOW. Women predicted to be less persistent by adherence score might be targeted for further intervention to promote adherence.



Observed vs. Predicted Persistence across Deciles of Predicted Risk

Disclosures: Jeffrey Curtis, Merck, 5; Amgen, 2; Merck, 2; Eli Lilly, 5; Amgen, 5; Roche, 2; Roche, 5; Novartis, 2; Proctor and Gamble, 2; Novartis, 5; Eli Lilly, 2
This study received funding from: Alliance for Better Bone Health

FR0446

Discontinuation of Denosumab and Associated Fracture Incidence: Analysis From the FREEDOM Trial. Jacques P. Brown^{*1}, Jens-Erik Beck Jensen², Nigel Gilchrist³, Chris Recknor⁴, Christian Roux⁵, Ove T'rring⁶, Matt Austin⁷, Andrea Wang⁷, Andreas Grauer⁷, Rachel B. Wagman⁷. ¹CHUQ-CHUL Research Centre, Canada, ²Hvidovre Hospital, Denmark, ³Canterbury Geriatric Medical Research Trust, New Zealand, ⁴United Osteoporosis Centers, USA, ⁵Paris Descartes University, France, ⁶Karolinska Institutet Sodersjukhuset, Sweden, ⁷Amgen Inc., USA

Denosumab (DMAb), a reversible RANKL inhibitor, decreases osteoclast formation, function, and survival. In the pivotal phase 3 fracture trial, FREEDOM, DMAB 60 mg administered every 6 months decreased the risk for new vertebral, nonvertebral, and hip fractures at 3 years compared with placebo (Cummings *NEJM* 2009). Osteoporosis is a chronic disease, and continued treatment is required to provide anti-fracture efficacy. While cessation of DMAB treatment has been associated with transient increases in bone remodeling and declines in bone mineral density (BMD) (Miller *Bone* 2008; Bone *JCEM* 2011), the effect on fracture risk is not as well characterized. To understand fracture incidence in an osteoporotic population after treatment cessation, we evaluated subjects in FREEDOM who discontinued treatment after receiving 2 to 5 doses of investigational product (IP), either DMAB or placebo, and continued study participation for ≥ 6 months since the last dose + 1-month study visit window (≥ 7 months). The off-treatment observation period began 7 months after the last dose of IP and lasted for approximately 6 to 24 months (for subjects who received 5 and 2 doses, respectively). This subgroup of 797 subjects (470 placebo, 327 DMAB) showed similar baseline characteristics for age, prevalent fracture, and lumbar spine and total hip BMD T-scores. During the treatment period, more subjects treated with placebo as compared with DMAB sustained a fracture and had significant decreases in BMD (Table). In addition, 42% of placebo-treated subjects vs 28% of DMAB-treated subjects initiated an alternative therapy after the last dose. After treatment discontinuation, similar percentages of subjects in both groups sustained a new fracture (9% placebo, 7% DMAB), resulting in a fracture rate per 100 subject-years of 13.5 for placebo and 9.7 for DMAB (HR 0.82; 95% CI: 0.49, 1.38), adjusted for age and total hip BMD T-score at baseline. There was no apparent difference in fracture occurrence pattern between the treatment groups during the off-treatment period (Figure). We conclude from this analysis that there was not an excess in fracture risk after treatment cessation with DMAB when compared with placebo during the off-treatment period for up to 24 months.

Table: Subject Characteristics at Treatment Discontinuation

	Placebo (N = 470)	Denosumab (N = 327)
Number of doses received		
2	114 (24)	86 (26)
3	138 (29)	99 (30)
4	90 (19)	68 (21)
5	128 (27)	74 (23)
Fracture during treatment*	90 (19)	36 (11)
Significant BMD reduction† during treatment*	80 (17)	4 (1)
Treatment discontinuation due to requiring alternative therapy or disease progression	116 (25)	29 (9)
Started alternative therapy after last dose	197 (42)	90 (28)

Values are number (%) of subjects. N = number of subjects who discontinued treatment after receiving 2 to 5 doses of investigational product, either denosumab or placebo, and continued study participation for ≥ 7 months after the last dose. *Treatment period = first dose through last dose + 7 months.

†Significant BMD reduction is defined as $\geq 7\%$ BMD reduction at total hip within any 12-month period, $\geq 10\%$ BMD reduction at total hip from baseline at any time point, or total hip BMD T-score < -4 at any time point.

Table 1

Figure: Time to First Osteoporotic Fracture During the Off-treatment Period

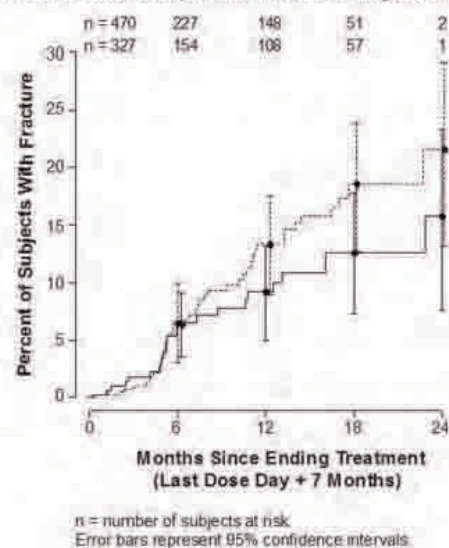


Figure 1

Disclosures: Jacques P. Brown, Amgen Inc., Eli Lilly, Merck, Novartis, sanofi-aventis, Warner Chilcott, 5; Abbott, Amgen Inc., Bristol-Myers Squibb, Eli Lilly, Merck, Novartis, Pfizer, Roche, sanofi-aventis, Servier and Warner Chilcott, 2; Amgen Inc., Eli Lilly, Novartis, 8

This study received funding from: Amgen Inc.

FR0448

Effect of a New Sustained-release Formulation of the Novel Cathepsin K Inhibitor, ONO-5334, on Serum and Urine Biochemical Markers of Bone Turnover in Healthy Post-menopausal Women. Shinichi Nagase¹, Yoshitaka Hashimoto², Maria Small¹, Mitchy Ohyama², JUNICHIRO MANAKO², Tomohiro Kuwayama¹, Stephen Deacon^{*3}. ¹Ono Pharma UK Ltd, United Kingdom, ²Ono Pharmaceutical Co., Ltd., Japan, ³Ono Pharma, United Kingdom

The novel cathepsin K inhibitor, ONO-5334, has been shown to effectively suppress bone resorption markers and increase BMD at a comparable level with alendronate [ALN] (with 300mg qd ONO-5334) in patients with osteoporosis [1]. In that study a twice daily formulation (50mg bd) showed equivalent or even better results compared to the once daily 100mg dose. This may suggest that a prolonged PK profile would allow greater suppression of bone resorption dose for dose. A sustained release tablet (SRT) was developed and compared to the immediate release tablet (IRT) dose that showed comparable results to ALN [1].

The single dose phase was a randomised, partial single-blind, crossover study where 50, 100 and 300mg SRT and 300mg IRT was administered as a single dose to 9 subjects. The multiple dose phase was a randomised, double-blind, placebo-controlled, parallel-group study where 100, 300mg SRT or placebo (PBO) was administered in repeated doses (on Day 1 then on Days 4-10) to two treatment groups of 12 subjects (9 active and 3 PBO). All subjects were post-menopausal women (aged 45-75y) and their status was confirmed by FSH >30 IU/L and Estradiol <92 pmol/L. PK, serum and urine bone resorption markers (CTX-I) (second morning void and 24h cumulative) were assessed.

After a single administration of 300mg SRT, median Tmax was delayed by 1.5h, mean Cmax was 3.3-fold lower, mean C24h was 5.4 times higher compared with 300mg IRT. Mean AUCinf was 0.83 fold compared to 300mg IRT and T1/2 was not significantly different. Repeated dosing of SRT was not considered to majorly affect PK. After a single dose of ONO-5334, serum CTX-I was suppressed by approx. 50% or more within 1h of administration reaching maximum suppression 6h post-dose (regardless of dose or formulation). Greater suppression was maintained for longer by 300mg SRT vs 300mg IRT. Second morning void and cumulative 24h urine CTX-I showed clear dose response effects for SRT with maximum suppression occurring at 24h for all treatments except for 300mg SRT in 24h cumulative urine where maximum suppression occurred in the 24-48h collection. With repeated dosing there appeared to be greater suppression in the 24h cumulative urine CTX-I.

Compared with the IRT, the SRT shows reduced Cmax, greater C24 but comparable overall AUCinf dose for dose. The SRT shows clear dose response suppression on bone resorption markers and greater efficacy dose for dose versus the IRT.

[1] Eastell R et al, JBMR 1 Feb 2011 [Epub]

Disclosures: Stephen Deacon, Ono Pharma UK Ltd, 3

This study received funding from: Ono Pharmaceutical Co Ltd, Osaka, Japan

FR0449

Effect of the Cathepsin K Inhibitor, ONO-5334, on Biochemical Markers of Bone Turnover in the Treatment of Postmenopausal Osteopenia or Osteoporosis: 2-Year Results from the OCEAN Study. Richard Eastell^{1*}, Shinichi Nagase², Maria Small², Steven Boonen³, Tim Spector⁴, Tomohiro Kuwayama², Stephen Deacon⁵. ¹University of Sheffield, United Kingdom, ²Ono Pharma UK Ltd, United Kingdom, ³Center for Metabolic Bone Disease & Division of Geriatric Medicine, Belgium, ⁴King's College London, United Kingdom, ⁵Ono Pharma, United Kingdom

The one year OCEAN results for ONO-5334, a Cathepsin K Inhibitor, have been previously reported. The aims of this extension study analysis were to observe whether ONO-5334 continued to increase BMD and decrease bone resorption markers (with little or no effect on bone formation). The effect of ONO-5334 (50mg bd, 100 or 300mg qd), on biochemical markers of bone turnover (BTM) was investigated in a randomised, placebo (PBO)-controlled, double-blind, 1y parallel-group study with a 1y extension, enrolling 285 postmenopausal women. Alendronate (ALN, 70mg qw) was used as an active reference. Patients were equally randomised to 5 treatment arms. Calcium and vitamin D were given to all patients. Subjects were 55-75 years old and had osteoporosis (with no fragility fractures) or osteopenia (with a fragility vertebral fracture). 197 women from the 1y base study continued into the 1y extension and 186 women completed 2y. Subjects and Investigators remained blinded to treatment allocation during the extension phase. We measured bone ALP, PINP, Osteocalcin and TRACP5b in serum(s) and CTX and NTX in urine(u) throughout the study. Lumbar spine (LS) and hip BMD were also assessed. 300mg ONO-5334 appeared to suppress bone resorption markers as potently as ALN (Table). Whilst ALN maintained suppression of bone formation markers after 2y at similar levels to 1y, ONO-5334 did not show suppression at 2y and even significant increases with lower doses. 50mg bd and 100mg qd showed significant increases in TRACP5b and no effect with 300mg qd. ALN maintained significant suppression of TRACP5b. All doses of ONO-5334 resulted in significant and dose-dependent increases in spine and hip BMD vs PBO. Mean \pm SE shown. At month 24, 300mg ONO-5334 increased lumbar spine (LS) BMD by 6.7% (\pm 0.6) ($p < 0.001$ vs. PBO 0.4% \pm 0.6), total hip BMD by 3.4% (\pm 0.4) ($p < 0.001$ vs. PBO 0.4% \pm 0.4) and femoral neck BMD by 3.7% (\pm 0.5) ($p < 0.001$ vs. PBO -0.5% \pm 0.5). ALN BMD results for LS, total hip and femoral hip were 6.3% \pm 0.6, 4.2% \pm 0.4 and 2.9% \pm 0.5, respectively ($p < 0.001$ vs. PBO). ALN continued to suppress all BTM at 2y whereas ONO-5334 showed no suppression of bone formation markers at 2y even at the highest dose and this differed from the 1y result. Thus, ONO-5334 continued to decrease bone resorption markers with little or no effect on bone formation. With comparable increases in BMD to ALN, this highlights a difference in the mechanism of action from bisphosphonates.

Table: Percentage change from baseline (95% CI) as a difference from PBO in BTMs

	Duration of Treatment	ONO-5334			ALN 70mg qw
		50mg bd	100mg qd	300mg qd	
uCTX/Cr	1y	-75 (-82, -64)***	-75 (-82, -64)***	-86 (-91, -79)***	-76 (-82, -66)***
	2y	-76 (-84, -68)***	-70 (-80, -55)***	-90 (-94, -84)***	-76 (-84, -64)***
uNTX/Cr	1y	-52 (-62, -39)***	-53 (-63, -41)***	-68 (-75, -60)***	-67 (-73, -58)***
	2y	-46 (-59, -29)***	-45 (-59, -28)***	-66 (-74, -56)***	-65 (-73, -54)***
sPINP	1y	6 (-13, 30)	16 (5, 42)	-28 (-41, -12)**	-65 (-71, -57)***
	2y	21 (-3, 51)	40 (13, 74)**	-2 (-21, 20)	-62 (-69, -52)***
sbone ALP	1y	2 (-9, 14)	9 (-3, 22)	-13 (-23, -3)*	-34 (-41, -26)***
	2y	12 (-3, 29)	17 (2, 35)*	-9 (-21, 5)	-37 (-45, -27)***
sOC	1y	1 (-15, 19)	2 (-14, 20)	-22 (-34, -8)**	-35 (-44, -23)***
	2y	5 (-10, 22)	-2 (-12, 18)	-8 (-20, 7)	-36 (-45, -26)***
sTRACP5b	1y	8 (-1, 18)	13 (4, 24)**	-6 (-13, 3)	-17 (-24, -9)***
	2y	18 (4, 34)*	22 (8, 38)**	6 (-6, 20)	-21 (-31, -11)***

Observed data/Full analysis set (* $p < 0.05$, ** $p < 0.01$, *** $p < 0.001$ vs. PBO as ratio of geometric means on log transformed markers). Cr: adjusted for creatinine

Eastell et al, ONO-5334 OCEAN 2y Abstract Table

Disclosures: Richard Eastell, Warner Chilcott, 2; Amgen, 5; Inverness Medical, 5; Novartis, 5; Fonterra Brands, 5; Lilly, 5; Medtronic, 5; Ono Pharma, 5; Unilever, 5; AstraZeneca, 5; Amgen, 2; Natch, 5; AstraZeneca, 2; Unipath, 5; GSK, 5; Past president ECTS, Member of MRC Efficacy and Mechanism Evaluation Board, 6; Sanofi Aventis, 5; Nestle, 5; Lilly, 2
This study received funding from: Ono Pharma Co, Osaka, Japan

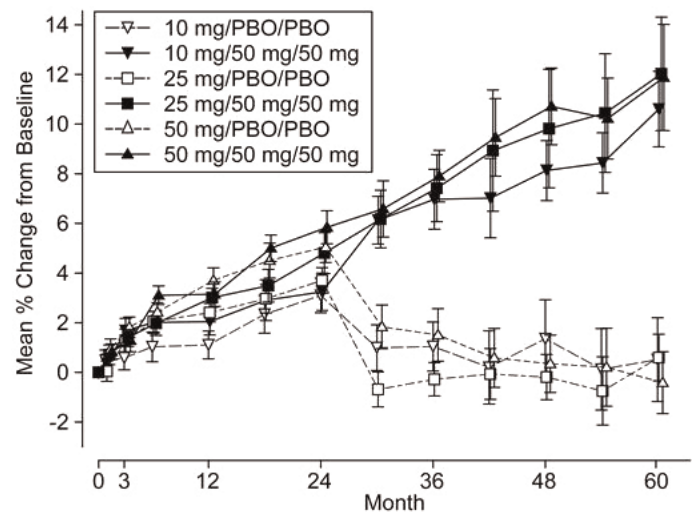
FR0453

Treatment with the Cathepsin K Inhibitor Odanacatib in Postmenopausal Women with Low BMD: 5 Year Results of a Phase 2 Trial. Neil Binkley^{1*}, Henry Bone², Nigel Gilchrist³, Bente Langdahl⁴, Heinrich Resch⁵, Jose Rodriguez-Portales⁶, Albert Leung⁷, Antonio Lombardi⁸, Celine Le Bailly De Tillegem⁹, Carolyn DaSilva⁸, Elizabeth Rosenberg⁸, Andrew Denker⁸. ¹University of Wisconsin, USA, ²Michigan Bone & Mineral Clinic, USA, ³Department of Orthopaedic Medicine & Surgery, Christchurch Hospital, New Zealand, ⁴Aarhus Sygehus, Aarhus University Hospital, Denmark, ⁵Medical University Vienna, Austria, ⁶Pontificia Universidad Catolica de Chile, Chile, ⁷Merck Research Laboratories, USA, ⁸Merck & Co., Inc., USA, ⁹Merck & Co., Inc., Belgium

The selective cathepsin K inhibitor odanacatib (ODN) progressively increased BMD at the spine and hip over the course of a 2-year trial and its 2-year extension. The trial extension is continuing, and we are reporting the results of an additional year. Postmenopausal women of mean age 63 years, with BMD T-scores initially between -2.0 and -3.5 at the lumbar spine or hip, received weekly placebo or ODN 3, 10, 25, or 50 mg for 2 years in addition to calcium, if needed, and vitamin D3. In year 3, women in each treatment group were re-randomized to ODN 50 mg or placebo. For years 4-5, women receiving placebo or ODN 3 mg in years 1-2 and placebo in year 3 were switched to ODN 50 mg; all others continued with their year 3 treatments. BMD at the lumbar spine (primary endpoint), femoral neck, trochanter, and 1/3 radius; bone turnover markers; and safety were assessed. Women entering the year 4-5 extension receiving placebo (n=41) or ODN 50 mg (n=100) had similar baseline characteristics. After 5 years, for women who received ODN 50 mg continuously from year 1 (n=13), mean % changes (SE) in BMD from baseline were: lumbar spine 11.9 (2.1) (Figure), femoral neck 9.8 (1.9), trochanter 10.9 (1.4), total hip 8.5 (1.0), and 1/3 radius -1.0 (1.3). In women who were switched from ODN 50 mg to placebo after 2 years (n=14), BMD mean % changes (SE) from baseline were: lumbar spine -0.4 (1.3) (Figure), femoral neck -1.6 (1.0), trochanter -1.0 (0.8), total hip -1.8 (0.8), and 1/3 radius -4.7 (1.7). After 5 years, for women continuously receiving ODN 50 mg (n=9-10), geometric mean % changes from baseline (SE) were -67.4 (10.1) for urine NTX/creatinine, but only -15.3 (5.9) for serum BSAP, whereas for women switched from ODN 50 mg to placebo after 2 years (n=10) these changes were 6.0 (7.6) and -11.9 (3.9), respectively. The administration of ODN over 5 years compared to placebo was generally well-tolerated. In summary, women who received ODN 50 mg for 5 years had a gain in spine and hip BMD over 5 years and showed a sustained reduction in urine NTX/creatinine and a smaller reduction in serum BSAP. As previously reported, discontinuation of odanacatib results in reversal of BMD gains.

Percent Change from Baseline in Lumbar Spine BMD (g/cm²) (Mean \pm SE)

Full-Analysis-Set Population - Last Observation Carried Forward



Figure

Disclosures: Neil Binkley, Merck, 2

This study received funding from: Merck Sharp & Dohme

FR0464

JTT-305 (MK-5442), an Orally Active Calcium-Sensing Receptor Antagonist, Stimulates Transient Parathyroid Hormone Release and Bone Formation. Shuichi Kimura*, Takashi Nakagawa, Yoshihisa Okamoto, Yuji Ishida, Yushi Matsuo, Yuko Shinagawa, MIKIO HAYASHI, Central Pharmaceutical Research Institute, JAPAN TOBACCO INC., Japan

Intermittent administration of parathyroid hormone (PTH) has a potent anabolic effect on bone in humans and animals. Calcium-sensing receptor (CaSR) antagonists stimulate endogenous PTH secretion through CaSRs on the surface of the parathyroid cells and thereby may be anabolic agents for osteoporosis. JTT-305 has been discovered as a potent, orally active CaSR antagonist. This study describes the pharmacological characteristics of JTT-305 (MK-5442). JTT-305 inhibited the increases in intracellular Ca^{2+} induced by extracellular calcium stimulation in COS-7 cells transiently transfected with human CaSR ($\text{IC}_{50} = 86 \text{ nM}$). JTT-305 stimulated PTH secretion from bovine parathyroid cells ($\text{EC}_{50} = 16 \text{ nM}$). Single doses of JTT-305 (0.3-3 mg/kg) were administered orally as a suspension in 0.5% aqueous methyl cellulose to male Sprague-Dawley (SD) rats. The pharmacokinetic and pharmacodynamic profiles were monitored over eight hours. Plasma levels of JTT-305 rapidly increased ($T_{\text{max}} = 30 \text{ min}$) and were cleared in a dose-dependent manner. Serum PTH levels rapidly increased in a dose-dependent manner ($T_{\text{max}} = 15\text{-}30 \text{ min}$, up to 7-8 fold above baseline) and returned to baseline in one to four hours. To evaluate the effect of JTT-305 on OVX-induced bone loss female SD rats, immediately after OVX, were administered JTT-305 (0.3, 1 or 3 mg/kg) orally once daily for 12 weeks. Both doses of JTT-305 prevented OVX-induced decreases in cancellous bone and total BMD at the proximal tibia. Compared to vehicle, JTT-305 increased bone volume, trabecular thickness, trabecular number, and trabecular bone pattern factor in microstructural analyses, and increased mineralizing surface and bone formation rate in histomorphometric analyses. In summary, JTT-305 is a potent, orally active CaSR antagonist that stimulates transient PTH release and prevents bone loss in OVX rats through stimulation of bone formation. These results suggest that JTT-305 is orally active and has the potential to be an anabolic agent for the treatment of osteoporosis.

Disclosures: Shuichi Kimura, JAPAN TOBACCO INC., 3
This study received funding from: JAPAN TOBACCO INC.

FR0465

Sclerostin Antibody Enhances Distraction Osteogenesis in Rats. David Little*¹, Oliver Birke¹, Michelle McDonald¹, Kathy Mikulec¹, Lauren Peacock¹, Alyson Morse¹, Min Liu², Hua Zhu Ke³. ¹The Children's Hospital At Westmead, Australia, ²Amgen, USA, ³Amgen, Inc., USA

Sclerostin is a negative regulator of osteoblast differentiation and bone formation, via antagonism of the Wnt/ β -catenin pathway and/or BMP activity. A sclerostin antibody (Scl-AbIII) has recently been shown to increase bone formation in ovariectomized rats and enhance fracture healing in rats. Distraction osteogenesis is widely used in limb lengthening and reconstruction surgery. Complications of this technique include disuse osteopenia and poor regenerate bone healing, both of which would benefit from pro-anabolic therapy.

A femoral osteotomy was stabilized externally in male Sprague Dawley rats. After a week of latency, the gap was distracted twice daily for 14 days to a total of 7mm. Saline or Scl-Ab (Scl-AbIII) was administered twice weekly throughout the distraction period and up to 4, 6 or 8 weeks post commencement of distraction. Three groups were examined, Saline, Continuous Scl-Ab (C Scl-Ab) and Delayed Scl-Ab with commencement after distraction was complete (D Scl-Ab).

DXA scans at 2 weeks revealed a 67% increase in regenerate BMC in the C Scl-Ab group over Saline ($p < 0.01$). By 6 weeks, regenerate BMC was increased 86% in C Scl-Ab ($p < 0.05$). Further, C Scl-Ab treatment increased BMC proximal to the regenerate compared to Saline at 2, 4, 6 and 8 weeks ($p < 0.05$). MicroCT scans of the regenerate revealed increases in bone volume of 89% with C Scl-Ab and 85% with D Scl-Ab compared to Saline at 6 weeks ($p < 0.05$). By 8 weeks these increases were 53% with C Scl-Ab ($p < 0.01$) and 30% with D Scl-Ab ($p < 0.05$). Further, BV/TV was increased 77% with C Scl-Ab and 82% with D Scl-Ab at 6 weeks compared to Saline ($p < 0.05$) and 40% with C Scl-Ab at 8 weeks ($p < 0.05$). Histology at 6 weeks confirmed MicroCT with 130% increases in BV/TV in the regenerate in C Scl-Ab and D Scl-Ab groups compared to Saline ($p < 0.05$). Analysis of mineral apposition rate showed increases of 56% in C Scl-Ab and 52% in D Scl-Ab over Saline ($p < 0.05$).

Scl-Ab treatment increased bone formation in this model of distraction osteogenesis resulting in a larger regenerate, with increased BMC and bone volume. We expect further studies to reveal increases in mechanical strength. C Scl-Ab and D Scl-Ab showed similar results by MicroCT, suggesting that timing of Scl-Ab is not pivotal. Scl-Ab is hence a candidate for clinical development to accelerate regenerate formation in distraction osteogenesis, which could shorten fixation time and decrease complications or re-fracture.

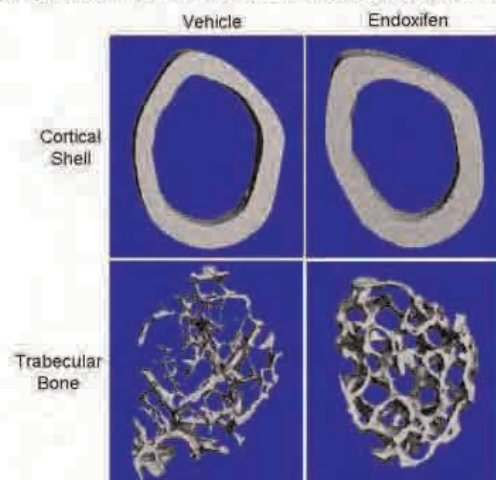
Disclosures: David Little, Amgen Inc, 2
This study received funding from: Amgen Inc

FR0466

The Tamoxifen Metabolite, Endoxifen, has Anabolic Actions on the Skeleton. John Hawse*¹, Malayannan Subramaniam², Muzaffer Cicek², Kevin Pite³, Kenneth Peters¹, Sarah Grygo¹, Xianglin Wu¹, Glenda Evans², James Ingle¹, Matthew Goetz¹, Thomas Spelsberg². ¹Mayo Clinic College of Medicine, USA, ²Mayo Clinic, USA, ³University of Minnesota, USA

Tamoxifen, an anti-estrogen, has been used for over 30 years as the primary therapy for the treatment of women with endocrine sensitive breast cancer. Recently, our laboratory has demonstrated that endoxifen is the active tamoxifen metabolite responsible for eliciting the anti-cancer effects of this drug. Based on these studies, clinical trials are now underway to treat breast cancer patients with endoxifen. For these reasons, it is imperative to understand the potential side effects of endoxifen on other endocrine sensitive organ systems such as the skeleton. As a first step, we examined the effects of endoxifen on both osteoblasts and osteoclasts in vitro. Endoxifen significantly induced the expression of critical bone marker genes such as Runx2, osterix, osteocalcin, osteoprotegerin and alkaline phosphatase in mouse bone marrow stromal cells and human osteoblasts. Induction of these genes occurred in a dose dependent manner and was associated with increased expression of estrogen receptor-beta ($\text{ER}\beta$), but not $\text{ER}\alpha$, suggesting that $\text{ER}\beta$ may primarily mediate endoxifen's effects on osteoblasts. Endoxifen was also shown to suppress the differentiation of osteoclast precursors derived from mouse bone marrow. We next administered endoxifen (50mg/kg) or vehicle control on a daily basis to 2 month old ovariectomized C57BL/6 mice ($n=10$) for 30 days. DXA analysis revealed significant increases in total body bone mineral density (BMD) (6%) and content (BMC) (9%), which was accompanied by a 23% decrease in fat tissue mass, in the endoxifen treated group. Dramatic increases in BMD (35%) and BMC (20%), as well as trabecular density (52%), cortical content (62%), cortical area (60%) and cortical thickness (78%), were also observed in the tibial metaphysis of endoxifen treated animals as assayed by pQCT. micro-CT analysis of the femoral metaphysis also revealed increases in bone volume/total volume (200%), trabecular number (38%) and trabecular thickness (18%), as well as decreased trabecular spacing (29%), following endoxifen treatment (see figure for representative image). These data are the first to demonstrate that endoxifen has anabolic effects on the skeleton and suggest that the use of endoxifen for the treatment of breast cancer may be more favorable than other new generation therapies which are known to have significant deleterious skeletal effects. Finally, endoxifen may also prove to be an effective therapy for the treatment and/or prevention of osteoporosis.

Representative micro-CT image of the femoral metaphysis following 30 days of vehicle control or endoxifen treatment of 2 month old ovariectomized C57BL/6 mice.



Figure

Disclosures: John Hawse, None.

FR0473

Differential Effects of Odanacatib and Alendronate on Bone Turnover in the Femoral Neck of Adult Ovariectomized Rhesus Monkeys. Tara Cusick*¹, Brenda Pennypacker², Maureen Pickarski¹, Le Thi Duong². ¹Merck & Co., Inc., USA, ²Merck Research Laboratories, USA

Odanacatib (ODN) is a selective, potent and reversible cathepsin K inhibitor in development for the treatment of osteoporosis. Here, we report the effects of ODN and alendronate (ALN) on bone mass and turnover in the femoral neck (FN) of OVX-rhesus monkeys after 20-months treatment. Monkeys (age 12-22 yrs; N=16/group) were dosed in prevention mode with either vehicle (Veh), ODN (2mg/kg/d, po), or ALN (30µg/kg/wk, sc). The ODN dose provided steady state exposure of 11µM·24h as compared to the equivalent clinical 50mg dose at a daily exposure of ~7µM·24h. A separate group of age- and BMD-matched intact monkeys (Int, N=12) was included as control. From *ex vivo* DXA, ODN and ALN displayed comparable trends of FN BMD increases by 5% (NS) compared to Veh. From shear strength test,

regression analysis of all groups showed that peak load of the FN was positively correlated to BMD ($R=0.705$; $p<0.0001$) and BMC ($R=0.740$; $p<0.0001$). Dynamic histomorphometry on both trabecular and periosteal surfaces was determined from 120 μ m-thick cross-sections from double fluorochrome labels, calcein (CAL, 8mg/kg, 15d, sc) at 12 mo. and tetracycline (TCY, 40mg/kg, 14d, IV) just prior to study end. Long-term (LT) bone formation (BF) was calculated based on the CAL-TCY labeling interval of ~228 days. In trabecular FN at both 12 and 20 mo. treatment, ODN tended to reduce and ALN significantly decreased short term (ST) mineralizing surface (MS/BS) vs. Veh. Whereas mineral apposition rate (MAR) remained unchanged, both agents significantly decreased BFR/BS at 12 mo. ($p<0.01$) and 20 mo. ($p<0.05$) vs. Veh. On the periosteal (Ps) cortical surface, all ST BF parameters were not affected by ODN or ALN treatment. However, ODN but not ALN significantly increased LT Ps. MS/BS and Ps.BFR/BS without affecting MAR compared to Veh. The increased LT BF by ODN resulted in a significant increase in cortical thickness by 23% ($p<0.05$) and cortical area per tissue area by 18% ($p<0.05$) and a decrease in marrow area per tissue area by 11% ($p<0.05$) vs. Veh. In summary, comparable to ALN, ODN treatment protected bone mass and maintained normal biomechanical property at the femoral neck of OVX monkeys. This study supports earlier findings that ODN effectively reduces trabecular bone remodeling, yet ODN differs from the bisphosphonates by simultaneously building cortical bone of the femoral neck, in part via stimulating periosteal bone formation.

Disclosures: Tara Cusick, Merck & Co., 3
This study received funding from: Merck & Co.

FR0475

Inhibition of GSK3 Modulates Early Biomarkers of Bone Turnover in Rats. Peter S Gilmour^{*1}, Witte Koopmann², Hitesh Sangane¹, Hiroki Wada¹, Ashwani Bahl¹, Stefan Kavanagh¹, Peter A Hall¹, Katherine Escott¹.
¹Astrazeneca R&D, United Kingdom, ²AstraZeneca, Sweden

Bone turnover is affected by a number of different mechanisms, including modulators of the wnt signaling pathway such as glycogen synthase kinase 3 (GSK3) inhibitors, anti-resorptive agents such as bisphosphonates, and bone anabolic agents such as parathyroid hormone (PTH1-34). Clinically, a variety of serum biomarkers have been used to measure early changes in bone resorption (e.g., tartrate-resistant acid phosphatase 5b, TRAcP-5b) and bone anabolism (e.g., procollagen type I N-terminal propeptide, PINP).

We investigated the utility of these serum biomarkers as early indicators of changes in bone turnover in rats in vivo. Eleven week old Sprague-Dawley rats were treated with vehicle, GSK3 inhibitors (AR28 and AZ241, po, UID), PTH1-34 (30 μ g/kg, s.c. every second day) or the bisphosphonate alendronate (30 μ g/kg, s.c. every second day). After 3 to 28 days treatment, rats were sacrificed and blood was taken for serum biomarker measurements using commercial assay kits for TRAcP-5b and PINP. Femurs were removed for histopathological assessment following formalin fixation, sectioning and H&E staining. A time course experiment was carried out with AR28 (30 μ mol/kg, po, UID), in which serum PINP was increased by 38% and 40% after 3 and 7 days dosing, respectively, and returned to baseline levels 14 days post-dosing. Serum TRAcP-5b was decreased by 48% at day 3, 65% at day 7 and 68% at day 28 with AR28. In a second experiment, after 7 days of treatment with AR28 (15 μ mol/kg, po, UID) or AZ241 (96 μ mol/kg, po, UID), TRAcP-5b was reduced by 60% and 79% and PINP increased by 37% and 100%, respectively. PTH1-34 produced an increase in PINP (30%) but did not affect TRAcP-5b at day 7. Alendronate inhibited TRAcP-5b (71%) but did not affect PINP at day 7. In contrast to PTH1-34 and alendronate, inhibitors of GSK3 altered both PINP and TRAcP-5b, suggesting both a reduction in bone resorption and an increase in bone formation. Evidence of increased bone formation was observed by histopathological assessment of femurs following treatment with AR28 and AZ241. The findings included trabecular and cortical bone hyperplasia, increased focal osteoid, and osteoblast hypertrophy from day 7 onwards. Thus, treatment with either AR28 or AZ241 led to a net increase in bone formation in rat femurs in vivo. In conclusion, changes in serum biomarkers of bone turnover, PINP and TRAcP-5b, are early indicators of bone turnover modulation in rats treated with GSK3 inhibitors.

Disclosures: Peter S Gilmour, None.

FR0482

Altered Balance between Chondrocyte Apoptosis and Proliferation is Associated with Growth Plate Fusion in Mice with a Specific Inactivation of AF-1 in Estrogen Receptor (ER)- α while Total Inactivation of ER α Results in Prolonged and Enhanced Longitudinal Bone Growth. Anna Borjesson^{*1}, Sara Windahl¹, Marie Lagerquist², Cecilia Engdahl³, Elham Karimian⁴, Emma E Eriksson⁴, Maria Cristina Antal⁵, Andree Krust⁵, Pierre Chambon⁵, Lars Savendahl⁴, Claes Ohlsson⁶.
¹Center for Bone & Arthritis Research, Sahlgrenska Academy, Sweden, ²Sahlgrenska University Hospital, Sweden, ³Centre for Bone & Arthritis Research, GU, Sahlgrenska Academy, Medicine, Sweden, ⁴Division of Pediatric Endocrinology, Department of Womens & Childrens Health, Karolinska Institutet, Sweden, ⁵Institut de Genetique et de Biologie Moleculaire et Cellulaire (CNRS, INSERM, UoS, College de France), Illkirch, France, ⁶Center for Bone Research At the Sahlgrenska Academy, Sweden

The key role for estrogen and estrogen receptor (ER)- α in the regulation of the growth plate and longitudinal bone growth is demonstrated by the findings that a nonfunctional ER α , or estrogen deficiency caused by a mutation in the aromatase gene, lead to continued growth after sexual maturation owing to non-fused growth plates. In rodents, the growth plates do not fuse directly after sexual maturation, but old mice have reduced growth plate heights and long-term high-dose estradiol treatment results in growth plate fusion.

ER α stimulates target gene transcription via two activation functions (AFs), AF-1 and AF-2. To evaluate the role of AF-1 for longitudinal skeletal growth and growth plate morphology, female mice with specific inactivation of AF-1 in ER α (ER α AF-1⁰) and mice with total inactivation of ER α (ER α ^{-/-}) were evaluated from a pre-pubertal age until they were old (16-19 months old).

Interestingly, the length- and growth plate phenotypes in the ER α ^{-/-} mice correspond with those found in patients with nonfunctional ER α or aromatase deficiency. Accordingly, old ER α ^{-/-} mice showed increased length of the appendicular skeleton (femur: +6.0%, tibia: +8.3%, $p<0.01$) and increased height of the proximal tibial growth plate (+18%, $p<0.05$) compared with WT mice, an effect that was not seen in young adult ER α ^{-/-} mice.

In contrast, the length of the appendicular skeleton was decreased in old ER α AF-1⁰ mice compared with WT mice (femur: -4.0%, tibia: -4.9%, $p<0.01$). Further, the proximal tibial growth plates were fused in all old ER α AF-1⁰ mice, while it was open in all WT mice. The proliferative zone of the growth plate was decreased already in the young adult ER α AF-1⁰ mice (proximal tibia: -17%, $p<0.01$). The fusion of the growth plate was associated with an altered balance between chondrocyte apoptosis and proliferation in the growth plate ($p<0.05$).

In conclusion, old mice with complete inactivation of ER α display a prolonged and enhanced longitudinal bone growth associated with increased growth plate height, resembling the appendicular bone phenotype of a patient lacking ER α . In contrast, specific inactivation of ER α AF-1 results in a hyperactive ER α , altering the balance between chondrocyte apoptosis and proliferation in the growth plate, leading to growth plate fusion.

Disclosures: Anna Borjesson, None.

FR0483

Androgen Directly Exerts Anabolic Action through Osteoblastic Androgen Receptor. Yuuki Imai^{*1}, Min-Young Youn¹, Min Ni², Kazuki Inoue¹, Shino Kondoh¹, Takahiro Matsumoto³, Myles Brown², Shigeaki Kato¹.
¹The University of Tokyo, Japan, ²University of Tokyo, Japan, ³Department of Medical Oncology, Dana-Farber Cancer Institute, USA, ³Tokushima University, Japan

Sex steroid hormones play important roles to maintain bone tissues through various mechanisms. However, it remains unclear whether androgen directly targets on bone tissue. To clarify physiological impact of AR in bone, we generated and analyzed osteoblast specific KO (*ObARKO*) and male, but not female, *ObARKO* mice exhibited decreased bone mineral density (BMD) in diaphysis of long bones and calvaria. Furthermore, bone histomorphometric analyses revealed that no apparent change was found in static parameters although dynamic parameters, such as MAR and BFR were reduced in both cortical and trabecular bone of *ObARKO*. These results suggested that AR in osteoblasts mediates androgen anabolic actions.

Therefore, to characterize the impact of AR in osteoblasts, gene expression microarray was performed using mRNA extracted from primary cultured calvarial osteoblasts from control and *ObARKO* mice. As a result, more than 500 genes were significantly changed in expression level. Moreover, gene ontology analysis of these genes reveals that categories of extracellular protein, growth factor activity and protein binding were highly ranked. Furthermore, to determine the direct target genes of AR in osteoblasts, a Chromatin Immunoprecipitation sequencing (ChIP-seq) was performed for an osteoblastic cell line, MC3T3E1, treated with DHT. ChIP-Seq analysis revealed 4018 AR binding sites in the mouse genome of MC3T3E1 cells with p value cut off of e^{-5} . Among these binding sites, 2329 Refseq genes have AR binding sites located between 10kb upstream of transcriptional start site to 10kb downstream from transcriptional terminate site. Twenty-four candidate genes of direct AR target in osteoblasts were raised from these two kinds of genome-wide data sets. Among the

candidate genes, Bmper was validated by qPCR. Bmper is the modulator of BMPs by binding with BMPs in extracellular spaces as reported. However, little is known about relationship between Bmper and androgen signaling. To answer this question, the effects of ORX were assessed for WT and Bmper heterozygous deficient male mice (*Bmper^{+/-}*), because of neonatal lethality of homozygous Bmper KO mice. As the results of BMD analysis, ORX failed to decrease BMD of *Bmper^{+/-}* although BMD of WT was significantly reduced by ORX.

These results indicate that AR can directly regulate the transcription of Bmper and androgen directly exerts anabolic action via osteoblastic AR by modulating BMP action.

Disclosures: Yuuki Imai, None.

FR0487

A Human BAC Transgene Containing the Vitamin D Receptor Gene Locus Humanizes the VDR-null Mouse and Rescues the Aberrant Biological Phenotype of VDR Deficiency. Seong-Min Lee^{*1}, Kathleen Bishop¹, Charles O'Brien², J. Pike¹. ¹University of Wisconsin-Madison, USA, ²University of Arkansas for Medical Science, USA

The biological actions of 1,25-dihydroxyvitamin D3 (1,25(OH)2D3) are mediated by the vitamin D receptor (VDR), a transcription factor expressed in a cell-type specific manner in the intestinal tract, kidney tubules, the parathyroid gland, skin and in bone cells, and regulated by hormones that include PTH, retinoic acid and 1,25(OH)2D3. Recent studies using genomic ChIP-chip and ChIP-seq together with recombinant BAC clone analyses have both defined the functional boundaries of the mouse and human VDR genes and identified a series of intronic and promoter-distal enhancers that contribute to the genes' basal as well as hormone-regulated expression in cultured cells. More recently, we have shown that when employed as transgenes in mice, these mouse and human VDR BAC clones are fully capable of recapitulating tissue-specific expression of the endogenous mouse VDR and directing bone cell-specific up-regulation of VDR in response to exogenous 1,25(OH)2D3 and cAMP. In the present studies, we crossed these transgenic mice with the VDR-null mouse and examined their ability to rescue the VDR-deficient phenotype. All aberrant parameters of systemic calcium and phosphate homeostasis in the VDR null mouse were normalized with each transgene, including a striking reduction in the high systemic levels of PTH inherent to VDR deficiency. Parathyroid hyperplasia apparent in the VDR-null mouse was also rescued. The two transgenes also normalized the expanded hypertrophic chondrocyte layer in the growth plate, corrected the tibia size-defect, and restored skeletal bone mineral density observed due to VDR deficiency. In the kidney, high levels of *Cyp27b1* and low levels of *Cyp24a1* expression in the VDR-null mouse were also restored. VDR action via transgenic expression also restored VDR-null defects in the skin, reducing the presence of dermal cysts and restoring postnatal hair cycling. Finally, VDR transgene expression also restored 1,25(OH)2D3's ability to induce expression of key genes in the intestine, kidney and bone. These studies demonstrate that BAC transgenes containing mouse and human VDR gene loci can direct tissue-specific expression of the VDR *in vivo* and fully rescue the VDR-null phenotype. Relative to the human transgene, this rescue results in the creation of a humanized VDR-null mouse. These studies will enable future identification of determinants of tissue-specific VDR expression and evaluation of VDR function *in vivo*.

Disclosures: Seong-Min Lee, None.

FR0492

DNA Methylation Levels of CYP2R1 and CYP24A1 Predict Vitamin D Dose-response Variation. Xiaojing Xu^{*1}, YU ZHOU², Fengxiao Bu², An Ye¹, Boting Zhou¹, Robert Recker¹, Joan Lappe¹, Lanjuan Zhao³. ¹Creighton University Osteoporosis Research Center, USA, ²CREIGHTON UNIVERSITY, USA, ³Creighton University Medical Center, USA

The wide variation of serum 25(OH)D in response to a given dose of vitamin D supplementation is a daunting challenge for vitamin D deficiency treatment. The goal of this study is to test whether DNA methylation levels of cytochrome P450 (CYP) enzymes (*CYP2R1*, *CYP27A1*, *CYP24A1*, and *CYP27B1*) are biomarkers predicting vitamin D dose-response variation.

Our preliminary data indicated that DNA methylation level of *CYP2R1* was associated with vitamin D dose-response variation in 18 responders and 18 non-responders, who were selected at two extreme tails of 12-month increase of serum 25(OH)D levels, from 446 white postmenopausal women who completed 12 months of a vitamin D3 (1100 IU/day) intervention. In this study, we further tested the importance of *CYP27A1*, *CYP24A1*, and *CYP27B1* in the 18 paired extreme samples. For each subject, genomic DNA at baseline and after the 12-month intervention was extracted from frozen serum. Methylation specific PCR (MSP) results in the promoter region of *CYP2R1*, *CYP27A1*, *CYP24A1*, and *CYP27B1* indicated that, compared to non-responders, responders have a significantly lower baseline DNA methylation level in the promoter region of *CYP2R1* (8% in responders, 30% in non-responders, $P=0.004$), and *CYP24A1* (13% in responders, 32% in non-responders, $P<0.0001$).

In order to validate our pilot results and identify specific CpG sites, pyrosequencing was conducted in 14 CpG sites of *CYP2R1* and 16 CpG sites of *CYP24A1* in

another independent 145 paired serum DNA samples. After the 12-month vitamin D3 intervention, all 14 CpG sites of *CYP2R1* became significantly lower methylated (average methylation level: 11% at 12-month vs 15% at baseline, $P<0.0001$). For *CYP2R1*, baseline DNA methylation levels at 8 CpG sites (-4C, +28C, +30C, +33C, +40C, +43C, +69C, +80C) were negatively associated with 12-month increase of serum 25(OH)D ($P<0.05$). For *CYP24A1*, baseline DNA methylation level at -342C and -293C were also negatively associated with vitamin D dose-response variation ($r=-0.151$, $P=0.011$; $r=-0.131$, $P=0.025$). These negative associations were consistent with our pilot MSP results. That is, high baseline DNA methylation levels of *CYP2R1* and *CYP24A1* gene were significantly associated with reduced conversion of vitamin D3 into 25(OH)D.

For the first time, our results indicated that DNA methylation levels of *CYP2R1* and *CYP24A1* at baseline may be potential biomarkers in predicting vitamin D dose-response variation.

Disclosures: Xiaojing Xu, None.

FR0493

Enhanced Vitamin D Synthesis in Osteoblasts Protects Against Age-Related Bone Loss. Paul Anderson^{*1}, Andrew Turner², Rebecca Sawyer¹, Peter O'Loughlin³, Gerald Atkins⁴, Howard Morris². ¹Musculoskeletal Biology Research, University of South Australia, Australia, ²SA Pathology, Australia, ³Chemical Pathology, SA Pathology, Australia, ⁴University of Adelaide, Australia

Age-related bone loss is associated with a change in bone remodeling characterized by an imbalance between bone formation and bone resorption. Our previous studies in rodents demonstrate that age-related bone loss occurs independently of sex hormone deficiency. While, the physiology of such age-related changes in bone volume remains unclear, ours and other studies suggest that vitamin D activity in the bone is critical for optimizing bone turnover and the prevention of osteoporosis. Furthermore while 1,25D treatment regulates osteoblast gene transcription, proliferation, differentiation and mineralization *in vitro*, the synthesis of 1,25D within osteoblasts also plays a critical role in the inhibition of cell proliferation, stimulating differentiation, and increasing matrix mineralisation by osteoblasts. To demonstrate the *in vivo* role for vitamin D synthesis within osteoblasts, we have created a transgenic mouse model in which transcription of the human *Cyp27b1* sequence is driven by the osteocalcin promoter (OSCyp27b1) only in mature osteoblasts. In primary osteoblasts cultures from OsCyp27b1 mice, increased 1,25D synthesis and enhanced mineralisation. Both male and female OsCyp27b1 mice demonstrate increased bone mineral volume due to increased trabecular number. Interestingly, while male OSCyp27b1 mice demonstrate increased bone from at least 7 weeks of age (12% increase in femoral trabecular BV/TV, $n=11$, $P<0.05$), female OSCyp27b1 mice demonstrate a marked increase in trabecular bone volume only at 20 weeks of age (19% increase femoral metaphyseal, $P<0.05$; 7% increase femoral epiphysis, $P<0.05$; 11% increase lumbar vertebrae $P<0.05$, $n=14$). These data suggest that in female mice increased CYP27B1 activity in osteoblasts protects against bone loss that occurs with aging. Consistent with this observation, TRAP-positive osteoclast numbers on trabecular surfaces are reduced by 26% in 20 week old OSCyp27b1 female mice when compared to WT ($n=3$ /grp). Thus our data strongly suggest that Cyp27b1 activity in mature osteoblasts and osteocytes modulates bone formation as well as resorption with an overall increase in bone mineral. Furthermore, the identification of CYP27B1 activity in osteoblasts as protective mechanism of age-related bone loss and provides a potential mechanism whereby a therapeutic intervention may be developed to improve bone formation and bone mass in the aging population.

Disclosures: Paul Anderson, None.

SA0001

Age-related Changes in the Activin A-myostatin-follistatin System within the Bone Marrow Microenvironment. Matthew Bowser¹, Norman Chutkan², John Martell¹, Raymond Corpe¹, Carlos Isales³, Mary Anne Park¹, Demetric Hillman¹, Mark Hamrick^{*1}. ¹Georgia Health Sciences University, USA, ²Georgia Health Sciences University, USA, ³Medical College of Georgia, USA

In vitro and in vivo studies have demonstrated that both activin A and its antagonist follistatin play important roles in bone formation. Activin A treatment can inhibit mineralization in cultured osteoblasts, whereas follistatin increases mineralization. Furthermore, inhibiting activin A in vivo using a decoy soluble activin A receptor (ActRIIA) increases bone formation in mice. Follistatin also antagonizes myostatin (GDF-8), and mice lacking myostatin show increased bone density. Thus, interactions among these factors are likely to be involved in the regulation of bone mass throughout growth, development and aging. Yet, changes in the relative levels of these factors within the bone marrow microenvironment with increasing age are not well understood. We investigated age-related changes in the activin A-myostatin-follistatin system using femoral bone marrow aspirates from young (12 months) and aged (24 months) mice, as well as bone marrow samples from young (<50 years) and older (>70 years) knee arthroplasty patients. Samples were processed using centrifugation to obtain bone marrow supernatant fluid from both mice and humans, since the soluble factors within the marrow supernatant in part define the extracellular milieu to which bone cells are regularly exposed. Supernatant samples were analyzed using ELISA. Results indicate that follistatin levels are not significantly altered with age in bone marrow supernatants from either mice or humans. Myostatin levels were significantly (+75%) increased in mouse bone marrow with age, but did not increase with age in human bone marrow. Activin A levels increased with age (+17%) in mouse bone marrow, and increased by more than 120% in human bone marrow. The marked increase in activin A levels with age in the patient samples was associated with a similar increase in the activin A: follistatin ratio. These findings suggest that activin A bioavailability is altered with age in the bone marrow microenvironment, and may therefore play a role in age-associated changes in bone metabolism. Funding for this research was provided by the Congressionally Directed Medical Research Programs (USAMRAA).

Disclosures: Mark Hamrick, None.

SA0002

See Friday Plenary Number FR0002.

SA0003

See Friday Plenary Number FR0003.

SA0004

See Friday Plenary Number FR0004.

SA0005

See Friday Plenary Number FR0005.

SA0006

Body Composition in Patients with Type 2 Diabetes Treated with Metformin and Incretin-Based Drugs. Olga Sukhareva, Irina Schmushkovich^{*}, Marina Shestakova, Tatyana Chernova. National Endocrinology Research Center, Russia

Background and goals: The main type 2 diabetes related issues, insulin resistance and impaired beta cell function, are often treated with metformin and incretin-based drugs, respectively. This combination therapy may have some additional benefits, too. One of the main problems in the therapy of such patients is excessive weight and obesity. The goal of this study was an assessment of patients' body composition and its dynamics for patients on such combination therapy.

Patients and methods: As a part of a bigger study we examined a subgroup of 16 patients, aged 45 to 74, with mean duration of T2D 5 years, with HbA1c level more than 7% and less than 10%. We performed the body composition analysis using DEXA Lunar Prodigy GE before and after 6 months of therapy. We analyzed body mass, fat, lean mass, and the percentage of tissue and regional fat in dynamics.

Results: the obtained results are following - mean body mass (kg) before therapy was 86,2310,41, after therapy - 83,4211,58 (P=0,023), fat mass (g) before therapy 32942,94950,16, after therapy - 30651,65721,39 (p=0,042), tissue fat (%) 39,776,49 before therapy and 38,176,41 after therapy (p=0,068). We also determines regional fat (%) before 38,496,29 and 36,916,25 after therapy (p=0,064) and lean mass (g), which

was 50465,59989,82 before and practically did not change after the therapy 49961,59931,08 (p=0,23).

Conclusion: During such therapy we obtained results showing a statistically significant decrease of body mass and body fat, while lean mass remained practically unchanged. These observations should be taken into account when choosing the diabetes therapy.

Changes in tissue and regional fat and A/G ratio observed in this study did not reach statistical significance. It should be noted that previously it had been shown that the change in these parameters lags behind the total fat decrease. Therefore, some trends may not be visible in the data obtained so far due to a short duration of this preliminary study.

Disclosures: Irina Schmushkovich, None.

SA0007

Diminished Mechanical Stimuli Following Transient Muscle Paralysis Are Not Associated with Acute Trabecular Bone Loss. Jitendra Prasad, Phillipe Huber, Steven Bain, Ted Gross^{*}. University of Washington, USA

Bone loss associated with muscle dysfunction (e.g., SCI, stroke) has been primarily attributed to diminished mechanical stimuli within the afflicted portion of the skeleton. Accordingly, we hypothesized that trabecular bone loss following transient muscle paralysis would be correlated to the loss of gait-induced mechanical stimuli. To test this hypothesis, C57 female mice (16 wk) were exposed to transient muscle paralysis of the quadriceps (Quad, n=6) or calf (Calf, n=6) via a single injection of botulinum toxin A (2 U/100g). Peak normal strains in the tibia during locomotion, calf muscle volume and trabecular bone morphology (BV/TV) of the proximal tibia were then quantified. To determine normal strains, hindlimb ground reaction forces were measured during spontaneous locomotion over a custom walkway with in-line force plate. Kinematic data were simultaneously collected and beam theory used to calculate peak normal strains at the tibia mid-diaphysis. All outcome measures were assessed at d 0 (prior to muscle paralysis) and d 12 (the time of maximal trabecular bone loss in this model). T-tests were used to detect significant differences (p<0.05) and Pearson correlations were used to assess the dependency of BV/TV on diminished normal strain and diminished muscle volume. Qualitatively, quadriceps paralysis induced a more severe gait defect than calf paralysis. Quantitative data supported this observation as peak normal strains in the Quad group were reduced -91.10.9% vs d 0 (p<0.001), while strains in the Calf group were diminished by -42.62.7% (p<0.001 vs. d 0 and p<0.001 vs Quad). In the Quad group, calf volume was significantly decreased (-13.62.6%, p<0.001). Atrophy in the Calf group was 2-fold greater than the Quad group (-26.62.2%, p<0.001 vs d 0, p<0.01 vs Quad). Independent of changes in normal strain and muscle volume, BV/TV was significantly and equivalently diminished in both Quad (-72.36.7%, p<0.001) and Calf groups (-65.33.5%, p<0.001). Consequently, neither diminished peak normal strains (r²=0.14) nor muscle atrophy (r²=0.04) accounted for acute trabecular bone degradation induced by muscle paralysis. We therefore conclude that these factors are unlikely to serve as the primary mediators of the observed bone degradation. Instead, these data emphasize consideration of alternative mechanisms underlying how muscle function modulates trabecular bone homeostasis.

Disclosures: Ted Gross, None.

SA0008

Effect of a Single Oral Dose of 600,000 IU of Cholecalciferol on Muscle Strength in Young Women with Vitamin D Deficiency: a Prospective Intervention Study. Cristiana Cipriani^{*1}, Elisabetta Romagnoli¹, Stefania Russo², Addolorata Scarpello², Claudia Castro², Roberta Pilotto², Federica De Lucia³, Jessica Pepe², Laura Lenge², Salvatore Minisola¹. ¹University of Rome, Italy, ²Department of Internal Medicine & Medical Specialties, University of Rome "Sapienza", Italy, ³Universita Di Roma "Sapienza, Italy

Purpose: The positive effects of vitamin D supplementation on muscle strength and tendency to fall is widely reported, particularly in the elderly. Few data are available in young people with low vitamin D status.

Methods: Eighteen young women (mean age 32.14.7 yrs, range 25-39; BMI 23.84.01 kg/m²) with vitamin D deficiency received a single oral dose of 600,000 IU of cholecalciferol. Isometric grip strength of the upper dominant limb was evaluated using a hand held dynamometer (Kayser Italia s.r.l., Livorno, Italy). Maximal voluntary contraction force (MVC, Newton, N) and speed of contraction (S, Newton/second, N/s) were measured in the sitting position in each subject at baseline and at day (d) 3, 15, 30, 60 and 90. Serum 25(OH)D, ionized calcium (Ca⁺⁺), phosphorus (P), PTH and 1,25(OH)₂D were measured at each time point.

Results: Mean MVC and S values did not change throughout the entire observation period. On the contrary, 25(OH)D levels significantly changed (p<0.001), with a rapid increase at d 3 (75.116.6 ng/mL; p<0.001) and up to d 90 (31.713.3; p<0.01), compared to baseline levels. A concomitant significant decrease in PTH concentration (p<0.01) was found, as soon as d 3 (-18.215.3 pg/mL; p<0.001) and up to d 90 (-19.812.9; p<0.001). A rapid increase in 1,25(OH)₂D serum levels, at d 3 (96.637.4 pg/mL, p<0.001) and up to d 60 (59.828.8; p<0.05) was observed. Mean Ca⁺⁺ levels did not change, whereas mean levels of P showed a significant increase at d 3 (3.80.6 mg/dL; p<0.05). Furthermore, no significant correlation was found between

both MVC and S with 25(OH)D, Ca⁺⁺, PTH and 1,25(OH)₂D levels at each time point. Interestingly, a positive significant correlation was found between both indices of muscle function and P levels at 60 d (MVC, r=0.546 and S, r=0.557 respectively; p<0.02 for both).

Conclusions: A single huge dose of 600,000 IU of cholecalciferol is not effective in enhancing skeletal muscle strength in young women with vitamin D deficiency. This finding could be partly due to the small sample study, and/or the relatively short period of follow-up. Another possibility is that the effect is not picked up exploring this group of muscles. However, our results are in line with recent data demonstrating that the effect of vitamin D on skeletal muscle is probably indirect since vitamin D receptor are absent in this tissue. An increase of serum phosphate could be a possible link between vitamin D administration and improvement of muscle function.

Disclosures: *Cristiana Cipriani, None.*

SA0009

See Friday Plenary Number FR0009.

SA0010

See Friday Plenary Number FR0010.

SA0011

See Friday Plenary Number FR0011.

SA0012

Lumbar Vertebral Bone Density is Positively Associated with Psoas Muscle Mass among Elderly Men. Lynn Marshall¹, Kathleen Holton¹, Joseph Zmuda², Jung Yoo¹, Nels Carlson¹, Yahtyng Sheu², Eric Orwoll¹. ¹Oregon Health & Science University, USA, ²University of Pittsburgh Graduate School of Public Health, USA

Muscle deterioration with aging is characterized by reduced mass, lipid accumulation within muscle fibers, and accretion of adipose tissue beneath the muscle fascia. These features of aging muscle could affect bone strength by altering loads to the skeleton, especially at muscle attachment sites. We evaluated the relation of vertebral volumetric bone mineral density (vBMD) and vertebral size to psoas and paraspinal muscle features. Data were from community dwelling men aged ≥ 65 years participating in the Osteoporotic Fractures in Men (MOS) study. At baseline, quantitative computed tomography (QCT) scans were obtained at the L1/L2 and L4/L5 levels. Vertebral integral and trabecular vBMD (g/cm³) and cross-sectional area (CSA) (cm²) were derived for L1 and L2 vertebrae. In a random sample of 667 men with L4/L5 scans, we derived psoas and paraspinal muscle measures. Muscle groups were manually segmented with contours drawn along the muscle fascia on both sides of the L4 vertebra. All voxels in each contour were summed to compute total volumes (cm³) for the psoas and paraspinal muscle groups separately. Muscle density, a marker of lipid accumulation, was computed as the average attenuation in Hounsfield units (HU) within the total volume of each muscle group. Intermuscular adipose tissue (IMAT) (cm³) volume in each muscle group was the sum of voxels in the HU range (-190 to -30) for AT. The analytic cohort included 510 men who all had the vertebral and muscle QCT measures. Generalized linear regression was used to estimate least square (LS) means and 95% confidence intervals (CI) of each vertebral measure within quartiles of the muscle parameter after adjusting for age, enrollment site, body mass index, and height. Terms for muscle volume and density were fit together; then terms for IMAT replaced those for density. Both integral and trabecular vBMD increased with psoas muscle volume (Table). However, the vBMD measures were unrelated to psoas muscle density or IMAT. Vertebral CSA was not associated with psoas muscle volume or IMAT, but was associated with psoas muscle density. LS means for CSA of L2 were 12.6 (95% CI: 12.1-13.0) in quartile 1 and 13.2 (95% CI: 12.8-13.6) in quartile 4 (p-trend=0.01). None of the vertebral measures was associated with paraspinal muscle volume, density, or IMAT. Among elderly men, vertebral measures that confer bone strength were positively associated with the size and density of psoas muscles, but with not paraspinal muscles.

Adjusted mean vertebral volumetric bone mineral density according to psoas muscle volume among 510 men aged ≥65 years.

Psoas muscle volume (cm ³)		Integral vBMD	Trabecular vBMD
Quartile	Range	LS Mean (95% CI)*	LS Mean (95% CI)*
1	4.6-9.0	0.210 (0.201-0.218)	0.099 (0.091-0.106)
2	9.1-10.7	0.221 (0.214-0.227)	0.106 (0.100-0.112)
3	10.8-12.6	0.226 (0.220-0.232)	0.113 (0.107-0.119)
4	12.7-19.6	0.230 (0.220-0.238)	0.114 (0.108-0.121)
p-trend		0.004	0.02

*Least square means and 95% confidence intervals from multiple linear regression adjusted for age, enrollment site, body mass index, and height.

Table.

Disclosures: *Lynn Marshall, None.*

SA0013

See Friday Plenary Number FR0013.

SA0014

Bone Responses to Body Fat Mass Loss Induced by an Exercise and Nutritional Program in Obese Rats. Maude Gerbaix¹, Lore Metz¹, Fabrice Mac-Way², Christelle Guillet³, Stephane Walrand³, Aurelie Masgraud³, Laurence Vico⁴, Daniel Courteix¹. ¹Universite Clermont Ferrand Laboratoire De Biologie Des APS, France, ²Hotel-Dieu de Quebec, Canada, ³INRA Universite d'Auvergne, France, ⁴University of St-Etienne, France

The association of a well-balanced diet with exercise is a key strategy to treat obesity. However, weight loss is linked to accelerated bone loss. On the other hand, exercise is known to induce beneficial effects on bone. The purpose of this study was to investigate the bone responses to body fat loss induced by an exercise and nutritional program in obese rats. Sixty Wistar male rats, aged 11 months, were previously fed with a high fat/high sucrose diet (HF/HS) for 4 months to induce obesity. Then, four regimens: Lipid and Sucrose Restrictive diet (LSR diet) plus exercise (treadmill: 50 min/day, 5 days/weeks); HF/HS diet plus exercise; LSR diet plus inactivity; HF/HS diet plus inactivity were initiated for 2 months. The body composition including specific central fat mass analysis was assessed by DXA. Visceral fat mass was evaluated by weighing perirenal and peri-epididymal adipose tissues. Lipid and hormonal profiles were assayed. Bone densitometry was assessed on tibia by Piximus. Bone histomorphometry was performed on the proximal metaphysis of tibia and L2 vertebrae (L2). Trabecular micro architectural parameters were measured on tibia and L2 by 3D microtomography. Osteocalcin and CTX were assayed to calculate the bone Uncoupling Index (UI). Global mass, global fat mass, central fat mass and ex-vivo fat mass were significantly lower (p<0.01) in exercised groups compared with sedentary groups. Except global mass, these parameters were significantly lower (p<0.05) in LSR diet groups than HF/HS diet groups. Trained rats showed significant lower triglyceride (p<0.05) and higher free fatty acids (p<0.01) levels than sedentary rats. LSR diet groups had significant higher triglyceride level than HF/HS groups. Both exercise and LSR diet had reduced significantly the leptin and adiponectin levels (p<0.05). BV Density and degree of anisotropy of tibia were lower in LSR diet groups (p<0.05) compared with HF/HS diet groups. Moreover, groups which were given LSR diet had significant lower BV/TV (p<0.001), MS/BS (p<0.001) and BFR/BS (p<0.05) in L2 compared with HF/HS groups. Exercise had increased significantly BMD of tibia and UI (p<0.05) but reduced significantly MAR of L2 vertebrae (p<0.05). In the present study a diet inducing fat mass loss had altered the bone tissue of obese rats. The moderate intensity exercise performed had increased BMD and UI but did not protect bone tissue from trabecular alterations.

Disclosures: *Maude Gerbaix, None.*

SA0015

HIV-Cox2-based, but not HIV-BMP4-based, In Vivo Gene Transfer Strategy Promotes Osteointegration in a Rat Model of Biceps Tenodesis. Shin-Tai Chen¹, Michael Coen², Jon Wergedal¹, Charles Rundle¹, Kin-Hing William Lau¹. ¹Jerry L. Pettis Memorial VA Medical Center, USA, ²Loma Linda University, USA

Lesions of the long head of the biceps tendon are a significant source of shoulder pain. Biceps tenodesis is a frequently used surgical option, which involves cutting the injured tendon at the site of its attachment into the labrum and reattaching it to the humerus. The success of the surgery depends on an effective bony incorporation of the graft (osteointegration) that would increase the return of its tensile strength. This study sought to determine if our HIV-Cox2-based gene transfer strategy would promote osteointegration, using our rat model of biceps tenodesis. We were interested in Cox2 because the Cox2 gene therapy is highly effective in promoting bony bridging of the fracture gap, which involves similar histologic transitions seen in osteointegration. BMP4 was included in this study for comparison. Briefly, a 1.14-mm diameter tunnel was drilled in the mid-groove of the humerus of adult Fischer 344 rats. The HIV-Cox2, BMP4, or β-gal control vector was applied directly into the bone tunnel and onto the end of the tendon graft, which was then pulled into the bone tunnel. A 1.1-mm diameter poly-L-lactide pin was press-fitted into the tunnel as interference fixation. Animals were sacrificed at 3 or 8 weeks for histology analysis of osteointegration. Both strategies enhanced chondrogenesis at the tendon/bone interface. The HIV-BMP4 treatment increased trabecular bone formation (BF) by 32% compared to the control (1,000.08 vs. 0,670.10 mm², p<0.05). In contrast, the effect of the HIV-Cox2 strategy on de novo BF was much smaller than that of the HIV-BMP4 strategy. The tendon/bone interface of the Cox2-treated tenodesis showed the well-characterized tendon-to-fibrocartilage-to-bone histologic transitions that are indicative of osteointegration. No such transitions were seen in the BMP4-treated graft. Thus, Cox2, but not BMP4, promoted osteointegration. To determine if the enhanced osteointegration would be translated into an improved mechanical property, the pull-out strength of the Cox2 and BMP4-treated tendon grafts was determined with our recently established mechanical testing that is suitable for the rat biceps tendon. Fig. 1 shows that the HIV-Cox2 strategy yielded a much better return of the pull-out strength of the tendon graft than the HIV-BMP4 strategy after 8

weeks. In conclusion, the HIV-Cox2-based, but not HIV-BMP4-based, gene transfer strategy enhanced osteointegration that improved return of the pull-out strength of the tendon graft.

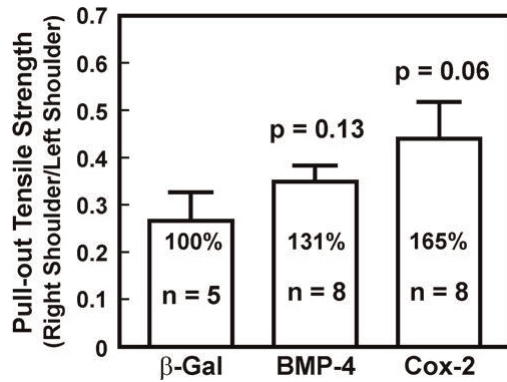


Figure 1.

Disclosures: Shin-Tai Chen, None.

SA0016

Is Vitamin D Level for Muscle Strength Improvement Higher Than That for Mobility Improvement for Japanese Pre-Frail Elderly Attending a Nursing Care Prevention Class? : Examination of Alfacalcidol Supplementation and Renal Function. JUNKO OKUNO¹, Shigeo Tamura², Takako Fukasaku³, Noriko Yabushita³, Mi-Ji Kim⁴, Tomohiro Okura³, Kivoji Tanaka³, Hisako Yanagi³. ¹UNIVERSITY OF TSUKUBA, Japan, ²Urawa University, Department of General Welfare, Japan, ³University of Tsukuba, Graduate School of Comprehensive Human Sciences, Japan, ⁴Tokyo Metropolitan Geriatric Hospital & Institute of Gerontology, Japan

A key characteristic of the pre-frail elderly is decreased mobility, which is reported to be associated with vitamin D levels and renal function. The aim of this study was to examine the association between physical fitness improvement which might have hierarchical levels and vitamin D levels by examining vitamin D supplementation and renal function in the pre-frail elderly. A longitudinal study was conducted in two towns (latitude 36 degree north) from June 2006 to December 2009 in Japan. Subjects consisted of 177 community-dwelling pre-frail elderly, aged 65 years and over (meanSD:76.45.5 yr) who attended a nursing care preventive exercise program for 3 months. A face-to-face interview was conducted based on a questionnaire. Serum levels of intact parathyroid hormone (iPTH), 25-hydroxyvitamin D (25(OH)D), 1,25-dihydroxyvitamin D (1,25(OH)₂D), creatinine, and calcium were measured. Estimated GFR (eGFR) (mL/min/1.73m²) was calculated using a new Japanese formula of 2008. Alfacalcidol 1μg/day was administered to elderly for three months and we assumed the elderly who took VD more than 80% a VD group. The following physical fitness tests were performed at baseline and at the end of a 3-month follow-up period: walking ability (timed up and go: TUG, a 5-meter walk), balance (functional reach: FR, one-legged stance with open eyes, tandem stance, tandem walk), and muscle strength (alternate step, 5-chair sit-to-stands). We conducted multiple linear regression analysis for the factors of physical fitness improvement. The prevalence of eGFR < 60.0 mL/min/1.73m² was about 24.3%, that of 25(OH)D < 50 nmol/L was 28.8%, and that of 25(OH)D < 75 nmol/L was 86.4%. Physical fitness tests except one-legged stance improved significantly in all subjects. Pre eGFR and pre 25(OH)D were significantly associated with improvement of timed up and go (TUG), vitamin D supplementation with FR, pre25(OH)D (<50nmol/L, >=50nmol/L) with tandem stance, post 1,25(OH)₂D with tandem walk, and pre 25(OH)D (<75nmol/L, >=75nmol/L) with alternate step and 5 chair sit-to-stands. Our data suggest that assessment of renal function and maintaining appropriate vitamin D levels seem to be significant for independent living in the pre-frail elderly and higher 25(OH)D level might be needed for improvement of muscle strength than mobility; if possible, a 25 (OH)D level greater than 75 nmol/L is preferable.

Disclosures: JUNKO OKUNO, None.

SA0017

The Effect of Sciatic Neurotomy and Nerve Repair on Cancellous Bone in Rat Femurs and Tibias. Glenda Evans¹, Huan Wang², Stephen Hodgson¹, M. Brett Runge², Anthony J. Windebank², Robert J. Spinner², Michael Yaszemski². ¹Mayo Clinic, USA, ²Mayo Clinic College of Medicine, USA

It is well established that bone loss occurs in the limbs of humans and animals following regional traumatic nerve resection and after surgically controlled unilateral sciatic neurotomy (USN) in animals. The mechanism of bone loss is presumably due to denervation muscle atrophy with resulting mechanical limb unloading.

Objective: Does reestablishment of neuronal function ameliorate and/or prevent bone loss due to denervation?

Methods: Unilateral left sciatic neurotomy was performed on three-month-old virgin female Lewis rats to create a 1-cm defect, which was immediately repaired by suturing the resected nerve ends to an intervening 1-cm polymer tube. The animals were allowed a recovery time of 16 weeks before sacrifice. Tibias and femurs were harvested and fixed in 70% ethanol and scanned at medium resolution (12um). Analysis was performed on 100 slices using micro computerized tomography (Scanco 35 μ CT). Continuity and quality of reattached nerves were evaluated by nerve conduction studies prior to sacrifice and muscle weights at sacrifice.

Results: The microCT revealed that bone loss occurred in all animals in the USN affected limb, greater in the tibia than femur (tibia -16%, femur -7%), when compared to tibias and femurs from the contralateral limb. The amount of bone loss inversely related to the magnitude of nerve conduction following reinnervation. Trabecular number decreased 11% in the tibia and 2% in the femur. Trabecular thickness decreased 14% in the tibia and 10% in the femur.

Conclusions: The system described above may represent a useful animal model for the study of effects of denervation and reinnervation on bone loss and for investigating potential preventive and therapeutic interventions of bone loss.

Disclosures: Glenda Evans, None.

SA0018

Effects of Laparoscopic Adjustable Gastric Banding and Weight Loss on Bone Turnover Markers in Morbidly Obese Adolescents. Marisa Censani¹, Ilene Fennoy¹, Shulamit Lerner¹, Rushika Conroy¹, Sharon Oberfield¹, Jeffrey Zitsman¹, Donald McMahon², Shonni Silverberg³. ¹Columbia University Medical Center, USA, ²Columbia University College of Physicians & Surgeons, USA, ³Columbia University, USA

The adolescent obesity rate has more than tripled in the United States over the past 30 years. Bariatric surgery is widely used in the morbidly obese adult population as an effective treatment for weight loss and is currently being evaluated in the adolescent population. While there are many reports in the adult literature on skeletal and mineral metabolism consequences of obesity and bariatric surgery, there are limited data on changes in bone turnover markers after rapid weight loss from bariatric surgery in adolescents.

Methods: The Center for Adolescent Bariatric Surgery is a multidisciplinary program of nutrition, medical care, and laparoscopic adjustable gastric banding (LAGB) for adolescents between the ages of 14-18 years who have BMI >40 kg/m² or >35 kg/m² and at least one co-morbidity. A pilot study in 12 adolescents (7 females, 5 males; mean age 16.5 ± 1.06 yrs; mean BMI 44.2 ± 7.26 kg/m²) assessed bone turnover markers (formation marker: osteocalcin and resorption marker: C-telopeptide [CTX]) at baseline and 12 months post-operatively. Comparison of within subject changes was performed using paired t-test and ANOVA with repeated measures and correlations between parameters of weight loss and bone turnover.

Results: By 12 months postoperatively (Table), mean BMI declined by 6.071.14 kg/m² (p=0.0003), with an absolute weight loss of 14.93 ± 2.69 kg (p=0.0002) and mean percent excess body weight loss of 28.39.0% (P=0.01). Bone turnover markers rose markedly after bariatric surgery, with osteocalcin rising 3.5-fold and C-telopeptide doubling by 12 months (p<0.001 for both). Change in osteocalcin tended to be inversely associated with percent excess body weight loss (adjusted r = -0.52; p<0.09).

Conclusions: In a pilot study of 12 morbidly obese adolescents, weight loss from LAGB was associated with marked increases in bone turnover. Significant increases were noted in markers of both formation and resorption 1 year after surgery. Despite our small numbers, the data suggest that the extent of increase in bone turnover may be associated with degree of weight loss. Whether the increased bone turnover will be associated with a decline in bone density in obese adolescent population undergoing bariatric surgery remains to be seen.

Variable	Baseline	12 m post LAGB
Age (years)	16.5 ± 1.06 (15.08-17.83)	
Weight (kg)	118.6 ± 28.59 (83.9-161.3)	105.8 ± 30.13 (66.7-153.2)
BMI (kg/m ²)	44.24 ± 7.26 (35.8-57.8)	39.08 ± 8.37 (28-52.7)
Excess Body wt (kg)	51.78 ± 22.85 (24-89.3)	39.04 ± 24.26 (8.2-79.5)
Serum osteocalcin (ng/ml)	8.92 ± 1.21 (0.51-16.55)	18.45 ± 1.21 (4.56-27.32)
Serum CTX (ng/ml)	0.18 ± 0.07 (0.06-0.37)	0.64 ± 0.07 (0.17-1.35)

Data are presented as Mean ± SEM (Range)

Table

Disclosures: Marisa Censani, None.

SA0019

Incident Vertebral Fractures among Children with Rheumatic Disorders 12 months Post-Glucocorticoid Initiation: a National Observational Study. L. M. Ward¹, C. Rodd², B. Lang³, N. Alos⁴, S. Atkinson⁵, D. Cabral⁶, R. Couch⁷, E. Cummings³, A. Huber³, P.M. Miettinen⁸, H. Nadel⁶, D. Stephure⁸, R. Stein⁹, S. Taback¹⁰, M. Matzinger¹, N. Shenouda¹, B. Lentle⁶, F. Rauch², K. Siminoski⁷, - and the Canadian STOPP Consortium¹¹. ¹University of Ottawa, Canada, ²McGill University, Canada, ³Dalhousie University, Canada, ⁴Universite de Montreal, Canada, ⁵McMaster University, Canada, ⁶University of British Columbia, Canada, ⁷University of Alberta, Canada, ⁸University of Calgary, Canada, ⁹University of Western Ontario, Canada, ¹⁰University of Manitoba, Canada, ¹¹Canadian Pediatric Bone Health Working Group, Canada

Background: Vertebral fractures are a potential complication of childhood rheumatic disorders or their treatment. The purpose of this study was to determine the frequency of incident (i.e. new) vertebral fractures (IVFs) 12 months after glucocorticoid (GC) initiation in children with rheumatic diseases and to describe the profile of children with IVFs compared to those without.

Methods: Children with rheumatic diseases initiating GCs were enrolled in a national, prospective observational study. Annual spine radiographs were evaluated using the Genant semi-quantitative method and spine areal bone mineral density (aBMD) was measured every 6 months. Clinical features, including GC exposure, back pain, disease and physical activity, calcium and vitamin D intake, and changes in spine aBMD Z-scores were also assessed.

Results: Of 118 children followed to 12 months post-GC initiation, 7 (6%) manifested IVFs. The diagnoses for these 7 children were: juvenile dermatomyositis (N=2), systemic lupus erythematosus (N=3), systemic vasculitis (N=1) and mixed connective tissue disease (N=1). The child with mixed connective tissue disease was excluded from the natural history analyses from 4 months onward because of the need for bisphosphonate therapy to treat multiple, painful IVFs at this time. Six children with natural history data to 12 months had a total of 7 IVFs (4 mild and 3 moderate; 5 thoracic and 2 lumbar). These children with IVFs received on average 50% more steroid over the 12 month period compared to those without as assessed by both cumulative GC dose (94523447 mg/m2 versus 62035181; p=0.030) and average GC dose (249 mg/m2/day versus 1613; p=0.044). At 6 months, the children with IVFs also had greater increases in body mass index (BMI) Z-scores (1.408 versus 0.508; p=0.010) and decrements in spine aBMD Z-scores (-0.805 versus -0.405; p=0.048). Four of 6 children (67%) with IVFs and natural history analyses to 12 months had spine aBMD Z-scores less than -2.0 at 12 months compared to 16% of children without (p=0.011).

Conclusions: IVFs were not frequent after one year of GC treatment in this cohort; however, children with IVFs at 12 months received more GC and manifested greater increases in BMI Z-scores and declines in spine aBMD Z-scores in the first 6 months of GC therapy.

Disclosures: L.M. Ward, None.

SA0020

See Friday Plenary Number FR0020.

SA0021

An Appropriate Animal Model for Studying Maternal Bone Changes during Pregnancy: A Model Resembling Winter Pregnancy in Youth. Negar Tabatabaei¹, Celia Rodd¹, Richard Kremer², Hope Weiler¹. ¹McGill University, Canada, ²McGill University, Royal Victoria Hospital, Canada

Establishing an appropriate animal model which would resemble human pregnancy in bone metabolism is crucial to examine bone physiology during this period. The objective of our study was to investigate the effect of pregnancy on maternal bone mass and metabolism using a guinea pig model. Female pigmented guinea pigs (n=44), 16 weeks of age, were randomized to isocaloric diets containing different dosages of vitamin D (0 IU/g (n=9), 0.25 IU/g (n=9), 0.5 IU/g (n=9), 1 IU/g (n=9) and 2 IU/g (n=8)) and then mated and maintained in a UV-free environment. Blood samples were drawn just before mating, d 21, d 42 of pregnancy and 24-36h after delivery. Plasma concentrations of 25(OH)D, deoxypyridinoline and total alkaline phosphatase were measured at all four time points. Whole body, spine (L1-L4), tibia and femur DXA scans were measured before mating and 24-36h after delivery. Statistical analyses were performed using a mixed model repeated measures ANOVA with a fixed effect of time and litter size and a random effect of sow and block. There was a strong dose-response effect of different dosages of dietary vitamin D on plasma 25(OH)D concentration (P<0.0001), but despite this effect, no differences were observed among the five different diets on plasma bone biomarkers and DXA measurements. Plasma concentrations of 25(OH)D decreased during pregnancy whereas deoxypyridinoline and alkaline phosphatase remained unchanged (Table 1). In post-partum blood 25OHD and alkaline phosphatase significantly decreased while deoxypyridinoline significantly increased compared to pre-delivery concentrations (Table 1). Compared to preconception indices postpartum whole body

BMD did not differ. Tibial and femoral BMD increased while the trend was different in L1-L4; showing a decrease in BMD (Table 2). Since plasma 25(OH)D concentrations were high at preconception and considering that guinea pigs at this age are still growing, this model may be suitable for studying the effect of pregnancy on adolescent bones in which conception is induced at the beginning of winter when 25(OH)D concentration are likely to be high. Changes in BMD at the femur, tibiae and spine early post-partum vs preconception suggest an increase in cortical bone and a decrease in trabeculae bone. Changes in post-partum bone markers suggest an uncoupling of bone resorption and formation. The decrease in maternal 25(OH)D likely reflects maternal-fetal transfer and physiological demands of reproduction.

Table 1. Maternal plasma 25(OH)D, deoxypyridinoline and total alkaline phosphatase at baseline, d21, d42 and post-partum of pregnancy

Outcome	Time-point				SEM	Effect of Time
	Pre-conception	d 21	d 42	Post-partum		
25(OH)D (nmol/L)	260.4 ^a	174.4 ^b	151.4 ^c	113.5 ^d	9.5	p<0.0001
Deoxypyridinoline (nmol/L)	10.2 ^a	11.4 ^a	14.9 ^a	26.2 ^b	6.5	p<0.02
Alkaline phosphatase (U/L)	104.3 ^a	99.3 ^a	105.2 ^a	44.4 ^b	6.6	p<0.0001

Data are estimated means ± SEM. Means reflect all diets combined. Means within a row with superscripts without a common letter differ, P<0.05.

Table 2. Maternal whole body, tibia, femur and spine (L1-L4) BMD at pre-conception and postpartum

Outcome (g cm ²)	Time-point		SEM	Effect of Time
	Pre-conception	Post-partum		
Whole Body BMD	0.228	0.229	0.002	p<0.10
Tibia BMD	0.286	0.291	0.004	p<0.01
Femur BMD	0.465	0.500	0.010	p<0.0001
Spine (L1-L4) BMD	0.282	0.271	0.004	p<0.0001

Data are estimated means ± SEM. Means reflect all diets combined. P<0.05 is significant.

An Appropriate Animal Model for Studying Maternal Bone Changes during Pregnancy

Disclosures: Negar Tabatabaei, None.

SA0022

Effect of Letrozole, an Aromatase Inhibitor, on Skeletal and Sexual Maturation in Rats. Rana Samadfam¹, Louise Pouliot², Keith Robinson², Paul Vancuntsem³, Marilynn Schneider⁴, Susan Y. Smith¹. ¹Charles River Laboratories, Canada, ²Charles River, Canada, ³Novartis, Germany, ⁴Novartis Pharmaceuticals Corporation, USA

Aromatase is the enzyme catalyzing the last step of estrogen production in the ovary and in peripheral tissues (males-converting testosterone to estrogen). Sex hormones are involved in the regulation of bone growth during puberty and maintaining bone mass in adulthood. The role of estrogen in the female reproductive system development has been well documented. Estrogen receptors are expressed in the male reproductive system during development, indicating roles for estrogen in regulating male tissue development and reproductive events. The objective of this study was to determine the effect of letrozole on bone growth and density when administered orally to juvenile rats (beginning on day 7 post partum) for up to 12 weeks followed by a 6 week recovery period. The effect on the reproductive system was also evaluated. Pups (20/sex/group) were assigned to four groups each receiving daily oral gavage of either vehicle control or letrozole at 0.003, 0.03 and 0.3 mg/kg/day. 10 per group were sacrificed at the end of the treatment period (day 92 pp) and the remaining animals were sacrificed following a 6 week recovery period (day 134 post partum). Decreases in bone length measured by radiography, area measured by DXA and total slice area measured by pQCT were observed for letrozole treated males relative to controls, while all these parameters were generally increased for females. The effects on bone length and area for both males and females, in most part correlated with the body weight gains (lower for males and higher for females). A significantly higher serum ALP level for females treated at 0.3 mg/kg/day compared to controls was consistent with increased bone formation. A statistically significant decrease in proximal tibia metaphyseal BMD was observed for females at the end of the treatment period. Withdrawal of treatment for up to 6 weeks showed evidence of recovery for both males and females treated at the low dose however recovery was less evident at the high dose. Evaluation of the reproductive system indicated delayed sexual maturation for both males and females consistent with the action of the compound to reduce sex hormones. In conclusion, the findings indicate that letrozole has the same effect in both males and females resulting in a delay in bone maturation and prevention of pubertal progression. These results provide unique insight into the effects of sex steroid hormones on bone growth and development in male and female rats.

Disclosures: Rana Samadfam, None.

SA0023

See Friday Plenary Number FR0023.

SA0024**High Bone Mass Radiographically Mimicking Osteopetrosis but with Rapid Skeletal Turnover and Maxillofacial Giant Cell Reparative Granuloma.**

Michael P. Whyte^{*1}, Katherine L. Madson², Steven Mumm¹, William H. McAlister³, Deborah V. Novack⁴, Deborah Wenkert², Joanne Blair⁵, Nicholas J. Shaw⁶. ¹Shriners Hospital for Children & Washington University School of Medicine, St. Louis, USA, ²Shriners Hospital for Children in St. Louis, USA, ³Department of Pediatric Radiology at the Mallinckrodt Institute of Radiology, St Louis Childrens Hospital at the Washington University School of Medicine, St. Louis, USA, ⁴Washington University in St. Louis School of Medicine, USA, ⁵Alder Hey Children's Hospital, United Kingdom, ⁶Birmingham Children's Hospital, United Kingdom

Disorders of high bone mass are important for revealing genes and signaling pathways that condition skeletal homeostasis. They can be divided into two main types, those due to osteoclast dysfunction (eg, osteopetrosis), and those due to excessive osteoblast activity (eg, sclerosteosis).

An 8-yr-old boy presented at age 2 years with a visual field defect for which an MRI scan identified a large mass in the perisellar region. Histology of the resected lesion showed features of a giant cell reparative granuloma. Radiographs showed evidence of dense bones with thick cortices and narrowing of the medullary spaces resembling osteopetrosis. However, bone turnover markers were markedly elevated with serum alkaline phosphatase > 5,000 iu/l (normal < 850 iu/l). Because of rapid regrowth of the tumor which appeared to contain osteoclasts he received pamidronate given intravenously and intermittently for three years which reduced, but did not normalize, the serum alkaline phosphatase level with no subsequent regrowth of the tumor.

Bone mineral density assessed by DXA showed a z-score in the lumbar spine of + 9.1 and in the hip of + 5.8. Radiographic skeletal survey before and after pamidronate treatment confirmed sclerotic bones with thickened cortices and narrow medullary cavities with interference of tubulation in many long bones similar to that seen in osteopetrosis. Two years after the last pamidronate dose, an iliac crest bone biopsy showed the majority of the bone to be trabecular with a large amount of osteoid containing an abundance of osteoblasts. Osteoclasts were readily seen with evidence of bone resorption. There was no retention of calcified cartilage as seen in osteopetrosis. Tetracycline labeling confirmed rapid bone remodeling. Mutation analysis excluded defects in the LRP5, RANKL, RANK, OPG, SQSTM1, TGFβ1, and sFRP1 genes which are known to cause various high bone mass disorders.

Our patient has a unique high bone mass disorder which radiographically resembled a form of osteopetrosis but on biochemistry and bone histology was instead consistent with rapid bone formation.

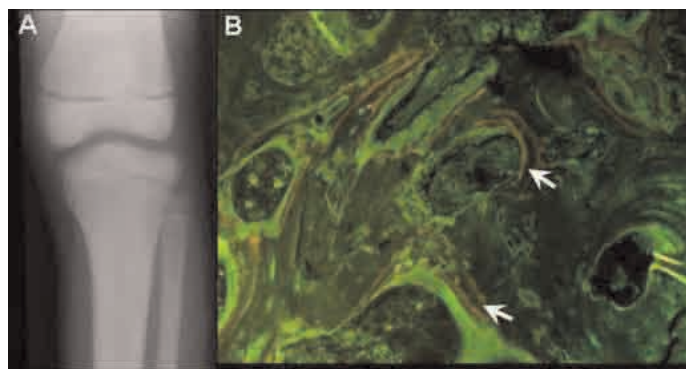


Figure A: Radiograph of the left knee two years after the previous dose of pamidronate. An Erlenmeyer flask deformity is apparent in the distal femoral metaphysis. The bones are radiographically dense and widened.

Figure B: Tetracycline double-labels (arrows) are apparent at this time in the iliac crest.

Figure

Disclosures: Michael P. Whyte, None.

SA0025

See Friday Plenary Number FR0025.

SA0026

See Friday Plenary Number FR0026.

SA0027**Limited Skeletal Deficits by Peripheral Quantitative Computed Tomography in Adolescents with Anorexia Nervosa.**

Amy DiVasta^{*1}, Natalie Stokes¹, Catherine Gordon². ¹Children's Hospital Boston, USA, ²Children's Hospital Boston & Harvard Medical School, USA

Purpose: Young women with anorexia nervosa (AN) commonly exhibit bone loss of the axial skeleton. We previously reported deficits in bone geometry and strength measured at the hip in adolescents with AN. However, the effects of AN on the peripheral skeleton are unknown. In the current study, we aimed to determine the effects of malnutrition on bone strength and geometry measured by pQCT in young women with AN.

Methods: Ten adolescents with AN and fifty healthy adolescents, aged 13-22 yr, were recruited from an adolescent medicine clinic. Volumetric bone mineral density (vBMD), cross-sectional area (CSA), cortical thickness (CTh), and strength-strain index (SSI) were measured by pQCT at the radius (4%, 50%, 66% site) and tibia (4%, 38%, 66% site). Anthropometrics were measured in all participants, and health history obtained by interview.

Results: Adolescents with AN were malnourished (BMI 17.5 1.6 kg/m²) compared to healthy young women (BMI 22.4 3.1 kg/m²; p<0.0001). All healthy subjects were regularly menstruating; girls with AN had been amenorrheic for a mean of 11.2 15.8 months (range 3-54 months). At the radius, significant differences in cortical thickness were demonstrated (50% site: AN 2.8 0.2 mm vs. Control 3.1 0.3 mm, p=0.03 and 66% site: AN 2.1 0.4 mm vs. Control 2.4 0.4 mm, p=0.04). At the tibia 4% site, both total CSA (846.4 99.3 mm vs. 955.8 140.3 mm, p=0.02) and trabecular CSA (659.9 96.9 mm vs. 765.6 127.5 mm, p=0.02) were significantly lower in girls with AN than controls. No difference in SSI or vBMD was noted between groups. The duration of amenorrhea was negatively correlated with total CSA at the radius, and with trabecular vBMD at the tibia (r= -0.63 to -0.78, p<0.05).

Conclusions: In young women with AN, cortical thickness and CSA measured at the radius and tibia by pQCT differed from that of healthy, age-matched control subjects. The duration of amenorrhea seen in the adolescents with AN was negatively associated with peripheral measures of skeletal health, particularly those at trabecular-rich skeletal sites. These results indicate that the impact of malnutrition and amenorrhea on the peripheral skeleton of young women with AN may differ from that of the axial skeleton.

Disclosures: Amy DiVasta, None.

SA0028**Reduced Volumetric Trabecular Bone Mineral Density of the Lumbar Spine in Adolescents with Anorexia Nervosa.**

Lily Wheeler^{*1}, M. Zulf Mughal², Jane Whittaker³, Judith Adams⁴, Sarah Ehtisham³. ¹University of Manchester, United Kingdom, ²The University of Manchester & Royal Manchester Children's Hospital, Endocrinology, United Kingdom, ³Royal Manchester Children's Hospital, United Kingdom, ⁴Manchester Royal Infirmary, United Kingdom

Introduction

It is well known that anorexia nervosa (AN) in adolescents is associated with reduced bone mineral density (BMD). Factors that contribute to low BMD in AN include low body mass index, secondary hypogonadism, resistance to growth hormone, low Insulin-Like Growth Factor-1 levels, high serum cortisol levels and alterations in various appetite-regulating hormones. Studies using high resolution quantitative computed tomography (QCT) have shown that adolescent girls with AN have lower distal radial trabecular bone volume, trabecular thickness and greater trabecular separation, compared with controls.

Objectives

A retrospective evaluation of patients with AN referred for endocrine and metabolic bone health assessment between February and September 2010 was made. Lumbar spine (LS) BMD was measured by dual-energy X-ray absorptiometry (DXA) and quantitative computed tomography (QCT). Distal radial total and trabecular BMD was measured by peripheral QCT (pQCT).

Methods

BMD of L1-L4 was measured by DXA. These data were expressed as bone mineral apparent density (BMAD; g/cm³) and values transformed to Z scores using local normative data (ADC;2007;92(1);53-9). Volumetric trabecular BMD (TBMD; mg/cm³) at L1-L3 was measured by QCT and values transformed to Z scores using Mindways softwareTM (Austin, Texas). Distal radial (4%) total and TBMD was measured by pQCT and values transformed to Z scores using local normative data (Osteoporos Int. 2009;20(8):1337-46).

Results

Twelve females and one male aged 13.6-16.9 years with a diagnosis of AN were evaluated. The mean duration of AN was 3.5 (0.7 to 8) years. Eleven of the females

had amenorrhoea; 2 primary, 9 secondary (mean duration 1.2 years). Mean BMI SDS was -1.74 (-4.2 to 0.19). A table of Z scores is shown below.

Conclusions

Results of this preliminary study suggest that adolescents with AN have reduced trabecular LS BMD. Further studies are needed to elucidate the reasons for reduction of trabecular BMD in the central, but not at the appendicular skeletal sites in this group of patients.

g/cm ³	Median Z score	Range Z scores	P value
DXA LS BMAD	-0.45	-2.36 to 0.79	<0.05
QCT LS TBMD	-1.91	-3.42 to -0.42	<0.001
Distal radius total BMD	0.06	-1.83 to 1.08	0.656
Distal radius trabecular BMD	-0.05	-1.91 to 0.81	0.416

A table of Z scores of LS BMAD, LS TBMD, distal radial total BMD and distal radial trabecular BMD.

Disclosures: Lily Wheeler, None.

SA0029

See Friday Plenary Number FR0029.

SA0030

See Friday Plenary Number FR0030.

SA0031

Denosumab Treatment of Fibrous Dysplasia of Bone. Alison M. Boyce^{*1}, Jack Yao², Marilyn H. Kelly³, Chris Chamberlain², William Chong⁴, Rachel Gafni², Alfredo Molinolo⁵, Natasha Cherman⁶, Nisan Bhattacharyya⁷, Michelle Ellsworth⁸, Josephine Kasa-Vubu⁸, Michael Collins². ¹NICHD, NIDCR, NIH, USA, ²National Institutes of Health, USA, ³SCSU, CSDB, NIDCR, NIH, USA, ⁴National Institute of Health, USA, ⁵OCBP, NIDCR, National Institutes of Health, USA, ⁶CSDB, NIDCR, NIH, USA, ⁷NIDCR, NIH, USA, ⁸University of Michigan Health Center, USA

Fibrous dysplasia (FD) is a benign fibroosseous skeletal disease caused by somatic activating mutations of the cAMP-regulating protein, Gsz. These mutations lead to replacement of normal bone by proliferative malfunctioning osteogenic precursors, leading to abnormal bone formation, deformity, fracture, and pain. Medical treatment has been ineffective in altering the disease course. Receptor activator of nuclear factor kappa-B ligand (RANKL) is a cell surface protein involved in many cellular processes, including osteoclastogenesis, and is reported to be overexpressed in FD-like bone cells. Denosumab is a humanized monoclonal antibody to RANKL approved for treatment of osteoporosis and prevention of skeletal-related events from bone metastases.

A 9-year-old boy with FD presented with rapid and dramatic expansion of FD in the right femur, not responsive to bisphosphonate therapy and necessitating amputation of the right lower extremity. Months later, the left thigh began a similar rapid and painful expansion, requiring daily narcotics, and a second amputation was planned. Immunohistochemical staining on a bone biopsy specimen taken prior to initiation of treatment revealed marked RANKL expression. A 12-month trial of denosumab was instituted to attempt to slow disease progression and prevent amputation. Denosumab was given by subcutaneous injection monthly at 1 mg/kg, with escalation to 1.25 mg/kg after 3 doses. Bone turnover markers were monitored monthly, and tumor volume was measured by CT 1 year prior to treatment, start of treatment, and after 3 months of therapy.

During the first 3 months of denosumab, pain resolved allowing discontinuation of all analgesics, and bone turnover markers declined significantly: alk phos 1683 U/L to 234 (86-315), P1NP 1300 mcg/L to 119 (22-105), B-CTX 1924 pg/mL to 251. Tumor volume 1 year prior to treatment was 170 cm³, and at treatment start had increased 56.5% to 266 cm³. While there were 13.5 months between studies, per report expansion began 6 weeks prior to treatment start. Assuming linear expansion over 13.5 months, the rate of growth was 4.2%/mo. Less conservative but likely more accurate estimates over 1.5 months show expansion of 37.5%/mo. After 3 months of denosumab, the volume was 277 cm³, representing a decreasing rate of expansion at 1.4%/mo.

Preliminary data after a 3-month treatment course suggests denosumab may be effective in slowing expansion of fibrous dysplasia.

Disclosures: Alison M. Boyce, None.

SA0032

See Friday Plenary Number FR0032.

SA0033

A Phantom for Calibrating Accuracy of DXA-Derived Femoral Neck Geometry. Thomas Beck¹, Ben Khoo², Roger Price³, Thomas Beck^{*1}, Richard Prince³, Roger Price³. ¹Quantum Medical Metrics, LLC, USA, ²Western Australian Health Department, Australia, ³Sir Charles Gairdner Hospital, Australia

There has been an increase in the use of structural geometry, measured by DXA and QCT methods to facilitate understanding of bone fragility. However, good methods for assessing and calibrating geometric accuracy are lacking. This study reports the development of a 3D anthropometric proximal femur phantom for calibration of femoral neck structural geometry. The phantom consists of a femoral shaft, head and seven interchangeable neck modules varying in size and shape to span the range of geometries commonly observed in adult femurs, with cortical thicknesses from 0.7 mm in a circular annulus (Module 1) to 3 mm and 8 mm in an asymmetric elliptical cross-section (Module 7).

Phantom was scanned (each module 10 times) in a water bath using Hologic Discovery DXA in hip-array mode and analysed using hip structural analysis (HSA) software at QMM.

All measured parameters were very highly correlated ($r=1.00$) with phantom dimensions but with some systematic errors as high as 98%. However, high correlations validate the use of the phantom as a calibration method. Linear prediction equations were generated for each variable (exponential for buckling ratio [BR]), then used to predict correct values using scan data. After calibration, maximum errors in the thinnest module (1) ranged from -22% in average cortical thickness (aCt) to +6% in aBMD. All variables in other modules showed a maximum error of 5% with most values <3%. Table summarises correlations and percentage differences between phantom geometry and HSA measurements for aBMD, cross-sectional area (CSA), cross-sectional moment of inertia (CSMI), outer diameter (OD) section modulus (Z), estimated aCt and Buckling Ratio (BR), after calibration with the pre-calibration value in parentheses.

Disclosures: Thomas Beck, None.

SA0034

Aging-Related Changes in Plasticity and Toughness of Human Cortical Bone at Multiple Length-Scales. Elizabeth Zimmermann^{*1}, Eric Schaible², Hrishikesh Bale², Holly Barth¹, Simon Tang³, Bjoern Busse¹, Tamara Alliston³, Joel Ager², Robert O. Ritchie¹. ¹University of California, Berkeley, USA, ²Lawrence Berkeley National Laboratory, USA, ³University of California, San Francisco, USA

The complex structure of human cortical bone evolves at multiple length-scales from its basic constituents of collagen molecules and hydroxyapatite crystals at the nanoscale to the osteonal (Haversian) structures at near-millimeter dimensions. Such a characteristic multi-scale structure provides the basis for its mechanical properties. With respect to resistance to fracture, toughness in bone is derived intrinsically, *i.e.*, from plastic deformation, at structural scales typically below a micrometer by such mechanisms as fibrillar sliding, whereas bone's extrinsic (crack-growth) toughness results from mechanisms such as crack deflection and bridging that are generated at much larger structural levels in the tens to hundreds of micrometers. Biological factors can degrade fracture resistance, such that the risk of bone fracture is markedly increased with aging. Although an important reason for the decreased fracture resistance is the loss of bone mass (or bone-mineral density) with age (*bone quantity*), we find here that significant aging-related changes in the bone-matrix structure can occur at multiple length-scales, which are detrimental to fracture resistance (*bone quality*). Specifically, non-enzymatic advanced glycation end-product measurements and (synchrotron) small-/wide-angle x-ray scattering (SAXS/WAXS) were used to characterize changes in the bone structure at sub-micrometer dimensions, while computed synchrotron x-ray tomography and *in situ* fracture toughness measurements in the environmental scanning electron microscope (ESEM) were used to characterize corresponding changes at micron-scale dimensions. Our results show how aging-related structural changes at differing size-scales can degrade both the intrinsic toughness by increased cross-linking at nanoscale dimensions, which acts to suppress plasticity, as well as the extrinsic toughness of bone by an increased osteonal density at the scale of tens to hundreds of micrometers, which acts to limit the potency of crack bridging mechanisms. The link between these processes is that the increased stiffness of the collagen fibrils from cross-linking requires energy to be absorbed by "plastic" deformation at higher structural levels; this is primarily achieved by the process of microcracking, which in turn has a profound effect on the mechanisms of extrinsic toughening in bone.

Disclosures: Elizabeth Zimmermann, None.

SA0035

Areal Bone Mineral Density and DXA Derived Geometrical Parameters at the Tibial Diaphysis Predict 3D Indexes of Bone Strength Assessed by HR-pQCT. Albrecht Popp^{*1}, Markus Windolf², Kurt Lippuner¹, Stefano Brianza², Andrea Tami², R.G. Richards², Damiano Schiama². ¹Osteoporosis Policlinic, University of Bern, Switzerland, ²AO Research Institute Davos, Switzerland

Background: The predictive value of areal bone mineral density (aBMD) at the distal tibia for fracture risk has been demonstrated in a population-based cohort of elderly women (Popp AW et al. Osteoporosis Int 2009). The tibial diaphysis applies as a model for bone strength assessment due to its geometrical structure and the high percentage of cortical bone. The aim of this study was to demonstrate that DXA at the tibial diaphysis is able to predict parameters of bone strength assessed by HR-pQCT.

Methods: Cadaveric tibias from female donors were scanned with DXA (Hologic QDR 4500 ATM, Hologic, Bedford, MA, USA) and high-resolution peripheral quantitative computed tomography (HR-pQCT, XtremeCTTM Scanco Medical, Brüttisellen, Switzerland). Parameters of interest were the total bone mineral density (vBMD) and the cortical thickness (CTH) obtained by HR-pQCT, the DXA derived CTH calculated with a Canny threshold-based DICOM analysis tool implemented in MATLABTM (MathWorks, Natick, MA, USA), and the product of BMD with the polar moment of inertia (pMOI), which was considered as index of bone strength.

Results: Sixty tibias from 35 female donors were included in this study corresponding to 25 pairs and 10 single tibias. The mean (SD) age of the donors was 78.5 ± 9.3 yr with mean height of 160.1 ± 7.8 cm and mean weight of 57.2 ± 11.4 kg. Ex vivo T-scores for distal tibial diaphysis and epiphysis were -2.0 SD and -2.3 SD, respectively. High correlation was found between parameters of bone strength, derived by DXA and HR-pQCT, respectively (table).

Conclusions: As a potential index of bone strength the product of aBMD with pMOI could be applied to a DXA cohort in order to assess its ability to predict fracture risk.

R ² _a	I	vBMD _a	CTH (HR-pQCT) _a	pMOI (HR-pQCT) _a	vBMD x pMOI (HR-pQCT) _a
aBMD _a		0.866_a	0.947_a	0.194_a	0.792_a
CTH (DXA) _a		0.045 _a	0.575_a	0.311_a	0.657_a
pMOI (DXA) _a		0.086 _a	0.240_a	0.623_a	0.551_a
aBMD x pMOI (DXA) _a		0.368_a	0.587_a	0.554_a	0.844_a

p<0.01 (bold/||)

areal BMD

Disclosures: Albrecht Popp, None.

SA0036

Association of QCT-Based Bone Strength Indices with Hip Fracture Risk among Older Men. Jan Borggreffe^{*1}, Timm de Buhr², Smriti Shrestha³, Carrie Nielson³, Eric Orwoll³, Lynn Marshall³, Dennis Black⁴, Claus-C Glueer⁵. ¹Klinik für Diagnostische Radiologie, Universitätsklinik Kiel, Germany, ²Klinik für Diagnostische Radiologie, Universitätsklinikum Schleswig Holstein, Campus Kiel, Germany, ³Oregon Health & Science University, USA, ⁴University of California, San Francisco, USA, ⁵Christian Albrechts Universität zu Kiel, Germany

Improved prediction of hip fracture risk and better understanding of relevant failure modes remain two key goals for osteoporosis research. We investigated the associations of biomechanically motivated strength indices of the proximal femur derived from quantitative computed tomography (QCT) with hip fracture risk among elderly men.

Using a case-cohort sampling design nested within the MrOS cohort, we evaluated QCT scans of 230 men (age 74.3 ± 6 years, 65 with confirmed hip fractures) with Mindways' QCTPRO BIT software. New failure mode specific bone strength indices for the femoral neck (FN) and for the trochanteric (TR) regions were defined, both for the respective entire cross sections and their quadrants. For FN and TR regions bending strength was estimated by minimum section modulus (Zmin) and quadrant bending index (QBI); buckling strength by buckling ratio (BR) and the local thinning index (LTI) of the quadrant of lowest strength. Integral and trabecular BMD were also derived for the two anatomic regions. Areal BMD (aBMD) of the total proximal femur from DXA is presented for comparison. Hip fractures occurring after enrolment through August 2010 (mean follow-up time: 7.4 yrs) were adjudicated centrally. Hazard ratios (HR) and 95% confidence intervals (CI) per standard deviation of the population variance were calculated from Cox proportional hazards models. Prentice weights were used to account for the case-cohort sampling design. All models were adjusted for age, BMI and center. Receiver operating characteristics areas under the curve (AUC) were calculated to characterize multivariate models.

Men with hip fractures were older than non-fx cases (77.1 ± 6.0 years vs. 73.3 ± 5.7 years, p<0.0001). HRs were significant for all indices tested except for TR LTI, with DXA aBMD being the strongest single predictor (see Table). In multivariate models, among QCT variables FN BR (HR=1.8; 1.2-2.8), TR BMD trab (HR=2.3; 1.4-4.0), and TR QBI (HR=2.4; 1.4-4.0) contributed independently (joint AUC=0.80), even in a model additionally including aBMD: FN BR (HR=1.6; 1.0-2.5), TR BMD trab (HR=2.0; 1.1-3.5), TR QBI (HR=2.1; 1.1-3.9), aBMD (HR=2.1; 1.1-4.0) (joint AUC=0.82).

QCT derived biomechanical indices of hip fracture risk add predictive value independent of DXA aBMD. These strength indices permit insight into the biomechanics of fracture risk: buckling of the FN and bending of the TR are relevant failure modes in older men not entirely captured by DXA.

Hip bone density or geometric measure	Adj. HR Mean (95% CI)	AUC
DXA aBMD total [g/cm ²]	4.3 (2.3, 8.2)	0.81
FN BMD integral [mg/cm ²]	3.4 (1.9, 5.9)	0.79
FN Zmin [cm ²]	2.0 (1.4, 3.0)	0.75
FN BR	2.4 (1.7, 3.6)	0.78
FN LTI [mg/cm]	2.0 (1.4, 2.9)	0.75
FN QBI [mg/cm]	1.7 (1.1, 2.6)	0.74
TR BMD trabecular [mg/cm ²]	2.8 (1.8, 4.6)	0.77
TR Zmin [cm ²]	2.0 (1.4, 3.1)	0.75
TR BR	1.5 (1.1, 2.1)	0.74
TR LTI [mg/cm]	1.3 (0.9, 1.8)	0.72
TR QBI [mg/cm]	2.0 (1.2, 3.2)	0.74

Table 1. Standardized Hazard Ratios (HR) for incident hip fractures, adjusted for age, BMI, center

Disclosures: Jan Borggreffe, None.

SA0037

Baseline Characteristics of Veterans Screened for VIVA-VA Study. Violet Lagari^{*1}, Orlando Gomez-Marin², Silvina Levis². ¹University of Miami, USA, ²University of Miami School of Medicine, USA

Purpose: Sedentary lifestyle is an important risk factor associated with the decline in physical performance that occurs with advancing age. Hypovitaminosis D (LoD) has been associated with age-related physical decline and an increased risk for falls. Studies have shown that older active individuals on small doses of vitamin D have improved results on isolated tests of physical performance, and nursing home residents with LoD show a significant reduction in the number of falls. The objective of this study is to test whether supplementation with 4000 IU of vitamin D3 (cholecalciferol) for 9 months will improve, or slow the decline of, the ability to perform physical tests which have been shown to be associated with the preservation of independence in the elderly.

Methods: We describe the study design and the baseline characteristics of the first 46 men screened in the VIVA-VA Study (Vitamin D In Vulnerable Adults in the VA), a 3-year, single-site, double-blind, placebo-controlled, randomized clinical trial that enrolls sedentary male veterans ages 65 to 90. The main inclusion criteria are 25-OH vitamin D (25OHD) levels ≥10 and ≤ 30 ng/ml and daily caloric expenditure ≤2600 (as assessed by CHAMPS questionnaire). The primary outcome of the study is the Short Performance Physical Battery (SPPB). Secondary outcomes include handgrip test and body composition by DXA. Subjects were recruited from the Miami Veterans Medical Center (MVAMC) clinics.

Results: The baseline characteristics (mean ± SD) of the 46 sedentary male veterans screened thus far are: age 75.5 ± 7.2 years; 25OHD 26 ± 9 ng/ml (range 10-51); systolic blood pressure (BP), 132.7 ± 17.8 and diastolic BP 75.6 ± 10.1 mm Hg; pulse rate 68.8 ± 11.7 beats per minute; waist circumference 107.1 ± 15.3 cm; and hip circumference 106.3 ± 13.9 cm. SPPB scores and its individual components are: total 6.5 ± 2.2 (range 2-10); balance test 3.1 ± 1.1; short walk test 1.9 ± 1.0; and 5 time chair sit to stand 1.4 ± 1.1. Mean hand grip was 35.8 ± 15.8 kg.

Conclusion: Thus far, the baseline characteristics observed of the first 46 men screened in the VIVA-VA Study are consistent with what is expected in a cohort of elderly frail men: low physical performance scores, including individual and total components of the SPPB and hand grip test, and low 25OHD levels despite living in South Florida. Recruitment is still underway and will continue through the upcoming months.

Disclosures: Violet Lagari, None.

SA0038

Bone Tissue Material Properties as Assessed by Reference Probe Indentation Are Associated with Proximal Femur Strength Independent of BMD. Sean Serell, Mary Bouxsein, Benjamin Roberts*. Beth Israel Deaconess Medical Center, USA

Whole bone strength is determined by bone mass, morphology, and bone tissue material properties. However, to date there are few techniques for direct assessment of bone material properties, and consequently little is known about the contribution of tissue-level mechanical properties to skeletal fragility. Reference probe microindentation is a new method for direct assessment of these properties. Our goal was to determine age- and sex- related differences in tissue-level mechanical properties, and whether these properties contribute to whole bone strength in human cadaveric femurs. **Methods:** We obtained 25 human proximal femora (16 women, 9 men, mean age=72.5 ± 9.3 yo). Following imaging with DXA (total femur aBMD, mg/cm²), femurs were mechanically tested in a sideways fall configuration. Cortical bone

material properties at the diaphysis were then assessed in the longitudinal direction with a microindentation system equipped with a tip sharpened to a 90 conical, 2.5µm radius (BioDent 1000, Active Life Technologies, Santa Barbara, CA). Five indentation tests per specimen were performed; outcomes included stiffness (N/µm), total indentation distance (TID, µm), indentation distance increase (IDI, µm), and creep indentation distance (CID, µm). Results: Women had 11% and 10% higher (ie worse) total ID and Creep ID, respectively, compared to men ($p<0.05$, table). Among microindentation properties, only CID significantly increased with age ($r=0.36$). Total femoral aBMD was negatively correlated with IDI ($r=-0.39$), CID ($r=-0.65$), and TID ($r=-0.74$). Femoral max force was moderately correlated with IDI ($r=-0.38$), CID ($r=-0.51$), and TID ($r=-0.64$). In a stepwise multiple regression vs. Max Force, only Creep ID significantly added to Max Force, increasing the correlation from $r^2=0.84$ to 0.87. Conclusion: After adjusting for BMD, some parameters from microindentation remain significantly correlated with femoral strength, showing that variation in material properties contributes in part to whole bone strength. These data illustrate provide strong rationale for further testing of in vivo microindentation to describe age- and sex-related differences in material properties, but also to determine their contribution to whole bone strength and fracture risk.

	Women	Men	Correl. w/ aBMD	Correl. w/ Max Force
IDI (µm)	29.59 (5.44)	26.18 (7.88)	-0.39	-0.38
Total ID (µm)	168.4 (16.7)*	151.5 (18.5)	-0.74	-0.64
Creep ID (µm)	4.72 (0.43)*	4.30 (0.54)	-0.48	-0.51
Stiffness (N/µm)	1.16 (0.12)	1.14 (0.13)	NS	NS

* $p<0.05$ men vs. women

Microindent Table

Disclosures: Benjamin Roberts, None.

SA0039

Changes in Tibial Density and Geometry in Infantry Trainees Following Initial Military Training. Rachel Izard¹, Julie Greeves², Charles Negus³, Craig Sale⁴, William Fraser⁵. ¹HQ ARTD, MOD, United Kingdom, ²HQ Army Recruiting & Training Division, United Kingdom, ³L-3 Applied Technologies, USA, ⁴Nottingham Trent University, United Kingdom, ⁵Norwich Medical School, University of East Anglia, UK, United Kingdom

Smaller cross-sectional area but higher density of the tibia, measured using peripheral computed tomography (pQCT), have been shown to increase the risk of tibial injuries in military trainees (Evans et al., 2010). The incidence of tibial injuries is typically higher during the initial phase of military training as bone responds to the rapid onset of increased loads. However, the functional adaptation of bone to initial military training has not been investigated. The purpose of this study was to monitor changes in tibial bone mass and geometry after 10 weeks of initial military training in male infantry recruits. Ninety recruits (mean±SD, age 21 + 3 y, height 1.78 + 0.06 m and body mass 73.95 + 9.76 kg) undertaking initial infantry training at the Infantry Training Centre (Catterick, UK) volunteered to take part. pQCT scans (XCT2000L, Stratec Pforzheim, Germany) were taken before (baseline) and after 10 weeks of training. Scans were performed at the 4% (trabecular bone), 38% and 66% (cortical bone) of the length measured from the distal end plate of the tibia. BAMPack software (L-3 Jaycor, San Diego, CA) was used to calculate whole and regional (60o sectors) bone parameters using previously described methods (Evans et al., 2008). Parameters included trabecular density (TbDn, mg/cm³), cortical density (CtDn, mg/cm³), cortical area (CtAr, mm²) and cortical thickness (CtTh, mm). Biomechanical strength indices were also recorded and included the bone strength index (BSI) and moment of inertia in the anterior – posterior (mmiAP) and medial – lateral (mmiML) planes. Wilcoxon-signed rank tests (SPSS v17.0) were used to analyse data. Statistical significance was set a-priori at $P<0.05$. Significant increases were observed in bone mineralisation (TbDn and CtDn) at all sites and bone geometry (CtAr and CtTh) and bone strength (mmi and BSI) at the 38 and 66% sites (Table 1). Changes were predominantly observed in the anterior, medial-anterior and anterior-posterior sectors. Increased mineralisation at the distal tibia and increased cortical area of the tibial shaft suggest that rapid and marked adaptations of bone take place within 10 weeks of military training. Further analysis will establish whether individuals who exhibit the greatest changes in, or have higher initial bone strength are better protected from tibial injury. This work was sponsored by the UK Ministry of Defence (Army).

Site	Parameter	Baseline	Week 10	P
4%	TbDn (mg cm ⁻³)	301.6 ± 27.8	304.4 ± 26.4	.000
	TbAr (mm ²)	1155.3 ± 175.2	1162.1 ± 170.2	.668
	CtDn (mg cm ⁻³)	1154.3 ± 24.3	1156.5 ± 21.8	.003
38%	CtAr (mm ²)	317.0 ± 35.1	319.0 ± 34.7	.000
	CtTh (mm)	5.16 ± 0.67	5.19 ± 0.66	.000
	mmiAP (mg cm ³)	301.4 ± 62.0	305.1 ± 63.1	.000
	mmiML (mg cm ³)	532.3 ± 106.9	537.9 ± 104.9	.000
	BSI (g cm ³)	3.53 ± 0.65	3.57 ± 0.65	.000
	CtDn (mg cm ⁻³)	1124.4 ± 21.5	1127.2 ± 19.3	.000
66%	CtAr (mm ²)	344.1 ± 38.3	345.2 ± 37.6	.026
	CtTh (mm)	4.20 ± 0.53	4.21 ± 0.51	.740
	mmiAP (mg cm ³)	458.7 ± 95.6	460.6 ± 96.1	.004
	mmiML (mg cm ³)	1061.9 ± 200.36	1072.1 ± 200.3	.000
	BSI (g cm ³)	6.38 ± 0.01	6.43 ± 0.05	.000

Table 1. Mean + 1SD pQCT data at baseline and week 10.

Disclosures: Rachel Izard, None.

SA0040

Effects of Multiple Exposures to Microgravity on the Femur of Adult Male Hindlimb Unloaded Rats. DERRICK MORGAN, JOSHUA DAVIS, Yasaman Shirazi-Fard, Josh Kupke, Joseph Marchetti, Alyssa McCue, Susan Bloomfield, Harry Hogan*. Texas A&M University, USA

Bone response to extended microgravity remains a concern for astronaut health. A particular question is how prior missions affect subsequent missions. Animal experiments were conducted to test the hypothesis that previous exposure to mechanical unloading would exacerbate the effects of a 2nd exposure. This study focused on the distal femur metaphysis (DFM) and femoral neck (FN).

Adult male Sprague-Dawley rats (6 mo.) were assigned to 2 groups: aging cage control (CC), hindlimb unloaded (HU). HU animals were further divided into subcategories: 1HU and 2HU. The 2HU group had 28d of HU at 6 mo. (2HU6), followed by 56d of recovery, and another 28d of HU (2HU9) starting at 9 mo. (day 84). The 1HU group had one bout of HU (1HU9) starting on day 84 (to match 2HU9). A group (n=15) was euthanized every 28d (days 0, 28, 56, 84, 112 & 168) from each of CC, 1HU, and 2HU groups. Excised femora were scanned by pQCT at the DFM and FN, and the FN was mechanically tested to failure.

Total (integral) BMC and vBMD for the DFM decreased significantly for 2HU6 (9% & 13%, resp.). Decreases for 2HU9 (second exposure) were less (2% & 7%, resp.), and only the latter was significant (7% for vBMD). Decreases for the age-matched single HU (1HU9) were quite similar to those for 2HU9 (3% & 6%, resp.), but once again, the decrease was significant for only vBMD (6%). Thus, for the DFM, negative effects were most prominent at the younger age (2HU6). HU effects at the older age (2HU9 & 1HU9) were milder and significant for only vBMD. The cross-sectional area of the cortical shell (Ct.Ar) at the DFM showed a similar response. Ct.Ar decreased 7.5% for 2HU6 (sig.) but only 2% for 2HU9 (n.s.) and 1.5% for 1HU9 (n.s.). Total BMC and vBMD for the FN were similar to results for the DFM. Both decreased significantly for 2HU6 (6.4% & 7.2%, resp.), with milder reductions (n.s.) for both 2HU9 and 1HU9 (from -3% to -5.5%). For mechanical strength of the FN, reductions due to HU were substantial (18-26%), significant, and similar regardless of age or prior HU exposure. The greatest reductions were at 9 mo. (26% for 2HU9, 22% for 1HU9), even though corresponding reductions in BMC and vBMD were mild (3-5.5%) and not significant.

These results are contrary to the initial hypothesis. Reductions in BMC and vBMD at the DFM and FN were affected by age but not prior HU. For strength of the FN, negative effects of HU were dramatic and similar in extent regardless of age or prior HU.

Disclosures: Harry Hogan, None.

SA0041

Evolution of Bone Strength with Age: A Large Micro-Finite Element Analysis in Women from the OFELY Cohort. Nicolas Vilayphiou¹, Stephanie Boutroy¹, Elisabeth Sornay-Rendu¹, Bert van Rietbergen², Roland Chapurlat¹. ¹INSERM UMR1033, Université de Lyon & Hospices Civils de Lyon, France, ²Department of Biomedical Engineering, Eindhoven University of Technology, Netherlands

Areal bone mineral density (aBMD) decreases with age in women, but our knowledge of the effect on bone biomechanical properties is limited. So, we have studied the decline of bone strength with age, with micro-finite element analysis (µFEA) using high resolution peripheral QCT (HR-pQCT) images.

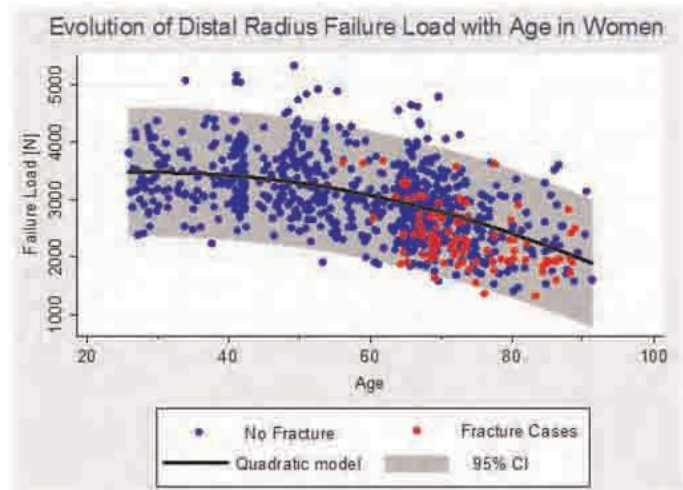
Our cross-sectional analysis has involved 831 women who had a valid HR-pQCT radius scan in the OFELY cohort. There were 228 pre- (preM) and 603 postmenopausal (postM) women, aged 407 and 679 years old respectively; 117 postM women have sustained fragility fractures before the visit.

Distal radius HR-pQCT scans were used to measure volumetric BMD (vBMD) and microarchitecture parameters, after segmentation of cortical (Ct) bone with

advanced algorithm (Burghardt, Buie et al. Bone 2010). Estimated failure load was assessed by μ FEA as the main outcome of radius bone strength, and permitted to derive the load to strength ratio Φ as an estimate of fracture risk. Total hip aBMD was recorded by DXA at the same visit. In preM women, most parameters did not vary with age. In postM women, Ct porosity and trabecular (Tb) heterogeneity significantly increased throughout the menopause, respectively from 0.7 to 3.4% and from 215 to 571 μ m. Total, Ct and Tb vBMD decreased with age, as well as Ct thickness and Tb number ($r=-0.41$ to -0.65 , $p<0.001$). The deterioration of microarchitecture with age resulted in a decrease of the μ FE-failure load with an overall loss of a third of bone strength throughout the postmenopausal period compared to preM women. A quadratic relationship between failure load and age was found (see Figure: $R^2=0.32$, $p<0.001$).

A total increase of Φ by 50% was observed, so that after the age of 70 more than half (60%) of the elderly women had a factor of risk $\Phi>1$. Considering Φ as a factor of risk for all fragility fractures, we compared the ROC curves of Φ and total hip aBMD, with respect to prevalent fractures. The area under the curves was slightly higher for Φ than for total hip aBMD (AUC [95%CI] =0.72 [0.66-0.78] and 0.69 [0.62-0.75], respectively). However, sensitivity and specificity for fracture of the mechanical criterion $\Phi>1$ were 73% and 58% respectively, whereas that of the T-score <-2.5 were 20% and 97% respectively.

To conclude, we observed a substantial decline of bone strength with age at the radius. We suggest that the calculated load to strength ratio Φ might be a relevant indicator of fracture risk, more sensitive than hip aBMD.



Figure

Disclosures: Nicolas Vilayphiou, None.

SA0042

Finite Element Prediction of Proximal Femur Fracture Profile Based on Anisotropic Behaviour Law Coupled to Damage. Awad Bettamer^{*1}, Ridha Hambli², Samir Allaoui². ¹L'Université d'Orléans, France, ²PRISME Institute, France

Introduction: A femoral fracture caused by the osteoporosis becomes increasingly important goal for both clinicians and biomedical researchers in order to evaluate and to prevent the risk of neck femur fracture. The purpose of this study was to develop a computed 3-D anisotropic model based on continuum damage mechanics to simulate the profile of the fractured area of proximal femur. The model was developed in term of anisotropic coupled behaviour law (strain-quasi-brittle damage) to describe the progressive crack initiation and propagation within proximal femoral. **Materials and methods:** The proposed model was implemented in ABAQUS/Standard FE software as a user subroutine. To illustrate the potential of the current approach, the right adult human femur previously investigated by Keyak et al., J.Medical Engineering & Physics. 781:7,2003 (Model B: male, age 61) was simulated till complete fracture under one-legged stance load. This proposed damaged model can be used successfully to simulate many different fracture patterns such as intracapsular (subcapital, transcervical and basal). In the current work our model is further applied on a patient aged 80 years, Konishiike T. et al., Journal of bone and joint surgery. 596:4,1999 in order to simulate its fracture type as well as to investigate how its crack was propagated. **Results:** The fracture profile was predicted (Fig.1-a) and the complete force-displacement curve from the beginning until complete fracture was predicted. The damage subsequent to the ultimate predicted force of (6 kN) with the assumption of brittle bone with () or (8 kN) with a brittle bone () result in a reduction of the mechanical properties in bone strength and stiffness of bone material that caused by the apparition of microcracks corresponds to crack displacement of (4.4 mm). The predicted fracture profile resulted can be registered as a type of Garden undisplaced fracture (stages 1 and 2). The obtained results were compared with similar clinical observed results (Fig.1-b) and (Fig.1-c). Good agreements were obtained and the model succeeded to predict the fracture profiles such as Garden undisplaced fracture (stages 1 and 2) as well as the displaced fracture (stages 3 and 4).

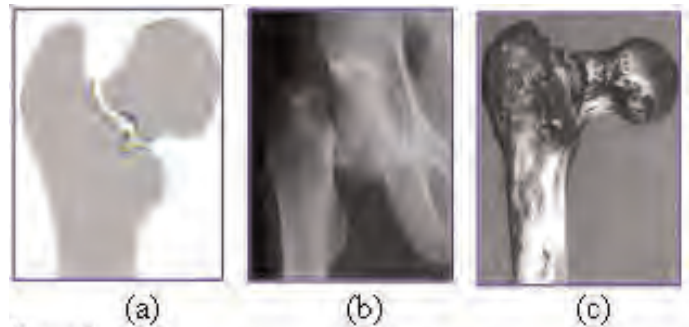


Figure 1.

- (a) Proposed damage fracture profile prediction model (Garden-stage 3: complete femoral neck fracture with full displacement).
(b) X-ray image of femur broken in a patient aged 80 years (Garden fracture stage 3).
(c) Example of a specimen after loading to failure of single leg Stance.

Figure 1

Disclosures: Awad Bettamer, None.

SA0043

High Resolution-pQCT Scanning of Radius and Tibia in Adult Patients with Osteogenesis Imperfecta. Roland Kocijan^{*1}, Christian Muschitz², Angela Trubrich², Christina Bittighofer², Franz Kainberger³, Heinrich Resch⁴. ¹St. Vincent Hospital Vienna, Austria, ²St. Vincent's Hospital, Austria, ³Medical University of Vienna, Austria, ⁴Medical University Vienna, Austria

Purpose Osteogenesis imperfecta (OI) is an inherited disorder characterized by increased bone fragility with recurrent fractures due to a defect in collagen metabolism. OI is also characterized by a low bone mass and a deterioration of cortical and trabecular bone microarchitecture. HR-pQCT is a non-invasive, radiological method for the analysis of bone structure and density. Recent studies have shown that the method can provide additional information about bone strength in patients with osteoporosis, however, the method has not yet been applied in patients with OI. **Methods** We performed HR-pQCT scans (XtremeCT, SCANCO Medical) in 10 patients with OI type I, III and IV by Sillence classification (OI, mean age 51.3 years) at the ultradistal radius and distal tibia. We assessed different density values and parameters of cortical and trabecular bone structure including trabecular volume (BV/TV), trabecular number (Tb.N), trabecular thickness (Tb.Th), trabecular separation (Tb.Sp), cortical thickness (Ct.Th) and inhomogeneity of the network (Tb.I/N.SD). The results were compared to a young, healthy control group at peak bone mass (CO, mean age 31.9 years). In addition, we compared the mild OI type I group to the severe, immobile OI III/IV group. **Results** We found significant changes ($p<0.05$) in different density parameters at the radius and the tibia between OI and CO. Trabecular structure parameters at the radius (Tb.N, Tb.Sp, Tb.I/N.SD) and tibia (Tb.N, Tb.Sp, Tb.I/N.SD, BV/TV) were significantly decreased in the total OI group. Ct.Th was markedly lower at the tibia and not at the radius in this group. In comparison to the controls all density and structure parameters were significantly decreased in the OI III/IV group except Tb.Th, whereas the mild form of OI I had no changes in Tb.Th and Ct.Th at both skeletal sites. Comparing the two OI subgroups Ct.Th was the most different parameter at both sites. **Conclusion** This is the first study so far applying HR-pQCT in patients with different classifications of OI. This non invasive imaging technique has the capability to display the structure alterations of bone architecture at cortical and trabecular sites.

Disclosures: Roland Kocijan, None.

SA0044

See Friday Plenary Number FR0044.

SA0045

See Friday Plenary Number FR0045.

SA0046

Marrow Recovery from Sub-Lethal Irradiation Is Evident Long Before Any Sign of Trabecular Bone Restoration. Danielle Green^{*1}, Benjamin Adler¹, Ete Meilin Chan¹, Clinton Rubin². ¹Stony Brook University, USA, ²State University of New York at Stony Brook, USA

Stem cell depletion and compromised bone marrow (BM) following radiation exposure inherently expedite long term detrimental effects on numerous physiologic systems including the skeletal system, ultimately increasing the risk of fractures due to osteoporosis. To study the interrelationship of a damaged BM cell population on trabecular microarchitecture, 8w & 16w C57BL/6 male mice were sub-lethally irradiated with 6 Gy of ¹³⁷Cs γ -rays, and adult stem cells residing in the BM, as well as bone quantity and quality, were evaluated in the proximal tibia following 2d, 10d & 8w, as compared to age-matched controls. Total extracted BM cells in the 8w mice, including hematopoietic stem cells (HSC), collapsed by 6511% after 2d, remaining at those suppressed levels at 10d, but showing full recovery by 8w. While the 16w mice showed a similar (6318%) cellular depletion after 2d & 10d, full recovery of the cell population had not been realized at 8w, remaining 129% below their age-matched controls. The rate of detriment and repair of the BM cells though was dependent on both the hematopoietic phenotype and the age of the mice. At 2d, the 16w mice showed an 897% collapse in lineage restricted lin-Sca-1+c-kit+ (LSK) progenitor cells, whereas the 8w mice showed no decline until 10d (616%). In contrast, the long term HSC (SP-LSK) in the 8w & 16w mice declined by 8710% and 895%, respectively at 2d, and showed no sign of recovery by 10d. By 8w, the LSK and SP-LSK cells returned to age-matched control levels for the younger mice, but the LSK and SP-LSK cells in the 16w mice remained 3914% and 2823% lower than age-matched controls. Evident as early as 10d following irradiation, 8w mice showed a 4112% and 334% decline in bone volume fraction and trabecular number respectively, and a 5010% increase in trabecular spacing as compared to controls, with compromised structure showing no sign of restoration even at 8w post-irradiation. Devastation of trabecular bone of the 16w mice was similar to the 8w mice, suggesting irradiation damage to bone structure is independent of skeletal maturity. Conceivably, efforts to recover the BM cell population following injury may restore bone architectural quality. However with such drastic declines in the BM and HSC populations at 2d & 10d, the drop in bone quality cannot solely be attributed to an active osteoclast response, but perhaps a physicochemical response enabled by irradiation compromises the bone matrix itself.

Disclosures: Danielle Green, None.

SA0047

Microarchitecture Is Impaired In Postmenopausal Caucasian Women With Fracture Independently Of Total Hip T-score - The MultiXCT Study. Stephanie Boutroy^{*1}, Sundeep Khosla², Elizabeth Sornay-Rendu³, Maria Belen Zanchetta⁴, Donald McMahon⁵, Chiyuan Zhang⁶, Roland Chapurlat⁷, Jose Ruben Zanchetta⁴, Emily Stein⁵, Cesar Bogado⁴, Sharmila Majumdar⁸, Andrew Burghardt⁸, Elizabeth Shane⁵. ¹Columbia University Medical Center, USA, ²College of Medicine, Mayo Clinic, USA, ³INSERM, France, ⁴Instituto de Investigaciones Metabolicas (IDIM), Argentina, ⁵Columbia University College of Physicians & Surgeons, USA, ⁶Columbia University, USA, ⁷E. Herriot Hospital, France, ⁸University of California, San Francisco, USA

As half of all postmenopausal fractures (FX) occur in women with T-scores <-2.5, there is interest in investigating the influence of bone microarchitecture assessed by HR-pQCT (Scanco Medical AG) on FX risk. As single-center studies have reported conflicting associations between microarchitecture and FX prevalence, we included HR-pQCT data from 4 centers worldwide into a large multicenter analysis of postmenopausal women with and without FX. Volumetric density (vBMD) and microarchitecture were assessed at the distal radius (DR) and tibia (DT) in 1250 Caucasian postmenopausal women (678 yr); 435 (35%) had at least one FX (171 vertebral, 183 forearm, 17 hip, 33 humerus...). All had lumbar spine (LS) and total hip (TH) BMD by DXA (Hologic or GE-Lunar). Age, height, weight, menopause age and total hip T-score differed across centers. Women with FX had higher BMI (26.75.3 vs 25.94.7 kg/m², p<0.01), were older (699 vs 668, p<0.001), and 1 year younger at menopause (487 vs 495, p<0.01). TH T-score was lower in the FX group (-1.21.0 vs -0.90.9, p<0.001) and LS T-score was similar (-1.41.4 vs -1.51.3). Logistic regression identified age, height and TH T-score as covariates for between-center differences. As DR and DT vBMD and/or microarchitecture also varied by center, center was added as a covariate in GLM models assessing center, FX status and FX by center interactions.

At the DR, total and trabecular (Tb) vBMD were significantly lower in FX women in 3/4 centers (by 7%-9% and 13%-14% respectively, p<0.05). Tb number and cortical thickness were also significantly lower in 2 centers (by 9% and 6%-9% respectively, p<0.05), and not in 2 other centers (lower by 4% and 2%-4% respectively). Similar results were found at the DT. When data from 4 centers were combined, however, women with FX had significantly lower total, Tb and cortical vBMD (by 1.2%-10.7%, p<0.05) and Tb microarchitectural deficits (lower Tb number and thickness by 2.9%-6.7%, p<0.05) than women without FX. Results were similar at DR and DT and remained significant after adjustment for TH T-score

In conclusion, we observed differences by center in the magnitude of FX/non FX differences at both the distal radius and tibia. However, when data were pooled across centers and the sample size increased, we observed significant and consistent deficits in

vBMD and microarchitecture independent of total hip T-score in postmenopausal Caucasian women with FX compared to women who never had a FX.

Overall percentage difference between Caucasian women with and without fracture

	% difference at the radius	% difference at the tibia
Total area	1.6	2.7 **
Total density	-6.1 ***	-5.0 ***
Cortical density	-1.2 *	-1.2 *
Cortical thickness	-4.9 **	-3.2 *
Tb density	-10.7 ***	-7.7 ***
Tb number	-6.7 ***	-2.9 *
Tb thickness	-4.3 ***	-4.9 **
Tb separation	10.1 **	4.7
Tb distribution	14.2 *	4.8

* p<0.05, ** p<0.01, *** p<0.001

Overall percentage difference between Caucasian women with and without fracture

Disclosures: Stephanie Boutroy, None.

SA0048

Microstructural and Mechanical Differences among Postmenopausal Caucasian, African, and Hispanic American Women. Bin Zhou^{*1}, Xiaowei Liu², Marcella Walker¹, Emily Stein², Thomas Nickolas³, Michael Yin¹, Donald McMahon², Elizabeth Shane², X Guo¹. ¹Columbia University, USA, ²Columbia University College of Physicians & Surgeons, USA, ³Columbia University Medical Center, USA

Many studies suggest that BMD is higher and fracture risk is lower in African American (AA) than Caucasian (CA) women. However, few data are available on three-dimensional trabecular bone microstructure and mechanical competence in AA, which may underlie these differences in BMD and fracture risk. Moreover, data on Hispanic (HISP) women of Caribbean origin, who manifest significant racial admixture and comprise a large proportion of the Latina population of the eastern US, are lacking. To explore racial/ethnic differences in trabecular bone microstructure in these underrepresented populations, we applied novel individual trabeculae segmentation (ITS) and micro finite element (μ FE) analyses to high resolution peripheral QCT (HR-pQCT; Xtreme CT, Scanco Medical) scans of postmenopausal women (27 CA age 623; 18 AA age 586; and 30 HISP age 597). At the distal radius (DR), total bone area for CA and HISP women was 15% and 12% lower than AA women, respectively (p<0.05). As a result, whole bone stiffness of CA and HISP women was 17% and 24% lower respectively than African-American women (p<0.05). At the distal tibia (DT), total bone area for HISP women was 10% and 11% lower than CA and AA women, respectively (p<0.05); cortical thickness of CA and HISP women was 25% and 6% lower than AA women, respectively (p<0.001), resulting in 16% and 21% lower whole bone stiffness than AA women (p<0.01). Trabecular microstructure was similar in three racial groups at DR. However, DT rod bone volume fraction (rBV/TV) of CA women was 24% and 26% higher, and rod trabecular number (rTb.N) 10% and 11% higher than AA and HISP women, respectively (p<0.05). Furthermore, rod-rod junction density of CA women was 43% and 41% higher than AA and HISP women (p<0.005). In addition, CA trabecular area was 15% higher and BV/TV was 15% higher than HISP (p<0.05), resulting in 30% lower trabecular stiffness in HISP compared with CA. These data suggest that HISP women more closely resemble CA than AA women in terms of whole bone size and strength. In contrast, however, trabecular bone microstructure of HISP women more closely resembles that of AA than CA women, in that both HISP and AA women have less "rod-like" microstructure than CA women. These results illustrate the importance of more complete characterization of bone microstructure and strength in premenopausal and postmenopausal CA and AA women, and HISP women of Caribbean descent.

Disclosures: Bin Zhou, None.

SA0049

See Friday Plenary Number FR0049.

SA0050

Porosity, Mineralization and Morphology Interactions At The Human Tibial Cortex. Naomi Hampson^{*1}, Remi Gendron², Guillermo Duarte², Surva R. Kalidindi¹, Karl Jepsen², Haviva Goldman³. ¹Drexel University, USA, ²Mount Sinai School of Medicine, USA, ³Drexel University College of Medicine, USA

Purpose: Previous studies of the human tibia have demonstrated a higher ash content amongst individuals with more slender bone phenotypes possibly as a compensatory mechanism to increase whole bone stiffness. We aimed to investigate the relationship between cortical porosity and ash content, relative to cross-sectional robustness in order to better understand the tissue level adaptations that may occur in the establishment of whole bone function.

Methods: 2.5mm cross-sections of 10 tibiae (age 37 +/- 8 yrs) were obtained from 38% and 66% from the distal articular surface, radially sectioned into 6 wedges, and

imaged using a Skyscan 1172 μ CT at 5 μ m resolution. Cortical tissue volume (TV) and canal volume (CV) were determined using Skyscan's CT Analyzer for each location and wedge to obtain a measure of %CV. Following μ CT imaging, each wedge was ashed. Tissue Mineral Density (TMD) for the entire cross section was obtained from pQCT of the adjacent block of tissue. Robustness was calculated as cross sectional area divided by tibial length.

Results: When adjusted for age and robustness, porosity values were significantly ($p < 0.05$) higher anteriorly (and to a lesser degree, posteriorly) relative to medial and lateral segments. At both locations, age had a significant ($p < 0.05$) effect on porosity distribution, while robustness had a significant effect only at 66%. Ash content was significantly ($p < 0.01$) lower anteriorly relative to all other wedges at both 38% and 66% locations. Porosity and ash content were non-linearly correlated, with the relationship driven primarily by the more slender individuals in the sample. Both were significantly correlated with TMD, with porosity explaining more of the variability in TMD ($r^2 = 0.51$) than ash content ($r^2 = 0.34$).

Conclusions: Significant differences were found around the cortex with respect to porosity and ash content, and both demonstrated relationships to TMD, robustness and age. Higher remodeling rates anteriorly (and to a lesser extent posteriorly) may reflect higher remodeling rates in these cortices, and relate to the A-P orientation of the axis of greatest bending rigidity. The non-linear relationship between porosity and ash content may indicate a novel biological strategy for establishing tissue quality through internal remodeling that is predictable based on the natural variation in skeletal robustness, which in turn may result in significant differences in bone aging between these bone phenotypes.

Disclosures: Naomi Hampson, None.

This study received funding from: DOD (DAMD 17-01-1-0806)

SA0051

Prediction of Forearm Impact Forces during Falls on the Outstretched Hand.

Chantal Kawalilak^{*1}, Joel L. Lanovaz², James D. Johnston², Adam D.G. Baxter-Jones², Saija Kontulainen². ¹College of Kinesiology, Can, ²University of Saskatchewan, Canada

Wrist and forearm fractures commonly result from a fall onto the outstretched forearm when the impact force exceeds bone strength. A commonly used mathematical model representing the response of the upper extremity and torso during a fall is the two-mass spring-damper model. This model is often used to predict the impact force experienced during a standing height fall, which can be related to image based estimates of bone strength to create an index of fracture risk (impact force: bone strength). However, the model has only been validated with experimental data for fall heights up to 5 cm. It is unknown whether the model will accurately predict impact forces at higher fall heights. Additionally, the relationship between impact force and forearm muscle cross sectional area (MCSA), which may influence the choice of model parameters, is unknown. The primary objective of this study was to compare experimentally measured forces in falls on an outstretched hand to forces predicted by the two-mass spring-damper model at heights greater than 5 cm. The second objective was to investigate the relationship between the experimental impact forces and forearm MCSA. Peak impact forces in the vertical direction were measured using a force platform for 10 healthy young adult males and females at 8 randomized fall heights from 1 to 25 cm. Forearm MCSA was measured using periperal quantitative computed tomography (pQCT). 2x8 factorial ANOVAs determined the difference between the experimental and model force peaks. Relationships between forearm MCSA and impact forces were investigated with Pearson's bivariate correlations. Recorded force patterns typically displayed an initial impact peak followed by a second peak corresponding to body deceleration. There were no significant differences between the model and experimental data ($p > 0.05$) for the first peak force across any fall heights. However, the model over predicted the second experimental peak force ($p < 0.05$) across all fall heights. Impact forces were related to MCSA ($r = 0.3-0.6$) and stature ($r = 0.4-0.6$); these relationships were stronger at higher fall heights. In conclusion, the two-mass spring-damper model appears capable of predicting the first impact force for fall heights up to, and including, 25 cm. Further research is needed to incorporate the observed associations between MCSA and peak forces within the model parameters.

Disclosures: Chantal Kawalilak, None.

SA0052

See Friday Plenary Number FR0052.

SA0053

Quantifying Bound and Pore Water in Cortical Bone with MRI. Adam Horch^{*1}, Dan Gochberg¹, Jeffry Nyman², Mark Does¹. ¹Vanderbilt University, USA, ²Vanderbilt University Medical Center, USA

Human cortical bone magnetic resonance imaging (MRI) has become clinically feasible with ultrashort-echo time (uTE) methods [1]. The cortical bone MRI signal arises from a combination of collagen-bound water and pore space water, which exhibit different transverse relaxation times (T2) [2]. Using a gold-standard CPMG, which is not clinically-compatible, bound and pore water signals have been directly ($r^2 = 0.68$) and inversely ($r^2 = 0.61$) correlated with peak stress (and other mechanical properties), respectively [3]. The net cortical bone water signal was poorly correlated

($r^2 = 0.06$), indicating that diagnostic MRI must discriminate bound from pore water. However, to date, MRI techniques have not been developed for such discrimination. This work demonstrates clinically-compatible cortical bone MRI methods for bound and pore water quantitation using bone T2 features.

Human cortical bone was obtained from medial midshafts of 14 human donor femurs (Mustuloskeletal Tissue Foundation, Edison, NJ). NMR measurements were performed on cortical bone specimens at 4.7T, consisting of 1) a non-imaging adiabatic inversion-recovery (AIR)-prepared uTE sequence, which isolates bound water by selectively inverting and then nulling the pore water via appropriate choice of AFP parameters and inversion time; and 2) a non-imaging double adiabatic full passage (DAFP) uTE sequence, which strongly attenuates bound water signals while leaving pore water signals largely intact. AIR and DAFP signals were converted to apparent 1H concentration by comparing signal size to that of a known water phantom. 3pt-bend mechanical testing (40 mm span) was performed to determine peak stress.

The AIR signal contains negligible signals in the pore water T2 spectral domain and is thus dominated by bound water (Fig 1). AIR-derived estimates of bound water concentration exhibited a moderate correlation to peak stress (Fig 2), although the correlation is weakened by one apparent outlier. Conversely, the DAFP signal is dominated by pore water (Fig 1), and DAFP-derived pore water concentration exhibited a moderately-strong correlation to peak stress. Importantly, the AIR and DAFP methods demonstrated here utilize clinically-compatible MRI parameters and are thus readily translatable for in vivo imaging. Given their bound/pore water specificity, these methods provide more utility than conventional uTE MRI.

1)Radiology 248(2008):824-833. 2)Magn.Reson.Med.64(2010):680-687. 3)PLoS One.2011 Jan 21;6(1):e16359.

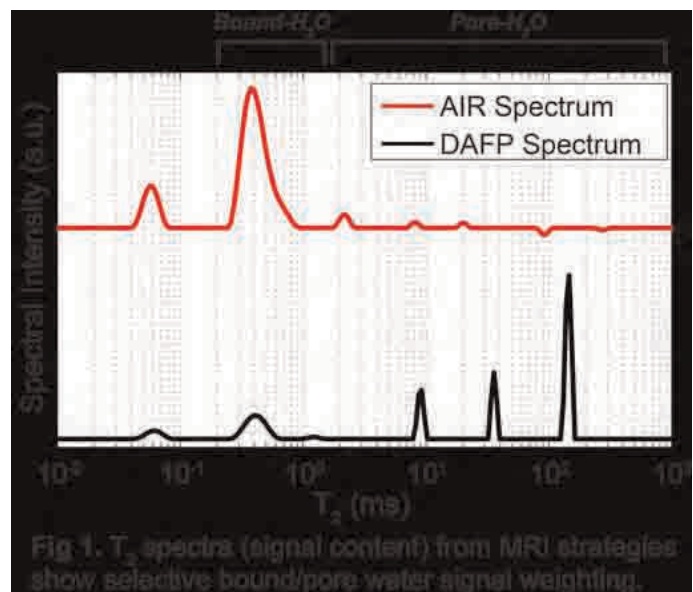


Figure 1

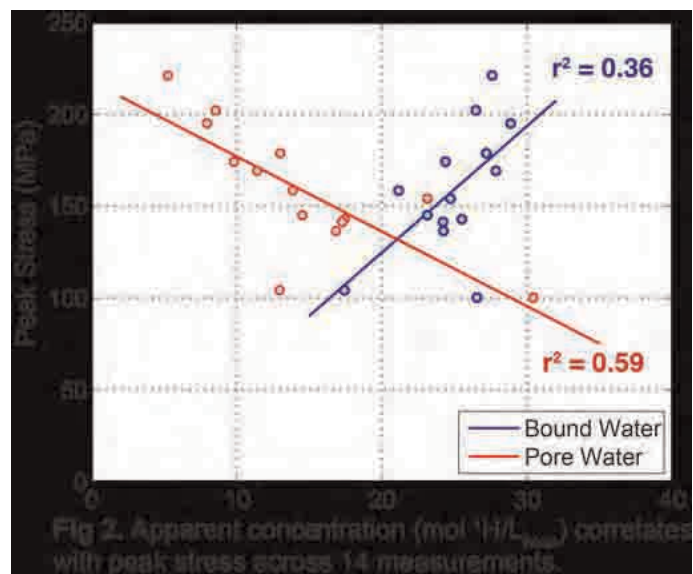


Figure 2

Disclosures: Adam Horch, None.

SA0054

Quantitative Computed Tomography-Based Nonlinear Finite Element Method is a More Sensitive Tool for the Assessment of Therapeutic Effects of Alendronate in Elderly Osteoporotic Women. MASAKO KANEKO¹, Isao Ohnishi², Masahiko Bessho², Takuya Matsumoto³, Satoru Ohashi³, Kenji Tobita³, Kozo Nakamura¹. ¹The University of Tokyo, Japan, ²Center for Clinical Medical Science International University of Health & Welfare, Japan, ³Department of Orthopaedic Surgery, University of Tokyo, Japan

Introduction

Quantitative computed tomography -based finite element methods (QCT/FEM) are reportedly able to accurately predict bone strength. We prospectively assessed the effects of alendronate(ALE) in patients with elderly osteoporosis by analyzing vertebral and proximal femur strengths using our originally developed QCT/FEM and calculated mean percent changes of bone strength at 6 and 12 months from baseline, and the data were compared to those from other existing bone densitometries.

Patients and Method

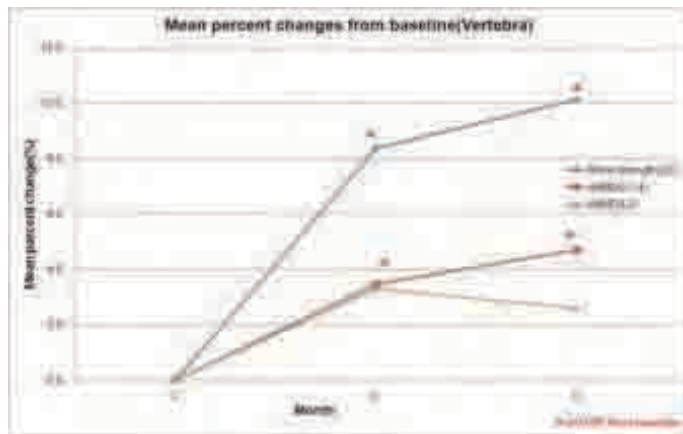
The inclusion criteria of patients included primary osteoporotic elderly Japanese women over 75 years of age. There were also exclusion criteria. The participants were treated using oral ALE at a dose of 35 mg/week. In patients who were enrolled in the study to assess the therapeutic effects of ALE, axial QCT with simultaneous scans of a calibration phantom containing hydroxyapatite rods, scans of the 2nd lumbar (L2) and proximal femur were obtained at baseline, 6, and 12 months. The bone strengths were analyzed using the QCT/FEM. The aBMD of the AP lumbar spine (L1-4) and the hip were measured by DXA at baseline, 6 and 12 months. The vBMD (L2) was analyzed using the QCT data (QCTpro). In the QCT/FEM analysis, a uniaxial compressive load with a uniform distribution and uniform load increment was applied for L2, and stance and fall configuration were applied for the proximal femur.

Results

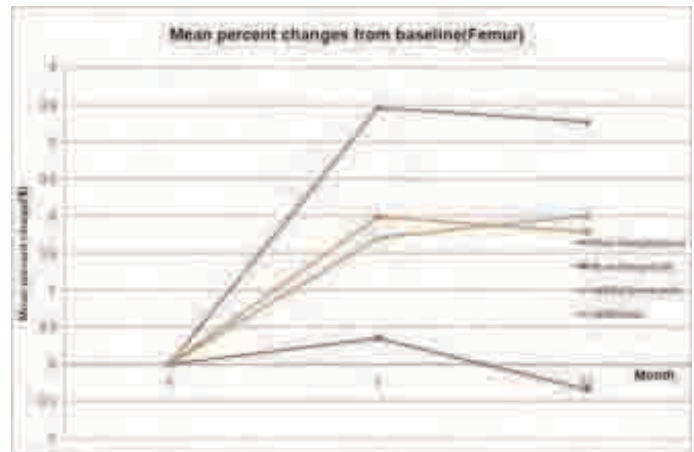
The participants were included 31 women (mean age, 79.5 years; range, 75-85 years). The proximal femur was analyzed in all and the lumbar spine in 25. 6 patients were excluded because a fragility fracture existed at L2. The mean percent changes from baseline in vertebral bone strength were +8.4% at 6 months, and +10.1% at 12 months, whereas they were +3.5%, and +4.7% in aBMD, and +3.3%, and +2.6% in vBMD. The mean percent changes from baseline in proximal femur strength under stance configuration were +3.5% at 6 months, and +3.3% at 12 months, and under fall configuration, were +0.36%, and -0.33%. The increases in aBMD (femoral neck) were +1.7%, and +2.0%, and those in aBMD (total hip) were +2.0%, and +1.8%, respectively.

Conclusions

In this study, vertebral bone strength by QCT/FEM was significantly more sensitive in evaluating the therapeutic effects of ALE than aBMD or vBMD. Proximal femur bone strength under stance configuration had greater sensitivity than aBMD. QCT/FEM is a highly useful and sensitive tool compared to existing densitometries.



graph1



graph2

Disclosures: MASAKO KANEKO, None.

SA0055

Relationships between Failure Patterns and Trabecular Architecture in the Thoracic Spine. Amira Hussein^{*}, Elise Morgan. Boston University, USA

Despite the high prevalence of vertebral fractures, their pathogenesis remains poorly understood. Studies have suggested that the mechanisms of vertebral fracture are closely linked to the substantial intra-vertebral heterogeneity in trabecular microstructure. However, this link has not been established. The overall goal of this study was to examine relationships between failure patterns and trabecular microstructure near the thoraco-lumbar junction.

Thirty, fresh-frozen vertebrae (15 T10, 15 T11) from 16 donors (age: 70-91 years; 8 male, 8 female) were scanned via μ CT (37 μ m/voxel). Volume fraction (Vf), apparent density (ρ_{app}), trabecular separation (Tb.Sp^{*}), trabecular number (Tb.N^{*}), connectivity density (ConnD), degree of anisotropy (DA) and structural model index (SMI) were calculated for contiguous, 5mm cubes within the centrum. The vertebrae were then compressed to failure, followed by a second μ CT scan. The pairs of pre- and post-test images were analyzed using digital volume correlation in order to quantify the failure patterns, as defined by the distributions of residual strains throughout the vertebral body. For statistical comparison via analysis of covariance, the microstructural values and residual strains for the cubes were grouped by anatomic location: 1) superior, middle, or inferior transverse plane; and 2) posterior, middle, or anterior coronal plane.

Residual strains were highest in the middle transverse plane ($p=0.002$), particularly in the anterior region of this plane. Near the superior endplates, higher residual strains occurred in the center as compared to the periphery; a similar, though milder, trend was found near the inferior endplate. High residual strains were associated with low values of SMI (more plate-like trabeculae) ($p=0.02$). Residual strains were also dependent on the interaction between anatomic location and each of Tb.N^{*} and Tb.Sp^{*} ($p\leq 0.002$).

These findings reveal failure patterns characterized by anterior wedge-type deformations and concomitant endplate biconcavity in response to axial compression. Although regions of sparse, rod-like trabeculae in the vertebra have often been hypothesized to be those at greatest risk for failure, our results instead indicate that failure patterns involve regions of more plate-like trabeculae. Together, these results suggest that the mechanisms of vertebral fracture relate to both the anatomic shape of the vertebra and the intra-vertebral distribution of trabecular architecture.

Disclosures: Amira Hussein, None.

SA0056

Strontium Ranelate Fully Prevents Alteration of Bone Mechanical Properties in Response to Cyclical Loading. Patrick Ammann^{*}¹, Rene Rizzoli².

¹Division of Bone Diseases, Switzerland, ²University Hospital, Switzerland

Microarchitecture and intrinsic bone tissue properties contribute independently and significantly to the improvement of bone strength induced by strontium ranelate (SrRan) treatment as evaluated by μ CT-based Finite Element Analysis. How improvement of bone material quality by SrRan could influence bone mechanical properties is unknown. One hypothesis is that SrRan present in bone tissue could prevent the formation of micro cracks and/or their propagation, thus influencing the capacity of the bones to cumulate micro-damage. The aim of the present study was to investigate whether SrRan could prevent alteration of bone mechanical properties in response to fatigue as evaluated at the level of vertebrae. Vertebrae of intact female rats treated 5 days a week over 12 weeks with SrRan at a dose-level of 625 mg/kg (corresponding approximately to the human SrRan exposure) or with a vehicle (control) were in silico cyclically loaded in axial compression under a controlled load for 100 cycles. The selected peak load corresponded to 5% of the maximal load of the adjacent vertebra, thus in the domain of elastic deformation. This peak load was determined to induce alteration of post yield load without any effects on vertebral

height i.e without fracture. The vertebrae were then loaded to failure. We compared the load/displacement curve of the cyclically loaded vertebra (L4) to the adjacent one (L3), not submitted to cyclic loading. Bone mechanical properties including post-yield load and deflection, which characterize post yield behaviour, were investigated. * $p < 0.05$ as compared to control unloaded adjacent vertebra (meanSEM). Maximal load was 26719 and 23320 (N) in unloaded SrRan and Control groups, respectively. Cyclic loading induced a deterioration of post Yield load (-40%) in control rats. This effect was fully prevented in SrRan-treated rats. The post Yield deflection was unaffected in either group. These results indicate that fatigue-induced alterations of post yield behaviour were fully prevented by SrRan treatment. They may also suggest that bone micro-damages could be less prominent in rats treated with SrRan (histological analysis is in progress). In conclusion, the improvement of bone intrinsic mechanical properties by SrRan could influence the response to cyclical loading (fatigue) and thus represents an original mechanism of action.

	Unloaded control	Fatigue control	Unloaded SrRan	Fatigue SrRan
Post Yield load (N)	19.61±3.36 (n=9)	11.80±2.03 (n=9)*	18.42±4.00 (n=8)	18.78±3.71 (n=8)
Post Yield deflection (mm)	0.067±0.007 (n=9)	0.073±0.017 (n=9)	0.063±0.011 (n=8)	0.072±0.012 (n=8)

table

Disclosures: Patrick Ammann, servier, 2
This study received funding from: Servier

SA0057

Synchrotron Radiation Micro-CT of Intra-Element Variation in Osteocyte Lacunar Volume and Density of the Human Femur. Yasmin Carter^{*1}, DAVID THOMAS², John G. Clement³, Andrew G. Peele⁴, Kevin Hannah⁴, David Cooper¹. ¹University of Saskatchewan, Canada, ²MELBOURNE DENTAL SCHOOL, Australia, ³University of Melbourne, Australia, ⁴LaTrobe University, Australia

In recent years there has been growing interest in the properties of osteocytes (including density and morphology) and how these potentially relate to adaptation, disease and aging. This interest has, in part, arisen from the availability of increasingly high resolution 3D imaging modalities such as synchrotron radiation (SR) micro-CT. As resolution increases, field of view generally decreases. Thus, while increasingly detailed spatial information is obtained, it is unclear how representative this information is of the skeleton or even the isolated bone. The purpose of this research was to describe intra-element variation in osteocyte lacunar density and volume within a healthy young (20 yr old male) human femur. Anterior, posterior, medial and lateral blocks (2 mm x 2 mm) were prepared from a diaphyseal ring of the proximal femoral shaft. These blocks (n=3, 3, 3 and 4, respectively) were SR micro-CT imaged using the 2BM beamline of the Advanced Photon Source synchrotron at 1.47µm pixel size. A cylindrical 0.786mm³ region of interest was analyzed for each block. SR micro-CT enabled tens of thousands of lacunae (mean of 31,461 per block) to be assessed in 3D. Average lacunar density (standard deviation) from the anterior, posterior, medial and lateral regions was 27,169/1935, 26,343/1262, 37,521/6416 and 33,972/2513 lacunae per mm³ of bone tissue, respectively. These values were significantly different between the medial and both the anterior and posterior regions ($p < 0.05$). The density of the combined anterior and posterior regions (26,756/1529) was also significantly lower ($p = 0.001$) than the combined density of the medial and lateral regions (35,493/4525). There were no significant differences ($p = 0.862$) between mean lacunar volumes (anterior 378µm³, posterior 400µm³, medial 409µm³ and lateral 408µm³). The results indicated that variation in osteocyte lacunar density, even within a single bone of a single individual, can be considerable (up to 30% between regions). The underlying functional significance of the observed variation in lacunar density is unclear, but it may relate to axes of mechanical loading - a hypothesis we believe warrants further study. Our findings demonstrate that the functional and pathological interpretations which are increasingly being drawn from high resolution imaging of osteocyte lacunae need to be better situated within the broader context of normal variation, including that which occurs within a single skeletal element.

Disclosures: Yasmin Carter, None.

SA0058

See Friday Plenary Number FR0058.

SA0059

See Friday Plenary Number FR0059.

SA0060

Type 1 Diabetes Mellitus Effects on Bone: Preliminary Results of Peripheral Quantitative Computed Tomography (pQCT) Analysis. Robert Recker¹, Diane Cullen², Laura Armas^{*2}. ¹Creighton University Osteoporosis Research Center, USA, ²Creighton University, USA

Diabetes Mellitus has a detrimental effect on the body's microvascular system affecting the kidneys, eyes and nerves. The effect on bone is less well known. Patients with Type 1 diabetes have lower bone mass and higher fracture risk than age and sex matched controls. The effect of diabetes on bone micro-architecture is not well elucidated. We report here preliminary results of 29 diabetic subjects (19 females, 10 males, ages 20-50) with Type 1 diabetes for a median of 19 years and 30 controls (20 females, 10 males, ages 20-46). The subjects were otherwise healthy without diabetic complications and the females were premenopausal. The Stratec XCT 3000 (Norland, White Plains NY) was used to measure the non-dominant distal tibia at the 4, 38 and 66% sites and at the 4 and 30% sites on the non-dominant radius. Measurements of the total bone area, total marrow area, cortical bone area, trabecular bone area, density and predicted strength density were obtained at these 4 sites. Descriptive statistics were calculated and ANOVA was used to test differences between diabetics and controls. Pearson correlation was used to find correlations between variables. There were no significant differences between diabetics and controls in cortical measurements at either the radius or the tibia. The trabecular bone density at the radius was diminished in the diabetics ($P = 0.009$). While the sample size was small, there was also a trend in the diabetic group for low total and trabecular area with decreased predicted bone strength at the 4% radius site ($P < 0.1$). Trabecular measures of density were highly correlated between the tibia and radius ($P < 0.001$) and a trend was also detected for lower trabecular density in the tibia 4% site of diabetic patients. In this group of healthy diabetics, the main effect of the disease is on the trabecular variables. The link between diabetic complications and bone fractures is unknown. Based on this sample of diabetics who have no known diabetic complications, there may be an early direct or indirect effect of diabetes on bone health.

Disclosures: Laura Armas, None.

SA0061

See Friday Plenary Number FR0061.

SA0062

See Friday Plenary Number FR0062.

SA0063

See Friday Plenary Number FR0063.

SA0064

Material Characterization of Bone Matrix in Rats: Effect of Treatment and Treatment Withdrawal. Daniel Nicoletta^{*1}, Ryan Potter¹, Don Moravits¹, Wei Yao², Nancy Lane². ¹Southwest Research Institute, USA, ²University of California, Davis Medical Center, USA

Bone strength depends on complex and interrelated characteristics of the bone matrix, the organization of the bone tissue, the shape of the bone, and bone density. The physicochemical and micromechanical properties of bone in aged rats subjected to various treatments and treatment-withdrawals were studied.

Methods. 12-month-old female rats were either ovariectomized (OVX) or sham operated and allowed to develop osteopenia for 2 months. The treatment groups studied were: 6 months OVX + vehicle (n=4) and 6 months post-sham operated (n=3), 4 months of treatment of either alendronate (OVX+ALN, n=4), Raloxifene (OVX+RAL, n=4), or hPTH (1-34) (OVX+PTH, n=4). Also, we characterized cortical and trabecular bone from animals from the following additional groups: 4 months treatment followed by both 4 and 8 months of treatment withdrawal from the sham, OVX, OVX+ALN, OVX+RAL, OVX+PTH groups. Using Raman spectroscopy, we measured the mineralization, carbonate substitution, crystallinity, and collagen cross links of bone matrix and nanoindentation was used to measure local bone modulus and hardness at the proximal tibia.

Results. Compared to the OVX group, matrix mineralization of the OVX+RAL treatment group was higher after 4 months of treatment (12.6 vs. 14.6, $p = 0.001$); the other groups were not different from the OVX group. 8 months after treatment withdrawal, tissue mineralization for the OVX+PTH treatment group was significantly lower than the OVX group (14.0 vs. 12.6, $p = 0.018$); all other groups were not different than OVX. Mineral crystallinity was significantly greater after 4 months of treatment in the OVX+PTH and OVX+RAL groups compared to OVX alone; at 8 months after treatment withdrawal, OVX+ALN, OVX+PTH, and OVX+RAL were greater than OVX. Tissue modulus was unchanged after 4 months treatment in all treatment groups compared to OVX; tissue hardness was greater in the OVX+ALN (0.995 GPa, $p = 0.006$) and OVX+RAL (0.947 GPa, $p = 0.046$) groups compared to OVX (0.83 GPa). 8 months after treatment withdrawal, tissue hardness increased in

the OVX (1.0GPa), $p=0.012$ group compared to the sham group (0.85 GPa). These data indicate that the effect of treatment and treatment-withdrawal on the bone matrix is complex and each treatment type and/or regimen alters the matrix differently. This data emphasizes that bone strength is not a function of a small number of traits or factors, but can be affected by combinations of traits/factors acting at multiple length scales.

Disclosures: Daniel Nicoletta, None.

SA0065

Risedronate Improves Bone Architecture in Goto-Kakizaki Rats, a Spontaneous Non-obese Model of type 2 Diabetes. Tetsuo Yano^{*1}, Mei Yamada¹, Tomoyuki Konda², Makoto Shiozaki¹, Daisuke Inoue³. ¹Ajinomoto Pharmaceuticals Co., LTD, Japan, ²Ajinomoto Pharmaceuticals Co., LTD., Japan, ³Teikyo University Chiba Medical Center, Japan

Background/Aim: Patients with type 2 diabetes exhibit decreased bone strength and increased fracture risk in part independently of bone mineral density (BMD). However, the molecular basis of the bone fragility and specific treatment for such diabetes-associated osteoporosis remain to be established. A previous report has demonstrated that alendronate (ALN) did increase BMD in patients with type 2 diabetes, but whether or not ALN and other bisphosphonates improve bone quality in diabetic subjects is unknown. The aim of the present study was to establish the ability of bisphosphonates to improve bone quality in type 2 diabetes by analyzing effect of risedronate (RIS) on bone architecture as compared to that of ALN in Goto-Kakizaki (GK) rats.

Methods: GK rats, a spontaneous non-obese model of type 2 diabetes, and Wistar rats as a control were used. Starting at 36 weeks of age the rats received treatment for 12 weeks with either vehicle, RIS, or ALN, subcutaneously, once a week. After 4 and 12 weeks of treatment, bone architecture in distal epiphysis of the femur and femoral diaphysis was examined by micro CT.

Results: Development of diabetes was confirmed just prior to the initiation of treatment, as blood glucose concentrations were significantly increased in GK rats compared with Wistar rats both under a fasting condition and after oral glucose challenge. In GK rats compared with Wistar rats, trabecular BMD (~25% at 12 weeks), bone volume fraction, trabecular number, trabecular separation (Tb.Sp) and connectivity density (Conn.D) were significantly decreased, and structure model index was significantly increased, indicating transition from plate-like architecture of trabeculae to a more rod-like structure. Analysis of cortical bone revealed increased periosteal perimeter, but there was no significant decrease in cortical thickness or BMD. We found that at 12 weeks RIS significantly improved Tb.Sp and Conn.D., while no significant effect of ALN was detected in any bone parameters measured. Neither RIS nor ALN had statistically significant effect on cortical bone architecture.

Conclusion: GK rats developed osteopenia predominantly in trabecular bone. And RIS significantly improved parameters of bone architecture. We therefore conclude that bisphosphonate, particularly RIS, can be effective treatment of osteoporosis associated with type 2 diabetes by improving both bone mass and quality.

Disclosures: Tetsuo Yano, Ajinomoto Pharmaceuticals, 3

SA0066

See Friday Plenary Number FR0066.

SA0067

See Friday Plenary Number FR0067.

SA0068

See Friday Plenary Number FR0068.

SA0069

See Friday Plenary Number FR0069.

SA0070

See Friday Plenary Number FR0070.

SA0071

See Friday Plenary Number FR0071.

SA0072

See Friday Plenary Number FR0072.

SA0073

See Friday Plenary Number FR0073.

SA0074

See Friday Plenary Number FR0074.

SA0075

Adenylyl Cyclase 6 Mediates In Vivo Mechanotransduction In Bone. Kristen Lee^{*1}, Dr. David A. Hoey¹, Dr. Tong Tang², Dr. H. Kirk Hammond², Christopher Jacobs¹. ¹Columbia University, USA, ²University of California San Diego, USA

Mechanical loading is an important stimulus that modulates bone development and adaptation. However the molecular mechanisms that regulate mechanotransduction in bone are unknown. Adenylyl cyclase 6 (AC6) is a membrane-bound enzyme isoform that is responsible for converting ATP into cAMP, a second messenger. Previously, we demonstrated that 2 minutes of oscillatory fluid flow induced a decrease in cAMP which was dependent on AC6 in MLO-Y4 osteocyte-like cells. This transient decrease in cAMP resulted in a subsequent increase in COX2, a gene involved in bone metabolism and turnover. The purpose of this study was to determine the in vivo role of AC6 in adult bone adaptation. Our hypothesis was that the loss of AC6 in vivo would inhibit mechanical load-induced bone formation. Virgin C57BL/6J transgenic mice with global deletion of AC6 and intact littermate controls were anesthetized and placed under compressive axial loading of the ulna characterized by 120 cycles per day with a 2Hz sine wave at 3N for Days 1-3. Right limbs were loaded while left limbs were not loaded and served as controls for normal cage activity. On Day 5 and 9, mice were subcutaneously injected with Calcein (10 mg/kg) and Alizarin Red (70 mg/kg), respectively. Mice were sacrificed on Day 15, and right and left ulnae were removed and embedded in PMMA. Sections were taken at the mid-shaft and images for histomorphometric analysis were captured using confocal microscopy (see Fig. 1). AC6 knockout mice (n=2) demonstrated a decreasing trend in relative MS/BS (%), MAR ($\mu\text{m}/\text{day}$), and BFR/BS ($\mu\text{m}^3/\mu\text{m}^2/\text{year}$) compared to control mice (n=3). Therefore our preliminary study indicates that AC6 is involved in mechanical loading-induced bone formation. Collectively, this data suggest that AC6 plays a role in the adaptation of adult bone to mechanical stimulus in vivo. Acknowledgements: Funding for this work was provided by NIH grants AR45989 and AR45156 and the NSF Graduate Research Fellowship.

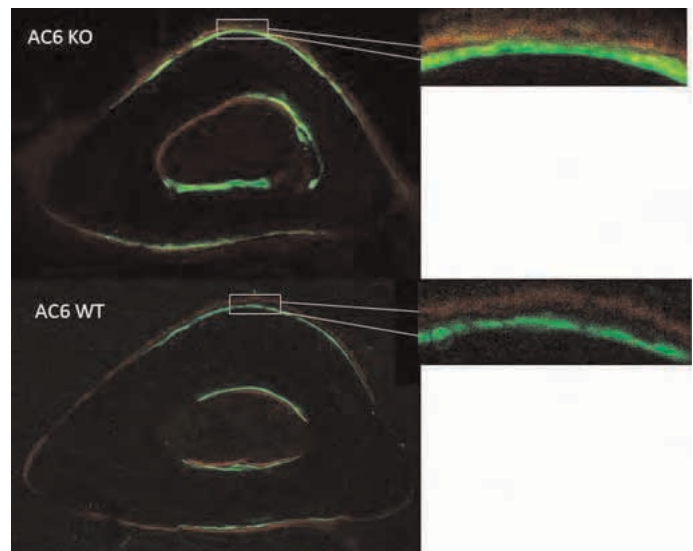


Figure 2: Dynamic histomorphometry images with Calcein (green) and Alizarin Red (red) labels in AC6 knockout and wildtype mice following ulna compressive loading.

Figure 2

SA0077

Effects of A 16-Week Obesogenic Diet Program on Bone Densitometry, Microarchitecture and Metabolism in Male Rat. Maude GERBAIX¹, Aurelie MASGRAU², Fabrice MAC WAY³, Christelle GUILLET², Stephane WALRAND², Marie Therese LINOSSIER³, Laurence Vico⁴, Daniel Courteix⁵, Lore METZ¹. ¹Laboratoire de Biologie des APS, EA 3533, PRES Clermont Université, Université Blaise Pascal, 24 avenue des Landais, France, ²Unité de Nutrition Humaine, UMR 1019, INRA/ Université d'Auvergne, France, ³Laboratoire de Biologie du Tissu Osseux, Inserm U890/IFR143, université de Lyon, France, ⁴University of St-Etienne, France, ⁵Université Clermont Ferrand Laboratoire De Biologie Des APS, France

A high-fat/high-sucrose acute diet has been shown to induce harmful effects on bone micro architecture and bone biomechanics of rat. If such chronic diet leads to obesity it may induce an improvement of biomechanical bone parameters.

The aim of this study was to assess the impact of a high-fat/high-sucrose diet on the body composition and its resulting effects on bone in male rats.

43 Wistar rats aged 7 months were split into 3 groups: 1 subjected to 16 weeks of high-fat/high-sucrose diet (HF/HS, n=14); 1 subjected to standard diet (Control, n=15) and 1 sacrificed before diet (BD, n=14). The body composition with specific central fat mass has been assessed by DXA every 3 weeks for the period of diet. One week before sacrifice, body composition, abdominal circumference and insulin sensitivity were measured. Visceral fat mass was assessed by weighing the total perirenal and peri-epididymal adipose tissues.

The bone mineral density (BMD) was analyzed at the whole body and tibiae by DXA. Microcomputed tomography and histomorphometric analysis were performed at L2 vertebrae and tibiae to study the trabecular and cortical bone structures and the bone cell activities. Osteocalcin and CTx were assayed to calculate the bone uncoupling index (UC) as suggested by Eastell et al.[1], in order to assess the relative balance of the formation and resorption processes of bone remodeling.

The HF/HS and Control groups had increased their total and abdominal fat mass and decreased bone parameters compared to BD group. The HF/HS group had higher body mass, global, central and visceral fat masses and abdominal circumference compared with Control group ($p < 0.001$). Insulin resistance appeared in HF/HS group. Bone mass ($p < 0.001$) and BMD ($p < 0.05$) were higher at the whole body and the cortical porosity was improved ($p < 0.05$) for HF/HS group vs. Controls. When adjusted for the total fat mass, all these differences disappeared. UC was positive (favor of bone formation) in HF/HS and negative (favor of bone resorption) in Controls.

The ageing process had increased the fat mass and produced deleterious effects on bone tissue in both groups. The HF/HS diet had induced obesity and insulin resistance also. These changes were linked to an improvement of quantitative and metabolic bone parameters. The fat mass increase partly explained these observations.

1 Eastell R, et al. Osteoporosis Int 1993; 3: 255-260.

Disclosures: Daniel Courteix, None.

SA0078

See Friday Plenary Number FR0078.

SA0079

See Friday Plenary Number FR0079.

SA0080

Translating the Strain Stimulus Equation from Animals to Humans. William Edwards, Karen Troy*. University of Illinois at Chicago, USA

Mechanical loads make an important contribution to bone health. The strain stimulus equation, $E = k \cdot \epsilon \cdot f$, was proposed to describe the relationship between mechanical loading environment and the resulting bone adaptive response. Here, ϵ is bone strain magnitude, f is the frequency of the loading waveform, and k is a proportionality constant. This equation appears to be valid in controlled animal experiments but has never been prospectively tested in humans.

Our purpose was to evaluate the applicability of the strain stimulus equation in humans. We hypothesized that subjects with larger strain stimulus values would experience greater increases in bone mineral content (BMC) after a 14-week mechanical loading regime.

Thirteen subjects (8 young and 5 postmenopausal women) participated in this institutionally approved study. Each applied an axially-directed force of 300 N to the palm of her non-dominant hand. With assistance from sound cues and visual feedback, subjects completed 50 cycles/day, 3 days/week. BMC was measured at weeks 0 and 14. Subjects applied either "rapid" or "slow" (i.e. high or low frequency) loading waveforms to achieve a range of strain stimuli.

Computed tomography data were acquired at baseline and validated techniques were used to generate subject-specific finite element (FE) models. These models, combined with load cell recordings, were used to calculate subject-specific values of

rBFR/BS

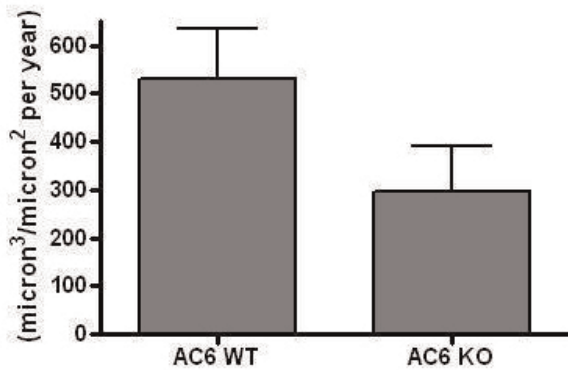


Figure 1. Relative BFR/BS of wildtype mouse and AC6 knockout mouse ulnae in response to mechanical loading in vivo (mean \pm SEM).

Figure 1

Disclosures: Kristen Lee, None.

SA0076

Diet and Exercise Affect Postcranial - but Not Cranial - Robusticity in Mice.

Lynn Copes¹, Margaret R. Brown¹, Elizabeth M. Dlugosz², Stefan Judex³, Svetlana Lublinsky³, Aleksandra Oldak⁴, Heidi Schutz⁴, Steven Tommasini³, Katie Whitmore¹, Theodore Garland². ¹Arizona State University, USA, ²University of California, USA, ³Stony Brook University, USA, ⁴California Polytechnic University, USA

Modern *Homo sapiens* show a recent, but dramatic, decrease in cranial vault thickness (CVT) relative to earlier hominin ancestral species. Two competing hypotheses for this hypertrophy involve 1) a hormonal increase mediated by exercise and causing systemic increases in skeletal robusticity, and 2) a localized effect of increased masticatory stress causing only an increase in CVT. We tested these hypotheses by manipulating the exercise and diet of several groups of mice.

In the exercise study, 50 female mice from lines artificially selected over 60 generations for endurance running ability and 50 female controls were split between cages with wheel access and no wheel access. The study began at weaning and lasted 3 months, after which skeletal elements were harvested at the conclusion of the experiment, and the humerus, femur, mandible, parietal and interparietal bones were scanned via desktop μ CT at 36 μ m. No significant differences in CVT were seen among groups, and no relationship between activity or hormone levels and CVT were found. Postcranial bones were significantly more robust in the selected mice than in controls, however.

A second experiment with similar parameters used 50 inbred and 50 wild-type female mice, divided at weaning into soft, cold, and control diet groups. The soft diet group was fed food the consistency of dough, while the cold group was housed in a 10C room in order to manipulate their food consumption by increasing resting metabolic rate. The inbred mice in the cold group had significantly lower CVT than other groups (0.19 mm mean vs. >0.21 mm; $p = 0.04$), but no other differences were found. While masseter mass differed significantly among the groups (soft < control < cold), its association with CVT was insignificant. Inbred and outbred strains showed identical variation in the trait, suggesting a very strong genetic control of its development. There were significant differences in postcranial robusticity, mostly related to differences in body mass. No relationship was found between hormone levels and CVT.

Our data suggest that the cranium is less sensitive than postcrania to environmental perturbations affecting muscle mass and hormone changes. Studies of morphological, hormonal, and behavioral correlates with cranial vault thickness in non-human primates and humans are needed to further establish the relative plasticity of the trait and its associations in our species.

Disclosures: Lynn Copes, None.

strain stimulus. Strain magnitude, ϵ , was assigned the peak strain predicted within the volume of the distal radius. This value was normalized and multiplied by a weighted sum from the frequency spectrum of the load cell signal. The constant k was assigned a value of 1. Pearson's correlations were calculated to compare change in BMC to strain stimulus.

Change in BMC was correlated with strain stimulus ($r=-0.735$, $P=0.004$, Figure 1). The greater the strain stimulus, the greater the resorptive response at 14 weeks. This is consistent with our previous reports of a temporary decrease in cancellous BMC in a separate group of subjects. High strain stimulus values may be associated with localized trabecular damage and the initiation of a remodeling and repair response that involves resorption. More data is needed to determine if strain stimulus is related to chronic changes in BMC.

In summary, we have developed methods to noninvasively quantify strain stimulus, and have shown that short-term changes in bone mass are related to strain stimulus in young and older women.

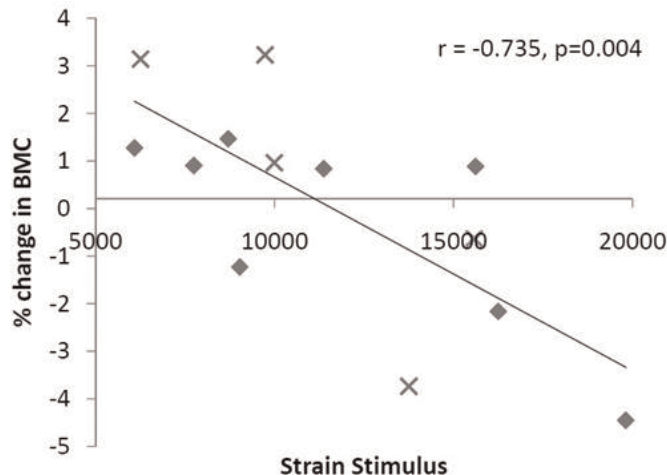


Figure 1 Strain stimulus versus change in BMC for 13 subjects. X symbols are for postmenopausal subjects and \blacklozenge is for younger subjects.

Figure 1

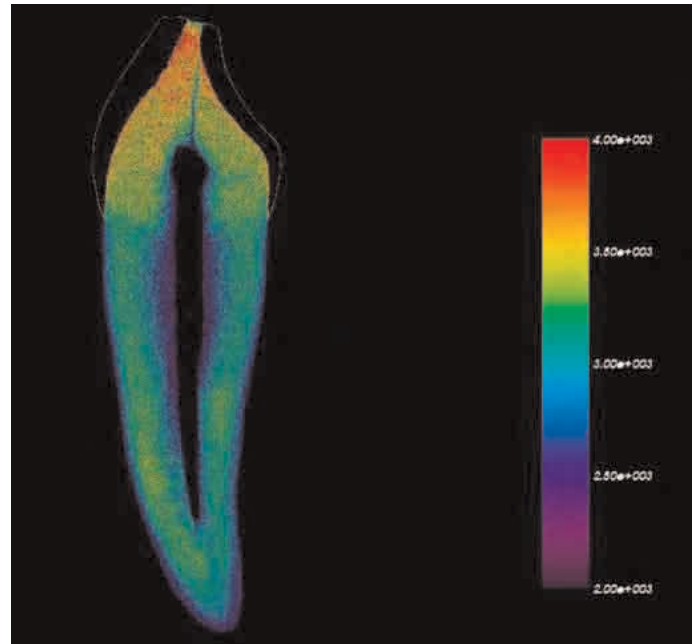
Disclosures: Karen Troy, None.

SA0081

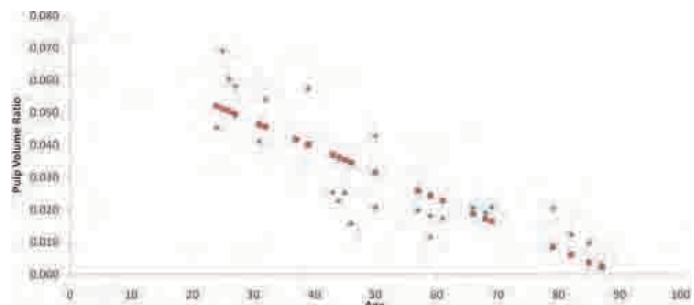
Advanced Imaging to Assess Age-Induced Mineralization Changes in Teeth.

Dana Begun¹, Rachel Caspari², Rihana Bokhari³, Kristina Galdes⁴, Steven Goldstein⁵. ¹University of Michigan Orthopaedic Research Lab, USA, ²Department of Anthropology, Central Michigan University, USA, ³University of Michigan, USA, ⁴University of Montana, USA, ⁵University of Michigan Orthopaedic Research Labs, USA

Dental remains are less susceptible to taphonomic changes, and thus are useful in estimation of age-at-death in forensic and archaeological inquiries. However, age estimates past dental maturity are often subjective and require destruction of the specimen. With aging, a number of alterations occur in the mineralization patterns of the teeth. Vascular root tubules become occluded with mineral deposit. The homogenization of density creates a translucent appearance when backlit. Another product of aging is the deposition of secondary dentine which results in a reduction of the pulp cavity volume. The purpose of this study is to validate the utility of micro-computed tomography and Raman spectroscopy in age estimation of teeth. The age-related parameters of root transparency, secondary dentine, root resorption, and enamel wear are quantified with these imaging modalities and accuracy of results compared to previous methods. With the development of these methods, regressions for the rate of modification with age can be elucidated and used to estimate ages in unknown remains. Medial and lateral incisors, as well as canines, were loaned by the University of Tennessee. The sample included 31 individuals of known age, ranging from 24 to 87. Previously developed manual measures of transparency, wear, and root attrition were taken by 3 individuals. Additionally, teeth were scanned in a specimen μ CT scanner (GE Healthcare Preclinical Imaging) at $27\mu\text{m}$ resolution. A global threshold was defined for dentine and enamel. A custom probe holder was used to take surface and offset Raman measures at increments along the tooth root. Manual measures of enamel wear did not accurately estimate age. Hand-taken transparency height was positively related to age (canines: $\beta=0.1073$, $p=5.977E-05$). However, due to inter-observer error, there was a high level of variance in multiple measures. μ CT measures of enamel and root attrition were not significantly related to age. Pulp volume ratio was inversely related to chronological age (canines: $\beta=-0.0008$, $p=1.972E-07$). Histogram analysis of Hounsfield values was also able to make similar transparency height estimates as those taken by hand. These methods provide more accurate and non-destructive approaches for assessing age in forensic and archaeological remains. Here we present results that establish the reliability of μ CT and Raman as substitutes for destructive and semi-quantitative techniques.



Gradient of tooth mineralization



Observed and expected values for canine pulp volume regression

Disclosures: Dana Begun, None.

SA0082

New Method for *in vitro* Glycation of Proteins. Grazyna Sroga*, Deepak Vashishth, Robert Davignon. Rensselaer Polytechnic Institute, USA

Glucose and other reducing sugars react with proteins *in vivo* and *in vitro* by a slow non-enzymatic process termed glycation. As a result crosslinks, known as advanced glycation end products (AGEs), are formed within and between proteins [1, 2]. The formation of AGEs in long-lived tissues such as bone mainly accounts for the increase of collagen crosslinking. This process accompanies normal aging and is accelerated in diabetes. Accumulation of AGEs causes age-related degradation of the bone's mechanical properties. The time-frame for *in vitro* glycation of bone samples using glucose ranges from a few weeks to several months [3]. The goal of the current work was to develop an efficient *in vitro* glycation method that uses glucose instead of more reactive ribose as a substrate and efficiently glycates a given protein within a few days.

Using a novel combination of several methods, we first attached glucose under *in vacuo* conditions to a protein, and then, converted it into pentosidine (PEN) within 8 to 9 days. Total AGEs were measured using fluorescent-based colorimetric assay and ultrahigh pressure liquid chromatography (UPLC) [4].

We determined that the amount of produced total AGEs increased over the experimental period and reached a plateau by the 7th day. PEN followed the same trend, but reached the plateau at the later time point.

In summary, we developed a new *in vitro* glycation method that uses less reactive sugar (glucose) than ribose and is more physiologically relevant. The novelty of our method lies in the introduction of *in vacuo* incubation of protein samples, with glucose as the first reaction step. This approach significantly speeds up the glycation process (2 weeks) as compared to a standard "in solution" method that takes over 5 months [3].

[1] Bank et al, *Biochem. J.* 330 (1998) 345-351. [2] Vashishth et al, *Bone* 28 (2001) 195-201. [3] Voziyan et al, *J. Biol. Chem.* 278 (2003) 46616-46624. [4] Sroga & Vashishth, *J. Chromatogr. B* 879 (2011) 379-385.

Disclosures: Grazyna Sroga, None.

SA0083

Bone Tissue Mineral Content Is Greater in the Subtrochanteric Cortex Than in the Trochanteric or Iliac Crest Cortices. Eve Donnelly*, Dennis Meredith, Joseph Nguyen, Adele Boskey. Hospital for Special Surgery, USA

Pathologic changes in bone composition with osteoporosis are typically assumed to occur throughout the skeleton, and not only at sites that fracture, as evidenced by the diagnostic use of biopsies of the iliac crest, a site that rarely fractures. However, the extent to which bone tissue composition varies across anatomic sites in normal or pathologic tissue is unknown. Our objective was to compare the composition of normal cortical and cancellous bone tissue across anatomic sites in the iliac crest and proximal femur. We hypothesized that the tissue composition of the iliac crest is representative of that of the proximal femur.

In an IRB-approved study, cadaveric tissue from 3 sites (iliac crest, greater trochanter, and sub-trochanter) was collected from 10 donors (sex: 3 M, 7 F; age: 53-90 y, mean 69 SD 12 y) with no history of bone disease. Cortical and cancellous regions were analyzed separately with Fourier transform infrared imaging (FTIRI) to assess the mineral:matrix ratio, carbonate:phosphate ratio, collagen cross-link maturity, and mineral crystallinity (XST). The pixel histograms of the FTIR images of each parameter were characterized by their mean and full width at half maximum (FWHM) values.

The mean mineral:matrix ratio was greater in the subtrochanteric cortex than in the cortices of the iliac crest (+20%) or the greater trochanter (+20%) (Table 1). There were also trends that did not reach statistical significance toward reduced width of the mineral:matrix distributions in the subtrochanteric cortex vs. iliac crest (-17%) and increased width of the XST distributions in the subtrochanteric trabeculae vs. iliac crest (+30%) and greater trochanter (+30%). The mean and FWHM values of all other FTIR parameter distributions were similar across sites.

Bone tissue composition differed across anatomic sites in the iliac crest and the proximal femur. In particular, bone mineral content was 20% greater in the subtrochanteric cortex than in the trochanteric or iliac crest cortices. Thus, in non-pathologic cadaveric bone, the cortex of the iliac crest has reduced mineral content relative to subtrochanteric tissue and may have limited utility as a surrogate for subtrochanteric bone.

Table 1: FTIR parameter distribution mean and full width at half maximum (FWHM) values reported as mean (SD) for iliac crest (IC), greater trochanter (GT), and subtrochanteric (ST) sites. * p < 0.05 vs. GT, ST; ^ p < 0.2 vs. GT, ST; ^^ p < 0.2 vs. GT by RM-ANOVA.

		Mineral: Matrix		Carbonate: Phosphate		Collagen Maturity		Crystallinity	
		Mean	FWHM	Mean	FWHM	Mean	FWHM	Mean	FWHM
		(SD)	(SD)	(SD)	(SD)	(SD)	(SD)	(SD)	(SD)
Cortical	IC	4.7	2.0	0.0092	0.0039	3.8	0.50	1.2	0.12
		(0.7)	(1.0)	(0.0009)	(0.0015)	(0.4)	(0.19)	(0.04)	(0.03)
	GT	4.7	2.1	0.0090	0.0037	3.7	0.52	1.2	0.15
		(0.6)	(0.6)	(0.0007)	(0.0006)	(0.3)	(0.14)	(0.04)	(0.05)
Trabecular	ST	5.7*	1.5^^	0.0092	0.0033	3.8	0.43	1.2	0.10
		(0.6)	(0.4)	(0.0010)	(0.0011)	(0.4)	(0.11)	(0.03)	(0.04)
	IC	4.1	2.2	0.0083	0.0042	3.8	0.54	1.2	0.13
		(0.5)	(0.5)	(0.0009)	(0.0010)	(0.5)	(0.22)	(0.03)	(0.01)
Trabecular	GT	4.4	1.8	0.0081	0.0035	3.8	0.48	1.2	0.13
		(0.8)	(0.4)	(0.0014)	(0.0019)	(0.4)	(0.13)	(0.04)	(0.02)
	ST	4.3	1.9	0.0088	0.0042	4.0	0.48	1.2	0.17*
		(0.5)	(0.4)	(0.0009)	(0.0012)	(0.3)	(0.12)	(0.04)	(0.03)

Table 1

Disclosures: Eve Donnelly, None.

SA0084

Mineral and Matrix Changes in Brlt/+ Bones and Teeth Provide Insight into Mineralization Mechanisms. Adele Boskey*¹, Lyudmila Spevak¹, Lyudmila Lukashova¹, Kostas Verdelis¹, Joan Marini². ¹Hospital for Special Surgery, USA, ²Bone & Extracellular Matrix Branch, NIH/NICHD, USA

The Brlt/+ mouse is a knock-in model for osteogenesis imperfecta (OI) type IV in which a Gly349Cys substitution was introduced into one colla1 allele, resulting in a phenotype representative of the disease. Changes in whole bone mechanical strength and collagen d- spacing in the Brlt/+ mice have previously been reported (Kozloff et al., 2004; Wallace et al., 2010). In this study we compared the bones and teeth of 2 month old wildtype (+/+) and Brlt/+ mice using micro-computed tomography (micro-CT; teeth) and infrared microscopic imaging (bones/teeth). The teeth of the Brlt/+ animals were visually different when examined by micro-CT with significant (p<0.05) increases in Brlt/+ crown total mineral density and decreased dentin, enamel, and root volumes, and decreased mineralized tissue volume/total volume in the roots; all indicative of delayed matrix formation. Fourier transform infrared imaging (FTIRI) showed mineral/matrix ratio was also increased in the Brlt/+ molars, which had previously been reported to have an odontogenesis imperfecta phenotype (Forlino et al., 1999). These data represent the first quantitative evaluations of the teeth in the Brlt/+ mice.

FTIRI was used to map the chemical composition of the bones at ~6 micron spatial resolution. While there were no statistically significant differences in global FTIRI parameters in the bones (tibias), the collagen spectra were broadened and differed in shape from the WT. To define the origin of the broadening, factor analysis of the collagen spectra from the trabecular region was used. An increase was noted in a subband at 1640 cm⁻¹; the ratio of the intensity of the 1640 cm⁻¹ subband to that of the major collagen band at 1660 cm⁻¹ varied from 0.800.02 in Brlt/+ to 0.770.02 in +/+ (p=0.02), with a similar but marginally significant trend (p=0.10) in cortical bone. This change suggests disruption of the collagen 310 helix in the Brlt/+ bones. The measured changes in FTIRI mineral/matrix ratio in both cortical and cancellous bone paralleled the bone mineralization density distribution (BMDD) measurements of Camean reported elsewhere. The increases in mineralization in the developing bones and teeth, along with the altered collagen structure imply that the hypermineralization in classical OI is associated with an abnormal collagen matrix, and provide one possible mechanism for the way these abnormal collagen matrices can affect initial mineralization.

Disclosures: Adele Boskey, None.

SA0085

Raman Microscopy Detection of Cyclic Mineralization Events in Perinatal Murine Calvaria. John-David McElderry*, Guisheng Zhao, Renny Franceschi, Michael Morris. University of Michigan, USA

Cyclic events, driven by clock genes in the hypothalamus, occur in many organs in the body. Cultured tissue separated from the brain can continue to display typical cyclic fluctuations for up to several days. Bone formation is thought to be regulated by clock genes through leptin hormone release and the sympathetic nervous system. Type I collagen deposition and osteocalcin blood levels both display diurnal cycles in the body confirming rhythmic influences in bone formation and turnover. Other processes in bone formation may also be regulated by clock genes.

Osteoblastic mineralization of the bone collagenous matrix is an extensively studied protein mediated process. However, current models for mineral deposition are not able to adequately describe apatitic crystal nucleation and propagation dynamics, both of which are essential for understanding mineral altering bone diseases. In the present study, intercollagenous deposition of apatitic mineral in ex vivo cultures of perinatal C57BL/6 murine calvaria (n=8) was monitored using a Raman microscope (830 nm laser) operated in an inverted configuration to accommodate a stage incubation chamber (5% CO₂, 37C, >90% humidity). Mineral deposition kinetics was measured in a 5x25 µm region at the occipital bone/anterior fontanel interface with a time resolution of 20 min. Mineral content in the tissue increased in periodically repeating intervals with near-diurnal frequency, while matrix components remained constant. Newly deposited mineral had the Raman spectral signature of small apatitic crystallites. A parallel study monitoring alkaline phosphatase (ALP) and inorganic phosphate (Pi) in medium of calvarial cultures using pups from the same litter (n=3) showed gradual decreasing levels of Pi, followed by near-synchronous fluctuations occurring over two days. ALP levels also showed large fluctuations but were asynchronous among pups. Our data suggests a bone mineral deposition mechanism that proceeds rapidly to the apatitic crystalline form and deposits in periodic steps probably regulated by clock gene expression. Video of tissue mineralization dynamics will be available during author presentation.

Disclosures: John-David McElderry, None.

SA0086

See Friday Plenary Number FR0086.

SA0087

See Friday Plenary Number FR0087.

SA0088

See Friday Plenary Number FR0088.

SA0089

See Friday Plenary Number FR0089.

SA0090

See Friday Plenary Number FR0090.

SA0091

Shh Secreted By Nucleus Pulposus Cells Is Required for the Maintenance of Postnatal Mouse Disc. Chitra Dahia*, Eric Mahoney, Christopher Wylie. Cincinnati Children's Hospital Medical Center, USA

Background: Degenerative disc disease is a major cause of lower back pain. However, the molecular signals that control normal growth and differentiation of the disc are not well defined. We hypothesize that nucleus pulposus (NP) cells, which originate from the embryonic notochord, provide signals that control growth and differentiation of the postnatal disc.

Methods: Postnatal day 4 mice IVDs were cultured in serum-free DMEM Ham/F12 medium at 37°C in 5% CO₂ for 2-5 days on type IV collagen-coated cell culture inserts. Cyclopamine (250 µM) was used as a Shh antagonist, and its specificity was tested by add-back experiments using 100 nM recombinant Shh (rShh). Cell proliferation was assayed using pulse-labelling with BrdU. 6 µm thick cryosections were immunostained (IHC) using antibodies specific to IVD differentiation markers, and Cy5 conjugated secondary antibodies. Imaging was carried out using confocal microscope. To test the role of Shh *in vivo*, triple transgenic mice [(tetO)7CMV-cre: R26 rtTA:Shh^{flx/flx}] were injected with 2 µg of doxycycline on postnatal day 4 to conditionally delete Shh, and the lumbar spine were collected 5 days later. Results were compared to vehicle treated controls.

Results: Both cyclopamine treatment *in vitro* and conditional Shh knockout *in vivo* caused rounding up and aggregation of the NP cells, and loss of orientation of the layers of the annulus fibrosus (AF). There was also a loss of expression of both NP and AF differentiation markers. BrdU incorporation studies showed loss of proliferation of NP cells. IHC for activated caspase-3 showed increased levels of apoptosis of NP cells rShh replacement reversed the cyclopamine phenotype *in vitro*.

Conclusions: These results show that Shh is essential for postnatal growth and differentiation of both the NP and AF.

Significance: Identification of signals controlling IVD growth and differentiation offers the opportunity for the development of biological repair as an alternative to surgery.

Disclosures: Chitra Dahia, None.

SA0092

See Friday Plenary Number FR0092.

SA0093

Time and Indentation Dependent Mechanical Response of Chondrocytes to Cyclic Loading. Cynthia Thomas¹, Nadeen Chahine², Craig Blanchette^{*3}, Gabriela Loots⁴, Todd Sulchek⁵. ¹LLNL, USA, ²Feinstein Institute for Medical Research, USA, ³Lawrence Livermore National Laboratories, USA, ⁴LLNLUC Merced, USA, ⁵Georgia Tech Research Institute, USA

Chondrocytes are responsible for the elaboration and maintenance of the extracellular matrix in articular cartilage. The biosynthetic responses of chondrocytes are known to be regulated by mechanical loading; therefore, mechanical properties of the cells play a pivotal role in the regulation of articular cartilage. In this study, the indentation and time-dependent mechanical response of individual chondrocytes was evaluated using atomic force microscopy (AFM). To measure the indentation-dependent response, chondrocytes were mechanically indented from 0.8 – 4 µm and the Young's modulus was calculated using the Hertzian model. The mechanical stiffness of chondrocytes isolated from 1 day old bovine was shown to dramatically increase between an indentation depth of 0.8 – 2 µm, and plateau at higher indentations. The time-dependent response of chondrocytes was evaluated as a function of the resting time between successive cyclic indentations (relax time). In these experiments, the compressive modulus of chondrocytes isolated from 1 day old bovine was shown to drastically decrease between a relax time of 0.5 s and 2 s. These results suggest that immediately after cyclic indentation, chondrocytes experienced a higher stiffness that decreases with increasing relaxation time. This relaxation behavior may be due to fluid pressurization inside the cell or viscoelastic elements in the membrane or organelles. To determine if these effects were dependent on the structural components of the cells, actin and/or intermediate filaments, these experiments were repeated in the presence of agents that disrupt the actin (cytochalasin B) and intermediate filaments (acrylamide) and the resulting mechanical response to cyclic loading were evaluated. In addition, to assess the effects of chondrocyte age on mechanical stiffness, the time and indentation dependent mechanical response of chondrocytes isolated from different aged bovine, immature (1-3 week old bovine calf), young (1-2 year old bovine) and aged (5-7 year old bovine), to cyclic loading was measured.

Disclosures: Craig Blanchette, None.

SA0094

See Friday Plenary Number FR0094.

SA0095

See Friday Plenary Number FR0095.

SA0096

Disruption of Aldehyde Dehydrogenase 2 Gene Resulted in Altered Cortical Bone Structure and Increased Cortical BMD without Affecting Bone Length and Trabecular BMD in Femurs of Mice. Takuto Tsuchiya*, Akinori Sakai, Toshiharu Mori, Kunitaka Menuki, Yoshinori Takeuchi, Shinkichi Kanoh, Hajime Utsunomiya, Teppei Murai, Toyohi Isse, Tsunehiro Oyama, Toshihiro Kawamoto, Toshitaka Nakamura. University of Occupational & Environmental Health, Japan

Aldehyde dehydrogenase 2 (ALDH2) is the enzyme which degrades and detoxifies acetaldehyde, which is in turn is metabolized from alcohol. More than 40% of Chinese and Japanese people have the inactive ALDH2 phenotype. In our previous study, trabecular bone volume decreased in ALDH2 knock-out (Aldh2^{-/-}) mice with alcohol drinking compared with wild type (Aldh2^{+/+}) mice. On the other hand, skeletal phenotype of ALDH2 gene except for alcohol factor remains unknown. The aim of this study is to clarify the skeletal phenotypic analysis of ALDH2 knock-out (Aldh2^{-/-}) mice at 12-weeks of age without alcohol drinking. We evaluated the femoral bone length and bone mineral density (BMD) was measured in the femur using peripheral quantitative computed tomography (pQCT). There were no significant differences in the femoral bone length and trabecular BMD in distal metaphysis of femurs between male and female Aldh2^{-/-} mice (n=8 in each group) and respective Aldh2^{+/+} mice (n=8 in each group). However, mid-shaft cortical BMD and cortical thickness were significantly increased, and cross-sectional area and bone marrow area were significantly decreased in femurs of male and female Aldh2^{-/-} mice compared with those in respective Aldh2^{+/+} mice. In Conclusion, disruption of ALDH2 gene resulted in altered cortical bone structure and increased cortical BMD without affecting bone length and trabecular BMD in femurs of mice.

Disclosures: Takuto Tsuchiya, None.

SA0097

Frzb is Dominant Regulator of Wnt Signaling During Early Fracture Healing in Mice. Travis Burgers^{*1}, Martin Hoffmann², Debra Sietsema³, Bart Williams⁴, Clifford Jones³, Jim Mason¹. ¹Van Andel Institute, USA, ²Grand Rapids Medical Education Partners, USA, ³Orthopaedic Associates of Michigan, USA, ⁴Van Andel Research Institute, USA

Purpose: Wnt signaling plays a role in normal and pathological bone healing and bone mass regulation through control of cell differentiation along the osteoblast or chondrocyte lineages. Here we hypothesize that Wnt signaling regulates bone healing in a stage-dependent manner through differential utilization of beta-catenin signal transduction.

Methods: Twelve-week-old male C57/BL6 mice were used in this study. A closed mid-diaphyseal femoral fracture was induced after retrograde insertion of a 23G intramedullary needle under sterile conditions (Figure 1). Two mice were sacrificed at 5, 14 and 21 days post-fracture (PF). The fracture callus and corresponding segment of the contralateral femur were harvested and the bone marrow removed under RNase-free conditions. RNA was extracted (QiaShredder, Qiagen Inc., Valencia, CA). Reverse transcriptase and real time polymerase chain reaction were performed (RT2 Nano PreAMP cDNA Synthesis Kit and Mouse WNT signaling pathway RT2 Profile PCR Array, SABiosciences). The increase in gene expression of the fracture callus with respect to a contralateral limb was calculated.

Results: At a minimum of one of the three time points, 19 different genes were up-regulated more than 10-fold in the fracture callus and nine genes more than 20-fold (Figure 2). Frzb (aka Sfrp3) was the most highly up-regulated gene. Many Wnts (1, 2b, 4, 5a, 5b, 7b, 8b, 11 and 16) were up-regulated at all three time points during healing. Wnt3a, 6 and 8a are all down-regulated on Day 5 PF and up-regulated on Day 21 PF. Wnt9a and 16 are up-regulated on Days 5 and 14 PF but down-regulated on Day 21 PF.

Conclusion: Frzb, Sfrp1, Sfrp2, Dkk1 and Wnt5a are negative regulators of canonical Wnt signaling that are initially up-regulated before returning to near-normal levels. Frzb has been shown to be related to endochondral bone formation [Enomoto-Iwamoto et al. Dev Biol. 2002] and pathologies in the chondrocyte lineage [Lories et al. Arthritis Rheum. 2007]. Anecdotally, when Sfrp1, one of the negative regulators for canonical Wnt signaling, was knocked out in a mouse, fracture healing was improved [Gaur et al. J Cell Physiol. 2009]. The results of this study demonstrate that knockout of Frzb (Sfrp3) may have an even more dramatic effect.

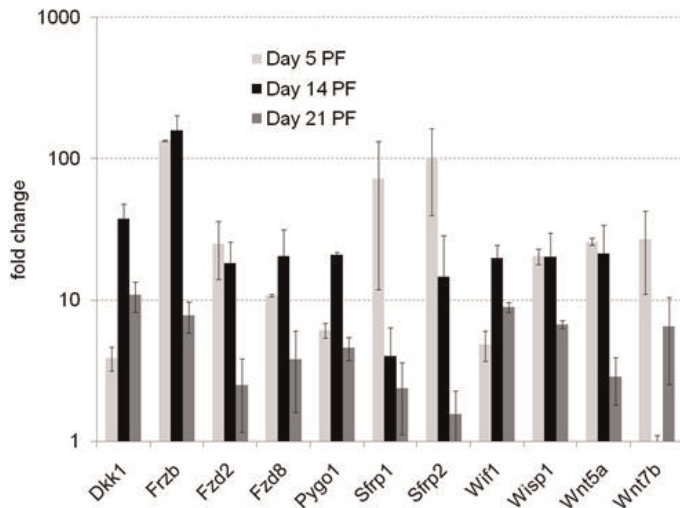


Figure 2: Gene expression in healing femoral callus compared to intact contralateral femur

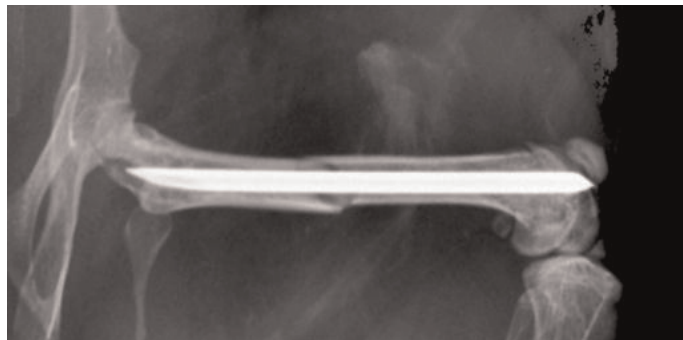


Figure 1: Fracture induced in mouse femur

Disclosures: Travis Burgers, None.

SA0098

See Friday Plenary Number FR0098.

SA0099

Immunohistochemical and Histological Study on Periodontal Tissue in GK Rat. Fumihiko Suwa¹, Akimichi Takemura¹, Naoko Yoshikawa^{*2}, Masatoshi Ueda³. ¹Osaka Dental University, Department of Anatomy, Japan, ²Osaka Dental University, Department of Periodontology, Japan, ³Osaka Dental University, Japan

It has been reported that 95 % of diabetes mellitus (DM) patients in Japan exhibit the non-insulin dependent type II disease. Diabetes is a risk factor for periodontitis, which is considered the sixth most common complication of the disease. It has been pointed out that bone metabolic abnormalities induced by diabetes include osteoporosis, and there is a relation between systemic bone metabolic disorders like osteoporosis and alveolar bone resorption in periodontitis. We investigated the relation between periodontal tissue and type 2 diabetes mellitus.

We used 9 eight month old Goto-Kakizaki (GK) rats, which is a type 2 DM model rat, as the experimental animals. 9 eight month old Wistar rats (NDM) were used as controls. We examined the development of connective tissue papillae in the free gingiva of external marginal epithelium on the lingual side of mandibular first molars using normal rats under light and scanning electron microscopy and immunohistochemically examined RANKL and OPG on alveolar bone. We also histochemically examined TRAP-positive cells and ALP-positive cells.

In observation of the specimen under a scanning electron microscope, the height of papillae of the DM was lower than that of the NDM. In histological measurement and statistical observation, the height and area of connective tissue showed smaller figures in the DM compared to the NDM, and significance difference was observed in both. However, neither showed difference in the number of connective tissue papillae. The development was poor in the DM compared to the NDM. There were distinct morphological differences.

In enzyme histochemical findings for TRAP and ALP, many TRAP positive multinucleated giant cells were observed in the alveolar bone around the root apex in NDM compared with DM, and many ALP were observed near the root apex in

NDM. In immunohistochemical findings for RANKL, many RANKL were observed from the alveolar bone in the mid portion root to the alveolar crests in NDM. In immunohistochemical findings for OPG, many OPG were observed from the alveolar bone in the mid portion root to the alveolar crests in DM.

These results suggest that diabetes may not only impair the development of connective tissue papillae by causing regressive changes and play an important role as a risk factor for low-turnover bone disease, but also delay periodontal tissue healing and aggravate periodontal diseases.

Disclosures: Naoko Yoshikawa, None.

SA0100

See Friday Plenary Number FR0100.

SA0101

Bioinspired Silicon Carbide Ceramics as Bone Substitute in an Experimental Bone Defect Rabbit Model. David Guede^{*1}, I Pereiro², E Solla², J Serra³, M Lopez-Pena⁴, F Munoz⁴, Antonio Gonzalez-Cantalapiedra⁴, Jose Caeiro⁵, PUo Gonzalez². ¹Trabeculae, S.L., Spain, ²Dept. Física Aplicada, Universidad de Vigo, Spain, ³Departamento de Física Aplicada, Universidade de Vigo, Spain, ⁴Departamento de Ciencias Clínicas Veterinarias, Universidade de Santiago de Compostela, Spain, ⁵Orthopaedic Surgeon, Spain

INTRODUCTION

The new generation of materials for medical implants must mimic the smart hierarchical structures present in nature and optimized by evolution. Bio-inspired silicon carbide (BioSiC) is a light and high-strength ceramic, produced from wood, presenting a natural structure similar to the one present in bone tissues, incorporating the unique property of interconnected porosity, which allows the internal growth of tissue and favors angiogenesis.

OBJECTIVES

The aim of this study was to test the osseointegration of BioSiC implants in femoral bone defects in an experimental rabbit model, and the possible enhancement of their bioactivity with a 50 nm surface coating of Si-substituted hydroxyapatite (Si-HA).

MATERIAL AND METHODS

BioSiC cylinders were manufactured from sapelli wood (Entandrophragma cylindricum) with the pyrolysis of selected wood at 1000C in inert atmosphere followed by the infiltration of the obtained carbon preform with molten silicon at 1550C. Of the 36 cylinders produced, 18 were coated with Si-HA (7.5 at. %) by pulsed laser deposition (PLD).

The cylinders were implanted in the femoral condyles of New Zealand rabbits. Animals were sacrificed at 1, 4 or 12 weeks after implantation resulting 3 subgroups for each type of implant. Samples were analyzed by histological examination using optical microscopy and by X-ray micro-computed tomography (micro-CT) to assess bone growth on the periphery and inside the pores of the implants. The statistical comparison was carried out by applying the Mann-Whitney U test and the relationship between both techniques was studied using Pearson correlation.

RESULTS

BioSiC implants showed a good osseointegration presenting both ongrowth and ingrowth. At 4 weeks of implantation the integration was nearly complete with no significant differences between 4 and 12 weeks in any of the analyzed parameters. The Si-HA coating did not significantly improve the value of any parameter with respect to uncoated implants. Histological parameters showed a good correlation with their analog micro-CT parameters.

CONCLUSIONS

BioSiC ceramics, fabricated from porous wood, present a good osseointegration when implanted and its interconnected porosity is colonized by bone tissue, together with lightweight and high strength for optimum biomechanical performance. Additionally, it does not require the bioactivity of a HA coating to improve the apposition of new-formed bone. Thus, BioSiC stands as a new material for biomedical applications.

Disclosure of Interest: None Declared

Disclosures: David Guede, None.

SA0102

Conditional Profilin1 Deficiency in Multiple Cell Lineages of Mesenchyme Origin Based on Prx1-Cre System Severely Disrupts Axial and Appendicular Skeletal Development. Daisuke Miyajima^{*1}, Tadayoshi Hayata², Takafumi Suzuki¹, Yoichi Ezura³, Tetsuya Nakamoto¹, Takuya Notomi⁴, Teruo Amagasa⁵, Ralph T Bottocher⁶, Reinhard Fässler⁶, Masaki Noda¹. ¹Tokyo Medical & Dental University, Japan, ²Medical Research Institute, Tokyo Medical & Dental University, Japan, ³Tokyo Medical & Dental University, Medical Research Institute, Japan, ⁴GCOE, Tokyo Medical & Dental University, Japan, ⁵Department of Maxillofacial Surgery, Tokyo Medical Dental University, Japan, ⁶Department of Molecular Medicine, Max Planck Institute of Biochemistry, Germany

Profilin1 (Pfn1), an actin monomer-binding protein, is thought to play key roles in cell activity through modulation of actin cytoskeleton during embryogenesis because Pfn1-null mice die as early as the two-cell stage. The analysis of cartilage-specific Pfn1-deficient mice demonstrated that Pfn1 is required for cytokinesis of chondrocytes (EMBO, 2009). However, the functions of Pfn1 in multi-cellular interplay involved in skeletal development have not been investigated. Since multi-cellular interaction is essential during skeletal development, we hypothesized that Pfn1 may play roles in this regard. To test this hypothesis, we conditionally inactivated Pfn1 by using Prx1-cre mice to examine the influences of Pfn1 deletion in multi cellular interaction during skeletal development. Mice with homozygous deletion of Pfn1 (Prx1-cre⁺; Pfn1^{fl/fl}, Prx1Pfn1) were born at the normal Mendelian ratio. They had complete cleft sternums and died shortly after birth due to inability to breathe. Newborn (P0) Prx1Pfn1 mice exhibited shorter limbs compared with control mice, though their body length was similar to the control. Histological analysis of P0 Prx1Pfn1-limbs revealed that the columnar structures of the growth plate were disorganized and that the hypertrophic zone, where average cell size was enlarged compared to those of control, was expanded to the other end, suggesting that the degradation of the cartilage matrix did not progress normally. In addition, the trabecular bone appearance of P0 Prx1Pfn1 was completely missing. Interestingly, blood cells and osteoclasts of P0 Prx1Pfn1 were localized only in mid-diaphysis. The invasion of blood vessels occurred in mid-diaphysis but the vascular ingrowth did not progress normally at this stage. In vitro experiment revealed that knockdown of Pfn1 by siRNA in MC3T3-E1 osteoblast-like cells inhibited cell migration and proliferation. Taken together, these findings indicate that Pfn1 is required for axial and appendicular skeletal development.

Disclosures: Daisuke Miyajima, None.

SA0103

Effects of Different Treatment Regimes on Collagen-Induced Arthritic Response in the Female Lewis Rat. CAROLINE RUH^{*1}, Richard Gregson¹, Aurore Varela², Susan Y. Smith², Richard Watson³. ¹Charles River, Canada, ²Charles River Laboratories, Canada, ³Revaliesio Corporation, USA

The collagen-induced arthritis (CIA) rat model is widely used to assess efficacy of potential drugs to treat rheumatoid arthritis. The study objective was to compare the arthritic response in female Lewis rats following treatment with vehicle controls via different routes of administration and dosing frequencies.

Type II porcine collagen (in IFA) was injected intradermally. As arthritis developed, rats were randomly assigned to 4 groups (10 rats/group). One group was treated daily for 42 days with saline intravenously (IV), one was treated weekly with saline subcutaneously (SC), one was treated daily with water by oral gavage (PO) and one was treated daily with Dexamethasone (Dex) as a positive control to give perspective to the magnitude of changes. Dosing was initiated the day after assignment to study. The following were performed: qualitative arthritis evaluation (AE), paw thickness (PT), C Telopeptide of Collagen type II (CTxII) in serum, X Ray evaluation of ankle joints, macroscopic and microscopic evaluation and paw weights (PW).

There were no notable differences between groups in CTxII, macroscopic observations or PW. The SC group had a higher incidence of disease-related clinical signs when compared to IV and PO. Statistically significant increases were obtained in mean AE results (at Day 43) and PT measurements (by Day 10) for SC when compared to IV and PO. The area under the curve (AUC) for PT was calculated and SC showed a 6% increase in AUC compared to IV or PO. X-Ray evaluation confirmed a higher score for SC with increases of 12 and 21% compared to IV and PO, respectively. Similarly, microscopic evaluation showed higher arthritis scores for SC compared to IV and PO with increases of 13 and 30%, respectively. There were no X Ray lesions or microscopic changes in Dex animals.

In summary, minimal differences in disease severity were observed between the 3 vehicle control treatment regimes, however animals treated once weekly SC were the most severely affected. Animals treated by daily oral gavage showed lower X-Ray and microscopic scores than animals treated by more invasive routes (SC or IV). These results provide intriguing evidence linking disease severity with stress levels that may be influenced by the frequency of manipulation and the ease of the dosing procedure. Thus, when assessing efficacy of a potential drug, the treatment regime for controls should be identical to drug-treated animals to avoid any possible bias associated with stress.

Disclosures: CAROLINE RUH, None.

SA0104

Human Perivascular Stem Cells and Nell-1 in Ectopic Bone Formation. Janette Zara^{*1}, Xinli Zhang², Aaron James², Mirko Corselli², Michael Chiang², Jonguk Chung², Kang Ting², Bruno Peault², Chia Soo². ¹UCLA, USA, ²University of California, Los Angeles, USA

Purpose: Conventional stem cell sources for bone regeneration such as bone marrow stem cells (BMSCs) or adipose derived stem cells (ASCs) have significant drawbacks such as donor site morbidity, low stem cell yield, or long culture derivation time. In comparison, perivascular stem cells (PSCs), a primitive origin of mesenchymal stem cells (MSCs), isolated through fluorescence activated cell sorting (FACS), are a more highly purified cell population that may be more effective in regenerating bone. The objectives of this study are to establish a novel source of stem cells for bone repair combined with potent osteogenic factors, and to compare the osteogenic potential of PSCs to human stromal vascular fraction (SVF) from adipose tissue.

Methods: FACS sorted PSCs (CD146⁺, CD34⁻, CD45⁻, CD56⁻) were derived from human liver, pancreas and adipose tissue, and their osteogenic capacity tested in vitro. In vivo bone formation was tested using 2.5 x 10⁵ PSCs mixed with a 100 uL demineralized bone matrix putty (DBX) and implanted in a nude mouse muscle pouch model. PSC-mediated bone formation was compared to bone formation by SVF + DBX, and DBX alone as control. Each group was also analyzed in the presence of the osteoinductive growth factor Nell-1. Analysis was by RT-PCR, in vivo PSC tracking, microCT, histology, immunohistochemistry, and histomorphometry.

Results: PSCs grown on standard culture ware or DBX scaffold exhibited osteogenic differentiation with elevated gene expression of osteogenic markers and alizarin red staining in vitro. In vivo, PSC implantation resulted in significantly higher bone formation compared to SVF and control, as shown by microCT analysis of bone volume and bone mineral density, histomorphometric analysis of serial sections of aniline blue slides, as well as increased bone sialoprotein (BSP) and osteocalcin (OCN) staining. Furthermore, addition of Nell-1 to PSC resulted in greater bone formation than PSC alone. Nell-1 also exhibited proangiogenic effects on PSCs, both in vitro and in vivo accompanied by elevated VEGF mRNA or protein expression and more small blood vessels throughout the implanted tissues.

Conclusions: These results indicate that human PSCs are a superior new source of stem cells for skeletal regenerative medicine in comparison to human SVF, and that Nell-1 protein is capable of stimulating and enhancing the osteogenic capacity of highly purified human PSCs as well as having proangiogenic effects to facilitate bone formation.

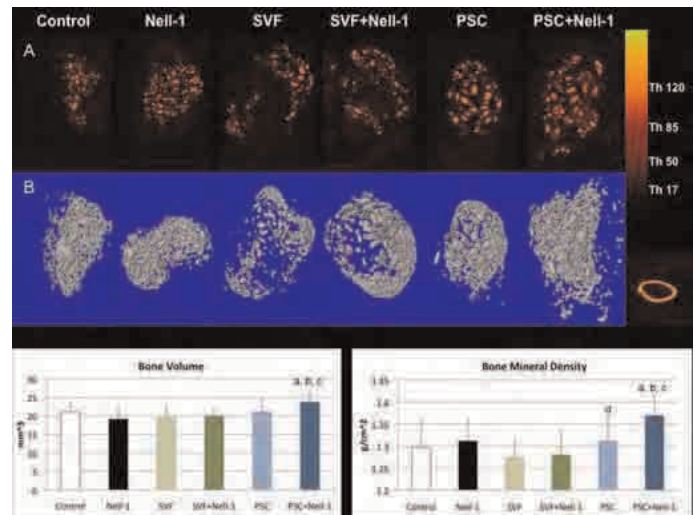


Figure 1: Color Density Figures, 3D reconstruction, and graphs of microCT analyses.

Disclosures: Janette Zara, None.

SA0105

In Vitro Testing of Biomaterial Scaffolds For Musculoskeletal Regenerative Medicine. Brya Matthews^{*}, Vieri Terreni, Sandy Lin, Karen Callon, David Musson, Ji-zhong Bai, Dorit Naot, Jillian Cornish. University of Auckland, New Zealand

Injuries to bone and tendons can cause major morbidity in healthy, active people, particularly if they heal slowly or fail to heal. Providing a scaffold that encourages appropriate cell attachment, growth, and ultimately tissue regeneration could improve the clinical outcomes from injuries such as rotator cuff tears and non-union fractures. We have tested several scaffold materials of both natural and synthetic origin to evaluate their biomaterial properties and their potential utility in musculoskeletal regenerative medicine.

Five different types of scaffolds were evaluated as biomaterials. The natural scaffolds tested were Endoform, a decellularized ovine forestomach matrix, Spidrex

543 spider silk fabric and hydroxyapatite (HA) particles derived from mussel shells and incorporated into collagen gels. Synthetic nanofibrous scaffolds were produced from polylactic acid (PLA) and polyethylene terephthalate (PET) using either electrospinning or a microfibrillar composite (MFC) technique. Attachment, growth and morphology of primary rat osteoblasts, MC3T3-E1 cells and primary rat tenocytes were analyzed using live-dead staining, alamar blue fluorescence and confocal microscopy. Scaffold structure and cell attachment were also evaluated using SEM. Cell differentiation was evaluated by calcein incorporation and gene expression.

Osteoblasts and tenocytes both successfully adhered to, and grew on the luminal and abluminal surfaces of Endoform, and on the silk. SEM examination of the synthetic scaffolds showed that both methods of production create three-dimensional networks. Electrospun scaffolds comprised of a fibrillar, cross-ply structure with 125 - 145 nm diameter fibrils, and MFC scaffolds consisted of an interconnected porous network with 70 - 75 nm fibril diameter. Osteoblast-like cells attached and grew on these scaffolds, with PLA scaffolds tending to show better cell growth than PET material. None of the HA particle preparations tested had a significant effect on osteoblast cell growth when incorporated into collagen gels at a concentration of 0.25%. Cells were able to form new mineralized areas in the presence of HA, and some preparations appeared to promote mineralization.

We have identified a number of scaffold materials that show potential for use in bone or tendon regeneration. More testing is required to determine if they support cell differentiation and appropriate tissue formation.

Disclosures: *Brya Matthews, None.*

SA0106

See Friday Plenary Number FR0106.

SA0107

Lymph Vessel-forming Factors and Receptors in Tooth Development in Mice. Shinya Takahashi^{*1}, Yuriko Moro¹, Hiroki Watanabe¹, Kimiharu Ambe², Toshihiro Nakagawa¹. ¹Ohu University School of Dentistry, Japan, ²OHU University, school of dentistry, Japan

Vascular endothelial growth factor (VEGF) is a family of factors that control angiogenesis and lymphangiogenesis. Factors playing important roles in lymph vessel formation have recently been clarified, such as VEGF-C and -D and their receptor, VEGF receptor 3 (VEGFR-3). In this study, we immunohistochemically investigated lymph vessel formation and control with tooth development in the mouse lower molars using antibodies against VEGF-C and -D and VEGFR-3. We also used von Willebrand factor (vWF) to distinguish between the blood vessels and lymph vessels. Mouse (C57BL/6L) dental papilla and pulp sections were immunohistochemically stained with specific antibodies for VEGF-C, VEGF-D, VEGFR-3 and vWF. In the cap-stage dental papilla after 14 days of gestational age, undifferentiated mesenchymal cells involved in blood and lymph vessel formation showed positive reactions to anti-VEGF-C and -D and VEGFR-3 and vWF antibodies. In the dental papilla in the uncalcified bell stage at 17 days of gestational age, positive undifferentiated mesenchymal cells increased, and lumen-forming endothelial cells also showed positive reactions, but anti-vWF showed a negative reaction. Positive undifferentiated mesenchymal and endothelial cells were also present in the coronal pulp at 0,3, and 7 days after birth, and the number of positive cells increased with aging. At 10 days of age, anti-VEGF-C, VEGF-D and VEGFR-3 staining showed many strongly positive undifferentiated mesenchymal and endothelial cells in the coronal and radicular pulp. The endothelial cells that showed weakly positive or positive reactions to anti-VEGF-C, -D, VEGFR-3 and vWF existed, but the numbers relatively decreased before 10 days of age. These findings suggest that VEGF-C and -D and VEGFR-3 are closely involved in lymph vessel formation on tooth development in mice.

Disclosures: *Shinya Takahashi, None.*

SA0108

Modulation of Trabecular Bone Formation by Dioxin Exposure and Aryl Hydrocarbon Receptor Ablation. Mikko Finnila^{*1}, Maria Herlin², Antti Aula³, Hanna Miettinen⁴, Merja Korkalainen⁴, Juha Tuukkanen¹, Timo Jamsa¹, Helen Hakansson², Matti Viluksela⁵. ¹University of Oulu, Finland, ²Karolinska Institutet, Sweden, ³University of Eastern Finland, Finland, ⁴National Institute for Health & Welfare, Finland, ⁵National Public Health Institute, Finland

Dioxins are a group of environmental contaminants able to interfere with bone modeling and remodeling. Exposure to these compounds has been shown to decrease bone strength, cortical area and mineralization. Most of the toxic effects of dioxins are suggested to be mediated through the Aryl hydrocarbon Receptor (AhR), a key regulator of cell metabolism, proliferation and differentiation. This study aims to characterize trabecular bone properties after dioxin exposure in wild type (*Ahr*^{+/+}) and AhR knockout (*Ahr*^{-/-}) mice.

Both genders of *Ahr*^{+/+} and *Ahr*^{-/-} mice were exposed once weekly either to the total dose of 200 µg/kg of 2,3,7,8-Tetrachlorodibenzo-p-dioxin or corn oil vehicle (controls) for 10 weeks by oral gavage. Samples were collected one week after the last dosing.

Tibia and L3 vertebra from each mouse were microCT scanned using voxel sizes of 4.7 µm and 9.9 µm, respectively. In tibia volume of interest was drawn starting 0.19 mm after the distal end of the growth plate and extended to 1.64mm towards the metaphysis. For vertebrae corresponding values were 0.1mm and 0.81mm.

Exposure to TCDD increased trabecular bone formation (BV/TV) in vertebra by 55% and 28% (p<0.05) in *Ahr*^{+/+} females and males, respectively, while no effects were seen in either male or female *Ahr*^{-/-}. These trabeculae were significantly thicker, closer to each other and have more plate-like structure. Also a negative trabecular pattern factor indicated that there are enclosed cavities within trabecular network in TCDD exposed *Ahr*^{+/+}. Tibial trabecular bone responded similarly to dioxin exposure, however, AhR ablation caused here site specific increase in trabecular bone formation. However, this increase was not further driven by TCDD exposure. The trabeculae in tibia of *Ahr*^{-/-} were also thicker and closer to each other and had a more plate-like structure, but there were no indications of closed cavities.

Previous observations on serum biomarkers indicated suppressed bone formation and increased bone resorption after TCDD exposure, whereas AhR ablation lead to increase in both formation and resorption markers, supporting the increased trabecular bone formation in *Ahr*^{-/-} presented here. These data suggests that dioxin exposure has opposite effect on trabecular bone than on cortical bone, for which we have previously shown decreased cortical bone area, increased porosity and decreased strength.

Disclosures: *Mikko Finnila, None.*

SA0109

Proteoglycan-4: A Dynamic Regulator of Skeletogenesis and PTH Skeletal Anabolism. Chad Novince^{*1}, Megan Michalski², Benjamin Sinder², Payam Entezami², Amy Koh², Matthew Eber², Thomas Rosol³, Thomas Wronski⁴, Kenneth Kozloff⁵, Laurie McCauley¹. ¹University of Michigan, School of Dentistry, USA, ²University of Michigan, USA, ³The Ohio State University, USA, ⁴University of Florida, USA, ⁵University of Michigan Department of Orthopaedic Surgery, USA

Proteoglycan-4 (*prg4*), known for its lubricating and protective actions in joints, is a strong candidate regulator of skeletal homeostasis and parathyroid hormone (PTH) anabolic actions in the skeleton. *Prg4* loss-of-function mutations result in the human condition camptodactyly-arthritis-coxa vara-pericarditis syndrome, which is characterized by precocious joint failure and osteopenia. The purpose of this study was to investigate the role of proteoglycan-4 as a regulator of skeletal development, remodeling, and PTH anabolic actions. C57BL/6 wildtype (WT) mice were subjected to a single PTH (1-34) injection, and bone marrow and liver were harvested at 1, 4, 8, 12 hours for real-time qPCR analysis. Acute PTH treatment regulated gene expression similarly in bone marrow and liver; decreasing PPR, increasing *prg4*, and increasing FGF-2. *Prg4* KO and WT mice were treated with daily intermittent PTH from 4-21d (young model) or 16-22wk (adult model). Joint range of motion and animal mobility were assessed prior to sacrifice. Static and dynamic histomorphometry were carried out in proximal tibiae and micro-CT performed in distal femurs. Bone marrow stromal cells (BMSCs) were analyzed for cell autonomous alterations, serum markers for bone turnover and mineral homeostasis were measured, and bone marrow and liver gene expression were evaluated by real-time qPCR. Young *prg4* KO mice had decreased growth plate hypertrophic zones, trabecular bone, and serum bone formation markers. Adult *prg4* KO mice had decreased trabecular and cortical bone, blunted PTH anabolic responses, but normal bone turnover. Joint range of motion and animal mobility were restricted in adult *prg4* KO mice. Adult *prg4* KO mice had reduced marrow and liver FGF-2 mRNA levels and reduced serum FGF-2 protein levels, which were normalized with PTH treatment. These data suggest proteoglycan-4 supports endochondral bone formation and the attainment of peak trabecular bone mass, while indirectly supporting cortical bone homeostasis via protecting joint function. FGF-2 is a candidate regulator of proteoglycan-4 actions in the support of basal bony trabecular numbers. Finally, blunted anabolic responses in adult *prg4* mutant mice are likely associated with the developmental reduction in bony trabeculae as well as reduced biomechanical impact. The novel finding that PTH similarly regulates gene expression in bone and liver strongly suggests that the liver plays a role in regulating PTH biologic actions.

Disclosures: *Chad Novince, None.*

SA0110

Tgf-β and Erg in Intervertebral Disc Development. Megan Cox^{*1}, Rosa Serra². ¹UAB, USA, ²University of Alabama at Birmingham, USA

Transforming growth factor β (Tgf-β) signaling plays an integral part in skeletal development. Conditional deletion of Tgf-β type II receptor (Tgfr2) from type II Collagen expressing cells has been shown to cause defects development of the intervertebral disk (IVD) specifically development of the annulus fibrosus was disrupted. We previously used microarray analysis to search for marker genes of IVD as well as transcription factors regulated by Tgf-β during IVD development. The transcription factor Erg was identified in the microarray screen as a candidate regulator of IVD development. To study the in vivo effects of Tgf-β over expression in axial skeleton development, we used the chick model system. Tgf-β soaked Affi-gel beads were placed into the lumbar region of the axial skeleton at stage HH 25. Within 5d post-implantation, we were able to see inhibition of cartilage formation as

determined by Alcian blue staining in the area surrounding the bead. This suggested that Tgf- β acts to suppress cartilage formation. We also showed that the beads soaked in Tgf- β induce mRNA expression of Versican, a marker of IVD development, and Erg, a disc enriched transcription factor, around the bead within 24h. As one of the candidate genes, we created an adenovirus to over-express Erg in primary sclerotomy micromass cultures. Over-expression of Erg led to a change in cell morphology and inhibition of differentiation into cartilage as seen by alcian blue staining. We also demonstrated an increase in expression of several IVD markers in the Erg expressing cultures, suggesting that these cells may be becoming more like annulus cells associated with the IVD. Overall, the data support a model in which Tgf- β acts to maintain the IVD and prevent differentiation into cartilage potentially through the transcription factor Erg. These experiments help to address fundamental questions about development of the axial skeleton and provide a basis for future studies aimed at disc repair or replacement.

Disclosures: Megan Cox, None.

SA0111

See Friday Plenary Number FR0111.

SA0112

In Vivo Analysis of Epithelial Dental and Bone Cell Cross-talks in Transgenic Mice: Experimental Models to Delineate Jaw Bone Specificity. Ariane Berdal¹, beatriz castadena², muriel de la dure molla³, chris mueller⁴, frederic lezot⁵. ¹University Paris-Diderot, France, ²INSERM UMRS 872 University Antioquia, France, ³INSERM UMRS 872 University Paris-Diderot, France, ⁴CNRS, UPR 9021 University Strasbourg, France, ⁵INSERM UMRS 957 University Nantes, France

Jaw bone shows a unique physiopathology, illustrated by regional osteonecrosis under anti-osteolytic agents. Our hypothesis is that Msx2/amelogenin/RANK pathway would play a part in this physiological specificity. Msx2 -/- (knock-in) mice harbour regional jaw osteopetrosis relied to epithelial dental cell (EDC) anomalies (Am J Pathol 177, 2516, 2011). Jaw osteoclast activation impacts EDC fate (targeted RANK overexpression in RANK-Tg mice; J. Cell Physiol., 226: 74, 2011). Msx2 knock-in line was crossed with RANK-Tg line to explore reciprocal EDC/bone cross-talks. Continuously growing incisor and growth-limited molars were analyzed from birth to 6 months. Analysis of microdissected dental and bone tissues by RT-qPCR, Western-blotting was associated with in situ RNA/protein mapping (Msx2, amelogenin, TRAP, PCNA, TNF?) as well as 2D- and 3D-morphology (micro-CT, histology). EDC harboured opposite expression for Msx2 and amelogenin (distribution patterns and relative levels in Msx2 +/-, Msx2 +/- and Msx2 -/- mice). Co-variations in the grade of EDC anomalies and osteoclast impairment characterized Msx2 -/- mice, culminating in the third molar which never erupted. There, EDC islands accumulated over months and overexpressed amelogenin. And, regional decreased RANK ligand and increased Runx2 expression levels (Msx2-/- versus Msx2 +/-) were measured. In the molar region of Msx2-/-; RANK-Tg double mutants, after a transient increase of EDC pool during growth, EDC anomalies and osteoclast impairment were normalised in adults. In contrast, incisor territories exhibited giant osteolytic and hyperproliferative epithelial tumour-like structures relied to increased TNF? expression. (1) From EDC to bone cells, Msx2-dependant amelogenins produced by dental cells would control, as established in the literature, Runx2 and RANK ligand levels and therefore osteoblast/osteoclast balance and (2) from bone to EDC, EDC growing niches were stimulated by activated resorption. Its impact followed specific frames (time-limited, continuous and inflammatory tumour-like growth). In conclusion, in contrast to vertebral and appendicular bones, cell network leading jaw bone balance would include additional EDC partners. According to EDC status which would vary in various bone physiopathological and inflammatory conditions, EDC would deliver specific signals to bone cells.

Disclosures: Ariane Berdal, None.

SA0113

Molecular Characterization of MMP7-BMP2 Complex and the Implications for Fracture Nonunion. Abdulhazef Selim¹, Hsiu Ying Sherry Wang², Ashraf Moharam³, Marina D'Angelo⁴. ¹Center for Chronic Disorders of Aging, PCOM, USA, ²Inspire Pharma, Egypt, ³Orthopaedic Surgery, Cairo University School of Medicine, Egypt, ⁴Philadelphia College of Osteopathic Medicine, USA

A delayed union or a nonunion of a fracture is a potentially adverse complication. Understanding the mechanisms of nonunion development may lead to improved treatment modalities. Proteases such as the matrix metalloproteinases (MMPs) play important roles in bone remodeling and repair, in which an imbalance or a nonfunctioning enzyme may lead to defects in bone healing (nonunion). MMP-7 and MMP-12 have been identified in fracture nonunion tissue and a role for them in direct binding to and degradation of bone morphogenetic protein-2 has been described. In this pilot study, we generated models of BMP2-MMP complexes and identified the interfacing residues in these complexes. MMP7-BMP2 complex has the following features; 1103.3 Å² interfacing area, Δ^1G -14.4 kcal/M (the solvation free energy gain

upon formation of the interface) indicating high affinity, Δ^1G p-value 0.34 indicating high specificity and 37 residues of MMP7 are interfacing 35 residues of BMP2. Interface analysis predicted formation of 9 hydrogen bonds between MMP7 and BMP2. No covalent bonds, disulphide bonds or salt bridges were predicted. This is the first study to characterize the nature of MMP7-BMP2 interaction at the molecular level. The data in this study will help to further understand the molecular pathology of fracture nonunion.



MMP7-BMP2 complex

Disclosures: Abdulhazef Selim, None.

SA0114

See Friday Plenary Number FR0114.

SA0115

See Friday Plenary Number FR0115.

SA0116

See Friday Plenary Number FR0116.

SA0117

Salmon Calcitonin Suppressed Chondrocyte Hypertrophy and Cartilage Calcification ex vivo. Pingping Chen¹, Kim Henriksen¹, Kim Vietz Andreassen¹, Morten Karsdal¹, Anne-Christine Bay-Jensen². ¹Nordic Bioscience A/S, Denmark, ²Nordic Bioscience, Denmark

Calcitonin is known as an anti-resorptive agent for the treatment of osteoporosis. However, the application of calcitonin in treatment of joint degenerative disease has likewise been investigated, but is less understood. A key event of cartilage degenerations is hypertrophy, which leads to cartilage calcification. The effect of calcitonin on cartilage hypertrophy and calcification is yet to be understood. The aim of our work was to investigate the effect of salmon calcitonin (sCT) on hypertrophic chondrocytes, in a validated ex vivo model.

Full depth cartilage (FDC) explants (from superficial to calcified cartilage) were isolated from bovine femoral condyle and hypertrophy was induced by culture for 13 days with triiodo-L-thyronine (T3) stimulation. Non-stimulated explants were cultured as control (W/O). Doses of sCT ranged from 1nM to 100nM were added from day 4 to day 13. Type X collagen (COL X) localization on hypertrophic chondrocytes and calcitonin receptor (CTR) expression were evaluated at day 4. Type II collagen (COL II) turnover and aggrecan degradation were measured by PIINP (formation), CIIM (degradation) and AGNx-II assay, respectively. Expression of markers of hypertrophic chondrocytes (Indian hedgehog (IHH), COL X, ALP and MMP-13) were evaluated using RT-PCR at day 13.

At day 4 induction of hypertrophy led to expression of COL X and a ~10 fold higher CTR expression level than W/O (p<0.05). sCT suppressed COL II degradation dose-dependently. In contrast, 10nM sCT showed positive effect on COL II formation whereas 1nM and 100nM sCT did not. Three doses of sCT all decreased aggrecan degradation, in which 1nM sCT had significant effect (p<0.05). The expression of COL X, ALP and MMP-13 were suppressed by doses of sCT, in which 1nM

suppressed COL X expression significantly ($p < 0.01$). 1nM sCT also decreased expression of IHH, whereas 10nM and 100nM sCT did not.

In conclusion, T3 induced hypertrophic chondrocytes. The calcitonin receptor was upregulated in hypertrophic chondrocytes compared to non-hypertrophic chondrocytes. Hypertrophy led to significantly increased levels of cartilage degradation measured by collagen and aggrecan. sCT suppressed expression of markers of hypertrophic chondrocytes, and cartilage degradation. This is the first model of hypertrophic chondrocytes that is an integrated part of the pathogenesis of OA. This model may be used to better understand the molecular mechanism leading to OA, and how to block these processes.

Disclosures: Kim Henriksen, None.

This study received funding from: The danish Research Foundation

SA0118

All-Trans-Retinoic Acid Inhibits Intestinal Phosphate Uptake and Type IIb Sodium-Dependent Phosphate Co-Transporter Gene Expression in Rat.

Hironroi Yamamoto^{*1}, Masashi Masuda¹, Mina Kozai¹, Sarasa Tanaka¹, Otoki Nakahashi¹, Shoko Ikeda¹, Hiroko Segawa², Yutaka Taketani¹, Ken-Ichi Miyamoto², Eiji Takeda¹. ¹Dept. Clinical Nutrition, University of Tokushima, Japan, ²Dept. Molecular Nutrition, University of Tokushima, Japan

The hyperphosphatemia is assumed to be one of the causes of the ectopic calcification in dialysis patients. Therefore, the phosphorus (Pi) management by the inhibition of the Pi uptake from small intestine using the Pi-binders and/or the Pi restricted diets is thought to be important by the CKD-MBD treatment and prevention. The type II sodium-dependent phosphate co-transporters family (Npt2a, Npt2b and Npt2c) play a critical role for the Pi homeostasis in kidney and intestine. Recently, we have reported that VAD (vitamin A-deficient) rats increased the levels of urine Pi and renal expression of Npt2a and Npt2c genes are transcriptionally up-regulated by ATRA (all-trans retinoic acid) and its receptors. However, the effect of vitamin A status on the intestinal Pi absorption remains unclear. In this study, we observed the effect of VAD diets and ATRA administration on the Pi homeostasis and Npt2b gene expression in small intestine.

Although plasma levels of Pi, calcium, 1,25-dihydroxyvitamin D and parathyroid hormone did not differ between VAD and control rats, VAD rats significantly decreased feces Pi excretion and increased intestinal Pi uptake activity. Western blots and quantitative RT-PCR analysis revealed that Npt2b protein and its mRNA expression were up-regulated in VAD rats. In contrast, the administration of ATRA significantly suppressed the Pi uptake activity and the Npt2b gene expression in VAD rat intestine. Promoter analysis with a luciferase assay revealed that transcriptional activity of a reporter gene containing the Npt2b promoter was markedly decreased by ATRA and a RAR (retinoic acid receptor)-specific analogue in retinoid receptors (RAR and RXR) overexpressing cells. Furthermore, we identified nRARE (negative retinoic acid responsive element) in the Npt2b gene promoter. These results suggest that ATRA inhibits the intestinal Pi uptake through the negative transcriptional regulation of Npt2b gene in small intestine.

Disclosures: Hironroi Yamamoto, None.

SA0119

See Friday Plenary Number FR0119.

SA0120

See Friday Plenary Number FR0120.

SA0121

See Friday Plenary Number FR0121.

SA0122

Study of the Phosphaturic Tumors that Cause Tumor-induced Osteomalacia Suggest that they Derive from Inducible Osteoprogenitor Cells. William Chong^{*1}, Rachel Gafni², Alfredo Molinolo³, Nisan Bhattacharyya⁴, Michael Collins². ¹National Institute of Health, USA, ²National Institutes of Health, USA, ³National Institutes of Health, National Institute of Dental & Craniofacial Research, USA, ⁴NIDCR, NIH, USA

Tumor-induced osteomalacia (TIO) is a rare disease characterized by renal phosphate wasting, hypophosphatemia and osteomalacia due to ectopic oversecretion of fibroblast growth factor-23 (FGF23). TIO tumors have been reported in diverse locations, and can occur in bone or soft tissue. Histologically, the majority of these tumors have been classified as hemangiopericytomas, implicating a potential role for pericytes in tumor development. Two lines of reasoning led us to hypothesize that

pericytes in these tumors may be induced by factors yet unknown to become osteoprogenitor-like cells: 1) TIO tumors commonly exhibit bone-related features (osteoclasts, chondroid matrix, and even lamellar bone), 2) the primary physiologic source of FGF23 is osteocytes. In addition, the mammalian target of rapamycin (mTOR) pathway is central to normal cell growth and proliferation, and dysregulation of this pathway has been implicated in tumorigenesis in some vascular-derived tumors. To better understand tumorigenesis in TIO, we investigated bone cell differentiation markers and components of the mTOR pathway.

Tumors from 10 patients with TIO, all of which met the criteria for phosphaturic mesenchymal tumor, but which included a spectrum of histopathologic findings were studied. Immunohistochemical staining for FGF23, bone-related markers and mTOR-pathway markers was performed.

Staining was positive for FGF23 in all of the tumors, consistent with the clinical diagnosis. Tumor cells were positive for CD146, a pericyte marker, RANKL, a marker of osteogenic cells capable of promoting osteoclastogenesis, osteopontin, a late marker in bone cell differentiation, and dentin matrix acidic phosphoprotein 1, a marker for fully differentiated osteocytes. Preliminary findings indicate that the mTOR pathway is activated in a subset of these tumors, suggesting that this may be the driving proliferative pathway for at least some of these tumors.

Based on the positive staining for FGF23 in all the tumors, and for skeletal markers indicative of various stages of differentiation, we suggest that these tumors are derived from cells (perhaps pericytes) that were induced to become osteogenic due to a change in the local environment, and that dysregulation of the mTOR pathway may play a role in TIO tumorigenesis. Increased understanding of the origins of these tumors may enhance understanding of FGF23 physiology and result in new diagnostic and therapeutic options for TIO.

Disclosures: William Chong, None.

SA0123

Comparative Gene Expression in Parathyroid Oxyphil and Chief Cells. Cynthia Ritter^{*1}, Bruce H Haughey², Brent Miller³, Alex Brown⁴.

¹Washington University School of Medicine, USA, ²Department of Otolaryngology - Head & Neck Surgery, USA, ³Renal Division, USA, ⁴Washington University in St. Louis School of Medicine, USA

The parathyroid glands (PTGs) of young adults are composed almost entirely of chief cells, but with age and stress another cell type appears: the oxyphil cell. These cells are thought to be derived by transdifferentiation of chief cells, but how and why they form, as well as their function, is totally unknown. Oxyphil cell number increases in PTGs of patients with chronic kidney disease (CKD) and increases further after treatment of hyperparathyroidism with calcitriol and cinacalcet (Lomonte, CJASN 2008). Here, we compared the gene expression in oxyphil and chief cells of PTGs of CKD patients by immunostaining for PTH, PTHrP, CaR, VDR and 25-hydroxyvitamin D-1 α -hydroxylase (1 α OHase or CYP27B1). Oxyphil cells, which are found in defined nodules or as diffuse, undefined "islands," were identified by H&E staining. Both oxyphil nodules and islands expressed PTH at a level equal to or greater than chief cells. PTHrP was most highly expressed in oxyphil islands, compared to lesser amounts in oxyphil nodules and chief cells. CaR was expressed in oxyphil islands at a level equal to or greater than in chief cells, but was virtually absent in oxyphil nodules. The VDR was expressed in both oxyphil nodules and oxyphil islands, at a level equal to or higher than in chief cells. The greatest difference was seen with the 1 α OHase, which was very highly expressed in oxyphil islands, with only trace levels in oxyphil nodules and virtually none in chief cells. The hypothesis that CaR activation by cinacalcet or calcitriol (indirect via Ca) is supported by our observation that incubation of normal rat parathyroid glands in high Ca medium led to the formation of oxyphilic cells. Studies are underway to further characterize and quantify the gene expression profile and secretome of parathyroid oxyphil cells, and to determine the role of these cells (positive or negative) in the morbidity and mortality of CKD patients.

Disclosures: Cynthia Ritter, Abbott Laboratories, 2

This study received funding from: Abbott Laboratories

SA0124

See Friday Plenary Number FR0124.

SA0125

P₁-Transport Links the Functions of PHOSPHO1 and TNAP During the Initiation of Skeletal Mineralization. Manisha Yadav^{*1}, Carmen Huesa², Tina Moreira³, Colin Farquharson⁴, Jose Luis Millan³. ¹Burnham Institute for Medical Research, USA, ²Roslin Institute University of Edinburgh, United Kingdom, ³Sanford-Burnham Medical Research Institute, USA, ⁴Roslin Institute, University of Edinburgh, United Kingdom

Endochondral ossification is a carefully orchestrated process mediated by promoters and inhibitors of mineralization. Tissue-nonspecific alkaline phosphatase (TNAP) plays a crucial role promoting mineralization of the extracellular matrix by restricting the concentration of the calcification inhibitor inorganic pyrophosphate (PPi). TNAP knockout mice (Akp2^{-/-}) faithfully mimic all the skeletal and dental

deficits characteristic of infantile hypophosphatasia. PHOSPHO1, a phosphatase with specificity for phosphoethanolamine (P-Etn) and phosphocholine (P-Cho), has a role in scavenging Pi from MV membrane phospholipids to favor intravesicular hydroxyapatite (HA) deposition. Phospho1^{-/-} mice display growth plate abnormalities, spontaneous fractures, bowed long bones, osteomalacia and scoliosis in early life^{1,2}. Importantly ablation of both TNAP and PHOSPHO1 function leads to complete absence of skeletal mineralization¹. Our working hypothesis is that transporter-mediated influx of extra-vesicular Pi, produced by the ATPase activity of TNAP, contributes to Pi accumulation and HA formation within MVs. This will occur even in the absence of PHOSPHO1 and explains why MVs from Phospho1^{-/-} mice still form mineral. Here, we have used ex vivo metatarsal cultures to provide an initial test for this premise. Metatarsals from E16.5 wild-type (WT) and Phospho1^{-/-} mice were cultured under mineralizing conditions for six days. Three different substrates were used: 4 mM ATP and 10 mM β -glycerolphosphate (β GP) (specific substrates for TNAP), and 3 mM P-Cho, which is hydrolyzed by both TNAP and PHOSPHO1. This experiment was also performed using foscarnet (phosphonoformic acid), an inhibitor of Pi-transporters, and MLS-026839, a specific inhibitor of PHOSPHO1. Mineralization of the WT metatarsals was significantly reduced with foscarnet when using ATP and β GP as substrates but remained unchanged when using P-Cho as substrate. PHOSPHO1 inhibitor MLS-026839 reduced mineralization of the WT metatarsals and adding foscarnet with MLS-026839 reduced it further. Phospho1^{-/-} metatarsals did not show any mineralization with foscarnet when using β GP as a substrate. Experiments are currently underway to confirm these ex vivo metatarsal data using in vitro chondrocytes and osteoblasts cultures as well as their isolated MVs. The data support the premise that Pi-transporters contribute to the PHOSPHO1-generated pool of intravesicular Pi for initiation of MV-mediated mineralization.

* Both authors contributed equally.

1. Yadav et al., J. Bone Miner. Res. 26: 286–297(2011).
2. Huesa et al., Bone (2011), doi:10.1016/j.bone.2011.01.010.
3. Ciancaglini et al., J. Bone Min. Res. 25: 716–723(2010).

Disclosures: Manisha Yadav, None.

SA0126

See Friday Plenary Number FR0126.

SA0127

Regulation of Bone Homeostasis by Transcription Factor Epiprotein. Takashi Nakamura^{*1}, Takahiro Okabe², Takanaga Ochiai³, Eiki Koyama⁴, Motomi Enomoto-Iwamoto⁵, Satoshi Fukumoto¹, Maurizio Pacifici⁴, Masahiro Iwamoto⁶, Yoshihiko Yamada⁷. ¹Tohoku University Graduate School of Dentistry, Japan, ²Nagano Hospital, Japan, ³Matsumoto dental university, Japan, ⁴Children's Hospital of Philadelphia, USA, ⁵The Children's Hospital of Philadelphia Research Institute, USA, ⁶The Children's Hospital of Philadelphia, USA, ⁷The Laboratory of Cell & Developmental Biology, NIDCR, USA

Formation, growth and homeostasis of skeletal elements are sustained through life by a fine balance between bone deposition and resorption and are regulated by systemic and local factors. Bone homeostasis is particularly important for normal skeletal function, biomechanical adaptation and quality of life and its crucial importance is widely appreciated, but much remains to be understood about its regulation, particularly at the molecular level. Parathyroid hormone (PTH) is a key systemic component of mechanisms regulating calcium homeostasis through its action on bone, kidneys and intestine. PTH is a polypeptide containing 84 amino acids and regulates blood calcium concentration by affecting bone resorption (osteoclastogenesis) and vitamin D action and by enhancing calcium reuptake in renal distal tubules and intestine. Recently we identified Epiprotein/Sp6 (Epf) as a zinc finger transcription factor belonging to the Sp family. *Epf* is preferentially expressed in developing ectodermal tissues such as teeth, and *Epf* ablation causes enamel defect and dentin abnormalities, formation of supernumerary teeth, and dental epithelial multilayering and hypercellularity. We also found that mutant mice are characterized by a severe decrease in bone density and volume in calvaria and other skeletal elements. Surprisingly the expression of *Epf* in bone, kidney or intestine tissues and cells was nearly undetectable. After further inquiry, we discovered that *Epf* is abundantly expressed in the parathyroid gland, but not in the thyroid gland or surrounding tissues. Interestingly, the parathyroid gland in mutant mice was enlarged and the parathyroid cells displayed abnormal cytological characteristics. Moreover PTH levels in blood serum of mutant mice were significantly increased compared with those of control littermates. These results suggest that *Epf* is a novel regulator of parathyroid development and function and bone homeostasis and abnormal development of the parathyroid and overproduction of PTH cause impaired bone formation in *Epf* deficient mice. *Epf* appears to act as a negative modulator or optimizer of PTH expression and could do so by binding the promoter region(s) of PTH gene under the control of calcium sensor receptor signaling.

Disclosures: Takashi Nakamura, None.

SA0128

See Friday Plenary Number FR0128.

SA0129

See Friday Plenary Number FR0129.

SA0130

The extra-long Gas variant XL α s Escapes Activation-Induced Subcellular Redistribution, Thus Leading to Sustained Production of Camp and Severe Impairment of Bone Differentiation. Zun Liu¹, Serap Turan¹, Vanessa Webbi², Jean-Pierre Vilardaga³, Murat Bastepe^{*1}. ¹Massachusetts General Hospital, Harvard Medical School, USA, ²University of Pittsburgh, USA, ³University of Pittsburgh, School of Medicine, USA

Murine models indicate that *G α s* and its extra-long variant XL α s, both of which are derived from *GNAS*, markedly differ regarding their cellular actions, but these differences are unknown. Here we investigated activation-induced trafficking of *G α s* and XL α s, using immunofluorescence microscopy and cell fractionation. In transfected cells XL α s remained localized to the plasma membrane, whereas *G α s* redistributed to the cytosol after activation by GTPase inhibiting mutations, cholera-toxin treatment, or isoproterenol. Total internal reflection fluorescence microscopy of live HEK293 cells transiently expressing type 1 PTH/PTHrP receptor (PTHR) and *G α s*-GFP or XL α s-GFP showed that *G α s*, but not XL α s, was depleted in the plasma membrane upon treatment with 10 nM PTH(1-34). Cholera toxin treatment of PC12 cells expressing *G α s* and XL α s endogenously led to an increased abundance of *G α s*, but not XL α s, in the soluble fraction. Mutational analyses revealed two conserved cysteines, and the highly charged domain as being critically involved in the plasma membrane anchoring of XL α s. An XL α s-*G α s* chimera in which a 72-bp portion of XL α s comprising these regions is added onto the N-terminus of *G α s* behaved similarly to XL α s regarding its subcellular localization upon mutational activation or cholera toxin treatment. Moreover, inhibition of palmitoylation by 2BP treatment resulted in the retardation of XL α s in the soluble fraction, suggesting that palmitoylation is required for the plasma membrane targeting of XL α s at the steady state. To determine whether the retention of activated XL α s in the plasma membrane correlates with enhanced adenylyl cyclase stimulation, we measured cAMP production in live cells by using a FRET-based assay. The cAMP response induced by M-PTH(1-14), a parathyroid hormone analog, terminated quickly in HEK293 cells stably expressing PTHR, whereas the response remained maximal for at least 6 min in cells that co-expressed PTHR and XL α s. Furthermore, a GTPase deficient XL α s mutant (R543H) found in certain tumors and patients with fibrous dysplasia of bone and McCune-Albright syndrome generated more basal cAMP accumulation in HEK293 cells and caused more severe impairment of osteoblastic differentiation of MC3T3-E1 cells than the cognate *G α s* mutant (R201H; *gsp* oncogene). Thus, activated XL α s and *G α s* traffic differently, and this may form the basis for the differences in their cellular actions.

Disclosures: Murat Bastepe, None.

This study received funding from: NIH/NIDDK

SA0131

See Friday Plenary Number FR0131.

SA0132

See Friday Plenary Number FR0132.

SA0133

See Friday Plenary Number FR0133.

SA0134

Halofuginone Reduces Bone Metastases:TGF- β dependent and Independent Effects. Patricia Juarez Camacho^{*1}, Khalid Mohammad¹, Ryan McKenna², Holly Davis², Xianghong Peng¹, Desiree Lane¹, Maryla Niewolna¹, Larry Suva³, John Chirgwin¹, Theresa Guise¹. ¹Indiana University, USA, ²University of Virginia, USA, ³University of Arkansas for Medical Sciences, USA

Transforming growth factor- β (TGF β) and bone morphogenic protein (BMP) control cellular processes to maintain homeostasis. Dysregulation of TGF β or BMP activity leads to developmental defects and diseases including bone metastases. Halofuginone (Hfg) is a plant alkaloid derivative with antiangiogenic and antiproliferative

ferative effects. Here we demonstrate that Hfg therapy decreases bone metastasis caused by breast & prostate cancer by inhibiting TGF β and BMP signaling.

Nude mice were inoculated into the left cardiac ventricle with MDA-MB-231/PC3 cancer cells and developed osteolytic bone metastases by 4 weeks. Mice treated with 5 μ g/d Hfg had significantly less osteolysis on x-ray compared with PBS-treated mice (2.11.2 vs 6.23.4mm² p<0.01). Bone histomorphometry showed less tumor in Hfg-treated mice compared to controls (4.31.5 vs 12.22.9mm² p<0.01). Hfg treatment (5 μ g) also decreased mammary fat pad tumor. Similar data were obtained with PC3 prostate cancer.

Further, in MDA-MB-231/PC3 cells, Hfg (100nM, 24h) significantly decreased TGF β -responsive reporter & genes, CXCR4, PTHrP & CTGF, important for bone metastases. Hfg increased Smad7 expression and decreased TGFBR2 levels, but Smad7 knockdown or TGFBR2 overexpression failed to prevent Hfg-inhibition of TGF β signaling. Thus, we studied Hfg effect on BMP signaling pathway. Treatment of MDA-MB-231/PC3 cells with Hfg inhibited BMP-reporter activity & ID1 expression induced by BMP7. Immunostaining of phosphorylated Smad2/3 & Smad1/5/8 showed that Hfg significantly reduced TGF β & BMP signaling in tumor cells from mouse bone metastases compared to control-treated mice.

We tested Hfg effect on bone of mice unaffected by cancer. Hfg (5 μ g) significantly decreased whole body BMD, trabecular & cortical volume and osteoblast number (175 vs 93 p<0.001). Bone marrow cultures from mice treated with Hfg increased TRAP+ osteoclast compared to placebo (1286 vs 803 p<0.001). Hfg effects on bone remodeling are in contrast with other TGF β inhibitors that increase bone mass suggesting that some effects of Hfg are independent of TGF β signaling and may be explained by inhibition of BMP signaling.

Halofuginone completed Phase II trials in sarcoma patients and could rapidly be brought to the clinic for the treatment of bone metastases in breast cancer patients. However, effects of Hfg on normal bone remodeling will need to be assessed in such patients, and measures taken to prevent bone loss at non-tumor-bearing sites.

Disclosures: Patricia Juarez, Camacho, None.

SA0135

See Friday Plenary Number FR0135.

SA0136

See Friday Plenary Number FR0136.

SA0137

See Friday Plenary Number FR0137.

SA0138

See Friday Plenary Number FR0138.

SA0139

See Friday Plenary Number FR0139.

SA0140

The Mechanotransduction Pathway Regulates Tumor Response to Rigidity and PTHrP Expression. Nazanin Ruppender¹, Alyssa Merkel¹, Scott Guelcher¹, Julie Sterling^{*2}. ¹Vanderbilt University, USA, ²Vanderbilt University Medical Center, USA

Breast cancer frequently metastasizes to bone where tumors promote bone resorption, pain, and fracture susceptibility. While the pathways regulating tumor-induced bone disease have been much studied, the reasons why tumor cells behave differently in bone versus other tissues has never been fully explained. Studies in soft tissue tumors have indicated that tumor cell behavior and gene expression change as tumors become more rigid. Since bone is several orders of magnitude more rigid than breast tissue or sites of soft tissue metastasis, we reasoned that this substantial difference in rigidity may regulate bone specific gene expression. Indeed, as we have recently published, the expression of parathyroid hormone related protein (PTHrP) and Gli2 (a Hedgehog transcription factor) were increased with increasing substrate rigidity, while other genes associated with tumor-induced bone disease were unchanged. Others have shown that tumors respond to the rigidity of their surrounding matrix through mechano-sensing pathways involving integrin signaling. Therefore, we hypothesized that tumor cell gene expression in response to rigidity is mediated through mechanotransduction signaling in an integrin-dependent manner, and utilized cells with alterations in the integrin-dependent mechanotransduction pathway. We found that inhibition of α v β 3 integrin using the integrin inhibitor LM609 blocked the rigidity-mediated increases in PTHrP and Gli2. Interestingly, this increase was mediated in a TGF- β (transforming growth factor- β)-dependent manner through the co-localization of α v β 3 with TGF- β Receptor type II (RII). Furthermore,

inhibition of down-stream mechanotransduction mediators, such as Src, reduced the rigidity-mediated increase in PTHrP. Additional studies revealed that the TGF- β dependent response was mediated through MAPK and not Smad signaling, since rigidity increased p38 phosphorylation but not Smad 2 or 3 phosphorylation. We have translated this approach to 3D matrices, where similar increases occur in PTHrP expression with increasing rigidity. The 3D matrices are well-tolerated in mice and in vivo experiments are currently underway in which tumor-seeded 3D scaffolds are implanted into the flank of athymic nude mice. In conclusion, these studies suggest that inhibition of mechanically transduced signaling pathways is a potential clinical target for the inhibition of tumor-induced bone disease.

Disclosures: Julie Sterling, None.

SA0141

The Relationship Between the Presence of Parathyroid Hormone-related Protein and Molecular Subtyping in Canine Mammary Tumors: A Good Model for Human Breast Cancer. Kristi Milley^{*1}, Chantal Denham², Judith Nimmo³, Samantha Richardson¹, Thomas John Martin⁴, Janine Danks¹. ¹School of Medical Sciences, RMIT University, Australia, ²St John of God Anatomical Pathology, Australia, ³ASAP Laboratory, Australia, ⁴St. Vincent's Institute of Medical Research, Australia

Parathyroid hormone-related protein (PTHrP) has been localized in 60% of primary breast tumors (Southby et al, Cancer Res. 50:7710, 1990) and in 11/13 bony metastases (Powell et al, Cancer Res. 51:3059, 1991). In clinical studies it has been shown that the presence of PTHrP in primary tumors gives a better patient prognosis and a lower rate of metastasis to any site (Henderson et al, Cancer Res. 66:2250, 2006).

In humans, better diagnostic and treatment tools have resulted in limited pathological material available for research and this has lead to a renewed search for new breast cancer models. Some groups have used transgenic animal models and others have suggested natural models, including canine mammary tumors (Rivera et al, Cancer Res. 69:8770, 2009). Dogs are considered a model of natural occurring breast cancer and they live in the same environment as humans and epidemiological, clinical, morphologic and prognostic features similar to human breast cancer.

In this study canine mammary tumors (CMT) have been collected from specialist veterinary pathologists and veterinary surgeons. The large amount of canine mammary tissue is collected as part of normal treatment and this has allowed a direct comparison of full tumor histopathological samples with tissue micro arrays (TMA). These tumours were classified histopathologically and subtyped using a panel of six antibodies using immunohistochemistry (IHC). Molecular subtyping has five subtypes: Luminal A, Luminal B, Basal-like, HER2+ and Normal-like. The antibodies are estrogen receptor (ER), progesterone receptor (PR), epidermal growth factor receptor (HER2), p63, CK5, vimentin, Ki67. This molecular subtypes have been suggested to better reflect patient prognosis (Perou et al, Nature 406:747, 2000) than the current typing by ER/PR status. Seventy-two benign and malignant CMTs had both PTHrP and parathyroid hormone receptor 1 (PTH1R) IHC carried out in both full tumor sections and TMAs. Polyclonal antisera to human PTHrP (1-14) and monoclonal antiserum to PTH1R were used and their presence in the CMTs indicated that there was a relationship between the presence of PTHrP and the molecular subtypes. Luminal subtypes have a better prognosis while Basal-like have a poor prognosis and the PTHrP presence in CMTs reflect this prognostic outlook. This could provide an explanation for the presence of PTHrP in the primary human breast cancers and its association with a better patient prognosis.

Disclosures: Kristi Milley, None.

SA0142

Validation Of In Vitro Assays For Identifying Compounds That Affect Breast And Prostate Cancer Cells. Katja Fagerlund^{*1}, Jukka Rissanen², Jani Seppanen¹, Mari Suominen¹, Heikki Vuorikoski¹, Jussi Hallee¹. ¹Pharmatest Services Ltd, Finland, ²Pharmatest Services, Limited, Finland

Breast and prostate cancer are among the most common types of cancer that metastasize to bone. Skeletal metastases can lead to severe pain, pathological fractures, paralysis and eventually increased morbidity. Although there is no curative medication for bone metastases, there are many treatments that can be used to treat the symptoms. Bone resorption inhibitors can be used to inhibit osteolysis, whereas chemotherapy drugs can be used to prevent cancer for spreading. However, the responses to treatments depend on the patient and the type of underlying cancer, and it is therefore of importance to know the direct response of treatment on cancer cells. We have optimized in vitro cancer cell culture models for testing the effects of new chemotherapy agents. MDA-MB-231 and MCF-7 breast cancer cells and PC-3 and LNCaP prostate cancer cells metastasizing to bone were used in the study. Seven known clinically used chemotherapy drugs with different modes of actions, including an alkylating agent N,N'-triethylenethiophosphoramide (ThioTEPA), a pyrimidine analog fluorouracil, an antimetabolic agent Cytosine arabinoside (Ara-C), a topoisomerase I inhibitor topotecan, an anthracycline antibiotic doxorubicin, a mitotic inhibitor paclitaxel and a nucleoside analog gemcitabine, were tested as reference compounds with the range of 1 nM to 1 μ M concentrations. The cells were cultured for 5 days and the effects of the chemotherapy drugs were identified by measuring proliferation of the cells at days 1, 3 and 5 using a commercial WST-1

based proliferation kit. ThioTEPA and fluorouracil showed no effect or only mild effects at 1 μ M concentration on the tested cell lines. Ara-C was a potent inhibitor at 1 μ M concentration, whereas topotecan and doxorubicin were potent inhibitors already at 100 nM concentration. The most potent inhibitors of cancer cell proliferation were paclitaxel and gemcitabine, which were potent inhibitors already at 10 nM concentration. There were no major differences of treatment responses between the cell lines, with the exception that gemcitabine was more potent to breast cancer cells than to prostate cancer cells. These results suggest that paclitaxel, gemcitabine, doxorubicin, topotecan and Ara-C inhibit cell proliferation of breast and prostate cancer cells in this cancer cell culture system. We conclude that this culture system can be used as a screening tool for finding new chemotherapy agents on bone metastatic cancer cells.

Disclosures: Katja Fagerlund, Pharmatest Services Ltd, 3; Pharmatest Services Ltd, 4

SA0143

Aggravation of Myeloma Growth and Its Drug Resistance By an Acidic Milieu Created in Myeloma-Osteoclast Interaction. Keiichi Watanabe^{*1}, Qu Cui², Masahiro Hiasa³, Makoto Kawatani⁴, Shiro Fujii², Takeshi Harada², Shingen Nakamura², Hirokazu Miki², Ayako Nakano⁵, Kumiko Kagawa², Kyoko Takeuchi², Hiroyuki Osada⁴, Eiji Tanaka⁶, Toshio Matsumoto⁷, Masahiro Abe⁸. ¹The University of Tokushima Graduate School of Oral Science, Japan, ²Department of Medicine & Bioregulatory Sciences, The University of Tokushima Graduate School, Japan, ³University of Tokushima Graduate School, Japan, ⁴Chemical Biology Core Facility, RIKEN Advanced Science Institute, Japan, ⁵University of Tokushima Graduate School of Medicine, Japan, ⁶Department of Orthodontics & Dentofacial Orthopedics, The University of Tokushima Graduate School of Oral Sciences, Japan, ⁷University of Tokushima Graduate School of Medical Sciences, Japan, ⁸University of Tokushima, Japan

Myeloma (MM) cells and osteoclasts (OCs) mutually interact in MM to confer aggressiveness and drug resistance in MM cells along with the progression of bone destruction. The MM-OC interaction appears to create a highly acidic milieu by proton produced by OCs and lactate by MM cells. Reveromycin A (RM-A), a novel anti-resorptive agent, permeates a cell membrane to induce apoptosis only in an acidic microenvironment. The present study was therefore undertaken to clarify the role of an acidic condition in MM tumor growth and drug resistance, and therapeutic effects of RM-A on tumor expansion and bone destruction in MM. Rabbit OCs on bone slices enhanced INA6 MM cell growth; however, blockade of acid release by the proton pump inhibitor concanamycin A partially but significantly reduced the enhancement of MM cell growth, suggesting the role of acid in MM growth. MM cell lines as well as primary MM cells constitutively express pH sensors including TDAG8, OGR1, G2A, and TRPV1 at various levels. MM cell growth was enhanced in media acidified by lactic acid to pH below 7.2. Interestingly, at pH7.0 or lower about a half of MM cells remained intact after treatment for 2 days with doxorubicin at 6 microM and the proteasome inhibitor bortezomib at 30 nM although intracellular accumulation of doxorubicin and subsequent generation of ROS in MM cells were not affected, whereas most cells quickly underwent apoptotic cell death at pH 7.4. Interestingly, MM cells showed up-regulation of Akt phosphorylation when cultured at pH 7.2 or lower, suggesting activation of Akt-mediated survival pathway. In contrast, RM-A marginally affected MM cell viability at pH 7.4, but potentially induced cell death along with caspase-3 activation in MM cells in acidic conditions. Furthermore, treatment with RM-A s.c. at 4 mg/kg twice daily or bortezomib s.c. at 0.5 mg/kg twice a week decreased the progression of tumor as well as osteolytic lesions in bones in human INA6 MM cell-bearing SCID-rab MM models. Of note, RM-A and bortezomib in combination almost completely eradicated MM cells and resumed bone formation. These results demonstrate that an acidic condition potentiates MM growth and confers resistance in MM cells to chemotherapeutic agents. RM-A is suggested to target not only OCs but also MM cells in a highly acidic milieu in MM bone lesions, and its anti-MM effects can be envisaged to be augmented in combination with bortezomib with anabolic actions which is active at non-acidic sites.

Disclosures: Keiichi Watanabe, None.

SA0144

Characterization of Bioluminescent Osteosarcoma Orthotopic Model Using Bioluminescent Imaging, Micro-computed Tomography and Histopathology. Rama Garimella*, Jeff Eskew, Priyanka Bhamidi, George Vielhauer, Yan Hong, H Clarke Anderson, Ossama Tawfik, Peter Rowe. University of Kansas Medical Center, USA

Osteosarcoma (OS) is the most common malignancy of bone, mainly affecting children, adolescents and young adults. It is a highly aggressive tumor and typically metastasizes to lungs. Despite aggressive chemotherapy and surgical treatments, the current survival rate is 60-70%. Hence there is a need for clinically relevant models to understand OS pathobiology, and to develop more efficacious treatment strategies. Our long term goal is to apply the bioluminescent orthotopic OS model to screen potential therapeutic agents that enhance the survival rates (especially in patients with

metastasis) by increasing responsiveness to standard cytotoxic drugs or by altering tumor biology. Bioluminescent imaging allows non-invasive tracking of tumor progression in real time. In this study, we developed a bioluminescent orthotopic OS model using the 143 B- OS cell line. We engineered 143B cells to express luciferase using retrovirus transduction techniques. Positive cells were selected in puromycin, expanded and assayed for luciferase activity. Exponentially growing 143B-luc cells were injected into the tibia of Nu/Nu mice, and tumor progression was monitored weekly using the IVIS system. Following intra-tibial injection, the 143B-luc cells formed tumors in the bones and spontaneously metastasized to lungs and kidneys, within four weeks. We detected the presence of m-cherry (fluorescent marker) positive 143B luc cells in the bone and lung sections (Figure 1 A-B). Histological examination showed the presence of actively dividing OS cells in tibias and lungs (Figure 1 C-F). In a defined region of interest at 10X magnification, we observed that the presence of tumor decreased the total bone volume by 19.5%. Segmental micro-computed tomography (μ -CT) analyses revealed a reduction in bone volume/tissue volume (BV/TV) in tumor bearing tibia vs. control (non-tumor) tibia, which needs to be further validated in a larger sample. Micro-CT analyses revealed changes in the bone architecture due to cortical penetration of the tumor in tumor bearing tibia vs. control tibia (Figure 2). Goldner staining on non-decalcified tibial sections indicated the presence of more osteoid in the tumor tissue compared to control, thereby indicating the presence of active osteoid secreting osteosarcoma cells. In conclusion, we have successfully established and characterized a bioluminescent orthotopic model that can be used to study OS pathobiology, and to evaluate potential therapeutic agents.

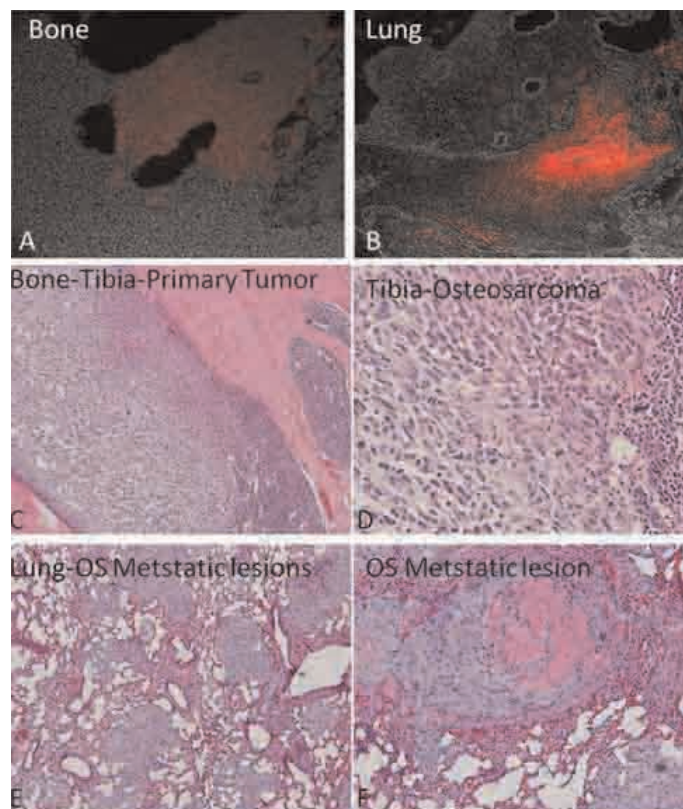


Figure 1. Photomicrograph illustration showing the presence of m-cherry positive 143B luciferase transduced cells in OS of bone and lung tissue (A-B); evidence of primary tumor in tibia (C-D) and OS metastatic lesions in lungs (E-F)

Figure1

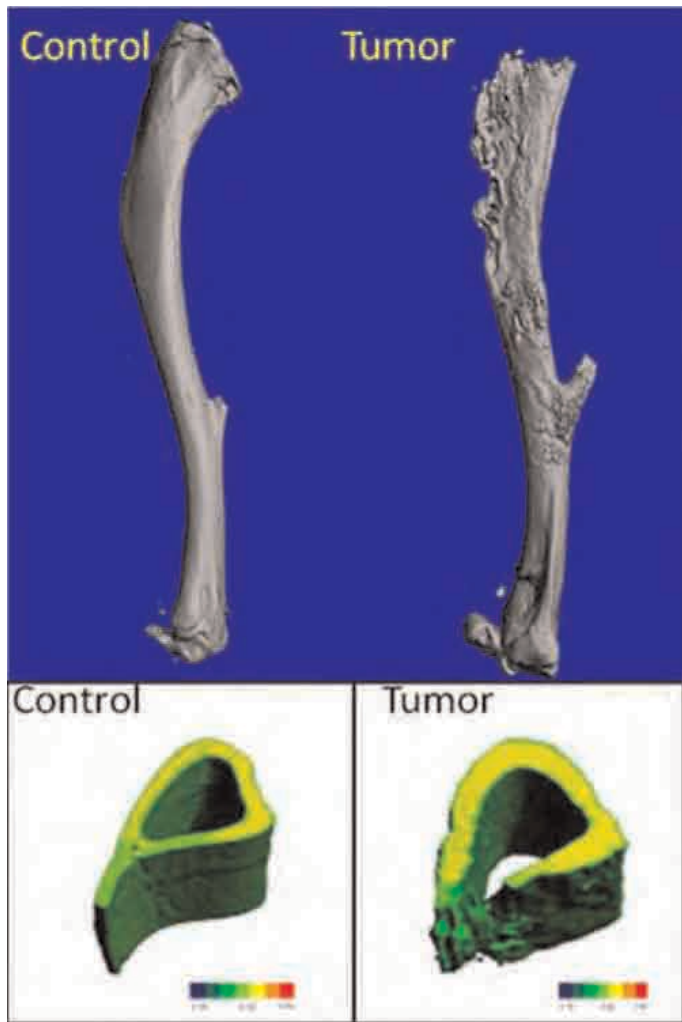


Figure 2: Changes in tibial bone architecture by μ -CT

Figure2

Disclosures: Rama Garimella, None.

SA0145

Characterization of Dkk-1 Expression in an Orthotopic Murine Model of Human Osteosarcoma. Tessa Grabinski, Bart Williams, Kevin Kampfschulte, Matthew Steensma*. Van Andel Research Institute, USA

The identification of factors leading to adoption of a metastatic phenotype represents a key area of research in osteosarcoma, as patients afflicted with metastatic disease experience greatly diminished survival. Upregulated Wnt/ β -Catenin signaling is thought to play an important role in osteosarcoma disease progression. The role of secreted Wnt inhibitors in this process has not been thoroughly evaluated. Elevated serum levels of Dickkopf-1 (Dkk-1) have been detected in patients with osteosarcoma, and correlate with tumor involvement in skeletal and non-skeletal sites. As such, Dkk-1 has been proposed as a suitable biomarker of disease burden. Mechanistically, Dkk-1 is known to play a role in the uncoupling of bone formation in osteolytic cancer, such as myeloma. Dkk-1 expression is Wnt/ β -catenin inducible as part of a negative feedback loop that is presumed to be aberrantly upregulated in osteosarcoma. Our goal is to characterize an animal model that recapitulates Dkk-1 expression in human osteosarcoma. In this way, specific hypotheses regarding the role of Dkk-1 expression as it relates to Wnt signaling can be tested. This model will also be useful for evaluating emerging, Wnt-specific diagnostic and therapeutic reagents.

An orthotopic tibial injection model of osteosarcoma was developed using GFP-expressing human osteosarcoma cell lines (MHOS and 143B; ATCC) that were previously demonstrated by ELISA to produce Dkk-1 in culture media. Following successful tumor induction, Dkk-1 serum levels were correlated with tumor size, quantitative *in vivo* fluorescence, as well as the degree of histologic necrosis in the developing primary tumor. *In vitro* modeling of the effects of Dkk-1 on proliferation (MTT assay), motility (scratch motility assay), osteoblastic differentiation and osteoclastogenesis (qPCR) were performed using an siRNA knockdown strategy for reducing Dkk-1 expression (Qiagen®).

Dkk-1 was readily detectable in mouse sera, and directly correlated with tumor size, intensity of *in vivo* fluorescence, and pulmonary metastasis. Additionally, histologic necrosis was associated with a relative decrease in Dkk-1. Minimal effects on proliferation or motility were observed in the siRNA Dkk-1 hypomorphic cell lines. Knockdown of Dkk-1 increased Axin2 expression indicating possible loss of negative feedback control. These data confirm the relevance of the orthotopic murine model with respect to Dkk-1, Wnt signaling and osteosarcoma disease progression.

Disclosures: Matthew Steensma, None.

SA0146

Genomic Promoter Occupancy of Runx2 Identifies Genes Involved in Cell Migration and Invasion in Osteosarcoma Cells. Margaretha van der Deen¹, David Lapointe¹, Sneha Gupta¹, Daniel Young¹, Martin Montecino², Jane Lian¹, Janet Stein¹, Gary Stein¹, Andre Van Wijnen^{*1}. ¹University of Massachusetts Medical School, USA, ²Universidad Andres Bello, Chile

Runx-related transcription factors (RUNX1, RUNX2 and RUNX3) are key lineage-specific regulators of progenitor cell growth and differentiation, but also function pathologically as cancer genes that contribute to tumorigenesis. RUNX2 attenuates growth and stimulates maturation of osteoblasts during bone formation, but is also robustly expressed in a subset of osteosarcomas, as well as in metastatic breast and prostate tumors. To assess the biological function of RUNX2 in tumorigenesis, we examined human genomic promoter interactions for RUNX2 using chromatin immunoprecipitation (ChIP)-microarray analysis in osteosarcoma cells (SAOS-2). Promoter binding of both RUNX2 and RNA Polymerase II (RNAPII) was compared with gene expression profiles of cells in which RUNX2 was depleted by RNA interference. The majority of RUNX2 bound loci (1550 of 2339 total) exhibit promoter occupancy by RNAPII and contain the RUNX consensus motif 5'[T/A/C]G[T/A/C]GG[T/G]. Gene ontology analysis indicates that RUNX2 controls components of multiple signaling pathways (e.g., WNT, TGF β , TNF α , and interleukins), as well as genes linked to cell adhesion, migration and/or invasion (e.g., the focal adhesion related genes FAK/PTK2 and TLN1). Trans-well studies reveal that RUNX2 depletion in osteosarcoma cells diminishes cellular invasion and migration. Hence, the metastatic potential of osteosarcomas and non-osseous tumors may be increased by pathological elevation of RUNX2.

Disclosures: Andre Van Wijnen, None.

SA0147

See Friday Plenary Number FR0147.

SA0148

See Friday Plenary Number FR0148.

SA0149

Impairment of Osteoblast Differentiation and Activity in Multiple Myeloma Bone Disease: Role of Sclerostin. Silvia Colucci^{*1}, Giacomina Brunetti², Angela Oranger¹, Giorgio Mori³, Giorgina Specchia⁴, Erminia Rinaldi⁴, Paola Curci⁴, Giovanni Passeri⁵, Alberta Zallone⁶, Rita Rizzi⁴, Maria Grano². ¹Department of Human Anatomy & Histology, University of Bari, Italy, ²University of Bari, Italy, ³Department of Biomedical Science, University of Foggia, Italy, ⁴Hematology Section, Bari University, Medical School, Italy, ⁵Department of Internal Medicine & Biomedical Sciences, Center for Metabolic Bone Diseases, University of Parma, Italy, ⁶University of Bari Medical School, Italy

Wnt signalling through the secretion of Wnt inhibitors DKK1, sFRP-2 and -3 plays a key role in the decreased osteoblast activity associated with multiple myeloma (MM) bone disease. We provide evidence that another Wnt antagonist, sclerostin, an osteocyte-expressed negative regulator of bone formation, is expressed by myeloma cells, i.e. human myeloma cell lines (HMCLs) and plasma cells (CD138+ cells) obtained from the bone marrow of a large number of MM patients with bone disease. We demonstrated that bone marrow stromal cells (BMSCs), differentiated into osteoblasts and co-cultured with HMCLs showed, compared with BMSCs alone, reduced expression of major osteoblastic specific proteins, decreased mineralized nodule formation, and attenuated expression of members of the AP-1 transcription factor family (Fra-1, Fra-2 and Jun-D). Moreover, in the same co-culture system the addition of neutralizing anti-sclerostin antibodies restored osteoblast functions by inducing nuclear accumulation of β -catenin. We further demonstrated that the up-regulation of RANKL and the down-regulation of OPG in osteoblasts were also sclerostin mediated. Our data indicated that sclerostin secretion by myeloma cells contribute to the suppression of bone formation in the osteolytic bone disease associated to MM.

Disclosures: Silvia Colucci, None.

SA0150

Longitudinal preclinical microCT scanning: Maintaining Biological Relevance in Non-Invasive Metastatic Burden and Osteolysis Monitoring. Ning Zhang¹, Jay Whalen¹, Anna Christensen^{*2}, Magdalena Bazalova³, Jeff Meganck¹, Ed Lim¹. ¹Caliper Life Sciences, USA, ²Caliper LifeSciences, USA, ³Stanford University, USA

Non-invasive imaging is commonly used in longitudinal studies of small animals. Biologically relevant models are essential in characterizing pathological processes and monitoring therapeutic responses. This has not been possible with earlier generation in vivo microCT systems that resulted in radiation doses high enough to potentially impact the underlying biology. New technologies in microCT have enabled true longitudinal assessment of disease with minimal radiation doses by minimizing the scan time. The following work will discuss the Gafchromic film dosimetry evaluation of the Quantum FX standalone microCT scanner for longitudinal monitoring of metastatic tumor burden and bone osteolysis non-invasively in biologically relevant conditions. Dosimetric evaluations showed a mean body dose starting at 8mGy per 17 second scan at 90KV. The dose range from the Quantum FX scanner allowed us to take multiple scanning time points to characterize the development of osteolysis without radiation artifact. The metastatic tumor burden of MDA-MB231 mammary carcinoma cells was concurrently monitored through bioluminescent optical imaging on an IVIS Spectrum validating the characteristic metastatic potential of this model for anatomical microCT assessment.

Disclosures: Anna Christensen, Caliper Life Sciences, 3
This study received funding from: Caliper Life Sciences

SA0151

Novel Bis-Cyclic Thioureas, Identified from Combinatorial Libraries, Inhibit the Proliferation and PTHrP Expression of Pancreatic Cancer Cells. Douglas Burton^{*1}, Randolph Hastings², Adel Nefzi³, Su Tu², Leonard Defetos⁴. ¹VA San Diego Healthcare System / University of California, San Diego, USA, ²VA San Diego Healthcare System / University of California San Diego, USA, ³Torrey Pines Institute for Molecular Studies, USA, ⁴Veterans Administration San Diego Healthcare System & University of California, USA

Background: PTHrP (parathyroid hormone related protein) is commonly expressed by pancreatic cancer cells and this oncoprotein can influence the progression of this malignancy. Recently we discovered, through combinatorial library screening, bis-cyclic thioureas compounds that inhibit lung cancer cell PTHrP expression and retard the growth of PTHrP-expressing lung cancer cells. The focus of this study was to evaluate these compounds for their effects on pancreatic cancer PTHrP expression and growth.

Methods: In vitro studies were conducted using human pancreatic cancer cell lines (BxPC-3 and CFPAC-1) treated with 2 µg/ml bis-cyclic thiourea compounds (#2 and #17). We measured PTHrP expression and cell growth over 7 days by immunoassays and MTT assays and compared the bis-cyclic thiourea treatment groups to the vehicle control (DMSO) treatment group.

Results: The bis-cyclic thiourea compounds significantly inhibited PTHrP expression and cell proliferation compared to the vehicle control treatment and the effects were directly proportional to the pancreatic cell basal PTHrP expression. The most dramatic inhibitory effects were observed in the BxPC-3 cells (>65% inhibition of PTHrP and growth). Less inhibitory effects were demonstrated on the CFPAC-1 cells (approx. 20% inhibition of PTHrP and growth). Compound #2 was more potent in both cell lines compared to compound #17.

Conclusions: Bis-cyclic thiourea molecules inhibit PTHrP expression and growth of PTHrP-producing pancreatic cancers. Cyclic thioureas could find clinical utility either as anti-neoplastic agents for innovative treatments of PTHrP expressing cancers or as treatments for hypercalcemia of malignancy.

Disclosures: Douglas Burton, None.

SA0152

See Friday Plenary Number FR0152.

SA0153

Opposing Survival Effects of Amino and Carboxyl-Terminal PTHrP in Non-Small Cell Lung Carcinoma Patients. Randolph Hastings^{*1}, Philippe Montgrain¹, Rick Quintana¹, Ann Tipps², Douglas Burton¹, Leonard Defetos³. ¹VA San Diego Healthcare System / University of California San Diego, USA, ²University of California San Diego, USA, ³Veterans Administration San Diego Healthcare System & University of California, USA

Introduction: From our previous work, we know that tumor expression of carboxyl-terminal PTHrP is a positive prognostic indicator in women with non-small

cell lung carcinoma (NSCLC). In contrast, a recent study suggests that amino-terminal PTHrP is associated with shorter survival in lung adenocarcinoma patients. The goal in this study was to tumor evaluate amino and carboxyl PTHrP immunoreactivity in the same group of NSCLC patients and investigate survival implications.

Methods: Amino PTHrP expression was assessed by immunohistochemistry in tumor samples from 165 patients with NSCLC. Carboxyl PTHrP had been determined previously in the same samples. A pathologist unaware of the clinical history classified specimens as PTHrP-positive or PTHrP-negative. The log-rank test and Cox regression were used to analyze survival as a function of PTHrP expression and other covariates.

Results: By odds of 6:1, lung carcinomas in males expressed amino and carboxyl PTHrP together rather than carboxyl PTHrP alone. A larger proportion of female carcinomas were solely carboxyl PTHrP positive. Amino PTHrP and carboxyl PTHrP were significant and independent negative and prognostic indicator with hazard ratios for death of 1.7 (P = 0.031) and 0.6 (P = 0.018), respectively. Patients with carboxyl PTHrP-positive/amino PTHrP-negative carcinoma had the longest survival overall and those that were amino positive/carboxyl negative had the shortest lifespans.

Conclusions: Amino and carboxyl PTHrP have independent and opposing associations with lung cancer patient survival. Dual expression of the two epitopes differs between male and female patients. This factor combined with the differing survival effects could explain the apparent restriction of a carboxyl PTHrP survival effect to females was associated with a survival advantage in female patients. Future work is indicated to determine whether the sex-based difference in lung cancer PTHrP peptide expression depends on variable processing of the prohormone and whether the effects could be targeted for therapeutic purposes

Disclosures: Randolph Hastings, None.

SA0154

Specific Receptor Tyrosine Kinases (RTKs) are Novel Therapeutic Targets for Osteosarcoma. Ashley Rettew^{*}, Mee Jee Lee, Patrick Getty, Edward Greenfield. Case Western Reserve University, USA

One-third of osteosarcoma patients succumb to pulmonary metastasis despite high-dose neoadjuvant chemotherapy protocols. These survival rates have not improved over the last 30 years. Tyrosine kinases have emerged as targets for new cancer therapies. Using phosphoproteomic screening of 42 individual RTKs, we identified 10 RTKs that were phosphorylated and previously unstudied in 143B and/or LM7 metastatic human osteosarcoma cell lines. An siRNA screen using pools of 4 individual duplexes to target each of the 10 activated RTKs demonstrated that 9 siRNA pools inhibited the in vitro phenotype (invasion, motility, cell growth and/or colony formation) of one or both cell lines. Since the major caveat of siRNA is the possibility for off-target effects, we individually tested the four siRNA duplexes to validate the pooled results. In these experiments, the pattern of phenotype inhibition replicated the pattern of knockdown by the individual duplexes for 6 of the 9 RTKs, indicating that those effects are consistent with on-target silencing. For example, in LM7 cells, the FGFR2 pool and two duplexes knocked down FGFR2 expression by >80% and inhibited motility and colony formation by ≥35% whereas the other two duplexes only reduced expression levels by <60% and had little to no effect on phenotype. To further validate the individual duplex experiments, approaches other than siRNA were used to inhibit the RTKs. Antisense-mediated knockdown targeting EphB2 or Ret significantly inhibited colony formation and motility in LM7 cells (p<0.05) demonstrating that the effects of EphB2 and Ret inhibition are on-target. Antisense-mediated knockdown of EphA2 demonstrated off-target effects in 143B cells. The translationally relevant small molecule inhibitors (SMIs) PD173074 and R428 were used to inhibit FGFRs or Axl, respectively. PD173074 inhibited motility and colony formation in both cell lines (p<0.001) and invasion in LM7 cells (p=0.03) in a dose-dependent manner. R428 reduced motility and colony formation in a dose-dependent manner in 143B cells (p<0.001). Moreover, R428 or PD173074 caused pre-formed colonies to undergo rapid changes in cell morphology consistent with cell death. In conclusion, our results indicate that specific RTKs (Axl, EphB2, FGFR2, FGFR3 and Ret) contribute to the in vitro behavior of metastatic osteosarcoma cell lines and are novel therapeutic targets for osteosarcoma.

Disclosures: Ashley Rettew, None.

SA0155

The Synthetic Inhibitor of ZZ Domain of Sequestosome-1/p62 Inhibits Both Stromal Cell Independent and Dependent Myeloma Cell Growth and Osteoclast Formation. Jumpei Teramachi^{*1}, Kyaw Ze Yar Myint², Rentian Feng², Xiang-Qun Xie², G. David Roodman³, Noriyoshi Kurihara⁴. ¹University of Pittsburgh & The Center for Bone Biology at UPMC, USA, ²University of Pittsburgh, Pharmaceutical Sciences, USA, ³University of Pittsburgh, The Center for Bone Biology at UPMC, & VA Pittsburgh Healthcare System, USA, ⁴University of Pittsburgh & The Center for Bone Biology, USA

The marrow microenvironment plays a critical supportive role in myeloma (MM), and enhances both tumor growth and bone destruction through MM cell derived TNFα activation of multiple signaling pathways in marrow stromal cells. We reported that sequestosome 1 (p62) plays a key role in the formation of signaling complexes

that result in NF- κ B, p38 MAPK and PI3K activation in the marrow stromal cells of patients with MM that result in enhanced MM growth and OCL formation. Recently, we generated deletion constructs of p62 that lacked specific p62 domains: PB1, ZZ, p38, TBS and UBA, to identify the domains of p62 responsible for increased MM cell growth and osteoclast (OCL) formation mediated by NF- κ B and p38 MAPK signaling, as a means to develop inhibitory peptides/molecules as potential therapeutic agents for MM. We transfected these constructs into a p62-knockout stromal cell-line and found that the ZZ domain is required for stromal cell support of increased MM cell growth, IL-6 production, VCAM-1 expression and OCL formation. These results suggest that dominant negative constructs or small molecules that target the ZZ domain of p62 should inhibit stromal cell support of MM cells and OCL formation by the marrow microenvironment. Therefore, we developed a p62-ZZ inhibitory small molecule (MW:363.5) and tested this compound for its capacity to block the enhanced myeloma cell growth, IL-6 production, VCAM-1 expression on stromal cells and OCL formation induced by TNF- α . TNF- α specifically induces PKC ζ phosphorylation that is activated via p62-ZZ. MM1.S myeloma cells or normal human CFU-GM, a source of OCL precursors, were co-cultured with human stromal cells in the presence or absence of the p62-ZZ inhibitor. The inhibitor (10 μ M) directly blocked MM cell growth by 90% compared to vehicle. VCAM-1 expression and IL-6 production by stromal cells induced by TNF- α was blocked by 30% and 90% respectively compared to vehicle controls. This compound at 10 μ M did not change the proliferation of stromal cells by the MTT assay. Further, the TNF- α induced PKC ζ phosphorylation in stromal cells and MM1.S was blocked when the cells were pre-treated with this p62-ZZ inhibitory compound for 3 hours. These results suggest that synthetic compounds that target the ZZ domain of p62 and can inhibit MM cell growth and OCL formation induced by the marrow microenvironment by blocking p62 function.

Disclosures: *Junpei Teramachi, None.*

SA0156

The Transcription Repressor Gfi1 Directly Interacts with the *Runx2* Gene In Osteoblast Precursors To Mediate Repression by Multiple Myeloma Cells Via TNF- α , Leading To Blocked Osteoblast Differentiation. Shunqian Jin^{*1}, Sonia D'Souza¹, Quanrong Sun¹, Benedicte Sammut¹, H. Leighton Grimes², G. David Roodman¹, Deborah L. Galson¹. ¹University of Pittsburgh, Medicine/Hematology-Oncology, The Center for Bone Biology of UPMC, & VA Pittsburgh Healthcare System, USA, ²University of Cincinnati College of Medicine/Division of Immunobiology, USA

Multiple myeloma (MM) is a plasma cell malignancy that is the most frequent cancer to involve the skeleton. MM bone disease is characterized by the formation of lytic bone lesions adjacent to MM cells that rarely heal even when patients are in long-term remission due to a persistent suppression of bone marrow stromal cell (BMSC) differentiation into osteoblasts (OB). We have previously reported that MM cells induce a long-lasting suppression of OB differentiation by repression of the *Runx2* gene, through elevated expression of the transcription repressor Gfi1. These changes were also mediated by TNF- α . Co-transfection reporter assays in MC-4 cells showed that the mouse *Runx2* promoter was repressed by MM cells and TNF- α , and was also repressed in a dose-dependent manner by cotransfection with wild-type (wt)-Gfi1 protein, and surprisingly, by the Gfi1N382S DNA-binding mutant, although not as efficiently as wt-Gfi1. We conducted detailed analyses to determine if Gfi1 directly represses the *Runx2* promoter and to identify the *Runx2* promoter sequences responsible for the Gfi1-mediated repression. Deletion analyses and biotin-oligonucleotide pull-down assays revealed that the -40~-1 region of the *Runx2* promoter is the main site of Gfi-1 binding, that the binding was specific by competition assays, and that the entire C-terminal Zn-finger region of Gfi1 is necessary and sufficient for binding. Importantly, these assays provided further proof that both wt-Gfi1 protein and the Gfi1N382S (albeit weaker) could bind directly to this region. The Gfi1 binding site was mapped within the -40~-1 region to an unusual palindromic double Gfi1 binding site, AAGCTT and confirmed by EMSA. Oligos with mutations of either AA or TT are still bound by wt-Gfi1, but not by Gfi1N382S, whereas mutation of both sides results in a complete lack of wt-Gfi1 binding. Luciferase assays with site-specific mutant *Runx2* promoter reporters demonstrated that this Gfi1 binding site is responsible for the Gfi1-mediated repression as well as part of the TNF- α -induced repression. Strikingly, chromatin immunoprecipitation revealed that Flag-Gfi1 binds within -111/+123 region of the endogenous *Runx2* promoter in MC-4 cells, confirming that Gfi1 binds the endogenous *Runx2* gene. Thus, these results indicate that MM cell secretion of TNF- α induces the transcription repressor Gfi1, which is directly involved in the repression of *Runx2* expression in OB precursor cells, thereby preventing OB differentiation.

Disclosures: *Shunqian Jin, None.*

SA0157

See Friday Plenary Number FR0157.

SA0158

See Friday Plenary Number FR0158.

SA0159

Soft Tissue Postraumatic Calcifications Associated with a New *FGF23* Gene Mutation: Clinicopathological and Molecular Genetic Study. Maria Luisa Brandi¹, Deobra Strigoli², Caterina Fossi², Cristiana Casentini², Gigliola Leoncini², Sergio Fabbri², Francesco Franceschelli², Gemma Marcucci², Loredana Cavalli¹, Francesca Giusti², Laura Masi^{*1}. ¹University of Florence, Italy, ²Metabolic Bone Diseases Unit, Italy

Extraskelatal calcifications of soft tissues are not rare radiographic finding. However, parts of these constitute a rare familial condition indicated as Tumoral Calcinosis (TC). It is a familial disease characterized by a phosphate disorder due to mutations of one of the genes coding phosphatonins (FGF23, GALNT3 or KLOTHO gene). Localized trauma can be responsible of deposition of calcium and phosphate in soft tissues with small nodules that may ulcerate, extruding a chalky with material identified as hydroxyapatite similarly with TC. In the literature, no phosphatonins gene mutations have been so far described in these patients. In the present study we evaluated the role of phosphatonins in a patient with postraumatic soft tissue calcifications. The patient is a man 44 yrs old with a history of traumatic fracture of the right tibia. Fracture was follow by a hemorrhage around the bone and the formation of nodule 10 cm diameter in the peroneal muscle. The histopathological analysis of the mass showed the deposits of calcium. The patient exhibited a normophosphatemia [2.9 mg/dL (n.v.: 2.7-4.5)], normocalcemia [9.6 mg/dL (n.v.: 8.2-10.7)]. Urine calcium and phosphate were in the normal range. A very low level of 25 hydroxyvitamin D3 was observed [5.7 ng/ml (n.v.:30-70)] with PTH circulating levels slightly upper normal range [8.1 pmol/L (n.v.: 1.3-7.6)]. Genomic DNA was extracted from peripheral blood collected from patient using the microvolume extraction method QIAamp DNA Mini Kit (Qiagen GmbH, Hilden, Germany), according to the manufacturer's instructions. Intact FGF23 serum level and C-terminal fragment were determined by ELISA. We found a new heterozygous (GGC>AGC) codon 240 Gly/Ser substitution in exon 3 of FGF23 gene. No mutations of the GALNT3 and KLOTHO genes were detected. Circulating intact and C-terminal fragment measurement showed a high level of inactive C-terminal fragment (90 RU/ml) a low level of active FGF23 (10.2 pg/ml). In conclusion we described a new mutation of FGF23 associated with formation of extraskelatal calcifications. C-terminal FGF23 fragment is usually very high in the serum of the patient after a bone fracture. However, the levels return in the normal range after 15-20 days. In the present case C-terminal fragment was measure after 6 months from the injury. We could speculate the FGF23 gene mutation could alter the normal production of FGF2 and may be favor the deposition of calcification after an injury.

Disclosures: *Laura Masi, None.*

SA0160

See Friday Plenary Number FR0160.

SA0161

Vitamin D Status in Ireland: Post IOM Interpretation. Malachi McKenna^{*1}, Barbara Murray¹, Mark Kilbane². ¹St. Michael's Hospital, Ireland, ²St. Vincent's University Hospital, Ireland

Background: The Institute of Medicine (IOM) in a recent public health report on dietary requirements for calcium and vitamin D in North America contained three important findings for clinicians: (1) a serum 25-hydroxyvitamin D (S-25OHD) level above 50 nmol/L meets the needs of 97.5% of the population for all life stages, (2) a S-25OHD level above 125 nmol/L could indicate those at risk of harm from over-replacement, and (3) a simulated dose-response formula is given for estimating the expected S-25OHD based on total oral vitamin D intake. We and others over the past 30 years have identified high prevalence of poor vitamin D status in Ireland. So we reviewed our recent experience of vitamin D status in the light of the IOM report both in healthy subjects and those with illnesses.

Methods: S-25OHD was measured in a diverse group of Irish subjects (n=1254): healthy adults during winter, patients with multiple sclerosis during winter; mothers at term and cord samples from their offspring; preterm infants at about 3 weeks old and again at about 15 weeks old; osteoporosis patients on low-dose vitamin D supplementation; and cystic fibrosis patients on low-dose vitamin D supplementation.

Results: In healthy adults during winter 33% were \geq 50 nmol/L compared to 28% of MS patients. Mothers at birth (45%) were more likely than their offspring (13%) to have levels \geq 50 nmol/L. Preterm infants at about 3 weeks were less likely to have levels \geq 50 nmol/L compared to same infants after prolonged augmented vitamin D intake of 400 IU/d (13% vs 86%), but of the later 25% were $>$ 100 nmol/L and 8% were $>$ 125 nmol/L. Osteoporosis patients on supplementation (723200 IU/d) achieved level \geq 50 nmol/L in 91% but cystic fibrosis patients on supplementation (1380447 IU/d) were less successful (Table 1). Using data from a previous study we calculated the dose-response to low-dose vitamin D and noted an increase 8.4 nmol/L/100 IU that is over fourfold higher than the oft quoted expected rise of 1.8 nmol/L/100 IU, but was similar to the IOM simulated dose-response.

Conclusion: The IOM offers a standard and a gauge for guaranteeing adequate vitamin D status in the Irish population but in our more northerly latitude we have an even greater dependence on oral intake in ensuring optimal vitamin D status. We found a high prevalence of poor vitamin D status in our unsupplemented groups; however for many infants 400 IU/d is excessive.

Groups	N	S-25OHD nmol/L				
		<30	30-49	≥50	>100	>125
Healthy adults during winter	229	21%	46%	33%	0%	0%
Multiple sclerosis patients during winter	331	40%	32%	28%	2%	1%
Healthy pregnant women at term	39	21%	34%	45%	3%	0%
Umbilical cord samples at term	39	59%	28%	13%	0%	0%
Preterm infants at 3 weeks	272	21%	65%	14%	1%	0%
Preterm infants at 15 weeks (supplemented)	148	3%	11%	86%	25%	8%
Osteoporosis outpatients (supplemented)	91	1%	8%	91%	20%	2%
Cystic fibrosis patients (supplemented)	105	23%	28%	49%	8%	3%

Table 1

Disclosures: Malachi McKenna, None.

SA0162

Epidemiology of Paget's Disease of Bone in the City of Recife, Brazil. Rainier Reis¹, MaÚra Poncell¹, Daniele Fontan², Erik Diniz², Francisco Bandeira³. ¹University of Pernambuco Medical School, Brazil, ²Division of Endocrinology, Agamenon Magalhaes Hospital, Brazil, ³UPE, Brazil

The aim of this study was to determine prevalence and incidence of Paget's disease of bone (PDB) between 2006 and 2009 in one institution in the city of Recife, Northeast Brazil. All patients aged 45 years and over attending the Pernambuco Osteoporosis Centre at the Endocrine and Diabetes Department were assessed. Serum alkaline phosphatase (SAP) was measured in all patients and pelvis X-rays taken previously for other medical reasons were also evaluated. When levels of SAP were elevated, bone scintigraphy was performed to identify possible affected sites. High bone turnover areas on scintigraphy were then examined using radiographies, which were used as gold standard for diagnosis of PDB. Period prevalence (PP) and incidence density (ID) were calculated for each year for males and females separately, with confidence intervals (CIs) and hypothesis test for difference between proportions. CIs for PP were estimated assuming a Binomial distribution, and expressed as percentage of every 1000 patients. Annual ID was computed as new cases arising from the beginning to the end of each year, divided by the assessed population and expressed as number per 10 000 person-years; CIs were calculated assuming a Poisson distribution. All statistical calculations were made using the MINITAB software Version 15. The present study was approved by the Research Ethics Committee of the Agamenon Magalhaes State Hospital.

A total of 7752 patients were assessed of which 53 presented with PDB. The age ranged from 53 to 90 years, with a mean of 69.53 ± 8.51 years. The total PP was 6.80/00 and a statistically significant increase from 4.20/00 in 2006 to 12.70/00 in 2009 was observed (p=0.013). The prevalence rates increased in both sexes during the period, although it did not reach statistical significance (p=0.058 for males and p=0.119 for females). Males were predominantly affected. The ID for PDB was 50.3 per 10 000 person-years for the period 2006-2009. A statistically significant increase from 34.6 in 2006 to 103.2 per 10 000 person-year in 2009 was observed (p=0.026). Males presented a statistically significant increase in the ID rates over this period (p=0.032). Such trend was not seen in females (p=0.307).

Our data show that prevalence and incidence rates of PDB in Recife are comparable to those from Southern Europe. No trends of decline either in prevalence or in incidence rates were observed. To our knowledge this is the first epidemiological study of PDB in South America.

Table 1. Period prevalence (PP) of Paget's disease of bone 2006-2009, in Recife, Brazil

Year	2006	2007	2008	2009	2006-2009
Total					
Number of cases of Paget's disease of bone	11	13	13	16	53
Assessed Population	2602	2175	1715	1260	7752
PP (%)	4.2	6.0	7.6	12.7	6.8
95% CI	2.1-7.6	3.2-10.2	4.0-12.9	7.2-20.5	3.1-8.9
Male data					
Number of cases of Paget's disease of bone	4	9	6	8	27
Assessed Population	590	516	440	336	1882
PP (%)	6.8	17.4	13.6	23.8	14.3
95% CI	1.9-17.3	8.0-32.5	5.6-29.4	10.3-46.4	9.3-20.8
Female data					
Number of cases of Paget's disease of bone	7	4	7	8	26
Assessed Population	2012	1659	1275	924	5870
PP (%)	3.5	2.4	5.5	8.7	4.4
95% CI	1.4-7.2	0.7-6.2	2.2-11.3	3.7-17.0	2.9-6.5

*Period Prevalence was calculated as the proportion (%) of the existing cases divided by the assessed population during the same period, expressed as number per 1,000 patients.

Table 1. Period prevalence (PP) of Paget's disease of bone 2006-2009, in Recife, Brazil

Table 1. Incidence density (ID) of Paget's disease of bone 2006-2009, in Recife, Brazil

	2006	2007	2008	2009	2006-2009
Total					
Diagnosed cases of Paget's disease of bone	8	8	8	13	37
Assessed Population	2602	2175	1715	1260	7752
ID*	34.6	41.4	46.6	103.2	50.3
95% CI	15.8-65.7	18.9-78.6	20.1-91.9	54.9-176.4	35.8-68.8
Male data					
Diagnosed cases of Paget's disease of bone	2	7	5	7	21
Assessed Population	590	516	440	336	1882
ID*	33.9	135.8	113.6	208.3	111.6
95% CI	4.1-122.4	54.5-279.5	36.9-263.2	83.8-439.2	69.1-170.6
Female data					
Diagnosed cases of Paget's disease of bone	7	2	3	6	18
Assessed Population	2012	1659	1275	924	5870
ID*	34.8	12.1	23.5	64.9	30.7
95% CI	14.0-71.7	1.4-43.3	4.8-68.8	23.8-141.3	18.2-48.5

*Incidence Density was calculated as the number of new cases each year divided by the total person-time of observation, expressed as number per 10 000 person-years.

Table 2. Incidence density (ID) of Paget's disease of bone 2006-2009, in Recife, Brazil

Disclosures: Francisco Bandeira, None.

SA0163

See Friday Plenary Number FR0163.

SA0164

See Friday Plenary Number FR0164.

SA0165

See Friday Plenary Number FR0165.

SA0166

See Friday Plenary Number FR0166.

SA0167

Bone Mineral Density (BMD) Assessment in Patients with Primary Hyperparathyroidism (PHPT) before and one year after Parathyroidectomy (PTX). Eugénie Koumakis¹, Jean-Claude Souberbielle², Didier Borderie³, Emile Sarfati⁴, Soueda El Kettani¹, Andre Kahan¹, Catherine Cormier⁵.

¹Rheumatology Department A, Cochin Hospital, APHP, Paris Descartes University, France, ²Laboratoire d'exploration fonctionnelles, Hôpital Necker-Enfants Malades, France, ³Laboratoire de Biochimie générale et spécialisée, Cochin Hospital, APHP, Paris Descartes University, France, ⁴Department of endocrine Surgery, APHP, Hôpital Saint-Louis, France, ⁵AP-HP Groupe Hospitalier Cochin, France

PHPT is a frequent cause of secondary osteoporosis. Increase in BMD following PTX has been reported in numerous studies. Subclinical PHPT is increasingly diagnosed in osteoporosis patients. It is unclear whether patients with a milder phenotype might benefit from PTX. This study was to investigate BMD changes in PHPT patients before and one year after PTX, and to compare BMD changes between patients with classic PHPT and a milder phenotype of PHPT.

Patients and Methods: single center longitudinal study of 55 PHPT patients aged 63.10 ± 6.6 years with mean T-score at the spine, femoral neck and total hip of -2.51 ± 0.29, -2.34 ± 0.74 and -1.80 ± 0.82 respectively. A history of fracture and osteoporosis were reported in 41.8% and 90.7% of cases, respectively. 23 patients had both an elevated pre-PTX serum total and ionized calcium level (group 1), while the remaining 32 had normal pre-PTX total and/or ionized calcium (group 2). All patients were operated on with complete resolution of PHPT (normal serum total and ionized calcium, phosphate, and PTH 3 months after PTX). BMD was evaluated using QDR 4500 (Hologic) before and one year after PTX. Paired data were assessed with the Wilcoxon rank test, and unpaired data were assessed with the Mann-Whitney test.

Results. In the 55 PHPT patients, BMD increased significantly one year after PTX by 3.25.1% at the spine (p=0.0001), 3.05.6% at the femoral neck (p=0.0002) and 3.35.3% at the total hip (p=0.0001). In group 1 patients, BMD increased significantly by 4.84.5% at the spine (p=0.0001), 4.65.9% at the femoral neck (p=0.0019), and 2.94.5% at the total hip (p=0.0005). In group 2, BMD increased significantly by

1.85.1% at the femoral neck ($p=0.031$) and 2.76.1% at the total hip ($p=0.048$) but not at the spine (2.05.2% gain, $p=0.098$). The BMD gain was more important at the spine in group 1 than in group 2 patients ($p=0.0076$), but there was no difference in BMD gain between the 2 groups at the femoral neck and total hip ($p=0.15$ and $P=0.16$ respectively). In group 2 patients, hyperplasia and multiple adenomas tended to be more frequent than in group 1 patients, although not significantly.

Conclusion. In these PHPT patients, BMD increased significantly after PTX at the spine and hip. Even in patients with normal pre PTX serum total and/or ionized calcium, a significant increase was observed at the hip. This highlights the need for a biological exploration in osteoporosis patients to exclude secondary causes of low bone mass.

Disclosures: Eugénie Koumakis, None.

SA0168

Carotid Plaque Calcification is Increased in Mild Primary Hyperparathyroidism. Marcella Walker^{*1}, Tatjana Rundek², James A. Lee³, Chiyuan Zhang¹, Donald J. McMahon¹, Ralph L. Sacco², Shonni J. Silverberg¹. ¹Columbia University, USA, ²University of Miami, USA

We have previously reported that patients with mild primary hyperparathyroidism (PHPT) have evidence of subclinical carotid atherosclerosis including increased carotid intima-media thickness and decreased vascular compliance. Although carotid plaque was no more common in PHPT compared to controls, recent advances in ultrasound imaging now allow for the determination of plaque morphologic composition including the degree of plaque calcification. Of 49 patients with mild PHPT, 20 (41%) had carotid plaque (age: 65.7; serum calcium 10.40.5 mg/dl; PTH 11358 pg/ml). We compared their plaque morphology with that in 27 age-, sex- and race-matched controls with plaque. Age, BMI, renal function, history of hypertension, diabetes, smoking, hypercholesterolemia, or myocardial infarction did not differ between the two groups. On carotid ultrasound, PHPT and controls had similar average plaque number (2.2 1.3 vs. 2.3 1.4, $p = 0.72$), maximal carotid plaque thickness (MCPT; 2.10.5 vs. 2.20.7 mm, $p=0.59$) and plaque area (17 14 vs. 19 16, $p = 0.70$), all estimates of the burden of atherosclerosis. Overall plaque composition (echogenicity, reflecting content of lipid-rich, calcified and mixed areas) was also similar (88 25 vs. 9229, $p=0.58$). However, within the echodense (calcified) portion of plaque, the degree of calcification was higher in PHPT (15891 vs. 10639, $p=0.02$). Degree of calcification did not correlate with PTH ($r = 0.23$, $p=0.35$) or serum calcium ($r=0.34$, $p=0.17$). Plaque did not become more echolucent (less calcified) after parathyroidectomy (PTX; $n=18$). Instead, echodensity increased (baseline 16064; 12 mo 21366, $p<0.005$; 24 mo 26378, $p<0.001$), as did maximum plaque thickness (baseline 2.10.2; 12 mo 2.20.2, $p=0.19$; 24 mo 2.30.3, $p=0.045$) and plaque area (baseline 18 7.7; 12 mo 22 7.9, $p=0.03$; 24 mo 269.2, $p=0.003$). In summary, although mild PHPT is not associated with a greater burden of carotid plaque, when plaque is present it is more highly calcified than plaque in controls. Since PTX did not prevent progression of plaque area, thickness, or calcification, surgery should not currently be recommended for the specific purpose of improving carotid plaque. Whether greater plaque calcification in PHPT patients represents plaque stabilization or is a marker for increased future cardiovascular risk requires further investigation.

Disclosures: Marcella Walker, None.

SA0169

Clinical and Biochemical Variables Determining BMD in Primary Hyperparathyroidism. Lars Rolighed^{*1}, Peter Vestergaard¹, Peer Christiansen², Lene Heickendorff³, Tanja Sikjaer¹, Lars Reinmark¹, Leif Mosekilde¹. ¹Aarhus University Hospital, Denmark, ²Department of Surgery P, Aarhus University Hospital, Denmark, ³Department of Biochemistry, Aarhus University Hospital, Denmark

Purpose: Primary hyperparathyroidism (PHPT) is a known cause of secondary osteoporosis. Decreased BMD is often present at the time of diagnosis especially at the hip and forearm. The purpose of this retrospective study was to analyze the association between different clinical and biochemical variables and BMD in a large series of PHPT patients.

Methods: We identified all 1391 consecutive patients undergoing parathyroid surgery at Aarhus University Hospital, Denmark in a 15 year period from 01.01.96 – 31.12.2009. We excluded patients operated for hyperparathyroidism secondary to renal disease and parathyroid implantation after thyroid surgery. With the unique Danish personal identification number we retrieved preoperative biochemical data including plasma levels of parathyroid hormone (PTH), ionized calcium (Ca^{2+}), creatinine and 25-hydroxyvitamin D (25OHD), height, weight and preoperative DXA measurements of the spine, hip and forearm. A complete set of biochemical data were available on 785 patients.

Results: Median age was 62 years (range 13-91) and 638 (81%) patients were women. PTH (mean SD) was 17.4 24.3 pmol/l and 25OHD was 56 30 nmol/l. Women had slightly lower Ca^{2+} (1.50 0.09 mmol/l) than men (1.53 0.12 mmol/l, $P < 0.001$) and also lower plasma creatinine compared with men ($P < 0.001$). Insufficient plasma 25OHD levels (< 50 nmol/l) were found in 365 (46%) patients. Associations with BMD were calculated in a multiple regression model. As expected BMD of the spine, hip and forearm were negatively associated with age ($P < 0.001$). PTH was inversely associated with BMD of the forearm ($P < 0.001$) but not associated with

total hip or spine BMD (NS). BMD of the spine, hip and forearm were not associated with 25OHD levels (NS). PTH was negatively associated with 25OHD ($P < 0.001$) and positively associated with creatinine ($P < 0.001$).

Conclusions: In PHPT patients, DXA of the forearm is recommended due to the negative association between PTH and BMD of the forearm and the higher prevalence of subnormal values. Plasma levels of 25OHD are inversely related to PTH. However, levels of 25OHD did not correlate to BMD of the spine, hip or forearm.

Disclosures: Lars Rolighed, None.

SA0170

Co-morbid Medical Conditions Associated with Prevalent Hypoparathyroidism: A Population-based Study. Bart Clarke^{*1}, Cynthia Leibson², Jane Emerson², Jeanine Ransom², Hjalmar Lagast³. ¹Mayo Clinic College of Medicine, USA, ²Mayo Clinic, USA, ³NPS Pharmaceuticals, USA

Hypoparathyroidism (HypoPARA) is a rare condition with widespread consequences, ranging from asymptomatic presentation to fatal hypocalcemia. Population estimates of prevalence of HypoPARA across the full range of disease and associated patient characteristics are lacking. Using unique longitudinal, population-based Rochester Epidemiology Project (REP) medical records linkage resources, we 1) identified all persons residing in Olmsted County, MN, in 2009 with any diagnosis of HypoPARA assigned by a REP provider since 1945, 2) reviewed detailed medical records to confirm diagnosis of HypoPARA and assign etiology, 3) assigned 2 age- and sex-matched controls per confirmed case, and 4) obtained all medical diagnoses from 2006 through 2008 to compare cases with controls for percent with any diagnosis in each chapter and subchapter of the International Classification of Diseases, Version 9, Clinical Modification (ICD-9-CM). There were 54 confirmed cases (prevalence=37/100,000; 71% female; mean age 5820 years); etiology=78% post-surgical, 9% secondary, 7% familial, 6% idiopathic. Cases were more likely than controls ($p<0.05$) to have ≥ 1 diagnosis within 7 of 17 chapters and 15 subchapters. Details on specific chapter and subchapter differences are provided in the table. These population-based data on confirmed HypoPARA prevalence and case characteristics reveal that, compared to unaffected peers, persons with HypoPARA exhibit a substantial burden of comorbid disease across multiple dimensions.

Table: Increased likelihood that persons with vs. those without confirmed diagnosis of HPT had any diagnosed medical condition within each ICD-9-CM chapter/subchapter.

Chapter Level Yes; (Subchapter Level) Yes
Infectious/Parasitic Diseases (Mycoses)
Neoplasms (Malignancies of Genitourinary Organs; Other/Unspecified Malignancies; Benign Neoplasms)
Endocrine/Nutritional/Metabolic/Immunity Disorders (Disorders of Thyroid Gland; Disorders of Other Endocrine Glands; Nutritional Deficiencies; Other Metabolic/Immunity Disorders)
Genitourinary System Diseases (Other Diseases of the Urinary System)
Diseases of the Skin/Subcutaneous Tissue (Other Diseases of the Skin/Subcutaneous Tissue)
Chapter Level Yes; (Subchapter Level) No
Respiratory Diseases; Congenital Anomalies
Chapter Level No; (Subchapter Level) Yes
Nervous System Diseases (Peripheral Nervous System Diseases)
Digestive Diseases; (Other Diseases of Intestine/Peritoneum)
Circulatory System Diseases (Ischemic Heart Disease; Other Heart Disease)
Musculoskeletal Diseases (Rheumatism Excluding the Back)
Chapter Level No; (Subchapter Level) No
Diseases of Blood/Blood Forming Organs; Mental Disorders; Pregnancy Complications; Perinatal Conditions; Symptoms/Signs; Injury/Poisoning

Table

Disclosures: Bart Clarke, NPS Pharmaceuticals, Inc., 2
This study received funding from: NPS Pharmaceuticals, Inc.

SA0171

Development of a Bioactive PTH (1-84) Specific Assay on the IDS-iSYS System. Craig Dixon^{*1}, Emma King², Christopher Fox², Jackie Tran³, David Laurie², Alex Barnes², Martha Garrity². ¹Immunodiagnostic Systems Ltd, United Kingdom, ²IDS Ltd, United Kingdom, ³IDS Ltd, USA

Introduction: Measurement of Parathyroid Hormone (PTH) is essential for the management of hyperparathyroidism and metabolic bone disease associated with chronic kidney disease (CKD-MBD). Currently available assays recognise either full-length PTH and large C-terminal fragments (Intact PTH) or are specific for only the full-length 84 amino acid molecule (Bioactive PTH). The cross-reactivity to non PTH (1-84) fragments recognised by Intact PTH assays can vary considerably, leading to significant variation in overall PTH results between analytical platforms. The 2009 KDIGO Clinical Practice Guideline for the Diagnosis, Evaluation, and Treatment of CKD-MBD indicates PTH should be measured from Stage 3 for diagnoses of abnormalities and rate of progression of CKD. Recognising the inter-laboratory differences in PTH assays, the guideline suggests clinical laboratories inform clinicians of the actual assay method in use and report any changes in methods, sample source (plasma or) serum, and handling specifications to facilitate the appropriate interpretation of biochemistry data. Consistent and accurate measurement of PTH levels is therefore vital. There is much discussion regarding which PTH assay represents the most reliable and sensitive method for PTH monitoring. In particular, whether Intact PTH can be used given the undefined biological activity of non-(1-84) fragments, opposed with the opinion that Intact PTH is still a robust indicator of overall PTH levels. The Bioactive PTH (1-84) assay will allow specific measurement of full-length PTH on the IDS-iSYS system and in combination with the available panel of bone and calcium metabolism tests, such as 25-OH-D and BAP, will allow clinicians to select treatment modality and monitor therapy efficacy.

Methods: The measurement of Bioactive PTH (1-84) is a two-site chemiluminescent immunoassay. PTH (1-84) is bound by Biotinylated C-terminal and Acridinium-conjugated N-terminal-specific antibodies. These complexes are captured by streptavidin-coated magnetic particles. Bound PTH (1-84) is measured in a high sensitivity luminometer, where signal generated by the acridinium conjugate is directly proportional to the concentration of PTH (1-84) in the sample.

Results: The Bioactive PTH (1-84) assay has a range of 4-1800pg/ml. Time to first result is 33 minutes. Analytical sensitivity is 1.8 pg/mL. Correlation with the IDS-iSYS Intact PTH assay gives a relationship of Bioactive PTH = 0.6 x Intact PTH values in EDTA plasma (n=59). Cross-reactivity with non PTH (1-84) fragments is clinically insignificant. Recovery was measured at 95%. Excellent linearity was observed across the full clinical decision range of CKD-MBD with an observed/expected value of 101%.

Conclusion: This assay has potential to provide accurate data for the specific measurement of PTH (1-84) across the full clinical range required for CKD-MBD monitoring.

Disclosures: Craig Dixon, IDS Ltd, 3
This study received funding from: IDS Ltd

SA0172

Genetic Analysis Of CDKN1B/p27^{Kip1} Gene in Familial Primary Hyperparathyroidism. Filomena Cetani^{*1}, Elena Pardi², Elena Paltrinieri², Simona Borsari², Benedetta Raspini², Federica Saponaro², Luisella Cianferotti¹, Antonella Picone², Chiara Banti², Edda Vignali², Claudio Marroccci¹. ¹University of Pisa, Italy, ²University of Pisa Department of Endocrinology & Metabolism, Italy

Primary hyperparathyroidism is usually a sporadic disorder, but in a minority of cases (<10%) occurs as part of hereditary syndromes, including multiple endocrine neoplasia types 1 and 2A (MEN1 and MEN2A), hyperparathyroidism-jaw tumor syndrome (HPT-JT), familial hypocalcemic hypercalcaemia (FHH) and familial isolated hyperparathyroidism (FIHP).

MEN 1 is an autosomal dominant disorder characterised by tumours in multiple endocrine glands, most commonly the parathyroid, enteropancreatic and anterior pituitary glands. To date over 1100 germline heterozygous mutations have been identified as the causative molecular defect of familial MEN1 disorders. However, there are no identifiable mutations in the menin coding sequence in approximately 20-30% of clinically proven MEN1 kindreds. FIHP can result either from incomplete expression of a syndromic form of familial primary hyperparathyroidism, or have still unrecognized causes. It has a heterogeneous molecular etiology, infact germline mutations of *MEN1* (25%); *HRPT2* (7%) and *CASR* (4%) genes were reported in a subset of FIHP families. Recently, a *cyclin dependent kinase inhibitor 1B* (*Cdkn1b*) germline frameshift mutation was identified in a rat colony as the cause of a recessive multiple endocrine neoplasia called MENX. Interestingly, germline mutations of the homologous human gene (*CDKN1B/p27^{Kip1}*) were identified in 6 kindreds with MEN1-like syndromes, clinical MEN1 without proven mutations in the MEN1 gene, thereby establishing a direct link between p27 alterations and tumor predisposition also in humans.

Our objective was to evaluate the role of *CDKN1B/p27^{Kip1}* gene in 11 MEN1 and 9 FIHP kindreds that were negative, respectively, for MEN1 gene and MEN1, HRPT2, CASR, genes germline mutations.

Genomic DNA from index cases was analyzed for germline mutations in the *CDKN1B/p27^{Kip1}* gene by PCR amplification and direct sequencing by a 16-capillaries automatic sequencer.

No mutations in the coding region of *CDKN1B/p27^{Kip1}* were detected. Our results indicate that *CDKN1B/p27^{Kip1}* mutations effectively happens in a small portion of MEN1 syndrome without known mutations in the MEN1 gene.

Disclosures: Filomena Cetani, None.

SA0173

Subclinical Hypoparathyroidism: A New Variant Based Upon a Cohort from MrOS. Natalie Cusano^{*1}, Patty Wang², Serge Cremers³, Elizabeth Haney², Douglas Bauer⁴, Eric Orwoll², John Bilezikian¹. ¹Columbia University College of Physicians & Surgeons, USA, ²Oregon Health & Science University, USA, ³Columbia University, USA, ⁴University of California, San Francisco, USA

Hypoparathyroidism (HypoPT), characterized by hypocalcemia and reduced PTH levels, occurs primarily as an autoimmune disorder or after neck surgery. Progressive loss of parathyroid function may occur over months to years. It follows that there may be a phase of HypoPT in which the serum calcium (Ca) level is still maintained but the PTH level is low. This phase is not likely to be recognized because PTH levels are rarely measured when the serum Ca concentration is normal. Subclinical HypoPT has surfaced when such patients are given bisphosphonates. With a mild lowering effect of bisphosphonate on serum Ca, symptomatic hypocalcemia can develop with inadequate parathyroid reserve. We hypothesized that individuals with subclinical HypoPT could be identified in an unselected population such as in The Osteoporotic Fractures in Men study (MrOS). MrOS consists of a cohort of US community-dwelling men ≥ 65 years at enrollment. We measured PTH levels (Scantibodies IRMA, inter-assay CV 8.4%, intra-assay CV 5.6%) in a random subset of 1593 men. 89 did not have serum Ca values and were excluded, leaving 1504 men for these analyses. Subclinical HypoPT was defined as a serum PTH below the reference range of the assay (<14 pg/ml) along with a normal albumin-adjusted serum Ca concentration. In this cohort, 25 subjects met these criteria for subclinical HypoPT (prevalence, 1.7%). There were no men with overt HypoPT (low serum Ca and PTH levels). The men with subclinical HypoPT had significantly higher phosphorus levels (3.5 vs. 3.2 mg/dl; $p<0.0001$) and 25-hydroxyvitamin D levels (28.5 vs. 25.1 pg/ml; $p=0.04$) than the others in the cohort. Daily calcium supplementation was significantly higher in the men with low PTH levels compared to the other subjects (617.7 vs. 347.2 mg/day; $p=0.002$) with the majority taking $\geq 1,000$ mg/day (52% vs. 23%; $p=0.0007$). Since this level of Ca supplementation in the setting of normal serum Ca does not suppress PTH to levels below the reference range, it is likely that higher Ca intake in these men represents greater calcium needs in the context of subclinical HypoPT. There were no significant differences between subjects with and without subclinical HypoPT in terms of: age, height, weight, BMI, bone turnover markers (P1NP, β CTX, TRAP5b), testosterone, estradiol, SHBG, lumbar spine or femoral neck BMD. The results provide evidence for the existence of a cohort of free-living community-dwelling individuals who have subclinical HypoPT.

Disclosures: Natalie Cusano, None.

SA0174

Vitamin D Status in Primary Hyperparathyroidism. Alfredo Scillitani^{*}. Casa Sollievo Della Sofferenza Scientific Institute, Italy

Hypovitaminosis D is common in patients with Primary Hyperparathyroidism (PHPT) and several mechanisms could theoretically predispose to vitamin D deficiency. Indeed the excess PTH induces an accelerated catabolism of 25 hydroxy-vitamin D (25OHD) by activating both renal 1 α -hydroxylase and liver 24 hydroxylase.

We evaluated vitamin D and DBP (vitamin D Binding Protein) serum levels in PHPT patients and compared them with 2 different groups of healthy family members: those sharing the same environment only—that are, in-law relatives (ILR) or those sharing genetic background and environment—namely, first degree relatives (FDR).

This study is part of a larger one in which an accurate evaluation of PHPT patients with matched FDR and ILR subjects is performed. Eighty-five PHPT subjects of 400 patients were initially collected because we had at least one FDR and one ILR subject (trios) for each patient. Subsequently 36 patients were excluded since they had reported taking vitamin D supplementations.

Finally we analyzed data on 49 families. Mean age SD of PHPT patients, FDR and ILR subjects was 59.6 9.9, 43.4 14.5 and 51.8 14.7 years, respectively. Serum 25OHD levels were 14.1 7.5, 21.5 11.4, 22.2 13.9 ng/ml, respectively and were significantly different between patients and either group of healthy subjects ($p<0.05$). Serum DBP levels were 347 64, 411 87, 408 88 ug/ml, respectively and were significantly different between patients and either group of healthy subjects ($p<0.05$).

Univariate analysis of variance by GLM was utilized in order to correct for other covariates (season, age and DBP). Serum 25OHD was lower in PHPT patients in respect the two groups of healthy subjects after adjustment for these covariates but the difference was not significant vs the FDR ($p=0.09$).

Our study confirms that, PHPT patients have lower 25OHDvitamin D levels than healthy subjects sharing the same environment and a similar genetic background.

Disclosures: Alfredo Scillitani, None.

SA0175

Calcium Carbonate Supplement Produces Positive Calcium Balance in Stage 3/4 Chronic Kidney Disease. Kathleen Hill¹, Berdine Martin², Meryl Wastney³, Sharon Martin Moe⁴, George McCabe², Connie Weaver², Munro Peacock⁵. ¹Indiana University School of Medicine, USA, ²Purdue University, USA, ³Metabolic Modeling Services, USA, ⁴Indiana University, USA, ⁵Indiana University Medical Center, USA

Background: Patients with chronic kidney disease (CKD) are often given a calcium carbonate supplement (CaCO₃) with meals both to bind dietary phosphate (Pi) and prevent negative skeletal calcium (Ca) balance. However, there are limited data on Ca balance and kinetics in CKD patients with or without CaCO₃. Purpose: To determine the state of Ca balance in CKD patients on an adequate Ca diet with and without CaCO₃. Methods: Three patients, of a projected eight, with stage 3/4 CKD participated in two 3wk Ca balance and kinetic studies using a randomized crossover design. Patients received 500 mg elemental Ca as CaCO₃ or placebo with meals 3x/d. Controlled diets consisted of 957 mg Ca/d. Wk 1 of each balance study was outpatient and considered an equilibration period. During wk 2 & 3, patients were inpatients, where they consumed the controlled diet, and collected all urine and feces. An oral and IV tracer (45Ca) were given on days 8 & 9, and serial blood drawn on days 8-21 for Ca kinetics estimated using a multi-compartmental model. Repeated measures ANOVA for crossover designs was used to determine differences between CaCO₃ and placebo. Results: Mean lumbar spine & femoral neck BMD t-scores were each -0.7. Mean fasting biochemistries did not differ between placebo and CaCO₃: serum Ca 9.3 & 9.5 mg/dL, Pi 4.2 & 4.2 mg/dL, Cr 2.4 & 2.6 mg/dL, PTH 73 & 60 pg/mL, FGF23 73 & 79 pg/mL, bone alkaline phosphatase 34 & 37 U/L, 25(OH)D 21 & 20 ng/mL, 1,25(OH)2D 48 & 43 pg/mL, urine Ca:Cr ratio 0.05 & 0.06. Ca balance was negative on placebo and positive on CaCO₃ (-111.6 & +105.6 mg/d); bone formation was higher on CaCO₃ than placebo (359 & 282 mg/d), and bone resorption was lower on CaCO₃ than placebo (254 & 394 mg/d); urinary Ca excretion was higher on CaCO₃ than placebo (136 & 102 mg/d); endogenous fecal Ca excretion was lower on CaCO₃ than placebo (138 & 167 mg/d); absolute Ca absorption was higher with CaCO₃ than placebo (380 & 158 mg/d) and fractional Ca absorption was lower on CaCO₃ than placebo (0.15 & 0.17). Conclusions: These preliminary studies suggest that patients with stage 3/4 CKD are in negative Ca balance while consuming a diet of 957 mg/d Ca, but are in positive Ca balance when given 1500 mg/d elemental Ca with meals, due to increased net Ca absorption and retention. The beneficial or adverse effects of chronic positive Ca balance on bone mass, extraskeletal mineralization and phosphate balance and homeostasis need to be established.

Disclosures: Kathleen Hill, None.
This study received funding from: Genzyme

SA0176

Cortical Abnormalities are Associated with Prevalent Fractures in Postmenopausal Women with Chronic Kidney Disease. Emily Stein¹, Thomas Nickolas², Donald McMahon¹, Adi Cohen², Xiaowei Liu¹, Mafo Kamanda-Kosse³, X Guo³, Elizabeth Shane¹. ¹Columbia University College of Physicians & Surgeons, USA, ²Columbia University Medical Center, USA, ³Columbia University, USA

Chronic kidney disease (CKD) is associated with increased fracture risk in postmenopausal women. We hypothesized that women with CKD and fragility fractures would have more cortical abnormalities than those with no fracture history. Postmenopausal women with stage 3 and 4 CKD (eGFR by MDRD 15-60ml/min) were enrolled. Women with significant bisphosphonate use (>1 yr) or any teriparatide use were excluded. Women with (FX, n=20) and without (C, n=33) a history of low trauma fracture after menopause had aBMD of the lumbar spine (LS), total hip, femoral neck, 1/3 radius and ultradistal radius (UDR) measured by DXA. Trabecular (Tb) and cortical (Ct) volumetric BMD (vBMD) and Tb microarchitecture were measured by high resolution peripheral computed tomography (HRpQCT, voxel size ~82 µm) of the radius and tibia.

Of 53 women enrolled (57% Caucasian, 36% Latina, mean age 717 years), mean eGFR was 414 ml/min and did not differ by fracture status. There was no difference in age, race, BMI, prevalence of hypertension or diabetes, use of estrogen, loop diuretics, calcitriol or parent vitamin D intake. Calcium intake tended to be higher among women with FX (995299 vs. 786401 mg/d; p=0.08). In FX subjects, mean T-scores were significantly lower at the UDR (-1.60.2 vs -0.80.2; p<0.03) and tended to be lower at the LS (-1.20.4 vs -0.60.2; p=0.14), but did not differ elsewhere. In contrast, HRpQCT revealed substantial microarchitectural differences (Table). At the radius, total area did not differ, but FX subjects had smaller Ct and larger Tb regions. FX subjects also had lower total density, tended to have lower Ct density, and had lower Ct thickness. Although Tb density did not differ, sub-cortical (outer) Tb density was lower in FX subjects. Tb number, separation and network heterogeneity did not differ. Similarly at the tibia, FX subjects had smaller Ct and greater Tb area. Total, Tb, and sub-cortical density were lower among FX subjects. While cortical density was not significantly lower at this site, Ct and Tb thickness were lower in FX subjects.

In conclusion, postmenopausal women with CKD and fractures have lower vBMD, primarily due to deficits in cortical bone. The smaller cortical area and lower sub-cortical density observed are consistent with endocortical cancellization. These changes along with lower cortical density and thickness suggest that excess PTH may be an important mediator of skeletal fragility in this population.

HRpQCT at the radius (RAD) and tibia (TIB) in women with CKD by fracture status

	RAD C	RAD FX	TIB C	TIB FX
Ct area (mm ²)	48 ± 2*	40 ± 2	92 ± 4**	71 ± 5
Tb area (mm ²)	172 ± 6 ^{0.09}	194 ± 11	567 ± 18*	632 ± 31
Total density (mgHA/ cm ³)	310 ± 12***	265 ± 14	249 ± 9**	210 ± 10
Ct density (mgHA/ cm ³)	843 ± 12 ^{0.09}	810 ± 14	774 ± 11	746 ± 18
Tb density (mgHA/cm ³)	141 ± 7	123 ± 9	150 ± 6 ^{0.06}	133 ± 7
Outer Tb density (mgHA/ cm ³)	206 ± 7*	185 ± 8	222 ± 6**	194 ± 8
Inner Tb density (mgHA/cm ³)	96 ± 8	81 ± 10	101 ± 6	92 ± 7
Ct thickness (microns)	752 ± 31**	619 ± 35	898 ± 48**	673 ± 52
Tb Number (1/mm)	1.9 ± 0.1	1.7 ± 0.1	1.7 ± 0.1	1.7 ± 0.1
Tb Thickness (microns)	62 ± 2	59 ± 2	72 ± 12*	65 ± 3

(mean±SE) *p<0.05, **p<0.01, ***p<0.001 vs FX

STEIN_CKD Abstract Table

Disclosures: Emily Stein, None.

SA0177

See Friday Plenary Number FR0177.

SA0178

See Friday Plenary Number FR0178.

SA0179

Identification of Pathological Bone Mineralization in Diabetic Osteomyelitis.

Karen Esmonde-White¹, Francis Esmonde-White², Crystal Holmes¹, Michael Morris², Blake Roessler¹. ¹University of Michigan Medical School, USA, ²University of Michigan, USA

Introduction: Diabetic osteomyelitis occurs when non-healing and infected wounds of plantar soft tissue spread to the underlying bone. Clinical and imaging tests show that whole tissue properties of bone, including hardness and mineralization, are directly affected by diabetic osteomyelitis. The assumption is that bone chemistry is altered to induce observable changes in tissue, however, these changes have never been examined in osteomyelitic bone. The objective of our study is to measure osteomyelitis-induced changes in bone composition. We used an optical method (Raman spectroscopy) to show that abnormal calcium phosphate minerals are present in diabetic foot osteomyelitis. Methods: All aspects of the clinical protocol were reviewed and approved by the University of Michigan Medical School Institutional Review Board. After informed consent, fragments of affected bone were collected from 4 human patients (Male 3, Female 1, mean age of 69 y) undergoing surgical treatment for diabetic osteomyelitis. We also examined bone fragments from cadaveric specimens as controls. Near infrared Raman spectra were collected at the surface of the bone fragments using a Raman equipped microscope. Raman spectra were compared with pathology, microbiology and clinical imaging results. Results: Osteomyelitis was indicated by clinical imaging in all 4 patients. Raman spectra showed presence of two calcium phosphate minerals not observed in normal bone tissue: uncarbonated calcium hydroxyapatite and dicalcium phosphate dihydrate (brushite). No atypical results were observed in the controls. Because brushite is only formed under acidic conditions, we hypothesize that the acidic environment of a diabetic foot wound bed accelerates dissolution of carbonated apatite and favors formation of other calcium phosphate minerals. Conclusions: We present preliminary results from a continuing study to characterize the chemical composition of bone infected by diabetic osteomyelitis. Our first results suggest pathological mineralization occurs in diabetic osteomyelitis, and mineral chemistry is significantly altered. While this study has focused on diabetic osteomyelitis, we anticipate that these findings can be generalized to bloodborne or post-surgical osteomyelitis. Translating this technique to the clinic may provide a predictive measurement of osteomyelitis infections based on identification of pathological mineral species when patients are still asymptomatic.

Disclosures: Karen Esmonde-White, None.

SA0180

ONO-5334, a Potent Cathepsin K Inhibitor, Suppresses Joint Destruction in the Monkey Collagen-induced Arthritis Model. Hiroshi Mori^{*}, Hiroyuki Yamada, Yasutomo Nakanishi, Akiko Kunishige, Satoshi Nishikawa, Yasuaki Hashimoto, Yasuo Ochi, Masafumi Sugitani, Kazuhito Kawabata. Ono Pharmaceutical Co., Ltd., Japan

Cathepsin K is highly expressed in osteoclasts, and plays a central role on bone degradation. It has been demonstrated that cathepsin K is also expressed in synovial fibroblasts and chondrocytes in rheumatoid arthritis (RA) patients that are implicated in cartilage degradation. Cathepsin K may be an attractive therapeutic target for joint

destruction in RA. In this study, we investigated the efficacy of ONO-5334, a novel small molecule inhibitor of cathepsin K, on joint destruction in the monkey collagen-induced arthritis model.

Arthritis was induced by immunizing with bovine type II collagen twice at 3-week intervals in female cynomolgus monkeys. Animals received either oral ONO-5334 (30 mg/kg, once daily), methotrexate (MTX, 10 mg/body, twice a week), combined treatment of ONO-5334 and MTX (ONO-5334/MTX) or vehicle (control) for 9 weeks from the day of the first immunization (4 groups, 9 animals/group).

In the control group, joint swelling score increased with time until week 7. Joint destruction was evaluated at week 9, and the findings such as joint space narrowing, bone atrophy, and bone erosion were observed at the phalangeal joints in X-ray examinations. ONO-5334 did not reduce joint swelling score. Joint swelling score in the MTX and ONO-5334/MTX was less than 50% of that in the control group at week 7 and 9, and the efficacy of these treatments was similar. ONO-5334 significantly decreased radiographic score, which indicates the affected joint number (48 joints per animal in total), by 65% compared to the control group ($p < 0.05$). MTX decreased radiographic score by 46%, but no significant difference compared to the control group. Radiographic score in the ONO-5334/MTX group showed further decrease and reached 74% suppression ($p < 0.05$ vs control). In the control group, the bone resorption marker, urinary CTX-I, and the cartilage degradation marker, urinary CTX-II, increased by 10-fold at week 7 and 7-fold at week 3 from baseline (median value), respectively. ONO-5334 and ONO-5334/MTX maintained both marker levels at near baseline (median value). CTX-I level in the MTX group was comparable at weeks 3, 5 and 9 or slightly lower at week 7 to the control group, but MTX maintained CTX-II levels at near baseline (median value).

These results suggest that ONO-5334 may be effective for the prevention of joint destruction. Concomitant use of ONO-5334 with MTX may help to reduce joint swelling and to augment suppressive effects on joint destruction in RA.

Disclosures: Hiroshi Mori, None.

SA0181

Relationship Between Periodontitis and Arthritis. Melissa Cantley*, David Haynes, Victor Marino, Peter Mark Bartold. University of Adelaide, Australia

Periodontitis (PD) and rheumatoid arthritis (RA) are similar chronic inflammatory diseases where bone loss is a major problem. Increasing evidence suggests that a relationship may exist between the two pathologies. Previous studies have demonstrated that PD is a risk factor for development of RA and it may also enhance RA severity. The aim was to investigate bone loss and the relationship between pre-existing PD and experimental arthritis similar to human disease in an animal model.

Periodontitis was induced in female balb/c mice by oral inoculations with live *P. gingivalis* bacteria (periodontal pathogen) over 36 days. Following this, collagen antibody induced arthritis (CAIA) was induced via intravenous injection of a mAb to type II collagen followed by injection of *E. coli* LPS two days later. These animals were compared to animals with PD alone, arthritis alone and no disease (controls) ($n=4$ per group). Visual changes in paw swelling were assessed for clinical development of arthritis. Alveolar bone and joint changes were assessed using live animal micro-CT analysis, histological analyses and immunohistochemistry. Serum levels of C-reactive protein (CRP) were used to monitor systemic inflammation.

Mice with pre-existing PD developed more severe arthritis at a markedly faster rate with significantly higher paw scores on days 6, 8, 9 and 10. There were also significantly higher CRP levels in the PD and arthritis group ($p < 0.05$). However, despite more rapid onset in animals with pre-existing PD there were no significant differences ($p > 0.05$) in bone loss in the radio carpal joints at day 10 (CT analysis). There was, however, more intense staining for RANKL in the PD and arthritis group compared to arthritis alone. Interestingly, mice with PD alone showed bone loss within the radio carpal joint and more intense RANKL staining than controls ($p < 0.01$). Similarly elevated RANKL expression and alveolar bone loss was seen in mice with arthritis alone in the gingival tissues.

Mice with pre-existing PD developed arthritis at a faster rate but bone loss was eventually similar to that seen in mice without PD. Interestingly, minor but significant bone loss was evident not only in the joints of PD mice but also in the alveolar bone of mice with arthritis. This demonstrates a relationship between PD and inflammatory joint disease. This unique model can be used to further investigate the relationship between PD and arthritis and test the effects of potential treatments.

Disclosures: Melissa Cantley, None.

SA0182

See Friday Plenary Number FR0182.

SA0183

Advanced Glycation End-Products-Induced Vascular Calcification Is Mediated By Oxidative Stress: Functional Roles of NAD(P)H-oxidase.

Yuko Tada*¹, Shozo Yano², Kyoko Okazaki¹, Noriko Ogawa¹, Miwa Morita¹, Ippei Kanazawa³, Toru Yamaguchi², Toshitsugu Sugimoto⁴. ¹Shimane University Faculty of Medicine, Japan, ²Shimane University Faculty of Medicine, Japan, ³McGill University, Canada, ⁴Shimane University School of Medicine, Japan

Background and aims: Vascular calcification is associated with increased morbidity and mortality in patients with diabetes mellitus and end-stage kidney disease. Especially, medial artery calcification, known as Monckeberg's type of calcification, is often detected in these patients. Growing evidence suggests that advanced glycation end-products (AGEs) are associated with vascular calcification, although their actions are still unclear. On the other hand, oxidative stress leads to vascular damage through diverse mechanisms. Thus, we investigated an *in vitro* study to elucidate the effects of AGEs and the roles of NAD(P)H oxidase in the pathogenesis of vascular calcification.

Materials and methods: Rat vascular smooth muscle cells (A7r5) were incubated in calcification medium with AGE3 to measure calcium deposition, to evaluate apoptosis (ELISA) and to determine mRNA expression levels of osteopontin (OPN), osteocalcin (OC), Runx2, Nox-1, Nox-4, and p22phox (real-time PCR).

Results: Calcium deposition was increased by AGE3 in a dose- and time-dependent manner in A7r5 cells. AGE3 was the most potent in calcium deposition among AGEs, which we had examined. Expression levels of the OPN, OC, and Runx2 mRNAs were significantly higher in AGE3 treatment than those in control BSA treatment, indicating the osteoblastic transdifferentiation of the vascular smooth muscle cells. In addition, apoptosis was enhanced within 24hrs in cells treated with AGE3, compared to that with control BSA. Increased expressions of Nox-1, Nox-4, and p22phox mRNAs (3 to 6 folds) were also observed in cells treated with AGE3, suggesting that AGEs most probably promote reactive oxidative species production resulting in the progression of calcium deposition. Therefore, we examined the effects of silencing of these mRNAs by using siRNA and found that AGE3-stimulated calcium deposition was significantly decreased in the cells transfected by either Nox-4 or p22phox siRNA. In contrast, no significant effect was shown in silencing of Nox-1.

Conclusion: The present findings indicate the involvement of osteoblastic transdifferentiation of the vascular smooth muscle cells and the apoptosis as well as oxidative stress in the pathogenesis of AGEs-induced vascular calcification. Activated NAD(P)H oxidase, which is induced by increased expression of Nox-4 and p22phox, may play important roles. These molecules could be a target of new strategy to prevent vascular calcification as well as vascular damage.

Disclosures: Yuko Tada, None.

SA0184

Aortic Arch Calcification Is Associated With Low Bone Mineral Density But Not Orthostatic Hypotension In Advanced Old Age. Jude Ryan*¹, Sheila Carew², Catriona O'Connell³, Teresa Donnelly², Catherine Peters², Aine Costelloe², Tina Sheehy², Declan Lyons².

¹Midwest Regional Hospital, Limerick, Ireland, ²Clinical Age Assessment Unit, Department of Medicine, Division of Ageing & Therapeutics, University of Limerick Medical School & Mid-West Regional Hospital, Ireland, ³Midwest regional Hospital, Ireland

Introduction

Vascular calcification has been associated with bone loss in previous epidemiological studies, suggesting a possible relationship between osteoporosis and age-related vascular stiffness. Orthostatic hypotension (OH) is a common age associated vasculopathic phenomenon. We investigated whether the presence of aortic arch calcification on chest x-ray may predict the co-existence of osteoporosis and orthostatic hypotension in advanced old age.

Methods

Patients who had a dual-energy-x-ray-absorptiometry (DEXA) scan, head up tilt test (HUT) and chest radiographs performed within a 1 year period were identified from our unit database. Radiographs were viewed by 2 experienced blinded clinicians to determine the presence/absence of aortic arch calcification. Results were correlated with bone mineral density (BMD) (hip) and blood pressure response to HUT.

Results

111 patients were studied, 88 female, mean age 85 years (range 80-95). 51/111 (45.9%) had aortic arch calcification. 70.6% of the total group had osteoporosis. 60.8% of the total group had a diagnosis of orthostatic hypotension on head-up tilt. Hip BMD was lower in the calcified compared to non calcified group (0.6830.02 V 0.7650.03g/cm²; $p=0.03$ unpaired t test). There was no difference in mean resting blood pressures between groups (144/764/2 V 148/784/2mmHg; $p=0.54$ unpaired t test). Change in systolic blood pressure in response to HUT was similar in both groups (-35.82.5 V -35.22.3 mmHg, $p=0.86$ unpaired t test).

Conclusion

The presence of aortic arch calcification is associated with a lower BMD, this lends support to a common mechanism for osteoporosis and large vessel calcification. In this study there doesn't appear to be any haemodynamic consequences associated with aortic arch calcification, specifically OH which would pose a significant risk of falling.

The lack of an association with OH is not surprising as the principal pathogenic site for this condition is the resistance vessel.

Disclosures: Jude Ryan, None.

SA0185

miRNA-125b is Involved in Calcification of Vascular Smooth Muscle Cells. Claudia Goettsch^{*1}, Martina Rauner², Lorenz Hofbauer³. ¹Brigham & Women's Hospital/Cardiovascular Division, USA, ²Medical Faculty of the TU Dresden, Germany, ³Dresden University Medical Center, Germany

Vascular calcification is a prominent feature of atherosclerosis and is closely linked to osteoporosis. Various microRNAs (miRNA) have been shown to regulate cell differentiation, including miR-125b, which is involved in osteoblast differentiation. However, no specific miRNA has been defined that modulates vascular calcification. Here, we assessed the impact of miR-125b in osteogenic transformation of vascular smooth muscle cells. Osteogenic transdifferentiation of human coronary artery smooth muscle cells (HCASMC) was induced by osteogenic medium (OM) and enhanced the formation of mineralized matrix resulting in a significantly higher mineral deposition after 21 days. The expression of miR-125b was time-dependently increased in HCASMC, and diminished during osteogenic transdifferentiation. At day 21, miR-125b was significantly reduced (-42%) compared to the untreated control. The miRNA processing enzymes DICER and DROSHA were also down-regulated. Furthermore, inhibition of endogenous miR-125b promoted osteogenic transdifferentiation as measured by an increased alkaline phosphatase activity and matrix mineralization. Expression analysis revealed the osteoblast transcription factor SP7 (osterix) as a target of miR-125b. In vivo, miR-125b was decreased in calcified aortas of ApoE knock out mice. In conclusion, our results suggest that miR-125b is involved in vascular calcification in vitro and in vivo at least partially by targeting SP7. Evaluating the role of miRNAs in arterial calcification in vivo may have important therapeutic implications.

Disclosures: Claudia Goettsch, None.

SA0186

See Friday Plenary Number FR0186.

SA0187

See Friday Plenary Number FR0187.

SA0188

Adaptation of Bone and Calcium Metabolism to Low Dietary Calcium (Ca) Intake is Affected by Genetic Background in Mice. Qiang Li^{*}, Rebecca McCreedy, James Fleet. Purdue University, USA

We tested the hypothesis that genetics control the ability of Ca and bone metabolism to adapt to low dietary Ca intake. Male mice from 11 inbred lines (129S1/SV1mJ, A/J, AKR/J, C3H/HeJ, C57BL/6J (B6), CAST/EiJ, CBA/J, DBA/2J, PWK/PhJ, SWR/J and WSB/EiJ) were fed AIN93G diets containing adequate (0.5%) or low (0.25%) Ca levels from weaning until 3 mo (n=8 mice from each line per diet group). Ca metabolism normally adapts to diet Ca restriction by increasing serum 1,25 dihydroxyvitamin D (1,25 D), causing upregulation of intestinal Ca absorption (Ca Abs), and protection of bone mass. Ca Abs was assessed using an oral gavage test (45Ca, 0.1 mM, 10 min) after an overnight fast. At sacrifice, serum was harvested for 1,25 D levels and femora were fixed for DEXA analysis of bone mineral density (BMD) and content (BMC). In mice fed the 0.5% Ca diet, significant differences were observed between the lines for all parameters measured (high 1,25 D in 129, A/J, C3H, CBA, SWR, WSB; high Ca Abs in A/J, C3H, CBA, SWR, WSB; high BMD/BMC in 129, AKR, C3H, CBA). This demonstrates that there is genetic control on these parameters. Ca restriction significantly increased 1,25 D in 129, C3H, B6, and SWR mice by 35-55%; increased Ca Abs in 129, B6, CAST, and SWR mice by 72-195%; reduced BMD in 6 lines of mice: A/J (-4.8%, p<0.1), AKR (-4.8%), CBA (-6.6%), C3H (-4.8%, p<0.1), CAST (-6.4%, p<0.1), and 129 (-9.0%). For A/J, AKR/J and CBA/J, the reduced BMD could be partly explained by their inability to increase serum 1,25 D and Ca absorption on low Ca intake. In contrast, the robust increase in Ca Abs in 129, CAST, and C3H mice did not protect them from bone loss, and PWK are able to protect BMD without a large increase in Ca absorption, suggesting mechanisms other than regulation of Ca absorption influence bone during low Ca intake. Collectively, these data show that genetic factors control a number of parameters relevant to Ca and bone metabolism and that there are genetic controls influencing the physiological adaptation of Ca metabolism to dietary Ca restriction that ultimately affect bone health. Future forward genetic approaches will be necessary to identify the genetic variation responsible for these physiological differences.

Disclosures: Qiang Li, None.

SA0189

See Friday Plenary Number FR0189.

SA0190

See Friday Plenary Number FR0190.

SA0191

See Friday Plenary Number FR0191.

SA0192

See Friday Plenary Number FR0192.

SA0193

See Friday Plenary Number FR0193.

SA0194

See Friday Plenary Number FR0194.

SA0195

See Friday Plenary Number FR0195.

SA0196

A Genome-wide Association Meta-analysis Identifies Two Loci for Cortical Thickness. Mattias Lorentzon^{*1}, Lavinia Paternoster², Terho Lehtimäki³, Mika Kahonen⁴, Olli Raitakari⁵, Marika Laaksonen⁶, Vera Mikkilä⁶, Jorma Viikari⁷, Leo-Pekka Lyytikäinen³, John P Kemp², Adrian Sayers⁸, Maria Nethander⁹, Liesbeth Vandenput¹⁰, Jon H Tobias², Claes Ohlsson¹, David M Evans². ¹Center for Bone Research at the Sahlgrenska Academy, Sweden, ²MRC CAiTE centre, School of Social & Community Medicine, University of Bristol, United Kingdom, ³Department of Clinical Chemistry, University of Tampere & Tampere University Hospital, Finland, ⁴Department of Clinical Physiology, University of Tampere & Tampere University Hospital, Finland, ⁵Research Centre of Applied & Preventive Cardiovascular Medicine, University of Turku & the Department of Clinical Physiology, Turku University Hospital, Finland, ⁶Department of Food & Environmental Sciences, University of Helsinki, Finland, ⁷Department of Medicine, University of Turku & Turku University Hospital, Finland, ⁸University of Bristol, United Kingdom, ⁹Center for Bone & Arthritis Research, Institute of Medicine, Sahlgrenska Academy, University of Gothenburg, Sweden, ¹⁰University of Gothenburg, Sweden

Several loci associated with areal bone mineral density (aBMD) (as measured by dual x-ray absorptiometry (DXA)) have previously been identified in large bone-related genome-wide association (GWA) studies. Though more direct measures of bone geometry and structure are related to fracture risk as strongly as aBMD, considerably less is known of their genetic determinants, and as of yet, no GWA studies have been performed searching for genetic signals for cortical thickness.

In order to determine genetic markers (Single Nucleotide Polymorphisms-SNPs) for cortical thickness, we performed a GWA study of this trait, as measured by peripheral quantitative computed tomography (pQCT) in the tibial diaphysis, among 5,952 Caucasian subjects from three cohorts (ALSPAC, aged ~15 years, n=3,456; GOOD, aged ~19 years, n=938 and YFS aged 31-46 years, n=1,558). We used an inverse variance weighted fixed-effect model meta-analysis of study-specific results. We identified genetic variants in two separate loci reaching genome wide significance ($p < 5 \times 10^{-8}$).

The top ranking SNP (rs9525638) was located in the *RANKL* (*TNFSF11*) locus on chromosome 13, had an effect size of 0.11 SD per allele and $p = 3.8 \times 10^{-10}$. In addition, we identified another genetic signal for cortical thickness in the *Wnt16* locus on chromosome 7 (rs2707466). This SNP had an effect size of 0.11 SD per allele and $p = 6.2 \times 10^{-9}$. *Wnt16* is a member of the wingless-type MMTV integration site family and has previously been shown to be involved in the regulation of bone turnover. Several previous GWA studies have identified the *RANKL* locus for aBMD and fracture, while only one previous study has implicated the locus near *Wnt16* as of importance for aBMD.

In conclusion, we identified two loci associated with cortical thickness. Our findings suggest that *RANKL* and *Wnt16* are involved in the regulation of cortical thickness.

Disclosures: Mattias Lorentzon, None.

SA0197

See Friday Plenary Number FR0197.

SA0198

Functionality of Bone-Specific Promoter SNPs in Human Bones In Vivo and Influence on the Phenotypic Variability of Osteogenesis Imperfecta (OI).

Aline Domingues¹, Marc delepine², Anne Boland², Diana Zelenika², Didier Hannouche³, Marie-Christine De Vernejoul⁴, Frederic Jehan^{*5}. ¹Inserm UMR 606 & University Paris-Diderot, Hopital Lariboisiere, France, ²Centre National de Genotypage (CNG), CEA, France, ³Department of Orthopaedic Surgery & Traumatology, AP-HP & University Paris-Diderot, France, ⁴Federation De Rhumatologie Et INSERM U606, France, ⁵INSERM Unit 606, France

In the bone field single nucleotide polymorphisms (SNPs) have been extensively tested in association studies on bone mineral density (BMD) and fractures, but for most SNPs little is known about their functionality in human bones. We have investigated the functionality of promoter SNPs that may be directly responsible for change on promoter activity, and we have search for associations with gene expression in bone. Around 95% of cells in cancellous bone are of the osteoblasts lineage and we have used RT-qPCR and genotyping techniques on RNA and DNA samples to perform our experiments. We have analyzed a first set of 40 cancellous bone samples (Caucasian patients) that were obtained under the tibial plateau removed during Knee-replacement surgeries at the Department of Orthopaedic Surgery and Traumatology. For gene expression normalization, we have tested 6 different reference genes and have selected the 3 that have a stable expression in bone (geNorm algorithm). All tested genes had a measured PCR efficiency over 90%. Candidate genes have been selected in the bone field for having SNPs with frequent variations in their regulatory region and significant association with BMD and/or fractures in the literature.

Among the 8 candidate genes we have tested on the 40 different bone samples we have found significant associations between promoter variants and gene expression (delta CT meanSD):

SOST: (rs851054 G/A) 6.7041.168 (n=14) for G+ vs. 7.6470.788 for G- alleles (n=24, p=0.0110)

RUNX2: (rs12197755 G/T in the P2 promoter) 4.1170.590 (n=15) for G/T vs. 4.5740.619 for G/G genotype (n=24, p=0.0284)

SFRP1: (rs921142 A/G) 5.6630.725 (n=33) for A+ vs. 4.3900.614 for A- alleles (n=7, p=0.0001)

FZD1: (rs10953043 A/C) of 4.8850.621 (n=19) for A/A vs. 5.3690.772 for A/C genotype (n=17, p=0.0431)

We have tested associations between these SNPs and BMD or occurrence of fracture in a cohort of 136 patients with OI (with type I collagen genes tested for mutations at the CNG, Evry, France). Preliminary results have shown significant associations with the occurrence of fractures for the SOST, RUNX2 and SFRP1 SNPs, and with BMD for SFRP1. These effects don't depend on the presence or absence of type I collagen mutation and are regardless on gender and age.

Taken together, our results show that promoter polymorphisms may influence gene expression in human bones, and that these functional polymorphisms may explain some of the variability observed in OI.

Disclosures: Frederic Jehan, None.

SA0199

See Friday Plenary Number FR0199.

SA0200

Dullard Is a Novel Common Negative Regulator of BMP Signaling in Osteoblasts and Chondrocytes Acting at Smad1 Level Independently of Caveolae-Proteasome Pathway. Tadayoshi Hayata^{*1}, Yoichi Ezura², Makoto Asashima³, Ryuichi Nishinakamura⁴, Masaki Noda⁵. ¹Medical Reserach Institute, Tokyo Medical & Dental University, Japan, ²Tokyo Medical & Dental University, Medical Research Insititute, Japan, ³Graduate School of Arts & Sciences, The University of Tokyo, Japan, ⁴Department of Kidney Development, Institute of Molecular Embryology & Genetics (IMEG), Kumamoto University, Japan, ⁵Tokyo Medical & Dental University, Japan

Bone morphogenetic protein (BMP) plays crucial roles during skeletal development. BMP activity is regulated negatively by many tissue- or stage-specific BMP inhibitors to maintain proper signal levels. However, the mechanism underlying regulation of the signaling by these BMP inhibitors during osteoblastic differentiation is not fully understood. Dullard is the newest member of BMP inhibitors that dephosphorylates activated type I BMP receptor and promotes type II BMP receptor degradation via ubiquitin pathway after caveolae-mediated internalization based on animal cap and C2C12 cells. However, in osteoblasts, we have shown that Dullard suppresses BMP signaling further downstream at Smad1 level independently of its

phosphatase activity, suggesting the presence of tissue-specific signaling system. In the present study, we investigated whether Dullard suppresses BMP signaling via caveolae-proteasome pathway in skeletal osteoblastic cells. Dullard suppressed BMP signaling in the presence of caveolae disrupters, Nystatin and methyl- α -cyclodextrin, and a proteasome inhibitor MG132 by BRE-luciferase assay. Immunofluorescent staining revealed that signals for Dullard and caveolin-1 only partially co-localized. To determine functional domain of Dullard, we performed Dullard deletion analysis based on luciferase assay. We found that Dullard functional domain is located in C-terminal domain but not N-terminal domain where conserved phosphatase motif is present. The transmembrane domain at N-terminus is also required for Dullard function. Immunohistochemistry analysis revealed that Dullard protein is detected in osteoblasts as well as in chondrocytes at all stages in growth plate in newborn mice. In chondrogenic cell ATDC5, the baseline of the BRE-luciferase activity was higher than MC3T3-E1, and under this condition, Dullard suppressed such BRE-luciferase activity. These results suggest that in skeletal cell system, Dullard plays a role in regulation of BMP signaling independently of caveolae-proteasome pathway.

Disclosures: Tadayoshi Hayata, None.

SA0201

See Friday Plenary Number FR0201.

SA0202

See Friday Plenary Number FR0202.

SA0203

FGF23 Affects the Lineage Fate Determination of Mesenchymal Stem Cells.

Xu He^{*}, Tobias Larsson², Jiaxue He³, Urban Lindgren², Yan Li². ¹a Karolinska Institute; b Jilin University, Sweden, ²Karolinska Institute, Sweden, ³a Karolinska Institute; b Jilin University, Sweden

Fibroblast growth factor 23 (FGF23) is a newly identified hormone, which is supposed to be produced in bone and integral for phosphorus- and vitamin D homeostasis. It is currently recognized as a strong predictor for the disease progression in patients with chronic kidney disease and a biomarker for health status in general population. Knowledge about the clinical significance of FGF23 expanded quickly during the past decade; however, how FGF23 is secreted and whether it has a direct local action in bone remain largely unknown. Bone remodelling is organized by the deliberated balance between bone formation by osteoblasts and resorption by osteoclasts. The osteoblasts are derived from the mesenchymal stem cells. They conduct matrix production during proliferation/ differentiation and in the end undergo apoptosis or turn into osteocytes/bone lining cells, which are supposed to be the major producers of FGF23.

The present study aims to clarify whether FGF23 can affect the differentiation of cells in osteoblastic lineage. We produced functional FGF23 by transfecting hFGF23-PcDNA3.1-V5-His TOPO plasmid into COS-7 cells. The expression of Klotho was detected in mouse mechymal stem cell line C3H10 cells by Western Blot and Real time PCR. For differentiation study, the cells were cultured in osteoblast inducing medium (α -MEM medium supplement with 10%FBS, β -glycerophosphate, α -ascorbic acid and dexamethasone) for 2 weeks with different concentrations of FGF23. Osteogenic markers, including RunX2, Osteocalcin, RANKL and OPG, and adipogenic specific marker PPAR-g were measured by real time PCR. To detect FGF23 signalling, the phosphorylation of P44/42 MAPK (ERK1/2) was detected by Western blot.

We found that Klotho was expressed at both mRNA and protein level in C3H10 cells, however, at a rather lower level compared with the kidney (Fig.1). FGF23 stimulated the expression of the osteoblastic marker genes in a dose-dependent manner, but did not significantly affect the expression of the adipocyte marker gene PPAR-g (Fig.2). We also found apparent phosphorylation of the P44/42 MAPK (ERK1/2) after 10 minutes treatment of FGF23 (2000 ng/ml) (Fig.3).

In conclusion, our data indicates that FGF23 might be produced by mature bone forming cells in order to induce the osteoblastic differentiation of their progenitors. Therefore, a paracrine function of FGF23 might exist and the direct action of FGF23-klotho axis on bone remodelling demands further investigation.

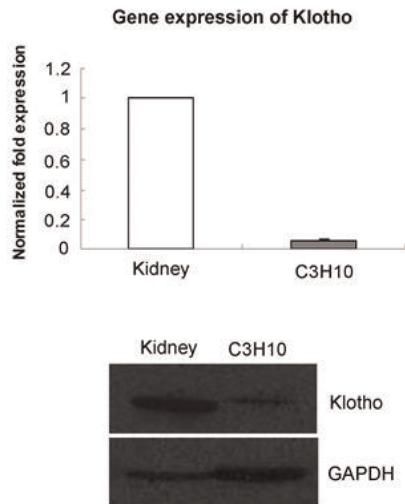


Fig.1

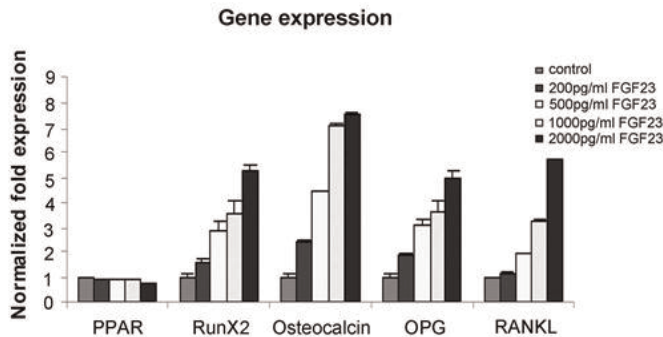


Fig.2

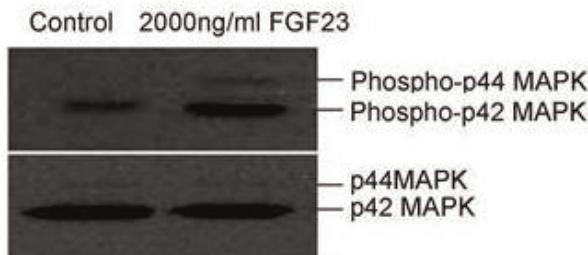


Fig.3

Disclosures: Xu He, None.

SA0204

HMWFGF2 Isoforms Regulate Bone Nodule Formation via Modulating FGFR/FGF23/ERK Signaling in BMSCs. Liping Xiao^{*1}, Alycia Eslinger¹, Marja Marie Hurley². ¹University of Connecticut Health Center, USA, ²University of Connecticut Health Center School of Medicine, USA

FGF23 is responsible for phosphate wasting and the phenotypic changes observed in human disease X-Linked Hypophosphatemia (XLH). However the mechanism(s) regulating FGF23 production by osteoblasts/osteocytes is not defined. Targeted over-expression of nuclear high molecular weight (HMW) FGF2 isoforms in osteoblasts resulted in a transgenic mouse with phenotypic changes similar to XLH including increased FGF23. HMWFGF2 also has phosphate independent effects on bone

formation in vitro mediated in part via FGF23. The goal of this study is to assess whether HMWFGF2 mediate effects on bone formation in vitro by modulating FGFR/FGF23/ERK signaling in bone marrow stromal cells (BMSCs).

To determine if decreased bone formation in cultures from HMW mice can be rescued by FGF23 neutralizing antibody, BMSCs harvested from Vector and HMWtg mice were cultured in osteogenic medium in the absence or presence of FGF23 neutralizing antibody (100 nM). Conditioned medium was collected on day 21 for FGF23 measurement by ELISA. To determine whether impaired mineralized nodule formation by HMWFGF2 over-expression can be abrogated by the FGF Receptor tyrosine kinase inhibitor SU5402 (25uM) or the MAP kinase inhibitor PD98059 (25uM), BMSCs from Vector and HMWtg were cultured in osteogenic medium and the inhibitors were added from day 14 to 21 of culture. The cells were harvested on day 21 to assess mineralized nodule formation by scanning of GFP and Xylenol Orange stained living cells and Alizarin Red staining to assess mineralized nodules. Parallel dishes were used for RNA and protein extraction. Gene and protein expression was assessed by qPCR and Western blot respectively.

FGF23 level in conditioned medium was dramatically increased in HMW-control IgG (229,6741.56 pg/mL) compared with Vector-control IgG (undetectable). In HMW-FGF23AB group FGF23 expression (close to zero) was comparable to Vector-control IgG. Mineralized nodule number was significantly decreased in HMW-control IgG compared with Vector-control IgG. The decreased nodule formation in HMW-control IgG was partially rescued by FGF23 neutralizing antibody. Decreased nodule formation in HMW cultures was also partially rescued by SU5402 and PD98059. Osteocalcin, RUNX2 and Osterix mRNA were also significantly decreased in HMW-Vehicle cultures compared with Vector-Vehicle and was partially rescued by SU5402 or PD98059 treatment.

We conclude that HMWFGF2 signals via FGFR/FGF23/MAPK to inhibit bone formation in vitro.

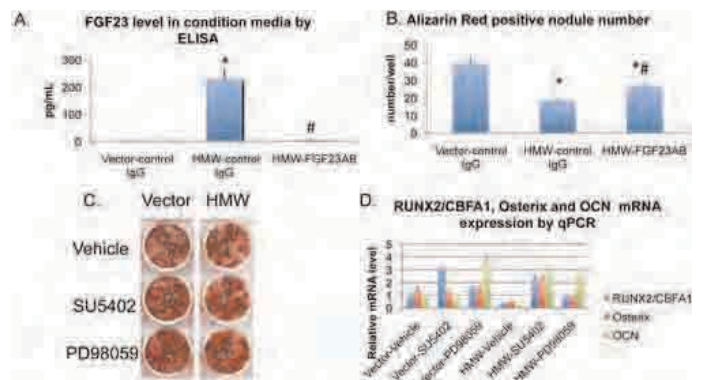


Figure 1. A) FGF23 level in condition media by ELISA. B) Alizarin Red positive nodule number per well. C) Alizarin Red stain. D) RUNX2/CBFA1, Osterix and OCN mRNA expression of BMSCs cultured for 21 days in osteogenic media. *: compared with Vector-control IgG p<0.05. #: compared with HMW-control IgG p<0.05.

Disclosures: Liping Xiao, None.

SA0205

See Friday Plenary Number FR0205.

SA0206

See Friday Plenary Number FR0206.

SA0207

EGFL6 Promotes Endothelial Cell Migration and Angiogenesis Through the Activation of ERK. Jennifer Tickner^{*1}, Shek Man Chim¹, Qin An¹, Ming Hao Zheng¹, Nathan Pavlos¹, Jiake Xu². ¹University of Western Australia, Australia, ²The University of Western Australia, Australia

Angiogenesis is required for bone development, growth, and repair. It is influenced by the local bone environment that involves cross-talk between endothelial cells and adjacent bone cells. However, data regarding factors that directly contribute to angiogenesis by bone cells remains poorly understood. Here, we report that EGFL6, a member of the epidermal growth factor (EGF) repeat superfamily proteins, induces angiogenesis by a paracrine mechanism in which EGFL6 is expressed in osteoblastic like cells but promotes migration and angiogenesis of endothelial cells. Co-immunoprecipitation assays revealed that EGFL6 is secreted in culture medium as a homodimer protein. Using scratch-wound healing and transwell assays, we found that conditioned medium containing EGFL6 potentiates SVEC endothelial cell migration. In addition, EGFL6 promotes the endothelial cell tubelike structure formation in Matrigel assays and angiogenesis in a chick embryo chorioallantoic membrane. Furthermore, we show that EGFL6 recombinant protein induces

phosphorylation of ERK in SVEC endothelial cells. Inhibition of ERK impaired EGFL6-induced ERK activation and endothelial cell migration. Together, these results demonstrate, for the first time, that osteoblastic like cells express EGFL6 that is capable of promoting endothelial cell migration and angiogenesis via ERK activation. Thus, the EGFL6 mediates a paracrine mechanism of cross-talk between vascular endothelial cells and osteoblastic like cells and might offer an important new target for the potential treatment of bone diseases, including osteonecrosis, osteoporosis and fracture healing.

Disclosures: Jennifer Tickner, None.

SA0208

See Friday Plenary Number FR0208.

SA0209

See Friday Plenary Number FR0209.

SA0210

See Friday Plenary Number FR0210.

SA0211

See Friday Plenary Number FR0211.

SA0212

Regucalcin Stimulates Osteoclastogenesis and Suppresses Osteoblastogenesis by NF- κ B Activation. Masayoshi Yamaguchi^{*1}, M. Neale Weitzmann². ¹Emory University School of Medicine, USA, ²Emory University School of Medicine & the Atlanta VA Medical Center, USA

Regucalcin plays a pivotal role in regulating intracellular calcium homeostasis and consequently has a profound effect on multiple intracellular signal transduction pathways. Regucalcin transgenic (RGN Tg) rat displays pronounced bone loss and bone marrow from these animals exhibits significantly elevated osteoclast formation. Consistent with these effects exogenous regucalcin promotes osteoclastogenesis in rat and mouse bone marrow cultures, but interestingly regucalcin suppresses the differentiation and mineralization of MC3T3 osteoblast precursors and down-regulates Runx2 and alkaline phosphatase expressions. However, the molecular mechanisms involved are presently unclear. As the NF- κ B signal transduction pathway is critical to osteoclastogenesis but inhibitory of osteoblastogenesis we hypothesized that regucalcin may promote osteoclastogenesis and suppresses osteoblastogenesis upregulating NF- κ B signal transduction. In this study we studied the effect of regucalcin on RANKL-induced osteoclast formation using RAW264.7 monocytic cell line and osteoblast formation using preosteoblastic cell line MC3T3.

As expected, culture with exogenous regucalcin was found to enhance RANKL-induced osteoclastogenesis. Consistent with this effect regucalcin increased basal and RANKL-induced NF- κ B activation as assessed by NF- κ B luciferase assay. The capacity of regucalcin to augment RANKL-induced NF- κ B activity was inhibited by menaquinone-7, a potent NF- κ B antagonist, while the Erk inhibitor PD98059 and staurosporine had no effect, demonstrating a specific effect on NF- κ B signaling.

By contrast, regucalcin inhibited mineralization in MC3T3 cells and enhanced TNF α -induced NF- κ B activation. As with NF- κ B induction in osteoclasts NF- κ B activation was abolished by addition of the NF- κ B antagonist menaquinone-7, but not PD98059 and staurosporine.

TGF- β and BMP-2 are potent early commitment and late osteoblast differentiation factors respectively and both mediate their actions through the Smad signal transduction pathway, a system that is extremely sensitive to and inhibited by TNF- α -induced NF- κ B. We consequently examined the effect of regucalcin on TGF- β - and BMP-2-induced Smad activation in the presence and absence of TNF- α . While regucalcin had no effect on basal Smad activation by TGF- β and BMP-2, it enhanced the suppressive effect of TNF- α on both TGF- β - and BMP-2-induced Smad activation.

Taken together our data suggest that regucalcin may induce bone loss in vivo by promoting osteoclasts and simultaneously suppressing osteoblasts through amplification of basal and/or cytokine-induced NF- κ B activation.

Disclosures: Masayoshi Yamaguchi, None.

SA0213

See Friday Plenary Number FR0213.

SA0214

See Friday Plenary Number FR0214.

SA0215

See Friday Plenary Number FR0215.

SA0216

TGF β Dependent Repression of MMP13 in Chondrocytes Via a Smad3 and Runx2 Dependent Pathway. Daniel Thuillier^{*1}, Carol Chen², Emily Chin², Tamara Alliston². ¹UCSF, USA, ²University of California, San Francisco, USA

In osteoarthritis, articular chondrocyte homeostasis is disrupted such that chondrocytes terminally differentiate and undergo hypertrophy. TGF β prevents chondrocyte hypertrophy in the growth plate, in part through its role in the perichondrium. Aberrant signaling of TGF β , Runx2, and Smad3 have each been associated with chondrocyte hypertrophy and osteoarthritis. However, molecular interactions of these factors in cartilage and the chondrocyte-intrinsic role of TGF β in hypertrophy remain unclear. In osteoblasts, TGF β activated Smad3 inhibits Runx2-inducible gene expression and terminal osteoblast differentiation. Therefore, we hypothesized that TGF β also inhibits terminal chondrocyte differentiation in a cell-intrinsic manner by Smad3-mediated repression of Runx2.

In Col2a1-Cre^{+/+};Smad3^{fl/fl} mice, deficient in Smad3 in chondrocytes but not in perichondrial cells, MMP13 protein expression was increased in growth plate hypertrophic chondrocytes by immunohistochemistry. Using ATDC5 chondroprogenitor cells, we examined if TGF β -mediated repression of MMP13 was also observed in vitro. Consistent with prior reports, TGF β induced MMP13 mRNA expression at 24 hrs and beyond. However, TGF β reproducibly repressed MMP13 induction at 8 hrs and earlier. Both effects were nullified by addition of a TGF β type I receptor inhibitor. Leveraging the well-studied MMP13 gene, we investigated mechanisms by which TGF β inhibits expression of a hypertrophic gene using gain and loss of function approaches. While overexpression of Runx2 in ATDC5 cells increased activity of an MMP13 promoter reporter construct, cotransfection of Smad3 or TGF β treatment repressed reporter activity dose-dependently. Accordingly, siRNA ablation of Runx2 impaired both the TGF β -mediated induction and repression of MMP13. However, when Smad3 was ablated, the rapid repression of MMP13 at 8hrs of TGF β exposure was lost and was replaced with induction. While our results are consistent with previously reported induction of MMP13 through TGF β -activated MAPK-signaling, we show here that TGF β also represses MMP13 expression in vivo, and in vitro through a chondrocyte-intrinsic Smad3 and Runx2 dependent pathway. As in other tissues, TGF β signaling through Smad3 may oppose non-Smad signaling in cartilage. By understanding the molecular pathways by which TGF β regulates expression of MMP13, this work sheds light on cell-intrinsic mechanisms utilized by TGF β to inhibit chondrocyte hypertrophy in vivo.

Disclosures: Daniel Thuillier, None.

SA0217

FoxO1 is a Bimodal Transcriptional Modulator of Bone Formation. Aruna Kode^{*}, Ioanna Mosialou, Charles Duncan, Barbara Silva, Stavroula Kousteni. Columbia University Medical Center, USA

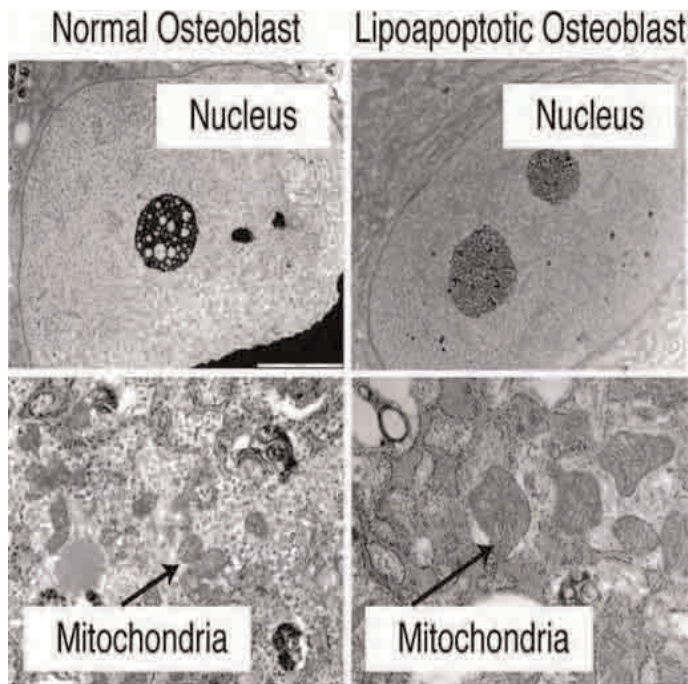
The Forkhead transcription factor FoxO1 is a known regulator of osteoblast function. Studies in mice with osteoblast specific deletion of FoxO1 have indicated that FoxO1 maintains osteoblast proliferation and bone formation by maintaining normal protein synthesis and redox balance in these cells. We show here that in spite of these proliferative effects, FoxO1 assumes a completely opposite role in the presence of high levels of serotonin, a hormone which when produced by the duodenum suppresses bone formation. Mouse models of high serotonin synthesis and cell culture experiments show that FoxO1 mediates the anti-proliferative actions of serotonin in osteoblasts. To understand this bimodal regulation we examined whether serotonin-activated FoxO1 interacts with a distinct set of proteins than those utilized under physiological conditions. We found that whereas both oxidative stress and serotonin induce nuclear localization of FoxO1, the first does so through AKT inactivation, whereas the latter suppresses PKA activity leading to an increase in the activity of JNK1. Activated JNK1 induces nuclear localization of FoxO1. In the nucleus FoxO1 can associate with either ATF4 or CREB. The association with ATF4 promotes FoxO1 transcriptional activity and thereby protein synthesis, it also maintains physiological oxidative stress levels. In contrast, association with CREB suppresses FoxO1 activity and does not affect protein synthesis or redox balance. Serotonin has no effect on the ATF4/FoxO1 complex but disrupts the FoxO1/CREB complex, an event which potentiates FoxO1 transcriptional activity. Enhancement of FoxO1 transcriptional activity is further reinforced by ATF4 and leads to suppression of cell cycle progression. These observations uncover a novel mechanism of regulation of osteoblast proliferation in which FoxO1 is the molecular node of an intricate transcriptional machinery in which different levels of FoxO1 transcriptional activity exert opposing effects on proliferation and bone formation.

Disclosures: Aruna Kode, None.

SA0218

Identification of Mechanisms of Lipopapoptosis in Normal Human Osteoblasts. Krishanthi Gunaratnam^{*1}, Christopher Vidal¹, Chris Thekkedam², Ross Boadle³, Gustavo Duque². ¹University of Sydney, Australia, ²Ageing Bone Research Program, University of Sydney, Australia, ³Millennium Research Institute, Australia

Although apoptosis plays an important role in the regulation of bone metabolism, the particular mechanisms of apoptosis in osteoblasts remain to be elucidated. We have previously demonstrated that osteoblasts undergo apoptosis after exposure to fatty acids suggesting a new model of lipopapoptosis in bone. In this study, we characterized the particular features and the mechanisms of lipopapoptosis in normal human osteoblasts (NHOs) after exposure to fatty acids. We hypothesized that, in contrast to "spontaneous" osteoblast apoptosis, lipopapoptosis is activated through a particular mechanism that should be identified in order to understand and prevent lipotoxicity in bone. NHOs were cultured in growth medium and induced to differentiate into osteoblast in the presence of either palmitic acid (100mM, 250mM and 500mM) or vehicle in the differentiation media for 24, 48 and 72h. Apoptosis was identified by TUNEL assay and electron microscopy. Additionally, the apoptotic pathways were identified using proteomic analysis of 43 apoptosis proteins (Human Apoptosis Array Kit, RayBiotech inc.). Finally, proteins showing a significant change were confirmed by western blot. TUNEL assay showed an increase in DNA fragmentation in palmitate-treated cells in a dose- and time-dependant manner. Electron microscopy showed predominantly early mitochondrial changes at 48h (Figure), which were more prevalent at higher concentration of palmitic acid. In addition, nuclear fragmentation was only observed at 72h. Later cellular changes (at 72h) included plasma membrane blebbing or budding and cell fragmentation into compact membrane-enclosed structures compatible with apoptotic bodies. Proteomic analysis identified 6 fold increase in Fas ligand ($p < 0.001$) and 2 fold increase in Bax and Cytochrome C ($p < 0.001$) expression in palmitate-treated cells (500 nM for 48 h) compared with untreated cells suggesting that, in agreement with the changes observed by electron microscopy, lipopapoptosis is induced through early activation of mitochondrial mechanisms following the activation of Fas-dependent pathways by palmitate, which in fact acts as a Fas-like compound. In summary, we have identified a previously unknown mitochondrial apoptotic pathway that is particular of lipotoxicity in osteoblasts. The regulation of fatty acid secretion and the inhibition of lipopapoptosis would protect osteoblasts against fat and could become a potential therapeutic target for osteoporosis in the future.



lipopapoptosis

Disclosures: Krishanthi Gunaratnam, None.

SA0219

Alcohol Consumption Delays Bone Healing in Association with Reduced Osteocalcin Expression after Drill Hole Injury. Yoshinori Takeuchi^{*1}, Akinori Sakai¹, Toshiharu Mori², Takuto Tsuchiya¹, Shinkichi Kanoh¹, Toshitaka Nakamura¹. ¹University of Occupational & Environmental Health, Japan, ²University of Occupational & Environmental Health, Jpn

Background: Alcohol consumption has been reported to delay fracture healing because of inhibiting osteoblast differentiation and function. However the effect of alcohol in vivo still remains unclear. The aim of this study is to clarify the effect of alcohol consumption on bone healing after drill hole injury.

Method: 8-week-old male mice (C57BL6J) were divided into two treatment groups: A) free-ingested water for 4 weeks B) free-ingested 5% ethanol for 4 weeks. At the age of 12 weeks, we made drill-hole injury, 1mm in diameter, at the anterior portion of the diaphysis of bilateral femurs. The femurs of each group were harvested before injury (day0) and at days 3, 5, 7, 10, 14 after injury. We performed bone histomorphometry at days 7, 14 after surgery and mRNA expression at days 0, 3, 5, 7, 10, 14.

Result: In bone histomorphometry, bone volume (BV/TV), OBs/BS at day7 was significantly decreased in alcohol group compared with that in water group, but there was no significant difference in BV/TV, OBs/BS at day 14 between two groups. Quantitative RT-PCR revealed osteocalcin mRNA expression significantly decreased in alcohol group at days 3, 5, 7.

Conclusion: Alcohol consumption inhibited bone regeneration and delayed bone healing in association with reduced osteocalcin expression after drill hole injury.

Disclosures: Yoshinori Takeuchi, None.

SA0220

Calcium Aluminate Scaffolds Covalently Linked with Melatonin Show Osteoconductivity and Osteoinductivity. William Clafshenkel¹, Rachelle Palchesko², Jared Romeo², James Rutkowski³, Kenneth McGowan⁴, Ellen Gawal², Paula Witt-Enderby^{*5}. ¹Duquesne University, Grad School of Pharmaceut Sci, USA, ²Duquesne University Bayer School of Natural & Environmental Sci, USA, ³Clarion Research Group, USA, ⁴Westmoreland Advanced Materials, LLC, USA, ⁵Duquesne University, School of Pharmacy, USA

One significant problem that the phosphate-based ceramic materials face is that they lack substantial mechanical integrity and are brittle and, as such, they require a high heat treatment so that they will develop the necessary strength. Another problem is that ceramic implants are only osteoconductive. Calcium aluminates (CAs) are composed of naturally hydratable mineral phases that form at room temperature. The objective of this study was to create novel CAs with regenerating and strength properties similar to natural bone that are moldable at room temperature and that display osteoconductive and osteoinductive properties. Recent evidence shows that melatonin enhances osteoblast differentiation, inhibits osteoclast-mediated bone resorption and is protective against bone loss. It was hypothesized that cooperative effects between calcium aluminate scaffolds (CAs) and melatonin occur to enhance bone regeneration in a model of calvarial (5x5mm²) defects. Our previous findings, in vivo, using female ovariectomized rats, show that melatonin-modified CA scaffolds (CA-Mel) are biocompatible and more osteoconductive compared to CA alone; the CA-Mel scaffolds showed greater bone remodeling within and around the CA-Mel scaffold/calvarial interface at 3 and 6 months as revealed by histochemistry and double fluorochrome labeling. To determine if the CA-Mel scaffolds were osteoinductive, in vitro studies were performed using human adult mesenchymal stem cells (hAMSCs) grown in culture. hAMSCs were plated over CA or CA-Mel scaffolds and then cultured in osteogenic medium for 7 days or 14 days; hAMSCs cultured under these conditions without scaffolds show differentiation into osteoblasts revealed by increases in alkaline phosphatase levels and alizarin red staining. The results from the in vitro studies reveal the presence of alkaline phosphatase within the CA-Mel scaffolds by 7 days in culture. These in vitro data show that hAMSCs grown on CA-Mel scaffolds induces their differentiation into osteoblasts, which is one indicator of osteoinductivity. These in vitro findings, showing increases in alkaline phosphatase levels within the CA-Mel scaffolds, also supports our in vivo findings about the osteoconductive nature of these scaffolds. These data support the hypothesis that CA-Mel scaffolds are both osteoconductive and osteoinductive. These findings are important and may lead to the development of a novel bioactive scaffold to enhance bone grating procedures.

Disclosures: Paula Witt-Enderby, None.

SA0221

Withdrawn

SA0222

Correction of the Haploinsufficient Hematopoietic Microenvironment is Sufficient to Normalize the Pathological Fracture Repair in Genetically Engineered Murine Model of Neurofibromatosis Type 1. Xiaohua Wu¹, Shi Chen¹, Yongzheng He¹, Steven Rhodes², Xiaohong Li¹, Xianlin Yang¹, Li Jiang¹, Grzegorz Nalepa¹, Khalid Mohammad², Alexander Robling², D. Wade Clapp¹, Simon Conway¹, Theresa Guise², Feng-Chun Yang².
¹Indiana University School of Medicine, USA, ²Indiana University, USA

Germline mutations in the NF1 tumor suppressor gene cause neurofibromatosis type 1 (NF1), a complex genetic disorder with a high predisposition to numerous skeletal dysplasias including short stature, osteoporosis and kyphoscoliosis. Understanding the pathogenesis of these sequelae has been difficult due to lack of appropriate orthologous genetic animal models.

In this study, Periostin promoter mediated Cre expression, which has been shown expressed in mesenchymal stem/progenitor cells (MSPCs) and osteoblasts, was introduced to the mouse model. PeriCre⁺ mice were intercrossed with mice bearing either systemic or conditional genetic targeting of the Nf1 allele (Nf1^{+/-} and Nf1flox/flox, respectively) to generate four experimental genotypes: PeriCre⁺;Nf1flox/flox (WT), PeriCre⁺;Nf1flox^{-/-} (Nf1^{+/-}), PeriCre⁺;Nf1flox/flox mice (Nf1 null in MSPCs and osteoblasts, otherwise systemically WT), and PeriCre⁺;Nf1flox^{-/-} mice (Nf1 null in MSPCs and osteoblasts, otherwise systemically Nf1 heterozygous). The skeletal phenotypes and fracture healing were evaluated by pDEXA, μ CT (for tibia or femur), TRACP staining, and McNeal's staining (for bone sections).

Our results showed that bone mineral density is significantly reduced in PeriCre⁺;Nf1flox^{-/-} mice as compared to other groups of mice. Furthermore, reduced trabecular bone formation and increased osteoclast activity in PeriCre⁺;Nf1flox^{-/-} mice are evidenced by μ CT analysis, McNeal's staining, and TRACP staining. PeriCre⁺;Nf1flox^{-/-} mice displayed an impaired fracture healing. These data suggest that the development of these skeletal manifestations requires a Nf1 haploinsufficient background in addition to nullizygous loss of Nf1 in MSPCs and their progenies. Moreover, the requirement of the hematopoietic bone marrow microenvironment is verified by adoptive transfer experiments. More importantly, transfer of WT bone marrow into PeriCre⁺;Nf1flox^{-/-} mice significantly improves fracture healing. These data provide the first evidence of a non-cell autonomous mechanism in non-malignant NF1 manifestations, specifically, skeletal manifestations.

Collectively, these data demonstrate a combinatory effect between nullizygous loss of Nf1 in osteoblast progenitors and haploinsufficiency in hematopoietic cells in the development of skeletal manifestations in NF1.

Disclosures: Xiaohua Wu, None.

SA0223

See Friday Plenary Number FR0223.

SA0224

See Friday Plenary Number FR0224.

SA0225

Forming Bone in Artificial Patterns Using Mother of Pearl. Ronke Olabisi*, Maude Rowland, Christy Franco, Joseph Hoffmann, Jennifer West. Rice University, USA

The purpose of this study was to direct osteoblast bone formation in specified patterns on surfaces of hydrogels using proteins extracted from mother of pearl (nacre). Neither biomimetics nor tissue engineering have yet produced a tissue biomechanically and structurally equivalent to authentic bone, and insights into developing better bone replacement materials may be obtained through studies of biomineralization. Water soluble proteins extracted from nacre initiated earlier biomineralization in MC3T3-E1 cells (1). Here we extract nacre proteins from the water soluble, urea soluble and EDTA soluble matrix (WSM, USM and ESM, respectively), then react them with poly(ethylene glycol)-succinimidyl valerate (PEG-SVA) to attach crosslinkable acrylated PEG polymers. Next, PEG hydrogels were formed containing PEGylated fibronectin to enable osteoblast attachment. PEGylated nacre proteins were combined with fluorescein o-acrylate (a fluorescent marker) and placed on the surface of hydrogels in all combinations of the 3 proteins (N=8: WSM, USM, ESM, WSM+USM, WSM+ESM, USM+ESM, WSM+USM+ESM, None). A patterned photomask was placed over the proteins and exposed to collimated white light in order to crosslink the PEGylated proteins to the hydrogel surface in the pattern. Murine osteoblasts (MC3T3-E1) were seeded on the surfaces of these hydrogels. On day 3, seeded hydrogels were imaged with phase and fluorescent microscopy and bone nodules were quantitated. On day 12, hydrogels were stained using the von Kossa method and imaged with phase microscopy. By day 3, mineralization occurred at a significantly greater rate ($p=0.019$) on the WSM hydrogel within or directly adjacent to areas containing WSM than areas devoid of the protein, as visualized by fluorescence of collocated fluorescein o-acrylate (Fig 1). von Kossa stains showed mineralized bone forming in the patterns on the surface of the WSM hydrogel (Fig 2). Hydrogels containing other proteins did not display this

phenomenon. While WSM proteins have been demonstrated to initiate bone formation by MC3T3-E1 cells, this is the first time this capacity has been demonstrated when the proteins have been covalently immobilized on a patterned hydrogel. Thus we have for the first time directed bone formation in a specified pattern. This may be the first step towards tissue engineering complex delicate bone structures, such as the stapes within the ear.

1. Rousseau M et al. Comp Biochem Phys B: Biochem Mol Biol 2003; 135(1):1-7.

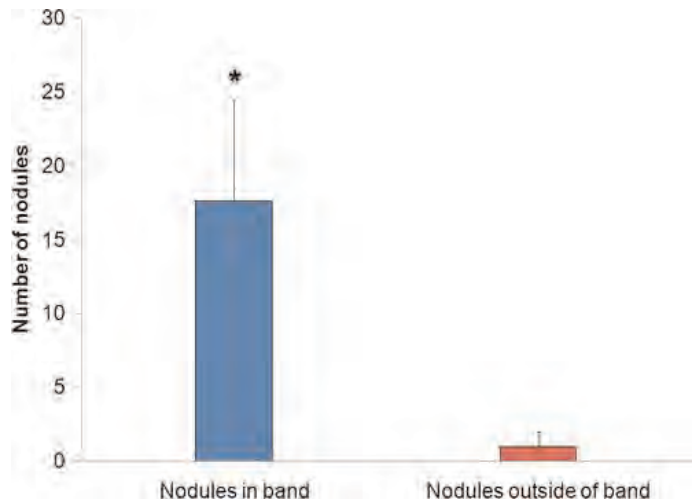


Figure 1. Tabulation of nodule formation on day 3.

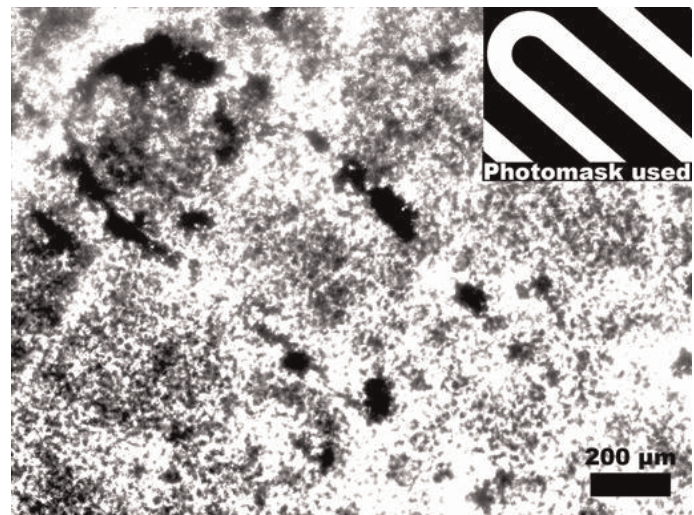


Figure 2. von Kossa stained phase contrast micrograph of patterned bone.

Disclosures: Ronke Olabisi, None.

SA0226

Impact of Omega-3 Polyunsaturated Fatty Acids on Bone During Chronic Simulated Resistance Training. Kaleigh Camp*, David Cunningham, Evelyn Yuen, Brandon Macias, Stuart Solomon, Harry Hogan, Susan Bloomfield. Texas A&M University, USA

Animals eating diets rich in omega-3 polyunsaturated fatty acids (n-3 PUFAs) exhibit enhanced bone formation. Eicosapentaenoic acid, an n-3 PUFA found in fish oil, competes with arachidonic acid, an omega-6 polyunsaturated fatty acid (n-6 PUFA), for the cyclooxygenase enzyme, modulating prostaglandin E2, a potent mediator of bone mechanotransduction. Whether this diet affects bone gains during chronic exercise is not well defined. The purpose of this study was to determine the impact of a diet rich in n-3 PUFAs on bone mass and geometry changes after simulated resistance training (SRT). We hypothesized rats consuming a high n-3 PUFA diet would gain more bone mass compared to the rats consuming a low n-3 PUFA diet in response to SRT. Virgin female Sprague-Dawley rats (5-mo-old, n=20) were assigned by body weight to one of two groups: diet with an n-6:n-3 dietary ratio of 23:1 (O6) or a diet rich in fish oil with an n-6:n-3 dietary ratio of 2:1 (O3) based on the AIN-93M purified diet. After 4 weeks' acclimation rats completed 9 SRT sessions on alternate days using stimulated muscle contractions under anesthesia at 75% peak isometric strength; each contraction included 1 sec isometric + 1 sec eccentric contraction. Cancellous and cortical density and geometric properties at the proximal and mid-shaft tibiae of both the exercised and non-exercised legs were quantified at

days -7 and 21 using *in vivo* peripheral quantitative CT. There were no significant differences in body weights among groups at baseline or after training. Rats on the O3 diet exhibited significant increases in total vBMD, total vBMC, and cortical BMD at the proximal tibia versus values in rats on the O6 diet ($p < 0.05$); however, the O3 diet had no effect on mid-shaft tibia cortical BMC, vBMD, or area. In both diet groups, SRT stimulated significant gains in total vBMD (6.3%) and cortical BMD (6.1%) at the proximal tibia, and cortical BMC (21.5%) and cortical area (19.8%) at the mid-shaft tibia. However, we could not detect any increased effect of the O3 diet on magnitude of these gains in bone mass or area with SRT. A diet high in n-3 PUFAs independently increases bone mass at the proximal tibia metaphysis; however, it does not further enhance gains in bone mass observed with simulated resistance training.

Disclosures: *Kaleigh Camp, None.*

This study received funding from: Huffines Institute of Sports Medicine and Human Performance, Texas A&M University

SA0227

Maintenance of Human Osteoblasts, Mesenchymal Stem Cells, and Bone Explants In Vitro Without the Use of Animal Derived Materials. *Mrs Carole Elford, Deborah Mason, Dr Jim Ralphs, Professor John W. Gregory, Dr Alastair J. Sloan, Bronwen Evans**. Cardiff University, United Kingdom

It is important to advance and implement the 3Rs i.e. replacing, reducing and refining the use of animals in research and testing. Furthermore, musculoskeletal cell or tissue replacement therapies require the use of chemically defined media, which do not contain animal derived materials. We investigated the use of a range of non-fetal calf serum (FCS) containing media on cell number (3 days; MTS assay) in human osteoblast lines (MG63, SaOS2). We have compared the current gold standard of DMEM containing 10% FCS with a range of test media: 1) DMEM with 10% human serum (Lonza), 2) DMEM with 10% human serum AB (Lonza) 3) DMEM with K/O serum replacement (10%, 15%; Invitrogen), and 4) TheraPEAK (defined medium; Lonza). We also investigated the effects of these media on multipotent, marrow-derived, human mesenchymal stem cell (MSC; Promocell) numbers and differentiation (3 days; ALP activity). Cells were either i) set up in control media and test media added the next day, or ii) set up in the test media. Furthermore, similar work was undertaken with explants derived from human bone.

With MG63 cells, human serum and K/O decreased (50-60%; $p < 0.001$), whereas TheraPEAK increased numbers (~130%; $p < 0.001$). With the more differentiated SaOS2, however, human serum increased (120%; $p < 0.01$) or had no effect, depending on the set up methodology used, K/O (15%) decreased (~35%; $p < 0.01$), whereas TheraPEAK increased numbers by 200 to 300% ($p < 0.001$). With undifferentiated MSCs, results were similar to those with MG63 cells, although reductions with human serum and K/O were ~25% and ~75% respectively ($p < 0.001$). Human serum and TheraPEAK stimulated (~250%; $p < 0.001$) differentiation (ALP activity) in MSCs. Human bone chips set up in different media resulted in the establishment of osteoblast cultures in all media, although FCS containing cultures exhibited most proliferation, whereas osteoblasts in human serum containing medium were the most differentiated. Very few cells were observed with TheraPEAK.

The work shows that cells at different stages of the osteoblast differentiation pathway respond differently to non-FCS containing media, and that it is possible to establish primary, human osteoblast cultures without using FCS. The results will guide our planned studies to design successful human osteoblast and osteocyte culture methods using media which do not contain animal derived materials.

Disclosures: *Bronwen Evans, None.*

SA0228

Mature Osteoclasts Produce S1P to Support Osteoblast Differentiation via S1P Receptor Engagement and RhoA Activation. *Patrick Quint**¹, *Moustapha Kassem*², *Jennifer Westendorf*³, *Sundeep Khosla*⁴, *Merry Jo Oursler*³. ¹Mayo Clinic Rochester, USA, ²Odense University Hospital, Denmark, ³Mayo Clinic, USA, ⁴College of Medicine, Mayo Clinic, USA

Bone is a dynamic tissue that continuously remodels and, under most conditions, resorbed bone is nearly precisely replaced in location and amount by new bone. It has long been recognized that bone resorption and formation are tightly coupled processes but the nature of the coupling factors remained unresolved. To study secreted osteoclast products that might recruit osteoblast lineage cells, we examined osteoclast precursor and mature osteoclast conditioned media (CM) influences on hMSC-TERT mesenchymal cells. A centrifuge filter unit with a nominal 10,000 dalton cut off was used to 10-fold concentrated conditioned media (CM) from mature osteoclasts. Osteoclast CM supported hMSC-TERT cell migration and mineralization compared to base media. The precursor CM also stimulated hMSC-TERT cells, but to a lesser extent than the mature osteoclast CM. Concentrated and unconcentrated CM stimulated hMSC-TERT cell migration and mineralization to nearly the same extent. These data indicated the possible presence of a low mass chemokine and we hypothesized that sphingosine-1-phosphate (S1P) was involved. There are two enzymes that produce S1P, Sphingosine-1-kinase (SPHK) 1 and SPHK2. During osteoclast differentiation, SPHK1 expression was up-regulated whereas SPHK2 expression remained constant. A luciferase reporter driven by the SPHK1 promoter confirmed promoter activation during osteoclast differentiation. Mass spectrometry

of the CM detected S1P in the CM from both osteoclast precursors and mature osteoclasts.

The hMSC-TERT cells expressed S1P receptors 1, 2 and 3 mRNAs. Targeted disruption of S1P interactions with S1P receptors 1 and 2, but not 3, blocked osteoclast precursor and mature osteoclast CM effects on mineralization and migration of hMSC-TERT cells. Combined blocking of receptors 1 and 2 was the most effective at blocking responses, supporting non-redundant roles for these receptors. To resolve the mechanisms by which S1P influences hMSC-TERT cells, we employed a pan-specific S1P receptor agonist to investigate influences of S1P on hMSC-TERT cells. Examination of Rho family GTPase activation revealed that Rho A, but not Rac1 or Cdc42, were activated following agonist treatment.

We conclude from these data that osteoclast precursor and mature osteoclast CM promote mesenchymal cells at least in part through production of the chemokine S1P, which stimulates mesenchymal cell RhoA activation to promote recruitment and differentiation.

Disclosures: *Patrick Quint, None.*

SA0229

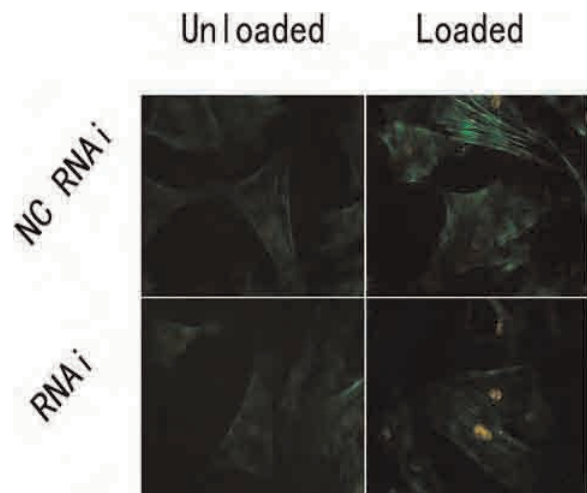
Mechanosensitivity of Osteoblasts Could Be Up-regulated by Inhibition of Cytoskeleton Reorganization. *Qiang Fu**, *Yun Shen*, *Yiping Zhang*, *Changjing Wu*, *Rui Chen*. School & Hospital of Stomatology, Sun Yat-sen University (present address is Shanghai Tenth People's Hospital, Shanghai), China

Evidence has proved that bone accommodates to steady mechanical loading by down-regulating its reaction induced by mechanical stimuli, inferring that bone cells can adapt their mechanosensitivity to a new mechanical environment. Cytoskeleton plays an important role in cellular mechanotransduction and would be reorganized in response to mechanical loading. In previous studies, we found that using RNAi against LIM domain kinase 2 (LIMK2) could inhibit the cytoskeleton reorganization induced by fluid shear stress in osteoblasts without structural or functional destruction of the cytoskeleton. Based on this, we proposed the hypothesis that the cytoskeleton reorganization of bone cells contributes to their adaptation to mechanical stimuli, and that the mechanosensitivity of bone cells would be manipulated by inhibition of the cytoskeleton reorganization.

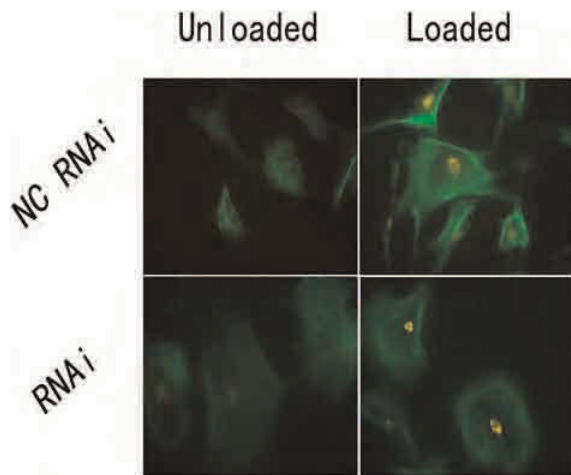
In the present study, we chose two significant molecules of c-Fos and cox-2 as the representatives of osteoblasts activity, and studied their expression levels under loading when cytoskeleton reorganization was inhibited. Mouse primary osteoblasts were pretreated with RNAi against LIMK2 and loaded by fluid shear stress at 12 dyne/cm² for 1/1.5h. Negative RNAi and cytochalasin D were also used to pretreat the cells as two control methods. C-Fos and cox-2 expression levels were examined by Real-time PCR, immunofluorescence and Western-blot.

We found that loaded cells treated with LIMK2 RNAi had 2.4- and 3.1-fold higher expression levels of c-Fos and cox-2 mRNA, respectively, compared with the negative RNAi controls and 1.3- and 1.6-fold higher c-Fos and cox-2 protein levels, respectively. In contrast, c-Fos and cox-2 expression levels induced by fluid shear stress were significantly reduced by 32% and 37%, respectively, in Cytochalasin D-treated cells.

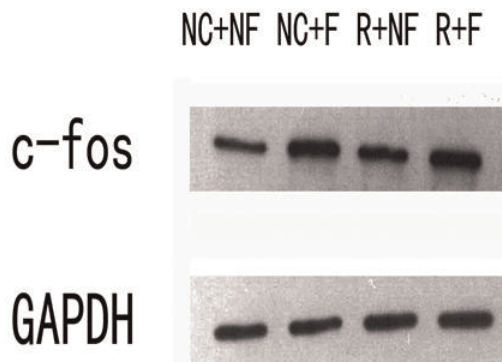
This study demonstrates that cytoskeleton integrity in osteoblasts is essential for the c-Fos and cox-2 genes expression induced by fluid shear stress, and when the cytoskeleton reorganization is inhibited their expression induced by fluid shear stress is promoted. So, from the point of view of these two important genes related with osteoblasts activity, it suggests that the mechanosensitivity of osteoblasts could be up-regulated by inhibition of cytoskeleton reorganization. The regulation of cytoskeleton should be a way to manipulate the mechanosensitivity of bone cells and even bone tissue.



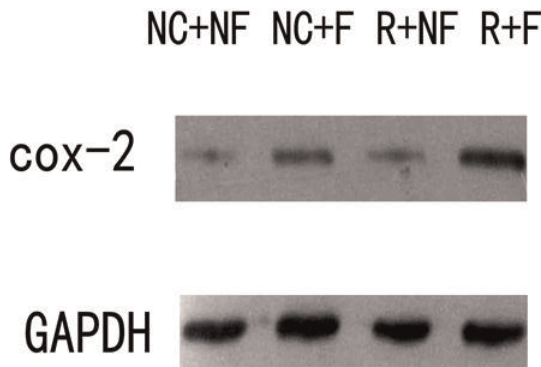
OBs immunofluorescence Density of c-Fos in RNAi group was higher than NC group after loading



OBs immunofluorescence Density of COX-2 in RNAi group was higher than NC group after loading



c-Fos expression level induced by fluid shear stress was promoted through RNAi



COX-2 expression level induced by fluid shear stress was promoted through RNAi

Disclosures: Qiang Fu, None.

This study received funding from: This work was funded by Science and Technology Planning Project of Guangdong Province (ID:2009B050700027) and Natural Science Foundation of Guangdong Province (ID:10151008901000140)

SA0230

Osteoblastic ephrinB2 Is Required for Normal Osteoblast Differentiation and Function *in vitro* and *in vivo*. Farzin Takyar¹, Stephen Tonna¹, Blessing Criméen-Irwin¹, T. John Martin¹, Natalie Sims². ¹St. Vincent's Institute of Medical Research, Australia, ²St. Vincent's Institute for Medical Research, Australia

Bidirectional signaling between EphB4 and ephrinB2 in osteoblasts leads to increased osteoblast differentiation *in vitro*, and interference with this interaction inhibits osteoblast differentiation. Furthermore, injection of PTH rapidly enhanced ephrinB2 expression in mouse and rat bone and isolated osteoblasts.

To determine the role of osteoblastic ephrinB2 in bone metabolism, we crossed *efnB2-flox* and osteoblast-specific tetracycline-regulatable *Osx1Cre* mice to delete *efnB2* from an early stage of osteoblast differentiation *in vivo*. Two groups of mice were studied: one where ephrinB2 was deleted constitutively, and one where mothers and pups were treated with doxycycline until 4 weeks of age, to allow ephrinB2 expression during

skeletal development. Tibiae from female 12 week old *Osx1Cre.efnB2^{fl/fl}* mice and controls (*Osx1Cre.efnB2^{wt/wt}*) were analyzed by histomorphometry.

No overt change in bone structure was observed in *Osx1Cre.efnB2^{fl/fl}* mice compared with *Osx1Cre.efnB2^{wt/wt}* regardless of whether ephrinB2 was deleted constitutively or after skeletal development. In *Osx1Cre.efnB2^{fl/fl}* mice treated with doxycycline until 4 weeks of age, we observed a significant (30%) increase in osteoblast number ($p=0.02$) compared to control animals, but osteoid and osteoclast parameters were unchanged. In *Osx1Cre.efnB2^{fl/fl}* mice with no exposure to doxycycline and therefore with ephrinB2 deletion throughout development, more dramatic alterations in bone formation were observed. With such lifetime deletion of ephrinB2, osteoblast surface, osteoblast number, and osteoid thickness were all significantly increased by ~30% in *Osx1Cre.efnB2^{fl/fl}* mice compared to controls ($p=0.03$, 0.003 , and 0.01 , respectively). Despite this, osteoid surface was not increased. Furthermore, in contrast to the increase in osteoblast number, a 30% decrease in mineralizing surface and 50% decrease in bone formation were observed in *Osx1Cre.efnB2^{fl/fl}* mice ($p=0.01$ and 0.03 , respectively). These data indicate that although their number is increased, ephrinB2-deficient osteoblasts have reduced mineralization ability. Osteoclast number was not significantly modified in *Osx1Cre.efnB2^{fl/fl}* mice.

These results provide *in vivo* evidence confirming *in vitro* findings indicating that ephrinB2 signaling within the osteoblast lineage is required for normal differentiation and function of osteoblasts in bone formation.

Disclosures: Farzin Takyar, None.

SA0231

See Friday Plenary Number FR0231.

SA0232

See Friday Plenary Number FR0232.

SA0233

See Friday Plenary Number FR0233.

SA0234

Time Course of Bone Response to Smoke Exposure in Cortical Bone. Diane Cullen^{*1}, Bryan Hackfort¹, Gwendolin Alvarez¹, Sara Rousch¹, Meredith Stein¹, Mohammed Akhter². ¹Creighton University, USA, ²Creighton University Osteoporosis Research Center, USA

Cigarette smoking is a risk factor for osteoporosis. In previous studies we have found bone loss, but inconsistent effects on bone formation in cortical bone. This may be due to the remodeling sequence and time frame for activation of osteoblasts and osteoclasts. We hypothesize that in mice, smoke exposure increases remodeling with early osteoclast activation and osteoblast suppression followed by an osteoblast increase secondary to osteoclast resorption. To test this, mice were divided into smoke exposure and control and then collected at baseline, after 3, 6, or 12 weeks treatment or after 12 wks treatment and 6 wks recovery. Mice were exposed for 3 hrs, 5 d/wk at an average smoke concentration of 103 mg/m³ TSP. To examine the interaction of smoking (catabolic treatment) with the Lrp5/Wnt pathway (anabolic pathway) we examined wild type C57Bl6 (W) mice, Lrp5 knockout (K) and HBM transgenic (H) mice. Differences were tested by three-way ANOVA for Time, Smoke, and Genotype (Figure). After 12 wks of treatment there was greater marrow area and lower bone strength in smoke exposed mice. In the control animals there was a decrease in bone formation rates with age. Periosteal bone formation rate (BFR) was further suppressed in all smoke groups at 3 and 6 wks of exposure and remained low at 12 wks. After smoke recovery, BFR was higher than in control. The endocortical BFR was suppressed at 3 wks and recovered to normal levels by 6 wks. At three weeks osteoblast activity is suppressed in all genotypes suggesting a negative effect of smoke on bone formation independent of Lrp5 expression. The recovery of formation by 6 wks, on the endocortical but not the periosteal surface is consistent with activation of osteoclasts and secondary osteoblast activation in remodeling. The periosteal surface in adult mice does not normally show remodeling and is perhaps the best indicator of direct smoke effects on the osteoblast which was consistent suppression. The periosteal recovery demonstrates the direct, acute effect of smoke exposure on osteoblasts. We conclude cigarette smoke suppresses osteoblast activity and that results from the endocortical surface are confounded by the coupling of osteoclasts and osteoblasts in remodeling.

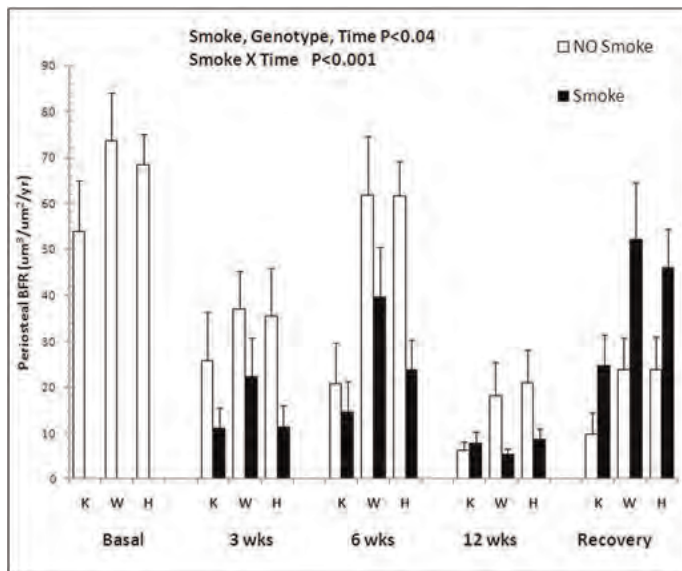


Figure 1

Disclosures: Diane Cullen, None.

SA0235

See Friday Plenary Number FR0235.

SA0236

A Program of MicroRNAs Controls Osteogenic Lineage Progression by Targeting Transcription Factor RUNX2. Ying Zhang^{*1}, Rong-lin Xie², Carlo Croce³, Janet Stein², Jane Lian², Andre Van Wijnen², Gary Stein². ¹Umass medical school, USA, ²University of Massachusetts Medical School, USA, ³The Ohio State University, USA

Lineage progression in osteoblasts and chondrocytes is stringently controlled by the cell-fate determining transcription factor Runx2. In this study we directly addressed whether small non-coding microRNAs (miRNAs), which inhibit mRNAs by binding to seed sites, control osteoblast maturation by modulating the osteogenic activity of Runx2. A panel of eleven Runx2-targeting miRNAs (miR-23a, miR-30c, miR-34c, miR-133a, miR-135a, miR-137, miR-204, miR-205, miR-217, miR-218 & miR-338) is expressed in a lineage-related pattern in mesenchymal cell types. During both osteogenic and chondrogenic differentiation, these miRNAs, in general, are inversely expressed relative to Runx2. Based on 3'UTR luciferase reporter and immuno-blot assays, each miRNA directly attenuates Runx2 protein accumulation. Runx2-targeting miRNAs differentially inhibit Runx2 protein expression in osteoblasts and chondrocytes and display different efficacies. Thus, cellular context contributes to miRNA mediated regulation of Runx2. All Runx2-targeting miRNAs (except miR-218) significantly impede osteoblast differentiation and their effects can be reversed by the corresponding anti-miRNAs. These findings demonstrate that osteoblastogenesis is limited by an elaborate network of functionally tested miRNAs that directly target the osteogenic master regulator Runx2.

Disclosures: Ying Zhang, None.

SA0237

Bone-specific Overexpression of NPY Modulates Osteogenic Differentiation. Igor Matic^{*1}, John Igwe², DARIO REPIC¹, SLAVICA PEJDA³, Tomislav Kizivat⁴, Douglas Adams¹, Ivo Kalajic¹. ¹University of Connecticut Health Center, USA, ²Department of Orthopedic Surgery, University of Connecticut Health Center, USA, ³University of Connecticut, USA, ⁴Croatia

Our previous work showed that neuropeptide Y (NPY) is expressed by osteoblast lineage cells and when administered in vitro can inhibit osteoblast lineage differentiation. We hypothesize that NPY, generated by mature osteoblast lineage cells, can control and modulate differentiation of osteoprogenitor cells. Therefore, in this study we have evaluated the effects of bone-specific overexpression by generating Col2.3NPY-ires GFP^{topaz} transgenic mice. As described in previous studies, this transgenic approach will direct NPY overexpression to mature osteoblasts and osteocytes. Real-time PCR analysis of bone-derived RNA showed increased expression of NPY in samples derived from Col2.3NPY mice compared to wild type. To characterize the Col2.3NPY mice phenotype in vivo, trabecular and cortical bone

morphometry was measured in three-month-old mice using µCT analysis. Lower trabecular and cortical bone mass and morphometric parameters were observed in both male and female mice, exhibiting 30-35% lower trabecular volume and 7-9% lower cortical volume, without differences in linear bone growth. Gene expression analysis in Col2.3NPY mice shows increased expression of OC when compared to wild type. No difference was detected in expression levels for BSP and DMP-1. Our preliminary data on dynamic histomorphometry has shown reduced mineral apposition rate in Col2.3NPY mice. This apparent discrepancy in bone mass and gene expression will be addressed by evaluating cellular parameters of bone lineage using histomorphometry and evaluation of the effects of NPY overexpression on proliferation and maturation of the osteoblast lineage cells in vivo. We have utilized primary culture to assess the effects of NPY overexpression. Markers of mature osteoblast lineage cells (BSP, OC, and DMP-1) in BMSCs derived from Col2.3NPY mice were enhanced compared to wild type. There was no difference in ALP activity or mineralization in MSC cultures derived from NPY versus wild type mice. In contrast to stromal cells, calvarial osteoblast derived from Col2.3NPY mice show a decrease in mineralization colonies. This difference between two culture models could be a result of the presence of more mature NPY producing cells driven by Col2.3 at the early days of calvarial osteoblast culture compared to BMSC. Further studies are required to clarify the bone phenotype of Col2.3NPY mice and to understand the mechanism by which bone derived NPY affects osteoprogenitor differentiation.

Disclosures: Igor Matic, None.

SA0238

Collagen-Mimetic Peptide of Adiponectin Accelerates Osteoblastic Differentiation. Aiko Kamada^{*}, Takashi Ikee, Yoshihiro Yoshikawa, Eisuke Domae, Seiji Goda, Isao Tamura. Osaka Dental University, Japan

Adiponectin, a adipocyte-derived biologically active molecule, abundantly present as a plasma protein, and exhibits various biological functions, such as regulating energy homeostasis and increasing insulin sensitivity in the liver and skeletal muscle. It is ~30-kDa polypeptide containing N-terminal signal sequence, variable domain, collagen-like domain, and C-terminal globular domain. Recent studies have demonstrated both a positive and negative action of adiponectin on bone formation, and it was thought that these different actions might be attributed to its multifunctional domains. Previously we demonstrated that functional domains of adiponectin act on osteoblasts through different manners, and the collagen-like domain may be involved to osteoblast differentiation. In this study we synthesized collagen-mimetic peptide designed from adiponectin functional domains, and investigated its effect on osteoblast differentiation.

Recombinant murine adiponectin collagen-like domain was designed and produced. Osteoblastic differentiation of a murine pro-osteoblastic cell line, MC3T3-E1 cells, was induced by differential medium including ascorbic acid and beta-glycerophosphate with or without the peptide. Gene expression was determined by real time RT-PCR analysis.

The collagen-mimetic peptide induced expression of genes related to various signaling pathways and BMP family involved to osteoblastic differentiation.

Our study suggests the collagen-mimetic peptide from adiponectin collagen-like domain may be useful for regeneration of calcified tissues.

Disclosures: Aiko Kamada, None.

SA0239

Differential Expression of Nuclear Receptors and Coregulators in Mouse Calvarial Osteoblast Differentiation and in Aged Mice. Matthew Roforth^{*1}, Sundeep Khosla², David Monroe³. ¹Mayo Clinic, USA, ²College of Medicine, Mayo Clinic, USA, ³Mayo Foundation, USA

A complex network of transcription factors contributes to the establishment and maintenance of the osteoblastic phenotype. Although relatively few transcription factors, such as Runx2 and osterix, are essential to the process of osteoblastic differentiation, others serve the purpose of fine-tuning in response to various environmental and hormonal cues. In this study we report the expression patterns of the entire nuclear receptor (NR) superfamily, select coregulator, and osteoblast marker genes during differentiation in a primary mouse calvarial cell model. Osteoblastic mineralization was visually apparent ten days following osteoblastic induction, as assessed by Alizarin red stain. Increases in the classical bone marker genes alkaline phosphatase, osteocalcin, Runx2 and osterix, were also observed. Interestingly, Sost, Dmp1, Fgf23, Phex and Mepe, all genes associated with osteocytic function, were increased suggesting the adoption of an osteocytic phenotype. Analysis of NR gene expression one day following induction revealed significant changes in a number of NR subfamilies and associated changes in select coregulators involved in NR signaling. Most notably upregulation of estrogen, retinoic acid and vitamin D receptors were observed within the first day of differentiation, supporting the role of these pathways in osteoblastic differentiation. Examination of NR and coregulator gene expression patterns at later stages of osteoblastic differentiation revealed that 78% of NRs and virtually all coregulators were downregulated. To place our findings in the context of age-related changes in bone metabolism, we next determined the NR and coregulator gene expression changes associated with age-related bone loss. Analysis of NR and coregulator gene expression in aged mice (18-22 month versus 6 month controls) revealed significant upregulation of Errα, Lxrα, Rorβ, Rev-erba/β and the p72 RNA helicase coactivator. Interestingly, all these NRs are associated with

either age-related bone loss or the support of adipogenesis. Collectively, these data demonstrate that large-scale changes in the nuclear receptor superfamily occur throughout osteoblastic differentiation and during the process of aging, leading to altered sensitivity to various hormonal cues. Whether these changes are prerequisite for osteoblast differentiation or a consequence of the induction of differentiation or the aging process remains an important area for further investigation.

Disclosures: *Matthew Roforth, None.*

SA0240

Effect of Nanocoating with Rhamnogalacturonan-I on Surface Properties and Osteoblasts Response. Katarzyna Gurzawska^{*1}, Rikke Svava², Susanne Syberg³, Yu Yihua⁴, Kenneth Brian Haugshøj⁵, Iben Damager⁶, Leif Højislet Christensen⁵, Peter Ulvskov Ulvskov⁶, Klaus Gotfredsen⁷, Niklas Jørgensen⁸. ¹Research Center for Ageing & Osteoporosis, University of Copenhagen, Glostrup Hospital, Denmark, ²Copenhagen Center for Glycomisc, Faculty of Health Sciences, University of Copenhagen, Denmark, ³Glostrup Hospital, Denmark, ⁴Microtechnology & surface analysis, Danish Technological Institute, Gregersensvej 3, 2630 Taastrup, Denmark, Denmark, ⁵Microtechnology & surface analysis, Danish Technological Institute, Denmark, ⁶Department of Plant Biology, Faculty of Life Sciences, University of Copenhagen, Denmark, ⁷Institute of Odontology, Faculty of Health Sciences, University of Copenhagen, Denmark, ⁸Copenhagen University Hospital Glostrup, Denmark

Long-term stability of titanium implants are dependent on a variety of factors. Nanocoating with organic molecules is one of the methods used to improve osseointegration. Therefore, the aim of this study was to evaluate the in vitro effect of nanocoating with pectic rhamnogalacturonan-I (RG-I) on surface properties and osteoblasts response.

Three different RG-Is from apple and lupin pectins were modified and coated on amino-functionalized tissue culture polystyrene plates (aminated TCPS). Surface properties were evaluated by scanning electron microscopy, contact angle measurement, atomic force microscopy and X-ray photoelectron spectroscopy. The effects of nanocoating on proliferation, matrix formation and mineralization, and expression of genes (real-time PCR) related to osteoblast differentiation and activity, were tested using human osteoblast-like SaOS-2 cells.

It was shown that RG-I coatings affected the surface properties. All three RG-I induced bone matrix formation and mineralization, which was also supported by the finding that gene expression levels of alkaline phosphatase, osteocalcin and collagen type-I were increased in cells cultured on the RG-I coated surface, indicating a more differentiated osteoblastic phenotype. This makes RG-I coating a promising and novel candidate for nanocoatings of implants.

Disclosures: *Katarzyna Gurzawska, None.*

SA0241

See Friday Plenary Number FR0241.

SA0242

See Friday Plenary Number FR0242.

SA0243

See Friday Plenary Number FR0243.

SA0244

Identification of a Common BMP-responsive Element in the Id1, Id2 and Id3 Genes. Masashi Shin^{*1}, Satoshi Ohte¹, Katsumi Yoneyama¹, Hiroki Sasanuma¹, Shoichiro Kokabu², Toru Fukuda³, Eiji Jimi⁴, Takenobu Katagiri⁵. ¹Saitama Medical University, Japan, ²Harvard School of Dental Medicine, USA, ³Keio University School of Medicine, Japan, ⁴Kyushu Dental College, Japan, ⁵Saitama Medical University Research Center for Genomic Medicine, Japan

Bone morphogenetic protein (BMP) induces several common early responsive genes in various types of cells, suggesting that the mechanism of these genes expression plays a central role in BMP signal transduction. Id1 through Id4, which are negative regulators of basic helix-loop-helix transcription factors, have been reported to be involved in myogenesis and in skeletal development regulated by BMPs. Previously we and others independently identified a BMP-responsive element (BRE) in the Id1 gene, which is a GC-rich element and recognized by a complex of Smad1/5 and Smad4 in response to BMP stimulation. Here we report the BREs in the Id2 and Id3 genes. First, we cloned the

5' flanking regions of the murine Id2 and Id3 genes up to -3 kb and a -6 kb, respectively, into a luciferase reporter plasmid. Both reporter activity was stimulated in response to BMP-4. Series of deletion plasmids revealed that the Id2 and the Id3 genes contained the BREs at -2.9 kb and at -3.3 kb regions, respectively. Sequence alignment of the BREs in the Id1, Id2 and Id3 genes identified a core sequence, which consisted of a common 6 base GC sequence recognized by a Smad1/4 complex in EMSA. Chromatin immunoprecipitation assay confirmed the physiological binding of Smad1 to the elements. These findings indicated that the 6 base GC sequences found in the Id1, Id2 and Id3 genes are the functional BREs in them, and the transcription of the Id genes may be activated by Smad1/5 and Smad4 in response to an activation of BMP receptors.

Disclosures: *Masashi Shin, None.*

SA0245

See Friday Plenary Number FR0245.

SA0246

Nanog Promotes Osteogenic Differentiation of Mesenchymal Cells By Modulating Bone Morphogenetic Protein (BMP) Signaling. Toru Ogasawara^{*1}, Shinsuke Ohba², Fumiko Yano³, Takahiro Abe¹, Hiroshi Kawaguchi⁴, Tsuyoshi Takato¹, Kazuto Hoshi¹. ¹University of Tokyo, Japan, ²The University of Tokyo Graduate School of Medicine, Japan, ³The University of Tokyo, Japan, ⁴University of Tokyo, Faculty of Medicine, Japan

How the pluripotency of stem cells is maintained and the role of transcription factors in this maintenance remain major questions. Nanog is a homeodomain transcription factor that maintains self-renewal of embryonic stem (ES) cells. In the present study, in order to clarify the mechanism underlying the pluripotency of somatic stem cells for the advancement of regenerative medicine, we examined the effect of forced Nanog expression in mesenchymal cells, with a particular focus on osteogenic differentiation. The human mesenchymal stromal cells (hMSCs) or mouse mesenchymal cell line C3H10T1/2 cells were transduced with the Nanog gene or control GFP gene by using retrovirus vectors. Short-term, forced Nanog gene expression had few effects on the terminal osteogenic differentiation of either hMSCs or C3H10T1/2 cells. To determine its long-term effects, we established C3H10T1/2 cells expressing Nanog constitutively. Constitutive Nanog expression strongly induced osteogenic differentiation of C3H10T1/2 cells. Nanog also enhanced osteocalcin and typeI collagen expression induced by the Runx2 or Osterix transfection. In regard to cell proliferation, constitutive Nanog expression promoted cell proliferation. However, Nanog repressed the proliferation of the cells treated with BMP-2. Western blot analysis revealed that constitutive Nanog expression enhanced phosphorylation of Smad1/5/8 and suppressed cyclinD1 and Cdk4. The promoter activities of both the osteocalcin and Id-1 genes were activated in cells expressing Nanog constitutively. These results indicate that Nanog functions as a modulator of BMP signaling in mesenchymal cells probably through a genome reprogramming process.

Disclosures: *Toru Ogasawara, None.*

SA0247

New AIS Candidate Gene Identification through Microarray Gene Expression Profiling. Khaled Fendri^{*1}, Shunmoogum Shunmoogum², Charlotte Zaouter³, Stefan Paent², Florina Moldovan⁴. ¹University of Montreal, Canada, ²University of Montreal, Canada, ³CHU Sainte-Justine, Canada, ⁴Montreal University, Canada

OBJECTIVES

We used a DNA microarray approach to evaluate gene expression profile of genes in Adolescent idiopathic scoliosis (AIS) individuals and identify genes that are differentially expressed (up- and down-regulated) as a result of estrogen exposure of non-AIS and AIS individuals.

METHODS

Gene expression profiling was investigated by microarray analysis in RNA samples isolated from osteoblasts derived from control (non-AIS) and AIS patients. We also evaluated gene expression levels in non-AIS and AIS osteoblasts following estrogen exposure: cells were cultured in absence or presence of 17 β -estradiol (E2) at different concentrations. Total RNA from osteoblasts were extracted, and then hybridized to DNA microarrays. Data analysis was performed. Genes that had at least 1.5-fold change in expression were considered differentially regulated relative to controls.

RESULTS

Microarray analysis revealed several genes that are differentially regulated in AIS osteoblasts compared to controls. Many of these genes are involved in different physiological pathways. We found that 2.6% of the examined genes were up-regulated in AIS osteoblasts, while 2.16% of them were down-regulated. We observed a roughly 3-fold increase in the transcripts of some genes in AIS osteoblasts. On the other hand, some genes were down-regulated by approximately 3-4-fold. When we compared the transcriptome profiling of estrogen-regulated genes between non-AIS and AIS osteoblasts, several genes were up- and down-regulated in response to estrogen. In presence of E2, we found a 3-4-fold increase in the expression of RBKS, OR8B4 and

RFC3 in AIS osteoblasts compared to non-AIS osteoblasts. Genes that were down-regulated by a considerable amount (3-4-fold) are MYT1, PSENEN and SCN1B.

CONCLUSION

More than one gene is likely responsible for AIS, and some of these genes are estrogen-regulated. In the absence of specific causative gene(s) for AIS, our study of gene expression by microarray pointed out putative biological pathways and genes to be carefully investigated.

Disclosures: Khaled Fendri, None.

This study received funding from: Fondation Yves Cotrel, Institut de France

SA0248

Odd-skipped Related1 and Odd-skipped Related2 are Mutually Regulated.

Shinji Kawai*, Atsuo Amano. Osaka University Graduate School of Dentistry, Japan

Zinc finger transcription factor Odd-skipped related (Osr) forms the gene family of Osr1 and Osr2, and they have high homology in the zinc finger region mutually. We previously reported on the function of Osr2 by using the transgenic mice of dominant negative Osr2. In this transgenic mice, delayed mineralization in calvarial and cortical bone tissues, distinctly increased radiolucency in soft X-ray analysis, reduced staining intensities with alcian blue and alizarin red in the skull and skeletal elements, and markedly thinner parietal and cortical bones are observed. The proliferation and differentiation of calvarial osteoblast decreased. Moreover, Osr2-deficient mice revealed that Osr2 play a critical role in secondary palate and teeth development. On the other hand, abnormality was seen in heart, kidney, and gonad in Osr1 knockout mice. In addition, it is shown that Osr1 and Osr2 take part in the formation of synovial joint.

In the present study, it aimed to clarify the interrelation of Osr1 and Osr2, and mutual expression regulations of Osr1 and Osr2 were examined. As a result, the expression of Osr1 was higher than Osr2 in fibroblastic C3H10T1/2 cells and osteoblastic MC3T3-E1 cells. Moreover, Osr1 increased the expression of Osr2, and Osr2 promotes the expression of Osr1. In addition, Osr1 and Osr2 regulated their expression by the specific region of promoter with deletion analysis of promoter.

We propose that Osr1 and Osr2 mutually regulate Osr2 and Osr1 expression, respectively, and participate in cellular proliferation and cellular differentiation of osteoblast.

Disclosures: Shinji Kawai, None.

SA0249

Osteoblast-specific Transcription Factor Osterix (Osx) Is an Upstream Regulator of Satb2 During Bone Formation. Chi Zhang*, Wanjin Tang, Yang Li, Lindsey Orsini. Bone Research Laboratory, Texas Scottish Rite Hospital, USA

Bone formation is a developmental process involving the differentiation of mesenchymal stem cells to osteoblasts. Osterix (Osx) is an osteoblast-specific transcription factor essential for osteoblast differentiation and bone formation. Osx knock-out mice lack bone completely. Satb2 is also critical for osteoblast differentiation as a special AT-rich binding transcription factor. It is not known how Satb2 is transcriptionally regulated during bone formation. In this study, microarray and real-time RT-PCR results demonstrated that Satb2 was dramatically downregulated in Osx-null calvaria. In stable C2C12 mesenchymal cells using Tet-off system, overexpression of Osx stimulated Satb2 expression. Moreover, inhibition of Osx by siRNA led to repression of Satb2 expression in osteoblasts. These results suggested that Osx controls Satb2 expression. Transient transfection assay showed that Osx activated 1kb Satb2 promoter reporter activity in a dose-dependent manner. To define the region of Satb2 promoter responsive to Osx activation, a series of deletion mutants of Satb2 constructs were made, and the minimal region was narrowed down to the proximal 130bp of Satb2 promoter. Further point mutation studies indicated that two GC-rich region mutations disrupted the Satb2 130bp promoter activation by Osx, suggesting that these GC-rich binding sites were responsible for Satb2 promoter activation by Osx. To examine physical association of Osx with Satb2 promoter in vivo, we performed Chromatin immunoprecipitation (ChIP) assays using primary osteoblasts from mouse calvaria. Endogenous Osx was shown to associate with native Satb2 promoter. Taken together, our findings conclude that Osx is an upstream regulator of Satb2 during bone formation. This reveals a new additional link of the transcriptional regulation mechanism that osteoblast-specific factor Osx controls bone formation.

Disclosures: Chi Zhang, None.

SA0250

See Friday Plenary Number FR0250.

SA0251

Regulation by TNF- α of Beta 2 Adrenergic Receptor Expression in Osteoblasts. Kyunghwa Baek*, Hyorin Hwang, Hyerim Lee, Hyunjung Park, Arang Kwon, Jeonghwa Baek. Seoul national university, School of dentistry, South Korea

TNF- α is a multifunctional cytokine whose level is elevated in inflammatory diseases such as atherosclerosis, diabetes and osteoporosis. Recent evidence has suggested that beta adrenergic receptor activation in osteoblasts suppress osteogenic activity. In the present study, we explored whether TNF- α modulates beta adrenoreceptor expression in osteoblastic cells and whether such a modulation is associated with a decrement in osteogenesis. First, increased beta 2 adrenergic receptor expression with TNF- α treatment was observed in various cell types including MC4, C2C12 osteoblastic cells and primary rat bone marrow stromal cells. Moreover, increased intracellular cyclic AMP level observed in C2C12 cells treated with isoproterenol, a beta adrenergic agonist, was further elevated with simultaneous TNF- α treatment, which indicates that TNF- α induced increments in beta adrenoreceptor expression actually increases intracellular beta adrenergic signaling in osteoblasts. TNF- α treatment suppression of alkaline phosphatase (ALP) activity and osteomarker gene expression, including ALP and osteocalcin, in BMP2 stimulated C2C12 cells was aggravated by isoproterenol. However, such a decrement induced by TNF- α was mitigated with propranolol treatment. TNF- α treatment also increased expression of sclerostin, a molecule preventing Wnt signaling pathway, in BMP2 stimulated C2C12 cells. This increase was aggravated with isoproterenol. Taken together, TNF- α increased beta 2 adrenergic receptor expression in osteoblasts and beta adrenergic signaling blockade mitigated TNF- α induced suppression in osteomarker gene expression. These findings suggest a crosstalk mechanism between TNF- α and beta adrenergic signaling pathways occurs in osteoblasts to modulate osteogenesis.

Disclosures: Kyunghwa Baek, None.

SA0252

See Friday Plenary Number FR0252.

SA0253

See Friday Plenary Number FR0253.

SA0254

See Friday Plenary Number FR0254.

SA0255

See Friday Plenary Number FR0255.

SA0256

In Vitro Hematopoiesis and osteoblastogenesis with Marrow from SAMP6 and SAMR1 mice. Regina O'Sullivan*, Joel Greenberger², Shaonan Cao³, Michael Epperly³, Julie Glowacki¹. ¹Brigham & Women's Hospital, USA, ²University of Pittsburgh School of Medicine, USA, ³University of Pittsburgh, USA

The SAM prone 6 (SAMP6) mouse develops osteoporosis with age and is an ideal model to investigate skeletal aging. The bone defect has been attributed to lower osteoblast potential in SAMP6. We compared *in vitro* hematopoiesis, proliferation, and osteoblastogenesis in marrow from SAMP6 and control SAMR1.

Methods: Long term bone marrow cultures (LTBMC) were established for hematopoiesis and for derivation of adherent Marrow Stromal Cells (MSCs). Growth curves were evaluated. Total RNA was extracted with Trizol reagent to determine constitutive expression. PCR products were separated by agarose gel electrophoresis and were quantified by densitometry. The MSCs were also grown in osteogenic media. The cells were grown to 90% confluence, the medium was changed from proliferation medium to osteogenic medium. Total RNA was extracted at intervals and was analyzed for expression of osteoblast markers Runx 2, Alkaline phosphatase (ALP), and Osteocalcin (Oc).

Results: SAMR1 LTBMC produce hematopoietic cells for a longer duration than the SAMP6 LTBMC. Cell expansion was slower in the SAMP6 cell line; cell population doubling time was 1.34-fold longer in cells from SAMP6 relative to SAMR1. This prolonged doubling time could be due, among other reasons, to prolonged G1 or G2 arrest. Consistent with age-related decreased proliferation the SAMP6 MSCs also exhibited induced expression of the inhibitors p16 and p19, and no significant differences in p53 and p21. There was constitutive expression of both ALP and Oc in the SAMP6 MSCs without osteogenic medium and there was up-regulation of PPAR γ in the SAMP6 cell line, compared with SAMR1. Runx 2

expression was similar in both cell lines. When cultured in osteogenic medium, there was greater Runx 2, ALP, and Oc expression in the SAMP6 cell line relative to the SAMR1 cell line

Conclusion: These *in vitro* results show that hematopoiesis in SAMP6 LTBMSC was shortened, compared with cells from SAMR1. The SAMP6 MSCs demonstrated constitutive expression of osteoblast signature genes relative to the SAMR1 cell line; both showed upregulation of osteoblast genes when cultured in osteoblastogenic medium. These unexpected findings suggest that *in vivo* factors may be important in suppressing osteoblast differentiation and function.

Disclosures: Regina O'Sullivan, None.

SA0257

A Novel Role of PlexinA2 in Regulation of BMP-2 Signaling and Osteoblast Differentiation. Yong Deok Lee*, Ji-Eun Oh, Hyung Joon Kim, Woo-Shin Kim, Youngkyun Lee, Hong-Hee Kim. Seoul National University, South Korea

PlexinA2 (PlxnA2) is a molecule previously characterized mediate axon guidance in neural development. In an effort to find new molecules involved in osteoblast differentiation by DNA microarray analyses, we found that PlxnA2 up-regulated during differentiation of mouse preosteoblastic cells induced by BMP-2. PlxnA2 also increased during the osteoblastic differentiation of human mesenchymal stem cells. Gene knock-down of PlxnA2 by using specific siRNA resulted in decreased osteoblast differentiation and mineralization, and suppressed the expression of Runx2, the master transcription factor for osteoblast differentiation. The type I BMP receptor was found in association with PlxnA2, suggesting a direct modulation of BMP-2 signaling at the receptor level by PlxnA2. Indeed PlxnA2 regulated both Smad and Akt signaling pathways of BMP-2. In addition, *ex vivo* cultures of mice calvariae with PlxnA2 siRNA displayed reduced osteoblastogenesis compared to the control siRNA, supporting that PlxnA2 has an *in vivo* role in osteoblast differentiation. In conclusion, our study discovered PlxnA2 as a novel regulator of osteoblast differentiation.

Disclosures: Yong Deok Lee, None.

SA0258

Challenges in Identifying Human Bone Cell Differentiation in Murine Models of Skeletal Repair. Xiaonan Xin*, Xi Jiang, Liping Wang, Alexander Lichtler, David Rowe. University of Connecticut Health Center, USA

Developing reliable osteoprogenitor cells from human sources will be a critical step in the clinical application of cell based skeletal repair. While demonstrating osteoblast differentiation of murine derived progenitor cells in models of skeletal repair that utilize GFP reporters has been quite reliable, we have not been as sanguine of the outcome when human osteoprogenitor cells from either adult bone marrow stroma or hES/iPS sources are used. Specifically, while bone formation within the calvarial repair model does occur, we have not been able to distinguish human cells at a stage of active mineralizing osteoid formation from cells that are trapped in a poorly formed mineralized matrix that may have been formed by murine host cells. To better understand the histology of human bone formation that occurs in a murine environment, we have closely examined the bone and cartilage that is formed within a teratoma derived from either hES or iPS cells. Developmentally, the bone has the appearance of a cortical structure that resembles the initial stages of perichondrial ossification of a cartilage core. While there is blood vessel investment of the forming bone and osteoclasts are evident, no bone marrow develops. Distinct mineralization lines are present, but instead of a row of AP positive cells overlying the mineralizing lines (a reliable feature of murine osteoblasts), a broad band of elongated AP positive cells extend over the mineralizing bone. Cells within the teratoma bone can be identified as human in origin with human specific mitochondrial and nuclear antibodies. A BSP antibody identifies extracellular deposits surrounding the cells within the mineralized bone and regions containing hypertrophic chondrocytes. While these antibodies do identify human cells within the mineralized tissue of the repair defect, they do not identify BSP deposition around these cells. A particular concern is the necessity of bone-marrow-dependent bone remodeling to produce the morphological features of mature bone. Because the mouse does not appear to develop marrow at sites of human bone formation, the histological features of mature bone derived from a human source may be difficult to demonstrate. Further modifications to the NOD/Scid/IL2rg null host mouse line, such as in breeding of a bone specific GFP reporter and humanizing the bone marrow may be required to definitively assess the extent of bone formation produced from a human osteoprogenitor source.

Disclosures: Xiaonan Xin, None.

SA0259

See Friday Plenary Number FR0259.

SA0260

See Friday Plenary Number FR0260.

SA0261

Development of a Fluorescent High-throughput CFU-O assay for a High Content Imaging Platform. Jeffrey Kiernan*, Cheryl Cui, William Stanford. University of Toronto, Canada

Intervention strategies for the treatment of osteoporosis (both type I and type II) are largely based around anti-resorptive drug therapy using bisphosphonates to prevent excessive bone resorption. Currently, there are only a few treatments based on increasing bone formation, mainly due to a lack of pharmacological modulators of osteoblasts. Drugs capable of increasing the commitment of mesenchymal stromal cells (MSCs) to osteoblasts, or the output of committed osteoblasts, could benefit both type I and type II osteoporosis. In drug discovery, high-throughput screening processes are usually followed up by validation with a low-throughput functional assay such as the CFU-O (Colony Forming Unit Osteoblast). Ideally, a high-throughput functional assay could streamline this process. The CFU-O, used to quantify bone nodule formation, is widely used to investigate the osteogenic potential of a given cell population. This assay, based on Von Kossa staining to label alkaline phosphatase activity and calcium deposition, however, it is not adaptable to high-throughput screens. Here, we introduce two fluorescence based high-throughput (fHT) assays that characterize the osteogenic potential of MSCs on a high content imaging platform (Cellomics). The first assay (static fHT-CFU-O) stains endogenous ALP activity with enzyme labeled fluorescent 97 (E197) dye, while calcium is stained with the dye calcium orange. The ALP positive area (Target 1) identifies the Region of Interest (ROI) in Channel 1, while Channel 2 identifies calcium positive areas (Target 2). Only those objects positive for calcium that lay within the ROI were counted as a bone nodule. The static fHT-CFU-O successfully quantified a similar number of bone nodules as compared to manual counting of Von Kossa stained nodules. For the second assay (kinetic fHT-CFU-O), we utilized the fluorescent properties of the osteotropic antibiotic tetracycline to develop a kinetic osteogenic assay able to track the growth rate of bone nodules. Tetracycline stained nodules were imaged at various time points during the calcification process to measure nodule formation and to quantify their growth rates. Objects from different time points were identified and tracked based on their locations in a particular field and further analyzed based on the rate of nodule growth over the time course. We currently utilizing these assays to investigate possible compounds that increase the osteogenic potential of MSCs.

Disclosures: Jeffrey Kiernan, None.

SA0262

See Friday Plenary Number FR0262.

SA0263

Immunohenotype and Functional Comparison of Osteoblast Progenitors from Human Embryonic Stem Cells and Bone Marrow. Melissa Stemig*, Mohammad Islam. University of Minnesota School of Dentistry, USA

Studies using human embryonic stem cells describe derivation of mesenchymal stem cells (hESMSC) based of CD73 expression. The purpose of our study is to compare immunophenotype and osteogenic potential of hESMSCs and human bone marrow derived mesenchymal stem cells (BMMSCs).

Materials and Methods: We isolated hESMSCs based on CD73 surface marker expression. Commercially available BMMSCs were used for comparison. We analyzed expression of cell surface markers CD73, CD90, CD105, CD31 and CD146 in hESMSC and BMMSCs. Osteogenesis was induced in both groups for 21 to 28 days. After this period, von Kossa staining for mineralized nodule formation and expression of osteogenic genes Runx2, bone sialoprotein (BSP), osteocalcin and collagen type I was compared. We also analyzed DNA methylation profile and lineage specific gene expression profile of hESMSCs using commercially available PCR arrays (SABiosciences). **Result:** Both hESMSCs and BMMSCs express MSC specific surface markers. They do not express endothelial marker CD31. Osteogenesis study showed that hESMSC form dark mineralized nodule in von Kossa staining. Osteogenic gene expression profile was also comparable. However, hESMSCs continue to proliferate during osteogenic differentiation, as demonstrated by cell count during differentiation. PCR array for stem cell transcription factor DNA methylation and lineage specific gene expression array showed differences in gene expression pattern between hESMSC and BMMSC. **Conclusion:** Standard methods for comparison of hESMSC and BMMSCs show that these two cell types are comparable. However, dissimilar DNA methylamine and lineage specific gene expression in these two groups suggests distinct character of hESMSCs.

Disclosures: Melissa Stemig, None.

SA0264

Ionizing Radiation-Induced Senescent Bone Marrow Stromal Cells Show Reduced Functions Essential for Hematopoietic Stem Cell Engraftment. Cynthia Carbonneau*, Christian Beausejour. Universite De Montreal - CHU Ste-Justine, Canada

The extent to which the integrity of the bone marrow stroma contributes to the success of hematopoietic cell transplantation is not well known. Alterations of the bone marrow microenvironment, which occur during aging or following genetic manipulations of telomere length, impair hematopoietic stem and progenitor cell (HSPC) engraftment and function. These results suggest that an increased number of senescent marrow stromal cells could affect niche function. We have shown that exposure to ionizing radiation (IR) impairs the bone marrow microenvironment by inducing senescence of the stromal cells, but the direct effects of such damage on transplantation is unknown. In this study, we investigated IR-induced alterations of bone marrow stromal cell functions susceptible to affect HSPC engraftment. High plasma levels of granulocyte colony-stimulating factor (G-CSF) were detected by ELISA in mice long-term post-IR. In vitro cultures of senescent bone marrow stromal cells with HSPC secrete more G-CSF compared to control cells. Migration assays showed that senescent stromal cells are less chemoattractive for HSPC in vitro. Also, less HSPC remained adhered to senescent stromal cells following a 3-hour co-culture compared to control cells. At the molecular level, we observed a down-regulation of N-cadherin mRNA and vascular cell adhesion molecule 1 (VCAM-1) protein in senescent stromal cells compared to control cells. In conclusion, senescent stromal cells could reduce HSPC engraftment (1) by mobilizing HSPC in blood due to G-CSF expression, (2) by limiting their recruitment to the bone marrow via reduced chemoattraction and (3) by limiting their retention in the niche via reduced adhesion molecules such as N-cadherin and VCAM-1.

Disclosures: Cynthia Carbonneau, None.

SA0265

Irradiation-induced DNA Damage Interferes with Mesenchymal Stem Cell Plasticity. Genevieve Despars*¹, Cynthia Carbonneau², Qanh Le³, Christian Beausejour³. ¹Centre De Recherche De L'Hopital St. Jus, Canada, ²Universite De Montreal - CHU Ste-Justine, Canada, ³Universite de Montreal, Canada

Mesenchymal stem cells (MSCs) give rise to chondrocytes, osteoblasts and adipocytes. Several transcription factors control lineage commitment in a cell-autonomous fashion, such as Runx2 and Osx/Sp7 in osteoblastogenesis and PPARγ for adipogenesis.

Exposure to ionizing irradiation (IR) can lead to the induction of cellular senescence, a process by which cells undergo permanent growth arrest and secrete a specific pattern of cytokines and inflammatory factors.

Here, we wanted to investigate whether the senescence phenotype could affect the differentiation potential of MSC. We found that IR-induced senescent MSCs were unable to form mineralised nodules *in vitro*, an effect we found could be due to their inability to adequately induce Runx2 and Osx/Sp7 following their culture with osteogenic factors. In contrast, IR-induced senescence of osteoblasts did not prevent the formation of mineralised nodules *in vitro*. Exposure to IR also prevented the differentiation of MSC into adipocytes despite that senescent MSC could upregulate PPARγ and SREBF1 at levels comparable to those observed in control non-irradiated MSC cultures. These results suggest a cell-autonomous defect in senescent MSC which cannot be bypassed by instructive differentiation factors.

Finally, we also investigated whether mineralisation of MSC could be affected in a paracrine manner by senescent cells. Unexpectedly, we found that mixed cultures of control and IR-induced senescent MSCs showed mineralisation. We hypothesize that IR-induced senescent MSC produce factors which increase mineralisation, or that irradiated MSC could revert to osteogenesis when in contact with control cells.

Overall, our results provide a rational on how exposure to IR could affect long-term bone formation; that is by preventing, in a specific manner, the differentiation and mineralisation of bone forming progenitor cells such as MSC.

Disclosures: Genevieve Despars, None.

SA0266

Mitochondrial Superoxide Dismutase Regulates Proliferation and Differentiation of Osteoblasts. Keiji Kobayashi*¹, Yoshitomo Saita², Hidetoshi Nojiri², Daichi Morikawa¹, Kenji Watanabe³, Kouichi Nakasone¹, Kazuo Kaneko², Takahiko Shimizu¹. ¹Morecular Gerontology, Tokyo Metropolitan Institute of Gerontology, Japan, ²Department of Orthopaedics, Juntendo Univ., Japan, ³Morecular Gerontology, Tokyo Metropolitan Institute of Gerontology, Japan

Reactive oxygen species (ROS) are mainly produced from mitochondria as metabolic products in cells. In particular, ROS reacts to oxidize cellular components, such as DNA, proteins and lipids leading to oxidative stress. Mn-superoxide dismutase (Mn-SOD) is localized in mitochondria to convert superoxide to hydrogen peroxide. In this context, Mn-SOD is considered to protect from mitochondrial

oxidative stress. Mitochondrial Mn-SOD (SOD2)-deficient mice showed perinatal death with increased mitochondrial oxidative stress, indicating that Mn-SOD is essential for maintenance of mitochondrial redox balance and murine lifespan. However, the physiological role of Mn-SOD in bone was not fully understood yet. In the present study, to evaluate it, we generated the time-specific Mn-SOD-deficient mice by crossbreeding tamoxifen-inducible Cre recombinase transgenic mice with Mn-SOD floxed mice.

To examine the effects of mitochondrial oxidative stress on a cellular level, we used osteoblasts derived from neonatal calvarial bone from mutant and wild-type mice. At first, we evaluated gene ablation, protein content, and ROS production in the presence of 4-hydroxytamoxifen (4-OHT) in vitro. 4-OHT treatment effectively deleted Mn-SOD gene and down-regulated Mn-SOD protein in mutant osteoblasts, indicating that tamoxifen-inducible cre system was effectively worked to manipulate the expression of Mn-SOD in osteoblasts in vitro. 4-OHT treatment also significantly enhanced the levels of ROS production detected by fluorescence dye after 7 days in culture, suggesting that Mn-SOD depletion would diminish mitochondrial antioxidant capacity leading to increased oxidative stress in osteoblasts. In the growth analysis, we found that treatment of 4-OHT significantly delayed the cell proliferation by 50% after 7 days in culture. Interestingly, we failed to detect any signs of apoptotic phenotype in the mutant cells. In differentiation analyses, ALP activity was decreased to nearly 20% lower in the presence of 4-OHT after 14 days in culture. With respect to the nodule formation, 4-OHT treatment decreased the ability to form mineralized nodule after 21 days in culture. These results indicate that Mn-SOD insufficiency suppressed both cell proliferation and differentiation of osteoblasts, suggesting that Mn-SOD plays a pivotal role in cell proliferation and differentiation by regulating the mitochondrial ROS metabolism in osteoblasts.

Disclosures: Keiji Kobayashi, None.

SA0267

See Friday Plenary Number FR0267.

SA0268

See Friday Plenary Number FR0268.

SA0269

See Friday Plenary Number FR0269.

SA0270

Estrogen Treatment Early in Differentiation Promotes Osteoblastic Nodule Formation in Murine Cortical Bone Cells. Kumar Chokalingam*¹, Sundeep Khosla², David Monroe³. ¹Mayo Clinic, USA, ²College of Medicine, Mayo Clinic, USA, ³Mayo Foundation, USA

Both clinical and experimental observations have demonstrated the importance of 17β-estradiol (E2) in maintaining bone mass. Although E2 has been shown to protect bone by increasing differentiation and function of osteoblasts, the effects of E2 on osteoblast differentiation in vitro are unclear. Recent in vivo studies using deletion of ERα specifically in osteoblasts (Almeida et al ASBMR 2010, 1113) indicate that ERα mainly plays a role in regulating cortical osteoblasts and the effects of E2 on these cells occur early in differentiation. The goals of this study were to identify a murine E2-sensitive in vitro cell system and to determine when E2 elicits its pro-differentiative signal during osteoblastic differentiation. Cortical bone cells (CBCs) obtained by collagenase digestion of flushed long bones of 4 month old mice were grown to confluence and then cultured in osteoblast differentiation (OB) media with and without E2 for 18 days. Robust mineralization was observed in controls, which was further enhanced with the addition of E2. To address the temporal effects of E2 on osteoblastic nodule formation, E2 was added for 28 days or after 7, 14 and 21 days to CBCs continuously cultured in OB media. Mineralization was increased in CBCs receiving E2 for the entire 28 days as compared to all other CBCs. Mineralization was similar between CBCs receiving E2 after 7, 14 and 21 days of differentiation and control. These data suggest that exposure of E2 during early osteoblastic differentiation is necessary for the enhanced mineralization. To further demonstrate this early effect of E2 during differentiation, E2 was added throughout for 28 days or withdrawn after 7, 14 and 21 days to CBCs continuously cultured in OB media. Mineralization was increased in all CBCs receiving E2 as compared to control; however mineralization was the same between CBCs receiving E2 for 7, 14, 21 and 28 days (Figure). These results confirm that exposure of E2 early in osteoblastic differentiation alone is sufficient for enhanced mineralization. Combined with the in vivo results of Almeida et al, our findings suggest the beneficial effects of E2 on cortical osteoblast mineralization occur early in the course of differentiation. In summary, our findings demonstrate that cells originating from the cortical bone compartment are sensitized to the effects of E2 in vitro and that treatment early in differentiation promotes an increase in osteoblastic nodule formation.

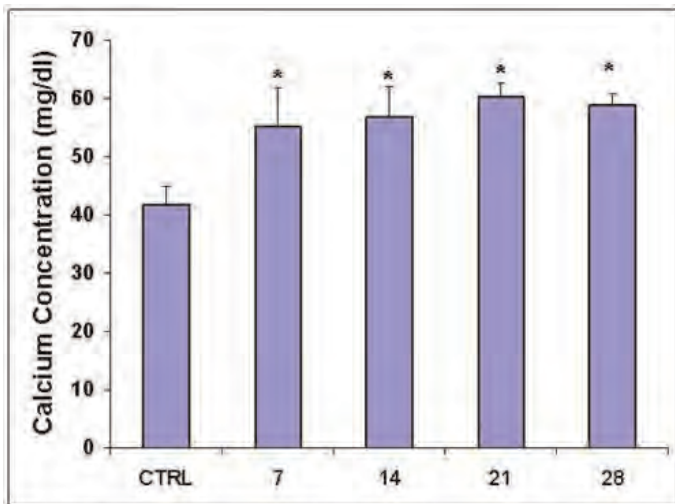


Figure. Calcium concentration in E2 treated groups is significantly higher than control. No difference was seen between the E2 treated groups. * $p < 0.05$

Disclosures: Kumar Chokalingam, None.

SA0271

Collagen as a Stop Signal for Osteoclastic Bone Resorption: an Extension of Chambers' Hypothesis. Kent Soe^{*1}, Ditte M.H. Merrild¹, Jean-Marie Delaisse². ¹Vejle Hospital, University of Southern Denmark, Denmark, ²Vejle Hospital, CSFU-IRS, University of Southern Denmark, Denmark

It is widely accepted that bone surface collagen prevents initiation of bone resorption activity of osteoclasts (OC), as first hypothesized by Chambers. Here we propose (i) that accumulation of undegraded demineralized collagen in the resorption pit itself similarly prevents continuation of ongoing OC resorption, (ii) so that the rate of collagenolysis relative to demineralization (C/D rate) determines arrest or continuation of resorption at a given resorption site.

We generated human OCs, and cultured them on cortical bone discs, in the presence or absence of inhibitors of collagenolysis (E64 and L873724) or demineralization (ethoxzolamide) in order to modulate C/D rates. Some assays were also performed on bone discs rendered anorganic through NaOCl. The efficiency of collagenolysis was monitored by assessing the thickness of the collagen fringes lining the excavations. Prevalence of continued vs. intermittent resorption (i.e. involving episodes of arrested resorption) was assessed as previously reported, by quantifying the number and surface of long continuous resorption "trenches" (i.e. continued resorption) vs. discrete round "pits" (i.e. intermittent resorption), as well as through assessment of resorption depths.

In all control culture conditions, pits were lined with a 3-5 μ m thick collagen fringe, whereas trenches did not show significant collagen leftovers. This suggests that the efficiency of collagen removal determines whether resorption stops or continues. Assays performed on anorganic bone showed a 2 to 5-fold increase in the trench surface/BS, supporting that resorption tends to continue in the absence of collagen. Furthermore, when we weakly inhibited demineralization, the trench surface/BS increased 2-fold and collagen leftovers decreased compared to controls. In contrast, when we inhibited collagenolysis, the trench surface/BS decreased 3-fold and 3-5 μ m thick fringes of demineralized collagen occurred at significantly lower resorption depths compared to controls. Thus, by modulating C/D rates through specific inhibition of demineralization or collagenolysis, we could push OC resorptive activity towards either continued or intermittent resorption.

We conclude that collagen may act as a stop signal for ongoing OC bone resorptive activity and that this signal is controlled by the balance between the rates of demineralization and collagenolysis.

Disclosures: Kent Soe, None.

SA0272

Genetic Ablation of CD68 Results in Increased Bone in Mice and Abnormal Osteoclasts *in Vitro*. Jason Ashley^{*1}, Zhenqi Shi¹, Haibo Zhao², Robert Kesterson¹, Xu Feng¹. ¹University of Alabama at Birmingham, USA, ²University of Arkansas for Medical Sciences, USA

Firm adhesion of osteoclasts to the bone surface by way of the sealing zone is a critical feature of efficient bone resorption. While there has been much study into mechanisms of sealing zone formation, understanding of the mediators of this attachment remains incomplete. To identify putative bone adhesion molecules, we screened a bone marrow macrophage cDNA bacteriophage display library for

proteins with an affinity for bone. Using this screen, we identified CD68 (also known as macrophage scavenger receptor class B type 1) as a molecule with high bone affinity. CD68 is a heavily glycosylated Lysosome-Associated Membrane Protein (LAMP) family member. Unlike most LAMPs, however, CD68 contains an O-glycosylated mucin-like domain that may give it protective functions similar to those of mucins. CD68 is a commonly-used marker for macrophage lineages, and we have confirmed that, while mouse bone marrow macrophages express high levels of CD68, mouse osteoblasts do not express any detectable amount. We hypothesize that CD68 serves an important function in osteoclasts. Consistent with this, CD68 expression is up-regulated during osteoclastogenesis in an M-CSF-dependant manner, and confocal microscopy of osteoclasts cultured on bone slices revealed that CD68 can be found in and around the sealing zone of resorbing osteoclasts. We also found that, when CD68 was inhibited *in vitro* with either an antibody or shRNA, macrophage attachment to bone slices was reduced as was *in vitro* bone resorption. These preliminary findings drove us to generate mice lacking expression of CD68. These mice appear healthy and fertile, but when compared to age and sex matched wild type mice, femurs from six-month-old CD68-null mice have a 160% increase in BV/TV ($p < .05$), a 20% increase in trabecular number ($p < .01$), and a 20% decrease in trabecular spacing ($p < .01$) measured by micro-computed tomography. Osteoclasts generated *in vitro* from CD68-null precursors have intracellular accumulations of a large number of vesicle-like structures not seen to such an extent in CD68-expressing cells. Furthermore, following tartrate resistant acid phosphatase staining of *in vitro* generated osteoclasts, 14% of wild type osteoclasts demonstrated retractions in their plasma membrane whereas retractions can be seen in over 40% of CD68-null osteoclasts ($p < .001$). These data indicate that CD68 plays a role in the function of osteoclasts, and we suspect that role is potentially one related to adhesion or sealing zone function.

Disclosures: Jason Ashley, None.

SA0273

Spatiotemporal Dynamics of Cytosolic Calcium in Osteoclasts: Distinct Patterns Associated with Lamellipod Extension and Uropod Retraction. Benjamin D. Wheel^{*1}, Natsuko Tanabe², S. Jeffrey Dixon¹, Stephen Sims¹. ¹The University of Western Ontario, Canada, ²Nihon University School of Dentistry, Japan

Osteoclasts are specialized cells that mediate the resorption of bone and other mineralized tissues. These cells are highly motile, with bone remodeling involving alternating cycles of migration and resorption. Osteoclast migration is characterized by extension of lamellipodia at the leading edge, lamellipodial attachment to the substrate and release of the uropod at the trailing edge of the cell. However, little is known regarding the role of cytosolic calcium in coordinating these distinct cellular events in osteoclasts. The purpose of this study was to characterize the spatial and temporal patterns of calcium changes associated with motility in osteoclasts. Subcellular calcium was monitored by digital fluorescence imaging of fura-2-loaded osteoclasts using alternating excitation wavelengths of 345/380 nm, with emission ratio at 510 nm corresponding to cytosolic calcium concentration. We first observed that osteoclasts exhibited a pattern of spatially restricted, transient elevations of calcium localized predominantly at the cell periphery, a phenomenon temporally associated with lamellipodial extension. The intracellular calcium chelator BAPTA completely abolished these transient elevations of calcium. The extracellular calcium chelator EGTA also abolished these calcium transients, indicating channel-mediated influx of calcium from the extracellular milieu. Consistent with this observation, the phospholipase C (PLC) inhibitor U73122 had no discernable effect on these transient elevations of calcium. In contrast, U73122 effectively blocked UTP-induced elevations of calcium, confirming its ability to inhibit PLC-mediated release of calcium from intracellular stores. A second distinct spatiotemporal pattern of calcium changes was also observed in osteoclasts. This consisted of a localized elevation of calcium in the trailing edge of migrating cells that coincided with uropod retraction. Interestingly, BAPTA-treated cells exhibited an elongated morphology, consistent with the inability of uropods to detach from the substrate and undergo retraction. Taken together, these findings reveal novel spatiotemporal patterns of cytosolic calcium changes in osteoclasts, with spatially restricted, transient elevations being associated with lamellipodial extension and more sustained elevations being required for uropod retraction. These studies provide new insights into the subcellular mechanisms underlying the regulation of osteoclast migration.

Disclosures: Benjamin D. Wheel, None.

SA0274

See Friday Plenary Number FR0274.

SA0275

Deletion of CD74, a Putative MIF Receptor, in Mice Enhances Osteoclastogenesis and Decreases Bone Mass. SE HWAN MUN^{*}, Paula Hernandez, Hector Aguila, Sun-Kyeong Lee. UNIVERSITY OF CONNECTICUT HEALTH CENTER, USA

CD74 is a type II transmembrane protein that can act as a receptor for macrophage migration inhibitory factor (MIF) and play a role in MIF-regulated responses. We have reported that MIF inhibited osteoclast formation and MIF KO

mice had decreased bone mass and increased osteoclasts. We therefore examined if CD74 was involved in the ability of MIF to alter osteoclastogenesis in cultured bone marrow (BM) from WT and CD74 deficient (KO) male mice. We also measured the bone phenotype of CD74 KO male mice. Osteoclast like cells (OCL) were identified as TRAP(+) multinucleated cells and granulocyte-macrophage colony-forming units (CFU-GM) were analyzed in semi-solid cultures. Bone mass in the femur of 8 week old mice was measured by micro-computed tomography and histomorphometry.

Bone marrow cells from CD74 KO mice formed 15% more OCL ($p<0.05$) with M-CSF and RANKL (both at 30 ng/ml) vs. WT. Addition of MIF to WT cultures inhibited OCL formation by 16% ($p<0.05$) but had no effect on CD74KO cultures. The number of CFU-GM in the bone marrow of CD74 KO mice was 26% greater ($P<0.05$) than in WT controls. However, flow cytometric analysis of bone marrow found no significant difference in the number of osteoclast precursors between WT and CD74 KO. Trabecular bone volume (TBV) in the femurs of CD74 KO male mice was decreased by 26% ($p=0.062$) compared to WT. In addition, cortical area and thickness were decreased by 14% and 11%, respectively ($p<0.05$ for both). Histomorphometric analysis demonstrated that TRAP (+) osteoclast number and osteoclast area were significantly increased ($p<0.05$) in CD74 KO by 35% and 43%, respectively compared to WT. We also measured serum CTX and osteocalcin levels in CD74KO mice. There was a trend for an increase in formation (osteocalcin) by 35% ($p=0.052$) while not significant changes in resorption (CTX). Finally, we examine the effect of MIF on RANKL-induced-signaling pathways in BMM cultures. MIF treatment decreased RANKL-induced NFATc1 and c-fos protein in BMM cultures by 44% and 32%, respectively ($p<0.05$).

Our data demonstrate that CD74 is required for MIF to affect in vitro osteoclastogenesis. Further, the bone phenotype of CD74 KO mice phenocopied that of MIF KO mice. MIF treatment of WT cultures suppressed RANKL-induced AP-1 expression, which resulted in decreased osteoclast differentiation in vitro. We speculate that CD74 play an important role in the effects of MIF on osteoclastogenesis.

Disclosures: SE HWAN MUN, None.

SA0276

IL-22 Promotes Osteoclastogenesis in Rheumatoid Arthritis Through Induction of RANKL from Synovial Fibroblasts. Kyoung-Woon Kim¹, Sang-Heon Lee^{*2}, Young-Il Seo³. ¹Konkuk University, South Korea, ²Konkuk University Medical Center, South Korea, ³Hallym University Medical Center, South Korea

This study aims to determine the regulatory role of IL-22 on the expression of receptor activator of NF- κ B ligand (RANKL) and the induction of osteoclastogenesis in rheumatoid arthritis (RA). The concentrations of IL-22 and RANKL in sera and synovial fluids (SF) of RA patients were measured using ELISA. After RA synovial fibroblasts were treated with rhIL-22, the expression of RANKL mRNA and protein was determined by real time PCR, western blot and intracellular immunostaining. IL-22 induced RANKL expression was also observed after inhibition of intracellular signaling molecules. Human monocytes were co-cultured with IL-22 pre-stimulated RA synovial fibroblasts and monocyte colony stimulating factor (M-CSF), and then osteoclastogenesis was determined by counting of TRAP-positive multinucleated cells. IL-22 concentration in RA SF was higher than that of OA patients. Serum IL-22 concentration was also higher in RA than that in OA patients and healthy subjects. Serum IL-22 concentration was correlated with serum rheumatoid factor titer, and SF IL-22 concentration was correlated with serum anti-cyclic citrullinated peptide antibody (anti-CCP) titer. When RA synovial fibroblasts were treated with rhIL-22, the expression of RANKL mRNA and protein were upregulated in a dose dependent manner. The IL-22 induced RANKL expression was significantly hampered by inhibition of p38 MAPK/NF- κ B and JAK-2/STAT3 signaling pathway. When human monocytes were cultured with IL-22 pre-stimulated RA synovial fibroblasts in the absence of RANKL, the monocytes were differentiated into osteoclasts, but this osteoclastogenesis was decreased after the inhibition of p38 MAPK/NF- κ B and JAK-2/STAT3. Our results reveal that IL-22 upregulates RANKL expression in RA synovial fibroblasts and it also induces osteoclastogenesis, which are mediated by p38 MAPK/NF- κ B and JAK-2/STAT3 pathways.

Disclosures: Sang-Heon Lee, None.

SA0277

Primary human CCR6+ memory Th17 cells activate synovial fibroblasts leading to a proinflammatory profile with joint destructive capacity. Erik Lubberts^{*1}, Nadine Davelaar², Jan Piet van Hamburg², Edgar Colin², Patrick Asmawidjaja². ¹Erasmus MC University Medical Center, The Netherlands, ²Erasmus MC University Medical Center, Netherlands

IL-17 is a proinflammatory cytokine and is a stimulator of osteoclastogenesis in vitro. It has been shown in arthritis models that IL-17 is an inducer of RANKL expression leading to loss of the RANKL/OPG balance, stimulating osteoclastogenesis and bone erosion in arthritis. Furthermore, it has been reported that neutralizing IL-17A in collagen-induced arthritis (CIA) ameliorated CIA including joint damage and reduced numbers of osteoclasts in the joint. Moreover, mouse Th17 cells (a new T helper subset that produce IL-17A) function as an osteoclastogenic T helper subset that links T cell activation and bone destruction. However, although human Th17 cells have been found in rheumatoid arthritis (RA) the contribution of these cells to joint damage is still unknown.

Here, we report that in peripheral blood of treatment-naïve early RA patients, the numbers of IL-17A/TNF- α -producing CCR6+CD45RO+ memory CD4+ T cells are increased. Functional co culture experiments with early RA synovial fibroblasts (RASf) revealed that these Th17-enriched CCR6+ memory T cells were potent inducers of IL-6, IL-8 and matrix metalloproteinase (MMP)-1 and MMP-3 in RASf. Interestingly, IL-17A production by CCR6+ memory T cells was markedly increased through this Th17-RASf interaction. Elevated expression of cathepsin K (CTSK) was found in the co culture condition compared to CCR6+ memory Th17 cells alone. Furthermore, condition media of these activated Th17-RASf co cultures induced a higher degree of fusion compared to condition media of activated Th17 cells alone during osteoclastogenesis in vitro. These data show the potential of primary human Th17 cells to activate synovial fibroblast leading to a proinflammatory profile with joint destructive capacity. Targeting human Th17 cell activity may be beneficial to prevent joint destruction in Th17 mediated disorders potentially by suppressing cell fusion during osteoclastogenesis.

Disclosures: Erik Lubberts, None.

SA0278

Regulatory Expression of Mitf-E as an Inducer of Osteoclastogenesis by the TGF- β family. Kumiko Asai¹, Masayuki Funaba², Ryo Ooishi¹, Masaru Murakami^{*1}. ¹Azabu University School of Veterinary Medicine, Japan, ²Kyoto University Graduate School of Agriculture, Japan

Microphthalmia-associated transcription factor (Mitf) is a tissue-specific transcription factor predominantly expressed in melanocytes, osteoclasts, mast cells, and heart. Mice with mutation of Mitf gene exhibit signs of osteopetrosis related to a lack of mature functional osteoclasts. Thus, Mitf is definitely involved in bone homeostasis, although the regulation of osteoclastogenesis by Mitf is not fully evaluated. There are at least nine Mitf isoforms differing in their transcriptional initiation site: Mitf-A, -B, -C, -D, -E, -H, -J, -M and -mc. Mitf isoforms are expressed in a cell type-specific manner, and their transcriptional activities are slightly but significantly different depending on the target gene. Here we specified Mitf isoform expressed during osteoclastogenesis induced by macrophage-colony stimulating factor (M-CSF) and receptor activator of NF- κ B ligand (RANKL), and explored the role of Mitf in the process. Expression of Mitf-E but not Mitf-A was induced in response to treatment with RANKL that stimulates osteoclast differentiation in primary bone marrow cells and RAW264.7 macrophage cells. Transfection with dsRNA for Mitf-E effectively inhibited the formation of osteoclasts and the expression of osteoclast-related genes, including tartrate-resistant acid phosphatase (Trap) and osteoclast-associated receptor (Oscar). Members of the transforming growth factor- β (TGF- β) family including TGF- β s, activins and bone morphogenetic proteins (BMPs) regulate a broad range of biological processes including osteoclastogenesis. TGF- β 1 and activin A but not BMP-2 enhanced RANKL-induced osteoclast formation in RAW264.7 cells; addition of TGF- β 1 or activin A to the culture medium containing RANKL increased the number of Trap-positive cells and expression of Trap and Oscar. TGF- β 1 and activin A also potentiated up-regulation of Mitf-E expression. The present results indicate that Mitf-E plays a crucial role in osteoclastogenesis, and that the expression of Mitf-E is positively regulated by the TGF- β family. Stimulatory activity of the TGF- β family on osteoclastogenesis may be partly elicited through up-regulation of Mitf-E.

Disclosures: Masaru Murakami, None.

This study received funding from: a Grant-in-Aid for Scientific Research from the Japan Society for the Promotion of Science, a Research Project Grant Awarded by the Azabu University

SA0279

See Friday Plenary Number FR0279.

SA0280

Analysis of Regulatory Mechanism of Mouse RANK Gene Expression through AP-1 Response Element. Riko Kitazawa^{*1}, Satomi Kinto¹, Junko Ishii¹, Takeshi Kondo¹, Kiyoshi Mori¹, Sohei Kitazawa². ¹Kobe University Graduate School of Medicine, Japan, ²Ehime University, Japan

Receptor activator of NF- κ B (RANK) expressed on osteoclasts and their precursors is a receptor for RANK Ligand (RANKL). Signals transduced by RANKL-RANK interaction induce genes essential for the differentiation and function of osteoclasts partly through the direct binding of NFATc1 to target gene promoters. We have cloned a 6-kb fragment containing the 5'-flanking region of the mouse RANK gene and have analyzed the binding elements of transcription factors such as PU.1 (-480), NFATc1 (-370) and MTF (-100). Here, we examined the regulatory mechanism of RANK gene transcription through the putative CRE/AP-1 binding site (-240).

RANK mRNA expression in primary cultured-bone marrow cells and pre-osteoclastic RAW cells was induced by PMA and suppressed by PKC inhibitor Calphostin C. On the other hand, forskolin and H89 showed no effect on RANK mRNA expression, suggesting that PKC, not PKA, signaling regulates the RANK gene. We then assessed the involvement of the AP-1 transcription factor, c-fos, in RANK gene transcription. In RAW cells, c-fos knockdown by siRNA nullified the

inducible effect of PMA on RANK expression. Transfection with a c-fos expression vector into RAW cells increased RANK mRNA expression. By EMSA, an oligonucleotide (-246/-238) showed DNA protein binding, the specificity of which was confirmed by block-shift with an anti-c-fos antibody and by the addition of the excess of a cold consensus probe. Co-transfection with a c-fos expression vector and the RANK promoter construct showed that c-fos increased RANK promoter activity 2-fold in RAW cells. Mutagenesis of the putative AP-1 site (-240) nullified the inducible effect of c-fos on promoter activity.

Taken together, these results indicate that during differentiation of bone marrow mono-nucleated cells into osteoclast precursors, RANK transcription is positively regulated by c-fos/AP-1 through the binding element of its gene promoter.

Disclosures: Riko Kitazawa, None.

SA0281

See Friday Plenary Number FR0281.

SA0282

Changes in Extracellular Calcium Concentration Affect Human Osteoclast Formation and Bone-Resorbing Activity. Francesca Hemingway¹, Xiaotong Cheng^{*2}, Nicholas Athanasou². ¹Nuffield Department of Orthopaedics, Rheumatology & Musculoskeletal Sciences, University of Oxford, United Kingdom, ²University of Oxford, United Kingdom

Osteoclasts are lysosome-rich multinucleated cells (MNCs) which resorb bone, releasing a large amount of calcium from the mineral component. The calcium concentration at the resorption site is very high, as much as 40 mM. Calcium in this region is removed into extracellular fluid by transcytosis. Previous studies in animals have shown variable effects of high extracellular calcium on osteoclast formation and activity, and no such studies have been carried out in man. Our study used human monocytes to examine the effect of high extracellular calcium and low extracellular calcium (in the case of hypocalcaemia) on osteoclast formation and osteoclast bone-resorbing activity.

CD14⁺ monocytes were isolated from human peripheral blood and cultured on glass coverslips or dentin slices with media containing 25ng/ml macrophage colony stimulating factor (M-CSF) and 50ng/ml receptor activator of nuclear factor kappa-B ligand (RANKL). Cells were cultured in media supplemented with CaCl₂ (final calcium concentrations in mM: 5, 7, 10, 15, 20), to study the effect of high extracellular calcium, or cultured in media with the calcium-chelating agent ethylene glycol tetraacetic acid (EGTA) (concentrations in mM: 0.5, 1.0, 1.5, 2.0) to study the effect of low extracellular calcium. CD14⁺ cells were cultured in above media for 12-14 days and osteoclast formation was assessed by counting the number of MNCs on tartrate resistant acid phosphatase (TRAP) staining. To study the effect on bone-resorbing activity, CD14⁺ monocytes were cultured with control media until osteoclasts formed then cells were cultured in high calcium media or media with EGTA for 3 days. The dentine slices were stained with toluidine blue to examine the extent of osteoclast resorption.

In 12-14 day cultures with high calcium media, the number of TRAP positive MNCs significantly decreased comparing to control (Figure 1). Similar results on osteoclast formation were found in 12-14 day cultures with EGTA, and the inhibition was recovered by adding the same amount of CaCl₂ in media (Figure 2). In 3-day cultures of mature osteoclast with high concentrations of calcium, the average area resorbed by MNCs increased comparing to control (Figure 3). Our findings indicate that both high and low concentrations of extracellular calcium inhibit human osteoclast formation, and that osteoclast bone-resorbing activity is enhanced in a high extracellular calcium environment.

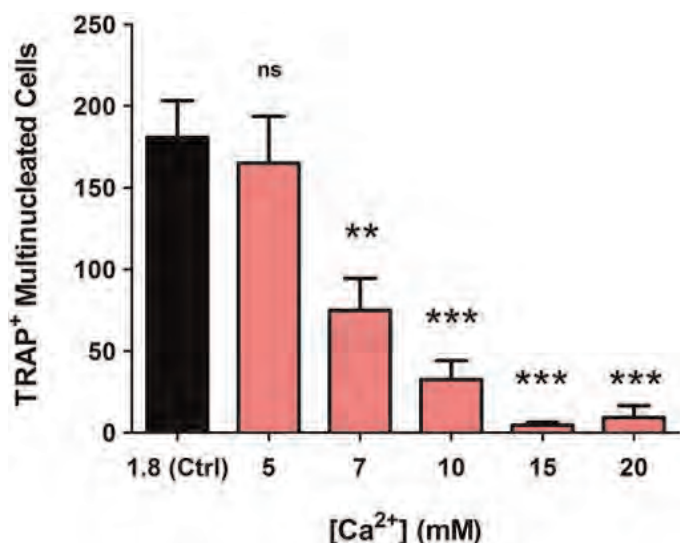


Figure 1

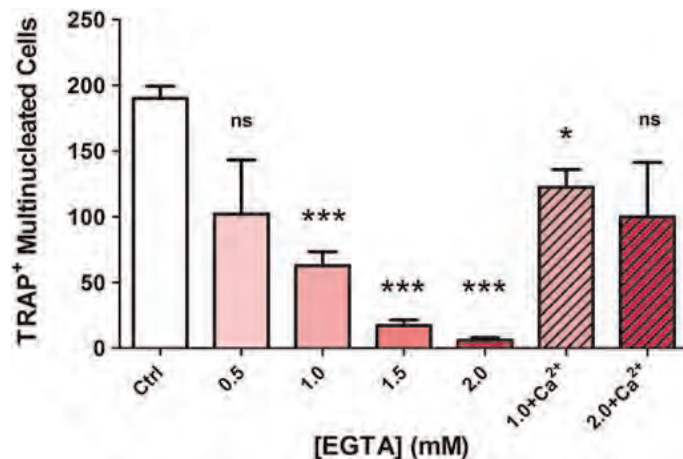


Figure 2

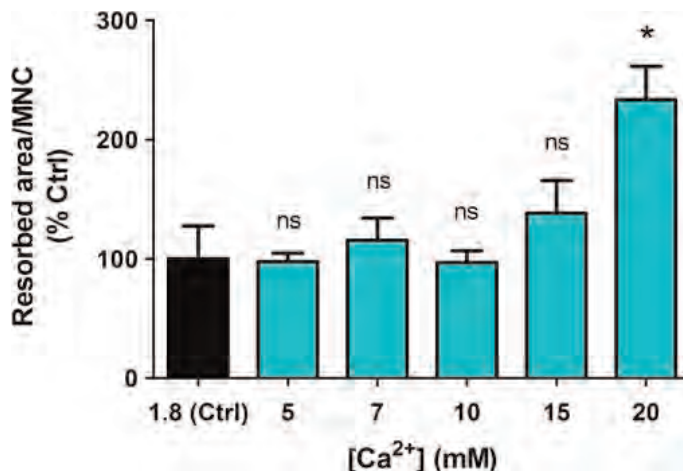


Figure 3

Disclosures: Xiaotong Cheng, None.

SA0283

See Friday Plenary Number FR0283.

SA0284

See Friday Plenary Number FR0284.

SA0285

See Friday Plenary Number FR0285.

SA0286

Effects of Dietary Amino Acids on Expression Levels of Markers of Osteoclastic Differentiation/Activity. Qing Zhong^{*1}, Ke-Hong Ding¹, Wendy Bollag¹, Hugh Nadeau¹, Karl Insogna², Norman Chutkan¹, Mark Hamrick¹, Carlos Isales³. ¹Georgia Health Sciences University, USA, ²Yale University School of Medicine, USA, ³Medical College of Georgia, USA

Increased dietary protein in humans has been reported to increase both bone formation and bone breakdown. We have previously shown that individual amino-acids, particularly those of the aromatic family (Tyrosine, Tryptophan and Phenylalanine) increase bone formation. Thus, we were interested in whether individual amino-acids could also have direct effects on osteoclasts and affect bone breakdown. To evaluate this possibility we used primary osteoclasts isolated from the bone marrow of C57Bl6 mice and examined the effects of twenty of the common amino-acids on four markers of osteoclast differentiation/activity: Carbonic anhydrase 2; Calcitonin receptor; Matrix metalloproteinase 9 and Cathepsin K.

Individual amino-acid levels were increased two-fold in the osteoclast culture medium to mimic post-prandial levels. Changes in mRNA were quantified using Real Time PCR. We found that: (1) Arginine (4.6 fold), Asparagine (4.0 fold), Isoleucine (2.6 fold), Alanine (2.5 fold) and Threonine (2.2 fold) had the largest effects on Carbonic anhydrase 2 expression; (2) Arginine (2.3 fold), Isoleucine (2.1 fold), Threonine (2.1 fold), and Histidine (1.9 fold) had the largest effects on Calcitonin receptor expression; (3) Arginine (2.3 fold), Isoleucine (2.3 fold), and Threonine (2.1 fold) had the largest effects on MMP9 expression; and (4) Arginine (3.0 fold), Methionine (2.1 fold), and Threonine (1.9 fold) had the largest effects on Cathepsin K expression. Thus, Arginine, Threonine and Isoleucine seem to consistently increase expression of osteoclastic differentiation. These amino-acids are distinct from those found to increase osteoblastic differentiation (e.g., Tyrosine, Tryptophan and Phenylalanine), suggesting that bone formation or breakdown may be preferentially activated depending on the composition of the protein ingested.

Disclosures: Qing Zhong, None.

SA0287

See Friday Plenary Number FR0287.

SA0288

Immunostimulatory Lipopeptides, Pam2CSK4 and Pam3CSK4, Enhance Osteoclast Differentiation. Jiseon Kim^{*1}, Jihyun Yang², Ok-Jin Park³, Cheol-Heui Yun⁴, Hong-Hee Kim¹, Seung Hyun Han³. ¹Seoul National University, South Korea, ²Department of Oral Microbiology & Immunology, DRI, & BK21 Program, School of Dentistry, Seoul National University, South Korea, ³School of Dentistry, Seoul National University, South Korea, ⁴Department of Agricultural Biotechnology & Research Institute for Agriculture & Life Sciences, Seoul National University, South Korea

Bacterial bone diseases including osteomyelitis and periodontitis are closely related with the excessive destruction of calcified matrix which is mainly caused by activation of osteoclasts. Since Gram-positive bacteria and Gram-negative bacteria preferentially express diacylated- and triacylated-lipoproteins, respectively, the immunostimulatory lipopeptides, Pam2CSK4 and Pam3CSK4, have been widely used as each of their lipoprotein models. In the present study, we investigated whether bacterial lipoproteins affect osteoclastogenesis in the committed osteoclasts using those two synthetic lipopeptides. Osteoclast precursors were prepared from C57BL/6 mouse bone marrow cells by treatment with macrophage colony stimulating factor (M-CSF) for three days. Then the cells were treated with M-CSF and receptor activator of nuclear factor κ B ligand (RANKL) for one additional day to differentiate them into the committed osteoclasts. When the committed osteoclasts were stimulated with the aforementioned lipopeptides in the presence of only M-CSF for two days, differentiation into mature osteoclasts was augmented concomitantly with an increase in the bone resorptive activity. When C57BL/6 mice were intraperitoneally administrated with Pam2CSK4 or Pam3CSK4, a decrease in the trabecular bone volume was also observed. Notably, such effects were not observed in the committed osteoclasts derived from TLR2- or MyD88-deficient mice. The lipopeptides also increased the expression of pro-inflammatory cytokines such as IL-6, IL-1 β and TNF- α . Furthermore, the lipopeptides enhanced phosphorylation of MAP kinases including ERK, p38 kinases, and JNK1, and the DNA-binding activity of AP-1, NF- κ B, and NF-AT in the committed osteoclasts. Collectively, these results suggest that the immunostimulatory lipopeptides enhance the osteoclast differentiation, which might at least partially contribute to the bone resorption.

Disclosures: Jiseon Kim, None.

SA0289

See Friday Plenary Number FR0289.

SA0290

See Friday Plenary Number FR0290.

SA0291

See Friday Plenary Number FR0291.

SA0292

See Friday Plenary Number FR0292.

SA0293

See Friday Plenary Number FR0293.

SA0294

The Alpha2 Integrin Minimally Impacts Osteoclast Differentiation and Adult Bone Homeostasis. Zhengyan Wang^{*1}, Grace Shin¹, Eric Everett², Xin Li³, Mary Zutter⁴, Laurie McCauley⁵. ¹University of Michigan, USA, ²University of North Carolina at Chapel Hill, USA, ³New York University, USA, ⁴Department of Pathology, Vanderbilt University Medical Center, USA, ⁵University of Michigan, School of Dentistry, USA

Collagen constitutes the most abundant protein in the bone extracellular matrix and triggers receptor mediated cell signaling. The α 2 β 1 integrin is a major collagen receptor on osteoblasts and osteoclasts and previous *in vitro* studies indicated that collagen- α 2 β 1 is essential for osteoblast differentiation. In osteoclasts, the α v β 3 integrin is known to mediate bone resorption; however, the role of α 2 β 1 integrin function is not known. The purpose of this study was to determine the role of α 2 β 1 integrin in osteoclastogenesis and function *in vitro* and *in vivo*. Bone marrow derived wild type osteoclasts showed increased cell surface expression of the α 2 integrin subunit during osteoclast differentiation *in vitro* as determined by flow cytometry and immunofluorescence. Stimulation of bone marrow derived osteoclasts with soluble type I collagen led to increased tyrosine phosphorylation, including src phosphorylation as detected via western blot analyses. This increased phosphorylation was reduced but not completely inhibited by α 2 β 1 blocking antibodies, suggesting that other collagen receptors may compensate in the absence of α 2 integrin signaling. Male C57BL/6 mice (10 wks) were examined via micro-computed tomography and bone histomorphometry. The α 2-/- mice had slight but significantly decreased femur length, diameter, and cortical bone density compared with wild-type littermates. There were no differences in other trabecular or cortical bone parameters including osteoclast number/perimeter evaluated in TRAP stained sections. Interestingly, α 2-/- osteoclasts had increased *in vitro* resorptive capacity as measured via resorption pit assay using Osteologic discs. Real time qPCR performed in cultures of differentiating osteoclasts revealed no differences in expression of osteoclast markers including β 3 integrin, calcitonin, cathepsin K, and *Nfatc-1*. There were no significant differences in serum TRAP levels in α 2-/- vs. wild type mice. In summary, these studies suggest that α 2-/- integrin is not essential for osteoclast differentiation or normal bone development and homeostasis. It is possible that other collagen receptors compensate for the lack of α 2, or the effects of α 2 integrin on osteoclasts are evident only in certain conditions.

Disclosures: Zhengyan Wang, None.

SA0295

Thrombospondin-1 Regulates Bone Density Through Effects on Nitric Oxide Signaling in Osteoclasts. Sarah Amend^{*1}, Ozge Uluckan², Michelle Hurchla¹, Hongju Deng², William Frazier², Katherine Weilbaecher². ¹Washington University in St. Louis, USA, ²Washington University in St. Louis School of Medicine, USA

Thrombospondin-1 (TSP1), recognized primarily for its role in angiogenesis, is a secreted glycoprotein and a ligand for at least 9 different receptors including β 3 integrin and CD47, essential proteins for maintaining bone homeostasis. There is phenotypic overlap among mouse models deficient for CD47, β 3, and TSP1. Interestingly, mice with a targeted disruption of CD47 have increased bone mass and defective OCs, rescued *in vitro* by inhibition of nitric oxide synthase (NOS). In vascular cells and platelets, TSP1 binding is sufficient to block nitric oxide (NO) signaling. A cell autonomous role for TSP1 signaling in OCs has not been elucidated. We demonstrate that TSP1 deficient mice (TSP1-/-) have increased bone mass due to an OC defect. TSP1-/- mice have 7% more trabecular bone volume compared to wild type (WT) littermates at six weeks of age as measured by microCT analysis of tibiae, a defect that intensifies with age, with 6 month old mice having 25% higher bone volume than controls. These data, coupled with decreased serum collagen breakdown products in TSP1-/- mice compared to WT, indicates a role for TSP1 in mediating OC function to maintain healthy bone. MCSF and RANK-L induced differentiation of OCs from bone marrow macrophages is disrupted upon TSP1 blockade as indicated by TRAP stain. In addition, bone marrow macrophage proliferation, measured by BrdU incorporation, is abrogated, both in TSP1-/- macrophages compared to control and upon administration of TSP1 neutralizing antibody in WT cultures. NO signaling is known to exert a "Goldilocks effect" on macrophage proliferation and OC formation, with signaling at high and low extremes having an inhibitory effect. TSP1 antagonism in OC cultures causes 30-fold increased expression of inducible NOS by quantitative reverse transcription PCR. The cultures also display elevated NO signaling, indicated by increased concentration of nitrite in cell culture supernatant in a Griess reagent assay. Inhibition of NOS using the pan-NOS inhibitor L-NAME rescues both the macrophage proliferation and the OC differentiation defect in the absence of TSP1. Our data show a cell-autonomous role for TSP1 in regulating OC formation, in part through inhibition of NO signaling. This data suggest that clinical modulation of NO levels, common in the treatment of cardiovascular disease, may decrease levels of bone resorption.

Disclosures: Sarah Amend, None.

SA0296

Type I Phosphoinositide-4 Phosphate 5 Kinase γ Regulates Osteoclasts in a Bifunctional Manner. Tingting Zhu^{*1}, Robert Mecham², Pietro De Camilli³, Jean Chappel¹, Steven Teitelbaum¹, Wei Zou¹. ¹Washington University in St. Louis-School of Medicine, USA, ²Washington University School of Medicine, USA, ³Yale University School of Medicine, USA

As in all cells, phosphoinositides (PI), including PI(4,5)P₂ (PIP₂), impact osteoclast formation and function. We therefore asked if an enzyme central to PIP₂ synthesis, namely type 1 phosphoinositide-4 phosphate 5 kinase γ (PIP5K1 γ), regulates the bone-resorptive cell. We find that PIP5K1 γ -/- precursors are resistant to RANK ligand (RANKL) as regards both osteoclast differentiation ($p < 0.001$) and activation of signals controlling the event including NFATc1, β 3 integrin, Akt, p38 and JNK. Confirming physiological relevance, osteoclastogenesis is reduced by more than half ($p < 0.01$) in PIP5K1 γ -/- mice, *in vivo*. On the other hand, PIP5K1 γ -/- osteoclasts spread normally, form actin rings and individually resorb bone as effectively as their WT counterparts, establishing compromised formation but not function. Because like PLC γ -deficiency, which compromises osteoclast formation and function, excess PIP5K1 γ likely yields increased PIP₂, we overexpressed PIP5K1 γ in osteoclast precursors. In fact, overexpression of PIP5K1 γ delays osteoclast differentiation and reduces cell number. Unlike its absence, excess PIP5K1 γ also disrupts the cytoskeleton in that the cells fail to spread or dynamically form actin rings. Consistent with a PIP₂-mediated event, the cytoskeleton-disruptive effects of excess PIP5K1 γ reflect its kinase activity but appear independent of adaptor function as a similar phenotype develops in cells transduced with splice variants capable or incapable of binding talin. The combined arrested differentiation and disorganized cytoskeleton of PIP5K1 γ -transduced osteoclasts compromises their bone resorptive capacity ($p < 0.001$). Thus, likely reflecting PIP₂ generation, optimal PIP5K1 γ expression by osteoclasts is essential for skeletal homeostasis, *in vitro* and *in vivo*.

Disclosures: Tingting Zhu, None.

SA0297

Calmodulin Interacts with Rab3D and Mediates Osteoclastic Bone Resorption. Jiaye Xu^{*1}, Taksum Cheng², Shek Man Chim², Jennifer Tickner², Estabelle Ang¹, Ming Hao Zheng², Nathan Pavlos². ¹The University of Western Australia, Australia, ²University of Western Australia, Australia

Calmodulin is a highly versatile protein that regulates intracellular calcium homeostasis and diverse cellular functions such as cardiac excitability, synaptic plasticity and signaling transduction. During osteoclastic bone resorption, calmodulin is concentrated at the ruffled border membrane of osteoclasts and has been implicated in the regulation of bone resorption. Here we show that calmodulin interacts with Rab3D, a molecule known to be important in osteoclast exocytic vesicle transport and bone homeostasis. By yeast two-hybrid screening, we identified a specific interaction between calmodulin and Rab3D, but not with other Rabs including Rab4, Rab5 and Rab6. This interaction was calcium-dependent as revealed by calmodulin sepharose pull-down assays *in vitro*. Consistently, expression of a calcium insensitive form of calmodulin (CaM1234) perturbed this interaction *in vivo* as monitored by bioluminescence resonance energy transfer (BRET) assays. Interestingly, the interaction of calmodulin and Rab3D was significantly enhanced when Rab3D was expressed and locked in its GTP-bound conformation (Rab3DQ81L) as compared to wild-type Rab3D, nucleotide lacking (Rab3DN135I) and prenylation deficient (Rab3DΔCXC) by BRET assays, suggesting that the interaction between calmodulin and Rab3D was nucleotide-dependent. During RANKL-induced osteoclast formation, calmodulin gene transcripts were constitutively expressed and paralleled with those of Rab3D. In mature osteoclasts, calmodulin co-fractionated with Rab3D at the plasma membrane during sucrose gradient sedimentation assays and colocalized with Rab3D in the ruffled border of bone-resorbing osteoclasts by confocal microscopy. Finally, functional blockade of this interaction by calmidazolium chloride resulted in a significant attenuation of osteoclastic bone resorption. Our data imply that calmodulin interacts with Rab3D at the ruffled border membrane to regulate efficient bone resorption by osteoclasts.

Disclosures: Jiaye Xu, None.

SA0298

Does Ovariectomy in Non-Resorbing Adult Mice Cause Bone Gain? Christian Thudium^{*1}, Carmen Flores², Ilana Moscatelli², Jesper Thomsen³, Mie Bruel⁴, Natalie Sims⁵, Maria Askmyr⁵, Thomas Martin⁵, Anita Neutsky-Wulff⁶, Vicki Jensen⁷, Gerling Langenbach⁸, Claus Christiansen⁷, Vincent Everts⁸, Morten Karsdal⁷, Johan Richter², Kim Henriksen⁷. ¹Nordic Bioscience, Denmark, ²Lund University, Sweden, ³University of Aarhus, Denmark, ⁴Institute of Anatomy, University of Aarhus, Denmark, ⁵St. Vincent's Institute for Medical Research, Australia, ⁶Nordic Bioscience & University of Copenhagen, Denmark, ⁷Nordic Bioscience A/S, Denmark, ⁸Dept. Oral Cell Biology, (ACTA), Universiteit van Amsterdam & Vrije Universiteit, Netherlands

Patients and mice with mutations reducing the ability of the osteoclasts to secrete acid have osteopetrosis, characterized by defective bone resorption, increased osteoclast numbers, and normal or even increased bone formation.

This has suggested that osteoclasts have at least two distinct functions, bone resorption and coupling signals stimulating bone formation. To investigate this hypothesis, we used adult mice, transplanted with acidification deficient osteoclasts in a standard OVX bone loss model.

We hypothesized that 1) ovariectomy (OVX) induced bone turnover could be rescued by preventive transplantation of oc/oc fetal liver cells and most importantly 2) that OVX in these mice would result in more rather than less bone in the OVX model.

Adult mice were irradiated and transplanted with fetal liver cells from wt or oc/oc mice (Ly5.2 background) by IV injection into wt mice (Ly5.1 background). Engraftment levels were assessed using flow cytometry of the Ly5.2/Ly5.1 ratio. OVX was performed 2 weeks post transplantation. Serum samples were collected every 4-6 weeks for measurement of bone turnover markers (CTX-I, ALP and TRACP 5b). At week 17 the animals were euthanized and bones were collected for histomorphometry, μ CT and mechanical tests.

An engraftment level >95% was obtained. The resorption marker CTX-I was reduced in the oc/oc groups compared to wt/wt and wt/wt OVX, while TRACP 5b was increased in the oc/oc groups compared to wt/wt and wt/wt OVX. ALP levels were unchanged between groups.

μ CT analyses of femurs and vertebrae showed a 50% increase in bone volume in trabecular and 20% in cortical compartments of oc/oc mice compared to wt/wt in pilot studies without OVX. Bone histomorphometry confirms the increased bone volume found in μ CT analysis. Furthermore, mechanical tests showed a 35% increase in bone strength in the femoral neck and diaphysis of oc/oc mice compared to wt/wt in the pilot study. μ CT analyses of femurs and vertebrae in the OVX study, biomechanical tests on femur and vertebrae, and bone histomorphometry of vertebrae are ongoing.

In conclusion, we here present data indicating that that bone formation is uncoupled from bone resorption in adult mice, when the osteoclasts are unable to acidify the resorption lacunae and that ovariectomy increases bone gain in mice with non-resorbing osteoclasts. These data highlight the different functions of osteoclasts.

Disclosures: Christian Thudium, None.

SA0299

See Friday Plenary Number FR0299.

SA0300

Lysophosphatidylinositol: Evidence for a Role in GPR55 Mediated Bone Resorption and Rheumatoid Arthritis. Lauren S. Whyte^{*}, Wendy R. Russell, Lynne Hocking, Michael Rogers, Ruth A. Ross, University of Aberdeen, United Kingdom

Male mice lacking the putative cannabinoid receptor GPR55 have a high bone mass phenotype due to a defect in osteoclast polarisation. Lysophosphatidylinositol (LPI), the endogenous ligand for GPR55, stimulates bone resorption *in vitro*, however it is not known whether osteoclasts produce LPI in response to GPR55 activation or whether levels of LPI are altered in response to cytokines known to modulate osteoclastic resorption. In addition, LPI is known to have a role in inflammation, but it remains to be determined whether levels of circulating LPI are altered in patients with rheumatoid arthritis (RA), an inflammatory condition associated with bone destruction.

Human osteoclasts were treated with the synthetic GPR55 agonist, O-1602, or the pro-inflammatory cytokines IL-1 or TNF α for 90 min. Cell pellets were extracted directly using acidified chloroform/methanol containing 1% acetic acid and prepared for LC-MS. The same LC-MS method was used to measure LPI in plasma collected from a cohort of patients with RA (n=14) and healthy controls (n = 6), with approval from the North of Scotland Research Ethics Committee. LPI was measured in triplicate for each sample.

Upon treatment of human osteoclasts with O-1602, levels of LPI were significantly increased relative to control cultures. Treatment of osteoclasts with IL-1, but not TNF α , resulted in a significant increase in LPI. These results suggest that activation of GPR55 results in an increase in production of the endogenous ligand. In

addition, LPI can also be produced in response to the pro-inflammatory cytokine IL-1 - most likely due to IL-1 induced activation of PLA2.

Having shown that LPI levels are altered upon treatment with IL-1, which is known to play an important role in bone erosion and cartilage destruction in arthritis models, we have also shown that plasma levels of LPI in a cohort of patients with RA were significantly higher than those measured in healthy controls. However, in the small number of patients studied so far, levels of LPI did not correlate with disease severity as assessed by DAS score.

These results suggest that LPI may play a role in IL-1 induced bone resorption via GPR55, further adding to the body of evidence that GPR55 antagonists may be of use in the treatment of bone diseases associated with excessive osteoclast activity. Furthermore, LPI may be a novel biomarker for RA.

Disclosures: Lauren S. Whyte, None.

SA0301

Silicon Nanocrystal Tracer for Real-Time Activity Bioassay of Single Osteoclasts. Naif Alsharif, Mark Birch, Benjamin Horrocks, Harish Datta*. Newcastle University, United Kingdom

There is a lack of suitable in vitro techniques for assaying osteoclastic (OC) resorptive activity in real-time, and existing assays for osteoclast resorptive activity are cumbersome, insensitive and retrospective. A variety of real-time assays have also been used that measure one or more of the products generated by OC during resorptive activity, such as superoxide anion, proton pump activity, calcium generation or enzyme release. An important disadvantage of these assays is that they estimate only one aspect of OC activity, which may or may not relate to the overall resorptive activity of these cells. To address these problems, we have developed an assay, which we show is easy to use, rapid, precise and allows the real-time resorption assay of a single OC. The assay is based on an artificial hydroxyapatite / collagen matrix containing a luminescent tracer. As the OC resorbs the matrix, the tracer is released and internalised by the cell which can be observed in a fluorescence microscope. The assay therefore determines the overall resorption activity of the OC, as in the pit assay, but with the sensitivity speed and convenience of fluorescence microscopy. In principle, many fluorescent dyes could be employed as the tracer; however there are important criteria the dye must satisfy to ensure the quality of the assay. In our previous studies we have shown that alkyl-capped nanocrystals (SiNCs) have appropriate properties for such application (1), are insoluble in water and therefore do not leach from the matrix and they have bright luminescence that is proportional to their concentration without evidence of the aggregation or self-quenching effects typical of molecular dyes. Silicon nanocrystals have advantages over other types of quantum dot for long duration experiments because they cannot leach heavy metal ion. In this in vitro assay, OC is inhibited by calcitonin (CT), methyl- β -cyclodextrin (MCD) and filipin, and stimulated by RANKL in the expected manner, and stimulants and inhibitors of OC activity can be easily distinguished from the real-time fluorescence data over a period of about 30 min. The kinetics of the assay exhibit a lag phase followed by a growth of cell fluorescent intensity and the whole time course was satisfactorily described by the logistic equation.

1. Alsharif, N. H., Berger, C. E. M., Varanasi, S. S., Chao, Y., Horrocks, B. R., and Datta, H. K. (2009) Small. 5(2), 221–228.

Disclosures: Harish Datta, None.

SA0302

Tctex-1, a Novel Interaction Partner of Rab3D, is Required for Osteoclastic Bone Resorption. Nathan Pavlos*, Taksum Cheng¹, An Qin¹, PeiYing Ng², Hao-Tian Feng², Estabelle Ang², Amerigo Carrello², Ching-Hwa Sung³, Reinhard Jahn⁴, Ming Hao Zheng¹, Jiak Xu². ¹University of Western Australia, Australia, ²The University of Western Australia, Australia, ³Cornell University, USA, ⁴Max-Planck-Institute for Biophysical Chemistry, Germany

Vesicular transport along microtubules must be strictly regulated to sustain the unique structural and functional polarisation of bone-resorbing osteoclasts. However, the molecular mechanisms bridging these vesicle-microtubule interactions remain largely obscure. Rab3D, a member of the Rab3 subfamily (Rab3A/B/C/D) of small exocytotic GTPases, represents a core component of the osteoclastic vesicle transport machinery. Here, we identify a new Rab3D-interacting partner, Tctex-1, a light chain of the cytoplasmic dynein microtubule motor complex by a yeast two-hybrid screen. We demonstrate that Tctex-1 binds specifically to Rab3D in a GTP-dependent manner and co-occupies Rab3D-bearing vesicles in bone-resorbing osteoclasts. Furthermore, we provide evidence that Tctex-1 and Rab3D intimately associate with the dynein motor complex and microtubules in osteoclasts. Finally, targeted disruption of Tctex-1 by RNA interference significantly impairs bone resorption capacity and mislocalizes Rab3D-vesicles in osteoclasts, attesting to the notion that components of the Rab3D-trafficking pathway contribute to the maintenance of osteoclastic resorptive function.

Disclosures: Nathan Pavlos, None.

SA0303

See Friday Plenary Number FR0303.

SA0304

TRAF family member-associated Nf-kappa B activator (Tank), Induced by RANKL, Negatively Regulates Osteoclast Survival and Function. Mengrui Wu*, Lianfu Deng², Yiping Wang³, Wei Chen⁴, Xu Feng⁴, Yi-Ping Li⁴.

¹Institute of Genetics, Life Science College, Zhejiang University & Department of Pathology, University of Alabama at Birmingham, China, ²Shanghai Key laboratory, Shanghai Institute of Trauma & Orthopaedics, Ruijin Hospital, School of Medicine, Shanghai Jiao-Tong University, China, ³Institute of Genetics, Life Science College, Zhejiang University, China, ⁴University of Alabama at Birmingham, USA

Precise control of osteoclast activity is required for bone homeostasis, so bone resorption needs to be “turned off” when it is no longer needed (a negative feedback loop). However, little is known about the mechanism that regulates the negative feedback loop. To test our hypothesis that certain signaling proteins induced in osteoclast differentiation negatively control osteoclast activity, we characterized the expression and function of such signaling proteins.

ChIPArray was performed for genome-wide analysis of genes expression before and after osteoclast maturation. Bone marrow monocytes (BMMs) transduced with Tank-siRNA lentivirus were induced by RANKL and M-CSF. TRAF family member-associated Nf-kappa B activator (Tank) knockdown was validated 48 hours after lentivirus transduction by western blot analysis. TRAP staining, acridine orange staining, and a scanning electronic microscope were respectively used to assess osteoclast formation, acid production, and number of resorption pits. Osteoclast survival was examined by TRAP-stained osteoclast morphological analysis at different timepoints during prolonged culture on bone slides.

Our results show that Tank expression increased 10-fold from RANKL stimulation during osteoclastogenesis according to our ChIPArray data. Tank was identified as a candidate regulator of negative feedback. Western blot and RT-PCR confirmed upregulation of Tank in RANKL-stimulated BMMs. One siRNA (Tank-shRNA-1) was shown to knockdown Tank expression by 85.6% in osteoclasts. No obvious differences were observed in the degree of osteoclastogenesis. However, the Tank-knockdown group had increased acid production and a 200% increase in the number of bone resorption pits compared to the control group. The survival rate of mature osteoclasts in the Tank-knockdown group was 3.5 times higher than the control group.

In conclusion, our data indicates that Tank expression is highly induced by RANKL and that Tank inhibits osteoclast activity and reduces osteoclast survival, functioning in a negative feedback loop in RANKL-induced bone resorption. Tank may negatively regulate RANKL signaling in osteoclasts by inhibiting Nf-kappa B (Nf- κ B) activity. This is the first report of Tank's function as a negative regulator in osteoclast function. These results may provide means for therapeutic intervention in diseases of excessive bone resorption.

Disclosures: Mengrui Wu, None.

SA0305

See Friday Plenary Number FR0305.

SA0306

See Friday Plenary Number FR0306.

SA0307

See Friday Plenary Number FR0307.

SA0308

Both VEGF Receptor 2 (VEGFR2) and the Parathyroid Hormone Type 1 Receptor (PTH1R) Mediate the Early Antiapoptotic Response to Mechanical Stimulation in MLO-Y4 Cells. Marta Mavcas*, Luis Fernandez de Castro¹, Beatriz Bravo¹, Cira Garcia de Durango¹, Jose Manuel Pozuelo¹, Pedro Esbrit², Arancha Gortazar³. ¹Universidad San Pablo CEU, Spain, ²FUNDACION JIMENEZ DIAZ, Spain, ³Universidad San Pablo-CEU School of Medicine Madrid Spain, Spain

Mechanical loading plays a key role in bone formation and maintenance. While unloading induces osteocyte apoptosis and bone loss in vivo, mechanical stimuli prevents osteocyte apoptosis through a mechanism involving β -catenin accumulation and ERK nuclear translocation. Both vascular endothelial growth factor (VEGF) and parathyroid hormone-related protein (PTHrP) have a crucial role in bone formation,

but their interaction with osteocytes is not completely understood. VEGF receptor 2 (VEGFR2) has recently been shown to mediate, at least in part, the mechanical response of endothelial cells in a VEGF-independent manner. On the other hand, activation of the PTH type 1 receptor (PTH1R) in osteocytes has recently been shown to increase periosteal bone formation by targeting the Wnt pathway. Of interest, in osteoblasts, VEGF-independent VEGFR2 activation appears to be in part responsible for the antiapoptotic effect of PTHrP. In this work, we aimed to evaluate the putative roles of the VEGF and PTHrP systems in early (10 min-1h) osteocyte mechanosensing. To this end, MLO-Y4 cells were subjected to mechanical strain by laminar fluid flow (FF) or hypotonic shock. Mechanical stimuli, VEGF165 (6 ng/ml) or PTHrP (1-36) (100 nM) similarly stimulated cell viability and β -catenin stabilization related to an increased membrane localization (assessed by western blot and immunocytochemistry). A VEGFR2 antagonist (SU5416) or transfection of a dominant negative VEGFR2 plasmid -in contrast to a VEGF neutralizing antibody- and the PTH type 1 receptor (PTH1R) antagonist PTHrP (7-34) all decreased these events. In contrast, VEGFR2 overexpression in MLOY4 cells mimicked the effect of FF on β -catenin and also nuclear ERK relocalization. Interestingly, we also observed that mechanical stimulation increased PTH1R in membrane. In conclusion, our *in vitro* findings strongly support the role of both VEGFR2, in a VEGF-independent manner, and the PTH1R in the mechanism whereby mechanical stimuli promote osteocyte viability.

Disclosures: Marta Maycas, None.

SA0309

See Friday Plenary Number FR0309.

SA0310

See Friday Plenary Number FR0310.

SA0311

See Friday Plenary Number FR0311.

SA0312

See Friday Plenary Number FR0312.

SA0313

Regulation of Osteocyte Apoptosis and ECM by PTHrP. Leonard Defetos^{*1}, Cheryl Chalberg², Su Tu², Douglas Burton², Lynda Bonewald³. ¹Veterans Administration San Diego Healthcare System & University of California, USA, ²VA San Diego Healthcare System / University of California San Diego, USA, ³University of Missouri - Kansas City, USA

Background: Although osteocytes are the most abundant cell type in bone, much of their biology remains enigmatic. Recent data reveal that osteocytes themselves act as endocrine cells that synthesize growth regulating factors and respond to other regulatory hormones. The signaling pathways among bone cells are complex and involve many factors, including parathyroid hormone-related protein (PTHrP). In this study, we evaluated the effects of PTHrP on osteocyte genes related to apoptosis and extracellular matrix (ECM).

Methods: The MLO-Y4 cells, derived from mature mouse osteocytes, were transfected for 24 hours with a mouse-specific PTHrP 1-139 expression plasmid and compared to cells transfected with a vector control plasmid. The PTHrP expression was measured by immunoassay and total RNA was purified. The mRNA samples were analyzed for genes related to apoptosis and ECM using qPCR arrays. A GFP expression plasmid was used to assess transfection efficiency.

Results: Positive GFP expression was observed in over 85% of the cells by fluorescence microscopy. PTHrP overexpression was confirmed in the PTHrP 1-139 transfected cells (4205 pg PTHrP/ ml media) compared to vector control transfected cells (81 pg PTHrP / ml media), respectively. Significant differences in apoptosis and ECM related genes were observed between the PTHrP 1-139 and vector control transfected groups. In general, PTHrP 1-139 was pro-apoptotic, increasing over 1.5-fold TNF ligand and receptor (*FasII*, *Tnf*, *Cd40lg*, *Cd40*) and CARD (*Card10*) family related genes and decreasing some of the anti-apoptosis related genes. Greater effects of PTHrP were observed in the ECM array. PTHrP 1-139 transfection increased several cell adhesion and ECM related markers over 2-fold (*Itgax*, *Cntn1*, *Cntna2*, *Sele*, *Adams2*, *Mmp10*) and decreased > 50% other ECM related genes (*Fnl1*, *Vcan*, *Adamts1*, *Col1a1*, *Col3a1*, *Col6a1*).

Conclusions: In this study, we have demonstrated that PTHrP can regulate osteocyte markers for apoptosis and ECM. Apoptosis plays a critical role in normal biological processes requiring cell removal including differentiation, development, and homeostasis and ECM play critical roles in normal processes such as cell growth, division, differentiation, and migration. The modulation of osteocyte growth and function by PTHrP identifies additional pathways for bone homeostasis. Exploring these pathways in detail can identify both basic and clinical relevance for the effects of PTHrP on osteocytes.

Disclosures: Leonard Defetos, None.

SA0314

Hypermineralization of Osteocyte Lacunae in the Aged Human Skeleton Leads to Underestimated Osteocyte Lacunar Densities. Vincent Carpentier, Jinquan Wong, Youwen Yeap, Cheryl Gan, Peter Sutton-Smith, Arash Badiei, Nicola Fazzalari, Julia Kuliwaba*. SA Pathology, Australia

Previous studies reporting on osteocyte density in the human skeleton (healthy vs pathological conditions) have underestimated 'true' osteocyte lacunar density, as hypermineralized osteocyte lacunae, a unique feature of the aging human skeleton, are not visible with standard histology. Therefore, the purpose of this study was to determine the extent of hypermineralized osteocyte lacunae in relation to bone mineralization for osteoporotic hip fracture (OP) and hip osteoarthritis (OA) patients, and non-pathological cadaveric controls (CTL). Intertrochanteric bone cores were obtained from patients at surgery for non-traumatic OP femoral neck fracture (10F, 4M, 65-94y) and for hip OA (7F, 8M, 62-87y), and femora at autopsy (CTL: 5F, 11M, 60-84y). Bone cores from the central region of L2 vertebrae were also obtained, from an independent cadaveric cohort (CVB: 3F, 6M, 53-83y). Bone samples were resin-embedded for quantitative backscattered electron imaging (qBEI). Bone tissue mineralization (wt %Ca) was not different between OP, OA, and CTL; but was greater in femoral CTL than in CVB (24.34 vs 22.95%; $p < 0.002$). Using a custom image-processing algorithm for qBEI images, lacunar, hypermineralized, and total lacunar densities were quantified. Percent hypermineralized lacunae relative to total number (HL/TL[%]) was greater in OP and OA than in CTL ($p < 0.005$). However, relative to bone mineral area, OP was characterized by increased hypermineralized lacunar density (HL.Dn[μm^{-2}]; $p < 0.02$); whereas OA was characterized by decreased lacunar density (L.Dn[μm^{-2}]; $p < 0.005$) and total lacunar density (TL.Dn[μm^{-2}]; $p < 0.02$). L.Dn was higher in CVB than in femoral CTL ($p < 0.04$). These study data suggest that even though the presence of hypermineralized lacunae is not specific to pathological bone, their proportionate number is increased in OP and OA. Further, these morphological data reiterate the fact that OP, OA, and CTL bone are different. Femoral trabecular bone was more mineralized with decreased lacunar density in comparison with vertebral trabecular bone, consistent with higher vertebral bone turnover. Further investigation is needed into whether the presence of hypermineralized lacunae in bone is detrimental to the quality of the osteocyte-canalicular cell network in terms of its mechanosensory role in bone adaptation, the ability to detect and repair microdamage, and its potential influence on bone material fracture strength and toughness.

Disclosures: Julia Kuliwaba, None.

SA0315

PTH Regulation of SOST and FGF23 in Novel Osteocytic Cell Lines. Jordan Spatz^{*1}, J Martorell², KJ Barry³, ER Edelman⁴, M Balcells⁵, Paola Pajevic Divieti⁶. ¹Harvard-MIT Division of Health Sciences & Technology (HST), USA, ²Massachusetts Institute of Technology & Institut Quimic de Sarria, Barcelona, Spain, USA, ³Endocrine Unit, Massachusetts General Hospital, Harvard Medical School, USA, ⁴Massachusetts Institute of Technology & Cardiovascular Division, Department of Medicine, Brigham & Women's Hospital, USA, ⁵Massachusetts Institute of Technology & Institut Quimic de Sarria, Barcelona, Spain, USA, ⁶MGH- Harvard Medical School, USA

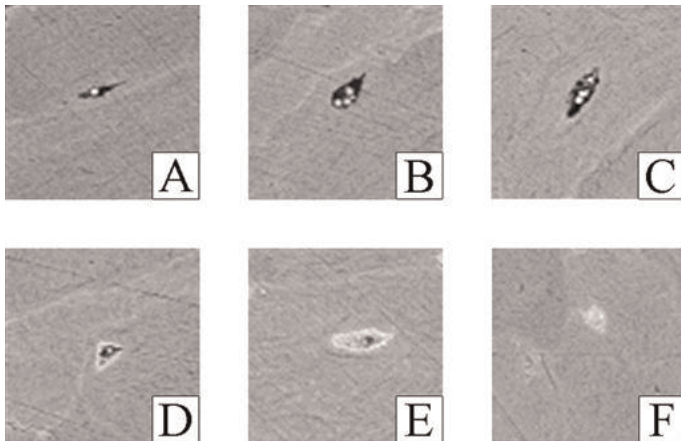
To date, *in vitro* studies of osteocyte function and regulation have relied upon limited immortalized osteocyte-like cell lines that have some, but not all of the characteristic phenotype of *in vivo* osteocytes. Specifically, no osteocytic cell lines are available that truly model the end-state differentiation of osteocytes. To this end mice expressing the green-fluorescent protein (GFP) under the control of Dentin Matrix (8KbDMP1-GFP) were mated with Immortomouse (Charles River) and osteocytes were isolated from calvaria and long bone of double transgenic offsprings. Cells were subjected to sequential collagenase digestions followed by FACS sorting for GFP-positive cells. GFP-positive sorted cells displayed the dendritic morphology characteristic of an osteocytic population. Selected clones were further characterized for the expression of osteocytic genes (PheX, E11, SOST, Cnx43, FGF23) and proteins (Sclerostin and FGF23) using semiquantitative rt-PCR (qPCR) and western blot, respectively. Notably, several of the clones expressed detectable levels of sclerostin and FGF23. In addition, all osteocytic clones were negative for alkaline phosphatase staining. Next, we assessed PGE₂ and SOST regulation after 4 hours of laminar fluid flow (16 dynes/cm²) to allow for comparison of PGE₂ responsiveness in our cells to MLO-Y4. Osteocytic cells exposed to fluid flow showed a greater than 15-20-fold increase in PGE₂ production and a 2-fold reduction in SOST mRNA expression compared to static controls. DMP1-GFP expression, as assessed by fluorescent microscopy, was also significantly increased in cells exposed to fluid flow. Lastly, we evaluated functional regulation of SOST and FGF23 mRNAs. Osteocytic cell showed a 2-30 fold up regulation of FGF23 and two-fold decrease in SOST mRNA expression, as assessed by qPCR, after 4-hour treatment with 100nM hPTH(1-34). Moreover, FGF23 was also significantly upregulated after treatment with 100 nM 1,25(OH)₂D₃ for 16hr or with 10mM forskolin for 4 hr. Likewise, treatment with forskolin also decreased SOST expression in a manner similar to PTH. Treatment with 20mM phosphate, on the other hand, had no effect on FGF23 gene expression suggesting osteocytes might not regulate FGF-23 expression in response to phosphate changes. In conclusion, we have established novel osteocytic cell lines from DMP1-GFP positive calvarias and long bones that will be a tool to further investigate fundamental osteocytic research avenues.

Disclosures: Jordan Spatz, None.

SA0316

The Formation and the Mineral Content of Hypermineralized Osteocyte Lacunae: the Phenomenon of Osteocyte Hypermineralization a Single State or a Matter of Degree?. Vincent T. Carpentier*, Jinquan Wong, Youwen Yeap, Cheryl Gan, Peter Sutton-Smith, Arash Badiei, Nicola L. Fazzalari, Julia S. Kuliwaba, SA Pathology & Hanson Institute, Australia

Hypermineralized osteocyte lacunae (HOL) have received little research attention as they are not visible with standard histologic techniques. No studies have investigated their formation or mineral content. Intertrochanteric trabecular bone cores were obtained from patients at surgery for osteoporotic (OP) femoral neck fracture (10F, 4M, 65-94y), and femora at autopsy (5F, 11M, 60-84y). Specimens were resin-embedded and carbon coated for quantitative backscattered electron imaging (qBEI) and energy dispersive X-Ray spectrometry (EDX). Using specimen observations under qBEI we describe different stages of intermediate HOL, between unmineralized black lacunae (grade I) and HOL (grade VII), which illustrate a phenomenon leading to HOL. The lacunae with a hypermineralized spherite (HS) (grade II; A) correspond to lacunae with a single HS. The lacunae with multiple HS (grade III; B) are characterised by the presence of several HS. The lacunae with wall-connected HS (grade IV; C) are lacunae with several HS where some merge with the lacunar wall. The partially HOL with HS (grade V; D) are lacunae with a hypermineralized lacunar ring associated with HS. The partially HOL (grade VI; E) are lacunae incompletely filled by hypermineralized substance, and without any presence of HS. The HOL (grade VII; F) are lacunae totally filled by hypermineralized substance. EDX analyses reveal that HOL are composed of Ca, P, Mg, and Na. Strikingly, the HOL mineral content ratios of Ca/Mg, P/Mg, and Na/Mg were higher than for the bone matrix in OP. Finally, in addition to the fact that one study reported that intermediate HOL are associated with the appearance of an apoptotic cell containing DNA under TEM (PMID:18615594), we report: 1) the fact that the osteocyte hypermineralization may be a multi-staged phenomenon; 2) the fact that HS look like "mineralized spheres" generated by osteoid-osteocytes (PMID:17115241). These findings strongly support the hypothesis that osteocyte hypermineralization is associated with osteocyte activity. We hypothesise that hypermineralization could happen in addition to osteocyte apoptosis. It appears that it is a possible specific osteocyte death which is different to apoptosis, necrosis or autophagy. Consequently, the relationship between hypermineralization and apoptosis needs to be further investigated. Unlike empty lacunae, HOL do not permit fluid circulation within the osteocyte network. Thus, their presence may modulate the quality of bone.



Stages of the phenomenon of osteocyte hypermineralization under qBEI at 400x.

Disclosures: Vincent T. Carpentier, None.

SA0317

See Friday Plenary Number FR0317.

SA0318

Evidence of Fibroblast Growth Factor as a Physiological Regulator of Osteocyte Differentiation; Lessons from Wildtype and Hyp Mice. Carolyn Macica*¹, Adam Kaye², Guoying Liang². ¹Yale University School of Medicine, USA, ²Yale University, USA

The osteocyte is the most abundant cell type in bone and is involved in both phosphate homeostasis and as the mechanical sensor that regulates bone turnover. In addition to the extensive dendritic processes of osteocytes that function to sense physiological changes in the environment, osteocytes also produce FGF23, a phosphatonin that regulates renal phosphate transport and underlies the phosphate wasting of familial X-linked hypophosphatemia (XLH). Osteocytes are derived from a subset of osteoblasts that become buried in unmineralized matrix or osteoid. However, the physiological factors that regulate the transition from osteoblast to osteocyte are unknown. We sought to determine the putative role of fibroblast growth factors by examining the expression of FGF receptors in both wildtype and Hyp mice,

a murine model of XLH, using histological techniques in the tibia and femur. Bone-lining osteoblasts of wildtype mice showed strong FGFR1 membrane staining. In addition, we found evidence of FGFR1 expression in osteoblastic osteocytes and osteoid osteocytes associated with unmineralized osteoid. A complete downregulation of FGFR1 was revealed in all preosteocytes and osteocytes; however, they were associated with robust upregulation of a constitutively active tyrosine-phosphorylated FGF receptor (anti-Phospho-FGFR pY653/654). Staining was localized not only to the soma of osteocytes but heavily stained throughout the processes and did not stain for FGFR3. We then examined the tibia/femur of Hyp mice which characteristically display hypomineralized periosteocytic lesions. While osteocytes of Hyp mice were positive for tyrosine-phosphorylated FGFR, FGFR1 staining abnormally persisted and was particularly evident in the osteocytes embedded in lacunae of unmineralized osteoid. FGFR1 staining was normalized in Hyp mice treated with oral phosphate and vitamin D. These data confirm that mineralization is an important cue in the terminal differentiation of osteocytes with further studies aimed at determining the potential autocrine role of osteocyte-derived FGF23 in FGFR signaling.

Disclosures: Carolyn Macica, None.

SA0319

See Friday Plenary Number FR0319.

SA0320

Functional Heterogeneity of Osteocytes in FGF23 Production Revealed by 3-Dimensional Fluorescence Morphometry. Ayako Nakane*¹, Rieko Tanabe², Mayu Haraikawa³, Takashi Watanabe¹, Hiroshi Kamioka⁴, Masae Goseki-Sone⁵, Yuzo Takagi⁶, Akira Yamaguchi⁷, Tadahiro Iimura¹. ¹Tokyo Medical & Dental University, Global Center of Excellence Program, Japan, ²Department of Food & Nutrition, Faculty of Human Sciences & Design, Japan Women's University, Japan, ³Graduate School of Human Life Science, Japan Women's University, Japan, ⁴Okayama University Graduate School of Medicine, Dentistry, & Pharmaceutical Sc, Japan, ⁵Japan Women's University, Japan, ⁶Developmental Oral Health Sciences, Tokyo Medical & Dental University, Japan, ⁷Tokyo Medical & Dental University, Japan

Osteocytes are the most abundant cells in bone and play important roles in bone metabolism through sensing mechanical loading and endocrine regulation of the serum level of phosphate. Though morphological diversity of osteocytes depending on the sites of bone tissues and pathological changes has been described, it is not well documented whether these cells are functionally homogeneous or heterogeneous. To access this issue, we took advantages of 3-dimensional fluorescence morphometry. After conducting immuno-fluorescence with antibodies against FGF23 and DMP1 on bone sections, optical sections at different levels along z-axis were obtained by confocal microscopes. Three dimensional reconstitution and image processing were conducted in silico. Measurements of fluorescence intensity and its 3-dimensional distribution enabled to quantify relative expression level of FGF23 in an osteocyte lacuna in situ. Comparative analysis of osteocytes between trabecular and cortical bones in rat tibiae demonstrated that cortical osteocytes expressed higher level of FGF23 protein than trabecular osteocytes. To know whether these differences are functionally relevant, we compared tibiae in ovariectomized rats and sham-operated ones. In this experiment, the serum level of FGF23 in ovariectomized rats was significantly reduced to almost half level compared to that in the sham-operated group. The fluorescence morphometry analyses showed that the level of FGF23 protein in cortical osteocytes in the ovariectomized group was significantly lower than that in the sham-operated group, whereas those levels in trabecular osteocytes show no significant difference. These observations suggested that cortical osteocytes are more responsible for the production of FGF23 in response to estrogen deficiency than trabecular osteocytes. Further detailed analysis in cortical bone in both groups showed that FGF23 was heterogeneously produced among osteocytes. The level of FGF23 production in each osteocyte was reciprocally correlated with the DMP1 protein level in osteocyte lacuna. Our observation using 3-dimensional fluorescence morphometry suggested that cortical osteocytes are more responsible for regulation of the serum level of phosphate than trabecular osteocytes and that functional heterogeneity among osteocytes involves locally regulated reciprocal levels of FGF23 and DMP1.

Disclosures: Ayako Nakane, None.

This study received funding from: Tokyo Medical and Dental University Global Center of Excellence Program

SA0321

Association Between Lipid Profile and Bone Turnover in Elderly Women and Men. Marija Tamulaitiene*¹, Rima Piliciauskiene², Vidmantas Alekna¹. ¹Vilnius University, Lithuania, ²State Research Institute Centre for Innovative Medicine, Lithuania

Background. Studies of bone markers and blood lipids are limited, and the results are conflicting.

Aim of study is to evaluate the relationship between the lipid profile and bone turnover markers.

Methods. This was a cross-sectional study on women and men aged 60 years and older who consecutively had visited the National Osteoporosis Center (Vilnius, Lithuania). Subjects who fractured during the last 12 months or have used medications known to affect bone metabolism were not included in this study. Blood samples were obtained between 9 and 11 am after overnight fasting. Total cholesterol, high-density lipoproteins (HDL), low-density lipoproteins (LDL) and triglycerides (TG) were analyzed. Serum bone resorption marker C-telopeptide of type I collagen crosslinks (s-CTX-I), type I procollagen amino-terminal propeptide (PINP) and parathyroid hormone (PTH) were measured by automated immunoassay (Cobas E411, Roche Diagnostic). Total body BMD was estimated by dual-energy X-ray absorptiometry (iDXA, GE Lunar). Mann-Whitney U test and Spearman's correlation methods were used for statistical analysis. Results. Participants included 69 men aged 71.236.85 y and 145 women aged 70.526.10 y. All the components of lipid profile were statistically significantly higher in women than in men. Total cholesterol was 6.071.23 mmol/l in women and 5.331.29 mmol/l in men ($p<0.001$), LDL - 3.831.07 mmol/l and 3.341.19 mmol/l ($p=0.001$), HDL - 1.660.44 mmol/l and 1.540.63 mmol/l ($p=0.011$) and TG - 1.370.61 mmol/l and 1.150.57 mmol/l ($p=0.002$), respectively. Total body BMD was higher in men than in women (1.1980.162 and 1.0320.132, respectively, $p<0.001$). PTH did not differ between genders: 49.9819.54 pg/ml in women and 47.9518.23 pg/ml in men. There was found weak correlation of HDL ($r=-0.20$, $p=0.022$) and LDL ($r=0.19$, $p=0.035$) with total body BMD in women. TG was statistically significantly negatively correlated to the s-CTX-I ($r=-0.23$, $p=0.007$) and PINP ($r=-0.25$, $p=0.002$) in women. No such relationship was found in men.

In conclusion we found that triglycerides negatively associated with bone turnover markers s-CTX-I and PINP only in women.

Disclosures: Marija Tamulaitiene, AMGEN, 8; AMGEN, 5; GSK, 8

SA0322

Evaluation of Undercarboxylated Osteocalcin (ucOC) in the Treatment for Osteoporosis: A Clinical Practice-Based Study. Yoichi Kishikawa*. Kishikawa Orthopedic Surgery, Japan

Purpose: Undercarboxylated osteocalcin (ucOC), which is a marker of deficiency of vitamin K2 (VK2), is an index of fracture risk independently on bone mineral density (BMD). The cut off values of serum ucOC for increased fractures risk have been determined as 4.5 ng/mL in patients without any medication for osteoporosis and 2.6 ng/mL in patients who are receiving bisphosphonate (BP) treatment. We evaluated serum ucOC levels in 255 patients (16 men and 239 women) with osteoporosis. Methods: The following information was obtained from all patients when serum ucOC levels were measured; age, sex, history of fractures, previous glucocorticoid use, BMD measured by a DXA, bone metabolism markers, and medication for osteoporosis for more than 3 months. Patients who were receiving glucocorticoid or BP treatment for more than 6 months were excluded from the analysis. Results: Serum ucOC levels were significantly lower in patients who were receiving BP treatment, but not raloxifene (RLX) or vitamin D (VD) treatment, than in those without any medication ($P<0.05$). In patients who were receiving BP or RLX treatment, but not VD treatment, ucOC levels were significantly correlated with serum NTX levels ($P<0.001$ and $P=0.007$, respectively). Among patients who were receiving BP treatment, the proportion of patients who showed serum ucOC levels less than 2.6 ng/mL was 51.3% despite lower serum NTX levels (<13.6 nmol BCE/L). A significant difference in serum ucOC levels was found between patients with lower serum NTX (<13.6 nmol BCE/L) and patients with higher serum NTX (13.6–16.5 nmol BCE/L). In patients who received combined treatment with BP or RLX and VK2, serum ucOC levels were significantly decreased than those with a single treatment with BP or RLX, and this reduction was greater in patients treated with BPs than those treated with RLX. Discussion: The present study showed that serum ucOC levels were significantly lower in patients who were receiving BP treatment than those without any medication for osteoporosis, and that serum ucOC was correlated with serum NTX in patients who were receiving BP or RLX treatment. We propose that when we use BPs, a two-step strategy utilizing bone metabolism markers is recommended. Firstly, the effect of BPs can be determined by measuring a bone resorption marker such as serum NTX. Secondly, fracture risk can also be determined measuring ucOC using a cut off value of 2.6 ng/mL.

Disclosures: Yoichi Kishikawa, None.

SA0323

Intravenous Zoledronate use in Adult Delayed Non-Union Fracture Healing. Nigel Gilchrist*, David Little², John McKie¹. ¹Department of Orthopaedic Medicine & Surgery, Christchurch Hospital, New Zealand, ²The Children's Hospital At Westmead, Australia

Introduction: Multiple surgical procedures are often required in patients with compound lower leg fractures with the result of either non-union or malunion with significant shortening and angulation.

Methods: We examined the effect of pulsed intravenous zoledronate, calcium and vitamin D supplements in such patients to assist bone healing. We included 7 patients who had malunion or non-union with shortening/angulation who required tibial revision surgery. Six males, age range between 42 – 68 years were included and 1

female aged 39. All subjects had undergone corrective revision surgery at least 2 – 3 years after their original compound fracture. All patients had been treated with an external fixator for deformity correction and lengthening but had failed to heal within 6 months of the revision surgery. All patients had biochemical/hormonal profile performed and technetium bone scans to assess ongoing local bone turnover. All patients except the 39 year old female had an active bone scan indicating ongoing local bone turnover and were therefore treated 6 weekly on 3 – 4 occasions with pulsed intravenous zoledronate and prior and post treatment with calcium and vitamin D. The dose of zoledronate 0.0125mg per Kg for the first dose and 0.025mg per Kg for subsequent dose and repeat doses were given on evidence of radiological healing.

Results: In all cases the fracture deficit healed allowing early (2 - 8 months) removal of the Taylor spatial frame. There were no adverse effects and no continuation of non-union at 6 month review.

Conclusion: It appears that pulsed low dose intravenous Zoledronate with Calcium and Vitamin D may aid healing of non-union fractures.

Disclosures: Nigel Gilchrist, None.

SA0324

Serum Sclerostin Level and its Association with Bone Turn-over Markers in Type 2 Diabetes. Megumi Shibata*, Atsushi Suzuki¹, Sahoko Sekiguchi-Ueda², Shogo Asano³, Yasumasa Yoshino², Masaki Makino², Nobuki Hayakawa³, Mitsuvasu Itoh³. ¹Fujita Health University, Division of Endocrinology, Japan, ²Fujita Health University, Japan, ³Toyokawa city hospital, Japan

Background: Accumulating evidences suggest that type 2 diabetes mellitus have an increased risk of fractures even with higher bone mineral density. In bone metabolism in diabetes patients, low bone formation seems to contribute to deteriorate so-called bone quality. Higher baseline levels of pentosidine and homocysteine are potential risk factors for osteoporotic fractures, but precise assessment of bone fragility in diabetes patients with a specific surrogate marker is still difficult. In the present study, we explored serum level of sclerostin, an inhibitor of bone formation, to assess its possible role to reflect bone metabolic disorder in diabetes patients.

Subjects and methods: We enrolled 49 patients (M/F= 26/23; age, 63.2 11.6 years) who visited our hospital for the treatment of type 2 diabetes mellitus. Mean HbA1c level was 6.8 0.9%. Serum sclerostin concentration was measured by ELISA (Biomedica GmbH, Wien, Austria).

Results: Mean serum sclerostin level was 28.1 21.1 pmol/l. Mean serum concentrations of iPTH, 25-OHD, serum NTx, BAP, homosistein, osteocalcin and pentosidine were 45.7 18.2 pg/ml, 25.1 7.5 ng/ml, 11.5 4.6nmolBCE/mmol, 22.3 6.3U/L, 11.3 5.8μmol/l, 3.8 1.9ng/ml and 0.06 0.06μg/ml, respectively. Sclerostin was not related to either iPTH, 25-OHD, serum NTx, BAP, homosistein or osteocalcin. On the other hand, serum sclerostin level was significantly associated with serum pentosidine concentration ($r=0.72$, $n=49$, $p<0.001$).

Conclusion: These results suggest that serum sclerostin could be another candidate to evaluate metabolic disorder in bone in type 2 diabetes.

Disclosures: Megumi Shibata, None.

SA0325

See Friday Plenary Number FR0325.

SA0326

Bone Loss in Ambulatory Patients with Multiple Sclerosis. Vit Zikan*, Michaela Tyblová², Ivan Raska¹, Eva Havrdová², Dana Michalská¹, Zdenek Telicka¹. ¹Department of Internal Medicine 3, Charles University Faculty of Medicine 1, Czech Republic, ²Department of Neurology, Charles University Faculty of Medicine 1, Czech Republic

Patients with multiple sclerosis (MS) have multiple risk factors for osteoporotic fractures, such as progressive immobilization, long-term glucocorticoids (GC) treatment or vitamin D deficiency. The aim of the present study was to investigate the relationships among the level of disability, GC use, vitamin D status, body composition and bone mineral density (BMD) in ambulatory patients with MS. Methods: We studied 90 men and 120 premenopausal ambulatory women with MS. Dual-energy X-ray absorptiometry was used to analyze body composition and BMD. Motor function of the patients was evaluated using the Kurtzke Expanded Disability Status Scale (EDSS). GC use was determined from medical records. Results: Our results showed that high proportion of patients with MS have low levels of 25-hydroxyvitamin D. Multiple regression analysis indicated that EDSS and Lean Mass were the most significant parameters associated with BMD in the proximal portions of the femur. Conclusion: In MS patients, both in men and premenopausal women, the level of disability and Lean Mass were the most significant parameters which correlated with the BMD at the proximal femur. Vitamin D insufficiency is common in patients with MS.

Disclosures: Vit Zikan, None.

SA0327

See Friday Plenary Number FR0327.

SA0328

See Friday Plenary Number FR0328.

SA0329

Estimation of Fracture Probability of Glucocorticoid-Induced Osteoporosis by a Logistic Regression Model. Ikuko Tanaka^{*1}, Shigenori Tamaki², Hisaji Oshima³. ¹National Center for Geriatrics & Gerontology, Japan, ²Nagoya Rheumatology Clinic, Japan, ³Tokyo Medical Center, Japan

[Background and purpose] FRAX made by WHO is a useful tool and is utilized all over the world. Input parameters for FRAX includes exposure to glucocorticoids but not dose of glucocorticoids which increases fracture risk. FRAX underestimates the possibility of fracture by glucocorticoid induced osteoporosis. The purpose of this study is to make a formula to calculate probability of fracture with BMD and dose of glucocorticoids. [Methods] Subjects were 220 patients with connective tissue diseases recruited in two years cohort study. Morphological incident fracture of the spine was measured with X-ray. A formula to calculate the two year probability of fracture was induced from the results of logistic regression analysis. Predictive accuracy of the fracture with this formula was compared to that with Japanese treatment guideline of glucocorticoid induced osteoporosis (JTG-GIOP). [Results] (1) Logistic regression analysis identified previous fracture, mean dose of glucocorticoids, %YAM, age, and sex as fracture risks. (2) A formula to calculate fracture probability was made. (3) Predictive accuracy of the formula and JTG-GIOP were 83.2% and 60.9%, respectively. [Conclusion] The probability formula is useful to predict fracture by glucocorticoid induced osteoporosis.

Disclosures: Ikuko Tanaka, None.**SA0330**

See Friday Plenary Number FR0330.

SA0331

See Friday Plenary Number FR0331.

SA0332

See Friday Plenary Number FR0332.

SA0333

Intra-rater Reliability of Dual Energy X-ray Absorptiometry-based Measures of Vertebral Height and Consistency of Vertebral Deformity Classification in Postmenopausal Women. Alison M. Bonnyman¹, Colin Webber², Paul W. Stratford¹, Norma MacIntyre^{*3}. ¹School of Rehabilitation Science, McMaster University, Canada, ²Hamilton Health Sciences, Canada, ³McMaster University, Canada

Purpose: Bone geometry adapts to site-specific mechanical forces. Few methods exist to assess change in mineral distribution in the spine. Dual-energy X-ray absorptiometry (DXA) can provide measures of vertebral height, in mm, however the reliability is unclear. The commercial software uses the ratios of vertebral height measures to grade each vertebral body shape in terms of deformity. The primary purpose of this study was to estimate intra-rater reliability of DXA-based vertebral height measures in postmenopausal women. A secondary purpose was to determine the consistency in vertebral deformity grade on duplicate analyses.

Methods: Vertebral fracture assessment images of spinal levels L4 to T4 were acquired for 32 postmenopausal women (mean(SD) age: 70.4(7)y) using DXA (Hologic Discovery A). Each image was analyzed twice (4 weeks apart) by a single rater. Hologic's semi-automated software and a pre-determined protocol were used to landmark superior and inferior endplates of each visible vertebral body in order to derive measures of anterior, middle, and posterior vertebral heights. A minimum sample size of 22 images was required given a desired reliability (intraclass correlation coefficient, ICC) ≥ 0.80 with a lower 95% confidence interval (CI) of 0.70. Grades of vertebral deformity (normal, mild fracture, moderate fracture, severe fracture) were generated in duplicate for 192 vertebrae. Level of agreement across all grades was characterized using Cohen's unweighted kappa (κ) and the observed proportion of agreement (Pobs). Pobs was also used to characterize agreement for each grade separately. For both statistics, perfect agreement = 1.

Results: Above T9, endplates were visible in ≤ 21 images (66%). For measures of vertebral height at L4 to T9, reliability was acceptable [0.87(95%CI: 0.74, 0.94) \leq ICC \leq 0.98(95%CI: 0.95, 0.99)] except for posterior vertebral height at T9 [ICC = 0.62 (95%CI: 0.15, 0.84)]. Table 1 compares the grade of vertebral deformity obtained on each analysis. Overall, κ (95%CI) = 0.50(0.28, 0.72) and Pobs(95%CI) = 0.91(0.85, 0.94). For normal, mild, moderate, and severe grades, Pobs(95%CI) = 0.92(0.86, 0.95), 0.24(0.08, 0.50), 0.36(0.12, 0.68) and 0.50(0.03, 0.97), respectively.

Conclusions: Excellent intra-rater reliability was achieved for vertebral height measures from T9 (excluding T9 posterior vertebral height) to L4 in postmenopausal women using the pre-determined protocol. Consistency in grading fracture deformities was poor.

		Analysis 2				Total
		Normal	Mild	Moderate	Severe	
Analysis 1	Normal	165	7	3	0	175
	Mild	4	4	0	0	8
	Moderate	1	2	4	0	7
	Severe	0	0	1	1	2
Total		170	13	8	1	192

Table 1. Vertebrae graded as normal, or fractured (mild, moderate, severe) on each analysis.

Disclosures: Norma MacIntyre, None.**SA0334**

Quantitative Morphometry on Spinal X-Rays: Long-Term Precision of a New Workflow Tool for Measuring Vertebral Body Height in Non-Fractured Vertebrae. Klaus Engelke^{*1}, Bernd Stampa¹, Peter Steiger², Thomas Fuerst³, Harry Genant⁴. ¹Synarc Inc, Germany, ²Optasia Medical, USA, ³Synarc, Inc., USA, ⁴UCSF/Synarc, USA

Vertebral body height assessed by 6-point quantitative morphometry (QM) provides useful information for the diagnosis of prevalent and incident vertebral fractures. The aim of this study was to evaluate the long-term longitudinal precision of a new QM tool (SpineAnalyzer, Optasia Medical Ltd, Cheadle, UK) in a research setting for the measurement of vertebral body height in non-fractured vertebrae.

In this study the default automatic placement provided by SpineAnalyzer was compared with a standard manual 6-point placement, which was used as a reference standard. In contrast to clinical routine, default automatic placements were not corrected by the reader even if they were obviously incorrect. Lateral lumbar and thoracic x-rays from 48 osteoporotic postmenopausal women (73.85.2 y, femoral neck T-score = -2.70.6) were retrospectively evaluated at two visits 3 years apart. None of the subjects had prevalent or incident fractures as evaluated by SQ reading. For each patient T4 to L4 levels were analyzed except for 8 vertebrae judged unreadable at one of the visits due to poor image quality. Standard QM was done by different operators and the automatic analysis was done by the same operator. Baseline and year 3 data were analyzed in separate sessions. Anterior (HA), mid (HM) and posterior (HP) heights were calculated from the 6 points using standard algorithms. The root mean square coefficient of variation (rmsCV) between the two visits was calculated independently for the automatic SpineAnalyzer and the standard QM analysis for each of the 3 heights and for each vertebral level.

Long-term mean rmsCV SD values (averaged over all vertebral levels) for standard QM were 4.40.8 % (HA), 4.00.7% (HM) and 4.70.7% (HP) compared to 3.9 0.9% (HA), 3.40.7% (HM) and 3.51.0% (HP) for the automatic analysis. Significant differences (paired T-tests) were found for all three heights of T10 and T8, and in addition for HP of T9, T11 and T12 and for HM of T11.

Overall the longitudinal precision of the automated analysis over a period of 3 years was slightly superior in some but not in all thoracic vertebrae in particular for the posterior heights. Precision was comparable in the lumbar vertebrae. The results show that the automated analysis using SpineAnalyzer works well in non-fractured vertebrae. However, the performance of the tool on fractured vertebrae has not been tested here.

Disclosures: Klaus Engelke, Synarc, 3**SA0335**

See Friday Plenary Number FR0335.

SA0336

Reproducibility of High Resolution Peripheral Quantitative Computed Tomography (HR-pQCT): Influence of Examination Site and Age on Measurement Variability. Margaret Paggiosi¹, Richard Eastell², Jennifer Walsh^{*1}. ¹Sheffield Teaching Hospitals NHS Foundation Trust, United Kingdom, ²University of Sheffield, United Kingdom

High resolution peripheral quantitative computed tomography (HR-pQCT) is a powerful tool for the assessment of densitometric and micro-architectural properties of trabecular and cortical bone. However, further evaluation of the measurement variability, for the variables obtained with this technique, is required.

The aims of this study were to i) assess the reproducibility of HR-pQCT measurement variables and ii) investigate differences in measurement variability with a) examination site and b) age.

We conducted a cross-sectional observational study of healthy men and women ages 30-32 years ('younger', n=60) and 70+ years ('older', n=60). Duplicate HR-pQCT examinations of the distal radius and distal tibia, with re-positioning, were performed using the XtremeCT (Scanco Medical AG, Zurich, Switzerland). All HR-pQCT images were processed using standard and extended cortical bone analysis techniques (Burghardt et al. 2010. Bone 47: 519-528). Measures of trabecular and cortical bone density, trabecular number and thickness, and cortical porosity were acquired. Percent short-term root mean square coefficient of variation (%RMSCV) for each of these variables was calculated. The influence of a) site and b) age, on variability was investigated by examining differences in the measurement variable SDs using variance ratio tests (F-tests), with P<0.05 indicating statistical significance.

Lower %RMSCVs were observed for the tibia rather than the radius measurement variables. Age-dependent differences in measurement variable SDs were detected for cortical bone density, and cortical porosity (P=0.023 to P=0.001), with greater measurement variability being observed for the older group. There were also site-dependent differences in measurement variable SDs for cortical measurements. Variability at the radius was greater than at the tibia for cortical bone density and cortical porosity (P<0.001 to P=0.001).

We conclude that differences in measurement variability in the cortex relate to examination site and age. Measurements for the tibia were less variable, than those for the radius, and this may be explained by the larger cortical bone volumes being examined. The greater measurement variability observed for older volunteers may be due to the loss of bone micro-architectural integrity with age.

Percent short-term root mean square coefficients of variation (%RMSCVs), for densitometric and micro-architectural measurement variables determined by high resolution peripheral computed tomography (HR-pQCT), in younger (30-32 years) and older (>70 years) men and women.

Measurement Variable	Examination Site	%RMSCV for younger volunteers	%RMSCV for older volunteers
Trabecular bone density	Radius	1.0	1.2
Trabecular number		5.8	5.8
Trabecular thickness		5.5	5.1
Cortical bone density †		1.9	2.4
Cortical porosity †*		13.3	13.4
Trabecular bone density	Tibia	0.5	0.5
Trabecular number		3.6	5.3
Trabecular thickness		3.6	5.2
Cortical bone density †*		0.3	0.4
Cortical porosity †*		5.2	6.3

† and * denote significant differences in measurement variable SDs when examining the effect of a) site and b) age, respectively. Significance testing was based on the variance ratio test (F test).

Table 1

Disclosures: Jennifer Walsh, None.

SA0337

Reproducibility of HR-pQCT measurements of the distal radius: influence of casting. Martijn de Kooter¹, Sandrine Bours^{*2}, Tineke Van Geel³, Chris Arts⁴, Paul Willems⁴, Joop Van Den Bergh⁵, Piet Geusens⁶, Bert Rietbergen⁷. ¹Eindhoven University of Technology, Netherlands, ²Maastricht University Medical Centre, The Netherlands, ³Maastricht University, The Netherlands, ⁴Maastricht University, Dept. of Orthopaedic Surgery, Netherlands, ⁵VieCuri MC Noord-Limburg & Maastricht UMC, USA, ⁶University Hasselt, Belgium, ⁷Eindhoven University of Technology, The Netherlands

Background: By using high resolution peripheral quantitative computed tomography (HR-pQCT), it is possible to obtain information of the cortical and trabecular microarchitecture of the bone. The reproducibility of HRpQCT measurements of the human radius in vitro is <3%. Subject motion is an important artifact affecting HRpQCT measurements. No data are available about the reproducibility with a synthetic cast.

Methods: The dominant radii of 15 healthy volunteers aged 20-40 year were scanned with the HRpQCT scanner (XtremeCT, Scanco) using the default in vivo settings given by the manufacturer, resulting in a voxel size of 82 µm. The length of the scan was extended to two stacks (220 slices), with a total duration of 5.8 minutes. Each volunteer had four scans, two with a synthetic cast and two without cast. CT Carpal X1 performed by Pearltec was used for fixation. In order to calculate short-term

precision, we used root-mean-square (RMS) averages of standard deviations of repeated measurements (SD). Precision errors were also expressed in coefficient of variation (CV). The data were tested to be normally distributed and a Pearson correlation test was applied, resulting in a coefficient of determination (R²). Reproducibility was assessed in two "groups": measurements without a cast (group 1) and measurements with a cast (group 2).

Results: In group 1, we found a RMS-CV of 0.98% (R² 0.99) for bone density and a RMS-CV of 3.77% (R² 0.90) and 3.49% (R² 0.94) for trabecular number (Tb.N) and trabecular thickness (Tb.Th), respectively. In group 2 the RMS-CV was 0.75% (R² 0.99), 2.56% (R² 0.95), 2.47% (R² 0.97) for density, Tb.N and Tb.Th, respectively. Linear regression analysis was performed to compare group 2 (with cast) with group 1 (without cast). The slope is 0.95 for density (R² 0.99), 0.91 for Ct.Th (R² 0.99), 0.87 for Tb.N (R² 0.92), 0.80 for Tb.Th (R² 0.96) respectively. Motion artifacts were found in 2 subjects without cast and in none with a cast.

Conclusions: The variation in each group was lower than 4%. With a synthetic cast we saw less variation, which is possibly due to better fixation with less movement artefacts than in the group without a cast. Motion artefacts occurred in 7% of measurements. A high correlation was found between measurements with and without a cast in young healthy volunteers.

Disclosures: Sandrine Bours, None.

SA0338

Calcaneal Quantitative Ultrasound Compared to Hip and Femoral Neck DXA in People with Spinal Cord Injury. Danielle Barkema^{*1}, Nicole Wysocki², Lisa Streff², Sheena Bhuvu³, Rachel Welbel⁴, Lisa Ruppert², Sarah Linn², Dorian Samuels², Keith Gordon¹, Thomas Schnitzer¹. ¹Northwestern University, USA, ²Rehabilitation Institute of Chicago, USA, ³Texas A&M Health Science Center, USA, ⁴Chicago Medical School, USA

Purpose: Obtaining DXA data in people with spinal cord injury (SCI) is difficult; use of calcaneal quantitative ultrasound (QUS) measurements could provide a useful means to screen if found to have acceptable sensitivity and specificity. This study was performed to compare calcaneal QUS measurements to those obtained by DXA at the hip and femoral neck in people with SCI and evaluate the utility of these measurements to screen for osteoporosis in this population.

Methods: A convenience sample of 36 individuals (age: 38.1 ± 15.2 yrs) with a mean duration since SCI of 4.8 ± 8.4 years underwent bone density evaluation using a Hologic QDR-4500A densitometer and a GE Lunar Achilles Express ultrasonometer. BMD T-scores were measured at the right and left total hip and femoral neck by DXA, whereas T-scores were measured at the right and left calcaneus by QUS.

Results: Mean BMD T-scores by DXA for the right and left total hip were -1.0 ± 1.6 and -1.3 ± 1.6, respectively. Mean QUS T-scores were -1.2 ± 2.1 for the right calcaneus and -1.1 ± 2.1 for the left calcaneus. Right and left hip DXA T-scores were strongly associated with corresponding right and left calcaneal QUS T-scores (Right: r=0.78, p<0.001; Left: r=0.75, p<0.001; Figure 1). Right and left femoral neck DXA T-scores also showed a fairly strong relationship with right and left calcaneal QUS T-scores (Right: r=0.70, p<0.001; Left: r=0.67, p<0.001). 14 individuals had calcaneal QUS T-score ≤ -2.5, whereas 12 individuals had hip or femoral neck DXA T-scores ≤ -2.5. Using a QUS T-score cut-off of -2.5, the sensitivity of calcaneal QUS to detect osteoporosis (DXA BMD T-score ≤ -2.5) at the hip or femoral neck was 0.93 with a specificity of 0.88; the positive predictive value of calcaneal QUS was 0.79; negative predictive value was 0.96; and the area under the ROC curve was 0.895.

Conclusions: Strong correlation exists between measurement of T-scores by QUS at the calcaneus and measurement of T-scores by DXA at the hip and femoral neck in people with SCI. Calcaneal QUS measurement has favorable characteristics for use as a screening tool for osteoporosis in SCI.

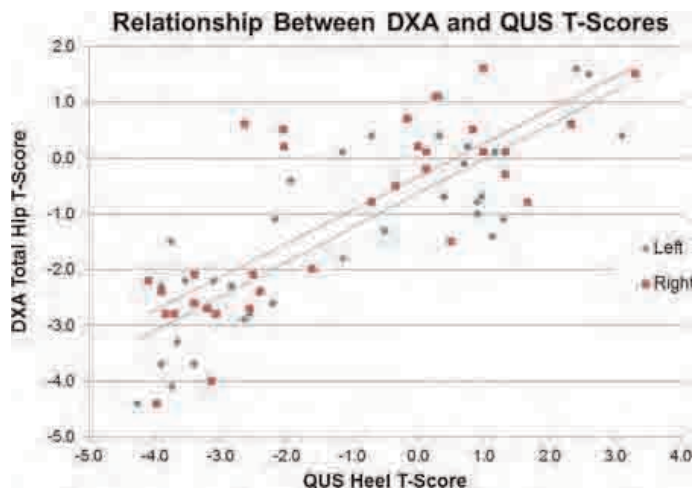


Figure 1

Disclosures: Danielle Barkema, None.

SA0339

See Friday Plenary Number FR0339.

SA0340

Quantitative Ultrasound Measurements at the Heel Predict the Risk of Fragility Fractures in Postmenopausal Women and would Save the use of Densitometry. María Jesus Gomez de Tejada¹, Pedro Saavedra¹, Diego Hernandez², Esther Gonzalez-Padilla², Manuel Sosa-Henriquez^{*3}.

¹Professor, Spain, ²Dr., Spain, ³University of Las Palmas de Gran Canaria, Spain

Introduction: Heel QUS have been used for screening patients to evaluate risk of osteoporotic fractures. The aim of this study was to evaluate the ability of QUS to identify women with low risk of osteoporotic fractures and to avoid them the performance of a densitometry with low possibility of error.

Methods: We studied 1,132 postmenopausal women. A previously validated questionnaire about risk factors for osteoporosis was filled and we also performed on them QUS heel measurements, DXA at the lumbar spine and proximal femur, X-Ray of the dorsal and lumbar spine and also registered the non-vertebral fractures. OC curve, sensibility, specificity, predictive values and likelihood ratios were estimated.

Results: A QUI value higher than 88.5 in postmenopausal women with an age higher than 58 years old would permit to avoid the performance of a DXA in 43.1% of our population. The area under ROC curve is high, 0.8363 (95% CI 0.8249; 0.8477). This provides a sensitivity of 88.8 (95% CI: 81.4; 93.5) with a negative predictive value of 93.8 (95% CI: 89.4; 96.4) with a high specificity: 70.4 (95% CI 64.6; 75.7).

Conclusion: A value of QUI higher than 88.5 in women aged more than 58 years old is associated to a very low risk of all fragility fractures, with a sensitivity that could reach to 93.5% and a negative predictive value as high as 96.4%. This could avoid the measurement of DXA in 43.1% of postmenopausal women.

Area under ROC curve (AUC)	0.8363 (0.8249; 0.8477)
Sensitivity	88.8 (81.4; 93.5)
Specificity	70.4 (64.6; 75.7)
Positive predictive value	55.6 (48.7; 62.6)
Negative predictive value	93.8 (89.4; 96.4)
Positive likelihood ratio	3.00 (2.45; 3.68)
Negative likelihood ratio	0.15 (0.08; 0.27)
Error rate	24.18 (20.56; 28.83)

Table 1. Area under ROC curve, Sensitivity, Specificity, Positive Predictive Value

Classification Tree for total fractures

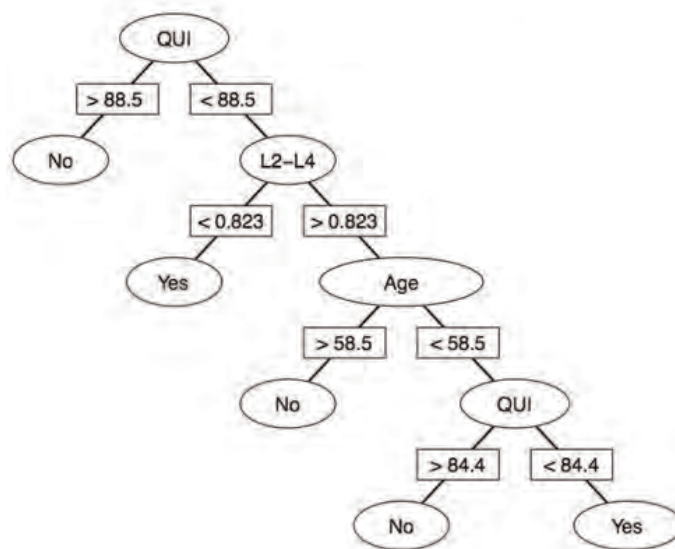


Figure 1. Classification tree for total fractures

Disclosures: Manuel Sosa-Henriquez, None.

SA0341

A Relationship Between Bone Mineral Density and Metabolic Syndrome in Koreans : The Chungju Metabolic Disease Cohort Study. Eun Hee Jang¹, Moo-Il Kang², Sun Hee Ko^{*3}, Ki-Hyun Baek¹. ¹Division of Endocrinology & Metabolism, Department of Internal Medicine, The Catholic University of Korea, South Korea, ²Seoul St. Mary's Hospital, South Korea, ³The Catholic University of Korea, South Korea

BACKGROUND Many studies have showed that the metabolic syndrome (MS) is associated with low-grade inflammation. In respect of bone, low-grade systemic inflammation activates bone resorption and may lead to reduce bone mineral density (BMD). The relationship between metabolic syndrome and bone mineral density has been actively investigated, but the results are inconsistent. This study aimed at identifying association between bone mineral density and metabolic syndrome in a community-based cohort in Korea. **MATERIALS AND METHODS** We evaluated a population-based, cross-sectional analysis of 2729 postmenopausal women and 1701 men aged 40 years and older in rural area of Chungju, Korea. Information on sociodemographic characteristics and diet intake were collected by an interviewer-administered standardized questionnaire. Bone mineral density was measured by central bone densitometry (Hologic QDR4500). MS was defined by American Heart Association/National Heart, Lung, and Blood Institute (AHA/NHLBI). **RESULTS** The prevalence of metabolic syndrome 36.5% in men and 55.2% in postmenopausal women. Men over 40 years and postmenopausal women with metabolic syndrome had higher femur and Lumbar spine BMD in the age-adjusted model. After multivariable adjustment, femur total BMD and femur neck were significantly lower among men with metabolic syndrome (0.746 g/cm², 0.891 g/cm²) than those without (0.759 g/cm²; p=0.035, 0.905 g/cm²; p=0.023). However, in postmenopausal women, there was no significant association between MS and bone mineral density. **CONCLUSION** In a community-based cohort in Korea, men older than 40 years with metabolic syndrome had lower femoral BMD, but there was no association between bone mineral density and MS in postmenopausal women.

Disclosures: Sun Hee Ko, None.

SA0342

Association of Bone Mineral Density with Insulin Sensitivity Indices in Normoglycemic Men and Women in the Fels Longitudinal Study. Naila Khalil^{*1}, Miryoung Lee², Audrey Choh¹, Keith Wurzbacher¹, Dana Duren¹, Cameron Wm Chumlea¹, Bradford Towne¹, Roger Siervogel², Stefan Czerwinski². ¹Wright State University, USA, ²Wright State University Boonshoft School of Medicine, USA

Purpose of the study: Insulin promotes collagen synthesis in osteoblasts in vitro, but it is not clear if this effect is impaired with the insulin resistance that often occurs prior to the onset of hyperglycemia. Few studies have examined the association between insulin resistance and bone mineral density (BMD) in healthy men and

women. The aim of our study was to explore relationships between BMD and insulin sensitivity, controlling for age and body composition.

Methods: We analyzed cross-sectional data from 673 apparently healthy adults (311 men; 362 women) aged ≥ 30 years (mean = 50 years) participating in the Fels Longitudinal Study. BMD (g/cm²) of the lumbar spine and femoral neck was measured using dual-energy x-ray absorptiometry. Fasting insulin and glucose were assayed using standard laboratory procedures. Insulin resistance was estimated by calculating both the glucose/insulin ratio and the Homeostasis Model Assessment-Insulin Resistance score (HOMA-IR). General linear models were used to evaluate the relationship between insulin resistance indices and BMD in each sex adjusting for age, weight, and stature. Each insulin resistance trait was divided into tertiles for analysis.

Results: In women, higher insulin levels were associated with significantly lower BMD in both the lumbar spine ($p=0.038$) and the femoral neck ($p<0.001$). A lower glucose/insulin ratio was also associated with lower BMD at both sites ($p<0.01$). For example, lumbar spine BMD was 0.980.01g/cm² in the lowest glucose/insulin ratio group compared to 1.030.01g/cm² in the highest group. Further, higher HOMA-IR levels were significantly associated with lower BMD in the femoral neck (0.760.1 vs. 0.790.01 vs. 0.800.01 g/cm², $p=0.007$). Among men, there were significant relationships between insulin resistance traits and BMD at the lumbar spine; both lower insulin levels and lower HOMA-IR scores were associated with increased BMD respectively.

Conclusions: These results suggest that even sub-clinical differences in insulin resistance are associated with BMD at different skeletal sites in a healthy sample of normoglycemic men and women.

Disclosures: Naila Khalil, None.

SA0343

Body Composition and Serum Cholesterol Play the Most Relevant Role on High Bone Mineral Density in Healthy Women, Regardless Physical Activity, Dietary Intake, Bone Remodeling and Menopausal and Vitamin D Status. Karin Sarkis*¹, Marcelo Pinheiro², Vera Szeinfeld³, Ligia Martini¹. ¹University of Sao Paulo, Brazil, ²Sao Paulo Federal University/ Unifesp/ Escola Paulista De Medicina, Brazil, ³UNIFESP/EPM, Brazil

Objective: The aim of this study was to evaluate the main aspects related to high bone mineral density (HBMD) in healthy women. **Patients and Methods:** From June 2005 to October 2010, all women that performed BMD measurements, from metropolitan area of Sao Paulo, Brazil, were enrolled in this cross-sectional study. After database review, almost 22000 bone scans were identified, of whom 421 (1.96%) had HBMD, defined as above 1.400 g/cm² at spine or above 1.200 g/cm² at femur and T-score above 2 SD in both sites. The exclusion criteria were aged 60 years or more, black background, pregnant, obesity and osteoarthritis at any site. Women with concomitant diseases or drugs that affect bone tissue were excluded. A total of 40 women with HBMD were included and matched to 40 healthy women with normal BMD, paired to age, ethnicity, BMI and menopausal status. All women answered a clinical questionnaire based on risk factors related to bone mass, including details about lifestyle and medical history. Dietary intake was assessed by a validated food frequency questionnaire. Besides, they performed body composition by DXA (DPX MD+, GE-Lunar) and thoracic and lumbar radiographs to better define spine's degenerative changes as well as exclude other causes of spine HBMD, including metastasis and Paget disease. Biochemical parameters included serum lipids, hormone and mineral profile, vitamin D status, bone markers and calcium metabolism. Using a forward selective linear regression model, the main variables associated with HBMD were investigated. Significant P value was set as 0.05. **Results:** There were not significant differences between groups regarding to physical activity, smoking, calcium and vitamin D intake, and lab exams, including serum CTx and hormone parameters. Nonetheless, HBMD women had higher intake of protein, phosphorus and zinc, adjusted to energy. Moreover, they had higher fat free mass ($p=0.03$) and skeletal lean mass (SLM) ($p<0.01$) than controls. After statistical adjustments, total fat mass (TFM) and LDL-cholesterol plays a negative role on BMD. On the other hand, SLM was considered as protective on bone mass, according the equation: [Femoral neck = 1.096 - 0.272 (TFM) - 0.396 (LDL-C) + 0.337 (SLM); R²adjusted = 34.7; $p<0.001$]. **Conclusion:** Our data demonstrate that the body composition and serum cholesterol are the main aspects related to HBMD, regardless physical activity, dietary intake, bone remodeling and menopausal and vitamin D status.

Disclosures: Karin Sarkis, None.
This study received funding from: FAPESP

SA0344

Correlates of Higher Bone Mineral Density in Inuit Preschoolers Living in the Arctic. Jessy Havek*, Hope Weiler, Grace Egeland. McGill University, Canada

Introduction: Aboriginal adults, but not newborns, have lower bone mineral density (BMD) compared to their white counterparts. Although 60-80% of peak bone mass is determined by genetics, nutrition and lifestyle factors can be modified to improve bone status, particularly in the first 2 or 3 decades of life.

Purpose: Investigate the effects of anthropometric, dietary, biochemical and lifestyle factors associated with higher BMD among Inuit preschoolers (3- 5 y) living in Arctic communities (56° 32'-72° 40'N).

Methods: Children were selected randomly in summer and early fall ($n = 282$). Dietary intake was assessed through the administration of a 24-h dietary recall and a food frequency questionnaire (FFQ). Anthropometry (height, weight) was measured using standardized procedures. Plasma 25-hydroxy vitamin D (25(OH)D) and parathyroid hormone was measured using a chemiluminescent assay (Liaison, Diasorin). Plasma alkaline phosphatase and total calcium were measured by Beckman Coulter. Heel BMD (g/cm²) was estimated using ultrasound (Sahara Sonometer, Hologic Inc.). Pearson's correlations, t-tests, ANOVA followed by Bonferroni and logistic regression were used to identify associations between BMD and its correlates.

Results: Heel BMD was not different by age groups (y), sex (M/F), calcium intake above or below the median (mg/d), vitamin D intake above or below the median ($\mu\text{g/d}$), number of milk servings (250 ml) above or below the median and plasma 25(OH)D concentration above or below the median (nmol/L). Higher BMD was observed among children in the third tertile of body mass index (BMI) percentiles using WHO categories and having intakes of monounsaturated fat and saturated fat above the median. However, when accounting for age, only saturated fat intake for 5 y children, and BMI categories across all age groups remained significant. Using logistic regression, BMD predictors among Inuit preschoolers were higher BMI, calcium intake above the adequate intake and lower latitude.

Conclusions: These data suggest that factors in support of bone mineral acquisition in young Inuit children are calcium intake, BMI and latitude as a proxy for year endogenous synthesis of vitamin D. Since the dietary data was mainly derived from the 24 h recall data, further investigation assessing usual intakes of traditional foods and nutrients affecting BMD using multiple 24 h recalls and FFQ along with serial assessment of vitamin D status of Inuit children across seasons is required.

Disclosures: Jessy Havek, None.

SA0345

High Prevalence of Osteoporosis in Female Patients Undergoing Total Knee Arthroplasty for Advanced Knee Osteoarthritis. Ja-Young Choi¹, Chong Bum Chang*², Tae Kyun Kim³, Eun Seok Seo³. ¹Seoul National University Hospital, South Korea, ²Seoul National University Bundang Hospital, Rok, ³Seoul National University Bundang Hospital, South Korea

Purpose: This study sought to determine whether elderly female patients with advanced knee osteoarthritis (OA) warranting total knee arthroplasty (TKA) differ in terms of bone mineral density (BMD) from community-based females without significant knee OA, and to determine whether preoperative clinical statuses are associated with BMD in females with advanced knee OA warranting TKA.

Methods: Study subjects were matched for age (486 subjects; 243 in each group), and separately for age and body mass index (424 subjects; 212 in each group). BMD T-scores of lumbar and proximal femurs were compared using the Student's t-test. Prevalences of osteoporosis (T score ≤ -2.5 SD) were compared using the chi-square test. In patients with advanced knee OA, regression analyses were performed to determine whether preoperative clinical statuses were associated with BMD.

Results: The prevalence of osteoporosis in the age-matched advanced knee OA group was significantly lower than that in age-matched controls (28% vs. 42%, $p=0.002$). However, the prevalences of osteoporosis in the age and body mass-matched advanced knee OA and control groups were not significantly different (40% vs. 41%, $p=0.629$). Advanced knee OA patients with poorer preoperative clinical scores were more likely to have lower BMD T-scores in the proximal femur and overall BMD T-scores.

Conclusions: This study documents that a considerable proportion of elderly female patients with advanced knee OA have osteoporosis. We found that advanced knee OA per se does not have a marked protective effect against osteoporosis. In addition, this study indicates that functional deteriorations in advanced knee OA adversely affect BMD. Based on our findings, we propose that knee surgeons should pay more attention to the identification and treatment of osteoporosis in elderly female patients with advanced knee OA warranting TKA.

Disclosures: Chong Bum Chang, None.
This study received funding from: Pfizer Global Pharmaceuticals

SA0346

Osteoporosis: Still A Neglected Condition Among Elderly Individuals Living In Nursing Homes. Ana Lirani-Galvao*¹, Patricia Zach¹, Adriana Silva¹, Gilmar Teixeira¹, Orivaldo Silva², Marise Lazaretti Castro³. ¹Universidade Federal de Sao Paulo, Brazil, ²Universidade de Sao Paulo, Brazil, ³Federal University of Sao Paulo, Brazil

Osteoporosis diagnosis and treatment are still neglected in patients living in nursing homes, despite their known high risk of fractures. The aim of the present study was to assess functional capacity and bone mass in ambulating elderly institutionalized individuals. Ninety seven aged (60 years or older) patients (47 women (age 79.39) and 50 men (age 73.67)) capable of deambulating, with or without walking devices, never diagnosed of bone metabolic diseases, residents of three long permanence institutions in the metropolitan area of Sao Paulo, Brazil, were submitted to bone densitometry exam and functional capacity assessment. Bone mineral density

(BMD, g/cm²) (lumbar spine, proximal femur and distal forearm) and body composition were measured by dual energy X-ray absorptiometry (Hologic, Discovery A). Timed-up-and-go test (TUG), Health Assessment Questionnaire Disability Index (HAQ-DI), pain diagram and general health related questions were also performed. In women, weight was correlated to L1-L4 ($r=0.51$), total femur ($r=0.48$) and femoral neck ($r=0.30$) BMD; age was correlated to distal forearm BMD ($r=-0.32$) and HAQ-DI score ($r=0.38$); and TUG was correlated to HAQ-DI score ($r=0.70$). In men, weight was correlated to L1-L4 ($r=0.34$), total femur ($r=0.47$) and femoral neck BMD ($r=0.57$); age was correlated to distal forearm BMD ($r=-0.34$); HAQ-DI score was correlated to number of pain regions ($r=0.52$) and TUG ($r=0.55$) (Spearman test, $p<0.05$). Osteoporosis was diagnosed in 69.9% of the women (T scores of respectively most prevalent sites: distal forearm -3.21; total femur -2.70.8; femoral neck -2.51.5; L1-L4 -2.41) and 42% of the men (T scores of respectively most prevalent sites: femoral neck -2.80.6; total femur -2.70.5; L1-L4 -2.81; distal forearm -2.62). Besides, 23.4% of the women and 48% of the men were diagnosed of osteopenia. None was receiving any treatment for osteoporosis. Among the individuals with low bone mass, 22.2% of men and 21.1% of women had at least one fall incident in the last six months; 26.6% of men and 44.7% of women reported back pain, 29% of men and women use walking devices, 26.6% of men and 42.1% of the women are sedentary and 42.2% of men and 21% of women smoke. The high prevalence of osteopenia and osteoporosis in this population should raise concern about fractures, considering the greater risk of falls and chronic reduction of mobility in institutionalized elderly patients.

Disclosures: Ana Lirani-Galvao, None.

SA0347

See Friday Plenary Number FR0347.

SA0348

Chronic Exposure to Natural Uranium Affects Bone Cortical Parameters and Both Osteoblast and Osteoclast Gene Expression in Growing Rats. Ndeye Marieme Wade-Gueye^{*1}, Olivia Delissen², Isabelle Dublaineau³, Patrick Gourmelon⁴, Maamar Souidi³. ¹IRSN, France, ²Institut de Radioprotection et de Surete Nucleaire (IRSN), DRPH, SRBE, LRTOX, Pierrelate, France, ³Institut de Radioprotection et de Surete Nucleaire (IRSN), DRPH, SRBE, LRTOX, Fontenay-aux-Roses, France, ⁴Institut de Radioprotection et de Surete Nucleaire (IRSN), DRPH, Fontenay aux roses, France

The presence of uranium in environment, either natural or due to civil and military use, may lead to life-long contamination of the public. Uranium is a natural radioactive heavy metal and its accumulation after a chronic contamination was reported in various organs. Bone is its most important site of accumulation. We previously showed that a chronic exposure to uranium has a biological effect on Vitamin D metabolism (Tissandie et al., BBA, 2007, 1770:266), a crucial hormone in mineral and bone homeostasis. In this context, we hypothesised that uranium contamination may have consequences on bone metabolism. We investigated the effects of a chronic exposure to natural uranium (NU) on bone quality and remodeling. Male Rats ($n=8$ /group) were exposed to NU at a concentration of 40mg.l⁻¹ (1 mg/rat/day), a non-nephrotoxic supra-environmental dose, in drinking water for 9 months, starting at 3 months of age (adult model: NU-Ad) or just after birth (post-natal model: NU-postnat) and compared to them to age-matched controls (CT). Data are given as meanSEM. We used Three-dimensional Microtomography (μ CT), bone histomorphometry of femur and RT-PCR to analyze gene expression involved in bone metabolism. After 9 months of contamination μ CT analysis showed that cortical morphometric and trabecular microarchitecture parameters, histomorphometric bone cell activity as well as gene expression did not differ between NU-Ad and controls. In contrast, in NU-Postnat, contamination decreased significantly by 13% cortical Bone Area (CT: 9.20.3mm² vs NU-Postnat: 8.00.2mm², $p=0.01$) and by 16% Cross sectional Area (CT: 15.30.3 mm² vs NU-Postnat: 12.70.5mm², $p=0.002$). Trabecular bone morphometric parameters, bone resorption parameters and osteoid surfaces were not affected by NU, while osteoid thickness (CT: 1.80.1 vs NU-Postnat: 2.40.1 μ m, $p=0.01$) was increased significantly by 25% by NU. Moreover expression of genes involved in bone turnover (OCN, TRAP), in osteoblast differentiation (Runx2, Osterix, BMP2), in the mineralization of the bone matrix (BSP, OPN, DMP1), and of Vitamin D receptor and TRPV5 were significantly decreased by NU. While the expression of genes involved in the regulation of bone resorption (OPG, RANKL), in the regulation of phosphate homeostasis (MEPE, FGF23), of calcium transport were not affected. In conclusion, we showed for the first time that a chronic exposure to NU at a supra-environmental dose for 9 months significantly affects the skeleton in the young rats while it has no detectable effects in older animals.

Disclosures: Ndeye Marieme Wade-Gueye, None.
This study received funding from: Institut de Radioprotection et de Surete Nucleaire (IRSN)

SA0349

Effects of Kale Supplementation on Bone Mineral Density and Bone Metabolic Markers in Postmenopausal Women. Noriaki Yamamoto*. Niigata rehabilitation hospital, Japan

Background: Kale contains a large amount of highly soluble calcium (Ca) and abundant vitamin K1. Its absorbability of Ca was equal to or better than that of milk, and it is expected to have efficacy on bone metabolism.

The purpose of this study is to determine the effects of oral intake of Kale in postmenopausal women for 1 year.

Methods: We conducted an open-label study with 13 postmenopausal women. All subjects take a beverage containing 9.5g of a powdered kale product (Ca: 126.6 \pm 5.4 mg/packet), 2 or 3 times a day for 12 months.

Serum Ca and bone metabolic markers (serum NTX, urinary NTX, serum OC, and serum BAP) are assessed at beginning, 3, 6, and 12 months of this study. Also bone mineral density in the lumbar spine (L2-4) and femoral neck are measured by dual-energy x-ray absorptiometry (DXA) at beginning, 6 and 12 months of this study.

Results: According to daily record of subjects, average Ca intake was 227.9~354.5 mg and vitamin K1 intake was 241.6~375.8 μ g.

Comparing to the baseline data, the serum NTX level had significantly decreased after 3 months ($p<0.05$), and maintained after 6 months and 12 months ($p<0.05$) of this study. The serum BAP level at 12 months had also significantly decreased ($p<0.05$). The urinary NTX had decreased .not significantly. The bone mineral density measurements showed a tendency of increase in the lumbar spine .

Conclusion: Improvement in both bone metabolic markers and bone mineral density was observed by oral intake of kale in postmenopausal women, which contains highly absorbable Ca and abundant vitamin K1.

Disclosures: Noriaki Yamamoto, None.

SA0350

Socioeconomic Status Over the Lifecourse and Adult Bone Mineral Density: The Midlife in the U.S. Study. Carolyn Crandall^{*1}, Sharon Stein Merkin¹, Neil Binkley², Gail Greendale¹, Teresa Seeman¹, Arun Karlamangla¹. ¹University of California, Los Angeles, USA, ²University of Wisconsin, USA

Purpose. To examine independent associations of adult and childhood socioeconomic status with bone mineral density (BMD) in participants of the MIDUS II Biomarker project, a sub-study of the Midlife in the U.S. Study of adults aged 25 to 74 years at baseline.

Methods. We used generalized linear mixed effects models to examine cross-sectional associations between socioeconomic advantage (from self-administered questionnaire) and BMD (by dual energy x-ray absorptiometry), adjusting for race, body weight, research center site, smoking, physical activity, menopausal transition stage (for women), and age (for men). Childhood socioeconomic advantage score was the sum of 3 items (total possible range 0 to 6): being on welfare in childhood (0 = yes, 2 = no) + childhood socioeconomic status relative to others (0 = worse off, 1 = same, 2 = better) + parent education (0 if < high school, 1 if high school or high school equivalent, 2 if some college or more). Adult socioeconomic advantage score was the sum of 5 items (total possible range 0 -10): participant education (high school or high school equivalent = 0, 1 = some college or associate's degree, 2 = college degree or more) + family-adjusted poverty to income ratio (0 if <300%, 1 if 300%-599%, 2 if \geq 600%) + self-assessed financial situation now (0 = worst, 1 = average, 2 = best) + money to meet needs (0 = not enough, 1 = just enough, 2 = more than enough) + difficulty paying bills (0 = very, 1 = not very, 2 = not at all).

Results. Data regarding socioeconomic advantage scores and BMD (lumbar spine and/or femoral neck) were available for 729 participants. Mean age of participants was 56.9 years, 51.6% were female, and 28% were non-White. After adjustment for race, body weight, menopause transition stage/age, smoking, and physical activity, childhood socioeconomic advantage score, but not adult socioeconomic advantage score, was statistically significantly associated with adult lumbar spine BMD. Independent of adult socioeconomic advantage score, for every point higher childhood socioeconomic advantage score, lumbar spine BMD was 0.011 g/cm² higher ($P=0.02$). Neither childhood nor adult disadvantage score were statistically significantly associated with adult femoral neck BMD.

Conclusions. Favorable childhood socioeconomic status is associated with higher adult lumbar spine BMD, independent of adult socioeconomic status. Childhood socioeconomic factors may influence attainment of peak trabecular BMD.

Table 1. Socioeconomic Advantage Scores and Lumbar Spine BMD		
	Model without smoking or physical activity (N=725)	Model with smoking and physical activity (N=647)
	Beta coefficient (SE)	Beta coefficient (SE)
Childhood Advantage Score	0.010 (0.004)*	0.011 (0.003)*
Adult Advantage Score	0.001 (0.002)	0.001 (0.002)
Score (non-white)	0.033 (0.006)***	0.034 (0.007)**
Body Weight	0.001 (0.0003)***	0.001 (0.0003)***
Menopausal transition stage/age		
Men, Age <50	Reference	Reference
Men, Age 50-59	-0.006 (0.020)	-0.009 (0.021)
Men, Age 60+	0.006 (0.004)***	0.005 (0.007)**
Pre-menopausal women	0.034 (0.025)	0.026 (0.026)
Early post-menopausal women	0.013 (0.034)	0.015 (0.035)
Late post-menopausal women (no hormone)	-0.033 (0.019)**	-0.034 (0.021)*
Postmen. taking hormones	0.026 (0.035)	0.044 (0.030)
Smoking (pack years)		-0.0004 (0.0004)
Physical Activity		
Age 14-18 (recreational)		-0.001 (0.004)
Age 14-18 (competitive)		0.003 (0.004)
Score, Age 20-13		0.0003 (0.0003)
Score, Current		0.00003 (0.00003)

Table 2. Socioeconomic Advantage Scores and Femoral Neck BMD		
	Model without smoking or physical activity (N=725)	Model with smoking and physical activity (N=645)
	Beta coefficient (SE)	Beta coefficient (SE)
Childhood Advantage Score	0.003 (0.003)	0.005 (0.003)
Adult Advantage Score	0.001 (0.002)	0.0003 (0.002)
Score (non-white)	0.040 (0.012)***	0.046 (0.013)***
Body Weight	0.002 (0.0002)***	0.002 (0.0002)***
Menopausal transition stage/age		
Men, Age <50	Reference	Reference
Men, Age 50-59	-0.040 (0.013)*	-0.040 (0.016)**
Men, Age 60+	-0.039 (0.014)*	-0.033 (0.018)*
Pre-menopausal women	0.021 (0.008)	0.016 (0.013)
Early post-menopausal women	-0.023 (0.019)	-0.024 (0.020)
Late post-menopausal women (no hormone)	-0.102 (0.014)***	-0.100 (0.013)***
Postmen. taking hormones	-0.040 (0.023)	-0.028 (0.027)
Smoking (pack years)		-0.0004 (0.0003)
Physical Activity		
Age 14-18 (recreational)		-0.001 (0.003)
Age 14-18 (competitive)		0.004 (0.003)
Score, Age 20-13		0.0003 (0.0003)*
Score, Current		0.000004 (0.000004)

* P-value < 0.05; ** P-value < 0.01; *** P-value < 0.001.

Tables

Disclosures: Carolyn Crandall, None.

SA0351

A Systematic Approach to Fragility Fracture Care and Prevention: Achieving a Consensus. Paul Mitchell¹, Alastair McLellan², Stephen Gallacher³, Andrew Gallagher⁴, Eamonn Brankin⁵, Alun Cooper⁶, Graham Davenport⁷, James Cooper⁸, Anne Thurston⁸, Femi Adekunle⁹, Emma Gilbert¹⁰. ¹University of Derby, United Kingdom, ²Western Infirmary, United Kingdom, ³Southern General Hospital, United Kingdom, ⁴Victoria Infirmary, United Kingdom, ⁵University of Glasgow, United Kingdom, ⁶Bridge Medical Centre, United Kingdom, ⁷Wrenbury Medical Centre, United Kingdom, ⁸National Osteoporosis Society, United Kingdom, ⁹Novartis Pharmaceuticals UK Ltd, United Kingdom, ¹⁰Amgen Limited, United Kingdom

Purpose: To describe development in the UK of a consensus shared by professional organisations, patient societies, policy makers and pharmaceutical manufacturers, and steps taken to implement a systematic approach to fragility fracture care and prevention of secondary fractures.

Methods: In 1999, professionals established an exemplar service, the Fracture Liaison Service (FLS), a new standard of care for fracture secondary prevention. In 2000, Scottish national audit found FLS achieves 7-9x higher rates of assessment/treatment for fracture secondary prevention than usual models of care. Key contributions from each group from 2000-2010 included:

Professional organisations: BOA-BGS Blue Book on the care of patients with fragility fracture, National Hip Fracture Database (NHFD) and Royal College of Physicians (RCP) National Audit of Falls and Bone Health

Patient societies: National Osteoporosis Society (NOS) Manifestoes and "Fighting for FLS" campaign

Policy makers: Falls and fracture section of Department of Health (DH) Prevention Package for Older People, Best Practice Tariff for hip fracture and Commissioning for Quality and Innovation payment framework

Pharmaceutical (and devices) manufacturers: FLS Resource Pack, FLS web modelling tool and unrestricted grants to support initial development of NHFD

Collaborative initiatives: NOS educational workshops to support local implementation of FLS in collaboration with DH in England, Amgen, Novartis and

Servier; Glasgow 'Preceptorships' (national education programme dedicated to sharing best practice on implementation of FLS and outcomes for clinicians and service managers); and Breaking Point Report (for parliamentarians, clinicians and service commissioners on the need and means to close the secondary prevention management gap).

Results: The 2008 RCP audit reported 29% of localities had established an FLS (update to be published in mid-2011). The 2010 NHFD Report identified progress in implementation of standards advocated in Blue Book and DH Prevention Package. On hospital admission, 10% of hip fracture patients received osteoporosis treatment; on discharge 75% were in process of receiving secondary preventive care.

Conclusions: Consensus has emerged on the need for a universal systematic approach to fragility fracture care and prevention in the UK. This provides an illustration of collaborative working across multiple specialities and sectors intended to improve healthcare quality and reduce associated costs.

Disclosures: Paul Mitchell, Novartis Pharmaceuticals UK Ltd, 8; GlaxoSmithKline, 5; Daiichi Sankyo UK Ltd, 5; Shire, 8; Amgen, 5; Novartis Pharmaceuticals UK Ltd, 5

SA0352

Accuracy of ICD-9 codes to identify Malunion and Nonunion & Developing an Algorithm to Improve Automated Case-Finding of Nonunion and Malunion. Denise Boudreau^{*1}, Onchee Yu¹, Leslie Spangler², Thy Do³, Monica Fujii¹, Susan Ott⁴, Cathy Critchlow⁵, Delia Scholes⁶. ¹Group Health Research Institute, USA, ²Group Health Cooperative, USA, ³Amgen Inc., USA, ⁴University of Washington, USA, ⁵Amgen, USA, ⁶Group Health Cooperative Group Health Research Institute, USA

Background/Aims: Automated health plan data are a potential source for observational studies of the prevalence and risk of fracture healing complications. However, misclassification of cases is possible since these codes may be used to rule out, follow up, or note delays or complications in healing. Our aims were: 1) evaluate the accuracy of using automated claims data to identify nonunions (NU) and malunions (MU) and; 2) explore a classification algorithm to improve the accuracy of case finding through use of additional automated data.

Methods: Using health plan data, we identified potential cases of NU (ICD-9 code 733.82; N=300) and MU (ICD-9 code 733.81; N=288) occurring during 2004-2008. Medical charts for all potential cases were reviewed. True NU cases were defined as evidence of NU and no evidence of MU in the chart (and vice versa for MUs) or clinician confirmed when chart evidence was unclear. To validate NU and MU status, positive predictive values (PPV) were calculated for each ICD-9 code compared to true cases. Using additional automated data on fracture site, subsequent diagnostic codes of NU or MU, procedures, place of ICD-9 code origin (ambulatory vs. inpatient), and type of provider, we conducted a classification and regression tree (CART) analysis to create case-finding algorithms for NU and MU.

Results: Compared to "true cases", the PPV of ICD-9 codes for identifying NU and MU was 77% and 37%. The best case-finding algorithm for NU contained three predictors: number of NU visits in the 12-months after the first NU code; fracture location; and provider specialty for the first NU code (Figure 1). Sensitivity of the algorithm was 74%, specificity 81%, PPV 93%, NPV 49%, and misclassification rate 24% (versus 30% using ICD-9 only). For the MU algorithm, fracture location and number of NU visits (predictor of non MU case) were the best predictors (Figure 2). Sensitivity of the MU case finding algorithm was 81%, specificity 60%, PPV 54%, NPV 84%, and misclassification rate 32% (versus 63% using ICD-9 only).

Conclusions: Identifying fracture healing complications in automated data with only ICD-9 codes is better for NU than MU, although algorithms incorporating additional data are needed for both to improve case-finding. Further research validating these algorithms in datasets from different populations is needed as well as further exploration of case-finding algorithms in a larger sample.

Figure 1. Algorithm for identifying intervention (NU) cases, Group Health development set

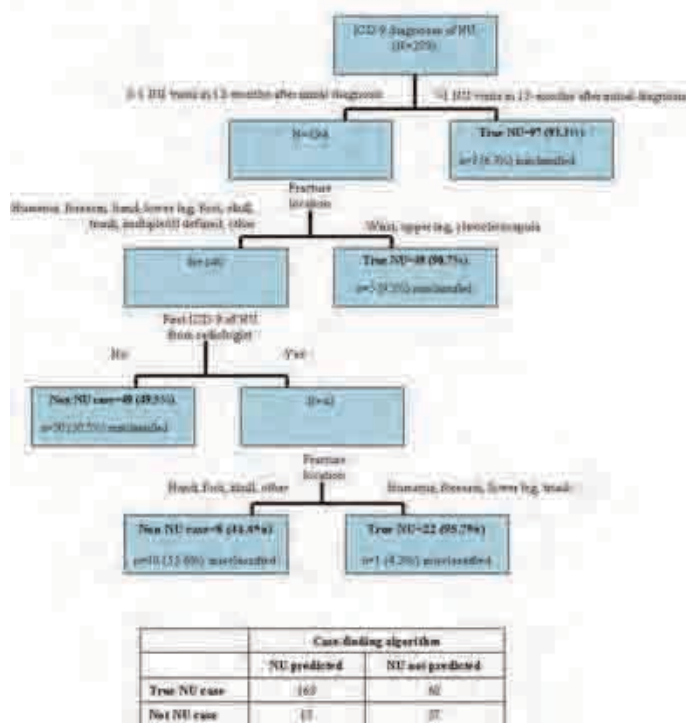
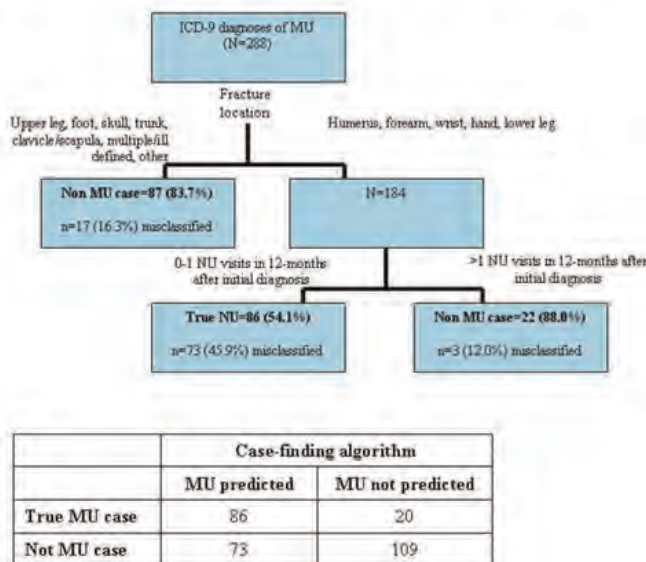


Figure 2. Algorithm for identifying malunion (MU) cases, Group Health development set



Disclosures: Denise Boudreau, Amgen, 2
This study received funding from: Amgen

SA0353

See Friday Plenary Number FR0353.

SA0354

See Friday Plenary Number FR0354.

SA0355

See Friday Plenary Number FR0355.

SA0356

Medical Care Resource Utilization and Costs Associated with Teriparatide Therapy in U.S. Patients. Russel Burge^{*1}, T. Kim Le¹, Yang Zhao¹, Jeffrey Curtis². ¹Eli Lilly & Company, USA, ²University of Alabama at Birmingham, USA

Objective: To examine all-cause healthcare utilization and costs among US patients during teriparatide (TPTD) usage. **Methods:** Employing a retrospective cohort study design on a large U.S. national healthcare claims database, patients aged 18+ who initiated TPTD in 2007 were identified. Initiation was defined as no prior TPTD use over the previous 12 months, where index date was first TPTD dispense date. All patients selected were required to have 12 months pre-index and minimum 12 to maximum 24 months post-index data. Four cohorts were constructed according to duration of TPTD therapy: <6 months, 6-11 months, 12-17 months, and 18-24 months. Descriptive statistics were summarized for patient demographics, comorbid medical conditions, prior medication use, and all-cause healthcare utilization and costs. Chi-square and Wilcoxon tests were used to make statistical comparisons between <6 months and ≥ 6 months of TPTD therapy. **Results:** The analysis included 2,461 TPTD patients. TPTD persistence for the four cohorts was: 21% (<6 months), 13% (6-11 months), 18% (12-17 months), and 48% (18-24 months). TPTD patients with <6 months of therapy were older (71 vs. 68 vs. 68 vs. 69 years, all p<0.05) compared to the other 3 cohorts. In the pre-index period, 31-33% of patients had a prevalent fracture, and 6-10% had rheumatoid arthritis. Patients with <6 months of TPTD therapy had more medical visits than those in the other cohorts over the 12 months pre-index period, and also had the highest prior 12-month total costs. Annualized mean number of medical visits per patient were lower after treatment initiation among all TPTD patients after 12 months of TPTD treatment vs. the pre-index period (26.0 vs. 23.8 for 12-17 months, 25.3 vs. 22.3 for 18-24 months, both p<0.05). In the TPTD cohort with <6 months of treatment, medical care costs (outpatient, emergency room, inpatient admission) per patient were higher than the pre-index costs. After 6 months of TPTD use, inpatient costs per patient decreased; and in the 18-24 month cohort the mean per patient costs were lower compared to the corresponding pre-index costs (inpatient: \$12,178 vs. \$22,826; outpatient: \$6,536 vs. \$7,280; emergency room: \$377 vs. \$635, all p<0.05). **Conclusion:** In this descriptive retrospective study, annualized total healthcare costs increased over time; however, lower inpatient costs were associated with longer TPTD exposure when compared to pre TPTD initiation levels.

Disclosures: Russel Burge, Eli Lilly & Company, 3
This study received funding from: Eli Lilly & Company

SA0357

See Friday Plenary Number FR0357.

SA0358

See Friday Plenary Number FR0358.

SA0359

See Friday Plenary Number FR0359.

SA0360

The Incidence of Femur Fractures Below Trochanter Increases Exponentially with Age. Lisa Strahm^{*1}, Albrecht Popp¹, Patrick Schwab², Christoph Senn¹, Romain Perrelet¹, Kurt Lippuner¹. ¹Osteoporosis Policlinic, University of Bern, Switzerland, ²Swiss Federal Statistical Office, Switzerland

Purpose:The incidence of femoral neck and pertrochanteric fractures increases exponentially with age. Little is known about the epidemiological characteristics of femoral fractures below trochanter.

Methods:The incidence of femoral fractures hospitalized in year 2008 was determined by ICD-10 code, sex, and 10-year age categories using the medical database and the Swiss population statistics of the Swiss Federal Statistical Office (SFSO) which encompassed 98.8% of all hospitalizations. Raw data were extrapolated to 100% and the age-specific incidence calculated per 100000 women or men aged 45 years or more.

Results:Femoral fractures below trochanter represented 13.1% and 13.9% of all femur fractures in women and men, respectively. The age-specific fracture incidences in women and men are shown in the table below.

Conclusions:The incidence of femoral fractures below trochanter increased exponentially with age both in women and men, following a pattern similar to that of femoral neck and pertrochanteric fractures. This observation suggests that femur fractures below trochanter should be regarded as osteoporotic fractures.

Women

Age (years)	45-54	55-64	65-74	75-84	85+
Femoral neck (S72.0) and pertrochanteric (S72.1) fractures	20.3	75.5	214.7	1007.6	2759.2
Subtrochanteric fractures (S72.2)	0.9	2.6	10.5	62.1	128.0
Fractures of the femoral shaft (S72.3)	3.4	6.3	18.6	44.2	129.7
Fractures of the distal femur (S72.4)	2.2	8.5	20.1	46.9	104.1
All femoral fractures below trochanter	6.5	17.4	49.2	153.3	361.9

Men

Age (years)	45-54	55-64	65-74	75-84	85+
Femoral neck (S72.0) and pertrochanteric (S72.1) fractures	31.4	67.1	132.9	500.7	1640.6
Subtrochanteric fractures (S72.2)	3.4	3.5	9.0	24.3	69.9
Fractures of the femoral shaft (S72.3)	7.3	7.9	12.9	22.6	81.5
Fractures of the distal femur (S72.4)	3.4	5.1	7.6	13.3	29.1
All femoral fractures below trochanter	14.0	16.5	29.5	60.3	180.6

Table

Disclosures: Lisa Strahm, None.

SA0361

The Profile of Diseases Had Previous Fractures of the Femur By Failing Into a Group of 40 Elderly Patients at the Hospital Public, Sao Paulo, Brazil. Roberto Queiroz¹, Ursula Karsch¹, Bianca Segantin¹, Fabiana Fonseca^{*2}, Thais Braga¹, Ana Elisa Rosa¹, Manuela Santos¹. ¹PUC - SP, Brazil, ²PUC Sp, Brazil

This article reveals the prevalence of existing diseases found in a search field with a group of 40 patients, from 60 years of age being 31 females and 9 males who suffered the fracture of femur treated in Hospital Public Server in Sao Paulo State with indication of surgical treatment. Patients from fall of own height, defined by Studensk, (2002): an unintentional displacement of the body to a level lower than the starting position, with inability to fix in a timely manner, as determined by various causes circumstances which compromise stability. According to studies carried out in Brazil by the Ministry of health (2010) the annual incidence of fractures in the country is 1 million and the single health system, spent about \$ 81 million with fractures in elderly in year 2009. Determine the profile of old pathologies fracture by fall is vital to try to prevent them, because some diseases can affect cognitive and motor coordination, is of fundamental importance provide contemplation by the quality of life of elderly people in Brazil.

Disclosures: Fabiana Fonseca, None.

SA0362

Trends in Hip Fracture Rates in Canada: An Age-Period-Cohort Analysis. Sonia Jean^{*1}, Siobhan O'Donnell², Claudia Lagace², Peter Walsh², Christina Bancej², Suzanne Morin³, Jacques Brown⁴, William Leslie⁵. ¹Institut National De Sante Publique Du Quebec, Canada, ²Public Health Agency of Canada, Canada, ³McGill University Health Centre, Canada, ⁴Laval University, Canada, ⁵University of Manitoba, Canada

Purpose: In Canada, age-standardized hip fracture rates have declined for males and females. This study explores whether these observed trends can be explained by period or cohort effects in order to identify the factors underlying these changes.

Methods: All hospitalizations during the study period 1985-2005 with a primary diagnosis of hip fracture (ICD-9-CM 820.x and ICD-10-CA S72.0-.2) were identified in a national database. Age- and sex-specific hip fracture rates (per 100 000 person-years) were calculated for nineteen age groups (from 0-4 to >85 years) and four calendar periods (from 1985 to 2004). This stratification resulted in twenty birth cohorts from 1905-09 through 2000-2004. Age-period-cohort (APC) models were fitted to the hip fracture rates using Poisson regression models.

Results: A total of 570,872 hospitalizations for hip fracture were identified (72.3% females and 27.7% males). Age-standardized hip fracture rates have progressively declined from 118.6 in 1985 to 80.9 in 2005 for females and from 68.2 to 51.1 for males. The annual linear decrease in rates per 5 year period were 12% for females and 7% for males (both $p < 0.0001$). Significant cohort effects were also observed for both sexes ($p < 0.0001$). Cohorts born prior to 1950 had a higher risk for hip fracture, while those born after 1954 had a lower risk. Table 1 shows a significant birth cohort effect, after adjustment for age and linear change (drift) for males ($p = 0.0126$) but not for females ($p = 0.9960$). In contrast, the period effect, after adjustment for age and linear change (drift) was significant for females ($p = 0.0373$) but not for males ($p = 0.2515$). For males, we observed no additional period effect after adjusting for age and cohort. For females, we observed no additional cohort effect after adjusting for age and period.

Conclusions: Although hip fractures rates have decreased in males and females, different factors may be contributing to these changes. In recent years, there have been more widespread preventive measures, diagnosis and treatment for osteoporosis. In addition to the linear decrease in rates, there is evidence of significant period effects in females and cohort effects in males. The causal factors underlying these changes remains uncertain.

Sex	Model	Deviance (df)	$\Delta D (\Delta df)$	p-value
Males	Age (A)	469.3012 (361)	Ref	Ref
	Age-drift (AD)	461.1777 (360)	8.1235 (1)	0.0044
	Age-period (AP)	463.9386 (358)	2.7609 (2)	0.2515
	Age-cohort (AC)	401.0704 (322)	60.1073 (38)	0.0126
	Age-period-cohort (APC)	401.6855 (319)	0.6151 (3)	0.8930
Females	Age (A)	422.3466 (361)	Ref	Ref
	Age-drift (AD)	409.7177 (360)	12.6289 (1)	0.0004
	Age-period (AP)	403.1398 (358)	6.5779 (2)	0.0373
	Age-cohort (AC)	390.8632 (322)	18.8545 (38)	0.9960
	Age-period-cohort (APC)	381.7467 (319)	21.3931 (39)**	0.9901

*Model APC versus AC

**Model APC versus AP

Table 1: Results for the age-period-cohort effects modelling

Disclosures: Sonia Jean, None.

SA0363

CIITA Polymorphisms Affecting Expression of MHCII are Associated to BMD, Bone Loss and Fracture. Maria Swanberg^{*1}, Fiona McGuigan², Mattias Callreus¹, Paul Gerdhem³, Kristina Akesson⁴. ¹Lund University, Sweden, ²University of Lund, Malmo, Skane University Hospital, Malmo, Sweden, ³Karolinska Institutet, Sweden, ⁴Skane University Hospital, Malmo, Sweden

Inflammatory factors such as cytokines, surface molecules and T lymphocytes affect osteoclast activity and thereby the fine balance between bone formation and resorption. After menopause, levels of the pro-inflammatory cytokine interferon-gamma (IFN γ) increase. IFN γ promotes T lymphocyte survival and stimulates their activity by inducing expression of MHCII molecules on antigen-presenting cells. This process is mediated by the MHC class II transactivator, encoded by the CIITA gene.

We investigated the effect of polymorphisms in CIITA previously associated with reduced expression of MHCII (rs3087456(G) and rs4774(C)) on BMD, bone loss and fracture risk in young and elderly Swedish women. In addition, 3 SNPs in CLEC-16A, reported to be in linkage disequilibrium (LD) with CIITA, and 3 SNPs in IFNG were analyzed. Phenotypes included BMD in 25- and 75 year-old women (PEAK-25 n=999, OPRA n=1003) and serum bone resorption markers, bone loss and fractures between age 75 and 80 (OPRA n=753 at age 80).

CIITA was not associated to BMD at peak bone mass, but at age 75 (lumbar spine, femoral neck, total hip, $p = 0.01-0.04$) and age 80 ($p = 0.02-0.04$). BMD was 1.8-3.4% higher in rs3087456(G)-carriers ($p = 0.009-0.02$), suggesting an increasing effect on BMD by reduced MHCII expression.

CIITA was also associated with increased rate of bone loss (femoral neck $p = 0.01$, total hip $p = 0.03$, total body $p = 4E-5$), but not serum bone resorption markers between age 75 and 80. Despite increased bone loss, rs3087456(G) was protective against

fracture comparing carriers and non-carriers (any fracture sustained in 28% vs 39%, $p=0.002$; osteoporotic fracture 23% vs 31%, $p=0.02$).

Polymorphisms in IFNG were weakly associated to lower total hip- ($p=0.04$) and lumbar spine BMD ($p=0.03$) at baseline, but not to bone loss or fracture.

CLEC16A, in partial LD with CITA, was associated to lower lumbar spine BMD at age 75 ($p=0.04$) and lower total body, total hip, and femoral neck BMD at age 80 ($p=0.04$ for all). CLEC16A was also associated to fractures between age 75 and 80, 31% of the rs725613(G) carriers had a fracture compared to 39% of the non-carriers ($p=0.02$).

In conclusion, CITA alleles inducing lower MHCII expression were associated to higher BMD and decreased fracture risk in elderly women. These results support the importance of MHCII expression levels and T lymphocyte activation in postmenopausal bone health and identify the CITA gene as a risk factor for osteoporosis and fracture.

Disclosures: Maria Swanberg, None.

SA0364

Bivariate Linkage Analysis Identifies a Genomic Region with Potential Pleiotropic Effects on Bone Mineral Density and Subclinical Cardiovascular Disease Indices. Allison Kuipers^{*1}, Candace Kammerer¹, Iva Miljkovic², Clareann H. Bunker², Alan L. Patrick³, Victor W. Wheeler³, Kim Sutton-Tyrrell², Joseph Zmuda¹. ¹University of Pittsburgh Graduate School of Public Health, USA, ²University of Pittsburgh, USA, ³Tobago Health Studies Office, Trinidad & Tobago

Subclinical measures of osteoporosis and cardiovascular disease are correlated in many populations, such that indices of adverse vascular health are associated with lower bone mineral density (BMD). We have recently demonstrated a significant genetic correlation between BMD and measures of vascular health in families suggesting that shared loci may explain in part the link between osteoporosis and CVD. To expand upon these findings, we performed bivariate genome-wide linkage analysis of subclinical CVD measures and BMD in 461 African ancestry individuals aged ≥ 18 years who belonged to 7 large, multigenerational families (mean family size 66; 3,414 relative pairs). Participants underwent carotid ultrasound scans to determine adventitial diameter (AD) and intima-media thickness (IMT). Dual-energy X-ray absorptiometry and peripheral quantitative computed tomography were used to determine BMD. Genotyping was completed by fluorescence-based methods using the Infinium HumanLinkage-12 BeadChip consisting of 6,090 single-nucleotide polymorphisms with average spacing of 0.58 cM across the genome. We conducted univariate and bivariate, multipoint quantitative trait linkage analyses using pedigree-based maximum likelihood methods. Models were adjusted for age, sex, weight, height, menopausal status, current smoking, alcohol intake and walking for exercise. Univariate linkage analysis identified a region on chromosome 14 linked to AD (LOD: 4.7) and another on chromosome 11 linked to trabecular BMD at the radius (LOD: 3.4). Bivariate analysis yielded strong evidence that the region on chromosome 14 might have pleiotropic effects on AD and cortical BMD at the tibia (LOD: 5.2). Our results suggest that the link between indices of CVD and osteoporosis may be due in part to genes with pleiotropic effects.

Disclosures: Allison Kuipers, None.

SA0365

Heritability of Prevalent Vertebral Fracture and Vertebral Volumetric Bone Mineral Density in Three Generations of the Framingham Heart Study. Ching-Ti Liu^{*1}, Yanhua Zhou², Mary Bouxsein³, Harry Genant⁴, Yi-Hsiang Hsu⁵, Kerry Broe⁶, Thomas Lang⁷, Serkalem Demissie¹, David Karasik⁸, Adrienne Cupples¹, Douglas Kiel⁸. ¹Boston University School of Public Health, USA, ²Boston University, USA, ³Beth Israel Deaconess Medical Center, USA, ⁴UCSF/Synarc, USA, ⁵Hebrew SeniorLife Institute for Aging Research & Harvard Medical School, USA, ⁶Hebrew Senior Life, USA, ⁷University of California, San Francisco, USA, ⁸Hebrew SeniorLife, USA

Background: Bone mineral density is an important risk factor for vertebral fractures, the most common osteoporotic fracture. Both environmental and genetic factors are suspected to contribute to the risk for vertebral fractures; however, there is a paucity of previous studies on the genetic contribution to vertebral volumetric bone mineral density (vBMD) and vertebral fracture. In fact the heritability (h^2) for vertebral fracture is not well established.

Objective: We aimed to estimate the h^2 of vertebral fracture and vBMD in Caucasian adult members of the Framingham Heart Study (FHS) families.

Methods: Members of the Original Framingham Cohort were assessed by lateral radiographs at 13 vertebral levels (T4-T12, L1-L4) in 1992-1993. In the Offspring and Generation 3, lateral QCT scout views were obtained in 2002-2005. In all cohorts, vertebral fracture status was measured using Genant's semi-quantitative (SQ) scale (grades 0-3). Fracture was defined as a SQ grade of 1 or higher at any vertebral level, in each participant. QCT scans from the Offspring and Generation 3 cohorts were also analyzed at the L3 level for integral (IBMD) and trabecular (TBMD) using custom

software developed by T. Lang. Heritability estimates were then calculated in SOLAR with and without adjustment for age, gender and cohort.

Results: For vertebral fracture, we analyzed 4,099 individuals including 2,082 women and 2,017 men with age ranging from 31 to 96 yrs. Among 665 vertebral fracture cases, 342 were present in men and 323 in women with age ranging from 32 to 96 yrs. Estimates of both crude and multivariable-adjusted h^2 were 0.205 ($p<0.0019$). For vBMD, we analyzed 3,129 individuals including 1,631 men and 1,498 women age ranging from 31 to 89 yrs. Estimates of crude h^2 ranged from 0.22 to 0.29 and multivariable-adjusted, ranged from 0.38 to 0.47 (all statistically significant).

Conclusion: Our study suggests both vertebral fracture and vertebral vBMD in Caucasian adults are heritable, although vertebral fracture heritability is not as high as related traits such as vBMD, underscoring the importance of further work to identify the specific variants underlying genetic susceptibility to vertebral fracture and its risk factors.

Phenotype	Model ^a	Heritability	SE	p-value
L3_IBMD	1	0.2913736	0.0379846	3.88E-18
	2	0.4652303	0.0423104	3.12E-35
L3_TBMD	1	0.2236174	0.0368283	7.03E-12
	2	0.3762544	0.0412855	3.12E-25
Vertebral Fracture	1	0.2047702	0.0721568	1.24E-03
	2	0.2027335	0.0809221	1.96E-03

Note: ^a Model 1: crude analysis; 2: multivariate adjusted

Heritability of vertebral fracture and vertebral vBMD

Disclosures: Ching-Ti Liu, None.

SA0366

See Friday Plenary Number FR0366.

SA0367

See Friday Plenary Number FR0367.

SA0368

See Friday Plenary Number FR0368.

SA0369

See Friday Plenary Number FR0369.

SA0370

Menopausal, but not Ethnic or Seasonal Differences in Serum C-telopeptide in UK Caucasian and South Asian Women. Andrea Darling^{*1}, Fatma Gossiel², Rosemary Hannon², Richard Eastell², Susan Lanham-New¹.

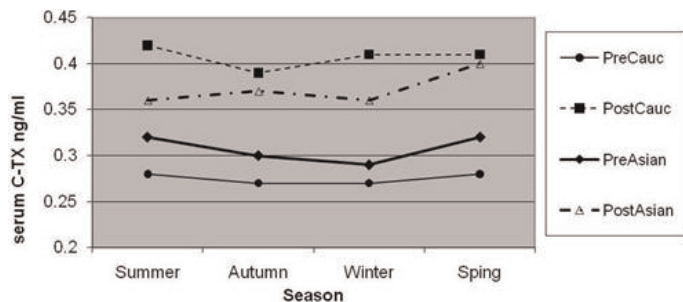
¹University of Surrey, United Kingdom, ²University of Sheffield, United Kingdom

Bone turnover is a well studied phenomenon, however it is still unclear as to whether bone shows a season driven rhythm over the course of the year, particularly in ethnic groups, such as South Asians. Indeed, some studies in Caucasian populations have found a significant seasonal variation in bone resorption markers¹ but others have not². This study aimed to establish if in younger or older women, bone turnover shows significant seasonal variation. The study also aimed to assess whether there are differences in bone resorption between South Asian and Caucasian women. This has practical implications in terms of the use of bone markers in diagnostics. The D-FINES study investigated 373 Surrey Caucasian (C) and Asian (A) women every season over a 12 month period (2006-2007). A random sub-sample of premenopausal C (n 18) and postmenopausal C (n 17); premenopausal A (n 13) and postmenopausal A (n 17) with blood samples for all seasons were selected. Serum C-telopeptide (sCTX) was determined by electrochemiluminescent immunoassay on a cobas e411 automated analyser on a cobas e411 automated analyser. A mixed between-within subjects ANOVA showed there was no significant main effect of season $F(3,59.0) = 1.467$, $p=0.233$. However, there was a significant between subjects effect of group $F(3,61) = 3.099$, $p=0.033$, with post hoc tests showing significant differences between the two C groups ($p=0.007$) and between the postmenopausal A and premenopausal C groups ($p=0.042$) but no significant differences between the other groups. Last, there was no significant interaction between season and group $F(9,143.741) = 0.540$, $p=0.843$. The lower sCTX in the younger premenopausal groups is as would be expected. However, unexpectedly, there was a non-significant trend in the postmenopausal groups for the A women to have a lower mean sCTX than the C women. In contrast, in the premenopausal women, the sCTX was lower in the C group. Therefore it appears that it is menopausal status, not ethnicity which is likely

the main reason for the group differences. Overall, no evidence for a seasonal variation in bone resorption was found here but there was evidence for a menopausal difference in bone resorption. However, numbers of participants in this preliminary analysis was small and further analysis with a larger sample is planned.

¹Hill, T. R., D. McCarthy, et al. (2007) *Int J Vitam Nutr Res* 77(5): 320-5.

²Zittermann, A., K. Scheld, et al. (1998) *EJC* 52(7): 501-506.



Serum C-Telopeptide By Ethnic/Menopausal Group and Season

Disclosures: Andrea Darling, None.

SA0371

A Study of the Risk Factors and Prevalence of Osteoporosis in Guayaquil, Ecuador. Augusto Focil*. California Hispanic Osteoporosis Foundation (CHOF), USA

This study aims to assess the incidence and risk factors of osteoporosis in Hispanics. A population-based cross-sectional study was conducted during November 2008 - November 2009 in Guayaquil, Ecuador. A total of 978 Ecuadorians (82% females, 18% males) underwent quantitative ultrasonography and were interviewed to find out the risk factors for osteoporosis. 456 (47%) were reported to be normal, 421 (43%) were osteopenic and 100 (10%) were osteoporotic. The mean age and standard deviation of the participants were 56 years +/- 12.0 years. In the univariate analysis, factors that were associated with osteoporosis/osteopenia included age, education, weight, marital status, use of cortisone/prednisone, and previous history of broken bone (p-value is less than 0.05). Using binary logistic regression, age, weight, sex, and education level were found to be independent predictors for osteoporosis/osteopenia as compared to normal individuals. The prevalence of osteoporosis and osteopenia is high among the study population of Guayaquil yet the understanding of the actual disease is shown to be low from our interviews and surveys.

Disclosures: Augusto Focil, None.

SA0372

Analysis of Clinical Risk Factors for Post-menopausal Osteoporosis Based on WHO Fracture Risk Assessment (FRAX) Tool. Sudhir Unni¹, Yiwen Yao¹, Karen Gunning¹, Jeffrey Curtis², Joanne LaFleur*. ¹University of Utah, USA, ²University of Alabama at Birmingham, USA

Purpose: Osteoporosis is highly under-diagnosed and under-treated. The development of the fracture risk assessment tool (FRAX) by WHO makes it possible to calculate the 10-year fracture risk in men and women using individual and clinical risk factors. The objective of this study was to determine whether FRAX scores could be calculated from risk factors captured from patient electronic medical record (EMR) data.

Methods: We conducted a cross-sectional analysis using data from the University of Utah Health Care System EPIC Electronic Medical Record. The database contains inpatient, outpatient, clinical and financial information for about 1.4 million patients. The study sample included female patients age 50 years and older between January 1, 2007 and December 31, 2008. Patient data related to FRAX risk factor constructs were identified and patients were categorized into four groups based on risk factor availability. FRAX scores were calculated using an automated program that directly queried the FRAX server. Sensitivity analyses were performed for cases where risk factor information was not available. Means, standard deviations, and ranges of FRAX scores were reported for each group as were the proportions of patients exceeding treatment thresholds defined by the National Osteoporosis Foundation. FRAX scores were estimated separately for patients that did and did not receive bisphosphonate therapy prior to study inclusion.

Results: There were 345 patients with all risk factors available of which 175 were bisphosphonate naive. The mean 10-year risk of any major fracture was 11.2% for the overall group and 10.4% for the untreated subset. The mean 10-year risk was 11.1% similar for the overall group and 9.1% for the untreated subset when bone mineral density (BMD) was used instead of body mass index (BMI) to estimate the FRAX score. The corresponding mean 10-year risk of hip fracture was 3.3% and 2.7% using BMI and 3% and 1.7% using BMD to estimate the FRAX score. FRAX treatment thresholds for major fracture were exceeded in approximately 14% of all patients and 9% of untreated patients in the two groups when scores were calculated using BMI

and 10% and 5% when using BMD. For hip fracture, the percentages were 37% and 31% using BMI and 33% and 17% using BMD.

Conclusion: Osteoporosis is undertreated and more than 25% of the patients in the study cohort were eligible for osteoporosis treatment.

Disclosures: Joanne LaFleur, Novartis, 2

This study received funding from: Novartis

SA0373

Anticonvulsant and Opioid Use and Fractures in Veterans with Spinal Cord Injury. Laura Carbone*, Amy Chin², Todd Lee², Stephen Burns³, Jelena Svircev⁴, Helen Hoenig⁵, Titilola Akhigbe¹, Frances Weaver². ¹University of Tennessee Health Science Center, USA, ²Edward J. Hines, Jr. VA Hospital, USA, ³VA Puget Sound Healthcare System, USA, ⁴VA Puget Sound, USA, ⁵VA Medical Center, USA

Purpose: Anticonvulsant and opioid use are associated with an increased risk for fracture in the general population. However, whether this also is true for patients with Spinal Cord Injury (SCI) has not been determined.

Methods: We utilized the Veterans Affairs Spinal Cord Disease Registry to identify all male Veterans with a traumatic SCI >two years duration from 2002-2007. Incident lower extremity fractures over during this time period and anticonvulsant and opioid use within five years prior to the fracture were identified. The association of anticonvulsant use overall, by type (enzyme inducing, non-enzyme inducing or both), by number (monotherapy vs. polytherapy) and by individual medication was determined. The relationship of benzodiazepine (BZD) use with overall fracture risk was determined. The relationship of opioid use to lower extremity fracture risk was also analyzed.

Results: There were 2964 anticonvulsant users and 4490 non users of these medications and 892 opioid users and 6562 non users of these medications. 892 Veterans developed an incident lower extremity fracture during this time period. After adjustment for covariates, there was no significant association between anticonvulsant use and lower extremity fractures (OR 0.96 (95% CI 0.82-1.11)). There was no significant association between type (p=0.79) or number of anticonvulsants (p=0.22) used and incident fractures. BZD use was not associated with fracture risk (OR 1.04 (95% CI 0.89-1.22)). Among individual anticonvulsants, topiramate (OR 1.93 (95% CI 1.18-3.18)) and temazepam (OR 1.44 (95% CI 1.12-1.85)) were positively and gabapentin (OR 0.83 (95% CI 0.69-0.99)) was negatively associated with fracture risk. After adjustment for covariates, there was no significant association between opioid use and lower extremity fractures (OR 1.01 (95% CI 0.86-1.17)). However, there was a significant positive association between hydromorphone (OR 1.91 (95% CI 1.12-3.26)), meperidine (OR 1.83 (95% CI 1.04-3.24)) and morphine use (OR 1.28 (95% CI 1.01-1.61)) and risk for lower extremity fractures.

Conclusions: The classes of anticonvulsant and opioid drugs are not associated with an increased risk for lower extremity fractures in males with SCI. However, the risk of fracture varies by individual anticonvulsant and opioid used. The selection of an anticonvulsant or an opioid for use in SCI patients at increased risk for fracture should be guided by the fracture risk associated with that particular drug.

Disclosures: Laura Carbone, None.

SA0374

Elevated Coronary Artery Calcium Scores Might be Related to Low Bone Mineral Density in Korean Women. Beom-hee Choi*, Kyu-nam Kim, Sang hyeon Je, Sang-man Kim, Nam-seok Joo, Duck-Joo Lee, Kwang-min Kim. Family Medicine, South Korea

Background; Decline of bone mineral density (BMD) is a character of aged women and coronary artery calcium deposit may be a risk factor of coronary artery diseases. However, little is known for the relationship between coronary artery calcium score (CACS) and BMD. The aim of this study was to evaluate that relationship in Korean women. **Methods;** We used the data of 634 Korean women who checked in a health promotion center of Cha and Ajou University, Republic of Korea, after excluding chronic diseases (kidney diseases, thyroid & parathyroid diseases, other autoimmune diseases), any cancers, history of coronary artery diseases. BMD was measured by the Dual Energy X-ray Absorptiometry (DEXA) and compared by CACS. CACS data was divided into two groups of group A (CACS=0) and group B (CACS>0). **Results;** Age, body mass index (BMI) and waist circumference were higher in group B than in group A. CACS showed positive correlation with age, BMI, and waist circumference. Lumbar, hip and neck BMD in group A was higher than in group B (p<0.05). After adjusting age, BMI, and waist circumference, group A still showed significantly higher BMD than group B (p<0.05). **Conclusions;** These results suggest that CACS may have inverse correlation with BMD and elevation of CACS may result from abnormal bone metabolism.

Disclosures: Beom-hee Choi, None.

SA0375

See Friday Plenary Number FR0375.

SA0376**Fat Mass Is Negatively Associated with Bone Mineral Content in Korean.**

Jung Hee Kim^{*1}, Hyung Jin Choi², Min Joo Kim², Jee Hyun An², Sang Wan Kim³, Seong Yeon Kim¹, Nam H. Cho⁴, Chan Soo Shin². ¹Seoul National University College of Medicine, South Korea, ²Department of Internal Medicine, Seoul National University College of Medicine, South Korea, ³Seoul National University Boramae Hospital, South Korea, ⁴Ajou University School of Medicine, South Korea

Obesity and osteoporosis, two disorders of body composition, have become increasingly important public health problems throughout the world. However, the effect of fat mass on bone mass remains controversial. This study investigates the effect of fat mass and regional fat distribution on bone mass within a community-dwelling cohort.

A total of 3042 subjects (1284 men, 362 premenopausal women, and 1396 postmenopausal women) were studied. Fat mass, percent fat mass, lean mass, percent lean mass, and bone mineral content (BMC) were measured by dual energy X-ray absorptiometry.

Fat mass and percent fat mass decreased significantly across increasing tertiles of BMC in all 3 subgroups (men, pre- and postmenopausal women). In contrast, lean mass and percent lean mass increased significantly across tertiles of BMC in men, and a similar trend was also identified in postmenopausal women. Interestingly, although correlation analysis showed a positive association between fat mass and BMC ($P < 0.05$), this association became negative after controlling for age and weight ($P < 0.05$). Finally, in pre- and postmenopausal women, subjects with the lowest waist circumference had the highest BMC in the higher three quartiles of percent fat mass after adjusting for age and weight ($P < 0.05$), indicating that abdominal obesity is associated with BMC independent of total fat mass.

This study demonstrated that fat mass was inversely related to BMC after removing the mechanical loading effect in Korean men and women. Moreover, abdominal obesity as measured by waist circumference was significantly associated with BMC independent of total fat mass.

Disclosures: Jung Hee Kim, None.

This study received funding from: National Genome Research Institute

SA0377

See Friday Plenary Number FR0377.

SA0378**High Serum Adiponectin Predicts Incident Fractures in Elderly Men. Mr OS**

Sweden. Helena Johansson^{*1}, Anders Oden², Ulf Lerner³, HANS JUTBERGER⁴, Mattias Lorentzon⁵, Elizabeth Barrett-Connor⁶, Magnus Karlsson⁷, Osten Ljunggren⁸, Ulf Smith⁹, Eugene McCloskey¹⁰, John Kanis¹¹, Claes Ohlsson⁵, Dan Mellstrom¹². ¹Swe, ²Centre for Bone & Arthritis Research (CBAR), Sahlgrenska Academy, University of Gothenburg, Sweden, Sweden, ³University of Umea, Sweden, ⁴UNIVERSITY HOSPITAL SAHLGRENSKA, Sweden, ⁵Center for Bone Research at the Sahlgrenska Academy, Sweden, ⁶University of California, San Diego, USA, ⁷Skane University Hospital Malmo, Lund University, Sweden, ⁸Uppsala University Hospital, Sweden, ⁹Lundberg Laboratory for Diabetes Research, University of Gothenburg, Sweden, ¹⁰University of Sheffield, United Kingdom, ¹¹University of Sheffield, Belgium, ¹²Sahlgrenska University Hospital, Sweden

An association between high serum adiponectin and increased risk of fracture in men is reported in a few studies. The aim of the present study was to determine whether high serum adiponectin was associated with an increase in the risk of fracture in elderly men, and if so, whether the relationship was non-linear in a multivariate analysis.

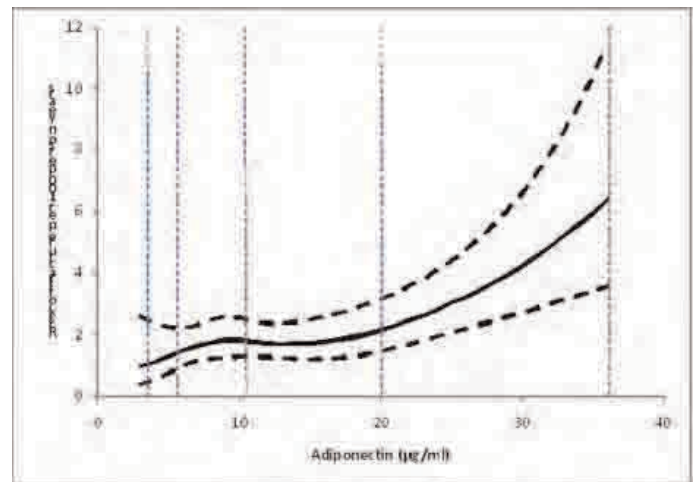
The relationship between serum adiponectin and the subsequent risk of fracture was examined in 999 elderly men drawn from the population recruited to the MrOS study in Gothenburg, Sweden. Baseline data included personal general health and life style questionnaires, BMI, BMD, serum adiponectin, osteocalcin, insulin and leptin. Serum adiponectin was analysed with an ELISA-kit (Linco Research, Missouri USA). Men were followed for up to 7.4 years (average 5.2 years). Poisson regression was used to investigate the relationship between serum adiponectin, other risk variables and the hazard function of fracture.

During follow up, 150 men sustained one or more fracture. The risk of fracture (adjusted for BMI, BMD, osteocalcin and insulin) increased by 32% for each SD increase in serum adiponectin (Gradient of risk = 1.32; 95% confidence interval = 1.15-1.52). When BMD was not adjusted for, the gradient of risk was 1.41 (95% confidence

interval = 1.23-1.61). The association between serum adiponectin and fracture risk did not significantly differ from linearity (Figure).

High serum adiponectin is associated with a significant excess risk of fracture in elderly men.

Figure. The hazard function of fracture (momentary risk) and 95% confidence intervals according to baseline serum adiponectin for a man where age was set to 75 years, the time since baseline was set to 2 years of follow up. Previous fracture was set to no and BMD and general health were set to the average value of the cohort. The vertical dashed lines represent the 1st, 10th, 50th, 90th and 99th percentile.



Figure

Disclosures: Helena Johansson, None.

SA0379**Inverse Associations between Abdominal Visceral Adipose Tissue and Bone**

Density. Miryoung Lee^{*1}, Audrey Choh¹, Keith Wurzbacher¹, Ellen Demerath², Richard Sherwood³, Dana Duren⁴, Roger Siervogel¹, Bradford Towne¹, Stefan Czerwinski¹. ¹Wright State University Boonshoft School of Medicine, USA, ²University of Minnesota School of Public Health Division of Epidemiology & Community Health, USA, ³Lifespan Health Research Center, Wright State University, USA, ⁴Wright State University, USA

Introduction and aim: Obesity is thought to beneficially influence bone density through mechanisms such as increased mechanical loading. A few recent studies, however, have inconsistently shown abdominal obesity, especially visceral adipose tissue (VAT), to be negatively associated with bone mineral density (BMD). The aim of this study was to determine whether VAT and abdominal subcutaneous adipose tissue (SAT) mass are related to BMD in healthy white adults, independent of total body adiposity and osteoporosis-related risk factors.

Methods: Our cross-sectional study sample consisted of 214 males and 249 females (age range 18-88 yr, mean age 45.4 yr) from the Fels Longitudinal Study. Total VAT and SAT mass (kg) were assessed using a multi-slice magnetic resonance imaging (MRI) protocol. Dual energy X-ray absorptiometry was used to estimate BMD of the femoral neck (NFBMD), lumbar spine L14 (LSBMD) and total body (TBBMD). Body mass index (BMI, kg/m²) was calculated from weight and height. Covariates included age, current smoking, physical activity levels, menopausal status for women, and diabetes status. Sex-stratified general linear regression models were used for statistical analysis adjusting for significant covariates of BMD.

Results: There were significant ($p < 0.05$) sex differences in VAT (men vs women, 3.92.6 vs 1.81.4 kg) and SAT (4.82.8 vs 5.63.4 kg). In men, VAT was negatively related to NFBMD and TBBMD in multiple regression models ($p < 0.001$); for example, a one SD increase in VAT was related to decreases of 0.39 g/cm² in NFBMD, and 0.54 g/cm² in TBBMD. Higher SAT levels were associated with lower NFBMD ($p = 0.005$) and TBBMD ($p = 0.025$). There were no significant relationships between either VAT or SAT with LSBMD. In women, higher VAT was significantly related to lower TBBMD ($p = 0.025$); a one SD increase in VAT was associated with a 0.22g/cm² decrease in TBBMD. VAT was not related to NFBMD or LSBMD. Higher SAT levels were related to lower NFBMD ($p = 0.001$) and TBBMD ($p = 0.003$).

Conclusion: Our results suggest that MRI-assessed abdominal adipose tissue mass (VAT and SAT) is inversely related to BMD at specific skeletal sites. These results reveal complexities of the relationship between fat and bone in white adults.

Disclosures: Miryoung Lee, None.

SA0380

See Friday Plenary Number FR0380.

SA0381

Prevalence of Higher Fracture Risk Using FRAX® in Community-Dwelling Japanese People. Yasuyo Abe^{*1}, Eugene McCloskey², Makoto Osaki¹, Kiyoshi Aoyagi¹. ¹Nagasaki University, Japan, ²University of Sheffield, United Kingdom

Diagnosis of osteoporosis has been based on bone mineral density (BMD). However, many fractures occur in individuals with BMD above the threshold for osteoporosis. Against this background, in 2008, a WHO Working Group developed FRAX® (<http://www.sheffield.ac.uk/FRAX>), a tool to evaluate 10-year fracture probability of individual patients based on clinical risk factors with or without femoral neck BMD. Using the FRAX® model for Japan, the Japan Osteoporosis Society is considering implementing an intervention threshold at or above a 10-year major osteoporosis fracture probability of 15% into a new version of the national guideline this year. The purpose of this study was to describe the potential burden of disease by assessing the prevalence of fracture risk above certain thresholds among community dwelling men and women, and the values of heel stiffness index in those identified at risk.

Study subjects included 128 men and 194 women aged 40 years and over participating in a community health checkup program in 2010. Major osteoporotic fracture risk was calculated from clinical risk factors alone using the Japan calculator in FRAX®. Heel stiffness index (SI) was also measured using a Lunar Achilles device. The prevalence of high fracture risk was calculated according to age group and gender for cut-off points of 5%, 10%, 15%, and 20%.

Major fracture probability was significantly higher in women than men (median; 11.4% vs. 6.1%, $p < 0.001$). Fracture probability increased with age in both genders, but at all ages and thresholds, the prevalence of high risk was substantially lower in men than women. For example, in men the prevalence at risk at or above the 15% threshold was only 1.9% at age 60-69 years whereas it was 20.0% in women of the same age. Among women, stiffness index was negatively correlated with age, but there was no significant correlation among men (women; $r = -0.53$, $p < 0.001$, men; $r = -0.09$, $p = 0.3$). In women the mean values of SI decreased with increasing stringency of the threshold used to define high risk (71.512.1 at 5-10% risk to 67.011.5 at 15-20% risk, $p < 0.001$). Similar association was observed in men (90.416.8 at 5-10% risk to 67.916.5 at 15-20% risk, $p = 0.01$).

Our results confirm that, when using FRAX® for screening high fracture risk individuals, the choice of cut-off points or thresholds will have a major impact on the apparent burden of disease. At any proposed threshold, treatment will be advocated in more women than men.

Disclosures: Yasuyo Abe, None.

SA0382

PTH Is a Predictor of Osteoporotic Fracture in older individuals: the Age, Gene/Environment Susceptibility (AGES)-Reykjavik Study. Vilundur Gudnason^{*1}, Kristin Siggeirsdottir¹, Thor Aspelund², Brynjolfur Jonsson³, Gunnar Sigurdsson⁴, Tamara Harris⁵. ¹Icelandic Heart Association Research Institute, Iceland, ²Icelandic Heart Association, Iceland, ³Malmo University Hospital, Sweden, ⁴Landspítali, Iceland, ⁵Intramural Research Program, National Institute on Aging, USA

Purpose

To investigate whether serum parathyroid hormone (PTH) improves risk calculator for major osteoporotic fractures in older persons.

Methods

In the AGES-Reykjavik Study, 1,897 participants (mean age 766) had serum PTH measured (Roche Diagnostics). The cohort was enrolled between September 2002 and February 2004 with 5 years of follow-up. Risk factors based on the FRAX® risk calculator included age, sex, weight, height, history of hip fracture in parent, smoking history, medication affecting BMD, alcohol use (g per week), and BMD of the hip. All previous and prospective fractures were identified from hospital and X-ray records. Risk of fracture was estimated using survival analysis and interactions between PTH and previous fracture history were considered. Hazard ratio for fracture per 1 SD change in PTH was estimated, the difference in area under the receiver operating curve, the Integrated Discrimination Improvement (IDI) and Net Reclassification Improvement (NRI) after adding PTH to a risk model with basic risk factors.

Results

There were 437 participants with previous fractures and 208 prospective fractures. Alcohol use was low in this population, on average less than 2 drinks per week, and had no effect on the results for risk of fracture. Interaction between PTH and previous of fracture was found to be statistically significant ($p = 0.013$). The hazard ratio of sustaining an incident fracture for 1 SD change in PTH for persons without previous fracture was 1.28 (95% CI 1.11 to 1.47). The hazard ratio for 1 SD change in PTH for persons with history of fracture (N=437) was non-significant 0.87 (95% CI 0.62 to 1.21). Use of PTH serum level did not lead to improvement in fracture risk prediction for subjects with previous fracture. For subjects without previous fracture (N=1460) the area under the curve changed from 0.705 to 0.712 ($p = 0.01$), the IDI was 0.012 ($p = 0.0007$), the relative IDI was 38%, and the NRI was 10% ($p = 0.0025$) applying cutoff thresholds of 5% and 10%.

Conclusion

Circulating PTH moderately improves risk prediction for major osteoporotic fracture in older free living individuals with no previous history of fracture compared to conventional risk factors. This suggests that PTH may have some clinical utility in short term fracture risk prediction.

Disclosures: Vilundur Gudnason, None.

SA0383

See Friday Plenary Number FR0383.

SA0384

See Friday Plenary Number FR0384.

SA0385

See Friday Plenary Number FR0385.

SA0386

The Association Between S-25-Hydroxyvitamin D and Total Femur BMD May Depend on Serum Concentrations of Retinol in Men. The Hordaland Health Study and The Oslo Health Study. Norwegian Epidemiologic Osteoporosis Studies (NOREPOS). Kristin Holvik^{*1}, Haakon E. Meyer², Glara G. Gjesdal³, Rune Blomhoff⁴, Grethe S. Tell¹. ¹Department of Public Health & Primary Health Care, University of Bergen, Norway, ²Department of Community Medicine, Institute of Health & Society, University of Oslo, & Division of Epidemiology, Norwegian Institute of Public Health, Norway, ³Department of Rheumatology, Haukeland University Hospital, & Institute of Medicine, University of Bergen, Norway, ⁴Department of Nutrition, Institute of Basic Medical Sciences, Medical Faculty, University of Oslo, Norway

A positive association between serum 25-hydroxyvitamin D (s-25(OH)D) levels and BMD is commonly seen in observational studies. It has been suggested that a positive effect of vitamin D on BMD may be counteracted by high concentrations of retinol.

In a sample of elderly men and women born 1924-27 who participated in two population-based osteoporosis health studies in Bergen (59N) and Oslo (60N), and who were randomly selected to the subcohort of a case-cohort study, 170 participants (72 men and 98 women) had BMD measurements performed by DXA in 1998-2001 (age at examination 71-77 years). DXA measurements of total femur were performed on two different densitometers (Lunar Expert and Lunar DPX-L) that were cross-calibrated for this purpose. Serum analyses of 25-hydroxyvitamin D and retinol were performed by respectively HPLC-APCI-MS and HPLC-UV, simultaneously in the same laboratory. Linear regression analyses were stratified by gender. Age, body mass index, and season of blood sampling were included as covariates.

Mean (SD) total femur BMD was 0.94 (0.15) g/cm² in men and 0.81 (0.11) g/cm² in women ($p < 0.001$). Mean (SD) s-25(OH)D and s-retinol was 58.1 (23.1) nmol/l and 2.49 (0.73) µmol/l, respectively, and not significantly different in women than men.

The association between s-25(OH)D and BMD was not significant. The interaction term between s-retinol and s-25(OH)D on BMD was statistically significant for men ($p = 0.016$) but not women ($p = 0.23$). In men, the coefficient for ΔBMD per 20 nmol/l increase in s-25(OH)D was reduced by 0.036 g/cm² (corresponding to 1/4 SD) for each µmol/l higher s-retinol.

The notion that a positive association between vitamin D status and BMD may be dependent on serum retinol levels was supported by these preliminary data in men, but not women.

Disclosures: Kristin Holvik, None.

SA0387

The Effect of Clinical Risk Factors (CRF) on Fracture Risk Decreases with Age. Diantha Howard, Edward Leib, Lynda Tilluckdharry*. University of Vermont, USA

Introduction: BMD combined with clinical risk factors (CRFs) such as in FRAX provide a better prediction of fracture risk. It is not clear however if the impact of CRFs on fracture risk varies with age.

Methods: We performed a retrospective analysis of a database of 15,033 PM women combining CRFs and BMD results utilizing a GELunar densitometer. Logistic regressions were performed at 10 year intervals, age 45-75, and individual CRFs and the odds ratio of risk of fracture were calculated.

Results: Of the total population studied, fractures occurred in 14.7%. CRFs including, smoking, current steroid use, steroid use for more than three months, rheumatoid arthritis (RA) and secondary causes of osteoporosis correlated with an increased risk of fracture. We did not find any correlation between fracture risk and parental history of a hip fracture; we did not survey for alcohol use and as fractures were historical, impact of previous fractures could not be ascertained. For every 5 year increase in age, there was a significant increase in fracture risk which was more apparent in women who did not have a clinical risk factor than for those that had the risk demonstrating that the presence of a clinical risk factor decreased the odds ratio of the impact of 5 year increments of age. However glucocorticoid use was sufficiently powerful to negate any significant effect of age. We looked at the risk of aging on the impact of a clinical risk factor at age 45, 55, 65, and 75. For the CRFs of smoking, RA, secondary osteoporosis and number of CRFs, the effect of the clinical risk factor declined with increasing age and by age 75 had no impact on risk of fracturing for any of the clinical risks.

Conclusion: Our findings from this large database of PM women demonstrate that the presence of clinical risk factors has a greater impact in younger individuals but in the elderly that effect disappears. The effect of age on fracture risk appears to be entirely negated in women on glucocorticoids. In elderly patients with CRFs, the calculated fracture risk would be increased by the presence of such factors and the impact in younger individuals may be greater than would be indicated in models such as FRAX.

Disclosures: Lynda Tilluckdharry, None.

SA0388

The Relationship of Bone Marrow Fat with Bone Geometry and Strength Differs By Diabetic Status. Yahtyng Sheu¹, Francesca Amati², Ann Schwartz³, Xiaojuan Li³, Christine Lee⁴, Christopher Gordon⁵, Bret Goodpaster⁶, Robert Boudreau⁶, Joseph Zmuda¹, Eric Orwoll⁷, Jane Cauley¹. ¹University of Pittsburgh Graduate School of Public Health, USA, ²University of Lausanne, Switzerland, ³University of California, San Francisco, USA, ⁴OHSU, USA, ⁵McMaster University, Canada, ⁶University of Pittsburgh, USA, ⁷Oregon Health & Science University, USA

Mechanism underlying the observation of high bone mineral density (BMD) and high fracture rate among diabetic (DM) individuals is not fully understood. Identifying new pathways for this paradoxical relationship is important. Osteoblasts and adipocytes share a common precursor cell, where its differentiation process favors adipocytes with aging. Recent studies have reported a negative association of bone marrow fat (BMF) with osteoporosis and BMD; however, its relationship with bone strength and geometry, especially among DM individuals, is unknown. Therefore, we hypothesized that higher BMF is associated with lower bone strength and geometry in 156 men aged 74-96 years old from the Osteoporotic Fracture in Men study. Spine BMF was measured using magnetic resonance spectroscopy. Peripheral quantitative computed tomography was used to obtain cortical strength and geometry measures at the radius and tibia, including cross-sectional area (CSA), thickness (THK), polar moment of inertia (PMI), cross-sectional moment of inertia (CSMI), section modulus (SM) and stress-strain index (SSI). BMF was expressed as lipid to "lipid+water" ratio (%). Pearson correlation and multivariable linear regression were used to test our hypothesis. All analyses were adjusted for age, weight and height. We found that men with DM had a significantly higher BMF than those without DM (59% vs. 55%; $p=0.04$). For the radius, modest and negative correlations were found between BMF and most, not all, of the strength indices in both DM and non-DM men (Table). However, all strength indices at the tibia were significantly correlated with BMF in the DM group only. For example, the correlation coefficient between BMF and CSMI at the tibia 33% site was -0.48 ($p<0.01$) in the DM group, compared to -0.04 ($p=0.69$) in the non-DM group. Additionally, in the DM group, one standard deviation increase in BMF was associated with a 12% reduction for CSMI at the same site. The relationship between BMF and bone strength at the radius was similar between men with and without DM. However, at the tibia, this association differed between groups. More studies are needed to further investigate the impact of bone marrow adiposity on bone strength and quality in diabetes.

	DM (n=38)		Non-DM (n=118)	
	Radius 33%	Tibia 33%	Radius 33%	Tibia 33%
CSA	-0.24	-0.33**	-0.23*	0.08
THK	-0.11	-0.21	-0.21*	0.06
CSMI	-0.34**	-0.48*	-0.22*	-0.04
PMI	-0.33**	-0.41*	-0.18**	0.02
SM	-0.36**	-0.43*	-0.15	0.12
SSI axial	-0.26	-0.43*	-0.18**	0.00
SSI polar	-0.37**	-0.45*	-0.14	0.06

* $p<0.05$; ** $p<0.01$

Disclosures: Yahtyng Sheu, None.

SA0389

Longitudinal Population-based Study Assessing Abdominal Aortic Calcification and Volumetric BMD in Postmenopausal Women. Louise Stuart¹, Elizabeth Atkinson¹, Jon Camp¹, Shreyasee Amin¹, Sundeeep Khosla², Ann Kearns¹. ¹Mayo Clinic, USA, ²College of Medicine, Mayo Clinic, USA

An association between atherosclerosis and osteoporosis has long been documented. However, few studies have longitudinally examined the progression of these disorders. To better define the relationship between these disorders, we have measured abdominal aortic calcifications (AAC) in postmenopausal women and compared the rate of AAC change to the rate of change in volumetric bone mineral density (vBMD) of the lumbar spine.

From an age-stratified random sample of community adults who had QCT scans of the lumbar spine, (which included views of the abdominal aorta), at baseline, 3 yrs, and 6 yrs, we studied 50 postmenopausal women (mean age [SD]: 66 yrs [11]) who had QCT scans at all three time points. We performed an assessment of AAC from QCT scans using Analyze (version 10) software. All three scans from each individual were registered to each other so that the same area of aorta was assessed over time. Quantification of AAC was performed using the Agatston scoring system. Lumbar spine vBMD was measured from QCT scans and rates of change calculated. The relationship between rates of change were assessed using Spearman correlations.

The median Agatston score standardized by slice increased over time from 3.8 at baseline to 15.2 at 6 yrs. The change was significantly correlated with baseline age ($r=0.42$, $p=0.003$), increasing more in older women. Lumbar spine vBMD decreased over time and also was significantly correlated with baseline age ($r=0.48$, $p<0.001$), declining more in younger women. The change in Agatston score did not correlate with the change in vBMD ($r=0.10$, $p=0.50$). Correlation adjusted for baseline age was $r=-0.13$ ($p=0.37$).

In postmenopausal women, AAC increases and vBMD of the lumbar spine decreases over time. The rates of change of both AAC and vBMD depend on baseline age. In light of previous cross-sectional data demonstrating age-independent associations between vascular calcification and bone mass, additional longitudinal studies in larger cohorts are needed to further evaluate possible relationships in the rates of change in these parameters.

Disclosures: Louise Stuart, None.

SA0390

The Serum Uric Acid Is Not Associated with Osteoporosis in Postmenopausal Women. Hee-Jeong Choi¹, Byung-Yeon Yu², Han Jin Oh³, ILWOO JOO⁴. ¹Department of Family Medicine, Eulji University School of Medicine, South Korea, ²Department of Family Medicine, Konyang University School of Medicine, South Korea, ³Kwandong University, College of Medicine, South Korea, ⁴Cheil General Hospital, Kwandong University, South Korea

Background: A recent study demonstrated that higher serum uric acid levels are associated with higher bone mineral density (BMD) at all skeletal sites and with a lower prevalence of vertebral and non-vertebral fractures in older men. Serum uric acid is a kind of endogenous antioxidants. Also the oxidative stress has been linked to osteoporosis. The objective of this study was to determine the relationships between the serum uric acid levels and the osteoporosis in postmenopausal women.

Methods: Subjects were healthy postmenopausal women who had visited the Health Promotion Center. Medical history and lifestyle data were collected by the questionnaire and history taking. Laboratory tests include renal function indices, serum C-telopeptide, osteocalcin, 25(OH)D, and uric acid levels. The lumbar spinal BMD (L1-4) was measured by dual-energy X-ray absorptiometry. Logistic regression analysis was used to determine the high level of uric acid affecting the lumbar spinal BMD.

Results: A total of 937 postmenopausal women were selected for this study. Mean age was 56.45.9 years old. The lumbar spinal BMD were significantly different according to tertiles of uric acid levels ($P=0.013$, P for trend=0.005): Lowest tertile (1.0090.178 mg/cm²), middle tertile (1.0160.164 g/cm²), highest tertile (1.0460.152 g/cm²). The proportion of osteoporosis (L1-4 T-score ≤ -2.5) was 25.7% in the lowest tertile of uric acid group. Otherwise, in the middle and highest tertile of uric acid group, the proportion of osteoporosis was 23.3% and 19.4%, respectively. Women with the highest tertile of uric acid were not significantly decreased the risk of osteoporosis (OR=0.78, 95% CI, 0.51-1.20) compared to those with the lowest tertile of uric acid after adjusting for age, body mass index, estimated glomerular filtration rate, alcohol drinking, current smoking, and exercise.

Conclusion: In healthy postmenopausal women with the highest tertile of uric acid levels, the lumbar spinal BMD is significantly higher than those with the lowest tertile of uric acid levels. However, the risk of osteoporosis is not significantly decreased in these women compared to those with the lowest tertile of uric acid levels.

Disclosures: Hee-Jeong Choi, None.

SA0391

See Friday Plenary Number FR0391.

SA0392

See Friday Plenary Number FR0392.

SA0393

Circulating Sclerostin Correlates to Bone Mineral Mass, Micro-Structure and Turnover in Healthy Elderly Men and Women. Claire Durosier^{*1}, Antoon Van Lierop², Serge Ferrari³, Thierry Chevalley⁴, Socrates Papapoulos², Rene Rizzoli⁵. ¹Hopitaux Universitaires De Geneve, Switzerland, ²Leiden University Medical Center, The Netherlands, ³Geneva University Hospital & Faculty of Medicine, Switzerland, ⁴University Hospitals of Geneva Division of Bone Diseases, Switzerland, ⁵University Hospital, Switzerland

Sclerostin is an osteocyte product which decreases bone formation and appears to be involved in the bone response to mechanical loading. However, the role and significance of circulating sclerostin (circ-SCL) is still poorly understood. We investigated circ-SCL using 2 immunological assays recognizing different epitopes in 190 healthy subjects (100 women and 90 men) aged 651 (xSD) years. Such a well homogenous group in terms of age allowed us to minimize the influence of age in the analysis. The relation between circ-SCL and whole body, spine and proximal femur bone mineral content/areal density (DXA), micro-structure (HR-pQCT, Scanco XtremCT) at weight-bearing and non weight-bearing sites, and turnover markers was assessed. Circ-SCL was positively correlated to whole body bone mineral content (WB-BMC) ($r=0.223-0.334$, $p=0.0001-0.002$) in men and in women, in both assays. A positive correlation of circ-SCL was also found with distal radius and tibia cortical area ($r=0.206-0.319$, $p=0.005-0.001$), cortical thickness ($r=0.148-0.285$, $p=0.0445-0.001$), relative cancellous bone volume (BV/TV) ($r=0.187-0.447$, $p=0.011-0.0001$), and trabecular number ($r=0.220-0.379$, $p=0.003-0.0001$). Circ-SCL was positively correlated to lumbar spine areal BMD ($r=0.370$, $p=0.0001$) in men and in women ($r=0.316$ and 0.389 , respectively, $p<0.002$). The relation between circ-SCL and cortical thickness lost significance after adjustment for WB-BMC, at the distal radius in both assays, but not at distal tibia in one assay, suggesting that mass rather than structure may primarily account for the association. The bone turnover markers PINP and CTX were negatively correlated to circ-SCL, even after adjustment for WB-BMC, in one assay. These results indicate that circ-SCL positively correlates to bone mass, as assessed by mineral content and/or micro-structure measurements. They thus suggest that circ-SCL may primarily reflect osteocyte cell number. Furthermore, the relation of turnover markers with circ-SCL, as determined in one of 2 assays, even after adjustment for bone mineral mass, suggests that circ-SCL may also be associated with bone remodeling. However, the detection of such an association seems to rely on the epitopes recognized by the immunological assays.

Disclosures: Claire Durosier, None.

SA0394

See Friday Plenary Number FR0394.

SA0395

Long-term Treatment with Raloxifene, but not Bisphosphonates, Reduces Circulating Sclerostin Levels in Postmenopausal Women. Hong-Hee Kim¹, Yun Ey Chung², Sun-Kyeong Lee³, Sun-Young Lee⁴, Seung Hun Lee^{*5}, Ghi Su Kim⁵, Shin-Yoon Kim⁶, Farval S. Mirza³, Jung-Min Koh⁷, Joseph A. Lorenzo³. ¹Seoul National University, South Korea, ²Department of Internal Medicine, Seoul Veterans Hospital, South Korea, ³Division of Endocrinology, University of Connecticut Health Center, USA, ⁴Asan Institute for Life Sciences, South Korea, ⁵Asan Medical Center, University of Ulsan College of Medicine, South Korea, ⁶Kyungpook National University Hospital, South Korea, ⁷Asan Medical Center, South Korea

Purpose: Circulating sclerostin concentrations are higher in postmenopausal than in premenopausal women, and estrogen treatment suppresses sclerostin levels in both men and women. We determined whether anti-resorptives may suppress the circulating sclerostin levels.

Methods: We conducted a retrospective observational study. Eighty postmenopausal women were treated with raloxifene for 19.4 7.7 months ($n = 16$), bisphosphonates for 19.2 6.7 months ($n = 32$), or were untreated ($n = 32$) for 17.1 4.6 months. Plasma sclerostin concentrations were measured before and after treatment.

Results: Plasma sclerostin levels after treatment were significantly lower in the raloxifene than in the control group (55.8 23.4 pmol/l vs. 92.1 50.4 pmol/l, $p = 0.046$), but were similar between the bisphosphonate and control groups. Relative to baseline,

raloxifene treatment markedly reduced plasma sclerostin concentration (-40.7 22.8%, $p < 0.001$), with respect to both control (-7.5 29.1%) and bisphosphonate (-3.1 35.2%) groups. Changes in bone-specific alkaline phosphatase and osteocalcin levels showed reverse associations with sclerostin concentration changes in the raloxifene ($\gamma = -0.505$, $p = 0.017$) and control ($\gamma = -0.410$, $p = 0.020$) groups.

Conclusions: Raloxifene, but not bisphosphonates, significantly suppressed circulating sclerostin concentration, suggesting that sclerostin may mediate the action of estrogen on bone metabolism, independently of their anti-resorptive effects.

Disclosures: Seung Hun Lee, None.

SA0396

See Friday Plenary Number FR0396.

SA0397

Histomorphometric Evaluation of Transiliac Bone Biopsies after Bariatric Surgery. Noortje Rabelink^{*1}, Nathalie Bravenboer¹, Dave Schweitzer², Coen Netelenbos³, Paul Lips¹. ¹VU University Medical Center, The Netherlands, ²Reinier de Graaf Gasthuis, Netherlands, ³VU Medical Center, The Netherlands

Purpose:

Patients who have undergone bariatric surgery (BS) are at increased risk for bone loss. This process of bone loss is not completely understood. We used bone histomorphometry to investigate changes at tissue level in these patients.

Methods:

In 8 patients (7 women) with an average age of 44 years (range 32-62) a transiliac bone biopsy was obtained while they were under general anaesthesia for plastic surgery. Patients were labeled with tetracycline prior to biopsy. Bone biopsies were embedded in methylmethacrylate without prior decalcification. Sections were stained with Goldner and tartrate-resitant acid phosphatase. Histomorphometry was performed with NIS-Elements AR 3.1 (Nikon GmbH, Dusseldorf, Germany) at 40 and 100 \times magnification. Dynamic parameters were measured only in 5 patients due to lack of double labelling in the other patients.

Results:

In patients after BS we found the following results; (Median [Interquartile range])

Bone volume 15.5% [9.2-19.8]
Bone surface 2.2 mm²/mm³ [1.8-3.1]
Osteoid thickness 10.9 μ m [9.0-14.8]
Osteoid volume 1.2% [0.8-1.6]
Osteoid surface 14.3% [8.4-24.0]
Trabecular thickness 127.4 μ m [116-166]
Trabecular number 1.0 mm [0.73-1.19]
Cortical thickness 1457 μ m [874-1757]
Cortical porosity 8.6 % [4.0-12.2]
Osteoclast number 0.3/mm² [0.2-1.0]
Mineral apposition rate 0.62 μ m/day [0.60-0.69]
Mineralisation surface 5.1% [3.3-7.1]
Bone formation rate (BFR) 0.033 μ m³/ μ m²/day [0.027-0.055]

Conclusion:

In our patients after BS, bone volume and trabecular number were low. This probably results from a low bone formation rate, while bone resorption continues.

Disclosures: Noortje Rabelink, None.

SA0398

Erythrocyte Fatty Acid Composition of Postmenopausal Women with and without Osteoporosis: Case-Control Study in Korea. Hyoun-Jung Moon¹, Yongsoon Park¹, Hae-Hyeog Lee², Kyo Il Suh³, Jin-Yong Yoo³, Hyeongkyu Park³, Tae-Hee Kim², Dongwon Byun^{*4}, Myung Hi Yoo³. ¹Hanyang University, South Korea, ²Soon Chun Hyang University Bucheon Hospital, South Korea, ³Soon Chun Hyang University Hospital, South Korea, ⁴Soon Chun Hyang University Hospital, South Korea

The purpose of the present study was to compare erythrocyte fatty acid composition between postmenopausal women with and without osteoporosis in Korea. Fifty cases and fifty control were participated in this study and osteoporosis was defined according to International Society for Clinical Densitometry guideline as <-2.5 standard deviation below the T-score for lumbar spine 1-4, femoral neck, or femoral total. The fatty acid composition of erythrocyte was analyzed by gas chromatography. Age, height, weight, and T-scores for lumbar spine 1-4, femoral neck and femoral total were significantly greater in controls than in osteoporosis cases, who also were significantly less likely to use calcium supplementation. However, age at menopause, exercise, smoking, drinking, and case of menopause did not differ significantly between cases and controls. In erythrocytes, plant source of omega-3 fatty acid, alpha-linolenic acid was significantly lower in case than control ($0.44 \pm 0.05\%$ vs $0.61 \pm 0.07\%$), while animal source of omega-3 fatty acid, docosapentaenoic acid was significantly higher in case than control ($2.53 \pm 0.07\%$ vs $2.26 \pm 0.09\%$). Other fatty acids, saturated fatty acids, monounsaturated fatty acids, polyunsaturated fatty acids,

trans fatty acid, and omega-3/omega-6 fatty acid ratio were not significantly different between case and control. Our results suggest that plant source of omega-3 fatty acids may decrease the risk for osteoporosis, but animal source of omega-3 fatty acids may increase the risk in the Korean menopausal women.

Disclosures: Dongwon Byun, None.

This study received funding from: the Korea Research Foundation Grant funded by the Korean Government (KRF-2008-313- C00279)

SA0399

Implications of Compromised Zinc Status on Bone Loss Associated with Low Grade Chronic Inflammation in C57BL/6 Mice. Elizabeth Rendina*, Yan Wang, Kelsey Hembree, MCKALE DAVIS, Barbara Stoecker, Stephen Clarke, Edralin Lucas, Brenda Smith, Oklahoma State University, USA

The trace element zinc is well-known for a broad range of physiological functions, including regulation of anabolic and catabolic activity of bone cells and various aspects of immunity. Compromised zinc status is common in older adults and has been associated with low bone mineral density (BMD) and increased risk of osteoporosis. Alterations in immune function in response to suboptimal zinc status parallel some of the immunological changes associated with aging. To begin to understand the relationship between zinc-induced immune changes and bone loss in a model of low grade chronic inflammation, 8 week old C57BL/6 male mice (n=32) were used in a 2 x 2 factorial design with dietary zinc (adequate = 35 ppm or inadequate = 5 ppm) and inflammation (0 or 0.1 mg LPS/kg bw). Diets were fed for 6 weeks prior to the 4 wk exposure to LPS by subcutaneously implanted slow release pellets. At the end of the study, complete blood counts were performed, tissue weights were recorded and bone specimens were collected. No differences in body weight due to treatments were observed during the course of the 10 week study. Thymus weight was increased in the cohort on the zinc adequate diet plus LPS, but the LPS-induced thymus hypertrophy was not observed in the zinc inadequate group. Spleen weight was unaltered by dietary and LPS treatments. Differential counts on whole blood smears revealed an increase in monocytes and a decrease in lymphocytes due to LPS in the zinc adequate cohort indicative of a chronic inflammatory response; however, these LPS-induced changes were ameliorated in the zinc deficient mice. Bone zinc content assessed using inductively coupled plasma (ICP) mass spectrometry was reduced ($p<0.05$) in the cohort receiving the 5 ppm zinc diet. This decrease in bone zinc was further exacerbated (11.1%) in the LPS treated mice on the zinc inadequate diet. BMD and microstructural analysis showed that LPS reduced ($p<0.05$) BMD and trabecular bone volume of the spine compared to the placebo in both diet groups, but the effect was not exacerbated by zinc status at the end of the 10 week study. Trabecular separation increased and trabecular thickness decreased in the LPS-treated cohorts irrespective of zinc status. No differences in cortical bone were observed between groups. Ongoing studies will evaluate the effects of zinc status and LPS on bone marrow lymphoid and myeloid populations, and future studies are needed to address the effects of age on this response.

Disclosures: Elizabeth Rendina, None.

SA0400

Rosiglitazone Decreased Muscle Cross-sectional Area and Increased %Fat While Maintaining Glycemic Control in Women with Type 2 Diabetes (T2D). Timothy Streeper^{*1}, Isra Saeed¹, Thomas Lang¹, John Kornak¹, Chengshi Jin¹, Allison R. Northcutt², Barbara Kravitz², Gitanjali Paul², Alexander R. Cobitz², Lorraine Fitzpatrick², Antonio J. Nino², ¹UC San Francisco, USA, ²GlaxoSmithKline Pharmaceuticals, USA

Rosiglitazone (RSG) stimulates stem cells to differentiate into fat cells and improves resistance to glucose, resulting in changes in muscle metabolism and body fat content. This study evaluated the effect on muscle mass and adiposity. This double blind study randomized postmenopausal women with T2D to RSG or metformin (MET) for 1 year followed by 6-month open-label MET. Markers of glycemic control and serum hormones were determined in all subjects; hip muscle lean cross-sectional area (CSA), percentage intermuscular fat in the muscle bed (%FAT), mean Hounsfield Unit of muscle tissue (LHU, a measure of intramuscular fat) and pelvic total lean body area (LBA) were assessed using hip QCT scans in a subset of subjects. In RSG, a 4.9% decrease (185.05 vs. 176.06 cm²) in CSA, and a 13.3% increase (0.15 vs. 0.17 %) in %FAT, were observed at 1y ($p<0.001$). LHU did not change. After discontinuation of RSG, CSA and %FAT showed partial recovery but still differed from baseline ($p=0.0009$ and $p=0.03$ respectively). In MET, 7.9% loss (43.09 vs. 39.68 HU) of LHU at 18 months ($p<0.01$) and a decrease of 2.6% LBA (212.06 vs. 206.46 cm²) ($p=0.03$) at 18 months were observed. Decreases from baseline (BL) to Week 52 in HbA1c were similar between treatment groups, fasting plasma glucose decreased from BL more in RSG compared to MET over time. HOMA-S increased from BL in RSG over time and decreased in MET. Serum estradiol decreased from BL to Wk52 and increased from Wk52 to Wk 76 in both treatment groups. Total testosterone increased from BL to Wk52 and decreased from Wk52 to Wk76 in both treatment groups but the change was greater in RSG. In this study, one year RSG treatment results in loss of lean hip muscle tissue and an increase of intermuscular fat, with no change in intramuscular fat. Changes trended to BL levels after discontinuation of RSG. RSG improved glycemic control and insulin sensitivity. These data highlight the relationship between metabolic and structural effects of RSG. These data support the hypothesis that RSG

promotes differentiation of stem cells to adipocytes in this population.

	Change from baseline to Week 52: Mean (SD)		Change from Week 52 to Week 76: Mean (SD)	
	RSG N=114	METFORMIN N=111	RSG N=114	METFORMIN N=111
HbA1c (%)	-0.50 (0.791)	-0.49 (0.719)	0.20 (0.704)	0.07 (0.782)
FPG (mg/dL)	-16.21 (34.537)	-11.38 (27.118)	7.69 (24.023)	5.71 (23.899)
% Change from Baseline Geo Mean (+SE, -SE) ^{1,2}				
HOMA-S (%)	16.77 (11.196, 22.633)	-5.15 (-9.259, - 0.861)	-16.72 (-20.815, - 12.415)	-12.03 (-15.213, - 8.732)
Serum Estradiol (pmol/L)	-3.453 [-17.0838, 12.4189]	-16.905 [-30.7981, -0.2237]	0.513 [-15.2056, 19.1447]	50.823 [29.3058, 75.9217]
Total Testosterone (nmol/L)	19.689 [14.1569, 25.4897]	1.932 [-4.8673, 9.2181]	-24.373 [-29.0307, - 19.4104]	-7.102 [-13.9923, 0.3411]

Changes in Glycemic and Sex Hormone Parameters

Disclosures: Timothy Streeper, GlaxoSmithKline Pharmaceuticals, 2

This study received funding from: GlaxoSmithKline Pharmaceuticals

SA0401

β -Cryptoxanthin, A Citrus Xanthophyll Carotenoid Prevents Inflammatory Bone Loss of Alveolar Bone in the Model for Periodontal Disease. Michiko Hirata*, Chiho Matsumoto, Tsukasa Tominari, Masaki Inada, Chisato Miyaura, Tokyo University of Agriculture & Technology, Japan

Periodontal disease is accompanied by inflammatory destruction of alveolar bone. Lipopolysaccharide (LPS) induces prostaglandin E2 (PGE2) synthesis and RANKL expression in osteoblasts, and leads osteoclastic bone resorption. Xanthophyll carotenoids were thought to be anti-inflammatory substance through anti-oxidization in tissues that is against various inflammatory diseases. β -Cryptoxanthin is a member of xanthophyll carotenoids included specifically in citrus fruits such as mandarin orange in Japan. Epidemiological studies have shown that the food intake of β -cryptoxanthin from citrus oranges is closely related to the level of serum β -cryptoxanthin and the markers for bone resorption in serum. In addition, bone loss was protected by the intake of citrus β -cryptoxanthin in Japanese women, and the effects were depending on serum levels of β -cryptoxanthin. In the previous study, bone loss in ovariectomized animal was partially recovered by the treatment with β -cryptoxanthin, however, effects of β -cryptoxanthin in inflammatory bone resorption is still unknown. In the present study, we investigated the effects of β -cryptoxanthin in the disease model of periodontitis. In the model, LPS from gram-negative bacteria induces inflammatory bone resorption of alveolar bone. We examined the effects of β -cryptoxanthin on PGE2 production by gingival fibroblasts, and bone resorption of mouse mandibular alveolar bone. In co-culture of mouse osteoblasts and bone marrow cells, β -cryptoxanthin suppressed the number of osteoclasts formed by inflammatory cytokines. The PGE2 production by gingival fibroblasts was markedly elevated by the treatment with LPS, and the PGE2 production was suppressed by adding β -cryptoxanthin. In organ cultures of mouse mandibular alveolar bone, β -cryptoxanthin clearly suppressed the LPS-induced bone resorption. In vivo model for periodontitis, we measured BMD of alveolar bone by DEXA and examined three-dimensional (3D) structure of mandible by micro-CT. LPS clearly decreased the BMD of alveolar bone, and the administration of β -cryptoxanthin recovered the bone loss and 3D structure of alveolar bone. Here we show that citrus β -cryptoxanthin is a possible candidate of natural components, which prevents alveolar bone loss associated with inflammation in periodontal disease.

Disclosures: Michiko Hirata, None.

SA0402

See Friday Plenary Number FR0402.

SA0403

Fractures Are Associated with Cortical Porosity at the Tibia: A Case-Control Study of Micro-Architectural Bone Parameters in Men with Idiopathic Osteoporosis. Agnes Ostertag¹, Martine Cohen-Solal², Sylvie Fernandez³, Eric Vicaut⁴, Marie-Christine De Vernejoul^{*5}, ¹U606 INSERM, France, ²Centre Viggo Petersen, France, ³Hopital Lariboisiere, France, ⁴Unite de Recherche Clinique Lariboisiere-St Louis Hospital Fernand Widal, France, ⁵Federation De Rhumatologie Et INSERM U606, France

Purpose: Idiopathic osteoporosis (OP) in men is a rare disorder that can induce fractures. The diagnosis is reached after exclusion of secondary OP in men aged 40 to 70 year-old with low bone mineral density (BMD) (Z-score < -2). Our objective was to determine biochemical, radiological and micro-architectural bone factors related to fragility fractures in these patients through a case-control study.

Methods: 40 to 70 yrs old men with a Z-score < -2 at one site (hip, lumbar or radius) were included. Men with secondary OP, treatment or any chronic inflammatory diseases were excluded. Cases were men with at least one fragility fracture (22 vertebrae, 5 hip, 8 rib, 3 wrist, 2 humerus) that occurred after the age of 40 (F+, n=32). Controls were men with OP without fracture (F-, n=36).

Data of previous fractures were collected using an interviewer-administered questionnaire, vertebral fractures were assessed on spine X-rays. Volumetric (v)BMD and bone micro-architectural indices at distal radius and tibia sites were measured with a HR-pQCT scan (X-treme, Scanco). Dual-energy X-ray absorptiometry measures were done at spine, hip and radius (Lunar). Urine and blood samples were collected in order to determine levels of bone-turnover markers, SHBG, bioavailable estradiol and testosterone, IGF-1 and homocysteine.

Student t-tests for independent groups were used to compare F+ and F-. Multiple linear regression models included age, height and weight as adjustment factors were conducted to compare the groups.

Results: F+ were significantly older than F- (58.8 vs. 53.9 yrs, $p=0.02$), but comparable in weight and height. BMD Z-score was identical at any site except at the total-hip where Z-score was significantly lower in F+ (-1.3 vs. -0.9, $p=0.02$). After adjustment on age, height and weight, micro-architectural parameters were not different at the radius. At distal tibia, cortical vBMD was significantly lower in F+ patients (801.74 vs. 857.61 mg HA/cm³, $p=0.02$) while cortical thickness was unchanged, suggesting that the decreased vBMD was related to increased porosity. Trabecular parameters, biochemical or hormonal parameters were not different in the 2 groups.

Conclusion: Our results confirm the role of cortical bone that differs according to the occurrence of fractures in men with idiopathic osteoporosis. This suggests that, in these particular patients, cortical porosity is associated with fractures in line with our previous histomorphometric data.

Disclosures: Marie-Christine De Vernejoul, None.

SA0404

A Comparative Randomized Trial of Levetiracetam and Older Antiepileptic Drugs: Bone Health and Related Outcomes. Tahir Hakami¹, Terence O'Brien¹, Sandra Petty², Jemma Christie¹, Susan Kantor¹, Marian Todaro³, John Wark³. ¹University of Melbourne, Australia, ²The University of Melbourne, Australia, ³Royal Melbourne Hospital, Australia

Antiepileptic drug (AED) therapy is associated with increased fracture risk but it is uncertain whether newer AEDs carry a similar risk to older AEDs. We compared bone mineral measures, body composition and hormones in patients who had substitution monotherapy with either levetiracetam (LEV) or an "older" generation drug, carbamazepine (CBZ) or sodium valproate (VPA). Patients with partial epilepsy on monotherapy with an older AED who had lack of efficacy or adverse effects were invited into a randomised open-label study with blinded endpoints. Those taking phenytoin (PHT) or CBZ were randomised to either LEV or VPA; those taking VPA were randomised to LEV or CBZ. Visits at 3 and 15 months included: areal bone mineral density (aBMD) at the lumbar spine, total hip, femoral neck, forearm and total body bone mineral content, soft tissue composition (Hologic 4500A, software version 5.73) including abdominal fat; peripheral quantitative computed tomography (pQCT: Stratec XCT 3000) of the radius and tibia, polar strength strain index (SSI_p); serum biochemistry and hormones; validated health and lifestyle surveys; blood pressure and anthropometry. Univariate and multiple regression analyses (SAS and SPSS) examined associations between change in bone measures and treatment group, age, sex, baseline height and weight, and follow-up interval. 84 patients [51 male (median age 40.1y, IQR 27.6-61.4), 33 female (36.8y, 23.8-51.8)] were enrolled. In most, AED substitution was within 3 months prior to baseline bone measures. 70 patients were reviewed at 12 months (40 LEV, 30 older AED group). Baseline anthropometry, bone mineral measures, fat distribution, serum biochemistry and hormones did not differ between treatment groups. At 12 months, there were increases in the older AED group in weight ($p=0.039$), BMI ($p=0.035$), % abdominal fat ($p=0.013$) and leptin ($p=0.032$) and a decrease in cortisol ($p=0.043$) with no difference in the LEV group, or between groups. There was no bone loss at any site by DXA or pQCT in either treatment group or between treatment groups. Substitution with older AED, but not with LEV, in patients previously treated for epilepsy caused significant increases in body weight and abdominal fat. There was no rapid bone change, nor any difference in the early bone response between groups when treated with LEV compared with CBZ or VPA. While this study provides reassurance, long-term follow-up may better characterize any AED effects on bone health.

Disclosures: John Wark, None.

This study received funding from: UCB Pharma

SA0405

See Friday Plenary Number FR0405.

SA0406

Aromatase Inhibitor Significantly Increased Circulating Sclerostin Level in Patients with Endocrine-responsive Breast Cancer. Yumie Rhee^{*1}, Yoon Jung Chung², Se Hwa Kim³, Sung-Kil Lim¹, Byeong Woo Park⁴.

¹Department of Internal Medicine, College of Medicine, Yonsei University, South Korea, ²Brain Korea 21 Project for Medical Science, Yonsei University, South Korea, ³Kwandong University College of Medicine, Myongji Hospital, South Korea, ⁴Department of Surgery, College of Medicine, Yonsei University, South Korea

BACKGROUND: Sclerostin, a Wnt inhibitor, product of osteocytes is known to decrease within 4 weeks of estrogen treatment in postmenopausal women. However, the level of sclerostin in endocrine-responsive breast cancer patients treated with aromatase inhibitor (AI) is still yet unknown. **OBJECTIVE:** The aim of the study was to analyze the changes in serum sclerostin levels in Korean women with endocrine-responsive breast cancer newly treated with AI assessing its relationship to estradiol, calcitropic hormones, bone turnover markers and bone mineral density (BMD). **DESIGN AND PARTICIPANTS:** We conducted a longitudinal prospective study of postmenopausal women with endocrine-responsive breast cancer ($n=45$) comparing with healthy premenopausal women ($n=36$). Patients with breast cancer were randomly assigned to either 5 mg of alendronate with 0.5 µg of calcitriol ($n=25$) or placebo ($n=20$) for 6 months to prevent bone loss associated with AI. **METHODS:** We analyzed serum sclerostin levels by ELISA (Biomedica Co., Austria) along with routine chemistry, bone markers including osteocalcin and C-telopeptide, and BMD by DXA. **RESULTS:** Premenopausal women were 27.9 years old in average, and postmenopausal women were 54.5 years old. Postmenopausal women showed significantly higher serum sclerostin levels (34.01.8 vs. 23.10.8 pmol/L, $p<0.05$). Interestingly, baseline sclerostin was positively correlated with either lumbar spine or total hip BMD ($r=0.498$, $p<0.001$ and $r=0.435$, $p<0.05$, respectively with age and Cr adjustment). There were no significant correlations between sclerostin level with bone markers but negative trend with PTH before starting AI ($r=-0.252$, $p=0.09$). Sclerostin levels after starting AI significantly increased by 31.1% in placebo group ($p<0.001$, paired t-test). It was only moderately increased in patients treated with alendronate by 16.7 % ($p=0.08$ vs placebo group). However, % changes of bone markers did not correlate with degree of sclerostin changes in either group. **CONCLUSIONS:** Our findings suggest that serum sclerostin level is indeed increased according to the level of estrogen deficiency in women either by menopause or AI use and somehow positively correlated with BMD at all sites. These findings need to be explored further in larger number of subjects.

Disclosures: Yumie Rhee, None.

SA0407

See Friday Plenary Number FR0407.

SA0408

Loss of Caspase-2 Alters Skeletal Stem Cell Properties and Results in Osteoporosis In Old C57BL/6 Mice. Ramaswamy Sharma^{*1}, Difernando Vanegas¹, Danielle Victor¹, Kathleen Woodruff¹, Marisa Lopez-Cruzan¹, Roberto Fajardo², Stephen Harris¹, Sherry Abboud Werner¹, Brian Herman¹. ¹University of Texas Health Sciences Center At San Antonio, USA, ²UT Health Science Center, San Antonio, USA

Caspase-2 is a cysteine protease involved in mitochondrial oxidative stress-induced apoptosis. Loss of caspase-2 results in premature aging, including a shortened maximum lifespan, impaired hair growth, reduced body fat content and, importantly, age-related osteoporosis. Dual energy X-ray absorptiometry (DXA) analysis of 24-26 month old *Casp2^{-/-}* mice indicated a significantly lower total body and femoral bone mineral density (BMD) as compared to wild type (WT) mice. Micro-computed tomography (µCT) analysis of *Casp2^{-/-}* femur indicated an abnormal growth plate and a lower number of secondary ossification centers that were less organized and had thinner inter-lacing trabecular bone. Reconstructed 3D-images of *Casp2^{-/-}* femur showed higher porosity, decreased bone mass and volume, wider metaphyseal compartment, significantly decreased trabecular numbers as well as decreased thickness of the bone cortex. Total indentation distance, average energy dissipated, and stiffness measurements also demonstrated decreased mechanical strength of *Casp2^{-/-}* bone. Collectively, these data demonstrate that *Casp2^{-/-}* mice become osteoporotic as they age.

Immunohistochemistry of bone sections from WT mice showed caspase-2 expression in bone marrow cells, osteoblasts, and lining cells in femur and tibia, at all ages tested. Specifically, caspase-2 is constitutively expressed in mesenchymal progenitor cells (also called skeletal stem cells) that differentiate into osteoblasts. Loss of caspase-2 in these cells resulted in decreased mineralization capacity as well as decreased sensitivity to oxidative stress-inducing agents. Interestingly, ELISA analysis of mesenchymal progenitor lysates from *Casp2^{-/-}* mice indicated a significant increase in CSF-1, which enhances differentiation of hematopoietic stem cells into osteoclasts. Taken together, we posit that loss of caspase-2 may result in altered skeletal stem cell differentiation and osteoblast function leading to decreased bone formation and increased bone resorption. Our data highlight a critical functional role for caspase-2 in male age-dependent osteoporosis. Because mortality following fracture is higher in older men as compared to women, our study suggests the use of caspase-2 as a diagnostic marker for osteoporosis as well as a putative target for treating osteoporotic disorders.

Disclosures: Ramaswamy Sharma, None.

SA0409

See Friday Plenary Number FR0409.

SA0410

See Friday Plenary Number FR0410.

SA0411

See Friday Plenary Number FR0411.

SA0412

Changes in Bone Turnover Markers After Weekly Teriparatide Administration in Postmenopausal Women with Osteoporosis. Toshitsugu Sugimoto^{*1}, Toshitaka Nakamura², Hideki Yoshikawa³, Masataka Shiraki⁴. ¹Shimane University School of Medicine, Japan, ²University of Occupational & Environmental Health, Japan, ³Osaka University Graduate School of Medicine, Japan, ⁴Research Institute & Practice for Involuntal Diseases, Japan

Background and Objective: Daily administration of teriparatide is known to result in increases in markers of both bone formation and bone resorption. In our research, a single injection of teriparatide (56.5 µg) was followed by a transient decrease in bone formation markers and then an increase over baseline levels up to 72 hr later, and lasting >7 days after administration, whereas bone resorption markers showed a transient increase after administration and then decreased to below baseline from 24 hr later and beyond. This study investigated the profile of changes in bone turnover markers over 24 weeks with weekly teriparatide administration and in the 24 hr after each dose, in order to assess effects on bone metabolism of teriparatide.

Methods: Postmenopausal women with osteoporosis between 65 and 79 years old were given subcutaneous injections of teriparatide (human PTH 1-34) at 56.5 µg once a week for 24 weeks. Measurements of bone turnover markers were taken before and within 24 hr after each dose at the start of administration and after 4, 12, and 24 weeks. BMD in L2 to L4 was also measured by DXA at the start of administration and 24 weeks later.

Results: Twenty-eight postmenopausal women with osteoporosis were enrolled. Analysis of the percent changes in bone turnover markers over the course of administration (Fig. 1) revealed that serum osteocalcin was higher throughout the 24-week period compared to baseline. Urine DPD, on the other hand, was lower throughout the 24-week period compared to baseline. Analysis of percent changes in bone turnover markers up to 24 hr post-dose relative to each pre-dose level (Fig. 2) revealed a transient decrease in serum PINP after teriparatide administration, returning to baseline levels within 24 hr post-dose. Urine NTX, on the other hand, underwent a transient increase after teriparatide administration and then returned to baseline within 24 hr post-dose. These responses were the same at every observation time point. BMD increased by approximately 2.6% after 24 weeks of administration. Weekly administration of teriparatide appeared to transiently decrease bone formation and transiently increase bone resorption, followed by a sustained increase in bone formation without increased bone resorption.

Conclusion: These results suggest that, unlike daily administration, weekly teriparatide administration enhances bone formation without enhancing bone resorption.

Disclosures: Toshitsugu Sugimoto, Daiichi Sankyo Co., 5; Asahi-Kasei Pharma Co., 5
This study received funding from: Asahi-Kasei Pharma Corporation

SA0413

See Friday Plenary Number FR0413.

SA0414

See Friday Plenary Number FR0414.

SA0415

See Friday Plenary Number FR0415.

SA0416

Once Weekly Teriparatide on Hip Structure and Biomechanical Properties. Masako Ito^{*1}, Masao Fukunaga², Teruki Sone², Toshitsugu Sugimoto³, Masataka Shiraki⁴, Yoshiki Nishizawa⁵, Toshitaka Nakamura⁶. ¹Nagasaki University Hospital, Japan, ²Kawasaki Medical School, Japan, ³Shimane University School of Medicine, Japan, ⁴Research Institute & Practice for Involuntal Diseases, Japan, ⁵Osaka City University, Japan, ⁶University of Occupational & Environmental Health, Japan

[INTRODUCTION] The effects of weekly administration of teriparatide (human PTH(1-34)) on volumetric bone mineral density (vBMD), bone geometry, and parameters of bone strength at the proximal femur were longitudinally investigated using clinical CT. This investigation was done in a subgroup of the participants in the randomized double-blind multicenter placebo-controlled clinical trial of once weekly teriparatide to evaluate the efficacy to prevent incident vertebral fracture. **[METHOD]** Sixty-six ambulatory patients with osteoporosis enrolled at 15 medical centers in Japan were randomly assigned to receive either weekly subcutaneous injection of 56.5 µg teriparatide (n=29, 74.25.1 years old) or placebo (n=37, 74.85.3 years old). **[RESULTS]** 1) teriparatide increased cortical thickness/area and total vBMD in femoral neck, inter-trochanter and shaft, 2) Cortical perimeter tended to decrease in teriparatide group, while it remained unchanged or increased in placebo group, 3) teriparatide decreased cortical vBMD in inter-trochanter, but not in femoral neck or shaft, 4) teriparatide improved biomechanical properties, i.e. increasing section modulus (SM) and decreasing buckling ratio (BR), 5) according to the distribution of percentage changes in SM or BR as a function of percentage changes in cortical thickness, teriparatide improved all three parameters while maintaining the relationship between changes in cortical thickness and other parameters as in placebo group. **[CONCLUSION]** Our longitudinal analysis of hip geometry by clinical CT revealed that once weekly administration of teriparatide exerts a similar effect to daily teriparatide injections; however, once weekly treatment for 72 weeks did not decrease cortical vBMD in femoral neck. Compared with the changes in placebo group, it is suggested that weekly teriparatide reverses age-related deteriorations in bone structure and strength, i.e. increasing cortical thickness/area and total vBMD, decreasing cortical perimeter, and improving biomechanical parameters.

Disclosures: Masako Ito, Chugai Pharmaceutical Company, 2; JT, 5; Asahi-Kasei Pharma, 5; Dai-ichi Sankyo, 5; Chugai Pharmaceutical Company, 5
This study received funding from: Asahi-Kasei Pharma

SA0417

Safety, Tolerability, Pharmacokinetics and Pharmacodynamics of Teriparatide Administered Transdermally in Japanese Postmenopausal Women. Masako Nakano^{*1}, Efrat Kochba², John Stock³, Leijui Hu³, Kazunori Uenaka⁴, Mika Tsujimoto⁴, Yael Kenan², Corina Lohrin³. ¹Eli Lilly Japan, Japan, ²TransPharma Medical Ltd., Israel, ³Eli Lilly & Company, USA, ⁴Eli Lilly Japan K.K., Japan

A system for transdermal (TD) delivery of teriparatide (TPTD) has been developed to alleviate the discomfort of subcutaneous (SC) injections and to improve acceptance and compliance. This study was the first clinical evaluation of TD TPTD application via the ViaDerm system in Japanese. The study purpose was to evaluate the safety, tolerability, pharmacokinetics (PK), and pharmacodynamics (PD) of TD TPTD in healthy Japanese postmenopausal females, and to compare PK and PD profiles with SC. Daily doses of 30-, 50-, or 80-ug TD TPTD, applied to the upper arm either by subjects or site personnel and kept on for 12 hr, or a daily dose of 20-ug SC TPTD were given for 28 days (single dose and 27 consecutive once-daily doses) in a subject/investigator blind, placebo-controlled, parallel group, dose-escalation study. Safety evaluations were performed and blood samples were collected to measure concentrations of TPTD and markers of bone formation (PINP) and resorption (CTX). A total of 61 subjects, median age 63 years, participated. The most common drug-related adverse events were increased serum ionized calcium (similar to SC) and application site reactions (pruritus, edema, erythema, and contact dermatitis), but they were not clinically significant. Application site evaluations (Draize scores) for most subjects showed no reactions or very slight erythema or edema. The visual analog scale (0 to 100 scale) for pain scored lower for TD compared to SC, with a maximum TD mean score of 3.0 (15.5 for SC). After TD application, TPTD was rapidly absorbed and absorption was essentially complete by 6 hr, with a median tmax of 2.0 hr (0.38 hr for SC). With TD, TPTD was eliminated rapidly, with a mean t1/2 of 1.65 hr (0.72 hr for SC). There was no apparent accumulation by 27 once-daily doses of TPTD. The AUC (0-6h) and Cmax after TD application increased generally in a dose-proportional manner over the 30- to 80-ug dose range. AUC was similar for 50- and 80-ug TD and 20-ug SC, though Cmax of TPTD was lower for TD compared to SC. Serum PINP increased approximately 2-fold from baseline for 50- and 80-ug TD after single and 27 once-daily doses (comparable to SC). Serum CTX showed a trend to increase after an initial decrease. In conclusion, once-daily TD applications of TPTD at dose levels of 30 to 80 ug were well tolerated by Japanese women. The results suggest that the TD TPTD system could be an alternative to SC injections and support further development of TD TPTD in Japan.

Disclosures: Masako Nakano, Eli Lilly Japan, 3
This study received funding from: Eli Lilly Japan

SA0418

See Friday Plenary Number FR0418.

SA0419

See Friday Plenary Number FR0419.

SA0420

Use of Teriparatide in Patients with Atypical Femur Fractures. Angela Cheung^{*1}, Lianne Tile², Neal Austin¹, Savannah Cardew², Heather McDonald-Blumer³, Rowena Ridout⁴, Robert Josse⁵, Judite Scher⁶, Jonathan Adachi⁷. ¹University Health Network, Canada, ²University of Toronto, Canada, ³Mount Sinai Hospital, Canada, ⁴Toronto Western Hospital, Canada, ⁵St. Michael's Hospital, University of Toronto, Canada, ⁶University Health Network, Canada, Canada, ⁷St. Joseph's Hospital, Canada

Purpose: The ASBMR task force on atypical femur fractures recently recommended the use of teriparatide for patients who have been on long term bisphosphonate therapy with atypical femur fractures. However, there is little empirical evidence that teriparatide use will help the healing of these fractures or prevent surgical intervention of incomplete fractures.

Methods: We prospectively examined 14 patients who were on long term bisphosphonate therapy and sustained atypical femur fractures. All subjects had to satisfy the major criteria as set forth by ASBMR. We measured their areal BMD at the total hip, femoral neck, lumbar spine and forearm by DXA (Hologic Discovery A, Hologic Inc.), as well as their volumetric BMD (total, cortical, trabecular) and geometric parameters by HRpQCT (Xtreme CT, Scanco Inc.) at baseline, 6, 12, 18 and 24 months. Plain radiographs were performed at regular intervals to assess fracture healing of the surgically repaired femur until healing was complete. Computed tomography scans were used to assess extent of incomplete fracture every 6 months. Outcomes, such as pain, mobility, and progression or regression of incomplete fracture as well as instability requiring surgical intervention, were noted.

Results: All 14 patients were postmenopausal women (79% Caucasians, 21% Asians) with mean age of 68.8 years, mean BMI of 25.9kg/cm² and a mean 25-hydroxyvitamin D level of 106.8nmol/L. All had normal ionized calcium and intact PTH. Average duration of bisphosphonate use was 10.5 years (range 3.0-21.0 years). Mean baseline BMD for lumbar spine, total hip and femoral neck were 0.82g/cm², 0.77g/cm², 0.62g/cm². Eleven had bilateral fractures. As of April 1, 2011, follow-up duration was 0.6 years (range: 1.4 to 22.0 months). Out of 14 patients, one discontinued therapy because of side effects, one died and 3 had to have surgical repair for their incomplete fracture despite teriparatide therapy. Patients reported variable effects with regard to pain and mobility after start of teriparatide.

Conclusions: Based on limited observational data, it is unclear whether teriparatide helps fracture healing in patients with atypical femur fractures. A randomized controlled trial examining the use of teriparatide in this population is urgently needed.

Disclosures: Angela Cheung, None.
This study received funding from: Eli Lilly

SA0421

See Friday Plenary Number FR0421.

SA0422

Atypical Subtrochanteric Fracture : An Easy to Find Situation in a Particular Patient with Compromised Bone Structure Treated for Osteoporosis. Carmen Barbu¹, Laura Chivu¹, Cristina Stefan², Suzana Florea³, Dariana Ionita³, Cristian Burnei¹, Dan Barbu¹, CATALINA POIANA^{*4}, Simona Fica¹. ¹Carol Davila University, Romania, ²Elias Hospital Endocrinology, Romania, ³Elias Hospital, Romania, ⁴AMGEN ROMANIA, Romania

Aim of the case report: underline the importance of the bone structure abnormalities in the etiology of the atypical subtrochanteric fracture (ATF) in a 38 yrs woman after 2 years of continuously antiresorptive treatment.

Medical history: at age of 20 yrs. had bone and joint generalized pain treated for short term with NSAIDs and prednisone 15mg daily (2 months). No clear etiology of the pain was revealed by investigations at that moment; at age of 28 yrs. was admitted in the hospital for went limp, pelvic pain. Radiographic findings: bilateral consolidated symphysis fractures, wedge-shaped vertebral body T5. L2-L4 DXA Zscore = -2.14SD. Bone scintigraphy - multiple areas of uptake in the ribs and vertebral bodies. Measurement of serum calcium and PTH ruled out the diagnosis of primary hyperparathyroidism (Ca=10 mg/dl, PTH=15pg/ml). No other endocrine disfunction was revealed by further investigations. An additional diagnosis of bilateral

spontaneous osteonecrosis of the femoral neck was made and bilateral prosthesis was recommended (postponed by the patient).

Oral bisphosphonate was started at age 29. In the next 5 years bilateral forearm fractures and 18 cm decreased in height occurred due to multiple vertebral fractures. At age 34 -histopathology showed generalized fibrous cystic osteitis.

Next 2 years treatment was stopped (pregnancy and nursing).

2009 first admitted in our department: reevaluation for endocrine diseases without abnormal results, skin biopsy - no histopathological changes of connective tissue, celiac disease test was negative, HIV test negative. Serum vitamin D, calcium, phosphate, PTH and IGF1 were normal. Bone resorption markers levels were near the upper normal limit.

2009-2010 - 5 mg intravenous zoledronic acid per year associated with strontium ranelate, and parenteral vitamin D3. During this period height and BMD measured by DXA were constant, no vertebral new fractures were revealed; the patient experienced a right forearm fracture in 2009 and a right ATF in february 2011.

Conclusion. In spite of not very typical features, all the data leads to the diagnosis of fibrous dysplasia. Intravenous 5 mg yearly zoledronic acid improved the clinical aspect and lowered significantly the fracture incidence. In our opinion, the background of the patient (progressive FD and osteonecrosis of the hips) claims a bigger impact on the ATF etiology comparing to a relative short period of continuous bisphosphonate (last 2 yrs) treatment.

Disclosures: CATALINA POIANA, None.

SA0423

See Friday Plenary Number FR0423.

SA0424

Combination Therapy with Ibandronate and Calcitriol Is Effective in Patients Following Liver Transplantation (LTX): A Three Year Prospective Controlled Study. Doris Wagner^{*1}, Karl Fenal², Hans Dimai¹, Harald Dobnig³, Karin Amrein¹, Daniela Kniepeiss¹, Philipp Stiegler¹, Astrid Fahrleitner-Pammer¹. ¹Medical University of Graz, Austria, ²Roche Austria GMBH, Austria, ³Diagnostikinstitut Univ.Prof.Dr.H.Dobnig GmbH, Aut

Transplantation bone disease is a well-known complication in patients after organ transplantation. Aim of this three year study was to investigate the influence of a combination therapy of iv. ibandronate and calcitriol on bone metabolism, bone mineral density and fracture status in patients following liver transplantation (LTX).

Thirty osteoporosis patients at least one year after LTX were assigned to the treatment group (IBN), 24 patients served as a control cohort (CTR). IBN patients received quarterly 2 mg ibandronate and daily 0.25 - 1.5 µg calcitriol. Control patients received daily 1200 mg calcium and 800 IU vitamin D. Laboratory analysis and dual energy absorptiometry (DXA) of the left hip were performed at baseline and every year. All participants underwent an X-ray of the spine at baseline and at study end.

The IBN group showed favourable changes in bone metabolism, a significant increase in BMD and a lower fracture incidence than the CTR group.

At baseline, 57% in the IBN group had vertebral fractures and at study end 7% had sustained new vertebral fractures. However at study end, in the control group, 23% had radiological evidence of new vertebral fractures, even though, none had had one at study start.

These results clearly indicate that osteoporosis remains an important issue in transplantation aftercare beyond the first 12 months. Antiresorptive treatment following LTX should be considered following transplantation. Because TX patients even with normal BMD are at high fracture risk, they might benefit from antiresorptive treatment.

Disclosures: Doris Wagner, None.

SA0425

Effect of Ibandronate for the Treatment of Osteonecrosis of the Knee: A Randomized, Double-Blind, Placebo-Controlled Trial. Christian Meier^{*1}, Claude Kraenzlin², Niklaus Friederich³, Thorsten Wischer⁴, Leticia Grize⁵, Christoph Meier⁶, Marius Kraenzlin¹. ¹Div. of Endocrinology, Diabetes & Metabolism, University Hospital Basel, Switzerland, ²Endocrine Clinic & Laboratory, Basel, Switzerland, ³Dept. of Orthopedic Surgery, Bruderholz, Switzerland, ⁴Dept. of Radiology, Merian Iselin Hospital, Basel, Switzerland, ⁵Biostatistics & Computational Sciences Unit, Dept. of Epidemiology, Swiss Tropical & Public Health Institute; University of Basel, Switzerland, ⁶Div. of Clinical Pharmacology & Toxicology, University Hospital Basel, Switzerland

Observational studies suggest beneficial effects of bisphosphonates in spontaneous osteonecrosis (ON) of the knee. We investigated whether ibandronate would improve clinical and radiological outcome in newly diagnosed ON.

In this randomized, double-blind, placebo-controlled trial, 30 patients (mean age, 57.310.7 yrs) with ON were assigned to receive either 12 mg of ibandronate or placebo

intravenously (divided into four doses within first 2 weeks). All subjects received additional treatment with oral diclofenac (70 mg) and supplementation with calcium carbonate (500 mg) and vitamin D (400 IU) to be taken daily for 12 weeks. Patients were followed for 48 weeks. The primary outcome was the change in pain score (visual analog scale, VAS) after 12 weeks. Secondary endpoints included changes in VAS, mobility (WOMAC and IKDC questionnaires), biochemical markers of bone turnover, and radiological outcome (MRI) after 24 and 48 weeks.

At baseline, both treatment groups (IBN, n=14; placebo, n=16) were comparable in relation to age, BMI, comorbidities, pain score, bone markers, and radiological grading (bone marrow edema, ON). Mean pain score was reduced in both ibandronate (mean change, -3.4; 95%CI, -4.7 to -2.2) and placebo (-3.2; 95%CI, -4.7 to -1.18) treated subjects after 12 weeks (between group comparison, p=ns). Except for significant decrease in bone resorption markers in ibandronate treated subjects (p<0.01), mean changes in all other outcome measures were comparable between treatment groups (after 24 and 48 weeks).

We conclude that in patients with spontaneous osteonecrosis of the knee bisphosphonate treatment (i.e. IV ibandronate) has no beneficial effect.

Disclosures: Christian Meier, None.

SA0426

Effects of Bisphosphonate on Bone Metabolic Markers, Bone Mineral Density and Vertebral Fractures in Young-Old or Old-Old Osteoporotic Patients. Yuji Kasukawa^{*1}, Naohisa Miyakoshi¹, Toshihito Ebina², Toshiaki Aizawa², Yoichi Shimada³. ¹Akita University Graduate School of Medicine, Japan, ²Kakunodate General Hospital, Japan, ³Akita University Graduate School of Medicine, Department of Orthopedic Surgery, Japan

Bisphosphonates improve bone mineral density (BMD) in osteoporotic patients and have preventive effects on osteoporotic fractures. Most of their effects have been demonstrated in postmenopausal osteoporotic women, but not in older osteoporotic patients, who have a high risk of fractures. The purpose of the present study was to evaluate the effects of bisphosphonates on bone metabolic markers, BMD, and incidence of vertebral fractures in young-old or old-old osteoporotic patients. Sixty-five osteoporotic women (mean age 77 years) were enrolled in this study. They were stratified into two groups: a young-old group (65–74 years old, n = 27); and an old-old group (≥75 years old, n = 38). Before and after 1-year treatment with a bisphosphonate, the following parameters were evaluated: serum markers of bone resorption (cross-linked N-telopeptide of type I collagen (NTX)) and bone formation (bone alkaline phosphatase (BAP)); and BMD, measured by dual-energy X-ray absorptiometry at the distal third of the forearm. Vertebral fractures of the thoracic and lumbar spine were detected by plain X-ray film. There were no significant differences in mean serum NTX and BAP between the two groups at baseline. The mean serum NTX and BAP were significantly decreased in the young-old group (p<.05 and p<.0001, respectively) and in the old-old group (p<.001 and p<.001, respectively) after 1-year treatment. Mean BMD (0.29 g/cm²; 59.4% young adult mean (YAM)) in the young-old group before treatment was lower than the BMD (0.25 g/cm², 52.8% YAM) in the old-old group (p=.06). BMD did not change significantly after treatment in either group. Only one new vertebral fracture occurred in the young-old group, but five occurred in the old-old group. Thus, bisphosphonates suppressed serum bone metabolic markers and maintained the BMD in both young-old and old-old groups. However, new vertebral fractures occurred more frequently in old-old patients than in young-old patients.

Disclosures: Yuji Kasukawa, None.

SA0427

Incidence of Fragility Fractures of the Femur, Including Subtrochanteric, up to 8 Years Since Initiation of Alendronate or Risedronate Treatment. Michael Pazianas^{*1}, Bo Abrahamsen², Yiting Wang³, Graham Russell¹. ¹University of Oxford, United Kingdom, ²Copenhagen University Hospital Gentofte, Denmark, ³Warner Chilcott Pharmaceuticals (former employee), USA

ABSTRACT

Few studies have acquired adequate data with prolonged follow-up on bisphosphonate users in the general population to evaluate their long-term effects on the risk of hip fractures including those in the subtrochanteric region. We explored this issue using a large USA medical claims database (Marketscan) to study the incidence of osteoporotic fractures of the femur according to therapy compliance and persistence of bisphosphonate use in the real-world setting.

Methods We compared patients with higher versus lower degrees of compliance. Radiographic adjudication of fracture site and features were not performed. Therefore the definition of atypical fractures proposed by the ASBMR was not used in this study. Hazard ratios (HR) for fracture were estimated using time-dependent Cox models. Restricted cubic splines (RCS) were used to plot fracture HRs against duration of therapy.

Results 3,655 incident cases of femoral fracture (764 subtrochanteric/shaft, 2,769 hip, 122 lower femur) were identified during 917,741 person-years of follow-up (median = 3 years) on 287,099 patients from the date when they initiated oral bisphosphonate therapy. The corresponding HRs (95% CI) for overall femoral fractures associated with each additional year of therapy were 0.93 (0.86-1.01) within

5 years, and 0.89 (0.77-1.03) beyond 5 years for risedronate and 0.86 (0.81-0.91) and 0.95 (0.84-1.07) for alendronate respectively. The corresponding estimates for subtrochanteric/shaft fractures were 1.05 (0.87-1.26) and 0.89 (0.60-1.33) for risedronate and 0.99 (0.92-1.05) and 1.05 (0.92-1.20) for alendronate respectively. The HRs (95% confidence interval) for overall femoral fractures associated with each additional year of alendronate or risedronate therapy within 5 and beyond 5 years were not significantly different.

Conclusion Our study showed evidence for a persistence of overall hip fracture protection with long-term use of alendronate or risedronate. Gaps in therapy of more than 90 days were associated with greater risk for all femur fractures (> 5 fold in all models).

Disclosures: Michael Pazianas, Warner Chilcott, 5
This study received funding from: Warner Chilcott

SA0428

Long Term Follow up of Patients on Drug Holiday from Bisphosphonates: Real World Setting. Jim Sinacore¹, Pauline Camacho², Lauren Myers^{*3}. ¹Loyola University Medical Center, USA, ²Loyola University of Chicago, USA, ³Loyola University Medical Center, Maywood, Illinois, USA

The ASBMR Task Force on Atypical Fractures recognized atypical femoral fractures to be a risk with prolonged bisphosphonate (BP) use. AACE recommends a drug holiday after 5 years of stability, but little data exists on the optimal duration. The FLEX study showed higher fracture risk at 5 years in patients who discontinued alendronate versus those who stayed on the drug. A follow up study (ASBMR 2010) showed that BMD changes did not predict who would fracture. Our aim was to describe the BMD and bone turnover marker (BTM) changes in a cohort of real world patients on BP holiday. This is a retrospective study of patients with low bone mass and osteoporosis at Loyola University Osteoporosis and Metabolic Bone Disease Center who were advised a holiday from 2005-2010. The demographic data, BP history, reports of fracture, DXA results, 25-hydroxy-vitamin D (25-OHD) and BSAP values were obtained from EMR data at the beginning of the holiday and yearly for 3 years. BSAP was chosen as the BTM due to reimbursement issues in Illinois with NTX and CTX. Comparative statistical analyses were used to compare DXA and BSAP results. Our cohort consisted of 139 patients; 123 females and 16 males, with a mean age of 6811 years and mean pretreatment length of 6.82.9 years. 70% of patients were on alendronate, 21% on risedronate and 9% on ibandronate. Baseline mean T scores were -1.81.0, and -1.31.4 in the lumbar spine BMD (LSBMD) and femoral neck (FBMD) and 25-OHD was 4516.4 ng/ml. 5 fractures occurred during the holiday. Over 3 years, there was no significant change in the mean LSBMD (1.070.25g/cm² baseline, 0.970.51g/cm² year 1, 1.030.23g/cm² year 2, 1.130.37g/cm² year 3) and femoral neck BMD (0.800.10g/cm² baseline, 0.780.09g/cm² year 1, 0.770.11g/cm² year 2, 0.850.13g/cm² year 3) There was a significant rise in BSAP starting at 6 months, (9.01.75 ug/L baseline, 10.92.78 ug/L year at 6 months). Neither the type of BP nor the duration of holiday significantly affected BMD and BTM. Vitamin D and calcium deficiency and other secondary cause of bone loss were corrected. In conclusion, this cohort of patients on BP holiday experienced stable bone density for 3 years. BSAP started to increase at 6 months but the number remained in the lower end of premenopausal range. Fractures do occur during the holiday; however, our study was not powered to assess fracture risk. Larger prospective studies are needed to adequately assess the optimal duration of holiday.

Disclosures: Lauren Myers, None.

SA0429

See Friday Plenary Number FR0429.

SA0430

Multiple Studies with Risedronate Demonstrate Consistent Bone Turnover Regardless of Dose. Robert Recker^{*1}, Louis-Georges Ste-Marie², Pascale Chavassieux³. ¹Creighton University Osteoporosis Research Center, USA, ²Hospital Saint-LucCHUM, Canada, ³INSERM UMR1033, Universite De Lyon, France

The purpose of this analysis was to study the validity and consistency of histomorphometric data from biopsies of post-menopausal women with osteoporosis (PMO) treated with risedronate at different dose levels and dosing frequency.

In a pivotal phase III randomized, placebo-controlled clinical study, patients were treated with either 5 mg of risedronate daily or placebo for 3 years. Analysis in paired biopsies showed that risedronate reduced mineralizing surface by 58% and activation frequency by 47%, which is consistent with its anti-resorptive activity¹. Of the 70 evaluable biopsies (33 placebo; 37 risedronate), double tetracycline labels, a reflection of on-going remodeling, were seen in all biopsies. In a subsequent 2-year extension study, double labels were identified in all paired biopsies indicating continuous bone remodeling² in patients treated with 5 mg/day for up to 5 years. Subsequently, three different regimens of risedronate were developed: 35 mg once-a-week (OAW) ³, one 75 mg dose on two-consecutive-days-a-month (2CDM)⁵, and 150 mg once-a-month (OAM)⁴. Non-inferiority of these new regimens compared to the daily 5 mg dose was demonstrated, based on a prospectively defined primary endpoint (Table). The 35 mg OAW study also included a 50 mg weekly dose. In all three studies, biopsies were taken at 24 months.

Double tetracycline labels were found in 97–100% biopsies (Table). Key histomorphometric variables were comparable across these studies. These data indicate that risedronate preserved bone structure and quality with continuous remodeling in all group regardless of dose and exposure.

The presence of double labels in 99% of all biopsies does not suggest compromise of bone remodeling during treatment with these established regimens, up to 5 years with 5 mg/day dose.

References: 1 E. Eriksen et al., Bone, 2002; 2LG Ste-Marie et al., CTI, 2004; 3R. Recker et al., ECTS, 2003; 4P. Chavassieux et al., ECTS, 2009; 5Warner Chilcott data on file.

Acknowledgement: Dr Eriksen performed some of the biopsy work reported here.

	Risedronate dose (mg)	# evaluable biopsies	# biopsies w/double label	% of double label
VERT-NA (36 months) ¹	5	37	37	100
VERT-NA (60 months) ²	5	13	13	100
OAW (24 months) ³	5	35	34	97
	35	29	29	100
	50	21	21	100
OAW (24 months) ⁴	5	35	34	97
	150	27	27	100
2CDM (24 months) ⁵	5	9	9	100
	75	5	5	100
PMO Total		211	209	99

Table

Disclosures: Robert Recker, NPS Allelix, 2; Procter & Gamble, 2; Merck, 5; GlaxoSmithKline, 5; Amgen, 2; Merck, 2; Roche, 5; Amgen, 5; Lilly, 2; Novartis, 2; Wyeth, 2; NPS Allelix, 5; Lilly, 5; Procter & Gamble, 5; Wyeth, 5; Novartis, 5; Roche, 2; GlaxoSmithKline, 2

This study received funding from: Warner Chilcott LLC, and sanofi-aventis, US

SA0431

Risedronate Improves Proximal Femur Bone Mineral Density and Geometry Parameters Over 3 Years in Patients with Osteoporosis or Osteopenia and Clinical Risk Factors of Fractures: A Practice-Based Observational Study. Masayuki Takakuwa^{*1}, Jun Iwamoto². ¹Takakuwa Orthopedic Nagayama Clinic, Japan, ²Keio University School of Medicine, Japan

Advanced Hip Assessment (AHA) software installed in a dual-energy X-ray absorptiometry (DXA, GE-Lunar) can be used to evaluate bone strength indices as well as bone mineral density (BMD) of the proximal femur. In particular, Femur Strength Index (FSI) is calculated using structural geometric properties, neck shaft angle, height, and body weight. The purpose of this study was to investigate the 3-year effects of risedronate treatment on AHA parameters of the proximal femur and BMD of the lumbar spine and proximal femur in patients with increased risk of fractures. In total, 174 patients (mean age: 67.8 yrs; 165 females and 9 males) with osteoporosis or osteopenia and clinical risk factors of fractures were treated with risedronate for 3 years in our outpatients clinic. AHA parameters of the proximal femur and BMD of the proximal femur and lumbar spine (L1-L4) were evaluated every 4 months over 3 years. The mean percentage changes from baseline in FSI after 4 months of risedronate treatment were 7.5% ($p < 0.001$) for the right femur and 4.3% ($p < 0.01$) for the left femur. The respective values for the right femur after 8, 12, 16, 20, 24, 28, 32, and 36 months of treatment were 5.8%, 10.0%, 12.6%, 13.6%, 15.2%, 15.7%, 13.4%, and 17.5% ($p < 0.001$) and those for the left femur were 7.7%, 8.2%, 11.5%, 10.2%, 12.9%, 16.9%, 16.7%, and 16.2% ($p < 0.001$). Cross-sectional moment of inertia (CSMI), cross-sectional area (CSA), mean neck width in the femoral neck, and BMD of the right and left proximal femur and BMD of the lumbar spine also continued to increase during 3 years of treatment. The increases in FSI and CSMI in the proximal femur at each time point were apparently greater than those in the proximal femur and lumbar spine BMD. These results suggest that risedronate treatment may more significantly improve femoral strength parameters than BMD of the proximal femur and lumbar spine over 3 years. Thus, it has been demonstrated that risedronate dose not only increase lumbar spine and proximal femur BMD, but also more significantly improves bone strength indices of the proximal femur in patient with increased risk of fractures.

Disclosures: Masayuki Takakuwa, None.

SA0432

ZOOM-NIS: Zoledronic acid - Osteoporosis Monitoring (a non-interventional study). Ruediger Moericke^{*1}, Christian Kasperk², Christine Kleinmond³. ¹Germany, ²University of Heidelberg, Germany, ³Novartis Pharma GmbH, Germany

Background: Annual iv infusion of zoledronic acid 5mg (ZOL) is an effective and welltolerated therapy for patients with osteoporosis; in patients with a recent low-trauma hip fracture and glucocorticoid-induced osteoporosis. Methods: The aim of the ZOOM-NIS is to evaluate the patient criteria that lead to the decision for the first-time treatment with ZOL 5mg, the characteristics of patients who are treated with ZOL 5mg, and the tolerability of the infusion in normal clinical setting. Further questions during the one-year observational period are pain reduction, change of general clinical presentation,

effects of therapy, adherence, and changes of quality of life assessed by questionnaire. Data are collected at baseline, at an optional follow up after 6 months, and at a final visit after 12 to 15 months. Results: Here we describe the results of an interim analysis of the first 1593 baseline visits with the ZOL 5 mg infusion. Population: female: 1347 (84.6), male: 212 (3.3%), not specified: 34 (2.1%). The mean age was 72.8 years (SD: 9.4; Median: 74.0; Min: 22.0; Max 96.0). In all, 818 (51.3%) of the patients had experienced at least one osteoporotic fracture (no fracture: 725, not specified: 50), and 1072 (67.3%) patients had received some treatment of osteoporosis (none: 427 [27.4%], not specified: 84 [5.3%]). The mean duration of the ZOL-infusion was 35.6 min (SD 18.0; Median 30.0 min, Min: 10, Max: 360). 91.7% of patients received adequate hydration (according to local SmPC), while 28.9% received prophylactic medical treatment of post-infusion syndrome, 63.7% with paracetamol. 84.2% of the patients received osteoporosis-related concomitant therapy: vitamin D 79.2%, calcium 73.2%, 14.6 % analgesics. Information on practicability was gathered by asking about the ease of preparation and safety of the infusion. More than 98% of the responses rated both categories as "very good" or "good". Regarding tolerability, there were no physician reports of AEs for 1460 (91.7%) of the patients. In total, 130 AEs were reported in 67 patients, of whom 14 patients experienced 44 serious AEs (30 assessed by the physician to be related 1 not related, and 13 were not specified). Summary: This non-interventional study is the first to collect information on the use of ZOL 5mg in the normal clinical setting. The interim analysis presented here describes the population and attests to the good tolerability of the infusion.

Disclosures: Ruediger Moericke, None.

This study received funding from: Novartis Pharma GmbH, Germany

SA0433

See Friday Plenary Number FR0433.

SA0434

Factors Related to Permanent Discontinuation of Osteoporosis Treatment. Ryan Outman¹, Jeffrey Curtis¹, Julie Locher¹, Meredith Kilgore², Kenneth Saag¹, Cornelis Van Den Bogert^{*1}, Amy Mudano¹, Elizabeth Kitchin¹, Lang Chen³.

¹University of Alabama at Birmingham, USA, ²University of Alabama At Birmingham School of Public Health, USA, ³UAB CERTs, USA

Purpose – To identify factors associated with non-persistence with osteoporosis treatment among community-dwelling individuals with osteoporosis or a prior fracture receiving home health services agency.

Methods – Eligible patients were contacted by phone; those agreeing to participate completed a computer-assisted telephone interview. We collected demographics, medical and fracture history, fall risk, osteoporosis treatment (current and past) and osteoporosis-related attitudes and beliefs using validated instruments informed by the Health Belief Model (osteoporosis knowledge, self-efficacy, perceived benefits and barriers to treatment and perceived severity of and susceptibility to osteoporosis). The primary outcome was past use of any prescription osteoporosis medication referent to current use of any medication. Stepwise logistic regression was used to identify factors associated with past vs. current use of osteoporosis treatment.

Results – Among 558 surveyed home health patients, we identified 88 past users (34.2%) and 169 current users (65.8%). Most common reasons for stop were 'took it as long as needed' (65.4%); 50% reported 'doctor told to stop', 'didn't feel it was helping/working' and 'don't like to take medications'. The most common medications among the persistent patients were Fosamax, Actonel and Reclast. Current users were more likely to have an osteoporosis diagnosis ($p = 0.02$) and to have higher perceived treatment benefits ($p = 0.01$), while past users were more likely to have higher perceived treatment barriers ($p = 0.02$). The individual items, "Would you still take your medication if the drug is expensive" ($p = 0.10$) and "Would you still take your medication if the drug upsets the stomach or causes other side effects" ($p = 0.01$) of the Self-Efficacy Scale, were positively associated with current use. In the multivariable model, osteoporosis and fracture diagnosis, treatment benefits and barriers and the individual efficacy subscale regarding side effects were significant (Table).

Conclusion – Patients with higher perceived prescription medication benefits, self-efficacy regarding side-effects and osteoporosis diagnosis are more likely to be persistent with osteoporosis medication, while perceived treatment barriers showed negative correlation with persistence. Opportunities exist to increase use of osteoporosis medication in this vulnerable population through interventions that incorporate these identified motivations and barriers.

Factors	C&S	OR	95% C.I.	P
Osteoporosis Diagnosis (no=ref)	0.019			
Yes		2.08	1.055-4.116	0.034
Fracture History (no=ref)	0.011			
Yes		0.57	0.298-1.098	0.089
Treatment benefits (low=ref)	0.033			0.04
Neutral		0.475	0.092, 2.452	0.374
High		1.174	0.249, 5.526	0.839
Treatment barriers (low=ref)	0.03			0.133
Neutral		0.756	0.4, 1.430	0.39
High		0.463	0.218, 0.982	0.045
Still using the drug if it causes side effects (disagree=ref)	0.045			0.016
Neutral		0.53	0.256, 1.097	0.087
Yes		0.333	0.146, 0.759	0.009

Used Abbreviations: ref = Reference Category; C&S = Univariate Cox & Snell R²; OR = Adjusted Odds Ratio; 95% C.I. = 95% confidence interval of the odds ratio.

Table. Multivariable Regression Model of Factors Associated with Treatment Continuation

Disclosures: Cornelis Van Den Bogert, None.

SA0435

Feasibility and Efficacy of Computer-assisted Quantitative Morphometry (MorphoXpress®) of Vertebral Fractures in Patients before, after and at 12 month Follow Up of Kyphoplasty Treatment. Jan Banzer^{*1}, Sebastian Radmer², Gerd Moeller³, Hans-Christof Schober⁴, Reimer Andresen⁵. ¹Charite Universitätsmedizin Berlin, Germany, ²Zentrum für Bewegungsheilkunde, Germany, ³Amgen (Europe) GmbH, Switzerland, ⁴Klinikum Sudstadt Rostock Klinik für Innere Medizin I, Germany, ⁵Westkuesten-klinikum Heide, Department of Radiology & Neuroradiology, Germany

Feasibility and Efficacy of computer-assisted quantitative Morphometry (MorphoXpress®) of vertebral fractures in patients before, after and at 12 month follow up of kyphoplasty treatment

J. Banzer, S. Radmer, G. Moeller, HC. Schober, R. Andresen

Introduction:

Balloon kyphoplasty (BKP) for treating fresh osteoporotic vertebral fractures (VF) has been established as a method of choice over the past years. Next to pain reduction it aims at height restoration (augmentation) VF.

Computer assisted quantitative vertebral morphometry using MorphoXpress® (cqVM) offers a validated objective method to assess the percentage of vertebral height reduction.

Goal of this study is to test the feasibility of cqVM in VF treated with BKP and to assess a possible augmentation immediately after the treatment and at 12 month follow-up in order to estimate and document the sustainability.

Patients and methods:

321 patients (230 f., 91 m., 48-91 years of age, mean age 70 y.) were examined: Vertebral heights were assessed by cqVM from lateral x-rays. Bone mineral density was measured using spinal quantitative CT. Fresh VF were identified by MRI.

VF were categorised using the AO classification system. Fracture types A.1.1., A.1.2. and A.1.3. were considered for BKP treatment.

Vertebral height was again assessed and documented post-interventionally and at 12 month follow-up.

Results:

In 120 of 321 patients BKP was performed in a total of 161 vertebral bodies. 85 patients presented single VF, 30 patients had two VF, and five patients suffered from more than two VF. QCT measurement identified a low BMD in all 120 patients (mean 46 mgHA/ml, range 3-112 mgHA/ml).

CqVM showed a mean vertebral height reduction of 43 % (range 12-82%) before BKP.

Mean augmentation of vertebral height was 9 % immediately after BKP (mean height reduction: 34 %, range 8-85%). At 12 month follow-up mean height reduction was 36 % (range 8-80%).

Discussion:

Computer assisted quantitative vertebral morphometry is a feasible tool for assessing vertebral height reduction and augmentation after balloon kyphoplasty.

Using cqVM we also show that BKP leads to a significant augmentation of VF. At 12 month follow up this augmentation remains fairly stable showing no significant height loss over time.

Computer assisted vertebral morphometry using MorphoXpress® seems to be an adequate tool for documentation of treatment success after BKP and for assessment of possible subsequent VF.

Disclosures: Jan Banzer, None.

SA0436

Patients Reject the Concept of Fragility Fracture - A New Understanding Based on Fracture Patients' Communication of their Fracture. Joanna Sale^{*1}, Monique Gignac², Lucy Frankel¹, Gillian Hawker³, Dorcas Beaton¹, Victoria Elliot-Gibson¹, Earl Bogoch¹. ¹St. Michael's Hospital, Canada, ²University Health Network, Canada, ³Women's College Hospital, Canada

Introduction and purpose: The reasons why fracture patients often do not associate their fragility fracture with low bone mass is important to the management of bone health. We examined patients' communication about fragility fractures to gain insight into the reason why some patients fail to perceive the connection between their fracture and low bone mass.

Methods: We conducted a descriptive phenomenological (qualitative) study. English-speaking male and female patients aged 65+ years who were high risk for future fracture based on their age, fracture status, and T-score were eligible for the study and screened for osteoporosis through an established screening program at an urban teaching hospital. During face-to-face interviews, participants described the experience of their fracture in detail, what they were doing when they sustained the injury, and the circumstances surrounding the fracture. Data analysis was guided by Giorgi's methodology.

Results: Participants were 21 females and 9 males, aged 65-88, who presented with a hip (n=11), wrist (n=11), shoulder (n=6), or other (n=2) fracture. Ten of the 30 fractures occurred inside the home and the remaining fractures occurred outside the home. Based on the interviews, sustaining a fragility fracture was perceived as a traumatic event, both physically and emotionally, for many older fracture patients. In general, participants used forceful, action-oriented words and referred to hard surfaces to describe the experience. Explanations for the fracture, other than bone quality, were often reported, especially that falls were "freak" or "fluke" events. Patients who fractured under more mundane circumstances (e.g. standing from a chair) seemed more likely to perceive a connection between the fracture and their bone health.

Conclusion: The term "fragility" or "low trauma" fracture was a misnomer for many older adults. This term, combined with participant perceptions that their fall was an isolated incident, seemed to result in many older fracture patients at high risk for future fracture not connecting their fracture with bone health and taking appropriate steps to reduce fracture risk.

Disclosures: Joanna Sale, None.

SA0437

Persistence and Compliance with Osteoporosis Medical Treatment - Analysis of a Large Scale, Representative, Longitudinal, German Database. Volker Ziller^{*1}, Karel Kostev², Ioannis Kyvernitis³, Jelena Boeckhof³, Peyman Hadji¹. ¹Philipps-University of Marburg, Germany, ²IMS HEALTH GmbH & Co. OHG, Germany, ³Philipps-University, Germany

Background

Osteoporosis can be effectively treated with a number of medications. However high persistence and compliance is required to assure efficacy.

Objective:

This study analysis persistence and compliance with a variety of medical interventions including oral, i.v. and s.c. administrations in Germany.

Methods:

This retrospective cohort study used a representative longitudinal database (IMS® LRX) comprising longitudinal prescription data for Germany from almost 80% of all German prescriptions of members of the German statutory health insurance.

Persistence is defined as the proportion of patients who remained on their initially prescribed therapy at 1 year. Compliance is measured indirectly based on the medication possession ratio (MPR).

Results: 1.107.482 patients were identified between 06/2006-05/2009 in the database with a prescription of a bisphosphonate, strontium or PTH. 268.568 of those fulfilled further inclusion criteria and had been included in the persistence analysis and 164.985 could be analysed concerning compliance. At 12 months rates of patients that remained on treatment were for Zoledronate 5mg 65.6%; Ibandronate iv 3mg 56.6%; PTH (Teriparatide and 1-84 PTH) 54.7 %, Ibandronate 150mg p.o. 51.0 %; Alendronate 70 mg 44.8 %; Etidronate 43.4%; Risedronate plus Calcium 42.3 %; Alendronate plus Vitamin D 37.8 %; Risedronate 35mg 35.2 %; Risedronate 5mg 30.6 %; Strontium ranelate 31.4 %; Alendronate 10mg 17.3 %.

Conclusion:

Persistence and Compliance in osteoporosis treatment is insufficient. I.v. treatments and PTH showed the highest persistence and compliance rates and daily oral bisphosphonates the lowest. More effort to improve treatment compliance and persistence is needed to assure clinical efficacy.

Disclosures: Volker Ziller, None.

This study received funding from: Nycomed Germany, unrestricted research grant

SA0438

See Friday Plenary Number FR0438.

SA0439

See Friday Plenary Number FR0439.

SA0440

The effect of enhanced Dual-energy Xray Absorptiometry (DXA) reports on osteoporosis care. Karen Barnard^{*1}, Cathleen Colon-Emeric². ¹Duke University Medical Center, Durham VAMC, USA, ²Duke University & Durham VAMC, USA

Purpose: To assess whether providers randomized to receive enhanced DXA reports that include an estimation of a patient's fracture risk and treatment recommendations plus an electronic order entry set for osteoporosis order more guideline-recommended osteoporosis therapy than those providers who receive usual DXA reports. **Methods:** An exploratory randomized controlled trial was conducted at the Durham VAMC from January 2010 to January 2011. Providers were randomized in a stratified fashion according to their DXA ordering frequency to either intervention or control groups. Subjects in the control group received the usual DXA reports and a handout on the indications for DXA. Subjects in the intervention group received the usual DXA report plus an assessment of their patient's fracture risk using the FRAX risk calculator, and guideline-based recommendations for laboratory evaluation non-pharmacologic and pharmacologic therapy. In addition, the intervention group had access to an electronic order entry screen which provided "point and click" ordering of recommended care. **Results:** Informed consent was obtained from 37 providers. A total of 161 DXA scans were ordered by the participating providers during the twelve month study period. The mean age of the patients was 62.5 years. There were 103 (64%) males and 58 (36%) females, 59 (37%) African Americans and 101 (63%) whites. Thirty seven patients (23%) had osteoporosis by T score, or osteopenia plus a FRAX score meeting recommended treatment thresholds (>20% for major osteoporotic fractures or >3% for hip fracture). Of these, 18 were in the control group and 19 were in the intervention group; representing 27% and 20% of total scans in each group respectively. **Results** are shown in table 1. **Conclusion:** In this small, exploratory study, enhanced bone density reports containing an assessment of the patient's fracture risk and recommendations for treatment did not result in improved osteoporosis care.

Therapy	Intervention (n=19)	Control (n=18)
Calcium and vitamin D	12 (63%)	10 (55%)
Bisphosphonate	10 (53%)	15 (83%)

Table 1. Proportion of patients meeting treatment criteria who received recommended therapy

Disclosures: Karen Barnard, None.

SA0441

Use of Pharmacologic Agents for the Prevention of Osteoporosis among Older Women with Low Bone Mass is Discordant with NOF Guidance. Jie Zhang^{*}, Jeffrey Curtis, Elizabeth Delzell, Kenneth Saag. University of Alabama at Birmingham, USA

Objective: To determine if treatment with pharmacologic agents among postmenopausal women with low bone mass (T score between -1.0 and -2.5) was in concordance with the current and recent National Osteoporosis Foundation (NOF) clinical guidelines.

Methods: Cross-sectional analysis from 2007 to 2009 among participants of the Global Longitudinal Study of Osteoporosis in Women (GLOW) recruited from the Birmingham, Alabama, site. Eligible subjects had a bone density test within 2 years prior to a GLOW survey and had their lowest T score (of either total hip, femoral neck, lumbar spine, or 1/3 radius) between -1.0 and -2.5. Those who reported a history of hip or spine fracture were excluded. Fracture risk factors and the use of anti-osteoporosis medications were self-reported. We examined the proportions of women managed in concordance with the NOF 2003 and 2008 guidelines, with concordance

defined as ever (current or past) received treatment among those recommended for treatment and never received treatment among those not recommended for treatment. Univariate odds ratios (ORs) and 95% confidence intervals (CIs) were calculated.

Results: Mean age among 770 eligible women was 70.7 years. When NOF 2003 guidelines were applied, 463 (61%) women were managed in concordance with the guidelines. Those who met NOF 2003 criteria were more likely to have ever received treatment (OR, 2.5; 95% CI, 1.9-3.4). Women with lower T scores were more likely to be treated (Table 1). Among those not recommended for treatment, women with T scores between -2.0 and -1.5 and absent of major risk factors were more likely to be treated than women with T scores between -1.5 and -1.0. Three hundred and nine (52%) women were managed in concordance with NOF 2008 guidelines. Those who met NOF 2008 criteria were not more likely to have ever received treatment (OR, 1.1; 95% CI, 0.8-1.6). Compared to women not recommended for treatment, those satisfying both NOF FRAX criteria were more likely to be treated (OR, 1.7; 95% CI, 1.1-2.6), while those satisfying only one of the criteria were not more likely to be treated (OR, 0.8; 95% CI, 0.5-1.4).

Conclusion: Up to 50% of the women with osteopenia were not treated in concordance with NOF guidelines. Those having one but not both of the NOF FRAX criteria for intervention were not more likely to be treated than those having neither. These results may reflect a lack of awareness of and insufficient dissemination of the guidelines among physicians.

Table 1. Univariate associations between meeting and not meeting National Osteoporosis Foundation criteria and having ever received anti-osteoporosis treatment

	N (%) Treated	Odds Ratio (95% Confidence Interval)
NOF 2003 Guidelines¹		
Overall		
Treatment recommended	262 (60.4)	2.5 (1.9-3.4)
Treatment not recommended	122 (37.8)	Reference
By BMD category and presence of major risk factors²		
Treatment recommended		
T score = -2.0	168 (63.9)	3.8 (2.6-5.7)
-2.0 < T score = -1.5 and presence of at least one of the following risk factors ³	94 (55.0)	2.7 (1.7-4.1)
Treatment not recommended		
-2.0 < T score = -1.5 and absent of the following risk factors ³	64 (46.0)	1.9 (1.2-2.9)
-1.5 < T score < -1.0	58 (31.5)	Reference
NOF 2008 Guidelines¹		
Overall		
Treatment recommended	168 (54.2)	1.1 (0.8-1.6)
Treatment not recommended	147 (51.0)	Reference
By FRAX risk score		
Treatment recommended		
10 year probability of hip fracture = 3% and 10 year probability of major osteoporotic fracture = 20%	98 (64.1)	1.7 (1.1-2.6)
Either 10 year probability of hip fracture = 3% or 10 year probability of major osteoporotic fracture = 20%, but not both	70 (44.6)	0.8 (0.5-1.4)
Treatment not recommended		
10 year probability of hip fracture < 3% and 10 year probability of major osteoporotic fracture < 20%	147 (51.0)	Reference

¹The NOF 2003 and 2008 criteria could not be evaluated in 13 and 172 women respectively due to missing values on key fracture risk factors.

²Risk factors include fracture since turning 45, parental hip fracture, body weight < 127 lbs, current smoking, and current glucocorticoid use

Table 1

Disclosures: Jie Zhang, Amgen, 2

SA0442

Evaluation of Effect of Raloxifene Hydrochloride on the Quality of Life of Patients with Postmenopausal Osteoporosis. Kousei Yoh¹, Etsuro Hamaya², Noriko Iikuni³, Noriko Takagaki², Takanori Yamamoto², Masanori Taketsuna², Akimitsu Miyauchi⁴, Hideaki Sowa⁵, Hisashi Urushihara², Kiyoshi Tanaka^{*6}. ¹Department of Orthopedic Surgery, Sasayama Hospital, Japan, ²Eli Lilly Japan KK, Japan, ³Eli Lilly & Company, USA, ⁴Miyauchi Medical Center, Japan, ⁵Lilly Research Laboratories Japan, Eli Lilly Japan K.K., Japan, ⁶Kyoto Women's University, Japan

[Aim] To evaluate the effects of treatment with raloxifene (RLX) on the quality of life (QOL) of patients with postmenopausal osteoporosis in daily practice. **[Subjects/Methods]** In patients with postmenopausal osteoporosis [based on Diagnostic Criteria for Primary Osteoporosis (rev. 2000)] treated with RLX in accordance with the package insert, a battery of QOL questionnaires [SF-8, EQ-5D and Japanese Osteoporosis Quality of Life Questionnaire (JOQOL) 2000] and the 10.0 cm-scale Visual Analogue Scale (VAS) for pain were administered at baseline and Weeks 8 and Week 24 of treatment. The changes in these scales from baseline were tested with paired t-test or Wilcoxon's signed rank test. Adverse reactions were also assessed. **[Results]** Of 536 patients enrolled in the study, 507 (mean age: 70.7 years) were included in the analyses. In comparison with baseline, all the SF-8, and physical and mental summary scores were significantly improved at Weeks 8 and 24 (p<0.001, t-test). The EQ-5D index score also significantly improved from baseline at both Weeks 8 and 24 (p<0.001, t-test). Furthermore, the total JOQOL 2000 score significantly improved at Week 24 (mean changeSD: 4.811.8, p<0.001, t-test). The VAS for pain

was significantly reduced at Weeks 8 (mean SD: -1.052.33 cm, $p<0.001$, t-test) and 24 (mean SD: -1.3 2.67 cm, $p<0.001$, t-test), with 2.0 cm or more reduction in over 30% of patients. In addition, a survey for pain frequency in the past four weeks revealed significant improvement ($p<0.001$, t-test). Adverse drug reactions were reported in 34 patients (6.71%) with the most commonly reported System Organ Class of gastrointestinal disorders in 10 patients. [Conclusion] In Japanese clinical setting, significant improvements in the QOL and pain were observed at Week 8 of treatment with RLX and maintained throughout the observation period. These results can provide the first evidence of effectiveness of RLX for osteoporosis patients in Japan.

Disclosures: Kiyoshi Tanaka, Eli Lilly Japan KK, S

This study received funding from: Eli Lilly Japan KK

SA0443

Cost Effectiveness Of A Targeted Intervention To Reduce Refracture Rates: Analysis Of A Four Year Prospective Controlled Study. Mark Cooper^{*1}, Kirtan Ganda², Andrew Palmer³, Markus J Seibel⁴. ¹University of Birmingham, United Kingdom, ²Australia, ³University of Tasmania, Australia, ⁴Bone Research Program, ANZAC Research Institute, University of Sydney, Australia

We recently reported the clinical effectiveness of a Minimal Trauma Fracture (MTF) service. The MTF intervention is offered on an outpatient basis to patients presenting with a minimal trauma fracture to Concord Repatriation General Hospital (CRGH) in New South Wales, Australia. In a 4-year prospective observational study, that was unique in having a control group treated in primary care, it was demonstrated that the MTF service significantly reduced the risk of refracture by 80%. The MTF service involves input from a specialist clinic and greater use of bone density assessment, laboratory tests and medications. It was thus unclear whether the benefits seen would be cost-effective. Our aim was therefore to determine the costs and improvements in quality-adjusted life years (QALYs) associated with the MTF service, allowing a comparison of value for money versus standard practice. We developed a Markov, 2nd-order Monte Carlo simulation model to project the 4-year clinical and cost outcomes to 10 years. The model accounted for hip, forearm and humerus fractures; their associated direct costs; changes in health utility; and in the case of hip fracture, increases in mortality. Fracture probabilities were calculated directly from the recently published clinical trial. Direct medical costs (expressed in 2010 Australian Dollars) for the MTF intervention and the control arm were derived from reported health resource consumption. Outcomes were discounted at 5% annually. Total 10-year costs (C), quality-adjusted life years (QALY) and incremental C/QALY-gained were calculated for MTF versus control. Extensive sensitivity analyses were performed e.g. varying anti-fracture effectiveness, intervention costs, number of patients treated and level of compliance with therapy.

Reducing recurrent fracture rates with the MTF service versus control led to an improvement of 0.08 QALYs per patient over 10 years. Despite higher treatment costs, total costs in the MTF treatment arm were only increased by \$1,480 per patient over the 10-year period, due to reduced costs from fractures avoided. The incremental cost-effectiveness ratio for the MTF service versus control was \$19,102/QALY gained, indicating that the MTF intervention represents excellent value for money. Sensitivity analysis demonstrated that the results were robust under all plausible assumptions.

The MTF service is thus a cost-effective intervention to reduce recurrent osteoporosis fractures in a high risk population.

Disclosures: Mark Cooper, None.

SA0444

Global Health Care Utilization Following a Fracture: The Global Longitudinal Study of Osteoporosis in Women. George Ioannidis^{*1}, Julie Flahive², Laura Pickard¹, Alexandra Papaioannou³, Roland Chapurlat⁴, Kenneth Saag⁵, Stuart Silverman⁶, Stephen Gehlbach⁷, Jonathan Adachi⁸. ¹McMaster University, Canada, ²University of Massachusetts Medical School, USA, ³Hamilton Health Sciences, Canada, ⁴E. Herriot Hospital, France, ⁵University of Alabama at Birmingham, USA, ⁶Cedars-Sinai/UCLA, USA, ⁷University of Massachusetts, USA, ⁸St. Joseph's Hospital, Canada

Purpose: Using the Global Longitudinal study of Osteoporosis in Women (GLOW) – an observational longitudinal study of non-institutionalized women aged ≥ 55 years recruited from 723 primary physician practices in 10 countries – we evaluated the direct medical health utilization associated with treating several types of fractures in different regions around the world.

Methods: Information was collected from GLOW via self-administered patient questionnaires at baseline and year 1 (N=51,491). From these tools, clinically recognized low trauma fractures at year 1 were classified into incident hip, spine, wrist/hand, arm/shoulder, and other fractures (included ankle, foot, knee, clavicle, elbow, coccyx, sternum, or neck.). Health care utilization data included whether the fractured patient was treated at a doctor's office/clinic, or at a hospital. Patients were also asked if they had undergone surgery and if they had been treated at a rehabilitation center or nursing home.

Results: The table shows the use of health care service for individual fracture types. In addition, patients with wrist/hand, arm/shoulder and other fractures were more

likely to be treated at a hospital in Southern (88.2%, 93.5%, 84.2%) and Northern European regions (92.3%, 86.7%, 84.3%) as compared with the USA (67.9, 71.0, 53.3%), respectively.

Conclusions: Patients who experience hip fractures use significant health care services. However, given the higher incident rates of the additional fracture types examined, all fracture types have an important impact on health care services. The resource utilization patterns identified in this study may assist health planners in developing future health care services.

Health care service used	New fracture at specific location, n/n (%)				
	Spine (n=195)	Hip (n=134)	Wrist/hand (n=419)	Arm/Shoulder (n=197)	Other ^a (n=658)
Office/clinic	121/165 (73)	76/124 (61)	270/379 (71)	130/181 (72)	456/596 (77)
Hospital	101/165 (61)	117/127 (92)	313/389 (80)	149/184 (81)	371/579 (64)
Overnight at hospital	57/95 (60)	102/111 (92)	85/281 (30)	66/138 (48)	115/339 (34)
Surgery	29/99 (29)	103/116 (89)	114/296 (39)	49/141 (35)	107/355 (30)
Rehabilitation center	24/161 (15)	69/122 (57)	47/357 (13)	43/176 (24)	64/563 (11)
Nursing home	8/153 (5.2)	19/116 (16)	8/349 (2.3)	12/168 (7.1)	13/534 (2.4)

Table 1

Disclosures: George Ioannidis, None.

This study received funding from: Financial support for the GLOW study is provided by Warner Chilcott Company, LLC and sanofi-aventis to the Center for Outcomes Research, University of Massachusetts Medical School

SA0445

Rates of Diagnosis and Treatment of Osteoporosis in Males Before and After Hip, Vertebral, and Non-Hip/Non-Vertebral (NHNV) Fractures. Susan Brennenman¹, Laura Christensen¹, Nicole Yurgin^{*2}. ¹Innovus, USA, ²Amgen Inc, USA

Purpose: To determine the proportion of male patients with closed fractures who were diagnosed (dx) or treated (tx) for osteoporosis before or after a closed fracture.

Method: Descriptive analysis was conducted on administrative claims from a large, national health plan. Subjects were males 45 or older with at least one medical claim for a new closed fracture at a single site (e.g., hip, vertebral) between January 1, 2005 and December 31, 2008, were continuously enrolled for 12 months before and after the fracture, and had at least two fracture-related outpatient visits in the follow-up. A closed fracture was considered 'new' if there were no health care claims for the fracture in the 12 month pre-fracture baseline period. For hip, femur, tibia and humerus fractures, individuals were excluded if they did not receive inpatient care. Commercially insured (COM) and Medicare Advantage Plan (MAP) members were analyzed separately. Osteoporosis treatment was defined as having at least one filled prescription for alendronate, risedronate, teriparatide, ibandronate, pamidronate, or zoledronate. Diagnosis of osteoporosis was defined as the presence of an ICD-9 diagnosis code of 733.0x on a medical claim.

Results: The sample mean age was 58 yrs and 74 yrs for COM and MAP, respectively. The study identified 18,917 (COM 16,191, MAP 2,726) new closed fractures during the study period. In the COM group, the pre-fracture dx and tx rates were 2.5% and 2.1%, respectively. After the men experienced a fracture, the mean dx and tx rates were 6.8% and 4.0%, respectively. The post-fracture dx rates by fracture type were: 14.4% for hip, 20.1% for vertebral, and 2.5% for NHNV. The post-fracture tx rates by fracture type were: 7.5% for hip, 11.8% for vertebral, and 1.5% for NHNV.

In the older MAP population, the pre-fracture dx and tx rates were 5.6%, and 2.4%, respectively. After the men experienced a fracture, the mean dx and tx rates were 17% and 6.8%, respectively. The post-fracture dx rates by fracture type were: 13.4% for hip, 31.3% for vertebral, and 7.1% for NHNV. The post-fracture tx rates by fracture type were: 3.2% for hip, 13.2% for vertebral, and 2.7% for NHNV.

Conclusion: Amongst males 45 and older, the rates of diagnosis and treatment for osteoporosis were higher after fracture. Nevertheless, the highest post-fracture diagnosis rate was still less than one-third of the fracture patients.

Disclosures: Nicole Yurgin, UnitedHealth Group, S

This study received funding from: Amgen Inc

SA0446

See Friday Plenary Number FR0446.

SA0447

Do our People Meet the IOM Recommendations on Calcium Dietary Intake?

Cristina Carbonell^{*1}, Daniel Prieto-Alhambra², Carmen Olmos³, Isabel Aymar⁴, Adolfo D  ez-Perez⁵, Xavier Nogues⁵. ¹Healthy Primary Care Via Roma Barcelona.Facultat de Medicina Universitat de Barcelona, Spain, ²Department of Internal Medicine, URFOA IMIM-Hospital del Mar, Parc de Salut Mar, Autonomous University of Barcelona, IDIAP Jordi Gol, Barcelona, Spain, Spain, ³Healthy Primary Care Via Roma Barcelona, Spain, ⁴Densitometry Unit. URFOA Hospital del Mar. Barcelona, Spain, ⁵Department of Internal Medicine, URFOA IMIM-Hospital, RETICEF (Red Tematica de Investigacion Cooperativa en Envejecimiento y Fragilidad), Instituto Carlos III, Barcelona, Spain del Mar, Parc de Salut Mar, Autonomous University of Barcelona,, Spain,, Spain

AIMS

Calcium is an important mineral for bone formation and cellular activity as second messenger with specific roles. We aimed to determine the percentage of people who meet an adequate intake of calcium in their diet according to the last IOM (Institute of Medicine) recommendations. Secondly, we determined predictors of calcium intake amongst the following: gender, age, education level and co-morbid conditions.

METHODS

Design: Observational, cross-sectional.

Subjects: consecutive sample of patients aged over 15 attending participant primary care consults in Barcelona (Spain) for any reason during the recruitment period (one week in January/2011). We excluded patients with osteoporosis or other bone metabolism conditions, those receiving antiresorptive drug/s or Calcium supplements, pregnant women and those with a history of renal stones.

Measurements: Validated weekly food frequency questionnaire of calcium intake. We collected age, sex, co-morbid conditions, educational level and nationality. Participants were considered to have sufficient calcium dietary intake if they reported ≥ 1100 mg daily in 15-19 years; ≥ 1000 in women 19 – 50 and in men aged 19 to 70; and ≥ 1200 mg/d in women older than 50 and men over 70.

Statistics: binomial test was used to calculate 95% Confidence Interval (95CI) for the proportion of patients meeting IOM recommendations. Multivariate linear regression models were fitted to study determinants of dietary calcium intake.

RESULTS

545 patients were eligible, 25 excluded and 520 included.186 were males (35.8%). Calcium intake was inadequate (low) in 276(53.1% (IC 95% 48.7- 57.4%)) patients. None were over the upper level intake. Significant predictors of dietary calcium intake were: age (adjusted beta per year 13.6 [95CI 0.76 to 26.5;p=0.038]), and educational level (adjusted beta 320.6 [95CI 42.0 to 599.2;p for linear trend=0.024]). We observed a borderline-significant trend to lower calcium intake for foreign nationality (adjusted beta -525.5;p=0.08) and for a history of COPD (adjusted beta -1270.8;p=0.057).

CONCLUSION

Only half of patients attending a primary care health center for any reason, excluding those with osteoporosis and/or bone metabolism diseases meet IOM recommendations for adequate dietary calcium intake. Patients with higher educational levels, and older participants, had a higher calcium intake. Immigrants and COPD patients might be at risk for insufficient calcium intake.

Disclosures: Cristina Carbonell, None.

SA0448

See Friday Plenary Number FR0448.

SA0449

See Friday Plenary Number FR0449.

SA0450

Effect of two years Dietary Hesperidin Supplementation on Bone Metabolism in Postmenopausal Women. Veronique Habauzit¹, Elizabeth Offord², Winnie Chee³, Lydia Jafrelo¹, Laurent Ameze², Gary Williamson⁴, Marie-noelle Horcajada^{*2}. ¹INRA, France, ²Nestle, Switzerland, ³National University of Malaysia, Malaysia, ⁴Nestle, France

Hesperidin (Hp), a major citrus flavonoid, has anti-inflammatory properties and prevents ovariectomized-induced bone loss in rodents. Here we report the results of the first clinical study to be conducted on the ability of Hp to protect against postmenopausal bone loss. The study was a parallel, placebo-controlled, double blind, 24-month randomized intervention trial assessing the effect of Hp on validated biomarkers of bone turnover and bone mineral density (BMD).

110 healthy Caucasian postmenopausal women, 50-65y, were randomized on their Ca intake and hip BMD and assigned to the Hp (500 mg Hp/day in 2 biscuits) or placebo (P) group (same biscuits without Hp). Subjects kept dietary records and minimized their citrus-rich food intake during the study period.

Both groups completed the study to a similar extent (87.5 % in P group, 91 % in Hp group). Demographics and baseline characteristics such as daily calcium intake (P: 884.7 276.2; Hp: 887.7 246.9 mg/day) or 25(OH)D (P: 82.0 38.3 ; Hp: 79.5 34.1 nmol/l) were not significantly different between the two groups. Evolution from baseline to 24 months of anthropometry, standard laboratory parameters was similar in the two groups. Concerning BMD, whatever bone site (total hip, femoral neck or lumbar spine), no statistically significant difference was found between groups based on mixed models with or without covariates in an ITT analysis. In the P group, from baseline to 24 months, the mean % change in BMD was between 2.48% and -1.15% depending on the bone site, and in the Hp group, changes ranged from 2.85% to 1.43%.

For serum b-ALP, serum CTX-1, serum PINP and calciuria, no statistically significant difference was seen between groups. However, a significant interaction group x time (p<0.05) was detected for bone turnover index: computed ratio b-ALP / CTX-1 and PINP / CTX-1. This significant effect could mainly be attributable to a higher value of the ratio at 18 and 21 months in the Hp group.

In conclusion, the yearly rates of bone loss (1-2%) were equivalent in the two groups. Evolution in BMD was not statistically different between the two groups. However, the hesperidin supplementation resulted in a significant modulation of biomarkers of bone remodeling after at least 18 months of exposure. As reflected by bone turnover index, the subjects consuming hesperidin daily presented a better balance in bone metabolism during the 2nd year of follow-up at the 18 and/or 21 month time-points.

Disclosures: Marie-noelle Horcajada, None.

This study received funding from: Nestle

SA0451

Effects of Strontium on the Quality of Bone Apatite Crystals.

Audrey Doublier^{*1}, Delphine Farlay¹, Xavier Jaurand², Ruben Vera³, Georges Boivin¹. ¹INSERM UMR1033; Universite De Lyon, France, ²Universite de Lyon, Centre technologique des microstructures, F-69622, France, ³Universite de Lyon, Centre de diffractometrie Henri Longchambon, F-69622, France

Interactions between strontium and bone mineral have been investigated at the tissue level in animals (1,2) and in women after 3 years of treatment with strontium ranelate (3-5). In treated women, strontium was exclusively present in bone formed during treatment, and degree of mineralization was maintained. The goal of this study was to assess the effect of strontium on the characteristics of apatite crystals. Ten paired iliac bone biopsies were taken from osteoporotic women before and after 3 years of treatment with either 2g per day of strontium ranelate (SrRan, n=7) or placebo (PLA, n=3), and then embedded in methyl methacrylate. By X-ray diffraction (XRD), position and full width at half-maximum of the apatite peaks (i.e., crystallinity) were measured on cortical and cancellous bone. Crystals' size was calculated by Scherrer's formula, as well as interplanar distances d002 and d310. d002 was also measured by selected area electron diffraction (SAED) in new and old bone (age of tissue). After treatment, the presence of strontium in new bone was verified by X-ray microanalysis in SrRan patients. The effects of treatment were assessed by a Wilcoxon test and difference between groups by a Kruskal-Wallis test (significant if p \leq 0.05). All spectra (PLA and SrRan) were characteristic of a biological apatite, and crystals were preferentially oriented along the organic matrix. Globally, in cortical and cancellous tissues, crystallinity (size and perfection of crystals), d002 (XRD and SEAD) and d310 (XRD) were not significantly modified neither by the duration (3 years versus before treatment) nor by the type of treatment (SrRan versus PLA). Moreover, d002 was similar in cortical and cancellous bone whatever the treatment group. To conclude, the quality of bone apatite crystals is maintained in a normal range in osteoporotic patients after 3 years of treatment with strontium ranelate. 1. Farlay et al. J Bone Miner Res 2005, 20:1569 ; 2. Bain et al. Osteoporos Int 2009, 20:1417 ; 3. Boivin et al. Osteoporos Int 2010, 21:667 ; 4. Li et al. J Bone Miner Res 2010, 25:968 ; 5. Doublier et al. J Bone Miner Res 2009, 24(Suppl 1):S41

Disclosures: Audrey Doublier, Servier Laboratories, 2

This study received funding from: Servier Laboratories

SA0452

Therapy With Strontium Ranelate Improves Bone Mineral Mass,Volumetric Bone Mineral Density and Geometrical Parameters of Bone in Postmenopausal Osteoporotic Women- 2Years Results. A Peripheral Quantitative Computed Tomography (PQCT) of the Tibia Study. Konstantinos Stathopoulos^{*1}, Erato Atsali¹, Ilias Bournazos², Aristidis B. Zoubos¹, Grigoris Skarantavos³. ¹"Attikon" Athens University Hospital, Greece, ²"Attikon" Athens University Hospital, Greece, ³Attikon University Hospital, Greece

Objective: We assessed the effects of strontium ranelate on bone mineral mass, volumetric bone mineral densities, geometrical properties of the bone and strength indexes in postmenopausal osteoporotic women using tibia pQCT.

Material and methods: We reviewed medical records of 32 women with postmenopausal osteoporosis who received strontium ranelate 2g sachets per os daily for 2 consecutive years. Inclusion criteria: 1) age \geq 50y 2) postmenopausal status \geq 2y, 3) DXA measurement (Spine/Hip) with Tscore \leq -2.5 SD 4) Tibia pQCT before, 1 y and 2 y

after treatment. Exclusion criteria: 1) Secondary osteoporosis' conditions 2) Other bone metabolic diseases 3) Previous use of bone anabolic agents 4) malignancies. Patients had tibia pQCT (Stratec Medizintechnik, Pforzheim, Germany), 3 slices were obtained at the 4% (trabecular), 14% (subcortical and cortical) and 38% (cortical bone) of tibia length sites. We studied 15 variables per slice, mainly total bone content (TOT_CNT), total density (TOT_DEN), trabecular content (TRB_CNT), trabecular density (TRB_DEN), cortical content (CRT_CNT), cortical density (CRT_DEN), subcortical content (CRTSUB_CNT), subcortical density (CRTSUB_DEN), cortical area (CRT_A), subcortical area (CRTSUB_A), mean cortical thickness (CRT_THK), and Stress Strength Indexes (SSIs) at the 14% and 38% sites. Results were corrected for strontium ranelate atomic weight. We performed statistical analysis (t-test, ANCOVA)-data expressed as meanstandard deviation (S.D.)

Results: Patients' mean age was 64.3 12.6y and mean tibia length 352.14 65.03mm. After 2 years treatment, we report increases at the 14% site in _CNT (181,0421,51 vs 183,0521,34, $p=0,006$), SUBCRT_CNT (168,6419,58 vs 170,4819,11, $p=0,005$), and CRT_CNT (62,9118,58 vs 66,6320,63, $p=0,021$). At the 38% site we report increases in TOT_CNT (276,4636,24 vs 278,9435,71, $p=0,09$), SUBCRT_CNT (205,8625,60 vs 208,5925,47, $p<0,000$), CRT_CNT (160,0931,19 vs 168,8432,62, $p<0,000$) and CRT_DEN (1192,4614,50 vs 1203,1517,05, $p<0,000$). We also report increases in CRT_A (134,1825,73 vs 140,1326,57, $p<0,000$) and mean CRT_THK (2,180,44 vs 2,280,46, $p=0,001$).

Conclusions: Our results indicate that 2 years of therapy with strontium ranelate increase significantly bone mineral mass, volumetric cortical densities, cortical area and mean cortical thickness in post menopausal osteoporotic women.

Disclosures: Konstantinos Stathopoulos, None.

SA0453

See Friday Plenary Number FR0453.

SA0454

Effects of Calcitonin Treatment in Patients with Osteoporosis Who Developed Acute Low Back Pain Due to a New Vertebral Fracture. Keiji Fujino¹, Naoto Endo², Shinya Tanaka³. ¹Fujino Orthopaedic Clinic, Japan, ²Niigata University, Japan, ³Saitama Medical University, Japan

Objectives Many elderly subjects have become bedridden or self-confined due to a vertebral fracture associated with osteoporosis. This study was performed to determine whether calcitonin treatment is effective for achieving early ambulation and preventing confinement to bed, in comparison with oral treatment with non-steroidal anti-inflammatory drugs (NSAIDs), in patients with osteoporosis who developed acute low back pain after suffering a new vertebral fracture.

Methods This was a multicenter, open-label, randomized study including female patients aged 65 years and over with primary osteoporosis who developed low back pain after suffering a new fragile fracture of the vertebrae. They were randomized either to receive intramuscular injection of calcitonin at 20 IU once weekly or oral treatment with NSAIDs. The study endpoints comprised the degree of low back pain assessed using the visual analog scale (VAS) and patients' quality of life (QOL) rated using the Roland Morris Questionnaire (RDQ) and the Japan Questionnaire for Osteoporotic Pain (JQ22).

Results The low back pain according to VAS assessment and QOL assessed using RDQ and JQ22 improved in both patients treated with calcitonin and those receiving oral NSAIDs at the end of Week 4 of study treatment. The assessment results were superior in these variables for the calcitonin group in comparison with the NSAIDs group, suggesting greater efficacy of calcitonin therapy as compared to oral treatment with NSAIDs.

Discussion Calcitonin has an analgesic effect via the central-nervous serotonergic system, which lasts a relatively long period, while lacking in a fast onset of effect like NSAIDs. Calcitonin injected once weekly is thus considered to be sufficient to provide pain control and improving patients' QOL. Calcitonin is considered to be essential in an early-stage treatment of pain due to a new vertebral fracture.

Disclosures: Shinya Tanaka, None.

This study received funding from: The Japanese Society for Musculoskeletal Rehabilitation (JSMR)

SA0455

Patient Education in the Digital Age. Jay Ginther*. Cedar Valley Bone Health Institute, USA

Communicating full information about osteoporosis prevention and treatment to patients and their families during the limited time of an office visit is virtually impossible. They will seek further information outside the office setting. The abundance of information aimed at the lay public available on the internet is impressive. Its accuracy is not. Our challenge is to supply abundant, scientifically accurate information, written for the lay public, to our patients. This poster presentation will detail the mix of paper handouts, office video, website, blog, CD, u-tube, and magazine articles used by Cedar Valley Bone Health Institute of Iowa.

Disclosures: Jay Ginther, Eli Lilly, 5; Eli Lilly, 8; BoneDocBlog.com, 4; Cedar Valley Bone Health Institute of Iowa, 4

SA0456

Relative Importance of Attributes that Influence Osteoporosis Decision-Making in Postmenopausal Women. Stuart Silverman¹, Andrew Calderon², Amy Mofield³, Wendy Brynildsen⁴, Michael Koenig², Kristina Kaw², Deborah Gold³. ¹Cedars-Sinai/UCLA, USA, ²OMC Research, USA, ³Duke University Medical Center, USA, ⁴Duke University, USA

Purpose: Patient preferences about medication attributes significantly influence osteoporosis (OP) medication decision making. Patients may decide to initiate, change, or stop therapies based on ranking of perceived attributes of the therapy and their personal rankings. Max-Diff is a form of conjoint analysis which allows participants to rank attributes by randomly presenting statements about these attributes. **Objective:** We examined the rank order of OP medication attributes using MaxDiff in a convenience sample of Caucasian postmenopausal (PM) women at risk of OP fracture. **Methods:** After conducting qualitative interviews with 13 postmenopausal women, we identified six major attributes that influence OP medication decision making: efficacy, short-term safety, long-term safety, cost, delivery system, and dosing interval. A sample of PM Caucasian women who were at risk of fracture based on FRAX (FRAX scores 3% risk hip fx or 20% major OP fx) were recruited to complete a laptop-based questionnaire to provide demographic data and to rank 39 statements about these attributes using Max-Diff. **Results:** We recruited a convenience sample of 82 PM Caucasian women (mean age=76.6 yrs, SD=5.83, range=65-89) at two US sites. Over half (53.7%) were not married (e.g. widowed, divorced or never married) and 54% had some post high school education. The majority of respondents considered their income at least enough to meet their needs (89.02%) and 93% reported to have a co-pay. 30% were currently taking an osteoporosis medication. Although interindividual variability was seen, these women rated efficacy (6 statements, mean importance score 6.63, range 5.88-7.16) twice as important as safety (14 statements, mean importance score 3.35, range 1.37-4.97). Safety (short- and long-term) was rated approximately threefold higher than cost (4 statements, mean 1.02, range 1.37-0.61). Cost was rated approximately 50% higher than either dosing interval (6 statements, mean importance 0.66, range 0.38-0.93) or delivery method (5 statements, mean importance score 0.54, range 0.08-0.65). **Conclusions:** A convenience sample of postmenopausal Caucasian women with risk of OP fractures rated efficacy and safety higher than cost, delivery system or dosing interval. This information may be helpful in structuring communication about osteoporosis medications to PM women. Ranking of attributes on an individual basis may allow the development of targeted communication to individual patients.

Disclosures: Deborah Gold, None.

This study received funding from: Novartis Pharmaceuticals

SA0457

Annual Bone Loss in Postmenopausal Women is Attenuated with 1000 IU but not 400 IU Daily Vitamin D3: A 1 Year Double Blind RCT Designed to Include Seasonal Effects at High Latitude. Adrian Wood¹, Lorna Aucott¹, Alexandra Mavroei², Karen Secombes¹, Alison Black³, William Fraser⁴, David Reid¹, Helen Macdonald⁵. ¹University of Aberdeen, United Kingdom, ²University of Aberdeen School of Medical Sciences College of Life Sciences, United Kingdom, ³Woolmanhill Hospital Aberdeen Osteoporosis Research Unit, United Kingdom, ⁴Royal Liverpool University Hospital, United Kingdom, ⁵University of Aberdeen Bone & Musculoskeletal Research Programme, United Kingdom

A number of trials have investigated the effect of vitamin D on bone health with mixed results. Subsequent meta-analyses have concluded that for beneficial effects either adequate calcium intake is also required or the daily vitamin D dose needs to be >800 IU. There may be confounding from the underlying effects of season, and the relationship between change in vitamin D status and bone status is unclear. The aim of this 1-year double blind placebo controlled RCT, designed to directly compare the seasonal changes in vitamin D status, was to determine whether vitamin D3 at daily doses of 400 IU or 1000 IU affected bone loss in postmenopausal women.

Three hundred and five women aged 60-70 y were randomised to receive either vitamin D or placebo in January-March 2009 and were seen at two-monthly intervals until January-March 2010 (87% attending the final visit). 25-hydroxyvitamin D [25(OH)D] was measured by dual tandem mass spectrometry using NIST aligned standard (Chromsystems UK). Bone mineral density (BMD) was measured at the hip and spine by Lunar iDXA.

The mean 25(OH)D change SD for the placebo, 400 IU and 1000 IU vitamin D groups was: -412 nmol/L, +3120 nmol/L and +4319 nmol/L, respectively. Figure 1 highlights a non-linear response showing that (i) the incremental increase in 25(OH)D for 1000 IU over 400 IU was small and (ii) the seasonal pattern for the placebo group was not followed for the vitamin D treatment groups. In contrast mean BMD loss at the hip was significantly less for the 1000 IU vitamin D group (-0.051.46%) compared to the 400 IU vitamin D and placebo groups (-0.571.33% and -0.601.67%, respectively) (P=0.02). There was no effect of treatment on BMD at the spine.

The discordance between the incremental increase in 25(OH)D when comparing the two doses of vitamin D and the effect on hip BMD suggests that serum 25(OH)D may not accurately reflect clinical outcome. It is not known whether the additional vitamin D was not converted to 25(OH)D because it was stored or degraded or whether it was not fully absorbed. Further research is required to explain whether the bone anabolic effect is confined to cortical bone or to particular sites, and whether the

increase in BMD is a result of transient increases in serum calcium after ingestion of the higher dose vitamin D, or if there are other explanations.

Effect of treatment on vitamin D status

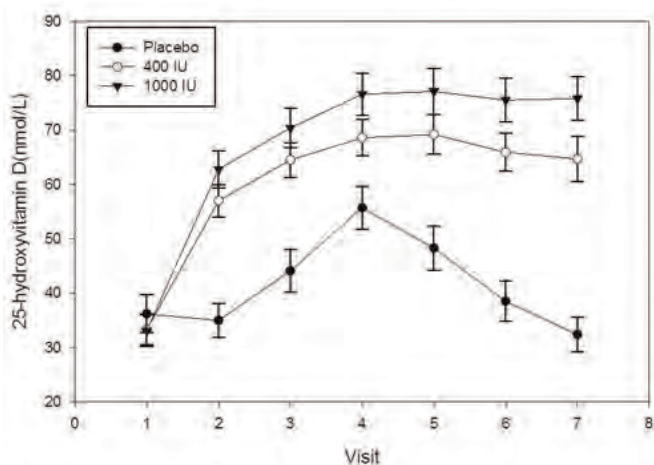


Figure 1

Disclosures: Helen Macdonald, None.

SA0458

Fermented Milk Enriched with Calcium and Vitamin D and Anthocyanins Improves Bone Metabolism in Postmenopausal Women. caroline puel¹, Veronique Coxam^{*2}, MJ Davicco³, patrice lebecque³, Yohann Wittrant⁴. ¹ELVIR, France, ²INRA Theix, France, ³INRA, France, ⁴Institut National de la Recherche Agronomique, France

Research in the field of nutrition allows considering the establishment of a real prevention of osteoporosis. The value of fruit and vegetables is discussed. A major reason is the recognition of their likely involvement in the prevention of various diseases associated with oxidative stress, such as osteoporosis. Red fruits are particularly interesting for their high anthocyanins content, endowed with anti-oxidant and anti-inflammatory properties.

The present clinical, controlled, randomized, double-blind placebo, prospective study, conducted over 3 months, aims to evaluate the possible osteoprotective effects of anthocyanins on bone metabolism, in postmenopausal women (less than 6 years).

In that purpose, fermented based blueberry extract milk, providing respectively 25% and 20% RDA of calcium and vitamin D, rich in anthocyanins, has been given to volunteers. Fifty six women aged 50 to 65 years, without HRT, were included in the study after a medical examination and a blood test. Throughout the study period, they kept their eating habits, limiting however the red fruits. They were randomized into 2 groups of 28 subjects receiving either 0 or 120 mg of anthocyanins per day. The intake of anthocyanins was conducted in the form of fermented milk containing 0 or 60 mg of active molecule / 100ml, with 2 bottles of 100 ml per day.

Consumption of a milk enriched in polyphenols significantly improved the serum bPAL activity, (an osteoblastic marker), without significant modification of CTX, a marker for bone resorption. This favorable orientation of bone metabolism could be explained by the contribution of anthocyanins from bilberry extract, the only noticeable difference between the 2 test foods. This finding is independent of the initial calcium and vitamin D consumption.

In conclusion, consumption of fermented milk containing blueberry, enriched with calcium and vitamin D for 3 months, has corrected the vitamin status of postmenopausal women for less than 5 years. In addition, it resulted in a favorable orientation of bone metabolism, as indicated by the rise of a biomarker of osteoblastic activity. This benefit is most likely related to the presence of blueberries (rich in polyphenols and phenolic acids).

Disclosures: Veronique Coxam, None.

SA0459

Vitamin D Serum Levels Influence Adequate Response To Bisphosphonate Treatment In Postmenopausal Osteoporosis. Angels Martinez-Ferrer^{*1}, Pilar Peris², Ana Monegal³, M. Jesus Martinez de Osaba⁴, Africa Mux⁵, Nuria Guanabens⁷. ¹Hospital Clinic Barcelona, Spain, ²Rheumatology. Hospital Clinic, Spain, ³Metabolic Bone Diseases Unit. Hospital Cl  nic. University of Barcelona., Spain, ⁴Hormonal Laboratory. Hospital Clinic., Spain, ⁵Universitat De Barcelona, Spain

It is not clear whether vitamin D sufficiency may optimize the response to bisphosphonates (BP) treatment in postmenopausal osteoporosis. Therefore, the aim of this study was to evaluate the role and possible mechanisms of vitamin D in adequate response to standard treatment with BP for postmenopausal osteoporosis.

Methods: We included 120 postmenopausal osteoporotic women (aged 688 years) treated with BP (alendronate or risedronate) at their annual follow-up visit. All patients underwent complete anamnesis, including treatment adherence, use of vitamin D supplements, and previous falls and fractures during the last year. Bone mineral density (BMD) evolution during this period was analyzed in all patients as was the bone mineral profile evaluating serum PTH and 25-OH vitamin D (25-OHD) and urinary NTx. In addition, muscular strength in lower limbs was measured in all patients. Patients were classified as inadequate responders to the antiosteoporotic treatment based on a BMD loss > 2% and/or the presence of fragility fractures during the last year.

Results: Thirty percent of patients showed inadequate response to BP treatment, with significantly lower levels of 25 OHD (22.41.3 vs. 26.60.3 ng/ml, p=0.01), a higher frequency of 25OHD levels < 30 ng/ml (91% vs. 69%, p=0.019) and higher urinary NTx (42.23.9 vs. 30.92.3 nM/mM, p=0.01). Inadequate responders also had an increase in lumbar (-3.70.7 vs. 3.50.4 %, p<0.001) and total femoral bone loss (-1.70.4 vs. 1.030.3 %, p<0.001) and in fragility fractures (p=0.007) when compared with adequate responders. No other significant differences were observed on comparing the two groups of patients. Patients with values of 25-OHD >30 ng/ml had a greater significant increase in lumbar BMD at the annual control than women with values <30 ng/ml (3.6 % vs. 0.8%, p<0.05). The probability of inadequate response was 4-fold higher in patients with 25-OHD levels < 30 (OR, 4.42; 95% CI, 1.22-15.97, p=0.02). Conclusions: Inadequate response to BP treatment is frequent in postmenopausal women with osteoporosis as is vitamin D insufficiency, despite vitamin D supplementation. Maintenance of vitamin D levels over 30 mg/ml is especially indicated for adequate response to BP treatment.

Disclosures: Angels Martinez-Ferrer, None.

SA0460

Determination of Intermittent PTH(1-34) Regimens Sufficient to Restore Trabecular Bone Mass in Adult Ovariectomized Osteopenic Rats. Jukka Morko^{*1}, ZhiQi Peng¹, Jukka Vaaranen¹, Mari Suominen¹, Katja Fagerlund¹, Tiina A. Suutari¹, Jukka P. Rissanen¹, Harrie C.M. Boonen², Trine S.R. Neerup³, Hanne H. Bak³, Jussi Halleen¹. ¹Pharmatest Services Ltd, Finland, ²Department of Pharmacology & Pharmacotherapy, University of Copenhagen, Denmark, ³Zealand Pharma A/S, Denmark

Recombinant human parathyroid hormone analog PTH(1-34) is the major bone anabolic agent in clinical practice. In preclinical studies, PTH(1-34) regimens have varied substantially and induced strong effects including osteosclerotic and hypercalcemic conditions. The purpose of this study was to identify intermittent PTH(1-34) regimens sufficient to restore trabecular bone mass in long bone and vertebra and to determine their effects on circulating calcium levels in adult osteopenic rats. Female Sprague-Dawley rats were ovariectomized (OVX) at the age of 6 months. After 6 weeks without treatment, a reduction in trabecular bone mineral density (Tb. BMD) was confirmed in their tibial metaphysis. Treatment was started at 7 weeks after the operations and continued once daily for 6 weeks. The osteopenic rats were treated subcutaneously with PTH(1-34) at 1.2, 4, 12, 40 and 120 µg/kg/d. During the treatment period, the reduction in Tb.BMD exacerbated in OVX rats treated with vehicle. At the end of the treatment period, their Tb.BMD and trabecular bone volume (BV/TV) were decreased by 70% in tibial metaphysis and by 35% in lumbar vertebra. Treatment with PTH(1-34) reversed these OVX-induced reductions at all doses in a dose-dependent manner. The doses 12 and 4 µg/kg/d were sufficient to restore Tb.BMD and BV/TV in tibial metaphysis and lumbar vertebra, respectively. These effects were associated with 100% increase in bone formation rate (BFR/BS) and 50% reduction in osteoclast number (N.Oc/B.Pm) in tibial metaphysis and with 60% increase in BFR/BS and 30% reduction in N.Oc/B.Pm in lumbar vertebra when compared with OVX rats treated with vehicle. Serum levels of total calcium (Ca) decreased and blood levels of ionized free calcium (Ca²⁺) remained unchanged in OVX rats treated with vehicle at 80 minutes after dosing at 5 weeks after the start of treatment. Treatment with PTH(1-34) reversed the OVX-induced reduction in serum Ca levels at 4-120 µg/kg/d and increased blood Ca²⁺ levels at all doses in a dose-dependent manner. The dose 4 µg/kg/d was sufficient to restore serum Ca levels and to increase blood Ca²⁺ levels transiently, whereas the dose 12 µg/kg/d induced a transient increase in both of these levels. This study demonstrated that intermittent subcutaneous treatments with PTH(1-34) at 12 and 4 µg/kg/d are sufficient to restore trabecular bone mass in long bone and vertebra, respectively, and that these doses induce a mild transient hypercalcemia in adult OVX rats.

Disclosures: Jukka Morko, Pharmatest Services Ltd, 3

SA0461

Effect of Estrogen Deficiency in Sclerostin Knockout Mice. Min Liu*, Pam Kurimoto, Qing-Tian Niu, Hua Zhu Ke, Amgen Inc., USA

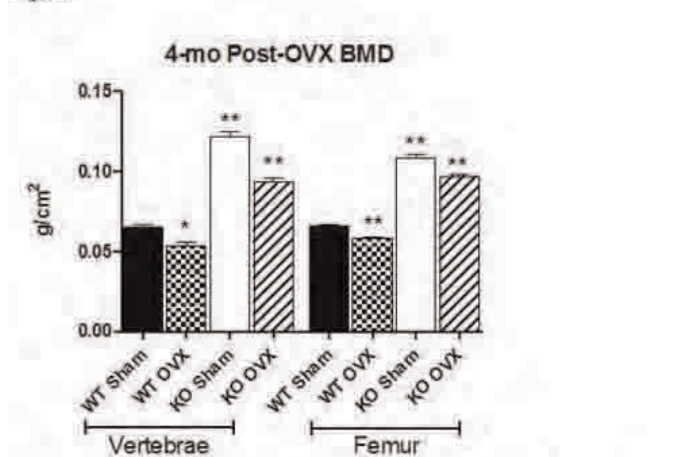
Estrogen deficiency is an important risk factor for postmenopausal osteoporosis, where bone resorption exceeds bone formation. Sclerostin (Scl) is a potent inhibitor of bone formation and sclerostin knockout (SOST KO) mice have a high bone mass phenotype. Here, we examined the effects of estrogen deficiency induced by ovariectomy (OVX) in SOST KO mice.

Eight-month old female mice underwent sham or OVX surgery and were sacrificed 4 months later. At baseline, SOST KO mice had a higher femoral (+36%) and spine (+44%) DXA BMD than wildtype (WT) mice. Following OVX, there was a decrease in bone mass in both WT and KO mice compared with their respective sham controls. Histomorphometry analysis of the femoral diaphyseal cortical bone and the 5th lumbar vertebral body trabecular bone demonstrated a significantly higher cross-sectional area, periosteal perimeter, cortical porosity area, and a significantly lower marrow cavity area in 12-month-old KO mice compared with WT mice. These changes led to a 122% increase in cortical bone area in KO mice. OVX induced a similar decrease in cortical bone mass independent of genotype. As for vertebral cancellous bone, KO mice had significantly higher trabecular bone volume and trabecular thickness than WT mice. OVX reduced both trabecular thickness (-16%) and trabecular number (-29%) in WT mice, and induced a greater decrease in trabecular thickness (-34%) than trabecular number (-15%) in SOST KO mice. However, at 4-months post OVX, femoral and vertebral bone mass were still significantly higher in OVX SOST KO mice than sham WT mice (Figure).

We also examined the vertebral bone dynamic change induced by 2 weeks of OVX in SOST KO mice compared with WT mice (4-month-old mice). In this short-term study, increased bone formation and bone resorption post-OVX were observed in both WT and KO mice.

These results demonstrated that SOST KO mice maintained higher cortical and trabecular bone mass at an older age. However, KO mice were not resistant to the systemic bone loss induced by estrogen deprivation. SOST depletion during skeletogenesis did not interfere with bone resorption mediated by estrogen deficiency. Additionally, although OVX induced bone loss in SOST KO mice, the bone mass in these mice was still significantly higher than that in WT sham controls after long-term OVX. This suggests that the higher bone mass in SOST KO mice present at the time of OVX provided protection against the deterioration of skeletal mass and structure induced by OVX.

Figure



*p<0.05 compared with WT Sham-OVX, **p<0.001 compared with WT Sham-OVX. N=11/group.

Figure

Disclosures: Min Liu, Amgen Inc., 1; Amgen Inc., 3
This study received funding from: Amgen Inc.

SA0462

Effect of Vitamin K₂ on Cortical and Cancellous Bone Mass and Hepatic Lipids in Rats with Combined Methionine-Choline Deficiency. Jun Iwamoto*¹, Azusa Seki², Hideo Matsumoto¹. ¹Keio University School of Medicine, Japan, ²Hamri Co., Ltd., Japan

The present study examined changes of cancellous and cortical bone in rats with combined methionine-choline deficiency (MCD). In addition, the effects of vitamin K₂ on cortical and cancellous bone mass and hepatic lipids were investigated in rats with MCD. Six-week-old male Sprague-Dawley rats were randomized into three groups of 10, including an age-matched control (standard diet) group, MCD diet group, and MCD diet + vitamin K₂ (menatetrenone at 30 mg/kg/day orally, five times a week) group. After the 1-month experimental period, histomorphometric analysis was performed on cortical and cancellous bone from the tibial diaphysis and proximal metaphysis, respectively, while histological examination of the liver was performed

after staining with hematoxylin & eosin and Oil Red O. MCD rats displayed weight loss, diffuse and centrilobular fatty changes of the liver, and a decrease of the cancellous bone volume per tissue volume (BV/TV) and percent cortical area (Ct Ar) as a result of decreased trabecular, periosteal, and endocortical bone formation along with increased trabecular and endocortical bone resorption. Administration of vitamin K₂ to rats with MCD attenuated weight loss, accelerated the decrease of cancellous BV/TV due to an increase of bone remodeling, and ameliorated the decrease of percent Ct Ar by increasing periosteal and endocortical bone formation. Vitamin K₂ administration also prevented MCD-induced diffuse fatty change of the liver. These findings suggest a beneficial effect of vitamin K₂ on cortical bone mass and hepatic lipid metabolism in rats with MCD. The loss of cancellous bone mass could possibly have been due to re-distribution of minerals to cortical bone.

Disclosures: Jun Iwamoto, None.

SA0463

Exported 18kDa Isoform of Fibroblast Growth Factor-2 Improved Bone Regeneration in Critical Size Mice Calvarial Defects. Daisuke Ueno*¹, Liping Xiao², Liisa Kuhn², Marja Marie Hurley³. ¹Tsurumi University, Japan, ²University of Connecticut Health Center, USA, ³University of Connecticut Health Center School of Medicine, USA

In this study we utilized Col3.6-18kDa FGF2-IRES-GFP sapphire transgenic (18kDa TgFGF2) mice in which a 3.6-kb fragment of the type 1 collagen 5' - regulatory region (Col3.6) is associated with green fluorescent protein-sapphire (GFP saph) expression combined with an induced over-expression of only the 18kDa isoform of FGF2. Vector only transgenic mice (Col3.6-IRES-GFPsaph, VTg) were utilized as controls. The purpose of this study was to analyze the bone regenerative capacity of the 18kDa TgFGF2 mice relative to vector only controls in a calvarial defect model. Bilateral calvarial defects (3.5 mm) were created in parietal bones of 18kDa TgFGF2 transgenic mice (n=5) and vector mice (n=4). A scaffold made of 70% type 1 collagen and 30% hydroxyapatite that was 3.5 mm in diameter and 1.5 mm thickness was placed into the defects. All mice were labeled with calcein and xylene orange on day 7 and day 2, respectively, before euthanasia. New bone was assessed by micro-CT of live animals (VIVA-CT) at 4, 6, 10, 16, 24 and 27 weeks post-surgery (Fig. 1). The experiment was terminated at 29 weeks post surgery and digital x-rays of the skulls were taken. The non-filled defect area was quantified from the x-ray images. There was a 47% significant decrease of the original defect area from 18kDa TgFGF2 mice compared with vector mice (3.020.31 cm² vs 5.710.73 cm² P< 0.008). Histologic analysis of the excised calvaria was performed. Samples were frozen, embedded and 7µm sections were taken through the middle of the defect to assess bone healing. Sections were scanned at 100x for GFPsaph, calcein, xylene orange and bright field using a Zeiss Axioplan 200 inverted microscope with a Zeiss AxioCam color digital camera. At all time points, the defect size was smaller in 18-kDa TgFGF2 mice compared with vector only mice indicating that the 18-kDa over-expression enhances bone defect repair. The majority of new bone formed at the defect edges with a few small islands of bone in the center of the defect. The double label distance of the new bone in the defect area was increased in 18kDa TgFGF2 mice compared with VTg (8.380.66µm vs 4.860.50µm) consistent with the observed increased bone formation (Fig. 2). The results of the present study demonstrate that FGF-2 over-expression can enhance bone healing and provides a rationale for the clinical application of a local gene therapy strategy to augment bone fracture healing.

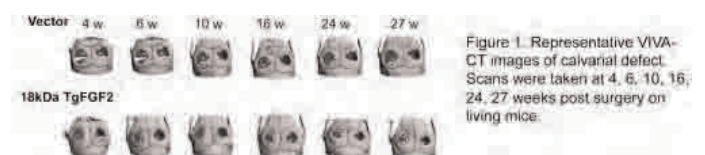


Figure 1. Representative VIVA-CT images of calvarial defect. Scans were taken at 4, 6, 10, 16, 24, 27 weeks post surgery on living mice.

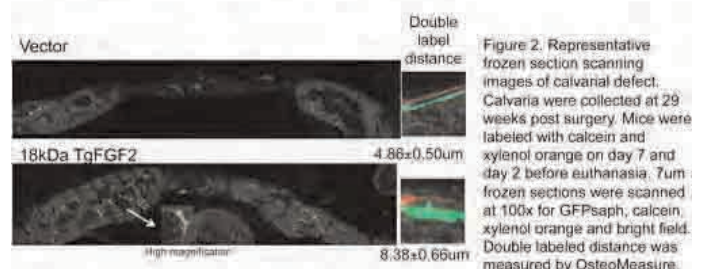


Figure 2. Representative frozen section scanning images of calvarial defect. Calvaria were collected at 29 weeks post surgery. Mice were labeled with calcein and xylene orange on day 7 and day 2 before euthanasia. 7µm frozen sections were scanned at 100x for GFPsaph, calcein, xylene orange and bright field. Double labeled distance was measured by OsteoMeasure.

Figure 1 and 2

Disclosures: Daisuke Ueno, None.

SA0464

See Friday Plenary Number FR0464.

SA0465

See Friday Plenary Number FR0465.

SA0466

See Friday Plenary Number FR0466.

SA0467

Correlations Between Serum Levels of TGF- β 1 and Bone Mineralization or Bone Strength Following Prolonged Bisphosphonate Treatments. Junjing Jia^{*1}, Wei Yao¹, Mohammad Shahnazari², Zhiqiang Cheng³, Sarah Amugongo⁴, Min Guan¹, Nancy Lane¹. ¹University of California, Davis Medical Center, USA, ²UCSF VA Medical Center, USA, ³University of California, San Francisco, USA, ⁴Department of Medicine, University of California Davis Medical Center, USA

Bisphosphonates (BPs) are the most common agents prescribed for the treatment for osteoporosis. While the anti-resorptive effects of the Bis are well documented, some investigators have reported that Bis may also have direct effects in regulating osteoblast differentiation through the involvement of TGF- β 1 signaling, and the reduction in TGF- β 1 signaling was shown to improve bone quality (Wu et al. Cell Stem cell 2010; Balooch et al. PNAS 2005). We hypothesize that Bis may alter TGF- β 1 serum levels, and this may be associated with overall bone quality and strength.

Serum levels of total serum TGF- β 1 levels, bone turnover, bone mineral density by microCT and biomechanical properties from bone cortical (tibiae) and trabecular bone (lumbar vertebral bodies) were obtained from three studies (Cheng & Shahnazari et al., JBMR 2008; 2011; Bone 2010): 1, Eighteen-month-old OVX rats received one iv injection of risendronate (500 μ g/kg) or zoledronic acid (100 μ g/kg). Rats were sacrificed on days 30, 60, 120 and 180. 2, Eighteen-month old OVX rats were treated with either risendronate (30 or 90 μ g/kg/month, sc. x3) or ibandronate (30 or 90 μ g/kg/month, sc x3) and were sacrificed at 24 months of age. 3, Six-month old OVX rats were either treated with continuous alendronate (OVX+Ale-Ale, 0.5 μ g/kg/3x/ week, sc) or alendronate for 3 months and then followed by vehicle (OVX+Ale-Veh). Rats were sacrificed on days 60, 150, 210 and 270. Correlation analyses were performed using Spearman Correlation test. We found 1, Single iv. BPs did not alter while continuous BP treatments dose-dependently increased total serum TGF- β 1 levels, which remained elevated even when BP treatment was withdrawn. 2, Total serum TGF- β 1 correlated with bone resorption (DPD/Cr). 3, No correlation was found between total serum TGF- β 1 levels with the degree of bone mineral density (DBM) of the trabecular bone or trabecular bone strength. 4, Total serum TGF- β 1 levels negatively correlated with DBM of the cortical bone and cortical bone strength; and every unit increase in TGF- β 1 accounted for a 4% decrease in the cortical DBM and a 10% decrease in cortical bone strength measured by 3-point bending of the tibiae.

In conclusion, prolonged BP treatments increased total serum TGF- β 1 levels and this appears to have negative effects on cortical bone mineralization and strength. Further studies are now warranted to elucidate how TGF- β 1 alters bone quality.

Disclosures: Junjing Jia, None.

This study received funding from: NIH/NIAM R01 AR043052 to NE Lane

SA0468

Effects of Endurance Running and Zoledronic Acid Treatment on Ovariectomy-induced Osteopenia in rats. Tsang-hai Huang^{*1}, Hsin-Shih Lin², Shen-Yu S Hsieh², Ming-Shi Chang³, Rong-Sen Yang⁴. ¹National Cheng-Kung University, Taiwan, ²National Taiwan Normal University, Taiwan, ³National Cheng Kung University, Taiwan, ⁴National Taiwan University Hospital, Taiwan

PURPOSE: To determine the effects of endurance running (EXE) and zoledronic acid (ZOL) treatment on bone histomorphometry and related serum markers. **METHODS:** Eight-four female Wistar rats (35 weeks old) were assigned to one sham operated group (SHAM) and six ovariectomized groups with different doses of zoledronic acid treatment and endurance running training, which were the OVX, EXE, LOW, HIGH, EXE+LOW, EXE+HIGH groups (n=12 for each group). A single injection of zoledronic acid (20 or 100 μ g/kg body weight) was done on the LOW and HIGH groups (with or without exercise training), respectively. Animals of exercise groups were subjected to treadmill running training by a protocol of 16m/min, 60min/day and 5 days/week for 10 weeks. Statistical analysis was preceded using one-way ANOVA. Fisher's LSD method was adopted for post hoc comparisons when statistical significance (p<0.05) was shown. **RESULTS:** In static histomorphometric analysis, four ZOL treated groups show significant higher bone volume ratio (BV/TV, %) and thicker trabeculae. Moreover, the EXE group showed significantly higher BV/TV as compared to the OVX. Osteoclast numbers were significantly higher in the OVX group as compared to other groups. Dynamic histomorphometric parameter of MS/BS (%) was significantly higher in the OVX and EXE groups as compared to the other groups. In serum marker assays, the EXE group and LOW+EXE groups revealed significantly higher serum phosphorus. C-terminal telopeptides of Type I collagen (CTX-I) showed no difference among groups. However, after normalized CTX-I by values of BV/TV, the OVX group showed a

significant higher modified CTX-I as compared to the EXE group, and, both them were significantly higher than all the other groups. In bone formation marker, the SHAM, OVX and EXE groups showed significantly higher serum osteocalcin as compared to the four ZOL treated groups. In addition, IGF-1 and IGFBP-3, were significant or marginally lower and higher, respectively, in the three exercise-trained groups as compared to the other four groups. Ratio between IGF-1 and IGFBP-3, which could served as another index of aging, showed significantly lower values in three exercise groups while the OVX group revealed the highest values in this index.

CONCLUSION: Exercise and zoledronic acid treatment seemed to protect ovariectomized induced bone degradation via different pathways. No synergistic effects were shown between exercise training and zoledronic acid treatment.

Disclosures: Tsang-hai Huang, None.

SA0469

Flaxseed Along with Low-Dose Estrogen Therapy Protects Bone Tissue by Favorably Influencing Bone Turnover in Ovariectomized Rats. Sandra Sacco^{*1}, Jianmin Chen², Bernhard Ganss², Lilian U. Thompson², Wendy Ward². ¹University of Toronto, Switzerland, ²University of Toronto, Canada

Background: Using the ovariectomized (OVX) rat model of postmenopausal osteoporosis, we previously demonstrated that flaxseed (FS), rich in phytoestrogens and n-3 polyunsaturated fatty acids, provides the greatest protection to bone mineral density (BMD), bone microarchitecture and strength at the lumbar vertebrae when combined with low-dose estrogen therapy (LD) compared to either treatment alone. We also showed that FS feeding results in the incorporation of phytoestrogen lignan and n-3 polyunsaturated fatty acids in skeletal tissue. These results suggest a potential role for FS to increase the effectiveness of LD during postmenopausal bone-loss.

Objective: To determine the effects of FS combined with LD on bone turnover in OVX rats to explain our previous findings.

Study Design: 3-month-old female Sprague-Dawley rats (OVX, n=56; SHAM, n=14) were randomized 3 weeks following ovariectomy or sham surgery to: 1) SHAM, 2) OVX, 3) OVX+FS, 4) OVX+LD or 5) OVX+FS+LD. Ground FS was added to the AIN-93M diet (100g/kg diet), and LD (0.42 μ g 17 β -estradiol/kg body weight per day) was delivered by a subcutaneous implant. After 2 weeks, rats were killed and the fifth lumbar vertebra and serum were collected. Histological analyses of vertebra were performed to determine bone volume fraction, osterix, osteocalcin, tartrate-resistant-acid-phosphatase-5 β (TRAP-5 β), osteoprotegerin (OPG) and receptor activator of NF- κ B ligand (RANKL). The following serum markers of bone metabolism were also measured: osteocalcin, TRAP-5 β , C-terminal peptides of type I collagen (CTX), OPG, RANKL and the ratio of OPG to RANKL.

Results: FS+LD resulted in higher bone volume fraction (p<0.05), OPG (p<0.001) and lower osteocalcin (p<0.01) at the lumbar vertebra compared to the OVX control. Serum analyses complemented these findings; FS+LD induced lower TRAP-5 β (p<0.05), CTX (p<0.001), osteocalcin (p<0.01), RANKL (p<0.05) and higher OPG (p<0.05) and OPG/RANKL ratio (p<0.05) compared to OVX control. FS resulted in higher osterix (p<0.05) and serum OPG (p<0.05) while the effects of LD in lumbar vertebra and serum were intermediate to both the SHAM and OVX control groups and did not differ significantly from FS+LD.

Conclusion: These findings suggest that LD and FS+LD, and less so with FS, protect against the deterioration of bone tissue due to a reduction in bone turnover but the specific mechanisms of action require further investigation.

Disclosures: Sandra Sacco, None.

SA0470

Green Tea Polyphenols Supplementation Improves Bone Microstructure and Quality on Long-term High-fat-diet-induced Obese Rats. Chwan-Li Shen^{*1}, Jay Cao², Raul Dagda¹, Samuel Chanjaplammootti³, Ming-Chien Chyu³, James Yeh⁴. ¹Texas Tech University Health Sciences Center, USA, ²USDA ARS, USA, ³Texas Tech University, USA, ⁴Winthrop-University Hospital, USA

We have demonstrated that green tea polyphenols (GTP) attenuate trabecular bone loss in various bone loss models. This study investigated the efficacy of GTP at bone microstructure and quality in high-fat-diet-induced obese rats. Thirty-six 3-month-old CD female rats were fed either a low-fat (LF, 10% energy as fat) diet (n=12) or a high-fat (HF, 45% energy as fat) diet (n= 24) at libitum for 4 months. Animals in the LF diet group continued in a LF diet for additional 4 months, while those in the HF diet group were divided into two groups: with or without GTP (0.5% wt/vol) in drinking water, in addition to a HF diet for another 4 months. Efficacy was evaluated in femur and tibia by dual-energy absorptiometry and histomorphometric analysis, respectively. In addition, bone strength using a 3-point bending test, body composition using a bioimpedance spectroscopy device, and serum leptin and insulin-like growth factor-I (IGF-I) concentrations using ELISA were also determined. Data were analyzed by one-way ANOVA followed by Fisher's LSD test. After 8 months of feeding study, compared to the rats in the LF diet (LF group), the rats in the HF diet (HF group) (i) had no impact on bone mineral density and strength at femur; (ii) increased trabecular separation, formation rate, and resorption rate, serum leptin and IGF-I levels, body weight, and fat mass; and (iii) decreased trabecular volume and thickness, femoral strength, and fat-free mass. Supplementation of GTP into the

drinking water for 4 months increased bone mineral density and strength, trabecular bone volume, thickness, and number, and fat-free mass, but decreased trabecular separation, formation rate, and resorption rate, fat mass, serum leptin and IGF-I in HF diet-induced obese rats. This study demonstrates that GTP supplementation in drinking water increased bone mineral density, strength, and microstructure through suppressing bone turnover rate. In addition, GTP supplementation also favored body composition through inhibiting leptin and IGF-I. The results from this animal model merit investigation of a potentially significant prophylactic role of green tea in bone health of obese humans.

Disclosures: Chwan-Li Shen, None.

SA0471

Icaritin Exerts Beneficial Effect on Skeletal Muscle Independent of Estrogen Receptor Pathway in Rats with Established Osteoporosis Induced By Ovariectomy. Baoting Zhang^{*1}, Baosheng GUO², Yixin HE³, Ling Qin⁴, Ge Zhang⁵. ¹Prince of Wales Hospital, The Chinese University of Hong Kong, Hong Kong, ²Prince of Wales Hospital, Hong Kong, ³The Chinese University of Hong Kong, Hong Kong, ⁴Musculoskeletal Research Laboratory, Department Of Orthopaedics & Traumatology, The Chinese University of Hong Kong, Hong Kong, China, Hong Kong, ⁵Prince of Wales Hospital, Hong Kong

We have reported that Icaritin prevents both bone loss and muscle dysfunction during osteoporosis development in ovariectomized rodents via estrogen-receptor (ER) -dependent and -independent pathways, respectively. This study aimed to examine the treatment effects of Icaritin on muscle and bone in rats with established osteoporosis induced by ovariectomy and its association with ER pathway. One hundred and ten 9-month-old female Wistar rats were either sham-operated (n=20) or ovariectomized (OVX) (n=90) and left untreated for 90 days. Before initial treatment, ten sham-operated and ten ovariectomized rats were sacrificed for verifying established osteoporosis. The remaining OVX rats were orally administered with vehicle (OVX-180) or Icaritin at low dose (Low-ICT) or Icaritin at middle dose (Middle-ICT) or Icaritin at high dose (High-ICT) or Icaritin combined with ER antagonist ICI 182780 (Low-ICT+ICI, Middle-ICT+ICI, High-ICT+ICI) or ICI 182780 only (ICI) for 90 days until sacrifice. The remaining sham-operated rats were served as control (Sham-180). After sacrifice, the femoral shaft was collected for microCT analysis (periosteal area, CSPA; endosteal area, CSEA; bone area, CSBA; cross-sectional moment of inertia, CSMI; volumetric bone mineral density, BMD) and for subsequent mechanical test (ultimate load and stiffness). The extensor digitorum longus (EDL) muscle was dissected for muscle contractile properties test (contraction time and peak tetanic force). For microCT analysis (Figure 1), OVX decreased CSBA, CSMI and BMD, and increased CSPA and CSEA. For mechanical test (Figure 2), OVX reduced the ultimate load and stiffness of the femoral shaft. For muscle functional test (Figure 3), OVX lowered peak tetanic force and prolonged contraction time and half-relaxation time. OVX-induced abnormalities in femoral shaft microstructure and mechanical properties were not changed by Icaritin at any dosage combined without or with ICI 182780. Interestingly, the peak tetanic force of EDL muscle was dose-dependently higher and the contraction and half-relaxation time was dose-dependently lower in the Icaritin-treated groups than that in the OVX-180 group. ER antagonist ICI 182780 didn't abolish the beneficial effect of icaritin on muscle contractile properties. It was concluded that Icaritin exerted beneficial effect on muscle independent of ER pathway in rats with established osteoporosis induced by ovariectomy.

(Support by Hong Kong GRF Ref CUHK478508)

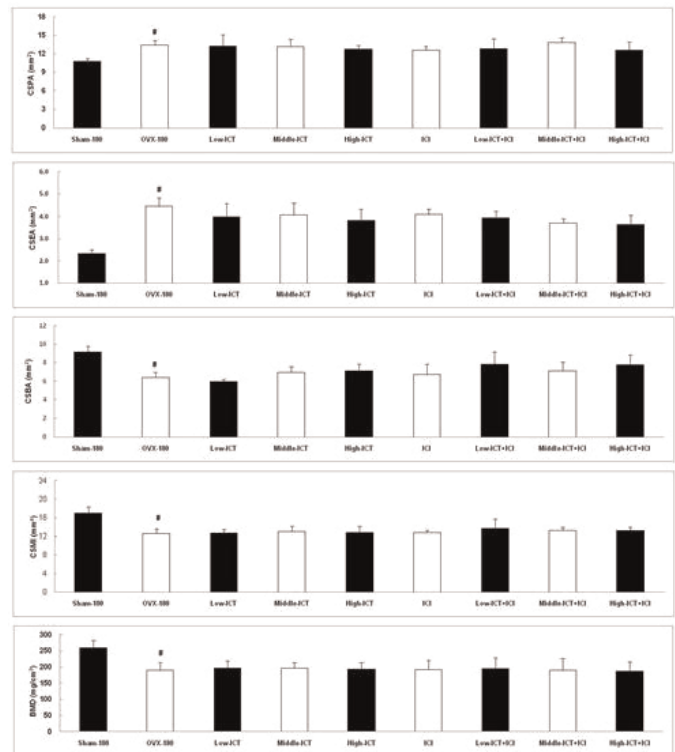


Figure 1 Bone micro-CT data. # P<0.05 between Sham-180 and OVX-180 groups. N=10 for each group.

Figure 1

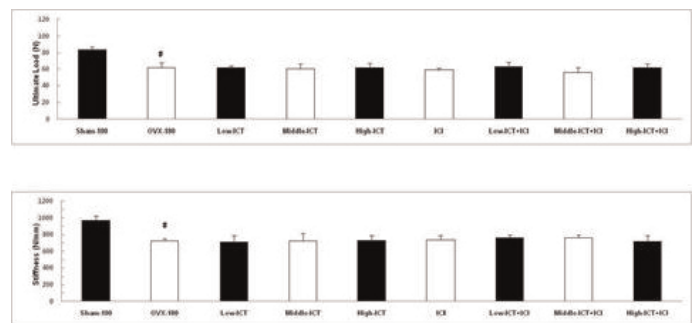


Figure 2 Bone mechanical data. # P<0.05 between Sham-180 and OVX-180 groups. N=10 for each group.

Figure 2

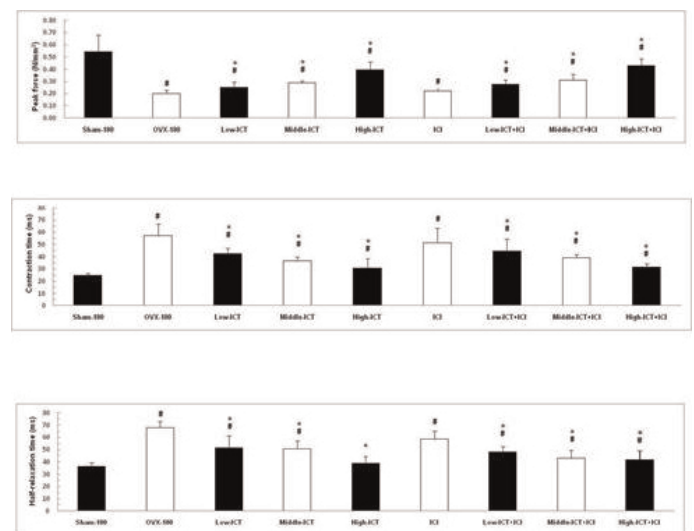


Figure 3 Muscle contractile data. # P<0.05 vs Sham-180 group, * P<0.05 vs OVX-180 group. N=10 for each group.

Figure 3

Disclosures: Baoting Zhang, None.

SA0472

Anti Osteoporotic Effects of 1,4-dihydroxy-2-naphthoic acid. Eiki Yamachika^{*1}, Masakazu Matsubara², Ken-ichiro Kita², Kiyofumi Takabatake², Yuki Fujita², Nobuyoshi Mizukawa², Tatsushi Matsumura², Hidetsugu Tsujigiwa³, Hitoshi Nagatsuka³, Seiji Iida².
¹Okayama University Hospital, Japan, ²Department of Oral & Maxillofacial Reconstructive Surgery, Okayama University, Japan, ³Department of Oral Pathology & Medicine, Okayama University, Japan

Introduction

Homeostasis of bone remodeling is regulated by the endocrine, nervous, and immune systems, and various bone diseases occur when this balance is disrupted. One such disease is osteoporosis. Several medications have been attempted to redress that unbalanced condition and vitamin K2 is often used for the treatment of steroid induced or postmenopausal osteoporosis. Since vitamin K2 facilitates bone formation and has a naphthoquinone skeleton, we focused on 1,4-dihydroxy-2-naphthoic acid (DHNA), a bacterial substance with a naphthoquinone skeleton. DHNA is the main component of the metabolic by-products of fermentation by *Propionibacterium freudenreichii* ET-3 (PC). In addition, DHNA has been reported as a bifidogenic growth stimulator that specifically facilitates the growth of *Lactobacillus bifidus*, part of the normal intestinal flora. We had reported the anti osteoporotic effects of DHNA from the experiments with using steroid induced osteoporosis mice. In the present study, DHNA was administered to ovariectomized (OVX) mice to confirm the anti osteoporotic effect of DHNA for postmenopausal osteoporosis.

Materials and methods

This study used 30 female ICR OVX mice and 5 female ICR sham operated mice. OVX mice were randomized into 6 groups: DHNA group, Vitamin K2(VK) group, Risedronate(Ris) group, Ris+VK group, Ris+DHNA group and control group. In each group, drugs were administered daily for 5 weeks. In each group, the right femur was collected and fixed in 4% paraformaldehyde. Fixed tissues were demineralized using 10% ethylenediaminetetraacetic acid for 30 days, and embedded in paraffin. Paraffinized tissue was stained using hematoxylin and eosin (HE).

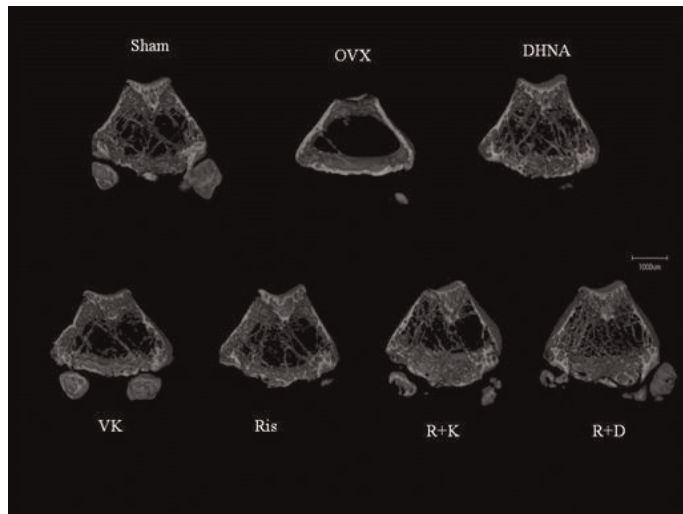
In addition, in each group, the left femur was collected for radiological analysis. Micro-CT machine (Scan X mate-A80; Scancom, Tokyo, Japan) was used to obtain 10- μ m sections of the distal epiphyseal femur. The resulting images were subjected to analysis using software (TRI/3D-BON; RATOC, Tokyo, Japan) to reconstruct 3D images for bone morphological analysis.

Results

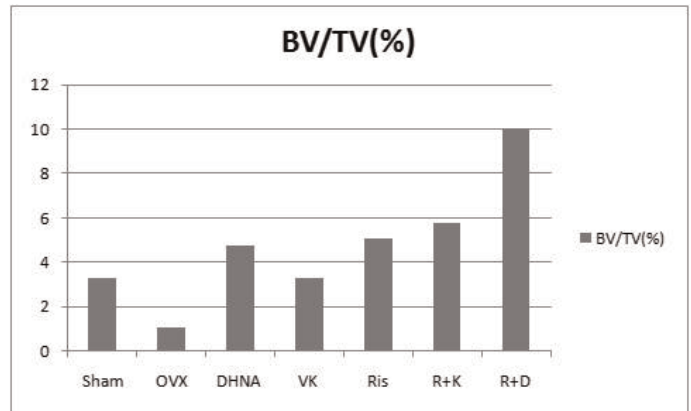
Histological and radiological analysis showed that in the OVX group, the trabecular bone was narrow and the bone marrow cavity was wide. But these osteoporotic changes were improved in DHNA group, Ris group, Ris+VK group and especially in Ris+DHNA group.

Conclusions and discussion

DHNA was effective for improving osteoporotic bone changes in not only steroid induced osteoporosis model mice but also postmenopausal osteoporosis model mice.



micro-CT



BVTV

Disclosures: Eiki Yamachika, None.

SA0473

See Friday Plenary Number FR0473.

SA0474

Effect of SBM on the Degree of Mineralization of Bone of OVX rats. Racquel LeGeros, Ning Jiang*. New York University College of Dentistry, USA

It is now accepted that bone quality (including degree of mineralization, DOM) is a better determinant of susceptibility to fracture associated with osteoporosis. A novel compound, described as MZF-CaP or synthetic bone mineral (SBM) with composition and crystallinity similar to that of bone mineral was recently developed [LeGeros 2004]. Our long-term goal was to demonstrate that this novel compound will be effective, safe and affordable for osteoporosis therapy and bone loss prevention. Objective: This study aimed to determine the effect of SBM on the degree of mineralization (DOM) of tibia bone in an ovariectomized (OVX) rat model. Methods: 40 Sprague Dawley rats were randomly divided into 4 groups (n=10/group): sham-operated on low mineral diet (LMD), OVX on LMD, OVX on LMD + SBM (126) and OVX on LMD + commercial calcium supplement (Caltrate). The rats were sacrificed after 2 months; tibia bones were separated, cleaned, and stored in alcohol. Bone sections were analyzed using backscattered electron (BSE) microscopy (SEM, Hitachi S3500N, Japan) operated at 20 kV. The image histograms were rescaled such that value 0 was the darkest and 255 was the brightest then further divided into eight equal intervals. For image display purposes, we designed a pseudo-color look-up table featuring the same eight classes (1-32 dark blue, 33-64 blue, 65-96 green, 97-128 yellow, 129-160 orange, 161-192 red, 193-224 pink and =>225 grey) [Boyde et al 1999]. Results: BSE images demonstrated that OVX rats had the lowest DOM and the SBM treated group had the highest average DOM in the tibia bone compared to sham-operated, OVX OVX on Caltrate. Conclusions: SBM (126) administered orally as a supplement, was effective in preventing bone loss induced by ovariectomy in a rat model, and may have a potential as a therapeutic compound.

Disclosures: Ning Jiang, None.

SA0475

See Friday Plenary Number FR0475.

SA0476

PTH 1-34 Rescues Impaired Fracture Healing in COX-2 Deficient Mice. Kiminori Yukata^{*1}, Chao Xie¹, Tian-Fang Li¹, Jennifer Jonason¹, Xinping Zhang², Edward Schwarz¹, Regis O'Keefe¹. ¹University of Rochester, USA, ²University of Rochester Medical Center, USA

Genetic ablation of cyclooxygenase-2 (COX-2) and its inhibition by non-steroidal anti-inflammatory drugs is known to impair fracture healing in mice. COX activity is essential for prostaglandin production, which activates PKA signaling through EP receptors. The parathyroid hormone receptor (PTH1R), similar to the EP receptors, is a G-coupled 7-transmembrane receptor that activates PKA signaling. PTH1R mediates the anabolic effect of Forteo (PTH 1-34) in osteoporosis patients via PKA signaling. Based on the similar signal transduction cascades induced by PGE2/EP4 and PTH/PTH1R, we hypothesized that PTH 1-34 rescues the defective fracture healing observed in COX-2 deficient (*Cox2*^{-/-}) mice. Here we tested this using a tibial fracture model. X-rays demonstrated that *Cox2*^{-/-} mice had decreased fracture callus formation and delayed healing. Micro-CT showed that *Cox2*^{-/-} mice treated with PTH 1-34 for 14 and 21 days had increased callus volume (2.22 and 4.02-fold, respectively;

$p < 0.05$) vs. untreated WT control. Quantitative histomorphometry showed that PTH 1-34 significantly increased both cartilage (day 7 and 10) and bone area (day 7, 10, 14 and 21) in *Cox2*^{-/-} mice ($p < 0.05$). Both chondrocyte (*coll10a1*) and osteoblast (*osteocalcin*) marker genes were increased in PTH 1-34 treated *Cox2*^{-/-} mice. PTH 1-34 treatment resulted in persistence of cartilage, consistent with a delay in endochondral bone formation in both genotypes. PTH 1-34 also increased both cell number (1.82 fold) and percentage of PCNA positive cells (11.7% vs. 0%) in the periosteum of *Cox2*^{-/-} mice on day 7 vs. untreated control. Consistent with these observations, *cyclin-D1* and β -catenin gene expression increased in *Cox2*^{-/-} fracture callus and in cell cultures of periosteal progenitor cells isolated from WT and *Cox2*^{-/-} callus. Finally, biomechanical testing showed that the maximum torque of fractured tibiae in treated *Cox2*^{-/-} mice was significantly increased vs. untreated control (166%, $p < 0.05$). Collectively, these results demonstrate that PTH 1-34 treatment rescues both structural and biomechanical fracture healing defects in *Cox2*^{-/-} mice, and suggest that PTH acts by increasing stem cell proliferation, chondrogenesis, and osteoblast differentiation. A more complete understanding of the effects of PTH 1-34 and its target cell populations will enhance the translation of this important anabolic agent into new treatments for bone repair.

Disclosures: Kiminori Yukata, None.

SA0477

Daily Administration of Eldecalcitol (ED-71), an Active Vitamin D Analog, Increases Bone Mineral Density by Suppressing RANKL Expression in Mouse Trabecular Bone. Suguru Harada^{*1}, Toshihide Mizoguchi², Yuko Nakamichi², Yasuhiro Kobayashi², Satoshi Takeda¹, Sadaoki Sakai¹, Fumiaki Takahashi¹, Hitoshi Saito¹, Hisataka Yasuda³, Nobuyuki Udagawa², Tatsuo Suda⁴, Naoyuki Takahashi². ¹Chugai Pharmaceutical Co., LTD., Japan, ²Matsumoto Dental University, Japan, ³Oriental Yeast Company, Limited, Japan, ⁴Research Center for Genomic Medicine Saitama Medical School, Japan

Eldecalcitol (ED-71) is a new vitamin D₃ derivative recently approved for the treatment of osteoporosis in Japan. Previous studies have shown that the daily administration of ED-71 increases bone mineral density (BMD) by suppressing bone resorption in various animal models. However, the mechanism of inhibition of in vivo bone resorption by ED-71 remains unknown. In this study, we examined how ED-71 suppresses bone resorption in vivo, using in vivo analyses of bone histomorphometry and osteoclastogenesis. Daily administration of ED-71 (50 ng/kg body weight) into mice for 2 and 4 weeks increased BMD in femoral metaphysis without causing hypercalcaemia. Bone and serum analyses revealed that the ED-71 administration inhibited both bone resorption and formation, indicating that the increase in BMD by ED-71 is due to the suppression of bone resorption. This suppression was associated with the decrease in the number of osteoclasts in trabecular bone. We previously identified cell cycle-arrested receptor activator of NF- κ B (RANK)-positive bone marrow cells as quiescent osteoclast precursors (QOPs) in vivo. Daily administration of ED-71 affected neither the number of RANK-positive cells in vivo, nor the number of osteoclasts formed from QOPs in ex vivo culture. In contrast, the ED-71 administration suppressed the expression of RANK ligand (RANKL) mRNA in tibiae. Immunohistochemical experiments also showed that the perimeter of RANKL-positive cell surface around the trabecular bone was significantly reduced in ED-71-treated mice than in the control mice. These results suggest that the daily administration of ED-71 increases BMD by suppressing RANKL expression in trabecular bone in vivo.

Disclosures: Suguru Harada, Chugai Pharmaceutical Co., LTD., 1

SA0478

Activating Mutation of the Calcium Sensing Receptor: A Single Centre Experience. Shaila Sukthankar^{*}, Sarah Ehtisham, Zulf Mughal. Royal Manchester Children's Hospital, United Kingdom

Introduction: Activating mutation of the calcium sensing receptor (CaSR), with gain in function in the renal tubule and the parathyroid gland, is associated with hypocalcaemic hypercalcaemia. Aggressive treatment to 'normalise' serum calcium level can lead to progressive hypercalcaemia and eventual nephrocalcinosis in the long term. It is important to recognise and distinguish this condition from other well-established aetiologies of primary hypoparathyroidism.

Aims and methods: We describe our single centre experience of symptoms, investigations and management of 6 children with activating mutation of the CaSR.

Results: Six children (3 boys) presenting with hypocalcaemia were found to have activating mutation of the CaSR. Four were asymptomatic. One had sensory neural deafness, autism and seizures for several years, with cerebral dysplasia. One had palpitations with flushing episodes, and incidental hypocalcaemia. Initial renal ultrasonography was normal in all. Five were started on oral 1- α hydroxycholecalciferol. Shortly after starting treatment, while serum calcium levels were still subnormal (1.8 - 2.1 mmol/L), there were sharp rises in the urinary calcium: creatinine (Ca:Cr) ratio (up to 1.4) - confirming hypocalcaemic hypercalcaemia. Genetic studies confirmed an activating mutation of the CaSR in all five tested. All children are currently asymptomatic (follow-up period 10 months - 9 years). Four have now developed nephrocalcinosis.

Conclusions: Activating mutation of the CaSR is an important cause of apparent primary hypoparathyroidism with hypocalcaemia. Our experience highlights that

contrary to literature reports, these children can have profoundly low/unrecordable parathyroid hormone (PTH) levels. The key to diagnosis is the close monitoring of urinary Ca:Cr ratio which starts increasing at relatively 'subnormal' serum calcium levels. Cautious treatment with active vitamin D analogues, and close monitoring for 'optimal' serum calcium levels to minimise hypercalcaemia will help delay the onset of nephrocalcinosis and consequent long term renal impairment.

Case	Sex/Age Years	Age at diagnosis Years	Family History	Ca mmol/L (2.2 - 2.4)	PTH pg/ml (10 - 60)	Urine Ca:Cr (< 0.56)	Nephrocalcinosis
1	M/16	15	Yes	1.99	11	0.58	Yes
2	M/3.5	1.5	Yes	1.68	<3	0.3	No
3	F/6	0.1	Yes	1.8	15	0.5	No
4	F/9	0.02	Yes	1.74	15	0.5	Yes
5	F/8	7	Yes	1.6	<3	0.5	No
6	M/11	10	Yes	2.03	<6	1.15	Yes

Clinical features

Disclosures: Shaila Sukthankar, None.

SA0479

Glucocorticoids Downregulate Gap Junction Function and Connexin Expression through Autophagy Dependent and Independent Pathways. Rekha Kar^{*1}, Manuel Riquelme², Wei Yao³, Nancy Lane⁴, Jean Jiang⁵. ¹The University of Texas Health Science Center, USA, ²University of Texas Health Science Center, USA, ³University of California, Davis Medical Center, USA, ⁴University of California at Davis, USA, ⁵University of Texas Health Science Center at San Antonio, USA

Glucocorticoid (GC) therapy is the most frequent cause of secondary osteoporosis and osteocytes are a major bone cell type affected by GCs. Gap junction channels formed by connexins play important roles in bone development and function. Connexin 43 (Cx43) is the major connexin expressed in osteocytes. We observed that treatment with GCs, dexamethasone (Dex) significantly decreased gap junction intercellular coupling in MLO-Y4 osteocyte cells determined by both scrape loading and microinjection dye transfer assays. In addition, Dex treatment decreased expression of Cx43 protein in a dose dependent manner. Interestingly, a similar decrease in Cx43 protein was also observed in osteocytes of bones from GC treated mice as opposed to the placebo (PL) controls. To determine the possible involvement of the glucocorticoid receptor pathway, we treated MLO-Y4 cells with the steroid receptor antagonist RU486. Dex-induced downregulation of Cx43 protein level was completely abolished by this antagonist. Dex treatment not only decreased Cx43 protein, but also caused a reduction in Cx43 mRNA expression. However, GCs did not have any effect on luciferase gene expression driven by a 2kb Cx43 promoter, suggesting lack of regulation at the gene transcriptional level. To explore the possibility of post-transcriptional regulation of Cx43 by Dex, we performed real time quantitative PCR to determine the quantity of Cx43 mRNA at different time points in the presence of actinomycin D, an inhibitor of gene transcription. Coincubation with Dex greatly reduced Cx43 mRNA level, suggesting that Dex decreases Cx43 mRNA stability. We reported previously that Dex induces the development of autophagy in MLO-Y4 cells. The autophagy inhibitor, Bafilomycin A, partially rescued Dex-induced decrease expression of Cx43 and also restored the gap junctional coupling between the osteocyte cells. Thus, apart from decreased mRNA stability, autophagy-dependent protein degradation also contributes to decreased Cx43 by Dex. Furthermore, the bone anabolic reagents PGE2, parathyroid hormone, conditioned media collected from fluid flow-treated osteocytes and alendronate failed to rescue Dex-induced decreased Cx43 expression. Taken together, our study, for the first time, demonstrates the regulation of gap junction mediated intercellular communication and Cx43 expression by GCs, which sheds new insight into mechanisms of bone loss by excess GC therapy.

Disclosures: Rekha Kar, None.

This study received funding from: NIH

SA0480

Regulation Of Osteoblastic 11 β -Hydroxysteroid Dehydrogenase Type 1 Expression By NF- κ B and p38 MAPK: Towards Osteoblast Specific Enzyme Inhibition. Rowan Hardy^{*}, Mohammad Ahasan, Chris Jones, Elizabeth Rabbitt, Karim Raza, Paul Stewart, Mark Cooper. University of Birmingham, United Kingdom

The 11 β -hydroxysteroid dehydrogenase type 1 (11 β -HSD1) enzyme is a tissue specific regulator of glucocorticoid (GC) action linked to the development of inflammation- and age-related osteoporosis. Systemic inhibition of 11 β -HSD1 activity has been proposed as a therapeutic option in these conditions. However, 11 β -HSD1 activity is also important in regulation of immune responses and the HPA axis. We previously demonstrated that proinflammatory cytokines, GCs and their combination dramatically increase 11 β -HSD1 expression and activity in osteoblasts. Expression in osteoblasts also increases with age.

We have now examined the mechanisms underlying regulation of 11 β -HSD1 activity in osteoblasts. Regulation was not due to any previously described

mechanism. The increase in activity induced by TNF α /IL-1 β was independent of new protein synthesis. 5' RACE and luciferase gene reporter studies showed that this effect was mediated via the classical HSD11B1 promoter. Chemical inhibitor studies showed that this increase in activity, along with basal enzyme activity, was mediated via NF- κ B. The involvement of classical NF- κ B signalling was confirmed using mouse embryonic fibroblasts (MEFs) where targeted deletion of p65/RelA, but not RelB, reduced basal expression and blocked cytokine induction of 11 β -HSD1. NF- κ B inhibitors had no effect on 11 β -HSD1 expression by other cell types e.g. hepatocytes. In lymphocytes GCs repress NF- κ B signalling by preventing nuclear translocation. However, translocation assays showed that GCs had no inhibitory effect on NF- κ B nuclear translocation in osteoblasts.

RelA KO studies also unmasked an inhibitory effect of TNF α /IL-1 β on 11 β -HSD1 expression. Chemical inhibitor studies showed that this effect was mediated through the p38 MAPK pathway. p38 MAPK inhibitors had the same synergistic effect on TNF α /IL-1 β induced 11 β -HSD1 expression as GCs. Cycloheximide studies showed the effect of GCs on p38 MAPK depended on new protein synthesis. Inhibitor and transgenic deletion studies confirmed the essential role of dual specificity MAPK phosphatase (DUSP1) in mediating the effect of GCs on p38 MAPK.

The mechanism by which expression of 11 β -HSD1 is regulated in osteoblasts is distinct from that in cells such as hepatocytes or lymphocytes. The finding that osteoblastic 11 β -HSD1 activity is regulated by NF- κ B and p38 MAPK pathways opens up new opportunities to inhibit or stimulate 11 β -HSD1 activity in an osteoblast restricted manner.

Disclosures: Rowan Hardy, None.

SA0481

Endogenous Parathyroid Hormone Is Associated with Reduced Cartilage Volume in Vivo in a Population-Based Sample of Adult Women. Sharon Brennan¹, Flavia Cicuttini², Geoff Nicholson³, Julie Pasco⁴, Mark Kotowicz⁵, Margaret Henry⁶, Anita Wluka^{*7}. ¹Department of Epidemiology & Preventive Medicine, Monash University 2. Northwest Academic Centre, Western Section, Department of Medicine, The University of Melbourne, Australia, ²Department of Epidemiology & Preventive Medicine, Monash University, Australia, ³Rural Clinical School, The University of Queensland, Australia, ⁴Deakin University, Australia, ⁵Barwon Health, Australia, ⁶School of Medicine, Deakin University, Australia, ⁷Monash University & Alfred Hospital, Australia

Purpose: Osteoarthritis (OA) affects the whole joint, including bone and cartilage. Parathyroid hormone (PTH) has complex actions on bone. Recent animal and in vitro studies also suggest that PTH may affect articular cartilage. However, little is known of the relationship between PTH and joint structure in vivo. Thus, the aim of this study was to examine the association between endogenous PTH and cartilage volume in vivo a healthy adult population with no symptoms of knee OA.

Methods: Magnetic resonance imaging of the dominant knee was performed on 101 asymptomatic females aged 35-49 years (2007-9), from which knee cartilage volume was determined. Blood samples were obtained 10 years prior (1994-7), and stored at -80C for random batch analyses. Serum intact PTH was quantified by chemiluminescent enzyme assay. Serum 25-hydroxyvitamin D (25(OH)D) was assayed using an equilibrium radioimmunoassay after extraction with acetonitrile.

Results: A 1-unit (pmol/L) increase in PTH was associated with reduced medial cartilage volume [regression coefficient (standard deviation, p value) (-0.70.3, p=0.03), after adjustment for age, BMI and bone area. Further adjustment for seasonal variation (-0.80.3, p=0.01), and 25(OH)D (-0.080.4, p=0.03), did not affect the results. All results remained significant (p<0.01) after excluding subjects with osteophytes to account for the possibility of pre-clinical osteoarthritis. No significant associations were observed with lateral cartilage volume (0.2 \leq p \leq 0.5).

Conclusions: This study suggests increased levels of PTH might be detrimental to cartilage in humans in vivo. Animal studies suggest that increased PTH may reduce the ability of cartilage to heal following minor injury. This may explain our results, particularly given the effect we observed in the medial compartment which is exposed to higher loads during weight bearing compared to the lateral compartment.

Disclosures: Anita Wluka, None.

SA0482

See Friday Plenary Number FR0482.

SA0483

See Friday Plenary Number FR0483.

SA0484

Estrogen Receptor-Related Receptor Gamma (ERR γ) Is a Regulator of Bone Turnover. Marco Cardelli^{*1}, Ruolin Guo², Jonathan Boetto¹, Ralph Zirngibl¹, Jane Aubin³. ¹University of Toronto, Canada, ²University of Rochester, USA, ³University of Toronto Faculty of Medicine, Canada

Sex steroids, such as estrogen, play a role in the onset and severity of symptoms in arthritis and osteoporosis. Estrogen exerts its activity via its receptors, estrogen receptor α and β , which are members of the nuclear receptor family. There are also members of the family for which ligands have not been identified, the so-called orphan receptors. Amongst these are the estrogen receptor-related receptors (ERRs), ERR α , ERR β , and ERR γ . Previously, we showed that ERR α is highly expressed in bone and cartilage and that it plays a functional role in osteogenesis and chondrogenesis in vitro (Bonnelye et al., 2001; Bonnelye et al., 2007). We have also found that ERR γ is expressed in skeletal cells and tissues, albeit at levels significantly lower than ERR α . Consistent with recent evidence from *in vitro* and ectopic bone formation experiments, suggesting that ERR γ is a negative regulator of osteogenesis, impinging on the BMP-Runx2 pathway (Jeong et al., 2009), we also found that knockdown of ERR γ in calvarial cell cultures increases osteoblast differentiation and bone nodule formation. To extend our *in vitro* findings to the whole animal level, we have utilized an ERR γ knockout line (Deltagen). Whole mount skeletal preparations of late embryonic/early postnatal stages revealed an increase in intramembraneous bone formation, but no significant difference in long bone length. By μ CT, we determined that several trabecular bone parameters are increased in 14 week and 6 month-old heterozygous male mice, and at 6 months there is also a significant decrease in SMI (indicative of a more plate-like trabecular structure) and a decrease in trabecular number. qPCR on mRNA isolated from trabecular bone of heterozygous 2 month-old male mice revealed an increase in osteoblast markers *Osx*, *Alp* and *Bsp*, as well as RankL and cathepsin K (*Ctsk*), markers of osteoclast differentiation and activity, respectively, suggesting an increase in bone turnover in ERR γ +/- compared to WT mice. To investigate the underlying cellular mechanisms, femoral bone marrow cells were isolated from 2 month-old male mice and cultured under osteoblast differentiation conditions. ALP- and von Kossa-positive colonies (number and area) were increased in ERR γ +/- compared to WT cultures. In silico analysis for ERRE consensus sequences identified *Alp*, *Bsp*, and *Ctsk* as putative ERR γ target genes. Collectively, our data indicate that ERR γ is a negative regulator of osteoblasts and osteoclasts, and further experiments are in progress to define how ERR γ impinges on the osteoblast-osteoclast signaling axis.

Disclosures: Marco Cardelli, None.

SA0485

Loss of ER α DNA Binding Suppresses Bone Gain In Vivo and In vitro Osteoblast Differentiation in the Context of a Wild-type or Null ER Alpha Allele. Orhan Oz^{*}, Asghar Hajibeigi. University of Texas Southwestern Medical Center, Dallas, USA

Estrogens regulate bone mass and metabolism through genomic and non-genomic pathways involving ER α . Mice have been created that harbor an ER α allele with a mutation in the DNA binding domain, the NERKI allele (N). We have previously reported that 129SvEv male mice with genotype +/-N have decreased bone mass and mechanical strength. To further understand the impact of the NERKI allele on bone metabolism we studied the prevention of bone loss and stimulation of bone gain in castrated male mice. WT and +/-N mice (n=5 or more/group) were castrated then immediately treated with estradiol pellets (0.1mg 21 day release) or after a 3 week washout. Bone mass was assessed by DEXA. The +/-N mice showed significantly less prevention of bone loss and lower bone gain compared to WT mice. Congenic B6 mice carrying the N allele were created by backcrossing 13 generations on the B6 JAX background. Male B6 -/N mice were created by mating with female ER α +/- mice. To study the impact of the N allele on in vitro osteoblastogenesis, bone marrow cells from +/-N and -/N male mice, grown in osteogenic medium, were tested for the ability to form alkaline phosphatase positive colonies and mineralized nodules versus WT or -/N marrow derived cells, respectively. The presence of the NERKI allele was associated with significantly fewer colonies and nodules. These data suggest that non-DNA binding activity of ER α may be involved in a pathway that suppresses osteoblastogenesis and bone formation.

Disclosures: Orhan Oz, None.

SA0486

A Cross talk between Prohibitin and Importin α 3 in Vitamin D signaling pathway- A novel implication in allergic airway inflammation. Tanupriya Agrawal^{*1}, Gaurav Gupta¹, Devendra Agrawal². ¹Creighton University, USA, ²Creighton University School of Medicine, USA

Purpose: Prohibitin is a ubiquitously expressed protein localized to the cell and mitochondrial membranes as well as the nucleus. Vitamin D has potent immunomodulatory properties including inhibition of proinflammatory cytokine production and induction of antimicrobial peptide synthesis in the cells of the innate immune system. NF- τ B is a transcriptional factor that activates many genes involved in inflammatory response. The nuclear import of p65 and p50 subunits of activated NF- τ B is

dependent on importin $\alpha 3$ (KPNA4) and importin $\alpha 4$ (KPNA3). We previously reported that calcitriol decreases the expression of importin $\alpha 3$ and nuclear translocation of NF- κ B in human bronchial smooth muscle cells (HBSMCs). TNF- α is a potent pro-inflammatory cytokine that plays a central role in systemic inflammation and airway hyperresponsiveness in asthma. In this study, we characterized the role of prohibitin in vitamin D receptor (VDR) function and identified prohibitin as a novel Vitamin D target gene which regulates the expression of importin $\alpha 3$. We also examined the effect of TNF- α on the expression of prohibitin with and without calcitriol.

Methods: HBSMCs were cultured in smooth muscle cell media containing 10% FBS. Cells in the passages 3-7 were stimulated with calcitriol (0.1-100nM) for different times (2- 36 hrs) and TNF- α (10ng/ml) for 12 hrs. Protein and mRNA expression of prohibitin were analyzed using Western Blot and qPCR, respectively.

Results: There was significant expression of mRNA and protein of prohibitin in HBSMCs. Treatment with increasing doses of calcitriol significantly increased mRNA and protein expression of prohibitin at 12hrs. There was a significant decrease in the mRNA and protein expression of prohibitin after stimulation with TNF- α for 12hrs and this effect was attenuated by calcitriol.

Conclusions: These data suggest that calcitriol increases the expression of prohibitin and this inhibits translocation of NF- κ B to nucleus by a novel mechanism of decreasing importin $\alpha 3$ expression. These results suggest a possible mechanism by which vitamin D may have a therapeutic effect in the treatment of allergic airway inflammation.

Disclosures: Tanupriya Agrawal, None.

SA0487

See Friday Plenary Number FR0487.

SA0488

A Role of Calcium in the Control of Hair Cycling. Leila J. Mady*¹, Dare V. Ajibade¹, Arnaud Teichert², Daniel Bikle³, Sylvia Christakos¹. ¹University of Medicine & Dentistry & New Jersey - New Jersey Medical School, USA, ²Department of Medicine, UCSF, USA, ³Endocrine Research Unit, Division of Endocrinology UCSF, USA

The skin has long been known as a target organ for vitamin D action. Although 1,25(OH)₂D₃ and calcium promote differentiation of keratinocytes, current literature does not suggest a role for 1,25(OH)₂D₃ and/or calcium in hair follicle development. Vitamin D receptor (VDR) deficient mice have been shown to develop alopecia and a role for unliganded VDR in hair follicle development has been reported. Whether 1,25(OH)₂D₃ and/or calcium have a direct effect on hair follicle development is, as yet, unresolved. Recent findings from our lab indicate that calbindin-D_{9k} nullmutant (KO) pups generated from calbindin-D_{9k} KO parents fed a vitamin D deficient, low calcium (0.4%) diet have alopecia. The pups appear phenotypically normal until 13 days of age, after which the coat begins to look ruffled and progressively sheds in a caudocephalic direction. This telogenic effluvium results in a truncal alopecia totalis at 20 - 23 days of age, sparing only the head and a tuft around the base of the tail. The alopecia is complete by 23 days with a spontaneous recovery completed by the end of the 4th wk. Histological and immunohistochemistry (IHC) examination of whole skin thickness were examined. During the late stages of catagen and early telogen (days 17 - 23) the hair follicles became markedly dystrophic and the hair shafts were lost. Histological studies indicate increased number of keratinocytes in the epidermis and hair follicle transformation toward utricle. IHC shows increased expression of Loricrin in the epidermis and atypical expression, suggesting altered differentiation. Unlike the VDR KO mice, there is permanent recovery of alopecia. Feeding the mothers a vitamin D deficient/high Ca²⁺ (2%), high lactose (20%) diet during lactation (from birth to post natal day 28) results in a delayed and less severe phenotype in the pups. The hair follicle defect was rescued when the pups were fostered to mothers on vitamin D (2,000 IU/D2/kg diet) and calcium (1%) in the diet. When wild type C57BL6 parents were fed a vitamin D deficient low calcium diet, a similar alopecia was observed but it was not consistent (it was observed in approx. 40% of the litters). Taken together our results show that vitamin D and calcium directly affect postmorphogenic hair follicle development and that deficiency of vitamin D and calcium leads to non-cicatricial alopecia, indicating for the first time a role of calcium in hair cycling.

Disclosures: Leila J. Mady, None.

SA0489

A Vitamin D₃ Analog, ED-71 Facilitates Vitamin D Receptor Degradation. Ken-ichi Takeyama^{*1}, Yumi Shiozaki¹, Yoko Yamamoto¹, Takeshi Kondo¹, Yuko Fukuda¹, Yuuki Imai¹, Suguru Harada², Naoki Tsuji², Fumiaki Takahashi², Hitoshi Saito² and Shigeaki Kato¹. ¹IMCB, Univ. of Tokyo, ²Chugai-pharm. Co., Japan

The active vitamin D₃ has a pivotal role in a many biological processes such as maintenance of calcium and phosphorous homeostasis, that are mediated by transcriptional regulation of target genes through nuclear vitamin D receptor (VDR). One of the vitamin D₃ analog, ED-71 has shown anabolic effect in bone, through the attenuation of bone resorption. Along with active vitamin D₃, ED-71 binds to VDR and induces the transactivation in the target genes. However, we never completely understood how ED-71 appears the attenuation of bone resorption through the VDR function, and its molecular mechanisms.

We have generated VDR deficient mice and analyzed its phenotype in bone. Intriguingly, heterozygous mutant mice of VDR (VDR+/-) only affect high bone mass phenotype, indicating that VDR function in bone negatively maintains, and rather, decreasing of VDR protein may facilitates bone volume and strength. Therefore, to test ED-71-mediated VDR function, we focused on the aspect of VDR protein in cells.

VDR protein levels in MG63 osteoblast like cell were significantly attenuated in the presence of ED-71. This attenuation of VDR protein was regulated by calpain which is calcium-dependent cysteine protease. Indeed, when a regulatory subunit of calpain, Capn1 was knocked down in the cells, the degradation of VDR protein was reduced, and ED-71-dependent VDR transactivation was significantly enhanced. Moreover, we could find that VDR protein levels in the ED-71-treated mouse bone were decreased, but not in other tissues. These findings indicate that ED-71 facilitates VDR degradation through the calpain protease, suggesting that ED-71-dependent anabolic effect in bone is mediated, at least in part, by VDR protein stability.

Disclosures: Ken-ichi Takeyama, None.

SA0490

Automated Measurement of Total 25 Vitamin D on the IDS-iSYS System. Etienne Cavalier*, Anne-Catherine Bekaert, Agnes Carlisi, Jean-Paul Chapelle. University of Liege, CHU Sart-Tilman, Belgium

Introduction: Most health professionals know vitamin D for its critical role in increasing the efficiency of dietary calcium absorption and preventing rickets in children. In the past decade, emerging research has also uncovered other important relationships between vitamin D and bone health as well as new information indicating it could potentially play a significant role in strengthening the body's defenses against chronic and autoimmune diseases and in controlling the growth of cells (both normal and cancerous). These new evidences have fuelled the global demand for 25-OH D testing. Clinical laboratories are under pressured to seek automated reliable platforms for 25-OH D analysis to keep up with the demanded volume.

Objective: Immunodiagnosics System (IDS, Boldon, UK) has commercialized a direct, fully automated, co-specific immunoassay for 25-OH D for use on the IDS-iSYS system. We seek to assess the analytical performance of the IDS-iSYS 25-OH D assay, and to compare this method to LC-MS/MS, DiaSorin Liaison, and DiaSorin RIA methods.

Methods: We determined the repeatability and reproducibility on 6 pools, ranging from 6.2 ng/mL to 71.2 ng/mL, the limit of quantification (LoQ) and the accuracy profile of the IDS-iSYS 25-OH D method. A total of 88 samples, selected to represent a wide range of 25-OH D concentrations [5.6-85.6 ng/mL], was assayed by each method.

Results: Intra and inter-assay coefficients of variation (CV) were <11% at 6.2 ng/mL and <8% at 71.25 ng/mL. The LoQ was established at 6.2 ng/mL. The accuracy profile between 6.2 and 71.2 ng/mL showed that the risk that one result falls out of the 30% acceptance limit is <5%, indicating that the method is completely validated in this range. The actual assay working range is 5 to 140 ng/mL. A comparison of IDS-iSYS 25-OH D with LC-MS/MS yielded the Passing Bablok fit equation: IDS-iSYS = 1.03 x (LC-MS/MS) + 1.50. The corresponding equation with Liaison was: IDS-iSYS = 0.94 x (Liaison) + 2.41, and with RIA: IDS-iSYS = 1.00 x (RIA) - 0.62.

Conclusions: The IDS-iSYS 25-OH D is a robust method, presenting analytical performances in accordance with the clinical expectations. The IDS-iSYS 25-OH D values were in excellent agreement with those determined with LC-MS/MS, DiaSorin Liaison and DiaSorin RIA. This method demonstrated suitable characteristics as a high throughput, fully automated, co-specific 25-OH D assay for clinical laboratories.

Disclosures: Etienne Cavalier, None.

SA0491

D Vitamin Levels in Children Born by Mothers with Vitamin D Deficiency. Ingrid Bergstrom^{*1}, Agneta Blanck², Lars Savendahl³. ¹Division of Endocrinology, Metabolism & Diabetes, Karolinska University Hospital, Huddinge, CLINTEC, Karolinska Institutet, Stockholm, Sweden, ²Unit for Obstetrics & Gynecology, Karolinska University Hospital, Huddinge, CLINTEC, Karolinska Institutet, Stockholm, Sweden, ³Division of Pediatric Endocrinology, Karolinska University Hospital, Solna, Department of Women's & Children's Health, Karolinska Institutet, Stockholm, Sweden, Sweden

It is important that the mother is vitamin D-sufficient enabling her to coop with the increased need of calcium during pregnancy when the fetus accretes large amounts of calcium. During pregnancy, vitamin D is transferred through the placenta to the fetus where it is stored. Consequently, the mother must increase her vitamin D intake to avoid deficiency. In the newborn, vitamin D stores are depleted by 8 weeks of age, if not supplemented. Breast fed infants are at risk of becoming deficient, as the amount of vitamin D taken up from the breast milk is low. In Sweden, it is recommended to supplement all infants with 10 micrograms of vitamin D3 daily starting from 2 weeks of age. We aimed to study if this recommendation is sufficient in infants of vitamin D deficient immigrant mothers. We characterized a cohort of 68 pregnant immigrant women living in Stockholm and compared their vitamin D levels with 51 controls born in Sweden of non-immigrant parents. The levels of 25 (OH) VitD3 was measured with a competitive RIA (Dia Sorin, Stillwater, MN). Intra-assay and inter-assay variations were 5% and 9%, respectively. Of the immigrant pregnant women, 77.9% had 25 (OH) VitD3 levels < 25 nmol/L and 29.4 % had levels <12 nmol/L. In contrast control subjects only 3.9% had vitamin D levels < 25 nmol/L and none had a level <12 nmol/L. We also made an attempt to monitor the infants of immigrant mothers and were able to follow 25 of the 64 infants up to the age of 6-12 months. Their mothers originated from Middle Asia (16), Africa (7) and South America (2). The table details 25 (OH) VitD3 levels in the pregnant mothers, in the umbilical cord at delivery, and in the infants at 6-12 months of age. Calcium levels in cord blood could only be measured in 11 out of 25 newborns, ranging between 2.3-3.0 mmol/L, which is normal. All newborns were normal and healthy. Their birth weight and Apgar score was normal. None of the children were reported to have a history of hypocalcemic seizures or any other condition leading to hospitalization. As shown in the table, most children had normal levels of vitamin D when assessed at 6-12 months of age (range 38-142 nmol/L) and none of them were severely deficient. We therefore conclude that the daily-recommended supplementation dose of 10 micrograms vitamin D3 is sufficient for children of vitamin D deficient immigrant women. Furthermore, our data suggest that compliance is good with the recommended vitamin D supplementation.

Table

	Mother; week 12 (n=25)	Mother; at delivery (n=12)	Umbilicus cord (n=12)	Infant; 6-12 mth (n=25)
25 OH vit D3 nmol/L (range)	14.8 (4.6) (10-28)	15.4 (8.7) (10-39)	23.3 (11.1) (20-54)	82.8 (29.7) (38-142)

Table

Disclosures: *Ingrid Bergstrom, None.*

SA0492

See Friday Plenary Number FR0492.

SA0493

See Friday Plenary Number FR0493.

SA0494

Hypercalcemia In The Elderly: Malignancy?. ALVARO PUIG^{*1}, Daisy Acevedo², Sanford Baim¹. ¹Miller School of Medicine, University of Miami, USA, ²University of Miami, USA

INTRODUCTION:

The majority of hypercalcemia cases are caused by hyperparathyroidism or malignancy. Less frequent etiologies for hypercalcemia include granulomatous diseases and drug-induced. The clinical history should also focus on the use of vitamins and over the counter preparations that the general population worldwide often consumes and are believed to be harmless. We describe a case of severe hypercalcemia in an elderly man caused by vitamin D supplementation prescribed by his physician.

CASE PRESENTATION:

An 86 year old Ecuadorian male presented with a two week history of lower extremity pain, polyuria, lethargy, abdominal pain, and 10 pound weight loss.

Initial laboratory testing revealed: serum total calcium 14.9 mg/dL (8.5-10.5), albumin 3.2mg/dL (3.9-5), PTH intact 7.81pg/mL (10-65). His evaluation to determine the underlying cause of hypercalcemia included the following negative tests: SPEP, UPEP, Skeletal survey and CT of Chest, abdomen and pelvis.

Additional laboratory testing revealed: 25-hydroxyvitamin D level >316 ng/mL (30-100), 1,25-dihydroxyvitamin D 74 pg/mL (18-72), PTHrP 11pg/mL (14-27).

Initial treatment of hypercalcemia consisted of IV normal saline and pamidronate 60 mg IV x1. Due to cardiac comorbidities, IV fluids were held with worsening serum calcium and development of metabolic acidosis.

Endocrinology was consulted and after extensive questioning it became evident the patient had taken one 600,000 IU ampoule of vitamin D each week PO (Raquiferol by Spedro Caillon Laboratories), that had been recommended by his physician in Ecuador for the past 6 weeks (total dose 3,600,000 IU).

The patient was restarted on IV hydration, furosemide, and a second dose of pamidronate 90 mg x1. Volume status was carefully monitored. His mental and physical condition gradually improved and he was able to ambulate with minimal assistance. The patient had been admitted to the hospital for a total of 1 month.

Upon discharge, he was encouraged to continue aggressive oral fluid intake. Calcium levels were closely observed with twice per week outpatient follow up.

CONCLUSION:

Patients commonly take over-the-counter medications as well as those prescribed by their clinician that may be unknown to the admitting physician, emphasizing the importance of a thorough historical evaluation. Hypercalcemia due to vitamin D intoxication may be an underlying cause for life-threatening complications.

Disclosures: *ALVARO PUIG, None.*

SA0495

The Effect of Mechanical Loading on the Regulation of 1 α -hydroxylase in Primary Human Bone Cells. Karen Van Der Meijden^{*1}, Astrid Bakker², Nathalie Bravenboer¹, Paul Lips¹. ¹VU University Medical Center, The Netherlands, ²ACTA - UVA & VU, RESEARCH INSTITUTE MOVE, Netherlands

1,25-dihydroxyvitamin D (1,25(OH)₂D) can change the response of bone cells to mechanical stimuli, which has important consequences for the maintenance of bone mass by mechanical loading. Bone cells express the 1 α -hydroxylase gene CYP27B1, and they can likely convert 25(OH)D into its' active metabolite 1,25(OH)₂D. However the regulation of 1 α -hydroxylase in bone cells is largely unknown. The aim of this study was to investigate whether 25(OH)D affects the response of primary human bone cells to mechanical loading, similar to 1,25(OH)₂D. Furthermore, we examined whether mechanical loading affects the conversion of 25(OH)D to 1,25(OH)₂D by human bone cells.

Primary human bone cells were incubated with 25(OH)D (0 or 400 nM) or 1,25(OH)₂D (0 or 100 nM) for 24h. Thereafter the cells were subjected to pulsating fluid flow (PFF; 0.7 0.3 Pa, 5 Hz) or kept under static conditions for 1h, and postincubated (0 or 3h) without PFF. The response to PFF was quantified by measuring nitric oxide (NO) using Griess reagent and ATP production using the bioluminescence (Roche). mRNA expression of mechano-regulated genes with a vitamin D response element, as well as CYP27B1 and CYP24 expression were quantified using RT-qPCR.

The stimulation of NO and ATP release by PFF was not influenced by incubation with 25(OH)D and 1,25(OH)₂D in human bone cells. PFF increased RANKL, FGF23 and MEPE mRNA expression 3 hours after PFF. Both 25(OH)D and 1,25(OH)₂D decreased the stimulating effect of PFF on RANKL, MEPE and FGF23. CYP27B1 mRNA was increased after PFF in the presence or absence of 25(OH)D or 1,25(OH)₂D, but CYP24 mRNA was not affected by PFF.

These data show that 25(OH)D affects the response of bone cells to mechanical loading in a similar manner to 1,25(OH)₂D, which suggests that 25(OH)D is hydroxylated into 1,25(OH)₂D in primary human bone cells. Interestingly, PFF increased mRNA expression of CYP27B1, suggesting that physical activity may enhance the availability of 1,25(OH)₂D to bone cells, thereby contributing to bone mass regulation.

Disclosures: *Karen Van Der Meijden, None.*

SU0001

A Muscle Derived Soluble Factor Activates PI3K/ β -catenin Signaling in Osteocytes. Nuria Lara*¹, Katharina Jaehn¹, Sandra Romero-Suarez¹, Chenlin Mo¹, Lynda Bonewald¹, Marco Brotto¹, Mark Johnson².
¹University of Missouri - Kansas City, USA, ²University of Missouri, Kansas City Dental School, USA

Osteoporosis and sarcopenia are major clinical problems in the aging population and in many patients these two conditions occur concurrently suggesting a molecular coupling of these diseases. Current dogma states that muscle applies load to bone and bone serves as an attachment site for muscle. We hypothesize that muscle releases myokines that condition osteocyte responsiveness to mechanical loading.

Osteocytes are considered the principle cell type in bone for sensing and responding mechanical loading. We have shown that mechanical loading stimulates the release of PGE2 from osteocytes leading to a 3-4 fold activation of PI3K/Akt pathway which ultimately leads to activation of β -catenin signaling, a key enhancer of bone formation. In the presence of muscle cell (C2C12 myotubes) conditioned media (CM) the load induced activation of the PI3K/Akt pathway was 7-8 fold increased. In this current study we examined the effect of muscle cell CM on the activation of the PI3K/Akt and β -catenin pathways in osteocytes under static conditions.

CM was collected from C2C12 cells induced to differentiate into myotubes (MTCM) or non-differentiated myoblasts (MBCM). HeLa cell CM was used as a control. MLO-Y4 osteocyte like cells and long bone primary osteocyte enriched cells were exposed to blank, control or CM for 15, 30, 60 and 120 minutes, the cells collected, and western blotting performed using antibodies against phospho-Akt, and the endogenous control, GAPDH. Translocation of β -catenin to the nucleus was studied using immunofluorescence with an antibody to the active form of β -catenin.

In the presence of 1% or 10% MTCM, the PI3K/Akt pathway was stimulated by 2-3 fold over control, in a transient manner peaking at 30min and returning to basal levels after 2h. HeLa cell CM had no effect. The addition of MTCM also resulted in β -catenin nuclear translocation at 1h post-addition. We did not observe this effect when cells were exposed to 10% MBCM. These data suggest that factors released by fully differentiated, mature muscle cells condition and/or regulate the response of osteocytes to loading. The identification of this factor could result in a new paradigm for enhancing the anabolic effects of loading on the aged or diseased skeleton.

Disclosures: Nuria Lara, None.

SU0002

Age-related Decreases in Anti-oxidative response, Autophagy and Osteogenesis -Gene Profiles Studies. Min Guan*, Wei Yao, Junjing Jia, Nancy Lane.
University of California, Davis Medical Center, USA

Introduction. Bone loss is a normal consequence of aging and occurs in both genders after peak bone mass has been obtained. Starting in the third decade, women lose 35% of their cortical bone and 50% of their trabecular bone, whereas men lose approximately two thirds of this amount over their respective lifetimes. The accelerated bone loss during post-menopausal period is associated with increased osteoclast activity due to declining estrogen levels. The more gradual bone loss observed with aging results from lower recruitment of osteoblasts to the bone surface and reduced osteoblast activity. In addition, oxidative stress in bone tissue was increased with age, and was associated with increased osteoblast apoptosis (Jilka, Aging Cell, 2010; Manolagas Endo Reviews, 2010) Based on these data we hypothesize that mesenchymal osteogenic activity and lifespan with aging is influenced by oxidation (Almeida, JBC, 2009) and cell autophagy, (Chen, Cell Death Differ. 2009),

Methods. We evaluated the age-dependent changes in gene-profiles of the oxidative stress responsive, autophagic and osteogenesis pathways (SABioscience) in three models: 1, Primary bone marrow cells culture from 3-, 12- and 28-week-old C57BL/6 female mice. 2, Distal femur cortical bone of 10-, 16 and 56-week-old C57BL/6 female mice. 3, Cortical bones of 6-, 12-, 18- and 24-month-old female Fisher rats. The gene-profiles obtained from the three studies were used to perform correlation analyses using Spearman Correlation test (SPSS 12.0). Correlations between gene expressions of anti-oxidation and autophagy were considered significant at the 0.05 level (2-tailed).

Results. 1, Aging is associated with decreased activation of gene expressions associated with anti-oxidative defense (1-5-fold decreases), autophagy (1-5-fold decreases) and osteogenesis(1-10-fold decreases) in bone marrow cells in vitro and cortical bone in vivo. 2, Anti-oxidative responses were positively correlated with increase osteogenesis ($R^2=0.02$, $p=0.04$) but were not correlated to activation of autophagy with aging.

Conclusion. Aging is associated with decreases in anti-oxidation and autophagy in the bone tissues in rodents. An intervention that augments the anti-oxidant defense potential represents a potential strategy to maintain osteogenesis and ameliorate age-related decrease in osteogenesis.

Disclosures: Min Guan, None.

This study received funding from: Endowment to NE Lane by UC Davis, NIH/NIAM R01 AR043052 to NE Lane.

SU0003

Analysis of Lipid and Lipoprotein Metabolism of the Skeleton Using Nanocrystals. Alexander Bartelt*¹, Barbara Freund¹, Harald Ittrich¹, Joerg Heeren¹, Andreas Niemeier¹, Oliver T. Bruns².
¹University Medical Center Hamburg-Eppendorf, Germany, ²Heinrich-Pette-Institute for Experimental Virology & Immunology, Germany

Objective

Lipids are transported via plasma lipoproteins, which can be either processed to release lipid constituents or can be taken up as whole particles. Next to triglycerides and cholesterol, also lipophilic vitamin K is delivered by lipoproteins. However, the contribution of the skeleton as a lipid storage organ to lipoprotein metabolism is poorly understood. Recently, we followed the fate of lipids using lipoproteins engineered with radioactive superparamagnetic iron oxide (SPIO) nanocrystals embedded within the hydrophobic lipoprotein core^{1,2}. Here we analyze lipoprotein uptake into bone with magnetic resonance imaging (MRI) in vivo in real-time and quantify the contribution of the skeleton to systemic lipoprotein metabolism.

Methods

Fasted FVB mice were injected with lipoproteins labeled with SPIOs and uptake was visualized by MRI at 3T. ⁵⁹Fe-SPIO and ³H-triolein labeled lipoproteins were injected to follow lipoprotein particle and fatty acid uptake simultaneously. Uptake was determined in organ extracts by scintillation counting. Animal models of defective lipoprotein function were used to elucidate molecular pathways responsible for lipid entry into bone.

Results

The liver and brown adipose tissue, two major organs in lipoprotein clearance, show greatly enhanced T2* contrast after SPIO lipoprotein injection which is indicative for lipoprotein uptake. Compared to liver and brown adipose tissue, the contrast increase in femur is low. However, femur displays a strong specific fatty acid uptake for ³H-triolein which is independent of lipoprotein receptor ligand apolipoprotein E and neither is blocked by pre-treatment with natural lipoproteins. In contrast to fatty acids, uptake of ⁵⁹Fe-SPIO core label into femur is low, and notably is blocked by pre-treatment with lipoproteins.

Conclusion

The majority of lipids are taken-up by 1. initial binding of lipoproteins, 2. hydrolysis of triglycerides and uptake of fatty acids and 3. clearance of remnant particles by liver and brown adipose tissue. Of note, when calculated for total organs, the skeleton plays a major quantitative role in triglyceride clearance. As the close relationship between glucose metabolism and the skeleton has been demonstrated recently, the uptake of fatty acids adds another piece of evidence that there is a complex interaction between systemic energy metabolism and the skeleton.

1. Bruns OT et al, Nat Nanotechnol. 2009 Mar;4(3):193-201.

2. Bartelt A et al, Nat Med. 2011 Feb;17(2):200-5.

Disclosures: Alexander Bartelt, None.

SU0004

Beta-ecdysone has Bone, Cartilage and Muscle Protective but no Estrogenic Effects in Ovariectomized Rats. Dana Seidlova-Wuttke¹, Wolfgang Wuttke*².
¹Robert-Koch-Str. 40, Germany, ²University of Goettingen, Germany

Purpose: Estrogens exert beneficial effects in the bone, joint cartilage and striated muscles. Their use however bears several risks. Therefore, intensive search for non-estrogenic alternatives is going on. By quantitative computer tomography we demonstrated that β -ecdysone can partially prevent osteoporosis following ovariectomy (ovx) of rats. Whether the bone protective effects can be confirmed by histomorphometric structure (STRUT) analysis and whether β -Ecd can also exert protective effects on joint cartilage and striated muscles is currently unknown and was therefore tested. **Methods:** Ovx rats were treated orally over a 3 months with no Ecd (control) or with 18 and 57mg Ecd/day/animal. Estradiol-17 β benzoate (E2) (159 μ g/day/animal) fed animals served as positive controls. STRUT analysis was performed in the upper metaphysis of tibia; cartilage thickness in the knee joint and thickness of muscle fibers in the M. gastrocnemius were determined histomorphometrically. **Results:** STRUT analysis demonstrated significantly better trabecular architecture: number of free ends (termini) were lower, number of nodes (cross sections of trabecles) were higher in E2 and Ecd treated animals in comparison to the ovx controls. Thickness of the knee joint cartilage was lowest in ovx, highest in E2 and at intermediate values in the Ecd treated animals. The muscle fiber diameter was lowest in ovx and significantly higher in Ecd and E2 treated animals. **Conclusions:** It is concluded that Ecd has similar osteo- and chondro-protective effects as E2 and that it stimulates muscle fiber diameter which, taken together, are beneficial effects in the musculo-skeletal unit.

Disclosures: Wolfgang Wuttke, None.

SU0005

Role of SKI-1 Protease in Osteoblast/Osteocyte Formation and Maintenance of Bone and Body Mass. Jeffrey Gorski^{*1}, Nichole T. Huffman¹, Annita Achilleos², Paul A. Trainor², Nabil G. Seidah³, Clifford Rosen⁴, Lynda Bonewald¹. ¹University of Missouri - Kansas City, USA, ²Stowers Institute for Medical Research, USA, ³Institut de Recherches Cliniques de Montreal, Canada, ⁴Maine Medical Center, USA

SKI-1 (subtilisin kexin-like or site-1) is an auto-catalytically activatable cis-Golgi serine protease required for activation of membrane embedded transcription factors and secreted proteins such as bone sialoprotein and BMP1 enhancer PCOLCE1. Germ-line disruption of SKI-1 is embryonically lethal whereas cartilage-specific knockout of SKI-1 displays a lack of endochondral ossification. Recently we showed in UMR106-01 cells that SKI-1 regulates transcription of 140 genes (including DMP1, Phex, COL11A1, fibronectin, and fibrillin-2) encoding key extracellular matrix proteins required for normal bone mineralization via release of endoplasmic reticulum bound transcription factors SREBP-1, SREBP-2, and OASIS. To clarify the role of SKI-1 in bone, we produced three separate bone knockouts using 3.6kb COL1 Cre, 2.3kb COL1 Cre, and 10kb DMP1 Cre. These three Cre transgenes cover distinct stages of osteoblast to osteocyte differentiation or ontogeny. SKI-1 cKO produced with 3.6kb COL1 [SKI-1 (flx/flx) x Cre (+/-)] exhibited hindlimb paralysis and spinal fusions at birth and diminished BMD at 10 days, while with 2.3kb COL1 Cre, SKI-1 cKO were dramatically smaller than controls. 3.6kb COL1 SKI-1 cKO embryos at E12 were deficient in fibrillin-2 in the posterior region, a gene regulated by SKI-1 in vitro. In contrast, DMP1 Cre SKI-1 cKO mice and control littermates showed no difference in BMD or in body weight at 5-11 weeks of age and expected ratios of the various genotypes were obtained. However, at 6-8 months of age, DMP1 SKI-1 cKO mice displayed an apparent decrease in BMD [cKO (males, n=6): 0.0616 g/cc +/- 0.0034 STD vs. controls (males, n=5): 0.0646 g/cc +/- 0.0030 STD; p=0.1666] and an apparent increase in body mass. Specifically, three out of six of the male SKI-1 cKO mice weighed 43-50 g vs. an average of 36 g for male controls. While total fat content as assessed by DEXA also increased in DMP1 SKI-1 cKO, the proportion of fat to body mass remained relatively constant. Our results indicate that deletion of SKI-1 early during bone development (3.6kb and 2.3kb COL1 Cre) can lead to dramatic changes in skeletal development while deletion later in osteocytes (DMP1 Cre) leads to a decrease in postnatal bone formation and an increase in body mass, the opposite of that predicted by Wolff's law. Our new hypothesis is that SKI-1 is required for bone formation during embryonic growth and for maintenance of not only bone mass but also body mass in adults.

Disclosures: Jeffrey Gorski, None.

SU0006

Approaches to Enhancing Sarco-osteoporosis Identification in Older Adults. Bjoern Buehring^{*1}, Diane Krueger¹, Neil Binkley². ¹University of Wisconsin, Madison, USA, ²University of Wisconsin, USA

Purpose: Chronologic age is a poor predictor of functional status. Nonetheless, age is currently included in the FRAX[®] fracture risk calculator but functional status and falls are not. Sarcopenia (SP) likely contributes to the increasing fracture risk currently attributed to age. Individuals with both osteoporosis (OP) and SP, so-called "sarco-osteoporosis" (SOP), may be at higher fracture risk than those with OP or SP alone. This study examined the overlap of OP and SP in older adults and the effect of advancing age on prevalence of SOP. Additionally, approaches to facilitate SOP identification, i.e., radius bone mineral density (BMD) measurement, and use of tallest historical, rather than current, height for SP diagnosis were explored.

Methods: BMD and total body composition data were acquired in community dwelling adults age 60+ by DXA using a GE Lunar iDXA densitometer. OP and SP were defined using standard criteria: T-score \leq -2.5 at the lumbar spine or hip and appendicular lean mass (ALM)/current height² $<$ 5.45 kg/m² (female) and 7.26 kg/m² (male). "Sensitive" OP criteria added the 1/3rd radius T-score, while "sensitive" SP criteria used historical tallest height instead of current height. The primary outcome was SOP prevalence by decade (60-69, 70-79, 80+). Fisher's Exact test was used to compare "sensitive" with standard criteria.

Results: 235 individuals (132 F/103 M) were included in this analysis. OP, SP and SOP prevalence was higher (p < 0.05) with the "sensitive" criteria and increased with advancing age. Prevalence of SOP was lower than OP or SP. Values for the SOP (standard/sensitive) criteria increased from 1.4%/3% in the 60-69 age group to 10.1%/25.6% in the 80+ age group. Prevalence of SP and OP increased from ~5%~10% to ~27%~47.5% in the same age groups.

Conclusions: Sarco-osteoporosis becomes more common with advancing age. The concept of sarco-osteoporosis might more accurately predict fracture risk than simple use of age. Similarly, use of 1/3rd radius BMD might improve fracture risk prediction in older adults. Use of historical tallest height and 1/3rd radius BMD may more appropriately identify those with sarco-osteoporosis. Future studies need to document whether those with SOP are at truly at higher fracture risk and explore the utility of 1/3rd radius BMD measurement and use of tallest height. Ultimately, sarco-osteoporosis might be integrated in fracture risk prediction models.

Disclosures: Bjoern Buehring, None.

SU0007

Are the Institute of Medicine Vitamin D Guidelines "Sufficient" for Frail Long Term Care Residents? MaryAnn Ferchak^{*1}, Megan Miller¹, Carroll Lee¹, Kimberly Zukowski¹, Subashan Perera², David Nace², Neil Resnick², Susan Greenspan³. ¹University of Pittsburgh, Division of Endocrinology, USA, ²University of Pittsburgh, Division of Geriatrics, USA, ³University of Pittsburgh, USA

Background: New Institute of Medicine (IOM) vitamin D guidelines suggest that levels of vitamin D above 20 ng/mL are sufficient for skeletal and muscle health.

Methods: To examine the impact of vitamin D deficiency and insufficiency for skeletal health and physical performance measures in frail elderly women, we measured 25 hydroxyvitamin D (liquid chromatography mass spectrophotometry) in 233 residents from long term care facilities, mean age 85 years. Vitamin D classification included: deficiency <20 ng/mL, insufficiency 20 \leq vitamin D <30 ng/mL, sufficiency \geq 30 ng/mL. Outcome measures included age, height, weight, body mass index (BMI), daily vitamin D and calcium intake, bone mineral density of the spine and hip (g/cm² and T-scores), Physical Activities of Daily Living (PADL), Instrumental Activities of Daily Living (IADL), Physical Performance Test (PPT includes timed 6 meter walk and sit to stand test), Duke Comorbidity Index (DCI), Short Verbal Mental Status Questionnaire (MSQ) and number of residents who fell in the past year.

Results: 19% of patients had vitamin D deficiency, 29% had insufficiency. By analysis of variance residents with vitamin D deficiency had lower serum calcium, higher serum PTH, longer sit to stand time and lower hip and femoral neck bone mineral density (Table). Vitamin D level was associated with the sit to stand time (p=0.024) with an estimated 0.4 second decrease for every 10 ng/mL increase in vitamin D. There were no significant differences in age, BMI, calcium or vitamin D intake, albumin, IADL, PADL, DCI, MSQ or history of falls. PTH levels were elevated (\geq 65 pg/mL) in 43%, 30% and 18%, respectively, among those with deficient, insufficient and sufficient serum vitamin D.

Conclusion: Higher levels of vitamin D are associated with greater BMD, walking and sit to stand performance measurements in frail residents of long term care. IOM guidelines may be "insufficient" for this cohort.

Variable	Vitamin D Deficiency	Vitamin Insufficiency	Vitamin D Sufficiency
N	44	68	121
Age (Years)	86.1 \pm 5.1	86.4 \pm 4.7	85.6 \pm 5.5
Calcium (mg/dl)*	9.2 \pm 0.3	9.4 \pm 0.4	9.4 \pm 0.4
PTH (pg/mL)*	84.5 \pm 65.5	53.4 \pm 30.6	44.4 \pm 28.5
T-score Spine (SD)	-0.94 \pm 1.82	-0.58 \pm 1.80	-0.78 \pm 1.70
Hip (SD)*	-2.37 \pm 1.19	-1.89 \pm 1.19	-2.00 \pm 0.94
Femoral neck (SD)*	-2.46 \pm 1.10	-1.93 \pm 1.10	-2.09 \pm 1.02
Sit to stand time (seconds)*	4.1 \pm 5.0	3.2 \pm 2.1	2.9 \pm 2.3
Walk time (seconds)	14.9 \pm 7.8	16.0 \pm 12.4	12.9 \pm 16.2
Mental Status	8.3 \pm 3.0	8.9 \pm 2.6	9.0 \pm 2.8
Fallers (%)	48.8%	40.6%	41.1%

*p<0.05 for at least one pairwise comparison

Table

Disclosures: MaryAnn Ferchak, None.

SU0008

Association of Spinal Muscle Composition and Prevalence of Hyperkyphosis in Healthy Community-Dwelling Older Men and Women. Wendy Katzman^{*1}, Peggy Cawthon², Greg Hicks³, Eric Vittinghoff⁴, John Shepherd⁴, Jane Cauley⁵, Tamara Harris⁶, Eleanor Simonsick⁷, Elsa Strotmeyer⁸, Catherine Womack⁹, Deborah Kado¹⁰. ¹University of California San Francisco, USA, ²California Pacific Medical Center Research Institute, USA, ³University of Delaware, USA, ⁴University of California, San Francisco, USA, ⁵University of Pittsburgh Graduate School of Public Health, USA, ⁶Intramural Research Program, National Institute on Aging, USA, ⁷Clinical Research Branch, National Institute on Aging, USA, ⁸University of Pittsburgh, USA, ⁹University of Tennessee, USA, ¹⁰University of California, Los Angeles, USA

Background: Older adults with hyperkyphosis are at increased risk of falls, fractures, and functional decline. Modifiable risk factors for hyperkyphosis have not been well studied. Our objective was to determine whether spinal muscle area and density are associated with hyperkyphosis, independent of age, race, sex, bone mineral density (BMD) and trunk fat. Methods: Using data from the Pittsburgh site of the Health, Aging and Body Composition study, we performed a baseline cross-sectional analysis. Participants were black and white men and women 70-79 years old (N=1172), independent in activities of daily living and able to walk 1/4 mile and up 10 steps without resting. We measured Cobb's angle of kyphosis from supine lateral scout computed tomography (CT) scans, and categorized hyperkyphosis as Cobb's angle $>$ 40 degrees. Axial images from lateral scout CT scans assessed spinal extensor muscle cross-sectional area and density (proxy for fat infiltration). Results: In our sample, 21% had hyperkyphosis. Prevalence of hyperkyphosis in black men was 11%; in white men, 17%; in black women, 26%; and in white women, 30%. In multivariate analysis, each standard deviation increase in muscle density was associated with a 29% reduction in the odds of hyperkyphosis, independent of covariates. Muscle area was

not significantly associated with hyperkyphosis. Conclusions: Lower spinal muscle density is associated with hyperkyphosis in healthy community-dwelling older men and women. This potentially modifiable risk factor could be targeted in exercise interventions. Randomized trials are needed to determine whether an exercise program targeting spinal muscle density reduces hyperkyphosis and in turn improves health outcomes.

Disclosures: Wendy Katzman, None.

SU0009

Effect of Vitamin D Supplementation on Cognitive Function in Older Adults with Mild Cognitive Impairment - A Randomized Trial. Leon Flicker^{*1}, Kathryn Greenop², Osvaldo Almeida³, Helman Alfonso³, Christopher Beer³, Keith Hill⁴, Caryl Nowson⁵, Samuel Vasikaran⁶, Nicola Lautenschlager⁷. ¹University of Western Australia, Australia, ²Telethon Institute for Child Health Research, Australia, ³Western Australian Centre for Health & Ageing, Australia, ⁴Latrobe University, Australia, ⁵Deakin University, Australia, ⁶Department of Core Clinical Pathology & Biochemistry, PathWest Laboratory Medicine, Royal Perth Hospital, Australia, ⁷Department of Psychiatry, University of Melbourne, Australia

Aims: Vitamin D insufficiency has been associated with reduced cognitive function in older people. The effect of vitamin D supplementation on cognitive function is currently unknown. The aim of this study was to determine whether vitamin D supplementation would improve cognitive function in older people with mild cognitive impairment.

Methods: Participants fulfilled criteria for mild cognitive impairment (MCI) but did not have dementia. All subjects scored 1.0 SD below age and sex matched norms on any of the tests of the CERAD test battery including verbal fluency, Boston Naming Test, word list (learning, delayed recall and recognition) and constructional praxis (including recall task). All subjects had a MMSE score of 24 or greater at study entry. In addition, participants had vitamin D insufficiency as determined by serum 25-hydroxyvitamin D (25-OHD) levels between 12.5 and 70 nmol/l. Participants were randomly assigned a daily tablet of 1000IU of cholecalciferol or placebo. Participants with calcium intake < 800 mg per day were treated with 600 mg of calcium carbonate. The primary outcome measure was the Cambridge Cognitive Score (CAMCOG). The Clinical Dementia Rating Scale (CDR) was scored with additional information from an informant.

Results: Mean age of subjects who entered the study was 73.2 years for the 59 subjects in the vitamin group and 73.5 for the 58 in the placebo group. Mean baseline 25-OHD levels were 49.1 and 53.2 nmol/l, respectively. The two groups were balanced for baseline age, 25-OHD levels, CAMCOG and MMSE scores. 52 subjects in the vitamin group and 51 in the placebo group completed the 18 month intervention. The difference between groups in 25-OHD levels at the 18 month timepoint was 25.4 nmol/l (95% CI: 17.3, 33.4). There was an apparent difference in the changes in CAMCOG score between groups at the 12 and 18 month time points with worse performance in the vitamin group (see Table 1 and Figure 1). Subjects in the vitamin group were 2.85 (95%CI 1.12-7.28) more likely than the placebo group to develop a worse CDR score at the 18 month timepoint.

Conclusion: Contrary to our hypothesis, vitamin D supplementation did not improve the cognitive outcomes of older people with MCI. In fact, our results suggest that treatment with vitamin D may be deleterious.

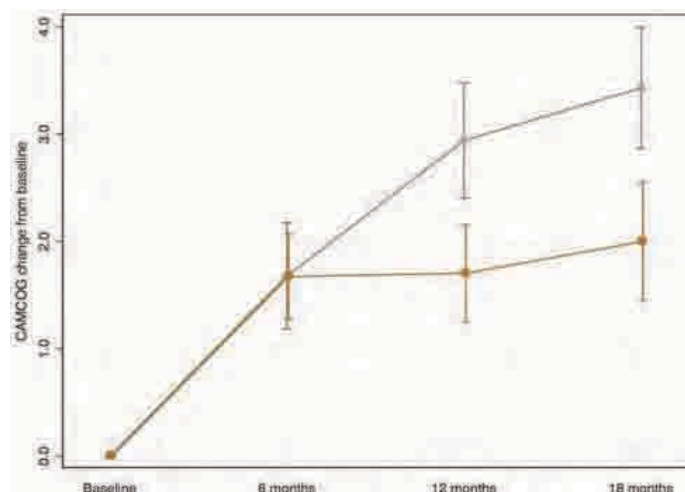


Figure 1

Table 1 Change in CAMCOG Scores
Follow-up score minus baseline score (SD)

	6 months	12 months	18 months
Vitamin D	1.8 (2.9)	1.7 (3.4)*	2.0 (4.1)*
Placebo	1.9 (3.9)	3.3 (3.8)	3.6 (3.9)

* P < 0.05 for comparison between groups

Table 1

Disclosures: Leon Flicker, None.

SU0010

Osteoporosis and Spinal Cord Injury in Patient with Ankylosing Spondylitis. Hyun-Sook Kim^{*}. Chosun University Hospital, South Korea

Objectives: Ankylosing spondylitis (AS) is an inflammatory disease involving the axial spine. Relating osteoporosis (OSP) is pathologic process of osteoclast activation and abnormal ankylosis. The spine is frequently kyphotic and has lost its flexibility. This is caused by a paravertebral benign ossification and sacroiliac joint. In the most severe form, these disease finally affects the entire spine including of cervical spine. We assess the OSP and related spinal injury sequelae in AS patients

Method: We present the atypical case of the severe OSP and related spinal traumatic neurological injury in AS patients

Result:

case1) Bilateral pedicle fracture in AS: A 63 year old man with 4 year history of AS was suddenly exacerbated low back pain. CT scan revealed bilateral L4 pedicle fracture accompanying spondylitis.

case2) Adjacent posterior element fracture in AS: A 54-year old man, with 10-year history of AS, had sudden onset back pain. CT scan confirm the transverse fracture through ossified posterior element below prior vertebroplasty.

case3) Epidural hematoma in AS: A 63-year old man, with 15-year history of AS suffered slip-down resulting paraplegia. lateral CT scanning revealed C7 interspinous fracture and intervertebral fracture. MRI confirmed the large epidural hematoma

Conclusion: Diffuse OSP responsible for bone fragility of AS is another feature established by recent data. The risk of vertebral fractures may be 7-fold increased compared with healthy individuals. The cervical spine in patient with long term AS has alteration in vertebral biomechanics that even minor trauma can cause fracture and serious neurological lesion

Disclosures: Hyun-Sook Kim, None.

SU0011

Prevalence of Sarcopenia and Osteopenia among 70-80-year Old Finnish Women. Kirsti Uusi-Rasi^{*}, Pekka Kannus, Saija Karinkanta, Matti Pasanen, Radhika Patil, Harri Sievanen. UKK Institute for Health Promotion Research, Finland

Aging is associated with decline in muscle mass and bone mass. The European Working Group on Sarcopenia in Older People recently devised a consensus algorithm to define sarcopenia on the basis of specific cut-off points for gait speed, handgrip strength and muscle mass index. The WHO definition of osteopenia rests on DXA-measured femur T-score. This study assessed the prevalence of sarcopenia and osteopenia among a population-based sample of 408 independently living 70 to 80-year-old Finnish women. They had normal or somewhat declined functional ability (Short Physical Performance Battery, SPPB ranging from 1 to 12).

Femoral BMD and body composition were measured with DXA. Skeletal muscle mass index was defined as ASM (appendicular skeletal muscle mass/height²). Four-meter gait speed and handgrip strength were used to assess physical performance and muscle strength. Gait speed provides a predictive value for the onset of disability, and low handgrip strength is a quick, simple clinical indicator of frailty and impaired mobility.

Of 408 women, 351 had no indication of sarcopenia (gait speed >0.8 m/s and grip strength >20 kg). Among the remaining 57 women, ASM was assessed in relation to the proposed cut-off point of 5.5 kg/m². In only 4 women (1% of the total sample) the ASM fell below the threshold of sarcopenia. Eight women had bilateral hip prosthesis leaving 400 women for femoral BMD analyses, 36% (n=144) of these women had femur T-score <-1. Three of the four sarcopenic women also had osteopenia.

Our study suggests that when using the above described definition, sarcopenia is very rare among older home-dwelling women while every third had osteopenia. Those with sarcopenia tend to have low bone mass.

Disclosures: Kirsti Uusi-Rasi, None.

SU0012

Prevalence of Sarcopenia in Older Men: The Geelong Osteoporosis Study. Julie Pasco^{*1}, Margaret J Henry¹, Mark Kotowicz², Geoff C Nicholson³.¹Deakin University, Australia, ²Barwon Health, Australia, ³The University of Queensland, Australia

Purpose: While sarcopenia develops in all individuals with advancing age, the extent varies on a continuum that progressively impacts on mobility, independence and frailty. We aimed to determine the prevalence of sarcopenia in older men living in south-eastern Australia. As recommended by the European Working Group on Sarcopenia in Older People (EWG-SOP), we defined sarcopenia in terms of both low muscle mass and low muscle function.

Methods: A random sample of 1540 men aged 20-97yr was selected from the population and enrolled in the Geelong Osteoporosis Study (GOS), 2001-6 (67% participation). Muscle mass was measured as total lean mass by DXA (Lunar) and expressed as a percentage of body mass; low lean mass was defined as more than 1SD below the mean for young adult men. The cut-off point derived from GOS men aged 20-39yr was 66.9%. Low muscle function was based on performance and identified using the timed up-&-go (TUG) test (distance 3m, cut-off point 10s). Dietary energy intakes and dietary protein intakes (adjusted for energy intake), were assessed using a food frequency questionnaire. Physical activity scores were determined using a questionnaire for the elderly. BMD at the femoral neck was measured using DXA (Lunar). Associations between sarcopenia and dietary intakes, physical activity and BMD were determined using multivariate linear regression.

Results: Among 624 men aged 60-97yr, 233 had low lean mass, 169 had TUG>10s and 81 had both, thus meeting criteria for sarcopenia. Age-specific prevalence for sarcopenia was 60-64yr 3.8%, 65-69yr 7.7%, 70-74yr 12.2%, 75-79yr 13.5%, 80-84yr 16.7% and 85+ 31.2%. Sarcopenia was associated with lower adjusted mean dietary energy intakes (by 10.8%), protein intakes (4.9%), physical activity scores (40.4%) and BMD (4.1%); all $p < 0.03$.

Conclusions: The prevalence of sarcopenia increased with age, affecting one-third of elderly men, aged 85+. Prevalence data age-standardised to national levels (2001) suggest that sarcopenia affects 10.6% of Australian men aged 60+. Cross-sectional analyses reveal that sarcopenia is associated with reduced caloric intakes that are relatively low in protein, and that men with sarcopenia are habitually less active and have lower BMD at the femoral neck. Prospective data are now being sought to identify risk factors for sarcopenia.

Disclosures: Julie Pasco, Speaker fees from Eli Lilly, Amgen, Sanofi Aventis, 8; NHMRC grants 454356 and 628582, 2

SU0013

The Association of Sarco-Osteopenia With Health Related Quality Of Life: A Population-Based Study In Estonia. Mart Kull^{*}, Riina Kallikorm, Margus Lember. University of Tartu, Estonia

Purpose. The aim of the study was to assess the association of a new sarco-osteopenia (SOP) phenotype, which was defined by decrements in both muscle functional and quantitative parameters with health related quality of life (HRQoL).

Methods: A population sample of 304 subjects aged 25-70 years was analysed with a Lunar DPX-IQ DXA machine and their HRQoL was assessed with the SF-36 questionnaire. SOP was defined as bone mineral density 1 standard deviation (SD) and height adjusted appendicular muscle mass 2SD and/or grip strength 2SD below the mean of 77 young individuals in the population sample (age 25-39). The impact of SOP on HRQoL was evaluated in the remainder (n=228) of the population sample with US norm based scoring. The study has Tartu University Ethics Committee approval and all patients signed a written informed consent. All study procedures were performed in accordance with the Declaration of Helsinki.

Results: The new SOP definition identifies 3-9% of middle aged (age 40-70 years) individuals as sarco-osteopenic. The prevalence of osteopenia/osteoporosis in the population group was considerably higher at 35-43%. Individuals who were sarco-osteopenic showed markedly lower scores in role-physical ($p=0.01$), vitality ($p=0.03$) and role-emotional ($p=0.02$) sub-scales of the SF-36 questionnaire (Figure). No difference in HRQoL was observed between osteopenic/osteoporotic and individuals with normal bone mineral density.

Conclusion: The new SOP definition identifies a population with significant decrements in both physical and mental health domains of HRQoL when compared with isolated osteopenia or osteoporosis subjects. We conclude that combining muscle as well as bone parameters under an umbrella diagnosis of sarco-osteopenia helps to isolate a more frail subpopulation than can be achieved utilising only bone density indices.

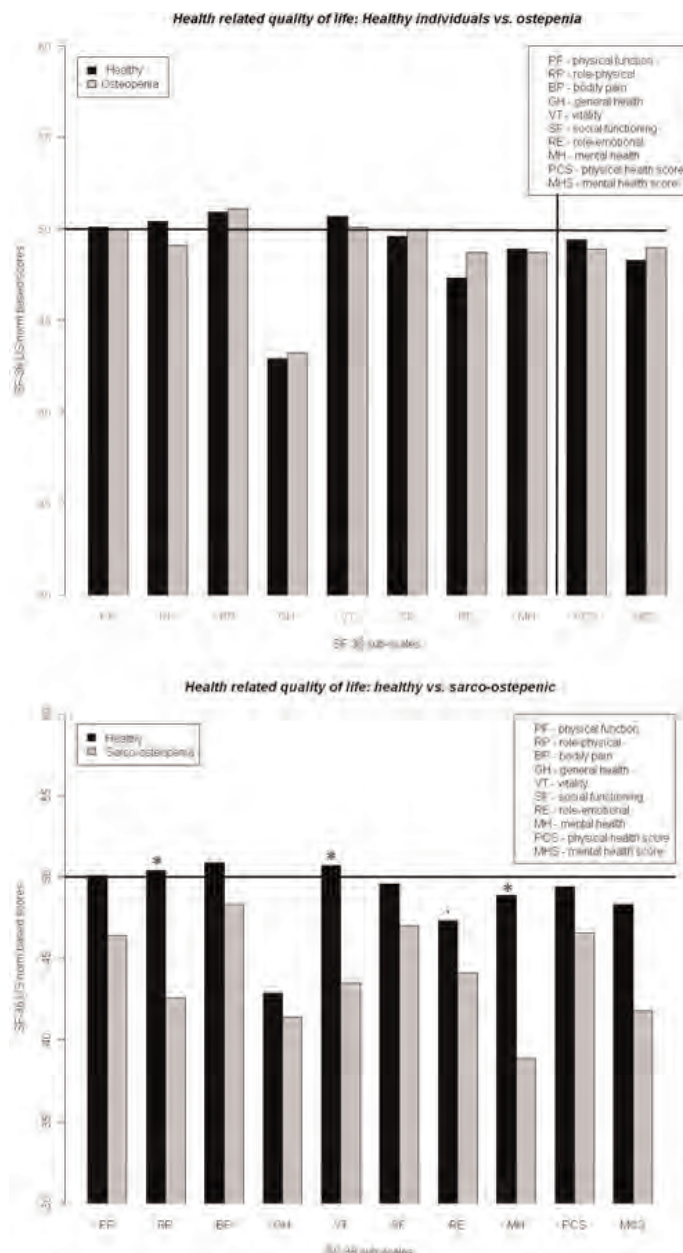


Figure. HRQoL of healthy individuals compared with osteopenic (above) and sarco-osteopenic (below)

Disclosures: Mart Kull, None.

SU0014

The Association of Sarcopenia and Sarcopenic-Obesity with Mobility Limitations in Older Men and Women: The Framingham Study. Alyssa Dufour^{*1}, Marian Hannan², Joanne Murabito³, Douglas Kiel¹, Robert McLean⁴. ¹Hebrew SeniorLife, USA, ²HSL Institute for Aging Research & Harvard Medical School, USA, ³Boston University School of Medicine & NHLBI's Framingham Heart Study, USA, ⁴Hebrew SeniorLife, Harvard Medical School, USA

Age-related loss of muscle mass and strength, termed sarcopenia, is common among older adults and associated with reduced mobility, functional disability and increased mortality. Our previous work suggested high % body fat was associated with mobility limitations (ML) in older adults, yet unexpectedly, low absolute lean mass and grip strength were not. New definitions of sarcopenia that account for body size and fat mass have since been proposed, as have measures of sarcopenic-obesity that assess the potential synergistic effects of combined low lean and high fat mass. We thus examined alternative definitions of sarcopenia and sarcopenic-obesity in relation to ML among 291 men and 513 women, who had information on ML and DXA, from the population-based Framingham Study Original Cohort. Whole body DXA (Lunar DPX-L) measured appendicular lean mass (ALM) and total fat mass in 1992-95.

Sarcopenia was defined using 2 published definitions: 1) $ALM/ht^2 > 2SD$ below young reference population; 2) lowest sex-specific quartile of residuals from regression of ALM on height and total fat mass. Obesity was defined as % body fat > 30 for men and > 40 for women, and combined with ALM/ht^2 to classify subjects into 4 sarcopenia-obesity groups: referent, obese, sarcopenic, sarcopenic-obese. Subjects reporting inability to walk 0.5 mi, walk up and down stairs, or perform heavy housework were defined as having ML. Sex-specific logistic regression calculated the odds of ML for sarcopenia and sarcopenia-obesity categories, adjusting for age (yrs), estrogen use (y/n), CVD (y/n), diabetes (y/n) and depression (CES-D). Mean age was 79 y (range 72-92). 18% of men and 30% of women had ML. In men, though CIs were wide, ALM/ht^2 and residuals sarcopenia were associated with 4-5 times the odds of ML (Table). Compared to referent men, the odds of ML for obese men was not significantly different, yet was 8-fold higher among sarcopenic men. Sarcopenic-obese men had only 4 times the odds of ML, suggesting no synergistic effect. In women, residuals sarcopenia, but not ALM/ht^2 , was associated with a 2-fold increase in the odds of ML, while there were no significant associations for sarcopenic-obesity. Our results support previous reports that lean mass sarcopenia definitions should consider body size and fat mass, and that lean and fat mass have different individual and combined effects on mobility in elders. Studies are needed to explore potential sex differences in these associations.

Table: Multivariable adjusted* odds ratios (OR) and 95% confidence intervals (CI) for association of sarcopenia and sarcopenia-obesity with mobility disability in 291 men and 313 women in the Framingham Study						
	Men			Women		
Sarcopenia	N	% limited	OR (95% CI)	N	% limited	OR (95% CI)
ALM/ht ²	60	36.67%	4.2 (2.06, 8.78)	65	33.85%	1.3 (0.72, 2.33)
Residuals	37	36.84%	4.5 (2.06, 9.81)	120	36.67%	1.7 (1.06, 2.69)
Sarcopenia-obesity						
Referent	108	9.26%	1.0	198	25.76%	1.0
Obese	123	15.45%	1.9 (0.81, 4.43)	250	32.80%	1.5 (0.94, 2.37)
Sarcopenic	35	42.86%	7.5 (2.80, 20.13)	44	34.09%	1.6 (0.75, 3.29)
Sarcopenic-obese	25	28.00%	4.2 (1.29, 13.32)	21	33.33%	1.7 (0.62, 4.74)

*Adjusted for age, estrogen use, CVD, diabetes, and depression.

*Adjusted for age, estrogen use, CVD, diabetes, and depression.

Table

Disclosures: Alyssa Dufour, None.

SU0015

Higher Premenarcheal Bone Mass in Elite Gymnasts is Maintained into Young Adulthood After Long-Term Retirement From Sport: A 14-year Follow-Up. Marta Erlandson¹, Saija Kontulainen², Phil Chilibeck², Cathy Arnold², Bob Faulkner², Adam Baxter-Jones². ¹University of Toronto, Canada, ²University of Saskatchewan, Canada

Purpose: Sports that impact load the skeleton during childhood and adolescence increase determinants of bone strength such as bone mineral content and density; however, it is unclear if these benefits are maintained after retirement from the sport. The purpose of this study was to assess whether the skeletal benefits of gymnastics training previously reported in premenarcheal girls were still apparent 10 years after the cessation of gymnastics participation.

Methods: In 1995, 22 elite premenarcheal gymnasts 8-15 years of age were measured and compared to 22 age-matched non-gymnasts. The same former gymnasts and non-gymnasts were measured again 14 years later (2009-2010). Gymnasts had been retired from gymnastics training and competition for an average of 10 years. Total body (TB), lumbar spine (LS), and femoral neck (FN) bone mineral content (BMC) was assessed at both measurement occasions by dual energy X-ray absorptiometry (DXA). MANCOVA was used to compare gymnasts' and non-gymnasts' BMC while controlling for differences in body size and maturation (covariates: age, height, weight, and years from menarche (1995) or age at menarche (2009/10)).

Results: Premenarcheal gymnasts had significantly ($p < 0.05$) greater size adjusted TB, LS, and FN BMC (15, 17, and 12%, respectively). After retirement, gymnasts maintained similar size adjusted TB, LS, and FN BMC significant differences ($p < 0.05$) (13, 19 and 13%, respectively) compared to non-gymnasts.

Conclusion: Higher bone mass related to gymnastics training before menarche was still apparent even after long-term removal of the gymnastics-loading stimulus.

Disclosures: Marta Erlandson, None.

SU0016

The Development of Neuromuscular Function in Pre-school Aged Children. Tom Hazel¹, Sarah Finch¹, Thu Trang Pham¹, Sonia Jean-Philippe¹, Catherine A. Vanstone¹, Sandra Dell'Elce¹, Atul K. Sharma², Hope Weiler¹, Celia Rodd¹. ¹McGill University, Canada, ²Montreal Children's Hospital, Canada

Childhood is a critical period for growth and development of the musculoskeletal system. However, the development of neuromuscular function in young children is not well established, as there are currently no data on children under the age of 6-7y. The objective of the current study was to measure neuromuscular function in pre-school children (3-5y of age) to provide data on their neuromuscular development. Using a

force plate (Kistler Instrument Corp., NY, USA), forty-nine children (26 boys, 23 girls; 3.71.1y) performed several neuromuscular function tests, including jumping (JMP), sit-to-stand (STS), and body sway tests. Children were grouped based on age, with $n=23$ at 3y, $n=11$ at 4y, and $n=15$ at 5y. One-way ANOVAs were used to compare age categories (3 vs 4 vs 5y) for indices of neuromuscular function (GraphPad Prism 5.00 for Windows, GraphPad Software, CA, USA). Mean (sd) height for age z-scores (3y: -0.10.8; 4y: -0.60.9; 5y: 0.41.5), and mean (sd) weight for age z-scores (3y: 0.50.7; 4y: -0.20.7; 5y: 0.51.1) were not different by age. Tables 1 and 2 summarize neuromuscular performance by age: JMP peak power ($P=0.01$) and normalized peak power (normalized for body weight, $P=0.05$), STS peak force ($P < 0.001$) and slope at 20-90% force (a proxy for muscle power; $P < 0.001$), and body sway amplitude ($P=0.03$) were all greater in 5y olds than in 3y olds. There were no age differences for JMP peak force, normalized peak force, or body sway velocity. These novel data demonstrate the progression of neuromuscular function in preschool aged children (3-5y of age), with significant differences observed in 5y old compared to 3y old children. Although originally developed for older children and adults, force-plate assessment of neuromuscular function is applicable in children as young as three years of age.

Table 1 Jumping (JMP) Performance				
Age (y)	Peak Force (N)	Normalized Peak Force (N/kg)	Peak Power (W)	Normalized Peak Power (W/kg)
3	272.7±44.5	18.7±3.2	119.3±112.1 ^a	7.7±6.5 ^a
4	341.5±89.9	20.0±5.1	210.2±119.8 ^a	12.5±7.2 ^a
5	323.2±87.4	17.3±3.7	288.5±210.1 ^b	15.0±10.7 ^b

Unlike superscript letters denote significant differences $P < 0.05$

Table 1

Table 2 STS				
Age (y)	Peak Force (N)	Slope 20-90% (N/s) (=power)	Amplitude (mm)	Velocity (mm/s)
3	158.0±37.8 ^a	762.2±493.8 ^a	1.7±1.5 ^a	11.8±12.4
4	219.4±28.6 ^b	1453.0±406.7 ^b	0.8±0.3 ^a	5.4±2.4
5	238.6±43.0 ^c	1579.3±397.3 ^c	0.7±0.2 ^b	6.6±4.7

Unlike superscript letters denote significant differences $P < 0.05$

Table 2

Disclosures: Tom Hazel, None.

SU0017

Use of the Safe Functional Motion-Short Form Test to Classify Risk in Individuals Following a Distal Radius Fracture. Norma MacIntyre¹, Joy C. MacDermid¹, Ruby Grewal², Julie Richardson¹. ¹McMaster University, Canada, ²Hand & Upper Limb Centre, St Joseph's Health Centre, Canada

Purpose: Long and short forms of the Safe Functional Motion test (SFM) have been used to measure body mechanics and functional motion during performance of everyday tasks in individuals at risk for osteoporotic fracture. The predicted probability of a prevalent vertebral or hip fracture for 1257 individuals seen in an osteoporosis specialty clinic increased by 18 to 21% for each 10% decrease in SFM score regardless of bone mineral density (aBMD, g/cm^2). For some individuals, distal radius fracture (DRF) may be the first clinical manifestation of osteoporosis. The purpose of this study was to determine the feasibility of using the short form of the SFM (SFM-short) to assess movement patterns in individuals with a recent DRF which may predict an increased risk for subsequent fracture.

Methods: The SFM-short, a performance-based assessment tool for quantifying habitual movement patterns during 6 typical daily tasks - removing/putting on footwear, picking up a newspaper from the ground, placing a container on an overhead shelf, getting down/up off the floor, carrying groceries up/down stairs and an emergency task that simulates getting up in the night (assessing vestibular components of the balance system), was administered to individuals seen in a tertiary care centre between March 2009 and March 2011 following DRF. Total SFM-short score is reported as a percentage of the maximum points associated with 6 domains. T-scores for lumbar spine and hip aBMD were recorded if available. Participants were asked about osteoporosis risk factors fracture and completed the SF-12 to determine physical health status.

Results: Of 83 patients with a recent DRF enrolled in a concurrent study, 67 (5 men) consented to complete the SFM-short. Only 61 patients (4 men; mean(SD) age = 61.2(7.5) y; mean(SD) weeks post DRF = 2.9(1.8); 13 treated surgically) completed all 6 tasks. Testing took approximately 15 minutes. Table 1 summarizes patient characteristics with respect to each outcome measure. The association between SFM-short and SF-13 was $r = 0.013$.

Conclusions: SFM-short scores, aBMD, and risk factor profiles concur in indicating that not everyone in the DRF population has an elevated risk for osteoporotic fracture but a substantial proportion do. SFM-short scores provide information that is distinct from self-reported physical health status. These findings suggest that further study of the predictive ability of this tool for future fracture in this population is warranted.

SU0019

The Effect of Obesity on Pediatric Fractures. Rushyuan J. Lee^{*1}, Colleen Cullen¹, Josephina Baca-Asher¹, Meredith Lazar-Antman¹, Arabella Leet².
¹Johns Hopkins University, USA, ²Johns Hopkins University School of Medicine, USA

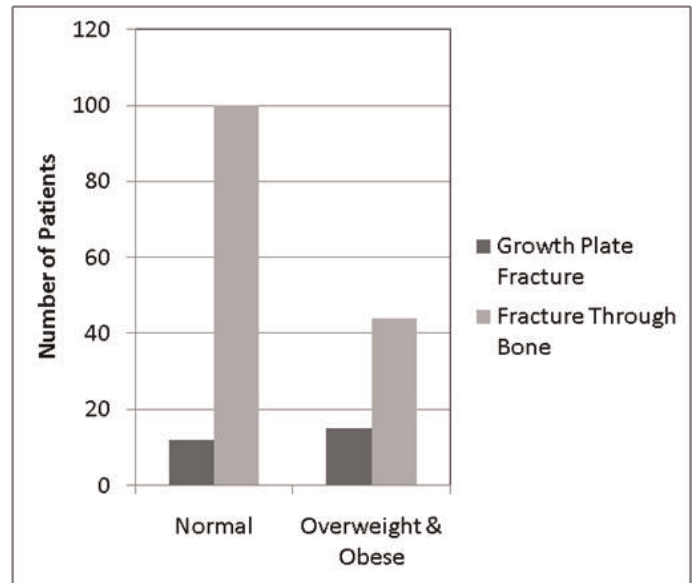
Purpose: Increasing obesity among children is a major health care concern. The purpose of this study is to examine children with fractures, comparing those who are normal weight with obese/overweight children.

Methods: 185 consecutive pediatric fracture patients were enrolled into an IRB approved registry. Information collected at the time of injury included: sex, age, height, weight, fracture location and pattern. Patients 2-16 years old were divided into two groups for comparison: (1) normal weight (2) obese/overweight (defined as > 85 %ile BMI for age). Statistical analysis was performed using Graph pad Prism 4 for Chi2 or Mann Whitney tests.

Results: The total population of 185 patients consisted of < 2 years of age (14), normal weight (112), and obese/overweight (59). Obese patients made up 22% of the entire population; obese/overweight combined were 34% of the study group. There was no difference between the mean ages in the normal weight group (9.4 yrs) compared with the overweight/obese group (9.0 yrs). There was a slight increase in numbers of girls in the obese group (16/59, 27%), compared with the normal weight children (27/112, 24%), but this was not statistically significant. The distribution of upper and lower extremity fractures was also comparable between groups. The normal weight group had a significantly higher rate of operative interventions compared to the overweight/obese group (33% vs 15%, $p < 0.05$). However, the overweight/obese group had a significantly higher rate of growth plate injuries (25% vs 10%, $p = 0.02$).

Conclusions: Twenty-two percent of children with fractures were obese which is higher than the expected prevalence of obesity in the general population. In contrast to the study by Rana, we report a lower number of operative cases in the heavier children(1). While Rana studied children from trauma registries, our patient population included both low and high energy mechanisms of injury. The growth plate is the weakest part of the bone, so the finding that obese/overweight children had a greater number of growth plate injuries is not surprising. Future studies include continued expansion of this database with the hope that understanding fracture patterns based on weight will lead to better injury protection strategies for obese children in the future.

Reference: 1. Rana A, et al., Childhood obesity: a risk factor for injuries observed at a level-1 trauma center, Journal of pediatric surgery 44, no. 8 (2009): 1601-1605.



Fractures Involving the Growth Plate

Variable	Frequency distribution
SFM-short Total Score (/100%) - Mean(SD)	80.5 (7.3)
SFM-short Domain Scores- Median(Min,Max)	
Spine loading (/6pts)	3 (0,5)
Balance (/17pts)	15 (10,17)
Upper body strength (/4pts)	4 (1,4)
Lower body strength (/4pts)	4 (2,4)
Upper body flexibility (/2pts)	2 (1,2)
Lower body flexibility (/4pts)	4 (2,4)
Lumbar Spine T-score, Mean(SD), n = 33	-1.00 (1.13)
Proximal Femur T-score Mean(SD), n = 32	-0.87 (0.92)
Fracture Risk Factor Profile (n)	
History of fracture other than current DRF	35
History of falling other than current DRF	7
Parent with hip fracture after age 50y	14
Weighs ≤ 125 lbs	10
Has rheumatoid arthritis	2
Has impaired vision after correction	6
Currently smokes	4
Currently takes bone sparing medications	6
SF-12 Physical Health, Mean(SD), n = 55	34.76 (11.70)

Table 1. Patient Characteristics

Disclosures: Norma MacIntyre, None.

SU0018

Assessment of Bone Mineral Status in Children with Noonan Syndrome: Another Consequence of Dysregulated RAS-MAPK Signaling? Monica Grover^{*1}, Kiran Choudhry¹, Alyssa Tran¹, Susan Carter¹, E. O' Brian Smith¹, Kenneth Ellis¹, Brendan Lee². ¹Baylor College of Medicine, USA, ²Baylor College of Medicine & Howard Hughes Medical Institute, USA

BACKGROUND: The RAS/mitogen activated protein kinase (MAPK) pathway is essential for regulation of cell differentiation and growth. However, its role in skeletal tissue development is unclear. Various skeletal abnormalities including low bone density in Neurofibromatosis (NF) 1, a disorder of dysregulated MAPK signaling, has given insight into its role in skeletal homeostasis. Noonan Syndrome (NS) is also a disorder of RAS-MAPK pathway, with clinical features of a skeletal dysplasia, but little information about the mineralization of bone.

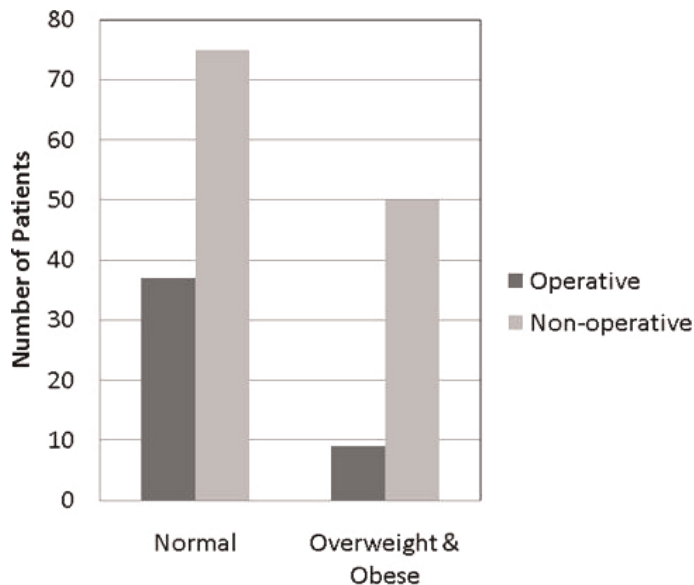
OBJECTIVE: We evaluated bone mineral status in children with NS.

DESIGN/METHODS: Using dual energy X-ray absorptiometry (DXA) bone status in 12 (9 males; 3 females) subjects (mean age 8.7 years) with NS was analyzed. The subjects were diagnosed with NS clinically and underwent genetic testing. 9 had mutation in PTPN11 gene, 1 in SOS1, and 2 patients had no mutations. As femur and lumbar BMD is unreliable at younger age, only total body measurements of bone were done. In subjects with low bone mass, indices of calcium-phosphate metabolism and bone turnover were obtained.

RESULTS: The mean height was low at 6.9 %ile. None of the subjects were on medications affecting bone metabolism or had history of fractures. BMC (bone mineral content) z-score calculations were based on age, gender, height, and ethnicity. Mean BMC z-scores were reduced at -0.89 gm (SEM +/-0.51) [95% CI -2.01; 0.23], P value 0.109. Whole body BMD (bone mineral density) z-scores were low. Mean total body BMD was -1.87g/cm2 (SEM +/-0.393), [95% CI -2.73; -1.0], P value 0.001. Most of our patients' height was < 2 SD for general population, we calculated total body BMD z-score based on height age. The mean adjusted total body BMD was -0.82g/cm2 (SEM +/-0.258), [95% CI -1.39; -0.25], P value 0.009. All biochemical parameters were within normal range. Serum IGF-1 and IGFBP3 were low normal.

CONCLUSIONS: We report low bone mineral density as compared to age and height matched controls and trend towards low bone mineral content as compared to age matched controls in NS. This is similar to the findings in the NF and indicates poor bone quality. The bone metabolism markers in our study indicated an absence of overt metabolic bone disease. Histomorphometric analysis of bone tissue from NS patients and mouse model of NS could further elucidate correlations between genetic defects in the RAS MAP kinase pathway and alterations in skeletal homeostasis.

Disclosures: Monica Grover, None.



Fractures Requiring Surgical Treatment

Disclosures: Rushyuan J. Lee, None.

SU0020

Youth School Physical Education Grades and Tibial Bone Traits in Adulthood. Vera Mikkilä¹, Marika Laaksonen¹, Olli Raitakari², Sanna Tolonen^{*1}, Harri Sievanen³, Terho Lehtimäki⁴, Mika Kahonen⁵, Jorma Viikari⁶. ¹University of Helsinki, Finland, ²Turku University Hospital & Research Centre of Applied & Preventive Cardiovascular Medicine, Finland, ³UKK Institute, Finland, ⁴Medical School & Tampere University Hospital, Finland, ⁵Tampere University Hospital, Finland, ⁶Turku University Central Hospital, Finland

Bone mass in adulthood is determined by peak bone mass attained in early life and the rate of bone loss during lifespan. High bone mass achieved in childhood may decrease the risk of osteoporosis later in life. We studied whether in 9-18 years old children (girls, n=655; boys, n=496) physical education grades at school (grades from 4 to 10; 10 being the highest) are associated with the structural peripheral quantitative computed tomography (pQCT) bone traits measured from tibia in adulthood approximately 25 years later. Results were adjusted with adult height and weight.

In girls, higher school physical education grades were associated with higher trabecular bone density, bone mineral content (BMC) and bone strength index (BSI) at the distal tibia (linear, P-values≤0.02), and total area, BMC, cortical strength index (CSI) and stress-strain index (SSI) at the tibial shaft (linear, P-values≤0.02). In boys, higher school physical education grades were associated with higher total area, BMC and BSI at the distal tibia (linear, P-values≤0.007), and total area, BMC, CSI and SSI at the tibial shaft (linear, P-values<0.001). These findings suggest that youth physical activity has a great influence on bone health later in life and may, therefore, reduce the risk of osteoporosis.

Disclosures: Sanna Tolonen, None.

SU0021

A Comparison of Trabecular Bone Microstructure at the Distal Radius Between Postpubertal Asian and Caucasian Adolescents: An HR-pQCT Study. SoJung Kim^{*1}, Lindsay Nettlefold¹, Christa Hoy¹, Sarah Moore¹, Meghan Donaldson², Heather Macdonald¹, Heather McKay¹. ¹University of British Columbia, Canada, ²San Francisco Coordinating Center, USA

Fracture incidence is lower among Asians compared with Caucasians; however, areal bone mineral density (BMD) is also lower in Asians than Caucasians. With these incongruities, it is important to investigate ethnic differences in three-dimensional properties of bone microstructure that contribute to bone strength during growth. Therefore, we used high-resolution peripheral QCT (HR-pQCT; isotropic voxel size 80µm) to directly assess bone trabecular microstructure at the non-dominant distal radius (7% site) in Asian (n=66) and Caucasian (n=78) boys and girls (17.6 ± 1.8 yrs). We used cross-sectional HR-pQCT data from the longitudinal Healthy Bones Study to compare trabecular bone volume fraction (BV/TV, %), trabecular thickness (Tb.Th, µm), trabecular number (Tb.N, 1/mm), and trabecular separation (Tb.Sp, µm) between Asian and Caucasian adolescents. Asian participants were those with either

both parents or all four grandparents born in Hong Kong or China, India, Philippines, Vietnam, Korea or Taiwan and Caucasian participants were those with parents born in North America or Europe. We assessed height and weight using standard protocols. We assessed physical activity (PA) and calcium intake (mg/day) by questionnaires. We conducted a separate analysis for boys and girls when comparing ethnic groups. We performed multiple regression analysis to evaluate the variance in trabecular bone microstructure explained by ethnicity, after adjusting for age (yrs), weight (kg), calcium (mg/day), PA (min/day), and radial length (mm). The magnitude of the difference for trabecular variables between ethnicities (Asian-Caucasian) adolescents was similar for both sexes (Boys: Tb.Sp ~ 8.7 %; Tb.N ~ -6.8%; Girls: Tb.Sp ~ 8%; Tb.N ~ -6.5%). However, ethnicity was only a significant predictor of trabecular bone variables for boys (Tb.N (p<0.05) and Tb.Sp (p<0.01)). The small sample size for girls may explain the sex difference in outcome. Differences in dietary calcium (both), PA (boys) and age (girls) may also contribute to these findings. Longitudinal data are needed to further clarify these differences and their implications.

Table 1. Descriptive characteristics of post-pubertal Asian and Caucasian boys and girls.

Variable	Boys		Girls	
	Asian (n=42)	Caucasian (n=44)	Asian (n=24)	Caucasian (n=34)
Age (yrs)	17.2±1.5	17.3±2.1	17.5±1.7	18.5±1.9
Height (cm)	173.2±6.2	176.9±9.7	158.8±5.6	167.3±6.2
Weight (kg)	64.9±12.8	67.5±11.9	56.7±8.5	62.0±10.9
Ca ²⁺ (mg/day)	833±682	1357±681	741±508	1136±685
PA (min/day)	72.0±50.3	89.4±86.2	56.6±48.7	55.0±37.9
Radial Length (mm)	283±16	288±17	250±10	264±13
BV/TV (%)	16±3	17±3	14±3	14±3
Tb.Th (µm)	84±14	85±14	76±11	75±11
Tb.N (1/mm)	1.87±0.26*	2.00±0.19	1.77±0.25	1.91±0.24
Tb.Sp (µm)	462±78*	421±44	499±84	456±71

Data are unadjusted mean±SD. Significant difference between Asians and Caucasians, at *p<0.05 and *p<0.01

Table 1

Disclosures: SoJung Kim, None.

This study received funding from: Canadian Institute for Health Research

SU0022

Negligible Influence Of Vitamin D Status On Cortical Bone Development In Childhood: Findings From A Large Prospective Cohort Study. Adrian Sayers^{*1}, Debbie Lawlor¹, William Fraser², J.H. Tobias³. ¹University of Bristol, United Kingdom, ²Royal Liverpool University Hospital, United Kingdom, ³Avon Orthopaedic Centre, United Kingdom

Background and aims: How vitamin D status affects bone development is unclear. In a prospective cohort study, we investigated relationships between vitamin D status in childhood (reflected by plasma levels of 25(OH)D2 and 25(OH)D3 at age 9.9) and subsequent development of cortical bone (measured by tibial pQCT at age 15.5).

Methods: 3260 children from the Avon Longitudinal Study of Parents and Children were included. The proportion of variation in pQCT parameters explained by 25(OH)D2 and 25(OH)D3 was estimated from r² derived from crude regressions with/without seasonal adjustment of 25(OH)D3. Further analyses were by bootstrap linear regression with additional adjustment for age, sex, body composition, social economic position and physical activity.

Results: 25(OH)D3 was positively skewed and seasonally patterned, mean(sd) 23.5 (8.4) ng.mL⁻¹, whereas 25(OH)D2 was positively skewed with no discernable seasonal patterning, mean(sd) 1.8(1.8) ng.mL⁻¹.

In crude analyses, 25(OH)D2 and 25(OH)D3 together explained only 0.4% of the variability in cortical bone mineral density (BMD_C), 0.7% in cortical thickness, 0.02% in periosteal circumference (PC), and 0.2% in cortical bone mineral content. Most of this explained variability represented seasonal variation; 25(OH)D3 explained 0.4% of the variability in cortical thickness in unadjusted models and after seasonal adjustment it only explained 0.04% of the variability.

25(OH)D2 and 25(OH)D3 differed in their associations with cortical bone outcomes in fully adjusted models: 25(OH)D2 was inversely related to BMD_C [-0.041 (-0.073,-0.008), P=0.01], whereas no association was observed with 25(OH)D3 [0.005 (-0.016,0.026), P=0.65, beta (with 95%CI) represents SD changes per doubling of vitamin D], P=0.02 for difference in associations with 25(OH)D2 and 25(OH)D3. 25(OH)D2 was unrelated to cortical thickness (calculated as inverse of endosteal circumference adjusted for PC) [-0.019(-0.046,0.009), P=0.18], whereas 25(OH)D3 was positively related to this parameter [0.024(0.008,0.04), p=0.0035], P = 0.007 for difference in associations.

Conclusions: Vitamin D status in children showed negligible association with subsequent cortical bone development, particularly after adjusting for confounders. These results suggest that population-based vitamin D supplementation is unlikely to improve bone development in childhood, even if based on D3, which unlike D2 showed, albeit weak, evidence of a protective effect.

Disclosures: Adrian Sayers, None.

SU0023

Non-Elite Gymnastics Induces Musculoskeletal Benefits in the Upper Limbs of Early Pubertal Girls: A 6-Month Study Using pQCT. Lauren Burt^{*1}, David Greene², Geraldine Naughton², Daniel Courteix³, Gaele Ducher⁴.

¹Centre of Physical Activity Across the Lifespan, Australian Catholic University, Australia, ²Centre of Physical Activity Across the Lifespan, School of Exercise Science, Australian Catholic University, Australia, ³Universite Clermont Ferrand Laboratoire De Biologie Des APS, France, ⁴Noll Laboratory, Department of Kinesiology, Penn State University, USA

Purpose

Little is known about the longitudinal musculoskeletal development of weight-bearing loading to the upper limbs of non-elite gymnasts during early pubertal growth. The purpose of this longitudinal study was to examine the effects of non-elite female gymnastics participation on upper body musculoskeletal parameters.

Methods

Eighty-four girls, (6-12 years, Tanner stages I to III) were divided into three groups based on their participation in gymnastics: high training (HGYM), 6-16 hr.wk⁻¹, low training (LGYM), 1-5 hr.wk⁻¹ and non-gymnasts (NONGYM). At baseline and 6 months, total density (ToD), bone mineral content (BMC), total and cortical area (ToA, CoA), bone strength (BSI and SSI) were assessed by pQCT at the 4% and 66% radius and ulna. DXA-derived BMC and lean mass in the arms, as well as pQCT-derived forearm muscle cross sectional area (MCSA) were also obtained. Upper body muscle function was assessed with generic assessments for explosive power, strength, and endurance.

Results

Growth rate (in height) over 6 months was not significantly different between groups. Arm lean mass, grip strength and muscle endurance, 66% BMC and ToA at radius 66% were the only bone parameters to increase over 6 months in NONGYM ($p<0.05$). Following body weight-adjustment, arm lean mass, SSI at the 66% forearm, ToA (66% radius), BMC and CoA (66% ulna), explosive power and muscle endurance, which were initially higher in gymnasts than NONGYM, remained higher at follow up. MCSA increased more in HGYM than both NONGYM and LGYM. At the 4% radius, HGYM had greater BMC, ToD and BSI than NONGYM at baseline, whereas LGYM had greater ToD ($p<0.05$). At 6 months, both groups of gymnasts had a greater increase in ToD at the 4% radius than NONGYM (LGYM +8% greater, HGYM +15% greater, $p<0.05$). HGYM had a greater increase in BMC and BSI at the 4% radius than both NONGYM (+25-45% greater, $p<0.01$) and LGYM (+20-28% greater, $p<0.05$).

Conclusion

At baseline, gymnasts had upper limb musculoskeletal benefits, potentially resulting from an average training history of three years. Benefits were maintained, and in some instances, increased over the duration of the study. Muscle function tests consistently showed superior skills among gymnasts, independent of hours of training. Although favorable skeletal gains were seen in LGYM, HGYM had the greatest gains. Musculoskeletal benefits beyond growth-induced effects exist following non-elite gymnastics participation during early puberty.

Disclosures: Lauren Burt, None.

SU0024

Optimizing Low-Magnitude, High-Frequency Vibration Parameters to Stimulate an Osteogenic Response in The mdx Mouse Model of Duchenne Muscular Dystrophy. Susan Novotny^{*1}, David J. Nuckley¹, Moiria Petit¹, Kristen A. Baltgalvis¹, Gordon L. Warren², Dawn A Lowe¹.

¹UNIVERSITY OF MINNESOTA, USA, ²Georgia State University, USA

Low-magnitude, high-frequency vibration prevents bone loss and stimulates bone formation in various populations. This modality of mechanical loading is particularly attractive to preserve skeletal health in Duchenne muscular dystrophy (DMD) because patients are advised to avoid traditional exercise. Prior to clinical usage, it is important to establish parameters for vibration (acceleration and frequency) that maximize osteogenic responses. Therefore, the purpose of this research was to use the mdx mouse model of DMD to determine the acceleration and frequency of vibration resulting in the greatest improvements in osteogenic gene expression and plasma osteocalcin (OC). Mdx mice were exposed to 14 days of vibration (15min/d) at an acceleration of either 0.3 or 0.6g at 30, 45, or 90Hz (n=6-8) and were compared amongst each other as well as to non-vibrated (control) mdx mice (n=8). RNA was extracted from tibiae for RT-PCR analysis of gene expression along the osteoblastic lineage (alkaline phosphatase (ALP), Runx2, bone morphogenetic protein 2, and collagen type-1 (COL1A1)) as well as genes known to inhibit and activate osteoclasts (osteoprotegerin (OPG) and RANKL). Osteoblast activity was assessed by plasma OC levels on day 14. RT-PCR and OC data were analyzed by two-way ANOVAs and post-hoc tests were used to compare against control mice; significance was set at $P<0.05$. Comparisons amongst the varying accelerations and frequencies showed that gene expression was not affected by the acceleration or frequency of vibration; there was however a trend for OPG to increase with higher frequencies (i.e., main effect of frequency $P=0.052$). Relative to control mice, the 45Hz at 0.6g mice had 31% upregulation in COL1A1 along with a trend toward greater ALP mRNA ($P=0.09$). Mice vibrated at 90Hz and 0.3g also had 40% upregulation of ALP compared to control mice ($P<0.05$). OC levels were similar across vibration conditions ($P>0.64$) and between vibrated and control mice ($P>0.28$). These results, similar to those found

in wildtype mice, indicate that acute vibration at 45Hz at 0.6g or 90Hz at 0.3g have a modest potential to elevate genes associated with osteoprogenitor cell proliferation and extracellular matrix mineralization in the mdx mouse. Despite these modest effects, improvements in bone strength have previously been realized with long-term vibration thus establishing the need of long-term studies in mdx mice to ensure improvements in skeletal health.

Disclosures: Susan Novotny, None.

SU0025

Racial Differences in Cortical Bone Mass, Size and Estimated Strength at the Tibial Diaphysis in Early Pubertal Children. Stuart Warden^{*1}, Ashley Ferira², Emma Laing², Kathleen Hill³, Berdine Martin⁴, Connie Weaver⁴, Munro Peacock⁵, Richard Lewis². ¹Indiana University, USA, ²The University of Georgia, USA, ³Indiana University School of Medicine, USA, ⁴Purdue University, USA, ⁵Indiana University Medical Center, USA

Osteoporotic fracture rates differ according to race, with blacks having up to half the rate of whites. The reduced fracture rate in blacks has been suggested to be due to their superior bone mass; however, mass is not the sole determinant of bone strength. Bone strength, and consequent fracture risk, is also influenced by how bone material is distributed or structured. It is likely bone structure also contributes to the lower incidence of fractures in blacks and that racial differences in bone structure have roots in childhood. The aim of this study was to assess the influence of race on pQCT-derived cortical bone mass, size and estimated strength at the tibial diaphysis in early pubertal children. 160 children were recruited, with equal subjects according to race (black, n=80; white, n=80) and sex (female, n=80; male, n=80). Subjects were at sexual maturation stages 2 or 3. Tomographic slices of the tibial diaphysis at 66% proximal from the medial malleolus were acquired using pQCT. Slices were assessed for cortical volumetric BMD (Ct.vBMD), cortical BMC (Ct.BMC), total (Tt.Ar) and cortical (Ct.Ar) area, density weighted maximum (I_{MAX}) and minimum (I_{MIN}) second moments of area, density-weighted polar strength-strain index (SSI_p), and muscle cross-sectional area (mCSA). Group differences were assessed by two-way analysis of covariance, with race (black vs. white) and sex (female vs. male) as independent variables. Covariates included predicted years from peak height velocity (maturity offset), tibial length and mCSA. There were no interactions between race and sex (all $P=0.50-0.98$) or main effect for sex (all $P=0.08-0.45$). Blacks had 15.7% more Ct.BMC, and 10.8-11.8% larger Tt.Ar and Ct.Ar than whites (all $P<0.001$). The greater enhancement of Ct.BMC relative to Ct.Ar resulted in blacks having 3.6% greater Ct.vBMD than whites ($P<0.001$). The combination of increased cortical bone mass, size and density in blacks contributed to enhanced estimated bone strength, with I_{MAX} , I_{MIN} and SSI_p being 20.0%, 34.5% and 25.2% greater in blacks than whites, respectively (all $P<0.001$). These data indicate that early pubertal black children have enhanced bone mass, size and estimated bone strength at the tibial diaphysis versus whites, independent of tibial length and mCSA. They suggest bone structural differences may contribute to observed racial differences in fracture rates and that structural divergence between races develops during childhood.

Disclosures: Stuart Warden, Eli Lilly, 5

SU0026

Sex Specific Effects of Physical Activity on Proximal Femur BMD in 8-9 Years Children. Graça Cardadeiro¹, Fatima Baptista^{*1}, Rui Ornelas², Luís B. Sardinha¹. ¹Exercise & Health Laboratory, Faculty of Human Movement, TU Lisbon, Portugal, ²Madeira University, Portugal

Mechanical loading by impact or via muscle forces is critical for skeletal growth and development in children and physical activity interventions are one way to target this important health-related outcome. The increase in femoral bone mass and strength in pre and pubertal children has been reported as a response to physical activity intervention programs, with the majority of studies showing that femoral neck sensitivity (as a surrogate of proximal femur sensitivity) to mechanical loading is higher in boys than in girls. Purpose: To investigate sex specific associations between everyday physical activity and mineralization of three regions of proximal femur in pre and early pubertal boys and girls aged 8-9 years. Methods: BMD in femoral neck, trochanter and intertrochanter regions, and lean mass of whole body were assessed using dual-energy x-ray absorptiometry in 161 girls (age: 9.70.3 yrs; body mass: 34.29.0 kg; body height: 137.20.1 cm) and 164 boys (age: 9.70.3 yrs; body mass: 34.17.1 kg; body height: 137.00.1 cm). Physical activity was assessed by accelerometry. Multiple linear regression analyses were used to investigate the ability of physical activity to explain the variance in BMD in the three regions of the proximal femur, after adjustment for body height, total lean mass, and pubertal status. Results: Physical activity explained 2-6% ($p<0.05$) in BMD variance in the three regions in both girls and boys, with differences between boys and girls for variance in bone regions BMD. An additional 10 minutes per day of vigorous physical activity (the best single predictor of BMD within physical activity variables) was associated with a ~2% higher trochanteric and intertrochanteric BMD in girls, while in boys it was related to a ~1% higher femoral neck, trochanter, and intertrochanteric BMD ($p<0.05$). Conclusions: Proximal femur response to weight-bearing physical activity may differ between boys and girls aged 8-9 years old, particularly in the femoral neck. Boys showed a more homogeneous response among the three regions of proximal femur, while a significant greater bone density in the trochanteric and intertrochanteric

regions was observed in the more active girls, compared with less active female participants.

Funded by Portuguese Science and Technology Foundation (SFRH/BD/38671/2007 and PTDC/DES/115607/2009).

Disclosures: Fatima Baptista, None.

SU0027

Vitamin D Insufficiency and Bone Mineral Status in Newcomer Immigrant and Refugee Children to Canada, an Emerging Public Health Problem. Hassanali Vatanparast^{*1}, Christine Nisbet². ¹University of Saskatchewan, Canada, ²University of Saskatchewan, Canada

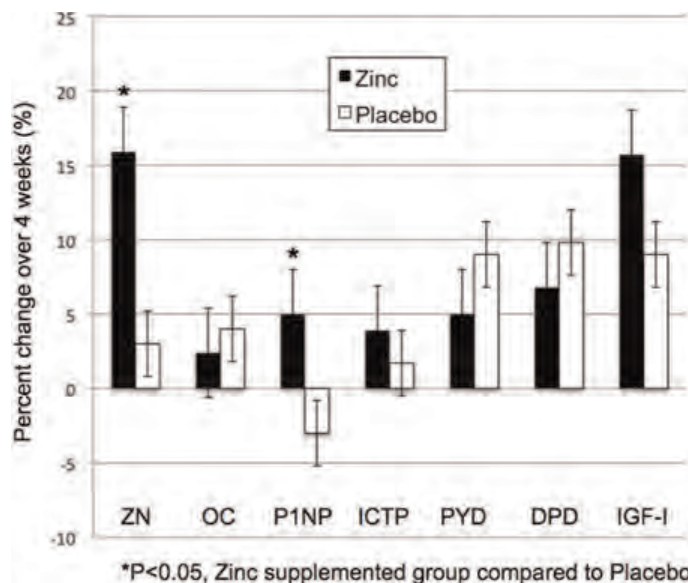
Nutrition and physical activity are two important factors influencing bone mineral mass accumulation during childhood and adolescence. Newcomer immigrant/refugee children are at a high risk of poor nutritional status and low level of physical activity. Vitamin D deficiency, in particular, and its related diseases is a major concern due to minimal sun exposure and limited dietary sources. No study is available in Canada to evaluate the relationship between nutrition, physical activity and bone mineral status on newcomer immigrant and refugee children. Objective: to evaluate the association between nutrition, physical activity and bone mineral status in immigrant and refugee newcomer children to Canada. Methods: In a cross-sectional design, we recruited 72 immigrant (n=33) and refugee (n=39) children aged 7-11 years who had been living in Saskatchewan, Canada for no more than five years. Measurements included serum 25OHD using LC-MS/MS method, total body bone mineral content (TBBMC) using DXA, dietary assessment using three 24-h recalls, physical activity questionnaire and food security using USDA questionnaire. Results: The mean age of children was 8.91.6 y. The rate of food insecurity was 38.5% and 57.1% in immigrants and refugees respectively. Most children (87.5%) were meeting the recommended level of physical activity (≥ 60 minutes/day). Fourteen percent of children had the TBBMC lower than the predicted values for their age, sex and ethnicity. We found 29% of participants were vitamin D deficient and another 44% had inadequate levels of serum vitamin D for bone health. Prevalence of inadequacy in vitamin D intake was 89%. In the regression model, after controlling for possible confounders including immigration status, food security, age, sex, ethnicity, physical activity level, total caloric intake, calcium intake, magnesium intake, phosphorus intake, sodium intake, and caffeine intake; height and serum vitamin D status were found to be determinants of TBBMC ($R^2=0.82$, $p<0.05$). Children who were taller and had greater serum vitamin D also had greater TBBMC with $\beta=0.95$ for height and $\beta=0.13$ for serum vitamin D. A considerably high rate of vitamin D deficiency and insufficiency in newcomer immigrant and refugee children and its association with bone mineral mass during this important stage of life requires immediate preventive interventions to minimize the risk of serious vitamin D related diseases.

Disclosures: Hassanali Vatanparast, None.

SU0028

Zinc Supplementation Improves Bone Formation in Early Pubertal Females. Richard Lewis^{*1}, Norman Pollock², Emma Laing¹, Paul Bernard³, Arthur Grider¹, Sue Shapses⁴, Kehong Ding², Carlos Isaacs³. ¹The University of Georgia, USA, ²Georgia Health Sciences University, USA, ³Medical College of Georgia, USA, ⁴Rutgers University, USA

Both animal and human studies show that beyond correcting skeletal and growth impairments under deficiency conditions, supplementation with zinc may have a bone health-promoting role. The purpose of this study was to determine if zinc supplementation (23 mg/d zinc sulfate) over 4 weeks altered serum zinc, markers of bone turnover [bone formation: osteocalcin (OC), procollagen type 1 amino propeptide (PINP); bone resorption: carboxyterminal telopeptide region of type 1 collagen (ICTP), pyridinoline (PYR), deoxypyridinoline (DPD)], and insulin-like growth factor-I (IGF-I) in early pubertal white and black females (9 to 11 years of age). A secondary aim was to determine if there was a race x treatment interaction among these variables. Early pubertal females of similar maturational status were randomized into a zinc supplementation group (ZN; n=75) or placebo group (CON; n=72), in a double-blind, placebo-controlled trial. Serum zinc was determined using atomic absorption spectrophotometry. OC, PINP and ICTP were assessed using RIA. PYR and DPD were determined using HPLC and IGF-I was determined by ELISA. Over 4 weeks, plasma zinc and PINP increased significantly more in the ZN vs CON group ($P<0.05$). There were no group differences in the other biomarkers (all $P>0.05$, see figure). No differences were observed by race. Findings from this study provide preliminary evidence that zinc may be a viable nutritional strategy for improving bone strength in young females. A long-term clinical bone trial is warranted to more definitively assess the potential for supplemental zinc to improve bone strength and to explore potential mechanisms involved.



Four-Week Changes in Biochemical Markers

Disclosures: Richard Lewis, None.

SU0029

Bioavailability of Vitamin D in Adolescents with Anorexia Nervosa. Amy DiVasta^{*1}, Michael Holick², Catherine Gordon³. ¹Children's Hospital Boston, USA, ²Boston University School of Medicine, USA, ³Children's Hospital Boston & Harvard Medical School, USA

Purpose: Young women with anorexia nervosa (AN) have a normal vitamin D status. Whether the bioavailability of vitamin D is different in states of malnutrition is not known. We sought to examine whether the serum response to oral vitamin D₂ is altered in young women with AN compared to normal-weight teens.

Methods: Twelve adolescents with AN (age 19.62.0 yr, BMI 16.51.4 kg/m² and 12 healthy controls matched by age and skin pigmentation (20.02.4 yr, 22.7 1.0 kg/m²) received a single oral capsule of vitamin D₂ 50,000 IU. Serum samples were collected pre-ingestion, 6h, 24h, and 1, 2, 3, and 4 wk following ingestion. Samples were analyzed for D₂, D₃, 25(OH)D, and 1,25(OH)₂D. Body composition was measured at baseline by dual-energy X-ray absorptiometry (DXA). The course of serum vitamin D concentrations over time was compared by repeated-measures ANOVA.

Results: The AN group was severely malnourished (77.26.3% median body weight), while controls were normal-weighted (106.26.2%). From a common baseline D₂ level (1.51.6 nmol/L, $p=0.34$) the groups diverged (time x group interaction $p=0.04$), reaching a peak of 7034 nmol/L at 6h in controls compared to 4328 nmol/L in AN subjects ($p=0.008$). The D₂ trajectories converged at 24 hr (57 nmol/L, $p=0.98$) and returned to near-baseline at 1 wk (3.11.6 nmol/L, $p=0.34$). D₃ was 3-4-fold higher in AN subjects at baseline (12.19.6 vs 3.12.3 nmol/L, $p<0.001$) and remained so throughout the study, despite a significant rise among controls at 1 wk (+1.41.7 nmol/L, $p=0.01$). 25(OH)D followed a common trajectory in AN and control subjects over the 4-wk study (time x group interaction $p=0.15$), rising from 3911 nmol/L pre-ingestion to a peak level of 4510 nmol/L at 24 hr and returning to baseline by wk 3 ($p=0.36$). 1,25(OH)₂D was lower in AN subjects at baseline (316 vs 548 pmol/L, $p=0.006$) and did not change at 4 wk in either group ($p>0.40$). Correlating the vitamin D levels with fat measures (BMI, body fat) in place of the AN-control comparison produced similar findings.

Conclusions: Despite severe malnutrition, young women with AN had a similar response to a single dose of oral ergocalciferol compared to healthy-weighted control subjects. These findings have implications for defining the baseline vitamin D requirements in AN. Based on our data, it appears that vitamin D dosing for patients suffering from malnutrition, irrespective of etiology, may not differ from that for normal-weighted adolescents.

Disclosures: Amy DiVasta, None.

SU0030

Leptin-directed Osteocalcin Regulation is Influenced by Health and Gender in Adolescents with Type 1 Diabetes. Shannon Haley¹, Mary Murray², Laurie Moyer-Mileur^{*2}, Kenny Helmandollar², Hillarie Slater², Kristine Jordan². ¹University of Utah School of Medicine, USA, ²University of Utah, USA

Background: Low bone density in adolescents with Type 1 diabetes (T1DM) has been established by our group and others. Leptin, produced by adipocytes, regulates carboxylation of osteocalcin (OC), a bone derived hormone that promotes bone formation. Undercarboxylated OC (ucOC) has low bone affinity, is the predominant

form in circulation with a positive effect on insulin sensitivity. Both serum leptin and OC levels are decreased in young adults with T1DM. The effect of T1DM on leptin-driven uOC, metabolic control, and bone mass is unclear. We tested relationships between serum leptin, OC, uOC, fasting glucose and insulin, body fat, and bone mass in adolescents with T1DM.

Methods: Adolescents age 12-15y with T1DM (n=14; 6M/8F) were compared to matched controls (CTL, n=12; 5M/7F). Subjects were admitted overnight and given a standardized diet. Height (cm), weight (g) as well as whole body minus head fat (%), bone area (BA, cm²), bone mineral content (BMC, g), and areal bone density (aBMD, g/cm²) by DXA (Hologic 4500A) were measured. Fasting blood samples were obtained with leptin, OC, and uOC determined by ELISA. Serum uOC was corrected for total serum OC. ANCOVA tested differences between groups controlling for gender and pubertal maturation; Pearson's R tested the relationships between serum, fat mass, and bone parameters (p<0.10).

Results: Age, maturation by Tanner stage, and body size were similar between groups and genders. Body fat (%) was lowest in T1DM males (group x gender interaction, p<0.10). T1DM subjects had higher serum leptin (16,915.7ng/ml T1DM vs. 11,510.0ng/ml CTL; p<0.05). In males, serum OC was higher in T1DM (60,413.2ng/ml T1DM vs. 42,320.2ng/ml CTL, p<0.10). Serum uOC values were greatest in CTL males compared T1DM males or CTL and T1DM females (p<0.10). Serum leptin was positively related to body fat% (R=0.60, p<0.01). In contrast serum leptin was negatively related to serum uOC (R=-0.46, p<0.10) as was serum OC to whole body BA and BMC (R=-0.33, p=0.10). Serum OC was positively related to fasting glucose (R=0.42, p<0.05).

Conclusions: In contrast to young adults, serum leptin and OC levels were elevated in adolescents with T1DM. Surprisingly, serum uOC did not reflect higher serum leptin. We speculate that the lower uOC in the presence of greater serum leptin may be due to health- and gender-divergent responses to leptin-driven osteocalcin regulation in adolescents with Type 1 diabetes.

Disclosures: Laurie Moyer-Mileur, None.

SU0031

The Interaction of Maternal Obesity and Neonatal Vitamin D Deficiency on Neonatal Anthropometrics. Jami Josefson^{*1}, Heather Price², Alfred Rademaker¹, Dinah Zeiss¹, Craig Langman². ¹Northwestern University, USA, ²Children's Memorial Hospital, USA

Maternal vitamin D deficiency (D-) is associated with low birth weight, while maternal obesity is associated with high birth weight. One study demonstrated that with increasing maternal obesity, mothers and newborns were more likely to be D-. In this study, we asked the question as to whether obese versus non-obese women, both without D-, would have newborns with similar vitamin D levels and differences in birth weight and anthropometry predicted by obesity alone. Obese [OB, pre-pregnancy BMI \geq 30 kg/m²] and healthy weight [HW, 18-25 kg/m²] pregnant women with a normal diabetes screening test were studied. All women had singleton, term pregnancies and were not hypertensive. Maternal fasting blood was collected at 36-38 weeks gestation and cord blood was collected at birth. Neonatal measurements, including length and body composition analysis by air displacement plethysmography to provide weight, fat mass, and % body fat were performed within 48 hours of birth. 23 OB and 38 HW mothers and their newborns completed the study. Maternal total 25(OH)D levels did not differ between the OB and HW groups (50 (mean) 23 (sd) vs. 46 17 ng/mL). The OB women had higher levels of fasting glucose (86.7 8.6 vs. 80.9 6.5 mg/dL, p=0.03), C-peptide (4.4 2.0 vs. 2.4 1.0 ng/mL, p<0.01), and leptin (54.1 14.5 vs. 25.0 12.7 ng/mL, p<0.001) compared to the HW women. Cord blood 25(OH)D levels were lower in neonates of OB women compared to HW women (20.8 10.3 vs. 27.5 10.0 ng/mL, p=0.02), and cord blood C-peptide levels were higher in OB newborns (1.2 0.7 vs. 0.9 0.3 ng/mL, p=0.04). In HW newborns, cord blood 25(OH)D levels were positively correlated to neonatal anthropometric measures of weight (r=0.45, p<0.01), length (r=0.43, p<0.01), fat mass (r=0.52, p<0.01), and % fat mass (r=0.46, p<0.01) but these correlations were not found in OB newborns. No differences were seen in any of the anthropometric measures of the OB vs. HW newborns or in their cord blood glucose, leptin, adiponectin or osteocalcin levels. Herein, we demonstrate that obese women without D- have neonates with lower cord blood 25(OH)D levels but not higher birth weight or other anthropometric evidence of obesity when compared to HW newborns. We suggest that maternal obesity may reduce the impact of vitamin D deficiency on low birth weight. The mechanism of vitamin D metabolism whereby OB offspring have lower vitamin D remains under investigation.

Disclosures: Jami Josefson, None.

SU0032

Hypophosphatasia (HPP): Iliac Crest Histomorphometry of Affected Children Given Subcutaneous Enzyme Replacement Therapy, ENB-0040. Michael P. Whyte^{*1}, Katherine L. Madson², Amy L. Reeves², Deborah Wenkert², Cheryl R. Greenberg³, Nerissa Kreher⁴, Hal Landy⁴, Frank Rauch⁵, Francis Glorieux⁶. ¹Shriners Hospital for Children & Washington University School of Medicine, St. Louis, USA, ²Shriners Hospital for Children, St. Louis, USA, ³University of Manitoba, Canada, ⁴Enobia Pharma, Inc, USA, ⁵Shriners Hospital for Children, St. Louis, Canada, ⁶Shriners Hospital for Children & McGill University, Canada

Background:

HPP is the heritable metabolic bone disease caused by inactivating mutation(s) in the gene that encodes the tissue-nonspecific isoenzyme of alkaline phosphatase (TNSALP). Impaired skeletal mineralization develops from extracellular accumulation of inorganic pyrophosphate (PPi), an inhibitor of hydroxyapatite crystal growth. ENB-0040 is a bone-targeted, recombinant TNSALP protein, delivered subcutaneously (SC), that has been reported in clinical trials to improve radiographic and functional outcomes in infants and children with HPP (Greenberg et al, ASHG 2010, abs. 13 & Whyte et al, ASBMR 2010, abs. 1016)

Objective:

Evaluate by iliac crest histomorphometry the effects of 6 months of treatment (Rx) with ENB-0040 on the skeletal findings of HPP in children.

Methods:

A 6-month, multi-center, open-label, historical control study of 13 children receiving ENB-0040 (2 or 3 mg/kg SC 3X weekly). Twelve of the 13 patients completed the study (one withdrew for elective scoliosis surgery). Iliac crest specimens were obtained, after tetracycline labeling, using a 5 mm diameter trephine at baseline and study completion. Specimens were analyzed "blindly" for osteoid indices, structural parameters, and dynamic parameters of bone formation. Wilcoxon testing was used for statistical comparisons.

Results:

Osteoid indices (thickness, surface per bone surface, volume per bone volume) were markedly elevated at baseline. In general, osteoid was "patchy" and not distributed evenly as commonly seen in other forms of rickets or osteomalacia. After Rx, median osteoid thickness had decreased significantly from 13.8 to 7.7 μ M (p=0.02), and osteoid surface per bone surface had decreased by 55% (p=0.04). Mineralization lag time was markedly elevated at baseline, and the median value almost halved [82.3 (25-75% 34.3, 126.0) vs. 44.0 (35.1, 58.0)] after Rx, but the change was not statistically significant (p=0.26), likely from the high variability of individual results. Structural parameters (bone volume per tissue volume, trabecular number, trabecular thickness) were similar to age-specific averages at baseline, and did not change significantly with Rx.

Conclusions:

Children with HPP manifest "patchy" accumulation of osteoid that seems different from other forms of rickets or osteomalacia. This osteoidosis improves after 6 months of Rx with ENB-0040. This tissue benefit parallels the radiographic and functional improvements reported in infants and children with HPP receiving ENB-0040.

Disclosures: Michael P. Whyte, Enobia Pharma, Inc, 2; Enobia Pharma, Inc, 5
This study received funding from: Enobia Pharma, Inc

SU0033

Accuracy of Histomorphometric Parameters to Quantify Trabecular Architecture: Comparison of 2D Thin Sections with 3D μ CT Data. Oleg Musevko¹, Robert Percy Marshall², Jing Lu¹, Georg Schett³, Michael Amling², Klaus Engelke^{*1}. ¹University of Erlangen, Germany, ²University Medical Center Hamburg-Eppendorf, Germany, ³Friedrich-Alexander University Medical School, France

Histomorphometry using 2D thin stained sections is the standard method to quantify trabecular bone architecture. However, the preparation is tedious and a single or even a few number of sections may not be representative for a 3D volume. Moreover the calculation of the structural parameters requires the assumption of a structural model such as the plate or rod model. 3D μ CT has increasingly replaced 2D stained sections as a full volume can be assessed. However, due to the lower spatial resolution compared to thin sections partial volume artifacts results that may impair the accuracy of the histomorphometric parameters.

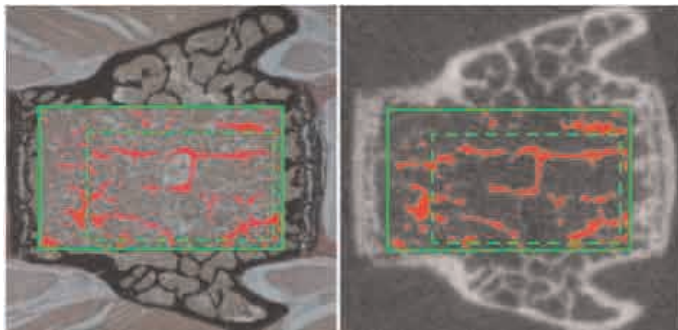
In this study 3D μ CT datasets (Scanco μ CT40, 15 μ m isotropic voxel size) were obtained from 7 vertebrae from 4 wild type mice. Afterwards two stained sections (3 μ m; von Kossa staining) were prepared for each vertebra. In order to directly compare the histomorphometric results the 2D sections were registered into the 3D μ CT volume using an affine transformation. As some stretching occurred during the preparation of the sections a simple rigid transformation gave unsatisfactory results. In the 2D sections the trabeculae were segmented using a global threshold whereas in the 3D μ CT datasets a local adaptive threshold was used in order to account for some of the partial volume artifacts. In addition in each μ CT dataset 6 slices neighboring the one corresponding exactly to the 2D section were analyzed. Also the size of the analysis ROI was varied (s. Fig).

The results shown in the table as means SD for the 7 vertebrae confirm that there is an accuracy error in the determination of histomorphometric parameters using

μ CT, in particular for Tb.Th. However, the variation from slice to slice that is not captured in 2D stained sections and even more so the choice of the analysis ROI in the 2D sections is comparable or even larger than the accuracy error. In this study a high resolution μ CT was used and the results may not be applicable at lower μ CT resolutions. Also the accuracy errors increased when global thresholds were used for the segmentation of the trabeculae in the μ CT datasets.

BV/TV	Tb.Th	Tb.Sp	Tb.N
%difference between 2D section and corresponding 2D slice in the μ CT dataset			
10.07 \pm 9.98	14.37 \pm 9.0	4.74 \pm 4.24	4.21 \pm 3.17
%difference among 7 slices of the μ CT dataset			
9.53 \pm 3.74	6.46 \pm 3.54	8.33 \pm 2.34	8.48 \pm 2.74
%difference between 2 analysis ROIs applied to the 2D sections			
24.28 \pm 15.76	10.42 \pm 5.63	16.46 \pm 12.04	24.22 \pm 22.88

Table



2D section and corresponding slice in microCT dataset

Disclosures: Klaus Engelke, None.

SU0034

Age and Gender Differences in Tibia Morphology and Estimated Bone Strength in Caucasians Using Serial pQCT Scans. Vanessa Sherk*, Debra Bembien. University of Oklahoma, USA

Variability in pQCT measurement sites limits direct result comparisons between studies. Further, it is unclear what estimates or surrogates of bone strength are most indicative of changes in fracture resistance due to aging, disease, or interventions. The purpose of this investigation was to compare pQCT-derived bone variables at multiple sites throughout the tibia in healthy men and women. Methods: Self-identifying Caucasian men (n=49) and women (n=56) ages 20-59 years had their non-dominant tibias assessed with pQCT (XCT 3000) at every 10% of the limb length from 5%-85% from distal to proximal. Participants were grouped by decade and by gender. Volumetric BMD, BMC, and area of the total, cortical and trabecular bone were determined. Also, periosteal (PeriC) and endosteal (EndoC) circumferences, cortical thickness (CTh), bone strength index (BSI), strength strain index (SSI), Imax, Imin, mass ratios, and strength to mass ratios were quantified. Results: Bone morphology and strength characteristics varied along the tibia in a nonlinear fashion. There were significant ($p < 0.01$) site effects for BMC, vBMD, area, strength (SSI, Imin, Imax, SSI:Tot.BMC ratio), PeriC and EndoC. Total vBMD peaked at the 35%, while cortical BMC peaked at 55% with minimums at 5% and 85%. Total BMC, SSI, SSI:Tot.BMC ratio, Imax all peaked at the 85% site. Gender differences (20-27.3%) in Tot. BMC were explained largely by differences in Tot.Area (19.3-23.7%), due to differences in Cort.BMC and area (20.3-25.3%) ($p < 0.01$). Gender differences ($p < 0.01$) in Imax, SSI, and SSI:Tot.BMC ratio were smallest at the 15% sites and increased through the diaphysis. Women had significantly ($p < 0.05$) greater Cort. vBMD than men. Men had significantly ($p < 0.01$) greater Tot.BMC ratios at 5%:35% and 5%:65%. Site*gender interaction effects were significant ($p < 0.05$) for area, BMC, circumference, and strength variables. CTh and total vBMD were lowest ($p < 0.05$) in 50-59 yr group, and many trends ($p < 0.10$) existed for BMC variables. EndoC was highest in the 50-59 yr group. Site*age interactions existed for Cort.vBMD, total and trabecular area, Tot.BMC, SSI, Imax, PeriC and EndoC. BMC ratios for 5:35% and 5:65% were highest ($p < 0.05$) in the 20-29 yr group. Conclusion: Gender differences were driven by bone size, whereas age differences were mostly due to density. The magnitude of age and gender differences varied by measurement site. Standardization of measurement sites is recommended.

Disclosures: Vanessa Sherk, None.

SU0035

Anatomically Confined Alterations in Collagen Cross-Links Coupled with Structural Changes Influence the Mechanical Properties of Whole Bone Independently of the Amount and Quality of Bone Mineral. Eleftherios Paschalis*¹, Dimitris Tatakis², Simon Robins³, Peter Fratzl⁴, Inderchad Manjubala⁴, Ruth Zoehrer¹, Sonja Gamsjaeger¹, Birgit Buchinger¹, Andreas Roschger¹, Roger Phipps⁵, Enrico Dall'Ara⁶, Peter Varga⁷, Philippe Zysset⁶, Klaus Klaushofer¹, Paul Roschger¹. ¹Ludwig Boltzmann Institute of Osteology at the Hanusch Hospital of WGKK & AUVA Trauma Centre Meidling, 1st Medical Department, Hanusch Hospital, Austria, ²Division of Periodontology, The Ohio State University, USA, ³Rowett Institute, United Kingdom, ⁴Max Planck Institute of Colloids & Interfaces, Department of Biomaterials, Research Campus Golm, Germany, ⁵Husson University School of Pharmacy, USA, ⁶Vienna University of Technology, Austria, ⁷Institut für Leichtbau und Struktur-Biomechanik, TU, Austria

In the present study a rat animal model of lathyrisms was employed to decipher whether anatomically confined alterations in collagen cross-links coupled with structural changes influence the mechanical properties of whole bone independently of amount and quality of mineral. Animal experiments were performed under an Ohio State University ethics committee approved protocol. Sixty-four female (47 day old) rats of equivalent weights were divided into four groups (16 per group): 2 control and 2 treatment groups. Controls were fed a semi-synthetic diet containing 0.6% calcium and 0.6% phosphorus for 2 or 4 weeks and β -APN treated animals were fed the same diet supplemented with β -aminopropionitrile (0.1% dry weight) for 2 or 4 weeks. At the end of this period the rats in the two groups were sacrificed, and L3-L6 vertebra were collected. Collagen cross-links were determined by both biochemical and spectroscopic Fourier transform infrared imaging (FTIRI) analyses. Mineral content and distribution was determined by quantitative backscattered imaging (qBEI), and mineral maturity / crystallinity by FTIRI techniques. Micro-CT was used to describe the architectural properties. Data were analyzed by two-way ANOVA with Bonferroni post-hoc tests. The results of the present study indicate a relationship between bone strength (determined by compression tests) and both bone structural properties (by micro-CT) and the amount and type of collagen cross-links (both by biochemical and FTIRI analyses), independently of the amount and quality of mineral (by qBEI and FTIRI). Microspectroscopic (FTIRI) analysis and nanoindentation mechanical tests reveal that the collagen cross-links alterations are confined in areas of primary mineralized bone exclusively. Interestingly, the collagen cross-link ratio in these areas had the same profile as seen in equivalent anatomical areas (in terms of tissue age and mineralization extent) in human iliac crest biopsies of both untreated high- and low- turnover osteoporotic patients, as well as of patients with fragility fractures unaccounted for by the classical clinical bone strength indicators such as bone mineral density and / biomarkers. Results of the present study suggest a considerable role of collagen cross-links in the determination of bone structural properties and strength, even when these changes are anatomically confined.

Disclosures: Eleftherios Paschalis, None.

SU0036

Association Between Prevalent Vertebral Fracture and Lumbar Vertebral Bone Density, Morphology, Geometry, and Compressive Strength in Men and Women: the Framingham QCT Study. Yoo Mee Kim*¹, Serkalem Demissie², Qiong Louie-Gao², Elizabeth Samelson³, Douglas Kiel⁴, Mary Bouxsein⁵. ¹Division of Endocrinology, MizMedi Hospital, South Korea, ²Department of Biostatistics, Boston University School of Public Health, USA, ³Hebrew SeniorLife, Harvard Medical School, USA, ⁴Hebrew SeniorLife, USA, ⁵Beth Israel Deaconess Medical Center, USA

There has been renewed interest in 3D bone measurements based on the possibility that these measures may provide additional predictive value for fracture risk. Although skeletal imaging with quantitative computed tomography (QCT) has been available for several decades, there are few studies comparing QCT measures and fracture risk using data from newer volumetric acquisitions. Thus, we aimed to determine the association between QCT-based bone density, morphology, geometry, compressive strength and prevalent vertebral fracture (VFX) in men and women in the Framingham Study. Methods: This cross-sectional study included 1,693 participants, 808 men and 885 women, age ≥ 50 years from the community-based Framingham CT Study. VFXs were identified from lateral CT scout views using Genant's SQ scale. QCT assessments at L3 included: integral (IvBMD), trabecular (TvBMD) and cortical volumetric BMD (CvBMD), cross-sectional area (CSA), and compressive strength (CStr) estimated using beam theory. We determined odds ratios for prevalent VFX, per SD decrease for each independent variable adjusted for age, height and weight. Results: We identified mild VFX in 141 (17%) men and 105 (12%) women, and moderate/severe VFX in 20 (2.5%) men and 16 (1.6%) women. Compared to persons without fracture, vBMD's were 3 to 8% lower in those with mild VFX and 8 to 30% lower in those with moderate/severe VFX ($p < 0.05$). Considering all fractures, decreased IvBMD and CvBMD were significantly associated with VFX in women and men (Table), although decreased TvBMD and CStr were only significant in men. In women, a lower CSA was protective of VFX. In those with moderate and severe

VFX, the associations with VFX were similar in men, although few reached statistical significance due to smaller sample size. However, in women with moderate and severe VFX, associations with low vBMD were stronger — for example, OR for a 1 SD decreased in integral vBMD was 7.18 (95% CI: 3.2-15.9). Conclusion: Decreased vBMD and CStr is associated with prevalent VFX in men and women. In women, but not men, lower CSA was unexpectedly associated with reduced risk of VFX. The association between vBMD of different compartments and risk of VFX differed somewhat in men and women, particularly among those with more severe VFX, suggesting that structural analysis by QCT may improve our understanding of sex-related differences in risk of VFX.

Table. Odds Ratio and 95% confidence intervals per 1 SD decrease of the independent variable for association with prevalent VFX in men and women (adjusted for age, height, and body weight)

	Men (n=151)	Women (n=114)	Men (n=151)	Women (n=114)
Int vBMD	1.50 (1.07-2.13)	1.38 (1.05-1.81)	1.54 (0.98-2.40)	1.59 (1.24-2.04)
Tr vBMD	1.29 (1.01-1.66)	1.04 (0.79-1.38)	1.48 (0.83-2.61)	1.27 (1.00-1.59)
Cv vBMD	1.40 (1.11-1.75)	1.58 (1.11-2.11)	1.56 (1.02-2.37)	1.69 (1.06-2.62)
CSA	1.02 (0.95-1.11)	0.73 (0.60-0.89)	0.81 (0.33-1.34)	0.55 (0.30-0.81)
CStr	1.26 (1.06-1.52)	1.11 (0.88-1.44)	1.27 (0.89-1.81)	1.26 (1.00-1.58)

Table.

Disclosures: Yoo Mee Kim, None.

SU0037

Bone Microarchitecture and Finite Element Analysis Measured with HR-pQCT can Identify Postmenopausal Women with and Without Forearm Fragility Fractures. Kyle Nishiyama^{*1}, Heather Macdonald², David Hanley¹, Steven Boyd¹. ¹University of Calgary, Canada, ²University of British Columbia, Canada

Measures of bone microstructure and estimates of bone strength can be obtained with high-resolution pQCT (HR-pQCT); however, it is unclear if these parameters can be used to identify people with fractures. Our objective was to determine if HR-pQCT measurements and finite element (FE) estimates of bone strength could identify women with and without low-trauma forearm fracture. We studied postmenopausal women in the Calgary cohort of the Canadian Multicentre Osteoporosis Study (CaMos) for whom we had 10-year fracture data and HR-pQCT (XtremeCT, Scanco Medical AG) scans at the completion of the study (Macdonald et al. 2011). During the follow-up, 14 women reported low trauma forearm fractures and were each randomly matched by age (+/- 1 year) to 2 women without fractures (Total N = 42, 72.9 ± 8.3 yrs.). In addition to standard HR-pQCT measurements (Boutroy et al. 2005), we measured cortical thickness, porosity (Bue et al. 2007; Nishiyama et al. 2010), finite element ultimate stress, and the portion of the load carried by the cortical and trabecular regions (MacNeil and Boyd 2007) in all subjects. We used DXA to measure femoral neck (FN) and lumbar spine (LS) areal BMD. Support vector machines (SVM; WEKA, University of Waikato) were used to classify women with and without fracture. A 10-fold cross validation scheme was used to gauge the accuracy and generalizability of the model. The first model was based on all HR-pQCT and FE parameters, the second model used FE measurements alone, and the third model used DXA aBMD (LS and FN) alone. The SVM based on all parameters correctly classified 35 of the 42 subjects in the cross validation (Accuracy = 83.3%, Sensitivity = 73.3%, Specificity = 88.9%, Kappa = 0.63, ROC AUC = 0.84). Using only FE parameters, 34 subjects were correctly classified (Accuracy = 81.0%, Sensitivity = 66.7%, Specificity = 91.7%, Kappa = 0.60, ROC AUC = 0.81). Areal BMD classified all subjects as controls resulting in 28 correct (Accuracy = 66.7%, Sensitivity = 66.7%, Specificity = 0.0%, Kappa = 0.00, ROC AUC = 0.50). Combined HR-pQCT and FE measurements and FE measurements alone had good accuracy identifying women with forearm fractures vs. age-matched controls, while DXA measurements failed to identify subjects. These models may help to predict individuals at risk of forearm fracture in a prospective study and form a basis to identify which parameters from HR-pQCT and FE analysis are critical for assessing fracture risk.

Disclosures: Kyle Nishiyama, None.

SU0038

Bone Tissue Quality Determination Using Novel Reference Point Indentation Technique. Oran Kennedy^{*1}, Matin Lendhe¹, Davis Brimer², Robert Majeska¹, Mitchell Schaffler¹. ¹The City College of New York, USA, ²Active Life Scientific, Inc., USA

Introduction: Deterioration of bone strength with age is associated with increased fracture risk. The toughness of bone, a parameter representing crack growth resistance, is critical in predicting fracture risk. Traditional toughness testing requires large sample size, obviating their use clinically. Recent data suggests a reference point indentation approach provides a novel toughness measurement of whole bones¹. Here, we evaluated the sensitivity of this method to discriminate small known differences in toughness between inbred mouse strains with small genetically based differences in mineralization². To do this we measured a new parameter called

Indentation Distance Increase (IDI) which is related to fracture toughness¹. We also characterized damage patterns beneath the indentation.

Methods: Femora from three genetically distinct mouse strains (A/J, C3H and B6) (n=5/group) were excised for testing. The reference point indenter (Biodent, Active Life Scientific, CA) consists of a two-probe assembly, one of which is fixed at the bone surface while the other moves cyclically to create an indent in the tissue, relative to that surface. Specifically, IDI is the distance between the indenter tip at the last cycle relative to the first. During testing femora were hydrated and clamped while two mid-diaphyseal indents were made at an interval of 500µm. Then samples were fixed and stained in basic fuchsin for damage visualization. Finally samples were embedded in PMMA and polished for SEM and fluorescence microscopy.

Results and Discussion: IDI was highest in A/J followed by C3H and then B6. These data precisely parallel reported bone phenotypes in these strains; A/J being most brittle, followed by C3H and B6 respectively². In all bones, a single or several small cracks formed under the indenter tip, suggesting that it is acting like an "opening-wedge". These cracks initiated in the transverse direction and were immediately blunted by diverting into the longitudinal direction; no differences in length were found. However, other toughening mechanisms were observed: Un-cracked ligament bridging in C3H bones, and extensive delamination in the B6 group, consistent with internal slippage in the mineralized collagen fibrils.

Conclusion: These data suggest that this is a suitable and sensitive method for detecting differences in toughness as a result of small differences in mineralization. This may have important clinical implications in the assessment of fracture risk.

Disclosures: Oran Kennedy, None.

SU0039

Calcium Phosphate Glass/Collagen: Preparation and Properties. Yu Zhang, Ning Jiang^{*}, Racquel LeGeros. New York University College of Dentistry, USA

Introduction: The human bone is a biologic composite consisting of an inorganic (hydroxyapatite crystals) and organic (collagen fibers) phases. Several calcium phosphate/collagen composites are explored as potential bone substitute materials. Objective: This study aimed to explore the potential of a novel Calcium Phosphate Glass/Collagen (CPG/COL) composite as potential biomaterials for bone repair. Methods: The CPG compositions from the system CaO-P2O5-MgO-ZnO were prepared according to methods previously described [LeGeros/Lee 2004]. The CPG/COL composite was prepared by mixing CPG (70%) and COL (30%) in a neutral salt solution maintained at 37°C to form CPG/COL gel and then freeze-dried. The CPG/COL composites were characterized using Scanning Electron Microscopy, Fourier Transform Infrared Spectroscopy and X-ray Diffraction Analysis, and Mechanical Testing. Degradation (dissolution) properties were evaluated in acidic buffer (0.1M KAc, pH 5, 37°C). Results: The results demonstrated that the morphological and structural features (i.e., porosity) and chemical composition of CPG/COL composite were very similar to that of bone. Conclusions: The composites showed physico-chemical properties similar to bone and may be potential materials as scaffolds for bone repair or in tissue engineering for bone regeneration. Future studies include: in vitro cell response and in vivo tissue response to the new composite.

Disclosures: Ning Jiang, None.

SU0040

Cell Based Gene Therapy for Fracture Healing on a Rat Femoral Critical Size Defect. Corinne Sonnet^{*1}, Ronke Olabisi², Kayleigh Sullivan¹, LaShan Simpson², John Hipp¹, ZaWaunyka Lazard¹, Zbigniew Gugala³, Francis Gannon¹, Steve Stice⁴, John Peroni⁴, Michael Weh⁴, Eva Sevik², Michael Heggeness¹, Alan Davis¹, Jennifer West², Elizabeth Olmsted-Davis¹. ¹Baylor College of Medicine, USA, ²Rice University, USA, ³University of Texas Medical Branch, USA, ⁴University of Georgia, USA, ⁵University of Texas, USA

Although bone is thought to possess the capacity to repair or remodel, often this process is ineffective when large amounts of bone must be rapidly regenerated, such as following traumatic injury. Thus orthopedic intervention to induce bone repair using autologous graft materials and osteoinductive agents is often the only option. However, in cases with substantial traumatic injury to hard and soft tissues, enhancing repair while suppressing destructive processes such as infection, are a significant challenge and may lead to loss of limb. We have developed a cell-based molecular therapy which induces rapid bone formation and healing at a targeted location in a femoral traumatic injury model in wild-type rats. In our model, an external fixation device is placed on the length of the femur and a critical size defect is made in the midshaft of the bone. Microencapsulated AdBMP2-transduced cells were injected into the defect at the time of surgery. The cells are microencapsulated within poly(ethylene) glycol diacrylate (PEGDA) hydrogel microspheres. At different time points post surgery, we radiologically evaluated bone formation and either allowed the healing to progress, or isolated the tissues for microCT, biomechanical and histological analysis.

We observed consistent bone formation at the targeted site after injection of the osteoinductive microspheres. The new bone formation was extensive enough to bridge the defect and appeared in many cases to be integrated with the skeletal bone as early as 2 weeks. This integrated bone appeared to be well fused, both radiologically (micro-

CT) and histologically to the adjacent skeletal bone with contiguous cartilage and bone within the defect site. Biomechanical analysis showed that the stiffness and strength of the repair bone were even greater than the contralateral control femur as early as 3 weeks postsurgery. In some cases, the external fixator was removed to confirm that the substantial well mineralized bone, as determined by x-ray, was able to support weight bearing and normal daily activity. In these experiments, the rats were able to ambulate normally, and no apparent additional fractures occurred in the callus region.

Thus, injection of the PEGDA hydrogel containing AdBMP2-transduced cells provides a novel method for inducing rapid repair of traumatic bone injuries, without the need for additional surgical intervention, autologous bone graft or a scaffold.

Disclosures: Corinne Sonnet, None.

SU0041

Changes in Human Vertebral Bone Microstructure from Infancy to Senescence. Jesper Thomsen^{*1}, Annemarie Bruel¹, Ellen Hauge². ¹University of Aarhus, Denmark, ²Aarhus University Hospital, Denmark

Introduction: During aging, not only is bone mass is lost, the bone structure also deteriorates: The volume fraction of bone and the number of connections in the trabecular network decrease. During growth, it is well known that the areal bone mineral density increases, whereas changes in trabecular bone microstructure are less well elucidated. Therefore we aimed at quantifying the changes in vertebral trabecular bone structure from infancy to senescence.

Methods: Age-related changes were investigated using third lumbar vertebral bodies obtained during routine autopsy procedures. The study comprised 119 individuals (51 women, 68 men), aged 0.2–95 years (median 59 years). The individuals had died suddenly from accidents or acute diseases. Individuals with known malignant, renal, or metabolic bone diseases were excluded as were vertebral bodies with known fractures. The vertebral bodies were rotated around a central craniocaudal axis and sawn into quarters. One randomly chosen quarter was embedded in methylmethacrylate and μ CT-scanned with a voxel size of $18.5 \times 18.5 \times 18.5 \mu\text{m}^3$. The reconstructed images were threshold-filtered with a constant value of 436 mgHA/cm and standard microstructure measures were computed. Data were analyzed by linear regression.

Results: Until peak bone mass (0–25 years), the connectivity density (CD) (r^2 ; B; p) (0.42; 12 1/mm; $p < 0.05$) and the structural modeling index (SMI) (0.62; 2.0; $p < 0.001$) decreased markedly. The CD continued to decrease (0.10; 8.0 1/mm³; $p < 0.01$) after peak bone mass, whereas SMI increased (0.37; 0.55; $p < 0.001$). Bone volume fraction (BV/TV) showed a non-significant increase until peak bone mass (0.18; 0.12%; $p = 0.05$), but a significant decrease after (0.47; 0.17%; $p < 0.001$). Trabecular separation (Tb.Sp*) increased before (0.51; 0.63 mm; $p < 0.001$) as well as after (0.35; 0.67 mm; $p < 0.001$) peak bone mass. Trabecular thickness (Tb.Th*) did not change significantly with age.

Conclusions: During growth (0–25 years), the architecture changes dramatically from a dense, highly connected network of rods to a less dense, less well connected network of plates, whereas the change in volume fraction of the trabecular network is less pronounced. During aging (>25 years), the architecture shifts to a less dense, less well connected network of rods accompanied by a loss of trabecular bone volume fraction. Interestingly, the mean trabecular thickness remains constant with throughout life.

Disclosures: Jesper Thomsen, None.

SU0042

Changes of Mechanical Properties of Lumbar Vertebrae in Ovariectomized Rats. ZhiQi Peng*, Jukka P. Rissanen, Jukka Vaaranemi, Heikki Vuorikoski, Jussi Halleen, Jukka Morko. Pharmatest Services Ltd, Finland

Ovariectomy (OVX) induces trabecular bone loss and decreases mechanical properties of femoral neck and lumbar vertebra in rats. However, it is not clear how OVX changes material properties of bone. We have demonstrated earlier that the decreased femoral neck strength in OVX rats was mainly due to elongation of the femoral neck, and OVX did not influence the bending strength in tibial diaphysis, suggesting that OVX did not influence material properties of rat bones. In order to understand the changes of the material properties of the lumbar vertebrae in OVX rats, we studied the compressive strength of the lumbar vertebral body with micro-CT analyzed vertebral samples. Eighteen young (3 months old) and 18 adult (6 months old) Sprague-Dawley rats were either OVX or sham operated. Lumbar vertebrae 5 (L5) of the young rats and lumbar vertebrae 4 (L4) of the adult rats were collected at 8 weeks after the operation and stored at -20°C. The lumbar vertebral bodies were trimmed by cutting from the pedicle of vertebral arch and pocketed by paraffin film for micro-CT scanning. After the micro-CT measurements, 4 mm long vertebral body cylinders were prepared for compressive test. Finally, the pressed vertebral bodies were embedded in plastic for sectioning to get the bone fracture morphometry. The micro-CT measurements and mechanical tests showed that the trabecular bone volume and maximal load of vertebral body were significantly decreased by OVX. The micro-CT analysis demonstrated that the minimum 2D cross-sectional bone area was in the cranial third of the artificially vertebral cylinder in all samples, and the fractures were found in this site or with some other sites. The stress of bone was calculated by maximal load to the minimum bone area. The stress was not affected by OVX. The modulus of bone was not affected either. The maximal load and the minimum bone

area correlated strongly both in L5 of young ($r = 0.807$, $p < 0.001$) and L4 of adult ($r = 0.766$, $p < 0.001$) rats. The study indicated that OVX did not influence the material properties of rat lumbar vertebral bone. Therefore, the changes of the bone mechanical properties in OVX rats were induced by bone structural changes due to the high bone turnover and the trabecular bone loss.

Disclosures: ZhiQi Peng, Pharmatest Services Ltd, 3

SU0043

Differences in Skeletal Micro-architecture in African-American and Caucasian Women. Melissa Putman^{*1}, Elaine Yu², Elizabeth Schindler², Alexander Taylor², Emily Cheston², Mary Boussein³, Robert Neer², Joel Finkelstein². ¹Massachusetts General Hospital Children's Hospital Boston, USA, ²Massachusetts General Hospital, USA, ³Beth Israel Deaconess Medical Center, USA

African-American women have a lower risk of fracture than Caucasian women, and this difference is only partially explained by differences in DXA-measured areal bone mineral density (aBMD). Little is known about possible ethnic differences in skeletal micro-architecture.

Methods: To evaluate potential factors underlying these racial differences in aBMD and fracture rates, we assessed cortical and trabecular volumetric bone mineral density (vBMD), cortical porosity, and measures of cortical and trabecular bone micro-architecture using high-resolution peripheral quantitative CT (HR-pQCT, Scanco Medical AG) in 222 peri- and post-menopausal African-American (n=79) and Caucasian (n=143) women participating in the Study of Women's Health Across the Nation (SWAN) in Boston, MA.

Results: On average, the women were 59.8 years old and experienced their final menstrual period 7.5 years earlier. 10.8% had used oral glucocorticoids, and 9.9% had been treated with anti-resorptive medications. Caucasian women had lower BMI (28.4 vs. 31.4 kg/m², $p < 0.01$), had higher vitamin D levels (27 vs. 17.9 ng/mL, $p < 0.01$), and were more likely to use hormone therapy (29.1 vs. 44.1%, $p = 0.03$). On unadjusted analysis, African-American women had greater cortical area, cortical thickness, and cortical vBMD at both the radius and tibia ($p < 0.05$ for all). These differences remained significant after adjusting for weight. Cortical porosity did not differ consistently between races. Even after multivariate adjustment, cortical area of radius and tibia, and cortical thickness of radius remained significantly higher in African-American women than in Caucasians. Similar results were obtained after excluding women with histories of glucocorticoid use, hormone therapy, or bisphosphonate use. There were no consistent differences in total vBMD, trabecular vBMD, trabecular number or trabecular thickness between groups.

Conclusions: African-American women have higher cortical volumetric density and greater cortical thickness and cortical area than Caucasian women. These differences are present in both weight-bearing and non-weight-bearing bones and persist even after adjustment for weight. Structurally advantageous differences in cortical bone may be a key factor that contributes to the higher BMD and lower fracture risk observed in African-American women.

	Radius		Tibia	
	African-American	Caucasian	African-American	Caucasian
Cort Area (mm ²)	55*	48	119*	104
Cort vBMD (mgHA/cm ³)	857*	835	846*	816
Cort Thickness (mm)	0.794*	0.703	1.143*	1.027
Cort Porosity (%)	2.32	2.66	6.46*	7.55
Trab vBMD (mgHA/cm ³)	159	148	165	162
Trab Number	1.87	1.85	1.88	1.87
Trab Thickness (mm)	0.071*	0.066	0.074	0.072

* $p < 0.05$ comparing African-American and Caucasian women

Table 1

Disclosures: Melissa Putman, None.

SU0044

Effect of a High-Fat Diet on Bone Strain in Adult Rat Femurs. Cheryl Druchok*, Andrew Don-Wauchope, Alison Holloway, Gregory Wohl. McMaster University, Canada

A diet high in fat adversely affects bone mechanical and material properties but it is unknown how these changes affect bone adaptation. Bone adaptation is thought to occur in response to strain-related mechanisms, and strain in the bone is affected by both structural and material properties. The purpose of this study was to compare the mechanical strain during loading in femurs from rats fed a high-fat (HF) or normal control (NC) diet. The Animal Research Ethics Board at McMaster University approved all animal experiments. At weaning (3 weeks of age), male and female Wistar rats were randomly assigned to receive a normal control diet (NC-5% fat; N=8 per gender) or high-fat diet (HF-41% fat; N=8 per gender) until termination (39 weeks of age). Post-mortem, right femurs were harvested and scanned by microCT (GE

Medical Systems, Toronto). Rosette strain gauges were then attached to the posterior aspect of the femoral mid diaphysis. Strains were recorded as femurs were loaded in 3-point bending to physiologic levels in the anterior-posterior direction. Femoral cross-sectional properties (bone area (XSA), moment of inertia) determined from microCT scans, were significantly greater in HF femurs vs. NC for males and females ($p<0.05$) (Fig 1a). At the applied loads there were no significant differences in measured principal longitudinal strains between HF and NC femurs for either the male or female rats (Fig 1b). Elastic modulus was calculated from the load and measured strain data and no difference was found between NC and HF femurs for either gender. Despite the significantly larger cross-sectional area properties between HF and NC male and female femurs, there was no significant difference in measured bone strain. However, when the HF femur strain was predicted using the average NC elastic modulus and the HF femur cross-sectional properties, there was a significant difference between the predicted HF strain (HF-Pred E=NC) and the measured NC strain (NC-Actual) ($p<0.05$) (Fig 1c). These findings suggest that the significantly greater femoral cross-sectional properties are a compensatory mechanism for deficient material properties in the HF bone, and is consistent with the notion that adaptive modeling is targeted to strain or a strain related phenomenon to preserve bone structural integrity.

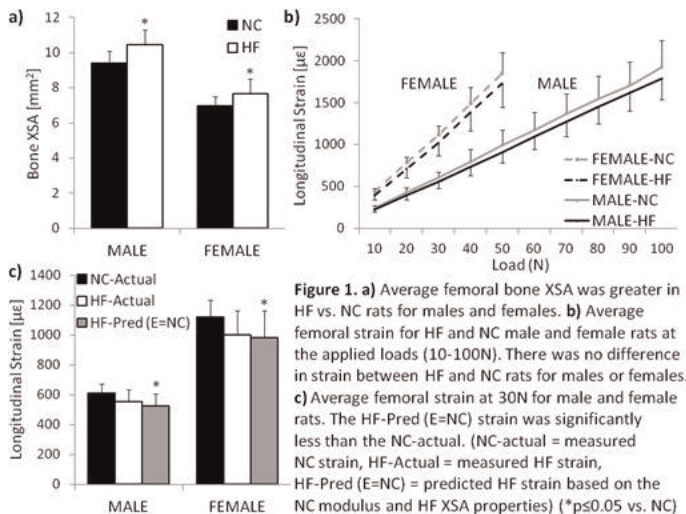


Figure 1

Disclosures: Cheryl Druchok, None.

SU0045

Effects of Cyclical Treatments with PTH and Alendronate on Trabecular Bone Mass and Strength. Sarah Amugongo¹, Wei Yao², Junjing Jia³, Daniel Walsh⁴, Mohammad Shahnazari⁵, Brian Panganiban⁶, Robert Ritchie⁶, Min Guan², Chin-Shang Li⁷, Nancy Lane². ¹University of California, Davis, USA, ²University of California, Davis Medical Center, USA, ³UCDavis, USA, ⁴UC Davis Medical Center, USA, ⁵UCSF VA Medical Center, USA, ⁶University of California Berkeley, USA, ⁷UC Davis, USA

Osteoporosis is currently treated with effective therapies that reduce fracture risk. While, the benefits of the individual agents are well known, the changes that occur following long-term sequential therapies in bone quantity and quality are not well understood. We evaluated these changes in an ovariectomized (OVX) rat model.

Methods: Six-month old female Sprague Dawley rats were either sham operated or OVX. The OVX rats were left untreated for two months to develop osteopenia then treated with subcutaneous injections of either vehicle (saline) 0.1ug/kg, 3x/wk; hPTH (1-34) 20ug/kg/d, 3x/wk; or alendronate (Ale) 0.5ug/kg/2x/wk. We studied three sequential treatment regimens in three 90 day cycles (Veh-Veh-Veh, PTH-Ale-Veh, Ale-PTH-Ale). Serum samples were collected for evaluation of biochemical markers of bone turnover, the 5th lumbar vertebrae were used for μ CT scans (microarchitecture and bone mineral density, BMD) and the 6th lumbar vertebrae were used for compression testing to determine bone strength (maximum (Max) load and stress).

Results: In OVX control group, bone turnover increased accompanied with decreases in BMD and strength from day 0-270 ($p<0.05$). In PTH-Ale-Veh group, PTH treatment day 0-90 increased Max load 81%, Max stress 70%, ($p<0.0001$); BMD 5% and Tb.Th 65% ($p<0.0001$) compared to OVX control. PTH-Ale treatment day 91-180 reduced bone strength parameters by an average of 9% ($p<0.005$) but maintained the increase in BMD and Tb.Th. PTH-Ale-Veh treatment day 181-270 further reduced strength by an average of 30%. However, at the end of treatment period Max load was 36% and BMD was 7% higher ($p<0.0001$) compared to baseline healthy rats. In Ale-PTH-Ale group, Ale treatment day 0-90 reduced DPD/Cr 67% ($p=0.0007$); increased Max load & stress ~40% ($p<0.05$) and did not change BMD compared to OVX control. Ale-PTH treatment day 91-180 increased DPD/Cr 47%, Max load & stress ~100%; BMD 8% and Tb.Th 100% ($p<0.000$). Ale-PTH-Ale treatment day 181-270 maintained the changes induced by PTH for all measured

parameters, which were higher compared to baseline healthy rats (Max load 88%, Max stress 53%, and BMD 8%, Tb.Th 53%).

Summary: Sequential treatment with PTH and Ale or Ale and PTH improve trabecular bone mass and strength. Additional studies are now being done to further evaluate the influence of cyclical therapies on cortical bone quality and quantity.

Disclosures: Sarah Amugongo, None.

SU0046

Evaluation of QCT Cortical Hip Parameters in a Clinical Trial with Rosiglitazone: The Potential for a New Study Endpoint? Colin G. Miller¹, Antonio J. Nino², John P. Bilezikian³, Barbara Kravitz², Gitanjali Paul², Alexander R. Cobitz², Allison R. Northcutt², Lorraine A. Fitzpatrick². ¹Bioclinica, USA, ²GlaxoSmithKline Pharmaceuticals, USA, ³Columbia University, College of Physicians & Surgeons, USA

Quantitative Computerized Tomography (QCT) measurements have been used extensively for ascertaining information about bone quality and density due to the 3D information it provides and its ability to segment out trabecular and cortical bone. This is particularly important for the evaluation of new therapeutic agents that affect bone metabolism and for the understanding of the role that each bone compartment plays in the pathogenesis and prognosis of fracture. However, precise assessments of the cortical bone remain elusive. This study was conducted to explore the effect of edge definition at different thresholds at the femoral neck (FN) in vBMD assessment.

We previously presented the Mechanism-of-Action Study1, assessing the effect of rosiglitazone (RSG) on bone mass and structure of the lumbar spine (LS) and FN DXA for areal Bone Mineral Density (aBMD) and with QCT1 for volumetric BMD (vBMD). We also presented an analysis of the cortical bone vBMD in FN quadrants (FNQ's). Here we present further evaluation of the FNQ's as measured by QCT.

This was a double-blind, randomized study in postmenopausal women with Type 2 Diabetes mellitus; BMD T-score >-2.5 at FN, LS, and total hip (TH). Subjects were randomized to RSG or metformin (MET) for 52 Weeks (Wk) followed by 24Wk of open-label MET. DXA T-scores: FN=-0.960.91; TH=-0.020.97; LS=-0.551.25

Using spiral multi-detector scanners with a standard acquisition technique, a subset of 79 subjects underwent QCT scans of the hip at baseline, after 52Wk of double blind treatment and after 24Wk of treatment with MET. All scans were evaluated centrally and analyzed using Mindways Software Inc. The % change in cortical vBMD and cortical thickness (mm) FNQ's is presented at 3 different thresholds: 350mg/cm³, 375mg/cm³, 400mg/cm³.

The results using different thresholds yielded changes in similar direction in cortical vBMD and cortical thickness at the superior-posterior quadrant. Cortical vBMD at the FN can be precisely segmented from trabecular bone and used to demonstrate therapeutic effect on this bone compartment. FNQ may provide utility as an endpoint in clinical trials for the elucidation of the therapeutic effect of new entities.

Refs

1. ASBMR 2010 poster # SA0035

A. % Change in Hip Cortical vBMD Via QCT at 3 Different Thresholds						
Superior-Posterior FN Quadrant Cortical vBMD (mg/cm ³)	350 mg/cm ³		375 mg/cm ³		400 mg/cm ³	
	Adjusted* % Change Mean(SE)		Adjusted* % Change Mean(SE)		Adjusted* % Change Mean(SE)	
	RSG	MET	RSG	MET	RSG	MET
BL to Wk52	-1.29 (1.18)	-0.10 (1.34)	-1.11 (0.77)	-0.21 (0.87)	-0.95 (0.74)	-0.13 (0.83)
BL to Wk76	-0.33 (1.14)	-0.32 (1.40)	-0.28 (0.70)	-0.81 (0.85)	-0.44 (0.68)	-0.82 (0.83)
Wk52 to Wk76	0.94 (0.98)	-0.01 (1.20)	0.73 (0.75)	-0.58 (0.91)	0.51 (0.73)	-0.64 (0.88)
Open label MET						
*Adjusted for BL, region and prior therapy. None of the treatment differences were statistically significant.						
B. Change in Hip Cortical Thickness Via QCT at 3 Different Thresholds						
Superior-Posterior FN Quadrant Cortical Thickness (mm)	350 mg/cm ³		375 mg/cm ³		400 mg/cm ³	
	Adjusted* Change Mean(SE)		Adjusted* Change Mean(SE)		Adjusted* Change Mean(SE)	
	RSG	MET	RSG	MET	RSG	MET
BL to Wk52	0.09 (0.07)	0.05 (0.08)	-0.10 (0.04)	0.06 (0.05)	-0.10 (0.04)	0.04 (0.05)
BL to Wk76	-0.06 (0.07)	0.02 (0.08)	-0.07 (0.04)	-0.03 (0.05)	-0.05 (0.04)	-0.03 (0.05)
Wk52 to Wk76	0.03 (0.06)	-0.02 (0.07)	0.03 (0.05)	-0.11 (0.08)	0.04 (0.05)	-0.09 (0.05)
Open label MET						
*Adjusted for baseline value, region and prior therapy. † p=0.0021 for treatment comparison (RSG-MET); ‡ p=0.0423 for treatment comparison (RSG-MET); § p=0.0137 for treatment comparison (RSG-MET); ¶ p=0.0459 for treatment comparison (RSG-MET)						

Changes in Hip Cortical vBMD and Hip Cortical Thickness via QCT

Disclosures: Colin G. Miller, GlaxoSmithKline Pharmaceuticals, 5
This study received funding from: GlaxoSmithKline Pharmaceuticals

SU0047

Fibula Osteotomy Model in the Sprague-Dawley Rat: Radiology, Densitometry, Biomechanics and histological characterization. Aurore Varela^{*1}, Luc Chouinard², Yannick Trudel³, CAROLINE RUH³, Iryna Primakova³, Gabrielle Boyd³, Katherine Escott⁴, Susan Y. Smith¹. ¹Charles River Laboratories, Canada, ²Charles River Laboratories, PCS Montreal, Canada, ³Charles River, Canada, ⁴Astrazeneca R&D, United Kingdom

The objective was to characterize the rat fibula osteotomy model using positive (PTH1-34 (PTH) and Alendronate (ALN)) and negative controls (Diclofenac (Dicl)). Male rats (18/group) were assigned to 4 groups and terminated 15 or 29 days after surgery. Five females were assigned as controls to assess gender effects (euthanized on Day 29). Animals received 0.5% methylcellulose and 0.025% Tween 20 orally daily or PTH (60 µg/kg/dose SC, 3/week) or ALN (0.03 mg/kg/dose SC 2/week) or Dicl (5 mg/kg/day orally daily). In addition, 45 females were assigned to control, PTH and ALN groups for histology. Osteotomy was performed at midshaft using a bone cutter. Clinical signs, body weights (BW) and food consumption (FC) were evaluated. X rays were taken after surgery at Weeks 1, 2, 3, 4 and Faxitron images obtained ex vivo. Callus area and BMC were measured by pQCT and Micro-CT ex vivo. Fibulae (osteotomized and intact) were tested in 4 point bending. Histologically, callus was scored for fibrous, cartilaginous or bone tissue relative percentages.

Animals recovered quickly, without signs of pain or effect on BW or FC. At Day 28, a similar radiological healing was observed between controls, PTH and ALN groups. In Dicl group, bone healing was lower with less cortical remodeling and bridging. Callus size measured by pQCT increased on PTH and ALN and decreased on Dicl at Day 14. Callus BMC showed a marked increase on ALN and a marked decrease on Dicl. At Day 28, similar differences between treatment groups were noted. Micro-CT changes in callus size and mineralization were similar. At Day 14, Peak load was increased 41% on ALN and decreased 35% on Dicl. At Day 28, peak load was decreased 25% on Dicl. At Day 28, peak load recovered to 50% relative to contralateral intact side in controls, PTH and ALN groups, and to 40% in Dicl group. No difference was noted between males and females. Histologically, callus was undergoing endochondral ossification with no meaningful effect of PTH. ALN treatment resulted in a slightly higher histologic score compared with controls.

The effects of PTH, ALN and Dicl in this model were consistent with the published data in rat bone healing models as determined by X-rays, densitometry, histology and biomechanics. Significant refinements using this model relative to other models include simple surgery, no immobilization, minimal limb stress, rapid healing and improved animal welfare.

Disclosures: Aurore Varela, None.

SU0048

Fracture Risk Classifiers based on Statistical Shape and Density Modeling of the Proximal Femur. Todd Bredbenner^{*1}, Robert L. Mason¹, Lorena M. Havill², Eric Orwoll³, Daniel P. Nicoletta¹. ¹Southwest Research Institute, USA, ²Texas Biomedical Research Institute, USA, ³Oregon Health & Science University, USA

The performance of fracture risk classifiers based on statistical shape and density modeling (SSDM) methods was investigated using a case-cohort sample of individuals from the Osteoporotic Fractures in Men (MrOS) study. Baseline QCT data of the right femur were obtained for 512 individuals, including 45 who fractured a hip (mean 6.9 year observation, validated by physician review) and a random sample of 472 men.

To date, QCT data were processed for 450 individuals (40 fracture cases and 410 non-cases; all processing was performed while blinded to fracture status) to develop volumetric models describing geometry and spatial BMD distribution of the 450 right proximal femurs. Each 3D model consisted of ~57,000 variables (i.e. spatial location and density at each mesh node located at corresponding anatomic positions for all femurs). Mean fracture and non-case models were created and complex variations in geometry and BMD distribution were demonstrated between the mean models (Figures 1a and 1b).

SSDM, based on Principal Component Analysis, was used to describe variation in 3D bone geometry and BMD distribution within the set of 450 individual femurs by reducing the ~57,000 highly correlated variables for each model to a set of 449 uncorrelated and independent principal components (e.g. composite geometry and BMD traits) without loss of information. Logistic regressions were used to model the relation of baseline hip aBMD (DXA QDR 4500W; Hologic) and principal component weighting factors to the occurrence of hip fracture. A classifier based on stepwise selection of 40 of the 449 weighting factors and adjusted for age and BMI had an area under the receiver operating characteristic (ROC) curve (AUC) of 0.994 and a classifier based on aBMD, age, and BMI had an AUC of 0.838. The SSDM-based classifier correctly identified 25 out of 40 cases compared to 7 out of 40 for the aBMD-based classifier in leave-one-out cross-validation analyses.

Fracture risk predictions based on SSDM outperformed that of aBMD in classification accuracy and AUC values, regardless of age and BMI inclusion. Principal components defined using SSDM identify complex combinations of structural bone traits (e.g. geometric and BMD distribution traits) that appear to indicate fracture risk. Finally, description of bone sample variation using SSDM allows investigation of important structural differences that may allow improved prediction of those at risk for future hip fracture.

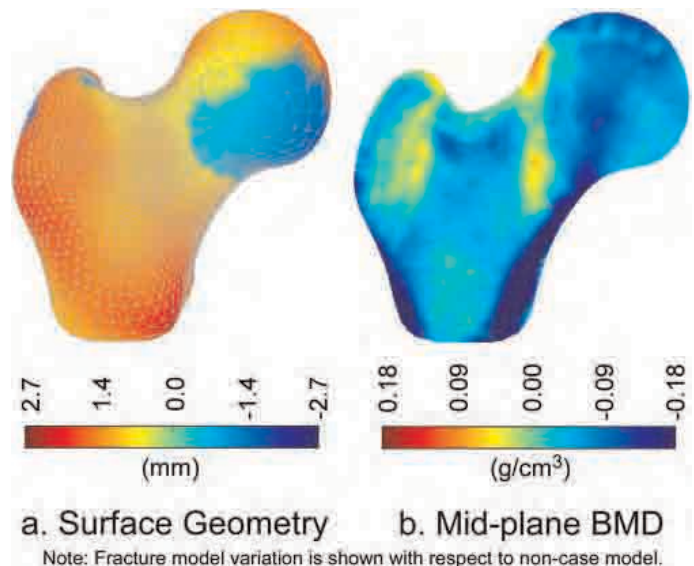


Figure 1: Variation between Mean Fracture Model and Mean Non-case Model

Disclosures: Todd Bredbenner, None.

SU0049

How Tough is Brittle Osteogenesis Imperfecta Mice Bone?. Alessandra Carriero^{*1}, Elizabeth Zimmermann², Bjoern Busse², Sandra J. Shefelbine¹, Robert O. Ritchie². ¹Imperial College London, United Kingdom, ²University of California, Berkeley, USA

Osteogenesis imperfecta (OI) or 'brittle bone disease' is a major birth defect occurring in approximately 1 in every 20,000 human births. It is caused by bone fragility and skeletal deformities due to mutation in the collagen type I genes. As bone fracture is the primary symptom of OI, it is crucial to understand how this mutation affects the initiation and growth of the crack on small length-scales as well as larger length-scales.

A mouse model of the disease, B6C3fe-a/acoli1a2oim/oim (oim), was used to characterize the toughness and crack propagation of oim bones in comparison to control (WT). Fresh frozen femora of contralateral sides of 9 oim and 11 WT mice were dissected and notched on the posterior surface of the mid-diaphysis with a razor blade irrigated with 0.5 µm diamond suspension. To characterize changes in bone toughness, the left femora were tested in three-point bending immersed in HBSS using an EnduraTec Elf 3200 machine. To determine the origin of toughness and define changes in crack path at the microstructural level, 2D crack propagation was observed in an environmental scanning electron microscope (ESEM); the right femora were polished on the periosteal surface, soaked in HBSS for at least 12 hours and tested in three-point bending using a GATAN in situ loading stage within an ESEM. All femora were loaded under displacement control at a rate of 0.001 mm/sec.

Results showed that oim bone exhibited classic brittle behavior with fracture occurring just after the yield point of the tissue. The area of stable crack growth and maximum loads were much smaller in oim bone. The coefficient of toughness k (calculated with the instability method) of oim bone was significantly lower than for WT bone ($p \leq 0.001$). High resolution real-time ESEM images of the crack propagation showed that in both oim and WT crack initiated at the notch root and propagated through the canals. Oim bone did not exhibit any mechanism to resist crack growth, and the crack propagated quickly and transversally. In the WT the crack deflected and resisted propagation with typical toughening mechanisms such as forming uncracked-ligament bridges. These results suggest that the lack of lamellar structure in oim bones may have implications for fracture toughness. We believe that differences between oim bone and WT bone nanostructure behavior may further help to explain the dramatic increase in fracture rates.

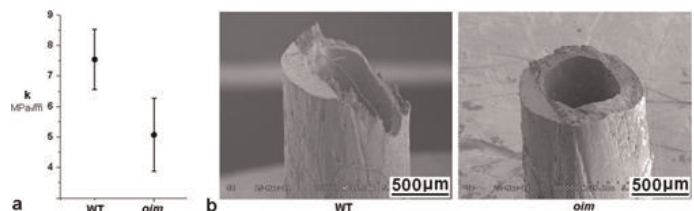


Figure 1.a. Toughness of oim and WT bone; b. Micrographs of the fracture surfaces of oim and WT bone

Disclosures: Alessandra Carriero, None.

SU0050

Image Quality Control for the Detection of Subject Motion in HR-pQCT. Yves Pauchard^{*1}, Anna-Maria Liphardt¹, Eva Szabo², Heather Macdonald³, David Hanley¹, Steven Boyd¹. ¹University of Calgary, Canada, ²Roger Jackson Center for Health & Wellness Research, University of Calgary, Canada, ³University of British Columbia, Canada

Subject motion during high-resolution peripheral quantitative computed tomography (HR-pQCT) causes image artifacts that affect morphological analysis of bone quality.

The aim of our study was to develop an automated quality control method and compare it to manual motion grading in vivo.

An automated technique was developed to measure in-plane translation (XYtrans) and rotation (XYrot) using CT projection data (Pauchard, et. al. IEEE ISBI 2009), as well as longitudinal translation (Ztrans). For validation, a phantom containing sections of distal cadaver radii was attached to a mechanical device and precisely controlled in-plane rotation and longitudinal translation was intentionally added during HR-pQCT data acquisition. Motion measured by the new technique was compared to applied motion, and morphological parameters were calculated to obtain percent error with respect to motion free images. Following validation, subject data was assessed for motion with both the new automated technique and manual grading (0=best, 4=worst) in N=137 image pairs (scan/re-scan) from Canadian Multicentre Osteoporosis Study (CaMos) Calgary cohort (Macdonald, et. al. JBMR, 2011). The coefficient of variation (CV) was calculated based on scan pairs below defined grading levels (see Table 1).

Morphological parameter error graphed as a function of measured motion shows a non-linear increase in parameter error with increased motion (Fig. 1). Paired t-tests showed that XYtrans is independent of bone type and robust to longitudinal motion ($p < 0.05$). CV results (Table 1) demonstrate improved reproducibility when only low motion images were included as determined by manual grading and automatic motion measurement. Consistent with previous data, Tt.BMD was most robust, Ct.Th decreased and Tb.N increased with increased motion.

Out of the three automated motion components considered, XYtrans was the most accurate and robust measure. Both automatic (XYtrans) and manual grading are suitable measures for image quality control in the presence of subject motion in vivo. To obtain reproducibility as reported earlier images should not exceed a manual grading of 2 or an automatic XYtrans grading of 1.2.

The automated technique provides fast and objective image quality control for subject motion in HR-pQCT scanning. It can be performed retrospectively based on original scan data. The technique is well suited for multicentre studies as well as any research where objective quality control is paramount.

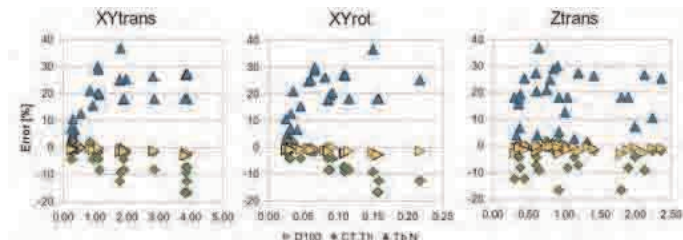


Fig. 1 Morphological error versus automatically detected motion type.

Manual	N	D100	Ct.Th	Tb.N	Automatic	N	D100	Ct.Th	Tb.N
≤ 1	4	1.66	2.85	1.48	≤ 0.5	4	1.17	2.99	5.68
≤ 2	32	0.94	2.29	4.81	≤ 1.2	33	0.91	1.97	5.84
≤ 3	84	1.2	2.93	9.37	≤ 2	80	1.2	2.75	8.11
≤ 4	137	1.63	4.27	10.9	≤ 27	137	1.63	4.27	10.9

Table 1: CV [%] based on manual and automatic (XYtrans) motion indices.

Disclosures: Yves Pauchard, None.

SU0051

Influence of Model Parameters in Large Scale Finite Element Simulations When Evaluating Stress Field in Human Trabecular Bone. Baptiste Depalle^{*1}, Roland Chapurlat², Benyebka Bou-Said³, Helene Follet⁴. ¹INSERM, UMR 1033 ; Universite de Lyon, France, ²E. Herriot Hospital, France, ³Universite de Lyon, CNRS, INSA-Lyon, LaMCoS UMR5259, France, ⁴INSERM, UMR1033 ; Universite De Lyon, Fra

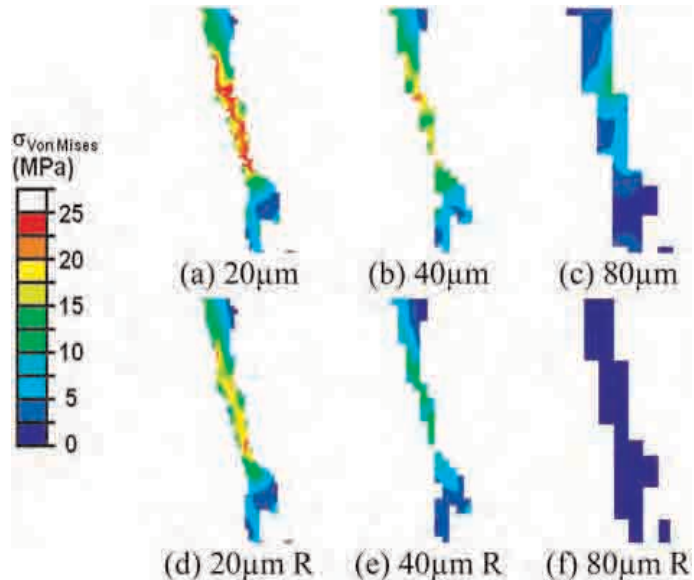
Numerical simulation using finite element models (FEM) has become more and more suitable to estimate the mechanical properties of trabecular bone. The size and kind of elements involved in the models, however, may influence the results. The purpose of this study is to analyze the influence of the element formulation on the evaluation of mechanical stress applied to trabeculae bone during the compression test simulation.

Trabecular bone cores (D=8.2mm, L=15mm) were extracted by necropsy from 18 L2 vertebrae (12 women and 6 men, mean age: 7611, BV/TV=7.51.9%). Samples were micro-CT scanned at 20µm isotropic voxel size. Micro-CT images have been sub-

sampled (20, 40 and 80µm) to create 5.6mm cubic FEM. For each sample, six models of a compression test have been created, two for each voxel size, with and without reduced integration formulation. Bone mechanical properties have been supposed isotropic, homogenous, following a linear elastic behavior law (Young modulus: 8GPa, Poisson ratio: 0.3).

Increasing voxel size led to micro-architecture modifications (loss of connectivity, trabeculae thickening) and changed stress distribution in bone tissue. Even if apparent mechanical properties were similar, stress concentrations were altered. Increasing the voxel size leads to a higher underestimation of stress magnitude and to a smoother distribution. This trend was amplified with reduced integration formulation. With 80µm size reduced elements, as used clinically, few stress variations were detectable (Figure). These observations also depended on trabecular thickness. Less than 2 elements within the trabeculae led to poor stress distribution assessment.

In conclusion, we found that the element size and the integration formulation influence trabecular mechanical behavior evaluation. This statement should be accounted for in clinical measurements.



Von Mises stresses in a trabeculae depending of both voxel size and elements formulation (R=reduced)

Disclosures: Baptiste Depalle, None.

SU0052

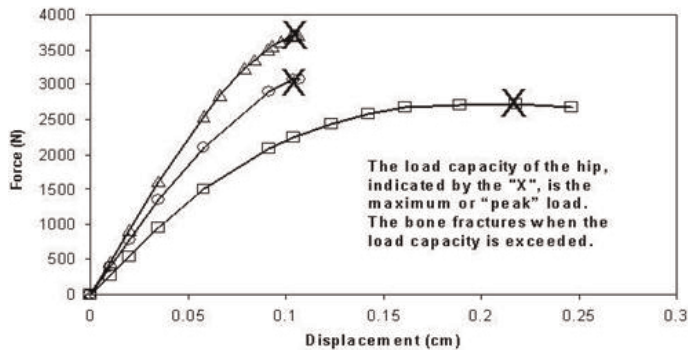
Modeling the Load Capacity of the Proximal Femur. Joyce Keyak^{*1}, Thomas Lang². ¹University of California, USA, ²University of California, San Francisco, USA

Purpose: Although finite element analysis (FEA) is used to evaluate hip strength, FEA strength is usually not the actual load capacity of the hip. Thus, we developed an FEA method to explicitly compute the hip's load capacity.

Methods: Quantitative computed tomography (QCT) scans of 17 matched pairs of cadaveric femora (age 52-92 yr) were obtained (GE 9800, 1.08mm pixels, 3mm slices, 80kVp, 280mAs). One femur from each pair was randomly selected for FEA and mechanical testing to failure under single-limb stance loading; the other was studied under posterolateral fall (Plfall) loading. Nonlinear mechanical properties, including post-failure strain-softening, were derived from QCT BMD. Displacement was applied to the femoral head, the shaft was constrained and, for fall loading, the greater trochanter surface was constrained. As displacement was incrementally applied, the FEA computed the femoral head reaction force, thereby producing a force-displacement curve and explicitly computing the load capacity (peak load) of the hip (Figure). Initially, to optimize material modeling, iterative analyses were used to maximize the correlation coefficient (R) between FEA and measured load capacity. For Plfall, 8 femurs were selected randomly for optimization; the other 9 were used to evaluate R independently. Stance loading was reported previously; results are included here for completeness. Precision in vivo was evaluated for stance, Plfall, lateral fall (Lfall), and posterior fall (Pfall) by performing repeat CT scans with repositioning and FEA of 9 postmenopausal women (age 47-71 yr), and calculating the root-mean-square percentage coefficient of variation (%COV). For comparison, % COV was computed for yield loads defined as the load at which 0.4cc had yielded.

Results: Compared with FEA yield loads, FEA peak loads were more strongly associated with measured peak loads for stance (peak, R=0.91-0.96; yield, R=0.78; published data) but similarly associated with measured peak loads for Pfall (peak, R=0.90; yield, R=0.93; for the 9 femurs). The %COV's were generally smaller for peak loads than for yield loads (%COV peak vs yield: Stance=1.6% vs 13.1%, Plfall=4.9% vs 6.4%, Lfall=5.4% vs 5.0%, Pfall=5.8% vs 9.5%).

Conclusions: The FEA-computed load capacity of the hip provides better reproducibility and equal or better predictions of measured peak loads compared with FEA yield loads. Thus, FEA-computed load capacity may be an improved measure for assessing hip fracture risk.



FEA-computed force versus displacement curves for 3 proximal femora.

Disclosures: Joyce Keyak, None.

SU0053

N-acetyl Cysteine Supplementation Mitigates Deterioration of Bone Microstructure in Mice Fed a High-Fat Diet. Brian Gregoire¹, Jay Cao^{*2}. ¹USDA ARS Grand Forks Human Nutrition Research Center, USA, ²USDA ARS, USA

Studies have demonstrated that obesity induced by high-fat diet increases bone resorption, decreases trabecular bone mass, and reduces bone strength in various animal models. This study investigated whether N-acetyl cysteine, an antioxidant, supplementation ameliorates deterioration of bone microstructure in mice fed a high-fat diet. Forty-eight 6-wk-old male C57BL/6 mice were randomly assigned to four treatment groups (n=12/group) and fed either a low-fat diet or a high-fat diet at libitum with or without N-acetyl cysteine supplementation (1 g/kg diet) for 3 months. Bone microarchitecture of distal femur was evaluated using micro-computed tomography. Body weight was recorded. Serum leptin concentrations were measured. Bone marrow cells were harvested for osteoclast formation. Compared to the low-fat diet, the high-fat diet increased body weight, serum leptin, osteoclast number, trabecular separation, and structural model index, while decreased bone mineral density, trabecular bone volume, connectivity density, and trabecular number. N-acetyl cysteine supplementation increased bone volume/total volume, connectivity density, and bone marrow osteoclast number in high-fat obese mice. These results indicate that antioxidant supplementation is beneficial to bone structure of obese mice induced by a high-fat by decreasing bone resorption.

Disclosures: Jay Cao, None.

SU0054

Non-invasive Quantification of Changes in Bone Micro-architecture and Strength: Three Year Follow-up at the Distal Radius. Ingrid Knippels^{*1}, L. Joseph Melton², Shreyasee Amin², Steven Boonen³, Sundeep Khosla⁴, Harry Van Lenthe⁵. ¹KULeuven, Belgium, ²Mayo Clinic, USA, ³Center for Metabolic Bone Disease & Division of Geriatric Medicine, Belgium, ⁴College of Medicine, Mayo Clinic, USA, ⁵Katholieke Universiteit Leuven, Belgium

With the introduction of high-resolution peripheral quantitative computed tomography scanners, detailed 3-dimensional *in vivo* imaging of human radii has become possible. Therefore, modeling and remodeling of bone in the distal radius can now be quantified in individual patients in terms of microstructural changes. The aim of this study was to measure changes in bone microarchitecture taking place during three years and to quantify the effects on bone strength.

In 119 adults (14 male, 105 female, age 6216) we scanned one of the distal radii twice with an interval of approximately 3 years (Mayo Clinic, Rochester, Minnesota, USA). Measurements at the first timepoint (TP1) were made with a prototype of the scanner while the measurements at TP2 were made using the XtremeCT (Scanco Medical AG, Brütisellen, Switzerland). Three-dimensional image registration [1] was performed to determine the bone volume common to both scans. 12 data sets had to be excluded for technical reasons, leaving 107 data sets for morphometry analysis. These analyses were performed on the volume that was present at both TPs using the standard evaluation protocol provided by the scanner manufacturer. Measures of volumetric bone mineral density (vBMD), trabecular bone volume fraction (BV/TV), trabecular number (Tb.N), trabecular separation (Tb.Sp) and cortical thickness (Ct.Th) were taken. Bone strength was determined from finite element (FE) analyses using a previously validated modeling approach [2]. All measurements of TP2 were corrected based on a cross-over study between the scanners used at TP1 and TP2 [3].

In this diverse group of adults, we found significant changes in vBMD, Ct.Th and Tb.N (Table 1). In individual subjects, up to 40% reductions in Ct.Th and 20% reduction in strength were found. Loss in vBMD was the best single predictor of bone strength reduction, although it only explained 31% of the variance.

In summary, we quantified changes in bone microarchitecture and strength at the distal radius occurring over a period of three years. Our data underline the strong patient-specific nature of longitudinal changes in bone.

References

- Schulte et al, *Bone*; doi:10.1016/j.bone.2010.10.007, 2010
- Knippels et al, *ESB 2010*, abstract 2010_0576
- Knippels et al, *ISB 2011*, abstract 1063

Acknowledgements

Funding from the European Union (VPHOP FP7-ICT2008-223865) and NIH (grant AR027065) is acknowledged. Computation time was provided by the Swiss National Supercomputing Centre (CSCS).

Table 1. Morphometric indices at two timepoints three years apart (TP1 and TP2) and their individual changes. Values expressed as: mean (standard deviation)

	TP1	TP2	Difference in percent	
vBMD (mgHA/cm ³)	348 (74)	340 (80)	-2.8 (5.3)	**
BV/TV (%)	12.6 (3.0)	12.7 (3.0)	0.6 (5.3)	ns
Tb.N (mm ⁻¹)	1.57 (0.34)	1.62 (0.35)	3.5 (7.8)	**
Tb.Sp (mm)	0.60 (0.22)	0.60 (0.21)	0.2 (9.4)	ns
Ct.Th (mm)	0.81 (0.20)	0.77 (0.22)	-5.9 (9.9)	**
Strength (N)	2708 (691)	2693 (703)	-0.5 (6.1)	ns

**p<0.01; paired t-test

Table 1

Disclosures: Ingrid Knippels, None.

SU0055

Paired Bone Biopsies - How Valid Are They? A Prospective Controlled Study. Doris Wagner¹, Hans Peter Dimai², Karin Amrein³, Thomas Pieber², Harald Dobnig⁴, Philipp Stiegler¹, Michael Sereinigg¹, Christine Beham-Schmid⁵, Astrid Fahrleitner-Pammer^{*6}. ¹Division for Transplantation, Department of Surgery, Medical University of Graz, Austria, ²Division of Endocrinology & Metabolism, Department of Internal medicine, Austria, ³Medical University of Graz, Austria, ⁴DiagnostikInstitut, Austria, ⁵Department of Pathology, Austria, ⁶Medical University Graz, Austria

Transiliac crest bone biopsy is a useful invasive means to assess bone histology. Accordingly, paired bone biopsies are also used to evaluate the effect of an osteoactive compound over an administration period. Data about a potentially existing side to side variance between paired biopsies are scarce.

Aim of the current study was to analyze the variance of paired transiliac crest biopsies that had been obtained under ideal conditions. Samples were taken in a population of brain-dead organ donors as part of explant surgery. The two biopsies were performed by the same surgeon directly after organ explantation. Consecutive organ donors between 10/2009 – 12/2010 were included into the study. The included donors were very carefully defined and healthy; donors with history of fractures or who had received any osteoporotic treatment or medication with impact on bone metabolism were excluded from the presented study. Histomorphometric analyses were performed in duplicates by the same technician who was blinded to patient's identity.

The total number of patients was 46 (27 males, 19 females) median age was 52.5 + 13 with a BMI of 23 + 2.1. All parameters investigated were comparable between men and women. Intraindividual variation coefficients ranged between 4.2 % (BV/TV) – 9.8 % (TbPf). The results of the histomorphometric analysis are listed in table 1. No differences between the sides of the paired biopsies were observed variance ranged from 0.9% (QS/BS) to 22% (ES/BS).

Histomorphometric analysis of bone biopsies – at least performed under standardized conditions - is a high sensitive approach to assess bone metabolism. As bone biopsies showed comparable results between both sides they might represent a possibility to investigate effects of specific medications even in small populations.

Table 1:

Left Right Delta (%) p-value	
BV/TV (%)	24.4 + 4 24.5 + 5 3 + 5 p = 0.79
BS/BV (%)	18 + 3 17 + 2 5 + 5 p = 0.14
OS/BS (%)	6.4 + 2.3 6.6 + 2.1 6 + 15 p = 0.32
ES/BS (%)	2.4 + 1 2.3 + 1 22 + 27 p = 0.79
QS/BS (%)	91 + 3 91 + 2 0.9 + 1 p = 0.74
Tb.N. (mm-1)	1.8 + 0.4 1.7 + 0.3 7 + 4 p = 0.37
Tb.Th (µm)	142 + 26 140 + 25 3.6 + 7 p = 0.22
Tb.Sp (µm)	420 + 87 426 + 100 4.5 + 7 p = 0.31

BV/TV (bone volume/tissue volume), BS/BV (bone surface/bone volume), OS/BS (osteoid surface/bone surface), ES/BS (eroded surface/bone surface), QS/BS (quiescent surface/bone surface), Tb.N (trabecular number), Tb.Th (trabecular thickness), Tb.Sp (trabecular separation rate)

Disclosures: Astrid Fahrleitner-Pammer, None.

This study received funding from: unrestricted research grant - Roche Austria

SU0056

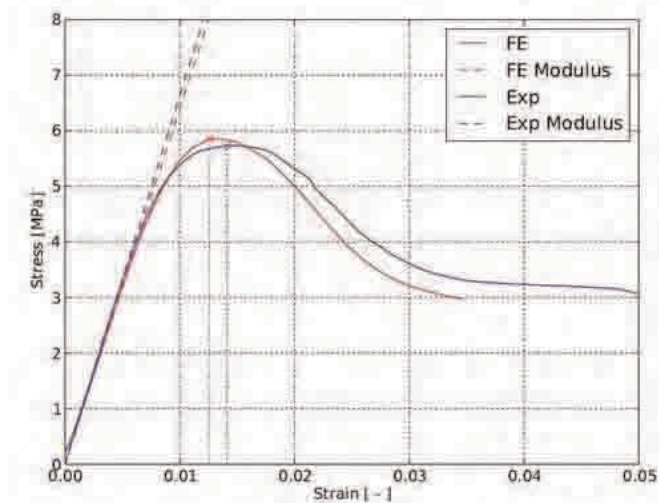
Prediction of Apparent Modulus, Ultimate Stress and Ultimate Strain of Human Vertebrae using a Viscous Damage Model with Softening. Jakob Schwiedrzik*, Enrico Dall'Ara, Philippe Zysset. Vienna University of Technology, Austria

Approximately 750000 osteoporosis-related vertebral compression fractures occur in the US every year. Quantitative computed tomography (QCT)-based finite element (FE) is an increasingly accepted method to assess vertebral strength in clinical studies. This work aimed at validating an improved QCT-based FE model featuring viscous damage and softening with in vitro experiments. The model was intended to extend the current predictions of apparent modulus (Y) and ultimate stress (σ_u) with the prediction of ultimate strain (ϵ_u) of vertebral bodies based on QCT scans obtained in vitro.

For the experiments, the endplates and posterior elements of 37 human thoracolumbar vertebral bodies (donors: 7 male, 3 female, 44-82 yrs) were removed. The vertebral sections were scanned with QCT and tested in monotonic compression at a rate of 5 mm/min. A ball joint allowed rotation of the loading plate during testing. The position of the upper loading plate was measured directly with 3 sensors to minimize the errors induced by machine compliance.

A nonlinear anatomy-specific FE model was generated for each vertebra from the vBMD-calibrated QCT images. Coarsened CT voxels were converted into finite elements with constant material orientation and BMD based material properties. Transverse isotropy in the cranial-caudal direction was assumed. Material parameters for viscous damage and softening were identified from the compression experiments optimizing the correspondence between FE predictions and experimental results. The FE models were loaded by a rigid loading plate, which motion reproduced the one recorded during the experiments.

Predicted Y, σ_u and ϵ_u were compared to the experimental data for each vertebral section. The FE model featuring viscous damage and softening predicted both Y ($p < 0.001$, $R^2 = 0.68$) and σ_u ($p < 0.001$, $R^2 = 0.77$) well. The correlation for ϵ_u was also significant ($p < 0.001$), however the R^2 was low ($R^2 = 0.37$) due to small range in ultimate strain. The predicted average ϵ_u was significantly lower than the experimental one ($p = 0.01$), but the relative difference was small ($< 10\%$). The linear regressions of the FE prediction for Y, σ_u and ϵ_u were close to the 1:1 relation. The model was able to predict vertebral Y, σ_u and ϵ_u of specific vertebrae under realistic boundary conditions with sufficient accuracy. It remains to be verified if the predictions remain accurate for in vivo scans which would make FE a possible predictive tool in future clinical studies.



Stress-strain curves of a compression test and the corresponding FE model

Disclosures: Jakob Schwiedrzik, None.

SU0057

Prediction of Forearm Failure Load in Women: the OFELY Study. Nicolas Vilayphiou*, Stephanie Boutroy¹, Elisabeth Sornay-Rendu¹, Bert van Rietbergen², Roland Chapurlat¹. ¹INSERM UMR1033, Université de Lyon & Hospices Civils de Lyon, France, ²Department of Biomedical Engineering, Eindhoven University of Technology, Netherlands

There is a growing interest for in vivo assessment of bone strength. However, the necessary technique for this evaluation - microfinite element analysis (μ FEA) - is highly demanding in computational resources. So, we sought to predict one of the outcomes of μ FEA by variables easily obtained by high resolution peripheral QCT (HR-pQCT) imaging of the distal radius.

Our cross-sectional analysis involved 831 women from the OFELY cohort who had a valid HR-pQCT radius scan. There were 228 pre- and 603 postmenopausal women, aged 407 and 679 years old respectively.

Distal radius HR-pQCT scans were used to measure volumetric BMD (vBMD), bone geometry and microarchitecture parameters, after segmentation of cortical (Ct) and trabecular (Tb) bone with advanced algorithm (Burghardt, Buie et al. Bone 2010). Estimated failure load for a fall on the outstretched hand was assessed on those segmented bone volumes by μ FEA. Areal BMD was measured at the ultradistal radius (UDR) by DXA at the same visit.

In premenopausal women, most parameters did not vary with age, thus they were used as reference data to calculate standardized T-scores for the variables included in the prediction model.

First, univariate regression models showed that the failure load was best predicted by UDR aBMD ($R^2 = 0.79$, $p < 0.001$). Among HR-pQCT parameters, it was the Ct area (CtAr) that was the best predictor of the failure load ($R^2 = 0.68$, $p < 0.001$). It was followed by total, Ct and Tb vBMD, and Ct thickness, with R^2 ranging from 0.49 to 0.61 ($p < 0.001$). Age and other microarchitectural or geometrical parameters were poor predictors of bone strength (all $R^2 < 0.31$, $p < 0.001$).

In ascending multivariable regressions using only HR-pQCT parameters, the best surrogate variables to predict failure load included only Ct.Ar and Tb.vBMD, with $R^2 = 0.85$ ($p < 0.001$). The addition of other microarchitectural parameters, age or UDR aBMD did not improve significantly the R^2 coefficient (up to $R^2 = 0.89$).

In conclusion, Ct.Ar combined with Tb.vBMD may be a surrogate variable of μ FEA estimated failure load. Without running μ FEA, this method could help to estimate indirectly and more quickly bone strength based only on HR-pQCT measurement in large datasets. Further validation will be needed regarding its use in fracture risk assessment.

Disclosures: Nicolas Vilayphiou, None.

SU0058

Radius and Tibia Strength Assessed by High Resolution pQCT Micro Finite Element Analysis: Effects of Age and Gender. Jennifer Walsh*, Margaret Paggiosi², Richard Eastell³. ¹NIHR Bone Biomedical Research Unit, United Kingdom, ²Sheffield Teaching Hospitals NHS Foundation Trust, United Kingdom, ³University of Sheffield, United Kingdom

We have previously reported that there are gender and age differences in cortical and trabecular microarchitecture assessed by HR-pQCT. Men have greater cortical perimeter than women at all ages. In men and women, cortical tissue mineral density is lower and cortical porosity is higher at age 16-18 and after age 70 compared to age 30-32. Micro-finite element modelling can be applied to HR-pQCT images to determine measures of bone strength. The aim of this study was to identify whether these differences in microarchitecture result in differences in bone strength between the end of longitudinal growth, peak bone mass and older age.

We conducted a cross-sectional observational study of 179 healthy men and women in three age groups; 16-18 (younger), 30-32 (peak bone mass) and 70+ (older). HR-pQCT images of the distal radius and distal tibia, acquired using the XtremeCT device (Scanco, Switzerland), were analysed with Imaging Processing Language software (Scanco) to obtain measures of stiffness and ultimate failure load in simulated compression. ANOVA with age group and gender as fixed factors and linear contrast were used to compare groups.

In all age groups, failure load and stiffness measures for the radius and tibia were greater in men than in women ($p < 0.001$). In men and women, failure load and stiffness measures for the radius and tibia were lower at older age than at peak bone mass.

In men, but not in women, radius failure load and stiffness were lower in younger adults than at peak bone mass. There were no significant differences in tibia failure load or stiffness between younger adults and peak bone mass in men or women.

We conclude that bone strength is greater in men than women which may be due to greater bone size. Despite different patterns of trabecular loss, both men and women demonstrate a reduction in bone strength with aging, and so the reduction in strength may be mostly due to cortical changes. The differences in radius stiffness and failure load between younger men and those at peak bone mass may reflect ongoing bone modelling with cortical consolidation. This may not have been apparent in women in this study due to the earlier onset and end of female puberty. There were no differences in tibia bone strength measures between the end of longitudinal growth and peak bone mass in men or women. This suggests that the age of completion of bone modelling may differ between weight-bearing and non-weight bearing sites.

		Radius		Tibia	
		Stiffness, kN/mm	Failure load, kN	Stiffness, N/mm	Failure load, kN
Women	16-18	71.7 (12.9)	3.67 (0.63)	215.9 (30.3)	10.93 (1.56)
	30-32	73.2 (12.2)	3.72 (0.60)	211.2 (32.3)	10.57 (1.52)
	70+	59.6* (13.9)	3.07* (0.69)	173.8* (33.7)	8.77* (1.62)
Men	16-18	95.5* (23.3)	4.90* (1.11)	294.7 (46.9)	14.93 (2.91)
	30-32	112.0 (22.8)	5.64 (1.04)	304.8 (46.9)	15.14 (2.24)
	70+	95.0* (20.7)	4.91* (0.99)	266.7* (43.7)	13.39* (2.10)

Results given as mean (SD)

*ANOVA with linear contrast; different from age 30-32 p<0.05

Results table

Disclosures: Jennifer Walsh, None.

SU0059

Role of Glycation in Microdamage Morphology in Cancellous and Cortical Bone. Lamya Karim*, Deepak Vashishth, Rensselaer Polytechnic Institute, USA

Factors other than low bone mass, such as changes in bone quality, may contribute to fracture risk. Non-enzymatic glycation (NEG) alters bone's extracellular matrix (ECM) and creates crosslinks known as advanced glycation end products (AGEs) that accumulate and increase bone fragility [1]. Elevated levels of AGEs may affect bone fracture resistance mechanisms such as the formation of microdamage since NEG stiffens bone's organic matrix and compromises its ability to dissipate energy. The goal of this study was to investigate the link between microdamage and NEG in both cancellous and cortical bone. 22 trabeculae were extracted from human cancellous bone cores that were mechanically tested and stained to detect microdamage [2]. Trabeculae were imaged with microcomputed tomography. Structure Model Index (SMI) was computed to categorize trabecular structure, and damaged surface area to volume ratio (DS/DV) for microdamage was calculated to characterize its morphology. Trabeculae were quantified for AGEs [3]. 9 human cortical bone beams were fatigue tested and stained with basic fuchsin to target microdamage. They were sectioned transversely into 4 μ m thick sections and mounted on membrane slides. Linear microcrack (LMC) and diffuse damage (DD) regions were laser-microdissected and collected in isolation caps. An extraction buffer was added to each tube and incubated to extract proteins (24 hours, 4C). Protein extracts were dialyzed against 1x PBS (24 hours, 4C), and extracts were used for AGEs quantification [4]. T-tests were run between AGEs quantity in LMC and DD regions while correlation tests were run between SMI and DS/DV; and between SMI and AGEs. Trabecular rods, which produced crack-like microdamage ($p<0.05$), were highly glycated ($p<0.05$) compared to trabecular plates. Similarly in cortical bone, regions of LMC were more glycated than regions of DD ($p=0.06$). Our results demonstrate that ECM property changes via NEG are responsible for the formation of specific morphologies of microdamage. This mechanism is similar in both cancellous and cortical bone where highly glycated regions of bone produce LMC that results in decreased fracture resistance.

1. SY Tang et al., *Bone*, 2007
 2. SY Tang and D Vashishth, *Bone*, 2010
 3. JF Woessner, *Arch. Biochem. Biophys.*, 1964
 4. GE Sroga and D Vashishth, *J. Chromatogr. B*, 2011
- Funding source: NIH-NIA AG0618 and NIH-NIGMS T32GM067545
Tissue source: NDRI via NIH 5 U42 RR006042

Disclosures: Lamya Karim, NIH-NIGMS T32GM067545, 2

SU0060

The Ability of Quantitative Ultrasound in Predicting the Principal Structural Orientation of Trabecular Bone. Liangjun Lin*¹, Christopher Lin², Frederick Serra-Hsu³, Jiqi Cheng¹, Yi-Xian Qin¹. ¹State University of New York at Stony Brook, USA, ²Ward Melville High School, USA, ³State University of New York, Stony Brook, USA

Introduction: Trabecular bone has the ability to adapt its microstructure to the loading environment [1]. The propagation of ultrasonic wave in trabecular bone is closely associated with the anisotropic mechanical properties and structural orientation [2]. The main objective of this study is to investigate the feasibility of using quantitative ultrasound to non-invasively predict the principal structural orientation of trabecular bone.

Materials and methods: A trabecular bone ball (diameter 25mm) was machined from bovine femur. Three main axes of superior-inferior (SI), antero-posterior (AP),

and medio-lateral (ML) orientations were marked on the surface of the bone ball. A quantitative ultrasound scanning system with 1MHz confocal transducers was used for the ultrasound tests. Ultrasound velocity (UV), attenuation (ATT) and broadband ultrasound attenuation (BUA) were recorded from the ultrasound test. The bone ball was rotated 10 degrees between ultrasound scans around each axis, resulting total $36 \times 3 = 108$ scans. To analyze the data, a 5×5 mm² region of interest (ROI) was selected in the center of the bone ball for each ultrasound image.

Results: Ultrasound scans around axis SI (Figure 1) did not showed particular results in any scanning direction for all three recorded parameters. But results around AP (Figure 2) and ML (Figure 3) axes showed that ultrasound signal in certain directions are stronger or weaker than in the others. In both AP and ML results, high peaks of BUA and UV curves appeared in the same scanning angle where low valleys appeared in the ATT results. And these high peaks and low valleys were symmetric: two peaks/valleys in every curve were located approximately 180 degrees from each other, indicating they were from the ultrasound scan along the same path in opposite directions.

Conclusion: Our quantitative ultrasound device provided the preliminary evidence that the results of ultrasound scans for trabecular bone are closely associated with different scanning directions. The symmetry of the data also revealed the repeatability and the validity of the results. The relation between the ultrasound results and the structural orientation needs to be further confirmed by computer tomography and mechanical testing in the future work.

1. Martin, R.B., *J Biomech*, 24 Suppl 1: p. 79-88, 1991.
2. Lin, W. et al., *J Acoust Soc Am*, 125(6): p. 4071-7, 2009.

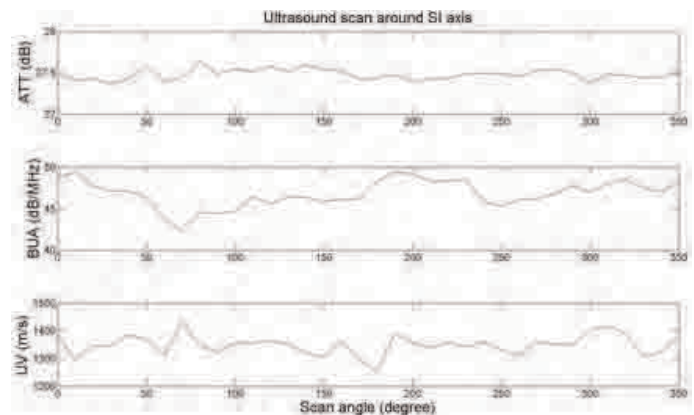


Figure 1 - ATT, BUA and UV results of ultrasound scan around SI axis

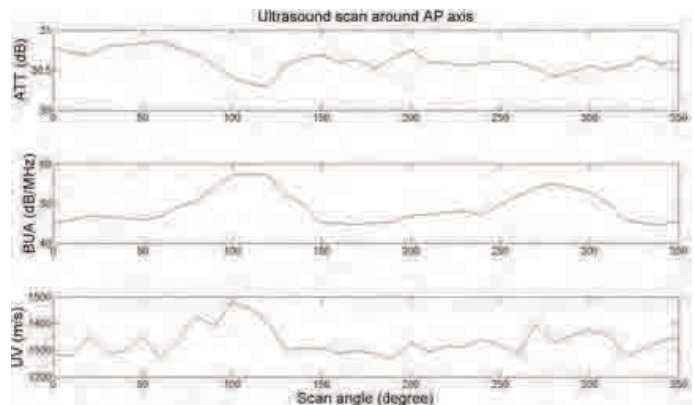


Figure 2 - ATT, BUA and UV results of ultrasound scan around AP axis

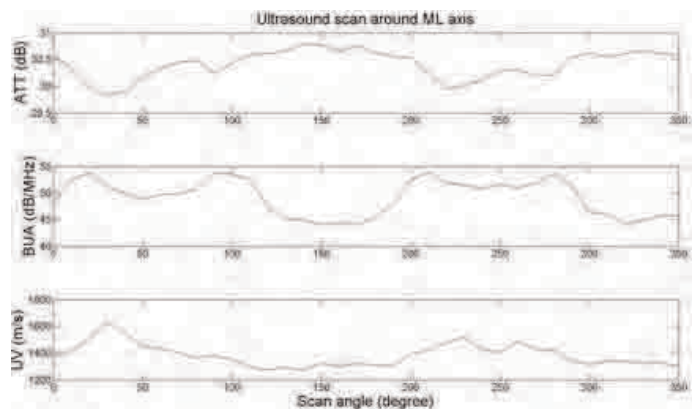


Figure 3 - ATT, BUA and UV results of ultrasound scan around ML axis

Disclosures: Liangjun Lin, None.

SU0061

Modulation of Bone's Mechanical Properties by its Architecture, Chemical Composition, and Age. Andrea Trinward^{*1}, Steven Tommasini¹, Alvin Acerbo², Lisa Miller³, Stefan Judex¹. ¹Stony Brook University, USA, ²Brookhaven National Laboratory, USA

Osteoporosis is associated with bone loss and a deterioration in tissue quality. Drugs such as alendronate (ALN), parathyroid hormone (PTH) and sodium fluoride (NaF) target bone loss differently leading to drug-specific changes in bone architecture, chemical composition, tissue age and ultimately, strength. To determine how drug-induced changes to bone quality relate to mechanical strength, we subjected OVX rats to 6mo of varying doses of ALN, PTH and NaF and analyzed cortical and trabecular bone through μ CT analysis, dynamic histomorphometry, FTIR and correlated to mechanical properties. Six mo old Sprague Dawley rats (n=10/group) were assigned to aged-matched controls (AM), OVX controls, OVX treated with high (H), medium (M) or low (L) doses of PTH (60, 15, or 0.3 μ g/kg/d), OVX treated with H, M or L-ALN (100, 10 or 1 μ g/kg/2xwk) or OVX treated with H or L-NaF (500 or 100ppm). At 12mo of age, OVX had 46% less trabecular bone in the L-4 vertebral body than AM. H- and M-doses of ALN, PTH and NaF maintained trabecular architecture while H-PTH increased cortical & trabecular thickness (Tb.Th) by 29% and 32% compared to AM (p<0.05). Mineral apposition rates increased by 35% in OVX and 55% in H-PTH (p<0.01), decreased by 74% in H-ALN (p<0.001), and were similar in H-NaF compared to AM controls. FTIR was performed on newly formed and pre-existing older bone. Compared to OVX, H-ALN rats had more phosphate in old bone and a greater mineral/matrix ratio in new trabecular bone (p<0.05). Crystallinity of NaF rats was greater than H-PTH in new cortical bone, greater than OVX and H-PTH in new trabecular bone, and greater than H-ALN and H-PTH rats in old trabecular bone (p<0.05). NaF rats also had higher phosphate levels in old cortical bone compared to AM, OVX and H-PTH. Tb.Th (r²=0.59) and mineral/matrix ratio (r²=0.33) were positively correlated to maximum load while apparent mineral density (μ CT) was not (r²=0.07). In summary, PTH treatment increased bone formation and Tb.Th, thereby producing newer, less mineralized bone. By maintaining existing bone, ALN caused more mineralized, older bone. In contrast, H-NaF maintained architecture with elevated phosphate and crystallinity. The correlations between chemical, histologic, and mechanical properties emphasize that bone volume and mineral density alone cannot predict fracture risk and that the modulation of bone strength by microarchitecture and chemical composition may be specific to any given drug intervention.

Disclosures: Andrea Trinward, None.

SU0062

Short-term Parathyroid Hormone Treatment Improves Cortical Bone Microstructure. Maria-Grazia Ascenzi^{*1}, Vivian Liao¹, Brittany Lee¹, Robert Lindsay², Felicia Cosman², Jeri Nieves³, John Bilezikian⁴, David Dempster³. ¹University of California, Los Angeles, USA, ²Helen Hayes Hospital, USA, ³Columbia University, USA, ⁴Columbia University College of Physicians & Surgeons, USA

We sought to identify cortical micro-structural features responsible for reduced fracture risk associated with short-term treatment with PTH. On 7 μ m-thin sections of iliac crest biopsies, we analyzed separately the architecture of type I collagen and the degree of calcification, which independently affects bone strength *in vitro*, in: 1] 8 postmenopausal patients with osteoporosis (mean SE, age 5410 years), pre- and post-treatment with recombinant human PTH (1-34); 2] 5 premenopausal patients with mild primary hyperparathyroidism (PHPT) (mean age 415 years), previously found to have preserved cancellous architecture; and 3] 5 healthy women (mean age 372 years). We measured i) collagen anisotropy by birefringence of circularly polarized light, ii) collagen orientation for specific birefringence by confocal and electron microscopy and iii) degree of calcification by micro-X-ray. For each input variable, a paired *t*-test established significance for pre- and post PTH treatment differences, while ANOVA and Tukey's post-hoc test established significant differences among the post-PTH, PHPT and healthy subject groups. Compared to the pre-PTH subjects, the post-PTH group exhibited a 12% decreased area of bright birefringence (p<0.01), a 38% increase in the number of osteons with bright and extinct lamellar alternation (p=0.03) and a 20% increase in lamellar thickness (p<0.03; Figure). These post-PTH parameters were not statistically different from those in the younger healthy group, but the percent area of bright birefringence was 17% greater (p=0.04) and lamellar thickness 24% greater (p<0.01) in the PHPT group compared to the healthy group. The collagen orientation with respect to the longitudinal direction showed predominant larger angles (4510) in birefringent bright, and smaller angles (23) in birefringent extinct regions. Both post-PTH and healthy groups showed a significantly higher percentage of osteons at initial rather than low-intermediate degree of calcification (p<0.04). Further, the post-PTH group showed a significant difference between low- and high-intermediate levels (p= 0.04) that the healthy group did not. In conclusion, PTH treatment restores tissue anisotropy, while the presence of PHPT shifts it away from a healthy premenopausal phenotype. If confirmed by a larger study at weight bearing locations, the observed anisotropy may help explain the change in fracture risk, reduced with post-PTH treatment and increased with PHPT.

Disclosures: Maria-Grazia Ascenzi, Micro-Generated Algorithms, 9

SU0063

The Effect of Zoledronic Acid on Cancellous and Cortical Bone Matrix Mineralization in Postmenopausal Osteoporotic Patients. Paul Roschger^{*1}, Barbara Misof¹, Daniela Gabriel¹, Eleftherios Paschalis¹, Erik Eriksen², Juerg Gasser³, Klaus Klaushofer¹. ¹Ludwig Boltzmann Institute of Osteology at the Hanusch Hospital of WGKK & AUVA Trauma Centre Meidling, 1st Medical Department, Hanusch Hospital, Vienna, Austria, ²Hormonlaboratoriet, AUS Aker Universitetssykehus Trondheimsveien, Oslo, Norway, ³Novartis Institutes for BioMedical Research, Basel, Switzerland

Background: Annual intravenous administration of zoledronic acid (ZOL) for 3 yrs has been shown to reduce fracture risk in postmenopausal women with osteoporosis (HORIZON pivotal fracture trial). Histomorphometric analysis of transiliacal bone biopsies of a subgroup of these patients revealed significantly improved trabecular architecture and reduced bone remodelling for the ZOL versus placebo treated patients. The aim of our study was to evaluate the mineralization of the bone matrix in these same biopsies.

Materials & Methods: We have measured entire transiliacal bone biopsy samples (previously used for the histomorphometric analysis) for cancellous and cortical bone mineralization density distribution (BMDD) by quantitative backscattered electron imaging (qBEI). Eighty-two patients were treated with ZOL (yearly doses of 5mg), 70 were treated with placebo and all received adequate Ca and VitD supplementation. To be enrolled in the study, the patients had to have a T-score \leq -2.5 or a T-score \leq -1.5 with evidence for at least 1 vertebral fracture. The patients were classified into 2 strata (I without concomitant treatment, II with concomitant other osteoporosis therapy, such as hormone replacement, selective estrogen receptor modulators, etc.).

Results: In both cancellous and cortical bone, all BMDD derived variables were significantly different between ZOL and placebo treatment (all p<0.001): the average (mean) and most frequent (mode) calcium concentrations (CaMean +3.2% and +2.7%; CaPeak +2.1% and +1.5%, cancellous and cortical bone, respectively) and the portion of highly mineralized bone areas (CaHigh +64% and +31%) were higher in ZOL than placebo, while the heterogeneity of mineralization (CaWidth -14% and -13%) and the percentage of areas undergoing primary mineralization were lower (CaLow -22% and -26%). Similar differences were observed when the study groups were considered for each stratum separately.

Discussion: The observed differences in BMDD vs. placebo are in excellent agreement with the strong reduction of bone turnover in the ZOL treated patients as reported by the histomorphometric results of the HORIZON study. A considerable and rapid decrease in bone turnover causes a reduction in the amount of new bone formation and a prolonged time for secondary mineralization of existing bone packets. Our findings demonstrate that both cancellous and cortical bone mineralization were affected by ZOL in a similar manner.

Disclosures: Paul Roschger, None.

SU0064

Viscoelastic Response of PTH, Ibandronate and Combination Treatment in Ovariectomized Rat Femur Correlating with BMD. Xiao Yang^{*}, Yong Hoow Chan, Padmalosini Muthukumaran, Taeyong Lee. National University of Singapore, Singapore

Aim

Viscoelastic response upon loading is one of the mechanical properties exhibited by bone. Little has been reported on viscosity changes existing in osteoporotic bone and with treatments. Since bone viscoelasticity correlates to load-bearing capacity, the aim of this study is to investigate the viscoelastic properties of ovariectomized and drug-treated rat femurs.

Methods

15 female SD rats were subjected to ovariectomy or sham surgery. They are divided into 5 groups: (1) SHM group with sham surgery; (2) OVX group underwent ovariectomy surgery and treated with vehicle saline; (3) PTH group: 10 μ g/kg PTH treated ovariectomized rats; (4) IBN group: 7 μ g/kg ibandronate treated ovariectomized rats; (5) COM group: ibandronate and PTH concurrent treatment on ovariectomized rats. Weekly treatments were administered subcutaneously from 4th week post-surgery. On week 12, all rats were euthanized. After metaphyseal region scanning by both μ CT and pQCT, femurs were embedded in epoxy and polished. After rehydration, nanoindentation was conducted using continuous stiffness measurement (CSM) to determine elastic modulus (E) and hardness (H). Basic creep test was also conducted using the Voigt model. Viscosity (η) is computed based on the curve fitting of creep displacement by non-linear regression.

Results

μ CT analysis suggested that IBN and COM group had a better effect than PTH in preserving trabecular bone properties in terms of BV/TV, Tb.Th, SMI, BS/BV, Tb.Sp and Tb.N. In BMD and viscosity, COM group were significantly higher than the other two monotherapy groups. In 12 wks, BMD and viscosity are positively correlated (R=0.94, p<0.05), whilst the BMD and E showed weak correlation (R=0.47). η had power-law correlation with E (p<0.05) in each group respectively. There was 18% increase in E and 44% increase in η for SHM compare to OVX.

Conclusions

Our results suggest that the osteoporotic deterioration do exist in bone viscosity while different drugs have varied ability to restore η . The source of creep may

contribute to the internal friction at cement lines [1]. Osteoporosis results in an increased number of newly formed cement lines. Thus more creep deformation (lower η) would take place under constant loading from daily activity. The strong positive correlation of η and BMD can be interpreted that the increase in the mineral portion of bone matrix may limit the interfibril motion of collagen which results in increased viscosity.



Figure 1 Visualization of bone loss in a transverse section of the metaphyseal femur of an rat from each group at 12th week

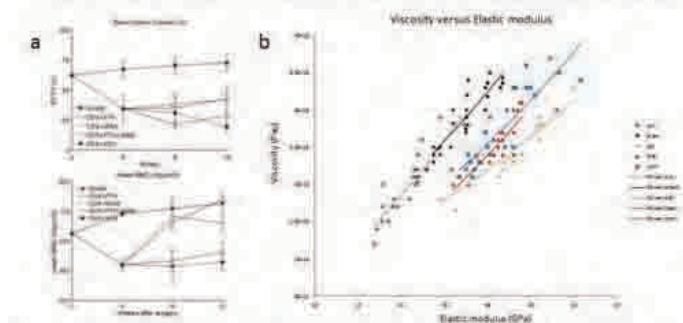


Figure 2 a) BV/TV, mBMD changes during 12wks; b) viscosity vs. elastic modulus in 12 wks for all groups.

Figure

Disclosures: Xiao Yang, None.

SU0065

Differences in Tibia Morphology Between the Lower Limbs of AFO-using Survivors of Stroke. Kyle Sherk¹, Vanessa Sherk¹, Mark Anderson², Debra Bembien¹, Michael Bembien¹. ¹University of Oklahoma, USA, ²University of Oklahoma Health Sciences Center, USA

Previous work has determined that bone losses occur on the affected side following a stroke, while the sound side may actually improve as it is heavily favored throughout the rehabilitation process for strength and stability. The use of gait aids in survivors of stroke is often mentioned in literature, but their effect on bone morphology has not been assessed. The purpose of this study was to examine the differences between the affected and sound lower limbs of ankle foot orthosis (AFO)-using chronic (>2 years post) survivors of stroke. Methods: 10 ambulatory survivors of stroke (ages 52-74 years) had their affected (6 left) and sound side tibias scanned at 4%, 38%, and 66% of the limb length with pQCT (XCT 3000) to assess volumetric BMD (vBMD), bone mineral content (BMC), and areas of the total, trabecular, and cortical bone. Periosteal (PeriC) and endosteal (EndoC) circumferences, cortical thickness (CTh), bone strength index (BSI) and strength strain index (SSI) were determined. Data were compared by paired t-tests in SPSS v18.0. Significance was set at $p \leq 0.05$. Results: Men ($n=6$) were taller than women ($n=4$) ($p < 0.001$). There were no gender differences in age, weight, time since stroke, or lapse of time from stroke to walking. Total BMC was greater on the sound side at all 3 sites ($p < 0.02$). Total vBMD was greater on the sound side at the 4% and 66% sites ($p < 0.001$). The 4% tibia site showed 22% greater trabecular BMC ($p < 0.01$) and 20% greater trabecular vBMD ($p < 0.01$). BSI at the 4% site was 41% smaller on the affected side ($p < 0.01$). The 38% site showed the total area to be 4% greater on the sound side ($p < 0.02$). Cortical area at the 38% and 66% sites were larger by 5% and 16%, respectively, on the sound side ($p < 0.05$) with larger CTh ($p < 0.001$). These resulted from smaller EndoC ($p < 0.01$) on the sound side at both sites. Cortical BMC was also larger on the sound side at both the 38% (8% difference) and 66% (15% difference) sites ($p < 0.02$). The 66% site revealed an 11% difference in SSI, with the sound side being greater ($p < 0.01$). Imin was only found to be greater at the 66% site ($p < 0.02$), leading to a significant difference ($p < 0.05$) in the Imax/Imin ratio with the affected side being the larger ratio. Conclusions: Hemiplegic side's trabecular and cortical tibia morphologies are affected following a stroke. It is still unknown if AFO use to maintain mobility accelerates or mediates these losses.

Disclosures: Kyle Sherk, None.

SU0066

Evaluation of HR-pQCT in Non-human Primates for Monitoring the Effect of Odanacatib on Bone Microarchitecture. Richa Jayakar¹, Antonio Cabal¹, John Szumiloski¹, Swanand Sardesai¹, Eual Phillips², Christopher Winkelmann¹, Paul McCracken³, Thomas Hangartner⁴, DON WILLIAMS⁵. ¹Merck & Co., Inc., USA, ²University of Pennsylvania, USA, ³Merck Research Laboratories, USA, ⁴Wright State University, USA, ⁵MERCK, USA

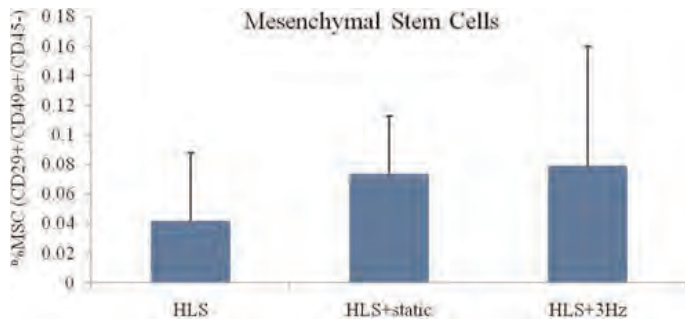
High Resolution peripheral Quantitative Computed Tomography (HR-pQCT) is gaining popularity in clinical studies for bone evaluation, but published literature in animal models is scarce. Pre-clinical studies are imperative for drug development and provide a test bed for designing clinical studies, but HR-pQCT performance in these smaller species needs to be evaluated. The objective of this study was to longitudinally evaluate HR-pQCT imaging (XtremeCT, Scanco Medical) for variability, stability, and sensitivity to change in an ovariectomized (OVX) non-human primate (NHP) model of bone loss, treated with odanacatib (ODN), a Cathepsin K inhibitor, being developed by Merck for treatment of osteoporosis. Rhesus monkeys were divided into 3 groups: Intact ($n=10$; non-ovariectomized), OVX-VEH ($n=11$; vehicle treated) and OVX-ODN ($n=10$; 30 mg/kg/day ODN). In-vivo scanning was performed at the ultradistal (UD) and distal 1/3 radius and tibia at 12 and 20 months post-OVX. The UD sites were located immediately distal to the growth plate of the radius and tibia, respectively. The distal 1/3 sites were located at 1/3 of the bone length measured from the distal end. Vendor software was used to analyze volumetric bone mineral density (vBMD) and micro-architectural parameters. Finite element analysis was performed on in-vivo images and the results validated by ex-vivo mechanical compression testing ($R^2=0.9$). To assess the test-retest variability of the imaging method, an off-study monkey and an excised radius and tibia were scanned five times during each scan period at the same anatomical sites. The coefficients of variation of various parameters in the off-study monkey and excised bones across all sites ranged from 0.1% to 7.4%. Pair-wise comparisons of OVX-VEH vs. Intact monkeys demonstrated a model effect showing decreases in parameters consistent with bone loss. Treatment effects were observed with pair wise comparisons of OVX-ODN vs. OVX-VEH at 20 months ($p < 0.05$) in vBMD (477 27 vs. 364 22 mg HA/cm³) and Cortical Thickness (CTh) (0.90 0.07 vs. 0.64 0.04 mm) at the UD radius, CTh (2.15 0.28 vs. 1.56 0.08 mm) at the distal 1/3 radius, and CTh (1.05 0.08 vs. 0.86 0.05 mm) at the UD tibia. We conclude that HR-pQCT serves as a reliable technique to longitudinally monitor osteoporosis treatment in rhesus monkeys; the OVX procedure results in bone loss, while ODN treatment increases bone mass, as evidenced by micro-architectural and density parameters.

Disclosures: Richa Jayakar, Merck, 3; Merck, 1
This study received funding from: Merck

SU0067

In Vivo Mesenchymal Stem Cell Proliferation Promoted by Dynamic Fluid Flow Stimulation. Minyi Hu¹, Robbin Yeh¹, Michelle Lien¹, Yi-Xian Qin². ¹Stony Brook University, USA, ²State University of New York at Stony Brook, USA

Osteoporosis gives rise to weaker bones that are more susceptible for fractures due to decreased bone mass and minerals. Our group has recently introduced a novel, non-invasive dynamic hydraulic stimulation (DHS) that enhanced bone structure, as 3Hz DHS inhibited disuse bone loss. Mesenchymal stem cells (MSCs) are able to self-renew and potentially differentiate into the cells that form tissues such as bone. To further illustrate the cellular effect of DHS and its potential mechanism in bone, the goal of this study was to quantify MSC populations in response to in vivo mechanical signals driven by DHS. Female Sprague-Dawley virgin rats (5m) were divided into 3 groups: hindlimb suspended (HLS, $n=10$), HLS+static ($n=6$), and HLS+3Hz ($n=4$). Stimulation were given to right tibia by an inflatable cuff with 30mmHg static +30mmHg dynamic pressures, for 10min on-5 min off-10min on, 5d/wk for 4 wks. Bone marrow was harvested from the right tibia at the end of the experiment. Quantification of MSC populations in the bone marrow was determined using flow cytometry. Red blood cells in the cell extracts were lysed by Pharmlyse (BD Bioscience). Appropriate antibodies (CD29, CD49e and CD45; BD Biosciences, BioLegend) with suggested concentrations were applied. Flow cytometry data were collected using FACS ARIA at Stony Brook Research Flow Cytometry Core Facility. Flow cytometric measurements indicated MSC population as represented by cells positive for CD29 and CD49e, and negative for CD45. DHS-treated animals (HLS +3Hz) had 88% ($p > 0.05$) increase in MSC population compared to HLS, while HLS +static had 74% ($p > 0.05$) increase. Previous studies had shown strong inhibition affect of DHS on disuse bone loss, indicating its enhancement on bone structural quality. This flow cytometry experiment suggests the ability of DHS in MSC proliferation to elicit phenotypic changes in the skeleton, which coincide our previous finding. The mechanical signals derived from DHS may bias the differentiation of MSCs towards osteoblastogenesis, promoting bone formation in disuse condition. MSCs express surface markers including CD29 and CD49e. CD45 was included as an HSC marker. The use of all these markers was to identify MSCs with higher specificity. This population showed an increase in response to DHS compared to HLS. Overall, these data indicate that the MSC pool, expressed by both positive and negative markers, has been positively influenced by mechanical signals driven by DHS.



Mesenchymal Stem Cells

Disclosures: Minyi Hu, None.

SU0068

Bone Mass And Microarchitecture Changes In Subchondral Bone During Osteoarthritis: Influence Of Prior Mechanical Loading?. Arnaud Boudenot^{*1}, Stephane Pallu², Nathalie Presle³, Christelle Jaffre⁴, Claude Laurent Benhamou⁵. ¹Inserm Unit U658, Hopital Porte Madeleine, France, ²INSERM U 658 / University of Orleans, France, ³UMR CNRS-UHP 7561, France, ⁴INSERM U658, Caracterisation du Tissu Osseux par Imagerie : Techniques et applications, France, ⁵INSERM Orleans-France, France

Although osteoarthritis (OA) is considered as a primary disorder of articular cartilage, the architecture and properties of the periarticular cortical and trabecular bone are also modified during the course of the disease. In an experimental model of OA, we have previously shown by DXA a bone loss in the epiphyseal area adjacent to the knee, and a protective effect of exercise on this parameter. The current study aimed to investigate changes in bone mass and trabecular microarchitecture in both the lateral and medial parts of rat knee joints in an OA model. Male Wistar rats (n=48) were divided into two groups: exercise (Ex) or non exercise (NEx). Ex rats were subjected to intermittent progressive training 1h/day, 5 d/week for 10 weeks. At the end of the training period, experimental OA was induced by intraarticular injection of 1 mg monoiodoacetate (MIA) in each half group (Ex-MIA and NEx-MIA). Rats in the other half were injected with saline as controls (Ex-C and NEx-C). Hematoxylin-eosin-safran and safranin-O-fast green stainings were performed on femoro-tibial joint sections to determine the severity of OA cartilage lesions. The proximal extremity of the tibia was imaged with Skyscan 1072 μ CT device. An analysis method has been developed to separate 2 ROIs, one from the lateral part, the other one from medial part. The ROI was a cylinder (volume: 2.13 mm³), the resolution was 12.02 μ m. Our data indicated that the lateral part of the knee joint exhibited significantly higher BV/TV and Tb.Th than the medial part. Exercise and OA did not alter the microarchitecture in the medial part. A lower BV/TV was found in the lateral part from rats injected with MIA (NEx-MIA vs Ex-C: 34.195.91 vs 42.213.34; p<0.01; Ex-MIA vs Ex-C: 32.816.31 vs 42.213.34; p<0.01). Lateral Tb.N was also reduced in both MIA groups (NEx-MIA vs Ex-C: 3.090.44 vs 3.610.25; p<0.01; Ex-MIA vs Ex-C: 3.040.38 vs 3.610.25; p<0.01), and lateral Tb.Th was significantly lower in the MIA groups compared to controls (NEx-MIA vs Ex-C: 0.110.01 vs 0.120.01; p<0.05; Ex-MIA vs Ex-C: 0.110.01 vs 0.120.01; p<0.05). Previous exercise had no effect on these parameters in this model. These data suggest that MIA-induced OA is associated with bone loss and changes in the trabecular subchondral bone from the load-bearing area of the knee joint. This chemical effect of the MIA seems finally differentially translated in the lateral vs medial part of subchondral OA bone, suggesting an interaction with mechanical properties of the rat knee.

Disclosures: Arnaud Boudenot, None.

SU0069

Effects of Pulsed Electromagnetic Field Stimulation on Transient Gene Expression Related to Bone Formation in Old Rats. Hiroyuki Tamaki^{*1}, Atsumu Yuki², Kounosuke Tomori³, kengo Yotani⁴, Hikari Kirimoto¹, Hideaki Onishi¹, Norikatsu Kasuga². ¹Niigata University of Health & Welfare, Japan, ²Aichi University of Education, Japan, ³Kanagawa University of Human Services, Japan, ⁴National Institute of Fitness & Sports, Japan

Aging is associated with bone loss resulting from low bone formation characterized by reductions in biological activity and numbers of osteoblasts. Pulsed magnetic stimulation (PMS) has been used to treat bone disorders and reportedly modifies differentiation, proliferation and mineralization of osteoblasts in vitro. We examined the in vivo effects of repetitive pulsed magnetic stimulation (rPMS) on bone formation in aged rat tibiae and femurs. Unilateral hindlimbs of male old rats (95-149 weeks) and young rats (6-8 weeks) were held on the table in the prone position and the PMS probe was placed 10-20 mm from the thigh and leg. Rats underwent rPMS at 25-

60% stimulation intensity at a frequency of 0.2-1 Hz, for 5-10 min. After sacrifice, tibiae were analyzed by quantitative histomorphometry and femora were used for analysis of bone morphogenetic protein (BMP)-2, transforming growth factor (TGF)- β 2, collagen (Col)-I, and osteocalcin (OC) mRNA expression by real-time reverse transcriptase-polymerase chain reaction (RT-PCR). Morphometric analysis was performed by micro-computed tomography and observation using a digital microscope comprising a video monitor and personal computer with image analysis software. Lower trabecular bone area and osteoid thickness were observed in old rats compared to young rats. RT-PCR showed that rPMS stimulated mRNA levels of BMP-2 and TGF- β 2 after 24 h of treatment compared to the contralateral hindlimb in young rats. In old rats, rPMS at higher intensity did not up-regulate mRNA expression levels of osteoblast marker genes. The beneficial effects of rPMS on gene expression levels related to bone formation may thus be associated with age and/or stimulation intensity.

Disclosures: Hiroyuki Tamaki, None.

SU0070

Fluid Flow Induced Early Response Genes Are Selectively Altered by Age. Leah Worton^{*1}, Ronald Kwon², Edith Gardiner¹, Ted Gross¹, Sundar Srinivasan¹. ¹The University of Washington, USA, ²La Jolla Bioengineering Institute, USA

There is controversy regarding whether bone's mechano-responsiveness is altered with age, as studies have noted enhanced, unchanged and muted tissue adaptation. To begin to explore whether and how aging might modulate mechanotransduction, we examined the early gene expression responses to fluid flow in cells derived from senescent (22 Mo, n = 5) and young adult female C57BL/6 mice (4 Mo, n = 5). Osteoblast/osteocyte cells were recovered from bone fragments from mice, were passaged, seeded and exposed to fluid flow-induced shear stress for 1h using a rocking platform (~0.5Hz, ~0.05Pa). Cells showed a 1.5-fold increase of COX-2 mRNA expression with flow vs. no flow regardless of animal age. Interestingly, both baseline and shear stress induced levels of COX-2 were lower in the cells from senescent vs. adult mice (p<0.05). While c-fos expression was also significantly increased in both groups by flow (11- and 18-fold in adult and senescent, respectively), neither baseline nor flow-induced levels of c-fos differed with age.

To explore the age-related differences in COX-2 and c-fos expression in response to shear stress, osteoblast and osteocyte expression markers were analyzed. Interestingly, cell cultures grown from senescent mice had greater expression of Runx2, Osx and ALP (1.8-, 2.2-, 2.1-fold higher vs. adult, respectively), but lower levels of the early osteocyte marker E11. The 'osteocytic' expression of genes involved in phosphate regulation was more complex; expression of DMP1 and PHEX was enhanced in senescent mice (2.7- and 4.4-fold vs. adult cells), while there was no age effect on the expression of FGF23 and MEPE. There was also no difference in expression of the late osteocyte marker SOST between these cell populations.

In combination, these data suggest that aging has the potential to selectively degrade early gene expression responses to mechanical stimuli. Further, while cell responses to fluid flow are undoubtedly governed by their baseline states, the differential responses observed could also arise due to differences in cell populations that emerged from the bones of senescent (more osteoblastic) vs. younger adult animals. An extension of this approach to examine higher-order cell functions downstream of interactions between degraded and intact pathways may definitively elucidate whether (and how) aging suppresses the osteogenic response to mechanical stimuli.

Disclosures: Leah Worton, None.

SU0071

Impact of Deleting the IGF-1 Receptor in Mature Osteoblasts on the Skeletal Response to Unloading and Reloading. Takuo Kubota^{*}, Hashem Elalieh, Muriel Babey, Yongmei Wang, Daniel Bikle. University of California San Francisco/VA Medical Center, USA

Mechanical loading has a prominent influence on bone remodeling. Insulin-like growth factor 1 (IGF-1) signaling also plays an important role in bone remodeling. IGF-1 production is increased in osteoblasts after mechanical load. In addition, skeletal unloading causes a decrease in bone mass with suppressed bone formation and enhanced bone resorption associated with resistance to the anabolic effect of IGF-1. Thus, we hypothesized that IGF-1 signaling mediates the skeletal response to unloading and reloading. In the present study, to prove our hypothesis, we assessed mice in which the IGF-1 receptor was deleted with osteocalcin-driven cre recombinase. These mice were hindlimb unloaded for two weeks and then reloaded after unloading for two weeks. Micro CT analysis showed that bone volume (BV/TV) in trabecular bone was reduced in knockout (KO) mice at baseline compared to that in control (CL) mice. The BV/TV in both KO and CL mice fell with unloading and then increased after reloading. The loss in BV/TV in KO female mice (92% reduction) tended to be more profound after unloading compared to that in CL female mice (78% reduction). Surprisingly the recovery of BV/TV with reloading was comparable. Bone histomorphometry showed that BV/TV and bone formation rate (BFR/BS) in trabecular bone was diminished at base line and after reloading in the KO mice compared to that in the CL mice, although there were no differences in osteoblast number between the KO and CL mice. Osteoclast number and eroded surfaces with osteoclasts tended to be reduced at base line and after reloading in the KO mice

compared to those in the CL mice. In addition, the KO mice exhibited a smaller and thinner cortical bone at baseline by micro CT analysis than the CL mice. The difference between the KO and CL mice in cortical bone was maintained after unloading and reloading. BFR/BS in the periosteal surface at the tibiofemoral junction of the KO mice after reloading remained suppressed (98% below the CL mice) unlike the partial recovery observed in the CL mice. These results suggest that the IGF-1 receptor in mature osteoblasts plays a modest role in the skeletal response to unloading and reloading, affecting both bone formation and resorption, but at least in trabecular bone IGF-1 resistance is likely manifested in less mature osteoblasts and osteoprogenitors which are responding normally in this mouse model.

Disclosures: Takuo Kubota, None.

SU0072

Pleiotropy Involving Skeletal, Vascular, and Reproductive Phenotype in Recombinant Congenic Mice via the Endothelin Signaling. Robert Blank¹, michael johnson², Jasmin Kristianto², Suzanne Litscher², Naomi Chesler², Zhijie Wang², Jacqueline Fisher². ¹University of Wisconsin, USA, ²University of Wisconsin-Madison, USA

There is a well established epidemiological association between skeletal fragility, atherosclerosis and low birth weight. Our lab has isolated pleiotropic quantitative trait loci (QTL) region in mouse chromosome 4 that is responsible for bone remodeling in response to loading via the study of recombinant congenic mice HcB-8 and HcB-23. Recombination during the strains' construction limits the QTL region to ~6.5 Mb and includes Ecel gene, encoding endothelin converting enzyme 1 (ECE1). We hypothesized that the QTL-mediated modeling differences in response to mechanical loading are shared between bones and blood vessels. The two strains harbor alternate genotypes for a chromosome 4 QTL that results in distinct bone phenotype between HcB-8 (low modeling) and HcB-23 (high modeling). HcB-8 carotid arteries have a smaller diameter at 90 mm Hg and are less compliant to increases in luminal pressure than HcB-23 carotids ($p=0.026$, $p=0.036$ respectively). Hence, we further hypothesized that the poor vascular modeling in HcB-8 may lead to lack of reproductive performance in comparison to HcB-23. HcB-8 litters are smaller than HcB-23 litters (4.4 ± 1.8 v 5.8 ± 2.0 , $p < 10^{-3}$) and HcB-8 pups are lighter at birth (1.2 ± 0.2 g v 1.5 ± 0.2 g, $p < 10^{-20}$). Based on CT scan data, all 4 pregnant HcB-8 females had at least 1 resorbed embryo while none were observed in HcB-23 ($N = 4$). Placental insufficiency may account for these differences. We also examined Ecel expression level in HcB-8 and HcB-23 heart and vessel tissues by real-time PCR and western blotting. At the mRNA level, HcB-23 expresses nearly 3-fold more Ecel ($p < 10^{-3}$), with the protein data showing a similar pattern. Immunohistochemistry of day 17 placentas shows higher ECE1 and NOS3 levels in HcB-23. Endothelin signaling through the B type receptor is known to induce Nos3, and endothelin signaling has also been shown to promote bone growth. These findings suggest that Ecel expression differences underlie the multi-system pleiotropy of the chromosome 4 QTL. In addition, the data indicate that the pleiotropy effect of chromosome 4 QTL extends beyond the skeletal system. Therefore, we propose that mechanically-induced modeling is the common mechanism linking the various traits controlled by the chromosome 4 QTL. We also speculate that the impaired response to mechanical loading may be a common underlying cause of intrauterine growth retardation.

Disclosures: Jasmin Kristianto, None.

SU0073

Prolonged Unloading in Growing Rats Reduces Cortical Osteocyte Lacunar Density and Volume in the Distal Tibia. Hayley Britz^{*1}, Yasmin Carter¹, Jarkko Jokihaara², Olli Leppanen³, Teppo Jarvinen⁴, George Belev⁵, David Cooper¹. ¹University of Saskatchewan, Canada, ²University of Tampere, Canada, ³University of Tampere, Finland, ⁴University of Tampere/IMT, Finland, ⁵Canadian Light Source, Canada

Load-related stimuli play an important role in the health of the skeleton which is able to dynamically adapt to the environmental demands placed upon it. It has been postulated that osteocytes sense changes in these stimuli and initiate adaptive responses, across a number of scales, through a process known as mechanotransduction. While gross morphological and tissue-level adaptation have been the focus of much research, relatively little is known regarding the relation between cellular-level features (e.g. osteocyte lacunar density, shape, volume) and loading. The increasing availability of high resolution 3D imaging modalities, including synchrotron-based technologies, has made studying 3D cellular-level morphology feasible on a scale not previously possible. The aim of this study was to experimentally test the hypothesis that unloading during growth results in altered osteocyte lacunar density and volume in the rat. Left tibial diaphyses from six female rats (30 weeks old) that had been immobilized by sciatic neurectomy for 27 weeks and those from six age and sex-matched controls were scanned with a 2 micron voxel size at the Canadian Light Source synchrotron. The Biomedical Imaging and Therapy bending magnet beamline (BMIT-BM; 05B1-1) was employed. Lacunar density and volume were quantitatively assessed within the complete distal diaphyses along 0.5 mm of their length. Qualitative observations of lacunar distribution in 3D revealed a marked regional variation about the tibial cross section. In some areas, the midcortical regions exhibited high concentrations of lacunae while periosteal bone tended to have fewer more regularly arranged lacunae. Overall lacunar density was found to be significantly ($p=0.039$)

higher in the control bones ($63,138 \pm 1,956$ lacunae per mm^3) than in the immobilized bones ($49,642 \pm 11,955$ lacunae per mm^3). It was also found that the mean lacunar volume for control bones ($284 \pm 28 \mu\text{m}^3$) was significantly higher ($p=0.039$) than for the immobilized bones ($209 \pm 72 \mu\text{m}^3$). Our results revealed that extreme differences in loading conditions, such as those created by paralysis, do indeed result in changes in osteocyte lacunar features. Further investigation is warranted to examine relations between these parameters and more subtle variation in loading as well as potential links to pathological states which have been linked to altered mechanotransduction.

Disclosures: Hayley Britz, None.

SU0074

Resistance to ER Stress Is Improved via Mechanical Input in MSC. Maya Styner^{*1}, Kornelia Galior¹, Natasha Case¹, Buer Sen², Zhihui Xie¹, Janet Rubin¹. ¹University of North Carolina, Chapel Hill, School of Medicine, USA, ²University of North Carolina At Chapel Hill, USA

Endoplasmic reticulum (ER) stress occurs in all cells when overwhelmed by misfolded proteins and is a common final pathway in diverse pathologic states including aging and oxidative stress. Exercise has been recently reported to protect against mutations that cause protein misfolding/dysfunction in the brain. Ablation of a key ER stress mediator, PERK, results in skeletal defects including deficient mineralization and osteoporosis suggesting a role for ER function and stress in bone formation. Given that mesenchymal stem cells (MSC) are responsible for bone formation, we hypothesized that mechanical input, analogous to exercise, might improve osteogenic capacity by decreasing MSC ER stress. C3H10T1/2 MSCs and/or marrow derived MSCs were cultured in the presence of the ER stress inducer tunicamycin. Mechanical stimuli were applied using a Flexcell device at 2%, 300 cycles per bout, 2 bouts per day, a regimen previously shown to repress MSC adipogenesis. Tunicamycin led to a rapid rise in the apoptosis marker CHOP at 6-8 hours followed by a steady decline. Spliced XBP1, another participant in ER stress, rose along with CHOP. The early increases in CHOP and XBP1s were followed by a rise in the chaperone BiP peaking at 24-48 hours. This pattern of increased BiP with decreasing CHOP is consistent with recovery from ER stress. Mechanical pre-treatment of MSC, dosed daily for 4 days, decreased ER stress. First the mechanical treatment increased the expression of the chaperone BiP 1.5-fold of control level suggesting induction of an increased ER capacity as BiP populates existent ER. Secondly, when ER stress was induced by tunicamycin (1 $\mu\text{g}/\text{ml}$), the untreated MSC demonstrated 2-fold higher elevations in CHOP compared to those pre-treated with mechanical stimulus. Our data suggests that MSC respond to mechanical input by expanding ER capacity, an effect which increases cellular resistance to multiple stressors. As such, mechanical regulation of ER stress in MSC is a mechanism by which exercise could improve skeletal health.

Disclosures: Maya Styner, None.

SU0075

A 14-week Initial Military Training Regimen Led to Distal Trabecularization and Diaphyseal Cortical Thickening in Tibiae of Men and Women. Charles Negus^{*1}, Rachel Izard², Julie Greeves³, William Fraser⁴. ¹L-3 Applied Technologies, USA, ²HQ ARTD, MOD, United Kingdom, ³HQ Army Recruiting & Training Division, United Kingdom, ⁴Norwich Medical School, University of East Anglia, UK, United Kingdom

Recent interventions by the British Army have reduced the incidence of medial tibial stress syndrome and lower limb stress fracture among recruits undertaking the 14-week Initial Training program. Women are still at higher risk of stress fracture than men and the effect of this intense training on the functional adaptation of bone in either sex is unknown. The purpose of this study was to compare tibial adaptations between men and women to 14 weeks of initial military training.

Of 248 recruits at Army Training Centre Pirbright who entered the study, 203 (82 men age 21.63 \pm 3.06 yrs; 121 women age 20.96 \pm 2.94 yrs) underwent pQCT (peripheral quantitative computed tomography) scans at both week 1 (pre) and 14 (post) of training. Scans were collected at 4%, 38%, and 66% of tibial length from the distal end plate. The Bone Alignment and Measurement Package (BAMpack) was used to align pre and post images of each subject, rotate images consistently, and calculate measures for the whole-cross section and in 60 sectors. Measures included Trabecular Density (TrDn), Cortical Density (CtDn), Bone Mineral Content (BMC), Trabecular Area (TrAr), Cortical Area (CtAr), Total Area (TtAr), Cortical Thickness (CtTh), Periosteal Perimeter (PPm), Endosteal Perimeter (EPPm), polar moment of inertia (I), mass moment of inertia (MMI), and Bone Strength Index (BSI). Only images with minimal motion artifacts and alignment error were used for statistical analysis at each site. Within-sex pre-post changes were assessed with paired t-tests, while sex-time interactions were assessed with repeated measures ANOVA analysis.

Results are summarized in Table 1. Both sexes experienced a significant pre-post increase in TrDn at 4% site (Figure 1), though women increased TrDn significantly more than men. At 38%, both men and women experienced significant increases in TtAr, CtAr and CtTh (primarily on the medial aspect), and PPm. The only significant change in CtDn at 38% was an increase in the anterior-posterior sectors of women. Adaptations at 66% were similar to the 38% site.

Both men and women increased mineralization at the distal tibia and exhibited signs of periosteal expansion in the cortical shaft. These adaptations are similar to

This work was sponsored by the UK Ministry of Defence (Army).



(+30.5%) weeks of full WB. A novel skeletonization algorithm implemented to define the topology of pore structures demonstrated that cortical pores became more interconnected on the affected side, as quantified by an increase in canal junctions (+37.6%, $p < 0.05$). Small decreases in BMD and Ct.BMD were detected following the non-WB period (-1.6% and -1.1%, $p < 0.05$), likely driven by the increase in Ct.Po. No changes in Ct.Po, pore structure, or densitometric parameters were detected on the contralateral side. Finite element analysis showed significant changes in biomechanics on the affected side following the non-WB period, including decreased stiffness and estimated failure load (-4.0% and -3.4%, $p < 0.05$). These biomechanical measures remained depressed following 6 and 12 weeks of full WB. Our results suggest that detectable microarchitectural and biomechanical degradation occurs as a result of non-WB and persists following return to normal loading. A better understanding of these microarchitectural changes and their short- and long-term influence on biomechanics may have clinical relevance in developing targeted countermeasures to prevent bone loss.

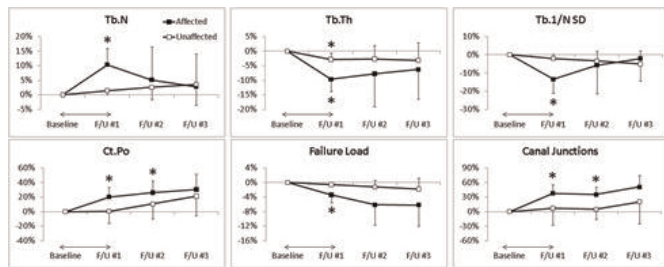


Figure 1. Longitudinal assessment of trabecular number (Tb.N), thickness (Tb.Th), and heterogeneity (Tb.L/N SD), cortical porosity (Ct.Po), estimated failure load, and canal junctions following a 6-week period of non-weight bearing (double arrows). Significant changes from baseline values are denoted with an asterisk ($p < 0.05$).

Figure 1

Disclosures: Galatea Kazakia, None.

SU0078

Non-invasive (pQCT) Analysis of Different Patterns of Structural/Bio-mechanical Relationships Along the Human Tibia in Healthy Volunteers and Long-Distance Runners. Ricardo Francisco Capozza¹, Sara Feldman², Pablo Mortarino¹, Paola Reina¹, Jose Ferretti^{3,4}, Joern Rittweger⁴, Gustavo Roberto Cointy¹. ¹Center of P-Ca Metabolism Studies (CEMFOC), Natl Univ of Rosario, Argentina, Argentina, ²Laboratory for Bone Biology & Emerging Therapies (LABOATEM), Natl Univ of Rosario, Argentina, ³National University of Rosario, Argentina, ⁴Div Space Physiology, Institute of Aerospace Medicine, German Space Agency (DLR), Germany

In a serial pQCT study of the leg (XCT-2000, Stratec, Germany) of sedentary healthy men and women aged 20-40 y ($n=10/10$, J Anat 216:470,2010) we had shown that bone mass distribution along the tibia reflected a structural adaptation to the variable stress pattern imposed by the mechanical usage of the limb. This study extends that observation to further 10/10 men and women of similar age chronically trained in long-distance running, aiming to analyze the interrelationships between indicators of bone mass (total and cortical BMC -ToC, CtC-, cortical cross-sectional area -CtA-, material "quality" (cortical vBMD -CtD-) and diaphyseal design (periosteal perimeter -PoPm-, thickness -CtTh-, circularity, and moments of inertia -MIs- of the CtA) as determined in slices taken at every 5% of height throughout the bone (sites S5 to S95), and of muscle force (maximal calf muscle cross-sectional area -MA-).

As previously observed, all the allometrically-related indicators (ToC, CtC, CtA, PoPm, MIs, MA) were higher, while CtD was lower, in men than women and in trained than in sedentary individuals ($p < 0.05$ - $p < 0.001$). All allometric bone indicators correlated positively with MA ($p < 0.05$ - $p < 0.01$). Circularity was maximal while ToC and MIs were minimal toward S15. ToC increased proximally, especially at sites closer to the knee. The MIs increased geometrically with bone height from S30 upwards. CtTh increased toward the central diaphysis and decrease more proximally. The analysis of all individuals together showed single-curve correlations between MIs and bone mass indicators, CtD and MA, with a maximal significance toward the central region of the bones. All these associations were independent of the degree of physical activity.

Results suggest that there would be three regions of the human tibia in which the structural features correspond specifically to three different patterns of usage-derived stress. In these regions the available bone mass would tend to be distinctly distributed in order to optimize predominantly the resistance to 1. uniaxial compression (distal end of the bone, approximately from S5 to S30), 2. anterior-posterior or lateral bending and torsion (central diaphysis, S30-S70), and 3. bi-axial compression (proximal end of the bone, S75-S95). This distribution would be highly oriented by the contractions of regional muscles, and were shown to be independent of the gender, anthropometric characteristics and degree of activity of the individual.

Disclosures: Jose Ferretti, None.

SU0079

Rapid Subchondral Bone Changes Immediately Following Non-Invasive Knee Injury In Mice. Blaine Christiansen*, Matthew J. Anderson, Joel C. Williams, Cassandra A. Lee, Dominik R. Haudenschild. University of California - Davis Medical Center, USA

Traumatic joint injuries commonly lead to osteoarthritis within 10-20 years after injury. Substantial changes to the subchondral bone can also occur during the development of post-traumatic osteoarthritis (PTOA), including thickening of the subchondral plate and degeneration of underlying trabecular bone. In animal models of PTOA, these changes occur within the first several months after injury. However, the time course of bone changes immediately after joint injury has not been defined. Early bone changes (<4 weeks) may predispose the joint to longer-term degeneration, and may help determine the "window of opportunity" for treatments aimed at delaying or preventing the onset of PTOA. In this study, we induced non-invasive knee injury in mice using tibial compression. This loading method causes anterior translation of the tibia relative to the distal femur, reproducibly injuring the soft tissues of the knee at compressive loads of 10-12 N. A single dynamic axial compressive load (1 mm/s loading rate) was applied to the right knee of mice, to a target compressive load of 12 N to induce knee injury. Mice were euthanized at 1, 3, 7, 14, 28, or 56 days after knee injury ($n=6$ mice/time point). Another 6 mice served as uninjured controls. Bilateral knees were scanned using micro-computed tomography (SCANCO μ CT 35, Bassersdorf, Switzerland). Trabecular bone was analyzed at the distal femoral epiphysis, proximal tibial epiphysis, and proximal tibial metaphysis. Cortical bone was analyzed at the tibial plateau. At the distal femoral epiphysis and proximal tibial epiphysis we observed a rapid and substantial loss of trabecular bone, reaching a minimum near 7 days post-injury (-44% BV/TV at the femoral epiphysis, -40% BV/TV at the tibial epiphysis). This was followed by a partial recovery of trabecular bone volume back to a new (but lower) steady state by 28 days (Fig. 1). There was a similar, but milder response in the contralateral limb, indicating a systemic effect, possibly due to the inflammatory response after injury. No significant changes were observed at the tibial metaphysis or tibial plateau cortical plate. This immediate loss of trabecular bone volume following injury is a novel and important observation, and may be crucial for determining the window of opportunity for treatments aimed at slowing the development of PTOA. If a similar change occurs in humans, it could fundamentally change treatment methods following traumatic knee injuries.

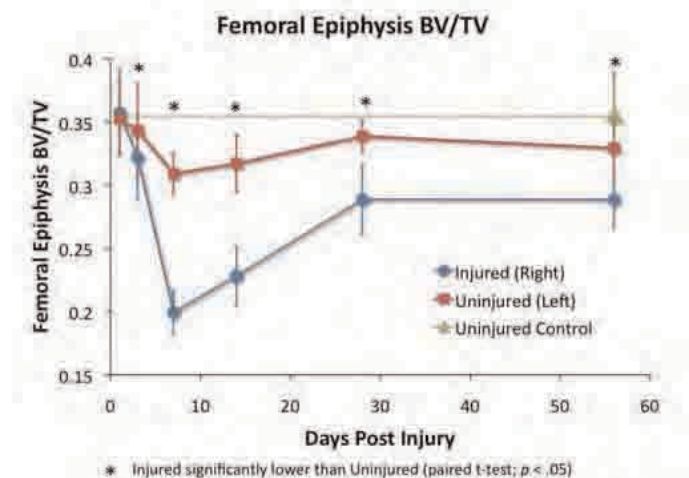


Figure 1: Changes in BV/TV of femoral epiphyseal trabecular bone after non-invasive knee injury.

Disclosures: Blaine Christiansen, None.

SU0080

Site-Specific Skeletal Advantages at the Proximal Femur and Forearm in Young Female Gymnasts. Jodi Dowthwaite*, Paula F. Rosenbaum¹, Tamara Scerpella². ¹SUNY Upstate Medical University, USA, ²University of Wisconsin, USA

Purpose:

We evaluated site-specific skeletal adaptation to loading during growth, comparing radius (RAD) and proximal femur (PF) DXA scans in young female gymnasts (GYM) and non-gymnasts (NON).

Methods:

Subjects from an ongoing longitudinal study (8-17 yrs old) underwent annual DXA scans (PF, forearm, total body) and anthropometry, completing maturity, nutrition and physical activity questionnaires. This cross-sectional analysis used the most recent data for which subjects met the following criteria: gynecological age ≤ 2.5

years (post-menarche); GYM annual mean gymnastic exposure ≥ 5.0 h/wk in the prior year. Maturity was coded as M1 (Tanner I breast), M2 (pre-menarche, \geq Tanner II breast) or M3 (post-menarche). Scans for 173 subjects were analyzed (Hologic software v.12.7), deriving bone geometric and strength indices via hip structural analysis (femoral narrow neck, NN) and similar RAD formulae (1/3 and Ultradistal (UD)). ANOVA and chi square compared descriptive data. Two factor ANCOVA adjusted for age and height, evaluating interactions and main effects for gymnastic exposure and maturity.

Results:

No differences were detected for GYM vs. NON in age, lean mass, arm length, Tanner breast stage or maturity ($p>0.05$). NON means were greater for height, weight, waist circumference and % body fat, whereas non-aquatic physical activity was greater in GYM ($p<0.05$). Maturity x activity interactions were detected for: BMC at all sites; aBMD (femoral neck (FN), NN & UD); 1/3 width & area; NN & 1/3 cCSA; NN cortical thickness (CT) & buckling ratio (BR); 1/3 Z; UDIBS ($p<0.05$). For RAD, all bone means were greater for GYM than NON (M1-3: $p<0.05$), with largest advantages in M3. At PF, in M1 & M3, GYM means were greater than NON for all but FN area, NN width & NN BR (NON > GYM, $p<0.05$). In M2 at PF, GYM bone means were similar to NON for all but: FN area, NN width, NN BR (NON > GYM); NN Z (GYM > NON) ($p<0.05$). Indices suggested greater bone strength in GYM than NON (M1-3: NN BR, Z (NN, 1/3), UDIBS, $p<0.05$).

Conclusions:

Maturity-specific comparisons suggest site-specific skeletal adaptation to loading during growth, with greater benefits at RAD than PF. At RAD, GYM advantages include bone width as well as cortical CSA and thickness; in contrast, at PF, GYM cortical CSA and thickness are greater, but bone width is less than NON. Thus, gymnasts gain skeletal strength through site-specific modes of geometric adaptation.

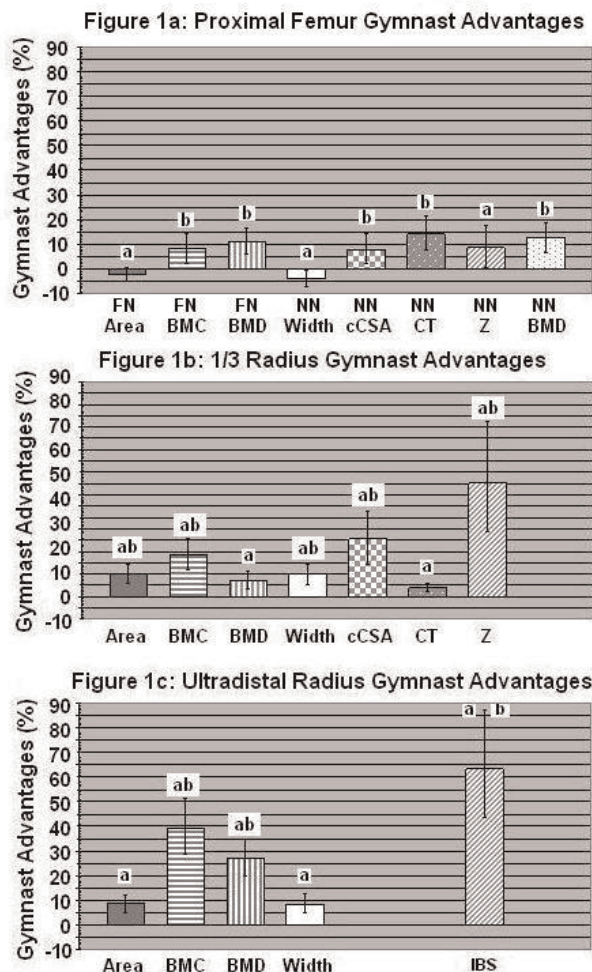


Figure 1: Main effects are depicted as percent differences in GYM vs. NON, with NON means as the zero reference.

- a Main effect for GYM vs. NON difference $p<0.05$
- b Gymnastics x Maturity Interaction $p<0.05$

SU0081

A Novel Imaging Technique and Mouse Model for Evaluation of Osteoarthritis. Zhechao Ruan^{*1}, Brian Dawson², Ming-Ming Jiang², Frank Gannon², Michael Heggenes², Brendan Lee³. ¹Baylor College of Medicine, USA, ²BCM, USA, ³Baylor College of Medicine & Howard Hughes Medical Institute, USA

Osteoarthritis (OA) is a common clinical condition with a prevalence of 40 million people in the United States, resulting in an annual cost of \$100 billion. It is characterized by degeneration of articular cartilage with intraarticular inflammation and synovitis, manifesting as pain and debilitation. In spite of the relative high frequency of OA, as of yet, no efficient treatment has been established. In part, implementation of new therapies has been limited due to a lack of a relevant mouse model of OA. In addition, evaluation of OA severity in the current available mouse models is difficult and not quantitative. Using a novel mouse model that mimics the human post-traumatic OA, we developed a grading system that is based on an imaging technique that combines phase-contrast optics with high resolution microCT, permitting three dimensional reconstructions of the knee joints including the cartilage. This technique allowed us to delineate and quantify histological changes in mouse knee joints including cartilage loss and bone remodeling for the first time. We correlated our OA imaging based grading with functional, behavioral studies and tissue histology. Hence, our data establishes novel technology for quantitatively assessing OA changes in articular cartilage in a surgical model in mice.

Disclosures: Zhechao Ruan, None.

SU0082

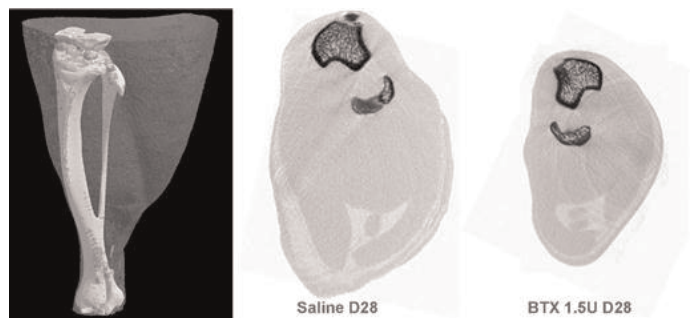
Muscle and Bone Loss after Botox Injection in the Rat (MicroCT study). Beatrice Bouvard^{*1}, Erick Legrand², Maurice Audran³, Daniel Chappard⁴. ¹university hospital of Angers, France, ²Centre Hospitalier d'Angers, France, ³Universite et CHU Angers; INSERM U922, France, ⁴INSERM, U922- LHEA, France

Bone and muscle grow in proportion to one another. Muscles impose large load on bone and skeletal unloading induces muscle loss and bone loss. Animal models for studying disuse use limb immobilization or tail suspension. Transient muscle paralysis using botulinum toxin A (BTX) has been shown to induce a remarkably rapid bone loss with the cessation of active muscle contraction and weight-bearing activity. The aim of our study was to evaluate the evolution of muscle and bone loss in Copenhagen rats by in vivo microcomputed tomography (microCT) after BTX injection.

Twenty-five 4-month-old female Copenhagen rats weighing about 180 grams were randomized in 5 groups. Rats were injected intramuscularly with 1.5 units BTX (Botox® Allergan, Inc.) dissolved in 0.2 mL physiological saline. Injections were performed under Isoflurane inhalation anesthesia in the quadriceps muscle of the right hindlimb in two anterior injection points and with saline in the left hindlimb which served as an internal control. Experimentation lasted 4 weeks and one group was sacrificed each week (D0, D7, D14, D21, and D28). After euthanasia, microCT was performed on each tibia and a stack of 2D-sections was obtained. Bone mass and microarchitecture were measured at the primary and the secondary spongiosa of the tibia. After reconstruction, 3D models from the stack of 2D sections were performed to create 2 models: one after bone thresholding, and the other after muscle thresholding. The two models were overlaid and a slice was done just under the growth plate of tibias, perpendicularly to the axis of tibia, to measure bone area and muscle area. Muscle area surface (MSA) was obtained subtracting bone area to muscle area for each tibia.

Gait dysfunction was detectable as soon as D1. At day 7, weight loss was about 3 % and was stable thereafter in each group. Significant differences in MSA and in bone trabecular volume (BV/TV) between right and left legs occurred at day 14. At day 28, MSA difference between right and left leg was 30% ($p<0.01$) and BV/TV difference was 47% ($p=0.01$). Differences in Tb.Th, Tb.N, Tb.Sp and Tb.Pf between left and right legs were also significant at D28.

This is the first study observing the effects of BTX on bone and muscle of Copenhagen rats. Muscle and bone loss were rapid and not recovered at D28. MicroCT is a useful tool to follow muscle and bone loss. Longer experiments are needed to study muscle and bone recovery.



3D and 2D models of tibia and muscle

Disclosures: Beatrice Bouvard, None.

SU0083

Osteoarthritis (OA)-Induced Pain Assessment. Rana Samadfam^{*1}, NANCY DOYLE², Luc Chouinard³, Susan Y. Smith¹. ¹Charles River Laboratories, Canada, ²CHARLES RIVER, Canada, ³Charles River Laboratories, PCS Montreal, Canada

Major findings in basic science of pain have failed to bring new drugs into clinical practice, partly due to the fact that the preclinical models used for pain assessments do not adequately represent the clinical condition. A potentially useful approach to evaluate antinociceptives is using animal models with diseases similar to humans such as OA. The objectives of this study were to determine the optimal dose of MIA (Monosodium Iodoacetate) to induce joint discomfort in rats and to develop/validate relevant pain endpoints. Measurement of dynamic weight bearing (DWB) has the advantage of quantifying a spontaneously emitted behavior, providing more clinically relevant results compared to reflexive measurements (Von Frey filament (VFF) or pinch). Adult rats were assigned to three groups, each receiving an intra-articular injection of saline or MIA at 1 or 3 mg/dose in the right knee. Osteoarthritis was confirmed and graded by histology evaluations. Pain was evaluated at Day 14 using: body position, gait, toe pinch, modified grip strength test VFF and DWB. Animals with more severe symptoms of OA were treated with Naproxen and pain was evaluated once predose, 4 and 6 hours post dose. Animals treated with MIA at 1 mg/dose generally had less severe OA symptoms but with normal body position and gait and only trends of an altered weight bearing of the right rear paw compared to controls. Animals treated with MIA at 3 mg/dose had more severe OA with normal gait but clearly showed signs of joint discomfort (right rear paw) as measured by DWB. Modified grip strength test indicated the right rear paw was weaker than the untreated left rear paw. The VFF test was the most sensitive endpoint for this model with significant differences between the right and left rear paws. Naproxen reduced pain in the majority of the 3 mg/dose animals as evidenced by balanced weight distribution and comparable use of both rear paws. These results indicate that reflexive pain measures were successfully measured at 1 mg/dose. However, the 3 mg/dose produced consistent quantitative changes and was considered the optimal dose of MIA to assess pain under more clinically relevant conditions (spontaneously emitted behavior) using DWB.

Disclosures: Rana Samadfam, None.

SU0084

Osteonectin Expression in Synovial Fluid of Artificial Hip Joints with Different Articular Couplings. Monica Montesi^{*1}, Alina Beraudi¹, Susanna Stea¹, Francesco Traina², Stefano Squarzone³, Stefano Falcioni¹, Aldo Toni². ¹Laboratorio di Tecnologia Medica, Istituto Ortopedico Rizzoli, Italy, ²Divisione di Ortopedia Traumatologia e Chirurgia Protesica e dei Reimpianti dell'anca e del ginocchio, Istituto Ortopedico Rizzoli, Italy, ³Istituto di Genetica Molecolare- CNR-, Italy

Osteonectin is an important matrix glycoprotein highly expressed in bone (1). In several in vitro and animal in vivo studies it is used as indicator of good integration and tolerance to biomaterials or implanted devices (2; 3; 4; 5). Up to now, not even one study was conducted ex vivo on humans, to investigate the expression of osteonectin in synovial fluid harvested from artificial hip joints with different couplings.

Aim of our study was to assess the expression of osteonectin in the synovial fluid of patients with metal-on-metal (MoM) and ceramic-on-ceramic (CoC) couplings, compared to that of natural hips from patients before a primary total hip arthroplasty. We evaluated also if osteonectin level was correlated with the age of patients, the life of the device and the presence of periprosthetic osteolysis and debris in synovial fluid.

The expression of osteonectin was evaluated by ELISA assay, while the presence of debris was assessed by digestion and EDX Spectroscopy of samples (6).

The expression of osteonectin in patients with CoC coupling was significantly higher (53,2 pg/ml) than in controls (16,9 pg/ml) and in MoM ones (19 pg/ml), while the values in MoM group was not significantly different compared to control (figure 1). The expression of osteonectin was not correlated with the age of patients, the life of the implanted device, and the presence of periprosthetic osteolysis and debris.

Our results suggested that the presence of an artificial hip joint could induce a high expression of osteonectin as indicator of healing and integration. Compared to the metal the ceramic increased the level of osteonectin as indicator of improved biocompatibility.

References

1. Termine JD, et al. Cell. 26, 99-105, 1981
2. Zreiqat H, et al. Biomaterials. 24, 337-346, 2003
3. Ko HC, et al. Dent Mater. 23, 1349-1355, 2007
4. Hu Z, et al. J Biomed Mater Res A. 95, 1048-1054, 2010
5. Roser K, et al. J Biomed Mater Res. 51(2):280-91, 2000
6. Toni A, et al. J Bone Joint Surg Am. 88 Suppl 4: 55-63, 2006

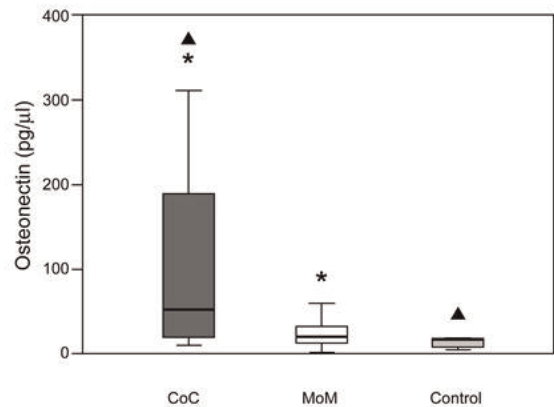


Figure 1
Median values of osteonectin levels (pg/ml) in the synovial fluid of patients with ceramic-on-ceramic (CoC), metal-on-metal (MoM) coupling and without hip prosthesis. The box-whisker plots indicate the median value (thick line) and the 25th (lower line of box) and 75th (upper line of box) percentile.

Figure 1

Disclosures: Monica Montesi, None.

SU0085

Mechanisms of Longitudinal Overgrowth Following Circumferential Periosteal Division of Rat Femur. Shinjiro Takata^{*1}, Tetsuya Enishi², Nori Sato², Mitsuhiro Takahashi², Natsuo Yasui². ¹Institute of Health Biosciences, University of Tokushima Graduate School, Japan, ²Tokushima University Hospital, Japan

INTRODUCTION

Circumferential periosteal division (CPD) of rat tibia produces an increase in its growth rate and in the activity of both the proliferative and hypertrophic zones (Taylor FJ et al. J Anat 151:221-231,1987). This study showed mechanisms of longitudinal overgrowth following CPD of femur of developing rat.

METHODS

Thirty-five Sprague-Dawley rats aged 8 weeks were used for this study. CPD was performed at the diaphysis of rat femur. Rats were sacrificed 2 weeks, 4 weeks and 6 weeks after CPD. The longitudinal length of femur (n=11), rate of longitudinal growth and bone turnover by bone histomorphometry 2 weeks (n=6), 4 weeks (n=6) and 6 weeks (n=6) after CPD, and the microarchitecture of trabecular bone by trabecular analysis of secondary spongiosa by micro CT 6 weeks after CPD (n=6) were compared with between ipsilateral and contralateral sides.

RESULTS

Longitudinal length of rat femur of ipsilateral and contralateral sides were 41.793 ±0.753 mm and 40.272 ±0.690 mm, respectively (p<0.0001), showing that CPD for 6 weeks produced an approximately 3.8% increase of rat femur compared with contralateral femur. Bone histomorphometry shows that the rate of longitudinal growth of femora of ipsilateral and contralateral sides 2 weeks after CPD was 97.17.8 and 84.37.2 µm/day, respectively (p=0.0003), 4 weeks after CPD was 92.35.3 and 54.44.6 µm/day, respectively (p<0.0001), and 6 weeks after CPD was 44.13.4 and 27.65.1 µm/day, respectively. Mineral apposition rate of femora of ipsilateral and contralateral sides 2 weeks after CPD was 4.680.63 and 3.330.44 µm/day, respectively (p<0.0001), 4 weeks after CPD was 3.900.38 and 3.070.25 µm/day, respectively (p=0.0004), and 6 weeks after CPD was 3.350.21 and 2.880.18 µm/day, respectively (p=0.0296).

Micro CT revealed that trabecular separation on ipsilateral and contralateral sides 6 weeks after CPD was 200.732.4 µm and 234.339.4 µm, respectively (p=0.0302), and that trabecular spacing on ipsilateral and contralateral sides was 263.730.3 µm and 300.337.6 µm, respectively (p=0.0261).

DISCUSSION

These results showed that unilateral CPD produces longitudinal overgrowth of ipsilateral femur compared with contralateral one of developing rats. The facts suggest that unilateral CPD stimulates endochondral ossification of ipsilateral femur, and that unilateral CPD might be a promising procedure to correct leg length discrepancy and bone atrophy.

Disclosures: Shinjiro Takata, None.

SU0086

Nitric Oxide Synthase (NOS) in Mouse Femur during Endochondral Ossification. Hiroki Watanabe, Toshihiro Nakagawa, Yuriko Moro, Shinya Takahashi, Kimihiaru Ambe*. Ohu University School of Dentistry, Japan

Recently it has become evident that Nitric oxide (NO) has a pleiotropic role, though NO was first identified as endogenous vasodilator factor (gas). NO plays an important role in several physiological processes, such as vascular relaxation, neurotransmission, and in immune regulation. NO is generated by nitric oxide synthase (NOS), which demonstrates three isoforms, a neuronal form (nNOS), an endothelial form (eNOS) and an inducible form (iNOS). We investigated the expression and cellular localization of NOS isoforms in mouse femur using immunohistochemistry and in situ hybridization in order to clarify its possible role in endochondral ossification. At postnatal 3 weeks, the immunoreactivity of nNOS was observed on chondrocytes from the resting zone to hypertrophic zone. The immunoreactivity of iNOS was localized to part of the chondrocytes in the proliferative zone and prehypertrophic zone, but the many chondrocytes in the prehypertrophic zone and hypertrophic zone were positive for anti-nNOS. The immunoreactivity of eNOS was observed on chondrocytes from the resting zone to hypertrophic zone. At postnatal 18 weeks, the proliferative zone and hypertrophic zone disappeared from the growth plate in femur, and the growth plate was not observed at the proliferation and differentiation of chondrocyte. There was no immunoreactivity for any of the NOS isoforms in chondrocytes. Expression of each NOS mRNA was not detected at chondrocytes. Osteoblasts and osteoclasts were positive for anti-nNOS, iNOS, eNOS until 18 weeks. Expression of NOS mRNA on in situ hybridization showed results approximately similar to those on immunohistochemistry. These findings suggest that each NOS may be related to trabecular bone growth and remodeling in the mouse femur. In addition, NO may play an important role in proliferation and differentiation in chondrocytes.

Disclosures: Kimihiaru Ambe, None.

SU0087

A Novel Double Fluorescent Strategy to Prospectively Isolate Label Retaining Chondrocytes at the Top of the Growth Plate. Noriaki Ono*¹, Takao Hirai², Henry Kronenberg³. ¹Massachusetts General Hospital & Harvard Medical School, USA, ²Kyoto Prefectural University of Medicine, Japan, ³Massachusetts General Hospital, USA

Slowly dividing cells at the top of the growth plate cartilage are the sources of all other chondrocytes in the growth plate and probably share some characteristics of postnatal stem cells. Slowly dividing cells retain nuclear labels longer than their more rapidly dividing progeny (label-retaining cells or LRCs). To prospectively isolate LRCs in the growth plate, we generated mice expressing a tetracycline-controlled transactivator under a type2 collagen promoter (Col2a1-tTA) and conducted a pulse-chase experiment based on a Tet-Off system and a histone 2B (H2B)-bound EGFP label. Col2a1-tTA; Col1a1-TRE-H2B-EGFP (a type1 collagen locus with Tet-responsive element (TRE)-H2B-EGFP cassette insertion) mice were fed with doxycycline for 5 weeks to shut off EGFP expression and sacrificed at 8 weeks of age. We found that the H2B-EGFP signal was largely abrogated in the growth plate region, and only a small fraction of cells near the top of the growth plate retained H2B-EGFP. However, we also found that a low level of H2B-EGFP signal persisted in osteoblasts/cytes even after the chase, perhaps because the TRE-H2B-EGFP cassette had been inserted in the Col1a1 locus. To distinguish the EGFP-labeled chondrocytes from osteoblasts/cytes, we attempted to label all chondrocytes in the growth plate with a red fluorochrome, using an inducible Col2a1-CreERT system that activated a Rosa26 cytomegalovirus enhancer/chicken beta-actin promoter (CAG)-tandem dimer (td) Tomato reporter locus. We confirmed that tamoxifen injection during a week earlier gave rise to Tomato(+) cells mostly within the growth plate. Col2a1-CreERT; Rosa26-CAG-tdTomato; Col2a1-tTA; Col1a1-TRE-H2B-EGFP quadruple mutant mice were fed with doxycycline for 5 weeks and injected with tamoxifen during a week prior to analysis at 8 weeks of age. We found that Tomato(+) chondrocytes near the top of the growth plate retained a higher level of H2B-EGFP expression. Epiphyses of long bones were dissected and serially digested by collagenase to release cells for flow cytometry. Growth plate chondrocytes defined as a Tomato(+) population represented 17% of non-hematopoietic cells. A Label-retaining population with >10⁴ unit of GFP (GFP^{high}) represented 1% of the Tomato(+) population. Distinct GFP^{mid} non-label-retaining and GFP^{low} populations were also observed. This study indicates the feasibility of our double fluorescent strategy to isolate label-retaining chondrocytes by cell sorting to study their gene profiles.

Disclosures: Noriaki Ono, None.

SU0088

Acceleration of Chondrocyte Differentiation with a Peptide Exhibiting Osteoclastogenesis Inhibitory Activity and Osteogenesis Stimulatory Activity. YURIKO FURUYA*, KOJI UCHIDA, HISATAKA YASUDA. ORIENTAL YEAST CO.,LTD, Japan

Introduction: A TNF α antagonistic peptide is known to inhibit osteoclastogenesis by blunting RANKL-RANK interaction. We reported that the peptide enhanced osteoblastic differentiation/mineralization in vitro and also increased bone formation in vivo in the previous meeting. Here we evaluated whether the peptide had a chondrocyte differentiative effect using mouse prechondrocytic ATDC5 cells and human mesenchymal stem cells (hMSCs).

Methods: ATDC5 cells and hMSCs were cultured in chondrocytic conditions with or without the peptide for 2 weeks and stained with alcian blue. The effect of the peptide was examined on 3 dimensional (3D) hMSC pellet cultures for 2 or 3 weeks. The synergistic effects of the peptide with TGF- β 3 or BMP-2 were examined in 3D hMSC pellet cultures. Formalin-fixed, paraffin-embedded 3D pellet sections were stained with safranin O and alcian blue, respectively, for detection of cartilage matrix. Gene expression in hMSCs treated with the peptide for 24, and 96 hr was examined by Gene chip assay.

Results: Alcian blue staining revealed that the peptide differentiated ATDC5 cells to chondrocytes in a dose-dependent manner. Similar observations were also found in hMSCs culture. The peptide enlarged markedly alcian blue-positive 3D hMSC pellets in a dose-dependent manner compared with the control. Simultaneous treatment of the 3D pellet cultures with the peptide and TGF- β 3 or BMP-2 markedly enhanced the alcian blue staining and safranin O staining, respectively, but TGF- β 3 or BMP-2 showed no additive effects on enlargement of the pellets cultured with the peptide. Gene expressions of cartilage matrix proteins and IGF-1 were significantly upregulated in hMSCs treated with the peptide for 24 and 96 hr.

Discussion: A peptide exhibiting osteoclastogenesis inhibitory activity and osteogenesis stimulatory activity induced chondrocytic differentiation in ATDC5 and hMSCs. The peptide also increased the production of cartilage matrix proteins and synergistically enhanced their production with TGF- β 3 or BMP-2. The peptide may be useful for and applicable to the treatment of chondropathy such as osteoarthritis and cartilage injury. The mechanism by which the peptide inhibits osteoclastogenesis and stimulates osteogenesis and chondrogenesis remained to be elucidated.

Disclosures: YURIKO FURUYA, ORIENTAL YEAST CO.,LTD., 3

SU0089

Activation of Wnt Planar Cell Polarity (PCP) Signaling Promotes Columnar Architecture of Growth Plate Chondrocytes In Vitro. Rachel Randall*¹, Yvonne Shao², Lai Wang¹, Robert Ballock³. ¹Cleveland Clinic, USA, ²CCF, USA, ³The Cleveland Clinic Foundation, USA

Background: Although the cellular and molecular mechanisms governing the morphogenesis of columnar growth plate cartilage are currently unknown, the activity of the Wnt Planar Cell Polarity (PCP) signaling pathway has been implicated in this process. We hypothesized that growth plate column formation can be recapitulated in vitro through activation of Wnt PCP signaling.

Methods: Epiphyseal chondrocytes were isolated from 4-day old Sprague-Dawley rats, digested, and transfected with plasmid DNA encoding the full-length Fzd7 receptor, or a deletion mutant of the Fzd7 receptor lacking the Wnt-binding domain, and cultured as three-dimensional cell pellets. Recombinant Wnt5a was added to the culture medium for up to three weeks. The alignment of cells into columns was assessed by histomorphometric measurements.

Results: Columnar architecture of growth plate chondrocytes was enhanced in cell pellets in which Wnt PCP signaling was activated by Fzd7 overexpression with addition of Wnt5a.

Conclusions: Activation of the Wnt PCP signaling pathway, through overexpression of the Fzd7 receptor and addition of exogenous Wnt5a, appears to promote columnar chondrocyte architecture of isolated growth plate chondrocytes in vitro.

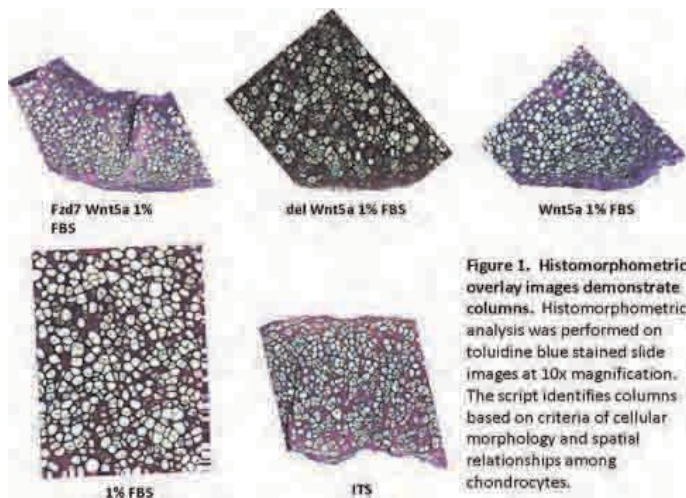


Figure 1

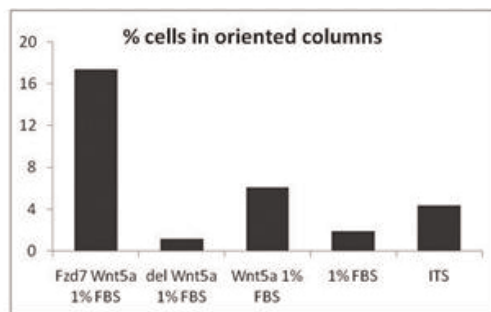


Figure 2. Percentage of cells in oriented columns. Histomorphometric analysis of toluidine blue stained images determined columns based on cellular morphology and spatial relationships among cells. Values shown are percentage of cells in the 10x image participating in columns of at least three cells and orientation between 65-115 degrees from a predetermined reference line. Treatment groups include isolated rat growth plate chondrocytes transfected with Fzd7, a deletion mutant of Fzd7 lacking the CRD, addition of exogenous Wnt5a, 1% FBS, or ITS (serum-free medium).

Figure 2

Disclosures: Rachel Randall, None.

SU0090

Essential Role of Cdc42 in Chondrogenesis and Interdigital Programmed Cell Death During Limb Development. Ryo Aizawa¹, Atsushi Yamada¹, Dai Suzuki², Hidetoshi Kassai³, Takeshi Harada³, Masayuki Tsukasaki¹, Gou Yamamoto¹, Tadahiyo Iimura⁴, Akira Yamaguchi⁵, Kazuki Nakao³, Matsuo Yamamoto¹, Atsu Aiba³, Ryutaro Kamiyo¹. ¹Showa University School of Dentistry, Japan, ²Showa University, Japan, ³The University of Tokyo, Japan, ⁴Tokyo Medical & Dental University, Global Center of Excellence Program, Japan, ⁵Tokyo Medical & Dental University, Japan

Cdc42, a member of the Rho family of small GTPases, is known to be a regulator of multiple cellular functions, including cytoskeletal organization, cell migration, proliferation, and apoptosis. However, its tissue-specific roles, especially in mammalian limb development, remain unclear. To investigate the physiological functions of Cdc42 during limb development, we generated a limb bud mesenchyme-specific inactivated Cdc42 mouse model (*Cdc42^{fl/fl}; Prx1-Cre*) by crossing *Cdc42^{fl/fl}* mice with *Prx1-Cre* transgenic mice, since *Cdc42^{-/-}* embryos die before embryonic day (E) 7.5. Although most of the *Cdc42^{fl/fl}; Prx1-Cre* mice were viable at birth, all died within 1 day. Anatomical analyses demonstrated that *Cdc42^{fl/fl}; Prx1-Cre* neonates had short limbs and body, skull hypoplasia, a complete cleft palate, disruption of the xiphoid process, and short and thick mineralized bone in the limbs as compared to *Cdc42^{fl/fl}* neonates. Detailed analyses of *Cdc42^{fl/fl}; Prx1-Cre* limbs revealed severely disorganized growth plates with a wider hypertrophic zone and altered cell shape of chondrocytes. In addition, *Cdc42^{fl/fl}; Prx1-Cre* mice presented with syndactyly characterized by fusion between the second and third phalanges. Defects in the expression patterns of *Sox9*, *Glil*, *Patched1*, and *Hoxd13* were apparent in *Cdc42^{fl/fl}; Prx1-Cre* mice as early as E12.5, consistent with the abnormal calcification and fusion of phalanges. Furthermore, cutaneous syndactyly with webbing of the interdigital skin

appeared in these mice. To determine whether webbing of the interdigital skin was due to a defect of interdigital programmed cell death, TUNEL assays were performed using limb buds obtained from E12.5-E14.5 mice, which demonstrated a significant reduction of interdigital programmed cell death. *Bmp2* expression was also down-regulated in the interdigital region of the limbs as compared to those of *Cdc42^{fl/fl}* mice, as were the expression of *Msx1* and *Msx2*, which are known as downstream target genes of BMP signaling and promote intense apoptosis in limb development. Taken together, these results demonstrate that Cdc42 is essential for chondrogenesis and interdigital programmed cell death during limb development.

Disclosures: Ryo Aizawa, None.

SU0091

Expression of Sclerostin in the Developing Zebrafish Brain and Skeleton. Melissa McNulty¹, THEODORE CRAIG¹, Victoria Bedell¹, Tammy Greenwood¹, Stephen Ekker¹, Rajiv Kumar². ¹Mayo Clinic, USA, ²Mayo Clinic College of Medicine, USA

Sclerostin (sost) is a secreted glycoprotein that influences skeletal development by modulating the activity of bone morphogenic proteins, LRP 5/6, *cyr61*, and the *erbB3* receptor. To gain insights into the ontogeny of zf sclerostin expression, we performed in situ hybridization with sense and anti-sense RNA probes 15-120 hpf. Embryos were fixed with paraformaldehyde, washed and treated with proteinase K. Approximately 400-500 bp-long digoxigenin-labeled sost RNA probes were hybridized to treated embryos. Following hybridization and extensive washing, zf embryos were treated with buffer containing 2 mg/mL BSA, and 2%-sheep serum. Digoxigenin antibody, 1/6000 dilution, pre-blocked with fish powder, was added and embryos incubated overnight. Embryos were washed with PBST and treated with AP buffer (Tris 100 mM, MgCl2 50 mM, NaCl 100 mM). AP substrate (NBT, BCIP) was added to the embryos. Substrate buffer was removed and embryos were washed with PBST. Localization of probes was visualized by light microscopy. Whole mount immunofluorescence was performed using polyclonal antibodies directed against zf sclerostin. Fixed embryos were digested with acetone or proteinase K. Embryos were blocked with 2% goat serum and 1% BSA in PBST. Anti-ZF-sclerostin antibodies (1:5000) were applied in blocking buffer. Following extensive washes, anti-rabbit Alexa Fluor555 antibodies (1:1000) were applied. Composite images of embryos were generated. Paraffin sections (4 µm) of adult zf were processed using the aforesaid antibodies.

Results: With an anti-sense sost probe, sost RNA was noted as early as the 12 somite stage. 20 hpf, sost RNA was detected in the nervous system (figure 1A). By 48 hpf, sost RNA was detected in the cartilage of the pharyngeal arches and the mandibular arch (figure 1B). Sost RNA was clearly seen in these structures 72 and 96 hpf, as well as, in developing dorsal fins (figure 1C and figure 1D). Experiments with sense probes showed no signal throughout the zf embryonic development. In 24 hpf embryos sclerostin epitopes were identified in the nervous system. In adult zf, sclerostin antibodies detected epitopes in osteoblasts of zf bone. **Conclusions:** Sclerostin RNA is detected in pharyngeal and mandibular cartilage of the developing zf demonstrating that it may play a role in cartilage development. In addition, sclerostin RNA is detected early in the developing neural system suggesting a role for this protein in nervous system physiology.

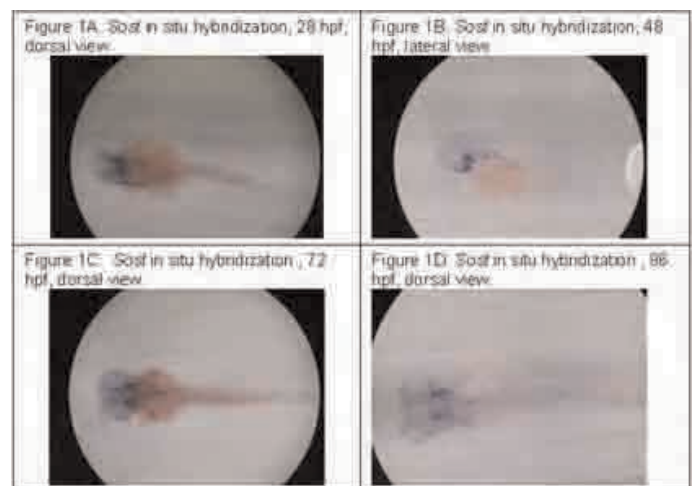


Figure 1

Disclosures: Rajiv Kumar, None.

SU0092

MEPE-ASARM Peptides: Novel Regulators of Growth Plate Mineralisation. Colin Farquharson¹, Vicky MacRae², Katherine Staines². ¹Roslin Institute, University of Edinburgh, United Kingdom, ²The Roslin Institute & R(D)SVS, The University of Edinburgh, United Kingdom

Advances in the understanding of hypophosphatemic disorders have identified a novel group of molecules (FGF23, PHEX, MEPE, DMP1) involved in phosphate homeostasis. The specific binding of PHEX to MEPE regulates the release of ASARM peptides, implicated in osteoblast mineralisation directly. Although the growth plates of MEPE transgenic display severe morphological disruption, the expression and function of MEPE in growth-plate mineralisation remains largely undefined.

Proximal tibiae from 3-week-old wild-type mice were analysed for *Mepe* expression by hybridisation and growth-plate microdissection. Gene expression by the ATDC5 chondrogenic cell-line was examined by RT-qPCR over a 20-day calcifying culture period. 20µM phosphorylated (pASARM) and non-phosphorylated ASARM (npASARM) peptides were added to ATDC5 cultures, and to embryonic metatarsal explants.

Mepe expression was abundant throughout the growth-plate as shown by *in situ* hybridisation. Microdissection of the growth-plate confirmed an increased expression of *Mepe* in the hypertrophic chondrocytes compared to proliferative chondrocytes ($P < 0.05$). ATDC5 cells showed an initial decrease in *Mepe* expression at day-10 of culture, after which expression increased at day-15. Treatment of ATDC5 cells with pASARM peptide caused an inhibition of mineralisation, determined by alizarin red staining ($P < 0.01$). Treatment with npASARM promoted mineralisation ($P < 0.01$). The growth rate of 15 and 17-day-old embryonic metatarsals and the proliferation of chondrocytes within were not affected by treatment with 20µM pASARM or npASARM peptides. This indicates that the peptides were not toxic and the bones were still viable after 7 days of culture. However, in 17-day-old embryonic metatarsals, the growth of the central diaphyseal mineralisation zone was inhibited in bones treated with 20µM pASARM ($P < 0.001$). In 15-day-old embryonic metatarsals, the central mineralised core only forms after 7 days in culture. Treatment with 20µM pASARM peptides completely prevented mineralisation. Alkaline phosphatase activity was unchanged between the treated and untreated bones, suggesting that the observed inhibition of mineralisation is not a result of decreased enzyme activity.

Our findings indicate that MEPE is expressed by growth-plate chondrocytes and that it is likely to have a developmental role in the inhibition of cartilage matrix mineralisation through its cleavage and subsequent phosphorylation of the ASARM peptide.

Disclosures: Katherine Staines, None.

SU0093

Notch Signaling during Chondrogenesis. Shan Chen^{*1}, Jianning Tao¹, Ming-Ming Jiang¹, Terry Bertin¹, Brendan Lee². ¹Baylor College of Medicine, USA, ²Baylor College of Medicine & Howard Hughes Medical Institute, USA

Notch signaling is critical during development directing binary cell fate between progenitors and differentiated cells. Aberrant Notch function causes several human skeletal diseases such as Spondylocostal dysostosis (SCDO) and Alagille syndrome. Recently, cartilage specific gain- or loss- of-function of Notch mouse models have been made in our and other laboratories. Although detailed phenotypic studies of these mice have been conducted, a full knowledge of the mechanisms of the pathway is still lacking. The canonical Notch pathway involves Rbpj as a co-factor to induce target gene expression. However several findings suggest Rbpj-independent mechanisms exist to promote Notch signaling transduction. Our goal is to unravel the molecular mechanisms by which Notch signaling controls cartilage development. We hypothesize that the function of Notch signaling is mediated by both the canonical and non-canonical pathways. To study the gain-of-function of Notch in cartilage, we crossed a Col2a1-cre line with a line having a conditionally activated allele of Notch1 intracellular domain (N1ICD). Resulting mutant mice have shortened limbs, undersized ribs, and virtual absence of the spine and tail. Decreased Alcian blue staining highlights the general defects of chondrogenesis. The decreased expression of Sox9, Col2, Col10 in the mutant suggests the inhibition of chondrocyte differentiation by Notch signaling. On the other hand, complete loss-of-function of Notch (achieved by deleting Presenilin 1/2 in cartilage) causes undersized and underdeveloped skeletal elements. The limbs and spine are about 40% shorter in the mutants at 3 weeks of age. Interestingly, cartilage specific deletion of Rbpj causes only a mild phenotype. The body weight and histology of cartilage appear to be normal at 3 weeks of age. To test whether Notch signal transduction depends on Rbpj, we made mice with deficient Rbpj on the Notch gain-of-function background. These mice have nearly normal limb structure but demonstrate irregular curvature of the spine with a shortened tail, suggestive of incomplete rescue. To completely map the Notch signaling pathway, we are identifying Notch targets by a CHIP-seq approach in the ATDC5 cells, a chondrocyte cell line. We have achieved high specificity and enrichment of the occupancy of the Notch targets using a tagged system. We hope to identify differential targets of canonical vs. noncanonical Notch signaling using this approach.

Disclosures: Shan Chen, None.

SU0094

PDGF-BB and CCL21 Mediate TGFβ-Induced Migration during Development of Dorsal Vertebrae. Ying Wang^{*}, Rosa Serra, University of Alabama at Birmingham, USA

During vertebrae development, sclerotome, a population of undifferentiated mesenchymal cells, differentiates and migrates to give rise to distinct parts of the vertebrae and ribs. Our laboratory has shown that deletion of TGFβ type II receptor (*Tgfr2*) in Col2a expressing tissue in mice results in small vertebrae and failure in the formation of the spinous process, mimicking spina bifida occulta, a common congenital malformation in humans. Mechanisms mediating closure of the dorsal vertebrae are not clear. In this study, we aimed to determine whether the missing dorsal structures in *Tgfr2* mutant mice are due to defects in migration of sclerotome and surrounding mesenchyme, and to further clarify the underlying mechanism of TGFβ-mediated migration.

We first crossed the Col2aCre mice to the Rosa26 reporter strain to show that TGFβ signaling is required for dorsal closure of vertebrae and formation of the spinous process, and that the disruption to development is evident by E16.5 days. We then used a chemotaxis migration assay to show that TGFβ signaling promotes the migration of embryonic sclerotome and associated mesenchyme, and this action is mediated by the downstream effector PDGF-BB. We found that PDGF-BB is mainly expressed in the sclerotome that forms future cartilage, whereas PDGFRβ is dominantly expressed in the surrounding mesenchyme. Previous studies have shown that PDGF signaling promotes migration of sclerotome associated mesenchymal cells, which secrete chondrogenic factors required to form dorsal cartilage. Using microarray technology, we also identified CC-chemokine ligand 21 as a downstream target of TGFβ signaling, which we propose is also involved in TGFβ-mediated migration and formation of the spinous process. Our study suggests that TGFβ signaling is required for dorsal closure of vertebrae and formation of the spinous process. This action is likely mediated by the downstream effectors PDGF-BB and CCL21 and their role in regulating migration of sclerotome and associated mesenchyme. These findings suggest that TGFβ potentially could be a therapeutic target for osteoarthritis or fracture repair, which also involve migration of chondrogenic mesenchymal cells.

Disclosures: Ying Wang, None.

SU0095

The Alk2 R206H (FOP) Mutation Causes Lower Limb Chondrodysplasia in Mice. Salin Chakkalakal^{*1}, Andria Culbert¹, Michael Convente¹, Devy Zhang¹, Frederick Kaplan², Eileen Shore¹. ¹University of Pennsylvania, USA, ²University of Pennsylvania Hospital, USA

Mutations in the ALK2 BMP type I receptor (encoded by the *ACVR1* gene) cause fibrodysplasia ossificans progressiva (FOP), a disabling human disease characterized by progressive heterotopic endochondral ossification and malformations of the great toe. Most individuals with FOP have the identical single nucleotide activating missense mutation (c.617G>A; R206H) in the GS regulatory subdomain of ALK2. We developed a heterozygous Alk2 R206H knock-in mouse in which the mutated allele is regulated by the endogenous *Acvr1* promoter. While mice chimeric for cells with the R206H mutation are viable and show all of the characteristic clinical features of FOP, germline transmission of the heterozygous mutant allele is perinatal lethal. By whole mount skeletal staining and microCT imaging, these one day old heterozygous Alk2 R206H mice have reduced body size compared to controls and exhibit malformations and joint ankylosis primarily affecting the tibia, fibula, and foot of the hind limbs, while, as with FOP patients, forelimbs were generally unaffected. Histological analysis of one-day old mutant mice showed defective growth plate morphology with expansion of proliferative chondrocytes, decreased hypertrophic and hypertrophic zones, and reduced metaphyseal ossification. Consistent with these altered patterns of chondrocyte differentiation and endochondral ossification, immunohistochemistry and/or quantitative RT-PCR revealed increased Sox 9 and collagen type II expression and decreased collagen type X and Runx2 expression. BrdU labeling of 18.5 dpc embryos showed increased proliferation of immature chondrocytes and an accumulation of labeled prehypertrophic chondrocytes (with limited progression to hypertrophic chondrocytes). Phosphorylated Smad1/5/8 was increased in both proliferating and hypertrophic chondrocytes, indicating enhanced BMP signaling in these cells. These studies indicate that the canonical Alk2 R206H FOP mutation in mice causes lower limb chondrodysplasia characterized by enhanced proliferation and accumulation of immature chondrocytes and decreased maturation and ossification of hypertrophic chondrocytes.

Disclosures: Salin Chakkalakal, None.

SU0096

The Role of Neogenin in Osteoarthritis Pathogenesis. Zheng Zhou^{*}, Lin Mei, Wencheng Xiong, Georgia Health Sciences University, USA

Osteoarthritis (OA) is the most common joint disease caused by aging, joint injury and heredity. However, molecular mechanisms underlying OA pathogenesis are largely unknown. Neogenin is identified as a member of cell surface receptor for neuronal axon guidance cue netrins and RGMs (repulsive guidance molecules), and is

involved in axon guidance, neuronal differentiation, and apoptosis. Recently, we have demonstrated that neogenin regulates endochondral bone development and iron homeostasis via BMP signaling. In light of these observations, we speculate a potential function of neogenin in articular chondrocyte differentiation and function, and loss of neogenin function may underlying OA pathogenesis. Here, we provide evidence from our preliminary studies that supports this hypothesis. Neogenin was expressed in articular chondrocytes. Neogenin heterozygous mice showed spontaneous OA-like phenotypes, including damage of articular cartilage, loss of proteoglycan, increased expression of degradative proteinases such as MMPs and ADAMTS. DMM (Destabilization of the medial meniscus) accelerated the OA-like phenotypes in neogenin heterozygous mice. The underlying molecular mechanism remains to be further investigated.

Disclosures: Zheng Zhou, None.

SU0097

Identification of Human Bone Cell Characteristic Transcripts and their Interactions Using Online Browser Based Search In a Giant Correlation Matrix. Sjur Reppe^{*1}, Daniel Sachse¹, Ole K. Olstad¹, Vigdis T. Gautvik², Paul Sanderson³, Harish Datta⁴, Jens P. Berg¹, Kaare Gautvik¹. ¹Oslo University Hospital, Norway, ²University of Oslo, Norway, ³Newcastle General Hospital, United Kingdom, ⁴Newcastle University, United Kingdom

Bone development, and remodeling is primarily dependent on complex interaction among 3 defined cell types: osteoblasts (OB) and osteocytes (Ocy) responsible for formation and osteoclasts (OC) causing resorption. To further understand the regulation of skeletogenesis it is important to have an overview of the characteristic cell-specific transcriptomes as well as of gene interactions and signaling pathways involved in the various physiological processes. Global gene expression analysis of iliac crest bone biopsies from 84 postmenopausal ethnic Norwegian women allowed defining the molecular skeletal phenotype through quantifications of ~23000 mRNA species. These mRNAs were inter-correlated giving an array containing >260 000 000 pairwise correlations with p- and Pearson r-values. An online browser was programmed for targeted search, thus enabling identification of transcripts which were correlated to those characteristic for Ocy, OB and OC. We found very high correlations between ensembles of known or uncharacterized transcripts linked to cell lineage-specific genes, and were able to define interacting molecular networks across the cell types. For validation of the browser based results we used experimentally proven interactions between the ubiquitous glucocorticoid receptor, the central bone transcription factors SATB2 or RUNX2 and their responsive genes. The matrix, recapitulated more than 92%, 81% and 55%, respectively, of documented interactions as significant correlations. A similar high degree of correlations related to bone cell characteristic transcripts were reproduced in a replica array originating from trabecular vertebral bone biopsies from British Caucasian males. The results provide a unique platform for the identification and further characterization of key functional and regulatory molecules in bone and possibly other tissues and cell types

Disclosures: Sjur Reppe, None.

SU0098

In Vivo Study of Mxsl Involvement in Alveolar Bone Growth. Sylvie Babajko^{*1}, Ibtisam Senussi², Fleur Meary³, Sophia Loidice⁴, Ariane Berdal⁵. ¹INSERM, France, ²Inserm U872 Université Paris 6, France, ³Inserm U872, France, ⁴Inserm U872 Université Paris 7, France, ⁵Université de Paris 7, France

Mxsl homeogenes play an important role in epithelial-mesenchymal interactions leading development. Mxsl is relevant for dental and craniofacial morphogenesis, as suggested by phenotypes of Mxsl mutations in human and Mxsl knock-out (KO) mice. During post-natal development and adulthood, Mxsl is still expressed in the skeleton where its role is largely unknown. Mxsl function in mandibular and maxillary bones was investigated by comparing the phenotype of Mxsl KO mice and a transgenic mouse line recently established for this study, with Mxsl expression under the control of the 2.3 kb collagen 1 alpha 1 promoter.

In the absence of Mxsl, mandible and alveolar bone morphology observed by micro-CT was affected suggesting Mxsl involvement in bone morphogenesis during embryonic development. On the other side, in Mxsl transgenic (Mxsl Tg), the overall morphology appeared similar even if the alveolar bone was thicker.

Histological analysis of the mandibles at one day after birth showed an accumulation of bone in Mxsl Tg mice compared to wild types. The greatest differences were observed in bone surrounding the incisor and the molars with an increased bone volume containing more trabeculae. On the contrary, Mxsl KO mice have already been shown to produce less alveolar bone. In parallel, our results showed that Mxsl increased cell proliferation as well as apoptosis investigated by caspase-3 expression and TUNEL activity assays. They suggest that Mxsl could be considered as a bone trophic factor leading to an increased cell number explaining the greater bone remodeling.

Disclosures: Sylvie Babajko, None.

SU0099

Is Serum Amyloid A3 (Saa3) a Link Between Hyperhomocysteinemia and the Development of Degenerative Skeletal Pathologies?. Roman Thaler^{*1}, Monika Rumpel², Silvia Spitzer², Eleftherios Paschalis³, Sonja Gamsjaeger², Klaus Klaushofer⁴, Franz Varga². ¹Ludwig Boltzmann Institute of Osteology, Austria, ²Ludwig Boltzmann Institute of Osteology at the Hanusch Hospital of WGKK & AUVA Trauma Centre Meidling, 1st Medical Department, Hanusch Hospital, Austria, ³Ludwig Boltzmann Institute for Osteology, Austria, ⁴Hanusch Hospital, Austria

Hyperhomocysteinemia is related to cardiovascular diseases, diabetes, osteoarthritis and bone fragility. We recently showed that homocysteine (Hcys) alters collagen cross-linking by hindering the expression of the collagen cross-linker lysyl-oxidase (Lox) through an epigenetic mechanism. In mice, Saa3 was identified as an inflammatory acute-phase reactant, while in rabbits SAA3 was shown to be highly up regulated in Ag-induced arthritis. In pre-osteoblastic MC3T3-E1 cells its mRNA expression is significantly upregulated by Hcys. C3H10T1/2, ST2, MC3T3-E1, 3T3-L1 and C2C12 cells were cultured up to 21 days with several Hcys conc. and/or inhibitors of signal transduction pathways. Osteoblastic cells were reseeded onto Hcys marred extra cellular matrix (ECM) produced by MC3T3-E1 cells. Gene expression was analyzed by GeneChip, qPCR and immuno-blotting. To study transcriptional regulation by Hcys, truncated and mutated variants of the Saa3 promoter were cloned into SEAP2-reporter vector, transfected into MC3T3-E1 cells, which were treated without or with Hcys. Promoter binding and localization of transcription factors were studied by chromatin immunoprecipitation (ChIP) assays and immunofluorescence. Collagen cross-links were measured by FTIR and collagen helix formation was analyzed by a discriminative antibody. Only osteoblastic cells showed a strong, time dependent up-regulation of Saa3 by Hcys treatment. Similarly, compared to untreated ECM, reseeding of MC3T3-E1 cells onto Hcys marred ECM increased Saa3 expression. Both conditions activated focal adhesion kinase and Paxillin and increased cytoplasmic accumulation of b-Catenin (bCat). Transfection of a cytoplasmic bCat-mutant increased strongly Saa3 expression which failed after mutation of a RELA site on Saa3 promoter. Comparison of Saa3 transfected and Hcys treated MC3T3-E1 cells to controls by GeneChip analysis revealed up regulation of Mmp13, the pro-apoptotic gene Fas and of several chemokines like Ccl2, 5, 7 and 9, Cxcl10, Il6 and Il33 in both cases. Mmp13 was up regulated via MAPK and AP-1. Hcys treatment changed collagen cross-linking and fibrillogenesis as shown by FTIR and immunofluorescence, respectively. Our results show that Hcys induces inflammatory genes via Saa3 by marred ECM. This regulation is mediated by FAK, Paxillin, bCat and RelA, as shown by ChIP. In conclusion, we propose Saa3 as new link between hyperhomocysteinemia and the development of degenerative skeletal diseases.

Disclosures: Roman Thaler, None.

SU0100

Pannexin 3 Plays a Critical Role for Odontoblast Differentiation. Tsutomu Iwamoto^{*}, YU SUGAWARA, Mariko Ono, Aya Yamada, Takashi Nakamura, Satoshi Fukumoto. Tohoku University Graduate School of Dentistry, Japan

Gap junction proteins play a crucial role in the development of tooth that has well-organized hard tissue structures in enamel and dentin. Pannexin (Panx) is a recently discovered gap junction protein in human and mouse genome. Here, we found that Panx3 was strongly expressed in tooth. Northern blotting revealed that Panx3 is preferentially expressed in tooth, compared to other tissues. In situ hybridization showed that Panx3 mRNA was expressed in preodontoblasts that are a responsible for a dentin formation. To analyze the function of Panx3, we used an odontoblastic cell line, mDP6. Expression of Panx3 was progressively induced in differentiating mDP6 cells after stimulation of BMP-2. Interestingly, overexpression of Panx3 inhibits cell proliferation and promotes their differentiation. Conversely, knockdown of endogenous Panx3 expression by siRNA inhibits BMP-2 induced odontoblast differentiation. Next, we examined whether Panx3 affect BMP-2-smad signaling. BMP-2 induced the phosphorylations of smad1/5/8 in mDP6 cells, but suppression of endogenous Panx3 reduced their phosphorylations levels. In conclusion, our results showed that Panx3 inhibits odontoblastic cell proliferation and promotes cell differentiation, indicating that Panx3 plays an important role in odontoblast differentiation.

Disclosures: Tsutomu Iwamoto, None.

SU0101

RNA Editing Occurs in the Bone and is Modulated by Dietary Fat Intake. Tongjun Gu, Cheryl Ackert-Bicknell, F. William Buaas, Allen Simons, Robert Braun, Matthew Hibbs^{*}. The Jackson Laboratory, USA

Studies have demonstrated that a high fat diet can influence bone mass, but the molecular mechanisms are not well characterized. RNA editing is a wide-spread, evolutionarily conserved RNA processing event that alters the sequence of RNA by changing single bases in transcripts. Edits can diversify the functionality of the

transcriptome (and then proteome) and non-coding edits can modulate protein regulation (e.g. modifications to miRNA target sites). In mammals, two classes of RNA editing have been characterized: adenosine to inosine (read as guanine; A->G), and cytidine to uridine (C->U). Editing has been primarily studied in the brain, where defects in editing are associated with several neurological disorders. Here we report one of the first studies that demonstrates RNA editing in bone. Further, we show that environmental perturbations can affect RNA editing in a tissue specific manner. Specifically, total RNA was isolated from femur, liver, and white adipose tissue from C57BL/6J female mice fed a either a low fat diet or a high fat diet from 8 to 16 weeks of age. Sequencing was performed using an Illumina GAIIX instrument, producing hundreds of millions of 75 base pair long, paired-end reads. These reads were aligned to the mouse reference genome using an algorithm that can tolerate mismatches due to editing. After filtering for read quality and base conservation, we identified genomic locations where aligned reads contained replicated mismatches as sites of RNA editing. We identified thousands of novel RNA editing sites across all three tissues, both common and unique. While many of these sites represent canonical editing, we have also observed significant numbers of non-canonical edits, such as U->G and A->C edits. We have experimentally verified over a dozen of these novel edit sites through Sanger sequencing and restriction fragment length polymorphism (RFLP) assays. By applying a multi-factor ANOVA model we determined that overall levels of RNA editing are significantly altered based on tissue, diet, and the interaction of tissue-by-diet. This work demonstrates that RNA editing occurs in the bone and is modulated by dietary fat; future efforts will continue to characterize the physiological implications of RNA editing in the bone.

Disclosures: Matthew Hibbs, None.

SU0102

Hox11 Genes in Musculoskeletal Patterning, Integration and Fracture Repair. Ilea Swinehart^{*1}, Kenneth Kozloff², Steven Goldstein³, Deneen Wellik⁴. ¹University of Michigan, USA, ²University of Michigan Department of Orthopaedic Surgery, USA, ³University of Michigan Orthopedic Research Labs, USA, ⁴University of Michigan Medical Center, USA

Development of the vertebrate musculoskeletal system requires precise coordination between muscles, tendons and bones to form an integrated and functional system. Recent data from our lab suggests that Hox genes play a key role in this process *in vivo*. Hox genes are established regulators of skeletal morphology. Loss-of-function mutation of the *Hox11* paralogous genes results in dramatic malformation of limb zeugopod elements (radius/ulna, tibia/fibula). Utilizing a *Hoxa11:eGFP* knock-in allele, our lab has demonstrated that *Hox11* gene expression is, surprisingly, excluded from skeletal elements. However, expression is observed in the outer perichondrium surrounding zeugopod elements, as well as in tendons and muscle connective tissue in the same region of the limb. Further, this expression is maintained through adult life, suggesting a role for these genes in the maintenance and repair of these tissues. Consistent with this expression data, *Hox11* mutants develop with significant muscle and tendon defects in addition to the skeletal defects. *Hox11* mutants display defects in muscle splitting as well as loss of muscle groups in the zeugopod region. Additionally, these genes are highly up-regulated following fracture injury in multiple cell types suggesting a role in fracture healing and remodeling responses. Taken together, these data clearly highlight a role for *Hox11* genes in the development and repair of the musculoskeletal system.

Disclosures: Ilea Swinehart, None.

SU0103

A Homozygous Lethal Mutation in Connexin 43 Leads to Abnormal Skeletal Development in Zebrafish. Juann-Huey Lin¹, Yvonne Matos¹, Matthew Goldsmith^{*2}. ¹Washington University in St. Louis, USA, ²Washington University School of Medicine, USA

Purpose: Mechanisms that regulate skeletal growth and homeostasis are protean and incompletely understood. We recently identified a new zebrafish mutant with short skeletal appendages. Because zebrafish harboring connexin 43 (*cxn43*) mutations have previously shown to have a similar short fin phenotype, we hypothesized that our newly identified mutant might represent a novel *cxn43* allele.

Methods: Based on a candidate gene approach, a single exon containing the entire *cxn43* coding sequence was amplified from both genomic and cDNA and sequenced (mutant and wild type). Skeletal histomorphometry, including Alcian blue, Alizarin red and calcein staining, along with microCT were used to further characterize the skeletal phenotype.

Results: An ENU-based forward genetic screen revealed a new zebrafish mutant with short skeletal appendages (fins). This short fin mutant has a decrease in both fin ray segment length and fin ray segment number when compared with unaffected siblings. Sequencing revealed a novel mutation (V96F) in the *cxn43* coding sequence. Unlike previously described zebrafish *cxn43* (*short fin*) mutants, homozygous *cxn43*^{V96F} mutants do not survive past 18 days of life, suggesting that V96F is a complete loss of function allele. Unlike mammals, early development of the axial skeleton appears normal in *cxn43*^{V96F} mutants.

Conclusions: We have identified a new *cxn43* allele. Unlike previously identified *cxn43* (*short fin*) mutants, *cxn43*^{V96F} appears to be homozygous lethal. However, that fact that *cxn43*^{V96F} survives until ~18 days of life may offer insight into the essentiality of *cxn43* function at various stages of development. Functional studies (membrane localization and dye coupling) of the V96F mutant CXN43 protein are currently underway. In addition, we are investigating the histomorphometric effects of several different *cxn43* mutations on development of the axial skeleton in post-larval and adult zebrafish.

Disclosures: Matthew Goldsmith, None.

SU0104

Allogenic Demineralized Dentin Matrix, an Ideal Bone Graft Biomaterial. Neema Bakhshalian^{*1}, Shirin Hooshmand¹, Sara Campbell², Bahram Arjmandi¹. ¹Florida State University, USA, ²Rutgers University, USA

The objective of this study was to evaluate the osteopromotive property of allogenic demineralized dentin matrix. There are different kinds of grafts and biomaterials being used for bone regeneration that are neither cost effective nor free of complications. Therefore, it would be ideal to utilize teeth that are extracted from other individuals (due to orthodontic treatments or wisdom teeth extractions, which are routinely discarded) to make an appropriate bone regenerative material, allogenic DDM. We hypothesized that allogenic DDM has bone regenerative properties. To test this hypothesis 30 New Zealand White rabbits were used. The rabbits were divided into four groups and sacrificed after 15, 30, 60, and 90 days. The thickness of bone specimens were measured before utilizing for micro-CT. Blood samples were collected from all rabbits at each time point. Average bone thickness was increased by 54% in experimental group and was significantly higher at all time points. Moreover, microstructural properties showed superior bone quality in experimental group. White blood cell count was numerically higher in control rabbits compared to experimental rabbits ruling out any inflammation or infection due to allogenic DDM. The results of the present study indicate that allogenic DDM significantly improves both bone quantity and quality through its osteoinductive and osteoconductive properties.

Disclosures: Neema Bakhshalian, None.

SU0105

Characterization of A Non-Invasive Model of Periodontitis and Alveolar Bone Loss in Rice Rats (*Oryzomys palustris*). J. Aguirre^{*1}, Mohammed Akhter², Donald Kimmel³, Jennifer Pingel⁴, Xuechun Xia⁴, Aly Williams⁵, Marda Jorgensen⁵, Kent Edmonds⁶, Ju-Youn Lee⁷, Lakshmyya Kesavalu⁷, Thomas Wronski¹. ¹University of Florida, USA, ²Osteoporosis Research Center, University of Florida, USA, ³Kimmel Consulting Services, USA, ⁴Department of Physiological Sciences, University of Florida, USA, ⁵Cell & Tissue Analysis Core, McKnight Brain Institute, University of Florida, USA, ⁶Department of Biology, Indiana University Southeast, USA, ⁷Department of Periodontology & Oral Biology, College of Dentistry, University of Florida, USA

The rice rat (*Oryzomys palustris*) develops periodontitis-like lesions when feeding a powdered diet high in sucrose and casein (H-SC). To our knowledge, no studies involving this animal species, in the context of dental research, have been reported in several decades. We aimed to reestablish whether this model can accurately and conveniently mimic the development of human periodontitis. For this purpose, 28 day-old rice rats (n=15/group; 10 males and 5 females) were randomly assigned to pelleted standard (STD) or H-SC diets. Animals were sacrificed after 6, 12 and 18 wks of diet feeding. Mandibles and maxillae were removed and processed for morphometric, histologic, histomorphometric and microCT analyses. We found mild to moderate periodontal lesions in the mandibles of rats fed the H-SC diet for 12 and 18 wks, respectively. Lesions were characterized by hyperplasia and/or ulceration of the gingival epithelium, leukocyte infiltration of the underlying connective tissue, and disruption of the transeptal fibers of the periodontal ligament. Morphometric analysis revealed a progressive increase in horizontal alveolar bone loss area with age in maxillae of males and females fed the STD diet. The H-SC diet exacerbated horizontal alveolar bone loss area at the lingual, but not the buccal surface, at 12 and 18 wks in both genders. No vertical alveolar bone loss at the interproximal space between the first and second molars occurred with age in males or females fed the STD diet. Conversely, significantly increased vertical bone loss was found in mandibles and maxillae of males and females fed the H-SC diet at 12 and/or 18 wks. Remarkably, the H-SC diet significantly increased mineralizing surface, mineral apposition rate, bone formation rate, eroded surface and osteoclast number, but did not alter bone volume, at the interproximal alveolar bone of rats fed for 6 wks, but not in those fed for longer periods. These findings indicate that the H-SC diet induced a transient increase in alveolar bone remodeling, which is followed by accelerated horizontal and vertical bone loss characteristic of moderate periodontitis. These data supports the use of rice rats fed a STD diet as a spontaneous animal model of horizontal alveolar bone loss (mild periodontitis) and a pelleted H-SC diet as an animal model for accelerated horizontal and vertical bone loss (moderate periodontitis).

Disclosures: J. Aguirre, None.

SU0106

Fourteen-month Changes in Volumetric BMD of Radius and Tibia upon Antidepressant Drug Administration in Young Depressive Patients. Laima Winterhalder¹, Jolanda Widmer², Prisca Eser², Peter M Villiger², Daniel Aeberli^{*3}. ¹Private psychiatric clinic Wyss, Switzerland, ²Dept. of Rheumatology/Clinical Immunology University Hospital Berne, Switzerland, ³Dept. of Rheumatology & Clinical Immunology/Allergy University Hospital, Switzerland

Background: Depression has been associated with lower areal BMD(aBMD) at the hip and spine and increased fracture risk compared to healthy controls. Cross-sectional studies in patients using antidepressant drugs, particularly selective Serotonin Reuptake Inhibitors (SSRI), also found lower aBMD and increased risk for osteoporotic fractures. However, because most of the previous studies included postmenopausal patients, the contribution of depression and use of antidepressant drugs to low bone strength compared to other confounding variables is unknown. Using peripheral quantitative computed tomography (pQCT), the aim of the present study was to determine the longitudinal changes in trabecular volumetric BMD (vBMD) in young depressive patients under therapy with either SSRI versus other antidepressants (such as tricyclics [TCA] or serotonin- norepinephrine reuptake inhibitors [SNRI]).

Methods: Consecutive male and female (premenopausal) patients on therapy with SSRI or non-SSRI (TCA or SNRI) seen at a private psychiatric clinic were recruited. pQCT measurements were performed at baseline and after 12 months at the distal 4% site of the radius and tibia. Of the epiphyseal bone scans cross-sectional area (CSA), total BMD and trabecular BMD (of the central 45% of total CSA) were analysed. Diaphyseal scans at the radius and tibia were performed at 66% from distal bone ends. From these, cortical CSA, total bone CSA, and cortical BMD were measured. Cortical wall thickness was calculated on the basis of a cylindrical model. Reproducibility measurements resulted in a smallest detectable difference for trabecular vBMD at the radius of 4.74 mg/cm³ and of 3.92 mg/cm³ at the tibia.

Results: A total of 40 patients (34 females and 6 males) were recruited, of whom 26 were on SSRI and 14 on non-SSRI (TCA and SNRI) therapy. Mean age was 37 years (range 18-55 years), and mean follow-up period 13.9 months (range 11.4-16.7 months). Age, follow-up period, sex ratio, and height were comparable between groups. Weight was significantly greater in the non-SSRI group (79.2 kg versus 68.6 kg in the SSRI group). Within the SSRI group, none of the bone parameters changed between baseline to follow-up measurement. Within the Non-SSRI group trabecular vBMD increased by 1.8% at the distal radius (p=0.021) and by 1.0% at the distal tibia (p=0.025). When longitudinal changes were compared between the two groups, trabecular vBMD at the distal radius and total vBMD at the distal tibia increased significantly more in the non-SSRI group (p=0.031 and 0.038, respectively).

Conclusion: This longitudinal prospective pQCT study of the radius and tibia in young patients on antidepressant drug therapy does not support previous findings that use of SSRI and/or depression leads to bone loss. Under therapy with TCA or SNRI a small increase in vBMD at the distal radius and tibia was noted.

Disclosures: Daniel Aeberli, None.

SU0107

Identification of Adipocyte Mediated Osteogenesis. Adam Taylor^{*1}, Alan Boyde², Jonathan Jarvis³, Lakshminarayan Ranganath³, James Gallagher¹. ¹University of Liverpool, United Kingdom, ²Institute of Dentistry, Barts & The London School of Medicine & Dentistry, United Kingdom, ³Musculoskeletal Biology, University of Liverpool, United Kingdom

It is the dominant concept that remodelling of bone is a process in which resorption is coupled with subsequent formation by osteoblasts. Using 3D SEM & qBSE-SEM, we have recently discovered non-coupled deposition of mineralised bone in patients with arthropathies. New structures appear in numerous forms including new bone packets and projections laid upon resting trabecular surfaces (Taylor, 2011). These appear in numerous types, are hypermineralised and often poorly integrated with pre-existing matrix. Others appear as partially resorbed trabeculae which have been smoothed over by new bone deposition. Further study was instigated by the outline and shape of some of these structures not being congruent with typical osteoblastic bone formation. This revealed a close association of adipocytes with some of these structures, which showed indented, rugged surfaces. Subsequent histological examination revealed that adipocytes exactly fitted the contours of the bone surfaces. A role for adipocytes as bone lining cells has been suggested previously (Boyde, 2006), but there is no literature proposing a role for adipocytes in templating or moulding the surface of bone. Immunohistochemistry shows that there is collagen VI in these excrescences. These results suggest that the deposition of the bone matrix within these mineralised excrescences is at least templated and modulated by adipocytes. However, the absence of osteoblasts from the forming surfaces raises the question of whether the matrix which is subsequently mineralised is partially synthesised by the adipocytes. Furthermore, it provides unequivocal evidence that adipocytes rather than inactive osteoblasts are the *de facto* lining cells on some bone surfaces. It is well recognised that adipocytes and osteoblasts can be derived from the same mesenchymal stem cells under the influence of different transcription factors. Furthermore there is evidence of

transdifferentiation between the cell types. However, this is the first report of an intimate role for adipocytes in osteogenesis. References: Taylor A, Boyde A, et al. (2011). Identification of trabecular excrescences, novel microanatomical structures, present in bone in osteoarthropathies. Submitted. Boyde A (2006) Three dimensional micro-anatomy of bone, with special reference to the mandible. J Oral Biosci (Japan) 48 Suppl 57-59.

Disclosures: Adam Taylor, None.

SU0108

Molecular Mechanism of CIZ Actions to Exacerbate Inflammation in Serum-induced Arthritis Based on Formation of Positive Feedback Loop with IL-1 Beta. Tetsuya Nakamoto^{*1}, Takayuki Motoyoshi², Makiri Kawasaki², Tomomi Sakuma¹, Tadayoshi Hayata³, Yoichi Ezura⁴, Masaki Noda¹. ¹Tokyo Medical & Dental University, Japan, ²Department of Molecular Pharmacology, Medical Research Institute, Tokyo Medical & Dental University, Japan, ³Medical Research Institute, Tokyo Medical & Dental University, Japan, ⁴Tokyo Medical & Dental University, Medical Research Institute, Japan

Rheumatoid arthritis deteriorates the quality of life in a large number of patients but the cause of this disease is still not understood. CIZ (Cis interacting zinc finger protein) is a transcription factor that regulates the transcription of MMPs. We have observed that CIZ deficiency suppressed the inflammation, cartilage destruction, osteoclast activation in serum-induced arthritis model in vivo, accompanied by the impaired induction of IL-1 beta, MMP-3, and RANKL in the joints. However, molecular bases were not known. Therefore, we investigated cellular and molecular bases to obtain mechanistic insights into the link between CIZ and IL-1 beta in inflammation. Primary chondrocytes from newborn mouse ribs expressed CIZ and the levels of the expression correlated with the chondrocyte differentiation. When chondrocytes were stimulated with IL-1 beta, the expression of CIZ increased up to 1.6 fold dose-dependently. Concurrently IL-1 beta also stimulated the expression of IL-1 beta itself and overexpression of CIZ in chondrocytes enhanced the upregulation of IL-1 beta in response to the stimulation by IL-1 beta, suggesting the role of CIZ in the transcriptional regulation of IL-1 beta. Therefore, we examined the effect of CIZ to IL-1 beta promoter. ChIP assay using anti-CIZ antibody confirmed that CIZ bound to sequences in the IL-1 beta promoter, which include CIZ-binding consensus sequences. Furthermore, overexpression of CIZ enhanced the promoter activity from the IL-1 beta promoter in osteoblastic cell line, MC3T3-E1 cells. To examine involvement of secreted IL-1 beta in induction of CIZ expression, we applied the blocking antibody to IL-1 beta to ATDC5 chondrocytic cell lines stimulated with LPS, and confirmed that CIZ upregulation was suppressed by the antibody. These in vitro results that (1) CIZ expression is induced by IL-1 beta and (2) the overexpressed CIZ enhances the expression of IL-1 beta, reveal the mechanism underlying CIZ actions to exacerbate arthritic inflammation.

Disclosures: Tetsuya Nakamoto, None.

SU0109

Standardization of proteoliposome systems containing Alkaline Phosphatase and Annexin V: kinetic characterization at physiological pH. Mayte Bolean^{*1}, Ana Maria Simao², Tina Moreira³, Marc Hoylaerts⁴, Jose Luis Millan³, Pietro Ciancaglini¹. ¹FFCLRP-USP, Brazil, ²University of Sao Paulo - USP, Brazil, ³Sanford-Burnham Medical Research Institute, USA, ⁴Center for Molecular & Vascular Biology, University of Leuven, Belgium

The biomineralization process is initiated inside matrix vesicles (MVs). The crystalline hydroxyapatite generation and its deposition is accomplished by the activities of proteins involved in Ca²⁺ and Pi homeostasis, among them Annexins (Anx V), Pi-transporters, PHOSPHO1 and tissue-nonspecific alkaline phosphatase (TNAP). Anx V mediates Ca²⁺ influx. TNAP hydrolyze phosphomonoester with release of Pi and alcohol. Dipalmitoylphosphatidylcholine (DPPC) and dipalmitoylphosphatidylserine (DPPS) are lipids found in the MV membranes that play a crucial role in the biomineralization process, regulating both Ca²⁺ entry into the MVs and formation of HA crystals. Since the presence of DPPS is necessary for the ability of Anx V to mediate Ca²⁺ flux across the membrane, but it reduces the activity of TNAP, we studied the best lipid composition to optimize the incorporation and functionality of both proteins. So, TNAP and Anx V were incorporated into liposomes of various lipid compositions, i.e. DPPC alone or DPPC:DPPS in different molar ratios (5, 10 and 15%). The presence of both proteins in the proteoliposomes was confirmed by Western blots. The kinetic parameters for the hydrolysis of ATP, ADP and PPI by TNAP, in the absence and presence of Anx V, were determined at physiological pH. DPPS-only liposome prevented the p-NPPase activity of TNAP. Hydrolysis of ATP was positively cooperative in all proteoliposomes and K_{0.5} values were similar (around 0.2 mM). The V_m values decreased by half with the increasing DPPS ratio. For ADP, negative cooperativity was observed in DPPC-proteoliposomes, but positive cooperativities were detected in the presence of DPPS. Lower K_{0.5} values were obtained for DPPC:DPPS-proteoliposomes (9.3 to 30.8 μM) when compared with the absence of DPPS (60.1 μM). The proteoliposome with DPPS 5% showed the highest V_m value (11.6 U/mg). It was observed negative cooperativities in all systems during PPI hydrolysis by TNAP-proteoliposomes. These vesicles showed the highest

K_{0.5} value (0.23 mM) and V_m values decreased strongly (46.2 to 24.8 U/mg) with the increase in DPPS ratio. Thus, the best catalytic efficiency was obtained with 10% DPPS, for all substrates, and with this condition we will examine the ability of AnxV-containing proteoliposome to flux Ca²⁺. Our ultimate goal is to evaluate the interplay of PHOSPHO1, AnxV, Pit-1, TNAP and NPP1 in a complex proteoliposome system that will mimic the initial events that lead to MV-mediated calcification.

Disclosures: Mayte Bolean, None.

SU0110

Determining the Function of WISP-1/CCN4 in Mineralized Tissue. Azusa Maeda^{*1}, Mitsuaki Ono¹, Tina Kiltz¹, Kenn Holmbeck², Karen Lyons³, Marian Young¹. ¹National Institutes of Health, USA, ²NIDCR, USA, ³University of California, Los Angeles, USA

WISP-1 (CCN4) is a CCN family member that is highly expressed in mineralizing tissues however its function in bone is unclear. To examine this we generated mice unable to make WISP-1 (WISP-1 KO) by gene targeting. Northern blotting, RT-PCR and western blotting confirmed that WISP-1 was depleted in the WISP-1 KO mice and their bones were subsequently analyzed by Dual Energy X-Ray Absorptiometry (DEXA) and micro computerized tomography (μCT). In 1 month-old WISP-1 KO mice there were no significant differences in the total bone mineral density (BMD) compared to normal (wild type/WT) mice, however, by 3 months of age the WISP-1 KO mice had significantly lower BMD compared to WT mice, and this persisted until 9 months of age. μCT analysis of 3 month-old femurs revealed numerous changes in the WISP-1 KO bones compared to WT bones. In the trabecular region, female KO mice had lower BMD, lower trabecular numbers and more trabecular separation, as well as greater bone surface/bone volume all indicating a decrease in bone mass. In the cortical bone, both male and female KO mice had decreased cortical area, decreased cross sectional area and decreased mean thickness, which is likely the basis for the decrease in total BMD noted from the DEXA scans in the WISP-1 KO animals. In addition to the changes in the trabecular and cortical bone character and architecture, the μCT analysis showed that the femurs from the WISP-1 KO male mice were shorter than WT controls. To understand the mechanism for these differences, osteogenic progenitors were obtained from the bone marrow (bone marrow stromal cells/BMSCs) of 6 week-old female mice and tested for their ability to differentiate towards osteogenesis. BMSCs from the WISP-1 KO mice had dramatically reduced levels of alkaline phosphatase, osteocalcin and bone sialoprotein mRNA that was accompanied by a significant reduction in Alizarin Red staining. To further understand the effects of WISP-1 depletion on BMSC, the ability of the cells to proliferate was examined and showed that WISP-1 KO mice had higher levels of BrdU incorporation compared to WT BMSCs, indicating they proliferated faster. Considering that in WISP-1 deficient BMSCs the differentiation of osteogenic progenitors was decreased while the proliferation levels were increased, it is proposed that WISP-1 potentially regulates bone mineral density and cortical bone thickness by balancing the proliferation and differentiation levels of osteogenic precursors.

Disclosures: Azusa Maeda, None.

SU0111

Withdrawn

SU0112

Fluid Osteocalcin Levels Correlate to Bone and Cartilage Matrix Measures in a Small Study of Men with Severe Osteoarthritis and Co-morbid Diabetes Mellitus. Karen King^{*1}, Trevor Oren², Allan Bucknell². ¹University of Colorado School of Medicine, USA, ²Eastern Colorado Health Care System, USA

Osteoarthritis patients with diabetes mellitus (DM) that receive total knee joint replacement (arthroplasty) are more vulnerable to complications, including aseptic loosening and need for revision surgery. To elucidate mechanisms related to arthroplasty failure in DM, we examined serum and synovial fluid biomarkers as well as collagen cross-links in bone and cartilage from twenty male patients (10 with DM, 10 without DM) undergoing this procedure at the Denver VAMC.

Subject age, HbA1c, and body mass index (BMI) were obtained from patient files. Bone alkaline phosphatase (BAP) and osteocalcin (OC) were measured in blood serum and index joint synovial fluid by ELISA. The contents of the cross-links hydroxylsypyrindinoline (HP), lysylpyrindinoline (LP), and pentosidine (Pen) were measured by HPLC in tissue obtained during the surgical procedure. Differences between groups and correlations between measures were analyzed ($\alpha < 0.050$ a priori).

Mean HbA1c was higher in the DM group (6.58 vs. 5.25, $P = 0.003$) while mean BMI was higher but not statistically significant (30.37 vs. 28.14, $P = 0.054$). Pen levels in joint tissues from the DM group were higher than non-DM group (significant in bone: $P = 0.050$; not significant in cartilage: $P = 0.075$). OC levels in synovial fluid were negatively correlated with HP levels in cartilage in all subjects when controlling for age and BMI ($\beta = -0.232$, $P = 0.033$). OC levels were also negatively correlated with Pen levels in cartilage when controlling for age and BMI, but only in the DM group ($\beta = -0.4750$, $P = 0.007$). The DM and non-DM groups differed in the direction of correlation between serum BAP and cartilage HP (DM: $r = -0.643$, $P = 0.045$; non-

DM: $r = 0.472$, $P = 0.168$). The relationship for the DM group, however, was not significant when adjusting for age and BMI ($\beta = -0.057$, $P = 0.065$).

These differences between the DM and non-DM groups suggest that a further relationship may exist between DM and OC. Returning to our data, an inverse relationship between serum OC and HbA1c was suggested by data in the DM group only, but this was not significant ($r = -0.466$, $P = 0.174$). The non-DM group data suggested an opposite effect ($r = 0.507$, $P = 0.134$). There was no such relationship between synovial fluid OC and HbA1c.

Data from this small study suggest a potential relationship between DM, OC, and joint tissues. However, further study is required elucidate the metabolic mechanism(s) for arthroplasty failure in patients with diabetes.

Disclosures: Karen King, DePuy Orthopaedics Inc., 2; Cerapedics, 5

SU0113

Periostin: A Novel Serum Marker of Cortical Bone Formation. Nicolas Bonnet^{*1}, Jean Charles Rousseau², Patrick Garnero³, Serge Ferrari⁴. ¹Division of Bone Diseases, Geneva University Hospital & Faculty of Medicine, S, Switzerland, ²INSERM UMR 1033, Université de Lyon, France, ³INSERM UMR 1033, Université de Lyon & Cistbio Bioassays, France, ⁴Geneva University Hospital & Faculty of Medicine, Switzerland

Biochemical markers are valuable tools to monitor the overall bone turnover, but they do not provide specific information on the modeling/remodeling rate in different compartment(s). Periostin is a matricellular protein which in bone is mainly expressed by periosteal cells and osteocytes and which regulates Sost expression. We previously reported that periostin-deficient mice (Postn^{-/-}) have low bone mass and a diminished anabolic response to loading and PTH. The aim of this study was to investigate changes in serum periostin, as measured by an in-house ELISA specific for the rodent protein in response to ovariectomy (OVX), PTH and androgens (DHT). Six month-old female mice were OVX or Sham-operated and administered intermittent PTH (40ug/kg/day), continuous DHT (7.5mg/kg) or vehicle (Veh) for 5 weeks. The relation between periostin levels and histomorphometrical and biochemical indices of bone turnover, including PINP and TRAP was also examined. In parallel, Postn mRNA levels were evaluated by qRT-PCR on whole femur extracts after 24h of treatment.

PTH significantly increased Postn mRNA expression (+62% vs Veh, $p < 0.01$) whereas OVX, and DHT did not change Postn gene expression. Compared to Sham, OVX decreased PINP (-23.4% vs +10.7%, $p < 0.05$) and TRAP (-20.8% vs +10.7%, $p < 0.05$) but not periostin. Compared to OVX Veh, PTH tend to reduce the decreased of PINP (-11.6%), and significantly increased TRAP (+10.7%, $p < 0.05$) without any changes in periostin, whereas DHT tend to reduce decreased of PINP (-15.8%), and significantly decreased TRAP (-72.5%, $p < 0.05$) and periostin (-29.5% in DHT vs -1.6% in Veh, $p < 0.01$). Regression analysis indicates that periostin changes were weakly correlated with changes of TRAP and PINP ($r = 0.27$ and $r = 0.18$, respectively, ns). Whereas serum PINP measured at sacrifice was better correlated than periostin with endocortical bone formation, periostin levels, but not PINP, correlated with periosteal BFR/BPm and MAR, as well as Ct.BV and the moment of inertia (table).

In conclusions, serum periostin levels were not affected by OVX or PTH, but decreased in response to DHT, and this effect was mostly independent of changes in PINP and TRAP.

Despite periostin ELISA were not able to detect increased in Postn gene expression induce by PTH, it revealed that compare to PINP, serum levels of periostin could reflect specific bone formation activities at the periosteal surface.

r^2	MAR Ec	BFR/BPm Ec	MAR Ps	BFR/BPm Ps	Ct.BV	M. inertia
Postn	0.11 ($p = 0.05$)	0.11 ($p = 0.05$)	0.14 ($p = 0.03$)	0.14 ($p = 0.02$)	0.15 ($p = 0.01$)	0.11 ($p = 0.05$)
PINP	0.17 ($p = 0.02$)	0.20 ($p = 0.01$)	0.014 ($p = 0.63$)	0.049 ($p = 0.23$)	0.025 ($p = 0.34$)	0.006 ($p = 0.63$)

table

Disclosures: Nicolas Bonnet, None.

SU0114

Quantitative Analysis of Fibronectin Fibril Assembly Dynamics in Living Osteoblast Cultures. Aditya Roshan^{*}, Ganesh Thiagarajan, Sarah Dallas. University of Missouri - Kansas City, USA

Fibronectin (FN) is an extracellular matrix (ECM) glycoprotein expressed in skeletal tissues. We have shown that FN regulates osteoblast differentiation and orchestrates the assembly of multiple bone ECM proteins. Understanding the mechanism of FN assembly is therefore key to understanding how bone matrix is formed. Our time lapse imaging studies in living osteoblasts have shown that FN assembly is a highly dynamic process that appears to be driven by cell motility. To further understand this process, time lapse movies of FN assembly were analyzed using a Digital Image Correlation technique to quantitate the mechanical strains experienced by FN fibrils during assembly and track their motion paths.

FN assembly was imaged in 2T3 osteoblasts by time lapse imaging over 48hr using an alexa555 labeled FN probe. FN was found to first assemble on the cell surface. Multiple cells then pool their surface assembled FN to build progressively larger fibrils. Pseudocoloring of forming fibrils showed that single fibrils receive contributions from up to 6-8 cells and as far away as 170μm. Cell motion continually stretches,

contracts and reorganizes the FN fibrils as the matrix matures. Movies were analyzed using a Digital Image Correlation (DIC) algorithm developed in Matlab that was manually validated. In this technique, markers are positioned on individual fibrils and the DIC algorithm compares each image to the previous image to match up image features within a defined search window and calculate fibril displacements and strains. Analysis of fibrils in the 24-36h movie segment showed strains ranging from -65,000 to 60,000 $\mu\epsilon$. The strains were intermittent, with fibrils repeatedly being subjected to tensile and compressive strains and not all points on the fibril moving in the same direction. Analysis of the same fibrils in the 36-48h segment showed strains from -27,500 to 42,415 $\mu\epsilon$ suggesting that fibrils are subjected to lower strain as the matrix matures. Individual fibrils showed distinct strain profiles over time, which were related to the underlying cell motion. These data suggest that during assembly, FN fibrils are subjected to strains generated by motile osteoblasts that are an order of magnitude higher than strains measured on bone surfaces during normal activity. Mechanical stretching of ECM fibrils may facilitate matrix assembly by exposing cryptic binding sites for ECM molecules and/or may alter cell behavior through "shedding" of ECM-bound growth factors.

Disclosures: Aditya Roshan, None.

SU0115

Moderate Joint Loading Downregulates MMPs 1, 3, and 13 in Mouse Articular Cartilage. Hiroki Yokota^{*1}, Daniel J. Leong², Robert Majeska³, Herb Sun². ¹Indiana University Purdue University Indianapolis, USA, ²Mount Sinai School of Medicine, USA, ³City College of New York, USA

Cartilage destruction is a hallmark of both osteoarthritis and rheumatoid arthritis. While the factors causing these diseases undoubtedly differ, the upregulation of the matrix metalloproteinases (MMPs) largely responsible for degrading cartilage extracellular matrix is common to both. We previously showed that mechanical loading, one of the most influential factors in maintaining cartilage homeostasis, is a potent modulator of MMP expression and activity. In vitro, moderate loading levels applied in several modalities (fluid shear, hydrostatic pressure and axial strain) downregulated MMPs 1 and 13 in normal and arthritic chondrocytes. We have also shown that passive joint rotation in vivo downregulates MMPs 1 and 3. Since chondrocytes are responsive to various types of mechanical stimuli, we hypothesize that a novel joint loading modality, which applies cyclic loads in the mediolateral direction and promotes bone formation throughout long bones, will downregulate several MMPs at the loaded joint. We first examined gene expression (by RT-PCR) and enzyme activity (by fluorogenic assay) in articular cartilage subjected either to elbow loading (0.2N to 2.0N, peak-to-peak) at 5 Hz, or to passive joint rotation (range of motion 65-125 at 2 cycles/min) both for 1 hour. The results showed that the effect of joint loading on MMP expression and activity in the ulna were loading intensity-dependent. Moderate loading at 0.2 N and 0.5 N downregulated mRNA expression of MMPs 1, 3, 8, 13 and decreased activities of gelatinase, collagenase, MMP-1 and MMP-13, with no effect on MMP-14. In contrast, higher levels of loading at 2 N did not change expression of MMPs 3, 8, 13, and 14 and activities of gelatinase and collagenase, and slightly upregulated MMP-1 expression and activity. In comparison, moderate joint rotation downregulated MMPs 1, 3, 13, but had no effect on MMP-8 expression. Together, our study suggests that moderate intensities of joint loading and joint rotation exert a potentially protective effect on articular cartilage by downregulating expression and activities of MMPs 1, 3 and 13. Given the fact that arthritis patients may have limited range of motion and pain due to joint motion, joint loading could offer an effective, anti-catabolic loading modality. Furthermore, in patients who do not have a restricted range of motion, the combination of both joint motion and joint loading may result in a synergistic effect, which will be tested in future studies.

Disclosures: Hiroki Yokota, None.

SU0116

Matrix Metalloproteinase-13-mediated Cortical Bone Remodeling Is Required for the Post-natal Maintenance of Bone Quality. Simon Tang^{*}, Tamara Alliston. University of California, San Francisco, USA

The maintenance of bone mass and quality throughout post-natal life is critical for the ability of bone to resist fracture. Although normal bone maintenance relies largely on the coupled activity of osteoclasts and osteoblasts, matrix metalloproteinases (MMP) may also contribute to the matrix remodeling of connective tissues. Specifically, MMP-13 is a collagenase expressed by hypertrophic chondrocytes, osteoblasts, and osteocytes that degrades collagen fibrils and has been implicated in bone development and fracture healing. However, much less is known about bone remodeling by osteoblasts and osteocytes. Therefore, this study examines the role of MMP-13 in post-natal bone remodeling and in the maintenance of bone quality using a murine knock-out model.

Mouse tibiae and femora were collected from 2-month old MMP-13 deficient (-/-) mice and their WT littermates (n=6-9). Immunohistochemistry (IHC) for anti-MMP-13 on WT bone shows the preferential localization of MMP-13 in the mid cortical region between the endo- and peri-osteal surfaces (Fig 1A). Strikingly, microCT analyses of the same regions in MMP-13 deficient mice show severe defects in the mineral distribution (Fig 1BCD), suggesting that the absence of MMP-13 results in mineral abnormalities. Unlike unresorbed calcified cartilage in cortical bone in previous reports, these hypermineralized zones do not resolve with age. These defects

were not accompanied by changes in osteoclast activity. Bone formation rates in WT and MMP-13^{-/-} animals were indistinguishable (p=0.734). The absence of MMP-13 did not affect osteoclast activity as measured by deoxypyridinoline (p=0.421), nor TRAP staining (p=0.313). Thus MMP-13-mediated, osteoclast-independent bone remodeling may be required to maintain the normal organization of mineral in cortical bone matrix. Failure to remodel cortical bone matrix in this way has adverse consequences on fracture resistance. MMP-13^{-/-} mice showed increased fragility through reduced post-yield work-to-fracture (p<0.001) under and reduced fracture toughness (p<0.001). These changes occurred in the absence of significant changes in the geometry of MMP-13 deficient bone.

Taken together, the loss of MMP-13 resulted in significant disruptions in the mineral distribution of bone that is associated with increased fragility without changes in osteoclast activity, revealing the importance of osteoclast-independent cortical bone remodeling for the maintenance of bone quality.

Disclosures: Simon Tang, None.

SU0117

Calcitonin Receptor Peptide: A Novel Peptide That Enhances Osteoblast Differentiation and Matrix Mineralization. David Komatsu^{*1}, Srinivas Pentyla², Julie Miller², Supriya Mishra², Kyle Urbanczyk², Sirish Kondabolu², Joshua J. Hinkle³, Michael Hadjiargyrou⁴. ¹Stony Brook University, Dept. of Orthopaedics, USA, ²Stony Brook University, Dept. of Anesthesiology, USA, ³Stony Brook University, Dept. of Biomedical Engineering, USA, ⁴State University of New York at Stony Brook, USA

Osteoporosis is one of the most prevalent musculoskeletal disorders with a global prevalence of ~168 million. Antiresorptives are the predominant treatment and while effective in arresting bone loss, they are not anabolic. The sole FDA approved anabolic treatment is Teriparatide, but its utility is hampered by daily injections and limited treatment duration. As such, an urgent need exists for new anabolic osteoporosis treatments. We recently used an algorithm and identified a potential bioactive peptide mapped to the C-terminal region of the calcitonin receptor termed, Calcitonin Receptor Peptide (CRP). A series of studies was conducted to study the effects of CRP on osteoblast proliferation and activity, as well as to try and identify endogenous forms of CRP. We used MC3T3 (mouse calvarial), and hFOB (human fetal osteoblast) cells to assess: 1) Osteoblast differentiation; 2) Matrix mineralization, and; 3) Simulated wound healing. Immunohistochemical (IHC) analyses of d10 rat calluses were also conducted. Western analyses showed that in the absence of CRP, osteocalcin (OC) levels were undetectable in hFOB, while CRP dose dependently induced OC expression. Consistent with these results, CRP also dose dependently increased the number and size of alizarin stained nodules in MC3T3 and hFOB cells. Quantification of eluted alizarin from the MC3T3 cells showed that treatment with 1 and 10 μ M CRP generated 1- and 10-fold increases in mineralization, respectively. Simulated wound healing was then studied in hFOB cells by scrapping a line through confluent cultures. 24 hours following scrapping, cultures treated with CRP were almost completely recolonized while untreated cultures showed few cells in scrapped areas. Lastly, IHC identified strong CRP labeling on woven bone surfaces in the hard callus (likely osteoclasts) and along the periosteum, with additional diffuse staining seen in regions of osteoid. Taken together, the in vitro results indicate CRP promotes osteoblast proliferation and matrix production, and may also stimulate proliferation or migration. As osteoblasts do not express the calcitonin receptor, these data suggest CRP acts independently of the receptor, possibly through direct stimulation of G-proteins. The IHC results intimate that, in addition to binding to the receptor, an endogenous form of CRP may be present in osteoid. We are currently working to identify the cellular localization of CRP binding, its binding partners, and its downstream signaling pathways, as well as seeking to identify any endogenous forms of CRP. In addition, a series of in vivo studies to assess the anabolic efficacy of CRP in vivo is ongoing. Completion of these studies will enable us to determine if CRP has the potential to facilitate the development of a new class of skeletal anabolic therapies for treating osteoporosis.

Disclosures: David Komatsu, None.

SU0118

Deletion of Cyp24a1 in Klotho-Null Mice Leads to Early Death. Xiuying Bai^{*1}, Dinghong Qiu¹, Rene St-Arnaud², David Goltzman³, Andrew Karaplis⁴. ¹Lady Davis Institute, Canada, ²Shriners Hospital for Children & McGill University, Canada, ³McGill University Health Centre, Canada, ⁴McGill University, Can

Mice homozygous for the null *Klotho* allele have a short lifespan and show biochemical and morphological features consistent with premature aging-like phenotype. In this study, we have used a mouse genetic approach to generate *Cyp24a1*^{-/-} mice and investigate *in vivo* the role of *Cyp24a1* in the *Klotho*-null background. *Cyp24a1*^{-/-} mice were sacrificed and serum and tissues were procured for analysis and comparison to *WT*, *Cyp24a1*^{-/-} and *Kt*^{-/-} controls.

At birth, there was no difference in body weight and gross appearance among *WT*, *Cyp24a1*^{-/-} and *Kt*^{-/-} controls and *Cyp24a1*^{-/-}*Kt*^{-/-} mice. However, by 48 hrs after birth (AB) *Cyp24a1*^{-/-}*Kt*^{-/-} and *Cyp24a1*^{-/-} mice displayed low body weights compared to their *WT* and *Kt*^{-/-} littermates. Although a number of *Cyp24a1*^{-/-}*Kt*^{-/-} mice survived up to 96 hrs, most of them died at 48-72 hrs AB.

When examining the changes in serum calcium from 12-72 hrs AB, an aberrant difference in *Cyp24^{-/-}/Kl^{-/-}* mice was observed. At 12 hrs AB, serum calcium level (mg/dl) was 5.62 0.50, higher than wild type (4.86 0.60). At 24 hrs AB, serum calcium level was 5.49 but ranged from 2.75 to 10.97. At 48 hrs AB, serum calcium level was 11.33 with a wide range from 8.94 to 14.33. At 72 hrs AB, in surviving animals, serum calcium level was 7.95 (range from 2.64 to 15.13).

From 24 hr AB onward until their demise, *Cyp24^{-/-}/Kl^{-/-}* mice constantly had higher serum inorganic phosphorus levels compared to WT mice.

At 24 hrs AB, serum FGF23 level was dramatically elevated in *Cyp24^{-/-}*, *Kl^{-/-}*, and *Cyp24^{-/-}/Kl^{-/-}* mice. Low serum 1,25 (OH)₂D₃ levels were exhibited in *Cyp24^{-/-}*, *Kl^{-/-}*, and *Cyp24^{-/-}/Kl^{-/-}* mice (219.7 17.33) (pmol/L) at 24 hrs AB compare to WT mice (351.3 31.52). However, by 48 hrs AB, serum 1,25 (OH)₂D₃ levels in *Cyp24^{-/-}/Kl^{-/-}* mice increased to 380.7 27.57, and examination of *Cyp27b1* expression in kidney at 24 hrs AB by Northern blot showed that *Cyp24^{-/-}* and *Cyp24^{-/-}/Kl^{-/-}* mice had low expression level of *Cyp27b1* compare to WT and *Kl^{-/-}* mice. Considering the absence of *Cyp24a1* and *Klotho*, *Cyp24^{-/-}/Kl^{-/-}* mice could produce more 1,25(OH)₂D₃ than WT and *Kl^{-/-}* mice. There was no significant change in serum PTH levels at 24 hrs AB.

In summary, *Cyp24^{-/-}/Kl^{-/-}* mice succumb to aberrant regulation in calcium and phosphate homeostasis. Our findings therefore substantiate *in vivo* the essential role of *Cyp24a1* in the *Klotho*-null phenotype as its ablation leads to early demise.

Disclosures: Xiuying Bai, None.

SU0119

Effect of Phosphate Overload on Podocyte of Glomerulus in the Kidney.

Sahoko Sekiguchi-Ueda¹, Shogo Asano², Megumi Shibata³, Yasumasa Yoshino⁴, Hiroyuki Hirai⁴, Yoshiteru Maeda⁴, Masaki Makino⁴, Nobuki Hayakawa⁴, Atsushi Suzuki⁵, Mitsuyasu Itoh⁴. ¹Fujita Health University, Division of Endocrinology, Jpn, ²Toyokawa City Hospital, Japan, ³Fujita Health University, Division of Endocrinology, Japan, ⁴Fujita Health University, Japan, ⁵Fujita Health University Division of Endocrinology, Japan

Phosphate (Pi) uptake at the cellular membrane is essential to maintain the cell activity because Pi has to be supplied for ATP synthesis. On the contrary, accumulating evidence suggests that Pi overload from the extracellular milieu would be stressful for the cells. We have previously reported Pi-induced damage of filtration barrier at glomerulus in the kidney of type III Pi transporter (Pit-1)-overexpressing rats (TG). In the present study, we further explore the effect of Pi overload on podocyte of glomerulus in the kidney.

Their podocytes lost their foot processes and underwent effacement in TG rats. Immunofluorescence microscopy showed that the markers of podocyte injury such as desmin and connexin43 in TG rats were more remarkable than WT in the early stage of the pathological proteinuria. On the other hand, there was little difference of the podocyte constituent proteins such as nephrin, podocin, synaptopodin and podocalyxin between WT and TG rats. TG rats showed higher Pi uptake of the primary cultured podocytes than WT rats, especially at low Pi concentration. However, Pi uptake of the podocytes from TG rats was finally caught up with those from WT at higher Pi concentration. In conclusion, these finding suggests us that even the small increase of extracellular Pi could affect podocyte function in the kidney, and self-limiting system to restrict the excess of Pi influx seems to exist in these cells.

Disclosures: Sahoko Sekiguchi-Ueda, None.

SU0120

PHEX and Fat Energy Metabolism across a Bone-Renal Axis. Peter Rowe¹, Anne-Marie Hedge², Yan Hong², Valentin David³, Lesya Zelenchuk². ¹University of Kansas Medical Center, USA, ²KUMC, USA, ³UTHSC, USA

PHEX defective mice (HYP) have hypophosphatemic rickets, abnormal vitamin D metabolism and increased FGF23. HYP mice are also hyperglycemic and hypoinsulinemic with increased osteoblastic, renal and hepatic gluconeogenesis. ASARM-peptides play a key role by decreasing cellular pH. Here we describe the changes in glucose metabolism and bone-renal mineralization following 28-day infusion of SPR4 peptide (4.2 kDa) in wild type (WT) and HYP mice. SPR4 competitively inhibits PHEX by binding to its physiological substrate, ASARM-peptide.

We infused vehicle (0.9% NaCl) or SPR4-peptide (276 nmol/hr/kg) into WT or HYP mice (n=5, male) for 28 days (osmotic-pumps). On day 28, mice were sacrificed after overnight metabolic-cage housing and serum-urine chemistries measured. Femurs and kidneys were scanned by micro computed tomography (μCT). Fat mass and aBMD were measured by DEXA on days 0 and 28.

HYP-mice SPR4-peptide treatment (HYPSPR4) corrected the HYP-mice (HYPVE) hyperglycemia (+78%; p<0.01) and hypoinsulinemia (-54%; p<0.01). Decreased serum leptin levels (-75%; p<0.01) occurred in HYPVE compared to wild type vehicle-mice (WTVE). Wild-type mice infused with SPR4-peptide (WTSPR4-mice) had reduced serum leptin (-60%; p<0.01) and osteocalcin (-32%; p<0.01) compared to WTVE-mice. HYPVE-mice had a 6 fold decrease (p<0.01) in bone glyceraldehyde phosphate dehydrogenase (GAPDH) expression compared to WTVE-mice. In contrast, HYPSPR4 and WTSPR4 mice had increased GAPDH of 68X and 6X respectively (p<0.01; Fig1). Also, increases in the fat-mass to weight ratio

occurred with HYPSPR4 (9.6X; p<0.01) and WTSPR4 (4.3X; P<0.01) mice over 28 days compared to the respective control vehicle-mice. Coordinate with these changes, HYPVE mice showed a 6X increase in bone SOST expression and levels compared to WTVE mice (p<0.01). In contrast, SPR4 peptide reduced bone SOST expression in wild type and HYP mice by 4X and 11X respectively (p<0.01), figure 1. Remarkably, these treated mice had significantly increased bone resorption, decreased bone volume, impaired mineralization and abnormal trabecular structure with increased PTH, osteopontin and FGF23 levels and expression. We propose a new model that integrates regulation of phosphate mineral homeostasis by the PHEX, FGF23 and ASARM axis to the established leptin, insulin and osteocalcin energy-metabolism pathway. SPR4-peptide and/or ASARM-peptides may be of clinical use in modulating this pathway.

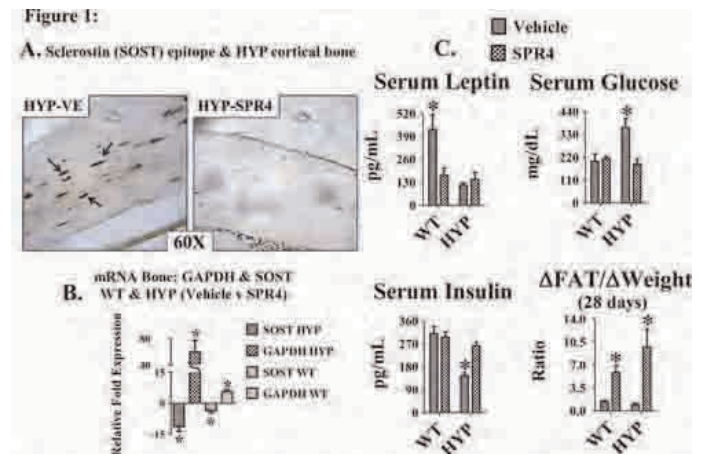


Fig 1 (A) immunohistochemistry of Sclerostin (SOST) epitopes in cortical bone, (B) Changes in mRNA expression of GAPDH & Sclerostin in HYP cortical bone following SPR4 treatment (C) Changes in serum markers and fat/weight ratio in WT & HYP mice treated with SPR4 peptide.

Table 1

Disclosures: Peter Rowe, None.

SU0121

Phosphate and Vitamin D Homeostasis after Live Donor Nephrectomy: Activation of the FGF-23 pathway. Ann Young¹, Anthony Hodsman¹, David Goltzman², Amit Garg¹, for the Donor Nephrectomy Outcomes Research (DONOR) Network¹. ¹University of Western Ontario, Canada, ²McGill University Health Centre, Canada

Living kidney donation offers a unique setting to study changes in phosphate and vitamin D homeostasis attributable to mild, isolated decrements in glomerular filtration rate (eGFR).

Methods: We performed a retrospective cohort study comparing biochemical markers of Chronic Kidney Disease-Mineralizing Bone Disorder in 198 Living Kidney Donors (LKD) and 98 Non-Donor Controls (NDC). Participants were recruited from 1140 eligible LKD and 421 potential donor-identified NDC from 9 transplant centres. Median follow-up time after donation was 5.3 (interquartile range: 3.8–8.4) years. Estimated GFR (eGFR) was calculated using the CKD-EPI formula.

Results: At assessment, LKD had a lower eGFR than NDC (7315 vs. 9814 mL/min/1.73m², p<0.0001), and were slightly older (44 vs. 41 yr., p=0.03). Within the LKD group, 68% had eGFR levels classifying them as Stage II CKD, and 18% as Stage III CKD; comparable data within the NDC group were 28% and 0% respectively. Serum fibroblast growth factor-23 (FGF-23) was significantly higher in LKD (38.115.7 vs. 29.710.6 pg/mL, p<0.0001). For every 10 mL/min/1.73 m² decline in eGFR, FGF-23 increased by 3.2 pg/mL (95%CI:2.0, 4.4). Compared to NDC, LKD showed higher renal tubular fractional inorganic phosphate excretion (FExPi) (17.87.9 vs. 12.35.2%, p<0.0001), lower serum Pi (0.970.16 vs. 1.020.21 mmol/L, p=0.03), and lower serum calcitriol (6321 vs. 7724 pmol/L, p<0.0001). Multivariable adjusted models indicated that serum FGF-23 was strongly correlated with serum Pi (z' = 0.20, p=0.004) and modestly correlated with renal FExPi (z' = 0.15, p=0.03). Furthermore, serum FGF-23 was inversely correlated with serum calcitriol (z' = -0.41, adjusted: 5.6 pmol/L decrease for every 10 pg/mL increase in FGF-23, p<0.0001). Plasma iPTH was significantly higher in donors (5.72.4 vs. 5.02.1 pmol/L, p=0.03). However, there was no significant linear correlation between serum FGF-23 and plasma iPTH (z' = 0.04, p=0.61), between serum Pi and plasma iPTH (z' = -0.11, p=0.06), or between serum calcitriol and plasma iPTH (z' = -0.04, p=0.56).

Conclusion: The FGF-23 pathway may be activated in living kidney donors who show early biochemical changes compatible with mineralizing bone disorder. In these subjects with early stages of CRF, serum FGF-23 was more clearly correlated with phosphate homeostasis than plasma PTH. Whether these changes influence bone mineral density and fracture rates after kidney donation warrants future study.

Disclosures: Anthony Hodsman, None.

SU0122

Administration of PTH1-34 Partially Rescues Hematopoietic Defects in Bmi1 Null Mice by Improving the Hematopoietic Microenvironment. Ruinan Lu^{*1}, Qian Wang¹, David Goltzman², Dengshun Miao³. ¹Nanjing Medical University, China, ²McGill University Health Centre, Canada, ³Nanjing Medical University, Peoples Republic of China

We assessed whether PTH administration could rescue hematopoietic defects in *Bmi1* null mice by activating the Notch pathway and improving the hematopoietic microenvironment. We treated *Bmi1*^{-/-} mice, with 80µg PTH1-34/Kg, sc, daily from 1 to 4 weeks of age and compared them with vehicle-treated *Bmi1*^{-/-} and wild-type (WT) mice. Using techniques of histopathology, immunohistochemistry, real-time RT-PCR, Western blots, immunofluorescent staining and flow cytometry, we examined osteoblastic bone formation, the numbers of total bone marrow cells, hematopoietic stem cells (HSC) and hematopoietic progenitor cells (HPC) in bone marrow and peripheral blood cells, and Notch signal pathway-related molecules. Vehicle-treated *Bmi1*^{-/-} mice exhibited a phenotype of premature osteoporosis characterized by decreased trabecular bone volume, decreased osteoblast number, decreased alkaline phosphatase (ALP)-positive, type I collagen-positive and osteopontin-positive bone matrix, down-regulation of ALP and osteocalcin gene expression and of Runx2, PTHR and IGF1 protein expression. In addition, there were increased numbers of adipocytes within bone marrow, which were associated with the up-regulation of PPAR γ protein expression. PTH1-34 administration significantly increased all parameters related to osteoblastic bone formation, and significantly reduced the number of adipocytes and PPAR γ protein expression, but these parameters did not reach the control levels observed in vehicle-treated WT mice. The total number of bone marrow cells, the numbers of Sca-1⁺c-kit⁺Lin⁻ HSC and Sca-1⁺c-kit⁺Lin⁺ HPC in each femur, and the number of white blood cells and lymphocytes in peripheral blood were all decreased significantly in vehicle-treated *Bmi1*^{-/-} mice. These parameters were all increased significantly in *Bmi1*^{-/-} mice by the administration of PTH1-34, but did not reach the control levels observed in vehicle-treated WT mice. The number of Notch ligand Jagged1 positive cells and percentage of Notch intracellular domain (NICD) positive bone marrow cells were decreased significantly in vehicle-treated *Bmi1*^{-/-} mice, and were all increased significantly in *Bmi1*^{-/-} mice by the administration of PTH1-34, but did not reach the control levels observed in vehicle-treated WT mice. Results from the present study indicate that the administration of PTH1-34 partially rescues hematopoietic defects in *Bmi1* deficient mice by improving hematopoietic microenvironment and activating the Notch pathway.

Disclosures: Ruinan Lu, None.

SU0123

Anabolic Skeletal Effects after Discontinuation of Human Synthetic Parathyroid Hormone 1-34 (PTH) Replacement Therapy in Hypoparathyroidism (HPT). Rachel Gafni^{*1}, C. Michele Christie², Marilyn H. Kelly³, Beth A. Brillante³, James Reynolds¹, Hua Zhou⁴, David W. Dempster⁵, Michael Collins¹. ¹National Institutes of Health, USA, ²Department of Pediatrics, Kaiser Permanente, USA, ³SCSU, CSDB, NIDCR, National Institutes of Health, USA, ⁴Helen Hayes Hospital, USA, ⁵Regional Bone Center, Helen Hayes Hospital, USA

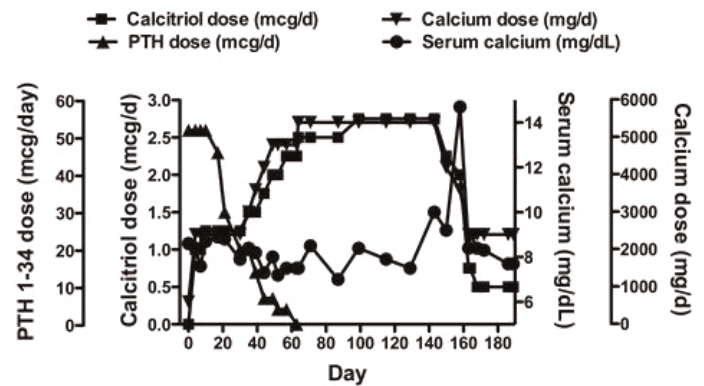
PTH 1-34 replacement therapy in hypoparathyroidism (HPT) maintains eucalcemia while converting quiescent bone to high turnover bone, as evidenced by bone markers and histomorphometry. However, the skeletal effects of PTH discontinuation are unknown.

Subject #1 is an 18 y/o man with congenital HPT who received PTH x 18 mos. Pre-PTH therapy was calcium (Ca) 1200 mg/d and calcitriol (1,25D) 0.75 mcg/d. At PTH start (15 1/2 y/o), he was in late puberty. Osteocalcin (OC), bone-specific alkaline phosphatase (BSAP), and N-telopeptide (NTX) were appropriately increased for age, and rose further with PTH. Iliac crest biopsy after 1 y of PTH showed increased bone volume, trabecular number, mineralizing perimeter and bone formation rate, compared to baseline. However, areal BMD by DXA changed little at most sites and declined at the radius. For 9 wk after stopping PTH, he required high doses of Ca and 1,25D to maintain serum Ca in the target range (7.6-9 mg/dL)-up to 4200 mg/d Ca and 1.5 mcg/d 1,25D. Doses were gradually weaned until he reached pre-PTH treatment doses 6 mos after stopping PTH. By 6 mos post-PTH, OC, BSAP, and NTX had declined to the adult normal range. BMD at 6 and 12 mos post-PTH rose markedly at the spine, hip, and total body with Z-score increases of 0.5-1 SD. Radial BMD also increased without Z-score change.

Subject #2 is a 43 y/o woman with surgical HPT who received PTH x 33 mos. Pre-PTH therapy was Ca 1200 mg/d and 1,25D 0.5 mcg/d. As in other HPT adults, PTH dramatically increased OC, BSAP, NTX, and hip BMD. Rather than stopping PTH abruptly, her PTH dose was weaned over 8 wk as oral Ca and 1,25D were increased to maintain serum Ca within the target range-up to 5400 mg/d Ca and 2.75 mcg/d 1,25D (Fig); doses were then weaned. Thirteen weeks after stopping PTH, she developed acute hypercalcemia (14.7 mg/dL) at doses of Ca 3600 mg/d and 1,25D 2 mcg/d. Supplements were stopped and she received treatment at her local hospital. She was restarted on Ca 2400 mg/d and 1,25D 0.5 mcg/d with stabilization of her serum Ca.

The transient increased Ca and 1,25D requirements accompanied by an increase in BMD Z-scores after cessation of long-term PTH therapy in HPT suggest an uncoupling of bone turnover favoring anabolic effects while transitioning from a high

turnover state. Further study and close monitoring of such patients is required to ensure safe transition to conventional therapy and to elucidate the physiological mechanism of this phenomenon.



Figure

Disclosures: Rachel Gafni, None.

SU0124

Dynamic formation of a PTH/PTHrP receptor-arrestin-Gs signaling complex in bone cells. Vanessa L. Wehbi^{*1}, Timothy N. Feinstein², Guillermo Romero², Jean-Pierre Vilardaga³. ¹University of Pittsburgh, USA, ²University of Pittsburgh, School of Medicine, Department of Pharmacology & Chemical Biology, USA, ³University of Pittsburgh, School of Medicine, USA

Arrestins and heterotrimeric G proteins ($G\alpha\beta\gamma$) regulate G-protein-coupled receptors (GPCRs) signaling and trafficking. Arrestins binding to activated GPCRs terminate receptor and G protein coupling, and promote receptor internalization. The binding of the β -arrestins and G proteins on activated GPCR is thought to be mutually exclusive. Here we show that β -arrestins prolong rather than shut down PTH/PTHrP receptor (PTHR) signaling. By using optical approaches (confocal microscopy, FRAP, TIRF, fluorescence correlation spectroscopy, and FRET) in bone- and kidney-cell derived lines (ROS 17/2.8 and HEK293) in real time we found that PTHR forms a ternary complex with β -arrestin1/2 and $G\beta\gamma$ subunits in response to PTH stimulation. We further confirmed the formation of a PTHR-arrestin- $G\beta\gamma$ complex in response to PTH(1-34) binding by coimmunoprecipitation assays. Additionally, we showed that the rapid ($t_{1/2} < 60$ s) assembly/disassembly dynamics formation of a multimeric receptor complex that contains PTH, PTHR, arrestin, and $G\beta\gamma$ subunits regulates cAMP levels in magnitude and duration. These data raise the novel model whereby the formation of a long-lived PTHR- $G\beta\gamma$ -arrestin ternary complex contributes to prolonged receptor signaling by mechanisms that presumably permit multiple rounds of $G\alpha\beta$ subunit coupling and activation.

Disclosures: Vanessa L. Wehbi, None.

SU0125

Elderly Men in Hong Kong Have Higher Serum Vitamin D and Lower Serum Parathormon Compared to Gothenburg. Mr Os. Ewa Waern^{*1}, Claes Ohlsson², R Chan³, Timothy Kwok³, PC Leung⁴, Egil Haug⁵, Magnus Karlsson⁶, Osten Ljunggren⁷, Dan Mellstrom¹. ¹Sahlgrenska University Hospital, Sweden, ²Center for Bone Research At the Sahlgrenska Academy, Sweden, ³The Chinese University of Hong Kong, Hong Kong, ⁴The Chinese University of Hong Kong, Hong Kong, ⁵Hormone Laboratory, Aker University Hospital, Norway, ⁶Skane University Hospital Malmö, Lund University, Sweden, ⁷Uppsala University Hospital, Sweden

Vitamin D is mainly produced in the skin in humans and increasing northern latitude, should influence both mean values and seasonal variation. However genetic, cultural, nutritional and anthropometric factors might have importance for the variation in serum vitamin D. The purpose of this study was to compare serum vitamin D and serum parathormon in Gothenburg (latitude 570 N) and Hong Kong (latitude 220 N).

Elderly men participated (69-80 years) in the population based Mr OS Sweden, Gothenburg (n = 1010) and Mr OS Hong Kong (n = 939).

Serum 25-hydroxyvitamin D (25 OH) and serum parathormon (PTH) was analysed at the same laboratory in Oslo, Norway.

25 OH was measured with competitive RIA (Dia Sorin, Stillwater, MN).

Intraassay and interassay variations were 5 % and 9 % respectively. PTH was measured with an immunoluminometric assay (Immulite 2000, Diagnostic Products Corporation, Los Angeles, USA). Intraassay variation was 5 % and interassay variation 9 %.

Vitamin D (25 OH) was higher in Hong Kong mean 78.3 (21.4) nmol/l compared to 66.7 (19.0) nmol/l in Gothenburg $p < 0.0001$.

Serum PTH was lower in Hong Kong 42.9 (22.7) ng/l compared to 51.9 (23.5) ng/l in Gothenburg ($p < 0.0001$). The correlation between 25 (OH) and PTH was ($r = -0.17$ $p < 0.0001$) in Hong Kong and ($r = -0.15$ $p < 0.0001$) in Gothenburg.

The mean body weight in Hong Kong was 61.7 (9.5) kg vs 80.9 (12.2) kg in Gothenburg $p < 0.0001$. The average height in Hong Kong was 163.1 cm vs 175.7 cm in Gothenburg $p < 0.0001$.

BMI was lower in Hong Kong 23.2 (3.2) vs Gothenburg 26.2 (3.5). BMI correlated to 25 (OH) in Hong Kong ($r = -0.08$ $p < 0.01$ and in Gothenburg ($r = -0.17$ $p < 0.0001$). In Hong Kong 1.7 % had obesity BMI > 30 vs 12.4 % in Gothenburg. Serum PTH correlated to body height in Gothenburg ($r = 0.07$ $p = 0.03$) but not in Hong Kong ($r = 0.01$ ns). The proportion of hyperparathyroidism PTH > 65 ng/l was in Gothenburg 21.1 % and in Hong Kong 11.4 %

$p < 0.0001$. In Hong Kong 51 % had 25 OH > 75 nmol/l vs 31 % in Gothenburg. Only 7 % had 25 (OH) < 50 nmol/l in Hong Kong vs 20 % in Gothenburg. Seasonal variation occurred in both cities. Figure.

We conclude that vitamin D is higher and PTH lower in Hong Kong compared with Gothenburg. Vitamin D correlated inversely to BMI. Hyperparathyroidism was more prevalent in Gothenburg.

Disclosures: Ewa Waern, None.

SU0126

Nuclear Actions of PTHrP Contribute to the Differentiation of the Mammary Mesenchyme. Kata Boras-Granic^{*1}, Pamela Dann¹, Andrew Karaplis², John Wysolmerski¹. ¹Yale University School of Medicine, USA, ²McGill University, Canada

Parathyroid hormone-related protein (PTHrP) is responsible for the clinical syndrome of humoral hypercalcemia of malignancy and it also contributes to osteolytic bone metastases from breast cancers. It is related to parathyroid hormone and binds to and activates a common type 1 PTH/PTHrP (PTHR1) receptor. Unlike PTH, PTHrP also contains canonical nuclear localization sequences in its mid-region and c-terminus that allow for its import into the nucleus. The functions of PTHrP in the nucleus is not known, but mice in which the native PTHrP gene has been replaced with a truncated form of PTHrP (1-86) (PTHrP (1-86)-knockin mice), that can be secreted but not enter the nucleus, are grossly normal at birth but fail to grow well and die at about 2 weeks of age. The exact cause of death in PTHrP (1-86)-knockin mice is unclear but they demonstrate widespread cell senescence. We examined the development of the mammary gland in PTHrP (1-86)-knockin mice. Global PTHrP and PTHR1 knockout mice demonstrate a failure of embryonic mammary development at the bud stage due to a failure of mammary mesenchyme development. One consequence of the disruption in mammary mesenchyme differentiation is a failure of the androgen-dependant destruction of the mammary bud. In PTHrP (1-86)-knockin embryos the mammary buds appeared grossly normal at E15. There appeared to be the initiation of ductal outgrowth in some buds, but the ducts were small and stunted compared to WT controls in PTHrP (1-86)-knockin neonates. Surprisingly, in male PTHrP (1-86)-knockin embryos, the mammary buds were retained at E15, suggesting a failure of the normal androgen response. This prompted us to examine markers of mammary mesenchyme differentiation. We found that loss of nuclear PTHrP led to a loss of mesenchymal estrogen receptor expression and reductions in the expression of beta-catenin and Lef1. These results partially phenocopy the results in global PTHrP and PTHR1 knockouts. Since PTHrP is only produced by epithelial cells and the PTHR1 is only expressed on mesenchymal cells, these results suggest that secreted PTHrP may bind to the PTHR1 receptor on mesenchymal cells and be internalized and traffic to the nucleus of these cells in order to modulate their differentiation.

Disclosures: Kata Boras-Granic, None.

SU0127

p85 α Subunit of PI3K Mediates Bone Loss Induced by Continuous PTH Infusion. Rajendra Kedlaya^{*1}, Reuben Kapur¹, Alexander Robling². ¹Indiana University School of Medicine, USA, ²Indiana University, USA

Osteoclastogenesis and activity is mediated by a number of signaling events, including M-CSF signaling through the M-CSF receptor, RANKL signaling through the RANK receptor, and integrin signaling through $\alpha\beta3$. A key downstream mediator of these receptors is the phosphoinositide-3 kinase (PI3K). Class 1A PI3Ks are heterodimers comprised of two subunits—a p110 catalytic subunit and a p85 regulatory unit. We showed previously that deletion of the p85 α subunit resulted in increased trabecular bone mass and architectural properties in mice. These mice also had elevated but functionally compromised osteoclasts, resulting in reduced resorption. Modulation of p85 α might present a viable target for mitigating osteoclast-mediated bone loss. To explore this proposal, we treated 12-wk female p85 α -/- mice with a pro-resorptive, catabolic stimulus by continuously infusing them with 40 μ g/kg/dy of PTH 1-34. Infusions lasted for 3 wks, and changes in bone mass

were measured using DEXA. In WT mice, 3 wks of vehicle infusion resulted in a 10.5% increase in whole body (WB) BMC, whereas PTH infusion resulted in a -1.2% decrease in WB BMC ($p < 0.05$). In p85 α -/- mice, vehicle infusion resulted in a 7.2% increase in WB BMC, whereas PTH infusion resulted in a 5.7% increase in WB BMC ($p = 0.74$). Similar results were found when the spine was analyzed in isolation. Having found that the p85 α -/- mice were resistant to the catabolic effects of continuous PTH, we assessed whether the anabolic effects of intermittent PTH were affected by p85 α deletion. PI3K mediates downstream signaling activity of many RTKs, including the IGF-1 receptor, which is crucially important for the anabolic effects of intermittent PTH. Male 10-wk old p85 α +/+ and p85 α -/- mice were given whole-body DEXA scans while under general anesthesia, then administered daily subQ injections of 40 μ g/kg/dy PTH, 7dy/wk, for 6 wks. In WT mice, 6 wks of vehicle treatment resulted in a 4.6% increase in WB BMC, whereas intermittent PTH resulted in a 18.0% increase in WB BMC ($p < 0.05$). In p85 α -/- mice, vehicle treatment resulted in a 12.1% increase in WB BMC, whereas intermittent PTH resulted in a 32.1% increase in WB BMC ($p < 0.05$). 2-way ANOVA yielded no significant interaction term, indicating that PTH induced similar anabolic effects regardless of genotype. In summary, the p85 α subunit of PI3K appears to modulate the catabolic effects of PTH signaling, but the same hormone maintains its anabolic properties in the absence of p85 α .

Disclosures: Rajendra Kedlaya, None.

SU0128

Parathyroid Hormone Reduces Oxidative Stress in Bone by Preventing Activation of p66^{Shc} and by Stimulating the Expression of Aldehyde Dehydrogenase 3a1. Robert Jilka^{*}, Annick DeLoose, Kanan Vyas, Maria Almeida, Stavros Manolagas, Center for Osteoporosis & Metabolic Bone Diseases, Central Arkansas Veterans Healthcare System, University of Arkansas for Medical Sciences, USA

Daily injections of PTH increase bone mass in postmenopausal women and elderly hypogonadal men, but the underlying mechanisms have not been established. It was shown previously that PTH-stimulated bone formation is greater in old as compared to young C57BL/6 mice, and is associated with reversal of the increased oxidative stress (OS) seen in the skeleton of aged mice. As shown elsewhere in this meeting, the level of OS in bone is determined in part by activation of p66^{Shc} - a redox sensitive adapter protein that amplifies the production of reactive oxygen species (ROS) by mitochondria. Lipid oxidation also contributes to OS via generation of 4-hydroxynonenal (4-HNE), which lowers the level of the important anti-oxidant glutathione. Oxidized lipids may also increase ROS levels by activating NADPH oxidase (Nox). Mechanistic studies have established that PTH suppresses the H₂O₂- and 4-HNE-stimulated increase in activated p66^{Shc} in osteoblastic cells via a protein kinase A- and protein kinase C-dependent mechanism. We now report that RNA and protein synthesis are also required as both actinomycin D and cycloheximide prevented the attenuating effect of PTH on H₂O₂-induced p66^{Shc} activation. Microarray studies revealed that PTH increased the expression of aldehyde dehydrogenase 3a1 (Aldh3a1) in murine vertebral bone by 10-fold, measured 1 h after injection of the hormone. Aldh3a1 detoxifies 4-HNE, and also produces NADPH needed for the synthesis of glutathione via the glutathione peroxidase/reductase system. Furthermore, PTH increased Aldh3a1 expression, and aldehyde dehydrogenase activity, in osteoblastic cells cultured from neonatal calvaria. On the other hand, PTH had little if any effect on the expression of other anti-oxidant enzymes including glutathione reductase and thioredoxin reductase, as well as peroxiredoxin and thioredoxin, in vivo or vitro. PTH also had no effect on the expression of Nox. We propose that intermittent PTH reduces OS, at least in part, by suppressing the activation of p66^{Shc} and by increasing the synthesis of Aldh3a1. Further studies are needed to establish the significance of the anti-oxidant property of PTH for its anabolic efficacy in the aged skeleton.

Disclosures: Robert Jilka, Radius Health, Inc., 1

SU0129

Persistently Elevated Parathormone after 12 months of Parathyroid Adenoma Surgery. Rabindera Mehrotra^{*}, Apollo Hospitals, India

We retrospectively analysed data of 25 patients who under went surgery for Primary Hyper Parathyroidism at our Hospital. 2 patients with multi gland disease (Hyperplasia) and 2 patients with associated CKD were excluded. For 11 patients data at 1 year was available for review.

Diagnosis of Primary hyper parathyroidism was based on elevated calcium with unsuppressed PTH. 10 were below 30 years of age. In all subjects single adenoma was localized in at least 1 of the imaging. Some subjects had markedly elevated levels of PTH (147-4560 ng/ml). Subjects with significant bone disease had markedly elevated PTH and higher values of alkaline phosphatase. Bone disease manifestation included X Ray evidence of sub periosteal re absorption and osteitis fibro cystica. At surgery all subjects had uni lateral exploration of neck. Effort was made to biopsy the remaining gland to confirm the diagnosis of Parathyroid adenoma. All 11 subjects had under gone neck exploration and single adenoma was removed. All biopsy reports were confirming to the diagnosis of parathyroid adenoma. In the post op period all subjects had significant hypo calcemia because of hungry bone disease. They were treated with oral and Intra venous calcium infusions. 125 Vit D3 analogues had to be used for a varied interval of time. Subjects with severe bone disease had more severe hypo calcemia They also received 4,000 units of chole claciferol every day. In follow

up there was symptomatic improvement, alkaline phosphatase started to decline and requirement of oral calcium supplements also declined. In some of the patients we had done DXA. BMD increase was noticed. The skeletal lesions healing was seen over a period of 6-12 months. 8 subjects had elevated PTH levels even after 1 year of follow up. All 8 subjects had normal calcium levels (even after correcting for albumin). In 3 subjects PTH even after 24 months PTH was elevated. No patient developed recurrent hyperparathyroidism. The elevated levels of PTH and ALP may be explained by continuing bone mineralization.

As these subjects were young and the skeleton had been demineralized because of hyperparathyroidism. They have increased requirement of calcium and Vitamin D for a prolonged period of time which may last for more than a year. Only dietary supplements would not be sufficient. The requirement is many times of RDA. Replacing Vitamin D and calcium in adequate dosages would help to recover the lost BMD.

Disclosures: Rabindera Mehrotra, None.

SU0130

PTH Skeletal and Bone Healing Efficacy in T-Cell Deficient and Normal Rats are Similar. Masahiko Sato¹, M.D. Adrian¹, Matt Hamang¹, Q.Q. Zeng¹, Yanfei Ma². ¹Lilly Research Labs, USA, ²Eli Lilly & Company, USA

T lymphocytes were shown previously to mediate the skeletal efficacy of PTH in mice, because nude mice exhibited a blunted skeletal response to PTH (M. Terauchi et al. 2008). The goal for this study was to compare the skeletal and bone healing responses to PTH in athymic nude and normal rats. Male, 14 week old, athymic nude rats (NIHRNU-M, NTac:NIH-Whn, Taconic), Hsd:RH-Foxn1nu (Harlan) and normal SD rats (Harlan) were maintained on a 12hr light/dark cycle at 22°C with ad lib access to food (TD 89222 with 0.5% Ca and 0.4%P, Teklad, Madison, WI) and water; and then were subjected to bilateral cortical defect surgery through both anterior and posterior cortices (D. Komatsu et al. 2009). Animals were weighed, and randomized into groups treated with 0, 5 or 30 µg/kg/d sc hPTH1-38 for 7 weeks of treatment, starting 8 days post-surgery. Relative to age-matched vehicle controls at necropsy, PTH dose-dependently enhanced BMD of the whole femoral diaphysis (24%, 60%, 35%) and the intramedullary spaces (95%, 401%, 243%) at the cortical defect site for NTac:NIH-Whn, Hsd:RH-Foxn1nu, and normal rats, respectively. Region specific analyses showed PTH enhanced healing of the anterior cortex for Hsd:RH-Foxn1nu (60%), but not for NTac:NIH-Whn or normal rats, relative to controls. Load to failure analyses at the cortical defect site showed dose dependent enhancement of femoral strength (17%, 39%) for NTac:NIH-Whn and Hsd:RH-Foxn1nu, respectively, but not for normal rat femoral diaphyses relative to controls. PTH dose-dependent efficacy was also observed at non-fractured sites as increased femoral neck strength (38%, 30%, 32%) and vertebral BMD (14%, 22%, 24%), for NTac:NIH-Whn, Hsd:RH-Foxn1nu, and normal rats, respectively. Longitudinal analyses showed that PTH enhanced bone healing by stimulating woven bone formation in the intramedullary spaces and stimulating endocortical mineral apposition resulting in stronger femora for 2 athymic rat strains in a manner that compared favorably to normal rats. Bone histomorphometric analyses showed higher mineralizing surface, mineral apposition rate, and bone formation rate in vertebra for both athymic rat strains. The data taken together also showed that systemic PTH skeletal efficacy in the athymic nude rats were also comparable to PTH efficacy in normal SD male animals, and that rats may differ from mice.

Disclosures: Masahiko Sato, Lilly Research Labs, 3

SU0131

The Effect of JTT-305 (MK-5442), an Orally Active Calcium-sensing Receptor Antagonist, on Calcium Metabolism in Parathyroidectomized Rats. MIKIO HAYASHI*, Takashi Nakagawa, Mariko Maekawa, Shuichi Kimura. Central Pharmaceutical Research Institute, JAPAN TOBACCO INC., Japan

JTT-305 (MK-5442) is a novel, orally active calcium-sensing receptor (CaSR) antagonist. In an in vitro study, JTT-305 showed specific binding ability to human CaSR (K_d: 6.2 nM) and inhibited the increase in intracellular Ca concentrations produced by extracellular Ca exposure in CaSR-transfected cells (IC₅₀: 86 nM). In an in vivo rat study, JTT-305 stimulated the transient secretion of endogenous parathyroid hormone (PTH) and prevented OVX-induced bone loss by stimulating bone formation. JTT-305 elevated serum Ca concentrations in a dose-dependent manner, while rat PTH(1-84) did not affect it.

The objective of this study was to examine the mechanism by which JTT-305 increases serum Ca in rats. In this study, parathyroidectomized (PTX) rats were used to investigate the effect of JTT-305 on Ca metabolism in the absence of parathyroid cells. After PTX, a micro-osmotic pump was implanted, and PTH was infused for 5 days in order to restore normal serum Ca levels. JTT-305 was administered at a dose of 10 mg/kg, and serum Ca was measured at 0.5, 1, 2, 4 and 8 hours after dosing. Urine was collected during 4, 8, and 24 hours, and urine Ca measured. Serum calcitonin was also measured in order to study the effect of JTT-305 administration on thyroid cells.

After administration of JTT-305, serum Ca was elevated from 0.5 hours to 8 hours in PTX rats. However, the changes in serum Ca concentrations in PTX rats were almost identical to those in intact rats. Conversely, urine Ca excretion was reduced

over the following 24 hours (vehicle vs. JTT-305: P<0.05). JTT-305 did not reduce serum calcitonin. Since CaSR is expressed in the parathyroid gland and the kidney, JTT-305 may increase serum Ca in rats via a renal mechanism. In summary, it is believed that the increase in serum Ca produced by JTT-305 is likely due to an effect on the renal CaSR and not to changes in endogenous PTH or calcitonin.

Disclosures: MIKIO HAYASHI, JAPAN TOBACCO INC., 3
This study received funding from: JAPAN TOBACCO INC.

SU0132

TWEAK and FN14 Signaling Through NFκB is Necessary for the RAS Effector Mutant Human Prostate Cancer Cell Line DU145/Ras^{V12G37} to Form Bone Metastasis. Kristin J Lastwika¹, Victoria Seng², Kirsten Tracy², Juan Juan Yin³, Kathleen Kelly². ¹George Washington University Institute for Biomedical Sciences, USA, ²Cell & Cancer Biology Branch, Center for Cancer Research, National Cancer Institute, USA, ³National Cancer Institute, USA

Prostate cancer is the third leading cause of cancer-related deaths in the Western world male population and bone metastases are the leading cause of mortality in prostate cancer patients. Understanding the mechanisms mediating this process is critical to the prevention of bone metastases. Our lab has previously reported that the *H-RAS* effector mutant DU145/G37 Ras^{V12G37} human prostate cancer cell line significantly increases bone metastatic capability. Three clones isolated from the bone metastasis showed a further increase in the rate of bone metastases. The bone clones and the parental DU145/G37 Ras^{V12G37} cell line were then compared by protein microarray to identify bone specific markers. All three of the metastatic bone clones had a significantly higher expression of the cytokine TNF-like weak inducer of apoptosis (*TWEAK*) and its receptor fibroblast growth factor-inducible 14 (*FN14*). Subsequent knockdown of *FN14* in the bone isolates decreased the number of bone metastasis to 30%, indicating that *FN14* expression is integral for these prostate cancer cells to colonize bone. *FN14* knockdown did not have an effect on brain metastases, suggesting that *FN14* expression is specific to bone metastatic growth. *TWEAK-FN14* binding has been shown to activate many different signaling cascades, including *PI3K*, *MAPK*, *NFκB* and *JNK*. In our system, the tumor bone clones use both the canonical and non-canonical *NFκB* signaling pathway to mediate their effects. We are currently investigating this *TWEAK-FN14* mediated *NFκB* pathway rescue and an *FN14* receptor rescue through *in vivo* experiments to monitor bone metastasis formation. The identification of this *TWEAK-FN14* signaling specific to prostate cancer cell growth in the bone microenvironment gives new insight into mechanisms mediating metastatic growth. These findings could potentially aid in the development of targeted therapeutics to prevent bone metastases.

Disclosures: Kristin J Lastwika, None.

SU0133

A Non-invasive Way to Target microRNA-21 and to Prevent Osteometastatic CSF-1 Expression by the Human Breast Cancer Cells via PTEN. Chandni Mandal¹, Triparna Ghosh-Choudhury², Goutam Ghosh Choudhury¹, Nandini Ghosh-Choudhury¹. ¹University of Texas Health Science Center at San Antonio, USA, ²Baylor College of Medicine, USA

Extravasation of circulating breast tumor cells produce micrometastasis to form osteolytic lesions in skeleton. We recently identified that fish oil diet targets and restores the expression of the tumor suppressor protein PTEN, a negative regulator of PI 3 kinase/Akt signaling, as one of the mechanisms to block growth and bone metastasis of MDA MB-231 breast cancer cell (MDA) *in vivo*. Here we report a novel mechanism for fish oil diet-induced PTEN expression and inhibition of osteolytic metastasis. Along with PTEN haploinsufficiency, oncomiR (oncogenic microRNAs) addition drives cancer metastasis. Interestingly, fish oil diet attenuated expression of miR-21 in mouse tumor xenografts. DHA and EPA, the key ω-3 fatty acids in fish oil, inhibited miR-21 expression in MDA. miR-21 expression increased migration of MDA and partially reversed DHA- or EPA-mediated migratory inhibition of MDA. PTEN mRNA 3'UTR contains miR-21 recognition element. Expression of miR-21 blocked the activity of PTEN 3'UTR-Luc reporter enzyme, indicating functional targeting of PTEN mRNA by miR-21 in MDA. Conversely plasmid-coded anti-miR-21 sequences (Sponge) increased PTEN 3'UTR-Luc activity. Moreover, expression of either miR-21 or miR-21 Sponge in MDA significantly suppressed or increased the expression of PTEN. Colonized breast cancer cells secrete osteoclastogenic cytokines, including colony stimulating factor-1 (CSF-1) to facilitate bone metastasis. qRT-PCR analysis of CSF-1 mRNA expression in the MDA-derived tumor xenografts showed significant inhibition by fish oil diet. *In vitro*, a direct correlation was observed for the CSF-1 mRNA and protein expressions and the bone metastatic potential of the breast cancer cells. DHA and EPA, inhibited CSF-1 mRNA and protein expression in MDA cells. We investigated the involvement of PTEN in CSF-1 expression by breast cancer cells. Cotransfection of the CSF-1 promoter-driven luciferase plasmid (CSF-1-Luc) in MDA with PTEN or dominant negative (DN) PI 3 kinase or DN Akt, inhibited the transcription of CSF-1. Next, we examined the involvement of miR-21 in regulating CSF-1 expression. Expression of miR-21 enhanced while miR-21 Sponge reduced abundance of CSF-1 mRNA via transcriptional regulation. Together these results uncover a novel function of fish oil, which beheads miR-21 signaling to increase

PTEN expression and in turn dampen expression of CSF-1 thus preventing osteoclastogenesis and osteolytic lesions in breast cancer bone metastasis.

Disclosures: Chandi Mandal, None.

SU0134

Breast Cancer Stem Cells Metastatize to Bone in a Human in Mice Model.

Lucia D'Amico^{*1}, Salvatore Patane², Cristina Grange³, Benedetta Bussolati³, Patrizia D'Amelio⁴, Giancarlo Isaia⁴, Riccardo Ferracini⁵, Ilaria Roato⁶. ¹Azienda Ospedaliero-Universitaria Molinette San Giovanni Battista, Italy, ²CeRMS, Italy, ³Department of Internal Medicine, Molecular Biotechnology Center, University of Turin, Italy, ⁴University of Torino, Italy, ⁵Department of Orthopaedics, A.O.U. San Giovanni Battista, Italy, ⁶A.O.U. San Giovanni Battista, Italy

Background. Bone metastases represent a common complication for breast cancer which is characterized by a selective bone tropism. Despite their clinical relevance, the mechanisms ruling bone metastatic process are not completely clear. Breast tumors are known to be composed of different cells, but it is not clear which of these cells contribute to tumor development and progression. The currently prevailing models explaining intratumor heterogeneity include the cancer stem cell hypothesis focused on a subset of tumor cells called cancer stem cells (CSCs), which are able to self renew and to differentiate in a heterogeneous tumor cell population. In breast cancer, CSCs were isolated and identified as a CD44+CD24- population. Many of the properties proposed for CSCs have identified them as candidates for mediating metastatic progression but no data are available on their ability to promote bone metastases.

Methods. We used a NOD/SCID human-in mice model. Briefly, we implanted fragments of human bone under the mice skin, then we injected CD44+CD24- breast CSCs transduced by luciferase-lentiviral vector to study their ability to metastatize to bone. Mice were divided according to the CSCs injection root: subcutaneously and intracardiac injection. After 8 weeks, mice were sacrificed and H&E staining was performed on bone and lung. Then CK, vimentin and EMA were studied by IHC. Moreover, we isolated and characterized by flow cytometry the metastatic breast CSCs from bone metastasis.

Results. Our model is a viable tool to study human bone metastases in animals, because H&E staining of the implanted bone showed its viability, activity and the presence of human neo-vascularization, detected by staining for human CD34. By in vivo imaging system we monitored the tumor growth and detected bone localization of breast CSC-Luc injection. H&E staining of bone showed the presence of bone metastatic lesions, with tumor cells positive for EMA, CK and vimentin. At last, we isolated from the implanted bone and characterized the breast metastatic CSCs, which exhibited a CD44-CD24+ phenotype.

Conclusions. We demonstrated the ability of breast CSCs to promote bone metastasis and we isolated for the first time the breast metastatic CSCs. This result opens new perspectives to define the precise nature of the cells that promote bone metastases.

Disclosures: Lucia D'Amico, None.

SU0135

Characterization of the Bone Metastatic Potential of Different Tumor Cell Lines.

Sophie Baret^{*}, Ingrid Stockmans, Riet Van Looveren, Geert Carmeliet. Katholieke Universiteit Leuven, Belgium

Bone metastasis is a major complication in patients with breast or prostate cancer. The use of preclinical models is of utmost importance to evaluate and validate the efficacy of novel therapeutic approaches. Intracardiac inoculation of tumor cells in mice is considered as the preclinical model of choice, but a thorough comparison between different tumor cell lines is still lacking.

We compared the bone metastatic potential and characteristics of 4 different tumor cell lines, which form predominantly osteolytic lesions. We used 3 breast tumor cell lines (human MDA-MB-231, human CN34-BoM2 and murine 4T1 cells) and 1 human prostate tumor cell line (PC3). Tumor cells were intracardially injected in mice and the development of bone metastasis was evaluated by μ CT imaging. The latency period before osteolytic lesions were first noticed, was longer for the PC3 and CN34 cells. The osteolytic pattern was clearly different in the PC3 cell line. Here, bone resorption was observed as separated round cavities scattered over the bone cortex whereas the breast tumor cell lines caused more diffuse osteolytic areas in the trabecular region. Histological data confirmed this pattern and revealed additional differences. The breast cancer cells expanded at first between the bone trabeculae and resorbed the metaphyseal bone before they destroyed the cortex. The CN34 and 4T1 cells showed a very infiltrative growth compared to the MDA cells. This growth pattern is in contrast with the prostate tumor cells which expanded radial in the cortex and formed multiple separated tumors. CD31 staining showed that PC3 metastases are surrounded by blood vessels with few vessels inside the tumor. In all the breast tumors abundant vessels were observed penetrating the tumor whereas the tumor borders were less marked off by vessels. TRAP staining revealed that osteoclasts encircled the PC3 tumors, whereas they were scattered at sites of contact between tumor cells and bone trabeculae in the breast tumor cell lines. In CN34 tumors TRAP positive cells were even noticed inside the tumor with no bone contact.

Our study revealed clear differences in the bone metastatic potential and characteristics of the different tumor cell lines. This information may help in

evaluating different anti-tumor therapies: potent therapeutics will be effective in the different models while others may seem to be more specific for a certain type of metastasis.

Disclosures: Sophie Baret, None.

SU0136

Current Practices of Screening, Prevention and Treatment of Androgen Deprivation Therapy (ADT) induced Osteoporosis in patients with Prostate Cancer.

Arthur Lau^{*1}, Humaid Al-Shamsi², Kartika Malik³, George Ioannidis¹, Jonathan Adachi⁴, Alexandra Papaioannou⁵. ¹McMaster University, Canada, ²McMaster University, Department of Medical Oncology, Canada, ³University of Toronto, Department of Geriatrics, Canada, ⁴St. Joseph's Hospital, Canada, ⁵Hamilton Health Sciences, Canada

Introduction:

In Ontario, Canada, prostate cancer is the most common cancer in men. Androgen deprivation therapy (ADT) is commonly used as an adjuvant for locally advanced and high risk localized disease. ADT's effects on bone metabolism are well documented. The goal of this study was to assess the care gap in this population regarding screening, prevention and treatment of osteoporosis. We also assessed the characteristics of the patients who were more likely to be screened for osteoporosis.

Methods:

Patients diagnosed with non-metastatic prostate cancer on ADT were assessed. Charts were assessed for utilization of DXA scan, prescription of calcium, vitamin D, calcitonin and bisphosphonates. Pre-specified osteoporosis risk factors were also abstracted. In addition, any new fractures incurred during the follow-up were also recorded. Bivariate analysis was used to determine the effect of numerous patient characteristics and likelihood for osteoporosis screening.

Results:

In total, 149 charts were assessed, with 3 year mean follow-up. 58.8% of men received a baseline DXA, of which 20.3% had a repeat DXA at any point within their individual follow-up periods. Bisphosphonates, calcium, vitamin D and calcitonin were prescribed to 12.7, 35.6, 36.9% and 1.3% respectively. In all, 28% were appropriately screened and managed for osteoporosis (received repeat DXA or bisphosphonate). During their follow-up, 0.7%, 2%, and 5.4% had a hip fracture, vertebral fracture and other fractures respectively.

In bivariate analysis, number of ADT injections was significantly associated with being screened. Mean number of injections in patients who received follow-up DXAs or bisphosphonates was 13.1 versus 7.9 ($p < 0.0001$). Age, Gleason score, and PSA at initial visit were not associated with increased screening.

Conclusions:

To prevent osteoporosis in patients on ADT, clinicians have been advised to screen patients prior to the initiation of ADT. Despite these recommendations, our study shows a care gap exists in the screening, prevention, and treatment of osteoporosis in this population. This is quite concerning since they're at high risk for bone loss and fractures. Patients with more ADT injections were more likely to be screened. Our results suggest more education is required for the physicians and healthcare providers treating prostate cancer to help prevent and treat osteoporosis in this susceptible population.

Disclosures: Arthur Lau, None.

SU0137

Dual Actions of Klotho in Breast Cancer Cells Cause Resistance to TGFbeta and Vitamin D.

Pierrick Fournier^{*}, Daniel Edwards, John Chirgwin.

Indiana University, USA

Klotho was discovered as an anti-aging gene and subsequently found to be the specific co-receptor for osteocyte-secreted FGF23. FGF23 signals via binding to klotho in the kidney to induce the transcription factor EGR1 and regulate phosphate homeostasis and vitamin D catabolism. Breast cancer expression of klotho increases with increasing tumor grade, and MCF7 human breast cancer cells, which cause bone metastases in nude mice, express klotho and the FGF receptor 1iic isoform. We previously reported that treating these cells with 100ng/ml recombinant FGF23 rapidly increased EGR-1 mRNA 30X by 1hr, followed at 2 hrs by a 10X increase in vitamin D-inactivating 24-hydroxylase, CYP24A1, while 1-alpha hydroxylase was unchanged. Treatment with 100nM 1,25-dihydroxyvitamin D3 for 6 days inhibited cell growth 90%, while FGF23 increased cell numbers by 215% ($p < 0.05$) in the presence of 1,25-dihydroxyvitamin D3.

FGF23 treatment of MCF7 cells rapidly increased mRNAs encoding the early response genes Cyr61 13X & CTGF 280X, respectively. Cyr61 & CTGF are related extracellular matrix proteins that stimulate growth of tumor and bone cells. Klotho is a 1012 aa C-terminally anchored transmembrane protein (mKL), which can be shed by extracellular proteolysis. The shed form consists of a two repeated domains and inhibits TGFbeta signaling by competing with nM affinity for ligand binding at the type II receptor subunit (Doi et al, JBC, 2011). Many cells also express an alternatively spliced transcript encoding a constitutively secreted, single-domain protein of 549 aa (sKL). We tested the effects of overexpression of mKL & sKL in MDA-MB-231 breast cancer cells, which respond to TGFbeta but express very low klotho mRNA. When cells were cotransfected with a TGFbeta reporter, (CAGA)

9-luciferase, sKL but not mKL, decreased TGFβ-induced luciferase activity from 270 to 160 RLU ($p < 0.05$; $n = 3$), indicating that single-domain sKL, like two-domain shed klotho, inhibits TGFβ signaling.

The data show that klotho plays two roles in metastatic tumor cells, acting in cis and in trans: 1) Membrane klotho confers tumor cell responsiveness to osteocyte-produced FGF23, activating early pro-metastatic gene expression (EGFR1, Cyr61, CTGF) and inactivating vitamin D metabolites (via Cyp24A1); 2) Secreted and shed forms of klotho inhibit TGFβ signaling, which can alter the bone phenotype at sites of metastases.

Disclosures: Pierrick Fournier, None.

SU0138

Induction of perlecan/HSPG2 Expression in Desmoplastic Bone Marrow Stromal Cells. Curtis Warren*, Daniel Carson, Mary Farach-Carson. Rice University, USA

Perlecan/HSPG2 is the most abundant heparan sulfate (HS) proteoglycan in bone marrow stroma, where prostate cancer (PCa) cells undergoing epithelial-mesenchymal transformation (EMT) find a metastatic niche in disease progression. HS is essential to growth factor signaling in PCa cell growth and angiogenesis, and perlecan expression increases in PCa-associated fibroblasts where it plays a key role in tumor growth. We hypothesized that the desmoplastic response that increases perlecan expression during PCa growth is driven by similar cell signaling processes in the bone marrow and prostate gland. To test this, we first studied perlecan regulation in reactive bone marrow stromal cells. An *in silico* analysis of conserved transcription factor binding sites in the proximal promoter region of the perlecan gene led to the hypothesis that growth factors and cytokines present in the tumor microenvironment activate transcription factors leading to perlecan promoter activation. This analysis revealed a conserved putative NFκB consensus element in the 2.6 kb proximal promoter region. Using the 2.6 kb human perlecan proximal promoter region to drive a firefly luciferase reporter, we found activation of the perlecan promoter by Tumor Necrosis Factor-α (TNFα) in the human bone marrow stromal cell line, HS-27a, a cell line used to model desmoplastic processes. Deletion analysis of the proximal promoter region in reporter assays demonstrated that the TNFα responsive *cis*-element is encoded in the distal portion of the 2.6 kb promoter region where a consensus NFκB binding site resides. Real-time RT-PCR and dot-blot based analysis of mRNA and protein extracts, respectively, of TNFα treated HS-27a cells confirmed an increase (2-3 fold) in steady state levels of both transcript and protein after 72 hours of TNFα treatment. Ongoing studies include mutation of the perlecan promoter construct to identify the active *cis* element(s) responding to TNFα treatment and further characterization of the intracellular mechanism of perlecan transcriptional activation in HS-27a, primary bone marrow stromal cells, and prostatic fibroblasts. Disruption of paracrine signaling interactions between PCa cells and surrounding stroma that increase perlecan expression during desmoplasia is expected to inhibit disease progression toward lethality.

Disclosures: Curtis Warren, None.

SU0139

Number Needed to Treat and Risk Benefit Analysis of Denosumab Versus Zoledronic Acid in the Treatment of Castrate-Resistant Prostate Cancer Patients with Bone Metastases. Andrew P Yu¹, Melissa Diener¹, Eric Q Wu¹, Madhav Namjoshi². ¹Analysis Group, Inc., USA, ²Novartis Oncology, USA

Purpose: Approximately 70% of patients with castrate-resistant prostate cancer (CRPC) experience bone metastases which lead to the development of skeletal related events (SREs) such as fractures. Zoledronic acid (ZOL) and denosumab (Dmab) have been shown to prevent or delay SREs in CRPC patients with bone metastases. A phase III trial (NCT00321620, Amgen) compared ZOL and Dmab in patients with CRPC. Results suggest that Dmab is superior in delaying time to SREs, whereas overall survival and disease progression rates are comparable, and ZOL appears to have better safety profile. The objective of this project was to conduct a risk-benefit analysis (RBA) comparing the number needed to treat (NNT) and the number needed to harm (NNH) for Dmab versus ZOL.

Methods: Results from the phase III trial were used to assess the benefits and risks of using Dmab versus ZOL. The NNT calculated the number of patients who would need to be treated with Dmab versus ZOL to prevent one additional fracture, whereas the NNH calculated the number of patients who would have to be treated with Dmab versus ZOL for one additional patient to experience a grade 3 or 4 adverse event (CTCAE3/4). The risk-benefit ratio (RBR), calculated as NNT/NNH, determines whether fewer patients will need to be treated to achieve a benefit than will be treated to experience one additional AE. A sensitivity analysis varied the treatment outcomes from pathological fracture to SRE, and the adverse event outcome from CTCAE3/4 to hypocalcaemia.

Results: For NNT analysis, 162.4 additional patients would need to be treated with Dmab versus ZOL to avoid one additional pathological fracture (absolute risk reduction 0.6% [95% CI: -2.6% to 3.8%]). NNH results showed that 18.4 more patients will experience a CTCAE3/4 with Dmab versus ZOL. The RBA of 8.8 indicates that over 8-fold more patients would need to be treated to prevent a pathological fracture than to have one additional CTCAE3/4. A sensitivity analysis showed that NNT for

any SRE was 21.3, whereas NNH for hypocalcaemia was 14.3, with RBA as 1.5, consistently indicating that the added risk of an AE is higher than the added benefit of SRE prevention by using Dmab.

Conclusion: The number needed to treat as well as the high risk-benefit ratio suggests that despite the better efficacy of Dmab, its benefits may not outweigh its added risks. Decision makers should therefore carefully consider these aspects prior to reimbursement decisions and formulary inclusion.

Disclosures: Madhav Namjoshi, None.

This study received funding from: Novartis Pharmaceuticals

SU0140

Osteoporosis-specific Quality of Life Change in the B-ABLE Cohort of Women on Aromatase Inhibitor Therapy: Predictors at 1-year Follow-up. Daniel Prieto-alhambra¹, Sonia Servitja², Laia Garrigos², Elisa Torres², Maria Martinez-Garcia², Josep Blanch³, Joan Albanell², Adolfo Diez-Perez⁴, Ignasi Tusquets², Xavier Nogues⁵. ¹Institut Municipal D'Investigacio Medica, Spain, ²Medical Oncology Department, Breast Cancer Unit. Molecular Therapeutics & Biomarkers in Breast Cancer, Cancer Research Program, IMIM-Hospital del Mar, Autonomous University of Barcelona, Barcelona, Spain, Spain, ³Rheumatology Department, Parc de Salut Mar, Barcelona (Spain), Spain, ⁴Department of Internal Medicine, URFOA IMIM-Hospital del Mar, Parc de Salut Mar, Autonomous University of Barcelona, RETICEF (Red Tematica de Investigacion Cooperativa en Envejecimiento y Fragilidad), Instituto Carlos III, Barcelona, Spain, Spain, ⁵RETICEF (Red Tematica de Investigacion Cooperativa en Envejecimiento y Fragilidad), Instituto Carlos III, Barcelona, Spain, Spain

PURPOSE Aromatase Inhibitors (AIs) are first-line therapies for early breast cancer. Their main side effects are increased bone loss and peripheral arthralgia, which can affect health-related quality of life. We aimed to study the patterns and predictors of bone-specific quality of life at three points in time: baseline (before AI initiation), at 3-months, and at 1-year.

METHODS Participants: 275 women with hormone-positive early breast cancer eligible for AI therapy were consecutively recruited in our hospital (Oncology and Bone Metabolism Units, Parc de Salut Mar, Barcelona (Spain)), and followed up for 1 year. Measurements: Drugs use, years since menopause, body mass index (BMI), previous chemotherapy, radiotherapy and tamoxifen use, smoking/drinking status and dietary calcium intake were collected at baseline. Self-reported osteoporosis-specific quality of life using the validated ECOS-16 questionnaire, arthralgia (using visual analogue scale) and serum Vitamin D (25-hydroxy-D) were measured at the three time points. Statistics: Wilcoxon signed rank tests for paired samples were used to compare ECOS-16 score at three time points. Uni and multivariate linear regression models were fitted to assess predictors of ECOS-16 change (as defined by follow-up minus baseline scores) at 3 months and 1 year. Models were adjusted for years since menopause, baseline Vitamin D and season when samples were drawn.

RESULTS Baseline ECOS-16 was significantly lower than 3-months (mean difference 3.35 [95%CI 2.19 to 4.50], $p < 0.001$) and 1-year scores (4.50 [95%CI 3.20 to 5.81], $p < 0.001$). By contrast, no significant differences were seen between ECOS-16 scores at 3 months and 1 year ($p = 0.13$). Main predictors of ECOS-16 change at 3 months were previous use of tamoxifen (adjusted beta (adjbeta) -3.80 [-6.49 to -1.12], $p = 0.006$), and arthralgia-related change in VAS score (adjbeta 0.50 [0.001 to 0.02], $p = 0.049$). Predictors at 1-year were Vitamin D at 1 year ≥ 30 mg/dl (adjbeta -6.6 [-10.67 to -2.51], $p = 0.002$ [see Figure 1]) and change in arthralgia score (adjbeta 1.60 [0.92 to 2.29], $p < 0.001$).

DISCUSSION Women with early breast cancer experience a significant loss in osteoporosis-specific quality of life after initiating AI therapy. This loss is produced mostly in the first 3 months of therapy, and highly driven by AI-related arthralgia. Previous tamoxifen use, and Vitamin D concentrations ≥ 30 mg/dl at 3 months protect from quality of life loss in this population.

SU0142

The Vitamin D Receptor Promotes Human Prostate Cancer Cell Growth via a Ligand Independent Pathway. Yu Zheng^{*1}, Difei Deng², Dennis Basel², Trupti Trivedi¹, Julian Kelly², Robert L Sutherland³, Colin Dunstan⁴, Dr. Hong Zhou⁵, Markus Seibel⁵. ¹Bone Research Program, ANZAC Research Institute, The University of Sydney, Australia, ²ANZAC Research Institute, The University of Sydney, Australia, ³Cancer Research Program, Garvan Institute of Medical Research, Australia, ⁴University of Sydney, Australia, ⁵Bone Research Program, ANZAC Research Institute, The University of Sydney, Australia

Prostate cancer is the most prevalent malignancy in men, with 20-40% of patients developing metastatic disease. Bone is a frequent site for metastasis. Epidemiological evidence suggests that vitamin D has a chemo-preventative role in prostate malignancy. We have previously reported that vitamin D deficiency promotes human prostate cancer cell growth in the bone microenvironment of nude mice. However, little is known about the role of the vitamin D receptor (VDR) in this context. The present study aimed to define the role of the VDR in human prostate cancer growth *in vitro* and *in vivo*.

VDR expression was knocked down by stable expression of shRNA in PC3 cells (PC3-VDR-KD), with non target cells (PC3-NT) generated as controls. mRNA knock down was 85% and induction of CYP24 mRNA expression by 1,25(OH)2D3, normally seen in VDR expressing cells, was abrogated in PC3-VDR-KD cells, indicating effective disruption of VDR signaling.

Treatment of PC3-NT cells with 1,25(OH)2D3 significantly reduced cell growth by up to 51% as compared to untreated PC3-NT cells. Surprisingly, growth of PC3-VDR-KD cells in ligand-free cultures was also reduced by 49% (compared to NT cells). Moreover, cell migration was increased by 10% in PC3-VDR-KD cells. Of note, PC3-VDR-KD cells did not respond to treatment with 1,25(OH)2D3. These *in vitro* results suggest that VDR knockdown in human prostate cancer cells results in reduced tumor cell growth and increased cell migration, providing evidence that the VDR may have ligand-independent functions in promoting proliferation and suppressing migration of cancer cells independent of its liganded form.

To further investigate the effects of VDR knockdown *in vivo*, PC3-NT and PC3-VDR-KD cells were implanted subcutaneously in nude mice, and tumor growth was monitored for 69 days. Compared to NT cells, VDR knockdown resulted in significantly smaller tumors from day 12 onwards ($p < 0.05$). Similarly, when PC3-NT or PC3-VDR-KD cells were implanted into the tibiae of vitamin D sufficient mice, disruption of VDR signaling resulted in significantly smaller osteolytic lesions from day 17 onwards ($p < 0.05$, by X-ray analysis).

In summary, our results suggest a novel ligand-independent role of the VDR in promoting prostate cancer cell growth and suppressing invasive cell potential. This novel function of the unliganded VDR contrasts with the known anti-proliferative actions of the liganded VDR and may offer new therapeutic approaches in cancer treatment.

Disclosures: Yu Zheng, None.

SU0143

TRPV6 Ion Channels Modulate Human Metastatic Prostate Cancer Cell Migration and Adhesion. Sarah McCarthy^{*}, Ronald R. Gomes. Penn State Hershey, USA

We have previously reported that intermittent parathyroid hormone 1-34 administration enhances the colonization of human osteoblastic prostate cancer cells to murine bone. While the mechanism is unknown, we propose that transient increases in serum calcium following parathyroid hormone 1-34 administration, confer a metastatic advantage to circulating prostate cancer cells, signaled, in part, via TRPV6 ion channels. We tested the hypothesis that TRPV6 ion channels are required for prostate cancer cell metastatic potential, *in vitro*. To test our hypothesis, shRNA lentiviral particles were employed to knock down TRPV6 expression in C4-2 prostate cancer cells. Knockdown was confirmed by qRT-PCR, Western blot analysis, and immunocytochemistry. Proliferation, transwell migration, and heterotypic cell adhesion (C4-2:human bone marrow endothelial (hbmE) cells) assays were employed to evaluate the metastatic potential of C4-2 cells with reduced levels of TRPV6 relative to wild type and control shRNA cells. QRT-PCR and Western blot analysis identified several clones that expressed reduced TRPV6 protein (40-63%). Confocal micrographs of paraformaldehyde fixed (4%) cells probed with TRPV6 specific antibodies, confirmed TRPV6 localization in knockdown clones was reduced at the cell surface. Relative to control cell lines, cells with decreased TRPV6 expression had a slower rate of proliferation. Transwell migration assays suggested that increased extracellular calcium (2.5 mM CaCl_2) enhanced migration of wild type and control cell lines; however, relative to controls, migration was reduced by 49% in knockdown clones treated similarly. Interestingly, heterotypic cell adhesion assays demonstrated cells with reduced TRPV6 expression were less adherent (-34%) to hbmE cells. Pre-treatment of prostate cancer cells with increased extracellular calcium (2.5 mM CaCl_2) did not alter their adhesion to hbmE cells. Surprisingly, pre-treatment of hbmE cells with 2.5 mM CaCl_2 enhanced adhesion of control cells by 78%; however, this response was abolished in TRPV6 knockdown clones. This is the first report employing shRNA to stably knockdown TRPV6 in a human osteoblastic prostate cancer cell line. Our observations support our hypothesis and suggest, for the first time, that TRPV6 may

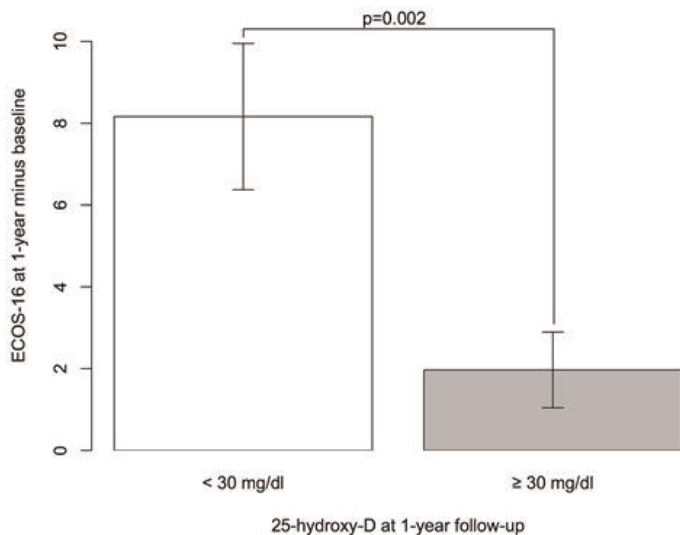


Fig 1. Change in ECOS-16 in subjects with 25-OH-VitD normal versus insufficient concentrations at 1 y

Disclosures: Daniel Prieto-alhambra, None.

SU0141

PTHrP Promotes Epithelial-To-Mesenchymal Transition and the Acquisition of Cancer Stem Cell-Like Properties in Prostate Cancer. Douglas Burton^{*1}, Weg Ongkeko², Alan Kiang³, Eric Abhold³, David Yi³, Leonard Deftos⁴. ¹VA San Diego Healthcare System / University of California, San Diego, USA, ²University of California San Diego / VMRF, USA, ³University of California San Diego, USA, ⁴Veterans Administration San Diego Healthcare System & University of California, USA

Background: The mechanism by which tumor cells become invasive and eventually metastatic is a crucial question in cancer biology. The metastatic process requires that a cell acquire a motile phenotype to penetrate tissue and reach the vasculature and lymphatics. Parathyroid hormone-related protein (PTHrP), an oncoprotein, has been implicated in the pathogenesis and progression of several cancers, including prostate cancer.

Methods: In this study, we compared the parental prostate cell lines with their corresponding derivatives that stably overexpress PTHrP *in vitro* and *in vivo*. We used qPCR, western blot analysis, and immunofluorescence to analyze EMT and stem cell markers, and an invasion assay to investigate PTHrP-mediated migration and invasion. GFP expression was used to monitor prostate cancer tumorigenesis, growth, and metastasis in the mouse model.

Results: We observed that PTHrP-overexpressing derivatives were 2-3 fold more invasive than their parental counterparts. PTHrP derivatives promoted epithelial-to-mesenchymal transition (EMT). Cells that overexpressed PTHrP had decreased levels of the epithelial marker, *E-cadherin*, increased levels of the mesenchymal marker, *vimentin*, and increased levels of the EMT regulator, *Snail*, as measured by qPCR. These results were supported by immunofluorescence data. Prostate cancer cells that had high levels of PTHrP also exhibited induction of the stem cell genes *CD133*, *Oct4*, and *Nanog*. In the mouse model of prostate cancer, DU 145 prostate cancer cells that normally are incapable of forming tumors when implanted subcutaneously into immunocompromised mice were transformed to highly tumorigenic cells when engineered to express high levels of PTHrP. In the orthotopic model, mice that were implanted with PTHrP overexpressing cells exhibited highly efficient tumorigenesis and metastasis compared to the parental cells in which there were very few, small discrete tumors. This finding was further confirmed in an intraosseous prostate model in which DU145 parental cells or those transfected with empty vector formed no tumor when injected into mice tibia while those that expressed PTHrP resulted in tumor formation, invasion, and destruction of bone.

Conclusions: Recent evidence suggests that the induction of EMT in cancer cells leads to the development of cancer stem cell traits. PTHrP appears to play an important role in EMT and acquisition of cancer stem cell properties in prostate cancer.

Disclosures: Douglas Burton, None.

serve an important role in modulating metastatic prostate cancer cell migration and adhesion to bone marrow endothelial cells, *in vitro*.

Disclosures: Sarah McCarthy, None.

SU0144

SQSTM1 Mutations Are not Common in Pagetic Osteosarcomas nor in High Grade Osteosarcomas. Pui Yan Jenny Chung¹, Piero Picci², Marco Alberghini³, Lars-gunnar Kindblom⁴, Patrick D'Haese¹, John-Paul Bogers¹, Leida Rozeman⁵, Pancras Hogendoorn⁵, Wim Van Hul^{*1}. ¹University of Antwerp, Belgium, ²Istituto ortopedica Rizzoli, Italy, ³Istituto Ortopedica Rizzoli, Italy, ⁴Royal Orthopedic Hospital, United Kingdom, ⁵Leiden University Medical Center, Netherlands

Paget's disease of bone (PDB) is, with a prevalence of 2-5% in the Caucasians above 55 years of age, the second most frequent metabolic bone disease, next to osteoporosis. Characteristics of PDB are bone lesions with an imbalanced bone remodelling, resulting in disorganised and non-fully-fledged new bone. The only disease-causing gene identified so far is the sequestosome1 (SQSTM1) gene. SQSTM1 mutations have been found in one third of families and in about 9% of isolated cases with PDB. All mutations are clustered in and around exon 7 and 8. Osteosarcomas are the most severe complications of PDB and occur more frequently in PDB patients, suggesting that PDB increases the risk for the development of an osteosarcoma. A previous study reported the presence of the recurrent SQSTM1 P392L mutation in 3 out of 5 osteosarcoma tissues from PDB patients, but not in adjacent normal tissues. In this study, we performed SQSTM1 mutation screening in 24 frozen osteosarcoma samples and 8 matching normal tissues from 22 PDB patients as well as in 26 frozen osteosarcoma samples and 10 matching normal tissues from 26 elderly patients with high grade osteosarcoma. At first, the samples were checked for the homogeneity of the tissue. If a tissue was not homogeneous, we either performed microdissection or laser capture microdissection, before DNA isolation. Then, mutation analysis of the exon 7 and 8 of SQSTM1 was performed by DNA-sequencing. In the Pagetic osteosarcoma tissues, we were able to detect, besides 2 unannotated intronic variants in 2 samples, the P392L mutation in only 1 sample out of the 24 tissues (4%). No normal tissue from this case was available. No SQSTM1 mutation was found in all pathological samples from elderly osteosarcoma patients. In conclusion, in this study we were not able to confirm a high frequency of SQSTM1 mutations in Pagetic osteosarcomas. Furthermore, SQSTM1 mutation seems not to be common in high grade osteosarcomas.

Disclosures: Wim Van Hul, None.

SU0145

Altered Bone Marrow Adiposity Following Localized Irradiation in Juvenile Mice. Lihini Keenawinna^{*1}, Megan Oest¹, Timothy Damron². ¹SUNY Upstate Medical University, USA, ²State University of New York Upstate Medical University, USA

Introduction: Clinical radiation therapy is often complicated by decreased bone strength and quality, often resulting in late-onset fracture.¹ Clinical radiology studies after radiotherapy typically show increasing marrow adiposity over time.^{2,3} The biological mechanisms mediating these adverse skeletal effects are not well understood, although we suspect differential effects on multipotent MSCs.

Hypothesis: We hypothesized that irradiated hindlimbs would demonstrate elevated marrow fat content compared to untreated hindlimbs.

Methods: Eight 4-week-old C57Bl/6 mice were anesthetized and exposed to unilateral, localized hindlimb irradiation at a dose of 20Gy (300kV, 10mA). One week post-irradiation, animals were euthanized for retrieval of tibias and femurs. Samples were fixed in 10% buffered formalin, then decalcified (12% buffered EDTA), and stained with 2% aqueous OsO₄. This process increases the radio-opacity of marrow lipids *in situ*, permitting micro-computed tomographic imaging using a 12 mm voxel resolution (Scanco Micro-CT 40). Total lipid volume of each bone was quantified using global digital thresholding.

Results: Contrary to our hypothesis, mean intraosseous lipid volume was lower after irradiation in femurs and tibias (Figure 1). However, statistical analysis detected no significant differences between treatment groups.

Discussion: Previous studies in our laboratory have qualitatively demonstrated increased marrow adiposity following localized skeletal irradiation in mice (Figure 2). Differing results between the studies could be due to the juvenile age of the current animals, as the earlier study used 12-week animals. MSCs from young donors exhibit greater plasticity and proliferative capacity and hence may be less susceptible to radiation-induced damage than mature animals. Additionally, the current animals were euthanized at 1 week post-irradiation whereas the previous animals were euthanized at 6 weeks. While cultured osteoblastic cells demonstrate decreased mineralization and proliferative capacities by one week post-irradiation,⁴ this may be insufficient time for effects to manifest in whole tissues. Ongoing studies with 26-week-old mice will allow us to determine if marrow adiposity subsequent to radiation therapy is an age-dependent outcome.

References: 1)Karsenty G., Nature (2003), 2)Garner HW et al, Radiographics (2009)

3)Mitchell MJ et al, Radiographics (1998), 4) Dudziak ME et al, Plastic and Reconstructive Surgery (2000)

Lipid Volume

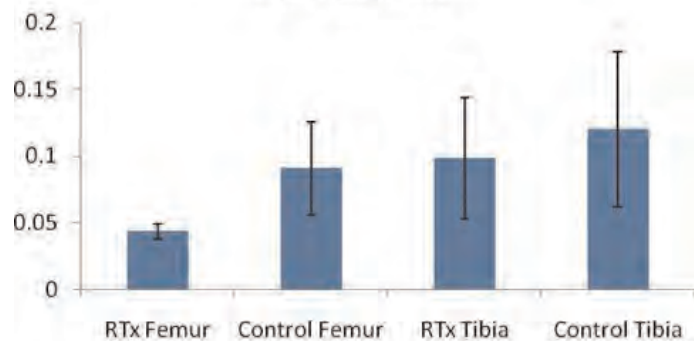
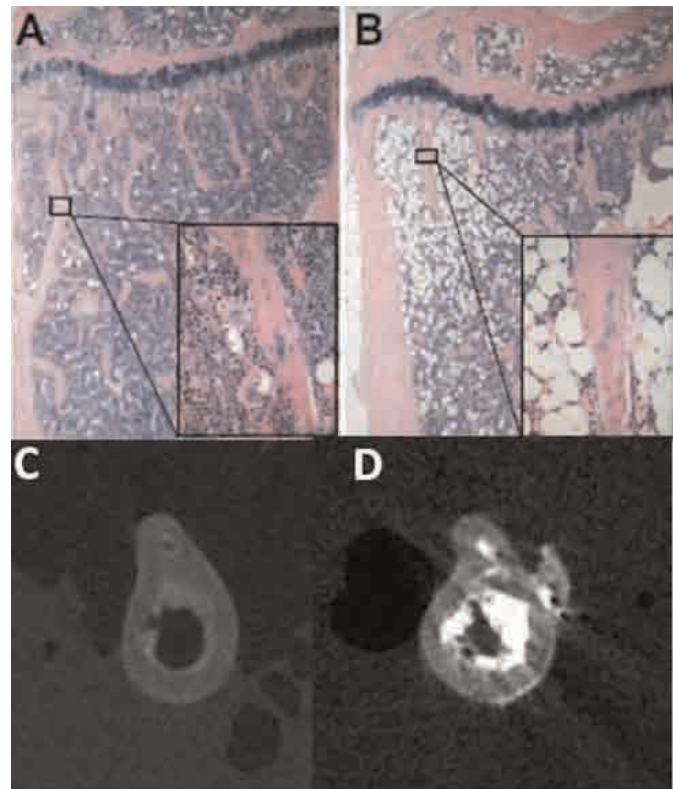


Figure 1. Hindlimb lipid volumes at 1 week post RTxa

Lipid Volume Graph



Representative histology (A,B, H&E stain) and μ CT images (C,D) of naïve (A,C) and irradiated (B,D) hindlimbs. White areas denote fat accumulation in μ CT images.

Histology and MicroCT images

Disclosures: Lihini Keenawinna, None.

SU0146

Cisplatin Treatment Inhibits Bone Healing: Implications for Osteosarcoma Surgery. Larry Suva^{*1}, Kimo Stine¹, Elizabeth Wahl¹, Lichu Liu¹, James Aronson¹, Robert Skinner¹, Kathryn Thrailkill², Corey Montgomery¹, John Fowlkes¹, David Becton¹, Charles Lumpkin¹. ¹University of Arkansas for Medical Sciences, USA, ²Arkansas Children's Hospital, USA

Osteosarcoma (OS) is the most common primary bone cancer that affects children and adolescents. The majority of patients are treated by a closely timed combination of chemotherapy and surgery, yet these patients continue to be at risk for postoperative complications especially in the area of bone repair. Cisplatin is a drug

commonly used for treatment of OS, yet the effects of cisplatin on bone regeneration are not well studied. As a result, the bone health of both childhood and adult OS survivors requires increased attention. Therefore, we tested the effects of two regimens of cisplatin dosing in a unique model of bone repair and regeneration, namely, distraction osteogenesis (DO) in mice. C57BL/6 male mice (n=20) underwent the standard DO protocol. Based on current clinical practices, cisplatin exposure can occur preoperatively, postoperatively, and even simultaneously with bone repair and/or regeneration. The dose of CDP was 60 mg/M2/day. Group 1 mice had surgery and started cisplatin simultaneously for 5 days; group 2 mice underwent DO surgery one week after receiving 2 doses of cisplatin; control mice received placebo. All mice were distracted for 11 days at a rate of 0.075 mm b.i.d. Animal weights at sacrifice were not significantly different. In Group 1, comparison of the distracted tibial radiographs demonstrated a dramatic and significant decrease in the mineralized area of distraction gaps of cisplatin-treated mice (3.6% + 2.1) versus vehicle treated (63.3% + 5.8) mice. Detailed histological analysis of the DO gaps confirmed the significant decrease in bone formation observed in the radiographs of the cisplatin-treated mice (7.6% + 7.0) versus the vehicle controls (75.4% + 5.5). Furthermore, microCT evaluation of the endosteal and periosteal bone volume in the DO gap demonstrated significant inhibition of both endosteal and periosteal new bone formation. Similarly in group 2, there was a significant decrease in the mineralized area of distracted gaps of cisplatin-treated mice (15.5% + 9.0) versus vehicle treated (42.8% + 12.6) mice that was also confirmed by microCT. These results demonstrate the severe inhibitory effects of cisplatin administration on bone healing and regeneration and suggest that increasing the time interval between the final cisplatin injection and any subsequent surgical intervention may be required for normal bone healing in surgical OS patients.

Disclosures: Larry Suva, None.

SU0147

Development and Validation of a Pre-clinical Model of Radiation Impaired Fracture Healing. Katarina Janic^{*1}, Fred Nicholls², Tom Willett³, Marc Grynpas³, Peter Ferguson⁴. ¹Mount Sinai Hospital, Samuel Lunenfeld Research Institute, Canada, ²University of Toronto, Department of Surgery, Division of Orthopedic Surgery, Canada, ³Samuel Lunenfeld Research Institute, Canada, ⁴Division of Orthopedic Surgery, Mount Sinai Hospital, Canada

Background: Currently, surgical excision combined with radiotherapy provides the best opportunity for local control in patients with soft tissue sarcoma. While there is increased benefit to combined modality therapy, complications are also increased. Pathologic fracture, one arising from no or minimal trauma, occurs within the site of irradiation in 2-10% of patients. Non union rates exceed 80% in these fractures, where after amputation is not uncommon and patient morbidity is increased.

Objectives: 1) Create an animal model for the study of non-union in patients undergoing multi-modal therapy for soft tissue sarcoma

2) Characterize the effect of combined modality therapy on bone biology

Method: 72 Wistar rats were randomized to 4 groups: I)Control, II)Radiotherapy, III)Periosteal Stripping, IV)Combination therapy. All groups underwent controlled fracture at nine weeks. Micro computed tomography, back scattered electron microscopy and static and dynamic histomorphometry were used to evaluate data.

Results: MicroCT results reveal greater bone volume, mineralized tissue and callus volume in control animals compared to any irradiated groups and periosteal stripped animals ($p < 0.001$). Histomorphometric analysis reveals increased osteoid and cartilage formation in control and periosteal stripped animals compared to both irradiated groups.

Conclusion: All animals that underwent radiotherapy failed to form callus and went on to form atrophic non-union. Future work will investigate the effects of a single implant of bone growth factor OP-1 into the intramedullary canal immediately prior to fracture.

Disclosures: Katarina Janic, None.

SU0148

Epigenetic Signatures of Osteosarcoma. Emma Baker^{*1}, Dario Strbenac², Thomas John Martin³, Louise Purton¹, Mark Robinson⁴, Carl Walkley¹. ¹St. Vincent's Institute, Australia, ²Garvan Institute of Medical Research, Australia, ³St. Vincent's Institute of Medical Research, Australia, ⁴WEHI, Australia

Purpose: Osteosarcoma (OS) is the most common malignancy of bone, and is the second leading cause of cancer related death in children. OS survival rates have plateaued since the 1980s. Patients presenting with metastatic or recurrent disease have less than 20% survival at 5 years. New therapeutic treatments are desperately needed to improve patient outcomes. It is clear that epigenetic changes play a major role in cancer initiation and progression, however the contribution of epigenetic instability to OS, especially metastatic disease, remains largely unknown. Understanding the specific epigenetic changes associated with OS disease onset, progression and metastasis will be important for developing new treatment options. **Methods:** We

have utilized low passage cell lines established from paired primary and metastatic tumours from a mouse model of OS¹, and normal osteoblasts derived by *in vitro* differentiation of Kusa4b10 cells² to identify epigenetic signatures that define OS. Genome-wide promoter maps of epigenetic modifications in OS and normal osteoblast cells were generated using NimbleGen ChIP-Chip arrays. **Results:** Gene expression profiling of OS cells and normal osteoblast cells showed a number of enzymes responsible for mediating epigenetic modifications are differentially expressed. Differences in expression were also apparent in cells derived from primary and metastatic tumours from the same mice. Genome-wide promoter mapping of modifications mediated by these enzymes identified an OS specific epigenetic signature that distinguishes the disease from normal osteoblasts. The signatures encompass both RefSeq annotated genes and miRNAs. **Conclusions:** Aberrant expression of epigenetic modifying enzymes in OS correlates with a specific epigenetic signature that distinguishes the disease from normal osteoblasts. Further profiling of the metastatic disease is warranted, as disease location appears to be associated with specific epigenetic enzyme gene expression. Identifying OS specific epigenetic signatures will provide invaluable knowledge of OS biology, potential markers of metastatic disease development and new therapeutic targets.

1. Walkley, C.R. et al, Genes Dev. 22: 1662, 2008.
2. Allan, E.H. et al, J Cell Biochem. 90: 158, 2003.

Disclosures: Emma Baker, None.

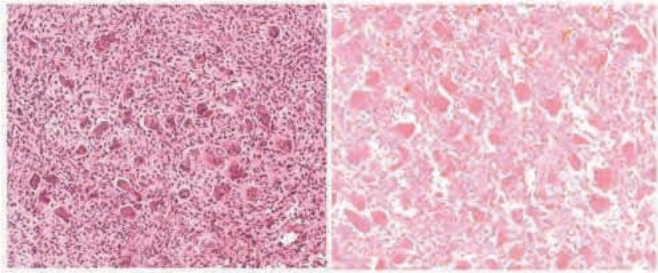
SU0149

Withdrawn

SU0150

Locally Administered Zoledronic Acid Therapy for Giant Cell Tumor of Bone. Toshihiko Nishisho^{*1}, Naoyoshi Hanaoka², Kenji Endo², Mitsuhiro Takahashi², Natsuo Yasui³. ¹The University of Tokushima, Institute of Health Bioscience, School of Medicine, Japan, ²Department of Orthopedics, The University of Tokushima, Japan, ³University, Japan

Giant cell tumor of bone (GCTB) is a locally aggressive tumor and typically occurs in the meta-epiphyseal region of long bones. Intralesional curettage alone has a high local recurrence rate. In the present study, zoledronic acid, a nitrogen-containing bisphosphonate, was administered locally as an adjuvant during a biopsy. An otherwise healthy 43-year-old male was admitted to our hospital with pain and swelling in the right knee following a fall 1 month earlier. Plain radiographs and MRI demonstrated an osteolytic tumor of the right proximal tibia. An open biopsy was performed and the intra-operative pathologic diagnosis was GCTB (Fig A). Following biopsy the defect was filled with beta-tricalcium phosphate (OSferion®), and 4 mg of zoledronic acid was locally administered into the tumor lesion. MRI performed 2 months after the biopsy demonstrated poor gadolinium enhancement of the residual tumor. Subsequently, curettage and bone grafting were performed. Sections were obtained during the curettage for histology, to evaluate the response to bisphosphonate treatment. Histologic examination revealed massive tumor cell death in the lesion in which both stromal cells and osteoclast-like giant cells were necrotic (Fig B). Curettage was performed and the defect was filled with a commercial preshaped hydroxyapatite-tricalcium phosphate (HAP/TCP) bone substitute (Cerattite®, Kobayashi Medical, Osaka, Japan). There were no serious complications directly associated with curettage or the local administration of zoledronic acid. Eighteen months after curettage, the patient had regained full range of motion and good function of the knee, and radiographs of 18 months after curettage revealed no recurrence of GCTB. Moreover, no side effects were observed during the treatment. In the present case, the local administration of zoledronic acid induced tumor cell death and may also have suppressed recurrence. This is the first report of local administration of bisphosphonates for the treatment of GCTB. This method of bisphosphonate administration may be suitable for other bone disorders such as metastatic bone disease. Written informed consent was obtained from a patient with GCTB and the treatment protocol was approved by the Ethics Committee of Tokushima University.



Fig

Disclosures: Toshihiko Nishisho, None.

SU0151

Mechanical Signals Partially Preserve Bone Quality in Animal Models of Ovarian Cancer While Promoting the Mesenchymal Progenitor Pool's Efficacy in Slowing Complications of the Disease. Gabriel Pagnotti^{*1}, Benjamin Adler¹, Danielle Green¹, Ete Meilin Chan¹, Wesley Beamer², Kenneth Shroyer³, Clinton Rubin⁴. ¹Stony Brook University, USA, ²The Jackson Laboratory, USA, ³Stony Brook University Medical Center, USA, ⁴State University of New York at Stony Brook, USA

The progression and subsequent treatment of cancer is often complicated by a rapid decline in bone quality, yet mounting concerns exist regarding the use of anabolic agents in preserving skeletal morphology as these factors may inadvertently exacerbate tumorigenesis. Low intensity vibration (LIV), a systemically-delivered, low magnitude mechanical signal that promotes osteoblastogenesis, could represent a non-invasive strategy to prevent cancer-induced skeletal atrophy but only if it does not facilitate disease progression.

Seventy 12w female F1-SWRxSJL mice, a strain highly susceptible to developing granulosa cell tumors, were randomly divided into baseline control (n=10), age-matched control (n=30), and LIV (n=30), which received mechanical signals (90Hz @ 0.3g) for 15m/d, 5d/w over the course of 1y. Survivability curves for both groups followed identical trends indicating longevity over the course of 1y was unaffected by LIV (9 lost/group). In those that survived 1y, μ CT of the proximal tibiae indicated trabecular bone volume was +25% (p=0.03) greater in LIV over control but had fallen markedly from baseline values (-40%; p<0.01). While primary ovarian lesions and peripheral metastases to lungs, lymph nodes, and liver were apparent in both study groups, the overall tumorigenic incidence was 37% lower in LIV-treated animals (NSD). FACS analysis detected shifts in mesenchymal stem cells (MSC) within the bone marrow, as MSC trends in LIV were 52% (p=0.01) lower than age-matched control and 31% (p=0.2) lower in non-pathologic mice, suggesting that decreased MSC levels are associated with suppressed pathology. Indeed, MSCs are known to contribute to neoplasias preceding tumorigenic events. These preliminary data indicate that mechanical signals, recognized as anabolic to bone, will not perturb the longevity index of animals that are highly susceptible to cancer. Further, these mechanical signals helped to preserve the bone quality of diseased animals, potentially contributing to a reduced risk of fracture. Perhaps these low intensity mechanical signals mimic the benefits of exercise in the preservation of clinically-relevant bone indices and, like exercise, contribute to a non-drug means of suppressing neoplastic endpoints.

Disclosures: Gabriel Pagnotti, None.

SU0152

Novel Biomarkers and Therapeutic Agents for Osteosarcoma Stem Cells. Vaibhav Saini^{*1}, Curtis Hose², Anne Monks², Mark Burkett², Bingnan Han², Dianne Newton³, Angelena Millione², Jalpa Shah², Melinda Holingshead³, Kunio Nagashima², Rene Delosh², Karen Hite², Thomas Silver², Dominic Scudiero², Paola Pajevic Divieti⁴, Robert Shoemaker³. ¹Research Fellow, MGH, Harvard Medical School, USA, ²SAIC, USA, ³NCI, USA, ⁴MGH- Harvard Medical School, USA

Osteosarcoma is the 6th most common pediatric tumor in the under 15 age group. Its 40% mortality rate has not improved since the 1970s. Osteosarcoma stem cells (OSCs) have been implicated in tumorigenesis and relapse. Thus, OSC ablation could improve treatment outcomes. Therefore, we hypothesized that characterizing OSCs could yield novel biomarkers and therapeutic targets. To obtain OSC-enriched sphere cultures, monolayer cultures of CHA59, HuO9, and Saos-2 osteosarcoma cell lines in fetal bovine serum (FBS) medium, previously implicated in promoting cancer stem cell differentiation, were transferred to stem cell enriching (SS) medium. Monolayers in FBS yielded

spheres in SS. Spheres demonstrated higher clonogenicity and tumorigenicity in NOD/SCID mice as compared with monolayers, indicating OSC enrichment in spheres. Spheres expressed osteosarcoma markers, such as alkaline phosphatase and osteocalcin, and produced osteoid as observed by H&E staining of xenograft sections. Transmission electron microscopy revealed organelle-devoid cells, previously reported as stem cells in breast cancer, in spheres and none in monolayers, confirming that sphere culture can recapitulate in vivo OSC features. Using the xCELLigence system, which monitors cell migration in real-time, we developed a novel kinetic 7-day assay, as opposed to the static 2-day boyden chamber assay, to compare sphere vs. monolayer migration ability. Individual cells derived from spheres migrated significantly more than those from monolayers towards the SS medium. After 7 days, we harvested spheres from the lower chamber that contained migrated cells, providing direct evidence that the cells migrating towards the SS medium are the sphere forming cells. Transcriptome, proteome, immunophenotyping, and bioinformatic analyses revealed significantly decreased CD326, CD24, CD44, and increased CBX3, ABCG2, ABCA5 (a newly discovered ABC transporter), aldehyde dehydrogenase expression in spheres as compared with monolayers. Upon high-throughput drug resistance analysis, spheres demonstrated higher resistance than monolayers to the majority of anti-tumor agents, except decitabine (DMNT inhibitor) and telomerase inhibitors. In summary, we identified two novel OSC-enrichment biomarkers (CBX3 and ABCA5), developed a kinetic 7-day migration assay, and identified epigenetic and anti-telomerase agents for targeted OSC ablation. With further research, these agents could be developed for translational osteosarcoma therapy.

Disclosures: Vaibhav Saini, None.

SU0153

Potential Risk Factors for Bisphosphonate-related Osteonecrosis of the Jaw: Retrospective Analysis of 576 Cancer Patients. Vivek Thumbigere-Math¹, Lam Tu¹, Sabrina Huckabay¹, Scott Lunos², Arkadiusz Dudek³, Karen Swenson⁴, Joseph Leach⁴, Pamela Hughes¹, David Basi¹, Raj Gopalakrishnan^{*5}. ¹University of Minnesota School of Dentistry, USA, ²University of Minnesota CTSI Academic Health Center, USA, ³University of Minnesota Cancer Center, USA, ⁴Park Nicollet Institute, USA, ⁵University of Minnesota, USA

We conducted a retrospective study to evaluate the frequency, risk factors, clinical presentation, and management of Bisphosphonate-Related Osteonecrosis of the Jaw (BRONJ) in cancer patients treated with intravenous Bisphosphonate (BP). Patients treated with intravenous BP therapy between January 2003 and December 2007 were identified through respective institute's pharmacy databases. Of the 576 identified patients, 18 (3.1%) developed BRONJ which included 8 of 190 (4.2%) patients with breast cancer, 6 of 83 (7.2%) patients with multiple myeloma, 2 of 84 (2.4%) patients with prostate cancer, 1 of 76 (1.3%) patients with lung cancer, 1 of 52 (1.9%) patients with renal cell carcinoma and in none of the 73 patients with other malignancies. Tooth extraction was the BRONJ inciting event in 10 patients (59%), whereas 7 (41%) patients reported no history of previous traumatic episode (missing data for one subject). BRONJ patients had received significantly higher number of mean BP infusions (38.119.06 vs 10.512.81, p<0.0001) and longer duration of BP treatment (months, 44.324.34 vs 14.618.09, p<0.0001) compared to patients without BRONJ. Diabetes (HR=3.40; 95% CI=1.11-10.11; p=0.028), hypothyroidism (HR=3.59; 95% CI=1.31-9.83; p=0.013), smoking (HR=3.44; 95% CI=1.28-9.26; p=0.015), and higher number of zoledronate infusions (HR=1.07; 95% CI=1.03-1.11; p=0.001) were found to be significant risk factors for developing BRONJ using multivariate Cox proportional hazards regression analysis. Based on the AAOMS staging system, one patient was initially diagnosed with Stage I lesion, 10 patients with Stage II and 4 with Stage III lesions. Initial management of BRONJ was non-surgical, with debridement performed at subsequent visits if needed. BRONJ lesions healed completely in 2 patients (11%), healed partially in 5 (28%), remained stable in 5 (28%), and progressed in 6 (33%). Among the identified risk factors, hypothyroidism is a novel finding contributing to BRONJ development. Further, increased cumulative doses and long-term intravenous BP treatment were found to be the most significant risk factors.

Disclosures: Raj Gopalakrishnan, None.

SU0154

Radiation Induced Bone Loss: A Dose Response PET-CT Study. Orhan Oz^{*1}, Jon Anderson², Rohama Khajia³, Keenan Brown³, Paul Medin². ¹University of Texas Southwestern Medical Center, Dallas, USA, ²UT Southwestern Medical Center at Dallas, USA, ³Mindway Software, USA

Radiosurgery of the spine is used to treat patients with spinal metastases and cord impingement from tumors. Recent clinical studies have shown increased fracture risk in patients treated with high doses of external irradiation. We are interested in knowing whether there is a dose response relationship between prescribe radiation and induced bone loss. In a study approved by the UT Southwestern Medical Center's Institutional Animal Care and Use Committee, three cervical vertebral bodies (C5-C7) of 10 ~50 week old Yucatan minipigs were irradiated with a 6 MV image-guided linear accelerator. Stereotactic targeting was performed using stereoscopic kV x-rays. Pigs were stratified into 2 dose groups of 16 (n=5) and 24 Gy (n=5). Dose was prescribed to the 90% isodose line. The mini-pigs were scanned on a Siemens Biograph 64 PET/CT scanner prior to irradiation, 1 month and 3 months after irradiation. Following

acquisition of the CT scans the mini-pigs were injected with ^{18}F FDG, a glucose analog. CT scans of C3 through T1 for each animal were analyzed using the Mindways "Bone Investigational Toolkit" ("BIT") version 2.0. BMD profiles approximately along the central axis for each vertebra were generated in BIT. Endplate-to-endplate distance was estimated by the distance between endplate peaks in the mass profiles. Total vertebral volume was estimated by the bone volume between endplate peaks. Average volumetric BMD and cross-sectional area were calculated for the central 75% of the distance between endplates. Volumetric BMD was estimated for both the total vertebral body and for the trabecular bone. A cortical threshold of 450 mg/cm³ was used to segment the bone into "cortical" and "trabecular" compartments. To date we have determined that trabecular bone loss is greater and occurs earlier in the group treated with the highest dose. ^{18}F FDG retention in the vertebral bodies was quantified as a standardized uptake value (SUV). Visually, there was decreased activity in the irradiated bones of the spines in both groups. Statistical evaluation of the mean SUV/treatment group and analysis of average volumetric BMD and cortical bone volume is underway.

Disclosures: Orhan Oz, None.

SU0155

Raman Spectroscopy Demonstrates Amifostine-Induced Protection of Bone Quality In The Irradiated Murine Mandible. Catherine Tchanque-Fossuo¹, Bo Gong², Behdod Poushanchi², K. Kelly Gallagher², Deniz Sarhaddi², Alexis Donneys², Sagar S. Deshpande², Michael Morris², Steven Goldstein³, Steven R. Buchman². ¹Plastic Surgery Research Fellow, USA, ²University of Michigan, USA, ³University of Michigan Orthopedic Research Labs, USA

Purpose: Adjuvant radiotherapy (XRT) in the management of head and neck cancer remains severely debilitating. Fortunately, newly developed agents aimed at decreasing XRT-induced damage have shown great promise. Amifostine (AMF) is a drug which confers radio-protection to the exposed normal tissues, such as bone. Our intent is to utilize Raman spectroscopy (RS) to demonstrate how AMF preserves the mineral composition of the murine mandible following human equivalent XRT.

Methods: 6 Sprague Dawley rats were randomly assigned into 2 groups: XRT (n=3), AMF (n=3). Both groups underwent bioequivalent XRT of 70Gy in 5 fractions to the left hemimandible. AMF was administered 45min prior to XRT. 56 days post-XRT, the hemimandibles were harvested, and Raman spectra with 4 cm⁻¹ spectral resolution taken in the region of interest spanning 5.1 mm posterior to the last molar. A contralateral hemimandible from XRT served as Control. Bone mineral and matrix-specific Raman bands were observed and analyzed using One-way Anova, with statistical significance at p<0.05.

Results: The XRT group exhibited greater signs of radiation-induced stress, including alopecia, mucositis and weight loss compared to AMF. Gross examination demonstrated a reduction in angular cortical density. Mineral crystallinity, determined by the width of the primary phosphate band, which is fitted to obtain the full-width half-maximal-FWHM was calculated. FWHM demonstrated significant difference between AMF and XRT (p=0.005) and XRT and Control (p=0.021). There was no difference between AMF and Control (p=0.901; Fig1). There was an important shift in the peak position of the major phosphate band to higher wavenumber. These results are consistent with XRT-induced changes in mineral composition and crystallinity. Additional computer-aided spectral subtraction further confirmed these results (Fig2). AMF was spectrally similar to the Control in the same region thus demonstrating AMF protective effect from XRT-induced mineral damage.

Conclusion: Our novel findings demonstrate that AMF prophylaxis maintains and protects bone quality in the setting of XRT. RS is an emerging and exceptionally attractive clinical translational technology to investigate and monitor both the destructive effects of XRT and the therapeutic remediation of AMF on the structural, physical and chemical quality of bone. With noninvasive fiberoptic probe this technology holds the potential for diagnostic use in humans.

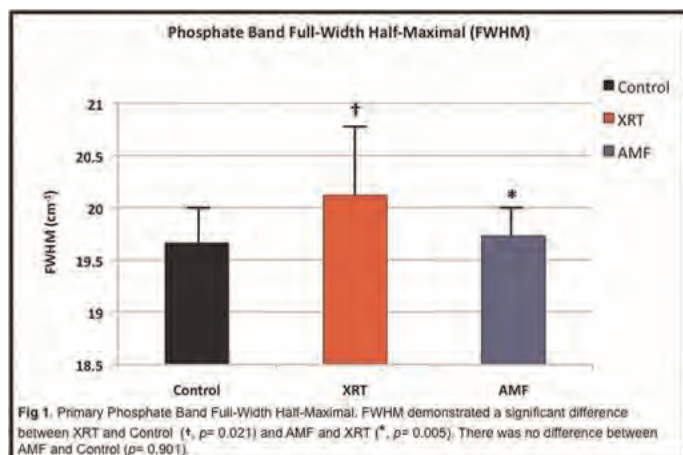


Figure 1

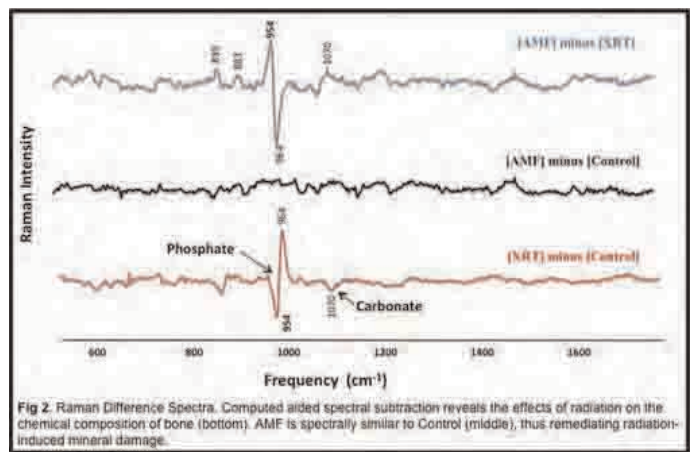


Figure 2

Disclosures: Catherine Tchanque-Fossuo, None.

SU0156

Role of CIZ in Melanoma Activity for Metastasis. Hiroaki Hemmi¹, Takuya Notomi², Tetsuya Nakamoto³, Tadayoshi Hayata⁴, Yoichi Ezura⁵, Tomomi Sakuma³, Masaki Noda³. ¹Immunology Frontier Research Center, Osaka University, Japan, ²GCOE, Tokyo Medical & Dental University, Japan, ³Tokyo Medical & Dental University, Japan, ⁴Medical Research Institute, Tokyo Medical & Dental University, Japan, ⁵Tokyo Medical & Dental University, Medical Research Institute, Japan

Bone Metastasis causes severe pain and multiple complications in locomotor system. However the mechanism of bone metastasis has not yet been fully understood. As bone metastasis is depend on diverse steps, which starts from the migration of the cells and metastasizing to the bone environment, attachment proteins would be involved in this process.

CIZ is a protein that has been known to be involved in regulation of genes related to metastasis such as MMPs. We examined the role of CIZ in B16 cells with respect to its actions for a migration and cell activities. CIZ expression levels in B16F10 were higher than those in B16 cells. This is correlating to the high metastatic activities in B16F10 than B16 cells. When we knocked down CIZ by using siRNA, B16 cells exhibited less migration activity upon the deletion of CIZ. In contrast enhanced expression of CIZ increased melanoma cell migrations. The size of migrated melanoma cells was also reduced by CIZ knocked down. By using intra-cardiac injection model, CIZ deficient host exhibited reduction in metastasis to bone, suggesting that the host CIZ may have a role in supporting the metastasis of B16 cells. With respect to cytokine, RANKL treatment enhanced CIZ expression in B16 cells. CIZ over expression activated the promoter of RANKL via the CIZ response elements located in RANKL gene. CIZ as well as RANKL promoted the migration of B16 melanoma cells and modulate cytoskeletal structures.

These observations suggested that CIZ regulates the property of metastatic B16 melanoma cells.

Disclosures: Tomomi Sakuma, None.

SU0157

Development of a High-throughput Screening (HTS) Assay for the Identification of Small Molecule Modulators of Gsa. Nisan Bhattacharyya¹, Dr. Catherine Chen², Dr. Wei Zheng², Dr. John K. Northup³, Dr. Susanne Neumann⁴, Dr. Michael T. Collins⁵. ¹NIDCR, NIH, USA, ²National Chemical Genomics Center, NHGRI, NIH, USA, ³Laboratory of Cell Biology, NIDCD, NIH, USA, ⁴Clinical Endocrinology Branch, NIDDK, NIH, USA, ⁵Skeletal Clinical Studies Unit, CSDB, NIDCR, NIH, USA

Somatic mis-sense mutations in the small subunit of the G-protein, Gs α (gsp), distributed in a mosaic pattern, are directly correlated with the occurrence of fibrous dysplasia of bone/McCune-Albright syndrome (FD/MAS), a disease that is defined by skeletal abnormalities that can be associated with various forms of hyperfunctioning endocrinopathies. The biochemical outcome of these mutations (R201H or R201C) is increased cAMP levels due to the impaired GTPase negative feedback regulatory step that converts active GTP-bound adenyl cyclase to the inactive GDP-bound form. Of interest is the fact that higher levels of cAMP may also correlate with the increased apoptosis that is observed in skeletal cells and is responsible for the age-related quiescence that is seen in FD. As such, certain endocrine tissues may benefit from gsp inhibition, while in skeletal tissue further gsp activation may speed apoptosis of mutation-bearing cells. The aim of this study is to develop an assay system that can be

used to discover small molecule inhibitors and activators specific for the mutated Gsx. Engineered CHO cells (Invitrogen) were stably transfected with either wild-type or mutated of Gsx (R201 and R201H). Several stable cell lines that showed equal expression of transfected Gsx were tested for cholera toxin-indifferent cAMP generation as the assay readout. One cell line from each set (WT9, C6 and H2), was selected for further studies and the assay optimized for use in a 1536 well format. The ability of activated Gsx to be inhibited and further stimulated was confirmed by testing with various adenylyl cyclase and adrenergic receptor inhibitors, and forskolin. Assay validation was carried out by screening the Library of 1280 Pharmacologically Active Compounds (LOPAC-1280) and a subset of 30976 compounds from the Molecular Library Probe Center Network (MLPCN) library. These validation screens showed hit rates of 0.16% and 0.5% against the LOPAC-1280 and partial MLPCN libraries, respectively. Screening of the full 300,000 compound Molecular Libraries is underway. Various bone- and endocrine-specific cell culture and animal models are in preparation for secondary and tertiary screening of compounds identified in HTS. Some of these compounds eventually may be developed into drugs for the treatment FD/MAS, as well as other gsp-mediated diseases.

Disclosures: Nisan Bhattacharyya, None.

SU0158

Elevated sclerostin in individuals with High Bone Mass. Celia Gregson^{*1}, Kenneth Poole², Susan Steel³, John Ayuk⁴, Emma Duncan⁵, Eugene McCloskey⁶, William Fraser⁷, J.H. Tobias⁸. ¹University of Bristol, United Kingdom, ²University of Cambridge, United Kingdom, ³Hull & E Yorks Hospital Trust, United Kingdom, ⁴University Hospitals Birmingham NHS Foundation Trust, United Kingdom, ⁵Royal Brisbane & Women's Hospital, Australia, ⁶University of Sheffield, United Kingdom, ⁷Norwich Medical School, University of East Anglia, United Kingdom, ⁸Avon Orthopaedic Centre, United Kingdom

Introduction

Sclerosteosis is a rare autosomal recessive disorder associated with High Bone Mass (HBM), caused by a loss-of-function mutation in the *SOST* gene encoding sclerostin, an osteocyte-derived inhibitor of bone formation. We recently recruited a large cohort of HBM individuals from systematically searching DXA databases around the UK; although to date sequencing has not identified any *SOST* gene mutations, we hypothesized that disordered sclerostin production might contribute to raised BMD in this context.

Methods

406 HBM index cases were identified by screening DXA databases from 4 UK centres (n=219,088). HBM was defined as a) L1 Z-score of $\geq +3.2$ plus total hip Z-score of $\geq +1.2$ or b) total hip Z-score $\geq +3.2$. Cases with significant osteoarthritis and/or other causes of raised BMD were excluded. Relatives & spouses were recruited, in whom HBM affection status was defined as L1 Z plus total hip Z-score $\geq +3.2$. Controls comprised unaffected relatives & spouses. Total body DXA and sclerostin measurements were performed in all. None had parathyroid disease. Analyses used multiple linear regression in Stata 11, adjusting for gender, menopausal status, weight & height and subsequently age.

Results

As expected, sclerostin increased with age in HBM cases (151 index cases + 47 affected relatives) (0.66 [0.15, 1.17] p=0.01), and controls (87 unaffected relatives + 36 spouses) (1.08 [0.68, 1.47] p<0.001) (results show adjusted beta coefficients with 95% confidence interval, per yearly increase in age). Sclerostin was higher in HBM cases than controls, mean (sd) 89.6 (40.7) vs. 66.4 (32.3) pmol/L, p<0.001, which persisted after adjustment, mean difference 23.9 (15.6, 32.2) pmol/L, p<0.001. After adjustment, sclerostin levels were positively related to total body BMD amongst HBM cases (12.3 [6.6, 17.9] p<0.001) to a greater extent than controls (6.6 [0.9, 12.2] p=0.02) (β equals sclerostin increase per 0.1mg/cm³ increase in BMD [95%CI]), interaction p=0.02.

Conclusion

We conclude that sclerostin concentrations are increased in HBM cases when compared with controls and that the relationship between bone density and sclerostin is stronger in HBM cases than controls. Elevated bone density in HBM does not fully explain the associated increase in sclerostin, suggesting other factors are implicated.

Funding: The Wellcome Trust, NIHR

Disclosures: Celia Gregson, None.

SU0159

Modest Reversal of Metabolic Syndrome Manifestations with Vitamin D Correction: A 12-month Prospective Study. Nasser Al-Daghri^{*}. King Saud University, Saudi Arabia

Background

Numerous cross-sectional studies have noted significant negative associations between circulating levels of vitamin D and cardio-metabolic risk factors, highlighting potential extra-skeletal functions of this steroid hormone. Prospective studies, however, have been limited and hence no cause and effect relations can be inferred. This study

aims to determine whether vitamin D correction can reverse already established manifestations of the metabolic syndrome (MetS).

Methods

A total of 59 adult non-diabetic, overweight and obese Saudis (65 males, 42 females) were randomly recruited in this prospective 1-year interventional study. Anthropometry and biochemical evaluation were performed, including determination of serum vitamin D, calcium and phosphorous concentrations, as well as fasting blood glucose and lipid profile. At the initial baseline visit, the prevalence of both low HDL-C and hypertension was significantly increased among patients with vitamin D deficiency (p<0.05), even after adjusting for gender and BMI. Subjects were advised to regularly expose themselves to sunlight and increase intake of vitamin D-rich foods. All measurements were repeated 6 and 12 months later.

Results

Overall prevalence of MetS patients by the modified NHANES ATP III definition decreased from 25.2 % to 13.0 % and this was largely due to a parallel decrease in the prevalence of low HDL-cholesterol, triglycerides and hypertension.

Conclusion

Optimization of vitamin D levels through sun exposure and increased intake of a vitamin D-rich diet can lead to an improved cardio-metabolic profile, offering a promising non-pharmacologic approach in the prevention of MetS manifestations.

Disclosures: Nasser Al-Daghri, None.

This study received funding from: King Abdulaziz City for Science and technology

SU0160

Severity of Knee Osteoarthritis Correlates with Estradiol and Leptin Levels in Serum and Synovial Fluid of Osteoarthritic Patients. Shirin Hooshmand^{*1}, Jenna Schmidt², Bahram Arjmandi¹. ¹Florida State University, USA, ²Florida State University, USA

Currently 21 million Americans are affected by osteoarthritis (OA) and to date, neither its etiology is well understood nor are effective therapies to prevent or halt OA available. Aside from inflammation, current evidence suggests that there is a relationship between estrogen and the development of OA. Evidence also suggests that loss of body fat is more important to decrease risk of OA than general weight loss emphasizing the role of fat tissue and its secretions and suggesting a metabolic link between obesity and OA. Therefore, the overall goal of this project is to improve cartilage health by exploring the relationship between synovial fluid and serum concentrations of leptin and estradiol and the degree of OA. To achieve this goal, a total of 80 mobile men and women, between the ages of 45 and 75 years with knee OA who were going under arthroscopic surgery or total knee replacement recruited. Blood samples and synovial fluid aspirated from their knee joints were obtained by an orthopedic surgeon as part of their surgery. Synovial fluid and serum samples were analyzed in duplicate using ELISA method to determine the concentration of leptin and estradiol. Our findings show a distinct correlation between BMI and serum leptin levels in both males and females (R=0.505, p=0.02; R=0.569, p=0.008). We found that in both men and women, the degree of OA was associated with serum leptin concentrations (R=0.487, p=0.02; R=0.498, p=0.04). Our data shows that females have higher levels of leptin in both serum and synovial fluid than males. In our study, as the severity of OA increased in females, the estrogen level in both serum and synovial fluid also tended to increase. However, this relationship was not found in male patients with OA. Women with severe OA had significantly higher levels of E₂ in their synovial fluid while E₂ levels in synovial fluid of men were not affected with degree of OA. In women, BMI was significantly correlated with level of estrogen in synovial fluid and tended to be significantly correlated with E₂ levels in serum (R=0.49, p=0.03; R=0.39, p=0.1). Although our results are promising in terms of relation among leptin and estradiol levels in synovial fluid and serum and the degree of OA, further studies are needed to investigate the exact role of leptin and estradiol in increasing the severity of OA.

Disclosures: Shirin Hooshmand, None.

SU0161

RANKL Over-Expression and Enhanced Bone Marrow Monocyte Response to RANKL Contribute to Low Bone Mass in Genetic Hypercalciuric Stone-Forming (GHS) Rats. Hongwei Wang^{*1}, Honggang Ye¹, Jinhua Wang¹, Soo Young Park¹, David Bushinsky², Murray Favus¹. ¹University of Chicago, USA, ²University of Rochester, USA

GHS rats are a useful model for human idiopathic hypercalciuria (IH), as both share increased intestinal Ca absorption and bone resorption, decreased renal tubule Ca reabsorption, Ca kidney stone formation and low BMD. Low bone mass is accompanied by changes in cortical bone that make it more brittle and fracture-prone. This study investigates the molecular mechanisms that may mediate low bone mass in GHS rats. Gene microarray analysis on bone marrow stromal cells (BMSC) revealed increased expression of several genes related to bone resorption including RANKL, RANK, GM-CSF, TNF α , and IL1, while genes related to bone formation (BMP2, Sppl, Sost) were decreased in GHS rats compared to Sprague Dawley (SD) control rats. Gene array analysis on splenic CD14⁺ monocytes from GHS and SD rats indicate that signaling pathways for VDR, TNF and IL-17 are up-regulated (CEBPB, CAMP, TNFR1 and IL-17R α). Real-time PCR results confirmed the microarray analyses. GHS rat bone marrow monocytes cultured in vitro with RANKL (100ng/

mL) showed greater stimulation of gene expression of osteoclast markers including integrin β , CAII, cathepsin K and TRAP. Mature osteoclast cell number increased 4.5 fold in GHS (vs SD) rats ($P < 0.05$). Mature osteoclasts from GHS rats were increased in number and individually larger compared to SD rats. Immunostaining demonstrated greater expression of RANKL in BMSCs from GHS rats. In conclusion, our results demonstrate that the low bone mass in GHS rats is due in part to greater RANKL expression in BMSCs, resulting in larger and more numerous osteoclasts. Suppression of osteoblast-specific genes suggests that decreased bone formation may also contribute to reduced BMD.

Disclosures: Hongwei Wang, None.

SU0162

Treatment of Tumor Induced Osteomalacia with CT-guided Percutaneous Ethanol Ablation and Percutaneous Cryoablation. Erik Olson, Sean Tutton, David King, Joseph Shaker*. Medical College of Wisconsin, USA

Tumor induced osteomalacia (TIO) is a rare condition often caused by a benign mesenchymal tumors (MT). Biochemical findings include hypophosphatemia (low P) with renal phosphate wasting (RPW) and 1,25(OH) $_2$ D levels which are lower than appropriate in the setting of low P. Production of FGF-23 by the tumor is often causal. In the absence of localization, medical therapy with phosphate salts and calcitriol results in improvement. When the tumor is found, resection results in biochemical and clinical resolution. Because of the risk of recurrence, wide excision (WE) has been advised.

A 51 YO M was evaluated in June, 2010. In February, 2008 he had a stress fracture of the right proximal femur which was treated with a total hip arthroplasty (THA). In February, 2010 he developed right knee pain and was found to have a stress fracture of the distal femur. He had weakness in his legs and slowing of gait. In January of 2009, he had a partial right nephrectomy for renal cell carcinoma. At that time, a lytic lesion was noted in the right iliac crest and was biopsied (consistent with reparative changes). On exam, he had weakness of the thigh flexors. There were no unusual skin lesions. The serum P was 1.4-1.7 mg/dl with RPW. The FGF-23 was high-normal. Reevaluation of the iliac lytic lesion was consistent with MT and immunocytochemistry was strongly positive for FGF-23. WE was advised, however, the prior THA complicated this option. The patient declined WE and opted for image-guided ablation (IA). He was treated with CT-guided percutaneous ethanol ablation (PEA) and cryoablation (PCA). This resulted in prompt normalization of P and FGF-23 as well as dramatic clinical improvement.

IA is established in the management of osteoid osteoma. In a prior report of IA for TIO, 2 ablations (RFA) were necessary and the 2nd RFA resulted in biochemical normalization. RFA uses radiofrequency energy to cause heating of tumor cells and has been associated with post-procedure pain. Many interventionalists have converted to PCA. We used a combination of PEA and PCA in an effort to prevent recurrence. Our patient appears to have had biochemical resolution, but will need long-term surveillance. In conclusion, we report a patient with a MT causing TIO who has had biochemical remission after IA. Although wide excision remains first-line therapy, IA may be an option in patients who cannot have or decline surgery.

Disclosures: Joseph Shaker, None.

SU0163

What Is the Minimal Serum 25-hydroxyvitamin D (25-OHD) Level for Optimal Skeletal Mineralization?. Sudhaker Rao*, Shijing Qiu, Tarlisha Eskridge, Nayana Parikh, Saroj Palnitkar. Henry Ford Hospital, USA

Background: There is currently an intense debate on optimal serum 25-OHD level for skeletal and non-skeletal health. Implicit in the recent IOM report was its reliance on evidence, but very little is known about the relationship between 25-OHD (the best available index of vitamin D nutrition) and osteoid indices (a measure of mineralization), in otherwise healthy individuals. Accordingly, we examined the relationship between 25-OHD and osteoid indices in 85 healthy women who were part of a study on bone effects of age and menopause.

Methods: Acquisition and analyses of relevant data are published. In this study we examined the prevalence of mineralization defect defined as Osteoid Thickness (O.Th) $> 12.5 \mu\text{m}$, or Osteoid Surface/Bone Surface (OS/BS) $> 20\%$, or Osteoid Volume/Bone Volume (OV/BV; derived from O.Th and OS/BS) $> 2\%$, cut-offs based on patients with osteomalacia (OM), an unambiguous condition with mineralization defect, or secondary hyperparathyroidism due to vitamin D depletion. Mineralization Index (MI), a composite index derived from OS, O.Th, OV, bone formation rate and osteoid maturation time, was also calculated; an MI > 10 suggests OM.

Results: In the entire group or in the sub-sets of ethnicity and menopause, there was no regression of O.Th, OS/BS, OV/BV, BFR or MI, or age on 25-OHD (range 12-55 ng/ml). Although the intercepts for each biopsy variable were different in the sub-sets, none of the differences were significant. PTH was inversely related to 25-OHD ($r = -0.24$; $p < 0.02$), but none had PTH $> 72 \text{ pg/ml}$, suggesting that lower 25-OHD ($< 20 \text{ ng/ml}$) in some women were of recent nature. In women with 25-OHD $< 20 \text{ ng/ml}$ none of the biopsies showed O.Th $> 12.5 \mu\text{m}$, except one ($12.6 \mu\text{m}$). Biopsies with OV/BV $> 2\%$ were distributed similarly among three 25-OHD groups: < 20 (n=17), 20-30 (n=21) or > 30 (n=13) ng/ml, but none $> 5\%$ (a conservative estimate of mineralization defect) in $> 30 \text{ ng/ml}$ group. Number of biopsies with OS/BS $> 20\%$ were similar in the 2 lower groups (n=13 & 17 respectively), but much less in $> 30 \text{ ng/ml}$ group (n=6). The

increase in OV/BV $> 2\%$ was mainly due to an increase in OS/BS but not in O.Th, hallmark of OM. Finally, MI was < 10 in all, which excludes OM.

Conclusions: In healthy women, a 25-OHD of $> 20 \text{ ng/ml}$ appears sufficient for bone mineralization, with small additional effect up to 30 ng/ml . None had OM implying that it is a function of both the degree and duration of vitamin D depletion.

Disclosures: Sudhaker Rao, None.

SU0164

Double Blind, Double Dummy, Randomized Controlled Trial of Oral Bisphosphonates (OB) in the Treatment of Active Pagets Bone Disease (PBD). Juan Carlos Barreira¹, Zulema Man², Claudia Gomez Acotto³, Emilio Roldan^{*4}. ¹Hospital Britanico, Argentina, ²Centro Medico TIEMPO, Argentina, ³Maimonides Univ., Argentina, ⁴Gador S.A., USA

The prevalence of PBD seems to be decreasing, notwithstanding subjects in the active phase (symptoms, plus abnormal biochemistry and positive scintigraphic images) demand intervention. Following previous criteria the suppression of bone resorption during 1-2 weeks promotes protracted post-treatment periods free of symptoms, and OB are adequate agents, but tolerability and a number of failures still cause concern. Hence olpadronate (OPD), the only soluble OB (crystal form A), showing previous rates of efficacy as high as I.V. therapies will be compared with the current accepted OB therapy in the country, pamidronate (APD), 400mg/day, during 4 months. OPD was administered at 200mg/day for only 12 days, randomized in a 1:2 schedule. Both formulations were double dummy with placebos in a group of 27 subjects with active PBD in spite of previous therapies. In a preliminary analysis 21 patients completed the protocol schedule, after 6 months mean bone sAP from basal was -39.4 % with APD, and -42.0 % with OPD (t test n.s.). Patients achieving normal values were 40.0 % with APD and 56.2% with OPD (Yates < 0.14). All patients with APD reported at least one digestive event, instead 39% of OPD patients were free of events (Fisher's $p < 0.05$). Although sample size limitations, because this is a rare condition, OPD performance, with a 10 fold shorter intervention, differs from APD being patients best controlled with the former compound. Hence, more patients are expected to benefit from this ultra short oral intervention with OPD.

Disclosures: Emilio Roldan, None.

This study received funding from: Gador SA

SU0165

Prediction of Paget's Disease of Bone Using Genetic Profiling. Omar Albagha^{*1}, W.D. Fraser², P.L. Selby³, Stuart Ralston¹. ¹University of Edinburgh, United Kingdom, ²Royal Liverpool University Hospital, United Kingdom, ³Manchester Royal Infirmary, United Kingdom

Paget's disease of bone (PDB) is characterised by focal increases in bone remodelling leading to bone pain and other clinical complications such as deformity, fracture, deafness, and osteoarthritis. Genetic factors are known to be important in PDB. Mutations in *SQSTM1* cause a high penetrance form of the disease but are only present in 10% of cases. In a recent genome wide association study we identified seven further loci that predispose to PDB risk on chromosomes 1p13, 7q33, 8q22, 10p13, 14q32, 15q24, and 18q21 by genome wide association study (Albagha *et al*, Nature Genetics, 2011 in press). Individually these loci increased the risk of PDB by 1.3 to 1.8 fold but together they had a large effect with a 10 fold difference in risk according to the number of risk alleles carried. Since PDB often presents after irreversible skeletal damage has already occurred, it would be advantageous to be able to identify high risk patients before the disease has become advanced so that prophylactic treatment can be given. The aim of this work was to evaluate the predictive power of genetic profiling in PDB using these markers, along with established risk factors such as family history and *SQSTM1* mutation status in 649 well-characterised PDB cases and 248 matched controls from the PRISM study. Each of these factors was entered into a predictive model and evaluated using receiver operating characteristic (ROC) curve analysis. Family history was found to predict the disease with a high specificity (97%) but poor sensitivity (13%) and accuracy (36%) and a total area under curve (AUC) of 0.55. Similarly, *SQSTM1* mutation status had high specificity (99.6%) but poor sensitivity (8%) and accuracy (33%) with an AUC of 0.54. The inclusion of both family history and *SQSTM1* mutation into the analysis was found to slightly improve the sensitivity (18%) and accuracy (40%) with limited changes in specificity (97%) and AUC (0.58). However, when risk allele scores were added to the analysis, we found a substantial improvement in both sensitivity (84%) and accuracy (70%) of the model with an AUC of 0.67, although specificity was lower (30%). This means that the combined model correctly identify the majority of true positive cases (84%), but a significant number of false positive cases were detected. This model was found to outperform the predictive value of bone mineral density with or without the FRAX algorithm in osteoporotic fracture prediction (AUC = 0.62 – 0.64; Bolland *et al*, JBMR, 2011). In conclusion our study has shown that genetic profiling may well be useful in predicting individuals at risk for developing PDB. Further studies are now indicated to investigate the feasibility of combining genetic testing with targeted therapeutic intervention to determine if this could prevent the development of morbidity in PDB.

Disclosures: Omar Albagha, None.

SU0166

Aortic Valve Calcification is Increased in Mild Primary Hyperparathyroidism. Marcella Walker*, Shinichi Iwata, Eiichi Hyodo, Zhezheng Jin, Rui Liu, Marco DiTullio, Shunichi Homma, Shonni J. Silverberg. Columbia University, USA

Aortic valve calcification is associated with cardiovascular death and myocardial infarction. Aortic valve calcification is a frequent complication of uremic secondary hyperparathyroidism, and although it was common in classical primary hyperparathyroidism (PHPT), little is known about aortic valve calcification in biochemically mild disease. 51 patients with mild PHPT (mean SD age: 617 yrs; serum calcium: 10.40.5 mg/dl; PTH: 8533 pg/ml) and 49 age- and sex-matched controls (age: 635 yrs) underwent echocardiography. Calcification area for each aortic valve leaflet was measured at mid-systole, and the sum of the calcification areas of all three aortic valve leaflets was calculated (aortic valve calcification area, AVCA) in both groups. Data were adjusted for cardiovascular risk factors. The peak transaortic pressure gradient was similar among PHPT patients and controls (62 vs. 62 mmHg; $p=0.2$). AVCA was, however, significantly higher in patients with PHPT (0.24 vs. 0.17 cm² $p<0.01$). AVCA was positively associated with PTH levels ($r=0.34$, $p<0.05$), while no association was found with serum calcium or 25-hydroxyvitamin D. Serum PTH level remained independently associated with AVCA after adjustment for cardiovascular risks known to affect aortic valve calcification (see table, Model R²=0.306; $p=0.037$). In this model, PTH was the only independently significant predictor, while traditional cardiovascular risk factors known to affect aortic valve calcification were not. PTH levels accounted for 17% of the known variance in AVCA. In summary, mild PHPT is associated with subclinical aortic valve calcification. PTH level, but not serum calcium concentration, is an independent predictor of AVCA. We conclude that in mild PHPT, PTH is a more important predictor of aortic valve calcification than well-accepted cardiovascular risk factors.

Variable	β	SE	p value
Parathyroid hormone	0.318	0.001	0.046
Male	0.214	0.049	0.162
Ever smoke	-0.225	0.036	0.110
Age	0.153	0.003	0.300
Body mass index	-0.254	0.005	0.127
Hypertension	0.130	0.045	0.417
Hypercholesterolemia	0.177	0.043	0.278
Glomerular filtration rate	-0.084	0.001	0.544

Disclosures: Marcella Walker, None.

SU0167

Asymptomatic Normocalcemic Primary Hyperparathyroidism: Characterization of a New Phenotype of Normocalcemic Primary Hyperparathyroidism. Natalie Cusano*, Patty Wang², Serge Cremers³, Elizabeth Haney⁴, Douglas Bauer⁵, Eric Orwoll⁴, John Bilezikian¹. ¹Columbia University College of Physicians & Surgeons, USA, ²Department of Medicine, Oregon Health & Science University, USA, ³Columbia University, USA, ⁴Oregon Health & Science University, USA, ⁵University of California, San Francisco, USA

Primary hyperparathyroidism (PHPT), a common endocrine disorder, is defined by elevated PTH and hypercalcemia. A newer presentation of PHPT has been described in which serum calcium (Ca) is normal and PTH is elevated, in the absence of secondary causes of hyperparathyroidism, such as renal disease or vitamin D deficiency. Recognition of this phenotype of PHPT, normocalcemic PHPT (NPHPT), supports a biphasic chronological time course, in which PTH levels are first elevated but serum Ca is normal, followed by the development of frank hypercalcemia. Although NPHPT was recognized by the Third International Workshop on the Management of Asymptomatic PHPT (JCEM, 2009), little is known about its epidemiology. Reports of NPHPT have largely come from referral centers in which subjects were seen for a metabolic bone disease. Our cohort of NPHPT came from patients referred to our metabolic bone disease unit and at diagnosis, 57% had osteoporosis by BMD and 11% had documented fragility fractures. We hypothesized that screening an unselected, non-referral population would identify asymptomatic subjects with NPHPT. The Osteoporotic Fractures in Men (MrOS) study is a cohort of US community-dwelling men ≥ 65 yrs at enrollment. We analyzed data from a random subset of 1504 men in whom PTH (Scantibodies IRMA, inter-assay CV 8.4%, intra-assay CV 5.6%) and serum Ca values were available. NPHPT was defined as serum PTH >66 pg/ml with normal albumin-adjusted serum Ca. 3 men were identified with hypercalcemic PHPT (excluded) and 45 had elevated PTH and normal serum Ca. We excluded all common secondary causes of hyperparathyroidism: renal

insufficiency (eGFR >40 cc/min, 12 excluded), vitamin D deficiency (<20 ng/mL, 17 excluded), and thiazide diuretic use (6 excluded). We identified 10 subjects (prevalence, 0.7%) with NPHPT as defined. There were no significant differences between subjects with and without NPHPT in terms of age, height, weight, BMI, phosphorus, bone turnover markers (P1NP, β CTX, TRAP5b), testosterone, estradiol, SHBG or femoral neck BMD (table). The men with NPHPT had a significantly higher lumbar spine BMD compared to the normal subjects (1.4 vs. 1.2 g/cm²; $p=0.01$), which may be due to the early anabolic effects of PTH on cancellous bone. The results identify an asymptomatic phenotype of NPHPT from an unselected community-dwelling cohort, which is distinctly different from previously described symptomatic cohorts.

Table. Characteristics of men with normocalcemic primary hyperparathyroidism (NPHPT) and comparison with normal men.

Parameter	Men with NPHPT (N = 10)		Normal men (N = 1481)		P value
	Mean \pm SD	Missing	Mean \pm SD	Missing	
Age (yr \pm SD)	75.9 \pm 7.0	0	73.7 \pm 5.9	0	0.24
Height (cm \pm SD)	174.8 \pm 8.2	0	174.3 \pm 6.9	0	0.82
Weight (kg \pm SD)	85.7 \pm 9.8	0	83.3 \pm 13.0	0	0.55
BMI (kg/m ² \pm SD)	28.0 \pm 2.5	0	27.4 \pm 3.7	0	0.58
White (%)	10 (100)	0	1354 (90.8)	0	0.31
Serum calcium adjusted for albumin (mg/dl \pm SD)	9.1 \pm 0.5	0	9.3 \pm 0.4	0	0.05
Intact PTH (pg/ml \pm SD) ¹	80.5 \pm 9.4	0	32.5 \pm 15.7	0	<0.0001
Serum phosphorus (mg/dl \pm SD)	3.1 \pm 0.4	0	3.2 \pm 0.4	0	0.42
25-Hydroxyvitamin D (pg/ml \pm SD) ²	26.6 \pm 5.1	0	25.2 \pm 8.0	0	0.58
P1NP (ng/ml \pm SD)	48.6 \pm 34.1	1	38.6 \pm 25.2	547	0.37
β CTX (ng/ml \pm SD)	0.4 \pm 0.3	1	0.4 \pm 0.2	546	0.72
TRAP5b (U/liter \pm SD)	3.5 \pm 0.9	1	3.2 \pm 1.0	552	0.33
SHBG (nmol/liter \pm SD)	54.5 \pm 19.0	0	49.4 \pm 19.8	15	0.42
Testosterone (ng/ml \pm SD)	435.1 \pm 207.2	0	405.1 \pm 170.9	19	0.58
Free Testosterone (ng/ml \pm SD)	7.9 \pm 3.0	0	7.9 \pm 2.9	31	0.94
Estradiol (pg/ml \pm SD)	26.6 \pm 7.7	0	22.5 \pm 6.6	18	0.13
Free Estradiol (pg/ml \pm SD)	0.6 \pm 0.1	0	0.5 \pm 0.2	37	0.34
Lumbar spine BMD (g/cm ² \pm SD)	1.4 \pm 0.2	0	1.2 \pm 0.2	13	0.01
Femoral neck BMD (g/cm ² \pm SD)	0.8 \pm 0.1	0	0.8 \pm 0.1	0	0.14

BMI, Body Mass Index; PTH, Parathyroid Hormone; P1NP, procollagen I N-terminal propeptide; CTX, C-telopeptide; TRAP, tartrate-resistant acid phosphatase; SHBG, Sex Hormone Binding Globulin; BMD, Bone Mineral Density.

¹By definition, PTH is >66 pg/ml in the individuals with NPHPT.

²By definition, 25-Hydroxyvitamin D is >20 pg/ml in the individuals with NPHPT.

Disclosures: Natalie Cusano, None.

SU0168

Basal Insulin Secretion is Correlated with Serum Undercarboxylated Osteocalcin (ucOC) Levels in Patients with Primary Hyperparathyroidism. Hisanori Suzuki*, Akira Takeshita¹, Megumi Miyakawa¹, Daishu Miura², Yasuhiro Takeuchi³. ¹Toranomon Hospital Endocrine Center, Japan, ²Department of Breast & Endocrine Surgery, Toranomon Hospital, Japan, ³Toranomon Hospital, Japan

Backgrounds: Osteocalcin (OC), a member of bone matrix proteins, is synthesized by mature osteoblasts. OC carboxylated by γ -carboxylase in a vitamin K-dependent manner is accumulated in bone matrix. Some OC molecules are not fully carboxylated or decarboxylated during bone resorption and released into circulation as undercarboxylated osteocalcin (ucOC) molecules. Recent animal studies have shown that ucOC could stimulate insulin secretion. However it remains unclear whether ucOC is actually involved in insulin secretion in humans. We have found serum ucOC levels are significantly higher in patients with primary hyperparathyroidism (pHPT) than controls.

Purpose: To clarify relationship between serum ucOC and insulin secretion in patients with pHPT.

Materials & Methods: We obtained data from clinical records of patients with pHPT who underwent parathyroidectomy at our hospital since April 2008. We analyzed data of fasting plasma glucose, insulin, biochemical bone markers [ucOC, OC, bone alkaline phosphatase, urine NTX], Ca, 1,25-dihydroxyvitamin D, intact PTH before surgery. Patients with diabetes mellitus or obesity (BMI more than 30) were excluded.

Results: We analyzed data of 22 patients in the present study. HOMA- β (homeostasis model assessment of β cell function) was significantly and positively correlated with ucOC, OC and bone alkaline phosphatase. HOMA- β had no correlations with BMI, age, Ca, intact PTH. HOMA-IR (homeostasis model assessment of insulin resistance) had no significant correlations with ucOC and OC. Among ucOC, OC and bone alkaline phosphatase, ucOC was indicated to be a predictor of HOMA- β with multiple regression analyses.

Conclusion: Basal insulin secretion estimated by HOMA- β is correlated with serum ucOC level at least in patients with pHPT. It is thus suggested that ucOC is involved in glucose metabolism via the regulation of basal insulin secretion in human.

Disclosures: Hisanori Suzuki, None.

SU0169

CDKN1B/p27^{kip1} Gene: Sequence Analysis in a Group of Sporadic Parathyroid Adenomas. Claudio Marcocci¹, Elena Pardi², Simona Borsari², Benedetta Raspini², Elena Paltrinieri², Federica Saponaro², Chiara Banti², Antonella Picone², Piero Berti³, Paolo Miccoli³, Filomena Cetani¹. ¹University of Pisa, Italy, ²University of Pisa Department of Endocrinology & Metabolism, Italy, ³University of Pisa Department of Surgery, Italy

Primary hyperparathyroidism (PHPT) is one of the most common endocrine disorders, especially in postmenopausal women, in whom it reaches a prevalence of 2-3%, and in the majority of cases has a sporadic presentation. Independent genetic events were associated with the development of a subset of these tumors, namely cyclin D1 overexpression (20-40%), loss of heterozygosity at chromosome 11q13 (40%) and/or somatic mutations of MEN1 gene (15-20%). A number of other genes have been studied for pathogenetic mutations in adenomas, but none has been found. Breaks in cell cycle control is a key event in tumorigenesis. Cyclin D1 promotes the G1-S-phase transition, probably by activating a cyclin-dependent kinase, and menin, the protein encoded by MEN1 gene, is also involved in the cell cycle control through its participation in functional dynamics of chromatin and regulation of transcription. Recently has been proved that menin directly regulates expression of the cyclin-dependent kinase inhibitors like p27Kip1. Inactivating mutations in *CDKN1B/p27^{kip1}* gene have been recently described in 6 families affected by MEN1-like syndromes or related states. The aim of our study was to evaluate the role of the *CDKN1B/p27^{kip1}* gene in a group of sporadic parathyroid adenomas (n = 102). Tissues were snap frozen after surgery. DNA from parathyroid tumors was prepared by a commercial kit that includes a preliminary proteinase K treatment. DNA was PCR amplified with primers for the two coding exons of *CDKN1B/p27^{kip1}* gene and direct sequencing was performed with a BigDye Terminator chemistry. No pathological variation in the coding region, nor in the splice site junctions of *CDKN1B/p27^{kip1}* were detected. We identified three, already reported, polymorphisms: a nucleotide substitution 79 bases before ATG (rs34330), a non synonymous mutation at codon 109, changing a valine for a glycine residue (rs2066827) and a silence mutation at codon 142 (Thr142Thr). We also reported a novel polymorphism 80 bases before ATG (c.1-80C>T). Our results exclude a role in sporadic parathyroid tumorigenesis for *CDKN1B/p27^{kip1}*, even if we can't exclude alterations of the regulatory region of the gene or post-transcriptional mechanisms, such as methylation, that could have a role in impairing protein function.

Disclosures: Claudio Marcocci, None.

SU0170

Depression in Primary Hyperparathyroidism: Prevalence and Sustained Benefit of Parathyroidectomy. Rachel Espiritu, Ann Kearns, Kristin Vickers, Douglass, Clive Grant, Euijung Ryu, Robert Wermers*. Mayo Clinic, USA

Context: Most patients with primary hyperparathyroidism (PHP) in the current era lack classical manifestations of the disease. However, often patients with PHP report nonspecific symptoms involving disturbances in neuromuscular function, cognition, and mood.

Objective: To determine the frequency of depression in an adult PHP cohort using a validated depression questionnaire and assess its response to parathyroidectomy.

Methods: A prospective case-control study utilizing the Patient Health Questionnaire-9 (PHQ-9) was performed in observed (n = 81) and surgically treated (n = 88) patients with PHP and patients with benign non-toxic surgical thyroid disease (n = 85). The PHQ-9 was performed at baseline then once again at 1 month, 3 months, 6 months, and 12 months after surgery or after the initial questionnaire in the observed PHP group. The associations between PHQ-9 scores and serum calcium, PTH, and PHP clinical feature as well as response to surgery were assessed.

Results: The three groups were similar with respect to gender, history of depression, antidepressant use, and psychotherapy, but PHP patients were older. Baseline PHQ-9 scores were 1.71 points higher in PHP patients than controls after adjusting for age and gender (p = .004). Clinically significant PHQ-9 scores (≥ 10) were twice as common in PHP subjects (31.4%) compared to thyroid surgery subjects (15.3%). Parathyroidectomy resulted in significant and sustained reductions in PHQ-9 scores in patients with PHP, which were greater than was seen in observed PHP subjects at all time points (p < .001). PHP patients with clinically significant PHQ-9 scores dropped to 7.4% (p < .001) and 7.6% (p < .001) at 1 month and 1 year after parathyroidectomy with declines that were also significantly greater than seen in observed PHP subjects. When compared to thyroid surgery, there were greater declines in PHQ-9 scores in surgical PHP patients at 1, 3, and 6 months (p < .001) and 1 year (p = .061).

Conclusions: Depressive symptoms are more common and severe in patients with PHP compared to those without the disease. Parathyroidectomy results in significant improvement in depressive indices in PHP compared to thyroid surgery and observed PHP subjects. The PHQ-9 questionnaire may be a useful tool in the evaluation of PHP patients, and scores of > 10 or ongoing depression may be appropriate indications for consideration of parathyroid surgery.

Disclosures: Robert Wermers, None.

SU0171

Establishment of Parathyroid hormone (PTH) Reference Range on 10 Different Assay Kits: Impact of the Recruitment of the Population. Etienne Cavalier¹, Jean-Claude Souberbielle². ¹University of LiegeCHU Sart-Tilman, Belgium, ²Hopital Necker-Enfants malades, France

Introduction: Reference values (Rv) for serum PTH levels are generally obtained by measuring PTH in a population of apparently healthy subjects. Exclusion criteria for this population are important and should correspond to any causes of altered PTH secretion, including vitamin D (VTD) insufficiency, which is very frequent in the general population and thus should be prevalent in an apparently healthy group. However, excluding VTD insufficient subjects from the reference group requires measuring the 25-hydroxy vitamin D (25OHD) level in all subjects, which was not considered in most studies which provided serum PTH Rv for different immunoassays. Some studies have shown that this could decrease the upper normal limit for PTH by 25-35% depending on the assay considered. Thus, for a given PTH assay, the Rv may significantly vary, depending on the reference population that has been recruited, and especially whether the VTD status has been taken into account.

Objective: We used the same reference population of VTD-replete normal subjects to establish Rv for 10 commercial PTH kits and compare them with those provided by the manufacturers. We thus selected 120 women (48.615.2 y., min-max: 20-79), and 120 men (51.517.5 y., min-max: 19-80). All were Caucasians and apparently healthy. Inclusion criteria were a 25OHD concentration (DiaSorin Liaison) ≥ 75 nmol/L, serum calcium and phosphate levels comprised between 2.15 and 2.60 and 0.74 and 1.51 mmol/L, respectively, and an estimated GFR (MDRD formula) ≥ 60 mL/min/1.73 m². The use of drugs known to influence bone and calcium/phosphorus metabolism was an exclusion criteria.

Results: There was no significant difference in PTH levels nor in age between men and women in our reference population. With all the tested PTH assays, the distribution of the concentrations was Gaussian. The results that we observed were lower than the Rv provided by the manufacturers with an upper normal limit only slightly different for 3 kits (Abbott Architect, DiaSorin Liaison N-tact and Ortho Vitros) but frankly lower (21 to 46.1 % lower) for the 7 other kits. The difference was most important for the Beckman Access kit (-46.1%), the DiaSorin N-tact IRMA (-33.9 %), and the DiaSorin Liaison 1-84 kit (-32.8 %).

Conclusions: An important multicentre work should be performed to recruit a very extensive reference population of vitamin D-replete, apparently healthy subjects in order to establish the PTH Rv for all the available kits.

Disclosures: Etienne Cavalier, None.

SU0172

Germline and Somatic DNA Variants in Cyclin-Dependent Kinase Inhibitor Genes in Sporadic Parathyroid Adenomas. Jessica Costa-Guda¹, Chen-Pang Soong², Andrew Arnold². ¹University of Connecticut Health Center, USA, ²University of Connecticut School of Medicine, USA

The molecular pathology of sporadic parathyroid adenomas remains incompletely understood. The possibility that alterations in genes encoding cyclin-dependent kinase inhibitors (CDKIs) might contribute to the development of sporadic adenomas was initially raised by discovery of cyclin D1's pathogenic role, and then by the finding of rare germline variants in several CDKI genes in patients with multiple endocrine neoplasia type 1 and related familial, syndromic and/or multiglandular hyperparathyroid disorders. Indeed, a recent report has implicated *CDKN1B*, encoding p27^{kip1}, in the pathogenesis of sporadic adenomas through the identification of both predisposing germline sequence alterations and clonal, tumor-specific mutation; however, other CDKI gene family members have not been similarly analyzed. We therefore sought to determine whether mutations/variants in *CDKN1A*, *CDKN2B* and *CDKN2C*, encoding the p21, p15 and p18 CDKIs respectively, might also contribute to the development of typical parathyroid adenomas. The coding regions and intron-exon boundaries of *CDKN1A*, *CDKN2B* and *CDKN2C* were sequenced in a series of 80 adenomas from patients with typical, sporadic presentations of primary hyperparathyroidism, and the germline/somatic status of each identified variant was determined by sequencing matched germline control DNA. DNA variants were identified in 5 adenomas (6%). Two tumors contained distinct heterozygous variants of *CDKN1A*, one germline and one somatic. One patient had a *CDKN2B* germline alteration, accompanied by loss of the normal allele in the tumor (LOH). Two distinct variants of *CDKN2C* were identified in two cases, one somatic and the other a germline change accompanied by LOH. None of the identified DNA changes were found in the latest build of dbSNP (132), which includes data from the 1000 Genomes Project, predicted to contain most genetic variants that have frequencies of at least 1% in the general population. The finding of somatic alterations in *CDKN1A* and *CDKN2C* suggests a directly conferred selective growth advantage in parathyroid tumorigenesis. The presence of germline variants of multiple CDKI-encoding genes in patients with sporadic presentations provides additional evidence for the concept that rare predisposing alleles in this gene family may collectively make an important contribution to the development of typical parathyroid adenomas.

Disclosures: Jessica Costa-Guda, None.

SU0173

Relative Prevalence of Normocalcemic and Hypercalcemic Hyperparathyroidism in a Community-Dwelling Cohort. Claudia Berger^{*1}, Lisa Langsetmo², David Hanley³, Jonathan Adachi⁴, Christopher Kovacs⁵, Jacques Brown⁶, Robert Josse⁷, David Goltzman⁸. ¹McGill University, Canada, ²Canadian Multicenter Osteoporosis Study, Canada, ³University of Calgary, Canada, ⁴St. Joseph's Hospital, Canada, ⁵Memorial University of Newfoundland, Canada, ⁶Laval University, Canada, ⁷St. Michael's Hospital, University of Toronto, Canada, ⁸McGill University Health Centre, Canada

We assessed the prevalence of primary hyperparathyroidism in a cross-sectional sample of 1305 women and 566 men, aged 31-97, participating in the population-based Canadian Multicentre Osteoporosis Study (CaMos) during study year 10 (2005-2007). Samples were analyzed for PTH and 25-hydroxyvitamin D [25(OH)D] with a Diasorin Liaison machine and for calcium and albumin using an autoanalyzer. Laboratory-specified reference ranges were 2.13 to 2.60 mmol/L for serum calcium levels, 17.3 to 72.9 pg/ml for PTH, and 34 to 48g/L for albumin. Serum calcium was corrected for albumin when albumin levels were outside the normal range. Among those who had blood samples at year 10, samples were also available from 300 participants at baseline and 691 participants at year 5.

There were 444 participants (315 women and 129 men) with increased serum PTH and normal serum calcium at year 10. In these participants, serum 25(OH)D was <50nmol/L in 132, 50 to 75 nmol/L in 182, and >75nmol/L in 130. Assuming a lower limit of 25(OH)D of 50nmol/L, 70.3% of the participants with high PTH and normal serum calcium had evidence of "normocalcemic hyperparathyroidism", which represents 16.7% of the study population at year 10 (17.4% of the women and 15.0% of the men).

There were 12 participants (0.6% of the population) with concomitantly high PTH and high serum calcium. In this group, 4 had serum 25(OH)D<50nmol/L, 5 had serum 25(OH)D between 50 and 75nmol/L, and 3 had serum 25(OH)D>75nmol/L. Among 7 with earlier blood samples, 6 had normal serum calcium and elevated PTH levels in earlier measurements (entry in the study or Year 5). These studies suggest that the normocalcemic hyperparathyroidism at baseline may have progressed to subsequent hypercalcemic hyperparathyroidism.

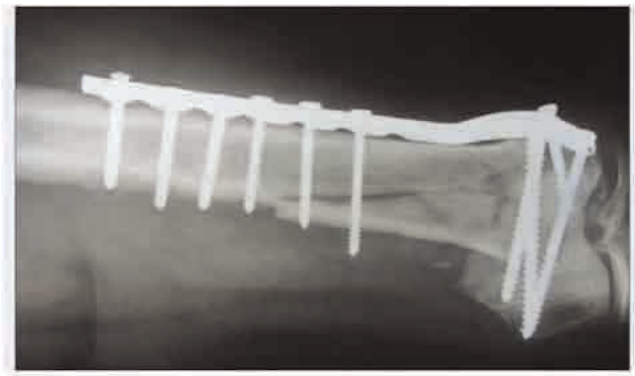
These results indicate that concomitant elevated serum PTH and calcium, suggestive of primary hyperparathyroidism, is rare in this cohort, but may be observed even in those with low serum 25(OH)D. Normocalcemic hyperparathyroidism, however, is 27 times as prevalent, but the morbidity associated with this condition requires further study.

Disclosures: Claudia Berger, None.

SU0174

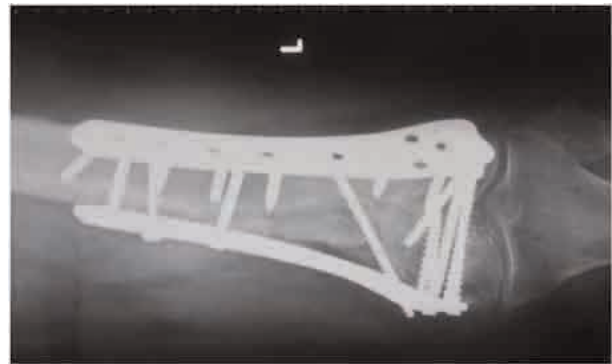
Repair of Fracture Nonunion Using a Combination of Low Dose rhFGF-2 and rhIGF-I; Case Report. Ashraf Moharam¹, Hsiu Ying Sherry Wang², Marina D'Angelo³, Abdulhafez Selim^{*4}. ¹Orthopedic Surgery, Cairo University School of Medicine, Egypt, ²Inspire Pharm, Egypt, ³Philadelphia College of Osteopathic Medicine, USA, ⁴Center for Chronic Disorders of Aging, PCOM, USA

Nonunion fractures present a challenge to orthopedics with no optimal solution. One of the greatest needs in the nonunion fractures field is a bioactive agent to stimulate bone formation. Fibroblast growth factor-2 (FGF-2) exhibited strong anabolic actions on angiogenesis and bone formation. IGF-I, another bone anabolic growth factor, is known to promote mesenchymal cell as well as osteoblast proliferation. Moreover, FGF-2 and IGF-I have synergistic effects of FGF-2 on the proliferation of human chondrocytes. Aiming at a clinical application, this study was undertaken to clarify the effect of a single local application of low doses of recombinant human FGF-2 and IGF-I on fracture healing. A fifty three year old healthy female was diagnosed with comminuted distal femur intercondylar fracture on May 2009. The patient was treated with fixation using single plate and nails. On May 2010, failure of fixation and evidence of nonunion was established by X-Ray and CT scan. Revision surgery was recommended. The patient was treated with fixation using double plating with synthetic calcium sulphate graft loaded with combination of rhFGF2 (500 microgram) and rhIGF-I (100 microgram). No side effects were observed postoperatively. Union was achieved 4 month postoperatively as evidenced by clinical and imaging. This is the first clinical case to show efficacy and safety of using low dose combination of FGF2 and IGF1 loaded on a synthetic carrier that had achieved union on a previously nonunion fracture.



Preoperative

Preoperative



Postoperative

Postoperative

Disclosures: Abdulhafez Selim, None.

SU0175

Daily Activity and Tests of Muscle Strength Are Associated With Fractures in Stage 3-5 Chronic Kidney Disease. Sarah West^{*1}, Charmaine E. Lok², Maryum Chaudhry², Scott G. Thomas¹, Sophie Jamal¹. ¹University of Toronto, Canada, ²Toronto General Hospital, Canada

Purpose: Fractures are common in patients with chronic kidney disease (CKD). Tests of neuromuscular function (NMT) discriminate well among fractured and non-fractured patients with stage 5 CKD on dialysis. The ability of NMT and daily activity to discriminate among fracture status in men and women with stages 3-5 CKD is unknown.

Methods: We utilized baseline data from an ongoing prospective study of patients, age ≥18 yrs, with stages 3-5 CKD (using NKF criteria by MDRD eGFR) to determine if NMT (the timed up and go test [TUG] and 6 minute walk test [6MW]), and/or daily activity (sedentary, light, or moderate/vigorous activity measured by triaxial accelerometry [StayHealthy, RT3]) could discriminate among those with and without fractures (self-reported low trauma fractures after age 40 and/or prevalent vertebral fractures identified by morphometry). Results are expressed as areas under the receiver operating characteristic curves (AUROC) with 95% confidence intervals (CI), adjusted for age and weight.

Results: Data was available for 128 men and 86 women; of these, 32 completed accelerometry. Compared to non-fractured patients (n=143), those with fractures (n=70) were older (5916 vs. 6914 yrs, p<0.001), had a reduced 6MW distance (335.587.1 vs. 289.9142.2 m, p=0.04), and participated in more sedentary and less light daily activity (min/day, p<0.05). All other demographic variables were similar among those with and without fractures. The mean weight of study subjects was 79.919.8 kg, most were Caucasian (70.0%), over 40% had diabetes, and 74% patients were categorized into stage 4 or 5 CKD. The mean duration of CKD was 8.010.3 yrs, and 30.2% reported a fall in the past 12 months. The TUG (mean 12.35.7 sec) was able to discriminate among those with and without fractures (AUROC: 0.70 [95% CI: 0.61-0.80]), as was the 6MW test with an AUROC: 0.69 (95% CI: 0.59-0.80). As determined by accelerometry, sedentary activity (min/day) was able to discriminate fracture status (AUROC: 0.71 [95% CI: 0.51-0.93]), as was light activity (min/day), which gave an AUROC of 0.76 (95% CI: 0.56-0.95).

Conclusions: NMT and accelerometry can discriminate among those with and without fractures. The AUROC was greater for more sensitive tests of daily activity, i.e. accelerometry, indicating that in early stages of CKD more sensitive tests of

physical function may be the best tool to discriminate among those with and without fractures. Further prospective studies are needed.

Disclosures: Sarah West, None.

SU0176

Evidences That PTH Can Be Directly Involved In The Regulation Of The Secreted Frizzled Related Proteins (sFRPs) And The Wnt Signaling Pathway. Natalia Carrillo-Lopez¹, Lucía Martín-Gutiérrez¹, Pablo Roman-García¹, Sara Panizo¹, Manuel Naves-DÚaz¹, Jorge Cannata Andía². ¹Bone & Mineral Research Unit. Hospital Universitario Central de Asturias. Instituto Reina Sofía de Investigación. REDinREN del ISCIII. Universidad de Oviedo. Oviedo, Asturias, Spain, ²Hospital Universitario Central de Asturias, Spain

PURPOSE: The aim of this study was to evaluate *in vivo* and *in vitro* the effect of different degrees of secondary hyperparathyroidism (sHPT) and different PTH concentrations on bone turnover-related and Wnt pathway signaling-related gene expression.

METHODS: In the *in vivo* study, chronic renal failure (CRF) was induced in 36 rats by 7/8 nephrectomy then, rats were divided in 2 groups, one was fed normal phosphorus (P) diet (NPD) (0.6% P) and other was fed high P diet (HPD) (0.9% P). A group with normal renal function and NPD diet was used as reference group. Rats were sacrificed at 8, 16 and 20 weeks. Blood samples were collected and the left tibia was removed to assess bone turnover-related and Wnt pathway-related gene expression. In the *in vitro* study, UMR-106 cells were grown in DMEM (with standard P concentration) with 10% FCS and then exposed to vehicle (ethanol) or different concentrations of PTH (1-34) (10^{-8} , 10^{-7} and 10^{-6} M) for 24 hours in the culture medium. Cells were collected and total RNA was extracted to study bone turnover-related and Wnt pathway signaling-related gene expression.

RESULTS: After 20 weeks, CRF rats fed HPD diet showed a remarkable significant increase in serum PTH and P levels, together with a significant decrease in serum calcium (table 1). The bone gene expression of bone turnover markers was significantly increased (table 2). Moreover, secreted Frizzled Related Protein (sFRP) 1, 2 and 4 and Dkk1 (inhibitors of the canonical signaling of Wnt pathway) were significantly over-expressed (table 2). In the *in vitro* study, cells exposed to PTH were able to significantly increase FGF23, osteocalcin, OPG, Cbfa1 and cathepsin K gene expression in a concentration dependent manner (table 3). As in the *in vivo* experiments, PTH was able also to significantly increase sFRP1, 2 and 4 gene expressions in a concentration dependent manner; however Lrp5 and Dkk1 did not show changes (table 3).

CONCLUSIONS: *In vivo*, the increase in PTH was associated with a significant increase of genes involved in bone turnover. In addition, an increased expression of the Wnt signaling pathway-related genes (including the inhibitors of the pathway) was observed. *In vitro* results confirmed part of the *in vivo* results, demonstrating for the first time that PTH directly increase the sFRPs, suggesting that PTH is directly involved in the sFRPs and Wnt pathway signaling regulation.

Table 3. FGF23, bone turnover and Wnt-related genes gene expression measured by qRT-PCR in UMR-106 cells treated with vehicle (Control) or PTH at different concentrations (10^{-8} , 10^{-7} , 10^{-6} M) for 24 hours. * $p < 0.05$ compared to Control group. R.U. : Relative Units vs. Control group.

	FGF23 (R.U.)	Osteocalcin (R.U.)	OPG (R.U.)	Cbfa1 (R.U.)	Cathepsin K (R.U.)
Control	1.00±0.00	1.00±0.00	1.00±0.00	1.00±0.00	1.00±0.00
10-8MPH	1.32±0.32	1.17±0.15	2.83±0.88*	1.45±0.06*	1.49±0.12*
10-7MPH	1.72±0.25*	1.71±0.47	9.87±2.16	2.05±0.53*	2.38±0.41*
10-6MPH	4.96±1.44*	2.66±0.85*	5.34±1.44*	1.60±0.19*	2.12±0.24*
	Lrp5 (R.U.)	Dkk1 (R.U.)	sFRP1 (R.U.)	sFRP2 (R.U.)	sFRP4 (R.U.)
Control	1.00±0.00	1.00±0.00	1.00±0.00	1.00±0.00	1.00±0.00
10-8MPH	0.89±0.17	1.10±0.15	1.52±0.54	1.56±0.43	1.93±0.37
10-7MPH	1.17±0.18	0.99±0.2	1.97±0.51*	5.90±1.68*	4.43±0.55*
10-6MPH	1.00±0.16	1.07±0.36	2.05±0.36*	11.01±0.86*	6.72±1.11*

Table 3

Table 2. Bone gene expression of bone turnover markers and Wnt-related gene expression measured by qRT-PCR in CRF rats fed NPD and HPD and the Reference group. * $p < 0.05$ compared to time-matched NPD group. * $p < 0.05$ compared to Reference group. R.U. : Relative Units vs. Reference group.

	Osteocalcin (R.U.)	OPG (R.U.)	Cbfa1 (R.U.)	Cathepsin K (R.U.)	Lrp5 (R.U.)	sFRP1 (R.U.)
8 weeks NPD	1.20±0.34	0.87±0.36	0.82±0.36	2.41±0.80	1.56±0.84	1.63±0.45
16 weeks NPD	0.73±0.59	0.83±0.28	0.81±0.18	2.57±1.36	0.95±0.39	2.73±0.93
20 weeks NPD	1.06±10.15	0.89±0.06	0.96±0.22	2.33±0.45	0.97±0.09	1.34±0.30
8 weeks HPD	2.27±0.98*,#	4.33±1.50*,#	2.81±0.88*,#	3.34±0.69*	1.33±0.41	5.89±1.62*,#
16 weeks HPD	8.84±1.43*,#	6.50±2.40*,#	3.73±1.70*,#	5.99±2.80*	1.75±0.96	8.51±2.69*,#
20 weeks HPD	13.06±3.75*,#	9.33±4.39*,#	5.96±1.50*,#	27.03±6.69*,#	1.20±0.36	17.87±2.99*,#
Reference group	1.00±0.50	1.00±0.31	1.00±0.15	1.00±0.36	1.00±0.26	1.00±0.21
	sFRP2 (R.U.)	sFRP4 (R.U.)	Dkk1 (R.U.)			
8 weeks NPD	1.90±0.91	0.96±0.22	1.75±0.54			
16 weeks NPD	1.17±0.38	1.25±0.29	1.30±0.36			
20 weeks NPD	1.47±0.40	1.07±0.09	0.98±0.04			
8 weeks HPD	2.12±0.38*	2.87±1.09	5.52±2.14*,#			
16 weeks HPD	19.13±10.30*,#	13.99±5.35*,#	3.05±1.62			
20 weeks HPD	8.59±2.59*,#	30.17±6.61*,#	4.57±1.57*,#			
Reference group	1.00±0.20	1.00±0.30	1.00±0.24			

Table 2

Table 1. Serum PTH, phosphorus and calcium levels in rats with CRF fed NPD and HPD and the Reference group. * $p < 0.05$ compared to time-matched NPD group.

	Serum PTH (pg/dL)	Serum Phosphorus (pg/dL)	Serum Calcium (mg/dL)
8 weeks NPD	37.8±22.0	5.7±1.2	12.1±0.2
16 weeks NPD	65.6±54.1	5.0±0.5	11.7±0.5
20 weeks NPD	82.2±57.6	5.6±0.7	12.5±0.6
8 weeks HPD	283.6±233.7*	8.7±0.8*	11.6±0.4*
16 weeks HPD	1314.0±781.7*	11.9±2.7*	11.3±2.1
20 weeks HPD	2461.2±717.0*	14.1±2.4*	10.9±0.1*
Reference group	44.2±39.1	4.9±0.9	11.5±0.6

Table 1

Disclosures: Natalia Carrillo-Lopez, None.

SU0177

Role of Akt-eNOS Signal Pathway in the Endothelial Dysfunction induced by Chronic Kidney Disease with Hyperphosphatemia. Tan Vu Van¹, Yutaka Taketani¹, Eriko Watari¹, Tomoyo Kitamura¹, Ken-Ichi Miyamoto², Hironori Yamamoto³, Eiji Takeda⁴. ¹University of Tokushima, Japan, ²Tokushima University School of Medicine, Japan, ³University of Tokushima, Japan, ⁴University of Tokushima School of Medicine, Japan

Generally, endothelial dysfunction plays a pivotal role in the development and progression of atherosclerosis, even in the chronic kidney disease (CKD) patients. Accumulation of endogenous inhibitor for endothelial nitric oxide synthase (eNOS) such as asymmetric dimethylarginine (ADMA) has been accused of accelerating progression of arteriosclerosis and increasing cardiovascular morbidity and mortality in CKD patients. In addition, recent studies have demonstrated that hyperphosphatemia can be involved in endothelial dysfunction as well as vascular calcification, suggesting that would be a linking mechanism between cardiovascular disease and CKD-MBD. However, it has not been clarified the detailed mechanism how hyperphosphatemia deteriorate endothelial function. In this study, we investigated the effect of lowering serum phosphate (P) level by dietary P restriction on the phosphorylation of eNOS and Akt in the adenine-induced CKD rats with hyperphosphatemia. Treatment with 0.75% adenine-containing diet for 3 weeks caused hyperphosphatemia, and decreased the phosphorylations of both eNOS at 1177 and Akt at 473 in the rat thoracic aorta with significant decrease in acetylcholine-dependent vasodilation. Lowering serum P levels by the treatment of

dietary P restriction for 2 weeks ameliorated not only the impaired vasodilation, but also the phosphorylations of eNOS at 1177 and Akt at 473. However serum ADMA, BUN, and creatinine levels were not improved by the ingestion of low P diet. These observations suggest that Akt-eNOS signal pathway plays an important role in the pathogenesis of endothelial dysfunction in CKD. In addition, hyperphosphatemia may be involved in the down-regulation of Akt-eNOS signal pathway in CKD. Treatment of hyperphosphatemia may be beneficial for vascular health by, at least, activating Akt-eNOS signal pathway.

Disclosures: Yutaka Taketani, None.

SU0178

Adipocytokines Affect the Bone Metabolism of Rheumatoid Arthritis Patients-TOMORROW study. Yuko Sugioka*, Tadashi Okano, Masahiro Tada, Tatsuya Koike. Osaka City University Medical School, Japan

Introduction: Adipocytokines may be implicated in the pathophysiology of rheumatoid arthritis (RA), but the relationship among adipocytokines, inflammation and bone metabolism remain unproven. We conducted a prospective cohort study to evaluate risk factors in RA patients associated with disease activity (Total Management Of Risk factors in Rheumatoid arthritis patients to IOWer morbidity and mortality: TOMORROW study, UMIN000003876). This study was designed to evaluate serum adipocytokines (adiponectin and leptin) concentrations in relation to inflammatory markers and bone mineral density in RA patients. Here we report the cross-sectional analysis at baseline.

Subjects and methods: Two hundred eight RA patients (112 patients received biologic agents and 96 patients received conventional therapy) and 205 age, sex-matched healthy volunteers (control) were enrolled in this study. Serum levels of adipocytokines and bone mineral density (whole body dual X-ray absorptiometry, Hologic QDR-4500) were measured.

Results: Subjects included 349 females and 64 males with a mean age of 57.9 (20.9-79.3) years. Serum level of both leptin and adiponectin were higher in RA patients than control ($p < 0.01$). Also RA patients showed higher fat rate, lower whole lean mass, and lower BMDs of spinal and extremities. Adiponectin levels inversely correlated with BMDs of thoracic vertebra and lower extremities ($r = -0.319$, $r = -0.364$, $p < 0.001$) and positively correlated with disease activity score (DAS) 28 ($r = 0.248$, $p = 0.003$). Serum adiponectin was negatively associated with thoracic spine ($\beta = -0.143$, $P = 0.022$) and leg ($\beta = -0.114$, $P = 0.034$) BMDs after adjusting for age, BMI, disease duration, DAS28-ESR, and whole lean mass (Table). In RA patients, leptin concentrations significantly correlated with % of fat rate ($r = 0.719$), but with neither disease activity nor bone mineral density.

Conclusion: The results confirm adiponectin concentrations were associated with the disease activity and bone mineral density. Whether adiponectin plays a pro-inflammatory role or simply concentrates in the presence of inflammation is unclear. Leptin has been reported to promote immune response. However, no correlation was identified between leptin and disease activity in our study. Leptin levels only reflected body composition. Further longitudinal study should give the insight for relationship of RA and adipocytokines.

Multivariate	RA	n=208
	β	p
Thoracic spine BMD	n=208	
Age (years)	-0.265	<0.001
BMI (kg/m ²)	-0.099	0.133
whole lean mass (kg)	0.466	<0.001
Disease duration (year)	0.044	0.465
DAS28-ESR	0.057	0.358
Adiponectin (μg/ml)	-0.143	0.022
Leg BMD (mg/cm³)	n=185	
Age (years)	-0.273	<0.001
BMI (kg/m ²)	-0.086	0.134
whole lean mass (kg)	0.595	<0.001
Disease duration (year)	-0.119	0.026
DAS28-ESR	-0.065	0.238
Adiponectin (μg/ml)	-0.114	0.034
Adiponectin (μg/ml)	n=208	
Age (years)	0.192	0.014
BMI (kg/m ²)	-0.154	0.045
disease duration (years)	0.030	0.670
DAS-ESR	0.147	0.043
whole lean mass (kg)	-0.158	0.038

Table

Disclosures: Yuko Sugioka, None.

SU0179

Bariatric Surgery Results in Significant Loss of Cortical Bone. Emily Stein^{*1}, Polly Chen², Angela Carrelli³, Donald McMahon¹, Kavita Pandit², Marc Bessler², Beth Schroppe², Elizabeth Shane¹, Shonni Silverberg². ¹Columbia University College of Physicians & Surgeons, USA, ²Columbia University, USA, ³New York Presbyterian- Columbia University, USA

Background: Substantial bone loss at weight bearing sites occurs after bariatric surgery, but the underlying mechanism and significance of this loss are not known. Recent reports of increased fractures following bariatric surgery raise concern that bone quality may be compromised.

Methods: This prospective study assessed changes in bone density and microarchitecture following bariatric surgery. Subjects undergoing Roux-en-Y gastric bypass (RYGB) and gastric banding (GB) were evaluated at the time of surgery and at 12 months post-operatively. Areal bone mineral density (aBMD) at the lumbar spine (LS), total hip (TH), femoral neck (FN) and 1/3 radius (1/3R) was measured by dual energy x-ray absorptiometry. Trabecular (Tb) and cortical (Ct) volumetric BMD and microstructure at the distal radius and tibia were measured by high resolution peripheral quantitative computed tomography (HRpQCT, voxel size ~82 μm).

Results: 14 women (age 43.10 yrs, 21% Caucasian, 64% Latina, 14% African American or mixed race, mean BMI 45.6 kg/m²) were enrolled. Ten subjects underwent RYGB and 4 GB. Mean weight loss was 283 kg ($p < 0.0001$). At baseline, mean T-scores were normal at all sites (LS:-0.10.3, TH:0.70.2, FN:0.10.2, 1/3R:0.10.3). aBMD decreased by 5.5% at the TH and 5.6% at the FN ($p < 0.01$ for both). There was no significant change in BMD at the LS or 1/3R. The amount of bone loss at the total hip was associated with the extent of weight loss ($r = 0.66$, $p < 0.01$). As expected, women who underwent RYGB had greater weight loss (RYGB:-34 kg vs GB:-16 kg; $p < 0.004$) and bone loss at the TH (RYGB:-8.1% vs GB:-0.9%; $p < 0.002$) and FN (RYGB:-8.2% vs GB:-0.8%; $p < 0.02$). Microarchitecture was assessed in RYGB. There were no significant changes at the radius on HRpQCT, mirroring the lack of change seen by DXA at non-weight bearing sites. However, HRpQCT revealed significant declines in cortical bone at the tibia. Ct area decreased by 3.3% ($p < 0.03$), Ct density by 2.2% ($p < 0.03$), and Ct thickness by 2.7% ($p < 0.04$). No significant changes in trabecular density or microstructure were observed.

Conclusions: Bone loss after bariatric surgery occurs at weight bearing sites by DXA (TH and FN but not LS or 1/3R) and HRpQCT (tibia but not radius). The small but consistent and significant microarchitectural changes we have observed suggest that cortical bone loss at weight bearing sites may explain the increased propensity to appendicular fractures in this population.

Disclosures: Emily Stein, None.

SU0180

Expression of DKK-1 and Sclerostin in Osteoarthritis. Allahdad Zarei^{*1}, Cyrus Cooper², Muhammad Javaid³, Afsie Sabokbar⁴. ¹Botnar Research Centre, University of Oxford, United Kingdom, ²University of Southampton, United Kingdom, ³University of Oxford, United Kingdom, ⁴University of Oxford, Botnar Research Centre, United Kingdom

Osteoarthritis (OA) is the commonest arthritis in the elderly, and the characteristic changes of OA involve both changes in subchondral bone as well as cartilage. The current phenotyping of the bone response in OA is incompletely understood but the Wnt pathway has been implicated in osteophyteogenesis. The purpose of this study was to assess and correlate the differential expression of Dickkopf-related protein 1 (DKK-1) and sclerostin (*SOST*), natural antagonists of the Wnt signalling pathway, in osteocytes in patients with end stage OA.

Bone core samples (6 x 15mm) were obtained from specific regions for each excised femoral head at the time of hip arthroplasty for OA. These regions were identified as F1: where complete absence of cartilage and deeply fissured subchondral bone was noted; F2: where there was margin of full thickness deficit; F3: this core sample was taken through the base of osteophyte and F4: represented the normal, macroscopic undamaged cartilage from the same femoral head. Bone samples were fixed in formalin, decalcified in EDTA, embedded in paraffin and 4μm sections were examined histologically and stained immuno-histochemically for DKK-1 and *SOST*.

Our data suggested that the expression of DKK-1 and *SOST* by osteocytes, inversely correlated with the local severity of OA within the same femoral head, as assessed using macroscopic, clinical and histological grading system. DKK-1 and *SOST* expression was most clearly noticeable in osteocytes in the normal/macroscopically undamaged bone or cartilage (F4 cores). In the complete absence of cartilage (F1 core) or samples taken from the base of the osteophytes (F3 cores), the expression of DKK-1 and *SOST* was not evident in osteocytes. In summary, we have shown that cortical and trabecular bone are active compartments in the disease process of OA and that DKK-1 and *SOST*, molecules involved in the down-regulation of bone formation, are differentially expressed in the same femoral OA hip. Furthermore, this is the first study to report DKK-1 expression by osteocytes in osteoarthritic bone.

Disclosures: Allahdad Zarei, None.

SU0181

Long Term Anti TNF α Therapy for Inflammatory Rheumatic Disease is Associated with Increased Bone Mineral Density and Paradoxical Elevation of TRAP5b Serum Levels. Eric Toussiot*¹, Laurent Mourot², Emilie Grandclement³, Daniel Wendling⁴, Gilles Dumoulin⁵. ¹University Hospital J Minjoz, France, ²EA3920 Physiopathologie Cardiovasculaire et Prevention, France, ³Explorations fonctionnelles et biochimie endocrinienne et metabolique, France, ⁴University Hospital Minjoz, France, ⁵Explorations fonctionnelles et biochimie hormonale et metabolique, France

Purpose: Rheumatoid arthritis (RA) and ankylosing spondylitis (AS) are inflammatory rheumatic diseases associated with increased risk of fractures, low bone mineral density (BMD) and increased levels of markers of bone resorption with normal or decreased values for bone formation markers. Anti-TNF α agents are very effective in treating clinical symptoms of RA and AS and suppressing inflammation.

Objectives: we evaluated the long term changes in bone mass and metabolic bone markers in patients with RA or AS while receiving anti-TNF α agent.

Patients and Methods: 20 patients (6 F) were evaluated (12 AS [modified NY criteria], age [mean SD]: 40.7 16.1 yrs; and 8 RA [ACR criteria], age 60.5 9.7 yrs; disease duration: 9.6 9.8 yrs). They all received anti-TNF α agent (adalimumab: 12; etanercept: 6; infliximab: 2). At baseline and at 1, 3, 6, 12, 18 and 24 months (M) after initiating anti-TNF α treatment, we measured both serum tartrate resistant acid phosphatase isoform 5b (TRAP5b, EIA, Quidel) and bone alkaline phosphatase (BAP, RIA, Beckman), as enzymatic markers of osteoclast and osteoblast, respectively, as well as serum beta CTX-I (EIA, IDS Nordic Bioscience), as marker of bone resorption. Serum osteocalcin (OC; RIA, Cisbio) and P1CP (Quidel) were measured as markers of bone formation. Osteoprotegerin (OPG, EIA, Quidel), an inhibitor of bone resorption was also evaluated. BMD at the lumbar spine and the hip was measured at baseline and after 6, 12 and 24 M by DEXA (iDXA, Lunar). No patients had bisphosphonate treatment. Nine patients were under low dose corticosteroids (< 10 mg prednisone).

Results: All the patients responded to the treatment with clinical improvement and decline in erythrocyte sedimentation rate ($p=0.006$) and CRP levels ($p=0.003$). Compared to baseline, lumbar spine and hip BMD at M24 increased (+ 6.3% and + 2.4% respectively), with significant changes at the spine ($p<0.001$). Beta CTX-I and OPG remained stable over the 24 M period while we observed a progressive and marked increase in TRAP5b (baseline: 1.21 0.74; M24: 2.44 1.05 U/L) ($p<0.001$). BAP also increased at M3 but not significantly. OC and P1CP similarly increased at M1 and M3 with significant change for P1CP ($p=0.04$), then returning to baseline values.

Conclusion: This study confirms the beneficial effects of anti-TNF α agents on BMD, mainly at the lumbar spine. On the contrary of previous study, we did not observe a decrease in bone resorption markers (beta CTX-I) but we found a paradoxical increase in TRAP5b. By contrast, bone formation markers (BAP, OC) were unchanged or transiently increased (P1CP). These results suggest that anti-TNF α agents may increase osteoclast activity, but without stimulation of bone resorption since there was no parallel increase of beta CTX-I and no deleterious effect on BMD. We conclude that prolonged treatment with TNF α blocking agents has a favorable effect on bone mass in patients with RA or AS.

Disclosures: Eric Toussiot, None.

SU0182

Safety of High Dose Vitamin D Therapy in Lung Transplant Recipients. Caroline Ball*¹, Daniel Dilling², Charles Alex², Pauline Camacho³. ¹Loyola University Chicago Stritch School of Medicine, USA, ²Loyola University Medical Center, USA, ³Loyola University of Chicago, USA

Introduction: Vitamin D deficiency is highly prevalent in lung transplant patients. We previously reported a prevalence of 80% among pre-transplant and 77% among post-transplant patients (ASBMR 2009). The standard therapy utilized in our institution is ergocalciferol at 50,000 IU weekly followed by every other week or lower doses determined by repeat levels at 3 months. We recommend 1200-1500 mg calcium per day. In non-transplant patients vitamin D toxicity as evidenced by hypercalcemia is virtually nonexistent at this dose. However, we have noted higher rates of hypercalcemia in transplant recipients. It is not clear whether this occurs due to interaction with transplant medications. No prior studies have looked at the safety of high dose vitamin D therapy after transplantation.

Methods: This is a retrospective study of 98 lung transplant patients from 2005 to 2010. Baseline information gathered from the electronic medical records included patient age and sex, reason for transplant, 25 OH-vitamin D, serum total and ionized calcium, PTH and creatinine. Treatment regimens with ergocalciferol and calcium were documented for 6 months following transplantation. Hypercalcemia was defined as serum calcium (CA) over 10.5 mg/dL or ionized calcium (ICA) over 1.3 mmol/L.

Results: 61 of the 98 (62%) lung transplant patients were treated for Vitamin D deficiency. One patient was excluded from the study because of sarcoidosis. The cohort consisted of 34 female and 27 male patients with a mean age of 51.57 14.37. Mean 25 OHD was 30.92 15.51 ng/mL, CA was 8.95 0.57 mg/dL, ICA was 1.20 0.11 mmol/L, PTH was 78.09 116.2 pg/mL and creatinine was 0.89 0.39 mg/dL. 6 patients (9.84%) treated for Vitamin D deficiency developed hypercalcemia, with a mean CA of 9.03 0.71 mg/dL and ICA of 1.32 0.05 mmol/L within 6 months of surgery. Of

these 6 patients 4 were female and 2 were male. The mean creatinine was 1.60 mg/dL. Hypercalcemia was documented at 74 41 days post-transplant. There were no demographic differences between patients who developed hypercalcemia and those who did not.

Conclusions: The data suggests that lung transplant recipients, in comparison to the general population are at a slightly higher risk of hypercalcemia with high dose vitamin D therapy, and in particular those who develop renal insufficiency post-transplant. Cautious utilization of vitamin D and monitoring of serum calcium and creatinine levels will help avoid vitamin D toxicity.

Disclosures: Caroline Ball, None.

SU0183

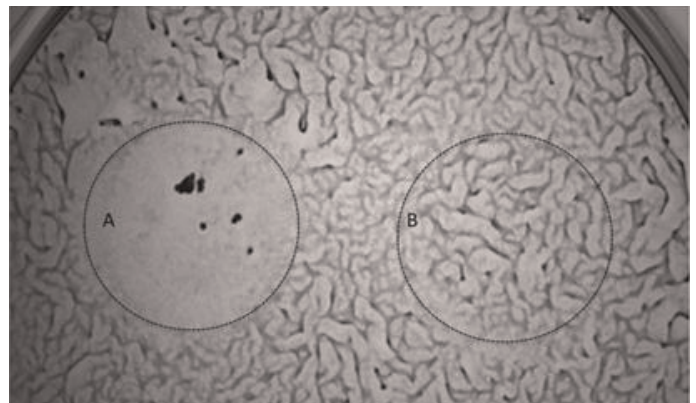
Cell Density Governs Self-Organization into Patterns in Calcifying Vascular Cells. Henry Cheng*¹, Aneela Reddy¹, Andrew Sage², Alan Garfinkel¹, Yin Tintut¹, Linda Demer³. ¹University of California, Los Angeles, USA, ²University of Cambridge, United Kingdom, ³David Geffen School of Medicine At University of California Los Angeles, USA

In embryonic development, formation of patterned biological structures such as bone and vasculature may occur via the phenomenon of reaction-diffusion, in which a morphogen pair (activator and inhibitor) guides cells into periodic patterns. This mechanism has been posited in bone development and vascular calcification, and recent studies identified the morphogen pair as BMP-2 and MGP. We previously showed that calcifying vascular cells, which undergo osteochondrogenic differentiation and mineralization, also self-organize into periodic patterns of swirls, spots, or labyrinths as computationally predicted by a reaction-diffusion model. To test the model prediction that local cell density affects cellular self-organization, we varied cell-plating density using cloning rings and monitored the rate of progression and types of patterns formed.

Calcifying vascular cells were seeded onto 6-well plates (2×10^4 cells/well). At confluence (2 days), a 1 cm cloning ring was placed in each well, and a second set of cells was plated (at range of densities from $2 - 32 \times 10^4$ cells/well) within the cloning rings. A second, control ring with no added cells was placed elsewhere in each well. After 2 days, the cloning rings were removed, and the pattern formation was monitored daily for 8 days by phase-contrast photomicrography.

Within the cloning ring site, cells organized at steady-state into a pattern of spots, consisting of discrete raised nodules, clearly distinct from the labyrinthine pattern formed in the surrounding monolayer and at the sites of the control rings, largely consistent with the model predictions. When the second layer was plated at a cell density of 2×10^4 , the cells progressed from a uniform monolayer at day 2 to a swirling pattern (local alignment) at day 4, a labyrinthine pattern at day 6, and discrete spots by day 7. The rate of pattern progression from swirls to spots increased with increasing cell density. The relationship between cell density and rate of pattern progression from swirls to spots was nonlinear. At a density of 16×10^4 the relationship between density and progression saturated.

These findings suggest that cell density strongly influences the rate of self-organization and pattern formation via reaction-diffusion in calcifying vascular cells, a type of osteoprogenitor cell. This phenomenon may contribute to mechanisms of embryonic development of patterned structures, such as the vasculature and skeletal bone.



Toluidine blue stain shows spot pattern in site of higher cell density (A) but labyrinthine pattern in control ring (B) and well monolayer.

Figure

Disclosures: Henry Cheng, None.

SU0184

Loss of Equilibrative Nucleoside Transporter 1 (ENT1) Leads to Progressive Hypermineralization of Paraspinal Tissues: A Novel Murine Model Resembling Diffuse Idiopathic Skeletal Hyperostosis (DISH) in Humans. Derek Bone, Sumeeta Warraich, Diana Quinonez, David Holdsworth, S. Jeffrey Dixon*, Cheryle Seguin, James Hammond. The University of Western Ontario, Canada

DISH is a non-inflammatory spondyloarthropathy, characterized by calcification of joint capsules, ligaments and entheses, especially in paraspinal tissues, that occurs in 6-12% of North Americans, most over the age of 50. Symptoms include spine pain and stiffness and, in severe cases, dysphagia and compression of the spinal cord and nerve roots. The etiology of DISH is unknown and there are no specific treatments. ENT1 is a protein that transfers hydrophilic nucleosides such as adenosine across the plasma membrane of many cell types. In mice lacking ENT1 (KO), we observed the development of calcified lesions with remarkable resemblance to DISH in humans. At 8-12 months of age, KO mice exhibited signs of spinal stiffness, hind limb dysfunction and eventually paralysis. MicroCT analyses of KO mice revealed hypermineralized lesions starting in the cervical-thoracic spine that extended to the lumbar region with advancing age. Eventually, aberrant mineralization (with density exceeding that of cortical bone) bridged the vertebrae. Histological examination of decalcified samples revealed large, irregular accumulations of eosinophilic, amorphous material in paraspinal and intervertebral regions with no apparent inflammation. Severe lesions involved intervertebral discs and impinged on the spinal cord, leading to compression that was likely the source of the paresis and paralysis observed in aged KO mice. We found no evidence for ectopic mineralization of appendicular joints or blood vessels, indicating tissue specificity. HPLC analyses of plasma showed a 2.8-fold increase in adenosine levels in KO compared to wild-type mice. In contrast, there were no significant differences in levels of the adenosine metabolites xanthine or uric acid, arguing against lesions being due to deposition of monosodium urate crystals. The large difference in plasma adenosine levels is consistent with loss of function of ENT1 – one of the primary uptake pathways for adenosine into cells. Together, the remarkable radiographic, histological and spatiotemporal similarity of lesions in KO mice and DISH patients suggests a link between loss of ENT1 function and development of DISH. Our findings validate the ENT1 KO mouse as a disease model, providing – for the first time – a means to investigate mechanisms underlying ectopic mineralization of paraspinal tissues and, eventually, to evaluate therapeutics for preventing pathological calcification in DISH and related disorders in the elderly.

Disclosures: S. Jeffrey Dixon, None.

SU0185

Severe Skeletal Toxicity from Protracted Etidronate Therapy for Generalized Arterial Calcification of Infancy (GACI). Gary S. Gottesman*¹, Jesse E. Otero², William H. McAlister³, Katherine L. Madson¹, Steven Mumm⁴, Michael P. Whyte⁴. ¹Shriners Hospital for Children, St. Louis, USA, ²Washington University in St. Louis School of Medicine, USA, ³Mallinckrodt Institute of Radiology, Washington University School of Medicine, St. Louis, USA, ⁴Shriners Hospital for Children & Washington University School of Medicine, St. Louis, USA

We report a 7-year-old boy with GACI (OMIM #208000) who was treated life-long with etidronate (EHDP) at another facility and was referred for severe skeletal dysmorphism. GACI is an autosomal recessive disease caused by loss-of-function mutations in the ectonucleotide pyrophosphatase/phosphodiesterase-1 gene (ENPP1: OMIM #173335). Decreased ENPP1 activity leads to low extracellular inorganic pyrophosphate (ePPi) and vascular mineralization with hydroxyapatite deposition in elastic fibers of arteries. If untreated with EHDP, 85% of patients die by age 6 months from cardiac ischemia and congestive heart failure. Survivors have normal skeletons although some arterial and peri-articular calcification may persist. Rickets can appear with chronic EHDP exposure.

EHDP, a 1st-generation bisphosphonate analog of PPI, inhibits both skeletal mineralization and resorption, eliminating arterial calcification in GACI by 2 weeks to 2 years of therapy. EHDP is then stopped. Our patient's arterial calcification resolved by age 6 months, yet intra- and peri-articular calcifications progressed. He remained on EHDP (200 mg/day).

At our research center, he had odynodysphagia, opioid-controlled body pain, facial asymmetry, plagiocephaly, proptosis, and joint contractures leaving him wheelchair bound. Biochemical parameters of mineral and skeletal homeostasis including serum calcium, phosphate, 1,25(OH)₂D, PTH, and total and bone-specific alkaline phosphatase were essentially normal. Osteocalcin was low suggesting reduced skeletal turnover. Radiographs revealed cranial synostosis, long-bone bowing, widened physes with osteosclerosis and "tongues" of radiolucency, along with metaphyseal cupping and fraying reminiscent of pediatric hypophosphatasia (Fig. A). Erlenmeyer flask deformity of the femurs, elevated serum creatine kinase (brain isoform) and TRAP-5b, and lumbar spine osteosclerosis along with a DEXA z-score of +5.7 suggested EHDP-induced osteopetrosis (Fig. C, D). ENPP1 gene analysis revealed an apparent homozygous mutation (c.653A>T, p.Asp218Val). Six weeks after cessation of EHDP his skeleton showed marked improvement (Fig. B).

Our patient with GACI, treated life-long with high-dose EHDP, showed profound but reversible inhibition of skeletal mineralization and decreased resorption. Although EHDP is life-saving in GACI, surveillance for resolution of arterial

calcification and the development of rickets is paramount to prevent severe skeletal toxicity.



Figure. EHDP-induced rickets in a boy with GACI.

(A) Left wrist at 6-11/12 years-of-age while taking EHDP. Here, features of hypophosphatasia include: 'tongues' of radiolucency (arrows), metaphyseal osteosclerosis, and irregularity in the provisional zones of calcification with widened physes (asterisks). Intra-articular calcification is noted (black arrow). (B) Six weeks after stopping EHDP, tongues of radiolucency are markedly improved, the provisional zone of calcification is more regular, physes have narrowed, while intra-articular calcification is unchanged (black arrow). (C) While taking EHDP, lateral lumbar spine demonstrates diffuse and end-plate sclerosis of the vertebrae with fusion of the posterior elements (arrows). (D) Left distal femur at 6-11/12 years shows Erlenmeyer flask-like deformity along with focal sclerosis and irregularity of the physal lines. (E) Lateral right knee demonstrates massive intra- and peri-articular calcification. Lucent areas with sclerotic borders are noted in distal femur and proximal tibia (arrow). Physes are irregular and widened (arrowheads). Femur shows severe bowing deformity.

Disclosures: Gary S. Gottesman, None.

SU0186

The Role of ApoE/Lrp5/6 in Aortic Valve Calcification: LDL-Density-Pressure Theory. Nalini Rajamannan*. Northwestern University Medical School, USA

Calcific Aortic Valve Disease is the number one indication for cardiac valve replacement in the US. The mechanisms of valve calcification are under intense investigation. Mutations in the low-density lipoprotein-related receptor 5 and 6 have been implicated in a number of disease processes in the field of bone, cancer, eye, neurodegenerative disease, congenital heart abnormalities and cardiovascular disease. This study proposes to test the effect of the LDL-Density-Pressure Receptor mechanism on the development of valvular heart disease. To test this hypothesis in an experimental hypercholesterolemia mouse model ApoE^{-/-}, Lrp5^{-/-}, ApoE^{-/-}/Lrp5^{-/-} mice (n=120) were tested. Group I (n=20) normal diet, Group II (n=20) 0.25% cholesterol(chol) diet (w/w), for the development of calcification. The aortic valve (AVA) was examined for calcification, and bone matrix markers. Bone formation was assessed by micro Computed Tomography (microCT), Lrp5, Lrp6, and cbfa-1 expression. Echocardiographic measurements were performed using the Vevo mouse echo machine to determine hemodynamic progression with the diets. Echocardiographic Peak Jet Velocity (control vs chol) ApoE^{-/-} 1.60.1m/sec vs 1.70.1m/sec, Lrp5^{-/-} 1.30.1m/sec vs 1.560.1m/sec, ApoE^{-/-}/Lrp5^{-/-} 1.840.3m/sec vs 2.030.3m/sec, (p>0.05 for all groups). Calcification analysis demonstrates increased calcification for the ApoE^{-/-}, and ApoE^{-/-}/Lrp5^{-/-} mice in the chol treatments but no evidence in calcification for the Lrp5^{-/-}, cholesterol treatments by MicroCT and Synchrotron measurements. RTPCR analysis demonstrates ApoE^{-/-} increase in Runx2 and Lrp5 in the chol treatment (p<0.05) Lrp5^{-/-} no change in Runx2 and no expression of Lrp5 in the chol treatment, ApoE^{-/-}/Lrp5^{-/-} increase in Runx2 and Lrp6 in the chol treatment (p<0.05). This data demonstrates ApoE, Lrp5 and Lrp6 are critical in the development of valve calcification and that a combination of these receptors play a unique role in the development of calcification in the aortic valve.

Disclosures: Nalini Rajamannan, None.

SU0187

Application of iPS Cells to the Research of Fibrodysplasia Ossificans Progressiva. Yoshihisa Matsumoto^{*1}, Makoto Ikeya², Akira Nasu², Isao Asaka², Takanobu Otsuka³, Edward Hsiao⁴, Junya Toguchida².

¹Department of Cell Growth & Differentiation, Center for iPS Cell Research & Application, Kyoto University, Department of Orthopedic Surgery, Graduate School of Medicine, Nagoya City University, Japan, ²Department of Cell Growth & Differentiation, Center for iPS Cell Research & Application, Kyoto University, Japan, ³Department of Orthopedic Surgery, Graduate School of Medicine, Nagoya City University, Japan, ⁴Gladstone Institute of Cardiovascular Disease, USA

Fibrodysplasia ossificans progressiva (FOP) is a rare genetic disease characterized by progressive ectopic ossification, which severely inhibits patients' ADL. The responsible gene for FOP is the ALK2 (activin like kinase 2) gene, which is one of type I receptors for BMP. Mutations found in patients transform ALK2 protein into a constitutive active form, which transduces the BMP signal without a ligand binding. This causes ectopic ossification in muscles, tendons, and ligaments, although precise mechanisms are not yet known. Harvesting target tissues from patients is strictly prohibited because tissue damage accelerates the ectopic ossification. This issue now can be overcome by using iPS cells derived from patients. We have established iPS cells from Japanese patients with FOP, from which cells in mesenchymal lineages are induced such as bone, cartilage, muscle, or tendon cells. We are currently analyzing the difference between wild type iPSCs and FOP-iPSCs during osteogenesis and chondrogenesis. We also try to recapitulate disease's phenotype in vitro by the stimulation with factors related to tissue damage. In this poster presentation, we will report our recent data and discuss the possibility of drug discovery by using our system.

Disclosures: Yoshihisa Matsumoto, None.

SU0188

A Transcriptomic Analysis of Type II Autosomal Dominant Osteopetrosis Osteoclasts : Identification of New Disease Markers. Amelie COUDERT^{*1}, Robert OLASO², Corinne COLLET¹, Marie-Christine De Vernejoul¹.

¹INSERM, France, ²CEA, France, ³Federation De Rhumatologie Et INSERM U606, France

Type II autosomal dominant osteopetrosis (ADO II) is a rare bone disorder characterized by an increased bone mass. About 80 % of ADO II are related to mutations in the chloride channel 7 gene (CLCN7), which encodes a chloride channel found on the ruffled border of the osteoclasts. The ADO II disease is characterized by a default in the resorption process. In order to gain insights in the mechanism of this default, we decided to carry out an analysis of the transcriptome of osteoclasts from ADO II patients versus the one from controls. Hence, we recruited 16 ADO II patients and 31 controls. Each patient was genotyped for CLCN7 mutations. Among our patients, we have found 2 yet undescribed CLCN7 mutations. PBMC from both osteopetrotic patients and controls were cultured with M-CSF and RANK-L to be differentiated into osteoclasts for 14 days. At the end of the culture, the number of multinucleated TRAP positive cells and the osteoclastic differentiation marker genes (TRAP, CATSK RANK) evaluated by qPCR were identical in the osteopetrotic and control cultures. We then hybridized RNA on the Illumina BeadChip. Microarray results showed a higher expression of ITGB5 (Integrin β 5) (x1.5). We therefore confirmed a significant higher expression of ITGB5 by qPCR. We also showed a higher expression of Integrin β 5 by western blot and by immunofluorescence with the expected intracytoplasmic localization. The mRNA of other integrins (Integrin β 3 and β 1) and members of the downstream pathway (vav3, src) were unchanged. In addition, we confirmed by qPCR several other genes that were differentially expressed in the microarray and we observed in ADO II patients a significantly higher expression of the mRNA of CES1 (1.5) and a lower expression of Perforin 1 (0.5), Serpine 2 (0.6) and WARS (0.7). In conclusion, our data showed higher expression of integrin β 5 in ADO II osteoclast and this can be associated with the low resorption capacity responsible of the bone phenotype of the patients. And the significant difference in several other gene expression in ADOII osteoclasts could defined them as new markers of osteoclast dysfunction in this disease.

Disclosures: Amelie COUDERT, None.

SU0189

Altered Transcript Pattern During Osteoblast Differentiation Associated With Improved Bone Phenotype In Homozygous Osteogenesis Imperfecta Brlt Mice. ADI REICH^{*}, Wayne A. Cabral, Joan Marini. National Institute of Child Health & Human Development, USA

Osteogenesis Imperfecta (OI), or "brittle bone disease", is a disorder of connective tissue characterized by skeletal fragility and deformity, and short stature. Most cases have autosomal dominant mutations in type I collagen. The Brlt knock-in mouse, with a G349C substitution in one COL1A1 allele, develops typical OI features, including osteoporosis, decreased BMD, fractures, and small size. Perinatal lethality

of heterozygous pups is 30%. Because it is typical that a dominant negative disorder is more severe in homozygous (HZ) than heterozygous (HET) form, we expected HZ Brlt mice to be lethal. Surprisingly, HZ survival was equal to WT, and their phenotype was intermediate between HET and WT. To investigate the amelioration in HZ phenotype, we compared the differentiation of cultured calvarial osteoblasts (OB) from WT, HZ & HET BRLT offspring over three weeks using Osteogenesis PCR Arrays and qPCR. Expression of OB differentiation markers was variably altered in HZ cells, rather than being restored to WT levels or expression intermediate between HET and WT. HZ OB displayed increased expression vs WT and HET OB of Cadherin 11, important for cell-cell adhesion, and Integrin α 2, that mediates cell attachment to the ECM. Paradoxically, the normal increase in gene expression on differentiation days 9-18 of Dmp1, Sost, Phex and Bmp2 by WT OB, associated with bone mineralization, was blunted in OI mice. Dmp1 and Bmp2 expression in HET and HZ cells, respectively, peaked at about half and 25% of WT, while Sost expression attained only 30% and 6% of WT levels. Phex expression in both OI genotypes increased minimally during differentiation. Furthermore Colla1, Colla2, Atp, Runx2, Tgfb1 expression were all consistently lower in HZ than HET or WT, throughout differentiation. In femoral tissue RNA from 2-month Het and HZ mice, Sost, Osx and Bmp2 expression was also decreased vs WT while Vegfa expression dramatically decreased in HZ mice. Immune staining of Dmp1 showed different localization and intensity patterns in the cortical bone of HET and HZ mice, in agreement with Dmp1 gene expression. These altered HZ expression patterns suggest that a compensation mechanism involving bone mineralization and remodeling as well as cell-matrix attachment, rather than a correction to WT patterns, improves the HZ bone phenotype. Cell-matrix exchange experiments are ongoing to determine the extent to which matrix structure and homogeneity influence OB cellular differentiation.

Disclosures: ADI REICH, None.

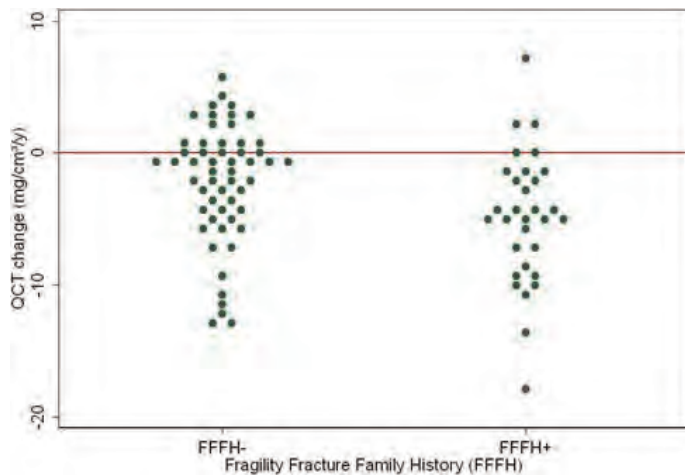
SU0190

Fragility Fracture Family History and Rate of Bone Loss—Volumetric Cancellous Spinal Bone Change in Premenopausal Women. Jerilyn Prior^{*1}, Christine Hitchcock¹, Yvette Vigna¹, Vanadin Seifert-Klauss². ¹University of British Columbia, Canada, ²Technical University of Munich, Germany

Numerous large and sophisticated genetic studies (candidate gene-focussed cohort studies, genome-wide association studies, etc.) are currently being performed to understand the heritable aspects of human osteoporosis. A person whose biological relative had a fragility fracture is known to be at increased risk of lower areal bone mineral density (BMD) and at a higher likelihood of fragility fracture. What is not known is whether a fragility fracture family history (FFFH+) is a risk factor for an increased rate of BMD loss. A post-ovariectomy sham-controlled rodent study showed widely varying rates of BMD loss or gain in different inbred strains suggesting that genetics influences rodent BMD change 1. However, several prospective human studies of BMD change by genetics or osteoporosis family history and found no clear 2-tailed differences²⁻⁵. Data were available on 1-yr quantitative computed tomography (QCT) spinal cancellous bone change in active, healthy premenopausal women from Vancouver, Canada (n=66) and 2-yr change in older, healthy premenopausal women from Munich, Germany (n=20). The Vancouver cohort was mean age 34, BMI 22 with FFFH+ present in 33%—all were initially ovulatory and 65% were runners. The Munich cohort was mean age 43.5, BMI 24 with FFFH+ present in 45%. Consistent with age differences, initial QCT values differed by center: Vancouver 15422, Munich 14221 mg/cm³ (95% CI of difference = -15, -12.8). QCT change/yr, however, did not differ: -3.55.1 Vancouver, -2.03.4 Munich (95% CI of difference = -3.9, 0.9). Within each cohort those with and without FFFH+ did not differ in any non-bone characteristic. However, in combined data, QCT annual change differed: FFFH-, -2.24.4; FFFH+, -4.95.0 mg/cm³/y (95% CI diff 0.7, 4.8) (Figure). By ANOVA, study center did not reach significance (F1, 83=2.41, P=0.124) but FFFH+ made a major contribution to annual QCT change (F1, 83=7.88 P=0.006). FFFH+ explained 7.7% of the variance in yearly QCT cancellous spinal bone change in these 86 premenopausal women. Thus, this prospective study in healthy premenopausal women from two cohorts shows clearly, for the first time, that having a biological relative with a fragility fracture is associated with a greater rate of human bone loss.

Reference List

1. Bouxsein ML JBMR 2005;20:1085-92.
2. Kelly JBMR 1993;11 3.
- Bainbridge K Osteo Int 2004;15:439
4. Sowers M, JBMR 1999;14:1411
5. Brot C J Int Med 1997;242:505



QCT Spine bone change by a Family History of Frailty Fracture

Disclosures: Jerilyn Prior, None.

SU0191

Heterozygous Carriers of the SOST Mutation Demonstrate Reduced Sclerostin and Increased PINP Concentrations. Antoon Van Lierop^{*1}, Herman Hamersma², Neveen Hamdy¹, Socrates Papapoulos¹. ¹Leiden University Medical Center, The Netherlands, ²Flora Clinic, Department of Ear-Nose-and_Throat, South Africa

Introduction

Homozygous null mutations of the SOST gene, encoding sclerostin, an osteocyte derived negative regulator of bone formation, lead to sclerosteosis, a rare sclerosing bone dysplasia. Heterozygous carriers of this mutation have no apparent bone phenotype, but demonstrate an increase in bone mineral density (BMD). We addressed the question whether this increase in BMD may be due to impaired sclerostin synthesis, leading to increased bone formation.

Method

We measured levels of sclerostin, PINP, and CTX in serum of 12 genetically confirmed sclerosteosis patients and 22 heterozygous carriers of the SOST mutation. Serum levels of these parameters compared between patients, carriers and 77 healthy controls.

Results

Sclerostin was undetectable in the serum of patients, but was measureable in all carriers (mean:15.5 pg/ml; 95%CI:13.7-17.2pg/ml), in whom it was significantly lower than in healthy controls (40.0pg/ml; 95%CI:36.9-42.7pg/ml; $p < 0.001$). PINP levels were highest in patients (132.5ng/ml; 95%CI:78.9-186.3ng/ml), but carriers also had significantly higher PINP levels (58.3ng/ml; 95%CI:46.8-69.8ng/ml) than controls (37.8ng/ml; 95%CI:34.9-42.0ng/ml; $p < 0.05$). Using linear regression analysis sclerostin levels were significantly correlated with those of PINP ($B = -0.41$, $p = 0.005$) in a pooled cohort of carriers and age and gender matched controls. Mean CTX levels were significantly higher in patients (0.40ng/ml; 95%CI:0.22-0.57ng/ml) than in carriers (0.13ng/ml; 95%CI:0.09-0.17), although this was no longer the case after correcting for age ($p = 0.15$). PINP levels were negatively correlated with age in patients ($r = -0.74$, $p = 0.006$), but not in carriers ($r = -0.19$, $p = 0.40$) or controls ($r = -0.07$, $p = 0.56$). Serum levels of PINP and CTX were significantly correlated in both patients ($r = 0.88$, $p < 0.001$) and carriers ($r = 0.64$, $p = 0.001$).

Conclusion

Our data show that heterozygous carriers of the SOST mutation demonstrate reduced circulating levels of sclerostin and increased levels of PINP compared to healthy controls, suggesting that the effect of sclerostin on bone formation can be titrated.

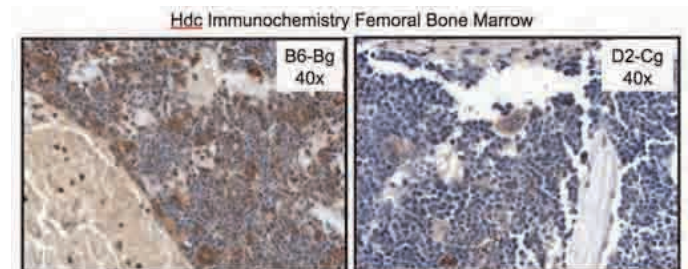
Disclosures: Antoon Van Lierop, None.

SU0192

Histidine Decarboxylase is a Candidate Gene for a Quantitative Trait Locus Affecting Peak Bone Density and Strength in Mice. Robert Klein^{*1}, Emily Larson², Wendy Wagoner², Amy Carlos², Terry Morgan². ¹Portland VA Medical Center, USA, ²Oregon Health & Science University, USA

The identification of genes underlying quantitative-trait loci (QTL) for complex diseases, such as osteoporosis, is a challenging and difficult task. We previously identified a QTL on chromosome 2 (chr 2) associated with variation in peak bone mineral density (BMD) in C57BL/6 (B6) and DBA/2 (D2) mice. Selective breeding was used to transfer the chromosomal fragment containing the chr 2 QTL interval (between 21 Mb and 152 Mb) from D2 onto a B6 genetic background (Bg). Comparison of the resulting D2 allele-bearing congenic (Cg) mouse strain with the B6 Bg strain established that the D2 genomic interval, in isolation, conferred increased

bone mass and strength. Peak whole body BMD, femoral BMD and vertebral BMD (determined by DXA in 20-wk-old mice) were 6%, 6% and 7% greater, respectively, in the Cg mice ($n = 50$) compared to the Bg mice ($n = 85$; $p < 0.01$). Consistent with the increased BMD, femoral mid-shaft failure load and stiffness (determined by 3-point bending) of the Cg mice were increased by 6% and 22%, respectively compared to the Bg mice ($p < 0.01$). A portion of the chr 2 introgressed region is homologous with a region in the human genome (15q21) that has been linked with variation in proximal femoral bone structure. Taking advantage of the synteny between human genome sequence and the murine chr 2 introgressed region, we identified histidine decarboxylase (Hdc), the rate-limiting enzyme in the biosynthesis of histamine, (residing at 15q21.2 in the human genome and at 126 Mb on chr 2 in the mouse genome) as a positional candidate gene for the observed variation in bone traits. Targeted deletion of Hdc in mice is known to increase bone formation and the expression of HDC in circulating monocytes is increased in osteoporotic women. Compared to Bg mice, bone marrow isolated from Cg mice had markedly reduced Hdc mRNA expression and Western immunoblotting and tissue immunohistochemistry confirmed reduced marrow Hdc protein expression in the Cg mice (see figure). Consistent with the differences in enzyme expression, marrow histamine levels were 81% lower in the Cg mice compared to the Bg mice ($p < 0.01$). We hypothesize that local histaminergic signaling is an important determinant of bone development in laboratory mice and that inherited variation in the activity of the enzyme responsible for histamine synthesis, HDC, may explain some proportion of the natural variation in peak bone density and strength in human populations.



HDC

Disclosures: Robert Klein, None.

SU0193

Microarray-based Copy Number Analysis Can Identify Genomic Disruptions of PHEX Causing X-linked Hypophosphatemic Rickets. Steven Mumm^{*1}, Deborah Wenkert², Margaret Huskey³, Valerie A. Wollberg², Michael P. Whyte¹. ¹Shriners Hospital for Children & Washington University School of Medicine, St. Louis, USA, ²Shriners Hospital for Children, St. Louis, USA, ³Washington University in St. Louis School of Medicine, USA

Heritable forms of hypophosphatemic rickets (HR) include X-linked dominant HR (XLH, caused by de-activating mutations in the PHEX gene), autosomal recessive HR (ARHR, caused by de-activating mutations in the DMP1 gene), and autosomal dominant HR (ADHR, caused by activating mutations in the FGF23 gene). Over the past 27 years, we have cared for 268 pediatric HR patients from throughout the United States. After excluding 12 patients with HR from McCune-Albright syndrome, epidermal nevus syndrome, tumor-induced rickets, or cystinosis, etc., there were 72 sporadic cases diagnosed clinically with XLH. We are investigating 30 of these 72 sporadic patients (those for whom DNA is available) to identify their genetic defect causing rickets. In 2009, we reported that no mutations in the DMP1 or FGF23 genes were identified among these 30 sporadic HR cases (Mumm et al, 2009 ASBMR meeting). We have now sequenced the PHEX gene in all 30 cases and identified mutations in 8 patients, and used microarray-based copy number analysis to identify apparent genomic disruptions in the PHEX gene for another 4 patients.

Genomic DNA was isolated from blood leukocytes. All 22 coding exons and adjacent mRNA splice sites of the PHEX gene were amplified by PCR and sequenced. The patients' DNA sequences were analyzed by alignment to a control sequence using VectorNTI AlignX software, and by examining DNA sequence electropherograms. For 8 patients, PHEX defects were found, including splice site and nonsense mutations, and small insertion/deletions. Genomic DNA was also subjected to microarray-based copy number analysis using Affymetrix SNP 6.0 arrays. Data analysis was performed with Partek Genomics Suite. Copy number changes, indicating genomic disruption of the PHEX gene, were found in 4 additional HR patients. One girl had a large heterozygous deletion that removed exons 13-22 and extended beyond the 3' end of the gene but did not appear to disrupt neighboring genes. Two unrelated male patients had an apparent copy number amplification of exons 13-15, and another boy had an apparent copy number amplification of exons 6-9. All of these disruptions must be confirmed using a complementary method. No copy number changes in PHEX, DMP1, or FGF23 were seen in the remaining sporadic HR patients.

After search for genetic defects in PHEX, DMP1, and FGF23, only 40% of our sporadic HR patients have PHEX mutations. For 60% of our sporadic HR patients, their underlying genetic defect remains unknown.

Disclosures: Steven Mumm, Shriners Hospital for Children, 2

SU0194

Osteoporosis Pseudoglioma Syndrome (OPPG): Severity of abnormal bone geometry varies with genotype. Sheila Ramirez¹, Mary Leonard², Rita Herskovitz², Elizabeth Streeten^{*3}. ¹University of Maryland, Endocrinology, USA, ²Children's Hospital of Philadelphia, USA, ³University of Maryland School of Medicine, USA

Introduction: OPPG is a rare autosomal recessive disorder of juvenile osteoporosis, due to reduced bone formation, and congenital blindness due to mutations in *LRP5*. We have observed fractures in OPPG after attainment of normal Z-scores by DXA after bisphosphonate (BP) treatment. We hypothesized that cortical bone geometry is abnormal in OPPG, even following longterm BP treatment and may be affected by genotype. No information is published on bone geometry in humans with OPPG. In our kindred of 12 affecteds, 2 different *LRP5* mutations have been found, both in exon 6, termed here A (W425X) and B (T409A).

Methods: We performed pQCT of the tibia on 6 patients with OPPG (Two AA homozygotes; 4 AB compound heterozygotes) and 11 unaffected first degree relatives (4 heterozygote A, 1 heterozygote B and 6 with unknown genotype). Age of OPPG affecteds was 8-22 yo (mean 14); unaffecteds 6-41 (mean 14.6). pQCT results were converted to race and sex specific Z-scores based on reference data in over 1000 healthy participants. Cortical geometry phenotypes were adjusted for tibial length. Comparisons were made for pQCT phenotypes between affecteds vs unaffecteds and between affecteds with AA vs AB genotype.

Results: Both affecteds and unaffected 1st degree relatives were shorter than reference normals, height Z -1.5+1.3 and -0.52+70 respectively. OPPG participants, compared to unaffecteds, had lower section modulus (SM) -2.4 + 0.83 vs 0.12 + 0.28, p=0.002 and lower periosteal circumference -2.45 + 0.79 vs 0.22 + 0.28, p=0.0011 but similar endosteal circumference -1.66 + 0.57 vs 0.71 + 0.25, p=0.09. Results for affecteds' Z-scores for cortical density (CD), trabecular density (TD), cortical diaphysis section modulus (SM), periosteal circumference (PC), and endosteal circumference (EC) are shown in the table below. The two AA OPPG patients had contemporaneous DXA-derived Z-scores in the hip of -1.8 and -0.6 (baseline Z-scores prior to BP -4.7, -2.9)

Conclusions: Patients with OPPG had extremely abnormal bone geometry, with low bending strength (SM), compared to unaffected relatives, attributable to low periosteal circumference. In AA genotype affecteds, pQCT identified severely low SM, more helpful clinical information than the normal DXA-derived Z-scores achieved after BP therapy. The high CD in AA patients was likely due to BP treatment. We conclude that pQCT is a useful tool to assess bone strength in OPPG in response to treatment.

	CD (Z-score)	TD (Z-score)	SM (Z-score)	PC (Z-score)	EC (Z-score)
AA (n=2)	1.84 ± 0.053	-2.03 ± 1.80	-4.96 ± 0.03	-4.88 ± 0.33	-3.03 ± 0.97
AB (n=4)	-1.43 ± 0.34	-1.52 ± 0.63	-1.15 ± 0.32	-1.23 ± 0.21	-0.6 ± 0.54
p value	0.029	0.75	0.0014	0.0006	0.082

Table 1. Geometry phenotype vs OPPG genotype

Disclosures: Elizabeth Streeten, None.

SU0195

Possible Hypophosphatasia in Personalized Medicine Research Project. Less Shrestha^{*1}, Fergus McKiernan¹, Richard Berg², Jay Fuehrer². ¹Marshfield Clinic, USA, ²Medical Bioinformatics, Marshfield Clinic Research Foundation, USA

PURPOSE: The purpose of our study was to identify subjects with possible hypophosphatasia (HPP) in the Personalized Medicine Research Project (PMRP).

BACKGROUND: PMRP is a population-based cohort of ~20,000 adult subjects recruited from among residents of a geographic region where a very high percentage of all healthcare encounters occur at Marshfield Clinic (MC). MC maintains a comprehensive, searchable electronic medical record that includes lab data since 1960, ICD-9 diagnosis codes since 1980 as well as stored DNA, plasma and serum for PMRP participants. HPP is a genetic metabolic disorder of skeletal mineralization with an estimated prevalence for severe disease of 1/100,000. We postulated that mild forms of HPP are more prevalent in an adult population than currently appreciated.

METHODS: The MC electronic medical record of all PMRP enrollees with recorded serum alkaline phosphatase (ALP) values mostly ≤ 30 IU/L (normal 40-120 IU/L) were manually searched for diagnostic terms, ICD-9 codes and laboratory values suggesting the presence of HPP. Individual radiographic reports and all available radiographs were reviewed for chondrocalcinosis and metatarsal stress fractures. Previously unrecognized HPP was considered possible when, in the judgment of the PIs, the available clinical, biochemical and radiographic evidence suggested its presence.

RESULTS: 21 subjects (14F/7M) were identified whose serum ALP was mostly ≤ 30 IU/L. Chondrocalcinosis was present in 7/21 and often characterized as extensive. 6/21 had suspected or proven acute crystalline arthritis or calcific tendinitis. 5/21 had calcaneal spurs or symptomatic foot exostoses. 4/21 had ≥ 1 metatarsal or femur shaft fracture. 2/21 had hip dysplasia. 2/3 subjects with available DXA scans had axial Z-scores ≥ +2.5. One subject each had kyphoscoliosis, mild hypermobility, clavicular

osteolysis or fibromyalgia. Onset of acute crystalline arthritis and metatarsal fractures was typically 20-40 years of age. No subject had alternate explanations for these conditions (e.g., hyperparathyroidism) or previously diagnosed HPP. At least 7 of 21 subjects in PMRP were considered likely to have previously unrecognized mild HPP.

CONCLUSION: Subjects with persistently low serum ALP appear to have significant musculoskeletal disease burden and some may have previously unrecognized HPP. Further clinical and biochemical investigation is warranted.

Disclosures: Less Shrestha, None.

SU0196

A Novel Gain-of-Function Mutation of the Calcium-Sensing Receptor Gene, *CaSR* D410E might be associated with Autosomal Dominant Hypocalcemia: A Series of Korean Hypoparathyroidism Registry Study (2). Byoungcho Choi^{*1}, Young Mi Kim², Yoon-Sok Chung³, Tae Sik Jung⁴, Chul Hoon Kim⁵, Suntaek Hong², Sihoon Lee¹. ¹Gachon University School of Medicine, South Korea, ²Gachon University of Medicine & Science, South Korea, ³Ajou University School of Medicine, South Korea, ⁴Gyeongsang National University School of Medicine, South Korea, ⁵Yonsei University College of Medicine, South Korea

Background: Autosomal dominant hypocalcemia (ADH) is a rare disorder characterized by benign hypocalcemia, inappropriately low parathyroid hormone (PTH) levels and mostly hypercalciuria. ADH can be caused by activating mutations of the calcium-sensing receptor (*CaSR*) gene located on chromosome 3q13.3-21. Calcium-sensing receptor plays a pivotal role in the regulation of calcium homeostasis and is abundantly expressed in parathyroid gland, thyroid C cell, and renal tubular system. Activation of *CaSR* by increased Ca^{2+} inhibits PTH secretion, stimulates calcitonin secretion, and promotes urinary Ca^{2+} excretion, and thereby maintains the Ca^{2+} at the normal level. Herein, we report a novel activating mutation in the *CaSR* gene in a Korean family with ADH.

Method: We identified a 55-yr-old woman with mild hypocalcemia (8.0 mg/dL) and hypercalciuria (24-hr urine Ca: 441 mg/d) caused by missense mutations of the *CaSR* gene. She showed low normal serum PTH level (10.14 pg/mL). We performed mutational analysis of the genes encoding GCMB, pre-pro-PTH, and *CaSR* using PCR-amplified genomic DNA from her family. The ability of wild-type and mutant *CaSR* to activate the MAPK signaling cascade was assessed by examining phosphorylation of ERK1/2.

Result: Direct sequencing analysis of the *CaSR* gene showed that the patient possesses a T to A transition at nucleotide 1230 resulting in a D410E missense mutation in exon 4 of the *CaSR* as well as R990G. *CaSR* R990G is already known to be one of the most frequently found SNP and is associated with gain-of-function. No mutation was detected in GCMB, Prepro-PTH. HEK293 cells were transfected with plasmids encoding wild-type, mutant A (D410E + R990G), mutant B (D410E), Mutant C (R990G) and Mutant D (P221L). Stepwise increase of the extracellular Ca^{2+} concentration from 0.5 to 5.0 mM resulted in increased phosphorylation of ERK1/2 in each mutant than wild-type indicated that D410E might be associated with ADH in this family.

Conclusion: Over 60 activating mutations in the *CaSR* gene have been identified to cause ADH so far. Here we add one more potential activating mutation that causes ADH. This could be of interest because this novel mutation occurred in the loop 3 region of the VFT domain in *CaSR* where little was known to be important in its function. Further study is undergoing to elucidate the molecular mechanisms about this novel mutation such as intracellular Ca^{2+} measurement by Fura-2.

Disclosures: Byoungcho Choi, None.

SU0197

A Novel Non-synonymous Coding Variant in the Frizzled-1 Gene is Associated with Enhanced Activation of the Canonical Wnt Signaling Pathway. Yingze Zhang^{*1}, Shibing Yu², Allison Kuipers³, Yanxia Chu¹, Cara Nestlerode¹, Joseph Zmuda³. ¹University of Pittsburgh, USA, ²University of Pittsburgh Medical Center, USA, ³University of Pittsburgh Graduate School of Public Health, USA

Frizzled-1 (FZD1) is a coreceptor for Wnt ligands. We have reported genetic associations of a novel non-synonymous SNP (c.190G>A/p.A64T) and BMD phenotypes among Afro-Caribbean men. However, the functional consequence of this FZD1 protein variant is not known. We cloned both the WT and the 64T variant of FZD1 (FZD1/64T) in expression vectors and analyzed their effects on the canonical Wnt signaling pathway using the Top-Flash system. In osteoblast-like, Saos2, cells, transient expression of both WT and FZD1/64T significantly increased the TOP-Flash luciferase activities. Addition of Wnt3A, a known Wnt ligand for FZD1, to the transfected cells dramatically enhanced the FZD1 dependent up-regulation of the TOP-Flash luciferase activity. Compared to WT, there was a 4.4 fold increase in TOP-Flash luciferase activity for FZD1/64T, while there was only a 1.2 fold increase in luciferase activity for the FOP-Flash plasmid. We further confirmed the FZD1 dependent up-regulation of the TOP-Flash luciferase activity in both HEK293 and cos7 cells, which are commonly used for studying gene regulation by transient expression. Compared to WT, there was a 4.9 and 2.0 fold increase in TOP-Flash

luciferase activity for FZD1/64T in cos7 and HEK293 cells, respectively. There were minimal effects detected for the luciferase activity with FOP-Flash plasmid in all cell lines for both of the WT and FZD1/64T plasmids. Our study suggests that A64T variation may lead to a more active protein associated with increased canonical Wnt signaling. This may be one of the molecular mechanisms of the genetic associations between the FZD1 c.190G>A/p.A64T variant and BMD observed in Afro-Caribbean men. Additional studies elucidating the molecular basis of the FZD1/64T variant mediated up-regulation of FZD1 function are underway.

Disclosures: Yingze Zhang, None.

SU0198

A Variant Near RUNX2 Is Associated with BMD and Cartilage Thickness. Martha Castano-Betancourt^{*1}, Karol Estrada¹, Hanneke Kerkhof², Albert Hofman³, Andre Uitterlinden⁴, Fernando Rivadeneira¹, Joyce Van Meurs⁵, GEFOS Consortium². ¹Erasmus University Medical Center, The Netherlands, ²Internal Medicine, Erasmus MC, Netherlands, ³Department of Epidemiology, Erasmus MC, Netherlands, ⁴Rm Ee 575, Genetic Laboratory, The Netherlands, ⁵Erasmus Medical Center, The Netherlands

Background. Osteoarthritis (OA), one of the most common locomotor disorders, is characterized by osteophyte formation and cartilage degradation, which is radiographically visualized as a reduction in the joint space width. OA has been associated with a systemically higher BMD. Recently, a meta-analysis of femoral neck (FN-) and lumbar spine (LS-) BMD within the GEFOS consortium identified 82 loci associated with BMD at suggestive or genome-wide significant (GWS) level. Aim. To determine whether the 82 BMD loci are associated with minimal joint space width (MJS), as a proxy for cartilage thickness.

Methods. This study is part of the Rotterdam study (RS); a large prospective population based cohort study of diseases in the elderly. We examined 4643 men and women of RSI and 1750 participants of RSII for replication, with radiographic measurements of minimal joint space width (Xray), anthropometry, FN- and LS-BMD (DXA) and GWAS data. Association of SNPs with MJS was tested in linear regression models adjusted for age and gender and as a secondary analysis additionally adjusting for height and BMD. Associations were significant at $P < 6.1E-04$ (Bonferroni correction).

Results. A SNP at chromosome 6p21.1 (minor allele frequency=0.42) mapping near RUNX2 was associated with MJS (beta minor allele: -0.067, se: 0.016, p: 4.93E-05). This association was significant in both men and women ($p=0.003$ and $p=0.001$). After correction for height and BMD the beta slightly decreased and the association remained significant (beta: -0.061, se: 0.015, p: 7.6 E-05). The association was also seen in subjects without OA ($p: 1.09E-04$), suggesting it is arising from cartilage thickness rather than cartilage degradation. The minor allele from this SNP was found associated with decreased BMD in the GEFOS consortium at GWS level. Another SNP, located 450 KB downstream and on moderate LD, was previously found associated with height within a large meta-analysis, indicating a pleiotropic role of this locus in skeletal cell differentiation.

Conclusions. We identified a SNP near RUNX2 associated with cartilage thickness. RUNX2 is an important transcription factor in skeletal system playing a major role in the development, growth and maturation of bone and cartilage. Further, this SNP and correlated variants have also been associated with BMD and height. These findings make RUNX2 a strong candidate for underlying the pleiotropic associations found in different skeletal traits.

Disclosures: Martha Castano-Betancourt, None.

SU0199

Genetic Control of Ca Absorption and BMC Differs Dependent on Dietary Calcium (Ca). Rebecca Replegle^{*1}, Libo Wang², Min Zhang², James Fleet¹. ¹Purdue University, USA, ²Purdue University Dept. of Statistics, USA

Genetic variation has been shown to influence bone phenotypes in mice and humans. However, it is unclear whether the penetrance of these genetic effects is influenced by low Ca stress or whether new variants affecting bone or Ca metabolism can be revealed under these conditions. We conducted a study to identify genetic loci controlling Ca/bone phenotypes in the BXD recombinant inbred mouse panel under normal and low dietary Ca conditions. Male mice from 51 BXD lines were placed on modified AIN93G diets containing 200 IU vitamin D and either 0.5% or 0.25% Ca at 4 wks of age ($n=8$ /line/diet). At 12 weeks of age Ca absorption (Ca Abs) was measured by Ca^{45} appearance in the blood 10 min after oral gavage, mice were then sacrificed and tissues collected. Bone mineral content (BMC) was assessed using DXA. Multiple linear regression identified significant covariates influencing BMC (femur length and body weight), and Ca Abs (femur length). Residuals were used for all further analyses. Linkage mapping was conducted using a Bayesian QTL method, loci with a Bayes factor >6 were considered significant. Narrow-sense heritability for Ca Abs was 0.37 and 0.56, and for BMC was 0.41 and 0.49 in mice fed the 0.5% and 0.25% Ca diets, respectively. Seven QTL affecting Ca Abs were identified in the 0.25% Ca group on ch 1, 2, 4, 5 (2), 7, 9 while 2 QTL were identified in the 0.5% Ca group on ch 4 and 8. Ca Abs was strongly correlated between the two Ca diets ($r=0.71$, $p<0.0001$) but only the ch 4 QTL was common across diet groups. With the exception of PTH near the ch 7 QTL and calbindin D9k near the ch 8 QTL, no Ca

homeostasis-regulating genes were found around these QTL suggesting the potential for novel gene discovery affecting Ca Abs. Six QTL affecting BMC were identified in the 0.25% Ca group on ch 5, 7, 11, 15 (2), 20 and 5 were identified in the 0.5% group on ch 2, 6, 9, 15, 20. BMC was correlated between the Ca diet groups ($r=0.81$, $p<0.0001$) but only two shared QTL were identified, on ch 15 and 20. The ch 15 locus is within 10cM of candidate genes VDR and Wnt10b but the ch 20 locus has not been identified previously. Our results indicate that baseline Ca-related phenotypes are influenced by genetics and that dietary Ca restriction reveals new QTL controlling these traits.

Disclosures: Rebecca Replegle, None.

SU0200

Casein Kinase II Activates Bone Morphogenetic Protein Receptor Type Ia in the Absence of Bone Morphogenetic Protein 2 Driving Osteoblast Differentiation. Beth Bragdon^{*1}, Oleksandra Moseychuk², Lauren Gurski², Hemanth Akkiraju², Jeremy Bonor², Anja Nohe². ¹University of Maine University of Delaware, USA, ²University of Delaware, USA

Bone Morphogenetic Protein 2 (BMP2) is a growth factor that is crucial for the proliferation and differentiation of osteoblasts. The absence of BMP2 can lead to the inability to heal spontaneous bone fractures in mice. Although BMP2 signaling is highly regulated we recently identified Casein Kinase II, CK2, to interact and regulate downstream BMP2 signaling. Three blocking peptides were developed to block the interaction between BMPRIa and CK2 which all led to increased BMP2 signaling and osteoblast differentiation in the absence of BMP2 with the cell line C2C12. In this study we were able to verify the specificity of the three blocking peptides by creating three different single point mutations of BMPRIa disrupting the each CK2 phosphorylation site. These mutants when overexpressed increased osteoblast differentiation and expression was determined by confocal microscopy. One mutant did show increased mineralization compared to the others, suggesting the role of one phosphorylation site is increased. Further the knockdown of BMPRIa eliminated all three blocking peptide effects on signaling. These results indicate the blocking peptides specifically inhibit the regulation by CK2 and allow for the activation of downstream signaling events leading to osteoblast differentiation without BMP2. The blocking peptide that correlated with the mutant with the increased mineralization was used for subcutaneous injections over mice calvaria. The blocking peptide injection led to increased bone area and bone mineral apposition rate. These results suggest osteoblast differentiation can be initiated through the BMP2 mechanism although BMP2 is absence.

Disclosures: Beth Bragdon, None.

SU0201

Wnt3a Stimulates Bmp2 Expression in Osteogenic Cells that Are Epigenetically Ready. Young-Dan Cho^{*}, Woo-Jin Kim, Won-Joon Yoon, Kyung Mi Woo, Jeong-Hwa Baek, Hyun-Mo Ryoo. Seoul National University, School of Dentistry, South Korea

Background: Wnt and Bmp are two of the most important extracellular signals that control osteoblast differentiation and bone mineralization. While there are many reports indicating the signal cross-talks between Wnt and Bmp downstream molecules, no direct evidence has been demonstrated that Wnt regulates Bmp expression or vice versa. Specific aim of this study was illuminating a possible cross-regulation between the two strongest osteogenic signals. Results: We found that a canonical Wnt pathway activator, Wnt3a, strongly stimulated *Bmp2* mRNA expression while Bmp2 could not stimulate *Wnt3a*. Overexpression or knockdown of canonical Wnt downstream molecules, β -catenin and Lef1, clearly indicated that they are positive regulators of *Bmp2* mRNA expression. In order to clarify a direct regulatory relationship, mouse *Bmp2* proximal promoter was analyzed. There are two strong Lef1 response elements and both are contributed Wnt3a-induced *Bmp2* transcription. The analysis of conditioned media of Wnt3a treated cells showed that Bmp2 protein level was highly increased so that the conditioned media treatment is good enough to stimulate Smad1/5/8 phosphorylation and Alp activation. Dkk1, a Wnt inhibitor, or noggin, a Bmp inhibitor, suppressed Alp staining or Alp mRNA level indicating both Wnt and Bmp signals are contributed to Alp expression and staining. Next question was addressed whether *Bmp2* induction by Wnt3a is a general phenomenon to all type of cells or is specific for osteogenic cells. *Bmp2* mRNA expression was increased 8 to 20 folds by Wnt3a treatment in cells having osteogenic potential such as MC3T3-E1, C2H10T1/2, ST2 and C2C12. Meanwhile, in cells having very low osteogenic potentials, 3T3-L1 or NIH3T3, *Bmp2* expression was not increased by Wnt3a. Other osteogenic marker genes, including *Alp*, expression showed similar pattern in the osteogenic and low osteogenic cell groups. We suspected that the difference came from their differences in epigenetic states because *Bmp2* or *Alp* mRNA level was increased by Wnt3a after trichostatin-A, a strong HDAC inhibitor. The analysis of acetylation and methylation state of histones in the promoter of Bmp2 and bone marker genes indicated that they are epigenetically not ready for expression. Conclusion: Wnt3a stimulated osteoblast differentiation directly through the canonical Wnt signaling and indirectly through Bmp2 induction in osteogenic cells. Meanwhile epigenetic modification would be required in nonosteogenic cells.

Disclosures: Young-Dan Cho, None.

SU0202

Expression of Subtilisin-like Proprotein Convertases (PCSKs) in FGF23 Producing Extravillous Trophoblast of Human Placenta. Masanori Takaiwa^{*1}, Koji Kadoya², Kosei Hasegawa³, Kunihiko Aya³, Hiroyuki Tanaka⁴, Tsuneo Morishima³, Motofumi Yokoyama⁵, Youichi Kondo¹, Nobuyuki Kodani¹. ¹Dept. of Pediatrics, Matsuyama Red Cross Hosp., Japan, ²Dept. of Pathology, Matsuyama Red Cross Hosp., Japan, ³Dept. of Pediatrics, Okayama University Graduate School of Medicine, Dentistry & Pharmaceutical Sciences, Japan, ⁴Okayama Saiseikai General Hospital, Japan, ⁵Dept. of Obstetrics & Gynecology, Matsuyama Red Cross Hosp., Japan

We have previously reported that circulating fibroblast growth factor 23 (FGF23) is predominantly inactivated in the human infant at birth. This observation suggested that a subtilisin-like proprotein convertases (PCSKs) dependent proteolysis plays crucial role in the physiological regulation of FGF23 activity during the perinatal period. We also demonstrated that FGF23 is expressed in the human placenta. As previously reported in a study regarding abundant FGF23 expression in non-calcified organs of rodent fetus, our observations reinforced that the inactivated FGF23 is substantially secreted from non-calcified organs including placenta in human fetus and neonates. Thus, it might be useful to study human placenta in order to seek an unidentified specific PCSK for the FGF23 inactivation in the physiological condition. In this study we analyzed mRNA and protein expressions of six PCSKs (PCSK1, PCSK2, FUR, PCSK4, PCSK5 and PACE4) in human placentas using RT-PCR, Western blot analysis and immuno-histochemical studies.

RT-PCR and Western blot analysis revealed that FGF23 and GALNT3 transcript and proteins are detectable in the samples prepared from whole human placentas. We also confirmed that expressions of PCSK1, PCSK4 and PCSK6 are abundant and those of FUR and PCSK5 are detectable at lower levels. In order to estimate the possible linkage between these PCSKs and FGF23 degradation in the placenta, we performed immuno-histochemical studies on paraffin embedded human placentas. As we previously demonstrated, positive staining of FGF23 was mainly localized in clusters of extravillous trophoblast of the Langerhans' fibrinoid layer that migrated in the chorionic plate of placenta. A specific antibody against PCSK1, but not those for PCSK4 and PCSK5 probed the clusters of extravillous trophoblast. Additionally, weaker positive staining for FUR and PCSK5 were observed in the chorionic plate of the placenta, resembling the distribution of the FGF23 positive trophoblasts. Thus, although further study is required, it will be useful to investigate whether PCSK1 is playing a crucial role in the enhanced FGF23 degradation specifically observed in the human newborns.

Disclosures: Masanori Takaiwa, None.

SU0203

Osteostatin Improves the Osteogenic Capacity of Fibroblast Growth Factor-2 Coated onto Si-Doped Hydroxyapatite in Osteoblastic Cells. Daniel Lozano^{*1}, MJ Feito², Sergio Portal-Nunez¹, RM Lozano³, MC Serrano⁴, M Vallet-Regu⁵, MT Portoles⁶, Pedro Esbrit⁷. ¹Instituto de Investigacion Sanitaria-Fundacion Jimenez DUaz, Spain, ²Dpto. de Bioquímica y Biología Molecular I, UCM, Spain, ³Centro de Investigaciones Biológicas, CSIC, Spain, ⁴Instituto de Ciencia de Materiales, CSIC, Spain, ⁵Departamento de Química Inorgánica y Bioinorgánica, UCM, Spain, ⁶Departamento de Bioquímica y Biología Molecular I, UCM, Spain, ⁷FUNDACION JIMENEZ DIAZ, Spain

Si-doped hydroxyapatites (Si-HA) have been proposed as matrices for the controlled release of biological agents to improve bone repair following skeletal injuries, namely fractures. Fibroblast growth factor (FGF)-1 and -2 are known modulators of osteoblastic proliferation and differentiation, as well as inducers of angiogenesis, an important process during bone repair. Recently, we demonstrated that these growth factors immobilized on powdered Si-HA and their scaffolds improve osteoblast adhesion and proliferation. In addition, we showed that parathyroid hormone-related protein (PTHrP) (107-111) (named osteostatin, OST) induces osteogenic features by directly acting on osteoblastic cell cultures and in vivo in rabbits. We aimed to evaluate and compare the efficacy of FGF-2 immobilized on powdered Si-HA, alone or combined with exogenous OST (100 nM), to affect osteoblastic growth and function. Osteoblastic MC3T3-E1 cells were grown in differentiation medium (α -MEM with 50 μ g/ml ascorbic acid, 10 mM β -glycerolphosphate and 10% FBS), with the tested materials for 4-12 days. Cell proliferation and viability (assessed by optical microscopy and flow cytometry), Ca^{2+} transients (by flow cytometry), mineralization (alizarin red), and gene expression analysis (by real-time PCR) were determined. Secreted vascular endothelial growth factor (VEGF) by MC3T3-E1 cells was determined by evaluating the proliferation of pig endothelial-like cells derived from endothelial progenitor cells (EPCs) induced by MC3T3-E1 conditioned-medium in the presence or absence of a VEGF neutralizing antibody. FGF-Si-HA, with or without soluble OST, similarly increased (50%) MC3T3-E1 cell proliferation. However, gene expression of both Runx2 and osteocalcin increased with FGF-Si-HA but was significantly higher (50%) in the presence of OST. VEGF (gene expression and secretion) and VEGF receptors 1 and 2 also increased (up to 2-fold) by OST. Similarly, the matrix mineralization capacity of this material was significantly

improved by the latter peptide. As an initial characterization of the underlying mechanism of the observed effects of OST, we found that this peptide induced a synergistic Ca^{2+} transient in MC3T3-E1 cells. In conclusion, these in vitro findings indicate that OST can improve the osteogenic efficacy of FGF-Si-HA biomaterial in osteoblastic cells. This supports the usefulness of these type of biomaterials for bone tissue repair.

Disclosures: Daniel Lozano, None.

SU0204

A Reappraisal of the Skeletal Phenotype of Leptin Signaling-Deficient Mice: Implications for the Physiological Role of Leptin as a Regulator of Bone Metabolism. Russell Turner^{*1}, Kenneth Philbrick¹, Satya P. Kalra², Urszula Iwaniec¹. ¹Oregon State University, USA, ²University of Florida McKnight Brain Institute, USA

The cellular basis for the skeletal phenotype of leptin signaling-deficient mice forms a cornerstone for the traditional model of neuronal regulation of bone metabolism. Leptin, by acting through a hypothalamic relay, is proposed to negatively regulate bone mass by suppressing bone formation. However, this antiosteogenic model of leptin action is not supported by long duration gene therapy studies which showed no detrimental effect of increased hypothalamic leptin levels on bone metabolism. We therefore sought to clarify the physiological actions of leptin on the skeleton by reevaluating the cellular mechanisms underlying changes in bone architecture in femur and vertebra of leptin receptor-deficient db/db, leptin-deficient ob/ob, and ob/ob mice treated with leptin. Decreases in bone growth, osteoblast perimeter and bone formation rate (please see table for representative data in db/db mice) were observed in leptin signaling-deficient mice. Also, indices of bone growth and turnover were greatly increased in ob/ob mice following short duration (3 weeks) sc administration of leptin or long-duration (15 weeks) hypothalamic leptin gene therapy. In spite of normal or increased osteoclast-lined bone perimeter, leptin signaling-deficient mice exhibited a mild but generalized osteopetrotic-like (calcified cartilage encased by bone) skeletal phenotype. Thus, impaired bone resorption rather than increased bone formation, as originally reported, is responsible for site-specific increases in bone volume of ob/ob and db/db mice. In summary, these data do not support the hypothesis that leptin reduces bone mass by inhibiting bone formation. Instead, they show that in the absence of leptin signaling bone fails to mature normally. We conclude that leptin, by enhancing bone growth, bone formation and bone turnover, plays an important physiological role in skeletal maturation.

Bone formation rate/bone perimeter ($\mu\text{m}^2/\mu\text{m}/\text{d}$) in 17-week-old female WT (C57/BL6) and db/db mice.

	WT	db/db
Femur diaphysis (endocortical bone)	468 \pm 128	93 \pm 85*
Femur metaphysis (cancellous bone)	209 \pm 31	65 \pm 21*
Femur epiphysis (cancellous bone)	92 \pm 19	28 \pm 11*
Lumbar vertebra (cancellous bone)	123 \pm 24	46 \pm 20*

Data are means \pm SE; *P < 0.05

Disclosures: Russell Turner, None.

SU0205

Acerogenins, a Natural Compound Isolated from *Acer nikoense* Maxim, Stimulates Osteoblast Differentiation through Bone Morphogenetic Protein Action. Ji-Won Lee^{*1}, Takayuki Yonezawa², Tasuku Kihara¹, Hiroyuki Akazawa³, Toshihiro Akihisa³, Akira Yamaguchi⁴, Je-Tae Woo⁵. ¹Section of Oral Pathology, Graduate School of Medical & Dental Sciences, Tokyo Medical & Dental University, Japan, ²The University of Tokyo, Japan, ³College of Science & Technology, Nihon University, Japan, ⁴Tokyo Medical & Dental University, Japan, ⁵Research Institute for Biological Functions, Chubu University, Japan

In the present study, we investigated the effects of eight compounds, which had been isolated from the stem barks of *Acer nikoense* Maxim, on osteoblastogenesis. Osteogenic activity of six diarylheptanoids, (1)acerogenin A, (2)(R)-acerogenin B, (3) aceroside I, (4)aceroside B1, (5)aceroside III and (6)(?)-centrolol and two phenolic compounds; (7)(+)-rhododendrol and (8)(+)-catechin was evaluated by measuring alkaline phosphatase (ALP) activity as a marker for early osteoblast differentiation. We found that the diphenyl ether-type cyclic diarylheptanoids [(1)-(5)] promoted ALP activity in MC3T3-E1 osteoblastic cells without affecting cell proliferation, but linear-type diarylheptanoids (6) and phenolic compounds (7) and (8) did not. Diphenyl ether-type cyclic diarypheptanoids (1)-(4) also increased protein production of osteocalcin, a late stage marker for osteoblast differentiation, and induced osteoblastic mineralization. Structure-activity relationships of these compounds demonstrated that the stimulatory efficacy of aglycones was higher than that of its glycosides. Among these compounds, acerogenin A stimulated the cell proliferation of RD-C6 osteoblastic cells (Runx2-deficient cell line) as well as MC3T3-E1 cells. It also increased ALP activity in MC3T3-E1 and RD-C6 cells and calvarial osteoblastic cells isolated from the newborn mice. Acerogenin A increased the expression of mRNAs

related to osteoblast differentiation, including Osteocalcin, Osterix and Runx2 in MC3T3-E1 cells and primary osteoblasts: it also stimulated Osteocalcin and Osterix mRNA expression in RD-C6 cells. The acrogenin A treatment for 3 days increased *Bmp-2*, *Bmp-4*, and *Bmp-7* mRNA expression levels in MC3T3-E1 cells. Adding noggin, a BMP specific-antagonist, inhibited the acrogenin A-induced increase in *osteocalcin*, *Osterix* and *Runx2* mRNA expression levels. These results indicated that acrogenin A stimulates osteoblast differentiation through BMP action, which is mediated by Runx2-dependent and Runx2-independent pathways.

Disclosures: Ji-Won Lee, None.

SU0206

Divergent Effects of Partial (*obl/+*) and Complete (*ob/ob*) Loss of Leptin Production on Cortical Bone. Kenneth Philbrick*, Russell Turner, Ursula Iwaniec. Oregon State University, USA

Morbidly obese leptin-deficient *ob/ob* mice cannot produce the adipokine leptin and develop a skeletal phenotype where, depending upon site and age, bone mass can be normal, increased, or decreased. Compared to wild type (WT) mice, heterozygous *obl/+* mice are heavier but produce leptin. We therefore evaluated bone metabolism in *obl/+* mice to determine whether reduced leptin production by adipocytes maintains a normal skeletal phenotype. This was accomplished by examining femora and lumbar vertebrae (LV5) in 7-week-old WT, *obl/+*, and *ob/ob* mice using DXA, μ CT, and histomorphometry. Selected results are summarized in the Table below. Body mass and abdominal white adipose tissue (WAT) mass were greater in the *obl/+* mice than in WT mice but lower than in *ob/ob* mice. Significant differences in serum leptin were not detected between *obl/+* and WT mice, suggesting that *obl/+* mice compensate for reduced leptin production by individual adipocytes by an increase in adipose tissue mass. Total femur length and bone mineral content (BMC) were greater in *obl/+* mice than in WT mice. In marked contrast to the low cortical bone mass observed in *ob/ob* mice, *obl/+* mice have higher than normal cortical bone mass. Cancellous bone volume adjusted for tissue volume (BV/TV) in distal femur metaphysis and vertebral body did not differ between *obl/+* and WT mice. Similarly (data not shown), significant difference in femoral and vertebral cancellous bone formation rates were not detected between *obl/+* and WT mice. Bone marrow adiposity (adipocyte area/tissue area, Ad.Ar/T.Ar), which is dramatically higher in distal femur metaphysis of leptin-deficient *ob/ob* mice, did not differ between *obl/+* and WT mice. In summary, *obl/+* mice have increased femoral length and cortical bone mass but normal cancellous bone mass and turnover. These findings suggest that increased body mass enhances the growth promoting effects of leptin on the mouse skeleton.

Endpoint	WT	<i>obl/+</i>	<i>ob/ob</i>	ANOVA (P <)*
Body Mass (g)	16.0 \pm 0.3	20.3 \pm 0.5 ^a	36.2 \pm 2.0 ^{a,b}	< 0.001
WAT Mass (mg)	370 \pm 20	640 \pm 60 ^a	3758 \pm 254 ^{a,b}	< 0.001
Serum Leptin (ng/ml)	6.7 \pm 0.5	4.9 \pm 0.4	ND ^{ab}	< 0.001
Femur Length (mm)	14.0 \pm 0.1	14.4 \pm 0.1 ^a	13.4 \pm 0.2 ^{a,b}	< 0.001
Femur BMC (mg)	13.8 \pm 0.3	16.3 \pm 0.5 ^a	11.5 \pm 0.7 ^{a,b}	< 0.001
Femur Metaphysis BV/TV (%)	12.5 \pm 0.9	10.3 \pm 0.7	8.4 \pm 1.0 ^a	0.017
Femur Metaphysis Ad.Ar/T.Ar (%)	1.3 \pm 0.2	0.8 \pm 0.5	9.0 \pm 1.5 ^{a,b}	<0.001
LV5 BV/TV (%)	15.1 \pm 0.4	15.2 \pm 0.8	18.2 \pm 0.7 ^{a,b}	0.010

Data are mean \pm SE; *An ANOVA followed by a Bonferroni post-hoc test was used to evaluate differences among groups. If ANOVA assumptions of homogeneity of variance were not met, a Kruskal-Wallis followed by a Tamhane post hoc test was used. ^aDifferent from WT, P<0.05; ^bDifferent from *obl/+*, P<0.05; ND, Not Detected.

Table

Disclosures: Kenneth Philbrick, None.

SU0207

Immune Cell Populations, Severely Compromised Following Long Term High Fat Diet, Are Partially Restored by Low Intensity Mechanical Signals. Ete Meilin Chan*, Benjamin Adler¹, Danielle Green¹, Ada H. Tsoi¹, Mario E. Botros¹, Clinton Rubin². ¹STONY BROOK UNIVERSITY, USA, ²State University of New York at Stony Brook, USA

Immune system dysfunction resulting from obesity, as reflected by a marked decrease in immune cell populations, precipitates a susceptibility to life-threatening diseases including osteoporosis. We examined here whether obesity damages the bone marrow niche where progenitors critical to bone remodeling and immunity originate. With evidence that low intensity vibration (LIV) can bias mesenchymal stem cell differentiation towards osteoblastogenesis, we further hypothesized that these mechanical signals would modulate other bone marrow cells types and, more specifically, help restore that population of immune cells placed at risk by a long-term high fat diet. Twenty male C57BL/6J mice, age 2 mo., were randomly assigned into four groups (n=5): regular diet (RD); RD+LIV; high fat diet (HFD); and HFD+LIV. Obesity was then established in each HFD groups using a high fat diet (45% kcal from fat). At 5 months of age, the RD+LIV and HFD+LIV were subjected to four months

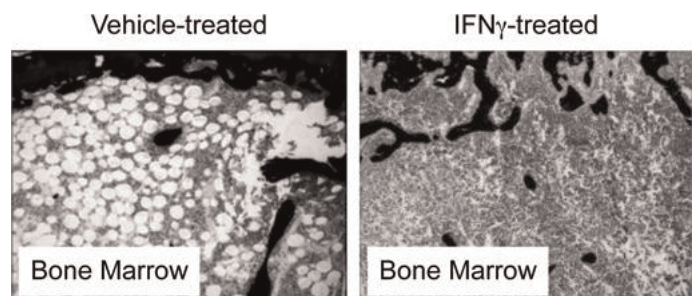
of LIV (0.2g, 90Hz, 15m/d, 5d/w), while RD and HFD were treated as sham controls. As compared to RD, 7-month HFD induced 41% higher body weight and 5-fold higher insulin resistance (p<0.01), representing a severely obese phenotype. B & T cells in blood and bone marrow were analyzed using FACS, and visceral adipose tissue volume (VAT) was measured by μ CT. VAT in HFD was significantly higher than both RD groups (+69.3%, p<0.01), while HFD+LIV was not different from RD (+44.5%, p=0.26). Circulating B cells in HFD were significantly lower than RD groups (-36%, p=0.01), while the HF+LIV circulating B cell population was higher than HFD (+57%, p=0.02), maintaining B cells to the level measured in RD (p=0.97). Although a HFD impact on circulating T cell and bone marrow T & B cells was not evident compared to RD (p=0.07, 0.36 & 0.11), both circulating (r=-0.52, p=0.04) and bone marrow B cells (r=-0.73, p=0.01) had a significant negative correlation with VAT. Also, circulating T cells (r=-0.61, p=0.01), but not bone marrow T cells (r=0.03, p=0.94), were negatively correlated with the VAT. An increasing adipose burden is associated with the decline of immune cells critical for immune surveillance and response. It is known that exercise is considered beneficial to the control of obesity and enhancing the immune system. In this study, LIV facilitated the recovery of the B-cell population, even in the face of obesity, potentially through modulating hematopoietic progenitors originated from the bone marrow.

Disclosures: Ete Meilin Chan, None.

SU0208

Interferon γ Inhibits Bone Marrow Adipogenesis. Sandra Bermeo-Serrato*, Christopher Vidal², Lee Wei Li³, Dao Chao Huang⁴, Richard Kremer⁵, Gustavo Duque⁶. ¹PhD Student, Australia, ²University of Sydney, Australia, ³University of Sydney, Nepean Clinical School, Australia, ⁴McGill University Royal Victoria Hospital, Canada, ⁵McGill University, Royal Victoria Hospital, Canada, ⁶Ageing Bone Research Program, University of Sydney, Australia

Interferon gamma (IFN γ) has been recently identified as to induce osteoblastogenesis *in vitro* and bone formation *in vivo*. Since this anabolic effect could be exerted by inducing osteoblast differentiation of mesenchymal stem cells (MSC) at the expense of adipogenesis, in this study we aimed to assess whether IFN γ has and anti-adipogenic effect both *in vitro* and *in vivo*. Human MSC were induced to differentiate into adipocytes for two weeks in the presence or absence of IFN γ (1, 10 and 100 ng/ml) in the media. Adipocyte differentiation was assessed by morphologic and enzymatic analysis and by quantification of protein expression and mRNA of adipogenic markers. Oil red O, was used to quantitate the extent of lipid accumulation within the MSC. By this morphologic criteria, IFN γ inhibited adipogenesis at a concentration of 100 ng/ml (p<0.001), the same dose that has been reported as strongly osteogenic *in vitro* (Duque et al, Stem Cells, 2009). This correlated with decreased levels of adipocyte specific enzymes and significantly lower expression of protein and mRNAs for PPAR γ and CEBP α (p<0.01), two major adipogenic factors. For our *in vivo* experiments, 8 week-old ovariectomized C57BL/6 mice were treated with osteogenic doses of IFN γ (2,000 and 10,000 IU, IP, 3 times a week for 6 weeks). After von Kossa staining of distal femur (Figure), treated mice showed significantly lower levels of fat volume/total volume (p<0.01), adipocyte number (p<0.01) and adipocyte diameter (p<0.01) as compared with the placebo treated mice. Together, these findings demonstrate that IFN acts as adipogenic antagonist supporting the hypothesis that the anabolic effect of IFN γ on bone involves the reciprocal regulation of adipogenesis and osteogenesis in the bone marrow microenvironment.



interferon and marrow fat

Disclosures: Sandra Bermeo-Serrato, None.

SU0209

Lipoteichoic Acid from *Enterococcus faecalis* Induces Chemokine Expression in Murine Macrophages via Toll-like Receptor 2/CD14/MyD88 Signaling Pathways. Ok-Jin Park^{*1}, Ji Young Han², Jung Eun Baik², Seulgie Choi², Jun Ho Jeon³, Cheol-Heui Yun³, Hong-Hee Kim⁴, Seung Hyun Han¹.

¹School of Dentistry, Seoul National University, South Korea,

²Department of Oral Microbiology & Immunology, DRI, & BK21 Program, School of Dentistry, Seoul National University, South Korea,

³Department of Agricultural Biotechnology & Research Institute for Agriculture & Life Sciences, Seoul National University, South Korea,

⁴Seoul National University, South Korea

Enterococcus faecalis is closely associated with refractory apical periodontitis often causing apical bone loss and its lipoteichoic acid (LTA) is considered as one of the major cell-wall virulence factor because of the inflammatory activity. It has been shown that chemokines facilitate differentiation of osteoclasts. In the present study, we purified LTA from *E. faecalis* and investigated the effect of LTA on the expression of chemokines in murine macrophages and used as an osteoclast precursor cell model. LTA from *E. faecalis* stimulated the expression of chemokines such as interferon- γ -inducible protein 10 (IP-10), macrophage inflammatory protein 1 α (MIP-1 α), and monocyte chemoattractant protein 1 (MCP-1) at both protein and mRNA levels. Toll-like receptor 2 (TLR2), CD14, and MyD88 appear to be essential for the expression of chemokines since such induction was not observed in the macrophages deficient in TLR2, CD14, or MyD88. Western blot analysis demonstrated that the LTA induced phosphorylation of MAP kinases including p38 kinase, JNK, and ERK. In addition, the LTA enhanced the DNA-binding activities of transcription factors, NF- κ B, AP-1, and NF-IL6, all of which are known to regulate the expression of chemokines. Further study using inhibitors demonstrated that the induction of IP-10 required ERK, JNK, p38 kinases, protein tyrosine kinases, phosphoinositide 3-kinases, and reactive oxygen species (ROS). However, interestingly, p38 kinases and ROS were not necessary for the induction of MCP-1 and MIP-1 α expressions while the other signaling molecules were required. These results suggest that *E. faecalis* LTA induces the expression of chemokines IP-10, MCP-1, and MIP-1 α , all of which require TLR2/CD14/MyD88, but through different signaling pathways in murine macrophages.

Disclosures: Ok-Jin Park, None.

SU0210

Nalp3 Inflammasome Activation Mediates Peri-implant Osteolysis. Ed Purdue^{*}, Nikolaus Binder, Krista Bohnert, Bryan Nestor, Thomas Sculco, F. Patrick Ross, Steven Goldring. Hospital for Special Surgery, USA

Aseptic loosening related to peri-implant osteolysis is the major cause of implant failure after total joint replacement surgery. The osteolytic process has been attributed to the release of implant particulate wear debris, inducing a granulomatous inflammatory reaction. Pro-inflammatory cytokines have been implicated as important mediators of particle-mediated inflammatory bone loss and, more recently, inflammasome and caspase-1 mediated processing and release of interleukin 1 beta (IL1 β) have been shown to be a significant component of myeloid cell responses to particulate danger signals such as those presented by orthopedic wear. Based on these observations we hypothesized that inflammasome signaling would contribute to osteolysis induced by particles of polymethylmethacrylate (PMMA) and ultra high molecular weight polyethylene (UHMWPE). Consistent with inflammasome signaling, LPS primed human peripheral blood monocytes and mouse bone marrow derived macrophages released IL1 β protein only after challenge with wear particles. This effect was dependent upon particle phagocytosis and caspase activity. Furthermore, macrophages deficient in components of the Nalp3 inflammasome (Nalp3, ASC, caspase-1) were defective in particle induced release of IL1 β , but unimpaired in production of TNF α and IL-6, neither of which requires activation of the inflammasome for their release. The pro-inflammatory effects of wear particles on IL1 β release from LPS primed cells were counterbalanced by repression of LPS induced expression of IL1 β mRNA by particle phagocytosis. This provides a possible mechanism for limiting inflammasome responses to particle phagocytosis. Macrophages lacking Nalp3, ASC or caspase-1 showed no defects in RANKL-induced osteoclastogenesis *in vitro*. In contrast, caspase-1 deficient mice were partially protected from orthopedic wear particle induced calvarial osteolysis. Our results provide evidence that the inflammasome pathway is activated in myeloid cells in response to orthopedic wear particles, resulting in caspase-1 dependent production of the pro-inflammatory cytokine IL1 β . Marked attenuation of osteolysis in caspase-1 deficient mice provides direct evidence *in vivo* implicating the inflammasome pathway in particle-mediated osteolysis. Inflammasome activation in response to orthopedic wear is also seen in human monocytes, providing evidence that this pathway represents a relevant therapeutic target in patients with periprosthetic osteolysis.

Disclosures: Ed Purdue, None.

SU0211

Platelet-derived Growth Factors (PDGFs) Functions in Tooth Development. YU SUGAWARA^{*}, Tsutomu Iwamoto, Masaharu Futagi, Mariko Ono, Aya Yamada, Takashi Nakamura, Satoshi Fukumoto. Tohoku University Graduate School of Dentistry, Japan

Tooth is a specific hard tissue, because the developmental process is well-regulated by reciprocal epithelial-mesenchymal interactions that are mediated by effective growth factor series. Platelet-derived growth factors (PDGFs) play crucial roles in organogenesis including tooth. Previously, we have reported that PDGFs regulates tooth size and shape during embryogenesis. However, the mechanisms of PDGFs during tooth development have not been clearly elucidated. Here, we focused on the identification of mechanisms of PDGFs on tooth cells including dental epithelial cells, ameloblasts, and dental mesenchymal cells, odontoblasts. RT-PCR and immunostaining revealed that PDGF ligands, PDGF-A and PDGF-B, and their receptors, PDGFR α , and PDGFR β , were expressed throughout the initial stages of tooth development. In organ culture of tooth germ, exogenous AG17, a tyrosine kinase inhibitor specific for PDGF signaling, suppressed the numbers of bromodeoxyuridine (BrdU) positive cells in both dental epithelium and mesenchyme. As the results, growth and cusp formation of molar tooth germ were inhibited. Next, we examined whether PDGF-AA or -BB affect dental epithelial cell differentiation. Dental epithelial cell line, SF2 cells were cultured with PDGF-AA or -BB. PDGF-AA, but not -BB, was strongly induced the expression of ameloblastin gene, a marker of differentiated ameloblasts. Further, we examined the effects of PDGF-AA and -BB on cell proliferation of the dental papilla cell line SP cells. PDGF-BB promoted SP cells proliferation, whereas PDGF-AA did not. In conclusion, our results indicate that PDGF-AA accelerates ameloblast differentiation and PDGF-BB promotes odontoblast proliferation, suggesting that PDGFs have important roles in tooth development.

Disclosures: YU SUGAWARA, None.

SU0212

PTH Stimulates Osteoblastic VEGF-A Expression in a Differentiation-Dependent Manner. Julianne Smith^{*1}, Jonathan Weber¹, Laura Calvi².

¹University of Rochester School of Medicine & Dentistry, USA,

²University of Rochester School of Medicine, USA

New vessel formation is required for both developmental bone growth and adult bone remodeling. The bone marrow (BM) sinusoidal vasculature is a key component of hematopoietic stem cell (HSC) trafficking and recovery from myeloablation. Osteoblastic activation of the PTH1R and systemic PTH treatment increase trabecular bone and expand HSCs. We hypothesized that PTH may exert its action on HSCs in part through effects on the BM microvasculature. In the tibial and femoral metaphyseal regions of c57/b6 mice, PTH increased microvessel number (16718.1 vs 34839.3 microvessels/hindlimb, n=5 mice per group, p= 0.0030) and vascular area (mm²): 0.1350.0194 vs 0.2810.00951, n=5 mice/group, p= 0.0001) measured by histomorphometry. To determine if PTH increases osteoblast-derived angiogenic signals, MC3T3 cells were differentiated in mineralizing media and treated with PTH(1-34) at various stages of maturation. Differentiation of MC3T3 cells did not affect baseline VEGF-a expression. PTH induced VEGF-a expression in day 7 cells at two hours, an effect that peaked at six hours (3.831.76 vs 50.79.72, n=3, p=0.0090) and was sustained 24 hours after treatment. The magnitude of the effect increased throughout differentiation and was maximal at 28 days. PTH also increased *in vitro* levels of secreted VEGF-A protein at corresponding time points (VEGF-A(pg/mL): 43.42.27 vs 46424.2, n=3, p< 0.0001). Surprisingly, *in vivo* BM plasma VEGF-A levels were decreased both in a transgenic mice with osteoblastic activation of the PTH1R (VEGF-A (pg/mL): 74.27.05 vs 44.03.67, n=3-5 mice per group, p=0.0054) and intermittent PTH treatment (VEGF-A (pg/mL): 1056.62 vs 78.64.95, n=9 mice per group, 2 independent experiments, p=0.0057), while serum VEGF-A levels were unchanged. VEGF-A bioavailability can be regulated by alternative splicing of VEGF-a pre-mRNA. Specifically, VEGF189 possesses endothelial mitogenic activity but is predominantly cell and matrix-bound. In MC3T3 cells, PTH strongly increased expression of the VEGF-a variant encoding VEGF189 six hours after treatment of maturing MC3T3 samples (1.701.100 vs 11325.1, n=2-3, p=0.0416). In conclusion, PTH increases marrow microvasculature *in vivo* in spite of decreased levels of BM soluble VEGF-A. Since PTH stimulates osteoblastic expression of matrix-bound VEGF-A, PTH-dependent proangiogenic signals in the BM microenvironment may be highly localized via modulation of VEGF-a pre-mRNA splicing in osteoblastic cells.

Disclosures: Julianne Smith, None.

SU0213

Synergistic Effects of Oncostatin M and IL-1 β in an Arthritic Chondrocyte Model. Liliana Mellor^{*}, Cheryl Jorcyk, Julia Oxford. Boise State University, USA

Osteoarthritis (OA) remains one of the few chronic diseases of aging without an effective treatment due to the lack of understanding of the underlying mechanisms leading to cartilage degeneration. Homeostasis between pro-inflammatory and anti-inflammatory cytokines that control the balance between matrix-degrading

metalloproteinases (MMPs) and tissue inhibitors of metalloproteinases (TIMPs) is essential to prevent increase in catabolic rate that leads to cartilage degradation. Oncostatin M (OSM), a member of the interleukin-6 (IL-6) cytokines family, and IL-1 β have been reported to act synergistically to induce gene expression of MMPs and ADAM-10 in articular cartilage, and elevated levels of both cytokines have been reported in the synovial fluid of patients with rheumatoid arthritis (RA) and OA. Our goal is to investigate the individual and synergistic effects and signaling pathways of OSM and IL-1 β on cartilage degradation. Using a cytokine array panel to detect over-expression of different cytokines and chemokines in the media of rat chondrosarcoma cells (RCS) treated with OSM, IL-1 β and OSM+IL-1 β , we found up-regulation of IL-8 (CINC-1), sICAM-1 and VEGF in all three conditions when compared to the untreated control. In addition, cells treated with both OSM and IL-1 β together showed expression of IL-6 and MIP-3 α (CCL20) while control cells and cells treated with OSM or IL-1 β alone showed no expression. These preliminary data suggests a novel synergistic effect of OSM and IL-1 β in chondrocytes that leads to cartilage degradation. In addition, IL-6 and MIP-3 α have also been found in the synovial fluid of arthritic patients, suggesting that the combination of IL-1 β and OSM may trigger a positive feedback mechanism in articular cartilage that leads to an increased catabolic rate. Future treatments for arthritis may be more efficient if both pro-inflammatory cytokines (IL-1 β and OSM) are targeted rather than individual treatments.

Disclosures: Liliana Mellor, None.

SU0214

System Engineering Approach to Optimize the Multi-cofactor Combination of Osteogenic Cocktail with Minimized BMP-2 Doses. Yoshitomo Honda¹, Xianting Ding², Federico Mussano³, Akira Wiberg⁴, Chih-ming Ho², Ichiro Nishimura⁵. ¹UCLA / Tohoku University, USA, ²Department of Mechanical & Aerospace Engineering, Center for Cell Control, UCLA, USA, ³UCLA School of Dentistry and University of Turin, Italy, USA, ⁴The Weintraub Center for Reconstructive Biotechnology, UCLA school of Dentistry, USA, ⁵University of California, Los Angeles, USA

Objectives: Bone morphogenetic protein 2 (BMP-2) is known to be a potent osteogenic factor. However, relatively supraphysiological concentrations are required to achieve its therapeutic effect, resulting in the healthcare cost and side effect issues that may prevent its routine clinical use in dental and orthopedic fields. Drug cocktails are often more effective than single drug administration, although the identification of such the optimal drug cocktail is extremely challenging due to the large number of possible combinations arising from multiple drugs and their doses. Recently, the feedback system control (FSC) technique using an engineering scheme has been shown useful as a tool to effectively search for the optimal drug combinations, rather than screening all the possible combinations by applying the traditional high-throughput screening. The objective of this study was to apply FSC to identify potent osteogenic drug cocktails including BMP-2 at lower concentrations. **Methods:** FSC was performed by repeating the following processes: 1) Preparation of various drug cocktails. BMP-2 and six selected co-factors at ten possible concentrations were mixed in the Dulbecco's Modified Eagle Medium with fetal bovine serum and antibiotic, which were utilized as the prototype of drug cocktails. 2) Bioassays. Bone marrow derived murine mesenchymal stem cell line (D1 cell) was stimulated by the drug cocktails. The level of alkaline phosphatase (ALP) and mineralization were measured at day 3 or 6, respectively, as indicator of the potency of each drug cocktail. 3) System engineering approach. The results of bioassay were fed into a stochastic search algorithm (Differential Evolution Algorithm) to elicit modified prospective drug combinations. **Results:** None of random selected drug cocktails induce obvious mineralization, while the candidate drug combinations started to emerge after 9 iterations of FSC with ALP assay and further 6 iterations with mineralization assay. One combination induced a 37% mineralization relative to that of high-dose BMP-2 (100 ng/ml) despite the concentration of BMP-2 in that cocktail reduced to 1/64. **Conclusion:** The result indicates that FSC successfully identified candidate drug cocktails that enhanced the ALP secretion and mineral deposition, out of a possible 10 million different combinations. FSC may serve as a useful tool for identifying potent osteogenic combinatory drugs for bone regenerative medicine.

Disclosures: Yoshitomo Honda, None.

This study received funding from: U19 AI67769 UCLA Center for Biological Radioprotectors, NIH/NIAID C06 RR014529, NIH/NCR

SU0215

The Level of Osterix Expression in Bone Is Important to Prevent Chronic Inflammation. Wook-Young Baek¹, Eun-Hye Lee¹, Tae-Hwan Kwon², Kwon-Moo Park³, Jung-Eun Kim⁴. ¹Cell & Matrix Research Institute, Department of Molecular Medicine, Kyungpook National University School of Medicine, South Korea, ²Cell & Matrix Research Institute, Department of Biochemistry & Cell Biology, Kyungpook National University School of Medicine, South Korea, ³Department of Anatomy, Kyungpook National University School of Medicine, South Korea, ⁴Kyungpook National University School of Medicine, South Korea

Osterix (Ox) is an essential transcription factor for osteoblast differentiation and bone formation. Ox null mutants died perinatally with a complete absence of bone formation and osteoblast-specific Ox conditional knockouts showed the osteopenic phenotype after birth. Even in Ox heterozygous mice with normal bone morphology, the reduced cortical thickness and osteoblast differentiation were observed by qCT and in vitro cell culture, respectively. This result exhibited that the level of Ox expression was still important for in vivo and in vitro bone formation. Here, we questioned whether physiological homeostasis is maintained by Ox expression. In Ox heterozygous mice with a low expression of Ox in bone, the expression levels of pro-inflammatory and anti-inflammatory cytokines were significantly altered, indicating that their body due to the reduced Ox expression may remain a chronic inflammatory state. Especially, the expression of IL-6, a key mediator of chronic inflammation, was increased in Ox heterozygotes and decreased in Ox overexpressed osteoblastic cells. Kidney as well as bone is one of the most important organs in order to maintain a physiological balance controlled by numerous endocrine factors. The cross-talk between the bone and kidney for physiological homeostasis has been studied for a long time. In Ox heterozygous mice compared to wild-type, no significant difference was observed in renal morphology and functions. However, the renal regeneration after ischemic damage was remarkably delayed in Ox heterozygous mice, as indicated by elevated blood urea nitrogen and creatinine levels, and morphological alterations consistent with acute tubular necrosis. Eventually, the low level of Ox expression caused a chronic inflammation in the body, resulting in the enhanced susceptibility to renal injury after ischemia/reperfusion. This study suggests that Ox expression in bone is important to prevent chronic inflammation and maintain physiological homeostasis.

Disclosures: Wook-Young Baek, None.

SU0216

New Mechanisms Accounting for a Fine Tuning Regulation of Osteoblast and Osteoclast Activity. Barbara Peruzzi¹, Alfredo Cappariello², Andrea Del Fattore², Nadia Rucci¹, Fabrizio De Benedetti², Anna Teti¹. ¹University of L'Aquila, Italy, ²Ospedale Pediatrico Bambino Gesù, Italy

The cytokine IL-6 and the tyrosine kinase c-Src reduce osteoblast (OB) activity *in vitro* and *in vivo*. Hence we hypothesized that they might establish a functional loop to maintain OBs in an immature status. In c-Src-inhibited OBs IL-6 mRNA was reduced by decreasing STAT3 transcription factor activation, suggesting that c-Src and STAT3 converge regulating IL-6 expression. To evaluate if this interplay has a role *in vivo*, WT, IL-6 overexpressing transgenic (TG) and inflammatory agents-treated mice were treated with the c-Src inhibitor CGP76030, which reduced STAT3 activation and mouse IL-6 mRNA in whole bones. Histomorphometric analysis showed that CGP76030 treatment significantly improved TG mice bone phenotype, demonstrating c-Src inhibitor anabolic and antiresorptive effects. Moreover, we evaluated IL-6 in mice carrying bone metastases induced by the human breast cancer MDA-MB231 cells. BALB/c-nu/nu mice intracardially injected with MDA-MB231 and treated with CGP76030 showed decreased incidence of bone metastases, with a reduction of both human (derived by MDA-MB231) and mouse IL-6 in sera and in the bone metastasis tissue. Therefore, c-Src exerts a leading role on IL-6 induced osteopenic phenotype *in vivo*. IL-6-treated OBs increased c-Src activation in long-term treatment, suggesting the involvement of mediators. Although IGF-1 could be instrumental to link IL-6 and c-Src pathways, IL-6-treated OBs showed no changes of IGF-1, while IGFBP5 mRNA was increased. IGFBP5-treated OBs showed increased c-Src activation, proving a direct role for IGFBP5 in IL-6/c-Src interplay in OBs. Since, unexpectedly, also c-Src inhibition increased IGFBP5 mRNA, we analysed the IGFBP5 promoter, identifying a responsive element for Runx2, that was up-regulated by c-Src inhibition. Consistently, Runx2-over-expression increased IGFBP5 mRNA in OBs. To test if this effect depended on OB maturation, IGFBP5 was administered to OBs at subconfluence (immature) and at overconfluence (mature). At variance with subconfluent cells, in overconfluent OBs c-Src was barely expressed and, hence, insensitive to IGFBP5-induced activation. To test if in this context other cells were targeted by IGFBP5, osteoclast (OC) precursors and mature OCs were treated with IGFBP5, which induced an increase of both osteoclastogenesis and bone resorption, thereby indicating a novel role for IGFBP-5 in bone homeostasis that could provide new insights in inflammation-related and cancer-related bone pathologies

Disclosures: Barbara Peruzzi, None.

SU0217

Aptamer-Functionalized Stable Nucleic Acid Lipid Particles for siRNA Cell-specific Delivery to Osteoblast Cells. Heng WU^{*1}, Tao Tang¹, Baosheng GUO², Baoting Zhang³, Zhiyun YANG⁴, Leungkim HUNG⁵, Ningsheng SHAO⁶, Lingqiang ZHANG⁷, Ling Qin⁸, Ge Zhang⁹. ¹The Chinese University of Hong Kong, Hong Kong, ²Prince of Wales Hospital, Hong Kong, ³Prince of Wales Hospital, The Chinese University of Hong Kong, Hong Kong, ⁴Hong Kong Baptist University, China, ⁵The Chinese University of Hong Kong, China, ⁶Beijing Institute of Basic Medical Sciences, China, ⁷Beijing Institute of Radiation Medicine, China, ⁸Chinese University of Hong Kong, Hong Kong, ⁹Prince of Wales Hospital, Hong Kong

Introduction: RNA interference could facilitate translation from negative regulator gene of bone formation to clinical treatment by knocking down the negative regulator genes. Unfortunately, systemic administration of small interference RNA (siRNA) requires greater therapeutic doses, which will carry a greater risk on non-bone tissues. Accordingly, the clinical application of therapeutic siRNA largely depends on specific delivery system, which possesses high selectivity for osteoblast and excellent transfection efficiency. Since aptamer could provide excellent alternatives to antibodies as cell-specific agents, so the objective of the present study is to prepare and evaluate stable nucleic acid lipid particles (SNALP) modified by L6-CELL-3 aptamer screened for rat osteoblast (ROS 17/28).

Methods: The L6-CELL-3 aptamer was attached to SNALP by post-insertion to form L6-SNALP, which was further optimized in terms of particle size, encapsulation efficiency and knockdown efficiency. The effect of L6-CELL-3 aptamer on binding and selectivity of L6-SNALP as well as the cellular uptake of CKIP-1 siRNA was determined by flow cytometry. The stability in serum and cytotoxicity of the L6-SNALP were also evaluated by agarose gel electrophoresis and MTT, respectively. After administration of L6-SNALP via tail vein injection, the rats were sacrificed at 4 hours and the distal femurs were dissected for immunohistochemistry analyses using ALP and RUNX2 antibodies as markers to evaluate the cell-specific delivery in vivo.

Results: After optimization, the average particle size of L6-SNALP was 906 nm and encapsulation efficiency was 864.6%. It demonstrated excellent knockdown efficiency at low concentration of 8 nM CKIP-1 siRNA. L6-SNALP also suggested selective binding and facilitated the cellular uptake of CKIP-1 siRNA in ROS17/28 cell compared with control-SNALP. In addition, it was stable in serum up to 12 h and possessed low cytotoxicity compared with traditional delivery system. The immunohistochemistry results suggested numerous instances of co-localization of the FAM-labeled siRNA with the RUNX2- or ALP-positive cells in L6-SNALP, which indicated this delivery system facilitated siRNA targeting osteoblast cell.

Conclusions: L6-SNALP suggested high knockdown efficiency at low siRNA dose and favorable targeting with osteoblast cell. It could be a potential cell-specific delivery system for targeting osteoblast cell with high efficiency, selectivity and low cytotoxicity.

Disclosures: Heng WU, None.

SU0218

Deficiency of Bax Expression Prevents Diabetes-induced Osteoblast Death and Bone Loss. Lindsay Martin-Coe^{*1}, Laura McCabe². ¹New York University College of Dentistry, USA, ²Michigan State University, USA

T1-diabetes is a metabolic disorder associated with bone loss. Both bone formation and density are decreased, however the exact mechanisms accounting for diabetic bone loss remain unknown. Previously, our lab reported an elevation in osteoblast apoptosis in diabetic mouse bones illustrated by increased TUNEL positive osteoblasts and Bax mRNA expression. Bax is a pro-apoptotic factor that mediates the intrinsic death pathway. Intrinsic apoptosis has also been associated with osteoblast death and bone loss in models of unloading and aging. Here we hypothesize that the diabetes-induced increase in Bax expression mediates osteoblast death. To test this, we examined the effect of diabetes on bones in Bax deficient mice. Diabetes was induced in 16-week-old male C57BL/6 Bax deficient and wild type littermates. Bones were examined for markers of osteoblast apoptosis, as well as bone formation and resorption. Our findings indicate that Bax deficiency protects osteoblasts from diabetes-induced osteoblast death. Decreases in trabecular BV/TV and markers of bone formation observed in diabetic bone were fully attenuated in Bax deficient diabetic mice compared to vehicle treated mice, while markers of bone resorption remained unchanged. Since diabetic marrow induces osteoblast apoptosis, we examined if Bax deficient osteoblasts were protected from diabetic marrow-induced osteoblast death. Co-culture studies demonstrate that Bax deficient osteoblasts are protected from diabetic marrow induced increases in osteoblast caspase 3 activity. Our results suggest a role for Bax in T1-diabetes-induced osteoblast death and bone loss. Therefore, targeting Bax expression through pharmaceuticals could prevent diabetes-induced osteoblast death and ultimately bone loss. One commonly used therapy for osteoporosis; bisphosphonates reduces osteoblast death while inhibiting osteoclast activity. Therefore we examined the effects of bisphosphonates on diabetic bone pathology. Our results illustrate that bisphosphonate therapy protects against diabetes-associated elevations in Bax mRNA levels and death, as well as bone loss. Taken together, our results suggest that inhibition of Bax-mediated osteoblast death prevents diabetes-induced bone loss.

Disclosures: Lindsay Martin-Coe, None.

SU0219

Vitamin C Administration Markedly Ameliorates Bone loss by Restoring the Osteoblastic Viability in Sod1-deficient Mice. Hidetoshi Nojiri^{*1}, Yoshitomo Saita², Daichi Morikawa³, Keiji Kobayashi⁴, Mitsuru Saito⁵, Kazuo Kaneko⁶, Takahiko Shimizu⁷. ¹Juntendo University, School of Medicine, Japan, ²Department of Orthopaedics, Juntendo University School of Medicine, Japan, ³Juntendo University, Japan, ⁴Molecular Gerontology, Tokyo Metropolitan Institute of Gerontology, Japan, ⁵Jikei University School of Medicine, Japan, ⁶Department of Orthopaedics, Juntendo University, Japan, ⁷Tokyo Metropolitan Institute of Gerontology, Japan

We have reported bone phenotypes in SOD1 deficiency, such as decreased bone mass and senescent cross-linking (Nojiri, H. et al. 2009 ASBMR and Saita, Y. et al. 2010 ASBMR). In comprehensive antioxidant treatments using Sod1-deficient mice for the rescue experiment, we found that several compounds, including vitamin C, were useful for improving the bone mass of Sod1-deficient mice (unpublished results). The mice were given 1% vitamin C (VC) in drinking water for 12 weeks from 4 weeks of age. In osteoblast culture, VC was added to produce a final concentration of 50 µg/ml for 24 hr for the ROS measurement and for 48 hr for the BrdU incorporation assay and cell death measurements. The oral administration of vitamin C completely restored the osteoporotic features of Sod1-/- mice, indicating that superoxide-induced bone loss could be improved by antioxidant treatment. These results also imply that the bone phenotypes in SOD1 deficiency were caused by excess oxidative stress, rather than by the lack of SOD1 itself. The total body BMD, as measured by DEXA; the BV/TV of the tibia, as measured by pQCT; and the femoral bone weight were significantly improved after vitamin C treatment, without any change in the length of the long bones. In addition, bone strength was markedly improved by VC administration. Interestingly, VC treatment also produced a partial improvement in the composition of collagen cross-links. In cellular experiments, VC treatment markedly suppressed the level of DCF-reactive ROS in Sod1-/- osteoblasts. In addition, the BrdU and TUNEL assays showed complete restoration of cell proliferation and apoptosis in Sod1-/- osteoblasts after the addition of VC. These results indicate that VC treatment completely restored osteoblast viability through the elimination of intracellular ROS, suggesting that VC treatment rescues osteopenia by restoring the osteoblastic viability in Sod1-/- mice.

These results imply that an intracellular redox imbalance caused by SOD1 deficiency plays a pivotal role in the development and progression of bone fragility both in vivo and in vitro.

Disclosures: Hidetoshi Nojiri, None.

SU0220

Angiotensin II induces osteoblast production of MMP-3 and MMP-13 via the AT₁ receptor. Kumiko Nakai^{*1}, Takayuki Kawato², Masafumi Motohashi³, Masao Maeno⁴. ¹Division of Oral Health Sciences, Japan, ²Nihon University School of Dentistry, Tokyo, Japan, ³Department of Oral Health Sciences, Nihon University School of Dentistry, Japan, ⁴Nihon University School of Dentistry, Japan

Objective: Angiotensin II (Ang II), which acts via Ang II type 1 (AT₁) and/or type 2 (AT₂) receptors, not only regulates systemic blood pressure through a direct vasoconstrictive effect but has also been shown to regulate bone metabolism by stimulating osteoblasts. However, the role of Ang II in the turnover of bone matrix proteins by osteoblasts is unclear. Therefore, we examined the effect of Ang II on the expression of matrix metalloproteinases (MMPs), plasminogen activators (PAs), and their inhibitors, including tissue inhibitors of metalloproteinases (TIMPs) and PA inhibitor-1 (PAI-1), in osteoblasts.

Methods: Rat ROS 17/2.8 osteoblast-like cells were cultured for up to 7 days with Ang II (0, 10⁻⁸ M, 10⁻⁷ M or 10⁻⁶ M) in the presence or absence of the AT₁ receptor blocker losartan (5 µM) or the AT₂ receptor blocker PD123319 (5 µM). Expression of the AT₁ and AT₂ receptors, MMPs, TIMPs, PAs, and PAI-1 was examined at the mRNA and protein levels by real-time PCR and Western blotting, respectively.

Results: Both the AT₁ and AT₂ receptors were expressed in ROS 17/2.8 cells. While cell proliferation was not affected by treatment with Ang II, alkaline phosphatase activity decreased. The expression of MMP-3 and MMP-13 increased significantly as a result of treatment with 10⁻⁶ M Ang II, whereas the expression of MMP-2, MMP-14, urokinase-type PA, tissue-type PA, TIMPs-1, -2, -3, and PAI-1 was unaffected by Ang II. Expression of MMP-1 and TIMP-4 was not detected. Losartan blocked Ang II-induced expression of MMP-3 and MMP-13, whereas PD123319 did not completely block these responses.

Conclusion: These results suggest that Ang II stimulates the resorption process that occurs during the turnover of osteoid by increasing the production of MMP-3 and MMP-13 in osteoblasts via the AT₁ receptor. Furthermore, they suggest that Ang II does not influence the plasminogen/plasmin pathway in osteoblasts.

Disclosures: Kumiko Nakai, None.

SU0221

Bone Size QTL Gene Located in Mouse Chromosome 4 is a Mechanoresponsive Gene. Jon Wergedal*, Chandrasekhar Kesavan, Subburaman Mohan, Jerry L. Pettis Memorial VA Medical Center, USA

Periosteal bone formation rate (BFR) is an important determinant of bone cross sectional size; and therefore of bone strength. Therefore, identification of genes that regulate periosteal bone expansion and elucidation of their molecular pathways are essential to develop strategies for a therapeutic strengthening of long bones. In previous work, we have identified a key bone size QTL on mouse chromosome (Chr) 4 using different inbred strain mouse crosses. Furthermore, we have demonstrated that a congenic line B6.C3H-4T-3 (4T3) of mice with a small region (129-139 Mbp) of Chr 4 from C3H/HeJ (C3H) in a C57/BL6 (B6) background exhibited an increased femur cross sectional size. We examined other bones and found the increased size phenotype in the tibia (242%, n=10, p<.01) and radius (122%, n=10, p<.01), indicating a general effect of the QTL gene on the bone size phenotype. Because mechanical strain is a known regulator of periosteal expansion, we hypothesized that the bone size QTL gene in Chr 4 is a mediator of mechanical strain response in the skeleton. To test this hypothesis, 11 4T3 congenic and 8 B6 control mice were subjected to external loading using a 4-point bending device. A 9n cyclic load was applied at a frequency of 2 hertz for 36 cycles. The force was applied to the tibia once daily for 6 days and the mice were euthanized on the 9th day. The mice were injected with tetracycline on day 4 and calcein on day 8 to label newly formed bone. Histomorphometric analysis revealed that the basal BFR in the externally unloaded left tibia was lower in the 4T3 congenic than in the B6 control mice (-3213%, p<.001) which was due to reduced bone forming surface (BFS) (-299%, p<.01). External loading significantly increased the BFR in the right tibia compared to the contralateral tibia in both 4T3 and B6 mice. However, the mechanical loading-induced increase in the BFR was 33% higher (p<.05) in 4T3 mice compared to B6 mice. This mechanical loading-induced increase in BFR was primarily due to a 37% increase in BFS (p<.05) in the 4T3 mice compared to the B6 mice. Conclusions: 1) The bone size QTL gene, located in the 129-139 Mbp of Chr 4, is a mediator of mechanical strain response in the skeleton. 2) Because the greater increase in the BFS in the 4T3 congenic mice in response to loading indicates an increased number of osteoblasts and because Wnt4, a known inducer of bone cell proliferation, is present in this Chr region, the Wnt4 gene could be a candidate for the Chr 4 bone size gene.

Disclosures: Jon Wergedal, None.

SU0222

Clopidogrel (Plavix®), a P2Y₁₂ Receptor Antagonist, Inhibits Osteoblast Function *in vitro* and Decreases Trabecular Bone *in vivo*. Isabel Orriss*¹, Susanne Syberg², Andrea Brandao-Burch¹, Mark Hajjawi¹, Timothy Arnett¹, Peter Schwarz³, Niklas Jorgensen⁴. ¹University College London, United Kingdom, ²Copenhagen University Hospital Glostrup, Denmark, ³Glostrup Hospital, Denmark, ⁴Copenhagen University Hospital Glostrup, Denmark

It is evident that extracellular nucleotides, signalling through P2 receptors (P2R), play a significant role in bone, modulating both osteoblast (OB) and osteoclast (OC) function. Clopidogrel (Plavix®) is a selective P2Y₁₂R antagonist and, currently, is the only P2R antagonist available for therapeutic use. It is an antithrombotic, prescribed to reduce the risk of heart attack and stroke, acting via inhibition of platelet aggregation. In this study, we investigated the effects of clopidogrel treatment on (1) OB formation, differentiation and activity *in vitro*; and, (2) trabecular and cortical bone parameters *in vivo*. OBs were obtained from rat calvaria and cultured with clopidogrel (1-50µM) for up to 14d. P2Y₁₂R expression was confirmed using qPCR and western blotting. ADP (≤100µM), an agonist at the P2Y₁₂R had no effect on OB differentiation and function. Clopidogrel at 10µM and 25µM inhibited mineralised bone nodule formation by 50% and >85%, respectively. Clopidogrel slowed OB proliferation with dose-dependent decreases in cell number of 25-40% in differentiating OBs (d7). One dose of 10-25µM clopidogrel to mature OB also decreased cell viability by 15%. At 14d, ≥10µM clopidogrel reduced ALP activity by ≤70% and collagen formation by 40%. Total E-NPP activity was unaffected. Activation of P2Y₁₂R receptors by ADP caused decreased intracellular cAMP levels; a single dose of 1-10µM clopidogrel to mature OB increased cAMP levels by 35%. qPCR array analysis of clopidogrel treated osteoblasts (14d) showed no change in ALP or collagen expression, however, levels of FGF1 and FGF3 were increased up to 9-fold. A second P2Y₁₂R antagonist, ARC-66096, exhibited similar effects on osteoblast function *in vitro*. 20-week old mice (n=10-12) were ovariectomised or sham treated and dosed orally with clopidogrel (1mg/kg) or vehicle (NaCl) daily for 4 weeks. DEXA analysis showed clopidogrel treated animals had decreases of 2% and 4% in whole body and femoral BMD, respectively. Detailed analysis of trabecular and cortical bone using µCT showed decreased trabecular bone volume (BV/TV) in the tibia (24%, p<0.05) and femur (18%, p<0.05) of clopidogrel-treated mice. Trabecular number was reduced 20% (p<0.01), whilst trabecular separation was increased up to 15% (p<0.05). Trabecular thickness and cortical bone parameters were unaffected. Combined, these findings indicate that long-term exposure of bone cells to clopidogrel *in vivo* could directly impact bone health.

Disclosures: Isabel Orriss, None.

SU0223

Deregulation of Wnt Signaling in the Fracture Callus Following Binge Alcohol Exposure is Attenuated by Lithium Chloride Treatment. Kristen Lauing*¹, Philip Roper², Rachel Nauer³, John Callaci⁴. ¹Loyola University Medical Center, USA, ²Loyola University Medical Center, Cell Biology, Neurobiology, & Anatomy Program, USA, ³Loyola University Medical Center, Department of Orthopaedic Surgery, USA, ⁴Loyola University of Chicago, USA

Binge alcohol consumption is a contributing factor in up to 40% of all orthopaedic trauma cases and is associated with delayed or incomplete fracture healing. The Wnt pathway, through strict temporal regulation of β-catenin, is essential for the formation of new bone and cartilage during repair. Lithium treatment (LiCl) is known to indirectly stimulate the Wnt pathway. We have previously shown that binge alcohol exposure decreases callus strength and quality, modulates the total expression of canonical Wnt transcriptional activation and downstream Wnt target gene expression, and perturbs the protein levels of β-catenin in the fracture callus. This study aims to investigate whether LiCl treatment can restore normal bone healing in a murine binge alcohol-tibial fracture model. Mice were administered alcohol (2 g/kg) or saline intraperitoneally once per day for 3 consecutive days, and subjected to a stabilized, mid-shaft tibial fracture. Four days post-fracture, mice were given either standard drinking water or 0.015M LiCl in water daily to examine the effects of exogenous Wnt pathway enhancement during healing. Mice were sacrificed 3, 6, 9, 14, or 21 days post-fracture.

Histological analysis revealed that alcohol was associated with decreased callus size and suppression of endochondral ossification with increased fibrous tissue formation, and inhibition of chondrocyte maturation and hypertrophy in the cartilaginous callus. The temporal expression of β-catenin in callus tissue was significantly disrupted by alcohol throughout day 21 of healing, which corresponds to previously observed alcohol-induced changes in Wnt transcriptional activity in the callus. Using a customized 4-point bending apparatus, we found that fracture calluses from binge-alcohol treated mice were significantly weaker than those from saline-treated controls. LiCl treatment attenuated alcohol-related damage to the fracture callus and Wnt signaling by augmenting β-catenin protein levels to those seen in saline-treated mice, restoring endochondral ossification, and increasing callus strength in alcohol-treated mice.

These data show that deficient fracture repair in alcohol-abusers may be due in part to deregulation of Wnt/β-catenin signaling during early stages of healing, leading to damaging effects on the biomechanical and cellular aspects of healing. Exogenous activation of the Wnt pathway during healing may improve fracture repair in patients at risk for alcohol-related complications.

Disclosures: Kristen Lauing, None.

SU0224

Effects of Focused Shock Wave (FSW) on Cementoblasts *in vitro*. Dawei Liu*. Marquette University School of Dentistry, USA

Root resorption (RR) is a pathological consequence of orthodontic treatment, which may cause mobility and eventual loss of teeth. How to prevent and repair RR is critical to the quality of orthodontic care. Similar to ultrasound therapy, focused shock wave (FSW) has been applied to enhance angiogenesis, growth and healing of bone, however its effects on RR have never been studied. The purpose of this study was to investigate the effects of FSW on cementoblasts, the cells forming and repairing cementum - the out layer of dental root, in attempt to find evidence to support potentially using FSW to treat RR. Based on current knowledge, we hypothesized that FSW at a certain level induces anabolic responses in cementoblasts. To test our hypothesis, OCCM.30 cementoblasts were prepared in suspension with a density of 10⁷/ml. One ml of the cell suspensions were prepared in eppendorf tubes which were geared to the FSW stimulator (Storz Medical AG, Switzerland). The cells were subjected to a single dose of 2000 impulses of FSW at 3 different dose levels (0.1mJ/mm², 0.25mJ/mm² and 0.5mJ/mm², respectively). Immediately after FSW, an aliquot of cell suspension was collected and spin to test ATP released - an early signal in bone metabolism. After 24 hours of post-incubation, the cells were centrifuged and lysed to test protein productions of sclerostin (SOST) - a negative regulator of bone formation and receptor activator of NFκB ligand (RANKL) - a direct stimulator of bone resorption. Controls were set under identical conditions without FSW application. To test the proteins, 50 micrograms of cell lysates were resolved through 10% SDS-PAGE, immunoblotted with the 1st antibodies against SOST and RANKL, followed by the 2nd antibody incubation and gel documentation. Densities of the gel bands of interest were equalized by that of a cytoskeletal protein vinculin. One-way ANOVA was used to compare the differences among the groups with p value set at 0.05. As results, ATP release was significantly increased in a dose-dependent manner (n=6, p=0.000). SOST protein was significantly decreased only at the dose level of 0.25mJ/mm² (n=3, p<0.05). RANKL protein was significantly increased at 0.1 and 0.5 (n=3, p<0.01) but not at 0.25mJ/mm² levels. Our data suggest (1) FSW at 0.25mJ/mm² level anabolically modulates bone remodeling by decreasing SOST production but not decreasing RANKL production; (2) FSW might potentially be used to treat root resorption in orthodontics.

Disclosures: Dawei Liu, None.

SU0225

Hairy and Enhancer of Split Related with YRPW Motif (Hey)2 Uncouples Bone Formation from Bone Resorption. Stefano Zanotti^{*}, Ernesto Canalis, St. Francis Hospital & Medical Center, USA

Notch signaling inhibits osteoblastogenesis and maintains bone marrow precursor cells in an undifferentiated state. In osteoblasts, Notch signaling induces the expression of proteins encoded by *Hairy and Enhancer of Split (Hes)1* and *Hes-related with YRPW motif (Hey)1*, *Hey2* and *HeyL*. Although the canonical signaling pathway mediates the actions of Notch in osteoblasts, the contributions of each target gene have been only partially explored. In fact, misexpression of *Hes1* in cells of the osteoblastic lineage does not phenocopy all the actions of Notch *in vivo* and *in vitro*, suggesting that alternate Notch targets mediate its activity in osteoblastic cells. *Hey1* misexpression has limited impact on skeletal homeostasis, and global *Hey2* inactivation is lethal, not allowing its study in the postnatal skeleton. In an effort to discern the skeletal activity of Notch targets, transgenics overexpressing *Hey2* under the control of a 3.6 kilobase fragment of the collagen type I $\alpha 1$ promoter were created in a tropism for Friend Virus-B genetic background. *Hey2* transgenics were viable and healthy, and bone microcomputed tomography revealed normal cancellous bone volume and trabecular microarchitecture. Bone histomorphometric analysis demonstrated a 40 to 50% decrease in mineralizing surface and bone formation rate, associated with a 20 to 30% increase in eroded surface and osteoclast number, demonstrating an uncoupling of bone formation from bone resorption in *Hey2* transgenic male mice. *Hey2* overexpression in female mice decreased osteoblast number and mineral apposition rate but had no effect on eroded surface or osteoclast number. To understand the mechanisms of *Hey2* action, osteoblasts were isolated from *Hey2* transgenics and control littermates. In agreement with the phenotype observed *in vivo*, *Hey2* inhibited alkaline phosphatase mRNA levels and activity, and suppressed osteocalcin transcripts. Osteoblasts from *Hey2* transgenic male or female mice induced resorption by co-cultured osteoclast precursors, suggesting that the resorptive phenotype in female mice was suppressed by estrogens. Since the *in vivo* and *in vitro* cellular effects were not translated in changes in skeletal microarchitecture, these results suggest that either the consequences of *Hey2* overexpression are transient, or that *Hey2* activates protective mechanism to preserve bone mass and skeletal integrity. In conclusion, overexpression of *Hey2* in osteoblasts uncouples bone resorption from bone formation.

Disclosures: Stefano Zanotti, None.

SU0226

Heparanase is a Physiologic Regulator of Bone Formation and Bone Mass. Vardit Kram^{*}¹, Eyal Zcharia², Orr Ofek¹, Alon Bajayo³, Malka Attar-Namdar¹, Yoav Smith¹, Jin-Ping Li⁴, Israel Vlodavsky², Itai Bab⁵. ¹Hebrew University of Jerusalem, Israel, ²Technion, Israel, ³Hebrew University Faculty of Dentistry, Israel, ⁴Uppsala University, Sweden, ⁵The Hebrew University, Israel

Heparanase (Hpse) is an endoglycosidase, which cleaves the heparan sulfate sugar moieties of heparan sulfate proteoglycans (HSPGs). Hpse has been implicated mostly in pathological processes. We have previously shown that Hpse is normally expressed in osteoblasts and promotes bone formation primarily by increasing osteoblast number. Hpse transgenic mice have a high bone mass phenotype attributable mainly to increased bone formation, with an additional spectrum of extraskeletal abnormalities. These mice also show decelerated skeletal elongation. By contrast, we show here that the only phenotype exhibited by Hpse deficient (*Hpse*^{-/-}) mice is skeletal, which mirrors the transgenic skeletal phenotype, namely, low bone mass (LBM) and accelerated longitudinal growth. The LBM is due to both reduced bone mass accrual and accelerated age-related bone loss and is manifested mainly in females; only the accelerated age-related bone loss is shared by *Hpse*^{-/-} males. Hpse-deficient osteoblasts have a reduced proliferative capacity, which is also demonstrable by wild type osteoblasts treated with a Hpse inhibitor. Although HSPGs regulate SMAD signaling, Hpse failed to activate this pathway in osteoblasts. A gene array analysis comparing *Hpse*^{-/-} and wild type osteoblasts suggests that the sexual dimorphism seen in the Hpse deficient animals could be related to androgen protection against reduced bone formation associated with impairments to the β -catenin pathway, such as increased caveolin-1 expression. The gene array analysis further shows the involvement of multiple growth and differentiation pathways in the *Hpse*^{-/-} skeletal phenotype. Both Hpse null males and females show marked decreases in *Ibsp* and *Ost-PTP* expression. The expression of both genes is highly upregulated in the Hpse transgenic animals. These changes are accompanied by a slight interference with energy metabolism. Because LBM is the only spontaneous phenotype so far identified in the Hpse mutant mice, it appears that the main physiologic involvement of Hpse is associated with a normal rate of bone mass accrual and maintaining bone remodeling at balance, thus protecting the skeleton against age-related LBM.

Disclosures: Vardit Kram, None.

SU0227

Mechanism of Formation of Novel Bone Forming Cells (monoosteophils) from LL-37 Treated Monocytes. Zhifang Zhang^{*}¹, John Shively². ¹City of hope, USA, ²Department of Immunology, City of Hope, USA

BACKGROUND: Bone generation and maintenance involve osteoblasts, osteoclasts, and osteocytes. However, an incomplete understanding of bone forming cells during wound healing has led to an unmet clinical need such as nonunion of bone fractures. Recently, our published paper showed that LL-37, the active peptide of human cathelicidin, has an ability to induce monocyte differentiation to a new type of bone forming cells (monoosteophils). We now have investigated the mechanism of monoosteophil formation. **RESULTS:** Treatment of monocytes from blood with LL-37 for 6 days resulted in their differentiation to monoosteophils. Monoosteophil on osteologic discs built bone-like nodules which consist of calcium and phosphorus. *In vivo* transplantation studies in NOD/SCID mice show that LL-37-differentiated monocytes form bone-like structures similar to endochondral bone formation. Monoosteophils are identified by up-regulation of integrin $\alpha 3$ and $\alpha 3 \beta 1$ and down-regulation of CD14, CD16, CD32, and CD163 on the membrane. Microarray analyses indicated the differential expression of 206 genes in the formation of monoosteophils. Among these genes we found elevated level of CCL22. **CONCLUSION:** Blood derived monocytes treated with LL-37 can be differentiated into a novel bone forming cell that functions both *in vitro* and *in vivo*. We propose the name monoosteophil to indicate their monocyte derived lineage and their bone forming phenotype. Integrin $\alpha 3$ and $\alpha 3 \beta 1$, CD14, CD16, CD32, and CD163 can be used as differentiation markers of monoosteophils and that the chemokine CCL22 may be involved in their formation.

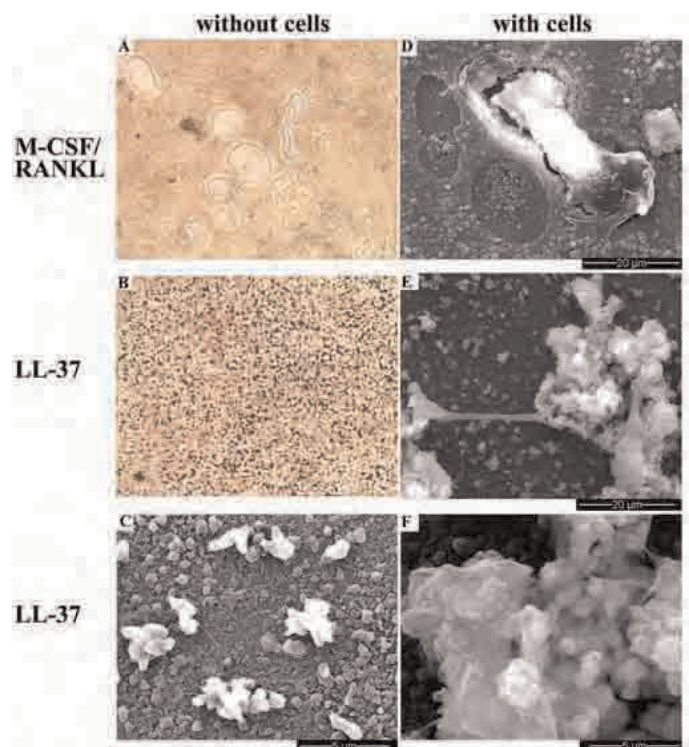


Fig 1. LL-37-differentiated monocytes built nodule-like structure on osteologic discs. Monocytes were incubated in the presence of M-CSF/RANKL (both at 25 ng/mL, A, D) or 5 μ M LL-37 (B,C,E,F) on BioCoat™ Osteologic™ Discs in 5% CO₂ atmosphere. After incubation for 3 weeks, cells were removed with bleach and observed by phase contrast microscopy (magnification $\times 200$, A, B) or scanning electron microscopy (SEM) (C). After incubation for 7 weeks, pit formation and osteoclast are shown on the disc incubated with M-CSF/RANKL-differentiated monocytes by using SEM (D), and built-up structures and cells are shown on the disc of LL-37-differentiated monocytes (E-F).

Fig 1

SU0229

Opto-Functional Control of Intracellular RANKL Transport/Secretion in Osteoblasts to Enhance Coupling With Osteoclasts Based on Photo-Energy Conversion of Molecularly-Engineered Channel-Rhodopsin. Takuya Notomi¹, Miyuki Kuno², Yoichi Ezura³, Masaki Noda⁴. ¹GCOE, Tokyo Medical & Dental University, Japan, ²Osaka City University, Japan, ³Tokyo Medical & Dental University, Medical Research Institute, Japan, ⁴Tokyo Medical & Dental University, Japan

Lysosomal vesicles (Lv) have a key role for transport of intracellular RANKL to membrane-bound RANKL (mBRANKL), however, its mechanism remains unclear. The Lv fusion is related to the change of membrane potential (MP). Thus, MP could regulate osteoblast (OB) function and RANKL secretion. So far little is known about the role of MP on bone physiology, because it is hard to control temporal patterns of MPs. To challenge this difficulty, we developed a genetic and cellular strategy to evoke light-inducible modulation of MP in OBs and show the novel mechanism of intracellular transport of RANKL via regulation of MP.

For controlling MP, we genetically modified OBs (MC3T3) by permanently transfecting Channel rhodopsin Wide Receiver (ChWR) which converts photo-energy (blue light) into channel activation and causes the permeation of cations. After establishing the stable cell lines of ChWR (WR) or control vector (C) expressing OBs, the MP was recorded under the whole cell clamp configuration. These cells were exposed to a series of blue light stimulus (BLS; (2" stimulus - 1" rest) × 10 times). We found that MPs in WR were depolarized immediately (< 20 msec) after the on-stimulus (AMP: 16.3 ± 1.1 mV) and were returned to the pre-stimulus potential after the off-stimulus. No changes were recorded in C. Thus, we established a new illumination system that enables us to optically control the temporal patterns of MP.

We went on to elucidate functional aspects of the relationship between RANKL secretion and MP in OBs. Although the BLS did not increase mBRANKL in RANKL-overexpressed (R-OE) C, mBRANKL was increased 5-fold in R-OE WR at 10 min after BLS. The BLS also increased the endogenous RANKL mRNA expression 5-fold at 120 min after BLS. For functional analysis, co-culture (RAW267.4 and R-OE WR or C) was subjected to BLS once a day for 5 days. No osteoclasts were observed in C. In contrast, biochemical TRAP activities in WR were increased 4-fold and the development of mature osteoclasts was observed. These results indicate that light-controlled membrane depolarization promotes osteoblastic RANKL expression in cell membrane that leads to enhanced coupling to stimulate osteoclastogenesis.

In conclusion, photo-energy conversion via ChWR regulates mBRANKL expression and osteoclast formation. Our system of photo energy conversion could trigger RANKL secretion whenever we need and provide a powerful tool to analyze osteoblastic control for osteoclasts during remodeling.

Disclosures: Takuya Notomi, None.

SU0230

Osteoblastic Wnts Regulate Postnatal Bone Remodeling through Maintaining BMSC and Inhibiting Inflammation. Wan Yong¹, Cheng Lu², Jingjing Cao², Zhengju Yao³, Gang Ma¹, Xizhi Guo¹. ¹Shanghai Jiao Tong University, Peoples Republic of China, ²colleague, China, ³mentor, China

Inflammatory bone loss is a puzzling and not well-defined process prevailing in arthritis. Previous study has shown that Wnt signaling plays an important role in embryonic osteoblastogenesis and bone formation. To understand the elaborate function of Wnts in postnatal bone homeostasis, we block the secretion of Wnts from osteoblasts through conditionally inactivating Wntless (Wls) gene by Col1(3.6kb)-Cre and Osteocalcin (Osc)-Cre. Most of the *Col1^{cre/+}*; *Wls^{cl}* displayed various defects of osteopenia, scoliosis and inflammation in bone marrow. The mutant mice showed high activity of bone turnover with increased bone resorption and decreased bone formation. *Osc^{cre/+}*; *Wls^{cl}* mice exhibited similar but milder defects as that of *Col1^{cre/+}*; *Wls^{cl}* mutant. In addition, the maintenance of bone marrow stem cell (BMSC) was impaired in *Col1^{cre/+}*; *Wls^{cl}* mutant. Extensive T cell infiltration was also detected in bone marrow upon inactivation of osteoblastic Wnts. IHC analysis revealed that Wnt5a and Wnt10b were the major osteoblastic Wnts that orchestrated postnatal bone remodeling, maintained BMSC capacity and protected from inflammatory bone loss.

Disclosures: Wan Yong, None.

This study received funding from: 973

SU0231

PTH1r and 5HT1b Receptors are Involved in Mediating the Action of n-3 Fatty Acids in Bone Cells. Hesam Tavakoli, Jose Candelario, Mirianas Chachivillits^{*}. La Jolla Bioengineering Institute, USA

The molecular pathway by which lipids interact with cells is yet to be established. There is evidence showing (1) lipids partake in bone metabolism and (2) parathyroid hormone type 1 receptor (PTH1R) and Serotonin Receptor B₁ (5HT1b) play a role in

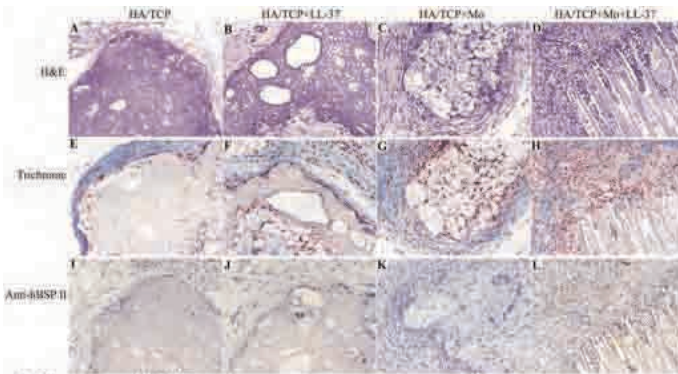


Fig 2. Bone formation of LL-37-differentiated monocytes in vivo. NOD/SCID mice were implanted subcutaneously with hydroxyapatite/tricalcium phosphate (HA/TCP) only (A-E), or with 5 μ M LL-37 (B, F, I), or with 5 $\times 10^5$ monocytes (C, G, K), or 5 μ M LL-37 plus 5 $\times 10^5$ monocytes (D, H, L). Implants were harvested 7 weeks later and sections stained with Hematoxylin and Eosin (A-D), Masson's Trichrome (E-H), and anti-human HSP110 (I-L) (1:1000).

Fig 2

Disclosures: Zhifang Zhang, None.

SU0228

Neuropeptide Y1 Receptor Antagonist Reduces Periosteal Bone Formation and Mitigates the Bone Response to Mechanical Loading. Edith Gardiner^{*}, Leah Worton, Steven Bain, Ted Gross, Sundar Srinivasan. University of Washington, USA

Reports indicating that neuropeptide Y (NPY) inhibits bone formation through osteoblastic Y1 receptor provide a basis for therapeutic targeting of NPY signaling. Furthermore, given evidence that NPY signaling is involved in bone cell mechanotransduction, we sought to explore whether suppression of endogenous inhibitory signaling (NPY) in the context of an anabolic stimulus (exogenous mechanical loading) would prove to be synergistic. We tested this concept by exposing mouse tibiae to exogenous mechanical loading with/without a Y1 receptor antagonist. Experimentally, the right tibiae of C57BL/6J mice were loaded (18 wk old, 8-11 per treatment group, 1600 μ s at 1 Hz, 50 cycles/day, 3 times/wk for 3 wk) and mice received the selective Y1 receptor antagonist BIBO3304 (0.12 or 0.4 mg/kg body weight, i.p.) or vehicle, 1 hr before (n=4 males, n=4 females/group) or 4 hr after (n=3 males/group) loading. Bone formation was assessed in contralateral and externally loaded tibiae by standard dynamic histomorphometry. Mean values for vehicle- and BIBO3304-treated groups were compared by t-test. Initial data analyses revealed no differences due to gender or pre/post loading treatment; all mice were therefore combined for statistical analyses. In contrast to genetic models in which Y1 gene deletion increased periosteal bone formation, both doses of BIBO3304 reduced periosteal mineralized surface (p.MS/BS, -73%) and bone formation rate (p.BFR/BS, -78%) vs vehicle on non-loaded contralateral limbs but did not alter periosteal mineral apposition rate (Table 1). Y1 antagonist treatment at the higher concentration also inhibited the loading-induced increase in p.MS/BS (-53%), p.BFR/BS (-53%), and mineral apposition rate (p.MAR, -37%). One possible reason for the unexpected mitigation of basal and mechanically induced bone formation is varied antagonist effects depending on osteoblastic maturity. Alternatively, BIBO3304-induced alterations in sympathetic tone may also contribute to the effects observed here. Clarifying the differences between the effects of constitutive gene deletion and those of acute pharmacological intervention will be critical in enabling therapeutic targeting of Y1 receptor to stimulate a robust bone anabolic response with or without exercise.

Table 1. BIBO3304 effects on periosteal bone formation in loaded and contralateral tibiae (n=8-11; mean \pm SE; *p<0.05).						
BIBO3304 Treatment	Non-loaded limb			Loaded limb		
	p.MS/BS (%)	p.MAR (um/d)	p.BFR/BS (um3/um2/d)	p.MS/BS (%)	p.MAR (um/d)	p.BFR/BS (um3/um2/d)
Veh (5% DMSO)	15.4 \pm 5.4	0.30 \pm 0.12	0.09 \pm 0.04	28.8 \pm 8.6	0.68 \pm 0.13	0.31 \pm 0.08
Low (0.12 mg/kg)	4.1 \pm 2.0*	0.19 \pm 0.10	0.02 \pm 0.01*	25.6 \pm 4.5	0.79 \pm 0.14	0.21 \pm 0.06
High (0.4 mg/kg)	4.3 \pm 2.2*	0.11 \pm 0.08	0.02 \pm 0.01*	13.4 \pm 4.1*	0.43 \pm 0.06*	0.14 \pm 0.03*

Table 1

Disclosures: Edith Gardiner, None.

bone metabolism. Using picosecond time-resolved fluorescence microscopy and G protein-coupled receptor conformation-sensitive fluorescence resonance energy transfer (FRET), we investigated conformational transitions in PTH1R and 5HT1b. Genetically engineered PTH1R and 5HT1b sensors containing an intramolecular FRET pair were used to enable the detection of conformational changes in single Human Embryonic Kidney (HEK) 293 cells in response to stimulation with different fatty acids. Downstream PTH1R and 5HT1b pathway activation was confirmed by monitoring ERK 1/2 phosphorylation through western blot analysis. (1) Stimulation of PTH1R and 5HT1b sensors with EPA or DHA caused significant conformational changes in the receptors. (2) The response to EPA stimulation in the PTH1R sensor was inhibited in the presence of the PTH1R antagonist [Nle8,18,Trp34]PTH(3-34). (3) Activation of PTH1R and 5HT1b downstream signaling with EPA or DHA resulted in a significant increase in ERK phosphorylation in western blot analysis. (4) ERK phosphorylation by activation of PTH1R with EPA or DHA was inhibited in the presence of PTH1R antagonist [Leu11-D-Trp12]PTH-rP(7-34). In conclusion, increased levels of EPA and DHA cause a change in the confirmation in PTH1R and 5HT1b receptors that leads to downstream activation and ultimately results in an increase of ERK phosphorylation. These results indicate that the fatty acids, EPA and DHA, can modulate the action of PTH1R and 5HT1b receptors and consequently provide a putative molecular mechanism for the anabolic effect of omega-3 fatty acids in bone

Disclosures: Mirianas Chachivilis, None.

SU0232

Recombinant Activated Protein C Stimulates Bone Nodule Formation and Osteocalcin Expression in Osteoblasts. Kaitlin Shen¹, Benjamin Chan², Meilang Xue³, Colin Dunstan⁴, Hala Zreikat⁴, Christopher Jackson³. ¹Kolling Institute of Medical Research/University of Sydney, Australia, ²Royal North Shore Hospital, Australia, ³Kolling Institute of Medical Research, Australia, ⁴University of Sydney, Australia

Introduction: Activated Protein C (APC) is a natural anticoagulant with strong anti-inflammatory and cytoprotective properties. It has a potential therapeutic role in rheumatoid arthritis (RA) by reducing activation of synovial fibroblasts and monocytes, however, the effects of APC on RA are not fully understood. This study aims to determine the effect of APC on bone turnover through its effects on osteoblast proliferation, differentiation and maturation.

Method: Human bone derived cells (HBDCs), isolated from RA or OA subchondral bone post knee replacement surgery and the mouse pre-osteoblast MC3T3-E1 cell line were used in this study. The expression of APC and its receptor, endothelial protein C receptor (EPCR) and type I collagen in HBDCs was determined by immunofluorescence/immunocytochemistry. The effect of recombinant human (rh) APC on HBDC and MC3T3-E1 proliferation was quantified by MTT assay and cell counts at 24, 48 and 72 hours. Reverse transcriptase qPCR was used to examine the mRNA transcripts of MC3T3-E1 cells modulated by rhAPC over 22 days. The effect of rhAPC on *in vitro* bone nodule formation was visualized by alizarin red staining.

Results: Immunofluorescence showed prominent expression and colocalization of APC and EPCR in HBDCs. Proliferation studies demonstrated that rhAPC significantly decreased MTT incorporation over 72 hours and also dose-dependently decreased cell count, by up to 40% when used at 10µg/mL. However, this suppression of proliferation was accompanied by a marked increase in type I collagen production over 24 hours after treatment with 10µg/mL of rhAPC, indicative of an early effect on osteoblast differentiation. The addition of rhAPC to MC3T3-E1 cells stimulated *in vitro* bone nodule formation by increasing both number of bone nodules (~30%) and alizarin red staining of calcified osteoblast monolayer. This effect may be partly explained by an average 32% upregulation of osteocalcin expression beyond 4 days of rhAPC treatment, suggesting that later stages of osteoblastic differentiation are maintained.

Conclusion: APC and EPCR are co-localized in osteoblasts and exogenous APC stimulates bone nodule formation possibly by increasing type I collagen and osteoblastic differentiation. Further investigations will determine the underlying mechanisms and implications for diseases such as rheumatoid arthritis.

Disclosures: Kaitlin Shen, None.

SU0233

Reduced Accumulation of Bone in Mice Lacking the *Men1* Gene in Osteoblasts. Ippei Kanazawa¹, Geeta Nayak², Lucie Canaff¹, Monzur Murshed¹, Geoffrey Hendy³. ¹McGill University, Canada, ²McGill University, Canada, ³McGill University, Royal Victoria Hospital, Canada

Homozygous inactivation of the multiple endocrine neoplasia type 1 (*Men1*) gene encoding menin in mice is embryonic lethal at 12 days and fetuses exhibit clear defects in cranial and facial development, whereas the heterozygous phenotype is similar to that of the *MEN1* syndrome in humans with endocrine tumors developing later in life. This suggested that menin plays a role in bone formation. *In vitro*, menin promotes the commitment of pluripotent mesenchymal stem cells to the osteoblast lineage, whereas, in mature osteoblasts, menin retards their later differentiation. To further understand the role of menin in bone development *in vivo* we are generating mouse models in which the expression of the *Men1* gene is altered only in bone cells.

Mice lacking *Men1* in osteoblasts were generated by crossing OC(Osteocalcin)-Cre mice with homozygous conditional mutants carrying modified *Men1* alleles with loxP

sites flanking exons 3 and 8. The OC-Cre^{+/+};Men1^{lox/lox} mice were viable and fertile and after a second round of mating, these mice (*Men1* KO) were compared with their control littermates (WT) lacking the OC-Cre transgene. There were no differences in growth rate between *Men1* KO and WT mice. In 9-month-old female mice while serum calcium and phosphate were normal, histomorphometric analysis showed that bone volume/total volume (BV/TV) (9.73 ± 0.35 n=5 vs. 14.10 ± 0.90 n=7, *P*=0.003) and bone surface/total volume (BS/TV) (7.28 ± 0.30 vs. 9.58 ± 0.66, *P*=0.019) were reduced in the *Men1* KO mice vs. WT mice.

To overexpress *Men1* specifically in osteoblasts, we made a *Col1a1*-*Men1* transgene construct in which a 2.3-kb *Col1a1* promoter fragment drives a Flag-tagged-menin cDNA. Two of the independent lines generated by mating each of seven *Col1a1*-*Men1* founder mice with WT mice demonstrated bone-specific transgenic expression. At three months of age, the *Flagmen1* mice (male and female) were not different from WT in growth rate, bone mineral density (DEXA), fat pad weight and serum calcium and phosphate levels.

Taken together, the data indicate that menin has a role in bone formation especially in older mice. Depletion of menin in the osteoblast leads to a reduction in bone whereas overexpression has no effect at least in younger mice. Hence, maintenance of menin expression and function in bone is important to avoid decreased bone formation. Therefore, menin is a potential target in combating the bone loss of disorders such as osteoporosis in the elderly.

Disclosures: Ippei Kanazawa, None.

SU0234

Resolution of Inflammation Modulates Wnt Signaling and Promotes Osteoblast-mediated Erosion Repair in Inflammatory Arthritis. Melissa Matzelle¹, Maxime Gallant², Keith Condon², Nicole Walsh³, Catherine Manning¹, Jane Lian¹, David Burr², Ellen Gravalles¹. ¹University of Massachusetts Medical School, USA, ²Indiana University School of Medicine, USA, ³St Vincent's Institute of Medical Research, Australia

Inflammation-induced bone loss results from an imbalance of bone resorption relative to bone formation. In rheumatoid arthritis, a disease characterized by inflammation-induced articular bone erosion, pro-inflammatory cytokines expressed by the synovium drive osteoclast-mediated bone resorption and simultaneously inhibit bone formation by osteoblasts. While effective therapies can halt the progression of bone erosion, repair is uncommon. To determine whether resolution of inflammation can promote anabolic osteoblast activity, inflammatory arthritis was induced by transfer of arthritogenic K/BxN serum to C57BL/6J mice and arthritis was allowed to resolve. Midfoot bones of the hind paws were evaluated by histology and histomorphometry; quantitative RT-PCR (qPCR) was performed on synovial tissue. In this model, inflammation peaked ten days after initial serum injection, with complete resolution of inflammation between days 28 and 38. qPCR of synovial tissue confirmed a 20-fold induction of IL-1β mRNA and 1.5-fold induction of TNF at day 10, both of which returned to non-arthritic levels by day 28. RANKL/OPG mRNA ratios also correlated with inflammation, favoring osteoclast-mediated resorption at day 10 and protection from resorption beginning as early as day 15. Dynamic histomorphometric analyses of fluorochrome incorporation at sites of erosion demonstrated that inflammation at the bone interface (day 10) was accompanied by a BFR similar to the rate in non-arthritic mice. However, resolution of inflammation from days 28 to 48 was accompanied by a significant increase in MS/BS, MAR, and BFR, correlating with striking repopulation of the bone surface by osteoblasts expressing alkaline phosphatase and osteocalcin. Modulation of inflammation was accompanied by dramatic changes in the synovial expression of components of the Wnt/β-catenin pathway. Inflammation induced gene expression of the Wnt antagonists sFRP1 and sFRP2. Furthermore, the downregulation of sFRP1 and sFRP2 expression with resolving inflammation paralleled the induction of the anabolic and pro-matrix mineralization factors Wnt10b and DKK2. Thus, in murine inflammatory arthritis, resolution of inflammation promotes osteoblast-mediated repair of articular bone erosions. As such, in diseases of inflammatory bone loss, strict control of inflammation may be essential for the creation of an anabolic microenvironment that supports bone formation and restoration of normal bone architecture.

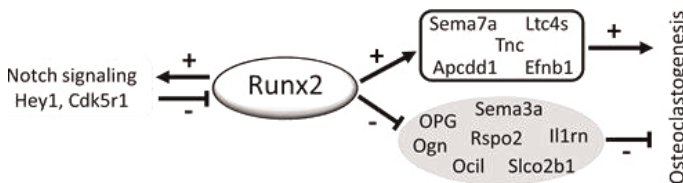
Disclosures: Melissa Matzelle, Abbott Bioresearch Center, 9

SU0235

Runx2 Promotes both Osteoblastogenesis and Novel Osteoclastogenic Signals in ST2 Mesenchymal Progenitor Cells. Sanjeev Baniwal¹, Parantu K. Shah², Yunfan Shi³, Josephine Haduong⁴, Yves DeClerck³, Yankel Gabet⁵, Baruch Frenkel¹. ¹University of Southern California, USA, ²Dana-Farber Cancer Institute, Harvard School of Public Health, USA, ³Keck School of Medicine, University of Southern California, USA, ⁴Keck School of Medicine, University of Southern California, USA, ⁵Tel Aviv University, Israel

In addition to being a master regulator for osteoblast differentiation, Runx2 controls osteoblast-driven osteoclastogenesis. Previous studies profiling gene expression during osteoblast differentiation had limited focus on Runx2 or paid little attention to its role in mediating osteoblast-driven bone resorption. ST2/Rx2^{dox}, a

bone marrow-derived mesenchymal pluripotent cell line that expresses Runx2 in response to Doxycycline (Dox) was used to profile Runx2-modulated gene expression. Runx2-induced osteoblast differentiation was assessed based on alkaline phosphatase staining and expression of classical marker genes. Osteoclastogenic potential was evaluated by TRAP staining of osteoclasts that differentiated from primary murine splenocytes co-cultured with the ST2/Rx2^{dox} cells. The BeadChip™ platform (Illumina) was used to interrogate genome-wide expression changes in ST2/Rx2^{dox} cultures after treatment with Dox or vehicle for 24 or 48 hours. Expression of selected genes was also measured by RT-qPCR. Dox-mediated Runx2 induction in ST2 cells stimulated their own differentiation along the osteoblast lineage and the differentiation of co-cultured splenocytes into osteoclasts. The latter was attributable to stimulation of osteoclastogenic genes such as *Sema7a*, *Ltc4s*, *Efnb1*, *Apccdd1* and *Tnc*, as well as inhibition of anti-osteoclastogenic genes such as *Tnfrsf11b* (OPG), *Sema3a*, *Slco2b1*, *Ogn*, *Clec2d* (Ocil), *Il1rn* and *Rspo2*. Control of osteoblast differentiation and concomitant paracrine control of osteoclast differentiation, both through the activity of Runx2 in pre-osteoblasts, constitute a novel mechanism with a potentially crucial role in coupling bone formation and resorption.



Runx2 control of osteoclastogenesis

Disclosures: Sanjeev Baniwal, None.

SU0236

Sef (IL17RD) is a Negative Regulator of Osteogenic Differentiation and Bone Formation. Qing He^{*1}, Xuehui Yang², Robert Friesel². ¹Maine Medical Center - Hospital, USA, ²Maine Medical Center Research Institute, USA

Fibroblast Growth Factor signaling plays a significant role in skeletal development and bone formation. Mutation in FGF Receptors in the human genome causes a variety of skeletal disorders including dwarfism and craniosynostosis. Knockout of FGFR3 in the mouse results in skeletal over-growth. Several feedback inhibitory pathways including Sprouty and Sef (IL17RD) negatively regulate FGFR signaling. Sprys have been demonstrated to regulate both osteoblast and chondrocyte differentiation. However, little is known about the role of Sef during skeletal development. In this study, we examined the function of Sef in osteogenic differentiation and bone formation using a Sef transgenic mouse model as well as a KST223-Sef knockout mouse model. RT q-PCR assays measuring expression of osteogenic marker genes, such as osteopontin, alkaline phosphatase, osteocalcin and runx2 indicated over-expression of Sef significantly inhibited osteogenic differentiation while loss of expression of Sef promoted osteogenic differentiation. Alkaline phosphatase staining and alizarin red staining of differentiated osteoblastic cells from Sef knockout and transgenic mice confirmed Sef negatively regulates osteogenic differentiation. Femurs from Sef knockout mice assessed by microtomography and histological analysis suggested loss of Sef increases bone formation in vivo. Furthermore, over-expression of Sef inhibited FGFR-ERK signal pathways during osteogenic differentiation by down regulating phosphorylation of Raf, MEK and ERK. Sef may also regulate the canonical Wnt/ β -catenin pathway by interacting with β -catenin. Collectively, our results suggest that Sef negatively regulates osteogenic differentiation and bone formation both in vivo and in vitro. Sef inhibits osteogenesis in part through inhibition of FGFR-ERK pathway and may also regulate canonical Wnt signaling.

Disclosures: Qing He, None.

SU0237

TRPV4 Deficiency Suppresses Fluid Flow Induced Activation of Calcium Oscillation in a Manner Dependent on Osteoblastic Differentiation. TAKAFUMI SUZUKI^{*1}, Takuya Notomi², Daisuke Miyajima¹, Yoichi Ezura³, Tetsuya Nakamoto¹, Tadavoshi Hayata⁴, Atsuko Mizuno⁵, Makoto Suzuki⁶, Fumitaka Mizoguchi¹, Yuichi Izumi⁷, Masaki Noda¹. ¹Tokyo Medical & Dental University, Japan, ²GCOE, Tokyo Medical & Dental University, Japan, ³Tokyo Medical & Dental University, Medical Research Institute, Japan, ⁴Medical Research Institute, Tokyo Medical & Dental University, Japan, ⁵Jichi Medical University, Japan, ⁶Department of Pharmacology, Jichi Medical School, Japan, ⁷Department of periodontology, Japan

Mechanical stress is an important factor to regulate bone homeostasis, and plays an important role in maintaining the bone structure and mass throughout life. TRPV4 is a Ca²⁺ and Mg²⁺ permeable non-selective cation channel, and activated by a variety of physical stimulation (cell swelling, heat, mechanical stress) and chemical reagents (endocannabinoids, arachidonic acid). TRPV4 is involved in bone formation

and remodeling as deficiency of TRPV4 suppresses unloading-induced osteoclast activation and osteoblast suppression. TRPV4 is expressed in osteoblasts and osteoclasts and plays a role in sensing mechanical stress and controlling bone remodeling in long bone. However, the function of TRPV4 in intracellular calcium regulation in osteoblasts is not known. The aim of our study is to investigate the possible role of TRPV4 in osteoblasts under mechanical stress.

We first examined TRPV4 expression level during osteoblastic differentiation. Osteoblasts were isolated from the calvaria of newborn WT and TRPV4 deficient mice, and cultured with osteogenic medium (100 μ g/ml ascorbic acid, 10mM β -glycerophosphate and 10n-100n-1 μ M dexamethasone). At 0-4-7 days, mRNAs were extracted and subjected to quantitative real-time PCR analysis. Under this condition, alkaline phosphatase expression was increased in a time dependent manner. We found that the expression of mRNA for TRPV4 was increased during the differentiation of osteoblastic cells.

Osteoblasts before changing osteogenic medium were seeded on BioFlux plate and loaded under fluid flow stress as mechanical stress. We adopted 5 dyn/cm² that is less than the rate used for endothelial experiments. Our results showed that the generation rate of calcium oscillation was markedly increased by fluid flow in WT osteoblasts ($p < 0.01$).

In addition, we examined osteoblasts after changing osteogenic medium. We found that the generation rate of calcium oscillation was significantly decreased in TRPV4 deficient osteoblasts ($p < 0.05$), suggesting that TRPV4 is involved in the generation of calcium oscillation during osteoblastogenesis.

In conclusion, we identified that expression of TRPV4 is developmentally regulated along with osteoblastic differentiation and this controls the generation of calcium oscillation.

Disclosures: TAKAFUMI SUZUKI, None.

SU0238

Age Related Changes in FGF2 and Beta-Catenin Expression in Osteoblasts from Young, Middle Aged and Elderly Female Patients. Maria Marie Hurley^{*1}, Alycia Eslinger², Liping Xiao², Gloria Gronowicz². ¹University of Connecticut Health Center School of Medicine, USA, ²University of Connecticut Health Center, USA

Fibroblast growth factor 2 (FGF2) stimulates pre-osteoblast replication and previous studies demonstrated that knockout of the Fgf2 gene in mice resulted in progressive osteopenia with age associated with decreased wnt signaling. In addition targeted expression of FGF2 in osteoblast progenitors resulted in increased bone mass in mice via modulation of wnt signaling. However the importance of FGF2 in the maintenance of bone mass in humans is not defined. We tested the hypothesis that there is a progressive reduction of FGF2 with age in human osteoblasts. Human osteoblasts cultures were derived from the discarded bone of orthopaedic surgeries according to an approved IRB protocol. Bone chips were prepared and cultured for 2 weeks in DMEM/F-12 medium with 10% fetal bovine serum and antibiotics. Outgrowth cells were trypsinized and replated at the same density for subsequent experiments. More than 95% of the cells express high levels of alkaline phosphatase and therefore, were considered osteoblasts. Cells were cultured until confluent and total RNA was extracted to assess Fgf2, Beta-Catenin and FGF receptors 1, 2 and 3 mRNA by qPCR, while protein was extracted for Western blots. As shown in Figure 1A, mRNA levels of Fgf2 and Beta-Catenin in human osteoblast cultures (passage 2 or less) from female patients ages 32, 47 and 66 years decreased with age. However, the receptors did not demonstrate an age-related decline. Western blot (Figure 1B) of FGF2 protein levels in human osteoblast cultures (passage 4 or less) from female patients of ages 29, 41 and 67 years old showed that FGF2 protein also decreases with age. One additional experiments with separate subjects demonstrated similar results. FGF2 was previously shown to activate Beta-catenin, which can upregulate bone formation. In conclusion, reduction in Fgf2 expression in osteoblasts could contribute to age-related bone loss in humans and Beta-Catenin may be involved in the signaling mechanisms that lead to FGF2-mediated bone loss.

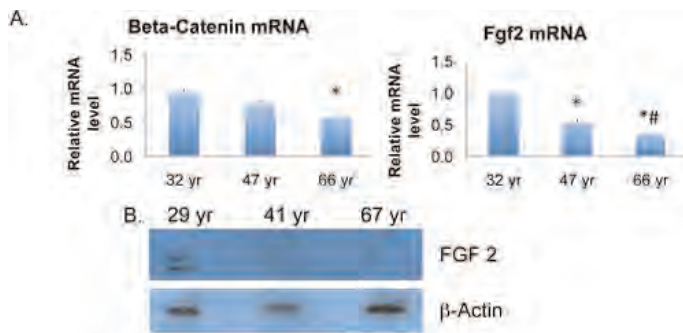


Fig. 1 (A) Beta-Catenin and Fgf2 mRNA in human osteoblast cultures from female patients ages 32, 47 and 66 years old were measured by qPCR. All Fgf2 groups were significantly different from each other (Student's t-test) and reduced with age. *: compared with 32 yr $p < 0.05$. #: compared with 47 yr $p < 0.05$.

(B) Western blot of FGF2 protein in human osteoblast cultures from female patients of ages 29, 41 and 67 years old. Equal amounts of protein were run per lane with β -actin as a loading control. An age-related decline was found.

Figure1

Disclosures: Marja Marie Hurley, None.

SU0239

Differential activation of the Alkaline Phosphatase promoter by pRB and p107. Stephen Flowers^{*1}, Elizabeth Moran². ¹NJMS-UH Cancer Center, University of Medicine of Dentistry of New Jersey, USA, ²University of Medicine & Dentistry of New Jersey, Cancer Center, USA

The retinoblastoma susceptibility gene, Rb1, is closely linked with osteosarcoma as well as retinoblastoma. Functional analysis of pRB and the related family members, p107 and p130, has tended to focus on repression of proliferation, but genetic evidence from our lab and others indicates an active requirement for pRB in osteoblast differentiation that correlates more directly with osteosarcoma susceptibility. pRB is linked with activation of the early osteoblast marker, alkaline phosphatase (the product of the *Alpl* gene). We have shown by chromatin immunoprecipitation (ChIP) that the active *Alpl* promoter is targeted directly by pRB and p107. pRB is required for several activation events, including displacing the histone demethylase, KDM5A, from the inactive promoter and recruiting the BRG1 subunit of the SWI/SNF complex to the active promoter. BRG1 in turn is necessary for the recruitment of RNA polymerase II.

The presence of p107 on the active *Alpl* promoter suggests it may also contribute to activation, but it is unknown if the function of p107 is redundant to the function of pRB. This issue is addressed with the use of shRNA to deplete p107 in the MC3T3-E1 preosteoblast line. Depletion of p107 resulted in impaired induction of alkaline phosphatase, demonstrating that it is also essential for activation. As with the pRB-depleted line, depletion of p107 resulted in failure of both BRG1 and RNA polymerase II to be recruited to the promoter. Transcription factors that target *Alpl* during activation have not been identified by ChIP, but SP1 and RUNX2 have been implicated. ChIP analysis, in parental cells, found both RUNX2 and SP1 bind the active promoter. Depletion of p107 did not affect the ability of either transactivator to associate with the promoter. In contrast, depletion of pRB resulted in the failure of both factors to be recruited. Unlike the pRB-depleted line, the p107-depleted line was able to displace KDM5A.

Our results reveal that pRB and p107 are both involved the activation of *Alpl* expression, but their roles at the promoter are not entirely redundant. Both pRB and p107 are needed for the recruitment of BRG1. However, p107 is dispensable for both the displacement of KDM5A and for the recruitment of both RUNX2 and SP1. Further study of the genes targeted in osteoblast by pRB and p107 during activation, and the contribution of each, will continue to increase our understanding of the specific role of pRB in suppression of osteosarcomas.

Disclosures: Stephen Flowers, None.

SU0240

ER Membrane Bound Transcription Factor ATF6 Is Involved in BMP2-induced Osteoblast Differentiation and Osteocalcin Transcription in MC3T3E1 Cells. Won Gu Jang¹, Eun Jung Kim¹, In Hong Kang^{*2}, Keun-Bae Lee¹, Hueng-Sik Choi¹, Jeong-Tae Koh¹. ¹Chonnam National University, South Korea, ²Interdisciplinary graduate program in molecular medicine, South Korea

Endoplasmic reticulum (ER)-bound transcription factor families are involved in the control of various metabolic pathways through the unfolded protein response (UPR). Bone morphogenetic protein 2 (BMP2) induces mild ER stress followed by the activation of major UPR transducers such as PERK/ATF4 and OASIS in osteoblast cells. ATF6 is also one of ER-bound bZIP transcription factors, which is cleaved and

translocated into nucleus by ER stress. However, involvement of ATF6 in BMP2-induced osteoblast differentiation has not been elucidated. In the present study, BMP2 treatment markedly induced the expression and activation of ATF6 with the increase in ALP and OC expression in MC3T3E1. However, the ATF6 activation by BMP2 was not observed in Runx2-/- primary calvarial osteoblasts and Runx2 overexpression recovered the BMP2 action. BMP2 stimulated ATF6 transcription through enhancing the direct binding of Runx2 to osteoblast-specific cis-acting element 2 (OSE2, ACCACA, -205 ~ -200 bp) motif of ATF6 promoter region. In addition, overexpression of ATF6 increased OC promoter activity with enhancing the direct binding to a putative ATF6 binding motif (TGACGT, -1126 ~ -1121 bp). Inhibition of ATF6 function with dominant negative form of ATF6 (DN-ATF6) blocked BMP2- or Runx2-induced OC expression. Of interest, OASIS, structurally very similar to ATF6, cannot induce the OC expression. ALP and Alizarin red staining results confirmed that BMP2-induced matrix mineralization was also dependent on ATF6 in vitro. Taken together, these results suggest that ER stress-activated transcriptional factor ATF6 mediates BMP2-induced osteoblast differentiation via regulating the osteocalcin gene expression.

Disclosures: In Hong Kang, None.

SU0241

Frizzled 1 Promoter Activity and Expression Is Regulated by E2F1 in Osteoblasts. Shihong Yu^{*1}, Laura Yerges-Armstrong², Yanxia Chu³, Joseph Zmuda⁴, Yingze Zhang⁵. ¹University of Pittsburgh Medical Center, USA, ²University of Maryland, USA, ³University of Pittsburgh, Department of Medicine, USA, ⁴University of Pittsburgh, Department of Epidemiology, USA, ⁵University of Pittsburgh, USA

Frizzled family members initiate Wnt signal transduction. Genetics studies by our group demonstrated significant associations of promoter polymorphisms and haplotypes in Frizzled-1 (FZD1) with bone mineral density and bone geometry phenotypes. However, little is known about the transcriptional regulation of FZD1 in osteoblasts. To define the molecular mechanisms involved in the regulation of FZD1 gene expression, we characterized the FZD1 promoter in the Osteoblast-like cell, Saos2, using a promoter reporter system and determining FZD1 protein expression. We demonstrated that E2F1, a critical transcription factor in osteoblasts, transactivated a FZD1 promoter specific reporter construct consisting of -655 to +71 of the translation start site. FZD1 promoter activity was increased by 10.4 fold in Saos2 and by 8.9 fold in cos7 when E2F1 was transiently expressed in these cells. In addition, a deletion construct of the FZD1 promoter consisting of -141 to +71 did not abolish the transactivation by E2F1. Transient expression of E2F1 in Saos2 and cos7 cells resulted in 9 fold and 7.8 fold increases in the promoter activity of the deletion promoter construct, respectively. To our knowledge, this is the first report identifying FZD1 to be a direct transcriptional target of E2F1. Further experiments are needed to determine the potential binding domains of E2F1 in the FZD1 promoter region and how FZD1 is regulated by E2F1.

Disclosures: Shihong Yu, None.

SU0242

Identification of a Small Molecule Kinase Inhibitor That Enhances Osteoblastic Differentiation and In Vivo Bone Formation of Human Skeletal (Mesenchymal) Stem Cells Through Regulation of BMP Signaling. Abbas Jafari^{*1}, Basem Abdallah², Diyako M. Qanie³, Li Chen⁴, Nicholas Ditzel⁴, Moustapha Kassem⁴. ¹University of Southern Denmark, Denmark, ²Odense University Hospital, University of South Denmark, Denmark, ³Institute of Clinical Research, University of Southern Denmark, Denmark, ⁴Odense University Hospital, Denmark

To identify novel anabolic targets for enhancing bone formation, we screened a commercially available Kinase Inhibitor Library (containing 80 known protein kinase inhibitors that covers a wide spectrum of signaling pathways) for their anabolic effects on human bone marrow derived-mesenchymal stem cells (hMSC) and we employed quantitative alkaline phosphatase activity (ALP) measurement as a readout for effects on osteoblast differentiation of hMSC. The screen identified the protein kinase inhibitor K1x that targets protein kinases A, C, and G, with reproducible and significant stimulatory effects on ALP activity of hMSC. Further studies, demonstrated that K1x increased, in a dose dependent fashion, gene expression of early (Runx2, collagen type I) and late (osteopontin, bone sialoprotein) osteoblast differentiation markers and enhanced ex vivo matrix mineralization of hMSC. Treatment of hMSC with K1x for 6 days followed by in vivo implantation subcutaneously in immune deficient mice, led to significant increase in ectopic bone formed by the cells. Microarray analysis of K1x-treated hMSC cultures versus control cultures, revealed up regulation of bone morphogenetic protein (BMP) signaling and BMP6 gene expression in K1x treated cultures. Silencing BMP6 expression by siRNA, abolished the enhancing effect of K1x on osteogenic differentiation of hMSC. In conclusion, our data demonstrate that K1x is a potent stimulator of osteoblast differentiation of hMSC in vitro and in vivo and its effect is mediated by BMP6. This kinase inhibitor may thus be developed as a novel drug for enhancing bone formation.

Disclosures: Abbas Jafari, None.

SU0243

Iron Decreases Osteoblastic Activity in Human MG 63 Cells. Mathilde Doyard*, Nadia Fatih, Marie-Laure Island, Patricia Leroyer, Gerard Chales, Olivier Loreal, Pascal Guggenbuhl, INSERM UMR 991, equipe Fer et foie : aspects physiologiques et pathologiques, Univ Rennes, France

Aim: iron overload in thalassemia and genetic hemochromatosis may cause osteoporosis. However, molecular mechanisms leading to iron-related bone loss are not fully characterized. Both, decrease osteoblasts and increase osteoclast activities have been suggested. Our aim was to analyze in vitro the impact of iron overload on human osteoblast cells.

Methods: MG-63 cell line from a human osteosarcoma was used as osteoblast model. Iron status was modulated by adding Ferric Ammonium Citrate (FAC) and/or Deferoxamine (DFO), an iron chelator. Quantitative RT-PCR was used to evaluate mRNA levels of: i) iron metabolism genes (Transferrin Receptor 1-TFRc-, hepcidin, hemojuvelin, ferroportin, and HFE), and ii) osteoblast phenotypic markers (alpha 1 collagen type I chain, osteocalcin and RUNX2). Ferritin level was evaluated by western-blot. Reactive oxygen species (ROS) level was quantified using cell-permeant fluorescent probe 2',7'-dichlorodihydrofluorescein diacetate (DCFH2-DA). Apoptosis was evaluated by measuring caspase 3 activity.

Results: MG-63 cells FAC exposure induced a dose-dependent decrease of TFRc mRNA level and an increase of intracellular ferritin level, reflecting the increase of intracellular iron. In addition, DFO alone increased TFRc mRNA and decreased ferritin levels; DFO added to FAC neutralized the iron impact on MG-63 cells. We found that ferroportin and HFE mRNAs were significantly expressed in basal conditions. Ferroportin mRNA level was induced by FAC whereas HFE mRNA level was slightly decreased. The mRNA levels of alpha 1 collagen type I chain, the major component of bone matrix, osteocalcin, a noncollagenous protein, and transcriptional factor RUNX2 were significantly decreased in presence of FAC. DFO addition to FAC, suppressed the iron impact. Iron exposure was responsible to ROS level increase in MG-63 cells. Such effect was prevented by concomitant DFO addition. Moreover FAC induced a caspase 3 activity increase.

Conclusion: our data in MG-63 cells showed that FAC exposure of human MG-63 cells: i) modulates intracellular iron status, ii) increases ferroportin mRNA expression level, iii) decreases the expression of genes associated to osteoblast phenotype. These effects are suppressed by DFO. In addition we found that: i) oxidative stress could contribute to these alterations and that iron favors MG-63 cells apoptosis. Taken together, our results support a role of osteoblast impairment in the iron-related osteoporosis.

Funded by the Societe Franaise de Rhumatologie

Disclosures: Mathilde Doyard, None.

SU0244

Mannosyltransferase Alg2 Is a downstream Regulator of Schnurri-3 in Osteoblast Differentiation. Katsuyuki Imamura¹, Yasuhiro Ishidou¹, Ichiro Kawamura², Masahiro Yokouchi¹, Setsuro Komiya¹, Shingo Maeda¹. ¹Graduate School of Medical & Dental Sciences, Kagoshima University, Japan, ²Dept. of Orthopaedic Surgery Kagoshima University, Japan

Shn3 (Shn3, also known as Hivep3, ZAS3, KRC) was shown to promote proteasomal degradation of Runx2 protein by recruiting E3 ubiquitin ligase Wwp1. It was reported that Shn3 knockout mice demonstrated accumulated Runx2 protein in osteoblasts, accelerated osteoblast differentiation, and high bone mass in adult bone. On the other hand, two groups reported that, forced expression of Runx2 in osteoblasts in vivo (Col1a1-driven Runx2 transgenic mice) resulted in accumulation of immature osteoblasts and lowered bone mass, osteopenia. The contrary bone phenotypes between these two lines of mice with high Runx2 protein level, led us to hypothesize that Shn3 should have other roles to regulate osteoblast maturation. Because Shn3 is a large zinc-finger protein, originally characterized as a transcription factor, we searched for genes expressed downstream of Shn3 in osteoblasts. siRNA mediated knockdown of Shn3 in MC3T3-E1 did not alter expression of Runx2 mRNA, whereas Runx2 protein was slightly accumulated. Expression of early osteoblast differentiation markers, *Osx* and *Alp*, were mildly enhanced, while maturation markers bone sialoprotein (Bsp) and osteocalcin (Ocn) were significantly attenuated by Shn3 knockdown. These results suggested a crucial inhibitory role of Shn3 in maturation of osteoblasts. We analyzed the expression profile of Shn3 siRNA-transfected MC3T3-E1 by microarray, and found eight genes to be differentially expressed after Shn3 knockdown. Among them, we focused on asparagine-linked glycosylation 2 homolog (*Alg2*), because it was highly expressed in MC3T3-E1 cells, and it was confirmed to be up-regulated by Shn3 overexpression. To study the possible roles of *Alg2* in osteoblast differentiation, we transfected siRNA for *Alg2* in MC3T3-E1 osteoblasts and ST-2 bone marrow stroma cells. *Alg2* siRNA did not affect expression of Runx2 nor Shn3. However, loss of *Alg2* showed significantly accelerated activity of *Alp* in MC3T3-E1. In addition, in ST-2, *Alg2* knockdown resulted in a promoted osteoblast differentiation, characterized by up-regulated expression of *Osx*, *Alp*, Bsp, and Ocn. *Alg2* is a mannosyltransferase crucial in the dolichol pathway of N-linked protein glycosylation. We speculated that *Alg2* regulates glycosylation and activity of protein which acts upstream of *Osx*. In conclusion, we identified *Alg2* gene as a downstream mediator of Shn3 to regulate osteoblast differentiation.

Disclosures: Katsuyuki Imamura, None.

SU0245

NR2C2 Gene Regulated Osteoblasts Bone Formation Activity through Runx2 Stability. Shen-chin Hsu¹, Hsin Chiu Ho², Huei-Ju Ting², Shinjen Lin³, Tian-Fang Li², Mo Chen⁴, Jonathan Holz², Tzong-Jen Sheu², J. Edward Puzas⁵, Min-jon Lin⁶. ¹Chung Shan Medical University Hospital Dept of Pharmacy, Taiwan, ²University of Rochester, USA, ³Univeristy of Rochester, USA, ⁴Columbia University, USA, ⁵University of Rochester School of Medicine, USA, ⁶Chung Shan Medical University Dept of Biomedical Sciences, Taiwan

BACKGROUND: NR2C2 (nuclear receptor subfamily 2, group C, member 2) belongs to a nuclear receptor superfamily without an identified ligand. NR2C2 is closely related to TR2 and RXRs (19). The expression of NR2C2 was found in all tissues tested including metabolic system, and cardiovascular system. NR2C2-/- mice have significant growth retardation, impaired cerebella function. NR2C2 is also highly expressed macrophages. However, its roles within the osteoblasts remain unknown. **RESULTS:** We generated several MC3T3-E1 stable cell lines which were pBabe-NR2C2, pBabe-NR2C2 RNAi, pBabe GFP, pBabe-NR2C2 MC3T3-E1 cells had been confirmed with four folds NR2C2 over-expression by real-time PCR and western blot methods. pBabe-NR2C2 RNAi MC3T3-E1 cells had 80% knock-down efficiency. pBabe-GFP MC3T3-E1 did not show significant NR2C2 expression level difference between pBabe-GFP and non-stabilized MC3T3-E1 cells. In the osteoblast differentiation assay, NR2C2 enhanced the alkaline phosphatase activity and mineralization. On the contrary, knock-down NR2C2 showed decrease alkaline phosphatase activity and mineralization. In order to further understand the possible mechanism, we screened several osteogenic genes. Only osteocalcin and collagen I showed time-course change with NR2C2 (increase) and NR2C2 RNAi (decrease). These gene expression results correlated with the osteoblast differentiation results. We also tested if NR2C2 can directly regulate the osteocalcin gene? In the pBabe NR2C2 cells, the NR2C2 and osteocalcin reporter gene assay results showed 10 folds increase in both reporters. However, In the NR2C2 knock-down cells, the results showed 60% decrease on both NR2C2 and osteocalcin reporter results. Therefore, we looked at the RNA and protein level of runx2 in both pBabe NR2C2 and NR2C2 RNAi cells. The RNA level of runx2 was similar between these two cells. This indicated NR2C2 did not alter the RNA expression but enhanced the protein level of runx2. These results also were confirmed with the runx2 functional reporter gene assay (6XOSE2-OC-Luc). NR2C2 regulated the runx2 protein stability and subsequently changed the osteocalcin amount. By the way, we also confirmed the cell lines results with the runx2 immunoassaying and osteocalcin ELISA assay in the NR2C2 knockout mice. **CONCLUSIONS:** Our data suggested that NR2C2 plays a pivotal role in fundamental bone formation through runx2 stability.

Disclosures: Shen-chin Hsu, None.

SU0246

Osteogenic Potential of Human Mesenchymal Stem Cells: Role of Specific Transcription Factors and Different Cell Culture Conditions. Elena Torreggiani¹, Elisabetta Lambertini², Letizia Penolazzi², Renata Vecchiati², Gina Lisignoli³, Claudio Nastruzzi⁴, Roberta Piva². ¹Department of Biochemistry & Molecular Biology, University of Ferrara, Ferrara, Italy; Department of Reconstructive Science, University of Connecticut Health Center, Italy, ²Department of Biochemistry & Molecular Biology, University of Ferrara, Italy, ³Laboratory of Immunorheumatology & Tissue Regeneration, Istituto Ortopedico Rizzoli, Italy, ⁴Department of Pharmaceutical Sciences, University of Ferrara, Italy

Bone regeneration by the means of induction of osteogenesis from mesenchymal osteoprogenitors (MSCs) offers a rational therapeutic option. Two of the most important challenges in this field are i. the development of novel culture systems of MSCs and ii. the identification of new factors with crucial role in the control of MSC differentiation program. In this context, the goals of our current work are to compare growth and differentiation of human MSCs cultured in different 3D systems including alginate beads, extracellular matrix (ECM) scaffold obtained from purified porcine urinary bladder matrix, and a rotating microgravity bioreactor (HARV technology), with cells cultured using standard 2D methodologies. We have immunophenotypically characterized hMSCs obtained from sources of different origin (bone marrow, PDL and umbilical cord Wharton's jelly) demonstrating that they are positive for CD90, CD73, CD105, CD146, but negative for CD31, CD3, CD14, CD34, CD45. The cells were assessed for viability with propidium iodide and Calcein-AM, analyzed for morphological changes by different microscopic techniques (optical microscopy, SEM, TEM), and analyzed for gene expression by qRT-PCR, immunocytochemistry, and Western blot. We demonstrated that 3D culture conditions and the use of Polymeric Micelles as delivery system for differentiating agents did not negatively affect viability and cell proliferation, enhanced cell adhesion and interaction, supported osteogenic differentiation positively affecting the expression of typical osteoblastic markers and deposition of mineralized matrix. Our data highlight the importance of the most appropriate combination between hMSCs and specific scaffolds.

In addition, we evaluated the effect of transcription factors (TFs) with crucial role in the control of hMSCs behaviour by using gene-silencing approach. We focused our

attention on Slug having identified it as TF promoting osteoblast maturation in an earlier study. We demonstrated that Slug has a novel crucial role for osteochondroprogenitor: in fact, its silencing leads to decreased hMSC migration, changes in the expression levels of Runx2, Sox5, Sox6, Sox9 and Stat1, and modulates the fate of the cells towards chondrocyte differentiation. These results encourage the development of alternative strategies to induce efficient differentiation of hMSCs for their clinical use in bone tissue engineering and repair.

Disclosures: Elena Torreggiani, None.

SU0247

Regulation of both Osteoblastic and Myogenic Differentiation by Proteasome Inhibitor Bortezomib. Maki Uyama*, Mari Sato, Masamitsu Kawanami, Masato Tamura, Hokkaido University, Japan

In eukaryotic cells, degradation of most intracellular proteins is realized by ubiquitin-proteasome pathway. The clinical efficacy of bortezomib (Bzb), a 26S proteasome inhibitor used in the frontline treatment of multiple myeloma as anticancer drug, has been linked to an increase in bone markers. Bzb has been recently reported to induce differentiation of osteoblast in vitro and in vivo. However, until now, little was known of the molecular basis of action of proteasome inhibitor such as Bzb on the regulation of cell differentiation. In the present study, we investigate that the effects of Bzb on differentiation of mesenchymal stem cells into osteoblasts or myotube. In myoblastic C2C12 cells in culture, Bzb inhibited myotube formation in low mitogen medium. Bzb also inhibited myogenic gene expression such as myogenin and muscle creatin kinase, and induced osteocalcin and alkaline phosphatase gene expression, indicating that Bzb have similar activities of BMP-2. To investigate the mechanisms by which Bzb activates osteocalcin transcription, transient transfection of osteocalcin (OG2) promoter-luciferase constructs into C2C12 cells with Bzb treatment resulted in a significant increase in luciferase activity. This result implies the presence of transcriptional machinery that is sensitive to interference by Bzb and that regulates transcriptional activity through interaction with the OG2 gene promoter via OSE1 and OSE2. Using reporter construct that have BMP-2 responsive elements of Id-1 gene, Bzb did not induce their transcription activities, suggesting that Bzb does not modulate Smad1/4-dependent BMP signaling pathway. In other hand, β -catenin is a well-known target of the ubiquitin-proteasome pathway. However, Bzb did not alter transcriptional activities of β -catenin dependent Top-flash reporter and canonical Wnt signaling target gene expression. These results show that the function of proteasome in controlling degradation of polyubiquitinated signaling molecules plays important role in decision of cell fate during differentiation such as osteoblasts or muscle cells.

Disclosures: Maki Uyama, None.

SU0248

The Orphan Nuclear Receptor COUP-TFII Negatively Regulates Osteoblast Differentiation through Inhibiting the Transcriptional Activity of Runx2. Kkot-nim Lee¹, Sin-Hye Oh¹, Hye-Ju Son², Won Gu Jang², In-Hong Kang², Sun-Hun Kim², Shee-Eun Lee², Jeong-Tae Koh^{*2}. ¹Chonnam National University School, South Korea, ²Chonnam National University, South Korea

Chicken Ovalbumin Upstream Promoter-Transcription Factor II (COUP-TFII; NR2F2) is an orphan nuclear receptor of the steroid-thyroid hormone receptor superfamily. COUP-TFII is widely expressed in multiple tissues and organs throughout embryonic development, and regulates cellular growth and differentiation and organ development. However, the role of COUP-TFII in osteoblast differentiation has not been elucidated. In this study, COUP-TFII was strongly expressed in multipotential mesenchymal cells and the endogenous expression level was decreased during osteoblast differentiation. Overexpression of COUP-TFII inhibited BMP2-induced osteoblastic genes expressions in C3H10T1/2 mesenchymal cell lines. The results of alkaline phosphatase and Alizarin-red staining and osteocalcin production assay showed that COUP-TFII overexpression blocked BMP2-induced osteoblast differentiation. In contrast, the down-regulation of COUP-TFII using shRNA synergistically induced BMP2-induced osteoblastic genes expressions and osteoblast differentiation. Furthermore, COUP-TFII significantly impaired the Runx2-dependent activation of osteocalcin promoter and immunoprecipitation assay showed the physical interaction between COUP-TFII and Runx2. In our chromatin immunoprecipitation assay, COUP-TFII repressed DNA binding of Runx2 on osteocalcin gene and blocked Runx2-induced osteoblast differentiation. Taken together, these results suggest that COUP-TFII negatively regulates osteoblast differentiation through inhibiting the transcriptional activity of Runx2.

Disclosures: Jeong-Tae Koh, None.

SU0249

The Transcription Factor Sox11 is Essential for the Early Osteoblast Development. Gadi Jogeswar^{*1}, Kwang Joon Kim², Ajita Jami³, Kyoung Min Kim², Hoon Choi⁴, Sung-Kil Lim². ¹Yonsei University College of Medicine Seoul South Korea, South Korea, ²Division of Endocrinology & Endocrine Research Institute, Department of Internal Medicine, Yonsei University College of Medicine, South Korea, ³Brain Korea 21 Project for medical sciences, Yonsei University College of Medicine, Seoul, Republic of Korea-120 752, South Korea, ⁴Inje University Sanggyepaik Hospital, South Korea

The high-mobility-group (HMG) domain containing gene, Sox11 has been shown to act as a transcriptional activator. Sox11 deficient mice exhibit severe developmental defects include heart defects, skeletal malformations with decreased bone size and bone density. Even though the studies on Sox11 deficient mice shows the significant effects on osteogenesis, the detailed functional role of Sox11 in osteoblast development has not yet been defined. We demonstrate here that Sox11 is expressed in different osteoblast cells and knock down of Sox11 significantly affects the proliferation and survival of primary calvarial and MC3T3-E1 osteoblast cells. Sox11 knockdown significantly affects the expression of osteoblast lineage transcription factors Runx2 and Osterix. In addition to this, we also identified the induced differentiation in osteoblast cells significantly decreased the expression of Sox11 after one week in differentiation medium, which suggested the role of Sox11 is restricted to the early stage of osteoblast development. From our studies, we hypothesize that Sox11 is necessary for the maintenance, proliferation and survival in the early steps of osteoblast development but not for the differentiation.

Disclosures: Gadi Jogeswar, None.

SU0250

Toward Understanding the Balance Between Osteoblastogenesis and Adipogenesis in Bone Marrow Microenvironment. Basem Abdallah^{*1}, Moustapha Kassem². ¹Odense University Hospital, University of South Denmark, Denmark, ²Odense University Hospital, Denmark

The majority of conditions associated with bone loss, including osteoporosis were shown to be accompanied by increased marrow adiposity due to shifting in the balance between osteoblast and adipocyte differentiation of bone marrow skeletal stem cells (MSC). However, little is known about how the balance between osteogenesis and adipogenesis is regulated in the bone marrow microenvironment. Recently, we proposed a novel molecular model for lineage fate determination of MSC that is regulated through the cross-talk between two unique populations of pre-committed osteoblasts (MSC-OB) and adipocytes (MSC-Adipo) rather than through changes in the differentiation pathway of multipotent MSC (Ref. 1&2). Thus, we aimed in this study to identify novel secreted factors that mediating the cross-talk between osteoblasts and adipocytes in bone marrow. For that purpose, we used a combination of microarray (GeneChip® MG430A 2.0 Array) and mass spectrometry-based proteomics (secretome) to identify secreted proteins by MSC-OB (only can differentiate into osteoblast) versus MSC-Adipo (only can differentiate into adipocyte). Transcriptome and secretome profiles of these two cell lines were compared using different criteria including bioinformatics, function annotation analysis, gene expression analysis and extensive literature survey. After excluding all previously studied factors in MSC differentiation, we identified 7 novel secreted proteins (three proteins by MSC-Adipo and other 4 by MSC-OB). Studying the molecular function of these proteins in MSC cells revealed a selection of 3 secreted factors with the potential to control the commitment of MSC into either osteoblast or adipocyte lineage. In conclusion, cross-talk exists between different populations of pre-committed osteoblast and adipocyte cells in bone marrow to regulate differentiation of multipotent MSC through novel secreted factors.

References:

- 1-Taipaleenmaki H, Abdallah BM, Aldamash A, Saamanen AM, Kassem M. Exp Cell Res. 2011 Apr 1;317(6):745-56
- 2- S. Post, B.M. Abdallah, J. F. Bentzon, and M. Kassem. Bone. 2008 Jul;43(1):32-9.

Disclosures: Basem Abdallah, None.

SU0251

A Novel Mechanism of Signal Transduction: Oxytocin Receptors Activated by the Ligand Translocate in the Nucleus to Enhance Osteoblast Specific Transcription. Adriana Di Benedetto¹, Stefania Dell'Endice², Graziana Colaiani¹, Roberto Tamma², Concetta Cuscito², Bice Nico², Bice Chini³, Damiana Calvano⁴, Carlo Zamboni⁴, Li Sun⁵, Mone Zaidi⁶, Alberta Zallone^{*1}. ¹University of Bari Medical School, Italy, ²Human Anatomy & Histology, University of Bari, Italy, ³Neuroscience, CNR, Milan, Italy, ⁴Department of Chemistry, University of Bari, Italy, ⁵Mount Sinai School of Medicine, USA, ⁶Mount Sinai Medical Center, USA

Oxytocin (OT), acting through a seven-transmembrane G-protein coupled receptor OTR, has a direct anabolic effect on bone (Tamma et al., 2009) upregulating the expression of osteoblast markers and transcription factors as Osterix, Schnurri 2 and 3, Atf-4, Osteocalcin and Osteopontin. Mice null for OT or OTR genes develop with time a reduced bone mass ascribable to a low turnover osteoporosis. OTRs activated by OT are known to signals through Gq/11, but after OT stimuli (15-30') we unexpectedly found OTRs largely relocated in osteoblast nuclei as identified by western blot analysis of cytoplasmic and nuclear extracts. These results were confirmed by immunogold identification of OTR in osteoblasts with TEM and by confocal immunofluorescence studies. Thus we asked the questions 1) how a GPCR receptor is transported to nuclei and 2) to do what.

Results 1) Within 2-3 min from OT treatment in primary osteoblasts OTRs were colocalized with β -arrestin1/2, thereafter, after β -arrestins detachment, were found colocalized with rab5 in the early endosomal compartment. Eventually the vesicles were taken in charge by transportin-1 and sorted to the nuclei. All these data were obtained by confocal microscopy of OTR-GFP in fixed and in living cells. MALDI-TOF analysis, performed on nuclear proteins, immunoprecipitated with anti-OTR 30' after OT treatment, revealed the presence of four peptides corresponding to OTR intracellular loops, further giving strong evidence to OTR nuclear localization.

Results 2) Both β -arrestin1/2 and Transportin-1 silencing in osteoblasts not only affected OTR nuclear localization but prevented OT induced up-regulation of several genes as ATF-4, Osterix and osteocalcin. Immunoprecipitation from nuclear lysates of OTR, or of the osteoblast transcription factor Runx2, and the transcription co-activator Schnurri-2 always demonstrated, but only after OT treatment, the three proteins immunoprecipitated together. Furthermore an OTR/Smad4 interaction was also found when osteoblasts were simultaneously stimulated with OT and BMP2.

Conclusion. Some OT anabolic effects on osteoblast activities are mediated by a novel mechanism involving OTR nuclear interaction with the BMP-2/ Runx2 pathway with an up-regulatory effect.

Disclosures: Alberta Zallone, None.

SU0252

Angiotensin II regulates RANKL:OPG ratio potentially through transactivation of ErbB receptors by EGF-like ligands. Kirsty MacRae^{*1}, Conrad Sernia², Walter Thomas³. ¹University of Queensland, Australia, ²Associate Professor, Australia, ³Professor, Australia

Angiotensin II (Ang II) is a potent pressor hormone and a dominant causative factor in cardiovascular disease. Elderly hypertensives show reduced bone mineral density that appears to implicate a higher AngII-induced RANKL:OPG ratio. The cellular pathways underpinning these changes are uncertain but one hypothesis - which we investigate in this study - involves the transactivation of epidermal growth factor receptors (ErbB receptors) by the angiotensin type 1 receptor (AT1R). This pathway features the activation of ErbB receptors by the AT1R through the shedding of EGF-like ligands by disintegrin and metalloproteases (ADAMs).

Methods; Serum-deprived UMR-106 osteoblast cells were stimulated with Ang II, and the EGFR ligands epidermal growth factor (EGF), heparin binding-EGF (HB-EGF), betacellulin (BTC) and neuregulin 1 β (NRG1 β). In addition, cells were treated with AG1478 (a selective ErbB1 inhibitor) or TAPI-1 (a non selective ADAM inhibitor) 45 minutes prior to adding Ang II. Total RNA was isolated with Trizol and OPG, RANKL, ErbB1, ErbB2, ErbB3, ErbB4, ADAM 17, EGF, HB-EGF, BTC and NRG1 β expression analysed semi-quantitatively by RT-PCR. ERK activation by Ang II was also evaluated by Western Blotting.

Results; We confirmed that UMR-106 cells express the four ErbB receptor subtypes (ErbB1, ErbB2, ErbB3 and ErbB4) and several of their ligands. Western Blotting revealed ERK activation 1-3 min of Ang II treatment and this affect may be partially attenuated with the addition of AG1478. Ang II (1x10⁻⁸M) increased ADAM 17 expression 2-fold. There was also up-regulation of EGF (3.1 fold), HB-EGF (3 fold), BTC (2.3 fold) and NRG1 β (2.3 fold). All four ErbB receptor subtypes expression increased by 2.1-2.6-fold. In keeping with our hypothesis, the EGF-like ligands (EGF, HB-EGF, BTC and NRG) induced a significant 2-3 fold down-regulation of OPG expression and a significant 2-3 fold up-regulation in RANKL expression; and these effects were partially prevented by inhibitors AG1478 and TAPI-1.

Conclusion; These data support our hypothesis that Ang II increases RANKL:OPG ratio partly via transactivation of ErbB receptors by the AT1R. This novel finding provides an insight into the mechanism through which AngII-associated hypertension induces lower bone mineralisation.

Disclosures: Kirsty MacRae, None.

SU0253

Duality of TRIP-1 Function in Regulating Osteoblast Activity *In Vitro*. Diana Metz-Estrella^{*1}, Tzong-Jen Shue¹, J. Edward Puzas². ¹University of Rochester, USA, ²University of Rochester School of Medicine, USA

The coupled processes of bone resorption and bone formation involve both a temporal and spatial component to maintain appropriate skeletal turnover. However, little is known about what controls the spatial component. We have put forward a hypothesis that molecules remaining at the reversal line during resorption can identify these sites for new bone formation. We posit that tartrate resistant acid phosphatase (TRAP) may be one of these molecules. TRAP has been shown to have an extremely high affinity for the TGF β receptor interacting protein (TRIP-1); an intracellular protein in osteoblasts. In this series of experiments we have characterized a dual role for TRIP-1 in mediating bone formation in osteoblasts. In the TGF β pathway TRIP-1 has been shown to be a regulator of gene expression. Our data with reporter assays show that TRIP-1 is essential for normal TGF β signaling. However, TRIP-1 is also known to be a subunit of the eIF3 complex; a complex involved in the initiation of protein translation. These facts imply that TRIP-1 has a dual role in the cell. Since TRIP-1 can be phosphorylated we believe the role of TRIP-1 in osteoblasts can be determined by its phosphorylation state. Examination under confocal microscopy showed that TRIP-1 can be localized in the nuclei of osteoblasts and its presence in the nucleus increased 44% following TGF β 1 treatment. Since TRIP-1 does not possess a nuclear localization signal we further investigated if it could enter the nucleus by interacting with Smads. Co-IP assays showed that TRIP-1 and Smad3 have a high affinity for each other, suggesting a possible mechanism for its nuclear internalization. To study the differential phosphorylation of TRIP-1 upon TGF β treatment we enriched cell lysates for phosphorylated proteins and then evaluated changes in phospho enriched TRIP-1 levels. Our results show that phospho-TRIP-1 levels are decreased 50% after treating osteoblasts with TGF β 1 for 30 minutes. In addition, phospho-TRIP-1 was mostly unchanged when osteoblasts were treated dually with okadaic acid and TGF β 1. This suggests that changes in TRIP-1 phosphorylation could be regulated at least in part by Ser/Thr phosphatases. Interestingly, a cell fractionation assay showed that phospho-TRIP-1 is almost exclusively present in the cytoplasmic fraction of osteoblasts. In conclusion, we believe that in the absence of TGF β 1, phosphorylated TRIP-1 is regulating protein translation in the cytoplasm. However, when TGF β 1 is present, phosphatases are activated and target cytoplasmic phospho-TRIP-1 allowing its nuclear translocation possibly through its interaction with Smad3. In the nucleus, unphosphorylated TRIP-1 will fulfill its role as a regulator of gene transcription.

Disclosures: Diana Metz-Estrella, None.

SU0254

Impaired Osteoblast Differentiation and PTH Response in Female Mice Lacking MAP Kinase Phosphatase-1. Chandrika Mahalingam¹, Tanuka Datta¹, Rashmi Patil¹, Jaclynn Kreider², Steven Goldstein², Abdul Abou-Samra¹, Nabanita Datta^{*1}. ¹Wayne State University School of Medicine, USA, ²University of Michigan, USA

Parathyroid hormone (PTH) is an important regulator of bone mass accrual that acts through PTH 1 receptor (PTH1R), and involves cAMP, PKC and MAPK pathways. MAPKs are negatively regulated by a family of dual-specificity phosphatases known as the MAPK phosphatases (MKPs). The role of MKP-1 in PTH anabolic action in bone is yet to be established. Previously, we have shown that female MKP-1 KO mice display osteopenia and PTH1R induction increases MKP-1 expression in differentiated osteoblasts both in vitro and in vivo. Here we show that primary calvarial osteoblasts derived from exon-2 deleted MKP-1 knock-out (KO) female mice display reduced and delayed expression of Alkaline Phosphatase (ALP), suggesting continued osteoblast proliferation and delayed differentiation. Genes associated with osteoblast maturation and functions were examined at basal state and after PTH treatment. Real-time PCR analysis showed significantly reduced ($p < 0.01$) levels of osteocalcin (OCN), osteonectin (ON) and Runx2 mRNA in osteoblasts isolated from KO females compared to those isolated from WT animals. PTH did not inhibit OCN, ALP, and Runx2 mRNA in cells from KO mice. In contrast to WT osteoblasts, ON expression was increased in MKP-1 null cells following PTH induction. To investigate the effect of MKP-1 deletion on the anabolic response to PTH in vivo, 4-day old WT and KO female mice were injected daily subcutaneously with 50 μ g/kg 1-34 hPTH or vehicle (0.9% saline) control for 21 days. Femora were isolated, dissected free of soft tissue, fixed and analyzed by micro-computed tomography. Images were reconstructed at 18 micron isotropic voxels. PTH significantly increased trabecular bone volume per total volume (BV/TV), trabecular thickness (TbTh) and trabecular number (TbN), by 85%, 33%, 27% respectively, in distal femora from WT mice compared to vehicle treated controls. The effect of PTH on BV/TV (45%), TbTh (23%) was less pronounced in KO animals relative to WT group when compared to respective controls. The increase in TbN (12%) between PTH and vehicle treated KO animals did not reach statistical significance. We conclude that MKP-1 is important for osteoblast differentiation and skeletal responsiveness to PTH.

Funding: NIDDK DK087848 to NSD

Disclosures: Nabanita Datta, None.

SU0255

Metabolic Acidosis-induced Stimulation of RANKL and Bone Resorption Requires G β Signaling. Nancy Kreiger^{*1}, Christopher Culbertson², David Bushinsky¹. ¹University of Rochester, USA, ²University of Rochester School of Medicine, USA

Chronic metabolic acidosis, an increase in proton concentration [H⁺] due to reduced [HCO₃], stimulates cell-mediated net calcium (Ca) efflux from bone. This efflux is mediated primarily through increased osteoblastic cyclooxygenase 2, leading to prostaglandin E₂-induced stimulation of RANKL and increased osteoclastic bone resorption. We and others have found that osteoblasts express OGR1, a H⁺-sensing G-protein coupled receptor (GPCR). We demonstrated that H⁺ activation of OGR1 increases intracellular Ca signaling in osteoblasts and that the OGR1 inhibitor, CuCl₂, blocks H⁺-induced bone resorption. Our findings suggest that OGR1, which is coupled to G β , is the sensor that detects the increased [H⁺] during metabolic acidosis and initiates subsequent osteoblastic signaling leading to increased osteoclastic bone resorption. We have recently found that metabolic acidosis inhibits osteoblastic RGS16, a regulator of G protein signaling which can limit GPCR activation. To further explore the regulation of this G-protein coupled signaling by acidosis we utilized gallein, a selective inhibitor of G β signaling activity. Neonatal mouse calvariae were incubated for 48h in physiologically neutral (Ntl, pH=7.50, Pco₂=34 mmHg, [HCO₃]=28 mM) or acid (Met, pH=7.17, Pco₂=33 mmHg, [HCO₃]=13 mM) medium 20 μ M gallein (Gal). Compared to incubation in Ntl (44280 nmol/bone/24h), Met induced net Ca efflux (133992, p<0.05); Gal did not alter Ca efflux in Ntl (21862) but blocked the increase with Met (264138, p<0.05 vs Met alone) (n=8/group, mean SE). To determine if Gal inhibited the acid-induced increase in RANKL, primary osteoblasts were isolated from neonatal mouse calvariae and incubated in Ntl (pH=7.43, Pco₂=39 mmHg, [HCO₃]=25 mM) or Met (pH=7.10, Pco₂=39 mmHg, [HCO₃]=15 mM) medium 20 μ M Gal. At 48h, cells were collected and RANKL mRNA levels were measured by real time PCR, normalized to RPL13A. Compared to incubation in Ntl (0.850.11), Met stimulated RANKL (1.2911, p<0.05); Gal did not alter RANKL in Ntl (0.690.06) but blocked the increase with Met (0.910.05, p<0.05 vs Met alone) (n=6/group). Thus gallein inhibited both acid stimulation of osteoblastic RANKL production and acid-induced net Ca efflux, a measure of bone resorption. These results, together with our previous finding of acid inhibition of RGS16, suggest that regulation of G β plays an important role in modulating the OGR1-mediated response of the osteoblast to metabolic acidosis.

Disclosures: Nancy Kreiger, None.

SU0256

The Role of Tmem119 in the BMP Signaling Pathway. Geoffrey Hendy¹, KENICHIRO TANAKA^{*2}, Lucie Canaff³, Toshitsugu Sugimoto², Hiroshi Kaji⁴, Riko Kitazawa⁵, Toshihisa Komori⁶, Susumu Seino⁷, Takenobu Katagiri⁸. ¹McGill University, Royal Victoria Hospital, Canada, ²Shimane University School of Medicine, Japan, ³McGill University, Canada, ⁴Kinki University Faculty of Medicine, Jpn, ⁵Kobe University, Japan, ⁶Nagasaki University Graduate School of Biomedical Sciences, Japan, ⁷Kobe University Graduate School of Medicine, Japan, ⁸Saitama Medical University Research Center for Genomic Medicine, Japan

Fibrodysplasia ossificans progressive (FOP) is a genetic disease in which heterotopic ossifications occurs in muscle tissue. The constitutively activating mutation (R206H) of the BMP type 1 receptor, ACVR1/ALK2 is thought to underlie the molecular pathogenesis of FOP. However, the details of the heterotopic ossification of muscle in FOP remain to be elucidated. We demonstrated that the Smad3 signaling rapidly induced by PTH, which is independent of TGF- β is important in bone anabolic effects. And we selected the bone formation-related factor, Tmem119 by comparative DNA microarray analysis between empty-vector-transfected mouse osteoblastic MC3T3-E1 cells and PD98059-treated stably Smad3-overexpressing MC3T3-E1 cells (JBC 2011). In the present study, we performed a comparative DNA microarray analysis between empty-vector- and ALK2 (R206H)-transfected mouse myoblastic C2C12 cells. Forty genes were identified whose expression was increased >3.5 times in the experimental groups versus the control. And this group included Tmem119. Stable Tmem119 overexpression induced the commitment and differentiation of myoblasts or mesenchymal cells into osteoblasts and mineralization. On the other hand, differentiation of myoblastic cells into myotubes was suppressed, and differentiation into chondrocytes was little affected. Moreover, transcriptional activity of the BMP-2 signaling molecules, Smad1/5 was increased in the absence of exogenous BMP-2 in C2C12 cells. Next, we analyzed the mechanism that Tmem119 induced the commitment and differentiation of myoblasts into osteoblasts using C2C12 cells. Tmem119 increased BMP-2 levels (Western, Real-time PCR), and Tmem119 siRNA antagonized BMP-2 levels. BMP-2/4 neutralizing antibody and dorsomorphin, an ALK2 inhibitor, antagonized Tmem119-enhanced ALP and OCN. Although Tmem119 interacts with Runx2, Smad1 and Smad5 physically and functionally, BMP-2 increased Tmem119 levels (Western, immunocytochemistry), Tmem119 siRNA antagonized the BMP-2-induced ALP and OCN, but not Runx2 and Osterix, mRNAs, in C2C12 cells. In this study, we showed that Tmem119 promotes the differentiation of myoblasts into osteoblasts induced by BMP-2 and the interaction with the BMP signaling pathway occurs downstream of Runx2 and Osterix in

myoblasts. Tmem119 may play a critical role in commitment of myoprogenitor cells to the osteoblast lineage.

Disclosures: KENICHIRO TANAKA, None.

SU0257

Additive Effects of TBT and TCDD on Bone Cell Differentiation. Antti Koskela^{*1}, Juha Tuukkanen¹, Matti Viluksela², Merja Korkalainen². ¹University of Oulu, Finland, ²National Institute for Health & Welfare, Finland

Important environmental contaminants, tributyltin (TBT) and 2,3,7,8-tetrachlorodibenzo-p-dioxin (TCDD), are wide-spread and persistent in nature. They accumulate in the food chain and they may participate in the toxicological burden on the development of osteoporosis. They are chemically different with different mechanism of action, but both have been shown to affect bone development. We utilized differentiation of mouse bone marrow stromal cells and hematopoietic stem cells of monocyte macrophage lineage to study the combined effects of TBT and TCDD on osteoblastogenesis and osteoclastogenesis respectively. Stem cells were isolated from the bone marrow of femurs and tibiae of male C57BL/6J mice, and differentiated to both osteoblasts or osteoclasts. Cells were exposed to 10⁻¹⁰ – 10⁻⁸ M TBT, 10⁻¹¹ – 10⁻⁹ M TCDD and 10⁻⁸ M TBT + 10⁻⁹ M TCDD. The combined treatment with TBT and TCDD additively decreased the mRNA expression of alkaline phosphatase and osteocalcin. Osteoclastogenesis was also affected and there was clear additive effect of TBT and TCDD on resorption pit formation. PCR array analysis revealed that TBT and TCDD evoked different gene expression patterns and in combined exposure they affected more genes than individual exposures. In conclusion, these results indicate that TBT and TCDD affect both bone formation and bone resorption with very low concentrations and the effect is additive.

Disclosures: Antti Koskela, None.

SU0258

Aged Perivascular Mesenchymal Stem Cells Derived from Adipose Tissue are Hyperproliferative and Resistant to the Induction of Osteogenic and Adipogenic Differentiation. Matthew Stern^{*1}, Amber Stern¹, Christopher Bergman², Stephen Kritchevsky³, Mark Van Dyke². ¹University of Missouri-Kansas City, USA, ²Wake Forest Institute for Regenerative Medicine, USA, ³Wake Forest Baptist Medical Center, Sticht Center on Aging, USA

Adipose derived stem cells (ADSCs) are multipotent mesenchymal stem cells that reside within the microvasculature of adipose tissue. ADSCs can differentiate into the osteogenic, chondrogenic, myogenic, and adipogenic lineages within the musculoskeletal system. Age-associated increases in tissue adiposity are observed during the development of sarcopenia in muscle and also within aging bone. Two questions regarding aged ADSCs that have not been adequately addressed are 1) whether the aging process adversely affects the potential of ADSCs for use in therapeutic applications and 2) whether age-related changes in ADSCs contribute to the increased tissue adiposity observed in aging individuals. To address these questions, we obtained ADSCs from young (4-6-month-old) and old (> 22-month-old) rats and compared their ability to proliferate and differentiate into multiple cell lineages. ADSCs obtained from young and old animals exhibited the same cell surface and gross morphological phenotype; however, old ADSCs were significantly more proliferative. When induced to undergo adipogenic or osteogenic differentiation, young ADSCs exhibited significantly greater levels of staining for indicators of terminal differentiation and greater changes in the expression of several genes involved in differentiation. Our results suggest that ADSCs are subject to cell-intrinsic aging mechanisms that render aged cells more proliferative and less responsive to differentiation cues than young cells, even when cultured under identical conditions, and suggest a role for Wnt signaling in this process. These findings raise concern over the potential use of autologous ADSCs in therapeutic applications for elderly individuals and suggest that hyperproliferative ADSCs could play a role in the accumulation of adipose and adipose-like tissue within the musculoskeletal system of aged individuals.

Disclosures: Matthew Stern, None.

SU0259

Biomimetic Calcium Silicate Support Differentiation of Human Orofacial Bone Marrow Stromal Cells. Sara Shah¹, Maria Giovanna Gandolfi², Ruoxue Feng¹, Carlo Prati², Sunday Akintoye^{*3}. ¹University of Pennsylvania, USA, ²University of Bologna, Italy, ³University of Pennsylvania School of Dental Medicine, USA

Introduction: Human orofacial bone marrow stromal cells (OFMSCs) from maxilla and mandible have robust osteogenic regenerative properties. Furthermore, a combination of OFMSCs with bioactive calcium-releasing scaffolds can potentially improve OFMSC multi-lineage differentiation abilities, but biocompatibility of calcium silicate cements with OFMSCs is still unclear. We tested the hypothesis that

material extracts of calcium-releasing calcium-silicate scaffolds support biomimetic microenvironment for survival and differentiation of human OFMSCs.

Methods: Two formulations of experimental calcium-silicate cements 1) calcium-silicate mineral powder (wTC) containing di- and tricalcium-silicate, calcium sulphate, and calcium chloride and 2) wTC doped with alpha-tricalcium phosphate (wTC- α TCP) were prepared. Cement setting times were assessed by Gilmore needles; ability to release calcium and hydroxyl ion was assessed by potentiometric methods and OFMSC attachment to calcium-silicate discs was assessed relative to tissue culture plastic. Calcium-silicate material extracts were tested for ability to support OFMSCs survival as well as *in vitro/in vivo* differentiation.

Results: Fewer OFMSCs attached to calcium-silicate discs relative to tissue culture plastic ($p=0.001$). Extracts of calcium-silicate cements sustained OFMSC survival, maintained steady state levels of vascular cell adhesion molecule-1, alkaline phosphatase and bone sialoprotein while upregulating their respective gene transcripts. Adipogenic and *in vivo* bone regenerative capacities of OFMSCs were also unaffected by calcium-silicate extracts.

Conclusions: Ion-releasing calcium-silicate cements support a biomimetic micro-environment conducive to survival and differentiation of OFMSCs. Combination of OFMSCs and calcium-silicate support hard tissue regeneration. This work was supported by USPHS/NIH/NCI grant 5K08CA120875-04.

Disclosures: Sunday Akintoye, None.

SU0260

Characterization of Murine Telomerase Reverse Transcriptase (mTERT) Immortalized Osteoblast Cell Lines Generated from Wild-type and Nmp4-null Mouse Bone Marrow Stromal Cells. Marta Alvarez¹, Paul Childress¹, Binu Philip¹, Rita Gerard-O'Riley¹, Michael Hanlon¹, Brittney-Shea Herbert¹, Alexander Robling², Fredrick Pavalko¹, Joseph Bidwell¹. ¹Indiana University School of Medicine, USA, ²Indiana University, USA

Intermittent parathyroid hormone (PTH) adds new bone to the osteoporotic skeleton; the transcription factor Nmp4/CIZ represses PTH-induced bone formation in mice and as a consequence is a potential drug target for improving hormone clinical efficacy. To explore the impact of Nmp4/CIZ on osteoblast phenotype, we immortalized bone marrow stromal cells from wildtype (WT) and Nmp4-knockout (KO) mice using murine telomerase reverse transcriptase. Clonal lines were initially chosen based on their staining for alkaline phosphatase and capacity for mineralization. Disabling Nmp4/CIZ had no gross impact on osteoblast phenotype. WT and KO clones exhibited sustained growth, reduced population doubling times, extended maintenance of the mature osteoblast phenotype, and competency for differentiating toward the osteoblast and adipocyte lineages. We recently demonstrated that PTH-induced c-fos femoral mRNA expression is enhanced in Nmp4-KO mice; unexpectedly in the present study we determined that null primary and clonal cells expressed significantly less PTH receptor than WT cells nevertheless hormone stimulated an equivalent increase in c-fos in both cells suggesting that the mature osteoblast is not responsible for the enhanced hormone-stimulated c-fos response *in vivo*. However, the null osteoblasts were hyper-responsive to bone morphogenetic protein 2 (BMP2)-induced changes in genes that support osteoblast differentiation, consistent with the previously observed enhanced BMP2-induced bone formation in null mice. We speculate that Nmp4 may repress PTH-induced bone formation, in part, by attenuating cell responsiveness to hormone-stimulated local increases in BMPs. These immortalized cell lines will provide a valuable tool for disentangling the complex functional roles underlying Nmp4/CIZ regulation of bone anabolism.

Disclosures: Marta Alvarez, None.

SU0261

Differential Effect of Arachidonic Acid and Beta-Cryptoxanthin on the Expression of Retinoic Acid Receptors Genes in Mesenchymal Stem Cells Differentiated to Osteoblasts and Adipocytes. Antonio Casado-Dúaz¹, Raquel Santiago-Mora², Jose Manuel Quesada Gomez³. ¹Hospital Reina Sofía, Spain, ²Universidad De Cordoba, Spain, ³Gabinete Quesper, Spain

The arachidonic acid (AA) is a ω -6 fatty acid which has the ability to favor the adipogenic differentiation of mesenchymal stem cells (MSC). The β -cryptoxanthin (β -Crx) is a carotenoid, abundant in quite a lot of fruits and vegetables that inhibits adipogenesis and enhances bone formation. These effects seem to be mediated by RARs and PPAR β/δ receptors. The high consumption of ω -6 in a large part of the population has a negative direct effect on bone health. The aim of this work is to study if β -Crx may decrease the adipogenic effect of AA in MSC induced to osteoblasts or adipocytes and its effect on the expression of the coding genes over their receptors.

Human MSCs were induced to differentiate to osteoblasts or to adipocytes. Additionally, MSC induced cultures were treated by using 20 μ M of AA and/or 10⁻⁶M or 10⁻⁵M of β -Crx. Osteogenic and adipogenic markers; the expressions of RAR α , β and γ , PPAR β/δ ; the cellular retinoic acid binding protein 2 (CRABP2) and Fatty acid-binding protein 5 (FABP5) genes were measured.

La β -Crx decreased the AA ability to increase adipogenesis in MSC induced to adipocytes, but not in MSC induced to osteoblast. The expression of RAR α and RAR γ in cells induced to adipocytes decreased in the presence of AA after 7 and 14 days of treatment, whereas it increased after 21 days. β -Crx prevented the inhibition of these two genes caused by the AA after 14 days. Oppositely, the expression of RAR β ,

PPAR β/δ , CRABP2 and FABP5 were increased by AA. Moreover, 10⁻⁶M of β -Crx, further enhanced the expression of these genes. In MSC induced to osteoblasts in presence of AA, appear adipocytes and the RAR α , β , γ and PPAR β/δ expression decreased. Additionally, CRABP2 decreased whereas FABP5 increased its expression after 7 days. The β -Crx promoted this increase even in presence of AA.

Our results show that RAR β are involved in the increase of adipogenic differentiation induced by AA, whereas RAR α and γ seem to be responsible for the diminution of the AA effect on adipogenesis mediated by β -Crx. The increase of CRABP2 and FABP5 expression in adipocytes with AA seem to indicate that their answer is mediated by a nuclear activation of RAR β and PPAR β/δ , which are coactivators, respectively. In MSC induced to osteoblasts, differentiation to adipocytes promoted by AA involves the inhibition of the 3 RARs genes, PPAR β/δ gene and the activation of FABP5 gene. This indicates a different mechanism for the induction of adipogenesis in these cultures.

Disclosures: Antonio Casado-Dúaz, None.

SU0262

Differential Requirement of SWI/SNF Chromatin Remodeling Complexes in Osteoblast Commitment and Differentiation *in vitro*. FUHUA XU¹, Stephen Flowers², Elizabeth Moran³. ¹New Jersey Medical School, UMDNJ, USA, ²NJMS-UH Cancer Center, University of Medicine of Dentistry of New Jersey, USA, ³University of Medicine & Dentistry of New Jersey, Cancer Center, USA

The commitment of the osteoblastic lineage, and further differentiation to osteoblasts and ultimately to mature osteocytes, is tightly regulated. Successive changes in gene expression patterns are controlled by specific transcription factors such as Runx2 and Osterix, acting in concert with histone modifiers and ATPase-dependent SWI/SNF chromatin remodeling complexes. BAF and PBAF, distinct subclasses of mammalian SWI/SNF complexes, share most subunits but are distinguished by unique subunits: ARID1A/B belong specifically to BAF and ARID2 is exclusive to PABF. The ATPase BRG1 can power either complex. Elucidating the mechanism of how BAF and PBAF differentially regulate genes required to osteoblast commitment and differentiation will be a significant step toward understanding bone development.

We have recently identified several gene expression patterns dependent on BRG1. Here we have considered whether these patterns segregate with BAF vs PBAF. Our results show induction of the osteogenic marker, alkaline phosphatase, is impaired in ARID1A or ARID1B depleted pre-osteoblasts in a milder version of the BRG1 depletion phenotype. ARID2 stable knockdown cells likewise fail to induce alkaline phosphatase and osteocalcin activity, implying non-redundant requirements for both BAF and PBAF in activation of osteogenic gene expression. Pre-osteoblasts express high levels of FGFR2, which is essential for maintaining osteoblast commitment status. Depletion of either BRG1 or ARID2 causes dramatic down-regulation of FGFR2 expression, suggesting PBAF is required for osteoblastic lineage commitment as well as for differentiation. Another phenotype of BRG1 depletion is inappropriate expression of the mature osteocyte markers Dmp1 and Phex in pre-osteoblasts, indicating that a BRG1 complex is required to repress premature expression of genes specific to the terminally differentiated osteocyte phenotype. Depletion of ARID2 does not cause premature expression of DMP1 or Phex, indicating that repression of osteocyte-specific genes in pre-osteoblasts is a BAF-specific function for which PBAF is not required. Collectively, these data identify some overlapping and some distinct functions for BAF and PBAF. To date, PBAF has segregated only with activation functions, while BAF participates in both activation and repression.

Disclosures: FUHUA XU, None.

SU0263

Distribution of Neural Crest-Derived Cells in Adult Mice and Their Induction into Osteoblastic Cells. Miki Ono¹, Masamichi Takami¹, Tetsuo Suzawa¹, Tomohiko Miyauchi¹, Atsushi Yamada¹, Junichi Watahiki¹, Kazuyoshi Baba¹, Masanori Nakamura¹, Kotaro Maki¹, Noriko Osumi², Ryutaro Kamijo¹. ¹Showa University School of Dentistry, Japan, ²Tohoku University Graduate School of Medicine, Japan

The neural crest is a type of embryonic tissue that transiently appears near the neural tubes during development. Neural crest cells migrate throughout the embryo and differentiate into various types of cells in different germ layers, including osteoblasts, neurocytes, myocytes, lipocytes, and cardiocytes. In adult tissues, subsets of neural crest-derived cells (NCCs) have been shown to reside as stem cells and are considered to be useful cell sources for regenerative medicine strategies. However, the distribution of NCCs in adults is not fully understood. To analyze the distribution and characteristics of NCCs in adult tissues, we utilized double transgenic mice in which NCCs expressed EGFP (enhanced green fluorescent protein) by mating protein 0 (a specific marker of the neural crest)-Cre transgenic mice with CAG-CAT-EGFP transgenic mice. GFP-positive cells were found in these double transgenic mice in a variety of tissues, such as the pancreas, stomach, skin, nasal conchae, palate, gingiva, oral vestibule, tongue, and buccal mucosa. On the basis of these findings, we focused on oral mucosa as a cell source for regenerative medicine, as buccal mucosal tissue abundantly exists and covers a broad area in the oral cavity and has a distinctive regenerative capacity. We surgically isolated buccal mucosa from the mice, then

digested the samples with collagenase and dispase to collect cells. A range of 1-4% of all buccal mucosa cells was found to be EGFP positive, indicating that they were identical to NCCs. We isolated EGFP-positive cells using a flow-cytometer equipped with a cell sorter and cultured them on low-adhesion culture plates. After 1 week, EGFP-positive cells formed spheres, typical cell clusters composed of stem cells, and expressed the stem cell marker *Musashi 1*, as well as the neural crest markers *p75*, *Twist*, and *Snail*, suggesting that the population contained neural crest-derived stem cells. Subsequently, we cultured EGFP-positive cells in osteoinductive medium with bone morphogenetic protein (BMP)-2 (100 ng/ml). After 14 days, those cells expressed alkaline phosphatase, and produced calcified substances detected by alizarin-red staining. These results suggest that NCCs reside in various regions throughout the body including buccal mucosa and possess a potential to differentiate into osteoblastic cells. Thus, NCCs may be a useful cell source for regenerative medicine strategies including bone regeneration.

Disclosures: Miki Ono, None.

SU0264

Hematopoiesis and Leukocyte Distribution Within Bone Marrow Are Rapidly Disrupted by a High Fat Diet, While Daily Bouts of Mechanical Signals Enhance the Hematopoietic Repair Response. Benjamin Adler^{*1}, Danielle Green¹, Ete Meilin Chan¹, Clinton Rubin². ¹Stony Brook University, USA, ²State University of New York at Stony Brook, USA

Obesity increases lifetime susceptibility to a host of chronic diseases, implicating a suppressed immune system. Obesity also biases bone marrow stromal cells (BMSCs) towards the formation of adipose tissue, compromising the bone marrow progenitor pool. In contrast, mechanical signals stimulate proliferation of BMSCs and drive their differentiation towards the formation of bone, while suppressing adipogenesis and adiposity. Considering the consequences of obesity – and the benefits of exercise – on BMSCs, we hypothesize that a high fat diet (HFD) will impair hematopoiesis, compromising immune populations, while mechanical signals will help preserve the reparative capacity of hematopoietic stem cells (HSC). Seven week old male C57BL/6J mice were fed either a high fat diet (HFD: 60% Kcal from fat) or regular chow diet. One group of HFD mice were subject to 15min/day, 5 days/wk of mechanical signals delivered via low intensity vibration (HFV), and compared to both high fat controls (HFC) and regular diet controls (RDC)(n=10 per group). Bone marrow was analyzed using flow cytometry at 1 and 6 weeks to characterize hematopoietic cell populations. Within one week, the HFD induced an "aged" phenotype in bone marrow leukocytes, with B-cell proportions reduced by -10% compared to RDC (p<0.05). By 6w of HFD the "aged" phenotype was completely manifested as B-cells had collapsed by -25% and T-cells reduced by -33%, while the myeloid cell fraction increased by +16% as compared to RDC (p<0.01). By 1w, hematopoietic progenitors central to the repair of the leukocyte pool had already elevated by +16% in HFC, and +25% in HFV relative to RDC (p<0.05). By 6w, the progenitor population in the HFC had regressed to control levels, yet the mechanically stimulated HFV animals retained a +25% increase relative to RDC (p<0.05). Hematopoiesis is vulnerable to even short-term exposure to a high fat diet, which disrupts leukocyte allocations threatening adaptive immunity. The rapid expansion of the HSC progenitor pool seen as early as 1w reflects the activation of a repair mechanism to restore the damaged leukocyte populations, a response which fails in HFC by 6w despite the continued disruption of hematopoiesis. Mechanical signals serve to perpetuate this reparative response, providing insight into the role of physical stimuli, and exercise in general, in regulating osteoimmunology.

Disclosures: Benjamin Adler, None.

SU0265

Stage-specific Embryonic Antigen-4 Identifies Human Dental Pulp Stem Cells. Noriaki Kawanabe^{*1}, Satoko Murata², Hiroaki Fukushima², Yoshihito Ishihara², Hiroshi Kurosaka², Hiroshi Kamioka³, Takashi Yamashiro². ¹Okayama University Hospital, Japan, ²Okayama University, Japan, ³Okayama University Graduate School of Medicine, Dentistry, & Pharmaceutical Sc, Japan

Embryonic stem cell-associated antigens are expressed in a variety of adult stem cells as well as embryonic stem cells. In the present study, we investigated whether stage-specific embryonic antigen (SSEA)-4 can be used to isolate dental pulp (DP) stem cells. In this study, DP cells showed plastic adherence, specific surface antigen expression, and multipotent differentiation potential, similar to mesenchymal stem cells (MSC), but did not display adipogenic differentiation potential. In addition, DP cells were positive for embryonic stem cell-associated antigens (SSEA-1, SSEA-3, SSEA-4, TRA-1-60, TRA-1-81, OCT4, NANOG, SOX2, and REX1) and alkaline phosphatase activity. Flow cytometric analysis demonstrated that 45.5% of the DP cells were SSEA-4+. When the DP cells were cultured in the presence of all-trans-retinoic acid, marked downregulation of SSEA-3 and SSEA-4 and the upregulation of SSEA-1 were observed. SSEA-4+ DP cells showed a greater telomere length and a higher growth rate compared to untagged and SSEA-4- cells. A clonal assay demonstrated that 65.5% of SSEA-4+ DP cells had osteogenic potential, and SSEA-4+ clonal DP cells showed multilineage differentiation potential toward osteoblasts, chondrocytes, and neurons. The presence of SSEA-4+ cells in DP tissue *in vivo* was also confirmed. Thus, our results suggest that SSEA-4 is a specific cell

surface antigen that can be used to identify DP stem cells. In addition, SSEA-4+ DP cells appear to be candidates for stem cells that can be used in regenerative therapy.

Disclosures: Noriaki Kawanabe, None.

SU0266

Therapeutic Potential of Glucocorticoid-Induced Leucine Zipper (GILZ) Protein in Rheumatoid Arthritis. Linlin He^{*1}, Nianlan Yang¹, Carlos Isaacs², Xing-Ming Shi². ¹Georgia Health Sciences University, USA, ²Medical College of Georgia, USA

Proinflammatory cytokines are known to inhibit osteoblastic differentiation and function while stimulating osteoclast differentiation and bone resorption. Steroid hormone glucocorticoids (GCs), which are superb anti-inflammatory agents, also cause bone loss resulting in osteoporosis. We showed previously that overexpression of a GC inducible protein Glucocorticoid-Induced Leucine Zipper (GILZ) can enhance osteogenic differentiation of bone marrow mesenchymal stem cells (MSCs). In this study we asked whether GILZ can override the inhibitory effect of tumor necrosis factor- α (TNF- α) on MSC osteogenic differentiation using both GILZ gain-of-function (retrovirus-mediated overexpression) and loss-of-function (lentivirus-mediated shRNA knockdown) approaches. Our results show that overexpression of GILZ antagonized the inhibitory effects of TNF- α on MSC mineralization and the levels of mRNA and protein of pivotal osteogenic regulators *Osx* and *Runx2*. Knockdown of GILZ had an opposite effect on MSC differentiation and gene expression. These actions appear to occur via mechanisms involving GILZ inhibition of TNF- α -induced mitogen-activated protein (MAP) kinase activation and E3 ubiquitin ligase-mediated protein degradation. Taken together, our studies show that GILZ has therapeutic potential for preventing bone loss caused by chronic inflammation such as rheumatoid arthritis.

Disclosures: Linlin He, None.

SU0267

Treatment of Skeletally Unloaded Mice With Sclerostin Antibody Increases Osteoblast Activity and Mineralization. Mohammad Shahnazari^{*1}, Vivian Chu², Marina Stolina³, Thomas Wronski⁴, Hua Zhu Ke³, Bernard Halloran⁵. ¹UCSF VA Medical Center, USA, ²VA Medical Center, USA, ³Amgen Inc., USA, ⁴University of Florida, USA, ⁵VA Medical Center (111N), USA

Sclerostin functions as an antagonist to Wnt signaling and has been shown to inhibit bone formation. Treatment with antibodies to sclerostin (Scl-Ab) stimulates bone formation and provides a means of treating patients with osteoporosis. Skeletal unloading or loss of weight is associated with a decrease in bone formation and bone loss. To determine the effect of Scl-Ab treatment on bone during skeletal unloading, male C57BL/6 mice (5 mo old) were hind limb unloaded or allowed normal ambulation and treated with Scl-ab (25mg/kg, day 1 and 4) or placebo (n=8/group) for 1 week. Bone marrow culture was performed after necropsies of the animals. Unloading induced a decrease in colony forming units (CFU) (-35%), alkaline phosphatase positive CFU (CFU-AP+) (-65%) and calcified nodules (-25%); and increased the population of TRAP+ multinucleated osteoclasts(+70%). Treatment of both unloaded and loaded mice with Scl-Ab increased CFU, CFU-AP+ and calcified nodules. Our data suggest that Scl-Ab treatment can prevent the loss of osteoprogenitors associated with skeletal unloading.

Disclosures: Mohammad Shahnazari, Amgen, 2
This study received funding from: Amgen

SU0268

VDR Is Required for Anti-proliferative and Pro-osteoblastogenic Effects of 1,25(OH)₂D₃ in Adult Human Mesenchymal Stem Cells. Shuo Geng, Shuanhu Zhou^{*}, Julie Glowacki, Brigham & Women's Hospital, USA

INTRODUCTION: Anti-proliferative and pro-differentiation effects of 1,25(OH)₂D₃ have been described for many tumor and normal cell types. Classically, 1,25(OH)₂D₃ mediates its actions through activation of the Vitamin D Receptor (VDR), a ligand-dependent transcription factor. Proliferation of some tumor cell, however, remained inhibitable by 1,25(OH)₂D₃ after VDR-silencing (BMC Genomics 2009;10:499). Mineralization abnormalities in growing VDR-KO mice were corrected with rescue diet, but some cellular defects persisted (Ann NY Acad Sci 2006;1068:204). Several novel and D-independent functions of VDR have been uncovered in normocalcemic VDR-KO mice. These studies test the hypothesis that VDR is required for actions of 1,25(OH)₂D₃ in human mesenchymal stem cells (hMSCs).

METHODS: Human MSCs were isolated by expansion of adherent, low-density progenitor cells from marrow discarded during surgery. Transient transfection of siRNA into hMSCs was performed by electroporation (Human MSC Nucleofector Kit, Lonza/Amazax Biosystems) and either VDR-siRNA (Invitrogen) or non-silencing control siRNA (NC, Santa Cruz Biotechnology, Inc.). Growth medium was phenol red-free α -MEM, 10% fetal bovine serum-heat-inactivated (FBS-HI) and antibiotics.

Osteoblastogenic medium (1% FBS-HI) had supplements (10 nM dexamethasone, 5 mM β -glycerophosphate, 50 μ g/mL ascorbate-2-phosphate).

RESULTS: RT-PCR revealed downregulation of VDR expression in cells transfected with VDR-siRNA. In a short-term proliferation assay (3-day), the number of NC hMSCs incubated with 1,25(OH) $_2$ D $_3$ was 65.8 \pm 3.3% of the number without 1,25(OH) $_2$ D $_3$ ($p < 0.0001$). In sharp contrast, the number of cells that had been transfected with VDR-siRNA was not affected by exposure to 1,25(OH) $_2$ D $_3$ (103.1 \pm 1.0%, compared with those not exposed to 1,25(OH) $_2$ D $_3$). Osteoblast differentiation was measured 3 days after change to osteoblastogenic medium 10 nM 1,25(OH) $_2$ D $_3$ by RT-PCR for alkaline phosphatase (ALP) mRNA. In control hMSCs, 1,25(OH) $_2$ D $_3$ stimulated ALP, 162% of untreated. In contrast, in hMSCs that had been transfected with VDR-siRNA, there was no stimulation of ALP by 1,25(OH) $_2$ D $_3$ (89% compared with those not exposed to 1,25(OH) $_2$ D $_3$).

CONCLUSION: There were substantial differences in the effects of 1,25(OH) $_2$ D $_3$ on hMSCs after transfection with VDR-siRNA and non-silencing control siRNA. These studies indicate that the anti-proliferative and pro-osteoblastogenic effects of 1,25(OH) $_2$ D $_3$ in hMSCs depend upon the VDR.

Disclosures: Shuanhu Zhou, None.

SU0269

Zinc Finger Targeting of Promoter-Reporter Constructs to a "Safe Haven" Site in Human Pluripotent Stem Cells to Facilitate Analysis and Therapy of Bone Disease. Xiaonan Xin*, Xi Jiang, Liping Wang, Mary Louise Stover, Hui-Chen Chan, Shuning Zhan, I-Ping Chen, Ernst Reichenberger, David Rowe, Alexander Lichtler. University of Connecticut Health Center, USA

Genetic bone diseases such as osteogenesis imperfecta (OI) and craniometaphyseal dysplasia (CMD) could be potentially studied and treated using induced pluripotent stem cells (iPSC) produced from patient cells. However, for this potential to be fully realized, it will be important to introduce ubiquitous and/or cell type specific marker genes into one or more site(s) in the human genome that both retain an active chromatin configuration and do not cause negative effects when constructs are inserted into them (referred to as "safe haven" sites). One such site is AAVS1, which is the insertion site of the common adeno-associated virus, which causes no known adverse effects. Because conventional gene targeting by homologous recombination in human embryonic stem cells (hESC) and iPEC is very inefficient, we are exploring zinc finger nuclease (ZFN) technology to increase the efficiency of homologous recombination at a specific site. We have delivered a construct containing the EF1 α promoter, which is widely expressed in cultured cells, driving an RFP-T2-puro expression cassette into H9 hESC AAVS1 site by co-transfection with AAVS1 site specific ZFN mRNA. Puromycin selection produced approximately 20 times as many colonies with the ZFN mRNA as without. We established colonies with more than 90% RFP expression. PCR demonstrated integration into the AAVS1 locus. Embryoid body formation showed that the EF1 α promoter is turned down in many differentiated cells. We plan to test the ubiquitin promoter for consistent expression in differentiated cells. To test the suitability of the AAVS1 site for supporting gene expression in osteoblasts, we used the Col2.3 promoter, which is most highly expressed in osteoblasts. Introducing Col2.3 promoter driven fluorescence protein expression into hESC/iPSC will be a useful tool for us to monitor hESC/iPSC differentiation into bone lineage. A Col2.3GFPmd construct has been introduced into hESC using ZFN technology, and targeted integration confirmed by PCR screening. Col2.3GFPmd expression in osteoblasts will be tested in teratomas, which we believe is currently the only method that reliably creates significant amounts of human cell-derived bone in mice. If results are positive, we will use these cells to test osteoblast differentiation protocols, which will be applied to iPSC. We are also developing reporter constructs that mark stages of mesoderm lineage progression toward different types of bone.

Disclosures: Xiaonan Xin, None.

SU0270

In Vitro Study on the Estradiol Dependent Changes on the Mechanical and Structural Properties of Human Fetal Osteoblasts cells. PADMALOSINI MUTHUKUMARAN*, Chwee Teck LIM, Taeyong Lee. National University of Singapore, Singapore

Aim

The most common form of osteoporosis is the postmenopausal osteoporosis, caused by estrogen deficiency. The pathogenesis of osteoporosis has been extensively studied in terms of the cellular and molecular effects of estrogen on osteoblasts and osteoblasts like cells. The aim of this study is to understand the mechanical basis of the pathogenesis of osteoporosis by assessing the direct effect of estradiol on the structural and mechanical properties of the human fetal osteoblasts (hFOB1.19).

Methods

The hFOB cells were seeded on sterile 13mm cover slips and allowed to reach confluency. The cells were then grown in either medium alone or medium supplemented with 10nM and 100nM β -Estradiol for 3 days. The cells were subjected to Atomic Force Microscopy (AFM) indentation. Hertz's contact equation was used to determine the apparent elastic modulus of the cell:

$$F(h) = (4/3) E^* h^{3/2}$$

where R = radius of probe, E* = apparent elastic modulus, h = indentation depth and F = indentation force. After treatment with estradiol the cells were stained with 0.1 μ g/ml TRITC-Phalloidin for F-Actin and imaged using confocal microscope. The cells were also tested for alkaline phosphatase (ALP) activity and mineralization.

Results

The cells treated with estradiol showed significantly lower apparent elastic modulus (10nM = 0.24kPa, 100nM = 0.26kPa) as compared to the control cells (0.42kPa) [Fig 1]. However there were no significant difference between the elastic moduli of 10nM Estradiol and 100nM Estradiol treated cells. The confocal images showed that the altered mechanical properties were associated with changes in the density of the actin filaments [Fig 2]. The quantified mineralization of all group cells remained the same. The ALP activity of estradiol treated cells significantly increased, concurring the literature data.

Conclusions

The results suggest that during the pathogenesis of osteoporosis the estrogen deficiency not only results in the changes in the physiological functions of osteoblasts but also is associated with changes in their elasticity. The confocal images showed that the changes in mechanical properties are due to changes in organization of actin filaments and not associated with difference in mineralization of the cells. Thus, this study shows that estradiol influences the mechanical properties of osteoblasts through cytoskeletal changes of the cells and that the mechanical property of the cells possibly influences their functions.

Figure 1: Apparent elastic modulus of control and Estradiol treated cells

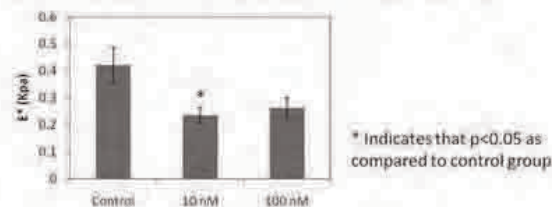
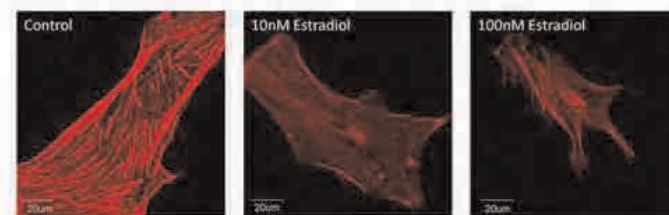


Figure 2: Confocal images of TRITC-Phalloidin stained cells



Disclosures: PADMALOSINI MUTHUKUMARAN, None.

SU0271

Characterization of Six Monoclonal Antibodies to Human Tartrate Resistant Acid Phosphatase (TRACP). Silvia D. Potenziani¹, Stephen Slone¹, Ranga Parthasarathy², Yi-Ying Wu³, Tsu-Yi Chao⁴, Lung Yam⁵, Anthony Jancik⁶. ¹Department of Pathology & Laboratory Medicine, University of Louisville, USA, ²Molecular Neuroscience & Bioinformatics, Robley Rex Louisville VA Medical Center, USA, ³Graduate Institute of Life Sciences, National Defense Medical Center, Taiwan, ⁴Department of Medicine, Taipei Medical University-Shuang Ho Hospital, Taiwan, ⁵Department of Medicine, University of Louisville, USA, ⁶Robley Rex Louisville VA Medical Center, USA

Purpose: Human serum TRACP5a is a potential marker for systemic macrophages and chronic inflammatory diseases. Serum TRACP5b is a marker of osteoclast number and bone resorption. In humans *Acp5* gene mutations with TRACP deficiency is causative for spondyloenchondrodysplasia (SPENCD), a disease of variable bone and autoimmune phenotype. Methods for immunoassay and immunodetection of TRACP isoforms are increasingly important. This study was undertaken to characterize six anti-TRACP monoclonal antibodies (mab) and determine their applications in various immunological methods.

Methods: Anti-TRACP mab9C5, 14G6, 162, 203, 220, and 89 were used as capture and detection antibodies in quantitative immunoassay, in western blot and in immunoprecipitation using serum TRACP5a and 5b and dendritic cell lysates as enzyme sources. Monoclonal antibodies were also tested for efficacy in immunohistochemistry of paraffin embedded tissues containing chronic inflammatory infiltrates. The clinical performance of mab14G6 for immunoassay of serum TRACP5b activity was compared to two commercial kit methods using sera from 20 patients with breast cancer and bone metastasis; 10 having clinical response to treatment and 10 with clinical progression. 15 patients without bone metastasis served as control.

Results: Mab9C5 reacted with a denatured epitope in the C-terminal portion of TRACP and was useful for western blot and IHC methods only. Mab14G6, 162, and 203 reacted with an epitope in the native conformation of both isoforms 5a and 5b.

They did not alter the pH optima of either TRACP5a or 5b, they had similar isoform specificity at pH 5.2 to 6.1 and may be similarly useful for quantitative immunoassay and immunoprecipitation of native TRACP. They were ineffective antibodies for western blot and IHC. Mab220 and 89 were specific for isoform 5a and useful in all applications. Both mabs increased the pH optimum and specific activity of serum TRACP5a in immunoassays. 14G6 performed equally to two commercial kit methods in terms of clinical sensitivity and specificity to detect clinical response or progression in breast cancer with bone metastasis.

Conclusion: Six monoclonal antibodies each had unique specificity for TRACP isoforms and were useful in selective applications. These antibodies will be important for clinical evaluation of disorders of bone metabolism and chronic inflammation. They also will aid in basic research of TRACP biochemistry and biology.

Disclosures: Anthony Jancikla, None.

SU0272

Small GTPases Rab14 and Rab4B are Required for Osteoclast Polarisation and Bone Resorption. Cecile Itzstein*, Denise Tosh, Miep Helfrich, Fraser Coxon, Michael Rogers. University of Aberdeen, United Kingdom

Osteoclasts are highly dependent on vesicular trafficking pathways to establish cell polarity and to degrade bone matrix. Ruffled border formation depends on polarised transport of acidic vesicles of the endocytic/lysosomal pathway, while degradation products are removed from the resorption lacuna by transcytosis. These vesicular trafficking pathways are regulated by the Rab family of GTPases. The expression profile and role of Rabs in osteoclasts is poorly understood.

We employed a proteomic approach to analyse the expression of abundant Rabs in human osteoclasts generated from peripheral blood monocytes. We identified nearly 20 Rabs, including Rab14 and Rab4B. These two GTPases are 58% homologous and both regulate endosomal trafficking pathways, particularly receptor recycling, for example of the transferrin receptor via their common effector RUFY1. Expression of Rab14 and Rab4B, analysed by qPCR, did not change during osteoclast differentiation. To determine the role of these two GTPases in osteoclast function, we knocked down their expression using siRNA. After expansion with M-CSF, human monocytes were cultured for 2 days with M-CSF and RANKL. The cells were then electroporated with 2 different Rab14 or Rab4B siRNAs, a GAPDH siRNA or a negative control siRNA. After 4 days of culture, osteoclasts were replated onto dentine discs and cultured for 48hr. Knockdown of Rab4B, Rab14 and GAPDH expression was confirmed by qPCR or western-blotting but had no effect on the formation of multinucleated osteoclasts. However, Rab4B knockdown caused a 40-70% decrease in both the number of polarised osteoclasts with actin rings and the amount of bone resorption. Similarly, Rab14 knockdown caused a 70-80% decrease in both these parameters. Moreover, when GFP-Rab14 was expressed in osteoclasts cultured on glass coverslips, the protein was found to colocalise in part with the endosomal marker EEA1 and the cis-golgi marker GM130, as previously described in other cell types. However, in 10% of the cells, GFP-Rab14 also colocalised with actin in podosomes. Our results indicate that both Rab4B and Rab14-regulated vesicular trafficking pathways are not involved in osteoclastogenesis but are required for osteoclast polarisation and activity. As Rab4 mediates integrin recycling in fibroblasts, Rab4B and Rab14 may both control $\alpha_v\beta_3$ recycling in osteoclasts, thereby regulating actin cytoskeleton reorganisation.

Disclosures: Cecile Itzstein, None.

SU0273

The Redundancy Between PTP Epsilon and PTP Alpha in Osteoclasts. Ari Elson, Eynat Finkelshtein*. Weizmann Institute of Science, Israel

Tyrosine phosphorylation plays a central role in regulation of cellular processes, among them bone structure and metabolism. We previously demonstrated that the non-receptor form of protein tyrosine phosphatase epsilon (PTPe), cyt-PTPe, is highly expressed in osteoclasts. Young female mice genetically lacking PTPe exhibit increased trabecular bone mass; their osteoclasts resorb bone less well in vitro and in vivo. These phenotypes are caused by reduced adhesion of PTPe-deficient osteoclast to bone, secondary to abnormal structure, stability and organization of podosomes, the adhesion structures of these cells. Most importantly, expressing cyt-PTPe in PTPe-deficient osteoclasts corrects the abnormal stability of podosomes in these cells. RPTPa is a very close structural relative of PTPe, and is also expressed at high levels in osteoclasts. However, our preliminary study of PTPa revealed no changes in bone matrix or osteoclast differentiation and their activity. Although the sequences of cyt-PTPe and RPTPa are very similar, Cyt-PTPe is predominantly cytosolic while RPTPa is an integral membrane protein. In order to determine if this difference prevented RPTPa from playing a significant role in osteoclasts we examined the ability of various forms of PTPe and PTPa to rescue the cellular phenotype of osteoclasts lacking PTPe, using podosomal organization as readout. We found that expression of cyt-PTPe or of an artificial cytosolic PTPa rescued the phenotype, while the receptor forms of PTPe (RPTPe) and PTPa (RPTPa) or of LCK-PTPe (a membrane-associated form of PTPe lacking an extracellular domain) cannot do so. We conclude that cytosolic localization of PTPe or PTPa catalytic activity is required to maintain proper organization and function of podosomes in osteoclasts.

Disclosures: Eynat Finkelshtein, None.

SU0274

Visualisation of the Apical Surface of Activated Osteoclasts. Kinga Szewczyk*, Karen Fuller¹, Raymond Moss¹, Timothy Chambers². ¹St. George's University of London, United Kingdom, ²St. George's Hospital Medical School, United Kingdom

Bone resorption occurs at the substrate-apposed, apical surface of osteoclasts, a surface that has not been accessible to direct visualisation. We have recently shown that it is the high affinity of bone mineral for vitronectin-receptor ligands that endows bone with the ability to activate osteoclasts. Consistent with this, osteoclasts secrete acid hydrolases and develop a ruffled border, as they do on bone, when they are incubated on vitronectin-coated plastic. Therefore, osteoclasts can be activated for resorption by substrates other than bone.

We have developed a novel approach to inspect the substrate-apposed surface of cells. To do this, cells are sedimented onto glass coverslips that have previously been coated with nail varnish. After incubation on such coverslips, the discs of nail varnish, with attached cells, are inverted onto a glass slide, and the nail varnish is removed with acetone. This exposes the underside of the cells, which can be inspected in the scanning electron microscope.

To analyse the substrate-apposed surface of activated osteoclasts, the nail varnish was coated with either vitronectin, or neonatal calf serum as a source of vitronectin. After incubation, the underside of osteoclasts showed a striking appearance. The whole undersurface was closely applied to the substrate, as it is on bone, in most osteoclasts. The central region was sometimes covered by fine, finger-like processes, often flattened against the substrate. More commonly the processes formed islands, or rings at the periphery of the central area. We also noted distinctive sucker-like structures of different sizes and shapes in almost all cells. Some of the central regions showed compartmentalisation, with compartmental walls similar in appearance to the stalks of 'suckers'. In some ruffled border regions we saw orifices, perhaps reflecting endocytic or exocytic processes.

The circumferential region appeared flat and featureless. However, if osmium tetroxide was omitted from fixation, rings, crescents and ridges of nodular protrusions, corresponding in position with podosomes, were observed circumferentially. The surface between and adjacent to podosomes, overlying the peri-podosomal cytoskeletal network, was extensively pitted.

This approach provides an exciting opportunity to characterise the morphological correlates of the resorptive process in osteoclasts.

Disclosures: Kinga Szewczyk, None.

SU0275

Activation of the Prostaglandin D₂ CRTH2 Receptor Induces Apoptosis of Human Osteoclasts by the Intrinsic Apoptosis Pathway. Li Yue, Artur De Brum-Fernandes*. Universite De Sherbrooke, Canada

Osteoclasts (OCs) are the multinucleated giant cells of hematopoietic origin and participate in several pathologies associated with bone loss. Induction of OC apoptosis leads to decrease in bone resorption and affects the rate of bone remodeling, which is important to maintain normal bone turnover. Prostaglandin D₂ (PGD₂), a lipid mediator synthesized from arachidonic acid, is involved in various pathophysiological processes and diseases; it activates through two known receptors, DP1 and CRTH2. Previous results from our laboratory showed that treatment with PGD₂ induced human OC apoptosis in vitro through activation of CRTH2, but not through activation of the DP1 receptor. However, it is unclear which apoptotic pathway (i.e., intrinsic and extrinsic pathway) is involved in the PGD₂-induced OC apoptosis, and the objective of the present study is to elucidate this issue. Human OCs differentiated from peripheral blood mononuclear cells in the presence of rhRANKL (60 ng/ml) and M-CSF (10 ng/ml) for 21 days were treated with PGD₂ in the presence or absence of specific receptor agonists and antagonists for 24 hours. Caspase fluorogenic substrates assay and western blot analysis were performed to determine the activities and levels of caspase-3, -8, and -9 in cell lysates. The levels/activities of caspase-3 and -9 were increased after incubation with 10 nM PGD₂ and 10 nM CRTH2 agonist (13,14-dihydro-15-keto-Prostaglandin D₂, DK-PGD₂), but not with 10 nM DP agonist compound BW 245C. Decreased caspase-3 and -9 activities were observed after incubation with 10 nM of the CRTH2 antagonist compound CAY10471, but not 10 nM of the DP antagonist compound BW A868C. All results after treatment with PGD₂, DK-PGD₂ or CAY10471 were statistically different from untreated controls (p<0.05). Interestingly, treatment with 2 nM and 10 nM of PGD₂, DP agonist (BW 245C), CRTH2 agonist (DK-PGD₂), DP antagonist (BW A868C) or CRTH2 antagonist (CAY10471) did not change caspase-8 activity. The induction of PGD₂-CRTH2 dependent apoptosis is associated with the activation of caspase-9, but not caspase-8, leading to caspase-3 cleavage in human differentiated OCs. These data show PGD₂ induces OC apoptosis through activating CRTH2-dependent-intrinsic apoptotic pathway.

Disclosures: Artur De Brum-Fernandes, None.

This study received funding from: Canadian Institutes of Health Research

SU0276

IL-23 Stimulates Human Osteoclast Formation and Bone Resorption In Vitro and IL-23 Neutralization Inhibits Bone Loss In Vivo. Iannis Adamopoulos^{*1}, Cheng-chi Chao², Eddie Bowman². ¹University of California, USA, ²Merck & Co., Inc., USA

We have recently shown that IL-23 is implicated in the pathogenesis of autoimmune arthritis, induces osteoclast differentiation in vivo in adult mice and IL-23p19 deficient mice have delayed osteoclast maturation. In this paper we translate our findings to an in vitro human system for direct relevance to human disease. We show that IL-23 induces the formation of multinucleated TRAP+ cells in human PBMC in vitro and dose dependently upregulates TRAF6 and NFATc1 message which are required for osteoclast differentiation. We also show that IL-23 induces the formation of F-actin rings and bone resorption in vitro. These effects correlate with a dose dependent upregulation of $\alpha\beta 3$ integrin and cortactin message which are required for osteoclast cytoskeletal organization. Moreover, we show that IL-23 neutralization in the collagen-induced arthritis model inhibits disease progression and arthritis-associated bone loss. Collectively our data suggest that IL-23 may be a promising target to combat pathological bone loss through osteoclast differentiation and activation in human autoimmune diseases.

Disclosures: Iannis Adamopoulos, Merck, 3
This study received funding from: Merck

SU0277

Interleukin-10 Regulates Bone Metabolism by Suppressing Osteoclastogenesis In Vivo. Gunwoo Kim¹, Seungwoo Han^{*2}, Younkwan Jung³, Eunjo Lee³. ¹Department of internal medicine, Daegu Fatima hospital, South Korea, ²Daegu Fatima Hospital, South Korea, ³Laboratory for arthritis & bone biology, Fatima research institute, South Korea

Background: Recent studies showed IL-10 may down-regulate osteoclastogenesis through inhibition of the expression of NFATc1, c-Fos and c-Jun and inhibition of calcium signaling downstream of RANK by inhibiting transcription of TREM-2. However, there has been no study about the role of IL-10 in osteoclastogenesis in vivo and under inflammatory condition such as TNF- α induced osteoclastogenesis. **Objective:** To elucidate the role of IL-10 in osteoclast formation under physiological and pathological condition. **Methods:** 3-month old male IL-10 KO and WT littermates were used (n = 7 mice/group). We compared the bone phenotype by microcomputed tomographic analysis, histologic analysis and TRAP staining. And we conducted in vitro induction of osteoclast formation by bone marrow monocytes from IL-10 KO and WT mice. **Results:** We analyzed the IL-10-/- mice for abnormal bone phenotypes. Microcomputed tomographic analyses showed that these mice had severe osteoporosis accompanied by markedly lower trabecular bone volume, number, and thickness, as well as a smaller number of bone nodules compared to wild-type mice. Histomorphometric analysis also revealed reduced bone mass in the IL-10-/- mice. Notably, TRAP stain showed higher osteoclast numbers and larger osteoclast surface areas in these mice. Moreover, we observed a higher rate of bone formation accompanying the accelerated bone resorption rate in the IL-10-/- mice, suggesting that their osteoporosis was caused by enhanced bone turnover and remodeling. We then attempted to investigate the roles of IL-10 in the processes underlying pathological bone destruction. We examined the effect of TNF- α on osteoclastogenesis using IL-10-/- precursors, because TNF- α is a major mediator of inflammation induced by TLRs and has been suggested to be able to induce osteoclastogenesis. Consistent with previous reports, TNF- α induced the development of a small number of osteoclasts in cultures of wild-type precursor cells. Notably, osteoclastogenesis was enhanced in cultures of IL-10-/- precursor cells treated with TNF- α . The mRNA expression levels of Nfatc1 and Acp5 in the IL-10-/- osteoclast precursors were also augmented by TNF- α , indicating that IL-10 also has a suppressive role in TNF- α -induced osteoclastogenesis. **Conclusion:** Our results show that IL-10 inhibits osteoclast formation under physiological and pathological conditions and suggest a model where downregulation of IL-10 contributes to RANKL-mediated osteoclastogenesis.

Disclosures: Seungwoo Han, None.

SU0278

Interplay Between Osteoclasts, Inflammatory Cells and Cytokines in the Pathogenesis of Periapical Bone Resorption. Lea da Silva¹, Sandra Fukada², Andiara De Rossi^{*3}, Marcos Rossi⁴. ¹Faculty of Dentistry of Ribeirao Preto, University of Sao Paulo, Brazil, ²Faculty of Pharmaceutical Sciences of Ribeirao Preto, University of Sao Paulo, Brazil, ³Faculty of Dentistry of Ribeirao Preto, University of Sao Paulo, Bra, ⁴Faculty of Medicine of Ribeirao Preto, University of Sao Paulo, Brazil

Endodontic infections occurs in consequence of polymicrobial infection of the dental pulp and root canal system, and ultimately results in destruction of periapical tissues including periodontal ligament, cementum and bone surrounding the tooth apex. However, the interplay between cells and cytokines involved in the destructive processes associated to inflammatory periapical bone loss has not been fully

elucidated. The aim of the present study was to evaluate the interplay between osteoclasts, inflammatory cells and osteoclastogenic factors in the progression of periapical lesions at different stages of development. Inflammatory periapical bone resorption was experimentally-induced in the lower first molars of male C57BL/6 wild-type mice, aging 6 to 8 weeks, by pulp exposure to the oral environment. Intact teeth were used as controls. At 0, 7, 21 and 42 days following pulp infection, the periapical region was evaluated under conventional microscopy (morphologic analysis), fluorescence microscopy (morphometric analysis), immunohistochemistry (neutrophils, macrophages and lymphocytes), immunofluorescence (RANK, RANKL and OPG), enzyme histochemistry (osteoclasts) and RT-PCR (RNA expression of IL-1 α , TNF- α , IL-10, IFN- γ , KC, IL-17, MIP-1 α , RANK, RANK-L, OPG and cathepsin K). Our results show a progressive increase in cementum and bone resorption, inflammatory cells and osteoclasts number, accompanied by enhanced mRNA levels of IL-1 α , IL-10, IFN- γ , KC, IL-17, MIP-1 α , RANK, RANKL, OPG and cathepsin K. This result suggests that these factors may be involved in the pathogenesis of periapical disease severity as modulator of cellular migration and osteoclasts differentiation and activity through RANK/RANKL/OPG signaling pathway. There was no significant enhancement in mRNA levels of TNF- α during all evaluated periods. Neutrophils were the most prevalent inflammatory cells at acute and chronic stages of the lesion development. **Conclusion:** our findings suggest that inflammatory periapical bone resorption are correlated with the osteoclasts and inflammatory cells number, and the severity of the lesions was directly correlated with the levels of IL-1 α , IFN- γ , IL-10, IL-17, KC, MIP-1 α , and cathepsin K, with RANK/RANKL/OPG pathway, but not with TNF- α .

Disclosures: Andiara De Rossi, None.
This study received funding from: FAPESP

SU0279

STAT3 Is a Novel Target for Treating Bone Resorption in Rheumatoid Arthritis. Yoshiaki Toyama, Akihiko Yoshimura, Tomoaki Mori^{*}, Takeshi Miyamoto. Keio University School of Medicine, Japan

Joint destruction is frequently seen in chronic inflammatory diseases, such as rheumatoid arthritis (RA). Osteoclasts are implicated in such joint destruction by their bone resorbing activity. However, the mechanisms underlying how joint destruction in RA develop and are sustained chronically remain largely unknown. In this study, we show that STAT3 is the key mediator of joint destruction in RA by inducing Receptor activator of nuclear factor kappa-B ligand (RANKL). In RA patients, pro-inflammatory cytokines, such as IL-1 β , TNF α and IL-6 are up-regulated and implicated in disease activity. We found that IL-6 cytokine family, such as IL-6, LIF, IL-11 and OSM, and RANKL were significantly up-regulated in osteoblastic cells by the treatment with these inflammatory cytokines, and such up-regulation were significantly suppressed in STAT3-/- MEF cells compared with WT. IL-1 β , TNF α or IL-6 activated STAT3 either directly or indirectly and in turn induced expression of IL-6 family cytokines, further activating STAT3 in osteoblastic cells. STAT3 activation also induced expression of RANKL, and thus STAT3 is considered a therapeutic target to treat inflammation and joint destruction. We screened STAT3 inhibitor, and identified two possible inhibitors of STAT3. STAT3 pharmacological inhibition promoted significant reduction in expression of both IL-6 cytokine family and RANKL and inhibited osteoclastogenesis in coculture system with primary osteoblasts and bone marrow cells. STAT3 inhibition was also effective in treating an RA model, collagen induced arthritis (CIA), in vivo, and joint destruction was completely improved. In CIA model, by STAT3 inhibition, significant reduction in expression of pSTAT3, IL-6 cytokine family and RANKL in the joints was evident by immunoblotting analysis, ELISA, fluorescent immunohistochemistry and RT-PCR. Furthermore, the serum level of IL-6 was reduced by the administration of STAT3 inhibitor in CIA model. Thus our data provide new insight into RA pathogenesis and provide evidence that inflammatory cytokines trigger a cytokine amplification loop via STAT3 that promotes sustained inflammation and joint destruction.

Disclosures: Tomoaki Mori, None.

SU0280

Choline Kinase Beta is an Important Regulator of Bone Homeostasis. Jasreen Kular^{*}, Jennifer Tickner, Nathan Pavlos, Baysie Lim, Tamara Abel, Ming Hao Zheng, Jiaka Xu. University of Western Australia, Australia

The maintenance of bone homeostasis requires a tight balance between bone formation and bone resorption by osteoblasts and osteoclasts. The molecular mechanism(s) underlying the fundamental activities of these cells still remains largely unclear. In search of novel molecules that potentially play an important role in bone homeostasis we screened a number of ENU-induced mutant mouse lines. We identify choline kinase beta, a kinase that phosphorylates the first reaction in the biosynthesis of phosphatidylcholine, as a novel candidate regulator of bone homeostasis. Choline kinase beta mutant mice exhibit an osteoporotic phenotype as evidenced by microCT and histological assessment. *In vivo* and *in vitro* analysis reveals elevated osteoclast numbers in the mutant mice. Osteoclast precursors, derived from the bone marrow of choline kinase beta mutant mice, have an increased sensitivity to RANKL during osteoclastogenesis. Furthermore, osteoclasts from choline kinase beta mutant mice exhibit increased resorptive activity as compared to those of littermate controls. Treatment with CDP-choline *in vivo* and *in vitro* reduces osteoclast numbers, thereby

rescuing the osteoclast phenotype. *In vitro* assays show a reduction in bone mineralisation in osteoblast cultures derived from the bone marrow of mutant mice. Taken together, our data document, for the first time, that choline kinase beta plays an important role in bone homeostasis by regulating both osteoclasts and osteoblasts.

Disclosures: Jasreen Kular, None.

SU0281

Double Stranded RNA Inhibits Osteoclast Differentiation via Interferon-beta/STAT1 Pathway and Increases Bone Mass in Osteoporosis Model Mice.

Arei Miyamoto^{*1}, Masamichi Takami², Yoichi Miyamoto³, Atsushi Yamada⁴, Mijung Yim⁵, Tomohiko Tamura⁶, Ryutaro Kamijo¹. ¹School of Dentistry, Showa University, Japan, ²Department of Biochemistry, School of Dentistry, Showa University, Japan, ³Showa University School of Dentistry, Japan, ⁴Showa University School of Dentistry, Jpn, ⁵College of Pharmacy, Sookmyung Women's University, South Korea, ⁶Department of Immunology, Graduate School of Medicine & Faculty of Medicine, Yokohama City University, Japan

Double stranded RNA, a ligand of Toll-like receptor (TLR) 3, is known to induce antiviral responses in the innate immune system. However, the effects of double stranded RNA on bone metabolism are unknown. We found that polyinosinic-polycytidylic acid [poly(I:C)], a double stranded RNA analog, markedly increased bone mass by inhibiting osteoclastogenesis. Six-week-old female mice were subjected to an ovariectomy (OVX) for an osteoporosis model or a sham operation for the control groups. After surgery, we intravenously administered poly(I:C) (250 µg) or PBS to the mice every 3 days for 4 weeks. Analysis of tibia using microcomputed tomography revealed that trabecular bone volume per tissue volume (BV/TV) in the sham/poly(I:C) group was significantly greater than that in the sham/PBS group (13.51.9% vs. 10.81.2%, $P < 0.05$). Similarly, BV/TV in the OVX/poly(I:C) group was significantly greater than that in the OVX/PBS group (13.51.4% vs. 8.30.6%, $P < 0.05$). Histomorphometric analysis of embedded femur sections revealed a significantly decreased number of osteoclasts in the OVX/poly(I:C) and sham/poly(I:C) groups as compared to the OVX/PBS and sham/PBS groups, respectively. To examine the effects of poly(I:C) on osteoclastogenesis, we cultured bone marrow-derived macrophages (BMMs) induced by M-CSF treatment for 3 days as osteoclast precursors in the presence of RANKL with or without poly(I:C). Osteoclastogenesis induced by RANKL was inhibited by poly(I:C) in a dose-dependent manner. We found that BMMs express TLR3 and produce interferon (IFN)-beta, an inhibitory factor of osteoclastogenesis, in response to poly(I:C). Next, we added antibodies for IFN-beta or its receptor to block IFN-beta stimulation of osteoclastogenesis. In the presence of these antibodies, osteoclastogenesis was successfully accomplished, even in the presence of poly(I:C). Subsequently, we prepared BMMs from mice deficient of STAT1, an intracellular signal transducer of IFN $\alpha\beta$ receptor, and cultured them with or without poly(I:C) in the presence of RANKL. Osteoclastogenesis of STAT1-deficient BMMs was not inhibited by poly(I:C). Furthermore, administration of poly(I:C) as well as PBS to STAT1-deficient mice did not increase bone mass in either the OVX or sham groups. These results suggest that poly(I:C) induces IFN-beta production in osteoclast precursors and inhibits osteoclastogenesis via the STAT1 signaling pathway, resulting in an increase of bone mass in both sham and OVX mice.

Disclosures: Arei Miyamoto, None.

SU0282

Human Osteoclastogenesis and Aging: Roles of PPAR γ and c-fos. Regina O'Sullivan^{*}, Ping-Lin Chung, Shuanhu Zhou, Meryl Leboff, Julie Glowacki. Brigham & Women's Hospital, USA

Age-related bone loss in humans results from more osteoclastic bone resorption relative to osteoblastic bone formation. It is known that c-fos is an essential mediator of osteoclastogenesis. Emerging evidence in mice suggests that PPAR γ regulates c-fos. We tested the hypothesis that PPAR γ and c-fos mediate the effect of age on human osteoclastogenesis.

Methods. We obtained discarded bone marrow from 19 patients (27 to 82 years) who underwent total hip replacement, with IRB approval. Mesenchymal and hematopoietic progenitors were enriched by density centrifugation with Ficoll/Histopaque 1077. Total RNA from low-density progenitor cells was extracted with Trizol reagent and PCR products were separated by agarose gel electrophoresis and were quantified by densitometry Image J software. Data were expressed by normalizing to GAPDH (internal control). Aliquots were cultured for 14 days (without added osteoclastogenic factors) in order to measure basal osteoclast differentiation by tartrate-resistant acid phosphatase (TRAP) expression. Low-density progenitor cells from old (PC^{OLD}) and young (PC^{YOUNG}) subjects were incubated overnight and treated with BADGE (PPAR γ antagonist), Rosiglitazone (Rosi, PPAR γ agonist) or vehicle (DMSO). Total RNA was extracted at intervals with Trizol reagent and were analyzed for endogenous PPAR γ and c-fos expression.

Results. There was an age-related increase in spontaneous osteoclastogenesis ($r = 0.60$, $p = 0.019$). Constitutive PPAR γ expression in fresh samples was 20.1-fold higher ($p = 0.0065$) from older subjects than younger subjects, with no difference in constitutive c-fos expression. In freshly-isolated PC^{YOUNG}, endogenous PPAR γ levels were undetectable; and BADGE reduced c-fos (64%, compared with vehicle) at 6

hours and Rosi upregulated c-fos (116%) at 12 hours. In PC^{OLD}, BADGE reduced endogenous PPAR γ (15%) and c-fos (43%) expression at 6 hours. In PC^{OLD}, Rosi had no effect on endogenous PPAR γ or c-fos levels.

Conclusions. There is an age-related increase in osteoclastogenic potential in human marrow progenitors. This study shows an age-related increase in constitutive expression of PPAR γ which may account for the age-related increase in human osteoclastogenesis. We show that PPAR γ -active agents modulated c-fos *in vitro*. The data suggest that PPAR γ may be an important factor in human skeletal aging, as has been reported in mice.

Disclosures: Regina O'Sullivan, None.

SU0283

Hyperfunctions of Osteoclasts in a Rheumatoid Arthritis Model. Kazuma Matsumoto^{*1}, Naozumi Ishimaru¹, Takashi Izawa², Masahiro Hiasa¹, Yoshio Hayashi¹, Eiji Tanaka¹. ¹University of Tokushima Graduate School, Japan, ²Washington University in St. Louis, USA

[Objectives] Although osteoclasts (OCs) are known to play a key role in the pathogenesis of rheumatoid arthritis (RA), the precise mechanism how OCs are activated in the development of RA has been still obscured. In this study, we investigated functions such as bone absorptivity, migration, and antigen presentation of OCs from MRL/lpr mouse, an animal model for human RA, bearing a mutant of Fas gene. [Methods] Bone dynamics of knee joints and distal femurs in control MRL+/+ and MRL/lpr mice was scanned using a micro CT system. Moreover, bone marrow-derived OCs from control and MRL/lpr mice were generated by the culture with M-CSF and RANKL, and then their phenotypes, gene expressions, and functions were analyzed by TRAP staining, flow cytometry, pit formation assay, real-time RT-PCR, migration assay and confocal microscopy. Furthermore, to know the *in vivo* function of MRL/lpr OCs, the precursors were transferred in knee joints, and the phenotypes of peripheral immune cells and pathology of RA were analyzed. [Results] The bone finding of MRL/lpr mice showed significantly decreased bone density compared with that of controls, resembling osteoporosis. Pit formation assay revealed that function of OCs from MRL/lpr mice was more enhanced than that from control mice. The mRNA expressions of differentiation or activation-related genes of MRL/lpr OCs were up-regulated compared with those of control OCs. In addition, the migratory response of MRL/lpr OCs to sphingosin-1-phosphate (S1P) was significantly enhanced compared with that of control OCs. Furthermore, *in vitro* and *in vivo* experiments showed more enhanced function of MRL/lpr OCs as antigen-presenting cells to activate peripheral T cells. [Conclusions] The hyperfunctions of OCs in MRL/lpr mice play a potent role in the pathogenesis for RA with bone destruction. Fas signaling of OCs may regulate the differentiation, activation, or important function of OCs.

Disclosures: Kazuma Matsumoto, None.

SU0284

Involvement and Regulatory Role of Membrane Nanotubes in Fusion of Osteoclast Precursors: A Possible Migration and Penetration of DC-STAMP Protein into Osteoclast Precursors through Inter-Cellular Bridges. Akira Takahashi^{*1}, Akiko Kukita², Yin-ji Li³, Hisayuki Nomiya⁴, Yasunori Ayukawa⁵, Kiyoshi Koyano³, Toshio Kukita⁶. ¹Kyushu University, Japan, ²Saga Medical School, Japan, ³Kyushu University, Japan, ⁴Kumamoto University, Japan, ⁵Kyushu University, Japan, ⁶Kyushu University, Faculty of Dental Science, Japan

The membrane nanotubes are intercellular bridges bearing cylindrical structure with small diameters (50–300nm) with length of 10–100µm or more. Membrane nanotubes play important roles in cell-to-cell communication in immune cells. Recently, M-Sec gene has been revealed to be an essential gene for the formation of membrane nanotubes. The one purpose of this study is to clarify an involvement of membrane nanotubes in the process of fusion of osteoclast precursors to form multinucleated osteoclasts. The other purpose is to verify that DC-STAMP, a membrane protein required for fusion of pre-osteoclast, could migrate between osteoclast precursors through membrane nanotubes in osteoclastogenesis. We confirmed the presence of numerous tubular bridges with small diameter between cells observed *in vitro* culture system for osteoclast differentiation. These intercellular structures contain actin fiber detected with TRITC-labeled phalloidin. These intercellular bridges were disappeared and formation of osteoclasts was markedly inhibited when cells were treated with Latrunculin B, an inhibitor of actin polymerization. These results demonstrate an involvement of membrane nanotubes in osteoclastogenesis. Time course analysis using RT-PCR revealed that expression of M-Sec gene was up-regulated as osteoclasts differentiated. Formation of osteoclasts was significantly suppressed by siRNA specific to M-Sec. Meanwhile, we co-cultured DiD (red fluorochrome)-labeled RAW-D cells with DC-STAMP-GFP (green fluorescence)-transfected RAW-D cells followed by extensive observation of the fusion process under fluorescence microscope. We have obtained evidence suggesting transportation of DC-STAMP-GFP protein expressed in RAW-D cells into DiD-labeled RAW-D cells by use of membrane nanotubes. Current study suggests an importance of membrane nanotubes in the regulatory process of fusion among osteoclast precursors.

Disclosures: Akira Takahashi, None.

This study received funding from: Kyushu University, Faculty of Dental Science

SU0285

Mapping the Transcription Factor Regulatory Network Involved in Osteoclast Differentiation. Heather Carey*, Fei Gu, Lyudmyla Sharma, Anand Merchant, Raksha Adhikari, Victor Jin, Sudarshana Sharma, Michael Ostrowski. The Ohio State University, USA

Osteoclasts are bone resorbing cells which differentiate from myeloid precursors. The crosstalk between osteoblasts, bone-forming cells, and osteoclasts tightly regulates bone remodeling which is a dynamic and continuous process in vertebrates. Improper regulation of this delicate balance can lead to debilitating diseases such as cancer metastasis to the bone, osteoporosis, and osteoarthritis. The signaling cascades originating from two cytokines, CSF1 and RANKL are necessary and sufficient to induce osteoclast differentiation *in vitro*. However, the downstream effectors of these pathways leading to the transcription of genes necessary for osteoclast function are not fully defined. Using a candidate gene-based approach, our lab has previously shown that MITF and PU.1 bind to the promoters of *Acp5* and *Ctsk* to regulate transcription of these two genes required for osteoclast function. NFATc1 aids in the maintenance of transcription of these genes. In this study, we are delineating the role of these three factors on a genome-wide scale using chromatin immunoprecipitation and next generation sequencing (ChIP-Seq). ChIP-Seq analysis demonstrated that there are at least 9000 regions in the mouse genome enriched for PU.1 binding. Preliminary analysis of regions bound by PU.1, MITF and NFATc1 indicated PU.1 as a primary transcription factor that is present irrespective of the stage of differentiation. Nevertheless, PU.1 may interact with other cofactors depending on signaling cues. Thus, we utilized these PU.1 enriched regions to analyze the most probable binding partners of PU.1 using ChIPMotifs. This analysis indicated members of the IRF family of transcription factors as the most probable binding partners of PU.1. Overlapping our ChIP-Seq data with microarray data for transcription factors that are differentially regulated during osteoclast differentiation enabled us to draw a transcription factor regulatory network. Furthermore, twenty four genes encoding transcription factors regulated by PU.1 and differentially expressed during osteoclast differentiation were implicated in volumetric bone mineral density. Our results indicate that one or multiple IRFs may play a central role in regulating the transcription factors that are important for osteoclast differentiation. Identifying the transcription factors that control osteoclast differentiation will aid in the development of more specific therapies for diseases caused by deregulated osteoclast function.

Disclosures: Heather Carey, None.

SU0286

Mechanisms for Radiation-Induced Bone Loss: Low Dose, Gamma Radiation Effects on Osteoclastogenesis and Osteoblastogenesis. Akhilesh Kumar*¹, Joshua Alwood¹, Luan Tran¹, Arundhati Balid¹, Charles Limoli², Ruth Globus¹. ¹NASA Ames Research Center, USA, ²University of California, USA

High total doses of ionizing radiation (here defined as $\geq 200\text{cGy}$) are known to cause bone loss both in humans and animals, although little is known about the cellular and molecular mechanisms involved. Furthermore, the potential influence of low dose radiation (radiation $\leq 10\text{cGy}$) on bone remodeling is not known. Here, we tested the hypothesis that low dose, low Linear Energy Transfer (LET) radiation can accelerate osteoclastogenesis and inhibit osteoblastogenesis of bone marrow-derived precursors. To induce osteoclast differentiation, non-adherent bone marrow cells isolated from C57BL/6J mice were treated with M-CSF (30 ng/ml) and RANKL (60 ng/ml), exposed to 10-200cGy of gamma radiation (Cs-137, 90 cGy/min) then cultured for 2-5 days. Osteoclastogenesis was assessed both by counting TRAP-positive, multinucleated cells and analyzing mRNA expression levels of osteoclast-related genes by RT-PCR. To assess osteoblast differentiation, adherent marrow cells grown with the addition of ascorbate (50 $\mu\text{g/ml}$) and beta-glycerolphosphosphate (10 mM), and were irradiated 2 days after plating. Osteoblastogenesis was assessed 15 days after irradiation by quantifying alizarin-red nodule formation and assessing expression levels of osteoblast-related genes. Both low dose (10cGy) and high dose (200cGy) radiation significantly increased the number of TRAP+ multinucleated osteoclasts (47% and 66%). Irradiation increased expression levels of differentiation (Nfatc1) and fusion-related genes (Atp6v0d2 and Tm7sf4), which were evident at an earlier time point (day 2) than sham-irradiated controls. In osteoblast cultures, high dose (200cGy) irradiation reduced mineralized nodule formation (61% decrease), compared to the sham-irradiated controls while lower doses (10cGy) had no effect. Similarly, the expression levels of differentiation-related genes (Runx2, Col1a1, Col1a2, Bglap, Ibsp) were lower than controls only in cultures irradiated with 200cGy. In sum, our results indicate that even low dose (10cGy) ionizing radiation stimulated osteoclastogenesis whereas osteoblastogenesis was not affected at this dose. Irradiation accelerated the expression of both differentiation and fusion-related genes by precursors to osteoclasts, providing a plausible explanation for the increased osteoclast number and bone loss observed acutely following irradiation *in vivo*. We conclude occupationally-relevant doses of ionizing radiation may influence bone health by stimulating osteoclastogenesis.

Disclosures: Akhilesh Kumar, None.

SU0287

Mesenchymal Stem Cells markedly suppressed Inflammatory Bone Destruction in Rats with Adjuvant-induced Arthritis. Toshio Takano*¹, Yin-ji Li¹, Akiko Kukita², Takayoshi Yamaza¹, Yasunori Ayukawa¹, Kiyoshi Koyano¹, Toshio Kukita³. ¹Kyushu University, Japan, ²Saga Medical School, Japan, ³Kyushu University, Faculty of Dental Science, Japan

Mesenchymal stem cells (MSCs) are known to have potential to differentiate into multiple cell lineages and have widely been applied to regenerative medicine as the useful cellular sources of various tissues. Recently, it has been revealed that MSCs also have anti-inflammatory and immuno-modulatory functions. In this report, we investigated on the regulatory function of MSCs for the development of inflammation and bone destruction in rats with adjuvant-induced arthritis (AA-rats). MSCs were isolated from rat bone marrow tissues and proliferated in the presence of basic FGF. Adjuvant arthritis was induced in Lewis rats by intradermal injection of the complete Freund adjuvant (CFA) at the base of the tail. MSCs were intraperitoneally injected into AA-rats (2×10^7 cells/rat). The swelling score of the fore and hind paw, swelling volume of the hind paw and the body weight were measured from day 7 to day 28 after CFA-injection. On day 28, hind paws were examined radiographically and histologically. Although MSC-injected group did not show significant effects on the parameter of the swelling volume, MSC-administration significantly suppressed the swelling score and prevented body weight loss. Radiographical evaluation showed that MSC significantly suppressed bone destruction. The control group (CFA-injected rats without MSCs) showed remarkable bone destruction, thickened synovial membrane and marked infiltration of inflammatory cells with extremely high number of osteoclasts. In contrast, only very low level of bone destruction was observed in MSC-injected group with almost normal morphology of the joint cavity. Furthermore osteoclastogenesis was markedly suppressed in MSC-injected group in comparison to the control group. These data showed that MSC significantly suppressed inflammation and bone destruction in AA-rats. Current study demonstrates the potential utility of MSCs for the treatment of inflammatory bone destruction.

Disclosures: Toshio Takano, None.

This study received funding from: Kyushu University, Faculty of Dental Science

SU0288

MicroRNA Targets of RANKL During Osteoclast Differentiation; miR-146a as a Lineage Determining Factor for Osteoclasts in Myeloid Precursors. Sudarshana Sharma*, Sankha Ghosh, Haritha Mathsvaraja, Jamie Wolf, Michael Ostrowski. Ohio State University, USA

The regulation of osteoclast (OCL) differentiation is a critical factor for normal bone remodeling and in bone related diseases such as osteoporosis, osteoarthritis and bone metastases. Two cytokines, CSF-1 and RANKL are sufficient to induce osteoclast differentiation *in vivo* and *in vitro*. While there are elegant studies about the signaling cascades and transcriptional regulators that are targets of these two cytokines and affect osteoclast differentiation, very little is known on the role of microRNAs (miRs), small noncoding RNAs which control expression of wide sets of genes. The objective of this study is to analyze the expression and regulation of differentially expressed miRs during osteoclast differentiation and their physiological significance.

We used a miR microarray to profile differentially expressed miRs. Validations were done using q-PCR assays. Transcriptional regulation of miRs was studied using ChIP seq and ChIP analysis. Knock down and overexpression of miRs were performed transiently in myeloid precursors using nucleofection procedure.

Global miR expression analysis recognized miR-146a as the only miRNA that is upregulated during osteoclast differentiation. However, ectopic expression of miR-146a in myeloid precursors resulted in decreased TRAF6 and IRAK1 protein levels, as well as attenuated osteoclast differentiation as represented by analysis of osteoclast specific markers. The regulation of miR-146a during osteoclast differentiation differed from the classical NF κ B dependent induction of miR-146a observed during inflammatory response in myeloid cells as demonstrated by ChIP. Further, knock down of IKK β which abrogated the LPS mediated miR-146a induction had no effect on RANKL mediated induction of miR-146a. The presence of conserved PU.1-Ebox binding sites prompted us to analyze association of MITF/PU.1 on this region by ChIP seq, as well as ChIP which confirmed association of MITF and PU.1 with this locus. This region exhibited the hallmark of an enhancer with high enrichment of monomethyl (K4) histone H3. The basal level of expression of miR-146a was maintained by EOS-CtBP corepressor complex which has been shown to be important in myeloid lineage determination. In conclusion our results indicate that miR-146a is regulated differentially to inflammatory signals from that of differentiation signals elicited by RANKL in myeloid cells and its expression in precursors inhibit osteoclast differentiation by TRAF6, IRAK1 downregulation.

Disclosures: Sudarshana Sharma, None.

SU0289

Negative Regulation of Osteoclastogenesis by beta2 Integrin-Bcl6 Axis. Kyung-Hyun Park-Min^{*1}, Eun-Young Lee², Nick Brownell¹, Neal Moskowitz³, LIONEL IVASHKIV¹. ¹Hospital for Special Surgery, USA, ²Seoul National University, South Korea, ³Arthritis group, USA

Integrins are receptors that mediate attachment between cells and the surrounding tissues, which may consist of cells and extracellular matrix (ECM). Extracellular matrix (ECM) proteins regulate various cell functions including cell adhesion, differentiation, proliferation, migration, invasion and survival. We hypothesized that the type or timing of integrin signaling generated by cell-matrix interactions influences the differentiation of osteoclast precursor cells (OCPs). The most well studied integrin receptor in osteoclasts is integrin $\alpha V\beta 3$, which is induced during RANKL-induced osteoclastogenesis and plays an essential role in bone resorption in mature osteoclasts. However, OCPs express various other integrin receptors, whose role in osteoclast differentiation is not well understood. Thus, we investigated the effect of integrin ligation in OCPs on subsequent osteoclastogenesis. Among the integrin receptors, the expression of integrins $\beta 2$ and $\beta 5$, which are highly expressed in OCPs, are suppressed after RANKL stimulation, suggesting a possible negative role in regulating osteoclast differentiation. We found that fibrinogen, a potent endogenous ligand of $\beta 2$ and $\beta 5$ integrins, significantly inhibited osteoclastogenesis in both human and mouse OCPs. Concomitantly, RANKL-induced NFATc1 expression was decreased and the expression of osteoclast specific genes was down-regulated by fibrinogen ligation. Fibrinogen inhibited osteoclastogenesis via the interaction with $\alpha M\beta 2$ integrins. Deletion of integrin $\alpha M\beta 2$ (Mac1) in mouse OCPs resulted in the reversal of fibrinogen-mediated inhibition of osteoclastogenesis. Similar results were obtained in fibrinogen-induced human osteoclastogenesis using integrin $\alpha M\beta 2$ (Mac1) blocking peptides. The mechanism of inhibition partially involved the induction of a transcriptional suppressor, B cell lymphoma 6, by fibrinogen ligation. Thus, in contrast to $\alpha V\beta 3$ integrins, which promote the late phases of osteoclast differentiation, $\alpha M\beta 2$ integrins suppress early steps of osteoclastogenesis in OCPs. These findings identify cell-matrix interactions that are suppressive for osteoclastogenesis and a potential homeostatic mechanism that limits osteoclast differentiation after extravasation of monocytes in physiological and inflammatory settings.

Disclosures: Kyung-Hyun Park-Min, None.

SU0290

Orai1-Mediated Calcium Entry Plays a Critical Role in Osteoclast Differentiation and Function by Regulating Activation of the Transcription Factor NFATc1. Sung-Yong Hwang^{*}, James Putney. National Institute of Environmental Health Sciences, USA

Bone diseases such as postmenopausal osteoporosis are primarily caused by excessive formation and activity of osteoclasts (OCL). Receptor activator of nuclear factor kappa B ligand (RANKL) is a key initiating cytokine for OCL differentiation and function. RANKL induces calcium (Ca^{2+}) oscillations, resulting in selective and robust induction of nuclear factor of activated T cells c1 (NFATc1), a Ca^{2+} -responsive transcription factor that drives osteoclastogenesis. Store-operated Ca^{2+} entry (SOCE) is a major Ca^{2+} influx pathway in most non-excitable cell types and is activated by any stimulus that depletes Ca^{2+} stores in the endoplasmic reticulum. Although the important role of Orai1, a store-operated Ca^{2+} entry channel in the plasma membrane, in maintaining Ca^{2+} oscillations and transactivation of NFAT in other cell types is well-known, its contribution to osteoclastogenesis remains unclear. We show here that silencing of the Orai1 gene with viral delivery of shRNA reduces SOCE and inhibits RANKL-induced osteoclastogenesis of RAW264.7 cells, a murine monocyte/macrophage cell line, by suppressing the induction of NFATc1. This was accompanied by defective induction of OCL-specific genes such as tartrate-resistant acid phosphatase and immunoreceptor OCL-associated receptor, which are known to be direct transcriptional targets of NFATc1 during osteoclastogenesis. In addition, maturation of OCLs was abrogated by defective cell fusion of pre-OCLs depleted of Orai1, consistent with defective RANKL-mediated induction of d2 isoform of vacuolar ATPase V_o domain that is involved in cell fusion of pre-OCLs. We found that the functional bone resorbing capacity was severely impaired in OCLs depleted of Orai1, potentially related to the observed decrease in the induction of cathepsin K, a major bone matrix degrading protease. We further investigated the role of Orai1 in OCL differentiation by using primary monocytes/macrophages isolated from bone marrow of Orai1-deficient (Orai1^{-/-}) mice. We found that monocytes/macrophages from Orai1^{-/-} mice lack SOCE. Consistent with the findings with the macrophage cell line, RANKL-induced osteoclastogenesis in vitro from Orai1^{-/-} mice was markedly impaired due to reduced fusion of pre-OCLs. Our results indicate that Orai1 plays a critical role in the differentiation and function of OCLs, suggesting that Orai1 might be a potential therapeutic target for the treatment or prevention of bone loss caused by OCLs.

Disclosures: Sung-Yong Hwang, None.

SU0291

Osteoclastogenesis is Highly Dependent on Exogenous Cholesterol, and Deficiency of Low Density Lipoprotein Receptor in Mice Causes Impaired Osteoclastic Cell Fusion and Increase in Bone Mass. Mari Okayasu^{*}, Chivomi Hayashida, Mai Nakayachi, Takuya Sato, Junta Ito, Naoto Suda, Yoshiyuki Hakeda. Meikai University School of Dentistry, Japan

Accumulating evidence indicates that dyslipidemia is closely associated with osteoporosis. However, the molecular mechanism of this association remains unclear. To clarify the relationship between lipid and bone metabolisms, we examined how cholesterol affected differentiation of osteoclasts by evaluating osteoclastogenesis in osteoclast progenitors isolated from low density lipoprotein receptor-knockout (LDLR-KO) mice. In vitro osteoclast formation in the culture medium with LDL-depleted FBS was suppressed compared to that in the medium with normal FBS. The down-regulation of osteoclastogenesis was restored by the addition of native LDL or oxidized LDL (ox-LDL) in a dose dependent manner. The restoration was seen in an additive manner. Supporting this finding, LDLR and scavenger receptor class A, which are receptors for native LDL and ox-LDL, respectively, were constitutively expressed and the expression levels did not change during the process of osteoclast formation regardless of RANKL stimulus. Osteoclastogenesis from LDLR-KO mice was significantly delayed than those of wild type (WT) littermate, and small-sized osteoclasts were noted in the culture of the former. The activation of Erk and Akt by RANKL, gene and protein expression of c-fos, NFATc1, TRAP and cathepsin K did not differ between cultures of both genotypes. Moreover, fusion index, represented as average number of nuclei per one multinucleated osteoclast, in culture from LDLR-KO mice, was about 20% of that in culture of WT mice, indicating the decreased osteoclast formation of gene-deficient mice is due to the impairment of cell fusion of mononuclear preosteoclasts to mature multinucleated osteoclasts. The expression of Atp6v0d2 and DC-STAMP mRNA, which are essential for cell-cell fusion of osteoclasts, did not differ between osteoclastic cells from genotypes, however, Atp6v0d2 in plasma membrane and lipid raft (cholesterol-rich micro domain in plasma membrane) of LDLR-KO osteoclasts was decreased compared to that of WT osteoclasts. Additionally, bone morphometric analysis showed that BV/TV and Tb.N were significantly increased. Taken together, osteoclast differentiation is highly dependent on exogenous cholesterol and the decrease in intracellular cholesterol level due to LDLR deficiency results in the reduction of cell-cell-fusion of preosteoclasts possibly via the impaired trafficking of osteoclast fusion protein such as Atp6v0d2 to the plasma membrane.

Disclosures: Mari Okayasu, None.

SU0292

Osteoclastogenic Potential of Mandible vs Long Bone Marrow. Thawinee Chaichanasakul^{*1}, Olga Bezouglia², Tara Aghaloo¹, Sotirios Tetradis³. ¹University of California, Los Angeles, USA, ²UCLA School of Dentistry, USA, ³UCLA, USA

Maxilla and mandible possess unique metabolic and functional properties and demonstrate discrete responses to homeostatic, mechanical and developmental stimuli. Specific bone pathologies such as cherubism and osteonecrosis of the jaws (ONJ) only affect the maxilla and mandible. Importantly, systemic diseases such as osteoporosis and malnutrition affect the jaws differently compared to other bones. Osteogenic potential of marrow stromal cells (MSCs) differs between mandible (MB) vs. long bones (LB). Furthermore, MB vs. LB derived osteoclasts (OCs) have different functional properties. Here, we hypothesized that MB vs. LB marrows have disparate osteoclastogenic potential at basal and stimulated conditions. To test our hypothesis, non-adherent marrow cells were isolated and differentiated in the presence of RANKL and M-CSF. TRAP staining showed increased number of TRAP+ multinucleated cells (MNCs) in MB vs. LB cultures. Additionally, osteologic disc resorption pit assays revealed a significantly higher resorbed area for MB vs. LB OCs. We then explored the ability of MB vs. LB MSCs to support osteoclastogenesis at basal and stimulated conditions. Confluent MSCs were cultured in osteogenic differentiation media in the presence of vehicle (veh), parathyroid hormone (PTH, 10 nM), 1 α ,25-dihydroxyvitamin D3 (D3, 10 nM), or dexamethasone (Dex, 100 nM), alone or in combination, for 1 or 2 weeks, and then RANKL and OPG mRNA levels were determined. No statistical difference on RANKL and OPG expression was observed at baseline. However, LB MSCs expressed significantly higher RANKL and lower OPG mRNA with a resultant increase in RANKL/OPG ratio in the presence of D3 alone, PTH+D3, and D3+Dex. Thus, LB MSCs appear to possess a significantly higher osteoclastogenic potential in stimulated conditions compared to MB MSCs. Finally, we isolated and cultured whole MB and LB marrow, containing both non-adherent and adherent cells, in the presence or absence of PTH and D3 and performed TRAP staining. No TRAP+ cells were observed at basal conditions. However, TRAP+ MNCs were significantly increased in LB vs. MB marrow. Collectively, our data demonstrate that although MB marrow contains increased number of OC precursors, under PTH, D3 and Dex stimulation LB marrow has higher osteoclastogenic potential. This appears to be, at least in part, due to the higher RANKL stimulation and OPG inhibition of long bone vs mandibular MSCs by these hormones.

Disclosures: Thawinee Chaichanasakul, None.

SU0293

Pam3CSK4, a TLR2 Agonist, Induces In Vitro Osteoclastogenesis RANKL-independently and Resorbs Alveolar Bone in Rats. Akiko Yano^{*1}, Keiko Suzuki², Tomio Morohashi², Takafumi Arimoto², Akiko Karakawa¹, Takeshi Igarashi², Hisashi Shinoda³, Matsuo Yamamoto¹, Shoji Yamada². ¹Showa University School of Dentistry, Japan, ²Showa University, Japan, ³Tohoku University Graduate School of Dentistry, Japan

Bacteria are a common cause of periodontitis, in which accelerated alveolar bone resorption may ultimately lead to tooth loss. It is well established that bacteria interact with host cells through components of their cell wall by binding to corresponding *Toll*-like receptors (TLRs). Among these, LPS, a component of gram-negative bacteria and a ligand for TLR4, is the most clearly defined molecule as a potent inducer of osteoclastogenesis and bone resorption. On the other hand, the fact that TLR2, in addition to TLR4, was prominently expressed in both precursors and differentiated osteoclasts, raised the possibility that components of gram-positive bacteria are involved in periodontitis-associated osteolysis. However, studies on the effects of TLR2 agonists, including diacylated lipopeptide and peptidoglycan, on osteoclastogenesis have been performed in coculture with osteoblasts, which secrete RANKL, or preosteoclasts (pOCs) in the presence of exogenously added RANKL. Therefore, the involvement of TLR2 ligation on osteoclastogenesis remains unclear.

To clarify the functional role of TLR2 agonist in osteoclastogenesis, we stimulated RAW 264.7 cells and pOCs, prepared from bone marrow cells by removing macrophages and stromal cells, with synthetic tri-acylated lipopeptide, Pam3CSK4. Furthermore, we studied whether Pam3CSK4 and *Streptococcus mutans* (*S. mutans*) 109c, a gram-positive oral bacterium, caused bone resorption in vivo. The results showed that: i) Pam3CSK4 induced osteoclastogenesis both in RAW264.7 cell and mouse pOC cultures, without adding RANKL exogenously; whereas, LPS (Re mutant), a specific ligand for TLR4, did not, ii) Pam3CSK4-induced osteoclastogenesis was mediated by p38, JNK, PI3K and NFkB pathways, iii) Quantitative RT-PCR analysis showed that Pam3CSK4 up-regulated TRACP and cathepsin K, but not RANK or RANKL, iv) Both Pam3CSK4 and *S. mutans* 109c injected into palate bone were able to cause alveolar bone resorption in rats.

Taken together, these results provide important findings as follows: i) Pam3CSK4 induces osteoclastogenesis in a RANKL-independent manner, ii) Pam3CSK4 also causes alveolar bone resorption in vivo, indicating that components of gram-positive bacteria, as well as those of gram-negative bacteria including LPS, may be a periodontal pathogen which causes alveolar osteolysis.

Disclosures: Akiko Yano, None.

SU0294

Role of the Fatty Acid Receptor GPR40 in Bone Remodeling. Fabien Wauquier^{*1}, claire philippe², laurent leotoing², sylvie mercier², Jerome Guicheux³, Veronique Coxam⁴, Yohann Wittrant⁵. ¹INRA, UMR 1019, UNH, CRNH Auvergne, F-63009 Clermont-Ferrand, France, France, ²INRA, France, ³Inserm ADR Grand Ouest, France, ⁴INRA Theix, France, ⁵Institut National de la Recherche Agronomique, France

In a context of increasing life expectancy, the prevalence of age-related diseases such as osteoporosis is becoming a major social and economical issue. While nutritional strategies appears to be an excellent alternative to conventional treatments, the study of nutrients' biological activities remains marginal for some tissues and certain types of molecules. This is particularly the case for bone and lipids, most notably fatty acids. Current literature, although growing in size, contains mainly descriptive studies that do not fully explain the mechanisms involved. Recently, the membrane receptor GPR40 (G Protein Coupled Receptor 40) has been highlighted for its interaction with long chain free fatty acids. Because, we demonstrated its expression in bone cells at the mRNA and protein level, we hypothesized that this receptor may play a role in mediating the effects of fatty acids on bone remodeling parameters.

In this study, the analysis by μ Computed Tomography of the femurs of mice invalidated for GPR40 reveals a marked osteoporotic phenotype that supports a protective role of this receptor for bone health.

In vitro, the effects of a specific agonist of GPR40, the GW9508 were analyzed. At high doses, this compound inhibits the proliferation of osteoclast precursors (Raw 264.7), whereas it has no effect on the viability of MC3T3-E1 osteoblast lineage. In addition, at lower doses, this compound blocks the osteoclastic differentiation of Raw 264.7 induced by RANKL, by inhibiting the activation of ERK and NF-kB pathways. GW9508 also stimulates the early stages of differentiation of osteoblastic MC3T3-E1, induce a rise in activity ALP (Alkaline phosphatase) and an increased expression of osteocalcin transcript. Moreover, the study of a line RAW264.7 invalidated by RNA interference (shRNA) together with analysis of the effect of GW9508 on induced-bone loss by ovariectomy in wild-type mice supports the working hypothesis.

In conclusion, these studies reveal for the first time a protective role of GPR40 in the bone tissues leading to a new insight in the bone and lipid relationships.

Disclosures: Fabien Wauquier, AMGEN, 9

SU0295

TNF α Induced HLA-B27 Upregulation in Osteoclast Precursors Affects Osteoclast Development in a Rat Model of Spondyloarthritis. Gerlinde Layh-Schmitt^{*1}, Eva Yang², Robert Colbert². ¹National Institutes of Health, USA, ²National Institutes of Health, NIAMS, USA

Purpose: Spondyloarthritis (SpA) are immune-mediated inflammatory diseases, mediated in part by TNF α , that involve both systemic bone loss and aberrant bone formation in the spine, which can lead to fusion of vertebrae. The HLA-B locus encodes a major susceptibility allele (B27). Upregulation of B27 exacerbates its tendency to misfold, and can lead to unfolded protein response (UPR) activation in macrophages. The UPR promotes the production of certain cytokines suggesting an 'upstream' pro-inflammatory role for B27. The goal of this project was to examine whether B27 also exerts 'downstream' effects in cells involved in bone homeostasis. Using B27 transgenic (B27-Tg) rats that develop SpA-like disease, we examined whether B27 expression affects osteoclast precursors and their development into osteoclasts.

Methods: Monocytes were derived from bone marrow (BMMo) of wild type (WT) and B27-Tg rats prior to onset of inflammatory disease. Monocytes were treated for five days with MCSF and RANKL (10, 30, 100 ng/ml) or TNF α (7.5, 15, 30 ng/ml). Osteoclasts were quantified by counting (>3 nuclei) TRAP positive cells. Resorption activity was measured by pit formation on corning osteo assay surface plates. Expression levels of B27 and UPR-specific genes like BiP, CHOP, XBP1 and XBP1-s were examined by RT-PCR, Western blot (B27 and BiP), and Immunofluorescence (B27 and BiP).

Results: We identified markedly (2-3 fold) enhanced TNF α -induced osteoclastogenesis of HLA-B27 BMMo compared to WT monocytes (p<0.05). RANKL had no differential effect on osteoclast numbers, but size was increased. B27-Tg rat derived osteoclasts were larger than wild type osteoclasts (>10 nuclei in 50% of B27-Tg cells vs. 10% of WT; p<0.05. Protein and mRNA expression levels of HLA-B27 (2- and 20-fold respectively) and BiP (1.5 and 3-fold, respectively) were increased after TNF α treatment and misfolded forms of HLA-B27 accumulated. In addition, TNF α induced XBP-1 splicing only in B27 expressing monocytes, suggesting acute UPR activation. We are presently investigating whether UPR induced cytokines such as IL-1 α or IFN β play a role in TNF α -induced osteoclastogenesis.

Conclusion: In summary, our preliminary analyses indicate that TNF α can induce a UPR activation in B27-expressing BMMo which may affect OC development and activity.

Disclosures: Gerlinde Layh-Schmitt, None.

SU0296

(-)-Epigallocatechin-3-gallate (EGCG), an AMPK Activator, Inhibits Ovariectomy-Induced Bone Loss by Suppressing Bone Resorption. Sook-Young Park¹, Shin-Yoon Kim², Hong-Hee Kim³, Sun Wook Cho⁴, Hyung Jin Choi⁴, Seung Hun Lee^{*5}, Ghi Su Kim⁶, Young-Sun Lee¹, Chan Soo Shin⁴, Beom-Jun Kim⁷, Sun-Young Lee¹, Jung-Min Koh⁷. ¹Asan Institute for Life Sciences, South Korea, ²Kyungpook National University Hospital, South Korea, ³Seoul National University, South Korea, ⁴Department of Internal Medicine, Seoul National University College of Medicine, South Korea, ⁵Asan Medical Center, University of Ulsan College of Medicine, South Korea, ⁶Division of Endocrinology & Metabolism, Asan Medical Center, University of Ulsan College of Medicine, South Korea, ⁷Asan Medical Center, South Korea

Purpose: Previously, we showed that AMP-activated protein kinase (AMPK) negatively regulates receptor activator of nuclear factor- κ B ligand-induced osteoclast formation in vitro. The present study aimed to investigate the effects of various AMPK activators on ovariectomy (OVX)-induced bone loss in mice.

Methods: Female mice subjected to OVX were administered various doses of AMPK activators, including (-)-epigallocatechin-3-gallate (EGCG), resveratrol (RES) and berberine, for 8 weeks. We performed micro-computed tomography (micro-CT) analysis of the tibia and bone histomorphometric examination of the femur. Western blot analysis was additionally performed to detect the levels of phosphorylated and total forms of AMPK- α in calvaria extracts.

Results: EGCG prevented OVX-induced body weight gain. Micro-CT experiments revealed that EGCG induced a significant increase in trabecular bone volume and trabecular number, and a decrease in trabecular spacing, compared to the OVX control. Histomorphometric analyses further showed that EGCG suppressed osteoclast surface, osteoclast number, and bone resorption rate. Phosphorylated AMPK expression was significantly elevated in bone, following EGCG treatment. RES and berberine did not have a significant effect on OVX-induced bone loss.

Conclusions: Our findings collectively indicate that EGCG, an AMPK activator, inhibits OVX-induced bone loss via suppression of bone resorption.

Disclosures: Seung Hun Lee, None.

SU0297

Anti-apoptotic Bcl-2 Family Member Mcl-1 Positively Regulates Cell Viability and Negatively Regulates Bone-resorbing Activity of Osteoclasts. Hironari Masuda^{*1}, Jun Hirose¹, Yasunori Omata¹, Hisataka Yasuda², Kozo Nakamura¹, Sakae Tanaka¹. ¹The University of Tokyo, Japan, ²Oriental Yeast Company, Limited, Japan

Mcl-1 is a member of Bcl-2 families that are known as regulators of apoptosis through mitochondrial pathway. Previous studies have suggested that an anti-apoptotic member Mcl-1 prolongs the cell viability of various cell types. However, only limited studies referred to the function of Mcl-1 in osteoclasts and it remains to be delineated. Our aim of this study was to elucidate the dynamics and the function of Mcl-1 in osteoclasts using techniques as overexpression, knockdown and knockout of Mcl-1 protein.

Mcl-1 protein levels in osteoclasts were increased in response to the addition of inflammatory cytokines such as TNF- α , IL-1 α and LPS. Mcl-1 exhibited a short half-life in osteoclasts, which was significantly prolonged by a proteasomal inhibitor MG132. We also found that Mcl-1 was markedly ubiquitinated, indicating the involvement of ubiquitin-proteasome pathways in the degradation process of Mcl-1 in osteoclasts.

When Mcl-1 expression was down-regulated by siRNA retrovirus introduction, osteoclasts had significantly shorter cell life than that of control osteoclasts, in spite of no significantly change in the cell differentiation or cytoskeletal organization. Conversely, Mcl-1 overexpression significantly prolonged cell life without showing significantly change in the cell differentiation.

We then examined the effect of Mcl-1 on the bone-resorbing activity of osteoclasts using pit-formation assay. Mcl-1 overexpressed osteoclasts by the adenovirus vector exhibited reduced bone resorbing area than control osteoclasts despite of their prolonged cell life. Mcl-1 knockout osteoclasts were generated by transducing Cre-recombinant adenovirus to osteoclasts from Mcl-1^{fllox/fllox} mice. Bone resorbing area of the Mcl-1 knockout osteoclasts was significantly increased despite of their short life time.

These results demonstrated that anti-apoptotic Bcl-2 family member Mcl-1 positively regulates cell viability and negatively regulates bone-resorbing activity of osteoclasts. Further studies are required to elucidate the role of Mcl-1 in physiological and pathological bone resorption by generating osteoclast-specific Mcl-1 knockout mice.

Disclosures: Hironari Masuda, None.

SU0298

Estrogen does not Promote Apoptosis of Avian Osteoclasts in Medullary Bone of Estrogen-Treated Male Japanese Quails. Shinji Hiyama^{*1}, Misa Takahashi², Aya Oda², Takashi Uchida³. ¹Hiroshima University Graduate School of Biomedical Sciences, Japan, ²Hiroshima University, Faculty of Dentistry, Japan, ³Hiroshima University, Graduate School of Biomedical Sciences, Japan

Medullary bone (MB) is a unique tissue of female birds, which is remodeled in the bone marrow cavity of long bones during the reproductive period. This bone remodeling is under the influence of circulating estrogen. Namely, when the concentration of estrogen declines, this bone is vigorously resorbed by osteoclasts. On the other hand, when the concentration of estrogen increases, osteoclasts are resting on the bone surface and osteoblasts form actively this bone. Although osteoclasts undergo apoptosis by estrogen in mammal, avian osteoclasts may not induce apoptosis, because the rapid remodeling of MB is necessary to reserve and provide for calcium of egg-shell. Therefore, in this study, we initially examined the effects of estrogen on the differentiation and apoptosis of avian osteoclasts derived from bone marrow cells (BMC) during MB formation in estrogen (E2)-treated male Japanese quails. After E2 administration in 0, 1, 2 & 3 days, BMC from femurs were cultured in the presence of RANKL/M-CSF and 17 β -estradiol (17-b). These cultures in each day were formed TRAP-positive multinucleated cells regardless the presence or the absence of 17-b. The expression level of Fas mRNA was down-regulated in osteoclasts derived from BMC of 3 days after E2 administration. Further, the expressions of Blimp1 and Bcl6 were decreased in same cultures. Bone resorption assay resulted that 17-b inhibited bone resorption in a concentration-dependent manner. To address the question of the effects of E2 to osteoclasts in vivo, the quails at day 5 after E2 administration when osteoclasts are appeared on the surface of MB were carried out E2 readministration. At day 0, 1, 2, & 3 after E2 readministration, BMC, but not osteoclasts on MB, showed positive reaction of apoptotic cells by histochemical analysis. These results suggest that estrogen has no effect on apoptosis and differentiation of osteoclasts, but rather suppress bone resorption in medullary bone.

Disclosures: Shinji Hiyama, None.

SU0299

High Knockdown of TCIRG1 Protein Expression Is Required for Resorption Deficiency in CD34+ Derived Human Osteoclasts. Christian Thudium^{*1}, Ilana Moscatelli², Johan Richter², Kim Henriksen³. ¹Nordic Bioscience, Denmark, ²Lund University, Sweden, ³Nordic Bioscience A/S, Denmark

Gene/protein function studies in human osteoclasts have been hampered as these terminally differentiated cells are hard to manipulate genetically. The aim of this study was to derive functional osteoclasts from CD34+ human cord blood cells and investigate whether lentiviral vectors can be used to overexpress and/or knock down genes in these cells, and what degree is needed to affect osteoclast function.

Human cord blood CD34+ cells were cultured for 2 weeks in the presence of a cytokine cocktail. The cells expanded approximately 500-fold, and FACS analysis revealed gradual loss of CD34 expression while 50% of cells became CD14+. Non-adherent cells were then incubated with M-CSF and RANKL on bone for 10 days, where they developed into fully functional osteoclasts expressing TRAP, releasing calcium, forming actin rings and generating resorption pits on boneslices.

Cord blood CD34+ cells were transduced using lentiviral vectors with shRNAs targeting TCIRG1. Cells were either selected using a puromycin resistance gene or sorted for GFP expression, and were then differentiated to mature osteoclasts. qPCR analysis revealed decreased levels of TCIRG1 mRNA and western blot revealed decreased protein levels in the transduced cells compared to controls, although levels varied through experiments. When high knock-down levels were observed the osteoclasts had a 40% increase in TRAP expression whereas calcium release, pit formation on bone slices and CTX-1 levels in the medium were all lower, in line with the known phenotype of infantile malignant osteopetrosis (IMO). However, in cells where the knockdown was less significant, a small increase in TRAP was observed, but no relevant effect was seen on calcium or CTX-I release.

In conclusion osteoclast differentiation from lentivirally transduced CD34+ cells poses a way to generate and manipulate osteoclasts in vitro, providing a novel tool to study osteoclast development and function. Furthermore, the knockdown of TCIRG1 in CD34+ cord blood cells provides a human *in vitro* model of IMO. However, a high degree of knockdown is vital to an effect on function, which possibly can be attributed to the haploinsufficient nature of TCIRG1, as neither humans nor mice that are heterozygous for TCIRG1 mutations have any phenotype.

Disclosures: Christian Thudium, None.

SU0300

Histone Deacetylase (HDAC) Expression and HDAC Inhibition in Different Pathogenic Bone Loss Diseases. Melissa Cantley^{*1}, David Fairlie², Peter Mark Bartold¹, Victor Marino², David Haynes¹. ¹University of Adelaide, Australia, ²University of Queensland, Australia

Inhibition of histone deacetylases (HDAC) is being investigated as a treatment for cancers and chronic inflammation. Class I HDACs are found in the nucleus and include 1,2,3 and 8 while class II are also found in the cytoplasm and include HDAC 4,5,6,7,9 and 10. We have recently reported that a novel HDACi compound targeting both HDAC classes, 1179.4b, suppressed human osteoclast resorption in vitro via down regulation of TRAF-6 during the late stages of development. This current study investigated the effect of 1179.4b on bone loss in animal models of human pathologies, periodontitis and peri-implant osteolysis. Expression of specific HDAC enzymes near sites of bone loss in periodontitis and peri-prosthetic osteolysis were also assessed in human tissues. In the peri-implant model, polyethylene particles were implanted onto the calvaria for 14 days to induce bone loss and 1179.4b was administered orally from day 7 (n=3 per group). For the mouse model of periodontitis, disease was induced via oral inoculations with *P.gingivalis* bacteria over 13 weeks. Once disease was established (week 7) mice were treated with 1179.4b daily for 6 weeks (n=4 per group). Live animal micro CT scanning was used to measure bone loss during the experiment. Expression of HDACs 1-10 mRNA was assessed by real time PCR. Human tissue samples from peri-implant tissues obtained during revision surgery (n=10) and osteoarthritic synovial tissues (n=5) from patients undergoing a primary implant at the Royal Adelaide Hospital were compared. Gingival tissue samples were obtained from patients with chronic periodontitis (n=9) and compared with normal gingival tissues (n=8).

1179.4b significantly (p<0.05) suppressed bone loss in the model of periodontitis despite not affecting inflammation. Interestingly, bone loss was not suppressed in the calvarial model by 1179.4b (p>0.05). Class I HDAC 1 was expressed at significantly higher levels in peri-implant tissues compared to OA tissues (p<0.05). In human periodontitis tissues HDACs from both classes I (1 and 8) and II (5 and 9) were highly expressed relative to normal tissue.

Differences in anti-resorptive activity of 1179.4b in the two pathologies may be due to different HDACs stimulating bone loss in each disease. This may also show differences in the importance of TRAF 6 signaling in the two diseases. This demonstrates developing HDAC therapies requires understanding the roles of individual HDACs in the pathology of specific diseases.

Disclosures: Melissa Cantley, None.

SU0301

Snx10: a Sortin Nexin Required for Osteoclast Differentiation and Function. Cui Hua Zhu^{*1}, Leslie Morse², Ricardo Battaglini¹. ¹The Forsyth Institute, USA, ²Department of Physical Medicine & Rehabilitation, Harvard Medical School & Spaulding Rehabilitation Hospital, USA

Osteoclasts are exceptionally dependent on vesicular trafficking in order to form the ruffled border, a process essential for bone resorption. Consequently, disruption (genetic or pharmacological) of osteoclastic vesicle transport abolishes cellular resorptive activity. We performed a genome-wide screening to identify genes that are up regulated during RANKL-stimulation of osteoclast precursor cells and may be involved in the process of differentiation and or activation. In this report we describe the expression and functional characterization of Sorting Nexin 10 (*snx10*). Snx10 belongs to the sorting nexin (SNX) family, a diverse group of proteins with a common feature: the PX domain. PX-containing yeast proteins are involved in vacuole sorting, suggesting that SNXs can regulate membrane trafficking and cargo sorting in endosomes. SNX10 can also induce formation of giant vacuoles in transfected cells and may be involved in the regulation of endosome homeostasis. *snx10* is strongly up regulated during RANKL-induced osteoclast differentiation in vitro and in vivo. qPCR analysis confirmed a significant increase in the expression of *snx10* in *in vitro*-derived osteoclasts, femur and calvaria. To visualize *in situ* expression, we performed immunohistochemical analysis of mouse embryo sections and detected expression in bone, calvariae and developing teeth, in cells that also expressed TRAP, demonstrating osteoclastic localization. Confocal immunofluorescence analysis revealed Snx10 localization in the cytoplasm with a pattern that partially overlaps with that of the endoplasmic reticulum (ER) marker protein disulfide isomerase (PDI). To study a possible role for *snx10* in osteoclast differentiation and function we silenced *snx10* expression and found that *snx10* silencing inhibits RANKL-induced osteoclast formation, osteoclast resorption on hydroxyapatite and also 50% inhibition in TRAP secretion. Taken together, these results confirm that *snx10* is expressed in osteoclasts and is required for osteoclast differentiation and activity *in vitro*. Since inhibition of vesicular trafficking is essential for osteoclast formation and activity and SNX10 is involved in intracellular vesicular trafficking, these studies may identify a new candidate gene involved in the development of human bone diseases including osteoporosis and bone loss associated estrogen deficiency.

Disclosures: Cui Hua Zhu, None.

SU0302

Syk Family Member ZAP70 Inhibits Syk-Mediated Osteoclast Function. Wei Zou^{*}, Tingting Zhu, Steven Teitelbaum. Washington University in St. Louis School of Medicine, USA

The $\alpha\text{v}\beta 3$ integrin stimulates the resorptive capacity of the differentiated osteoclast (OC) by organizing its cytoskeleton via the tyrosine kinase Syk. Thus, Syk-deficient OCs fail to spread or form actin rings, in vitro and in vivo. These cytoskeletal defects of Syk^{-/-} OCs arrest their bone resorptive capacity resulting in enhanced bone mass.

The Syk family of tyrosine kinases consist of Syk itself and ZAP70 which are expressed by different cell types. Syk appears in all myeloid cells and ZAP70 is primarily found in T-lymphocytes and NK cells. Because of their structural similarity we asked if ZAP70 can compensate for absence of Syk in OCs. To this end, we retrovirally transduced Syk^{-/-} macrophages (MΦ) with WT Syk or ZAP70 and cultured them into OCs. As expected, expression of Syk normalizes the cytoskeletal abnormalities of Syk^{-/-} OCs. ZAP70, however, fails to do so. In keeping with this observation, Syk, but not ZAP70, rescues $\alpha\text{v}\beta 3$ integrin-induced SLP76 phosphorylation in Syk^{-/-} OCs. These results suggest that Syk but not ZAP70 is capable of regulating OC function.

Both Syk and ZAP70 contain tandem SH2 domain and kinase domain. To determine the role of these motifs in OC function, we transduced Syk^{-/-} MΦ with 2 chimeras namely 1) Syk(SH2)-ZAP70(Kinase) and 2) ZAP70(SH2)-Syk(Kinase). While Syk(SH2)-ZAP70(Kinase) is ineffective in Syk^{-/-} OCs, ZAP70(SH2)-Syk(Kinase) substantially rescues their resorptive activity, establishing that Syk's kinase, but not adaptor function is required for OC activity. Consistent with these results, kinase-inactive but not SH2 domain mutant Syk, inhibits WT OC spreading and resorption.

While ZAP-70 fails to compensate for absence of Syk in OCs their structural similarity suggests ZAP-70 may inhibit Syk activity in WT cells. The relevance of this conjecture is underscored by the fact that Syk inhibitors are presently in clinical trial for treatment of inflammatory osteolysis. To address this issue, we retrovirally transduced ZAP70 into WT MΦ. Similar to kinase-inactive Syk, expression of ZAP70 inhibits WT OC spreading, actin ring formation and bone resorptive activity, but not differentiation. In keeping with arrested cytoskeletal organization, ZAP70 blocks integrin-activated endogenous Syk, SLP76 and Vav3 phosphorylation. Thus, the kinase domain of Syk is uniquely required for OC function. Furthermore, the apparent dominant/negative effects of ZAP70 suggest its candidacy as a therapeutic Syk inhibitor in osteolytic disorders.

Disclosures: Wei Zou, None.

SU0303

Transcription Factor E47 Regulates Homeostatic Bone Remodeling Through Upregulation of Inhibitor CD38 in Osteoclast Precursors. Courtney Long^{*1}, Xiao-Hong Sun², Mary Beth Humphrey¹. ¹The University of Oklahoma Health Sciences Center, USA, ²Oklahoma Medical Research Foundation, USA

Osteoclast differentiation and bone resorption are activated through temporally spaced transcription factors that subsequently turn on genes involved in these processes. Here we elucidated a role for the basic Helix-loop-Helix (bHLH) transcription factor, E47, in osteoclast regulation. To do so, we analyzed the baseline bone mass of a transgenic mouse model, termed ET2, expressing a myeloid specific E47 gain-of-function transgene. By microcomputed tomography (microCT), ET2 mice have significantly increased bone volume/tissue volume (BV/TV) compared to controls. Thus, we hypothesized that E47 gain-of-function altered osteoclast maturation, survival or function. To analyze E47 gain-of-function changes in pre-osteoclasts at the molecular level, we stimulated precursors with RANKL for 24 hours, isolated RNA, and then measured differential expression of total RNA transcripts by Solid Sequencing. CD38, a known inhibitor of osteoclastogenesis, was among the genes upregulated in ET2 osteoclast precursors as compared to control precursors. Compared to control, CD11b+ ET2 osteoclast precursors had increased CD38 expression determined by flow cytometry. In vitro analysis of osteoclast assays revealed fewer but more complex ET2-derived osteoclasts compared to controls; whereas, ET2 and control osteoclasts exhibited similar resorption. These results suggested that ET2 pre-osteoclasts expressed more inhibitory CD38, and thus had a greater threshold to overcome to proceed towards osteoclast maturation. To determine if this inhibition could be overcome in vivo, we performed two studies of osteoclast activation: 1) direct stimulation of osteoclastogenesis through RANKL injections or 2) indirect stimulation of osteoclastogenesis through LPS injections. In both models, microCT analysis of pre- versus post- injections showed a significant decrease in bone volume in control and ET2 mice. These data indicate that increased E47 in myeloid cells negatively regulates basal osteoclastogenesis and that strong osteoclastic stimulation, as seen in our two models, can overcome this inhibition to drive functional osteoclasts. Our results suggest the role of E47 in vivo is to inhibit early osteoclast differentiation through upregulation of CD38, an osteoclast inhibitory protein.

Disclosures: Courtney Long, None.

SU0304

A Novel Identification Schema For Osteoclast Progenitors In Mice And In Humans. Monique Bethel^{*1}, Brahmananda Chitteti¹, Yinghua Cheng¹, Angela Bruzzaniti², Edward Srouf¹, Melissa Kacena¹. ¹Indiana University School of Medicine, USA, ²Indiana University School of Dentistry, USA

There are a number of skeletal disorders in which alterations in osteoclast (OC) activity contribute to disease pathology, such as osteoporosis and the inflammatory bone disorders, rheumatoid arthritis and juvenile idiopathic arthritis. Identification of novel OC markers and functional cell surface receptors is critical for the development of innovative therapies for these disorders. Here we show for the first time that murine and human OC progenitors express CD110 (c-mpl), the receptor for thrombopoietin (TPO), which was previously thought to be restricted to cells of the megakaryocyte lineage. Using flow cytometry, we isolated cells expressing CD11b+ or CD14+, which are commonly used as markers of human OC progenitors, and further separated these cells based on the expression of CD110. Importantly, isolated cells from both CD11b+CD110+ and CD14+CD110+ populations resulted in robust generation of mature, TRAP+ OCs with >3 nuclei (855138 and 1150155 OCs/well, respectively), whereas the number of mature OCs generated by CD11b+CD110- and CD14+CD110- cells was almost undetectable, although precursor cell viability was unaltered. Interestingly, approximately 90% of OC progenitors defined as CD11b+CD110+ or CD14+CD110+ cells also expressed CD14+ or CD11b+, respectively. These findings suggest that utilization of CD110 in combination with traditional OC markers, either CD11b and/or CD14, results in a significant enrichment in OC progenitors. Indeed, CD14+CD11b+CD110+ cells gave rise to significantly more mature OCs than that observed in all other populations tested. We next determined the effect of CD110 activation on OC differentiation and function. Our data demonstrate that treatment of OC progenitors with the CD110 ligand, TPO, results in a significant dose-dependent increase in mature OC number, with 100 ng/ml of TPO inducing up to a 6-fold increase in OC number (p<0.01) relative to untreated control cultures. TPO also significantly increased the bone resorbing activity of mature OCs on dentin in vitro (p<0.05). The regulation of OCs by TPO highlights a novel therapeutic target for bone loss diseases and may be important to consider in the numerous hematologic disorders associated with alterations in TPO/c-mpl signaling as well as in the bone destruction associated with inflammatory bone disorders.

Disclosures: Monique Bethel, None.

SU0305

A Unique Cytoplasmic Domain in RANK Induces Long-term Signaling Required for Osteoclast Differentiation. Yuu Taguchi*, Jin Gohda, Jun-ichiro Inoue. The Institute of Medical Science, The University of Tokyo, Japan

Receptor Activator of NF- κ B (RANK) is a member of the TNF-receptor superfamily, and the signal transduction of RANK is mediated by the adaptor molecule, TRAF6, as with CD40. It is known that RANK, but not CD40, can induce osteoclastogenesis efficiently, which led us to think that a specific domain in the cytoplasmic tail of RANK in concert with the TRAF6-binding site may promote osteoclastogenesis. Here we identify such a domain, *highly conserved domain* in RANK (HCR), which is dispensable for the early phase activation of RANK signaling but is essential for their late phase signaling including sustained activation of NF- κ B and PLC γ 2 leading to induction of NFATc1, a master transcriptional factor in osteoclastogenesis. Moreover, we found that the HCR recruited an adaptor protein, Gab2, which further associated with PLC γ 2 in the late phase. Our experiment also revealed that Gab2 binds to TRAF6. These results suggest that the HCR provides a platform for forming the novel signal complex including Gab2, PLC γ 2 and TRAF6, and the formation of such a complex could account for the sustained activation of NF- κ B and PLC γ 2.

In a therapeutic point of view, we also found that expression of the HCR-peptide composed of 62 amino acids severely inhibited RANKL-induced activation of NF- κ B/ MAPKs and RANKL-induced formation of multinucleated TRAP-positive cells. These results indicate that the HCR peptide is a potent inhibitor of osteoclastogenesis presumably by quenching Gab2-containing signal complexes. Furthermore, expression of the amino- or carboxyl-terminal half on HCR-peptide also inhibited osteoclastogenesis, respectively. However, Gab2 could bind to only the carboxyl-terminal half on HCR-peptide, but not to amino-terminal half. Therefore, we think that HCR is comprised of two functionally distinct regions, and that peptides from each region are very useful for developing drugs to inhibit osteoclastogenesis. Because our search of the GenBank database did not hit any proteins homologous to the primary structure of HCR amino acid-sequences, the HCR-mediated signal complex may be a good target for developing drugs to treat bone diseases with minimal side effects.

Disclosures: Yuu Taguchi, None.

SU0306

Lysosomal Degradation of TRAF3 Is Important for RANKL/NF- κ B - mediated Osteoclastogenesis. Yan Xiu*¹, Zhenqiang Yao², Yoshikazu Morita², Lianping Xing², Brendan Boyce¹. ¹University of Rochester Medical Center, USA, ²University of Rochester, USA

Osteoclast (OC) formation is regulated by many factors including RANKL and TNF, which activate NF- κ B signaling using TNF receptor-associated factor (TRAF) complexes in OC precursors (OCPs) and mediate joint erosion in patients with rheumatoid arthritis. TNF limits OC formation through the inhibitory NF- κ B p100 protein and TRAF3. TNF increases and RANKL decreases p100 and TRAF3 protein levels in OCPs. However, the mechanisms by which cytokines control TRAF3 levels in OCPs are unknown. We report that TRAF3 expression levels decrease progressively during RANKL- but not TNF-induced OC formation suggesting that RANKL promotes TRAF3 degradation. TRAF3 retroviral over-expression in WT OCPs reduced OC numbers 2-fold suggesting that TRAF3 is a negative regulator of RANKL-induced OC formation. To explore this further, we examined protein levels of several NF- κ B components in TRAF3 over-expressing OCPs in response to RANKL and found reduced RelA, RelB, and NIK levels accompanied by decreased processing of NF κ B2/p100 to p52, while TRAF3 basal levels are significantly increased in RelB/p52 double knockout mouse OCPs, indicating a regulatory loop between TRAF3 and NF- κ B components. To examine how RANKL induces TRAF3 degradation, we treated bone marrow-derived OCPs with RANKL and the proteasome inhibitor MG132 or the lysosome inhibitors NH₄Cl or chloroquine (CQ) and found that only the lysosome inhibitors were effective. We next co-transfected 293T cells with RANK and WT or TRAF3 deletion mutants, treated them with RANKL, and found that the TRAF3 ring finger domain is required for RANKL-induced TRAF3 degradation. We then over-expressed a TRAF3-GFP fusion protein in OCPs and found using confocal immunostaining that TRAF3 co-localized with the lysosomal protein LAMP2. RANKL increased co-localization of TRAF3 and LAMP2 (242% vs 81% control) and this effect was prevented by CQ (91.5%). Our data indicate that TRAF3 negatively regulates RANKL-induced OC formation by suppressing both canonical (RelA and NIK) and non-canonical (RelB and p52) NF κ B signaling and that RANKL-induced lysosomal degradation of TRAF3 is an important step in RANKL-induced activation of NF- κ B pathways in OCPs. Mechanisms to increase cellular TRAF3 levels in OCPs, including inhibition of its lysosomal degradation by drugs such as CQ may thus limit NF κ B-dependent RANKL-induced OC formation and bone destruction in common bone diseases.

Disclosures: Yan Xiu, None.

SU0307

Protein Kinase D Regulates Osteoclast Differentiation. Eric Jensen*, Lan Pham, Raj Gopalakrishnan, Kim Mansky. University of Minnesota, USA

Osteoclasts, which are bone resorbing cells vital for skeletal homeostasis, are large multinucleated cells generated by fusion of precursor cells derived from the monocyte/macrophage lineage. One of the factors required for osteoclast differentiation is bone morphogenic proteins. Increased levels of BMP signaling *in vivo* leads to increased osteoclast activity, resulting in osteopenia, while blockage of BMP signaling prevents their formation *in vitro*. An important unresolved question is which molecular signaling pathways are required for this effect.

BMPs activate intracellular signal transduction pathways including SMADs, MAP kinases and protein kinase D. To characterize the molecular mechanisms through which BMPs regulate osteoclast formation, we examined the role of PKD. We find that BMP signaling stimulates protein kinase D activation in osteoclasts. Suppression of PKD expression or activity inhibits *in vitro* osteoclast formation, while overexpression of PKD enhances osteoclastogenesis. These data establish PKD as an important regulator of osteoclasts.

Disclosures: Eric Jensen, None.

SU0308

3D Visualization of Osteocyte Lacunae in the entire long bone. Yoshihiro Takeda¹, Yasunari Takada², Kazuhiko Omote¹, Koichi Matsuo². ¹Rigaku Corporation, Japan, ²School of Medicine, Keio University, Japan

The osteocyte is an important cell type responsible for bone metabolism. In recent years, sub-micron resolution x-ray computed tomography (CT) has been employed to analyze the three-dimensional shape of osteocyte lacuna and to measure lacunar volume. However, due to trade-offs between high resolution and a small field of view, it is difficult to obtain sufficient information by focusing on a partial bone area, which contains only a small population of osteocytes. Therefore, we investigated the micro structure of an entire mouse femur at submicron resolution. To achieve this goal, we developed an x-ray microscope capable of measuring large objects with submicron pixel size. The microscope consists of a high power x-ray source, a high resolution camera and motorized stages. Using this system, we obtained CT images of the entire femur (length ca. 10 mm) isolated from 7-week-old mice. The total number of voxels of each CT image was greater than 3,300 x 3,300 x 16,000 with the voxel size of 0.6 micron. CT images clearly depicted bone marrow, fine blood vessels, and osteocyte lacunae. Within cortical bone in a 6-mm diaphysis of the femur, more than 20,000 osteocyte lacunae were detected at the average density of 50,000 / mm³. Curiously, the lacunar density was periodically altered along the longitudinal axis. To our knowledge, this is the first report of periodicity in osteocyte lacunar density along the long bone.

Disclosures: Yoshihiro Takeda, None.

SU0309

An In Vitro Model for Osteocyte Differentiation. Ken Watanabe¹, Hirovuki Aburatani², Kyoji Ikeda¹. ¹National Center for Geriatrics & Gerontology, Japan, ²RCAT, The University of Tokyo, Japan

Osteocytes, terminally differentiated osteoblastic cells, have been suggested to play important roles in the regulation of bone metabolism. Evidences for *in vivo* function of osteocytes or their products have been accumulating from human as well as mouse genetics studies, while the mechanism underlying the terminal differentiation of osteocytes from osteoblasts remains to be defined at the molecular level. MC3T3-E1 is a pre-osteoblastic cell line that is widely distributed and utilized for bone research. MC3T3-E1 cells differentiate into mature osteoblasts, as evidenced by mineralization of extracellular matrix and expression of osteoblastic signature genes such as osteocalcin and bone sialoprotein. When the mineralizing culture was extended up to 7-9 weeks, expression of osteocytic genes, such as *Sost*, *Mepe* and *Fg23*, was observed, suggesting that the long-term culture recapitulates osteocytogenesis or osteocytic differentiation from osteoblasts. Using this mineralizing long-term culture (MLC) system, RNA was isolated at day 3, week 3 and 9, and the gene expression profiling was performed by microarray analysis. Expression of phosphate-regulating genes, *Phe*, *Enpp1* and *Phospho1*, was highly expressed at 8 weeks of MLC. Expression of known osteocytic genes, *Dmp1* and *Ibsp*, was also substantially increased in the MLC. In addition to *Sost*, another Wnt antagonist *Wif1* was expressed at 8 weeks of MLC. The expression of *Pthr1* encoding PTH receptor was increased during osteocytogenesis, and expression of *Sost* and *Axin2* was down- and up-regulated, respectively, by PTH treatment of MLC, suggesting that the MLC can mimic PTH response in osteocytes *in vivo*.

Sp7, encoding Osterix, has been demonstrated to play a critical role in terminal differentiation of osteoblasts into osteocytes. In addition to *Sp7*, genes encoding transcription factors such as *Dlx3*, *Tcf7*, *Mef2c* and *Epas1*, were upregulated during the osteocytic differentiation in MLC. Overexpression of these genes in MC3T3-E1 accelerated osteocytogenesis, as determined by osteocytic gene signature, while knockdown of *Dlx3* or *Mef2c* genes attenuated the transition from osteoblasts to osteocytes, suggesting that *Dlx3* and *Mef2c* may play roles in osteocytic differentiation. Thus, the MLC of MC3T3-E1 faithfully recapitulates osteocytic gene expression signature, and may provide a useful tool as an *in vitro* model for osteocytogenesis.

Disclosures: Ken Watanabe, None.

SU0310

Connexin 43 Hemichannels Protect Osteocytes against Oxidative Stress Induced Cell Death. Rekha Kar^{*1}, Manuel Riquelme², Sherry Werner², Jean Jiang³. ¹The University of Texas Health Science Center, USA, ²University of Texas Health Science Center, USA, ³University of Texas Health Science Center at San Antonio, USA

Recent studies suggest that oxidative stress is a primary, underlying mechanism of aged-related bone mass and strength loss. The increasing osteocyte death during aging and oxidative stress is thought to be the principal cause contributing to the impairment of bone quality. However, the molecular mechanism of oxidative stress on osteocytes is poorly understood. Here, we treated MLO-Y4 osteocyte cells with different doses of oxidant, H₂O₂. H₂O₂ induced cell death of MLO-Y4 cells as shown by a dose-dependent increase of PI positive cells. Interestingly, H₂O₂ also caused a dose-dependent decrease in gap junction/hemichannel forming connexin 43 (Cx43) expression. Similar to our *in vitro* finding, the osteocytes in the bone sections from 20 month old mice showed much less Cx43 expression as opposed to the 5 week young animals. Microinjection dye transfer assay was performed to examine whether decreased Cx43 expression resulting from H₂O₂ treatment also affected the gap junction intercellular communication (GJIC). GJIC was evaluated using the alexafluor 488 coupling assay. Intercellular transfer of alexa fluor 488 from the microinjected cell to neighboring cells was reduced progressively after 30 min of H₂O₂ treatment in addition to complete uncoupling after 70 min. To evaluate the effect of H₂O₂ on Cx43 hemichannels, we measured uptake of ethidium (Etd) bromide by time lapse recording under resting conditions (basal) and after the addition of different concentrations of H₂O₂. In contrast to the effect on gap junctions, with increasing concentrations of H₂O₂, there was a dose-dependent increase of hemichannel function. To elucidate the functional role of increased hemichannel activity during oxidative stress, we blocked Cx43 hemichannel activity using the Cx43 (E2) antibody, a potent antibody which specifically blocks Cx43 hemichannel activity but not gap junction or any other channel activity. Cx43 (E2) antibody completely blocked dye uptake induced by H₂O₂ and further exacerbated H₂O₂ induced death of MLO-Y4 cells. This result suggests a protective role of Cx43 hemichannel against oxidative stress. Together, our study provides novel cell protective mechanism mediated by osteocytic Cx43 hemichannels against oxidative stress and aging.

Disclosures: Rekha Kar, None.

This study received funding from: NIH

SU0311

Cox-2 Inhibition Suppresses the Response to Short Term Tibial Compression in Mice. Bryan Hackfort^{*1}, Gwendolin Alvarez¹, Mohammed Akhter², Diane Cullen¹. ¹Creighton University, USA, ²Creighton University Osteoporosis Research Center, USA

Osteoporosis is a disease that can lead to fractures and substantial morbidity. Anabolic treatments are necessary to help reverse the structural deterioration related to osteoporosis, yet we need to first understand the interaction of pathways on bone formation. PGE₂ and mechanical loading are known stimulators of bone formation. Previous studies have shown inhibition of prostaglandins with a selective Cox-2 inhibitor (NS-398) blocks the bone formation response in rats to a single mechanical load. NS-398 also blocks the prostaglandin response to fluid flow. Previously we looked at the long term adaption of bone to tibial compression *in vivo* (10 sessions, 3 weeks) while inhibiting the prostaglandin pathway with NS-398 in mice. As compared to the vehicle group, the NS-398 treatment resulted in a greater bone formation response to mechanical loading. These unexpected results prompted us to question the use of the mouse model in exploring the interaction of prostaglandins and mechanical loading. In this study, we used the tibial compression model to test the response of WT C57Bl/6 mice to a one time high mechanical load while injecting a Cox-2 inhibitor to block prostaglandins. The tibial compression model applies forces through the knee and ankle avoiding injury to the bone. We hypothesize that NS-398 will reduce the amount of bone formation stimulated by a single mechanical load using the tibial compression model in mice. Adult, female mice were injected 3 hours prior to mechanical loading with 10mg/kg NS-398, DMSO, or Saline. Mice were loaded at 11N (1430µe) for 360 cycles at 2Hz. Calcein was injected on days 5 and 9 with collection on day 12. Tibiae were fixed in 70% EtOH, dehydrated, and embedded in methyl methacrylate. Sections were cut at 80µm, 1-3 mm proximal to the TFJ region and mounted for histomorphometry. The net load response was calculated as Load-noLoad and differences due to drug treatment analyzed by planned contrasts (P<0.05). The differences due to loading in periosteal mineralizing surface (MS/BS) was reduced in the NS-398 treated group (4.40 2.71%) compared to its DMSO control group (17.49 4.03%). DMSO showed no effects on MS/BS compared to saline treatment (10.37 3.56%). In conclusion, the mouse model mimics the rat response to Cox-2 inhibition in short term tibial compression. These results suggest the response to Cox-2 inhibition may be different in short term vs. long term mechanical loading.

Disclosures: Bryan Hackfort, None.

SU0312

Load responsive Genes and Inflammation-Associated Genes are elevated in Dmp1 null Osteocytes while Genes associated with Bone Formation are Suppressed. Stephen Harris^{*1}, Marie Harris¹, Yong Cui², Lynda Bonewald³, Jian Feng⁴, Jelica Gluhak-Heinrich¹. ¹University of Texas Health Science Center at San Antonio, USA, ²UTHSCSA, USA, ³University of Missouri - Kansas City, USA, ⁴Texas A&M Health Science Center, USA

It has been proposed that the osteocyte lacunocanalicular network acts in an endocrine fashion to target tissues distant from bone. Osteocytes in Dentin Matrix Protein1, Dmp1, null bone highly express FGF23, osteocalcin, E11/gp38, Sost, and other osteoblast/osteocyte markers. To identify other regulatory factors produced by these cells, full genome expression microarray analyses were performed using *ex vivo* culture of calvarial bone fragments from WT and Dmp1 null animals, in which the osteoblasts were removed by serial collagenase-trypsin digestions and fragments cultured overnight in 10% FBS. Illumina Mouse-6 v2 arrays, Genome Studio-RNA expression module for normalization-statistic of n=2 arrays per group, David Bioinformatic, and Ingenuity Pathway Analysis for construction of literature based pathways and networks were used. Several mechanically responsive genes, such as Igf1, Mepe, Ccl7, 2 (MCP3,1) and Prostaglandin E synthetase were highly elevated suggesting osteocytes in the DMP1 null bones are experiencing elevated strain due to the hypomineralized "soft" matrix surrounding the cells. A massive increase (3 to 50 fold) in cytokines/chemokines involved in immune-inflammatory pathways and macrophage biology, such as CCL2, 7, 3, 14, CXCL1, 3, and ATF3 was also observed. Although, E11/GP38, involved in osteocyte embedding/dendrite formation was also increased, many genes involved in "tube" formation related to branching were reduced in the DMP1null osteocytes, including Csf1, Cx43, VegfA, and Ihh/Gli2, 3 genes. These may play a role in the formation of the lacunocanalicular system. Many of the semaphorins involved in axon guidance, normally highly expressed in osteocytes, were also reduced. In addition, a large number of genes in the Wnt pathway including Wnt1, 7b, axin1, Tcf7, and three calcium-calcineurin transcription factors, Nfatc1, 2, and 3 were reduced. 145 genes involved in transcription, including Sp7, Osterix, a key transcription factor in bone, were reduced in DMP1null osteocytes, (Sp7 over 7 fold), suggesting major alterations in the genetic program of the DMP1null osteocytes. Gene expression levels of Sp7, Ccl7, and Igf1 have been validated by *in situ* hybridization in WT and DMP1null animals (2 mo old). These studies have implications regarding the potential elevation of circulating cytokines in patients with hypophosphatemic rickets and design of potential treatment and preventive therapies.

Disclosures: Stephen Harris, None.

SU0313

MT1-MMP Affects the Mechanosensitivity of Osteocytes. Rishikesh N. Kulkarni¹, Astrid D. Bakker¹, Elisabeth V. Gruber², Thomas D. Chae³, Joris B. B. Veldkamp¹, Vincent Everts¹, Jenneke Klein-Nulend^{*1}. ¹ACTA-University of Amsterdam & VU University Amsterdam, Dept Oral Cell Biology, Research Institute MOVE, Netherlands, ²Medical University of Vienna, Bernhard Gottlieb School of Dentistry, Bone Research Group, Austria, ³Columbia University College of Dental Medicine, USA

Bone mass and architecture are continuously adapted to the prevailing mechanical loads. It is generally assumed that osteocytes act as key regulators of bone mass in response to mechanical cues that are perceived via their cell processes. Since matrix metalloproteinase-14 (MT1-MMP) is essential for osteocyte cell process formation *in vivo*, and also affects bone mass, we aimed to investigate whether MT1-MMP affects the osteocyte response to mechanical loading.

MT1-MMP positive and knockdown (siRNA) osteocytes were either or not stimulated by 1h pulsating fluid flow (PFF; 0.70.3Pa, 5Hz). The pulsating fluid flow-response was quantified by measuring c-jun, c-fos, and MT1-MMP mRNA expression, and nitric oxide (NO) production. Focal adhesions were visualized by paxillin immunostaining. Osteocyte number, number of empty lacunae, and length-to-width ratio of osteocyte lacunae were measured in long bones of MT1-MMP^{+/+} and MT1-MMP^{-/-} mice aged 14-50 days.

Pulsating fluid flow decreased MT1-MMP mRNA expression by 2.2-fold in MT1-MMP positive osteocytes, suggesting that mechanical loading affects pericellular matrix remodeling by osteocytes. Pulsating fluid flow increased NO production by 3.5-fold within 5 minutes in MT1-MMP positive osteocytes, whereas pulsating fluid flow increased NO production by 8.1-fold compared to static control conditions in MT1-MMP knockdown osteocytes. Pulsating fluid flow upregulated c-jun gene expression by 1.8-fold, and c-fos gene expression by 1.9-fold in MT1-MMP knockdown osteocytes, but not in MT1-MMP positive osteocytes. Interestingly, MT1-MMP knockdown increased number of focal adhesions in osteocytes. MT1-MMP deficiency enhanced osteocyte elongation and increased the number of osteocytes by 1.5-fold, and decreased the number of empty lacunae by 1.6-fold. The elongated osteocytes in MT1-MMP^{-/-} bone followed the principle loading direction, suggesting that they can sense mechanical loading despite lack of cell processes. This was supported by a low number of empty lacunae in MT1-MMP^{-/-} bone, as osteocytes lacking mechanical stimuli tend to undergo apoptosis.

In conclusion, MT1-MMP knockdown increased the osteocyte response to mechanical stimuli, demonstrating a novel and unexpected role for MT1-MMP in mechanosensing. Our results shed new light on the process of mechanosensing by

osteocytes and warrant further research in this direction, since this will undoubtedly contribute to new perspectives of bone tissue physiology.

Disclosures: Jenneke Klein-Nulend, University of Amsterdam, 2

SU0314

Osteogenic Transcriptome Regulation in MLO-Y4 Osteocytes Exposed to Fluid Flow. Peter Govey¹, Norman Karin², Henry Donahue³. ¹Penn State College of Medicine, USA, ²Pacific Northwest National Laboratory, USA, ³The Pennsylvania State University College of Medicine, USA

The lacuno-canalicular niche of osteocytes positions them as prime candidates to transduce fluid shear stress to regulate bone remodeling. The purpose of this study is to establish the utility of high-throughput approaches, specifically gene transcript microarrays, to investigate this intricate response of osteocytes exposed to fluid flow. We hypothesize that gene expression levels in MLO-Y4 osteocyte-like cells exposed to fluid flow will reflect regulation of known mechano-sensitive signaling pathways.

MLO-Y4 were cultured on collagen I-coated glass slides two days prior to flow. Cells were then exposed to 2 hours oscillating fluid flow in parallel plate flow chambers, inducing 10 dynes/cm² shear stress at 1 Hz. Paired sham controls were maintained in identical, static chambers. Triplicates of both flowed and static cells were collected immediately (time 0) and following 2, 8, and 24 hours post-flow incubation in fresh media. Total RNA was isolated, biotin-labeled cRNA synthesized and fragmented, hybridized to Mouse Genome 430A 2.0 GeneChips and scanned. Gene set enrichment for gene ontology biological process annotation was calculated to identify the most significant cellular processes affected by flow.

After detection of approximately 14,000 gene expression levels, 788 gene products increased or decreased by at least 1.25-fold in flowed vs. non-flowed MLO-Y4. Importantly, regulation of these gene products corresponds with previously implicated osteogenic signaling pathways. Ptg2, which encodes osteogenic COX-2, increases 1.45-fold at 2 hours post-flow. Expression of LRP5, shown by others to be up regulated by flow, increased 1.25-fold immediately after flow. Anabolic LRP5 is a receptor in the Wnt/beta-catenin signaling pathway; inhibitors of this pathway, Dkk2 and Dkk3, decreased 1.37-fold and 1.27-fold at 8 hours, respectively. These changes are consistent with an anabolic effect of flow on osteocytes and demonstrate the power of this approach in revealing global gene expression pathways. Gene ontology assessment yielded statistically significant activity in cell metabolism, connective tissue function, and cell-to-cell signaling activity.

These results identify a composite mechano-sensitive response in flowed MLO-Y4. Furthermore, the transcriptome will provide context to explore novel mechano-sensitive pathways. Proteomic analysis will be useful in assessing post-transcriptional and post-translational regulation of these gene products.

Disclosures: Peter Govey, None.

SU0315

Quasi-3D Dynamics of Actin and Microtubule Networks in Individual MLO-Y4 Osteocytes under Steady and Oscillatory Flow. Andrew Baik¹, Jun Qiu², Elizabeth Hillman¹, Cheng Dong³, X Guo¹. ¹Columbia University, USA, ²Tsinghua University, China, ³Penn State University, USA

Purpose: Osteocytes in vivo experience complex fluid shear flow patterns to activate biochemical pathways and the actin and microtubule (MT) cytoskeletal networks play mechanical roles to regulate this process. Due to high intercellular variability, the actin and MT networks were tracked in two orthogonal planes (dubbed quasi-3D) simultaneously in the same cell to observe the spatiotemporal differences of the two networks under fluid shear loading.

Methods: A quasi-3D two-microscope system consisting of an upright and inverted microscopes with individual cameras and beamsplitters allowed simultaneous 3D measurement of two fluorescent dyes in two orthogonal planes (bottom-view and a side-view) of a single cell. MLO-Y4 cells were transfected with TagCFP-Lifeact and mKate2-EMTB to visualize the F-actin networks in cyan and the microtubule networks in far-red. Cells were then plated in a flow and imaging chamber for a short period to ensure a rounded cell body that mimics the in vivo osteocyte shape (Fig. 1A). Steady (n=8) or 1 Hz oscillatory flow (n=7) with a wall shear stress of 1 Pa were applied to cells and imaged. Intracellular cytoskeletal strains were calculated using a digital image correlation technique. Paired t-tests were used to determine significant differences between the two networks' deformational behavior within single cells.

Results: Steady flow had a viscoelastic effect of creep and creep recovery on both the actin and microtubule networks (Fig. 1B), while oscillatory flow produced mainly "elastic" behavior (Fig. 1C). Steady flow developed higher shear strains in the cell body than in oscillatory flow. Under steady flow, actin normal strains were higher in the leading edge to flow compared to the MT normal strains in those areas at the end of the loading period (p<.05). Side-view shear Exz strain was higher in the actin networks in the basal part of the cell closer to the coverslip, possibly due to the presence of focal adhesions. Oscillatory flow strains left no visible residual strains after flow, further emphasizing the different nature of the two flow patterns.

Conclusion: These results demonstrate for the first time a dual simultaneous tracking of both actin and microtubule strains at the single cell level to our knowledge. The high temporal resolution of the quasi-3D system allowed full mapping of differences in the network deformational responses under steady and oscillatory fluid flow profiles.

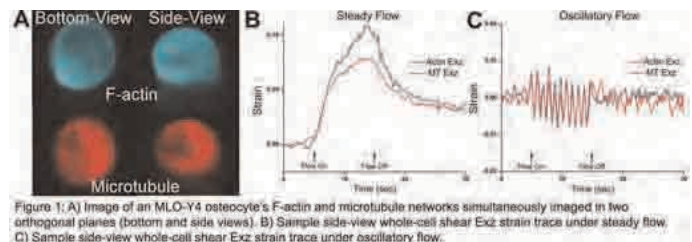


Figure 1

Disclosures: Andrew Baik, None.

SU0316

Radiation-Induced Bone Loss: Role of the Osteocyte. Jeroen Buijs¹, Laura Tedeschi², Marc Mendonca¹, Teresita Bellido², Ted Bateman³, Khalid Mohammad¹, Theresa Guise¹. ¹Indiana University, USA, ²Indiana University School of Medicine, USA, ³University of North Carolina, USA

Patients with tumors in the pelvic region frequently receive radiation therapy, and as a result, bystander bone may experience adverse effects, including bone loss and increased fracture risk, particularly at the hip region. Earlier reports demonstrated that radiation-induced bone loss occurs via increased osteoclast activation in a mouse model. However, the exact mechanism through which osteoclasts are activated is unclear. Apoptosis of Osteocytes has been shown to trigger osteoclast progenitor recruitment and differentiation, and limited reports suggest that osteocytes might be radiosensitive. We hypothesized that radiation induces osteocyte apoptosis leading to increased osteoclastogenesis and subsequent bone loss.

We evaluated the effects of radiation on MLO-Y4 (osteocytes), MC3T3-E1 (osteoblast progenitor) and UMR-106-01 (osteoblast-like/osteosarcoma) cell lines. Osteocytes were exposed to doses of 2 to 10 Gy radiation, and cell death and apoptosis were determined by trypan blue exclusion and by caspase-3 activation and annexin-V expression using flow cytometry, respectively.

Radiation with 2Gy significantly increased the number of trypan blue positive MLO-Y4 cells up to 14.9%, 15.5% and 14.6% after 6, 24 and 48 hours respectively (vs 5.1-7.8% at Co levels), and 10Gy further increased these numbers up to 16.0%, 19.7% and 21.4%. The increase in trypan blue positive UMR-106-01 and MC3T3-E1 cells were most prominent 24 hours after 10Gy radiation (41.5% and 42.1% respectively).

While a marginal induction of apoptosis in MLO-Y4 cells was observed with 2Gy radiation, higher doses of radiation resulted in a much greater induction of apoptosis. At later time points (48hr + 7d), 10Gy radiation induced expression of the apoptotic markers in 50-60% of the MLO-Y4 cells. Similar trends were found for UMR-106-01 and MC3T3-E1 cells.

In conclusion, our findings demonstrate that radiation increases cell death and apoptosis in MLO-Y4 osteocytic cells, in a time and dose dependent fashion. Further studies are underway to functionally test whether radiation-induced bone loss is mediated via osteocytes. This may lead to rapid implementation of therapeutic interventions that can reduce bone loss and fracture risk in patients receiving radiation therapy.

Disclosures: Jeroen Buijs, None.

SU0317

Dose-dependent Effects of Glucocorticoid on Anti-Oxidation, Autophagy and Apoptosis. Junjing Jia¹, Wei Yao¹, Min Guan¹, Weiwei Dai², Jean Jiang³, Lynda Bonewald⁴, Nancy Lane¹. ¹University of California, Davis Medical Center, USA, ²Department of Medicine, University of California at Davis Medical Center Sacramento, CA, USA, ³University of Texas Health Science Center at San Antonio, USA, ⁴University of Missouri - Kansas City, USA

In response to stress such as oxidation, cells may be activated to undergo necrosis, apoptosis, or undergo a stress metabolism and autophagy, and the cell may go onto survive or go onto apoptosis depending on the duration and severity of the insult. As glucocorticoids (GCs) have been shown to induce both "a high oxidative state and osteocyte apoptosis and autophagy, we sought to determine if osteocyte cell fate in the presence of GCs was dose dependent using in vivo and in vitro approaches. We performed in vitro studies with MLO-Y4 cells that were transfected with the GFP-LC3 and then cultured with dexamethasone at 10⁻⁸-10⁻⁵ M doses for 24 hours. We also performed an in vivo experiment using three-month-old male Swiss-Webster mice were treated with slow release pellets prednisolone that delivered a day GC dose at 0 (placebo, PL), 1.4, 2.8 or 5.6 mg/kg/d for 28 days. RNA was extracted from cells or the femurs to perform RT-PCR gene arrays for anti-oxidant, autophagy and apoptosis. The prevalence of osteocyte autophagy and apoptosis were quantitated in vivo by immunohistochemistry in both trabecular and cortical regions. We found that in MLO-Y4 cells, GC exposure did not change their anti-oxidant responses but increased activation of autophagy associated genes, especially at the lower dose levels (10⁻⁷-10⁻⁶M). GC treatment in mice dose-dependently decreased the activations of the anti-oxidant, autophagic and anti-apoptotic gene pathways. The presence of osteocyte

autophagy, detected by immunostaining for LC3, increased about 50% in the distal femur cortical bone site at two lower dose levels (1.4 and 2.8mg/kg/d). There was no GC dose response association with osteocyte autophagy in trabecular bone. The percentage of apoptotic osteocytes dose dependently increased in the cortical bone and was the most significant at the highest dose (5.6 mg/kg/d). In conclusion, GCs appear to have a dose dependent effect on osteocyte cell fate, with lower doses favoring autophagy and higher doses favoring apoptosis. GC dose-dependently decreased both the anti-oxidant defense and autophagy in vivo. The anti-oxidant gene expressions were positively correlated to the activation of genes associated with autophagy but not apoptosis. Our findings suggest interventions that alter autophagy and oxidative stress as therapeutic approach to reduce GC induced bone fragility.

Disclosures: Junjing Jia, None.

This study received funding from: R01 AR043052 (to NEL); PO1 AR46798 (to L.F.B. and J.X.J.) and Welch Foundation Grant AQ-1507 (to J.X.J.)

SU0318

Mediators of Osteocyte Apoptosis in Chronic Kidney Disease. Renata Pereira^{*1}, Thomas Lisse², Harald Jueppner³, Isidro Salusky⁴, Katherine Wesseling⁵. ¹UCLA, USA, ²UCLA/Orthopaedic Hospital Research Center, USA, ³Harvard Medical School & Mass. General Hospital, USA, ⁴University of California, Los Angeles School of Medicine, USA, ⁵UCLA Medical Center, USA

Renal osteodystrophy (ROD), a condition marked by increased bone fragility and deformities, is characterized by osteocyte dysfunction, as evidenced by abnormal mineralization and increased osteocytic FGF-23 and DMP1 expression (Pereira et al. Bone 2009). Although osteocyte viability plays a major role in the maintenance of bone homeostasis and integrity, the factors regulating this process in chronic kidney disease (CKD) are unknown. Thus, the rate of osteocyte apoptosis was evaluated in bone biopsy specimens from 14 pediatric patients with CKD stages 3-5 with the following biochemical variables: Ca: 9.1±0.2mg/dl, P: 5.1±0.4 mg/dl, Alk P:tase: 364±70 IU/l, PTH (1st IMA, Immotopics): 357±100 pg/ml, C-term GF-23 (2nd generation, Immotopics): 1106±295 RU/ml. Bone histology was OF (n=1), mixed (n=4), adynamic (n=4), OM (n=2), and normal (n=3). Apoptosis in bone sections was assessed via in situ nick-end labeling (TUNEL) reaction using Klenow terminal deoxynucleotidyl transferase per manufacturer's instructions (Oncogene Research Products). Apoptotic osteoblasts and osteocytes were not detected in bone from CKD patients while 10-20% of osteocytes were apoptotic in normal controls. To assess potential mechanisms underlying this decreased apoptotic rate in CKD bone, the murine osteocyte cell line MLO-Y4 was cultured in serum-free conditions with either normal (1 mM Pi) or phosphate enriched (8 mM Pi) media in the presence of FGF-23 (50 or 100 ng/ml), DMP1 (40 or 100 ng/ml), or 1,25(OH)₂vitamin D (1, 10, or 100 nM) for 24 and 48 hours. Cell death was assessed by acridine orange/ethidium bromide and trypan blue staining and caspase-3 activity (Biovision) was measured in cell lysates. Higher Pi and the addition of 1,25(OH)₂vitamin D increased MLO-Y4 cell apoptosis as measured both by proportion of dead cells and by caspase-3 activity, the effect of Pi and vitamin D was additive. By contrast, FGF-23 decreased MLO-Y4 cell apoptosis at 24 and 48 hours; this effect was stronger in the presence of high phosphate. DMP1 had no effect on cell life span. In conclusion, osteocyte function is altered in patients with CKD and factors intrinsic to bone (such as FGF-23) and extrinsic to bone (such as circulating phosphate and 1,25(OH)₂vitamin D) influence osteocyte viability. Further studies are warranted to define the genes and mechanisms responsible for alterations in osteocyte cell cycle in CKD; defining this process will have implications for the treatment of ROD.

Disclosures: Renata Pereira, None.

SU0319

Ex-vivo Imaging of the Autonomous Intracellular Ca²⁺ Oscillations of Osteoblasts and Osteocytes in Bone. Yoshihito Ishihara^{*1}, Yasuyo Sugawara², Hiroshi Kamioka³, Noriaki Kawanabe⁴, Hiroshi Kurosaka⁵, Keiji Naruse⁶, Takashi Yamashiro³. ¹Okayama University, Japan, ²Okayama University Graduate School of Medicine, Dentistry, & Pharmaceutical Sc, Japan, ³Okayama University Graduate School of Medicine, Dentistry, & Pharmaceutical Sc, Japan, ⁴Okayama University Hospital, Japan, ⁵Okayama University Graduate School of Medicine, Dentistry, & Pharmaceutical Sciences, Japan, ⁶Okayama University Graduate School of Medicine, Dentistry, & Pharmaceutical Science, Japan

Ca²⁺ is a ubiquitous second messenger in various physiological cellular processes. Bone cells form a complex three-dimensional network consisting of different types of osteoblasts and osteocytes embedded in mineralized extracellular matrices. Previous in vitro study indicated that the intermittent rise in intracellular Ca²⁺ concentration ([Ca²⁺]_i) oscillation has been observed in isolated osteoblasts. However, it has not been entirely clear whether the same [Ca²⁺]_i responses take place when the cells remain in the integrated system. In the present study, we developed for the first time an ex-vivo live Ca²⁺ imaging system that allows the dynamics of the [Ca²⁺]_i responses occurring in intact chick calvaria explants without damaging the complicate network of the bone. Our live imaging analysis revealed that both osteoblasts and osteocytes showed repetitive and autonomous [Ca²⁺]_i oscillations. In addition, thapsigargin, an inhibitor of

the endoplasmic reticular which empties intracellular Ca²⁺ stores, abolished the such [Ca²⁺]_i response both in osteoblasts and osteocytes. These results indicated that Ca²⁺ release from intracellular stores plays a key role in the oscillation of these bone cells in intact bone explants. Since calcium waves were propagated, at least in part, by gap junctional communication in other organs. We further investigate the possible roles of gap junctions in maintenance of such autonomous [Ca²⁺]_i oscillations in intact bones. Treatment with 18 α-GA, a reversible inhibitor of gap junctional intercellular communication, significantly reduced the ratio of the responsive osteocytes, but the relative calcium increase and the frequency of the [Ca²⁺]_i oscillations were not affected. In contrast, the gap junction inhibitor did not affect [Ca²⁺]_i oscillations in osteoblasts. These findings indicated that gap junction is specifically important in the maintenance of the responsive osteocytes in [Ca²⁺]_i oscillation. Taken together, we found that bone cells in intact bone explants showed autonomous [Ca²⁺]_i oscillation that require release of intracellular calcium stores. In addition, osteocytes specifically propagated intercellular calcium waves with cell-cell communication by gap junction, which maintains the responsive cells of the oscillation in bone.

Disclosures: Yoshihito Ishihara, None.

SU0320

Effects of Ovariectomy and PTH(1-34) on Osteocyte Lacunar Properties in Adult Rats. Donald Kimmel^{*1}, Tiffany Fong², Mohammed Akhter³, Thomas Wronski⁴. ¹Kimmel Consulting Services, USA, ²Xradia, Inc., USA, ³Creighton University Osteoporosis Research Center, USA, ⁴University of Florida, USA

Estrogen loss may increase osteocyte (Ot) apoptosis, reducing Ot lacunar (Ot.La) density. Parathyroid hormone (PTH) raises serum Ca by multiple means including Ot activity to increase Ot.La size. Synchrotron radiation (SR) microscopy achieves ~0.7μm pixel resolution (PR), resolving whole Ot.La in 3D images of intact mouse bone. Current laboratory 3D-imaging devices have difficulty resolving Ot.La in intact bones. We report Ot.La volume, density, and separation in PTH-treated, ovariectomized (OVX) rats, from measurement of 3D images acquired on a lab-based instrument that attains SR-like resolution (3D X-Ray Microscope; MicroXCT-200).

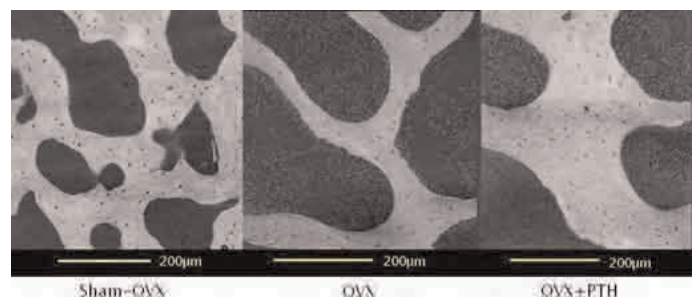
Female rats aged 13wks were OVXd (N=24) or Sham-OVXd. After 6wks, OVX rats were treated for 16wks with 0 [Veh] or 0.05 mg/kg PTH (1-34) [PTH] 5d/wk. Tibiae and L2 vertebrae (LV2) were fixed (70% ethanol). Histomorphometry showed typical OVX and PTH-induced changes in tibial bone. LV2 (4/grp) was trimmed of processes and embedded in methacrylate. 2X2X8mm sagittal samples of the LV2 body were scanned at 5μm PR in the central trabecular region just caudal to the cranial growth plate. Sub-volumes of interest (VOIs) were selected for non-destructive scanning by local 3D x-ray microscopy at ~0.6μm PR. 3D images of each sub-VOI were analyzed by RatoC Segmentation Software (RSS; Tokyo, JP) for Ot.La density (Ot.LaD) and volume (Ot.LaV). BaryCenter of each Ot.La was determined by RSS; separation of Ot.La was calculated (Ot.La.Sp). Ot.La were defined as discrete bone tissue voids >50 and <400μm³.

Data are presented (Table and Figure). OVX+Veh rats have smaller and fewer lacunae than Sham-OVX rats. PTH-treated OVX rats tend to have larger, more numerous lacunae than OVX rats. Bone marrow space is dark in the Figure.

Complete evaluation of bone quality is an unmet need in current fracture risk evaluation. Bone tissue with fewer, smaller Ot.La for early microcracks to encounter, could have reduced ability to slow microcrack propagation, leading to increased bone fragility. Lacunar properties may be yet another bone quality not addressed by current bone measurement methods. Our osteocyte lacunar data, resembling those from human biopsy specimens, may provide new information about bone quality that could explain an additional portion of increased bone fragility related to estrogen deficiency. These data also confirm past studies of Ot.LaV in PTH-treated rats, possibly suggesting a new effect of PTH on bone quality.

Variable	Units	Sham-OVX	OVX+Vehicle	OVX+PTH
Ot.LaD	m.m ⁻³	44795±15390*	15163±7770	35064±14274*
Ot.LaV	μm ³	132.8±36.0*	81.1±6.8	123.7±32.6*
Ot.LaV/BV	%	0.626±0.324*	0.124±0.078	0.450±0.236*
Ot.LaSp	μm	18.2±4.0	17.6±4.1	18.3±4.5
Mean±SD; different from OVX+Vehicle (*P<.05; *P<.10)				

Table



Figure

Disclosures: Donald Kimmel, Xradia, Inc., 5
This study received funding from: Xradia, Inc.

SU0321

A Novel ELISA Assay for Detecting the Active Form of Cathepsin K in Human Serum. Yujia Ding¹, Qinlong Zheng¹, Morten Karsdal², Kim Henriksen^{*2}. ¹Nordic Bioscience Beijing, China, ²Nordic Bioscience A/S, Denmark

Cathepsin K plays essential roles in bone resorption and is an intensely investigated as a therapeutic target for the treatment of osteoporosis. Assessment cathepsin K may provide important biological information in many diseases in which increased bone erosion is a central part of the pathology such as osteoporosis, cancer and rheumatoid arthritis.

Presently there are no robust assays for the assessment of cathepsin K in serum. We focused on developing an ELISA-based assay specifically detecting active cathepsin K in serum samples from humans, rats and mice.

Mice were immunized with a peptide comprising the first 10 aminoacids of active cathepsin K linked to KLH. The antibody was IgG purified and HRP-labelled using commercial systems. A competitive ELISA was setup using a biotinylated coater peptide and a non-labelled peptide as the standard curve. Supernatants from human osteoclasts generated using CD14 magnetic bead sorting and culture were used as positive control. Recombinant cathepsin K, S and L were activated using low pH cysteine-containing buffers.

The inter and intra assay variations of the assay were below 10%. The dilution recovery was 95% until 1:4 dilution.

By using latent and activated Cathepsin K the assay was demonstrated to specifically detect activated cathepsin K. No cross-reactivity to the activated forms of the closely related cathepsin S and L was observed. Using immunoprecipitation it was shown that the antibody only recognizes native cathepsin K.

Quantification of the levels of active cathepsin K in supernatants of purified human osteoclasts compared to corresponding macrophages showed a 30-fold induction ($p < 0.001$).

Active cathepsin K was assessed in serum samples from rats collected at baseline and three weeks after ovariectomy. A 75% significant increase ($p < 0.01$) in active cathepsin K after OVX was observed, which correlated to the increase in bone resorption (CTX-I) ($R^2 = 0.4$, $p < 0.001$). A comparison of the levels of active cathepsin K were quantified in serum samples from patients with osteoclast-rich osteopetrosis (ADOI) and age and sex-matched controls, showed a 100% elevation in ADOI ($p = 0.05$).

In summary, we have developed a robust and sensitive assay specifically detecting the active form of cathepsin K. As cathepsin K is the primary protease in bone resorption, we speculate that the levels of active cathepsin K will prove useful for prediction of future bone loss.

Disclosures: Kim Henriksen, None.

This study received funding from: The Danish Research Foundation

SU0322

Circulating OPG In Femoral Osteoporotic Fracture-Healing. Costantino Corradini^{*1}, Jacopo Bernieri², Vittorio Macchi², Emiliano Malagoli², Cesare Verdoia². ¹State University of Milan, Italy, ²University of Milan, Italy

Objective: Circulating OPG has been measured in different physiological and pathological processes. The main action remains probably the regulation of osteoclastogenesis. Recent studies have revealed opposite OPG serum levels at 6 and 12 months after assumption of antiosteoporotic drugs. Moreover it is still uncertain its role in osteoporotic fractures. The aim of this study was to assess serum OPG levels in elderly patients affected by a femoral osteoporotic fracture. **Material and Methods:** 58 females between 63 and 81 years old with osteoporosis but without important cardiovascular, renal and bowel co-morbidity were recruited. They were divided in two homogeneous groups for number and age on the basis of a presence or less at the moment of hospitalization of proximal femoral fracture treated with proximal femoral nail. Circulating OPG levels were measured in both groups by sandwich enzymelinked immunoassay at 0, 1, 3 and 6 month. **Results:** There is not a normality range of OPG but it was increased for decade and fractured patients revealed a further significant increase. This increase was more evident in the first period of fractures during healing process. During the period of 6 months there was a significant difference in serum OPG levels between fractured patients and unfractured patients. However circulating OPG was higher in fractured patients during the first 3 months, while at 6th month no statistical differences with unfractured were detected. **Conclusion:** the clinical relevance of this study is the increase of serum OPG levels in fractured vs unfractured osteoporotic population. Even if further study are necessary to define range of OPG in only osteoporotic patients and fractured ones, this study suggests an involving of OPG in fracture healing processes. **References:** Dobnig H. Osteop Int 2006 Dundar U. JBMM 2009 Marchelli D. J Orthop Traumatol 2009 Reyes-Garcia R. Menopause 2010

Disclosures: Costantino Corradini, None.

SU0323

Ketonuria's Metabolic Benefits on Bone Metabolism in Korean Women. SANG HYEON JE^{*1}, Nam-Seok Joo², KYU-NAM KIM³, Kwang-Min Kim², Duck Joo Lee⁴. ¹Ajou University Hospital, Department of Family Medicine, South Korea, ²Ajou University Hospital, South Korea, ³Ajou University, South Korea, ⁴Ajou University School of Medicine, South Korea

Recent studies have reported that Ketonuria is related to obesity-related metabolic parameters such as body weight, waist circumference, body mass index (BMI), blood glucose, high density lipoprotein (HDL) cholesterol, triglyceride, blood pressure and insulin. Osteoporosis is a result of combination of diverse interactions in these parameters. In a cross-sectional study, we examined metabolic characteristics, including bone mineral density (BMD), in Korean women with ketonuria after a minimum 8 hr fast ($n = 14,193$).

The ketonuria group showed more favorable BMD than non-ketonuria group did. The ketonuria group also had lower prevalence of lower levels of body weight, triglyceride, fasting blood glucose, blood pressure, and homocysteine; and higher HDL cholesterol than the non-ketonuria group had. The correlation analyses showed that BMD and HDL cholesterol were significantly associated with ketonuria ($r = 0.128$ and $r = 0.151$, respectively). In the linear regression analyses adjusted for age and risk factors of atherosclerosis, BMD was significantly positively associated with risk of ketonuria (Odd ratios (OR), 1.88, 95% CI 1.57-2.24), but BMI was associated with a lower risk of ketonuria (OR 0.88, 95% CI 0.82-0.94).

The presence of ketonuria after at least an 8 hr fast may have metabolic benefits even in the bone mineral metabolism, other than obesity-related metabolism.

Disclosures: SANG HYEON JE, None.

SU0324

Serum PINP Predicts Changes Caused by Intermittent PTH(1-34) Treatment in Mechanical Properties and Other Bone Parameters in Adult Ovariectomized Osteopenic Rats. Jussi Halleen^{*1}, ZhiQi Peng¹, Katja Fagerlund¹, Tiina Suutari¹, Jukka Vaaranen¹, Mari Suominen¹, Jukka Rissanen², Harrie Boonen³, Trine Neerup⁴, Hanne Bak⁴, Jukka Morko¹. ¹Pharmatest Services Ltd, Finland, ²Pharmatest Services, Limited, Finland, ³University of Copenhagen, Denmark, ⁴Zealand Pharma A/S, Denmark

Procollagen I N-terminal propeptide (PINP) is a sensitive marker of bone formation for monitoring the efficacy of treatment with recombinant human parathyroid hormone (1-34) analog (PTH) in osteoporotic patients. We evaluated the value of serum PINP for predicting changes in bone parameters caused by intermittent PTH treatment in adult ovariectomized (OVX) osteopenic rats. Study groups included a sham-operated control group, an OVX-operated control group receiving vehicle, and OVX-operated groups receiving daily subcutaneous injections of 1.2, 4.0, 12.0, 40.0 and 120.0 µg/kg human PTH. Each group contained 12 animals that were 6 months of age at the time of the operations. Dosing was started at 7 weeks after OVX and continued for 6 weeks. PINP and other bone turnover markers C-terminal cross-linked telopeptides of type I collagen (CTX) and tartrate-resistant acid phosphatase 5b (TRACP 5b) were determined in serum before the start of treatment, at 2 weeks after the start of treatment, and at the end of the study. Bone parameters were determined in long bones and vertebra by peripheral quantitative computed tomography (pQCT), static and dynamic histomorphometry and biomechanical testing. PTH treatment showed strong anabolic effects and serum PINP values showed a strong dose-dependent increase by PTH treatment both at 2 weeks and at the end of the study. The PINP values showed strong correlations both at 2 weeks and at the end of the study with parameters of pQCT, including trabecular bone mineral density in tibial metaphysis and vertebra and cortical thickness in tibial diaphysis, with parameters of bone histomorphometry, including trabecular bone volume/tissue volume (BV/TV) and trabecular thickness (Tb.Th.) in tibial metaphysis and vertebra, and bone formation rate as determined by dynamic histomorphometry in vertebra, tibial metaphysis, and periosteal and endosteal surfaces of tibial diaphysis, and with serum TRACP 5b values, but not with serum CTX values. Most importantly, serum PINP values correlated strongly with mechanical properties of bones, including maximal load in femoral neck as determined by cantilever bending test, in tibial diaphysis as determined by three-point bending test and in vertebra as determined with compression test. These results demonstrate that serum PINP values predict changes caused by intermittent PTH treatment in mechanical properties and other bone parameters in adult ovariectomized osteopenic rats.

Disclosures: Jussi Halleen, Pharmatest Services Ltd, 3; Pharmatest Services Ltd, 4; IDS Ltd, 5

SU0325

Usability of Serum Tartrate-resistant Acid Phosphatase Type 5b (TRACP-5b) in Rat Ovariectomy Model. Wataru Kikuchi¹, Yasuaki Namatame¹, Yuri Matsuki¹, Iwao Kiyokawa¹, Fumio Nomura², Kimimitsu Oda³, Toshihide Miura¹. ¹Nittobo Medical Co., Ltd., Japan, ²Department of Molecular Diagnosis, Graduate School of Medicine, Chiba University, Japan, ³Department of Oral Life Science, Graduate School of Medical & Dental Sciences, Niigata University, Japan

Background: We had developed a new EIA assay kit for TRACP-5b in rat serum, and reported the basic performance for the kit in ASBMR 2009 Annual Meeting. This time, we studied about the behavior of serum TRACP-5b levels in rat ovariectomy (OVX) model. And we had also evaluated the usefulness of monitoring TRACP-5b as a bone turnover marker with some drugs.

Methods: Twelve weeks old of female Wister rats were divided into five groups. Group 1 (Control group): sham operated given placebo. Group 2: OVX operated given placebo, Group 3: OVX operated given 17 β -Estradiol (E2), Group 4: OVX operated given Alendronate (ALN), Group 5: OVX operated given Calcitonin (CT). Blood was withdrawn before operation and every week after operation, and serum TRACP-5b and CTX was measured. All of rats were killed at the 5th week, and femur was harvested for measurement of pQCT analysis.

Result: A TRACP-5b level of OVX group (Group 2) was significantly declined compared with Sham group (Group1). This TRACP-5b change was opposite of changing in postmenopausal women. Reducing activity of TRACP-5b was inhibited with treatment of E2 (Group 3). These data suggested that deficient secretion of estrogen leads reducing of serum TRACP-5b in rat.

The result of pQCT analysis indicated that treatment of ALN (Group4) and CT (Group5) can significantly prevent the bone loss. Treatment of ALN reduced the level of TRACP-5b and CTX in a week. TRACP-5b kept 5 weeks on low levels, but CTX shifted to increase at the third week. In ALN-treated group, the level of BUN on 5th week was significantly higher than non-treated group. This may suggested that increasing of CTX is caused by declining of renal function.

Conclusions: TRACP-5b changed in early stage, and kept reflecting bone resorption significantly with some drugs. We conclude that TRACP-5b is very useful marker of bone resorption in rat model.

Disclosures: Wataru Kikuchi, None.

SU0326

Central DXA Utilization in Medicare Beneficiaries in the Wake of Reimbursement Changes. Jie Zhang¹, Elizabeth Delzell¹, Hong Zhao¹, Andrew Laster², Kenneth Saag¹, Meredith Kilgore³, Michael Morrisey¹, Nicole Wright¹, Huifeng Yun¹, Jeffrey Curtis¹. ¹University of Alabama at Birmingham, USA, ²Arthritis & Osteoporosis Consultants of the Carolinas, USA, ³University of Alabama At Birmingham School of Public Health, USA

Purpose: Medicare gradually reduced payments for physician office based dual energy X-ray absorptiometry (DXA) services from an average of \$139 in 2006 to \$72 in 2009. In contrast, reimbursement for hospital based DXA services was unaffected. We investigated the utilization of central DXA services in the Medicare population before and after the reduction.

Methods: We identified individual from the 5% random sample of Medicare beneficiaries who were ≥ 65 years of age and continuously enrolled in Medicare Parts A and B but not in a Medicare Advantage plan for at least one full calendar year from 2002 through 2009. The first central DXA test for these beneficiaries in each calendar year was identified using Current Procedural Terminology codes. We classified each test as a facility (hospital based) or a non-facility (physician office based) DXA. For each calendar year, we calculated the proportion of beneficiaries who had at least one central DXA and the proportions of facility versus non-facility DXAs of all DXAs performed. The total number of DXA tests was multiplied by 20 to extrapolate to the entire nation's Medicare fee-for-service population.

Results: In 2009, the average age of all Medicare beneficiaries was 75.7 years; 58% were female; and 88% were Caucasians. From 2002 to 2006, the proportion of beneficiaries who had at least one central DXA increased from 7.7% to 9.6% at an average annual rate of 0.4%. The proportion continued to climb and peaked in 2008 at 9.9% and remained unchanged in 2009. Between 2007 and 2009, the annual rate of increase was 0.1% (Figure 1). Compared to 2006, in which 1,643,720 (69%) of DXAs were performed in physician offices, the absolute number and proportion of office based DXAs declined to 1,534,240 (66%) by 2009 (Figure 2). This decline was offset by an increase in the number of facility DXAs, which increased from 719,780 (31%) in 2006 to 804,000 (34%) in 2009.

Conclusions: Between 2007 and 2009, reductions in Medicare payment for physician office based central DXA services was associated with a slight slowing in the annual rate of growth in the overall number of DXAs performed and a modest shift in DXA use away from office based to hospital based DXAs in the Medicare fee for service population.

Figure 1 Proportion of beneficiaries who received at least one central DXA by calendar year

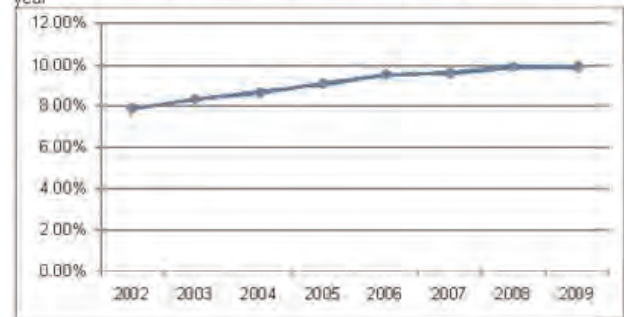
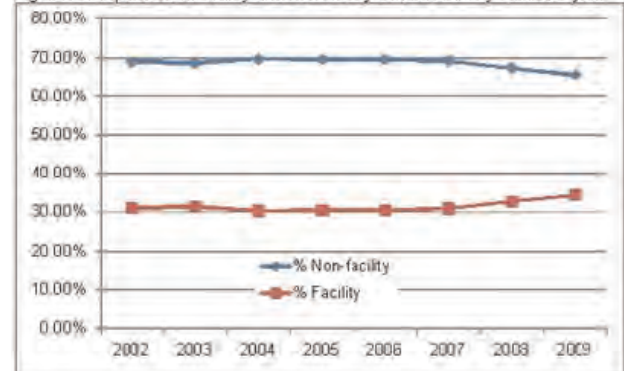


Figure 2 Proportions of facility and non-facility central DXA by calendar year



Disclosures: Jie Zhang, Amgen, 2

This study received funding from: Amgen

SU0327

Comparison Of The Effect Of Surrounding Fat On Measurements Of BMD By DXA And High Resolution Quantitative Computerized Tomography. Edward Colt¹, Muhammad Akram², Fahad Javed¹, Elizabeth Shane³, Stephanie Boutroy⁴. ¹Columbia University & St. Luke's-Roosevelt Hospital, USA, ²St. Luke's-Roosevelt Hospital, USA, ³Columbia University College of Physicians & Surgeons, USA, ⁴Columbia University Medical Center, USA

Quantity of soft tissue may affect bone mineral density (BMD) measurements by dual energy X-ray absorptiometry (DXA). The purpose of the study was to compare the effect of surrounding fat on the measurement of bone density by High Resolution peripheral Quantitative Computerized Tomography (HRpQCT, Scanco Medical AG) and by iDXA (GE-Lunar).

We conducted two experiments, one with a thin lamb diaphyseal bone and 3 layers of lard, each of approximately 0.7-0.8 cm thickness and one with a thick beef diaphyseal bone and 1 layer of lard of 1.5 cm. The bones were scanned, surrounded or not by several layers of lard, 3 times each. Acquisition modes were the standard tibia acquisition for HRpQCT and whole body scan mode for iDXA.

On the lamb bone (Table), we observed that higher number of lard layers decreased measured areal BMD (aBMD) by DXA and total and cortical volumetric BMD (vBMD) by HRpQCT. The effect of lard was more marked on DXA results. Measurement of cortical thickness was minimally affected by fat. On the thicker beef bone, a single layer of surrounding lard decreased total and cortical vBMD by 4.5% and 6.7% respectively and cortical thickness by 0.3%. In contrast, aBMD increased by 7.4% with a layer of lard.

In conclusion, measurements of BMD were slightly affected by the amount of fat tissue surrounding bone, whether assessed three-dimensionally by HRpQCT or two-dimensionally by DXA. The effects of surrounding fat on DXA measurements were substantially greater than on HRpQCT measurements. A future analysis on a diaphysis will allow us to study the effect of surrounding fat tissue on trabecular density and microarchitecture. The discrepancy observed between the effect of fat on aBMD of thin lamb and thick beef bones by DXA requires further investigation

Areal and volumetric BMD of lamb bone surrounding by different layers

	mean value no. layer	% difference from no. layer		
		1 layer	2 layers	3 layers
Lamb bone				
Total density (mg HA/cm ³)	595 ± 0.05	-1.9%	-4.9%	-11.2%
Cortical density (mg HA/cm ³)	1074 ± 0.04	-1.2%	-4.4%	-10.2%
Cortical thickness (mm)	2.04 ± 0.01	1.0%	0.0%	-2.0%
aBMD by DXA (g/cm ²)	0.777 ± 0.002	-9.5%	-8.5%	-19.6%
Beef bone				
Total density (mg HA/cm ³)	840 ± 0.50	-4.6%		
Cortical density (mg HA/cm ³)	1204 ± 0.40	-6.7%		
Cortical thickness (mm)	0.29 ± 0.01	-0.3%		
aBMD by DXA (g/cm ²)	2.542 ± 0.013	7.4%		

Table

Disclosures: Edward Colt, None.

SU0328

DXA and HR-pQCT Detect Minimal Bone Loss After Kidney Transplantation with Early Corticosteroid Withdrawal. Lucas Nikkel^{1*}, Chivuan Zhang², Sumit Mohan³, Bekir Tanriover³, David Cohen³, Lloyd Ratner³, Geoffrey Dube³, Stephanie Boutroy¹, Xiaowei Liu³, Donald McMahon³, Elizabeth Shane³, Thomas Nickolas¹. ¹Columbia University Medical Center, USA, ²Columbia University, USA, ³Columbia University College of Physicians & Surgeons, USA

With corticosteroid (CS)-based immunosuppression, areal bone mineral density (aBMD) declines by 4-9% during the first 3-6 months (m) after kidney transplant (KTx), particularly at trabecular (Tb) rich sites, such as the lumbar spine (LS). Moreover, fracture rates are very high at both spine and hip. Early corticosteroid withdrawal (ECSW) protocols, primarily based on calcineurin inhibitors (CNI), are increasingly utilized for immunosuppression after KTx. We hypothesized that KTx recipients managed with ECSW would not experience significant bone loss.

Included were KTx recipients ≥18 yrs and managed with ECSW after 4 days of induction solumedrol. At baseline, 3m and 6m post-KTx, we measured aBMD by dual energy X-ray absorptiometry (DXA) at predominantly Tb sites, including the LS and ultradistal radius (UDR), and cortical (Ct) sites, the total hip (TH), femoral neck (FN) and 1/3 radius (1/3R). High resolution peripheral quantitative computed tomography (HR-pQCT; XtremeCT; Scanco Medical, voxel size=82µm) was used to measure total, Ct and Tb volumetric BMD (vBMD); Ct thickness (CtTh); and Tb number (TbN), thickness (TbTh) and separation (TbSp) at the distal radius (RAD) and tibia (TIB). Comparisons were made using paired T-tests; results are expressed as MeansSD.

Of 55 subjects enrolled, 26 and 16 completed 3m and 6m of observation respectively. Age was 5013 years; 31% were women and 73% were white. BMI was 297 Kg/m². Mean baseline T-Scores were > -2.5 at all sites. At 3m, aBMD declined significantly only at the TH (-1.6%, p<0.001; mean T-score decrease -0.2SD, p<0.001), with recovery by 6m (p=0.15 compared to baseline). However, 6m UDR aBMD decreased by -3.7% (p<0.01; mean T score decrease -0.3SD, p<0.01). By HR-pQCT at 6m, RAD total vBMD decreased by -1.6% (p=0.03), Tb vBMD decreased by -2.6% (p=0.003), TbTh decreased by -5.6% (p<0.01) and there was a non-significant 1.6% decrease in TIB vBMD (p=0.06). TbN and TbSp were unchanged at both RAD and TIB at 6m.

After KTx, ECSW was associated with minimal bone loss at the LS, FN, TH and 1/3R, lower than previously reported for patients on CS. In contrast, significant bone loss occurred at the UDR. At the RAD, HR-pQCT suggested that Tb bone loss is due to Tb thinning rather than drop out. At the TIB, the mechanism of bone loss was unclear. Larger and longer studies are needed to assess the effects of ECSW protocols on bone mass microstructure and stiffness and fracture rates in KTx recipients.

Disclosures: Lucas Nikkel, None.

SU0329

Influence of Vertebral Fracture Assessment on Osteoporosis Treatment. Violaine Carcasses^{1*}, Jacques Fechtenbaum², Christine Bonnet³, Pascale Vergne-Salle³, Alexandra Poinas³, Philippe Bertin³. ¹Hospital center, France, ²Centre D'Evaluation, Des Maladies Osseuses, France, ³University hospital center, France

Vertebral fracture is a severe complication of osteoporosis. Despite its common severity and its value to predict further osteoporotic fractures, vertebral fractures (VF) are underdiagnosed. Performing spine radiographs in all patients screened for osteoporosis is not thinkable according to time and cost parameters. With the last generation of dual energy X-ray absorptiometer, thoracic and lumbar spine scan are possible. Evaluation of vertebral fracture status on these images is called Vertebral Fracture Assessment (VFA). At present the place of VFA is not well definite in Europe in osteoporosis management and more specially in postmenopausal osteoporosis management.

The aim of the study was to evaluate if VFA among postmenopausal osteopenic or osteoporotic women naive of osteoporosis treatment could change therapeutic management according to french osteoporosis recommendations published in 2006.

Methods : This prospective study was realized from January to June 2010, on osteopenic or osteoporotic postmenopausal women, aged from 50 to 80 years old, referred for bone mineral density testing. Fracture evaluation (L4-T7) was performed semi-quantitatively using the Genant classification. Classic osteoporotic risk factors (tobacco use, age of menopause, personal and family history of fragility fracture..) were listed. Patients with neoplastic history, corticosteroid significant traitement or prior VF were excluded. Spine radiographs was made in case of VF or incertain diagnostic to confirm it and to eliminate secondary etiology.

Results : 42 patients were included. The percentage of readable vertebrae was 94.8% and prevalence rate fracture was 7%. For 5 patients VFA was considered as non informative due to unreadable vertebrae. For 37 patients, we could identify those with (3 patients (7%)) or with not (34 patients (81%)) management change. The management change consisted in anti-osteoporotic treatment indication thanks to VF diagnostic. The table summarize the densitometric status and impact of VFA on therapeutic management for the 37 patients.

Conclusions : we confirmed the easy realisation of this exam as a daily practice with a good percentage of readable vertebrae notably. The small effective and the low VF prevalence rate contributed to underestimate the main objective. Nevertheless 7% of the population included did profit of therapeutic proposition thanks to this exam and VF diagnostic which is consequent.

	Osteopenia	osteoporosis	All
Change therapeutic management	1	2	3
No change therapeutic management :			
- Treatment recommended before VFA	2	6	8
- No treatment confirmation	21	5	26

Table : Osteoporosis was defined by a T score at the lumbar spine or hip < -2.5; osteopenia by a lowest T score at the lumbar spine or hip between -2.5 and -1.

Disclosures: Violaine Carcasses, None.

SU0330

Measurement of Bone Mineral Density and Bone Mineral Content Under an Oxford Hemi-Knee Arthroplasty Device – Precision Study. Allison Heard¹, Gary Hooper², Rachel March¹, Rod Maxwell², Christopher Frampton³, Ian Penny², Nigel Gilchrist^{4*}, Patricia Maguire¹. ¹CGM Research Trust, Christchurch, New Zealand, ²Department of Orthopaedic Surgery, Christchurch Hospital, New Zealand, ³Department of Medicine, Christchurch School of Medicine & Health Sciences, University of Otago, New Zealand, ⁴Department of Orthopaedic Medicine & Surgery, Christchurch Hospital, New Zealand

Introduction: Uni-compartment knee replacements are becoming more common. It is proposed that they preserve more bone, are less painful; require a shorter hospital stay with improved function and recovery, compared to total knee replacements. The development of the Lunar i-DXA bone densitometer with near xray quality images and better resolution enabled us to measure areas around the tibial component of an Oxford hemi-knee arthroplasty.

Methods: The study used the Lunar i-DXA densitometer with Version 13.1 software. A developmental orthopaedic knee software was used to complete and analyse tibial component bone mineral density (BMD) in each patient. Ethics Committee approval was obtained. Both knees in 20 patients were measured 3 times in the supine position with repositioning between each scan. The patient was centred on the table parallel to the long axis of the table with the patella upwards. Foam cushions were positioned under the scanned knee to flex the knee so that the tibial base plate was perpendicular to the direction of the beam, the ankle was then strapped. The i-DXA measurement commenced 10cm below the patella. We chose 7 regions of interest to evaluate the bone density under and beside the implant. Areas 1 and 2 were directly under the implant and the other areas were either adjacent or distal to the implant. Once a template was established this was used on the contra lateral knee, which was also scanned and compared.

Results: Twenty patients with the mean age of 69 years (13 females and 7 males) were scanned. Small but significant differences between the implant and non-implanted knee were noticed with the non-implanted knee having slightly higher BMD and bone mineral content (BMC) in areas 1 – 3 (p = <0.001) and area 6 (p = 0.002). There was higher BMD in area 4 (p = 0.028). The precision for BMD in the 7 areas of interest in the implanted knee varied between 0.55% - 4.04% and BMC 1.8% - 5.3%. There was no significant difference in the precision between the non-implanted and implanted knees.

Conclusion: We have established that with a dedicated knee software using i-DXA we can obtain very accurate and precise measurements of BMD and BMC underneath and around an Oxford hemi-knee replacement. We have a prospective study underway to assess the issue of stress loading and bone loss or gain, adjacent to these implants before and after surgery.

Disclosures: Nigel Gilchrist, None.

SU0331

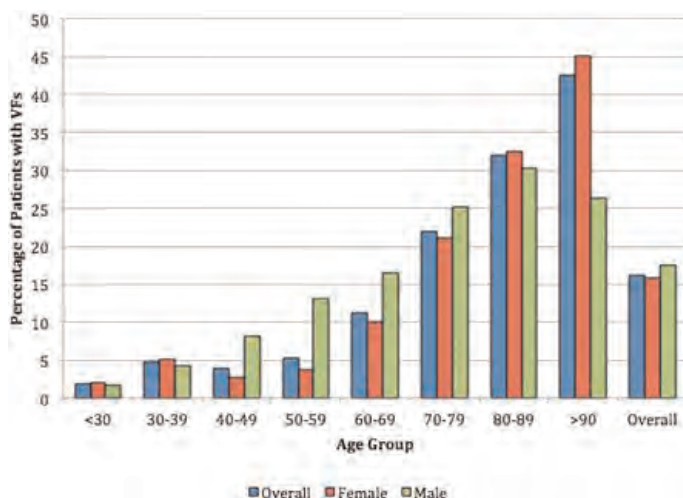
The Prevalence of Vertebral fractures in Irish patient attending for Dual Emission X-ray Absorptiometry (DXA) using Lateral Vertebral Assessment (LVA). Bill Walsh¹, David Crosby¹, Kara Fitzgerald², Georgina Steen¹, Miriam Casey¹, James Walsh³, Joseph Browne^{*1}. ¹Bone Health & Osteoporosis Unit, St James's Hospital, Ireland, ²Bone Health & Osteoporosis Unit, St James's Hospital, Ireland, ³Trinity College Dublin, The University of Dublin, Ireland

Bone mineral density (BMD) alone underestimates the severity of osteoporosis in patients with previously undiagnosed vertebral fractures. Lateral vertebral assessment (LVA) may be used as a diagnostic tool for the identification of vertebral fractures (VFs) in patients attending for DXA and highlights patients who require additional assessment and treatment for optimal bone health. Additional risk factor assessment may highlight patients who are unaware that they have vertebral fractures.

The LVAs of patients attending for DXA were retrospectively reviewed at an Osteoporosis Clinic in Dublin, Ireland over a 6 year period between 2003 to 2008. An LVA was performed from T4 to L4 using a GE Lunar Prodigy DXA. Deformities were reviewed by 2 trained reviewers independently.

4248 patients attended for DXA and 152 (3.7%) patients excluded due to issues analysing their LVAs. Of the remaining 4096 patients (818 (19.96%) men and 3278 (80.04%) women), the mean age was 65.13 (+/-16.98) yrs (age range: 18 – 102). 3390 (63.35%) patients were 60 years or older. Semiquantitative measurements of the LVAs identified 664 (16.2%) patients with VFs with T8, T12 and L1 being the most common vertebrae to be fractured. VFs were more prevalent in older groups ($P < 0.001$). Younger male patients (40-49, 50-59 and 60-69 year old groups) had a higher prevalence of vertebral fractures compared to similar aged female patients ($p=0.02$, $p=0.001$ and $p=0.022$, respectively). Older female patients had a higher prevalence of VFs, with 45.08% women over 90 years identified with at least one VF. Patients with a history of a low trauma hip fracture had the highest prevalence of VFs (38.1%; age-adjusted OR 1.74, 95% CI 1.32 – 3.02; $p<0.001$), although they were comparatively older ($p<0.001$). Patients with a history of glucocorticoid use had a higher vertebral fracture prevalence and the risk increased two-fold over similar age-matched patients who were not on glucocorticoid therapy (OR 2.04, 95% CI 1.83 – 2.21, $p<0.01$). Other osteoporosis risk factors such as smoking, height loss and reduced BMI were associated with VFs ($p<0.001$).

There is a high prevalence of vertebral fractures identified on LVA in patients who attended our unit for DXA examination, particularly in those with significant risk factors for osteoporosis such as a previous fracture or a history of glucocorticoid use. Lateral vertebral assessments should be performed on all patients attending for a DXA scan.



Percentage Prevalence of Vertebral Fractures identified according to Age Group

Disclosures: Joseph Browne, None.

SU0332

Utility of FRAX and Q-fracture in the evaluation of T2DM patients. Pedro Rozas-Moreno¹, Rebeca Reyes-García², Antonia García-Martín^{*2}, Ines Luque-Fernandez², Miguel Aguirre³, Manuel Munoz-Torres⁴. ¹Endocrinology Division, Hospital General de Ciudad Real, Ciudad Real, Spain., Spain, ²Bone Metabolic Unit (RETICEF), Endocrinology Division, Hospital Universitario San Cecilio, Granada, Spain., Spain, ³Endocrinology Division, Hospital General de Ciudad Real, Ciudad Real, Spain., Spain, ⁴University Hospital, Spain

CONTEXT: The World Health Organization fracture risk assessment tool (FRAX) is implemented in several guidelines and most widely used at present, although the presence of diabetes is not included as a risk factor. Q fracture includes the presence of

diabetes, and could be better in the evaluation of patients with diabetes. Our objective was to evaluate the performance of FRAX tool and Q-fracture in a group of T2DM patients.

DESIGN, SETTING AND STUDY SUBJECTS: Cross-sectional study including 78 patients with T2DM. Lumbar spine and femoral BMD were measured by dual X-Ray absorptiometry (Hologic QDR 4500). Ten-year major osteoporotic fracture risk and hip fracture risk were calculated using FRAX tool and Q fracture. Results were analyzed using SPSS 15.0.

RESULTS: Mean age was 57.8 years (57.86.4). 44.8% were females (n=35) and 55.2% males (n=43). 22.4% of patients have densitometric criteria for osteoporosis and 9% had a previous fracture. Prevalent radiographic vertebral fractures were detected in 27.7%. Medium FRAX index was 2.521.95 for major osteoporotic fractures and 0.350.40 for hip fractures. If BMD values was added to calculation medium FRAX index was 2.772.38 for major osteoporotic fractures and 0.350.59 for hip fractures. There were no differences between medium FRAX index calculated with or without BMD. When treatment thresholds were applied (7% ten-year probability for major osteoporotic fracture and 3% ten-year probability for hip fracture) few patients were selected for treatment. 2.6% of patients had a ten-year probability for major osteoporotic fracture >7% and the percentage raised to 5.1% when femoral neck BMD was added ($p = 0.002$). No patients had a ten-year probability for hip fracture >3% and 2.6% meet criteria when femoral neck BMD was added. Using Q fracture, 3.8% of patients had high risk fracture and 1.3 % high risk of hip fracture.

CONCLUSIONS: In our group of T2DM patients a low percentage of T2DM patients are selected for treatment by FRAX tool or by Q fracture despite the high risk of fracture demonstrated by high vertebral fracture rate. Additional studies are needed to establish the performance of those scales in the evaluation of fracture risk in T2DM patients.

Disclosures: Antonia García-Martín, None.

SU0333

Assessment of Microarchitectural Parameters in Transiliac Bone Biopsies of Females and Males with Fragility Fractures. Angela Trubrich^{*1}, Christian Muschitz², Roland Kocian³, Christina Bittighofer⁴, Thomas Pirker⁵, Thomas Gross⁶, Philippe Zysset⁷, Heinrich Resch⁸. ¹Austria, ²St. Vincent's Hospital, Austria, ³St. Vincent Hospital Vienna, Austria, ⁴Krankenhaus Barmherzige Schwestern, Austria, ⁵The VINFORCE Study Group - St. Vincent Hospital - Medical Department II, Austria, ⁶Institute of Lightweight Design & Structural Biomechanics, Technical University Vienna, Austria, ⁷Vienna University of Technology, Austria, ⁸Medical University Vienna, Austria

Purpose: Biomechanical characteristics of bone are not only determined by bone mass, but also by the geometry of cortical and trabecular microarchitecture and intrinsic material properties. Patients who sustain fragility fractures probably have reduced bone mass and alterations in their bone structure. Furthermore gender specific discrepancies are considered.

Methods: In this retrospective study we evaluated transiliac bone biopsies of 48 male patients (aged 18 to 71 years) and 36 female patients (aged 17 to 73 years), who sustained fragility fractures. All Samples were analysed by micro-tomographic imaging system (μ CT40, Scanco Medical AG, Brüttisellen, Switzerland). The following morphometric indices were determined: VOX-TV, VOX – BV, VOX-BV/TV, Conn-Dens., TRI-SMI, Dt-TbN, Dt-TbTh, Dt-Tb Sp, Dt-Tb(1/N).SD, Dt-Tb TH SD, Dt-Tb Sp SD, Apparent Density and Tissue Density. The total group was divided into age-related quartiles (<35.9; 35.9 – 43.11; >43.11-<54.71; >54.71yrs) and split in gender groups. Additionally, BMD and T-score of lumbar spine and hip, prevalent fracture status and previous medication were recorded. Laboratory tests did not reveal any evidence metabolic disorder or vitamin D deficiency.

Results: Despite significant differences in BMD of the total hip ($p=0.005$) in the total group we did not find significant gender specific differences in the microarchitectural parameters. Even the age quartiles showed no differences in the indices except the youngest and the oldest quartile. In these subgroups significant gender-specific changes in BMD of the total hip ($p=0.028$) were detected, furthermore VOX-BV/TV ($p=0.035$), Apparent Density ($p=0.041$) and Tissue Density ($p=0.029$) demonstrated significant differences in the youngest subgroup, but not in the other quartiles

Fracture status and previous medication demonstrated no distinctions in the subgroups and the total group.

Conclusions: According to our results we could not obtain significant genderspecific alterations in microarchitectural parameters in males and females with fragility fractures. Nevertheless there were significant changes in the BMD of the total hip. However these result did not correlate with the any values of the microarchitectural parameters. Our findings and the lack of gender specific differences seem to be not due to different patterns of microstructure but due to changes at the material level.

Disclosures: Angela Trubrich, None.

SU0334

Conception and Validation of a Non-Threshold based Processing and Analysis of Bone Images. Roger Zebaze^{*1}, Ali Ghasem-Zadeh¹, Sandra Iuliano-Burns¹, Kylie King¹, Aloys Mballa², Ego Seeman¹. ¹Austin Health, University of Melbourne, Australia, ²Strax Corp, Australia

Background- Assessment of bone architectural and material composition requires two steps — (i.) image acquisition and (ii.) processing and analyses of the acquired image. Both steps are critical. We propose that difficulties to accurately quantify bone architecture are at least in large part, due to suboptimal image processing. For example, most if not all, image processing algorithms use thresholding at some stage of the processing. However, there is no universally acceptable thresholds that allow robust processing of all images without loss of information given the heterogeneity of bone material composition and structure. We test hypotheses that (i.) accurate segmentation and analysis can be achieved without thresholding (ii.) The results of such processing can be used to more accurately identify individuals with fractures.

Methods- Analyses of the radial density profile around the perimeter of the bone was used to achieve a non-threshold based segmentation of bone into compact-appearing cortex (CC), transition zone (TZ) and trabecular compartment. The algorithm was implemented in a software (StrAx1.0). Micrograph of bone from the hip with differing degree of porosity were collected. HR-pQCT images of 35 women with distal radius fracture (fx; n=35) and their age-matched peers (n=40) were analysed using StrAx1.0 to measure total, cortical and trabecular densities (TvbMD, CtBMD and TrvBMD) and porosity (CtPo) of the total cortex (CC+TZ). Standard HR-pQCT parameters were also measured.

Results- Porosity measured directly from micrographs correlated with porosity measured using StrAx1.0 ($r^2=0.85$). TvbMD, CtBMD and TrvBMD as measured by StrAx1.0 were lower in fx than in non-fx respectively 20.7% $p<0.0001$; 10.3% $p<0.007$; and 55.7% $p<0.0001$. Differences in these parameters between fx and non-fx were also observed with methods but were less TvbMD 15.6% $P=0.01$; CtBMD 1.89% $p=NS$ and TrvBMD 21.6% $P=0.004$. CtPo measured with StrAx1.0 was 14.6% $p=0.007$ higher in fx than non-fx cases.

Conclusion- Bone images can be accurately processed without using thresholding. This approach is robust and allows better identification of individuals at risk for fracture.

Disclosures: Roger Zebaze, None.

SU0335

Effect of Age on Femoral Neck Bone Strength using Quantitative CT, DXA, and Biochemical Markers of Bone Metabolism of the Normal Postmenopausal Women. Shigeharu Uchiyama^{*1}, Shota Ikegami², Mikio Kamimura³, Yoshiyuki Sasaki⁴, Mitsutoshi Sugano⁵, Yoshikazu Ido⁶, Akiko Takata⁶, Kiichi Nonaka⁷, Toshihiko Imaeda⁸, Yukihiko Hata⁶, Hiroyuki Kato⁹. ¹Shinshu University, School of Medicine, Japan, ²Department of Orthopaedic, Japan, ³Kamimura Clinic, Japan, ⁴Radiology Division, Shinshu University Hospital, Japan, ⁵Laboratory Medicine, Shinshu University Hospital, Japan, ⁶Rehabilitation Center, Shinshu University Hospital, Japan, ⁷Elk Corporation, Japan, ⁸Department of Food & Nutritional Environment, Kinjo Gakuin University, Japan, ⁹Department of Orthopaedic Surgery, Shinshu University School of Medicine, Japan

The risk of femoral neck fracture has been previously assessed by examining the bone mineral density (BMD), bone geometry, as well as certain biochemical markers of bone metabolism. For effective assessment of the risk of fragility fracture, these different methodologies should preferably be combined. Thus, this cross-sectional study aimed at assessing the age-related trends in hip structure analyses using quantitative computed tomography (QCT), 12 biochemical markers of bone metabolism, and dual-energy X-ray absorptiometry (DXA)-derived BMD. [Methods] We recruited 79 healthy postmenopausal women who did not have any history of systemic diseases or fragility fractures. QCT of the femoral neck was performed, and the images were analyzed using Mindways QCT-PRO BIT software. The total cross-sectional area (total CSA), cortical cross-sectional area (cortical CSA), and average cortical thickness (ave cort thick) were considered as the geometrical parameters and measured; and the cross-sectional moment of inertia (CSMI), section modulus (SM), and buckling ratio (BR) were calculated as the measurements of bending strength and risk of buckling. DXA-derived BMDs of the proximal femur and lumbar spine were also calculated. Serum bone-specific alkaline phosphatase, osteocalcin, and under-carboxylated osteocalcin; serum and urinary pentosidine; plasma homocysteine, whole parathyroid hormone (wPTH), 1,25-(OH)₂ vitamin D, and 25-(OH) vitamin D; serum tartrate-resistant acid phosphatase 5b (TRACP); and urinary deoxypyridinoline (DPD) and N-terminal cross-linked telopeptide of type I collagen were measured as the biochemical markers of bone metabolism. Regression analysis was used to measure the effect of age on all the geometric and mechanical parameters and biochemical markers. In addition, correlation of each parameter was evaluated. [Results] DXA-derived femoral neck BMD, cortical CSA, ave cort thick, CSMI, and SM had significantly negative correlations with age and significantly positive correlations with BR. Those correlations were weak to moderate. Age did not affect

the total CSA ($p = 0.75$). A wide range of values for BR were observed when the BMDs were low. TRACP, serum pentosidine, homocysteine(weak) and DPD (moderate) were positively correlated with age. None of the biochemical markers were correlated with CSMI or SM. BR had weak positive correlation with TRACP or osteocalcin. Data obtained in each decade are presented in the table. [Conclusion] The geometric and mechanical parameters of femoral neck QCT, and the biochemical markers are affected by age, but correlation is weak to moderate. Further studies are required to assess whether DXA and QCT when used with the biochemical markers of bone metabolism can provide a more detailed risk assessment of bone fragility fracture.

Table.

Average values of parameters of DXA, QCT, and biochemical markers.

Age yrs			50~59	60~69	70~79	80~
number			31	27	15	6
DXA	BMD	g/cm ²	0.82	0.76	0.68	0.60
	CSA	cm ²	8.04	8.1	8.4	8.4
QCT	cortical CSA	cm ²	2.2	1.9	1.7	1.3
	Ave. cort thick	mm	2.8	2.4	2.1	1.7
	Section modulus (Z)	cm ³	0.99	0.88	0.84	0.81
	Max. CSMI	cm ⁴	1.4	1.2	1.2	1.1
	Buckling Ratio		6.7	7.9	8.8	10.6
	BAP	μg/L	16.3	16.2	16.0	18.9
serum	TRACP-5b	mU/dL	366	352	419	571
	Osteocalcin	ng/mL	7.1	6.9	8.0	7.0
	ucOC	ng/mL	4.8	3.6	4.4	4.7
	Pentosidine	μg/mL	0.0227	0.0266	0.0235	0.0326
	Whole PTH	pg/mL	24.2	30.0	25.8	26.5
	1-25(OH) ₂ Vit D	pg/mL	55.9	66.7	60.0	67.1
	25(OH) Vit D	ng/mL	20.1	21.4	19.9	18.8
	Homocysteine	nmol/mL	7.6	7.7	7.7	11
	NTx	nmolBCE/nmol·CRE	45.0	42.4	43.5	49.9
	DPD	nmol/nmol·CRE	4.8	5.1	5.5	9.6
urine	Pentocidine	μg/mg·CRE	0.046	0.0432	0.044	0.0324

Table

Disclosures: Shigeharu Uchiyama, None.

SU0336

Ethnic Variability in Bone Geometry as Assessed by Hip Structure Analysis: Study of Women Across the Nation (SWAN). Michelle Danielson^{*1}, Thomas Beck², Yinjuan Lian¹, Kristine Ruppert¹, Gail Greendale³, Arun Karlamangla³, Jane Cauley⁴. ¹University of Pittsburgh, USA, ²Quantum Medical Metrics, LLC, USA, ³University of California, Los Angeles, USA, ⁴University of Pittsburgh Graduate School of Public Health, USA

Racial/ethnic variation in bone mineral density (BMD) does not fully account for differences in fracture rates; indeed, some racial/ethnic groups with lower areal BMD have fewer fractures. This paradox may be explained, in part, by racial/ethnic differences in femoral hip geometry. To test this hypothesis, we conducted Hip Structure Analysis (HSA) on 1942 baseline DXA scans from SWAN participants. Women were pre-/early peri-menopause, mean age 46.4 y, and none were taking hormone therapy. Racial/ethnic composition was: Caucasian (n=966), African American (n=517), Chinese (n=220) and Japanese (n=239). We assessed HSA BMD (g/cm²), cross-sectional area (CSA, cm²), outer diameter (OD, cm), section modulus (SM, cm³) and buckling ratio (BR) at the femoral narrow neck and inter-trochanter regions; neck shaft angle (NSA, °) and neck length (NL, cm) were also measured. Higher values of BMD, CSA and SM are considered protective while higher values of OD, BR, NSA and NL are deemed detrimental to fracture risk. Multiple linear regression models, adjusted for covariates including age, height, weight, menopausal status, physical activity, smoking, dietary calcium, calcium supplement use, vitamin D supplement use, daily alcohol consumption, corticosteroid use, diabetic status, arthritis and study site, were used to compare mean values of HSA measures in each racial/ethnic group to those of the Caucasian referent. NL was adjusted for height only; NSA is not body size dependent so was not adjusted for height and weight. Shown in the Table, African American women had a significantly greater HSA BMD, CSA and SM, a smaller OD and NSA, and a lower BR. Japanese women also had a significantly greater HSA BMD, CSA, and SM and a lower BR. Chinese women had a significantly lower BMD, CSA and SM and a higher BR. These results support that, compared to Caucasian women, African American and Japanese women have greater, while Chinese women have lesser, geometric hip strength, independent of their body

size. We conclude that these geometric differences may help explain the racial/ethnic differences in hip fracture rates generally observed among women. **ACKNOWLEDGEMENTS:** SWAN is supported by NIH/DHHS (NR004061, AG012505, AG012535, AG012531, AG012539, AG012546, AG012553, AG012554, and AG012495). The content of this abstract is solely the responsibility of the authors and does not necessarily represent the official views of the NIA, NINR, ORWH or the NIH.

Table: Multivariable* adjusted mean of hip structure analysis (HSA) indices by race/ethnicity

	Caucasian	African American	% Diff **	Chinese	% Diff **	Japanese	% Diff **
Narrow Neck							
BMD (g/cm ²)	0.95	1.03 [§]	+8	0.86 [§]	-9	1.13 [§]	+19
Cross-Sectional Area (cm ²)	2.68	2.88 [§]	+7	2.40 [§]	-10	3.28 [§]	+22
Outer Diameter (cm)	2.96	2.92 [§]	-1	2.93 [§]	-1	3.07 [§]	+4
Section Modulus (cm ³)	1.22	1.27 [§]	+4	1.06 [§]	-13	1.62 [§]	+33
Buckling Ratio	8.91	8.06 [§]	-10	9.93 [§]	+11	7.40 [§]	-17
Inter-trochanter							
BMD (g/cm ²)	0.93	0.98 [§]	+5	0.84 [§]	-10	1.11 [§]	+19
Cross-Sectional Area (cm ²)	4.54	4.69 [§]	+3	3.99 [§]	-12	5.63 [§]	+24
Outer Diameter (cm)	5.10	5.03 [§]	-1	4.94 [§]	-3	5.35 [§]	+5
Section Modulus (cm ³)	3.72	3.69 [§]	-1	3.13 [§]	-16	4.94 [§]	+33
Buckling Ratio	7.68	7.33 [§]	-4	8.28 [§]	+8	6.16 [§]	-19
Neck Shaft Angle (%)	131.5	130.5 [§]	-0.8	132.1	+0.5	129.4 [§]	-1.6
Neck Length (cm)	4.83	4.87	+1	4.65 [§]	-4	4.97 [§]	+3

* Adjusted for age, weight, height, menopausal status, physical activity, smoking, daily dietary calcium intake, calcium supplement, vitamin D supplement, daily alcohol consumption, corticosteroid use, diabetic status, arthritis, and study site; neck length is adjusted for height only; neck shaft angle is unadjusted; ** Percent difference vs. Caucasian; † p<0.05; ‡ p<0.001; § p<0.0001 vs. Caucasian.

Table

Disclosures: Michelle Danielson, None.

SU0337

Evaluation of a Novel Approach for Automatic Delineation of Vertebral Contours in Radiographs. Peter Mvsling¹, Kersten Peter², Mads Nielsen², Martin Lillholm³. ¹Synarc Imaging Technologies & University of Copenhagen, Denmark, ²University of Copenhagen, Denmark, ³Synarc Imaging Technologies, Denmark

Purpose: Accurate measurement of vertebral shape is important in the development of novel procedures for quantitative vertebral fracture assessment. The purpose of this work was to investigate the feasibility of a novel, computational, fully automatic approach for measurement of vertebral shape in lateral radiographs.

Methods: We evaluated the technique on a data set of 157 manually annotated radiographs of the lumbar spine. The acquired radiographs were a subset of the Prospective Epidemiological Risk Factor (PERF) study cohort, containing a combination of baseline and follow-up images of postmenopausal women. Manual annotations of the vertebrae were performed by trained, blinded radiologists for the L1-L4 vertebrae. First, the radiologists were requested to place six points corresponding to the vertebra corners and end-plate mid-points. Subsequently, the same radiologist was requested to delineate the full vertebra contour by a polygonal line of an arbitrary number of landmarks. In cases of ambiguity because of double contours, the radiologists were requested to consistently annotate the lower contour. The evaluated technique detects the vertebral outlines in a hierarchical manner, moving from a coarse estimate of the spine alignment to a detailed description of the individual vertebral shapes. The technique was based on a statistical model of the vertebral shape and appearance and centered around a sampling-based segmentation scheme. The technique was evaluated in terms of the average point-to-contour errors and the average error in estimating the posterior, medial, and anterior vertebral heights, with respect to the manual annotations of the radiologists.

Results: Our experiments showed an average point-to-contour error of 0.81 mm (+/- 0.053, SEM), which compares favourably to the current state-of-the-art. Moreover, we were able to estimate the vertebral heights with an average error of 1.36 mm (+/- 0.076, SEM) and a coefficient of variation from the ground truth annotations of 5.1%.

Conclusion: Our experiments showed that the accuracy of the evaluated technique compares favorably to the current state-of-the-art in automatic vertebra segmentation. The automatic procedure was able to estimate the vertebral heights with considerable accuracy. We believe that our technique could be relevant in vertebral fracture detection and in the development of novel, automatic osteoporosis biomarkers based on vertebral morphometry.

Disclosures: Martin Lillholm, None.

This study received funding from: Synarc

SU0338

Effect of Whole-Body Vibration on Calcaneal Quantitative Ultrasound Parameters in Osteopenic Postmenopausal Women: A Randomized Controlled Trial. Lubomira Slatkova¹, Shabbir Alibhai¹, Joseph Bevene², Queenie Wong¹, Angela Cheung¹. ¹University Health Network, Canada, ²McMaster University, Canada

Purpose: Effect of whole-body vibration (WBV) on calcaneal quantitative ultrasound (QUS) parameters has never been examined. We conducted a 12-month

randomized controlled trial with calcaneal QUS outcomes as prespecified secondary endpoints.

Methods: Postmenopausal women with primary osteopenia not on bone medications were randomized to one of three groups: 0.3g WBV at 90 Hz (90Hz, n=67), 0.3g WBV at 30 Hz (30Hz, n=68) and control (CON, n=67). Participants in 90Hz and 30Hz groups were asked to stand on a WBV platform 20 minutes a day at home and adherence was recorded by each platform. All participants were provided calcium and vitamin D supplements. QUS broadband attenuation (BUA), speed of sound (SOS) and QUS index (QUI) were obtained at the calcaneus at baseline and 12 months using a Hologic Sahara Clinical Bone Sonometer. Between-group differences in absolute 12-month change (final - baseline) in BUA, SOS and QUI were examined using one-way ANOVA with prespecified all pair-wise contrasts at p<0.05, and using intent-to-treat and per protocol approaches. Prespecified subgroups were also examined (≥80% adherent, <65 kg in mass, ≤60 years old or ≤10 years since menopause).

Results: QUS outcomes were missing or compromised in 27 participants due to drop-out (n=7), unattained final measurement (n=4), unsuccessful calibration (n=7), invalid measurement (n=7) or taking hormone therapy during study (n=2), and were thus imputed in the intent-to-treat approach but excluded from per protocol analyses (90Hz, n=58; 30Hz, n=60; CON, n=57). Median adherence to WBV ranged between 65-79% depending on definition used. After 12 months of WBV, BUA decreased in 90Hz (-0.4 dB·MHz⁻¹ / -0.2%) and 30Hz (-0.7 dB·MHz⁻¹ / -0.6%) groups and increased in controls (1.3 dB·MHz⁻¹ / 2.0%), leading to a significant between-group difference using the intent-to-treat but not per protocol approach. Pair-wise contrasts revealed significant decreases in BUA in 30Hz versus CON group using both intent-to-treat and per-protocol analyses, and in 90Hz versus CON group in the ≥80% adherent and <65 kg subgroups. Changes in SOS and QUI were similar between groups.

Conclusions: WBV produced statistically significant though clinically small decreases in calcaneal BUA in osteopenic postmenopausal women. Future studies are needed to confirm these unanticipated findings and to elucidate potential mechanisms.

Disclosures: Lubomira Slatkova, None.

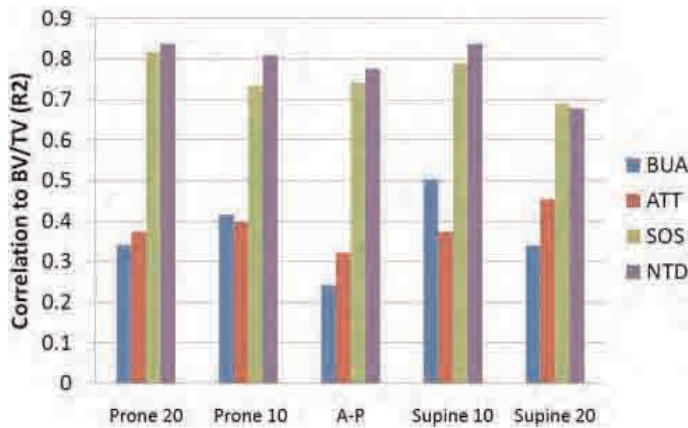
SU0339

Quantitative Ultrasound for Bone Loss at a Critical Fracture Site; the Distal Radius. Frederick Serra-Hsu¹, Jiqi Cheng², Yi-Xian Qin³. ¹State University of New York, Stony Brook, USA, ²SUNY Stony Brook, USA, ³State University of New York at Stony Brook, USA

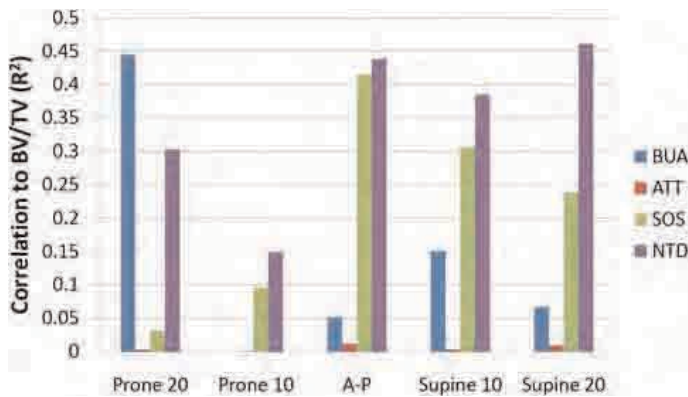
In the US, osteoporosis is responsible for nearly 1.5 million fractures annually. The most typical fracture sites are the hip, spine, wrist (distal radius) and ribs. [NOF.org, 2005] Osteoporosis is characterized by a silent painless bone loss and alteration of bone micro-architecture. Mass loss and architecture changes result in altered load distribution through bone. Quantitative ultrasound (QUS) at the calcaneus has been shown to correlate well to both fracture risk and mechanical properties. [Xia, et al 2005] This research aims to expand QUS to the distal radius, a critical fracture site. Specifically, wave propagation must be investigated to determine which QUS parameters, if any can provide the most accurate picture of bone health. Le Floch et al. in 2008 showed that 2D simulated ultrasound propagation through a slice of the distal radius can yield ultrasound parameters that are related to structural properties of the bone. Here we have taken 23 fixed cadaver distal forearms for analysis. Structural properties were obtained with a SCANCO vivaCT. Wave3000 software was used to perform 3D wave propagation simulations to obtain theoretical QUS parameters that can be correlated to internal structural parameters. Simulations were run at 5 different angles of penetration. After simulations the cadaver forearms were scanned with current scanning QUS technology at the same penetration angles, and the same ultrasound parameters were calculated. In simulations, Net-Time-Delay and Speed-Of-Sound in bone correlate very well to structural parameters such as SMI, Tb, Sp., and density estimates such as BV/TV. Despite highly linear BUA frequency bands (p<0.001), BUA only moderately correlates to bone properties. At 10 supine penetration R² values for BV/TV to NTD and BUA are 0.84 and 0.50, respectively. Simulations show NTD correlated to SMI (a trabecular layout metric) with greater than R²=0.68 across all angles. Experimental QUS shows reduced predictive capability. At 10 supine penetration R² values for BV/TV to NTD and BUA are 0.22 and 0.16, respectively. NTD remains the best predictor of structural parameters at the wrist. The current data suggest that QUS at the distal radius is subject to complex bone geometry and wave propagation schemes. The data is being investigated for additional metrics of internal structure at this clinical fracture site. Mechanical testing will provide failure loads which can be used to determine true fracture risk predictability.



Simulation Geometry and Ultrasound Propagation



Simulation QUS vs. BV/TV Results



Experimental QUS vs. BV/TV Results

Disclosures: Frederick Serra-Hsu, None.

SU0340

Ultrasonic Assessment of the Ultra-Distal Radius. Jonathan Kaufman¹, Gangming Luo¹, Xiaowei Liu², Fernando Rosete², Polly Chen³, Mafo Kamanda-Kosse², Donald McMahon², Emily Stein², Elizabeth Shane², Robert Siffert⁴. ¹CyberLogic, Inc., USA, ²Columbia University College of Physicians & Surgeons, USA, ³Columbia University, USA, ⁴The Mount Sinai School of Medicine, USA

The overall objective of this research is to develop an ultrasonic method for non-invasive assessment of the ultradistal radius (UDR). The specific objective was to examine the propagation of ultrasound through the UDR using 3D computer simulations, and to determine the relationships between bone mass and ultrasound, as well as the ability of ultrasound to discriminate between fracture and non-fracture cases. High-resolution peripheral-QCT (HR-pQCT) 3D images were obtained from a set of 110 adult female subjects that were part of a larger study on osteoporosis. Twenty-three of the subjects had experienced a UDR fracture within the past two years; the other 87 subjects served as age-matched controls. Each 3D image was used to simulate ultrasound measurements that would result from propagation through the UDR, from its posterior to its anterior surfaces. The simulation was carried out using Wave3000 (CyberLogic, Inc., New York, USA), which solves the full 3D viscoelastic wave equation using a finite difference time domain method. Bone mineral density at the UDR associated with each subject was computed from the HR-pQCT image and also determined using DXA at the UDR. An ultrasound parameter, known as the net time delay (NTD) was evaluated using the simulated measurements. NTD has been shown to be highly correlated with total bone mass in both *in vitro* and clinical studies. The *t*-test and area under the receiver operating characteristic (ROC) curve (AUC) were used to assess the ability of ultrasound to distinguish between fracture and non-fracture cases. Significant correlation was found between NTD and total bone mass (Fig. 1, $R^2=0.91$, $p<0.001$). The data also showed a statistically significant difference in ultrasound derived parameters for the fracture and non-fracture cases. In particular, the NTD ($t=3.80$) discriminated the fracture and non-fracture cases better than DXA ($t=2.95$), but not as well as the volumetric trabecular BMD as determined by HR-pQCT ($t=4.35$). However, when NTD was combined with a measure of UDR size (NTD/size), it provided the highest *t*-value of all ($t=4.60$). The AUC of the NTD/size, HR-pQCT trabecular density and DXA-UDR were 0.79, 0.78, and 0.74, respectively. On-going work involves imaging additional subjects with HR-pQCT and DXA-UDR, and obtaining clinical ultrasonic data with a new desktop device. This study suggests that bone mass and fracture risk can be assessed through ultrasonic measurement of the UDR.

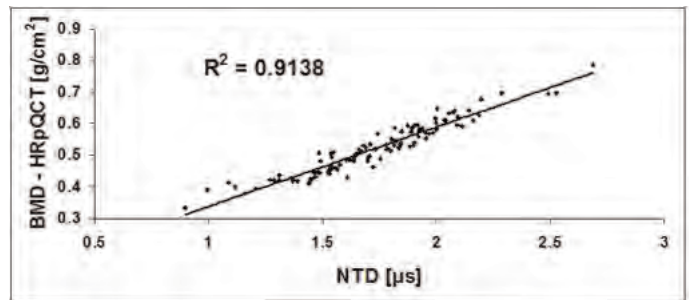


Fig. 1. BMD as determined by HR-pQCT vs. the ultrasonic NTD.

Disclosures: Jonathan Kaufman, CyberLogic, Inc., 4; CyberLogic, Inc., 3

This study received funding from: The kind support of the National Institute of Aging of the National Institutes of Health through the Small Business Innovative Research Program (Grant Number 9R44AG036879-04) is gratefully acknowledged.

SU0341

Bone Mineral Density Is Cross Sectionally Associated with Cartilage Volume in Healthy, Asymptomatic Adult Females: Geelong Osteoporosis Study. Sharon Brennan¹, Julie Pasco², Flavia Cicuttini³, Margaret Henry⁴, Mark Kotowicz⁵, Geoff Nicholson⁶, Anita Wluka⁷. ¹Department of Epidemiology & Preventive Medicine, Monash University ²Northwest Academic Centre, Department of Medicine, The University of Melbourne, Australia, ³Deakin University, Australia, ⁴Department of Epidemiology & Preventive Medicine, Monash University, Australia, ⁵School of Medicine, Deakin University, Australia, ⁶Barwon Health, Australia, ⁷Rural Clinical School Research Centre I School of Medicine I The University of Queensland, Australia, ⁷Monash University & Alfred Hospital, Australia

Purpose: The association between osteoporosis and osteoarthritis is controversial. Whilst previous studies have shown an association between bone mineral density (BMD) and cartilage volume to be positively associated, and some data exist of the relationship between local BMD and knee structures, the association between distant site-specific measures of BMD and other knee structures is unknown. The aim of this study was to determine the associations between BMD at eight skeletal sites and knee structure in asymptomatic young to middle-aged females without any clinical signs of osteoarthritis.

Methods: One hundred and sixty healthy, females (29-50yr) without symptoms of osteoarthritis underwent magnetic resonance imaging of the knee. BMD was measured at the spine, hip, total body and forearm by dual energy x-ray absorptiometry, and SoS, BUA and SI were measured at the calcaneus by quantitative ultrasound (QUS). BMD was tested for an association with cartilage volume, defects, and bone marrow lesions (BMLs).

Results: Medial cartilage volume was positively associated with BMD at the total body, femoral neck, and Ward's triangle (all $p<0.05$). Non-significant associations in the same direction existed at the spine ($p=0.07$), and trochanter ($p=0.10$). Findings in the lateral compartment were similar. The presence of medial cartilage defects showed a non-significant association with BMD at the spine ($p=0.05$). BMD was not associated with lateral cartilage defects or BMLs. No associations were observed with QUS measures at the calcaneus.

Conclusions: Whilst site-specific BMD is associated with cartilage volume at the knee in asymptomatic females aged 29-50yr, peripheral BMD measures, and QUS measures of the calcaneus, showed no associations with knee structure. These data suggest that the association between cartilage volume and axial/ lower limb BMD may relate to common local, possibly biomechanical, factors.

Disclosures: Anita Wluka, None.

SU0342

Bone Mineral Density Screening and Osteoporosis Rates in Veterans. Robert Adler¹, Joanne LaFleur², Jonathan Nebeker³, Candace Hayden³, Scott DuVall³, Thomas Ginter³. ¹McGuire VA Medical Center, USA, ²University of Utah, USA, ³VA Salt Lake City Healthcare System, USA

Background: Osteoporosis is under-recognized and under-treated in men.

Purpose: The purpose of this analysis was to characterize the prevalence of bone density (BMD) screening among veterans age 65 and older and, among screened veterans, to estimate the prevalence and incidence of osteoporosis and osteopenia.

Methods: We identified all veterans age 65 and older in the Veterans Integrated Service Network (VISN) 19, the Rocky Mountain Region of the United States, who had outpatient encounters between 1999 and 2008 using administrative datasets. The date of the first outpatient encounter identified after age 65 was defined as the index date. For identified patients, BMD screening results were captured from radiology report using natural language processing (NLP) tools.

Results: There were 80,516 veterans with outpatient encounters included in the analysis. The mean (SD) age of the cohort was 72.3 (6.4). The prevalence of BMD screenings as of baseline was 0.23%. In the follow-up period, 1,471 patients (1.8%) went on to have BMD screens over an average follow-up period of 3.43 years, corresponding to an incidence of 5.3 screenings per 1000 person-years. Among screened patients, the mean (SD) T-score was -0.67 (SD 2.63). The incidences of osteoporosis and osteopenia at any site were 11.0 and 202.0 per 1000 person-years, respectively.

Conclusions: Although BMD screening is taking place among men, the rates are low.

Disclosures: Joanne LaFleur, None.

SU0343

Epidemiologic Study on Osteoporosis in Polish Women: RAC-OST-POL. Wojciech Pluskiewicz^{*1}, Bogna Drozdowska¹, Aleksandra Czekajlo², Władysław Grzeszczak¹, Piotr Adamczyk¹. ¹Medical University of Silesia, Katowice, Poland, ²Nefrolux, Siemianowice, Poland, Poland

Purpose. The aim of epidemiologic study was to establish the prevalence of risk factors for osteoporosis and osteoporotic fractures, assess skeletal status and ten-year fracture risk and therapy used in population studied.

Method. The study was conducted in women aged over 55 y. from a district of Raciborz, Poland. In whole district was 17,500 such women and we randomly selected 10% of them. We collected data in questionnaire and BMD was measured at proximal femur using Lunar DPX (GE, USA). Skeletal status was also established using quantitative ultrasound at hand phalanges using DBM Sonic 1200 (IGEA, Italy); measured parameter Ad-SoS, m/s. Ten-year fracture risk was calculated using FRAX algorithm for US Caucasian and German population, and Garvan nomogram.

Results. 625 women were studied (35.7%). Mean age was 66.377.83 y, menopause 48.984.82 y, height 155.55.99 cm, weight 75.514.15 kg, BMI 31.235.53 kg/m². Osteoporotic fracture was reported by 176 women (28.16%), and forearm fracture was the most common (108 fractures). Paternal hip fracture was present in 47 subjects (7.52%). Other risk factors included: falls in last 12 months (324 falls in 211 women, 33.8%), secondary risk factors (n=74, 11.84%), smoking (n=70, 11.36%), rheumatoid arthritis (n=40, 6.4%), steroid use (n=30, 4.8%), alcohol use (n=4, 0.64%). Mean FN T-score was -1.260.92 and total hip T-score -0.481.19. T-score less than -2.5 for FN was in 23 women (3.72%) and for total hip T-score in 59 women (9.54%). Ad-SoS was 1951.254 m/s, T-score -3.421.09, Z-score 0.541.0. Ad-SoS correlated with FN BMD (r=0.30, p<0.0001). Ten-year fracture risk values were for any fracture for US, German, Garvan 12.086.02%, 8.416.1%, 18.113.1%, respectively. For hip fracture adequate values were: 2.444.06%, 2.484.06, 5.379.64%. Ad-SoS negatively correlated with ten-year fracture risk for any and hip fracture (r ranged from -0.145 to -0.225, p<0.0001). Antiresorptive therapy for osteoporosis (excluding HRT) was used in 97 women (15.52%), and the most commonly used was alendronate (n=42, 6.72%). 94 women reported use of calcium (15.04%), 84 vit. D (13.44%). HRT was prescribed in 135 women (21.6%).

Conclusion. In the study was presented the current status of osteoporosis epidemiology in Polish women aged over 55 y.

Disclosures: Wojciech Pluskiewicz, None.

SU0344

How Frequent Is Premenopausal Osteoporosis In Clinical Practice?. Alicia Bagur^{*}, Silvina Mastaglia, Diana Gonzalez, Candela Fernandez, Beatriz Oliveri, Carlos Mautalen, Centro de Osteopatías Médicas, Buenos Aires, Argentina

Premenopausal (preMP) osteoporosis (OP) may be idiopathic or due to diseases or treatments that affect bone mineral density (BMD). Aim: To identify the frequency and clinical characteristics of women with preMP OP in clinical practice. We reviewed the clinical records of 61 preMP women who were referred during the last 3 years for evaluation of OP or low BMD to an Institute of Metabolic Bone Diseases. Patients were either self-referred due to concern for the disease or referred from other physician mainly on the basis of a previous BMD measurement. The preMP OP represents ~0.3% of the total number of consultations for OP seen during that period. We analyzed the clinical relevant information such as personal and familiar history of fractures (Fx), BMD, biochemical bone markers, the final diagnosis and their treatments. BMD was considered normal as a Z score above -2.0 in the lumbar spine and/or total femur. Results: 23 out 61 (38%) were in the BMD osteoporotic values. In 9 out of 23 (39%) a diagnosis of idiopathic or primary (1♂) OP was made. Fourteen patients (61%) had secondary (2♂) OP due to the following diseases: pregnancy (3), celiac disease (2), hypercalciuria (2), 1♂ hyperparathyroidism (1), anorexia nervosa (1), hypothalamic amenorrhea (1), glucocorticoid (1), osteogenesis imperfecta (1), excess of T4 (1), and congenital adrenal hyperplasia (1). None of the women with 1♂ OP had Fx. Four out 14 women (29%) with 2♂ OP had Fx at the following site: wrist (2), vertebrae (1), and metatarsal (1). Five (55%) of the 1♂ OP women and 3 (21%) with 2♂ OP had a familiar history of Fx. The only differences between 1♂ and 2♂ OP were: Age was lower in 2♂ vs 1♂ OP (29.29 vs. 42.06, p<0.0001 respectively) and serum calcium was lower in 1♂ vs. 2♂ OP (9.10.3 vs. 9.50.3, p<0.03 respectively). PTH, 25OHD, CTX and BAP were similar in both groups. The 1♂ OP patients received the following treatments: Calcium and vitamin D (Ca+D) (6), bisphosphonate (B) (2), without treatment (1). Secondary OP patients received: Ca+D and

treatment according to the underlying disease. The PreMP visits represent ~0.3% of the total number of consultations for OP in our Center. Less than a half of preMP women who consult to evaluate their BMD have OP and ~40% of them are idiopathic. In the remaining 60% 2♂ OP was recognized. It is therefore important to rule out diseases and drugs that can affect BMD in these young women.

Disclosures: Alicia Bagur, None.

SU0345

Occurrence of Falls in Elderly People in Brazil, There Is Something that Health Professionals Can do to Avoid?. Thais Braga, Roberto Queiroz, Fabiana Fonseca^{*}, Bianca Segantin, Manuela Santos, Ursula Karsch, Ana Elisa Segantin. PUC - SP, Brazil

According to a study conducted by the health department of the state of Sao Paulo between 2000 and 2008 rose from 7,600 to 28,400 the number of deaths per year in the elderly due to falls. This field study aimed to describe the occurrence of falls during the 01 years before the current fracture, in 40 elderly patients aged from 60 years in 2010 in the pre-operative femur surgery at the Hospital Server Public State of Sao Paulo. 77% of seniors reported that they often fell, and 32% of this group of elderly people suffered fractures different from today, over 05 years. Suggest specific and complex tests for balance and posture. Identify the possibility of falling is the duty of the health professional in order to have effectiveness in preventing falls and even decreased mortality of elderly individuals and our duty to the possible improvement of the quality of the biopsychosocial and elderly community.

Disclosures: Fabiana Fonseca, None.

SU0346

Sclerostin is Associated with Age, BMI and Bone Mineral Content, but not Gender or Physical Activity in Healthy Adults. Karin Amrein^{*1}, Astrid Fahrleitner-Pammer², Steven Amrein³, Camilla Drexler⁴, Hans Dimai², Thomas R. Pieber⁵, Andreas Tomaschitz⁵, Harald Dobnig⁶. ¹Medical University of Graz, Austria, ²Medical University Graz, Austria, ³Medical University of Graz, Austria, Department of Anaesthesiology & Intensive Care Medicine, Austria, ⁴Medical University of Graz, Austria, University Clinic of Blood Group Serology & Transfusion Medicine, Austria, ⁵Medical University of Graz, Austria, Division of Endocrinology & Metabolism, Department of Internal Medicine, Austria, ⁶Diagnostikinstitut Univ.Prof.Dr.H.Dobnig GmbH, Aut

Introduction

Sclerostin is produced by osteocytes and potently inhibits bone formation through the Wnt/Ö-catenin signalling pathway. While the potential of sclerostin inhibition with a monoclonal antibody (Scl-Ab) is currently under investigation, limited data is available on the association of circulating sclerostin levels with important clinical parameters such as age, gender and bone mineral density (BMD) in humans.

Objective

We aimed to evaluate the gender specific distribution of circulating sclerostin levels and its correlation to age, BMD and physical activity (PA) in healthy adult men and premenopausal women with normal renal function.

Methods

In 161 healthy adults (21% premenopausal women) aged 19 to 64 years, serum sclerostin levels were measured with a quantitative sandwich enzyme-linked immunosorbent assay (Biomedica, Vienna, Austria). Body composition and BMD were measured by DXA (GE Lunar) and physical activity was assessed by a standardized questionnaire.

Results

The mean serum sclerostin level was 47.1 17.8 pmol/L (range 17.8 to 114.4). As shown in Figure 1A and 1B, there was a positive correlation between age and sclerostin in both men (r=0.37; p<0.001) and premenopausal women (r=0.66; p<0.001). Men had significantly higher sclerostin levels than women (49.8 17.6 vs. 37.2 15.2 pmol/L, p < 0.001), however, after adjustment for age and bone mineral content the difference of sclerostin levels did not reach statistical significance (47.3 in men vs. 46.4 pmol/L in women, p=0.817). Overall, we did not find a relevant association between the degree of physical activity and sclerostin levels. Partial correlation analysis revealed a significant positive correlation between sclerostin levels and bone mineral content (BMC), BMD at the lumbar spine and the left hip and body mass index (age and gender adjusted correlation coefficients 0.235, 0.215, 0.266 and 0.228 respectively), but not between sclerostin levels and estimated glomerular filtration rate.

Conclusion

Our data demonstrate that there is a significant relationship of serum sclerostin levels with age, BMI and BMD. Surprisingly however, no significant association between sclerostin and gender or PA was seen in this healthy population. Further studies are needed to confirm our findings and to evaluate whether circulating sclerostin levels accurately reflect sclerostin activity on tissue level.

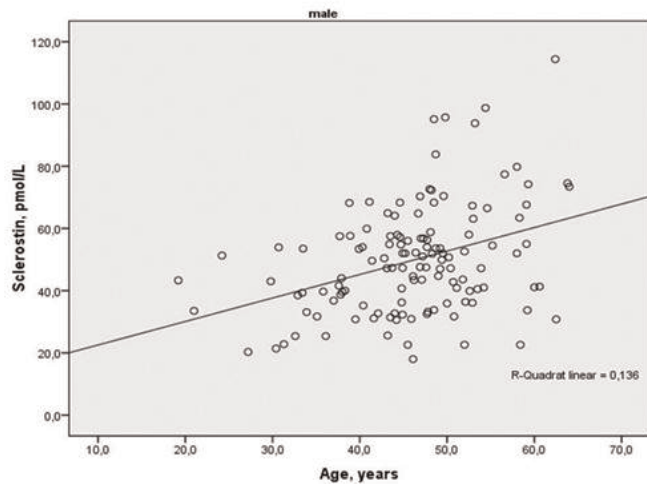


Figure 1A

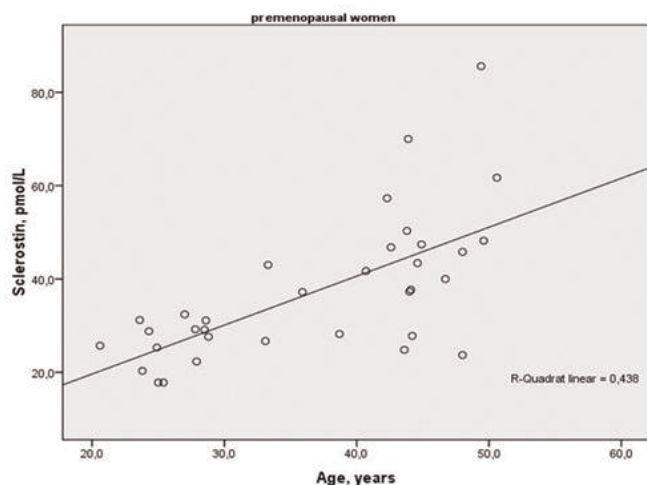


Figure 1B

Disclosures: Karin Amrein, None.

SU0347

The Relationship Between Inflammatory Bowel Disease and Bone Mineral Density. Results of a Population-Based Study. Laura Targownik*, Zoann Nugent, Charles Bernstein, William Leslie. University of Manitoba, Canada

Introduction: Patients with inflammatory bowel disease (IBD) are at higher risk of osteoporosis and related fractures. Most studies on IBD and BMD are from selected referral centres and do not delineate what aspects of IBD contribute to lower BMD

Methods: We created a linkage between the University of Manitoba IBD Epidemiologic Database, and the Manitoba BMD Database, which respectively capture virtually all persons in Manitoba, Canada, with diagnosed IBD and all persons with clinical DXA measurements, respectively. BMD was assessed at each of the lumbar spine (L1-L4), total hip, femoral neck, and greater trochanter. Multivariate linear and logistic regression were performed to determine the independent effect of an IBD diagnosis on T-scores and on the likelihood of having an osteoporotic T-score (-2.5 or lower) at each of the four BMD sites. We developed both a partially adjusted model (for age, sex, and body mass index [BMI]) and fully adjusted model (additionally adjusted for hormone replacement therapy [HRT], osteoprotective therapy [OTX], and recent systemic glucocorticoid [GC] use).

Results: 45714 patients age 20 and older underwent baseline BMD testing between 1997 and 2008, 1230 of whom had IBD. Compared with non-IBD subjects, subjects with IBD were more likely to be younger, male, and have lower BMI. IBD patients were significantly more likely to be recent GC users (26% vs 6%). When adjusted for age, sex, and BMI, IBD was associated with lower T-scores at each of the four assessment sites (Table 1). IBD was also associated with having an osteoporotic T-score at the L1-L4 and the total hip (Table 1). However, when the model was further adjusted for exposure to GCs, HRT, and OTX, IBD was associated with only a marginal reduction in T-scores at the total and the greater trochanter. Moreover, IBD

was not associated with a higher risk of having an osteoporotic T-score at any of the four sites in the fully adjusted model.

Conclusion: While patients with IBD are at higher risk for lower BMD and for osteoporosis, this effect is not seen after adjusting for exposure to GCs and other medications. This suggests that the deleterious effects of IBD on BMD are predominantly related to GCs rather than to the IBD itself. Further work is required to delineate the independent effects of IBD, inflammatory activity, and its therapies on BMD and fracture risk.

Table 1: Relationship between IBD and T-scores at Anatomic Sites of BMD Evaluation

BMD Evaluation Site	Partially Adjusted Model			Fully Adjusted Model		
	Predicted Change in T-score due to IBD	Lower Limit 95% CI	Upper Limit 95% CI	Predicted Change in T-score due to IBD	Lower Limit 95% CI	Upper Limit 95% CI
L1-L4	-0.15	-0.23	-0.07	-0.05	-0.13	0.03
Femoral Neck	-0.12	-0.18	-0.08	-0.05	-0.10	0.00
Total Hip	-0.20	-0.26	-0.14	-0.08	-0.14	-0.02
Greater Trochanter	-0.21	-0.28	-0.16	-0.10	-0.16	0.04

*Partially adjusted model: adjusted for age, sex, BMI

Fully adjusted model: adjusted for age, sex, BMI, hormone replacement therapy, osteoprotective medications, and corticosteroids.

Table 2: Association between IBD and Osteoporosis (T-score <-2.5) at Anatomic Sites of BMD Evaluation

BMD Evaluation Site	Partially Adjusted Model			Fully Adjusted Model		
	Odds Ratio	Lower Limit 95% CI	Upper Limit 95% CI	Odds Ratio	Lower Limit 95% CI	Upper Limit 95% CI
L1-L4	1.23	1.03	1.47	1.17	0.97	1.40
Femoral Neck	1.17	0.93	1.48	0.99	0.78	1.25
Total Hip	1.52	1.24	1.85	1.16	0.95	1.42
Greater Trochanter	1.30	0.997	1.69	1.02	0.78	1.33

*Partially adjusted model: adjusted for age, sex, BMI

Fully adjusted model: adjusted for age, sex, BMI, hormone replacement therapy, osteoprotective medications, and corticosteroids.

Disclosures: Laura Targownik, None.

SU0348

What Is The Value of Laboratory Testing to Identify Possible Secondary Contributors to Osteoporosis in Older Men? Howard Fink^{*1}, Stephanie Litwack-Harrison², Kristine Ensrud³, Eric Orwoll⁴, Douglas Bauer⁵.

¹GRECC, Minneapolis VA Medical Center, USA, ²San Francisco Coordinating Center, California Pacific Medical Center, USA, ³Minneapolis VA Medical Center / University of Minnesota, USA, ⁴Oregon Health & Science University, USA, ⁵University of California, San Francisco, USA

The value of laboratory testing to identify possible secondary conditions in osteoporotic (OP) men is unknown.

Cross-sectional analyses were performed using baseline data from the MrOS study, a prospective cohort of 5,994 community-dwelling men age ≥ 65 years. Men were defined as having OP by DXA BMD T-score of ≤ -2.5 at total hip, femoral neck, or lumbar spine. Laboratory data were available from 1571 men selected randomly from the cohort. Possible secondary conditions evaluated were low testosterone (total T < 250 ng/dl), vitamin D deficiency (25-OH-D < 20 ng/ml), renal insufficiency (estimated GFR [eGFR] < 60 ml/min/1.73m²), hypercalciuria (urine calcium/creatinine ratio > 0.14), hypothyroidism (TSH > 4.5 mU/L), hyperthyroidism (TSH < 0.5 mU/L), low estradiol (total E ≤ 16 pg/ml), and hyperparathyroidism (intact PTH > 66 pg/ml). Prevalence of each laboratory abnormality was calculated in OP and non-OP groups. Age and weight-adjusted risk (aOR) of each laboratory abnormality as a function of OP status was estimated using logistic regression, overall and in analyses stratified by median age (< 73 vs. ≥ 73 yr) and weight (< 82.6 vs. ≥ 82.6 kg), and by Z-score (< -2.0 vs. ≥ -2.0).

Within the random cohort, 163 men (10.4%) had OP. In these OP men, prevalence of possible secondary conditions varied widely by condition (Table). 64.9% of OP men had at least one laboratory abnormality and 27.6% had multiple abnormalities. However, only vitamin D deficiency (aOR 1.5, 95%CI 1.02-2.1) and low estradiol (aOR 1.8, 95%CI 1.3-2.7) were significantly more common in the OP men. OP men with lower weight also were significantly more likely to have low T (aOR 2.0, 95%CI 1.1-3.7). Only 10 men had a Z-score < -2.0 .

Laboratory testing older OP men identified many abnormalities, but few of these lab abnormalities were significantly more prevalent than in non-OP men. Testing yield may be higher in lower weight men. To further assess the value of laboratory testing in OP men, future studies will need to evaluate whether treatment of possible secondary conditions in OP men reduces fractures, and whether effects of OP treatments differ between men with secondary factors versus those without them.

Table II: Age, Height and Bone Mineral density at proximal femur in women.

	OP %	Non-OP %	aOR (95%CI)
Low T	15.2	13.6	1.5 (0.9-2.3)
Vitamin D deficient	30.7	24.8	1.5 (1.02-2.1)
eGFR < 60	17.1	17.9	0.8 (0.5-1.4)
Hypercalciuria	17.3	12.5	1.5 (0.9-2.3)
Hypothyroid	11.7	9.5	1.2 (0.7-2.0)
Hyperthyroid	2.5	2.0	1.4 (0.5-4.0)
Low E	28.9	18.2	1.8 (1.3-2.7)
Hyperparathyroid	6.2	3.4	1.9 (0.9-4.0)

Disclosures: Howard Fink, None.

SU0349

Bone Mineral Density was Similar in Spanish Medieval Women and Higher in Medieval Men Compared to Actual Spanish Population. Belen Lopez¹, Carlos Gomez^{2*}, Pablo Manrique¹, Ana Gomez¹, Serafin Costilla³, Jorge Cannata Andia⁴. ¹Physical Anthropology, Department of Biology of Organisms & Systems, University of Oviedo, Spain, ²Hospital Universitario Central de Asturias, Spain, ³Department of Radiology, Hospital Universitario Central de Asturias University of Oviedo., Spain, ⁴Hospital Universitario Central de Asturias, Spain

Life span, lifestyle and survival to chronic diseases explain the epidemiology of osteoporosis in the last years. On the other hand bone mass is strongly linked to population genetic load.

Purpose: The aim of the study was to assess the possible differences in bone mineral density between a medieval population and the current Spanish population, both from the northern Spain.

Methods: The medieval skeletons came from the excavation of a cemetery in San Andres del Arroyo (Palencia, Spain) dated on 11th -12th century. From the 98 exhumed people we selected those subjects with 20 years-old or more. We also excluded those with impaired both femora (n = 5) or those with radiological presence of sand inside the bone (n = 4). Age, sex and height of the medieval sample were assessed using standard archaeological methods. For each one of the 37 people finally selected, we randomly chose two age and sex matched controls from our normative database (participants in the Spanish Normative Bone Mineral Density Study). Bone mineral density (BMD) was performed at proximal femur with the same DXA device (Hologic QDR-1000) according to the International Society of Clinical Densitometry rules. Isolated femora were placed in a box with 25 cm height of wheat flour to facilitate their placement and provide a similar soft tissue density around.

Results: Medieval male population had a significant lower height than current controls. Nevertheless BMD values trend to be higher with significant differences in trochanter and total hip (Table I). Medieval female population had also a significant lower height than their current controls (with a more relative difference than in males) but they had a similar BMD at all three regions of interest (Table II). The distribution according to the BMD categories using the WHO classification was similar in both populations. Fractures were present in four medieval men (2 clavicle, 1 vertebra and 1 fibula) and in two medieval women (1 clavicle and 1 vertebra) with no relationship with low BMD. One of the medieval women had bone deformities and histological evidence of osteomalacia.

Conclusions: Bone mineral density is similar in our contemporary women with regards ancestor medieval female population, whereas in males our medieval ancestors had a higher BMD. Perhaps, it could be explained by a more intense physical activity in medieval population and a higher reproductive effort (pregnancy and lactation) in the case of medieval women.

Table II: Age, Height and Bone Mineral density at proximal femur in women.

	Women		
	Medieval (n=13)	Controls (n=26)	P value
Age (years)	45,1 ± 11,1	45,3 ± 11,2	
Height (cm)	151,96 ± 5,95	159,16 ± 7,07	,004
Femoral neck (g/cm2)	0,781 ± 0,099	0,812 ± 0,108	,395
Trochanter (g/cm2)	0,732 ± 0,127	0,672 ± 0,089	,102
Intertrochanter (g/cm2)	1,051 ± 0,157	1,060 ± 0,125	,857
Total hip (g/cm2)	0,913 ± 0,125	0,902 ± 0,106	,781

Table I

	Women		
	Medieval (n=13)	Controls (n=26)	P value
Age (years)	45,1 ± 11,1	45,3 ± 11,2	
Height (cm)	151,96 ± 5,95	159,16 ± 7,07	,004
Femoral neck (g/cm2)	0,781 ± 0,099	0,812 ± 0,108	,395
Trochanter (g/cm2)	0,732 ± 0,127	0,672 ± 0,089	,102
Intertrochanter (g/cm2)	1,051 ± 0,157	1,060 ± 0,125	,857
Total hip (g/cm2)	0,913 ± 0,125	0,902 ± 0,106	,781

Table II

Disclosures: Carlos Gomez, None.

SU0350

Calcium and Vitamin D intakes in Canadian Youth Ages 16-24 years: the Canadian Multicentre Osteoporosis Study (CaMos). Wei Zhou^{1*}, Lisa Langsetmo², Claudie Berger³, Suzette Poliquin³, David Goltzman¹, Stephanie Kaiser⁴, Jerilyn Prior⁵, Robert Josse⁶, Tanveer Towheed⁷, Tassos Anastasiadis⁷, K. Shawn Davison⁸, Christopher Kovacs⁹, Manny Papadimitropoulos¹⁰, Nancy Kreiger¹¹. ¹McGill University Health Centre, Canada, ²Canadian Multicentre Osteoporosis Study, Canada, ³McGill University, Canada, ⁴Dalhousie University, Canada, ⁵University of British Columbia, Canada, ⁶St. Michael's Hospital, University of Toronto, Canada, ⁷Queen's University, Canada, ⁸Laval University, Canada, ⁹Memorial University of Newfoundland, Canada, ¹⁰Eli Lilly Canada Inc., Canada, ¹¹University of Toronto, Canada

Calcium and vitamin D are nutrients essential for overall health, optimal bone mass, and prevention of osteoporosis and fractures in adulthood. Our objective was to estimate calcium and vitamin D intake among Canadian youth. CaMos recruited 1001 participants ages 16-24, randomly selected from within a 50 km radius of 9 cities across Canada in 2004-2006. A short interviewer-administered semi-quantitative food frequency questionnaire was given at baseline and Year 2 (2006-2008). Calcium intake from both diet and supplements, and vitamin D intake from milk and beverage fortification as well as supplements, were estimated cross-sectionally and longitudinally. Estimates of mean daily intakes for calcium and vitamin D were stratified by sex and age (16-18 years, 19-24 years). The study sample included 487 women and 458 men at baseline, and 396 women and 347 men at Year 2. The mean (standard error (SE)) daily intakes for calcium were 1077 (28) mg for women and 1361 (38) mg for men at baseline, and were 1083 (33) and 1276 (45) mg for women and men respectively at Year 2. For vitamin D, mean (SE) daily intakes were 4.0 (0.2) µg and 6.1 (0.3) µg for women and men respectively at baseline, and were 5.1 (0.3) and 6.6 (0.3) µg at Year 2. Participants reported no vitamin D supplement intake at baseline. Detailed baseline intake by age and sex is shown in Table 1, along with comparison to 2010 IOM dietary reference intakes. Median calcium intakes were above the estimated average requirement (EAR) in men and in women in the younger age group but not in women in the older group. Median intakes of vitamin D were well below the EAR. The resulting prevalence of youth below the EAR ranges from 29% to 47% for calcium, and 71% to 95% for vitamin D. The change of calcium intake in these groups over two years was only different from zero in the younger age group of women, in which calcium intake decreased by 184 (95% confidence interval (CI): 67, 301) mg/day. The mean changes of daily vitamin D intakes were 1.6 (95% CI: 0.7, 2.4) µg in the older group of women and 1.0 (95% CI: 0.2, 1.8) µg in the older group of men; but were not different than zero in the younger group in either sex. We observed a high prevalence of Canadian youth that did not meet the EAR established for calcium and vitamin D in the recent IOM report. Adoption of the new guidelines would have policy implications, as the goal would be to increase intake among those not currently meeting the EAR.

Age (years)	N	Calcium (mg/day) ^b			Vitamin D (µg/day) ^c		
		Mean (SE)	Median (IQR)	Above EAR ^a % (SE)	Mean (SE)	Median (IQR)	Above EAR % (SE)
Women							
16-18	200	1186 (49)	1051 (705, 1526)	53 (3.5)	4.8 (0.3)	3.8 (1.4, 7.5)	13 (2.4)
19-24	287	1002 (33)	924 (593, 1350)	57 (2.9)	3.4 (0.2)	2.8 (0.9, 5.0)	5 (1.2)
Men							
16-18	195	1484 (63)	1345 (796, 1954)	66 (3.4)	7.2 (0.4)	6.3 (2.6, 10.0)	29 (3.2)
19-24	263	1269 (47)	1116 (712, 1628)	71 (2.8)	5.3 (0.3)	4.1 (1.4, 7.6)	18 (2.4)

^a EAR: Estimated Average Requirement, RDA: Recommended Dietary Allowance

^b EAR for calcium for women and men: age 14-18, 1100 (mg/day); age 19-30, 800 (mg/day); RDA for calcium for women and men: age 14-18, 1300 (mg/day); age 19-30, 1000 (mg/day)

^c EAR for vitamin D for women and men: age 14-30, 10 (µg/day); RDA for vitamin D for women and men: age 14-30, 15 (µg/day)

Table 1. Calcium and Vitamin D Intake by Gender and Age Group - Baseline

Disclosures: Wei Zhou, None.

SU0351

Dairy Calcium Intake Accompanied with Higher Intake of Vitamin D Could Efficiently Decrease Body Fat Mass and Increase Lean Mass without Decreasing BMD During Moderate Weight Loss in Normal Weight Young Japanese Women. Takako Hirota^{*1}, Izumi Kawasaki², Kenji Hirota³. ¹Kyoto Koka Women's University, Japan, ²Tsui Academy of Nutrition, Japan, ³Hanwa Sumiyoshi General Hospital, Japan

This study investigated whether intake of dairy calcium or vitamin D affected changes in body fat, lean mass, and bone mineral density (BMD) during weight reduction in normal weight young women.

One hundred female students (ages; 23-25 years, BMI; 21.5-23.3 kg/m², calcium intake; 4741.96 mg/d) who wanted to lose weight were randomly assigned either to drink milk (>200 ml/d; milk group, n=52) before dinner or were given no instructions on milk intake (control, n=48). All were advised to consume a moderately energy-restricted diet and to increase physical activity for 4 months. Their energy intake decrease (-2203.97 kcal/d) and the duration of physical activity were similar between the groups. All were asked to keep a diary of body weight, dairy intake, and physical activity. Baseline milk intake was 1161.15 ml/d. Body fat, lean mass, and BMD by DXA, blood pressure, and serum lipid profiles were measured at baseline and after 4 months.

Moderate energy restriction for 4 months resulted in significant decreases in weight (-0.91.8 kg), L2-L4 BMD, waist and hip circumferences, and blood pressure to the same extent in both the milk and control groups. Serum lipid profiles did not change in either group. Baseline calcium intakes were not associated with body weight, fat, or lean mass. However, body fat mass in the milk group was significantly decreased (-1.242.64 kg cf. -0.363.04 kg in the control group) and the body lean mass was increased (+0.272.03 kg cf. -0.452.62 kg) after intervention. Higher tertiles of milk intake were associated with increased fat mass loss (-0.48, -0.74, and -2.40 kg; p<0.05) and associated with increased lean mass gain (-0.10, -0.08, and +0.95 kg). Higher intake of vitamin D (>200 IU/d; median) increased the additional changes in the highest tertile of milk intake, although vitamin D levels did not affect the control group. The gain in lean mass was strongly correlated with a decrease in fat mass (r=-0.78), and an even stronger correlation (r=-0.85) was observed in the subjects with higher intake of vitamin D. Changes in lean mass were correlated with changes in L2-L4 BMD (p=0.05). The highest quartile of lean mass gain in the milk group did not decrease in L2-L4 BMD.

Intake of higher dairy calcium together with higher vitamin D is recommended to decrease body fat mass and to increase lean body mass without decreasing BMD during weight loss, to help prevent metabolic syndromes and osteoporosis.

Disclosures: Takako Hirota, None.

SU0352

Red Blood Cell n-3 and n-6 Fatty Acid Concentrations as Predictors of Inflammatory Markers in The Women's Health Initiative. Steven Ing^{*1}, Tonya Orchard¹, Andrea Lacroix², Charles Kooperberg², Aaron Aragaki², Martha Belury¹, Bo Lu¹, Rebecca Jackson¹. ¹The Ohio State University, USA, ²Fred Hutchinson Cancer Research Center, USA

Background: Inflammatory biomarkers, tumor necrosis factor-α soluble receptor (TNFα-sR) 1 and 2 are positively associated with incident total fracture. Diets high in n-3 polyunsaturated fatty acids (PUFA) may shift the balance of eicosanoid

production leading to decreased inflammation and bone turnover, thereby contributing to lower fracture risk.

Methods: A nested case-control study from the Women's Health Initiative Clinical Trial and Observational Study of hip fracture cases and matched controls (293 pairs matched on age, race, self reported or randomization to hormone therapy, and latitude). Baseline serum TNFα-sR1, TNFα-sR2 concentrations were previously measured and comprise the outcome variables of this study. We measured predictor variables - red blood cell (RBC) concentrations of total n-3, eicosapentaenoic acid (EPA), docosahexaenoic acid (DHA), and alpha linolenic acid (ALA) using gas chromatography in frozen samples obtained at the baseline screening visit. The relationship between predictor and outcome variables was analyzed using a linear mixed model accounting for the paired design.

Results: In 586 cases and controls, TNFα-sR1 (n=271), TNFα-sR2 (n=271) and RBC fatty acid levels (n=208) were available for analysis, in part due to degradation leaving a final sample size of 208. Total n-3 PUFA by tertiles was negatively associated with TNFα-sR1 (p=0.0004) and TNFα-sR2 (p=0.0003). EPA+DHA, but not ALA, was negatively associated with TNFα-sR1 (p=0.0002) and TNFα-sR2 (p=0.0002).

Conclusion: Higher dietary fatty acid intakes of total n-3 PUFA and EPA+DHA are associated with decreased inflammatory markers in postmenopausal women and may modulate hip fracture risk.

Table: Inflammatory markers by fatty acids

RBC Fatty Acid	TNFα-sR1 ¹		TNFα-sR2	
	Mean (SE) ²	p ³	Mean (SE)	p
Total n-3		0.0004		0.0003
T1	1790 (66)		3448 (89)	
T2	1598 (67)		3228 (90)	
T3	1444 (60)		2970 (81)	
ALA		0.7932		0.6541
T1	1606 (72)		3234 (98)	
T2	1562 (66)		3196 (89)	
T3	1627 (64)		3175 (86)	
EPA+DHA		0.0002		0.0002
T1	1794 (64)		3483 (86)	
T2	1595 (70)		3140 (94)	
T3	1428 (61)		2991 (82)	

¹ TNFα-sR1, tumor necrosis factor alpha soluble receptor 1; TNFα-sR2, tumor necrosis factor alpha soluble receptor 2; n=208

² pg/ml; SE, standard error

³ p-values are from tests for linear trend.

Table: Inflammatory markers by fatty acids

Disclosures: Steven Ing, None.

SU0353

Reduced T and Z Scores at the Femoral Neck and Lumbar Spine Are Associated With Increased Dietary Protein Intakes In UK Dwelling South Asian and Caucasian Postmenopausal Women. Andrea Darling^{*}, Kathryn Hart, Susan Lanham-New. University of Surrey, United Kingdom

There is a long standing controversy as to whether dietary protein is beneficial or detrimental to bone health. Dietary protein has known anabolic effects on bone via hormones (e.g.IGF1) and may increase dietary calcium absorption¹. However, high dietary protein intake may also increase physiological acid load and thus may increase urinary excretion of calcium and bone resorption². In Autumn 2006, n=38 postmenopausal South Asian (mean age 58+/-4 years) and n=138 postmenopausal Caucasian women (mean age 61+/-4.5 years) took part in the D-FINES study. A Dual X-ray Absorptiometry (DXA) scan (Hologic) was undertaken as well as completion of 4 day diet diaries. Relevant anthropometric and lifestyle information and serum 25 (OH)D were also obtained. Partial correlations were run using PASW 18.0 to examine associations between protein intake (adjusted per Kg body weight) and T and Z score bone indices. For the fully adjusted model (model 2), in both ethnic groups there was a significant (p<0.05) negative correlation between protein intake and T scores at the femoral neck (T-FN) and lumbar spine (T-LS), although in Caucasians this was only of borderline statistical significance. Also, for both groups a significant negative association between protein intake and Z scores at the femoral neck (Z-FN) and lumbar spine (Z-LS) was found. In comparison, model 1 shows the data that was not adjusted for micronutrients, which was only statistically significant in Asian for Z-FN and Caucasians for T-FN and Z-FN. There was no significant difference (p>0.05) in protein intake per Kg between the Asian and Caucasian groups (Asian mean= 0.98g/Kg body weight, sd=0.37) (Caucasian mean=1.07g/Kg body weight, sd=0.27). This negative relationship is very surprising considering most epidemiological studies and a recent meta-analysis³ have shown a positive association between dietary protein and bone health. Also, controlling for dietary vitamin C, Na, K, P and Mg (model 2) actually strengthened the association, not weakened it. Overall the strong negative association between dietary protein and bone indices found here in this group of older Asian and Caucasian women was unexpected and has not been examined before in the literature.

1Kerstetter JE, O'Brien KO, Insogna KL (1998) Am J Clin Nutr 68, 859-865.
2Kerstetter JE, Mitnick ME, Gundberg MC et al (1999) J Clin Endocrinol Metab 84, 1052-1055. 3Darling AL, Millward DJ, Torgerson DJ et al (2009) Am J Clin Nutr 90, 1674-1692.

	Model 1*				Model 2**			
Asian n=21	T-FN	Z-FN	T-LS	Z-LS	T-FN	Z-FN	T-LS	Z-LS
r	-0.48	-0.54	-0.36	-0.41	-0.815	-0.863	-0.728	-0.788
p	0.07	0.04	0.19	0.13	<0.01	<0.01	0.02	<0.01
Caucasian n=123	T-FN	Z-FN	T-LS	Z-LS	T-FN	Z-FN	T-LS	Z-LS
r	-0.21	-0.21	-0.10	-0.16	-0.26	-0.26	-0.19	-0.26
p	0.03	0.03	0.29	0.11	0.01	0.01	0.06	0.01

*Model 1-controlling for log age, log deprivation index, log physical activity, height, dietary Ca, log 25(OH)D status and energy intake; **Model 2-controlling for log age, log deprivation index, log physical activity, height, dietary Ca, log 25(OH)D status, energy intake, log dietary vitamin C, log dietary Na, log dietary K, dietary P and Mg

Partial correlations between protein intake (per Kg body weight) and T and Z scores

Disclosures: Andrea Darling, None.

SU0354

Dietary Vitamin D Intake and the Risk of Fracture and Osteoporosis. Greta Snellman¹, Eva Warensjö-Lemming², Liisa Byberg², Karl Michaelsson².

¹Department of surgical sciences, Uppsala University, Sweden, ²Uppsala Clinical Research Center, Sweden

Background: Vitamin D is important for optimal calcium absorption. Since calcium is needed for mineralization of bone, vitamin D insufficiency may lead to osteoporosis and fracture. Whilst supplemental vitamin D can decrease the risk of fracture among old frail women, less is known about the benefit of dietary vitamin D intake in community-dwelling women.

Method: 61,433 women, in the population-based Swedish Mammography Cohort were followed for 19 years. All fractures were identified from registry data. In a sub-cohort of 5,022 women, Swedish Mammography Cohort Clinical, osteoporosis was diagnosed by Dual-Energy-X-ray-Absorptiometry. Diet and supplemental vitamin use was assessed by repeated food-frequency-questionnaires. Associations between vitamin D intake, fracture and osteoporosis were determined.

Results: Mean age of the women at study start was 54 years (range 38-76). Mean vitamin D intake was 4.4 µg (SD 1.3). During follow-up, 14,738 women experienced any type of first fracture, and 3,871 of these were hip fractures. Twenty percent of the women in the subcohort were classified as osteoporotic. The multivariable-adjusted hazard ratio (HR) and 95% confidence interval (CI) for any first fracture were 1.06 (1.01-1.12) for the lowest (median intake 2.8 µg) and 1.07 (1.02-1.13) for highest quintile (median intake 6.3 µg) compared to the third quintile, that was set as a reference. The corresponding values for a first hip fracture were 1.05 (0.94-1.16) and 1.04 (0.94-1.15). The odds ratios for osteoporosis within lowest and highest quintiles of vitamin D intake was 1.03 (0.77-1.38) and 1.01 (0.81-1.27), respectively. Conclusions: We conclude that the dietary intake of vitamin D is of minor importance for the risk of osteoporosis and osteoporotic fractures in Swedish middle aged and elderly women.

Figure legend: Multivariable adjusted spline curve for the association between dietary vitamin D intake and risk of any type of first time fracture.

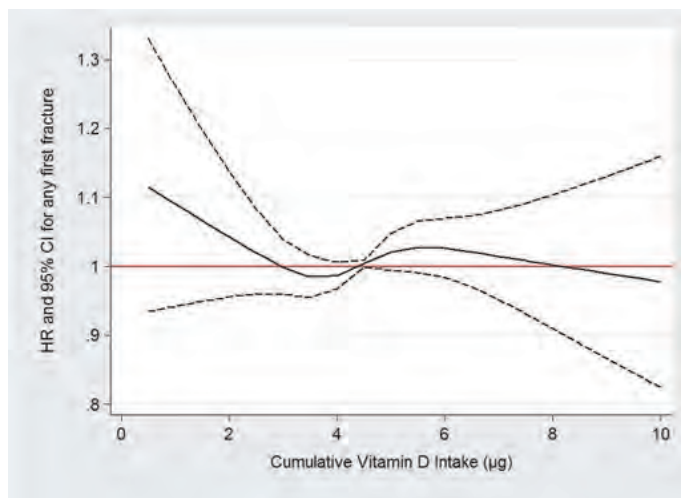


Figure 1

Disclosures: Greta Snellman, None.

SU0355

Final Results from a Population-Based Post-Fracture Intervention Based Upon Administrative Health Data: A Randomized Controlled Trial. William Leslie¹, Lisa Labine², Darlene Drelich², Penny Klassen², Patricia Caetano². ¹University of Manitoba, Canada, ²Manitoba Health, Canada

Post-fracture care is suboptimal and strategies to address this major "care gap" are urgently required. Case management is effective but is resource-intensive and difficult to deliver to a widely scattered population. HYPOTHESIS: Post-fracture mail notification to physicians and/or patients will lead to improved osteoporosis care. METHODS: An RCT (NCT00594789) was conducted across the Province of Manitoba, Canada, from June 2008 to May 2010, in which men and women age 50 or older with recently reported fracture (hip, spine, humerus, and forearm) from medical claims data, and without recent BMD testing (three years) or osteoporosis therapy (last year), were randomized to three groups: Group 1 (control) received usual care; Group 2 (MD only) had mailed notification to the reporting and primary care physicians (alert letter, BMD requisition, management flow chart); Group 3 (MD & Patient) had physician notifications and patient notification (alert letter). BMD testing and/or osteoporosis medication initiation to 12m was documented from population-based data sources. RESULTS: 5,349 fracture patients meeting the inclusion criteria were randomized. Group 1 (usual care) interventions at 12m were 15.3% in women and 6.6% in men (combined 12.3%). There was a significant improvement (P<.001) in all outcome measures for groups 2 (MD only) and 3 (MD & Patient), with no significant differences between Groups 2 and 3 (i.e., no additive benefit from patient notification). At 12m the absolute improvement in interventions for women and men combined was 13.9% (Group 2) and 14.9% (Group 3), with Number Needed to Notify=7. The adjusted odds ratio (aOR) for either intervention in Group 2 was 2.6 (95% CI 2.2-3.1) and in Group 3 was 2.8 (95% CI 2.3-3.3; P=0.409 for Group 2 vs 3). In addition to randomized group, factors associated with treatment initiation included sex (aOR men 0.4 [95% CI 0.4-0.5] versus women), age (aOR age 60-69 1.5 [1.2-1.8], age 70-79 1.7 [1.4-2.1] versus age 50-59) and fracture site (aOR spine 1.7 [1.3-2.0] versus forearm). CONCLUSIONS: This post-fracture intervention, based upon medical claims data, provides an easy way to enhance post-fracture care. The approach is scalable, can be delivered to a widely scattered population, and requires minimal infrastructure. This low cost intervention can complement more resource-intensive programs based on case managers.

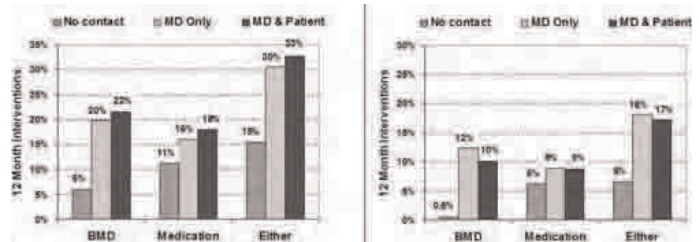


Figure: Post fracture intervention rates at 12 months.

Disclosures: William Leslie, None.

SU0356

Hip Extensor Lean Cross-Sectional Area Is Associated with Incident Hip Fracture: The Age/Gene/Environment Susceptibility Study-Reykjavik. Thomas Lang¹, Sigurdur Sigurdsson², KRISTIN SIGGEIRSDOTTIR³, Gyda Karlsdottir², Gudny Eiriksdottir², Joyce Keyak⁴, Vilundur Gudnason³, Tamara Harris⁵.

¹University of California, San Francisco, USA, ²Icelandic Heart Association, Iceland, ³ICELANDIC HEART ASSOCIATION RESEARCH INSTITUTE, Iceland, ⁴University of California, USA, ⁵National Institute on Aging, USA

Quantitative computed tomography (QCT) provides measures of proximal femoral density, structure and strength that are established predictors of hip fracture. QCT images also provide information on the cross-sectional area (CSA) and attenuation of the muscles surrounding the hip, and these measures may affect fracture risk through both an effect on hip strength and an effect on frailty-related risk factors for falling. There is no information about the association of these measures with incident fractures of the hip. We hypothesized that smaller CSA and lower attenuation would increase hip fracture risk independently of reduced muscle strength and slow gait. We analyzed CT scans of the hip for bone and muscle variables in 4000 subjects aged 65-90 years, 43% of them male, who were enrolled in the Age/Gene Environment Susceptibility Study - Reykjavik, a study of community-dwelling men and women in the Reykjavik area. CT scans were analyzed to obtain the lean cross-sectional area (ECSA) and mean attenuation of the hip extensor group as well as the volumetric bone mineral density of the total hip (vBMD). To assess fall-related measures of physical function and lifestyle, we measured the time to complete the Timed Up and Go (TUGO) test, as well as lifestyle factors including alcohol consumption, smoking, self-reported health status, and physical activity. We computed odds ratios (OR) (per standard deviation (SD) for hip fracture using three multi-variate logistic regression models relating vBMD, ECSA and attenuation to incident hip fracture (Table). Model A was adjusted for age and gender. Model B

added adjustments for height and BMI, and Model C added TUGO and lifestyle factors. Over a 7-year followup, 190 hip fractures occurred. ECOSA and vBMD, but not muscle attenuation, were independent hip fracture predictors in Models A and B. ECOSA was only of borderline significance after adjustment for TUGO and lifestyle factors, while vBMD remained strongly predictive of fracture. In conclusion, a one-SD reduction in ECOSA increased the risk of hip fracture by a third, even when vBMD was taken into account, and lifestyle factors attenuated this relationship. The combination of vBMD with a quantitative muscle assessment assessed from the same scan may improve estimation of hip fracture risk compared to vBMD alone.

	Model A	Model B	C
vBMD	2.30 (1.91, 2.79)	2.28 (1.88, 2.77)	2.11 (1.73, 2.58)
LCOSA	1.32 (1.05, 1.63)	1.32 (1.04, 1.71)	1.23 (0.94, 1.60)

Table: OR for Hip Fracture (95% Confidence Interval) per one SD decrease

Disclosures: Thomas Lang, Merck, 2; Glaxo-SmithKline, 2

SU0357

Hospitalizations for Hip Fractures and Femur Fractures below Trochanter Follow Similar Trends in Women. Kurt Lippuner¹, Lisa Strahm¹, Albrecht Popp¹, Patrick Schwab², Christoph Senn¹, Romain Perrelet¹. ¹Osteoporosis Polyclinic, University of Bern, Switzerland, ²Swiss Federal Statistical Office, Switzerland

Purpose: It has recently been reported that hip (femoral neck and pertrochanteric) fracture incidence had declined between 1996 and 2006 in the US while the incidence of the more rare femur fractures distal to the lesser trochanter had remained stable over time (Nieves et al 2010). Whether similar trends exist in Switzerland is unknown.

Methods: The incidence of femoral fractures hospitalized in years 2000-2008 was determined by ICD-10 code, sex, and 10-year age categories using the medical database of the Swiss Federal Statistical Office (SFSO) which covered 81.2% (year 2000) to 98.8% (year 2008) of all hospitalizations. Raw data were extrapolated to 100%. The age-standardized incidence per 100000 women aged 45 years or older was calculated by 5-year age groups for each calendar year, using the Swiss population statistics of the SFSO. The standardized incidence rate ratio (IRR) and corresponding 95% confidence intervals were calculated for year 2008 compared to year 2000. Linear trends between 2000 and 2008 were analyzed by simple linear regression.

Results: The age-standardized incidence of hospitalizations for femur fractures by localization is shown in the table below. Hip fracture incidence decreased significantly by 18% with a significant trend over time ($p < 0.001$). Subtrochanteric fractures and total fractures below trochanter decreased significantly by 11% (p -value for trend = 0.004) and 9% ($p = 0.043$), respectively. The proportion of hospitalized hip fractures, below trochanter fractures, and other fractures remained stable over time at approximately 84%, 12%, and 4%, respectively.

Conclusions: Hip fractures and femur fractures below trochanter followed similar hospitalization trends between 2000 and 2008 in Swiss women.

Year	2000	2001	2002	2003	2004	2005	2006	2007	2008	Standardized IRR (95%CI)	p value for trend
Fracture of the femoral neck (S72.0)	266	281	259	255	236	222	218	220	206	0.77 (0.74-0.81)	<0.001
Pertrochanteric fracture (S72.1)	212	228	212	203	194	188	190	187	188	0.89 (0.85-0.93)	0.002
Total hip fractures	478	509	471	458	430	410	407	407	394	0.82 (0.80-0.85)	<0.001
Subtrochanteric fracture (S72.2)	23.0	23.8	24.1	22.2	22.0	20.2	19.1	20.2	20.5	0.89 (0.77-1.03)	0.004
Fracture of the femoral shaft (S72.3)	24.9	25.4	22.1	24.7	20.7	19.1	23.3	22.2	21.5	0.86 (0.75-1.00)	0.107
Fracture of the distal femur (S72.4)	20.9	20.6	19.8	24.5	20.9	15.8	17.6	18.5	20.6	0.99 (0.85-1.15)	0.309
Total femur fractures below trochanter	68.5	69.7	65.9	71.5	63.6	55.2	60.1	61.2	62.5	0.91 (0.84-0.99)	0.043
Total other femur fractures*	23.6	27.8	25.4	21.4	20.9	22.7	19.1	18.3	15.7	0.66 (0.57-0.78)	0.002

* multiple (S72.7), other (S72.8), no further mention (S72.9)

Table

Disclosures: Lisa Strahm, None.

SU0358

Hyperkyphosis and Incident Fractures Older Community Dwelling Women: The Study of Osteoporotic Fractures (SOF). Deborah Kado¹, Dana Miller-Martinez², Lily Lui³, Kristine Ensrud⁴, Teresa Hillier⁵, Howard Fink⁶, Marc Hochberg⁷, Peggy Cawthon³. ¹University of California, Los Angeles, USA, ²David Geffen School of Medicine at UCLA, USA, ³California Pacific Medical Center Research Institute, USA, ⁴Minneapolis VA Medical Center / University of Minnesota, USA, ⁵Kaiser Center for Health Research, USA, ⁶GRECC, Minneapolis VA Medical Center, USA, ⁷University of Maryland School of Medicine, USA

While hyperkyphosis is strongly associated with osteoporosis, it is not known whether increased thoracic spine curvature, independent of vertebral fractures, may itself be a risk factor for future fracture. Therefore, we used data from the Study of Osteoporotic Fractures to assess whether women aged 65 and older with increased kyphosis may be at risk for non-spine fractures. We used the digitized Cobb angle (T4 – T12) derived from supine lateral thoracic spine radiographs to calculate the degree of kyphosis in 940 randomly selected women from the parent cohort who were then followed for an average of 17.7 years. Incident non-spine fractures were ascertained from postcard follow-up every 4 months and were confirmed by radiographic report ($n = 464$ women). At the baseline visit, participants were an average of 69.4 (SD = 4.0) years old and had a mean kyphosis angle of 44.9 (SD = 11.8) degrees. Multivariable Cox proportional hazards analyses were used to assess whether greater degrees of kyphosis, measured continuously or by the top quartile, were associated with an increased risk of non-spine fracture. In age and clinic adjusted models, with each 10 degree increase in kyphosis, there was a 1.13-fold increased risk of future non-spine fracture (95% CI: 1.04 – 1.22). After further adjustment for calcaneal bone mineral density, history of previous fracture and morphometric prevalent vertebral fracture, the risk was not substantially changed (H.R. = 1.09; 95% CI: 1.01 – 1.19). Consideration of other potential confounders including body mass index, self-reported health, and physical activity made no difference in the results. Although there is no widely accepted hyperkyphosis angle threshold, it is estimated that about 25% of the older population may be affected by accentuated thoracic curvature. In SOF, women in the top quartile of kyphosis (Cobb angle kyphosis of >53 degrees compared to the lower three quartiles) had a 1.32-fold increased risk of non-spine fracture (multivariate-adjusted 95% CI: 1.07 – 1.63). We conclude that older women with hyperkyphosis are at an increased risk of subsequent osteoporotic fractures, independent of a history of prior fracture, prevalent vertebral fractures, and bone mineral density.

Disclosures: Deborah Kado, None.

SU0359

Incidence of Fractures after Cardiac and Lung transplantation: A Single Center Experience. Aileen Hariman^{*}, Charles Alex, Biljana Pavlovic-Suriancev, Alain Heroux, Pauline Camacho. Loyola University of Chicago, USA

BACKGROUND: Osteoporotic fractures are well-known complications of organ transplantation. Reports in the early 1990s documented fracture rates up to 35% following heart and lung transplantations. More recent studies demonstrated fracture rates as low as 7.6% following heart transplantation and 12% following lung transplantation. At Loyola University Medical Center, pre-transplant protocols routinely include DXA scans and aggressive vitamin D screening prior to and immediately post-transplantation. Antiresorptive medications are widely utilized. The aim of this study was to assess the incidence of fragility fractures following cardiac or lung transplantation.

METHODS: In a retrospective observational study conducted from 2005-2010, 210 patients who underwent lung transplantation (110 men, 100 women) and 105 heart transplantation (88 men, 17 women) at Loyola University Medical Center were analyzed through electronic medical records. Both clinical and radiographic fractures through review of medical records were recorded.

RESULTS: Out of 210 lung transplant recipients, 17 patients (8.0%) had fractures post-transplantation and out of 105 heart transplant patients, 9 patients (8.57%) had fractures. The incidence of fracture in lung transplant patients in years 1 to 5 were 4.76%, 0.95%, 0.00%, 0.95%, and 1.90%, respectively. The median time to the first fracture was 8 months and the mean time was 19.11 +/- 21.0 months. The incidence of fracture in heart transplant patients in years 1 to 5 were 3.81%, 1.43%, 1.90%, 0.48%, and 0.48%, respectively. The median time to the first fracture was 12 months and the mean time was 18.41 months. Heart transplant recipients who fractured were significantly older than those who did not (60.78 +/- 7.84 yrs vs 52.66 +/- 12.13, $p = 0.016$). A similar finding was seen in lung transplant patients (54.65 +/- 7.97 yrs vs 52.53 +/- 13.41, $p = 0.048$). The use of bisphosphonates in fracture and non-fracture groups did not differ in heart (55.56% vs. 33.33%, $p = 0.362$) or in lung transplant patients (52.94% vs. 28.87%, $p = .909$).

CONCLUSION: Our findings demonstrate a much lower incidence of fractures post-transplantation in heart and lung transplant recipients in comparison to earlier reports. Comprehensive bone care, including DXA scans, screening for vitamin D deficiency, and early initiation of antiresorptive therapy at the pre-transplant or

immediate post-transplant period, are possible contributors to these improved outcomes.

Disclosures: Aileen Hariman, None.

SU0360

Incidence of Osteoporotic Fracture in Patients with High Plasma Homocysteine Level. Naohisa Miyakoshi¹, Yuji Kasukawa¹, Koji Nozaka^{*2}. ¹Akita University Graduate School of Medicine, Japan, ²Akita City Hospital, Japan

[Background]High plasma homocysteine(Hcy) levels, which are a useful surrogate marker for detecting osteoporosis caused by deterioration of bone quality, may also be a bone quality marker that enables predicting the risk of fracture, which cannot be assessed by bone mineral density alone. However, details on patients with high plasma Hcy levels undergoing clinical treatment for fractures remain unclear.[Objective]To retrospectively investigate patients with high plasma Hcy levels in order to elucidate: 1) the proportion of patients who have high plasma Hcy levels; 2) the incidence of fractures among patients with high plasma Hcy levels; and 3) the types of fractures among patients with high plasma Hcy levels.[Subjects and methods]Subjects were 137 patients who underwent plasma Hcy measurement (standard values: 3.7-13.5 nmol/ml) upon admission to our department or when visiting the outpatient department from among the 1639 patients for whom bone mineral density was measured at our hospital in 2009. "High plasma Hcy levels" were defined as plasma Hcy levels above the upper limit of the standard values, i.e., 13.6 nmol/ml.[Results]A total of 20.4% (28/137) of patients had high plasma Hcy levels. These patients included 8 men and 20 women, and had a mean age of 76.4 years (range, 54-94 years), mean plasma Hcy level of 18.8 nmol/ml (13.6-40.7 nmol/ml), and mean bone mineral density (%YAM) of 57.9% (29-88%; >70% of the YAM, n=6; <70% of the YAM, n=22). The incidence of fractures among patients with high plasma Hcy levels was 92.9% (26/28). The 26 fractures included vertebral fracture (n=14) of one vertebra (n=2) or multiple vertebrae (n=12). A total of 12 patients had non-vertebral fractures, and surgery was indicated for each of these patients. These fractures included hip fracture (n=5; surgery performed, n=3), tibial plateau fracture (n=3; surgery performed, n=2), distal tibia fracture (n=1; surgery performed, n=1), distal radius fracture (n=2), and proximal humerus fracture (n=1). A total of 24 of 26 (92.3%) patients had experienced fractures at multiple sites, and all 26 patients had low-trauma or non-traumatic fragility fractures.[Discussion]The incidence of fractures among patients with high plasma Hcy levels was 92.9%, which was much higher than anticipated, and many of the patients had a history of multiple fractures. Plasma Hcy measurement is a useful predictive marker of osteoporotic fractures.

Disclosures: Koji Nozaka, None.

SU0361

Morbidity and Mortality After Hip Fracture with Using Jeju Cohort in South Korea : A Minimum 5 Year Follow-Up. Jae-Suk Chang¹, Yong-Chan Ha^{*2}, Young-Kyun Lee³, Hyun-Koo Yoon⁴, Deog-Yoon Kim⁵. ¹Ulsan University, Asan Medical Center, South Korea, ²Chung-Ang University College of Medicine, South Korea, ³Seoul National University Bundang Hospital, South Korea, ⁴Cheil General Hospital & Women's Healthcare Center, South Korea, ⁵Department of Nuclear Medicine, Kyung Hee University Medical Center, South Korea

Introduction: Since 2002, the author has been performing epidemiologic study in Jeju island South Korea. Jeju Island is geographically isolated from main land and patients with hip fractures typically require hospitalization, which makes ascertainment easier and much reliable than other types of fractures. This prospective study was performed to estimate the morbidity and mortality after hip fractures of people over 50 years of age, in Jeju island, South Korea.

Methods: Eight hundreds nine patients(820 hips) over 50 years of age who sustained a femoral neck or intertrochanteric fracture from 2002 to 2006 were followed-up for minimum 5 years (range; 5-8 years). Crude and standardized annual mortality ratio was calculated and comparison of mortality was made between hip fractured patients and general population in Jeju island. We accessed functional capacity before and after injury, including independence in activities of daily living and walking ability.

Results: The mean age of the patients at the time of fracture was 77.8 years (71.3 years in 179 men, 79.9 years in 630 women). Accumulated mortality was 52.3% (79/151 patients) at 8 years, 43.3%(350/809 patients) at 5 years, 16.2%(131/809 patients) at 1 year, respectively. Standardized mortality ratio at 5 year follow-up was 2.8 times of the general population. Patients who could recover preoperative activity after treatment were only 40.4%(190/470 patients) at the final follow-up.

Conclusion: Considering high mortality and poor activity at the minimum 5 years follow-up period, the hip fracture in older patients is life threatening factors. Prevention of falling and reduction of hip fracture risk are necessary.

Disclosures: Yong-Chan Ha, None.

SU0362

Quality of Life in Community-Dwelling Elderly Women: The Impact of Asymptomatic Vertebral Fractures. JAQUELINE LOPES^{*1}, Leandro Fung², Carolina Cha², Camille Figueiredo², Liliam Takayama², Valeria Caparbo², Rosa Pereira³. ¹Faculdade de Medicina da Universidade de Sao Paulo, Sao Paulo, Brazil, ²Division of Rheumatology (Bone Mineral Metabolism Laboratory), Faculdade de Medicina da Universidade de Sao Paulo, Brazil, ³Faculdade de Medicina da Universidade de Sao Paulo, Brazil

Purpose: To investigate the impact of asymptomatic vertebral fractures in the quality of life (QOL) of community-dwelling elderly women.

Methods: 180 elderly women with 65 years or older from community were evaluated. The Quality of Life Questionnaire of the European Foundation for Osteoporosis (QUALEFFO) was administered to all subjects. Total domain score was computed by summing the scores of all questions and submitting the sum to a linear transformation to a scale of 100. A low score domain indicates worse health and a high score indicates better health. Anthropometric data was obtained by physical examination and body mass index (BMI) was calculated. The participants underwent bone mineral density (BMD) measurements by DXA of the lumbar spine and hip, as well as thoracolumbar spine X-ray to identify asymptomatic vertebral fractures. According to the ISCD definition, subjects were classified in normal BMD, osteopenia, and osteoporosis. Vertebral fractures were diagnosed using semiquantitative method (Genant-1993).

Results: 41 (22.8%) elderly women presented asymptomatic vertebral fractures. QOL was inversely correlated with age (R²=0.02, p=0.03) and IMC (R²=0.05, p<0.01). The women with vertebral fractures had lower QUALEFFO score [64.3 (16.1) vs. 77.3 (15.0), p=0.02] and worse physical function domain [69.5 (20.1) vs. 77.2 (17.1), p=0.01]. Comparing women with normal BMD, osteopenia and osteoporosis, a significant difference was found only for physical function domain (p=0.04, by Kruskal-wallis). After, we separated both osteopenic and osteoporotic women according to whether or not they had vertebral fractures, and a significant difference was found only in osteoporotic patients for physical function domain [71.3 (17.1) vs. 79.9 (18.8), p=0.03] and total QUALEFFO score [65.2 (13.5) vs. 71.8 (16.6) p<0.03]. Stepwise multiple logistic regression analysis of the whole sample showed that older individuals (p=0.03), high BMI (p=0.04) and vertebral fractures (p=0.02) impair QOL physical function.

Conclusions: Our results showed that physical function of QOL appears to be impaired in patients with asymptomatic vertebral fractures.

Disclosures: JAQUELINE LOPES, None.

SU0363

Review of Lower Extremity Fractures in Veterans with Spinal Cord Injury. Helen Hoenig¹, Titilola Akhigbe^{*2}, Amy Chin¹, Stephen Burns³, Jelena Svircev⁴, Helen Hoenig¹, Frances Weaver⁵, Kim Seunghyun², Laura Carbone². ¹Department of Veterans Affairs, USA, ²University of Tennessee Health Science Center, USA, ³Puget Sound, USA, ⁴VA Puget Sound, USA, ⁵Edward Hines Jr. VA Hospital, USA

Purpose: The purpose of this study was to describe fracture circumstances and examine morbidities, receipt of pharmacological therapies to prevent future fracture and changes in functional status in the one year time period following an incident lower extremity fracture in Veterans with Spinal Cord Injury (SCI).

Methods: We used the VA Spinal Cord Disorders Registry and the National Patient Care Database to identify all Veterans with a traumatic SCI who sustained an incident lower extremity fracture from 2002-2007 who received care at one of the four sites of our study (Durham, Hines, Memphis, Puget Sound). Retrospective medical record reviews of these fracture cases were performed at each site.

Results: There were 155 incident lower extremity fractures in 136 Veterans. The majority of incident fractures occurred in the femur (n=49) or tibia/fibula (n=80). 99% of the fracture cases were male; 36% had a prevalent fracture, 52% were ASIA A, 20% ASIA B, and 4% ASIA C or D with the remainder unknown. Approximately 1/3 were current users of tobacco or alcohol. The majority (44%) of these fractures occurred while using a wheelchair. 15% of fractures required surgical treatment. In the first year following the fracture, approximately 21% of Veterans received additional treatment to prevent future fractures (20% calcium, 16% vitamin D supplements, 6% bisphosphonates, <1% other). Morbidity complications occurred in the majority of Veterans following fracture, principally urinary tract infections (55%), pressure ulcerations (45%), fracture non-union (13%) and amputation (6%). Pre and post fracture residences were unknown in 4% and 6% of patients respectively. Of the remainder, more individuals were at home without home health care prior to fracture than post fracture (58.52% vs.46.67%), whereas all categories requiring more services, including home health care services (32.59% vs. 34.07%), assisted living (2.96% vs.5.19%) and nursing home residence (2.22% vs.3.7%) increased following the fracture.

Conclusions. Wheelchair use is a common mechanism for lower extremity fractures in Veterans with SCI. Surgery is required for approximately 15% of these fractures. These fractures have a substantial impact on Veterans. However, only a minority receive pharmacological therapies for fracture prevention following fracture. Future studies are needed to determine whether strategies that focus on safe wheelchair use might prevent fractures in this population.

Disclosures: Titilola Akhigbe, None.

SU0364

Review of Radiological Scoring Methods of Osteoporotic Vertebral Fractures for Clinical and Research Settings. Felisia Ly^{*1}, Ling Oei², Carola Zillikens¹, Andre Uitterlinden³, Gabriel Krestin¹, Fernando Rivadeneira², Edwin Oei¹. ¹Erasmus MC, Netherlands, ²Erasmus University Medical Center, The Netherlands, ³Rm Ee 575, Genetic Laboratory, The Netherlands

Osteoporosis is characterised by decreased bone density and bone quality resulting in an increased risk of fragility fractures. Vertebral fractures (VFX) are the most common osteoporotic fractures. There have been many publications on different criteria that are used to assess VFX. Such grading definitions are currently under debate. The purposes of this review are to high-light benefits and limitations across methods in terms of vertebral fracture (VFX); to illustrate how prevalence of VFX is influenced by different assessment methods; to discuss the application of scoring methods in scientific research and clinical practice.

Image examples from a population-based study will be used to illustrate different radiological scoring methods. We will discuss Quantitative morphometry (QM) and semi-quantitative (SQ) methods, which were developed to overcome the subjectivity of traditional visual diagnosis. QM ratios derived from exact measurements of the anterior, middle and posterior heights of vertebral bodies are used to define deformities, e.g. McCloskey-Kanis. SQ visual grading of VFX is done by trained readers according to height and area reduction, e.g. Genant. However, not all vertebral deformities are osteoporotic VFX. A newer algorithm-based qualitative (ABQ) method introduced a scheme to systematically rule out non-fracture deformities and diagnoses osteoporotic VFX based on endplate depression alone, regardless of vertebral height reduction. The methods discussed were developed based on conventional radiography, however they are also applicable to lateral dual-emission X-ray absorptiometry (DXA), magnetic resonance imaging (MRI) and X-ray computed tomography (CT).

As different scoring methods use different definitions of VFX diagnosis and severity, this may have implications for patient care and scientific research. So a standardized and accurate scoring method for osteoporotic VFX is desirable. Available standardized scoring methods for osteoporotic VFX can be implemented for different imaging modalities.

Disclosures: Felisia Ly, None.

SU0365

Serum Vitamin D Level and Functional Outcomes in Patients with Fragility Fractures, Shifting the Paradigm. Lohrasb Ahmadian^{*}, Joseph Lane. Hospital for Special Surgery, USA

Introduction: The goal of this study is to emphasize the importance of scientific measurement paradigm in testing the relationship of functional outcomes and serum vitamin D in patients with fragility fracture. **Methods:** We designed a cross-sectional study of community-living persons with the history of fragility fracture and/or low bone density. Lowest quartile of vitamin D concentration among study subjects was defined (<35 ng/ml). All self-reported functional outcomes were estimated using both standard method of summing Likert-type scores and Rasch analysis. Rasch analyses adjusted by age, sex, and comorbidity were performed on the responses to all functional and (QoL) measures. A series of multivariable linear and logistic regression models were used to evaluate the association between specific cutoff points of vitamin D concentration and functional and QoL outcomes. Odds ratios (ORs) were calculated for the lowest quartile of serum Vitamin D using other quartiles combined as the reference group. Finally, classification and regression tree (CART) analysis was performed to identify a hierarchical order of and potentially complex interactions between vitamin D level (continuous) and other variables. **Results:** The sample included 190 participants with average age of 71 (SD 11). The mean level of vitamin D was 43.7 ng/ml (SD 15.8 ng/ml), with 25% less than 35 ng/ml. Only raw scores of mental domain of QoL measures (SF12) in both unadjusted (OR, 3.42; CI, 1.25-9.24; p=.02) and adjusted models were significantly associated with the low level of vitamin D (<35 ng/ml vs ≥35 ng/ml). In all other unadjusted analyses, low level of vitamin D was not associated with the level of QoL, functional disability, ambulation, and fall risk measures. Most of the functional and QoL scales investigated showed valid acceptable person separation reliability but poor targeting and item performance. The Rasch person-item map showed that most of the items in functional and QoL measures have not good range and are not well centered with respect to the person measure distribution in patients with fragility fractures. **Conclusion:** We can conclude that the observed poor predictive relationship of low vitamin D and functional outcomes is the consequence of measurement insufficiency and major mismatch between self-reported item measures and person measures. To investigate the dose-response relationship of vitamin D and functional outcomes, the selected measures need to be adequate to describe the functional ability of the subjects in the study.

Disclosures: Lohrasb Ahmadian, None.

SU0366

A Novel MECOM Gene Predisposing to Osteoporotic Fracture Identified by a Combined Meta-analysis and Functional Effects. Joo-Yeon Hwang^{*1}, Seung Hun Lee², Min Jin Go³, Beom-Jun Kim⁴, Shiro Ikegawa⁵, Kou Ikuvo⁵, Unnur Styrkarsdottir⁶, Soumya Raychaudhuri⁷, Young Jin Kim³, Dong-Joon Kim³, Ji Hee Oh³, Heejo Koo³, My-Jung Cha³, Min Hye Lee³, Ji Young Yun³, Hye-Sook Yoo³, Young-Ah Kang³, Ki Won Oh⁸, Moo Il Kang⁹, Ho Young Son⁹, Shin-Yoon Kim¹⁰, Ghi Su Kim¹¹, Bok-Ghee Han³, Yoon Shin Cho³, Jong-Young Lee³, Jung-Min Koh⁴. ¹Korea National Institute of Health, Center for Genome Science, South Korea, ²Asan Medical Center, University of Ulsan College of Medicine, South Korea, ³Center for Genome Science, KNIH, South Korea, ⁴Asan Medical Center, South Korea, ⁵RIKEN, Japan, ⁶Decode Genetics, Iceland, ⁷Broad Institute, USA, ⁸Sungkyunkwan university, South Korea, ⁹CMC, South Korea, ¹⁰Kyungpook National University Hospital, South Korea, ¹¹University of Ulsan, South Korea

Osteoporotic fracture (OF) has become a matter of substantial morbidity and mortality in demographic changes of an aging populations. However, genetic contributions to OF risk assessment remain undetermined for the assignment of preventive measures. Although bone mineral density is a valuable parameter to predict OF risk, identifying a genetic susceptibility for OF itself as an end point would be more important. In an attempt to detect genetic liability to OF in East Asian populations, we conducted a GWAS as a screening in epidemiological cohort study (Korea Association Resource, KARE, n = 1,427). The lead SNP was replicated in hospital-based independent women, Korean (ACMC, n = 1,372) and Japanese (RIKEN, n = 929), respectively. In combined meta-analysis of osteoporotic vertebral fracture from a discovery cohort (KARE) and two de novo replication sets (ACMC and RIKEN), we found the most significant association in the same direction. Functionally, real-time PCR revealed that the differentiated osteoclasts expressed more of its transcript than pre-osteoclasts. Knock-down by MECOM siRNA suppressed osteoclastogenesis and expressions of marker genes for differentiated osteoclasts. These suggest that MECOM may stimulate osteoclastogenesis, resulting in the increased bone resorption. Bioinformatic analyses based on the identified SNP suggest functional connectivity underlying the suppressive effect in RANK signaling. Taken together, our observations suggest that the MECOM polymorphism represents a strong genetic determinant for OF risk in the East Asian individuals, and that the gene has a critical role on bone metabolism.

Disclosures: Joo-Yeon Hwang, None.

SU0367

Assessment of Gene-by-sex Interaction Effect on Bone Mineral Density. Ching-Ti Liu^{*1}, Yi-Hsiang Hsu², Karol Estrada³, Vangelis Evangelou⁴, Yanhua Zhou⁵, Laura Yerges-Armstrong⁶, Najaf Amin⁷, Nicole Glazer⁸, Ryan Minster⁹, Gudmar Thorleifsson¹⁰, Jane Cauley¹¹, CM van Duijn¹², Tamara Harris¹³, John Ioannidis⁴, Yongmei Liu¹⁴, Braxton Mitchell¹⁵, Jeffery R O'Connell¹⁶, John Robbins¹⁷, Elizabeth Streeten¹⁶, Unnur Styrkarsdottir¹⁸, Andre Uitterlinden¹⁹, M Zillikens²⁰, Fernando Rivadeneira³, David Karasik²¹, L Adrienne Cupples¹, Douglas Kiel²¹.

¹Boston University School of Public Health, USA, ²Hebrew SeniorLife Institute for Aging Research & Harvard Medical School, USA, ³Erasmus University Medical Center, The Netherlands, ⁴University of Ioannina School of Medicine, Greece, ⁵Boston University, USA, ⁶University of Maryland, USA, ⁷Erasmus University Medical Center, Netherlands, ⁸Boston University School of Medicine, USA, ⁹University of Pittsburgh, USA, ¹⁰deCODE Genetics, Reykjavík, Iceland, Ireland, ¹¹University of Pittsburgh Graduate School of Public Health, USA, ¹²Erasmus University Medical Center, Ireland, ¹³Intramural Research Program, National Institute on Aging, USA, ¹⁴Wake Forest University School of Medicine, USA, ¹⁵University of Maryland, Baltimore, USA, ¹⁶University of Maryland School of Medicine, USA, ¹⁷University of California, Davis Medical Center, USA, ¹⁸deCODE Genetics, Reykjavík, Iceland, Iceland, ¹⁹Rm Ee 575, Genetic Laboratory, The Netherlands, ²⁰Erasmus MC Rotterdam, The Netherlands, ²¹Hebrew SeniorLife, USA

Aim: Bone mineral density (BMD), a heritable trait, is one of the major determinants of bone strength and a key predictor of osteoporotic fracture. Sexual dimorphism in various bone phenotypes is widely observed, which in genome-wide association studies (GWAS) meta-analyses can hamper the discovery of sex-specific effects. Such sex-specific genetic determinants influencing BMD variation will not rank high in GWAS combining sexes. Therefore we specifically examined genome-wide gene-sex interactions for BMD traits, seeking the identification of variants with opposing and/or sex specific effects.

Methods: We conducted a GWAS meta-analysis under the framework of the Genetic Factors of Osteoporosis (GEFOS) Consortium including ~25,000 individuals

(36% male) from seven cohorts. SNP-by-sex interaction on lumbar spine (LS-) and femoral neck (FN-) BMD, was modeled additively for ~2.5 million imputed SNPs across the genome using multivariable linear regression models with a statistical interaction (SNP*sex) term. Inverse variance weighted fixed effects meta-analysis was used to aggregate results from each study. A genome-wide significance (GWS) threshold was set at $P \leq 5 \times 10^{-8}$ and suggestive at $P \leq 1 \times 10^{-5}$. Sex-specific associations for the identified top SNPs were tested using a corrected $P < 0.0042$ as the significant threshold.

Results: We detected one novel genome-wide significant interaction associated with LS-BMD at the Chr3p26.1-p25.1 locus, near the GRM7 gene (male p -value = 3.0×10^{-5} ; female p -value = 3.3×10^{-2}) and eleven suggestive loci associated with either FN- or LS-BMD. All associations displayed opposite effect directions in men compared to women. Significance of association was attained in only one gender in all but one locus (XCL2 gene at Chr 1q24.2, significant in both genders, p -value = 5.7×10^{-4} and 1.2×10^{-4} for male and female, separately).

Conclusion: This collaborative work identified twelve loci suggestive of sex-specific effects on FN- and LS-BMD and corroborated sexual dimorphism of bone. These results are currently being replicated in an additional 4,600 male and 12,000 female Caucasian samples (the GENOMOS Consortium).

RefGene	CHR	Trait	Alleles ¹	EAF ²	Interaction Result		Male		Female	
					Effect	SE	Effect	SE	Effect	SE
GRM7	3	LSBMD	C/G	0.11	0.034	0.006	3.41E-08	0.020	0.005	3.03E-05
XCL2	2	LSBMD	A/G	0.65	0.021	0.004	7.42E-08	0.011	0.003	5.75E-04
C4orf52	4	LSBMD	A/G	0.13	-0.028	0.006	7.98E-07	-0.021	0.005	5.64E-06
GALR1	18	LSBMD	A/G	0.44	-0.019	0.004	1.50E-06	-0.012	0.003	2.74E-04
REL1	4	LSBMD	T/C	0.83	0.023	0.005	1.89E-06	0.018	0.004	1.99E-06
CRABP1	15	LSBMD	T/C	0.12	-0.028	0.006	6.20E-06	-0.019	0.005	7.56E-05
UBE4B	1	LSBMD	A/T	0.62	0.019	0.004	8.60E-06	0.011	0.003	3.77E-04
DOC4S	8	LSBMD	C/T	0.49	0.015	0.003	8.99E-06	0.009	0.003	1.35E-03
UGCG	9	FNEMD	A/G	0.85	0.017	0.003	5.42E-07	0.007	0.003	1.18E-02
TYRP1	9	FNEMD	T/G	0.43	0.011	0.002	5.76E-06	0.006	0.002	3.08E-03
SERPINA1	14	FNEMD	A/C	0.15	-0.016	0.004	7.39E-06	-0.009	0.003	1.09E-03
MAT2B	5	FNEMD	T/C	0.38	-0.011	0.002	7.50E-06	-0.008	0.002	1.69E-05

Note: ¹ Effect Allele/Other Allele ² Effect Allele Frequency

Table 1. Interaction and gender-specific result

Disclosures: Ching-Ti Liu, None.

SU0368

Genome-Wide Association Meta-Analysis of Cortical Volumetric BMD Identifies Three Known and One Novel Bone-Related Loci. Claes Ohlsson^{*1}, Lavinia Paternoster², Terho Lehtimäki³, Mika Kahonen⁴, Olli Raitakari⁵, Marika Laaksonen⁶, Vera Mikkilä⁶, Jorma Viikari⁷, Leo-Pekka Lyytikäinen³, John P Kemp², Adrian Sayers⁸, Maria Nethander⁹, Liesbeth Vandenput¹⁰, Jon H Tobias¹¹, Mattias Lorentzon¹, David M Evans². ¹Center for Bone Research At the Sahlgrenska Academy, Sweden, ²MRC Centre for Causal Analyses in Translational Epidemiology, University of Bristol; School of Social & Community Medicine, University of Bristol, United Kingdom, ³Department of Clinical Chemistry, University of Tampere & Tampere University Hospital, Finland, ⁴Department of Clinical Physiology, University of Tampere & Tampere University Hospital, Finland, ⁵Research Centre of Applied & Preventive Cardiovascular Medicine, University of Turku & the Department of Clinical Physiology, Turku University Hospital, Finland, ⁶Department of Food & Environmental Sciences, University of Helsinki, Finland, ⁷Department of Medicine, University of Turku & Turku University Hospital, Finland, ⁸University of Bristol, United Kingdom, ⁹Genomics Core Facility, University of Gothenburg, Sweden, ¹⁰University of Gothenburg, Sweden, ¹¹School of Clinical Sciences, University of Bristol, United Kingdom

Previous bone-related genome-wide association (GWA) studies have mainly focused on the identification of SNPs associated with areal bone mineral density (aBMD) as analysed by dual energy x-ray absorptiometry (DXA). However, this measure is influenced by several different skeletal parameters such as periosteal expansion, cortical volumetric BMD (cvBMD), cortical thickness, trabecular number and trabecular thickness, which may be under distinct biological and genetic control. Interestingly, cvBMD displays a weak correlation with femoral neck aBMD ($r_s = 0.039$ in the GOOD cohort), suggesting that the genetic determinants of cvBMD may differ from the earlier published genetic determinants of aBMD.

We, therefore, performed a GWA study of cvBMD, as measured by peripheral quantitative computed tomography (pQCT) in the tibial diaphysis, among 5,952 Caucasian subjects from three cohorts (ALSPAC, aged ~15 years, $n=3,456$; GOOD, aged ~19 years, $n=938$ and YFS 31-46 years of age, $n=1,558$). Inverse variance weighted fixed-effect model meta-analysis of study-specific results was performed. We identified genetic variants in four separate loci reaching genome wide significance. Three of these loci (RANKL, OPG and estrogen receptor- α) have earlier been reported to be associated with aBMD. We identified two strong hits (rs1021188, $p=1.5 \times 10^{-12}$, effect size 0.15 SD per allele and rs1325798, $p=4.1 \times 10^{-10}$, effect size 0.10 SD per allele), with $r^2 < 0.2$, in the RANKL (TNFSF11) locus, suggesting that there may be two independent signals in this locus. We have previously, in a small-scale meta-analysis, reported that the rs1021188 SNP is associated with cvBMD. The other two signals in known bone-related genes were located close to OPG (TNFRSF11B, rs7839059,

$p=4.1 \times 10^{-9}$, effect size 0.10 SD per allele) and estrogen receptor- α (rs6909279, $p=1.0 \times 10^{-8}$, effect size 0.09 SD per allele). Importantly, we identified one novel bone-related signal, located on chromosome 6 in the region of LOC285735 ($p=2.9 \times 10^{-11}$, effect size 0.11 SD per allele), to be consistently associated with cvBMD.

In conclusion, we identified genetic variants in one novel and three known bone-related loci to be associated with cvBMD. The three known loci include RANKL, OPG and estrogen receptor- α , strongly suggesting that the RANK/RANKL/OPG pathway and estrogen signalling are involved in the regulation of cvBMD. The mechanism/pathway for the influence of the novel chromosome 6 hit on cvBMD remains to be determined.

Disclosures: Claes Ohlsson, None.

SU0369

Genome-wide Association Study of Hip Fracture Suggests Loci in Biological Pathways Associated with Bone Remodeling. Rebecca Jackson^{*1}, Andrea LaCroix², Aaron Aragaki², David Duggan³, Chris Carlson⁴, Brent Richards⁵, Zari Dastani⁵, Tim Spector⁶, John Eisman⁷, Tuan Nguyen⁷, Stuart Ralston⁸, Eugene McCloskey⁹, Emma Duncan¹⁰, Geoffrey Nicholson¹¹, William Leslie¹², David Goltzman¹³, Subha Krishnan³, Charles Kooperberg². ¹The Ohio State University, USA, ²Fred Hutchinson Cancer Research Center, USA, ³Translational Genomics Research Institute, USA, ⁴University of Washington, USA, ⁵McGill University, Canada, ⁶King's College London, United Kingdom, ⁷Garvan Institute of Medical Research, Australia, ⁸University of Edinburgh, United Kingdom, ⁹University of Sheffield, United Kingdom, ¹⁰Royal Brisbane & Women's Hospital, Australia, ¹¹The University of Queensland, Australia, ¹²University of Manitoba, Canada, ¹³McGill University Health Centre, Canada

Background: Hip fractures are the most serious outcome of osteoporosis and one of the most disabling consequences of aging in women. Although twin and family studies suggest that up to half the variance of hip fracture is due to genetic effects, no genetic loci have been reported to be associated with hip fracture risk.

Methods: A genome-wide association study of hip fracture was conducted with individual genotyping (Illumina 550 and 610K) on 4432 postmenopausal European American women drawn from the Women's Health Initiative; 2055 hip fracture cases and 2377 controls with no history of postmenopausal fracture at baseline, matched to cases on age (+/-1 yr), year of enrollment, and clinical trial treatment group for the Hormone Therapy (HT) and Calcium plus vitamin D Trials. For cases not enrolled in the HT Trial, we matched on current estrogen use at baseline. Case definition was defined as an incident hip fracture: all hip fractures were centrally verified by masked review of radiographic and/or surgical reports. All controls had no prevalent or incident hip fracture by the end of follow up. Analyses used an additive regression model with age, height, weight and the first four principal components in the final model. Genome-wide Significance (GWS) was set at $P \leq 5 \times 10^{-8}$ and suggestive at $5 \times 10^{-8} < P < 5 \times 10^{-6}$. Replication involved *de-novo* genotyping (iSELECT) the 384 most strongly associated SNPs identified from the hip fracture discovery GWAS based on p values and linkage disequilibrium in 3776 independent samples including 1784 hip fracture cases and 1992 controls. Separate regression models were then fit for each cohort included in replication and results were combined via meta-analysis.

Results: We identified 5 loci (0 GWS and 5 suggestive) on chromosomes 2, 3, and 12 associated with incident hip fracture. Two of these loci map within or near genes involved in pathways that regulate bone resorption (NFKB1 and SPTBN1). There was no evidence of an age x SNP interaction. No SNP reached GWS when data were analyzed by fracture type (femoral neck versus intertrochanteric fracture). Further *in silico* replication of the top 384 SNPs is underway.

Conclusion: This large hip fracture GWAS has identified several suggestive loci involving pathways associated with bone remodeling. Meta-analyses with inclusion of carefully phenotyped incident hip fracture cases will help to further explore these findings.

Disclosures: Rebecca Jackson, None.

SU0370

Increased Physical Activity Associated with Longitudinal Decrease in Weight, and Increase in Bone Mineral Density: The Canadian Multicentre Osteoporosis Study (CaMos). Lisa Langsetmo^{*1}, Christine Hitchcock², Elaine Kingwell², K. Shawn Davison³, Siri Forsmo⁴, Wei Zhou⁵, Claudie Berger⁶, Nancy Kreiger⁷, Jerilynn Prior². ¹Canadian Multicenter Osteoporosis Study, Canada, ²University of British Columbia, Canada, ³Laval University, Canada, ⁴Norwegian University of Science & Technology, Norway, ⁵McGill University Health Centre, Canada, ⁶McGill University, Canada, ⁷University of Toronto, Canada

Background: Physical activity (PA) has been identified as a modifiable factor for both weight (hence body mass index or BMI) and bone mineral density (BMD). Weight is strongly predictive of BMD. Our aim was to determine the cross-sectional and prospective associations between PA and BMD, taking weight into account.

Methods: The Canadian Multicentre Osteoporosis Study (CaMos) is a random, population-based, prospective cohort study of Canadian women and men. PA was determined from interviewer-administered questionnaires at Years 0 and 5 as daily energy expenditure, summarized as metabolic equivalent of task multiplied by minutes/day (MET*m/d). Height, weight, and total hip BMD were measured at Years 0 and 5. BMD was calibrated between centers and over time. General linear models were used to assess relationships between physical activity and BMD, both cross-sectionally (Year 0 PA with Year 0 BMD) and longitudinally (average PA and 5-y change in PA with 5-y change in BMD). Confidence intervals are denoted as CI. Weight was considered as a secondary outcome and mediating factor. Potential confounders included age, center, education, caffeine, alcohol, smoking, history of weight-cycling, and for women, age at menarche, past use of oral contraceptives, history of >3 months missed menstruation, menopausal status, and antiresorptive use (estrogen, bisphosphonates).

Results: The study sample included 2855 men and 6442 women. Cross-sectionally, higher PA was associated with lower weight, and longitudinally, 5-y increase in PA was associated with 5-y decrease in weight: 1.27 (95% CI: 0.69, 1.85) kg loss per 1000 MET*m/d PA increase (men) and 1.05 (95% CI: 0.61, 1.49) kg loss per 1000 MET*m/d increase (women). Weight was strongly associated with BMD; weight change was strongly predictive of BMD change ($p < 0.001$). However, despite previously noted relationships, 5-y increase in PA (no weight change adjustment) was associated with small 5-y increase in BMD: 0.004 (95% CI: 0.000-0.008) g/cm² per 1000 MET*m/d increase (men) and 0.003 (95% CI: 0.000-0.007) g/cm² per 1000 MET*m/d increase (women). Average PA was associated with a small, non-significant increase in BMD in men, but essentially no change in women.

Conclusion: An increase in PA over time was associated with a decrease in weight and a slight increase in total hip BMD, suggesting that population level measures to increase PA may be favorable for bone health.

Disclosures: Lisa Langsetmo, None.

SU0371

Effect of Menopause on Bone Loss in HIV-infected Women. Michael Yin^{*1}, Chiyuan Zhang¹, Polly Chen¹, Ivelisse Colon², Donald McMahon³, David Ferris⁴, Emily Stein³, Phyllis Tien⁵, Elizabeth Shane³. ¹Columbia University, USA, ²Columbia University Medical Center, USA, ³Columbia University College of Physicians & Surgeons, USA, ⁴Bronx Lebanon Hospital Center, USA, ⁵University of California, San Francisco, USA

Purpose: HIV infection is associated with chronic T cell activation and increased production of pro-inflammatory, pro-resorptive cytokines. Cytokine levels decline but do not completely normalize on antiretroviral therapy (ART). Since estrogen downregulates T cell activation and cytokine production, we hypothesized that bone loss will be accelerated in HIV-infected (HIV+) women after menopause.

Methods: We measured bone mineral density (BMD) by DXA and serum cytokines and a resorption marker, N-telopeptide (NTX), in two separate cohorts: 168 (100HIV+, 68HIV-) premenopausal (PreM) women and 187 (92 HIV+, 95 HIV-) postmenopausal (PM) women at baseline and 2 years. Premenopausal women were enrolled in the Women's Interagency HIV Study (WIHS) and PM women were from a New York City cohort.

Results: PreM HIV+ women were older (40±5 vs 36±7, $p < 0.01$), but had similar body mass index (BMI; 29±7 vs 30±7 kg/m²) and race than HIV- PreM women. PM HIV+ women were younger (56±1 vs 60±1, $p < 0.01$), had lower BMI (27±1 vs 31±1 kg/m², $p < 0.01$) and were more likely to be African American (37% vs 20%, $p < 0.05$) than PM HIV- women. Mean CD4 count was 438±273 cells/ul and 474±326 cells/ul in PreM and PM HIV+ women respectively; 59% and 78% were on ART, respectively. Baseline Tumor Necrosis Factor- α (TNF α) and NTX levels were higher in PM but not PreM HIV+ versus HIV- women (Table). In PreM women, annualized % change in BMD (Δ BMD) at the lumbar spine (LS) and femoral neck (FN) did not differ between HIV+ and HIV- groups, before or after adjustment for age, BMI, and baseline BMD. In PM women, annualized % Δ BMD in HIV+ women was similar at the LS and FN, but 2.2-fold and 3.7-fold greater at the total hip (TH) and distal radius (DR) respectively, before and after adjustment for age, race, BMI, and baseline BMD.

Conclusions: Serum TNF α and NTX were higher in HIV+ than HIV- PM but not PreM women. Rates of LS and FN bone loss did not differ by HIV status in either PreM or PM women. At the TH and DR, rates of loss were higher in HIV+ than HIV- PM. Although limited by lack of TH and DR data in WIHS, these results demonstrate that estrogen deficient PM HIV+ women are at greater risk for site-specific bone loss than HIV- PM. The mechanism of HIV-associated bone loss in PM women may be related to higher bone turnover secondary to upregulation of pro-resorptive cytokines.

Table	PreM			PM		
	HIV+	HIV-	P value	HIV+	HIV-	P value
NTX (nmol/BCE/L)	11.3±4.3	10.4±3.2	0.17	19.4±1.0	16.6±0.6	0.02
TNF- α (pg/ml)	3.7±6.5	2.8±4.0	0.36	43.1±2.9	30.5±1.6	<0.001
% Δ LS BMD	-0.7±0.3	-0.5±0.3	0.54	-1.2±0.3	-0.5±0.4	0.14
% Δ TH BMD	NA	NA		-1.6±0.4	-0.7±0.2	0.045
% Δ FN BMD	-0.6±0.2	-0.4±0.3	0.34	-1.2±0.3	-0.8±0.4	0.42
% Δ DR BMD	NA	NA		-1.1±0.2	-0.3±0.2	0.007

Table

Disclosures: Michael Yin, None.

SU0372

Pleiotropic Genetic Determinants of BMD and Ages at Menarche and Natural Menopause: Multivariate Genome-Wide Association Meta-Analyses.

Yi-Hsiang Hsu^{*1}, Xing Chen², Douglas Kiel², Brent Richards³, Cathy Elks⁴, Jane Cauley⁵, Karol Estrada⁶, Michael Econs⁷, Kathryn Lunetta⁸, Ken Ong⁹, John Perry¹⁰, Fernando Rivadeneira⁶, Lisette Stolk¹¹, Tim Spector¹², Andre Uitterlinden¹³, M Zillikens¹⁴, Joanne Murabito¹⁵, David Karasik². ¹Hebrew SeniorLife Institute for Aging Research & Harvard Medical School, USA, ²Hebrew SeniorLife, USA, ³McGill University, Canada, ⁴Inst of Metabolic Sci, Addenbrooke's Hosp, United Kingdom, ⁵University of Pittsburgh Graduate School of Public Health, USA, ⁶Erasmus University Medical Center, The Netherlands, ⁷Indiana University School of Medicine, USA, ⁸Boston Uni Sch Public Health, USA, ⁹Paediatrics, University of Cambridge, United Kingdom, ¹⁰Inst Biomedical Clinical Science, Peninsula Med Sch, United Kingdom, ¹¹Departments of Internal Medicine, Erasmus MC, Netherlands, ¹²King's College London, United Kingdom, ¹³Rm Ee 575, Genetic Laboratory, The Netherlands, ¹⁴Erasmus MC Rotterdam, The Netherlands, ¹⁵Boston Uni Sch Med, USA

Reproductive aging and menopause in women are associated with the risk of osteoporosis that may be due to the changes in ovarian hormone production that affects bone health. Previously, we conducted univariate genome-wide association studies (GWAS) and identified novel genetic variants that associated with reproductive aging (age at menarche and age at natural menopause from ReproGen consortium) and associated with BMD (lumbar spine and femoral neck, from GEFOS consortium) in women of European descent. To identify pleiotropic genetic variants that associated with both reproductive aging and BMD, we performed multivariate GWAS meta-analyses on ~2.5 million SNPs across genome. METH-ODS: To model age at menarche and BMD simultaneously (as well as age at natural menopause and BMD), multivariate GWAS were performed using an empirical-weighted linear-combined test statistics (eLC) approach. Results from univariate GWAS meta-analyses were obtained from the GEFOS consortium for BMD (23,678 women, mean age ~60.5 yrs) and from the ReproGen consortium for age at menarche and age at natural menopause (87,802 women and 38,968 women, respectively; excluding women with age at menarche < 9 years old and age at menopause < 40 or > 60 years). The eLC approach directly combines test statistics from each univariate meta-analysis while accounting for the correlation among phenotypes, providing an unbiased estimation of multivariate test statistics. Multivariate p-values $\leq 5 \times 10^{-8}$ were considered genome-wide significant. Only loci with multivariate p-values significantly less than univariate p-values (for the same SNPs) were considered as potential pleiotropic loci. RESULTS: We identified 11 genome-wide significant pleiotropic loci from multivariate GWAS analyses, including previously reported loci for BMD such as MEPE, C6orf97 (near ESRI) and WNT4. Novel genome-wide significant pleiotropic loci included genes located in chr. 6q22.3, 7p12.2, 11p13, 11p14-p13 and 16q12.1 for age at menarche and BMD; and chr11p14.1 and 22q13.1 for age at natural menopause and BMD. Gene-set enrichment analysis showed significant enrichment in steroid synthesis ($p = 3.5 \times 10^{-6}$) and generation of germ cells ($p = 1.1 \times 10^{-6}$). CONCLUSION: Using a multivariate GWAS approach, we discovered potentially-pleiotropic loci that may be involved in the regulation of bone density and reproductive aging. A replication and eQTL analysis are underway to further validate these findings.

Disclosures: Yi-Hsiang Hsu, None.

SU0373

Relative Contributions of Estradiol and Testosterone to the Determination of Bone Mineral Density in Vietnamese Men and Women. Lan T Ho-Pham^{*1}, Thai Q. Lai², Nguyen Nguyen³, Tuan Nguyen³. ¹Pham Ngoc Thach University of Medicine, Vietnam, ²People's Hospital 115, Vietnam, ³Garvan Institute of Medical Research, Australia

Estrogen is known as an important determinant of bone mass in women. However, recent studies in Caucasian populations indicated that estrogen is also an important determinant of bone mineral density (BMD) in men. The present study was designed to examine the relative contribution of estrogen and testosterone to the determination of BMD in Vietnamese men and women.

The study was designed as a cross-sectional investigation, which involved 200 men and 415 women aged between 18 and 89 years (median: 47 years), who were randomly selected from various districts within the Ho Chi Minh City (Vietnam) by a simple random sampling process. Bone mineral density at the spine and femoral neck was measured by DXA (Hologic QDR4500, Bedford, MA, USA) by a ICSD-certified technician. Serum concentrations of total testosterone (TT) and estradiol (E2) were measured by competitive electrochemiluminescence immunoassays on the 10100/201 Elecsys autoanalyzer (Roche Diagnostics, Indianapolis, IN). The association between TT, E2, and BMD was analyzed by the multiple linear regression model.

The mean E2 in men and women was 28 pg/mL (SD 42) and 80 pg/mL (SD 237), respectively. The mean TT in men and women was 487 ng/dL (SD 208) and 20 ng/dL (SD 32), respectively. Serum levels of E2 declined with advancing age more in women than in men. In women, after adjusting for age and body weight (or BMI), higher serum concentrations of E2, but not TT, were significantly associated with greater BMD at the femoral neck ($r=0.48$; $P<0.001$) and lumbar spine ($r=0.49$; $P<0.001$). In men, E2, but not TT, was significantly associated with femoral neck BMD ($r=0.19$; $P<0.009$). In the multiple linear regression model, age, body weight and E2 accounted for 50-55% variance in femoral neck BMD, and 25% (in men) and 48% (in women) variance in lumbar spine BMD. In the presence of age and weight, variation in the serum concentrations of E2 contributed between 1 and 2% of total variance in femoral neck and lumbar spine BMD.

Thus, these results indicate that estrogen may be more important than testosterone in the determination of age-related bone loss in Vietnamese men and women. However, the relative contributions of estrogen to the variance in BMD is likely to be modest.

Disclosures: Lan T Ho-Pham, None.

SU0374

4-year Follow-up of the Bone Fracture Risk with FRAX in Patients not Treated with Antifracture Medicines. Pomost study. Jerzy Przedlacki^{*}, Krystyna Ksiezczepolska-Or^{oowska}, Artur Grodzki, Andrzej Swirski, Jan Musia^o, Ewa Loth, Pawe^o Teter, Andrzej asiewicz. National Center of Osteoporosis, Poland

It is not recommended not to use FRAX® in the follow-up of the fracture risk in patients treated with vitamin D and calcium.

The aim of the study was to assess the changes of 10-year fracture risk (10-FR) of the main bones with the use of FRAX® in patients not treated with antifracture medicines and the use of FRAX® in making therapeutic decisions in osteoporosis in these patients.

The study was performed in 107 patients (23 males and 84 females) aged 66.86.9 years not treated with antifracture medicines, and with 10-FR of the main bones $\leq 20\%$ (low and medium 10-FR) calculated with British version of FRAX®. Their age and T-score of femoral neck were changed during observation. Patients were supplemented with vitamin D (400-800 IU daily) and calcium (500-1000 mg daily).

There were not any new bone fracture and any other new clinical risk factors during observation. Baseline 10-FR was 9.03.7% (3.1-19%, median 8.6%). The controlled 10-FR was assessed in 70 patients after 1, in 56 after 2, in 51 after 3 and in 26 after 4 years. There was increase of 10-FR after 1-year in 39 patients (0.1-4.0 percentage points – PP; median 1 PP), after 2 in 39 patients (0.1-6.0 PP, median 1.0 PP), after 3 in 40 patients (0.3-9.0 PP, median 1.4 PP) and after 4 years in 25 patients (0.1-8.0 PP, median 1.5 PP). There was decrease of 10-FR after 1 year in 20 patients (0.2-7.1 PP, median 0.9 PP), after 2 years in 10 patients (0.1-2.2 PP, median 0.75 PP), after 3 years in 7 patients (0.5-4.0 PP, median 1.0 PP) and after 4 years in anybody. There was no change in 10-FR after 1 year in 12 patients, after 2 years in 4, after 3 years in 2 and after 4 years in 6 patients. There was change from low to medium 10-FR after 1 year in 2 patients (baseline 10-FR 18% and 19%), after 2 years in anyone, after 3 years in 1 (10-FR 17%) and after 4 years in 1 patient (10-FR 19%). Nobody had change of 10-FR from low to high during the whole observation.

There is not indication for the repeated DXA exam after up-to 4 years at least, in making decision on the treatment with antifracture medicines in patients with baseline low and medium (up to 16% in our study) 10-FR and any new clinical bone fracture risk factors. In patients with 10-FR in upper range of medium 10-FR ($\geq 17\%$ in our study) controlled DXA exam even after 1 year should be considered.

Disclosures: Jerzy Przedlacki, None.

SU0375

Depressive Symptoms on Balance Function and Osteoporosis: Result from CMC Study. Ki-Hyun Baek¹, Moo-Il Kang², Hyeon-Woo Yim³, Sun-Hee Ko², Seong-Su Lee⁴, Eunhee Jang^{*5}, Ki-Won Oh⁶. ¹St. Mary's Hospital, South Korea, ²Seoul St. Mary's Hospital, South Korea, ³Department of Preventive Medicine, The Catholic University of Korea, South Korea, ⁴Catholic medical college, South Korea, ⁵St.Mary's Hospital, Republic of Korea, ⁶Kangbuk Samsung Hospital, Sungkyunkwan University, South Korea

Objectives: Previous epidemiological study has suggested that depression might be associated declining physical function and lower BMD in older age. We aimed to investigate the impact of depressive symptoms score on balance test and BMD from community acquired cohort study in rural areas of Chungju, Korea.

Methods: One thousand six hundred sixty-four community dwelling subjects (Men:596/Women:1068) aged over 40 years old participated in the study by the stratified random cluster sampling in the Chungju, Korea. Anthropometric data, sociodemographic parameters and diet intake were collected by an skilled interviewer-administered standardized questionnaire. Depressive symptoms were assessed using the Center for Epidemiologic Studies Depression Scale (CES-D). Bone mineral density were measured by central bone densitometry (Hologic QDR4500). Balance function was estimated with one-leg-stand test (OLST) in all participants.

Results: Mean age of participants was 66.9 years old (meansSD), their mean BMI was 22.93 kg/m². After age adjustment, CES-D score showed negative correlation with OLST (male $r=-0.366$, female $r=-0.208$), not BMD in an elderly Korean population. Results were not substantially altered when adjusted for potential confounders (body weight, medical history, calcium intake). In multiple regression analysis, age and CES-D score persisted negative influence on balance function regardless of gender (male $R^2=0.089$, female $R^2=0.142$).

Conclusions: We concluded that depressive symptoms score was more correlated with balance function, not BMD in our study.

Disclosures: Eunhee Jang, None.

SU0376

Genome-wide Copy Number Variation Analysis on the Risk of Osteoporotic Fractures in Caucasian Men and Women: The Framingham Osteoporosis study. Kannabiran Nandakumar^{*1}, Ching-Lung Cheung², Huanvui Zhou³, Ching-Ti Liu⁴, Serkalem Demissie⁵, David Karasik⁶, Adrienne Cupples⁵, Douglas Kiel⁶, Yi-Hsiang Hsu⁷. ¹Hebrew Senior Life Harvard Medical School, USA, ²The University of Hong Kong, Hong Kong, ³Hebrew Rehabilitation Center, USA, ⁴Boston University School of Public Health, USA, ⁵BUSPH, USA, ⁶Hebrew SeniorLife, USA, ⁷Hebrew SeniorLife Institute for Aging Research & Harvard Medical School, USA

Copy number variations (CNVs) are sequence structure variations that are commonly found in the human genome. Studies have reported association between CNVs and cis-transcript levels that are not explained by SNPs. Although, GWAS have successfully discovered novel SNP variants associated with bone health phenotypes, up to date, those common SNP variants only explain 10% of BMD variability in Caucasians. To discover additional genetic determinants of bone health phenotypes, we conducted a genome-wide CNV association analysis on osteoporotic fractures in 8,700 adult men and women from the Framingham Study. The CNVs were called from Affymetrix 500K chip by PennCnv package and then confirmed by GoldenHelix SVS CNV module. A total of 112,745 CNV events were estimated in the Framingham population. Non-vertebral osteoporotic fractures (excluding high-impact trauma, fractures at head, spine, fingers and toes) were either ascertained by medical records/X-ray images or self-reported. There are 1,671 men and 2,160 women with at least one non-vertebral osteoporotic fracture. Association analysis was performed by using a burden test for rare/low frequent CNV regions (frequency $< 1\%$). From the burden test we found chromosomes 8, 9 and 15 significant based on the number of segments and proportion of samples with one or more segments. To further identify rare events, regional tests were performed for cnv regions in each chromosome. One of the regions in the region 15q11.2 was shown to be significantly associated with non-vertebral fracture. In conclusion, we identified a CNV that may increase susceptibility to osteoporotic fracture risks.

Disclosures: Kannabiran Nandakumar, None.

SU0377

Hypovitaminosis D in Postmenopausal Women with a Distal Radius Fracture. Woo Young Chang, Hyun Sik Gong^{*}, Cheol Ho Song. Seoul National University Bundang Hospital, South Korea

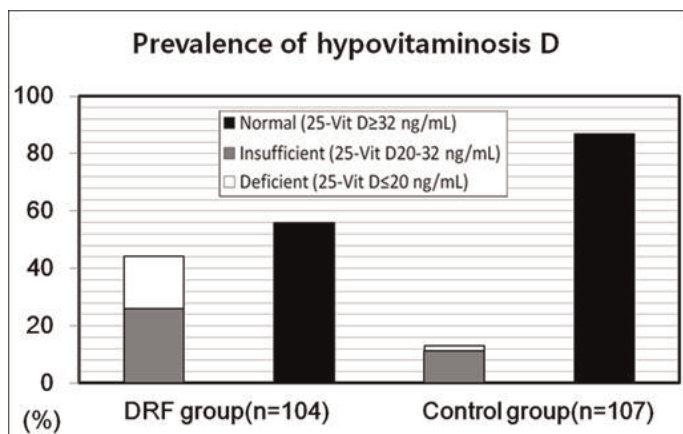
Purpose: Although hypovitaminosis D is reported to be common in the general population, few reports have examined vitamin D levels in patients with a distal radius

fracture (DRF). The authors hypothesized that postmenopausal women with a DRF may have depressed vitamin D levels.

Methods: The data of 104 postmenopausal women treated for a distal radius fracture (DRF group) and 107 age-matched control patients with soft tissue disease, such as tenosynovitis or lateral epicondylitis (control group) were compared. Serum vitamin D levels (25-hydroxycholecalciferol, 25(OH)D3) and the levels of several bone metabolism markers including serum parathyroid hormone, osteocalcin, C-telopeptide, and urine N-telopeptide were sampled and compared.

Results: Mean levels of the serum 25(OH)D3 in the DRF and control groups were 36.38 20.48 ng/mL and 47.16 17.69 ng/mL, respectively, and this difference was significant ($p < 0.001$). In particular, patients in their sixth and seventh deciles in the DRF group had significantly lower vitamin D levels than patients in the control group. Twenty-seven patients (26%) and 19 patients (18%) in the DRF group were vitamin D insufficient (defined as a serum level of 20-32 ng/mL) or vitamin D deficient (defined as a serum level of < 20 ng/mL), respectively, as compared with 12 patients (11%) and 2 patients (2%) in the control group (Figure 1). A weak positive correlation was found between femur neck BMD and serum 25(OH)D3 levels in the DRF group ($r = 0.22$, $p = 0.02$). However, the levels of the assessed markers of bone metabolism were similar in the two groups.

Conclusions: Postmenopausal women with a DRF were found to have significantly lower serum vitamin D levels than the control. Since vitamin D is required for bone metabolism and musculoskeletal function, further studies are warranted to determine whether hypovitaminosis D is a risk factor for DRF and whether vitamin D supplementation helps rehabilitation and the prevention of future fractures in patients with a DRF.



Prevalences of hypovitaminosis D in the DRF and Control groups

Disclosures: Hyun Sik Gong, None.

SU0378

Incidence of Multiple Falls and Risk Factors in a Longitudinal Population-Based Cohort Study in Japan: The ROAD Study. Shigeyuki Muraki¹, Toru Akune¹, Hiroyuki Oka¹, Kozo Nakamura², Hiroshi Kawaguchi³, Noriko Yoshimura¹. ¹22nd Century Medical & Research Center, University of Tokyo, Japan, ²The University of Tokyo, Japan, ³University of Tokyo, Faculty of Medicine, Japan

Multiple falls are the most serious cause of fractures in the elderly; therefore, it is important to identify subjects with risk factors for multiple falls. The objective of the present study was to determine the incidence of multiple falls and the risk factors. Among the 3,040 participants in the baseline study of the Research on Osteoarthritis/osteoporosis Against Disability (ROAD) study, 2,485 subjects (81.7%) participated in the follow-up study. Among the 2,485 subjects, 2,215 subjects (745 men and 1,470 women; mean age, 68.0 years) were analyzed. These subjects filled questionnaires regarding their falls between the baseline study and the follow-up study and questionnaires regarding their knee and lower back pain in the baseline study. Multiple falls was defined as 2 or more falls. They underwent radiography of the knee and the lumbar spine, and their physical abilities were measured in the baseline study. At the baseline, physical ability was estimated by measuring the grip strength and the walking speed at the usual pace. Knee osteoarthritis (OA) and lumbar spondylosis were defined as Kellgren/Lawrence grade ≥ 3 . The mean duration between the baseline and follow-up studies was 3.3 0.6 years. During this period, 261 subjects (11.8%; 84 men and 177 women) fell multiple times. A logistic regression analysis without adjustment showed that age (odds ratio [OR], 1.02; 95% confidence interval [CI], 1.01-1.03), grip strength (OR, 0.98; 95% CI, 0.97-1.00), walking speed [m/min] (OR, 0.98; 95% CI, 0.97-0.99), radiographic knee OA (OR, 1.86; 95% CI, 1.35-2.52), and knee pain (OR, 2.07; 95% CI, 1.56-2.73) were significantly associated with multiple falls, while radiographic lumbar spondylosis (OR, 0.93; 95% CI, 0.72-1.21) and lower back pain (OR, 1.21; 95% CI, 0.88-1.66) were not. Next, to determine the independent associations of each variable with multiple falls, a multiple logistic regression analysis was performed with age, gender, grip strength, walking speed, radiographic knee OA, and knee pain as independent variables. Walking speed [m/min] (OR, 0.98; 95% CI, 0.98-0.99) and knee pain (OR, 1.27; 95% CI, 1.08-1.48) were found to be independently associated with multiple falls. In conclusion, this longitudinal study

showed that lower walking speed at usual pace and knee pain were risk factors for multiple falls; these findings indicated that multiple falls may be prevented by walking as an exercise and by treating the knee pain.

Disclosures: Shigeyuki Muraki, None.

SU0379

Lack of Evidence Defining Vitamin D Inadequacy as Less than 30 ng/ml of Serum 25(OH)D. Sena Hwang¹, Han Seok Choi², Kyoung Min Kim³, Kwang Joon Kim³, Yumie Rhee¹, Sung-Kil Lim¹. ¹Yonsei University College of Medicine, South Korea, ²Division of Endocrinology & Metabolism, Department of Internal Medicine Dongguk University Ilsan Hospital, South Korea, ³Institute of Endocrine Research, & Brain Korea 21 Project for Medical Sciences, South Korea

Background: It is well known that vitamin D is important for metabolism for various organs as well as bones. However, the Institute of Medicine (IOM) gave a skeptical response for maintaining serum 25(OH)D levels over 30 ng/mL because the current evidence does not support beneficial effects on skeletal and nonskeletal health. We want to determine the association of 25(OH)D and clinical disorders and the optimal level of serum 25(OH)D for skeletal and non-skeletal health. **Methods:** This is a cross-sectional analysis of vitamin D and clinical disorders in 10,562 volunteers (10 to 95 years, male 4759, female 5803) participated in KNHANES, and nationally representative survey to assess the health and nutritional status from 2008 to 2009. We grouped according to 25(OH)D level follows as 25(OH)D < 12 ng/mL for group 1, $12 \leq$ group 2 < 20 , $20 \leq$ group 3 < 30 , and ≥ 30 ng/dL for group 4. **Results:** Serum 25(OH)D was below 12 ng/mL in 14.8%, below 20 ng/mL in 60%, below 30 ng/mL in 91.7%, and above 30 ng/mL in 8.3%. In skeletal health analyzed by bone geometry, cross sectional area, cross sectional moment of inertia and cortical thickness in femoral neck were significantly increased with serum 25(OH)D and cortical buckling ratio was decreased with serum 25(OH)D over all age groups in males ($p < 0.05$). However, in females, it was significant only over 50 age groups. In addition, in males, BMD values in group 4 were higher than those in group 2 or 3 ($p < 0.01$). In females, it was significant only age group of over 20 years ($p < 0.05$). There were no significant differences in vertebra. In non-skeletal health, there were significant differences in HOMA-IR, lipid profile (total cholesterol, HDL-, LDL-Cholesterol, triglyceride) according to 25(OH)D groups. In concomitant diseases, the risk of pulmonary tuberculosis was increased in group 1 compared to group 4. Of interest, there were no significant differences in all factors of skeletal and non-skeletal health between 25(OH)D 20-30 ng/mL group and 25(OH)D ≥ 30 ng/mL group. **Conclusion:** We demonstrated vitamin D was important not only for skeletal but also non-skeletal health. However, maintaining serum 25(OH)D with 20-30 ng/mL may be appropriate for proper skeletal and non-skeletal health without any complications with excessive supplement of vitamin D.

Disclosures: Sena Hwang, None.

SU0380

Non-traumatic Fractures and the Treatment Care Gap in Individuals with Diabetes: the Canadian Multicentre Osteoporosis Study. Lisa-Ann Fraser¹, Jonathan Adachi², Alexandra Papaioannou³, Lehana Thabane³. ¹University of Western Ontario/McMaster University, Canada, ²St. Joseph's Hospital, Canada, ³McMaster University, Canada

Purpose: Individuals with diabetes have been found to be at increased risk of non-traumatic fracture. A fracture is strongly predictive of future fracture risk and therefore pharmacologic intervention is usually indicated. Diabetes is not a disease that has been classically associated with increased osteoporosis or fracture risk; therefore it is unclear if individuals with diabetes are being identified and treated for skeletal protection. We aimed to describe fracture prevalence and bisphosphonate use in men and women with insulin-dependent and non-insulin-dependent diabetes in a large population-based Canadian cohort study.

Methods: 7741 Canadian men and women over 50 years of age were examined, including 506 individuals with non-insulin-dependent diabetes and 98 with insulin-dependent diabetes. History of non-traumatic fracture was investigated and a logistic regression model was created to identify factors associated with bisphosphonate use at any time during a 10 year period of the CaMos study.

Results: Individuals with diabetes were more likely to have a history of fracture than non-diabetic CaMos participants (odds ratio [OR]=1.21, 95% confidence interval [CI] 1.00-1.46, $p=0.04$). Other factors that were found to be associated with a history of fracture ($p < 0.05$) were: femoral neck T-score (OR: 0.79), rheumatoid arthritis (OR: 1.34) family history of osteoporosis (OR: 1.26), female gender (OR: 1.11) and increased age (OR 1.01). Despite the association with increased fracture rates, individuals with diabetes were less likely to be on bisphosphonate therapy at any point over 10 years of CaMos compared to other CaMos subjects (OR: 0.58; 95% CI 0.46-0.75, $p < 0.001$). Increased femoral neck T-score was also associated with decreased bisphosphonate use (OR: 0.40; 95% CI 0.40-0.44, $p < 0.001$). Variables associated with increased bisphosphonate use included: rheumatoid arthritis (OR: 1.28, 95% CI 1.04-1.58, $p=0.02$), family history of osteoporosis (OR: 1.25, 95% CI 1.07-1.45, $p=0.004$), female gender (OR: 3.04, 95% CI 2.62-3.51, $p=0.003$), and history of non-traumatic fracture (OR: 1.20, 95% CI 1.06-1.36, $p=0.004$).

Conclusions: Despite having an increased prevalence of non-traumatic fractures, we found individuals with diabetes were less likely to be treated with a bisphosphonate than those without diabetes. These findings point to a care gap in the treatment of non-traumatic fractures in individuals with diabetes.

Disclosures: Lisa-Ann Fraser, None.

SU0381

Prediction of Fractures over 6 Years from FRAX® in Older Women: Recent Falls History as a Further Independent Risk Factor. Judith Finigan^{*}¹, Claus-C Glueer², Dieter Felsenberg³, David Reid⁴, Christian Roux⁵, Richard Eastell¹.

¹University of Sheffield, United Kingdom, ²Christian Albrechts Universitaet zu Kiel, Germany, ³Charite - Campus Benjamin Franklin, Germany, ⁴University of Aberdeen, United Kingdom, ⁵Hospital Cochin, France

FRAX®, the WHO Fracture Risk Assessment Tool, calculates the 10-year probability of osteoporotic or hip fracture from 11 risk factors and, optionally, femoral neck (FN) BMD. We aimed to examine associations between the FRAX-derived percentage probabilities of fracture and the 6-year incidence of any non-vertebral, major osteoporotic, or vertebral fracture in a postmenopausal population, and to investigate whether recent falls were an further risk factor.

Women over age 55 years were recruited at 5 European centres (the OPUS study). Medical and lifestyle data were obtained at baseline including any falls in the previous year. Non-vertebral fractures since baseline were self-reported and verified at 6-year follow-up. In addition, lateral spine radiographs were obtained at both visits for diagnosis of incident vertebral fractures. Subjects were only included in the analysis if they had complete data on FRAX risk factors and falls at baseline and incident fracture data and radiographs at follow up. FRAX probabilities were calculated individually, based on each subject's details, history and FN BMD. Multivariate logistic regression, with the calculated FRAX probabilities and falls history as co-variables, was used to calculate odds ratios of incident fracture.

The inclusion criteria were fulfilled by 1410 subjects, of whom 220 sustained an incident fracture at any site: 175 had a non-vertebral, 60 a vertebral and 129 a major osteoporotic fracture (vertebra, hip, wrist or humerus). In the year before baseline 402 women had one or more falls, of whom 90 had 3 or more. By stepwise multivariate regression the most significant FRAX probability scores for predicting fractures, those with FN BMD, were identified for each fracture category. Any recent fall was an additional independent predictor of non-vertebral fractures (adjusted OR 1.50 (1.07, 2.10)) but the number of falls was not. Conversely neither osteoporotic nor vertebral fractures were additionally predicted by a recent fall ($p > 0.05$) but women with 3 or more falls were at greater risk (adjusted ORs 2.29 (1.27, 4.11) and 3.15 (1.51, 6.56), $p < 0.01$).

We conclude that the 10-year percentage risk of osteoporotic fracture calculated by FRAX, including FN BMD, also predicts different categories of fracture over 6 years in postmenopausal women. Recent prior falls are a further risk factor for non-vertebral fractures but the risk of osteoporotic and vertebral fractures is increased only with multiple falls.

Disclosures: Judith Finigan, None.

SU0382

Risk Factors for Vertebral Fractures in Frail, Long Term Care Residents. Mary Anne Ferchak, Megan Miller, Kimberly Zukowski, Carroll Lee^{*}, Subashan Perera, David Nace, Gail Fiorito, Neil Resnick, Susan Greenspan. University of Pittsburgh, USA

Background: Studies suggest a sideways fall, low hip bone mineral density, low BMI and poor mobility are associated with hip fracture in frail nursing home residents. However, little data are available on risk factors associated with vertebral fractures (VF) in this population.

Methods: To examine this question we assessed bone mineral density (hip or spine, DXA or heel ultrasound), calcium and vitamin D intake, Physical Performance Test (PPT), Physical Activities of Daily Living (PADL), Instrumental Activities of Daily Living (IADLs), Duke Comorbidity Index (DCI), mental status, falls history (in the last year) in 233 residents from long term care institutions on no medications for osteoporosis. Vertebral fractures included those reported as clinical vertebral fractures (medical record verified) or by DXA-derived Vertebral Fracture Assessment (moderate to severe fractures Genant classification).

Results: Mean age was 86.0 years. 30.5% of patients had a vertebral fracture, including 17.6% of patients who had an unknown, silent or moderate to severe vertebral fracture. Bone mineral density at the lateral spine or femoral neck was significantly lower, height shorter, and weight lower in patients with vertebral fracture compared to those without ($p < 0.05$, Table). The association with falls was marginally significant. Measures of heel ultrasound, calcium and vitamin D intake, PPT, PADL, IADL, DCI, mental status or osteoporosis diagnosis by BMD (T-score ≤ -2.5 at spine or hip) did not differ between the groups.

Conclusion: Low bone mineral density at the spine/hip, low body weight and history of falls are risk factors for vertebral fracture in residents of long term care. The association of bone mineral density and vertebral fracture in this cohort suggest that therapeutic intervention to improve bone mass should be pursued. Future studies are needed to examine which factors are associated with prospective changes in bone mineral density and incident vertebral fractures.

Variable	Vertebral fracture present	Vertebral fracture absent
N	71	162
Age (years)	86.3 ± 4.3	85.8 ± 5.6
BMI (kg/m ²)	26.7 ± 5.5	28.0 ± 5.4
Height (m) **	1.55 ± 2	1.57 ± 0.06
Weight (kg) **	64.1 ± 13.9	69.0 ± 13.4
BMD (g/cm ³) PA spine *	0.93 ± 0.19	0.98 ± 0.19
Lateral spine **	0.59 ± 0.11	0.65 ± 0.13
Total hip *	0.67 ± 0.14	0.70 ± 0.13
Femoral neck **	0.59 ± 0.11	0.63 ± 0.12
T-score (SD) PA spine *	-1.09 ± 1.74	-0.60 ± 1.74
Lateral spine **	-2.87 ± 1.35	-2.12 ± 1.53
Total hip *	-2.24 ± 1.12	-1.94 ± 1.04
Femoral neck **	-2.34 ± 1.03	-2.01 ± 1.08
Osteoporosis Dx by BMD (%)	43.5%	40.1%
Falls Reported (%) *	52.2%	38.1%

* $p < 0.10$ and ** $p < 0.05$ Vertebral fracture present vs absent

Table

Disclosures: Carroll Lee, None.

SU0383

Six Year Follow up in Patients with Previous Osteoporotic Fracture of Proximal Femur. Vaclav Vyskocil^{*}¹, Tomas Pavelka², Monika Honnerova³. ¹Center for Metabolic Bone Diseases, Czech Republic, ²Department of Orthopaedic Surgery, Czech Republic, ³Department of Bone Disease, Czech Republic

The authors observed 231 patients with low-trauma osteoporotic fractures, 87 in the area of proximal femur, 84 vertebral fractures and 60 fractures of distal forearm and proximal humerus, which had been treated in the Plzen University Hospital Clinic of Orthopedics and Traumatology in 2004. After hospital discharge densitometric measurement was performed and according to the results anti-osteoporotic pharmacotherapy was started. Bone mineral density (BMD) was measured in hip and spine.

In patients with spine injury was found significantly lower vertebral BMD, T-score -2.14 in area of L1-L4 and -1.6 in hip. The situation was opposite in patients with hip fractures: T-score -1.6 in L1-L4 and -2.02 in hip. In patients with fracture of proximal humerus and forearm was found less significant standard deviation from the norm T-score -1.3 in both areas. Average age of patients with fracture of distal forearm was 62, for vertebral fractures 67 and hip fractures 70. Relatively lower average age of patients with hip fractures was driven by the fact that those patients were able to come to densitometric measurement and all of them underwent surgical treatment of fracture. Treatment of distal forearm, proximal humerus and vertebral fractures was considering the patient age predominantly conservative.

Patients were treated despite the high fracture risk mostly by calcium and vitamin D. Only patients with lower BMD than -2.5 T score with low-trauma hip or vertebral fracture received an antiresorptive therapy at the specialized center. Although all patients were educated about the risk of another fracture, only 5% of them agreed to take the antiresorptive therapy. 15% of patients who refused the treatment suffered from another hip fracture contra-laterally within one year period and 35% within 3-year period after the first fracture.

After six years follow up of patients with the hip fracture (set of 87 patients), more than 43.7% of patients experienced contralateral fracture or other type of fracture. The authors also performed the monitoring of the same parameters in set of patients with vertebral fractures and distal forearm fractures and from the original densitometric measurements calculated FRAX index and they compare the risk of fracture with the actual incidence of fractures.

Disclosures: Vaclav Vyskocil, None.

SU0384

Ten Year Probability of Fractures Estimation with the WHO Fracture Risk Assessment Algorithm in Subjects with Osteopenia Naive to Treatment in the Latin America Vertebral Osteoporosis Study (LAVOS) Population, Puerto Rico Site. Rafael Gonzalez^{*}¹, Leticia Hernandez¹, Lillian Haddock-Suarez². ¹University of Puerto Rico, School of Medicine, Puerto Rico, ²University of Puerto Rico School of Medicine, Puerto Rico

There is limited information in literature regarding the prevalence of osteopenia or osteoporosis risk factors in the Puerto Rican population. The Latin American Vertebral Osteoporosis Study (LAVOS) was the first population-based study of vertebral fractures in Puerto Rico. The prevalence of vertebral fractures was estimated to be 11.9%. In 2008, the National Osteoporosis Foundation (NOF) published a revised Clinical Guide for the Prevention and Treatment of Osteoporosis. Treatment in patients with osteopenia (T-score between -1.0 and -2.5) is recommended if the 10-year hip fracture probability is 3% or higher and/or if the 10-year major osteoporosis-related fracture probability is 20% or higher, based on the World Health Organization (WHO) FRAX® algorithm. The aim of this study was to determine the prevalence of osteopenia in the LAVOS population and of the risk factors used in the FRAX

algorithm, along with the proportion of subjects who were treatment candidates by the new NOF guide.

The prevalence of osteopenia and risk factors used in the new NOF FRAX-based Guide was estimated using data from 398 female subjects between 50-90 years old collected in LAVOS. Osteopenic subjects were identified according to the WHO definition, (T-score between -1.0 and -2.4). The proportion of postmenopausal women age 50+ years who are treatment candidates by the new NOF Guide was calculated as well as the prevalence of risk factors taken in consideration in the WHO FRAX algorithm. Subjects were sub-classified in 4 age strata as follows: (1) 50-59, (2) 60-69, (3) 70-79 and (4) 80+ years.

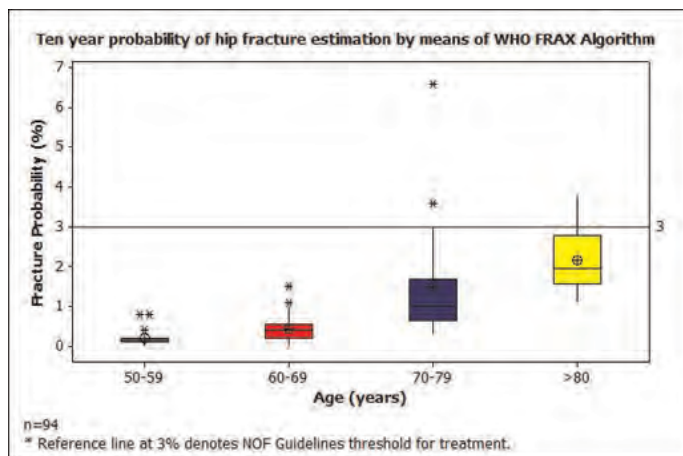
One hundred and seventy one (171) subjects were found to be osteopenic (42.96%). Ninety four (94) of these subjects were identified as osteopenic and naive to treatment, meeting inclusion criteria for our study. The prevalences of individual risk factors are shown in Table 1. After estimation of FRAX Score only 4 subjects (4.26%) met treatment criteria. Two subjects were 70-79 and 2 subjects older than 80 years old. No individuals met treatment criteria taking into consideration their 10 year major osteoporotic fracture probability.

Conclusion: Only 4 (4.26%) postmenopausal women were eligible for treatment according to their 10 year hip fracture probability and all were older than 70 yrs. These results are in accordance with previous studies showing that the new NOF FRAX-based Guide favors treatment in older women mostly based in their 10 yr probability of hip fracture.

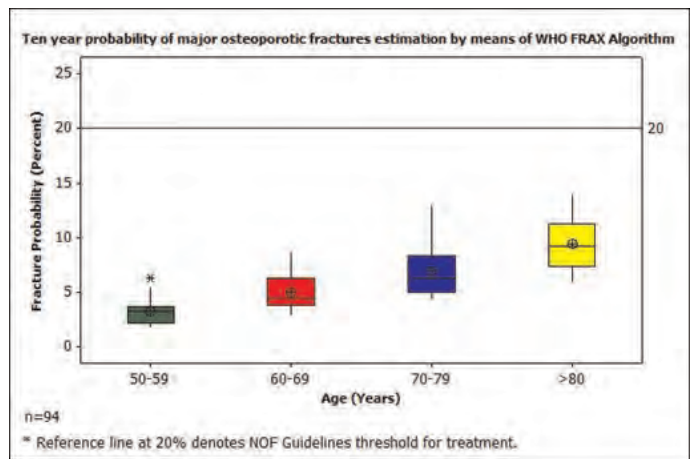
Table 1. Prevalence of individual risk factors in the WHO FRAX algorithm in a sample of osteopenic and naive to treatment women in the Municipality of San Juan, Puerto Rico.

Risk Factor	N	%	Mean	SD	SEM
Age (years)	94	100	65.48	8.95	1.03
50-59 years	27	28.72	-	-	-
60-69 years	32	34.04	-	-	-
70-79 years	25	26.60	-	-	-
80+ years	10	10.64	-	-	-
BMI (kg/m²)					
50-59 years	27		29.30	4.34	0.83
60-69 years	32		31.27	4.04	0.71
70-79 years	25		31.09	5.22	1.04
80+ years	10		30.34	2.90	0.92
Previous fracture (excluding hip or spine)	15	15.96	-	-	-
50-59 years	3	3.19	-	-	-
60-69 years	3	3.19	-	-	-
70-79 years	5	5.32	-	-	-
80+ years	4	4.25	-	-	-
Parent Hip Fracture	3	3.19	-	-	-
50-59 years	0	0	-	-	-
60-69 years	2	2.13	-	-	-
70-79 years	1	1.06	-	-	-
80+ years	0	0	-	-	-
Current Smoking	18	19.15	-	-	-
50-59 years	5	5.32	-	-	-
60-69 years	10	10.63	-	-	-
70-79 years	1	1.06	-	-	-
80+ years	2	2.13	-	-	-
Alcohol (more than 3 units/day)	0	0	-	-	-
Rheumatoid Arthritis	7	7.45	-	-	-
50-59 years	1	1.06	-	-	-
60-69 years	1	1.06	-	-	-
70-79 years	2	2.13	-	-	-
80+ years	3	3.19	-	-	-
Corticosteroids	0	0	-	-	-

Prevalence of individual risk factors in the WHO FRAX Algorithm



Estimation of 10 year probability of hip fractures by means of the WHO FRAX Algorithm



Estimation of 10 year probability of major osteoporotic fractures by means of the WHO FRAX Algorithm

Disclosures: Rafael Gonzalez, None.

SU0385

The Association Between Newer Anticonvulsants and Bone Mineral Density. Richard Lee^{*1}, Kenneth Lyles², Richard Sloane², Cathleen Colon-Emeric². ¹Duke University, USA, ²Duke University Medical Center, USA

Background: Newer anticonvulsant medications, such as levetiracetam, lamotrigine, and gabapentin, have been increasingly prescribed for the treatment of seizure disorders, neuropathic pain and mood disorders. Observational studies have reported an association between anticonvulsant use and reduced bone mineral density (BMD), but have largely been limited to traditional anticonvulsants, such as phenobarbital and phenytoin.

Objective: To examine the effect of newer anticonvulsant medications on BMD compared to traditional anticonvulsants.

Method: We performed a retrospective cohort study of patients at the Durham VA Medical Center. All patients who had a DXA between May 2006 and January 2010 were included. Cumulative exposure to anticonvulsant medications during the 10 years prior to DXA was determined from the computerized pharmacy record, including drug class, dose and duration. Patient demographics, comorbidities, and laboratory data were abstracted from the electronic medical record. Logistic regression modeling was used.

Results: There were 1779 BMD assessments within the study period. The most prescribed newer anticonvulsants were lamotrigine and gabapentin. Phenobarbital was the most prescribed traditional anticonvulsant. Use of newer anticonvulsants was associated with a lower risk of osteopenia or osteoporosis at the total hip or femoral neck (OR 0.72, 95% CI: 0.57 – 0.92) and lumbar spine (OR 0.74, 95% CI: 0.58 – 0.95). After adjustment for age, gender, BMI, and concurrent medications (including corticosteroids and bisphosphonates), the association between newer anticonvulsants and osteopenia or osteoporosis at the total hip or femoral neck was no longer statistically significant ($p = 0.08$). However, the association at the lumbar spine remained ($p = 0.02$).

Conclusion: Use of newer anticonvulsants, such as lamotrigine and gabapentin, is associated with a lower risk of osteoporosis or osteopenia by BMD at the lumbar spine.

Disclosures: Richard Lee, None.

SU0386

The Importance of Morphometric Radiographic Vertebral Fracture Assessment for the Detection of Patients Who Need Pharmacological Treatment of Osteoporosis among Postmenopausal Diabetic Korean Women. Yong Jun Choi^{*1}, Seoung-Oh Yang², Chan Soo Shin³, Yoon-Sok Chung¹. ¹Ajou University School of Medicine, South Korea, ²Asia Cancer Center, South Korea, ³Department of Internal Medicine, Seoul National University College of Medicine, South Korea

Purpose: Vertebral fracture assessment (VFA) is important for identifying patients who need pharmacologic therapy for osteoporosis. However, many patients with VFs remain undiagnosed and untreated. This study evaluated the number of patients who would be candidates for osteoporosis treatment according to the National Osteoporosis Foundation (NOF) Clinician's Guidelines to the Prevention and Treatment of Osteoporosis, among postmenopausal diabetic Korean women with morphometric VFs, assumed to have no radiographic diagnosis of VFs.

Methods: A total of 873 postmenopausal type 2 diabetic women were enrolled. Lateral plain radiographs of the thoracolumbar spine, and total hip BMD were obtained. The FRAX[®] probability was computed using the algorithm available online

at <http://www.shef.ac.uk/FRAX> (South Korea version). The subjects were classified with and without VFs into candidates for osteoporosis treatment [Tx(+)] and not candidates for osteoporosis treatment [Tx(-)] according to the NOF pharmacologic treatment guidelines, regardless of the presence of VFs.

Results: Among the subjects with morphometric VFs, only 2% of the patients had previously diagnosed VFs by medical doctors. There were 33.6% of the patients with current back pain that had VFs. However, 73.6% of the patients with VFs were not included in the Tx(+) group, given the assumption of no radiographic diagnosis of VFs.

Conclusions: With regard to increased risk of VFs in postmenopausal Korean women with type 2 diabetes mellitus, radiographic VFA would be useful for the clinical identification of treatment for osteoporosis and fractures.

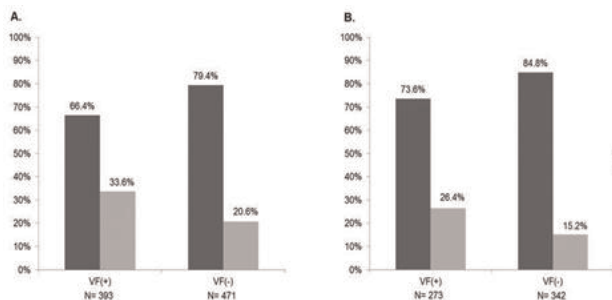


Figure. The number of women that were candidates for treatment [NOF Tx(+)] and not candidates for pharmacologic treatment [NOF Tx(-)] with [VF(+)] and without [VF(-)] vertebral fractures according to the National Osteoporosis Foundation (NOF) Guidelines: (A) After excluding the patients with a previous history of vertebral fractures (B) After excluding the patients with a previous history of vertebral fractures that were on pharmacological treatment for osteoporosis.

Disclosures: Yong Jun Choi, None.

This study received funding from: Sanofi-Aventis Korea

SU0387

Utilization of osteoporosis Medications in Women With and Without Diabetes Mellitus. Nicole Wright*, Elizabeth Delzell, Paul Muntner, Jeffrey Curtis, April Carson, Monika Safford. University of Alabama at Birmingham, USA

Purpose: Individuals with diabetes mellitus (DM) have an increased fracture risk. They also have multiple medical problems that compete for physician attention, potentially resulting in sub-optimal use of osteoporosis medications. Using baseline data from the Reasons for Geographic And Racial Differences in Stroke (REGARDS) study, the objectives were to compare fracture risk and utilization of osteoporosis medications among women with and without DM.

Methods: REGARDS is a population-based nationwide cohort study of 30,239 Caucasian and African American adults age >45 years in the US. DM was defined by self-report of physician or other healthcare provider diagnosis. Women without DM included those who did not self-report and did not have a fasting glucose >126 mg/dL or non-fasting glucose ≥200 mg/dL. Fracture risk was calculated using the World Health Organization fracture assessment tool (FRAX), and women were considered at high fracture risk if hip FRAX scores were ≥3%, major osteoporotic FRAX scores were ≥20%, or if they reported having a previous fracture at 45 years of age or older. Logistic regression models were used to evaluate associations between DM and osteoporosis medication use among women with high fracture risk.

Results: This study included 14,679 women with a mean (SD) age of 64.3 (9.4) years, of which 45% were African American. At baseline, 3,148 (21.5 %) women had DM. The proportion of women at high fracture risk was substantial, but lower ($p < 0.001$) in women with DM (26.8%) than women without DM (35.6%). Among women with a high fracture risk ($n = 4,888$), only 21.0% without DM and 10.6% with DM used osteoporosis medications. Several socio-demographic and co-morbidity variables were associated with osteoporosis medication use, including: age, body mass index, race, income, education, smoking, insurance, self-reported health, steroid use, number of cardiovascular conditions, and number of prescriptions. In the high fracture risk group, women with DM were less likely than women without DM to be taking osteoporosis medications after adjusting for other factors related to osteoporosis medication use [adjusted Odds Ratio (95% CI) = 0.72 (0.53-0.98)].

Conclusion: Overall, only one in five women with high fracture risk in the REGARDS study received osteoporosis medications and only one in 10 women with DM did so. Interventions to improve osteoporosis awareness and treatment targeted at high risk women with DM may be warranted.

Disclosures: Nicole Wright, Amgen, 2

SU0388

Vertebral Morphometry and its Heterogeneity Predict Lumbar Vertebral Fracture in Postmenopausal Women. The OFELY Study. Safaa Belghali, Jean-Paul Roux*, Elisabeth Sornay-Rendu, Roland Chapurlat, INSERM, UMR 1033, Université de Lyon, France

Vertebral morphometry is widely used to depict vertebral fracture but its utility for their prediction is poorly documented. The aim of our study was to analyze the vertebral morphometry and its heterogeneity in post menopausal women before incident vertebral fracture.

A case control study from the OFELY cohort was performed, including 29 postmenopausal women with incident lumbar vertebral fractures (mean age 71.9 years, mean time until fractures 9.4 years) age-matched with 57 controls without any incident fracture. Body height was not significantly different between groups. The distribution of vertebral fractures was: 7 (L4), 7 (L3), 5 (L2), 16 (L1), six women sustained more than one vertebral fracture. Digital scans were performed on lateral X-rays of lumbar spine (T12 to L4) at baseline with a spatial resolution of 0.26mm/pixel. From these radiographs, the following parameters were measured from six digitized points using Morpho Expert software (Explora Nova, la Rochelle, France): 1) the posterior, middle and anterior vertebral height, 2) the heterogeneity of heights evaluated by the coefficient of variation of these three values. All measurements were done by two observers, intra and inter observers reproducibility were excellent with an ICC of 0.99 and 0.97 respectively.

Mean vertebral heights were significantly lower in the fracture group vs the control one (33.43 vs 34.53mm; $p = 0.049$). The posterior heights did not differ between the two groups. Only the anterior and middle heights were significantly different between the two groups in L4 and L3 vertebrae. No significant differences were found in L1-L2 and T12. The mean heterogeneity of vertebral height was significantly greater in the fracture group (6 vs 5%; $p = 0.003$).

In summary, our study confirms the association between vertebral height and occurrence of fracture in postmenopausal women. The heterogeneity of vertebral heights seems to be a relevant variable associated with fracture, with a good reproducibility.

	Mean vertebral heights	Mean heterogeneity of heights (CV%)	L4			L3		
			ant. height	mid. Height	post. Height	ant. Height	mid. Height	post. Height
Fractures	33.43	6	35.89	33.56	34.17	36.21	32.71	35.89
Controls	34.53	5	36.75	34.68	34.93	37.11	34.07	36.43
p*	0.049	0.003	NS	0.02	NS	0.02	0.03	NS

*Mann Whitney test. Heights (mm).

No significant differences were found in L1-L2-T12.

Disclosures: Jean-Paul Roux, None.

SU0389

Circulating Sclerostin Demonstrates a Circadian Rhythm in Young Healthy Men. Shankar Narayan H Santosh*, Frank Joseph², Amanda Hamilton³, Brian Durham⁴, Anna Robinson⁴, Jonathan Tang³, Jiten P Vora³, William D Fraser⁵. ¹Royal Liverpool University Hospital, GBR, ²Countess of Chester Hospital NHS Trust, United Kingdom, ³Royal Liverpool University Hospital, United Kingdom, ⁴University of Liverpool, United Kingdom, ⁵Department of Clinical Chemistry, University of Liverpool, United Kingdom

Introduction: Sclerostin is secreted predominantly by the osteocytes, and is a physiological inhibitor of bone formation. By binding to LRP5/6 receptor it inhibits the Wnt signalling pathway and limits bone formation. A cross-sectional study was undertaken to ascertain whether true endogenous sclerostin circadian rhythmicity exists in healthy individuals.

Subjects and Methods: 6 healthy young men with normal BMD were recruited. Blood samples were collected every hour. Samples were centrifuged immediately, and serum/plasma was separated to be frozen at -700C for later analysis. Sclerostin was measured by an enzyme linked immunoassay (Biomedica, Austria). All samples were assayed in duplicates. The inter and intra assay CV% being 12.3% and <5% respectively with a detection limit of 8.9pmol/L.

Statistical Analysis: Individual and population mean cosinor analysis was performed using CHRONOLAB 3.0 (Universidade de Vigo, Vigo, Spain), a software package for analyzing biological time series by least squares estimation. Circadian rhythm parameters evaluated were: 1) midline estimate statistic of rhythm (MESOR), rhythm-adjusted mean; 2) amplitude and 3) acrophase were measured. A p value for the rejection of the zero-amplitude (no rhythm) assumption is also determined for each individual series and for the group.

Results: Significant circadian rhythm was observed for sclerostin in the study population ($p = 0.028$). The mean sclerostin (MESOR) was 84.41.4pmol/L. Circulating sclerostin demonstrated a nocturnal peak (time of onset 0100h) with concentrations remaining above mean over 4 hours. A small but ill sustained increase is noted at 0700h which culminates in a steep descent to a trough (at 0800h) the levels remain low throughout the morning till midday (1200h). The maximum percentage increase in the sclerostin concentration between 0100h and 0700h [(value at each time point - 0100h value) / 0100h value x 100] was 19.7%.

Conclusion: These results confirm a definite circadian rhythm for circulating sclerostin. This is the first demonstration of a circadian rhythm for sclerostin secretion in young healthy men.

SU0391

Take Two to Tango: Estrogen Deficiency and Increased Iron in Postmenopausal Osteoporosis. Qing Yang¹, Jinlong Jian¹, Florence Huang², Xi Huang^{*3}. ¹New York University Medical Center, USA, ²Bergen County Academy, USA, ³New York University School of Medicine, USA

Women during menopausal transition experience not only estrogen deficiency but also iron accumulation as a result of cessation of menstruation. Menopause initiates a rapid transit phase of bone loss at the early stage, which is reversible by hormone replacement therapy, and a subsequent slow phase of bone loss independent of estrogen deficiency. In the present study, we have investigated whether, in addition to estrogen deficiency, which promotes bone resorption, increased iron causes bone formation slowdown. We have found that hepcidin, a negative regulator of iron uptake, contains an estrogen responsive element. Estrogen deficiency by ovariectomy in mice initiates an increase in hepcidin, which temporarily causes an iron increase in the bone tissue because of iron excretion shutdown through its binding to ferroportin, an iron exporter. This estrogen deficiency-induced increase in iron in the bone could contribute to the early phase of bone loss. At the later stage, complete cessation of menstruation leads to a slow systemic increase in iron. We have found that iron inhibits alkaline phosphatase in osteoblast progenitor cells by enhancing hypoxia-inducible factor-2 α through an iron responsive element/iron regulatory protein system. Secondly, in the presence of iron, hemojuvelin (HJV), a co-receptor of bone morphogenetic proteins (BMP) receptors, is shed into the extracellular media. Solubilized HJV binds to BMPs and, thus, antagonizes the BMP signaling. Similar effects could be true with hemochromatosis Fe (HFE), another iron membrane protein. Taken together, our results suggest that iron accumulation is a previously ignored factor that could orchestrate the scenario of bone resorption outpacing bone formation with estrogen deficiency, leading to postmenopausal osteoporosis development.

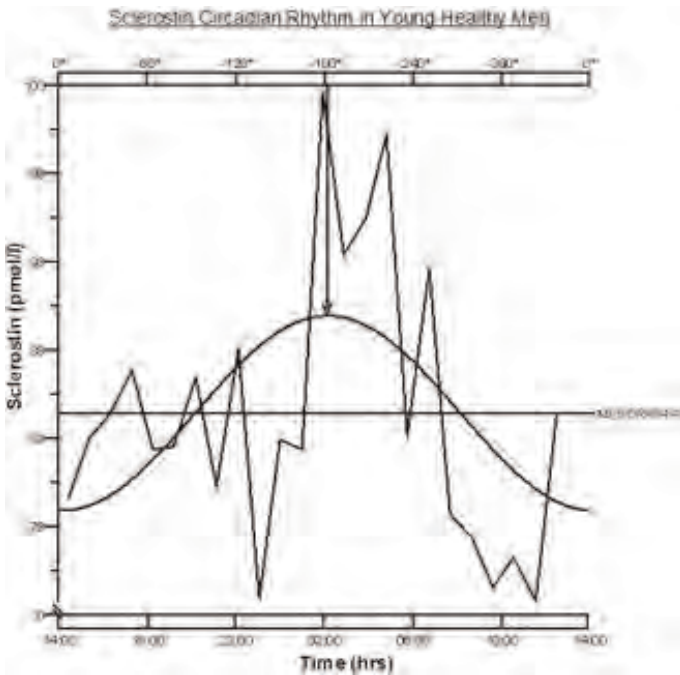
Disclosures: Xi Huang, None.

SU0392

Central IL-1 Signaling Regulates Bone Mass Via Parasympathetic Skeletal Innervation. Alon Bajayo^{*1}, Arik Bar², Adam Denes³, Marilyn Bachar², Vardit Kram², Malka Attar-Namdar², Alberta Zallone⁴, Raz Yirmiya², Itai Bab⁵. ¹Hebrew University Faculty of Dentistry, Israel, ²Hebrew University of Jerusalem, Israel, ³University of Manchester, United Kingdom, ⁴University of Bari Medical School, Italy, ⁵The Hebrew University, Israel

We have previously observed that central IL-1 stimulates bone mass accrual by favoring bone formation over bone resorption. This activity appears to oppose the adrenergic skeletal tone, which restrains bone formation and enhances bone resorption. Hence, we hypothesized that the central IL-1 signals are communicated to the skeleton by the parasympathetic nervous system (PSNS). Indeed, we show here osteoclastic nicotinic acetylcholine (ACh) receptors (nAChRs) consisting mainly of $\alpha 2$, $\beta 2$ and $\beta 4$ subunits, whereas osteoblasts express mainly muscular nAChRs subunits. Muscarinic ACh receptors were undetectable in either cell type. nAChR agonists inhibit bone resorption by inducing premature osteoclastogenesis and osteoclast apoptosis. The same agonists also stimulate osteoblast number. $\alpha 2$ subunit deficient mice have a markedly low bone mass phenotype due mainly to increased bone resorption. Additional parasympathetic components present in the skeleton are ACh as well as parasympathetic nerve fibers immunohistochemically positive for choline acetyltransferase and the vesicular ACh transporter (VAcHT). These fibers receive parasympathetic inputs from the central nervous system via the sacral intermediolateral cell column, shown by retrograde transneuronal tracing with a recombinant pseudorabies virus inoculated into the distal femoral metaphysis. The membrane bound and soluble ACh esterases (AChEs), the ACh degrading enzymes, are also present in bone cells. Taken together, these data establish the occurrence of skeletal parasympathetic innervation. PSNS activation by administering the peripheral AChE inhibitor pyridostigmine (PS) to mice during bone mass accrual leads to increased skeletal ACh content and a marked stimulation of bone mass consequent to decreased bone resorption. Mice with silenced central IL-1 signaling show high turnover low bone mass, almost complete inhibition of skeletal VAcHT expression and decreased ACh content, which cannot be rescued by PS. These findings demonstrate that during bone mass accrual central IL-1 signaling maintains a positive bone remodeling balance by controlling a skeletal parasympathetic tone.

Disclosures: Alon Bajayo, None.



Sclerostin Circadian Rhythm in Young Healthy Men

Disclosures: Shankar Narayan H Santosh, None.

SU0390

FSH Correlates with Trabecular Bone Loss in Rats Transitioning to Ovarian Failure. Ashley Lukefahr¹, Jennifer B. Frye¹, Laura Wright², Janet Funk^{*3}. ¹University of Arizona, USA, ²The University of Arizona, USA, ³University of Arizona Health Sciences Center, USA

Elevated follicle-stimulating hormone (FSH) correlates with low trabecular bone mineral density (BMD) in women during the perimenopause, an estrogen-sufficient period. A similar estrogen-replete state with elevated FSH occurs in rats during persistent estrus, an acyclic period that precedes ovarian failure. To examine the hypothesis that elevated FSH can drive perimenopausal trabecular bone loss, trabecular bone was assessed prospectively (by serial DXA measurement of distal femoral and proximal tibial BMD) in female Sprague Dawley rats undergoing normal ovarian senescence or treated with VCD, an industrial chemical known to accelerate the natural process of ovarian follicular atresia. As anticipated, serum 17 β -estradiol levels remained unchanged during natural or VCD-induced persistent estrus. In control rats naturally transitioning to ovarian senescence, BMD of the proximal tibial and distal femoral were unchanged, relative to peak BMD attained at 5 months of age, during a 6-month period from age 14-20 months when serum FSH was elevated 3.5-fold relative to young cycling animals. Administration of VCD to 1-month old animals accelerated the onset (age 5 months) of increased FSH. FSH levels in these rats were dose-dependently increased by VCD and exceeded those documented in animals undergoing natural senescence, being 5 to 12-fold elevated as compared to young cycling animals. FSH elevations in these rats preceded significant 4-13% decreases in BMD as compared to age-matched controls. Overall, BMD was significantly decreased in VCD-treated groups whose average cumulative FSH exposure (area under the curve [AUC], age 2-12 months) was > 3.8-fold higher than age-matched controls. When assessed at multiple time points across the transition to ovarian failure in control and VCD-treated animals (age 2-13 months), FSH levels were significantly and inversely correlated with BMD ($r^2 = 0.19$, $p < 0.0002$). Inhibin A levels across the transition correlated inversely with FSH ($r^2 = 0.27$, $p < 0.0001$) but did not correlate with BMD unless normally cycling (2-month old) animals were excluded ($r^2 = 0.13$, $p < 0.006$). To our knowledge, these results provide the first in vivo evidence of a correlation between trabecular bone loss, elevated FSH and decreased inhibin in estrogen-replete rodents transitioning to ovarian failure, lending further support to the prevailing hypothesis that non-estrogenic hormonal changes drive trabecular bone loss during perimenopause.

Disclosures: Janet Funk, None.

SU0393

Preliminary Evidence for Acute Post-Burn Bone Resorption in Sheep. Gordon Klein^{*1}, Minyi Hu², Liangjun Lin², Yi-Xian Qin², Cherry Croft³, Larry R Sumpter³, X Zhou³, H Qing⁴, Lynda Bonewald⁵.

¹University of Kentucky College of Medicine, USA, ²State University of New York at Stony Brook, USA, ³University of Kentucky, USA, ⁴University of Missouri Dental School, USA, ⁵University of Missouri - Kansas City, USA

Bone becomes adynamic by two weeks after severe burns in children. This occurs due to apoptosis of osteoblasts and, presumably, osteocytes caused by excessive endogenous glucocorticoid production and pro-inflammatory cytokines derived from the systemic inflammatory response that can cause osteoclastogenesis and acute bone resorption by stimulating the osteoblasts/osteocytes to produce RANK Ligand (RANKL). Thus it is possible that inflammatory cytokines and endogenous glucocorticoids together may be able to explain substantial resorptive bone loss by two weeks post-burn. If so we may be able to explain why acute administration of the bisphosphonate pamidronate is able to prevent significant post-burn bone loss. The aim of our study was to determine if osteoclasts are activated during this post-burn period. We obtained 1 cm² samples of iliac crest from six adult female cross-breed sheep weighing 30-40 kg. The specimens were fixated, dehydrated, and embedded in methylmethacrylate before being subjected to backscatter scanning electron microscopy (BS-SEM). When compared to specimens taken from uninjured sheep the burned sheep had less bone with enlarged osteocytic lacunae and substantial scalloping. The latter is considered a result of active bone resorption. To substantiate this finding TRAcP staining and osteoclast counts of two samples from each iliac crest section revealed an osteoclast count in the burned sample (n=1) that was 3.3 times higher in the burned specimen than in control specimens (n=3). To determine biomechanical properties, two trabecular bone cubes (average diameter 5x5x5 mm³) were cut from each sample using a low-speed diamond blade saw with continuous water irrigation. Compression testing was performed on a MTS Mini Bionix (MTS Corp, Minneapolis MN) axial load frame with Test Star II control software. Failure loading test was used to analyze the result of the mechanical testing, and compared to control samples (n=3), the experimental sample (n=1) showed a 28% decrease in elastic modulus (p<0.065). Thus we have preliminary evidence in sheep bones supporting acute resorption with attendant decrease in biomechanical stiffness acutely following burn injury. If further studies confirm these findings we have additional evidence supporting the early use of bisphosphonates to prevent post-burn bone loss.

Disclosures: Gordon Klein, None.

SU0394

Regulation of Parathyroid Hormone Secretion By Caffeine-Potential Impact on Osteoporosis. Ming Lu^{*}, Lars-Ove Farnebo, Robert Branstrom, Catharina Larsson. Karolinska Institutet, Sweden

Caffeine is a highly consumed psychoactive substance present in our daily drinks. Independent studies have reported associations between caffeine consumption, low bone mineral density and urinary calcium loss, as well as impaired bone development in vitro and in vivo. Besides calcium (Ca²⁺) and vitamin D, secretion of parathyroid hormone (PTH) is known as a critical regulator of bone remodeling. One study also observed a negative correlation between serum levels of intact PTH and coffee consumption, suggesting a potential association between caffeine and parathyroid gland function. However, the effect of caffeine on parathyroid hormone secretion in parathyroid cell has never been explored. In this study, we showed that 200µM and higher doses of caffeine inhibited intact PTH secretion in human parathyroid adenoma cells using perfusion technique. However, intracellular Ca²⁺ determined by Fura-2 was not affected by caffeine at any of the doses (50, 200, 500µM or 5mM). Protein expression of two main caffeine targets, adenosine receptors A1 and A2A, was demonstrated in human normal parathyroid and parathyroid adenomas. Measurements of intracellular cAMP showed decreased cAMP at 50µM caffeine, and gradually increased cAMP at higher concentrations. In conclusion, high doses of caffeine inhibit PTH secretion in human parathyroid cells independent of intracellular Ca²⁺ and cAMP level. The inhibition of PTH secretion caused by high doses of caffeine may contribute to bone loss in human.

Disclosures: Ming Lu, None.

SU0395

Response Of Bone Turnover Biomarkers Following Ovariectomy In A Model Of Low Birth Weight In The Female Sprague-Dawley Rat. Thomas P Royals^{*}, Michael B Manigrasso¹, Norma B Ojeda², Michelle A Tucci³, Barbara T Alexander¹. ¹University of Mississippi School of Medicine, Department of Physiology, USA, ²University of Mississippi School of Medicine, Department of Pediatrics, USA, ³University of Mississippi School of Medicine, Department of Orthopedics, USA

Osteoporosis is the most common type of bone disease, with postmenopausal bone loss as the most prevalent cause. Ovariectomy (OVX) in the female Sprague-Dawley (SD) rat creates an ovarian hormone deficient animal model that mimics accelerated

bone loss observed in postmenopausal women. Low birth weight (LBW) also compromises adult bone structure and increases the risk of osteoporosis. Utilizing a model of LBW induced by placental insufficiency, the aim of this study was to test the hypothesis that bone loss due to estrogen deficiency would be exacerbated in female LBW or intrauterine growth restricted (IUGR) offspring as evaluated by serum bone remodeling biomarkers. Birth weight was significantly reduced in IUGR (n=10) compared to normal birth weight (NBW; n=12) offspring (5.11 ± 0.06g vs. 5.91 ± 0.09g respectively; p<0.05). At 12 weeks of age a subgroup of IUGR and control rats underwent OVX or SHAM OVX. Blood was collected at the day of surgery, day 0, and days 7, 14, 28, and 42 post OVX or SHAM OVX and three bone turnover biomarkers were evaluated: N-terminal propeptide of type I collagen (PINP), C-terminal telopeptide of type I collagen (CTX-1), and tartrate resistant acid phosphatase 5b (TRACP 5b). PINP, a bone formation marker, was increased in NBW OVX relative to IUGR OVX at days 7 and 14 post OVX. Whereas CTX-1, a marker of osteoclast activity, was increased in IUGR OVX relative to NBW OVX at 14 and 28 days post OVX. TRACP 5b, a marker of osteoclast number, was significantly reduced in both IUGR OVX and NBW OVX compared to their SHAM counterparts at all time points following ovariectomy. In addition the resorption index (RI), an indicator of mean osteoclast activity, CTX-1/TRACP 5b remained elevated above baseline in the IUGR OVX while their NBW counterparts had returned to baseline levels at 28 days post OVX. Thus, these data indicate that IUGR may lead to an increase in osteoclast activity and an increase in bone resorption following estrogen withdrawal compared to their NBW counterparts, thereby accelerating postmenopausal bone loss. Therefore low birth weight women not only have compromised adult bone structure and increased risk for osteoporosis, but their risk for postmenopausal osteoporosis may be further increased as well.

	PINP (ng/mL)		CTX-1 (ng/mL)		TRACP 5b (U/L)		CTX-1/TRACP 5b (mcg/U)	
	Day 0	Day 14	Day 0	Day 28	Day 0	Day 28	Day 0	Day 28
NBW SHAM n=3-4	10.71 ± 0.62	8.13 ± 0.53*	10.95 ± 1.32	9.12 ± 0.24	1.06 ± 0.13*	1.42 ± 0.27*	10.61 ± 1.39	8.02 ± 2.45*
IUGR SHAM n=3	9.47 ± 1.06	12.16 ± 0.24*	10.09 ± 1.11	6.43 ± 1.11	1.70 ± 0.27*	2.02 ± 0.23*	7.15 ± 1.61	3.18 ± 0.49*
NBW OVX n=5-8	18.91 ± 4.18	43.15 ± 8.60*	13.76 ± 2.23	17.95 ± 3.38	1.06 ± 0.11*	1.01 ± 0.11*	14.94 ± 3.50	13.70 ± 2.16*
IUGR OVX n=4-7	11.15 ± 3.45	35.10 ± 4.65*	14.10 ± 1.59	20.91 ± 4.04	1.01 ± 0.03*	1.06 ± 0.09*	14.69 ± 0.07	16.39 ± 2.41*

*P<0.05 vs all other groups at same time point

Serum Bone Remodeling Biomarker Levels Following OVX or SHAM OVX

Disclosures: Thomas P Royals, None.

SU0396

Effects of Various Bone Loss Factors on Bone Micro Architecture in Female Rats. Keiko Iwaki, Tomoko Hanaoka, Yasue Nishii, Hidetaka Imagita, Susumu Sakata, Akira Minematsu*. Kio University, Japan

There are various factors to cause bone loss. This study was investigated the effects of estrogen deficiency, immobilization and low calcium insufficiency on bone mineral density (BMD) and trabecular bone micro structure in female rats. Twenty-four Wistar female rats aged 10 week-old were divided into 4 groups randomly; sham-operated (SHAM), ovariectomy (OVX), sciatic denervation (DN) and low calcium intake (LC) groups. They were bred for 6 months and allowed at libitum feeding (standard laboratory diet; Ca 1.12g/100g or LC diet; Ca 1.18mg/100g) and drinking. After this experiment, all tibias of the rats were dissected out. Micro CT scanning was used to determine morphological indices of BMD and trabecular bone structure in the metaphysical region of the proximal tibia. This region spanned 2 mm, with the first slice starting from 1 mm under the growth plate. BMD and trabecular bone structure as bone volume fraction (BV/TV), trabecular thickness (Tb.Th), trabecular number (Tb.N), trabecular separation (Tb.Sp), trabecular width (Tb.W), connectivity density (Conn.D), trabecular bone pattern factor (Tb.Pf), the structural model index (SMI), and osteoporotic degree of marrow space (Vm) and trabecular (Vt) of bones were measured with bone analysis soft. This study was carried out in accordance with the Guide for Animal Experimentation and the Committee of Research Facilities of Laboratory Animal Science of Kio University. BMD of all groups decreased significantly compared with SHAM group (trabecular bone; range -12.3% to -16.8%, p<0.001, cortical bone; range -6.2% to -26.0%, p<0.0001), and decreased most in LC group. Though bone loss was occurred in OVX, DN and LC groups, bone micro structure parameters showed the different changes among these factors. Reduction of BV/TV was induced by decrease of BV in OVX group, but increase of TV in DN and LC groups (range -27.3% to -68.3%, p<0.0001). All micro structure parameters of OVX, DN and LC groups showed the negative changes compared with SHAM group. Tb.N, Tb.Sp, Tb.Pf, SMI, Vm and Vt of OVX group, Tb.Th, Tb.Sp, Tb.W, Tb.Pf, Vm and Vt of DN group, and Tb.N, Tb.Sp and Vm of LC group had significance to those of SHAM group. It was concluded that OVX, DN and LC occurred to decrease of BMD and increase of Tb.Sp, and the general factor like estrogen deficiency and lack of Ca affected Tb.N, and local factor like immobilization affected Tb.Th and Tb.W. The process of bone loss was different by its cause.

Disclosures: Akira Minematsu, None.

SU0397

Influence of Vitamin D on Bone Micro-Structural and Biomechanical Properties in Patients with Hip Fracture. Cristina Miranda^{*1}, M^a Jose Montoya², Mercedes Giner³, M^a Angeles Vazquez², Ramon Perez-Cano¹.

¹University of Seville, Spain, ²Virgen Macarena Hospital, Spain, ³Virgen Macarena Hospital/Seville University, Spain

Introduction: Vitamin D is essential for muscle-skeletal health. Insufficient levels of 25(OH)D are associated with PTH and bone remodelling increase, bone mass decrease and mineralization defects.

Objective: The aim of this study was to evaluate serum levels of 25(OH)D, hormones with influence on bone metabolism (PTH and IGF-I), bone remodelling markers (β -CrossLaps and PINP), bone mass density (BMD) and bone micro-structural and biomechanical properties of femoral neck of patients with osteoporotic hip fracture that required hip arthroplasty (OP) compared to patients with osteoarthritis admitted for elective hip arthroplasty without osteoporotic fractures antecedents (OA).

M&M: We studied 29 OP patients and 14 OA patients, all of them over 50 years old. Hormones serum levels, bone remodelling markers (immunoassay, electrochemical-luminiscence), femur BMD (Hologic-Discover densitometre), microstructural (SkyScan 1172 computerized microtomography) and biomechanical (IGFA system, monoaxe compression essay) properties were measured. Ethical approval was obtained from the local Research Ethic Committee, as well as the informed consents from all the patients included in this study. Results were statistically analyzed with SPSS 17.0 software.

Results: OP patients showed 25(OH)D ($p = 0.02$) and femur BMD ($p = 0.029$) levels significantly lower than OA patients, but PTH ($p=0.029$) and β -CrossLaps ($p=0.04$) levels significantly higher. 25(OH)D levels were positively correlated with IGF-I ($r=0.338$, $p=0.044$) but negatively with β -CrossLaps ($r=-0.483$, $p=0.003$). PTH levels were negatively correlated with femur BMD ($r = -0.617$, $p=0.005$) and positively with trabecular separation ($r=0.530$, $p=0.006$). Patients with 25(OH)D levels lower than 20ng/mL (with comparable antropometrics parameters) showed significantly higher β -CrossLaps levels ($p=0.006$), lower IGF-I levels ($p=0.007$) and smaller trabecular thickness ($p=0.04$) than patients over 20ng/mL.

Conclusion: Both pathologies showed low vitamin D levels, especially in OP patients, high PTH and bone remodelling markers levels and decreased BMD levels. Patients with 25(OH)D levels lower than 20ng/mL showed high bone remodelling levels, low IGF-I levels and bone structural disorders (trabecular thickness), which may be related with an increased fracture risk.

Disclosures: Cristina Miranda, None.

SU0398

Calcium Intake Affects Body Composition, Bone Metabolism and Insuline Resistance in Spontaneously Obese Rats. Clarisa Marotte^{*1}, Gabriel Brvk², MarÚa Catalina Olguin³, Diego MartÚn Lucero⁴, Laura Schreier⁴, Silvia MarÚa Friedman⁵, MarÚa Luz Portela⁶, Susana NoemÚ Zeni⁷.

¹Seccion OsteopatÚas Medicas, Hospital de CIÚnicas, Universidad de Buenos Aires. Catedra de BioquÚmica General y Bucal, Facultad de OdontologÚa, Universidad de Buenos Aires. Consejo Nacional de Investigaciones CientÚficas y Tecnicas, Argentina, ²Seccion OsteopatÚas Medicas, Hospital de CIÚnicas, Universidad de Buenos Aires. Catedra de BioquÚmica General y Bucal, Facultad de OdontologÚa, Universidad de Buenos Aires, Argentina, ³Universidad Nacional de Rosario, Argentina, ⁴Laboratorio de LÚpidos y LipoproteÚnas, Departamento de BioquÚmica CIÚnica, Hospital de CIÚnicas, Universidad de Buenos Aires, Argentina, ⁵Catedra de BioquÚmica General y Bucal, Facultad de OdontologÚa, Universidad de Buenos Aires, Argentina, ⁶Catedra de Nutricion y BromatologÚa, Facultad de Farmacia y BioquÚmica, Universidad de Buenos Aires, Argentina, ⁷Seccion OsteopatÚas Medicas, Hospital de CIÚnicas, Universidad de Buenos Aires. Catedra de BioquÚmica General y Bucal, Facultad de OdontologÚa, Universidad de Buenos Aires. Consejo Nacional de Investigaciones CientÚficas y Tecnicas (CONICET), Argentina

MB Zemel theory postulated in 2004: "A high CaI would be a preventive factor for Ob/OW development". **Objective:** to evaluate the effect of feeding different Ca content diet on body composition, bone metabolism and insulin-resistance in rats that spontaneously develop Ob in adolescent state. Female IIMbb rats fed from pregnancy one of 3 isocaloric diets only varied in Ca content: 0.9g% (HG), 0.5g% (NG) and 0.2g% (LG). At weaning male offspring continued feeding the same mother diet till 50 days of age (Tf). Results (mean SD), groups HG, NG & LG, respectively are shown in the Table 1.

Different letters: $p<0.05$. LG increased BW by the increment in body fat. An inverse relationship between CaI and insulin resistance was observed. **Conclusions:** The low CaI not only affects bone metabolism but also body composition and insulin resistance in spontaneous obese rats. UBACyT091.

	HG	NG	LG	Method
Food intake	13.51±1.55	12.26±1.80	13.69±1.63	-
Ca intake (Cal)	221.0±15.0a	126.0±44.0b	46.0±9.0c	-
% Ca Absorption	84±8a	87±1b	91±9c	[(ICa-Fecal)/ICa] x100.
Body Weight (BW) (g)	185±9a	227±13b	262±7c	-
%Water	69.2±4.2	70.0±2.8	66.7±3.3	AOAC
%Protein (g/100g BW)	14.3±1.7	14.2±1.9	15.9±2.1	AOAC
%Fat	14.2±0.9a	13.7±0.8a	15.9±0.6b	AOAC
BMC (g/100g BW)	1.09±0.02a	1.29±0.08b	0.83±0.03c	DXA
P (mg/100g BW)	532±22a	520±31a	882±15b	UV-Colorimetry
BGP (ng/dl)	279±73a	375±46b	478±45c	EUSA
sCTX (mg/dl)	84.9±22.5a	71.9±12.4ab	80.6±14.1b	EUSA
Glucose (mg/dl)	111.8±25.5a	151.9±21.9b	207.0±11.0c	Colorimetry
Insulin (ng/ml)	1.92±0.75a	4.07±0.93b	6.87±2.24c	EUSA

TABLE 1

Disclosures: Clarisa Marotte, None.

SU0399

Dietary Iron Deficiency is Associated with Impaired Mineralization and Osteogenic Gene Expression in Weanling Sprague Dawley Rats. Edralin Lucas, MCKALE DAVIS, Yan Wang, Elizabeth Rendina, Stephen Clarke, Brenda Smith, Krista Shawron^{*}. Oklahoma State University, USA

Recent studies have demonstrated an intriguing connection between iron deficiency and negative alterations in BMD, leading to the speculation that iron plays a role in the regulation of normal bone metabolism. Due to these observations linking iron status and osteoporosis, examination of the mechanisms contributing to iron-dependent alterations in bone metabolism is warranted. Our objective was to explore the effects of iron deficiency on BMD and bone microarchitecture in the tibia and spine in an animal model of iron deficiency. Weanling Sprague Dawley rats were assigned to one of three groups for 35 days ($n=10-12$ /group): (1) iron deficient (ID; < 5 mg Fe/kg diet), (2) control (C; 50 mg Fe/kg diet) or (3) pair-fed (PF) the control diet to the level of intake as the ID group. BMD and microarchitecture were examined by DXA and microCT in both the tibia and spine. Total RNA was isolated from a metaphyseal region of the femur and used to synthesize cDNA to examine gene expression by qPCR.

Due to differences in food intake and body weight, only data for PF and ID are presented here. BMD of both the tibia and spine in ID animals was lower ($p<0.05$). Further examination of the tibia by microCT indicated that trabecular tissue was unaffected in response to iron deficiency, though cortical thickness was significantly decreased in ID animals ($p<0.05$). In contrast to the tibia, BV/TV, TbTh, and TbN were decreased in the spines of ID animals ($p<0.001$). To examine the extent to which alterations in osteogenic gene expression contributed to impaired microarchitecture in ID animals, RNA from the femur was extracted and used for gene expression analyses by qPCR. Osteocalcin, BMP-2, and Col1a1 expression was repressed in the ID group ($p<0.05$), suggesting an impairment in bone formation and mineralization in response to iron deficiency. Runx2 expression was repressed in ID animals ($p<0.05$) and associated with a decrease in osterix expression. The expression of genes related to osteoclast differentiation and activity, including CTSK, NFATc1, and TRAP were unaltered in response to iron deficiency. Thus, these data suggest that iron deficiency is associated with an impairment in osteoblast differentiation or function. Additional studies are currently in progress focused on examining the mechanisms through which iron deficiency impairs osteogenic gene expression and/or osteoblastogenesis.

Disclosures: Krista Shawron, None.

SU0400

The Effect of Weight Loss and Dietary Macronutrient Composition on Bone Mineral Density - Results of a Randomized Controlled Trial. Amir Tirosh¹, Vincent Carey¹, Frank Sacks¹, George Bray², Steven R. Smith², Meryl Leboff¹. ¹Brigham & Women's Hospital, USA, ²Pennington Biomedical Research Center of the Louisiana State University System, USA

Purpose: The effects of weight loss diets and different macronutrient compositions on bone mineral density (BMD) in overweight and obese individuals have not been fully elucidated, although there are concerns regarding the potential deleterious effects of low-carbohydrate high-proteins diet on BMD and fracture risk. **Methods:** The Preventing Overweight Using Novel Dietary Strategies (Pounds Lost), is a randomized controlled trial of 811 overweight and obese adults randomly assigned to 4 diets with targeted percentages of energy derived from fat, protein, and carbohydrates of: 20, 15, and 65%; 20, 25, and 55%; 40, 15, and 45%; and 40, 25, and 35%, respectively (N Engl J Med. 360:859, 2009). In 424 Pounds Lost participants (mean age 529 years, 57% females) from 2 centers (Boston and Baton Rouge). BMD was measured at the spine, total hip and femoral neck (FN) at baseline, 6, and 24 months of intervention using DXA machines (QDR 4500A, Hologic, Bedford MA). Reproducibility of the spine and femoral neck BMD were 1.21% and 1.74% respectively. **Results:** The overall average weight loss after 6 and 24 months of intervention was 6.9 and 6.1 kg, corresponding to a 7.9% and a 6.9% weight loss of the initial body weight, respectively. Retention rates were 78% and 56% at 6 and 24 months. There were no significant differences in the magnitude of weight loss among the 4 diet groups. Despite significant weight loss, the change from baseline in spine, total hip and FN BMDs at 6 months was 0.0005 (p=0.07), -0.001 (p<0.001), and -0.007 (p=0.016) gm/cm² and at 24 months was 0.005 (p=0.04), -0.014 (p<0.001), and -0.014 (p<0.001) gm/cm², respectively. In a multivariate model adjusted for age, sex, baseline BMD, diet group and baseline anthropometric measurements, for every 1% of body weight loss, there was a small but significant change in BMD of -0.00155 and -0.00121 gm/cm² at the total hip and FN (p<0.0001), with no change at the spine over 2 years. High protein diets were not associated with greater bone loss as compared with the low-protein groups. **Conclusions:** Dietary interventions to reduce weight loss can result in a small amount of bone loss, possibly related to the DXA measures or other mechanisms. This effect can become clinically significant with higher percentages of weight loss over time. All 4 interventions, including the low-carbohydrate-high-protein diets resulted in similar amounts of bone loss in this large, prospective randomized trial.

Disclosures: Amir Tirosh, None.

SU0401

Bone Quality Is Negatively Affected by Glucocorticoid-induced Changes in the Geometry of Osteoclast Resorption Cavities. Jozef Vanderroost¹, Kent Soe², DITTE MARIE MERRILD², Jean-Marie Delaie³, Harry Van Lenthe⁴. ¹K.U.Leuven, Belgium, ²Vejle Hospital, University of Southern Denmark, Denmark, ³Vejle Hospital, CSFU-IRS, University of Southern Denmark, Denmark, ⁴Katholieke Universiteit Leuven, Belgium

Loss of bone strength and prevention of fractures is a major concern for clinicians dealing with bone pathologies, such as postmenopausal osteoporosis (PMOP) and glucocorticoid-induced osteoporosis (GIO). Unlike for PMOP, bone mineral density (BMD) is a poor predictor of fracture risk for GIO. We have recently found that glucocorticoid (GC) causes osteoclasts (OCs) to change their resorptive behavior, making large elongated resorption cavities instead of circular resorption cavities, without affecting the total eroded surface (S/Se et al. JBMR 2010). The aim of this study was to determine whether this change in resorptive behavior of OCs can explain the increase in fracture risk as seen in GIO.

The three-dimensional characteristics of resorption cavities generated in vitro by human OCs in the presence or absence of GC were recorded. The impact of GC-induced resorption on the mechanical properties of bone was modeled using the beam-shell finite element model of trabecular bone (Vanderroost et al. J Biomech 2011). Resorption cavities with a distribution of cavity dimensions taken from the in vitro measurements were added; the eroded surface was kept constant at 2% of the bone surface. Trabecular bone samples originated from 40 patients and three anatomical sites (4th lumbar vertebra, femoral neck and iliac crest) covering a wide range of trabecular bone properties. Uniaxial compression tests were used to quantify bone apparent stiffness as a measure of bone quality.

The model showed that, when compared to the control case, resorption cavities generated in the presence of GC, caused a statistically significant loss of stiffness (Table 1). The largest stiffness reduction was found for lumbar spine samples with mostly rod-like trabeculae, the lowest for femoral samples with mostly plate-like trabeculae (Table 1).

We conclude that the altered resorptive behavior of the OCs due to GC-exposure negatively affects bone stiffness and likely increases bone fracture risk independent of the extent of eroded surface. In vivo, this effect is likely to be stronger, because several OCs can resorb bone at the same cavity; hence, the excavation in vivo is likely to be deeper than the ones we observed in vitro after 72hrs of culture. Since deeper cavities can cause trabecular rupture or perforation, the expected stiffness loss in vivo is larger. These findings demonstrate that the dimensions of OC resorption cavities are one of the factors determining bone quality.

Stiffness loss (%)	Control	Glucocorticoids
4 th lumbar spine	0.315	0.336
Femoral head	0.084 ^a	0.111 ^a
Iliac crest	0.217 ^a	0.276 ^a
All data pooled	0.205 ^a	0.240 ^a

Table 1: average stiffness loss, t-test for GC effect. a: p < .001

Disclosures: Harry Van Lenthe, None.

SU0402

Age-Related Changes in Proximal Humerus Bone Health in White Males. Robyn Fuchs*, Sara Mantila Roosa, Andrea Hurd, Stuart Warden. Indiana University, USA

The proximal humerus is a common site for osteoporotic fracture during aging, accounting for up to 5% of fractures to the appendicular skeleton. While falls onto an outstretched hand are usually physically responsible for proximal humerus fractures, the ability of the underlying bone to resist applied loads must also play a role. Few studies have assessed proximal humerus bone health with aging. The aim of the current study was to explore age-related bone changes at the proximal humerus in men. A cross-sectional study design was used to assess peripheral quantitative computed tomography (pQCT)-derived bone properties of the proximal humerus in a cohort of 112 white males (age range = 30-85 yrs). A tomographic slice of the non-dominant upper extremity was acquired at 80% of humeral length proximal from its distal end-a location corresponding to the surgical neck of the humerus. Images were assessed for cortical (Ct.BMC) and trabecular (Tb.BMC) BMC, total (Tt.Ar), cortical (Ct.Ar) and medullary (Me.Ar) area, periosteal (Ps.Pm) and endosteal (Es.Pm) perimeter, cortical thickness (Ct.Th), and bone strength index for compression (BSI_c). BSI_c was calculated as the product of Tt.Ar and the square of total volumetric BMD. Data were plotted against age and linear regression lines assessed for their slope. Slopes were subsequently converted to percent change in the bone property per year. During aging, the proximal humerus expanded with Tt.Ar and Ps.Pm increasing at rates of 0.40%/yr and 0.19%/yr, respectively. However, Me.Ar (0.62%/yr) and Es.Pm (0.34%/yr) expanded at faster rates such that there was net loss of both Ct.BMC (-0.23%/yr) and Tb.BMC (-1.08%/yr). Also, the more rapid expansion of Me.Ar relative to Tt.Ar meant that Ct.Ar (-0.15%/yr) and Ct.Th (-0.34%/yr) both decreased with age. The net result of these mass and structural changes was progressive loss of bone strength with age, as indicated by a 0.44%/yr decline in BSI_c. These data provide a picture of bone changes at the proximal humerus during aging. They suggest that between age 30 and 80 yrs, approximately 54% and 11% of Tb.BMC and Ct.BMC at the proximal humerus is lost, respectively. They also suggest that compressive strength of the proximal humerus declines by 22% between age 30 and 80 years. These declines in proximal humerus bone health have implications for fracture risk at this location during aging.

Disclosures: Robyn Fuchs, None.

SU0403

Poor Bone Microarchitecture in Older Men with Low Muscle Mass and Grip Strength - The STRAMBO Study. Stephanie BLAIZOT¹, Stephanie Boutroy², Nicolas Vilaythiou³, Roland Chapurlat⁴, Pawel Szulc⁵. ¹INSERM UMR 1033, Université de Lyon, France, ²Columbia University Medical Center, USA, ³INSERM UMR1033, Université de Lyon & Hospices Civils de Lyon, France, ⁴E. Herriot Hospital, France, ⁵Hopital E. Herriot, Pavillon F, France

We have shown that low relative appendicular muscle mass (RASM, kg/m²) is associated with lower bone width in men (Szulc, JBMR, 2005). Our aim was to assess the association of bone microarchitecture with RASM and grip strength in 810 men aged ≥60 yr. Bone microarchitecture was assessed at the distal radius and tibia by high resolution peripheral QCT (XtremeCT Scanco). RASM was assessed by DXA. Statistical analyses were adjusted for age, height, fat mass, sex steroids, lifestyle factors and co-morbidities. At the distal radius and tibia, men in the lowest RASM quartile (Q1) had lower cross-sectional area (CSA), trabecular area and cortical thickness (Ct.Th) than men in the highest (Q4) quartile (6 to 11%, 0.33-0.64 SD, p<0.01-0.001, p_{trend}<0.05-0.001). At the distal tibia, they also had lower total and trabecular volumetric BMD (vBMD) and lower trabecular number (TbN) (Q1 vs Q4: 7 to 9%, 0.34-0.60 SD, p<0.05-0.005, p_{trend}<0.05) as well as more heterogeneous trabecular distribution (TbSpSD) (p<0.001). At the distal radius, men in the lowest quartile of grip strength had lower CSA, total and trabecular vBMD, TbN and Ct.Th than men in the highest quartile (4 to 10%, 0.29-0.45 SD, p<0.05-0.001, p_{trend}<0.05-0.005). They also had 8% higher TbSpSD (p_{trend}<0.005). After adjustment on arm muscle mass, differences remained significant for total and trabecular vBMD, TbN and TbSpSD. At the tibia, men in the lowest quartile of grip strength had lower total and cortical vBMD and lower Ct.Th (3 to 8%, 0.33 SD, p<0.05, p_{trend}<0.05). In multivariate models including both grip strength and arm muscle mass, total CSA and

trabecular area were associated with muscle mass ($r^2=3-7\%$, $p<0.001$), not grip strength. Cortical vBMD correlated with grip strength ($r^2=3\%$, $p<0.01$). Trabecular parameters were associated weakly with muscle mass ($r^2=1-3\%$) and grip strength ($r^2\leq 1\%$). Men having both low arm muscle mass and low grip strength (lowest tertiles) had 9% lower TbN (0.61 SD, $p<0.005$) and 5% higher TbSpSD (0.49 SD, $p<0.05$) than men in the highest tertiles of both variables.

In older men, low RASM and low grip strength are associated with poor cortical and trabecular microarchitecture. The associations remaining significant after adjustment for confounders including body size suggest direct association. Muscle mass and force are associated jointly and partly independently with bone microarchitecture, suggesting different mechanisms of linkage.

Disclosures: Stephanie BLAIZOT, None.

SU0404

Bone Mineral Density and Skeletal Microarchitecture in Small-Fiber Polyneuropathy. Anne Louise Oaklander¹, Ruchit Kumbhani², Erica Siwila-Sackman², Heather Downs¹, Benjamin Leder³. ¹Department of Neurology, Massachusetts General Hospital, USA, ²Endocrine Unit, Massachusetts General Hospital, USA, ³Massachusetts General Hospital/Harvard Medical School, USA

Skeletal metabolism is regulated by both the central and peripheral nervous system in humans and animals. Most studies in this area have focused on the effects on the autonomic nervous system or damage to the large-diameter myelinated peripheral nerves, but almost all bone innervation is by small-diameter somatic and autonomic axons. Small-fiber polyneuropathy (SFPN) is a peripheral nerve disease that usually presents with burning pain in the distal lower extremity and has been associated with numerous underlying etiologies. Patients with SFPN can present with underlying local bone destruction but effects on skeletal health have not been systematically studied. To assess the skeletal effects of SFPN, we performed high-resolution peripheral quantitative computed tomography (HR-pQCT) of the distal tibia, DXA of the hip and spine, and measured serum CTX and PINP (BTMs) in 12 men with SFPN (age 30-60) and in 12 healthy, age-matched controls. The presence and severity of small-fiber losses was quantified using distal-leg skin biopsies immunolabeled against PGP9.5 and standard methods for clinical diagnosis. Subjects with DM, calcium regulatory disorders, hypogonadism, recent fracture, or using bone-active medications were excluded. Comparison between patients and their age-matched controls was performed by paired t-test. As shown below, mean (SD) density of epidermal nerve fibers was significantly lower in SFPN patients compared to controls whereas other clinical parameters were similar. Despite extensive peripheral nerve damage, tibial BMD, compartmental BMD, cortical thickness and trabecular microarchitecture (Tb.Th, Tb.N, Tb.Sp) did not significantly differ between groups. DXA-derived central BMD and BTMs were also similar (data not shown for trabecular microarchitecture and BTMs).

In summary, compared to healthy age-matched controls, men with SFPN have similar skeletal parameters both peripherally (tibia by HR-pQCT) and centrally (hip and spine by DXA). While this small study cannot exclude a modest influence of peripheral axonal damage on the skeleton, there does not appear to be a substantial or consistent skeletal phenotype in SFPN, even in the specific skeletal sites that correspond with the anatomical distribution of the axonal damage observed.

	Age (years)	Axonal Density (n/mm ²)	Testosterone (ng/dl)	25-(OH)VitD (mg/dl)	Calcium (mg/dl)	Creatinine (mg/ml)
Patients	48 ± 6	51 ± 17	403 ± 145	33 ± 10	9.0 ± 0.4	0.9 ± 0.1
Controls	47 ± 7	235 ± 13	323 ± 141	27 ± 8	9.1 ± 0.4	1.0 ± 0.2
P value	0.93	<0.0001	0.15	0.12	0.48	0.66

	HR-pQCT (tibia)			DXA			
	BMD (tot) mg/cm ³	BMD (trab) mg/cm ³	BMD (cort) mg/cm ³	Cort Th mm	PA Spine gm/cm ²	Fem Neck gm/cm ²	Total Hip gm/cm ²
Patients	305 ± 63	191 ± 46	858 ± 50	1.21 ± 0.27	1.07 ± 0.15	0.84 ± 0.15	1.03 ± 0.20
Controls	333 ± 48	200 ± 30	874 ± 38	1.38 ± 0.25	1.07 ± 0.17	0.84 ± 0.07	1.04 ± 0.09
P value	0.31	0.61	0.45	0.20	0.96	0.98	0.97

Table:

Disclosures: Benjamin Leder, None.

SU0405

Bone Mineralization Is Not Different in Women With Long-Standing Type 2 Diabetes: A Microscopy Investigation with Quantitative Backscattered Electron Imaging (qBEI). Janet Pritchard¹, Cora Tomowich¹, Alexandra Papaioannou², Jonathan Adachi³, Stephanie Atkinson¹, Lora Giangregorio⁴, Karen Beattie¹, Justin DeBeer¹, Mitchell Winemaker¹, Victoria Avram¹, Henry Schwarcz¹. ¹McMaster University, Canada, ²Hamilton Health Sciences, Canada, ³St. Joseph's Hospital, Canada, ⁴University of Waterloo, Canada

Purpose: Adults with type 2 diabetes (T2D) are at greater risk of osteoporotic fracture, despite normal or elevated bone mineral density (BMD). Suppressed bone

turnover in these patients has been reported and may lead to hypermineralized bone, contributing to bone fragility. The purpose of this study was to replicate the bone mineral density distribution (BMDD) methodology developed by Roschger and colleagues (1), and to determine if BMDD is different in bone specimens from women with T2D compared to non-diabetic controls.

Methods: Using sections of fresh excised proximal femur from elective total hip replacement patients, we assessed BMDD in women >65 years who had T2D for more than 5 years, and women without T2D. A 5.0mm thick slice of bone was taken from the neck of the femur of the specimen, fixed in glutaraldehyde, embedded in epoxy, polished and coated with carbon. The sample was imaged using quantitative backscattered electron imaging (qBEI) with a scanning electron microscope (Vega, TESCAN USA), using previously described scanning parameters (1). Daily instrument variation was assessed using C, Al, MgO and enamel standards over 8 days, and the average %CV was 3.6%. Several regions of interest were randomly identified for each specimen and mean and standard deviation for BMDD variables (C_{MEAN}, C_{PEAK}, C_{LOW}, C_{WIDTH}) were derived using ImageJ (version 1.44o, NIH, USA)(1). This study was approved by Hamilton Health Sciences/FHS at McMaster University REB.

Results: These preliminary results include 3 specimens from women with T2D (mean age 74.0 years) and 2 specimens from controls (mean age 85.5 years). The average number of years since T2D diagnosis was 11.85.0 years. Women with T2D had a greater BMI (31.2 kg/m², versus 26.3 kg/m²). Analysis of bone specimens revealed that mean calcium concentration (C_{MEAN}) in samples from patients with T2D (22.30%wtCa) and controls (22.20%wtCa) were similar, however the C_{MEAN} for the control group was closer to the normative C_{MEAN} reported previously (22.20 wt %Ca)(2). Additional BMDD variables were also similar between groups.

Conclusions: Given the suppression of bone turnover in adults with T2D, as reported by others, mineralization characteristics, assessed using qBEI with SEM may have important implications related to the mechanisms acting to affect bone turnover in this high-fracture risk population.

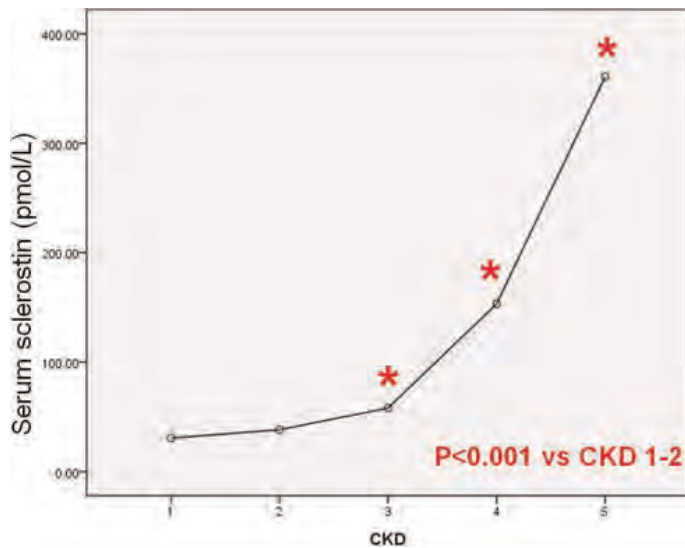
References: 1) Roschger P et al. *Bone*. 1998;23. 2) Roschger P et al. *Bone*. 2003;32

Disclosures: Janet Pritchard, None.

SU0406

Decreased Renal Function but not Liver Function Overpowers the Circulating Sclerostin Level. Se Hwa Kim¹, Hyeong Jin Kim¹, Soo Young Yoon², Sang Chol Lee², Sung-Kil Lim³, Yumie Rhee⁴. ¹Kwandong University College of Medicine, Myongji Hospital, South Korea, ²Department of Internal Medicine, College of Medicine, Kwandong University, Myongji Hospital, South Korea, ³Yonsei University College of Medicine, South Korea, ⁴Department of Internal Medicine, College of Medicine, Yonsei University, South Korea

BACKGROUND: Sclerostin is a Wnt inhibitor produced specifically by osteocytes and its circulating level is known to be negatively associated with estrogen and parathyroid hormone. However, basic relation to kidney or liver function with circulating sclerostin level is yet unrevealed. OBJECTIVE: The aim of the study was to compare serum sclerostin levels in Korean women and men to evaluate its relationship to age, gender, renal and liver function. METHODS: We conducted a cross-sectional observational study of 376 people from population based sampling of pre-(n=40) and post-menopausal women(n=176), and men(n=160). The patients with diabetes and hepatitis were included in these samples. We analyzed serum sclerostin levels by ELISA (Biomedica Co., Austria) and correlated with age, gender estimated GFR and liver function with Child-Pugh scores (CPS). RESULTS: 1) Gender difference: serum sclerostin level was definitely higher in males (105.98.6 pmol/L) vs females (60.45.6 pmol/L), we then analyzed gender-specifically hereafter. 2) In pre- and post-menopausal women, and men, sclerostin levels were positively associated with age ($r=0.22$ & $r=0.24$, respectively, $p<0.005$). There was a stronger relation between sclerostin level with renal function presented as serum creatinine (Cr) and estimated GFR, in both gender (Cr; $r=0.940$ and 0.875 , eGFR; $r=-0.623$ and -0.722 , respectively in females and males, $p<0.001$). Sclerostin level was dramatically increased in patients with CKD stage 3 and more (Fig). 3) The liver function measured by aspartate and alanine aminotransferase (AST/ALT) was only negatively related in females ($r=-0.220$ and -0.226 , $p<0.05$). Furthermore, we have assessed the sclerostin level according to CPS which better represents degree of chronic liver disease graded into A-C. The sclerostin level seemed to be higher in CPS class B-C, but after adjusting with Cr, there was no difference related to hepatic dysfunction. Decreased renal function was significantly associated with increased sclerostin level even after the adjustment for age, fasting glucose, and AST/ALT (standardized $\beta=-0.841$, $t=-12.8$, in females and $\beta=-0.864$, $t=-15.8$, in males, $p<0.0001$, respectively). CONCLUSIONS: Our findings suggest that serum sclerostin is higher in males and is metabolized mainly via kidney but not by liver. Therefore, in order to use or analyze the circulating sclerostin levels, the renal function should be considered as a main confounding factor.



Circulating sclerostin level according to CKD stage

Disclosures: Se Hwa Kim, None.

SU0407

Effects of Preoperative Renal Function on the Postoperative ADL of Patients with Osteoporotic Vertebral Collapse with Neurological Deficits. Masafumi Kashii¹, Ryoji Yamazaki², Tomoya Yamashita³, Takahito Fujimori¹, Yukitaka Nagamoto¹, Shinya Okuda², Takenori Oda², Tetsuo Ohwada³, Motoki Iwasaki², Hideki Yoshikawa¹. ¹Osaka University Graduate School of Medicine, Japan, ²Department of Orthopedic surgery, Osaka Rousai Hospital, Japan, ³Department of Orthopedic surgery, Kansai Rousai Hospital, Japan

Surgical treatment of osteoporotic vertebral collapse (OVC) with neurological deficits has some significant clinical challenges and problems because elder patients with extremely bone fragility often have serious medical comorbidities. The objective of this study is to minutely examine patients' background containing concurrent commodities and individual severity of osteoporosis in OVC patients with neurological deficits, and to investigate prognostic factors which affect postoperative patients' ADL.

We retrospectively reviewed 88 patients with OVC with neurological deficits who underwent three kinds of surgical procedures. Clinical results regarding neurological deficits and patient's ADL were assessed by the modified Frankel performance grade and the criteria of bedridden established by Ministry of Health, Labour and Welfare (J1-C2: eight-grade system), respectively. The prognostic factor of postoperative patients' ADL was examined using the univariate analysis and the multivariate analysis.

Improvement rate of neurological impairment and ADL was 60.2% and 55.0%, respectively. There were no significant differences in pain relief and improvement rate of neurological impairment and ADL among these three procedures. The multiple logistic regression analysis was performed using age, sex and two explanatory variables (the decrease of estimated glomerular filtration rate (eGFR) and high serum ALP) taken from the univariate analysis. Decrease of eGFR (OR=1.08; 95%CI, 1.03-1.13; p=0.0001) and high serum ALP level (OR=0.989; 95%CI, 0.979-0.997; p=0.0007) were the strong prognostic factors to predict deterioration of postoperative ADL in OVC patients with neurological deficits.

The majority of patients with poor postoperative ADL are in the condition with advanced-stage CKD with high bone turnover as well as bone fragility. It is important to fully recognize that osteoporosis is a systemic disorder and there is a hidden pathogenesis of osteoporosis such as CKD-MBD (Chronic Kidney Disease with Mineral and Bone Disorder). Decline of renal function and high serum ALP found in this study seems to be valuable markers to evaluate both patients' general health and severity of osteoporosis, when we choose the surgical procedure.

Disclosures: Masafumi Kashii, None.

SU0408

Estrogen Prevents TZDs-induced Apoptosis in Osteoblasts. Hui Sheng*. Shanghai, Fudan University, Peoples Republic of China

Thiazolidinediones (TZDs), as insulin sensitizers, are used in clinics for type 2 diabetes patients. Recent studies showed that TZDs exert bone damage, which is characterized by inhibiting bone formation. Our previous studies showed that TZDs induced osteoblasts apoptosis in vitro and in vivo models, indicating that osteoblasts apoptosis is one of the important mechanisms in this pathophysiology. Clinical data

showed older diabetic women are more susceptible to TZDs-induced bone loss, implying estrogen may have protective effects. This study aims to investigate the effects of estrogen on pioglitazone-induced osteoblasts apoptosis.

Primary rat calvaria osteoblasts and mice MC3T3-E1 osteoblasts were used and treated by 17 β -estradiol and pioglitazone hydrochloride (Pio). Osteoblasts apoptosis was tested by flow cytometry and Terminal deoxynucleotidyl transferase dUTP nick end labeling (TUNEL) assay. Glycogen synthase kinase 3 β (GSK3 β) was assayed by Western blot. siRNA for GSK3 β were used for underlying mechanism exploration.

Pio induced osteoblasts apoptosis in a dose-dependent manner, and the apoptosis rate increased from 4.5% in control group to 12.2%, 18.2%, 25.5%, in 5 μ M, 10 μ M and 20 μ M Pio- treated groups. Simultaneous treatment with Pio and 17 β -estradiol prevented osteoblasts apoptosis, the apoptosis rate decreased to 15%, 10.4%, and 6% after 17 β -estradiol treatment (0.001nM, 0.01nM, 0.1nM) in 10 μ M Pio group. Western blot results showed that Pio induced osteoblasts apoptosis with activation of GSK3 β , and 17 β -estradiol addition reduced the activity of GSK3 β . siRNA for GSK3 β could also improve Pio-induced osteoblasts apoptosis. The similar results were also confirmed in primary rat osteoblasts.

Estrogen could prevent Pio-induced osteoblasts apoptosis in vitro study. GSK3 β plays an important role in Pio-induced osteoblasts apoptosis. This study could at least partly explain the clinical observation that older diabetic women are more susceptible to TZDs-induced bone loss.

Aknowledgements This study was supported by Shanghai Pujiang Program (09PJ1410300), NSFC(30900698) and Ph.D. Programs Foundation of Ministry of Education of China(20090072120020).

Disclosures: Hui Sheng, None.

SU0409

Osteocalcin and Residual β -Cell Function in Type 1 Diabetes. Annarita Maurizi, Rocky Strollo, Paolo Pozzilli, Nicola Napoli*. University Campus Biomedico, Italy

The skeleton is an important target of diabetes complications. The relationship between type 1 diabetes (T1D) and bone metabolism appears to be complex and the mechanisms leading to bone loss in T1D remain unclear. It is reported that not only poor glycemic control has negative effects on bone metabolism, but also the rate of bone turnover may in turn regulate glucose homeostasis.

Aim of the present study was the evaluation of the relationship between markers of bone formation [osteocalcin (OC), bone alkaline phosphatase (bALP)], bone mineral density (BMD) and body composition] and metabolic control in T1D patients. A total of 45 patients affected by T1D aged 18-50 years (29 males 16 females) and 37 age and gender-matched healthy subjects underwent assessment of biochemical bone formation markers (OC and bALP), BMD and measurement of body composition using dual energy X-ray absorptiometry. In T1D patients HbA1c, fasting C-peptide and daily insulin requirement (I.R.) were also evaluated. A two-sides paired T-test was used to assess differences between patients with T1D and controls. Pearson's correlation coefficients were used for assessing the association between two continuous variables. No differences were observed in OC and bALP levels between the two groups. T1D patients and controls showed also similar fat mass and BMD at all sites. In T1D patients fat distribution, expressed as abdominal fat/total fat ratio, was positively correlated with HbA1c levels ($r=0.5$, $p=0.032$) and with I.R. ($r=0.4$, $p=0.02$). Finally, a positive correlation between osteocalcin and fasting C-peptide was observed in T1D patients ($r=0.5$, $p<0.001$). In conclusion, patients affected by T1D show minor differences in body composition and no difference in BMD compared with normal subjects. The novel finding of a positive correlation between osteocalcin and residual C-peptide observed in T1D is consistent with experimental models, suggesting a direct effect of this osteoblast-derived protein on β -cell function

Disclosures: Nicola Napoli, None.

SU0410

Serum Sclerostin Levels Correlate Positively with Bone Mineral Density at Multiple Skeletal Sites in Postmenopausal Women. Farayal Mirza*, Anne Kenny², Pamela Taxel¹, Joseph Lorenzo¹. ¹University of Connecticut Health Center, USA, ²University of Connecticut, USA

Sclerostin is a negative regulator of Wnt signaling and bone formation. We previously reported that serum estrogen levels inversely correlate with serum sclerostin levels in postmenopausal women. In this study, we examined the effect of aging on serum sclerostin levels and the relationship between serum sclerostin levels and bone mineral density (BMD) in postmenopausal women. We evaluated 100 postmenopausal women, 45 to 95 years of age, in a cross sectional study. Serum sclerostin levels were measured along with levels of estradiol (E2), estrone (E1), sex hormone binding globulin (SHBG) and serum and urine bone formation and resorption markers. Free estrogen index (FEI) was calculated as (E2+E1) (pmol/l)/SHBG. BMD was measured using dual x-ray absorptiometry in 88 subjects. Pearson product moment correlations were used to evaluate the relationships between age, serum sclerostin level and bone density.

Mean age of the subjects was 70.11 years. Mean body mass index (BMI) was 28.6. Mean serum sclerostin level was 48.20 ng/ml and mean FEI was 3.72 pmol/nmol. Serum sclerostin level correlated positively and significantly with age ($r = 0.316$, $p =$

0.001). However, although this relationship persisted after adjusting for FEI ($r = 0.315$, $p = 0.001$) it disappeared after adjusting for body mass index (BMI). In contrast, after adjusting for age, BMI, FEI and parathyroid hormone (PTH) levels, serum sclerostin correlated positively with BMD at the lumbar spine ($r = 0.386$, $p = 0.001$), mean total hip ($r = 0.437$, $p < 0.001$), mean trochanter ($r = 0.401$, $p < 0.001$), and total body BMD ($r = 0.461$, $p < 0.001$). There were no significant relationships between serum sclerostin levels and bone formation markers (bone specific alkaline phosphatase and osteocalcin, OC) or bone resorption markers (serum N-telopeptide, NTX). However, there was a trend for a negative relationship between serum sclerostin and the ratio of NTX to OC ($r = -0.224$, $p = 0.093$) after adjusting for age, BMI, FEI and PTH.

Our findings demonstrate that in multivariate analysis serum sclerostin levels correlate positively with bone density at multiple skeletal sites in postmenopausal women. We speculate that this association results from a relationship between serum sclerostin and bone turnover as reflected by the ratio of NTX to OC. Serum sclerostin levels are an easily obtainable independent marker of bone mass in postmenopausal women, which may have clinical utility.

Disclosures: Faryal Mirza, None.

SU0411

The Associations of Serum Serotonin with Bone Traits Are Age- and Gender-specific. Qin Wang^{*1}, Leiting Xu², Decai Chen¹, Alen Markku³, Sulin Cheng². ¹Dept. Endocrinology of West China Hospital, Sichuan University, China, ²University of Jyväskylä, Finland, ³Department of Medical Rehabilitation, Oulu University Hospital & Institute of Health Sciences, University of Oulu, Finland

Objective: This study is aimed to investigate the associations between serum serotonin and bone traits at multiple sites in women and men.

Subjects and Methods: The study population of this report is a part of the CALEX-family study. In brief, 235 young women (mean age 18.3 yrs), 121 premenopausal (mean age 46.1 yrs) and 124 postmenopausal women (mean age 66.5 yrs), as well as 112 men under 60 yrs old (mean age 50.0 yrs) and 56 men over 60 yrs old (mean age 72.9 yrs) were included in this report. Body composition was assessed using DXA. Areal bone mineral density (aBMD) of whole body (WB), lumbar spine (L2-4), femoral neck (FN) and total femur (TF) were assessed by DXA. In addition, pQCT was used to assess bone mineral content (BMC), and total, cortical and trabecular volumetric bone mineral density (vBMD) at distal radius and tibial shaft. Fasting serum concentration of serotonin was determined using a competitive enzyme-linked immunosorbent assay.

Results: The serotonin concentration declined with advancing age both in females and males (all $p < 0.01$). Serotonin was negatively correlated with weight, BMI, lean and fat mass in women ($r = -0.22$ to -0.39 , all $p < 0.001$), but positively with height and lean mass in men (all $p < 0.01$). In young and premenopausal women, serotonin concentration was negatively correlated with aBMD of WB and L2-4 ($r = -0.21$ and -0.23 , respectively, all $p < 0.05$), but the statistical significance disappeared after adjusted for weight. Conversely, in postmenopausal women, serotonin was positively correlated with aBMD of WB, TF and FN, as well as with total BMC and vBMD of the distal radius ($r = 0.20$ to 0.30 , all $p < 0.05$). After adjusted for weight, the positive correlations remained or became even more pronounced. In men, no significant associations were found between serotonin and bone traits at multiple sites.

Conclusion: Serum concentration of serotonin was positively associated with bone traits only in postmenopausal women not in premenopausal women or men. The associations between serotonin and bone traits are gender- and age-specific.

Disclosures: Qin Wang, None.

SU0412

Comparison of the Effect of Teriparatide in Japanese and Non-Japanese Patients with Osteoporosis - Bridging Strategy. Mika Tsujimoto, Kazunori Uenaka, Atsuko Iwata, Yoshihiro Higashiuchi, Hideaki Sowa^{*}. Lilly Research Laboratories Japan, Eli Lilly Japan K.K., Japan

Background/Objective: Teriparatide is an anabolic therapy for osteoporosis approved in the United States since 2002 and European Union since 2003. However, as with many other drugs, approval in Japan had lagged significantly at the time a phase 1 study was planned in Japan in 2003. A strategy for addressing the lag in drug approval by bridging data from large foreign studies with smaller domestic studies is described in the International Conference on Harmonization (ICH) E5 guideline. This bridging strategy was used to accelerate the new drug application, which led to Japan approval in 2010.

Methods: Analyses were made according to the ICH E5 guideline to support bridging between Japanese studies and the large Fracture Prevention Trial (ClinicalTrials.gov identifier: NCT00670501; FPT). We analyzed data from a single dosing study in healthy Japanese and Caucasian postmenopausal women (Phase 1, pharmacokinetics, Study identifier: GHCO; J-PK) as well as data from studies of 6 months (Phase 2, dose ranging, ClinicalTrials.gov identifier: NCT00191867; J-Ph2)

and 12 months (Phase 3, efficacy and safety, ClinicalTrials.gov identifier: NCT00433160; J-Ph3) randomized, placebo-controlled, once-daily treatment in Japanese patients with osteoporosis at high risk of fracture.

Results: In J-PK, apparent AUC and C_{max} were up to 40% greater in Japanese versus Caucasians; however body weight-adjusted values were comparable between populations. Age and time since menopause were similar in the FPT and Japanese studies, but bone mineral density (BMD) at lumbar spine (L1-L4) as well as body weight and proportion of smokers and drinkers were lower for Japanese at baseline. With teriparatide 20 µg/day, statistically significant increases in BMD compared with placebo were observed at 12 months in both FPT and J-Ph3. Furthermore, percent and actual changes in BMD were comparable between studies suggesting that Japanese and non-Japanese populations are similar in terms of BMD response. Dose-response at 6 months and changes in bone turnover markers were broadly comparable across populations. No novel safety signals were identified in Japanese subjects.

Conclusion: These results show that the teriparatide clinical data met ICH E5 criteria for bridging. Findings from foreign trials including the FPT, such as fracture prevention and bone microstructure improvement, can thus be extrapolated to anticipate response in Japanese subjects treated with teriparatide.

Disclosures: Hideaki Sowa, Eli Lilly Japan K.K., 3

SU0413

Evidence for Bone Reversal Properties of KoAct™, a Novel Dietary Supplement. Bahram Arjmandi^{*1}, Shirin Hooshmand¹, Jennifer Gu², Sara Campbell³. ¹Florida State University, USA, ²AIDP, Inc., USA, ³Rutgers University, USA

Menopause drastically increases the risk of osteoporosis, and although drug therapies are available, having an efficacious dietary supplement as an alternative to a prescription drug is highly desirable. Recent findings suggest that KoAct™, a calcium-collagen chelate, is highly effective in modulating bone mass in rat models of osteoporosis. Based on these findings, we hypothesize consumption of KoAct™ reverses bone loss in postmenopausal women with osteopenia as early as three months. We screened 90 women, 1 to 5 years postmenopausal, not on hormone replacement therapy or any other prescribed medication known to influence bone metabolism. Twenty qualified participants were randomly assigned to one of two treatment groups: 1) control and 2) KoAct™ as a dietary supplement intervention daily for three months. Control group received 500 mg of elemental calcium in the form of calcium carbonate, while the KoAct™ group received 5 g of KoAct™ which also contained 500 mg elemental calcium. Additionally both groups received 200 IU vitamin D daily. Bone mineral density of lumbar spine, forearm, hip, and whole body were assessed at baseline and the end of the study using dual-energy x-ray absorptiometry. Blood and urine samples were collected at baseline and after 3 months to assess bone biomarkers of bone metabolism. Physical activity recall and three-day food frequency questionnaire were completed at baseline and after 3 months to examine physical activity and dietary confounders as potential covariates. KoAct™ significantly increased BMD of total body in comparison to the control group (1% vs. baseline; p value = 0.021). In comparison with corresponding baseline values, KoAct™ tended to increase bone-specific alkaline phosphatase activity and decrease tartrate resistant acid phosphatase-5b after three months. These preliminary data suggested that KoAct™ enhances bone mass by increasing bone formation and suppressing bone resorption.

Disclosures: Bahram Arjmandi, None.

This study received funding from: AIDP, Inc.

SU0414

High Resolution Peripheral Quantitative Computed Tomography (HRpQCT) Detects Improved Trabecular Volumetric BMD and Microarchitecture in Premenopausal Women with Idiopathic Osteoporosis Treated with Teriparatide. Adi Cohen^{*1}, Stephanie Boutroy¹, Emily Stein², Xiaowei Liu², Joan Lappe³, Robert Recker³, David Dempster⁴, Hua Zhou⁵, Donald McMahon², Chiyuan Zhang⁴, Polly Chen⁴, Bin Zhou⁴, Ji Wang⁴, X. Edward Guo⁴, Elizabeth Shane². ¹Columbia University Medical Center, USA, ²Columbia University College of Physicians & Surgeons, USA, ³Creighton University Osteoporosis Research Center, USA, ⁴Columbia University, USA, ⁵Helen Hayes Hospital, USA

Idiopathic osteoporosis (IOP) in premenopausal (preM) women is a disorder of uncertain pathogenesis in which fragility fractures and/or low BMD occur in otherwise healthy women with intact gonadal function. Both HRpQCT and transiliac bone biopsy (Bx) revealed thinner cortices, fewer, thinner, more widely separated and heterogeneously distributed trabeculae, and reduced stiffness in women with IOP than controls. Although dynamic remodeling parameters were heterogeneous and did not differ between subjects and controls, subsets of women with IOP had low or high bone turnover assessed by bone formation rate/bone surface (BFR/BS). We hypothesized that teriparatide (TPTD), which directly increases osteoblast activity, would improve volumetric BMD (vBMD), bone microarchitecture and stiffness in women with IOP. Herein, we report interim results of an open-label pilot study of 22 preM women with IOP treated with TPTD 20 mcg SC daily. HRpQCT (Scanco Medical AG) of the distal radius (DR) and tibia (DT) was performed at baseline and 12-18 months in 18

women (age 415 yrs; 14 with fractures). Measurements were more variable at the DR than DT. Trabecular (Tb) vBMD increased significantly by 5.2% at the DR and 2.3% at the DT (Table), with larger increases in the inner than outer Tb compartment. Cortical (Ct) vBMD and thickness did not change at either site. At the DT, there were significant increases in Tb number and decreases in Tb separation and heterogeneity of the Tb network; similar directional changes at the DR were not significant. Stiffness (Tb elastic modulus) by FEA did not change significantly at either site. Changes in Tb and Ct vBMD did not correlate with %change in spine or hip BMD by DXA or baseline serum bone turnover markers. At the DR, %change in Tb vBMD correlated directly with baseline endocortical wall width (WWi) on transiliac Bx, a measure of osteoblast productivity ($r=0.502$; $p=0.04$). Percent change in DR Ct vBMD correlated directly with baseline cancellous osteoid width (OWi; $r=0.638$; $p=0.006$), as did DT CT vBMD with intracortical OWi ($r=0.484$; $p=0.049$). In conclusion, HRpQCT detected significant improvements in vBMD (DR and DT) and Tb microarchitecture (DT only) in preM women with IOP treated with TPTD. Baseline static parameters of osteoblast function (OWi, WWi) on transiliac Bx predicted responses in Tb and Ct vBMD, suggesting that osteoblast function is an important determinant of response to TPTD in preM women with IOP.

	Radius		Tibia	
% Common Region Between Scans	92.3 ± 6.4%		95.5 ± 3.7%	
	% Change	p	% Change	p
Total vBMD	2.7 ± 7.3	0.2	1.3 ± 1.6	0.003
Ct vBMD	-0.2 ± 1.5	0.6	-0.1 ± 1.5	0.8
Tb vBMD	5.2 ± 8.3	0.04	2.3 ± 2.7	0.002
Inner Tb vBMD	14.4 ± 28.3	0.09	4.1 ± 4.2	0.0006
Outer (Meta) Tb vBMD	2.8 ± 4.1	0.01	1.5 ± 2.4	0.02
Cortical Thickness	2.5 ± 9.9	0.3	0.9 ± 2.8	0.2
Tb Number	2.5 ± 7.4	0.2	3.6 ± 5.4	0.02
Tb Thickness	2.5 ± 9.2	0.2	-0.7 ± 6.1	0.6
Tb Separation	-2.4 ± 7.2	0.1	-3.3 ± 4.7	0.006
Tb Distribution (Tb Separation SD)	-1.1 ± 8.7	0.7	-2.9 ± 4.4	0.02
Estimated Stiffness (Elastic Modulus) by FEA: E _{xx} (longitudinal)	18.3 ± 59.9	0.2	2.2 ± 17.4	0.99

Table

Disclosures: *Adi Cohen, None.*

This study received funding from: Eli Lilly and Company

SU0415

How to Predict a Suboptimal Response to Recombinant Parathyroid Hormone Treatment in Osteoporosis. Najia Siddique^{*1}, Martin Healy², Choon Guan Chan³, Nessa Fallon⁴, John Brown Walsh³, Miriam Catherine Casey³. ¹St James University Hospital, Ireland, ²central pathology lab, St.James Hospital, Ireland, ³Bone health services, St.James hospital, Ireland, ⁴osteoporosis & bone health clinic, St.James Hospital, Ireland

Introduction:

Recombinant PTH is an anabolic agent with a unique mechanism to increase bone mineral density and reduce fractures in postmenopausal women. However, little attention has been paid to what constitutes a poor response to rPTH treatment. Better understanding of indicators predicting response to it may lead to improved management and better clinical outcomes. This study therefore investigates the baseline characteristics of the patients who failed to respond to rPTH treatment despite being compliant to it.

Design: A retrospective study.

Methods:

Data on 234 patients with postmenopausal osteoporosis (mean age 68yrs) was collected, who were treated with PTH 1-34 for 18 months at Osteoporosis clinic in ST. JAMES Hospital, Dublin, Ireland. (60% were on bisphosphonates for ≥6 mths). Out of these, data on 160 patients who were compliant was selected for analysis. Patients were divided into two main groups as responders vs nonresponders. Patients with a <3% gain in BMD at lumbar spine or a new vertebral fracture at 18mth were considered as non responders to the treatment. A statistical comparison of the baseline characteristics and biochemical values at baseline, 3mths and 12 mths on rPTH was made between the groups using T-test and Wilcoxon rank sum test.

Results:

There was no significant difference in responders vs non responders for GFR, Serum PTH, Calcium, 25(OH)Vitamin D, Alk Phos and 24hr Urinary Ca at baseline, 3mth and 12mth on treatment. There was no significant difference in Bone markers including serum CTX, Osteocalcin and PINP at baseline. But a trend was observed towards a greater PINP rise in responders at 3mth. Two more significant findings are detailed below in Table 1.

Conclusion: This was a comprehensive study analysing a large population on rPTH to identify the predictors of a poor response to it. Of interest the non responders had significantly greater BMI vs responders. This group therefore could have poor dietary habits or metabolic syndrome however; this abstract doesn't investigate into it. Thus, Screening for lifestyle, dietary habits and metabolic syndrome could refine the selection of patients for rPTH treatment for Osteoporosis. This data analysis also identified a lesser PINP rise at 3mths as compared to the responder group. Therefore, PINP measurement at 3 months could somehow predict who is going to respond and vice versa. Very little else predicts response to this treatment especially when this analysis is independent of 25 (OH) vitamin D levels.

Table1.

	Responders Median and CI	Non-responders Median and CI	p-value
BMD at baseline	0.70 (0.64, 0.78)	0.80 (0.74, 0.89)	0.0003
BMD gain	12.4 (7.8, 18.3)	0.84 (-1.08, 1.92)	<0.001
BMI	20.5 (15.0, 26.8)	29.2 (21.1, 32.9)	0.005

Baseline BMI, BMD and BMD gain at 18mths

Disclosures: *Najia Siddique, None.*

SU0416

Once Yearly Zoledronic Acid After 18 months of Parathyroid Hormone (1-84) for Severe Osteoporosis. Marco Invernizzi^{*1}, Stefano Carda², Alessio Baricich², Maurizio Bevilacqua³, Carlo Cisarì². ¹University of Eastern Piedmont, Novara, Italy, ²Department of Clinical & Experimental Medicine, University of Eastern Piedmont "A. Avogadro", Italy, ³Endocrinology & Diabetes Unit, Department of Medicine, Luigi Sacco Hospital (Vialba)-University of Milan, Italy

INTRODUCTION: Since the use of full-length parathyroid hormone (PTH1-84) as a treatment for severe osteoporosis is limited to 18 months, important questions remain regarding management strategy after this treatment.

Previous studies investigate the use of alendronate after 1 year of PTH1-84 alone, showing further gains in Bone Mineral Density (BMD). However these gains in BMD were lost if PTH1-84 was not followed by an antiresorptive agent. At present time evidences about antiresorptive therapies other than alendronate after PTH1-84 are lacking.

AIM: to determine whether once yearly 5mg of intravenous zoledronic acid (ZOL) can maintain or increase gains in BMD at hip site after 18 months of therapy with PTH1-84.

METHODS: 18 severe osteoporotic postmenopausal women who had received PTH1-84 monotherapy (100 µg daily) for 18 months were treated with 5mg zoledronic acid two months after having ended PTH1-84 therapy. BMD at femoral neck and total hip were assessed with the use of dual-energy x-ray absorptiometry at baseline, after 18 months of treatment and 1 year after zoledronic acid infusion. Bone biochemical turnover markers (serum CTX, OC and B-ALP) were assessed at baseline, every 6 month during PTH treatment and 1 year after zoledronic acid infusion. Tolerability was evaluated by adverse experience (AE) reporting.

RESULTS: At femoral neck BMD increased by 6.4% (2.2% after PTH1-84 and 4.4% after ZOL respectively) and an analogue improvement was observed at total hip. After PTH1-84 treatment there were significant increases at 6, 12 and 18 months of OC (+232.5%, +212.5%, +190% respectively), serum CTX (+151%, +236%, +244%) and B-ALP (+131%, +210%, +198%; $p<0.01$ for all vs. basal). On the other hand, after zoledronic acid infusion we observed a decrease in OC (-58%), serum CTX (-70.4%) and B-ALP (-30.6%). None of the patients experienced severe adverse events during PTH1-84 treatment, while 7 (38.8%) of patients experienced a self-limiting acute phase reaction after ZOL.

CONCLUSIONS:

Our data show that after 18 months of PTH1-84, ZOL is a safe and effective option to not only to maintain but also to increase BMD at the hip site. These results have clinical implications for therapeutic choices after the discontinuation of PTH1-84.

Disclosures: *Marco Invernizzi, None.*

SU0417

PTH (1-84) Acutely and Transiently Augments Vasodilation in the Bone Vasculature and Diminishes Osteoclast Activity in Rats. Rhonda Prisby^{*}, Jeremiah Campbell, Thomas Menezes. University of Texas at Arlington, USA

Intermittent parathyroid hormone (PTH) administration augments bone mass and is a treatment for osteoporosis. In addition, 15 days of PTH enhanced vasodilation of the femoral principal nutrient artery (PNA), the primary conduit for blood flow to long bones. Adequate circulation to bone is requisite for normal growth, remodeling and repair, yet the acute response of the bone vascular system to PTH remains unknown. The purpose of the study was to determine which system, vascular or skeletal, is foremost affected by PTH. **METHODS:** Male Wistar rats (3-4 mon) were administered 100 µg/kg of PTH 1-84 and sacrificed at 1H (n=6) and 4H (n=8). A control (CON; n=7) group received PBS. Right PNAs were dissected and cannulated to assess endothelium-dependent (acetylcholine [ACh]: 10⁻⁹ – 10⁻⁴ M) and endothelium-independent (sodium nitroprusside [SNP]: 10⁻¹⁰ – 10⁻⁴ M) vasodilation. Right femora were analyzed by bone histomorphometry to determine bone microarchitectural (i.e., bone volume to total volume ratio [BV/TV; %], trabecular thickness [Tb.Th; µm], trabecular number [Tb.N/mm], and trabecular separation [Tb.S; µm]) and bone static (i.e., osteoid surface to bone surface [OS/BS; %], osteoblast surface to bone surface [Ob.S/BS, %], osteoclast surface to bone surface [Oc.S/BS; %], osteoclast number per total bone area [N.Oc/TA/mm], and osteoclast number per bone perimeter [Oc.N/BPm/mm]) properties. **RESULTS:** Endothelium-dependent vasodilation was augmented by 41% 1H subsequent to PTH, which normalized to

CON values by 4H. No differences among groups exist in endothelium-independent vasodilation to SNP. As expected, bone microarchitectural properties were similar among groups. Data indicate no change in Ob.S/BS; however, PTH diminished Oc.S/BS by 48% and 62% at 1H and 4H, respectively, vs. CON. In addition, N.Oc/Tar was also significantly reduced vs. CON. CONCLUSIONS: A single dose of PTH 1-84 acutely (1H) augmented endothelium-dependent vasodilation of the femoral PNA. Intriguingly, these early modifications in bone vasomotor function were associated with reduced osteoclast activity; i.e., bone resorbing cells. Acute effects of PTH (1H and 4H) were not evident in osteoblast activity. Currently, the question as to which system is first modified by PTH remains to be resolved. Future studies (i.e., an earlier time point of analysis) and determination of bone perfusion are requisite to answer this question.

Supported by University of Texas Arlington Research Enhancement Program.

Disclosures: Rhonda Prishy, None.

SU0418

Treatment with PTH 1-84 in Male Patients with Severe Osteoporosis - Results from a Prospective 24 month Open-Label Trial. Christian Muschitz¹, Judith Haschka^{*2}, Roland Kocijan², Astrid Fahrleitner-Pammer³, Guenther Nirnberger⁴, Angela Trubrich⁵, Christina Bittighofer⁵, Heinrich Resch⁶. ¹St. Vincent's Hospital, Austria, ²St. Vincent Hospital Vienna, Austria, ³Medical University Graz, Austria, ⁴Bioconsult Ltd, Austria, ⁵The VINFORCE Study Group - St. Vincent Hospital - Medical Department II, Austria, ⁶Medical University Vienna, Austria

Purpose: Osteoporosis in men is an important and often underestimated problem. Generally accepted is the administration of antiresorptives which influence bone metabolism by reducing bone resorption and increasing bone mineral density (BMD). Usually Anabolic treatment by Parathyroid hormone (PTH) is reimbursed when new osteoporotic fractures occur during antiresorptive treatment, in glucocorticoid induced osteoporosis (GIOP) and in patients with low BMD and multiple clinical risk factors (CRF).

Methods: We prospectively assigned 26 men (mean age 63.3 14.3 ys) to daily subcutaneous injections of 100µg of PTH 1-84 for 24 months. All pts received daily supplementation of 1000mg calcium and 800IU vitamin D. Mean T-score was -3.24 0.92 at L1-L4 and -2.31 0.94 at hip. 81% had prevalent fractures including vertebral fractures (20 pts, mean 3 1.8), non vertebral fractures (11 pts) and hip fractures (5 pts). 6 pts had long term steroid medication (9.3 5.3 ys). 20 pts had prior antiresorptive treatment (6.3 2.6 ys) and 6 were treatment naive (low BMD, ≥ 2 CRFs).

Primary objectives were the gain of BMD at lumbar spine and hip and the changes of bone turnover markers (PINP, S-CTX). Secondary objectives were reduction of new osteoporotic fractures and the evaluation of safety and tolerability.

Patients had BMD measurements (DXA), X-ray of spine, assessment of PINP, S-CTX at baseline and at months 6, 12, 18 and 24. A visual analogue scale (VAS) was assessed for general health.

Results: The increase of lumbar BMD at month 12 was 6.51% and at month 24 finally 13.98%, at femoral neck from 1.17% and 8.5% and at total hip 1.5% and 7.72% compared to baseline (P<0.0001 for all). PINP rapidly increased up to 421% at month 12 and remained till to the end of the observation period; S-CTX increased between 181% and 322% (maximum 347% at month 12) [P<0.001 for all].

One patient (GIOP) had a new morphometric vertebral fracture and one patient sustained a hip fracture after a major trauma (accident).

PTH 1-84 was generally well tolerated. VAS score declined from 7.5 to 3.2 (P<0.05).

Conclusions: Our data suggest that PTH 1-84 rapidly increases BMD at different skeletal sites regardless of prior long-term treatment with bisphosphonates or steroid medication. The bisphosphonate induced suppression of the bone turnover does not seem to reduce the anabolic effect of PTH in male patients with severe osteoporosis

Disclosures: Judith Haschka, None.

SU0419

Atypical Diaphyseal Femoral Fractures Associated With Bisphosphonate Use and Severe Curved Femur: A Case Series. Satoshi Sasaki^{*1}, Yuji Kasukawa², Yoichi Shimada², Michio Hongo², Naohisa Miyakoshi². ¹Yuri-kumiai General Hospital, Japan, ²Akita University Graduate School of Medicine, Japan

Purpose: Recent reports have raised concerns about atypical subtrochanteric and diaphyseal femoral fractures after long-term bisphosphonate treatment, which may be associated with severely suppressed bone turnover (SSBT). However, diaphyseal femoral fractures without bisphosphonate treatment have also been reported in patients with severely curved femur, which are not rare in the elderly. The purpose of this study was therefore to investigate associations between occurrence of such fractures, bisphosphonate use, and curvature of the femur.

Methods: Nine consecutive elderly patients treated for atypical diaphyseal femoral fractures between 2005 and 2010 were retrospectively reviewed. Three patients sustained bilateral fractures. Eight patients were administered bisphosphonates and

one patient was administered raloxifene. Duration of osteoporosis treatment, type of fractures, surgical procedure, and curvature of opposite femur were evaluated.

Results: The mean duration of drug administration was 3.6 years. All fractures showed similar X-ray patterns of simple transverse fracture with medial spike. Nine femurs showed thickening of the femoral cortex. One case was treated with locking plate fixation, while the other cases were operated with intramedullary nails (9 antegrade nails, 2 retrograde nails). One femur treated with retrograde nail showed delayed bone union. Femoral curvature tended to show larger values in cases without cortical thickening than those with cortical thickening, however, it was not significant.

Conclusions: Our experience suggests that 2 types of atypical diaphyseal femoral fracture should be considered in the elderly: fracture resulting SSBT and showing thickening of the femoral cortex; and pathological fracture due to malalignment of the femur without cortical thickening.

Disclosures: Satoshi Sasaki, None.

SU0420

Atypical Femoral Fractures: From the Pain without Fracture to the Fracture without Pain. Enrique Casado^{*}, Ivonne Vazquez, Marta Larrosa, MarÚa GarcÚa-Manrique, Jose Antonio Gonzalez, Jordi Gratacos. University Institute Parc TaulÚ, Spain

Purpose: To describe the clinical and radiological features of patients with atypical femoral fractures diagnosed in the last three years at the Hospital of Sabadell (Barcelona, Spain).

Methods: Descriptive study. All consecutive patients admitted to the Orthopedics Department, Hospital of Sabadell (reference population 400,000) from January 2008 to December 2010 were reviewed. After the confirmation of an atypical fracture of the femur (major features) the patient clinical chart was reviewed, collecting some data about patient demographics, osteoporosis treatment and phospho-calcium metabolism parameters on admission.

Results: Eight atypical fractures of the femur in six patients were registered. All patients were female. Mean age 76.710.1 years (range 60-91). In all cases the fracture was located in the femoral shaft. In two patients the fracture was bilateral and in four patients unilateral (2 right, 2 left). Six out of eight fractures were transverse and two were oblique. Two patients had no previous symptoms and four patients had previous limb pain (lasting 1-8 months). All patients except one were receiving bisphosphonates: alendronate (2 patients), ibandronate (2 patients), risedronate (1 patient). Patients under risedronate and ibandronate had previously received other bisphosphonates for more than 7 years. The time of treatment with bisphosphonates in each patient ranged between 3 and 12 years. Five patients (83%) had hypovitaminosis D (25 (OH)D <25 ng/ml), with a mean of 25(OH)D of 185.4 ng/ml. The only patient with normal vitamin D levels was receiving chronic treatment with glucocorticoids for pulmonary fibrosis.

Conclusions: Atypical fractures of the femur in our series were located in the diaphysis and occurred in women over 60 years with hypovitaminosis D and treated with bisphosphonates for more than 3 years. The clinical presentation of these fractures was variable: some patients had an incomplete fracture with previous limb pain and other patients had a complete fracture without any previous symptoms.

Reference:

1Shane E, Burr D, Ebeling PR, et al. Atypical subtrochanteric and femoral diaphyseal fractures: Report of a task force of the American Society for Bone and Mineral Research. J Bone Miner Res 2010; 25:2267-2294.

Disclosures: Enrique Casado, None.

SU0421

Bone Safety of a Novel Delayed-release Risedronate 35 mg Once-a-Week Assessed by Bone Histology and Histomorphometry. Robert Recker^{*1}, Ivo Valter², Katre Maasalu³, Clelia Magaril⁴, Zulema Man⁵, Jose Ruben Zanchetta⁶, Carlos Mautalen⁷, Kadri-Liina Vahula⁸, Paul Miller⁹, Dietrich Wenderoth¹⁰, Michael McClung¹¹. ¹Creighton University Osteoporosis Research Center, USA, ²Center for Clinical & Basic Research, Estonia, ³OCRC, Tartu University Hospital, Estonia, ⁴IMAI-Research, Argentina, ⁵Centro Medico TIEMPO, Argentina, ⁶Instituto de Investigaciones Metabolicas (IDIM), Argentina, ⁷Centro de OsteopatÚas Medicas, Argentina, ⁸KLV Medical Office, Estonia, ⁹Colorado Center for Bone Research, USA, ¹⁰Warner Chilcott Deutschland GmbH, Germany, ¹¹Oregon Osteoporosis Center, USA

Bisphosphonates (BPs) are the standard of care for postmenopausal osteoporosis. The dosing instructions of oral BPs per their approved labels require that they be taken on an empty stomach at least 30 to 60 minutes before the first food or drink or other medications. The 2-year efficacy and safety results of a novel delayed-release (DR) formulation of risedronate 35 mg once-a-week (OaW) that can be taken with or without breakfast are available. The results of the bone histology and histomorphometry of the corresponding study are presented.

The primary objective of this randomized, double blind, active controlled study was to determine the non-inferiority, based on the percent change in lumbar spine BMD from baseline to Endpoint/Week 52, of risedronate 35 mg OaW DR taken before or after breakfast compared to 5 mg daily immediate release (IR), in 923 randomized postmenopausal (PM) women, at least 50 years of age, with a lumbar spine or total hip BMD T-score < -2.5 or a T-score < -2.0 with at least one prevalent vertebral fracture. 722 of the 923 randomized subjects completed 2 years of treatment. 45 subjects (risedronate 35 mg OaW DR following breakfast (FB) n=15/307, risedronate 35 mg OaW DR at least 30 minutes before breakfast (BB) n=12/308, risedronate 5 mg IR daily n=18/307) consented to undergo a single transiliac bone biopsy at Week 104. Bone biopsy samples were examined by qualitative histology and quantitative histomorphometry.

After 2 years of treatment, no histological abnormalities were observed in any of the risedronate-treated groups and double tetracycline label was detected in all 45 biopsies. Results for key bone turnover parameters were similar across treated groups, indicating comparable remodeling activities as well as bone mineralization parameters showing that mineralization was not impaired by the 35 mg DR formulation. The histomorphometric results seen with 5 mg IR daily in this study are consistent with the results seen in previous 5 mg IR studies in subjects with PMO.

Overall 35 mg Risedronate DR weekly regimens preserve normal bone quality and maintain bone remodeling and mineralization at a level similar to the 5 mg IR daily regimen and within the normal pre-and post-menopausal range.

1. C.L Benhamou et al., Osteoporosis Int (2011) 22 (Suppl 1):S337-S338

Disclosures: Robert Recker, GSK, 2; GSK, 5; Procter & Gamble, 5; Roche, 5; Roche, 2; Lilly, 5; Amgen, 2; Procter & Gamble, 2; Lilly, 2; Merck, 5; NPS Allelix, 2; Novartis, 5; Wyeth, 2; Amgen, 5; sanofi-aventis, 2; NPS Allelix, 5; Novartis, 2; Merck, 2; Wyeth, 5
This study received funding from: Warner Chilcott Company, LLC

SU0422

Effects of Antiresorptive Therapies on Glucose Metabolism: Results from the FIT, HORIZON and FREEDOM Trials. Ann Schwartz¹, Anne Schafer², Andrew Grey³, Ian Reid³, Li-Yung Lui⁴, Lisa Palermo¹, Dennis Black¹, Douglas Bauer¹, Eric Vittinghoff¹, Robert B. Wallace⁵, Steven Cummings⁶.
¹University of California, San Francisco, USA, ²University of California, San Francisco & the San Francisco VA Medical Center, USA, ³University of Auckland, New Zealand, ⁴California Pacific Medical Center Research Institute, USA, ⁵University of Iowa, USA, ⁶San Francisco Coordinating Center, USA

Osteocalcin (OC) knock-out mice have increased fat mass and insulin resistance, and are more likely to develop diabetes (DM) on a high fat diet. Antiresorptive therapies reduce circulating levels of total OC by 40-50%. Reductions in under-carboxylated OC have been shown with alendronate. To test whether these therapies increase the risk of weight gain, glucose intolerance or DM, we used data from randomized placebo-controlled trials, the Fracture Intervention Trial (FIT) of alendronate (ALN), the Health Outcomes and Reduced Incidence with Zoledronic Acid (ZOL) Once Yearly (HORIZON) trial, and the Fracture Reduction Evaluation of Denosumab (DMAB) in Osteoporosis every 6 months (FREEDOM) trial. Analyses excluded women with probable baseline DM or with unknown status, based on self-report, DM medication use, or an elevated fasting glucose (FG)(>126 mg/dl) or non-fasting glucose (>200 mg/dl). Incident DM was identified based on adverse events, new use of DM medication, or at least 2 elevated glucose results. Changes in weight and FG were compared with linear mixed models. The rate of incident DM was compared with proportional hazards (FIT, FREEDOM) or logistic regression (HORIZON) models. In FIT 6459 postmenopausal women with femoral neck (FN) T-score < -1.6 received daily ALN or placebo (PBO) for up to 4 years; 308 were excluded. Weight (N=6151) and serum glucose (N=1073) were measured annually. In HORIZON 7736 postmenopausal women with osteoporosis based on FN T-score and/or baseline vertebral fracture received a once-yearly infusion of ZOL or PBO for up to 3 years; 623 were excluded. Weight (N=7113) and FG (N=5213) were measured annually. In FREEDOM 7762 postmenopausal women with T-score < -2.5 received DMAB or PBO every 6 mos for up to 3 years; 686 were excluded. Weight (N=7076) was measured annually. FG (N=7048) was measured at baseline, 1-mo, 6-mos, and every 6 mos thereafter. ALN and DMAB, but not ZOL, were associated with less weight loss than PBO but differences were modest (Table). FG changes and the rate of incident DM did not differ between any therapy and PBO. Gain in total bone with antiresorptive therapy may account for some, but not all, of the differences in weight change, a finding that warrants further investigation. We found no change in fasting glucose or diabetes incidence with antiresorptive therapy in postmenopausal women. Lowering OC with antiresorptive therapy does not appear to have a clinically important effect on glucose homeostasis.

Table. Effects of antiresorptive therapies on glucose metabolism after 3-4 years

	ALN	PBO	ZOL	PBO	DMAB	PBO
Mean weight change (kg)	0.26*	-0.06	-0.35	-0.50	-0.13*	-0.44
Mean FG change (mg/dl)	3.41	3.87	0.71	0.52	1.83	1.74
	69	72	68	75	66	78
Incident DM (N(%))	(2.3%)	(2.4%)	(2.0%)	(2.1%)	(1.9%)	(2.2%)
Incident DM (RR (95% CI) for TMT vs PBO)	0.96 (0.69, 1.33)		0.91 (0.65, 1.27)		0.85 (0.61, 1.17)	

*p-value < 0.05 , comparing treatment and placebo (PBO)

Table

Disclosures: Ann Schwartz, Merck, GlaxoSmithKline, 2; Amgen, GlaxoSmithKline, 5
This study received funding from: Novartis Pharmaceuticals

SU0423

Effects of Combination therapy (Alendronate with Alfacalcidol) on Osteoporotic Fractures for Postmenopausal Japanese Women: The Japanese Osteoporosis Intervention Trial (JOINT) - 02. Hiroaki Ohta¹, Masataka Shiraki², Toshitaka Nakamura³, Masao Fukunaga⁴, Takayuki Hosoi⁵, Yukari Uemura⁶, Tatsuhiko Kuroda⁷, Nobuaki Miyakawa⁷, Yasuo Ohashi⁶, Hajime Orimo⁸.
¹Tokyo Women's Medical University Sanno Medical Center, Japan, ²Research Institute & Practice for Involuntary Diseases, Japan, ³University of Occupational & Environmental Health, Japan, ⁴Kawasaki Medical School, Japan, ⁵National Center for Geriatrics & Gerontology, Japan, ⁶Department of Biostatistics, School of Public Health, The University of Tokyo, Japan, ⁷Public Health Research Foundation, Japan, ⁸Japan Osteoporosis Foundation, Japan

Objectives The Japanese Osteoporosis Intervention Trial (JOINT) - 02 was conducted a randomized controlled trial to clarify the efficacy and safety of alendronate with alfacalcidol versus alendronate alone in a clinical practice. Eligible patients were postmenopausal women with severe osteoporosis who were aged 70 years or older and had several risk factors for incident fractures. The primary endpoint was prevention of incident fractures, and the anti-fracture efficacy was evaluated in relation to the baseline serum level of 25-hydroxycholecalciferol [25(OH)D]. Research design and methods A total of 2164 patients were randomized to alendronate with alfacalcidol (combination therapy group) or alendronate alone (monotherapy group). The efficacy was evaluated for 2022 patients (combination therapy group, 995; monotherapy group, 1027) and the safety 2053 patients (1019 and 1034, respectively). Results The combination therapy group had a significantly reduced risk of vertebral fractures after the first 6 months (HR, 0.53; 95% CI, 0.28 to 0.99). In subgroup analyses, the combination therapy group was superior in the strata of number of prevalent vertebral fractures of ≥ 2 (HR, 0.51; 95% CI, 0.32 to 0.84) and grade 3 of prevalent vertebral fractures (HR, 0.55; 95% CI, 0.38 to 0.94). The rate of non-vertebral weight-bearing bone fractures, which mainly consisted of proximal femur fractures, was significantly lower in the combination therapy group than in the monotherapy group during the follow-up period (HR, 0.31; 95% CI, 0.10 to 0.96). A lower baseline 25(OH)D level was associated with a higher incidence of non-vertebral weight-bearing bone fractures (HR, 3.34; 95% CI, 1.21 to 9.25) after adjustment for age, prevalent vertebral fractures and BMD despite alendronate use. Although one patient given the combination therapy had mild hypercalcemia, serious hypercalcemia and unknown adverse events were not encountered in either group. Conclusions In conclusion, combination therapy of alendronate with alfacalcidol was more effective for fracture prevention, especially for non-vertebral weight-bearing bone sites, than alendronate alone in elderly osteoporosis patients with multiple risks. Alendronate combined with alfacalcidol in a promising treatment for postmenopausal osteoporosis.

Disclosures: Hiroaki Ohta, None.

This study received funding from: Public Health Research Foundation

SU0424

Effects of Monthly Risedronate with Cholecalciferol on 25-hydroxyvitamin D Level and Bone Markers in Korean Patients with Osteoporosis. Sung-hwan Moon¹, HYOUNG MOO PARK², Chan Soo Shin³, Ho-Yeon Chung⁴, Yoon-Sok Chung⁵, Byung-koo Yoon⁶, Jae-Suk Chang⁷, Moo-Il Kang⁸, Jin-Young Park⁹, Hyun-Koo Yoon¹⁰.
¹Yonsei University, South Korea, ²CHUNG-ANG UNIV. OB&GYN, Republic of Korea, ³Department of Internal Medicine, Seoul National University College of Medicine, South Korea, ⁴Kyung Hee University, South Korea, ⁵Ajou University School of Medicine, South Korea, ⁶Sungkyunkwan University, South Korea, ⁷Ulsan University, Asan Medical Center, South Korea, ⁸Seoul St. Mary's Hospital, South Korea, ⁹Konkuk University, South Korea, ¹⁰Cheil General Hospital & Women's Healthcare Center, South Korea

Introduction: We performed a randomized, double-blind, prospective, 16-week clinical trial to evaluate the efficacy and safety of monthly risedronate with and without cholecalciferol on 25-hydroxyvitamin D [25(OH)D] levels and bone markers in Korean patients with osteoporosis.

Methods We randomly assigned 150 adults with osteoporosis to one of two treatment groups: RSD+ (monthly risedronate 150 mg and cholecalciferol 30,000 IU combined in a single pill, n=74) or RSD (monthly risedronate 150 mg alone, n=76). We measured serum levels of 25(OH)D, parathyroid hormone (PTH), and bone markers and performed muscle function tests, at baseline and after 16 weeks of treatment.

Results: After 16 weeks of treatment, mean serum 25(OH)D increased significantly from 17.8 to 24.3 ng/mL in the RSD+ group and declined significantly from 18.1 to 15.8 ng/mL in the RSD group. The RSD+ groups had significant decreases in serum PTH from 46 to 36.7 pg/mL during the study, but the RSD group showed increasing tendency of PTH from 38 to 40.6 pg/mL. In both groups, serum bone-specific alkaline

phosphatase (BSAP) and C-terminal telopeptide (CTX) declined rapidly and significantly during the treatment; there were no significant differences between groups. There was also no significant difference between groups in lower-extremity function tests. The overall incidence of clinical adverse events was not significantly different between groups.

Conclusion In patients with osteoporosis, a once-monthly pill of risendronate and cholecalciferol provided equivalent anti-resorptive efficacy to risendronate alone in terms of bone turnover and improved 25(OH)D level over a 16-week treatment period without significant adverse events.

Disclosures: Ho-Yeon Chung, None.

This study received funding from: Hanlim pharmaceutical Co.Ltd

SU0425

Efficacy of Intravenous Ibandronate in Postmenopausal Women with an Inadequate Response to Oral Bisphosphonate. Ha Young Kim^{*1}, Sung Jin Bae², Beom-Jun Kim², Seung Hun Lee³, Jung-Min Koh², Ghi Su Kim³.

¹Wonkwang University Sanbon Hospital, South Korea, ²Asan Medical Center, South Korea, ³Asan Medical Center, University of Ulsan College of Medicine, South Korea

Objective: Oral bisphosphonate (BP) therapy is a mainstay for treatment of post-menopausal osteoporosis. However, it has been reported that the number of inadequate responders to oral BP is up to 25% in treated post-menopausal women. The mechanism behind inadequate responses to oral BP have to be detailed and clarified. In this study, we evaluated the efficacy of intravenous BP using biochemical bone turnover markers in post-menopausal women with an inadequate response to oral BP.

Material and Methods: We measured serum C-telopeptide (CTX) levels after 6 months of therapy in 172 post-menopausal women who have received uninterrupted oral BP therapy (Alendronate, 10mg/day and 70mg/week; Risedronate, 5mg/day and 35mg/week; Ibandronate, 150mg/month) for at least 3 months. Inadequate responders were defined as patients who did not show more than a 51% reduction of serum CTX compared with pre-treated levels or whose serum CTX did not fall to below the pre-menopausal mean level. Identified inadequate responders were classified into two groups: Continuous Oral BP Treatment and Change to IV Ibandronate Treatment. After 3 months and 12 months of treatment, we measured serum CTX levels.

Result: At the baseline, there was no significant difference in age, years since menopause, height and weight between the alendronate treatment group (n=88) and the risedronate treatment group (n=84). We identified 28 inadequate responders (16.3%; 11(12.5%) in the alendronate group and 17 (20.2%) in the risedronate group. The alendronate group showed a higher tendency in therapeutic response ($P=0.169$). Among the subjects who were changed to IV ibandronate therapy (n=13), serum CTX levels measured 7 days after the second injection (0.191 0.110 ng/mL) and again just prior to the fifth injection (0.274 0.159 ng/mL) showed a significant decrease compared to pre-treatment levels (0.450 0.134 ng/mL) ($P < 0.001$ and $P = 0.004$, respectively).

Conclusion: Inadequate response to oral BP may result from decreased absorption in the intestine and/or binding with food-containing materials. Therefore, the change to intravenous BP could be a good alternative for inadequate responders.

Disclosures: Ha Young Kim, None.

SU0426

Lessons Learned From Setting Up a Community Based IV Bisphosphonate Service. Eamonn Brankin^{*1}, Robin Munro², Wendy Feeney², Margaret Yates², Paul Mitchell³, John Hinnie⁴, Andrew Gallagher⁵, Janet Horner¹, Stephen Gallacher⁶. ¹NHS Lanarkshire, United Kingdom, ²NHS Lanarkshire Osteoporosis Service, United Kingdom, ³University of Derby, United Kingdom, ⁴South Glasgow Osteoporosis Service, United Kingdom, ⁵Victoria Infirmary, United Kingdom, ⁶Southern General Hospital, United Kingdom

In 2010 we presented set up of an IV bisphosphonate infusion service. We now share lessons learned to aid colleagues wishing to follow suit. During the process the financial situation within the NHS changed resulting in significant service implementation delay. Historically, various services – rheumatology, orthopaedics, care of the elderly and family medicine each treated patients in isolation. We aimed to progress to a unified service. Lessons learned: -Establish a unified drug budget. Lack of a drug budget was our biggest hurdle -Enlist senior NHS pharmacist help at outset. -To achieve NHS funding approval a protocol must be submitted to budget holders very early in the process -Sourcing Vitamin D was difficult requiring additional approval as an unlicensed use -Many patients in care homes have mental health/consent issues. This causes delay in treatment -For financial reasons funding approval for the use of zoledronic acid was restricted to hip fracture patients initially. Limiting treatment numbers improves chances of initial funding approval -A significant number of patients died shortly post fracture. As such it is beneficial to delay IV treatment for a period of time post fracture -Developing a patient identification system is essential -Inconsistencies with data retrieval from IT systems causes issues. -Access to past medical/drug histories is variable. Access to the NHS emergency care summary across primary/secondary care would be optimal. Some care homes are

reluctant to release notes -Care home staff may be too busy to help staff assess patients and some patients with more severe dementia did not tolerate cannulation -Setting up the service required close networking with care homes, care home liaison and mental health staff, pharmacy, falls/elderly care teams. The patient pathway improved as other services are now aware of how to access the service -Timing issues – political and financial, are important as is mentoring/training of nurses in IV cannulation and drug administration -It is optimal to have an IT system which records patient consultations. Working between primary/secondary care makes careful choice of an appropriate IT system essential, but again takes time -Liaison with medical physics is essential. Lightweight ambulatory infusion pumps are optimal for community use. This may not fit with corporate purchasing policy. Pumps have to be 'fit for purpose' as patients with dementia may not be able to sit for the duration of the infusion

Disclosures: Eamonn Brankin, Roche, 2; Novartis, 2

This study received funding from: Novartis

SU0427

Osteoporosis Treatment Patterns Among Medicare Beneficiaries. Huifeng Yun^{*1}, Jeffrey Curtis¹, Robert Matthews¹, Meredith Kilgore², Michael Morrissey¹, Nicole Wright¹, Kenneth Saag¹, David Becker¹, Elizabeth Delzell¹. ¹University of Alabama at Birmingham, USA, ²University of Alabama At Birmingham School of Public Health, USA

Background: Low adherence to bisphosphonates (BPs) is associated with increased fracture risk. Standard measures of adherence, which often classify patients as non-persistent (i.e., discontinuing) if they switch to other osteoporosis (OP) treatments or restart therapy at a later time, may underestimate adherence and hinder identification of factors associated with discontinuation.

Objectives: To identify OP medication discontinuation and switching patterns among Medicare beneficiaries and factors associated with discontinuation.

Method: We used a 5% sample of Medicare beneficiaries with at least 30 months of fee-for-service and part D drug coverage from 2006 through 2008. We identified a cohort of new BP users who initiated treatment after a 12 month baseline period with no BP prescriptions filled. We classified medication status at the end of 18 months of follow-up as: continued same BP drug without a treatment gap (≥ 90 days after end of days' supply), discontinued all OP drugs (≥ 90 days with no subsequent prescription for an OP med), restarted same drug after a gap, switched to another BP or non-BP drug without a gap, or switched to another drug with a gap. We used multinomial logistic regression to identify factors associated with medication status at the end of follow-up.

Results: Among 5,069 new BP users, after 18 months of follow-up, 35.5% continued the same BP, 37.0% completely discontinued, 15.3% restarted the same drug after a gap ≥ 90 days, and 12.1% switched to another BP or non-BP drug, either with (3.9%) or without (8.2%) a gap. With non-persistence defined as total discontinuation, having a gap in BP therapy ≥ 90 days or switching, 64.4% of patients would have been considered non-persistent. Lower income, more comorbidity, and no DXA during baseline were significantly associated with total discontinuation of BPs within 18 months.

Conclusion: Among new BP users, switching between BPs, switching out of the BP treatment class, and having treatment gaps are common. Discontinuation and switching patterns should be considered in order to characterize adherence more accurately in future OP studies.

Disclosures: Huifeng Yun, Amgen, 2

This study received funding from: Amgen

SU0428

Relationship Between Change in Total Hip BMD in Response to Zoledronic Acid 5 mg and Pre-treatment Change in Total Hip BMD: the HORIZON-PFT Extension Study. Richard Eastell^{*1}, Lisa Palermo², Steven Boonen³, Felicia Cosman⁴, Ian Reid⁵, Steven Cummings⁶, Dennis Black². ¹University of Sheffield, United Kingdom, ²University of California, San Francisco, USA, ³Center for Metabolic Bone Disease & Division of Geriatric Medicine, Belgium, ⁴Helen Hayes Hospital, USA, ⁵University of Auckland, New Zealand, ⁶San Francisco Coordinating Center, USA

Several studies have shown the high bone turnover is associated with 1) greater rates of bone loss and 2) greater BMD response to anti-resorptive therapy in postmenopausal osteoporosis. However, it is not known whether greater rates of bone loss prior to therapy are associated with greater BMD response to anti-resorptive therapy. In the HORIZON-PFT Extension study, one group of women who were randomized to receive placebo for 3 years (years 1, 2 and 3), were then all treated with Zoledronic Acid 5 mg annually for up to three injections (years 4, 5 and 6, P3Z3 Study) (n=1223). We measured total hip BMD at baseline, 1, 2 and 3 years on placebo and at 4.5 and 6 years on zoledronic acid. BMD was measured by DXA and total PINP by automated immunoassay analyser. The PINP was measured at 3, 4.5 and 6

years, but results were excluded if patients had a fracture in the past year (PINP increases for up to a year following a fracture). Also, by design not all subjects were followed for as long as 6 years, so this analysis will focus on the results at 4.5 years.

The change in total hip BMD in years 0-3 was related to the change in total hip BMD on zoledronic acid at 4.5 years ($r = -0.39$, $P < 0.0001$). Thus, those with greater loss during years 0-3 had greater gain during years 3-4.5. In order to test whether this last result was robust, we repeated the analysis with hip BMD at 6 years ($r = -0.24$, $P < 0.0001$) and we repeated the analysis with change in hip BMD at 2 years ($r = -0.09$, $P < 0.01$). The change in total hip BMD in years 0-3 on placebo was related to the serum PINP at the end of the 3-year period ($r = -0.24$, $P < 0.0001$). The change in total hip BMD on zoledronic acid from year 3 to 4.5 was related to the serum PINP at the end of the 3-year period ($r = 0.26$, $P < 0.0001$). We conclude that BMD response to zoledronic acid is greater in postmenopausal women who had larger loss prior to treatment. The likely mechanism for this association is that higher bone turnover is associated with both greater BMD response to zoledronic acid and greater bone loss on placebo.

Disclosures: Richard Eastell, Warner Chilcott, Amgen, Eli Lilly, AstraZeneca, 2; AstraZeneca, Amgen, GlaxoSmithKline, Medtronic, Nasteck, Nestle, Fonterra Brands, Novartis, Ono Pharma, Eli Lilly, Sanofi Aventis, Tethys, Unilever, Unipath, Inverness Medical, 5

This study received funding from: Novartis Pharmaceuticals

SU0429

The Effect of One Year Bi-monthly Ibandronate on Bone Mineral Density and Bone Turn Over Marker in Korean Postmenopausal Women. Young Goo Shin*. Wonju College of Medicine, South Korea

Background: Osteoporosis is the condition of fragile bone, which is easy to fracture with minor trauma. Bisphosphonates are widely prescribed worldwide, today. Among these bisphosphonates, the oral monthly ibandronate is the least frequent dosing in postmenopausal osteoporosis, approved by USA-FDA. But, in Korea, the HIRA (public health assurance) cover the drug cost with only 6 month during one year and only in patients just T-score less than -3.0 regardless the kinds of drugs for osteoporosis. So, in Korea, physician should prescribe the drugs for osteoporosis by the above guideline or the other 6 months-prescribing should be done without public health assurance coverage. So, I review the efficacy of ibandronate with the change BMD and bone marker during one year treatment between monthly and bi-monthly dosing.

Methods: About 200 patients were enrolled. The patients were divided to 2 groups, monthly dosing and bi-monthly dosing. Patients were tested for L2-4 spine BMD, femur neck BMD, total hip BMD, serum osteocalcin and CTx at baseline and 1 year after dosing.

Results: The patients for monthly dosing were 78 and for bimonthly dosing were 48. The age was older with monthly (62.5 vs 59.5, $p = 0.031$). The basal BMD (g/cm²) were significant higher with bi-monthly; L2-4 (0.860 vs 0.967), femur neck (0.720 vs 0.797), total hip (0.762 vs 0.861).

With monthly dosing, there were significant increasing BMD at all site and decreasing bone marker after ibandronate treatment by paired t-test. The BMD (g/cm²) was increased as follows: L2-4 0.860 to 0.899, femur neck 0.720 to 0.744, total hip 0.762 to 0.789. The osteocalcin (ng/ml) 27.12 decreased to 14.89, and the CTx (ng/ml) 0.74 decreased to 0.23.

With bi-monthly dosing, the BMD was only significant increasing in lumbar spine BMD, and the others also have tendency to increase but not significant by paired t-test. The changes of BMD (g/cm²) as follows: L2-4 0.967 to 1.011, femur neck 0.797 to 0.803, total hip 0.861 to 0.865. The changes of bone markers also significant decrease in this group by paired t-test. The osteocalcin (ng/ml) 24.6 decreased to 18.05, and the CTx (ng/ml) 0.61 decreased to 0.32.

But these significant changes were disappeared with repeated measured ANOVA, adjusted with age, height and weight.

Conclusion: The ibandronate therapy was effective to Korean postmenopausal women in both groups, monthly or bi-monthly dosing. And there was not differ between the 2 dosing treatments.

Limitation of this study: There was some selection bias because the patients were not conditioned. So, I had tendency to prescribe the drug monthly to weaker bone, bi-monthly to relative strong bone.

Table 1. Basal characteristics in both groups

	Monthly (n=78)	Bi-monthly (n=48)	p
Age (years)	62.55 ± 7.72	59.50 ± 7.90	0.031*
Height (cm)	151.29 ± 6.44	152.43 ± 6.16	0.261
Weight (kg)	56.92 ± 8.83	58.40 ± 8.38	0.356
Serum Osteocalcin (ng/ml)	27.05 ± 14.73	24.70 ± 13.58	0.432
Serum CTx (ng/ml)	0.73 ± 0.43	0.60 ± 0.38	0.143
ALP (U/L)	91.45 ± 37.09	93.59 ± 39.35	0.779
Calcium (mg/dL)	9.49 ± 0.47	9.44 ± 0.43	0.818
Phosphate (mg/dL)	4.01 ± 0.40	4.39 ± 0.72	0.155
Lumbar (L2-4) BMD (g/cm ²)	0.860 ± 0.124	0.966 ± 0.099*	0.000*
Total Hip BMD (g/cm ²)	0.762 ± 0.105	0.861 ± 0.123*	0.000*
Femur neck BMD (g/cm ²)	0.720 ± 0.100	0.797 ± 0.107*	0.000*

Data expressed as mean ± SD. * = 0.05 compared to Group1 with t-test.

Table 2. Changes of calcium, phosphate, bone turnover markers and bone densitometry before and after treatment in both groups

	Monthly			Bi-monthly		
	Before	After	P*	Before	After	P**
OC	27.12 ± 14.73	14.89 ± 7.03	0.000	24.60 ± 13.92	18.05 ± 10.90	0.000
CTx	0.74 ± 0.42	0.23 ± 0.13	0.000	0.61 ± 0.39	0.32 ± 0.25	0.000
ALP	90.90 ± 37.20	66.43 ± 23.50	0.000	91.74 ± 38.37	72.92 ± 19.35	0.000
LS	0.860 ± 0.124	0.899 ± 0.131	0.000	0.967 ± 0.099	1.011 ± 0.113	0.000
TH	0.720 ± 0.100	0.744 ± 0.109	0.002	0.797 ± 0.109	0.803 ± 0.109	0.154
TH	0.762 ± 0.105	0.789 ± 0.104	0.000	0.861 ± 0.125	0.865 ± 0.126	0.510
Ca	9.52 ± 0.46	9.44 ± 0.50	0.309	9.67 ± 0.39	9.43 ± 0.29	0.001
P	3.90 ± 0.57	3.71 ± 0.59	0.006	4.23 ± 0.73	3.75 ± 0.41	0.000

Data expressed as mean ± SD.

P* = 0.05 paired t-test.

P** = repeated measured ANOVA. The data adjusted with age, height and weight.

OC: osteocalcin (ng/ml); CTx: serum C-telopeptide (ng/ml); ALP: serum alkaline phosphatase (U/L); LS: Lumbar (L2-4) BMD (g/cm²); TH: Femur neck BMD (g/cm²); TH: Total Hip BMD (g/cm²); Ca: Calcium (mg/dL); P: Phosphate (mg/dL).

Disclosures: Young Goo Shin, None.

SU0430

Weekly Alendronate Versus a Single Infusion of Zoledronic Acid: Effects on Bone Turnover Markers, Areal and Volumetric BMD and Bone Microarchitecture During the First Year After Heart or Liver Transplantation. Adi Cohen*¹, Emily Stein², Stephanie Boutry¹, Donald McMahon², Chiyuan Zhang³, Polly Chen³, Kavita Pandit¹, Donna Mancini¹, Robert Brown¹, Susan Restaino¹, Elizabeth Shane². ¹Columbia University Medical Center, USA, ²Columbia University College of Physicians & Surgeons, USA, ³Columbia University, USA

Bone loss and vertebral fractures occur during the first year after heart (HTX) or liver (LTX) transplant. Alendronate (ALN) prevents bone loss in HTX recipients and 3 month (3M) infusions of zoledronic acid (ZA) prevent bone loss in LTX recipients. We conducted a 12M, double-masked, active comparator, non-inferiority trial in 84 HTX or LTX recipients randomized to ALN 70 mg/week or a single infusion of ZA 5 mg, both initiated 258 days post-TX. We compared 12M change in serum C-telopeptide (CTx), BMD at the lumbar spine (LS), femoral neck (FN) and total hip (TH) by DXA, and in a subset, volumetric BMD (vBMD) and microarchitecture at the radius (RAD) and tibia (TIB) by HRpQCT. A nonrandomized reference group (REF, n=25; T score ≥ -1.5) was also enrolled. In the REF group, CTx fell by 21% ($p = \text{NS}$). BMD fell by 1.71.1% (SD; $p = 0.12$) at the LS, 2.00.8% ($p = 0.01$) at the TH and 1.91.0% ($p = 0.07$) at the FN. TIB trabecular (Tb) vBMD fell by 2.17.0% ($p = 0.04$) and Tb number (Tb.N) fell by 3.513.4% ($p = 0.07$), with no significant changes at the RAD. Cortical (Ct) parameters were stable. By 2M, CTx declined significantly more ($p < 0.05$) in the ZA (-69%); 0.656 to 0.201 pg/ml; $p < 0.02$) than the ALN group (-35%); 0.554 to 0.360 pg/ml; $p < 0.13$) and remained lower all year. 12M LS aBMD increased in the ZA group (1.80.7%; $p = 0.03$) with no change in the ALN group (-0.30.7%; $p = 0.9$). TH and FN aBMD did not change in either group. When HTX and LTX recipients were analyzed together, no DXA or HRpQCT parameter differed between ALN and ZA groups. However, HTX recipients randomized to ALN had more LS bone loss than those randomized to ZA (-2.80.9 vs +1.30.9%; $p = 0.013$). In LTX recipients randomized to ALN, RAD Tb vBMD fell by -3.88.0% ($p = 0.01$) and Tb.N fell by -8.716.1% ($p = 0.03$); neither measure changed in the ZA group (between-groups $p < 0.04$). In HTX recipients, TIB Ct thickness declined by -1.54.5% in the ALN group ($p = 0.09$), with no change in the ZA group (+0.44.0%, $p = \text{NS}$). In summary, ZA suppresses CTx more than ALN after HTX or LTX. There was no LS, FN or TH bone loss in HTX/LTX recipients treated with either drug. However, ZA provided greater protection than ALN for LS aBMD in HTX recipients and RAD Tb vBMD and Tb.N in LTX recipients. We conclude that a single infusion of ZA provides more suppression of CTx and is non-inferior to weekly ALN in preventing bone loss during the first 12M after HTX/LTX.

Disclosures: Adi Cohen, None.

This study received funding from: Novartis

SU0431

Bisphosphonate Prescribing, Persistence and Cumulative Exposure in Ontario, Canada. Andrea Burden^{*1}, J. Michael Paterson², Daniel Solomon³, Muhammad Mamdani¹, David N. Juurlink¹, Suzanne Cadarette¹. ¹University of Toronto, Canada, ²Institute for Clinical Evaluative Sciences, Canada, ³Harvard Medical School, USA

Purpose:

To describe bisphosphonate prescribing, persistence and cumulative exposure among seniors in Ontario, Canada.

Method:

We used Ontario Drug Benefit pharmacy claims to identify residents aged ≥ 66 years who initiated oral bisphosphonate therapy between April 1996 and March 2009. The first date of bisphosphonate dispensing was considered the index date. Persistence with therapy was defined as continuous treatment with no interruption exceeding 60 days. We examined persistence with therapy and the number of extended gaps (>60 days) between prescriptions over time periods ranging from one to nine years. We also identified the proportion of patients filling only a single prescription and switching to a different bisphosphonate, and calculated the median days of exposure irrespective of gaps in therapy.

Results:

451,113 eligible new bisphosphonate users were identified: mean age=75.6 years (SD=6.9), 84% female, and median follow-up length=4.7 years. Persistence with therapy declined from 63% at one year to 46% at two years and 12% at nine years. Among those with at least five years of follow-up (n=213,029), 61% had one or more extended gaps in bisphosphonate therapy. Overall, 10% of patients filled only a single prescription, 37% switched to a different bisphosphonate and the median exposure was 2.2 years.

Conclusion:

Less than half of patients persisted with bisphosphonate therapy for two years and interruptions in therapy were common, with most patients experiencing two or more >60 day gaps in therapy. Interventions are needed to improve persistence with bisphosphonate therapy and reduce the frequency of gaps in treatment.

Disclosures: Andrea Burden, None.

SU0432

Case Study: Osteoporosis in Cosenza (Clabria, Italy). Alfonso Reda^{*1}, Claudia Carbone², Luisa Gallo², Maria Gabriella Bartoletti³, Brunella Piro⁴. ¹Italy, ²Servizio Farmaceutico Territoriale, Italy, ³Centro Riabilitazione Biolife, Italy, ⁴Ufficio di Farmacovigilanza Servizio Farmaceutico, Italy

Introduction. The osteoporosis is a disease characterized by underdiagnosis and undertreatment. We want to see if it is true in our referring population. **Method.** We have considered the population from the district of Cosenza in Calabria (Italy). The whole population is 291'086, the women are 149'246 (51.3%) and the men are 141'790 (48.7%). Particularly the women above 50 years hold are 89'994 (60.3%). We have considered two years 2009 – 2010 and all the patients treated with an active drug for osteoporosis (sold in chemistry). Teriparatide, parathyroid hormone, raloxifene, alendronyc acid (only with colcalciferole), ibandronic acid, ricedronic acid, strontium ranelate. **Results.** All treated women are above 50 years hold and they are 11094 (12.33 % of the women above 50 years hold). 84 (0.75% of the treated women above 50 years hold) women took the teriparatide. Two women took parathyroid hormone (0.018% of the women treated above 50 years hold). We have to say that the prescription of teriparatide, parathyroid hormone, is under a restrictive criteria. 317 women took raloxifene (2.86% of the treated women above 50 years hold). 4610 (41.55 % of the treated women above 50 years hold) women took alendronyc acid (only with colcalciferole). 1082 (9.75 % of the treated women above 50 years hold) women took ibandronic acid. 2649 (23.87% of the treated women above 50 years hold) women took ricedronic acid. 2350 (21.18 % of the treated women above 50 years hold) women took strontium ranelate. **Conclusions.** Our observation confirms the underdiagnosis and undertreatment of the osteoporosis. This is one of the greatest problem of Italian health system.

Disclosures: Alfonso Reda, None.

SU0433

Comparative Analysis of Clinical Outcomes in Patients with Osteoporotic Vertebral Compression Fractures (OVCF); Conservative Treatment Vs Balloon Kyphoplasty. Seong-Hwang Moon¹, Seung Woo Suh², Hwan Mo Lee¹, Si Young Park^{*3}, Jae Young Hong². ¹Yonsei University College of Medicine, South Korea, ²Korea University, College of Medicine, South Korea, ³Korea University, Medical College, South Korea

Introduction

Almost OVCF can be treated conservatively. Recently Kyphoplasty has become a common treatment for painful osteoporotic compression fractures. It has shown numerous benefits including early pain control and height restoration of vertebral body. In spite of simple procedure, numerous complications related to kyphoplasty have been reported. Moreover there is limited evidence to support its superiority.

Methods

Prospectively, we assigned 259 patients who had one or two acute painful OVCF confirmed by MRI. All patients were treated conservatively in initial three weeks. Kyphoplasty was performed in 98 patients who complained sustained back pain and disability in spite of conservative treatment for initial 3 weeks. Participant were stratified according to age, sex, level, number of fractures, BMD, BMI, collapse rates and past history of spine fractures. Pain score using VAS and Oswestry disability index were assessed at 1 week and at 1,3,6 and 12 months.

Results

A total of 259 patients were enrolled and 238 (89 of 98 in Kyphoplasty group, and 149 of 161 in conservative treatment group) completed the 1 year follow up. About 62% of patients were treated successfully with conservative treatment. Risk factors of failure of 3 weeks conservative treatment were older age (over 80), severe osteoporosis (less than -3.0 of t-score), overweight (over 25 of BMI) and larger collapse rates (over 35%). There were significant reductions in VAS and ODI score in both groups at each follow up assessment. At 1 month, better clinical results were assessed in Kyphoplasty group. However, there were not significant differences in outcome measures between two groups at 3,6,12 months. 13 subsequent compression fractures (8 in Kyphoplasty group, 5 in conservative treatment group) occurred during the 1 year follow up period.

Conclusion

Both treatments of OVCF showed successful clinical results at 1 year follow up period. Kyphoplasty showed better outcomes in only 1st month. At the result, in case of the patient with OVCF has no risk factors for failure of conservative treatment, Kyphoplasty might not be indicated. Trial of conservative treatment for 3 weeks will be beneficial.

Disclosures: Si Young Park, None.

SU0434

Compliance with Intravenous Zoledronate in Elderly Patients with Osteoporosis. Young-Kyun Lee^{*1}, Yong-Chan Ha², Deog-Yoon Kim³, Jae-Suk Chang⁴, Hyun-Koo Yoon⁵, Kyung-Hoi Koo¹. ¹Seoul National University Bundang Hospital, South Korea, ²Chung-Ang University Hospital, South Korea, ³Kyung Hee University Hospital, South Korea, ⁴Ulsan University, Asan Medical Center, South Korea, ⁵Cheil General Hospital & Women's Healthcare Center, South Korea

Purpose; Although bisphosphonate is effective for the prevention and treatment of osteoporosis, this therapy obviously work only when patients with osteoporosis take it with good compliance. Intravenous zoledronate, which is administrated annually, has shown the good efficacy of osteoporosis therapy and has ensured its effectiveness for one year. On the contrary to poor compliance with oral bisphosphonate, annual administration of zoledronate seems to overcome the weak point of oral bisphosphonate. However, there is little information available concerning compliance with intravenous zoledronate for osteoporosis in the usual care setting. The aim of this study was to assess intravenous zoledronate compliance after the first administration, and to evaluate the factors contributing to compliance with zoledronate.

Methods; A questionnaire survey about the second administration of zoledronate was performed in 259 patients, whom the first intravenous zoledronate had been administered between January 2009 and December 2009, at the second visit. The questionnaire asked whether the patients were administered zoledronate or not, and why they refused the second injection in non-compliance patients.

Results; One hundred thirty six patients revisited our outpatient clinic at the second year, and the second administration was performed on 89 patients (34.4%, 89/259). Of 79 patients completed the questionnaire, thirteen patients refused the second administration and wanted to exchange into oral bisphosphonate. A post-infusion syndrome was the reason why the six patients out of thirteen (46.2%, 6/13) refused the second administration (46.2%, 6/13).

Conclusion; Although it is guaranteed that the effect of annual intravenous administration of zoledronate will last for a year, the compliance to the second administration was only a third, which was comparable with oral bisphosphonate after a year. The post-infusion syndrome was the factor contributing compliance with intravenous zoledronate in real setting.

Disclosures: Young-Kyun Lee, None.

SU0435

Does FRAX® change Treatment Decision in Patients visiting a German University Hospital?. Susanne Rendl¹, Peter Schneider^{*2}. ¹University Clinic Würzburg, Germany, ²Clinic for Nuclear Medicine, Germany

Purpose: FRAX derived 10-years fracture probability incorporates femur neck BMD as risk factor modulating a small range of the fracture probability forecast, thus giving BMD a minor weight as compared with T-score definition alone. We wanted to see whether or not FRAX influenced our treatment recommendations for use of level Ia or Ib agents in clinical routine.

Methods: 100 consecutive patients (26 men, age 65.18.2, 74 women, age 62.311.4) were scanned within 6 weeks using DXA at both hips and the spine (GE Prodigy) and pQCT at the distal radius (Stratec XCT2000). Risk factors were assessed and entered in compliance with FRAX risk factor definition. The lower of the dual femur neck density values was entered. Treatment decision was met using propriety software to project the calculated probabilities on the decision diagram [1] (fig.1). The decision was "yes" if one of the probabilities for general osteoporotic or hip fracture exceeded the threshold. FRAX based neck T-score was compared with German (D) normal data base T-scores for radius, spine and neck. Correlations were determined, $p < 0.05$ was considered significant.

Results: Correlations for the T-scores $\text{neck}_{\text{FRAX}}/\text{neck}_D$ were $r=0.96$, for the T-scores $\text{spine}_D/\text{neck}_D$ $r=0.49$, and, for T-scores $\text{radius}_D/\text{neck}_D$ $r=0.60$, all significant. The mean FRAX derived T-Score was 0.12 lower (not signif.) than the D. Percentages of treatment candidates according to a T-score threshold of ≤ -2.5 or to the FRAX risk assessment tool are shown in fig.2. The correlation between the neck T-score $\text{neck}_{\text{FRAX}}$ and the FRAX_{risks} derived treatment decision (yes/no) was weak ($r=0.38$, $p < 0.01$). The $\text{neck}_{\text{FRAX}}$ T-score correlated with the probability for major osteoporotic fractures by $r=0.62$ ($p < 0.01$). 3% of the patients with a $\text{neck}_D \leq -2.4$ and 16% with a $\text{neck}_D > -2.5$ received a treatment recommendation. For the FRAX-derived neck T-score it was the same rate, but included different individuals (T-Score range: $-0.5 \dots -3.4$, $r=0.95$) due to the impact of their risk profile.

Conclusion: FRAX as a very useful tool is leading to different treatment decisions as compared with a solely T-score based decision. However, it provides a more convincing justification, which is far less dependent on known systematic DXA errors, particularly evident in spine DXA.

[1] Kanis et al., Osteoporos Int 2008; 19

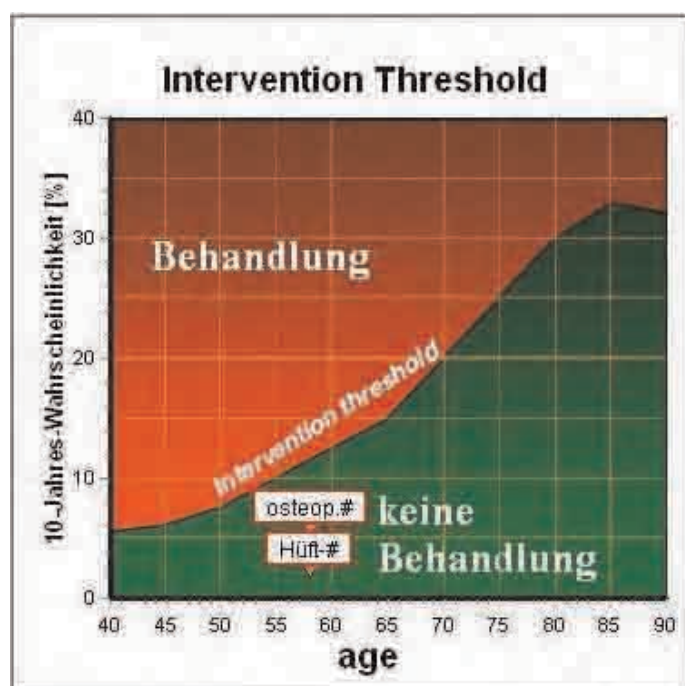


Fig. 1

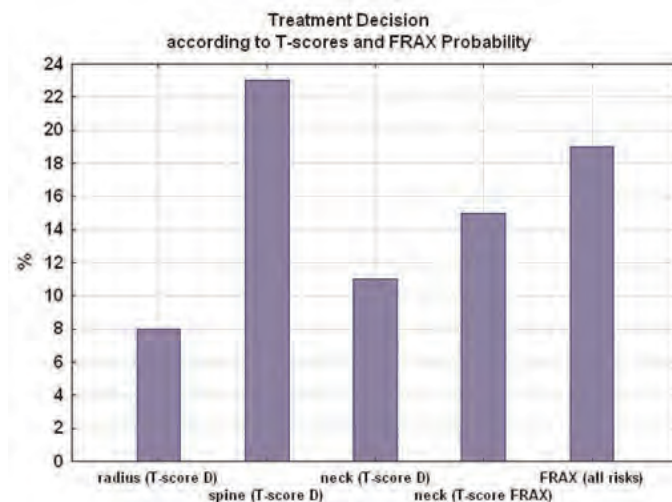


Fig. 2

Disclosures: Peter Schneider, None.

SU0436

Osteoporosis Medication Prescribing in British Columbia and Ontario: Impact of Public Drug Coverage. Suzanne Cadarette^{*1}, Diana Baek¹, Nadia Gunraj², Greg Carney³, Michael Paterson², Colin Dormuth³. ¹University of Toronto, Canada, ²Institute for Clinical Evaluative Sciences, Canada, ³University of British Columbia, Canada

Background: Approved therapies for treating osteoporosis in Canada include bisphosphonates, calcitonin, denosumab, raloxifene and teriparatide. However, significant variation in public drug access to these medications exists across Canada. We sought to compare patterns of osteoporosis medication prescribing between British Columbia (BC) and Ontario.

Methods: Using dispensing data from BC (PharmaNet) and Ontario (Ontario Drug Benefits), we identified all new users of osteoporosis medications aged 66 or more years from 1995/96-2008/09. We summarized the number of new users by fiscal year, sex and index drug for each province. BC data were also stratified as provincial PharmaCare accepted or not.

Results: We identified 578,254 ($n=122,653$ BC) eligible new users. Overall patterns of prescribing were similar between provinces: 1) most received an oral bisphosphonate (94% BC and 99% in Ontario); 2) etidronate prescribing declined after 2001/02, reaching a low of 41% in BC and 10% in Ontario in 2008/09; and 3) the proportion of males treated increased over time, from 8% of new users in 1995/96, to 25% of new users in 2008/09. We note differences in access to second-generation bisphosphonates (alendronate or risendronate) in BC when stratified by whether or not drugs were covered by BC PharmaCare; $<2\%$ (PharmaCare) versus 79% (non-PharmaCare) of medications dispensed were for second-generation bisphosphonates.

Conclusions: Oral bisphosphonates are the primary drugs used to treat osteoporosis in Canada. Prescribing practices changed over time as newer medications came to market, yet access to second-generation bisphosphonates through BC PharmaCare was limited. Implications of differential access to oral bisphosphonates warrants further study.

Disclosures: Suzanne Cadarette, None.

SU0437

Osteoporosis Telephonic Intervention to Improve Medication Adherence (OPTIMA): A Large Pragmatic Randomized Controlled Trial. Daniel Solomon^{*1}, Maura Iversen², Jerry Avorn², Timothy Gleeson², Alan Brookhart³, Amanda Patrick², Laura Rekedal², William Shrank², Joyce Liu², Elena Losina², Jeffrey Katz². ¹Harvard Medical School, USA, ²Brigham & Women's Hospital, USA, ³University of North Carolina, USA

Purpose: Multiple studies have demonstrated poor adherence with medications prescribed for chronic illnesses, including osteoporosis. Few interventions have been proven to improve adherence. We conducted a randomized controlled trial of telephone counseling based on motivational interviewing to improve medication adherence for osteoporosis.

Methods: We collaborated with a pharmacy benefit program for Medicare beneficiaries in one US state and invited persons newly prescribed a medication for osteoporosis to participate. Consenting persons were randomized to either a one-year program of telephone-based counseling ($n = 1,046$) using a motivational interviewing framework or a control group ($n = 1,041$) that received intermittent mailed educational materials. Medication adherence was the primary outcome and was

measured as the median (interquartile range, IQR) medication possession ratio (MPR), calculated as the ratio of days with filled prescriptions to total days of follow-up. The median MPR was compared across treatment arms.

Results: The groups were well balanced at baseline, with a mean age of 78 years; 94% were female. In an intention-to-treat analysis, median adherence was 48.8% (IQR 6.9, 87.9) in the intervention arm and 40.6% (1.5, 86.0) in the control arm ($P = 0.074$ by Kruskal-Wallis test) (see Table). The completer analysis showed similar effects ($P = 0.019$). Subjects 65-74 years old had a larger intervention effect than those 75 or over (P for interaction = 0.045). There were no differences in self-reported fractures.

Conclusions: A telephonic motivational interviewing intervention provided improvement in osteoporosis medication adherence that did not reach statistical significance. Such counseling-based programs may be a useful tool to improve adherence to medications for chronic conditions.

	Intervention		Control		P value [†]
	N	MPR (IQR)	N	MPR (IQR)	
Intention to treat	1046	48.8 (6.9, 87.9)	1041	40.6 (1.5, 86.0)	0.074
Completer analysis*	1008	51.3 (6.9, 88.8)	1040	40.6 (1.4, 86.2)	0.019
Subgroup analyses					P value (interaction)
Age, years					0.045
65-74	346	48.4 (7.4, 87.4)	362	30.5 (0.0, 80.0)	
75 and over	700	49.0 (6.2, 87.9)	679	45.6 (1.7, 89.7)	
Gender					0.27
Female	986	50.0 (6.9, 88.4)	971	40.6 (1.7, 86.2)	
Male	60	20.3 (0.0, 80.7)	70	38.4 (0.0, 83.0)	
Prior fracture					0.058
Yes	303	45.8 (6.9, 86.5)	285	51.2 (11.6, 85.0)	
No	723	49.5 (6.9, 88.4)	708	34.5 (0.0, 86.0)	
Marital status					0.17
Married	228	52.2 (6.9, 89.8)	231	31.8 (0.0, 83.0)	
Other**	818	48.2 (6.9, 86.9)	810	43.7 (3.0, 86.7)	
Race					0.065
White	942	50.4 (6.9, 89.7)	909	39.7 (0.0, 86.7)	
Non-white	104	35.0 (3.6, 76.1)	132	42.6 (10.8, 79.3)	

MPR, medication possession ratio; IQR, interquartile range

* The completer analysis censors subjects when they drop out of the trial. Some subjects never filled a bisphosphonate after the start of follow-up and were not included in the analysis (intervention, $n = 38$; control, $n = 1$).

[†] P-values derived from Wilcoxon Rank Sum test.

** Other refers to widowed, divorced, or single.

Table

Disclosures: Daniel Solomon, Amgen, 2

SU0438

Post Fracture Osteoporosis Treatment Program, is it Efficient? Elena Segal^{*1}, Marina Nodelman¹, Doron Norman¹, Michael Soudry¹, Daniela Militianu¹, Sophia Ish-Shalom². ¹Rambam Health Care Campus, Israel, ²Rambam Health Care Campus, Technion Faculty of Medicine, Israel

Low trauma events are common in the elderly. Patients with fragility fractures have a fivefold risk for further osteoporotic fractures. Orthopedic care usually does not include initiation of fracture prevention treatment.

Patients/methods: Fractures Prevention Program (FPP) was initiated in Rambam Health Care Campus in March 2009. All patients (pts) with fragility fractures were referred from the Department of Orthopedic Surgery to the Bone and Mineral Metabolism Unit for fracture prevention treatment (consult during hospitalization and outpatient clinic after discharge).

Results: 900 pts, aged 50-107 (75.1811.7), 247 (27.4%) men, 653 (72.6%) women. There were 593 (66%) hip fractures, 60 (7%) vertebral fractures, 247 (27%) other fractures (humerus, wrist, tibia, fibula); 155 (17%) pts had previous fragility fractures.

All hip radiographs were retrospectively assessed by a bone radiologist; 5 (0.8%) met the atypical fractures criteria. All were treated with alendronate for 2-9 years. They were not diagnosed during hospitalization.

Prior to hospitalization 156 pts (17.3%) received a fracture prevention treatment: 152 (23.2%) women [134 (88.2%) oral bisphosphonates; 10 (6.5%) – raloxifene, 5 (3.3%) – teriparatide]; 4 (1.6%) men – alendronate. 250Hd serum level prior to hospitalization was available for 239 (26.5%) pts. Mean 250Hd was 26.514.7 (4-118) ng/ml; in 85 (35.6%) pts 250Hd ≤ 20 ng/ml, 25 (10.5%) 250Hd ≤ 10 ng/ml.

154 (17.1%) pts [23 (9.3%) men, 131 (20.1%) women] adhered to the FPP. 98 (63.6%) pts had

femoral (neck and midshaft) fractures, 56 (36.4%) – other fractures. 746 (82.9%) pts stayed out of the FPP: 52 (10.6%) women continued, 1 (0.3%) man started the treatment in the community. 693 (92.8%) pts refused to join the FPP and remain untreated, 18 (2.4%) died. 207 (23%) pts are currently treated, including 53 in the community: 80 (38.6%) receive alendronate, 46 (22.2%) – risendronate, 5 (2.4%) – raloxifene, 32 (15.4%) – zoledronate, 28 (13.5%) – teriparatide, 16 (7.7%) – calcium and vitamin D prior to starting bisphosphonate. Four patients with atypical fractures were switched to teriparatide, 1 – refused.

Conclusion: Majority of elderly pts remain untreated after fragility fractures. Hospital based FPP increased by 8% the rate of post fracture treatment. Diagnosis of atypical fractures deserves special clinical and radiologic attention during hospitalization.

Disclosures: Elena Segal, Novartis, 9; Eli Lilly, 9; Merck, 3

SU0439

Psychometric Properties of the Osteoporosis-Specific Morisky Medication Adherence Scale (OS-MMAS) in Postmenopausal Women With Osteoporosis (OP) Treated with Bisphosphonates (BP). Kristi Reynolds^{*1}, Hema Viswanathan², Cynthia O'Malley², Paul Muntner³, Teresa Harrison¹, T. Craig Cheatham⁴, Jin-Wen Hsu¹, Deborah Gold⁵, Stuart Silverman⁶, Andreas Grauer⁷, Donald Morisky⁸. ¹Kaiser Permanente Southern California, USA, ²Amgen Inc., USA, ³University of Alabama at Birmingham, USA, ⁴Kaiser Permanente Pharmacy Analytic Services, USA, ⁵Duke University Medical Center, USA, ⁶Cedars-Sinai/UCLA, USA, ⁷Amgen Health Center, USA, ⁸University of California, Los Angeles, USA

Purpose: Low adherence to BPs in women with OP is common and can lead to poor outcomes. The objective of this study was to examine the psychometric properties of the recently developed OS-MMAS in postmenopausal women newly prescribed BPs.

Methods: This was a cross-sectional survey of women aged ≥ 55 yrs with OP who were newly initiated on daily or weekly BPs between 5/15/10 and 8/15/10 and enrolled in Kaiser Permanente Southern California (KPSC). KPSC is a large integrated healthcare delivery system with over 3.2 million members. Eligible women were randomly selected and mailed a self-administered survey that included: the 8-item OS-MMAS, Self-Efficacy for Appropriate Medication Use Scale (SEAMS), Beliefs about Medicines Questionnaire (BMQ), Treatment Satisfaction Questionnaire for Medicines (TSQM), Gastrointestinal Symptom Rating Scale (GSRs), 12-item Short Form Health Survey (SF12), and clinical and sociodemographic questions. OS-MMAS scores range from 0 to 8; higher scores indicate better medication adherence. Test-retest reliability was assessed using a subset of respondents surveyed within 7 to 21 days of the initial survey. Women reporting discontinuation of BP therapy were excluded. Reliability was assessed using Cronbach's α and intraclass correlation coefficients (ICCs). Convergent validity was assessed using correlations between OS-MMAS and related measures with Bonferroni adjustment, and confirmatory factor analysis (CFA).

Results: Of 195 respondents, 150 were included. The mean (SD) age was 71 (9) years; 61% were white, and 30% had a prior fracture. Overall, 31%, 33% and 36% had low (<6), medium (6 to <8) and high (8) OS-MMAS scores, respectively. The OS-MMAS had high internal consistency (Cronbach's $\alpha = 0.79$) and demonstrated good test-retest reliability with a weighted Kappa statistic of 0.61 (95% CI, 0.48-0.75) and an ICC of 0.77 (95% CI, 0.58-0.84). The directionality of correlations was consistent with our expectations. Convergent validity was supported by significant correlations with the SEAMS, BMQ necessity and TSQM scores. No significant correlations were found between OS-MMAS and BMQ concerns, GSRs, and SF-12. In CFA, validity was supported by measurement of a single underlying factor of medication adherence.

Conclusion: The OS-MMAS showed strong psychometric properties among women newly prescribed BPs. Further evaluation of validity based on pharmacy data is ongoing to evaluate the utility of the tool in the clinic setting.

Measures	Correlation With the 8-Item OS-MMAS	P-value
Self-Efficacy for Appropriate Medication Use Scale	0.40	< 0.0001
Beliefs about Medicines Questionnaire		
Necessity Score	0.31	0.0001
Concerns Score	-0.22	0.0073
Treatment Satisfaction Questionnaire for Medicines		
Effectiveness Score	0.39	< 0.0001
Convenience Score	0.42	< 0.0001
Side-Effects Score	0.27	0.0009
Satisfaction Score	0.32	< 0.0001
Gastrointestinal Symptom Rating Scale		
Abdominal pain score	-0.13	0.10
Reflux syndrome score	-0.13	0.12
Diarrhea syndrome score	-0.03	0.74
Indigestion syndrome score	-0.09	0.28
Constipation syndrome score	-0.03	0.75
12-item Short Form Health Survey		
Global health status	-0.06	0.47
Physical component	0.05	0.58
Mental Health component	-0.01	0.95

Table 1

Disclosures: Kristi Reynolds, Amgen Inc., 2
This study received funding from: Amgen Inc.

SU0440

Reduced BMD and Osteoporosis in Men Treated for Hypogonadism. Mario Rui Mascarenhas¹, Ana Paula Barbosa², Antonio Gouveia de Oliveira³, Ana Gonçaves⁴, Vera Simoes⁵, David Santos Pinto⁶, M Bicho⁷, Isabel do Carmo⁸. ¹Faculdade de Medicina Lisboa, Portugal, ²Endocrinology University Clinic & Metabolism & Endocrinology Center, Genetics Laboratory (FMUL), CEDML - Endocrinology, Diabetes & Metabolism Clinic, Lda., Endocrinology, Diabetes & Metabolism Department, Santa Maria Hospital, CHLN-EPE, Portugal, ³Biostatistics Department, FCMUNL, Portugal, ⁴Endocrinology, Diabetes & Metabolism Department, Santa Maria Hospital, CHLN-EPE, Romania, ⁵Metabolism & Endocrinology Center, Genetics Laboratory (FMUL), CEDML - Endocrinology, Diabetes & Metabolism Clinic, Lda., Portugal, ⁶CEDML - Endocrinology, Diabetes & Metabolism Clinic, Lda., Portugal, ⁷Metabolism & Endocrinology Center, Genetics Laboratory (FMUL), Portugal, ⁸Endocrinology, Diabetes & Metabolism Department, Santa Maria Hospital, CHLN-EPE, Portugal

OBJECTIVE

To study the impact of the therapy of male hypogonadism in patients with low bone mineral density (BMD) and osteoporosis.

MATERIALS AND METHODS

A group of 26 non-treated hypogonadal men (17 with hypogonadotropic hypogonadism, 7 with hypergonadotropic hypogonadism and 2 with eugonadotropic hypogonadism) were evaluated with DXA scans before and during therapy for the disease: these exams were repeated after starting treatment, between 1-8 years: mean 3.1 (2.3) years (treated hypogonadal men group).

The BMD at the lumbar spine and at the hip (femoral neck and total) as well as the total body fat and lean masses were accessed by using the QDR Discovery-W densitometer (Hologic Inc.). The weight, height and BMI were also determined. Blood was collected for measurement of the LH, FSH, PRL, estradiol and total testosterone levels in the peripheral blood.

Descriptive, Anova and regression analysis statistical tests were used; statistical significance was considered for $P < 0.05$.

RESULTS

The mean BMD, T-scores and Z-scores were lower at the lumbar spine in the no treated male hypogonadism group as compared with the treated hypogonadism group, but the mean BMD, T-scores and Z-scores at the total hip were similar between the groups. The bone mass qualification is in Table 1.

TABLE1. Prevalence of normal BMD, reduced BMD and osteoporosis in the no treated and treated male hypogonadism groups.

A small increment was detected in the mean total body lean mass during hypogonadism treatment ($P > 0.05$) as well as a decrease in the mean total body fat mass ($P > 0.05$).

CONCLUSIONS

The data of this study may suggest that a late therapy of male hypogonadism may influence the weak response at the cortical bone. However, the increase in the cortical BMD to hypogonadism treatment may be higher in men with initial low BMD at the lumbar spine and at the femoral neck.

The increment of the BMD was greater in men with the lowest total testosterone levels.

Finally, it remains unclear whether the low BMD of hypogonadal men can be restored to normal, after a long-term androgen or the etiological therapy of the male hypogonadism.

However, other associated measures, to increase bone mass, may have clinical indication in order to reduce the early osteoporosis development risk.

TABLE1. Prevalence of normal BMD, reduced BMD and osteoporosis in the no treated and treated male hypogonadism groups.

Groups:	NO TREATED HYPOGONADISM n = 26 (100%)	TREATED HYPOGONADISM n = 26 (100%)
BMD		
Normal	6 (23.1%)	8 (30.8%)
Reduced	12 (46.1%)	11 (42.3%)
Osteoporosis	8 (30.8%)	7 (26.9%)

Table 1.

Disclosures: Mario Rui Mascarenhas, None.

SU0441

The Efficacy of Bazedoxifene in Postmenopausal Women is Independent from Kidney Function. Rene Rizzoli¹, Silvano Adami², Amy Levine³, Santosh Sutradhar⁴, Arkadi Chines⁴. ¹University Hospital, Switzerland, ²University of Verona, Italy, ³Pfizer, USA, ⁴Pfizer Inc, USA

Purpose: Two global, randomized, double-blind, placebo- (PBO) and active-controlled phase 3 studies (2-year prevention [N = 1583] and 3-year treatment [N = 7492]) have shown that bazedoxifene (BZA) is safe and effective for prevention and treatment of osteoporosis in postmenopausal women. We investigated whether kidney function, which generally worsens with age, influences the effects of BZA. The efficacy

of BZA was evaluated in relation to baseline glomerular filtration rate (GFR) in women enrolled in these studies.

Methods: Data for the BZA 20- and 40-mg and PBO groups from both studies were integrated, and bone turnover markers (osteocalcin and C-telopeptide [CTx]) and bone mineral density (BMD) were assessed. In the treatment study, the incidence of fractures was assessed for all fractures (morphometric vertebral and clinical) for the 2 BZA doses combined because of the small number of events. GFR was estimated by the Modification of Diet in Renal Disease Study equation. Women were categorized by GFR in mL/min per 1.73 m²: normal (GFR ≥ 90 ; n = 1477), mild impairment (60 \leq GFR < 90 ; n = 4617), or moderate/severe impairment (GFR < 60 ; n = 549).

Results: Across all renal subgroups, BZA 20 and 40 mg reduced osteocalcin (median percent change from baseline; -34.7% to -41.5%) and CTx (-42.8% to -49.6%) at Month 12 versus PBO (-18.7% to -20.4%; $P < 0.0001$ and -23.4% to -24.9%; $P < 0.0001$, respectively). Improvements in lumbar spine BMD (mean percent change from baseline) at Month 24 were greater for BZA 20 mg (1.4%-1.8%) and BZA 40 mg (1.6%-2.1%) versus PBO (0%-0.1%; $P < 0.0001$) for the normal and mild renal impairment subgroups; a similar trend was observed in the moderate/severe renal impairment subgroup but the increases with BZA versus PBO were not statistically significant. Changes in total hip BMD from baseline to Month 24 were greater for BZA 20 mg (0.8%-1.1%) and BZA 40 mg (0.9%-1.1%) versus PBO (-0.3%; $P < 0.0001$) in the normal and mild renal impairment subgroups, as well as for BZA 40 mg (1.1%) versus PBO (-0.3%; $P < 0.001$) in the moderate/severe renal impairment subgroup. The effect of BZA treatment on all fractures did not appear to be affected by kidney function, as evidenced by overall consistent trends (hazard ratios < 1) across GFR categories and no treatment by GFR interaction ($P = 0.766$).

Conclusion: Kidney function did not appear to affect the efficacy of BZA on bone turnover, BMD, and fractures in postmenopausal women.

Disclosures: Rene Rizzoli, Nestle, Amgen, Novartis, Servier, Roche, 8; Danone, Servier, Amgen, Novartis, Roche, Nycomed, 5
This study received funding from: Pfizer Inc

SU0442

Adherence to Osteoporosis Medications in Men: A Systematic Review of the Literature. Robyn VonMaltzahn¹, Heather Wiewer¹, Seema Patel¹, Nicole Yurgin². ¹HERON Evidence Development Ltd, United Kingdom, ²Amgen Inc, USA

Male osteoporosis is recognized as a growing but under-managed problem. Adherence to therapy is important in understanding real-life effectiveness and how this may be improved. We conducted a systematic review to identify information on adherence to osteoporotic medication in men, including typical adherence rates, and the factors and consequences associated with adherence. MEDLINE and Embase were searched using keywords and MeSH terms from 1998-2010 and recent conference proceedings (2008-2010) were also screened. Studies were included if they were in English and reported osteoporosis related adherence data from actual clinical practice for male populations.

Fourteen studies were identified which reported male-specific information. Of these, eight studies reported adherence rates specific to men, indicating a paucity of research in this population. Disparate methods of measurement and reporting were used, hindering comparison between results. Medication Possession Ratios (MPRs) were calculated from insurance database records in four studies. One US study reported MPRs at one year ranging between 70% [for monthly bisphosphonates (BPs)] and 41% (for daily BPs). Another US study reported more than 40% of men were non-adherent (MPR $< 80\%$) to alendronate (ALN) at one year. Persistence with newly prescribed medication was reported to be as low as 54% for weekly oral ALN after one year of treatment in a study from Germany. In a small study of men in the UK who were prescribed teriparatide injections, persistence was reported to be as high as 77% after one year. Where reported, results were conflicting with regard to gender differences in adherence. No significant association between adherence and risk of fracture was shown in one 2-year study in men treated with ALN but the number of fractures may have been too small to reliably demonstrate lack of association. In the same study, adherent men (MPR $\geq 80\%$) showed a significantly greater increase in lumbar spine bone mineral density compared with those who were non-adherent.

Where available for males, adherence and persistence estimates varied widely, perhaps due to differences in methodology, geography, and/or treatments. Nevertheless, the available studies indicate that a substantial number of male osteoporotic patients do not optimally use currently prescribed osteoporotic medications. Further research is needed to characterize adherence in men and to identify the impact of adherence on fracture risk in men.

Disclosures: Nicole Yurgin, Amgen Inc, 5
This study received funding from: Amgen Inc

SU0443

Medication Adherence in Patients on Osteoporosis Therapy: Physician Perceptions Versus Patient Behavior. Qian Cai¹, Jeffrey Curtis², Sally Wade³, Hema Viswanathan⁴, Jeff White⁵, Akhila Balasubramanian⁴, Joel Kallich⁴, John Adams⁶, Brad Stolshek⁴. ¹HealthCore, Inc, USA, ²University of Alabama at Birmingham, USA, ³Wade Otucomes Research & Consulting, USA, ⁴Amgen Inc., USA, ⁵Wellpoint, USA, ⁶RAND Corporation, USA

Purpose

Adherence to osteoporosis medication regimens is a key determinant of clinical benefit (fracture risk reduction). This study compares physicians' estimates of medication possession ratios (MPR) for their patients with MPR calculated from pharmacy claims for those same patients.

Methods

Administrative claims data from a large, U.S. commercial health plan were used to identify females, \geq age 45, with \geq 1 osteoporosis pharmacy claim between 1/1/2005 and 8/31/2008, and continuous coverage for \geq 12 months before and after first (index) medication claim in the study period. Patients with pre-index Paget's disease or malignant neoplasm, and those in a skilled nursing facility or on combination therapy at index were excluded. Prescribing physicians treating \geq 5 study patients were invited to complete a 26-item IRB-approved online or paper survey covering physician characteristics, estimated adherence levels for their patient panel, and patient management approaches. Claims-based MPR was calculated for the 12-month post-index period for each patient. Physicians were classified as optimistic (overestimated % of their patients achieving MPR \geq 0.8 by \geq 10%) or non-optimistic based on absolute differences. Logistic regression was used to assess physician characteristics associated with optimism.

Results

The analysis included survey data from 376 of the 2184 invited physicians (62% female; 58% age 45-60 years; 55% with $>$ 20 years in practice; 35% in academic setting) and claims data for 2748 patients [mean age (SD) of 62.0 (10.6) years]. On average, physicians estimated 67% of patients to have MPR \geq 0.8, yet only 40% of their eligible patients had claims-based MPR \geq 0.8. Optimistic physicians (n=277, 74%) estimated 70% of patients to have MPR \geq 0.8; yet, only 32% of their patients had claims-based MPR \geq 0.8. On average, non-optimistic physicians (n=99, 26%) underestimated the percent of patients with MPR \geq 0.8 by 8 percentage points (54% vs. 62%). Physicians in academic settings were more likely to be optimistic than community-based physicians (OR 1.69, 95% CI: 1.01, 2.85).

Conclusion

Physicians treating postmenopausal osteoporosis patients in a commercial health plan tended to overestimate the proportion of patients in their practices who had MPR \geq 0.8 for osteoporosis medications. Overestimating adherence may impede physicians' ability to support patients' efforts to adhere to medication regimens.

Disclosures: Brad Stolshek, HealthCore, 3
This study received funding from: Amgen Inc

SU0444

Womens Attitudes toward Screening for Osteoporosis (Risk-stratified Osteoporosis Strategy Evaluation). Mette Rothmann^{*1}, Lotte Huniche², Jette Ammentorp³, Kim Brixen⁴, Anne Pernille Hermann⁵. ¹Denmark, ²Institute of Public Health, University of Southern Denmark, Denmark, ³Institute of Regional Health Services Research, University of Southern Denmark, Denmark, ⁴Institute for Clinical Research, Denmark, ⁵Department of Endocrinology, Odense University Hospital, Institute of Regional Health Services Research, University of Southern Denmark, Denmark

Purpose: A large-scale trial on risk-stratified screening for osteoporosis in the Region of Southern Denmark has been initiated to test if risk-stratified screening in women aged 65-80 years is effective with respect to preventing fractures. Before a screening program is to be implemented WHO recommends that ethics and psychological issues and participant's perspective are investigated. The aim of this study was to investigate womens perspectives on the actual screening program.

Methods: In order to obtain in depth and nuanced insight into womens attitudes toward screening for osteoporosis, qualitative interviews were carried out. Data were generated using focus group interviews (4 groups, n=15) and in-depth interviews (n=3). To ensure group dynamics the focus groups were divided with respect to age (65-72 and 73-80). The focus group discussions were facilitated by photos, statements and participants' comments. Both focus groups and in-depth interviews were semi-structured.

Result: Generally, the women were positive about screening for osteoporosis. Attitudes toward screening were influenced by age, experiences with illness, and knowledge on osteoporosis. Screening was perceived as an opportunity to take care of personal health. In general, women did not find screening for osteoporosis ethically

and psychologically problematic due to disease severity. In contrast, reasons for non-attendance were lack of relevance due to a healthy life situation, confidence in bodily experiences of illness and a resistance to be medicalised. A screening program seems to entail a number of issues important in women's everyday lives such as; to be sick or healthy, to be at risk, and knowledge on osteoporosis.

Conclusions: Knowledge on women's attitudes and perspectives on the actual screening program is important to the evaluation of the program according to WHO recommendations. Generally the women display acceptance of the screening program. No major ethical issues or psychological consequences were detected. However, awareness of fracture risk was described as affecting everyday life such as physical activity. A minority of the women question the relevance and usefulness of screening affecting the willingness to participate in the program. Significantly, non-attendance was described as a deliberate decision based on personal considerations. This contrasts widespread assumptions of non-attendance as caused by lack of knowledge or disregard of general health recommendations.

Disclosures: Mette Rothmann, None.

SU0445

Baseline Fracture Probabilities Using the WHO FRAX® Tool in a Phase 3 Study of a Novel Oral Recombinant Salmon Calcitonin. John Kanis¹, Helena Johansson¹, Christine Buben², James Gilligan², David Krause^{*2}. ¹WHO Collaborating Centre for Metabolic Bone Diseases, United Kingdom, ²Tarsa Therapeutics, USA

BACKGROUND: The WHO FRAX® tool is a population based model designed to evaluate fracture risk of individual patients (pts). It is based on individual pt models that integrate the risks associated with clinical risk factors as well as bone mineral density (BMD) at the femoral neck. ORACAL is a recently completed phase 3 trial of a novel oral recombinant salmon calcitonin. The objective of this study was to determine fracture probabilities at baseline of women recruited to this trial, using FRAX. **METHODS:** In this multinational, randomized, active and placebo controlled trial, 565 postmenopausal women with osteoporosis were randomized 4:3:2 to oral calcitonin tablets and placebo nasal spray, nasal calcitonin spray and placebo tablets, or placebo tablets and nasal spray. The intended treatment exposure was for 48 weeks. Replicate DXA scans were obtained at baseline, Week 24 and Week 48; images were read centrally by blinded readers. The study was undertaken at multiple sites in the US, UK, Bulgaria, Poland, Hungary and South Africa. Demographic and risk factor data were provided by the sponsor to a central database for purposes of risk calculation. The data were anonymised and blinded to treatment allocation. For each pt the 10 year probability of a major osteoporotic fracture (clinical spine, hip, forearm and humerus) was calculated with and without BMD for the country chosen. Version 3.1 of the FRAX models was used. **RESULTS:** The mean age/BMI was 66.5y/25.7 kg/m². The mean probability of a major fracture was 11.9% and, for a hip fracture was 3.2% when BMD was used in the FRAX model. The overall effect of excluding information on BMD was to increase hip fracture risk slightly; however, the addition of BMD to the FRAX model increased the estimated hip fracture probability up to the age of 70 years. At the age 70-89 years, the hip fracture probability calculated with BMD was lower than that calculated without BMD. Most pts were Caucasian. Very high risk was demonstrated for US Caucasian pts (N=69). High risk was represented by the Bulgaria, Poland, South Africa (Caucasian), UK, US (Black) and US (Asian) pts (N=434). Moderate risk was represented by pts in Hungary (N=54). Fracture probabilities increased progressively with age. **CONCLUSIONS:** Although not an entrance criterion, the WHO FRAX tool confirmed that ORACAL enrolled a multinational population of postmenopausal women at high risk of fracture.

Disclosures: David Krause, None.

This study received funding from: Tarsa Therapeutics

SU0446

Bone Loss Caused by Anticonvulsants: BMD Improvement Using Strontium Ranelate. Ilenia Pepe^{*1}, Giuseppin Campisi¹, F Scozzari¹, Nicola Napoli², Giovambattista Rini³, Gaetana Di Fede¹. ¹University of Palermo, Italy, ²University Campus Biomedico, Italy, ³Department of Clinical Medicine, Italy

Certain anticonvulsants may cause bone loss, mostly phenytoin, phenobarbital, carbamazepine, and primidone. It has been reported that bone loss nearly doubled in those receiving anti-epileptic drugs, compared to the general population.

These antiepileptic drug are all potent inducers of CYP-450 isoenzymes, leading to rapid metabolism of vitamin D, and possibly, estrogen. anti-epileptic drugs are also associated with decreased fractional calcium absorption, secondary hyperparathyroidism, and increased bone turnover.

Clinical cases: from 2008 to 2009 we have observed 4 patients attending to the Bone Health Program at University of Palermo (3 females and 1 male, age 54.24.3) treated from 2 to 5 years with anticonvulsants. Their serum biochemistry showed a typical osteomalacia pattern: 25(OH)vitamin D 10.41.2 ng/ml, Ca 8.20.4 mg/dl, PTH 1552.1 ng/ml. BMD measured by DEXA was in the osteoporosis range in all four patients (<-2.5 SD at lumbar spine, femoral neck and total femur). Patients were treated for

6 months with calcitriol (1 mcg/day), calcium (1000 mg/day) and strontium ranelate 2g/day.

At a six months clinical control, vitamin D, Ca and PTH were in the normal range and we observed also a slight BMD increase at lumbar spine (+2%), femoral neck (+1.5%) and total femur (+2%).

Conclusions, the National Institute for Health and Clinical Excellence in UK, recommend a strict monitoring of vitamin D, PTH and calcium serum levels. However, Vitamin D and calcium supplementation should be taken in consideration in order to avoid osteomalacia. In this preliminary study we showed for the first time that strontium ranelate treatment may be helpful together with calcitriol and calcium supplementation to revert anticonvulsants related bone loss. Patients healed quickly and without side effects.

Disclosures: *Ilenia Pepe, None.*

SU0447

Delayed Healing of a Sub-Prosthetic Fracture of the Femoral Shaft after Prolonged Alendronate Therapy: Treatment with Teriparatide. Emanuela Raimondo¹, Marco Massarotti², Carlo Eugenio Zaolino³, Andrea Fossali³, Luca Pietrogrande^{*4}. ¹A.O. San Paolo, Italy, ²IRCCS Humanitas Clinical Institute, Italy, ³Università Statale degli Studi di Milano, Italy, ⁴Università degli Studi di Milano, Italy

Background. Many recent reports describe cases of atypical femoral fractures of the proximal femur without efficient trauma associated with long-term therapy with alendronate. It is not yet clear the dimension of the problem and the pathophysiological bases, nor the way of treatment of these fractures.

Methods. We report a case of a 68-year-old woman that after 12 years of therapy with alendronate, for a low energy hip fracture treated with total hip arthroplasty (THA), incurred in a transverse fracture of the femoral diaphysis just below the tip of the stem after a very low energy trauma. The fracture was correctly treated with plating, but 6 months after surgical treatment there was the rupture of the plate for non-union. The fracture was fixed again with an LCP plate and a strut bone-graft with cerclages.

After 18 months there still was pain in the fracture site during weight-bearing and the radiographic appearance showed an atrophic non-union of the fracture. The bone turnover markers shown a very low remodelling rate. A treatment with teriparatide (1-34 PTH) was started and after 18 months the fracture was healed at the clinical, radiographic and bone scan evaluation.

Discussion. The minimal energy that caused the fracture and its radiographic appearance are similar to that present in described low bone turnover atypical subtrochanteric femoral fractures. The difficult healing, despite a correct surgical treatment, suggest a role of the low bone turnover.

Conclusions.

Fractures in bones with a severe suppression of the turnover are an emerging challenge to the orthopaedic surgeons, only the association of an anabolic therapy with a correct surgical treatment of these fractures seems to guarantee a success, as already reported. The routinely use of PTH in these kind of fracture is recommended.

Disclosures: *Luca Pietrogrande, None.*

SU0448

Effects of Folic Acid and B Vitamin Supplementation on Fracture Risk in Women: Results of a Large Randomized Trial. Douglas Bauer^{*1}, JoAnn Manson², Li-Yung Lui³, Deborah Kado⁴, William G. Christen⁵, Ara Sarkissian⁵, Margarette Haubourg⁵, Steven Cummings⁶, Katie Stone⁷. ¹University of California, San Francisco, USA, ²Harvard Medical School, USA, ³California Pacific Medical Center Research Institute, USA, ⁴University of California, Los Angeles, USA, ⁵Harvard University, USA, ⁶San Francisco Coordinating Center, USA, ⁷California Pacific Medical Center-Research Institute, USA

Elevated homocysteine and low vitamin B12 levels are associated with a greater risk of fracture in some but not all observational studies. The skeletal benefits of vitamin supplementation to lower homocysteine and increase B12 levels are unknown. To address this question we collected fracture outcomes in a large cardiovascular endpoint trial of vitamin supplementation.

We retrospectively reviewed and adjudicated fracture outcomes among 5442 women over age 42 with existing cardiovascular disease or 3 or more risk factors enrolled in the Women's Antioxidant and Folic Acid Cardiovascular Study (WAFACS). Participants were randomized to either the combination of daily folic acid (2.5 mg), vitamin B6 (50 mg) and vitamin B12 (1 mg) or matching placebo, and followed for an average of 7.0 yrs. After completion of study follow-up but before unblinding, participants were queried about the occurrence of clinical fractures during the trial. Radiographic reports or other clinical documentation for each reported fracture were reviewed centrally without knowledge of treatment assignment; women with inadequate fracture documentation were excluded. Following an intention-to-treat analysis, we assessed the effect of vitamin therapy vs. placebo on fracture risk

using Cox models. Subgroup analyses defined by age, B vitamin supplement use, and hormone therapy use were also done.

The vitamin and placebo groups were well matched at baseline with regards to age (62.6 vs. 62.5), postmenopausal status (91.3% vs. 91.5), previous fracture (37.1% vs. 37.5) and estrogen replacement (51.8% vs. 51.8%). 80% of women reported >66% compliance during the trial. Of the 1229 women reporting fractures, adequate documentation was available for 597, and 349 women had confirmed non-spine fractures (including 22 hip and 67 wrist fractures). The risk of any non-spine fracture was similar among those randomized to vitamins or placebo (RH=1.08, 95% CI: 0.88, 1.34), as were rates of hip (RH=0.99, CI: 0.43, 2.29) and wrist fracture (RH=1.30, CI: 0.80, 2.11). Non-spine fracture results were similar among those who were 100% compliant (RH=1.05, CI: 0.82, 1.35) and among baseline subgroups defined above (interaction p values>0.05).

We conclude that in this large double-blinded randomized trial of women with existing cardiovascular disease or multiple risk factors, the combination of daily folic acid, B6 and B12 treatment had no significant effect on non-spine fracture risk.

Disclosures: *Douglas Bauer, None.*

SU0449

Effects of Vitamin K or Bisphosphonate on Serum Undercarboxylated Osteocalcin In Osteoporosis Patients. Hiroshi Yonezu^{*}. Department of orthopaedic surgery, Mitoyo General Hospital, Japan

(INTRODUCTION) Undercarboxylated osteocalcin (ucOC) is a marker of vitamin K deficiency in bone formation, and an increased ucOC level is a predictor of hip fracture. On the other hand, ucOC is reportedly affected by bone turnover, and bisphosphonate or steroid administration may reduce the serum ucOC level. In this study we evaluated the effect of vitamin K or bisphosphonate administration on serum ucOC levels.

(PATIENTS AND METHODS) We measured serum ucOC levels in 321 patients with osteoporosis (average age 76.4 years). Fifty-seven patients had been taking vitamin D, 31 bisphosphonate, 19 bisphosphonate + vitamin D, and 15 vitamin D + vitamin K. These treatments had been taken for at least 6 months. One hundred ninety-nine patients had received no therapy for osteoporosis. Patients whose serum ucOC level was above the normal range (upper limit 4.5 ng/ml) were prescribed additional vitamin K or bisphosphonate for 6 months.

(RESULTS) The average serum ucOC level was 6.966.31 ng/ml. The serum ucOC level exceeded the upper limit of normal in 57.0% of our patients, but was low those who had taken vitamin K or bisphosphonate. There was a significant correlation between the ucOC level and NTX. There was no significant difference in lumbar BMD between patients with normal and abnormal ucOC levels. The serum ucOC level normalized in 64.6% of patients after receiving additional vitamin K medication, but was high in those with high bone turnover. The serum ucOC level normalized in 31.9% of patients after receiving additional bisphosphonate medication. Vitamin K reduced the serum ucOC level, but did not alter bone turnover or lumbar BMD. On the other hand, bisphosphonate reduced the serum ucOC level, via decreased bone turnover and increased lumbar BMD.

(DISCUSSION) It has been reported that vitamin K treatment reduces ucOC but does not alter bone turn over, density or geometry in healthy postmenopausal women. On the other hand, the effect of bisphosphonate on the serum ucOC level is controversial. It was recently reported that bisphosphonate may interfere with vitamin K activation in bone cells. However, whether bisphosphonate treatment decreases the carboxylation of osteocalcin is uncertain. Further study is needed to resolve this issue.

(CONCLUSION) Our results support the suggestion that vitamin K decreases the ucOC level when taken as a supplement to treat vitamin K deficiency, and that bisphosphonate decreases the serum ucOC level by decreasing bone turnover.

Disclosures: *Hiroshi Yonezu, None.*

SU0450

Long-term Effects of Angiotensin Converting Enzyme Inhibitor (ACEI) on Femur Neck BMD of Men in the Health Aging and Body Composition Study. Nahid Rianon^{*1}, Claudia Pedroza², Melissa Garcia³, Ann Schwartz⁴, Frances Tykavsky⁵, Jane Cauley⁶, Brendan Lee⁷, Tamara Harris⁸. ¹UTHealth The University of Texas Medical School at Houston, USA, ²UT Houston Medical School, USA, ³NIA/NIH, USA, ⁴University of California, San Francisco, USA, ⁵University of Tennessee, Memphis, USA, ⁶University of Pittsburgh Graduate School of Public Health, USA, ⁷Baylor College of Medicine & Howard Hughes Medical Institute, USA, ⁸Intramural Research Program, National Institute on Aging, USA

Background: A large proportion of older adults in the U.S. are under antihypertensive treatment. Animal studies indicate that antihypertensive medications affecting the renin-angiotensin system (RAS) may have positive effects on bone. Preliminary data from the Health Aging and Body Composition (Health ABC) study showed a positive cross-sectional association in men between femur neck bone mineral density (FNeckBMD) and RAS related medications, e.g., angiotensin converting enzyme inhibitors (ACEI). In this study we investigate if long-term use of ACEI can reduce risk for age-related bone loss in older men.

Methods: We used regression analysis to examine associations between year 10 FNckBMD and long-term (4 years) ACEI use in 913 men of the Health ABC study. Long-term ACEI use was defined as ACEI medications used at both years 5 and 10 examinations. Models were adjusted for year 5 report of age, weight, height, race, exercise and current smoking, HTN and diabetes mellitus (defined as self-reported and/or medication use), and use of steroid, calcium and vitamin D supplements. In addition, we controlled for thiazide and bone promoting medication (BoneMeds) use for 4 years. We also investigated associations between annual percent change in FNckBMD from year 5 to year 10 and long-term ACEI use in the same men using a similar regression model.

Results: Mean (standard deviation) age for men at year 10 was 833 (range 78-89) years. About 23% of men were using ACEI at both Year 5 and Year 10. Mean year-10 FNckBMD was 0.780.15 gm/cm² for ACEI users and was 0.750.14 for non ACEI users. Average annual bone loss among ACEI users and non-users were 3.035% and 2.736%, in order. The year-10 FNckBMD among men with long-term ACEI use was 0.039 gm/cm² higher (95% confidence interval: 0.004 to 0.074, $p < 0.05$) than those not using ACEI. However, there was no significant association between annual percent change of FNckBMD and ACEI use in these men. BoneMeds use was a significant predictor of year-10 FNckBMD in both models ($p < 0.05$).

Conclusions: Long-term (4 years) ACEI use was associated with FNckBMD in older men in the Health ABC study at Year 10 but not with change between Year 5 and Year 10. Very small percent change in FNckBMD or a smaller effect of ACEI than BoneMeds and a small sample size may have impacted our results.

Disclosures: Nahid Rianon, None.

SU0451

Prevention of Hip Fractures with a Multifactorial Educational Program in Elderly Finnish Women: A Population-Based, Long-Term Controlled Clinical Trial. Tuula Pekkarinen^{*1}, Eliisa Loyttyniemi², Matti Valimäki³. ¹Peijas Hospital, Finland, ²Turku University, Finland, ³Helsinki University Central Hospital, Finland

Non-pharmacological approaches to reduce osteoporotic fracture risk are of great importance both economically and individually.

We assessed effectiveness of a multifactorial educational program in prevention of osteoporotic hip fractures among community-dwelling elderly women. Inclusion criteria were female gender, age 60-70 years and living in Uusimaa region in southern Finland. A random sample of women with these criteria was drawn from the population register.

A total of 2178 women (52% of the cohort) were recruited between 1996 and 2000 and randomized in intervention group (IG, n=1004) and control group (CG, n=1174). The intervention started with a one-week period at a rehabilitation center followed by two one-day sessions during the ten-year follow-up and included counseling on physical activity, balance training, nutrition, hip protectors, home hazards and medications and illnesses related with falls. The CG received usual information through media and health care system. At baseline and at years 2, 5, 8 and 10 both groups filled in a questionnaire regarding factors related to osteoporosis (e.g. current medication, life-style and fractures). All fractures during the study were confirmed from a radiologists report. A hip fracture was the primary end-point of the study.

At baseline mean age was 65.3 (SD 3.1) years in the IG and 65.3 (SD 3.1) in the CG ($p = 0.62$), and mean BMI 26.9 kg/m² (SD 4.5) and 26.1 (SD 4.1), $p < 0.0001$ respectively. At baseline subjects in the IG reported having sustained more often major fractures (23% vs 19%, $p = 0.03$) and falls within 3 months (13% vs 12%, $p = 0.04$), used more often vitamin D (55% vs 49%, $p = 0.003$) and calcium supplementation (47% vs 39%, $p < 0.0001$) than subjects in the CG. Dietary calcium intake was greater, mean 827mg (SD 469) in the IG vs 787mg (SD 464) in the CG, $p = 0.03$. At baseline estrogen use did not differ between the groups, but smoking was more common in the CG (current+ ex-smokers 30% vs 27% in IG, $p = 0.04$). Together 218 women died during the follow-up, 89 (9%) in the IG and 129 (11%) in the CG, $p = 0.12$. During the ten year follow-up, 6 women (0.6%) in the IG sustained hip fracture vs 18 women (1.5%) in the CG, $p = 0.04$.

As compared with usual care, this multifactorial educational program appears to be a viable option to prevent osteoporotic hip fractures among elderly women.

Disclosures: Tuula Pekkarinen, None.

SU0452

The Effect of Vitamins K on Bone Density and Fractures in Postmenopausal Women: Should There Be More Studies? Olga Gajic-Veljanoski^{*1}, George Tomlinson², Ahmed M. Bayoumi³, Zoe Agnidis¹, Angela Cheung¹. ¹University Health Network, Canada, ²University of Toronto & University Health Network, Toronto, Canada, ³University of Toronto & St. Michael's Hospital, Toronto, Canada

Studies in different populations have shown variable effects of vitamins K2 and K1 on bone mineral density (BMD) and fractures. We performed a systematic review to examine the clinical effectiveness of vitamins K on BMD and fractures in postmenopausal women and to determine whether future studies are worthwhile.

We systematically searched electronic databases (Medline, EMBASE, CINAHL, AMED, International Pharmaceutical Abstracts:1950- March 2011) and bibliographies, screened 4749 and reviewed 130 potentially eligible studies. We included

randomized-controlled trials (RCTs) assessing the effects of vitamins K2 or K1 on the lumbar spine (LS), total hip (TH) and femoral neck (FN) BMDs or on the risk of clinical, vertebral and non-vertebral fractures in postmenopausal women. Two reviewers used the Cochrane Risk of Bias tool to assess the methodological quality of 19 relevant RCTs. Bayesian random-effects meta-analyses were used to synthesize the evidence from trials comparing vitamin K2 (0.36mg/d-1 RCT, 45mg/d-11 RCTs, 5647 women), vitamin K1 (0.08-5mg/d, 6 RCTs, 1133 women) or both (1 and 45mg/d, 1 RCT, 381 women) against control treatments. The outcomes were mean difference (MD) (difference in the mean % change) for BMD, population odds ratio (OR) for fractures and posterior probabilities of benefit (MD > 0 or OR < 1) in favor of vitamins K in current and future studies.

Vitamin K2 increased LS BMD by 1.59% (95% Credible Interval (CrI): 0.31, 2.93). The probability of any increase in LS BMD was 99.1% in current and 84.3% in future studies. Vitamin K2 did not change TH and FN BMDs (the probabilities of benefit: 25.4% and 57.3% in current and 31.9% and 56.5% in future studies for TH and FN BMDs, respectively). Vitamin K1 had no effect on LS (MD: -0.17%, 95%CrI: -0.81, 0.49), TH or FN BMDs. The probabilities of benefit of vitamin K1 on LS, TH and FN BMDs were 28.7%, 71.2% and 63.3% in current and 35.6%, 69.3% and 57.1% in future studies, respectively. Vitamin K2 was not associated with significant reductions of clinical (current OR: 0.61, 95%CrI: 0.18, 1.41; future OR: 0.55, 95%CrI: 0.04, 5.35), vertebral and non-vertebral fractures, but the probabilities of benefit were 89.9-93.6% in current and 71.6- 78.1% in future studies.

In conclusion, we found moderate-to-high probabilities of beneficial effect in favor of vitamins K2 and K1 on BMD and fractures in postmenopausal women. Further trials are required to determine the effect of vitamins K on fractures.

Disclosures: Olga Gajic-Veljanoski, None.

SU0453

Acute Bone Marker Responses to Whole-Body Vibration and Resistance Exercise in Young Women. Debra Bemben^{*}, Vanessa Sherk, Carmen Chrisman, Kaelin Young, Jessica Smith, Harshvardhan Singh, Michael Bemben. University of Oklahoma, USA

Whole-body vibration (WBV) is a type of mechanical stimulus that has been shown to acutely increase anabolic hormone responses; however, its acute effects on bone metabolic markers have not been determined. The purpose of this study was to examine bone marker responses to single bouts of high intensity resistance exercise (RE) and high intensity resistance exercise combined with WBV (WBV + RE) in women ages 20-30 years. Subjects (n=10) were not resistance trained, and they were taking oral contraceptives to control for menstrual phase variations in bone marker levels. We used a randomized, cross-over repeated measures design as subjects performed both conditions in random order 2 weeks apart. The RE session involved 6 isotonic exercises 3 sets of 10 repetitions at 80% of maximal strength. The WBV + RE session exposed subjects to 5 minutes of vibration (5 1 minute repetitions, 20 Hz, 1mm amplitude separated by 1 minute of rest) standing barefoot on a vibration platform (Vibraflex, Orthometrics, Inc.) with knees bent at 30 degrees. After a 3 minute rest, subjects then performed the RE protocol. All sessions were in the morning and fasting blood samples were obtained before, immediately post WBV, immediately post RE, and 30 minutes post RE. Bone-specific alkaline phosphatase (Bone ALP), tartrate-resistant acid phosphatase (TRAP5b), and C-terminal Telopeptides of Type I collagen (CTX) were measured using commercial ELISA kits. Bone ALP did not have significant condition or time effects, nor did it change from the pre vibration to post vibration time points. In contrast, bone resorption markers showed significant acute responses. TRAP5b significantly ($p < 0.05$) increased from the pre to post vibration time points, then decreased from immediately post RE to 30 minutes post RE for both conditions. Correcting the TRAP5b concentrations for plasma volume changes eliminated these significant responses. There was a significant ($p < 0.05$) condition \times time interaction effect for CTX, which decreased from pre to post vibration and from pre to 30 minutes post exercise only for the WBV + RE condition. Plasma volume corrections did not alter these responses. Also, the WBV + RE condition showed a greater relative decrease in CTX levels than RE (-12.6 4.7% and -1.13 3.5%, respectively). In conclusion, a low amplitude whole-body vibration exposure was associated with an acute decrease in CTX levels not elicited with resistance exercise alone in young women.

Disclosures: Debra Bemben, None.

SU0454

Balloon-Sacroplasty on Patients with Osteoporotic Fatigue Fractures. Reimer Andresen^{*1}, Sebastian Radmer², Peter Kamusella³, Christian Wissgott³, Jan Banzer⁴, Hans-Christof Schober⁵. ¹Westkustenklinikum Heide, Germany, ²Zentrum für Bewegungsheilkunde, Berlin, Germany, ³Westkustenklinikum Heide Westkustenklinikum Heide, Germany, ⁴Charité Universitätsmedizin Berlin, Germany, ⁵Klinikum Sudstadt Rostock, Germany

Introduction:

In patients with calcipenic osteopathy, fatigue fractures of the Os sacrum are relatively common and are typically accompanied by strong, disabling pain. The aim of our study was to verify the feasibility and safety of Sacroplasty by using a balloon catheter as well as the outcome of pain after the intervention.

Material and Methods:

25 patients (20 women with an average age of 72.6 years, 5 men with an average age of 68.4 years) were diagnosed in a CT to have an Os sacrum fracture, in 12 women the fracture was unilateral, in the remaining patients bilateral. As a manifestation from an extant bone reconstruction process, all patients, through MRT strong T2 weighted images, were found to have distinctive oedema. In QCT results, all patients were found to have strong demineralisation of the vertebrae column with results from max 63mg/dl to min 13mg/dl, clinically, extreme pain is significant. On all patients, a CT controlled balloon sacroplasty was performed. During the intervention, the patient is in a ventral position, to enable the cement to be dispensed in a longitudinal angle to the fracture, and the balloon catheter is directed through a hollow needle in the Os sacrum either from the caudal to the cranial or from the craniodorsal to the caudoventral. The balloon catheter was accordingly deflated 1-3 times along the fracture in the appropriate direction, thus causing a cavity that was then filled with PMMA-cement under low pressure. A control-CT as well as a conventional X-ray was then carried out. The pain intensity was defined by means of VAS before the intervention, on the second day, after 6 and 12 months.

Results:

The balloon-sacroplasty enabled a good technical performance on every patient. The control-CT and the X-Ray control of the Os sacrum showed an adequate distribution of the cement, a cement leakage was not detected. Before the operation, the average pain encountered was according to the VAS 8.3. On the second postoperative day, a considerable reduction with an average of 2.7 was reported, this was still stable with an average of 2.5 after 6 and 12 months.

Discussion:

The Balloon-Sacroplasty is an effective treatment method for immediate pain relief and remobilisation in patients with fatigue fractures of the Os sacrum. Different approaches as well as the utilisation of a balloon enables preferably large cement streams in the longitudinal direction of the fracture in the Os sacrum.

Disclosures: Reimer Andresen, None.

SU0455

Development of a Comorbidity Index Using the FREEDOM Trial in Women With Postmenopausal Osteoporosis. Stuart Silverman^{*1}, Andrea Wang², Hema Viswanathan², Yu-Ching Yang², Cesar Libanati³, Michelle Geller², Luanda Graetz⁴, Andreas Grauer⁵, David Macarios², Michael Nevitt⁶, Dennis Revicki⁷, Ethel Siris⁸, Steven Boonen⁹. ¹Cedars-Sinai/UCLA, USA, ²Amgen Inc., USA, ³Amgen Inc, USA, ⁴University of Southern California, USA, ⁵Amgen Health Center, USA, ⁶University of California, San Francisco, USA, ⁷United BioSource Corporation, USA, ⁸Columbia University College of Physicians & Surgeons, USA, ⁹Center for Metabolic Bone Disease & Division of Geriatric Medicine, Belgium

Purpose: Comorbidities are often important for adjusting for risk of outcomes in clinical trials, especially in pooled analyses using clinical trial data. Existing comorbidity indices offer little assistance in this regard as they are not designed for use with data commonly collected in a clinical trial. We developed a comorbidity index by adapting and applying two published algorithms to subjects' medical history from the FREEDOM trial (Cummings, NJEM 2009) in postmenopausal women with osteoporosis.

Methods: The FREEDOM trial enrolled women aged 60 to 90 years with a total hip or lumbar spine DXA T-score ≤ -2.5 and not ≤ -4.0 at either site. Comorbidity indices were calculated using methods described by Wolfe et al. (Wolfe, J Rheumatol 2010) and Sangha et al. (Sangha, Arthritis Rheum 2003). Here, we present results based on the method by Wolfe et al. as it allowed for weighting and inclusion of previous fractures. The index included pulmonary and cardiovascular conditions, hypertension, diabetes, previous fractures, depression, gastrointestinal ulcer or disorders, and cancer. The range for the index is 0 to 9, with higher scores indicating greater comorbidity. Four clinicians independently reviewed subjects' medical history data using MedDRA preferred terms corresponding to specific comorbid condition categories. In cases where there was lack of agreement, discrepancies were adjudicated by a fifth clinician who facilitated a panel discussion to reach consensus. Spearman correlations between the index and subject characteristics expected to be associated with comorbidities were examined.

Results: A total of 7,808 subjects were included; 60% of subjects had either zero or one comorbidity. The mean modified Wolfe comorbidity index was 1.4 (SD: 1.3) for all subjects. The comorbidity index distribution was as follows: 0, 29.2% of the population; 1, 29.9%; 2, 23.5%; 3, 10.8%; 4, 4.5%; 5, 1.7%; and ≥ 6 , 0.3%. The correlation between the indices using the two methods was 0.9. Correlations between the modified Wolfe comorbidity index and baseline characteristics are shown in the table.

Conclusions: The Wolfe et al. algorithm may be adapted for clinical trial data to assess comorbidities. As expected, the index was found to be significantly correlated with variables including the number of medications and impaired health status at baseline. This comorbidity index allows for the categorization and understanding of co-morbid conditions in clinical trial populations.

Baseline Characteristics	Correlation With the Modified Wolfe Comorbidity Index	P-value
Number of medications	0.54	< 0.0001
Osteoporosis Assessment Questionnaire (OPAQ) physical function	-0.28	< 0.0001
OPAQ emotional status	-0.28	< 0.0001
EQ-5D Visual Analog Scale score	-0.28	< 0.0001
OPAQ back pain	-0.22	< 0.0001
Body mass index (kg/m ²)	0.16	< 0.0001
Age (years)	0.16	< 0.0001

Table 1

Disclosures: Stuart Silverman, Amgen Inc, Genentech, Eli Lilly, Novartis, Pfizer, Wyeth, Roche Pharmaceuticals, Roche Diagnostics, Warner Chilcott, 5; Eli Lilly, Pfizer, Wyeth, Warner Chilcott, 2; Amgen Inc, Eli Lilly, Novartis, Pfizer, Wyeth, Roche Pharmaceuticals, 8

This study received funding from: Amgen Inc

SU0456

Effects of Maitake Mushroom VitaminD₂ Supplementation on Serum vitamin D Level and Bone Metabolic Markers in Postmenopausal Women. Noriaki Yamamoto^{*}. Niigata rehabilitation hospital, Japan

Background: Maitake is a kind of mushroom contains a large amount of vitamin D₂.

The purpose of this study is to determine the effects of oral intake of Maitake mushroom supplementation in postmenopausal women for 1 year.

Methods: We conducted an open-label study with 31 postmenopausal women. All subjects take Maitake mushroom supplementation (Ichimasa kamaboko Co.,Ltd) containing 1600IU of vitamin D₂ everyday for 6 months. After 6 months of this study, all subjects were divided into 2 subgroup. Group A, 17 women continued to take supplementation for another 6 months and Group B, 14 women stop the supplementation. Serum Ca and bone metabolic markers (urinary NTX, serum BAP, 25OHD) were assessed at beginning, 6, and 12 months of this study.

Results: Comparing to the baseline, 6 months supplementation of Maitake mushroom significantly increased serum 25OHD level from 21.26 ng/mL to 31.14 ng/mL ($p < 0.01$). Another 6 months of treatment, 25OHD level was maintained 31.34 ng/mL ($p < 0.01$) in group A until 12 months of this study. However 25OHD level went down to 21.56 ng/mL after 6 months from the cessation of supplementation, in group B.

The serum BAP, Ca, and urinary NTX/Cre, level showed no significant changes during this study.

Conclusion: Improvement in 25OHD level in postmenopausal women was achieved by receiving Maitake mushroom supplementation which containing 1600IU of vitamin D₂ without adverse events.

Disclosures: Noriaki Yamamoto, None.

SU0457

Evaluation of a 1,25D-Dihydroxy Vitamin D Assay on the IDS-iSYS Automated System. Sybil Bergmann^{*1}, Michael Gardner², Chris Roffe², Chris Fox², Zoltan Seres², David Laurie². ¹TUD UKD Institute of Clinical Chemistry & Laboratory Medicine, Germany, ²Immunodiagnostic Systems Limited, United Kingdom

1,25-dihydroxyvitamin D (1,25D) is one of the major regulators of calcium metabolism. Measurement of 1,25D is used in conjunction with 25-hydroxyvitamin D (25D) and parathyroid hormone (PTH) in the differential diagnosis of various bone diseases. However, 1,25D circulates at very low (pg/mL) concentrations compared to 25D (ng/mL) and both are bound to the vitamin D binding protein. Specific and accurate measurement of 1,25D is thus difficult requiring some sort of sample extraction (immunoextraction or C18) and immunoassay.

As a result 1,25D assays currently available to laboratories are manual RIA or EIA versions which are time consuming relative to the number of samples that can be processed. To our knowledge no semi or fully automated 1,25D assays exist.

A new 1,25D assay was evaluated where 1,25D was extracted from delipidated samples by the current IDS immunoextraction technology and reconstituted samples were run directly on the IDS-iSYS system. Sample 1,25D competed with 1,25D-Acridinium (1,25D-ACR) for a limited amount of biotinylated polyclonal anti-1,25D antibody sites. Bound complexes were captured by use of streptavidin-coated magnetic particles. Following washing and addition of Trigger reagents, bound 1,25D-ACR was measured in a luminometer where signal generated was inversely proportional to the 1,25D concentration in the sample. Total time to first result (immunoextraction and immunoassay) was 4hr 30min.

The 1,25D assay had an assay range of 5 to 415pg/mL. Analytical sensitivity (mean -2SD of 'A' calibrator, n=20) was 6.4pg/mL. Intra-assay precision was 12%, 7% and 7% for samples at 22, 76 and 317pg/mL, (n=20). Inter-assay precision was 11 to 16% (samples 17 to 318pg/mL, n=8). An excellent correlation (n=55) with a slope of 1.29, intercept 0.9pg/mL and an R² of 0.86 was demonstrated to the commercially available IDS RIA.

These are the first laboratory results from a semi-automated 1,25D assay. The combination of immunoextraction and the IDS-iSYS system will allow laboratories to accurately analyse larger numbers of samples per day. With an expanded assay range,

excellent precision and good correlation to current methods the IDS-iSYS 1,25D assay will be a valuable tool in clinical laboratories for the accurate measurement of 1,25D in human sera or plasma.

Disclosures: Sybille Bergmann, None.

SU0458

Vitamin D Deficiency and Repletion: Effect of Ethnicity and BMI. Amer Budayr*¹, Joan Lo², Rita Hui², Ashley Coates², Moxie Stratton-Loeffler², Malini Chandra², Jerome Minkoff². ¹Permanent Medical Group, USA, ²Kaiser Permanente, USA

While the optimal level of vitamin D (25-OH-D) continues to be debated, the prevalence of vitamin D deficiency in adults is very high. We examined trends in use of prescription strength vitamin D (receipt of ergocalciferol 50,000 IU) and testing (25-OH-D) in the setting of a large integrated health care delivery system over an interval of 4 years (2007-2010). With the increased public awareness and ongoing physician education efforts over the period of the study, we wanted to examine the quantitative impact of this "epidemic" on the utilization of pharmacy and laboratory services. The broader goal of this study was aimed at examining optimal regimens of vitamin D replacement and the effect of demographic and clinical characteristics on the rate of successful vit D repletion.

METHODS: We ascertained the number of patients with new vitamin D prescriptions for each year, excluding patients with Vitamin D prescription in the prior 12 months. Among these patients, we examined the frequency of Vitamin D repeat testing between 6-52 weeks after receiving the first prescription. The rate of successful repletion was defined by a 25-OH-D level of 30 ng/ml or higher in the repeat testing.

RESULTS: We identified a total of 110,220 (76% female, mean age 59 +/- 16 years) patients initiating pharmacologic vitamin D during the study period. Across the 4 years of study, the number of patients with new prescriptions for vitamin D increased 6-fold from 6893 in 2007 to 42,858 in 2010. For the first prescription, 75% received a total of 0.45 – 0.60 M IU. We found an initial 69 % rate of repeat testing. The rate of successful repletion was in obese individuals and those of African American race.

CONCLUSION: We observed increasing population trends in the treatment of Vitamin D deficiency within a large integrated health care delivery system that parallel efforts to increase awareness of Vitamin D deficiency among healthcare providers and patients. Race/ethnicity and body mass index may be associated with differential rates of successful repletion. A significant proportion of patients may require additional therapy to achieve optimal levels of Vitamin D during follow-up testing.

Disclosures: Amer Budayr, None.

SU0459

Vitamin D Status does not Affect Bone Mineral Density Response to Raloxifene with Co-administration of Alfacalcidol. Itsuo Gorai*¹, Yasuhisa Iwaoki². ¹Sanikukai Hori Hospital, Japan, ²Department of Obstetrics & Gynecology, JA Yoshida General Hospital, Japan

Purpose: The persistent increase in PTH caused by vitamin D insufficiency reduces bone density response to anti-resorptive agents in postmenopausal women with osteoporosis. Vitamin D status at initiation of therapy did not affect bone mineral density (BMD)'s response to both alendronate and raloxifene with co-administration of cholecalciferol and calcium. We tried to assess whether vitamin D status at randomization could modify the subsequent BMD response to raloxifene with co-administration of alfacalcidol in postmenopausal Japanese women with osteoporosis or osteopenia (<-2.0 SD). **Method:** A total of 169 subjects (64.76.9 yrs) were randomly assigned to groups receiving 60 mg raloxifene (R), or 1 µg alfacalcidol (D), or a combination of both (R+D) for 2 yrs. Serum 25(OH)D was measured at randomization. We compared the groups using a Turkey-Kramer test for changes in L- and TH-BMD and calcium metabolism when significant differences were found using one-way ANOVA. The parameters in each group were analyzed by means of paired-t tests. **Result:** Baseline 25(OH)D was 23.7 ng/ml and 67.6% had vitamin D insufficiency (I) [20ng/ml<25(OH)D<32ng/ml] and 24.2% had vitamin D deficiency (D) (≤20ng/ml). I-PTH was 38.7pg/ml and 6.3% had asymptomatic hyperparathyroidism (i-PTH>65pg/ml). In the D+R group there was a significant increase in L-BMD (+4.6% at 1 yr and +5.8% at 2 yrs, P<0.0001), and the increase was significant compared with that in the R-group (vs. +2.6% at 2 yrs, P<0.05). In both R- and R+D groups there were no significant differences in the background characteristics except for corrected serum Ca of the R+D groups (I>D) between each vitamin D category. We found no significant differences in the changes in L-BMD at 2 yrs between I and D categories in both R- and R+D groups (4.0% vs. 1.8%, 5.6% vs. 5.9%, respectively). In each vitamin D category, there were no significant differences in the backgrounds between the R- and the R+D groups. Irrespective of vitamin D status, i-PTH showed an increase in the R-group and a decrease in the R+D group. In I category supplementation of alfacalcidol to raloxifene showed non-significant increases in L-BMD at 6, 12 and 18 months (4.4%, 5.0% and 4.9%) and a significant increase at 24 months (5.9%, P=0.0095) compared to the raloxifene alone group (1.6%, 2.3%, 2.8% and 1.8%, respectively). **Conclusion:** Vitamin D status at randomization did not

affect the subsequent BMD response to raloxifene with co-administration of alfacalcidol.

Disclosures: Itsuo Gorai, None.

SU0460

Inhibition Of Gut Serotonin Synthesis Normalizes Bone Mass In Lrp5-Deficient Mice And Other Models Of Osteoporosis. Hiroyuki Inose¹, Bin Zhou², Vijay Yadav², X Guo², Gerard Karsenty², Patricia Ducy*². ¹Tokyo Medical & Dental University, Japan, ²Columbia University, USA

A proof-of-concept study recently showed that decreasing synthesis of gut serotonin through the use of a small molecule inhibitor of Tph1 could prevent and treat ovariectomy-induced osteoporosis in rodents. Since the role of gut-derived serotonin in the control of bone formation arose from the study of Lrp5-deficient mice it was important to verify the usefulness of this treatment in these mutant mice as well as in other models of osteoporosis. To address the first question we compared the efficacy of the small inhibitor of Tph1 to LiCl. While both drugs could normalize bone formation parameters we noted that LiCl also increased significantly bone resorption parameters, an unwanted effect in the treatment of osteoporosis. Next, we showed that Tph1 inhibition could cure ovariectomy-induced osteoporosis in one year-old mice. We noted also that the anabolic effect of Tph1 inhibition persisted up to 6 weeks after the arrest of the treatment in mice. Lastly, we gathered evidence that Tph1 inhibition could work well in concert with an anti-resorptive agent to increase bone mass in ovariectomized mice. Taken collectively these data underscore the potential therapeutic importance of the inhibition of gut serotonin synthesis for the treatment of osteoporosis.

Disclosures: Patricia Ducy, None.

SU0461

Development of an Osteopenic Bone Fracture Model. Kellie Brune*¹, Hong Liu¹, Christopher Bull¹, Jeffrey Wolos², Rachel Reams¹. ¹Covance Laboratories, Inc., USA, ²Scientific Consultant, USA

The purpose of developing this osteopenic rat fracture model was to provide an early (as short as 42 days) and longitudinal assessment tool for osteopenic bone regeneration. An in-house computer analysis program for computed tomography (CT) images was designed to specifically analyze the healing process at the fracture site.

A total of 36 virgin Sprague Dawley rats were ovariectomized at 6 months of age. Following ovariectomy, a 2 month window was allowed for bone loss to occur. 8 – 10 weeks post ovariectomy, an external fixator was secured in place on both femurs using stainless steel screws. Each femur was then cut transversely (mid-diaphysis) using a micro saw blade. After the surgery, the rats were divided into three groups: two groups treated with 5 or 30 mcg/kg/day parathyroid hormone (PTH), and a vehicle treated group. 3D images were collected at selected time points using Volumetric Computed Tomography (VCT). The VCT image gray level at each voxel within a 5 mm thick stack at the osteotomy site was quantified and converted as callus BMD (bone mineral density). The region of interest in each slice in the stack was then determined by an elastic wrapping algorithm. Statistical density distributions of callus BMD for each group were extracted at Days 7, 42, 63 and 84. Quantitative measures that reflect bone regeneration quality based on these distributions were given as Total Mineral, Mean Intensity, High Density Fraction and Total Mineral above 815 BMD.

Data from this 12 week validation study demonstrated a constant increase of bone regeneration across all three groups. The regeneration as indicated by our VCT measurements was statistically significantly stronger in the 30 mcg/kg/day group than in the 5 mcg/kg/day group which in turn was significantly stronger than the vehicle group. These statistically significant, dose-responsive alterations were noted as early as Day 42. In addition, Total Mineral above 815 BMD at Day 42 correlated well to the biomechanical strength measured at Day 84 (Pearson CC=0.7512 with p<0.0001). Our data support the utility of this model as an early and longitudinal assessment of bone regeneration that provides data that are complementary to, or potential a replacement for, traditional endpoints such as mechanical strength or histopathology. This model provides a robust higher-throughput screening tool to compare the pharmacological efficacy between benchmark compounds such as PTH, and other agents.

Disclosures: Kellie Brune, None.

SU0462

Effect of PTH 1-84 on the Remodeling, Microstructure and Bone Mass In Male Orchidectomized Rats. Marta MartÍN-Fernandez^{*1}, Manuel DÚaz-Curiel², David Guede³, Jose Ramon Caeiro⁴, Concha de la Piedra¹, Elena Martínez⁵. ¹Bioquímica Investigacion, Instituto de Investigacion Sanitaria Fundacion Jimenez DÚaz, Spain, ²Internal Medicine, Instituto de Investigacion Sanitaria Fundacion Jimenez DÚaz, Spain, ³Trabeculae, Parque Tecnológico de Galicia, Spain, ⁴Cirugía ortopedica y Traumatología, Complejo Hospital Universitario de Santiago de Compostela, Spain, ⁵Director Medico, Spain

Androgenic depletion due to hypogonadism affects bone metabolism, causing osteopenia. Although its utility in the treatment of postmenopausal osteoporosis has been established, there is limited evidence on the effect of PTH 1-84 in male osteoporosis.

Purpose: To study the effect of PTH 1-84 in an experimental model of orchidectomized male rats, measuring the changes in bone mineral density (BMD), remodeling markers and bone microstructure.

Material and Methods: 4 groups of 10 6-month-old male Wistar rats. SHAM: n=10, simulated intervention; OQX: n=10, orchidectomized; OQX+PTH1: n=10, orchidectomized and treated with PTH 10 mcg/Kg; OQX+PTH2: n=10 orchidectomized and treated with PTH 50 mcg/Kg. The treatment was started 3 months after orchidectomy, and was maintained for 3 months. After sacrifice, BGP, FTR 5b and beta-CTX bone remodeling markers, BMD of the lumbar spine and femur, and a femoral microstructure analysis by microCT scan were measured.

Results: A statistically significant reduction in vertebral and femoral BMD was evidenced in the OQX group versus the SHAM group, which partially reverted with the low dose of PTH, and completely reverted with the high dose. A significant increase of the CTX/FTR ratio was seen in the OQX group versus the SHAM group, which was maintained in the treated groups. The level of BGP did not show any changes in the OQX group, although a significant dose/response increase was seen in the treated groups. A relative reduction of BV/TV was seen in the OQX group, a decrease in the number of trabeculae and an increase in their separation. PTH treatment (both doses) restored baseline values of BV/TV, partially reducing separation and increasing trabecular number with the low dose, completely restoring both parameters with the high dose. Trabecular pattern factor increased in OQX, it was restored with the low PTH dose, and it became lower than in the SHAM group with the high dose. The structure model index (SMI) experienced a significant reduction in the high-dose group, compared to the OQX rats.

Conclusions: In an animal model of osteoporosis by androgenic deprivation, treatment with PTH 1-84 has shown to have a bone-forming effect, reflected by an increase in bone formation markers, and increased lumbar and femoral BMD and a partial or total recovery of microstructural parameters.

Disclosures: Marta MartÍN-Fernandez, None.

This study received funding from: Nycomed Pharma

SU0463

Increased Alveolar Bone Mass in Sclerostin Knockout Mice. Min Liu^{*1}, Xianglong Han², Pam Kurimoto¹, Jerry Feng², Paul Dechow², Hua Zhu Ke¹. ¹Amgen Inc., USA, ²Baylor College of Dentistry, Texas A & M Health Science Center, USA

It has been postulated that osteoporosis and oral bone loss are associated among the elderly, although the evidence for this relationship is mostly preliminary. During development, most long bones develop endochondrally, whereas bones of the skull and face generally develop through intramembranous ossification. Sclerostin (Scl), acting through antagonizing BMP and Wnt signaling, is a potent inhibitor of bone formation. Sclerostin knockout (SOST KO) mice show a high bone mass phenotype in various skeletal regions (eg, vertebrae and long bones). In the current study, we analyzed the jaw bone phenotype of SOST KO mice. Methods included radiography, quantitative μ CT, mechanical testing, and histological analysis.

We first investigated the expression pattern of Scl in the periodontium of young and adult wildtype (WT) mice. Strong Scl expression was observed in WT mandibular odontoblasts, osteocytes and cementoblasts, although there were no significant differences in TRAP staining and osteocyte apoptosis between WT and SOST KO mice. Radiography and μ CT assessment revealed that 10-month old WT mice had age-related mandibular bone loss while aged-matched SOST KO mice did not; the mandible bone in SOST KOs was well-preserved, even in 24-month-old mice. Quantitative μ CT analyses showed that increases in bone volume fraction (BVF) in SOST KO mice varied regionally in the mandible. Compared to WT, SOST KO mice had increases of 18%, 12.5% and 4% in alveolar bone, condylar head, and condylar neck BVF respectively, which was correlated with variations in WT BVF among regions; areas with lower BVF showed greater increases in BVF and bone density. In line with elevated bone mass, mechanical testing showed significantly stronger mandibular bone in SOST KO mice (+61%, $p < 0.02$) than WT mice. The increase in total alveolar bone volume in SOST KO mice coincided with osteon formation, which does not normally exist in small animals. Lastly, in spite of the high bone mass phenotype in the mandible, teeth developed normally in the SOST KOs.

In conclusion, SOST KO mice preserved mandibular bone at old ages and had higher alveolar bone mass and stronger mandibles compared with WT mice. The overall increase in bone strength in the mandible suggests a systemic effect, while the relative regional differences in jaw bone mass increases suggest local mechanical effects.

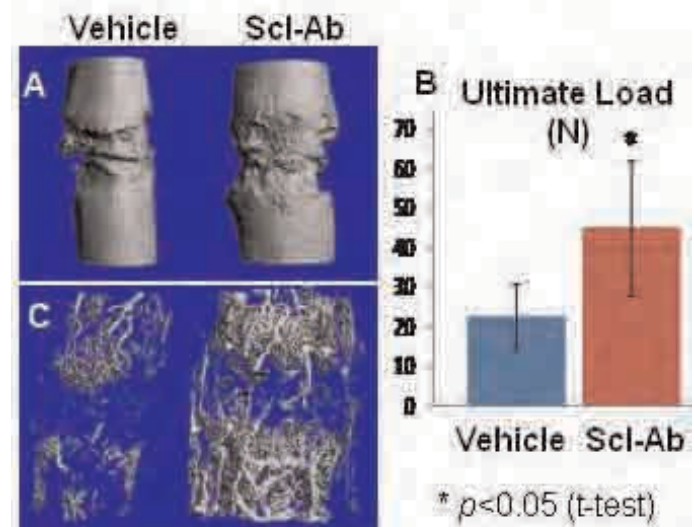
Disclosures: Min Liu, Amgen Inc., 3; Amgen Inc., 1

This study received funding from: Amgen Inc.

SU0464

Inhibition of Sclerostin by Monoclonal Antibody Enhances Bone Healing in a Rat Osteotomy Model. Yi-Xin He^{*1}, Zhong Liu¹, Tao Tang¹, Li-Zhen Zheng¹, Chi-Wai Man¹, Chao-Yang Li², Ge Zhang¹, Hua-Zhu Ke², Ling Qin¹. ¹The Chinese University of Hong Kong, Hong Kong, ²Amgen Inc., USA

Sclerostin is a negative regulator of bone formation and treatment with a sclerostin monoclonal antibody (Scl-Ab) results in increased bone formation, bone mass and bone strength in animal models of bone loss and fracture repair. The objective of this study was to investigate the effects of systemic administration of Scl-Ab on fracture repair in an open fracture model in rat femur. Sixty 6-month-old SD rats were randomly divided into Scl-Ab groups and vehicle groups after a transverse osteotomy performed at the mid-shaft of the right femur. One day post-surgery, rats were treated with Scl-Ab (s.c. injection, 25 mg/kg, 2 times per week) or vehicle for 3 or 6 weeks. The fractured femora were dissected for microCT scanning, mechanical testing, histology and angiography. MicroCT showed that the Scl-Ab groups had significantly higher callus volume fraction and BMD in both 3 and 6 weeks (Figure 1A) post-fracture compared to vehicle groups. Four-point bending testing showed significantly higher ultimate load (+98%) in Scl-Ab group than vehicle group with stiffness and energy to failure also trending higher in the Scl-Ab group at 6 weeks post fracture (Figure 1B). The increased callus bone volume fraction and fractured femoral bending strength with Scl-Ab treatment suggest that enhanced bone repair was achieved by inhibiting sclerostin. H&E staining showed more granulation tissues at 3 weeks and more woven bone at 6 weeks in the Scl-Ab treated calluses than in vehicle treated calluses. Fracture repair is complex, involving a coordinated sequence of biological processes that includes angiogenesis. Consistent with the enhanced fracture repair, we also observed an increase in callus vascularization (microCT based angiography) at the 3 week time point in the Scl-Ab treated animals as compared to vehicle treated animals (Figure 1C). Our data, showing enhanced fracture repair in rat osteotomy model support the potential of systemic Scl-Ab administration to enhance open fracture healing in patients.



Disclosures: Yi-Xin He, Amgen Inc., 2

This study received funding from: Amgen Inc.

SU0465

Vitamin K₂ Improves Renal Function and Increases Femoral Bone Strength in Rats with Renal Insufficiency. Jun Iwamoto^{*1}, Azusa Seki², Hideo Matsumoto¹. ¹Keio University School of Medicine, Japan, ²Hamri Co., Ltd, Japan

Renal insufficiency induces cortical bone loss in rats. The purpose of the present study was to examine the effects of vitamin K₂ on renal function and cortical bone

mass and bone strength in rats with renal insufficiency. Thirty male Sprague-Dawley rats, 8 weeks of age, were randomized by the stratified weight method into the following three treatment groups of 10 rats each: sham-operation (control), 5/6 nephrectomy (NX), and 5/6 NX + vitamin K₂ administration (30 mg/kg, 5 days/week, orally). Nine days after the surgery, serum and urine samples were collected to assess renal function and the treatment was initiated next day. After 6 weeks of treatment, the serum and urine samples, femora, and tibiae were obtained. Renal function was re-evaluated, bone histomorphometric analysis was performed on the tibial diaphysis, the length and wet weight of the femur were measured, and the bone mineral density (BMD) and mechanical strength of the femoral diaphysis were determined by peripheral quantitative computed tomography and three-point bending test, respectively. NX did not only induce renal dysfunction as indicated by the increased serum creatinine and urea nitrogen levels and the decreased creatinine clearance, but also decreased the femoral wet weight and femoral diaphyseal BMD without significantly affecting the femoral length, tibial diaphyseal cortical and marrow areas, and femoral diaphyseal bone strength. Vitamin K₂ improved renal function parameters, but did not significantly influence the femoral length, femoral wet weight, and femoral diaphyseal BMD. However, vitamin K₂ decreased the marrow area of the tibial diaphysis and increased the stiffness of the femoral diaphysis. These findings suggest that vitamin K₂ appears to improve renal function and increase bone strength without improving BMD in the cortical bone of rats with renal insufficiency.

Disclosures: Jun Iwamoto, None.

SU0466

Alendronate Systemic Administration: Effects on Bone and Mineralized Dental Structures. Marilia Lucisano¹, Raquel Silva^{*2}, Roberto Silva³, Raquel Gerlach¹, Paulo Nelson-Filho¹, Ricardo Battaglini⁴, Monica Serra¹, Leslie Morse⁵, Lea Silva¹. ¹School of Dentistry of Ribeirao Preto - University of Sao Paulo, Brazil, ²School of Dentistry of Ribeirao Preto - University of Sao Paulo, Brazil, ³School of Pharmaceutical Sciences of Ribeirao Preto - University of Sao Paulo, Brazil, ⁴The Forsyth Institute, USA, ⁵Harvard Medical School, USA

The objective of this study was to evaluate the effect of the systemic use of sodium alendronate in rats *in vivo*. Forty-five Wistar rats aged 36-42 days and weighing 200-230 g were assigned to two groups: experimental (n= 25) and control (n= 20). The experimental group received two weekly doses of 1 mg/kg of chemically pure sodium alendronate, while the animals of the control group received distilled water. After 60 days, the animals were sacrificed, the maxillary incisors were extracted and the tibias were removed. We determined bone mineral density, by radiographic optical densitometry and dual-energy x-ray absorptiometry (DXA); the mineralized dental structures of murine incisors, by analysis of infrared (IR) spectrometry, fluorescence spectroscopy, cross-sectional microhardness (CSMH), scanning electron microscopy (SEM) and polarized light microscopy (PLM). The results were subjected to statistical analysis by the Kruskal-Wallis non-parametric test, using the SAS (Statistical Analysis System) software for Windows version 9.1.3 (significance level of 5%). The experimental group presented higher mineral bone density (p<0.05) than the control group, by radiographic optical densitometry and DXA. The chemical analysis by IR spectrometry and fluorescence spectroscopy revealed the presence of alendronate in the mineralized dental structure of the specimens of the experimental group, with a percentage of incorporation of 0.0018% per tooth. The results of enamel and dentin CSMH did not show statistically significant difference between the experimental and control groups (p>0.05). There were no significant morphological differences among the specimens of the groups by SEM and PLM. Based on the obtained results, it may be concluded that the treatment with sodium alendronate caused an increase in the mineral bone density of the proximal tibial metaphysis, and that alendronate was incorporated in the mineralized dental structures without causing significant effects in the enamel and dentin microhardness and morphology of rat incisors.

Disclosures: Raquel Silva, None.

SU0467

Is Alendronate Effective in Improving Material Properties of Frail Cortical Bone in Inactive Model Rats? Mitsutoshi Suto¹, Kouji Naruse¹, Kentaro Uchida¹, Kaori Suto¹, Ken Urabe¹, Moritoshi Itoman², Yuko Mikuni-Takagaki^{*3}. ¹Department of Orthopedic Surgery, Kitasato University School of Medicine, Japan, ²Kyushu Rosai Hospital, Japan, ³Kanagawa Dental College & Graduate School of Dentistry, Japan

Age, hormones, diseases, medications, and physical activity all affect the bones of elderly people, some of whom suffer from osteoporosis. Bisphosphonates are now widely prescribed to treat osteoporosis, and they are effective. However, new evidence suggests that people who take bisphosphonates may be at greater risk of a subtrochanteric or proximal diaphyseal femur fractures from a low-energy event. With a new inactive rat model, (J Bone Miner Metab, in press), we studied the effect of alendronate (ALN) to answer key questions related to these atypical fractures. At 40 weeks female Wistar rats underwent surgery, either an ovariectomy (OVX) or a sham operation, and were then kept for 5 weeks. For the next 13 weeks, we forced some rats inactive by housing them in cages that allow free access to water and food but do not permit the rats to rise up or walk. Dissected femur were analyzed by ?CT,

pQCT, confocal Raman microspectroscopy, and three point bending test. Our results show that alendronate effectively prevents cortical bone loss in osteoporotic OVX rats but not in inactive rats. Results of pQCT also showed that a geometry parameter, cross sectional moment of inertia, CSMI, of Inactive+ALN is smaller than that of Walking (Sham). Matrix parameters such as Amide I and Amide III showed that Inactive rat cortical bone has significantly lower intensity values than those of Walking and OVX+ALN rats and that values of Inactive rats and Inactive+ALN rats are not significantly different. Mineral parameters such as PO43- ?4 also showed a significant difference between OVX+ALN and Inactive rats. Both mineral and matrix are deficient in the cortical bone of inactive rat, and ALN does not seem to restore the deficiency. Measurements of bone strength showed that the breaking force of both Inactive and Inactive+ALN rat femur is significantly smaller than that of WalkingALN and OVX+ALN rats, and that ultimate force of Inactive+ALN rat femur is significantly smaller than that of OVX+ALN rat. ALN may have made these parameters of cortical bone in the inactive rats worse. Association of atypical fractures with the physical inactivity of patients treated with bisphosphonates may be worth examining.

Disclosures: Yuko Mikuni-Takagaki, None.

SU0468

First-In-Human Study of Transdermal Salmon Calcitonin - Pharmacokinetics and Pharmacodynamics. Yael Kenan^{*1}, Efrat Kochba², Galit Levin³, Keren Greenfeld-Barsky², Keren Mevorat², Hagit Sacks², Hana Gadasi², Yael Leshem², Francis Berenbaum⁴, Virginia Kraus⁵. ¹TRANSPhARMA MEDICAL LTD., Israel, ²TransPharma Medical, Israel, ³Transpharma Medical, Israel, ⁴Saint-Antoine hospital, AP-HP, France, ⁵Duke University Medical Center, USA

Salmon calcitonin (sCT) has been shown to reduce the bone resorption and cartilage degradation associated with osteoarthritis. TransPharma Medical has developed a transdermal (TD) delivery system of synthetic sCT to alleviate the discomfort of subcutaneous (SC) injections and to improve reliability of delivery, patients' acceptance and compliance. The system creates MicroChannels in the upper skin layers, allowing rapid diffusion of the peptide from a subsequently-applied drug patch into the inner skin and systemic circulation (Ish Shalom et al., ASBMR2010). The aim of this phase I study was to assess safety, tolerability, pharmacokinetics (PK; serum sCT), and pharmacodynamics (PD; CTX-I, CTX-II/cr) of ascending doses of TD sCT in an open-label, cross-over, single-center study in 20 healthy postmenopausal women age 45-75 y. CTX-I and CTX-II are biomarkers for bone resorption and cartilage degradation, respectively. In Part A, 12 women received sCT SC 100 IU (Salco; Genmedix.Ltd) and sCT TD 300 µg. In Part B, 14 women (including 6 from part A) received sCT SC 100 IU (Mialcalcin; Novartis) and 60, 100, 150 µg sCT TD. There was a wash-out period of 1 week after each dose. PK and PD were evaluated from samples collected postdose for up to 24 h in Part A and up to 7 days in Part B. Evaluation of the daily biological variability of CTX biomarkers was assessed for 24 h predose. Skin and general safety assessments were performed. TD delivery of sCT was safe and tolerable; there were no clinically significant differences across study groups in adverse events. Cmax of TD sCT was delayed compared to SC. A dose-response in Cmax was observed for TD 60, 100 and 150 µg sCT; relative bioavailability ranged from 18 to 25%. In Parts A & B, the changes from predose to maximal reduction in CTX-I and CTX-II were similar between TD and SC delivery of sCT; these reductions in biomarkers were significantly greater than those observed with diurnal variation. Biomarker data also demonstrated a comparable PD profile between TD and SC for all doses in the relative percent change from predose to 12 h postdose (Table), and 24 h and 7 days postdose (data not shown). In conclusion, this first-in-human, dose-range finding study of transdermal sCT demonstrated significant reductions in markers of bone resorption and cartilage degradation that were comparable to subcutaneously administered sCT. Delivery of both TD and SC sCT was well-tolerated.

Table. Relative percent change from predose to 12 hour postdose for serum CTX-I and urine CTX-II by salmon calcitonin delivered transdermally (TD) or by subcutaneous (SC) injection.

	Serum CTX-I (ng/ml)	Urine CTX-II (ng/ml-mmol Cr)
Part A		
TD 2x150 µg	-95.1 (-96.0, -91.1) (n=12)	-79.2 (-84.4, -68.2) (n=12)
SC 100 IU	-80.2 (-84.6, -71.6) (n=12)	-66.0 (-78.6, -28.2) (n=12)
Part B		
Control*	-19.6 (-26.6, -10.3) (n=14)	-28.8 (-46.2, -14.1) (n=14)
TD 60 µg	-90.2 (-94.4, -80.9) (n=14)	-74.1 (-79.5, -55.0) (n=14)
TD 100 µg	-93.3 (-98.7, -79.6) (n=12)	-72.9 (-77.9, -48.6) (n=12)
TD 150 µg	-93.8 (-96.7, -86.8) (n=11)	-72.5 (-83.8, -49.5) (n=11)
SC 100 IU	-93.4 (-95.4, -92.3) (n=11)	-59.2 (-73.7, -53.3) (n=11)

Data presented as median % change from predose, (95% CIs),
(number of participants)

*Control - Diurnal variability assessed for 24 h predose

SU0470

Non-nuclear ERα Signaling Prevents Oxidative Stress and the Loss of Bone, but not the Loss of Uterine Weight, in OVX Mice. Shoshana M. Bartell^{1,*}, Li Han¹, Srividhya Iyer¹, Aaron Warren¹, Randal S. Shelton¹, Robert W. Bradsher¹, Sung H. Kim², Benita S. Katzenellenbogen², Ken L. Chambliss³, Philip W. Shaul³, John A. Katzenellenbogen², Paula K. Roberson¹, Robert S. Weinstein¹, Charles A. O'Brien¹, Robert L. Jilka¹, Maria Jose S. Almeida¹, Stavros C. Manolagas¹. ¹Center for Osteoporosis & Metabolic Bone Diseases, Central Arkansas Veterans Healthcare System, University of Arkansas for Medical Sciences, USA, ²University of Illinois, USA, ³University of Texas Southwestern Medical Center, USA

Sex steroid deficiency in mice, similar to aging, increases the generation of reactive oxygen species (ROS) and the activity of p66shc, an isoform of the growth factor adapter Shc that amplifies ROS production in the mitochondria. Moreover, the adverse effects of the acute loss of ovarian function on bone can be prevented by antioxidants. Conversely, estrogens decrease ROS and p66Shc activation, antagonize ROS-induced osteoblast apoptosis, and attenuate the pro-survival effects of RANKL on osteoclasts also via anti-oxidant mechanisms. These effects of estrogens are fully preserved in a mouse model bearing an estrogen receptor (ER) α knock-in mutation that prevents binding to DNA. In addition, a 17 β -estradiol (E2) dendrimer conjugate (EDC) that is not capable of stimulating the nuclear-initiated actions of ER is as potent as E2 in attenuating p66shc phosphorylation and osteoblast apoptosis, as well as promoting osteoclast apoptosis in vitro. Prompted by these observations and the demonstration that ER α non-nuclear signaling induced by the EDC promotes cardiovascular protection, but not uterine or breast cancer growth in mice (Chambliss et al, JCI 2010), we have examined here the effects of this compound on the skeleton of ovariectomized (OVX) mice. For these experiments, 17 week-old C57BL/6 female mice were OVX or sham-operated and implanted with mini-pumps delivering vehicle, a dendrimer control (DC), or equimolar concentrations of E2 or the EDC for 6 weeks. The EDC prevented the OVX-induced oxidative stress (as determined by ROS and glutathione levels in the bone marrow and p66shc phosphorylation in vertebral bone) to the same extent as E2; was as potent as E2 in preventing bone loss at the spine (DEXA); and significantly attenuated loss of cortical bone as determined in the vertebrae or femur (micro-CT). Further, EDC was as potent as E2 in preventing the OVX-induced increase in both osteoclast and osteoblast progenitors, as assayed by the number of bone marrow-derived TRAP-positive cells and CFU-OB, respectively. In sharp contrast, the OVX-induced decrease in uterine weight was fully restored by E2 but was unaltered by the EDC. DC- and vehicle-treated OVX mice were indistinguishable in all these measures. These results demonstrate unequivocally that at least several effects of estrogens on bone, including their anti-oxidant properties, are mediated by a mechanism distinct from their classical genotropic action on reproductive organs.

Disclosures: Shoshana M. Bartell, None.

SU0471

Effects of Low Intensity Pulsed Ultrasound on OVX Induced Bone Mass Decrease in Mice. Yoshitsugu Kojima¹, Takayuki Watanabe¹, Hiroki Yazawa¹, Hiroyoshi Nishi², Nobuo Izumo², Yoshihiro Nishimura^{1,*}. ¹Nippon Sigmax Co., Ltd., Japan, ²Yokohama College of Pharmacy, Japan

Low intensity pulsed ultrasound (LIPUS) has been widely used for bone fracture healing. Effects of LIPUS on bone fracture site have been revealed recently. Yet mechanism of LIPUS on osteoporosis is less well understood. The aim of this study is to test the effects of LIPUS on bone loss model of OVX model mouse. ICR mice, 14-week-old, were ovariectomized or sham operated. Ovariectomized mice were divided into ultrasound exposed group and unexposed group. LIPUS was exposed for 20min/day, and 5day/week at 2MHz, duty 20%. Bone density and bone mineral content (BMC) were measured with LCT-100Lite, Hitachi Aloka Medical, Ltd, on pre-exposed, one month and two month after beginning of LIPUS exposure. At three month, all mice were sacrificed. Tibia, ovary and serum were collected. The bone density and BMC of right tibia were measured. Sera were used for ELISA of osteopontin (OPN) and TRAP. At three month ovary weight was significantly decreased to 15% of sham group on both OVX and LIPUS exposed groups. Bone density was significantly decreased on OVX mouse against sham mouse at 1, 2 and 3 month after OVX operation. BMC was significantly decreased on OVX group against sham group at 1 and 2 month. However, BMC was not showed significant difference on LIPUS group. Moreover, at 3 month, BMC of LIPUS group was significantly higher than that of OVX group. OPN expression level in serum was significantly increased on LIPUS group. On the other hand, TRAP level was decreased on both LIPUS and OVX groups against sham group. In this study, the effects of LIPUS on BMC were indicated. The results of ELISA suggested the effect of LIPUS on osteoblastic cells. Our next step is to elucidate the mechanism of osteogenic responses by LIPUS with western blot and real-time PCR.

Disclosures: Yoshihiro Nishimura, Nippon Sigmax Co., Ltd., 3

Table

Disclosures: Yael Kenan, Transpharma Medical, Ltd, 3; Transpharma Medical, Ltd, 1

This study received funding from: Transdermal Medical, Ltd

SU0469

Interaction of Calcium Intake and Vitamin D Status throughout Young Adulthood and OVX-Induced Estrogen Deficiency on Bone and Calcium Metabolism. Clara Park^{*}, James Fleet, George McCabe, Connie Weaver, Purdue University, USA

Calcium (Ca) intake and vitamin D (VD) status may affect the progression of bone loss through menopause in women. We investigated this in female Sprague Dawley rats. Initially weanling rats were fed a diet with 0.4% Ca and 100 IU VD/kg diet for 5 wks in a UV-free environment, targeting the average Ca and VD status of US adolescents. Bones were labeled with ⁴⁵Ca and 24-hour urine collections were done weekly thereafter to assess bone loss. At 8 wks of age, rats were fed diets containing either 0.2 % or 1.0 % Ca and 50, 100, or 1000 IU VD/kg diet (14-16 rats/treatment diet, 2 x 3 factorial design). Ovariectomy (OVX) was performed at 12 wks of age. Rats were sacrificed at 7 mo of age and tibias and femurs were excised. Urinary ⁴⁵Ca excretion was measured by liquid scintillation, 4-day metabolic Ca balance (at 3 mo post-OVX or older) and bone Ca content were determined by atomic absorption spectrometry and inductively coupled plasma optical emission spectrometry, bone length and width by digital calipers, bone density by underwater weighing, bone structure by μ CT, and bone strength by 3-point bone breaking. One-way or 2-way ANOVA was used to analyze the data. Urinary ⁴⁵Ca increased after OVX in all rats, but rats on the 1.0 % Ca diet excreted less starting 4 wks after OVX, regardless of VD intake. VD improved net Ca absorption in rats fed 0.2 % but not 1.0 % Ca. A Ca x VD interaction affected Ca content in tibia but not femur. In tibia, Ca content was highest in the 1.0 % Ca + 100 IU VD/kg diet group, however, no diet effect was observed for bone length, width, density, or bone strength. In the femur, higher VD intakes increased bone width and improved mechanical strength (higher energy to failure). Ca intake increased tibia trabecular (Tb) number and reduced Tb spacing, while higher VD reduced Tb spacing. No diet effect was seen in cortical bone. We conclude that high Ca intake prevents bone turnover after OVX regardless of VD status, but VD can increase Ca absorption at low Ca intakes. Increased VD intake affects bone width and strength only in the femur. In the tibia, Ca and VD interact on bone Ca content, but Ca and VD promote trabecular bone independently. Thus Ca metabolism and bone health during estrogen deficiency is affected by the habitual input of Ca and VD during later growth and adulthood through the individual and interactive effects of these nutrients.

Disclosures: Clara Park, None.

SU0472

Effects of Parathyroid Hormone, Alendronate and Their Combination Regimen on Bone Mass and Turnover in Ovariectomized Cathepsin K Null Mice. Michael Gentile^{*1}, Carlyle Horrell¹, Maureen Pickarski¹, Le Thi Duong². ¹Merck & Co., Inc., USA, ²Merck Research Laboratories, USA

Cathepsin K (CatK) is a cysteine proteinase highly expressed in osteoclasts and plays a major role in bone resorption. Inhibition of CatK prevents bone loss while preserving bone formation in ovariectomized (OVX) mice, rabbits and monkeys. Treatment with the CatK inhibitor odanacatib has been shown to increase bone mineral density (BMD) at the spine and hip in postmenopausal osteoporosis. Parathyroid hormone (PTH) is the currently approved osteoanabolic agent for the treatment of osteoporosis. The goal of this study is to compare efficacy of hPTH1-34 (40µg/kg, daily, 5x week), ALN (0.3mg/kg, wkly) and their combined effects in OVX-wild type (WT) vs. -KO mice. Treatment of skeletal mature OVX-mice (surgery at age 12 weeks) was initiated at 3-months post surgery for 12-weeks total. *In vivo* DEXA was performed at baseline, 6 and 12 weeks during treatment, and calcein was administered 7 and 2 days prior to necropsy. Although whole body BMD of KO is significantly higher than WT at baseline, OVX resulted in significant lumbar vertebrae (LV) bone loss in WT by 12.0% (p<0.001, one way ANOVA, Fisher's PLSD) and KO by 10.9% (p<0.001) versus the respective Sham-OVX. Lumbar vertebra (LV4-6) and whole femur (WF) were evaluated *ex vivo* for BMD and dynamic histomorphometry. In OVX-WT mice, PTH and ALN increased LVBMD (p<0.001) by 13.3% and 24.0%; and WF BMD (p<0.001) by 14.8% and 18.5%, respectively vs. vehicle. In OVX-KO, PTH and ALN increased LVBMD (p<0.001) by 19.2% and 23.0%; and WF BMD (p<0.001) by 28.3% and 11.6%, respectively. Interestingly, combination of PTH and ALN additionally increased LVBMD (p<0.001) by 42.2 % and WFBMD by 29.6 % in OVX-WT and increased LVBMD (p<0.001) by 51.9 % and WFBMD by 35.0 % in OVX-KO with total BMD gains in KO significantly higher than that in WT. From dynamic histomorphometry, bone formation rate (BFR) in Sham and OVX-KO is ~3-4 fold higher than that in Sham and OVX-WT. While ALN treatment alone diminished overall bone turnover and BFR, PTH increased trabecular BFR in both OVX-WT and -KO. In combination with PTH, ALN partially reduced PTH induced gains in BFR in both OVX-WT, and -KO with the KO groups displaying increased BFR relative to WT in all treatment regimens. Taken together, the combination regimen of PTH and ALN resulted in higher gains of bone mass with less suppression of bone formation in response to estrogen deficiency in CatK KO as compared to that in wild type mice.

Disclosures: Michael Gentile, None.

SU0473

Efficacy of ONO-5334, a Cathepsin K Inhibitor, on Bone Mineral Density, Geometry and Bone Strength in the Radius in Ovariectomized Cynomolgus Monkeys. Satoshi Nishiwaka*, Hiroyuki Yamada, Yasutomo Nakanishi, Akiko Kunishige, Yasuaki Hashimoto, Hiroshi Mori, Yasuo Ochi, Masafumi Sugitani, Kazuhito Kawabata. Ono Pharmaceutical Co., Ltd., Japan

ONO-5334 is a small molecule and an orally-active inhibitor of cathepsin K, which plays an important role in osteoclast-mediated bone resorption. We have previously reported that ONO-5334 increased areal BMD in the radius as well as the lumbar vertebra in ovariectomized (OVX) monkeys ¹⁾. In this study, we evaluated the efficacy of ONO-5334 on trabecular and cortical bone, and bone strength in the radius.

Female cynomolgus monkeys were assigned to one of the following 6 groups (20 animals/group): sham operated, OVX control treated with vehicle, ONO-5334 1.2, 6 or 30 mg/kg, or alendronate (ALN) 0.05 mg/kg. ONO-5334 was orally administered once daily from the day following OVX surgery for 16 months. ALN was administered i.v. once every 2 weeks. After necropsy, distal and mid radius (5 and 50% of total radius length from the distal end, respectively) were scanned using pQCT to measure volumetric BMD (vBMD) and geometric parameters, followed by a 3-point bend test at the mid radius.

In the distal radius, OVX caused a significant decrease in trabecular vBMD (p<0.01), but there were no changes in integral and cortical vBMD and geometric parameters such as cortical thickness, periosteal and endosteal perimeter compared to the sham group. ONO-5334 at 6 and 30 mg/kg significantly increased integral vBMD (41, 48% resp.) and cortical vBMD (23, 22% resp.), and cortical thickness (51, 59%), vs the OVX control group (all p<0.01). ONO-5334 at 6 and 30 mg/kg significantly decreased endosteal perimeter (p<0.01 vs OVX), but did not affect periosteal perimeter. ONO-5334 at 30 mg/kg increased trabecular vBMD over sham level (p<0.01 vs OVX). In the mid radius, OVX induced a significant decrease in cortical vBMD (p<0.01 vs sham), but there were no changes in geometric parameters. All ONO-5334 doses significantly increased cortical vBMD and thickness (except for cortical thickness of 1.2 mg/kg) (p<0.05 vs OVX). Periosteal and endosteal perimeters were not affected by ONO-5334. Bone strength (maximum load) at the mid radius decreased due to OVX (p<0.05 vs sham), and significantly increased by ONO-5334 at 6 and 30 mg/kg (p<0.05 vs OVX). ALN did not affect any pQCT parameters or bone strength in the radius.

In summary, ONO-5334 increases BMD by affecting cortical bone predominantly as well as trabecular bone in the radius. In addition, ONO-5334 has a positive effect on bone strength in the mid radius, where cortical bone predominates.

¹⁾ ASBMR 2009, FR0420

Disclosures: Satoshi Nishiwaka, None.

SU0474

MIV-711, a Potent and Selective Oral Once Daily Cathepsin K Inhibitor, Reduces Markers of Bone Resorption While Maintaining Carboxylated and Undercarboxylated Osteocalcin Levels in Dogs Subjected to Partial Medial Meniscectomy, an Experimental Model of Osteoarthritis. Erik Lindstrom¹, Lotta Vrang¹, Susanne Sedig¹, Ylva Terelius¹, Kristina Wikstrom¹, Britt-Louise Sahlberg², Timothy Chambers³, Don Mau⁴, Alison Bende⁵, Urszula Grabowska^{*6}. ¹Medivir AB, Sweden, ²Medivir, Sweden, ³St. George's Hospital Medical School, United Kingdom, ⁴Pre-Clinical Research Services, USA, ⁵Bolder Biopath, USA, ⁶Medivir, United Kingdom

Background and Aims

Cathepsin K, produced by osteoclasts, degrades type I collagen in bone and cathepsin K inhibitors act as anti-bone resorptives. Although agents are now available that suppress bone loss, anti-resorptive treatment typically suppresses bone formation, and thus prevents the replacement of lost bone. We have recently evaluated MIV-711, a potent and selective cathepsin K inhibitor, in an experimental dog model of osteoarthritis (OA) on markers of bone resorption and bone formation.

Methods

Female beagle dogs, subjected to partial medial meniscectomy, were treated with either vehicle (n=15) or MIV-711 (n=15) at 30 µmol/kg once daily (q.d.) starting the day before surgery. Treatment continued for 28 days after surgery followed by necropsy on day 29. Plasma and urinary samples were collected at various time points during the experiment and at necropsy. Biomarkers were measured using commercially available ELISA kits.

Results

MIV-711 reduced CTX-I levels (marker of bone resorption) in plasma (max effect: 46-67%, effect at trough: 30-37%) and in urine (79-86%) compared to baseline. CTX-I levels did not change in response to vehicle. The plasma levels of undercarboxylated and carboxylated osteocalcin (a marker of bone formation) did not differ between vehicle and MIV-711-treated groups at sacrifice.

Conclusions

In summary, markers of bone resorption in OA dogs were reduced by the selective cathepsin K inhibitor MIV-711 compared to vehicle while the bone formation markers measured did not differ from vehicle despite the prominent inhibition of bone resorption. Taken together, these data suggest MIV-711 may be beneficial not only for osteoporosis but also for OA.

Disclosures: Urszula Grabowska, None.

SU0475

Pre-operative Intermittent Administration of Human Parathyroid Hormone Enhances Bone Union at the Site of Cancellous Bone Osteotomy in Ovariectomized Rats. Hiroyuki Tsuchie*, Naohisa Miyakoshi, Yuji Kasukawa, Hiroshi Aonuma, Toyohito Segawa, Daisuke Kudo, Yoichi Shimada. Akita University Graduate School of Medicine, Japan

Purpose: Surgery for osteoporotic fracture occasionally requires several days of pretreatment to control various complications. If postoperative bone union is promoted by intermittent administration of PTH during this preoperative waiting period, the duration of post-operative bed rest may be decreased. Therefore, we evaluated the effects of preoperative PTH treatment on bone union and its mechanism of cancellous bone fracture. Method: Seven-month-old female Sprague-Dawley rats underwent ovariectomy (OVX) followed by osteotomy of the proximal tibia four weeks after OVX, then the tibiae were fixed with wire one week after osteotomy. Animals were divided into the following 6 groups (n=10-11 in each group at different time points) according to the method of human PTH administration (hPTH, 30 µg/kg body weight) or vehicle (3 times a week) before and after wiring: (1) pre-operative vehicle-treated control group (V); (2) pre-operative PTH-treated control group (P); (3) pre- and post-operative vehicle-treated group (V-V); (4) pre-operative vehicle- and post-operative PTH-treated group (V-P); (5) pre-operative PTH- and post-operative vehicle-treated group (P-V); and (6) pre- and post-operative PTH-treated group (P-P). Tibiae from the V-V, V-P, P-V, and P-P groups were harvested 2 or 4 weeks after osteotomy. Decalcified hematoxylin/eosin stained sections were used to evaluate bone union, bone volume per tissue volume (BV/TV), osteoid surface (OS/BS) and eroded surface (ES/BS). Alcian blue/hematoxylin stained sections were used to evaluate cartilage volume. Sections immunostained with PCNA, Sox9 or Runx2 were used to evaluate cell differentiation and proliferation. Result: PTH treatment significantly increased BV/TV and OS/BS, and decreased ES/BS. At 1 and 2 weeks after osteotomy, the percentages of bone union in P, P-V and P-P groups were significantly greater than these in the V, V-V and V-P (P<0.05, respectively). Cartilage volume in the P group was significantly greater than that in the V group (P<0.01). P-P group showed significantly increased percentages of cell positive for PCNA (p<0.05) and Runx2 (p<0.01), but not Sox9, compared to the V-V group at 4 and 2 weeks after osteotomy, respectively. Conclusions: Pre-operative intermittent administration of hPTH enhances bone union by promoting cartilage formation and cell differentiation to osteoblast, but not by promoting cell proliferation.

Disclosures: Hiroyuki Tsuchie, None.

This study received funding from: Asahi Kasei Pharma Co., Ltd., Tokyo, Japan

SU0476

Strontium Ranelate Rebalances Adipogenesis and Osteoblastogenesis and Attenuates Bone Loss in Senescent Osteopenic Mice through NFATc/Maf and Wnt Signalling. Zuzana Saidak¹, Eric Hay², Caroline Marty¹, Alain Barbara¹, Pierre Marie^{*3}. ¹Inserm U606 & University Paris Diderot, France, ²INSERM 4606, France, ³INSERM Unit 606 & University Paris Diderot, France

Age-related bone loss is associated with a continuous decrease in bone forming activity associated with a preferential differentiation of mesenchymal stromal cells (MSC) into adipocytes. We previously showed that the anti-osteoporotic drug strontium ranelate (SrRan) activates osteoblastic cell replication, differentiation and survival through Wnt/NFATc signaling activation. Here, we investigated whether SrRan controls MSC adipogenic differentiation *in vitro* and *in vivo*. We showed that SrRan (3 mM) increased Runx2 expression and osteogenesis and decreased PPARgamma2 expression and adipogenesis in murine C3H10T1/2 and human primary MSC, indicating that SrRan regulates adipocyte/osteoblast differentiation. We then tested the effect of SrRan in senescent osteopenic SAMP6 mice which exhibit decreased osteoblastogenesis and increased adipogenesis. SAMP6 mice were administered with SrRan 5 days per week for 10 weeks at a dose-level (1800 mg/kg) providing serum Sr level equivalent to the known clinical exposition in osteoporotic treated women. DEXA and microCT analyses showed that SrRan increased tibial bone volume, trabecular thickness and number and decreased trabecular separation, resulting in higher connective density (+38%, $P < 0.05$) compared to control mice. Histomorphometric analysis confirmed that SrRan increased femoral bone volume (+38 %, $P < 0.01$) as a result of increased bone formation rate (+45%, $P < 0.001$) and decreased TRAP+ osteoclast surface and number (-31%, $P < 0.05$). Remarkably, SrRan decreased adipocyte volume (-43%, $P < 0.05$) and size (-55 %, $P < 0.05$) in the bone marrow compared to control mice. Gene expression analysis of the mice bone marrow stroma showed that SrRan increased Wnt5a mRNA level by 2-fold compared to control mice. Furthermore, SrRan increased bone marrow stroma expression of Maf, a NFATc-regulated transcription factor controlling the bifurcation between osteoblasts or adipocytes. The results show that SrRan has the potential to act on the switch between adipocyte and osteoblast differentiation of mesenchymal stromal cells *in vivo*, and suggest the implication of Wnt and NFATc/Maf signaling cascade in this effect. Restoration of the balance between osteogenesis and adipogenesis by SrRan resulted in attenuation of bone loss and improved bone microarchitecture in senescent osteopenic mice.

Disclosures: Pierre Marie, Servier, 2
This study received funding from: Servier

SU0477

Elcalcitol (ED-71) Increases Bone Formation and Strength of Cortical Bone in Osteoporotic Mouse Model. Sadaoki Sakai^{*}, Koichi Endo, Keisuke Tanaka, Masahiko Mihara. Chugai Pharmaceutical Co., Ltd., Japan

The primary aim of osteoporosis treatment is to reduce bone fracture. A phase III clinical trial showed that in osteoporotic patients with sufficient vitamin D supply, elcalcitol (ED-71; a 2β-hydroxypropyloxy derivative of 1α,25(OH)₂D₃) was superior to alfacalcidol in decreasing bone resorption and reducing incidence of vertebral and non-vertebral fractures, such as wrist fractures, with safety equivalent to that of alfacalcidol (ASBMR2010, #1248). The aim of the current study was to investigate the mechanisms of ED-71 on the recovery of cancellous and cortical bone. For this purpose, we induced osteoporosis in mice by injecting them with GST-RANKL, a fusion protein of glutathione S-transferase and the extracellular domain of human receptor activator of NF-κB ligand. Two i.p. injections of GST-RANKL (each 1 mg/kg, 24h intervals) significantly reduced distal femur cancellous bone volume/tissue volume (BV/TV). Mice were given ED-71 (0.05 μg/kg, p.o.) once daily for 11 days from 3 days after the first GST-RANKL injection. On the day after the last ED-71 administration we assessed the structure, morphology, and midshaft strength of the femur. Micro-CT analysis revealed that ED-71 recovered BV/TV of both distal cancellous and midshaft cortical bone and also increased midshaft cortical thickness and strength. Morphological analysis revealed that ED-71 decreased Osteoclast surface/bone surface (Oc.S/BS) but did not change mineralizing surface/bone surface (MS/BS) or bone formation rate (BFR) of cancellous bone. However, ED-71 increased MS/BS of both periosteal and endosteal cortical bone. As a consequence of these alterations in morphology, cortical thickness and midshaft strength were increased. In summary, ED-71 treatment recovered femur BV/TV of both distal cancellous and midshaft cortical bone in GST-RANKL-induced osteoporotic mice. The morphological analyses revealed some differences in the mechanisms of ED-71 with respect to cancellous and cortical bone. In cancellous bone, ED-71 reduced bone resorption, whereas in cortical bone, ED-71 upregulated bone formation, thereby elevating cortical thickness and bone strength. This action of ED-71 on cortical bone might be one mechanism behind the reduction of non-vertebral fractures observed in osteoporotic patients treated with ED-71.

Disclosures: Sadaoki Sakai, CHUGAI PHARMACEUTICAL CO., LTD, 3

SU0478

Impact of Allosteric Modulators of the Extracellular Calcium-Sensing Receptor on Human Calcitonin-Secreting C-cells. Hee Chang Mun^{*1}, Arthur Cristopoulos², Arthur Conigrave¹. ¹University of Sydney, Australia, ²Monash University, Australia

The extracellular Ca²⁺-sensing receptors (CaR) is a class C G-protein coupled receptor that plays a central role in calcium homeostasis by regulating parathyroid hormone (PTH) and calcitonin (CT) secretion. We previously demonstrated that L-amino acids (1) and γ-Glutamyl peptides (2) allosterically activate the CaR in CaR-expressing HEK-293 cells and normal human parathyroid cells. In normal parathyroid cells, L-Phenylalanine (L-Phe) and S-methylglutathione (SMG) activate intracellular Ca²⁺ mobilization and suppress PTH secretion. In the current study, we have investigated the impact of CaR activation by positive allosteric modulators including L-Phe, SMG, cinacalcet as well as the calcilytic NPS 2143 on intracellular Ca²⁺ mobilization and CT secretion from human calcitonin-secreting TT cells. TT cells were cultured in F12-K nutrient medium with 10% FBS in the presence of 100 ng mL⁻¹ human interleukin-1 beta (hIL-1β) for 48 h (3). For the analysis of intracellular Ca²⁺ mobilization, TT cells were cultured on coverslips, loaded with the Ca²⁺-sensitive dye fura-2 AM (5 μM; 1.5 h) and then analyzed for sensitivity to elevated Ca²⁺ concentration or allosteric modulators. For analysis of CT secretion, TT cells were cultured in 24-well plates with hIL-1β as above and then incubated with extracellular Ca²⁺ (0.5 to 1.5 mM) in the presence of allosteric modulators for various times (0 – 20 min). In fura-2 loaded cells, allosteric modulators (10 mM L-Phe, 30 μM SMG and 10 μM cinacalcet) enhanced intracellular Ca²⁺ mobilization in the presence of extracellular Ca²⁺ (2.0 mM) and these effects were suppressed by 20 μM NPS 2143. In experiments on CT release, we also observed enhanced sensitivity to elevated Ca²⁺ concentration in the presence of L-Phe, SMG and cinacalcet and a threshold Ca²⁺ concentration was identified at around 1.0 mM. In addition, CT secretion was suppressed in response to all these modulators by 20 μM NPS 2143. We find that positive allosteric modulators of the CaR promote intracellular Ca²⁺ mobilization and CT secretion from CT-secreting cells and that these effects are suppressed by the calcilytic NPS 2143.

1. Conigrave AD et al. J. Biol. Chem. (2004) 279:38151 – 38159
2. Broadhead GK et al. J. Biol. Chem. (2011) 286:8786 – 8797
3. Canaff L & Hendy GN. J. Biol. Chem. (2005) 280:14177 - 14188

Disclosures: Hee Chang Mun, None.

SU0479

Bone Mineral Values And Sex Hormones Related To Maturity In Adolescent Females. Rita Gruodyte^{*1}, Jaak Jurimae², Toivo Jurimae², Adam Baxter-Jones¹. ¹University of Saskatchewan, Canada, ²University of Tartu, Estonia

Although the role of estradiol in bone health is well established, relatively little is known with regards to the role of progesterone. The aim of this study was to evaluate the relationships of estradiol and progesterone with bone mineral density (BMD) and content (BMC) in adolescent females. In a cross-sectional sample of healthy 13-15-year-old girls (n=202), total body (TB) BMC (g) and BMD (g/cm²) as well as at femoral neck (FN) and lumbar spine (L2-L4) (LS) BMD were measured using DXA. Venous blood samples were drawn after an overnight fasting to determine the concentration of estradiol and progesterone. Years from Peak Height Velocity (PHV) was used as an indicator of biological age and was estimated using anthropometric equation parameters. Maturity groups (early, average and late maturing) were developed using a tertile split based on predicted age at PHV (APHV). When subdivided by maturity, early maturers TB BMC was inversely correlated to estradiol ($r = -0.27$; $p < 0.05$), although after adjusting for Body Mass Index (BMI), these associations disappeared ($p > 0.05$). In the average maturing group, significant correlations ($r = 0.33$, $p < 0.05$) were found between TB BMD and estradiol, whereas progesterone correlated with the TB BMC ($r = 0.32$, $p < 0.05$) and FN BMD ($r = 0.40$, $p < 0.01$). Partial correlation analysis, while controlling for BMI, confirmed these associations. In the late maturers no relationships were observed between bone parameters and sex hormones. Stepwise multiple regression analysis indicated that, in average maturers only, estradiol alone explained 8.7% and 9.1% of the total variance at TB and LS BMD, respectively. Accordingly, progesterone explained 10% and 15.6% of the total variance at TB BMC and FN BMD, respectively. Estradiol and progesterone together explained 24.5% of the total variance at the FN BMD in the average maturing group only. In conclusion positive influences of estradiol and progesterone to bone mineral variables appear to be maturity dependant.

Disclosures: Rita Gruodyte, None.

SU0480

Estrogens Attenuate Osteocyte Apoptosis via Activation of the NO/cGMP/ PKG Pathway. Nisha Marathe^{*}, Hema Rangaswami, Gerry Boss, Renate Pilz. UCSD, USA

Estrogens exert a positive effect on bone health through both genomic and extra-genomic effects. They protect osteoblasts and osteocytes from apoptosis via binding to a membrane-bound estrogen receptor and rapidly activating protein kinase B (Akt)

and the mitogen-activated protein kinases Erk-1/2. Estradiol has also been shown to rapidly increase intracellular nitric oxide (NO) and cGMP concentrations. We recently found NO/cGMP-dependent activation of Src and Erk-1/2 in mechanically-stimulated osteoblasts; therefore, we explored the role of the NO/cGMP signaling pathway in estrogen regulation of osteocyte survival.

To study the anti-apoptotic effects of estrogens, we examined etoposide-induced cell death in MLO-Y4 osteocyte-like cells by trypan blue staining, caspase-3 cleavage, and TUNEL assays. Apoptosis was completely prevented when cells were treated with estradiol, and we found that this protective effect was mimicked when cells were pre-treated with the membrane-permeable cGMP analog 8-CPT-cGMP. Pharmacological inhibition of NO synthase, soluble guanylate cyclase, or cGMP-dependent protein kinases (PKGs) reversed the anti-apoptotic effects of estradiol, supporting a requirement for NO/cGMP/PKG signaling downstream of estrogen. siRNA-mediated knock-down and viral reconstitution of individual PKG isoforms demonstrated that the anti-apoptotic effects of estradiol and cGMP were mediated by PKG I α and PKG II. We found that Akt and Erk-1/2 activation by estradiol required PKG II, and that cGMP mimicked the effects of estradiol on Akt and Erk, including induction of Erk nuclear translocation. Osteocyte apoptosis is regulated by interaction of the death-promoting protein BAD with the anti-apoptotic protein Bcl-2. The ability of BAD to interact with Bcl-2 and induce apoptosis is negatively regulated by BAD phosphorylation on Ser¹³⁶ and Ser¹⁵⁵, with Akt phosphorylating BAD on Ser¹³⁶. We found that cGMP increased BAD Ser¹⁵⁵ phosphorylation in intact osteocytes, and that PKG I phosphorylated this site in vitro. Experiments with phosphorylation-deficient BAD mutants demonstrated that the anti-apoptotic effects of cGMP and estradiol required BAD phosphorylation on Ser¹³⁶ and Ser¹⁵⁵.

In conclusion, estradiol protects osteocytes against apoptosis by activating the NO/cGMP/PKG cascade; PKG II is required for estradiol-induced activation of Erk and Akt, and PKG I α contributes to pro-survival signaling by directly phosphorylating BAD.

This study was funded by NIH R01 AR51300 (PI-R.B.Pilz) and T32HL007251 (N.M.)

Disclosures: Nisha Marathe, None.

SU0481

Flaxseed, Alone or Combined with Low-Dose Estrogen Therapy Has No Adverse Effect on Uterus Health in Ovariectomized Rats. Sandra Sacco^{*1}, Jessica J.M. Jiang², Lilian U. Thompson², Wendy Ward². ¹University of Toronto, Switzerland, ²University of Toronto, Canada

Background: The risk of adverse events associated with the use of standard-dose hormone therapy (conjugated equine estrogen + medroxyprogesterone acetate) may be reduced by using low-dose transdermal estrogen monotherapy (LD). Thus, LD may be appropriate for use by postmenopausal women with an intact uterus. Previously, we showed using ovariectomized (OVX) rats that flaxseed (FS), rich in phytoestrogen lignan and n-3 polyunsaturated fatty acids, protects against bone loss and deterioration of bone microarchitecture and strength at the lumbar vertebrae when combined with LD compared to either treatment alone. However, their combined effects on uterine tissue are unknown.

Objective: To determine the effects of FS combined with LD on markers of uterine health in OVX rats.

Study Design: 3 weeks following ovariectomy or SHAM surgery, 3-month-old female Sprague-Dawley rats (OVX, n=48; SHAM, n=12) were randomized to: 1) SHAM, 2) OVX, 3) OVX+FS, 4) OVX+LD or 5) OVX+FS+LD. Ground FS was added to the AIN-93M diet (100g/kg diet), and LD was delivered using a subcutaneous implant to deliver 0.42 μ g 17 β -estradiol/kg body weight per day, mimicking LD in postmenopausal women. After 12 weeks, uterus wet weight was determined and histological analyses of the luminal epithelium were performed to determine morphological characteristics and cell proliferation.

Results: As expected, SHAM had a significantly higher relative uterus weight (p<0.001) compared to all other groups. However, no significant differences in uterus weight were observed among OVX groups. Qualitative analyses demonstrated that luminal epithelia in the OVX group were flattened or cuboidal cells organized in a single layer while FS, LD and FS+LD treatments resulted in a single layer of elongated luminal epithelia that were columnar in shape. SHAM resulted in higher cell proliferation (p<0.05) of the luminal epithelium compared to the OVX, FS, LD and FS+LD groups. No other differences in cell proliferation were observed.

Conclusion: FS, alone and in combination with LD, does not affect uterine weight and cell proliferation at the luminal epithelium in the OVX rat model of postmenopausal osteoporosis. The observation that FS, alone and combined with LD, induces a small estrogen-like effect on the morphology of the luminal epithelium which is lower in magnitude to SHAM, suggests that FS both alone and combined with LD are not significant modulators of uterine carcinoma risk in this OVX rat model.

Disclosures: Sandra Sacco, None.

SU0482

Gender-Specific Effects of Estrogen and Androgen on Gene Expression in Human Monocyte-Derived Osteoclasts. Jun Wang¹, Paula Stern^{*2}. ¹Northwestern University, USA, ²Northwestern University Medical School, USA

Estrogen and androgen are both critical for the maintenance of bone, but the target cells, mechanisms and responses could be sex-specific. To compare sex-specific actions of estrogen and androgen on osteoclasts, human peripheral blood mononuclear precursor cells from adult Caucasian males (n=3) and females (n=3) were differentiated into osteoclasts and then treated for 24 hr with 10 nM 17 β -estradiol or testosterone. Gene expression was studied with a custom designed qPCR-based array containing 94 target genes related to bone and hormone action. In untreated osteoclasts, only 4 genes showed significant gender differences, with the largest difference being a 776-fold greater expression of the tumor necrosis factor family member APO2L in the cells from the male donors. Treatment with 17 β -estradiol significantly affected 12 genes in osteoclasts from females and 6 genes in osteoclasts from males. Fifteen of the 18 genes responsive to 17 β -estradiol were different in the cells from the two sexes, and 2 of the genes affected by 17 β -estradiol in both sexes were regulated oppositely in the male and female-derived cells. Among the genes most highly stimulated (greater than 100-fold) by 17 β -estradiol in the cells from the female donors were integrin alpha 1, osteonectin, caspase 2 and Fas ligand. None of these genes was significantly stimulated by 17 β -estradiol in the cells from the male donors. Fas was the most highly stimulated gene (greater than 2000-fold) by 17 β -estradiol in the cells from the male donors only. Testosterone treatment significantly affected 6 genes in osteoclasts from females and 2 genes in osteoclasts from males; all except one were different in the two sexes. Among the genes most highly stimulated (greater than 100-fold) by testosterone in the cells from the female donors only were transforming growth factor beta 3, phosphatase and tensin homolog (PTEN), and intercellular adhesion molecule 1 (ICAM1). The findings indicate that although osteoclasts from both sexes respond to both 17 β -estradiol and testosterone, the cells from the two sexes respond differently to each of the hormones. The apoptotic effects may be mediated differently. The results also suggest that there are aromatase-independent effects of testosterone on the osteoclasts that are not mimicked by 17 β -estradiol. An understanding of the sex-selective skeletal responses to other stimuli including therapeutic agents could lead to more personalized and efficacious therapy.

Disclosures: Paula Stern, None.

SU0483

Reduced Bone Mass and Muscle Strength in Male 5 α -Reductase Type 1 Inactivated Mice. Sara Windahl¹, Klara Sjogren^{*2}, Niklas Andersson³, Anna Borjesson¹, Charlotte Swanson², Johan Svensson², Sofia Moverare Skrtic⁴, Marie Lagerquist⁵, Claes Ohlsson⁶. ¹Center for Bone & Arthritis Research, Sahlgrenska Academy, Sweden, ²Centre for Bone & Arthritis Research, Sweden, ³Sahlgrenska University Hospital, Sweden, ⁴Center for Bone & Arthritis Research at the Sahlgrenska Academy, Sweden, ⁵Center for Bone & Arthritis Research, Sweden, ⁶Center for Bone Research At the Sahlgrenska Academy, Sweden

Androgens are important regulators of bone mass but the relative importance of testosterone (T) versus dihydrotestosterone (DHT) for the activation of the androgen receptor (AR) in bone is unknown. 5 α -reductase is responsible for the irreversible conversion of T to the more potent AR activator DHT. There are two well established isoenzymes of 5 α -reductase (type 1 and type 2), encoded by separate genes (*Srd5a1* and *Srd5a2*). 5 α -reductase type 2 is predominantly expressed in male reproductive tissues whereas 5 α -reductase type 1 is highly expressed in liver and moderately expressed in several other tissues including bone. The aim of the present study was to investigate the role of 5 α -reductase type 1 for bone mass and muscle using *Srd5a1*-/- mice.

Four-month-old male *Srd5a1*-/- mice had reduced trabecular bone mineral density (-36%, p<0.05) and cortical bone mineral content (-15%, p<0.05) but unchanged serum androgen levels compared with wild type (WT) mice. The cortical bone dimensions were reduced in the male *Srd5a1*-/- mice as a result of a reduced cortical periosteal circumference compared with WT mice. T treatment increased the cortical periosteal circumference (p<0.05) in orchidectomized WT mice but not in orchidectomized *Srd5a1*-/- mice. Male *Srd5a1*-/- mice demonstrated a reduced forelimb muscle grip strength compared with WT mice (p<0.05). Female *Srd5a1*-/- mice had slightly increased cortical bone mass associated with elevated circulating levels of androgens.

In conclusion, 5 α -reductase type 1 inactivated male mice have reduced bone mass and forelimb muscle grip strength and we propose that these effects are due to the lack of 5 α -reductase type 1 expression in bone and muscle. In contrast, the increased cortical bone mass in female *Srd5a1*-/- mice, is an indirect effect mediated by elevated circulating androgen levels.

Disclosures: Klara Sjogren, None.

SU0484

24,25(OH)₂ Vitamin D Levels Are Elevated in Dialysis Patients. Marta Christov^{*1}, Nigel Clarke², Richard Reitz², Julia Wenger¹, Ravi Thadhani¹, Harald Jueppner¹. ¹Massachusetts General Hospital, USA, ²Quest Diagnostics, Inc., Nichols Institute, USA

25(OH) vitamin D (25D) deficiency is common in patients with chronic kidney disease (CKD) and in patients treated with dialysis, and this deficiency may contribute to the adverse outcomes observed in these cohorts. In addition, in these groups of patients increased FGF23 levels are thought to inhibit the renal 1- α hydroxylase and stimulate the 24-hydroxylase thus contributing to diminished 1,25(OH)₂ vitamin D (1,25D) levels and to the development of secondary hyperparathyroidism. Recent data suggest the presence of increased amounts of the vitamin D catabolic enzyme 24 hydroxylase (CYP24) in the kidney of humans and animals with CKD, which may contribute to both 25D deficiency (by direct modification and subsequent metabolism into inactive analogs) as well as 1,25D deficiency (by "siphoning off" of the precursor 25D and direct modification of 1,25D). The absolute levels of 24,25(OH)₂ vitamin D (24,25D) in the CKD/dialysis population, and thus the level of 24-hydroxylase activity, are unknown. Using a novel mass spectrometry approach, we measured 24,25D levels in the circulation of 120 individuals with no known renal dysfunction and 60 patients initiating hemodialysis. In the controls, 24,25D levels were correlated with 25D status, i.e. individuals with lower total 25D levels had lower 24,25D levels. For example, the mean 24,25D level in individuals with 25D levels <20 ng/mL was 1.270.3 ng/mL (meanSEM), while in individuals with 25D levels >30 ng/mL it was 6.10.56 ng/mL (meanSEM). In the dialysis population the ratio of 24,25D to 25D levels was significantly elevated; patients with baseline 25D levels <20 ng/mL had an increased 24,25D level of 9.01.26 ng/mL (meanSEM), at times rising above the absolute 25D level in individual patients. 24,25D levels correlated positively with 25D, calcium and albumin. Treatment with an active vitamin D analog did not increase 24,25D levels and neither did the dialysis procedure itself. Given that FGF23 is a strong inducer of the 24-hydroxylase, studies to assess the correlation between 24,25D and FGF23 levels are ongoing. In summary, 24,25D levels in dialysis patients are increased compared with those in the control population, which may reflect increased 24-hydroxylase activity and contribute to 25D deficiency.

Disclosures: Marta Christov, None.

SU0485

An Immunoassay for Free 25 Hydroxy Vitamin D. Mike Martens^{*1}, Frans Rosmalen², Leon Swinkels¹, Erik Harbers³, George Parsons⁴. ¹Future Diagnostics, The Netherlands, ²Future Diagnostics BV, The Netherlands, ³Future Diagnostics, Netherlands, ⁴Parsons Group LLC, USA

The objective of this study was to develop an immunoassay for free 25 Hydroxy Vitamin D [25(OH)VitD]. Binding proteins for 25 Hydroxy Vitamin D₂ and D₃ are altered by some of the same factors that control thyroid hormone binding protein levels. Pregnancy and oral contraceptive use increase both thyroid and 25(OH)VitD binding proteins and the corresponding total analyte concentrations may give misleading results. Liver disease decreases both thyroid and 25 (OH)VitD binding protein levels and total 25(OH)VitD. Total 25(OH)VitD levels may underestimate vitamin levels. End stage renal disease and dialysis also represent interesting challenges for measurement of free versus total 25(OH)VitD.

Binding protein levels may play an important role in 25(OH)VitD bioavailability, and current assays destroy that information with sample pretreatment steps before the actual assay begins.

Our novel Free 25(OH)VitD assay captures information on both the total 25(OH)VitD levels and the serum binding protein status in a simple, easily automatable format. Antibodies reactive with 25(OH)VitD are immobilized on traditional solid phases such as microtiter wells or superparamagnetic particles. Standards, controls and patient samples are exposed to these antibodies in a simple buffer and allowed to react. Free 25(OH)VitD is captured on the antibody and accumulated during a 90-minute incubation. The solid phase is then washed and a labeled analog of 25(OH)VitD is allowed to react with the remaining antibody in a second incubation. This incubation is followed by another wash and quantitation of the signal, which is inversely proportional to the level of free 25(OH)VitD in the sample. The assay was calibrated against a symmetric dialysis method.

Measurements of free 25(OH)VitD in samples from third trimester pregnancy confirmed a significantly higher total 25(OH)VitD than in controls. The free 25(OH)VitD in these subjects was comparable or even lower than in controls.

We have developed a free 25(OH)VitD assay capable of determining the actual Vitamin D status in critical patient groups.

Disclosures: Mike Martens, Future Diagnostics, 4; Future Diagnostics, 3

SU0486

Immunoassay for 25 hydroxy vitamin D. Leon Swinkels^{*1}, Antwan Maas², Mike Martens¹, Frans Rosmalen³. ¹Future Diagnostics, The Netherlands, ²Future Diagnostics, Netherlands, ³Future Diagnostics BV, The Netherlands

The objective of this study was to develop an immunoassay for 25(OH)Vitamin D [25(OH)VitD]. About 85% of the circulating 25(OH)VitD is bound to Vitamin D binding Protein (DBP) with a relatively high affinity. The accuracy of 25(OH) Vitamin D measurement in serum by immunoassay depends among others on the efficiency of the release of endogenous 25(OH)Vit D from DBP.

There are several approaches to eliminate the effect of DBP in the assay for 25 (OH)Vit D. Organic solvents may be used to solubilize and separate 25(OH)Vit D from its binding protein. For this purpose ethanol can be used, but this method requires centrifugation of the denatured protein and therefore is not suitable for automation. Methods that do not require a separation step, may rely on competitive displacement using compounds such as Anilino Sulfonic Acid (ANS), or on displacement of bound 25(OH)Vit D by lowering the pH.

We propose an alternative method for the release of 25(OH)Vit D based on fluoro-alkyl surfactants. We used an antibody that recognized 25(OH)Vit D₂ as well as 25 (OH)Vit D₃.

The surfactant effectively releases 25(OH)Vit D from DBP. The efficacy of the release was compared with the efficiency of displacement using a combination of methanol and ANS. The displacement was monitored using 3H-25(OH)Vit D. The apparent residual binding was less using the fluoro-alkyl surfactant than with methanol/ANS.

The results of the assay using the alternative release composition were compared with the results obtained by LCMS. A good correlation was observed (r=0.945, n=40, range 6-60 ng/ml).

We conclude that this alternative release approach is an effective, easily automatable method for the assay of 25(OH)Vit D.

Disclosures: Leon Swinkels, future diagnostics, 3

SU0487

Mechanisms Involved in Altered Calcium Homeostasis in the Klotho Knockout Mouse. Leila J. Mady^{*1}, Puneet Dhawan², Angela Porta³, Makoto Kuro-o⁴, Sylvia Christakos¹. ¹University of Medicine & Dentistry & New Jersey - New Jersey Medical School, USA, ²UMDNJ, USA, ³Kean University, USA, ⁴The University of Texas Southwestern Medical Center at Dallas, USA

Klotho is a multifunctional protein and cofactor for FGF23 involved in phosphate and calcium homeostasis. A premature aging phenotype has been described in klotho deficient mice. Klotho knock out (KO) mice have increased serum calcium, renal 1 α (OH)ase and serum 1,25(OH)₂D₃ and decreased serum PTH. In klotho KO mice upregulation of 24(OH)ase by 1,25(OH)₂D₃ is significantly reduced by 6 weeks of age. To understand the mechanisms of the premature aging phenotype we examined genes and transcription factors involved in calcium homeostasis and the activity of VDR and VDR coactivators by in vivo ChIP. Since studies from our lab indicate that CARM1 [a methyltransferase that methylates histone 3 at arginine 17 (H3R17)] is a coactivator with VDR of 24(OH)ase transcription and ChIP-seq analysis identified 1,25(OH)₂D₃ dependent genome wide co-occurrence of VDR binding and H3R17 methylation in kidney cells, in vivo ChIP assays were done examining VDR binding and H3R17 methylation in response to 1,25(OH)₂D₃. In vivo ChIP revealed a significant 2-4 fold decrease in VDR binding and H3R17 methylation at the 1,25 (OH)₂D₃ regulatory regions of the 24(OH)ase gene in kidney of 6 week old klotho KO mice compared to WT mice and aging 50 week old mice respectively, suggesting that in kidney prolonged exposure to high levels of 1,25(OH)₂D₃ results in desensitization to 1,25(OH)₂D₃. In klotho KO mice we also found a significant decrease in renal C/EBP β (3 fold compared to WT). Since C/EBP β is a transcription factor that inhibits 1 α (OH)ase transcription, our findings suggest that decreased renal C/EBP β is one factor involved in the increase in 1 α (OH)ase in klotho KO mice. In klotho KO mice intestine there is an induction of TRPV6 and calbindin-D_{9k} and an increase in intestinal calcium absorption. Calbindin-D_{9k} is increased in all regions of the intestine (6-46 fold compared to WT; highest induction in ileum, cecum and colon). In vivo ChIP in the klotho KO mouse intestine indicates enhanced binding of cdx2 at the cdx2 regulatory regions in the calbindin-D_{9k} gene. In the aging 50 week old mouse there is a marked decline in calbindin and in intestinal calcium absorption. These findings, which indicate that the mechanisms involved in the phenotype of klotho KO mice are in contrast to changes observed in aging mice, highlight the importance of klotho in the regulation of calcium homeostasis and provide new insight into molecular mechanisms related to the phenotype of the klotho KO mouse.

Disclosures: Leila J. Mady, None.

SU0488

Multiple Sclerosis and Chronic Diseases Is More Frequent in Young Adults Born in Summer Versus Winter – An Effect of Vitamin D Status?. Susanna Streyms Thomsen*, Lars Rejnmark, Leif Mosekilde, Peter Vestergaard. Aarhus University Hospital, Denmark

Background: Development of diseases such as type 1 diabetes mellitus (T1D), infections and multiple sclerosis (MS) is believed to result from the interaction between imprinting of genes and environmental factors, including vitamin D status at the time of conception, intrauterine growth or time of birth. Vitamin D status is among other factors dependent on maternal exposure to sunlight and therefore dependent on season of the year.

Hypothesis: Occurrence of later diseases such as T1D, infection and MS is influenced by time of gestation or time of birth.

Aim: To investigate relations between T1D, infections, MS and season of gestation and intrauterine growth in people living in Denmark.

Design: Cohort studies in Denmark using 3 birth cohorts followed until December 31, 2009.

Material and Methods: Data were obtained from 1) all children born in 1940 (n=72.839), 2) all children born in 1977 (n=89.570) and 3) all children born in 1996 (n=74.015). Information on death and migrations were obtained from the central person register along with all contacts to hospitals (1977-2009) which were obtained from the National Hospital Discharge Register. The main exposure variable was month of birth (subdivided into: summer, i.e. April-September and winter, i.e. October-March) and the main outcome variable was occurrence of T1DM, occurrence of MS, or hospitalization due to infections.

Statistical analyses were done using one sided Fishers Exact test and Kaplan-Meier survival plots using IBM SPSS version 19.

Results: There were no associations between T1D or infection in terms of time of birth in any of the three birth cohorts. There was an association between MS and time of birth, as 60.2% (n=62) with the diagnosis of MS was born in summertime and 39.8% (n=41) were born in wintertime (p=0.046) in the 1977 cohort. Fig. 1 shows the Kaplan-Meier survival curve, diseases of free survival. However, no association between time of birth and MS was present in the 1940 cohort. In the 1996 cohort, too few cases of MS were present for analysis.

Conclusion: MS in subjects less than 35 years of age may be related to season of birth and thus maternal vitamin D exposure. In subjects older than 35 years (the 1940 cohort, which was followed from 1977 and onwards) the effect of season could not be confirmed. Decreased exposure to sun in the winter time leading to low vitamin D levels during pregnancy is a possible explanation and this needs further research.

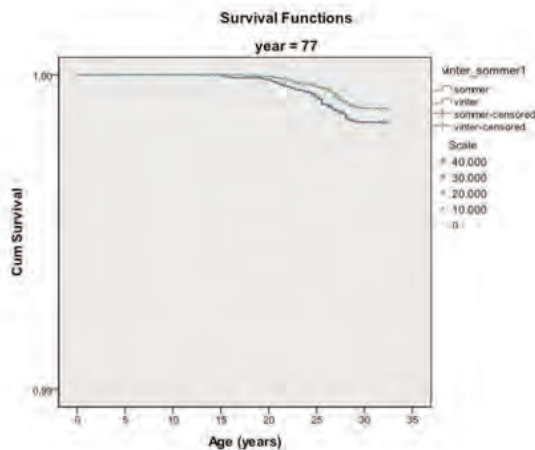


Fig 1: Kaplan-Meier survival curve

Disclosures: *Susanna Streyms Thomsen, None.*

SU0489

Novel Mechanism of Negative Regulation of 1,25-Dihydroxyvitamin D₃ Induced 24(OH)ase Transcription: Epigenetic Modification Involving Cross-talk Between Protein Arginine Methyltransferase 5 and the SWI/SNF Complex. Sneha Joshi*¹, Tanya Seth², Puneet Dhawan³, Said Sif⁴, Sylvia Christakos². ¹UMDNJ-NJMS, USA, ²University of Medicine & Dentistry & New Jersey - New Jersey Medical School, USA, ³UMDNJ, USA, ⁴Ohio State University, USA

The mammalian SWI/SNF chromatin remodeling complex facilitates gene transcription by remodeling chromatin using the energy of ATP hydrolysis. Each SWI/SNF contains two homologous ATPases, BRG-1 and BRM. Recent studies have indicated an interplay between histone modifying enzymes and chromatin remodeling factors. Among the histone modifying enzymes are the protein arginine methyltransferases (PRMTs) which have been implicated in transcriptional activation or repression. Little is known however about the role of SWI/SNF and PRMTs in vitamin D receptor (VDR) mediated transcription. Using SW13 and C33A cells, which are deficient in BRM and BRG-1, we found that 1,25(OH)₂D₃ induction of 24(OH)ase transcription is markedly reduced (6 – 10 fold), suggesting that the SWI/SNF complex is an important component of VDR mediated transcription. Activation of transcription was restored in these cells preferentially by BRG-1. In UMR osteoblastic cells the N-terminal region of BRG-1 (BRG-1-N), that acts as a dominant negative inhibitor, inhibits 1,25(OH)₂D₃ induction of 24(OH)ase expression 2 fold as indicated by Western blot analysis. Mutant BRG-1 also inhibits C/EBPβ enhancement of VDR mediated 24(OH)ase transcription and expression. Immunoprecipitation assays indicate that BRG-1 associates with C/EBPβ. Chromatin immunoprecipitation assays show that C/EBPβ and BRG-1 bind simultaneously to the 24(OH)ase promoter. BRG-1 enhancement of VDR mediated transcription is not observed using a 24(OH)ase promoter construct with the C/EBP site mutated. Here we further show that PRMT5, a type II PRMT that dimethylates histone 3 at arginine 8 (H3R8) and histone 4 at arginine 3 (H4R3) inhibits BRG-1 and C/EBPβ enhancement of 1,25(OH)₂D₃ induced 24(OH)ase transcription. In the presence of PRMT5 (100ng) the 3 fold enhancement of VDR mediated 24(OH)ase transcription observed in the presence of BRG-1 and the 5 fold enhancement in the presence of both BRG-1 and C/EBPβ (100ng each) are inhibited. 1,25(OH)₂D₃ induction of 24(OH)ase transcription is also inhibited (2 fold) by PRMT5 (p<0.05 transcriptional activation in the presence or absence of PRMT5). Using a catalytically inactive PRMT5 (methylation of H3 and H4 is lost) negative regulation of 24(OH)ase transcription is not observed. ChIP assays show that PRMT5 associates with BRG-1 at the C/EBP site. These studies define epigenetic events linked to a novel mechanism of negative regulation of VDR mediated transcription.

Disclosures: *Sneha Joshi, None.*

SU0490

Role of TAF12 in the Increased VDR Activity in Paget's Disease of Bone. Jumpei Teramachi¹, Huiling Cao¹, Jolene Windle², G. David Roodman³, Noriyo Kurihara¹. ¹University of Pittsburgh & The Center for Bone Biology at UPMC, USA, ²Virginia Commonwealth University, USA, ³University of Pittsburgh, The Center for Bone Biology at UPMC, & VA Pittsburgh Healthcare System, USA

We reported that osteoclast precursors (OCL-P) from Paget's (PD) patients expressing measles virus nucleocapsid protein (MVNP) are hypersensitive to 1,25-(OH)₂D₃ (1,25-D₃) and form OCLs at physiologic rather than pharmacologic levels of 1,25-D₃. The increased 1,25-D₃ sensitivity was mediated by TAF12, a coactivator of VDR, which is expressed at higher levels in PD OCL than normals. These results suggest TAF12 plays an important role in the abnormal OCL activity in PD. We then generated transgenic mice in which TAF12 expression is targeted to the OCL lineage (TAF12 mice). OCL-P from TAF12 mice formed OCL at very low levels of 1,25-D₃, and had a similar responsiveness to RANKL as wild type (WT) mice. However, TAF12-OCL-P did not form hyper-multinucleated OCL characteristic of PD. In contrast, inhibition of TAF12 with a specific TAF12 antisense construct decreased OCL formation and OCL-P sensitivity to 1,25-D₃ in PD bone marrow samples. Thus, TAF12 plays an important role in induction of the 1,25-D₃ hypersensitivity of OCL-P from PD patients. However, the molecular mechanisms underlying both 1,25-D₃'s effects on OCL formation and the contribution of TAF12 to these effects in both normals and PD patients are undefined. Therefore, we performed ChIP analysis, using an anti-TAF12 antibody, and demonstrated TAF12 binds the 24-hydroxylase (Cyp24a1) promoter, which contains two functional VDREs in the presence of 1,25-D₃. Since TAF12 in kidney cells directly interacts with ATF7 and potentiates ATF7-induced transcriptional activation of ATF7-driven genes, we determined if TAF12 is a functional partner of ATF7 in OCL-P. Interestingly, ATF7 was also increased in OCL-P from mice expressing MVNP in their OCL. ATF7 expression was detected in OCL-P lysates from MVNP mice and was not further increased by 1,25-D₃. Expression of TAF4 was not affected by MVNP. Immunoprecipitation of lysates from either WT or MVNP expressing OCL-P with an anti-TAF12 antibody and blotting with an anti-ATF7 antibody or vice versa revealed that TAF12 and ATF7 physically interact in OCL-P. Importantly, TAF12-dependent ATF7-regulated transcriptional activation was inhibited by TAF4, which binds both ATF7 and TAF12. We also showed that knockdown of ATF7 decreased Cyp24 sensitivity to 1,25-D₃ as well as TAF12 levels in MVNP-expressing cells. These results show that

ATF7 interacts with TAF12 and may be involved in the upregulation of TAF12 and the hypersensitivity of OCL-P to 1,25-D₃ in PD.

Disclosures: *Junpei Teramachi, None.*

SU0491

Serum 25OHD Changes Following High Rates of Sun Exposure in Young Subjects with Pigmented Skin Living in the Tropics. Estela Carvalho¹, Amanda Melo¹, Lara Voss¹, Daniele Fontan², Narriane Holanda³, Francisco Bandeira^{*4}. ¹Agamenon Magalhaes Hospital, Brazil, ²Brazil, ³Agamenon Magalhaes Hospital, Bra, ⁴UPE, Brazil

Objective: To Evaluate the changes in serum 25OHD levels after prolonged (from 6-10 am) sunlight exposure :in 10 healthy subjects (7 females and 3 males, mean age 33.7.4 years, body mass index(BMI) 23.7. 3.32 kg/m², with a exposed body surface area of 73.8. 22.7%, mean of PTH levels 47.9933.69, mean of calcium levels 9.520.43, mean of albumin levels 4.210.24, mean of creatinine levels 0.790.17) who were evaluated on beaches along the coast of Recife(8°S). Regarding the skin phototype(Fitzpatrick classification), 80% had type 3 or more. **Methods:** Anthropometric data and information on skin phototype and sun exposure x fraction of body surface area exposed (BSA) were collected and, serum 25OHD was measured before and after sunlight exposure without sunscreen. **Results:** The mean estimated irradiance at the 4h period was 4.0602.107 watts/m². Mean serum 25OHD increased from 22.595.45 ng/ml to 24.396.60 ng/ml(p<0.05) at the end of 4h period; and to 25.80 5.81 ng/ml one week after sun exposure(NS). **Conclusion:** Although statistically significant, the changes in serum 25OHD levels were minimal in absolute terms (mean of 3ng/ml) for the very large amount of UV received. Considering the harmful effects of this amount of sun exposure on skin health, our data demonstrated that oral vitamin D supplementation may be a preferable approach to achieve optimal serum 25OHD concentration.

Disclosures: *Francisco Bandeira, None.*

SU0492

The Efficacy of High-Dose Oral Vitamin D₃ Administered Once a Year: Is the Increased Risk of Falls Attributable To Changes in Muscle Strength? Kerrie Sanders^{*1}, Amanda L Stuart¹, Elizabeth J Williamson¹, Julie A Simpson¹, Mark Kotowicz², Geoffrey Nicholson³. ¹University of Melbourne, Australia, ²Barwon Health, Australia, ³The University of Queensland, Australia

We have previously reported an increased rate of falls and fractures in a RCT using a single annual dose of 500,000IU cholecalciferol administered orally to 2,256 older women in fall or winter for 3 to 5 years¹. The increased rate of falling in the vitamin D group was higher in the first 3 months following dosing (p=0.017) suggesting an adverse mechanism in the immediate post-dose period. Serial biochemistry and physical assessments were done on a sub-study of 97 randomly selected participants. Serum 25-hydroxyvitamin D (25D) was measured using DiaSorin immunoassay. Muscle strength was measured at the hip flexion, quadriceps and hip abduction using a NicholasTM Manual Muscle Tester and is reported at 3-month post dose, ≥2 years after recruitment. The peak force (kg) required to break an isometric muscle contraction was measured as the examiner applied force against the participant. For each participant 3 trials were performed and averaged for each muscle group.

The median baseline serum 25D was 49nmol/L. The vitamin D group, 1-, 3- and 12-month median post dose levels were 124, 93 and 62nmol/L, respectively. Our post-hoc analysis used a linear regression model for hip flexion strength at 3-months post-dose and included age, baseline strength and change in 25D as covariates. The analysis was stratified by whether or not the change in 25D was more than 150% of the baseline serum 25D. For the group with smaller increases in 25D (<150%), increases in 25D were associated with progressively increased hip flexion strength whereas the group with larger increases in 25D (>150%) were associated with decreasing strength (estimated mean change in hip flexion strength associated with a 10 nmol/L unit increase in 25D = 0.38 kg {95% CI: 0.1, 0.7} vs -0.26 kg {95% CI: -0.6, 0.06}; Group<150% vs Group>150% increase in 25D, respectively). There was heterogeneity of the two effects (p=0.003). For quadriceps and hip abduction, the direction of effects in the two strata followed similar patterns, but the p-values for heterogeneity were not significant.

These findings suggest a threshold effect of vitamin D status and are consistent with a U-shaped association reported between frailty status and 25D levels². Analysis of muscle biomarkers and vitamin D metabolites will further progress our understanding of a mechanism underlying the occurrence of increased falls following annual high-dose vitamin D supplementation.

¹Sanders KM et al, JAMA 2010

²Ensrud KE et al, JCEM 2010

Disclosures: *Kerrie Sanders, None.*

SU0493

The Vitamin D Analog Eldecalcitol (ED-71) Is a Potent Regulator of Intestinal Phosphate Absorption and NaPi-IIb. Alex Brown^{*1}, Cynthia Ritter². ¹Washington University in St. Louis School of Medicine, USA, ²Washington University School of Medicine, USA

The vitamin D analog eldecalcitol [1α,25-dihydroxy-2β-(3-hydroxypropyloxy) vitamin D3] has been developed for treatment of osteoporosis. We have previously reported that this analog has greater potency than calcitriol, the natural vitamin D hormone, on intestinal calcium and phosphate (Pi) absorption. In the present study, we further investigated the actions of eldecalcitol on Pi absorption and induction of the intestinal sodium/phosphate cotransporters. Vitamin D-deficient rats were treated orally with 0, 20, 50 or 150 pmol of eldecalcitol or calcitriol q.o.d. for 12 days. Serum phosphate levels rose slightly, but not significantly, with eldecalcitol, while they were unchanged by calcitriol. Duodenal Pi absorption, measured by the in situ loop method, was increased maximally by 8-fold increase with the 20 pmol dose of eldecalcitol, while none of the doses of calcitriol were effective. This action of eldecalcitol was attributable to a dramatic 24-fold induction of NaPi-IIb (SLC34A2) mRNA in the duodenum; Pit-1 (SLC20A1) and Pit-2 (SLC20A2) mRNA levels were not increased. An additional experiment with a shorter treatment period confirmed the induction of NaPi-IIb mRNA in the duodenum and jejunum, but not the ileum, while calcitriol was ineffective in all segments. Surprisingly, lung NaPi-IIb was not increased by eldecalcitol, despite its co-expression with the VDR in alveolar type II cells. These studies indicated that chronic oral administration of eldecalcitol potentially stimulates intestinal Pi absorption via induction of NaPi-IIb. Further investigation of the mechanism for the induction, and cell specificity, is underway.

Disclosures: *Alex Brown, Chugai Pharmaceuticals, 2*

This study received funding from: Chugai Pharmaceuticals

SU0494

The Association Between Mortality and Vitamin D Levels is U-shaped: A Study from the Primary Health Care, Denmark. Darshana Durup^{*1}, Henrik J Jørgensen², Peter Schwarz³, Anne-Marie Heegaard¹, Bent Lind⁴. ¹Faculty of Pharmaceutical Sciences, University of Copenhagen, Denmark, ²Department of Clinical Biochemistry, Bispebjerg Hospital, Denmark, ³Glostrup Hospital, Denmark, ⁴Copenhagen General Practitioners Laboratory, Denmark

Aim

The aim of this investigation was 1) to determine the prevalence of vitamin D deficiency and secondary hyperparathyroidism (SHPT); 2) to investigate the association of mortality with the levels of 25-hydroxyvitamin D (25(OH)D), calcium and parathyroid hormone (PTH) in the primary health care

Methods

Vitamin D results from 247,546 subjects referred from the general practitioners in the Copenhagen area (population 1.1 mill) and s-PTH (n=34,990) and s-calcium (n=111,524) results from the subjects were included in the study. Blood samples were collected from 2004 to 2010. The 3-year mortality associated with SHPT was studied by Kaplan-Meier analysis. The association between 3-year mortality and 25-hydroxy vitamin D, calcium and PTH serum levels was graphed and the odds ratios were calculated. The study protocol was approved by the Danish Data Protection Agency

Results

The prevalence of vitamin D deficiency, based on serum 25-hydroxyvitamin D (s-25(OH)D), were as follows; s-25(OH)D < 50 nmol/L: 53.3 %; s-25(OH)D < 25 nmol/L: 20.5 %; and s-25(OH)D < 12.5 nmol/L: 5.4 %. Mean age was 50.8 (females) and 51.4 years (males). 11.08% suffered from SHPT (n=29,939). Analysis of mortality as a function of serum 25(OH)D, calcium (s-calcium) and PTH (s-PTH) levels showed a U-shaped association for all three parameters. The lowest mortality was observed in subjects with s-25(OH)D ranging 60-70 nM. When compared to the overall mortality at the 60 nM s-25(OH)D level, the odds ratios were 1.78 for 25(OH)D levels ≤10nM and 1.86 for levels ≥140 nM. The corresponding numbers for subjects above 60 years of age (n=91,195) were 2.82 and 2.22, respectively. When compared to the overall mortality at the 4 pM serum PTH level, odds ratios were 2.62 for serum PTH levels ≤1 pM and 7.32 for levels ≥14 pM. When compared to the overall mortality at the 2.4 mM serum calcium level, odds ratios were 18.75 for levels ≤2 mM and 4.63 for levels ≥2.7 mM

Conclusion

In the general population vitamin D deficiency was not only prevalent (53.3%), but also severe; 11.2 % of the vitamin D deficient subjects also suffered from SHPT. Both high and low serum levels of 25(OH)D, calcium and PTH were associated with increased mortality. Attention must be paid to this U-shaped correlation.

Further investigations specifically aimed at elucidating causal relationships between s-25(OH)D and mortality and morbidity are needed to make recommendations more evidence-based.

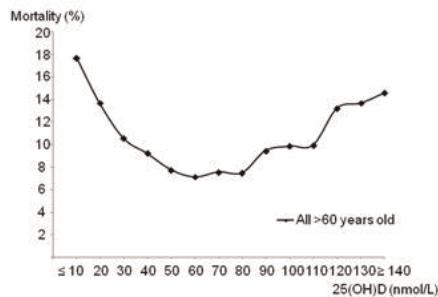


Fig 1: Association of 25-hydroxyvitamin D (25(OH)D) serum levels with mortality.

Disclosures: Darshana Durup, None.

SU0495

Vitamin D Binding Protein and Monocyte Responsivity to 25-hydroxyvitamin D and 1,25-Dihydroxyvitamin D: Analysis by Mathematical Modeling. Rene Chun^{*}¹, Brad Peercy², Arthur Sherman³, John Adams⁴, Martin Hewison⁵.
¹Orthopedic Hospital Research Center UCLA, USA, ²Dept. Mathematics & Statistics, University of Maryland at Baltimore County, USA, ³NIDDK - LBM - Math Cell Modelling Section, USA, ⁴University of California, Los Angeles, USA, ⁵UCLA, USA

Studies *in vitro* have shown that vitamin D can regulate many biological activities. However, the relevance of these activities is unclear because binding of both 25-hydroxyvitamin D (25OHD) and 1,25-dihydroxyvitamin D (1,25(OH)₂D) to the serum vitamin D binding protein (DBP) will be greater *in vivo* than in cell culture. We hypothesize that DBP is a key determinant of the tissue bioavailability of 25OHD and its subsequent metabolism to 1,25(OH)₂D by the enzyme 1 α -hydroxylase (CYP27B1). DBP exists in allelic forms (GC1F, GC1S, GC2) that circulate at different levels (GC1F>GC1S>GC2) and exhibit differing affinities for vitamin D metabolites (GC1F>GC1S>GC2). To predict the impact of DBP level/genotype on biological activity *in vivo*, we developed a 'steady state' mathematical model to estimate levels of free 25OHD and 1,25(OH)₂D under different DBP conditions. Results with this model show that in 100% serum with 50 nM 25OHD and 100 pM 1,25(OH)₂D, <0.05 nM 25OHD (0.1%) and <1.5 pM 1,25(OH)₂D (1.5%) are 'free'. Levels of free 25OHD and 1,25(OH)₂D increase 3-fold from GC1F/1F to GC2/2 given the same total ligand concentrations. To explore the biological impact of DBP, a 'dynamic' mathematical model was generated incorporating localized CYP27B1 activity and binding of 1,25(OH)₂D to the vitamin D receptor (VDR). This model was based on published biochemical data and *in vitro* data for 25OHD/1,25(OH)₂D-mediated induction of the antibacterial cathelicidin gene product (CAMP) in human monocytes. Using this model, we predicted the induction of CAMP expression *in vivo* under various activation parameters relative to DBP levels and genotype. Induction of CAMP was minimal in unactivated conditions. However, enhanced expression of VDR (5-fold) and CYP27B1 (10-fold) supported 25OHD-mediated induction of CAMP (greater than 5-fold). Intracellular metabolism of 25OHD to 1,25(OH)₂D (opposed to exogenous 1,25(OH)₂D) was the most viable mode for vitamin D-mediated induction of CAMP *in vivo*. As with the 'steady state' model, the 'dynamic' model predicted *in vivo* induction of CAMP by 25OHD would be lower for high affinity forms of DBP (e.g. GC1F). These new models underline the importance of DBP as a determinant of vitamin D 'status.' In particular, DBP affinity data have implications for circulating 25OHD and 1,25(OH)₂D levels and subsequent vitamin D supplementation strategies in patients with specific DBP genotypes.

Disclosures: Rene Chun, None.

MO0001

Analyses of Gene Expression in hMSC Indicate Age-Associated Loss of Self-Regeneration and Function. Peggy Benisch^{*1}, Sonke Frey², Lothar Seefried¹, Ludger Klein-Hitpass³, Moustapha Kassem⁴, Regina Ebert⁵, Franz Jakob¹. ¹University of Würzburg, Orthopedic Center for Musculoskeletal Research, Germany, ²Hospital University Würzburg, Department of Trauma-, Hand-, Plastic- & Reconstructive Surgery, Germany, ³Hospital University Essen, Institute of Cell Biology, Germany, ⁴Odense University Hospital, Denmark, ⁵University of Würzburg, Orthopedic Center for Musculoskeletal Research, Germany

Mesenchymal stem cells represent the basis of bone formation, because as multipotent cells they can differentiate into many cell types important for bone homeostasis, e.g. osteoblasts. During aging an imbalance between bone formation and bone resorption occurs, which results in reduced bone mass. It is still unclear whether MSC biology is directly involved in reduced bone formation associated with age or osteoporosis, e.g. by accumulating malfunctions or by entering replicative senescence.

In this study, age-associated changes in gene expression of human MSC (hMSC) were determined by performing microarray hybridizations and data analyses with SAM. RNA of hMSC isolated from patients of old age (+ 80 years) was compared to control hMSC from patients of younger age (45-57 years). Moreover, the gene expression patterns of *in vitro* aged, senescent hMSC was compared to the pattern of hMSC from patients of old age to perform a comparison between *ex-vivo* and *in vivo* aging. Human MSC of patients diagnosed with primary osteoporosis were also examined because osteoporosis is a polygenetic disease of aged bone.

Systems biology based interpretation of the microarray data revealed that senescent hMSC, *in vivo* aged hMSC as well as hMSC from patients with osteoporosis showed deficiency in proliferation, differentiation capacity and migration despite the fact that all three hMSC populations exhibited only few similarities in gene expression pattern. Genes that were lower expressed (42 in total) in all three different hMSC populations were linked to chromosome condensation and DNA repair.

Furthermore, in hMSC from patients with osteoporosis we detected genes responsible for enhanced osteoclastogenesis (CSF1, COX2, ANGPTL4) and promising candidates for osteoporosis with respect to inhibition of osteogenesis. SOST as an inhibitor for WNT signaling, as well as MAB21L2 as an inhibitor for BMP signaling were higher expressed in those cells.

In summary, our findings suggest that *in vivo* aging does not necessarily result in senescent stem cells, because the aging of an organism is a multicellular process, which is influenced by many other factors, e.g. accumulation of mutations and tumor defense. Furthermore reduced bone formation in osteoporosis could be connected to autoinhibition of the stem cells, as well as reduced differentiation capacity and migration. We can hypothesize that hMSC serve less efficiently as a regenerative source for osteogenesis in aged-associated bone loss.

Disclosures: Peggy Benisch, None.

MO0002

Borage and Fish Oils Lifelong Supplementations Decrease Inflammation and Improve Bone Health in a Murine Model of Senile Osteoporosis. Fabien Wauquier^{*1}, Laurent Leotoing², Claire Philippe², Elisabeth Miot Noiraull³, Veronique Coxam⁴, Yohann Wittrant⁵. ¹INRA, UMR 1019, UNH, CRNH Auvergne, F-63009 Clermont-Ferrand, France, France, ²INRA, France, ³INSERM, France, ⁴INRA Theix, France, ⁵Institut National de la Recherche Agronomique, France

Fats are prevalent in western diets; they have known deleterious effects on muscle insulin resistance and may contribute to bone loss. However, relationships between fatty acids and locomotor system dysfunctions in elderly population remain controversial. The aim of this study was to analyze the impact of fatty acid quality on the age related evolution of the locomotor system and to understand which aging mechanisms are involved. In order to analyze age related complications, the SAMP8 mouse strain was chosen as a progeria model as compared to the SAMR1 control strain. Then, two months old mice were divided in different groups and subjected to the following diets : (1) standard "growth" diet - (2) "sunflower" diet (high $\omega 6/\omega 3$ ratio) - (3) "borage" diet (high γ -linolenic acid) - (4) "fish" diet (high in long chain $\omega 3$). Mice were fed *ad libitum* through the whole protocol. At 12 months old, mice were sacrificed and tissues were harvested for bone studies, fat and muscle mass measures, inflammation parameters and bone cells markers expression. We demonstrated for the first time that borage and fish diets restored inflammation and bone parameters using an original model of senile osteoporosis that mimics clinical features of aging in humans. Therefore, our study strongly encourages nutritional approaches as relevant and promising strategies for preventing aged-related locomotor dysfunctions.

Disclosures: Fabien Wauquier, None.

MO0003

Botulinum Toxin Type A Does Not Directly Affect Bone Cell Viability or Differentiation. Susan Grimston^{*}, Marcus Watkins, Roberto Civitelli. Washington University in St. Louis School of Medicine, USA

Botulinum toxin Type A (BtxA) has been used recently to model disuse bone loss, as a single intramuscular injection of BtxA results in muscle paralysis rapidly followed by profound bone loss, attended by sharply increased osteoclast number and bone resorption. However, it can be argued that the BtxA-induced bone loss might be attributed in part to a direct effect of BtxA on bone cells. We tested this hypothesis in macrophages derived from bone marrow of mouse tibiae and femora (as an osteoclast model), and in the MC3T3 osteoblastic cell line. For osteoclast differentiation, non-adherent bone marrow cells, which include macrophages, were cultured in the presence of M-CSF and Rankl to promote osteoclast differentiation. Osteoclasts were visible after 4-5 days in culture as TRAP+ multinucleated cells. Osteoblast like MC3T3 cells were cultured in α -MEM without ascorbic acid. Both osteoblast and osteoclast cultures were incubated with BtxA for 24 hours at concentrations ranging from 12.5mU/100 μ l to 200mU/100 μ l. Cell viability, assessed by the MTT method, was not affected by BtxA in either MC3T3 (93.0225.1% to 135.5428.5% of non-treated control cultures) or macrophage/osteoclast cultures (82.5414.52% to 119.6132.22% of control). By contrast, 10 μ M tamoxifen caused osteoclast cell death and 10% EtOH caused MC3T3 cell death, 1.282.2% and 3.271.2% viability of control, respectively. Importantly we detected no effects of BtxA at any concentrations on the number of TRAP positive cells. Furthermore, exposure of macrophage cultures to BtxA during differentiation into osteoclasts showed no effect of treatment on either osteoclast differentiation or cell viability (83.028.7% to 127.1710.18% of controls); and BtxA did not promote osteoclast differentiation in the absence of Rankl. These data demonstrate that BtxA does not affect bone cell viability at concentrations used in mice *in vivo*, and does not affect the differentiation of macrophages into osteoclasts. Therefore it is unlikely that a direct effect of BtxA on osteoclast viability or differentiation may explain the sharp increase in endocortical bone resorption, osteoclast activation and bone loss occurring after intramuscular BtxA injection in mice. Bone loss in this model is more likely due to local muscle paralysis and its resulting decreased force production. The BtxA model of bone loss is therefore an effective tool for modeling disuse osteoporosis.

Disclosures: Susan Grimston, None.

MO0004

Muscle Strength and its Relationship to Inflammation Markers and Antioxidants Intake in Elderly Women. Patr cia Genaro^{*1}, Marcelo Pinheiro², Ligia Martini³, Vera Szejnfeld⁴. ¹Universidade Federal de Sao Paulo, Brazil, ²Sao Paulo Federal University/ Unifesp/ Escola Paulista De Medicina, Brazil, ³University of Sao Paulo, Brazil, ⁴UNIFESP/EPM, Brazil

Inflammation markers are associated with physical decline and this association may point to a role of inflammation in age-related decline in muscle mass and strength. On the other hand, diet plays an important function by contributing to muscle protein turnover and an antioxidant system as well. The aim of the present study is to evaluate the relationship between muscle mass and strength, antioxidant intake and inflammatory markers in elderly women. This cross-sectional study comprised 177 free-living elderly, mean age 71.2 years old (5.1). Dietary intakes were assessed by three-day dietary records. The Nutrition Data System software (Minneapolis, MN) was used to evaluate nutrient intakes (vitamin C, vitamin E, selenium and zinc). Body composition was measured in all participants using dual-energy X-ray absorptiometry (DXA, Lunar). Grip strength assessed by dynamometer (Jamar[®]) was used as a measure of muscle strength. Inflammation markers measured in 12h fasting blood samples included interleukin-6 (IL-6), C-reactive protein and tumor necrosis factor-alpha (TNF- α). Skeletal muscle mass was significantly higher in women who were in the last tertile of muscle strength, compared with women who were in the first tertile [14.7 kg (1.9) vs 13.0 kg (1.9), p=0.000] respectively. There was no significant difference between antioxidants intake among tertiles of muscle strength. Muscle strength was negatively correlated with IL-6 (r = - 0.201; p=0.007). In addition, this cytokine appears to contribute negatively to the muscular strength regardless of age, muscle mass, fat mass, physical activity, smoking, consumption of protein and calcium and vitamin D supplementation (r²=0.271; p=0.000). In conclusion, there was no association between antioxidant intake and muscle strength. On the other hand, interleukin-6 appears to contribute negatively to muscle strength in elderly women.

Disclosures: Patr cia Genaro, None.

MO0005

Skeletal Muscle Cells Secrete Factor(s) Protecting Bone Cells from Glucocorticoid Induced Cell Death. Katharina Jaehn^{*1}, Leticia Brotto¹, Nuria Lara¹, Chenglin Mo¹, Mark Johnson², Marco Brotto¹, Lynda Bonewald¹. ¹University of Missouri - Kansas City, USA, ²University of Missouri, Kansas City Dental School, USA

Prolonged glucocorticoid (GC) management of inflammatory diseases is the leading cause for secondary osteoporosis potentially through osteoblast and osteocyte cell death. As we have recently shown that muscle cells produce factors that enhance osteocyte responsiveness to mechanical loading and that mechanical loading of MLO-Y4 osteocyte cells blocks GC induced cell death, we hypothesized that muscle factors may also play a role in the protective effects of loading on bone cell viability. Dexamethasone (dex) treated MC3T3 osteoblast, MLO-Y4 osteocyte, and primary isolated osteocyte-enriched cells from 7 day-old mice were used to assess the effect of conditioned media (CM) derived from C2C12 myotubes or from *ex vivo* contracted extensor digitorum longus (EDL) or soleus muscle from 4 month-old mice. Both the trypan blue exclusion for cell death and nuclear fragmentation assay for apoptosis were used. C2C12 myotube CM, but not undifferentiated C2C12 myoblast CM prevented dex-induced cell death and apoptosis in MC3T3, MLO-Y4, and primary osteocyte cells. The effect of C2C12 myotube CM media was effective down to 0.1% and the active factor(s) were found to be smaller than 10kD, stable to freezing and heating, destroyed by UV, extractable in ethyl acetate under both neutral and acidic conditions and volatile.

EDL is composed mainly of fast-twitch, glycolytic, type IIB/IIx, fatigable muscle fibers that are lost with aging while the soleus muscle represents a muscle composed of slow-twitch, oxidative, type I/IIa, fatigue resistant fibers that are less affected by age. Primary EDL and soleus muscle CM prevented dex induced MLO-Y4 cell death. The CM derived from the EDL muscle contracted under high frequency of 80Hz was more potent in prevention of dex-induced osteocyte death than CM from soleus muscle (app. 10 fold), and more potent than CM produced during low frequency contraction of 1Hz (app. 10 fold). This would suggest that type II fibers are superior to type I fibers in protecting and maintaining osteocyte viability.

We conclude that muscle cells naturally secrete factor(s) that prevent apoptosis in osteoblasts and osteocytes stressed by glucocorticoid exposure. Identification of this factor could have far reaching consequences for the prevention of glucocorticoid induced secondary osteoporosis.

Disclosures: Katharina Jaehn, None.

MO0006

Assessment of Muscle Mass Changes and Nerve Conduction Velocity in the Rat Orchidectomy Model. NANCY DOYLE^{*1}, Aurore Varela², Elisabeth Lesage², Solomon Haile¹, Joseph Arezzo³, Susan Y. Smith², Hitoshi Saito⁴. ¹CHARLES RIVER, Canada, ²Charles River Laboratories, Canada, ³Albert Einstein College of Medicine, Departments of Neuroscience & Neurology, USA, ⁴Chugai Pharmaceutical Company, Limited, Japan

Androgens may indirectly affect musculoskeletal homeostasis through interaction with body growth, body composition and the GH-IGF-I axis. The purpose of this study was to evaluate the effects of orchidectomy (ORX) and subsequent testosterone depletion on muscle and peripheral nerve conduction velocity in mature Sprague-Dawley rats over a 3-month period.

Six-month-old male rats were randomly assigned to 2 groups by body weight (BW). Ten rats underwent either ORX or Sham operation and were observed for 13 weeks after surgery. Bone densitometry and fat/lean analysis by pQCT was measured at 0, 6 and 13 weeks. pQCT scans were obtained at the proximal tibia metaphysis and diaphysis. Body weights and food consumption were measured weekly and muscle weights were recorded at necropsy. In addition, conduction velocity was recorded in the mixed caudal nerve, the sensory digital nerve, and the distal motor branches of the tibial nerve innervating plantar muscles of the foot at 0, 6 and 12 weeks.

Following surgery, food consumption of ORX rats was lower than Shams by up to 10% between Weeks 5 and 13, which resulted in lower body weight gains and a reduced body weight of 5% at the end of the study. This was associated with decreases in muscle area (measured by pQCT), relative to Shams of 6% and 13% at Weeks 6 and 13, respectively, with no significant changes in muscle density or fat area. Paired muscle weights measured at necropsy were also consistent with these observations, showing trends for lower gastrocnemius and extensor digitorum longus weights by 4.5% and 4.0% respectively, for ORX rats compared to Shams. The induced changes in muscle were not associated with slowing of either sensory or motor nerve conduction velocity.

The ORX rat is an established model for the evaluation of the effects of experimental treatments on bone mass; the present study indicates that this model can also be valuable in tracing direct effects of compounds on muscle mass which are independent of peripheral neuropathy.

Disclosures: NANCY DOYLE, None.

MO0007

Characterization of Bone Status in a Premature Aging Mouse Model. Sergio Portal^{*1}, Rashed Manassra², Daniel Lozano³, Alicia Acitores⁴, Monica De la Fuente², Pedro Esbrit⁵. ¹Spain, ²Dpto. de Fisiología Animal (Fisiología Animal II), UCM, Spain, ³Instituto de Investigación Sanitaria-Fundación Jiménez Dúaz, Spain, ⁴Laboratorio de Metabolismo Nutrición y Hormonas, Instituto de Investigación Sanitaria-Fundación Jiménez Dúaz, Spain, ⁵FUNDACION JIMENEZ DIAZ, Spain

Bone frailty and subsequent bone fractures are associated with aging-related osteopenia. Research in this field uses animal models as source of information. However, animal aging and frailty models are usually difficult to obtain. Here, we describe the bone status of a premature aging mouse (PAM) model that spontaneously develops from normal female ICR-CD1 mice. These mice take longer to explore a T-shaped maze; they have high anxiety levels and similar neurochemical parameters than those of aging mice, a decreased immune function and a lower life span. Adult PAM (292 weeks), old PAM (722 weeks), and their NoPAM counterparts (n=6 per age/type) were analyzed. After assessing bone densitometry (by PIXImus), mice were euthanized, long bones were extracted for Q-PCR (femur), western blot analysis (tibia), and histomorphometry (femur) studies. At sacrifice, body weight decreased in old NoPAM (p<0.05); whereas glycemia increased in both old NoPAM and PAM (p<0.05). With aging, the % fat in total body, and in tissue surrounding vertebrae (L1-L4) and long bones significantly increased only in NoPAM (p<0.05). Adult PAM showed higher BMD and BMC values than NoPAM in the tibiae (p<0.05). Consistently, % BV/TV showed a trend to be higher, related to significantly (p<0.05) higher Tb.N. and lower (p<0.05) Tb.Sp., in adult PAM mice. Runx2 expression was significantly downregulated with aging in both types of mice studied (p<0.05). There were no significant changes in the OPG/RANKL system with age in these mice. A significant increase in the adipogenic markers PPAR γ and Ap2 and in the oxidative stress marker FOXO-1 gene expression occurred in adult PAM and in both old groups; in contrast, exploring the expression of genes related with the Wnt-pathway, we found that Cyclin-D1 (final target gene) expression was significantly downregulated in these mice. A significant downregulation in Dkk-1 (inhibitor) was observed in both types of old mice (p<0.05). β -catenin protein levels were similar in both types of adult mice, but dramatically decreased in the long bones with age in both groups. Meanwhile, sclerostin was decreased in both PAM groups. In conclusion, these results support the notion that PAM might be a useful model for bone frailty studies, including exploring the role of oxidative stress in the mechanisms of age-related osteopenia.

Disclosures: Sergio Portal, None.

MO0008

Community-dwelling Female Fallers Have Lower Leg Muscle Density, and Similar Forearm Muscle Density and Distal Radius Bone Parameters Relative to Non-fallers: Evidence from the Saskatoon CaMos Cohort. Andrew Frank^{*1}, Jonathan Farthing², Philip Chilibeck², W.P. Olszynski³, Saija Kontulainen⁴. ¹The University of Saskatchewan, Canada, ²College of Kinesiology, University of Saskatchewan, Canada, ³Midtown Medical Center (#103), Canada, ⁴University of Saskatchewan, Canada

Falls result in an estimated 1.7 million distal radius fractures globally, and muscle function is a major contributing factor to fall incidence. Low muscle density reflects higher muscle adiposity, which is associated with poor lower extremity performance, the development of mobility impairments, frailty, bone fragility and fracture. These associations may relate to falls, yet no studies have compared muscle density and distal radius bone parameters between community-dwelling fallers and non-fallers. Our primary objective was to determine whether peripheral quantitative computed tomography (pQCT)-derived lower leg and forearm muscle density and cross-sectional area (MCSA) differ between community-dwelling elderly women grouped as fallers (one or more falls in the past year) and non-fallers. Additionally we sought to determine whether pQCT derived distal radius total bone mineral content (ToC), density (ToD), area (ToA), compression bone strength index (BSIc), and trabecular bone content (TrC), density (TrD) and area (TrA) differ between the two groups. Women (N=140), age 60 or older (mean 74.2 SD 7.8y) were recruited from a random sample of community-dwelling residents. pQCT scans of the 66% non-dominant lower leg and 65% forearm were acquired to determine muscle density and MCSA. The 4% distal radius was scanned to obtain ToC, ToD, ToA, BSIc TrC, TrD and TrA. Basic functional mobility (Timed Up and Go Test [TUG]), and handgrip strength were also measured. All variables were screened for violations of normality and equality of variance. Independent t-tests, Mann-Whitney U tests, and analyses of covariance were used to compare (P<0.05) variables between groups. The lower leg muscle density of Fallers (n=36) was 3.2% lower (P=0.044, mean rank difference of -15.3) than non-fallers (n=99). Forearm MCSA was 5.3% higher (P=0.038, mean rank difference of 15.9) in fallers (n=36) than non-fallers (n=100). Age, height, weight, body mass index, TUG, handgrip strength, forearm muscle density, and all radius bone parameters (adjusted for forearm MCSA) did not differ between fallers and non-fallers. Differences in muscle density appear to be localized to the lower extremity and may serve as a physiological marker in the assessment of lower leg muscular health and fall risk in community-dwelling elderly women. The clinically relevant distal radius bones appear to be similar between community-dwelling female fallers and non-fallers.

Disclosures: Andrew Frank, None.

MO0009

Development of an Immunoassay for the Quantitative Determination of Myostatin (GDF-8). Karl Florian Wintgens*, Corinna Berger, Stanka Stoeva, Franz Paul Armbruster. Immundiagnostik AG, Germany

The TGF-beta superfamily member Myostatin, also known as Growth Differentiation Factor-8 (GDF-8), is an important regulator of muscle mass. Myostatin inhibits muscle growth and promotes muscle protein degradation in mammals and other vertebrates. In many conditions associated with muscle loss, such as old age, prolonged bed rest, liver cirrhosis, uremia, cancer, and HIV infection, Myostatin levels are increased.

The aim of this study was to develop an immunoassay for the quantitative detection of human Myostatin. For this purpose, recombinant human Myostatin was expressed in HEK293-EBNA cells and used to immunize rabbits. The resulting polyclonal rabbit antiserum was characterized by Western Blot and immunohistochemistry. The antiserum detects all subunits of Myostatin, the propeptide, the c-terminal mature protein as well as the protein dimer. In sections of human skeletal muscle, Myostatin can be visualized around the myonuclei and near the cell borders.

A competitive enzyme immunoassay (EIA) was established using the polyclonal anti-Myostatin antibody. The Myostatin EIA does not cross-react with GDF-11, Myoglobin, Follistatin or Follistatin-related gene protein. The limit of detection is 0.273 ng/ml as determined by repeated measurements of a blank sample. The mean coefficient of variation was determined to be < 10 % for intraassay variance and 15 % for interassay variance. Using the Myostatin EIA a reference range was established in a healthy population subdivided according to age and gender. To our knowledge, this is the first commercially available Myostatin immunoassay. It is a suitable tool for the sensitive and precise quantification of Myostatin.

Disclosures: Karl Florian Wintgens, Immundiagnostik AG, 3
This study received funding from: Immundiagnostik AG

MO0010

Forearm Muscle and Cortical Bone Predict Fracture Load. Jenny Zhao*¹, Ruchun Dai¹, Zhehao Dai¹, Jon Jacobson¹, Harry Genant², Peter Augat³, Yebin Jiang¹. ¹Osteoporosis & Arthritis Lab, University of Michigan, USA, ²University of California, USA, ³Biomechanics Research Laboratory, Germany

Investigation of muscle and bone interaction is of considerable research interest. The largest loads applied to bones during daily activities come from the muscles. We investigated the relationships between muscle and bone and used an in vitro fracture model to identify how bone and muscle predicted fracture load.

Cross-sectional area (CA) of cortical bone and muscles, cross-sectional moments of inertia (CSMIs) of the cortical bone were determined from MR images of 20 fresh human cadaveric forearms that were also evaluated using a peripheral quantitative CT (pQCT) scanner at 15% of the length of the forearm. The specimens were randomly assigned to different loading patterns with wrist either in a neutral position or extended/dorsiflexion 45 adjusted between the axes of the radius and the third metacarpal confirmed on radiographs. The load to fracture was applied at a displacement rate of 75 mm/second, mimicking an impact from a fall.

There was no significant difference in the maximum load between dorsiflexion (23881685 N) and neutral position (27821104 N). The pressure sensitive films showed focal pressure concentration in the center of the radiocarpal joint in neutral upright loading configuration, and in an equally distributed pressure pattern across the radiocarpal joint in extended-wrist situation. Correlations (r^2) were 0.61 ($p < 0.0001$) between MRI muscle CA and cortical bone CA, and 0.52 ($p < 0.0001$) between MRI muscle CA and pQCT BMC at the 15% site. Correlations (r^2) between MRI and pQCT at the 15% site were 0.89 and 0.90 ($p < 0.0001$) for polar CSMI and CA, respectively. The fracture load could be predicted by MRI cortical CA, MRI muscle CA, and pQCT cortical BMC at the 15% site with r^2 of 0.85, 0.57, and 0.84 ($p < 0.0001$), respectively. Similar strong correlations with the fracture load were found after adjustment for bone size.

The muscle and bone are significantly associated. The properties of cortical bone and the muscle in the distal radius contribute significantly to its biomechanical competence and predict strength and risk of forearm fractures. Rather than directly influencing fracture load, the different loading configurations influenced the load transfer pattern from the carpal bones into the radius.

Disclosures: Jenny Zhao, None.

MO0011

pQCT Measures of Bone and Muscle Are Independently Associated With Falls in Women – A Principal Components Analysis of Morphometric Measures. Andy Kin On Wong*¹, Aakash Bhargava¹, Karen Beattie¹, Christopher Gordon¹, Laura Pickard¹, Colin Webber², Alexandra Papaioannou², Jonathan Adachi³. ¹McMaster University, Canada, ²Hamilton Health Sciences, Canada, ³St. Joseph's Hospital, Canada

Individuals who fall lack muscle strength, which may also affect bone. Objective: To determine the association between fallers and morphometric measures of bone and muscle using peripheral quantitative computed tomography (pQCT).

Methods: Women ≥ 50 years of age completed grip strength, timed 'up-and-go' (TUG) tests, and responded to a questionnaire on self-reported falls in the last year, and duration of vitamin D supplementation. pQCT scans were obtained at the 66% site of the tibia with a single slice thickness of 2.3–0.5 mm. Muscle was segmented from bone to yield measures of bone and muscle macrostructure, density as well as bone mechanical parameters using manufacturer software. Principal components analysis (PCA) was performed using Varimax transformation to extract components (PC) explaining the largest percent of variance in bone variables above an Eigenvalue cutoff of 1.0. Binary logistic regression determined the relationship between 1-year prevalence of falls and each of bone PC's, individual bone and muscle parameters. Regression models were adjusted for anthropometrics, physical function and duration of vitamin D use, as shown in Table 2. Odds ratios per standard deviation increase in variables were reported with 95% confidence intervals (CI). Regression model fit was ascertained by Hosmer-Lemeshow tests. Receiver-operator characteristics (ROC) analyses for falls was examined for the same variables reporting areas under the curve (AUC) tested against 0.50.

Results: Of 49 women (mean age: 74.56 \pm 8.4 years; BMI: 26.5 \pm 4.2 kg/m²), 14 (28.6%) fell at least once. PCA identified 7 pQCT bone PC's explaining 93.51% of variance in 60 variables. Only PC1-PC3 providing component loading correlations larger than 0.80 were further analyzed (Table 1). Combined, muscle and bone volumetric density showed reduced odds for falls (0.846 (0.726, 0.987)), not significant after accounting for covariates. Only a larger PC2 was associated with reduced odds for falls by as much as 90% after accounting for covariates (Table 2). pQCT PC2 exhibited a significant AUC of 0.714 (95% CI: 0.547, 0.881) with 71.4% sensitivity and 72.2% specificity for falls discrimination.

Conclusions: pQCT bone characteristics associated with peri- and endosteal geometry, marrow area and mass at the mid-tibia (PC2) were independent discriminants of falls in women. Combined with smaller muscle area and density, poor mid-tibial bone geometry is associated with fallers.

Table 1. Principal components of pQCT-derived bone macrostructural measures at the 66% tibia. Extraction of 7 PC's with significant variance explanation (Eigenvalues (EV) > 1.0) and with 3 PC's containing variables with component loading correlation coefficients > 0.80. Subscripts: P = polar.

PC	EV	% of Variance Explained	Cumulative % of Variance	Variables with Component Loading Correlations (R) > 0.80
1	21.32	38.08	38.08	Moments of inertia _{xx} (cortical, total), bending resistance _{xx} (cortical), bone mineral content (cortical, total)
2	14.72	26.29	64.36	Endosteal and periosteal circumference, marrow area and mass
3	4.57	8.17	72.53	Density-weighted moment of inertia _{yy}
4	3.94	7.03	79.56	N/A
5	3.67	6.55	86.11	N/A
6	2.27	4.05	90.16	N/A
7	1.87	3.35	93.51	N/A

Table 2. Odds for falls in women explained by pQCT bone measures. Principal component 2 for pQCT bone parameters was examined for an association with falls and was further examined in conjunction with muscle area and density (Models 4-9), adjusting for anthropometrics (age, BMI), duration of vitamin (Vit) D use and physical function (maximum grip strength (GSM_{max}), timed 'up-and-go' (TUG) time).

Model	Covariates	OR	Lower CI	Upper CI	P-value
	None	0.444	0.209	0.942	0.034
Model1	Age, BMI	0.327	0.111	0.961	0.042
Model2	Model1+GSM _{max} , TUG Time	0.092	0.010	0.858	0.036
Model3	Model2+Duration Vit D use	0.104	0.012	0.931	0.043
Model4	Model1+Muscle area	0.328 ^a	0.110	0.980	0.046
Model5	Model1+Muscle density	0.184	0.043	0.791	0.023
Model6	Model2+Muscle area	0.087	0.008	0.897	0.040
Model7	Model2+Muscle density	0.040	0.002	0.940	0.046
Model8	Model3+Muscle area	0.100	0.010	0.973	0.047
Model9	Model3+Muscle density	0.030	0.001	1.118	0.058

^a indicates poor fit of regression model based on Hosmer-Lemeshow test at 90% CI

Disclosures: Andy Kin On Wong, None.

MO0012

Retest Reliability of Muscle Function Testing in Older Adults. Bjoern Buehring^{*1}, Ellen Fidler¹, Diane Krueger¹, Neil Binkley². ¹University of Wisconsin, Madison, USA, ²University of Wisconsin, USA

Background: Sarcopenia is a risk factor for falls and fractures. As muscle performance (strength and power) predicts disability, morbidity and mortality better than muscle mass, it is appropriate that a recent consensus definition of sarcopenia included measuring both mass and function. Clinical trials of sarcopenia prevention/treatment require sensitive quantitative tools to evaluate muscle function. Jumping mechanography (JM) may be one such tool. However, it is necessary to evaluate whether muscle performance as measured by JM in older adults is reproducible over time and correlates with classical functional assessment tools. Thus, the purposes of this study was to evaluate reproducibility of JM parameters over time and correlate these measures with current functional tests.

Methods: Community dwelling individuals age 70 and older who volunteered and met inclusion/exclusion criteria performed a battery of muscle function tests including the short physical performance battery (SPPB), grip strength, and JM. JM uses maximal counter-movement jumps performed on a force plate. With this methodology, force is recorded and body weight corrected peak power and jump height are calculated. To examine reliability over time, these measures were performed at a screening visit, a baseline visit a few days later and at 2 weeks and 3 months. Intraclass correlation (ICC) and coefficient of variation (CV) were used to examine retest reliability.

Results: 49 females and 48 males (average age of 80.6, range 70 – 95) with and without osteoporosis and sarcopenia participated. Muscle function testing was generally well tolerated; no participant sustained a JM related injury. Jump power, jump height and grip strength had excellent ICCs (0.94, 0.89, and 0.95 respectively) CV was 6.8% for jump power, 13.5% for jump height and 13.6% for grip strength. ICC and CV for SPPB components varied among tests (ICC: 0.37 for total balance score to 0.81 for repeated chair rise time, CV: 9.5% for gait time to 23.4% for total balance score).

Conclusion: JM appears to have an excellent retest reliability in older adults with and without sarcopenia. No apparent learning effect was observed. In this study JM was comparable to grip strength and possibly better than measures included in the SPPB. JM is a promising tool for muscle power assessment in older adults and likely comparable to classical function assessment tools for longitudinal interventional studies.

Disclosures: Bjoern Buehring, None.

MO0013

The Association Between Serum 25-Hydroxyvitamin D and Obesity and Sarcopenia in Elderly Men. Vidmantas Alekna^{*}, Asta Mastaviciute, Marija Tamulaitiene. Vilnius University, Lithuania

Background: A combination of excess weight and reduced muscle mass, and strength is called as sarcopenic-obesity. There are not sufficient data about vitamin D status in sarcopenic-obesity.

Purpose: The aim of this study was to investigate serum 25-hydroxyvitamin D in obese, sarcopenic and sarcopenic-obese elderly men.

Methods: Subjects for this cross-sectional study were 58 men aged 60 years and more. Exclusion criteria were conditions and current use of any medication known to affect muscle and lipid metabolism, or taking vitamin D supplements. DXA was used to measure fat mass, body fat percentage, and lean mass (iDXA, GE Lunar). Sarcopenia was defined as condition when appendicular skeletal muscle mass divided by stature squared was $<7.26 \text{ kg/m}^2$ and gait speed was $<0.8 \text{ m/s}$. Obesity was based on the relative fat mass and was defined as percentage of body fat greater than 27% and BMI greater than 30 kg/m^2 . In case of the combination of sarcopenia and obesity subjects were classified as sarcopenic-obese. Serum levels of 25-hydroxyvitamin D were measured by automated immunoassay (Cobas E411, Roche Diagnostics).

Results: Of all men investigated 35 subjects were obese, 15 - sarcopenic and 8 men were defined as sarcopenic-obese. The mean 25-hydroxyvitamin D was $15.485.8 \text{ ng/ml}$ in obese subjects, $11.36.24 \text{ ng/ml}$ in sarcopenic, and $9.084.17 \text{ ng/ml}$ in sarcopenic-obese men. Using one-way ANOVA test statistically significant 25-hydroxyvitamin D status difference was found between body composition groups investigated ($p=0.036$). Post hoc analysis revealed the statistically significant difference of serum 25-hydroxyvitamin D between obese and sarcopenic men as well as between obese and sarcopenic-obese groups ($p=0.04$ and $p=0.02$, respectively). There was weak correlation of 25-hydroxyvitamin D with obesity ($r=0.215$, $p=0.004$).

Conclusions: Serum 25-hydroxyvitamin D is associated with obesity in men. The lowest serum 25-hydroxyvitamin D was found in sarcopenic-obese men. Larger cohorts of subjects studied are needed to clarify the significance of our finding.

Disclosures: Vidmantas Alekna, Amgen, 8; Amgen, 5; Amgen, 2; Novartis, 8; GSK, 8

MO0014

Bone Micro-Architecture, Muscle Strength, and Undercarboxylated Osteocalcin in Middle-Aged Men. Itamar Levinger^{*1}, Roger Zebaze², Ali Ghasem-Zadeh², George Jerums³, David Hare³, Steve Selig⁴, Ego Seeman². ¹Victoria University, Australia, ²Austin Health, University of Melbourne, Australia, ³Austin Health, Australia, ⁴Deakin University, Australia

Background: Serum undercarboxylated osteocalcin (unOC) has been shown to play a role in energy metabolism in mice. There is also a growing number of correlative evidence to suggest that unOC play a role in glycaemic control in humans. Remodelling is surface dependent – there must be a surface for remodelling to be initiated upon before matrix can be remodelled. We tested the hypothesis that bone assembled with a larger surface/tissue volume configuration (therefore high porosity, lower volumetric bone density, vBMD) will be associated with higher serum unOC. We also tested whether muscle strength is negatively correlated with bone porosity.

Methods: We examined the associations between bone micro-architecture in the distal tibia and distal radius, by using high-resolution peripheral quantitative computed tomography (HR-pQCT) and serum unOC and muscle strength, in 29 middle-aged men (age 52.9 ± 1.3 yrs BMI $=32.00.9 \text{ kg-m}^2$ mean SEM). Correlations between bone measures and serum unOC and muscle strength were adjusted for age and BMI.

Results: unOC correlated with porosity of the entire tibia ($r=0.59$, $p=0.001$) and radius ($r=0.52$, $p=0.005$), and so correlated negatively with total vBMD of the entire tibia ($r=-0.56$, $p=0.002$) and radius ($r=-0.49$, $p=0.008$). unOC was also correlated with cortical porosity in the tibia and radius ($r=0.57$, $p=0.001$ and $r=0.60$, $p=0.001$, respectively). Muscle strength correlated negatively with porosity of the tibia ($r=-0.36$, $p=0.04$) and directly with total vBMD of the tibia ($r=0.42$, $p=0.019$) and radius ($r=0.35$, $p=0.046$).

Conclusion: Increased bone porosity is associated with higher serum unOC while higher bone density is associated with lower serum unOC in middle-aged man. Serum unOC is surface dependent. Greater muscle strength is associated with lower bone porosity and so higher vBMD. Interventions aimed to increase muscle strength may have favourable effects on bone quality in ageing man.

Disclosures: Itamar Levinger, None.

MO0015

Reambulation After Disuse Causes Differential Age-Dependent Responses in Bone Strength and Bone Formation in Trabecular and Cortical Bone. Tristan Fowler^{*1}, Thomas Williams¹, Nisreen Akel¹, William Hogue¹, Frances Swain¹, Esther Dupont-Versteegden², Larry Suva¹, Dana Gaddy¹. ¹University of Arkansas for Medical Sciences, USA, ²University of Kentucky, USA

We and others have demonstrated the deleterious effects of age and disuse on trabecular bone mass and strength. The goal of the present study was to investigate the effects of disuse on cortical bone geometry and strength, the capacity for bone restoration by reambulation (RE), and the impact of age on these skeletal changes. Using the well established hindlimb suspension (HS) model of musculoskeletal disuse, male rats 6 mo. and 32 mo. of age were assigned to control groups, HS for 14 days, and HS + RE for either 7 or 14 days. To determine if HS and/or RE effects were the result of changes in bone formation, rats were injected with calcein and Alizarin red and tibiae were analyzed via dynamic histomorphometry to determine bone formation rate (BFR) and mineral apposition rate (MAR) in both trabecular and cortical bone compartments. Femoral cortical bone strength was determined by three-point bending. Load-displacement curves were recorded and analyzed yielding measurements of stiffness, load at yield, peak load, load at failure, total displacement, energy to yield, and energy to failure. MicroCT analysis revealed no significant differences in cortical bone geometry by HS or RE in the tibial mid-shaft within any age group. Dynamic histomorphometry in the cortex revealed that HS reduced both endosteal and periosteal BFR and MAR in both the 6 and 32 mo. old rats. Neither 7 nor 14 days of RE affected the HS-induced decreases in dynamic cortical bone formation indices. These cortical results contrast with the findings in trabecular bone where MAR and BFR were completely restored with 7 days of RE in 6 mo. rats, and 14 days of RE in 32 mo. old rats. The cortical histomorphometry results paralleled mechanical testing data that demonstrated 32 mo. old bones had decreased stiffness and peak load not restored by RE. In 6 month old rats, HS caused a decrease in stiffness, but no change in peak load, or energy to yield or failure. The decrease in stiffness was restored by RE. Collectively, these findings demonstrate that HS compromises cortical bone strength in both 6 and 32 mo. old rats, and that skeletal recovery by RE is age-dependent. Unlike aged trabecular bone that has delayed bone formation recovery potential, aged cortical bone had no recovery potential. These findings suggest that ambulation in the elderly may selectively protect trabecular bone while having a more limited benefit for the protection of cortical bone.

Disclosures: Tristan Fowler, None.

MO0016

Yoga Spinal Flexion Positions and Vertebral Compression Fracture in Osteopenia of Spine. Mehrsheed Sinaki^{*1}, Bart L Clarke¹, Elisabeth Preisinger², Vahab Fatourehchi¹. ¹Mayo Clinic, USA, ²Univ Vienna, Austria

Abstract: That yoga has a positive effect on balance, posture, flexibility, and quality of life is well-known. The objective of this report is to raise awareness of the effect of strenuous yoga flexion poses on the osteopenic (OP) spine. Flexibility of the spine achieved with yoga in older individuals can be an affliction rather than a blessing. Back strengthening exercises are important to reduce bone loss related vertebral compression fractures (fx) (VCF's). We previously reported on subjects with known osteoporosis who developed VCF's after spine flexion exercises (SFE's), and recommended that SFE's not to be prescribed in patients with osteoporosis of the spine.

We report 3 cases of healthy individuals with low bone mass, yoga-induced pain and/or fx.

Patient #1: An 87 y/o healthy woman with osteopenia developed severe back pain while performing strenuous spine flexion exercises during yoga with instructor supervision. Spine x-rays: L2 VCF and mild anterior wedging of several thoracic vertebrae. BMD Spine: T score -1.4; hips R/L : -1.2/-1.6.

Patient #2: A 61 y/o woman with osteopenia developed severe back pain while performing strenuous SFE's during yoga poses. Spine x-rays: VCF of superior end plate of T4. BMD Spine: T score -1.8.

Patient #3: A 70 y/o woman with osteopenia and degenerative joint disease of the cervical spine developed severe neck and back pain after performing common yoga spinal flexion position exercises. BMD: T Score: Spine -1.3; BMD hips:-1/-0.9. Spine x-rays: Advanced osteopenia. Degenerative cervical spondylosis, most significant at C4-7. Degenerative changes in the thoracic spine with anterior wedging of T8 and T9.

SUMMARY: OP is characterized by low bone mass, loss of bone microstructure and ↑ fx risk. OP musculoskeletal rehabilitation is a non-pharmacologic approach to reduce vertebral fx. Although exercise has been shown to be an effective method for improving BMD and ↓ fx risk, our subjects developed VCF's, neck and back pain while engaged in Yoga exercises. This suggests that factors other than bone mass should be considered for exercise counseling in patients with OP. The ↑ torque pressure applied to vertebral bodies during SFE's may be one such risk and requires consideration.

CONCLUSION: Although exercise is effective and important in the treatment of OP, fx risk assessment in individuals with bone loss performing SFE's and other high impact exercises is an important clinical consideration.

Disclosures: Mehrsheed Sinaki, None.

MO0017

Bone Densitometry Evaluations in Juvenile Dogs. Rana Samadfam^{*1}, Maria Adamo², Aurore Varela¹, Keith Robinson², Susan Y. Smith¹. ¹Charles River Laboratories, Canada, ²Charles River, Canada

Effects on skeletal development and mineralization during neonatal and juvenile periods could have long lasting consequences later in adult life. The aim of this study was to establish procedures to evaluate the effects of drugs on skeletal development and density in non-clinical pediatric studies in beagle dog pups, the primary non-rodent species used in post-natal and juvenile studies. The techniques evaluated included radiography, DXA and pQCT. These imaging techniques were performed repeatedly on the same animals, from neonatal pups to juvenile animals of several months of age. DXA provided measurements for area, bone mineral content (BMC) and bone mineral density (BMD) of large areas of the skeletal system. pQCT provided volumetric measurements of area, BMC and BMD of the total slice, trabecular and cortical bone as well as geometry parameters. Radiograph images were used to assess skeletal abnormalities and epiphyseal closure during growth. These images were also used to measure length of the femur, tibia and lumbar spine. Beagle pups were scanned at weeks 1, 2, 3, 4, 5, 13, 17, 20 and/or 26 postpartum. Reproducible data were obtained for in vivo DXA scanning of the whole body, lumbar spine and whole right femur of weanling pups. Due to low bone density, manual bone mapping was required at 4 weeks and occasionally at 13 weeks of age. At 4 weeks, pQCT was performed at the radius proximal metaphysis and diaphysis. A single scan was acquired at the diaphysis using 40% of the bone length. The metaphysis scans were acquired at 18% of the total bone length. Changes in skeletal morphology during growth necessitated adjustment of slice positioning at the metaphysis over the course of the study. Increases in bone length measured by radiology were consistent with increases in body weight and increases in area parameters (DXA and pQCT). The results of these investigations indicate that radiography, DXA and pQCT provide reproducible and repeated non-invasive measurements of skeletal growth in vivo in skeletally immature dog pups at axial and appendicular sites. These data, combined with routine histology, provide a comprehensive assessment of the developing skeleton supporting use of these end-points in this model in drug development.

Disclosures: Rana Samadfam, None.

MO0018

In Vivo and Ex Vivo Measurements of Post Natal Skeletal Development in Rodents Non-Clinical Reproductive Toxicology and Pediatric Studies. Aurore Varela^{*1}, Maria Adamo², Jacquelin Jolette³, Luc Chouinard⁴, Rana Samadfam¹, Keith Robinson², Susan Y. Smith¹. ¹Charles River Laboratories, Canada, ²Charles River, Canada, ³Charles River Laboratories, Preclinical Services Montreal, Canada, ⁴Charles River Laboratories, PCS Montreal, Canada

The aim of this work was to establish procedures to evaluate the effects of drugs on skeletal development in non-clinical pediatric studies in rats, the primary rodent species used in post-natal and juvenile studies. The techniques evaluated included radiography, DXA, pQCT, histology and histomorphometry. Sprague-Dawley pups starting at 7-day old were used.

Radiographs were taken under anesthesia to measure the femur, tibia and lumbar spine (L1-L6) lengths. Positioning and anatomical landmarks selected were reliable for repeat measurements of the same animal with coefficient of variation (CV%), not exceeding 1.7% at 14 days of age. CV% between age groups ranged from 0.7 to 4.7% across all sites evaluated and were similar for males and females at 14, 21, 28 and 35 days old. Bone length increased at each site with age, consistently with longitudinal bone growth. The details of the radiographs allowed evaluation of skeletal abnormalities including those of the physis. Peripheral QCT was performed in vivo as early as 7 days post-partum at the tibial proximal metaphysis and diaphysis. DXA scanning of the whole body, lumbar spine (L1-L4) and of the whole right femur of weanling rats (28 and 35 days of age) was performed using manual bone mapping. These imaging techniques were performed repeatedly on the same animals, from neonatal pups to juvenile animals of several months of age. pQCT provided information on the trabecular and cortical bone compartments and bone geometry. For pQCT, reproducible data was acquired using single or multiple scan slices set at 15% of the total bone length for females and 13% in males. Changes in skeletal morphology during growth, for animals more than 7 weeks of age, necessitated adjustment of slice positioning during the study. Histology provided cellular and microscopic architecture information. Histomorphometry measurements, including growth plate thickness in 35 day old rats, was used to evaluate effects of drug upon the cartilaginous scaffold and its mineralization, and to provide structural and dynamic bone turnover variables.

These results indicate that radiography, DXA and pQCT provide reproducible and repeated non-invasive measurements of skeletal growth in vivo in skeletally immature rats at axial and appendicular sites. These data, combined with histology and histomorphometry ex vivo evaluations, provide a comprehensive assessment of the developing skeleton supporting use of these end-points for drug development.

Disclosures: Aurore Varela, None.

MO0019

Increasing Incidence of Nutritional Rickets in Olmsted County, Minnesota, since 1970. Tom Thacher^{*1}, Philip Fischer¹, Peter Tebben², Ravinder Singh¹, Stephen Cha¹, Barbara Yawn³. ¹Mayo Clinic, USA, ²Mercy Health, USA, ³Olmsted Medical Center, USA

Background: Concern has been expressed regarding the persistence and possibly increasing incidence of nutritional rickets in the United States. It is unclear if the incidence is related to an increased prevalence of vitamin D deficiency or an artifact of increased 25(OH)D measurements or rising immigrant population. The aim of this study was to determine if the incidence of nutritional rickets has increased.

Methods: We identified all children (<18 years) residing in Olmsted County, MN between 1970 and 2009 with diagnostic codes of rickets, vitamin D deficiency, hypovitaminosis D, rachitis, osteomalacia, genu varum, genu valgum, craniotabes, hypocalcemia, hypocalcemic seizure, and tetany in the Rochester Epidemiology Project databases. Data abstraction was performed to select subjects with X-ray confirmation of rickets. Nutritional rickets was defined as X-ray evidence of rickets without evidence of inherited, genetic, or other secondary causes of rickets.

Results: Of 778 children with eligible diagnostic codes, 25 had radiographic evidence of rickets, and 17 were attributed to nutritional rickets. Fifteen (88%) were aged 6-24 months, 13 (76%) were black or non-Caucasian. Clinical presentation included poor growth (12), leg deformity (8), motor delay (5), leg pain (3), weakness (3), and hypocalcemia or tetany (2). Of the 13 who had 25(OH)D measurements, 5 (38%) had vitamin D deficiency (≤12 ng/ml). In consecutive 10-year intervals from 1970 to 2009, the mean incidence rates of nutritional rickets in children under 3 years of age were 0, 2.2, 3.7, and 24.1 per 100,000, respectively (P=0.003).

Conclusion: The incidence of nutritional rickets has increased significantly during the past four decades in Olmsted County, MN, and not all cases can be attributed to vitamin D deficiency.

Disclosures: Tom Thacher, None.

MO0020

Age-Related Changes in Cortical Bone Geometry in the Human Tibial Diaphysis: A Whole-Bone Perspective. Zachariah Hubbell¹, James Gosman¹, Colin Shaw², Timothy Ryan². ¹The Ohio State University, USA, ²Pennsylvania State University, USA

Previous research has revealed distinct developmental trajectories for trabecular and cortical bone structures in the long bones of humans. Mature configuration of trabecular microarchitecture is achieved by late childhood, while development of cortical bone geometry extends into late adolescence. The purpose of this research is to test the hypothesis that the ontogenetic pattern of change in cortical cross sectional geometry from the whole-bone diaphyseal perspective is age- and anatomical site-specific. Tibiae ranging developmentally from neonatal to skeletally mature were obtained from the Norris Farms no. 36 skeletal series, a collection of skeletons recovered from an Oneota Native American cemetery dating to approximately A.D. 1300. Whole tibiae underwent high resolution x-ray CT scanning at the Penn State Center for Quantitative Imaging with resolutions ranging from 0.013 to 0.094 mm depending on specimen size. Cortical bone cross-sectional geometric properties were calculated for entire tibial diaphyses using the BoneJ plugin for ImageJ. From these results, Imax/Imin ratios (a measure of cross-sectional shape) were calculated for each CT slice (between 983 and 2277 slices per bone) for the whole diaphysis of each tibia and were then plotted against percent diaphyseal length (Figure 1). For each tibia, average values of Imax/Imin were calculated for five regions of the diaphysis of equal length (Region 1 being most distal, Region 5 being most proximal); these averages were correlated with age. Correlation results and associated p-values are presented as a table in Figure 2. The distribution of Imax/Imin values indicate that in general, cross-sectional shape follows a trend of decreasing 'roundness' with increasing age, especially toward the proximal end of the diaphysis (represented by Region 4, 60% to 80% of diaphyseal length). These changes in shape correspond to patterns of site-specific bone accretion that likely reflect combined genetic patterning, linear growth, and mechanical/locomotor influences. Notably, Imax/Imin values in Region 4 appear to increase markedly for individuals age 9 years and older, while remaining relatively homogeneous for individuals age 5 years and younger. Further investigation of this age-related anatomical divergence may elucidate the regional significance of diaphyseal cortical bone accrual during growth as well as the potential factors that influence the shift toward mature cortical bone structural configuration.

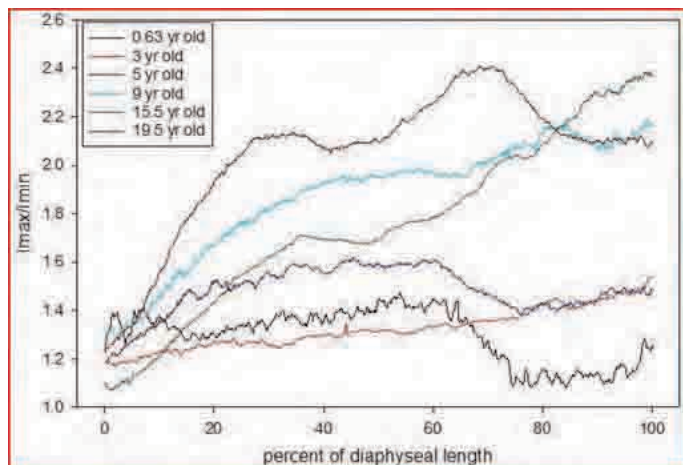


Figure 1. Age-specific Imax/Imin values by percent tibial diaphysis.

Age (yrs)	Imax/Imin Averages				
	Region 1	Region 2	Region 3	Region 4	Region 5
0.63	1.33	1.35	1.41	1.26	1.15
3	1.22	1.27	1.31	1.36	1.45
5	1.36	1.54	1.59	1.48	1.45
9	1.46	1.81	1.96	2.02	2.12
15.5	1.23	1.61	1.72	1.94	2.26
19.5	1.56	2.08	2.13	2.33	2.11
Pearson's Correlation	0.483	0.848	0.841	0.94	0.885
P-value	0.056	0.058	0.059	0.057	0.058

Note: Reported p-values are likely influenced by small initial sample size and may reach significance after analyzing a larger number of specimens.

Figure 2. Average values of Imax/Imin and age correlations for each region of the tibial diaphysis.

Disclosures: Zachariah Hubbell, None.

MO0021

A Comparison of Trabecular Bone Microstructure at the Distal Radius and Distal Tibia Between Healthy Weight and Overweight Adolescents: An HR-pQCT Study. Christa Hoy¹, Lindsay Nettlefold¹, Sarah Moore¹, Sojung Kim¹, Meghan Donaldson², Heather Macdonald¹, Heather McKay¹. ¹University of British Columbia, Canada, ²San Francisco Coordinating Center, USA

Obesity prevalence has increased drastically in recent years and is known to be associated with many chronic conditions. Although overweight children have greater bone mass than their healthy weight peers, they sustain more fractures. Thus, there is a need to better understand the relation between overweight status and three-dimensional properties of bone microstructure that influence bone strength. We aimed to examine this relation in this cross-sectional study using high-resolution pQCT (HR-pQCT) in adolescent boys and girls in the Healthy Bones Study cohort. We categorized boys (n=100; 17.41.6yrs) and girls (n=84; 17.81.8yrs) into body mass index (BMI) groups using the CDC BMI for age curves (Overweight (OW) \geq 85th percentile, 14 boys, 15 girls; Healthy Weight (HW) < 85th percentile, 86 boys, 69 girls). We used HR-pQCT and standard protocols to assess the non-dominant distal radius (7% site) and left distal tibia (8% site). Bone outcomes for tibia and radius were: trabecular number (Tb.N, 1/mm), trabecular thickness (Tb.Th, mm), trabecular bone volume to tissue volume (BV/TV, %) and trabecular separation (Tb.Sp, mm). We used multiple regression to evaluate the variance in trabecular bone microstructure explained by weight status after adjusting for age (yrs), ethnicity (Asian vs. Caucasian), physical activity (min/day) and radius or tibia length (mm). For girls, OW was not a significant predictor of trabecular bone microstructure at either site. However, in boys OW was a significant positive predictor of BV/TV ($p < 0.01$, 13.7% greater than HW) and Tb.N ($p < 0.05$, 9.3% greater than HW) and negative predictor of Tb.Sp ($p < 0.01$, 11.9% less than HW) at the distal radius. At the distal tibia in boys, weight status was a positive predictor of Tb.N ($p < 0.01$, 15.2% greater than HW) and negative predictor of Tb.Th ($p < 0.05$, 7.5% less than HW) and Tb.Sp ($p < 0.01$, 15.7% less than HW). Thus, an apparent paradox exists where OW positively influences BV/TV and Tb.N in boys; however, trabeculae are thinner at the distal tibia suggesting a negative effect of excess body weight on bone microstructure. Further research with a larger cohort over a longer time period is needed to clarify these sex-specific relations and their implications.

Table 1. Descriptives for healthy weight (HW) and overweight (OW) boys and girls and bone microstructure variables as measured by HR-pQCT at the distal radius and tibia.

Variable	Boys		Girls	
	HW (n=86)	OW (n=14)	HW (n=69)	OW (n=15)
Age (yrs)	17.4 (1.6)	17.3 (1.6)	17.8 (1.8)	17.8 (1.8)
Tibia length (mm)	420 (25)	431 (36)	381 (23)	390 (29)
Radius length (mm)	265 (15)	262 (15)	257 (13)	261 (16)
Physical activity (min/day)	80.5 (11.8)	53.6 (39.1)	81.4 (42.1)	33.3 (35.3)
Ethnicity (% Asian/Caucasian)	(48/52)	(5/9)	(53/16)	(4/11)
Radius BV/TV (%)	15.7 (3.3)	17.7 (2.5)	13.3 (2.8)	13.7 (2.6)
Radius Tb.N (1/mm)	1.93 (0.25)	2.04 (0.14)	1.85 (0.27)	1.88 (0.19)
Radius Tb.Th (mm)	0.054 (0.014)	0.056 (0.015)	0.054 (0.012)	0.053 (0.009)
Radius Tb.Sp (mm)	0.444 (0.073)	0.397 (0.036)	0.474 (0.095)	0.464 (0.047)
Tibia BV/TV (%)	17.2 (2.5)	19.0 (2.3)	16.1 (2.9)	16.8 (3.1)
Tibia Tb.N (1/mm)	1.86 (0.26)	2.15 (0.25)	1.75 (0.26)	1.82 (0.22)
Tibia Tb.Th (mm)	0.050 (0.011)	0.055 (0.012)	0.050 (0.014)	0.048 (0.011)
Tibia Tb.Sp (mm)	0.458 (0.055)	0.398 (0.047)	0.491 (0.061)	0.419 (0.041)

Data are Mean (SD); means are unadjusted.

Table 1

Disclosures: Christa Hoy, None.

This study received funding from: Canadian Institute for Health Research

MO0022

Accumulation of Bone Marrow Adipose Tissue in Childhood May Adversely Affect Skeletal Strength. Krista Casazza¹, Lynae Hanks¹, Harry Hu². ¹UAB, USA, ²USC, USA

Although appositional relationship between body fat and bone mineral content (BMC) in the pediatric population is often reported, obesity is overrepresented in childhood fracture cases thus challenging a beneficial contribution of adiposity to bone health. Further, whereas, insulin resistant children tend to have higher bone mass compared with the general population, they paradoxically remain unprotected from fractures. Assessment of the bone marrow compartment particularly during growth and development represents a viable avenue in which to explore the allocation of resources between fat and bone as it is here that undifferentiated cells capable of multiple lineages (i.e. osteoblasts, adipocytes) meet their fate. The objective of this study was to evaluate the association between bone marrow adipose tissue (BMAT) and BMC in growing children and to determine the extent to which total body adiposity and insulin may influence this relationship. Ninety-five pre-pubertal children age 4-10 years ($\mu = 6.8 \pm 0.2$) participated. BMC and total body mass were assessed by DXA, bone marrow adipose tissue by MRI and fasting insulin by venipuncture. A positive relationship between BMAT and BMC was observed ($p < 0.001$); however, inclusion of total body fat or fasting insulin attenuated the relationship ($p = 0.19$, 0.58 , respectively). Stratification by percent fat cut-points (25% for boys, 30% for girls), revealed greater BMAT, BMC and insulin among those with greater adiposity. However, a differential contribution of adiposity to the

BMAT-BMC relationship was observed such that among children with normal adiposity the relationship was not significant ($p=0.37$) whereas, among those with excess adiposity BMAT was inversely associated with BMC ($p=0.03$) and the relationship was at least in part mediated by insulin. Accumulation of BMAT may adversely affects skeletal strength and the effect may be exacerbated in children with excess adiposity and impaired insulin dynamics. Revelation of factors contributing to bone integrity within the bone marrow cavity during childhood is a key determinant in body composition trajectory over the life course with numerous health implications.

Disclosures: Krista Casazza, None.

MO0023

Bone Biomarkers and Mineral Biochemistries in Early Pubertal Black and White Adolescent Boys and Girls. Kathleen Hill¹, Berdine Martin², Emma Laing³, Stuart Warden⁴, George McCabe², Richard Lewis³, Connie Weaver², Munro Peacock⁵. ¹Indiana University School of Medicine, USA, ²Purdue University, USA, ³The University of Georgia, USA, ⁴Indiana University, USA, ⁵Indiana University Medical Center, USA

Purpose: To describe mineral biochemistries and bone metabolism biomarkers in healthy early pubertal adolescents and to determine differences in these measures among blacks, whites, boys, and girls. **Methods:** Baseline fasting blood and urine from 247 healthy early pubertal (Tanner stage 2-3) US adolescents (black girls $n = 55$, black boys $n = 51$, white girls $n = 64$, white boys $n = 77$) participating in a randomized controlled trial of vitamin D supplementation were measured for serum osteocalcin (OC), bone alkaline phosphatase (BAP), parathyroid hormone (PTH), calcium (Ca), phosphate (Pi), creatinine (Cr) and urine Ca, Pi, Cr, and N-telopeptide cross-links (NTx). Differences in these variables among blacks, whites, boys, and girls were analyzed using ANOVA with SAS 9.2 (Cary, NC) and significance set at $\alpha = 0.05$. Pearson correlations were used to assess associations among variables. Variables were inspected for normal distribution and transformed when appropriate. **Results:** OC was higher in blacks than whites (37 vs. 30 ng/mL), and did not differ between boys and girls. NTx was lower in blacks than whites (529 vs. 613 nM/mM) and higher in girls than boys (600 vs. 556 nM BCE/mM Cr). BAP was higher in black girls than white girls (235 vs. 201 U/L). Serum Pi was higher in blacks than whites (5.2 vs. 5.0 mg/dL), serum Ca was higher in black boys than white boys (9.9 vs. 9.8 mg/dL) and there were no sex differences in serum Ca or Pi. Serum Cr was higher in blacks than whites (0.67 vs. 0.62 mg/dL) and in boys than girls (0.66 vs. 0.62 mg/dL). Urine Ca/Cr mg ratio was higher in whites than blacks (0.07 vs. 0.04) and was higher in black boys than black girls (0.05 vs. 0.03). Urine Pi/Cr mg ratio was higher in whites than blacks (3.69 vs. 3.17) but there was no sex difference. Positive correlations existed among OC, BAP and NTx. Additionally, serum PTH and Pi were positively associated with bone turnover, serum PTH was negatively associated with urine Ca/Cr, and urine Ca/Cr and P/Cr were negatively correlated with bone turnover. **Conclusions:** Black children had different mean values for bone turnover markers compared with whites, but the direction of the difference varied by marker, and bone turnover markers were most strongly associated with serum Pi. Blacks had lower urinary calcium excretion than whites, which was most strongly associated with serum PTH.

Disclosures: Kathleen Hill, None.

MO0024

Influence of Bone Age and Diet-induced Weight Loss on Bone Mineral Density in Prepubertal Obese Children. Guillermo Martinez Diaz-Guerra¹, Gabriel Martos², Sonsoles Guadalix³, Jesus Argente², Federico Hawkins⁴. ¹University Hospital 12 Octubre, Spain, ²Hospital Infantil Universitario Nino Jesus, Spain, ³University Hospital 12 de Octubre, Spain, ⁴Hospital Universitario, Spain

Background: The effects of obesity and weight loss after caloric restriction in bone mass of young obese children have been insufficiently studied to date.

The aims of this study were: 1) To compare the standardized spine BMD (LS-BMD) of a group of obese children according to both their chronological (CA) and their bone age (BA). 2) To evaluate the effect of diet-induced weight loss on BMD in childhood obesity.

Patients and Methods: Prospective study in 25 prepubertal obese children (19 boys/6 girls; mean age 8.71.5 years; mean BMI 4.71.3 SDS). BA was estimated according Greulich & Pyle method at baseline. Spine BMD (L1-L4) measurements and body composition analysis were performed at baseline and 12 months (Hologic QDR 4500) after reducing their BMI in more than 1.5 SDS. Therapeutic plan included caloric restriction, self-registered physical activity and behavioural management.

Results: BA was significantly higher than CA in obese children (9.5 2.0 vs 8.7 1.5 years; $p < 0.001$). Standardized LS BMD was significantly higher if referred to CA (2.04 1.24 SDS) than to BA (1.32 1.27 SDS; $p < 0.001$). According to CA, 56% of patients had high bone mass (defined as BMD > 2 SDS) whereas according to BA, 28% had high bone mass.

Weight loss determined a reduction of the raw (41.4 2.9 vs. 36.6 4.4%) and standardized (3.9 0.7 vs. 2.9 0.8 SDS) percentage of body fat (both $p < 0.001$). In contrast, a significant increase in LS BMD (0.714 0.070 vs. 0.764 0.099 g/cm²; $p < 0.001$) was observed without changes in standardized LS BMD (2.0 1.2 vs. 2.3 1.5 SDS).

Conclusions 1) Obese prepubertal children show an advance in skeletal development. 2) Referral of BMD to CA overestimates bone mass in these children. 3) Properly controlled weight reduction does not alter BMD acquisition in prepubertal obese children.

Disclosures: Guillermo Martinez Diaz-Guerra, None.

MO0025

Insulin Inhibits Cortical Bone Development Independently of Body Composition: Findings From a Cross Sectional Analysis of pQCT Parameters in Adolescents. Adrian Sayers¹, Debbie Lawlor¹, Naveed Sattar², J.H. Tobias³. ¹University of Bristol, United Kingdom, ²University of Glasgow, United Kingdom, ³Avon Orthopaedic Centre, United Kingdom

Background / Aim: Hyperinsulinaemia may be a risk factor for low bone mineral density, possibly reflecting a lipotoxic effect of intra-muscular fat deposition on bone. We aimed to determine if insulin is related to bone development, and if so whether this effect is independent or mediated by changes in body composition including intra-muscular fat deposition.

Methods: A total of 2784 boys and girls (mean age 15.5 years) from the Avon Longitudinal Study of Parents and Children participated in the study. Blood samples were taken after an overnight or minimal 8-hour fast and insulin levels were measured using a Mercodia ELISA which does not cross-react with pro-insulin. Periosteal circumference and cortical bone mineral density was measured at the 50% tibial site using peripheral quantitative computed tomography. Subcutaneous fat area, muscle density (inversely related to intramuscular fat), and muscle cross sectional area (MCSA) were also calculated.

Results: Insulin was positively associated with PC in minimally adjusted (age/sex) analyses [β 0.015 (95%CI:0.003,0.027), $P=0.015$] (β = change per 50% increase in insulin), but there was an inverse association following further adjustment for height, MSCA, subcutaneous fat and muscle density [β -0.013 (95%CI:-0.022,-0.003), $P=0.008$]. Insulin was inversely related to BMD_C in both minimal and more completely adjusted analyses [β -0.018 (95%CI:-0.030,-0.006), $P<0.0001$, more completely adjusted model].

Path analyses revealed inverse associations between insulin and PC via a direct path [β -0.012 (95%CI:-0.022,-0.003), $P=0.01$], and an indirect path through muscle density [β -0.002 (95%CI:-0.004,-0.001), $P=0.0004$]. Positive indirect associations were also seen between insulin and PC via subcutaneous fat [β 0.013 (95%CI:0.009,0.016), $P<0.0001$] and MCSA [β 0.015 (95%CI:0.010,0.020), $P<0.0001$].

Conclusions: The relationship between insulin and PC via intramuscular fat provides evidence of a lipotoxic effect on bone. However, an inverse association between insulin and bone parameters persisted after adjusting for body composition, suggesting insulin also acts to inhibit bone development via a direct pathway yet to be elucidated.

Disclosures: Adrian Sayers, None.

MO0026

Skeletal Muscle Fat Content is Inversely Associated with Bone Strength in Young Girls. Joshua Farr¹, Janet Funk², Zhao Chen³, Jeffrey Lisse⁴, Robert Blew⁵, Vinson Lee⁵, Monica Laudermilk⁵, Timothy Lohman⁴, Scott Going⁴. ¹Mayo Clinic, USA, ²University of Arizona Health Sciences Center, USA, ³University of Arizona College of Public Health, USA, ⁴University of Arizona, USA, ⁵The University of Arizona, USA

Childhood obesity is an established risk factor for insulin resistance and type 2 diabetes mellitus. Its influence on bone development, however, remains controversial, and may depend on the regional pattern of fat deposition. Consequently, we examined associations of regional fat compartments (calf and thigh) with weight-bearing bone parameters in girls. Data from 444 girls aged 9–12 years from the “Jump-In: Building Better Bones” study were analyzed. Peripheral quantitative computed tomography (pQCT) was used to assess volumetric bone mineral density (vBMD, mg/cm³), bone geometry, and indices of bone strength at metaphyseal and diaphyseal sites of the femur and tibia along with subcutaneous adipose tissue (SAT, mm²) and muscle density (mg/cm³), an index of skeletal muscle fat content. As expected, SAT was positively correlated with total body fat mass ($r = 0.87-0.89$, $p < 0.001$) and muscle density was inversely correlated with total body fat mass ($r = -0.24$ to -0.28 , $p < 0.001$), supporting that pQCT provides useful measures of regional adiposity. Multiple linear regression with muscle density, SAT, muscle cross-sectional area, bone length, maturity offset, and ethnicity as independent variables gave significant associations between muscle density and trabecular vBMD ($\beta = 0.11-0.26$, $p < 0.05$) and bone strength index ($\beta = 0.13-0.19$, $p < 0.001$) at metaphyseal regions of the femur and tibia. In contrast, associations between muscle density and trabecular area at metaphyseal regions of the femur and tibia were non-significant ($p > 0.05$). Positive associations were observed between muscle density and cortical vBMD ($\beta = 0.08-0.17$) and area ($\beta = 0.06-0.08$) at diaphyseal regions of the femur and tibia, whereas associations between muscle density and endosteal and periosteal circumferences at diaphyseal regions of femur and tibia were lower and non-significant (all p values > 0.05). In addition, significant associations were observed between muscle density and strength-strain index ($\beta = 0.06-0.09$, $p < 0.01$) at diaphyseal regions of the femur and tibia, whereas associations between SAT and bone parameters were non-significant at all skeletal sites (all p values > 0.05), except metaphyseal bone strength index of the tibia ($\beta = 0.09$, $p = 0.029$). In conclusion, our results suggest that excess skeletal

muscle fat content of the calf and thigh may be detrimental to the development of weight-bearing bones in young girls.

Disclosures: Joshua Farr, None.

MO0027

Lumbar Bone Mineral Density (BMD) in Children with Duchenne Muscular Dystrophy Treated with Corticosteroids. Cristina Tau^{*1}, Gisela Viterbo², Soledad Monges³, Juliana Castagneto¹. ¹Metabolismo Calcico, Endocrinolog  a, Hospital de Pediatria Garrahan, Argentina, ²Endocrinolog  a, Hospital de Pediatria Garrahan, Argentina, ³Neurolog  a, Hospital de Pediatria Garrahan, Argentina

Reduced mobility and glucocorticoids as adjunctive therapy may cause osteoporosis and fractures in children with Duchenne muscular dystrophy (DMD). We analyzed the BMD in 16 boys with DMD treated with deflazacort or methylprednisone, age, time of immobilization, treatment duration, and cumulative dose of corticosteroids therapy. Lumbar L2-L4 BMD was measured by dual-energy X-ray absorptiometry (Lunar, Prodigy). Mean age was (SD) 11.53 years (range, 6.3-18.2). All children received deflazacort (0.9mg/kg/day, n=10) or methylprednisone (0.75mg/kg/day, n=6) during 3.82.1 years (range, 0.75-7), with vitamin D (300 to 2400 IU), and calcium supplement (0.25 to 1 g/day). Calcium intake by dairy products was 594221 mg/day. Serum calcium (Ca), phosphate (P), alkaline phosphatase (AP), PTH, and urinary calcium and D-Pyridoline/creatinine (uD-Pyr) were measured. Weight (Z-Score) was -0.151.16 (-1.70 to 2.65), height was -1.690.95 (n:9; -2.7 to -0.08). Eight patients were wheelchair-bound (mean age: 13.42.6 years), and the mean age for walking incapacity was 10.9+/-1.5 years. Time of their immobilization was 2.32.2 years. Two patients had long bone fractures, seven patients had vertebral crush fractures (two of them could walk). The cumulative corticosteroids dose was 28,520.3 g (range, 6.3-68.4). Mean BMD Z-score was -2.51.6 ranging from -5.9 to -0.4. BMD Z-score was <-2 in nine patients (56%), and between -1 and -2 in four patients (25%). BMD-Z-score was inversely correlated with age (p<0.000), time of immobilization (p<0.02), and duration of corticosteroid therapy (p<0.001). BMD-Z-score was also inversely correlated with cumulative dose of corticosteroids both in patients receiving deflazacort and those receiving methylprednisone (p<0.000). Patients with vertebral crush fractures had lower BMD (Z-score: -3.781.26, p<0.006). The number of fractures was positively correlated with cumulative corticosteroids dose. Ca, P, AP and PTH were within the normal range. Urinary calcium was increased in six patients (four were wheelchair-bound) and four other patients had increased uD-Pyr (three of them were immobilized). In summary, severe osteoporosis was found in children with DMD. Lowest BMD was correlated with treatment duration, cumulative corticosteroids dose, and time of immobilization.

Disclosures: Cristina Tau, None.

MO0028

Idiopathic Infantile Hypercalcemia. Stepan Kutilek^{*1}, Sylva Skalova², Josef Gut³, Milan Bayer². ¹Pardubice Hospital; Faculty of Health Studies; University of Pardubice, Czech Republic, ²Department of Paediatrics in Hradec Kralove, Faculty of Medicine in Hradec Kralove, Charles University in Prague, Czech Republic, ³Dept. of Pediatrics, Ceska Lipa Hospital, Czech Republic

Idiopathic infantile hypercalcemia (IIH) is a rare cause of hypercalcemia in the first year of life. IIH has an estimated incidence of approximately 1 in 47,000 live births. We present three patients with IIH, where other causes of hypercalcemia were clearly ruled out. In two girls aged 1.5 and 5 months, the S-Ca peaked to 5.2 and 4.3 mmol/L, respectively. Hypercalcaemia resolved after furosemide and glucocorticoid application. In the third patient, a 5-months old boy, S-Ca reached 5 mmol/L, and two doses of intravenous pamidronate were necessary due to poor effect of steroids and furosemide.

IIH was originally described during a period of high-dose vitamin D fortification in England in the 1950s. The diagnosis of IIH can be established only after the exclusion of other conditions that cause hypercalcemia in the first year of life, such as Williams syndrome, benign familial hypocalciuric hypercalcemia, severe neonatal hyperparathyroidism, Janssensmetaphyseal dysplasia, primary hyperparathyroidism, vitamin D intoxication, granulomatous diseases, thyroid disease, malignancy. Identification of the gene for Williams syndrome (WS) now allows a clear separation of IIH from WS. The inheritance and pathogenesis of IIH remains largely unknown, with only sporadic cases reported to date. Familial occurrence has been also documented. IIH presents between the ages of 3 and 7 months with nonspecific signs and symptoms such as lethargy, thirst, hypotonia, poor feeding, failure to thrive, dehydration, constipation and respiratory distress, all due to hypercalcemia. Hypercalciuria with nephrocalcinosis is also common finding in IIH. Only limited published data exist on the natural history of IIH, with case reports suggesting that hypercalcaemia spontaneously resolves when the child is approximately 12 months of age. Treatment consists of furosemide (given only after rehydration), glucocorticoids, and eventually calcitonin. The application of pamidronate in our patient is a first report of such treatment in IIH, as until now pamidronate has not been used in IIH, but only in one patient with WS. In conclusion, IIH is a rare condition of uncertain pathogenesis and natural history. Appropriate treatment improves outcome of patients with IIH.

Disclosures: Stepan Kutilek, None.

MO0029

Mechanical-Tactile Stimulation Increases Tibial Bone Strength in Preterm Infants. Laurie Moyer-Mileur¹, Hillarie Slater¹, Kimberly Neff¹, Joanna Beachy¹, Sandra Smith¹, Chelsea Evans¹, Brett Barrett¹, Shannon Haley^{*2}. ¹University of Utah, USA, ²University of Utah School of Medicine, USA

Preterm delivery (<37 wks post-menstrual age) is associated with suboptimal bone mass. Preterm infants experience numerous stressful events. Stress decreases insulin-like growth factor-I and in turn, osteoblast number and bone mass. We have reported improved stress response in preterm infants who received mechanical-tactile stimulation (MTS) consisting of kinesthetic movement and tactile stimulation. We hypothesized that twice daily MTS would increase bone formation and bone strength in preterm infants. Furthermore, we predicted that increased bone formation and bone strength would be associated with improved stress response and circulating IGF-1 levels. Preterm, AGA infants (29-32 wks, 10th-90th%ile) were randomly assigned to MTS (N=15) or Control (N=17). Twice daily, 20 min sessions of DMT were provided by a licensed massage therapist, 6 d/wk, for up to 4 wks. Control infants received the same care without MTS treatment. Treatment was masked to parents, health care providers, and study personnel. Baseline and weekly measures were collected for tibia speed of sound (tSOS, m/sec), a surrogate for bone strength, by quantitative ultrasound (Sunlight8000); serum IGF-1; urine markers of bone resorption (pyridinium crosslinks) and urine levels of osteocalcin (Glu-OC). Data are reported comparing changes from baseline to Day 15 on study by repeated measures with gender, weight gain, and corrected age a cofactors. Infant characteristics at birth and study entry as well as energy/nutrient intake were similar between MTS and Control. MTS intervention maintained tSOS values and prevented the decrease in tSOS observed in Control infants (p<0.001). MTS infants also experienced greater increases in serum IGF-1 as well as urine osteocalcin (Glu-OC; P<0.05). The markers of bone resorption, urinary deoxypyridinoline and pyridinoline, were not significantly different between groups. MTS improves bone strength in premature infants by attenuating the decrease that normally follows preterm birth. Further, MTS increased circulating IGF-1 levels as well as urinary osteocalcin (Glu-OC). Taken together, we speculate that MTS improves bone mineralization.

Disclosures: Shannon Haley, None.

MO0030

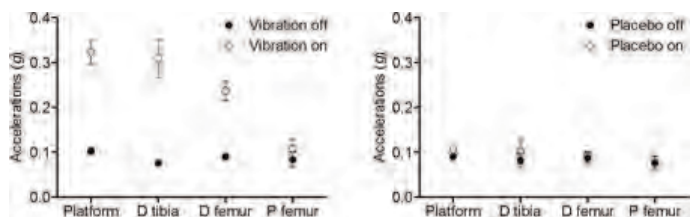
Transmission of a Floor-based Vibration Stimulus Across the Tibia and Femur in Children with Osteogenesis Imperfecta. Christopher Modlesky^{*1}, Marcus Spera¹, Kurt Manal¹, Brianne Mulrooney¹, Lauren Davey², Erica Hartman¹, Michael Bober². ¹University of Delaware, USA, ²A.I. DuPont Hospital for Children, USA

Purpose: There is evidence that a high-frequency, low-magnitude vibration (HLV) treatment administered daily increases bone mass and improves bone structure. It is plausible that the effect of the treatment is dictated by the degree to which the HLV stimulus reaches a bone site. The aim of this pilot study was to determine the degree to which an HLV signal emitted by a floor-based platform transmits across the tibia and femur of children with osteogenesis imperfecta (OI), a group that is very susceptible to fracture.

Methods: Seven children with mild OI (Type 1; 5-10 y) were randomly assigned to stand on a platform that emits an HLV (0.3 g, 30 Hz; n = 4; Juvent Medical, Inc, Somerset, NJ) or a platform that makes a similar sound but does not emit an HLV (n = 3). Tri-axial accelerometers (CXL10GP3; Crossbow, Technology, Inc, San Jose, CA) were placed on the medial aspect of the distal tibia (D tibia), the lateral condyle of the distal femur (D femur), the greater trochanter of the proximal femur (P femur) and on the platform. Accelerations were assessed for 30 seconds while the platform was off and for 30 seconds while the platform was on.

Results: Relative to the platform, acceleration transmission (mean SD) was 95 10% at the D tibia, 74 10% at D femur and 34 7% at P femur (see Figure). On the other hand, no notable differences were observed at any site in the placebo group.

Conclusions: The findings suggest that of the bone sites evaluated in the tibia and femur, the maximum effect of a floor-based HLV treatment should be at the distal tibia.



Figure

Disclosures: Christopher Modlesky, None.

MO0031

Active Shape Modelling of Bilateral Knee Osteoarthritis in the Osteoarthritis Initiative. Jennifer Gregory, Richard Aspden, David Reid, Rebecca J Barr, Fiona Saunders*. University of Aberdeen, United Kingdom

Purpose: To determine the changes in osteoarthritis (OA) by active appearance modelling (AAM) of a bilateral model of the knees.

Dataset: The male participants of Image group B from the Osteoarthritis Initiative (OAI) were selected. They were matched to suitable controls by age, height and weight after previous selection for beam angle (10 2.5).

Methods: This model was based on an active shape model of a single knee used in previous studies. A template of 186 points was constructed using a single image from the OAI image set using AAM software to describe the shape of the knees. The coordinates of the points were found semi-automatically in all images and principal components analysis (PCA) was used to reduce these variables to a small number of independent variables (modes). Here we describe the correlation between various measured parameters such as joint space narrowing and joint alignment in relation to shape and appearance mode 1. Correlations were carried out using Pearson's correlation in SPSS v18.0.

Results: Table 1 shows that the Image B cohort and the controls were well matched using the height and weight parameters ($p = 0.914$ and $p = 0.980$ respectively); however the age matching was less successful due to non-Gaussian distribution.

Correlations show that hip-knee angle, medial joint space narrowing and joint alignment were highly correlated to mode 1 in both shape and appearance (table 2). This was clearly shown by the model, as large changes in the distance between the knees were observed, with the joint alignment measurement and hip knee angle also being tied in with these observations. Medial joint space narrowing was also associated with these parameters. Osteophytes, a typical radiographic indicator of osteoarthritis were found not to be correlated until higher modes of shape and appearance variation (table 2). Other parameters such as symptomatic OA were found to be correlated with higher modes of change in shape and appearance. In addition to the shape changes described above, appearance mode 1 also showed sclerosis where there was evidence of joint space narrowing.

Conclusions: The data shows that the new bilateral knee model shown here is a strong model which correlates common anatomical features of OA such as joint space narrowing with changes in shape and appearance.

Table 1: Characteristics of Image B modelling cohort and matched controls

Variable	Image B cohort	Matched Controls	p value
Age	64 (52-72)	63 (52-71)	0.275†
Height (mm)	1771.3 ± 68.5	1772.5 ± 68.0	0.914
Weight (kg)	94.8 ± 13.7	94.7 ± 13.6	0.980
BMI	30.2 ± 3.7	30.1 ± 3.8	0.942
Beam Angle [degrees]	10.9 ± 2.4	11.11 ± 1.1	0.686

Analysed using paired t test except †Wilcoxon Signed Rank Test, mean ± SD except age which is median and interquartile range

Table 2: Correlation with selected OA parameters in mode 1

Variable	Shape mode 1 correlation (p value)	Appearance mode 1 correlation (p value)
Hip-knee angle (right)	0.558 (0.01)	0.565 (0.01)
Hip-knee angle (left)	0.507 (0.01)	0.523 (0.01)
Medial Joint space narrowing (right)	-0.348 (0.01)	-0.332 (0.01)
Medial Joint space narrowing (left)	0.367 (0.01)	0.370 (0.01)
Osteophytes (right)	0.725	0.835
Osteophytes (left)	N.D.	N.D.
Alignment (right)	-0.397 (0.01)	-0.391 (0.01)
Alignment (left)	-0.350 (0.01)	-0.346 (0.01)

Analysed using Pearson's correlation, N.D. not determined

Disclosures: Fiona Saunders, None.

This study received funding from: Medical Research Council

MO0032

Are Raman Spectroscopic and MicroCT Compositional Measurements Commensurate?. Gurjit Mandair^{*1}, Jason P. Long², Jessica Lopez¹, Steven A. Goldstein², Michael D. Morris¹. ¹University of Michigan, Department of Chemistry, USA, ²University of Michigan, Orthopaedic Research Labs, USA

Purpose: This study examines whether bone tissue composition as measured by Raman spectroscopic mapping is commensurate with volumetric bone mineral density (vBMD) as measured by micro-computed tomography (microCT). **Methods:** Tibiae from a skeletally-mature, female beagle were obtained and the proximal metaphyses were removed for analysis. Specimens were dehydrated and embedded in polymethylmethacrylate. Distal and proximal cortical surfaces were mapped using Raman spectroscopy (six Raman maps per cortical bone type). MicroCT-scans were acquired (29 µm voxel size) and vBMD (mg/cc) values calculated at the same locations (ROI depths of 175 microns and 1.5 mm). Mean mineral-to-matrix (M/M) and carbonate-to-mineral (C/M) ratios were calculated from the pixel histograms of the corresponding Raman maps. Full-width at half-maximum (FWHM) of the Gaussian-fitted compositional histograms were used as measures of bone mineral heterogeneity. Similar data were obtained for cancellous bone along the proximal metaphyses (30 Raman maps). Correlations between Raman compositional parameters and vBMD, including FWHM were investigated. **Results:** By using 1.5 mm deep ROIs, moderate correlations were observed between distal vBMD and M/M ratios ($R^2 = 0.61$), the latter performed slightly better when compared to proximal bone ($R^2 = 0.43$). Correlations between vBMD and C/M for distal and proximal bone were moderate but improved significantly when the distal and proximal datasets were pooled together ($R^2 = 0.82$, $p \leq 0.001$). From FWHM studies, the strongest correlation was found between distal C/M and FWHM ($R^2 = 0.95$) and a partial correlation between distal M/M and FWHM ($R^2 = 0.41$). Raman analyses showed that cortical and cancellous bone composition along the proximal metaphyses were identical in terms of M/M ratios ($p \geq 0.8$) and C/M ratios ($p \geq 0.15$). In ongoing studies, we have observed similar moderate correlations in human specimens. **Conclusions:** As expected only moderate linear correlations between Raman compositional parameters and vBMD were found. Raman compositional parameters include information that is not directly related to calcium content. A better approach is to consider the techniques complementary measures of bone mineral content because Raman spectroscopy reports directly on ion substitutions within the mineral crystallites, while vBMD does not. Non-linear correlative methods may work better and these approaches are currently under development.

Disclosures: Gurjit Mandair, None.

This study received funding from: NIH

MO0033

Biomechanical Role of Collagen Cross-Links in Bone Strength: Finite Element Study. Abdelwahed Barkaoui^{*1}, Ridha Hamblé¹, Awad Bettamer². ¹PRISME Institute, EA4229, University of Orleans, France, ²L'Université d'Orleans, France

Collagen cross-linking, a major post-translational modification of collagen, plays important roles in biomechanical features of bone. The aim of this work is to use a 3D FE model of collagen microfibril and to investigate the important roles of cross-links in the expression of bone strength and its capacity to absorb energy. Studies in vitro and in vivo have reported that increases in cross-linking are associated with enhancement of some mechanical properties (strength and stiffness) and reductions of others (energy absorption). These experimental data are limited in their ability to define individual biomechanical effects of cross-linking. In the present work the study of the effect of cross-links is more realistic that's because the proposed FE model succeed to combines the collagen, mineral and cross-links furthermore been able to varying the mechanical properties of each phase and to visualize their influence on corresponding properties of the collagen microfibril. FE model of microfibril with symmetric and periodic boundary conditions is considered here, with an array of five TC cross-linked together, the all is put into a mineral matrix. A parametric study was performed in order to investigate the influence of varying number of cross-links on the mechanical behaviour of the microfibril. This Finite element model was coupled to a UMAT to calculate the equivalent proprieties of microfibrils. From a FE point of view, spring elements can be used to model connections between two different regions to couple a force with a relative displacement representing the elasticity of the physical connecting constituents. In this study results were obtained under tensile loading with symmetric and periodic boundary conditions. These results show that the number of cross-links has a most influence on the increase in the elastic and failure properties, at constant Young's modulus, if the number of cross-link N increase the bone material will be more stronger, however when $N > 20$ fracture stress does not depend on the cross-link number and it remains at plateau value, same observation has been also found by M.J.Buehler in his molecular multi-scale study. Where it is found that fracture stress depend on the cross-link density β only when $\beta < 25$. This plateau can be explained by the fact that whenever the number of cross link increases their stiffness increases up a threshold value hence the behaviour of all collagen-cross-links becomes insensitive to the number N.

Disclosures: Abdelwahed Barkaoui, None.

This study received funding from: French National Research Agency (ANR) through TecSan program (Project MoDos, nANR-09-TECS-018).

MO0034

Bone Mineral Density (BMD) and Microarchitecture Assessment by Trabecular Bone Score (TBS) at the Spine in Patients with Rheumatoid Arthritis (RA) and Systemic Sclerosis (SSc). Eugenie Koumakis^{*1}, Emese Toth¹, Marine Meunier¹, Emilie Maury², Andre Kahan¹, Yannick Allanore¹, Catherine Cormier³. ¹Rheumatology Department A, Cochin Hospital, APHP, Paris Descartes University, France, ²Service De Rhumatologie A, AP-HP Groupe Hospitalier Cochin - Saint Vincent De Pa, France, ³AP-HP Groupe Hospitalier Cochin, France

RA is a frequent chronic inflammatory rheumatic disease, and a frequent cause of secondary osteoporosis, due to a chronic inflammatory state and long-term glucocorticoid therapy (GC). In SSc, the risk of osteoporosis may be less important because of milder inflammation and fewer patients receiving glucocorticoids. The aims of our study were to examine BMD and bone microarchitecture by TBS in female patients with RA and SSc, to assess their associations with GC use and prevalent fractures and to compare these parameters between these 2 populations and with a control population of same age and sex.

Cross-sectional study of 82 female RA and 38 female SSc patients with mean age of 62.69.3 and 61.10.1 years, mean BMI of 24.44.4 and 26.53.7kg/m², mean disease duration of 17.613.2 and 9.78.6 years, mean CRP of 14.319.7 and 8.69.1mg/l, respectively. In the combined RA and SSc population (n=120), 104 were receiving GC (mean total dose of 3354626117mg in RA and 862111524mg in SSc). 35.3% of RA patients and 36.8% of SSc patients had a history of fracture. BMD and TBS were assessed at AP Spine (L1-L4) with DXA Prodigy (GE-Lunar) and TBS iNsight® (Med-Imaps).

In the combined RA and SSc population, TBS and BMD were significantly lower in patients with a history of fracture (n=43) than in non fractured patients (p=0.006 and p=0.03 respectively). 16 out of these 43 fractured patients had a spine and/or hip BMD in the osteopenia zone (T-score between -1 and -2.5), and TBS was below 1.35 (threshold defining microarchitectural alteration in studies of postmenopausal women) in 11/16 (68.8%) patients. In RA and SSc patients receiving more than 5mg/day of GC (n=55) TBS and BMD were significantly lower than in controls (p=0.007 and p=0.04 respectively), whereas there was no difference with patients receiving less than 5mg/day. Among SSc and RA patients with GC, SSc patients tended to have lower TBS than RA patients (not significant) despite lower total GC dose (p=0.01), higher BMI (p=0.03), and no difference in CRP between the 2 groups.

Microarchitecture assessment by TBS helped to differentiate between patients with and without fractures and between patients with GC and controls. TBS detected 68.8% of fractured patients in the osteopenia zone on BMD. TBS tended to be lower in SSc than in RA suggesting that in SSc there may be additional risk factors for osteoporosis other than glucocorticoid therapy and systemic inflammation, such as vascular alterations and fibrosis.

Disclosures: Eugenie Koumakis, None.

MO0035

Changes in Osteocyte Density in Postmenopausal Women with Prodromal Bone Deterioration (PBD) in Femoral Shaft after Long Term Bisphosphonate Therapy. D. Sudhaker Rao, Shijing Qiu*, Saroj Palnitkar. Henry Ford Hospital, USA

In recent years, there is growing concern about atypical femoral fractures in patients on long-term bisphosphonate (BP) therapy. Such atypical fracture is often preceded by the presence of sub-periosteal new bone and fissure fracture line(s) in lateral femoral cortex, which we refer to as prodromal bone deterioration (PBD). We have previously demonstrated that bone fragility was increased in postmenopausal women with lower osteocyte density. In this study, we investigated whether the PBD resulting from long-term BP treatment is associated with compromised osteocyte integrity.

Trans-iliac bone biopsies were obtained from 4 age matched normal postmenopausal women and 4 postmenopausal PBD patients who had received >5 years of BP treatment. From toluidine blue stained sections, we measured numbers of osteocytes (Ot.N), empty lacunae (EL.N) and total lacunae (Tt.L.N) in osteonal and interstitial areas in cortical bone. Table 1 shows the differences in osteocyte-related variables between PBD patients and normal women. In both osteons and interstitial bone, the densities of osteocytes and total lacunae as well as the percentage of osteocyte occupied lacunae were significantly decreased in PBD patients, whereas the increase in empty lacunar density in PBD patients was seen only in osteons.

The results suggest that patients with PBD (or atypical fracture) have lower osteocyte density. Moreover, the severely suppressed bone turnover induced by long term BP therapy may exacerbate osteocyte deficit. The loss of osteocytes integrity would interfere with microdamage repair, increasing bone fragility and the risk of fracture.

Disclosures: Shijing Qiu, None.

MO0036

Chinese Women Have Greater Cortical Bone Density at the Hip Compared to White Women. Marcella Walker^{*1}, Isra Saeed², Donald McMahon¹, Julia Udesky¹, George Liu³, Thomas Lang², John Bilezikian⁴. ¹Columbia University, USA, ²University of California, San Francisco, USA, ³New York Downtown Hospital, USA, ⁴Columbia University College of Physicians & Surgeons, USA

Chinese women have lower rates of hip and forearm fracture than white women despite lower areal bone density (aBMD) by dual x-ray absorptiometry (DXA). We recently reported higher cortical bone density as well as greater trabecular and cortical thickness, but smaller bone area at the forearm and tibia as measured by high resolution peripheral quantitative computed tomography in Chinese (CH) compared to white women. Premenopausal, but not postmenopausal Chinese women, also had higher trabecular bone density compared to white women. It is unclear whether the differences in skeletal structure observed at peripheral sites are relevant to the central skeleton (lumbar spine and hip). This study was designed to assess this question by comparing racial differences at the lumbar spine (LS) and hip by quantitative computed tomography (QCT). Bone size and volumetric density (vBMD) in pre (PreM; n=83) and postmenopausal (PostM; n=50) CH and white women were determined by QCT. L1-L2 measures included vertebral cross-sectional area (VBSCA) and mid vertebra integral (INT) and trabecular (Tb) vBMD. QCT hip measures included INT, Tb and cortical (Ct) vBMD at the femoral neck (FN) and total hip (TH), FN cross-sectional area (FNCS) and the ratio of tissue volume in Ct regions to total tissue volume within the periosteal boundaries (C/I), a measure of Ct thickness. Age did not differ in either the preM or postM groups: PreM CH 354 vs. white 344yrs and PostM CH 612 vs. white 623 yrs. aBMD by DXA did not differ at the LS or TH in either the PreM or PostM groups. At the LS, VBSCA was smaller in CH compared to white women among PostM but not PreM women. There were no racial differences in INT or Tb vBMD in either age group at the LS. At the hip, FNCS was lower in CH than in white women: 6.5% lower (p=0.02) in preM CH and 8.2% lower (p=0.008) in postM Chinese. Cortical vBMD was 3.6% greater at the TH (p=0.02) in preM CH vs. white women, but there were no differences in Ct vBMD at the FN. Among PostM women, Ct vBMD was 4% greater in CH compared to white women at both the FN (p=0.04) and TH (p=0.03). There were no differences in INT or Tb vBMD or C/I at any hip site in either age group. Similar to the peripheral skeleton, we observed smaller bone size but greater cortical BMD at the hip in Chinese versus white women. The denser cortical compartment in Chinese versus white women may provide greater bone strength and therefore a lower risk of fracture despite smaller bone size.

Disclosures: Marcella Walker, None.

MO0037

Differentiation of Treatment Effects of Odanacatib from Alendronate in Ovariectomized Rhesus Monkeys Using Voxel Based Morphometry of Quantitative Computed Tomography Images. Sangeetha Somayajula^{*1}, Seetha R. Kummari², Todd Bredbenner³, Belma Dogdas⁴, John Szumiloski⁵, Mona L Purcell⁶, Paul McCracken⁷, DON WILLIAMS⁸, Le Thi Duong⁷, Sherri L Motzel⁹, Antonio Cabal¹⁰. ¹USA, ²Case Western Reserve University, USA, ³Southwest Research Institute, USA, ⁴Informatics -IT, Merck Research Laboratories, USA, ⁵Biometrics Research, Merck Research Laboratories, USA, ⁶Imaging, Merck Research Laboratories, USA, ⁷Merck Research Laboratories, USA, ⁸MERCK, USA, ⁹Lab Animal Resources, Merck Research Laboratories, USA, ¹⁰Merck & Co., Inc., USA

Preclinical evaluation of disease burden and treatment efficacy is critical to the development of new therapies for osteoporosis. Quantitative computed tomography (QCT) is a clinically translatable in vivo imaging modality that produces three-dimensional (3D) images of volumetric bone mineral density (vBMD). This enables localization of longitudinal changes in vBMD at each voxel using voxel based morphometry (VBM). Here, VBM was used to evaluate the local effects of odanacatib (ODN) and alendronate (ALN) in comparison to Vehicle (VEH) in ovariectomized (OVX) rhesus monkey. QCT data were obtained (spatial resolution 500 µm) for three groups (n=16 each) of OVX animals treated with VEH, 2 mg/kg ODN daily, and 15 µg/kg twice weekly ALN. Longitudinal QCT measurements were made at 0, 6, 9, 12, and 18 months post-treatment. Femurs were semi-automatically segmented from QCT images, and a statistical shape and density model was generated from all the subjects at each time point, leading to corresponding tetrahedral meshes describing proximal femur geometry with vBMD values assigned at each node of the mesh. In this corresponding representation, the longitudinal change of vBMD at each node is tracked, and the spatial distribution of density changes for each treatment group was obtained. Longitudinal changes in femoral neck vBMD are shown in Fig 1. We also performed a paired t-test (p=0.05, false discovery rate threshold 0.05) between baseline and 18 months for each group to find the nodes that have a significant increase in vBMD compared to baseline. The total number of nodes that showed significant increase was 782 for ODN, 475 for ALN, and 0 for VEH group (Fig.2). The distribution of distances of the interior significant nodes from the surface nodes is shown in Figure 3. While ALN had a nearly uniform distribution of significant nodes up to about 4 mm from the surface, ODN showed an approximately Rayleigh distribution with a peak around 2.5 mm (average cortical thickness is 2.2 mm). We

verified that this distribution is different from that obtained by a random sampling of interior nodes, confirming that the difference is due to treatment effect, and not by chance. This work shows that ODN is efficacious in increasing vBMD (femoral neck vBMD and number of significant nodes), and that the effect of ODN is more cortical compared to ALN. These findings are supported by data from other modalities and anatomic locations.

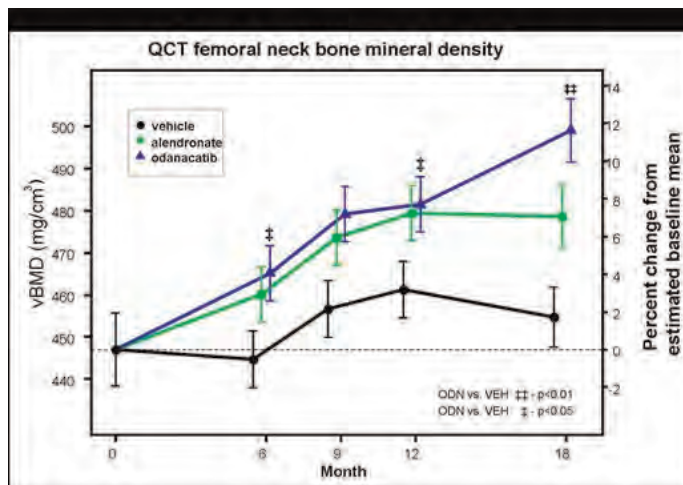


Figure1: Model means and relative standard errors of QCT femoral neck vBMD

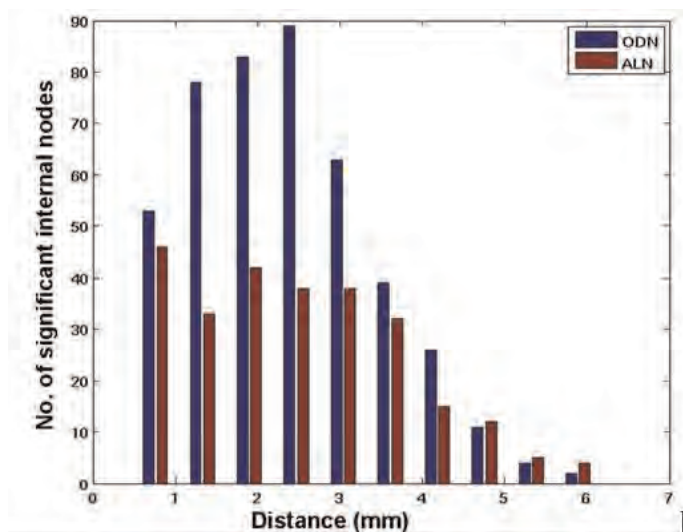


Figure 3: Histogram of distances of significant internal nodes from surface nodes

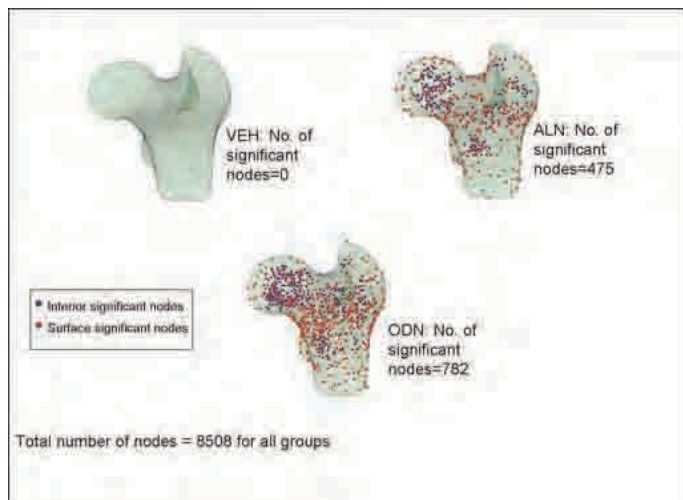


Figure 2: Nodes showing significant increase in BMD from baseline to 18 months

Disclosures: Sangeetha Somayajula, None.

MO0038

Hip Fracture in Older Women: Association with the Femoral Strength as Assessed by Finite Element Analysis of Qct Scans. Lang Yang*, Will J M Udall, Eugene V McCloskey, Richard Eastell. University of Sheffield, United Kingdom

Bone fractures only when loaded beyond its strength. Although conventional BMD by DXA predicts hip fracture well, it is not a specific measure of the bone strength. The purpose of this study was to determine the association of femoral strength, as estimated by finite element (FE) analysis of QCT scans, with hip fracture in comparison to femoral neck (FN) and total hip (TH) BMD.

We recruited 50 postmenopausal women (55-89 yrs) who had sustained hip fractures (37 intracapsular (IC) and 13 extracapsular (EC)) due to low-energy trauma. QCT scans were performed within 3 months of the fracture. For each fracture case a postmenopausal women, matched by age (5 yrs), weight (5 kg) and height (5 cm) was recruited as a control.

We performed linear-elastic FE analysis to simulate a sideways fall. The elastic modulus and yield stress of elements were calculated from the element vBMD. Femoral strength was defined as the impact force that caused the von Mises stress in a volume of at least 125 mm³ that's made up of contiguous elements to exceed the element yield stress. Odds ratio (OR) of hip fracture for one standard deviation change was derived from conditional logistic regression and area under the curve (AUC) from analysis of receiver operating characteristics. Significance level was chosen at $p < 0.05$.

As expected, the fracture group had lower FN BMD (0.568 SD 0.100 v. 0.659 SD 0.105 g/cm²), TH BMD (0.693 SD 0.136 v. 0.803 SD 0.125 g/cm²) and strength (2702 SD 746 v. 3664 SD 812 N) than the controls. The strength was highly correlated to the FN and TH BMDs ($r = 0.64$ & 0.72 , $p < 0.0001$). The hip BMDs and strength were significantly associated with hip fracture (see Table). Strength alone discriminated hip fracture significantly better than TH BMD. Bivariate logistic regression showed that strength was associated independently with hip fracture and significant larger AUCs than that of TH BMD were obtained by combining BMDs and strength.

In conclusion, femoral strength derived from the FE analysis of QCT scans has the potential to discriminate hip fracture better than BMD alone.

	OR (95% CI)	AUC (95% CI)
Univariate logistic regression		
FN BMD	4.3 (1.9, 9.5)	0.73 (0.63, 0.82)
TH BMD	5.5 (2.2, 13.9)	0.72 (0.62, 0.82)
Strength	5.1 (2.2, 11.6)	0.82 (0.73, 0.90) ^a
Bivariate logistic regression		
1. FN BMD	2.6 (1.1, 6.5)	0.81 (0.72, 0.89) ^{ab}
Strength	4.1 (1.6, 10.3)	
2. TH BMD	2.4 (0.8, 6.9)	0.79 (0.70, 0.88) ^b
Strength	3.6 (1.4, 9.1)	

Note: AUC with subscript a and b were significantly larger than that of FN and TH BMDs at $p < 0.05$, respectively.

OR for 1 SD decrease and AUC

Disclosures: Lang Yang, None.

MO0039

Insulin resistance, Diabetes, and Composite Indices of Femoral Neck Strength: Findings from The Hip Strength Across the Menopausal Transition Study. Shinya Ishii¹, Jane Cauley², Preethi Srikanthan³, Carolyn Crandall³, Mei-Hua Huang⁴, Michelle Danielson⁵, Gail Greendale³, Arun Karlamangla³. ¹UCLA, VA, USA, ²University of Pittsburgh Graduate School of Public Health, USA, ³University of California, Los Angeles, USA, ⁴UCLA, USA, ⁵University of Pittsburgh, USA

Diabetes mellitus (DM) has been associated with increased fracture risk, despite being associated with higher areal bone mineral density (aBMD). We hypothesized that this disparity is, at least partly, due to DM associations with bone size (which affects bone strength) and body size (which determines the forces on bone during a fall), and that composite indices of femoral neck strength, which integrate dual energy x-ray absorptiometry (DXA) derived aBMD, femoral neck width (FNW) and femoral neck axis length (FNAL) with body weight and height, and are inversely associated with hip fracture risk, would be lower in diabetic and pre-diabetic women than in women with neither condition. We also hypothesized that the strength indices would be inversely related to insulin resistance, the primary pathology in type 2 diabetes.

We analyzed data from 1887 women (from 4 ethnic groups: Caucasian, African American, Chinese and Japanese) from the baseline visit of the Study of Women's Health Across the Nation (SWAN), when participants were in either pre- or early peri menopause. Composite indices for femoral neck strength in different failure modes were created as $aBMD \times FNW / \text{weight}$ for compression strength index (CSI), $aBMD \times (FNW)^2 / FNAL$ for bending strength index (BSI), and $aBMD \times FNW \times FNAL / \text{height} \times \text{weight}$ for impact strength index (ISI). Women were categorized into DM (n=81), pre-diabetes (n=291), and normal groups (n=1515) based on fasting glucose

measurements, self-report of DM, and review of medications. Homeostasis model assessment of insulin resistance (HOMA-IR) was calculated from fasting values of glucose and insulin, and log-transformed for analysis. Multiple linear regression models were used to adjust for age, race/ethnicity, menopausal stage, body mass index (BMI), smoking status, and study site.

Areal BMD was higher and yet all three composite strength indices were lower in women with DM and pre-diabetes than in women who were normal (Table). There were graded inverse relationships between HOMA-IR and all three strength indices in LOESS plots; these inverse relationships persisted after adjusting for covariates in linear regression. (Table).

Relative to the loads they bear, diabetic women have lower femoral neck strength, consistent with their documented higher rates of fracture. Insulin resistance appears to play an important role in the reduction in bone strength in diabetes.

Effects of diabetes status and insulin resistance

	Pre-diabetic vs. normal	Diabetic vs. normal	Per unit increase in ln(HOMA-IR)
Femoral Neck:			
aBMD: unadjusted	+0.046***	+0.134***	+0.077***
adjusted	-0.001	+0.037**	+0.009
CSI: unadjusted	-0.27***	-0.57***	-0.45***
adjusted	-0.06	-0.13*	-0.12***
BSI: unadjusted	-0.035***	-0.085***	-0.067***
adjusted	-0.008	-0.021*	-0.022***
ISI: unadjusted	-0.031***	-0.065***	-0.052***
adjusted	-0.007	-0.015*	-0.014***

*, **, *** denote $p < 5\%$, 1% , 0.1% level, respectively

Table

Disclosures: Shinya Ishii, None.

MO0040

Measuring Apparent Trabecular Structure with the Stratec pQCT: A Comparison with HR-pQCT. Deena Lala^{*1}, Angela Cheung², Kayla Hummel¹, Dean Inglis³, Christopher Gordon³, Lora Giangregorio¹. ¹University of Waterloo, Canada, ²University Health Network, Canada, ³McMaster University, Canada

Background/Objective: Peripheral quantitative computed tomography (pQCT) is used to assess bone density and cortical bone structure. Previous work suggests that the Stratec pQCT can be used to estimate apparent trabecular structure, but it is unknown how this technique compares to comparatively newer methods with improved spatial resolution such as high-resolution pQCT (HR-pQCT). We examined the accuracy of pQCT-based measurements of cortical thickness, density and apparent trabecular structure at the ultra-distal tibia, using HR-pQCT as a gold standard.

Methods: Fifteen dry human tibia specimens were immersed in saline in a sealed cylinder and scanned 22.5mm from the distal tibia plateau using pQCT (one slice; thickness: 2.2mm; pixel size 0.2mm x 0.2mm; Stratec XCT2000), and HR-pQCT (simultaneous acquisition of 110 slices; thickness: 9.02mm; isometric voxel size 82µm; Scanco XtremeCT). Pearson correlations were used to examine relationships between the techniques for apparent trabecular structure variables (average hole size, H_A ; trabecular spacing, TbSp; bone volume to total volume, BV/TV; trabecular volumetric bone mineral density, TDen; trabecular area, TbA; total area, TotA) and cortical thickness (CTH) and density (CDen). pQCT measures of H_A , BV/TV, TbSp, were assessed using custom developed software, while Stratec software was used to obtain TDen, TbA, TotA, and CDen, and CTH was obtained using both. H_A was compared to TbSp to establish convergent validity. Bland-Altman analyses were performed to qualitatively investigate measurement bias between pQCT and HRpQCT. All analyses were performed using SAS 9.2.

Results: All variables were well correlated ($r^2=0.50-0.98$, Table 1). pQCT estimates of H_A , TbSp, BV/TV, TDen, TbA, CTH (custom), CDen, and TotA were overestimated, while CTH (Stratec) was underestimated compared to HRpQCT (Table 1). Additionally, as values of H_A , BV/TV, TotA increased, the difference in methods increased, however as values of CTH (Stratec) increased, the difference in methods decreased. There were no proportional differences for TbSp, TbA, CDen, CTH (custom software), and TDen.

Conclusion: pQCT-based measurements of cortical thickness, density and apparent trabecular structure at the ultra-distal tibia were well correlated with HR-pQCT estimates. pQCT yielded higher values for H_A , TbSp, BV/TV, TDen, TbA, CTH (custom), CDen, TotA, and lower values for CTH (Stratec).

Bone Variable	r^2	Bias	95% Limits of Agreement	
			Lower	Upper
H_A	0.9204	-0.125	-0.559	0.309
TbSp, mm	0.5047	-0.2480	-0.319	-0.178
BV/TV	0.8262	-0.420	-0.493	-0.348
TDen, mg/cm ³	0.6047	-32.140	-87.980	23.700
TbA, mm ²	0.7247	-21.435	-200.314	157.445
CTH, mm (custom software)	0.8275	-0.057	-0.295	0.180
CTH, mm (Stratec software)	0.9769	0.268	0.053	0.483
CDen, mg/cm ³	0.9059	-110.927	-153.197	-68.656
TotA, mm ²	0.9337	-176.955	-249.048	-104.862

Table 1

Disclosures: Deena Lala, None.

MO0041

Morphometric Assessment of Vertebral Fracture Risk in Postmenopausal Women using Vertebral Shape Models and Discriminative Shape Alignment. Alessandro Crimi¹, Marco Loog², Marleen de Bruijne³, Mads Nielsen⁴, Martin Lillholm^{*5}. ¹Nordic Bioscience & University of Copenhagen, Denmark, ²Delft University of Technology, Netherlands, ³University Medical Center Rotterdam, Netherlands, ⁴University of Copenhagen, Denmark, ⁵Synarc Imaging Technologies, Denmark

Purpose

The FRAX index summarizes osteoporosis risk factors, such as, prevalent vertebral fractures and BMD into a 10-year risk of major osteoporotic fractures. Vertebral deformities below accepted fracture thresholds are, however, not normally considered. This work investigated to which extent vertebral pre-fracture morphometric changes offer risk segregation in addition to standard OP risk factors.

Methods

A case group of 19 postmenopausal women was selected as the subset of an epidemiological study population (PERF) that had no vertebral fractures at baseline and developed at least one incident fracture in the lumbar region (T12-L4) by follow-up (6.3 years). 91 controls that remained fracture free throughout were matched to the case group based on BMD, BMI, age, and other standard OP risk factors. Lateral radiographs were acquired at baseline and follow-up. Vertebral fracture status was assessed, using Genant's semi-quantitative method, by an experienced radiologist. Subsequently, the corner and mid-points of the two vertebral end-plates were annotated for each lumbar vertebra using a computer-program.

A shape model was trained on the spine/vertebral shapes represented by the lumbar height points using Discriminative Shape alignment (DSA) and each shape represented using 2-4 eigenmodes. The ability to separate cases from controls at baseline was tested using a linear classifier. The performance was estimated using unbiased cross-validation. The inter-annotator reproducibility was assessed through repeat annotations by two trained x-ray technicians.

Results

Based on the ROC-curves for separation of cases and controls at baseline, results are reported as the area under the curve (AUC) and a Delong p-value indicating significance of performance relative to chance. The AUC for the radiologist was AUC = 0.73, $p=0.01$. For the two repeat annotations, the values were AUC=0.70, $p=0.02$ and AUC=0.70, $p=0.01$ respectively, yielding an inter-annotator CV of 2.4%.

Conclusion

For groups matched for standard OP risk factors, the suggested methodology was able to segregate lumbar fracture risk using pre-fracture vertebral deformities measured at baseline. The inter-annotator reproducibility between radiologist and technicians was good. Inclusion criteria for OP clinical trials, such as, BMD and prevalent vertebral fractures could be supplemented by a morphometric measure of fracture risk and potentially improve statistical power or reduce required samples sizes.

Disclosures: Martin Lillholm, CCBR Synarc, 2
This study received funding from: CCBR Synarc

MO0042

Nanoindentation Shows Significantly Increased E, H and Viscosity for Sclerotic Bone Healing Response, Corresponding well with Micro-CT and pQCT Results. Xiuli Chen^{*1}, Yong Hoow Chan², Sungyun Park², James Goh³, Shamal Das De³, Richie Soong⁴, Taeyong Lee¹. ¹National University of Singapore, Singapore, ²Division of Bioengineering, National University of Singapore, Singapore, ³Department of Orthopaedic Surgery, National University Hospital, Singapore, ⁴Department of Pathology, National University of Singapore, Singapore

Purpose

Sclerotic bone formation, which was found in some rodent bones with osteolytic W256 mammary carcinoma cells induced, is similar to the development of lytic lesions into sclerotic for benign tumors. The aim of this study is to quantify changes in bone

micro-mechanical, micro-structural and materials properties of localized sclerotic healing response.

Methods

28 female SD rats were inoculated with W256 cells in the left femur, 5 mm away from distal metaphysis. 9 SD rats were sham operated in the left femur. Localized sclerotic bone formation away from surgical site was observed from histological evaluation at 10, 30, 50 day time points. At 50 day, femurs were harvested and subjected to microCT, pQCT scanning. Following that, the bones were embedded in epoxy, polished and rehydrated for nano-indentation. A Berkovich tip was used to indent on the bone using CSM (Continuous Stiffness Measurement) mode at 45Hz. Forty indentations were made per bone specimen and creep test was carried out at maximum load of 6.3mN for 400s. Viscosity (η) was evaluated using Voigt model.

Results

Histological observation of localized woven bone formation was concurred in pQCT images (Figure 1). Significant increases in BMD % change (Figure 2A), cortical density % change, BMC % change (compared to intact RF) were observed as compared to sham groups ($p < 0.05$). Similarly, nanoindentation results showed significant increases in elastic modulus (E) (Figure 2B), hardness (H) and viscosity (η) (Figure 2C) in sclerotic cortical bone in the same ROI as compared to the normal bone. This is not unexpected since increase in mineralization (as indicated from increases in BMC and BMD) increases E. In sclerotic bone, significant Pearson correlation was also found between h and H ($R = 0.540$, $p = 0.009$) and a weaker correlation between h and E ($R = 0.414$, $p = 0.055$). These results correspond well with previous study [2], where there were positive relationships of h with E and H .

Conclusions

Nanoindentation was able to quantify localized mechanical property changes for sclerotic healing response, which complemented micro-structural and material property changes monitored by microCT and pQCT. Similar sclerotic bone formation found in other benign tumor cases can change the local mechanical properties of bone with increase in E , H and h . This study helps to demonstrate the use of nanoindentation for the study of diseased bone and localized drug effect.

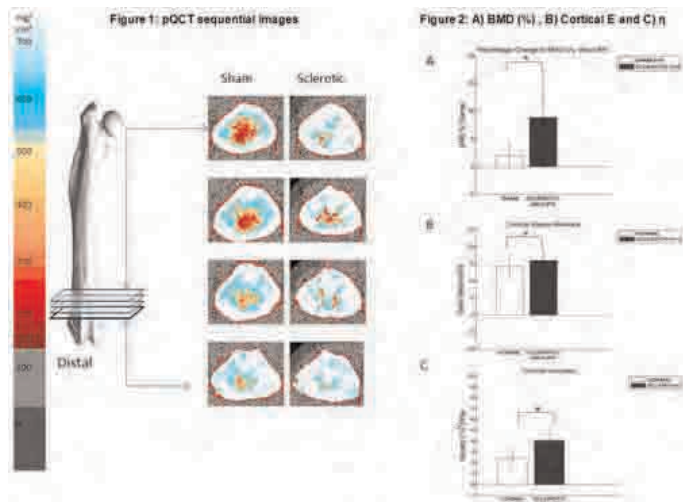


Figure 1 and 2

Disclosures: Xiuli Chen, None.

MO0043

Physical Exercise Programs in a Female Rat Model: What Is the Most Osteogenic? Priscilla C. AVELINE*, Eric LESPESSAILLES, Claude-Laurent BENHAMOU, Gael Rochefort, INSERM U658, France

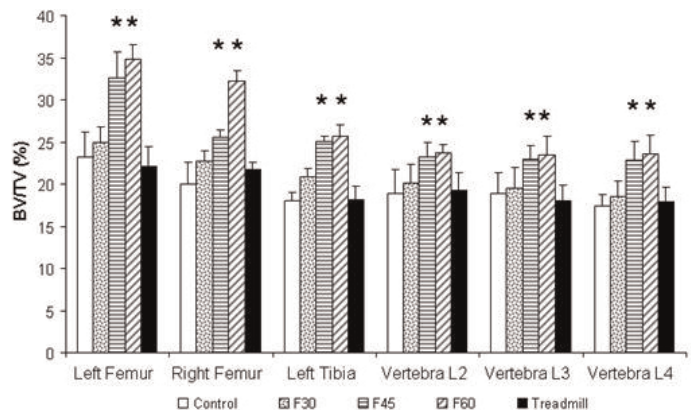
Physical exercise is a well-recognized intervention to adapt the skeleton and to increase bone density and bone mass by changing bone architectural, remodeling and mechanical properties. Exercise triggers an osteogenic response increasing bone strength. The aim of this study was to determine in a female rat population what is the best physical exercise to improve bone quality.

In this study, four different exercise groups were studied: fall impact 30 cm (F30), fall impact 45 cm (F45), fall impact 60 cm (F60), a treadmill (T) group and a sedentary group. Each group included 10 female Wistar rats, 8 weeks old at baseline. Animals were subjected to 10 impacts per day from different heights, 5 days a week or run on a treadmill: 1h a day, 5 days a week during 8 weeks. Bone mineral density (BMD) and content (BMC) (whole body and left femurs) were measured by DXA (Hologic Discovery) at different time of the study (week 0, week 4 and week 8). Morphological properties of the trabecular bone from tibias, femurs and L2 to L4 vertebrae were analyzed by micro-computerized tomography (Skyscan 1072) and mechanical properties were recorded.

BMD and BMC on whole body and left femurs increased all groups versus baseline but differences between groups were not significant. In terms of bone mass (BV/TV), the F45 and F60 groups had significantly higher values than the 5 groups, while the F30 and T groups had no higher values than the 5 groups. The profile was

similar concerning Tb.N, Tb.Th, while Tb.Sp, Tb.Pf and SMI were significantly lower in the F45 and F60 groups. For mechanical properties, F45 were significantly superior to the other groups concerning the Young modulus.

These data suggest that the treadmill exercise and the impact 30 cm (with this specific intensity) are not beneficial on bone status, while impacts from 45 and 60 cm appear the most osteogenic, and impact 45 cm gives the best mechanical results.



μ CT results on the percent of bone volume (BV/TV) from femurs, tibias and vertebrae after different physical exercises, compared to sedentary.

Fall impact 45 cm (F45) or fall impact 60 cm (F60) were significantly (*) increased compared to control (C), fall impact 30 cm (F30) or treadmill (T). These results showed that the impact 45cm and 60cm exercises induced a higher rise of bone volume than the other exercise. Physical exercise had also different effect on bone sites.

Fig 1

Disclosures: Priscilla C. AVELINE, None.

MO0044

Pre- and Post-Menopausal Differences in Bone Density, Microstructure, and Mechanical Competence in Chinese-American and Caucasian Women. Xiaowei Liu^{*1}, Marcella Walker², Emily Stein¹, Bin Zhou², Julia Udesky², George Liu³, Donald McMahon¹, Elizabeth Shane¹, John Bilezikian¹, X Guo². ¹Columbia University College of Physicians & Surgeons, USA, ²Columbia University, USA, ³New York Downtown Hospital, USA

Despite lower areal BMD (aBMD) by DXA, Chinese-American (CH) women have fewer fractures than Caucasian (CA) women. We applied individual trabeculae segmentation (ITS) and finite element analysis to high-resolution peripheral QCT images of the distal radius (DR) in pre- (PreM; n=95) and post-menopausal (PostM; n=97) CH and CA women to quantify trabecular (Tb) plate- and rod-microarchitecture and bone stiffness.

Age did not differ between PreM groups (CH 367 vs. CA 357 yrs) but was lower in PostM CH (CH 612 vs. CA 643 yrs). Height and weight were lower in the CH vs. CA groups (PreM: CH 162cm 57kg vs. CA 165cm 63kg; PostM: CH 157cm 58kg vs. CA 163 cm 66kg, $p < 0.05$). aBMD did not differ at the spine, hip or 1/3 radius in either age group. At DR, PreM CH had 14% greater Tb vBMD (Dtrab), 65% higher Tb plate vs. rod ratio (P-R Ratio), 46% higher plate bone volume fraction (pBV/TV), and 23% greater plate-plate junction density (P-P Junc.D, indicating intactness of Tb network) compared to PreM CA women ($p < 0.001$). Despite smaller bone size (-9%, $p = 0.03$), greater cortical thickness and vBMD (Ct.Th & Dcort, 18% & 4%, $p < 0.001$) and more Tb plates led to 14% greater whole bone stiffness ($p < 0.05$) in PreM CH vs. CA women. In contrast, PostM CH had similar Dtrab, pBV/TV, and P-P Junc.D, yet 38% higher P-R Ratio ($p = 0.01$) compared to PostM CA women. Despite smaller bone size (-10%, $p = 0.008$), PostM CH women had greater Ct.Th & Dcort (18% & 6%, $p < 0.01$) and relatively intact Tb plate, resulting in similar bone stiffness compared to CA women.

The aBMD at each site, and Ct.Th and Dcort at DR were significantly lower in PostM vs. PreM, and the PreM-PostM differences were similar between CH and CA women. Whole bone stiffness, Dtrab, and Tb plate parameters were also significantly lower in PostM vs. PreM women. Moreover, the PreM-PostM differences in Dtrab and pBV/TV were significantly greater ($p < 0.05$) in CH and the differences in stiffness, P-R ratio, and P-P Junc.D tended to be greater in CH vs. CA women ($p = 0.06$, Table 1).

The data show greater microstructural advantages in both Ct and Tb bone in PreM CH women. However, differences between the PreM-PostM groups suggest greater loss in plate-like Tb bone in PostM CH women. Nevertheless, advantages such as thicker cortices and more plate-like Tb bone remain in PostM CH. The results provide greater insight into the microstructural advantages of the CH vs. CA skeleton in both pre- and postmenopausal states.

PostM vs. PreM	CH (%)	CA (%)	p-value (PreM-PostM differences in CH vs. CA)
DXA			
aBMD at LS	-12.3*	-9.6*	0.47
aBMD at TH	-8.4*	-12.1*	0.28
aBMD at FN	-11.8*	-15.7*	0.22
aBMD at 1/3 Radius	-11.5*	-11.5*	0.99
HRpQCT (DR)			
Bone Area	-4.7	-3.3	0.86
Dtrab	-27.8*	-12.6*	0.01
Dcort	-4.8*	-6.6*	0.40
Ct.Th	-11.1*	-11.4*	0.78
P-R Ratio	-29.1*	-15.3	0.06
pBV/TV	-36.5*	-21.6*	0.02
P-P Junc.D	-34.9*	-22.2*	0.06
Whole Bone Stiffness	-23.9*	-17.1*	0.07

Table 1. % differences (PostM vs. PreM) in CH and CA women.
* indicates significant difference in PostM vs. PreM.

Table 1

Disclosures: Xiaowei Liu, None.

MO0045

Pyridoxamine and Sorbinil Do Not Prevent Bone Mechanical and Tissue Deterioration in a Rat Model of Type 2 Diabetes. Maxime Gallant^{*1}, Kathleen Hill¹, Benjamin Rowland¹, Matthew Allen¹, Richard G. Peterson², David Burr¹. ¹Indiana University School of Medicine, USA, ²PreClinOmics Inc., USA

Type 2 diabetes mellitus (T2DM) is metabolic disorder characterized by high blood glucose levels and insulin resistance. The hyperglycemia in T2DM causes an increase in advanced glycation end products which are known to negatively affect bone tissue, resulting in a more brittle bone phenotype. We hypothesized that pharmacologically interfering in the glucose and fructose-induced glycation pathways with the vitamin B6 vitamer pyridoxamine (PM) or the aldose reductase inhibitor sorbinil (Sorb), respectively, would prevent bone tissue deterioration in a rat model of T2DM.

Fifteen week-old Zucker Diabetic Sprague-Dawley (ZDSD) and control CD rats were fed a high-fat diet (Purina 55CA) for 3 wks to induce T2DM and were treated with PM (100 mg/kg, s.c.), Sorb (65 mg/kg, p.o.) or respective vehicles for 15 wks. A baseline group of both strains was analyzed at 15 wks of age, before the diet-induced initiation of T2DM. Bones were analyzed post-mortem for changes in density, architecture, and mechanical properties. Blood chemistries were also performed. Two-way ANOVAs were performed to look at strain and diet effect between the baseline and control animals, and strain and treatment between the controls, PM and Sorb groups.

At baseline, the ZDSD and CD rats had similar BMD, BV/TV and vertebral mechanical and tissue properties. However, the ZDSD had significantly stronger and stiffer femurs but lower energy absorption capacity compared to CD controls. These differences in whole bone mechanical properties remained after correction for differences in geometry indicating the differences exist at the tissue level.

The high-fat diet induced T2DM in ZDSD rats but not CD rats, as expected, and significantly decreased BMD, bone mechanical and material properties at both the femur and vertebra compared to the control CD rats.

Treatment with pyridoxamine had no beneficial effect on any bone parameter and in some cases reduced properties compared to untreated controls (e.g. decreased vertebral strength). Sorbinil increased femur toughness, but only in CD rats; no beneficial effect of sorbinil was observed in ZDSD rats.

These results show that pyridoxamine does not positively affect bone properties in a rat model of T2DM or in control rats. Sorbinil had some positive effects on bone, but seemed to be effective only in control CD rats. The rapid onset of T2DM in the ZDSD rat model may reduce the potential therapeutic window available to improve bone mechanical properties.

Disclosures: Maxime Gallant, None.

MO0046

Quantitative Bone Micro-Architecture in Young Adults Using Multi-Detector CT Imaging and Volumetric Topological Analysis – A Feasibility Study. Punam K. Saha^{*}, Yinxiao Liu, Cynthia Pauley, Trudy Burns, James Turner, Steven Levy. University of Iowa, USA

Background: Adult bone diseases, especially osteoporosis, lead to increased risk of fracture associated with substantial morbidity, mortality, and financial costs. Clinically, osteoporosis is defined by low bone mineral density (BMD). However, evidence suggests trabecular bone (TB) micro-architecture is an important determinant of bone strength and fracture risk. Multi-detector CT (MDCT) shows promise for peripheral TB imaging at an acceptable radiation dose that avoids invasive bone biopsies with conventional histomorphometry. Volumetric topological analysis (VTA), developed in our laboratory, assesses topology of individual trabeculae on

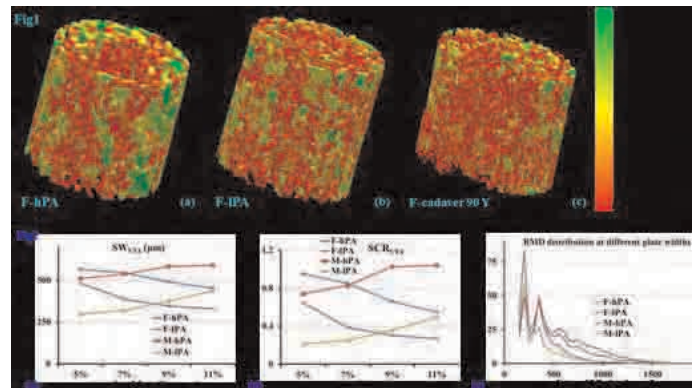
the continuum between a perfect plate and a perfect rod (Fig1), and provides a unique measurement of BMD distribution at different TB plate widths (Fig2). We conducted a feasibility study of TB micro-architecture in young adults using MDCT and VTA.

Methods: Four age-similar (18-23Y) volunteers – 1 male/1 female each with high/low physical-activity (PA) (hPA/iPA) participated. MDCT scans of the distal tibia were acquired on a 128 slice Siemens Flash scanner at 120kV, 200mAs, pitch: 1.0, slice thickness: 0.3mm and scan length: 10cm (total effective dose:17 mrem \approx 20 days of environmental radiation). An INTableTM Calibration Phantom was used to calibrate CT Hounsfield units into BMD (mg/cc).

Results: Fig1 compares color-coded TB plate/rod classification for the female volunteers with high (F-hPA) and low (F-lPA) PA to a 90Y female cadaver specimen. The TB core of F-hPA has more plates (green). The cadaver has significantly fewer plates and more rods (red). Fig2 summarizes the surface-width (SWVTA) (2a), surface-to-curve-ratio (SCRVTa) (2b) and BMD distribution (2c) at different plate widths over 5-11% of tibial length from the distal endplate. Volunteers with hPA show higher architectural parameters (SWVTA, SCRVTa). PA level is a less meaningful predictor of BMD distribution over more rod-like trabeculae (<500 μ m), but is more strongly associated with the plate width range 500-1000 μ m (2c). The rate of change of TB geometry along the tibial axis is gender-dependent.

Conclusion: MDCT with VTA detected effects of PA in vivo and is suited for longitudinal and cross-sectional clinical studies related to bone diseases.

Acknowledgement: This research study was supported by the NIH grants: R01 AR054439 and R01 DE012101.



Figures 1 and 2

Disclosures: Punam K. Saha, None.

MO0047

Recent Hip Fracture Does Not Account for Polar and Radial Distribution of Cortical Density At Tibial Mid-Diaphysis. Ari Heinonen^{*1}, Timo Rantalainen², Johanna Koskinen³, Marja Arkela-Kautiainen⁴, Mauri Kallinen⁴, Sarianna Sipilä³. ¹Department of Health Sciences, University of Jyväskylä, Fin, ²Department of Mechanical Engineering, Lappeenranta University of Technology & Neuromuscular Research Center, Department of Biology of Physical Activity, University of Jyväskylä, Finland, ³Gerontology Research Centre, Department of Health Sciences, University of Jyväskylä, Finland, ⁴Central Finland Central Hospital, Finland

It is well established that cortical volumetric density (vBMD, mg/cm³) varies around the bone cross-section as well as along the axial length of the bone. Changes in vBMD distribution have been attributed to growth and aging, whereas it is unclear whether lower limb vBMD distribution is modulated by recent hip fracture. This study evaluated the tibial side-to-side differences in polar and radial vBMD distributions as well as differences in vBMD (mg/cm³), cortical area (CoA, mm²) and density weighted section modulus (SSI, mm³) among 68 hip fracture patients (mean age: 79.7 years, height: 161.9 cm, weight: 66.1 kg). 78% of the participants were women and 9% current smokers. The majority (80%) of fractures occurred as the consequence of a fall. The participants had sustained a femoral neck or trochanteric fracture 6 to 16 weeks earlier. Bone cross-sections at the tibial mid-diaphysis were assessed with peripheral quantitative computed tomography (pQCT). Polar and radial vBMD distributions were analyzed in 36 sectors and 3 divisions, respectively. The innermost and outermost layers of pixels were excluded from the analysis to avoid partial volume effect (Fig. 1). The side-to-side differences (fractured vs. non-fractured side) in the tibial vBMD (-0.34.3 %), CoA (-0.85.6 %) and SSI (-1.08.9 %) were not statistically significant. No significant differences were observed in polar vBMD distribution (MANOVA, P = 0.787) or in radial vBMD division (P = 0.758) between the fractured and non-fractured side (Fig.1). In conclusion, a recent proximal femoral fracture has no effect on polar and radial cortical density distributions or bone mineral mass and strength in the tibial bone. This suggests that previously reported bone mass and geometry decline after hip fracture is caused by the disuse following the injury.

References:

1. Mikkola T, Sipilä S, Portegijs E, Kallinen M, Alen M, Kiviranta I, Pekkonen M, Heinonen A. Impaired geometric properties of tibia in older women with hip fracture history. Osteoporos Int 2007 18:1083-1090.

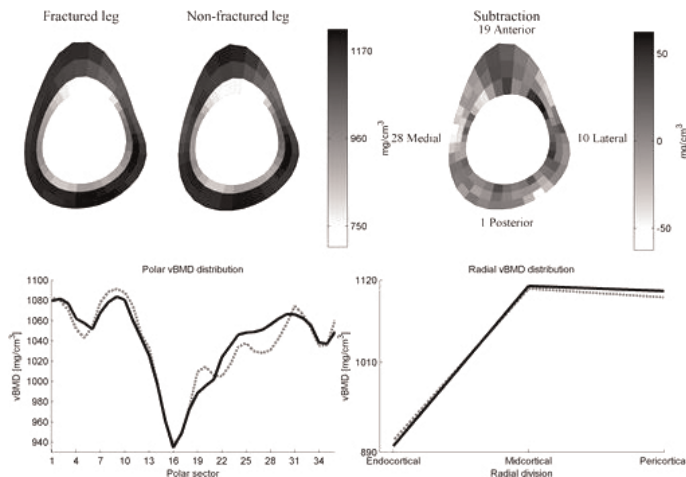


FIGURE 1. Illustration of the mean leg's cortical density distributions from the tibial mid-shaft al

Disclosures: Ari Heinonen, None.

MO0048

Reference Point Indentation: A new paradigm for characterization of visco-elastic materials. Alexander Proctor*, Davis Brimer. Active Life Scientific, Inc., USA

Reference Point Indentation (RPI) is an emerging microindentation technology with novel translational research capabilities, including both ex vivo and in vivo measurement of Bone Material Strength (BMS). Here we characterize the performance of an improved RPI instrument optimized for pre-clinical bone research (BioDent, Active Life Scientific, Inc., Santa Barbara, CA). The improved BioDent is a load-controlled RPI with cyclical indentation capabilities. The novel arrangement of a Test Probe and a Reference Point enable quantitative measurements of mechanical properties at a local site on the bone without the need for a rigid load frame. The instrument can indent a material at forces ranging from 2.0N to 12.0N at frequencies ranging from 0.1Hz to 5.0Hz. Each measurement may consist of up to 100 cyclical indentations at the same location. For this study a calibration phantom, poly-methyl methacrylate (PMMA), was measured using various combinations of input parameters. PMMA is often used as a calibration phantom because it exhibits similar mechanical properties to bone during indentation testing. To characterize the performance of BioDent, 20 different indentation forces were selected that evenly span the operating range of the instrument (2.0N-12.0N) and 6 different indentation frequencies were selected that evenly span the operating range (0.1Hz-5.0Hz). Each of these measurements consisted of 10, 50, or 100 indentations cycles. A total of 360 measurements were made on PMMA. For each combination of input parameters, measured outputs were tabulated and evaluated for consistency and reproducibility. Additionally, performance characteristics were calculated during each measurement (force resolution, distance resolution, and compliance). For each combination of input parameters BioDent showed an average variation of less than 10-15% between each measurement. Maximum force varies by less than 10% for all indentation forces. Based on these results, it is clear that the improved RPI instrument, optimized for pre-clinical bone research, can consistently and quantitatively measure material strength of visco-elastic materials.

Disclosures: Alexander Proctor, Active Life Scientific, Inc., 3
This study received funding from: Active Life Scientific, Inc.

MO0049

Regional Variation in Cortical Microarchitecture of the Distal Radius and Tibia. Galateia Kazakia¹, Gregory Bernstein², Miki Sode³, Andrew Burghardt¹, Sharmila Majumdar¹. ¹University of California, San Francisco, USA, ²University of California, USA, ³University of California San Francisco & Berkeley, USA

Cortical structure is vital to the mechanical integrity of long bones, and can be influenced by age, disease, and therapeutic intervention. Quantification of cortical structure parameters is critical to fracture risk prediction in the context of these effects, but conventional analysis techniques obscure potentially important regional parameter variations. Therefore, the objective of this study was to characterize spatial variability in cortical microstructure and geometry at the distal radius and tibia. High resolution peripheral QCT images were acquired from 142 healthy individuals (50 M 92 F, 20-78 y). Periosteal and endosteal boundaries and haversian porosity within the cortical compartment were identified using an automated segmentation technique. Cortical thickness (Ct.Th), porosity (Ct.Po), pore diameter (Po.Dm), and heterogeneity of pore size (Po.Dm SD) were calculated by direct 3D methods. Four regions were defined based on anatomic axes. Regional variations were examined with respect to global means, and compared between male/female and young/elderly subjects. At

both the radius and tibia, substantial regional variation was found. Overall in the radius, Ct.Po varied from +38% (medial) to -39% (anterior). Radius Po.Dm and Po.Dm SD followed the same pattern, with increased and more heterogeneous pore size at the medial quadrant, and reduced and less heterogeneous pore size at the anterior quadrant. Radius Ct.Th varied +10% (posterior) to -18% (lateral). At the radius, age differences were most pronounced in the lateral quadrant, where Ct.Po was 357% higher in elderly (65-78) vs young (20-29) women (1.5x the global mean difference). Age related increases in Po.Dm and Po.Dm SD were also most pronounced in the lateral quadrant of the radius. Overall in the tibia, Ct.Po varied from +18% (posterior) to -30% (anterior). Tibia Ct.Th varied +9% (lateral) to -5% (posterior). At the tibia, age differences were most pronounced in the anterior quadrant, where Ct.Po was 443% higher in elderly vs young women (1.5x the global mean difference). In elderly women, both the radius and tibia displayed the highest Ct.Po within the quadrant adjacent to the secondary bone: the lateral quadrant in the tibia, the medial (ulnar) quadrant in the radius. These data illustrate that substantial regional variation exists in cortical microstructure. Investigation of regional changes in addition to global trends may lead to more sensitive analysis of age-related skeletal changes.

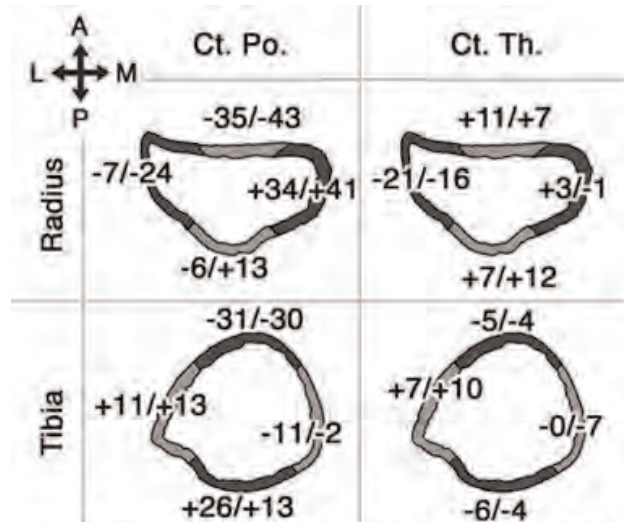


Figure: Regional variation in cortical porosity (Ct.Po) and thickness (Ct.Th) expressed as mean % difference from the global mean for males/females.

Figure

Disclosures: Galateia Kazakia, None.

MO0050

Risedronate Improves Bone Architecture and Strength Faster Than Alendronate in Ovariectomized Rats on a Low Calcium Diet. Tetsuo Yano¹, Mei Yamada¹, Tomoyuki Konda¹, Makoto Shiozaki¹, Daisuke Inoue². ¹Ajinomoto Pharmaceuticals Co., LTD, Japan, ²Teikyo University Chiba Medical Center, Japan

Background/Aim: Several studies have suggested that clinical dose of risedronate (RIS) is less potent in suppressing bone turnover and in increasing bone mineral density (BMD) than alendronate (ALN). Nevertheless, RIS does reduce bone fracture risk as potently as ALN from the early phase of treatment. Such differences in clinical efficacy between bisphosphonates may arise from unique pharmacological properties of each compound, but the mechanism remains unclear. In the present study, we tested a hypothesis that RIS improves bone quality, especially bone architecture, faster than alendronate, using ovariectomized (OVX) rats.

Methods: Female Sprague Dawley (SD) rats at 24 weeks of age were divided into sham-operated and ovariectomized groups and fed a low calcium (0.05%) diet under paired feeding. Three months after surgery, OVX rats were divided into five groups (vehicle, RIS (3.5, 17.5 µg/kg/week s.c.) and ALN (7, 35 µg/kg/week s.c.)) based on serum parameters of bone turnover, such as NTx and ALP. Six or eight weeks after treatment, the rats were sacrificed and bone architecture and strength of the left femur were evaluated using micro-CT and a three-point-bending biomechanical testing apparatus, respectively.

Result: Trabecular BMD (-47% at 8 weeks), trabecular number and trabecular thickness were significantly decreased in OVX rats, compared with the sham-operated group. Similarly, cortical BMD, cortical bone area (Ct.Ar, -9% at 6 weeks) and cortical thickness (Ct.Th) were also decreased in OVX rats. RIS significantly improved Ct.Ar (+8%) and Ct.Th (+9%) at 6 weeks. In contrast, ALN only caused a significant improvement in Ct.Ar (+8% at 6 weeks) with the higher dose. At 8 weeks, both RIS and ALN significantly increased trabecular BMD (+46%) compared to the vehicle controls. Bone strength using three-point bending method showed a good and significant overall correlation with Ct.Ar and Ct.Th. In bone strength test, only RIS, but not ALN, significantly improved maximum load at 6 weeks, consistent with the better improvement in the cortical architecture by RIS.

Conclusion: Consistent with our hypothesis, in a relatively early phase of treatment in OVX rats on a low calcium diet, RIS showed a superior effect on cortical bone architecture and strength to ALN. These results further suggest that RIS has a relatively predominant effect on bone quality compared to ALN.

Disclosures: Tetsuo Yano, Ajinomoto Pharmaceuticals, 3

MO0051

Skeletal Fragility and Hip Geometry: The Fracture Is "Behind the Angle".

Monica Celi^{*1}, Irene Cerocchi², Alessandro Scialdoni³, Luca Saturnino³, Umberto Tarantino⁴. ¹University of Rome Tor Vergata, Italy, ²Università Di Roma Tor Vergata, Italy, ³University of Tor Vergata, Italy, ⁴Azienda Ospedaliera PTV, Italy

Aim: To assess how differences in the proximal femur geometry (PFG) can influence hip fracture risk.

Methods: We studied 224 postmenopausal women aged 50 – 95 years who had sustained a fragility fracture and who resulted osteoporotic either at the proximal femur or at the lumbar spine or both. Bone Mineral Density (BMD) was evaluated by Dual X-Ray absorptiometry (Lunar i-DXA, GE Healthcare) and in addition to the conventional densitometry measurements, structural variables were determined using the Hip Strength Analysis program, including hip axis length (HAL), neck-shaft angle (NSA) and the femur strength index (FSI) calculated as the ratio of estimated compressive yield strength of the femoral neck to the expected compressive stress of a fall on the greater trochanter. Patients were divided into two groups based on fracture site (hip fracture group, n=112; non-hip fracture group n=112). Non-hip fracture included vertebral, humeral, wrist and ankle fractures due to low-energy trauma. Age, height, weight, Body Mass Index (BMI), femoral neck BMD and structural variables were compared between the two groups using t test.

Results: femoral neck BMD and PFG parameters (i.e. NSA, HAL and FSI) were different when groups were compared by t test. Differences regarding age and anthropometric parameters were not statistically significant. We found that patients in the hip fracture group had longer HAL than the non-hip fracture group (mean value 103.7 mm vs 101.4 mm, $p < 0.05$) and wider NSA (mean value 126.3 vs 123.2, $p < 0.01$). Significant differences were also found in the hip fracture group between patients with lateral fractures and patients with medial fractures. In particular, HAL resulted greater in the medial fracture group with respect to subjects with a lateral fracture (mean value 105.2 mm vs 99.3 mm, $p < 0.01$). Moreover, medial fracture patients were generally taller than those with a lateral fracture (mean body height 159.8 cm vs 156.44 cm, $p < 0.05$).

Conclusions: These data indicate that differences in PFG parameters might have a role in predisposing to hip fracture instead of non-hip fracture following low-energy trauma in women of the same age. PFG and anthropometric parameters seem to also influence hip fracture type (lateral or medial).

Disclosures: Monica Celi, None.

MO0052

Statistical Power in Measures of Microscopic Tissue Damage in Cancellous Bone. Katherine Ehler^{*1}, Ralph G. O'Brien², Christopher Hernandez¹.

¹Cornell University, USA, ²Case Western Reserve University, USA

The accumulation of microscopic cracks and other microscopic damage has been implicated as a characteristic of bone that may influence whole bone strength and resistance to fracture. While there have been a number of studies of naturally-occurring and experimentally generated microscopic tissue damage in cancellous bone, most reports show high variability as indicated by coefficient of variation (SD/ Mean, typically 50-100%). High measurement variability limits the ability to detect differences between groups. Variability in measures of microscopic tissue damage is caused by both sampling methodology (stereology, number of sections, amount of specimen, etc.) as well as biological variability among specimens. Here we present a statistical model to express how sampling methodology influences measures of microscopic tissue damage and statistical power. A statistical model using a Poisson distribution to simulate microscopic tissue damage events (individual cracks or regions of diffuse damage) was generated. The model used the results from published measures of microscopic tissue damage (DV/BV, Cr.Dn) achieved with 2D histology/ stereology or 3D approaches (lead uranyl acetate staining). The statistical model suggests that when using stereology, error in measures within the sample can be minimized by examining a cross-sectional area equivalent to 2 or more slices of an 8 mm diameter cancellous bone core. Specimen bone volume fraction and the mean amount of microscopic tissue damage present in the specimen have only a minor influence on this measurement error. The amount of variance found when using stereology is typically large, however, and is estimated to require 67 specimens/group to detect a 30% difference between groups with a power of 0.80. In contrast, 3D measures of microscopic tissue damage (as demonstrated using lead uranyl acetate staining or fluorescence-based serial milling) do not have as much measurement error because they examine the entire specimen and hence are estimated to require only 6 specimens/group to achieve the same statistical power for the situation above (Fig. 1). Stereology-based measures of microscopic tissue damage in cancellous bone are highly variable and require very large sample sizes to detect all but the most drastic differences between study groups. Three-dimensional measures of microdamage have the potential to detect more subtle differences between groups.

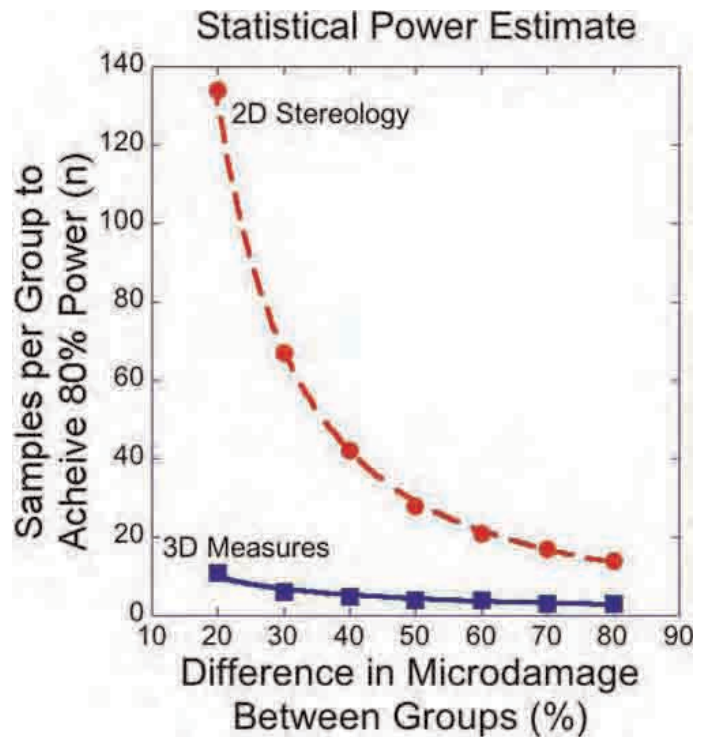


Figure 1

Disclosures: Katherine Ehler, None.

MO0053

The Correlation Between Bone Mineral Density Values With Insertion Torque of Pedicle Screws In Posterior Lumbar Pedicle Screw Fixation. Jae Hyup Lee^{*1}, Young-Ho Shin², Ji-Ho Lee², Jae Woo Park², Hye Soo Lee².

¹Seoul National University, College of Medicine, South Korea,

²Department of Orthopedic Surgery, Seoul National University College of Medicine, SMG-SNU Boramae Medical Center, South Korea

In a pedicle screw fixation, the degree of osseointegration between a screw and the bone is an essential factor for the stability and fusion. The purpose of this study was to predict the initial fixation force of a pedicle screw prior to the surgery, to identify the correlation between the BMD and the torque during a pedicle screw fixation and to clarify the predictable torque depending on the BMD. A total of 181 patients enrolled prospectively from November of 2006 to December of 2009; received the posterior lumbar instrumentation using a pedicle screw by a single surgeon; and intraoperatively had an insertion torque of pedicle screw measured by digital torque gauge. Conventional 6.5mm diameter by 40 to 45mm length pedicle screw was placed. In regard to the maximal insertion torque, an analysis was performed using Pearson's correlation coefficient for the BMD at the corresponding surgical vertebrae, mean BMD at the lumbar vertebrae and mean BMD in the proximal femur. A simple regression analysis was also performed to evaluate the correlation between the BMD and the predicted insertion torque generated during a pedicle screw fixation. In regard to the insertion torque during a pedicle screw fixation, there was a positive correlation with the BMD at the surgical vertebrae ($r=0.49$), T-value at the surgical vertebrae ($r=0.52$), mean BMD in the lumbar vertebrae ($r=0.32$), mean T-value in the lumbar vertebrae ($r=0.50$), mean BMD in the proximal femur ($r=0.45$) and mean T-value in the proximal femur ($r=0.42$). In patients with osteoporosis, the insertion torque had positive correlations with the BMD in the lumbar vertebrae. The insertion torque was significantly lower in patients with osteoporosis and those with osteopenia as compared with normal patients. Besides, a regression analysis formula for the insertion torque (kgf·cm) was found to be $-1.3 + 16.1 \times$ (the BMD at the surgical vertebrae) and $9.6 + 7.87 \times$ (mean BMD in the lumbar vertebrae). The BMD therefore be used in predicting the accurate degree of a pedicle screw fixation. Because there is a positive correlation between the BMD and the fixation force of a pedicle screw, however, it can therefore be inferred that the assessment of BMD would be useful in determining the fixation of device and the number of fusion segments in patients who are suspected to have osteoporosis and indicated in a pedicle screw fixation.

Disclosures: Jae Hyup Lee, None.

MO0054

The Effect of Advanced Glycation Endproducts on Cortical Bone Mechanical Properties. Sibi Sutti¹, Christopher Tranquada², Marc Grynpas¹, Thomas Willett^{*3}. ¹Samuel Lunenfeld Research Institute, Canada, ²University of Toronto, Canada, ³Mount Sinai Hospital, Canada

Advanced glycation endproduct (AGE) accumulation in bone may contribute to skeletal fragility in aging, diabetes, and various other diseases and conditions. Recent literature suggests that AGEs may deteriorate cortical bone toughness and post-yield properties. Fatigue resistance of cortical bone is more physiologically meaningful and more sensitive to changes in bone collagen. The effect of AGEs on cortical bone fatigue has not been studied.

Objective: Determine the sensitivity of cortical bone fatigue resistance to AGEs using a controlled in vitro model where only the collagen is modified through AGE formation.

Objective A: Test phosphate buffered saline (PBS) vs. simulated body fluid (SBF) to determine which best maintains bone properties during incubation.

Hypothesis A: SBF will maintain the mineral phase and mechanical properties better than PBS.

Objective B: Test the effect of in vitro AGE accumulation on bone mechanical properties and fatigue resistance.

Hypothesis B: AGE accumulation will reduce bone toughness and fatigue resistance.

Matched triplet beams corresponding to ASTM D790 were cut from 10 steer metatarsi; one was a non-incubated control (kept at -20°C), and two were incubated in either SBF 0.6M ribose or PBS 0.6M ribose at 37°C for 14 days. Ribose causes AGE formation. BMD was measured with DEXA. Static three-point bending failure tests were performed to test the incubation buffers and the effect of AGE accumulation. AGE contents were measured using HPLC. Fatigue testing of specimens (10 triplets) incubated in SBF 0.6M ribose and matched non-incubated controls was performed under both low-cycle and high-cycle conditions in three-point bending.

PBS incubation led to BMD loss (3-4%) and variations in mechanical properties whereas SBF incubation maintained BMD, reduced variation and eliminated detectable differences in mechanical properties between non-incubated controls and incubated controls. The post-yield toughness of the SBF+ribose specimens was 21% lower than non-incubated controls and incubated controls, supported by decreased damage fraction and increased secant modulus at failure. We were unable to confirm an effect of AGEs on fatigue resistance in this model.

SBF is a better buffer for long-term incubation of bone specimens. Static tests performed on cortical bone beams incubated in SBF+ribose suggest that AGEs may deteriorate bone toughness. On the other hand, our fatigue data has not confirmed an effect on fatigue resistance.

Disclosures: Thomas Willett, None.

MO0055

Validation of a Novel Microindenter for Bone Material Strength Measurement. Robert Guerri Fernandez^{*1}, Adolfo Diez-Perez², Xavier Nogues³, Daniel Prieto-alhambra³, Leonardo Mellibovsky⁴, Daniel Bridges⁵, Connor Randall⁶, Paul Hansma⁷. ¹Fundacio IMIM, Spain, ²Autonomous University of Barcelona, Spain, ³Institut Municipal D'Investigacio Medica, Spain, ⁴Internal Medicine / Infectious Diseases, Hospital del Mar, IMIM, Spain, ⁵University of California Santa Barbara, USA, ⁶UCSB, USA, ⁷University of California, Santa Barbara, USA

Fracture has been the only direct measurement of bone strength in clinics. Reference Point Indentation (RPI) provides an in vivo method for assessing bone material properties (1). A new handheld pocket-size RPI instrument (Osteoprobe®) (2) measures bone's resistance to fractures caused by impacts. Here we report the first validation study.

Methods: we carried out a case-control study including a consecutive sample of hip fracture cases and controls who accepted to participate. Measurements are made at the tibial midshaft after local anesthesia. The instrument applies impacts of 18N with a rise time of order 1 msec to a sharpened probe that has been inserted through the skin and soft tissue into the bone surface with a first force of 11N. Test time is about 2 minutes and painless. We perform 5 indentations for the patient and then 5 indentations into a PMMA calibration phantom (PMMA). The raw data obtained from the test is the indentation distance increase from the impact. The Bone Material Strength (BMS) a normalized parameter, is defined as 100 times the ratio of the average indentation distance increase from the impact into the calibration PMMA phantom divided by the indentation distance increase from the impact into the bone.

To compare BMS in cases and controls adjusted for age differences we used multivariate logistic regression.

Results: 21 cases (age 826) and 12 controls without fractures (age 778) were assessed. Age-adjusted analysis was performed using univariate logistic regression.

The BMS was significantly lower for the fracture vs. no fracture cases (795 vs. 916), which stood for adjustment for age (OR per increase in one Standard Deviation of BMS 18.42[1.5to226.26];p=0.023)(see Figure).

These results are consistent with the previous results with a cyclic-loading microindentation instrument (1,2). This new RPI instrument uses impacts and test conditions that mimics the trauma conditions for fractures and it is simple and convenient since it is handheld and gives just one, normalized, measurement that may provide a direct measurement of bone material propensity to fracture. We conclude that BMS determined from impact microindentation testing discriminates between fracture and no fracture cases. Bone material properties measured by microindentation may be highly relevant to measure fracture risk in the clinical setting. (1) JBMR 2010; 25:1877; (2) Active Life Scientific, Santa Barbara, CA.

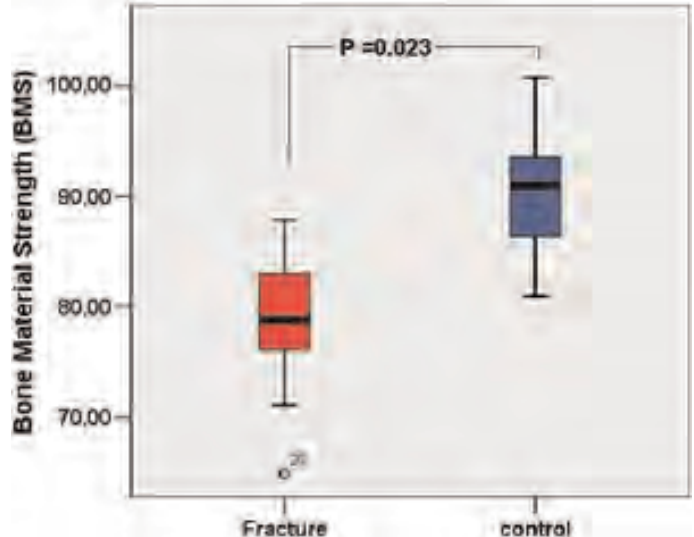


Figure 1

Disclosures: Robert Guerri Fernandez, None.

MO0056

Volumetric Bone Mineral Density Estimation using a 3D Reconstruction Method from Dual-energy X-ray Absorptiometry. Tristan Whitmarsh¹, Ludovic Humbert², Luis Del Rio^{*3}, Alejandro Frangi⁴. ¹Universitat Pompeu Fabra, Spain, ²Ph, Spain, ³Cetir Centre Medical, Spain, ⁴PhD, Spain

Volumetric BMD (vBMD) has been shown to be strongly related to bone strength and osteoporotic hip fracture. This can be estimated for the femoral neck from Dual-energy X-ray absorptiometry (DXA) by using the projected area as: $vBMD = BMC/A^2$ where BMC is the bone mineral content and A the projected area on the DXA image. However, such approximation cannot be used for other critical locations, such as the trochanteric and adjacent shaft region. An accurate quantification of the vBMD can be obtained from Quantitative Computed Tomography (QCT), however, this modality subjects the patient to a high radiation dose and is not as widely available as DXA central devices.

In this work an estimation of the vBMD from a DXA image is presented by using a 3D reconstruction method. The reconstruction method uses a 3D statistical model, constructed from a dataset of QCT scans which describes the statistical variations in shape and BMD distribution. The 3D statistical model is registered onto the 2D DXA image of the patient so that the projection of the model matches the DXA image. The result of this reconstruction process is a patient specific volumetric reconstruction of the BMD distribution onto which the vBMD can then be extracted for specific regions.

Reconstructions were subsequently obtained from the DXA images of 30 patients (15 male and 15 females with an average age of 5013 years). The vBMD of the femoral neck and the trochanteric region was extracted from the reconstructions and the vBMD in the corresponding regions of the QCT scans of the same subjects were considered the ground truth. The linear correlation with the ground truth vBMD then indicates the vBMD estimation accuracy. For the trochanteric and shaft region, our method achieved a strong correlation with a correlation coefficient of 0.94 and 0.93 and a Mean Average Error (MAE) of 15.3 and 21.8mg/cm³ respectively. In addition, the proposed method resulted in a MAE of 17.2mg/cm³ and a correlation coefficient of 0.92 for the femoral neck region whereas the vBMD, estimated using the projected area, resulted in a correlation coefficient of 0.91.

These results indicate that our proposed method accurately estimates the vBMD of the trochanteric, shaft and femoral neck region from DXA. This potentially allows for an improved fracture risk estimation while maintaining DXA as the current standard modality.

Disclosures: Luis Del Rio, None.

MO0057

Changes in the 3D Osteocyte Lacunar Network Induced by Estrogen Withdrawal and Pharmaceutical Treatment of Osteoporosis as Detected by Synchrotron Micro-CT. Steven Tommasini¹, Andrea Trinward¹, Alvin Acerbo², Lisa Miller³, Stefan Judex¹. ¹Stony Brook University, USA, ²Brookhaven National Laboratory, USA, ³Brookhaven National Laboratory, USA

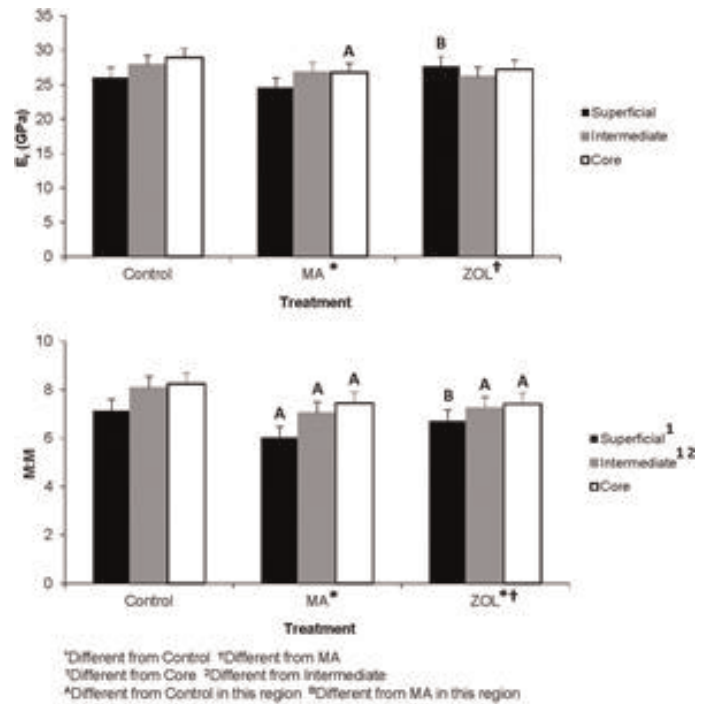
Osteocyte lacunar size may increase in rodents that were either ovariectomized (OVX) or treated with parathyroid hormone (PTH). As this evidence was largely limited to 2D methods, the aim of this study was to quantify changes in the 3D osteocyte-lacunar network induced by estrogen withdrawal and 2 different osteoporosis treatments. Unlike 2D measurements, this data collected via synchrotron radiation-based μ CT (0.75 μ m resolution) can describe the size and 3D spatial distribution of a large number of osteocyte lacunae within cortical bone. Six-month old female Sprague-Dawley rats were separated (n=6/group) into 1) age-matched control, 2) untreated OVX, 3) OVX treated with PTH, or 4) OVX treated with Alendronate (ALN). Intracortical microporosity of the medial quadrant of the femoral diaphysis was quantified at endosteal, intracortical, and periosteal regions of the samples, allowing the quantification of osteocyte lacunae that were formed primarily before and after the start of treatment. Average osteocyte lacunar volume (Lc.V) of untreated OVX rats was significantly greater ($p<0.01$) in the periosteal region compared to endosteal and intracortical regions indicating that, in bone formed after estrogen withdrawal, there was an increase in osteocyte lacunar size. However, Lc.V in bone formed after the start of both treatments was similar to controls. The number of lacunae per bone volume was significantly higher in the periosteal region for ALN and PTH treatments compared to age-matched controls and untreated OVX ($p<0.05$) suggesting that bone formed on the periosteal surface after the start of treatment had more osteocytes per bone volume. Thus, activity of osteoblasts was different compared to before treatment. There also was a significant increase in the size and number of small pores in the intracortical region for PTH compared to controls, but not for ALN. This is consistent with previous reports. Additionally, small porosities may be related to improved bone strength with PTH treatment, as smaller osteocyte lacunae may be better able to absorb shear forces than larger lacunae. Together, these changes may not only directly influence the mechanical properties of bone tissue, but also may affect the osteocyte's role as mechanosensors. Further associations of this data with detailed spatial mechanical and chemical matrix data will improve our understanding of the relationship between osteoporosis treatments, osteocyte biology, and bone quality.

Disclosures: Steven Tommasini, None.

MO0058

Gradients in Mineralization and Nanomechanical Properties Across Trabeculae are Altered with Zoledronate Treatment in an Ovine Model of Osteoporosis. Jayme Burket¹, Jennifer MacLeay², Shefford Baker¹, Adele Boskey³, Marjolien Van Der Meulen¹. ¹Cornell University, USA, ²Hill's Pet Nutrition, Inc., USA, ³Hospital For Special Surgery, USA

Trabeculae from healthy human bone show gradients in tissue stiffness from edge to center paralleling gradients in mineralization. Increased turnover with osteoporosis decreases tissue mineralization and may affect mineral properties and their tissue distribution. Ovine metabolic acidosis (MA), unlike OVX, increases turnover and produces similar mineral changes as human osteoporosis, allowing us to examine disease and treatment effects on cancellous tissue composition and mechanical properties. Cancellous bone was obtained from distal femora of skeletally mature ewes. Controls (CONT) were fed a normal diet for 12 months (n=5); treatment groups were fed a diet to induce MA for 6 months and then treated with either Zoledronate (ZOL, n=6) or vehicle (n=6) while maintaining the diet for another 6 months. Reduced modulus (E_r) and hardness (H) were assessed with nanoindentation along lines spanning the width of 3 trabeculae/sample, with indents placed at the center of lamellae (n=10-17/trabecula). Mineral:matrix (M:M), carbonate:phosphate (C:P) and crystallinity (XST) were characterized by Raman spectroscopy at indent locations. Effects of treatment, region (superficial, intermediate, or core of trabecula), and their interaction were tested by multifactor, nested ANOVAs with Tukey post-hoc. Relative to CONT, MA decreased M:M in all regions (mean -13%); with ZOL, only core regions had lower M:M, and the positive mineralization gradient from superficial to core tissue was reduced (MA Δ 10% vs. CONT Δ 16%). E_r followed mineralization, decreasing in all regions with MA (-6% vs. CONT), and increasing only in superficial regions with ZOL (+13% vs. MA). ZOL restored E_r to CONT levels in all regions, but the gradient from superficial to core of trabeculae was not recovered. H was similar to E_r . C:P increased in core regions with MA (+6% vs. CONT) and increased in all regions with ZOL (+6% vs. CONT). XST increased in all regions with MA and ZOL (+8% vs. CONT). Changes in tissue mineralization with MA in sheep were similar to those of high-turnover osteoporosis in humans. ZOL restored mineralization levels, stiffness, and hardness but did not recover gradients present in healthy tissue and mineral crystal properties were altered. The role of gradients in trabeculae is unknown. Restoring tissue stiffness at the periphery of trabeculae may be most critical to resist bending and buckling loads, two dominant failure modes of trabeculae within cancellous bone.



Er and M:M vs. Treatment and Region of Trabeculae

Disclosures: Jayme Burket, None.

MO0059

Mechanical Property and Tissue Mineral Density Differences Among Severely Suppressed Bone Turnover (SSBT) Patients, Osteoporotic Patients, and Normal Subjects. Crystal Tjhia¹, Clarita Odvina², Sudhaker Rao³, Susan Stover¹, Xiang Wang¹, David Fyhrie¹. ¹University of California Davis, USA, ²University of Texas Southwestern Medical Center, Dallas, USA, ³Henry Ford Hospital, USA

We hypothesized that tissue-level mechanical properties and mineralization of the iliac crest would differ among 1) a subset of osteoporotic patients with atypical fractures and severely suppressed bone turnover associated with long-term bisphosphonate use (SSBT), 2) age-matched, bisphosphonate-naïve osteoporotic patients with vertebral fracture, 3) age-matched normals and 4) younger normals. Large differences in tissue-level mechanical properties or mineralization among these groups could help explain the occurrence of fracture in the 2 patient groups. Elastic modulus, hardness and tissue mineral densities of cortical and trabecular bone regions of 55 iliac crest biopsies were measured using nanoindentation and quantitative backscattered electron microscopy. Twelve SSBT patients (SSBT group), 11 untreated osteoporotic patients with vertebral fracture (Osteoporotic group), 12 age-matched subjects without fracture (Older Normal group), and 20 younger subjects without fracture (Younger Normal group) were examined (Table 1). Elastic modulus, hardness, and mineral density of trabecular bone were different among the groups ($p<0.05$, Fig. 1). The SSBT group had harder trabecular bone compared to the other three groups and stiffer trabecular bone compared to the osteoporotic and younger normal groups. SSBT trabecular bone was more highly mineralized than that of the older normals and osteoporotics. Among the osteoporotics, younger normals and older normals, trabecular bone mechanical properties were not different from each other, and trabecular bone mineral density was only slightly higher in younger normals than older normals and osteoporotics. Cortical bone mechanical properties and mineralization were not different among groups. The largest difference in mechanical properties or mineralization was that SSBT trabecular bone was 17.8% harder than that of younger normals. In contrast, the differences in bone formation rate (BFR; previously measured) among the groups were much greater, with the osteoporotic, younger normal and older normal groups having greater BFR than the SSBT group by 5400%, 4400% and 4800%, respectively. The differences in mechanical properties and mineral densities were consistent with differences in BFR, but the magnitudes of the mechanical property and mineral density differences were small. We conclude that differences in tissue mechanical and mineral properties among the groups are consistent with normal aging and differences in BFR.

MO0061

The Decrease in Cortical Bone Volumetric Mineral Density Induced by Teriparatide in Postmenopausal Osteoporotic Women is Associated With an Increase in Cortical Porosity as Assessed by High Resolution Peripheral Computerized Tomography (HR-pQCT). Cesar Bogado^{*1}, Fernando Silveira¹, David Dempster², Hua Zhou³, Ursula Masiukiewicz⁴, Cecilia Fosse⁴, Jose Ruben Zanchetta¹. ¹Instituto de Investigaciones Metabolicas (IDIM), Argentina, ²Columbia University, USA, ³Helen Hayes Hospital, USA, ⁴Pfizer, Inc., USA

We have previously reported that daily injections of 20 µg teriparatide for 12 months in a group of 20 postmenopausal women with osteoporosis resulted in a decrease in cortical vBMD at the distal radius and tibia, as assessed by HR-pQCT (1).

To test the hypothesis that the decrease in vBMD was related to an increase in cortical porosity, HR-pQCT scans of the distal tibia obtained during our previous study were analyzed using an automated segmentation technique developed to identify the periosteal and endosteal margins and detect intracortical pore space morphologically consistent with Haversian canals (2). Cortical bone vBMD and porosity (Co. Po) were measured at baseline and month 3, 6 and 12 following teriparatide administration. Bone turnover rate was estimated measuring serum CTX and PINP.

Percent changes over time are depicted in Table1. The changes in cortical vBMD were almost identical to those obtained in our previous study using the standard analysis technique (1). Co.Po significantly increases at month 6 and continues to increase subsequently. This increase in cortical porosity is in agreement with the findings in paired iliac crest bone biopsies obtained in 11 of these patients, showing a 68.3% (95% CI 7.77, 162.70; p= 0.026) increase in cortical porosity area at month 12, compared to baseline. The increase in Co.Po at month 6 is coincident with the increase in overall bone turnover rate, indicated by the significant rise in serum CTX levels, after a period of bone formation stimulation reflected by the serum PINP changes at month 3. There was a strong linear negative correlation (R-squared= 0.46; p= 0.0013) between the changes in vBMD and Co.Po at month 12. That correlation was maintained after adjusting for baseline vBMD (R-squared 0.45; p= 0.0016).

In conclusion, our results suggest that the decrease in cortical vBMD induced by teriparatide is related to an increase in cortical porosity and that those changes in porosity can be estimated by non-invasive imaging techniques like HR-pQCT.

References

- 1- C.E. Bogado, J. Zanchetta, H. Zhou, et al. J Bone Miner Res 24 (Suppl 1). Available at <http://www.asbmr.org/Meetings/AnnualMeeting/AbstractDetail.aspx?aid=8024c14d-c2f2-4a0d-bd3c-0584c85b91ad> (2009)
- 2- A.J. Burghardt, H. R. Buie, A. Laib, et al. Bone 47(3):519-28 (2010)

Table 1. Percent change from baseline at month 3, 6 and 12 in HRpQCT variables and biochemical markers of bone turnover.

	Month 3		Month 6		Month 12	
	Mean (%)	95% CI (%)	Mean (%)	95% CI (%)	Mean (%)	95% CI (%)
Ct.vBMD	-0.44	-1.10, 0.22	-1.74#	-2.70, -0.78	-2.74#	-4.37, -1.11
Ct.Po	1.96	-3.41, 7.33	6.40*	0.55, 12.24	11.47*	0.94, 22.00
sCTX	1.65	-20.43, 23.68	49.34#	10.41, 101.73	73.34#	27.54, 135.31
sPINP	95.44#	62.45, 135.14	137.14#	81.33, 193.93	177.45#	102.31, 280.50

* p < 0.05 versus baseline; # p < 0.01 versus baseline; # p < 0.001 versus baseline

Ct.vBMD: Cortical bone volumetric bone mineral density; Ct.Po: Cortical porosity, relative voxel-based measure of the volume of the intracortical pore space normalized by the sum of the pore and cortical bone volume; sCTX: Serum carboxyterminal cross-linking telopeptide of bone collagen, a marker of bone resorption; sPINP: Serum procollagen type I N-terminal propeptide, a marker of bone formation.

Table 1

Disclosures: Cesar Bogado, None.

MO0062

Integrated Finite Element Modeling of Upper Femur Behavior With Ageing: From Cellular Activities Toward Fracture. Ridha Hamblil^{*1}, Abdelwahed Barkaoui², Romain Rieger¹, Eric Lespessailles³, Claude Laurent Benhamou⁴, Awad Bettamer⁵. ¹PRISME Institute, France, ²PRISME Institute, EA4229, University of Orleans, France, ³Centre Hospitalier Regional, France, ⁴INSERM Orleans-France, France, ⁵L'Universite d'Orleans, France

Introduction: Bone models offer the opportunity to simulate bone behaviour (remodeling, resistance, fracture, ...). Current works focused either on bone mechanical induced reactions or biological cells activities in a given bone site without considering the synergic interactions between mechanical stimulus and the biological machinery of bone cells. We have developed a finite element model integrating coupled mechanical and biological aspects in order to simulate the upper femur behaviour starting from a remodeling cycle (under cyclic load and frequency for a given period of time) followed by a fracture prediction (under a monotonic excessive load) to predict the maximum force at fracture and the fracture pattern of the femur. **Material and Method:** The initial 3D geometry model (standardized femur model

Group	N	Age	Mean Age (SD)	Bone formation rate [µm ³ /µm ² /yr]
Younger Normal	20	20-40	31.6 (5.6)	13.5 (6.9)
Older Normal	12	49-74	63.8 (8.5)	14.8 (13.7)
Osteoporotic	11	53-76	65.5 (7.7)	16.7 (19.4)
SSBT	12	49-77	64.1 (9.3)	0.3 (0.4)

Table 1

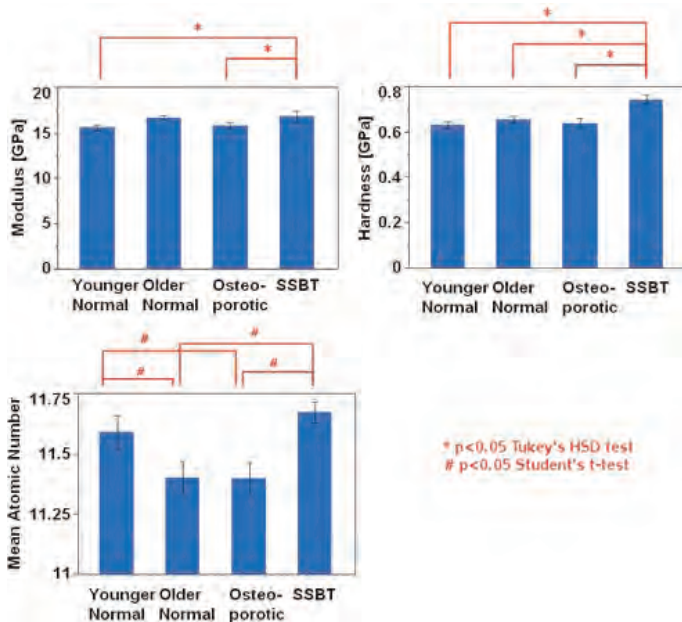


Fig. 1

Disclosures: Crystal Tjha, None.

MO0060

Prediction Of Mechanical Bone Strength From In Vivo Bone Density And Biomarkers In A Rat Experiment - An Individual Model Using Automatic Learning. Joseph Zarka^{*1}, Eric Lespessailles², Su Hua Leow¹, ZAHRA ACHIOU³, Claude Laurent Benhamou⁴. ¹JZ SARL, France, ²Centre Hospitalier Regional, France, ³INSERM, France, ⁴INSERM Orleans-France, France

We have previously analyzed the combined effects on bone tissue of zoledronic acid (Z) and physical activity (PA) in an ovariectomized (OVX) rat model. Although the treadmill running exercise was shown to preserve the bone strength, the combined effects of Z and PA did not produce any additive effect. In the present study we aimed to explore the ability of an Automatic Learning software (SEA of Ecole Polytechnique, CADLM, France) to predict bone biomechanical properties from body composition, bone density measurements and bone biomarkers obtained in vivo.

The study included 5 groups of 12 female rats (6 months old at baseline): 1) sham, 2) OVX, 3) OVX + PA, 4) OVX + Z, 5) OVX + Z + PA. Body weight, lean body mass, fat mass, whole body mineral content and density were measured by DXA before sacrifice, such as biomarkers of bone remodelling: serum osteocalcin and collagen cross links (CTX). We have extracted from the database each rat separately and treated all the parameters on the whole group. The criteria to be predicted are the Young's Modulus, the ultimate force and stress to failure. Ten cases have been randomly excluded from the study group and the predictive model has been retested in this sub-group.

As every software of Automatic Learning, the results with the SEA software are expressed by the quantification of errors obtained by the model. The maximum relative errors were evaluated at 8% for the ultimate force, 8% for the stress at failure and 20% for the Young's Modulus.

These data suggest that it seems possible to estimate bone biomechanical properties from in vivo non invasive measurements like DXA and bone biomarkers by this software of automatic learning working. All this work is produced on an individual basis, suggesting an interest in "personalized" prediction of the bone status. This model is currently tested with another group of rats.

Disclosures: Joseph Zarka, None.

from <http://www.biomedtown.org>) has been implemented with the averaged properties of a 75 yrs femur. Local material properties was assigned (BV/TV, elastic modulus, strain at fracture, biological cells activities parameters). The remodeling process is simulated based on the reaction of the osteoblasts-osteoclasts-osteocytes balance. Formation and resorption of bone are respectively performed by the osteoblasts and the osteoclasts. The BMUs behaviour has been incorporated into the finite element model based on previously published validated models. The 3D femur model has been submitted to two cycles (one and two years period) of remodeling process under cyclic loading with low (2000 N) and high (3400 N) physical activities applied at angle of 20 from the vertical. The frequency was fixed at 6000 cycles/day in both cases. At the end of every remodeling cycle, fracture FE simulation were performed to assess the fracture conditions (force and fracture profile) in relation with the remodeling-predicted bone adaptation. Results: Our predicted results show that the maximum fracture force and fracture profile of the upper femur depends mainly on the remodeling process conditions (amplitude of the remodeling force and duration). Indeed, The predicted maximum fracture forces corresponding to the different cases was: Low force-1 yr remodeling : F= 4000N, Low force-2 yrs remodeling : F= 3400N, High force-1 yr remodeling : F= 4400N, High force-2 yrs remodeling : F= 5200N. The proposed unified remodeling-to-fracture model can be applied to study the effects of remodeling factors (force, frequency, cells activities) on the strength of human femur.

Disclosures: *Ridha Hambli, None.*

MO0063

Positive Association Between Circulating Sclerostin and Bone Mass in Chronic Spinal Cord Injury: Evidence Against Sclerostin as a Target to Treat Chronic Disuse Osteoporosis. Leslie Morse^{*1}, Supreetha Sudhakar², Valery Danilack³, Carlos Tun⁴, Antonio Lazzari⁵, David Gagnon⁶, Eric Garshick⁷, Ricardo Battaglini⁸. ¹Department of Physical Medicine & Rehabilitation, Harvard Medical School, Spaulding Rehabilitation Hospital, USA, ²Spaulding Rehabilitation Hospital, USA, ³Programs in Research at VA Boston, USA, ⁴Rehabilitation Medicine Service, USA, ⁵Primary Care Section, VA Boston Healthcare System & Boston University School of Medicine, USA, ⁶VA Cooperative Studies Program, VA Boston Healthcare System, Department of Biostatistics, Boston University School of Public Health, USA, ⁷Pulmonary & Critical Care Medicine Section, Medical Service, VA Boston Healthcare System, Channing Laboratory, Department of Medicine, Brigham & Women's Hospital, Harvard Medical School, USA, ⁸The Forsyth Institute, USA

Spinal cord injury (SCI) results in profound bone loss due to muscle paralysis and the inability to ambulate. Sclerostin, a Wnt signaling pathway antagonist produced by osteocytes, is a potent inhibitor of bone formation. Short-term studies in rodent models have demonstrated increased sclerostin in response to mechanical unloading that is reversed with reloading. These studies suggest that complete spinal cord injury, a condition resulting in mechanical unloading of the paralyzed lower extremities, will be associated with high sclerostin levels. We assessed the relationship between circulating sclerostin and bone density in 39 subjects with chronic SCI and 10 without SCI. We found that greater total limb bone mineral content was significantly associated with greater circulating levels of sclerostin. Sclerostin levels were reduced, not elevated, in subjects unable to walk due to SCI compared to persons who walked regularly. The ability to walk regularly, not injury severity, was also significantly associated with greater bone density at SCI-specific, sublesional skeletal sites (distal femur and proximal tibia). These findings suggest that circulating sclerostin is a biomarker of osteoporosis severity, not a mediator of ongoing bone loss, in long-term, chronic paraplegia. This is in contrast to the acute sclerostin-mediated bone loss demonstrated in animal models of mechanical unloading where high sclerostin levels suppress bone formation. As these data indicate important differences in the relationship between mechanical unloading, sclerostin, and bone mineral content in chronic SCI compared to short-term rodent models, it is likely that sclerostin is not a good therapeutic target to treat chronic SCI-induced osteoporosis.

Disclosures: *Leslie Morse, None.*

MO0064

Extracellular High Glucose Levels Modulate Bone Cell Mechanotransduction. Mia Thi^{*}, David C. Spray, Sylvia O. Suadicani. Albert Einstein College of Medicine, USA

Although it has been shown that patients with insulin dependent diabetes mellitus (IDDM; Type 1 diabetes) display higher bone loss and increased risk for osteoporosis and related bone fractures, the underlying mechanisms are still not well understood. Given that the maintenance of skeletal integrity in response to daily physical activity relies on the regulation of the bone forming cells, osteoblasts, and the primary load sensing cells, osteocytes, we hypothesized that bone loss in diabetes is due to compromised ability of bone cells to perceive and respond to mechanical loading as a result of changes in structure of bone cells pericellular matrix (PCM) and altered expression of specific purinergic receptors (P2Rs) and pannexin1 (Panx1) channels. To simulate in vitro the extracellular glucose levels to which bone cells are exposed in

healthy vs. diabetic bones, we cultured MOB-C (osteoblastic cells) and MLO-Y4 (osteocytic cells) for 10 days in α -MEM containing 100 mg/dL (5.5 mM) and 450 mg/dL (25 mM) glucose. Cells were subjected to oscillatory fluid shear stress [FSS - low level unidirectional mean flow ($\tau = 0.5$ dyne/cm²) superimposed with a sinusoidal oscillating flow ($\tau = 10$ dyne/cm²) at 1 Hz] in a parallel plate flow chamber with a closed flow loop. We observed that high glucose (HG) exposure altered the thickness of PCM determined by heparan sulfate proteoglycan immunolabeling in both MOB-C and MLO-Y4 cells. While P2Y₁R expression remained the same, HG exposure differentially regulated the expression of P2Y₂R, P2Y₄R and P2X₇R subtypes and Panx1 in MLO-Y4 and MOB-C. The P2X₇R and Panx1 in MLO-Y4 was substantially downregulated in HG while the P2Y₂R and P2Y₄R in MOB-C were significantly upregulated. Moreover, FSS-induced ATP release under control conditions was substantially reduced after HG exposure in both MLO-Y4 and MOB-C. Likewise, FSS-induced Ca²⁺ transients in both cell types were also lower in HG compared to control condition. These findings indicate that HG-induced thickening of bone PCM and altered P2R and Panx1 expression impairs proper sensing and transduction of physiological FSS, which ultimately impairs the adaptive response of osteocytes/osteoblasts to mechanical loading.

Disclosures: *Mia Thi, None.*

MO0065

Fluid Shear Modulates COX2 mRNA Expression but not Mineralization during Oscillatory Motions. Gunes Uzer^{*1}, Sarah Manske¹, Ete Meilin Chan¹, Yi-Xian Qin², Clinton Rubin², Stefan Judex¹. ¹Stony Brook University, USA, ²State University of New York at Stony Brook, USA

When applied at high frequencies, bone can sense and respond to mechanical signals of extremely small magnitude. During the application of low-level vibrations, cell populations within the bone are likely subjected not only to acceleratory motions but also to fluid shear as a result of fluid-cell interactions. Here, we tested whether COX2 mRNA expression and the level of calcification is modulated by the magnitude of vibration induced fluid shear. To this end, we developed a combined cell culture/analytical model in which finite element (FE) modeling determined peak fluid shear stresses acting on a monolayer of cells during high-frequency oscillations. Fluid shear was modulated both in vitro as well as analytically by increasing the acceleration magnitude and/or increasing the viscosity of the fluid via the addition of dextran. Osteoblast-like MC3T3-E1 cells were vibrated at 0.15g or 1g peak accelerations at 60Hz for 30min/day in mediums with dextran concentrations of 0%, 3%, 6% or 9% for 1, 7, or 14 days (n=3-4, each). Increase of dextran concentration from 0% to 9% resulted in a 4.5-fold increase in estimated fluid shear. Similarly, increasing acceleration from 0.15g to 1g increased fluid shear 6.7-fold. COX2 mRNA expression was determined by RT-PCR at day 1 and calcification levels were determined at days 14 and 21. Compared to controls, cells subjected to 1g peak acceleration elicited greater increases in COX2 expression than cells subjected to 0.15g. The only group in which COX2 levels were not up-regulated was the 0.15g, 0% dextran group (45% down-regulated compared to controls). Increasing fluid shear via dextran or acceleration magnitude resulted in a logarithmic increase of COX2 expression ($R^2=0.8$). Differences in COX2 expression as a function of fluid shear were not mirrored by calcification data obtained after either one or two weeks of vibration. Vibration exposure at 0.15g or 1g vibration equally increased ($p<0.05$) calcification compared to non-vibrated controls, independent of the viscosity level of the medium. This data suggests that cells are able to respond to very low levels of fluid shear (0.02Pa – 0.08Pa) when exposed to an oscillatory frequency of 60Hz. That the non-linear increase in COX2 mRNA with fluid shear was not matched by a similar relation between fluid shear and calcification suggests that fluid shear does not regulate the level of vibration-induced mineralization.

Disclosures: *Gunes Uzer, None.*

MO0066

Withdrawn

MO0067

Microscale Fluid-Flow Analysis in Osteocyte Canaliculi Using High-Resolution Image-Based Models. Hiroshi Kamioka^{*1}, Yoshitaka Kameo², Yuichi Imai³, Astrid Bakker⁴, Rommel Bacabac⁵, Takashi Yamashiro³, Taiji Adachi⁶, Jenneke Klein-Nulend⁷. ¹Okayama University Graduate School of Medicine, Dentistry, & Pharmaceutical Sc, Japan, ²Department of Mechanical Engineering, Graduate School of Engineering, Osaka Prefecture University, Japan, ³Department of Orthodontics, Okayama University Graduate School of Medicine, Dentistry, & Pharmaceutical Sciences, Japan, ⁴Department of Oral Cell Biology, ACTA-University of Amsterdam & VU University Amsterdam, Research Institute MOVE, Netherlands, ⁵Medical Biophysics group, University of San Carlos, Philippines, ⁶Department of Biomechanics, Research Center for Nano Medical Engineering, Institute for Frontier Medical Sciences, Japan, ⁷ACTA-VU University Amsterdam Dept Oral Cell Biology (Rm # 11N-63), The Netherlands

A number of fascinating studies suggest that osteocytes play a key role in the regulation of bone mass and structure by mechanical stimuli, thereby designating osteocytes as important mediators of bone fracture resistance. It is generally thought that mechanical loading-induced matrix strains cause a flow of interstitial fluid over the osteocyte processes, but how this fluid flow subsequently activates the osteocyte is still a matter of much debate. Several theories exist, but their value of these theories is somewhat limited since they are not based on actual three-dimensional (3D) morphologies of the osteocyte canaliculi, while microscopic fluid flow analysis using detailed morphological data of the osteocyte canaliculi in the bone matrix is essential for the quantitative estimation of the fluid-induced shear stress acting on the cell processes. In the current study we aimed to construct a realistic 3D model of the pericellular space between the osteocyte cell membrane and the canalicular wall for microscale flow analysis. We observed detailed structures of both osteocyte cell processes and canaliculi. Furthermore, using the 3D image-based model of a single canaliculus, fluid dynamics was numerically analyzed using the Lattice Boltzmann method. We found that the microscopic surface asperity of the osteocytic processes and canalicular wall strongly influenced the flow profiles, demonstrating the applicability of high-resolution image-based models for quantitative flow analysis in the canaliculus. Our simulation assumed the steady-state Newtonian flow in a canaliculus at 602 nm in length. However, whether this assumption holds at micro-scale fluid flow as well as the estimation of the influence of the fluid mechanical properties and the boundary conditions on the shear stress acting on the surface of cell processes needs further discussion. This study was partially supported by the Nanotechnology Network Project at the Research Center for Ultrahigh Voltage Electron Microscopy, Osaka University, from the Ministry of Education, Culture, Sports, Science and Technology (MEXT) of Japan.

Disclosures: Hiroshi Kamioka, None.

MO0068

Molecular Factors Involved in the Early Response of Bone and Skeletal Muscle to Mechanical Unloading. Maria Squire^{*1}, Jason Stankiewicz², Melissa Monaghan³, Anil Dhundale⁴, Stefan Judex⁵. ¹Department of Biology, The University of Scranton, USA, ²Biochemistry Program, The University of Scranton, USA, ³OSI Pharmaceuticals, LLC, USA, ⁴LIHTI & SBU Business Incubators, Stony Brook University, USA, ⁵Biomedical Engineering Department, Stony Brook University, USA

Bone and skeletal muscle are mechanosensitive tissues, remodeling their structures to accommodate to changes in their mechanical loading environments. In rodents, hindlimb unloading significantly decreases the quantity of bone and skeletal muscle within as little as 2 weeks. Functional relationships between bone and muscle have been proposed, but whether their initial molecular responses to altered mechanical loading are similar or distinct is largely unknown. In this study, we examined gene expression in bone and muscle following short-term hindlimb unloading. Total RNA was extracted from the whole proximal tibia and soleus of adult (4 mo) female F1 crossbred (BALB/cByJ x C3H/HeJ) mice following 4 d of normal cage activity (control) or hindlimb unloading (n=5 each). Reference samples were hybridized with either a control or unloaded sample onto custom oligonucleotide arrays (n=5 per group) containing 16,442 ESTs (70mer oligos) from the Operon mouse genome library (v2). Following normalization and filtering, 164 (tibia) and 115 (soleus) differentially regulated genes were identified (p<0.05), with only 3 genes common to both lists. Of the three genes affected in both tissues, one was a transcription factor (transcription factor AP-4 (Tfap4)) and another was a known modulator of transcription factor activity (protein inhibitor of activated STAT 2 (Pias2)). Both were significantly up-regulated in bone (64% and 38%) and muscle (68% and 52%). Classification of the differentially regulated genes in bone revealed that unloading down-regulated mRNA levels of runt-related transcription factor 2 (Runx2a, -38%) and a number of extracellular matrix genes including collagen type I α 1 (-30%) and biglycan (-45%). qPCR analyses confirmed the down-regulation of biglycan (-49%) as well as the down-regulation of asporin (-41%) and decorin (-41%), all of which belong to class I small leucine rich proteoglycans. In skeletal muscle, the gene encoding for MAD homolog 7 (Drosophila) (SMAD7), a protein with a known role in skeletal muscle cell differentiation, was down-regulated by 57% following unloading and qPCR studies are ongoing to validate this finding. Taken

together, the results suggest that although there may be some overlap in the molecular mechanisms that mediate the early response of bone and skeletal muscle to mechanical unloading, most of the genes are tissue-specific.

Disclosures: Maria Squire, None.

MO0069

The Effect of Vibratory Forces on the Rate of The Tooth Movement in Rats. Zana Kalajzic^{*1}, Elizabeth Blake¹, Achint Utreja¹, Manshan Xu¹, Jing Chen¹, Flavio Uribe¹, Ravindra Nanda¹, Douglas Adams¹, Sunil Wadhwa². ¹University of Connecticut Health Center, USA, ²University of Connecticut, USA

Orthodontic tooth movement requires external orthodontic forces to be converted to cellular signals that result in coordinated removal of bone by osteoclasts (compression side), and the formation of new bone by osteoblasts (tension side). Recently, vibratory forces have been shown to increase the rate of tooth movement in rodent models. The objective of this study was to examine potential mechanisms behind this action. Seven week old Sprague Dawley female rats were used in this study. The animals were divided into three groups. The control group (A) received only the orthodontic spring which was activated from the left maxillary first molar to the maxillary left incisor. The experimental group (B) received the spring and additional occlusal vibratory stimulation of 0.4 N compression at 30Hz for 10 minutes twice a week. The third group (C) received the vibratory stimulation only. The duration of the experiments was 2 weeks. The amount of tooth movement and alveolar bone parameters were measured using microCT analysis. Dissected maxillae were processed for paraffin and frozen embedding. Sagittal sections were stained for TRAP, Von Kossa and immunostained for TUNNEL. Vibratory forces significantly decreased the amount of tooth movement (50%) in the experimental group B compared to the control group A. We did not notice any changes in osteoclast number, localization or mineralization of the PDL between those 2 groups. Vibration alone in group C did not cause any change of osteoclast number and their localization nor any change in bone parameters: total volume, bone volume and tissue density. However, the number of apoptotic cells within the PDL was higher in the experimental group B than in control groups A and C. Future studies will need to address the possible role of PDL cell apoptosis in the tooth movement.

Disclosures: Zana Kalajzic, None.

This study received funding from: Ortoaccel

MO0070

TNF α Partly Controls Fluid Pressure Induced Osteolysis. Anna Fahlgren^{*1}, Denis Nam¹, Goran Andersson². ¹Hospital for Special Surgery, USA, ²Karolinska Institute, Sweden

In contrast to the well-understood pathway by which implant-derived particles induce bone resorption, little is known about the recently-described process in which loosening is generated as a result of force-induced mechanical stimulus at the bone-implant interface (Fahlgren et al, 2010). Specifically, there is no knowledge as to what cells or signaling pathways couple mechanical stimuli to bone resorption in context of loosening. We showed previously that pressure-induced osteoclast activation was associated with lower levels of inflammatory cytokines compared to particle-induced osteolysis. Thus, mRNA expression of TNF α (0,330.07 versus 0,470,16) and RANKL (3,72,3 versus 11,49,6) was significantly lower after fluid pressure compared to wear particles. Never the less, we found the same number of osteoclasts per unit area in both models. These findings suggest that in both circumstances levels of TNF α are sufficient to induce maximal osteoclastogenesis in the presence of priming levels of RANKL (Lam et al, 2003). To test this hypothesis we used our established model of pressure-induced bone loss in rats in the absence of wear particles. To block TNF α function we administered Enbrel 4mg/kg (TNF α Ra) (n=9), or saline (n=8), every third day, starting 2 days prior to initiation of the pressure stimuli. As a positive control similar groups of experimental or control animals were given dexamethasone 2mg/kg (n=10), to suppress activation of the innate immune system. Our primary readout was the number of cathepsin K positive osteoclasts. Five days of pressurization resulted in suppression of Cathepsin K positive osteoclast by both dexamethasone (64%) and Enbrel (50%) (Figure 1). These results suggest that a) pressure induced osteolysis is mediated only in part of TNF α , and b) additional inflammatory cytokines are required for osteoclast activation.

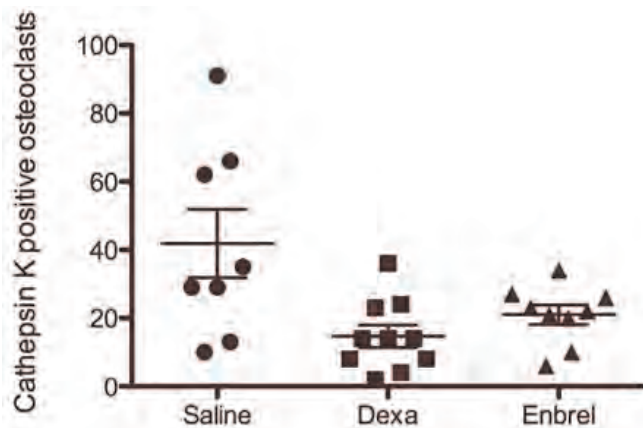


Figure 1. Inhibition of pressure induced osteoclast activation by dexamethasone (Dexa) and Enbrel (TNFaRa) treatment.

Disclosures: Anna Fahlgren, None.

MO0071

Bone Geometry and Strength is Preserved in Adults Following Bariatric Surgery. Lesley Scibora^{*1}, Sayeed Ikramuddin¹, Henry Buchwald¹, Thomas Beck², Moira Petit¹. ¹University of Minnesota, USA, ²Quantum Medical Metrics, LLC, USA

Bone loss is an accepted consequence of bariatric surgery based on areal bone mineral density outcomes. No known studies have prospectively explored the effects of bariatric surgery on bone strength indices in morbidly obese adults using peripheral quantitative computed tomography. Purpose: To describe changes in tibial and radial bone geometry, volumetric density, and estimates of bone strength from baseline (pre-surgery) to 12 months following bariatric surgery in morbidly obese adults. Methods: Bone geometry and strength were assessed by peripheral quantitative computed tomography (pQCT) in 10 obese (mean BMI 49.4 (SD 5.6) kg/m²; mean age 42.3 (SD 15.5) years) adults. Total volumetric bone mineral density (ToD, mg/mm³), total bone area (ToA, mm²), and bone compressive strength (bone strength index (BSI)) were assessed at the distal (4%) sites of the tibia and radius. ToA and cortical bone area (CoA, mm²), cortical volumetric density (CoD, mg/mm³), cortical thickness (CoTh, mm), and bone bending strength (polar strength strain index (SSIp), mm³) were measured at the midshaft sites of the tibia (66%) and radius (50%). Air displacement plethysmography was used to assess body composition (fat mass and fat-free mass (kg)). Results: On average, at 12 months following bariatric surgery body weight decreased 23% ($p < 0.01$), reducing BMI to 38.5 (SD 9.9) kg/m². Weight loss was primarily fat mass (-38.5%, $p < 0.01$), rather than fat-free mass (-5.7%, $p < 0.05$). The fat mass to fat-free mass loss ratio at 3, 6, and 12 months was 4.7:1, 7.5:1, and 7:1, respectively. After 12 months, changes in bone parameters were marginal (<1.0%) at radius (50%) and tibia (66%) midshaft sites, with non-significant increases in BSI at the distal radius (+1.7%) and tibia (+2.5%). Conclusions: Morbidly obese adults who underwent bariatric surgery experienced rapid and substantial weight loss, primarily due to fat mass loss, compared to a small reduction of fat-free mass. However, participants did not suffer short-term deleterious effects on estimates of bone strength at either weight-bearing or non weight-bearing sites. Our results contrast with DXA-based studies that demonstrated reductions up to 14% at hip sites, but not at the radius. Although participants remained obese, they lost little fat-free mass; this may have preserved bone strength. Future studies should examine longer-term effects of bariatric surgical procedures on bone geometry and strength.

Disclosures: Lesley Scibora, None.

MO0072

Effect of Carbohydrate Feeding on the Bone Metabolic Response to Exhaustive Running. Craig Sale^{*1}, Julie Greeves², Thomas Jones³, Ian Varley¹, Ruth Hobson¹, John Dutton⁴, William Fraser⁵. ¹Nottingham Trent University, United Kingdom, ²HQ Army Recruiting & Training Division, United Kingdom, ³Northumbria University, United Kingdom, ⁴University of Liverpool, United Kingdom, ⁵University of East Anglia, United Kingdom

There is a proposed link between carbohydrate (CHO) feeding and bone metabolism at rest, which suggests a potential strategy to attenuate the increase in bone resorption often shown following strenuous exercise (Scott et al. 2010, *JCEM*, 95, 3918-25). We examined the bone metabolic response to CHO ingestion during exhaustive running.

Ten healthy males (mean SD, age 23.2 y, height 1.75 ± 0.08 m, body mass 72.93 ± 7.54 kg, body fat percentage 14.2% and $\text{VO}_{2\text{max}}$ 55.49 ± 6.53 ml·kg⁻¹·min⁻¹) completed two repeated measures, counterbalanced 7 d trials involving a bout of 120 min of running at 70% $\text{VO}_{2\text{max}}$, once with CHO feeding at the start and every 20 minutes of exercise (total glucose ingestion was 102.10 ± 10.56 g) and once with a matched placebo (P). From days 1 to 3, participants refrained from exercise and maintained dietary control. On day 4, venous blood was withdrawn prior to exercise, with subsequent samples being withdrawn immediately post-exercise and after 60 and 120 min of recovery. Participants also provided blood samples at rest on three follow-up days (5, 6 and 7). Markers of bone resorption (β -CTX) and bone formation (PINP), osteoprotegerin (OPG), parathyroid hormone (PTH), glucose and lactate were measured. Bone marker data were analysed using area under the curve (AUC) and paired samples t-tests, with other data being analysed using two-way ANOVA.

CHO feeding resulted in a significantly increased plasma glucose concentration at the cessation of exercise ($P \leq 0.001$) and reduced lactate concentrations across the trial period ($P \leq 0.05$). In P, β -CTX concentrations were increased to ~120% of baseline on days 5 to 7. With CHO feeding, these increases in β -CTX were abolished (~100% of baseline on days 5 to 7). The AUC for β -CTX, calculated from baseline and follow-up day data only, was significantly lower in CHO than in P ($P \leq 0.05$). CHO feeding had no significant effect on AUC for PINP or on PTH and OPG concentrations at any time point.

CHO feeding attenuated the increase in bone resorption observed with strenuous running, suggesting a strategy for reducing the negative effect of repeated exhaustive exercise on bone. However, CHO feeding had no significant effect on bone formation. The effect of CHO feeding on bone resorption was not explained by changes in either OPG or PTH.

This work was sponsored by the UK Ministry of Defence (Army).

Disclosures: Craig Sale, None.

MO0073

Heterogeneity in Mechanosensitivity Among Canadian Postmenopausal Women With and Without Fractures. Celeste Hamilton^{*1}, Thomas Beck², Alia Khaled³, Sophie Jamal⁴, Jonathan Adachi⁵, Jacques Brown⁶, Kenneth S. Davison⁷. ¹Women's College Hospital/University of Toronto, Canada, ²Quantum Medical Metrics, LLC, USA, ³Department of Electrical & Computer Engineering, Johns Hopkins University, USA, ⁴The University of Toronto, Canada, ⁵St. Joseph's Hospital, Canada, ⁶Laval University, Canada, ⁷Department of Medicine, Laval University, Canada

The function of bone's adaptation to mechanical load is to adjust the amount and distribution of bone tissue, such that strains experienced within the bone are kept within certain physiological limits. Genetic differences may cause heterogeneity in load response (mechanosensitivity), such that equivalent loads would generate higher or lower strains depending on load sensitivity. Individuals who are less sensitive to load stimuli should therefore require higher strains to generate an adaptive response and should consequently have weaker bones and be more susceptible to fracture. The purpose of the current study was to determine if stresses (proportional to strains) at the femoral neck under equivalent physiologic loads were higher in postmenopausal women with a history of fractures than in women without fractures. We studied 2922 postmenopausal women who participated in the Canadian Multicentre Osteoporosis Study (CaMos) and who had available Hip Structure Analysis (HSA) data from dual energy x-ray absorptiometry (DXA) scans. Women were categorized into 3 groups based on the number of self-reported fractures at baseline (no fractures, 1-2 fractures and 3 or more fractures). We computed stress (megapascals=MPa) at the infero-medial margin of the femoral neck in a one-legged stance mode using a 2-D engineering beam analysis incorporating dimensions and geometry from DXA scans using the HSA method. We used general linear models (SAS 9.1) after first evaluating significant confounding effects of parameters in Table 1 to determine associations between stance stress and the number of reported fractures based on fracture groupings. Women with 1-2 fractures had higher stress than women with no fractures (10.892.39 vs. 10.622.11 MPa; $p=0.0028$) and women with 3 or more fractures had higher stress than women with 1-2 fractures (11.422.35 vs. 10.892.39 MPa; $p=0.0162$). Because the infero-medial margin of the femoral neck is a site that is normally loaded under compression during upright walking, where the cortex is relatively well preserved with age, these findings are consistent with the theory that individuals who fracture may be more likely to have an underlying genetic difference causing decreased mechanosensitivity. This has important clinical implications in terms of treatment selection, as those with compromised mechanosensitivity may respond best to metabolic agents which would increase their response to load stimuli.

Table 1. Subject characteristics by fracture group.

Variable	No fractures (n=1683)	Fracture Group 1-2 fractures (n=1114)	3 or more fractures (n=125)
		Mean(SD)	
Age (years)	65.2 (9.1)	66.2 (9.3)	68.8 (9.3)
Weight (kg)	68.5 (13.4)	69.5 (13.3)	69.6 (13.7)
Years since menopause	18.5 (10.3)	20.3 (10.3)	23.0 (10.8)
Hours per week of strenuous sports	1.3 (0.7)	1.3 (0.8)	1.3 (0.9)
Hours per week of vigorous work	1.3 (0.8)	1.3 (0.8)	1.2 (0.8)
Hours per week of moderate activity	5.3 (1.6)	5.2 (1.7)	4.9 (1.6)
		Frequency (%)	
Current estrogen use	527 (31.3)	352 (31.6)	35 (28.0)
Previous estrogen use	338 (20.1)	246 (22.1)	28 (22.4)
Never used estrogen	818 (48.6)	516 (46.3)	62 (49.6)
Low trauma fracture at age 50+ years	Not applicable	442 (39.7)	79 (63.2)
Strenuous sports: jogging, bicycling on hills, tennis, racquetball, swimming laps, aerobics; vigorous work: moving heavy furniture, loading or unloading trucks, shoveling, weight lifting, or equivalent manual labour; moderate activity: housework, brisk walking, golfing, bowling, bicycling on level ground, gardening.			

Table 1

Disclosures: Celeste Hamilton, None.

MO0074

Increased Microcracks and Nanoindentation Modulus in the Subchondral Region of the Femoral Head Following Ischemic Necrosis. Olumide Aruwajoye¹, Mihir Patel², Matthew Allen³, Pranesh Aswath², Harry Kim⁴. ¹Texas Scottish Rite Hospital, USA, ²University of Texas at Arlington, USA, ³Indiana University School of Medicine, USA, ⁴Scottish Rite Hospital for Children, USA

Ischemic necrosis (IN) of the immature femoral head initially produces subchondral fracture and subsequent femoral head deformity. Interestingly, even before bone resorption or repair occurs, a decrease in the indentation stiffness of the femoral head and its bony components has been reported. Furthermore, increased mineralization of the necrotic bone has been found suggesting that the material properties of the bone are altered following IN. We hypothesize that the increased mineralization of the necrotic bone leads to increased subchondral brittleness and an increase in the microdamage, resulting in the compromise of the mechanical properties of the subchondral region following IN. The purpose of this investigation was to determine the nanoindentation properties and to assess the presence of microcracks in the subchondral region 2 weeks post IN induction in a well established piglet model of IN. This model has been shown to develop a subchondral fracture and femoral head deformity resembling juvenile femoral head osteonecrosis. Five animals were used for the nanoindentation and microcrack assessments. The left femoral head of each animal was used as a normal control, while the right side had a surgical IN induction by ligating the femoral neck vessels with a ligature. Two 2 mm sections were obtained from each femoral head for the assessments. Measurements included crack length and number, with calculations of crack density, crack surface density, hardness, and reduced modulus. A bony area of the subchondral region was randomly selected for nanoindentation. On average, 44 indentations per 3600 μm^2 were obtained. Nanoindentation for the normal side showed a modulus of 12.23.6 GPa and corresponding hardness of 456187 MPa, while the ischemic side showed a significant increase in the modulus and hardness, 17.16.5 GPa and 626310 MPa, respectively ($p < 0.001$). Crack density in the ischemic side (mean 3.2 cracks/ mm^2) was significantly higher compared to the normal side (mean 0.27 cracks/ mm^2) in the subchondral region ($p < 0.001$). Taken together, these results suggest that IN of the immature femoral head increases the brittleness of the subchondral trabecular bone and makes it more susceptible to microcracks. We postulate that continued loading of the hip joint when there is a lack of bone cells to repair the microcracks due to IN leads to an accumulation of the microcracks and subsequent subchondral fracture.

Disclosures: Olumide Aruwajoye, None.

MO0075

Low Intensity Pulsed Ultrasound as Targeted Therapy towards Bone Loss. Sardar Uddin¹, Yi-Xian Qin². ¹Stony Brook University, USA, ²State University of New York at Stony Brook, USA

Osteoporosis and microgravity has been known to cause adverse effect on bone quality leading to decrease in bone mass density (BMD) in load-bearing bones (Lang T.F et al 2006). Therapeutic approaches using drugs and different growth factors have been considered to maintain bone mass with limitations of high costs and difficulty to maintain over longer periods of time besides the systematic effects of such treatments (Hughes-Fulford M. 2002). To reverse the adverse effects on bone physiology, it is important to provide cells with physical stimulus which can maintain essential mechanical signal for cells to counter the bone loss. Ultrasound generated local acoustic pressure vibrations can be readily applied *in vivo* for human therapeutics as a non-invasive modality and more target specific treatment related loading profiles. The objective of this study was then to evaluate the systematic effects of low intensity pulsed ultrasound (LIPUS) on a disused bone model.

C5BL/6 mice were hind limb suspended for 4 weeks. Animals were distributed into 5 groups, Age-Match(AM), Non-Suspended Sham(NS), Non-Suspended-LIPUS

(NU), Suspended Sham (SS) and Suspended - LIPUS(SU). NU and SU animals' tibia were exposed to LIPUS at 30mW/cm² for 20min/day for 5 days/week.

After 4 weeks of loading animals were euthanized and tibia were collected. Bone quality was assessed using mCT with resolution of 12mm. MicroCT data showed significant increase in bone mineral density (mmHg/cc, $p = 0.02$), Trabecular Thickness (mm, $p = 0.05$) and Bone surface/volume (mm²/mm³, $p = 0.05$) (Table 1). Analyses of right (non LIPUS treated) and left (LIPUS treated) tibia of NU don't show any changes. Right tibia of SU mice doesn't show any anabolic effects of LIPUS exposure as observed in left tibia (Fig 1).

LIPUS anabolic effects are localized and show no systematic effects suggesting LIPUS treatment as localized noninvasive therapy inhibited bone loss induced by disuse. Further work includes on-going histomorphometry and molecular analyses to understand the mechanotransductive pathways activated by LIPUS stimulation.

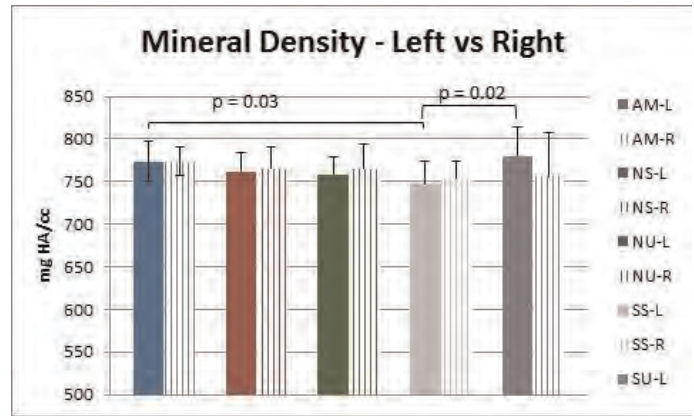


Fig 1: LIPUS as localized bone loss therapy.

Group	BV/TV	Mean1	Mean2	Tb.N	Tb.Th	ConDen	BS/BV
AM	0.086±0.027	188.09±24.39	773.43±24.82	4.83±0.49	0.039±0.003	79.76±48.31	71.72±6.66
NS	0.085±0.019	186.56±16.67	762.04±21.80	4.92±0.41	0.036±0.003	83.76±32.74	73.95±5.66
NU	0.080±0.02	179.08±25.58	758.85±19.99	4.64±0.47	0.036±0.003	81.84±47.15	76.45±9.22
SS	0.055±0.02	156.35±28.01	747.86±26.49	4.37±0.62	0.034±0.001	41.43±31.03	85.42±6.96
SU	0.062±0.02	160.98±20.76	779.98±34.77	4.25±0.55	0.036±0.004	45.77±31.11	75.98±3.25

Table 1: Significant increase in bone quality parameters in disuse model with LIPUS treatment

Disclosures: Sardar Uddin, None.

MO0076

Short Term Physical Activity May Induce Changes In Bone Density And Geometry Even After Bone Maturation In Talented Female Athletes. Beatrice FERRY¹, Eric Lespessailles², Gaele Ducher³, Martine DUCLOS⁴, Pierre ROCHCONGAR⁵, Geraldine NAUGHTON⁶, Daniel Courteix⁷. ¹Clermont Universite, Universite Blaise Pascal, EA 3533, Laboratoire de Biologie des Activites Physiques et Sportives, BP 10448, F-63000; ²Universite de Limoges, Faculte des Sciences et Techniques, Departement STAPS, F-87060 LIMOGES, France, ³Centre Hospitalier Regional, France, ⁴Penn State University, USA, ⁵Service de Medecine du Sport et des Explorations Fonctionnelles, France, ⁶Unite de biologie et medecine du sport, CHU Pontchaillou, France, ⁷Centre of Physical Activity Across the Lifespan Australian Catholic University, Australia, ⁸Universite Clermont Ferrand Laboratoire De Biologie Des APS, France

The benefits of exercise on bone geometry and density are linked to the history and modalities of sports participation. The period of late adolescence, characterized either by a minimal increase or a plateau in bone maturation has not been plainly investigated. The aim of the present study was to assess changes in hip structural parameters and bone mineral density, in high level adolescent soccer and swimmers.

Fifty-eight girls swimmers (SWIM: n=26, aged 15.9 ± 2 years) or soccer players (SOC: n=32, aged 16.2 ± 0.7 years) were investigated before and after an 8-month training season. Fifteen non active age-matched adolescents were enrolled at baseline to serve as a reference group. Body composition and areal bone mineral density were measured at the total body, lumbar spine and total hip by DXA. Indices of bone geometry were extracted from DXA scans using the hip structure analysis (HSA) method. Anatomical (cross sectional area-CSA, endocortical diameter-ED and periosteal diameter-WIDTH) and mechanical parameters (CSMI, Z and buckling ratio-BR) were analyzed. A one way ANOVA with repeated measures was performed.

After eight month of training, SOC increased their density at all traditional bone sites whereas SWIM did not. The SOC's changes are associated with an increase of whole body lean mass. At the neck and total hip, SWIM kept their baseline low Z-score values and SOC remained above the normal. The most important changes in HSA parameters were observed at the femoral shaft. When comparing the T-score to the control group at this section, SWIM who were normal for ED and WIDTH and below for CSA, did not change after the season. For the SOC group who started

already above the average range, CSA and WIDTH still improve during this period. The T-score showed an improvement of CSMI and Z at FS section for SOC ($p < 0.001$), without any change in the SWIM group. Remarkably SWIM had improved the T-score of BR ($p < 0.005$) while SOC did not.

A season of training for sport characterized by impact (SOC) is associated with bone geometry improvement in late adolescent female despite expectations that this period of growth represents a plateau in bone maturation. This study adds to the existing literature describing intensive swimming practice as lacking an osteogenic effect when assessed by DXA. Weight bearing physical activity can be an important contributor to bone strength at the end of adolescence, as observed during childhood.

Disclosures: Beatrice FERRY, None.

MO0077

β -Adrenergic Receptor Antagonist Suppresses Occlusal Force Unloading-Induced Alveolar Bone Loss in Rats. Yasuhiro Shimizu^{*1}, Jun Hosomichi², Sawa Kaneko¹, Takashi Ono¹. ¹Orthodontic Science, Department of Orofacial Development & Function, Division of Oral Health Science, Graduate School, Tokyo Medical & Dental University, Japan, ²Department of Orthodontics & Pediatric Dentistry, School of Dentistry, University of Michigan, Orthodontic Science, Department of Orofacial Development & Function, Division of Oral Health Science, Graduate School, Tokyo Medical & Dental University, USA

Mechanical stress to bone plays a crucial role in the maintenance of bone homeostasis, and prolonged lack of mechanical stimuli leads to disuse osteoporosis. Unloading of occlusal force upon alveolar bone, occlusal hypofunction, suppresses the formation of bone and results in atrophic changes of alveolar bone. Sympathetic nervous system controls bone resorption by increasing production of RANKL, via β -adrenergic receptors in leptin-dependent neuronal regulation of bone formation. Sympathetic nervous system mediates unloading-induced bone loss by reduction in osteoblastic cell activity and enhancement of osteoclastic cell activity. Therefore, we hypothesized that the modulation of sympathetic nervous system via β -adrenergic receptors is involved in the metabolism of the alveolar bone. We focused on the effect of sympathetic nervous tone on occlusal force unloading-induced alveolar bone loss in rats using a non-selective β -adrenergic receptor antagonist.

Twenty-four 5-week-old male Wistar rats were randomly divided into 4 groups; Group C was an untreated group, Group H was an occlusal hypofunction group, Group B was a group administered a non-selective β -adrenergic receptor antagonist, propranolol hydrochloride, and rats in Group HB received water with the same dose of propranolol as in Group B under the hypofunctional condition in the molar area. Occlusal hypofunction in the molar area was produced by attaching appliances to rat maxillary and mandibular incisors. In addition, propranolol was administered orally to rats in drinking water to pharmacologically suppress sympathetic nervous activity. After 1 week, alveolar bones were examined by micro-CT, histomorphometry and histology to determine their trabecular bone phenotypes and histological changes.

The marrow spaces of the interdental alveolar bone of rat mandibular first molars (M1) increased in Group H but not in Group C, while these decreased in Group HB. Bone volume/tissue volume, trabecular thickness and trabecular number for interdental alveolar bone of M1 in Group H were significantly lower than those in Group C, whereas those in Group HB remained as high as those in Group C. The number of TRAP-positive cells in Group H increased compared to that in Group C, whereas it significantly decreased in Group HB. Findings from our study suggest that β -adrenergic receptors in the sympathetic nervous system are the target of occlusal force unloading-induced alveolar bone loss.

Disclosures: Yasuhiro Shimizu, None.

MO0078

Collagen Enzymatic Cross-links Deficiency and Bone Quality. Delphine Farlay^{*1}, Marie-Eve DUCLOS², Evelyne Ginevys³, Cindy BERTHOLON¹, Stephanie VIGUET-CARRIN¹, Thierry ROGER⁴, Daniel HARTMANN⁵, Roland Chapurlat⁶, Helene Follet⁷, Georges Boivin⁸. ¹INSERM, UMR1033; Universite De Lyon, France, ²Universite de Lyon, UPSP 2007-03-135 RTI2B, VetAgroSup, France, ³Universite De Lyon, France, ⁴VetAgroSup, France, ⁵Universite de Lyon, UPSP 2007-03-135 RTI2B, France, ⁶E. Herriot Hospital, France, ⁷INSERM, UMR1033 ; Universite De Lyon, Fra, ⁸INSERM, UMR 1033 ; Universite de Lyon, France

A collagen enzymatic cross-link (ECL) deficiency, such as pyridinium ECL, alters the mechanical properties of bone organic matrix. However, the influence of such a deficiency on mineral characteristics is not well documented. Our hypothesis was that a decrease in pyridinium ECL modifies the arrangement of collagen fibers and consequently disrupts the mineral characteristics of bone mineral. To investigate the relationship between ECL and mineral phase, a model of lathyritic rats was designed. This model consists to inhibit the lysyl oxidase, enzyme catalyzing the ECL formation, by using a lathyrogen agent such as α -aminopropionitrile (α APN). Twenty Wistar rats (28 day-old) received either 666 mg/kg/day of α APN (LATH) or vehicle (CTL) twice daily during 30 days. After sacrifice, left tibia and radii were embedded in

PMMA for histomorphometry and Fourier Transform Infrared Microspectroscopy (FTIRM). By the latter, mineral maturity (age of mineral, 1030/1110 cm⁻¹ area ratio), crystallinity index (crystal size/strains, FWHM 604 cm⁻¹) were measured. Right tibia and radii were frozen at -20°C for biochemical dosage (HPLC) of ECL, pyridinoline (PYD) and desoxypyridinoline (DPD). Histomorphometry and FTIRM were performed on radii in which the decrease of ECL was higher than in tibia. Non-parametric tests (U Mann-Whitney) were performed. Results: a significant body weight loss was observed in all LATH animals, after the 14th day of injection, compared to CTL rats. In LATH rats, significant decreases of both ECL and collagen synthesis were observed compared to CTL. Moreover, a significant decrease of BV/TV, an increase in growth plate thickness and cortical porosity were observed. Cortical thickness was not modified. Mineral maturity and crystallinity index were unchanged in LATH animals. In conclusion, an ECL deficiency does not affect the quality of bone mineral phase.

1- Oxlund et al, Bone 1995, 17 365S-371S ; 2- Farlay et al, 2010 J Bone Miner Res 25 (Suppl 1) SU0065.

Disclosures: Delphine Farlay, None.

MO0079

Polarization Control of Raman Spectroscopy Optimizes Measures of Bone Quality. Alexander Makowski^{*1}, Chetan Patil¹, Lacey Gorocho¹, Anita Mahadevan-Jansen¹, Jeffry Nyman². ¹Vanderbilt University, USA, ²Vanderbilt University Medical Center, USA

Interest in the concurrent assessment of both mineral and collagen phases of bone composition and matrix organization has led to novel techniques that modulate laser polarization while conducting Raman Spectroscopy (RS). Since bone is inherently birefringent, polarization will affect the light path through the tissue and hence the Raman spectra. Moreover, polarization bias from RS system components could affect measurements of mineral to collagen ratios, crystallinity, and carbonate substitution. We modulated source and collection polarization in a commercial instrument to test the hypothesis that matching the polarization behavior of individual Raman peaks would isolate the quantification of organization from the quantification of compositional properties while minimizing variance in traditional Raman properties of bone.

To demonstrate the effect of polarization on compositional differences between osteonal and interstitial bone, we collected spectra from multiple osteons and neighboring interstitial sites of a transverse section of human cortical bone (medial quadrant of the femur mid-shaft) before and after 90 degree sample rotation. To analyze sensitivity of spectral components to the light orientation, spectra were collected on the same sample and similar tissue sites after adding an excitation arm (isolator) and a collection arm (analyzer) polarizers. With a fixed sample orientation at each site, spectra were collected at analyzer rotation angles of 0:180 degrees per 15.

Bone rotation studies revealed lower coefficients of variation for the collagen marker Proline than the traditional Amide I, and it yielded more consistent measures of osteonal-interstitial tissue differences in mineral to collagen ratio, regardless of bone orientation. Exploring underlying causes, sinusoidal modeling of the peak intensities vs. polarization angle revealed that the established quantity ν_1 Phosphate/Amide I contains a bias in bone orientation relative to laser polarization, making it suitable for structural analysis, while the alternative ν_1 Phosphate/Proline corrects for polarization bias, and thus can assess composition independent of polarization angle (Fig.1). These results support differential optimization of RS quantities for analysis of structure or composition. Careful consideration of polarization bias for instrumentation and experimental protocols can prevent spurious correlation, ensuring Raman provides meaningful insight into bone's resistance to fracture.

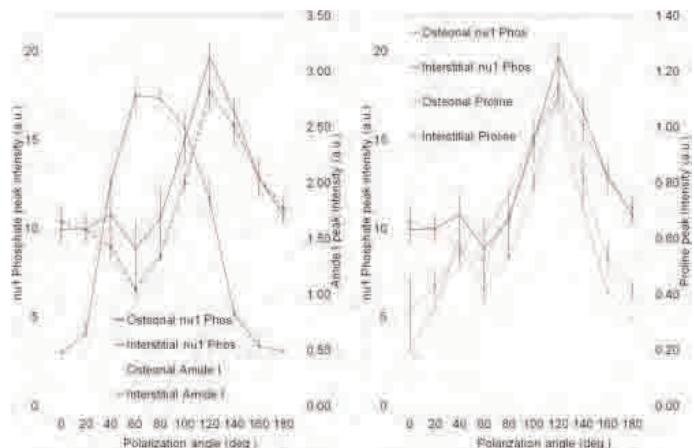


Fig1. Peak intensity vs. polarization shows bias (Amide I, left) and correction (Proline, right)

Disclosures: Alexander Makowski, None.

MO0080

Calcified Cartilage in Mature Rat Cortical Bone. Fiona Linnea Bach-Gansmo¹, Jesper Thomsen², Annemarie Bruel², Henrik Birkedal^{*1}.¹Aarhus University, Denmark, ²University of Aarhus, Denmark

Bone remodeling of cortical bone in humans involves Haversian remodeling. However, this mode of remodeling is very scarce in rodents such as rats [1, 2]. Indeed, why Haversian remodeling is used in some animals but not in others remains an unresolved question.

Using backscatter electron imaging, we found islands of brighter contrast, reflecting a higher degree of mineralization, in the center of mid-femoral rat cortical bone. The islands typically had rounded borders, often concave with an osteocyte located nearby, in a manner suggesting that the island had not been turned into bone, when an osteoblast matured into the osteocyte. This observation suggested that these islands could be remnant calcified cartilage. This hypothesis was confirmed by toluidine blue staining and by immuno-labelling against collagen type II. The degree of mineralization was mapped by qBEI [3], which clearly established that these areas were more highly mineralized than the surrounding tissue. This was further confirmed by energy dispersive X-ray analysis mapping. The mechanical properties of the cartilage islands were probed by nanoindentation using an indentation protocol similar to the one in [4]. As expected from the higher degree of mineralization, both the indentation modulus and hardness were significantly higher in the calcified cartilage than in surrounding bone.

The islands were elongated in the longitudinal direction of the femur. Our present observations explain previous biochemical results showing that collagen type II is present in rat cortical bone [5].

We suggest that the cartilage islands are leftovers from the bone formation process. As such they represent archaic mineralized tissue that is unlikely to sense and react appropriately to microcracks etc. Further work is needed in order to establish, whether their presence leads to reduced mechanical performance. We speculate that avoiding their presence may be an additional reason for Haversian remodeling in larger animals.

[1] D. B. Kimmel in Principles of Bone Biology (J. P. Bilezikian, L. G. Raisz, G. A. Rodan, eds.) pp. 1635-1655.

[2] J. D. Currey. Bones, Structure and Mechanics. Princeton University Press, 2 ed. 2006..

[3] P. Roschger, E. P. Paschalis, P. Fratzl & K. Klaushofer, Bone, 42, 456-466, 2008.

[4] A.-M. Bruel et al., Calc. Tissue. Int., 88, 142-152, 2011.

[5] M.A. Schreivewis et al., J. Cell. Biochem., 101, 466-476, 2007.

Disclosures: Henrik Birkedal, None.

MO0081

Thermodynamic Properties and Characterization of Proteoliposomes Rich in Microdomains Carrying Alkaline Phosphatase. Mayte Bolean^{*1}, Ana Maria Simao¹, Bruno Favarin¹, Jose Luis Millan², Pietro Ciancaglini³.¹Department of Chemistry, FFCLRP-USP, Brazil, ²Sanford-Burnham Medical Research Institute, USA, ³FFCLRP-USP, Brazil

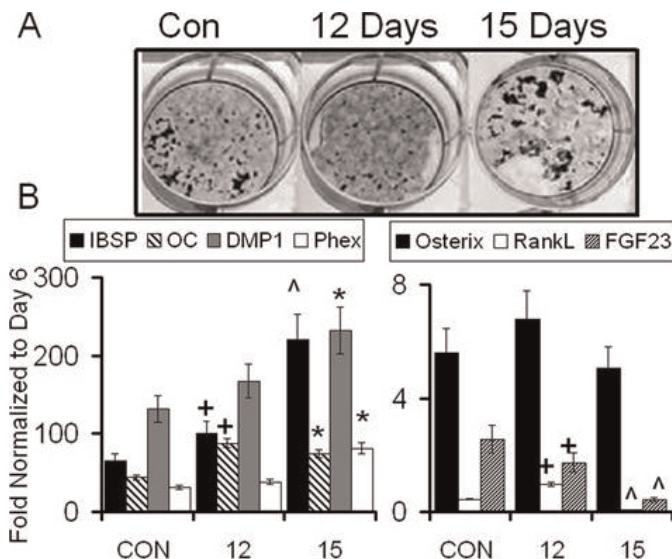
Tissue-nonspecific alkaline phosphatase (TNAP) is associated to the plasma membrane via a GPI-anchor and plays a key role in the biomineralization process. In plasma membranes, most GPI-anchored proteins are associated with "lipid rafts", ordered microdomains enriched in sphingolipids, glycosphingolipids and cholesterol. In order to better understand the role of lipids present in rafts and their interactions with GPI-anchored proteins, the insertion of TNAP into different lipid raft models was studied using dipalmitoylphosphatidylcholine (DPPC), cholesterol (Chol), sphingomyelin (SM) and ganglioside (GM1). The membrane models studied were binary systems (9:1 molar ratio) containing DPPC:Chol, DPPC:SM and DPPC:GM1; ternary systems (8:1:1 molar ratio) containing DPPC:Chol:SM, DPPC:Chol:GM1 and DPPC:SM:GM1 and finally, a quaternary system (7:1:1:1 molar ratio) containing DPPC:Chol:SM:GM1. Calorimetry analysis of the liposomes and proteoliposomes revealed lateral phase segregation only in the presence of cholesterol, with the formation of cholesterol-rich microdomains centered above T_c=41.5°C. The presence of GM1 and SM into DPPC-liposomes influenced mainly ΔH and Δt_{1/2} values. The gradual increase in the complexity of the systems decreased the activity of the enzyme incorporated. The presence of the enzyme also fluidifies the systems, as seen by the intense reduction in ΔH values, but do not alter T_c values significantly. The study of these microdomains will contribute to our understanding of the interactions between the lipids present in MVs and GPI-anchored TNAP.

Disclosures: Mayte Bolean, None.

MO0082

Vascular Endothelial Cells Produce Factors that Promote Osteogenic Differentiation of MSCs but Inhibit Mineral Deposition and Terminal Osteocyte Differentiation. Jennifer Fitch¹, James Birkhead², Elle Nugent², Louis Gerstenfeld^{*1}. ¹Boston University School of Medicine, USA, ²Pervasis Therapeutics, USA

Skeletal development after injury or surgery is co-dependent on vascularization. While this co-dependency is often thought of in terms of the skeletal tissue's need for appropriate nutrition and oxygen, vascular morphogenesis also provides the structural template around which the Haversian and trabecular bone units develop. These phenomena suggest that development and mineralization of skeletal tissue is tightly coordinated with vascular ingrowth. In order to define the nature of the signals between skeletal and vascular tissues, human endothelial cells (EC) embedded in a collagen carrier were co-cultured in transwell culture chambers with murine bone marrow stromal cells (MSCs). After a six day selection for the adherent MSCs, the cells were grown in a 50/50 MSC/EC culture media mixture supplemented with osteogenic levels of ascorbate and beta-glycerophosphate. Co-cultures were either grown for up to 15 days continuously in the presence of ECs or only for 6 days after initial selection. Continuous co-culture prevented mineral nodule formation but enhanced osteogenic differentiation based on the induction of osteonin and elevated osteocalcin and RankL mRNA expression compared to control no co-culture. Co-culture for only six days and assay of the cultures after an additional 12 or 15 days of growth showed that shorter co-culture periods delayed nodule formation but after additional time nodule formation caught up to control cultures. Assay of osteogenic differentiation (OC, BSP and RANKL) showed statistically significant increases in expression at 12 days, while assay of genes associated with terminal osteocyte differentiation (DMP1, Phex and FGF23) that are known to control mineral deposition showed delayed onset for the expression of DMP1 and Phex but enhanced the expression of FGF23. At 15 days both DMP1 and Phex were expressed at statistically higher levels than control cultures while FGF23 levels were decreased well below those seen in either the control or day 12 cultures. The decreased expression of FGF23 that is known to inhibit mineral deposition and elevated expression of DMP1 and Phex that promote matrix mineralization suggest a mechanism for the delay in mineralization related to the control of phosphate metabolism. The data suggest that factors produced by EC will promote early osteogenic differentiation but prevent premature mineralization during the period when newly formed blood vessels are growing into the developing bone tissue.



Effect of EC Co-Culture on MSCs. A) Nodule formation. Con = Control No Co Culture; 12 or 15 Days= (6 days Co-culture and 12 or 15 days in osteoinductive media). **B) qRT-PCR of RNAs values normalized to Day 6** when cultures are removed from Co Culture + = sig between Day 12 and con. * = Sig between Day 15 and Day 12. ^ = sig Between both Day 15, Day 12 and con. P=0.05

Co_Culture of Endothelial Cells with MSCs

Disclosures: Louis Gerstenfeld, Pervasis Therapeutics, 2
This study received funding from: Pervasis Therapeutics

MO0083

***Pknox2* Is Identified as a Regulator for Ulna and Deltoid Tuberosity Formation During Limb Development.** Wenrong ZHOU^{*1}, Zhu Huang², Haixia Zhao², Jingjing Cao³, Wan Yong², Jun Yang⁴, Gang Ma², Ruijiang Zhou³, Xizhi Guo². ¹Shanghai JiaoTong University, Peoples Republic of China, ²Shanghai Jiao Tong University, Peoples Republic of China, ³Bio-X Center, Shanghai Jiao Tong University, China, 200240, China, ⁴Shanghai Jiao Tong University, China

Pknox2 encodes a homeodomain-containing transcription factor as a member of Pknox subfamily of TALE (Three Amino acid Loop Extension) family. Its expression was confined in presumptive zuegopod and partial stylopod domain in murine limb at E10.5 or E11.5; after E12.5 it was specifically expressed at joint region of limb bud. To analysis the *Pknox2* function in vivo, we ectopically activated *Pknox2* expression in chondrocyte or osteoblast through generating *Col2a1-Pknox2* and *Col1a1-Pknox2* transgenic mice. The *Col2a1-Pknox2* transgenic embryos displayed a twisted radius and disorganized ulna with missing olecranon at the elbow joint in forelimb, while the hind limb was relatively normal. Histochemistry analysis showed that chondrocyte differentiation and osteogenesis program was exclusively abrogated in the ulna of *Col2a1-Pknox2* mutant at 15.5. Interestingly, ectopic ossified nodals on the first lumbar was also detected, indicating an alteration of the axial formula. In addition, *Col1a1-Pknox2* transgenic mice exhibited relatively normal skeletons except with loss of deltoid tuberosity. Preliminary data also suggested a potential modulation of Hox10/11 protein family and Wnt/ β -catenin signaling by *Pknox2* in regulating ulna identity and deltoid tuberosity development. More evidence is coming out to elucidate the mechanism of *Pknox2* in limb development.

Disclosures: Wenrong ZHOU, None.

MO0084

Activation of IGF- β Signaling Regulates Joint and Tendon Marker Expressions in Isolated Joint Developing TGF- β Type II Receptor Expressing Cells. Tieshi Li^{*1}, Lara Longobardi¹, Froilan Granero-Molto¹, Timothy Myers², Ying Li¹, Douglas Mortlock³, Anna Spagnoli¹. ¹University of North Carolina at Chapel Hill, USA, ²University of North Carolina, USA, ³Vanderbilt University Medical Center, USA

TGF- β type II receptor (*Tgfr2*) signaling plays an essential role in joint and tendon development as indicated by the lack of these skeletal elements in the *Tgfr2*^{PRX-1KO} mouse, in which the *Tgfr2* is conditionally inactivated in developing limbs. (Spagnoli A et al, J Cell Biol, 2007; Schweitzer R et al, Development, 2009). In our previous studies we also showed the specific expressing domains of Tgfr2 within the developing limbs. (T. Li et al, ASBMR-2010). This study is to investigate the gene expression profile in embryonic limb mesenchymal Tgbr2 expressing cells and whether those cells provide signaling for joint and tendon marker expression. We isolated Tgfr2 expressing cells (1-2%) from developing (E13.5 and E14.5) limb mesenchyme digits of *Tgfr2*- β -Gal-GFP-Bac, a GFP-LacZ reporter mouse for Tgbr2 expression, of via GFP FACS sorting and treated isolated cells with TGF- β . Statistical significance was set at $p < 0.05$. qRT-PCR measurements showed that Tgfr2 positive cells compared to negative cells express more tendon markers such as Scleraxis (SCX) and Notch1 as a stem cell related gene, but less Collagen I and Collagen II. Comparing gene expression in E13.5 Tgfr2 positive cells vs E14.5 we found that joint marker genes such as GDF5, Sulf-1 and Gli3 increased with time. These results are consistent with our previous immunohistochemistry studies in which we showed the co-localization of Tgfr2 with these markers in developing joints (T. Li et al; ASBMR-2010). When placed in cultures, Tgfr2 expressing cells failed to form micromasses. Activation of Tgfr2 signaling in Tgfr2 expressing cells with Tgfb1 treatment (10 ng/ml; for 16 hours), when compared with untreated cells, up-regulated tendon-related gene expressions such as SCX and Tenomodulin as well as joint and stem cell markers such as GDF5, Noggin, Sulf-1, Notch1 while down-regulated collagen I, collagen II, Wnt9a, Gli3 and Tbx5. We further evaluated in Tgbr2 expressing cells, the expression patterns of genes related to mesenchyme stem cells. We found that 100% of Tgfr2 expressing cells express CD29; while around 20-30% express CD44, CD166, CD73 and CD105. Our studies provide evidence that the joint developing Tgfr2 expressing cells can be isolated, express joint and tendon markers and such expression is regulated by the activation of the TGF β signaling.

Disclosures: Tieshi Li, None.

MO0085

Delayed Bone Fracture Healing In Mice Due to Tamoxifen-induced Knockout of IGF1R Gene In Chondrocyte. Zhiqiang Cheng^{*1}, Hanson Ho², Fuqing Song², Alfred Li³, Christian Santa Maria², Yongmei Wang⁴, Michael You³, Chialing Tu³, Daniel Bikle⁵, Wenhan Chang¹. ¹University of California, San Francisco, USA, ²VAMC, UCSF, USA, ³VAMC, UCSF, USA, ⁴Endocrine Unit, University of California, San Francisco/VA Medical Center, USA, ⁵Endocrine Research Unit, Division of Endocrinology UCSF, USA

Fracture healing is delayed in mice due to tamoxifen-inducible knockout IGF1R gene in the chondrocyte. Z. Cheng, H. Ho, F. Song, Alfred Li, Christian Y. Santa Maria, C. Tu, D. Bikle, W. Chang. Endocrine Research Unit, Department of Veterans Affairs Medical Center, NCIRE, University of California, San Francisco, CA, USA. Many studies showed that IGF1R is important in the normal endochondral bone formation in the growth plate during development, starting from embryonic stages. Specific deletion of IGF1R in chondrocytes showed cell hypoproliferation, delayed differentiation and shortened hypertrophic zone. Although the majority of fracture heal is endochondral ossification parallel those that take place in growth plate, the process is more complex in fracture healing. To assess the role of IGF1R in this process, we fractured the chondrocyte-specific knockout of IGF1R mice by using three-point bending. Since cartilage-specific IGF1R Knockout mice died shortly after birth, we generated Tamoxifen-inducible expression of Cre under the control of the type II collagen promoter. We injected Tamoxifen one day before fracture at the age of 3 months, keeping injection for 6 days. We investigated the callus of these mice, 4 Wild Type (WT) vs. 3 Knockout (KO), after non-fixed tibia fracture over 10 days by using gene expression analyses and by bone histomorphometry. Callus gene expression confirmed IGF1R expression is significantly reduced in KO mice with the higher level of IGF1. It showed the early differentiation marker—Agg and Col (II) were increased in KO mice compared to WT, the late terminally differentiation marker—OPN is decreased in KO mice, but Col(X) is increased in KO. The osteoblast marker—Clo(I) and OCN were different between two group. Histomorphometric analysis demonstrated that there were a moderate increased on BV/TV (22.4% vs. 18.5%, +21% $p=0.062$). A significant increase in WT were seen on total callus volume (TV) (8.6% vs. 5.2%, +65.4% $p=0.0009$), terminal differentiative chondrocytes volume (TDCV/CV) (56.2% vs. 48.0%, +17.1% $p=0.014$) and new bone thickness (BTh) (10.9% vs. 9.7%, +12.4% $p=0.016$). The cartilage volume in the callus (CV) was decreased in WT compare to KO (20.4% vs. 34.4%, -68.6% $p=0.0012$). The increased CV, but reduced hypertrophic chondrocytes as well as decreased BV/TV in the callus of the IGF1R KO mice indicated that the deletion of IGF1R in cartilage could extended the process of chondrocytes maturation from the resting phase to the terminal differentiation, and lead to delayed ossification, eventually reduced new bone formation. This study revealed that the conditional knockout IGF1R in the chondrocyte exerts impaired fracture healing of mice. It implicated the IGF1R also playing a key roles during the endochondral bone formation of fracture repair process, just like its function in normal bone development.

Disclosures: Zhiqiang Cheng, None.

MO0086

Developing GFP Reporters for Assessing Lineage Progression Within Articular and Fibroarticular Tissues. Sumit Yadav^{*}, Xi Jiang, Jianping Huang, Peter Maye, Ivo Kalajzic, David Rowe. University of Connecticut Health Center, USA

Mapping the early cellular response to cartilage injury has been difficult to construct because stages of lineage progression are not well defined. We are utilizing GFP reporters that are active in different types of cartilaginous tissues and have found significant differences in expression between fibrocartilage, articular cartilage and growth plate cartilage. While Col2A1 and Col10A1 reporters show activity in the expected cellular locations in the three tissue types, other reporters appear to have unique patterns of expression. A Dkk3-GFP reporter was active in the superficial pre-chondrocytic articular cells of fibrocartilage (temporal mandibular joint, TMJ) and articular cartilage. Also common to both tissues are the synovial lining cells that express lubricin GFP, while deeper cells within the cartilage matrix that are tenascin C GFP positive. Articular cartilage cells of young animals express GDF5-GFP in the groove of Ranvier, and Dlk1-GFP in the superficial cells along the lateral articular surface prior to the more central location of Dkk3 cells. In contrast, TMJ shows reporter expression of osterix, BSP and Col1A1 after Dkk3 activation and prior to the onset of Col2A1 expression. None of these pre-chondrocytic reporters are observed in growth plate chondrocytes. Most striking is the activity of a SMAA-CreERT2 driver, which demonstrates that the mature cells within the fibrocartilage develop from a SMAA progenitor, a lineage that is not observed in articular or growth plate chondrocytes. A pathway of lineage progression of SMAA \rightarrow Dkk3 \rightarrow Col3.6/BSP \rightarrow Col2A1 \rightarrow Col10A1 is observed in all fibrochondrocytic tissues including the TMJ, intervertebral disc and endplate, sternum, multiple tendon/ligament entheses and fracture callus. These reporters have proven useful in developing conditions for maintaining chondrocyte differentiation in primary culture, particularly under low oxygen culture conditions, and for isolating subpopulations of cells either directly from articular surfaces or primary culture for microarray characterization based on their GFP expression. As more molecular and cellular detail is assembled to validate the meaning of these reporters within the context of cartilage biology, a better

understanding of the signals that control lineage progression will emerge, and reporter mice can be assembled to better map the consequence of injury, repair or degeneration to articular and fibrocartilagenous tissues.

Disclosures: *Sumit Yadav, None.*

MO0087

Essential Role of the Runx2-Cbf- β Transcription Complex for Endochondral Bone Formation. Kyung-eun Lim¹, Jung-eun Kim², Ichiro Taniuchi³, Na-rae Park^{*1}, Suk-Chul Bae⁴, Je-Yong Choi⁵. ¹Department of Biochemistry & Cell Biology, Skeletal Diseases Genome Research Center, School of Medicine, WCU Program, Cell & Matrix Research Institute, Kyungpook National University, South Korea, ²Depat. of Molecular Medicine, Kyungpook National University School of Medicine, South Korea, ³Laboratory for Transcriptional Regulation, RIKEN Research Center for Allergy & Immunology, Japan, ⁴Department of Biochemistry, School of Medicine, Institute for Tumor Research, Chungbuk National University, South Korea, ⁵Kyungpook National University, School of Medicine, South Korea

Endochondral bone formation requires expression of Runx2 in prehypertrophic and hypertrophic chondrocytes. Core binding factor- β (Cbf- β) is a partner protein of Runx family transcription factor. Here, we showed that chondrocyte-specific deficiency of Cbf- β inhibited endochondral bone formation. Cbf- β /fl mice died immediately after birth. However, Cbf- β /+ mice showed no difference in longevity and skeletal tissues compared with wild type mice. From embryonic days 15.5 (E15.5) to birth, Cbf- β /fl mice showed delayed chondrocyte maturation and decreased Runx2 expression in chondrocytes compared with wild type. Besides, Runx2 protein levels from primary chondrocyte (E15.5), mouse embryonic fibroblast (E12.5), and mesenchymal cell (E11.5) in Cbf- β /fl mice were dramatically reduced without change of its mRNA levels. These findings indicate that Cbf- β is essential for Runx2 mediated endochondral bone formation by regulating Runx2 protein stability.

Disclosures: *Na-rae Park, None.*

MO0088

Expression of Ift88, a Cilia Component Gene, is Under Temporal Regulation Along with the Differentiation of Chondrocytic Cell Line ATDC5. Makiri Kawasaki^{*1}, Tetsuya Nakamoto¹, Takuya Notomi², Tadayoshi Hayata³, Yoichi Ezura⁴, Masaki Noda¹. ¹Tokyo Medical & Dental University, Japan, ²GCOE, Tokyo Medical & Dental University, Japan, ³Medical Research Institute, Tokyo Medical & Dental University, Japan, ⁴Tokyo Medical & Dental University, Medical Research Institute, Japan

Primary cilium, a non-motile, microtubule-based structure which protrudes from the cell surface, is observed in most of the eukaryotic cells. Now it is revealing that this organelle has a role as a mechanosensor and it is involved in multiple signaling pathways, however the function of primary cilia in chondrocytes is scarcely known. Intraflagellar transport (IFT) is required for the cilia assembly and Ift88/Tg737 is one of the IFT particles moving anterogradely along the cilium. It has been shown that the deletion of Ift88/Tg737 causes loss of cilia. In this research, we examined whether or not Ift88 is expressed in the mouse chondrocytic cell line ATDC5 and its expression is regulated along with the differentiation of ATDC5. After 10 days in culture, ATDC5 cells started to form nodules and expressed chondrocyte specific extracellular matrix. During this period, Ift88 expression was dramatically increased four-fold compared to day 7 of culture. The Ift 88 expression peaked on day 14 and the level of its expression was maintained up to day 17. This expression pattern of Ift88 was corresponding to that of type 2 collagen. In the meanwhile, Runx2 and OSX expression were also increased on day 10 three-fold and two-fold, respectively. However these two genes showed a decreasing tendency in expression after day 14 of culture. These results indicate that Ift88 expression is regulated along with chondrocyte differentiation.

Disclosures: *Makiri Kawasaki, None.*

MO0089

Neurofibromin Is Required for Normal Endochondral Ossification. Koichiro Ono^{*1}, Weixi Wang², Jean Ndong³, Heather Eleanor³, Xiangli Yang², Florent Elefteriou². ¹Center for Bone Biology, USA, ²Vanderbilt University, USA, ³Vanderbilt University Medical Center, USA

Most genetically linked human skeletal abnormalities are caused by dysregulation of endochondral ossification. Studies of achondroplasia have focused on FGFR3 signal transduction pathways, including signaling through STAT1 and ERK. Mutations in Nf1, the gene encoding the RAS GTPase protein neurofibromin, cause constitutive ERK activation. Neurofibromin is expressed by pre-hypertrophic and hypertrophic chondrocytes, as determined by immunohistochemical analysis. Based on these observations, we hypothesized that proper regulation of endochondral

ossification may require neurofibromin. To address the role of Nf1 in this process, we generated Nf1 conditional knockout mice lacking Nf1 in chondrocytes, using the mouse type2 collagen promoter-cre mice (Nf1col2^{-/-} mice). Histological analyses showed that although growth plate develops normally till E15.5, the hypertrophic zone in Nf1col2^{-/-} mice become progressively shorter than WT littermates afterwards. Nf1col2^{-/-} mice are born with a normal body but their growth is impaired postnatally, leading to a 50% size reduction by 5 weeks of age. This growth phenotype starts to develop when primary ossification centers appear, leading us to hypothesize that lack of Nf1 in chondrocytes mainly impairs the formation of primary ossification centers rather than chondrocyte proliferation or differentiation. To support this notion, in vivo BrdU incorporation and in situ hybridization assays did not reveal significant changes in chondrocyte proliferation or expression of Indian hedgehog (Ihh), a critical determinant of chondrocyte proliferation in the growth plate of Nf1col2^{-/-} pups. In addition, blood vessel invasion of primary ossification centers was not affected by lack of Nf1. On the other hand, qPCR analyses using both chondrocyte micromass cultures and growth plate cartilage from WT and Nf1col2^{-/-} mice showed a significant increase in Opn and Rankl expression in mutant chondrocytes, suggesting that Nf1 inhibits early osteoclastogenesis. Supporting this data, TRAP staining indicated that osteoclast number at the osteochondral border in Nf1col2^{-/-} newborns was significantly increased. In addition, WT splenocytes plated on primary chondrocytes from Nf1col2^{-/-} mice formed more osteoclasts than WT splenocytes plated on WT chondrocytes. These results collectively indicate that neurofibromin function in chondrocyte is required for proper longitudinal growth and inhibits osteoclast differentiation at the osteochondral border.

Disclosures: *Koichiro Ono, None.*

MO0090

Sirt6 Regulates Chondrocyte Proliferation and Differentiation during Endochondral Ossification. Jinying Piao^{*1}, Hiroki Ochi², Kunikazu Tsuji³, Daisuke Koga⁴, Atsushi Okawa⁴, Sadao Morita¹, Shu Takeda², Yoshinori Asou⁴. ¹Department of Rehabilitation Medicine, Graduate School, Tokyo Medical & Dental University, Japan, ²Section of Nephrology, Endocrinology & Metabolism, Department of Internal Medicine, School of Medicine, Keio University, Japan, ³Section of Orthopedic Surgery, Division of Bio-Matrix, Graduate School, Tokyo Medical & Dental University, Japan, ⁴Department of Orthopaedics Surgery, Tokyo Medical & Dental University, Japan

Members of the sirtuin (SIRT) family of NAD-dependent deacetylases promote longevity in multiple organisms. Deficiency of mammalian Sirt6 leads to growth retardation, shortened life span (die around p24) and an aging-like phenotype in mice. SIRT6^{-/-} mice fail to thrive and exhibit osteopenia, with 30% reduction in bone mineral density and lordokyphosis at 3.5 weeks of age. However, the roles of Sirt6 in bone and cartilage metabolism are unclear. The aim of this study is to investigate the Sirt6 signal pathway in the maintenance of cartilage. For this purpose, histological evaluation was performed in Sirt6^{-/-} mice and WT littermates. Sirt6 was expressed in articular chondrocyte and growth plate chondrocyte. At birth, the length of tibiae and femur was 10-20% shorter in Sirt6^{-/-} compared to wild-type littermates. In the growth plate (GP), PCNA expression was reduced in Sirt6^{-/-} mice. The number of TUNEL positive cells was comparative between Sirt6^{-/-} and littermate at this stage. At two weeks after birth, growth retardation was apparent in Sirt6^{-/-}, with reduced proliferating zone in GP, delayed formation of secondary ossification center and decreased primary spongiosa. Col2 mRNA expression was reduced in Sirt6^{-/-} primary chondrocyte, indicating chondrocyte differentiation was retarded by Sirt6 deficiency. Sirt6^{-/-} mice is reported to exhibit severe metabolic defects with precipitous drops in serum glucose and IGF-1 levels. Thus, to evaluate the involvement of exogenous glucose and IGF-1 in the prevention of chondrocyte differentiation, Sirt6 was knocked-down by siRNA in primary chondrocyte and chondrocyte-like cell line ATDC5. Real time PCR analysis revealed the expression of chondrocyte marker genes, including Col2, Col10 and aggrecan, were reduced in vitro. Interestingly, autologous IGF-1 expression in chondrocyte was not affected by Sirt6 deficiency. Our data indicate that Sirt6 controls cell growth and differentiation in embryonic and postnatal chondrocytes.

Disclosures: *Jinying Piao, None.*

MO0091

TGF- β -induced SnoN Prevents BMP Signaling and Hypertrophic Conversion of Chondrocytes. Ichiro Kawamura^{*}, Yasuhiro Ishidou, Katsuyuki Imamura, Masahiro Yokouchi, Seturo Komiya, Shingo Maeda. Graduate School of Medical & Dental Sciences, Kagoshima University, Japan

(Objective)

Loss of TGF- β signaling in mice leads to the promoted hypertrophic differentiation of articular chondrocytes, which process is suggested to be an important step in progression of osteoarthritis (OA). However, the molecular mechanisms of which TGF- β inhibits chondrocyte maturation remain unclear. We screened for target genes downstream of TGF- β signaling to inhibit chondrocyte hypertrophy.

(Methods)

To assess the impact of endogenous TGF- β signaling in chondrocyte maturation, we treated ATDC5 cells with a TGF- β type I receptor inhibitor compound SB431542, and induced differentiation with BMP-2. Maturation of chondrocytes was evaluated by real-time reverse transcription polymerase chain reaction (RT-PCR) and ALP staining. The function of the purified gene was studied by stable overexpression and siRNA-knockdown approaches.

(Results)

BMP-induced expression of Col10a1 gene, a specific marker for hypertrophic chondrocytes, was further up-regulated dramatically, upon treatment with SB431542. Although the phosphorylation (activated status) of BMP-Smads-1/5/8 was not influenced by SB431542 application, expression of Id1 gene, the direct target of BMP Smads, was enhanced by SB431542. Thus, BMP signaling seemed to be inhibited by TGF- β signaling at the level beneath the phosphorylation process of BMP-Smads. We studied expression profile of candidates for BMP signal-inhibitors, and found that SnoN was the only gene which expression was induced upon TGF- β treatment, while was inhibited by SB431542 application. Importantly, knock down of SnoN resulted in enhanced maturation of ATDC5, and overexpression of SnoN suppressed it. Finally, the immunohistochemistry revealed that the expression of SnoN was positive only in prehypertrophic zone of mouse growth plate. In human OA cartilage, SnoN was detected around degenerated hypertrophic chondrocytes of moderate OA cartilages. However, SnoN was absent in severe-grade OA cartilages.

(Conclusion)

Our results suggest that SnoN suppresses hypertrophic transition of chondrocytes, as an effector of TGF- β signaling, to prevent the progression of OA.

Disclosures: Ichiro Kawamura, None.

MO0092

The Critical Role of the Epidermal Growth Factor Receptor in Endochondral Ossification. Xianrong Zhang^{*1}, Valerie Siclari², Shenghui Lan³, Ji Zhu¹, Frank Beier⁴, Ling Qin². ¹University of Pennsylvania, School of Medicine, USA, ²University of Pennsylvania, USA, ³Union Hospital, Tongji Medical College, Huazhong University of Science & Technology, China, ⁴University of Western Ontario, Canada

Loss of epidermal growth factor receptor (EGFR) activity in mice alters growth plate development, impairs endochondral ossification, and retards growth. However, the detailed mechanism by which EGFR regulates endochondral bone formation is unknown. Here, we used an EGFR-specific small molecule inhibitor, gefitinib, in a rat model to study long bone growth. Administration of this inhibitor into 1-month-old rats by oral gavage for 7 days produced profound defects in long bone growth plate cartilage characterized by epiphyseal growth plate thickening, massive accumulation of hypertrophic chondrocytes, and decreased hypertrophic cartilage mineralization. Immunostaining demonstrated that growth plate chondrocytes express EGFR but endothelial cells and osteoclasts have low to no expression. BrdU labeling and mRNA expression analysis of chondrocyte differentiation markers revealed that gefitinib did not alter chondrocyte proliferation or differentiation in the growth plate. H&E staining did not identify any overt difference in the number, location, orientation, or morphology of blood vessels underneath the growth plate in gefitinib-treated rats. However, we observed a 50% decrease in the number of TRAP+ cells at the chondro-osseous junction, but not in the primary spongiosa, in gefitinib-treated rats. This decrease in osteoclast number was due to attenuated RANKL expression in the growth plate. Moreover, gefitinib treatment inhibited the expression of matrix metalloproteinases (MMP9 and 13), increased the amount of collagen fibrils, and decreased degraded extracellular matrix products in the growth plate. In vitro, TGF α , an EGFR ligand, strongly stimulated RANKL, MMP9 and MMP13 expression and suppressed OPG expression in primary chondrocytes. Furthermore, chondrocyte-specific EGFR-deficient mice exhibited a similar phenotype as gefitinib-treated rats with enlarged hypertrophic zones in the growth plate, indicating that chondrogenic EGFR expression is responsible for normal growth plate development. Together, our data demonstrate that EGFR signaling supports osteoclastogenesis at the chondro-osseous junction and promotes chondrogenic expression of MMPs in the growth plate. Therefore, we conclude that EGFR signaling plays an essential role in the remodeling of growth plate cartilage extracellular matrix into bone during endochondral ossification.

Disclosures: Xianrong Zhang, None.

MO0093

The Differentiation Capacity of the Mesenchymal Stem Cells into Intervertebral Disc Under the Hypoxia Condition. Hwan-Mo Lee¹, Seong-Hwang Moon², Young-Mi Kang^{*1}. ¹Yonsei university, South Korea, ²Yonsei University College of Medicine, South Korea

INTRODUCTION

Human mesenchymal stem cells (hMSCs) from the bone marrow represent a potential source of pluripotent cells for autogenous bone tissue engineering. Aggrecan is since this major extracellular matrix which permits the intervertebral disc (IVD) to withstand compressive loads. GLUT-1 expression is also stimulated in a variety of cells under hypoxic condition, a response that is mediated by the transcription factor HIF-1 α . Among various phenotypes, HIF-1 α and glucose transporter-1 (GLUT-1)

proved to be phenotypical signature of nucleus pulposus. Therefore, the objective of this study is to evaluate possibility that hMSCs induce the IVD in hypoxia condition.

MATERIALS AND METHODS

Human bone marrows were collected during surgery from patients (age range 45-67 years) with lumbar spinal stenosis. hMSCs were purified by density gradient centrifugation in Ficoll/Hypaque and maintained in the condition medium until one passage. The hMSCs were seeded in collagen type I sponge at a cell density of 5×10^5 cell per each one for protein and RNA isolation in hypoxia condition (1% O₂, 5% CO₂, 37 °C) and normal condition (5% CO₂, 37 °C) for three days. Human disc cells were used as a control. For expression of HIF-1 α and GLUT-1 at the mRNA and protein level, RT-PCR and western blot were performed according to the manufacturing protocol.

RESULTS AND DISCUSSION

The expression of aggrecan mRNA was increased in hypoxia condition as comparing with normal condition. Also the expression of GLUT-1 mRNA on the MSCs is higher than on the disc cells. Hypoxic condition on the MSCs rendered increase in aggrecan and GLUT-1 mRNA expression, which also provide phenotypical stabilization under the hypoxic condition. Furthermore, expression of GLUT at protein level was increased comparing with others. Glucose is needed both for glycolytic metabolism and the synthesis of glycoproteins and glycosaminoglycans. The uptake of glucose by disc cells is a fundamental process that has been neglected in most studies of IVD metabolism. Our study suggests that the MSCs can be differentiated into IVD although further work is required to confirm this observation.

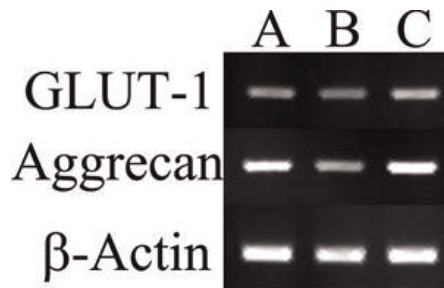


Figure 1. GLUT-1 and aggrecan mRNA expression.

A; MSCs in hypoxia condition B; MSCs in normal condition C; Discs in hypoxia condition

Disclosures: Young-Mi Kang, None.

This study received funding from: This research was supported in part by Brain Korea 21 project.

MO0094

Understanding the Mechanisms of Radius and Ulna Deformation in Neonatal Chk β Mutant Mice. Zhuo (Bill) Li^{*}. University of Alberta, Canada

Choline kinase (CK) has two isoforms: Chk α and Chk β . CK is the first enzyme in Kennedy pathway to make phosphatidylcholine and it converts choline to phosphocholine. Inactivation of Chk α in mice results in embryonic lethality, whereas Chk β mutant mice display hindlimb muscular dystrophy and neonatal forelimb bone deformation. Previous study has been demonstrated that impaired phosphatidylcholine biosynthesis contributes to hindlimb muscular dystrophy phenotype, but the mechanisms for neonatal forelimb bone deformation are still unknown. To understand the mechanisms of bone deformation phenotype, we characterized the major long bones of forelimb and hindlimb both at embryonic and neonatal stages by various histology techniques. We found that the deformation is only specific to radius and ulna. While humerus and femur in mutant mice still maintain relative normal growth plate structure, radius, ulna and tibia have bone developmental and growth plate defect. In details, at embryonic stage, we found that in mutant mice radius, ulna and tibia have delayed formation of primary ossification center, which is accompanied by premature chondrocyte hypertrophy leading to increased hypertrophic zone and decreased proliferation zone. In addition, we also found that in mutant mice radius and ulna display unorganized proliferative columns and abnormal cell morphology at distal end of growth plate but tibia doesn't. At neonatal stage, radius and ulna in mutant mice are much shorter and totally lose the proliferation zone at the distal end growth plate and they still suffer from enlarged hypertrophic zone and decreased proliferation zone at proximal end. In mutant mice tibia at neonatal stage is also much shorter and continues to show increased hypertrophic zone and reduced proliferation zone at both proximal and distal ends of the growth plate, but it maintains relative good growth plate structure and normal cell morphology at both ends. In conclusion, our study shows that (1) Chk β deficiency affects the development of distal limb long bones including radius, ulna and tibia (2) that the cartilage and growth plate defect observed in mutant mice radius and ulna could be the main cause for their structure deformation (3) and that the less severe growth plate defect observed in mutant mice tibia compared to radius and ulna may explain why deformation only occurs in radius and ulna but not tibia.

Disclosures: Zhuo (Bill) Li, None.

MO0095

Annexin a5 Expression Regulates Periodontal Tissue and Cementum Formation. Akemi Shimada^{*1}, Koichiro Komatsu¹, Kazuhisa Nakashima¹, Norio Amizuka², Bent Brachvogel³, Akira Nifuji¹.
¹Tsurumi University School of Dental Medicine, Japan, ²Hokkaido University School of Dentistry, Japan, ³Universitat Zu Koln, Germany

Objectives: Periodontal ligament connects tooth cementum and alveolar bone to maintain and support teeth in situ and preserve tissue homeostasis. The progenitor cells for periodontal tissues and their molecular markers have not yet been identified. Pericytes have been suggested to be progenitor cells for periodontal tissues and one molecule that is specifically expressed in the pericytes is annexin A5 (Anxa5). In this study, we examined whether Anxa5 is expressed in progenitor cells in periodontal tissues and functions in their homeostasis by using anxa5 knockout /LacZ knock-in mice.

Methods: We used Anxa5 knockout /LacZ knock-in mice which contain a LacZ (β -galactosidase) reporter gene fused in-frame with the Anxa5 gene. The maxillae dissected from the Anxa5-LacZ^{+/+}, Anxa5-LacZ^{+/-}, and Anxa5-LacZ^{-/-} mice at 1, 4, 7, and 8 weeks of age were fixed and subjected to LacZ histochemistry and immunohistochemistry using anti-annexin A5 antibody. The morphology of the first molar and its periodontal tissues were analyzed by micro computed tomography (micro CT) and histology.

Results: At the 1 week old of age, LacZ gene expression was detected around the area forming tooth roots. After tooth eruption at 4 to 8 weeks of age, LacZ gene expression was detected in all over the periodontal ligament, specifically intensive in the periodontal ligament around the root apices and cervical areas. Intensive LacZ gene expression was also observed in the cementoblast at the root apices, periosteal cells of the alveolar bone, and putative pericytes around the blood vessels in the periodontal ligament. Immunohistochemistry using anti-annexin A5 antibody showed consistent results with LacZ histochemistry. The histological and micro CT analyses showed that smaller amount of cementum formation at the mesial root apex was observed in the Anxa5^{-/-} mice than in the wild mice. In addition, the width of periodontal ligament of Anxa5^{-/-} mice was significantly narrower than that of wild mice ($p < 0.001$).

Conclusion: These results suggest that Anxa5 is expressed in the periodontal tissue cells including pericytes and functions for periodontal tissues and cementum formation.

Disclosures: Akemi Shimada, None.

This study received funding from: Ministry of Education, Culture, Sports, Science, and Technology of Japan

MO0096

Novel Genes Critical for Bone Formation. Yunxia (Yesha) Lundberg^{*1}, Mohammed Akhter², Liping Yang¹, Hui Zhang¹, Hua Yang¹, Xing Zhao¹, Yinfang Xu¹, Yan Zhang¹. ¹Boys Town National Research Hospital, USA, ²Creighton University, USA

We have identified novel genes (identity to be revealed at the ASBMR meeting due to possible patent application) that critically affect bone formation. Examination of respective knockout and functional null mutant mice for these genes shows morphological and histological abnormalities in bone. Detailed micro-CT analyses of trabecular bone at the distal femur have been done using 16 μ m scan resolution (1.5 mm region of interest proximal to the growth plate). Compared to that in wildtype mice (n=11), trabecular bone in mutant mice (n=9-10) show significant reductions in many parameters including apparent volumetric mineral density (App-vBMD), bone connectivity/density (ConD), bone volume over total volume (BV/TV), and trabecular bone number (TrabN), with a concomitant increase in trabecular spacing (TrabSp). Preliminary histological and molecular studies suggest that the bone abnormalities likely arise from altered numbers of osteoblasts and osteoclasts, and that these genes may function through inter-linking and overlapping mechanisms.

Disclosures: Yunxia (Yesha) Lundberg, None.

MO0097

Pax9, a Transcription Factor That Is Expressed in Ligament Cells Derived From Ligamentum Flavum of Patients with Lumbar Spinal Canal Stenosis. Ken Watanabe^{*}, Yoshihito Sakai, Shumpei Niida, Atsushi Harada. National Center for Geriatrics & Gerontology, Japan

Lumbar spinal canal stenosis, a condition that spinal canal narrows causing compression of the nerves, is seen more in and reduces activity of daily living of elderly. Although the etiology has not been clarified yet, it has been suggested that the stenosis is caused by congenital narrow canal and acquired hypertrophy of ligamentum flavum. Molecular and cellular mechanism underlying hypertrophy of ligamentum flavum is not yet to be elucidated. To determine the molecular basis of ligamentum flavum cells, gene expression profiling was performed. The primary ligament (LF) cells were prepared from the ligament flavum removed from the surgery of the patients by collagenase treatment. For the control, human osteoblasts (hOST), mesenchymal stem cells (hMSC), and skin fibroblasts (MJ90) were used. RNA was

isolated from the cells from 3 patients diagnosed as lumbar spinal canal stenosis, as well as the control cells, and the gene expression was analyzed by microarray technique. Scleraxis (SCX) and Mohawk (MKX), genes known to be expressed in ligaments and tendons, were extracted as genes encoding transcription factors predominantly expressed in the LF cells. In addition to these genes, PAX9, ME0X2, and TP63 were identified. To determine the function of the transcription factors, the genes were introduced in 10T1/2. Whereas mock-transfected 10T1/2 cells deposited lipid droplets in the 2 wk culture, the deposition was significantly suppressed in MKX-, ME0X2-, PAX9-, and ETV4-transfected cells. The cell accumulation was observed in the PAX9-transfected cells, suggesting that the proliferation was upregulated. This observation was supported by BrdU incorporation assay. Since HDAC9 was extracted as a gene expressed in LF cells, the expression of Hdac9 was determined in the transfected cells. Hdac9 was specifically upregulated in PAX9-transfected cells but not in others. HDAC9 encodes a type II histone deacetylase and its activity was inhibited by HDAC inhibitors, such as sodium butyrate (SB) and Trichostatin A (TSA). TSA, as well as SB, significantly reduced the proliferation both of the cells in a dose-dependent manner. Thus, PAX9-induced proliferation may be mediated by upregulation of HDAC activity at least in part. Since, in some cases, ligament cells were focally accumulated in hypertrophied ligamentum flavum in the patients, the PAX9-HDAC9 pathway may be participated in the hypertrophy of ligamentum flavum.

Disclosures: Ken Watanabe, None.

MO0098

Phenotypic Analysis of Transgenic Mice Overexpressing Mx1 in Oral Bones. Ibtisam Senussi^{*1}, Ariane Berald², Sylvie Babajko³. ¹Inserm U872, France, ²University Paris-Diderot, France, ³INSERM, France

Homeobox gene Mx1 encodes for a transcription factor widely expressed during embryogenesis and postnatal development involved in epithelio-mesenchymal interactions. Thus, Mx1 is particularly important in limb and tooth development, and could control progenitor cells and terminal differentiation of mineralized tissue forming cells like osteoblasts and odontoblasts. Mutations in this gene in humans are associated to cleft palate and/or tooth agenesis. Similar phenotype is observed in mice presenting an invalidation of Mx1 gene. As null mutant mice died at birth, it is difficult to study the role of Mx1 in vivo. Thus, we decided to generate a transgenic mouse line with Mx1 expression targeted in mineral matrix secreting cells by 2.3 Kb collagen 1 alpha 1 promoter.

Histological analysis of the mandibles at one day after birth showed an accumulation of bone in Mx1 transgenic (Mx1 Tg) mice compared to wild types. The greatest differences were observed in bone surrounding the incisor and the molars. Osteoblast and osteoclast metabolism was analyzed by TRAP (tartrate-resistant acid phosphatase) activity and collagen 1 alpha 1 ISH (in situ hybridization) respectively. Both of them showed an increased number of labelled cells in Mx1 Tg mice reflecting active bone remodeling.

Analysis of caspase-3 expression associated to apoptosis was carried out by IHC (Immunohistochemistry) using a specific antibody directed against caspase-3. Our results showed stronger staining and ten times more caspase-3 expressing osteoblasts in transgenic mice compared to wild-type mice. This could explain the fact that it was not possible to evidence Mx1 over-expression by RT-Q-PCR.

These results are in accordance with Mx1 function that probably increases the pool of progenitor cells. In addition, increased Mx1 expression is associated with high bone remodeling.

These results could be interesting for gene or cell therapy for bone reconstruction using Mx1

Disclosures: Ibtisam Senussi, None.

MO0099

Skeletal Phenotyping of Chibby Knockout Mice. David Komatsu^{*1}, Joshua J. Hinkle², Mohanlall Narine², Feng-Qian Li³, Ken-Ichi Takemaru³, Michael Hadjiargyrou⁴. ¹Stony Brook University, Dept. of Orthopaedics, USA, ²Stony Brook University, Dept. of Biomedical Engineering, USA, ³Stony Brook University, Dept. of Pharmacology, USA, ⁴State University of New York at Stony Brook, USA

Chibby (Cby) is a highly conserved 14 kDa protein that both antagonizes canonical Wnt/ β -catenin signaling and facilitates the formation of motile and primary cilia. Mice with global Cby deletion (Cby^{-/-}) are undistinguishable from wild-type (Cby^{+/+}) littermates at birth, but by post-natal day (P) 14 develop anemia, reductions in subcutaneous fat, and runting. By P25 the majority of Cby^{-/-} mice die, for unknown reasons, and survivors develop chronic sinusitis and remain runted. This study examined the skeletal phenotype of a cohort of Cby^{-/-} mice that survived into adulthood (N=5) and were sacrificed at 3 months, and compared these mice to a group of age-matched Cby^{+/+} controls (N=5). MicroCT analyses revealed that Cby^{-/-} femurs were 16% shorter than those from Cby^{+/+} mice. Consistent with reduced length, cortical and periosteal areas were reduced by 33 and 21% in Cby^{-/-} mice, respectively. Similarly, Cby^{-/-} mice had reductions of 61% in bone volume (BV), 23% in total volume (TV), 49% in BV/TV, 17% in trabecular thickness, and 38% in connectivity density, concomitant with a 23% increase in trabecular spacing. H&E staining revealed thinner cortices, fewer trabeculae, and smaller growth plates in

Cby^{-/-} tibiae, as well as a reduction in the number of hypertrophic chondrocytes. IHC staining of Cby^{+/+} tibiae with Cby antibodies showed positive staining of osteocytes within the cortices, and lower intensity diffuse staining within the growth plates that could not be resolved to specific cell types. Quantitative RT-PCR analysis of osteocalcin (OC) showed it to be up-regulated ~3-fold in Cby^{-/-} samples. Given the smaller size of Cby^{-/-} mice, the findings of shorter femora with thinner cortices and less trabecular bone were fully expected. However, while histological observations of smaller tibiae in Cby^{-/-} mice are consistent with smaller bones, the reduction in hypertrophic chondrocytes suggests that Cby may also have direct effects on skeletal development. The increase in OC expression in Cby^{-/-} mice provides further evidence that Cby directly affects the skeleton. As OC expression is down-regulated by Wnt signaling, these data are consistent with the function of Cby as a Wnt antagonist, but difficult to reconcile with the low bone mass phenotype of these mice. In order to clarify these issues, we are in the process of analyzing newborn Cby^{-/-} mice, as well as adult Cby^{+/+} mice, which are not runted. The further characterization of these mice is expected to provide new insights into the role of not only Wnt signaling, but also the role of cilia in skeletal development and homeostasis.

Disclosures: David Komatsu, None.

MO0100

Trps1 Plays Distinct Roles in the Development and Function of Mineralizing Tissues. Dobrawa Napierala^{*1}, Brian Dawson², Terry Bertin³, Chad Shaw³, Anne Poliard⁴, Odile Kellerman⁵, Brendan Lee⁶. ¹University of Alabama at Birmingham School of Dentistry, USA, ²Baylor College of Medicine, Howard Hughes Medical Institute, USA, ³Baylor College of Medicine, USA, ⁴Faculte de Chirurgie Dentaire, et UMR-S 747, Universite Paris Descartes, France, ⁵INSERM, Universite Rene Descartes, France, ⁶Baylor College of Medicine & Howard Hughes Medical Institute, USA

The transcription factor Trps1 is highly expressed in developing cells destined to produce mineralizing matrix. Interestingly, the onset of mineralization coincides with diminished Trps1 expression, which suggests that Trps1 is involved in maturation of these cells, but may negatively affect the function of mature cells. Previously we have demonstrated that deficiency of Trps1 in mice results in advanced mineralization of perichondrium due to insufficient repression of the Runx2 transcription factor. Our recent studies of Trps1 transgenic mice specifically expressing Trps1 in osteoblasts and odontoblasts revealed severe impairment of dentin mineralization. Thus the *in vivo* data suggest that Trps1 acts as a repressor of mineralization. To understand the role of Trps1 in differentiation and function of cells producing mineralized matrix, and to identify genes regulated by Trps1 in these cells we used the 17H1A11 preodontoblastic cell line, a cellular model of mineralization. We generated both Trps1-deficient and Trps1-overexpressing 17H1A11 cell lines. Effects of Trps1 on the mineralization of the generated cell lines were evaluated by alkaline phosphatase, von Kossa and alizarin red staining. As predicted, based on our previous *in vivo* data, delayed mineralization of Trps1-overexpressing cells was observed when compared to control cells. Interestingly, 17H1A11 Trps1-deficient cells lose their characteristic alkaline phosphatase activity and ability to mineralize. Global gene expression studies using the Affimetrix Mouse Exon 1.0 ST Array were performed to identify genes regulated by Trps1 in 17H1A11 cells. These analyses identified genes involved in several signaling pathways as well as components of the extracellular matrix. Genes with a previously demonstrated function in mineralization were also identified. In conclusion, our studies demonstrate that while Trps1 represses mineralization, it is required for the terminal differentiation of cells destined to produce mineralizing matrix, and it executes this function by regulating genes involved in mineralization.

Disclosures: Dobrawa Napierala, None.

MO0101

Absence of P2X7 Nucleotide Receptors Leads to Abnormal Fat Distribution in Mice. Kim Beaucage^{*}, Andrew Xiao, Matthew Grol, David Holdsworth, Stephen Sims, Mark Darling, S. Jeffrey Dixon. The University of Western Ontario, Canada

Extracellular nucleotides such as ATP signal through two subfamilies of P2 nucleotide receptors – P2Y (G protein-coupled receptors) and P2X (ATP-gated nonselective cation channels) – in many cell types. The P2X7 receptor is expressed by both osteoblasts and osteoclasts. In this regard, mice lacking P2X7 exhibit reduced bone formation and excessive bone resorption. We have shown previously that deletion of the P2X7 receptor results in downregulation of osteogenic markers and upregulation of adipogenic markers in calvarial cell cultures, indicating that P2X7 may regulate bone and fat lineage determination from a common mesenchymal progenitor. Given these effects of P2X7, our purpose was to assess whether the skeletal changes observed in mice lacking this receptor are associated with altered adipose tissue distribution and lipid accumulation *in vivo*. Two, 6, 9 and 12-month-old, male wild-type (WT; P2rx7^{+/+}) and P2X7 knockout (KO; P2rx7^{-/-}) mice (n=10) were fasted for 6 hours, sacrificed and weighed. Blood samples were obtained by cardiac puncture. Selected tissues were weighed and prepared for histological analyses. KO mice exhibited a significantly greater overall body weight than WT at 9 months of age. In this regard, epididymal fat pad weight in KO mice was also significantly greater at 9 months, consistent with a role for P2X7 in regulation of metabolism and adipose tissue development. Morphometric analysis revealed no

significant difference in the size of epididymal fat pad cells, consistent with adipocyte hyperplasia rather than hypertrophy. Histological examination revealed increased accumulation of lipid droplets and/or increased numbers of adipocytes in several tissues in 9 and 12-month-old KO mice, including kidneys and several exocrine glands, but not liver, heart or skeletal muscle. Specifically, extraorbital lacrimal glands and pancreas from KO mice exhibited a greater number of adipocytes in perivascular, periductal and acinar regions. Lipid accumulations were also apparent in the renal tubular epithelium and acini of the submandibular salivary gland. Blood plasma analyses revealed diminished total cholesterol levels and greater triglyceride levels in 9-month-old KO compared to WT mice, reflecting disrupted lipid metabolism. Taken together, these data indicate that P2X7 regulates systemic adipose distribution and metabolism, and are consistent with an inhibitory effect of the P2X7 receptor on fat lineage determination and adipogenesis.

Disclosures: Kim Beaucage, None.

MO0102

Alkaline pH Increases Phosphate Production by Proteoliposomes Carrying Alkaline Phosphatase and Nucleotide Pyrophosphatase/ Phosphodiesterase-1. Ana Maria Simao^{*1}, Mayte Bolean², Jose Luis Millan³, Marc Hoylaerts⁴, Pietro Ciancaglini². ¹University of Sao Paulo - USP, Brazil, ²FFCLRP-USP, Brazil, ³Sanford-Burnham Medical Research Institute, USA, ⁴Center for Molecular & Vascular Biology, University of Leuven, Belgium

Endochondral calcification is mediated by chondrocyte- and osteoblast-derived matrix vesicles (MVs). The primary function of tissue-nonspecific alkaline phosphatase (TNAP) is to degrade extracellular inorganic pyrophosphate (ePPi), a mineralization inhibitor produced by nucleotide pyrophosphatase/ phosphodiesterase-1 (NPP1), thus restricting the concentration of ePPi to maintain a Pi/PPi ratio permissive for normal bone mineralization. In this study, either TNAP, recombinant NPP1 or both together were reconstituted in dipalmitoylphosphatidylcholine (DPPC) liposomes as previously standardized¹, as an osteoblast-derived MVs biomimetic, and the hydrolysis of ATP, ADP, AMP and PPi by these proteoliposomes was studied at pH 9, by measuring the amount of inorganic phosphate (Pi) liberated as a function of time¹, since it has been shown that the pH may play a regulatory role during the mineralization process. Hydrolyzed ATP and ADP nucleotide intermediates were separated and quantified by HPLC¹. All substrates were hydrolyzed by TNAP, NPP1- and TNAP plus NPP1-containing proteoliposomes. NPP1 plus TNAP additively hydrolyzed the substrates, but TNAP appeared more active in adenosine formation than NPP1. Cooperative effects were observed for all substrates studied and the catalytic efficiencies were higher for TNAP-containing proteoliposomes. Affinity constants were lower for NPP1-containing proteoliposomes, except for ADP. Also, at pH 9, catalytic efficiencies were higher for ATP and PPi hydrolysis when compared with physiologic pH1, for both TNAP- and NPP1-proteoliposomes. Therefore, the reconstitution of TNAP and NPP1 into proteoliposome membranes generates a phospholipid microenvironment that enables the complementary hydrolysis of natural phospho-substrates and their intermediates at pH 9, leading to very efficient phosphate accumulation in the immediate microenvironment of the phospholipid membrane surface. More detailed studies of those catalytic processes at different pH will allow us to understand the fine regulatory role that changes in pH may play during the mineralization process by modulating both the microenvironment composition and Pi production by the proteins involved in this process.

¹Simao et al., Proteoliposomes harboring alkaline phosphatase and nucleotide pyrophosphatase as matrix vesicle biomimetics. J. Biol. Chem. 285: 7598-7609 (2010).

Disclosures: Ana Maria Simao, None.

MO0103

Bone Regeneration Potential of Polypropylene Fumarate Scaffolds Coated with Osteoconductive Agents. Theresa Hefferan^{*1}, M. Brett Runge¹, Mahrokh Dadsetan¹, James Herrick¹, Donna Jewison¹, Glenda Evans², Viviane Luangphakdy³, Kentaro Shinohara³, Hui Pan³, George Muschler⁴, Michael Yaszemski¹. ¹Mayo Clinic College of Medicine, USA, ²Mayo Clinic, USA, ³Cleveland Clinic, USA, ⁴Cleveland Clinic Foundation, USA

Traumatic injury and surgical resection can result in large segmental bone defects for which there are limited options for reconstruction and bone regeneration. In order to expand the treatment options, our laboratory has developed a biocompatible, biodegradable synthetic bone substitute - polypropylene fumarate (PPF). PPF is a polyester polymer with mechanical properties similar to bone and a slow rate of degradation. The objective of this study was to assess the bone regenerative capacity of PPF scaffolds with an osteoconductive coating in a canine femoral multi-defect model. A Viper Si2 stereolithography system was used to fabricate 3-dimensional porous PPF scaffold cylinders with an overall size of 9.9 mm diameter x 15 mm height. The pores were 1mm x 1mm channels, separated by 500 um walls. To promote bone regeneration, the scaffolds were coated by spray deposition with either hydroxyapatite (HA) or tri-calcium phosphate (TCP). The canine femoral multi-defect model was used to assess bone regeneration and the scaffolds were harvested after 4 weeks. Bone regeneration was assessed by micro-CT scanning and quantitative histology. First, the scaffolds were fixed and scanned using a GE Locus micro-CT scanner at 45 micron resolution and subsequently processed for histology. After embedding the scaffolds in methyl methacrylate, they were sectioned at 5 microns and stained. A modified

Goldner trichrome stain was used to delineate mineralized bone and osteoid formation within the scaffold. The Goldner stained slides were scanned using a NanoZoomer Digital Pathology System (Hamamatsu) and the slides were analyzed using the software package IHC Score (Bacus Labs) to measure bone growth into the implant, cellular matrix, and residual polymer. The results are reported as a percentage of the total area for the residual scaffolds, and as a percentage of the pore area in the scaffold for the bone and cell matrix. After 4 weeks, 58.8% + 6.9% (PPF-HA) and 62.2% + 2.4% (PPF-TCP) of the total area contained scaffold. The scaffold pores were filled with 25.1% + 1% (PPF-HA) and 29.2% + 12.8% (PPF-TCP) bone; and 74.9% + 1% (PPF-HA), 70.8% + 12.8% (PPF-TCP) cellular matrix. New bone was formed along scaffold surfaces, while the scaffold pores in the pericortical region were nearly completely filled with new bone. This short-term study in a large animal model demonstrates the bone regenerative potential for porous PPF scaffolds coated with the osteoconductive agents HA or TCP.

Disclosures: Theresa Hefferan, None.

MO0104

CD59 - A Novel Role in Bone Homeostasis. Anja Bloom¹, Carole Elford¹, Robert J van 't Hof², B Paul Morgan¹, Bronwen AJ Evans¹, Daniel Aeschlimann¹, Anwen S Williams¹. ¹Cardiff University, United Kingdom, ²University of Edinburgh, United Kingdom

The complement (C) system has crucial functions in host defence; regulating the inflammatory response, mammalian development, tissue repair, angiogenesis, liver regeneration and neurone refinement. Novel data by Tu et al. recently described a role for C-components in osteoclastogenesis (OC-genesis). CD59a is a regulator of the terminal C pathway in mice; the purpose of the study was to investigate the importance of CD59a in bone homeostasis. Methodology: Femurs and spines were collected from 8-10 week old wild-type (WT) and CD59a deficient (CD59a^{-/-}) mice. Bone architecture and bone resorption parameters were analysed by μ CT and Aniline blue/TRAP staining respectively (n= 12 per group). For mechanistic studies, bone marrow cells from WT (n=8) and CD59a^{-/-} (n=6) mice were cultured in osteoclast (OC) differentiation medium for 7 days, and the OC stained and counted. The chemokine mKc was quantified in OC assay supernatants by ELISA. Results: In male mice femoral length was increased in CD59a^{-/-} versus WT mice (4%, p<0.05). Cortical bone volume was increased (26%, p<0.01) whilst BMD was reduced (7%, p<0.01) in CD59a^{-/-} versus WT. Trabecular bone analysis of the distal femur showed increased BV/TV (90%, p<0.005), Tb.Th (18%, p<0.005) and Tb.N (57%, p<0.005) in CD59a^{-/-} over WT. In vitro, OC-genesis was increased by 29% (p<0.05) and mKc levels were elevated by 283% (p<0.001) in CD59a^{-/-} over WT. Finally, sections of distal femurs were analysed for OC numbers and resorption surfaces by histomorphometry. OC/BS (77%, p<0.05) and OC.S/BS (71%, p<0.01) were increased in the trabecular bone of CD59a^{-/-} over WT mice. In female mice, there was no difference in femoral length; no histomorphometric changes and no difference in OC-genesis (CD59a^{-/-} versus WT). Conclusions: Changes in bone histomorphometry related to CD59a gene deletion are gender specific. Our study identifies CD59a as a potentially important regulator of OCs which is necessary for maintaining healthy bone in young adult male mice. More studies are necessary to establish whether CD59 is an important homeostatic regulator in bone in humans. Since aberrant CD59 expression has been noted in human arthritic joints, CD59 could also augment adverse bone pathology in diseases such as rheumatoid arthritis and osteoarthritis.

Disclosures: Anja Bloom, None.

MO0105

Dental Pulp Cells Exhibit High Performance as a Biomaterial for Bone Formation Through Expression of Annexin A8. Yuko Nakamichi¹, Takahiro Hagihara¹, Midori Nakamura¹, Asayo Imaoka², Yoshimitsu Abiko², Hiroshi Nakamura¹, Naoyuki Takahashi¹, Nobuyuki Udagawa¹. ¹Matsumoto Dental University, Japan, ²Nihon University, Japan

Dental pulp cells are considered to be a promising tool for the regeneration of hard tissues, due to their multipotency. The goal of the present study is to establish a simple method of regenerating hard tissues using dental pulp cells. Toward this end, we characterized dental pulp cells in comparison with osteoblasts and explored the mechanisms of calcification. The survival of cultured dental pulp cells completely depended on cell density. The densely cultured dental pulp cells exhibited 60-times stronger ALP activity than osteoblasts. Dental pulp cells remarkably induced extracellular matrix (ECM) calcification even in the absence of exogenous BMP-2, or in the presence of a pan-BMP antagonist, Noggin. On the other hand, ECM calcification in osteoblast culture was completely suppressed by the addition of Noggin. A Genechip analysis showed the overall gene expression in dental pulp cells to be similar to that in osteoblasts, though dental pulp cells expressed higher levels of BMPs, annexin A8 (a Ca channel), and solute carrier protein 20a2 (Slc20a2) (a Pi transporter) than osteoblasts. Furthermore, dental pulp cells exhibited extremely lower expression levels of ectonucleotide phosphodiesterase/pyrophosphatase-1 (ENPP-1) and matrix Gla protein (MGP), calcification inhibitors. These results may explain why ECM calcification in dental pulp cell culture was not suppressed by the pan-BMP antagonist Noggin. Overexpression of either annexin A8 or Slc20a2 in osteoblasts induced ECM calcification even in the absence of exogenous BMPs. Especially, the effect of annexin A8 was dominant. In contrast, knockdown of either

annexin A8 or Slc20a2 using siRNAs suppressed ECM calcification in dental pulp cell culture. Finally, we examined the ability of the cultured dental pulp cells to form hard tissues. We transplanted three-dimensional culture of dental pulp cells with denatured type I collagen sponges (GelfoamTM) and semi-solid type I collagen (Cellmatrix Type I-ATM) into immunocompromised mice. At 8 weeks after transplantation, the grafts generated bone in which hematopoiesis was carried out. Taken together, these results suggest that transplanted dental pulp cells exert bone regenerative activity through the expression of annexin A8.

Disclosures: Yuko Nakamichi, None.

MO0106

Effect of AMD3100 on MSC Mobilization and Bone Regeneration in the Mouse. Margaret McNulty^{*}, Kent W. Christopherson, Robin R. Frank, Amarjit Viridi, D. Rick Sumner. Rush University Medical Center, USA

Enhancement of intramembranous bone repair is likely to improve the long-term success of distraction osteogenesis, joint replacement, and rigid fracture fixation. Mobilized adult stem cells have great potential for regenerative medicine and represent an important strategy for enhancing bone repair. Stem cells can be mobilized from the bone marrow to the peripheral blood using drugs that affect the CXCR4/SDF-1 axis, including AMD3100, a direct antagonist of CXCR4. The purpose of this study was to examine the effect of AMD3100 treatment on bone regeneration following marrow ablation in mice. Ten week old female C57/Bl6 mice received a single injection of AMD3100 (5mg/kg; n=7) or saline (n=8) and were sacrificed one hour after injection. Peripheral blood (PB) was collected for CFU-F assays immediately after sacrifice. Cells from all mice in each group were pooled, and 0.5X10⁶ cells were plated in triplicate at 37°C, 5%CO₂, 5%O₂, 100% humidity for 7 days. In addition, a second group of 11-week old female C57/Bl6 mice underwent femoral bone marrow ablation surgery in the left femur (n=57). These mice received a single injection of AMD3100 (5mg/kg) or saline 3 hours after surgery and were sacrificed after 7, 14, or 21 days (n=9-10/group). Trabecular bone volume (BV), total volume (TV), and BV/TV were assayed by μ CT in the distal 50% of the femur, 0.5mm proximal to the growth plate. A significant increase in WBCs in the PB was found in AMD3100 treated mice one hour after injection (p=0.004). The average number of CFU-F colonies increased in the PB of the AMD3100 mice (196.5 CFU/mL) compared to saline treated mice (4.8 CFU/mL). BV was significantly elevated in the ablated femurs of AMD3100 treated mice compared to saline injected mice at 7 days post-surgery (p=0.022), however BV/TV was not significantly different (p=0.063). BV and BV/TV were also elevated in the AMD3100 treated mice at 21 days, but neither of these differences were significant (p=0.052 and p=0.090, respectively). This study shows that AMD3100 is capable of mobilizing MSCs to the peripheral blood, and has the potential to improve bone regeneration at early time points following femoral bone marrow ablation in the mouse.

Disclosures: Margaret McNulty, Musculoskeletal Transplant Foundation, 2

MO0107

Loss of Prolyl-3-Hydroxylation at Position 986 of Type I Collagen in Transgenic Mice Has A Negative Effect on Bone Mass and Structure. Ingo Grafe¹, Dustin Baldrige¹, Erica Homan¹, Terry Bertin¹, Yuqing Chen¹, Mary-Ann Weis², Dobrawa Napierala¹, Tao Yang¹, Brian Dawson¹, Caressa Lietman¹, Elda Munivez¹, Shan Chen¹, Monica Grover¹, Ming-Ming Jiang¹, David Eyre², Brendan Lee¹. ¹Department of Molecular & Human Genetics, Baylor College of Medicine, USA, ²Department of Orthopaedics & Sports Medicine, University of Washington, USA

Purpose

Cartilage associated protein (CRTAP) is required for prolyl-3-hydroxylation (3-Hyp) at position 986 of the triple helical domain of fibrillar collagens *in vivo*. It has been shown that loss of CRTAP results in recessive Osteogenesis Imperfecta (OI), but it is unclear if the concomitant loss of 3-Hyp directly contributes to the bone phenotype. Therefore, this study investigates if loss of 3-Hyp at position 986 of the α 1(I) collagen chain has a negative impact on bone tissue through use of a transgenic mouse model.

Methods

Transgenic mice with overexpression of mutated *Colla1* gene in bone have been generated. Specifically, a point mutation was introduced in the *Colla1* DNA, resulting in a proline to alanine change at position 986. Alanine cannot be 3-hydroxylated and as it is the second most common amino acid in the X-position of the collagen Gly-X-Y triplet, the P986A substitution is predicted not to disrupt folding or stability of the collagen triple helix. The P986A *Colla1* gene is expressed in transgenic mice (P986A-Tg) under control of the osteoblast specific 2.3kb *Colla1* promoter. Similarly, transgenic mice with overexpression of the wildtype *Colla1* gene were generated as controls (Control-Tg). Expression levels of *Colla1* mRNA were quantified by RT-PCR and 6 week old female P986A-Tg and Control-Tg mice with similar expression were chosen for further studies.

Results

In bone of P986A-Tg mice, mass spectrometry confirmed a 20% expression of the alanine form of total α 1(I) collagen chains. As compared to non-transgenic littermates the P986-Tg mice had a 8% reduced weight (p<0.05). MicroCT analysis of vertebral body L4 demonstrated a reduced BV/TV (-11.1%;p<0.05), reduced trabecular number

(-9.6%; $p<0.05$), increased trabecular separation (+14.2%; $p<0.05$) and a slightly reduced BMD (-8.3%; $p=0.054$). No significant differences regarding these parameters were observed in Control-Tg mice compared to non-transgenic littermates.

Conclusion

Our results indicate that bone specific expression of $\alpha 1(I)$ collagen chains lacking 3-Hyp at position 986 affects bone mass and structure in a dominant negative manner. This suggests that 3-Hyp is required for the formation of normal bone and that loss of 3-Hyp, at least in part, may contribute to the OI phenotype related to loss of function of Crtap.

Disclosures: Ingo Grafe, None.

MO0108

Peripheral Nerve Regulation of Early Heterotopic Ossification. Elizabeth Salisbury*, Eric Rodenberg, Corinne Sonnet, ZaWaunya Lazard, John Hipp, Francis Gannon, Tegv Vadakkan, Mary Dickinson, Elizabeth Olmsted-Davis, Alan Davis. Baylor College of Medicine, USA

Heterotopic ossification (HO), or bone formation in nonskeletal sites, is often the result of traumatic injury. The release of BMP2 (bone morphogenetic protein 2) upon injury has been linked to this process. Here we examine the role of the peripheral nerves in HO. As BMP2 has been shown to stimulate release of the neuro-inflammatory molecules substance P (SP) and calcitonin gene-related peptide (CGRP) from peripheral, sensory neurons, we examined this process in our cell-based gene therapy model of HO. Isolation of proteins from mouse hind limb tissues after injection of AdBMP2 transduced cells reveals an increase in expression of SP and CGRP. Animals lacking functional sensory neurons (TRPV1 $-/-$) display impaired release of SP and CGRP, and microCT shows the resultant HO in these animals is significantly inhibited. One major outcome of neuroinflammation is the recruitment of mast cells. Toluidine blue staining reveals an increase in the number of mast cells after induction of HO that appear to localize to the peripheral nerve structures, presumably for nerve tissue remodeling. If mast cell degranulation is blocked using cromolyn, heterotopic bone volume is substantially reduced. Immunohistochemistry also reveals expression of the stem cell markers nanog and Klf4, as well as the osteoblast marker osterix, within the peripheral nerves of these tissues. The data suggests that BMP2 can act on sensory neurons to induce neuroinflammation, resulting in nerve remodeling and the release of osteogenic stem cells from the nerve. Intriguingly, mast cell degranulation also induces the rapid and transient production of brown adipose, which plays a key role in bone patterning. Degranulating mast cells release serotonin locally, which, in this model, induces sympathetic signaling and the rapid increase of both $\beta 3$ -adrenergic receptor and uncoupling protein 1 (UCP1) gene expression. Immunofluorescence reveals expression of the brown adipose marker UCP1 associated with the peripheral nerve upon BMP2 induction. Blocking mast cell degranulation with cromolyn appears to block local sympathetic signaling, as UCP1 gene expression is no longer elevated in the tissues undergoing bone formation. Together, these data support the hypothesis that BMP2 induced heterotopic bone formation is mediated by peripheral nerve signaling. Further, mast cells appear to play a crucial role in the process through both nerve remodeling and activation of sympathetic signaling.

Disclosures: Elizabeth Salisbury, None.

MO0109

PHOSPHO1 Overexpression Promotes Extracellular Matrix Mineralization in Osteoblast Cultures. Carmen Huesa¹, Manisha Yadav², Elaine Seawright³, Tina Moreira⁴, Jose Luis Millan⁴, Colin Farquharson⁵. ¹Roslin institute/University of Edinburgh, United Kingdom, ²Burnham Institute for Medical Research, USA, ³Roslin Institute, University of Edinburgh, United Kingdom, ⁴Sanford-Burnham Medical Research Institute, USA, ⁵Roslin Institute, University of Edinburgh, United Kingdom

During the process of bone formation, osteoblasts mineralize their extracellular matrix (ECM) by promoting the initial formation of crystalline hydroxyapatite inside matrix vesicles. Bone alkaline phosphatase (TNAP) is important for ECM mineralization yet TNAP null (*Akp2*^{-/-}) mice are born with a normal mineralized skeleton. The phosphatase, PHOSPHO1, is highly expressed by osteoblasts and chondrocytes and its developmental expression profile coincides with the initial stages of mineralization. Membrane phospholipids, phosphatidylethanolamine (P-Etn) and phosphatidylcholine (P-Cho) have been identified as putative substrates for PHOSPHO1. The skeleton of *Phospho1*^{-/-} mice is characterized by osteoidosis, which results in altered material and mechanical properties, greenstick fractures and scoliosis. In this study we examined the effects of PHOSPHO1 overexpression in osteoblast-like cells in the presence of various substrates to further characterize the function of this phosphatase in the mineralization process. Two subclones of the MC3T3-E1 cell line previously characterized as mineralizing (clone 14) and non-mineralizing (clone 24) were used. Over a 21-day culture, ECM mineralization by clone 14 was first noted at day 11 when beta-glycerol phosphate (BGP) and P-Cho were substrates. No mineralization was noted with P-Etn. ECM mineralization of clone 24 was less than that noted in clone 14 and was first noted at day 11 (BGP), 14 (P-Cho) and 21 (P-Etn). Clone 14 expressed 10 times more PHOSPHO1 protein than

clone 24, which may explain the greater ECM mineralization noted in clone 14. A lentiviral vector was constructed to induce the overexpression of mouse recombinant PHOSPHO1. An empty vector was used as control. PHOSPHO1 overexpression in clone 14 resulted in a 20% increase in PHOSPHO1 protein levels and no alteration in ECM mineralization at day 14 in the presence of BGP, P-Etn or P-Cho. PHOSPHO1 overexpression in clone 24 showed an 80% increase in PHOSPHO1 expression when compared to the control cells and a 10-fold increase in mineralization with BGP, P-Etn and P-Cho as substrate. These data highlight the importance of PHOSPHO1 in the control of osteoblast ECM mineralization. Work on primary osteoblasts from wild type, *Phospho1*^{-/-}, and *Akp2*^{-/-} mice, is in progress to uncover the mechanisms of action of this phosphatase and its functional interaction with TNAP.

Disclosures: Carmen Huesa, None.

MO0110

Sexual Dimorphisms in Bone Mineral Density in Sprague-Dawley Rats from 8 to 20 Weeks of Age. Jason DeGuire*, Hope Weiler. McGill University, Canada

Peak bone mass is said to be achieved by 12 wk of age in rodents, but sexual dimorphisms according to bone site are unclear. Therefore, the objective of this study was to serially measure bone mineral density (BMD) in growing healthy rats from sexual maturity to middle-age. Sixty Sprague-Dawley rats (30 male, 30 female) were fed an AIN-93 diet from weaning and measured at 8, 12 and 20 wk of age for whole body, lumbar spine vertebrae (L4) and femur using dual-energy x-ray absorptiometry and analyzed with small animal software (QDR 4500A, Hologic Inc). Mixed model repeated measures ANOVA was used to test for sex and time effects with post hoc Tukey testing and significance set at $P<0.05$. Male (8 wk: 308, 12 wk: 465, 20 wk: 615 g) and female (8 wk: 208, 12 wk: 269, 20 wk: 323 g) rats were of normal body weight. For all BMD measurements, a sex by time interaction was observed. Whole body and lumbar spine BMD increased significantly at each time point ($P<0.0001$; Table 1), but was not different between sexes until week 16 ($P<0.0001$). However, femur BMD in females increased significantly from 8 to 12 wk ($P<0.0001$), but was not different at 12 and 20 wk whereas in males, BMD increased at each time ($P<0.0001$). At 8 wk, sex differences were not detected for femur BMD, but were evident at both 12 and 20 wk ($P<0.0001$). These data suggest that peak bone mass is not consistently reached by 12 wk of age in male and female rats and that age at attainment of peak bone mass is likely site specific as is the case for humans.

Table 1: Estimated mean bone mineral density \pm SE (g/cm³) at 8, 12 and 20 weeks of age.

Age (wk)	Sex	Whole Body	Lumbar Spine	Femur
8	Male	0.120 \pm 0.001 ^a	0.194 \pm 0.003 ^a	0.280 \pm 0.006 ^a
	Female	0.122 \pm 0.001 ^a	0.230 \pm 0.003 ^b	0.272 \pm 0.006 ^b
12	Male	0.148 \pm 0.001 ^a	0.250 \pm 0.003 ^a	0.402 \pm 0.006 ^a
	Female	0.146 \pm 0.001 ^b	0.275 \pm 0.003 ^b	0.368 \pm 0.006 ^c
20	Male	0.173 \pm 0.001 ^a	0.304 \pm 0.003 ^a	0.485 \pm 0.006 ^a
	Female	0.163 \pm 0.001 ^d	0.309 \pm 0.003 ^d	0.385 \pm 0.006 ^c

Within columns, differences among means are indicated by different superscripts, $P<0.0001$.

Table 1

Disclosures: Jason DeGuire, None.

This study received funding from: NSERC

MO0111

Whitetail Deer Antlerogenic Progenitor Cells Show Robust Mineralization in a Murine Ossicle Growth Model. Ethan Daley¹, Amy Koh-Paige¹, Laurie McCauley², Steven Goldstein³. ¹University of Michigan, USA, ²University of Michigan, School of Dentistry, USA, ³University of Michigan Orthopedic Research Labs, USA

The deer's annual cycle of antler regeneration is unique among mammals and enabled by some of the highest bone formation and resorption rates in nature. This cycle is driven by antlerogenic progenitor cells (APCs) residing in niches in the permanent pedicle and antler tip. How APCs conform to models of mesenchymal stromal (MSC) cell behavior and how they differ from other bone-forming, cervid MSCs is poorly understood. Here, we present the initial results of an ongoing *in vitro* and *in vivo* functional characterization of APCs and cervid marrow-derived MSCs (cmMSCs).

In vitro assays: Two mature whitetail stags (*Odocoileus virginianus*) were acquired during the rapid growth phase of antler regeneration. APCs were harvested from the antler reserve mesenchyme and perichondrium and cmMSCs from the phalanx medullary canal. Adherent cells were cultured using standard methods and frozen. Animal-matched cmMSCs and perichondrial APCs were thawed and the viability (>90%) measured. Cell number was measured over 264 hours using a fluorescent nuclear dye and CFU-F assays were used to estimate clonogenicity.

In vivo assays: cmMSCs and perichondrial APCs, as well as murine MSCs harvested from C57/BL6 mice (for method validation) were seeded onto 17 gelatin scaffolds (97500-1x10⁶ cells/scaffold) and implanted subcutaneously in 4 athymic mice (6 BL6-seeded scaffolds, 2 APC, 9 cmMSC.) At 4 and 6 weeks, ossicles were analyzed

using micro-computed tomography. Four week ossicles were paraffin-embedded, sectioned and stained for manual cell counts.

Results: cmMSCs colony counts and cell numbers at most plating densities were greater than those of paired APCs. However, APC-seeded ossicles had greater cellularity in both cortical and interior regions than paired cmMSCs. APC-seeded ossicles also had similar bone mineral content and bone/tissue volume as BL6 ossicles, despite seeding densities 1/5-2/3 that of the latter. CmMSC-seeded scaffolds showed comparatively low BMC and BV/TV, even at 6 weeks.

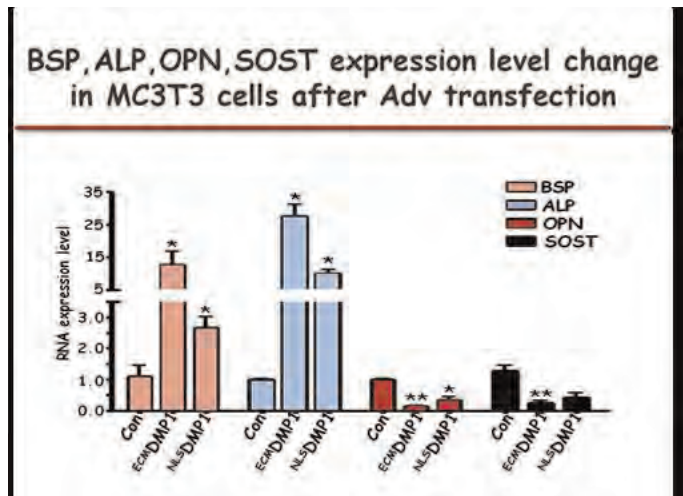
Conclusions: Implanted APCs gave rise to more mineralized ossicles compared to matched cervid MSCs. While APCs *in vitro* were less proliferative and colony-forming than cmMSCs, APCs *in vivo* formed more cellular ossicles. The latter could be due to rapid APC proliferation in the presence of unidentified factors available in a corporal but not *in vitro* environment. Or, perhaps APCs themselves secrete factors more conducive to host cell homing and/or proliferation.

Disclosures: Ethan Daley, None.

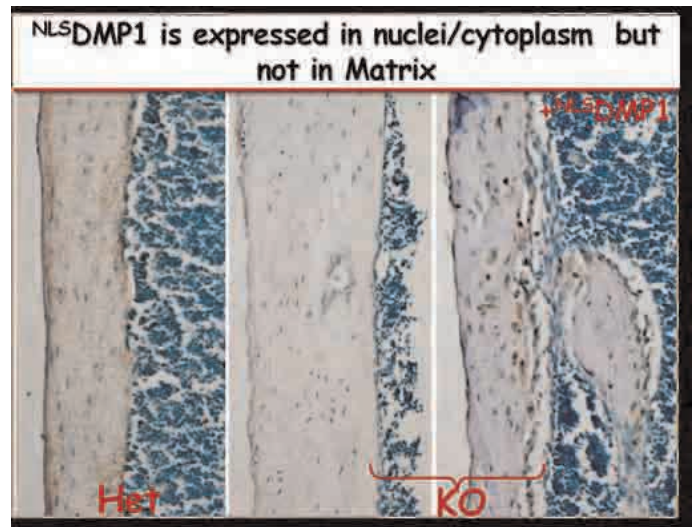
MO0112

DMP1 Does Not Function As A Co-transcriptional Factor. Baozhi Yuan¹, Shuxian Lin², Zhengguo Cao³, Ying Liu³, Yongbo Lu⁴, Marc Drezner⁵, Jian Feng⁶, Qi Zhang², Tian Gao³. ¹University of Wisconsin, Madison, USA, ²Baylor College of Dentistry, USA, ³Baylor College of Dentistry, Texas A&M Health Science Center, USA, ⁴University of Missouri, Kansas City, USA, ⁵University of Wisconsin, USA, ⁶Texas A&M Health Science Center, USA

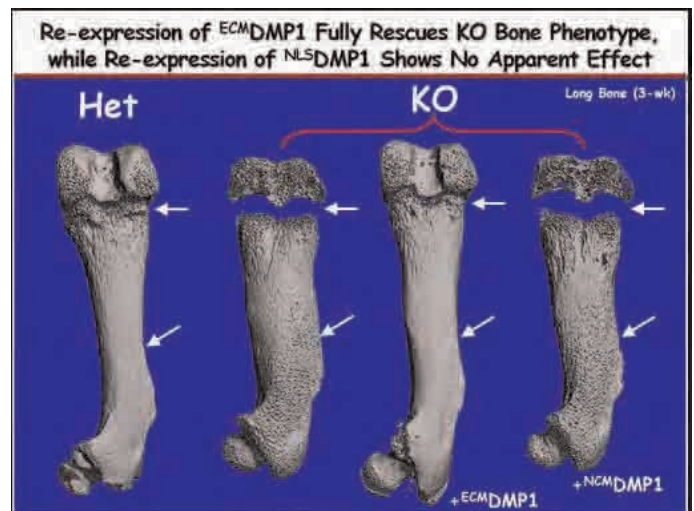
DMP1 plays a key role in the differentiation of osteoblasts into osteocytes. The identification of DMP1 mutations in humans has led to the discovery of autosomal recessive hypophosphatemic rickets. Currently, there are two hypotheses: 1) DMP1 is a matrix protein that functions via MAP kinase signaling (JBMR 2010); and 2) DMP1 acts as co-transcriptional factor (JBC, 2002). This study was designed to test whether DMP1 could function as a transcription factor both *in vivo* and *in vitro*. First we generated two Adenovirus CMV constructs: natural form of DMP1, containing a signal peptide that directs the extracellular transport of DMP1; and nlsDMP1 transgene, in which the signaling peptide is replaced with a Nucleus Localization Signal peptide that directs DMP1 into the nucleus only. Both Ad-CMV-construction increased expressions of BSP and ALP with no apparent difference when infected into the MC3T3 osteoblast cell line. Next, these constructs were driven by a 3.6 kb rat Col 1 α 1 promoter for generations of transgenic lines separately. Three to five independent lines were generated from each transgene. Immunohistochemistry assay showed that the natural DMP1 was expressed in bone matrix but not in the nucleus; and that the nlsDMP1 was expressed in osteoblast/osteocyte nucleus only. Different analyzing methods, including X-ray, μ CT, histology and immunohistochemistry, showed that none of the transgene displayed an apparent phenotype in the WT background. Interestingly, the natural DMP1 fully rescued the Dmp1-KO phenotype when crossed into the Dmp1 KO knockout background, including biochemistry parameters (FGF23, Pi), rickets and osteomalacia in 2 independent-rescue-lines. In contrast, the nlsDMP1 failed to rescue the Dmp1-KO phenotype. **CONCLUSIONS:** No rescue of Dmp1-KO mice by the targeted re-expression of the nlsDMP1 in osteoblast-osteocyte supports the concept that DMP1 is not a co-transcription factor but an extracellular matrix protein.



Both Ad-CMV-construction increased expressions of BSP and ALP



Immunohistochemistry assay showed the expression of natural DMP1 and nlsDMP1



micro-CT picture of femurs from mouse with different genotypes

Disclosures: Shuxian Lin, None.

This study received funding from: NIH/DE015209

MO0113

Thrombospondin-2 Promotes Collagen Fiber Assembly and Stability in the Osteoblast-Derived Extracellular Matrix. Andrea Alford*, Anita Reddy. University of Michigan, USA

Our published data suggest that thrombospondin-2 (TSP2) RNAi affects collagen in the extracellular matrix (ECM) of MC-3T3-E1 cells. We have extended these observations by examining the effects of a total genetic absence of TSP2 on levels and distribution of type I collagen in primary marrow stromal cells (MSC) undergoing osteoblastic differentiation. We harvested MSC from the long bones of 8-week old male TSP2-null and wild-type (WT) littermates and cultured them under osteogenic conditions. After 9 days, conditioned medium and 0.5 M acetic acid-soluble matrix fractions were collected and collagen was quantified using a Sirius red dye-binding assay. DNA was quantified in parallel wells by UV spectrophotometry. Our data suggest that WT cells secrete more total collagen than TSP2-null cells, and that it is distributed differently between the medium and matrix compartments in the two cell-types. While the conditioned medium of WT MSC contains more collagen than that of TSP2-null cells (10.1 \pm 0.53 vs. 5.6 \pm 0.045 ng per μ g DNA in WT vs TSP2-null cultures, respectively; $p < 0.001$), collagen levels in the acid-soluble matrix are similar (1.4 \pm 0.1 vs 1.2 \pm 0.1 ng per μ g DNA in WT and TSP2-null cultures, respectively; $p = 0.057$). Relative levels of mature fibrillar collagen in the acid-insoluble matrix were estimated by heat-denaturing it to gelatin. On a per DNA basis, the acid-insoluble matrix of WT cells contained about twice as much collagen as that of TSP2-null cells (1.0 \pm 0.15 and 0.48 \pm 0.046 for WT and TSP2-null cultures, respectively; $p < 0.05$). After 30 days, WT cells had accumulated a collagen-rich acid insoluble matrix, whereas the TSP2-null cultures still displayed relatively low levels (1.0 \pm 0.12 and 0.19 \pm 0.08 for WT and TSP2-null cultures, respectively; $p < 0.0001$). We conducted western blot analysis of conditioned medium using an antibody that recognizes pro- α 1(I)-collagen, as well as the pro-peptide processed forms. Our preliminary data show that

type I pro-collagen appears in the medium sooner in WT than in TSP2-null cultures, but that removal of the pro-peptides from type I pro-collagen occurs in both cell types. Together, our data suggest that TSP2 may promote the synthesis or secretion of collagen, as well as facilitate its proper assembly into fibrils during the initial stages of osteoblast differentiation, and that TSP2 may also affect the stability of matrix collagen fibers in the mature, mineralizing matrix.

Disclosures: Andrea Alford, None.

MO0114

Conditional Loss of MT-MMP Activity in Perivascular Tissues Leads to Disruption of Skeletal Growth. Joanne Shi*, Susan Yamada, Emily Purcell, Pamela Robey, Kenn Holmbeck. National Institute of Dental & Craniofacial Research, USA

Purpose: Multipotent skeletal progenitor cells residing in the bone marrow proper (including the subset associated with marrow vasculature) express membrane-type matrix metalloproteinases (MT-MMPs). We have previously shown that universal loss of MT-MMP activity in adulthood leads to severe perturbation of the skeletal homeostasis with dramatic bone loss and exuberant osteoclast activity, fibrosis, joint erosion and arthritis. MT-MMPs are expressed in a wide variety of cells in the skeleton and the contribution of specific skeletal cell populations to the development of disease is therefore difficult to assess. To work around this obstacle, we have employed a strategy of cell-specific ablation of MT-MMP activity. Here we investigate the role of MT-MMP activity in a subset of vascular-associated cells expressing these proteases.

Methods: A mouse strain carrying a floxed conditional null allele for MT1-MMP was crossed to mice expressing Cre-recombinase under the control of the SM22a promoter to excise of the MT1-MMP gene in perivascular cells.

Results: We demonstrate that selective ablation of MT1-MMP in the SM22a-expressing subset of cells caused significant diminution of skeletal bone content in both the craniofacial and appendicular skeleton. In the skull, fibrosis of the sutures was pronounced and the bone of the cranial vault was thin with overt endosteal fibrosis. In long bones, SM22a-specific loss of MT1-MMP led to substantial loss of trabecular bone, diminished cortical thickness and atrophy of the epiphyseal growth plate.

Conclusion: The specific loss of MT-MMP activity in cells associated with the vasculature led to overt reduction of bone content in mice. We propose based on these observations that the peri-vascular environment is a significant repository of skeletal progenitor cells with potential to populate several tissues of the skeleton including the craniofacial bone, sutures and cartilages. In summary, our data provide compelling evidence that vascular-associated multipotent progenitor cells contribute substantially to skeletal development.

Disclosures: Joanne Shi, None.

MO0115

Chronic MAPK Inhibition in Hyp Mice Rescues Disordered Vitamin D Metabolism and Skeletal Mineralization Defect. Martin Zhang¹, Daniel Ranch², Anthony Portale¹, Farzana Perwad^{*3}. ¹University of California, San Francisco, USA, ²Univ. Texas Health Science Center, San Antonio, USA, ³University of California San Francisco, USA

The X-linked hypophosphatemic (Hyp) mouse carries a loss-of-function mutation in the *PheX* gene, which results in hypophosphatemia due to renal phosphate (Pi) wasting, inappropriately suppressed 1,25(OH)₂D production, and rachitic bone disease. Increased circulating fibroblast growth factor-23 (FGF-23) is responsible for the disordered metabolism of Pi and 1,25(OH)₂D. We previously showed in Hyp mice that activation of the mitogen-activated protein kinase (MAPK) signaling pathway mediates FGF-23-induced suppression of renal Pi reabsorption and 1,25(OH)₂D synthesis, and this suppression is reversed when MAPK signaling is acutely inhibited. In the present study, we tested the hypothesis that chronic MAPK inhibition in Hyp mice can reverse their metabolic derangements and rachitic bone disease. Hyp mice were fed the MAPK inhibitor, PD0325901 (PD901) (7.5 mg/kg) or vehicle orally, 5 days/week for 4 weeks. After 4 weeks of treatment, weight gain was greater than in vehicle-treated mice (2.4±0.2 vs 0.5±0.2 gm, mean ± SEM, P<0.05). In Hyp mice, PD901 induced 15-fold and 2-fold increases in renal 1α-hydroxylase mRNA and protein abundance, respectively (P<0.05) and thereby higher serum 1,25(OH)₂D levels (115±13 vs 70±16 pg/ml, P<0.05), compared to values in vehicle-treated Hyp mice. With PD901, serum Pi levels (5.1±0.5 vs 3±0.2 mg/dl, P<0.05) and Npt2a brush-border membrane protein abundance (P<0.05) were higher than in vehicle-treated mice. Hyp mice typically develop rachitic bone disease characterized by shortened long bones, increased unmineralized osteoid volume, widened epiphyses, and disrupted growth plates. In the PD901-treated Hyp compared to vehicle-treated Hyp mice: Histomorphometric analysis of distal femur showed significant mineralization of cortical and trabecular bone, lower osteoid volume (24.3±2.3 vs 73.7±3.7%), and lower osteoid thickness (7.8±1.6 vs 18.42±2.6 μm (P<0.05); microCT analysis showed a substantial increase in cortical bone volume (0.31±0.005 vs 0.27±0.003 %, p<0.05), cortical thickness (0.11 ±0.003 vs 0.09±0.002μm, P<0.5) and

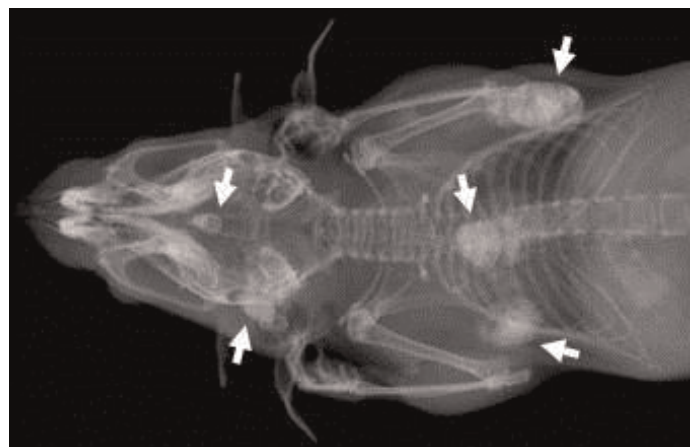
femur length (11.79±0.15 vs 11.21 ±0.36 mm, P=0.2). These findings provide evidence that in Hyp mice, activation of the MAPK pathway is critical for FGF23-mediated suppression of renal Pi reabsorption and 1,25(OH)₂D production, and chronic MAPK inhibition reverses disordered Pi and 1,25(OH)₂D metabolism and significantly improves the rachitic bone disease.

Disclosures: Farzana Perwad, None.

MO0116

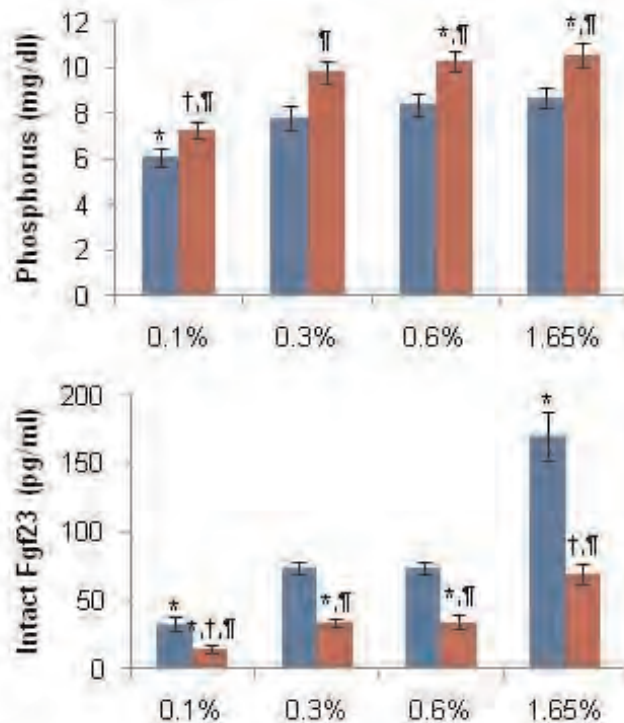
Dietary Phosphate Intake Modulates Phenotype of a Mouse Model of Familial Tumoral Calcinosis. Shoji Ichikawa*, Amie K. Gray, Anthony M. Austin, Leah R. Padgett, Michael Econs. Indiana University School of Medicine, USA

Mutations in the *GALNT3* gene cause familial tumoral calcinosis characterized by ectopic calcifications due to hyperphosphatemia and hyperostosis-hyperphosphatemia syndrome presenting with recurrent swelling of the long bones. We recently developed *Galnt3* knockout mice, which had hyperphosphatemia with increased bone mineral density (BMD) and infertility in males. To test the effect of dietary phosphate intake on their phenotype, *Galnt3* knockout mice were fed various phosphate diets: 0.1% (low), 0.3% (low normal), 0.6% (normal), and 1.65% (high). Serums were analyzed for calcium, phosphorus, alkaline phosphatase, creatinine, blood urine nitrogen, and a phosphaturic hormone, fibroblast growth factor 23 (Fgf23). Femurs were evaluated by dual-energy X-ray absorptiometry. On all four phosphate diets, *Galnt3* knockout mice had consistently higher phosphorus levels and lower alkaline phosphatase and intact Fgf23 concentrations than littermate controls. The low phosphate diet normalized serum phosphorus, alkaline phosphatase, and areal BMD in *Galnt3* knockout mice. However, normophosphatemia failed to correct male infertility in *Galnt3* knockout mice. The high phosphate diet did not increase serum phosphorus concentration due to compensatory increase in intact Fgf23 levels. However, increased phosphate intake induced the development of large ectopic calcifications, reminiscent of tumoral calcinosis in humans. In conclusion, the low phosphate diet normalizes biochemical and skeletal phenotypes of *Galnt3* knockout mice, indicating that dietary phosphate restriction can be an effective therapy for tumoral calcinosis. In contrast, the high phosphate diet brings out a more severe phenotype in *Galnt3* knockout mice, making them an excellent animal model of tumoral calcinosis.



White arrows denote ectopic calcifications.

Ectopic calcifications.



Blue, control and red, *Galnt3* knockout mice. N = 8-12 per group. P < 0.05: * vs. control on the 0.6% diet; †, vs. *Galnt3* knockout mice on the 0.6% diet (comparisons limited to *Galnt3* knockout mice); ¶, vs. control on the same diet.

Serum biochemistries.

Disclosures: Shoji Ichikawa, None.

MO0117

Evaluation of a New Automated Chemiluminescence Immunoassay for FGF23. Yuichiro Shimizu*, Seiji Fukumoto, Toshiro Fujita. University of Tokyo Hospital, Japan

Fibroblast growth factor 23 (FGF23) is a hormone regulating phosphate and vitamin D metabolism. Excess and deficient FGF23 actions result in several kinds of hypophosphatemic rickets/osteomalacia and familial hyperphosphatemic tumoral calcinosis, respectively. We have previously established an enzyme-linked immunosorbent assay (ELISA) for full-length active FGF23. Using this assay, we have shown that hypophosphatemia with FGF23 levels of more than 30 pg/ml indicates the disease caused by excess actions of FGF23. However, this ELISA has a rather narrow assay range (3 to 800 pg/ml). In addition, it was pointed out that the assay performance of this ELISA was not satisfactory when automatic washing machine was used. Therefore, we have evaluated the basic performance and clinical utility of a newly developed automated chemiluminescence immunoassay for FGF23. This assay uses the same monoclonal antibodies for FGF23 as the previous ELISA and a fully automated chemiluminescence system (CL-JACK, Kyowa Medex, Japan). The assay requires 10 µl of serum or plasma samples and needs 20 minutes for the first result. The detection limit using 2 standard deviations of blank sample was 1 pg/ml and the good linearity was proven up to 15,000 pg/ml. The coefficient of variations using samples with FGF23 levels of 10 to 2500 pg/ml were less than 5%. When FGF23 levels in more than 200 samples from hypophosphatemic patients with various cases were measured by this assay and the previous ELISA, there was a good correlation with R^2 of more than 0.9. In addition, when these samples were divided into two groups with FGF23 levels of higher or lower than 30 pg/ml, there was no discrepancy in the discrimination of samples using these two assays. These results indicate that this new chemiluminescence immunoassay for FGF23 has a wider assay range and a lower detection limit than those of the previous ELISA. This assay also showed good repeatability, requires less amount of samples and shorter time to get the first result. Therefore, this assay seems to be ideal for both clinical use and clinical studies especially measuring many samples with high FGF23 levels.

Disclosures: Yuichiro Shimizu, None.

MO0118

Fibroblast Growth Factor 23 (FGF23) Alters Gene Expression of Isolated Cardiac Ventricular Muscle. Michael Wacker*, Vladimir Tchikrizov², Jaime Mannix², Chad Touchberry², Jason Stubbs³, Lynda Bonewald². ¹University of Missouri-Kansas City School of Medicine, USA, ²University of Missouri - Kansas City, USA, ³University of Kansas Medical Center, USA

Fibroblast growth factor 23 (FGF23) is a hormone primarily released by osteocytes in bone that regulates phosphate and vitamin D metabolism to create a bone-kidney-gut axis. Recent observational studies in humans suggest circulating FGF23 levels to be independently and positively associated with cardiac morbidity and mortality, but the mechanisms responsible remain unclear. FGF23 levels are markedly elevated in patients with several inherited forms of hypophosphatemic rickets and in patients with chronic kidney disease (CKD), yet it is unclear if FGF23 directly contributes to changes in cardiac function. To begin to determine if FGF23 has a direct effect, heart weight to body weight ratios (HW/BW) of two animal models with high serum FGF23 levels were analyzed and the independent effects of recombinant FGF23 on isolated wild-type cardiac muscle strips were examined. The *Dmp1* null mouse model which has high serum FGF23 due to disruption of *Dmp1* expression in osteocytes had a 17% increase in HW/BW compared to wild-type at 24 weeks of age (n=5-6). The *Col4a3* null mouse, a murine model of human Alport disease that develops progressive proteinuric kidney disease and exhibits high levels of serum FGF23, demonstrated a 22% increase in HW/BW compared to wild-type at 10 weeks of age (n=4-5). In order to determine if FGF23 could have a direct receptor-mediated effect on cardiac muscle to induce hypertrophy, we performed quantitative RT-PCR analysis of right ventricular RNA for FGF receptor 1 (FGFR1) and the co-receptor *klf10*. We observed FGFR1 mRNA to be expressed at 6.7 1.0 cycles greater than the β -actin housekeeping gene in all 4 control strips. For *klf10*, mRNA was detectable in 2 of 4 control strips with expression at 15.6 0.2 cycles higher than β -actin. In addition, right ventricular muscle strips were treated for 24 hrs with 900 pg/ml FGF23 or vehicle. Gene expression levels of atrial natriuretic peptide (ANP) and brain natriuretic peptide (BNP), markers of cardiac hypertrophy, were found to be increased 18 and 6 fold respectively from vehicle levels (n=4). In summary, our data indicate that two distinct mouse models exhibiting FGF23 overexpression demonstrate cardiac hypertrophy. Furthermore, treatment of isolated mouse cardiac muscle with FGF23 causes a significant increase in ANP and BNP gene expression. These data provide support for the hypothesis that FGF23 may be a direct contributor to the development of cardiac hypertrophy.

Disclosures: Michael Wacker, None.

MO0119

Absence of the Mid-region, Nuclear Localization Sequence, and C-terminus of PTHrP Alters the Osteogenic, Adipogenic, Chondrogenic, and Myogenic Differentiation of Murine Bone Marrow Stromal Cells. Blake Hildreth*, Krista M. Hernon, Brandlyn N. Marlow, John Leong, Thomas Rosol, Ramiro Toribio. The Ohio State University, USA

Since the roles of the mid-region, nuclear localization sequence (NLS), and C-terminus of parathyroid hormone-related protein (PTHrP) in the differentiation of bone marrow stromal cells (BMSC) is currently unknown, we investigated the effects of deletion of these regions on their multi-lineage differentiation. It is established that the N-terminal domain promotes bone and cartilage differentiation from BMSC, while concurrently inhibiting adipogenesis. However, little information exists regarding the role of PTHrP in myogenesis. BMSC were isolated from mice lacking the mid-region, NLS, and C-terminus of PTHrP (*Pthrp*^{Δ1/Δ}) and wild-type (control) littermates. Cells were grown in differentiation media both in monolayer (osteo-, adipo-, and myogenesis) and in pellet cultures (chondrogenesis) for 24 days. Secreted biomarkers were analyzed every 6 days and compared with a 2-way RM-ANOVA. Lineage-specific mRNA at day 12 and 24, and histochemical/morphological indices at day 24 were measured and compared with an unpaired t-test at $P < 0.05$. *Pthrp*^{Δ1/Δ} BMSC had greater alkaline phosphatase (ALP) activity ($P < 0.0001$). However, *Pthrp*^{Δ1/Δ} BMSC ultimately had reduced osteoblast maturation, demonstrated by decreased mineralization and osteocalcin secretion at day 24 ($P = 0.016$ and 0.029). Similarly, *Pthrp*^{Δ1/Δ} BMSC-derived cartilage pellets were smaller ($P < 0.0001$) and expressed greater *Ihh* ($P = 0.035$) but less *Sox9* at day 24 ($P = 0.042$). Although *Pthrp*^{Δ1/Δ} BMSC produced greater numbers of adipocytes ($P = 0.023$) with increased *Pparγ* expression at day 24 ($P = 0.087$), both genotypes had similar adipogenic gene expression profiles. Interestingly, *Pthrp*^{Δ1/Δ} BMSC produced a larger number of myocytes ($P < 0.0001$) and expressed more *desmin* and *myogenin* at day 24 ($P = 0.002$ and 0.031). In conclusion, regions distinct from the N-terminus influence BMSC differentiation. Increased ALP and *Ihh* by *Pthrp*^{Δ1/Δ} BMSC, but less bone and cartilage formation, indicates that the mid-region, NLS, and C-terminus inhibit proliferation, but promote osteoblast and chondrocyte maturation. This is the first time that these regions of PTHrP have been implicated in regulating adipocyte and myocyte formation, and they complement the inhibitory function of the N-terminus. Similarities in adipogenic gene expression profiles, despite a greater number of *Pthrp*^{Δ1/Δ} BMSC-derived adipocytes, suggest alterations in energy metabolism, which may contribute to the perinatal lethality in *Pthrp*^{Δ1/Δ} mice.

Disclosures: Blake Hildreth, None.

MO0120

Acute Decline in Serum Sclerostin in Response to PTH Infusion in Healthy Men. Elaine Yu^{*1}, Ruchit Kumbhani², Erica Siwila-Sackman², Benjamin Leder³. ¹Massachusetts General Hospital, USA, ²MGH Endocrine Unit, USA, ³Massachusetts General Hospital/Harvard Medical School, USA

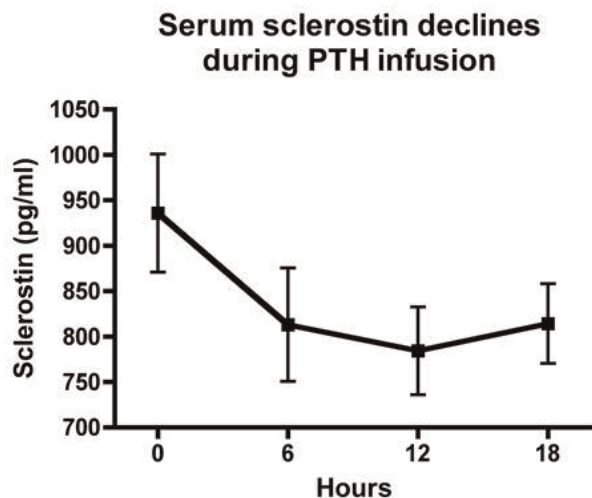
Background: Animal models suggest that the osteoblast-stimulating actions of parathyroid hormone (PTH) are mediated by acute suppression of sclerostin, an inhibitor of the anabolic Wnt pathway. Conflicting data exist on the effect of intermittent subcutaneous PTH therapy on serum sclerostin, but the immediate physiologic changes in serum sclerostin in response to acute PTH administration have not been reported in human studies.

Objective: We sought to determine the physiologic effects of acute PTH infusion on serum sclerostin and bone turnover markers in healthy adult men.

Methods: 53 healthy adult men underwent an 18-hour intravenous infusion of hPTH(1-34) at a dose of 0.55 U/kg-h. Serum levels of ionized calcium, sclerostin, and markers of bone formation (osteocalcin, PINP) and bone resorption (CTX, NTX) were obtained at 0, 6, 12, and 18 hours.

Results: Serum ionized calcium, CTX and NTX increased, and OC and PINP fell linearly throughout the PTH infusion ($p < 0.01$ for all). Average (SEM) sclerostin levels declined from 936 (65) pg/ml to 813 (63) pg/ml at 6 hours ($p < 0.01$) and remained stably suppressed for the duration of the PTH infusion. We did not observe any significant correlations between change in sclerostin and change in bone turnover markers.

Conclusion: Serum sclerostin declined in response to acute PTH infusion within 6 hours in healthy adult men. The early plateau in sclerostin suppression by PTH contrasts with the linear changes seen in bone turnover markers, and may indicate that maximal stimulation of the Wnt pathway is achieved quickly after exposure to PTH. This finding might partially explain the opposing effects of intermittent and continuous PTH.



Change in Sclerostin during PTH infusion

Disclosures: Elaine Yu, None.

MO0121

Greater Increase in Urinary Calcium in Response to 1,25(OH)₂D₃ in Genetic Hypercalciuric Stone-Forming Rats than in Controls. Kevin Frick^{*1}, John Asplin², Christopher Culbertson¹, Daniel Asplin², Nancy Kreiger¹, David Bushinsky¹. ¹University of Rochester, USA, ²Litholink Corporation, USA

Genetic hypercalciuric stone-forming (GHS) rats, selectively bred to maximize urine (U) calcium (Ca) excretion, demonstrate increased intestinal Ca absorption, increased bone resorption and reduced renal tubular Ca reabsorption, all leading to a marked increase in UCa compared to control Sprague-Dawley rats and all form kidney stones. The GHS rats express an increased number of vitamin D receptors (VDR) at these sites of disordered Ca transport. To determine if the excess VDR is biologically active, we fed GHS rats a Ca replete diet (1.2% Ca) and injected 1,25(OH)₂D₃ (1,25D, 25 ng/d) or vehicle (veh) for 9 d. With 1,25D, UCa in SD increased from 1.70.3 mg/d to 24.41.2 mg/d and in GHS from 10.50.7 to 41.90.7 and PTH was suppressed to undetectable levels in both groups (all groups n=8, mean SEM, all comparisons $p < 0.01$). To determine if GHS rats would continue to have an augmented increase in UCa in the absence of 1,25D induced intestinal Ca absorption, GHS and SD rats were fed a low Ca diet (0.02%) and again injected with 1,25D or veh for 9 d. With 1,25D, UCa in SD increased from 1.30.1 mg/d to 9.40.9 mg/d and in GHS from 4.70.3 to 21.50.9 and PTH was again suppressed in both groups (all groups n=8, all comparisons $p < 0.02$). In both studies the marked increase in UCa with 1,25D in GHS, which exceeded the increase in SD, indicates that the enhanced number of

VDR in GHS results in greater biological response to administered 1,25D. To help understand the greater increase in UCa in response to 1,25D in GHS than SD, we measured RNA expression of a number of components of renal tubular Ca transport in the low Ca diet study. We found that expression of the distal luminal renal Ca transporter TRPV5 and the transcellular Ca transport protein calbindin D_{28k} were both elevated by 1,25D in SD but not GHS rats. These findings indicate the potential for less renal tubular Ca reabsorption in GHS than SD resulting in greater hypercalciuria. Thus, the increased VDR found in the GHS rats is biologically active and results in a greater increase in UCa as compared to SD rats. In the absence of appreciable dietary Ca, the greater UCa in the GHS rats compared to SD may be secondary to a decrease in distal renal tubular Ca reabsorption mediated by TRPV5.

Disclosures: Kevin Frick, None.

MO0122

High Prevalence of Vitamin D Deficiency Among Pregnant Women at Term and Their Neonates in Thessaloniki, Northern Greece. Gkastaris Konstantinos, Karras Spiros, Papadopoulos Foteini^{*}. Panagia General Hospital, Thessaloniki, Greece

Introduction: Maternal vitamin D status is integral to fetal development. There are few data from Greece, a country with abundant sunshine, regarding the prevalence of vitamin D deficiency in pregnancy. Our aim was to assess vitamin D status of women at term and their neonates in a region of Northern Greece.

Methods: Maternal serum and cord blood levels of calcium (Ca), 25-hydroxyvitamin D (25-OH-D), alkaline phosphatase (ALP), phosphorus (P) and parathyroid hormone (PTH) were studied in 60 mother-newborn pairs at term. The study was conducted between February 2010 - March 2011. Dietary habits and skin phototype (Fitzpatrick's classification) were studied.

Results: Mean level of maternal serum 25(OH) D was 10.11 (6.2-21.2) ng/ml, significantly lower ($P < 0.001$ -paired samples test) than that of cord blood 14.2 (9.5-23.8) ng/ml. Maternal serum 25-OH-D correlated positively with cord blood 25-OH-D ($r = 0.79$, $P < 0.001$) (Spearman's correlation). According criteria defining vitamin D deficiency, 82.3% of mothers and 62.5% of neonates were vitamin D deficient, respectively. Umbilical venous blood P was significantly ($P < 0.001$) higher than maternal blood levels [5.2 (3.8-5.9) vs. 3.6 (2.9-3.8) mg/dl], while umbilical PTH levels were significantly lower ($P < 0.001$) than maternal levels [4.5 (2.5-7.1) vs. 22.19 (6.5-36.2) pg/ml]. No differences were found between maternal and cord blood Ca and ALP levels ($p = 0.710$). The intake of Ca and vitamin D was uniformly low [283103 mg/d and 4824 IU/d], respectively. Mothers who delivered during winter and spring had lower 25-OH-D levels ($P < 0.001$), than those who delivered in summer and autumn [8.9 (5.1-11.1) vs. 9.6 (5.8-15.4)]. Finally, women with fair phototype had higher 25-OH-D ($P < 0.001$) than women with darker phototypes.

Conclusion: We observed a high prevalence of hypovitaminosis D among pregnant women and their newborns in Northern Greece. Further public health intervention and vitamin D supplementation is needed to improve maternal and neonatal vitamin D status.

Disclosures: Papadopoulos Foteini, None.

MO0123

Intermittent PTH Therapy is Anabolic in the Temporomandibular Joint in Young Growing Mice. Yosuke Kamiya^{*1}, Jing Chen¹, Manshan Xu¹, Achint Utreja¹, Kyeong Lee¹, Hector Aguila¹, Carol Pilbeam¹, Sunil Wadhwa². ¹University of Connecticut Health Center, USA, ²University of Connecticut, USA

Intermittent PTH treatment is a common therapy for the treatment of osteoporosis and unlike other osteoporosis therapies is able to cause an anabolic response in the periosteum. The temporomandibular joint is composed of the mandibular condyle, the articular portion of the temporal bone and a disc that are covered by fibrocartilage. Unlike other joints, the cartilage of the mandibular condyle is derived from periosteum. Therefore, the goal of this study was to examine if similar to bone, intermittent PTH therapy is anabolic in the temporomandibular joint (TMJ). Intermittent PTH (80µg/kg) or vehicle was injected to young mice (6-7 weeks old male C57BL/6) for 14 days. Gene expression of chondrocyte maturation markers, proliferation and condylar cartilage thickness was evaluated in the mandibular condyle from both treatment groups. In young growing mice, intermittent PTH therapy caused a significant increase in the mandibular condylar cartilage thickness, no changes in proliferation and a trend for increased Collagen type 2 expression ($p = .10$) compared to the vehicle treated group. Intermittent PTH treatment caused increased condylar cartilage thickness in young growing mice. Future studies are needed in order to evaluate the effects of intermittent PTH treatment in the temporomandibular joint in adult non-growing mice.

Disclosures: Yosuke Kamiya, None.

MO0124

Parathyroid Hormone-Vitamin D Relationship is Mediated by Weight Status. Lynae Hanks^{*1}, Krista Casazza², Ambika Ashraf¹, Timothy Mark Beasley¹, Jessica Alvarez¹, Jose Fernandez¹. ¹University of Alabama at Birmingham, USA, ²UAB, USA

Obesity has been associated with low levels of 25-hydroxy vitamin D (25OHD) and high levels of parathyroid hormone (PTH), two antagonistic hormones intricately involved in skeletal health. Whereas, PTH secretion increases to adapt to higher rate of bone formation associated with growth, fat as the main reservoir of vitamin D may affect 25OHD bioavailability thereby perturbing the PTH-25OHD relationship. This has particular relevance during in females as they approach reproductive maturity as it is then that peak bone mass is attained. The aim of this study was to identify the 25OHD nadir resulting in PTH stimulation by weight status. One-hundred normal (n=60) and overweight (n=40) females ages 5-15 years were included. Despite similar 25OHD levels, the relationship between D and PTH differed by weight status (controlling for reproductive maturity). Loess regression analysis indicated 27.2ng/dL (p=0.002) as the level of 25OHD necessary to stimulate PTH secretion in normal weight girls, whereas 14.4ng/dL was the level identified in overweight girls (although the trend and the post-threshold relationship in the overweight group was not significant). This data suggests a weight-dependence in inflection point; or more specifically, that the vitamin D decrement to stimulate PTH secretion is likely of lower magnitude in normal weight girls. This can have profound implications in terms of skeletal health during this sensitive period of development.

Disclosures: Lynae Hanks, None.

MO0125

Parathyroidectomy Improves Bone Geometry and Microarchitecture in Female Patients with Primary Hyperparathyroidism. A 1-year Prospective, Controlled Study using High Resolution Peripheral Quantitative Computed Tomography. Stinus Hansen^{*1}, Ellen M Hauge², Jens Erik Beck Jensen³, Kim Brixen⁴. ¹Dept. of Endocrinology, Odense University Hospital, Denmark, ²Department of Rheumatology, Aarhus University Hospital, Denmark, ³Osteoporosis Research Clinic, Hvidovre University Hospital, Denmark, ⁴Institute of Clinical Research, University of Southern Denmark, Denmark

Objective.

Following parathyroidectomy (PTX), bone mineral density (BMD) increases in patients with primary hyperparathyroidism (PHPT), yet information is scarce concerning changes in bone structure following normalization of parathyroid hormone levels post-surgery. In this 1-year prospective, controlled study high resolution peripheral quantitative computed tomography (HR-pQCT) was used to evaluate alterations of bone geometry, volumetric BMD (vBMD) and trabecular microarchitecture in female patients with PHPT before and one year after PTX, compared to age- and sex-matched healthy control subjects.

Subjects and Methods

At baseline and after one year of follow up, 26 women with PHPT, in whom PTX was successful (median age 62, range 44-75 years), and 31 female controls (median age 63, range 40-76 years), recruited by random sampling from the background population, were studied using HR-pQCT (Scanco Medical) of the distal radius and tibia providing 82 µm isotropic voxel size images. Changes from baseline to follow-up were assessed with a two group mean comparison t-test of delta values.

Results

Results are shown in Table 1. The two groups were comparable regarding age, height, weight and menopausal status (not shown). At one year, cortical (Ct.) area, Ct. thickness and Ct. vBMD increased in radius in patients (0.09%, 0.68% and 0.50%, respectively) opposed to decreases in controls (-3.35%, -2.64% and -0.76%, respectively) (all p<0.01). A similar pattern was observed in tibia with increases in patients (Ct. area 2.87%, Ct. thickness 10.51%, Ct. vBMD 0.80%) contrasting decreases in controls (-0.30%, -1.10%, -0.43%, respectively) (all p<0.05). Trabecular (Tb.) bone changes were only observed in radius. In patients, Tb. vBMD and Tb. bone volume per tissue volume (BV/TV) increased (2.01% and 1.44%, respectively) along with decreased Tb. spacing (3.97%). In controls, Tb. vBMD and Tb. BV/TV decreased (-0.37% and -0.64%, respectively) whereas Tb. spacing increased (1.53%) (all p<0.01). No significant differences were found for Tb. number or Tb. thickness or any trabecular parameter in tibia.

Conclusion

In patients with PHPT, normalization of PTH levels induces significant alterations of cortical bone in both radius and tibia, reversing or alleviating age-related changes observed in controls. In radius, trabecular bone volumetric BMD increased while trabecular spacing decreased. These changes suggest that bone strength increases.

Table 1: Baseline and one year follow-up value for patients and control subjects. Data are presented as mean±SD

HR-pQCT parameter	PHPT (n=26)		Control subjects (n=31)		p-values*
	Baseline	Follow-up	Baseline	Follow-up	
Radius					
Cortical area (mm2)	54±10	54±10	58±11	56±11	0.001
Trabecular area (mm2)	216±48	216±48	202±45	204±45	0.001
Cortical thickness (mm)	0.82±0.19	0.82±0.20	0.91±0.20	0.89±0.19	0.01
Cortical vBMD (mmg/ccm)	844±76	848±69	884±62	877±68	0.01
Trabecular vBMD (mmg/ccm)	106±45	108±45	131±38	130±38	0.01
Trabecular BV/TV (%)	8.88±3.80	9.03±3.76	10.88±3.14	10.83±3.14	0.01
Trabecular spacing (mm)	0.715±0.340	0.687±0.320	0.547±0.270	0.556±0.306	0.01
Tibia					
Cortical area (mm2)	101±20	104±22	103±18	102±19	0.01
Trabecular area (mm2)	653±133	651±133	651±130	650±129	0.23
Cortical thickness (mm)	1.00±0.24	1.10±0.24	1.01±0.20	1.00±0.21	0.01
Cortical vBMD (mmg/ccm)	799±88	805±75	815±66	811±69	0.03
Trabecular vBMD (mmg/ccm)	127±37	130±36	148±33	148±33	0.08
Trabecular BV/TV (%)	10.57±3.12	10.87±2.98	12.29±2.74	12.34±2.73	0.08
Trabecular Spacing (mm)	0.616±0.277	0.603±0.271	0.483±0.098	0.482±0.103	0.44

* Unpaired t-test comparing delta values between groups

Table 1

Disclosures: Stinus Hansen, None.

MO0126

Phospholipase C Signaling through the PTH/PTHrP Receptor Is Required for Serum Phosphate Homeostasis but not for Serum 1,25(OH)2D3. Jun Guo^{*1}, Hiroko Segawa², Lige Song¹, Minlin Liu¹, F. Richard Bringham¹, Ken-Ichi Miyamoto³, Henry Kronenberg¹, Harald Jueppner¹. ¹Massachusetts General Hospital, USA, ²University of Tokushima Graduate School, Japan, ³Tokushima University School of Medicine, Japan

Parathyroid hormone (PTH) regulates phosphate (Pi) homeostasis by reducing renal Pi reabsorption. To determine which second messengers mediate this action in vivo the effect of continuous PTH infusion was assessed in wild-type (Wt) and in DD mice expressing a mutant PTH/PTHrP receptor (PPR) that activates adenyl cyclase normally but cannot activate phospholipase C (PLC). Mice at 7 wk of age were infused (s.c.) with vehicle or hPTH(1-34) (40 µg/kg/day) for 8 days. Blood and urine were collected before and 1, 2, 4, and 8 days after infusion. PTH infusion caused a persistent decrease in serum Pi (by 50%) in Wt mice, whereas DD mice exhibited lowered serum Pi only transiently for the first 2 days before returning to the basal level. Fractional excretion index of Pi (FEi-Pi) was increased initially in Wt and DD mice, but did not persist in DD mice. To determine the roles of NaPi2a (2a) and NaPi2c (2c), the proximal tubule phosphate transporters, in mediating the PTH actions in Wt and DD mice, mice that are null for each transporter in either Wt or DD background were tested. PTH infusion caused a persistent decrease in serum Pi in Wt/2c-/- mice, which was similar to the response in Wt mice. Interestingly, the PTH effect was less pronounced in DD/2c-/- mice than in DD mice. From lower baseline levels, in Wt/2a-/- mice PTH infusion led to a further persistent decrease in serum Pi. The Pi lowering effect of PTH observed in Wt/2a-/- mice was somewhat attenuated in DD/2a-/- mice. In mice null for 2a and 2c, continuous PTH had no effect on serum Pi or FEi-Pi. PTH administration led to an almost 2-fold increase in serum 1,25(OH)2D3 in both Wt and DD mice with or without 2a or 2c. However, continuous PTH administration had no effect on the already elevated serum 1,25(OH)2D3 levels in Wt or DD mice lacking both transporters. PTH infusion increased serum FGF23 (C-Term ELISA kit) in sera collected after 8 days of infusion by 50% in all groups of mice. In addition, PTH infusion dramatically elevated blood ionized calcium in all groups of mice regardless of basal levels. Our data indicate that the PPR/PLC signaling pathway contributes to PTH-dependent regulation of Pi homeostasis, but not to the regulation of 1,25(OH)2D3, FGF23, and blood calcium levels. Both 2a and 2c are essential targets of PTH action on Pi homeostasis.

Disclosures: Jun Guo, None.

MO0127

PTH Activates BMP Signaling by Inducing Endocytosis of BMP Extracellular Antagonists. Bing Yu^{*1}, Xiaoli Zhao², Chaozhe Yang³, William Lu², Mei Wan⁴, Xu Cao¹. ¹Johns Hopkins University, USA, ²Department of Orthopaedics & Traumatology, The University of Hong Kong, China, ³Department of Orthopaedic Surgery, The Johns Hopkins University, USA, ⁴Johns Hopkins University School of Medicine, USA

More than 20 members in the BMP subfamily transduce their signals using the same BMP receptors. The activity and specificity of different BMPs are achieved by various extracellular antagonists that regulate their binding to their receptors. PTH

has been shown to induce Smad1 phosphorylation effectively, suggesting that PTH regulate the activities of BMP extracellular antagonists. We found that PTH stimulated the level of phosphorylated Smad1 (p-Smad1) in osteoblastic cells on the bone surface of 8-wk old mice in 30 min after single dose injection. Moreover, PTH increased p-Smad1+ MSCs from 12.1% to 81.2% at 30 min in vivo. PTH also stimulated BMP-2-induced phosphorylation of p38, another downstream target of BMP signaling pathway. Importantly, noggin abrogated the PTH-induced phosphorylation of Smad1, indicating PTH activates Smad1 signaling through regulation of extracellular BMP antagonists. PTH lost its effect on Smad1 phosphorylation in PTH1R-/- OC59 cells. These data demonstrate that PTH activation of BMP signaling is PTH1R-dependent and extracellular BMP antagonist noggin negatively regulates the activation.

We therefore examined whether PTH increases the access of BMP ligands to their receptors with 125I labeled BMP2. PTH stimulated 125I-BMP2 cell surface binding in a dose- and time-dependent manner. When PTH-induced PTH1R endocytosis was blocked by knockdown of β -arrestin using siRNA, PTH-elevated phosphorylation of both Smad1 and ERK1/2 was inhibited. Moreover, chlorpromazine, an endocytosis inhibitor, also inhibited the PTH-enhanced phosphorylation of Smad1. We further examined how PTH-induced endocytosis stimulates phosphorylation of Smad1. LRP6 binds to noggin and sclerostin, the antagonists of BMPs, and they form a complex, indicating that LRP6 may organize an extracellular network of BMP antagonists that prevent access of BMPs to BMP receptors. Indeed, deletion of endogenous LRP6 in the MSCs isolated from floxed LRP6 mice by adenovirus-mediated Cre expression elevated PTH-stimulated Smad1 phosphorylation. Furthermore, PTH induces endocytosis of LRP6 in disruption of the antagonist inhibition, but does not induce endocytosis of BMP receptor (BMPRII). As a result, PTH increased the exposure of BMPRII significantly in a cell surface protein biotinylation assay. Collectively, our data demonstrate that PTH stimulates phosphorylation of Smad1 by increase of binding of BMPs to their receptors to induce osteoblast differentiation of MSCs.

Disclosures: Bing Yu, None.

MO0128

Regulation of Renal Sodium-Dependent Phosphate Co-Transporters During Lipopolysaccharide-Induced Acute Inflammation. Shoko Ikeda^{*1}, Hironori Yamamoto¹, Mina Kozai¹, Masashi Masuda¹, Sarasa Tanaka¹, Otoki Nakahashi¹, Hiroko Segawa², Yutaka Taketani¹, Ken-Ichi Miyamoto², Eiji Takeda¹. ¹Dept. Clinical Nutrition, University of Tokushima, Japan, ²Dept. Molecular Nutrition, University of Tokushima, Japan

Type II sodium-dependent phosphate (NaPi) co-transporters Npt2a and Npt2c play a critical role in renal Pi homeostasis, and their brush border membrane (BBM) expression is down-regulated by parathyroid hormone (PTH) and fibroblast growth factor 23 (FGF23). Sepsis is the systemic inflammatory response syndrome (SIRS) that occurs during severe infection and is often associated with electrolyte disorder. Indeed, it has been reported that endotoxin induces plasma PTH levels, hypocalciuria and hyperphosphaturia. However, the mechanism of regulation of Pi homeostasis during acute inflammation is still unclear. In this study, we investigated the regulation of renal Pi metabolism and its mechanism under the acute systemic inflammation using lipopolysaccharide (LPS; E.coli 055:B5) treated animals.

C57BL/6J mice in 3hr after LPS (2-20mg/kg, i.p.) challenge indicated dose-dependently increase the levels of plasma Pi and PTH and urinary Pi excretion, in contrast, urinary Ca excretion was significantly decreased. However, C3H/HeJ mice carrying a Toll-like receptor 4 mutation did not show these changes by LPS. We also observed LPS stimulated PTH levels in a time-dependent manner but plasma FGF23 levels were transiently-increased at 3 hr. Western blot analysis using kidney BBM demonstrated that renal expression of Npt2a but not Npt2c was down-regulated at 3 hr after LPS injection. Furthermore, TNF- α treatment also increased plasma PTH levels and decreased renal BBM Npt2a protein levels. Surprisingly, parathyroidectomized (PTX) rats had impaired LPS responsiveness of urinary Pi excretion and renal Npt2a expression. However, plasma FGF23 levels were significantly increased in both sham and PTX rats after 3 hr of LPS treatment. These results suggest that the alteration of Pi homeostasis during LPS-induced acute inflammation is mediated the down-regulation of renal Npt2a gene expression by PTH.

Disclosures: Shoko Ikeda, None.

MO0129

The Immediate PTH Anabolic Action on Bone Marrow Mesenchymal Progenitor Cells. Valerie Siclari^{*1}, Ji Zhu², Fei Liu¹, Abhishek Chandra¹, Ling Qin¹. ¹University of Pennsylvania, USA, ²University of Pennsylvania, School of Medicine, USA

Intermittent injection of parathyroid hormone (PTH 1-34) is an effective anabolic treatment for osteoporosis. Long-term, it dramatically increases trabecular bone mass but the exact mechanism, especially its early action on bone, is not completely understood. Recently, we established a novel method to isolate mesenchymal progenitors (MP) from trabecular bone marrow (BM) and identified a rapid effect of PTH on these cells. The current method to isolate MPs from rodents is to culture BM flushed from long bones. However, histology revealed that it only released BM from the cortical mid-shaft but not BM entrapped within the trabecular bone. To obtain trabecular MPs, long bones were cleaned of soft tissue and periosteum.

Cortical BM was flushed out of the bone and then the bones were cut in half, washed, and digested in collagenase/trypsin solution to release the trabecular BM cells. In vitro, these cells generated both alkaline phosphatase (AKP)⁺ and ⁺ colonies and could differentiate into osteoblasts and adipocytes, suggesting that they include mesenchymal stem cells and osteoprogenitors. The frequency of MPs from trabecular BM was about 3-fold more than that from cortical BM. Interestingly, a single PTH1-34 injection (80 ug/kg) in rats increased the number of trabecular MPs 1.9-, 2.2-, and 3.0-fold after 2, 4, and 24 hrs, respectively. A similar effect was observed in mice. PTH1-34 treatment increased CFU-AKP⁺ colony diameter, suggesting that PTH stimulates the proliferative ability of trabecular AKP⁺ MPs. PTH1-31 (activating PKA pathway), but not 3-34 (activating PKC pathway), produced similar effects. Continuous PTH1-34 (40 ug/kg/day), which leads to bone loss, did not have any effect on the trabecular MPs. Bone resorption was not required for the PTH-induced increase in the number of trabecular MPs. Enhanced proliferation alone cannot explain why PTH increases trabecular MP numbers within 2-4 hrs. Chemotaxis assays demonstrated that conditioned media (CM) from PTH-treated osteoblasts resulted in a 2-fold increase in the migration of MP cells compared to CM from vehicle-treated cells but PTH alone had no effect on the migration. This suggests that PTH stimulates osteoblasts to secrete chemotactic factors which subsequently induce MP migration toward the trabecular bone. In summary, our studies identify an early step in anabolic PTH action on bone in which PTH rapidly stimulates MP proliferation and migration.

Disclosures: Valerie Siclari, None.

MO0130

Treatment of Non-healing Fractures with Parathyroid -hormone (1-34). Thomas Westphal¹, Dirk Ganzer², Kathrin Baessgen¹, Guido Schroeder¹, Hans-Christof Schober^{*3}. ¹Klinikum Sudstadt, Germany, ²Dietrich Bonhoeffer Klinikum, Germany, ³Klinikum Sudstadt RostockKlinik Fur Innere Medizin I, Germany

Introduction: Non-healing fractures remains a major challenge in orthopaedic surgery. Numerous surgical interventions and the disability of the patients are causing high individual and economic burden. Case reports have shown some effectiveness of Teriparatid 1- 34 (Forsteo®) in non - unions and delayed healing of bone fracture .

In the study presented, we aimed to induce fracture healing and to improve the clinical situation by short term treatment with rhPTH 1-34.

Methods: 8 patients: age 49 - 74 y; gender: 4 male, 4 female, fracture site: femur (1x), proximal tibia (3x) and pilon -tibial (4x), time duration of non -unions: 9 - 32 months.

Number of surgical interventions: 2 - 7 times with autogenous bone grafting. X-ray: before, 3 and 6 months after treatment; Laboratory testing: Calcium, Phosphorus, alkaline phosphatase, bone specific alkaline phosphatase, Vitamin D, tartrate resistant alkaline phosphatase 5b before and after 3 weeks of treatment.

Treatment: 2 months rh PTH 1- 34 (Forsteo®) 20µg subcutaneously once daily.

Results: In all cases except one a fracture healing could be observed. Radiological signs of fracture healing were usually detected after 3 months. Calcium levels did not increase. Changes in the markers of bone turnover were inconsistent.

Conclusion: 2 months administration of 20 µg recombinant parathyroid hormone 1 - 34 seems to induce stable consolidation of the bone in non-unions and delayed healing of bone fractures despite inconsistent changes in bone turnover markers. Therefore PTH could be an alternative option in the treatment of non healing fractures of long bones.

Disclosures: Hans-Christof Schober, None.

MO0131

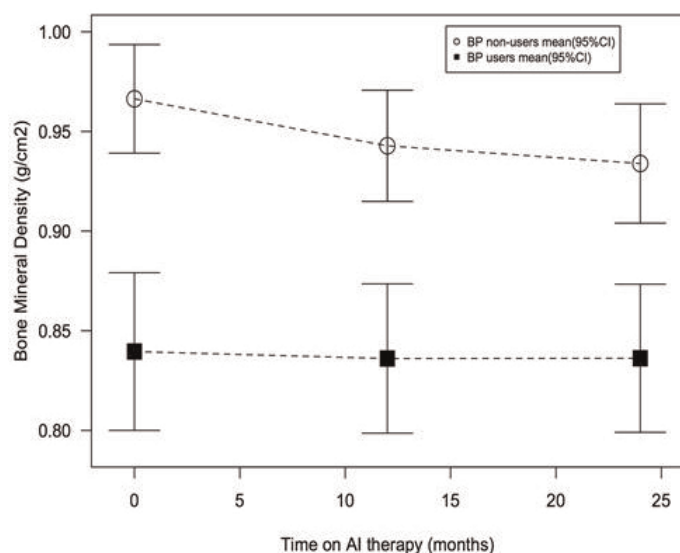
Bone Loss in the B-ABLE Clinical Cohort of Women Completing Aromatase Inhibitor 2-year therapy after Tamoxifen: Patterns and Determinants. Daniel Prieto-alhambra^{*1}, Sonia Servitja², Laia Garrigos², Elisa Torres³, Maria Martinez-Garcia², Joan Albanell², Adolfo Diez-Perez⁴, Ignasi Tusquets², Xavier Nogues⁴. ¹Institut Municipal D'Investigacio Medica, Spain, ²Medical Oncology Department, Breast Cancer Unit. Molecular Therapeutics & Biomarkers in Breast Cancer, Cancer Research Program, IMIM-Hospital del Mar, Autonomous University of Barcelona, Barcelona, Spain, ³Department of Internal Medicine, URFOA IMIM-Hospital, RETICEF(Red Tematica de Investigacion Cooperativa en Envejecimiento y Fragilidad), Instituto Carlos III, Barcelona, Spain del Mar, Parc de Salut Mar, Autonomous University of Barcelona, Spain, ⁴Department of Internal Medicine, URFOA IMIM-Hospital del Mar, Parc de Salut Mar, Autonomous University of Barcelona, RETICEF(Red Tematica de Investigacion Cooperativa en Envejecimiento y Fragilidad), Instituto Carlos III, Barcelona, Spain, Spain

PURPOSE Aromatase inhibitors (AI) are first-line agents in hormone-positive early breast cancer. Data on AI-related bone loss is scarce, and comes mostly from randomised clinical trials. We aimed to quantify and to determine the predictors of bone loss after a pre-specified 2-year AI therapy, in the B-ABLE prospective clinical cohort.

METHODS We recruited in our hospital (Oncology and Bone Metabolism Units, Parc de Salut Mar, Barcelona (Spain)) a consecutive sample of women eligible to switch from tamoxifen to AI therapy. BMD was measured at baseline and yearly using DXA. Serum 25-hydroxy-vitamin D levels (25(OH)D) were assessed at baseline, 3 months and 1-year. Patients started on Exemestane or Letrozole according to current guidelines. Participants with osteoporosis or a T-score <-2.0 with fracture risk factors were started on bisphosphonates. All received daily vitamin D3 (800 IU) with calcium, and women with baseline 25(OH)D<30 ng/ml received additional 8,000 IU D3 weekly. Paired T-test was used to quantify bone loss. Multivariate regression models were fitted to determine predictors of bone loss (adjusted for BMI, radio and chemotherapy, baseline 25(OH)D and age). All the analyses were stratified on bisphosphonate use (BPU).

RESULTS To date 85 participants have completed the pre-specified 2-year AI therapy: 56(65.9%) Exemestane, 29 (34.1%) Letrozole. Bisphosphonates were given to 31(36.5%). Bisphosphonate non-users (BPNU) experienced a significant bone loss vs. baseline throughout the 2-years follow-up (3.36% [95%CI 2.00% to 4.71%; p<0.001], which occurred mainly in the first year: 2.37% [1.19% to 3.56%; p<0.001]. BPU showed non-significant bone loss: 0.14% [-2.10% to 2.38%;p=0.70]. (see Fig 1) Type of AI was predictive of bone loss at year 1 (adjusted beta (ab) for letrozole vs exemestane 2.74, p=0.011) but not at year 2. Serum 25(OH)D levels at month 3 were predictive of bone loss both at years 1 and 2: ab per 10ng/ml -0.69 (p=0.003) and -0.49 (p=0.043) respectively. Years since menopause predicted 2-year bone loss: ab per year -0.54 (p<0.001).

CONCLUSIONS Bisphosphonate non-users experience a significant decline in BMD, which is highest in the first year of AI therapy. BPU prevents this. Vitamin D repletion reduces bone loss in BPNU.



BMD at baseline and after 2 years on AI therapy: bisphosphonate users and non-users.

Disclosures: Daniel Prieto-alhambra, None.

MO0132

CT-based Rigidity Analysis Affects Treatment of Patients with Appendicular Metastasis. Ara Nazarian^{*1}, Vahid Entezari¹, Robert Turcotte², Megan Anderson¹, Albert Aboulafia³, Patrick Lin⁴, Edward Cheng⁵, Richard Terek⁶, Mark Gebhardt¹, Timothy Damron⁷, Brian Snyder⁸. ¹Beth Israel Deaconess Medical Center, USA, ²McGill Medical Centre, Canada, ³Sinai Hospital, USA, ⁴MDACC, USA, ⁵UMN, USA, ⁶RI hospital, USA, ⁷State University of New York Upstate Medical University, USA, ⁸Children's Hospital Boston/Harvard Medical School, USA

INTRODUCTION: Clinicians make subjective assessments regarding fracture risk using clinical and radiographic guidelines that are sensitive but poorly specific. We have developed and validated a CT-based method to monitor the fracture risk associated with metastatic lesions. This study aims to evaluate whether patient's treatment based on clinical and radiographic guidelines was changed by CT-based Structural Rigidity Analysis (CTRA).

PATIENTS AND METHODS: Patients with uni/bilateral metastasis to appendicular skeleton were enrolled prospectively into the study. Biplanar radiographs and transaxial CT scans (with hydroxyapatite phantom) of involved bones were obtained on all patients. The orthopedic oncologist was asked to select a treatment (observation, chemotherapy, radiation, surgical stabilization, intercalary allograft and/or prosthetic replacement) based on the fracture risk assessment using Mirels score and then again after CTRA.

RESULTS: 86 patients (male/female= 0.86, Age =60.3 ±14.4) with metastasis to appendicular skeleton were enrolled into the study. Lung, breast, multiple myeloma,

kidney and prostate were major sources of metastasis. There were total of 100 lesions of the femur, humerus, acetabulum and clavicle which 62% were lytic, 28% were mixed and the rest was blastic in nature. The median total Mirels score for the lesions was 9 (range:7-12). Considering the full range of treatments options, CTRA would have changed the initial treatment plan in 26% (n=21) of the times. Based on the Mirels criteria alone (Score <9), 68% of lesions (n=55) were at high risk for fracture. According to physicians' initial judgment, 44% of these lesions (n=36) needed surgical fixation, while CTRA alone recommended surgery in 40% (n=33) of lesions.

DISCUSSION: The results suggest that more than 25% of the clinical treatment recommendations would potentially be altered by use of CTRA. Treatment plans were similar in cases where there was either marked bony destruction or minimal bone involvement.

Disclosures: Ara Nazarian, None.

MO0133

Curcuminoids Decrease Osteolytic Breast Cancer Bone Metastases Separate from Effects on Tumor Cell Growth. Laura Wright^{*1}, Theresa Guise², Khalid Mohammad², Janet Funk³. ¹The University of Arizona, USA, ²Indiana University, USA, ³University of Arizona Health Sciences Center, USA

Curcuminoids are polyphenolic compounds isolated from the rhizome of turmeric (*Curcuma longa* L.), a botanical commonly used in Ayurvedic medicine. We previously found that curcuminoid-containing turmeric extracts inhibited osteoclast-mediated bone resorption in a translational model of rheumatoid arthritis and prevented rheumatoid synovocyte expression of parathyroid hormone-related protein (PTHrP), a bone-resorptive peptide in rheumatic joints. Because PTHrP is also a critical breast cancer-derived mediator of lytic bone metastases, curcuminoid effects on osteolytic breast cancer bone metastases were tested. Four-week old female nude mice (n = 11/group) were inoculated with MDA-MB-231 cells (1 x 10⁵) into the left cardiac ventricle and treated ip every other day with a curcuminoid-enriched extract (25 mg curcuminoids/kg/dose) or vehicle. Evidence of lytic bone lesions in the hind limbs was evaluated prospectively for 3 weeks by x-ray. Curcuminoid-treated mice had significantly less osteolytic bone lesion area compared to vehicle-treated mice (2.0 ±1.0 mm² vs. 11.1 ±2.1 mm²; p < 0.05). In a separate study, four-week old female nude mice were inoculated with MDA-MB-231 cells (1 x 10⁶) into the left mammary fat pad. Using an identical dosing regime, orthotopic tumor volume was not significantly reduced by curcuminoid treatment relative to vehicle-treated mice (500 ±85 mm³ vs. 769 ±120 mm³; p > 0.05) in four-week old female nude mice (n = 7/group). *In vitro*, when MDA-MB-231 cells were pre-treated with curcuminoids (0.3-10 mg/ml) and stimulated with TGF-β (5 ng/ml) for 24 hours, PTHrP secretion, as measured by radioimmunoassay, was inhibited by curcuminoids (IC₅₀ = 2.1 mg/ml) independent of effects on cell proliferation and survival. These initial data suggest that curcuminoids may decrease lytic bone metastases in breast cancer through inhibition of breast cancer cell expression of PTHrP.

Disclosures: Laura Wright, None.

MO0134

Effect of Exercise on Bone Strength, Body Composition and Physical Performance in Breast Cancer Patients- A 12-month RCT. Riku Nikander^{*1}, Harri Sievanen², Katriina Ojala³, Pirkko-Liisa Kellokumpu-Lehtinen⁴, Tiina Palva⁵, Carl Blomqvist⁶, Riitta Luoto³, Tiina Saarto⁶. ¹Metropolia University of Applied Sciences, Helsinki, Finland, Finland, ²UKK Institute, Finland, ³UKK Institute for Health Promotion Research, Finland, ⁴Tampere University Hospital, Finland, ⁵Pirkanmaa Cancer Society, Finland, ⁶Helsinki University Central Hospital, Finland

Breast cancer is the most common malignant disease of women in Western countries. This 12-month randomized controlled examiner-blinded trial aimed to explore whether vigorous aerobic exercise could facilitate survivors' recovery from breast cancer by enhancing their body composition, physical performance and bone strength.

A total of 86 patients were randomly assigned into the training or control group after the adjuvant chemo- and/ or radiotherapy. Body composition and bone traits were assessed by DXA and pQCT. Physical performance was also assessed. Training effects on outcome variables were estimated by ANCOVA.

While bone loss occurred in both groups, bone strength was better maintained among the trainees. At the femoral neck, the distribution of trainees' bone mass

remained unchanged in contrast to controls who lost bone from their upper region of the femoral neck (2%, $p < 0.05$). In addition, the total cross-sectional area and bone structural strength improved 1% and 2% compared to controls among the postmenopausal trainees at the tibial diaphysis ($p < 0.05$). Small positive training effects of physical performance were observed in agility (between-group difference 3%, $p < 0.05$).

In conclusion, a 12-month vigorous aerobic exercise training regimen helped to maintain bone structural strength and slightly improved physical performance of breast cancer patients.

Disclosures: Riku Nikander, None.

MO0135

Osteocyte-derived FGF23 Stimulates Klotho-Positive Prostate Cancer Cells.

Pierrick Fournier^{*1}, Erik Imel², Daniel Edwards¹, James Knight¹, Noah Hahn¹, John Chirgwin¹. ¹Indiana University, USA, ²Indiana University School of Medicine, USA

Prostate cancers metastasize to bone more frequently than other solid tumors, often causing osteoblastic responses via local interactions with the bone microenvironment. Bone is the sole source of fibroblast growth factor 23, an endocrine hormone that acts on kidney cells expressing its receptor (klotho+FGFR1) to increase the transcription factor EGR1 and alter metabolism of vitamin D. This pathway normally controls kidney handling of phosphate. Expression of klotho by other tumor types has been reported, suggesting FGF23 might act on bone-metastatic prostate cancers.

Eight human prostate cancer lines tested all expressed mRNAs for klotho & FGFR1iic. DU145 cells, which cause bone lesions in nude mice, were treated with 100ng/ml recombinant human FGF23 and analyzed by real-time PCR ($n=3$). EGR1 mRNA increased 3 X at 1hr ($p < 0.0001$) and returned to baseline after 2 hrs. Expression of mRNAs encoding the vitamin D-inactivating 24-hydroxylase, CYP24A1 and TRPV6 Ca channel increased 2X at 2 hrs ($p < 0.05$) and returned to baseline by 4 hrs. Two other early-response genes, CTGF & Cyr61, were significantly increased by FGF23. Parallel results were seen with C4-2B cells, where treatment with 100ng/ml FGF23 for 6 days increased cell number by 40% ($p < 0.05$) in the face of growth-inhibiting concentrations of 1,25-dihydroxyvitamin D3. This response was not seen with MDA-MB-231 breast cancer cells, which have very low klotho expression. FGF23/klotho signaling may contribute to tumor growth in bone through targets downstream of EGR1, such as Cyp24A1 & TRPV6, which regulate prostate cancer responsiveness to 1,25-dihydroxyvitamin D3.

Following case reports of altered FGF23 concentrations in patients with prostate cancer, we measured circulating intact FGF23 in bisphosphonate-naïve prostate cancer patients: 27 with bone metastases, and 12 without. Serum FGF23 concentrations did not differ between groups: 32.5 19.1 in the bone metastasis group and 39.0 20.7 in the group without bone metastases ($p=0.35$).

The data suggest that a local FGF23/klotho/EGR-1 axis may be active in prostate cancer bone metastases, where signaling could alter tumor growth and vitamin D resistance. FGF23 binding to klotho on prostate cancer cells may provide a novel target for therapeutic intervention against bone metastases.

Disclosures: Pierrick Fournier, None.

MO0136

Runx2 ChIP-seq. Gillian Little*, Ben Berman, Sanjeev Baniwal, Gerhard Coetzee, Baruch Frenkel. University of Southern California, USA

Runx2 plays important roles in both bone and cancer biology. In bone, it controls both osteoblastogenesis and osteoblast-driven osteoclastogenesis. In cancer, attention has increasingly moved to the role of Runx2 in bone metastasis. Runx2 is subjected to multiple negative feedback mechanisms, whereby its expression and activity are inhibited in response to its own activation. These self-limiting mechanisms impede the detection of Runx2 DNA-binding and stimulation of target genes in living cells that are not synchronized for Runx2 activation. To overcome this experimental impediment, we transduced mesenchymal stem cells, primary osteoblasts, breast cancer and prostate cancer cells with lentiviruses encoding Doxycycline (Dox)-inducible Runx2. Dox treatment resulted in synchronous activation of Runx2 and robust stimulation of target genes. In C4-2B prostate cancer cells, Dox treatment resulted in expression of Runx2 to levels seen in more aggressive metastatic cells such as PC3, reaching a steady state at 12h. Despite this, Runx2 chromatin immunoprecipitation (ChIP) assays at known Runx2-occupied regions (R2ORs) demonstrated cyclical recruitment of Runx2 with a periodicity of about 4h (Figure 1). We selected the 20h time point to capture what is to our knowledge the first true genome-wide Runx2 DNA-binding landscape in living cells. Massively parallel sequencing of the Runx2 ChIP (ChIP-seq) revealed 5,413 robust and highly significant R2ORs, many of which were located close to genes we identified by expression microarray analysis as differentially regulated by Runx2 in C4-2B cells. These include known R2ORs near the *CSF2* and *KLK2* genes, and novel regions including those near *WNT4*, *TCF7L2*, *LRP6*, *GSK3B*, *WISP1*, *WIF1*, *DKK2*, *TGFB2*, *TGFBR3*, *IGF2R*, *DLX1*, *BMP6*, *FGF13*, *PIP* and *RUNX1* genes (see Figure 2 for examples). Less than 5% of R2ORs were within 2kb of a transcription start site and more than 90% were located within introns or intergenic regions, suggesting Runx2 likely occupies predominantly enhancer and not promoter regions. Functional annotation analysis of R2ORs revealed significant enrichment in cell motility and migration pathways and motif analysis using several methods revealed RUNX as the strongest of several very highly

enriched motifs within R2ORs. High throughput characterization of Runx2 genomic occupancy and activation of target genes will open new avenues in understanding the role of this transcription factor in both cancer and bone biology.

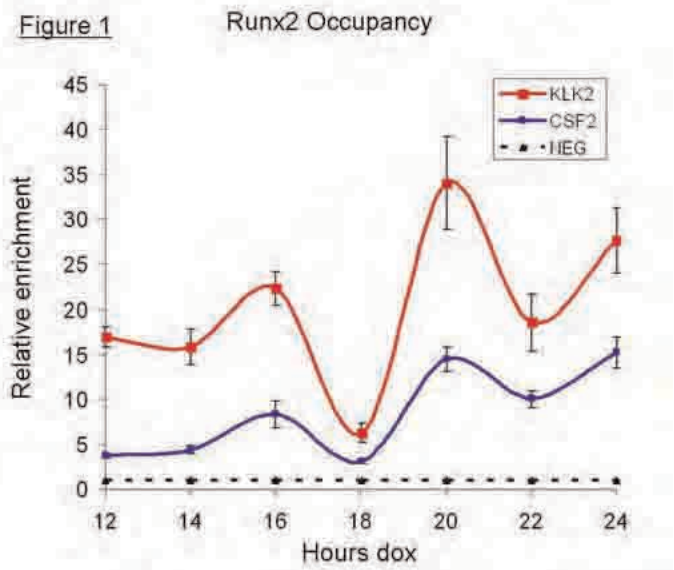


Figure 1

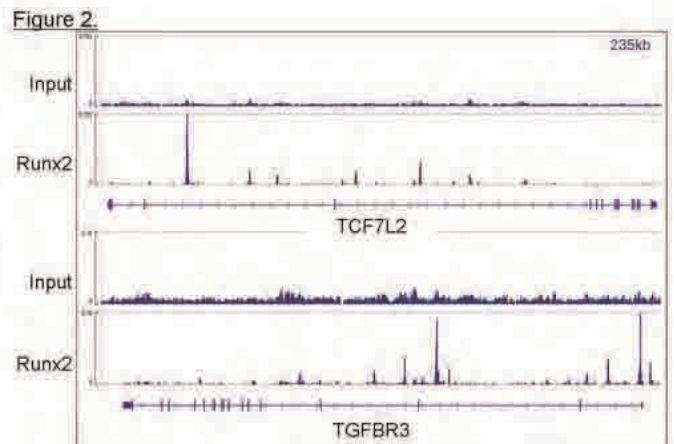


Figure 2

Disclosures: Gillian Little, None.

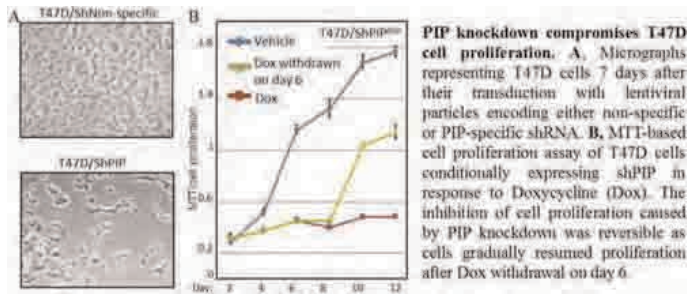
MO0137

Runx2 Controls a Positive Feedback Loop between Androgen Signaling and Prolactin-induced Protein (PIP) in promoting T47D Cell Proliferation.

Sanjeev Baniwal*, Gillian Little, Nyam-Osor Chimgé, Baruch Frenkel. University of Southern California, USA

PIP is a small polypeptide expressed by advanced breast and prostate cancer (BCa, PCa) cells. However, both the regulation of PIP expression and its function in cancer cells are poorly understood. Using breast and prostate cancer cells, we found that Runx2, a pro-metastatic transcription factor, functionally interacts with the Androgen Receptor (AR) to regulate PIP expression. In C4-2B/Rx2^{dox} and LNCaP/Rx2^{dox} PCa cells, Doxycycline (Dox)-induced Runx2 synergized with AR to promote PIP expression. In T47D BCa cells, which express endogenous Runx2 and PIP, basal as well as hormone stimulated PIP expression was abrogated by shRNA-mediated Runx2 knockdown. Chromatin immunoprecipitation (ChIP) assays showed that Runx2 and AR occupied an enhancer element located ~11kb upstream of the PIP open reading frame, and that Runx2 facilitated AR recruitment to the enhancer. Dox-induced PIP knockdown using shRNA arrested proliferation that was driven by either a mixture of serum growth factors or dihydrotestosterone (DHT) alone. PIP knockdown compromised DHT-stimulated expression of multiple AR target genes including PSA, FKBP5, FASN, and SGK1. The inhibition of AR activity due to loss of PIP was attributable at least in part to abrogation of its nuclear translocation. Our data suggest that Runx2 controls a positive feedback loop between androgen signaling and PIP in promoting carcinogenesis. PIP may explain at least in part the oncogenic properties of AR and Runx2, and pharmacological inhibition of PIP may offer a novel therapeutic approach for the treatment of a subset of prostate and breast cancer

patients.



Runx2 Regulates PIP

Disclosures: Sanjeev Baniwal, None.

MO0138

The Vitamin D Receptor has a Ligand-Independent Role in Human Breast Cancer Cell Growth. Trupti Trivedi¹, Yu Zheng¹, Li Laine Ooi¹, Colette Fong-Yee¹, Colin Dunstan², Markus Seibel¹, Dr. Hong Zhou¹. ¹Bone Research Program, ANZAC Research Institute, The University of Sydney, Australia, ²University of Sydney, Australia

We have previously reported that vitamin D deficiency promotes human breast cancer growth in murine bone. While this effect seems to be mediated mainly through the bone micro-environment, vitamin D and the vitamin D receptor (VDR) may also have direct actions on cancer growth in bone. The current study aimed to define the role of the VDR in human breast cancer growth *in vitro* and *in vivo*.

Using stable shRNA expression, VDR expression was knocked down by 85% and 80% in MDA-MB-231 (MDA-VDRshRNA) and MCF-7 (MCF7-VDRshRNA) cells, respectively. Non-target (NT) cells served as controls. The induction of CYP24 mRNA expression by 1,25(OH)2D3, normally seen in VDR expressing cells, was completely abrogated in VDR-knock-down cells, indicating effective disruption of VDR signaling.

Compared to untreated NT cells, treatment of MDA-NT and MCF7-NT cells with 10⁻⁸ M 1,25(OH)2D3 significantly reduced cell growth by 37% and 48%, resp., and induced a 2 to 3-fold increase in apoptosis. Surprisingly, MDA-VDRshRNA and MCF7-VDRshRNA cells also exhibited reduced growth rates (-40% & -53%, resp.) and increased apoptosis (6 to 7-fold) compared to the corresponding NT cells cultured in ligand free conditions. Treatment of either knockdown cell line with 1,25(OH)2D3 treatment had no effect on growth or apoptosis. In MDA-VDRshRNA cells, the reduced cell growth was associated with decreased β -catenin protein and its target gene, cyclin D1, when compared to MDA-NT cells.

To investigate tumor growth *in vivo*, MDA-VDRshRNA and NT cells were xenografted orthotopically into the mammary fat pad of nude mice. Again, VDR knockdown significantly reduced tumor growth from day 12 onwards. At day 33 post implantation, tumour weight was reduced by 40% and apoptosis was significantly increased in VDRshRNA compared to NT tumours ($p < 0.05$). Similarly when MDA-NT and VDRshRNA cells were implanted into the tibiae of nude mice, lytic lesion size at endpoint (day 21) was significantly smaller in mice implanted with VDRshNA than with NT cells ($p < 0.05$).

We conclude that the VDR has ligand-independent functions in regulating breast cancer cell growth which contrast its ligand-dependent, anti-proliferative and pro-apoptotic effects. It appears that the ligand-independent actions of the VDR are mediated through the β -catenin signalling pathway.

Disclosures: Trupti Trivedi, None.

MO0139

Treatment with Interleukin 6 Receptor Antibodies Inhibits Prostate Cancer Growth in a Murine Model of Bone Metastasis. Dennis Basel¹, Yu Zheng², Julian Kelly¹, Frank Buttgerit³, Robert L Sutherland⁴, Colin Dunstan⁵, Dr. Hong Zhou⁶, Markus Seibel⁶. ¹ANZAC Research Institute, the University of Sydney, Australia, ²Bone Research Program, ANZAC Research Institute, The University of Sydney, Australia, ³Department of Rheumatology & Clinical Immunology, Charite University Medicine (CCM), Germany, ⁴Cancer Research Program, Garvan Institute of Medical Research, Australia, ⁵University of Sydney, Australia, ⁶Bone Research Program, ANZAC Research Institute, The University of Sydney, Australia

In patients with metastatic prostate cancer, high circulating interleukin-6 (IL-6) levels have been associated with disease progression and poor prognosis. In human prostate cancer cells, expression of IL-6 has been linked to a more aggressive phenotype and progression of hormone refractory prostate cancer. We previously demonstrated a correlation between increasing or decreasing bone resorption activity and corresponding changes in metastatic tumor IL-6 expression and tumor growth in

murine models of breast and prostate cancer. These data indicate that IL-6 may play a role in metastatic cancer growth in bone. In the present study, we investigated the effect of the IL-6 on human prostate cancer growth *in vitro* and *in vivo*.

In vitro studies: Treatment of the human prostate cancer cell line, PC3, with RANKL up-regulated IL-6 mRNA expression 2-fold within 4 hrs. Interestingly, treatment of PC3 cells with IL-6, in turn, increased RANK expression 2-fold, and PTHrP expression 4-fold. The effects of IL-6 on RANKL expression were blocked by treatment of PC3 cells with the anti-human IL-6 receptor (IL-6R) antibody, tocilizumab (Tmab). These data suggest that RANKL, IL-6 and RANK (or PTHrP) may form a "feed-forward" loop that promotes cancer growth in bone.

In vivo studies: PC3 cells were implanted intra-tibially into five week-old BALB/c nu/nu male mice. Mice were then randomized into 2 groups (n= 8 each), receiving either Tmab (50mg/kg/3d) or vehicle. Zoledronic acid (ZA) was co-administered at a dose of 100 μ g/kg every 3 days in a subset of mice (n=8) to determine the contribution of the bone microenvironment to tumor growth. Tibiae were monitored by X-ray imaging on days 17, 24 and 30 (sacrifice). Compared to controls, treatment with Tmab significantly inhibited radiographic osteolysis from d17 onwards (d17: 0.110.04 vs. 0.370.10 mm²; d24: 0.440.13 vs. 0.900.14 mm²; d30: 0.800.24 vs. 1.460.22 mm², $p < 0.05$). Co-treatment with ZA completely prevented osteolysis.

As tumor-derived IL-6 increased tumor cell RANK expression, and bone-derived RANKL increased tumor cell IL-6 expression, the inhibitory effects of Tmab on tumor growth may be due to the interruption of a "feed-forward" loop between tumor and bone cells which involves RANKL, IL-6 and RANK (or PTHrP). Our data indicate that IL-6 plays an important role in the metastatic growth of prostate cancer cells in bone and may be a potential therapeutic target in prostate cancer bone metastasis.

Disclosures: Markus Seibel, None.

MO0140

TWIST WR/Runx Domain Synergizes NF- κ B Activity and Promotes Cellular Invasiveness through IL-8 Production. Karen Aboody¹, Shan Li², Raquel Raices³, Stephen Kendall⁴, GINA LOWE⁵, Carlotta Glackin⁶. ¹City of Hope Medical Center, USA, ²Beckman Research Institute Graduate School, USA, ³Stem Cell Technologies, USA, ⁴Fluidigm, USA, ⁵CITY OF HOPE/BECKMAN RESEARCH INSTITUTE, USA, ⁶Beckman Research Institute at City of Hope, USA

Metastasis is the major cause of mortality among cancer patients. One potential mechanism of metastatic spread centers the concept of epithelial-to-mesenchymal transition (EMT). In adenocarcinomas, EMT describes the processes that differentiated cells lose epithelial features, acquire mesenchymal properties and attain the ability to invade the basement membrane, leading to dissemination of cancer cells. More recently, tumor cells undergoing EMT were also reported to display stem cell-like phenotype, which relates EMT to the cellular potential of tumor relapse and metastatic re-growth. Multiple EMT regulators identified to date are primarily based on their ability to repress E-cadherin expression, a hallmark of EMT. Many of these regulators have a role in early morphogenesis, such as Zeb2, Snail and the master regulator of mesenchymal lineages, Twist, emphasizing the important role of EMT in the pathology of metastasis.

Here we describe the unique property of the C-terminal WR/Runx domain of Twist in mediating NF- κ B activation and breast cancer cell invasion through the expression of interleukin 8 (IL8). We discovered that IL8 production is induced by Twist expression in a cis-binding independent mechanism. In this mechanism, Twist activates the IL8 promoter by stimulating and synergizing NF- κ B transcriptional activity through interactions of NF- κ B subunit RELA with the WR protein binding domain. Activated NF- κ B exhibits enhanced IL8 promoter binding affinity, leading to increased IL8 cytokine production. Finally, we demonstrate that the IL8 autocrine pathway in breast cells increases cellular invasiveness by promoting production and activation of metalloproteinases. Given the important roles of NF- κ B in cancer progression, as well as the many significant functions of IL8 in angiogenesis, chemotaxis, proliferation and invasion, Twist-expressing cells can indirectly activate and synergize a series of complex biological responses through the WR domain among cancer cells, in addition to the immune and circulatory system, thereby triggering cancer cell dissemination.

In order to test the therapeutic role of Twist inhibition of IL-8 in metastasis, Soluble Twist Inhibitors (STIs) are being evaluated as novel therapeutics to selectively reduce tumor cell invasion, allowing progression toward a normal differentiated or apoptotic phenotype. The impact of STIs as novel therapeutics may serve as proof-of-principle for reducing aggressive tumor metastases *in vivo*.

Disclosures: Carlotta Glackin, None.

MO0141

VEGFR3 Expression in Human Breast Cancers and Effects of VEGFR3 Antibody in a Mouse Model of Metastatic Breast Cancer. Yoshikazu Morita¹, Lei Shu², Kristina Subik², Ping Tang², Brendan Boyce², Lianping Xing¹. ¹University of Rochester, USA, ²University of Rochester Medical Center, USA

VEGF-mediated angiogenesis plays an important role in cancer development and metastasis. The VEGF family contains multiple members, including VEGF-A, B, C,

and D. VEGF-C and D are growth factors for lymphatic endothelium and signal through VEGFR3, a receptor specific for VEGF-C and D. Breast cancer cells and osteoclasts express high levels of VEGF-C, which could have a role in bone metastasis. However, the VEGF-C/VEGFR3 system has not been investigated in breast cancer bone metastasis. Here, we examined VEGFR3 expression using immunohistochemistry in a tissue microarray containing cores from breast cancer and normal breast tissue from 116 patient samples. We found that most breast cancer samples (70%; 84/116 cases) are VEGFR3 positive, while normal breast tissue is mainly negative (87%, 96/110 cases). VEGFR3 expression correlated positively with estrogen receptor (ER+ or ER+/PR- (progesterone receptor) expression status, tumor type, and lymph node metastasis compared to VEGFR3 negative tumors, i.e. ER+: 56% vs 26%; ER+/PR-: 73% vs 27%; infiltrating ductal carcinoma: 74% vs 26%; lymph node metastasis: 87% vs 13%. Furthermore, VEGFR3 positive staining correlated with tumor size (<1 cm: 26% positive vs 74%, 1-2 cm: 81% vs 19%, >2cm: 80% vs 20% in VEGFR3-negative tumors). To examine the effect of VEGFR3 blockade on breast cancer bone metastasis, we injected MDA-MB-231 cells, which express high levels of VEGF-C, into the left vehicle of nude mice. The mice were given VEGFR3 neutralizing antibody (VEGFR3 NA) (0.8mg/mouse, twice a week, ip) for 4 weeks, a regime that inhibits lymphangiogenesis around inflamed joints of TNF transgenic mice. We found that mice that given VEGFR3 NA were healthier and heavier (body weight: 21+2g vs 19+1) than mice given IgG control. They also had a lower death rate than the IgG-treated mice (# dead: 1/9 vs 4/6). However, X-ray and histology indicated that VEGFR3 NA did not affect the number and size of bone metastases or bone volume in recipient mice. In summary, 1) most breast cancers express VEGFR3; 2) VEGFR3 expression is positively associated with ER status, tumor size and lymph node metastases; 3) VEGFR3 blockade improves the general health and survival of tumor-bearing mice. Thus, VEGFR3 is a potential prognostic indicator for breast cancer, and further studies are warranted to determine how VEGFR3 blockade improves survival of tumor-bearing mice if it reduces bone metastases in combination with other anti-cancer treatments.

Disclosures: Yoshikazu Morita, None.

MO0142

Vertebral Fractures and Trabecular Microstructure in Men with Prostate Cancer on Androgen Deprivation Therapy. Julie Wagner*, Karen Vujevich, Megan Miller, Subashan Perera, Joel Nelson, Neil Resnick, Susan Greenspan. University of Pittsburgh, USA

Background: Although bone mineral density (BMD) assessed by conventional dual energy x-ray absorptiometry (DXA) is the gold standard to determine fracture risk, BMD does not assess for vertebral fractures (VF). High resolution microMRI (HR-MRI) assesses bone microarchitecture and may provide additional information in men with VF. Androgen deprivation therapy (ADT), a common treatment for prostate cancer, is associated with bone loss and fractures.

Methods: To determine if identification of VF increased the diagnosis of osteoporosis beyond BMD and if HR-MRI demonstrated skeletal deterioration in men with VF, we enrolled 137 men ≥ 60 years with nonmetastatic prostate cancer on ADT for ≥ 6 months. BMD of the spine and hip were assessed by DXA. Vertebral fracture assessment (VFA) by DXA was confirmed with conventional lateral x-ray and classified by Genant criteria (mild, moderate, severe VF). HR-MRI of the wrist included bone volume to total volume (BV/TV), surface density (trabecular plates), surface/curve ratio (plates/rods) and erosion index (higher depicts deterioration).

Results: Silent (unknown) VF were found in 37% of men. The duration of ADT was associated with lower BMD at the spine ($r = -0.21$), total hip ($r = -0.20$), and 1/3 distal radius ($r = -0.32$, all $p < 0.05$). 7% of total participants were classified as having osteoporosis by BMD. 37% of men without osteoporosis by BMD had VF identified by VFA and conventional x-rays. This suggests that 82% of patients with clinically defined osteoporosis would have been misclassified by BMD alone. By ANOVA comparison across VF grades, the BV/TV was lower, surface density was lower and erosion index was higher in men with moderate-severe VF compared to lesser grades (Table, all $p < 0.05$). Conventional BMD at the spine, hip and 1/3 distal radius were also significantly lower ($p < 0.05$) in men with the more severe grade of VF ($p < 0.05$). Indices of HR-MRI were associated with BMD at the ultra distal radius ($r = 0.46-0.65$, $p < 0.01$), total hip ($r = 0.34-0.49$, $p < 0.01$) and some with spine ($r = 0.22-0.37$, $p < 0.05$).

Conclusions: ADT for men with prostate cancer is associated with silent VF in 37% of men. Measurement of BMD alone leads to misclassifications of osteoporosis which can be avoided by assessment for VF. HR-MRI provides a novel technique to assess the deterioration of structural integrity in men with VF and adds additional information to conventional BMD.

	No Vertebral Fracture	Mild Vertebral Fracture	Mod-Severe Vertebral Fracture
N	86	41	10
Age (years)	73.5 \pm 0.8	74.2 \pm 1.1	79.7 \pm 2.1
BMI (kg/m ²)	29.6 \pm 0.4	29.7 \pm 0.8	28.7 \pm 1.4
Duration ADT (months)	47.3 \pm 5.6	49.5 \pm 7.8	63.6 \pm 18.0
PSA (ng/mL)	2.0 \pm 0.5	4.4 \pm 2.5	1.5 \pm 0.5
BMD(g/cm ²)			
PA spine*	1.118 \pm 0.019	1.120 \pm 0.031	0.964 \pm 0.065
Total hip*	0.957 \pm 0.014	0.967 \pm 0.020	0.847 \pm 0.046
Femoral neck*	0.782 \pm 0.013	0.771 \pm 0.020	0.668 \pm 0.038
1/3 Distal radius*	0.739 \pm 0.009	0.760 \pm 0.013	0.670 \pm 0.043
High Resolution MicroMRI			
BV/TV (%) *	12.877 \pm 0.264	12.938 \pm 0.293	10.950 \pm 0.520
Surface density*	0.062 \pm 0.002	0.062 \pm 0.002	0.050 \pm 0.003
Surface/curve*	11.015 \pm 0.554	11.039 \pm 0.630	7.774 \pm 0.886
Erosion index*	0.884 \pm 0.029	0.866 \pm 0.032	1.070 \pm 0.066
Results as mean \pm SEM, * $p < 0.05$, # $p < 0.1$, ANOVA across VF grades			

Table

Disclosures: Julie Wagner, None.

This study received funding from: US Department of Defense

MO0143

10 Years of Balloon Kyphoplasty in Malignant Vertebral Body Lesions - Critical Analysis of Benefits and Complications. Dr. Max Markmiller*. Klinikum Kempten, Germany

Purpose of the study: Affection of the spine by metastases threatens the patients with pain, loss of mobility and neurologic defects. Treatment options have to meet concerns of the short term prognosis, the limited operability and should allow quick mobilisation and short hospital stay. An answer is the minimally-invasive percutaneous augmentation of the vertebra by CT – guided dilatation and injection of bone cement (methylmethacrylate). Benefits are immediate mobilization after the procedure, minimized surgical trauma and no need of an additional orthosis. Cement leakage rates are increased compared to kyphoplasty procedures of osteoporotic fractures, but no oncologic patient required a surgical revision.

Methods: The patients were documented prospectively by ASA – Score, Karnovsky – Index, Visual Analog Scale (VAS) and Oswestry Disability Index (ODI). Percutaneous kyphoplasty was guided with CT and combined with fluoroscopy. All patients were aftertreated functionally with early mobilisation. Epidural tumor involvement was no contraindication.

Results: From 05/2000 to 05/2011 out of 1117 kyphoplasties 115 patients with metastatic lesions were treated. The localisation favorites the thoracolumbar junction. The subjective evaluation using the VAS showed a decrease of the pain level of 60 % in 80% of the patients. All patients were mobile without orthosis after the procedure. The clinical and radiological followups after 6 and 12 months confirmed the good results in the ODI however 24 patients had died in between. Radiologically, all survivors showed an unaltered mechanical sufficient bone cement material. The complication rate is on the lower limit of the literature, but increased compared to kyphoplasty procedures of osteoporotic fractures. Complications refer to paravasations of the bone cement (40 patients, 35 %): eight patients showed temporary radiculopathy, 31 patients with intervertebral, vascular or paravertebral paravasation stayed asymptomatic. 9 patients showed epidural paravasation without neurological impairment, no oncologic patient required surgical revision.

Conclusion: Percutaneous kyphoplasty is an excellent method of palliation for pain relief and mobility in oncologic patients with cancer metastases of the spine.

Disclosures: Dr. Max Markmiller, None.

MO0144

A New Murine Model of Medulloblastoma Bone Metastasis. Jessica Grunda*, James Mobley, Gregory Clines. University of Alabama at Birmingham, USA

Purpose: Medulloblastoma is the most commonly diagnosed pediatric primary brain neoplasm, comprising 20 to 25% of all childhood CNS tumors. Approximately 13% of these patients will develop extra-neural brain metastases, of which bone is the most prevalent site of metastasis (84%), followed by bone marrow (27%), lymph nodes (15%), lung (6%), and liver (6%). Although recent meta-analyses indicate that these extra-CNS metastases significantly diminish patient survival, response to therapy and quality of life, no studies exist investigating mechanisms underlying medulloblastoma extra-neural metastasis or treatment, highlighting the critical need for research in this area. The purpose of the herein described study was to generate and characterize murine models of medulloblastoma bone metastasis, which would greatly facilitate the elucidation of new treatment strategies.

Methods: The human DAOY and D283 Med medulloblastoma cell lines were inoculated into the intratibial space of athymic nude mice. Development of bone metastases and tumor burden were monitored through radiographic imaging and quantified by computerized image analysis. Total bone area, tumor area, osteoclast and osteoblast cell numbers of bone lesions and control bone were assessed through

histomorphometric analysis. Potential molecular pathways involved in bone metastasis were explored.

Results: Lytic and mixed lytic / blastic lesions were radiographically detected in mice 30 and 34 days post Daoy and D283 Med tumor cell injection respectively. Histomorphometric analysis of various bone parameters confirmed these observed bone phenotypes. Subsequent molecular analysis of bone lesions and *in vitro* medulloblastoma cell cultures identified several signaling pathways potentially driving the development of medulloblastoma skeletal metastases and bone remodeling.

Conclusions: The new mouse models of medulloblastoma osseous metastasis described herein are a critical first step in the investigation of mechanisms driving the extra-neural metastasis of medulloblastoma to the bone. Results from this and future studies utilizing these models should aid in the development of tumor-specific bone metastases treatments. Furthermore, findings may also facilitate the development of novel therapies targeting bone metastases from other types of cancers as well, such as prostate, breast and lung.

Disclosures: Jessica Grunda, None.

MO0145

BTK Mediates SDF-1-Induced Migration of Myeloma Cells and Osteoclast Precursors, Osteoclastogenesis and Myeloma Cell Clonogenicity. RAKESH BAM*, Angela Pennisi, Upparahalli Sathisha, Xin Li, Sharmin Khan, Yuping Wang, Wen Ling, Bart Barlogie, John Shaughnessy, Shmuel Yaccoby. University of Arkansas for Medical Sciences, USA

Multiple myeloma (MM) cells typically grow in bone, recruit osteoclast precursors and induce their differentiation in areas adjacent to tumor foci. Bruton's tyrosine kinase (BTK), a nonreceptor tyrosine kinase of the TEC family, is preferentially expressed in the hematopoietic cells and known to regulate B-lymphocyte function, osteoclastogenesis and induction of chemotaxis by SDF-1. The aims of the study were to evaluate expression of BTK in MM cells and osteoclast precursors, determine its role in migration of these cells towards SDF-1, osteoclast differentiation, and clonogenicity of myeloma cells. Our clinical microarray data indicate that primary MM cells express BTK and that relative to normal plasma cells, BTK expression is upregulated in myeloma cells molecularly classified in the CD-1, CD-2, HY, LB and MF subtypes. Expression of BTK at the RNA and proteins levels in MM cells and osteoclast precursors was validated using qRT-PCR and Western Blot. SDF-1 (30 nM) induced migration of MM cells (n=5) by >2.5 folds, an effect that was significantly inhibited by the small molecule BTK inhibitor, LFM-A13 (25-50 μ M). Using FACSARIA flow cytometry we found that CXCR4-positive, but not CXCR4-negative, sorted myeloma cells express BTK, indicating that BTK expression is restricted to a subset of MM cells and that CXCR4 and BTK signaling are linked. LFM-A13 or siRNA against BTK inhibited clonogenic potential of myeloma cell lines using a 2-week methylcellulose assay. LFM-A13 reduced migration of osteoclast precursors towards SDF-1 and dose dependently (10-40 μ M) inhibited formation of multinucleated osteoclasts in cultures supplemented with RANKL and M-CSF. *In vivo*, SCID-rab mice were engrafted with BTK-expressing MM cells. Upon establishment of MM growth as assessed by measurement of circulating human immunoglobulins, hosts were intraperitoneally treated with 40 mg/kg LFM-A13 or vehicle (10 mice/group) twice a day for 3 weeks. Whereas in the control group bone mineral density (BMD) of the implanted bone was reduced by 154% from pretreatment levels, it remained unchanged in the LFM-A13 treated hosts (p<0.01). LFM-A13 prevented induction of osteolytic lesions and reduced the number of osteoclasts in myelomatous bones. At the end of the experiment, tumor burden was insignificantly lower in hosts treated with the LFM-A13. We conclude that BTK plays critical role in MM cell homing and clonogenicity, and in homing and differentiation of osteoclast precursors.

Disclosures: RAKESH BAM, None.

MO0146

Functional Inhibition of Osteoblastic Cells in an In Vivo Mouse Model of Myeloid Leukemia. Benjamin Frisch*¹, John Ashton², Lianping Xing³, Michael Becker², Craig Jordan², Laura Calvi¹. ¹University of Rochester School of Medicine, USA, ²University of Rochester School of Medicine & Dentistry, USA, ³University of Rochester, USA

The mechanisms by which leukemic cells shape their bone microenvironment have currently been evaluated only in xenograft or irradiated models where non-hematopoietic cells are abnormal. Normal osteoblastic cells play a crucial role in hematopoiesis, thus we hypothesized that leukemia-dependent disruption of osteoblastic cells may contribute to impairment of normal hematopoiesis in acute leukemias. To define effects of leukemic cells on the bone microenvironment we employed an immunocompetent syngeneic murine model of acute myeloid leukemia in which leukemia develops in WT C57/B6 mice within 10 days. Leukemic mice had significant trabecular and cortical bone loss by micro-CT analysis (0.23 \pm 0.13 \pm 0.01 tibia trabecular BV/TV Normal(N) vs Leukemic(L) p<0.001 n=5 mice/group). In leukemic mice TRAP+ osteoclastic cells were mildly increased at day 6 but decreased at day 10 (d6: 50.8 \pm 3.6 vs 64.4 \pm 3.2; d10: 33.8 \pm 4.7 cells/ histological section N vs L p<0.05 n=5 mice/group) however the resorption marker CTX did not change. Treatment with zoledronic acid rescued leukemia-induced trabecular but not cortical bone loss (0.24 \pm 0.02 vs 0.10 \pm 0.01 cortical BV/TV N vs L p<0.001 n=4 mice/group)

and disease course was unaffected. Leukemic mice had severe reduction in osteocalcin (OC) mRNA in non-hematopoietic CD45- marrow cells (1290 \pm 124.7 vs 440.1 \pm 34 relative expression N vs L p<0.001 n=5 mice/group) even at early time points when the leukemia was only detectable in the marrow. Osteoprogenitor cells were also decreased (5.8 \pm 1.2 vs 0.9 \pm 0.3 CFU-OBs/1x10⁶ marrow cells N vs L p=0.005 n=7-10 mice/group). Immuno-staining indicated decreased endosteal-lining Osteopontin+ cells in leukemic mice. Leukemic mice had severe systemic decrease in OC levels (92.6 \pm 11.6 vs 25.9 \pm 4.4 ng/ml N vs L p<0.0001 n=8-12 mice/group). CCL-3 mRNA was increased 16 fold in CD45+ marrow cells from leukemic mice compared to normal controls (p<0.005 n=5 mice/group). CCL-3 was reported to increase osteoclastogenesis, inhibit osteoblastic function, and downregulate OC expression in multiple myeloma. We are currently investigating if CCL3 mediates the leukemia-dependent osteoblastic inhibition. These data demonstrate the impact of leukemic cells on the marrow microenvironment particularly osteoblasts. Therapeutic mitigation of leukemia-induced osteoblastic dysfunction may represent a novel approach to promote normal hematopoiesis in patients with myeloid neoplasms.

Disclosures: Benjamin Frisch, None.

MO0147

Localized Tumor Growth in Bone: Quantification of Tumor Burden, Bone Destruction, and Weight Bearing. Subba Chintalacheruvu*¹, Jeffrey Wolos², Elizabeth Misener¹, Christopher Bull¹, Li Li¹, Kellie Brune¹. ¹Covance Laboratories, Inc., USA, ²Scientific Consultant, USA

Metastatic bone disease is common in patients with multiple myeloma, breast, prostate, and lung cancer, and is a frequent cause of morbidity in advanced cancer patients. Metastatic bone tumors destroy bone and cause severe bone remodeling, leading to structural weakening and bone fractures in a large percentage of patients, and often resulting in severe bone pain.

We have implemented multiple imaging modalities to examine tumor growth, bone erosion, and pain in a nude rat model. A surgical defect was created in the tibia, exposing the marrow cavity. Luciferase-expressing MDA-MB-231 mammary tumor cells were injected into the exposed bone cavity. Rats inoculated with tumor cells were treated with either doxorubicin (3 mg/kg/week, iv) or risendronate (80 μ g/kg/day, ip). Animals were monitored weekly for tumor burden by optical imaging and for bone erosion by CT. In addition to clinical observations, pain in weight bearing paws was measured by an incapacitance machine. Compared to controls, rats treated with doxorubicin demonstrated a significant decrease in luminescence, indicating tumor growth inhibition (bone protection). Decreased luminescence correlated with sparing of the bone as measured by CT. In contrast, risendronate had limited effect on tumor growth, but preserved bone integrity. In both treatments, protection of bone was associated with normalization of weight bearing. This finding supports the premise that pain in metastatic bone cancer is due to bone loss (destruction) and remodeling. Weight-bearing data correlated directly with clinical observations. This model, leveraging multiple imaging modalities, enables longitudinal and quantitative assessment of tumor growth, bone loss, remodeling and weight-bearing in test animals and therefore provides a sensitive and robust screening tool to evaluate compounds for anti-tumor, bone-sparing and pain amelioration effects.

Disclosures: Subba Chintalacheruvu, None.

MO0148

Longitudinal Monitoring of Osteolytic Bone Tumors with Integrated Optical-MicroCT Imaging. Jeff Meganck*, Ning Zhang, Heng Xu, Ed Lim, Stanley Liang, Victor Ninov, Jay Whalen, Chainey Kuo, Tammy Troy, Qing Feng, JaeBeom Kim, Brad Rice. Caliper Life Sciences, USA

Tumor metastases in the vicinity of bone tissue may cause osteolytic lesions and further exacerbate the pathological condition. Longitudinal *in vivo* bioluminescence imaging studies are commonly applied to detect the onset of metastases and monitor tumor burden over time due to the high sensitivity and simplicity of these methods. MicroCT has also been extensively used to monitor the bone loss that occurs with osteolytic lesions; these methods are accurate as long as the radiation dose is managed to minimize the impact on tumor biology. Because these two modalities monitor the pathological process from different perspectives, but need to be interpreted together, the purpose of this study is to explore the utility of a new integrated optical-MicroCT system to simultaneously track metastasis and osteolytic lesion development with the human mammary tumor MDA-MB231-luc2 cell line.

Systemic tumor metastases were established via intracardiac injection of MDA-MB231-luc2 cells into Nu/Nu mice. Injections were confirmed at Day 0 via bioluminescence imaging. Bioluminescence and MicroCT images were sequentially acquired at 1week intervals until animal death (4-8 weeks). For all bioluminescence images, acquisition occurred approximately 10 minutes after an intraperitoneal injection of luciferin. To visualize an overlay of the two images and simplify interpretation, a correction was applied to the optical images to account for inherent distortion in the lens used to acquire the optical images. Next, the MicroCT image was registered with the photograph. Finally, the skin surface of the mouse is extracted and input into 3D diffuse optical tomography algorithms to reconstruct the 3D optical signal. Preliminary data indicate that the 3D bioluminescence signal can be accurately overlaid with the MicroCT image. In addition, quantification of the bioluminescence signal shows increases that are consistent with exponential cell growth. Quantifying bone volume in the distal femur of the MicroCT image indicates a decrease in bone volume that

happens simultaneously with this increased cellular growth. This study established the utility of multimodality optical/microCT imaging within a single system for quantifying tumor metastases and bone degeneration in a complex pathological setting.

Disclosures: Jeff Meganck, Caliper Life Sciences, 3
This study received funding from: Caliper Life Sciences

MO0149

Partial Weightbearing for 21-Days and Low Dose High Energy Radiation Results In Cancellous and Cortical Bone Loss. Brandon Macias^{*1}, Florence Lima¹, Yasaman Shirazi-Fard¹, David Cunningham¹, Evelyn Yuen¹, Kaleigh Camp¹, Michael Wiggs¹, James D Fluckey¹, Elizabeth S Greene¹, Matthew Allen², Leslie A Braby¹, Harry Hogan¹, Susan Bloomfield¹. ¹Texas A&M University, USA, ²Indiana University School of Medicine, USA

Astronauts on exploration missions, such as to the moon, may experience whole body radiation doses of ~1.0 Gy per mission. No data exist testing radiation effects in combination with Lunar gravity levels of weightbearing (WB) which approximate 1/6th those of Earth. We hypothesized modeled galactic cosmic radiation during simulated Lunar gravity (G/6) would exacerbate bone loss seen during G/6 without radiation exposure. Female BALB/cByJ mice (4-mo-old, n=9/group) were randomly assigned to cage control (1G), 1/6th gravity (G/6), or 1/6th gravity+radiation (G/6+R) for a 21-d partial WB suspension protocol. Both 1G and G/6 mice were exposed to ²⁸Si (300MeV/u) under one of three conditions: 0.5Gy (Day-0), 0.17Gy (Day-0) or fractionated 0.5Gy dose (0.17Gy on Days 0, 2 and 7). Femoral cancellous architecture and cortical geometry were assessed by microCT; bone formation rate (BFR), mineral apposition rate (MAR) and mineralizing surface (MS/BS) were quantified by dynamic histomorphometry. Load to failure of the femoral neck (FN) was measured using an Instron 3345. Relative to the 1G group, distal femur BV/TV and Tb.N were significantly lower in the 1G+0.5Gy (-14%, -14%, respectively) and G/6+0.5Gy (-26%, -15%, respectively) groups at day 21. Cortical cross-sectional thickness, cross-sectional bone area, and polar moment of inertia were significantly lower in the G/6 groups compared to the 1G groups. Endocortical and periosteal bone formation rates were both lower in G/6 groups, with and without radiation exposure. FN load to failure, in 1G and G/6 groups receiving a single 0.17Gy dose were significantly lower (-33% and -17%, respectively) vs. SHAM controls. Interestingly, there was an intermediate decrement of load to failure in both the single and fractionated 0.5Gy 1G groups (-17% and -16%, respectively); however, the 0.5Gy single or fractionated ²⁸Si dose groups during G/6 show a higher load to failure (29% and 33%, respectively) vs. SHAM controls. Serum TRAP5b was significantly higher in all G/6 groups compared to 1G controls; no independent effect of ²⁸Si exposure was detected on this marker of osteoclast number. In support of our hypothesis, low dose high energy radiation exposure during partial WB conditions exacerbates cancellous bone loss. However, the higher load to failure of FN in partial WB mice receiving 0.5Gy exposures suggests that bone loss may not be consistent in all metaphyseal bone sites or may not accurately predict changes in bone strength.

Disclosures: Brandon Macias, None.

MO0150

RANK Ligand Regulation of Autophagy in Oral Squamous Cell Carcinoma Tumor Cells. Yuvaraj Sambandam^{*1}, Kumaran Sundaram², William Ries¹, Sakamuri Reddy². ¹Medical University of South Carolina, USA, ²Charles P. Darby Children's Research Institute, USA

Head and neck squamous cell carcinomas (HNSCC) are the most common malignant neoplasm estimated to be greater than 40,000 cases annually in the US. Oral squamous cell carcinoma (OSCC), which contributes to >40% of all HNSCC, is associated with mucosal surfaces of the oral cavity and oropharynx. We recently reported OSCC tumor invasion of bone and osteolysis in mice. Autophagy is a cellular self-consumption process for degradation of damaged/ dysfunctional cellular organelles, protein aggregates and plays an important role in malignant tumor progression and resistance to anti-cancer therapies. We showed OSCC cells express high levels of RANK ligand (RANKL), a potent osteolytic factor; however a functional role for RANKL in autophagy is unknown. We demonstrated RANK expression in OSCC tumor cells by confocal and histochemical analysis. Formation of autophagosomes involves autophagy proteins (Atg) and conversion of cytoplasmic microtubule-associated protein 1 light chain 3 (LC3-I) into the membrane form of LC3-II. We identified high levels of LC3-II expression in OSCC tumor cells (SCC-1, SCC-12 & SCC-14a) compared to normal human epithelial (RWPE-1) cells. Further, we showed increased levels of LC3-II and Atg5 expression in OSCC tumor specimens from human subjects and OSCC tumors on calvaria from athymic mice by immunohistochemistry. Interestingly, Western blot analysis of total cell lysates obtained from OSCC cells stimulated with RANKL (0-100 ng/ml) for 24 h demonstrated a dose dependent increase in LC3-II and RANKL expression which indicates an autoregulation of RANKL expression and autophagosome formation in OSCC cells. Thus our results implicate a novel function for RANK-RANKL signaling that may play an important role in autophagy modulation of OSCC tumor progression/osteolysis.

Disclosures: Yuvaraj Sambandam, None.
This study received funding from: NIH

MO0151

RNA-Dependent Protein Kinase is Essential for 2-Methoxyestradiol-Induced Autophagy in Osteosarcoma Cells. Caihong Yang, Kristen Shogren, Ribu Goyal, Michael Yaszemski, Avudaiappan Maran^{*}. Mayo Clinic College of Medicine, USA

Autophagy is a multi-step process that leads to sequestration and degradation of organelles and macromolecules within lysosomes. Autophagy, which regulates cell death in normal and pathophysiological conditions, has been implicated in tumor suppressor pathways. Osteosarcoma is the most common primary malignant bone tumor that affects children and young adults. Surgical resection and adjunctive chemotherapy are widely used in the treatment of osteosarcoma. Although surgery and chemotherapy have improved survival in the last decades, many patients diagnosed with osteosarcoma develop metastatic diseases. The anti-tumor compound 2-Methoxyestradiol (2-ME) triggers cell death through the induction of apoptosis in osteosarcoma cells, but not in normal osteoblasts. The goal of this study is to investigate whether autophagy plays a role in the anti-tumor effects of 2-ME in osteosarcoma cells. Our analysis of osteosarcoma cells using transmission electron microscopy shows that 2-ME treatment leads to the accumulation of autophagosomes. The results also show that 2-ME induces the conversion of the microtubule-associated protein LC3-I to LC3-II, a biochemical marker of autophagy that is correlated with the formation of autophagosomes. Furthermore, 2-ME does not induce accumulation of autophagosomes in osteosarcoma cells that stably express the dominant negative mutant RNA-dependent protein kinase (PKR) protein and are resistant to the anti-proliferative and anti-tumor effects of 2-ME. Thus, our study shows that 2-ME treatment induces autophagy in a PKR-dependent manner in human osteosarcoma cells, and that the induction of autophagy could lead to anti-tumor pathways in 2-ME-treated osteosarcoma cells. Taken together, these results demonstrate that treatment strategies that increase PKR expression and positively control autophagy could be useful in clinically controlling osteosarcoma growth in patients.

Disclosures: Avudaiappan Maran, None.

MO0152

Selective Targeting of the Ubiquitin Ligase Cbl Reduces Receptor Tyrosine Kinases Signaling and Osteosarcoma Tumorigenesis. Nicolas Severe^{*1}, François-Xavier Dieudonne¹, Caroline Marty¹, Olivia Fromiguet¹, Pierre Marie². ¹INSERM U606 & University Paris Diderot, France, ²INSERM Unit 606 & University Paris Diderot, France

Receptor tyrosine kinases (RTKs) are cell surface transmembrane proteins responsible for intracellular signal transduction. Over-expression of RTKs are often associated to human cancers, resulting in tumor cell growth and metastasis. Although RTKs represent pivotal targets in approaches of cancer therapy, strategies using anti-RTKs are not optimally efficient in clinics. Ubiquitin ligase-dependent degradation downregulation of RTKs is a critical step for modulating their activity. We previously showed that the ubiquitin ligase c-Cbl positively controls mesenchymal cell differentiation into osteoblasts via negative regulation of RTKs. In this study, we hypothesized that genetic manipulation of c-Cbl might reduce RTK signaling and tumorigenesis in osteosarcoma cells. Western blot analyses showed that c-Cbl and Cbl-b were inversely expressed in various human and murine osteosarcoma cells, in line with the basal expression of RTKs in these cells. We overexpressed c-Cbl in human (U2OS) and murine (K7M2) osteosarcoma cells with wild type (WT) c-Cbl. c-Cbl overexpression slightly (50 %) reduced cell replication and markedly (80 %) induced cell apoptosis in both U2OS and K7M2 cells in vitro, as shown by BrdU, MTT, caspases activity and TUNEL analysis. These effects were associated with c-Cbl-induced downregulation of RTKs, indicating that selective targeting of Cbl can reduce RTK-dependent osteosarcoma cell growth and survival. Additionally, c-Cbl overexpression reduced U2OS cell migration and invasion, as shown by conventional assays. To investigate whether the negative effect of c-Cbl overexpression on cancer cells may translate in reduced tumorigenesis in vivo, murine K7M2 osteosarcoma cells were transduced with c-Cbl or control vector and transplanted intramuscularly in BALB/C mice. Analysis of tumor size showed that c-Cbl overexpression in K7M2 cells reduced tumor growth by 50 % after 3 weeks compared to control tumors (P<0.05). Overall, the results provide the first demonstration that targeted overexpression of c-Cbl in osteosarcoma cells reduces RTK expression, inhibits cell growth, promotes cell apoptosis and reduces cell migration and invasion in vitro. In vivo, this effect translates into reduced tumorigenesis in this aggressive type of cancer. This study provides the proof-of-concept that selective targeting of the ubiquitin ligase Cbl reduces RTK signalling and osteosarcoma tumorigenesis.

Disclosures: Nicolas Severe, None.

MO0153

Serum 25-hydroxyvitamin D and Nuclear Grade in Patients with Ductal Carcinoma In Situ. Mercedes Gacad^{*1}, Nancy Greep¹, Deborah Cunningham¹, Jaime Shamoni², Myung-Shin Sim¹, Dave Hoon¹, Armando Giuliano¹, Frederick Singer¹. ¹John Wayne Cancer Institute, USA, ²Saint John's Health Center, USA

Epidemiologic studies suggest that vitamin D deficiency may play a role in the development and clinical course of invasive breast cancer. In this pilot study we examine the possibility that vitamin D deficiency may be a factor in the expression of ductal carcinoma in situ (DCIS), a non-obligate precursor of invasive breast carcinoma. We have evaluated serum 25-hydroxyvitamin D levels and tumor characteristics in 64 patients who had surgery for (DCIS). After informed consent blood was taken from patients prior to surgery between 2000 and 2010. The sera were stored at -80 degrees centigrade and subsequently evaluated in a batch assay at Heartland Assays utilizing the DiaSorin Liaison Assay. The mean serum 25-hydroxyvitamin D +/- SD was 26.5 +/- 11.5 ng/ml with a range of 4.2 - 66.7 ng/ml. While there is controversy in defining vitamin D sufficiency, we classified levels of <20 ng/ml as deficient, 20-30 ng/ml as insufficient and >30 ng/ml as sufficient. In the 64 patients 27% were classified as vitamin D deficient, 44% as insufficient and 29% as sufficient. Nuclear grade has been used to classify and predict the clinical course of DCIS. The nuclear grade of the patients lesions were classified as low, intermediate, or high. Using Student's T test we compared mean serum 25-hydroxyvitamin D levels in patients who had low grade to patients with intermediate and high grade nuclear scores and found that the low nuclear grade patients had higher serum 25-hydroxyvitamin D levels (n=11; mean +/- SD= 32.9 +/- 14.7 ng/ml) than intermediate grade patients (n=13; mean +/- SD= 24.0 +/- 9.7, p= 0.09) and high grade patients (n=40; Mean +/- SD= 25.5 +/- 10.7; p= 0.07) although the differences were not quite significant. An increase in sample size of the intermediate and high nuclear grade patients may provide stronger evidence of the effect of vitamin D deficiency on DCIS. Further analyses including Ki67 seem warranted to help determine whether vitamin D deficiency has an impact on cell replication in patients with DCIS

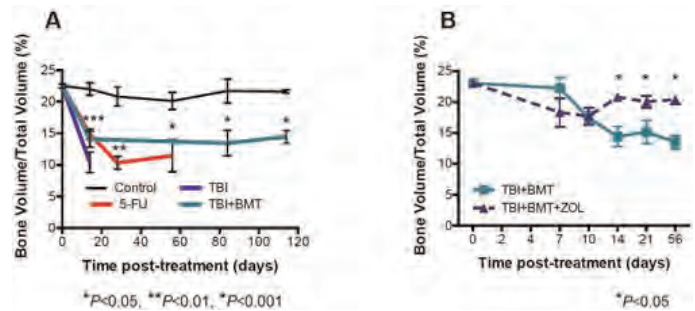
Disclosures: Mercedes Gacad, None.

MO0154

Single Cytotoxic Agents Directly Cause Bone Loss due to Increased Osteoclastogenesis: Implications for Preventing Bone Loss in Cancer Patients. Julie Quach^{*1}, Maria Askmyr¹, Tanja Jovic¹, Kirby White¹, Emma Baker¹, Nicole Walsh², Louise Purton¹. ¹St. Vincent's Institute, Australia, ²St Vincent's Institute of Medical Research, Australia

Purpose: Reduced bone mass is one of the most common side effects occurring in long-term survivors of cancer therapies. Aside from osteolytic lesions occurring in response to some cancers, the bone loss is most commonly attributed to the use of corticosteroids as part of the anti-cancer (cytotoxic) treatment regime. In this study we sought to determine 1) the effects that common cytotoxic therapies have on bone in the absence of corticosteroids and 2) whether zoledronic acid (ZOL) could protect against cytotoxic therapy-induced bone loss. **Methods:** We treated cohorts of eight-week old male mice with three different cytotoxic therapies: 1) lethal total body irradiation (TBI); 2) lethal TBI with bone marrow transplantation (BMT) or 3) a single dose (150mg/kg) of the chemotherapy agent, 5-fluorouracil (5-FU). In a separate study we also investigated the effects of a single dose of ZOL (10µg/kg) injected 3 days prior to BMT. Bone parameters were compared to those of non-treated age-matched littermate controls. **Results:** All three cytotoxic treatments caused rapid, irreversible loss of trabecular bone compared to controls as assessed by µCT and histomorphometry (Figure A). In all three therapies this bone loss correlated with significant increases in the numbers and size of osteoclasts at 4 to 7 days post-treatment, and elevated osteoclast activity as shown by significantly increased levels of serum carboxy-terminal collagen-1. Increased mRNA expression of inflammatory cytokines, including TNFα, IL-1β and IL-6, was observed in F480+CD11b+ macrophages purified from BM after cytotoxic therapies by fluorescence-activated cell sorting (FACS). These inflammatory cytokines preceded elevated expression of RANK in osteoclast precursors and increased RANKL expression in FACS-purified osteoblastic cells (1). Treatment of mice with a single dose of ZOL prevented the bone loss that occurred in the BMT mouse model (Figure B). **Conclusions:** Bone loss occurs in response to a range of cytotoxic therapies independent of corticosteroid use. This is likely due to inflammation occurring in response to cytotoxic therapies, which in turn causes increased osteoclastogenesis. Furthermore, a single dose of ZOL prevented the bone loss observed after BMT. Collectively these studies suggest that blocking osteoclast activity prior to commencing cytotoxic therapies may prevent the long-term bone loss that occurs in cancer patients.

1. Semerad, C.L., et al. Blood 106, 3020-3027 (2005).



Figure

Disclosures: Julie Quach, None.

MO0155

The Role of VEGF in the Progression of Human Osteosarcoma. Paul Daft^{*1}, Jennifer Paige-Robinson², Majd Zayzafoon³. ¹The University of Alabama At Birmingham, USA, ²University of Alabama-Birmingham, USA, ³University of Alabama at Birmingham, USA

Osteosarcoma is the most common primary bone tumor found in children and young adults. These malignant tumors are characterized by the production of tumor osteoid, and demonstrate aggressive local and distant metastasis. Angiogenesis is a complex process by which new blood vessels arise from the pre-existing vasculature. Most tumor types overexpress Vascular Endothelial Growth Factor (VEGF), directly correlating with regions of angiogenesis. We previously demonstrated the ability of Ca2+/Calmodulin kinase two alpha (CaMKIIα) to regulate the growth and metastasis of osteosarcoma in vivo. In order to determine whether the observed effects of CaMKIIα were due to its ability to regulate VEGF, expression we examined the role of VEGF in the growth of osteosarcoma. Here we show that the levels of VEGF gene expression are positively correlated with the in vitro growth and motility of different osteosarcoma cell lines. A two-fold increase in VEGF mRNA expression was observed in the more aggressive osteosarcoma cells when compared to the less aggressive cells. VEGF protein levels were measured using Enzyme-Linked Immunosorbent Assay, demonstrating a four-fold increase in VEGF protein secretion in the highly aggressive 143B cell line when compared to the less aggressive MG-63 cell line. Conditioned media from 143B cells resulted in increased tube formation in an endothelial cell tube formation assay when compared to MG-63 cells. In order to examine whether CaMKIIα regulates VEGF expression and secretion, we genetically inhibited CaMKIIα with shRNA, and pharmacologically with KN-93. Both MG-63 and 143B CaMKIIα deficient cells resulted in an 80% decrease of both VEGF gene expression and protein levels of its main transcription factor, hypoxia inducible factor one alpha (HIF-1α). In order to identify the signaling pathways by which VEGF controls the growth of osteosarcoma, we treated 143B cells with the VEGF inhibitor, CBO-P11. VEGF inhibition resulted in decreased survival of 143B cells, demonstrated by an 80% reduction in the levels of the phosphorylated pro-survival protein Akt (P-AKT), while increased cellular apoptosis was shown by an increase in the pro-apoptotic cleaved caspase-3. Taken together our data suggest that the ability of CaMKIIα to control VEGF expression and secretion may be critical for the growth of human osteosarcoma.

Disclosures: Paul Daft, None.

MO0156

The Skeletal Effects of the Tyrosine Kinase Inhibitor Nilotinib. Susannah O'Sullivan^{*}, Jian-Ming Lin, Maureen Watson, Karen Callon, Dorit Naot, Pak Cheung Tong, Anne Horne, Opetia Aati, Fran Porteous, Greg Gamble, Jillian Cornish, Peter Browett, Andrew Grey. University of Auckland, New Zealand

Nilotinib is a tyrosine kinase inhibitor (TKI) developed to manage imatinib-resistance in patients with chronic myeloid leukaemia (CML). It inhibits similar molecular targets to imatinib, but is a significantly more potent inhibitor of Bcr-Abl. Nilotinib exhibits off-target effects in other tissues, and of relevance to bone metabolism, hypophosphataemia has been reported in up to 30% of patients receiving nilotinib. We have assessed the effects of nilotinib on bone cells in vitro and on bone metabolism in patients receiving nilotinib for treatment of CML. We firstly investigated the effects of nilotinib on proliferating and differentiating osteoblastic cells, and on osteoclastogenesis in murine bone marrow cultures and RAW264.7 cells. Nilotinib potently inhibited osteoblast proliferation (0.01-1µM), through inhibition of the platelet-derived growth factor (PDGFR). There was a biphasic effect on osteoblast differentiation such that it was reduced by lower concentrations of nilotinib (0.1-0.5µM), with no effect at higher concentrations (1µM). Nilotinib also potently inhibited osteoclastogenesis, predominantly by stromal-cell dependent mechanisms. Thus, nilotinib decreased osteoclast development in murine bone marrow cultures, but did not affect osteoclastogenesis in RAW264.7 cells. Nilotinib treatment of osteoblastic cells increased expression and secretion of OPG and decreased expression of RANKL. In 10 patients receiving nilotinib, levels of bone

turnover markers were in the low-normal range, despite secondary hyperparathyroidism, findings that are similar to those in patients treated with imatinib. Bone density tended to be higher than age and gender-matched normal values. These data suggest that nilotinib may have important effects on bone metabolism. Prospective studies should be conducted to determine the long-term effects of nilotinib on bone density and calcium metabolism.

Disclosures: *Susannah O'Sullivan, None.*

MO0157

Bone-seeking Labels as Markers for Bone Formation in Sclerostin Knockout Mice. Nicole Collette^{*1}, Darren Hillegonds², Kenneth Turteltaub¹, Gabriela Loots³. ¹Lawrence Livermore National Laboratory, USA, ²Lawrence Livermore National Library, USA, ³LLNLUC Merced, USA

The gold standard approach for evaluating bone turnover rates is dynamic histomorphometry, a laborious approach with limited clinical application. Calcium (Ca) tracer kinetic studies can be used to determine bone formation and resorption rates. To validate isotopic approaches to bone metabolism we used ⁴¹Ca as a tracer to measure the net bone calcium balance in animal models of high (Sost KO) and low (Lrp5 KO) bone mass. Unlike other stable Ca isotopes, ⁴¹Ca is radiologically benign, has low natural abundance, and a small dose remains distinctly quantifiable in body fluids and excreta for many years. To determine the metabolic profile of ⁴¹Ca in mice, we measured ⁴¹Ca/Ca after an IP dose and found that the resorbing bone is the dominant source of tracer, 21 days (d) post dosing (>200 days in humans). At d28 post dosing the total tracer accumulation in tibia and femur (1.60.8% of administered dose) was >1600X higher than that in blood, heart and kidney, confirming high bone Ca retention and fast soft tissue elimination. To demonstrate the potential of ⁴¹Ca as an assay of dynamic bone turnover we collected weekly urine from 5 adult males for up to 10 weeks from three distinct genetic backgrounds: wildtype (B6; reference bone metabolism), Lrp5 KO (low anabolic bone activity/osteopenic) and Sost-/- mice (high anabolic bone activity/high bone mass). All measurements of ⁴¹Ca/Ca were obtained on the Center for Accelerator Mass Spectrometry's (AMS) 10MV FN-class tandem electrostatic AMS system at LLNL, and were corrected for instrumental drift and analytical ⁴¹Ca backgrounds with concurrently processed and analyzed isotope ratio standards and ⁴¹Ca-free blanks. Whereas we observed a significant reduction of ⁴¹Ca/Ca ratio excretion in Sost KO mice at every time point up to d35, the most dramatic reduction was at 7-days post injection. This 40% reduction in urine ⁴¹Ca/Ca (p<0.01 versus WT) in Sost KO mice suggests that high bone formation rates is reflected by a significantly higher initial uptake of ⁴¹Ca. Therefore our preliminary data suggests that AMS ⁴¹Ca/Ca can be used to distinguish mice with different bone turnover rates. The successful implementation of ⁴¹Ca assays in genetic screens and in patients with bone disease could have wide benefits, including improved risk assessment, monitoring treatment, and early detection.

Disclosures: *Nicole Collette, None.*

MO0158

Cellular Dysregulation of Gene Expression May Contribute to Matrix Hypermineralization in Osteogenesis Imperfecta. Wayne Cabral^{*1}, Nadja Fratzl-Zelman², Paul Roschger³, Klaus Klaushofer⁴, Adele Boskey⁵, Joan Marini⁶. ¹NIH, NICHD, USA, ²Ludwig-Boltzmann Institute of Osteology, Austria, ³L. Boltzmann Institute of Osteology, Austria, ⁴Hanusch Hospital, Austria, ⁵Hospital for Special Surgery, USA, ⁶National Institute of Child Health & Human Development, USA

Classical Osteogenesis Imperfecta is an autosomal dominant disorder caused by mutations in *COL1A1* and *COL1A2*. Affected individuals have increased susceptibility to fracture. The Brlt mouse is heterozygous for a *Col1a1* G349C mutation and reproduces the moderately severe OI phenotype. We previously demonstrated that adaptations in Brlt femoral strength and stiffness occur through changes in material properties, with potential alterations in bone mineral composition. To investigate the role of mineral and organic components in OI bone fragility, we analyzed Brlt femurs by qBEI and FTIR and quantitated expression of genes involved in matrix mineralization. Femurs from 2- and 6-month Brlt mice show BMDD changes characteristic of OI, with significantly higher matrix mineralization of both cancellous metaphyseal and mid-diaphyseal cortical bone than wt littermates. In cancellous and cortical bone, the typical mineralization density (CaPeak) was increased ~2%. Brlt cortical bone mineral heterogeneity (CaWidth) decreased at 6 months vs 2 months (~ -8%). At six months of age, Brlt CaWidth was lower (~ -11%) than wild-type femurs. Consistent with BMDD, FTIR on 2-month Brlt femurs yielded a trend toward increased mineral/matrix index in trabecular bone.

In RNA from whole femurs of Brlt vs WT 2-month mice, measurement of transcripts of late osteoblastic and osteocyte markers by real time RT-PCR revealed significant increases of *Dmp1* (1.8x) and *Phex* (1.3x) expression. On Osteogenesis PCR arrays, *Bmp2* transcripts were decreased 2.4x, while *Sost* expression was unchanged in Brlt vs WT femurs. During differentiation of newborn calvarial osteoblasts in culture, the increase in *Dmp1* and *Phex* transcripts seen in WT cells was delayed several days in Brlt. Transcripts for *Sost* and *Bmp2* were decreased over 3-fold in newborn Brlt vs WT calvarial osteoblasts throughout in vitro differentiation. Furthermore, alizarin red staining detected increased deposition of mineral by Brlt vs WT cultured osteoblasts, with and without BMP2 treatment. Preliminary cell-matrix exchange experiments

support a contribution of matrix composition to delayed Brlt cellular development, because expression of *Dmp1*, *Phex*, *Sost* and *Bmp2* is decreased in both WT and Brlt cells grown on Brlt matrix. Our data suggest that OI bone hypermineralization may be caused in part by differentiation defects of osteoblasts or osteocytes which alter expression of noncollagenous proteins involved in control of mineralization.

Disclosures: *Wayne Cabral, None.*

MO0159

Generation of iPS Cells from Fibroblasts and Peripheral Blood Cells of CMD Patients. I-Ping Chen^{*1}, Xiaonan Xin¹, Mary-Louise Stover¹, Hui-Chen Chan¹, Keiichi Fukuda², Noemi Fusaki³, Akihiro Iida³, Mamoru Hasegawa³, Ernst Reichenberger¹, Alexander Lichter¹. ¹University of Connecticut Health Center, USA, ²Keio University School of Medicine, Japan, ³DNAVEC Corporation, Japan

Craniofacial dysplasia (CMD) is a monogenic human disorder characterized by hyperostosis of craniofacial bones concurrent with abnormal shape of long bones. Its lifelong progression leads to life-threatening consequences in some patients. To date, there is no treatment other than repetitive surgery. Mutations for autosomal dominant CMD have been identified in the ANK gene (ANKH). We previously revealed osteoclast (OC) defects in a knock-in (KI) mouse model (AnkKI/KI mice) carrying a CMD-causing Ank mutation. Our long-term goal is to use the patient-specific inducible pluripotent stem cells (iPSCs) to study the mutational effects of ANKH on CMD with a focus on OCs. We have reported the reprogramming of somatic cells into human iPSCs using retroviral transduction of OCT3/4, SOX2, KLF4, c-MYC and Lin28. The retroviral method did not fully reprogram CMD fibroblasts to iPSCs and some retrovirally derived-iPSCs showed incomplete vector silencing which may hinder the differentiation process. Here, we show the derivation of iPSCs from skin fibroblasts and from peripheral blood mononuclear cells (PBMCs) of CMD patients and healthy controls. We used a floxed lentiviral "stem cell cassette" (STEMCCA) combining OCT3/4, SOX2, KLF4, c-MYC in a single polycistronic vector or four separate Sendai virus vectors encoding OCT3/4, SOX2, KLF4, c-MYC. The STEMCCA allows simultaneous transfer of reprogramming factors to achieve higher reprogramming efficiency and produce transgene free iPSCs upon exposure to Cre recombinase. The Sendai virus, a cytoplasmic RNA vector, can produce iPSCs which are free of vector integration into chromosomes. The derived iPSCs have similar morphology to human embryonic stem cells (hESCs) and express pluripotency-related factors shown by gene expression analysis and immunocytochemistry. Assays for testing differentiation capability of these iPSCs by embryoid body and teratoma formation are in progress. We have derived OC-like cells from hESCs using the hESCs-OP9 cocultures. This protocol results in the formation of multinucleated cells which were TRAP positive, with actin belts at the periphery and capable of resorbing calcium-phosphate coated discs. Next, we will apply the same method to differentiate OCs from iPSCs. We expect this tool will allow us to study the molecular mechanisms, by which ANKH mutations cause impaired osteoclastogenesis in human CMD.

Disclosures: *I-Ping Chen, None.*

MO0160

The High Bone Mass Phenotype is Characterised by Increased Subcutaneous and Intra-muscular Fat, but Decreased Marrow Fat. Celia Gregson^{*1}, Adrian Sayers¹, Victor Lazar², Sue Steel², Joern Rittweger³, Jon Tobias⁴. ¹University of Bristol, United Kingdom, ²Hull Royal Infirmary, United Kingdom, ³Institute of Aerospace Medicine, German Aerospace Center, Germany, ⁴Musculoskeletal Research Unit, University of Bristol, United Kingdom

In our unique case-control study of High Bone Mass (HBM), cases have previously been found to have greater total body fat mass, reduced exercise tolerance and lower platelet levels compared to controls. To explore inter-relationships between fat, bone and bone marrow suggested by these results, we aimed to characterise adipose tissue distribution in HBM individuals using a novel application of tibial pQCT.

196 HBM index cases were identified by screening a hospital DXA database (n=105,333). HBM was defined as a) L1 Z-score of 3.2 or more and total hip Z-score of 1.2 or more, or b) total hip Z-score 3.2 or more. Cases with significant osteoarthritis and/or other causes of raised BMD were excluded. Relatives and spouses were recruited, in whom HBM affection status was defined as L1 Z plus total hip Z-scores of 3.2 or more. Controls comprised unaffected relatives and spouses. pQCT was performed at the tibial diaphysis (66% of its length), using a Stratec XCT2000L. Cases were compared with controls using linear regression, adjusting for age, gender, height and menopausal status.

98 HBM cases (71 index, 27 affected relatives) & 65 controls (43 unaffected relatives, 22 spouses) underwent pQCT; 81.6% & 50.8% were female, mean age 58 & 55 years, height 167 & 171 cm, weight 86 & 82 kg respectively; all Caucasian. As shown in the table below, compared with controls, HBM cases had 22% more intra-muscular fat and considerably greater calf muscle and subcutaneous fat areas; however, marrow cavity area was reduced at the expense of marrow fat rather than other X-ray attenuating tissue (such as haemopoietic tissue). Interestingly, after

further adjustment for body weight, HBM cases still had greater intra-muscular fat than controls (mean difference 1.79 [0.22, 3.37]cm², p=0.025) and marrow results remained unchanged.

In summary, HBM individuals have greater subcutaneous and intra-muscular fat tissue, whilst in contrast marrow fat is reduced, possibly reflecting a mechanism to maintain haemopoietic function within the reduced marrow cavity of HBM long bones. Whether increased intra-muscular fat in HBM cases has a detrimental effect on muscle function, so explaining the reduction in exercise tolerance previously observed amongst HBM cases, remains to be determined.

Table: Calf pQCT measures taken from the 66% tibia in High Bone Mass cases and family controls; all values adjusted for age, gender, height & menopausal status amongst women

66% TIBIA	HBM Cases	Controls	Adj. p
Area measures (cm ²)	(n=98) [95% CI]	(n=65) [95% CI]	value
Total bone area	7.1 (6.8, 7.4)	6.8 (6.6, 7.1)	0.05
Calf muscle	84.1 (79.7, 88.5)	79.9 (76.1, 83.8)	0.02
Subcutaneous fat	33.2 (27.6, 38.8)	28.4 (23.4, 33.3)	0.03
Intra-muscular fat	19.1 (16.7, 21.5)	15.8 (13.7, 17.9)	<0.01
Marrow cavity	2.15 (1.89, 2.41)	2.40 (2.17, 2.63)	0.02
Haemopoietic tissue	1.08 (0.92, 1.25)	1.15 (1.01, 1.29)	0.30
Marrow fat	1.07 (0.90, 1.24)	1.25 (1.09, 1.40)	<0.01

Mean areas measured in cm². Adjusted linear regression p value shown

HBM: High Bone Mass, CI: Confidence Interval

All marrow cavity tissue with density between 200 and -250 mg/cm³ was measured. Haemopoietic tissue defined as that unfiltered by Stratec F07 fat filter, whilst marrow fat defined as that filtered by F07 fat filter.

Disclosures: Celia Gregson, None.

MO0161

Assessment of Bone Associated Pain in the Aged Osteomalacic Rat. Darshana Durup¹, Jesper Ryhl Plovst¹, Erik Frandsen², Solveig Petersen², Lars Thorbjørn Jensen², Niklas Jørgensen³, Anne-Marie Heegaard^{1*}.
¹Faculty of Pharmaceutical Sciences, University of Copenhagen, Denmark, ²Glostrup Hospital, Denmark, ³Copenhagen University Hospital Glostrup, Denmark

Background: Adult patients with severe vitamin D deficiency, where the mineralization of the bone is affected (osteomalacia) often suffer from musculoskeletal pain; however, the underlying mechanisms of bone pain are unknown.

The aim of this project was to develop an animal model for osteomalacia in mature rats and to quantify bone associated pressure pain threshold.

Methods: 6 months old Sprague Dawley female rats were fed either a vitamin D (vit D) deficient diet (n=25) or a control diet (n=25). After 4 months on the vit D deficient diet the phosphorus content of the diet was decreased to 0.16% (Ca:P ratio 5.85). Blood samples were taken monthly and 25-hydroxy vitamin D (25(OH)D), parathyroid hormone (PTH), total calcium, phosphorus, magnesium, albumin and alkaline phosphatase were measured. Bone associated pressure threshold was measured with the Randall Selitto test at 7 different bone-near sites. Acute pain threshold was measured by the hot plate test and von Frey filaments. Degree of calcine label and osteoid was determined by histology. The experiment was approved by the Danish Animal Experiments Inspectorate.

Results: After 4 months on a vit D deficient diet, the 10 months old rats were vitamin D deficient: 25(OH)D serum levels were 57.7 4.35 nM and 15.1 3.37 nM in rats receiving control diet and vit D deficient diet, respectively. However, no effect of the diet was observed on any of the other biochemical markers measured and no increase in osteoid was found. Also, there was no difference among the two groups of rats in any of the pain-related tests. The phosphorus (P) content in the diet was hereafter decreased to 0.16%, which, after 1 month, resulted in an increased amount of osteoid. Compared to the aged-matched rats on the control diet, the rats on the low vit D and P diet had decreased serum levels of 25(OH)D (92.1 6.26 nM vs 11.8 1.8 nM); phosphorus (1.4 0.16 mM vs. 0.53 0.12 mM), and PTH (445.4 78.7 pg/ml vs. 58.5 11.2 pg/ml). Pressure pain thresholds measured by Randall Selitto were significantly higher in the vit D and P deficient rats but no difference was found in the hot plate test and the von Frey test

Conclusion: A vitamin D deficiency diet in six-month-old female rats was not sufficient to induce osteomalacia and had no effect on pain-related behaviors. However, an additional decrease of phosphorus content lead to the development of osteomalacia. Surprisingly the osteomalacic rats had higher bone associated pressure pain threshold



Bone Scintigraphy

Disclosures: Anne-Marie Heegaard, None.

MO0162

How High Dose(s) of Oral Vitamin D3 Can Correct Insufficiency in a Non Supplemented Rheumatologic Population? Olivier Lamy¹, Didier Hans^{2*}, Marc-Antoine Krieg³, Jean Dudler¹, Berengere Aubry-rozier³, Delphine Stoll¹. ¹CHUV, Switzerland, ²Lausanne University Hospital, Switzerland, ³University Hospital, Switzerland

Introduction

700 to 1000 UI Vitamin D/day prevent 20% of fall and fracture. Higher dosage could prevent other health problems, such as immune diseases. Adherence to oral daily vitamin D supplementation is low. There is no guideline on how to supplement patients with rheumatic diseases. We evaluated if 1-2 dose(s) of 300'000 UI oral vitamin D3 was enough to reach an optimal level of 25-OH vitamin D in late winter in patients with insufficiency.

Methods

During November 2009 (M0) patients attending our Rheumatology Outpatient Clinic had a blood test to measure 25-OH vitamin D. Results were classified as: deficiency <10µg/l, insufficiency 10µg/l to 30µg/l and normal >30µg/l. Patients on daily oral vitamin D3 or who received a single high dose of vitamin D3 in the last 6 months and patients with deficiency or normal results were excluded.

Patients included received a single dose of 300'000 IU of oral vitamin D3 and were asked to come back for a blood test for 25-OH vitamin D after 3 (M3) and 6 months (M6). If they were still insufficient at M3, they received a second high dose of 300'000 IU of oral vitamin D3.

Results

292 patients had their level of 25-OH vitamin D determined at M0. 141 patients (70% women) had vitamin D insufficiency (18.5µg/l (10.2-29.1)) and received a prescription for a single dose of 300'000 IU of oral vitamin D3. Men and women were not statistically different in term of age and 25-OH vitamin D level at M0.

124/141 (88%) patients had a blood test at M3. 2/124 (2%) had deficiency (8.1µg/l (7.5-8.7)), 50/124 (40%) normal results (36.7µg/l (30.5-56.5)). 58% (72/124) were insufficient (23.6µg/l (13.8-29.8)) and received a second prescription for 300'000 IU of oral vitamin D3.

Of the 50/124 patients who had normal results at M3 and did not receive a second prescription, 36 (72%) had a test at M6. 47% (17/36) had normal results (34.8µg/l (30.3-42.8)), 53% (19/36) were insufficient (25.6µg/l (15.2-29.9)).

Out of the 54/72 (75%) patients who received a second prescription, 28/54 (52%) had insufficiency (23.2µg/l (12.8-28.7)) and 26/54 (48%) had normal results (33.8µg/l (30.0-43.7)) at M6.

(figure 1)

Discussion

This real life study has shown that one or two oral bolus of 300'000 IU of vitamin D3 in autumn and winter was not enough to completely correct hypovitaminosis D but was a good way of preventing a nadir of 25-OH vitamin D usually observed in spring in a Swiss rheumatologic population.

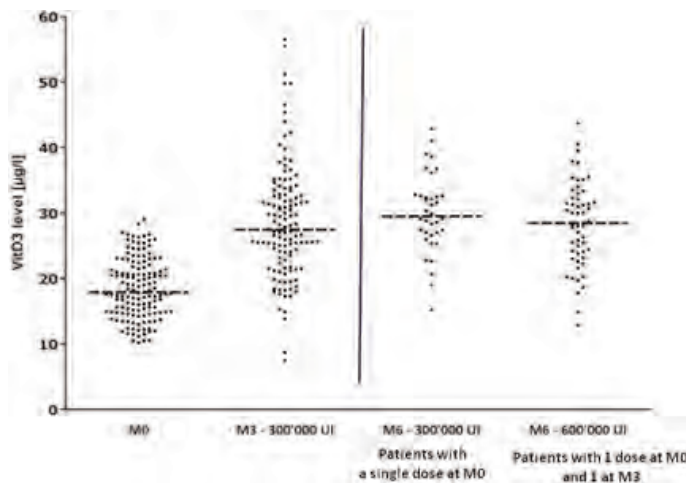


figure 1

Disclosures: Didier Hans, None.

MO0163

Identification of Susceptibility Loci to Giant Cell Tumor and Paget's Disease of Bone. Daniela Merlotti¹*, Fernando Gianfrancesco², Domenico Rendina³, Teresa Esposito², Alessandra Mingione², Daniela Formicola², Riccardo Muscarello³, Pasquale Strazzullo³, Ranuccio Nuti¹, Luigi Gennari¹. ¹University of Siena, Italy, ²Institute of Genetics & Biophysics, CNR, Italy, ³Department of Clinical & Experimental Medicine, Federico II University of Naples, Italy

Paget's disease of bone (PDB) is a common skeletal disorder with a strong genetic component. Recently, mutations in SQSTM1 gene have been identified in up to 10% and 40% of sporadic and familial PDB cases, respectively. Even though patients with SQSTM1 mutations generally show an increased disease severity than SQSTM1-negative patients, we recently identified SQSTM1-negative families with a severe phenotype and the presence of peculiar phenotypic characteristics, including the occurrence of giant cell tumor (GCT). This complication may be multifocal and aggressive, leading to increased morbidity and mortality of patients. Patients with extensive, recurrent, and/or biologically more aggressive tumors may require wide excision, and generally do not respond to bisphosphonates or other antiresorptive agents commonly in use to treat classical PDB. Importantly, both familial clustering and the evidence that GCT occurs with higher prevalence in PDB patients from Campania (accounting for up to 50% of all GCT cases) even if they have lived for several years in other countries strongly suggests the hypothesis of a genetic factor in the etiology of this complication. In this study we performed a genome-wide scan in a large kindred with PDB and GCT. All the 14 affected patients had polyostotic PDB (with a mean of 5.72.6 affected skeletal sites, range 2-12) with a preferential localization of axial bones, and 4 of them had GCT. We used Affymetrix Genome-Wide Human SNP Array 6.0, containing more than 1.8 million genetic markers, including more than 906,600 single nucleotide polymorphisms (SNPs) and more than 946,000 probes for the detection of copy number variation (CNV). Parametric and non-parametric analysis identified 2 major regions on chromosomes 8 and 10 (Zmax=6.2; LODmax=2.2), while an additional region was identified on chromosome 20 by parametric analysis (LOD=2.3). Interestingly the linkage peak on chromosome 10 is just downstream from a new candidate region within the OPTN gene, recently evidenced in a large genome-wide association study on PDB, while the peak on chromosome 8 is next to the TNFRSF11B gene, encoding osteoprotegerin. Whilst further work will be required to identify the functional variants as well as the pathogenic mechanisms, the present study has provided new insights into the genetic cause of GCT in PDB.

Disclosures: Daniela Merlotti, None.

MO0164

A Prospective Study of Dietary Calcium and the Risk for Primary Hyperparathyroidism. Gary Curhan¹, Julie Paik¹*, Eric Taylor². ¹Brigham & Women's Hospital, USA, ²Maine Medical Center, USA

Purpose: Primary hyperparathyroidism (PHPT) affects at least 2% of postmenopausal women and is associated with morbidities and costly sequelae, including decreased bone mineral density, fractures, and kidney stones. However, little is known about risk factors for PHPT. Low calcium diets in humans raise PTH level and in animals produce higher parathyroid hormone (PTH) level and cellular proliferation in the parathyroid gland. However, no study to date has prospectively examined the association between dietary calcium intake and risk for PHPT in women.

Methods: We conducted a prospective study of the relation between dietary calcium intake and the risk of primary hyperparathyroidism in a cohort of 60,502 women, 37-65 years of age in 1984 with no history of PHPT, participating in the Nurses' Health Study. Dietary calcium was measured by a semiquantitative food-frequency questionnaire in 1984, 1986, 1990, 1994, 1998, 2002, and 2006. Supplemental calcium use was also measured during those years. All cases of PHPT were confirmed by medical record review. Between 1984 and 2008, 281 cases of PHPT were documented.

Results: After adjustment for age, dietary calcium intake was inversely associated with PHPT risk; the relative risk of PHPT for women in the highest compared with the lowest quintile group for calcium intake was 0.57 (95% confidence interval, 0.41 to 0.88, p for trend < 0.01). After further adjustment for other potential risk factors, including calcium supplement use, body mass index, alcohol consumption, smoking status, caffeine intake, dietary intakes of phosphorus, vitamin D, protein, vitamin A, and magnesium, the relative risk of PHPT for women in the highest compared with the lowest quintile group for dietary calcium intake was 0.52 (95% confidence interval 0.30 to 0.91).

Conclusions: A low dietary calcium intake increases the risk of developing primary hyperparathyroidism in women.

Disclosures: Julie Paik, None.

MO0165

Aryl Hydrocarbon Receptor Interacting Protein (AIP) Gene Mutations in a Subset of Sporadic Parathyroid Adenomas. Filomena Cetani¹*, Simona Borsari², Elena Pardi², Elena Paltrinieri², Benedetta Raspini², Federica Saponaro², Antonella Picone², Piero Berti³, Paolo Miccoli³, Claudio Marcocci¹. ¹University of Pisa, Italy, ²University of Pisa Department of Endocrinology & Metabolism, Italy, ³University of Pisa Department of Surgery, Italy

Primary hyperparathyroidism (PHPT) is caused by excessive, incompletely regulated secretion of parathyroid hormone (PTH) from one or more of the four parathyroid glands. It is due to a benign parathyroid adenoma in 80% of cases and multiglandular involvement in 15-20% of cases. The molecular events involved in the formation of parathyroid lesions are poorly understood. Two genes, cyclin D1 (CCND1) and MEN1, have been established as having major roles in parathyroid tumorigenesis, but account for a rather small number of cases. Recently, Vierimaa *et al.* reported that inactivating mutations of the gene encoding aryl hydrocarbon receptor interacting protein (AIP) on chromosome 11q13.3 occurred in patients with pituitary tumors in the familial and sporadic settings. To address the potential role of AIP mutations in the pathogenesis of sporadic parathyroid adenomas, we undertook a genetic screening of AIP gene in a large cohort of apparently sporadic parathyroid tumors (n=100). Coding regions and splice junctions of AIP gene from somatic DNA were sequenced for mutations. Mutation screening revealed an AIP mutation in two apparently unrelated patients, a heterozygous missense mutation in exon 6 (c.911G>A) that brings to a substitution of an arginine to a glutamine residue at codon 304 (R304Q). This codon, situated in a CpG islet, is considered a mutational hotspot, R304X being also described. Unexpectedly this mutation was also present in the germline cells in both cases.

Pathogenic role of R304Q mutation is supported by the presence of this mutation in many familial isolated pituitary adenomas (FIPA) families, as well as in sporadic pituitary GH-secreting adenomas and is not present in a large group of healthy subjects.

In conclusion, in this study we identified a well-known mutation of AIP gene in a minority of sporadic parathyroid adenomas (2%).

Disclosures: Filomena Cetani, None.

MO0166

Case Report: Severe Renal Osteodystrophy in a 40 Year Old Female with End Stage Renal Disease. Maria Princess Landicho¹*, Thelma Crisostomo¹, Pauline Camacho². ¹Makati Medical Center, Philippines, ²Loyola University of Chicago, USA

Background: Metabolic bone changes from chronic kidney disease can have a wide range of presentation. Clinical presentation can be mild or at the extreme end is severe renal osteodystrophy which can present with osteoporosis, osteitis fibrosa cystica, bone resorption, soft tissue and vascular calcification, and the rarely seen uremic leontiasis ossea. This patient illustrates dramatic bony deformities from severe renal osteodystrophy.

Case: We report a case of the most severe form of renal osteodystrophy in a 40 year old female with a 7 year history of undertreated ESRD due to glomerulonephritis. At age 38, she experienced occasional gum bleeding with increase in palate size. At 39, the gum bleeding became frequent, her palate expanded gradually, the gaps in-between her teeth became wider, and she started to have difficulty in eating resulting in weight loss. Her height decreased as she developed a pigeon breast due to compression deformity of the spine. Her Intact PTH then was at 4,444 pg/ml, with normal ionized calcium (1.18 meq/L), increased phosphorus (8 mg/dl) and sestamibi scan showed right parathyroid mass. BMD with T scores of -6.4 spine, -5.2 hip, and -6.9 wrist. She was offered parathyroidectomy but refused.

She was seen in the endocrine clinic at age 40. At this time, she had lost 20 cms in height, 25 kgs in weight. Her palate has expanded downward almost occupying $\frac{1}{4}$ of her oral cavity. Likewise, her maxilla and mandible had expanded forward and downward with looks similar to leontine facies. Her AV fistula was tortuous, severely calcified and enlarged. Her PTH was at 1,508 pg/ml, with normal ionized calcium (1.18 meq/L), more elevated phosphorus (8.54 mg/dl), high alkaline phosphatase (2,604 mg/dl) and creatinine (7.9mg/dl), low vitamin D (12.5 mg/dl). Skeletal survey showed skull with granular deossification, lamina dura of the teeth is gone, massive thickening of the facial bone, C5 and C6 with brown tumors, compression deformity with rugger-jersey spine of thoracolumbar, subperiosteal erosions of bilateral humerus, radius, ulna, and phalangeal bones. Extensive calcific deposits in the soft tissue of the left arm and calcified interdigital vessels. MRI showed generalized thickening of the calvarium, upper and lower jaws, with loss of the lamina propria around the roots of the teeth. Neck ultrasound showed 4 parathyroid masses. Parathyroid scintigraphy showed right parathyroid adenoma.

A multi disciplinary team of doctors discussed approach of treatment. The general consensus was she is high risk for surgery due to poor nutritional status and high anesthesia risk (Mallampati 4). The decision was to defer surgery, treat her with cinacalcet, paricalcitol, sevelamer and improve her nutritional status in preparation for surgery. However, intake of medications was erratic due to economic issues. The patient expired from hemorrhage from her palatal mass.

Conclusion: This case describes a classic severe case of renal osteodystrophy with a marked and progressive growth in the palate and severe bone deformities.



Figure 1. Transition in patient's appearance



Figure 2. Uremic leontiasis ossea, lateral view



Figure 3. Uremic leontiasis ossea



Figure 4. Pigeon chest



Figure 5. Soft tissue and vascular calcification

Disclosures: Maria Princess Landicho, None.

MO0167

Cushing's Disease-Induced Osteoporosis: Evaluation at Diagnosis and Two, Five and Ten Years after Hypercortisolism Resolution. Wallace Holanda-Miranda^{*1}, Sergio Luchini Batista², Aline Ramos¹, Paula Elias¹, Francisco Pereira³, Margaret Castro¹, Avrton Moreira¹, Francisco Jose De Paula⁴. ¹School of Medicine of Ribeirao Preto, USP, Brazil, ²School of Medicine of Ribeirao Preto, University of Sao Paulo, Brazil, ³University of Sergipe, School of Medicine of Sergipe, Brazil, ⁴School of Medicine of Ribeirao Preto - USP, Brazil

Introduction: Glucocorticoid-induced osteoporosis (GIO) is considered to be the most important cause of secondary osteoporosis. Clinical guidelines have clearly established effective strategies to prevent and treat GIO. However, these protocols do not include patients harboring endogenous hypercortisolism, who usually have a hormonal profile distinct from that observed in patients with exogenous hypercortisolism. The aim of the present transversal study was to evaluate bone mineral density (BMD) and bone remodeling in Cushing's disease at diagnosis and in patients after different periods of hypercortisolism resolution. **Subjects and methods:** We studied 11 control individuals (C), 17 patients with Cushing's disease at diagnosis (D) and 28 post-treatment patients with Cushing's disease, divided into 3 subgroups: 2 years (PT2, n=8), 5 years (PT5, n=10) and 10 years (PT10, n=10) after successful treatment, respectively. All groups were matched by age and body mass index. All patients were submitted to the determination of Bone Mineral Density (BMD) in lumbar spine, femoral neck and total hip. The C and D groups were submitted to bone remodeling evaluation [osteocalcin (OC) and deoxypyridinoline (DPD)]. **Results:** Patients at the diagnosis of Cushing syndrome presented significantly lower lumbar spine (C = 0.955 \pm 0.101 vs D = 0.877 \pm 0.121 g/cm², P < 0.05) and femoral neck (C = 0.887 \pm 0.097 vs D = 0.789 \pm 0.107 g/cm², P < 0.05) BMD than controls. Serum OC levels were markedly decreased in these patients (C = 41.1 \pm 26.1 vs D = 4.0 \pm 4.2 ng/ml P < 0.0001), whereas urinary DPD levels were similar to control (C = 5.4 \pm 4.3 vs D = 6.4 \pm 2.5 nmol/mmol of creatinine). At long term, cure of endogenous hypercortisolism induced an improvement in BMD Z-score in lumbar spine (Lumbar spine Z-score: 2 years = -1.13 \pm 0.67 SD, 5 years = -1.25 \pm 0.83 SD and 10 years = -0.15 \pm 1.41 SD). **Discussion:** Our data show that Cushing's disease has a great impact on BMD, which is rescued by successful treatment (after 10 years). Reduced bone formation is the main mechanism involved in bone loss associated with Cushing's disease. The study encourages further investigation to determine fracture risk and the beneficial effect of preventive therapy in Cushing's disease-induced osteoporosis. **Financial support:** National Council for Scientific and Technological Development (CNPq), Brazil.

Disclosures: Wallace Holanda-Miranda, None.

MO0168

Effect of Long Term Stable Hypercalcemia on Kidney Function in the Elderly. Sharon Lahiri¹, Nayana Parikh¹, Sudhaker Rao¹, Manjari Devidi^{*2}. ¹Henry Ford Hospital, USA, ²St. Joseph Hospital, USA

Background: Age is a well known risk factor for declining renal function, but the additional effect of stable hypercalcemia due to primary hyperparathyroidism (PHPT) is unknown. It is argued that elderly patients are less likely to have parathyroidectomy (PTX) because of concern about surgical risk, but very little is known about the effect of untreated PHPT in this group of patients. Accordingly, we retrospectively reviewed the effect of chronic stable moderate to severe hypercalcemia on renal function as assessed by serum creatinine (Cr) in the elderly.

Materials & Methods: Twelve patients, all women, >75 years (mean age of 84 \pm 5 years) and with a disease duration of >10 years were followed for 11-21 years. Serum calcium (Ca; adjusted for albumin), ionized Ca (iCa), PTH, and Cr were measured periodically to monitor the disease. Three of the 12 patients had previous failed surgeries (1-3 PTXs) in expert hands and refused further surgery. Nine women did not want opt for PTX believing that they were "well and did not need intervention" despite repeated urging. None of the 12 had kidney stones or skeletal fractures despite moderate to severe hypercalcemia and low bone density.

Results: The mean serum Ca over the mean follow-up of 17 \pm 4 years was 11.2 \pm 0.71 mg/dl, iCa was 1.47 \pm 0.08 mmol/l, and Cr was 1.03 \pm 0.26 mg/dl with no regression of Cr on serum Ca, iCa or PTH, or age. None developed any of the known complications traditionally associated with PHPT nor hypercalcemic crisis. All were on adequate calcium and vitamin D supplements (mean serum 25-OHD was 34.3 \pm 11.9 ng/ml), and the mean PTH was 131 \pm 72 pg/ml. Mean lowest BMD T-score (spine or femoral neck) was -2.4 \pm 1.3 SD.

Conclusions: Despite traditional concerns, there does not appear to be adverse effects of stable hypercalcemia on renal function in the elderly. Our study is limited by the small sample size and lack of more sensitive measures of renal function. It is likely that adequate Ca and vitamin D supplements may have mitigated some the adverse effects. Finally, there does not appear to be compelling reason to warrant PTX in the absence of overt symptoms since the benefits of PTX may not outweigh the potential risks of surgery in these elderly subjects, especially after failed parathyroidectomy.

Disclosures: Manjari Devidi, None.

MO0169

Long Term Safety of Vitamin D Replacement in Mild Primary Hyperparathyroidism. Shila Begum¹, Jacqueline Berry², Peter Selby^{*2}. ¹Manchester Royal Infirmary, United Kingdom, ²Manchester University, United Kingdom

Primary hyperparathyroidism (PHP) is one of the most common endocrine disorders. It leads to increased catabolism of vitamin D and hence vitamin D deficiency and PHP frequently co-exist. There has been clinical hesitation to replace vitamin D in PHP for fear that this may lead to further increase in plasma calcium concentration. Short term studies have suggested that this may not be the case and we now report the long term safety of vitamin D replacement in patients with PHP and vitamin D deficiency.

Nineteen patients (1 male) with PHP diagnosed on standard biochemical criteria were studied. All had been found to have vitamin D deficiency (serum 25OHD <10ng/ml; n=8) or markedly insufficient (<20ng/ml) and were treated with 1.25mg (50 000iu) ergocalciferol daily for 10 days and then once a month thereafter. Six of the patient had previously been treated with bisphosphonates. Blood samples were obtained before treatment and after 12 months.

Before treatment mean 25OHD was 10.9 (SE 1.1) ng/ml; this increased to 32.6 (4.2) ng/ml after 1 year of ergocalciferol (p<0.001). Over the same period plasma calcium remained stable at 2.77 mmol/l before treatment and 2.72 afterwards. Plasma PTH fell non-significantly with the greatest fall in PTH occurring with the greatest change in 25OHD. No adverse events were recorded in relation to treatment.

We conclude that restoration of 25OHD to the normal range in patients with PHP is safe and ought to be undertaken as part of routine clinical management.

Disclosures: Peter Selby, None.

MO0170

Medical Care Costs for Persons with and without Prevalent Hypoparathyroidism: A Population-based Study. Cynthia Leibson^{*1}, Bart Clarke², Jeanine Ransom¹, Hjalmar Lagast³. ¹Mayo Clinic, Department of Health Sciences Research, USA, ²Mayo Clinic College of Medicine, USA, ³NPS Pharmaceuticals, USA

Hypoparathyroidism (HypoPARA) is a rare condition which may last from a few days to an entire lifetime and with consequences ranging from asymptomatic presentation to fatal hypocalcemia. Population estimates of prevalence of HypoPARA and associated medical care costs are lacking. We addressed these issues using unique population-based, longitudinal, medical-records-linkage resources of the Rochester Epidemiology Project (REP) to 1) identify all persons residing in Olmsted County in 2009 with any diagnosis of HypoPARA ever assigned by a REP provider since 1945, 2) review detailed medical records to confirm diagnosis of HypoPARA and assign etiology, 3) assign 2 age- and sex-matched controls per confirmed case, and 4) censor follow-up for every case/control set member at shortest follow-up for each member. Since 1987, REP resources also include provider-linked line item billing data for essentially all medical services and procedures received by residents of Olmsted County, MN, with the capacity to assign nationally standardized wage- and inflation-adjusted dollar estimates. Data on outpatient prescription costs are excluded. Using these resources, we obtained all medical care costs for each year 2006 through 2008 to compare cases with controls for 2009 estimated dollar costs. There were 54 confirmed cases (71% female; mean age 5820 years; etiology=78% post-surgical, 9% secondary, 7% familial, 6% idiopathic). The prevalence of 37/100,000 translates to approximately 100,000 persons with HypoPARA in the US in 2010. Results of cost comparisons for 2006-8 are provided in the Table. In each year, mean (median) costs for HypoPARA cases [12,696 (1,062); 10,861 (1,911); 7,607 (2,716)] were approximately 3 times those for controls [4,669 (328); 3,697 (584); 2,817 (557)]. These population-based data on confirmed HypoPARA prevalence over the full range of disease and associated medical care costs reveal that, although a relatively rare condition, the burden of costs associated with HypoPARA is substantial and consistent. Additional investigation is needed to elucidate the source of excess costs.

Annual medical care costs for prevalent confirmed cases with HypoPARA and age-, sex- matched controls in 2009 \$							
Year		N	Mean	25 th Pctl	Median	75 th Pctl	Maximum
2006	Control	108	4669	0	328	2019	89329
	Case	54	12696	196	1062	6198	235046
2007	Control	108	3697	0	584	1516	161447
	Case	54	10861	800	1911	8025	170656
2008	Control	108	2817	137	557	1998	54712
	Case	54	7607	843	2716	7304	57612

Medical care costs HypoPARA cases vs. controls

Disclosures: Cynthia Leibson, None.

This study received funding from: NPS Pharmaceuticals

MO0171

PTH (1-84) Replacement Therapy in Hypoparathyroidism: Effects on Bone Metabolism and Structure. Tanja Sikjaer¹, Lars Rejnmark¹, Annemarie Bruel², Jesper Thomsen², Leif Mosekilde¹. ¹Aarhus University Hospital, Denmark, ²University of Aarhus, Denmark

Conventional treatment of hypoparathyroidism (hypoPT) with calcium supplements and active vitamin D analogues causes reduced bone turnover and over-mineralized bone.

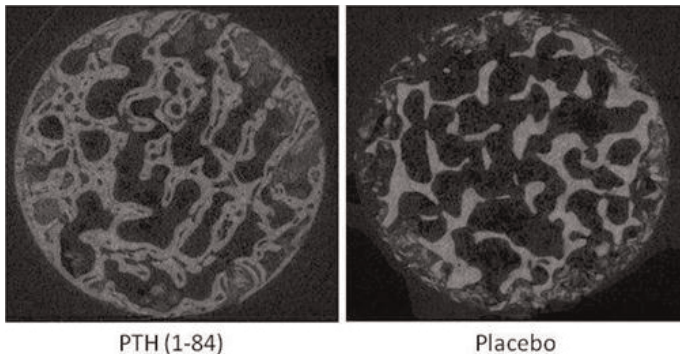
We studied 62 patients with known hypoPT randomized into 2 groups of treatment with either PTH (1-84) 100 µg/d s.c. or placebo, as an add-on therapy.

We investigated the changes in bone structure and density using µCT in 44 iliac crest bone biopsies (23 on PTH treatment) obtained after 24-wks of treatment. Trabecular tunnelling was evident in 11 (48%) biopsies from the PTH-group, whereas no tunnelling was detected in the placebo group. Patients showing tunnelling had significantly higher levels of biochemical markers of bone resorption (NTX and CTX) and formation (osteocalcin, bone specific alkaline phosphatase, PINP). Compared with placebo, PTH-treatment resulted in lower trabecular thickness (Tb.Th*) ($p < 0.01$), and trabecular bone tissue density ($p < 0.01$), whereas connectivity density (CD) was higher ($p < 0.05$) and structural modelling index tended to be lower indicating a change in trabecular architecture from a rod-like to a more plate like structure. The changes in Tb.Th* and CD can be explained by the intratrabecular tunnelling.

Cortical porosity tended to be higher in PTH-treated patients, especially in those with tunnelling. Occurrence of tunnelling was not associated with etiology, length of disease, concentration of PTH, ionized calcium, or 1,25-hydroxy vitamin D.

Quantitative computed tomography (QCT) at the spine and hip were performed at baseline and at week 24 in 31 patients. At the lumbar spine (L1+L2), the increase in trabecular vBMD over the study period was significantly ($p = 0.02$) higher in the PTH group (+12.2%) than in the placebo group (-0.7%). On the contrary, total vBMD decreased more in the PTH than in the placebo group at the total hip (-1.83% vs 0.43%, $p < 0.05$), at the trochanteric region vBMD (-3.28% vs 0.46%, $p < 0.03$), and at the femoral neck (-3.3% vs -0.84%, $p = 0.12$). At all three sites, there was a tendency towards an increased trabecular and a decreased cortical vBMD in the PTH treated patients.

The effect of PTH (1-84)-treatment in hypoPT is an increased bone turn-over with a decreased vBMD at cortical sites, and an increased vBMD at the trabecular sites, which is related to morphological changes in the bone microstructure with intratrabecular tunnelling and increased cortical porosity.



Disclosures: Tanja Sikjaer, None.

MO0172

PTH(1-84) Lowers Circulating Sclerostin Levels in Hypoparathyroidism. Aline Costa¹, Mishaella Rubin¹, Jim Sliney Jr², Zachary Lenane¹, Rebecca Ives², Chiyuan Zhang¹, Donald McMahon³, Serge Cremers¹, John Bilezikian³. ¹Columbia University, USA, ²Columbia University Medical Center, USA, ³Columbia University College of Physicians & Surgeons, USA

The inhibitory actions of PTH on sclerostin function are seen *in vivo* but there are little human data. Hypoparathyroidism (HYPOPT), a disorder characterized by low PTH, is an ideal clinical situation to test the hypothesis that PTH regulates sclerostin in human subjects. We investigated the effect of PTH(1-84) [PTH] administration on circulating sclerostin in HYPOPT. 42 subjects with HYPOPT (11 men, 13 post- and 18 pre-menopausal women) were treated for 12 months with PTH, 100µg every other day by subcutaneous injection. Blood samples were collected prior to PTH injection, and bone markers and serum sclerostin [measured by ELISA (TECOMedical)] were assessed at baseline and throughout the treatment period: months 1, 2, 3, 6 and 12. Mean age of subjects was 48.12 yrs and HYPOPT had been diagnosed for 16.13 yrs. Baseline values: serum calcium (8.50.9mg/dL; nl: 8.5–10.4); PTH (54 pg/mL; nl: 10–65) and sclerostin: 0.8400.37 ng/mL (nl men: 0.74; postmenopausal: 0.69; premenopausal: 0.56). Baseline sclerostin was different among the gender subgroups with men showing higher sclerostin levels than the other 2 groups (1.191 vs 0.794ng/mL, $p < 0.005$

postmenopausal; vs 0.659 ng/mL, $p < 0.0001$ premenopausal women). Post- and premenopausal women did not differ from each other. As expected, bone turnover markers started to increase with PTH treatment by month 1. After month 1, the entire cohort showed a progressive decline in sclerostin reaching significantly lower values at month 6 (0.840 to 0.778ng/mL; $p < 0.05$). The PTH-associated lower sclerostin concentration was sustained thereafter, to month 12 (0.840 to 0.777ng/mL; $p < 0.05$). Among the different subgroups, postmenopausal women first showed differences in sclerostin levels from month 1 to month 2 (0.861 to 0.741, $p < 0.05$). A time-dependent, progressive decline in sclerostin levels was seen in men (1.191 to 1.041ng/dL; $p < 0.05$), and less so in pre- (0.659 to 0.618ng/dL; $p = 0.5$) and post-menopausal women (0.790 to 0.774 ng/dL; $p = 0.7$). However, the overall sclerostin response to PTH was similar among the 3 groups. The results indicate that administration of PTH in HYPOPT is associated with reduced circulating sclerostin in human subjects. The concomitant increase in bone turnover markers, a characteristic of PTH administration, may be directly related to the associated effect of PTH to reduce sclerostin levels.

Disclosures: Aline Costa, None.

MO0173

Relationships Between Pharmacokinetic Profile of Human PTH(1-84) and Serum Calcium Response in Postmenopausal Women Following 4 Different Methods of Administration. John Fox^{*}, David Wells, Roger Garceau. NPS Pharmaceuticals, USA

Recombinant full-length human PTH [rhPTH(1-84)] is approved in the EU to treat postmenopausal osteoporosis (PMO) and is currently being developed as a hormone-replacement therapy in hypoparathyroidism. In PMO the optimal pharmacokinetic (PK) profile is for the sc injection to result in a transient increase in plasma PTH levels. This maximizes the anabolic response in bone and minimizes side-effects such as increased serum Ca. In contrast, in hypoparathyroidism where increased serum Ca is a required endpoint, a more-prolonged PK profile may be preferable. We have investigated the relationship between the PK profile of PTH following administration of 100 µg rhPTH(1-84) and the serum Ca response in normal postmenopausal women using 4 different dosing methods [15-min iv infusion; sc injection in abdomen or thigh, intradermal injection (1.5 mm depth) in abdomen]. Mean data are shown in the Table. The highest PTH level was achieved with iv infusion but rapid clearance resulted in the fastest restoration of preinfusion PTH levels and the smallest and shortest duration of increased serum Ca. Lower maximum PTH levels occurred later following sc injection in abdomen and PTH exposure was only 55% of that with the infusion. Predose PTH levels were not re-established until 9 h and the serum Ca response was greater with normal Ca levels not restored until 14–24 h. In contrast, sc injection in thigh resulted in a smaller but more-prolonged PTH increase and a larger and longer serum Ca response, despite a 15% lower PTH exposure vs. abdomen. Intradermal injection resulted in a shorter PTH profile and serum Ca response than with sc injection. In conclusion, the magnitude and duration of the serum Ca response to the sc administration of rhPTH(1-84) in the thigh is greater than when given sc or id in the abdomen, or iv. This has significant therapeutic implications for the various potential indications for PTH therapy, such as hypoparathyroidism.

Route (n)	Plasma PTH(1-84)			Serum Total Ca		
	Max (h)	C _{max} (pg/mL)	Time to return to predose levels (h)	Max (h)	Max increase (mg/dL)	Time to return to predose levels (h)
Intravenous (12)	0.25	8162	3	2	0.38	10
SC-Abdomen (16)	1.1	402	9	7	0.62	14,24
SC-Thigh (18)	1.0	326	12	11	0.81	>24
Intradermal (19)	0.08	440	6	6	0.82	16

Table 1

Disclosures: John Fox, NPS Pharmaceuticals, 1; NPS Pharmaceuticals, 5
This study received funding from: NPS Pharmaceuticals

MO0174

Simultaneous Quantitative Analysis of Vitamin D Receptor (VDR), Calcium Sensing Receptor (CaSR), Parathyroid Hormone (PTH) and Cyclin D1 mRNAs in Moderate to Severe Primary Hyperparathyroidism (PHPT) in Asian Indians. Shweta Varshnay¹, Sanjay Bhadada², Sudhaker Rao³, Uma Nahar¹, Anil Bhansali⁴, Arunanshu Behera¹, Ambrish Mithal⁵, Sadhna Sharma¹. ¹PGIMER, Chandigarh, India, ²PGIMER, Chandigarh, Ind, ³Henry Ford Health System, USA, ⁴PGIMER, Chandigarh, India, ⁵Medicity Hospital, Gurgaon, India

Background: PHPT has varied presentation in different parts of the world and its pathogenesis remains elusive. We previously reported reduced VDR & CaSR in sporadic parathyroid adenomas in mild to moderate PHPT, but such data is lacking in moderate to severe PHPT. In addition, the relationship between PTH secretion and cell proliferation, and adenoma size has not been fully elucidated. Accordingly, we simultaneously measured VDR and CaSR mRNAs, as well as mRNAs of PTH (marker of PTH secretion) and Cyclin D1 (marker of cell proliferation) in moderate to

severe PHPT and correlated with indices of the disease (serum Ca& PTH and adenoma weight) to better understand the varied pattern of presentation of PHPT.

Material & Methods: mRNA expressions (VDR, CaSR, PTH, and Cyclin D1) were assessed by quantitative RT-PCR in 50 surgically confirmed parathyroid adenomas and 10 normal parathyroid samples. The relative mRNA expression (mean of duplicate RT-PCR assays) was assessed by 2-^{-ΔΔCp} Method. The results are expressed as % change (up or down) after adjusting for the traditional housekeeping gene, GAPDH.

Results: Consistent with our previous immunohistochemistry findings and other reports of mRNA studies, both VDR and CaSR mRNAs were reduced by 65% and 58% respectively ($p < 0.001$ for both) in adenomatous compared to normal parathyroid tissue. In contrast, mRNAs of PTH and Cyclin D1 were increased by 17.2& 10.3 fold respectively ($p \leq 0.001$ for both). Although the PTH mRNA did not correlate with adenoma weight, there was a significant correlation between Cyclin D1 mRNA and adenoma weight ($r = 0.78$; $p < 0.001$). Also, PTH mRNA correlated with serum iPTH levels ($r = 0.86$; $p < 0.001$), but there were no correlations between VDR and CaSR mRNA levels either with indices of disease (serum Ca&PTH) or with serum 25-OHD levels. There was no relationship between decreased VDR and CaSR mRNA expression and increased PTH and Cyclin D1 mRNA expression. This implies that the reduction in VDR and CaSR gene expression may depend on parathyroid cell proliferation rather than on indices of disease (serum Ca&PTH) or vitamin D nutrition (25-OHD).

Conclusions: We reaffirmed the reduced VDR & CaSR expression in moderate to severe PHPT in Asian Indians just as in mild PHPT in the west. In addition, we demonstrated greatly increased expression of PTH and Cyclin D1 mRNAs, and the latter correlated with adenoma weight. The implications of our findings to the clinical expression of the disease and its pathogenesis deserve further study.

Disclosures: Shweta Varshnay, None.

This study received funding from: Indian Council of Medical research

MO0175

Vitamin D Toxicity in a Patient with Surgical Hypoparathyroidism. Chae Kim, Heather Hofflich*. University of California, San Diego, USA

Purpose: Case Report

A 35-year-old female presented to our clinic. Patient's medical history was significant for papillary thyroid cancer diagnosed at age 19, for which she was treated with a total thyroidectomy followed by radioiodine therapy. She was diagnosed with hypoparathyroidism due to persistent hypocalcemia following thyroidectomy. Our patient was taking 50,000 alternating with 100,000 IU of Vitamin D2 (drisdol) daily. She was taking 1500 mg of calcium carbonate daily. Patient presented with symptoms of polydipsia, polyuria, muscle pain, numbness of extremities, constipation, and a 20lb weight loss over the last year. On presentation to our clinic, patient's 25-OH vitamin D level was found to be 284 ng/mL (reference range: 30-80 ng/mL) and serum calcium level was 8.9 mg/dL (reference range: 8.6-10.5 mg/dL) (ARUP labs were used). One month after stopping the vitamin D, the 25(OH) vitamin D level was 87 ng/mL and our patient was asymptomatic.

Conclusion: Different formulations of vitamin D can be used to treat hypoparathyroidism. Although calcitriol is preferred over vitamin D2 or D3 because of rapid onset and offset, daily doses of 25,000-100,000 IU of Vitamin D2 or D3 is also an accepted and less expensive way to treat hypoparathyroidism. Because of the long half-life, it is recommended to adjust the dose by checking serum levels of calcium, albumin, phosphorous, and creatinine. (1) However, it is also crucial to regularly monitor 25(OH) vitamin D levels in all patients on high dose Vitamin D supplements. This was not performed in our patient on a regular basis.

In our review of the literature, most cases of vitamin D toxicity present with elevated serum calcium levels.(2,3) Our patient had symptoms and findings of hypercalcemia, but had normal serum calcium levels throughout her clinical course. This is most likely due to her acquired hypoparathyroidism. We do know that calcium levels of 9.0-9.4 mg/dL can be high for a patient with hypoparathyroidism. We want clinicians to be aware to also look at the 24 hour urine calcium levels, especially in patient's with hypoparathyroidism.

1. Shoback D. Hypoparathyroidism. The New England Journal of Medicine. 2008;359:391-403.

2. Klontz KC, Acheson DW. Dietary Supplement-Induced Vitamin D Intoxication. The New England Journal of Medicine. 2007;357:308-309

3. Koutkia P, Chen TC, Holick MF. Vitamin D Intoxication Associated with an Over-the-Counter Supplement. The New England Journal of Medicine. 2001;345:66-67

	Ref. Range	04/26/10	05/26/10 Initial Presentation	06/04/10	06/16/10	06/30/10
BUN	6-20 mg/dL	12	12	14		
CREATININE	0.51-0.95 mg/dL	0.91	0.90	0.89		
CALCIUM	8.6-10.5 mg/dL	9.0	9.4	9.2	8.5 (L)	9.0
CALCIUM, IONIZED	1.13-1.32 mEq/L	1.12 (L)	1.12 (L)			
PHOSPHOROUS	2.7-4.5 mg/dL		4.4	4.1		
PTH INTACT	15-65 pg/mL		9 (L)			
VITAMIN D, 1,25-DIHYDROXY	15-75 pg/mL	40	54			
VITAMIN D, 25-HYDROXY	30-80 ng/mL	284(H)	144 (H)	143 (H)	96 (H)	87 (H)
ALBUMIN	3.5-5.2 gm/dL	3.5 4/29/2010	4.6			4.4 6/24/2010
24 hour urine calcium	420 mg/dL					

lab values for our patient

Disclosures: Heather Hofflich, None.

MO0176

Decreased Trabecular Tissue Mineralization Is Associated with Fracture in Patients with Kidney Disease. Thomas Nickolas^{*1}, Xiaowei Liu², Emily Stein², Mafo Kamanda-Kosse³, Ivelisse Colon¹, Serge Cremers³, Lucas Nikkel¹, Chiyuan Zhang³, Donald McMahon², Elizabeth Shane². ¹Columbia University Medical Center, USA, ²Columbia University College of Physicians & Surgeons, USA, ³Columbia University, USA

In renal osteodystrophy (ROD), abnormal Vitamin D metabolism and remodeling cause tissue mineralization defects. As degree of mineralization, or tissue mineral density (TMD), affects tissue-level mechanical properties, abnormal TMD may contribute to the high fracture (Fx) risk in chronic kidney disease (CKD) patients. Previously, invasive iliac bone biopsy was required to evaluate tissue mineralization. We have now measured TMD on non-invasively acquired high resolution peripheral QCT (HRpQCT) scans of the distal radius (DR) and tibia (DT). We hypothesized trabecular (Tb) TMD is lower in CKD patients with fracture (Fx) than both CKD patients without Fx and healthy Controls. We also hypothesized Tb TMD is inversely related to calciotropic hormones and bone turnover markers (BTM).

We performed HRpQCT (Scanco Medical, AG; voxel size 82µm) of the DR and DT in 47 patients with CKD (n=23 Fx; 24 nonFx) and 21 healthy Controls without Fx, matched for age, sex, race. By digital topological analysis (DTA), we classified Tb bone voxels as belonging to one of 3 envelopes: surface Tb bone, central Tb bone and intervening (middle) Tb bone occupying the envelope between surface and central Tb bone (Fig 1). TMD was calculated for surface (sTMD), central (cTMD), and middle (mTMD) envelopes. We also measured serum iPTH, 25-OHD and bone formation (BSAP, PINP) and resorption (CTX, Trap5b) markers.

CKD-Fx, CKD-nonFx, and Controls were well matched for age (68 yrs; F-test NS), female sex (60%, 58% and 68%, $p = \text{NS}$) and white race (28%, 29%, 32%, $p = \text{NS}$). Tb TMD was significantly lower in CKD-Fx than Controls. At the DR, sTMD and mTMD were lower by 2.6% and 3.0%, respectively (all $p < 0.05$). At the DT, sTMD, mTMD and cTMD were lower by 2.2%, 2.6% and 3.1%, respectively (all $p < 0.05$). Tb TMD in CKD-nonFx was intermediate between CKD-Fx and Controls but did not differ significantly from either. At the DT, each standard deviation decrease in s-, m- and cTMD was associated with 1.7%, 1.4% and 1.1% increased odds of Fx ($p < 0.05$ for all). Higher levels of iPTH, BSAP, PINP and CTX, were inversely and significantly correlated with s-, m- and cTMD; r values ranged from -0.40 for PINP vs DT sTMD ($p < 0.009$) to -0.53 for iPTH vs DR sTMD ($p < 0.0005$).

CKD patients with Fx have low Tb TMD, likely related to secondary hyperparathyroidism and high bone turnover. HRpQCT may provide a non-invasive approach to measurement of Tb TMD in CKD; validation against iliac crest bone biopsy is needed.

MO0178

The Influence of Growth Hormone Treatment on Bone Matrix Mineralization in Children with Chronic Kidney Disease. Kamilla Nawrot-Wawrzyniak^{*1}, Nadja Fratzl-Zelman¹, Barbara M. Misof¹, Paul Roschger¹, Sonja Lueger¹, Małgorzata Pancyk-Tomaszewska², Helena Ziółkowska², Klaus Klaushofer¹. ¹Ludwig Boltzmann Institute of Osteology at Hanusch Hospital of WGKK & AUVA Trauma Centre Meidling, 1st Medical Department; Hanusch Hospital Vienna, Austria, ²Department of Pediatrics & Nephrology Medical University of Warsaw, Poland

Patients with chronic kidney disease (CKD) develop renal osteodystrophy (ROD) that is classified by the turnover/mineralization/volume-system. Treatment with recombinant human growth hormone (rhGH) was shown to be a safe and efficacious method to improve height deficits in children with CKD. The influence of rhGH treatment on bone matrix mineralization, an important determinant of bone material quality, is unknown.

We studied bone histomorphometry and matrix mineralization in 20 children (4-16 years) with CKD before and after treatment with rhGH in paired transiliac bone biopsies (with informed consent from the parents). Bone mineralization density distribution (BMDD) was determined by quantitative backscattered electron imaging. Following parameters were used to characterize the BMDD curve: weighted mean mineral concentration (Ca_{Mean}), most frequently measured mineral concentration (Ca_{Peak}), heterogeneity of mineralization (Ca_{Width}) and portion of fully (Ca_{High}) and low (Ca_{Low}) mineralized bone areas. All BMDD data were compared to previously published reference data of healthy children.

Before rhGH-treatment the bone samples were classified to adynamic bone disease (ABD, n=5), osteomalacia (OM, n=2), normal bone (NB, n=4), mixed uraemic osteodystrophy (MUO, n=9) and osteitis fibrosa (OF, n=0). In general indices of bone formation and bone resorption were decreased or normal, while bone matrix mineralization was normal or increased.

After rhGH-treatment ROD classification was: ABD (n=1), OM (n=1), NB (n=6), MUO (n=11), OF (n=1) and bone turnover indices were normal or increased. The BMDD results showed that Ca_{Mean} (-4.1%, $p<0.03$), Ca_{Peak} (-4.4%, $p<0.01$) and Ca_{High} (-70.6%, $p<0.001$) were decreased, whereas Ca_{Width} (+16.6%, $p<0.01$) was increased compared to before treatment. There were significant correlations between bone turnover variables (BFR/BS, MS/BS) and BMDD parameters. In particular, the correlations within the former ABD subgroup were remarkably strong: Spearman coefficients ranged from -0.71 to -0.88 for Ca_{Mean} , Ca_{Peak} , Ca_{High} , and from 0.74 to 0.88 for Ca_{Width} and Ca_{Low} (p -value from <0.001 to <0.05) after treatment.

The results revealed an anabolic effect of rhGH on bone. In particular in the ABD group with abnormally high bone matrix mineralization, there was a shift towards normal BMDD. In conclusion, rhGH-treatment in pediatric CKD patients seems to improve bone material quality.

Disclosures: Kamilla Nawrot-Wawrzyniak, None.

MO0179

Bone Metabolism in Diabetic Patient with or without Metabolic Syndrome. Ran Cui^{*1}, Shen Qu², Hui Sheng³. ¹Tenth People's Hospital of Tongji University, Peoples Republic of China, ²Tongji University School of Medicine, Peoples Republic of China, ³Shanghai, Fudan University, Peoples Republic of China

The features of bone metabolism in patients with diabetes and metabolic syndrome (MS) remain unclear; here we are going to explore the relationship of osteoporosis and metabolic syndrome in diabetic patients. 107 male (32-85 years) and 136 postmenopausal female patients (44-87 years) with type 2 diabetes were recruited. The patients were divided to two groups according to the diagnosis criteria of MS by IDF 2004. Each patient accepted the bone mineral density (BMD) measured by Dual Energy X-ray Absorptiometry (DEXA) and the serum bone metabolic markers including type I collagen (β -CTX), parathyroid hormone (PTH), osteocalcin (OC), calcitonin (CT). Bone specific alkaline phosphatase (BAP) and Vitamin D (VD) were measured at same time. The components of MS including fasting plasma glucose, serum insulin, blood pressure and lipid were determined. In males, the diabetic patients with MS have a higher BMD in femur neck (FN) (95%CI: (0.012, 0.110), $P=0.015$) and a lower β -CTX and OC level (95%CI (-0.223, -0.051), $P=0.002$; (-6.93, -5.7), $P=0.021$ respectively). In females, no significant differences were found in patients with or without MS. Multiple linear stepwise regression in the MS group showed the BMD of right hip (RH) and FN in males and lumbar (L) in females had positive correlations with weight ($\beta=0.382$, $P=0.023$; $\beta=0.318$, $P=0.018$; $\beta=0.446$, $P=0.000$) after adjusted for age. Waist circumference (WC) was negatively correlated with lumbar BMD ($\beta=-0.289$, $P=0.016$) and positively with FN ($\beta=0.249$, $P=0.015$). The triglyceride (TG) level was positively related to FN ($\beta=0.270$, $P=0.044$) in males, LDL was positive related to RH ($\beta=0.217$, $P=0.027$) and Total cholesterol (TC) was negative related to FN ($\beta=-0.220$, $P=0.026$) in females. Diastolic blood pressure (DBP) was positive related with RH ($\beta=0.310$, $P=0.002$) in females. In males, the BMD in diabetic patients with MS was higher in lumbar with the lower bone turnover level but there was no significant difference in females in these parameters. Weight was a positive factor on BMD in both males and females. Other components of MS, such as the blood pressure, lipid and insulin resist had dissimilar effect on different gender, more studied were expected.

Disclosures: Ran Cui, None.

This study received funding from: Shanghai PJ1408400

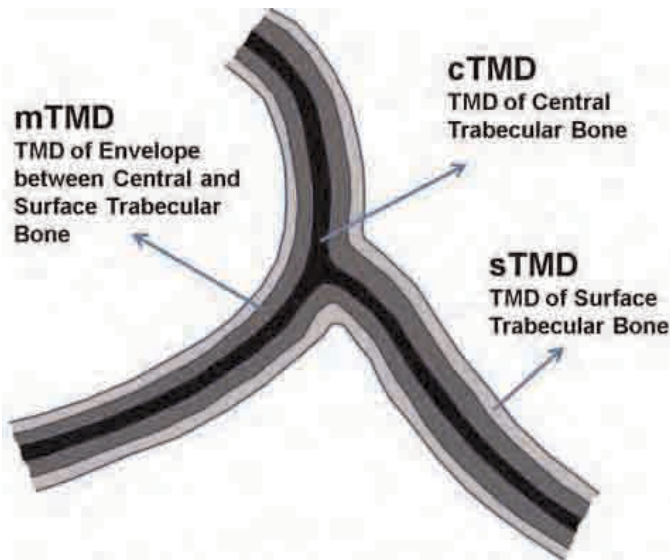


Figure 1. Classifications of surface Tb bone (sTMD), central Tb bone (cTMD) and intervening Tb bone (mTMD) occupying the envelope between surface and central Tb bone.

Figure 1

Disclosures: Thomas Nickolas, None.

MO0177

Tests of Bone Density and Structure are Associated with Fractures in Stage 3-5 Chronic Kidney Disease. Sophie Jamal^{*1}, Sarah West², Angela Cheung³, Charmaine E. Lok⁴. ¹The University of Toronto, Canada, ²University of Toronto, Canada, ³University Health Network, Canada, ⁴Toronto General Hospital, Canada

Purpose: Fractures are common in patients with chronic kidney disease (CKD). Previous studies showed that bone mineral density (BMD) by dual x-ray absorptiometry (DXA) does not discriminate well (hip BMD AUROC: 0.56) among fractured and non-fractured patients with stage 5 CKD on dialysis. However, the ability of BMD by DXA and bone structure by high-resolution peripheral quantitated computed tomography (HR-pQCT) to discriminate fracture status among pre-dialysis patients with stages 3-5 CKD has not been well studied.

Methods: We utilized baseline data from an ongoing observational study in patients, age ≥ 18 yrs, with stage 3-5 CKD (using NKF criteria by MDRD eGFR) to determine if BMD by DXA (Hologic) at the lumbar spine (LS), total hip (TH), ultradistal radius (UDR); and/or cortical area, density & thickness, trabecular area, density & separation by HR-pQCT (XtremeCT) at the radius could discriminate between those with and without fracture (self-reported low trauma fractures occurring after age 40 and/or prevalent vertebral fractures identified by morphometry). Results are expressed as areas under the receiver operating characteristic curves (AUROC) with 95% confidence intervals (CI), adjusted for age and weight.

Results: Data was available for 128 men and 86 women. Compared to those without fractures (n=143), those with fractures (n=70) were older (5916 vs. 6914 yrs, $p<0.001$). There were no other differences in demographics by fracture status. The mean weight was 79.919.8 kg, most were Caucasian (70.0%), over 40% had diabetes, and most (74%) subjects had stage 4 or 5 CKD. The mean duration of CKD was 8.010.3 yrs, and 30.2% reported a fall in the last 12 months. BMD by DXA was able to discriminate among those with and without fractures (AUROC for LS: 0.70 [95% CI: 0.62-0.78]; TH: 0.69 [95% CI: 0.61-0.77]; UDR: 0.71 [95% CI: 0.63-0.78]). HR-pQCT also performed well for cortical measures (AUROC for area: 0.67 [95% CI: 0.59-0.76]; density: 0.70 [95% CI: 0.63-0.78] and thickness: 0.70 [95% CI: 0.62-0.78]) and trabecular measures (AUROC for area: 0.70 [95% CI: 0.62-0.78]; density: 0.70 [95% CI: 0.63-0.78]; and separation: 0.70 [0.63-0.78]).

Conclusions: BMD by DXA and HR-pQCT parameters are able to discriminate fracture status in stage 3-5 CKD pre-dialysis patients, which is different than what has been reported in patients with stage 5 CKD on dialysis. Prospective studies are needed to evaluate the fracture predictive ability of BMD and HR-pQCT.

Disclosures: Sophie Jamal, None.

MO0180

Gene Expression Changes in Femoral Head Necrosis of Human Bone Tissue. Janos Kosa^{*1}, Bernadett Balla¹, Csaba Pinter², Janos Podani³, Laszlo Kiss⁴, Istvan Takacs⁵, Gabor Speer¹, Zsolt Nagy⁵, Balazs Horvath², Laszlo Koranyi⁶, Peter Lakatos⁵. ¹Semmelweis University, Hungary, ²Csolnoky Ferenc Veszprem County Hospital, Hungary, ³Eotvos Lorand University, Hungary, ⁴Hetenyi Geza County Hospital, Hungary, ⁵Semmelweis University Medical School, Hungary, ⁶Drug Research Center, Hungary

Osteonecrosis of the femoral head (ONFH) is the result of an interruption of the local circulation and the injury of vascular supply of bone. Multiple factors have been implicated in the development of the disease. However the mechanism of ischemia and necrosis in non-traumatic ONFH is not clear. The aim of our investigation was to identify genes that are differently expressed in ONFH vs. non-ONFH human bone and to describe the relationships between these genes using multivariate data analysis. Six bone tissue samples from ONFH male patients and 8 bone tissue samples from non-ONFH men were examined. The expression differences of selected 117 genes were analyzed by TaqMan probe-based quantitative real-time RT-PCR system. The significance test indicated marked differences in the expression of nine genes between ONFH and non-ONFH individuals. These altered genes code for collagen molecules, an extracellular matrix digesting metalloproteinase, a transcription factor, an adhesion molecule, and a growth factor. Canonical variates analysis demonstrated that ONFH and non-ONFH bone tissues can be distinguished by the multiple expression profile analysis of numerous genes controlled via canonical TGFB pathway as well as genes coding for extracellular matrix composing collagen type molecules. The markedly altered gene expression profile observed in the ONFH of human bone tissue may provide further insight into the pathogenetic process of osteonecrotic degeneration of bone.

Disclosures: Janos Kosa, None.

MO0181

Increased Visceral Adiposity during Anti TNF α Treatment for Inflammatory Rheumatic Disease is Associated with Various Changes on Serum Adipokines: A 2 years Prospective Study. Eric Toussiot^{*1}, Laurent Mourou², Nhu uyen Nguyen³, Malika Bouhaddi³, Daniel Wendling⁴, Gilles Dumoulin⁵. ¹University Hospital J Minjoz, France, ²EA3920 Physiopathologie Cardiovasculaire et Prevention, France, ³Explorations fonctionnelles Physiologie, Minjoz Hospital, France, ⁴University Hospital Minjoz, France, ⁵Explorations fonctionnelles biochimie endocrinienne et metabolique Minjoz Hospital, France

Introduction: TNF α blocking agents are very effective in rheumatoid arthritis (RA) or ankylosing spondylitis (AS) and has been associated with weight gain. Adipokines are proteins produced by the adipose tissue with many physiologic functions and can also influence the inflammatory response. Certain adipokines could represent a link between the immune response, the metabolic functions and the nutritional status.

Objectives: we evaluated the long term effects of anti TNF α treatment on body weight, body composition and distribution. The changes on the serum levels of adipokines (leptin, adiponectin and resistin) and ghrelin, a gastric peptide involved in appetite regulation were also studied.

Patients and methods: 20 patients (6F) were evaluated (12 AS [modified NY criteria], age [mean SD]: 40.7 16.1 yrs; and 8 RA [ACR criteria], age 60.5 9.7 yrs; mean disease duration: 9.6 9.8 yrs). They received infliximab (2), etanercept (6) or adalimumab (12). Body weight, body mass index (BMI), serum levels of adipokines and ghrelin were measured (IRMA) at baseline and then at months (M) 1, 3, 6, 12, 18 and 24. Body composition was evaluated at baseline and then at M6, 12 and 24. Total and regional body fat and lean masses were measured by total body DEXA (Lunar iDXA). Adiposity was calculated as the ratio between total fat tissue and total lean mass + total fat tissue. Fat distribution was evaluated as the relative proportion of fat tissue in the android (central) and the gynoid (hip and thigh) regions.

Results: there was a slight but significant increase in body weight (+ 1.35 kg) and BMI (+ 0.55 kg/cm²) (p<0.005). All the patients responded to the treatment with clinical improvement and decline of erythrocyte sedimentation rate and CRP (p<0.01). Although fluctuating during the study, leptin and resistin levels did not significantly change. By contrast, adiponectin increased at M1, and then decreased slowly and reached lower values at M24 compared to baseline (baseline: 12.1 4.8; M24: 11.4 5.4 ?g/ml; p= 0.01). We also observed a rapid decline in ghrelin which remained low until the end of the study (baseline: 1256 387; M24: 1117 429 pg/ml; p= 0.035). Lean mass and fat mass in the gynoid region did not change while there was a significant increase at M24 in adiposity (+ 1.36%; NS), in total fat mass (+ 2.4 kg; p= 0.003) and in fat tissue located in the android region (+ 366 g; p= 0.025).

Conclusion: long term administration of TNF α blocking agents was associated with gain of body weight and BMI. Leptin and resistin levels fluctuated while ghrelin decreased. However, TNF α blockade is associated with a modest but significant gain in total fat and especially fat in the android region. It is known that abdominal or visceral adipose tissue is associated with the development of atherosclerosis. These changes, together with the decrease in adiponectin serum levels, could negatively influence the cardiovascular risk of these patients.

Disclosures: Eric Toussiot, None.

MO0182

Toll-like Receptor 2 Heterodimer, TLR1/2 and TLR 2/6, Induces Inflammatory Bone Loss via PGE₂ Production by Osteoblasts. Chiho Matsumoto^{*}, Tsukasa Tominari, Toshio Oda, Michiko Hirata, Masaki Inada, Chisato Miyaura. Tokyo University of Agriculture & Technology, Japan

Toll-like receptors (TLRs), TLR1-TLR13, play critical roles in innate immunity, and various ligands for respective TLR are thought to regulate host defense mechanisms against pathogens. TLRs are divided into two major subgroups, one group is consist of TLR1, 2, 4, 5, 6 and 11, which are expressed on cell surfaces, and the other is composed of TLR3, 7, 8 and 9, which are mainly expressed in intracellular vesicles. TLR4 was identified as the receptor for lipopolysaccharide (LPS), which is an outer membrane component of gram-negative bacteria and known as a pathogen for periodontitis. We have reported that LPS binds to TLR4 expressed in osteoblasts, and the TLR4 signal induces prostaglandin E₂ (PGE₂) synthesis and RANKL expression in osteoblasts, leading to subsequent bone resorption in mouse alveolar bone. Recently, TLR2 is known to form heterodimers with TLR1 and TLR6, but the roles of TLR2 heterodimer signals in bone are not known. TLR1-TLR2 heterodimer (TLR1/2) is known to recognize triacylated lipopeptides from gram-negative bacteria as a specific ligand. On the other hand, TLR2-TLR6 heterodimer (TLR2/6) recognizes diacylated lipopeptides from gram-positive bacteria. Using the respective ligand for TLR1/2 and TLR2/6, we examined the effects of TLR2 heterodimer signals on bone resorption. In co-cultures of mouse bone marrow cells and osteoblasts, TLR2/6 ligand markedly induced osteoclast formation, the potency was similar to that of TLR4 ligand LPS. TLR1/2 ligand also induced osteoclast formation, but the effect was less than that of TLR2/6. Both TLR1/2 and TLR 2/6 ligands induced PGE production and the expression of RANKL mRNA in osteoblasts, and elicited bone resorption in mouse calvarial organ cultures. We detected the expression of TLR1, 2, 4, and 6 mRNAs in osteoblasts, and the level of TLR2 expression was enhanced by the treatment with TLR1/2 or TLR 2/6 ligand, but not by TLR4 ligand LPS. Then, it is possible that the TLR2 heterodimer signal potentiates the other TLR2 signal each other in osteoblasts. Both TLR1/2 and TLR2/6 ligands induced bone resorption of mandibular alveolar bone in organ cultures, and the potency was TLR2/6>TLR1/2. Here, we show that TLR2 signals mediated by TLR2/6 and TLR1/2 may play a key role in PGE-mediated inflammatory bone loss in periodontal disease.

Disclosures: Chiho Matsumoto, Tokyo University of Agriculture and Technology, 3 This study received funding from: Tokyo University of Agriculture and Technology

MO0183

Vertebral Deformity in Patients with End Stage Renal Disease. Eual Phillips^{*1}, Mary Leonard², Chamith Rajapakse³, Michael Wald⁴, Yusuf Bhagat¹, Felix Werner Wehrli⁴. ¹University of Pennsylvania, USA, ²Children's Hospital of Philadelphia, USA, ³University of Pennsylvania School of Medicine, USA, ⁴University of Pennsylvania Medical Center, USA

Early detection of vertebral deformity is important in organ transplant recipients due to known elevated risk for further fractures. Although DXA BMD measurements are clinically accepted as a noninvasive means for fracture risk assessment in the general population, BMD is a poor predictor of fracture risk in renal transplant patients. Here, we evaluated vertebral deformity in patients with end stage renal disease (ESRD) who were candidates for renal transplantation. The study comprised of 43 adults (24 men, 19 women) with ESRD (mean age: 40 years, $\sigma = 10.1$) and 46 healthy controls (18 men, 28 women; mean age: 37 years, $\sigma = 7.6$, p=NS). Multi-slice sagittal MR images of the midline spine were acquired at 1.5-T (Siemens Sonata) scanner using the manufacturer's surface array coil and a turbo spin-echo sequence. Acquired spine images were taken as input to a custom-built semi-automatic software tool designed for quantitative spine morphometry. Using a six-point operator-guided labeling method, anterior height (H_a), posterior height (H_p), and middle height (H_m) of each vertebral body were computed by taking the Euclidian distance between landmark points. Three types of vertebral deformities - wedge (W), biconcavity (B), and compression (C) - were calculated for each vertebra by adapting an approach developed by Eastell. A continuous measure of deformity, vertebral deformity index (VDI), was computed for the hypothoracolumbar vertebral column (T8-L5) using the sum of each deformity per vertebrae ($VDI = \sum(W_i + B_i + C_i)$). Intervertebral disc (IVD) heights were also calculated using the Dabbs height method, which is the average of the anterior and posterior IVD heights. Compared to controls, women with ESRD had greater vertebral deformity (2.5%, p < 0.0005), while the group difference in VDI of men was non-significant. H_a and H_p were higher in both men (9%, p < 0.005) and women (6%, p < 0.05) with ESRD. IVD heights were lower in both men (15%, p < 0.005) and women (22%, p < 0.0005) with ESRD. Results from vertebral and IVD heights potentially indicate disc degeneration. The increased spinal deformity reflects the markedly increased fracture incidence in the ESRD compared to the general population. We conclude that MRI-based spinal morphometry can reliably differentiate patients with ESRD from controls. Finally, we are not aware of prior observations on the effects of ESRD on the IVD, reported here.

Disclosures: Eual Phillips, None.

MO0184

Cellular Cholesterol Metabolism is required for Vascular Cell Calcification. Jeff Hsu^{*1}, Yifan Geng¹, Jinxiu Lu¹, Linda Demer², Yin Tintut¹.
¹University of California, Los Angeles, USA, ²David Geffen School of Medicine At University of California Los Angeles, USA

Vascular calcification impairs vessel compliance and increases the risk of cardiovascular events. We previously found that activation of the PKA pathway induces osteogenic differentiation and matrix mineralization of vascular smooth muscle cells (VSMCs), and that agonists of liver X receptor (LXR), which regulates homeostasis of intracellular cholesterol, enhance the effects of PKA. Since cholesterol is an integral component of matrix vesicles that are involved in mineralization, we examined the roles of cellular cholesterol biosynthesis and cholesterol uptake via low-density lipoprotein receptors (LDLR) in vascular cell calcification.

Results showed that aortic VSMC isolated from Ldlr^{-/-} mice had 2.5 to 4-fold less alkaline phosphatase (ALP) activity and matrix mineralization than those from WT mice. A PKA activator, forskolin, increased the ALP activity at day 4 and matrix mineralization at day 10 in Ldlr^{-/-} cells to the levels seen in forskolin-treated WT cells. This effect may be due to a compensatory increase in cholesterol synthesis, since forskolin treatment for 7 days upregulated expression of the rate-limiting enzyme for cholesterol biosynthesis, HMG-CoA reductase, only in Ldlr^{-/-} cells.

In WT cells, inhibition of HMG-CoA reductase activity with mevastatin failed to attenuate matrix mineralization. This lack of effect may be due to a compensatory increase in cholesterol uptake since mevastatin upregulated LDL receptor expression by 4-fold and increased intracellular cholesterol accumulation by 1.5-fold, as measured by a fluorometric assay. Inhibition of cholesterol uptake by culture with lipoprotein deficient serum (LPDS) completely inhibited matrix mineralization in WT cells. This inhibitory effect of LPDS on matrix mineralization was partially reversed by the addition of cell permeable cholesterol, a cyclodextrin-cholesterol complex.

In conclusion, these results suggest that upregulation of cholesterol metabolism is essential for forskolin-induced matrix mineralization by vascular cells.

Disclosures: Jeff Hsu, None.

MO0185

The Appearance and Modulation of Osteocyte Marker Expression During Calcification of Vascular Smooth Muscle Cells. Dongxing Zhu¹, Neil Mackenzie¹, Jose Luis Millan², Colin Farquharson^{*3}, Vicky Macrae¹.
¹The Roslin Institute, University of Edinburgh, United Kingdom, ²Sanford-Burnham Medical Research Institute, USA, ³Roslin Institute, University of Edinburgh, United Kingdom

Vascular calcification is an indicator of elevated cardiovascular risk. Vascular smooth muscle cells (VSMCs), the predominant cell type involved in medial vascular calcification, can undergo phenotypic transition to both osteoblastic and chondrocytic cells within a calcifying environment. In vitro VSMC calcification studies in conjunction with ex vivo analyses of vascular tissue from Enpp1^{-/-} - a mouse model of idiopathic infantile arterial calcification, showed that vascular calcification is associated with the expression of osteocyte phenotype markers. The culture of murine aortic VSMCs in calcifying medium (medium containing α -glycerolphosphate and ascorbic acid), confirmed that calcifying VSMCs had increased alkaline phosphatase activity and Pit-1 expression, which are recognized markers of vascular calcification. Expression of DMP-1, E11 and sclerostin mRNA was also upregulated during VSMC calcification in vitro indicating the presence of cells of the osteocyte phenotype. Increased protein expression of E11, an early osteocyte marker, and sclerostin, expressed by more mature osteocytes was also observed in the calcified media of Enpp1^{-/-} mouse aortic tissue. Control wild-type tissue showed no positive staining. The reliability of these findings were confirmed by studying the terminal differentiation of murine calvarial osteoblasts into osteocytes under identical culturing conditions was also, as expected, associated with increased expression of the osteocyte markers DMP-1, E11 and sclerostin. This study has demonstrated the up-regulation of key osteocytic genes and proteins during vascular calcification. A fuller understanding of the functional role of osteocyte formation and specifically sclerostin and E11 expression in the vascular calcification process may identify novel potential therapeutic targets for clinical intervention.

Disclosures: Colin Farquharson, None.

MO0186

Bone Geometry, Density and Microarchitecture in Patients with Type I Osteogenesis Imperfecta Compared with Age and Sex Matched Healthy Controls Utilizing High-Resolution Peripheral Quantitative Computed Tomography. Lars Folkestad^{*1}, Jannie Dahl Hald², Stinus Hansen³, Jeppe Gram⁴, Bente Langdahl⁵, Bo Abrahamsen⁶, Kim Brixen⁷.
¹Department of Endocrinology, Odense University Hospital / 3Department of Endocrinology, Hospital of Southwest Denmark / Institute of Clinical Research, University of Southern Denmark, Denmark, ²Department of Endocrinology & Internal Medicine, Aarhus University Hospital, Denmark, ³Department of Endocrinology, Odense University Hospital / Institute of Clinical Research, University of Southern Denmark /, Denmark, ⁴Department of Endocrinology, Hospital of Southwest Denmark, Denmark, ⁵Department of Endocrinology & Internal Medicine, Denmark, ⁶Department of Internal Medicine, Gentofte Hospital / Institute of Clinical Research, University of Southern Denmark, Denmark, ⁷Department of Endocrinology, Odense University Hospital / Institute of Clinical Research, University of Southern Denmark, Denmark

Background: Osteogenesis imperfecta (OI) is a hereditary, heterogeneous disease characterized by defects in the biosynthesis of collagen type I resulting in increased risk of fractures. Both bone mineral density (BMD) and bone quality is affected in OI. Only a few studies have investigated the bone architecture, geometry and volumetric BMD (vBMD) in patients with type-I OI (T1-OI). High-resolution peripheral quantitative computed tomography (HR-pQCT) allows *in vivo* assessment of cortical thickness (Ct.Th), trabecular thickness (Tb.Th), trabecular number (Tb.N) and trabecular separation (Tb.Sp) without discomfort for the patients. To investigate bone microstructure in T1-OI, we compared HR-pQCT parameters in OI patients and healthy age- and gender matched controls.

Methods and material: From our clinical database and through the *Danish OI Patient Society*, a total of 155 patients with OI were invited and 21 patients with clinical T1-OI and no known other metabolic bone disease were included in this study. Twenty-one age- and sex-matched healthy controls were invited at random from the background population through the national civil registry. All participants had both ultra distal radius and tibia investigated using a Scanco Medical Xtreme CT. We present the data as meanSD. Between-group differences are analyzed with Wilcoxon's nonparametric rank-sum test, due to a non Gaussian distribution. p-values are two-sided and the statistical significance level was set at .05.

Results: Six men and 15 women participated in each group. The mean age was 47.5 (range 21-75) years. Results are summarized in table 1. Patients with T1-OI had significantly lower number of trabeculae and increased Tb.Sp in both tibia and radius. In the tibia, patients had significantly thinner trabeculae. Moreover, vBMD was significantly lower in the cortical compartment in both regions. In the tibia, patients had significantly lower total vBMD. Finally, cortical area was significantly lower in the tibia, but not in the radius.

Conclusion: Patients with OI have altered micro-architecture in both tibia and radius and have low vBMD compared with healthy age- and gender-matched controls. This indicates that the increased fracture risk in OI patients may be the result of both low bone mass and altered bone structure.

Geometry	Radius			Tibia		
	T1OI	Controls	p-value	T1OI	Controls	p-value
Total area (mm ²)	257.4±60.5	285.7±78.5	N.S	767.7±202.0	768.5±183.9	N.S
Cortical area (mm ²)	53.8±11.3	60.8±19.7	N.S	95.9±22.5	121.3±39.3	<0.05
Trabecular area (mm ²)	199.0±52.5	220.3±71.6	N.S	665.1±189.6	641.3±177.4	N.S
Density						
Total (mg HA/ccm)	288.4±58.3	319.0±86.7	N.S	209.0±51.7	283.2±67.7	<0.001
Cortical (mg HA/ccm)	905.2±48.6	877.6±78.9	N.S	862.5±67.0	847.9±79.1	N.S
Trabecular (mg HA/ccm)	101.7±38.1	141.1±51.8	<0.05	103.3±32.0	164.8±46.0	<0.001
Trabecular BV/TV (%)	8.5 ± 3.2	11.6 ± 4.3	<0.05	8.6 ± 2.7	13.7 ± 3.8	<0.001
Micro-architecture						
Tb.N (1/mm)	1.262±0.512	1.797±0.455	<0.05	1.231±0.441	1.913±0.344	<0.001
Tb.Th (mm)	0.071±0.020	0.064±0.012	N.S	0.074±0.019	0.071±0.013	N.S
Tb.Sp (mm)	0.381±0.560	0.537±0.199	<0.05	0.890±0.454	0.468±0.101	<0.001
Ct.Th (mm)	0.779±0.117	0.866±0.270	N.S	0.886±0.198	1.118±0.344	<0.05

Table 1 - Results

Disclosures: Lars Folkestad, None.

MO0187

Dental Phenotype in a Mouse Model for Craniometaphyseal Dysplasia. Eliane Dutra*, I-Ping Chen, Peter Maye, Ernst Reichenberger. University of Connecticut Health Center, USA

Craniometaphyseal dysplasia (CMD) is a genetic disorder characterized by hyperostosis of craniofacial bones and flaring metaphyses of the long bones. Mice carrying a knock-in mutation (Phe377del) in the Ank gene replicate many skeletal characteristics of human CMD as well as dental abnormalities. A known function of the transmembrane protein ANK is to transport intracellular pyrophosphate (PPi) into the extracellular environment. Although the morphologies of erupted molars and incisors appear to be normal, AnkKI/KI mice have abnormal cervical loop positioning of the lower incisors and excessive cementum deposition of molars and incisors. We hypothesize that a combination of mechanisms may contribute to the abnormal tooth development in AnkKI/KI mice: 1) reduced bone resorption and impaired function of stem cells may contribute to the abnormal development of the incisors and 2) altered Pi/PPi may cause excessive cementum formation. Cementoblasts and osteoclasts are known to express IBSP and TRAP, respectively. In order to examine the mutational effects of a CMD-causing Ank mutation on these two cell types, we crossed AnkKI/KI mice with transgenic fluorescent reporter mice expressing Ibsp-Topaz/Dmp1-mCherry and Trap-ECFP. Histology of the AnkKI/KI/Ibsp-Topaz+Dmp1-mCherry mice revealed increased Ibsp-positive cells around the roots of the molars in comparison to the Ank+/+ mice, suggesting increased numbers of cementoblasts. Characterization of the AnkKI/KI/Trap-ECFP showed increased ECFP expression, indicating more TRAP-positive mononuclear and multinucleated cells in the mandibles of the AnkKI/KI mice. Interestingly, quantification of osteoclast number and osteoclast surface of TRAP-stained paraffin sections using Osteomeasure software revealed decreased numbers of osteoclasts in the apical end of the AnkKI/KI incisor. Our data suggest that bone resorption activity may be reduced around the cervical loop of the AnkKI/KI incisor due to decreased numbers of mature osteoclasts although more TRAP-positive cells are present in this region. Our previous data showed increased apoptosis in the stellate reticulum and decreased proliferation of odontoblast precursors in the apical end of AnkKI/KI incisors. We are currently investigating gene expression in the cervical loop to determine whether the incisor phenotype is caused by a cervical loop deficiency or is secondary to reduced bone resorption.

Disclosures: Eliane Dutra, None.

MO0188

Determination and Comparison of Serum and Plasma Sclerostin Concentrations by Commercially Available Enzyme-Linked Immunoassays. Melissa McNulty¹, Ravinder Singh¹, Eric Bergstralh¹, Xujian Li¹, Rajiv Kumar^{*2}. ¹Mayo Clinic, USA, ²Mayo Clinic College of Medicine, USA

Sclerostin alters bone formation. The precise and reproducible measurement of sclerostin concentrations in biological samples could potentially be important for assessment of metabolic bone disease. We compared sclerostin concentrations in serum and plasma using two commercially available enzyme-linked immunoassays. Serum or heparin-plasma was obtained from 25 normal human subjects. Sclerostin was measured in these samples using two commercial ELISAs available from Biomedica Medizinprodukte GmbH and TECOmedical AG following the manufacturers instructions.

With the Biomedica assay, serum sclerostin concentrations were 0.99 ± 0.12 ng/mL (mean ± SEM) and plasma concentrations were 1.47 ± 0.13 ng/mL (paired t-test, P < 0.001). With the TECO assay, serum sclerostin levels were 0.71 ± 0.05 ng/mL and plasma sclerostin concentrations were 0.80 ± 0.06 ng/mL (paired t-test, P < 0.001) (Table 1). Serum and plasma sclerostin concentrations were significantly different when determined by the two assays (serum, P = 0.015; plasma, P < 0.001). To determine whether the recovery of added exogenous sclerostin was quantitative, we obtained recombinant sclerostin produced in mammalian cells from R & D Systems, and added a known amount to serum or plasma samples. Recovery of added recombinant sclerostin to serum was less than expected with both Biomedica and TECO assays (P < 0.001, paired t-test) (Table 1).

Conclusions: The concentrations of sclerostin in serum and plasma are different when determined by the two assays. The recovery of exogenously added sclerostin is not quantitative suggesting that presence of binding proteins in serum or plasma. Serum or plasma sclerostin concentrations with current assays should be interpreted with caution. Our data suggest that the same assay should be used for comparing groups of patients or patients being followed longitudinally. Standardization of sclerostin assays is required prior to their being introduced into general clinical laboratory use.

Table 1					
Biomedica Assay			TECO Assay		
Serum sclerostin, ng/mL, N = 25, mean ± SEM	Heparin Plasma sclerostin, ng/mL, N = 25, mean ± SEM	P-value	Serum sclerostin, ng/mL, N = 25, mean ± SEM	Heparin Plasma sclerostin, ng/mL, N = 25, mean ± SEM	P-value
0.99 ± 0.12	1.47 ± 0.13	<0.001	0.71 ± 0.05	0.80 ± 0.05	<0.001
Recovery ^a			Recovery ^a		
Expected serum sclerostin, ng/mL, N = 25, mean ± SEM	Observed serum sclerostin, ng/mL, N = 25, mean ± SEM	P-value	Expected serum sclerostin, ng/mL, N = 25, mean ± SEM	Observed serum sclerostin, ng/mL, N = 25, mean ± SEM	P-value
3.95 ± 0.11	2.93 ± 0.15	<0.001	3.69 ± 0.05	3.21 ± 0.08	<0.001
1:2 dilution			1:2 dilution		
Expected serum sclerostin, ng/mL, N = 25, mean ± SEM	Observed serum sclerostin, ng/mL, N = 25, mean ± SEM	P-value	Expected serum sclerostin, ng/mL, N = 25, mean ± SEM	Observed serum sclerostin, ng/mL, N = 25, mean ± SEM	P-value
0.99 ± 0.12	0.90 ± 0.13	0.33	0.71 ± 0.05	0.81 ± 0.07	0.005

Table 1

Disclosures: Rajiv Kumar, None.

MO0189

Epidemiogenetic Study of French Families Affected by Paget's Disease of Bone. Laetitia Michou^{*1}, Corinne Collet², Jean Morissette¹, Maurice Audran³, Thierry Thomas⁴, Edith R. Gagnon¹, Jean-Marie Launay², Jean-Louis Laplanche², Jacques Brown⁵, Philippe Orce⁶. ¹Centre De Recherche Du CHUQ - CHUL, Canada, ²Service de biochimie et biologie moleculaire, Hopital Lariboisiere, APHP, France, ³Universite et CHU Angers; INSERM U922, France, ⁴Hopital Nord - CHU de St-Etienne, France, ⁵Laval University, Canada, ⁶University Paris Diderot, France

Purpose: To search for association between environmental factors and Paget's disease of bone (PDB) and to determine the frequency of *SQSTM1* gene mutations and haplotypes in French families affected by PDB.

Methods: Unrelated PDB patients were recruited in three French Rheumatology departments. All patients had monostotic or polyostotic PDB, as defined by increased bone radionuclide uptake with typical radiographic lesions. First- and second-degree relatives of each index case completed a questionnaire and had a clinical examination, blood taken for DNA extraction and biochemical measurements, and a whole-body bone scan or X-ray. Exons 7 and 8 and exon-intron boundaries of *SQSTM1* gene were PCR amplified before sequencing. In patient carriers of a *P392L* mutation, haplotypes were determined by genotyping six intragenic markers. Prevalence of PDB was estimated in first-degree relatives and siblings. Comparisons of clinical characteristics and exposure to environmental factors between PDB patients and healthy relatives were performed.

Results: We investigated 18 families affected by PDB, totalling 83 individuals: 20 patients with known PDB, three relatives newly diagnosed with PDB and 60 healthy relatives. Four (22.2%) out of the 18 families had familial PDB. The prevalence of PDB was 8.8% among first degree relatives, and 15.4% among siblings. Index cases and/or relatives affected by Dupuytren's disease were found in eight (44.4%) out of the 18 families. Comparison of exposure to environmental factors between PDB affected patients and healthy relatives provided no statistically significant difference, but 43% of PDB patients were former or current tobacco users versus 18% of healthy relatives (p=0.02; OR=3.37 (1.04-11.09)). Five index cases (27.8%) were carriers of *SQSTM1* mutations: three carried the *P392L* mutation, one carried *P392L* and *A390X* double mutation and one carried an *A390X* mutation. Haplotype analysis revealed that the *P392L* mutation was carried by haplotype 2 in the four index cases carrier of this mutation. Dupuytren's phenotype was not associated with *SQSTM1* mutation.

Conclusions: Accurate phenotype assessment of 63 relatives of 18 French PDB patients allowed for a new diagnosis of PDB in three asymptomatic relatives. There was evidence for an aggregation of Dupuytren's disease in families of PDB, and an association between PDB and tobacco exposure. Half of PDB familial forms carried a *SQSTM1* mutation, the *P392L* mutation being the most frequent.

Disclosures: Laetitia Michou, Warner Chilcott, 8; Eli Lilly, 8; Eli Lilly, 2; Amgen, 8; CIHR, 2; Roche, 8

MO0190

Implication of Gender Difference in the Association between Bone-specific Alkaline Phosphatase Activity and Serum Biochemical Parameters or Dietary Nutrients. Mayu Haraikawa¹, Rieko Tanabe², Natsuko Sogabe³, Aoi Sugimoto⁴, Toshimi Michigami⁵, Takayuki Hosoi⁶, Masae Goseki-Sone⁷.

¹Graduate School of Human Life Science, Japan Women's University, Japan, ²Division of Nutrition, Department of Food & Nutrition, Faculty of Human Sciences & Design, Japan Women's University, Japan, ³Department of Health & Nutrition Sciences, Faculty of Human Health, Komazawa Women's University, Japan, ⁴Graduate School of Human Sciences & Design, Division of Food & Nutrition, Japan Women's University, Japan, ⁵Osaka Medical Center, Research Institute for Maternal & Child Health, Japan, ⁶National Center for Geriatrics & Gerontology, Japan, ⁷Japan Women's University, Japan

Alkaline phosphatase (ALP) hydrolyzes a variety of monophosphate esters into inorganic acid and alcohol at a high optimum pH (pH 8-10). Tissue non-specific ALP (TNSALP) is associated with skeletal mineralization. Hypophosphatasia (HPP) is a rare inherited systemic bone disease caused by the presence of either one or two pathologic mutations in the TNSALP gene, and is characterized by the defective mineralization of bone and/or teeth in the presence of low serum and bone ALP activity. Clinical features range from stillbirth without mineralized bone to pathologic fractures of the lower extremities in later adulthood. Nutritional management based on the characteristic pathology of HPP seems to be important for the control and treatment of this disease. In this study, we aimed to clarify the effect of dietary nutrients on bone-specific ALP (BAP) activity in young adults in order to obtain basic information for planning a desirable nutritional management program in HPP. Serum biochemical parameters, such as serum ALP, BAP, 1 α , 25(OH)2D3, and osteocalcin were measured in healthy young males (n=97, age: 22.3 \pm 1.7 y, mean \pm standard deviation) and females (n=96, age: 21.8 \pm 1.8 y). Dietary nutrient intakes were measured based on 3-day food records before the day of blood examinations. TNSALP gene mutations were analyzed in the DNA of peripheral blood leukocytes. All subjects were unrelated volunteers and provided informed consent before the study. Through the analysis of BAP activity and other biochemical parameters, a significant positive correlation was revealed between BAP and serum 1 α , 25(OH)2D3 or osteocalcin in male subjects. However, there was no significant correlation between BAP and the other serum biochemical parameters in female subjects. As a result of 3-day food records, there was a significant positive correlation between serum 1 α , 25(OH)2D3, and Ca/P intake in female subjects ($r=0.250$, $p=0.014$). In addition, 1559delT mutation, which has been reported the most frequent in Japanese HPP, was not detected in all subjects (n=193). Our results suggest that gender difference should be considered in planning the strategies for the nutritional management of HPP.

Disclosures: Masae Goseki-Sone, None.

MO0191

Mutations in NOTCH2 in Patients with Hajdu-Cheney Syndrome. Michael Mannstadt¹, Wenping Zhao², Karen Miller², Rachel Gafni³, Michael Collins³, Margaret Seton², Harald Jueppner². ¹Massachusetts General Hospital Harvard Medical School, USA, ²Massachusetts General Hospital, USA, ³National Institutes of Health, USA

Purpose: Hajdu-Cheney Syndrome (HCS) is a rare disorder characterized by acroosteolysis of the distal phalanges, severe osteoporosis, dental abnormalities and a variety of other findings, including renal cysts. It occurs sporadically or can be transmitted in an autosomal-dominant fashion. Recently, heterozygous disease-causing mutations were identified in NOTCH2 (Simpson et al. and Isidor et al., Nature Genetics 2011). Here, we describe phenotypic and genetic findings in sporadic and familial HCS cases.

Methods: We studied 3 affected members of one family with an autosomal-dominant form (HCS1) and 5 patients with the sporadic form (HCS2-6). NOTCH2 exon 34 was sequenced and nucleotide sequence variations were compared to public databases.

Results: Patients had clinical findings consistent with HCS, which were of variable severity. Direct sequence analysis of NOTCH2 exon 34 revealed heterozygous mutations in all 8 HCS patients (see table). Five of the mutations are novel; the nonsense mutation c.7198C>T has been described (Simpson et al., Nature Genetics 2011).

Of the six different mutations, two are nonsense mutations; four are deletion mutations leading to a shift in reading frame and a premature stop codon. Because these mutations are located in the last exon, the resulting mRNA is predicted to escape nonsense mediated decay. All six mutations lead to the deletion of the carboxyl-terminal PEST sequence.

Conclusions: We identified heterozygous mutations in NOTCH2 exon 34 in each of our HCS patients; five of these mutations are novel. All six mutations are predicted to lead to a loss of a PEST sequence. The deletion of this protein-destabilizing motif is predicted to lead to a longer half-life of the NOTCH2 protein and the identified mutations are therefore likely to represent "gain-of-function" mutations. Our findings confirm that heterozygous NOTCH2 mutations are the cause of HCS and the findings in our patients expand the mutational spectrum of this disorder.

Individual	Mutation	Protein
HCS1_301/302/202	c.6450delT	Val2151X
HCS2_201	c.6586C>T	Gln2196X
HCS3_207	c.6662-6663delTG	Val2221GlufsX22
HCS4_205	c.6578-6588delTCCATGCCAG	Val2193AlafsX7
HCS5_203	c.6383delG	Gly2128GlufsX2
HCS6_202	c.7198C>T	Arg2400X

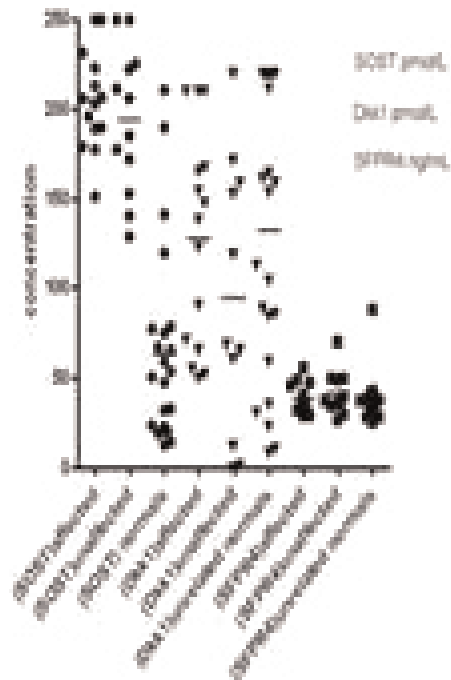
Mutations in NOTCH2 in patients with Hajdu-Cheney Syndrome

Disclosures: Michael Mannstadt, None.

MO0192

Serum Levels of Dkk1, Sclerostin and Secreted Frizzled Related Protein 4 are not Changed in Individuals with Gain-of-function Mutations in LRP5. Christine Simpson*, Grace Lee, Dinah Foer, Benhua Sun, Joseph Belsky, Karl Insogna. Yale University School of Medicine, USA

It is thought that gain of function mutations in LRP5 result in high bone mass syndromes because these allelic variants confer resistance to the actions of endogenous inhibitors, in particular Dkk1. Not uncommonly, resistance syndromes are associated with increased expression of the inhibitor. We therefore wondered if circulating levels of known Wnt inhibitors might be altered in patients with gain-of-function mutations in LRP5. We collected fresh serum samples from 15 individuals (60+21 yrs) with known high bone mass and mutations in LRP5 (G171V or N198S), 11 unaffected individuals (42+21 yrs) in the same kindreds and 25 normal age-matched controls (56+24 yrs). Serum levels of sclerostin (SOST), Dickkopf-related protein 1 (Dkk1), secreted frizzled protein 4 (SFRP4), c-terminal telopeptide of type 1 collagen (CTX) and serum procollagen type 1 amino-terminal propeptide (P1NP) were measured using commercially available assays. As summarized in the graph below, there were no significant differences in serum levels of SOST, Dkk1, or SFRP4 in affected vs. unaffected individuals from different kindreds. When analyzed by genetic mutation, again there were no observed differences. Further, when compared to age-matched, unrelated, normal individuals there were no differences in the levels of the three inhibitors in the individuals with LRP5 mutations. When the unaffected and normal control individuals were analyzed as a group, there was no correlation of SOST, Dkk1, SFRP4 with either CTX or P1NP, albeit the sample size was small. These data suggest that either gain-of-function in LRP5 is not reflected in circulating levels of these three inhibitors, or that the mechanism of action of the LRP5 mutations is mediated by other molecular pathways *in vivo*.



Serum Levels of Dkk1, SOST and SFR4 in the Three Study Groups

Disclosures: Christine Simpson, None.

MO0193

The Bone Tissue Defect in Children with Hypophosphatasia: Histomorphometric Study. Frank Rauch^{*1}, Cheryl Greenberg², Michael Whyte³, Hal Landy⁴, Rose Travers⁵, Francis Glorieux⁶. ¹Shriners Hospital for Children, St. Louis, Canada, ²University of Manitoba, Children's Hospital, Canada, ³Shriners Hospital for Children, USA, ⁴Enobia Pharma, Canada, ⁵Shriners Hospital for Children, Canada, ⁶Shriners Hospital for Children & McGill University, Canada

INTRODUCTION: Hypophosphatasia (HPP) is the inherited skeletal disorder caused by loss-of-function mutation(s) in the gene that encodes the tissue-nonspecific isoenzyme of alkaline phosphatase. The characteristics of HPP have not been assessed in detail in many affected children at the bone tissue level.

OBJECTIVE: To determine the bone tissue abnormalities of children with HPP.

METHODS: Static and dynamic histomorphometric analyses were performed in the trabecular compartment of transiliac bone biopsy samples that had been obtained from 12 children (age 6.0 to 12.5 years) with HPP as the baseline measure of an enzyme replacement trial. Results were expressed as percentages of the means of age-specific reference ranges from our laboratory.

RESULTS: Structural parameters (bone volume per tissue volume, trabecular number, trabecular thickness) were close to the age-specific average of the reference range, whereas osteoid indices (osteoid thickness, osteoid surface per bone surface, osteoid volume per bone volume) were markedly elevated (Table). Among dynamic parameters of bone formation (based on tetracycline double labeling), mineralizing surface related to bone surface was below the age-specific average of the reference range. Mineral apposition rate was slightly elevated, whereas bone formation rate per bone surface was below the expected average for age. Mineralization lag time was markedly elevated.

Qualitative evaluation suggested that the accumulation of osteoid was not distributed evenly, but rather was patchy. In many locations, trabeculae were covered by osteoid of normal thickness, whereas in some trabeculae a large proportion of the diameter seemed to consist of osteoid mixed with calcified cartilage (presumably unremodeled growth plate material).

CONCLUSION: Children with HPP have a mineralization defect that fulfills the histomorphometric criteria for osteomalacia. In addition, there are distinctive patches of unmineralized bone containing cartilage fragments.

	N	median (IQR)	P*
Bone volume/tissue volume	7	121 (116; 136)	0.03
Trabecular number	7	117 (92; 138)	0.10
Trabecular thickness	12	100 (93; 126)	0.20
Osteoid thickness	12	221 (194; 247)	<0.001
Osteoid surface/bone surface	12	204 (170; 248)	<0.001
Osteoid volume/bone volume	12	396 (276; 567)	<0.001
Mineralizing surface/bone surface	12	62 (34; 143)	0.44
Mineralizing surface/osteoid surface	12	29 (17; 63)	<0.001
Mineral apposition rate	12	108 (103; 157)	0.01
Bone Formation Rate/bone surface	12	63 (43; 175)	0.69
Mineralization lag time	12	527 (237; 895)	0.003

Results given as percentages of age-specific mean value of reference range
IQR: Interquartile range. *Significance of the difference from 100%

Disclosures: Frank Rauch, Enobia Pharma, 2

This study received funding from: Enobia Pharma

MO0194

Determining the Repertoire of Human Genes Bound by Osterix (SP7). Kurt Hankenson^{*1}, Jianhua Zhao², Fengchang Zhu¹, Struan Grant². ¹University of Pennsylvania, USA, ²Children's Hospital of Philadelphia, USA

Candidate gene and genome wide association studies (GWAS) have revealed a number of loci encoding transcription factors that are very strongly associated with endocrine-related traits, including *Osterix* (*Sp7*), *VDR*, and *TCF7L2* with bone mineral density (BMD), osteoporosis and type 2 diabetes, respectively. The combination of chromatin immunoprecipitation (ChIP) and massively parallel sequencing (ChIP-seq) can be used to directly identify the DNA sequences bound by transcription factors genome wide *in vivo*, including strength of binding, in order to determine the network of genes they regulate. We previously reported the mapping of the genomic regions bound by TCF7L2 using ChIP-seq and found that the list of genes bound by this transcription factor harbor a highly significant over-representation of loci uncovered in GWAS of metabolic and cardiovascular disease. Further support for our conclusions came from a subsequent VDR ChIP-seq study that gave a similar enrichment of GWAS-discovered genes, albeit for immune and cancer related traits. As such, it is our hypothesis that a substantial set of genes bound by GWAS-implicated transcription factors will also harbor genetic variants associated with a given trait of interest. With these facts in mind, we aimed to determine a set of human genes bound by Osterix. Osterix was both overexpressed and knocked-down using

adenovirus in human primary marrow-derived mesenchymal stem cells (hMSC). Cells were induced to become osteoblasts with BMP6. Knockdown inhibited terminal differentiation while *Osterix* overexpression promoted differentiation. Microarray analysis revealed a set of genes, either directly or indirectly regulated by Osterix, involved in extracellular matrix assembly and terminal osteoblast differentiation. Specifically Osterix regulates the expression of a cluster of proteoglycans on human chromosome 9, including osteomodulin (*OMD*), asporin (*ASPN*) and osteoglycin (*OGN*). Next we used ChIP to identify genomic segments bound by Osterix, revealing a promoter segment located downstream of *OMD* and upstream of *OGN*, thus demonstrating a direct interaction between Osterix and this proteoglycan locus. In summary, we have distilled loci bound by Osterix and have gained an insight in to the gene networks regulated by this key transcription factor. Our future work will utilize ChIP-seq, with this identified genomic segment acting as a positive control, to identify novel loci genome wide directly bound by Osterix.

Disclosures: Kurt Hankenson, None.

MO0195

Genome-Wide Association Analysis of Hip Structure Phenotypes in the Fels Longitudinal Study. Stefan Czerwinski^{*1}, Miryoung Lee¹, Bradford Towne¹, Joanne Curran², Thomas Dyer², Audrey Choh¹, John Blangero², Roger Siervogel¹. ¹Wright State University Boonshoft School of Medicine, USA, ²Texas Biomedical Research Institute Department of Genetics, USA

Introduction: Bone structure is important in assessing fracture risk and is moderately to highly heritable. Several recent genome-wide analyses have identified SNPs linked or associated with bone mineral density and fracture risk. However, less is known about the genetic influences on hip geometric parameters related to bone strength. In this study, we conducted an initial genome-wide association analysis of hip geometric parameters on white adults in the Fels Longitudinal Study.

Methods: The study sample includes 1,227 participants (men 569, women 658, mean age 45.4yr) aged between 18 and 91 yrs. Hip geometric parameters were obtained from existing dual energy X-ray absorptiometry scans using Hip Structure Analysis (HSA) software (Hologic, Waltham, MA). Our analyses focused on femoral neck shaft angle and three HSA phenotypes (i.e., cortical buckling ratio (BR), cross-sectional area (CSA), and section modulus (Z)) collected at three regions of the femoral neck (i.e., the shaft, intertrochanteric and narrow neck). Each participant has been genotyped with the Illumina Human 610-Quad BeadChip containing more than 550,000 SNPs. Association analyses were conducted using measured genotype analysis implemented in the software program SOLAR allowing for residual non-independence among relatives. In this sample, genome-wide significance was indicated by a chi-square > 27.85 and suggestive evidence by a chi-square > 22.70.

Results: We observed a significant association for SNP rs4314247 (chromosome (ch) 4, chi-square 30.15) and highly suggestive associations for rs1041350 (ch 9, chi-square 27.39) with shaft angle. rs4314247 lies within the intron region of a gene coding for Palladin, a cytoskeletal associated protein on ch 4q32.3. We found 19 SNPs that were suggestively associated with HSA phenotypes in the three regions. A total of 8 suggestive SNPs were associated with more than one HSA trait for the same region. In the shaft region, a highly suggestive association for rs1198121 with BR was observed (ch10, chi-square 27.03). SNP rs6549288 (ch3, chi-square 25.2) and rs7614990 (ch3, chi-square 24.6) were associated with CSA and Z. In the intertrochanteric region, five SNPs on ch 16 were suggestive with both CSA and Z.

Conclusion: In summary, we identified several significant and suggestive SNPs associated with hip geometric parameters. Further research aimed at replicating these results in other populations is planned.

Disclosures: Stefan Czerwinski, None.

MO0196

Heterogeneous Stock Rat: a Unique Genetic Resource for Rapid and Efficient Discovery of the Genetic Determinants of Bone Fragility. Imranul Alam^{*1}, Daniel Koller¹, Sun Qiwei¹, Ryan Roeder², Toni Canete³, Gloria Blazquez³, Regina Lopez-Aumatell⁴, Esther Martınez-Membrives³, Elia Vicens-Costa⁵, Carme Mont³, Sira Dıaz³, Adolf Tobena³, Alberto Fernandez-Teruel³, Adam Whitley⁴, Pernilla Strid⁶, Margarita Diez⁶, Martina Johannesson⁴, Jonathan Flint⁴, Michael Econs¹, Charles Turner⁷, Tatiana Foroud⁸. ¹Indiana University School of Medicine, USA, ²University of Notre Dame, USA, ³Autonomous University of Barcelona, Spain, ⁴Wellcome Trust Center for Human Genetics, United Kingdom, ⁵Autonomous University of Barcelona, Spain, ⁶Karolinska Institutet, Sweden, ⁷Orthopaedic Surgery, USA, ⁸Indiana University Purdue University Indianapolis, USA

Osteoporosis is a common polygenic disorder with reduced bone mineral density (BMD) and increased susceptibility to fracture at multiple skeletal sites. BMD, structure and strength are the primary skeletal determinants of osteoporotic fracture risk and are under substantial genetic control. Previously, we demonstrated that these skeletal determinants vary considerably among 11 different inbred rat strains. Subsequently, we performed quantitative trait loci (QTL) analysis in 4 inbred rat

strains (F344, LEW, COP and DA) for different bone phenotypes and identified several candidate genes influencing various bone traits. The standard approach to narrowing QTL intervals down to a few candidate genes typically employs the generation of congenic lines, which is time consuming and often not successful. A potential alternative approach is to use a highly genetically informative animal model resource capable of delivering very high-resolution gene mapping such as Heterogeneous stock (HS) rat. HS rat was derived from eight inbred progenitors: ACI/N, BN/SsN, BUF/N, F344/N, M520/N, MR/N, WKY/N and WN/N. The genetic recombination pattern generated across 50 generations in these rats has been shown to deliver ultra-high even gene-level resolution for complex genetic studies. We investigated the usefulness of the HS rat model for fine mapping and identification of genes underlying bone fragility phenotypes. We compared bone geometry, density and strength phenotypes at multiple skeletal sites in HS rats with those obtained from 5 of the 8 progenitor inbred strains. In addition, we estimated the heritability for different bone phenotypes in these rats and employed principal component analysis to explore relationships among bone phenotypes in the HS rats. Our study demonstrated that significant variability exists for different skeletal phenotypes in HS rats compared with their inbred progenitors. In addition, we estimated high heritability for several bone phenotypes and biologically interpretable factors explaining significant overall variability, suggesting that the HS rat model could be a unique genetic resource for rapid and efficient discovery of the genetic determinants of bone fragility. Currently, we are undertaking a genome-wide association study for over 1500 HS rats using 20,000 SNPs to narrow the candidate genes considerably, which will greatly enhance our ability to identify causative genes that affect bone fragility phenotypes.

Disclosures: Imranul Alam, None.

MO0197

Identification of *Lpin1* as a Candidate Gene for a Quantitative Trait Locus for Bone Mineral Density. Cheryl Ackert-Bicknell¹, Dana Godfrey¹, Yaoyu Chen², Beverly Paigen¹. ¹The Jackson Laboratory, USA, ²University of Massachusetts Medical School, USA

Genome wide association studies have identified a number of loci associated with bone mineral density (BMD) in human subjects. Collectively, these loci explain a very small fraction of the variance in this phenotype, suggesting the existence of additional, yet unidentified loci for BMD. Due to the development of new resources and analysis methods, there has been increased success in finding the genes associated with BMD using mouse models. In this study, we have identified *Lpin1* as a candidate gene for a quantitative trait locus (QTL) for BMD in mice. Specifically, we mapped 7 QTLs for whole body areal BMD in an F2 cross between the C57BL/6J (B6) and NZW/LacJ (NZW) inbred strains. We identified two highly significant QTL: on Chromosome (Chr) 1 at 73.9 cM and on Chr 12 at 8.7 cM. Statistically suggestive QTL were identified on Chrs 5 (at 45.4 cM), 10 (1.9 cM), 14 (at 34.7 cM), 15 at 8.4 cM and 17 (at 12.0 cM). The confidence interval for the Chr 12 QTL extended from 2.7 to 18.7 cM and this QTL is coincident for a femoral volumetric BMD QTL mapped in MRLxSJL (at 5.5 cM) and a femoral volumetric BMD QTL mapped in B6xC3H (at 2.94 cM). Using block haplotyping, we were able to reduced this QTL to 5 genes: *Apob*, *Lpin1*, *Myt1l*, *Sntg2* and *Hdac9*. Of these genes, only *Lpin1* and *Hdac9* are expressed in bone. The fatty liver dystrophy (*fld*) strain of mice carry a spontaneous deletion of the 2nd and 3rd exons of the *Lpin1* gene which arose on a BALB/cByJ (BALB) strain background. Mice homozygous for the *fld* allele lack normal adipocytes and have greatly reduced white adipose tissue mass. Furthermore, these mice have abnormal energy expenditure in muscle. We wished to evaluate if *Lpin1* was a candidate gene for this QTL in the absence of the lipodystrophy observed in the null mutant mice. In order to do this, we bred *fld/fld* mice to wildtype BALB mice to make *Lpin1* haploinsufficient mice (*fld/+*). Female, 11 week old *fld/+* mice had normal percent body fat compared to age matched BALB controls (*fld/+* = 16.47 ± 0.24% vs. *+/+* = 16.01 ± 0.39%, *P* = 0.449). However, these mice did have reduced whole body areal BMD (*fld/+* = 0.0480 ± 0.0002, *+/+* = 0.0510 ± 0.0007, *P* = 0.007). In sum, using genetic mapping and bioinformatics methods, we have identified *Lpin1* as a candidate gene for a BMD QTL on mouse Chr 12, such that a reduction in *Lpin1* levels is associated with decreased bone mass.

Disclosures: Cheryl Ackert-Bicknell, None.

MO0198

Meta-Analysis of Genome-Wide Association Study Identifies Three Loci Influencing Serum Osteoprotegerin Levels. Ching-Lung Cheung^{*1}, Yi-Hsiang Hsu², Joel Eriksson³, Johnny Kwan⁴, David Karasik⁵, Emelia Benjamin⁶, Joao Fontes⁷, Douglas Kiel⁵, Mattias Lorentzon⁸, Martin Larson⁹, Annie Kung¹⁰, Claes Ohlsson⁸, Pak-Chung Sham¹¹, Josee Dupuis¹². ¹The University of Hong Kong, Hong Kong, ²Hebrew SeniorLife Institute for Aging Research & Harvard Medical School, USA, ³Center for Bone & Arthritis Research, Departments of Internal Medicine & Geriatrics, Sahlgrenska Academy, University of Gothenburg, Sweden, ⁴Hong Kong University, Hong Kong, ⁵Hebrew SeniorLife, USA, ⁶Department of Medicine, Boston University Schools of Medicine; Dept of Epidemiology, Boston University School of Public Health, Boston, MA; Framingham Heart Study of the National, Heart, Lung, & Blood Institute & Boston University, Framingham, USA, ⁷Cardiology Section, Boston University Schools of Medicine, Boston; Framingham Heart Study of the National, Heart, Lung, & Blood Institute & Boston University, Framingham, USA, ⁸Center for Bone Research at the Sahlgrenska Academy, Sweden, ⁹Framingham Heart Study of the National, Heart, Lung, & Blood Institute & Boston University, Framingham; Department of Mathematics & Statistics, Boston University, Boston, USA, ¹⁰Dr. Kung-Wai Chee Clinic, Hong Kong, ¹¹Department of Psychiatry, the University of Hong Kong, Hong Kong, ¹²Framingham Heart Study of the National, Heart, Lung, & Blood Institute & Boston University, Framingham; Department of Biostatistics, Boston University School of Public Health, Boston, USA

Osteoprotegerin (OPG) is an osteoblast-secreted decoy receptor that is crucial for bone metabolism. There is evidence that OPG is also involved in non-skeletal disease pathology, such as cardiovascular diseases and metabolic syndrome, and that it is a predictor of mortality. In addition to age, gender, body mass index and menopause status, determinants of circulating levels of OPG remain poorly understood. However, the moderate heritability of serum OPG suggests that genetic factors play an important role. To identify common genetic variants affecting serum OPG levels, we conducted a meta-analysis of genome-wide association studies of natural log transformed serum OPG, using ~2.5 million genotyped and imputed common single nucleotide polymorphisms (SNPs) on autosomes and sex chromosomes in 8,545 participants of European and Chinese descent from the Framingham Heart Study (*n* = 3,223 and 3,685 European ancestry men and women, respectively), GOOD Study (*n* = 935 European ancestry men), and Hong Kong Osteoporosis Study (*n* = 702 Chinese women). All cohorts performed GWA analyses on genotyped and imputed data adjusting for age, age² and sex. An additive regression model was applied. Summary statistics from the individual studies were combined using fixed-effects inverse-variance weighted meta-analysis. Evidence of genome-wide significance (GWS) was set at *P* < 5 × 10⁻⁸ after a genomic control correction. Variants at 2 loci reached GWS for association with serum OPG concentrations: 8q23-q24.1 (*p* = 2.8 × 10⁻¹⁴ near *MAL2*, *COLEC10* and *OPG*), and 14q21.1 (*p* = 3.0 × 10⁻⁹ near *LRFN5*). Sex-specific meta-analysis revealed an additional locus on 15q26.2 (*p* = 3.5 × 10⁻⁸ near *MCTP2*). In summary, we identified 3 novel loci that are associated with serum OPG levels in populations of European and Chinese descent. Follow-up replication, fine-mapping, and functional studies of these genomic loci may provide additional insights into the regulation of serum OPG levels.

Disclosures: Ching-Lung Cheung, None.

MO0199

BMP Signaling Inhibits Myogenesis and Induces Osteoblastic Differentiation in Satellite Cells During Muscle Regeneration. Hiroki Sasanuma¹, Katsumi Yoneyama¹, Satoshi Ohte², Masashi Shin², Shoichiro Kokabu¹, Toru Fukuda¹, Takenobu Katagiri^{*3}. ¹Saitama Medical University RCGM, Japan, ²Saitama Medical University, Japan, ³Saitama Medical University Research Center for Genomic Medicine, Japan

Bone morphogenetic proteins (BMPs) induce heterotopic bone formation in skeletal muscle. Fibrodysplasia ossificans progressiva (FOP) is a rare inherited disorder characterized by progressive ectopic bone formation in skeletal muscles. Several mutations in one of BMP type I receptors, ALK2, have been identified in patients with FOP. In FOP, muscle injury induces acute heterotopic bone formation in skeletal muscle. Skeletal muscle satellite cells are quiescent progenitors located underneath the basal lamina that surrounds muscle fibers and play central roles in postnatal muscle growth and regeneration. Recently, it was reported that BMP signaling plays important role in muscle regeneration. In this study, we examined a role of BMP signaling on differentiation of primary satellite cells in vitro. We induced muscle regeneration by injecting snake venom into tibialis anterior muscle in mice. Necrotic myofibers were detected during the first 2 days, and then many mononuclear cells were gradually invaded into the muscle tissue until on day 3 after the injury. On day 5 to 7, regenerative myofibers appeared in the tissue. The numbers of satellite cells increased 2- to 3-fold than that in uninjured muscles. To examine the impact of BMP

signaling on satellite cell function, freshly sorted cells were stimulated with BMP-4. Myogenic differentiation of satellite cells was inhibited by the BMP treatment. In contrast, ALP activity of BMP was induced by BMP-4 in a dose-dependent manner. These findings suggest that satellite cells are the potential target of BMP signaling to induce heterotopic bone formation during muscle regeneration in FOP.

Disclosures: Takenobu Katagiri, None.

MO0200

Increasing canonical Wnt signaling does not rescue the fracture phenotype of mice lacking Bmp2. Giuseppe Intini*, Luciane Capelo, Karen Cox, Vicki Rosen. Harvard School of Dental Medicine, USA

BMP signaling and Wnt signaling are active during fracture repair but whether these pathways work in tandem to promote healing is unknown. Mice lacking limb-specific expression of Bmp2 (Bmp2cko) display two fracture-related phenotypes: bones of the appendicular limb skeleton spontaneously fracture as the mice age; once fractured, limb bones are unable to initiate fracture repair. Among the components of the Wnt signal transduction pathway analyzed during fracture repair, Dkk1 has been identified as a negative regulator of fracture healing in mice and in humans, increased Dkk1 transcript levels are found in patients with nonunion fractures. Since BMP2 has been shown to regulate Dkk1 in the developing limb, we hypothesized that the Bmp2 fracture phenotypes might be the result of altered Dkk1 activity. Here we show that Bmp2cko mice have elevated levels of bone Dkk1 transcripts at 8 and 15 weeks of age, consistent with the lack of fracture healing we observe in these mice. Surprisingly, when we reduce Dkk1 levels (Bmp2cko;Dkk1^{-/-}), the Bmp2cko fracture phenotypes are unaffected. Spontaneous fractures occur at the same rate in Bmp2cko;Dkk1^{-/-} mice and Bmp2cko mice, and there is no initiation of healing in either mouse genotype. As we can rescue the lack of healing in Bmp2cko mice by local injection of recombinant human BMP2 at the fracture site, we believe that the periosteal progenitor cell population needed to initiate repair is resident but remains in a quiescent state in the absence of BMP2. Increasing Wnt signaling does not influence periosteal cells to initiate repair when BMP2 is absent. We believe our data suggest that BMP signaling and Wnt signaling have distinct cellular targets in adult bone, where BMPs activate periosteal progenitors required for healing while Wnts activate more mature bone cells to enhance bone formation.

Disclosures: Giuseppe Intini, None.

MO0201

The Pattern of CXCR2-related Chemokine Gene Expression by FGF2 in the Osteoblast and Endothelial Cells Supports the Mobilization of Hematopoietic Stem and Progenitor Cells. Je-Yoel Cho¹, Kyung-Ae Yoon^{*2}, Hey-Sim Cho³. ¹School of Dentistry, Kyungpook National University, South Korea, ²Kyungpook National University, South Korea, ³School of dentistry, Kyungpook National University, South Korea

The maintenance of stem cells requires a specific microenvironment. HSC (hematopoietic stem cell) niche could be mainly derived into the osteoblast (OB) niche that maintains a quiescent HSC microenvironment and the vascular niche that regulates the proliferation, differentiation, and mobilization of HSC. SDF1-CXCR4 signaling is known to be important for hematopoiesis. Recent report showed that the reduction of SDF-1 were affected the expression of OB niche-related factors in bone marrow (BM) stromal cells of the conditioned knockout mice model. Systemic administration of FGF2 failed normal hematopoiesis in the BM by the reduced SDF-1. However, FGF2 signaling was an important regulator of endothelial cell angiogenesis by increasing SDF-1. Therefore, we hypothesized FGF2 induces a change of HSCs migration in BM and investigated important factors of HSCs migration using microarray chip. We firstly confirmed FGF2 decreased the expression of HSC niche-related genes in the primary OB but not in C166 cells. We selected the regulated genes that function in extracellular region during FGF2 treatment from the gene chip analysis. We confirmed the selected genes by qRT-PCR and identified CXCR2-related chemokine candidate, CXCL5. Chemotaxis assay showed CXCL5 induced the migration of hematopoietic stem and progenitor cells (HSPCs). According to these results, FGF2 induced the change of chemokine expression, of CXCL5. Finally, the difference action of FGF2 on the OB and C166 cells affected the mobilization of HSPCs in the BM.

Disclosures: Kyung-Ae Yoon, None.

This study received funding from: Korea Science and Engineering Foundation (KOSEF) grant(2009-0077615)

MO0202

A Novel Role for the Estrogen Responsive Cytokine, Lipocalin-2, in Bone. Muzaffer Cicek^{*1}, John Hawse², Sarah Grygo³, Kevin Pitel⁴, Kenneth Peters³, Nalini Rajamannan⁵, Malayannan Subramaniam¹, Thomas Spelsberg¹. ¹Mayo Clinic, USA, ²Mayo Clinic College of Medicine, USA, ³Mayo Clinic College of Medicine, USA, ⁴University of Minnesota, USA, ⁵Northwestern University Medical School, USA

Neutrophil Gelatinase-associated Lipocalin-2 (LCN2) is a member of the secreted lipocalin family of cytokines which function as modulators of many different physiological processes including cell differentiation, proliferation and apoptosis. Expression of LCN2 is primarily ubiquitous with the highest levels observed in bone marrow. Despite its high expression in bone marrow, the role of LCN2 in the skeleton has yet to be studied. To begin to elucidate its role in bone, we first investigated the changes in the expression levels of LCN2 during the course of calvarial cell mineralization. These studies revealed that LCN2 expression significantly increases, upwards of 250 fold, during the course of osteoblast differentiation. Since LCN2 has been shown to be regulated by estrogen in other tissues, and since estrogen is an important anabolic hormone in bone, we next investigated the regulation of LCN2 by estrogen in bone cells. U2OS osteosarcoma cells expressing either ER α or ER β were treated with estrogen over the course of 24 hours. LCN2 was shown to be induced by approximately 5 fold after 4 hours of treatment only in cells expressing ER α . Interestingly, ovariectomy of C57BL/6 mice also resulted in increased expression of LCN2 in the cortical shell of long bones which was further magnified following estrogen replacement. These data suggest that LCN2 may in part mediate estrogen effects in bone. To further extend our investigations, we also examined LCN2 expression in hematopoietic osteoclast progenitors isolated from bone marrow following treatment with MCSF. These studies revealed that LCN2 expression was significantly elevated in the non-adherent population compared to adherent stromal cells. The addition of RANKL and MCSF to the non-adherent cells decreased the expression of LCN2 at day 0 and completely suppressed the expression of this gene in mature osteoclasts. The same patterns of LCN2 expression were also observed in RAW264.7 cells. Treatment of osteoclast precursors with a LCN2 antibody also suppressed fusion and differentiation of osteoclast. Taken together, these data suggest that expression of LCN2 is essential during early stages of osteoclast differentiation. These studies are the first to implicate an important role for LCN2 in mediating both osteoblast and osteoclast function and suggest that this estrogen responsive cytokine may also serve as a novel coupling factor contributing to bone homeostasis.

Disclosures: Muzaffer Cicek, None.

MO0203

Alveolar Bone Repair under Homeostatic Conditions: Modulation of Inflammatory and Osteogenic Processes by IL-10 and TNF- α . Andreia Vieira^{*1}, Carlos Eduardo Repeke², Elcia Maria Silveira³, Carolina Favaro Francisconi³, Raissa Goncalves Carneiro Spera Andrade³, Ana Paula Favaro Trombone³, Gerson Francisco Assis³, Rumio Taga³, Gustavo Pompermaier Garlet³. ¹Bauru School of Dentistry - University of Sao Paulo, Brazil, ²Bauru School of Dentistry - University of Sao Paulo (FOB - USP), Brazil, ³Bauru School of Dentistry - University of Sao Paulo (FOB - USP), Brazil

Cytokines have been implicated in inflammatory bone loss process, however its role in bone repair process remains unknown. The objective of this study was to characterize the role of IL-10 and TNF- α (anti- and pro-inflammatory cytokines, respectively) in alveolar bone healing process after tooth extraction in IL-10KO and TNFp55KO strains compared to C57BL/6 (WT) mice. Following the extraction of the right upper incisor, the maxilla containing the remaining alveolus was collected 0, 7, 14, 21, 28 and 42 days after extraction for molecular (RealTimePCR) analysis and histomorphometric analysis descriptive and quantitative for fibers, fibroblasts, blood vessels, bone matrix, inflammatory cells, osteoblasts, osteoclasts and clot. The results demonstrated that in WT mice the initial formation of clot (0 hours) was followed by the transient appearance of foci of inflammatory infiltrate (7 days) and gradual (7-42 days) formation of connective tissue, vessels and bone. The IL10KO strain showed an increased density of inflammatory cells associated with higher levels of pro-inflammatory cytokines and chemokines (IL-1 β , TNF- α , KC/CXCL1, MCP-1/CCL-2 and MIP-1 α /CCL3) in the initial periods with lower density of the clot. It was followed by lower density of the fibroblasts, blood vessel and bone matrix, indicating a significant delay in bone repair associated with lower expression of CBFA-1, ALP, OCN and PHEX and higher density of osteoclasts. On the other hand, TNFp55KO strain presented intense increase in counts of inflammatory cells, in spite of a slight decrease of the KC/CXCL1, MCP-1/CCL-2, MIP-1 α /CCL3 and IL-10 expression. TNFp55KO also presented a delay in angiogenesis and in transition of granulation to bone tissue, associated with increased COL-I and a discreet presence of newly formed bone tissue associated with decreased CBFA-1, ALP, OCN and PHEX expression, in opposite of the higher proportion of osteoclasts in the late periods of the repair process. The results show that both cytokines interferes in alveolar bone repair through mechanisms that involve the control of inflammatory cell migration and modulation of osteogenic markers expression, since that the absence of IL-10 is associated with higher inflammatory activity and bone resorption concomitant with

lower bone formation, while the deficiency of TNF- α affect the recruitment of inflammatory infiltrates and the kinetics of alveolar bone healing.

Disclosures: Andreia Vieira, None.

MO0204

Hedgehog Signaling Pathway Implicated in Oxysterol-Mediated Osteogenesis in Rabbit Bone Marrow Stromal Cells. Sarah Sorice^{*1}, Akishige Hokugo¹, Kenneth Fan¹, Vicente Meliton², Patricia Zuk¹, Weibiao Huang³, Timothy Miller¹, Farhad Parhami², Reza Jarrahy¹. ¹Division of Plastic & Reconstructive Surgery, David Geffen School of Medicine at UCLA, USA, ²Department of Medicine, David Geffen School of Medicine at UCLA, USA, ³Plastic Surgery Section, VA Greater LA Healthcare System, Division of Plastic Surgery, USA

Purpose: To determine the osteogenic capacity of a novel growth factor on rabbit bone marrow stromal cells

Background: Both autologous bone grafts and alloplastic materials are commonly used in the reconstruction of complex craniofacial osseous defects, but both are associated with significant morbidity profiles. Tissue engineering solutions offer an alternative to these techniques. Bone morphogenetic protein (BMP) is an effective osteoinductive growth factor, but its clinical application is limited by exorbitant cost and undesirable side effects. Oxysterols are naturally occurring cholesterol oxidation products that are capable of inducing osteogenic differentiation. The effects of oxysterol on rabbit-bone marrow stromal cells (BMSC) have not been described.

Methods: Rabbit BMSCs were incubated with various concentrations of a novel oxysterol or BMP-2. Alkaline phosphatase (ALP) activity, expression of markers of osteogenic differentiation, and *in vitro* calcification assays were performed. To determine the mechanism of action of oxysterol, rabbit BMSC conditioned with oxysterol were incubated with various concentrations of the Hedgehog (Hh) inhibitor cyclopamine and ALP activity was measured.

Results: ALP activity in rabbit BMSCs treated with oxysterol was significantly higher than in controls and was equivalent to activity in cells treated with BMP-2. Gene expression of osteogenic markers in BMSCs treated with oxysterol was significantly higher than in control groups. Addition of cyclopamine to cultures negated the positive effect of oxysterol on ALP activity.

Conclusion: Oxysterols can induce osteogenesis *in vitro* in rabbit BMSCs with an efficacy similar to BMP-2. This osteogenic activity is in part mediated through the Hh signaling pathway. Oxysterols may represent a viable alternative to BMP-2 in bone tissue engineering models.

Disclosures: Sarah Sorice, None.

MO0205

Withdrawn

MO0206

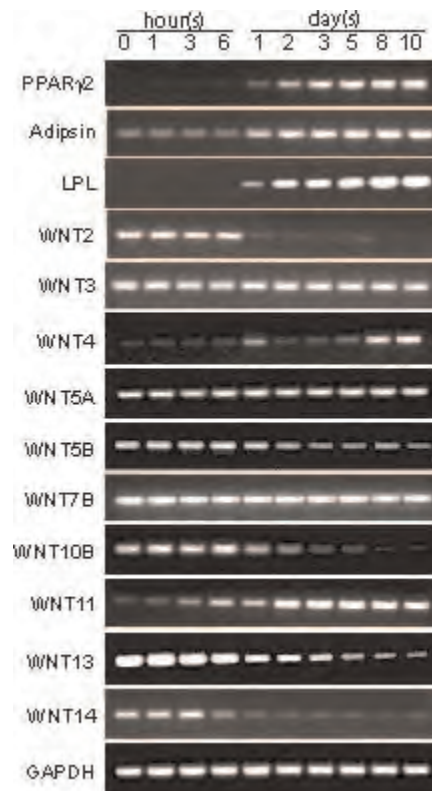
Inhibition of Adipocytogenesis by Canonical WNT Signaling in Human Mesenchymal Stem Cells. Longxiang Shen¹, Julie Glowacki², Shuanhu Zhou^{*2}. ¹Brigham & Women's Hospital, USA, ²Brigham & Women's Hospital, USA

INTRODUCTION: Adult human mesenchymal stem cells (hMSCs), also known as marrow stromal cells, have the capacity to differentiate into adipocytes, osteoblasts, and chondrocytes. The WNT signaling pathway plays important roles in the self-renewal and differentiation of mesenchymal stem cells (MSCs). Differentiation of murine adipocytes requires Wnt4 and Wnt5a and is negatively regulated by Wnt10b. Because little is known about WNT signaling in adipocyte differentiation of human MSCs, we tested the hypotheses that canonical and non-canonical WNTs differentially regulate *in vitro* adipocytogenesis of human MSCs.

METHODS: Human MSCs were isolated by expansion of adherent, low-density progenitor cells from marrow discarded during orthopedic surgery. Growth medium was phenol red-free α -MEM, 10% fetal bovine serum-heat-inactivated (FBS-HI), and antibiotics. Adipocytogenic medium had supplements (1 μ M dexamethasone, 0.5 mM 1-methyl-3-isobutylxanthine and 10 μ g/ml insulin) with 1% FBS-HI. Transient transfection of siRNA into hMSCs was performed by electroporation with the Human MSC Nucleofector Kit (Lonza/Amara Biosystems) and either human β -catenin-siRNA (Invitrogen) or non-silencing control siRNA (NC, Santa Cruz Biotechnology, Inc.) as described (Zhou S. J Cell Biochem. 2011 Feb 22. doi:10.1002/jcb.23079).

RESULTS: The expression of adipocyte genes (*PPAR γ 2*, *lipoprotein lipase*, *adipsin*) increased during adipocytogenesis of hMSCs. Simultaneously, the expression of canonical *WNT2*, *10B*, *13*, and *14* decreased, whereas non-canonical *WNT4* and *11* increased, and *WNT5A* was unchanged (Figure). Activation of Wnt/ β -catenin signaling with highly selective inhibitor of GSK-3 β , SB-216763, increased accumulation of β -catenin protein as assessed with Western immunoblotting, inhibited induction of adipocyte genes as well as non-canonical *Wnt4* and *11* gene expression and inhibited adipocytogenesis as demonstrated with Oil-Red-O staining. In contrast, knockdown of β -catenin with siRNA resulted in spontaneous adipocytogenesis.

CONCLUSION: These findings support the view that canonical WNT signaling inhibits and non-canonical WNT signaling promotes adipocytogenesis in adult human marrow-derived mesenchymal stem cells.



Figure

Disclosures: Shuanhu Zhou, None.

MO0207

Microarray Analysis of Fracture Gene Expression in Response to Cox-2 Gene Therapy Identifies Novel Angiogenic Genes. Charles Rundle^{*}, Nicoleta Popa, Subburaman Mohan, K-H. William Lau, Jerry L. Pettis Memorial VA Medical Center, USA

Cyclo-oxygenase (Cox)-2 gene therapy is one of the very few therapies that has been demonstrated to promote the bony union of the fracture callus and thereby accelerate fracture repair. To elucidate the mechanism for Cox2 regulation of fracture callus cartilage conversion, we performed a microarray analysis of gene expression in the mouse femur fracture callus in response to Cox-2 transgene expression. Gene expression was determined in femur fractures injected 1 day post-fracture at the periosteum with murine leukemia virus (MLV)-Cox2 (N=3) or MLV-B-galactosidase control (N=3) vectors. RNA was harvested from fracture calluses at 10 days post-fracture, a time coinciding with cartilage conversion to bone. Microarray hybridization utilized the Affymetrix ST-1.0 mouse exon array. Of the genes that displayed significant changes in expression ($p < 0.05$), 237 were more than 1.2-fold up-regulated, while 473 were more than 1.2-fold down-regulated. Although few of the growth factor families traditionally associated with bone formation or remodeling were represented, pathway analysis identified 2 key pathways modulated by Cox2 expression: inflammation and angiogenesis. Among the differentially expressed inflammatory genes, the chemokines Ccl7, Ccl8, Cxcl9 and Cxcl10 were between 1.6 and 3-fold up-regulated, suggesting that Cox2 promotes chemotaxis. Some inflammatory genes were up-regulated, including IL6 (1.4-fold), but many inflammatory genes were down-regulated, indicating that Cox2 regulation of cartilage conversion is complex and can be counter to its normal pro-inflammatory role. Surprisingly, the better-characterized families of angiogenic growth factors, such as VEGF, did not display significant changes in gene expression at a time when they would be expected to promote bony union of the fracture callus. Several angiogenic genes did display significant changes in expression. Angiopoietin-like (ANGPTL)-1 and ANGPTL2 were up-regulated 1.3-fold and 1.2-fold respectively, while ANGPTL7 was down-regulated 1.4-fold. These ANGPTL genes have been associated with oxidative stress, and blood vessel branching and remodeling during angiogenesis. Thrombospondins 3 and 4 were also up-regulated, suggesting that Cox2 regulates cell adhesion. We conclude that Cox2 promotes bony union of the fracture callus through 1) inflammatory pathway recruitment of osteoblasts and osteoclasts that remodel fracture cartilage to bone, and 2) angiogenesis regulated by novel angiogenic genes.

Disclosures: Charles Rundle, None.

MO0208

Nerve Growth Factor (NGF) Promotes Dental Epithelial Cell Proliferation. Mariko Ono*, Tsutomu Iwamoto, YU SUGAWARA, Aya Yamada, Takashi Nakamura, Satoshi Fukumoto. Tohoku University Graduate School of Dentistry, Japan

Enamel, the outer layer of tooth, is the hardest tissue in body and is formed by dental epithelial cell, ameloblast. Nerve growth factor (NGF), a member of neurotrophins, is expressed in dental epithelial cells, but their biological functions in ameloblasts differentiation have not been cleared. Here, we report that NGF positively regulates the proliferation of undifferentiated ameloblasts. NGF activates two types of receptors: tyrosine kinase receptor A (TrkA) and p75. RT-PCR and immunohistochemistry revealed that p75 was expressed in inner dental epithelium cells during early developmental stage of ameloblasts. On the other hand, TrkA was absent in tooth germ. To analyze the function of NGF in dental epithelium, a rat dental epithelial cell line, SF2, was used in this study. Exogenous NGF increased the number of SF2 cells and the incorporation of bromodeoxyuridine (BrdU), indicating that NGF promotes proliferation of SF2 cells. Immunostaining of p75 in cultured SF2 cells showed the different expression, compared to ameloblastin expression, indicating that p75 is expressed in undifferentiated SF2 cells, but not in differentiated SF2 cells. Further, NGF induced the phosphorylation of ERK1/2, but not of both I κ B and p38. U0126, a MEK inhibitor, inhibited NGF induced SF2 cell proliferation. Taken together, these results suggest that NGF regulates dental epithelial cell proliferation via p75-ERK1/2 pathway.

Disclosures: Mariko Ono, None.

MO0209

Oncostatin M Is a Potent Regulator of Interleukin-6 and RANKL Expression in Mouse Synovial Fibroblasts and Synergises with Interleukin-1. Benoit Le Goff¹, Brett A. Tonkin¹, Sofie Singbrant¹, T. John Martin¹, Evange Romas², Natalie Sims³, Nicole Walsh^{*1}. ¹St Vincent's Institute of Medical Research, Australia, ²Department of Medicine, St Vincent's Hospital, University of Melbourne, Australia, ³St. Vincent's Institute for Medical Research, Australia

Oncostatin M (OSM) is a multipotent cytokine expressed in the synovium of rheumatoid arthritis (RA) patients. OSM alone, or in concert with pro-inflammatory cytokines like IL-1, can stimulate expression of genes that promote inflammation and joint destruction. This study determined the acute effects of OSM, IL-1, and their combination on expression of IL-6 and RANKL in synovial fibroblasts (SFs). For this study, SFs were isolated from non-arthritis mouse hind paws and stimulated with mouse OSM (2 ng/mL), mouse IL-1 (10 ng/mL), or their combination for 1, 6 and 24 hours. RNA was isolated for quantitative RT-PCR analyses. OSM and IL-1 both increased IL-6 mRNA expression, with induction by OSM being more rapid and sustained compared with induction by IL-1: 135 fold vs. 40-fold at 24 hrs. Profound synergistic upregulation of IL-6 expression was observed when suboptimal doses of OSM and IL-1 were combined (>1000-fold at 6 and 24 hrs). Both OSM and IL-1 increased RANKL mRNA expression by 6 hrs (8-fold and 3-fold, respectively) but only OSM further increased RANKL expression at 24 hrs (20-fold). Combining suboptimal doses of OSM and IL-1 significantly enhanced RANKL expression by 24 hrs (100-fold). Cells lacking OSMR expression showed no induction of IL-6 or RANKL mRNA expression in response to OSM treatment, but responded to IL-1 treatment in a similar manner to matched wild type SFs. In wild type SFs, OSM stimulated expression of its co-receptors (OSMR, 6-fold at 6 and 24 hrs, and gp130, 3-fold at 24 hrs). Furthermore, OSM increased IL-1 receptor mRNA expression at 6 and 24 hrs (5-fold) and increased IL-1 receptor protein expression at 24 hrs as determined by flow cytometry. IL-1 did not regulate its own receptor, but induced a 3-fold increase in OSMR mRNA expression at 6 and 24 hrs. Finally, immunostaining showed protein expression of OSM and its co-receptors in the synovium in normal mouse knee joints; this expression was increased in antigen-induced arthritis. Together our data shows that OSM, acting alone or in synergy with IL-1, is a potent regulator of IL-6 and RANKL expression in SFs. The ability of OSM and IL-1 to cross-regulate expression of their respective receptors likely explains their synergistic effects on SFs. The results identify a significant role for OSM, acting through OSMR, in mediating inflammation and bone destruction in arthritic joints. OSM signaling via OSMR is therefore a potential therapeutic target in the treatment of RA.

Disclosures: Nicole Walsh, None.

MO0210

Protease-Activated Receptor-2 is Required for Normal Skeletal Growth and Repair. Smitha R Georgy¹, Charles N. Pagel¹, Natalie Sims², Eleanor Mackie^{*3}. ¹School of Veterinary Science, University of Melbourne, Australia, ²St. Vincent's Institute for Medical Research, Australia, ³University of Melbourne, Australia

The G-protein-coupled receptor, protease-activated receptor-2 (PAR₂), is expressed by many cell types including osteoblasts and monocytes, and activated by proteases including coagulation factors, mast cell tryptase and kallikreins, which are

likely to be present in bone at sites of injury, inflammation or cancer metastasis. Moreover, PAR₂ antagonists are currently being developed for the treatment of inflammatory conditions in a number of tissues, thus it is important to understand how activation of this receptor influences bone metabolism. The aim of the current study was to investigate the role of PAR₂ in skeletal growth and bone repair using wild type (WT) and PAR₂ knockout (KO) mice. Tibiae were isolated from male WT and KO mice at 50 days of age and analysed by static and dynamic histomorphometry. To identify the role of PAR₂ in bone repair, a hole was drilled through the tibiae of 14-week-old WT and KO mice then the mice were killed at various times after surgery for histological analysis of the injured bone. Bone marrow isolated from the bones of WT and KO mice was cultured and investigated for the presence of alkaline phosphatase (ALP)-positive fibroblastic colonies; osteoclasts (TRAP-positive multinucleate cells) were counted in bone marrow cultures treated with M-CSF and RANKL. Trabecular bone volume (BV/TV) was significantly greater in the tibiae of PAR₂ KO mice than in those of WT mice at 50 days of age. This high bone volume in KO mice was associated with greater trabecular number and thickness. Osteoclast surface was significantly lower in KO than in WT mice, but osteoblast surface and osteoid volume were also significantly lower in KO than in WT mice. In mice subjected to bone injury, there were significantly fewer cells in the drill site of KO mice compared to WT mice 3 days post-surgery, although macrophage numbers did not differ between genotypes. There was significantly less new bone in the drill site in PAR₂ KO mice compared to WT mice 7 days post-surgery; there were also fewer osteoclasts in KO than in WT drill sites at this stage. Bone marrow cultures from KO mice showed fewer ALP-positive colony-forming units and osteoclasts compared to cultures from WT mice. These results suggest that PAR₂ activation contributes to the determination of cells of both the osteoblast and osteoclast lineages within bone marrow, and thereby participates in the regulation of skeletal growth and bone repair.

Disclosures: Eleanor Mackie, None.

MO0211

Skeletal Phenotype of the Leptin Receptor-Deficient Db/Db Mouse. Garry Williams^{*1}, Karen Callon¹, Maureen Watson¹, Jessica Costa², Yaoyao Ding¹, Michelle Dickinson¹, Yu Wang³, Dorit Nao¹, Ian Reid¹, Jillian Cornish¹. ¹University of Auckland, New Zealand, ²University of Auckland, Nzl, ³University of Hong Kong, Hong Kong

Leptin, a major hormonal product of the adipocyte regulates appetite and reproductive function through its hypothalamic receptors. The leptin receptor is present in osteoblasts and chondrocytes and previously we have shown leptin to be an anabolic bone factor in vitro, stimulating osteoblast proliferation and inhibiting osteoclastogenesis. Leptin increases bone mass and reduces bone fragility when administered peripherally but can also indirectly reduce bone mass when administered into the central nervous system. However, data from animal models deficient in either leptin (ob/ob) or its receptor (db/db) remain contradictory. We compared the bone phenotype of leptin receptor-deficient (db/db) and wild-type (WT) mice using micro-computed tomography (μ CT) analysis of the proximal tibiae and vertebrae. In the tibia, db/db mice had reduced percent trabecular bone volume (13.0 1.62% in WT vs 6.01 0.601% in db/db, $p = 0.002$) and cortical bone volume (411 21.5 μm^3 vs 316 3.53 μm^3 , $p = 0.0014$), trabecular thickness (48.4 0.0107 μm vs 45.1 0.929 μm , $p = 0.041$) and trabecular number (2.68 0.319 mm^{-1} vs 1.34 0.148 mm^{-1} , $p = 0.0034$). In the 5th lumbar vertebral body the trabecular thickness and cortical thickness were decreased in the db/db vs WT (0.053 0.0011 mm vs 0.047 0.0013 mm, $p = 0.0002$) and (0.062 0.00054 mm vs 0.056 0.0009 mm, $p = 0.0001$) respectively whereas the trabecular and cortical percent bone volume and trabecular number did not reach significance. The total (endosteal and periosteal) cortical perimeter (12.2 0.19mm vs 13.2 0.30mm, $p = 0.01$) was increased. The serum osteocalcin levels were reduced in the db/db mouse, suggesting that bone formation rates are decreased. The material properties of db/db femora were determined by three-point bending and nanoindentation, showing decreased bone strength (13.3 0.280 N vs 7.99 0.984 N, $p = 0.0074$), and material stiffness (28.5 0.280 GPa vs 25.8 0.281 GPa, $p < 0.0001$).

Disclosures: Garry Williams, None.

MO0212

Study on Structure and Function of Sclerostin by Site Directed Mutagenesis of Cysteine- Knot and Finger 2 residues. Kwang Joon Kim¹, Ajitha Jami², Kyoung Min Kim¹, Sung-Kil Lim¹, Gadi Jogeswar^{*3}, Eun Jin Kim⁴, Sena Hwang¹. ¹Division of Endocrinology & Endocrine Research Institute, Department of Internal Medicine, Yonsei University College of Medicine, South Korea, ²Brain Korea 21 Project for medical sciences, Yonsei University College of Medicine, South Korea, ³Yonsei University College of Medicine Seoul South Korea, South Korea, ⁴Severance Biomedical Science Institute, Yonsei University College of Medicine, South Korea

Sclerostin is a secreted glycoprotein, expressed and secreted by osteocytes and acts as a negative regulator of bone formation using Wnt signaling. The inhibitory action of Sclerostin in Wnt signaling is due to the binding of Wnt co-receptor LRP5. Inhibition of Sclerostin binding to Wnt receptor can enhance the Wnt signaling makes it as a highly interesting target for diseases related to bone loss such as osteoporosis.

Recent studies shows that the first missense mutation in the human Sclerostin (SOST) gene results in the exchange of a cysteine residue of the cysteine-knot motif of Sclerostin for a non-cysteine amino acid, a defect that leads to a complete loss of function of Sclerostin due to retention of the mutated protein in the ER. In order to identify the key cysteine knot motif residues contributing for the Sclerostin structure and function, we choose site directed mutagenesis method and substituted the cysteine residues with alanine. After the expression of the pcDNA3.1/Sost-mycHis (wild type) and pcDNA3.1/mut-Sost-mycHis in MC3T3-E1 cells, we found that the Sclerostin expression in the cell lysate and culture medium was significantly different in the cysteine mutants compared to wild type, we also found that the secretion into the culture medium was significantly reduced in the mutants compared with the wild type Sclerostin. The functionality of wild type and mutant Sclerostin will be determined by the Wnt signaling activity, which is measured by super-Top MC3T3-E1 stable cell lines treated with wild type and mutant Sclerostin conditioned medium. This study is crucial to elucidate the key residues essential for the structure and function of Sclerostin, which will further helpful to design molecules targeting to Sclerostin for the enhancement of bone formation.

Disclosures: Gadi Jogeswar, None.

MO0213

Systemic Bone Metabolism and Inflammation in RA Patients Receiving TNF Inhibiting Therapy. Won Park^{*1}, Mie Jin Lim², Seong Ryul Kwon¹, Kowoon Ju¹, Min Jung Son¹. ¹Inha University Hospital, South Korea, ²Division of Rheumatology, Department of Internal medicine, Inha University, South Korea

Background: Etanercept is soluble Tumor Necrosis Factor (TNF)- α receptor which is effective in suppressing inflammation in Rheumatoid Arthritis (RA). However bone metabolism is not yet known after etanercept therapy.

Objective: Our aim is to assess bone metabolism along with inflammation in RA patients after etanercept treatment for 3 months and to compare bone turnover markers in RA patients with age, sex matched control group.

Methods: Twenty-two patients (20 women and 2 men; age 47.05 \pm 11.87 years) with active RA were included. Etanercept was administered at standard dose, twice a week. Age and sex matched control group were recruited. Venous blood was drawn at baseline and after 12-14 weeks of etanercept use in RA patient. Bone metabolism was assessed using bone specific alkaline phosphatase (BSAP), osteoprotegerin (OPG), sclerostin for bone formation and receptor activator for nuclear factor κ B ligand (RANKL), serum c-telopeptide (CTX) for bone resorption. Serum level of inflammatory mediators including ESR, CRP, TNF- α and IL-6 were also determined. TNF RNA expression was measured by real time RT-PCR.

Differences between two groups were examined by Wilcoxon signed ranks test. A p value of less than 0.05 was denoted statistically significant.

Results: At baseline both serum sclerostin and CTX level was significantly lower in RA patients than in control group but sclerostin increased markedly after etanercept treatment while CTX rose marginally (Table 1). BSAP and OPG were least affected by etanercept. RANKL decreased mildly after treatment.

Inflammatory mediators responded to the treatment as ESR, CRP and IL-6 all significantly decreased (Table 2). However, serum TNF- α increased to > 32 pg/mL in all RA patients after treatment and TNF RNA expression also showed concordant increase (2.04 \pm 1.38, p = 0.002).

Conclusions: Our study showed significantly lower serum CTX and sclerostin level in RA patients than in control group which increased after etanercept treatment. Thus we postulate that in addition of suppressing inflammation due to RA, etanercept normalize bone metabolism which was suppressed in RA patients and increased serum TNF level along with high TNF RNA expression after etanercept treatment seem to play some role in it.

	Age, sex matched control	RA patients Baseline	P (control vs. RA patients Baseline)	week 12-14 after etanercept	P (RA patients Baseline vs. Week 12-14)
Sclerostin (pg/mL)	2.2 \pm 1.61	1.76 \pm 2.29	0.019	3.04 \pm 4.1	0.036
Serum CTX (ng/mL)	0.4 \pm 0.19	0.28 \pm 0.13	0.016	0.34 \pm 0.17	0.108

Table 1

	Baseline	Week 12-14 after etanercept	p
ESR (mm/hr)	39 \pm 30.5	28 \pm 26.9	0.039
CRP (mg/dL)	0.94 \pm 0.86	0.51 \pm 1.15	0.044
IL-6 (pg/mL)	3.72 \pm 4.34	0.68 \pm 0.66	< 0.001
OPG (pmol/L)	2.36 \pm 1.081	2.2 \pm 0.786	0.619
BSAP (U/L)	20 \pm 6.97	20.3 \pm 7.45	0.887
RANKL (pmol/L)	0.25 \pm 0.37	0.22 \pm 0.422	0.07

Table 2

Disclosures: Won Park, None.

MO0214

Targeted Deletion of Chemokine Receptor (Ccr)-3 Increases Trabecular Bone Density in Mice. Bouchra Edderkaoui^{*}, Yan Hu, Anil Kapoor, Subburaman Mohan, Jerry L. Pettis Memorial VA Medical Center, USA

Chemokines are now recognized to be the major factors in inflammation-induced bone loss. The functions of chemokines are mediated by members of Ccr family. Chemokines and their receptors are known to be expressed in cells of both osteoblastic and osteoclastic lineage. Accordingly, disruption of Ccr1 in mice leads to osteopenia caused by impaired osteoclast and osteoblast functions. In contrast, Ccr2 knockout (KO) mice exhibit increased bone mass caused by deficiency in osteoclast functions. Since little is known on Ccr3 functions in bone, we evaluated the expression of Ccr3 during RANKL-induced differentiation of mouse monocyte RAW-264.7 cells into TRAP-positive multinucleated osteoclasts in vitro. We found Ccr3 expression was increased by 4-, 10- and 30-fold (all P < 0.01) compared to control cultures after 1 day, 2 and 3 days treatment with RANKL, respectively. Based on these data and the findings that Ccr3 is expressed in both osteoclast and osteoblast cells and it binds to chemokines known to influence osteoclast function, we tested the hypothesis that Ccr3 regulates peak bone mass. Heterozygous Ccr3^{+/-} mice were bred to generate homozygous KO and their corresponding littermate wild type (WT) mice. BMD measurements by PIXImus revealed significant increases in femur BMD in Ccr3-KO mice at 5 and 8 weeks of age compared to WT control mice. Micro-CT measurements revealed that trabecular (Tb) bone volume/total volume was increased by 19% (P = 0.03) in female KO mice at 10 weeks of age which was caused by both an increase in Tb thickness and a reduction in Tb separation. Accordingly, Tb BMD was increased by 15% in the KO mice compared to WT mice. To determine the mechanism for high bone mass in the KO mice, we evaluated the expression level of osteoblast and osteoclast marker genes. While the expression level of RANK in bones was not significantly different between KO mice and WT mice, Runx2 expression was increased by 2-fold (P = 0.03) in the KO mice. **Conclusions:** 1) Targeted disruption of Ccr3 increases trabecular bone density by influencing Tb thickness and Tb separation, consistent with effects on both bone formation and resorption. 2) Our data and other published data suggest complex functions for Ccrs that influence both osteoclasts and osteoblasts and thereby regulate bone mass either positively or negatively.

Disclosures: Bouchra Edderkaoui, None.

MO0215

Circulating Liver Derived IGF-1 is Dispensable for the Osteogenic Response to Mechanical Loading in Female Mice. Johan Svensson¹, Sara Windahl², Leanne Saxon³, Klara Sjogren¹, Joanna Price⁴, Lance Lanyon³, Claes Ohlsson⁵. ¹Center for Bone & Arthritis Research, Sweden, ²Center for Bone & Arthritis Research, Sahlgrenska Academy, Sweden, ³Royal Veterinary College, United Kingdom, ⁴University of Bristol, United Kingdom, ⁵Center for Bone Research At the Sahlgrenska Academy, Sweden

IGF-I is a key regulator of bone mass and its expression is regulated in response to mechanical loading. Conditional depletion of IGF-I in osteoblasts inhibits the bone anabolic effect of mechanical loading. 1 Serum IGF-I is mainly liver-derived and low serum IGF-I is associated with increased fracture risk. 2, 3. Mice with conditional liver-specific IGF I inactivation (LI-IGF-I mice) display reduced cortical bone mass. 4. The aim of the present study was to determine the role of liver-derived IGF-I for the osteogenic response to mechanical loading in mice.

We evaluated the osteogenic response in LI-IGF-I mice. At either 6 (adult) or 19 (aged) months of age, the right tibia was subjected to short periods of axial cyclic compressive loading, three times a week for two weeks (40 cycles, peak strains of either 2800 or 3500 μ ε for the adult and aged mice, respectively). Peripheral computed

tomography (pQCT) was used to assess the osteogenic response in the cortical and cancellous bone of the loaded (right) versus the non-loaded (left) tibia ((R-L)/L*100; n=7-11).

Mechanical loading increased the trabecular bone mineral density (BMD; adult 123%; aged 119% over non-loaded tibia, $p<0.001$) and cortical cross sectional bone area (adult 28%; aged 26% over non-loaded tibia, $p<0.001$) similarly in adult and aged wild type mice. LI-IGF-I mice had a 70% reduction of serum IGF-I ($p<0.001$), resulting in a reduced cortical cross sectional bone area ($p<0.05$). However, in contrast to the osteoblast specific IGF-I inactivated mice, which do not respond to mechanical loading, LI-IGF-I mice responded normally to mechanical loading in both the trabecular (trabecular BMD, adult 170%, aged 77% over non-loaded tibia, $p<0.001$) and cortical (cortical cross sectional bone area, adult 28%, aged 31% over non-loaded tibia, $p<0.001$) bone compartments.

These findings demonstrate that although liver-derived IGF-I regulates cortical bone mass, it does not mediate the osteogenic response to mechanical loading in female mice. We therefore propose that IGF-I produced locally in the bone, but not circulating liver-derived IGF-I, modulates the osteogenic response to mechanical loading in bone.

References

- 1) Kesavan et al 2009 J Bone Miner Res 24 (Suppl 1):1119
- 2) Ohlsson et al 2009 Endocrine Reviews 30:494-535
- 3) Ohlsson et al 2011 J Bone Miner Res 26:865-72
- 4) Sjogren et al 2002 J Bone Miner Res 17(11) 1977-82

Disclosures: Sara Windahl, None.

MO0216

Adhesion to Apatite Surfaces Is Capable of Manipulating MAPK signaling and Osteogenesis in Human Adipose-derived Stem Cells. Patricia Zuk^{*1}, Benjamin Wu², Christopher Arakawa², Eric Tsang². ¹University of California, Los Angeles, USA, ²UCLA Dept of Bioengineering, USA

Background: In the past, combining pro-osteogenic growth factors with human adipose-derived stem cells (ASCs) has been proposed as a means to augment their osteogenic capacity. As an alternative to upstream growth factors, direct manipulation of downstream signaling pathways may represent another option. As such, this study explores the use of apatite surfaces in the manipulation of MAPK signaling and ASC osteogenic capacity.

Results: MAPK signaling and ASC osteogenesis were first characterized on tissue culture polystyrene (TCPS), using exogenous inhibitors to ERK, p38MAPK and JNK activation. ERK and JNK inhibitors, administered at the start of osteogenic differentiation, significantly inhibited AP activity and extracellular mineral production, suggesting that these kinases may promote osteogenic commitment. Consistent with this, altered mineralization levels were also observed upon transduction of osteo-induced ASCs with shRNA lentiviruses for ERK1/2 or JNK1/2 knockdown. Administration of these inhibitors continuously throughout the induction period also resulted in decreased osteogenesis, albeit with distinct stage- and kinase-specific effects, implying a complex role for MAPK signaling in ASC osteogenesis. Distinct changes to MAPK activity and osteogenesis were also measured upon culturing of ASCs on 2D apatite surfaces. Specifically, the apatite surface significantly increased both AP activity and mineral deposition, when compared to TCPS, suggesting that apatites can be osteoinductive to ASCs. The effect of ASC adhesion to apatites and ERK signaling was found to depend on the crystallinity of the apatite or its modification via protein adsorption. Highly crystalline surfaces were found to promote ERK activity in comparison to TCPS, while poorly crystalline surfaces decreased its activity. Adsorption of the serum protein albumin, or the matrix proteins fibronectin or collagen type I to the apatite increased ERK activity, beyond that measured on unmodified controls. ERK activation could be eliminated upon adsorption of the fibronectin peptide RDGS or recombinant osteonectin.

Conclusion: MAPK signaling appears to play a complex role in ASC osteogenesis. Its signaling can be directly manipulated through the ASC adhesion to crystalline apatite surfaces modified through protein or peptide adsorption. As such, adhesion to apatite surfaces may represent an alternative way of altering ASC osteogenesis through manipulation of the MAPK cascade.

Disclosures: Patricia Zuk, None.

MO0217

Salubrinol Reduces Apoptosis of Mesenchymal Stem Cells and Osteoblasts Induced by Stress to the Endoplasmic Reticulum. Liming Zhao¹, Hiroki Yokota^{*2}. ¹Purdue University School of Indianapolis, USA, ²Indiana University Purdue University Indianapolis, USA

Salubrinol is a small, synthetic chemical agent, known to prevent dephosphorylation of eukaryotic initiation factor 2, alpha subunit (eIF2a). We previously demonstrated that local administration of salubrinol stimulated bone formation and accelerated healing of bone wounds. To understand the mechanism of salubrinol action, we examine its effects on apoptosis. We hypothesized that salubrinol would reduce cellular apoptosis induced by stress to the endoplasmic reticulum (ER).

To test this hypothesis, we employed primary MSCs isolated from mouse bone marrow and MC3T3 osteoblast-like cells. Cells were pre-incubated with 20 microM

salubrinol for 6 h, and then exposed to stress inducers such as thapsigargin, tunicamycin, and dexamethasone for 18 h. Thapsigargin and tunicamycin are the inducers of stress to the ER through the inhibitions of ATPase and glycosylation, respectively. Dexamethasone is a steroid, known to induce catabolic responses and apoptosis. The results demonstrated that pre-incubation with salubrinol reduced apoptosis caused by thapsigargin and tunicamycin. In response to incubation with 5 microM thapsigargin in MC3T3 cells, for instance, cell death was increased to 12.4 4.8% with elevation of an active form of caspase 3. This increase was reduced to 1.6 1.2% by pre-treatment with salubrinol. Similarly, in response to incubation with 1 mg/ml tunicamycin, pre-incubation with salubrinol reduced cell death from 10.9 3.6 % to 2.5 1.1%. For cell death induced by dexamethasone, however, salubrinol did not improve cell viability. The results suggest that salubrinol is a specific suppressor of cellular death, which was induced by stress to the ER. Studies during the last decade demonstrated that apoptosis is as important as mitosis for the growth and maintenance of the skeleton. Stress to the ER is often caused by an accumulation of unfolded or misfolded proteins and induces apoptosis. Through the elevation of eIF2a phosphorylation, salubrinol decreases translational efficiency of a majority of proteins except for a group of proteins such as ATF4 that is one of the critical transcription factors for bone formation. Further investigation of the mechanism of salubrinol-mediated bone formation and suppression of apoptosis is our future studies.

Disclosures: Hiroki Yokota, None.

MO0218

Abnormal Mechanical Environment Affects the Morphology, Cytoskeleton and Cytoskeleton-Associated Proteins Expression in Bone Cells. Airong Qian^{*1}, Lifang Hu², Xiang Gao², Wei Zhang², Shengmeng Di², Peng Shang². ¹Northwestern Polytechnical University, Peoples Republic of China, ²Northwestern Polytechnical University, China

Osteocytes are believed to be the mechanosensors of bone and can regulate its effector cell such as osteoblasts and osteoclasts to respond to mechanical stresses. Osteoblasts, which are responsible for bone formation, may directly sense and respond to mechanical stimulation (e.g., fluid flow). The purpose of this study is to investigate the effects of abnormal mechanical environment on the proliferation, morphology, cytoskeleton architecture, cytoskeleton-associated proteins expression in cultured bone cells, and whether osteocytes have regulatory roles in osteoblasts function.

Murine osteoblast-like cell line MC3T3-E1 and osteocyte-like cell line MLO-Y4 were cultured in the bore of a superconducting magnet with large gradient high magnetic field (LG-HMF), which can simulate three apparent gravity levels [μ -g (diamagnetic levitation), 1-g, and 2-g] for 24 or 48 hrs. And then electron microscope (EM), atomic force microscope (AFM) and laser scanning confocal microscope (LSCM) were used to investigate the changes in morphology and cytoskeleton. Western blotting was used to examine the expression of cytoskeleton-associated proteins. MTT assay was employed to detect the effects of conditioned medium (CM) of osteocytes on osteoblasts proliferation.

The results showed that LG-HMF treatment of 24 or 48 hours had no acute lethal effects on both osteoblast-like and osteocyte-like cells. Compared to the natural 1-g control, simulated μ -g environment significantly altered MC3T3-E1 shape, cytoskeleton structure and decreased the expression of h2-calponin, a gene known to response to changes in mechanical environment. The elongated shape, reduced cell extension, reorganized cytoskeleton architecture (F-actin, microtubule and intermediate filament) and decreased expression of cytoskeleton-associated proteins, such as paxillin, talin, vinculin and microtubule actin crosslinker factor (MACF1) were also found in osteocyte-like cells after 48 h - exposure to simulated μ -g environment. CM of osteocytes exposed to simulated μ -g environment promoted osteoblasts proliferation. In contrast, LG-HMF-simulated 1-g and 2-g apparent gravity did not have such effects.

Our findings indicate that that bone cells are sensitive to abnormal mechanical environment, cytoskeleton-associated proteins may be involved in the interaction of bone cells with their mechanical environment and osteocytes have an a regulatory role in osteoblast function.

Disclosures: Airong Qian, None.

MO0219

Afamin, Secreted from Non-Resorbing Osteoclasts, Acts as a Chemokine for Preosteoblasts via Akt and G_i-coupled Receptor Signaling Pathway. Beom-Jun Kim^{*1}, Sun-Young Lee², Young-Sun Lee², Seung Hun Lee³, Sung Jin Bae¹, Ha Young Kim⁴, Jung-Min Koh¹, Hong-Hee Kim⁵, Shin-Yoon Kim⁶, Ghi Su Kim⁷. ¹Asan Medical Center, South Korea, ²Asan Institute for Life Sciences, South Korea, ³Asan Medical Center, University of Ulsan College of Medicine, South Korea, ⁴Wonkwang University Sanbon Hospital, South Korea, ⁵Seoul National University, South Korea, ⁶Kyungpook National University Hospital, South Korea, ⁷University of Ulsan, South Korea

In spite of the possible effects of osteoclasts on bone formation by signaling to osteoblasts, questions remain as to when coupling factors are produced during osteoclastogenesis and which stage of osteoblastogenesis is affected by these factors.

To clarify these questions, we established in vitro system for coupling phenomenon. We obtained supernatants of osteoclast culture in the stages of early and late differentiation and resorption, and then the collected conditioned media (CM) were treated on preosteoblastic MC3T3-E1 cells to evaluate influence on migration, viability and proliferation of osteoblasts. We found that secreted coupling factor from early osteoclast differentiation can stimulate recruitment of preosteoblasts. By further performing fractional analyses of the CM with liquid chromatography-tandem mass spectrometry, we identified afamin, known to have binding activity with vitamin E, as one of osteoclast-derived chemokines for preosteoblasts. Chemotactic responses were measured with Boyden chamber and wound healing assay. When we transfected Raw264.7 cell with siRNA against afamin and tested the CM of siRNA-treated osteoclasts for chemotactic activity, osteoclast-induced chemotaxis for preosteoblasts was significantly suppressed. To identify the possible mechanisms of afamin as a chemokine, we focused on several signaling pathways related to cell migration. The phosphorylation of Akt was remarkably increased after afamin treatment on MC3T3-E1 cells, whereas Akt inhibitor LY009242 significantly blocked afamin-induced preosteoblasts migration. In addition, pertussis toxin (PTX), a specific inhibitor of Gi-coupled receptor signaling, significantly diminished afamin-induced preosteoblasts recruitment. However, the level of afamin-induced phosphorylated Akt was not affected by PTX, indicating that Akt and Gi-coupled receptor pathways independently mediate afamin-induced chemotaxis. When we investigated the effect of afamin on osteoclasts themselves, it stimulated osteoclast formation in a dose-dependent manner, based on TRAP staining, and increased bone resorption by 2.8-fold compared with untreated control. In conclusion, we identified afamin as one of osteoclast-derived chemokines for preosteoblasts through activation of Akt and Gi-coupled receptor pathways. We also showed that afamin can act as an autocrine manner by increasing differentiation and resorptive activity of osteoclasts, indicating that it can cause high bone turnover state.

Disclosures: Beom-Jun Kim, None.

MO0220

Bone Sialoprotein and Runx2 Are Interdependent during Osteogenic Differentiation of Adult Mesenchymal Stem Cells. Qinghua Lu, Marianna Rodova, James Bernard, Jinxi Wang*. University of Kansas Medical Center, USA

Bone sialoprotein (BSP) is one of the major non-collagenous phosphoproteins in bone and dentin. Our previous study revealed that implantation of BSP stimulates osteogenesis in surgically created rat calvarial defects, but not in rat thoracic subcutaneous tissue. The mechanisms of the tissue-specific response to BSP treatment remain unclear. This study aimed to test our hypothesis that the effect of BSP on osteogenic differentiation is principally dependent on the characteristics of responding cells. We first performed gene expression analyses by quantitative real-time PCR (qPCR) and found that the expression level of Runx2, a transcriptional activator of osteoblast differentiation, was significantly higher in normal dura and periosteum at the cranial site than in normal thoracic subcutaneous tissue of rats/mice. However, there were no significant differences in expression level of osteocalcin between these tissues. To examine if Runx2 and BSP are interdependent during osteogenic differentiation of adult mesenchymal stem cells, we performed loss- and gain-of-function analyses in cell cultures. Primary mesenchymal cells isolated from the dura (the primary source of BSP-responsive cells in vivo) or thoracic subcutaneous tissues of 3-month-old mice were cultivated in the same conditions of α -MEM media. When the cells reached ~70% confluence, they were transfected with Runx2/BSP-specific expression or RNAi lentiviral vectors with the addition of 50 μ g/ml ascorbic acid and 5 mM β -glycerolphosphate. The effects of Runx2/BSP on osteogenesis were determined by qPCR analysis of the expression level of osteoblast marker genes (e.g., osteocalcin) and histomorphometric analysis of the number of bone-like nodules in the cultures. The results revealed that: 1) knockdown of Runx2 by RNAi suppressed BSP-stimulated osteogenesis in cultured dural cells, while forced expression of Runx2 enhanced this process; and 2) forced Runx2 expression or BSP treatment alone failed to achieve osteogenesis, while forced Runx2 expression plus BSP treatment stimulated osteogenesis in cultured thoracic subcutaneous cells. These results suggest that BSP and Runx2 are interdependent during osteogenic differentiation of adult mesenchymal stem cells. BSP elicits osteogenesis in cranial defects but not in thoracic subcutaneous tissue due mainly to the lack of Runx2 expression in the latter. However, Runx2-expressing cells do not spontaneously differentiate to functional osteoblasts without BSP.

Disclosures: Jinxi Wang, None.

MO0221

Both TNF- α and RANKL Antagonist Peptide Stimulates Bone Formation In TNF- α Deficient Mice to the Same Extent As In Wild Type Mice. Masud Khan*, Neil Alles², Kenichi Nagano³, YURIKO FURUYA⁴, Hisataka Yasuda⁵, Keiichi Ohya³, Kazuhiro Aoki³. ¹Tokyo Medical & Dental University G-COE, Japan, ²JSPS, Tokyo Medical & Dental University, Japan, ³Tokyo Medical & Dental University, Japan, ⁴ORIENTAL YEAST CO.,LTD, Japan, ⁵Oriental Yeast Company, Limited, Japan

PURPOSE:

W9 peptide (W9) is originally designed as TNF (tumor necrosis factor) - α antagonist by using a ligand-recognition-site-structure on TNF-type1-receptor

(TNFR1). Recently we found the stimulatory effects of W9 on bone formation. Since TNF- α is proven to inhibit bone formation, we hypothesized that W9 might promote bone formation under the TNF- α dependent mechanism. In this study, we tested whether the stimulatory effects of W9 on bone formation is TNF- α dependent or regulated by the other mechanism.

METHODS:

Five weeks old male TNFR1 deficient, TNF- α deficient mice (C57BL/6 background) and the wild type (WT) mice were used. Type1-bovine-collagen discs were used as a carrier of BMP-2 and W9. Collagen discs containing either BMP-2 (1 μ g) alone or BMP-2 (1 μ g) with 0.56 mg W9 were freeze-dried, and were implanted into the mice back muscle. Mice were sacrificed on day 12 after implant, and radiological analyses were performed.

RESULTS:

Three dimensional μ -CT images showed that larger size of ectopic bone was observed in BMP-2 with W9 group compare to BMP-2 alone in WT mice. Surprisingly, W9 also increased ectopic bone formation in both TNFR1 deficient and TNF- α deficient mice. These findings were confirmed by the quantitative analysis using DXA. In WT mice, W9 increased bone mineral content (BMC) of ectopic bone by 2.6 fold more compare to the ectopic bone induced by BMP-2 alone. W9 also increased bone mineral content of ectopic bone induced by BMP-2 in both TNFR1 deficient and TNF- α deficient mice to the same extent as in WT mice (by 3.4-fold and 2.7-fold, respectively).

DISCUSSION AND CONCLUSION:

W9 is proven to bind to receptor activator of NF- κ B ligand (RANKL) as well as TNF- α . We speculated that the stimulatory effects of W9 on BMP-induced bone formation might be regulated by the other mechanism such as RANKL-related signaling not TNF- α .

Disclosures: Masud Khan, None.

This study received funding from: Oriental Yeast CoLTD

MO0222

CD47 is an Integral Modulator of Osteoblastogenesis. Victoria Demambro*, Laura Maile², Casey Doucette¹, Phuong Le¹, Wesley Beamer³, David Clemmons², Clifford Rosen⁴. ¹Maine Medical Center Research Institute, USA, ²University of North Carolina Chapel Hill, USA, ³The Jackson Laboratory, USA, ⁴Maine Medical Center, USA

We reported that CD47 is a critical molecule for osteoclastogenesis through its association with SHPS-1. However $Cd47^{-/-}$ mice have decreases in body weight, aBMD, femoral length, cortical thickness, BV/TV and trabecular thickness vs $Cd47^{+/+}$ controls. To confirm the presence of a defect in osteoblast function, histomorphometry was performed on 16 wk $Cd47^{-/-}$ and $Cd47^{+/+}$ controls. $Cd47^{-/-}$ mice had reduced bone formation rates ($p < 0.05$), mineral apposition rates ($p < 0.01$), and osteoblast numbers ($p < 0.01$) vs $Cd47^{+/+}$. Serum N-terminal propeptide of type I procollagen (PINP) a marker of bone formation was reduced by ~20% ($p = 0.03$) in $Cd47^{-/-}$ mice vs $Cd47^{+/+}$ consistent with the histomorphometric findings. In vitro analysis of bone marrow stromal cell (BMSC) cultures revealed decreases in alkaline phosphatase activity at Days 7, 14 and 21 suggesting a defect in cell proliferation in the $Cd47^{-/-}$ cultures. Likewise the amount of mineral apparent by von Kossa staining was significantly reduced in the $Cd47^{-/-}$ cultures in line with the histomorphometric findings in vivo. RANKL expression was significantly greater (2 fold, $p = 0.005$) in $Cd47^{-/-}$ Day 7 BMSC pre-osteoblast cultures compared to $Cd47^{+/+}$. OPG expression was decreased by 20% ($p = .005$) resulting in a 2.5 fold increase in the RANKL/OPG ratio in the $Cd47^{-/-}$ cultures. Despite these increases, bone marrow cultures treated with either Vit D or PTH revealed significant reductions (~38%) in the number of TRAP5b staining osteoclasts (>3 nuclei), suggesting that both osteoclast and osteoblast defects in $Cd47^{-/-}$ mice are cell autonomous in nature. Two subclones of MC3T3 calvarial osteoblast cell lines, one with high osteoblast potential (Clone 4) and one with low osteoblast potential (Clone 24) were then examined. Intact CD47 levels and alkaline phosphatase staining were decreased by 40% in the low osteoblast cell line. Addition of thrombospondin-1 (TS-1) an extracellular matrix protein shown to protect CD47 from degradation increased the intact CD47 levels and alkaline phosphatase staining in the Clone 24 cells, thus confirming the importance of intact CD47 in osteoblastogenesis. In summary we have shown that CD47 is a critical factor for both bone formation and bone resorption. The low bone turnover in $Cd47^{-/-}$ is due to a defect in osteoblast proliferation/differentiation as well as osteoclastogenesis. Further studies are needed to define how CD47 affects the growth and differentiation of osteoblasts.

Disclosures: Victoria Demambro, None.

MO0223

Delayed Fracture Repair in mice lacking the dystrophin gene. Celine Colnot¹, Shirley Lieu², Yan Yiu Yu*, Theodore Miclau². ¹INSERM, France, ²University of California, San Francisco, USA, ³UCSF, USA

Introduction: Many clinical and experimental observations have suggested that muscle plays a role in bone regeneration. To functionally assess the role of muscle in bone repair, we assessed fracture healing in Dmd^{mdx} mice, which lack of dystrophin gene. Dmd^{mdx} mice exhibit progressive muscle degeneration due to structural defects in muscle fibers. Although this phenotype is often associated with osteoporosis in

human, mice carrying this mutation are not osteoporotic, allowing us to determine the unique effects of muscle degeneration on bone repair.

Methods: Tibial fractures were created in anesthetized *Dmd^{mdx}* mice. Callus tissues were collected at different time points during fracture repair. Safranin-O and Trichrome staining were used to quantify callus, cartilage and bone volume via histomorphometry. PECAM immunohistochemistry and Tartrate-resistant acid phosphatase (TRAP) staining were used to quantify blood vessels and TRAP-positive cells via stereology.

Results: Histomorphometric analyses (Fig 1) showed that cartilage volume and the proportion of cartilage volume were comparable between wild type and *Dmd^{mdx}* mice during fracture repair. Total bone volume (BV) and the proportion of bone in the callus were significantly decreased in *Dmd^{mdx}* compared to wild type mice at day 7 post-fracture (p.f.). BV peaked at day 14 and gradually decreased until day 28 p.f. in wild type mice, but was significant increased in *Dmd^{mdx}* mice at day 21 p.f. Total callus size was comparable between the two groups from days 7 to 14 p.f. but was significantly increased in *Dmd^{mdx}* compared to wild type mice at day 21 p.f. PECAM immunohistochemistry showed that blood vessels were stained near the periosteum at the fracture site at day 5 p.f. and blood vessel surface density was significant decreased in *Dmd^{mdx}* compared to wild type mice. TRAP-positive cells were found within bone marrow and near the periosteum at the fracture site at day 5 p.f. and was significant increased in *Dmd^{mdx}* compared to wild type mice.

Conclusion: Muscle degeneration in *Dmd^{mdx}* mice affects fracture repair. During the early stage of healing, bone formation and angiogenesis are inhibited, while osteoclastogenesis is enhanced in *Dmd^{mdx}* mice compared to wild-type mice. At later stage, callus and bone remodeling are delayed in *Dmd^{mdx}* mice. Muscle may play a supporting role during fracture repair by allowing vascularization of the callus.

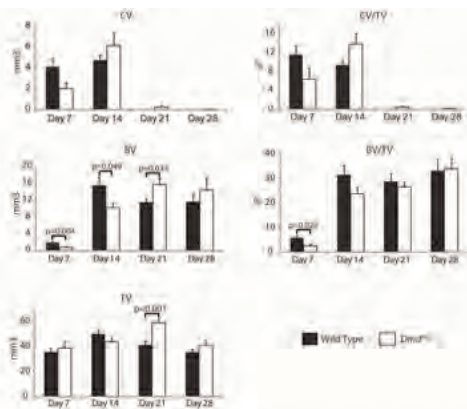


Figure 1

Histomorphometric measurements of total cartilage volume (CV), total cartilage volume as a proportion of total callus volume (CV/TV), total bone volume (BV), total bone volume as a proportion of total callus volume (BV/TV), and total callus volume (TV) during tibial fracture repair in wild type and *Dmd^{mdx}* mice. There is a statistically significant decrease in BV and BV/TV in the callus of *Dmd^{mdx}* mice compared to wild type mice at day 7 post-fracture, a statistically significant decrease in BV in the callus of *Dmd^{mdx}* mice at day 14 post-fracture. There is a statistically significant increase in BV and TV in *Dmd^{mdx}* mice compared to wild type mice at day 21 post-fracture.

Figure 1

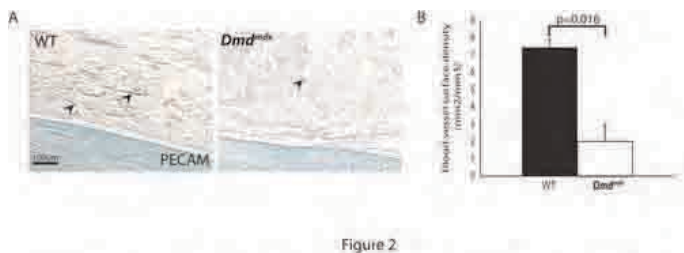


Figure 2

(A) PECAM immunostaining (arrows) in fracture calluses of WT and *Dmd^{mdx}* mice at day 5 post-fracture. (B) Stereological analyses of blood vessels within the callus in WT and *Dmd^{mdx}* mice. There is a statistically significant decrease in blood vessel surface density in *Dmd^{mdx}* compared to WT mice at day 5 post-fracture.

Figure 2

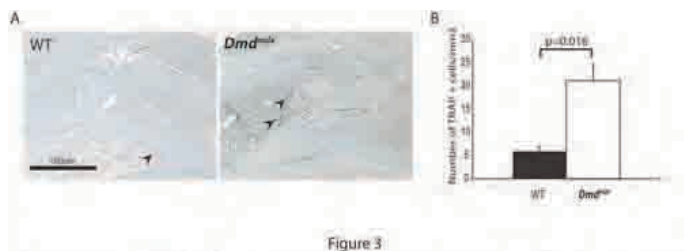


Figure 3

(A) TRAP staining (arrows) in fracture calluses of WT and *Dmd^{mdx}* mice at day 5 post-fracture. (B) Stereological analyses of TRAP positive cells within the callus in WT and *Dmd^{mdx}* mice. There is a statistically significant increase in the number of TRAP positive in *Dmd^{mdx}* compared to WT mice at day 5 post-fracture.

Figure 3

Disclosures: Yan Yiu Yu, None.

MO0224

Epigenetic Mechanisms Modulate the Expression of Genes Controlling Osteoclast Differentiation. Jesus Delgado-Calle¹, Carolina Sanudo², Agustin F. Fernandez³, Raul Garcia-Renedo⁴, Mario F. Fraga³, Jose Riancho⁵. ¹IFIMAV-H.U. Marques de Valdecilla-University of Cantabria, Spain, ²Department of Internal Medicine. Hospital U.M. Valdecilla-IFIMAV-University of Cantabria. RETICEF. Santander, Spain, Spain, ³Cancer Epigenetics Laboratory. Instituto Universitario de Oncología del Principado de Asturias (IUOPA), HUCA, University of Oviedo. Oviedo, Spain, Spain, ⁴Department of Orthopaedic surgery & Traumatology. Hospital U.M. Valdecilla. Santander, Spain, Spain, ⁵University of Cantabria, Spain

DNA methylation is increasingly recognized as a major mechanism to regulate gene expression. However, there is still scanty information about its role in bone remodeling. The aim of this study was to investigate the role of CpG methylation in the transcriptional levels of two osteoblast-derived critical factors in the regulation of osteoclastogenesis: the receptor activator of nuclear factor NF- κ B ligand (RANKL) and its soluble decoy receptor osteoprotegerin (OPG).

Bioinformatic analysis was performed to identify CpG islands within regulatory regions of both genes. RANKL (isoform I) and OPG gene expression was studied by RT-quantitative real time PCR in human primary osteoblasts (hOBs), osteoblastic (MG-63) and non-osteoblastic (HEK-293) human cell lines. DNA methylation was explored by quantitative methyl specific PCR (qMSP) and pyrosequencing.

Two CpG islands were found in the RANKL gene (region 1 and region 2) and one in the OPG gene. hOBs and MG-63 cells expressed much higher amounts of RANKL than kidney-derived HEK-293 cells. Similarly, OPG transcripts were much more abundant in osteoblastic cells than in kidney cells. qMPS and pyrosequencing analysis showed that the methylation in the region 1, but no in region 2, was inversely correlated with RANKL gene expression. On the other hand, OPG transcript abundance also correlated inversely with DNA methylation in the explored area. In addition, treatment with the DNA demethylating agent 5-azadeoxycytidine promoted a 170-fold induction of RANKL, and a 20-fold induction of OPG expression in HEK-293 cells.

Transcriptional levels of both genes were also explored in bone tissue samples from patients with hip fractures or hip osteoarthritis. RANKL transcript abundance and the RANKL:OPG transcript ratio were significantly higher in samples from patients with fractures than in those with osteoarthritis (RANKL: 0.780.23 vs 0.240.08, $p=0.014$; RANKL:OPG: 11.654.94 vs 0.900.19, $p=0.005$). However, no between-group differences in DNA methylation were found.

In conclusion, the correlation between DNA methylation and RANKL and OPG expression strongly suggests that methylation-dependent mechanisms regulate the transcriptional levels of these genes. However, other mechanisms appear to be responsible for the increased RANKL/OPG ratio of patients with osteoporotic fractures.

Disclosures: Jesus Delgado-Calle, None.

MO0225

Fate of the Chondrocyte-Like Cells in Chondroid Bone during Distraction Osteogenesis in the Rabbits. Mitsuhiro Takahashi¹, Tetsuya Enishi², Shinjiro Takata³, Toshihiko Nishisho⁴, Takao Tsuneki¹, Natsuo Yasui⁵. ¹Orthopedics, Japan, ²The University of Tokushima Faculty of Medicine, Japan, ³Institute of Health Biosciences, University of Tokushima Graduate School, Japan, ⁴The University of Tokushima, Institute of Health Bioscience, School of Medicine, Japan, ⁵University, Japan

Distraction osteogenesis is currently a standard method of bone lengthening. Mechanical stimulation by distraction induces ossification, biological responses of skeletal regeneration which are accomplished by a cascade of biologic processes including differentiation of multipotent tissue, angiogenesis, mineralization, and remodeling. Chondroid bone, a tissue intermediate between bone and cartilage, was formed directly by chondrocyte-like cells, with transition from fibrous tissue to bone occurring gradually and consecutively. Transchondroid bone formation is difficult to research due to its restricted localization. Little is known about the chondrocyte-like cells in chondroid bone, especially about the fate of them.

The purpose of this study is to investigate the cell death of the chondrocyte-like cells in chondroid bone during transchondroid bone formation.

To study this, we used 10 Japanese white rabbits, ranging from 2.2 to 2.7 kg of body weight. Mid-diaphyseal tibial lengthening was performed. Transverse osteotomy was performed below the tibio-fibular junction between the second and third screw, using a thread wire saw. A 1-week lag phase after the osteotomy was followed by 2 weeks of distraction at a rate of 0.7 mm every 12 h (1.4 mm/day). After achieving approximately 20 mm of lengthening, rabbits were sacrificed. Histological findings demonstrated that new bone was formed by endochondral ossification at the proximal and distal ends of the distracted callus, and chondroid bone was observed at the boundary between fibrous tissue and bone. The chondroid bone was detected by expressing both type I and type II collagen using immunohistochemistry and in situ hybridization. We examined the fate of hypertrophic chondrocytes and chondrocyte-like cells by immunohistochemistry for caspase-3. Although most hypertrophic chondrocytes in endochondral bone formation were caspase-3 positive, some

chondrocytes-like cells were caspase-3 negative during transchondroid bone formation, furthermore there were no caspase-3 positive cells in chondrocyte-like cells embedded in the newly formed bone trabeculae.

In conclusion, some chondrocytes-like cells in transchondroid bone formation survive in the newly formed bone trabeculae, while most hypertrophic chondrocytes in endochondral bone formation undergo apoptosis.

Disclosures: Tetsuya Enishi, None.

MO0226

Glutathione Role on Specific Markers of the Bone Remodeling. Cecilia Romagnoli*, Gemma Marcucci, Roberto Zonefrati, Carmelo Mavilia, Gianna Galli, Annalisa Tanini, Teresa Iantomasi, Maria Teresa Vincenzini, Maria Luisa Brandi. University of Florence, Italy

Reactive oxygen species and GSH have been recently linked to bone metabolism and remodeling but molecular mechanisms related to these events are little known.

Aim of this study was to evaluate the GSH role and changes in intracellular oxidative state on the mineralization and specific parameters related to osteoblast differentiation and osteoclastogenic process.

Methods: in order to modulate intracellular oxidative state SaOS-2 cells, with phenotypic properties of osteoblastic cells, were treated with buthionine sulfoximine (BSO), specific inhibitor of GSH synthesis, or with GSH itself. GSH and GSSG levels were measured by HPLC assay and calcium deposits by alizarin red S assay. Specific marker mRNA was determined by quantitative PCR.

Results: increases of GSH/GSSG ratio, index of intracellular redox state, obtained by cell treatment with GSH, enhanced the calcium production, whereas this was inhibited in GSH depleted cells. GSH was able to eliminate BSO effect, and the mineralization increase in BSO plus GSH treated cells was also observed. Indeed, we previously found a relationship between changes in alkaline phosphatase activity and intracellular oxidative state. Similarly, the GSH/GSSG ratio levels were related to marker gene expression of osteoblast differentiation and mineralization such as RUNX-2 and osteocalcin (OCN). A high oxidative state decreased RUNX-2 and OCN expression which enhanced when the oxidative state was reduced.

The expression of the receptor activator of nuclear factor κ B ligand (RANKL) and osteoprotegerin (OPG), osteoclastogenesis markers produced in osteoblasts, were also studied. OPG expression levels decreased in BSO treated cells, and GSH was able both to eliminate BSO effect and to increase OPG expression. Differently, redox alterations did not affect RANKL expression. Thereafter, RANKL/OPG ratio, a key factor in the osteoclastogenesis, was also affected by changes in oxidative state, a relationship with changes in GSH/GSSG ratio being found.

Conclusions: a high oxidative state decreases osteoblast differentiation and mineralization process, differently it induces osteoclastogenesis; GSH reverses these effects by the maintenance and increase of intracellular reduced status. These results may provide informations on GSH role in the bone remodeling and be useful to develop novel therapies in bone redox-dysregulated diseases such as osteoporosis, rheumatoid arthritis and bone inflammation diseases.

Disclosures: Cecilia Romagnoli, None.

This study received funding from: MIUR, Ente Fondazione Cassa di Risparmio di Firenze

MO0227

Ibuprofen Administered Pre- or Post- Simulated Resistance Exercise Training Does Not Diminish Gains in Bone Formation or Bone Mass. David Arthur Cunningham*, Kaleigh Camp, Evelyn Yuen, Brandon Macias, Stuart Solomon, Harry Hogan, Susan Bloomfield. Texas A&M University, USA

INTRODUCTION: Non-steroidal anti-inflammatory drugs (NSAIDs) have been shown to suppress bone formation when administered before, but not if administered after, an acute bout of mechanical load. The NSAID ibuprofen inhibits cyclooxygenase-2 enzyme, effectively reducing mechanically induced prostaglandin E2. Whether this affects eventual bone mass gains after multiple sessions of a more physiological mechanical loading regimen is unclear. Therefore, the aim of this study was to test the hypothesis that gains in bone mass and size will be diminished in adult rats given ibuprofen before, but not after, each exercise bout during 20 days of simulated resistance training (SRT). **METHODS:** Virgin female Sprague-Dawley rats (5-month-old, n=29) completed 9 SRT sessions using stimulated muscle contractions under anesthesia at 75% peak isometric strength on alternate days; each of 20 contractions included 1 sec isometric + 1 sec eccentric contraction. Animals were blocked assigned by body weight to one of three groups: (1) ibuprofen (30mg/kg) before exercise, placebo after (I:P)(n=9), (2) placebo before, ibuprofen after (P:I) (n=10) and (3) placebo before and after (P:P)(n=10). *In vivo* pQCT scans measured changes in total volumetric bone mineral density (vBMD) and total bone mineral content (BMC) at the proximal tibia (cancellous), and total vBMD, total BMC and total area at midshaft tibia on days -7 and 21. Dynamic histomorphometry on both midshaft tibiae (exercised and non-exercised legs) determined mineralizing surface (MS/BS), mineral apposition rate (MAR) and bone formation rate (BFR) on the periosteal surface. **RESULTS:** There were no differences in body weights among groups. There were significant gains due to the SRT but not ibuprofen treatment in total BMC (10.50 S.D. 8.15%) and total vBMD (5.29 S.D. 3.41%) at the proximal tibia. The midshaft tibia exhibited significant gains in total vBMD (6.68 S.D. 3.03%), total BMC

(19.18 S.D. 5.51%) and total area (11.68 S.D. 5.49%) due solely to SRT. Furthermore, there were significant increases in periosteal MS/BS, MAR & BFR at the midshaft tibia in the exercised vs. non-exercised legs in all groups but no effect of ibuprofen regimen was detected on these indices of bone formation. **CONCLUSION:** Ibuprofen given before or after exercise during simulated resistance training, performed at intensities similar to those used by humans, does not reduce robust increases in BFR or bone mass in cortical or cancellous bone.

Disclosures: David Arthur Cunningham, None.

MO0228

Influence Of Antiplatelet Drugs In the Pathogenesis Of Experimental Periodontitis And Periodontal Repair In Rats. Leila Coimbra*¹, Carlos Rossa Junior², Morgana Rodrigues Guimaraes², Raquel Fernanda Gerlach³, Marcelo Nicolas Muscara⁴, Denise Madalena Palomari Spolidorio², Bruno Schneider Herrera², Luis Carlos Spolidorio². ¹University of Sao Paulo State, Brazil, ²Araraquara Dental School, Brazil, ³Ribeirao Preto Dentistry School, Brazil, ⁴Institute of Biomedical Sciences, Brazil

Background: Platelets contain an array of biological mediators that can modulate inflammation and repair processes. Previous studies have shown that periodontitis and periodontal repair are associated with platelet activation. We hypothesized that drug-induced platelet inactivation might interfere in the processes of inflammation and repair in experimental periodontitis in rats by suppressing the release of biological mediators from platelets to the site of injury.

Methods: To measure the effects on periodontal disease, 40 rats were randomly distributed in four equal groups (n=10). Ligatures were placed around lower first molars in three groups and Aspirin (Asp) (30 mg/kg), Clopidogrel (Clo) (75 mg/kg) or Saline (NaCl 0.9%) were given intragastrically, by gavage, once daily for 15 days. Periodontitis was assessed by histological analysis and Interleukin-6 (IL-6), Tumor Necrosis Factor-alpha (TNF-alpha) and Thromboxane A2 (TXA-2) levels measured by ELISA. To evaluate the effects of antiplatelet drugs on periodontal repair, 50 rats were randomly distributed in five equal groups (n=10). Ligatures were placed in four groups, and the negative control group and one group with periodontitis were sacrificed 15 days after the insertion of the ligatures. The remaining three groups had the ligatures from both sides removed after 15 days of periodontitis induction and Asp, Clo or Saline were administered beginning in the following day for 15 days. Periodontal repair was assessed by micro-computed tomography (μ CT) and histological analysis.

Results: On periodontitis phase, Asp and Clo significantly reduced levels of TNF-alpha and IL-6 ($p < 0.05$), but only Asp decreased TXA-2 ($p < 0.05$). Asp and Clo decreased inflammatory infiltration, however this reduction was more pronounced with Clo treatment ($p < 0.05$). Histometric analysis showed that Asp and Clo impaired alveolar bone resorption. During the repair process and after removal of the ligatures, μ CT analysis demonstrated that treatment with Asp and Clo did not impair alveolar bone repair. In the histological analysis, there was repair of the alveolar bone and gingival tissue represented by the restoration of tissue architecture of the epithelium and connective tissue in the experimental groups.

Conclusion: Systemic administration of Asp and Clo attenuates the inflammatory process associated with periodontitis without affecting the repair process when stimulus is removed.

Disclosures: Leila Coimbra, None.

This study received funding from: Funda o de Aux lio a Pesquisa do Estado de Sao Paulo (FAPESP); CNPq

MO0229

Osteoblast Targeted Deletion of FIP200, an Essential Component of Mammalian Autophagy Leads to Osteopenia in Mice. Dongye Yang¹, Jaclynn Kreider¹, Paul Krebsbach², Steven Goldstein³, Jun-Lin Guan¹, Fei Liu⁴. ¹University of Michigan, USA, ²Univ of Michigan, Sch of Dentistry, USA, ³University of Michigan Orthopedic Research Labs, USA, ⁴University of Michigan School of Dentistry, USA

FIP200 (200-kDa FAK-family interacting protein) plays important roles in mammalian autophagy and other cellular functions, but its role in bone cells has not been examined. To determine to what extent FIP200/autophagy regulates bone homeostasis, we conditionally deleted FIP200 in osteoblasts in vivo with *Ox-Cre* transgenic mice. MicroCT analysis revealed that FIP200 conditional knockout (CKO) male mice had severe osteopenia demonstrated by decreased bone volume/tissue volume (9.7% \pm 5.1% in CKO vs 22.8% \pm 2.5% in control, n=6-7), decreased trabecular number, decreased trabecular thickness and decreased cortical thickness in femora at 1 month. The osteopenic phenotype was also observed in 2 month and 6 month old male and female CKO mice. Four-point bending tests showed that mutant bones had compromised mechanical properties. Histomorphometry analysis corroborated MicroCT data. Interestingly, both osteoblast and osteoclast number and surface per bone surface were not altered in mutant bone. However, the bone formation rate in CKO mice was decreased to less than half of that in control mice. Alizarin red staining indicated that bone marrow cells isolated from CKO mice had significantly compromised mineralization. The mRNA levels of osteoblast differentiation markers

(ALP, BSP, OCN, Runx2, Osx) were significantly decreased in the CKO group. We also isolated bone marrow cells from FIP200F/F mice and infected them with adenovirus encoding Cre (Ad-Cre) or LacZ after 7 days osteogenic culture. In the FIP200-null group (Ad-Cre), terminal differentiation was significantly compromised, suggesting that FIP200 plays an important role at a later differentiation stage. Similarly, we found that FIP200 null primary calvarial osteoblasts had significantly compromised terminal differentiation. However, the proliferation (shown by Ki67 immunostaining and cell number counting) and early differentiation (shown by alkaline phosphatase staining and alkaline phosphatase mRNA expression) appeared to be normal. Consistent with the essential role of FIP200 in autophagy, we found that 36h nutrient-deprivation induced nearly 100% cell death in FIP200-null primary calvaria osteoblasts compared to less than 10% in control cells. Furthermore, large ubiquitin-positive aggregates were found in the osteoblasts of CKO mice, another indication of abnormal autophagy activity. In conclusion, our data suggest that FIP200 positively regulates bone mass possibly through its autophagic role.

Disclosures: Fei Liu, None.

MO0230

T Cell Subsets Differently Regulate Osteogenic Differentiation of Human Mesenchymal Stromal Cells. Francesco Grassi^{*1}, Luca Cattini², Anna Piacentini², Cristina Manferdini², Elena Gabusi², Andrea Facchini², Gina Lisignoli². ¹Istituti Ortopedici Rizzoli, Italy, ²Ramses Lab. Rizzoli Orthopedic Institute, Italy

The interplay of immune cells and bone cells plays a fundamental role in inflammatory and post-traumatic lesions of bone tissue. In particular, activated T cells were shown to be a key source of osteoclastogenic cytokines and to drive the increase of osteoclast differentiation typical of post-menopausal osteoporosis as well as erosive diseases of bone following acute inflammation. Recent findings suggest that T cells can also regulate the pool of mesenchymal stromal cells (MSC) and its potential to give rise to fully differentiated osteoblasts; in particular, T cells in mouse were found to play a key permissive role for MSC to respond to PTH anabolic stimulation of bone. However, whether unstimulated T cells secrete sufficient osteogenic factors to regulate the fate of MSC is still unclear. In this study we investigated whether T cells secreted factors can support MSC osteogenic differentiation in vitro and if any differential stimulation is present between CD4 and CD8 cells. Unstimulated total T cells, CD4+ and CD8+ T cells were isolated by means of immunomagnetic negative selection by human peripheral blood obtaining a purity of $\geq 98\%$ for each of the subsets. The three subsets were cultured in RPMI medium for 72 hours; conditioned medium (CM) was then collected, filtered and added to human primary MSC cultured in osteogenic medium at a 50:50 ratio (T cells CM/?-MEM supplemented with ascorbic acid, ?-glycerophosphate and dexametazone). Osteogenic differentiation of MSC was evaluated by a) Real Time-PCR quantification of osteogenic factors expression (collagen I and XV, BSP, ALP, OC, RUNX2) at days 14 and 21 and b) functional assays of mineralization by means of Alizarin S and Von Kossa staining of cultures after 21 days. Compared to control cultures, MSC cultured in the presence of total T cells CM showed increased mineral apposition (40% increase relative to control in Alizarin S assays) as well as significantly increased expression of Collagen I, collagen XV, BSP and ALP at day 14. Interestingly, CM obtained from CD4 or CD8 differently regulated MSC differentiation: CD8-derived CM was significantly more effective in inducing mRNA upregulation of Collagens XV, ALP and BSP and induced greater mineralization in functional assays than CD4-derived CM, suggesting that CD8 T cells secrete soluble factors which can effectively support osteogenic differentiation of MSC. Our data provide preliminary evidence for a role of unstimulated T cells, and in particular CD8+ T cells, in inducing MSC osteogenic differentiation and can provide novel tools for improving the bone repair process through regulation of host to graft interaction in regenerative medicine.

Disclosures: Francesco Grassi, None.

MO0231

The Role of the Extracellular Signal-Regulated Kinase (Erk)-Mapk Pathway In Osteoblasts During Post-Natal Bone Healing. Jason Long^{*1}, Xiang Zhao², Christopher D. Beale¹, Casey A. Boyle¹, Steven Goldstein³, Renny Franceschi¹. ¹University of Michigan, USA, ²University of Michigan, School of Dentistry, USA, ³University of Michigan Orthopedic Research Labs, USA

Using a transgenic approach, the extracellular signal-regulated kinase (ERK)/mitogen-activated protein kinase (MAPK) pathway was previously found to affect embryonic skeletal development when expressed in osteoblasts using a murine 0.6 kb mOG2 promoter.¹ Specifically, constitutively active MAPK/ERK1 (TgMEK-SP) expression accelerated bone development and dominant-negative (TgMEK-DN) was inhibitory. These effects are explained in part by ERK/MAPK-dependent activation of RUNX2. While bone healing recapitulates aspects of skeletal development, the role of the ERK-MAPK pathway on osteoblast function during post-natal repair is unknown. We investigated the influence of MEK1 transgenic expression in two experimental models: 1) tibial fracture (pre-dominantly endochondral healing) and 2) sub-critical drill hole defects (intramembraneous healing). We hypothesize that TgMek-sp expression will accelerate healing and TgMek-dn will be inhibitory compared to WT controls. **Methods:** Adult C57BL/6 mice (male and female; TgMek-

sp^{het}, TgMek-dn^{het} and WT) were enrolled into one of two experiments. For one group, left tibiae were fractured following pre-nailing of the medullary canals; for the other, 0.9mm drill holes were placed in the right, proximal tibial metaphyses and the left femoral mid-diaphyses. All animals were euthanized 14 days post-surgery. Following harvest, specimens were scanned and evaluated using micro-computed tomography. Specimens were then sectioned and stained with safranin-O/ fast green for measuring cartilage content. **Results:** Comparing fracture calluses, the TgMek-dn males had significantly higher density and bone volume fraction than the other male genotypes. For the same specimens, the TgMek-dn mice had significantly lower cartilage content than the TgMek-sp mice. Comparing the drill hole specimens, the TgMek-dn males had significantly higher neo-tissue density in the metaphysis than the other male genotypes; no significant differences were identified in the diaphysis. Similar trends, though none significant, were observed among female specimens. **Conclusions:** Contrary to our expectation, TgMek-dn males had accelerated bone formation compared to TgMek-sp and WT males based upon two mechanistically different healing experiments. The basis for these observations is yet understood, but may be due to differences in rate-limiting cell populations during development versus healing.

References: 1) Ge C et al., J Cell Biology, 156:10, 2007

Disclosures: Jason Long, None.

MO0232

Ursodeoxycholic Acid Neutralizes the Detrimental Effects of Lithocholic Acid and Bilirubin on Osteoblasts. Silvia Ruiz-Gaspa^{*1}, Marta Dubreuil¹, Angels Martinez-Ferrer², Anna Enjuanes³, Pilar Peris⁴, M^aJesús Martínez de Osaba³, Luisa Alvarez¹, Ana Monegal³, Andres Combaliá³, Albert Pares¹, Nuria Guanabens⁵. ¹CIBERehd, Hospital Clinic, IDIBAPS, University of Barcelona., Spain, ²Hospital Clinic Barcelona, Spain, ³Hospital Clinic, IDIBAPS, University of Barcelona., Spain, ⁴Hospital Clinic of Barcelona, Spain, ⁵Universitat De Barcelona, Spain

Background and aims: Osteoporosis resulting from decreased bone formation is a common complication in patients with chronic cholestasis. Lithocholic acid (LCA) and bilirubin may play a role in osteoporosis given that both substances have detrimental effects on survival of human osteoblasts (hOB). Since ursodeoxycholic acid (UDCA) improves cholestasis we have assessed if this bile acid may neutralize the harmful effects of LCA and bilirubin on bone formation.

Methods: The experiments were performed in cultured human primary osteoblasts and a human osteosarcoma cell line (SAOS-2) at different times and concentrations of UDCA, LCA, cholic acid (CA) and bilirubin to assess cell viability using a colorimetric assay (Wst-1), osteoblast differentiation using alkaline phosphatase activity assay (ALP) and osteoblast mineralization by Alizarin Red assay. The differentiation experiments were performed with vitamin D (10-7M) in the culture media.

Results: Both LCA (10-4 M) and bilirubin (50 µM) decreased cell viability. UDCA significantly decreased cell survival at concentrations 10 times higher (10-3 M) to that observed with LCA, and CA did not decrease survival. Cell differentiation was not influenced by LCA and CA but was increased by UDCA. UDCA (10-4M) neutralized the detrimental effects of LCA (10-4M) and bilirubin (50 µM) on osteoblast survival at 48 and 72 h. Moreover, UDCA (10-6M and 10-5M) increased osteoblast differentiation in cells treated with toxic concentrations of LCA (30% and 35%, respectively) or bilirubin (60% and 40%, respectively), effects which were partially prevented by the presence of 10% FBS (4% and 8% for LCA and 0% and 8% for bilirubin). LCA and UDCA increased osteoblast mineralization (61% and 63% respectively) after 21 days in culture. By contrast, bilirubin (50 µM) resulted in a decreased mineralization (-60%), effect which was neutralized by UDCA (10-4M) (2%).

Conclusions: Ursodeoxycholic acid increases osteoblast differentiation and mineralization, and neutralizes the detrimental effects of LCA acid and bilirubin on osteoblastic cells. Therefore, UDCA may exert a favorable effect on bone formation in patients with chronic cholestasis.

Disclosures: Silvia Ruiz-Gaspa, None.

MO0233

Y1 Receptor Antagonism Increases Bone Formation in Mice. Daniela Sousa^{*1}, Ron Enriquez², Amanda Sainsbury², Paul A. Baldock², Meriem Lamghari¹, Herbert Herzog². ¹INEB - Instituto de Engenharia Biomedica, Portugal, ²Garvan Institute of Medical Research, Australia

Several lines of evidence have highlighted the critical role of the neuropeptide Y (NPY) system as a key regulator of bone metabolism. Specifically the involvement of Y1 receptor signaling in osteoblasts has been shown to be important for this process suggesting that an anti-receptor strategy may be a useful approach to prevent and/or reverse bone loss. In order to test this hypothesis, we analyzed the effects of a highly selective Y1 receptor antagonist BIBO3304 in wild-type mice.

10-week-old wild-type mice (n =6-10 per group) were treated daily with a low (500nM) or a high dose (5µM) of BIBO3304 for 8 weeks. The drug was incorporated into a jelly and administered orally to mice. Jelly without the drug was used as control. Food intake and metabolic parameters were monitored throughout the treatment. Bone remodeling alterations were analyzed by micro-CT and histomorphometry analysis on isolated femurs.

8 weeks of treatment with a dose of 500nM BIBO3304 mice showed a trend to increase bone mass but this did not reach significance. However, treatment of mice with the 5µM BIBO3304 dose resulted in significant greater femoral cancellous bone volume (8.66 0.58 vs 13.07 0.67%, $p<0.001$), trabecular number (3.28 0.15 vs 4.12 0.23/mm, $p<0.01$) and trabecular thickness (26.38 1.41 vs 32.12 2.20 µm, $p=0.05$). This was associated with an increase in mineral apposition rate (MAR) (1.61 0.06 vs 2.00 0.11 µm/day, $p<0.01$). Bone resorption rate was also elevated as shown by an increased in osteoclast number (2.20 0.22 vs 3.19 0.32/mm, $p<0.05$) and osteoclast surface (5.18 0.56 vs 7.40 0.80 %, $p=0.05$). These results are consistent with data previously described for the germ line Y1 receptor knockout mice. Furthermore, 5µM BIBO3304-treated mice showed a smaller marrow volume (1.24 0.03 vs 1.12 0.04 mm³, $p<0.05$) along with a trend towards reduced tissue volume (2.32 0.05 vs 2.20 0.05 mm³, $p=0.09$), albeit with no change in cortical volume and thickness or in endocortical MAR. Importantly, 8-week treatment with BIBO3304 did not induce significant changes on either body weight or energy metabolism, suggesting no adverse effects on other peripheral or brain functions.

Together, these findings demonstrate that the systemic BIBO3304 treatment increases bone turnover resulting in a greater bone mass *in vivo* suggesting the possible therapeutic application of BIBO3304 for treatment of bone diseases, such as osteoporosis.

Disclosures: Daniela Sousa, None.

MO0234

Beta1 Integrin Expression In Osteoblast Progenitors Is Required for Bone Formation. Nina Kawelke, Matthaeus Vassel, Carina Wuerfel, Christine Hoffmann, Inaam Nakchbandi*. Max-Planck Institute for Biochemistry & University of Heidelberg, Germany

Integrins are cell surface receptors involved in transmitting pericellular signals into the cell. Their activation results in a variety of intracellular effects depending on the signal and receptor involved. Integrins are expressed as dimers of one α and one β subunit. Osteoblasts express mainly integrins containing $\beta 1$ subunit, while osteoclasts express mostly $\beta 1$ and $\beta 3$ containing integrins.

Deletion of $\beta 1$ integrin in differentiated osteoblasts using the collagen- $\alpha 1(I)$ 2.3 kb promoter resulted in only small defects in osteoblast function without affecting bone mineral density (BMD). This was surprising because of the critical role of integrins and the predominance of $\beta 1$ integrins in osteoblasts. To examine the role of $\beta 1$ integrin in bone further we used mice homozygote for the floxed gene of $\beta 1$ integrin and that carry the Mx promoter attached to cre. Mx is expressed in many cell types and has to be activated in mice to induce cre expression. The Mx promoter can delete floxed genes in osteoclasts and in early progenitors of osteoblasts. Deletion of $\beta 1$ integrin using the Mx promoter resulted in a decrease in $\beta 1$ integrin expression by more than 95% in peripheral blood and bone marrow *in vivo*, and by more than 90% in osteoblasts *in vitro*. BMD was significantly diminished in mice at the age of 8 weeks, 4 weeks after activation of cre with a drop in trabecular BMD by 23% in conditional knockout (cKO) mice compared to littermate controls (CT) (CT: 1511 vs. cKO: 1197 g/cm³, $p<0.0001$, $n=13$) and a drop of 14% in total BMD (CT: 52613 vs. cKO: 4529 g/cm³, $p<0.0001$). To determine the reason for this change we performed dynamic and static histomorphometry and found a decrease in bone formation (Bone formation rate; BFR/BS: CT: 0.440.08 vs. cKO: 0.140.06 mm²/mm/y, $p<0.05$, $n=4$) despite an increase in osteoblast numbers (CT: 19.70.4 vs. cKO: 28.80.1, $p<0.01$). The osteoblasts were thus dysfunctional with a delay in mineralization (Mineralization lag time, Mlt: CT: 1.90.4 vs. cKO: 8.92.0 days, $p<0.05$). In contrast, the osteoclasts did not show any defect. Thus the decrease in BMD is due to a decrease in bone formation.

In summary, loss of $\beta 1$ integrin in osteoblast progenitors is detrimental to their function resulting in a delay in mineralization despite an increase in osteoblast number. This then leads to a decrease in bone mineral density. This points to a critical role for integrins in modulating osteoblast behavior and bone mineral density.

Disclosures: Inaam Nakchbandi, None.

MO0235

Y-Tocotrienol inhibits RANKL Gene Expression and Reduces Osteoclast Formation by an HMG-CoA Reductase Dependent Mechanism. Wenxi Li*, Yuedi Ding, Jun Fan, Ying Peng, Runlin Yang, Lili Deng, Xiaohua Qiu, Tingting Shu, Qiang Fu. Key Laboratory of Nuclear Medicine, Ministry of Health; Jiangsu Key Laboratory of Molecular Nuclear Medicine; Jiangsu Institute of Nuclear Medicine., China

Vitamin E analogs, collectively called tocopherols, are comprised of α -, β -, γ - and δ -tocopherol and α -, β -, γ - and δ -tocotrienol. α -tocopherol is the most commonly used vitamin E supplement and the most abundant vitamin E isoform in human and animal tissues. Tocopherols exert their biological effects not only by virtue of their antioxidant properties but also by inhibiting the enzyme hydroxy-methyl-glutaryl-coenzyme A (HMG-CoA) reductase. Studies have shown that free radicals affect bone remodeling by regulating osteoclast activity, and that HMG-CoA reductase inhibitors increasing bone mass by enhancing osteoblast viability and differentiation. compared to other tocopherols, γ -tocotrienol (GT3), one of the isoforms of vitamin E which possess an isoprenoid side chain with three unsaturated bonds, has more powerful antioxidant activity and stronger inhibitor effects on HMG-CoA reductase. Based on this, we

investigated the bone protection of GT3 in ovariectomized C57BL/6 mice. We found that in mice which were one time injected subcutaneously with 100mg/kg GT3, the receptor activator of NF- κ B ligand (RANKL) expression in bone tissues induced by dibutylryl-cAMP (db-cAMP) was inhibited and the inhibition was sustained for at least 14 days after GT3 administration. The bone marrow cells harvested from GT3 treated mice had lower osteoclast formation in co-culture of osteoblast and bone marrow cells induced by PTH. Supplementation with 100mg/kg GT3 via subcutaneous injection once per month for three months significantly prevented bone loss in ovariectomized C57BL/6 mice. These beneficial effects of GT3 for bone tissues were reversible by mevalonate, the product of the reaction catalyzed by HMG-CoA reductase. Our results demonstrate the inhibition of GT3 for RANKL gene expression and osteoclast formation via an HMG-CoA reductase dependent mechanism, suggesting GT3 may have therapeutic value for treating and preventing bone loss.

Disclosures: Wenxi Li, None.

MO0236

Cbf- β has a Positive Role on Postnatal Bone Formation by Regulating Runx2 Stability. Suk-Chul Bae¹, Ichiro Taniuchi², Shin-Yoon Kim³, Jung-Eun Kim⁴, MIN-SU HAN⁵, NARAE PARK⁶, Kyung-eun Lim^{7*}, Jae-Hwan Jeong⁷, Je-Yong Choi⁷. ¹5Depat. of Biochemistry, School of Medicine, Institute for Tumor Research, Chungbuk National University, South Korea, ²Institute of Physical & Chemical Research, Research Center for Allergy & Immunology, Japan, ³Kyungpook National University Hospital, South Korea, ⁴Kyungpook National University School of Medicine, South Korea, ⁵Republic of Korea, ⁶Kyungpook National University, Republic of Korea, ⁷Kyungpook National University, School of Medicine, South Korea

Bone formation requires intact Runx2 function during skeletogenesis. The core binding factor-beta (Cbf- β) is the partner protein of Runx family transcription factors. It has been known that Cbf- β binds Runx2 and enhances Runx2 function through upregulation of DNA binding. Because of embryonic lethality of Cbf- β knockout mice, function of Cbf- β has not been determined in skeletal tissue specifically. In this study, Cbf- β floxed mice were crossed with 2.3 kb Col1-Cre mice to determine the function of Cbf- β in osteoblasts specifically. The osteoblast-specific deletion of Cbf- β showed normal growth and development except bone mass at 5 and 12 weeks after birth. In μ -CT analysis, bone mass and cortical bone thickness were reduced in femur and humerus of Cbf- $\beta^{Aob/Aob}$ mice. In dynamic histomorphometric analysis, mineral apposition rate was also reduced in long bone. Although the number of osteoblasts was not changed, the population of flat-shaped one was increased in Cbf- $\beta^{Aob/Aob}$ mice. In histochemical and real-time Q-PCR analyses, Osterix, Osteocalcin and Osteopontin were decreased in Cbf- $\beta^{Aob/Aob}$ mice. Reduction of these osteogenic markers was due to the decrease of Runx2. Mechanistically, Cbf- β increased Runx2 protein stability by inhibition of its ubiquitination. It suggests that loss of bone mass in adult stage of Cbf- $\beta^{Aob/Aob}$ mice is due in part to the proteasome dependent Runx2 degradation. Collectively, these results indicate that Cbf- β has a positive role on mature osteoblasts by direct regulation of Runx2 stability *in vivo*.

Disclosures: Kyung-eun Lim, None.

MO0237

Cnot3, a Crucial Factor of mRNA Stability, Controls Osteoblastic Differentiation. Chiho Watanabe¹, Masahiro Morita², Yoichi Ezura³, Tetsuya Nakamoto⁴, Tadayoshi Hayata⁴, Hiroaki Hemmi⁵, Takuya Notomi⁶, Keiji Moriyama¹, Tadashi Yamamoto², Masaki Noda¹. ¹Tokyo Medical & Dental University, Japan, ²Division of Oncology, Institute of Medical Science, University of Tokyo, Japan, ³Tokyo Medical & Dental University, Medical Research Institute, Japan, ⁴Medical Research Institute, Tokyo Medical & Dental University, Japan, ⁵Immunology Frontier Research Center, Osaka University, Japan, ⁶GCOE, Tokyo Medical & Dental University, Japan

Regulation by both transcription and epigenetic control is critical to determine bone mass. Messenger RNA stability can provide the rapid and flexible control of gene expression. Recently, new molecules which control mRNA stability have been identified, such as DCP1-DCP2 complex and PAN2-PAN3 complex (Nat Rev Immunol.2010). However, the roles of regulation of mRNA stability in the regulation of bone remodeling has not been fully understood. Among the new molecules, we focused on Cnot3. Cnot3 is a component of CCR4-NOT complex and is implicated in mRNA stability in eukaryotic cells. We observed that Cnot3+/- mice exhibited low bone mass compared to wild-type. In these Cnot3+/- mice BV/TV was decreased more in aged compared to young adult mice. To elucidate the role of Cnot3 at cellular level, we used siRNA to knockdown Cnot3 in MC3T3-E1 cells. Cnot3 mRNA was reduced by 60%. ALP activity was increased when the cells was treated with rh-BMP2 in control cells, while siCnot3-treated-MC3T3-E1 cells showed significant decrease. RT-PCR analysis revealed that gene expression level of type I collagen was down-regulated about 1/3-fold in siCnot3-treated-MC3T3-E1 cells relative to control. In

conclusion, our data indicates that Cnot3 controls osteoblastic differentiation that is critical for the maintenance of bone mass.

Disclosures: Chiho Watanabe, None.

MO0238

Essential role of Intraflagellar transport 80 in osteoblast differentiation through regulating Ihh/Gli and Wnt signaling pathways. Changdong Wang¹, Shuying Yang². ¹State University of New York at Buffalo, USA, ²State University of New York at Buffalo, USA

Intraflagellar transport (IFT) proteins are microtubule based transport machinery, which are essential for the assembly and maintenance of all eukaryotic motile cilia and flagella and nonmotile sensory cilia. Recent findings have demonstrated IFT controls gene expression, cell proliferation and differentiation, and animal development. IFT80 is newly-defined IFT protein. Mutation of IFT80 in human causes a disease, Jeune asphyxiating thoracic dystrophy (JATD) with abnormal skeletal development such as a long, narrow thorax with short ribs, shortened long bones and occasional polydactyl. However, the role and mechanism of IFT80 in osteoblast differentiation is unknown. To gain insight into the role of IFT80 in osteoblast differentiation, we first analyzed the expression pattern of IFT80 by western blot and found that IFT80 is highly expressed in mouse long bone, skull, heart and lung tissues. It was also expressed in mouse muscle, ear and eye, but to a far less extent. RT-PCR results further showed that IFT80 transcripts slightly decrease during osteoblast differentiation. To demonstrate the importance of IFT80 function in osteoblast differentiation, we used lentivirus-mediated RNA interference (RNAi) technology to knock down IFT80 expression in an embryonic mesenchymal cell line C3H10T1/2 induced with ascorbic acid (AA)/ β -glycerol-phosphate (β -g-p). In contrast to the wild-type cells, we found that the cells infected with IFT80 shRNA lentivirus contain undetectable IFT80 protein. Immunostaining and scanning electron microscope (SEM) results showed that silence of IFT80 leads to either shortening or loss of cilia and decrease of Arl13b expression. Western blotting results showed that IFT80 silencing blocks the expression of Gli2, a critical transcriptional factor in Ihh signaling pathway. By performing ALP activity assay, Alzilian Red staining and von kossa staining, we further found that IFT80 silencing in C3H10T1/2 cells not only markedly blocks the expression of osteoblast markers such as RUNX2, OCN and Col I, but also significantly inhibits ALP activity and cell mineralization. Overexpression of Gli2 can rescue the deficiency of osteoblast differentiation from IFT80-silenced cells, as well as dramatically promote the control cells to differentiate into osteoblasts. Moreover, Transcription of cAMP-dependent protein kinase A (PKA), a negative regulator of the Hh signaling pathway, is dramatically increased; on the contrary, Ihh is markedly decreased in IFT80 silenced cells. Interestingly, we also found that silence of IFT80 down-regulates GSK-beta3 and up-regulates beta-catenin transcription. Thus, these results suggested that IFT80 plays an important role in osteoblast differentiation likely through regulating Ihh/Gli and Wnt signal pathways. We have generated Col24x1 knockout model and are analyzing the role and mechanism of IFT80 in bone formation in vivo.

Disclosures: Shuying Yang, None.

MO0239

Foxo1 Mediates IGF1/Insulin Regulation of Osteocalcin Expression by Antagonizing Runx2 in osteoblasts. Shengyong Yang¹, Haiyan Xu², Shibing Yu³, Huiling Cao⁴, Jie Fan⁵, Chunxi Ge⁵, Renny Franceschi⁶, Henry Dong⁷, Guozhi Xiao⁴. ¹VA Pittsburgh Healthcare System, USA, ²Rhode Island Hospital, Brown Medical School, USA, ³University of Pittsburgh Medical Center, USA, ⁴University of Pittsburgh School of Medicine, USA, ⁵University of Michigan School of Dentistry, USA, ⁶University of Michigan, USA, ⁷Children's Hospital of Pittsburgh, University of Pittsburgh, USA

In this study, we determined the molecular mechanisms whereby forkhead transcription factor Foxo1, a key downstream signaling molecule of insulin-like growth factor 1 (IGF1)/insulin actions, regulates Runx2 activity and expression of the mouse osteocalcin gene 2 (Bglap2) in osteoblasts in vitro. We showed that Foxo1 inhibited Runx2-dependent transcriptional activity and osteocalcin mRNA expression and Bglap2 promoter activity in MC-4 preosteoblasts. Co-immunoprecipitation assay showed that Foxo1 physically interacted with Runx2 via its C-terminal region in osteoblasts or when coexpressed in COS-7 cells. Electrophoretic mobility shift assay demonstrated that Foxo1 suppressed Runx2 binding to its cognate site within the Bglap2 promoter. IGF1 and insulin prevented Foxo1 from inhibiting Runx2 activity by promoting Foxo1 phosphorylation and nuclear exclusion. In contrast, a neutralizing anti-IGF1 antibody decreased Runx2 activity and osteocalcin expression in osteoblasts. Chromatin immunoprecipitation assay revealed that IGF1 increased Runx2 interaction with a chromatin fragment of the proximal Bglap2 promoter in a PI3K/AKT-dependent manner. Conversely, knockdown of Foxo1 decreased Runx2 interaction with the promoter. This study establishes that Foxo1 is a novel negative regulator of osteoblast-specific transcription factor Runx2 and modulates IGF1/insulin-dependent regulation of osteocalcin expression in osteoblasts.

Disclosures: Shengyong Yang, None.

MO0240

Genome-wide Analysis of Epigenetic Transcriptional Control by Runx2 During Osteogenesis. Hai Wu*, Jonathan Gordon, Troy Whitfield, Seungchan Yang, Jason Dobson, Phillip Tai, Andre Van Wijnen, Janet Stein, Jane Lian, Gary Stein. University of Massachusetts Medical School, USA

Runx2 is a master regulator of osteogenesis that coordinates expression of many osteoblast-related genes. It organizes gene regulatory complexes with several classes of co-factors (histone modifying enzymes and receptor mediators of signaling pathways) in nuclear microenvironments. In addition to its role as a transcriptional regulator, Runx2 has other key functions that support bone formation. Runx2 is also involved in epigenetic bookmarking at the onset of lineage commitment and initiates chromatin remodeling events required for osteoblast-specific gene expression. However, the epigenetic mechanisms controlled by Runx2 to regulate the bone-specific reorganization of chromatin during osteoblastogenesis remain to be explored. Therefore, we employed Chromatin Immunoprecipitation coupled with high-throughput sequencing (ChIP-Seq) to profile the occupancy of Runx2 and specific epigenetic marks (histone modifications) across the mouse genome in pre-osteoblasts at defined stages of osteogenesis: pre-osteoblastogenesis (day 0, proliferation), early osteoblastogenesis (day 9, matrix deposition), and late osteoblastogenesis (day 28, mineralized). We detected ~10,000 Runx2 binding regions in the proximal promoters of genes in osteoblasts, but an even greater number (>30,000) in distal promoter regions, intronic regions, and intergenic regions. These data sets were further analyzed in relation to transcriptome and proteome profiles to identify Runx2-responsive genes and proteins. Our results provide a signature of Runx2 mediated genomic interactions that support epigenetic control during osteoblast differentiation. We propose that Runx2 is a global organizer of chromatin context during osteoblastogenesis and mediates interactions that are both short-range (proximal promoter-related) and long-range (related to enhancers, introns and intergenic regulatory regions) to maintain higher order chromatin structure in Runx2 related subnuclear domains to modulate temporal expression of osteoblast-related genes.

Disclosures: Hai Wu, None.

MO0241

Global Transcriptome Analysis of Osteoblasts in Transgenic Models of Manipulated G Protein Signaling. Lalita Wattanachanya¹, Susan M. Millard², Weidar Lu¹, Dylan O'Carroll¹, Peter Mailhot¹, Edward Hsiao³, Bruce R. Conklin⁴, Robert Nissenson¹. ¹VA Medical Center & University of California, San Francisco, USA, ²University of Queensland, Australia, ³University of California, San Francisco, USA, ⁴Gladstone Institute of Cardiovascular Disease, University of California, San Francisco, USA

The balance of Gs and Gi G protein coupled receptor (GPCR) signaling is an important regulator of bone formation. We have previously described a number of transgenic mouse models in which G protein coupled signaling has been manipulated in vivo in osteoblasts (OBs) that express the 2.3 kb-Col I promoter. These models include OB-specific expression of an engineered constitutively active Gs-coupled receptor, Rs1, and OB-specific expression of pertussis toxin (PTX) to block Gi signaling; both of which demonstrate an anabolic bone phenotype. To investigate the cellular basis for these effects, we developed a strategy to examine alterations in the OB transcriptome. Identification of OBs for isolation was achieved by OB-specific expression of Histone2B-GFP in vivo either alone or together with Rs1 or PTX under control of the same promoter. OBs were isolated from calvariae of 7 day old mice and flow cytometry was used to sort OBs based on GFP fluorescence. Expression analysis using the Affymetrix Mouse Gene 1.0 ST Array was performed on three OB preparations of RNA from each genotype. We identified 361 and 763 genes whose expression was altered in Rs1 and PTX model, compare to control, respectively (p<0.01). Significantly regulated genes were clustered using the Gene Ontology Tree Machine, and pathway analysis was done with GO-Elite software. Both models demonstrated up-regulation of a large number of genes associated with mitosis and cytokinesis. Contrary to this trend, the mitosis-associated gene FGF9 was down-regulated in both models. Decreased FGF9 was validated by real time PCR and functionally verified in primary mouse osteoblasts where FGF9 was markedly down-regulated after treatment with forskolin or PTH (-64% and -72% respectively, p<0.05). When added continuously to mouse BMSCs grown under osteogenic conditions, FGF9 suppressed (by>80%) the formation of mineralized nodules. These findings indicate that in these models of manipulated G protein signaling in osteoblasts, bone anabolism may be associated with an increase in the relative number of proliferating osteoblasts. They further demonstrate that increased Gs coupled signaling activity down-regulates FGF9 expression, and suggest that this could contribute to the observed increase in bone formation.

Disclosures: Lalita Wattanachanya, None.

MO0242

Increased Expression of Thrombospondin 1 in Runx2 Transgenic Mice. Guillaume de la Houssaye*, Valerie Geoffroy, INSERM Unit 606, France

Thrombospondin 1 (THBS1) is a transmembrane protein with a well known anti-angiogenic activity. Recently, its role in the regulation of resorption activity of osteoclasts and in the inhibition of mineralized nodules formation by osteoblasts has been demonstrated *in vitro*.

The Runx2 gene is essential to the function and differentiation of osteoblasts. Runx2 overexpression blunts terminal differentiation of osteoblasts and leads to an increase in bone resorption *in vivo* and to a defective formation of mineralized nodules *in vitro*.

The aim of our study is to demonstrate the involvement of THBS1 in the mineralization defect observed *in vivo* and *in vitro* in Runx2 mice. Our hypothesis is that overexpression of Runx2 increases directly or indirectly expression of THBS1 during osteoblast differentiation. We performed a comparative gene expression analysis (microarray) of primary osteoblasts isolated from transgenic mice overexpressing Runx2 (Runx2 mice) and control mice (WT) at different stages of culture. After 14 days of culture, the expression of thrombospondin is 3 times greater in the osteoblasts from Runx2 mice compared to WT. This result was validated by qPCR. We showed that expression of THBS1 is decreased during differentiation of WT primary osteoblasts. In contrast, THBS1 expression in osteoblasts isolated from Runx2 mice is stable throughout differentiation which results after 14 days of culture (d14) in a higher expression level of THBS1 in osteoblasts overexpressing Runx2 compared to WT. At the later stage of differentiation (d14), THBS1 protein expression assessed by immunoblotting is greater in Runx2 primary osteoblast than in WT. In WT mice, expression of THBS1 increases until 8 months of age and remains stable until 30 months of age. In aged Runx2 mice, the decrease in bone mineral density is inversely correlated with the expression of THBS1. Furthermore, in transient transfection experiments in MC3T3-E1, overexpression of Runx2 is responsible for a significant increase of the THBS1 promoter activity, indicating a possible transcriptional control of THBS1 by Runx2.

In conclusion, we demonstrated that overexpression of Runx2 leads to an increased expression of thrombospondin 1 *in vivo* and *in vitro*. Our results could partly explain the low bone mass observed in Runx2 mice. Ongoing experiments are being performed *in vivo* and *in vitro* to test this hypothesis.

Disclosures: Guillaume de la Houssaye, None.

MO0243

Interaction of Prx-1 with Runx2 Suppresses Osterix Transcription. Linda Gilbert¹, Xanghuai Lu², Hong Chen², Mark Nanes^{*3}. ¹VA Medical Center, USA, ²Emory University, USA, ³VA Medical Center & Emory University, USA

Osterix (Ox, Sp7) expression is required for differentiation of osteoblasts. We previously showed that TNF inhibition of OB differentiation was due, in part, to suppression of Ox transcription. Using the TNF response element of the Ox promoter as bait, a suppressor protein complex was identified using mass spectroscopy that contained the homeodomain-like protein Prx-1. Prx is required for limb bud formation early embryogenesis and then levels are reduced. However, TNF stimulates Prx-1 expression in adult tissues where it acts as a suppressor of OB differentiation (Lu et al, JBMR 26:209 2011). Here we report that Prx binding to the TNF response element of the Ox promoter occurs indirectly through protein-protein interactions that involve binding to RUNX2. Evaluation of the Ox promoter sequence revealed a homeobox consensus upstream of the TNF response element that is contiguous with a known RUNX2 binding site. Electrophoretic mobility shift studies using two Prx antibodies revealed that Prx-1b and Prx-2, but not Prx-1a, isoforms bind the TNF element, consistent with the isoform-specific suppression of Ox transcription. Binding of Prx to the TNF element required nuclear extract, suggesting that protein-protein interaction was required for incorporation of Prx into the suppressor complex on the promoter. Prx bound the upstream homeobox site without added nuclear extract, indicating that the homeobox site was a preferred binding site with subsequent interaction of Prx with the TNF suppressor protein complex. Since the homeobox site was contiguous with a RUNX2 binding site, we considered that PRX might interact with RUNX2. To test this hypothesis, co-immunoprecipitation studies were done using nuclear extract from C3H10T1/2 cells. Prx-1 and RUNX2 were co-immunoprecipitated using specific antibodies suggesting interaction of these proteins. We conclude that Prx1 binds the Ox promoter at a classic homeodomain binding site where it interferes with the RUNX2 organizer. The Prx anchored at this site then interacts with proteins on the TNF response element just downstream to render suppressor function to this transcriptional complex. This mechanism may contribute to suppression of OB differentiation and bone formation in inflammatory arthritis and aging.

Disclosures: Mark Nanes, None.

MO0244

Interactions between ERK1/2 and p38 MAP Kinase Pathways Control RUNX2 Phosphorylation and Transcriptional Activity. Chunxi Ge^{*1}, Qian Yang¹, Guisheng Zhao¹, Hong Yu², Keith Kirkwood³, Renny Franceschi⁴.

¹University of Michigan School of Dentistry, USA, ²Department of Craniofacial Biology, Medical University of South Carolina, USA, ³Medical University of South Carolina, USA, ⁴Dept of Periodontics & Oral Medicine, University of Michigan School of Dentistry, USA

The RUNX2 transcription factor is a master regulator of osteoblast formation and bone development. Both ERK1/2 and p38 MAP kinases phosphorylate RUNX2 and stimulate its transcriptional activity. However, the relative contribution of each pathway to RUNX2-dependent transcription is not known. In this study, a combination of genetic and pharmacological approaches were used to compare ERK1/2 and p38 α /p38 β MAP kinase regulation of RUNX2 phosphorylation and activity. Because phosphorylation of RUNX2 at S319 is required for activation by both ERK and p38, we developed an antibody to monitor phosphorylation at this site and compared phosphorylation levels with transcriptional activity. ERK1, p38 α and p38 β all stimulated RUNX2 S319 phosphorylation and transcriptional activity. However, under optimal conditions, ERK1 was ten times more active than p38 α and four times more active than p38 β . ERK1 and p38 β were found to physically and functionally compete for a common docking site on RUNX2; mutation of this site abolished the ability of either kinase to stimulate transcription. One consequence of this competition is that RUNX2 phosphorylation and transcriptional activity is actually lower in the presence of both activated kinases than with ERK1 alone, due to displacement of ERK1 by the less active p38 β . Pharmacologic and genetic inhibition studies showed that ERK1/2 and p38 activities are regulated in a reciprocal manner. For example, inhibition of P-p38 with SB203580 or dominant-negative MKK6 increased P-ERK, RUNX2-S319-P and transcriptional activity while ERK inhibition increased P-p38 and reduced RUNX2 S319-P. Similarly, calvarial osteoblasts from transgenic mice over-expressing a constitutively active MEK1 had elevated P-ERK, suppressed P-p38 and elevated RUNX2-S319-P while cells from mice harboring a dominant-negative MEK had reduced P-ERK, elevated P-p38 and reduced RUNX2 S319-P. Lastly, evidence was obtained that ERK1/2 and p38 MAPKs have different roles in osteoblast differentiation. Ascorbic acid-induced osteoblast differentiation, which is known to be dependent on collagen matrix activation of α 2 β 1 integrins, is associated with parallel increases in P-ERK and RUNX2-S319-P in the absence of any changes in P-p38. In this system, ERK inhibition blocked RUNX2 S319-P and transcriptional activity while a p38 inhibitor was without effect. In contrast, when cells were treated with AA and BMP2/7, the strongly synergistic induction of RUNX2-dependent transcriptional activity was blocked by both ERK and p38 inhibition suggesting that the BMP-dependent component of the transcriptional response is at least partly dependent on p38.

Disclosures: Chunxi Ge, None.

MO0245

Mechanism of Akt and Erk Activation in Mechanically-stimulated Osteoblasts: Cross-talk Between Calcium and cGMP. Hema Rangaswami^{*1}, Raphaela Schwappacher², Nisha Marathe², Darren Casteel², Sanford Shattil², Gerry Boss², Renate Pilz². ¹University of California, San Diego, USA, ²UCSD, USA

Weight bearing and locomotion stimulate interstitial fluid flow through the bone canalicular system, and the resultant shear stress is thought to be a major mechanism whereby mechanical forces stimulate osteoblast growth and differentiation. Fluid shear stress (FSS) increases intracellular calcium, leading to increased NO and cGMP synthesis, and activation of cGMP-dependent protein kinases (PKG). We previously showed that NO/cGMP/PKG II signaling is required for ERK-mediated activation of *fos* family genes and proliferation in fluid shear-stressed osteoblasts. Membrane-bound PKG II directly phosphorylates and activates Shp-1, leading to activation of Src and Erk. PKG II-null mice demonstrated defective Src-Erk signaling and decreased Erk-dependent *fos* family gene expression in bone. Others showed that focal adhesion kinase (FAK) is required for Erk and Akt activation in fluid shear-stressed osteoblasts. How FAK is activated and how FAK and Src relate to each other in osteoblast mechano-transduction is unknown.

We have used biochemical and genetic approaches to order the signaling events leading to activation of Akt and Erk in mechanically stimulated osteoblasts. FSS-induced Akt and Erk activation required both calcium and NO/cGMP/PKG II signaling. Treatment with a calcium ionophore mimicked the effects of FSS on Akt and Erk; calcium effects were only partially prevented by the NO synthase inhibitor N-nitro-L-arginine methyl ester (L-NAME), although this agent completely blocked calcium-induced NO synthesis. NO/cGMP-dependent and -independent pathways activated by calcium worked at least additively to increase Akt and Erk activity. In the presence of L-NAME, calcium activated FAK and Src independently of each other; in contrast, NO/cGMP only activated Src. siRNA-mediated knock-down of either FAK or Src blocked FSS- and calcium-induced Akt and Erk activation, whereas cGMP-induced Akt and Erk activation required only Src, indicating that direct activation of PKG II can bypass FAK.

In conclusion, elevation of intracellular calcium by FSS activates FAK independently of NO/cGMP, and Src through both NO/cGMP-dependent and -independent pathways; FAK and Src cooperate in activating Erk and Akt, providing

crucial signals for osteoblast proliferation. Our results establish an important role of NO/cGMP/PKG II signaling in osteoblast mechano-transduction and support using PKG-activating drugs as mechano-mimetics for the treatment of osteoporosis.

Disclosures: Hema Rangaswami, None.

MO0246

Withdrawn

MO0247

Protein Inhibitors of Activated STAT (PIAS) Proteins Regulate Runx2 Transactivation Activity. Masataka Nakamura, Noriko Funato*. Tokyo Medical & Dental University, Japan

Protein inhibitors of activated STAT (PIAS) proteins were initially identified as specific cofactors inhibiting DNA binding and transcriptional activation by the STAT family of transcription factors. PIAS family genes are expressed in osteoblasts. However, it still remains unknown whether any member of the PIAS family has any specific action on osteoblast differentiation. Here we report that PIAS proteins regulate the transcription factor Runx2, a master regulator of osteoblast differentiation. PIAS proteins inhibit Runx2 transactivation activity. PIAS proteins and Runx2 showed colocalization to the same intranuclear regions in cotransfected COS cells. Histone deacetylases (HDACs) are also known to directly interact with Runx2 and inhibit its transactivation activity; however, PIAS-mediated repression was unaffected by the HDAC inhibitor TSA, suggesting that the repression was independent of HDAC catalytic activity. These results indicate that PIAS proteins function as new negative regulators of Runx2.

Disclosures: Noriko Funato, None.

This study received funding from: The Ichiro Kanehara Foundation

MO0248

Sclerostin Expression Is Induced by BMPs in Human Saos-2 Osteosarcoma Cells but Not Through Direct Effects on Its Promoter or ECR5 Element. Longchuan Yu*, Marissa van der Valk, Jin Cao, Chun-Ya E. Han, Todd Juan, Michael B. Bass, Chetan Deshpande, Michael A. Damore, Richard Stanton, Philip Babij. Amgen, Inc., USA

Sclerostin is a negative regulator in the Wnt signaling pathway and plays a key role in the control of bone mass. The expression of sclerostin is mostly restricted to mature osteocytes but the transcriptional regulation of sclerostin is not well understood.

Both sclerostin mRNA and protein were increased in human Saos-2 osteosarcoma cells and rat primary calvaria cells following treatment with BMP2, BMP4 and BMP7. The increase in sclerostin expression was correlated with increases in mineralization markers, including ALP activity, osteocalcin and calcium content.

Deletion mutants of the -7.4kb upstream region of the human sclerostin promoter were examined in Saos-2 cells and no direct response from any of the promoter regions was observed to BMPs, Wnt3a or PTH treatment. The ECR5 downstream element did not have enhancer activity in Saos-2 cells and had no direct response to BMPs or PTH treatment.

The increased expression of several transcription factors with putative consensus DNA binding sites in the sclerostin promoter was identified through genome-wide microarray analysis of Saos-2 cells treated with BMP2. Among these transcription factors, the DLX family, MSX2, HEY1, SMAD6/7 and MEF2A/2C showed a range of inhibitory activity whereas SMAD9 showed no activity. However, MEF2B exhibited a positive effect on both the promoter and ECR5 element.

These observations indicate that the inducing effects of BMPs on sclerostin expression in Saos-2 cells and rat primary calvaria cells are indirect. Furthermore the dramatic increase of sclerostin expression in both types of cells is associated with the late stage differentiation of osteoblasts and the mineralization process.

Disclosures: Longchuan Yu, Amgen, Inc., 1

This study received funding from: Amgen, Inc.

MO0249

Statin Suppresses Excess Runx2 Expression in Human Osteoblastic Osteosarcoma Cells. Takashi Ikeo*, Aiko Kamada¹, Yoshihiro Yoshikawa¹, Eisuke Domaie¹, Seiji Goda¹, Isao Tamura¹, Yoshitomo Takaishi², Takuo Fujita³. ¹Osaka Dental University, Japan, ²Takaishi Dental Clinic, Japan, ³Katsuragi Hospital, Japan

Statins, the cholesterol-lowering drug, activate the promoter of the BMP-2 gene, and stimulate bone formation. However, the mechanism of the stimulation of bone metabolism by statins is not precisely clarified. Runx2/Cbfa1 and Dlx5, osteogenic master transcription factors, are known as a downstream target of BMP-2. Previously, we compared the gene expression of the human osteoblastic osteosarcoma cell line, SaOS-2, cells and normal human osteoblasts, and demonstrated continuous excess expression of Runx2 in SaOS-2, though the expression was hardly observed in normal differentiated osteoblasts. It was considered that the excess expression of Runx2

inhibited mineralization of the osteosarcoma cells. In this study, we investigated whether statins effect the expression of Runx2 and Dlx5, using SaOS-2 cells.

Real time RT-PCR analysis confirmed that compactin (mevastatin) induced BMP-2 mRNA expression in the osteosarcoma cells once on day 3, and time-dependent increase in the type I collagen. When the osteosarcoma cells were incubated with compactin, there was a significant decrease in mRNA level of Runx2 compared with controls ($p < 0.01$). There appeared to be no overall changes in Dlx5. The mineralized matrix produced by the cultured osteoblasts was visualized by von Kossa staining. Non-stimulated control cells did not form a mineralized matrix, but the cells stimulated by compactin were formed.

It is known that Runx2 is essential for the initial osteoblastic differentiation, but it inhibits the final differentiation. Our observations indicate that statins enhance the mineralization of human osteosarcoma cells through suppression of the excess Runx2 expression. Hence, it is indicated that statins promote not only the initial osteoblastic differentiation but also the final differentiation through regulation of transcription factors.

Disclosures: Takashi Ikeo, None.

MO0250

ATP stimulates Caveolar Endocytosis of P2X₇ Receptors in MC3T3-E1 Osteoblasts. Vimal Gangadharan*, Anja Nohe, Randall Duncan. University of Delaware, USA

Purinergic signaling plays a critical role in mechanotransduction in bone. We have shown that nucleotides are rapidly released by osteoblasts and osteocytes in response to mechanical stimulation to initiate a cascade of signaling events in osteoblasts through P2X₇ receptor (P2X₇R) activation. This activation ultimately leads to increased bone formation. However bone rapidly becomes desensitized to loading and we hypothesize that this loss of sensitivity results from internalization of the P2X₇R via endocytosis by caveolin-1. Using sucrose gradient fractionation following detergent-free isolation of lipid rafts, we demonstrated that P2X₇R was co-fractionated with caveolin-1. Further, treatment of these cells with ATP resulted in a shift of caveolin-1 and P2X₇R to the denser fractions indicative of endocytosis. To visualize the caveolar endocytosis in response to ATP treatment, MC3T3-E1 preosteoblastic cells were transfected with caveolin-1 GFP and visualized under Zeiss 5 Live confocal microscope. Using AF-555 albumin as a (fluorescent) selective marker for caveolar endocytosis, MC3T3-E1 cells were treated with 250μM ATP for 40 minutes. We found increased AF-555 albumin uptake with ATP stimulation and its co-localization with caveolin-1 GFP indicated endocytosis via caveolae. These data suggest ATP stimulation induces internalization of caveolin-1 from the membrane lipid rafts into the cytosol. Presence of P2X₇ receptors in the same fraction as caveolin-1 indicates an association with caveolae of MC3T3-E1 osteoblasts and that ATP stimulation may induce caveolar endocytosis of P2X₇ receptor. However we have found that caveolin-1 and P2X₇R do not co-immunoprecipitate. This association suggests that, upon purinergic stimulation, P2X₇R may be internalized, but when caveolin-1 is absent, this receptor stays on the cell surface. This postulate may explain why caveolin-1 null mice have a higher bone density than their wild-type counterparts. These data also suggest that caveolae are a major signaling hub in mammalian cells and that it's function in response to ATP stimulation could be a vital process in mechanotransduction in osteoblasts.

Disclosures: Vimal Gangadharan, None.

MO0251

Gα₁₁ Over-expression in Osteoblasts of Growing Mice Results in Osteopenia. Ariana Dela Cruz*, Michael Mattocks¹, Kim Sugamori¹, Marc Grynpas², Jane Mitchell¹. ¹University of Toronto, Canada, ²Samuel Lunenfeld Research Institute, Canada

Gα₁₁, a member of the heterotrimeric Gq protein family, mediates phospholipase C-dependent signaling downstream of G protein-coupled receptors including the parathyroid hormone 1 receptor (PTH1R). Our group has previously demonstrated that dexamethasone, a potent glucocorticoid, increases Gα₁₁ expression in osteoblasts and can therefore enhance parathyroid hormone (PTH) signaling through the PTH1R. To determine the effects of increased Gα₁₁ in bone, we developed a transgenic mouse model that over-expresses Gα₁₁ (+G11) in osteoblasts under control of the 3.6kb Col1A1 promoter.

Characterization of young (3- to 8-week) +G11 mice mid-diaphysis femur and lumbar vertebrae by DEXA and microCT scans revealed significant reductions in bone mineral density (BMD), trabecular thickness, and cross-sectional geometry. We further investigated the effects of skeletal Gα₁₁ over-expression on response to secondary hyperparathyroidism induced with a low-calcium diet regimen. Femoral aBMD was significantly reduced in both wild-type and +G11 mice and remained significantly lower in +G11 mice.

Bone marrow stromal cells isolated from +G11 mice proliferate at a normal rate, but showed reduced survival and exhibit decreased mineralization with a distinct expression profile of osteoblastic genes when compared to cells from wild-type animals. +G11 bone marrow stromal cells were also more susceptible to apoptosis induced by oxidative stress.

Together, our results show that overexpression of Gα₁₁ in osteoblasts results in an osteopenic phenotype in growing mice.

Disclosures: Ariana Dela Cruz, None.

MO0252

Insulin Resistance Takes Place in Bone of Type 2 Diabetic Mice. Jianwen Wei*, Mathieu Ferron, Patricia Ducy, Gerard Karsenty. Columbia University, USA

The recent realization that bone is an insulin target tissue involved in the control of whole-body glucose homeostasis raises the following question: is bone also a site of insulin resistance in the case of type 2 diabetes induced by high fat diet? To answer this question wild type (WT) mice were fed a high fat diet (HFD) for 8 weeks so that they could develop glucose intolerance and insulin insensitivity. Remarkably HFD fed WT mice develop several features observed in mice lacking insulin signaling in osteoblasts, that include decreased bone resorption, increased expression of Opg and decreased circulating level of the active form of osteocalcin. To investigate the molecular bases of the insulin resistance occurring in bone, we performed cell culture experiments and treated primary osteoblasts in the presence or absence of palmitic acid (100 μ M), the most abundant saturated fatty acid we identified in the serum of HFD fed WT mice. Remarkably palmitate impaired insulin-induced phosphorylation of FoxO1 at ser256 and AKT at Thr308 and Ser473. It also increased expression of Opg. Taken together, this study provides strong experimental evidence that bone is a site of insulin resistance in animals fed a HFD. This occurs because a HFD diet raises the level of circulating free fatty acid, which in turn hampers insulin signaling in osteoblasts, as a result bone resorption is decreased and osteocalcin activation is inhibited. These results further underscore the importance of the skeleton in the control of glucose metabolism.

Disclosures: Jianwen Wei, None.

MO0253

Phospholipase Cgamma1 and Inositol Hexakisphosphate Kinase 1/2 are Required for the Cx43-dependent Amplification of the Osteoblast Response to FGF2. Corinne Niger, Maria Luciotti, Joseph Stains*. University of Maryland School of Medicine, USA

Connexin43 (Cx43) plays a critical role in osteoblast function and, ultimately, the achievement of peak bone mass. However, the identity of the second messengers being transmitted by Cx43 gap junctions, the molecular targets of these second messengers and the manner by which they regulate osteoblast function remain largely unknown. We have previously shown that alterations of Cx43 expression in an osteoblast cell line can impact the responsiveness to FGF2, by modulating the transcriptional activity of Runx2.

In the present studies, we examine the contribution of the phospholipase Cgamma1/inositol polyphosphate cascade to the Cx43-dependent transcriptional response of MC3T3 osteoblasts to FGF2. Inhibition of PLCgamma1 activity with dominant negative constructs, pharmacological inhibitors or siRNA can abrogate the ability of Cx43 to potentiate FGF2-induced signaling through Runx2. Conversely, stabilization of 1,2-diacylglycerol levels with a DAG-lipase inhibitor fails to amplify the response to FGF2. Instead, we find that the activity of the inositol polyphosphate cascade, which converts inositol 1,4,5-triphosphate (InsP3) to higher order inositol poly- and pyrophosphates, such as InsP6 or (PP)₂InsP4, is required for the effect of Cx43 on osteoblast transcription from a Runx2-binding element. Knockdown of inositol polyphosphate multikinase (IPMK), which can convert InsP3 to InsP4 and InsP4 to InsP5, partially attenuates the Cx43-dependent potentiation of transcription in response to FGF2. Similarly, chemical inhibition of the inositol hexakisphosphate kinases, which generate inositol pyrophosphates from InsP4 or InsP6, with 10microM TNP abrogates the Cx43-dependent potentiation of transcription. Likewise siRNA-mediated knockdown of either IP6K1 or IP6K2 can inhibit the effect of Cx43 on Runx2-mediated transcription.

In summary, these data implicate PLC activity and the water-soluble inositol pyrophosphates as mediators of the Cx43-dependent amplification of the osteoblast response to FGF2. Accordingly, our data suggest that these low molecular weight second messengers may be biologically relevant mediators of osteoblast function that are communicated by Cx43-gap junctions. In total, our data establish the FGF2/PLCgamma1/inositol pyrophosphate/PKCdelta/Runx2 pathway as a modulator of osteoblast function that is influenced by Cx43 expression.

Disclosures: Joseph Stains, None.

MO0254

Serum Osteocalcin Is Not Associated with Energy Expenditure or Glucose Metabolism in a Cohort of Low and High Fatness Families. Sulin Cheng*¹, Kaisa K. Ivaska², Leiting Xu¹, Kalervo H. Vaananen², The Calex-family study group³. ¹University of Jyväskylä, Finland, ²Department of Cell Biology & Anatomy, Institute of Biomedicine, University of Turku, Finland, ³Department of Health Sciences, University of Jyväskylä, Finland

It has been suggested that bone may have a regulatory role in energy metabolism via osteocalcin which has been shown to affect insulin secretion and sensitivity in mice. To study whether the skeleton regulates energy metabolism also in humans, we evaluated the associations between glucose metabolism, energy expenditure, body composition and different forms of osteocalcin in low and high fatness families

consisting of 16 mother-daughter-father trios (18 subjects from 6 low fatness trios, mean total body fat =23.8%; and 30 subjects from 10 high fatness trios, mean fat =38.8%). Low and high fatness were here defined as all three members of the family trio falling in either the lowest or highest tertiles for body fat % as determined in a larger family dataset of which the current subjects were a subset. Serum concentrations of total and carboxylated osteocalcin (tOC, cOC) were determined. Uncarboxylated osteocalcin (ucOC) was indirectly calculated as the difference between tOC and cOC. An oral glucose tolerance test was performed. Insulin resistance was indicated by HOMA-IR. Total body bone mass (BM), lean mass (LM) and fat mass (FM) were measured by DXA. Total energy expenditure (TEE) was measured by doubly labeled water and rest energy expenditure (REE) by calorimetry. The high fatness families had significantly higher mean values of weight, FM, fasting, 1-hr and 2-hr insulin and HOMA-IR than the low fatness families (p<0.001 for all). No differences were found between low and high fatness families in age, height, fasting glucose, TEE, REE, LM and BM as well as in tOC, cOC, and uOC. Furthermore, tOC, cOC and uOC were not associated with fasting, 1-hr or 2-hr glucose and insulin, HOMA-IR, TEE, REE, BM, LM or FM. However, cOC was negatively associated with fasting glucose (r=-0.387, p=0.008) but this association disappeared after adjustment for age and gender. TEE and REE were positively correlated with LM (r=0.704 p<0.001, r=0.701 p<0.001) and BM (r=0.713 p<0.001, r=0.651 p<0.001). No associations were found between TEE and glucose metabolism and body fat. We conclude that osteocalcin is not associated with glucose metabolism, total energy expenditure and fat accumulation. These results challenge the view that bone has a direct regulatory role in energy metabolism in humans.

Disclosures: Sulin Cheng, None.

MO0255

The Protein Kinase Inhibitor (PKI) Gene Family Decreases Osteoblast Differentiation by Terminating Protein Kinase A (PKA) Signaling. Edward Greenfield¹, Guang Zhou¹, Shunichi Murakami¹, Guangbin Luo¹, Janet Rubin², Erik Schnaser¹, Bryan Hausman¹, Xin Chen*¹. ¹Case Western Reserve University, USA, ²University of North Carolina, Chapel Hill, School of Medicine, USA

PKA signaling stimulates osteoblast differentiation. The PKI gene family (α , β , and γ) inactivates PKA in the nucleus and thereby terminates PKA-induced gene expression. We previously showed that γ is the primary PKI expressed in osteoblastic and fibroblastic cell lines. We also showed that γ knockdown by siRNA or antisense significantly increases the magnitude and extends the duration of effects of PTH or forskolin (FSK) on PKA activation, immediate-early (IE) gene expression, and inhibition of apoptosis. The goal of this study was therefore to determine whether PKI regulates stimulation of osteoblast differentiation by PKA signaling. We found that γ is also the primary PKI expressed in murine femoral metaphyses and calvarial osteoblasts (γ > α > β). We therefore generated γ -/- mice and compared their skeletal and cellular phenotypes to wild-type mice. PKA activation and IE gene expression induced by FSK are increased in magnitude (3-8 fold, p<0.03) and substantially increased in duration in γ -/- murine embryonic fibroblasts (MEFs). Alkaline phosphatase activity in MEFs in osteogenic media is increased by FSK or γ deficiency (8 or 6 fold respectively, p<0.001) and is further increased by the combination of FSK treatment and γ deficiency (19 fold, p<0.001). Alkaline phosphatase and osteocalcin mRNA levels induced by FSK are also increased in γ -/- MEFs (9-12 fold, p<0.001). In contrast to the dramatic effects in MEFs, γ -/- had little or no effect on IE gene expression induced either by PTH or FSK in isolated calvarial osteoblasts or by PTH in vivo. The bone phenotype of γ -/- mice was also not different from wildtype as assessed by uCT at 5 weeks. This lack of an in vivo phenotype may in part be due to the compensatory upregulation of PKI α mRNA that occurs in the γ -/- calvarial osteoblasts (2 fold, p<0.005, n=3) and the γ -/- femoral metaphyses (1.6 fold, p=0.054, n=5-6) but not in the γ -/- MEFs (p>0.3, n=4). To assess whether α and γ act together, we performed siRNA experiments in a murine marrow-derived mesenchymal stem cell line. Alkaline phosphatase mRNA levels induced by FSK are significantly increased by knockdown of either α or γ (10 or 5 fold respectively, p<0.005) and are further increased by double knockdown of both α and γ (20 fold, p<0.001). Our results strongly support the conclusion that the PKI gene family decreases osteoblast differentiation by terminating PKA signaling and may therefore be useful targets for enhancing repair of bone defects.

Disclosures: Xin Chen, None.

MO0256

A Comparison of Murine Long Bone Segmental Defect Repair Models. Liping Wang*¹, Xi Jiang¹, Nathan Dymant², Aditva Chaubey², David Butler², David Rowe¹. ¹University of Connecticut Health Center, USA, ²University of Cincinnati, USA

Using a calvarial repair defect model that employs a variety of GFP reporter mice, we found that the type of donor-derived bone that was formed differed when the source of donor cells came from bone marrow stromal cells (BMSC->cortical with marrow) or neonatal calvarial osteoblasts (nCOB->membraneous without marrow). In the process of developing a long bone segmental defect model to test the relative contribution of each cell source to the repair process, we evaluated a variety of external fixation methods versus an approach based on internal fixation utilizing non-

radiopaque materials. Two key differences in the host repair response were observed. First, the circumferential periosteal metallic bands that are used to attach the external fixative devices to the bone flanking the defect site significantly blunt the periosteal response to the critical defect. Second, a pseudoarthrosis is initiated when the periosteal response fills the marrow space and caps the ends of the defect area instead of forming a cortical bridge across the defect zone. This unfavorable outcome can be blocked with an intramedullary pin that prevents the formation of the capping structure. Building on these two observations, a surgical model was developed in NOD/Scid/IL2rg null mice that inserts a 0.8 x 14 mm plastic triangular shaped pin within the intramedullary space at the time the segmental defect is generated. The stability is augmented by a 1.0 x 1.4 x 8 mm rectangular pin that is secured to the periosteal surface with a resorbable suture. This support allows the repair to maintain good alignment and normal animal ambulation for 8 weeks after induction of a 3-4 mm critical defect. When the defect area is less than 2 mm or when a critical size defect is loaded with BMSC derived progenitor cells, full cortical bridging is obtained without the development of the capping process. Donor derived BMSCs contribute significantly to the bridging process by integrating with the host's periosteal response, while nCOB failed to generate the bridge and instead formed a non-integrating bony mass. This model is attractive because radiographs of the repair process are easier to interpret in the absence of obstructing hardware, and the histology of the repair can be obtained without removing the hardware thus preserving alignment. Because the mice are immunocompromized, they can be engrafted irrespective of the genotype of the mouse and with human derived bone progenitor cells.

Disclosures: Liping Wang, None.

MO0257

Copper Stimulated Differentiation of Mesenchymal Stem Cells. Ines Burghardt¹, Frank Luthen¹, Cornelia Prinz², Hans-Georg Neumann², Joachim Rychly^{*1}. ¹University of Rostock, Germany, ²DOT GmbH, Germany

In context with the design of medical implants which both stimulate the regeneration of bone tissue and are suitable to prevent infection due to bacteria, we have been interested in the effects of copper ions on the osteogenic differentiation of human mesenchymal stem cells (MSC). We hypothesized that the release of copper from an implant surface can induce bacterial death. However, because of the known physiological role of copper, lower concentration in a later phase after implant incorporation or at greater distances from the implant surface could have a stimulating effect on stem cells. Mineralization of cells as a marker for osteogenic differentiation was measured by calcein bound to extracellular calcium phosphate and visualized by laser scanning microscopy. We found that the critical concentration of copper ions for the survival of human bone marrow derived MSC was 0.5 mM. Therefore we studied the effect of copper on the osteogenic differentiation below this concentration. We found that when adding CuSO₄ into osteogenic differentiation medium for 28 days, copper ions stimulated the osteogenic differentiation of adherent cells with a maximum at a concentration of 0.3 mM. Copper in the culture medium induced a stronger mineralization when the cells were cultured on cell culture polystyrene than on titanium oxide or titanium surfaces. To see, whether copper implemented into implant materials induces an osteogenic differentiation of MSC, cells were cultured on calcium phosphate surfaces containing copper salts. These surfaces enhanced the osteogenic differentiation of adherent MSC compared with copper free surfaces. Because copper is a cofactor for the enzyme lysyl-oxidase (Lox) which catalyzes cross-links of extracellular collagen and elastin we studied components of cell adhesion. We found that copper decreased the expression of different integrin subunits. The strength of cell adhesion was slightly decreased at a low copper concentration but increased again at 0.3 mM.

We conclude that copper containing implants are suitable to promote bone regeneration by the stimulating effect on the osteogenic differentiation of mesenchymal stem cells.

Disclosures: Joachim Rychly, None.

MO0258

Dietary Amino Acids Activate the MAPK Pathway In Bone Marrow Stromal Cells. Ke-Hong Ding^{*1}, Qing Zhong¹, Xing-Ming Shi², Wendy Bollag¹, Michael Cain¹, Clare Bergson¹, Erin Fynan¹, William Hill¹, Mona Elrefaey¹, Karl Insogna², Norman Chutkan¹, Monte Hunter¹, Mark Hamrick¹, Carlos Isaacs². ¹Georgia Health Sciences University, USA, ²Medical College of Georgia, USA, ³Yale University School of Medicine, USA

We have previously shown that amino-acid supplementation prevented bone loss in aging C57Bl6 mice placed on a low protein diet. These findings are consistent with epidemiologic data demonstrating an association between low protein intake and fractures in the elderly population. Conigrave et al. (2000) demonstrated L-type amino-acid binding to the extracellular calcium receptor. Work from our laboratory was consistent with individual amino acids binding and activating this extracellular calcium receptor in osteoprogenitor/bone marrow stromal cells (BMSCs). Since BMSCs differentiate into the bone forming or osteoblastic cells they would appear to be natural targets for any bone anabolic activity associated with dietary protein ingestion. In order to better elucidate the intracellular signaling pathways activated by these individual amino acids we used BMSCs isolated from C57Bl6 mice and tested

all twenty of the common amino-acids. We found that: (1) Aromatic amino-acids (Tyrosine, Tryptophan and Phenylalanine at 100 μ M) were the most potent in increasing intracellular calcium as measured by single cell calcium measurements with Fura-2; (2) in addition, Tryptophan and Tyrosine induced the largest increases in phospho c-Raf (7.5 and 29 fold respectively) as measured by Western blot and (3) Tryptophan and Tyrosine increased phospho MEK 1/2 (2.6 and 1.4 fold respectively); further (4) all three aromatic amino-acids transiently increased ERK phosphorylation (up at 10 minutes and down to baseline by 30 minutes) and combining two aromatic amino acids did not have an additive effect on ERK phosphorylation; and (5) Tyrosine and Tryptophan induced BMSC proliferation (measured by thymidine uptake). Taken together our data are consistent with aromatic amino-acids activating the MAPK pathway, potentially resulting in BMSC proliferation and differentiation down the osteoblastic pathway.

Disclosures: Ke-Hong Ding, None.

MO0259

Ebf1: An Essential Regulator of Mesenchymal Lineage Allocation and Osteoblast Differentiation. Jackie Fretz^{*1}, Tracy Nelson², Mark Horowitz². ¹Yale School of Medicine, USA, ²Yale University School of Medicine, USA

While the osteoblast (Ob) is defined as the anabolic cell in bone capable of laying down and mineralizing new matrix, it exists along a continuum of differentiation flowing from immature mesenchymal precursors to the mature mineral-encased osteocyte. We have reported previously that Ob progenitors express Ebf1 and while bones of Ebf1^{-/-} mice have unusually large numbers of Obs and osteoid, they exhibit low bone mass. Our preliminary studies indicate that this does not appear to be a complete block in mineralization, but instead a delay in ossification. This is supported by mineralization delay observed at select sites in the skeletons of newborn pups, increased osteoblast numbers on bone surfaces accompanied by accumulation of non-mineralized osteoid in the skeletons of Ebf1^{-/-} animals, and μ CT of femora that revealed a significant lack of mineralized bone in the 4 week old Ebf1^{-/-} mice that was reversed by the time the animals were 3 months old. Mineralization defects were also seen *in vitro* from primary bone marrow, isolated MSCs, and calvarial osteoblasts deficient in Ebf1. Investigation into the mechanism underlying this phenomenon has identified two independent points at which the absence of Ebf1 results in an inhibition of Ob maturation and function. First, very early progenitor populations are reduced in number in the BM, form reduced numbers of ALP⁺ colonies, and exhibit reduced SMAD signaling. Second, when more mature Obs are induced to form bone nodules *in vitro*, they exhibit normal numbers of early to intermediate markers of Ob maturation, and equal numbers of ALP⁺ colonies, but fail to express markers of progression to late-stage Obs. The earliest of these markers that fails to be upregulated is Dentin matrix protein 1 (DMP1) which functions as transcription factor within the cell and a nucleator for mineralization when it is secreted. ChIP and luciferase assays confirm that DMP1 is directly regulated by Ebf1 though several enhancers conserved across species. Multiple transcription factors, including Runx2 and Osterix, are required for the progression of Ob cell fate along this continuum. Our data indicate that Ebf1 is also a member of this critical group.

Disclosures: Jackie Fretz, None.

MO0260

Ectonucleotide Pyrophosphate/Phosphodiesterase-1 (Enpp1) Promotes Osteoblast Differentiation Through a Catalytic Independent Mechanism. Hwa Kyung Nam, Jin Liu, Nan Hatch^{*}. University of Michigan, USA

Purpose: Enpp1 (ectonucleotide pyrophosphate/phosphodiesterase-1) is an established regulator of tissue mineralization. Previous studies demonstrated that Enpp1 is expressed in differentiated osteoblasts and that Enpp1 influences matrix mineralization by increasing extracellular levels of inorganic pyrophosphate. Enpp1 is also expressed in pre-osteoblasts when stimulated with FGF2 and is expressed in mesenchymal precursor cells of developing molars several days prior to mineralization, but the role of Enpp1 in pre-osteoblastic and other precursor cells is unknown. Here we investigate the function of Enpp1 in pre-osteoblasts. Methods: Enpp1 expression was inhibited in MC3T3E1(C4) cells by lentiviral transduction with Enpp1 specific shRNA and by isolation of cells from Enpp1 knockout mice. Wild type and catalytic inactive Enpp1 expression was increased in MC3T3E1(C4) cells by retroviral transduction with Enpp1 and Enpp1/T238A cDNA. Enpp1 expression was measured by western blot and real time PCR. Enpp1 enzyme activity was measured by NTPPPH assay. The expression of genes associated with osteoblast maturation, including OCN, BSP, TNAP and Col1a1, was compared in Enpp1 deficient, control, Enpp1 over-expressing and Enpp1/T238A over-expressing cells by real time PCR. To determine if Enpp1 influences osteoblastic gene expression by altering extracellular levels of inorganic phosphate or pyrophosphate, OCN, BSP, TNAP and OPN mRNA levels were compared in control and Enpp1-overexpressing cells upon treatment with phosphate or pyrophosphate. Results: Enpp1 deficient cells exhibited defective osteoblastic differentiation, as indicated by a lack of cellular morphological change, a lack of osteoblastic gene expression and an inability to mineralize matrix. MC3T3E1(C4) cells in which Enpp1 or Enpp1/T238A expression was increased exhibited an increased tendency to differentiate, as exhibited by increased expression of osteoblastic genes. Notably, treatment of cells with inorganic phosphate or pyrophosphate inhibited, as opposed to enhanced, expression of BSP, a gene that is expressed in association with osteoblast differentiation, matrix deposition and mineralization.

Conclusions: Taken together, our results indicate that Enpp1 plays multiple and distinct roles in the development of mineralized tissues and that the influence of Enpp1 on osteoblast differentiation and gene expression includes a mechanism that is independent of its catalytic activity.

Disclosures: Nan Hatch, None.

MO0261

Effects of Rosiglitazone on Circulating Osteoblast and Osteoclast Cell Populations in Postmenopausal Women With Type 2 Diabetes Mellitus. Mishaela Rubin¹, John Sanil Manavalan¹, Donald McMahon², Antonio Nino³, Allison Northcutt⁴, Barbara Kravitz⁵, Paul Gitajali⁵, Lorraine Fitzpatrick⁵, John Bilezikian^{*2}. ¹Columbia University, USA, ²Columbia University College of Physicians & Surgeons, USA, ³GSK, USA, ⁴GlaxoSmithKline, USA, ⁵GlaxoSmithKline Pharmaceuticals, USA

The increase in fractures in women seen with Rosiglitazone (RSG), a PPAR- γ activator, is accompanied by a reduction in bone formation and an increase in bone resorption markers. One mechanism for these changes in bone turnover markers could be an effect of PPAR- γ activation to divert mesenchymal stem cell development from the osteoblast to the adipocyte lineage pathway. We hypothesized that circulating osteogenic and osteoclast precursor cells would be altered by RSG in Type 2 Diabetes Mellitus (T2D). A convenient comparator drug is Metformin (MET) which is not known to affect the skeleton. Two hundred and twenty six subjects with T2D were randomized to RSG or MET for 52 weeks (Wk) (double-blind period), followed by 24 Wk of MET in all (open-label period). Using flow cytometry, in 73 subjects we sorted peripheral blood mononuclear cells (PBMC) and characterized them with the osteoblast-specific ligand osteocalcin (OCN), as well as early osteoblastic stem cell markers CD34 and CD146. CD14+ PBMCs were also sorted, cultured for 8 days with M-CSF and RANK-L and stained for TRAP, a marker of osteoclast activity. There were no significant differences between RSG and MET in total osteogenic or osteoclast populations. However, with RSG, the most mature osteogenic cell sub-populations, lacking expression of CD34 and CD146 markers (OCN+/CD34-/CD146-) increased from 67.2% at Wk0 to 73.7% at Wk52 ($p=0.006$). After switching to MET, this more mature cell population returned to baseline (67.3%) by Wk76. Similarly, cells that had lost CD34 but retained CD146 (OCN+/CD34-/CD146+) fell from 7.9% at Wk0 to 4.8% at Wk52, ($p=NS$) and increased towards baseline after stopping RSG at Wk76 (9.8%; $p=0.07$). Similarly, cells that retained the CD34 marker but did not retain the CD146 marker fell from 20.8% at Wk0 to 17.0% at Wk52 ($p=0.03$). This population was stable through Wk76. Circulating osteoclast cells increased in both RSG and MET groups at Wk52, with RSG increasing from 2.9% to 14.0% ($p=0.001$) and MET increasing from 3.3% to 16.7% ($p=0.001$). The results show that RSG is associated with a change in peripheral osteogenic cells that favors a maturation sequence from earlier osteogenic forms. This pattern tends to reverse toward baseline values when RSG is discontinued. Osteoclast activity increased with both RSG and MET. These studies provide new insights into mechanisms by which RSG may affect the skeleton.

Disclosures: John Bilezikian, GSK, 2

This study received funding from: GlaxoSmithKline

MO0262

Epigenetic Control of Fetal Bone Development through HoxA10 in the Rat. Jin-Ran Chen^{*1}, Jian Zhang¹, Oxana P. Lazarenko¹, Rebecca A. Wynne², Michael L. Blackburn¹, Martin J. Ronis¹, Kartik Shankar¹, Thomas M. Badger¹. ¹University of Arkansas for Medical Science, Arkansas Children's Nutrition Center, USA, ²ACNC, USA

Epidemiological studies show that quality of nutrition during intrauterine and early postnatal life impact the risk of low bone mass and fracture later in life. Maternal consumption of high-fat diets has been demonstrated to affect health outcomes, such as: brain development; obesity; insulin resistance; and hypertension. Here, we show that fetal rat osteogenic calvarial cells (FOCC) from obese rat dams fed a high fat diet (HFD) have significantly less potential to develop into mature osteoblasts compared to cells from AIN-93G diet-fed controls. These FOCCs taken from E18.5 embryos from obese rat dams express lower levels of alkaline phosphatase (ALP), but higher levels of PPAR- γ compared to fetal cells from control dams fed low fat diets ($p<0.05$). Profiling of transcriptional genes for osteogenesis revealed a 15-fold decrease in the homeodomain-containing factor A10 (HoxA10) in these FOCCs from HFD offspring. Significant methylation of the HoxA10 promoter was found in these FOCCs, as well as in ST2 cells treated with a mixture of free fatty acids (palmitic, stearic, oleic, linoleic and arachidonic acid in the ratio of 5:1:2:3:1 similar to that found in rat serum from HFD rats), this was accompanied by lower expression of alkaline phosphatase (ALP), but higher levels of PPAR- γ . Silencing of the HoxA10 gene ex vivo in control FOCCs produced effects similar to those observed in FOCCs from HFD offspring. Treatment of FOCCs from control rats and ST2 cells with an artificial mixture of free fatty acid, significantly down regulated the HoxA10 protein expression and cells exhibit triglyceride accumulation as measured by Oil Red O staining. These results suggest that maternal obesity may affect fetal skeletal development through down regulation of the HoxA10 gene by altered free fatty acid composition in the maternal circulation, which may lead to an increase of the prevalence of low bone mass in their offspring later in life. Supported in part by ARS CRIS #6251-51000-005-03S.

Disclosures: Jin-Ran Chen, None.

MO0263

Epigenetic Regulation of Human Mesenchymal Stem Cell Differentiation by Cyclin-Dependent Kinase-9 and the Histone H2B Ubiquitin Ligase RNF40. Oleksandra Karpiuk^{*1}, Andrei Shchebet¹, Zeynab Najafova¹, Moustapha Kassem², Steven Johnsen¹. ¹Georg-August University, Dept. of Molecular Oncology, Germany, ²Odense University Hospital, Denmark

Human bone marrow-derived mesenchymal stem cells (hMSCs) are multipotent cells which can differentiate into various mesenchymal cell lineages including osteoblasts, adipocytes and chondrocytes. Importantly, diseases such as osteoporosis are characterized by increased adipogenesis at the expense of decreased osteogenesis suggesting a shift in the differentiation of hMSCs from the osteoblastic to the adipocytic lineage. The differentiation of pluripotent and multipotent cells is largely controlled by epigenetic mechanisms. Cyclin-dependent kinase-9 (CDK9) is one factor that controls multiple differentiation pathways including adipocytic differentiation. Since we recently showed that CDK9 activity is essential for maintaining the global levels of histone H2B monoubiquitination (H2Bub1) we hypothesized that CDK9 may epigenetically program hMSC differentiation by directing H2Bub1. Therefore we investigated the levels of H2Bub1 during both adipocytic and osteoblastic differentiation using telomerase-immortalized hMSCs. While the levels of H2Bub1 were very low in undifferentiated hMSCs, differentiation into either lineage resulted in a dramatic time-dependent increase in H2Bub1. Consistently, CDK9 activity was also increased in a similar manner. In order to determine whether CDK9 and H2Bub1 play essential roles in determining lineage-specific differentiation we performed siRNA knockdown studies of either CDK9 or the H2B ubiquitin ligase RNF40 and induced hMSC differentiation. Knockdown of either CDK9 or RNF40 dramatically decreased osteoblast and adipocyte differentiation as assessed by von Kossa or Oil Red O staining and the expression of osteocalcin and PPAR- γ , respectively. Finally, in order to determine the global effects of H2Bub1 on hMSC differentiation, we performed transcriptome-wide gene expression microarray studies following RNF40 knockdown. While RNF40 knockdown had very little effect on the gene expression profile of undifferentiated hMSCs, the change in gene expression profile induced by differentiation to either the adipocytic or osteoblastic lineages was dramatically impaired. Thus we conclude that CDK9-dependent increases in H2Bub1 are essential for hMSC differentiation. These studies suggest that the development of small molecule inhibitors or activators which influence lineage-specific epigenetic regulation may provide a more specific and viable treatment for diseases such as osteoporosis.

Disclosures: Oleksandra Karpiuk, None.

MO0264

Identification of the Differentially Methylated Promoter and Intragenic CpG-Cytosines in the Human Synovium and Bone Marrow Derived Mesenchymal Stem Cells. Yoichi Ezura^{*1}, Tadayoshi Hayata², Tetsuya Nakamoto³, Takuya Notomi⁴, Ichiro Sekiya³, Takeshi Muneta³, Masaki Noda³. ¹Tokyo Medical & Dental University, Medical Research Institute, Japan, ²Medical Research Institute, Tokyo Medical & Dental University, Japan, ³Tokyo Medical & Dental University, Japan, ⁴GCOE, Tokyo Medical & Dental University, Japan

Stromal progenitor cells existing in various adult tissues, including bone marrow, adipose and synovial tissues possesses multi-potency for differentiation into various cell types, and thus called as mesenchymal stem cells (MSCs). Basic characterization of the human and mouse MSCs including cell surface marker expression has shown that the cells from different origin share a common feature. However, detailed comparison also has shown that there are consistent differences among them. The synovial derived human MSCs (hMSCs) are most potent for chondrogenesis by pellet culture, whereas the osteogenesis is best reported by bone marrow derived MSCs. Basic origin of these differences have not been clarified yet. Previously we compared gene expression profiles of various hMSCs with different tissue origin, showing that there are slight differences. Here, to investigate the epigenetic ground of the differential gene expression, we compared CpG-cytosine methylation status of MSCs using single-base extension method on the beads-array (Infinium[®] assay) for bisulfite-converted DNA. Analysis of 27,551 CpG-sites showed that methylation status of synovium and bone marrow derived hMSCs was basically similar globally. However, about 6% of the CpG-sites were differentially methylated more than 20% (%-methylation), representing as differentially methylated regions (DMRs). Comparison of the methylation status and gene expression revealed that 20-30% of the differentially methylated CpG-Cites were associated with decreased gene expression, in comparison to the most CpG-cites with no difference in gene expression (about 60-70%) and the sites with opposite trend (less than 8%). In addition to the observation that the selected DMRs negatively correlated with gene expression sometimes included multiple CpG-sites, those genes included key transcription factors known to be important for chondrogenesis and maturation. The data indicated that the origin of the different gene expression with deviated differentiation features of hMSCs from different tissues includes epigenetic differences based on promoter-/intronic-CpG methylation, at least in part. Clarification of the basic cause of deviated differentiation potential of hMSCs would be beneficial for better protocol for the tissue-engineering therapies.

Disclosures: Yoichi Ezura, None.

MO0265

Interleukin-3 Promotes Osteoblast Differentiation and Bone Formation of Human Mesenchymal Stem Cells. Amruta P. Barhanpurkar¹, Navita Gupta¹, Rupesh K. Srivastava¹, Geetanjali B. Tomar², Sameer P. Naik¹, Satish T. Pote¹, Gyan C. Mishra¹, Mohan Wani^{*1}. ¹National Centre for Cell Science, India, ²National Center for Cell Science, India

Interleukin-3 (IL-3) is an important cytokine that stimulates the proliferation, differentiation and survival of pluripotent hematopoietic stem cells. IL-3 potently inhibits osteoclast differentiation and bone resorption from hematopoietic precursors. However, its role in osteoblast differentiation is not yet known. In this study, we investigated the role of human IL-3 on osteoblast differentiation using purified population of human bone marrow-derived mesenchymal stem cells (MSCs). We found that IL-3 in a dose-dependent manner increased osteoblast differentiation and matrix mineralization in human MSCs, and significantly enhanced the expression of osteoblast specific genes such as alkaline phosphatase, collagen type-I, osteocalcin and osteopontin. In addition, expression of key osteogenic transcription factors, Runx-2 and osterix was significantly increased by IL-3.

Moreover, IL-3 induced the expression of bone morphogenetic protein-2 in a dose-dependent manner, and activated smad1/5/8. AG490, a specific inhibitor of JAK2 abolished stimulatory effect of IL-3 on matrix mineralization suggesting the possible involvement of JAK/STAT pathway in IL-3 action on osteoblast differentiation. Interestingly, IL-3 stimulated *in vivo* bone regeneration ability of MSCs in immunocompromised mice. Furthermore, migration and wound healing abilities of human MSCs were increased in presence of IL-3. IL-3 showed no effect on differentiation of MSCs into adipocytes. Thus, our studies reveal the novel role of IL-3 to promote osteoblast differentiation and bone formation. We suggest that IL-3 may be used as putative anabolic agent for bone formation in osteoporosis and other bone diseases.

Disclosures: Mohan Wani, None.

MO0266

Involvement of Changes in Subcellular Localization of Runx2 and Osterix in Osteoblast Differentiation Revealed by 3-dimensional Fluorescence Morphometry. Takashi Watanabe^{*1}, Ayako Nakane¹, Akiyoshi Hoshino², Yuji Makino³, Akira Yamaguchi⁴, Tadahiro Iimura¹. ¹Tokyo Medical & Dental University, Global Center of Excellence Program, Japan, ²National Center for Global Health & Medicine, Japan, ³Juntendo University Graduate School of Medicine, Department of Orthopedic Surgery, Japan, ⁴Tokyo Medical & Dental University, Japan

Runx2 and Osterix are essential transcriptional factors for osteoblast commitment and differentiation. Their transcriptional regulations have been well studied. However, their protein expression and subcellular localization associated with osteoblast differentiation were not well documented. To access this issue, we took advantages of 3-dimensional fluorescence morphometry after conducting immunofluorescence with antibodies against Runx2 and Osterix on cultured osteoblastic cells MC3T3-E1 and bone sections. Three-dimensional confocal microscopy and image processing enabled to quantify relative expression level and subcellular distribution pattern of Runx2 and Osterix *in situ*. During the course of MC3T3-E1 cells culture, the transcriptions of Runx2 and Osterix showed the highest expression on day 6 and day 12, respectively, by RT-PCR. Osteocalcin transcription was augmented on days 6 and 12 compared to that on day 2. Fluorescence morphometry analysis demonstrated that Runx2 protein expression per single cell showed the highest expression on day 2 and localized largely in nuclei, however, its expression on days 6 and 12 were faintly detected in cytoplasm. Osterix protein expression per single cell also exhibited the highest expression on day 2 and largely localized in nuclei with lower detection in cytoplasm. On days 6 and 12, lower level of Osterix was detected mainly in cytoplasm. We further analyzed protein levels and subcellular distributions of these transcriptional factors in developing rat femurs. Large numbers of Runx2 protein- and Osterix protein-positive cells were detected in trabecular bone area. Detailed analysis demonstrated that Runx2-positive cells in nuclei were detected in some cells in bone marrow and osteoblasts on trabecular bone surface, whereas some osteoblasts on the bone surface exhibited Runx2 protein in cytoplasm. Osterix-positive cells in nuclei were also observed in some cells in bone marrow and osteoblasts on the bone surface, whereas some osteoid osteocytes showed its protein expression in their cytoplasm. Our *in vitro* and *in vivo* analyses suggested that protein expression levels and subcellular localizations of Runx2 and Osterix were spatiotemporally regulated and their functional roles in nuclei were temporarily limited in early phase of osteoblast differentiation.

Disclosures: Takashi Watanabe, None.

This study received funding from: Tokyo Medical and Dental University, Global Center of Excellence Program

MO0267

MAN-1, a Novel Target to Stimulate Osteoblastogenesis and Bone Formation. Christopher Vidal^{*1}, Jessica Tong², Lee Wei Li³, Li Sze Yeo⁴, Diane Fatkin², Gustavo Duque⁵. ¹University of Sydney, Australia, ²Faculty of Medicine, University of New South Wales, Australia, ³University of Sydney, Nepean Clinical School, Australia, ⁴Victor Chang Cardiac Research Institute, Australia, ⁵Ageing Bone Research Program, University of Sydney, Australia

Apart from being a structural border to the nucleus, the nuclear membrane also plays an important role in the regulation of cell differentiation and function. MAN-1 is an inner nuclear membrane protein that is known to sequester R-Smads in fibroblasts. Loss-of-function mutations in the human *MAN-1* (*hMAN-1*) gene result in phenotypes characterized by hyperostosis. In this study we investigated the role of MAN-1 in mesenchymal stem cell (MSC) differentiation into osteoblasts both *in vitro* and *ex-vivo*. We hypothesized that MAN-1 plays an important role as a regulator of osteoblastogenesis. Initially, we performed siRNA of *hMAN-1* in osteogenic differentiating human MSC using 33 and 66 nM final concentrations of oligonucleotides. Transfections were repeated every three days. On day 9, proteins and RNA were extracted and cells were stained for mineralization using Alizarin red. Mineralization was significantly higher in *hMAN-1* siRNA-treated cells when compared to the negative siRNA control ($p < 0.001$). Quantitative real-time PCR showed 75% knockdown of *hMAN-1* and significantly increased levels of mRNA for Runx2 (28%) and for the osteoblastic genes osteopontin (2.3-fold) and alkaline phosphatase (56%) ($p < 0.05$), suggesting that the expression of these osteogenic genes is facilitated in absence of *hMAN-1*. We then assessed whether siRNA of *hMAN-1* would be associated with high levels of β -catenin expression in nuclear extracts, which would indicate an easy transit from the cytoplasm to the nucleus and constitutes a potent osteogenic stimulus. Western blot analysis of nuclear extracts suggested that in absence of *hMAN-1*, β -catenin is free to translocate to the nucleus in a significant manner ($p < 0.01$). For our *ex vivo* experiments, and since MAN-1 expression is increased in absence of lamin A/C, we performed confocal microscopy using *ex-vivo* cultured MSC derived from lamin A/C knockout (*lnna^{-/-}*) mice. A higher level of nuclear colocalization of Runx2 and MAN-1 was observed in the *lnna^{-/-}* MSC nuclei when compared to wild-type controls ($p < 0.01$). In conclusion, we demonstrate that MAN-1 plays an important role in the regulation of osteoblastogenesis and bone formation, most likely by sequestering molecules that are essential for the transcription of osteogenic genes. Due to its potent osteogenic effect, the inhibition of MAN-1 in MSC could become a novel therapeutic approach to osteoporosis.

Disclosures: Christopher Vidal, None.

MO0268

Osteogenic Differentiation in Adipose Tissue Mesenchymal Stem Cells: Effect of Strontium Ion. Sergio Fabbri, Valeria Nardone, Simone Ciuffi, Francesca Marini, Gianna Galli, Carmelo Mavilia, Roberto Zonefrati, Anna Maria Carossino, Annalisa Tanini, Maria Luisa Brandi^{*}. University of Florence, Italy

Introduction and purpose:

Adipose tissue derived mesenchymal stem cells (AMSCs) are able to differentiate into osteoblasts with analogous characteristics to bone marrow mesenchymal stem cells producing alkaline phosphatase (ALP) and calcified nodules, mainly composed by hydroxyapatite (HA), collagen and osteocalcin. These characteristics, combined with the greater achievable quantity and the lower invasivity of the tissue drawing, compared with bone marrow, give the adipose tissue as an optimum source of stem cells to use in bone regeneration processes. As strontium, the active principle of the drug strontium ranelate, acts on bone metabolism by bone formation and bone resorption, the aim of our study was to evaluate the effects of different concentrations of Sr²⁺ on osteogenic differentiation of AMSCs.

Methods:

Long-term primary cultures of AMSCs were obtained from adipose tissue of seven normal subjects. The cells were cultured in growth medium (GM): Ham's F12 Coon's modification medium supplemented with 10% fetal calf serum. Cells were differentiated to osteogenic phenotype by use of osteogenic medium (OM): GM supplemented with 10 nM dexamethasone, 10 mM β -glycerophosphate and 50 μ g/ml 2-phospho-L-ascorbic acid trisodium salt. Different SrCl₂·6H₂O concentrations (0.5-100 μ g/ml) were added at different time points from 0 to 30 days. The differentiation was evaluated by quantitative fluorometric assay for ALP and HA and analysis of some specific genes expression. The total RNA was extracted, reverted to cDNA and the expression was analyzed in qPCR.

Results:

Significant increases of HA production were observed for the lower SrCl₂·6H₂O concentrations (0.5-1 μ g/ml) from 14, 21 or 28 days of induction depending on the cell line. ALP production was significantly increased for the higher SrCl₂ concentrations (50-100 μ g/ml) from 7, 14 or 21 days of induction depending on the cell line. Sr²⁺ induced an increase of the expression of almost all the genes analyzed (table 1).

Conclusions:

Our preliminary results confirm that SrCl₂·6H₂O promotes the production of early markers of differentiation as ALP at higher concentrations (50-100 μ g/ml) and the formation of bone matrix at lower concentrations (0.5-1 μ g/ml). These data show that Sr²⁺ ion can play a role in the increase of AMSCs osteogenic differentiation, promoting the formation of bone tissue from AMSCs with good perspectives for next applications in the field of cell therapy.

Table 1

		GENES EVALUATED					
		ALP	OCN	OPN	OPG	RANK-L	RUNX-2
0 Day	OM+Sr ²⁺ 1µg/ml vs OM	0	0	0	+	0	0
	OM+Sr ²⁺ 10µg/ml vs OM	0	0	0	+	0	0
	OM+Sr ²⁺ 100µg/ml vs OM	0	0	+	+	0	0
	GM+Sr ²⁺ 1µg/ml vs GM	0	0	0	+	0	0
	GM+Sr ²⁺ 10µg/ml vs GM	0	0	0	0	0	0
	GM+Sr ²⁺ 100µg/ml vs GM	0	0	0	0	0	0
15 Day	OM+Sr ²⁺ 1µg/ml vs OM	0	0	0	++	0	++
	OM+Sr ²⁺ 10µg/ml vs OM	0	0	0	++	0	++
	OM+Sr ²⁺ 100µg/ml vs OM	0	++	+	++	0	++
	GM+Sr ²⁺ 1µg/ml vs GM	0	+	0	0	0	0
	GM+Sr ²⁺ 10µg/ml vs GM	0	0	0	0	0	0
	GM+Sr ²⁺ 100µg/ml vs GM	0	+	-	+	0	0
30 Day	OM+Sr ²⁺ 1µg/ml vs OM	+	++	0	+	0	+
	OM+Sr ²⁺ 10µg/ml vs OM	++	++	0	+	0	++
	OM+Sr ²⁺ 100µg/ml vs OM	++	++	0	0	0	++
	GM+Sr ²⁺ 1µg/ml vs GM	0	+	-	+	0	0
	GM+Sr ²⁺ 10µg/ml vs GM	0	0	0	+	0	0
	GM+Sr ²⁺ 100µg/ml vs GM	0	+	0	+	0	0

0: no modulation ++: increased expression with p<0.01
 +: increased expression with p<0.05 -: decreased expression with p<0.05

Table 1

Disclosures: Maria Luisa Brandi, None.

This study received funding from: Istituto Farnaco Biologico Stroder s.r.l. (Italy), Les Laboratoires Servier (France)

MO0269

p53 is Required for TNF α to Inhibit Osteoblast Proliferation and Differentiation. Nicole Fleming¹, Decorian Williams¹, Christine Eischen¹, Charles Lumpkin², Daniel Perrien³. ¹Vanderbilt University, USA, ²University of Arkansas for Medical Sciences, USA, ³Vanderbilt University Medical Center, USA

Tumor Necrosis Factor alpha (TNF α) is a well documented inhibitor of osteoblast differentiation and proliferation. Preclinical models have demonstrated that overexpression of TNF α is a common mechanism of delayed bone repair in a number of comorbid conditions including diabetes, aging, and alcohol abuse making TNF α signaling an attractive target to prevent nonunions in challenging populations. We have recently described that p21 is required for TNF α to inhibit bone regeneration in vivo. This finding led to the hypothesis that p53, an immediate upstream regulator of p21 activity, is required for TNF α to inhibit osteoblast differentiation and proliferation. To test whether TNF α requires p53 to inhibit Ob differentiation, murine embryonic fibroblasts were harvested from wildtype or p53^{-/-} embryos at E12.5. Osteoblast differentiation was induced by ascorbic acid and cells were maintained for 14 days in the presence or absence of 4 ng/ml TNF α . Differentiation was measured by alkaline phosphatase staining and calculation of the percentage of AP⁺ colonies per well. The effects of TNF α on osteoblast proliferation in WT and p53^{-/-} calvarial osteoblasts were measured by BrdU incorporation in cells incubated in osteogenic media alone or containing 0.5 ng/ml - 8 ng/ml TNF α . In wildtype MEF's, TNF α significantly reduced the %AP⁺ colonies (Con = 30.4% +/- 17.3% vs 0% in TNF; p<0.0001) and significantly reduced BrdU incorporation at all doses tested (p<0.01 vs control media at all doses of TNF α). In contrast, neither the differentiation nor proliferation of p53^{-/-} cells was significantly affected by TNF α at any dose. These results demonstrate that p53 mediates the inhibitory effects of TNF α on osteoblastic differentiation of MEFs and proliferation of calvarial osteoblasts. This role of p53 in the TNF α signaling pathway in osteoblasts suggests that additional upstream effectors of p53 may be useful targets to enhance bone repair.

Disclosures: Daniel Perrien, None.

MO0270

Thyroid Hormone Antagonist NH3 Inhibits Osteoblast Differentiation in Human Calvaria Periosteal Mesenchymal Stem Cell. Cristiane Costa^{*1}, Roberto Fanganiello², Thomas Scanlan³, Maria Rita Passos-Bueno², Cecilia Gouveia⁴. ¹Institute of Biomedical Science, Brazil, ²Institute of Biosciences, University of Sao Paulo, Brazil, ³Oregon Health & Science University, USA, ⁴University of Sao Paulo, Institute of Biomedical Sciences, Brazil

Thyroid Hormone (T3) exerts a variety of effects on bone development, growth and metabolism. It has been shown that T3 inhibits osteoblastic proliferation and stimulates osteoblast differentiation in animal cell cultures. These actions results from T3 interaction with its nuclear receptors (TRs). NH3 is a recently developed T3 antagonist that binds TRs and impairs T3-TR interaction. A previous study showed that NH3 has TR antagonist properties on T3-responsive parameters. The aim of this study was to evaluate the effect of T3 and NH3 in the formation of mineralized nodules (analysed by absorbance) and on the mRNA expression of RUNX2 (by real-time PCR) to evaluate osteoblast differentiation. Cells were maintained in osteoblast differentiation media in the presence of T3 (10⁻⁸M), NH3 (10⁻⁸M), T3+NH3 (10⁻⁸M for both) or left untreated (control cells) for 21 days. T3 stimulated mineralized nodules formation (2.3-fold versus control, p<0.05) and NH3 blocked this T3 effect. Accordingly, T3 induced RUNX2 mRNA expression in these cells (3-fold versus control, p<0.05), while NH3 blocked this effect and tended to decrease RUNX2 mRNA expression. These results show that T3 induces the differentiation of human calvaria periosteal mesenchymal stem cells to osteoblasts and that NH3 blocks this effect. Our findings suggest that NH3 could be used as a pharmacological tool to study the involvement of thyroid hormone on osteoblast differentiation in diseases where this process is accelerated, such as craniosynostosis.

Disclosures: Cristiane Costa, None.

MO0271

Human And Mouse Osteoclastogenesis Are Inhibited By Cysteine Proteinase Inhibitors Through Interference With Rank Signaling. Fredrik Stralberg^{*1}, Petra Henning², Inger Gjertsson³, Pedro Souza⁴, Magnus Abrahamson⁵, Franciszek Kasprzykowski⁶, Anders Grubb⁷, Ulf Lerner⁸. ¹Molecular Periodontology, Umea University, Sweden, ²CENTRE FOR BONE & ARTHRITIS RESEARCH, Sweden, ³Department of Rheumatology & Inflammation Research, Goteborg University, Sweden, ⁴Department of Physiology & Pathology, Sao Paulo State University, Brazil, ⁵Laboratory Medicine, Division of Clinical Chemistry & Pharmacology, Lund University, Sweden, ⁶Department of Organic Chemistry, University of Gdansk, Poland, ⁷Clinical Chemistry & Pharmacology, Sweden, ⁸University of Umea, Sweden

We have previously reported that the cysteine proteinase inhibitor cystatin C inhibits osteoclast formation in both crude bone marrow and spleen cell cultures. In the present study, we show that osteoclast progenitor cells are the target cells for cystatin C. Cystatin C (EC₅₀ 0.3µM) inhibited the formation of TRAP⁺MuOCL in purified mouse bone marrow macrophage (BMM) cultures stimulated by M-CSF and RANKL. This effect was associated with decreased mRNA expression of osteoclast-specific genes such as *Acp5*, *Calcr*, *Ctsk*, *Mmp-9*, *Itgb3*, *Atp6i*, and total TRAP activity. Cystatin C did not affect proliferation or apoptosis. The effect of cystatin C on osteoclast formation and gene expression was concentration dependent with half maximal inhibition at 0.3µM. Cystatin C also inhibited osteoclast formation, resorption pits, and release of CTX when BMMs were cultured on bone slices. BMMs stimulated by RANKL and cystatin C retained macrophagic characteristics as assessed by phagocytosis of FITC-labelled zymosanA particles, and increased expression of the macrophage transcription factor *Irf-8*. Three other cysteine proteinase inhibitors, cystatin D, Z-RLVG-CHN₂, and E-64, also inhibited osteoclast differentiation of RANKL stimulated BMMs and formation of osteoclasts; however, the MMP inhibitor TIMP-1 was without effect. Cystatin C, Z-RLVG-CHN₂, and E-64 also inhibited osteoclast formation when RANKL stimulated human CD14⁺ monocytes were cultured on plastic or bone. The effect on BMM differentiation by cystatin C was exerted at an early stage (1-3h) after RANKL stimulation and was associated with decreased RNA and protein expression of c-Fos and NFATc1 and downregulated mRNA expression of *JunB* and *Fra-2*. Furthermore, cystatin C also decreased NFkB activation as assessed by decreasing RANKL induced expression of *p52*, *RelB*, and *Ikb α* mRNA. Cystatin C also gradually decreased *Tnfrsf1a* (*Rank*) mRNA and RANK protein without any effect on *Csflr* (*c-Fms*) mRNA expression. However, inhibition of osteoclast formation by cystatin C was also observed in lentivirus transfected BMM overexpressing RANK. Together, these data show that cystatin C inhibits osteoclast differentiation and formation by interfering intracellularly with signaling pathways downstream RANK, most likely through inhibition of intracellular cysteine proteinases of importance for osteoclast formation.

Disclosures: Fredrik Stralberg, None.

MO0272

Lyn and other Src-family Tyrosine Kinases cannot rescue the cytoskeletal phenotype of Src-/- Osteoclasts. Takuma Matsubara^{*1}, Lynn Neff², William Horne², Roland Baron³. ¹Oral Medicine, Infection & Immunity Harvard School of Dental Medicine, USA, ²Harvard School of Dental Medicine, USA, ³Harvard School of Medicine & of Dental Medicine, USA

c-Src is ubiquitously expressed, but germline deletion effects are predominantly restricted to osteoclasts (OCs), disrupting their cytoskeletal organization and reducing bone resorbing activity, leading to osteopetrosis. In contrast, while OCs express several Src family kinases (SFKs), single KO of other SFKs in mice does not alter OCs cytoskeleton and function. Thus, other SFKs do not compensate for the loss of Src, suggesting that Src performs a critical function not only unique among SFKs but also essentially restricted to OCs.

Although we have previously shown that both the kinase domain and the SH2 and SH3 domains of Src are required to rescue the OC phenotype, the specific feature(s) of one or more of these domains that makes Src unique has not been identified. The aim of this study is to identify this unique function of Src in OCs and the domain in which it resides. To approach this question, we measured the expression of SFKs in wild type (WT) and Src-/- OCs by rtPCR. In WT OCs, expression of Src and Lyn was similarly high. Fyn and Hck expression were respectively 1/3 and 1/10 of Src. Expression of other SFKs was very low. In Src-/- OCs, Fyn expression decreased by ~80%, Hck expression increased ~7-fold, approaching the level of Src in WT OCs, and Lyn expression further increased ~5-fold. Since both Hck and Lyn are highly expressed in Src-/- OCs, these results suggest that neither Hck nor Lyn can compensate for Src deletion. To confirm this and further investigate the roles of SFKs in OCs, we tested the ability of constitutively active forms (mutated C-terminal tyrosine) of each SFK to rescue the ability to form a podosome belt (actin ring) at the cell periphery of Src-/- OCs in vitro, first verifying that expression of Src in Src-/- OCs restored the belt. Like Src, Fyn, which is 75% homologous to Src, rescued belt formation, while Hck, Fgr or Blk only partially rescued and Lyn had no effect on belt formation. These results suggest that Fyn fails to compensate for Src's absence mostly due to its low expression in Src-/- OCLs, but that differences in the binding properties of the SH2 and SH3 domains of Src, on the one hand, and Hck, Blk, Fgr and particularly Lyn on the other, account for the failure of these SFKs to compensate for Src's absence. Thus, the unique function of Src in OCs is due to specific motifs in Src that are not found in Lyn. Domain swapping between these two SFKs should allow identification of this unique feature(s) of Src.

Disclosures: Takuma Matsubara, None.

MO0273

The activity of Dock5, an Osteoclast Specific Activator of the GTPase Rac, is Necessary for the Endochondral Ossification of Mouse Bones. Heiani Touaitahuata¹, Gaelle Cres², Anne Blangy^{*1}. ¹CNRS UMR 5237 CRBM, France, ²Centre De Recherche De Biochimie Macromoléculaire, France

During embryogenesis and after birth, endochondral ossification is the process by which the cartilaginous model of long bones is progressively replaced by bone. The cartilaginous bone primordial contains chondrocytes that are less mature at the end of the bone and more mature when looking toward the middle of the bone. These mature hypertrophic chondrocytes are characteristic of the hypertrophic cartilage that will be progressively mineralized and replaced by bone. Mineralization of the bone requires cartilage matrix remodeling in which osteoclasts are essential players.

We reported previously that osteoclasts lacking Dock5, an activator of the GTPase Rac, are defective for bone resorption due to abnormal podosome organization and absence of sealing zone formation. As a consequence, Dock5-/- adult mice have increased bone mass (Vives et al, JBMR, in press). Dock5-/- osteoclasts express all characteristic differentiation markers in culture and Dock5-/- mice have normal number of osteoclasts. We used Dock5-/- mice to further investigate how the lack of sealing zone in osteoclasts could impact the development of bones. For this we performed histomorphometry on long bones of embryonic and newborn mice. We found no obvious difference in the formation of the cartilage model of bones between Dock5-/- and Dock5+/+ embryos. But interestingly, whole embryo staining indicated a marked reduction of mineralization in Dock5-/- embryos visible from E17.5. Further histomorphometry indicated that the lack of Dock5 leads to a dramatically elongation of the hypertrophic cartilage zone in all long bones. Dock5-/- embryos retained more cartilage and showed reduced mineralization in the central part of the bone corresponding to the primary center of ossification.

These observations show that Dock5 is essential during embryonic development to ensure efficient endochondral ossification of long bones. They further suggest that during ossification, osteoclasts are not only a source of metalloproteases to degrade the cartilaginous bone primordial. The proper organization of osteoclast adhesion structures, which is essential for mineralized bone resorption, also appears as an important determinant of cartilage resorption to ensure efficient ossification of long bones.

Disclosures: Anne Blangy, None.

MO0274

Cytokine Release and Osteoclast Formation from Peripheral Blood Mononuclear Cells from Patients With Chronic Periodontitis. Bruno Herrera^{*1}, Alliny Souza Bastos¹, Leila Santana Coimbra¹, Simone Aparecida Teixeira², Marcelo Nicolas Muscara², Luis Carlos Spolidorio¹. ¹Department of Physiology & Pathology, Araraquara Dental School, UNESP, Brazil, ²Department of Pharmacology, Institute of Biomedical Sciences, USP, Brazil

Introduction: Periodontitis (P), a chronic inflammation of periodontal tissues, leads to unwanted alveolar bone loss in response to inflammatory cytokines, which reflects an increased osteoclast (OCs) formation and activity.

Objectives: To investigate whether mononuclear leukocytes from peripheral blood (PBMCs) collected from patients with chronic periodontitis (CP) differ from those from periodontally healthy patients (control group) in terms of their capacity to express pro/anti-inflammatory cytokines and chemokines under lipopolysaccharide (LPS, E. coli) stimulation and their ability to form OCs and resorpt bone.

Methods: PBMC were isolated in both male patients with CP (n=10; according to American Academy of Periodontology) and without CP (n=9; control) by Ficoll density gradient and, stimulated or not with LPS for 20h. The supernatants were collected and the pool was analyzed for protein cytokines with an array panel (52 cytokines). For OC culture, cells were isolated from PBMC with CD14-labeled magnetic bead and cultured in the presence of RANKL alone or with MCSF and counted 14 days later following TRAP staining for differentiation, and after 21 days on osteologic plate for activity; cells with three or more nuclei were considered OCs and data are presented as the proportion of the culture dish area covered by OCs.

Results: Supernatants from non-stimulated MCs from the CP group expressed interleukin (IL)-1 α , IL-1 β , interferon (IFN) γ -induced protein (CXCL10) and macrophage inflammatory protein (MIP)-1 β , and higher levels (~5-fold) of IFN- γ , IL-1 α , monocyte chemoattractant protein (MCP)-1 when compared with controls. In the presence of LPS, MCs from both groups released more cytokines, but only the CP group showed tumor necrosis factor (TNF)- α and higher levels (~2.4-fold) of IFN- γ , IL-1 α , -1 β , -1 γ , CXCL10, macrophage migration inhibitory factor (MIF), MIP-1 α , and -1 β . There were no differences in OC formation and activity when stimulated with RANKL and MCSF (CP: 39.46.2% vs. control: 37.211.1%), but PBMC's CP patients resulted in a higher number of OCs in the presence of RANKL alone (28.49.2% vs. control: 3.22.1%, p<0.05) and increased resorption pit counts (to a degree comparable with increased OC growth).

Conclusion: PBMCs from patients with CP are more responsive to LPS and do not need M-CSF priming to become OC-like cells, thus suggesting that the presence of periodontitis can increase the reactivity of circulating human mononuclear cells.

Disclosures: Bruno Herrera, None.

This study received funding from: FAPESP (grants n^o 08/02893-4 and 09/1515-0) and CNPq

MO0275

IL-17A and IL-17F, but not IL-17B-E, Stimulate Bone Resorption in Mouse Calvarial Bones by Enhancing RANKL. Pedro P. C. Souza^{*1}, Catharina Lindholm², Howard Conaway³, Ulf Lerner⁴. ¹Sao Paulo State University, Brazil, ²Center for Bone Research, Sweden, ³University of Arkansas for Medical Sciences, USA, ⁴University of Umea, Sweden

Th17 cells have been implicated in inflammation induced bone resorption. In the present study, we have used mouse calvarial osteoblasts and bones to determine which IL-17 peptides in the IL-17 family increase RANKL and stimulate bone breakdown. IL-17A time- and concentration-dependently enhanced release of ⁴⁵Ca and the collagen degradation fragment CTX from calvarial bones, effects inhibited by the bisphosphonate zoledronic acid. IL-17A also enhanced mRNA expression of TRAP and cathepsin K, and the number of multinucleated cathepsin K⁺ osteoclasts in the calvarial bones. The stimulatory effect on ⁴⁵Ca release was seen after culturing bones with IL-17A and IL-17F, but not after culture with IL-17B, IL-17C, IL-17D, or IL-17E. IL-17A and IL-17F, but not IL-17B-E, enhanced *rankl* mRNA and RANKL protein in calvarial bones. IL-17A and F slightly increased *opg* mRNA, but decreased OPG protein in the calvarial bones. The stimulatory effect of IL-17A on ⁴⁵Ca release was inhibited by exogenous recombinant OPG. Calvarial osteoblasts expressed *il-17a*, *il-17c*, and *il-17e* receptor mRNA. IL-17A and IL-17F, but not IL-17B-E, enhanced *rankl* mRNA, but had no effect on *opg* mRNA in calvarial osteoblasts. In the calvarial bones, IL-17A and IL-17F, but not IL-17B-E, increased the mRNA expression of *cox-2* and *il-1b*, but had no effect on *il-6* or *tnf- α* mRNA. In calvarial osteoblasts, IL-17A and IL-17F, but not IL-17B-E, enhanced *il-6* mRNA and slightly increased *cox-2* and *tnf- α* mRNA expression without affecting *il-1b* mRNA. IL-1 receptor antagonistic protein and indomethacin strongly inhibited the stimulatory effect of IL-17A on *rankl* mRNA expression in calvarial bones. These data suggest that IL-17A and IL-17F stimulate bone resorption by increasing RANKL, a response mediated by IL-1b and prostaglandins.

Disclosures: Pedro P. C. Souza, None.

MO0276

Osteoprotegerin Prevents Infection-induced Bone Loss. Yasunari Takada*, Koichi Matsuo. School of Medicine, Keio University, Japan

We reported previously that RANKL is reduced and osteoprotegerin (OPG) is increased in the peripheral blood of mice injected with bacterial lipopolysaccharide (LPS). These activities cannot be attributed to osteoblasts because expression of RANKL and OPG is induced and reduced, respectively, in osteoblasts stimulated with LPS. In this study, we focused on the mechanism and biological significance of OPG production in response to infection. Peripheral blood OPG levels were elevated in mice infected with microorganisms such as *Salmonella*, *Staphylococcus*, *Mycobacterium* and influenza virus. Moreover, injection of mice with LPS induced OPG production specifically in lymph nodes, especially in high endothelial venule cells, but not in other organs. OPG production was suppressed in c-Fos-deficient mice and enhanced in Fra-1 transgenic mice, indicating that OPG production is regulated by AP-1 transcription factors. Loss of OPG in mice did not affect either their survival or *Salmonella* proliferation in spleen and liver after infection with virulent strains of *Salmonella*. Interestingly, however, when wild-type mice were infected with an avirulent *Salmonella* strain, which can induce OPG, osteoclast development was suppressed and bone mineral density was increased. These data reveal for the first time that lymph nodes protect bones from infection-induced bone loss through OPG production.

Disclosures: Yasunari Takada, None.

MO0277

TGF- β Represses S1P Production in Osteoclasts to Reduce Osteoblast Recruitment. Kuniaki Ota*¹, Patrick Quint², Moustapha Kassem³, Jennifer Westendorf¹, Sundeeep Khosla⁴, Merry Jo Oursler¹. ¹Mayo Clinic, USA, ²Mayo Clinic Rochester, USA, ³Odense University Hospital, Denmark, ⁴College of Medicine, Mayo Clinic, USA

In young adults new bone formation nearly precisely replaces bone resorbed by osteoclasts, coupling bone resorption to formation. Recent studies have begun to elucidate osteoclast and matrix-derived factors that recruit osteoblast lineage cells and promote mineralization. Transforming growth factor- β (TGF- β) released from the bone matrix by osteoclasts is involved in recruitment of osteoblast lineage cells and the coupling of bone resorption to bone formation. With aging and following menopause, the rate of bone resorption increases. Coupling of resorption to formation breaks down during aging, as bone formation no longer replaces all of the resorbed bone, leading to decreased bone with aging. Although the rate of bone formation increases along with resorption, it is unable to keep pace with bone loss. The reasons for this uncoupling remain unresolved. Because increased bone resorption leads to locally elevated release and activation of TGF- β , TGF- β may be involved in the increase in bone formation observed with aging. In this study we investigated whether TGF- β also regulates osteoclast coupling factor production. We have shown that osteoclasts secrete the chemokine Sphingosine 1 Phosphate (S1P) to promote osteoblast recruitment and differentiation, coupling bone resorption to subsequent bone formation. We utilized an *in vitro* model in which marrow-derived osteoclast conditioned media promotes migration and mineralization of hMSC-TERT mesenchymal cells. TGF- β had no influence on hMSC-TERT cell migration or mineralization whereas conditioned media from TGF- β treated osteoclasts reduced osteoblast migration and mineralization. Sphingosine 1 Kinase (SPHK1) and SPHK2 produce S1P in osteoclasts. TGF- β treatment suppressed SPHK1 and SPHK2 mRNA and protein expression. Mass spectrometry measurements confirm reduced S1P levels in the conditioned medium from TGF- β treated osteoclasts.

We conclude from these data that the elevated TGF- β resulting from increased resorption in aging bone suppresses coupling factor production by osteoclasts, mitigating direct TGF- β recruitment of osteoblast lineage cells. Thus, the elevated bone formation and the breakdown of coupling of resorption to formation may both be due to elevated TGF- β levels.

Disclosures: Kuniaki Ota, None.

MO0278

TNF- α Induces RANKL Expression in Gingival Epithelium through PKA Signaling. Michihiko Usui*, Ryoichi Fujihara, Akiko Yano, Akihiro Saito, Matsuo Yamamoto. Showa University School of Dentistry, Japan

Periodontitis is an inflammatory disorder of the supporting tissue of teeth, which is composed of the gingival soft tissue, the cementum covering the tooth root, the alveolar bone, and the periodontal ligament. Recent clinical studies indicate that levels of RANKL in gingival crevicular fluid are increased, while OPG level is decreased in periodontitis. Although gingival sulcus is composed of gingival tissue, RANKL expression in gingival epithelial cells (GECs) has not been fully understood.

To investigate the expression of RANKL in GECs, we examined Ca9-22 cells (human cell line), Ho-1-u-1 cells (mouse cell line) and human primary GECs. RT-PCR analysis showed RANKL mRNA was expressed by these GECs. To confirm protein levels of RANKL expression, we performed western blotting analysis using these GECs. Similar to mRNA expression, protein expression of RANKL was also detected in them. To examine RANKL expression *in vivo*, we did immunostaining of gingival epithelium

of mouse. RANKL protein expression can be seen in periodontal ligament cells and osteoblasts as reported previously. Intriguingly, RANKL positive cells exist in junctional epithelium, sulcular epithelium and oral gingival epithelium of gingival. Which factors regulate RANKL expression in GECs? TNF- α , pro-inflammatory cytokine has been reported to increase RANKL expression in periodontal ligament cells. Furthermore, TNF- α is known to be expressed in junctional epithelial cells. To examine the effect of TNF- α on RANKL expression in GECs, we treated GECs with TNF- α . Similar to periodontal ligament cells, TNF- α increases the levels of RANKL mRNA and protein expression. To investigate mechanism TNF- α induces RANKL expression, we examined the effect of both H89 and PKI (PKA inhibitors) of TNF- α -induced RANKL expression in GECs. H89 and PKI inhibit RANKL expression activated by TNF- α approximately 60%. These data indicated that TNF- α induced RANKL expression is mediated partially via PKA signaling. Finally, we performed *in vitro* osteoclast formation assays using bone marrow-derived murine osteoclast (OC) precursors to determine if GECs can directly promote differentiation of OC precursors to mature OCs. Although GECs without TNF- α in co-culture system also can very few OCs, TNF- α treatment strongly induces OC formation. These observations suggest that TNF- α induces RANKL expression in GECs, which may play a role of osteoclastogenesis in progression of alveolar bone destruction by periodontitis.

Disclosures: Michihiko Usui, None.

MO0279

***In Vivo* Migration of Osteoclast Progenitors to the Bone Marrow and Peripheral Tissues in a Competitive Reconstitution Mouse Model.** Christian Jacome*, Sun-Kyeong Lee, Joseph Lorenzo, Hector Aguila. University of Connecticut Health Center, USA

It has been proposed that bone marrow contains a population of osteoclast progenitors (OCP) that circulate via the bloodstream and repopulate a peripheral pool of macrophages and dendritic cells while still retaining their potential to become osteoclasts (OC). We have characterized and isolated cells with OCP activity from bone marrow and spleen. These cells can differentiate clonally into macrophages, dendritic cells and OC. Using pOBCol3.6-GFP transgenic mice, which express GFP in OC, we studied the *in vivo* migration of OCP. In competitive reconstitution experiments, we transferred OCP (B220-CD3-CD11b^{low}CD115⁺CD117⁺) from the BM of pOBCol3.6 GFP CD45.2 donor mice into lethally irradiated C57BL/6 CD45.1 (WT) recipient mice. Mice were co-transferred with a radio protective source of HSC (Lin-c-Kit+Sca-1+, LKS) from WT mice. Controls included transfer of OCP from the BM of transgenic mice into non-irradiated WT mice and LKS from transgenic mice into irradiated WT recipient mice. Engraftment, assessed by histology and flow cytometry, showed that WT irradiated recipients receiving OCP from transgenic BM of donor mice had engraftment in the BM and spleen (1 and 0.2% of total CD45.2, respectively). In addition, frozen sections of femur showed fluorescent OCLs associated with the endosteal bone surfaces of irradiated but not of non-irradiated mice. We have also transferred splenic OCP (LYM-CD11b+Gr1+CD115+) from transgenic mice into irradiated WT mice and found engraftment of CD45.2 cells in the BM and spleen. Finally, we developed a new OCL labeling system by crossing Cathepsin K-Cre "knock-in" mice with a reporter mouse (LoxP-Rosa-TdTomato FP transgenic mice), which expresses red fluorescent protein (RFP) in cells only after expression of Cre. This system has greater OCL-specific fluorescent protein expression than pOBCol3.6-GFP mice. OCP isolated from the BM of these mice had red fluorescent cells *in vitro* only after stimulation with M-CSF and RANKL. We are currently using this model in transfer experiments. In summary, this work showed that BM-derived OCP transplanted into lethally irradiated mice have the ability to home to the BM and migrate to the spleen after lethal irradiation. These experiments suggest that OCP generated in the BM can circulate to peripheral tissues and become resident in spleen. These findings also demonstrate important new tools to study the development and migration of OCP *in vivo* in normal and pathological conditions.

Disclosures: Christian Jacome, None.

MO0280

***In Vitro* Osteoclastogenesis is Impaired in Cells from +/R740S Osteopetrotic Mice.** Irina Voronov*¹, Noelle Ochotny¹, Celeste Owen², Morris Manolson³, Jane Aubin⁴. ¹University of Toronto, Canada, ²Centre for Modeling Human Disease, Samuel Lunenfeld Research Institute, Mt Sinai Hospital, Canada, ³University of Toronto, Can, ⁴University of Toronto Faculty of Medicine, Canada

Vacuolar H⁺-ATPase (V-ATPase), the multimeric enzyme at the ruffled border of osteoclasts, is necessary for acidification of the resorption lacunae. V-ATPases consist of 14 subunits, one of which, the "a3" subunit, is highly enriched in osteoclasts. Heterozygous mice with an R740S mutation in "a3" (+/R740S) have defective V-ATPase activity resulting in mild osteopetrosis. Osteoclast number is increased in +/R740S bones; however, *in vitro*, osteoclast number and size are decreased compared to wild type (+/+) cells, and this decrease was not due to increased cell death as demonstrated by TUNEL assay. These results suggest that "a3" is not only important for acidification, but also plays a role in osteoclast differentiation *in vitro*.

Gene expression analysis of +/R740S and +/+ bone marrow-derived osteoclasts showed that mRNA levels of key osteoclast markers (TRAP, cathepsin K, OSCAR,

DC-STAMP, "d2" subunit of V-ATPase, and NFATc1), while not affected at day 4 of culture, were significantly decreased in +/R740S cells at day 6. Immunoblotting confirmed the decrease of "d2", NFATc1, and "a3" protein levels, while the levels of ubiquitous V-ATPase E subunit were not changed. To rescue impaired osteoclastogenesis, bone marrow-derived osteoclasts were co-cultured with neonatal calvarial osteoblasts. A co-culture with +/R740S but not +/+ osteoblasts rescued impaired osteoclastogenesis, as well as gene expression of osteoclast markers measured above.

As gene expression of these key osteoclast markers is under NFATc1 control, its nuclear translocation was assessed by immunofluorescence. In +/R740S osteoclasts, the percent of nuclei per cell with NFATc1 nuclear translocation was decreased compared to +/+ cells suggesting that NFATc1 activation is affected in +/R740S osteoclasts.

A decrease in NFATc1 activation, as well as the ability of calvarial osteoblasts to rescue impaired osteoclastogenesis, points to other known V-ATPase functions such as vesicular traffic. Receptor-mediated endocytosis of transferrin did not visually appear affected in +/R740S cells as determined by immunofluorescence. Future experiments will determine whether the R740S mutation affects vesicular traffic and intracellular pH in osteoclasts. These studies will help to elucidate precise roles of the V-ATPase "a3" subunit in osteoclast maturation and activity.

Disclosures: Irina Voronov, None.

MO0281

DR3 and TL1A – Effect on Osteoclast Differentiation and Function. Eddie Wang, Anwen Williams, Fraser Collins*, Anja Bloom. Cardiff University, United Kingdom

Death Receptor 3 (DR3) and its only known ligand TNF-like protein 1A (TL1A) are involved in a variety of inflammatory diseases including experimental arthritis where bone pathology was exacerbated (1). The aim of this study was to evaluate the role of DR3 in osteoclast (OC) formation and function *in vitro*.

Bone marrow cells were obtained from the femora of wild-type (WT) and DR3-deficient (DR3^{-/-}) mice (DBA-1). Cells were grown on ivory discs for 10 days in medium containing macrophage colony stimulating factor (M-CSF) and receptor activator for nuclear factor κ B ligand (RANKL). TL1A, OC number and size as well as resorption pit numbers were quantified. Gelatinase activity was observed by zymography.

In order to demonstrate a direct role of DR3 in OCgenesis we compared WT and DR3^{-/-} cultures. WT OC showed a significant increase in resorptive capacity over DR3^{-/-} OC ($p < 0.01$); a greater number of resorption pits/mm² were observed in the WT (9/mm²) compared to a negligible number in the DR3^{-/-} (0.2/mm²). OC numbers per mm² and size were comparable in the WT and DR3^{-/-} cultures. Overall a 30 fold increase ($p = 0.02$) in the number of resorption pits/OC/mm² was observed in WT (0.3 pits/OC/mm²) versus DR3^{-/-} (0.01 pits/OC/mm²). Levels of active MMP 9 were increased in WT cultures compared to DR3^{-/-} cultures.

In order to define the role of TL1A in OC function, add-back experiments were performed. Addition of TL1A to WT cultures lead to a threefold decrease in the number of resorption pits/mm² (3/mm²) compared to WT cultures without TL1A (9/mm²) and a significant decrease ($p = 0.02$) in OC/mm² (from 30/mm² to 24/mm²). TL1A did not affect the number of resorption pits/OC/mm² (0.3 pits/OC/mm²); therefore, did not significantly affect OC resorptive capacity. CCL2, a chemokine that is involved in the recruitment of monocytes and their fusion (2), was reduced in WT+TL1A cultures compared to WT-TL1A cultures. OC parameters were comparable in DR3^{-/-} cultures TL1A.

Conclusion:

Our results show that DR3 has an important regulatory function on OC; it increased OC-driven resorption a function that may be mediated by MMP9. TL1A inhibited OCgenesis, this function may be CCL2 dependent. These results highlight an important potential role for DR3 and TL1A in diseases that affect bone.

1: Bull MJ and Williams AS et al. Journal of Experimental Medicine. 2008.

2: Kim et al. Journal of Biological Chemistry. 2005

Disclosures: Fraser Collins, None.

MO0282

Epigenetic Regulation of Osteoclast Differentiation: Possible Involvement of Jmjd3 in the Histone Demethylation of Nfatc1. Jun Hirose*, Tetsuro Yasui², Takumi Matsumoto¹, Hironari Masuda¹, Kozo Nakamura¹, Sakae Tanaka¹. ¹The University of Tokyo, Japan, ²University of Tokyo, Japan

Recent studies have revealed that gene expression is controlled by epigenetic mechanisms such as chromatin histone modifications and DNA methylation, and that the expression of key developmental genes tend to be regulated by the trimethylation and demethylation of histone H3 lysine 4 (H3K4me3) and lysine 27 (H3K27me3). Osteoclast differentiation is tightly controlled by two essential cytokines, macrophage colony-stimulating factor and receptor activator of nuclear factor kappa B ligand (RANKL). However, the role of epigenetic regulation in osteoclast differentiation is poorly understood.

We applied massively parallel sequencing of the chromatin immunoprecipitation products using the Illumina cluster station and 1G Analyzer to investigate the H3K4me3 and H3K27me3 modification patterns around the transcription start site (TSS) of several transcription factors known to be important for osteoclastogenesis, i.e. Mitf, Nfkb1, Nfkb2, Mitf, Fos, and Nfatc1. H3K4me3 was present in both osteoclast precursors and osteoclasts in TSS of all of these transcription factors, except for Mitf. The H3K27me3 marks were present in a relatively broad peak centered on the TSS of Nfatc1, but not of the other transcription factors. Following the treatment with RANKL and subsequent osteoclast differentiation, a marked reduction in the level of H3K27me3 at the Nfatc1 locus was observed. Since the most likely explanation of H3K27me3 demethylation at the Nfatc1 locus is the involvement of H3K27me3 demethylases, we examined the expression of H3K27me3 demethylases during osteoclast differentiation. The expression of Jumonji domain containing-3 (Jmjd3), but not Utx, was time-dependently increased in osteoclast precursors and recruited in the vicinity of the TSS of Nfatc1 after stimulation with RANKL. In addition, gene silencing of the Jmjd3 gene by short hairpin RNA reduced demethylation of H3K27me3 around the TSS of Nfatc1 and markedly suppressed RANKL-induced osteoclastogenesis.

These results suggest that demethylation of H3K27me3 in the vicinity of the TSS of the Nfatc1, regulated by Jmjd3, plays a key role in RANKL-induced osteoclast differentiation.

Disclosures: Jun Hirose, None.

MO0283

Evidence that ITAM Related Factors in Synovial Tissue and Vasculature of Active Rheumatoid Arthritis may be Involved in Modulating Local Bone Erosion. Tania Crotti*, Ekram Alias², Kencana Dharmapatri², Helen Weedon³, Andrew Zannettino⁴, Malcolm Smith⁵, David Haynes⁶.

¹University of Adelaide, Australia, ²Discipline of Anatomy & Pathology, University of Adelaide, Australia, ³Rheumatology Unit, Repatriation General Hospital, Flinders University, Australia, ⁴Myeloma Research Laboratory, Centre for Cancer Biology, SA Pathology & Department of Medicine, University of Adelaide, Australia, ⁵Rheumatology Research Unit, Repatriation General Hospital, Flinders University, Australia, ⁶Discipline of Anatomy & Pathology, School of Medical Sciences, Australia

Elevated receptor activator NF kappa B ligand (RANKL) in active rheumatoid arthritis (RA) is associated with increased osteoclast differentiation and resorption activity. RANKL-RANK signaling induces the transcription factor nuclear factor of activated T cells (NFATc1) that is central to osteoclast formation and plays a role in the immune system. The immunoreceptor tyrosine-based activation motif (ITAM) pathway provides osteoclast co-stimulatory signals and regulates proliferation, survival and differentiation of effector immune cells. In the osteoclast, the receptors TREM2 and OSCAR and their respective adaptor proteins, DAP 12 and FcR γ , mediate ITAM signals and induce calcium signaling. NFATc1 induces OSCAR expression and they then interact via a positive feedback loop. We propose that increased expression of ITAM factors in active RA augments osteoclastogenesis and focal bone erosion development. Thus, we examined the expression of osteoclast markers, ITAM related factors and NFATc1 in human synovial tissues by immunohistochemistry. The proportions of positive cells were scored using a semi-quantitative 5-point grading system and the number of NFATc1 positive lymphoid aggregates was scored. The expression of ITAM factors was examined in cytokine stimulated HUVEC cells. Soluble OSCAR was measured by ELISA in RA and OA patient synovial fluids. NFATc1-positive cells were predominantly lymphocytic and found in aggregates with significantly higher positive aggregates in active RA versus normal synovia. The proportion of OSCAR, FcR γ , DAP12 and TREM2 positive cells was significantly higher in active RA tissues compared to the normal synovia. TREM2 and DAP12 staining was associated with synovial macrophages in the synovial lining and within lymphoid aggregates and multinuclear cells of the sub-lining. Of note, TREM2 staining was also associated with endothelial cells. OSCAR expression was mainly associated with macrophage-like cells in the subsynovial tissue. Interestingly, OSCAR was strongly expressed in the microvasculature of RA tissue (9/9) but weakly in OA and normal tissues. This was in contrast to our previous findings, where OPG (the RANKL decoy receptor), was high in microvasculature of normal tissue but weak in RA tissues. Synovial fluids from RA and OA contained 45-147ng/ml sOSCAR. Increased levels of ITAM factors in synovial tissues from RA patients support a role for ITAM factors and NFATc1 induction in the pathophysiology of RA.

Disclosures: Tania Crotti, None.

MO0284

Functional Study of the RANKL Promoter Regions and the Effect of Hormone and Cytokine Treatments. Guy Yoskovitz*¹, Natalia Garcia-Giral¹, Roberto Guerri¹, Daniel Prieto-Alhambra¹, Patricia Sarrion², Roser Urreiziti², Leonardo Mellibovsky¹, Luis Perez-Edo³, Susana Balcells², Daniel Grinberg², Adolfo Diez-Perez¹, Xavier Nogues¹. ¹URFOA, IMIM, RETICEF, Hospital del Mar, Autonomous University of Barcelona, Spain, ²Genetics Dept, University of Barcelona, CIBERER, IBUB, Barcelona, Spain, ³Hospital Ntra Sra Del Mar, Spain

Aim: The bone remodelling, which determines the bone mineral density and microarchitecture, is in part regulated by the RANK/RANKL/OPG system. An imbalance in their equilibrium affects bone and may result in various pathological states, among them osteoporosis. Receptor Activator of Nuclear Factor kappa-B (RANK) and its interaction with its ligand (RANKL) is one of the main triggers of osteoclast differentiation and survival, hence plays a major role in bone remodelling. In this work we studied the functionality of the RANKL promoter.

Methods: The proximal 2015 bp region of the RANKL promoter was cloned into pUC19 vector and subsequently into pGL3 basic vector. Following, by deleting segments from the 2015 bp promoter a total of 4 structures were designed: P1 (-2015 bp promoter), P2 (-1347 bp), P3 (-1038 bp) and P4 (-330 bp) and transfected into U2OS (Human Osteosarcoma cell line) with renilla vector as control. Luciferase and renilla activities were measured after 24 hours incubation. To achieve an overall view of the promoter functionality, we treated the cells with cytokines, hormones and growth factors (Transforming Growth Factor beta (TGF- β) 10^{-7} M, Vitamin D 10^{-7} M, 17β -Estradiol 10^{-6} M, Dexamethasone 10^{-6} M, Tumor Necrosis Factor alpha (rHTNF α) 100ng/ml, Parathyroid Hormone (PTH) 10^{-7} M and Interleukin-1 (IL-1) 10ng/ml) 6 hours after transfection followed by a 16 hours incubation period.

Results: Analysis of the non-treated promoter structures showed a significantly higher luciferase expression levels for P4 comparing to the other promoters structures ($p < 0.05$) while P1, P2 and P3 presented similar expression levels.

Preliminary results of the treatments applied to the culture showed higher expression levels induced by 17β -Estradiol and PTH, while IL-1, rHTNF α and TGF- β down regulated the reporter gene expression in all structures tested in comparison to the non-treated transfected cells. On the other hand, vitamin D and Dexamethasone seemed to have no effect on any promoter structure.

Conclusions: P1, P2 and P3 structures have inhibitory elements that are able to regulate the basal promoter (P4). Furthermore, this basal promoter harbours cytokines and hormones response elements that regulate the RANKL expression.

Disclosures: Guy Yoskovitz, None.

MO0285

Gamma-Radiation Causes Trabecular Bone Loss Similar to Skeletal Aging and Stimulates Resorptive Activity In Vitro. Joshua Alwood*¹, Akhilesh Kumar¹, Luan Tran¹, Angela Wang¹, Charles Limoli², Ruth Globus¹. ¹NASA Ames Research Center, USA, ²UC Irvine, USA

Occupational exposure to ionizing radiation may pose a risk to long-term skeletal health. Gamma-irradiation at high doses (defined here as ≥ 100 cGy) causes trabecular osteopenia in humans and mice, although the influence of lower doses during subsequent aging is not known. We hypothesize low dose (≤ 10 cGy), total body irradiation accelerates skeletal changes that are characteristic of normal skeletal aging by increasing the number and activity of osteoclasts. To begin to address this, C57BL/6J mice (10wk old, male) were irradiated (IR) (10 or 100cGy 137 Cs, 90cGy/min) or were sham-irradiated (0cGy-controls). Tissues were harvested on the day of IR (basal), 1 or 4 mo. later ($n=8$ /gp). Microcomputed tomography was used to quantify 3D cancellous microarchitecture of proximal tibia metaphyses. To determine *in vitro* effects of IR on osteoclast formation and function, RAW 264.7 cells treated with RANKL (15-100 ng/mL), were irradiated within 48hrs (0, 10, 200cGy), then TRAP+, multinuclear cells counted (d5) and resorption pits quantified (BD Osteologic mineral substrate) (d14). Irradiation did not affect body weights at any dose or time post-IR. In sham-IR control mice, trabecular bone volume/total volume (BV/TV), trabecular number (TbN), and connectivity density (CnD) did not change between 0 and 1mo. post-IR ($p > 0.05$). Cancellous bone subsequently underwent an age-related decline between 1 and 4 mo. in BV/TV (-13%), TbN (-17%) and CnD (-41%) ($p < 0.05$). In 10cGy-IR mice, bone loss did not differ from 0cGy-controls. In 100cGy-IR mice, TbN and CnD declined faster between 0 and 1 mo. post-IR (-20% and -36%, respectively; $p < 0.05$, ANCOVA for slope differences between groups) compared to age-matched controls, and then remained constant between 1 and 4 mo. post-IR. *In vitro*, IR (200cGy) of RAW 264.7 cells caused an increase ($p < 0.05$) in the number of TRAP+ cells (d5) and IR (10 or 200cGy) caused an apparent increase in resorption pit area (d14). In sum, a low dose of gamma-radiation (10cGy) did not induce osteopenia relative to age-matched controls, although a higher dose (100cGy) accelerated trabecular bone loss at a rate comparable to later skeletal aging in 0cGy-IR controls. In conclusion, irradiation above a threshold of 10 cGy appears to accelerate skeletal aging by stimulating resorption of cancellous tissue.

Disclosures: Joshua Alwood, None.

MO0286

Hypoxia-Related Regulation of Osteoclast Formation by Pyruvate Kinase M2. Youngho Kim¹, Lexie Holliday², Edgardo Toro³, SEONG SIK KIM*⁴. ¹South Korea, ²University of Florida College of Dentistry, USA, ³University of Florida, USA, ⁴Pusan National University, USA

Hypoxic stress could enhance osteoclast differentiation. Previous study shows that osteoclastogenesis is associated with expression of increased levels of several glycolytic enzymes and with the expression of PKM2. A small molecule activator of PKM2 (NCGC00185916-01; ref. 1) at a concentration of 1 micromolar increased the number of osteoclasts (tartrate-resistant acid phosphatase expressing multinuclear cells) formed during differentiation of RAW 264.7 cells stimulated by RANKL and mouse marrow osteoclasts stimulated by calcitriol by from 1.5 to 5-fold. In this study, we have investigated (1) Pyruvate Kinase M2 expression during osteoclast formation from RAW264.7 cells with RANKL differentiation under hypoxia (1% O₂), and (2) bone resorption activity of Mouse Bone Marrow Cells with calcitriol differentiation under hypoxia. The expression levels of Pyruvate Kinase M2 (PKM2) increased at 24 hours hypoxia (1% O₂) condition with time-dependent manner, however, PKM2 expression decreased at 48 hours hypoxia. For 48 hours hypoxia induced RAW264.7 cells apoptosis and cell cycle arrest at G0/G1 phase. A small molecule activator of PKM2 under hypoxia enhances osteoclastogenesis of RAW264.7 in response to sRANKL, and mouse marrow in response to calcitriol. A small molecule activator of PKM2 stimulated osteoclastic resorption 2- to 3-fold in assays of lacunar bone resorption under hypoxia than normoxia, without affecting osteoclast viability. These results demonstrate that the small molecule activator may disrupt normal coupling and inhibit bone resorption, however, hypoxia may have a role in regulating coupling of glycolysis to V-ATPase proton pumping activity in bone resorbing osteoclasts. 1. Boxer, M. B., Jiang, J. K., Vander Heiden, M. G., Shen, M., Skoumbourdis, A. P., Southall, N., Veith, H., Leister, W., Austin, C. P., Park, H. W., Ingles, J., Cantley, L. C., Auld, D. S., and Thomas, C. J. (2010) J. Med. Chem. 53, 1048-1055.

Disclosures: SEONG SIK KIM, None.

MO0287

Identification and Isolation of Transplantable Osteoclast Progenitors from Human Pluripotent Stem Cells. Sierra Root*¹, Hector Aguila. University of Connecticut Health Center, USA

Osteoclasts (OC) are hematopoietic cells that differentiate from monocyte progenitors into bone resorbing cells during bone remodeling. Their development is tightly linked to osteogenesis and restricted to bone marrow microenvironments that support the generation of progenitors and the conditions for their terminal differentiation. In mice we have identified clonal OC progenitors (OCP) that, after injection into preconditioned recipients, engraft and form OC that localize on endosteal surfaces. The evidence of transplantable OCP and the restriction on their development led us to propose that OC could serve as restricted cellular vectors to deliver bioactive molecules to the bone marrow microenvironment. The implementation of this approach to humans is limited by the fact that OCP have not been faithfully characterized making difficult their isolation and testing for engraftment properties. Human pluripotent stem cells can serve as a renewable source for these progenitors, and they can be modified genetically to allow the expression of defined molecules under the control of OC specific promoters. We have developed an efficient method to generate active mature osteoclasts from human embryonic stem cells through the generation of embryoid bodies in the presence of hematopoietic cytokines. Characterization and isolation of candidate progenitors has been done by flow cytometry. Dissection of hematopoietic derivatives expressing CD45 showed cells expressing multiple markers of lymphoid and myeloid progenitors. OCP activity, measured by the *in vitro* formation of TRAP+ multinucleated cells after culturing with MCSF plus RANKL, was contained mostly within a fraction negative for CD14 and CD11b. This population could be further dissected in the context of CD115 and CX3CR1, two markers of transplantable murine monocyte progenitors. CD115 is expressed in around 10% of the cells and about 70% of them co express CX3CR1. Finer dissection is being done using these additional markers. We have also developed transgenic hESCs expressing GFPs, to evaluate derivatives for their ability to engraft in immuno compromised NOG mice expressing the col2.3ATK transgene, that permits the opening of hematopoietic niches after depletion of osteoblasts with gancyclovir treatment. Engraftment will be measured by the presence of GFP positive TRAP positive cells on the endosteal surface of recipient bones, or in pre-established human bone ossicles.

Funded by NIH/NHLBI Grant 1RC1HL100569-01

Disclosures: Sierra Root, None.

MO0288

Identification of the Promoter Region that Mediates Colony Stimulating Factor 1 Induction of the Jun Dimerization Protein 2 Gene. Gang-Qing Yao*¹, Karl Insogna. Yale University School of Medicine, USA

In addition to its critical role in osteoclastogenesis, Colony Stimulating Factor 1 (CSF1) also regulates mature osteoclast function. Thus, CSF1 stimulates motility, augments the activity of the Na/HCO₃- co-transporter, NBCn1 (and relevant to this

work) induces c-fos gene transcription in mature osteoclasts. As part of a microarray screen designed to identify targets for CSF1's actions in mature osteoclasts, we found that expression of Jun dimerization protein 2 (JDP2) was induced by the cytokine. This finding was confirmed by qPCR using RNA isolated from CSF1 treated osteoclast-like cells. JDP2 is an AP-1 repressor protein. Thus, as is often the case, a ligand (CSF1) induces a stimulatory signal (c-fos, part of the AP-1 complex) and also stimulates the inhibitor (JDP2) so that the agonist signal can be modulated. JDP2 has a critical role in osteoclastogenesis since suppressing its expression blocks osteoclast differentiation. Regulatory elements in the JDP2 gene have not been reported presumably because the 5' UTR of this gene is very GC rich, making cloning extremely difficult. We were able to clone a 3297 bp fragment of the JDP2 gene from -2612 to +682 (relative to the transcription start site). To approximate the locations of CSF1-responsive elements in this fragment, a series of 5'-deletions were generated and fused to a luciferase reporter gene in the pGL3 vector. Basal and CSF1-inducible activity of the deletion constructs were analyzed by transiently expressing them in p-zen cells, a fibroblast cell line overexpressing the CSF1 receptor, c-fms. We found that the JDP2 promoter region from -261 to -52 bp is required for both basal activity and CSF1 transcriptional activation. Several canonical transcription-binding sites are located in this region including AP2, STRE, CREB, GATA-1, MZF1, Ik-2, KLF4/GKLF and an SP1 site. Since it is known that CSF1-induced transcriptional activation of the VEGF gene is Sp1 dependent, we mutated the Sp1 site in the JDP2 promoter. This did not affect basal promoter activity or the ability of CSF1 to induce transcriptional activation. We conclude that CSF1 stimulates JDP2 expression via cis regulatory element(s) located in the sequence from -261 to -52 bp. Since none of the identified cis-elements (except Sp1) located in this region are regulated by CSF1, the control of JDP2 expression by CSF1 appears to involve a novel, as yet uncharacterized, DNA sequence.

Disclosures: Gang-Qing Yao, None.

MO0289

M-CSF Induces Osteoclastogenesis Resistance In CD31⁺/Ly6C⁺ Osteoclast Precursors; An Effect Not Occurring In The Presence Of Bone. Teun De Vries¹, Ton Schoenmaker², Pieter J.M. Leenen³, Vincent Everts^{*4}. ¹ACTA, University of Amsterdam & VU University, The Netherlands, ²Dept Periodontology, ACTA, Netherlands, ³Dept. Immunology, Erasmus MC, Netherlands, ⁴ACTA, Vrije Universiteit, The Netherlands

We recently demonstrated that osteoclasts can differentiate from mouse bone marrow precursors of various stages of maturity (J. Leukocyte Biol. 85: 919-927, 2009). Since M-CSF may play a role in priming osteoclast precursors, we assessed how pre-incubation with M-CSF affects osteoclast formation. Successive myeloid developmental stages were isolated from mouse bone marrow. Unfractionated bone marrow, early blasts (CD31hi/Ly-6C-), myeloid blasts (CD31+/Ly-6C+) and monocytes (CD31-/Ly-6Chi) were primed for 1 to 4 days with M-CSF, followed by incubation with M-CSF + RANKL for another 4 days. M-CSF priming for 2 days significantly increased osteoclast formation from early blasts and monocytes and these cells retained their capacity to develop into osteoclasts also when primed for 4 days. Surprisingly, M-CSF primed myeloid blasts, the osteoclast precursor that differentiates fastest into osteoclasts with M-CSF and RANKL, lost this potential over time. Myeloid blasts cultured for 4 days with M-CSF and then 4 days with M-CSF + RANKL remained mononuclear and TRACP-negative and positive for mouse monocyte/macrophage markers Mac-1 and F4/80. Priming of myeloid blasts with M-CSF followed by M-CSF + RANKL did not affect RANK expression, but osteoclast-related mRNA for TRACP, calcitonin receptor and DC-STAMP were down-regulated. A completely different situation occurred when myeloid blasts were cultured on cortical bone slices. Here, priming with M-CSF followed by M-CSF + RANKL resulted in abundant osteoclast formation. Interestingly, osteoclasts formation was also evoked in myeloid blasts grown on plastic next to the bone slices. Thus, bone itself or cells grown on bone may elicit factors that drive osteoclast formation.

Our results imply that early and late stages (early blasts and monocytes, respectively) in myeloid differentiation represent a route of osteoclast differentiation which is not inhibited by M-CSF priming. Cells in the myeloid blast fraction appear to be primed for osteoclast generation, but lose this preference upon M-CSF stimulation, unless they are in the vicinity of bone. In vivo, transition of myeloid precursors to an osteoclastogenesis-resistant stage could be functional when travelling away from bone towards organs where no osteoclasts are needed. Possibly, in the vicinity of bone the formation of such osteoclastogenesis-resistant cells is prevented.

Disclosures: Vincent Everts, None.

MO0290

PAMM Expression During Osteoclastogenesis Is Mediated by Akt Activation. Li Zhang¹, Liang Ye², Leslie Morse³, Raquel Silva⁴, Yan Xu⁵, Ricardo Battaglini^{*1}. ¹The Forsyth Institute, USA, ²Harvard School of Dental Medicine, USA, ³Harvard Medical School, USA, ⁴School of Dentistry of Ribeirao Preto - University of Sao Paulo, Brazil, ⁵Kunming Medical University, China

Reactive oxygen species (ROS) play a central role in osteoclast differentiation and in skeletal homeostasis. ROS stimulate osteoclast differentiation and function whereas

free radical scavengers and antioxidants have the opposite effect. We identified and characterized PAMM (Peroxiredoxin expressed in M-CSF Activated Monocytes) a protein with peroxidase activity, expressed during osteoclast differentiation. In RAW 264.7 cells, PAMM over-expression prevented the reduction of GSH/GSSG induced by RANKL. Concurrently, PAMM expression completely abolished RANKL-induced osteoclast differentiation. In human Peripheral Blood Mononuclear Cells (PBMC), M-CSF was able to induce PAMM expression, while addition of RANKL resulted in decreased PAMM expression. The purpose of this study was to elucidate the molecular pathway/s mediating expression of PAMM in response to M-CSF and M-CSF/RANKL stimulation. We found that M-CSF induced both, PAMM expression and activation of Akt (by phosphorylation in Ser 473). PI3Kinase activity is required for Akt activation. Wortmannin, a specific PI3Kinase inhibitor, blocked PAMM expression in response to M-CSF. Activated Akt can, in turn, directly phosphorylate mTOR in a rapamycin-sensitive way. Rapamycin could also block M-CSF-induced PAMM expression. Stimulation of PBMC with M-CSF and RANKL, on the other hand, resulted in inhibition of Akt activation and PAMM expression. The addition of Rapamycin enhanced the effect of RANKL on PAMM expression as well as on the formation of TRAP positive osteoclasts. Akt provides a survival signal that protects cells from apoptosis induced by growth factor withdrawal and oxidative stress. This pathway involves the activity of PI3 kinase and is, therefore, wortmannin-sensitive. Our results clearly indicate that M-CSF-induced PAMM expression is mediated by Akt and suggest that RANKL-induced osteoclast formation requires downregulation of PAMM. These observations suggest that PAMM expression could play a dual role in osteoclastogenesis: inhibiting osteoclast differentiation while stimulating proliferation of osteoclast precursors by regulating the levels of intracellular ROS. These findings also point to PAMM as a potential candidate for Akt-mediated protection against oxidative stress.

Disclosures: Ricardo Battaglini, None.

MO0291

Potent Inhibitory Effect of Foeniculum Vulgare Miller Extract on Osteoclast Differentiation and Ovariectomy-Induced Bone Loss. Tae-Ho Kim^{*1}, Eui Kyun Park², Hyun-Ju Kim¹, Sang-Han Lee³, Shin-Yoon Kim⁴. ¹Kyungpook National University School of Medicine, South Korea, ²Kyungpook National University School of Dentistry, South Korea, ³Department of Food Science & Biotechnology, Kyungpook National Univ., South Korea, ⁴Kyungpook National University Hospital, South Korea

Inhibition of osteoclast differentiation and bone resorption is considered as an effective therapeutic approach to the treatment of postmenopausal bone loss. To find natural compounds that may osteoclastogenesis, we screened medicinal herb extracts on bone marrow culture system. In this study, we found that aqueous extract of Foeniculum vulgare Miller (FvMs), which has traditionally been used as a treatment for variety of complaints, inhibited osteoclast differentiation and bone resorptive activity of mature osteoclasts at low concentration. We further investigated the effects of FvMs on ovariectomy (OVX) -induced bone loss using micro-computed tomography, biomechanical tests and serum markers assay for bone remodeling. Oral administration of FvMs (30mg or 100mg/kg/day) for 6 weeks had an intermediary effect on prevention of femoral BMD, BMC, and other parameters when compared to OVX controls. In addition, FvMs slightly decreased bone turnover markers that were accelerated by OVX. The bone protective effects of FvMs may be due to suppression of OVX-induced increase in bone turnover. In summary, our findings indicate that Foeniculum vulgare extract has the potential for prevention of bone loss in postmenopausal osteoporosis by reducing both osteoclast differentiation and function.

Disclosures: Tae-Ho Kim, None.

MO0292

The Corning® Osteo Assay Surface for Osteoclast Differentiation and Bone Resorption. A Fawad Faruqi^{*}. Corning Life Sciences, USA

Bone related diseases such as osteoporosis, multiple myeloma, and bone metastasis from prostate and breast cancer tumors represent a significant challenge for both research and drug development. In vitro assays that can measure both the formation and function of osteoclasts are critical for furthering our understanding of the biology of normal bone remodeling. Current systems for assaying osteoclast activity using bone or dentine slices are time consuming and difficult to quantify. An inorganic coating has been developed on standard polystyrene multi-well plates by Corning® that can be used for the study of bone cell biology.

The Corning Osteo Assay Surface has been evaluated for osteoclast differentiation and bone resorption. We have compared the surface to dentine discs using cultures of primary human osteoclast precursors and found that osteoclast differentiation and activity can be assessed rapidly and accurately on the Corning Osteo Assay surface whereas use of dentine discs remains problematic. We have also demonstrated that the surface provides a convenient platform for bone related drug screening. Additionally, the surface provides a useful tool for migration and co-culture studies in combination with Transwell® permeable supports.

In summary, both osteoclast differentiation and activity can be readily measured with Corning Osteo Assay Surface, which provides consistent and reproducible results

in assays using osteoclast precursors and also provides a platform for bone related drug screening.

Disclosures: A Fawad Faruqi, None.

MO0293

Two RANK TRAF-binding Motifs Play a Pivotal Role in TNF- and IL-1-mediated Osteoclastogenesis via functional crosstalk with the IVVY motif in the RANK Cytoplasmic Domain. Joel Jules*, Zhengqi Shi, Jianzhong Liu, Shi Wei, Xu Feng. University of Alabama at Birmingham, USA

The receptor activator of NF- κ B (RANK) ligand (RANKL) promotes osteoclast formation, survival and function by activating its receptor RANK, which recruits TNFR associated factors (TRAF) via three intracellular motifs (PFQEP369-373: Motif 1; PVQEET559-564: Motif 2 and PVQEQG604-609: Motif 3). RANK also possesses a TRAF-binding motif (IVVY535-538) which plays a vital role in osteoclastogenesis by committing bone marrow macrophages (BMMs) to the osteoclast lineage. Intriguingly, mutation of the IVVY motif exerts no impact on the activation of the TRAF-binding site-mediated signaling pathways (NF- κ B, Akt, ERK, JNK and p38) in BMMs. Moreover, the IVVY motif plays a critical role in the lineage commitment not through activating any of the NF- κ B, Akt, ERK, JNK and p38 pathways. Thus, we hypothesized that the TRAF-binding sites and the IVVY motif are functionally independent. However, when these two distinct types of functional motifs were simultaneously activated in the same cells using two different chimeric receptors in which either TRAF-binding sites or the IVVY motif were mutated, we found, unexpectedly, that concurrent activation of the two chimeric receptors failed to promote osteoclastogenesis. This unexpected finding indicates that the TRAF-binding sites and the IVVY motif in the RANK cytoplasmic domain have to be present in the same RANK molecule to be functional, suggesting that one or more TRAF-binding sites functionally crosstalk with the IVVY motif. To address this possibility, we investigated the involvement of the RANK TRAF-binding motifs in TNF- and IL-1-mediated osteoclastogenesis since we have recently demonstrated that the IVVY motif plays a crucial role in TNF- and IL-1-mediated osteoclastogenesis. Motifs 2 and 3, but not Motif 1, are significantly involved in TNF- and IL-1-mediated osteoclastogenesis. Mutation of both Motif 2 and Motif 3 dramatically blocked osteoclastogenesis. Mechanistically, Motif 2 and Motif 3 play an important role in osteoclastogenesis by activating the expression of four osteoclast genes, which were previously shown to be critically regulated by the IVVY motif, in TNF- and IL-1-mediated osteoclastogenesis. Thus, our data indicate that Motif 2 and Motif 3 play a critical role in osteoclastogenesis via a functional crosstalk with the IVVY motif, and these two TRAF-binding motifs have the potential to serve as novel therapeutic strategies for preventing and treating osteoporosis and inflammatory bone loss.

Disclosures: Joel Jules, None.

MO0294

A Computational Model to Examine Osteocytes' Potential to Regulate Osteoclastic Resorption. Lyndsey Schutte*, Jeffrey Hollinger. Carnegie Mellon University, USA

Medical treatment of osteoporosis and other bone diseases is limited by the lack of understanding of how bones function as a complex system. There is a disconnect between the basic science and the clinic. The purpose of this research is to develop a computational framework for integrating the known information about bone cells and their signaling pathways into one model so that the emergent behavior of bone can be better understood and predicted. As a first step towards this, an agent-based model was built to include trabecular structures, osteocytes and osteoclasts capable of forming resorption pits. The model then examined the potential capabilities of osteocytes to regulate the resorption of bone through a disuse threshold.

Using an agent-based model, the osteocytes were placed in a trabecular structure at a physiological population density, and were given the ability to produce a signaling molecule when the local mechanical stress in the surrounding mineralized matrix increased above a certain threshold. Below this threshold, the bone would be in 'disuse' and could be resorbed. At the locations where the volume of bone decreased, the local stress would increase, potentially rising above the osteocytes' threshold. The signal generated by the osteocytes would then prevent any osteoclast activity wherever the osteoclasts came in contact with it. When the osteoclasts did not receive the signal, they continued resorbing the bone. The simulation would stop when the system reached steady state-either through the whole trabecula being shielded by the osteocytes or by the bone being resorbed.

This model showed that osteocytes were able to control the remodeling of the bone to a minimal required size with just one signaling molecule and one local mechanical threshold. Increasing the population density of the osteocytes decreased the variance of the final volume of bone and significantly reduced the risk of the osteoclasts resorbing through the full thickness of the trabeculae. When bone-lining cells were added in a syncytial manner to the osteocytes, the remodeled edges became smoother and the variance in final trabecular width was also reduced.

Based on these results, it is reasonable to hypothesize that osteocytes are physiologically capable of controlling the spatial locations of bone resorption, potentially with the assistance of bone-lining cells.

Disclosures: Lyndsey Schutte, None.

MO0295

Effect of Rac GTPase Deletion on Osteoclast Cytoskeletal Organization. Monica Croke*, Wei Zou², Steven Teitelbaum². ¹Washington University School of Medicine, USA, ²Washington University in St. Louis School of Medicine, USA

Osteoclastic bone resorption requires reorganization of the osteoclast (OC) actin cytoskeleton, which we have shown is mediated by Rac, a member of the Rho family of GTPases. Rac is activated by stimulation of the OC surface receptors c-Fms and α v β 3 integrin, leading to cellular polarization, formation of the actin ring, and resorption of the bone matrix.

To study the effect of Rac GTPases on actin ring organization and bone matrix resorption, we utilized mice lacking Rac1 and 2, the isoforms expressed in the OC and its myeloid precursor. Mice lacking both isoforms (Rac dKO), in combination, develop severe osteopetrosis with bone matrix occupying one-third of the marrow cavity. Marrow cells isolated from the Rac dKO mice differentiate into TRAP-positive OCs when cultured in the presence of M-CSF and RANKL and express OC markers such as c-Src and Cathepsin K at levels comparable to WT. Rac dKO OCs fail to organize their cytoskeleton when generated on bone as manifest by a non-polarized phenotype and complete absence of actin rings. These morphological abnormalities translate into dysfunctional resorption, exemplified by absence of pit formation on bone and diminished release of collagen degradation products into the culture medium. Consistent with in vivo data from the Rac1 or 2 single knockout animals, the in vitro phenotype of Rac dKO OCs is rescued by exogenous expression of either Rac1 or 2.

We have observed a consistent decrease in β 3 integrin protein levels during early osteoclast differentiation in Rac dKO cells despite abundant mRNA. We are investigating the role of Rac in the regulation of β 3 integrin translation, stability, and cellular localization during osteoclastogenesis.

Our studies show that Rac1 and 2, through a complex network of effector proteins, are required for the dynamic process of actin ring formation in the resorptive osteoclast. Additionally, we have identified Rac as a possible mediator of β 3 integrin protein expression in the osteoclast.

Disclosures: Monica Croke, None.

MO0296

Functional Involvement of the Microtubule-Binding Dynein-Dynactin Complex in Osteoclast Formation and Bone Resorption. Pei Ying Ng*, Haotian Feng², Ee Cheng Khor¹, Shiqiao Ye³, Haibo Zhao³, Ming Hao Zheng², Jiakie Xu¹, Nathan Pavlos². ¹The University of Western Australia, Australia, ²University of Western Australia, Australia, ³University of Arkansas for Medical Sciences, USA

Bone resorption by osteoclasts relies on the co-ordinated interplay between acidified carrier vesicles laden with osteolytic enzymes (e.g. Cathepsin K), motor proteins and the underlying cytoskeleton in order to sustain the specialized structural and functional segregation of the ruffled border membrane. Cytoplasmic dynein, a processive mechanochemical motor comprising heavy, intermediate and light chains coupled to the dynactin co-factor complex, powers retrograde motility of diverse cargoes to microtubule minus-ends. Despite its crucial involvement in a wide range of fundamental cellular processes, the contribution of the dynein-dynactin motor complex in osteoclasts remains unknown. Here, using a combination of complementary biochemical and morphological assays, we have dissected the intracellular localization and function of the dynein-dynactin complex in osteoclasts. By subcellular fractionation and immunofluorescence confocal microscopy we demonstrate that the dynein-dynactin complex is highly expressed in mature osteoclasts and is intimately coupled to microtubules, undergoing dramatic reorganization upon the onset of osteoclastic polarization. In bone-resorbing osteoclasts, p150^{Gluc} and CLIP-170, both major constituents of the dynactin and CAP-Gly domain-containing microtubule plus end-associated proteins, exhibit distinct polarization at the osteoclastic resorptive front, thus orientating the ruffled border as the microtubule plus-end domain. Interestingly, disruption of the dynein-dynactin complex via p50/dynactin-over-expression retards the formation and maturation of osteoclasts, owing to a delay in mitotic stasis of mononuclear progenitor cells. Moreover, uncoupling of the dynein-dynactin motor from microtubules coincides with a drastic redistribution of key osteoclastic intracellular organelles, including the Golgi and lysosomes. Finally, we provide evidence that the dynein-dynactin complex is required for the targeted positioning and delivery of Cathepsin K to the ruffled border membrane, and thus constitutes an integral component of the osteoclastic bone resorption machinery. Together, these data unveil an unexpected yet versatile role for the dynein-dynactin motor in osteoclast formation and function.

Disclosures: Pei Ying Ng, None.

MO0297

Oligomerization of the Osteoclastic Chloride Transporter CIC-7 Demonstrated by Bioluminescence Resonance Energy Transfer (BRET). Vicki Jensen*, Morten Karsdal, Kim Henriksen. Nordic Bioscience A/S, Denmark

The lysosomal chloride-proton antiporter CIC-7 plays an important role in acid secretion into the osteoclastic resorption lacunae, through its co-operation with the osteoclastic V-ATPase. Autosomal dominant mutations in CIC-7 lead to osteopetrosis, suggesting that functional CIC-7 is a homodimer, in accordance with other CLC family members; however, evidence proving the interaction for CIC-7 is absent. An important interaction partner of CIC-7 is Ostm1, which is believed to protect CIC-7 against degradation.

In this study, we investigated whether CIC-7 forms homooligomers and whether CIC-7 dimerization is specific using the Bioluminescence Resonance Energy Transfer (BRET) technique, and how this interaction is affected by Ostm1.

Recombinant proteins of CIC-7, CIC-6 and Ostm1 were fused to either green fluorescent protein (GFP) or luciferase (Luc) and co-transfected into HEK293 cells. When in close proximity the Luc-tagged proteins excite the GFP-tagged proteins upon addition of the substrate coelenterazine. The BRET signal is a ratio calculation between GFP and Luc signal. As negative control a BRET cold protein was engineered by tagging CIC-7 recombinant protein with haemagglutinin (HA). The known interaction of CIC-7 with Ostm1 was used as positive control. The expression levels were confirmed by western blotting. The BRET assays were performed in microsome membranes purified from HEK293 cells expressing the recombinant proteins.

Co-transfection of a constant amount of Luc-CIC7 and increasing amounts of GFP-CIC7 produced a dose dependent BRET signal at low levels of GFP-CIC7, while a saturation of the signal was seen at a 1:6 ratio of Luc:GFP and above, indicating specificity of the interaction. The specificity of the CIC-7-CIC-7 interaction was confirmed as no interactions of CIC-7 with fusion proteins of the closely related CIC-6 were observed. When adding different ratios of cold tagged Ostm1 to the CIC-7 homooligomer no effect was seen on the stability of the CIC-7 oligo interaction.

Taken together human CIC-7 was shown to form stable homooligomers independent of Ostm1 interaction. The establishment of CIC-7/CIC-7 BRET assay allows characterization of the CIC-7 oligomerization in the absence of protein crystallization data, and allows mutation studies delineating the interaction surfaces. This technique opens the possibility for studying molecules disrupting the CIC-7 oligomer interaction and thus will aid further molecular characterization of CIC-7.

Disclosures: Vicki Jensen, None.

This study received funding from: The Danish Research fund

MO0298

Osthole Inhibits Osteoclastogenesis through Activation of β -Catenin-OPG Signaling. De-Zhi Tang*¹, Zhou Yang¹, Qi Shi¹, Di Chen², Yong-Jun Wang¹. ¹Spine Research Institute, Shanghai University of Traditional Chinese Medicine, China, ²University of Rochester Medical Center, USA

Osthole, a coumarin-like derivative extracted from Chinese herbs, which has been used as the treatment of bone diseases for thousands of years. It has been shown to stimulate osteoblast differentiation by increasing the expression of Bmp2 in MG-63 cells. Our published paper showed that osthole stimulated osteoblast differentiation and bone formation by activation of β -catenin-Bmp signaling. But there is no evidence to indicate the effect of Osthole on osteoclast formation and bone resorption recently. To figure out the effect of Osthole on osteoclastogenesis and underlying mechanism, we performed this study. Our in-vivo study showed that Osthole at a dose of 5 mg/kg/day increased bone mass in OPG-/- mice by stimulating bone formation, not by inhibiting bone resorption. Osteoclast number was not reduced in OPG-/- mice after the treatment of Osthole. These data suggested that OPG may be the target gene of Osthole to affect osteoclastogenesis. To test this hypothesis, we analyzed the role of Osthole on the OPG gene expression in bone marrow stromal cells. qPCR data showed that Osthole significantly increased the expression of OPG mRNA in a dose-dependent manner, especially at the concentration of 100 μ M. These data indicated that Osthole may inhibit osteoclast formation by stimulating OPG expression. To further identify our hypothesis, bone marrow stromal cells were isolated from OPG-/- mice and its littermates of OPG+/+ mice, induced to form osteoclast by M-CSF and RANKL, and treated with or without Osthole at the concentration of 100 μ M. TRAP staining data showed that Osthole reduced the number of osteoclast dramatically in OPG+/+ mice but its effect was blocked totally in OPG-/- mice, which demonstrated that Osthole inhibited osteoclast formation in an OPG-dependent manner. Since activation of β -catenin signaling promoted the expression of OPG, to determine if Osthole induced OPG expression through β -catenin signaling, the rescue assays were performed. We found that the deletion of the OPG gene did not affect β -catenin expression and the deletion of the β -catenin gene inhibited OPG expression in bone marrow stromal cells, which demonstrated that Osthole stimulated the expression of OPG through activation of β -catenin signaling in bone marrow stromal cells. Taken together, our findings verified that Osthole inhibited osteoclast formation by activation of β -catenin signaling and could be a potential agent to inhibit bone resorption.

Disclosures: De-Zhi Tang, None.

MO0299

Polarized Osteoclasts Put Marks of Tartrate-Resistant Acid Phosphatase on Dentin Slices-A Simple Method for Identifying Polarized Osteoclasts. Nakayama TAKAHIRO*¹, Mizoguchi Toshihide², Uehara Shunsuke², Yamashita Teruhito², Kawahara Ichiro², Kobayashi Yasuhiro², Udagawa Nobuyuki², Takahashi Naoyuki². ¹Matsumoto Dental University, Japan, ²Matsumoto Dental University, Japan

Osteoclasts form ruffled borders and sealing zones toward bone surfaces to resorb bone. Sealing zones are defined as ringed structures of F-actin dots (actin rings). Polarized osteoclasts secrete protons to bone surfaces via vacuolar proton ATPase through ruffled borders. Catabolic enzymes such as tartrate resistant-acid phosphatase (TRAP) and cathepsin K are also secreted to bone surfaces. Here we show a simple method of identifying functional vestiges of polarized osteoclasts. Osteoclasts obtained from cocultures of murine osteoblasts and bone marrow cells were cultured for 48 hr on dentin slices. Cultures were then fixed and stained for TRAP to identify osteoclasts on the slices. Cells were removed from the slices with cotton swabs, and the slices subjected to TRAP and Myer's hematoxylin staining. Small TRAP-positive spots (TRAP-marks) were detected in the resorption pits stained with Myer's hematoxylin. Pitted areas were not always located in the places of osteoclasts, but osteoclasts existed on all TRAP-marks. A time course experiment showed that the number of TRAP-marks was maintained, while the number of resorption pits increased with the culture period. The position of actin rings formed in osteoclasts corresponded to that of TRAP-marks on dentin slices. Immunostaining of dentin slices showed that cathepsin K and vacuolar proton ATPase were colocalized with the TRAP-marks. Treatment of osteoclast cultures with alendronate, a bisphosphonate, suppressed the formation of TRAP-marks and resorption pits. Calcitonin induced the disappearance of both actin rings and TRAP-marks in osteoclast cultures. These results suggest that TRAP-marks are vestiges of polarized osteoclasts.

Disclosures: Nakayama TAKAHIRO, None.

MO0300

Protein Kinase C- δ Regulates Osteoclastic Bone Resorption. Ee Cheng Khor*¹, Tamara Abel², Jennifer Tickner², Taksum Cheng², Keiichi Nakayama³, Keiko Nakayama⁴, Nathan Pavlos², Ming Hao Zheng², Jiaye Xu¹. ¹The University of Western Australia, Australia, ²University of Western Australia, Australia, ³Kyushu University, Japan, ⁴Tohoku University Graduate School of Medicine, Japan

The serine threonine kinase family, Protein Kinase C (PKC), consists of 10 isoforms classed into 3 groups: the classical (Phospholipid, DAG and Ca²⁺ dependent) PKC- α , - β I, - β II and - γ ; novel (Phospholipid and DAG dependent) PKC- δ , - ϵ , - η and - ζ ; and atypical (Phospholipid dependent) PKC- λ /I and - ζ . PKCs are involved in many signalling pathways including cell proliferation, differentiation and apoptosis. Previously, PKC- δ deficient mice displayed a defect in embryonic bone formation due to reduced osteoblast differentiation [1]. Here we have identified PKC- δ as a regulator of osteoclastic bone resorption that is independent of osteoblast activity. We showed that PKC- δ deficient mice were osteopetrotic as evident by increased trabecular bone volume and the presence of residual cartilaginous bars within the trabecular bone, characteristic of osteopetrosis. Osteoclasts from PKC- δ null mice have reduced bone resorption activity. The defective bone resorption is also observed in LPS-induced model of osteolysis in which osteoclasts are accumulated on the bone surface but failed to resorb bone in PKC- δ null mice. As a possible compensating mechanism for defective bone resorption, RANKL-induced osteoclastogenesis *in vitro* was enhanced in PKC- δ null mice. In addition, treatment of Rottlerin, an inhibitor PKC- δ was able to block LPS-induced bone resorption *in vivo*. In short, our data show that PKC- δ regulates osteoclastic bone resorption and thus may be a potential therapeutic target.

1. Noncanonical Wnt Signaling through G Protein-Linked PKC δ Activation Promotes Bone Formation, Developmental Cell. 12:1, 2007.

Disclosures: Ee Cheng Khor, None.

MO0301

Versatile Roles of V-ATPase Accessory Subunit Ac45 in Osteoclast Formation and Function. An Qin¹, Taksum Cheng², Ke Rong Dai³, Ming Hao Zheng⁴, Qing Jiang⁵, Nathan Pavlos², Jiaye Xu². ¹Shanghai Jiao Tong University; The University of Western Australia, Australia, ²The University of Western Australia, Australia, ³Shanghai Jiao Tong University, China, ⁴University of Western Australia, Australia, ⁵Nanjing University, China

Vacuolar-type H⁺-ATPases (V-ATPases) are macromolecular proton pumps that acidify intracellular cargos and deliver protons across the plasma membrane of a variety of specialized cells, including bone-resorbing osteoclasts. Extracellular acidification is crucial for osteoclastic bone resorption, a process that initiates the dissolution of mineralized bone matrix. While the importance of V-ATPases in osteoclastic resorptive function is well-defined, whether V-ATPases facilitate

additional aspects of osteoclast function and/or formation remains largely obscure. Here we report that the V-ATPase accessory subunit Ac45 participates in both osteoclast formation and function. Using a siRNA-based approach, we show that targeted suppression of Ac45 impairs intracellular acidification and endocytosis, both are prerequisite for osteoclastic bone resorptive function *in vitro*. Interestingly, we find that knockdown of Ac45 also attenuates osteoclastogenesis owing to a reduced fusion capacity of osteoclastic precursor cells. Finally, in an effort to gain more detailed insights into the functional role of Ac45 in osteoclasts, we attempted to generate osteoclast-specific Ac45 conditional knockout mice using a Cre-LoxP system. Surprisingly, however, insertion of the neomycin cassette in the Ac45-FloxNeo mice resulted in marked disturbances in CNS development and ensuing embryonic lethality thus precluding functional assessment of Ac45 in osteoclasts and peripheral bone tissues. Based on these unexpected findings we propose that, in addition to its canonical function in V-ATPase-mediated acidification, Ac45 plays versatile roles during osteoclast formation and function.

Disclosures: Ming Hao Zheng, None.
This study received funding from: NH&MRC

MO0302

α -tocotrienol Inhibits Osteoclastic Bone Resorption by Suppressing RANKL Expression and Signaling and Bone Resorbing Activity. Hyunil Ha¹, Jong-Ho Lee², Ha-Neui Kim¹, Jung-Wook Kim³, Zang Hee Lee⁴. ¹Seoul National University, South Korea, ²Department of Cell & Developmental Biology, School of Dentistry, Seoul National University, South Korea, ³Department of Pediatric Dentistry, School of Dentistry, Seoul National University, South Korea, ⁴Seoul National University School of Dentistry, South Korea

α -tocotrienol, osteoclasts, bone resorption, RANKL Vitamin E, an essential nutrient with powerful antioxidant activity, is the mixture of two classes of compounds, tocopherols (TPs) and tocotrienols (TTs). Although TTs exhibit better bone protective activity than α -TP, the underlying mechanism is poorly understood. In this study, we investigated whether α -TT and α -TP can modulate osteoclastic bone resorption. We found that α -TT but not α -TP inhibits osteoclastogenesis in coculture of osteoblasts and bone marrow cells induced by either IL-1 or combined treatment with 1 α ,25(OH)₂ vitamin D₃ and prostaglandin E₂. In accordance with this, only α -TT inhibited receptor activator of NF- κ B ligand (RANKL) expression in osteoblasts. In addition, α -TT but not α -TP inhibited RANKL-induced osteoclast differentiation from precursors by suppression of c-Fos expression, possibly through inhibiting ERK and NF- κ B activation. This anti-osteoclastogenic effect was reversed when c-Fos or an active form of NFATc1, a critical downstream of c-Fos during osteoclastogenesis, was overexpressed. Furthermore, only α -TT reduced bone resorbing activity of mature osteoclasts without affecting their survival. Overall, our results demonstrate that α -TT but not α -TP has anti-bone resorptive properties by inhibiting osteoclast differentiation and activation, suggesting that α -TT may have therapeutic value for treating and preventing bone diseases characterized by excessive bone destruction.

Disclosures: Zang Hee Lee, None.

MO0303

Class IA Phosphatidylinositol 3-kinase Regulates Osteoclastic Bone Resorption. Masahiro Shinohara^{*1}, Sakae Tanaka², Hiroshi Takayanagi³. ¹Tokyo Medical & Dental University, Jpn, ²The University of Tokyo, Japan, ³Tokyo Medical & Dental University, Japan

Osteoclasts are multinucleated giant cells which are able to resorb bone because they are polarized and have specialized machinery to attach to and degrade the mineralized matrix. Differentiation of monocyte/macrophage lineage precursor cells into mature osteoclasts is induced by a TNF family cytokine RANKL in the presences of M-CSF, which provides an activatory as well as survival signal to the osteoclast lineage. Osteoclasts secrete protons and matrix-degrading enzymes such as cathepsin K and MMPs through the ruffled border membrane into this space, enabling the efficient decalcification and degradation of bone matrix. Thus, these specialized structures, the sealing zone and ruffled border, are required for the bone resorbing activity of osteoclasts.

Class IA phosphoinositide 3-kinases (PI3Ks) are activated by growth factor receptors and regulate a wide range of cellular processes. In osteoclasts, they are activated downstream of α v β 3 integrin or c-Fms and thought to be involved in the regulation of osteoclastic bone resorbing activity. However, most of the reports are based on *in vitro* studies using PI3K inhibitors, which inhibit all classes of PI3K, and precise role of class IA PI3K in osteoclasts have not been elucidated. Here, we show that the osteoclast-specific deletion of the p85 genes encoding regulatory subunits of class IA PI3K results in a severe osteopetrotic phenotype caused by a defect in osteoclastic bone resorbing activity. We also showed that although class IA PI3K has an important role in M-CSF-induced activation of Rac and Akt, Akt rather than Rac is essential for class IA PI3K-mediated bone resorption. Electron microscopic analysis revealed that class IA PI3K is required for the formation of the ruffled border and vesicle transport, but not the formation of the sealing zone. This study identifies the role of class IA PI3K-Akt pathway regulates osteoclastic bone resorption by regulating the vesicle transport, and may provide attractive therapeutic strategies

against bone diseases such as rheumatoid arthritis and osteoporosis by targeting osteoclast-specific signaling pathway.

Disclosures: Masahiro Shinohara, None.

MO0304

Osteopontin Signals through Calcium-NFAT in Osteoclasts: A Novel RGD-dependent Pathway Promoting Cell Survival. Natsuko Tanabe^{*1}, Benjamin D. Wheel², Ryan Shugg², Hong H. Chen², Stephen M. Sims², Harvey Goldberg³, S. Jeffrey Dixon². ¹Nihon University School of Dentistry, Japan, ²The University of Western Ontario, Canada, ³University of Western Ontario, Canada

Osteopontin (OPN), an integrin-binding, phosphorylated, extracellular matrix glycoprotein, enhances osteoclast activity; however, its mechanisms of action are elusive. The calcium-dependent transcription factor NFATc1 is essential for osteoclast differentiation. Activation of NFATc1 involves its dephosphorylation by calcineurin and subsequent translocation from the cytoplasm to the nuclei. The purpose of this study was to determine the effects of OPN on NFATc1 activation and survival of osteoclasts. Native OPN (nOPN, post-translationally modified) from rat bones and rat recombinant OPN (rOPN, prokaryotically expressed without post-translational modifications) were purified to homogeneity using FPLC. Osteoclasts were isolated from the long bones of neonatal rabbits and rats, and plated on coverslips – uncoated or coated with nOPN, rOPN or bovine albumin. NFATc1 activation was assessed by immunofluorescence as the percentage of osteoclasts demonstrating nuclear localization of NFATc1. Apoptosis and survival were quantified following 6 and 18 h incubation, respectively. After 3 h, nuclear localization of NFATc1 was significantly enhanced in osteoclasts plated on nOPN or rOPN, but not albumin. Activity of both nOPN and rOPN indicates that post-translational modifications are not essential for causing translocation of NFATc1. In contrast, rOPN had no significant effect of nuclear localization of NF- κ B, indicating specificity. An RGD-containing, integrin-blocking peptide prevented the translocation of NFATc1 induced by rOPN. Moreover, mutant rOPN lacking RGD failed to induce translocation of NFATc1. Thus, activation of NFATc1 is dependent on integrin binding through RGD. Using fluorescence imaging, rOPN was found to increase the proportion of osteoclasts exhibiting transient elevations in cytosolic calcium (oscillations). rOPN also suppressed apoptosis and enhanced the survival of osteoclasts. The intracellular calcium chelator BAPTA abolished calcium oscillations and inhibited the increases in NFATc1 translocation and survival induced by rOPN. Furthermore, a specific, cell-permeable peptide inhibitor of NFAT activation blocked the effects of rOPN on NFATc1 translocation and osteoclast survival. This is the first demonstration that OPN activates NFATc1 and enhances osteoclast survival through a calcium-NFAT-dependent pathway. Increased NFATc1 activity and enhanced osteoclast survival may account for the stimulatory effects of OPN on osteoclast function *in vivo*.

Disclosures: Natsuko Tanabe, None.

MO0305

Poly-ubiquitination of NF- κ B Pathway Mediates Inflammatory Osteolysis. Kannan Karuppaiah, Yousef Abu-Amer^{*}. Washington University in St. Louis School of Medicine, USA

Inflammatory osteolysis is a devastating clinical challenge that undermines skeletal stability. One of the principal causes of inflammatory osteolysis that attends orthopedic implant failure is implant-derived wear debris, in the form of polymethylmethacrylate (PMMA) particles, which activate and recruit macrophages and osteoclasts around and at the implant-host interface. The ensuing bone resorption around the implant leads to loosening and implant failure. Recent work has identified important cellular entities and secreted factors that contribute to inflammatory osteolysis. In previous work, we have shown that PMMA particles contribute to inflammatory osteolysis through stimulation of major pathways in monocytes/macrophages, primarily NF- κ B and MAP kinases. The former pathway requires assembly of large IKK complex encompassing IKK1, IKK2, and IKK γ /NEMO. Interfering with the NF- κ B and MAPK activation pathways, through introduction of inhibitors and decoy molecules, impedes PMMA-induced inflammation and osteolysis in mouse models of experimental calvarial osteolysis and inflammatory arthritis. In this study, we report that PMMA particles activate the upstream transforming growth factor beta activated kinase-1 (TAK1) which is a key regulator of signal transduction cascades leading to activation of NF- κ B and AP-1 factors. More importantly, we found that PMMA particles induce TAK1 binding to NEMO and UBC13. In addition, we show that PMMA particles induce TRAF6 and UBC13 binding to NEMO and that lack of TRAF6 or TAK1 significantly attenuates NEMO ubiquitination. Supporting a key role for this signaling complex as mediator of osteolysis, we identified Lysine 392 residue in NEMO as crucial mediator of PMMA particle-induced inflammatory osteoclastogenesis and osteolysis. Using mice in which NEMO-K392R mutation has been introduced, we provide evidence that PMMA-induced osteoclasts and osteolytic responses are impaired. Furthermore, we show that this impairment is likely due to poor activation of NF- κ B and Erk, but not other MAP kinases. Altogether, our observations suggest that PMMA particles induce ubiquitination of NEMO, an event likely mediated by TRAF6, TAK1 and UBC13. Furthermore, NEMO Lysine392, a well-established K63-linked poly-ubiquitination site, is an important mediator of PMMA-induced osteolysis. Our findings provide

important information for better understanding of the mechanisms underlying PMMA particle-induced inflammatory responses.

Disclosures: Yousef Abu-Amer, None.

MO0306

RANK Regulates the Osteoclast Cytoskeleton in a c-Src/ α v β 3 Dependent Manner. Takashi Izawa^{*1}, Wei Zou², Steven Teitelbaum². ¹Washington University in St. Louis, USA, ²Washington University in St. Louis School of Medicine, USA

Organization of the osteoclast cytoskeleton depends upon RANKL-induced differentiation characterized by expression of the α v β 3 integrin. This integrin, when occupied, activates a canonical signaling pathway which includes c-Src, Syk, Dap12, SLP-76, the guanine nucleotide exchange factor Vav3 and its target the small GTPase, Rac. In addition to its effects on osteoclast differentiation, however, RANKL, by mechanisms unknown, also directly activates the mature polykaryon to resorb bone by organizing its cytoskeleton. Because c-Src is the most proximal known signaling molecule in the integrin-activated pathway we asked if the tyrosine kinase also mediates RANK-stimulated osteoclast activity. We find transfected c-Src and RANK associate in 293T cells and more importantly, endogenous c-Src and RANK co-precipitate in pre-fusion osteoclasts derived from marrow or spleen. This association, which occurs in lipid rafts, is dependent upon the presence of the α v β 3 suggesting a collaborative relationship between the integrin, kinase and cytokine receptor. We next transfected 293T cells with HA-RANK and various c-Src constructs and found the first myristoylation and SH2, but not SH3, domains of the kinase recognize RANK. The same obtains with endogenous RANK in c-Src-/- pre-osteoclasts retrovirally transduced with the same c-Src constructs and stimulated by RANKL. As expected, WT c-Src rescues the cytoskeleton and resorptive capacity of c-Src-/- osteoclasts and the same obtains regarding Δ SH3. In contrast, absence of the first myristoylation (Δ MYR) or Δ SH2 fail to normalize osteoclast spreading or bone degradation. These events are mirrored by RANKL activation of Syk, SLP76, c-Src itself, Vav3, and Rac. Thus, RANKL-mediated stimulation of osteoclast function is mediated by RANK/c-Src binding via the latter's first myristoylation and SH2 domains in an α v β 3 integrin-dependent manner.

Disclosures: Takashi Izawa, None.

This study received funding from: NIH

MO0307

Assessment Of The GPCR Landscape in Osteocytes Reveals Novel Candidate Regulators of Bone Homeostasis. Christine Halleux^{*1}, Frederic Bassilana², Ina Kramer¹, Hansjoerg Keller¹, Frederic Morvan¹, Olivier Leupin¹, Klaus Seuwen¹, Michaela Kneissel¹. ¹Novartis Institutes for Biomedical Research, Switzerland, ²Novartis Institutes for Biomedical Research, Switzerland

Osteocytes emerged in recent years as critical regulators of bone homeostasis. Moreover a rising number of osteocyte endocrine functions are identified such as regulation of mineral homeostasis and putatively lipid and energy metabolism. However the molecular mechanisms underlying these functions are only starting to be revealed. Since G protein coupled receptors (GPCRs) are critical to physiological processes and are targets of about 30% of all medicinal drugs including anti-osteoporotic drugs, we focused here on the elucidation of the GPCR expression profile of these cells. To this end we extracted RNA from GFP+ osteocytes and GFP-osteoblasts from newborn calvaria of *Dmp1-Cre;GFP* mice. Real time PCR was performed using a mouse GPCR array monitoring most (343) non-sensory GPCRs. A number of GPCRs were found to be highly expressed in osteoblasts and -cytes (e.g. *Pthr1*) and 14 were further enriched in osteocytes compared to -blasts. Expression of most was confirmed in RNA extracted from osteocyte enriched human hip cortical bone. Some of the upregulated receptors are associated with bone biology such as cannabinoid receptor 1 (*Cnr1*) or calcitonin receptor-like receptor (*Calcr*). The latter was co-regulated with *Ramp1*, indicating increased expression of functional CGRP receptors in osteocytes. Further examples of receptors, which have been implicated in bone homeostasis or skeletal development are the Wnt signaling mediator frizzled homolog 5 (*Fzd5*), lysophosphatidic acid receptor 1 (*Lpar1*) and endothelin 1 receptor (*Ednra*). Among the orphan GPCRs highly expressed in osteoblasts and further enriched in osteocytes, is *Gpr133*, which has been recently associated with human height. Moreover *Gpr153*, which has not been implicated in bone biology so far, was expressed at comparable levels as *Pthr1*. Immunohistochemistry confirmed protein expression in mouse bone osteocytes. Interestingly, we found this orphan GPCR to be upregulated during osteoblastic differentiation of human mesenchymal stem cells. This translated to the tissue level, as *GPR153* was expressed in human hip cortical bone and immunohistochemistry confirmed protein expression. As we detected no distinct bone mass alterations in the skeleton of *Gpr153* KO mice the role of osteocyte expressed GPR153 remains to be elucidated. In summary the described GPCR expression profile is consistent with critical roles of these cells for bone homeostasis and identifies novel candidate regulators of osteocyte function.

Disclosures: Christine Halleux, None.

MO0308

CSF-1 Deficiency in CSF-1KO Mice Leads to Osteocyte Defects. Sherry Abboud Werner^{*1}, Diane Horn², Kathleen Woodruff², Rekha Kar³, Xiaodu Wang⁴, Jean Jiang¹, Marie Harris¹, Stephen Harris¹. ¹University of Texas Health Science Center at San Antonio, USA, ²University of Texas Health Science Center, USA, ³The University of Texas Health Science Center, USA, ⁴University of Texas at San Antonio, USA

CSF-1, a key determinant of osteoclast-mediated bone remodeling, is expressed in osteoblasts/osteocytes and bone matrix. Osteoblasts differentiate into osteocytes that have dendritic processes that enable cell contact with adjacent osteocytes, osteoblasts and preosteoclasts. We have shown that global CSF-1 deficiency in *Meox2Cre-CSF-1KO* mice decreases osteoclasts and results in an osteopetrotic phenotype. However, little is known regarding the effect of CSF-1 on osteoblasts/osteocytes and bone formation. To address this issue, bones from 3 wk CSF-1KO and WT mice were tested for material properties by nanoindentation. Histologic preparations were stained with H&E, CD31, Tunel and examined under polarized light to assess morphology, vascularity, apoptosis and collagen fibrils, respectively. Undecalcified samples were processed for TEM to visualize osteocytes and mineral. Connexin43(Cx43), the major gap junction/hemichannel forming protein in osteocytes, was examined by Western blot and immunostaining and microarray analysis was performed for osteocyte markers. Compared to WT, CSF-1KO bones showed decreased modulus of elasticity and hardness. Osteoblasts in CSF-1KO were disorganized with loss of polarity and showed early entrapment in matrix. The transition of osteoblasts to form osteocytes was impaired in CSF-1KO and abnormal clusters of osteocytes within lacunar spaces were identified. Vascular sinusoids were compromised with narrow lumens. CSF-1KO cortical bone was thin and showed decreased collagen fibrils that lacked lamellar structure with randomly scattered osteocytes. Little apoptosis was identified in WT bone, whereas increased apoptotic osteocytes were detected in CSF-1KO. Osteocyte loss in CSF-1KO was associated with micropetrosis and by TEM osteocytes showed blunted dendrites and resided in patchy mineralized matrix likely due to decreased E11/GP38 and DMP1 expression. Morphologic defects in CSF-1KO osteocytes correlated with decreased Cx43 and altered gene profile by microarray with 10-fold reduction in *Sost*. These findings suggest that CSF-1 is crucial for osteoblast polarity, directional matrix deposition, formation of osteocytes, matrix mineralization and hydration. Loss of osteocyte dendrite contacts in CSF-1KO mice may exacerbate osteoblast and osteoclast defects. Importantly, our data provide a novel link between CSF-1 and osteocyte survival/function that is essential for maintaining bone mass and strength during skeletal development and aging.

Disclosures: Sherry Abboud Werner, None.

MO0309

Effects of Pioglitazone on Serum Levels of Sclerostin and Bone Turnover Markers in Male Patients with Type 2 Diabetes Mellitus. Antoon Van Lierop^{*1}, Neveen Hamdy¹, Rutger van der Meer², Jacqueline Jonker², Michaela Diamant³, Luuk Rijzewijk³, A de Roos², Johannes Romijn⁴, Jan Smit², Socrates Papapoulos¹. ¹Leiden University Medical Center, The Netherlands, ²Leiden University Medical Center, Netherlands, ³VU University Medical Center, Netherlands, ⁴Amsterdam Medical Center, Netherlands

Introduction

Thiazolidinediones are of proven benefit in the management of patients with type 2 diabetes mellitus (T2DM), but their use has been associated with an increased risk of fractures. This increased fracture risk may be due to activation of the peroxisome proliferator-activated receptor γ (PPAR γ) in mesenchymal stem cells, favouring differentiation into adipocytes rather than into osteoblasts. A recent in vitro study showed that TZDs also stimulate the expression of sclerostin, a negative regulator of bone formation, synthesised by osteocytes, the up-regulation of which could contribute to decreased bone formation and increased fracture risk.

Methods

We measured sclerostin, PINP, and CTX levels in stored samples of 71 male patients with T2DM, collected at baseline and at the end of a 24 weeks double blind randomised controlled study, in which patients received either pioglitazone (PIO) 30 mg once daily, or metformin (MET) 1000mg twice daily. Percentage changes in serum sclerostin, PINP and CTX were compared between the pioglitazone and metformin treated group.

Results

At baseline there was no significant difference in sclerostin levels between patients, randomised to use pioglitazone or metformin (PIO: 58.5 pg/ml, MET: 62.4 pg/ml, $p=0.42$). After 24 weeks of treatment sclerostin levels increased by on average 11% (95%CI:2.3%-19.8%) in PIO-treated patients, and decreased by 1.8% (95%CI:-8.8%-5.0%) in MET-treated patients ($p=0.027$). Intriguingly, serum PINP levels also increased by 3.7% (95%CI:-3.9%-11.3%) in the PIO group, and decreased by 19.1% (95%CI:-25.5%-12.8%) in the MET group ($p<0.001$). CTX increased by 16.8% (95%CI:4.4%-29.1%) in the PIO group, and decreased by 19.0% (95%CI:-27.1%-10.9%) in the MET group ($p<0.001$). Whereas there was no significant relation between changes in serum sclerostin and changes in serum PINP, changes in serum sclerostin did significantly correlated with changes in serum CTX in the whole population studied ($r=0.34$, $p=0.004$), and in the PIO group ($r=0.39$, $p=0.023$), but not in the MET group ($r=0.03$, $p=0.084$).

Conclusion

Our data show a small increase in sclerostin levels after 24 weeks of treatment with pioglitazone. There was however no evident change in PINP levels. The potential contribution of pioglitazone induced increased sclerostin to increased fractures risk remains unclear.

Disclosures: Antoon Van Lierop, None.

MO0310

IL-6 Affects Signaling Molecule Production by Osteocytes Resulting in Inhibition of Osteoblast Differentiation. Astrid D Bakker^{*1}, Rishikesh N Kulkarni¹, Willem F Lems², Jenneke Klein-Nulend¹. ¹ACTA - University of Amsterdam & VU University Amsterdam, Research Institute MOVE, Netherlands, ²VU University Medical Center, Research Institute MOVE, Netherlands

During inflammation TNF α reduces bone mass by stimulating osteoclastic bone resorption and inhibiting osteoblastic bone formation, and by modulating the osteocyte response to mechanical loading. IL-6 produced during inflammation also affects bone mass, but conflicting reports exist regarding its' effect on bone resorption, and whether IL-6 affects the function of osteocytes is unknown. We tested whether IL-6 modulates the production of signaling molecules by osteocytes either or not subjected to mechanical loading, resulting in modulation of osteoblast differentiation or osteoclastogenesis.

MLO-Y4 osteocytes were incubated for 24h with IL-6 (10 pg/ml), sIL-6R (40 ng/ml), or control medium, and subjected to 1h mechanical loading by pulsating fluid flow (PFF; 0.70.3 Pa, 5 Hz). The cellular response was quantified by measuring nitric oxide (NO; Griess) and prostaglandin E2 (PGE2) production (ELISA), and expression of IL-6, TNF α , COX2, Rankl, Opg, and M-CSF (PCR). Osteocyte apoptosis was assessed by Caspase-Glo 3/7 assay. Osteocyte-conditioned medium was added to MC3T3-E1 osteoblasts for 5 days, and ALP activity and expression of Ki67, Runx2, and Osteocalcin were measured as differentiation parameters. Mouse bone marrow cells were cultured for 7 days on TNF α (0.1 ng/ml) or IL-6-treated osteocytes, and multinucleated TRACP+ osteoclasts were counted.

IL-6 increased expression of TNF α (2.2-fold) and IL-6 (3.0-fold) in osteocytes. It enhanced the stimulating effect of PFF on COX-2 expression but did not affect PFF-stimulated NO and PGE2 production. IL-6-treated osteocytes enhanced expression of proliferation marker ki67 (3.8-fold), but reduced Runx2 and Osteocalcin expression and ALP activity by osteoblasts. Interestingly, PFF reversed the negative effect of IL-6-treated osteocytes on Osteocalcin expression by osteoblasts. TNF α , but not IL-6, enhanced osteocyte-stimulated osteoclastogenesis. IL-6 did not affect RANKL or M-CSF expression, but reduced Opg expression and osteocyte apoptosis, resp. stimulating and inhibiting osteoclastogenesis.

In conclusion, IL-6 did not affect signaling molecule production by osteocytes in response to mechanical loading, nor osteocyte-stimulated osteoclastogenesis, which is in sharp contrast to the known actions of TNF α . However, IL-6 triggered osteocytes to produce soluble factors that strongly inhibit osteoblast differentiation, suggesting that IL-6 production during inflammation reduces bone mass by inhibiting bone formation.

Disclosures: Astrid D Bakker, None.

MO0311

Responses of Osteocytes to Microdamage in vitro. Chao Liu^{*1}, Lidan You². ¹University of Toronto, Canada, ²Mechanical & Industrial Engineering, University of Toronto, Canada

Purpose: Physiological loading of the bone creates microdamage, which has been shown to cause damage to osteocytes embedded within the bone [1]. The damaged osteocytes may signal bone remodeling of the damage site. This process may be inflammatory in nature and unlikely to be the same as unloading-induced remodeling, which involves osteocyte apoptosis, since in vivo evidence suggested that mechanical loading is required for the repair of microdamage in bone [2] and inflammatory cytokines such as TNF α were upregulated [3]. We hypothesize that MLO-Y4 cells damaged by physical trauma similar to microdamage would release increased levels of TNF α , and this response can be mechanically regulated.

Methods: MLO-Y4 osteocyte-like cells (gift from Dr. Lynda Bonewald, University of Missouri) were cultured in α -MEM supplemented with 5% FBS, 5% CS, and 1% P/S on type I rat tail collagen-coated glass slides at 37 $^{\circ}$ C and 5% CO₂. An array of 9 equally spaced 20G needles were used to mechanically damage the cells. Apoptosis were induced with serum-starvation. The cells were then incubated at 37 $^{\circ}$ C and 5% CO₂ for 4 time points: 5 minutes, 15 minutes, 30 minutes, and 1 hour. After incubation, total RNA was isolated and Q-PCR was performed to quantify TNF α mRNA level. Student's t-test was used to assess significance ($P < 0.05$).

Results: The TNF α mRNA level in MLO-Y4 cells did not change from baseline values 5 min, 15 min, or 30 min after mechanical damaged. However TNF α mRNA level was reduced by 36% at 1 hr after microdamage. In contrast, serum starvation has reduced TNF α mRNA level in 15 min. (Figure 1.)

Conclusions: This study has shown that mechanical damage to osteocyte decreases TNF α mRNA level, and it is time-dependent. In comparison with mechanical damage induced effects, serum-starved induced apoptotic osteocytes showed an earlier decrease from the cell culture. As opposed to our hypothesis, the decreased TNF α levels suggest that microdamage-initiated remodeling may not be inflammatory in nature. Also, since TNF α suppresses osteogenic differentiation, the decrease in TNF α level may suggest

increased osteogenic differentiation by mesenchymal stem cells. Future work includes investigating how mechanical loading affect osteocyte apoptosis and responses to damage.

References: [1]. Taylor, D., et al., Nat. Mater., 2007. 6(4): p. 263-268. [2]. Waldorff, E.I., et al., J. Bone Miner. Res., 25(4): p. 734-745. [3]. Kidd, L.J., et al., Bone, 2010. 46(2): p. 369-378.

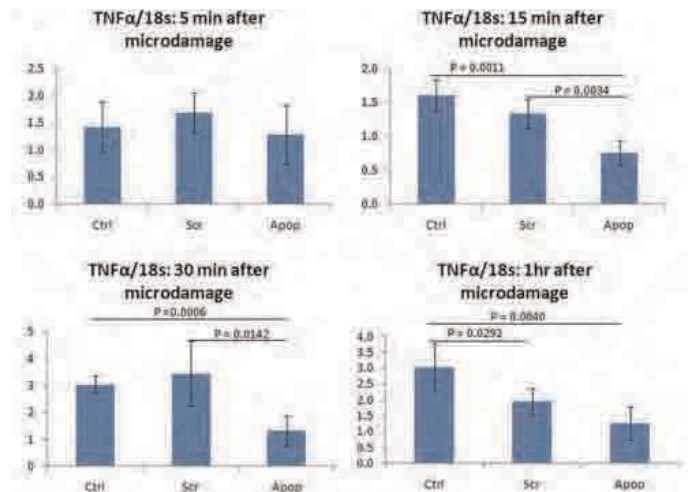


Figure 1. The time-dependent response of TNF α mRNA level after microdamage (n = 6). Non-damaged MLO-Y4 cells were used as control (Ctrl). The mechanical damage has been applied to the cells with an array of 20G needles (Scr). The Ctrl and Scr groups have been compared against cells cultured without serum (Apop), which has been shown to induce apoptosis.

Figure 1

Disclosures: Chao Liu, None.

MO0312

Sclerostin Antibody Enhances Bone Repair in a Rat Femoral Defect Model. Farhang Alaei^{*1}, Amy Tang¹, Michael Ominsky², Hua Zhu Ke³, Marina Stolina⁴, Denise Dwyer⁵, Jay Lieberman¹. ¹University of Connecticut Health Center, USA, ²Amgen, Incorporated, USA, ³Amgen, Inc., USA, ⁴Amgen Inc, USA, ⁵Amgen Inc., USA

Systemic sclerostin-neutralizing monoclonal antibody (Scl Ab) has been shown to increase callus density and strength in murine and primate models. We tested Scl Ab in a 3 mm femoral defect in 12 w/o male Sprague Dawley rats to evaluate its potential in bone healing. There were 5 groups, each containing 15 rats. Scl Ab (25 mg/kg/dose twice weekly, sc) or PBS was injected in the following groups: I: Continuous Scl Ab (Scl Ab for 12 weeks), II: D-Scl Ab (Scl Ab for 10 weeks starting 2 weeks post-op), III: Vehicle 6w (PBS for 6 weeks), IV: Scl Ab 6w (Scl Ab for 6 weeks) and V: Vehicle (PBS for 12 weeks). The rats were sacrificed upon completion of the treatment. Serum bone biomarkers were measured and radiographic, μ -CT and histological analyses were performed. Union was observed in 3/15 in D-Scl Ab, 2/15 in Scl Ab, and 1/15 in Vehicle and Scl Ab 6w groups. Osteocalcin, a bone formation marker, was elevated in response to treatment, but levels of PINP (bone formation) and TRACP 5b (bone resorption) were not significantly different compared to vehicle alone. Radiographic scoring of defect healing from 0 to 5 (Fig1A) and μ -CT-based BV/TV of bone in the defect (Fig 1B) only showed significant increases in D-Scl Ab (Score: 3.07 \pm 0.06, BV/TV: 35.0% \pm 4.7) vs. Vehicle (Score: 2.53 \pm 0.13, BV/TV: 21.1% \pm 2.4, $P < 0.05$). Histomorphometric analysis showed no significant differences in defect BV/TV between the treatment vs. Vehicle at 6 or 12 weeks. μ -CT-based BV/TV of the extra-cortical new bone formed outside the defect (Fig1C) showed significantly increased amounts in both Scl Ab (71.0% \pm 1.4) and D-Scl Ab (73.3% \pm 0.8) compared to the Vehicle (61.9% \pm 1.4) ($P < 0.05$). In the contralateral femurs, Scl Ab and D-Scl Ab showed similar increases in distal femur BV/TV, trabecular thickness, and femoral shaft cortical thickness relative to Vehicle (Table 1). Distal femur BV/TV and trabecular thickness in the operated legs were also increased in treatment vs. Vehicle at 6 and 12 weeks (Table 2) ($P < 0.05$). In conclusion we demonstrated that Scl Ab can enhance new bone formation in a defect model. The more uniform response to Scl Ab outside the defect could reflect the lower number or delayed participation of Scl Ab responsive cells in the defect. In contrast a previous 6 mm defect study in Lewis rats demonstrated that continuous Scl Ab improved both radiographic scores and defect BV/TV. This difference in results may be secondary to the use of different rat strains.

age-related differences in mechanosensitivity, their function in diseases such as osteoporosis, and in genetic disease. This novel methodology should prove useful to advance knowledge regarding the role of mature osteocytes in health and disease.

Disclosures: Amber Stern, None.

MO0314

Ultrastructural Evidence for Continued Synthetic Activity in Osteocytes. Ruairidh, I. Watson¹, Eman Azzam¹, Jenny, S. Gregory¹, Miep Helfrich². ¹Musculoskeletal Programme, School of Medicine & Dentistry, University of Aberdeen, United Kingdom, ²University of Aberdeen, United Kingdom

Osteocytes play an important role in the regulation of mineralisation, bone formation, phosphate metabolism, and overall energy metabolism. To do this, they produce and secrete proteins and signalling factors. Paradoxically, while such activities indicate osteocytes are metabolically active cells, they are generally described as "small, with little cytoplasm and few organelles" and "to contain 70% less cytoplasm than osteoblasts". We asked whether the transition from osteoblast to osteocyte is associated with upregulation of autophagy to recycle organelles no longer required. We used high pressure freezing (HPF) of calvarial bones from newborn mice to prepare tissue for ultrastructural examination and studied expression of the autophagy-related proteins LC3 and p62 by immunohistochemistry (IHC) in demineralised wax-embedded sections of newborn mouse and rabbit bone. Ultrastructural analysis of more than 50 cells showed that osteocytes appeared like osteoblasts with abundant rough endoplasmic reticulum (RER), mitochondria and cytoplasm. Cellular features were then measured in randomly selected osteocytes and osteoblasts (n=10 for each) and revealed no statistically significant differences between cell types in cytoplasmic area, area occupied by RER and numbers of mitochondria. Power calculations showed that a minimum of 150 cells would be required to have a chance of detecting a difference for cytoplasmic area or RER and more than 3000 cells to detect a difference in mitochondria. Osteocytes did contain significantly more autophagosomes than osteoblasts (4 vs 2 per cross section; p<0.006), but the variation between individual osteocytes was large (2-11 per cross section) and we are currently repeating this analysis with more cells and multiple layers per cell. IHC showed strong staining for LC3 and p62 in osteoclast and hypertrophic chondrocytes. Staining was also present in osteoblasts, not detected in transition cells and only in individual osteocytes, in keeping with the large variation seen in the autophagosome count in the ultrastructural analysis. In conclusion, osteocytes in calvarial bone in young animals maintain extensive synthetic capacity and the transition from osteoblast to osteocyte is not associated with systematic induction of autophagy. We suggest that osteocyte ultrastructure, including in cortical bone in adult animals, is re-examined in HPF bone and results interpreted alongside the newly discovered information on osteocyte function.

Disclosures: Miep Helfrich, None.

MO0315

Histochemical Examination on the Distribution of DMP-1, MGP and Osteocalcin in *Klotho*^{-/-} Mice. Muneteru Sasaki¹, Chihiro Tabata¹, Tomoka Hasegawa¹, Minqi Li¹, Tsuneyuki Yamamoto¹, Nobuo Inoue¹, Norio Amizuka². ¹Hokkaido University, Japan, ²Hokkaido University School of Dentistry, Japan

[Introduction]

It is likely that osteocytes and their canaliculi, i.e., osteocytic lacunar canalicular system (OLCS) would play a pivotal role in regulating minerals such as calcium and phosphates in bone. However, *klotho* deficiency has been reported to cause hyperphosphatemia and hypercalcemia, due to disrupted function of kidney. Therefore, it seems of importance to examine the osteocytic functions in the abnormal state of hyperphosphatemia in *klotho*^{-/-} mice. In this study, we have examined the distribution of OLCS and synthesis of dentin matrix protein 1 (DMP1), osteocalcin and matrix gla protein (MGP).

[Materials and Methods]

Six 5 weeks-old *klotho*-deficient male mice and the age-matched wild-type littermates were fixed with paraformaldehyde, and their tibiae were extracted for histochemical and ultrastructural examination. Von Kossa's staining, immunohistochemistry for DMP-1, MGP and osteocalcin, which have an affinity of calcium, and double staining of ALP and TRAP were performed on the tibial paraffin sections of both mice. We employed immuno-gold technique to localize DMP-1 onto the wild-type and *klotho*^{-/-} bone under transmission electron microscope.

[Result and Discussion]

Wild-type mice showed the regularly-arranged OLCS, while the OLCS of *klotho*^{-/-} mice were disorganized. Wild-type metaphyseal trabeculae revealed even mineralization in bone, whereas *klotho*^{-/-} metaphysis demonstrated the unmineralized patchy area despite many ALP-positive osteoblasts covering the bone surface. MGP, which has been reported to inhibit mineralization, was localized at the boundary of cartilage core and surrounding bone matrix of metaphyseal mixed spicules, although the wild-type metaphysis hardly showed immunoreactivity for MGP. Abundant DMP-1 was associated with *klotho*^{-/-} osteocytes, compared with that in the wild-type specimens. Osteocalcin were found in some osteocytic lacunae and cement lines in bone, while the wild-type bone displayed osteocalcin mainly at the bone surface and cement lines.

Figure 1. A) Radiographic score in the gap defect. Data expressed as mean \pm SE (n=15/group). *P<0.05 vs. Vehicle and Sci Ab groups. B) μ -CT-based BV/TV in the gap defect. Data expressed as mean \pm SE (n=15/group). *P<0.05 vs. Vehicle. C) μ -CT-based BV/TV outside the defect showing significantly increased BV and BV/TV outside the defect area between the most proximal and the most distal pins in treatment groups compared to Vehicle group at 12 weeks. Data expressed as mean \pm SE (n is variable). *P<0.05 vs. Vehicle.

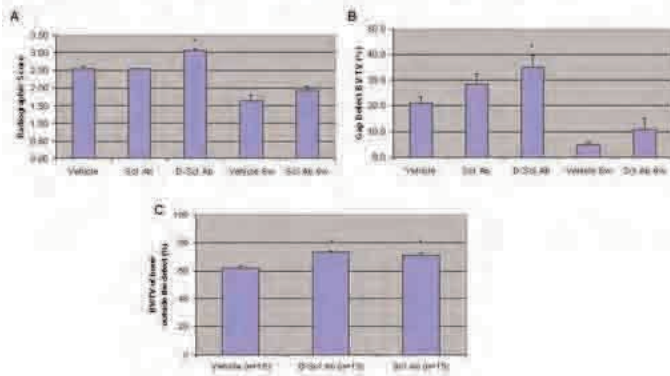


Figure 1

Group	Distal Femur Tb. BV/TV (%)	Distal Femur Tb. Thickness (μm)	Femur Shaft Ct. Thickness (mm)
Vehicle	13.9 \pm 1.7	87 \pm 6	0.80 \pm 0.02
Sci Ab	34.2 \pm 4.4*	135 \pm 9*	0.97 \pm 0.03*
D-Sci Ab	35.9 \pm 2.7*	161 \pm 6*	0.94 \pm 0.01*

Table 1: μ -CT-based analysis of the contralateral femur showing significantly increased distal Tb. BV/TV and thickness as well as mid-shaft cortical thickness in treatment groups compared to Vehicle group at 12 weeks. Data expressed as mean \pm SE (n=5/group). *P<0.05 vs. Vehicle

Table 1

Group	Distal Operated Femur Tb. BV/TV (%)	Distal Operated Femur Tb. Thickness (μm)
Vehicle (n=13)	10.8 \pm 0.9	91.4 \pm 2.4
Sci Ab (n=13)	25.5 \pm 2.1*	153.3 \pm 4.5*
D-Sci Ab (n=12)	23.9 \pm 2.1*	153.4 \pm 4.5*
Vehicle 6w (n=15)	8.8 \pm 1.1	86.5 \pm 4.9
Sci Ab 6w (n=12)	16.4 \pm 2.3†	119.8 \pm 5.2†

Table 2: μ -CT-based analysis of the distal operated femur showing significantly increased Tb. BV/TV and thickness in treatment groups compared to Vehicle groups at 6 and 12 weeks. Data expressed as mean \pm SE (n is variable). *P<0.05 vs. Vehicle †P<0.05 vs. Vehicle 6w

Table 2

Disclosures: Farhang Alaei, None.

This study received funding from: Amgen, Inc. & UCB

MO0313

The Isolation and Culture of Primary Osteocytes from the Long Bones of Skeletally Mature and Aged Mice. Amber Stern¹, Matthew Stern², Mark Van Dyke³, Lynda Bonewald¹. ¹University of Missouri - Kansas City, USA, ²University of Missouri-Kansas City, USA, ³Wake Forest University, USA

Isolation and retrieval of osteocytes from mature, highly mineralized bone matrix has been difficult to achieve, unlike isolation from immature, hypomineralized bone such as chick calvaria or post-natal mice. Therefore, even though osteocytes are the most abundant cell type within adult bone, little is known about their function. While their location makes them ideally situated to sense bone strain, it also makes their observation and study in vivo difficult. The purpose of the work presented here was to adapt previously published osteocyte isolation techniques using immature bone to enable the study of primary osteocytes procured from skeletally mature young (4-month-old) and old (24-month-old) mice. Osteocytes were isolated from the long bones of the mice through a process of extended enzymatic digestions using collagenase (300 units/mL) followed by decalcification using 5 mM EDTA solution. The bone chips were subjected to a total of nine digestions. Following the final digestion, a tissue homogenizer was employed to reduce the remaining bone chips to a suspension of bone particles that were cultured resulting in an outgrowth of osteocyte-like cells. All of the isolated cells in the final digestion that displayed an osteocyte-like morphology (essentially 100%) also stained positive for E11/gp38, confirming the osteocyte phenotype which was further confirmed by negative staining for alkaline phosphatase. In line with previously reported data, the percentage of osteocyte-like cells increased, while the percentage of fibroblast and osteoblast-like cells decreased with each serial digestion. We are currently in the process of characterizing the secondary outgrowths of the bone particles. This technique resulted in an improved osteocyte yield over previously reported methodologies as well as facilitated the study of osteocytes procured from skeletally mature young (4-month-old) and old (24-month-old) mice. With the additional capability of isolating and culturing osteocytes from young and old mice, it is now possible to directly compare osteocytes obtained from not only immature, but also young adult and aged adult bone with regards to

Thus, an excessive amount of DMP-1 and abundant osteocalcin were accumulated in osteocytic lacunae of *klotho*^{-/-} mice. Taken together, the excessive amount of osteocyte-producing molecules appears to inhibit mineralization rather than to induce proper mineralization in *klotho*^{-/-} bone.

Disclosures: Muneteru Sasaki, None.

MO0316

1,25(OH)₂D and PTH Up-regulate *Rankl* while Down-regulate *Phex* and *Dmp1* in Primary Osteocytes Isolated from Mouse Bones. Kazuaki Miyagawa^{*1}, Keiichi Ozono², Kanako Tachikawa¹, Masanobu Kawai¹, Yuko Mikuni-Takagaki³, Mikihiro Kogo⁴, Toshimi Michigami¹. ¹Department of Bone & Mineral Research, Osaka Medical Center & Research Institute for Maternal & Child Health, Japan, ²Osaka University Graduate School of Medicine, Japan, ³Kanagawa Dental College & Graduate School of Dentistry, Japan, ⁴Osaka University Graduate School of Dentistry, Japan

Osteocytes are the terminally differentiated cells of the osteoblastic lineage. In addition to their roles in the control of bone mass, those in phosphate metabolism are now getting attention. Among the molecules responsible for hereditary hypophosphatemic rickets, FGF23, PHEX and DMP1 are expressed in osteocytes. However, the regulatory mechanisms for the expression of these molecules remain still unclear, partly due to the lack of appropriate cell models. Therefore, in the current study, we utilized primary osteocytes isolated from mouse bones to address this issue. Mouse long bones were minced and subjected to sequential digestion with collagenase and decalcification with EGTA for fractionation of osteoblasts and osteocytes. Since strong expression of *Dmp1* and *Sost* was detected in fractions 6-9 among the isolated 9 fractions, we considered them as osteocyte-rich fractions. To verify that the isolated osteocytes retain the gene expression *in vivo*, we compared the gene expression in the cells isolated from wild-type mouse and *Hyp* mouse, a homologue of human X-linked hypophosphatemic rickets (XLH), with a 3' deletion in the *Phex* gene. The expression of *Sost* in isolated osteocytes was comparable between the genotypes, while that of *Fgf23* and *Dmp1* was elevated in *Hyp*-derived osteocytes. These results were consistent with those in immunohistochemistry, confirming that the isolated osteocytes kept the gene expression *in vivo*. Next, we investigated the effects of 1,25(OH)₂D and PTH on gene expression in isolated osteocytes. The primary osteocytes isolated from wild-type mice were embedded in type I collagen matrix, and cultured in the presence or absence of 10⁻⁸ M 1,25(OH)₂D or 10⁻⁶ M PTH for 48 hours before RNA was extracted for analyses. The expression of *Sost* was retained after 48-hr culture, confirming the osteocytic phenotype of the cells. Treatment with 1,25(OH)₂D markedly increased the expression of receptor activator of NF-κB ligand (*Rankl*). On the other hand, the expression of *Phex* and *Dmp1* was reduced by treatment with 1,25(OH)₂D. PTH also increased the expression of *Rankl*, while decreased that of *Phex* and *Dmp1*. These results provide the evidence that 1,25(OH)₂D and PTH exert their effects directly on osteocytes to regulate genes involved in bone homeostasis and phosphate metabolism.

Disclosures: Kazuaki Miyagawa, None.

MO0317

Characteristics of Osteocyte Lacunae in Patients with Renal Hyperparathyroidism. Aiji Yajima^{*1}, Shigeru Satoh², Yoshihiro Tominaga³, Shigeru Otsubo⁴, Masaaki Inaba⁵, Kosaku Nitta⁶, Akemi Ito⁷. ¹Towa Hospital, Japan, ²Division of Renal Replacement Therapeutic Science, Akita University School of Medicine, Japan, ³Department of Transplant Surgery, Nagoya Second Red Cross Hospital, Japan, ⁴Department of Nephrology, Sangenjaya Hospital, Japan, ⁵Department of Internal Medicine, Metabolism, Endocrinology & Molecular Medicine, Osaka City University Graduate School of Medicine, Japan, ⁶Department of Medicine, Kidney Center, Tokyo Women's Medical University, Japan, ⁷Ito Bone Histomorphometry Institute, Japan

The type 1 parathyroid hormone (PTH)/PTH related peptide (PTHrP) receptor (PTHrP) in osteocyte plays an important role in mobilizing calcium (Ca) by the osteocytes in lactating mice as there is a high Ca demand and PTHrP levels are elevated in these mice (Hai Q, et al. JBMR Suppl 2010). In addition, a great deal of mineralization was observed around the lacunar wall through the osteocyte-canalicular system after parathyroidectomy (PTX) for renal hyperparathyroidism (Yajima A, et al. JBMR 2010). As a result, osteocytic osteolysis and bone mineralization by the osteocytes were demonstrated in these reports. Therefore, we observed the shape of osteocyte lacunar walls to investigate the osteocyte function in renal patients with high PTH before PTX. Transiliac bone biopsy specimens were obtained from 45 hemodialysis (HD) patients (age; 57.0 ± 8.6 yrs, duration of HD; 14.8 ± 7.3 yrs) and 19 subjects without renal insufficiency (age; 59.0 ± 11.9 yrs). We regarded the eroded surface-predominant lacunae (ES.Lc) as the resorption lacunae of the patients. In addition, the osteoid surface-predominant lacunae (OS.Lc) was thought to be the formative lacunae and the quiescent surface-predominant lacunae (QS.Lc) was thought to be the lacunae without both any active bone resorption and formation. We calculated the number of ES.Lc per bone volume (BV) (N.ES.Lc/BV), the number

of OS.Lc per BV (N.OS.Lc/BV), and the number of QS.Lc per BV (N.QS.Lc/BV) in these 2 groups. In HD patients with high PTH, N.ES.Lc/BV was greater than N.OS.Lc/BV (272.3 ± 91.4 vs 10.3 ± 18.0 N/mm² (P < 0.001)) and N.ES.Lc/BV was greater in HD patients than normal controls (272.3 ± 91.4 vs 23.5 ± 12.5 N/mm² (P < 0.001)). In addition, total lacunar volume of each type of lacunae was calculated. The volume of ES.Lc per BV (ES.Lc.V/BV), the volume of OS.Lc per BV (OS.Lc.V/BV) and the volume of QS.Lc per BV (QS.Lc.V/BV) was 1.17 ± 0.38, 0.49 ± 1.02 and 0.44 ± 0.11 %, respectively, in patients with high PTH. ES.Lc.V/BV was greater than both OS.Lc.V/BV (P < 0.001) and QS.Lc.V/BV (P < 0.001) significantly. In addition, ES.Lc.V/BV was greater in HD patients with high PTH than normal controls (1.17 ± 0.38 vs 0.13 ± 0.09 %, P < 0.001). These data suggest that an increase of serum Ca level and the reduction of bone mass are caused by an increase of osteocytic osteolysis and a decrease of bone formation by the osteocytes as well as osteoclastic resorption in patients with renal hyperparathyroidism.

Disclosures: Aiji Yajima, Chugai, 5

MO0318

Menopause-related Changes in Osteocyte Lacunar Density, Volume, and Separation in Adult Human Trabecular Bone. Mohammed Akhter^{*1}, Robert Recker¹, Tiffany Fong², Donald Kimmel³. ¹Creighton University Osteoporosis Research Center, USA, ²Xradia, Inc., USA, ³Kimmel Consulting Services, USA

Synchrotron radiation (SR) microscopy (0.7μm pixel resolution [PR]) facilitates 3D imaging of whole Ot lacunae (Ot.La). The smallness of Ot.La creates difficulty for current laboratory-based 3D imaging devices to resolve them and study their properties in sizable samples of intact bone. Though osteocytes (Ot) alter their lacunar volume in response to pharmacologic/mechanical stimuli, less is known about lacunar density and separation. We report the effect of estrogen status on Ot.La volume (Ot.LaV), density (Ot.LaD), and separation (Ot.LaSp) in human trabecular and cortical bone, using measurements taken on 3-D images obtained with a laboratory instrument that achieves SR-like resolution.

Biopsy specimens were taken from opposite ilia of a healthy woman before (PRE) and at one year after (POST) her last menses, then embedded undecalcified in plastic. Activation frequency was 7X higher POST-menopause. A portion of each specimen that remained after thin-sectioning was trimmed to 2X2X8mm and scanned at 5μm PR with a laboratory-based 3D XRay microscope (MicroXCT-200). Twelve trabecular or cortical bone sub-volumes of interest (sub-VOIs; 1.3mm diameter X 0.7mm long; 6 PRE/6 POST) were selected and scanned at ~0.97μm PR. Ten additional trabecular bone sub-VOIs (0.9mm diameter X 0.5mm long; 4 PRE/6 POST) were scanned at ~0.6μm PR. Ot.La were defined as bone tissue voids >50 and <500μm³. The 3D image from each ~0.97μm PR VOI was analyzed by Ratoc Segmentation Software (RSS; Tokyo, JP) for Ot.LaD and Ot.LaV. BaryCenter (centroid) was determined by RSS for each Ot.La in all 0.6μm PR sub-VOIs. The distance of each lacuna to its nearest neighbor was calculated (Ot.LaSp). Each 0.6μm PR sub-VOI was also analyzed for Ot.LaV.

Regions with a total of >50,000 Ot.La were studied. Data are shown in the table. Study of these and other transmenopausal pairs continues.

Our data indicate that Ot.LaD decreases with menopause in trabecular bone, but not cortical bone. The data also suggest that Ot.LaV decreases with menopause in both types of bone. Ot.LaSp, the mean distance from one lacuna to the next nearest one, is ~27.51.3μm. Bone tissue with smaller, less numerous Ot.La could have reduced ability to intercept propagating microcracks. These properties may be bone qualities that change, increasing bone fragility in a way not detected by current measurements. These findings parallel data showing reduced Ot.LaV and Ot.LaD in trabecular bone of estrogen-deficient rats.

Variable	Region	PR (μm)	Units	PRE	POST
Ot.LaV	T	~0.97	μm ³	183±10	156±14*
Ot.LaV	C	~0.97	μm ³	186±9	165±3*
Ot.LaD	T	~0.97	mm ⁻³	13063±1583	10033±2187*
Ot.LaD	C	~0.97	mm ⁻³	14464±445	15069±127
Ot.LaV	T	~0.6	μm ³	171±121	156±108*
Ot.LaSp	T	~0.6	μm	26.7±0.8	29.0±1.8*

Mean±SD; T-trabecular; C-Cortical; PR- Pixel Resolution; diff from PRE-menopause (*P<.02; *P<.01)

Table

Disclosures: Mohammed Akhter, Xradia, Inc., 5
This study received funding from: Xradia, Inc

MO0319

Skeletal Unloading Changes Phosphate (Pi) Homeostasis. Rong Zhang^{*1}, X Han², Baozhi Yuan³, Marc Drezner⁴, Lynda Bonewald⁵, Jian Feng⁶.
¹School of Stomatology, Fourth Military Medical University, Peoples Republic of China, ²Baylor College of Dentistry, USA, ³University of Wisconsin, Madison, USA, ⁴University of Wisconsin, USA, ⁵University of Missouri - Kansas City, USA, ⁶Texas A&M Health Science Center, USA

Osteocytes are mechanosensors that also act as endocrine cells to regulate Pi homeostasis through FGF23 production. Deletion of dentin matrix protein1 (DMP1) in mice or DMP1 mutations in humans leads to elevated FGF23 and hypophosphatemic rickets. To test the hypothesis that the bone malformations in this disease model of osteomalacia would be corrected in unloaded bones, both wild-type and Dmp-1 null mice were tail suspended for 30 days. In Dmp1 null mice, a dramatic improvement of osteomalacia in not only the unloaded hindlimb occurred as expected but also an improvement in morphology of the loaded forelimb was observed as determined by x-ray uCT, fluorochrome labeling, and histology. A partial improvement of protein expression, such as SOST, PHEX and FGF23 as determined by immunohistochemistry, was also observed along with increased osteoclast number. In the wild-type control mice, tail suspension also led to a significant increase of serum Pi (from 8.610.63 to 11.971.217mg/dl), and bone loss not only in the unloaded hindlimb, but also in the loaded forelimb. Bone marrow cells isolated from the loaded forelimbs and the unloaded hindlimbs had a significant increase in RANKL expression and RANKL/OPG ratio as determined by RT-PCR. Finally, healthy human subjects subjected to head down tilted bed rest (n=6) showed a significant increase in serum Pi (from 3.310.25 to 4.037mg/dl), but not calcium after 30 day period. Our data shows that chronic unloading results in an increase in serum Pi in addition to bone loss due to unloading. In Dmp1 null animals, this increased serum Pi (from 5.320.25 to 6.990.517mg/dl) is beneficial. This study has clinical relevance with regards to treatment of immobilized, chronically ill patients and astronauts.

Disclosures: Rong Zhang, None.

MO0320

A New Sandwich ELISA of Mouse Periostin for in-vitro and in-vivo Animal Studies. Jean-Charles Rousseau^{*1}, Marjorie Thomas², Blandine Merle¹, Cindy Bertholon¹, Olivier Borel¹, Evelyne Gineyts¹, Patrick Garnero³.
¹INSERM UMR 1033, Université de Lyon, France, ²INSERM UMR 1033, Université de Lyon, France, ³INSERM UMR 1033, Université de Lyon & Cisbio Bioassays, France

Purpose: Periostin (POSTN) is an adhesion Gla-containing protein mainly expressed in the periosteum that plays an important role in regulating bone formation. The measurement of POSTN may be useful as a biological marker of periosteal surface activity. The aim of this study was to develop a sensitive and specific ELISA for mouse POSTN and measure its concentration in the serum and in the supernatants of periosteal cell culture.

Methods: We developed a sandwich ELISA using a goat antibody directed against recombinant mouse POSTN and a rabbit polyclonal antibody raised against a synthetic peptide of 22 amino acids located in the C-terminal part of POSTN which is common to all POSTN isoforms. The ELISA was calibrated using mouse recombinant POSTN. POSTN was measured with this new ELISA in the serum of 37 Balb/c mice and in the culture medium of periosteal cells isolated from long bones of mice (C57BL/6) aged of 4 weeks.

Results: Western blot analyses show that the two antibodies recognized in mouse serum a POSTN immunoreactive form co-migrating with recombinant POSTN. The intra and inter-assay precisions of the ELISA for both serum and culture supernatant was below 6 and 12%, the mean dilution recovery was 105% and the mean spiking test was 99%, allowing accurate measurements of POSTN from 1 (detection limit) to 50 ng/ml. Serum POSTN was stable for up to 5 of thaw/freezing cycles and at least 2 hours at room temperature. In mice, serum POSTN levels ranged from 5.9 to 14.7 ng/ml (mean: 9.1 +/- 2.04 ng/ml). For the measurement of POSTN in cell culture supernatant, the protocol was modified to increase the sensitivity of the ELISA. As expected we found that the concentration of POSTN decreased with advancing stage of periosteal cell differentiation, in agreement with the qPCR data.

Conclusions: The new ELISA for mouse POSTN is specific, sensitive and reproducible. It should be useful for the investigation of periosteal metabolism in in-vitro and in-vivo animal models of osteoporosis and other metabolic bone diseases, including bone metastases.

Disclosures: Jean-Charles Rousseau, None.

MO0321

Correlations of Urinary ⁴¹Ca with Biomarkers and Minerals in Post-Menopausal Women. George Jackson^{*}, WangHee Lee, Berdine Martin, Connie Weaver, Purdue University, USA

Urinary ⁴¹Ca measurement, expressed as the ratio of ⁴¹Ca to normal calcium (⁴¹Ca:Ca), has been used to follow the long-term changes in bone metabolism due to its significantly long half-life (T_{1/2} = 10⁵ years). We correlated the ⁴¹Ca:Ca ratio with traditional markers of bone metabolism and minerals in both the serum and urine. In particular, we looked for correlations with osteocalcin (ng/ml), bone alkaline phosphatase (ng/ml), parathyroid hormone (pg/ml), 25-hydroxy vitamin-D (ng/ml), serum alkaline phosphatase (U/L), fasting N-terminal telopeptide (nM BCE/mM Cr), fasting deoxy-pyridinoline (nM/mM Cr), fasting calcium (mg/dL), fasting creatinine (mg/dL), and fasting phosphate (mg/dL). Thirty subjects that received similar doses of ⁴¹Ca (50 or 100 nCi) were used for correlation analysis. We used data from two studies where estradiol, alendronate, and other interventions showed statistically significant effects on the measured ratio increasing the likelihood of detecting meaningful correlations. ⁴¹Ca was assayed at a different frequency than the biomarkers or minerals, but we only correlated data that was collected on the same day. Since ⁴¹Ca can be detected for many years after dose and the ratio is decreasing as the tracer is excreted from the body, care needs to be taken in how the correlations are performed. Because timing of both ⁴¹Ca dose and urinary measurement contribute to large variations, we compensated for these effects by fitting the ⁴¹Ca data with two different models (compartmental and a mathematical fit) and used the residues for correlations. However, these methods did not compensate for variation caused by the carry over effect of some treatments and individual differences. Thus, we statistically considered the subjects to offset variations among subjects and correlated the difference in consecutive biomarkers with the difference in consecutive ratios. The difference in consecutive osteocalcin (ng/ml) and NTx/Cr (nM BCE/mM Cr) concentrations were positively correlated with the consecutive differences in ratio (p values of 0.0091 and 0.0118 respectively) with all other biomarkers and minerals not being significantly correlated with ⁴¹Ca.

Disclosures: George Jackson, None.

MO0322

Effectiveness of Urinary Gamma-Glutamyltransferase as Screening for Osteoporosis. Shinya Tanaka^{*1}, Sawako Moriwaki², Kazuhiro Uenishi³, Nobuo Koinuma⁴, Kiyoshi Tanaka⁵, Yoshitaka Ikeda⁶, Shumpei Niida⁷.
¹Saitama Medical University, Japan, ²Laboratory of Genomics & Proteomics, National, Japan, ³Laboratory of Physiological Nutrition, Kagawa Nutrition University, Japan, ⁴Department of Health Administration & Policy, Tohoku University Graduate School of Medicine, Japan, ⁵Department of Food & Nutrition, Kyoto Women's University, Japan, ⁶Department of Biomolecular Sciences, Faculty of Medicine, Saga University, Japan, ⁷National Center for Geriatrics & Gerontology, Japan

[Background and Aims] To undergo the osteoporosis test is effective to prevent osteoporotic fractures. In Japan, a public osteoporosis screening program has been executed to alert individuals having osteoporosis risk. However, cost of this program puts pressure on local government finance. We have previously developed a low-cost test for osteoporosis using urinary concentration of gamma-glutamyltransferase (u-GGT) which is a potent index of bone absorption. Thus, to assess the effectiveness of this new screening test for osteoporosis, we performed group examinations and analyzed the relative operating characteristic (ROC), specificity, sensitivity, and accuracy. [Materials and Methods] 1. Four-hundred one women, from 40 to 78 y-o, living in Higashiura town or Obu city, Aichi, Japan were included. The correlations between u-GGT and urinary concentration of deoxypyridinoline (u-DPD) were statistically analyzed about respective region and total regions. 2. ROC analysis was performed with use of the bone mineral density (BMD) at lumbar spine (L2-4) made on the subjects less than 70% of the young adult mean (YAM) (17 osteoporosis women) and 111 non-osteoporosis women. [Results] The correlations between u-GGT and u-DPD were 0.2833 in Higashiura (p=0.0000), 0.0211 in Obu (p=0.8297), and 0.1336 in total (p=0.0184). Weak correlation was seen in the Higashiura data. From ROC analysis, 46IU/gCr was given as a desirable cutoff point for diagnosis of osteoporosis were 100% in Higashiura, 80.0% in Obu, and 82.35% in total. Specificities of 46IU/gCr were 57.45%, 59.38%, and 58.56% respectively. Accuracies were 44.90%, 48.10%, and 46.88% respectively. 46IU/gCr had high sensitivity for osteoporosis diagnosis. [Conclusion] We confirmed that 46IU/gCr was affordable to screen osteoporosis in group examinations.

Disclosures: Shinya Tanaka, None.

MO0323

Magnesium and Osteoporosis: A Clinical Profile of Hypomagnesaemic Patients Attending a Bone Health Clinic. James Mahon^{*1}, Joseph McAndrew², Lorraine O' Keeffe², James Walsh³, Miriam Casey². ¹St James's Hospital, Ireland, ²St. James's Hospital, Ireland, ³Trinity College Dublin, The University of Dublin, Ireland

Introduction: Magnesium deficiency is associated with a number of clinical disorders including osteoporosis. Animal studies have shown magnesium deficiency leads to increased cytokine production and osteoclastic bone resorption (1). Magnesium disorders can also cause hypocalcaemia (2). St. James's Hospital Dublin Osteoporosis and Bone Health Clinic, a tertiary referral centre, has been in operation since 2004. It has compiled a database of 3,600 patients. As part of initial assessment, magnesium levels have been measured since 2008.

Methods: We interrogated our database from Jan 2008 to Dec 2010 to identify patients who had serum magnesium (Mg) levels measured at presentation. We created clinical profiles to include age, sex, T-scores, prior history of fracture, bisphosphonate use, as well as serum markers 25-OH vitamin D, parathyroid hormone (PTH), calcium (Ca), osteocalcin, Procollagen type 1 N-terminal propeptide (PINP) and CTX-telopeptide (CTX). We further compared hypomagnesaemic to normomagnesaemic patients.

Results: We identified 487 patients (83 male, 404 female) for whom Mg was measured. Descriptive statistical means were generated: Age 64 years (SD 14.3); T-score hip -1.5 (SD 1.2), T-score spine -1.8 (SD 1.6); Mg 0.85 mmol/L (SD 0.09); Ca 2.22 mmol/L (SD 0.12); 25-OH vitamin D 56 nmol/L (SD 27), PTH 43 pg/mL (SD 27), osteocalcin 23.6 ng/mL (SD 15.3); PINP 50.0 ng/mL (SD 35.1); CTX 0.33 ng/mL (SD 0.2). 66% had prior history of fracture, and 28% were taking bisphosphonates. 18 patients (4% of total group) were hypomagnesaemic (Mg <0.70 mmol/L). Analysis of this subgroup showed mean T-score hip -2.0 (SD 0.8), T-score spine -1.8 (SD 1.3), and a 71% prevalence of prior fractures. We did not find strong coefficients of correlation between Mg and other parameters.

Conclusions: In this elderly population, we found a low prevalence of hypomagnesaemia. While we did find increased presence of hip fractures and lower T-scores in the hypomagnesaemic subgroup, the absolute number of hypomagnesaemic patients was too small to attribute statistical significance. Continuing collection of these data will further characterise hypomagnesaemia in the context of osteoporosis, and help determine appropriate intervention in the treatment of an elderly, osteoporotic population.

References:

¹ Skeletal and hormonal effects of magnesium deficiency (J Am Coll Nutr. 2009 Apr;28(2):131-41)

² Magnesium metabolism and its disorders (Clin Biochem Rev. 2003 May;24(2):47-66)

Disclosures: James Mahon, None.

MO0324

Serum Osteocalcin and Undercarboxylated Osteocalcin Levels Are Associated with Renal Function and Vascular Complications in Type 2 Diabetes. Atsushi Suzuki^{*1}, Junnichi Ishii², Sahoko Sekiguchi-Ueda¹, Megumi Shibata³, Yasumasa Yoshino¹, Shogo Asano⁴, Fumihiko Kitagawa², Toshiaki Sakuishi², Takashi Fujita², Takashi Ishikawa², Masaki Makino¹, Nobuki Hayakawa¹, Mitsuyasu Itoh¹. ¹Fujita Health University Division of Endocrinology, Japan, ²Department of Joint Research Laboratory of Clinical Medicine Fujita Health University, Japan, ³Fujita Health University, Division of Endocrinology, Japan, ⁴Toyokawa City Hospital, Japan

Diabetes and osteoporosis are both aging-related disease, and recent findings showed that glucose intolerance is closely associated with bone metabolism. Among bone turn over markers, osteocalcin (OC) and its inactive form, undercarboxylated osteocalcin (uOC) have been reported to affect insulin secretion and sensitivity. At the same time, both OC and uOC levels are affected by renal function, which is often damaged in diabetes patients. In the present study, we evaluated OC and uOC levels in type 2 diabetes patients, and their association with clinical complications with diabetes.

We enrolled 351 type 2 diabetes outpatients (M/F=211/140; Mean age, 65.311.5 years). Mean serum OC and uOC levels were 4.073.4 ng/ml and 3.223.6 ng/ml, respectively. Both OC and uOC levels were closely related to estimated GFR and urinary albumin concentration (UAE), but not with HbA1c. OC and uOC levels were significantly higher in the patients with severe proliferative retinopathy and chronic renal failure, and the levels of OC and uOC were higher in CKD stages 3, 4, and 5 compared with CKD stage 1 and 2. In CKD stages 1 and 2 (n=241), eGFR was not related to either OC or uOC levels, while HbA1c was inversely associated not with uOC but with OC (r=0.13, p=0.04) level. OC and uOC levels were higher in the patients with the past history of cardiovascular disease, even in CKD stages 1 and 2. On the contrary, either OC or uOC were not related to highly sensitive CRP, N-terminal BNP or troponin T levels in CKD stages 1 and 2. In conclusion, serum OC and uOC concentrations were affected by renal function, but seem to have some association with vascular complications of type 2 diabetes.

Disclosures: Atsushi Suzuki, None.

MO0325

Bone loss in Patients with COPD – 3 years of Follow-up. Dorte Brask-Lindemann^{*1}, Suzanne Cadarette², Dr. Peter Eskildsen³, Bo Abrahamsen⁴. ¹Copenhagen University Hospital K1/2, Denmark, ²University of Toronto, Canada, ³Koege Hospital, Denmark, ⁴Copenhagen University Hospital Gentofte, Denmark

Background: Patients with chronic obstructive pulmonary disease (COPD) are at increased risk of osteoporosis and fractures. Several factors may contribute to this, including inadequate physical activity, vitamin D deficiency, low body mass index, and long-term use of glucocorticoids. However, it is unclear if patients have greater bone loss rates once they are diagnosed with COPD and treated for this, compared with subjects without COPD. **Aim:** To explore bone loss progression over a 3-year period in patients with COPD compared to age and gender matched pulmonary healthy controls referred for DXA examination. **Methods:** Patients with moderate to severe COPD referred for a pulmonary rehabilitation programme were consecutively recruited for the study and an age and gender matched non-COPD control group was identified in the osteoporosis clinic database. Pulmonary function was assessed by spirometry and categorized according to GOLD guidelines. DXA examination was performed using the same dual energy X-ray absorptiometry machine (DXA - Hologic Discovery A). Change in bone mineral density (BMD) over time was computed as the change in lowest T-score of the hip or spine between baseline and end of follow up period. Descriptive statistics, paired t-test and chi-square were used in statistical analysis.

Results: A total of 152 patients with COPD were included and 81 (53.3%) were alive and available for follow up three years later. Of 156 included controls, 113 (72.4%) were available for follow up in the same time period. Baseline BMD (mean of lowest T-score of hip or spine) in patients was -2.0 (SD 1.2) and in controls -1.9 (SD 1.2) (p=0.3). In patients with 3 years follow up (n=81) baseline BMD was higher (T-score -1.74 (SD 1.2) but not significantly (p=0.5), while lowest baseline T-score for controls (n=113) was unchanged. At follow up, no significant differences in bone loss progression rate in or between (p=0.5) the two groups were revealed (Patients t-score -1.74 (SD 1.2) to -1.8 (SD 1.1) (p=0.8) and controls t-score -1.9 (SD 1.1) to -1.8 (SD 1.0) (p=0.3)). **Conclusion:** These results confirm a high prevalence of low BMD in patients with moderate to severe COPD but do not suggest a COPD-associated increased rate of bone loss progression.

Disclosures: Dorte Brask-Lindemann, None.

MO0326

Evaluation of FRAX Analysis in Patients with Glucocorticoid-Induced Osteoporosis of Connective Tissue Diseases (CTD). Ikuko Tanaka^{*1}, Shigenori Tamaki², Hisaji Oshima³. ¹National Center for Geriatrics & Gerontology, Japan, ²Nagoya Rheumatology Clinic, Japan, ³Tokyo Medical Center, Japan

Objective: We evaluated FRAX in patients with CTD, where severe secondary osteoporosis such as glucocorticoid-induced and arthritis related osteoporosis particularly at the spine. **Subjects & Methods:** One hundred and five outpatients (female; 90, average age; 65) in the rheumatology clinic were recruited by following criteria; i) more than 40 years old of age, ii) no therapeutic agents for osteoporosis. BMD data of the hip were not available. After 2 years of follow-up, incident fractures were identified with the spine X-ray. **Results:** Sixty five subjects were taking glucocorticoid (average daily dose: 5.1 mg of prednisolone) and 20 had RA. Other elements for FRAX analysis were 154 cm on average body height and 51 kg on average body weight. Ten had a history of bone fracture and 5 had the parental history. Smokers were 20, drinkers were 5, and 5 had the secondary osteoporosis. The FRAX predictive values for the incidence of major osteoporotic fracture (10 years) (FRAX-MO) and hip fracture (FRAX-HF) were 15.9% and 5.5%, respectively. Although hip fractures were not actually observed in the two-years observation, 30 showed the vertebral fractures (29%) diagnosed by X-ray. The mean of the FRAX-MO in subjects with the vertebral fracture (24.1%) was higher than those without the fracture (12.6%), but statistically not significant (p=0.110). Forty patients showed low FRAX-MO (<7%) values, but still had high incidence (5 subjects; 12.5%) of the vertebral fractures. **Conclusion:** In patients with CTD, FRAX was valuable to predict new fracture. However, more frequent morphological fractures were observed possibly due to no information of glucocorticoid dosage in FRAX. These results suggested that FRAX might be underestimated in CTD patients.

Disclosures: Ikuko Tanaka, None.

MO0327

First Demonstration of Microdamages in Vivo in Computerized Magnified Radiographs of the Dental Alveolar Bone and Their Association with Vertebral Fracture and BMD. Yoshitomo Takaishi^{*1}, Aiko Kamada², Takashi Ikeo², Takami Miki³, Takuo Fujita⁴. ¹Takaishi Dental Clinic, Japan, ²Osaka Dental University, Japan, ³Osaka City University Medical School, Japan, ⁴Katsuragi Hospital, Japan

< Purpose >

Microdamages and microfractures, small fractures in bone subjected to mechanical stress, serve as markers of responses bone to external force and their repair, but have

so far been detected only in histological sections and never in radiograms in vivo. Attempts were therefore made to demonstrate microdamages in the computerized and highly magnified radiogram by Bone Right Method, to explore their relationship with spinal fracture and risk factors.

< Method >

In 33 subjects ranging between 50 and 69 years of age, microdamages were found in the magnified stereoscopic radiogram obtained by computed radiograms (Bone Right). Association among these was tested. Lumbar bone mineral density (LBMD) was measured by DXA, and vertebral fracture assessed by X-ray, and body mass index (BMI) calculated from weight and height. Dental examination consisted of pocket depth and alveolar thickness measurement and alveolar bone density (al-BMD).

< Results >

Number of microdamages in the uppermost part of alveolar bone of the first premolar showed a significant positive correlation with vertebral fracture with correlation coefficient (CV) of 0.722 ($p < 0.01$) and age with CV of 0.462 ($p < 0.01$), along with negative correlation with LBMD (CV-0.651, $p < 0.01$) and al-BMD (CV-0.63, $p < 0.01$).

< Conclusion >

Microdamages were detected in the dental alveolar bone for the first time in the computed, magnified and stereoscopic radiogram of the upper alveolar bone. The number of microdamages showed significant positive correlation with vertebral fracture and age, and negative correlation with LBMD and al-BMD.

Factors	Age	BMI	L-BMD	Pocket Depth	Alveolar Thickness	al-BMD	Microdamage	Fracture
Age	1	-0.334	-0.604**	0.028	-0.456**	-0.458**	0.462**	0.448*
BMI		1	0.289	0.117	0.40*	0.273	-0.88	-0.227
L-BMD			1	-0.242	0.418*	0.703**	-0.651**	-0.490**
PocketDepth				1	-0.242	-0.514**	0.289	0.213
Alveolar Thickness					1		-0.277	-0.418*
al-BMD						1	-0.637**	-0.615**
Microdamage							1	0.722**
Fracture								1

** $p < 0.01$ * $p < 0.05$

Table Correlations among al-BMD (al,T,V) in postmenopausal women

Disclosures: Yoshitomo Takaishi, None.

MO0328

Knowledge and Perception of Osteoporosis and Fracture Risk Among Post-Menopausal Canadian Women. Alexandra Papaioannou^{1*}, Suzanne Morin², Jonathan Adachi³, Alan Bell⁴, Sidney Feldman⁵, Heather Frame⁶, Stephanie Kaiser⁷. ¹Hamilton Health Sciences, Canada, ²McGill University Health Centre, Canada, ³St. Joseph's Hospital, Canada, ⁴University of Toronto, Canada, ⁵Baycrest Geriatrics Health Care System, Canada, ⁶Assiniboine Medical Clinic, Canada, ⁷Dalhousie University, Canada

Purpose: To explore the attitudes and knowledge related to post-menopausal osteoporosis (PMO) among Canadian women over 55, with and without diagnosed PMO, including understanding of prior fracture as a key factor for increased risk.

Methods: A survey was conducted online and via telephone with women across Canada in October 2010. Potential participants, from a database of individuals who consented to participate in surveys, were screened to confirm post-menopausal status. Only completed surveys were analyzed. The survey includes responses to questions about the potential or actual impact of PMO on their lives, understanding of PMO risk factors and experience with fractures. In parallel, another survey of awareness and assessment of PMO was conducted with 404 Canadian family physicians (FPs).

Results: Of 910 women completing the survey (445 had diagnosed PMO and 465 did not. Of women without a diagnosis, 9% stated they were very concerned about PMO. A majority of women had a good understanding of the major risk factors for PMO (e.g. low bone density, age, previous fracture) (Figures), but less than half felt it strongly impacted quality of life. Only 49% of undiagnosed women reported being tested for osteoporosis, and only 35% had discussed osteoporosis with their doctor. However, 18% of these women reported a fracture or broken bone after age 45, a key risk factor for PMO and future fractures. As 36% of these reported fractures were attributed to falls from standing or low height, it appears that ~7% of total undiagnosed women had experienced fragility fractures that might prompt further clinical evaluation. Few FPs (18%) say they routinely ask about fractures, and most (71%) were less than "fully confident" they would receive a report from the hospital regarding a patient's fracture. In the FP survey, 51% indicated that they were "very concerned" that their 55+ year female patients would develop PMO, and 36% felt their patients of this age were also "very concerned".

Conclusion: Although women without a diagnosis of PMO appear familiar with the disease and its risk factors, few reported they were greatly concerned about their own risk. Our findings suggest the awareness of fracture as a key risk factor predicting increased risk of future fracture is low in both women 55+ and FPs. As such, routine screening for patients' fracture history may not be incorporated effectively in risk assessment practice.

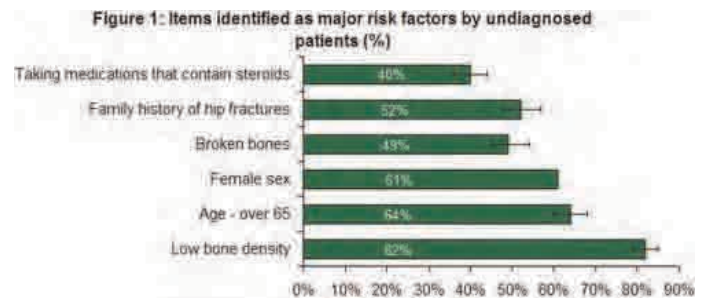


Figure 1

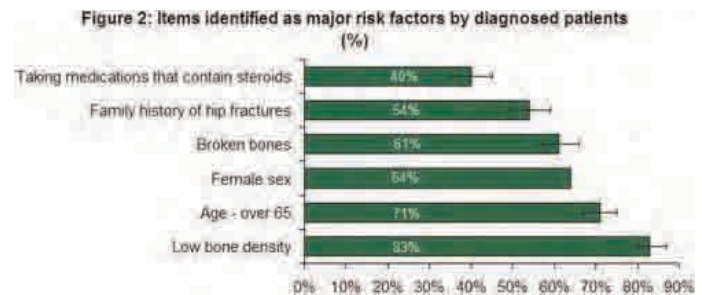


Figure 2

Disclosures: Alexandra Papaioannou, Novartis, 8; Eli Lilly, 5; Amgen, 8; Amgen, 5; Novartis, 5; Amgen, 2; Warner Chilcott, 5

This study received funding from: Amgen Canada and Osteoporosis Canada

MO0329

Osteoporosis Intervention Threshold based on BMD versus FRAX. Peter Jackuliak¹, Eva Lalcikova¹, Juraj Payer², Zdenko Killingner^{1*}. ¹University Hospital, Bratislava, Slovakia, ²University Hospital, Ruzinov, Slovakia

Objectives: Currently, indication of antiprotective treatment in Slovakia is based on low bone mineral density (T-score below -2.5 SD). According to epidemiological data more than a half of fractures occur in patients with osteopenia. These patients are currently not treated. It seems crucial to identify these high-risk osteopenic patients using the FRAX (Fracture risk assessment tool).

Aim of the study: 1) To calculate the 10-year probability of fracture in patients sent to BMD (bone mineral density) testing according to the ISCD criteria. 2) To compare two different approaches in initiation of antiprotective treatment - one based on BMD T-score below -2.5 and another based on FRAX outcomes.

Methods and patients: We calculated the 10-year absolute risk of hip fracture and major osteoporotic fracture of 379 patients sent to the Osteocenter at University Hospital using FRAX (Austrian population). The mean age of our group was 63 years. We measured BMD at the femoral neck and lumbar spine.

Results: The absolute 10-year risk was 12% for a major osteoporotic fracture and 4.3% for hip fracture. Mean T score was -1.5 SD at the femoral neck and -1.85 at lumbar spine. 98 patients were classified as osteoporotic, 184 patients were osteopenic and 97 had their BMD in normal range. Based on BMD (T-score -2.5 and below) 98 osteoporotic patients are currently indicated for antiprotective treatment. Based on FRAX outcomes and thresholds proposed by the NOF (National Osteoporosis Foundation) (20% for a major osteoporotic fracture and 3% for hip fracture), the number of treated patients would rise to 157 (90 osteopenic, 62 osteoporotic patients and 5 patients with normal BMD).

Conclusions: Based on the FRAX tool outcomes and the NOF treatment thresholds we would identify 157 patients at high risk for osteoporotic fractures. The use of this intervention threshold in clinical practice would significantly increase (twice) the number of treated patients with considerable impact on the health-care system.

Disclosures: Zdenko Killingner, None.

MO0330

The 3/2 Power of Bone Mineral Apparent Density. Xiaohai Wan^{*}, John Krege. Eli Lilly & Company, USA

Objective: Dual-energy X-ray Absorptiometry (DXA) and Quantitative Computed Tomography (QCT) are techniques used clinically to measure bone mineral density (BMD) to evaluate the status of the skeleton. DXA, the gold standard to diagnose and monitor patients with osteoporosis, measures areal BMD (aBMD, g/cm²) via a projected radiography technique and hence cannot directly consider the thickness of the assessed bone. aBMD is calculated as bone mineral content (BMC) divided by bone area (BA). QCT provides the opportunity to assess 3-dimensional volumetric BMD (vBMD, g/cm³) measurements. The purpose of this analysis was to assess the relationship between aBMD and vBMD using data from Lilly clinical trials. On

theoretical grounds, a bone mineral apparent density (BMAD), calculated as $BMC/BA^{1.5}$ should approximate vBMD.

Methods: The analysis includes postmenopausal women with osteoporosis who participated in two clinical trials ($N_1 = 203$, $N_2 = 198$). DXA measurements collected included bone mineral content (BMC), bone area (BA) and aBMD. QCT measurements collected included vBMD. Nonlinear regression was used to estimate three parameters (a_0 , a_1 and a_2) in the following formula: $E(vBMD|BMC,BA) = a_0 + a_1 \cdot BMC/BA^{1.5}$. Linear regressions were applied to assess the relationships between BMC, BA, vBMD, aBMD and BMAD.

Results: The exponent parameter a_2 in the nonlinear regression model was estimated to be very close to the value of $3/2$ ($p < 0.01$) as in the theoretical definition of BMAD at femoral neck, hip and lumbar spine.

Conclusion: We showed through nonlinear regression technique that the BMAD formula allows 2-dimensional aBMD data to be converted to an approximation of volumetric BMD in osteoporosis patients.

Disclosures: Xiaohai Wan, Eli Lilly & Co, 3; Eli Lilly & Co, 1
This study received funding from: Eli Lilly and Company

MO0331

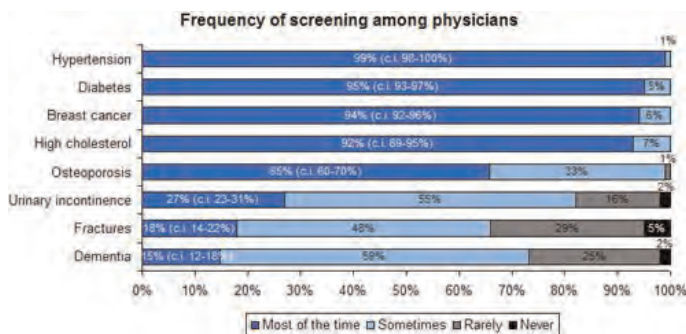
Variability in Screening for Post-menopausal Osteoporosis by Canadian Family Physicians. Suzanne Morin^{*1}, Alexandra Papaioannou², Andre Belanger³, Jacques Brown³, Angela Cheung⁴, David Hanley⁵, David Kendler⁶, Daniel Ngui⁷. ¹McGill University Health Centre, Canada, ²Hamilton Health Sciences, Canada, ³Laval University, Canada, ⁴University Health Network, Canada, ⁵University of Calgary, Canada, ⁶Osteoporosis Research Centre, Canada, ⁷University of British Columbia, Canada

Purpose: To explore the attitudes and screening practices of Canadian family physicians (FPs) regarding post-menopausal osteoporosis (PMO) and its management.

Methods: In October 2010, 2594 eligible FPs, identified from a database of physicians from across Canada who had consented to participate in surveys, were invited to complete this survey. FPs were included if they routinely saw >100 patients/month, of whom $\geq 15\%$ were age 55+, and wrote ≥ 15 prescriptions per month for PMO medications. Only completed surveys were analyzed. The survey included FP responses to questions about the impact of PMO, their concern with chronic diseases and their approach to assessing patients' risk of PMO.

Results: Of 404 FPs completing the survey, 35% indicated they were "very concerned" about the quality of life (QoL) impact of PMO in their patients. However, chronic conditions judged to be of greater concern included dementia, cerebral vascular disease, breast cancer, heart disease and diabetes. Only 65% and 18% of FPs regularly screened for osteoporosis and fractures, respectively, as compared to 99% for hypertension and 95% for diabetes during routine examination of women in this age group (Figure). Despite the fact that 71% of FPs were "somewhat to not at all confident" that the hospital would inform them of a patient's fracture, FPs surveyed do not routinely ask their patients if they experienced a fracture since they were last seen. Many (42%) believe up to one-fourth of their patients have undiagnosed and untreated fragility fractures. Most FPs (68%) were aware that absolute fracture risk models, including that endorsed by the Canadian Association of Radiologists and Osteoporosis Canada (CAROC), were available, but 58% said they still relied on the DXA T-score alone for the diagnosis of PMO.

Conclusion: This survey suggests that FPs may not adequately consider fragility fractures in their PMO patients and underestimate the potential long-term impact of these fractures on women's functional status. Hip fractures, for instance, are estimated to occur at an annual rate of 86.4/100,000 women in Canada and cause lasting deficits in women's global QoL, mobility, and self-care. The new Osteoporosis Canada Guidelines emphasize fracture risk assessment over DXA-based diagnosis. However, based on the high usage of DXA alone, FPs may benefit from education in the use of predictive models of PMO, which incorporate prior fracture history and other established risk factors.



Figure

Disclosures: Suzanne Morin, Novartis, 5; Novartis, 8; Amgen, 2; Eli Lilly, 5; Amgen, 8; Warner-Chilcott, 5; Amgen, 5
This study received funding from: Amgen Canada and Osteoporosis Canada

MO0332

Abnormal Cortical and Trabecular Parameters in Persons with Epilepsy. Alison Pack^{*1}, Rebecca B. Bausell¹, Stephanie Boutroy², Donald McMahon³, Elizabeth Shane³. ¹Columbia University, USA, ²Columbia University Medical Center, USA, ³Columbia University College of Physicians & Surgeons, USA

Persons with epilepsy have a 2-6 fold increased risk of fracture. Both low BMD and abnormal microarchitecture are associated with fracture. Therefore, we evaluated areal BMD (aBMD) by DXA, and volumetric BMD (vBMD) and bone microarchitecture by high resolution peripheral QCT (HRpQCT) in 111 persons with epilepsy on various antiepileptic drugs: 39 older men (587), 50 premenopausal (PreM) women (377) and 22 postmenopausal (PM) women (615). Excluded were subjects with bone disease or with illnesses or on medications that affect the skeleton. aBMD was measured by DXA (Hologic QDR 4500) at the spine (LS), total hip (TH), femoral neck (FN), and 1/3 radius (1/3R). vBMD and trabecular (Tb) and cortical (Ct) microarchitecture were measured at the nondominant distal radius (RAD) and tibia (TIB) by XtremeCT (SCANCO Medical AG; voxel size ~82µm). DXA sex-specific Z-scores were compared to reference population normative values provided by Hologic Corp. HR-pQCT sex-specific Z-scores were compared to normative values provided by Boutroy for PreM and PM women and by Chaitou et al. (JBMR, 2010) for older men. DXA Z-scores did not differ from normative values at any site for men (Table). For PM women DXA Z-scores did not differ at LS, TH or FN, but were significantly higher at the 1/3R. For PreM women, FN Z score was below and 1/3R Z score was above normative values, while LS and TH were normal. At the RAD, cross-sectional area (CSA) was low in men and PM women. Total vBMD was normal in all groups, Ct vBMD were high in men and normal in PreM and PM women, and Ct thickness (CtTh) was normal in all. Tb vBMD was low in PreM women, but not PM women or men. There were consistent increases in Tb number (TbN) and decreases in Tb thickness (TbTh) in all groups. At the TIB, CSA was normal in men and PM women and high in PreM women. All groups had low Ct vBMD and CtTh and normal Tb vBMD. As at the RAD, TbN was higher and TbTh lower in all groups. In summary, compared to age-matched and gender norms, aBMD by DXA was low only at the FN and only in premenopausal women. HR-pQCT differences were most marked and consistent at the Tibia where persons with epilepsy had smaller bones with thinner, less dense cortices. Tb vBMD was normal, likely because higher TbN compensated for lower TbTh higher TbTh. These differences in bone quality, smaller bones with thinner, less dense cortices and thinner trabeculae, could contribute to increased fracture risk.

Mean±SEM *p<0.05		PreM Women Z-score	PM Women Z-score	Men Z-score
DXA	LS	0.03±0.15	0.46±0.23	-0.06±0.21
	TH	-0.14±0.12	0.21±0.19	-0.03±0.13
	FN	-0.45±0.14*	-0.01±0.17	-0.19±0.13
	1/3R	0.37±0.13*	0.89±0.21*	0.26±0.20*
Radius	CSA	-0.26±0.15	-0.52±0.17*	-0.92±0.16*
	Ct vBMD	0.20±0.21	0.10±0.18	0.54±0.18*
	CtTh	0.05±0.19	0.29±0.19	0.32±0.17
	Tb vBMD	-0.37±0.17*	-0.04±0.22	-0.34±0.17*
	TbN	0.93±0.22*	0.72±0.28*	0.44±0.21*
	TbTh	-1.22±0.15*	-0.82±0.21*	-0.89±0.18*
Tibia	CSA	0.53±0.13*	0.20±0.18	0.28±0.15
	Dcomp	-0.62±0.13*	-0.77±0.20*	-0.66±0.17*
	CtTh	-0.69±0.14*	-0.48±0.17*	-0.50±0.17*
	Dtrab	-0.23±0.15	0.20±0.23	-0.01±0.16
	TbN	1.00±0.16*	1.05±0.27*	0.76±0.16*
	TbTh	-1.09±0.12*	-0.72±0.20*	-0.72±0.16*

Disclosures: Alison Pack, None.

MO0333

Estimation of Cortical Density with Clinical CT. Graham Treece^{*}, Kenneth Poole, Andrew Gee. University of Cambridge, United Kingdom

There is growing evidence that focal thinning of cortical bone in the proximal femur is critical in determining resistance to fracture. Accurately assessing cortices thinner than 2.5 mm in clinical MDCT is challenging, since they are corrupted by imaging blur. We recently proposed a model-fitting technique for accurate estimation down to 0.3 mm (Treece et al. Medical Image Analysis, 2010). The technique assumes a patient-specific, fixed value for true cortical density, estimated from CT data of thick cortices below the lesser trochanter. Using this technique, we have shown, for 65 osteoporotic women, precisely where in the proximal femur new bone is laid down following treatment with hPTH(1-34) (Poole et al. Plos One, 2011). We now aim to provide an improved density estimate which is more representative of the entire proximal femur, is available from incomplete CT data or patients with thin cortices, and has associated confidence intervals.

If the true cortical density is substantially constant, and the imaging blur is Gaussian, we can derive the expected distribution of peak cortical density with thickness (solid line in figure 1), which depends only on the imaging blur, true cortical

density, and background density. We sample the peak cortical density, measured in clinical CT data, at many points over the proximal femur, and compare this with the expected distribution. Modelled blur, cortical and background density are adjusted to minimise the difference between measured and expected distributions, leading to mean and 95% confidence limits for the true cortical density. Figure 1 shows typical outcomes from three different subjects in the hPTH study. The measured and expected distribution are in close agreement in figure 1(a). Figure 1(b) is a more difficult case where the model accurately predicts a true cortical density which is not apparent in the measured data. In figure 1(c), the cortex is very thin and the density estimate is hence less reliable: this is reflected in the increased confidence limits of 25 HU. Nevertheless, using the new technique on the hPTH data, the worst case confidence limits were only 38 HU, and all cases were deemed to give acceptable estimates of cortical density. The resulting baseline population cortical bone mineral density was 1185.1 67.9 mg/cm³ decreasing to 1133.6 78.1 mg/cm³ ($p < 0.001$) after 24 months' treatment.

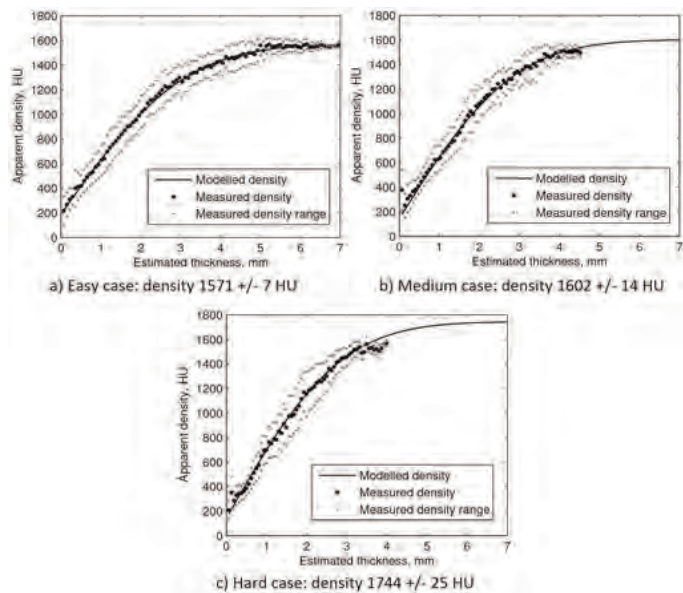


Figure 1: The distribution of cortical density against thickness for typical clinical MDCT data.

Disclosures: Graham Treece, None.

MO0334

Low BMD Is not Necessarily a Measure of Bone Fragility; The Structural Basis of Areal Bone Mineral Density. Ali Ghasem-Zadeh*, Thuy Vu, Qingju Wang, Roger Zebaze, Ego Seeman. Austin Health, University of Melbourne, Australia

Background Bone mineral density (BMD) is commonly used in clinical and research to identify individuals at risk for fracture. However, it lacks sensitivity and specificity, in part, because the BMD measurement is 'blind' to the spatial organization of bone. In an attempt to quantify the material and structural basis of a BMD measurement, whether 'low' or 'high' we examined bone microarchitecture and hypothesized that, as 80% of bone is cortical at peripheral sites, the variance in BMD will mostly be explained by variance in cortical structure.

Material & Methods We studied 66 male mean age 41 yr and 99 women mean age 58 yr (range 18 to 85). High resolution peripheral computed tomography (HRpQCT) images were obtained at the distal radius and total volumetric bone mineral density (TbBMD), cortical vBMD (Ct vBMD) and area (Ct Area), trabecular vBMD (TrvBMD) and area (TrArea) and total cross sectional area (T-CSA) were measured using the manufacturer's software. BMD was measured at the same location using Lunar Prodigy.

Results In males, only Ct Area, T-CSA and TrvBMD were independent predictors of BMD explaining 93.6% of its variance. Ct Area was the best determinant of BMD explaining 80.8% of its variance whereas T-CSA and TrvBMD explained respectively 11.6% and 1.2% of the variance. In females, only Ct Area, and TrvBMD were independent predictors of BMD explaining 85.4% of its variance. Ct Area was the best determinant of BMD explaining 72% followed by TrvBMD which explained 13.4% of the variance in BMD. In both sexes, Ct vBMD correlated with BMD in univariate model but not after accounting for Ct Area.

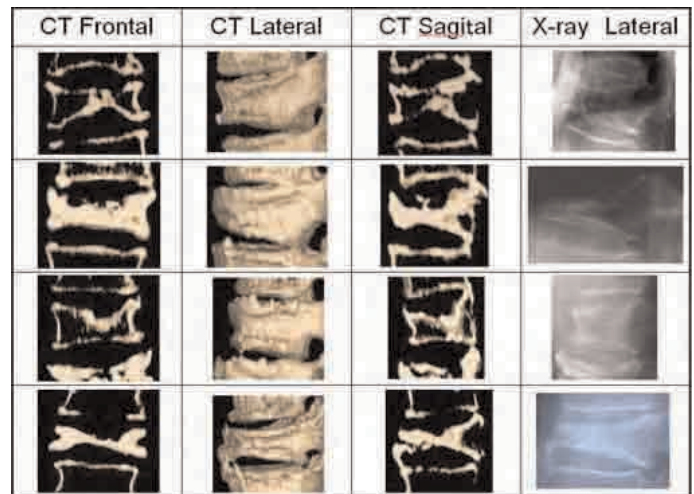
Conclusion At peripheral sites such as the distal radius, BMD largely reflects cortical area but fails to identify persons with normal BMD at risk for fracture risk due to architectural deterioration or persons with osteoporosis by BMD with normal microarchitecture. Understanding bone fragility requires the study of bone morphology.

Disclosures: Ali Ghasem-Zadeh, None.

MO0335

The Involvement of Two Forces in Osteoporotic Vertebral Fracture - Pressures of the vertebral rim or disk and their involvement in fish shaped and wedge type fractures. Hitoshi Noguchi¹, Sumiaki Okamoto², Sumitada Okamoto³, Hirovuki Suzuki⁴, Akira Itabashi⁵. ¹Noguchi hospital, Japan, ²Okamoto Clinic SORF, Japan, ³KS Okamoto Naika, Japan, ⁴Suzuki Orthodontic Clinic, Japan, ⁵SCBR, Japan

The forces that cause the vertebral fractures have seldom been discussed. The vertebral endplates neither shrink by themselves to concave shape nor are compressed by divine powers. The question is, why the fracture lines of fish-shaped vertebra are uneven, while those of wedge-type vertebra are straight. The mechanism remains uncertain due to lack of proper reading of the concave fracture lines. TV-X ray fluoroscopy was performed in 136 normal volunteers and 2,740 female osteoporosis patients. Also we created computerized 3-D renderings of 1,540 cases by Helical CT (Asteion Super 4 edition Toshiba). To make the X-ray pass through straight on the vertebral bodies, we asked the patients in an upright position to adjust their postures so that the distal and proximal edges of each vertebra would coincide. In 37 young female volunteers, the mean Central to Posterior height ratios coincide with previously reported autopsy data. When observed in 3-D CT renderings, the C/P ratio is smaller than the Anterior to Posterior height ratio in 99% of the "wedge shaped" fractures observed. Conventional diagnostic criteria for a fish shaped fracture is a C/P ratio of 80%, and the criteria for a wedge shaped fracture is a A/P ratio of 75%. But in reality, the centers of the vertebral endplates are far more compressed than the anterior vertebral rim in almost every case. Consequently, the C/P ratio has a higher recognizing power for wedge fractures than the A/P ratio. The nucleus pulposus of intervertebral disc bears the burden of vertebra, and that pressure concaves the center of the vertebral body terminal endplate. When the vertebral body become deformed into fish-shaped vertebra, fracture lines are rarely smooth but consist of the mixture of many perforated indentations, or Schmorl nodes, while the vertebral rim lines remain intact which eventually come closer together. At that time the fulcrum, posterior intervertebral joints, which have remained strong, cause enough stress to crush the anterior part of the vertebra. Eventually, the pressure of rim against rim forces the vertebra into a straightly lined "wedge type" change. None of the textbooks or guidelines has so far made any mention of this simple observation due to the fact that most of the diagnoses are based on outdated or inadequate X-ray images in which the compression of the fractured endplates cannot be observed, or due to the incompetence of the radiologist who failed to acknowledge it.



Wedge shaped vertebra almost always present terminal plate indentations

Disclosures: Sumiaki Okamoto, None.

MO0336

Ultrashort TE Imaging and Bi-Component Analysis of Bound and Free Water Components in Bovine Cortical Bone - Validation with Sequential Drying. Reni Biswas*, Won Bae, Eric Diaz, Christine Chung, Graeme Bydder, Jiang Du. University of California, San Diego, USA

Purpose: To evaluate the bound and free water components in bovine cortical bone as well as changes to these two components after sequential air-drying at room temperature using Ultrashort TE (UTE) imaging.

Methods: Ten bovine fragments with approximate dimensions of 20 mm long x 8 mm wide x 4 mm thick were cut from fresh mature bovine femur obtained from a local slaughterhouse, and imaged using a UTE sequence with a minimum nominal TE of 8 μ s on a clinical 3T MR scanner. UTE T2* images were repeatedly acquired after every one percent (in weight) bone water loss after air-drying at room temperature using the following imaging protocol: TR = 200 ms, FOV = 4 cm, matrix = 256 x 256, flip angle = 10, short hard pulse (32 μ s in duration), bandwidth = 62.5 kHz, 20 TEs ranging from 8 μ s to 10 ms. The drying process was terminated after three days. In-house bi-

component fitting software was used to calculate $T2^*$ and fractions of the shorter $T2^*$ (bound water) and longer $T2^*$ (free water) components. The changes in $T2^*$ as well as the fractions of bound and free water components were displayed as a function of drying time. For one sample, UTE imaging with two TRs of 100 ms and 1000 ms were also performed to investigate the effect of T1 on bi-component analysis. Free water is lost faster than bound water at room temperature.

Results: Excellent bi-component fitting was achieved for all 10 bovine cortical bone samples. Figure 1 shows typical UTE imaging and bi-component analysis of a wet bovine bone sample and the same sample after air-drying for three days. At room temperature wet bone had a 75-80% bound water, and a 20-25% free water. The free water component gradually decreased to near zero after three days of air-drying. Both $T2^*$ and the fractions of bound and free water components remained unchanged with two different TRs of 100 ms and 1000 ms.

Conclusion: The results show that UTE imaging with bi-component analysis can be used to estimate bound and free water in cortical bone, and chemical exchange between bound and free water is much slower than T1 but much faster than $T2^*$. Modeling T1 with a single component and $T2^*$ with bi-component appears appropriate.

Clinical Relevance UTE imaging and bi-component analysis can quantify the free and bound water components in cortical bone. The free water component may be used to estimate bone porosity, and bound water component may be used to evaluate collagen matrix.

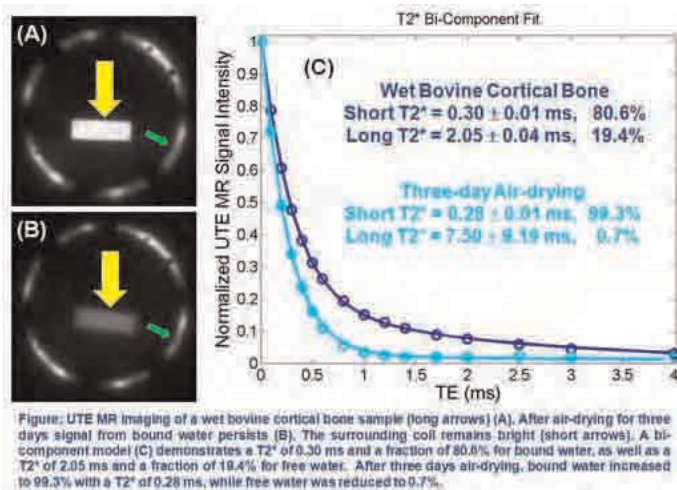


Figure 1

Disclosures: Reni Biswas, None.

MO0337

Body Composition and Sex Hormones Differently Influence Quantitative Ultrasound Parameters at Calcaneus and at Phalanges in Elderly Women. Stefano Gonnelli*, Carla Caffarelli, Loredana Tanzilli, Daniela Merlotti, Luigi Gennari, Barbara Lucani, Stella Campagna, Beatrice Franci, Ranuccio Nuti. University of Siena, Italy

Quantitative ultrasound (QUS) has been applied to the assessment of bone status for almost two decades. A crucial point for a larger use of QUS in the evaluation of bone status and the assessment of fragility fracture risk is represented by the necessary definition of whether the main determinants of BMD in postmenopausal women could have a similar or a different impact on QUS parameters.

This study aimed to evaluate the influence of body composition parameters, Vitamin D and sex hormones on QUS parameters.

In 897 postmenopausal women (64.1 ± 6.6 yrs) we measured QUS at calcaneus (Stiffness) by Achilles-GE and at phalanges (amplitude dependent speed of sound [AD-SoS], bone transmission time [BTT] and ultrasound bone profile index [UBPI]) by Bone Profiler-IGEA. In all we measured fat mass (FM), lean mass (LM), android and gynoid fat by DXA. In all subjects we also assessed serum testosterone (T), estradiol (E), sex-hormone binding globulin (SHBG), free estrogen index (FEI), free androgen index (FAI), 25-hydroxyvitamin D (25OHD), and bone alkaline phosphatase (B-ALP).

No significant relationships were found between T and QUS. Estradiol was significantly correlated with Stiffness ($r=0.11$; $p<0.05$), AD-SoS ($r=0.09$; $p<0.05$) and BTT ($r=0.12$; $p<0.05$), whereas FEI showed a significant correlation with all QUS parameters. By grouping the patients according to FEI quartiles, we found that women in the lowest FEI quartile had the lowest mean QUS values and those in the highest quartile had the highest mean QUS values. This trend was statistically significant for BTT ($p=0.014$), AD-SoS ($p=0.043$) and Stiffness ($p=0.048$). BMI and LM were positively correlated with Stiffness ($r=0.14$; $p<0.01$ and $r=0.17$; $p<0.01$ respectively), whereas BMI and FM showed negative correlations with AD-SoS, BTT and UBPI. 25OHD showed positive relationships ($p<0.05$) with Stiffness and AD-SoS. In multivariate models after adjusting for all confounders LM remained independently associated with Stiffness whereas only age and E were significant

predictors of BTT. AD-SoS was negatively associated with FM and B-ALP, but positively with E and 25OHD.

In postmenopausal women QUS parameters at calcaneus and at phalanges are significantly, but diversely, influenced by body composition, sex hormones, 25OHD and bone turnover markers. This finding may increase the potential of QUS in the evaluation of bone status.

Disclosures: Stefano Gonnelli, None.

MO0338

Correlation between QUS of Phalanx and DXA in Assessment of Bone Structure in Hemodialysed Patients. Zohreh Hamidi*, Dr. Sima Maziar*, Dr. Mitra Mahdavi-Mazdeh*, Dr. Abbas Ali Keshtkar*, Dr. Ghassan Maalouf*, Dr. Bagher Larijani*. ¹Endocrinology & Metabolism Research Center of Tehran University of Medical Sci, Iran, ²Tehran University of Medical Sciences, Iran, ³St George University Hospital, Lebanon

Many hemodialysing patients, have reduced BMD. Dual X-ray absorptiometry (DXA), standard method for assessing BMD, is not always available. So this study compares the quantitative ultrasound (QUS) of phalanx (an inexpensive, mobile, and radiation-free method) with DXA in detecting bone changes in such patients.

In 64 patients, axial BMD measured by a GE-Lunar DXA device (DPX-MD) and a DBM-Sonic 1200 device used for QUS of phalanx.

Osteoporosis found in 31.3% of patients, Using DXA and in 28.1% of them, using QUS. Using ROC curve, sensitivities of T-score ≤ -2.5 of phalanx for diagnosing of osteoporosis in neck and total of hip and L2-L4 were respectively 37.5% and 50% and 80% and specificities were respectively 75% and 77% and 76%. Area under curve for neck, total and spine regions were 0.692 (Pvalue=0.022), 0.701 (Pvalue=0.031), 0.809 (Pvalue=0.023), respectively.

It seems QUS of phalanx can be recommended for screening osteoporosis among hemodialysed patients.

Disclosures: Zohreh Hamidi, None.

MO0339

Novel Density Index Method for Osteoporosis Diagnostics at Primary Healthcare. Juha Toivras*, Janne Karjalainen*, Ossi Riekkinen*, Heikki Kroger*, Jukka Jurvelin*. ¹Kuopio University Hospital, Finland, ²University of Eastern Finland, Finland

Osteoporosis is diagnosed using the axial DXA technique. However, the DXA is a X-ray method that is non-portable, uses ionizing radiation and has significant costs. Therefore, it is not suitable for primary healthcare level. Today, there are 200 million osteoporotic patients worldwide and most of them are not diagnosed until several fractures have occurred (annual cost 36 billion/EU). It is estimated that over 75% of osteoporotic patients are not diagnosed nor receive treatment for their pathological condition. At the moment, the peripheral techniques, e.g., heel ultrasound or heel DXA, which are designed for small practices, predict only moderately the results of current diagnostic standard, axial DXA ($r = 0.2 - 0.6$). Therefore, these techniques alone are not suitable for diagnosis of osteoporosis. It is approximated that 40-60% of patients screened with the peripheral techniques need an additional axial DXA measurement.

In this study, a prototype of multi-site pulse-echo (PE) ultrasound method combined with subject characteristics (i.e. density index, DI, patent pending) is proposed for osteoporosis diagnostics. Forty elderly (74 ± 3 years) women were examined *in vivo* using PE ultrasound (at 2.25 MHz) to measure cortical bone thickness in proximal and distal tibia. Further, bone mineral density in the femoral neck (BMD_{neck}) was determined by axial DXA. In addition, the DI and BMD_{neck} were inserted into FRAX® (World Health Organization fracture risk assessment tool) along with the subject questionnaire to obtain treatment proposals (available for UK population in FRAX).

Cortical bone thickness at distal and proximal tibia combined with age and weight of the subject (DI), provided a significant estimate of BMD_{neck} ($r = 0.84$, $p = 0.001$, $n = 40$). The FRAX® with DI indicated the same treatment proposal as the FRAX® with BMD_{neck} at the sensitivity and specificity of 82% and 90%, respectively. In addition, provided that FRAX® treatment proposals were calculated first using body mass index only and then, if needed, with BMD_{neck} (60% of patients) or DI, the sensitivity and specificity for treatment proposals were 100% and 89%, respectively.

Due to high correlation between the DI and BMD_{neck} and high agreement for treatment proposals using FRAX®, only few subjects would require additional axial DXA measurements. This result is encouraging and suggests that DI may improve significantly the accessibility of osteoporosis diagnostics.

Disclosures: Janne Karjalainen, None.

MO0340

Bone Mineral Density Does Not Differ Between Ethnic Groups in Preschool Aged Children Attending Daycares. Thu Trang Pham*, Sarah Finch, Sandra Dell'Elce, Sonia Jean-Philippe, Tom Hazell, Sherry Agellon, Celia Rodd, Catherine Vanstone, Hope Weiler. McGill University, Canada

The Canadian national surveillance data from 2007-2009 raises concerns that non-white individuals, due to their darker skin-pigmentation, have lower vitamin D status which is associated with lower bone mineral density (BMD). Differences have been reported for vitamin D status and BMD between ethnicities and immigration status in adolescents and adults.

The objective of this study is to determine whether BMD in young children is related to darker skin pigmentation, ethnicity and immigration status.

A cross-sectional study was conducted with 287 children (boys=161, girls=126). Sampling was done in randomly selected daycares in Montreal regions between June and December 2010. Skin colour was measured using a spectrophotometer (CM-700d/600d, Konica Minolta, Ramsey, NJ, USA). Individual typological angle (ITA) was calculated with the L* and b* values given by spectrophotometer. Forearm BMD was measured using a peripheral bone densitometer (PIXI, GE Lunar, USA). Ethnicity and immigration status were reported by parents. Capillary blood was sampled to measure plasma total 25(OH)D using a chemiluminescent immunoassay (Liaison, Diasorin, ON, Canada). Data was statistically analyzed using Pearson's correlations with log transformations where applicable. Differences in ethnicity, immigration status, plasma 25(OH)D and BMD were analysed by ANOVA. Significance was set at $p < 0.05$.

Mean age was 3.61.0 y; height for age Z-score, 0.01.03; weight for age Z-score, 0.360.92 and BMI for age Z-score, 0.780.88. Plasma 25(OH)D <75 nmol/L were seen in 47% of children. After accounting for age and sex, ITA was weakly correlated with plasma 25(OH)D ($R=0.18$, $P=0.002$), but not with BMD ($R=-0.06$, $P=0.296$). Compared to white children, 25(OH)D was lower in Black ($P=0.05$) and higher in Arab ($P=0.04$) children whereas BMD was not different (Table 1). BMD ($P=0.187$) and 25(OH)D ($P=0.822$) did not differ by immigration status. Although not significant, there was an observed trend of lower BMD in immigrant ($\mu=0.382 \text{ g/cm}^2$) compared to non-immigrant children ($\mu=0.411 \text{ g/cm}^2$).

This study is on-going and a final sample size of 500 is anticipated. The lower vitamin D status in children with darker pigmentation does not appear to compromise BMD in this age group. Future analyses including dietary assessment will clarify if endogenous synthesis or exogenous intakes underpin the lower vitamin D status. (Supported by the Dairy Farmers of Canada).

TABLE 1

Ethnicity	n	Age±SD (y)	Girls (%)	25(OH)D±SD (nmol/L)	BMD±SD (g/cm^2)
White	176	3.7±1.0	42	84.8±29.4	0.232±0.033
Black	21	3.6±1.1	67	72.8±23.8*	0.241±0.045
Arab	20	3.5±1.0*	55	92.3±31.4*	0.233±0.036
Asian	8	3.8±0.6	38	67.0±24.9	0.229±0.031
Latin America	3	3.6±0.8	67	74.2±26.5	0.254±0.029
Mixed	59	3.6±1.0	37	85.8±31.8	0.242±0.033

* $P < 0.05$ vs white

Table 1

Disclosures: Thu Trang Pham, None.

This study received funding from: Dairy Farmers of Canada

MO0341

Circulating Sclerostin Levels in a Cohort of Adolescent and Young Adult Women: Cross-Sectional Associations with Age and Bone Mass. Delia Scholes*¹, Laura Ichikawa², Andrea LaCroix³, Thy Do⁴, Puneet Arora⁵, Susan Ott⁶. ¹Group Health Cooperative/Group Health Research Institute, USA, ²Group Health Research Institute, USA, ³Women's Health Initiative, USA, ⁴Amgen, Inc., USA, ⁵Amgen Inc., USA, ⁶University of Washington Medical Center, USA

Background: Sclerostin has been identified as an important Wnt signaling pathway inhibitor that acts to inhibit bone formation. However, relatively little is known about the role of circulating sclerostin in human biology. Sclerostin serum concentrations in younger populations who are in the process of gaining bone are largely unevaluated. Thus, we assessed circulating sclerostin in a cohort of adolescent and young adult women aged 14-30 years to 1) identify factors associated with circulating sclerostin levels and 2) examine the association between sclerostin and bone measures (BMD, BMC).

Methods: Serum samples were obtained from 300 women who were part of a large cohort recruited in a defined HMO population. Serum sclerostin levels (in pg/mL) were measured using an electrochemiluminescence sandwich assay (%CV ≤ 15%; LLOQ 50 pg/mL). BMD and BMC were measured at the hip, spine, and whole body using DXA (Hologic Delphi).

Results: Mean sclerostin (+SEM) levels were 254± 8 pg/mL for adolescents ages 14-19 years, 208±13 for ages 20-23, and 261±11 for ages 24-30 ($p=0.004$ for between-group differences). An examination of sclerostin by age revealed a U-shaped pattern, with sclerostin trending downward at ages 14-20, and upward trends at ages 24-30. A quadratic term was significant ($\Delta^2=1.06$, $p=0.0012$) (Figure). Fracture risk factors including race/ethnicity, current smoking, BMI, physical activity score, calcium intake, gravidity and oral contraceptive use were not associated with sclerostin level, either by age group or overall after age adjustment. An examination of the association between sclerostin and BMD and BMC found significant positive correlations at the spine for BMD and BMC and whole body BMD in 24-30 year-old women, but not in younger women (Table).

Conclusion: In this cohort of young women, age was the factor most strongly associated with circulating sclerostin levels, with lower levels at ages 19-23 years and higher values on either side (ages 14-18 and 24-30 years). Circulating sclerostin was positively correlated with bone measures (BMD, BMC) at the spine and whole body in women ages 24-30 years, showing higher values at ages when bone growth is slowing.

Table. Correlation of baseline circulating sclerostin and bone measures, by age group

	Age 14-19		Age 20-23		Age 24-30	
	BMD	BMC	BMD	BMC	BMD	BMC
Total hip	0.001	-0.02	0.10	0.03	0.18	0.16
Spine	0.07	0.09	0.08	0.11	0.31*	0.32*
Whole body	0.02	0.02	0.16	-0.01	0.22*	0.19

BMD = Bone mineral density, BMC = Bone mineral content
* $p < 0.05$

Table

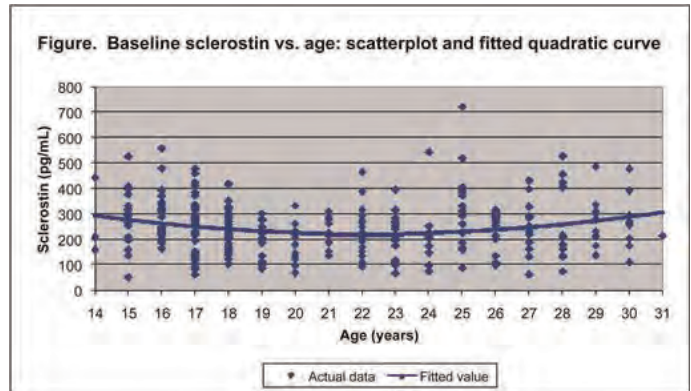


Figure 1

Disclosures: Delia Scholes, None.

This study received funding from: Amgen, Inc.

MO0342

Effects of Age, Gender and Body Composition on Bone Mineral Density and Vitamin D metabolism. Shuanhu Zhou, Nithya Setty, Julie Glowacki, Meryl Leboff*. Brigham & Women's Hospital, USA

Low vitamin D levels have been reported in older adults and in obese individuals. We previously found that expression of vitamin D hydroxylases in human marrow stromal cells (hMSCs) are influenced by the vitamin D status of the individual from whom the hMSCs were obtained (Endocrinology 151:14, 2010). Because little is known about metabolism of vitamin D in obese subjects, we tested the hypotheses that age, gender, and body composition (body mass index, BMI, and fat mass index, FMI) influence bone mineral density (BMD) and vitamin D metabolism in hMSCs. Body composition including BMD and FMI ($\text{FM}/\text{height}^2$) were measured by DXA (Hologic, Discovery). Discarded femoral heads were obtained from 54 consented subjects whose 25OHD was obtained prior to hip surgery. Human MSCs were obtained by expansion of adherent low-density marrow mononuclear cells; RNA was extracted for measurement of constitutive gene expression.

First, among all consented subjects (32 women and 22 men), FN T-scores, BMI and FMI were inversely correlated with age; and FN T-scores were correlated with BMI and FMI. For the women, FN T-scores were correlated with BMI ($r=0.73$, $p<0.0001$) and FMI ($r=0.58$, $p=0.0028$), and inversely correlated with age ($r=-0.60$, $p=0.0009$). For the men, FN T-scores were not significantly correlated with BMI or

age, except for a trend correlation with FMI ($r=0.53$, $p=0.055$). Second, we assessed the relationship between vitamin D enzymes in hMSCs and clinical characteristics of the individual from whom the hMSCs were obtained. Constitutive expression of CYP27A1/25OHDase in hMSCs was inversely correlated with serum 25OHD ($n=26$, $r=-0.42$, $p=0.031$). Obese women ($BMI>30 \text{ kg/m}^2$) had lower serum 25OHD levels (16.04 ng/ml) than their non-obese counterparts (30.44 ng/ml) ($p=0.037$, unpaired t-test); ages of obese (656) and non-obese (683) women were similar. Cells from obese women ($n=5$), but not men, expressed higher CYP27A1 levels than non-obese women ($n=7$) ($p=0.02$). These preliminary data suggest that obese females may have a better response to vitamin D₃ than non-obese females; this may be due to the higher CYP27A1 in their bone marrow cells possibly as a result of lower serum 25OHD. In sum, our data in female subjects indicate that low BMD is associated with advanced age, low BMI or FMI. We speculate that increased expression of CYP27A1/25OHDase in marrow stromal cells in obese women may potentially contribute to autocrine actions of vitamin D on bone.

Disclosures: Meryl Leboff, None.

MO0343

Femoral Volumetric Bone Density and Dimensions in Relation to Serum 25-Hydroxy Vitamin D Levels Among Elderly Men. Elizabeth Martin^{*1}, Elizabeth Haney¹, Jackie Shannon¹, Jane Cauley², Kristine Ensrud¹, Joseph Zmuda², Eric Orwoll¹, Lynn Marshall¹. ¹Oregon Health & Science University, USA, ²University of Pittsburgh Graduate School of Public Health, USA, ³Minneapolis VA Medical Center / University of Minnesota, USA

Greater femoral neck BMD estimated with DXA is associated with higher serum 25-hydroxyvitamin D (25(OH)D) levels. However, the associations of femoral neck bone density distribution in cortical and trabecular compartments or of bone size with serum 25(OH)D are not well understood. We evaluated variation in femoral neck volumetric BMD (vBMD) and femoral neck size with serum 25(OH)D in men ages ≥ 65 years from the Osteoporotic Fractures in Men Study (MrOS). Baseline fasting serum 25(OH)D levels were measured by liquid chromatography/mass spectrometry (LC/MS) assays in a large randomly selected sample. Latitude of clinic site was defined as high latitude (40 degrees and higher) or low latitude (less than 40 degrees). Season of visit was divided into winter (January-March), spring (April-June), summer (July-September) and fall (October-December). Femoral neck measures obtained from quantitative computed tomography (QCT) were integral, cortical and trabecular vBMD; cross-sectional area; and integral, cortical, and percent cortical volume. QCT image processing was completed centrally without knowledge of 25(OH)D status. The analytic cohort was comprised of 888 men with both serum 25(OH)D and femoral neck measures. Multivariable linear regression models with adjustments for age, race, BMI, height, latitude of clinic site and season of visit were used to estimate adjusted means of femoral neck measures and their 95% confidence limits (CI) within quartiles of vitamin D, with quartile 4 (highest) as the referent. Tests of linear trend were performed for each femoral neck measure across increasing serum 25(OH)D concentrations. On average, femoral neck vBMD measures all increased with increasing 25(OH)D concentration (Table). Overall femoral neck size, as represented by cross-sectional area and integral volume did not vary according to serum 25(OH)D concentration. However, both cortical volume and cortical volume as a percent of integral volume increased significantly with increasing 25(OH)D concentration. We observed positive associations of femoral neck cortical and trabecular vBMD and percent cortical bone volume to serum 25(OH)D among elderly men. These data suggest that higher serum vitamin D levels may inhibit endosteal resorption.

Table: Distribution of QCT measurements of the femoral neck within Vitamin D quartiles (N=888)

	25(OH)D Quartile				p-trend
	Q1 [11.1-19.7 ng/ml]	Q2 [19.7-24.4 ng/ml]	Q3 [24.4-29.6 ng/ml]	Q4 [29.7-55.8 ng/ml]	
Femoral Neck Measures	Adjusted Means* and 95% CI of outcome measures within quartiles				
n	221	219	226	222	
Integral BMD (g/cm ³)	0.289 (0.282, 0.296)	0.289 (0.281, 0.298)	0.300 (0.293, 0.307)	0.308 (0.299, 0.318)	<0.001
Cortical BMD (g/cm ³)	0.528 (0.519, 0.538)	0.525 (0.515, 0.534)	0.534 (0.525, 0.544)	0.540 (0.529, 0.550)	0.03
Trabecular BMD (g/cm ³)	0.075 (0.069, 0.081)	0.075 (0.068, 0.082)	0.084 (0.078, 0.091)	0.084 (0.077, 0.091)	0.01
Cross-Sectional Area (cm ²)	12.4 (12.2, 12.6)	12.4 (12.2, 12.7)	12.5 (12.2, 12.7)	12.5 (12.2, 12.8)	0.42
Integral Volume (cm ³)	20.7 (20.3, 21.0)	20.6 (20.2, 21.0)	20.5 (20.1, 20.9)	20.4 (20.0, 20.9)	0.35
Cortical Volume (cm ³)	9.0 (8.8, 9.2)	9.1 (8.8, 9.3)	9.2 (9.0, 9.4)	9.4 (9.1, 9.6)	0.01
Percent Cortical Volume	44.2 (43.2, 45.1)	44.4 (43.4, 45.4)	45.1 (44.3, 46.3)	46.5 (45.4, 47.6)	<0.001

* Least square means and 95% Confidence Interval (CI) estimate from generalized linear regression for each outcome variable after adjustment for age, race, latitude of study site, season of visit, height and BMI

Table

Disclosures: Elizabeth Martin, None.

MO0344

Occurrences of Falls in Elderly People within the Domicile. Bianca Segantin¹, Fabiana Fonseca^{*2}, Manuela Santos¹, Thais Sabbag¹, Ana Elisa Rosa¹, Ursula Karsch¹, Roberto Queiroz¹. ¹PUC - SP, Brazil, ²PUC Sp, Brazil

The falls are the leading cause of accidents in the elderly and in most cases occur in the home, being responsible for 70% of accidental deaths in this group of citizens and the 6th leading cause of death in the elderly (Edelberg, 2001). This study is based on

field research, the data were collected with semi structured interview on 40 patients aged from 60s, interned in orthopedics Hospital public server Sao Paulo State, Brazil. In the year 2010 with the goal of revealing the location of fall of elderly hospitalized with fracture of femur, and therefore in need of surgical support. 23% of patients surveyed suffered the fall outside his domicile (bus, walk, work, etc). And 77% suffered the fall in his home. The local prevalence of falls in the home for the elderly was fourth with 32%, followed by 12%, 10%, 10% in ladder lounge, 5% in the bathroom, 2% on laundry, 2% in the service area in the yard, 2% and 2% by nearest domestic pet. Which begs the need for environmental adaptation and permanent education for care not to suffer falls.

Disclosures: Fabiana Fonseca, None.

MO0345

Reduction in Hip Bone Mass in Elderly Women Is More Related to Loss of Cortical Bone Than Trabecular Bone. ZhiFeng Yu¹, Keenan Brown², Ben Khoo³, Kun Zhu⁴, Marie Pollock⁵, Colin Binns⁶, Deborah Kerr⁶, Vicky Solah⁶, Amanda Devine⁷, Richard Prince^{*5}. ¹School of Medicine, University of Western Australia, Australia, ²Mindways Software, USA, ³Western Australian Health Department, Australia, ⁴University of Western Australia, Sir Charles Gairdner Hospital, Australia, ⁵Sir Charles Gairdner Hospital, Australia, ⁶Curtin University, Australia, ⁷Edith Cowan University, Australia

Quantitative computed tomography (QCT) is able to discriminate cortical and trabecular bone compartments. This study compares the difference in cortical and trabecular bone compartments over 2 years in elderly women.

135 females mean age 74.1 (SD 2.6) were recruited from the general population to participate in a 2 year study of protein supplementation. At baseline height was 160.2 (SD 5.9) cm and weight 68.4 (SD 10.7) kg. Subjects were scanned on a Phillips Brilliance 64 MDCT with 1mm in plane resolution. The image was analysed with Mindways CTX Hip software. Segmentation of cortical and trabecular compartments used a 300 mg/cm³ threshold.

Cortical mass and volume decreased but density remained constant. Trabecular mass decreased but without significant reduction in volume or density.

Reduction in total hip density obscures a substantial loss of cortical bone volume but not density in aging with relative preservation of remaining trabecular bone.

Disclosures: Richard Prince, None.

MO0346

Risk Factors for Osteoporosis in Greek Male Population. George Trovas^{*}. Greece

Introduction: Although not as common as in women, osteoporosis remains a significant health care problem in men. Data concerning risk factors for low Bone Mineral Density (BMD) and fractures are lacking for Greek male population. The objective of the current cross-sectional study was to determine the factors associated with BMD in Greek men.

Methods: A total of 1084 men (age range 50-93 years) from 92 sites all over Greece, participated in the present study. Demographic, medical, family history and life style information were obtained by interview and physical examination and anthropometric data by examination. Spine and hip BMD was measured using dual-energy x-ray absorptiometry. Univariate, multivariate and logistic regression analyses were performed.

Results: The prevalence of osteoporosis and osteopenia were 48,1% and 27,9% respectively. A number of nutritional, life style characteristics and medical conditions were associated with BMD. The multiple regression analysis found that age, Rheumatoid arthritis (RA), Chronic Obstructive Pulmonary Disease (COPD) and family history of osteoporosis were independently associated to the osteoporosis status and on the other hand BMI and exercise until 30years of age, were associated with higher BMD.

Conclusions: Aging, Rheumatoid Arthritis, Chronic Obstructive Pulmonary Disease and family history of osteoporosis are the main risks factors associated with osteoporosis in a population of Greek adult men.

Disclosures: George Trovas, None.

This study received funding from: sanofi-aventis Greece

MO0347

The Association of Bone Marrow Fat with Areal and Volumetric Bone Mineral Density Differs by Diabetic Status. Yahtyng Sheu^{*1}, Francesca Amati², Ann Schwartz³, Xiaojuan Li³, Christine Lee⁴, Christopher Gordon⁵, Bret Goodpaster⁶, Robert Boudreau⁶, Joseph Zmuda¹, Jane Cauley¹. ¹University of Pittsburgh Graduate School of Public Health, USA, ²University of Lausanne, Switzerland, ³University of California, San Francisco, USA, ⁴OHSU, USA, ⁵McMaster University, Canada, ⁶University of Pittsburgh, USA

Osteoblasts and adipocytes share a common precursor cell. During normal aging process, differentiation of these precursor cells in the bone marrow compartment is thought to favor adipogenesis. Recent small studies have shown a negative association between bone marrow fat (BMF) and areal BMD (aBMD) in both men and women. However, little is known about this relationship among older adults and whether results are similar for volumetric BMD (vBMD). We recruited 156 men aged 74-96 years old from the Osteoporotic Fracture in Men study to test whether BMF is inversely correlated with both aBMD and vBMD. All men underwent measures of spine BMF using magnetic resonance spectroscopy, spine and hip aBMD by dual-energy x-ray absorptiometry, and cortical (CRT) and trabecular (TRAB) vBMD at the radius and tibia by peripheral quantitative computed tomography (pQCT). BMF was expressed as lipid to "lipid + water" ratio (%). Pearson correlation and multivariable linear regression were used to examine our hypothesis. All analyses were adjusted for age, weight and height. The mean BMF was 55.6 % (ranged 23.5%-76.4%). We observed no significant correlation between BMF and aBMD at both hip and spine. For vBMD, the correlation was only significant for CRT vBMD at the tibia 66% site. However, the prevalence of diabetes (DM) was significantly higher in higher quartile of BMF (lowest: 18% vs. highest: 41%). Thus, we stratified our results by DM status: the correlations were significant for total hip aBMD (DM group) and CRT vBMD at the tibia 66% site (non-DM group). Moreover, one standard deviation (SD) increase in BMF was associated with 5.8% lower hip aBMD in DM group and 1.2 % lower CRT vBMD at the tibia 66% site for the non-DM group. We found no association between BMF and aBMD until analyses were stratified by DM status. Using pQCT, our study demonstrates for the first time a negative correlation between BMF and cortical, but not trabecular, vBMD. In addition, our study is also the first to identify differences in the relation of BMF and BMD by DM status. Further investigation on the role of DM in the BMF and bone connection may provide a better understanding of the high fracture rates among DM individuals despite their high BMD.

Table: Correlation coefficients between BMF and BMD in older men

	All	DM (n=38)	Non-DM (n=118)
aBMD, g/cm ²			
Femoral neck	-0.07	-0.27	-0.03
Total Hip	-0.11	-0.35*	-0.04
Total Spine	-0.09	-0.05	-0.17
vBMD, mg/cm ³ *			
T4% TRAB	-0.08	-0.20	-0.07
T33% CRT	-0.10	0.05	-0.16 [†]
T66% CRT	-0.22*	-0.12	-0.29*

* p<0.05; [†] 0.05< p<0.1; [‡] only results for tibia were shown

Disclosures: Yahtyng Sheu, None.

MO0348

Are Plasma Concentrations of B Vitamins or Homocysteine Associated with Bone Volumetric Density and Size? The Framingham Study. Robert McLean^{*1}, Shivani Sahni², Paul Jacques³, Jacob Selhub⁴, Kerry Broe⁵, Mary Bouxsein⁶, Douglas Kiel⁷. ¹Hebrew SeniorLife, Harvard Medical School, USA, ²Hebrew SeniorLife, Institute for Aging Research, USA, ³Jean Mayer U.S. Dept of Agriculture Human Nutrition Research Center on Aging at Tufts University, USA, ⁴Jean Mayer U.S. Dept of Agriculture Human Nutrition Research Center on Aging at Tufts University, USA, ⁵Hebrew Senior Life, USA, ⁶Beth Israel Deaconess Medical Center, USA

Decreased bone mineral density (BMD) has been hypothesized as one potential mechanism linking low B vitamin status and related elevated homocysteine (Hcy) with increased fracture risk, yet blood concentrations of B vitamins and Hcy have been inconsistently associated with DXA-based BMD across population-based studies. Areal BMD, however, does not provide information on volumetric and compartment specific bone density or bone geometry, which are important determinants of bone strength. We thus determined the cross-sectional associations of plasma concentrations of folate, vitamin B12, vitamin B6 and Hcy with QCT measures of spinal bone density among community-dwelling middle-aged and older adults. We hypothesized that plasma B vitamin concentrations would be positively associated, and Hcy concentrations negatively associated, with volumetric BMD. Participants included 615 men and 665 women from the Framingham Offspring cohort who had plasma B vitamins and Hcy measured in 1998-2001 and QCT scans of the lumbar spine in 2002-06. Plasma folate (nmol/L), vitamin B12 (pmol/L), vitamin B6 (nmol/L) and Hcy (μmol/L) were measured from fasting blood samples. Trabecular volumetric BMD (Tb.vBMD, g/cm³), integral volumetric BMD (Int.vBMD, g/cm³) and cross-sectional

area (CSA, cm²) at L3 were measured from QCT scans using custom software. Separately for men and women, multivariable linear regression determined the associations (β coefficient) of log-transformed B vitamins and Hcy with each bone measure, adjusting for age (yrs), height (in), BMI (kg/m²), smoking (y/n), alcohol (oz/wk), osteoporosis medication use (y/n), and estrogen use (y/n) and menopause status (y/n) in women. Mean age was 64 yrs (range 41-86). B vitamins and Hcy were not associated with QCT measures in men (Table). In women, folate and vitamin B6 were not associated with QCT measures. Though vitamin B12 was not associated with volumetric BMD, there was a borderline statistically significant positive association with CSA (β=0.271, P=0.04). Hcy in women tended to be positively associated with Int.vBMD (β=0.010, P=0.05), but not with Tb.vBMD or CSA. Our results suggest that plasma B vitamins and Hcy are not associated with volumetric bone density and geometry of the lumbar spine. Longitudinal studies that include additional bone sites are needed to confirm our results, and alternate mechanisms linking B vitamins and Hcy to fracture risk should be explored.

QCT measure	Folate (nmol/L)		Vitamin B12 (pmol/L)		Vitamin B6 (nmol/L)		Hcy (μmol/L)	
	β	P-value	β	P-value	β	P-value	β	P-value
Men								
Int.vBMD, g/cm ³	-0.001	0.83	0.006	0.16	0.001	0.60	0.002	0.73
Tb.vBMD, g/cm ³	0.001	0.71	0.007	0.10	-0.001	0.73	0.001	0.80
CSA, cm ²	-0.066	0.47	-0.156	0.23	-0.018	0.80	-0.091	0.60
Women								
Int.vBMD, g/cm ³	-0.001	0.70	0.001	0.74	0.002	0.32	0.010	0.05
Tb.vBMD, g/cm ³	0.0004	0.86	0.006	0.15	0.001	0.50	0.009	0.12
CSA, cm ²	0.051	0.56	0.271	0.04	0.107	0.10	-0.207	0.24

* Adjusted for age, height, BMI, smoking, alcohol, osteoporosis medications, and in women, estrogen use and menopause status

Table

Disclosures: Robert McLean, None.

MO0349

Distribution and Determinants of Serum 25-hydroxyvitamin D (25[OH]D) Levels and Change in Serum 25[OH]D Levels in Older Women: Data from the Study of Osteoporotic Fractures. Marc Hochberg^{*1}, Li-Yung Lui², Jane Cauley³, Kristine Ensrud⁴, Lisa Fredman⁵, Teresa Hillier⁶, Erin LeBlanc⁷, Steven Cummings⁸. ¹University of Maryland School of Medicine, USA, ²California Pacific Medical Center Research Institute, USA, ³University of Pittsburgh Graduate School of Public Health, USA, ⁴Minneapolis VA Medical Center / University of Minnesota, USA, ⁵Boston University School of Public Health, USA, ⁶Kaiser Center for Health Research, USA, ⁷Oregon Health Sciences University School of Medicine, USA, ⁸San Francisco Coordinating Center, USA

Purpose: To examine the distribution and determinants of serum 25-hydroxyvitamin D (25[OH]D) levels and change in serum 25[OH]D levels in older women. **Methods:** Serum 25[OH]D levels were measured using liquid chromatography tandem mass spectroscopy (LC-MS/MS) (ThermoFisher Scientific, Franklin, MA and Applied Biosystems-MDS Sciex, Foster City, CA) at the Mayo Clinic in 1297 randomly selected women who participated in the 6th biannual visit (V6) in the Study of Osteoporotic Fractures (January 1997 to January 1999). The distribution of serum 25[OH] levels was examined and cutpoints were identified at the quartiles. Characteristics of subjects by category of 25[OH]D were compared using analysis of variance for continuous and chi-square tests for categorical data. Multiple linear regression analysis was performed including age, clinic and all variables with P < 0.10 in bivariate analysis. Change in serum 25[OH]D levels since the 4th biannual visit (V4) (March 1992 to December 1994) was calculated for the 1044 white women with longitudinal data. Characteristics of subjects according to tertiles were compared as above and multiple logistic regression analysis was performed. Results: The 1297 women had a mean (SD) age of 79.5 (4.6) years and 130 (10%) were African-American; mean (SD) serum 25[OH]D level was 24.4 (10.1) ng/ml (interquartile range: 17, 31). Factors associated with categories of serum 25[OH]D in bivariate analysis are shown in Table 1. Multiple regression analysis showed that Caucasian race, lower body mass index, use of calcium and vitamin D supplements as well as estrogen and thiazide diuretics were all significantly associated with higher 25[OH]D levels. Among 1044 white women with serial data (mean [SD] 4.5 [0.6] years apart), the mean (SD) change in serum 25[OH]D level was 2.0 (9.8) ng/ml (interquartile range: -3.6, 7.0). Factors associated with categories of change in serum 25[OH]D levels in bivariate analysis are shown in Table 2. Multiple regression analysis showed that women who used vitamin D supplements were significantly more likely to have an increase in 25[OH]D levels while those with a history of stroke were significantly more likely to have a decline in 25[OH]D levels. Conclusion: These data demonstrate that older white women have higher adjusted serum 25[OH]D levels than older African-American women, and that use of vitamin D supplements is associated with an increase in serum 25[OH]D levels over time in older white women.

Characteristics of 1297 Women by Category of Serum 25(OH)D Level

Variable	≤ 16 ng/ml N = 327	17-23 ng/ml N = 328	24-30 ng/ml N = 296	≥ 31 ng/ml N = 346	P value
African-American	63 (19.3%)	42 (12.8%)	13 (4.4%)	12 (3.5%)	<0.0001
Calcium use	118 (36.1%)	146 (44.5%)	168 (55.5%)	243 (70.2%)	<0.0001
Vitamin D use	73 (22.3%)	173 (52.7%)	190 (64.2%)	293 (84.7%)	<0.0001
BMI kg/m ² mean(SD)	27.8 (5.8)	27.3 (5.0)	26.6 (4.5)	25.6 (4.4)	<0.0001
Estrogen use	39 (11.9%)	65 (19.8%)	60 (20.3%)	94 (27.2%)	<0.0001
Thiazide use	75 (22.9%)	84 (25.6%)	54 (18.2%)	95 (27.5)	0.04

Table 1

Characteristics of 1044 White Women by Category of Change in Serum 25(OH)D Level

Variable	≤ -1.1 ng/ml N = 342	-1.1 – 4.9 ng/ml N = 336	≥ 4.9 ng/ml N = 366	P value
Calcium use @ V6	168 (49.1%)	181 (53.9%)	228 (62.3%)	0.002
Vitamin D use @ V6	159 (46.5%)	204 (60.7%)	257 (70.2%)	<0.0001
BMI kg/m ² mean(SD)	26.7 (4.7)	26.6 (4.7)	26.3 (4.3)	0.42
Estrogen use	65 (19.0%)	65 (19.4%)	70 (19.1%)	0.99
History of stroke	21 (6.1%)	10 (3.0%)	9 (2.5%)	0.02

Table 2

Disclosures: Marc Hochberg, Theralogix LLC, 5; Theralogix LLC, 1

BAP (p= 0.002). Among non-users, higher dietary alpha-tocopherol intake was associated with lower uNTx/Cr (p=0.001).

Conclusions: Higher serum levels of gamma-tocopherol are associated with increased bone formation among supplement users, while higher intake of alpha-tocopherol was associated with increased bone resorption. This may be because high intake of alpha-tocopherol, due to supplement intake, suppresses serum gamma-tocopherol level. More studies are needed to confirm these findings.

Disclosures: Maryam Hamidi, None.

MO0351

Physical Activity Patterns and Preferences in Women with Low Bone Mass. Carly Skidmore^{*1}, Michel Saccone¹, Nicole Mittmann², Lora Giangregorio¹. ¹University of Waterloo, Canada, ²Sunnybrook Health Sciences Centre, Canada

Objectives: Balance and resistance training can reduce fall risk and positively impact bone density and geometry among persons with low bone mass, whereas there is less evidence that walking can reduce fall risk or influence bone strength. It is not known whether physical activity participation in this population is consistent with current evidence or physical activity guidelines. Further, future research or community programs should consider patient preferences and willingness to pay. The current study characterized physical activity patterns and preferences of women with low bone mass. **Methods:** Women ≥50 years old were recruited from 3 osteoporosis support groups. The Community Healthy Activities Model Program questionnaire was used to characterize physical activity. A Physical Activity Preferences questionnaire developed and pilot tested by our team was used to assess activity preferences and willingness to pay for exercise instruction. **Participant characteristics and outcomes** are summarized using descriptive statistics. **Results:** 54 women (mean [SD] age 73.8 [7.47] years) participated; 39 (72%) and 14 (26%) reported having osteoporosis or osteopenia, respectively. Mean (SD) total frequency and hours per week of moderate intensity weight-bearing or resistance exercise were 5.2 (3.6) times a week and 3.7 (3.2) hours, respectively. Walking was reported most frequently (62% [n=31] engaged in uphill or brisk walking), followed by light (using <5lbs) resistance training, reported by 44% of participants. Only 24% reported resistance training with weight ≥5lbs. Half of the participants reported doing balance exercises. 71% of participants reported moderate intensity weight bearing exercise ≥ 3 times per week, but it dropped to 53% when walking/jogging was removed. 35.2% reported that they prefer a combination of individual and group exercise, with the rest being divided between the two. Many (42.6%) were not interested or not willing to pay for individualized exercise prescription. 68.5% received exercise recommendations from a physician, with walking being the most common recommendation (31.5%). **Conclusions:** Many, but not all of our sample reported regular moderate intensity weight-bearing exercise. Further, participation in interventions for which there is strongest evidence, namely resistance and balance training, are practiced much less frequently. Finally, cost may be a barrier in delivering evidence-based exercise prescription.

Disclosures: Carly Skidmore, None.

MO0352

Positive Association of Total Dairy and Milk Intake with Bone Mineral Density (BMD): Results from the Framingham Offspring Study. Shivani Sahni^{*1}, Katherine Tucker², Douglas Kiel³, Lien Quach⁴, Virginia Casey⁴, Marian Hannan⁵. ¹Hebrew SeniorLife, Institute for Aging Research, USA, ²Northeastern University, USA, ³Hebrew SeniorLife, USA, ⁴Institute for Aging Research, Hebrew SeniorLife, USA, ⁵HSL Institute for Aging Research & Harvard Medical School, USA

Objective: Health effects of dairy foods may be due to more than a single nutrient. We evaluated the association of intake of milk, yogurt, cheese, cream and total dairy intake (with/without inclusion of cream since cream has high fat content) with bone mineral density (BMD) at the hip [femoral neck (FN), trochanter (TR)] and spine (lumbar spine, LS) in the Framingham Offspring Study.

Methods: 2,733 men and women completed a food frequency questionnaire (FFQ) in 1992-95 or 1995-98 (baseline exam) and a BMD assessment of hip and spine completed in 1996-2001 using dual-energy X-ray absorptiometry. We used linear regression to estimate mean BMD for men and women separately and combined, by quartile/categories of dairy intake (servings/week) with adjustment for age, sex, total energy intake, weight, height, menopause and estrogen use in women alone, calcium supplement use and vitamin D supplement use. Final models simultaneously included dairy items adjusting for each other.

Results: Mean age was 55y (SD: 9.6, range: 26-86) at the baseline exam. In the combined sample of men and women, total dairy (excluding cream and ice cream) was positively associated with hip and spine BMD (Table 1) while total dairy (including cream and ice cream) was associated only with FN and TR but not LS-BMD. Milk intake was associated with hip and spine BMD. However, cream intake tended to be negatively associated with FN but not with other BMD sites. Subjects with high yogurt intake (>4 servings/week) had higher BMD compared to those with no intake. Although not significant, a similar trend was seen for cheese intake. When milk, yogurt, cheese and cream were included simultaneously in the model, milk and high

Effects of Dietary and Serum Alpha-tocopherol versus Serum Gamma-tocopherol Levels on Bone Turnover Markers among US Postmenopausal Women. Maryam Hamidi^{*1}, Paul N Corey², Valerie Tarasuk², Angela Cheung³. ¹University of Toronto/University Health Network-TGH, Can, ²University of Toronto, Canada, ³University Health Network, Canada

Background: Alpha- and gamma-tocopherol are different forms of vitamin E. In vitro and animal studies suggest that gamma-tocopherol may have an anabolic effect on bone, while alpha-tocopherol may have anti-bone resorptive properties. Human studies are limited. We examined the associations between alpha-tocopherol intake (dietary or supplements), serum alpha- and gamma-tocopherol levels and bone turnover markers (BTMs) among postmenopausal women in the United States.

Methods: We used cross-sectional data from the National Health and Nutrition Examination Survey 1999-2002 cycles. We included 518 postmenopausal women aged ≥ 45 years who were not taking steroids, estrogen, osteoporosis treatment medications; were free from kidney and liver disease, cancer, rheumatoid arthritis; and were fasting > 9 hours prior to examination. Data for dietary gamma-tocopherol intake was not available. Natural logarithmic transformation of all biomarkers and dietary data was performed to reduce the within sample variability and to avoid inappropriate exclusion of outliers. Multiple regression models with adjustments for relevant confounders were used to examine the relationship between the vitamin E variables and serum bone-specific alkaline phosphatase (BAP, a biomarker of bone formation) and urinary N-Telopeptides/Creatinine (uNTx/Cr, a biomarker of bone resorption).

Results: The geometric means (95% CI) for dietary alpha-tocopherol, serum alpha- and gamma-tocopherol levels were 4.45 (4.06, 4.89) mg/day, 1482.97 (1428.91, 1539.06) mcg/dL and 194.06 (177.77, 211.84) mcg/dL respectively. 44% of women took vitamin E (alpha-tocopherol) supplements. We found that the association between dietary alpha-tocopherol intake and serum gamma-tocopherol and BTMs varied among vitamin E supplement users and non-users. Among vitamin E supplement users, higher dietary alpha-tocopherol intake was associated with higher uNTx/Cr (p= 0.001); and higher serum gamma-tocopherol was associated with higher

yogurt intake remained positively associated with BMD while cream remained negatively associated with hip and spine BMD (Table 2). The positive associations for cheese did not reach significance.

Conclusion: Total dairy intake, specifically milk and yogurt intake, were significantly associated with BMD at hip and spine in men and women, while cream adversely influenced BMD suggesting that not all dairy products are equally beneficial on the skeleton.

Table 2: Association of dairy intake (servings/week) with BMD (g/cm³) adjusting for other dairy products in men and women from the Framingham Offspring Cohort.

n=2479	FN-BMD			TR-BMD			LS-BMD		
	β	SE	p-value	β	SE	p-value	β	SE	p-value
Milk (serv./wk)	0.00096	0.001	0.02	0.00065	0.0004	0.11	0.00052	0.0006	0.42
Yogurt, No intake	Ref			Ref			Ref		
Medium intake (=4 serv./wk)	-0.00001	0.005	0.99	0.00695	0.005	0.18	0.00707	0.008	0.39
High intake (>4 serv./wk)	0.02045	0.010	0.05	0.02489	0.010	0.02	0.01862	0.017	0.26
Cheese, Low intake (<2 serv./wk)	Ref			Ref			Ref		
Medium intake (2-4 serv./wk)	0.00038	0.006	0.94	-0.00417	0.006	0.46	-0.0051	0.009	0.57
High intake (>4 serv./wk)	0.00547	0.006	0.39	0.00448	0.006	0.49	0.01404	0.010	0.17
Cream, (serv./wk)	-0.00082	0.0003	0.02	-0.00078	0.0003	0.04	-0.00109	0.0006	0.05

Model adjusted simultaneously for milk, yogurt, cheese, cream, age, sex, total energy intake, weight, height and menopause, estrogen, calcium supplement use, and vitamin D supplement use

Table 2

Table 1: Association of dairy intake (servings/week) with BMD (g/cm³) in men and women from the Framingham Offspring Cohort.

Mean \pm SE ¹ (n=2479)	FN-BMD	TR-BMD	LS-BMD
Milk (serv./wk), Q1 (Lowest)	Ref	Ref	Ref
Q2	-0.00652 \pm 0.007	-0.00101 \pm 0.007	-0.00462 \pm 0.011
Q3	0.00552 \pm 0.007	0.01238 \pm 0.007 [†]	0.01800 \pm 0.010
Q4 (Highest)	0.01435 \pm 0.007*	0.01308 \pm 0.007*	0.01554 \pm 0.010
P trend	0.007	0.009	0.03
Yogurt (serv./wk), No intake	Ref	Ref	Ref
Medium intake (=4 serv./wk)	0.00074 \pm 0.005	0.00823 \pm 0.005	0.00838 \pm 0.008
High intake (>4 serv./wk)	0.02304 \pm 0.010*	0.02628 \pm 0.010*	0.02218 \pm 0.016
P trend	0.12	0.006	0.11
Cheese (serv./wk), Low intake	Ref	Ref	Ref
Medium intake (2-4 serv./wk)	0.00217 \pm 0.005	-0.00214 \pm 0.005	-0.00347 \pm 0.009
High intake (>4 serv./wk)	0.00612 \pm 0.006	0.00575 \pm 0.006	0.01542 \pm 0.009
P trend	0.33	0.44	0.18
Cream (serv./wk), Q1 (Lowest)	Ref	Ref	Ref
Q2	-0.00328 \pm 0.007	0.00117 \pm 0.007	-0.01319 \pm 0.011
Q3	-0.00736 \pm 0.007	-0.00963 \pm 0.007	-0.02078 \pm 0.011
Q4 (Highest)	-0.01150 \pm 0.007 [†]	-0.00751 \pm 0.007	-0.01404 \pm 0.010
P trend	0.07	0.11	0.16
Total Dairy (without cream & ice cream, serv./wk), Q1 (Lowest)	Ref	Ref	Ref
Q2	-0.00171 \pm 0.007	-0.00064 \pm 0.007	0.01389 \pm 0.010
Q3	0.01750 \pm 0.007*	0.01383 \pm 0.007*	0.02819 \pm 0.010*
Q4 (Highest)	0.02383 \pm 0.007*	0.02461 \pm 0.007*	0.03431 \pm 0.010*
P trend	<0.001	<0.001	0.0005
Total Dairy (with cream & ice cream serv./wk), Q1 (Lowest)	Ref	Ref	Ref
Q2	-0.00912 \pm 0.007	-0.01604 \pm 0.007*	-0.00658 \pm 0.010
Q3	0.01707 \pm 0.007*	0.01625 \pm 0.007*	0.02445 \pm 0.010*
Q4 (Highest)	0.00803 \pm 0.007	0.00605 \pm 0.007	0.00705 \pm 0.010
P trend	0.02	0.02	0.12

[†] Means \pm SE represent the mean difference in BMD compared to the reference quartile (Q1). Means are significantly different from means of Q1: * P<0.05, [†] P=0.1

Table 1

Disclosures: Shivani Sahni, None.

This study received funding from: General Mills Bell Institute

MO0353

Atypical Humeral Fractures and Bisphosphonate Use. Maria Yavropoulou¹, Andrea Giusti², Sharita Ramautar¹, Sanders Dijkstra³, Neveen Hamdy⁴, Socrates Papapoulos⁴. ¹Leiden University Medical Center, Department of Endocrinology & Metabolism, Netherlands, ²Galliera Hospital, Italy, ³Leiden University Medical Center, Department of Orthopedic Surgery, Netherlands, ⁴Leiden University Medical Center, The Netherlands

Background: Atypical fractures of the femur have been reported to occur in patients on long-term treatment with bisphosphonates (BPs) but causality has not been proven and it is not known whether similar fractures may occur in other long bones. We have addressed this issue by examining the relationship between humeral shaft fractures and BP use. Patients and Methods: We identified all patients aged ≥ 50 years consecutively admitted to a single center with a new humeral fracture over a 9-year period. All individual radiographs were examined and fracture site was classified according to the Muller AO classification of Fractures of Long Bones. A case-control study was undertaken in patients with humeral shaft fractures using as controls sex and age matched patients with proximal humeral fractures in a 1:4 ratio. Patients with shaft fractures and radiographic characteristics similar to those of atypical femoral

fractures, including cortical thickening and unicortical beaking, were compared with those with ordinary shaft fractures. The relationship of "atypical" fractures and BP or GCs use was examined. Results: One hundred and ninety eight patients had a low-energy fracture of the humerus and in 20 of those this was a shaft fracture (10%). These 20 patients (cases) were matched with 80 patients with proximal fractures (controls). BPs were used by 5% of cases and by 6.3% of controls (OR, 0.80; 95%CI, 0.09-6.85) and GCs were used by 10% of cases and 8.8% of controls (OR, 1.15; 95% CI 0.23-5.83). There was no difference in cortical thickness between cases and controls and BP or GCs users and non-users. Four of the 20 patients with shaft fractures had "atypical" radiographic features (20%). None of these patients had ever been treated with BPs or GCs and two of them had diabetes type 2. Conclusions: Data of our study suggest that low-energy "atypical" fractures of the humeral shaft are infrequent (2% of low energy humeral fractures) and are not associated with the use of BPs or GCs.

Disclosures: Maria Yavropoulou, None.

MO0354

Fracture Risk Is Increased in Young Women with Rheumatoid Arthritis. Shreyasee Amin*, Sherine Gabriel, Sara Achenbach, Elizabeth Atkinson, L. Joseph Melton. Mayo Clinic, USA

Rheumatoid arthritis [RA] is the only cause of secondary osteoporosis singled out in the WHO's fracture [fx] prediction algorithm, FRAX[®]. Nevertheless, the risk for fx among younger women and men with RA is not well established. We examined the risk for fx by sex and by age at diagnosis in a population-based RA cohort.

We studied Olmsted County, MN residents (age ≥ 18 yrs) first diagnosed with RA between 1955-2007, all of whom met 1987 American College of Rheumatology criteria for RA, and an equal number of age- and sex-matched controls. All incident fxs were identified through a complete review (inpatient and outpatient) of medical records. Excluding fxs resulting from severe trauma, the risk for first osteoporotic fx [OP fx] (hip, spine, wrist and proximal humerus), and for any first fx following their RA diagnosis was compared with their matched control, stratified by sex, using a Cox proportional hazards model, where follow-up time (until death or last known follow-up) ended at the first date reached by either within a pair. We then stratified by age at RA diagnosis (<50 yrs, ≥ 50 yrs). For those <50 yrs, we examined the risk for fx over all available follow-up as well as until age 50 yrs.

In 1155 RA cases (810 women and 345 men, mean age at RA diagnosis SD: 56 16 yrs and 58 14 yrs, respectively) followed for 12,585 person-yrs [p-y], 205 women (25%, 23 per 1000 p-y) and 67 men (19%, 19 per 1000 p-y) had an OP fx, while 276 women (34%, 31 per 1000 p-y) and 87 men (25%, 24 per 1000 p-y) had any fx. Women and men with RA were at increased risk for fx relative to controls, regardless of age at diagnosis [see table]. When follow-up was limited to age 50 yrs in the 304 women <50 yrs with RA (mean age at RA diagnosis: 39 yrs), the hazard ratio [HR] for OP fx was 6.7 (95% CI: 1.5, 29.5), with 13 women having at least one OP fx (7 per 1000 p-y) vs. 2 (1 per 1000 p-y) in matched controls; the HR for any fx was 1.9 (95% CI: 1.04, 3.4), with 31 women with RA having at least one fx (16 per 1000 p-y) vs. 17 (9 per 1000 p-y) in matched controls. In men <50 yrs with RA (N=109, mean age: 41 yrs), too few had a fx before age 50 yrs (N=2 with OP fx; N=5 for any fx) for any robust conclusion on fx risk relative to controls.

Women and men with RA, including those younger than age 50 yrs when diagnosed, have an increased fx risk. Furthermore, we have identified that young women with RA are at an increased risk for fx occurring even before age 50 yrs.

Hazard Ratio (95% CI) by Age at RA Diagnosis			
Women	Any Age	<50 yrs**	≥ 50 yrs
OP Fx*	1.7 (1.4, 2.2)	4.3 (2.4, 7.8)	1.4 (1.1, 1.8)
Any Fx*	1.6 (1.3, 1.9)	2.4 (1.6, 3.5)	1.4 (1.1, 1.7)
Men			
OP Fx*	1.6 (1.1, 2.4)	1.4 (0.7, 3.0)	1.8 (1.1, 2.8)
Any Fx*	1.4 (1.02, 1.9)	1.7 (0.9, 3.2)	1.4 (0.9, 2.0)

*excludes any severe trauma fx

**based on all available follow-up

Table

Disclosures: Shreyasee Amin, Merck & Co., 5

MO0355

Incidence of Subsequent Fractures According to Age and Site of Initial Non-Vertebral Fractures: The First 3 Years of the OPTIMUS Initiative. Fran ois Cabana¹, Michele Beaulieu², Dominique Lambert³, Pierre-Yves C  te⁴, Marc Vaillancourt⁵, Marie-Claude Beaulieu⁶, Sophie Roux⁷, Gilles Boire⁸. ¹Centre hospitalier universitaire de Sherbrooke, Division of Orthopaedics, Canada, ²Merck Canada - Medical Liaison, Canada, ³Warner-Chilcott Canada Co., Canada, ⁴Amgen Canada, Canada, ⁵Novartis Canada, Canada, ⁶Universit  de Sherbrooke- Department of Family Medicine, Canada, ⁷University of Sherbrooke, Canada, ⁸Centre Hospitalier Universitaire De Sherbrooke, Canada

Introduction: Although a previous fragility fracture (FF) is a well-documented risk for subsequent fracture, the impacts of sex, age, and site of non-vertebral FF on subsequent fracture risk are less well known.

Objectives: To describe the rates of subsequent fractures over the first 3 years following a non-vertebral FF according to age group and site of initial FF.

Methods: An ongoing prospective cohort of men and women over 50 years of age was followed up in the OPTIMUS study, a placebo-controlled intervention aimed at increasing the rate of initiation and persistence on osteoporosis treatment after an incident non-vertebral FF leading to an orthopaedic consultation. After inclusion, the consenting participants were counselled about osteoporosis and its relationship to FF. A letter also informed their Family Physician (FP) to stress the importance of treating osteoporosis unmasked by a FF according to the 10-year fracture risk, with reminders sent to the FP of patients still untreated at the time of regular phone follow-up. At year 1, the delivery of anti-osteoporosis medication was confirmed with the patients' pharmacists (56% were then compliant with an appropriate treatment). The occurrence of novel FF was obtained from patients during phone follow-ups.

Results: From January 2007 to December 2010, 1043 patients (861 women, 182 men) with non-vertebral FF were included in the OPTIMUS intervention, including 200 control patients. Consent was obtained from 80% of the targeted population. Up to 43% (451) of the patients were younger than 65 (mean age 57); the mean age of patients 65 and over was 77 years. Follow up was obtained from 788/841 (93.7%), 587/634 (92.6%) and 289/346 (83.5%) surviving patients at year 1, 2, and 3, respectively. The rates of FF following inclusion according to age and site of FF are shown (Table). Ankle FF, the only FF site more frequent in younger patients, was associated with a lower but significant 3-year risk for recurrent FF. Rates of recurrent FF were not statistically different between younger and older age groups.

Conclusions. Our data suggest that any non-vertebral FF indicates a high risk for new FF over the following 3 years, even when fractures occurred before the age of 65 and at sites considered as Minor (i.e. other than hip, wrist or proximal humerus). This risk is underestimated as it applies to FF patients who were apt to consent, who survived at least one year and of which more than 50% were treated at year 1.

Site of the initial fracture (Number of patients with fracture)	Incidence of New fractures per 100 person-years (Number of new fractures/Total person-years)		
	All patients	< 65 years	≥ 65 years
Any fragility fracture (n= 1043)	5.1 (79/1545)	4.4 (29/661)	5.7 (50/884)
Hip (n= 214)	6.5 (20/309)	11.6 (5/43)	5.6 (15/266)
Wrist (n= 327)	4.9 (23/471)	5.0 (11/218)	4.7 (12/253)
Ankle (n= 206)	3.6 (11/307)	3.1 (6/196)	4.5 (5/111)
Proximal humerus (n= 187)	4.7 (13/278)	2.5 (3/121)	6.4 (10/157)
Other nonvertebral sites* (n= 109)	6.7 (12/180)	4.8 (4/83)	8.2 (8/97)

*Upper limb (50), Lower limb (35), Clavicle (10), Pelvis (11), Scapula (2) and Ribs (1).

Table. Incidence of recurrent fractures according to age and site

Disclosures: Gilles Boire, Merck Canada; Alliance for Better Bone Health (sanofi-aventis Canada and Warner-Chilcott Canada Co.); Amgen Canada; Novartis Canada; Servier Canada, 2

This study received funding from: Merck Canada; Alliance for Better Bone Health (sanofi-aventis Canada and Warner-Chilcott Canada Co.); Amgen Canada; Novartis Canada; Servier Canada

MO0356

Mortality after Vertebral Fracture in Korea : Analysis of the National Claim Registry. Young-Kyun Lee¹, Yong-Chan Ha², Jae-Suk Chang³, Hyun-Koo Yoon⁴, Deog-Yoon Kim⁵. ¹Seoul National University Bundang Hospital, South Korea, ²Chung-Ang University Hospital, South Korea, ³Ulsan University, Asan Medical Center, South Korea, ⁴Cheil General Hospital & Women's Healthcare Center, South Korea, ⁵Kyung Hee University Hospital, South Korea

Purpose: A vertebral compression fracture is a serious complication associated with osteoporosis of the spine. We evaluated the incidence of vertebral fracture and subsequent mortality in Korea, using nationwide data from the Health Insurance Review Agency (HIRA).

Methods: The used HIRA database was the National Korean Health Insurance claims database, which covered about 97% of the Korean populations. All clinics and

hospitals submit data on inpatients and outpatients, including data on diagnosis and medical costs, for claims. Therefore, virtually all information about patients and diseases is available from the Korean HIRA database, which has been used on several occasions for epidemiological studies. All new visits or admissions to clinics or hospitals for fractures were recorded in nationwide cohort by the Korean HIRA using ICD-10 code. The incidence of vertebral fracture and excess mortality associated with vertebral fracture were evaluated, in men and women aged 50 years or more between 2005 and 2008. Standardized mortality ratio (SMR) was calculated to determine excess mortality associated with vertebral fracture.

Results: The crude overall incidence of vertebral fractures was 984 per 100,000 person years from 2005 to 2008. The overall mortality rate at 3, 6 months, 1 year, and 2 years after vertebral fracture in men (55.6 %, 94.1 %, 146.1 %, and 206.1 %, respectively) were higher than women (24.1 %, 43.6 %, 71.6 %, and 104.8 %, respectively). In both genders, the age-specific mortality rates were more than those of the general population. The SMR was highest during the first 3 months and gradually declined to 2.53 in men and 1.86 in women at the 2-year period.(Figure 1)

Conclusions: The incidence of vertebral fracture in Korea was comparable with other countries such as Switzerland, and the mortality after vertebral fracture is higher than that of normal populations. The incidence of osteoporotic vertebral fracture and following high mortality are likely to become serious socioeconomic problems.

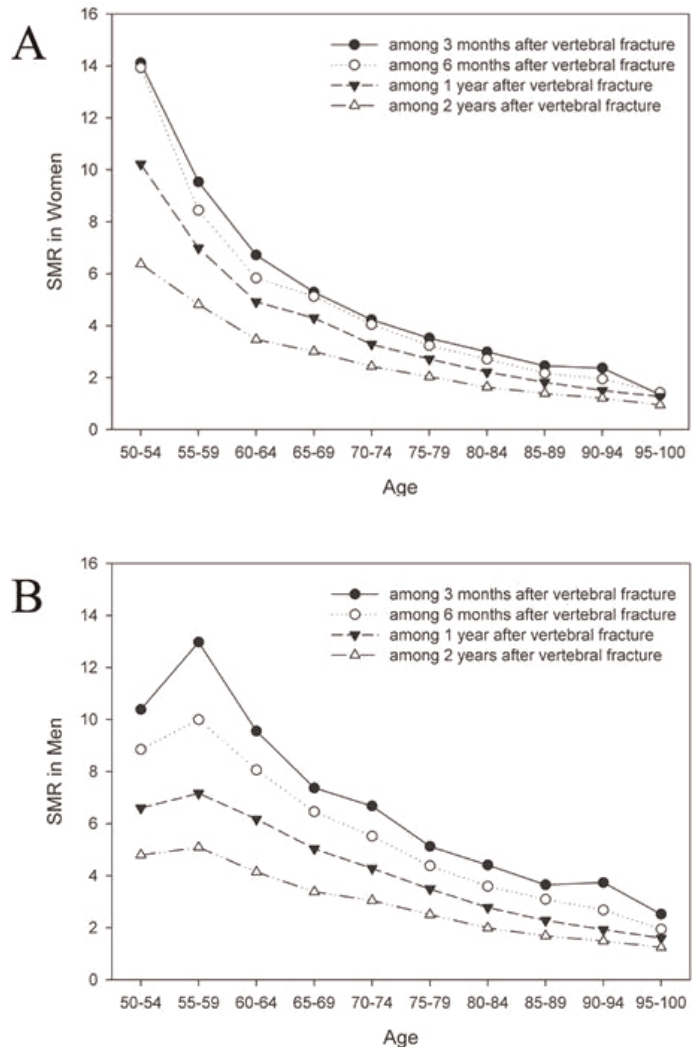


Figure 1

Disclosures: Young-Kyun Lee, None.

MO0357

Myocardial Infarction and Stroke Predict Fractures - A 13-Year Follow-Up Study in Men and Women. Kerstin Landin-Wilhelmsen^{*1}, Penelope Trimppou², Anders Lindahl³, Goran Lindstedt³, Goran Olerod³, Per-Olof Hansson⁴, Anders Oden⁵, Lars Wilhelmsen⁴. ¹Sahlgrenska University Hospital, Sweden, ²Section for Endocrinology, Department of Internal Medicine, Sahlgrenska University Hospital, Sweden, Swe, ³Department of Clinical Chemistry, Sahlgrenska University Hospital, Sweden, ⁴Department of Medicine, Sahlgrenska University Hospital, Sweden, ⁵Department of Mathematical Sciences, Chalmers University of Technology, Sweden

Purpose Fractures and cardiovascular disease (CVD) are a burden to society. The purpose was to study prospectively a possible link between fractures and CVD, especially myocardial infarction and stroke during 13 years of follow-up.

Methods A random population sample of Gothenburg, Sweden; 410 men and women, aged 25-64 years in 1995, from the WHO MONICA Project, was re-studied in 2008. Calcaneal Quantitative Ultrasound (QUS) and physical examination were performed. CVD, lifestyle factors and medical treatment were retrieved via medical records and questionnaires. Fractures were verified by X-ray. Blood samples were taken in fertile women on cycle day 7-9.

Results Since 1995, 26% of the subjects had fractured (women 29%, men 17%). Myocardial infarction, stroke, total CVD ($p=0.001$), low QUS, physical inactivity, low sex hormone levels in women, and use of antidiabetics and tranquilizers in 1995, predicted future fractures. In subjects with fractures, CVD, mainly stroke ($p=0.0005$), and higher cholesterol levels but less treatment with lipid-lowering agents were more common than in subjects without fractures in 2008.

After adjustment for age and BMI, changes in QUS were positively correlated with changes in serum estradiol and negatively correlated with changes in cholesterol levels in women. HRT decreased from 31% in 1995 to 8% in 2008, along with serum estradiol. Use of calcium/vitamin D (0-10%), anti-osteoporotics (0-3%), tranquilizers (15-29%), and lipid-lowering agents (0-15%) was increased in all subjects. Total cholesterol decreased, irrespective of treatment.

Conclusions Myocardial infarction, stroke, diabetes, tranquilizers and a sedentary lifestyle predicted future fractures. Fractured subjects had higher cholesterol levels but fewer lipid-lowering agents than subjects without fractures. Use of anti-osteoporotics was low at 13 years of follow-up, indicating undertreatment. The results point towards a link between metabolic bone disease and cardiovascular disease.

Disclosures: Kerstin Landin-Wilhelmsen, None.

MO0358

Nitrate Use For Angina Is Not Associated with a Reduction in Osteoporotic Fractures in Elderly Women. Yasuyo Abe^{*1}, Helena Johansson², Kiyoshi Aoyagi¹, Anders Oden³, Diane Charlesworth³, Monique Beneton³, Jenny Cliffe³, Linda Kersh³, Carol McGurk³, John Kanis⁴, Eugene McCloskey⁵. ¹Nagasaki University, Japan, ²Swedish University of Agricultural Sciences, The Biomedical Center, Sweden, ³WHO Collaborating Centre for Metabolic Bone Diseases, United Kingdom, ⁴University of Sheffield, Belgium, ⁵University of Sheffield, United Kingdom

Nitric oxide stimulates bone formation, inhibits bone resorption and prevents bone loss in postmenopausal women. The impact of nitric oxide donors on fracture risk is controversial.

We studied 5212 women, aged 75 years and older, randomly selected from the local population regardless of the presence or absence of osteoporosis. Hip BMD and other risk factors were captured at entry to a randomized, double-blind, placebo controlled trial of daily oral clodronate. At baseline, concomitant medications and conditions were documented including nitrate use and angina. The incidence of hip or any osteoporotic fractures was captured during a median of 4 years follow-up.

Overall, 951 women took intermittent ($n=351$, largely glyceryl trinitrate) or continuous ($n=600$, daily oral or patch) nitrate donors. Compared to 4261 women without nitrate use, those exposed to nitrates were slightly but significantly older, reported recent multiple falls more frequently (6% vs. 3%), more frequently took or had taken glucocorticoids (12% vs. 9%) and more frequently had difficulty in the sit-to-stand test (40% vs. 29%) at baseline. However, they had higher body mass index and higher femoral neck bone mineral density (BMD) at baseline. In total, 749 incident fractures including 186 hip fractures occurred during follow-up. When adjusted for age, time since baseline and study treatment, nitrate use was associated with a non-significant reduction in the risk of any fracture or hip fracture (HR 0.87, 95%CI 0.61-1.25 and 0.85, 0.39-1.83 respectively, both $p>0.3$). No difference was observed between continuous and intermittent users. Further adjustment for falls (or sit-to-stand), glucocorticoid use and femoral neck BMD showed no significant effect of nitrates on any fracture or hip fracture.

Our study demonstrates that population cohort studies of nitrate use and fracture rates are likely to be confounded by other risk factors. Our results suggest little or no impact of nitrates on fracture in women with angina. Further, large intervention trials are required of nitrates in men and women without angina.

Disclosures: Yasuyo Abe, None.

MO0359

Prevalence of Back Pain in Postmenopausal Osteoporosis and Associations with Multiple Spinal Factors. Naohisa Miyakoshi^{*1}, Michio Hongo¹, Hiroyuki Kodama², Akira Horikawa³, Yoichi Shimada¹. ¹Akita University Graduate School of Medicine, Japan, ²Minamiakita Orthopedic Clinic, Japan, ³Igarashi Memorial Hospital, Japan

Introduction: Back pain is a major source of morbidity among patients with osteoporosis. Although back pain in osteoporosis is often attributed to vertebral fractures (VFs), the cause of back pain in osteoporosis has been suggested as likely to show relationships with multiple factors. However, concomitant prevalences of back pain and multiple spinal factors in patients with osteoporosis have not yet been reported. The present study evaluated: 1) prevalence of back pain in patients with postmenopausal osteoporosis; and 2) associations of back pain to multiple spinal factors such as VFs, spinal alignment, mobility, and back extensor strength (BES) in these patients.

Methods: A total of 174 postmenopausal women with osteoporosis (mean age, 68 years) who visited their practitioner were asked whether they had clinically relevant back pain, and bone mineral density (BMD), number of VFs, kyphosis angle and range of motion (ROM) of the thoracic and lumbar spine, and isometric BES were evaluated. As patients with documented VFs within the last 6 months were not included, back pain for patients enrolled in this study indicated chronic back pain not attributable to fresh VFs. Measured variables were compared between subjects with back pain (BP group) and without back pain (non-BP group). In the BP group, associations between back pain intensity and other measured variables were further evaluated.

Results: Prevalence of back pain was 91.4% ($n=159$). No significant differences were seen between BP and non-BP groups with regard to age, BMD, number of VFs, thoracic and lumbar kyphosis angles, and thoracic and lumbar ROMs. However, BES was significantly less in the BP group than in the non-BP group ($p=0.013$). In the BP group, pain intensity showed a significant positive correlation with number of VFs ($r=0.171$, $p=0.031$), and negative correlations with lumbar spinal ROM ($r=-0.264$, $p<0.001$) and BES ($r=-0.268$, $p<0.001$). However, no significant correlations were observed between pain intensity and age, BMD, thoracic or lumbar kyphosis angles, or thoracic spinal ROM. Multiple regression analysis for pain intensity revealed lumbar spinal ROM ($p=0.017$) and BES ($p=0.014$) as significant contributors to pain intensity.

Conclusion: Prevalence of back pain in women with postmenopausal osteoporosis is high and the pain is significantly related to limited lumbar spinal mobility and decreased BES.

Disclosures: Naohisa Miyakoshi, None.

MO0360

Prevalence of vertebral fractures in Venezuela. Preliminary report from the Latin American Vertebral Osteoporosis Study (LAVOS). Gregorio Riera-Espinoza^{*1}, Jennv Ramos², Ada Colmenares³, Patricia Clark⁴, Fidencio Cons Molina⁵, J.O Talavera⁶. ¹Unidad Metabolica. CEAM, Venezuela, ²Unidad Metabolica, CEAM, Venezuela, ³INE Venezuela, Venezuela, ⁴Laboratorios Clinicos De Puebla, Mexico, ⁵Centro De Investigacion En Artritis Y Osteoporosis, Mexico, ⁶CMN Siglo XXI-IMSS, Mexico

The prevalence of vertebral fractures in women from Latin-America (Brazil, Argentina, Mexico, Puerto Rico and Colombia) has been shown to be similar to the rest of the world according to the population-based study LAVOS. The present study reports and expand the information of vertebral fractures in Latin America adding the prevalence of vertebral fractures in Venezuela using the same protocol as reported in the first LAVOS study.

A Population based sampling frame was obtained from the city of Valencia in Venezuela in women 50 years and older. Using the LAVOS design an age-stratified random sample of (50-59, 60-69, 70-79 and 80+) of 368 women in Valencia, Venezuela participated in the study. A questionnaire to get information on demographics, osteoporosis conventional risk factors, and some life styles characteristics was applied in all participants. BMD in two regions and lateral dorsal/lumbar X rays were obtain in all cases accordingly with LAVOS protocol to be able to have cross-national comparisons. Digital Morphometry was used to determine vertebral deformities by modified Eastell criterion. Morphometry and BMD readings were concentrated in one center

Results: A total of 383 women from Venezuela were included, however x rays of 15 cases were excluded due to position errors. Therefore the present report is based in 368 women. The overall prevalence of vertebral fractures was 14.4%. Over 50% of the women 80 and over contacted were unable to participate due to several reasons. The overall prevalence of Women from Venezuela is similar than the one reported as pooled prevalence in the LAVOS study.

Conclusion: The prevalence of vertebral fractures in Venezuela is similar as in the other Latin American Countries using the same methodology.

Age	LAVOS Venezuela n=368	Fx vs no fx	Prevalence 95% CI	LAVOS pooled data, n=1902*
50-59	96 (26.1)	14/82	14.58 (7.3 – 21.7)	6.9 (4.6-9.10)
60-69	111 (30.2)	13/98	11.71 (5.6 – 17.7)	10.2 (7.6-12.8)
70-79	105 (28.5)	18/87	17.14 (9.8 – 24.4)	18.0 (14.7-21.3)
≥80	56 (15.2)	8/48	14.29 (4.8 – 23.7)	27.8 (23.1-32.4)

Lavos Venezuela. Prevalence of vertebral fractures

Disclosures: Gregorio Riera-Espinoza, None.

MO0361

Risk Factors Associated with Secondary Fractures & Mortality in Fracture Patients Managed by a Fracture Liaison Service. Alastair McLellan^{*1}, Mayrine Fraser¹, Frances Lovell². ¹Western Infirmary, United Kingdom, ²Royal Infirmary, United Kingdom

The Fracture Liaison Service (FLS) delivers systematic identification & assessment for treatment for prevention of secondary fractures to women & men age 50+yr who present with 'low trauma' fractures or are reported to have a vertebral fracture. 11727 patients (incl. 2944 men) in whom dates of incident fractures & dates of death (if occurred) were recorded were subject to survival analysis to ascertain outcomes incl. rates of secondary fractures & mortality; logistic regression was performed to identify associated risk factors (RF). In the first 5yr of the FLS, 19% of women & 16% of men sustained a secondary fracture; 13% of women & 19% of men died. The 5yr secondary fracture rate (5yrSFR mean(95%CI)) & mortality rate (MR) in the context of site of index fracture, prevalence of osteoporosis (OP) & treatment (treated (bisphosphonate + calcium/vit D(CaD) (total incl. CaD only)) are shown in table. Using logistic regression, in men, after adjustment, site of fracture, fracture history, alcohol excess, recurrent falls, being seldom on feet, low weight, low FNBMd were all associated with significantly increased secondary fracture risk (OR 1.59 to 4.17) (the greatest being history of 4+ fractures (compared to 1 fracture). Treatment was associated with OR of secondary fracture of 0.5(0.35to0.70). In women, in addition to the above, early menopause & height loss were also associated with significantly increased fracture risk with OR 1.16 to 2.09 (greatest risk being associated with fracture history of 4+ fractures (versus 1 fracture). Treatment (typically with BP/CaD) was associated with OR of secondary fracture of 0.65(0.55-0.77). RFs significantly associated with mortality are male gender, increasing age, alcohol excess, smoking, low weight, low FNBMd & fractures at specific sites (hip, humerus and 'other sites'), the most influential being male gender OR 1.94(1.67-2.26). Treatment with BP has no influence on mortality after correction for the above RFs. Conclusion: An FLS effects high rates of treatment for fracture secondary prevention, that are associated with 35-50% reduction in secondary fracture incidence. Treatment does not alter mortality rate. Despite these interventions, widely differing secondary fracture rates & mortality accompany fractures at different sites in women & men.

	Index fx	Hip	Humerus	'other'	Radius/ulna	Hand/foot	Ankle
Women	n	983	1170	1076	3106	1425	1023
	Treated(%)	81(92)	58(64)	67 (74)	54(60)	42(47)	37(43)
	OP(%)	72	45	54	42	31	26
	MR(%)	26	14	19	10	8	7
	5yrSFR(%)	27(24-34)	22(19-25)	26(22-29)	19(17-21)	16(13-19)	13(11-16)
Men	n	404	454	570	640	478	398
	Treated(%)	75(88)	48(54)	50(58)	33(40)	30(35)	23(29)
	OP(%)	53	35	34	24	20	16
	MR(%)	37	18	22	14	13	10
	5yrSFR(%)	27(20-34)	26(20-32)	16(11-20)	13(10-16)	9(5-13)	9(6-13)

Outcomes of FLS

Disclosures: Alastair McLellan, None.

MO0362

Secondary Prevention of Osteoporotic Fracture: A Systematic Approach to Case-finding in Brazil. Adriana Machado^{*1}, Wellington Monteiro Machado¹, Regina Celia Popim², Maria Virg nia M Alves², Angela M A Zeller³, Paul James Mitchell⁴. ¹Internal Medicine Department - Univ. Estadual Paulista, Brazil, ²Nurse Department - Univ. Estadual Paulista, Brazil, ³Nutrition Service - Univ. Estadual Paulista, Brazil, ⁴Auckland, New Zealand & University of Derby, UK, New Zealand

It is widely known that a significant care gap exists in relation to the secondary prevention of osteoporotic fractures. To fill this gap in our city, we started a clinic to assess people who have sustained a probable osteoporotic fracture and assess their

bone health and their risk of falls with further education and treatment. The clinic is based in the rehabilitation unit of a University Hospital (430 beds) in a median size city (130,000 habitants) in the inner of Sao Paulo State, Brazil. It is an initiative of the Geriatrics Discipline and has one geriatrician, two nurses, one nutritionist and one physiotherapist. The clinic is held once a week and accepts referral from any part of the hospital, in particular from the orthopaedic ward and outpatient's clinic and the emergency department. The referral criteria are patients aged 50 or above, both genders, with history of an atraumatic or a low impact fracture (with focus on hip, wrist, vertebra and humerus). When a new patient comes, they have an appointment with the geriatrician, who will check the clinical risk factors, the circumstances of the fall, and will request the bone densitometry measurement and the laboratory tests (full blood count, glycaemia, creatinine, albumin, sodium, potassium, magnesium, serum calcium, serum phosphate, urinary calcium, vitamin D, PTH and TSH levels). Subsequently, a nurse will assess independence in the activities of daily living, the eye test (Snellen chart) and the walking ability (timed up and go - TUG test). The nutritionist will assess the whole nutritional status, with a special focus on calcium and vitamin D. Based on these assessments, further referrals to physiotherapist will happen when needed. Everyone in the team is engaged in education aspects - life style changes, falls prevention and diet. A second visit will be arranged with the geriatrician to check the laboratory exams and the bone densitometry results, and a proposal of treatment. During the first year, the patient will have repeated appointments with the nurse every 4 months to check compliance with therapy, falls and new fractures. Our pilot program provides one of the first examples of a systematic approach to case-finding of fragility fracture patients in Brazil. Post-fracture coordinator models have been advocated by professional associations, patient societies and policymakers throughout the world. Our programme will be audited in an ongoing fashion which will inform future publications.

Disclosures: Adriana Machado, None.

MO0363

Vertebral Fracture Assessment: A Valid Tool to Detect Vertebral Fractures in Elderly Community. Diogo Domiciano^{*1}, JAQUELINE LOPES², Camille Figueiredo¹, Valeria Caparbo¹, Liliam Takayama¹, Rosa Pereira¹. ¹Faculdade de Medicina da Universidade de Sao Paulo, Brazil, ²Faculdade de Medicina da Universidade de Sao Paulo, Sao Paulo, Brazil, Brazil

Introduction: Vertebral fractures (VFX) are associated with higher morbidity and mortality, increasing the risk of incident fractures. Although only 30% of the VFX cause symptoms, this finding is a relevant issue for managing patients with high fracture risk, as well prevention of new fractures, independently of bone mineral density. Studies have shown effectiveness of Vertebral Fracture Assessment (VFA) to detect prevalent VFX comparable to the spine X-ray, considered as gold standard method. The aim of this study was to compare the performance between VFA and X-ray to identify VFX in healthy elderly men and women from community. Patients and Methods: 429 non-institutionalized subjects (60% women), aged over 65 years, from community (Butanta area, Sao Paulo, Brazil) were enrolled in this cohort. VFA by DXA measurements and spine X-ray (T4 to L4) were analyzed according to semiquantitative method (Genant HK, 1993). The first one was evaluated by two expert rheumatologists by consensus between them. The second one was evaluated by one expert radiologist. The interobserver correlation between VFA and spine X-ray to identify VFX was analyzed by kappa (k) scores. P<0.05 was set as significant. Results: The prevalence of VFX in both methods was 29.4%, without significant difference between men and women. Unavailable vertebrae were significantly lower in spine X-ray than VFA (1% and 5.5% respectively, p<0.001), especially among T4-T6. According to VFA, 5013 (96%) vertebrae were considered as normal, 144 (2.7%) had grade 1 fractures, 58 (1.1%) with grade 2 fractures and 12 (0.2) grade 3 fractures. To identify VFX, the sensitivity of VFA was 73% and the specificity was 99.1%. After excluding deformities grade 1, the sensitivity increased to 93% and specificity to 99.6%. The correlation between VFA and X-ray was good (k=0.74). Again, without grade 1, the agreement was also better (k=0.84). The correlation vertebrae by vertebrae between VFA and spine X-ray was lower in T5-T7. There was not significant difference between methods, according by gender (k=0.72 in men, k=0.75 in women).

Conclusion. In elderly community, VFA had similar performance to conventional spine X-ray to identify VFX in visible vertebrae. The sensitivity increased after excluding of mild deformities. Thus, this methodology is easy and feasible to be performed during routine DXA measurements, in order to improve the management of patients with higher risk of osteoporotic fractures.

Disclosures: Diogo Domiciano, None.

This study received funding from: FAPESP

MO0364

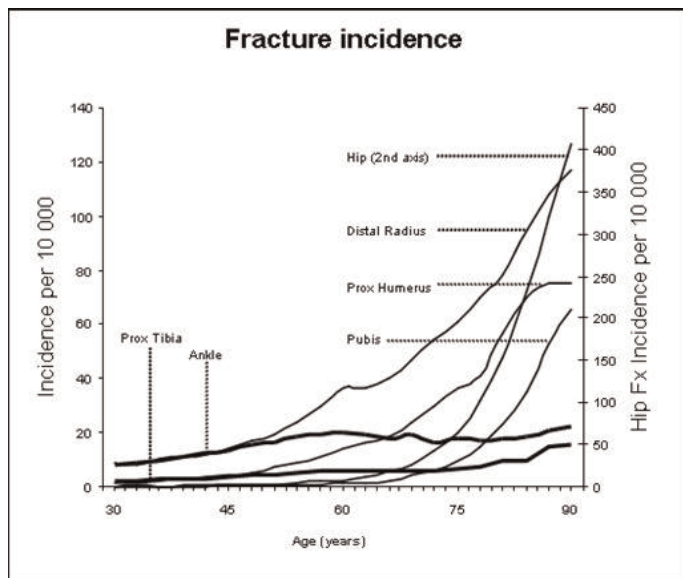
Which Types of Fractures Should in General be Regarded as Related to Osteoporosis? Bjorn Rosengren¹, Ingemar Peterson², Magnus Karlsson¹, Martin Englund². ¹Skane University Hospital Malmö, Lund University, Sweden, ²Musculoskeletal Sciences, Department of Orthopedics, Clinical Sciences Lund, Lund University, Lund, Sweden, Sweden

Purpose: In epidemiological studies, fractures of the hip, os pubis, proximal humerus, wrist, proximal tibia, and the ankle are often considered as typical osteoporotic fractures when occurring in individuals aged 50 years or older. However, it is currently unclear if all these fractures actually follow an age trend influenced by osteoporosis, i.e., showing a stable incidence during adulthood until age 50-60 years, followed by an exponential increase into older age.

Methods: Through the Skane Health Care Register, a diagnosis-based register covering all in- and outpatient health care data of residents in the County of Skane in Sweden (1.2 million inhabitants), we included adult men and women (aged 20-95 years) and registered all fractures of the hip (n=31 872), os pubis (n=4 388), proximal humerus (n=13 674), wrist (n=28 842), proximal tibia (n=4 769) and ankle (n=15 179) from year 1998 until 2009 (9.8 million person-years). We calculated age and sex-specific annual incidence estimates using the mid-year adult population as the population at risk for each calendar year, respectively. These estimates were then averaged over the 12-year study period to obtain age- and sex-specific incidence figures over a one-year time frame.

Results: A pattern typical for osteoporosis-related fractures (as detailed above) was seen for fractures of the hip, os pubis, proximal humerus, and the wrist (Figure). The increment with advancing age was more prominent in women than in men. In contrast, the incidences of fractures of the ankle and proximal tibia were fairly stable throughout life with only a slight increase in incidence of proximal tibial fractures in persons at about 90 years of age (Figure).

Conclusion: The incidence of hip, os pubis, proximal humerus, and wrist fractures follows an age pattern suggesting a clear influence by osteoporosis, while fractures of the ankle and proximal tibia show a relatively stable age-related incidence pattern. This knowledge is essential when deciding which fracture sites should be regarded as related to osteoporosis in epidemiological studies, and also when predicting the future demand for health care resources.



Figure

Disclosures: Bjorn Rosengren, None.

MO0365

A Genome-wide Screen of Gene-Gene Interactions for Osteoporosis Susceptibility. Tie-Lin Yang¹, Yan Guo¹, Hui Shen², Qing Tian², Hong-Wen Deng². ¹Xi'an Jiaotong University, China, ²Tulane University, USA

Osteoporosis is a typical complex disease determined by both actions and interactions of multiple genes. Bone mineral density (BMD) is the most important risk phenotype for osteoporosis. Recent genome-wide association studies (GWAS) identified several genes for their independent effects on osteoporosis. However, no studies have been performed to identify gene-gene interactions in GWAS analyses. Here, we performed a genome-wide gene-gene interaction analysis for osteoporosis susceptibility in two independent US Caucasian populations. Sample 1 consisted of 916 unrelated subjects with extreme hip BMD Z-scores (458 high and 458 low) selected from a 2286 subjects. Sample 2 consisted of 400 unrelated subjects with extreme hip BMD Z-scores (200 high and 200 low) selected from 1000 subjects. Combining results from these two samples, we detected one SNP-interaction pair

(rs8047431 and rs1975460) significantly associated with hip BMD after FDR adjustment for multiple testing, with the original P value of 1.88×10^{-10} . SNP rs8047431 was located at WW domain-containing oxidoreductase (WWOX) gene, which encodes a tumor suppressor. WWOX functionally suppressed RUNX2 transactivation ability in osteoblasts. Wwox^{-/-} mice exhibited a delay in bone formation and developed metabolic bone disease. The evidence suggested that WWOX might be a potential candidate gene for BMD. SNP rs1975460 located at 16q23.1, the nearest gene was ribosomal protein L36a pseudogene (RPL36AP46). In addition, we detected some other interaction pairs of SNPs showing suggestive association with osteoporosis susceptibility ($P = 3.77 \times 10^{-8}$ to 4.85×10^{-9}), such as SNPs in LNX1 and TMEM132D, and SNPs in SOX6 and HAUS6. In summary, our findings suggest that gene-gene interactions may play a role in osteoporosis susceptibility.

Disclosures: Hong-Wen Deng, None.

MO0366

Allelic Determinants of Vitamin D Insufficiency, Bone Mineral Density and Past and Prospective Bone Fractures. Olivia Trummer¹, Elisabeth Wehr¹, Verena Schwetz¹, Daniela Walter¹, Markus Gugatschka¹, Wilfried Renner¹, Astrid Fahrleitner-Pammer², Harald Dobnig³, Thomas Pieber¹, Barbara Obermayer-Pietsch^{*2}. ¹Medical University, Austria, ²Medical University Graz, Austria, ³Diagnostikinstitut Univ.Prof.Dr.H.Dobnig GmbH, Aut

Purpose: Low 25-hydroxyvitamin D (vitamin D) status is known to play an important role in many diseases with focus on bone health. Based on recently reported genetic determinants of vitamin D insufficiency we investigated GC, DHCR7 and CYP2R1 variants for their potential role in predicting vitamin D and bone mineral density (BMD) status as well as bone fractures.

Methods: Replication was performed in two cohorts, a cross sectional BMD and fracture study in 541 elderly unrelated subjects (mean age 56.13 years) and in a prospective cohort study on bone fractures in 1119 very old nursing home patients (mean age 84.6 years), both with clinical and biochemical patient characterisation.

Results: Mean vitamin D level was 33.13 ng/ml in the elderly and 9.6 ng/ml in the nursing home population. The GC genotype was significantly associated with lower mean vitamin D levels in both cohorts ($p=0.001$ and $p=0.048$, respectively). CYP2R1 and DHCR7 variants showed only a trend, but a linear gene-dose-effect in both cohorts.

There was no association with BMD in any of the genotypes at all sites measured and no relationship to the various types of past fractures. However, prospective fractures were significantly different between DHCR7 ($p=0.01$) and GC ($p=0.02$) genotypes, but did not differ between CYP2R1 groups. Moreover, DHCR7 genotypes differed significantly in prospective hip fracture cases (overall $n=48$) compared to persons without fractures ($n=923$; $p<0.001$) and GC genotypes in prospective radius fracture cases (overall $n=23$) compared to participants without fractures ($n=950$, $p<0.001$). DHCR7 variants were significantly associated with months to hip fracture ($p=0.04$, risk ratio of recurrence (RR) 0.73 [95% CI 0.53-0.99]) and were significantly associated with time to fracture by Kaplan-Meier analysis.

Conclusions

In our cohorts, GC, and probably DHCR7 and CYP2R1 variants were associated with vitamin D status even in view of markedly low mean vitamin D levels in the nursing home cohort, but not with BMD. However, prospective fracture risk might be related to these gene variants. Further studies in large cohorts are warranted to confirm our findings.

Disclosures: Barbara Obermayer-Pietsch, None.

This study received funding from: FFG Austria K-Projekt 471230

MO0367

Association of Common Variants in Obesity Related Genes with Osteoporosis and Fracture among Swedish Women. Jitender Kumar¹, Fiona McGuigan^{*2}, Mattias Callreus¹, Paul Gerdhem³, Kristina Akesson⁴. ¹Lund University, Sweden, ²University of Lund, Malmö, Skane University Hospital, Malmö, Sweden, ³Karolinska Institutet, Sweden, ⁴Skane University Hospital, Malmö, Sweden

Purpose: The opposing phenotypes of osteoporosis and obesity are complex disorders of body composition, whose consequences are a worldwide public health concern. Bone mineral density (BMD) and body mass index (BMI) are used as surrogate markers for osteoporosis and obesity respectively. Body composition, particularly fat mass and lean mass, are established determinants of BMD, although recent studies highlight the complexity of interactions between bone-fat. In this study we analyzed associations between single nucleotide polymorphisms (SNPs) from three obesity related genes with osteoporosis and fracture. **Methods:** Two population-based cohorts of women from Sweden: PEAK-25 (all aged 25 years, $n=1005$) and OPRA (all aged 75 years, $n=1010$) were utilized. Five SNPs (rs9939609, rs1121980, rs17782313, rsrs1770633, rs7566605) from three obesity associated genes involved in energy metabolism and identified through genome-wide association studies (Fat mass and obesity associated, FTO; Melanocortin 4 receptor, MC4R; and Insulin induced gene 2, INSIG2) were genotyped in both cohorts to determine age related effects on bone

phenotypes and fracture. Results: Total body (TB) fat mass and TB lean mass were the strongest determinants of BMD in OPRA and PEAK-25 respectively. SNP rs9939609 from the FTO gene showed significant association with BMI and TB fat mass ($p=0.004$) in PEAK-25. Individuals carrying the minor allele had increased BMI and TB fat mass. There was no association with BMD however regression analysis showed association with fracture ($p=0.04$) independent of BMD and fat mass in the OPRA cohort. Carriers of the minor allele had fewer fractures. SNP rs17782313 from the MC4R gene showed significant association with bone ultrasound (QUS) measurements in the OPRA cohort ($p<0.007$) – carriers of the minor allele had higher values of all QUS parameters. No association with BMD or fracture was found. INSIG2 SNPs failed to reach significance for any of the parameters studied. Conclusion: We have identified associations between SNPs from obesity related genes, bone quality and fracture. Association of FTO SNPs with fat mass was age dependent, suggesting interaction with environmental factors. The association between MC4R and bone quality is supported by rat studies whereby the absence of Mc4r leads to decreased bone resorption and increased BMD. Further studies are warranted to reveal the exact mechanism of the role of these genes on osteoporosis and fractures.

Disclosures: Fiona McGuigan, None.

MO0368

Linkage Analysis in an Australian Cohort Identifies a Region Associated with Femoral Neck BMD. Sing Nguyen*, Jacqueline Center, John Eisman, Tuan Nguyen. Garvan Institute of Medical Research, Australia

Genome-wide association studies, with their large cohorts and dense sequencing coverage, have been extremely successful at identifying the gene regions which influence many different traits, including bone mineral density (BMD). Whilst they continue to be useful, the numbers needed to detect and replicate signals is at times prohibitively large. Given the high heritability of BMD traits, linkage studies using related individuals represent a cost-effective alternative for detecting regions associated with variation in BMD. A moderately-sized linkage study using related individuals can have the same power to detect gene regions as a much larger association study using unrelated individuals.

Here we perform a linkage analysis for BMD at the femoral neck, lumbar spine and total body in 500 people across 90 extended pedigrees from the Dubbo Osteoporosis Genetics Study (DOGS). This study is a sister study of the Dubbo Osteoporosis Epidemiology Study (DOES), and is a multi-generational family study with ongoing recruitment and follow-up.

Using a multipoint linkage scan, we find evidence for linkage at chromosome 3q25 with respect to variation in femoral neck BMD (but not lumbar spine or total body BMD). Furthermore we find evidence for suggestive linkage at regions previously identified in other linkage and association studies looking at BMD. Overall there is reason to once again pursue linkage as a study design for identifying gene regions associated with BMD traits.

Disclosures: Sing Nguyen, None.

MO0369

Factors Associated with Use of Anti-Osteoporosis Medication. The Global Longitudinal Study of Osteoporosis in Women (GLOW). Stephen Gehlbach*, Pamela Guggina², Frederick Hooen³, Julie Flahive⁴, Steven Boonen⁵, Juliet Compston⁶, Cyrus Cooper⁷, Adolfo Diez-Perez⁸, Susan Greenspan⁹, Robert Lindsay¹⁰, Coen Netelenbos¹¹, Philip Sambrook¹², Stuart Silverman¹³, Nelson Watts¹⁴. ¹University of Massachusetts, USA, ²University of Massachusetts School of Public Health, USA, ³University of Massachusetts Medical School, USA, ⁴UMass Medical School, USA, ⁵Center for Metabolic Bone Disease & Division of Geriatric Medicine, Belgium, ⁶University of Cambridge School of Clinical Medicine, United Kingdom, ⁷University of Southampton, United Kingdom, ⁸Autonomous University of Barcelona, Spain, ⁹University of Pittsburgh, USA, ¹⁰Helen Hayes Hospital, USA, ¹¹VU Medical Center, The Netherlands, ¹²Royal North Shore Hospital, Australia, ¹³Cedars-Sinai/UCLA, USA, ¹⁴University of Cincinnati Bone Health & Osteoporosis Center, USA

Osteoporosis is a common condition for which there are effective medications. Many women at high risk for fracture are not treated, while some low-risk women are on anti-osteoporosis medications (AOMs).

Aim: To identify characteristics associated with AOM treatment and determine whether these characteristics differ between high- and low-risk women.

Methods: The Global Longitudinal Study of Osteoporosis in Women (GLOW) is a multinational prospective cohort study involving 60,393 women aged ≥ 55 yr. Data were collected via self-administered questionnaires at baseline and annually for 3 years. Women were eligible if they had visited the practice within the previous 2 years, were non-institutionalized and had no barriers to completing a questionnaire. The high-risk category contained women ≥ 65 yr with a prior fracture or ≥ 2 FRAX risk factors (history of fracture, low bone mineral density, low body mass index, oral glucocorticoid, rheumatoid arthritis, risk factors for secondary osteoporosis, parental history of hip fracture, tobacco use and ≥ 3 alcoholic drinks/day). The low-risk

category contained women <65 yr with no FRAX risk factors. Variables included were diagnosis of osteoporosis/osteopenia, education, age, comorbidities, prescription drugs, concern about osteoporosis, self-perception of fracture risk and vitality score. The outcome of interest was AOM use.

Results: 3645 women were in the low-risk group; 941 reported osteopenia, 335 osteoporosis and 2369 neither. 3759 women were in the high-risk group; 872 had osteopenia, 1322 osteoporosis and 1565 neither. 14.2% of low-risk women and 35.7% of high-risk women were treated ($p<0.0001$). Characteristics associated with AOM are listed in the Table. Diagnosis of osteoporosis was the most significant. The odds ratio (OR) was 69.4 in the low-risk group and 17.9 among high-risk women. An osteopenia diagnosis was also significant, with an OR of 18.7 among the low-risk women and 6.2 for those at high risk. Age was associated with treatment among high-risk women while prescription drug coverage was associated with treatment among the low-risk group. Education level was not related to treatment.

Conclusion: While a diagnosis of osteoporosis or osteopenia is most strongly associated with treatment with AOM in both high and low risk women, several other factors are also associated with treatment, including presence of comorbid conditions, concern about osteoporosis, perceived fracture risk and vitality.

Variable	Low risk OR (95% CI)	High risk OR (95% CI)
Age by 5-year increment	1.3 (1.0, 1.7)	1.2 (1.1, 1.3)
Diagnosis of osteoporosis vs. neither	69.4 (45.2, 106.4)	17.9 (13.9, 22.9)
Diagnosis of osteopenia vs. neither	18.7 (13.0, 27.1)	6.2 (4.8, 8.0)
More than high-school education vs. high-school education or less	1.3 (0.9, 1.8)	1.2 (1.0, 1.5)
No comorbidities vs. at least 1 comorbidity	1.4 (1.1, 1.8)	1.5 (1.1, 1.9)
Prescription drug coverage vs. no drug coverage	5.6 (2.3, 13.5)	1.0 (0.7, 1.5)
Osteoporosis concern: very/somewhat vs. not at all	2.1 (1.1, 4.3)	1.9 (1.3, 2.7)
Perceived fracture risk: higher vs. same/lower than others	2.0 (1.5, 2.6)	1.6 (1.3, 1.9)
Vitality, above vs. below median	1.7 (1.3, 2.2)	1.7 (1.4, 2.0)

Table. Characteristics associated with AOM use in low- and high-risk women (adjusted for study site)

Disclosures: Stephen Gehlbach, None.

This study received funding from: Warner Chilcott Company, LLC and sanofi-aventis

MO0370

Secular Trends in Fractures and Sex Hormones in Men and Women. Penelope Trimpou^{*1}, Anders Lindahl², Goran Lindstedt², Goran Olerod², Lars Wilhelmsen², Kerstin Landin-Wilhelmsen². ¹Section for Endocrinology, Department of Internal Medicine, Sahlgrenska University Hospital, Sweden, Swe, ²Sahlgrenska University Hospital, Sweden

Purpose Age, hormones and life style are determinants for many conditions and diseases. The purpose was to study secular trends in fractures, sex hormones and life-style factors in a random population sample of men and women, during 13 years.

Methods This is a prospective, longitudinal study in a random sample of the general population of Gothenburg, Sweden. Totally 1257 men and women, aged 35-64 years, from the WHO, MONICA Project, Goteborg 1995 was restudied in 2008. Subjects with a mean age of 40, 50 and 60 years were compared at similar ages 13 years apart. Body composition was measured with bioimpedance and bone mass with calcaneal ultrasound. Life-style factors were estimated via questionnaires. Fasting serum hormones were measured in every 4th subject from the 1995 year cohort. In fertile women collections were made in cycle day interval 7-9. Fractures were X-ray verified.

Results When comparing men from 1995 with men of similar age in 2008, body composition, physical activity and fracture incidence were similar. Postmenopausal women 45-64 years, had increased physical activity during leisure time and bone mass but decreased physical activity at work in 2008 the fracture incidence in the same age groups increased from 17 to 28% between 1995-2008 ($p<0.001$). The majority was fall fractures i.e. radius, upper arm and ankle. Vertebral crush increased in postmenopausal women in 2008, from 9% to 28% of all fractures ($p=0.0085$). Estrogen replacement therapy (HRT) declined from 28% to 7% ($p<0.0001$) as did serum estradiol.

Conclusions Secular trends were seen both in fracture incidence and fracture type in postmenopausal women but not in men during 13 years. A decrease in HRT use concomitant with an increase in leisure time physical activity might explain the results.

Disclosures: Penelope Trimpou, None.

MO0371

The Relationship Between Circulating Soluble RANK Ligand and Breast Arterial Calcification in Japanese Postmenopausal Women. Fuminori Hirano^{*1}, Hiroshi Wada², Hideo Nishimura¹. ¹Asahikawa Medical Center, Japan, ²Wada women's clinic, Japan

Breast arterial calcification (BAC) is common but unreported findings on routine screening mammography. BAC is reported to be associated with an increased

MO0373

Association of Red Blood Cell n-3 and n-6 Fatty Acids and Hip Fracture.
Tonya Orchard¹, Steven Ing¹, Bo Lu¹, Martha Belury¹, Andrea Lacroix², Charles Kooperberg², Aaron Aragaki², Rebecca Jackson¹. ¹The Ohio State University, USA, ²Fred Hutchinson Cancer Research Center, USA

Title: Association of Red Blood Cell n-3 and n-6 Fatty Acids and Hip Fracture

Purpose: The objective of this research was to examine red blood cell (RBC) n-3 and n-6 fatty acids (FAs) as a biological marker of hip fracture in postmenopausal women and to investigate the relation of these FAs to regulators of bone turnover.

Methods: A nested case-control study (n=400 pairs) was completed within the Women's Health Initiative (WHI) prospective cohort. RBCs and serum were collected from blood drawn at the baseline screening visit. RBC FAs were analyzed using gas chromatography. Bone biomarkers (osteoprotegerin (OPG) / receptor activator of NF κ B ligand (RANKL) ratio) in serum were analyzed in an on-going WHI study. Serial measures of bone mineral density (BMD) were obtained at baseline, year 3 and year 6. Hip fractures were confirmed by medical record review. Cox proportional hazard models were constructed to estimate risk of fracture. The association of FAs to OPG/RANKL and BMD was estimated using generalized linear models.

Results: After exclusion of 116 samples due to potential RBC degradation and their corresponding case-control match (n=98), 293 matched pairs were included in statistical analysis. Higher alpha linolenic acid (ALA) was associated with lower hip fracture risk in multivariate analysis [Hazard Ratio (HR) for tertile 3: 0.39; 95% CI: 0.19-0.78; p for linear trend 0.04] and a 7-fold higher OPG/RANKL ratio (Tertile 3 mean: 489.79; SEM: 149; p for linear trend 0.07). HR for hip fracture based on the highest tertile of the n-3 index [%eicosapentaenoic acid (EPA) +docosahexaenoic acid (DHA) in RBCs] was 0.53; 95% CI: 0.28-1.01; p for linear trend 0.09, and based on highest tertile of total n-3 FAs HR was 0.53; 95% CI: 0.28-0.99; p for linear trend 0.07. There was no association between n-3 and n-6 FAs and BMD. Although total n-6 FAs tended to decrease the OPG/RANKL ratio (Tertile 3 mean: 95.71; SEM: 150; p for linear trend 0.0508), there were no associations between n-6 FAs in RBCs and risk of hip fracture. However, HR for hip fracture increased with an n-6/n-3 ratio > 6.01 in RBCs (HR tertile 3: 2.31; 95% CI: 1.03-5.16; p for linear trend 0.05).

Conclusions: The n-3 FA, ALA, in RBCs was inversely associated with hip fracture risk, potentially related to a more favorable OPG/RANKL ratio. Higher total n-6 FAs tended to be associated with lower OPG/RANKL and an n-6/n-3 ratio >6.01 in RBCs more than doubled relative risk of hip fracture in these postmenopausal women.

Table 4a: Hazard ratios for risk of hip fracture based on n-3 and n-6 polyunsaturated fatty acids in red blood cells¹

n-3 fatty acids	n	Unadjusted			HR	Adjusted ²			n-6 fatty acids	n	Unadjusted			HR	Adjusted ²		
		HR	95% CI	P		HR	95% CI	P			HR	95% CI	P		HR	95% CI	P
Total n-3 ³									Total n-6								
T1(1.57-4.50)	194	1.00			1.00				T1(24.36-35.89)	194	1.00			1.00			
T2(4.50-8.87)	199	0.88	(0.56-1.31)	0.47	0.87	(0.35-1.26)			T2(35.89-135.57)	199	0.91	(0.61-1.35)	0.96	(0.54-1.70)			
T3(8.87-16.44)	193	0.85	(0.56-1.28)	0.55	0.55	(0.28-0.99)			T3(135.57-23.91)	193	1.10	(0.71-1.68)	1.46	(0.76-2.84)			
ALA					0.40				LA					0.08			0.66
T1(0.07-0.21)	194	1.00			1.00				T1(0.05-0.22)	194	1.00			1.00			
T2(0.21-0.26)	199	0.79	(0.53-1.18)	0.70	0.70	(0.38-1.28)			T2(0.22-0.33)	199	0.88	(0.58-1.33)	0.80	(0.34-1.94)			
T3(0.26-0.69)	193	0.60	(0.38-0.96)	0.30	0.30	(0.19-0.76)			T3(0.33-1.00)	193	0.88	(0.57-1.36)	0.80	(0.42-1.63)			
EPA+DHA					0.30				AA					0.24			0.26
T1(1.86-1.94)	194	1.00			1.00				T1(0.66-1.92)	194	1.00			1.00			
T2(1.94-4.40)	199	0.94	(0.63-1.40)	0.45	0.45	(0.35-1.21)			T2(1.96-16.37)	199	0.94	(0.63-1.40)	0.80	(0.46-1.50)			
T3(4.40-11.67)	193	0.86	(0.56-1.31)	0.53	0.33	(0.28-1.03)			T3(16.37-20.89)	193	1.27	(0.82-1.96)	1.36	(0.76-2.45)			

¹ Percent fatty acids from total of the following RBC fatty acids: arachidonic acid, alpha linolenic acid, docosahexaenoic acid, docosapentaenoic acid, eicosapentaenoic acid, eicosatetraenoic acid, gamma linolenic acid, linolenic acid, myristic acid, palmitic acid, palmitoleic acid, stearic acid.

² Hazard ratios (HRs) are obtained from Cox Proportional Hazards models.

³ Values are from tests for linear trend.

⁴ Model adjusted for potential history of fracture, fracture after age 54, height, weight, corticosteroid use, diabetes, and weekly exercise.

⁵ (A) Alpha-linolenic acid, (EPA) eicosapentaenoic acid, (DHA) docosahexaenoic acid, (DPA) docosapentaenoic acid.

Red blood cell PUFAs and hazard ratio for hip fracture

Disclosures: Tonya Orchard, None.

MO0374

Body Mass Index and Bone Mineral Density in Adults over 50: Results from NHANES 2005-2008. Jennifer Lloyd¹, Dawn Alley¹, William Hawkes¹, Shari Waldstein², Marc Hochberg³, Denise Orwig¹. ¹University of Maryland, Baltimore, USA, ²University of Maryland, Baltimore County, USA, ³University of Maryland School of Medicine, USA

The objective of this study is to examine variation in bone mineral density (BMD) across body mass index (BMI) groups among older adults using recent, nationally representative data. Although previous studies have reported a positive relationship between BMI and BMD, this relationship hasn't been examined in more recent cohorts. Using data from the National Health and Nutrition Examination Survey (2005-2008), we examined the association between BMI and low BMD and osteoporosis (defined as >1 SD and >2.5 SD below young, sex-specific mean, respectively). There were 3,801 adults >50 years (mean 63 years), predominately female (52%), white (83%), and overweight or obese (72%), with a mean femoral neck

prevalence of both cardiovascular risk factors and cardiovascular morbidity. Moreover, osteoprotegerin (OPG) and soluble RANK ligand (sRANKL) have been consistently associated with the incidence and prevalence of coronary artery disease. However, little is known about serum OPG and sRANKL levels in postmenopausal women with breast arterial calcification. The purpose of this study is to clarify the relationship between plasma OPG and sRANKL levels and breast arterial calcification in Japanese osteoporotic postmenopausal women. This study was carried out in fifty-one postmenopausal women aged 46-82 years who underwent screening mammography. Each mammogram was reviewed for the presence of arterial calcifications. Participants were divided into four groups of the number of calcified vessels including, 0BAC: no calcification, 1BAC: one calcified vessel, 2BAC: two calcified vessels and >3BAC: more than 3 calcified vessels. Serum OPG, sRANKL, alkaline phosphatase (Alp), low density lipoprotein-cholesterol (LDL-C), high density lipoprotein-cholesterol (HDL-C) and urinary type-I collagen cross-linked-N-telopeptide (uNTX) were measured. The mean age of these 51 women was 64.5 ± 1.1 years-old, 0BAC; n=25, 1BAC; n=11, 2BAC; n=8 and >3BAC; n=7. The prevalence of low bone density (osteopenia) and osteoporosis was 33.3% and 56.9%, respectively. The prevalence of BAC was 58.6% in osteoporosis and 47.1% in osteopenia higher than 20.0% in women without osteopenia and osteoporosis. In the subgroups of BAC, BMD in >3BAC group was clearly decreased, and serum OPG and sRANKL levels were significantly increased in >3BAC group compared with those in 0BAC group. In addition, sRANKL/OPG ratio was pivotally higher in 2BAC and >3BAC groups compared with that in 0BAC group. In contrast, serum Alp, the ratio of LDL-C/HDL-C and uNTX were not significantly changed, increasing the number of BAC in postmenopausal women. In conclusion, the prevalence of BAC in Japanese postmenopausal women was remarkably high in osteopenia and osteoporosis. Especially, the result in the subgroups of BAC showed that sRANKL/OPG ratio was increased in severe calcification of breast artery, suggesting that BAC may be associated with surrogate markers of reduced BMD and subclinical cardiovascular disease including coronary artery calcification.

Disclosures: Fuminori Hirano, None.

MO0372

Aging Males' Symptoms (AMS) Scale and Bone Mineral Density in HIV Positive Males Treated with Highly Active Anti-Retroviral Therapy (HAART). Jessica Pepe¹, Andrea Isidori¹, Mario Falciano¹, Giancarlo Iaiani¹, Emilia Sbardella¹, Romano Del Fiacco², Addolorata Scarpello¹, STEFANIA RUSSO³, Cristiana Cipriani⁴, Elisabetta Romagnoli⁴, Salvatore Minisola⁴. ¹Sapienza, University of Rome, Italy, ²University "Sapienza" - Rome, Italy, ³UNIVERSITY SAPIENZA OF ROME (ITALY), Italy, ⁴University of Rome, Italy

Background: HIV infection is frequently associated with osteoporosis which is considered mostly attributable to hypogonadism; this last has been considered secondary to HAART.

Aim: We administered the Aging Males' Symptoms (AMS) questionnaire (currently used to clinically evaluate partial androgen deficiency of aging men) to HIV patients and concomitantly investigated their skeletal health.

Methods: We studied 50 men with HIV type-1 (mean age: 48.79 ± 4 yrs; diagnosis: 10.1 ± 5.9 yrs; CD4, cells/microL: 626.266; HIV RNA, copies/mL: 55.425.9) and 27 age-matched HIV negative men (49.18 ± 3 yrs). We measured main parameters of mineral metabolism and hormonal status; each subject underwent lumbar and femoral DXA densitometry (iDXA, GE Medical Systems Lunar, Madison WI, USA) and quantitative ultrasound of the proximal phalanges using DMB Sonic 1200 device (IGEA, Carpi, Italy). Ultrasonometric parameters considered were speed of propagation of ultrasound dependent on the amplitude of the ultrasound wave crossing bone tissue (Amplitude-Dependent Speed of Sound, ADSoS) and a parameter calculated by computer analysis of dynamic parameters of ultrasound signal (Ultrasound Bone Profile Index, UBPI).

Results: 31.5% of HIV patients were osteoporotic at the lumbar and/or femoral sites compared with 3.7% of control subjects (p = 0.02). Mean ADSoS values of HIV patients were significantly reduced (206775 vs 212189 m/s, p < 0.01). HIV patients were characterized by a higher prevalence of biochemical hypogonadism compared with controls (26% vs 4%, p = 0.04), as determined by free testosterone levels. 62% of HIV patients (40.7% of controls, p = 0.04) had values of AMS above the pathological threshold (≥ 27). Among HIV-infected population, AMS score was negatively correlated with neck BMD (r = -0.36, p = 0.016) and with both ADSoS values and UBPI (r = -0.47, p = 0.009, r = -0.39, p = 0.002, respectively), even after adjusting for covariates (age and BMI).

Conclusion: There is a significant prevalence of hypogonadism in HIV men, which is also accurately reflected by AMS scores. The correlation between AMS score and neck BMD, might support the use of this questionnaire as a screening tool for low bone mass in this condition. The significantly reduced ultrasonometric parameters in HIV positive patients suggests, for the first time, a qualitative other than quantitative involvement of skeletal tissue, strongly related to the hypogonadism.

Disclosures: Salvatore Minisola, None.

BMD of 0.772 gm/cm² (SD=0.14). Both overweight and obese persons had significantly lower odds of low BMD (OR=0.56 CI: 0.37-0.84; and OR=0.19, 95% CI: 0.08, 0.44, respectively) and osteoporosis (OR=0.22, 95% CI: 0.15, 0.33; and OR=0.21, 95% CI: 0.08, 0.59, respectively). Gender and race were not significant effect modifiers. Stratified analysis examined gender and race/ethnic groups to determine if the BMI and BMD association was linear. Including a BMI squared term in stratified analysis indicated a possible significant curvilinear relationship among some racial/ethnic groups and among men. Results demonstrate the strong positive association between BMI and BMD, consistent with prior research. Although, there may be a threshold for the protective effects of high BMI after which additional weight does not continue increase BMD.

Disclosures: Jennifer Lloyd, None.

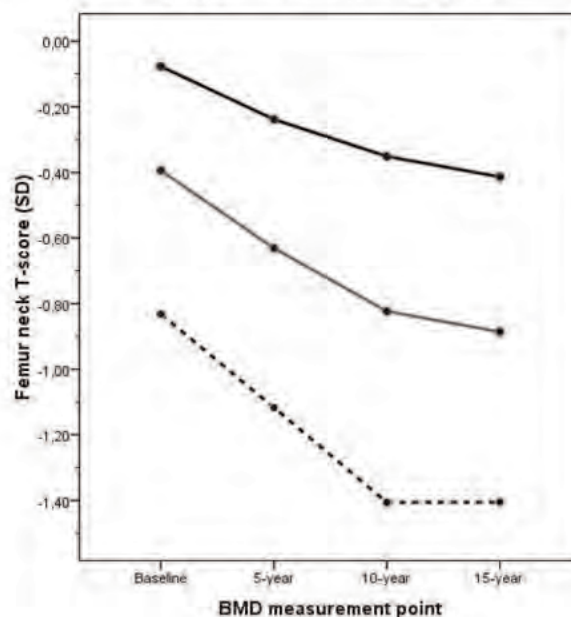
MO0375

Does Optimal Risk Factor Profile Guarantee Better Bone Health During The Postmenopause? - A 15-Year Population Based Study. Joonas Sirola^{*1}, Toni Rikkinen², Marjo Tuppurainen³, Risto Honkanen⁴, Heikki Kroger³.

¹University of Eastern Finland / Kuopio, Finland, ²Researcher, University of Eastern Finland, Finland, ³Professor, Kuopio university hospital, Finland, ⁴Adjunct Professor, University of Eastern Finland, Finland

Aim: To investigate long-term effects of selected modifiable and non-modifiable risk-factors on the development of osteoporosis. **Methods:** The study population consisted of 1895 postmenopausal women from Osteoporosis Risk Factor and Prevention (OSTPRE) -study cohort (n=14 220), Kuopio, Finland. Risk-factor inquiry and femoral neck (FN) bone mineral density (BMD) measurements were performed between and 2004 at 5-year intervals. Low-trauma energy fractures during the follow-up were validated from medical records. The study population was categorized into: 1) quartiles of score calculated based on presence of modifiable osteoporosis risk-factors (BMI, smoking, alcohol intake, physical activity, use of HT and calcium intake) and 2) number of non-modifiable osteoporosis risk-factors (age, glucocorticoid use, rheumatoid arthritis, insulin dependent diabetes, coeliac disease, chronic liver disease, early menopause or biovariectomy and fracture history) 3) three groups of total risk based on number of both modifiable and non-modifiable risk factors. All risk-factors were selected 'a priori' to analyses based on current clinical conception of osteoporosis risk and preventive factors. **Results:** Women with highest modifiable risk (group A) had T-score -0.59 SD at baseline and T-score -1.13SD at 15-year while women with lowest modifiable risk (group B) had FN T-score -0.21 SD at baseline and -0.57 SD at 15-year (p<0.001 vs. group A in ANOVA). Women with three or more non-modifiable risk-factors for osteoporosis (group C) had baseline T-score -0.65 SD and 15-year T-score -1.20 SD whereas women with no non-modifiable risk factors (group D) had baseline T-score -0.26 SD and 15-year T-score -0.73 SD (p<0.01 vs. group C in ANOVA). Women with the highest total risk (group E) had baseline T-score -0.83 SD and 15-year T-score -1.41 SD whereas women with the lowest total risk (group F) had baseline T-score -0.08 SD and 15-year T-score -0.41 SD (p<0.001 vs. group E in ANOVA, see Figure). In logistic regression model groups A/C/E had 1.8/3.0/4.7 higher odds of suffering follow-up fracture in comparison to groups B/D/F, respectively (p<0.001, see table). **Conclusions:** Both modifiable and non-modifiable factors have clinically significant impact on development of low BMD and low trauma energy fractures. All risk-factors selected for the present study accounted for a 1 SD difference in FN T-score and 5 fold odds' difference in fracture risk during the 15-year follow-up.

Figure. Change in FN T-score according to total risk during the follow-up. (Grey dotted line=highest total risk (group E), Black line=lowest total risk (group F))



Figure

Table. Effect of modifiable, non-modifiable and total risk-score on fracture risk.

	OR	95 % CI		P-value
A.Modifiable risk quartile		Lower	Upper	
4 (Highestrisk, group A)	1.78	1.30	2.45	<0.001
3	1.65	1.21	2.24	0.001
2	1.45	1.07	1.97	0.016
1 (Lowestrisk, group B,reference group)	1	1	1	0.002
B.Non-modifiable risk group				
4 (Highestrisk, Group C)	3.03	1.89	4.87	<0.001
3	2.39	1.77	3.22	<0.001
2	1.73	1.35	2.20	<0.001
1 (Lowestrisk, Group D, reference group)	1	1	1	<0.001
C.Totalrisk group				
3 (Highestrisk, Group E)	4.74	2.80	8.03	<0.001
2	1.98	1.34	2.91	0.001
1 (Lowestrisk, Group F,reference group)	1	1	1	<0.001

Table

Disclosures: Joonas Sirola, None.

MO0376

Does Work Disability Predict Fractures? Paivi Rauma^{*1}, Risto Honkanen², Marjo Tuppurainen³, Heli Koivumaa-Honkanen⁴, Heikki Kroger⁵.

¹University of Eastern Finland, Finland, ²BCRU & Public Health, University of Eastern Finland, Finland, ³Kuopio University Central Hospital, Finland, ⁴University of Oulu, Finland, ⁵BCRU, University of Eastern Finland, Finland

The purpose was to examine if disability before old age is related to osteoporotic fractures and if this relationship varies according to fracture site and cause of disability. The study population consisted of the 9759 women (born in 1932-41) of the Kuopio Osteoporosis Risk Factor and Prevention (OSTPRE) Study cohort who responded to enquiries in 1989, 1994, 1999 and 2004. Information on work disability pensions was obtained from the national register which covered all pensions in Finland. Pensions allowed before March 1996 (n=3240) were included. The ICDIX diagnosis displayed the cause of disability. Self-reported fractures in 1999-2004 were validated by perusal of radiological reports. Fracture risks were estimated with logistic

regression. The risks were adjusted for age, height, weight, year of menopause, fracture history, estrogen use and medication.

A total of 905 women had sustained a fracture and 461 women an osteoporotic fracture (wrist 351, humerus 67, clinical spine 56 and hip 30). A pension increased the overall fracture risk by 18% ($p=0.019$), the risk of osteoporotic fracture by 9% ($p=0.224$) and the risk of non-osteoporotic fracture by 27% ($p=0.016$). It decreased the risk of wrist fracture by 13% ($p=0.224$). It increased the risks of hip fracture by 202% ($p=0.002$) and humerus fracture by 201% ($p<0.001$), while the spine fracture risk change was slight (+30%) ($p=0.332$). Pensions due to mental (626), neurological (134), cardiovascular (395), musculoskeletal (1621) disorders or injury (102) did not increase the overall fracture risk, while respiratory disease (150) increased it by 98% ($p=0.002$). Neurological disease increased hip fracture risk by 419% ($p=0.013$) and respiratory disease the humerus fracture risk by 431% ($p<0.001$). Mental disorders increased the risk of hip fracture by 193% ($p=0.022$) and depression the risk of humerus fracture by 257% ($p=0.004$). Adjustments (Cf. above) weakened predictions to about half. When the medication variable was dropped from the model, the predictions resumed most of their original strength.

In women before old age, disability increases the risks of hip and humerus fracture but not that of wrist fracture. Wrist fracture dominance may mask fracture risk increasing effects of disability.

Disclosures: Paivi Rauma, None.

MO0377

Effect of Co-Morbidities on Fracture Risk: Findings from The Global Longitudinal Study of Osteoporosis in Women. Juliet Compston^{*1}, Melissa Premaor², Julie Flahive³, Ethel Siris⁴, Stephen Gehlbach⁵, Jonathan Adachi⁶, Steven Boonen⁷, Roland Chapurlat⁸, Adolfo Diez-Perez⁹, Fredrick Hooven¹⁰, Andrea Lacroix¹¹, Coen Netelenbos¹², Johannes Pfeilschifter¹³, Maurizio Rossini¹⁴, Christian Roux¹⁵, Kenneth Saag¹⁶, Philip Sambrook¹⁷, Stuart Silverman¹⁸, Nelson Watts¹⁹, Susan Greenspan²⁰, Elaine Dennison²¹, Cyrus Cooper²². ¹University of Cambridge School of Clinical Medicine, United Kingdom, ²Federal University of Santa Maria, Brazil, ³UMass Medical School, USA, ⁴Columbia University College of Physicians & Surgeons, USA, ⁵University of Massachusetts, USA, ⁶St. Joseph's Hospital, Canada, ⁷Center for Metabolic Bone Disease & Division of Geriatric Medicine, Belgium, ⁸E. Herriot Hospital, France, ⁹Autonomous University of Barcelona, Spain, ¹⁰University of Massachusetts Medical School, USA, ¹¹Fred Hutchinson Cancer Research Center, USA, ¹²VU Medical Center, The Netherlands, ¹³Alfried Krupp Krankenhaus Steele, Germany, ¹⁴University of Verona, Italy, ¹⁵Hospital Cochin, France, ¹⁶University of Alabama at Birmingham, USA, ¹⁷Royal North Shore Hospital, Australia, ¹⁸Cedars-Sinai/UCLA, USA, ¹⁹University of Cincinnati Bone Health & Osteoporosis Center, USA, ²⁰University of Pittsburgh, USA, ²¹MRC Epidemiology Resource Centre, United Kingdom, ²²University of Southampton, United Kingdom

Introduction: Fracture prediction algorithms such as FRAX[®] are available worldwide, and are in constant evolution. It has been suggested that greater awareness of the relationship between specific co-morbidities and fracture risk might improve fracture prediction. We utilised data from a large, multinational cohort study to investigate the effect of single or multiple co-morbidities on fracture risk.

Methods: 52,960 women were recruited from the Global Longitudinal Study of Osteoporosis in Women (GLOW). GLOW is an observational prospective study of women aged 55 years and older recruited through 723 primary physician practices in 17 sites in 10 countries. All non-institutionalized women visiting a practice within the prior 2 years were eligible. At baseline, women completed a questionnaire detailing medical history, including co-morbidity history and fracture. They were re-contacted annually thereafter and incident clinical fracture history was elicited and validated. A co-morbidity index, defined as number of co-morbidities reported at baseline from the following medical conditions, was derived: high blood pressure, high cholesterol, heart disease, stroke, asthma, chronic obstructive pulmonary disease (COPD), arthritis (reported osteoarthritis and rheumatoid arthritis), inflammatory bowel disease, coeliac disease, cancer, diabetes, multiple sclerosis and Parkinson's disease.

Results: 3224 (6.1%) women sustained an incident fracture over the 2 years of follow-up. Co-morbidities were common, with 26,215 women (49.5%) reporting hypertension, and 26,084 women (49.3%) reporting high cholesterol levels. All recorded co-morbidities were significantly associated with fracture except high cholesterol, and coeliac disease; the strongest association was seen with Parkinson's disease [hazard ratio 2.13 (95% CI 1.51-3.01), $p<0.0001$]. The hazard ratio of fracture increased with increasing co-morbidity index (Table). A stepwise model of incident fractures found that the co-morbidities that contributed most to fracture prediction, in order of importance, were: arthritis, Parkinson's disease, COPD, diabetes and multiple sclerosis.

Conclusion: Co-morbidities, particularly arthritis and Parkinson's disease, contribute significantly to fracture risk. Increasing co-morbidity index was associated with increasing fracture risk. The mechanism of this effect is unclear but might be related in part to increased risk of falling.

Table 1. Hazard ratios for the adjusted model according to co-morbidity index (adjusting for age, BMI, prior fracture, alcohol ≥ 3 drinks/day and current smoking)

Co-morbidity index	HR (95% CI)
1 vs 0	1.08 (0.94, 1.26)
2 vs 0	1.24 (1.08, 1.43)
3 vs 0	1.21 (1.04, 1.41)
4+ vs 0	1.35 (1.12, 1.61)

Table

Disclosures: Juliet Compston, None.

This study received funding from: Warner Chilcott Company, LLC and sanofi-aventis

MO0378

Fragility Fracture and Osteoarthritis: Interaction between Bone Mineral and Bone Mass Index. Mei Chan^{*1}, Tuan Nguyen², Jacqueline Center², John Eisman², Nguyen Nguyen². ¹Osteoporosis & Bone Biology, Australia, ²Garvan Institute of Medical Research, Australia

Increased bone mineral density (BMD) and bone mass index (BMI) are associated with increased risk of osteoarthritis (OA) and reduced risk of fragility fracture. However, little is known about the relationship between fragility fracture and osteoarthritis. In this study, we sought to examine the interactions between BMD and BMI in the determination of the OA-fracture relationship. The study was part of the on-going Dubbo Osteoporosis Epidemiology Study, which involved 2,412 women and 1,452 men aged between 46 to 99 years. The individuals had been followed up for a median of 7 years (range: 0.1 to 21 years). Baseline BMD was measured at femoral neck (FNBMD) and lumbar spine (LSBMD) by dual energy X-ray absorptiometry (GE-Lunar, Madison, WI). Osteoarthritis was ascertained by self-report. The incidence of fragility fracture was ascertained by X-ray report during the follow-up period. In addition, data concerning demographic characteristics, clinical history, and lifestyle factors were obtained by a structured questionnaire. A total of 1,077 participants (691 women and 386 men) had reported a diagnosis of OA. Overall, the risk of OA was associated significantly with increased LSBMD in men (odds ratio [OR] 1.34, 95%CI, 1.19-1.52) and women (1.20; 1.09-1.32). Elevation in FNBMD was significantly associated with increased risk of OA in men (OR 1.16; 1.02-1.32), but not in women. When stratified by BMI, significant association remained between OA risk and high LSBMD amongst women with BMI < 25kg/m² (OR 1.26; 1.07-1.47) and BMI >30kg/m² (1.26; 1.05-1.51); and in men with BMI < 25kg/m² (OR 1.75; 1.37-2.27) or BMI 25-30kg/m² (1.21; 1.02-1.43). OA was associated with an increased risk of fracture. After adjusting for LSBMD women with OA had significant increased fracture risk (1.41; 1.16-1.72); however, the association was not significant in men (OR 0.96; 0.69-1.32). Moreover, the association between OA and fracture risk was particularly pronounced in women with BMI 25-30kg/m² (OR 1.45; 1.05-1.99, adjusted for LSBMD). These data suggest that high BMD is associated with a greater risk of OA in both men and women, particularly those with low BMI. The results also suggest that BMD could be a useful measure for identifying individuals at high risk of OA, particularly among those at lower BMI spectrum. Despite having higher bone density, women with self-reported OA, especially those overweight, have an increased risk of fragility fracture, suggesting that the OA-fracture association is mediated via non-BMD factors.

Disclosures: Mei Chan, None.

MO0379

Insulin Resistance Independently Had the Negative Association with the Bone Mineral Density in Normal Fasting Glucose Tolerance and Impaired Fasting Glucose Not in Diabetes. Sangmo Hong^{*1}, Chang Beom Lee¹, Yong Soo Park¹, Dong Sun Kim¹, You Hern Ahn¹, Tae Wha Kim¹, Woong Choi². ¹Endocrinology & metabolism, Hanyang University College of medicine, South Korea, ²Hanyang University Hospital, South Korea

The relationships between insulin resistance and BMD are not clear. Therefore, we conducted a cross-sectional study to examine the relationship between insulin resistance and BMD among Korean population which was divided with glucose level. This study is based on the Korea National Health and Nutrition Examination Survey (KNHANES) IV (2008). BMD and body composition were measured by DXA method. Insulin resistances were obtained by HOMA-IR equation. We divided the population according to fasting glucose level (NGT, IFG, DM). The relationship between BMD and HOMA-IR were analyzed with multiple regression models which were adjusted with age, body weight, body fat mass, body lean mass, alcohol drink, exercise level and 25(OH) vitamin D level. Among 3290 persons, 1368(41.6%) persons were men and 1922(58.4%) persons were women. In whole population, HOMA-IR showed positive correlations with total body BMD and lumbar BMD in men but not femur BMD in men and all BMD in women. However, NGT group showed negative correlation with all site BMD in both gender (table 1) and IFG group also have negative relations with BMD in total body BMD of men ($B=-0.007$, $p<0.001$) and

serum specimens from all 435 men who experienced any non-vertebral fracture from baseline until February 2007 (average follow-up 4.7 years), all 168 men with first hip fracture from baseline until August 2010 (average follow-up 7.6 years), and a sample of 1602 men randomly selected from the cohort. Cystatin C was measured using a particle-enhanced immunonephelometric assay (inter- and intra-assay CV 3.1% and 2.8%, respectively). Fractures were confirmed with x-ray reports. Modified proportional hazards models were used to estimate the relative hazards (RH) of fracture in men across quartiles of cystatin C (cutpoints 0.80, 0.90, 1.03 mg/L). In a model adjusted for age, race, site and body mass index, higher cystatin C was not related to risk of nonvertebral fracture (p-trend 0.88), but was associated with an increased risk of hip fracture (RH (95% CI): 1.0 [Q1, referent group]; 0.9 (0.5-1.7) [Q2]; 1.1 (0.6-1.9) [Q3]; and 1.6 (0.9-2.8) [Q4]; p-trend 0.04). The majority of the effect of cystatin C on hip fracture was observed among men in Q4 who had a 1.6-fold (95% CI 1.1-2.3) increase in risk compared with men in Q1-3 (Table). Adding potential confounders (including fall history, prior fracture, prevalent cardiovascular disease, frailty status and total hip BMD) one at a time to the base model modestly attenuated the association, with frailty status having the greatest impact. After simultaneous adjustment for multiple confounders, the association no longer reached significance (RH (95% CI) Q4 versus Q1-3: 1.3 (0.9-1.9)). In conclusion, older men with higher serum cystatin C are at increased risk of hip (but not any nonvertebral) fracture. The association between cystatin C and hip fracture is due at least in part to the greater prevalence of frailty among men with higher cystatin C levels.

Table. Association between Cystatin C and Risk of Hip Fracture

	Relative Hazard of Hip Fracture (95% CI)			
	Model 1 (Base)	Model 2 [†]	Model 3 [‡]	Model 4 [§]
Quartile 4	1.6 (1.1-2.3)	1.5 (1.0-2.2)	1.4 (1.0-2.0)	1.3 (0.9-1.9)
Quartiles 1-3	1.0 (referent)	1.0 (referent)	1.0 (referent)	1.0 (referent)

[†]Base model adjusted for age, race, site and body mass index

[‡]Base model + total hip BMD

[§]Base model + frailty status

[§]Final model adjusted for age, race, site, body mass index, fall history, prior fracture, prevalent cardiovascular disease, frailty status and total hip BMD

Association between Cystatin C and Risk of Hip Fracture

Disclosures: Kristine Ensrud, None.

MO0383

The Presence of Arteriosclerosis is a Risk Factor for Vertebral Fracture in Patients with Type 2 Diabetes. Masahiro Yamamoto^{*1}, Toru Yamaguchi¹, Mika Yamauchi¹, Shozo Yano¹, Toshitsugu Sugimoto². ¹Shimane University Faculty of Medicine, Japan, ²Shimane University School of Medicine, Japan

Purpose: We previously reported that patients with type 2 diabetes (T2DM) have an increased risk for vertebral fractures (VFs) compared to non-T2DM controls independent of bone mineral density (BMD) (JBMR 2009). However, it is still unclear what kind of variables could become risk factors for VFs in T2DM. It is well known that low BMD is associated with prevalent cardiovascular disease in the general population, suggesting that bone fragility may be linked to atherosclerosis. The aim of this study is to investigate whether or not atherosclerosis is a risk factor for VFs in T2DM patients.

Methods: We compared parameters for atherosclerosis including maximal intima-media thickness (Max IMT), carotid plaque score (PS) and brachial-ankle pulse wave velocity (baPWV) as well as bone metabolic markers and BMD values at the lumbar spine, femoral neck and one-third of radius between Japanese T2DM patients with and without VFs (203 men over 50 years old and 171 postmenopausal women), whose creatinine levels are within normal range.

Results: Comparison between patients with and without prevalent VFs revealed no significant differences in baPWV, HbA1c, BMD values at any site, or bone metabolic markers in either sex. In contrast, Max IMT and PS in those with VFs were significantly higher than the parameters in those without VFs in each sex (Men: 2.29 1.30 mm vs. 2.68 1.30 mm, P = 0.03, 5.9 4.5 vs. 8.1 5.0, P < 0.01; Women: 2.03 0.90 mm vs. 2.61 1.37 mm, P < 0.01, 5.7 4.2 vs. 9.0 6.3, P < 0.01, respectively). Multivariate logistic regression analysis adjusted for age, BMI, HbA1c, serum creatinine, duration of diabetes, LDL-cholesterol, systolic blood pressure levels, smoking habits, and lumbar spine BMD showed that the presence of prevalent VFs was significantly associated with PS in each sex [Men: Odds ratio (OR)=1.63, 95% CI=1.09-2.43, P = 0.02; Women OR=1.85, 95%CI=1.17-2.93, P = 0.01], and with Max IMT in women (OR=1.61, 95%CI=1.04-2.49, P = 0.03).

Conclusion: These findings showed that atherosclerotic parameters were associated with prevalent VFs independent of BMD in T2DM patients, suggesting that atherosclerosis may be linked to deteriorating bone quality and become a risk factor for VFs in the population.

Disclosures: Masahiro Yamamoto, None.

MO0384

Thyroid Function, Bone Loss, and Fracture in Older Men: The MrOS Study. Douglas Bauer^{*1}, Stephanie Harrison², Howard Fink³, Mary H. Samuels⁴, Peggy Cawthon⁵, Avantika Waring¹, Joseph Zmuda⁶, Eric Orwoll⁴.

¹University of California, San Francisco, USA, ²San Francisco Coordinating Center, USA, ³GRECC, Minneapolis VA Medical Center, USA, ⁴Oregon Health & Science University, USA, ⁵California Pacific Medical Center Research Institute, USA, ⁶University of Pittsburgh Graduate School of Public Health, USA

Excess thyroid hormone is associated with increased bone loss and fracture risk in older women, but there are few data in men. We performed a prospective study to determine if thyroid function, as assessed by thyroid stimulating hormone (TSH) and free thyroxine (FT4), were independently associated with bone loss and fracture risk in the Osteoporotic Fractures in Men Study (MrOS).

At the baseline MrOS visit hip DXA (Hologic QDR4500) was measured and fasting serum was archived at -80C in 5994 men over 65. Repeat hip DXA was obtained in 4418 men after a mean follow-up of 4.6 yr., and incident non-spine fractures were centrally adjudicated. We used baseline serum to measure TSH and FT4 (ADVIA Centaur, Siemens Diagnostics, Deerfield, IL) in 436 men with confirmed non-spine fracture (including 168 hip fractures) and 1604 randomly selected men. TSH and FT4 were analyzed as both continuous and categorical variable using the manufacture's normal range (TSH 0.55-4.78 mIU/L, FT4 0.70-1.85 ng/dL). Bone loss was examined using age-adjusted multivariate regression models in 1604 randomly selected men, and fractures were examined using clinic and age-adjusted hazard models that account for the case-cohort sampling and further adjusted for BMI, race, self-reported health and thyroid hormone use.

In the randomly selected subgroup, 123 (7.7%) men reported thyroid hormone use at baseline and mean (+/-SD) values of TSH and FT4 were 2.54 (2.23) and 0.99 (0.16), respectively. Compared to those without fracture, men with non-spine fracture during follow-up were significantly older (75.5 yr vs. 73.8), had lower total hip BMD (0.89 gm/cm² vs. 0.95) and were more likely to be Caucasian (95% vs. 91%), but TSH and FT4 levels were similar (TSH: 2.542.63 vs. 2.54 2.23, p=0.70, FT4: 0.980.17 vs. 0.980.16, p=0.99). In fully adjusted analyses of TSH as a continuous variable, lower TSH (indicating thyroid excess) was associated with an increased risk of the hip fracture (relative hazard=1.35 per SD decrease, 95% CI: 1.03, 1.77) but fracture risk did not differ significantly by TSH category (Table). FT4 was not associated with fracture risk and neither TSH nor FT4 were associated with bone loss (data not shown).

We conclude that in this cohort of older men lower TSH is weakly associated with an increase in hip fracture risk, but neither abnormal TSH nor FT4 are associated with bone loss or a significant increase in hip or non-spine fractures.

Fracture Outcome	Adjusted Relative Hazard (95% CI)		
	TSH<0.55 (n=52)	0.55<TSH<4.78 (n=1757)	TSH >4.78 (n=164)
Any Non-spine	1.02 (0.53, 1.94)	1.0 (referent)	0.80 (0.54, 1.19)
Hip	0.69 (0.21, 2.27)	1.0 (referent)	0.67 (0.36, 1.25)

Table

Disclosures: Douglas Bauer, None.

MO0385

Vitamin D Insufficiency and Occurrence of Osteoporosis and Disability: The ROAD Study. Noriko Yoshimura^{*1}, Shigeyuki Muraki¹, Hiroyuki Oka¹, Hiroshi Kawaguchi², Kozo Nakamura³, Toru Akune¹. ¹22nd Century Medical & Research Center, University of Tokyo, Japan, ²University of Tokyo, Faculty of Medicine, Japan, ³The University of Tokyo, Japan

The aim of this study is to clarify predictive capacity of the levels of serum 25(OH)D with occurrence of osteoporosis (OP) and disability in the general population. We initiated ROAD (Research on Osteoarthritis/osteoporosis Against Disability), a large-scale population-based cohort study in urban, mountainous and seaside areas of Japan in 2005-7, and a total of 3,040 participants were registered at baseline. The present study enrolled 1,690 subjects (596 men; 1,094 women, mean age 65.2 yrs) in the mountainous and coastal areas. Of them, 1,439 (85.1%) individuals participated in the second surveillance visit in 2008-10 and 1,384 subjects (446 men, 918 women; mean age, 63.9 yrs) underwent BMD examination by DXA (Hologic Discovery) of lumbar spine (L2-4) and femoral neck (FN) at both visits. The cumulative incidence over 3 years of OP was estimated in 1,384 completers. The information of occurrence of disability, certified by a committee consisted of clinical experts, of the 967 subjects (368 men, 599 women) with 65 years and older at baseline was collected. Serum 25 (OH)D levels of all subjects were measured and VD insufficiency was characterised as a serum level of 25(OH)D <30 ng/mL. The mean levels (SD) of serum 25(OH)D of baseline participants were 25.7 (6.5) ng/mL in men and 22.0 (6.2) ng/mL in women. The prevalence of VD insufficiency was 44.4% in men and 69.0% in women (men vs. women, p<0.001). The cumulative incidence over 3 years of OP at L2-4 and FN was 2.2%/3yrs (men, 0.9%/3yrs; women, 3.0%/3yrs) and 5.8%/3yrs (men, 2.2%/3yrs; women, 7.9%/3yrs). A logistic regression analysis using occurrence of OP as an objective factor and serum levels of 25(OH)D as an explanatory factor, after

adjustment for age, weight (kg) and menstrual status (0: pre- and perimenopause, 1: menopause) in women, showed serum 25(OH)D concentration was significantly associated with occurrence of FN OP in women (+1SD, odds ratio, 0.70; 95% confidence interval (CI), 0.51-0.95, $p<0.05$). We confirmed occurrence of disability in 87 individuals (28 men, 59 women) and the incidence was estimated as 2.35/100 person-year (men, 1.96/100 person-year; women, 2.58/100 person-year). Cox's proportional hazards analysis using the incidence as an objective factor and serum levels of 25(OH)D as an explanatory factor, after adjustment for age, gender and weight showed that serum 25(OH)D level was associated with occurrence of FN OP in women (+1SD; hazard ratio, 0.75; 95%CI, 0.61-0.93, $p<0.01$). In conclusion, this longitudinal study showed that high serum 25(OH)D levels could be preventive factors for OP occurrence in women and for disability in both genders in the near future.

Disclosures: Noriko Yoshimura, None.

MO0386

What Are the Risk Factors for Bone Loss in Lupus Patients?. Ioana Moldovan*, Emmanuel Katsaros, Loma Linda University, USA

The purpose of this study was to study risk factors associated with low bone density in a lupus cohort from our university clinic. The charts of 120 patients that fulfilled the American College of Rheumatology criteria for SLE (systemic lupus erythematosus) were reviewed. Forty patients had bone mineral density (BMD) assessed by dual absorptiometry scan (DXA) and their charts were reviewed in detail. Age, race, body mass index (BMI) and disease duration were recorded. Disease activity was assessed by the SLEDAI (SLE disease activity index) score. Laboratory test results were reviewed, including erythrocyte sedimentation rate (ESR), presence of double stranded DNA (dsDNA), complement levels, complete blood counts and presence of proteinuria. Vitamin D levels were included when available. Medications were recorded, including glucocorticoids, immunosuppressants, osteoporosis medications, calcium and vitamin D. The patients were aged from 21 to 76 years, with a median of 44 years old. 23 patients (57.5%) were premenopausal and 17 (42.5%) were postmenopausal. In the premenopausal group, the patients had moderate disease activity, as opposed to the postmenopausal group, where disease activity was low. 8 patients (20%) had osteoporosis, 22 (55%) had osteopenia and 10 (25%) had normal bone density. No racial predominance was observed in any of the three groups. The majority of patients were on chronic low dose glucocorticoids, however only approximately half were taking osteoporosis-preventing medications. The patients with BMD within normal and osteopenic ranges were younger and had moderate disease activity. A higher prevalence of dsDNA antibodies was also observed, supporting the higher disease activity in those groups. The patients with osteoporosis were older, in majority postmenopausal, had longer disease duration and low disease activity. ESR and vitamin D levels were not significantly different in the three groups. BMI was higher, in the overweight range, for the patients with normal BMD, and normal in the osteopenic and osteoporotic groups. In conclusion, in our study, the main determinants for low bone density were lupus disease duration and postmenopausal status. Disease activity and inflammation at the time of obtaining the DXA did not seem to play a major role in bone density. Higher BMI seemed to have a protective effect. Larger, prospective studies would be necessary to better define the risk factors associated with low bone density in lupus patients.

Disclosures: Ioana Moldovan, None.

MO0387

Comparison of Comparison of Histomorphometric Parameters of Bone Structure in the Femoral Neck in Osteoporosis and Osteoarthritis. Yasemin Cinar¹, Funda Atamaz Calis², Yesim Kirazli³, Basak Doganavsargil³, Murat Sezak⁴, Nadir Ozkayin⁴, Semih Aydogdu⁴, Kemal Aktuglu⁴. ¹Ege University Medical Faculty, Physical Therapy & Rehabilitation, Turkey, ²Ege University Medical Faculty, Turkey, ³Ege University Medical Faculty, Pathology, Turkey, ⁴Ege University Medical Faculty, Orthopaedic Surgery, Turkey

Background: Osteoarthritis (OA) and osteoporosis (OP) are common disorders resulting in significant morbidity and an extensive use of health-care resources with the aging of population. Although they have been studied in detailed, the association of OA and OP has always been debated. In this study, we compared the histomorphometric parameters of bone structure in the femoral neck taken from patients who sustained an osteoporotic hip fracture compared with patients with OA. In addition, we aimed to assess the association between the histomorphometric parameters and bone mineral density (BMD) values. **Method:** Femoral head specimens were obtained from 18 patients (11W/ 7M) with OA and 17 patients (12W/ 5M) with femoral neck fracture due to OP during total hip arthroplasty. Histomorphometric analysis was performed by using Zeiss AxioVision LE, Rel. 4.6 (Carl Zeiss micro-imaging Inc., North America) software program to measure trabecular area (Tb.a, mm²), trabecular thickness (Tb.th, μ m) and trabecular separation (Tb.s, μ m). BMDs of lumbar spine (L1-L4) and proximal femur were measured by dual-energy X-ray absorptiometry (DXA) using a Hologic QDR 4500A apparatus (Hologic, Waltham, MA). Also, urine deoxypyridinoline (DPD), serum osteocalcin, 25(OH)D, PTH, calcium and phosphate were measured in all patients. **Results:** The mean age was 68.6 7.8 and 79.1 5.7 for OA and OP patients, respectively. While the Tb.a and Tb.th parameters were significantly higher in the OA

group (Tb.a was 23.2 9.8 vs 13.6 5.5 and Tb.th was 282.2 92.3 vs 123.6 27.5, $p<0.05$), Tb.s was 1084.8 366.1 in the OP group with a significant difference when compared with OA group (496.2 136.1, $p<0.05$). Among the biochemical and hormonal parameters, urine DPD was significantly higher in OP patients (17.5 9.8 vs 9.8 4.3, $p<0.05$). All histomorphometric parameters were highly correlated with the BMDs of lumbar spine and proximal femur ($p<0.01$). **Conclusion:** We observed significant differences in histomorphometric parameters between the patients with OA and OP suggesting that the loss of the trabecular bone plays an important role in the osteoporotic hip fracture. In addition, the high correlations between histomorphometric parameters and BMDs support the value of DEXA measurement in the detection of OP.

Disclosures: Yesim Kirazli, None.

MO0388

Determinants of Circulating Vitamin D and Bone Density in a Young Adult Physician Population. Terri Washington, Buvana Manickam*, Aaron Benjamin, Elena Barengolts, Elizabeth Villagrana, Subhash Kukreja, University of Illinois, USA

Introduction: In this prospective cohort study, we examined determinants of serum 25-hydroxyvitamin D (25OHD) level and bone mineral density (BMD) in young physicians.

Materials and Methods: We evaluated lifestyle, serum 25OHD, parathyroid hormone (PTH) and calcium levels as well as BMD by dual-energy X-ray absorptiometry in apparently healthy resident physicians and medical students including Caucasian subjects (CS), Asian (South and East Asians) subjects (AS), and other ethnic (Hispanic and Black) subjects (OS) working at an urban hospital.

Results: Among 104 participants 75% were females and 42% were whites. Prevalence of 25OHD deficiency (25OHD<20 ng/ml), insufficiency (25OHD 20-29 ng/ml), and sufficiency (25OHD \geq 30 ng/ml) was 48%, 29%, and 23% respectively. Prevalence of normal BMD, osteopenia, and osteoporosis was 63%, 31%, and 6% respectively. Table summarizes the distribution of risk factors and clinical characteristics according to the ethnic groups. Caucasians were taller and had higher serum 25OHD level than AS and OS groups ($p=0.023$ and $p<0.0001$, respectively). Serum 25OHD level was higher in CS than in AS and OS but PTH level and proportion of physicians with relative secondary hyperparathyroidism (PTH >43 pg/ml) were similar among the groups. There was a significant negative linear association between serum 25OHD and PTH in Caucasians ($r=-0.48$, $p=0.008$) and Asians ($r=-0.38$, $p=0.02$) but not in OS ($r=-0.46$, $p=0.26$).

Subjects with vitamin D deficiency were more likely to be of Asian ethnicity (67.4%, $p=0.003$), had higher prevalence of family history of osteoporosis (65.8%, $p=0.01$), were less likely to take vitamin D supplements (61.2%, $p=0.03$) but more likely to be exercising (62.3%, $p=0.01$).

In multiple regression analysis of the entire group, independent determinants ($p<0.05$ for all) of serum 25OHD level included age, race, family history of osteoporosis, use of vitamin D supplements, and sun exposure. These parameters explained 49% of serum 25OHD level variation ($r^2=0.49$). Sun exposure was associated with 25OHD level in CS and AS but not in OS group. Significant determinants of low BMD (osteopenia plus osteoporosis) included gender ($p=0.005$) and BMI ($p<0.0001$).

Conclusion: Young resident physicians and medical students have relatively high prevalence of low serum vitamin D and low BMD despite of healthy lifestyle. Serum 25OHD level in this population is determined in part by modifiable risk factors such as vitamin D supplements and sun exposure.

Characteristics of subjects according to the ethnic group			
Characteristic	Caucasian	Asian	Other
Number (N)	44 (42)	48 (49)	12 (12)
Gender: female	32 (72.7)	36 (75.0)	10 (83.3)
Age, yr	28.0 (2.1)	27.8 (2.1)	26.1 (2.0)
Height, cm	166 (5)	156 (5)	162 (3)
Weight, kg	66.6 (12.4)	62.1 (12.2)	60.8 (14.4)
BMI	23.4 (2.5)	22.7 (2.3)	22.2 (4.3)
Non-smokers	42 (95.5)	46 (95.8)	10 (83.3)
Alcohol intake >20 mg/day	28 (63.6)	25 (52.1)	11 (91.7)
Caffeine intake >200 mg/day	31 (70.5)	36 (75.0)	11 (91.7)
Family history of osteoporosis	16 (36.4)	21 (43.8)	5 (41.7)
Ca supplements >1000 mg/day	22 (50.0)	27 (56.3)	5 (41.7)
Vitamin D supplements >400 IU/day	25 (56.8)	22 (45.8)	4 (33.3)
Exercise >2 times/week	21 (47.7)	29 (60.4)	7 (58.3)
Sun exposure >30 min/day	25 (56.8)	32 (66.7)	9 (75.0)
Serum calcium, mg/dL	9.4 (0.2)	9.4 (0.4)	9.5 (0.3)
Serum 25(OH)D, ng/mL	27.3 (10.8)	15.8 (6.4)	22.7 (11.7)
Serum PTH, pg/mL	36.4 (20.0)	44.7 (26.1)	40.7 (23.2)
Spine BMD, g/cm ³	1.054 (0.107)	0.940 (0.145)	1.040 (0.125)
Femoral neck BMD, g/cm ³	0.953 (0.105)	0.937 (0.137)	0.941 (0.145)
Hip BMD, g/cm ³	0.994 (0.107)	0.930 (0.130)	0.922 (0.151)
Trabecular BMD, g/cm ³	0.746 (0.069)	0.716 (0.116)	0.716 (0.116)
25OHD <20 ng/mL	12 (27.3)	26 (54.2)	5 (41.7)
25OHD 20-29 ng/mL	10 (22.7)	3 (6.3)	3 (25.0)
PTH >43 pg/mL	11 (25.0)	16 (33.3)	6 (50.0)
Normal BMD	32 (72.7)	27 (56.3)	9 (75.0)
Tb.a are mean (SD) or median (N)			
Data available for 95 subjects			
Data available for 98 subjects			
*p<0.05, **p<0.01, ***p<0.001			

Characteristics of subjects

Disclosures: Buvana Manickam, None.

MO0389

Effect of Voluntary Exercise and Energy Restriction on Bone Mineral Density in Female Rat Model. Kaoru Yanaka^{*1}, Mitsuru Higuchi², Yoshiko Ishimi¹. ¹Waseda University & National Institute of Health & Nutrition, Japan, ²Waseda University, Japan

Female Athlete Triad is a syndrome of that involves disordered eating, amenorrhea, and low bone mass/osteoporosis in female athletes. The main pathophysiologic mechanism that leads low bone mass is low energy availability and functional hypothalamic amenorrhea. The aim of the present study was to establish animal model of osteoporosis for female athlete. We have designed to investigate the effect of long-term energy restriction on bone mineral density (BMD), and 17 β -estradiol (E2), and luteinizing hormone (LH) levels in voluntary wheel running female rats. Fourteen female Sprague-Dawley rats (8 wk old) were randomly assigned to two groups, running group (n=8) or sedentary group (n=6). Water and diet were available to all rats initial 10-wk baseline period. Running group were free access to wheels throughout the study. At 18 wk of age, the rats in running group were randomized into two groups: Run-Control-fed (ad lib-fed) group (RC group, n=4) or Run-Restricted-fed (30 % energy restriction for 14-wk) group (RR group, n=4). Daily food intake, body weight, and running distance were collected throughout the 24-wk experimental periods. Serum E2 and LH concentration were measured by ELISA. Femoral BMD were determined by dual-energy X-ray absorptiometry (DXA). Histomorphometric analysis of the femur was performed with an image analyzing system linked to a light microscope. The food intake and body weight, in RR group were significantly decreased during food restricted phase. The running distance was not different in both running groups. The BMD in the RR group was significantly lower than RC and sedentary groups. Histomorphometric analysis showed that the bone volume (BV/TV) in distal femoral cancellous bone was lower in the RR group than that in the sedentary group. Serum E2 levels were significantly low in the RR and RC groups than sedentary group. Furthermore, LH level was markedly reduced in RR group compared with RC and sedentary groups. These distinct endocrine profiles in this model suggest that energy restriction with voluntary exercise disturbs the hypothalamic-pituitary-ovary axis. The present study indicated that the long term energy restriction in voluntary wheel running induced bone loss in female rats with intact ovary. This may establish a foundation for osteoporosis for female athlete rat model caused by the dysfunction of reproductive system.

Disclosures: Kaoru Yanaka, None.

MO0390

Bone Turnover Markers in Subclinical Hyperthyroidism. Ana Paula Barbosa^{*1}, Mario Rui Mascarenhas², Antonio Gouveia de Oliveira³, Vera Simoes⁴, Ana Gonçaves⁵, David Santos Pinto⁶, Manuel Bicho⁷, Isabel do Carmo⁵. ¹Endocrinology University Clinic & Metabolism & Endocrinology Center, Genetics Laboratory (FMUL), CEDML - Endocrinology, Diabetes & Metabolism Clinic, Lda., Endocrinology, Diabetes & Metabolism Department, Santa Maria Hospital, CHLN-EPE, Portugal, ²Faculdade de Medicina Lisboa, Portugal, ³Biostatistics Department, FCMUNL, Portugal, ⁴Metabolism & Endocrinology Center, Genetics Laboratory (FMUL), CEDML - Endocrinology, Diabetes & Metabolism Clinic, Lda., Portugal, ⁵Endocrinology, Diabetes & Metabolism Department, Santa Maria Hospital, CHLN-EPE, Portugal, ⁶CEDML - Endocrinology, Diabetes & Metabolism Clinic, Lda., Portugal, ⁷Metabolism & Endocrinology Center, Genetics Laboratory (FMUL), Portugal

Subclinical hyperthyroidism, a clinical condition defined by a low TSH level with normal T4 and T3, can predispose to reduced bone mineral density (BMD), osteoporosis and fragility fractures. Recently, the data of some studies suggest that TSH is a direct negative regulator of bone remodeling, inhibiting both formation and survival of osteoclasts and inhibiting the differentiation of osteoblasts.

PURPOSE

To evaluate the relationships between the bone turnover markers plasma levels, the hormones affecting bone metabolism and BMD, in patients with subclinical hyperthyroidism.

MATERIAL AND METHODS

In a group of 32 subclinical hyperthyroid postmenopausal patients the plasma bone turnover markers osteocalcin, CTX, and bone alkaline phosphatase, as well as the blood concentrations of the thyroid hormones, TSH, PTH, IGF-1, calcium, SHBG and 25(OH)vitamin D were measured.

The BMD (g/cm²) at the lumbar spine (L1-L4), at the proximal femur, at the distal radius and at the whole body and the total body soft tissues composition (lean and fat masses, Kg) were evaluated by dual X-ray absorptiometry, using the Hologic QDR Discovery W densitometer.

No patient was previously treated for hyperthyroidism and/or OP.

Descriptive and regression tests were used and statistical significance was considered for P < 0.05.

RESULTS

These women with subclinical hyperthyroidism presented a mean age (SD) of 59.1 (12.5) years and the mean height was 1.56 (0.06) m, the mean weight was 70.1 (11.4) kg and the mean BMI was 28.8 (4.1) kg/m².

The CTX plasma levels were significantly correlated to PTH and IGF-1 plasma levels. The TSH plasma levels were significantly related with the PTH and the 25(OH) vitamin D plasma levels. Finally, the osteocalcin plasma levels were significantly related with the bone alkaline phosphatase blood concentrations.

CONCLUSIONS

These results may suggest that in subclinical hyperthyroidism the bone turnover markers and some of the hormones involved in bone metabolism are already modified even before the increase of the thyroid hormone levels, indicating a possible important isolated role for the TSH in bone tissue. Thus, the measures for changing life style, namely the increase in calcium intake and the sun exposure, should be precociously instituted, in order to minimize the bone mass loss and the possible increase of osteoporotic fractures risk.

Disclosures: Ana Paula Barbosa, None.

MO0391

Idiopathic Osteoporosis in Premenopausal Women: Bone Turnover Provides Clues to Pathogenesis. Adi Cohen^{*1}, Emily Stein², David Dempster³, Hua Zhou⁴, Serge Cremers³, Clifford Rosen⁵, Thomas Nickolas¹, Thomas Kohler⁶, Andreas Wirth⁷, Harry Van Lenthe⁸, Ralph Muller⁶, Polly Chen¹, Robert Recker⁹, Joan Lappe¹⁰, Elizabeth Shane². ¹Columbia University Medical Center, USA, ²Columbia University College of Physicians & Surgeons, USA, ³Columbia University, USA, ⁴Helen Hayes Hospital, USA, ⁵Maine Medical Center, USA, ⁶ETH Zurich, Switzerland, ⁷Institute for Biomechanics, ETH Zurich, Switzerland, ⁸Katholieke Universiteit Leuven, Belgium, ⁹Creighton University Osteoporosis Research Center, USA, ¹⁰Creighton University, USA

Idiopathic osteoporosis (IOP) in premenopausal women is an uncommon disorder in which fragility fractures occur in otherwise healthy women with intact gonadal function. Whether women with idiopathic low bone mineral density (BMD) and no fractures truly have IOP is uncertain. To investigate the pathogenesis of IOP, we conducted a case-control study of premenopausal women with IOP: 45 with fractures, 19 with low BMD (Z score < -2.0), and 40 controls. All had tetracycline-labeled transiliac biopsies analyzed by 2D histomorphometry and micro-CT, and stiffness estimated by finite element analysis. Women with IOP had lower BMI than Controls, but serum/urine calcium, estradiol, vitamin D metabolites, IGF-1 and most bone turnover markers (BTMs) were similar. Only serum PTH (2912 vs 229 pg/ml) and the resorption marker, TRAP5b (2.312 vs 1.610 U/l), were significantly higher in Subjects than Controls (both p < 0.01). Compared to Controls, women with IOP had thinner cortices, fewer, thinner, more widely spaced and unevenly distributed trabeculae and lower stiffness. Static remodeling parameters reflecting osteoblast synthesis of osteoid were lower in Subjects than Controls; osteoid width (OWi) was 12% lower (p = 0.02) and mean wall width (WWi) 4% and 6% lower at endocortical and intracortical surfaces, respectively (p < 0.02). Dynamic parameters, bone formation rate (BFR/BS), mineral apposition rate and activation frequency were variable, but comparable on average to Controls. All biochemical and histomorphometric parameters were indistinguishable between IOP subjects with and without fractures. Hypothesizing that the pathogenesis of IOP may differ between women with low and high bone turnover, we analyzed subjects by tertiles of BFR/BS (Table). Women in the low BFR/BS group had significantly lower BTMs, OWi, WWi, Bone Volume Fraction (BV/TV) and stiffness than those in the high tertile. The low BFR/BS group also had higher age adjusted IGF-1 than the upper two tertiles (195+43 vs 170+43; p = 0.04), suggesting osteoblast dysfunction and resistance to IGF-1. Women in the high tertile had higher serum 1,25(OH)₂D and a trend toward higher PTH (p = 0.06) and urine calcium (p = 0.07), suggestive of mild idiopathic hypercalciuria. In conclusion, diagnosis of IOP in premenopausal women should not require a history of fracture. Bone turnover is heterogeneous in women with IOP and the pathogenesis of IOP may differ according to whether bone turnover is high, normal or low.

	Controls	Low Tertile	High Tertile
Cn BFR/BS	0.008±0.007	0.003±0.002	0.017±0.010
BV/TV (%)	23.7 ± 7.7	16.7 ± 4.5 ²	21.3 ± 5.7 ^B
Stiffness (MPa)	545 ± 350	273 ± 173 ²	398 ± 217 ^A
Cn O.Wi (# lam)	4.1 ± 1.0	3.1 ± 1.4 ²	3.8 ± 0.7 ^A
Cn W.Wi (µm)	35.0 ± 3.6	32.6 ± 4.2 ¹	35.5 ± 3.3 ^A
PTH (pg/ml)	22 ± 9	24 ± 10	31 ± 10 ²
1,25(OH) ₂ D	49 ± 11	49 ± 20	60 ± 12 ^{2, A}
24H Urine Ca	162 ± 68	177 ± 80	230 ± 101 ²
Osteocalcin (ng/ml)	15.4 ± 7.9	11.7 ± 5.4	19.8 ± 8.3 ^B
CTX (ng/ml)	0.287 ± 0.19	0.255 ± 0.15	0.434 ± 0.21 ^B
TRAP5b (U/l)	1.6 ± 1.0	1.8 ± 1.1	2.8 ± 1.1 ^{3, B}
1 p<0.05, 2 p<0.01, 3 p<0.0001 Controls vs Tertiles (Low, High) A p<0.05, B p<0.01 Low vs High Tertile.			

Characteristics by Tertile of Bone Turnover

Disclosures: Adi Cohen, None.

MO0392

Preliminary Clinical Study Regarding Improvement Of Dental Implants Stability In Osteoporosis. Horia Barbu^{*1}, Andreea Brehar¹, Monica Comaneanu¹, Adi Lorean², Doina Ghergic¹, Constantin Dumitrache¹.
¹Romania, ²Israel

Purpose: There is a general concern for finding practical solutions that allow for the best possible primary stability of dental implants, an essential condition for a favorable long-term prognosis of implant-prosthetic treatments and improving patient's quality of life. The aim of our study is to investigate and increase stability of the inserted implants in patients with osteoporosis, according to their size and shape, but also to the biomechanical properties of bone.

Methods: We studied two groups of patients, group A consisting of patients without osteoporosis and group B consisting of patients with osteoporosis. Bone quality and risk of implant failure assessment were evaluated by several investigations, including bone turnover using telopeptides Beta Crosslaps (B-ctx) measurement. For group A, surgical protocols specific for clinically healthy patients were applied. In group B, the classic bisphosphonate treatment was replaced with strontium ranelate for 3-12 months, in order to avoid complications such as osteonecrosis of the jaw. Surgical procedures for insertion of dental implants were performed after the B-ctx value passed the 150 pg/mL threshold. We used Resonance Frequency Analysis (RFA) every 3 weeks to monitor variations in the curve drawn by ISQ (implant stability quotient) values from the beginning (primary stability), to the moment of obtaining osseointegration. After prosthetic loading, records of ISQ values were done every three months for one year.

Results: Although the original ISQ index had a greater value (69-87 in group A, 51-64 in group B, respectively), it was observed that in the first 2 months after implant insertion, ISQ value shows a significant decline and over the next 4-6 months implant stability quotient increases, but fails to reach baseline. Those initial values are equaled, or even surpassed 8-10 months after prosthetic loading.

Conclusions: Interdisciplinary collaboration is essential to improve long-term predictability of implant-prosthetic treatment applied to patients with osteoporosis. Strontium ranelate intake for 9-12 months has clearly improved primary stability in subjects belonging to group B and no case of osteonecrosis was found. Inserted implant macro-geometry has a decisive role in obtaining a rigid mechanical fixation in osteoporotic bone and good results are achieved with implants with rough and bioactive surfaces. RFA is a noninvasive, atraumatic and very reliable method of investigation.

Disclosures: Horia Barbu, None.

MO0393

Reduction in Circulating Estrogen and Increase in Postprandial Serotonin Levels in Subjects with Helicobacter Pylori CagA+ Infection: Effects on Circadian Rhythm of Bone Turnover and Skeletal Health. Luigi Gennari^{*1}, Daniela Merlotti¹, Natale Figura², Maria Stella Campagna², Maria Beatrice Franci², Anna Calabro², Annalisa Avanzati², Barbara Lucani², Stefania Lardiello², Leonardo Vaglio², Konstantinos Stolkakis², Ranuccio Nuti¹.
¹University of Siena, Italy, ²Department of Internal Medicine, Endocrine-Metabolic Sciences & Biochemistry, University of Siena, Italy

Helicobacter pylori (HP) is a gram-negative bacterium that affects more than 30% of the world population and elicits a chronic inflammatory response in the gastric mucosa. Several lines of evidence indicate that HP is a major cofactor for the development of upper gastrointestinal disorders but more recent studies also indicated that HP may influence the clinical course of other chronic, age-related conditions such as atherosclerosis and glucose tolerance. In a preliminary analysis in elderly men we demonstrated that infection by HP strains bearing the cytotoxin associated gene A (CagA, that is associated with enhanced inflammatory response) increases bone resorption and is more prevalent in osteoporotic than non-osteoporotic subjects. Here we confirm these results in an extended population-based analysis showing a consistent association between seropositivity for CagA bearing HP strains and osteoporosis or fractures in a large cohort of 1109 elderly male and female subjects. In order to provide further insight on the potential mechanisms underlying this association, we explored the relationship between HP infection and bone turnover markers (bone alkaline phosphatase and serum CTX), 25OH vitamin D, PTH, sex hormone and SHBG levels, as well as other gastrointestinal peptides such as adiponectin, ghrelin and serotonin. Half of the patients underwent all measurements at 8.00 am in a fasting state while the remaining half underwent blood sampling post-feeding, at 3.00 pm, in order to uncover potential effects on circadian rhythms. Consistent with our previous preliminary observation we observed reduced total and free estradiol levels in both male and female subjects affected by HP CagA positive strains, with an higher and statistically significant difference in the fasting state. Moreover, in CagA positive patients circulating ghrelin was significantly lower than in CagA negative or non-affected subjects. Interestingly, while serum CTX significantly decreased after feeding in all subjects, we observed a statistically significant decrease in postprandial levels of bone alkaline phosphatase only in CagA positive subjects that was associated with an increase in serum and plasma serotonin levels. In conclusion, the presence of chronic HP infection by strains expressing CagA may be considered a risk factor for osteoporosis and fractures in males as well as in females. The underlying pathogenetic mechanisms may include variation in estrogen and other gastrointestinal peptides and need to be clarified in further studies.

Disclosures: Luigi Gennari, None.

MO0394

Aging of Iliac Cortical Bone in Normal Women and Men. ANNE-SOPHIE BRAVO MARTIN^{*1}, Jean-Charles Giunta¹, Roland Chapurlat², Georges Boivin³.
¹INSERM, UMR 1033 ; Université de Lyon, France, ²E. Herriot Hospital, France, ³INSERM, UMR 1033 ; Université de Lyon, France

In Human, bone structural changes with age have been mainly described rather in cancellous bone than in cortical bone. Yet, about 80% of all fractures with aging occur at sites mainly cortical (1). Cortical bone organization depends on bone remodeling (2) which is unbalanced with aging in favor of bone resorption leading to bone loss and fragility (3,4). The aim of this study is to evaluate, in a normal human population, the structural changes with aging in cortical bone. Iliac bone samples were taken at necropsy from 99 men and 68 women aged from 17 to 91 years, who died suddenly without apparent bone disease. This population is well distributed with similar numbers of women before and after 50 years, and with 2/3 of men between 17 and 49 years. Undecalcified 100 µm-thick bone sections perpendicular to Haversian canals were microradiographed (5). Cortical thickness, cortical porosity, number of intact osteons, number of fragments of osteons, Haversian canal diameter, cortical mean wall thickness (MWT) and degree of mineralization (DMB) were measured on calcified cortical bone tissue. Cortical thickness decreases ($p < 0.01$) and its porosity increases ($p < 0.02$) with age in both sexes. These are explained by an increase of bone resorption with time leading to enlarged cavities incompletely refilled. The increase of cortical porosity with age can also be partly due to an augmentation of the number of Haversian canals in men (number of intact osteons, $p < 0.05$), and by the enlargement of Haversian canals in women ($p < 0.01$), especially after 50 years. In women, the increase of the number of fragments of osteons ($p < 0.0001$), more marked from 50 years, results from increased bone remodeling, leading to extension of interstitial bone. To the contrary of trabecular MWT (8) but in agreement with data on rib cortical osteons (2), iliac cortical MWT doesn't change significantly with age in men and women. Cortical DMB increases with age in both sexes, but significantly only in men ($p < 0.0001$). To conclude, in women and men, aging and unbalanced bone remodeling lead to cortical thinning, extended cortical porosity and increased amount of interstitial bone.

1-Zebaze *et al.*, Lancet. 375:1729, 2010

2-Frost, Calcif Tissue Res. 3:211, 1969

3-Courpron *et al.* In: Meunier PJ ed., Bone histomorphometry, 2nd Int Workshop, Lyon, 1976

4-Arlot *et al.*, Osteoporos Int. 1:41, 1990

5-Boivin and Meunier, Calcif Tissue Int. 70:503, 2002

6-Lips *et al.*, Calcif Tissue Int. 26:13, 1978

Disclosures: ANNE-SOPHIE BRAVO MARTIN, None.

MO0395

The Interaction Between Calcium and Vitamin D Intake on PTH and Bone Biomarkers. Mageda Mikhail*. Winthrop University Hospital, USA

Background: Adequate calcium and vitamin D are needed to maintain calcium homeostasis and to support skeletal health. **Objective:** To examine the influence of calcium supplementation and vitamin D supplementation separately as well as their interaction and their combined effect on serum PTH and bone biomarkers in healthy postmenopausal women. **Design:** Healthy women, age 45 and older who were menopausal for over 1 year were recruited to participate in a 6-month study. Participants were randomly assigned one of four groups: 1) placebo, 2) vitamin D 100 mcg daily alone, 3) calcium 1200 mg daily alone, 4) vitamin D 100 mcg + calcium 1200 mg daily. Fasting serum calcium, PTH, 25-OHD, 1,25-OH2D, CTX, P1NP, and urine calcium/creatinine ratio were measured at baseline, and at 15 and 28 weeks after baseline. Results: One hundred and fifty nine participants were randomized, with an average age of 60 years and average BMI of 27 kg/m², and 120 participants completed the study. After adjusting for baseline differences and time, the three active treatments all significantly reduced the fasting PTH levels from baseline. The reduction in PTH was highest in the combined calcium + vitamin D treatment group. Using the stringent analysis for multiple comparisons, calcium + vitamin D treatment significantly lowered PTH compared to placebo. For CTX and P1NP, the largest and most significant drop occurred with the use of calcium. Using the stringent analysis for multiple comparisons, either calcium treatment or calcium + vitamin D treatment significantly lowered CTX, compared to placebo. For P1NP, however, only calcium treatment significantly lowered it. A table of mean declines from baseline of PTH, CTX, and P1NP by treatment group is provided. **Conclusion:** Calcium plus vitamin D treatment caused the most significant lowering of PTH compared to placebo, while calcium treatment alone caused the most significant lowering of CTX and P1NP compared to placebo.

Mean Declines (from Baseline) of PTH, P1NP and CTX, by Treatment Group

Group	PTH (pg/ml)	p-value	P1NP (ug/L)	p-value	CTX (ng/ml)	p-value
Vitamin D	-3.59	0.0193	-0.284	0.8698	0.059	0.0093
Placebo	-0.74	0.6837	0.523	0.8068	0.049	0.0732
Calcium + D	-8.67	< 0.0001	-5.115	0.0008	-0.046	0.0456
Calcium	-4.40	0.0139	-7.896	0.0002	-0.077	0.0042

Note: A negative sign indicates a decline.

By a stringent analysis for multiple pair-wise comparisons, we find the following group differences ($p < 0.05$): For PTH, there was a significant difference in decline for Calcium + D vs. Placebo. For P1NP, there were significant differences in declines for Calcium vs. Vitamin D and Calcium vs. Placebo. For CTX, there were significant differences in declines for Calcium vs. Vitamin D and Calcium vs. Placebo. For CTX, there were significant differences in declines for Calcium + D vs. Vitamin D and Calcium + D vs. Placebo.

Mean Declines of PTH, PINP and CTX, by Treatment Group

Disclosures: *Mageda Mikhail, None.*

This study received funding from: Merck

MO0396

Bone Mineral Density (BMD) Loss Due to Weight Reduction Differs in Obese and Overweight: The Contribution of Fat and Lean Tissue. Sue Shapses¹, Claudia Pop¹, Deeptha Sukumar¹, Robert Zurfluh¹, Steven Heymsfield², Yvette Schluskel¹. ¹Rutgers University, USA, ²Pennington biomedical Research Center, USA

Changes in soft tissue composition accompany voluntary weight reduction but whether the loss in these tissue compartments can predict the change in BMD by obesity status is not clear. We examined pooled data from 231 overweight and obese women and men 24-74 years of age who were assigned to six months of a weight loss (WL, > 2.5% loss) or weight maintenance (WM) intervention from 1995-2010. Participants were asked to maintain their usual physical activity level. Body composition, BMD and hormones were measured. Multiple regression analysis was performed to examine whether soft tissue changes could explain the variance in BMD loss using body mass index (BMI) definitions of overweight (25-29.9 kg/m²) or obese (> 30 kg/m²) classification in the model. Results: Total fat loss explained the variance for BMD loss at the trochanter, and ultra distal (UD) and 33% radius ($r^2 = 2-6\%$; $p < 0.05$), whereas lean tissue loss explained the variance for total body BMD (TBBMD, $r^2 = 10\%$, $p < 0.001$) and there was no difference due to BMI classification. 157 individuals lost 7.2 4.8% of their weight and 74 maintained their weight (0.1 2.3%). Compared to the WM group, the WL group lost more BMD ($p < 0.05$) at the 33% radius (-1.2 3.0%) and trochanter (-0.8 3.8%). Due to baseline differences in the population, we also analyzed a subset of postmenopausal women ($n=121$) and found that total fat loss remained a predictor of the UD radius and lean tissue remained a predictor of TBBMD ($r^2=14\%$). BMI classification explained ($r^2 = 5-6\%$) the BMD loss at the 33% radius and trochanter. Two-way ANOVA (WL/WM by BMI classification) shows a greater reduction in fat:lean tissue in the overweight (3:1) than obese (1:1) women despite similar weight loss of 6.0 2.9 kg. Surprisingly, at the 33% radius, BMD loss was greater in the obese compared to overweight, irrespective of weight loss. In contrast, only the overweight showed weight-loss induced BMD loss (-2.1 4.3% at trochanter; $p < 0.005$). These findings show that fat loss explains most of the loss in BMD at sites vulnerable to fracture in the entire population, and that bone and soft tissue loss occurs differently in obese and overweight women. Loss of BMD at the 33% radius (non-weight bearing) is vulnerable to bone loss irrespective of weight reduction in the obese, whereas overweight women attempting to lose moderate weight are at greater risk of bone loss despite attenuated loss of lean tissue.

Disclosures: *Sue Shapses, None.*

MO0397

Determination of Serum Sclerostin Levels in Women with Anorexia Nervosa. Christina Bittighefer¹, Julia Wild², Angela Trubrich¹, Judith Haschka³, Roland Kocian⁴, Wolfgang Woloszczuk⁵, Stylianios Kapiotis⁶, Sebastian Dinu⁶, Christian Muschitz³, Heinrich Resch⁷. ¹The VINFORCE Study Group - St. Vincent Hospital – Medical Department II, Academic Teaching Hospital of the Medical University of Vienna, Austria, ²Medical University of Vienna, Department of Obstetrics & Gynecology, Austria, ³St. Vincent's Hospital, Austria, ⁴St. Vincent Hospital Vienna, Austria, ⁵Biomarker Design ForschungsGmbH, Vienna, Austria, ⁶Central Laboratory St. Vincent Group, Austria, ⁷Medical University Vienna, Austria

Purpose: Bone metabolism is severely altered in patients with anorexia nervosa (AN) causing bone loss and consequently an increased fracture risk. However, the pathophysiology is still under debate. AN is classified into two subgroups, the restricting type (increased physical activity, rejection of eating) and the binge/purging type (self-induced vomiting, misuse of laxatives, diuretics, or enemas). It has been recently recognized that sclerostin (scl), a glycoprotein expressed by osteocytes, regulates bone mass by inhibiting Wnt signaling and bone formation. However, the importance of sclerostin in patients with AN and low bone mass is unknown. Methods: We compared serum scl levels in 18 patients (pts) with AN (mean age 23.3 4.3 ys; mean BMI 14.8 1.2 kg/m²). Subsequently we allocated the AN pts into the restricting type ($n=8$; mean age 20.8 2.5 ys; mean BMI 14.2 1.2 kg/m²) and the binge/purging type ($n=10$; mean age 24.4 4.4 ys, mean BMI 15.2 1.1 kg/m²). Pts were

compared with 21 healthy premenopausal women (mean age 27.1 2.7 ys; mean BMI 21.8 2.9 kg/m²). Sclerostin was determined by a quantitative sandwich ELISA assay (Biomedica, Vienna, Austria). Scl levels were correlated with demographic data, female sex hormones and BMD measurements at hip and lumbar spine. Results: Scl levels were significantly lower in women with AN compared to controls (12.7 4.8 pmol/L vs 17.0 7.4 pmol/L, $p=0.03$). Particularly pts in the restricting subgroup showed lower scl levels than women in the binge/purging subgroup (9.8 2.0 pmol/L vs 14.4 5.2 pmol/L, $p=0.03$). The restricting type had significantly lower scl levels ($p=0.01$) compared to healthy women, whereas the scl levels in the binge/purging type were similar to scl levels in the control group. Serum scl levels were positively correlated with BMI in women with AN ($r=0.49$, 95% CI 0.5595; 0.7763; $p=0.03$), but not with female sex hormones and BMD values. Conclusion: Our data clearly show significantly decreased scl levels in pts with AN compared to healthy, age-matched female controls. Within the two AN subgroups the restricting type showed significantly lower scl levels, most likely caused by the hyperactivity in this AN type as a possible explanation for these differences. Furthermore, there seems to be no relationship between estrogen levels and scl secretion, giving evidence of an uncoupling in bone remodeling.

Disclosures: *Christina Bittighefer, None.*

MO0398

Factors Associated with Fractional Calcium Absorption (FCA) in Postmenopausal Women. Karen Hansen¹, Andrea Jones², Lisa Davis¹, Elizabeth Crone¹, Christina Lemon¹, Diane Burroughs¹, Martin Shafer³. ¹University of Wisconsin, USA, ²University of Wisconsin School of Medicine & Public Health, USA, ³Wisconsin State Lab of Hygiene, USA

Introduction: Increasing calcium absorption efficiency was associated with higher femoral neck bone mineral density and lower risk of hip fracture in the Study of Osteoporotic Fractures. In a post-hoc analysis of three separate calcium absorption studies, we evaluated associations between demographic, dietary and laboratory characteristics and FCA in postmenopausal women.

Methods: 50 postmenopausal women were recruited for studies evaluating changes in calcium absorption related to correction of vitamin D insufficiency ($n=19$), use of proton pump inhibitors ($n=21$) and use of aromatase inhibitors to treat breast cancer ($n=10$). The baseline calcium absorption visit was used for the current analysis. Levels of dual stable isotopes in a 24-hour urine collection were used to calculate FCA. Food during each 25-hour inpatient study replicated subjects' outpatient diet based on analysis of 7-day diet diaries. Demographic variables included race, age, height, weight and body mass index. Dietary variables included the average daily intake of kilocalories, carbohydrates, protein, fat, fiber, calcium, vitamin D, magnesium, iron, sodium, caffeine and oxalate. Laboratory variables included serum calcium, creatinine, parathyroid hormone, 25(OH)D and 1,25(OH)₂D levels. We used Pearson's correlation coefficients, independent sample t-tests and multivariate linear models to assess characteristics associated with FCA.

Results: 50 women with a mean (SD) age of 60 (8) years and FCA of 20% (8%) of were studied. FCA was significantly lower in Caucasian compared to non-Caucasian women (19% versus 29%, $p=0.001$). Table 1 presents a comparison of variables in women with FCA above and below the median. FCA correlated negatively with age ($r = -0.48$, $p < 0.001$), calcium intake through diet and supplements ($r = -0.53$, $p < 0.001$), dietary protein ($r = -0.35$, $p = 0.02$), dietary magnesium ($r = -0.38$, $p = 0.008$), and serum 25 (OH)D levels ($r = -0.50$, $p < 0.001$). In multivariate models, age and calcium intake accounted for 42% of the variance in calcium absorption, with no improvement in the model with the addition of other variables.

Conclusions: In this cross-sectional assessment of variables associated with FCA postmenopausal women, increasing age and increasing calcium intake were inversely associated with FCA and accounted for 42% of the variance in FCA. Interventions to increase FCA in postmenopausal women might be of limited benefit in the elderly or in women with high calcium intake.

Table: Characteristics of women with fractional calcium absorption above and below the median

Variable	Mean (SD) or % for Subjects with FCA Below the Median (n=23)	Mean (SD) or % for Subjects with FCA Above the Median (n=25)	p-value
Demographic Variables			
Age, years	64 (7)	56 (7)	<0.001
Caucasian Race	100%	72%	0.01
Height, inches	64 (2)	65 (2)	0.750
Weight, kg	76 (14)	80 (16)	0.269
Body Mass Index, kg/m ²	28 (4)	30 (5)	0.237
Nutritional Variables			
Kilocalories	1940 (400)	1730 (410)	0.084
Protein, grams	85 (18)	73 (21)	0.051
Fat, grams	82 (28)	68 (24)	0.077
Carbohydrates, grams	228 (56)	213 (64)	0.366
Fiber, grams	22 (9)	17 (8)	0.031
Calcium, mg	1686 (623)	909 (351)	<0.0001
Vitamin D, IU	175 (73)	124 (121)	0.092
Magnesium, mg	372 (89)	274 (113)	0.002
Iron, mg	14 (5)	12 (5)	0.241
Sodium, mg	2556 (998)	2700 (813)	0.588
Oxalate, servings	1.4 (1.1)	0.7 (0.7)	0.017
Serum Laboratory Variables			
Calcium, mg/dL	9.3 (0.5)	9.2 (0.4)	0.781
Creatinine, mg/dL	0.80 (0.1)	0.8 (0.1)	0.405
GFR, mL/minute	80 (17)	87 (18)	0.138
Parathyroid, pg/dL	45 (21)	54 (21)	0.166
25(OH)D, ng/mL	34 (9)	22 (9)	<0.0001
1,25(OH) ₂ D, pg/dL	45 (23)	42 (18)	0.576

Data exclude two outliers, one with an FCA of 5% and the other with an FCA of 41%. Dietary variables are presented as the average intake per day, based on analysis of seven-day diet diaries. Calcium intake includes both dietary and supplemental intake.

Table

Disclosures: Karen Hansen, None.

MO0399

Physiological Supplementation of Sex Steroids Suppresses Bone Turnover in Male But Not Female Gonadectomized Mice. Alexandra Heyny*, Carmen Streicher, Reinhold Erben. University of Veterinary Medicine, Austria

Although mice are very often used as models of estrogen and androgen deficiency-induced bone loss, the existing data about the bony effects of a physiological supplementation of estradiol (E2) and testosterone in gonadectomized (GX) mice are scarce. It was the aim of this study to assess the skeletal effects of physiological doses of sex hormones in GX C57BL/6 mice. Physiological doses were defined by estrogenic and androgenic effects on typical target organs such as the uterus in females and seminal vesicles in males. Twelve-week-old male and female C57BL/6 mice were ovariectomized (OVX) or orchietomized (ORX). OVX mice received vehicle (benzylbenzoate/ricinus oil 1:5, v/v, B/R) or daily doses of 1.25, 2.5, 5, and 10 µg/kg E2 five times per week. ORX mice were treated with vehicle (B/R) or 20, 30, and 40 mg/kg testosterone undecanoate (TUD) twice weekly. All mice were killed 4 weeks post-GX after in vivo calcein labeling. Ten µg/kg estradiol in OVX mice, and 30 mg/kg TUD in ORX mice completely prevented uterine and seminal gland atrophy, respectively. Peripheral quantitative computed tomography (pQCT) and µ-CT analysis revealed femoral and lumbar vertebral cortical and cancellous bone loss in vehicle-treated OVX and ORX mice at 1 month post-GX. Osteopenia in male mice was associated with increased cancellous bone formation rate, higher osteoclast numbers, and augmented urinary excretion of collagen crosslinks, whereas vehicle-treated OVX mice did not show an increase in bone turnover, relative to sham-operated mice. In both ORX and OVX mice, the doses of E2 and TUD which prevented uterine and seminal gland atrophy also completely prevented post-GX bone loss. However, 30 mg/kg TUD in ORX mice suppressed bone formation rate, osteoclast numbers, and urinary collagen crosslink excretion relative to vehicle-treated ORX mice, whereas 10 µg/kg E2 lacked a suppressive effect on bone turnover in OVX mice. We conclude that male C57BL/6 mice show a typical high turnover osteopenia after androgen withdrawal at 1 month post-ORX which is suppressed by physiological doses of testosterone. In contrast, post-OVX bone loss in female C57BL/6 mice is not associated with increased bone turnover at 1 month post-OVX, and supplementation of OVX mice with physiological doses of E2 does not suppress bone turnover.

Disclosures: Alexandra Heyny, None.

MO0400

Sclerostin Production Decreases after Ovariectomy in Mouse Bones in Association with an Increase in Bone Formation. Sandra Jastrzebski¹, Judith Kalinowski¹, Yurong Fei¹, Shilpa Choudhary¹, Carol Pilbeam¹, Farayal Mirza¹, Maria Marie Hurley², Joseph Lorenzo^{*1}. ¹University of Connecticut Health Center, USA, ²University of Connecticut Health Center School of Medicine, USA

Sclerostin (SOST) is a negative regulator of Wnt signaling and bone formation. In postmenopausal women SOST and serum estrogen (E) levels negatively correlate. We examined if ovariectomy (OVX) altered bone SOST production and bone turnover in mice. 8-wk-old C57BL/6 females were either sham-operated (SHAM) or OVX. In this model bone loss begins 3 wks after OVX and is maximal after 5 wks. Femurs and calvaria were examined for SOST mRNA and protein by qRT-PCR and western blotting. Bone turnover was determined by serum CTX and osteocalcin (OC) ELISA. In vitro osteoclastogenesis in bone marrow cells was induced with M-CSF and RANKL for 6 d. We also cultured murine bone marrow cells for 16 days in osteogenic conditions +/- E (estradiol 10 nM) and measured medium SOST by ELISA and SOST and alkaline phosphatase (AP) mRNA by qRT-PCR. Our ELISA can measure murine SOST in medium but not in serum because of interfering substances.

The effects of OVX on SOST mRNA and protein differed between skeletal sites. In calvaria there was a trend for a 33% decrease in SOST mRNA with OVX (p=0.09) at 3 wks. At 6 wks the decrease in calvaria SOST mRNA was 52 % (p<0.01). In femurs SOST mRNA decreased by 53% (p<0.01) with OVX at 3 wks but was not different from SHAM at 6 wks. SOST protein in calvaria decreased with OVX by 62 % at 3 wks and 42 % at 6 wks (p<0.01 for both). There was no difference in SOST protein in femurs between SHAM and OVX at either time point. Bone turnover also differed with time. Formation (OC) increased by 36% at 3 wks and 34 % at 6 wks (p<0.01 for both). However, resorption (CTX) was increased at 3 wks (by 33%, p<0.01) but not at 6 wks. Similar to CTX, in vitro osteoclastogenesis increased by 38% in cells from 3 wk OVX mice (p<0.01) but not from 6 wk OVX mice. SOST protein was detected in the medium of osteogenic cultures at d 12 and was maximal at d 14-16. SOST and AP mRNA levels at d 16 were similar and E treatment did not alter SOST protein or mRNA.

These results demonstrate that after 3 and 6 wks OVX had inhibitory effects on SOST production in mouse bones, which varied with the time and site examined. The effect of E on SOST appeared to be indirect since it was not reproduced by E treatment of primary cultures. However, it was associated with an increase in bone formation at both times but not resorption, which increased at 3 but not 6 wks. We speculate that a decrease in SOST is a mechanism by which bone formation increases after OVX.

Disclosures: Joseph Lorenzo, None.

MO0401

Myostatin Serum Concentrations in Men – Age-Related Changes and Correlates– the STRAMBO Study. Pawel Szulc^{*1}, Claudia Goetsch², Michael Schoppert³, Roland Chapurlat⁴, Lorenz Hofbauer⁵. ¹Hopital E. Herriot, Pavillon F, France, ²University of Dresden, Germany, ³University of Marburg, Germany, ⁴E. Herriot Hospital, France, ⁵Dresden University Medical Center, Germany

Serum myostatin levels in men and its determinants have not been defined. We measured serum myostatin in 1,153 men aged 20 to 87 using an ELISA detecting the dimeric full-length peptide and its C-terminal active protein (Immundiagnostik AG, Bensheim, Germany). We assessed lumbar aortic calcification (AC) on the Vertebral Fracture Assessment scans and relative appendicular muscle mass (RASM, kg/m²) by DXA. Between 20 and 60 years of age, circulating myostatin increased by 28% (n=353, r=0.16, p<0.005), whereas RASM was stable. After 60 years, serum myostatin and RASM decreased (n=800, r= -0.12 and r= -0.21, p<0.001). We analyzed data in 780 men aged ≥60, who did not take vitamin D or calcium supplements, using the multivariate analysis of covariance. Men having aortic calcifications had lower myostatin levels (3.3%, 0.23 SD, p<0.005). Men in the highest myostatin quartile (>39.5 mg/L) had lower average AC score compared with the three lower quartiles combined (p<0.005 adjusted for confounders). In multivariate models, prevalence of AC decreased with increasing myostatin levels (OR=0.76 per 1SD decrease, 95%CI: 0.64-0.91, p<0.001). AC prevalence was lower (OR=0.48, 95%CI: 0.33-0.68, p<0.001) in the highest quartile vs three lower quartiles combined. Serum levels of myostatin and 25-hydroxyvitamin D (25OHD) were positively correlated (partial r=0.20, p<0.001). Serum myostatin levels were 12% higher (0.76 SD, p<0.001) in 45 men with 25OHD>40 ng/mL compared with 369 men with 25OHD<20 ng/mL. In multivariate models, low calcium intake (<590 mg/day, lowest quartile) was associated with 11% lower (0.37 SD, p<0.01) serum myostatin vs three higher quartiles combined. Elevated concentration of C-reactive protein (CRP, >3.27 mg/L, highest quartile) was associated with 4.3% lower (0.30 SD, p<0.001) serum myostatin levels compared with the three lower quartiles combined. Serum myostatin levels were 5% lower (0.43 SD, p<0.05) in 45 current mild smokers (median: 8 cigarettes/day) compared with non-smokers. Men who drank >110 g alcohol/week (median) had 12% lower (0.41 SD, p<0.001) myostatin level compared with men who drank less.

Thus, in men serum myostatin concentrations increased until the age of 60, then decreased. In older men, aortic calcification, lower 25OHD level, low calcium intake,

higher CRP level, current smoking, and higher alcohol intake were all independently associated with lower myostatin levels.

Disclosures: Pawel Szulc, None.

MO0402

Relationship Between Serum Testosterone and Fracture Risk in Men: A Comparison of Radioimmunoassay Versus Liquid Chromatography Tandem Mass Spectrometry. Thach Son Tran^{*1}, Nguyen Nguyen¹, Jacqueline Center¹, Markus Seibel², John Eisman¹, Tuan Nguyen¹. ¹Garvan Institute of Medical Research, Australia, ²Bone Research Program, ANZAC Research Institute, The University of Sydney, Australia

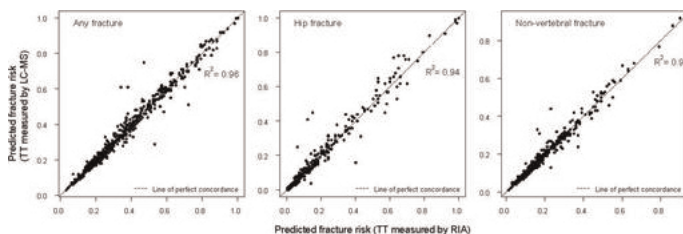
Low serum levels of testosterone are associated with fracture risk in elderly men. Serum levels of testosterone can be measured by several laboratory methods, including the liquid chromatography tandem mass spectrometry (LC-MS) and radioimmunoassay (RIA) method. This study was designed to determine whether the testosterone-fracture relationship is affected by methods of measurement at the population and individual level.

The study was part of the on-going Dubbo Osteoporosis Epidemiology Study, which was initiated in 1989. Total testosterone (TT) was measured by LC-MS and RIA methods from serum samples collected from 609 men, whose incidence of fractures had been continuously ascertained (by X-ray reports) from 1989 to 2010. Baseline clinical risk factors were obtained by a structured questionnaire. The concordance in serum levels of TT between LC-MS (MS-TT) and RIA (RIA-TT) methods was evaluated by the Deming regression model. The association between TT and fracture risk was assessed by the Cox's proportional hazards model.

On average, MS-TT was higher than RIA-TT by 26 ng/dL (95% confidence interval [CI]: 11 to 41). The coefficient of concordance between MS-TT and RIA-TT was 0.70 (95% CI: 0.66 to 0.74). Using the threshold of TT ≤ 300 ng/dL, 25% and 28% of the men were classified as hypogonadal by MS-TT and RIA-TT, respectively. The Deming's equation linking the two measurements was: MS-TT = 0.91 + 0.86*RIA-TT, R² = 0.50.

Among 560 men with complete data, 103 had sustained at least one fragility fracture during the median duration of follow-up of 5.8 years. After adjusting for age, weight, bone mineral density, fracture history, smoking status, calcium intake, and sex hormone-binding globulin, TT was significantly associated with fracture risk. The hazard ratio of fracture per standard deviation decrease in TT was 1.29 (95%CI: 1.09 to 1.52) for MS-TT, and 1.26 (95% CI: 1.06 to 1.48) for RIA-TT. The correlation between predicted probabilities of fracture by MS-TT and RIA-TT was R² = 0.99 (Figure), with average difference in the predicted probability of fracture being 0.01% (95%CI: -6.1% to 6.2%) for any fracture.

These results indicate that lower serum levels of total testosterone was associated with increased risk of fracture in elderly men. Despite the modest concordance between methods of measurement, TT measured by RIA could predict fracture risk as good as LC-MS method.



Ten-year predicted probability of fracture based on serum testosterone measured by LC-MS and RIA

Disclosures: Thach Son Tran, None.

MO0403

Contribution of Enzymatic and Non-Enzymatic Collagen Crosslinks to Femoral Neck Fragility. Comparison Between Osteoporosis and Osteoarthritis. Evelyn Gineyts^{*1}, Nathalie R Portero-Muzy¹, Hubert Blain², Roland D Chapurlat¹, Pascale M Chavassieux¹. ¹INSERM, UMR 1033, Université de Lyon, France, ²Department of Geriatrics, CHU of Montpellier, France

We have previously shown that the relative protection of patient with hip osteoarthritis (OA) against fracture may be due to cortical thickening and preservation of the trabecular microarchitecture at the femoral neck (Blain et al, 2008). Changes in collagen crosslinks concentrations may also contribute to skeletal fragility. We have investigated the collagen crosslinks composition in the ultradistal part of femoral necks collected during hip replacement in 16 hip OA patients (668 yrs) and 16 osteoporotic (OP; 799 yrs) postmenopausal women. Mature enzymatic crosslinks pyridinoline (PYD), deoxypyridinoline (DPD) and the non-enzymatic crosslink pentosidine (PEN) were analyzed by reverse phase-HPLC in the cortical and trabecular bone. When compared to OA, trabecular bone in OP was characterized by significant higher amounts of PYD (+38%), DPD (+32%) and PEN (+43%) (p<0.001)

but without change of the PYD/DPD ratio. In cortical bone, only PEN was significantly greater in OP than in OA (+43%; p<0.001). The magnitude of collagen crosslinks contents increase in OP was greater than previously reported with ageing (Saito et al, 1987). In OA, PYD and the PYD/DPD ratio were significantly lower in the superior quadrant than in the 3 others. In contrast, in OP, the distributions between the four quadrants were similar. Trabecular PYD, PEN and PYR/DPD ratio were significantly correlated with 2D-histomorphometric parameters of bone mass BV/TV (r²=0.59, 0.58, 0.46 respectively; p<0.01) and trabecular connectivity TBPf (r²=0.52, 0.58, 0.39; p<0.03). In conclusion, modifications of the enzymatic and non-enzymatic collagen crosslinks may contribute to femoral neck fragility in OP and to the relative resistance in OA.

Blain H et al. Bone 2008;43:862-868

Saito et al. Anal Chem 1987;253:26-32

Disclosures: Evelyn Gineyts, None.

MO0404

Increased Expression of the Purinergic P2Y2 Receptor Results in Increased Resorption and Decreased Bone in vivo. Ning Wang¹, Peter Schwarz², Susanne Syberg^{*2}, Solveig Petersen³, Cansu Agca⁴, Niklas Jorgensen⁵, Yuksel Agca⁶, Alison Gartland⁷. ¹The University of Sheffield, United Kingdom, ²Glostrup Hospital, Denmark, ³Laboratory Technician, Denmark, ⁴Research Scientist, postdoc, USA, ⁵Copenhagen University Hospital Glostrup, Denmark, ⁶Prof, Assoc, USA, ⁷The Mellanby Centre for Bone Research, The University of Sheffield, United Kingdom

Nucleotides such as adenosine triphosphate (ATP) are released from bone cells in response to a number of stimuli including fluid shear stress. They act on P2 purinergic receptors. The P2Y2 subtype is a G-protein coupled receptor and is expressed in osteoblasts and osteoclasts. In vitro activation of the receptor nucleotides results in inhibition of alkaline phosphatase production and of matrix mineralization. The aim of this study was therefore to investigate whether increased expression of the receptor affects bone mass and structure in vivo. Ten wildtype (WT) and 10 P2Y2 overexpressing (P2Y2R) female nullipara rats were sacrificed at age 3 months. At -10 and -2 days before sacrifice, bones were labelled by injection with Alizarin Red 30 mg/kg body weight i.p. Bones were collected for bone mass measurements on a Piximus densitometer, for micro-CT of bone microstructure, and for histomorphometry. Serum was collected for bone marker analysis. Bone mineral density (BMD) was reduced in P2Y2R compared to WT, meanSEM: 0.181 (0.003) g/cm² vs. 0.190 (0.002) g/cm², respectively (p<0.05). This was partially due to an increase in area: 2.26 (0.03) cm² vs. 2.12 (0.04) cm², (p<0.05). In addition, femurs of P2Y2R were slightly longer than WT (3.52 (0.02) cm vs. 3.46 (0.01) cm, (p<0.01). Micro-CT showed reduced trabecular thickness in the P2Y2R (0.057 (0.0005) U vs. 0.059 (0.0005) U), and increased structure model index (1.45 (0.05) vs. 1.23 (0.08)). The reduced bone mass was supported by an increase in bone resorption measured as TRAP-5b in P2Y2R vs. WT (2.1 (0.2) U vs. 1.5 (0.1) U, p<0.01), while no differences could be detected for bone formation. Finally, the increased resorptive activity was confirmed by histomorphometry, where P2Y2R showed increased erosive surfaces with ES/BS% of 18.6 (0.5) % vs. 16.9 (0.5) % (p<0.05). In contrast, the number of actively forming surfaces (MS/BS %) was decreased in the P2Y2R (56.9 (0.5) % vs. 60.6 (1.0) %, p<0.01). In conclusion, P2Y2 receptor overexpression in rats results in decreased BMD, but not BMC. This is partially due to increased bone resorption, and decreased formation. Furthermore, P2Y2R have slightly increased length growth compared to WT. This is consistent with previously published in vitro effects of P2Y2 receptor activation in osteoblasts. Further studies will show whether P2Y2 receptor inhibition could increase bone mass and thus be a potential pharmacological target for treatment of bone loss.

Disclosures: Susanne Syberg, None.

MO0405

Normal Histomorphometric Reference Ranges for Cortical Bone Width and Cortical Porosity in Adult Females. Donna Jewison^{*1}, Robert Wermers², Stephen Hodgson², Thomas J. Sebo³, Michael Yaszemski⁴, Theresa Hefferan². ¹Mayo Clinic Rochester, MN, USA, ²Mayo Clinic, USA, ³Mayo Clinic Rochester, USA, ⁴Mayo Clinic College of Medicine, USA

Cortical bone porosity and cortical bone thickness are known determinants of bone strength and fracture susceptibility. Whenever bone histology is evaluated quantitatively, it is necessary to compare the results with data from a properly controlled group. Histomorphometric quantitation of cortical bone in metabolic bone disorders is important to provide insight into the underlying pathophysiology of the disease process. The purpose of this study was to generate a unique histomorphometric-based reference range for cortical width and cortical porosity from a population of normal healthy females. Archived transiliac crest biopsies from the Institutional Review Board (IRB) approved studies were used to generate the normal reference ranges. The biopsies were obtained from 13 premenopausal women, 30-45 years old, and 33 postmenopausal women, 50-70 years old. The results were reported from the combined premenopausal and postmenopausal data (n=46). The biopsies were embedded in glycol methacrylate and 5 micron thick sections were stained with a modified Goldner's trichrome. These sections were used for quantitative static

histomorphometry using an OsteoMeasure analysis system with the following cortical parameters measured: cortical width, cortical area and cortical porosity. The mean cortical width was 879.1 ± 291.9 microns with a range of 369.0 – 1699.2 microns, mean cortical area was 11.89 ± 3.74 mm² with a range of 6.09 – 24.53 mm² and mean cortical porosity was $10.22 \pm 6.37\%$ with a range of 2.59 – 31.87%. Although data analysis by Pearson correlation coefficient revealed no correlation with age and cortical width ($r=0.2115$, $p=0.1583$), cortical area ($r=0.2571$, $p=0.0845$) or cortical porosity ($r=0.1982$, $p=0.1868$), there was a trend towards a decrease in cortical width and an increase in cortical porosity in advancing age ($r=0.2571$, $p=0.0845$). Cortical bone may be directly impacted by metabolic bone diseases; therefore it is necessary to compare the results to a normal reference range, which we have defined here.

Disclosures: Donna Jewison, None.

MO0406

Osteoblastic Differentiation is Inhibited by Warfarin and 18- α -glycyrrhetic Acid. Dong Jin Chung^{*1}, Yun-Hey Jin², Dong Hyeok Cho¹, Hyung Min Jeong², Jin Ook Chung¹, Min Young Chung¹, Kwang Youl Lee².

¹Chonnam National University Medical School, South Korea, ²College of Pharmacy & Research Institute of Drug Development, Chonnam National University, South Korea

Anticoagulation therapy with vitamin K antagonists such as warfarin is widely used to prevent and treat stroke in patients with chronic atrial fibrillation or mechanical heart valves. Because vitamin K is an essential factor for γ -carboxylation of osteocalcin, vitamin K antagonists might cause bone loss. Although the association between warfarin use and bone metabolism is still controversial, several studies show that bone mineral density is decreased and fracture risk is increased with warfarin therapy. Meanwhile, attenuation of gap junctional communication (GJC) by warfarin is reported in rat liver epithelial cells. However, the effect of warfarin on osteoblasts, in which GJC is important for osteoblastic differentiation, remains unknown. Here we investigated whether warfarin has an inhibitory effect on osteoblastic differentiation using an osteoblastic cell line (C2C12). Warfarin and 18- α -glycyrrhetic acid (AGA), which is known as a nontoxic reversible GJC inhibitor, had the same effect on osteoblastic differentiation. Warfarin and AGA inhibited the bone morphogenetic protein (BMP)2-induced mRNA levels of alkaline phosphatase (ALP), collagen I α 1 (col1 α 1), osteocalcin (OC) and osteonin, which are specific markers for osteoblastic differentiation, in a dose-dependent manner. Moreover, the activities of OC- and ALP-luciferase reporters, which are induced by BMP2, and the transcriptional activity of Runx2 on OC and ALP promoters were inhibited by warfarin and AGA. The amount and activity of alkaline phosphatase (ALP) induced by BMP2 were also decreased by warfarin and AGA. These results suggest that warfarin and AGA, a GJC inhibitor, have an inhibitory effect on osteoblastic differentiation.

Disclosures: Dong Jin Chung, None.

MO0407

Total and Carboxylated Osteocalcin Associate with Serum Insulin and Bone Mineral Density in Young Adults. Paivi Maria Paldanius^{*1}, Kaisa Ivaska², Petteri Hovi¹, Sture Andersson¹, Johan Eriksson³, Kalervo Vaananen⁴, Eero Kajantie¹, Outi Maki¹. ¹Children's Hospital, Helsinki University Hospital, Finland, ²University of Turku, Department of Cell Biology & Anatomy, Finland, ³Department of General Practice & Primary Health Care, University of Helsinki, Finland, ⁴University of Eastern Finland, Finland

Serum osteocalcin (OC) is an osteoblast-derived protein with a role in the regulation of glucose and energy metabolism. The regulatory role of OC is most likely exerted via uncarboxylated OC, which in mice induces expression of adiponectin, insulin, and markers of pancreatic islet cell proliferation. Young adults born with very low birth weight (VLBW) have altered glucose regulation and lower bone mineral density (BMD) when compared with those born at term. The aim of this study was to explore the association between bone and glucose metabolism by evaluating OC, carboxylated osteocalcin (cOC) and markers of glucose metabolism at fasting and during a 75-g oral glucose tolerance test, in apparently healthy young adults. The cohort comprised 332 normoglycemic young adults (age range, 18 to 27 years) born either with VLBW ($n=163$; 92 females, 71 males) or at term ($n=169$; 101 females, 68 males). The mean adult weight, height and BMD were significantly lower in VLBW subjects. They also had higher fasting levels of OC (ANOVA, $p=0.027$) and cOC ($p=0.005$) than the term-borns and their mean lumbar spine Z score was significantly lower (-0.94) than in those born at term (-0.42 , $p<0.001$). OC and BMD were inversely correlated in all subjects ($r=-0.239$, $p<0.001$). Subjects with VLBW had higher 2-hour insulin ($p=0.001$) and 2-hour glucose concentrations ($p=0.037$) and marginally elevated fasting insulin ($p=0.068$). The glucose load induced a significant reduction in total OC and cOC levels in all subjects, mean (95% CI) decreases being -17.4% (-19.0 , -15.8) and -18.5% (-20.0 , -16.9) for OC and cOC, respectively. This reduction in OC was not associated with OGTT-induced increases in insulin ($p=0.54$) but weakly with increase in glucose levels ($r=0.13$, $p=0.022$). Total OC and cOC were, however, negatively correlated with fasting insulin after adjustment for age, gender, BMD and VLBW status ($r=-0.182$, $p=0.009$ and $r=-0.283$, $p<0.001$, respectively). The study shows that fasting insulin and VLBW status predicted cOC values, whereas OC

and cOC correlated only weakly with glucose values at 120 min. Changes in OC during OGTT were not associated with changes in insulin suggesting that serum OC is associated with long-term glucose regulation whereas acute changes during OGTT are mediated via other mechanisms. Increased OC and cOC may partly explain reduced BMD and decreased insulin sensitivity in subjects with VLBW.

Disclosures: Paivi Maria Paldanius, Novartis, 1; Novartis, 3

MO0408

Vertebral Marrow Fat and Body Composition in Older Men and Women: Preliminary results from the AGES-BMA study. Trisha Hue^{*1}, Xiaojuan Li¹, Clifford Rosen², Vilundur Gudnason³, Thomas Lang¹, Sigurdur Sigurdsson³, KRISTIN SIGGEIRSDOTTIR³, Gunnar Sigurdsson⁴, Keerthi Shet¹, Tamara Harris⁵, Lisa Palermo¹, Ann Schwartz¹. ¹University of California, San Francisco, USA, ²Maine Medical Center, USA, ³Icelandic Heart Association Research Institute, Iceland, ⁴Landsþítali, Iceland, ⁵Intramural Research Program, National Institute on Aging, USA

Bone marrow fat (MF) increases with age, and in older adults, the total volume of MF is approximately the same as that of visceral fat. Although MF is a relatively large fat depot, little is known about the mechanisms regulating accumulation. In young women with anorexia nervosa, MF increases even as other fat depots are depleted. However, previous studies in healthy men and women have generally found no association between MF and body mass index (BMI), subcutaneous adipose tissue (SAT), or total adipose tissue (TAT). Only one study in premenopausal women demonstrated a positive correlation between MF and visceral adipose tissue (VAT).

We assessed the association of MF and body composition in men (means: 79.9 years, BMI 27.1) and women (means: 78.5 years, BMI 29.0) in the Bone Marrow Adiposity, Bone and Body Composition (BMA) study. BMA is a cross-sectional ancillary study to Age Gene/Environment Susceptibility-Reykjavik (AGES-Reykjavik), an ongoing population-based cohort study in Iceland. BMA enrollment is currently ongoing and this preliminary analysis includes the first set of participants, excluding those with diabetes, users of bisphosphonates, glucocorticoids, or hormone therapy. Measures include vertebral (L1-L4) marrow fat content estimated from single voxel proton magnetic resonance spectroscopy; total body fat percent (BF%), fat and lean mass by dual-energy X-ray absorptiometry; VAT, SAT, and TAT by quantitative computed tomography; and BMI. General linear models were adjusted for age and evaluated for significance. To assess for effect modification by sex and BMI, interaction terms were included in the models. With $\alpha < 0.10$, the models including the sex interaction term with SAT ($p=0.06$) and TAT ($p=0.07$) resulted in possible interaction. Therefore, results are stratified by gender (see table).

These preliminary results suggest that in older men, vertebral MF is associated with SAT, TAT, and BF%. In contrast, no significant associations were found in the older women. Consistent with other studies, we did not find any association between MF and BMI. Our data suggest that the association of MF with body composition in older adults may be modified by gender and may be fat-depot specific. Future analyses are planned when enrollment is completed.

	Men (n=37)		Women (n=44)	
	β (SE)	p-value	β (SE)	p-value
Body mass index (BMI, kg/m ²)	2.09 (1.57)	0.19	0.88 (1.23)	0.48
Visceral adipose tissue (VAT, g)	2.94 (1.57)	0.07	0.19 (1.24)	0.88
Subcutaneous adipose tissue (SAT, g)	3.26 (1.57)	0.045	-0.12 (1.24)	0.92
Total adipose tissue (TAT, g)	3.61 (1.54)	0.026	0.04 (1.24)	0.98
VAT/TAT	0.34 (1.83)	0.84	0.40 (1.25)	0.75
Total body fat (%)	3.30 (1.59)	0.046	1.27 (1.21)	0.30
Fat mass (g)	2.89 (1.58)	0.05	0.42 (1.24)	0.74
Lean mass (g)	-0.08 (1.59)	0.96	-0.95 (1.20)	0.42

Table

Disclosures: Trisha Hue, None.

MO0409

Clinical Development of An Orally Delivered Recombinant PTH Analog. Nozer Mehta^{*1}, Roxanne Tavakkol², Kristine Erickson², Bill Stern², Tamara James², Seymour Fein², Sheela Mitta², Amy Sturmer², Paul Shields², Andy Rasums², Lorraine Fitzpatrick³. ¹Unigene Laboratories, Incorporated, USA, ²Unigene Laboratories, USA, ³GlaxoSmithKline, USA

An oral tablet formulation of a PTH analog has been developed and initially optimized in a dog model. The PTH analog was produced by recombinant expression in *E. coli*. An initial rising dose pharmacokinetic (PK) study in postmenopausal women examined PTH levels following administration of tablets containing 2, 4, 6 and 8 mg of the PTH analog. A linear dose-dependent response was seen at the three higher doses. A second two-period replicate dose PK study was then carried out to evaluate the safety as well as the inter- and intra-subject variability of two dosing

regimens in an open label study in postmenopausal women. Blood samples were collected over a 6 hour period following dosing and PTH levels were quantified using a specific sandwich ELISA. The C_{max} values with both the 6 mg and 2x4 mg tablets were in the 200 to 300 pg/mL range, and hence achieved or exceeded blood levels that have been shown to be anabolic with an existing injectable formulation. The PK profiles were consistent with the requirement for bone anabolic activity, with an elimination $t_{1/2}$ of 13-21 minutes. Both the inter- and intra-subject variability was deemed to be more desirable with the 6 mg dose. There were no clinically significant changes in serum calcium, phosphate, magnesium or endogenous PTH activity and no serious adverse events were reported. A phase 2 study has been initiated at the appropriate dose in postmenopausal osteoporotic women to further evaluate the safety and efficacy of the oral PTH formulation. This 24 week double blind, randomized, repeat dose parallel group study will evaluate the oral PTH formulation or a placebo tablet. The study also includes an open label active comparator Forsteo® arm. The study will measure the change in bone mineral density at the lumbar spine, compared to baseline, in the three arms of the study. Serum markers of bone formation and resorption will also be measured as a secondary endpoint.

Disclosures: Nozer Mehta, Unigene Laboratories, 3
This study received funding from: Unigene Laboratories

MO0410

Cumulative Doses of PTH (1-84) Stimulates Vasodilation in the Bone Vasculature of Rats: the Role of VEGF and NO Signaling Pathways.
Rhonda Prishby*, Jeremiah Campbell, Thomas Menezes. University of Texas at Arlington, USA

Parathyroid hormone (PTH) is a vasodilator in several vascular beds. In cultured human umbilical cord vein endothelial cells, PTH stimulates eNOS through PKA and PKC pathways. Since intermittent PTH administration augments bone mass and is a treatment for osteoporosis, it is paramount to determine the effects of PTH on the bone vasculature. Previous data demonstrate that 15 days of intermittent PTH augments ACh-induced vasodilation in the femoral principal nutrient artery (PNA), the primary conduit for blood flow to long bones. Further, this modification is related to vascular endothelial growth factor (VEGF). To date, it is unknown whether PTH directly stimulates vasodilation of the bone vasculature. Therefore, the purposes of the study were to 1) determine whether PTH augments vasodilation of the femoral PNA and 2) determine the signaling mechanism(s) responsible for mediating the presumed vasodilation. **METHODS:** Right femoral PNAs were dissected from male Wistar rats and cannulated to assess vasodilation to PTH 1-84 (10-13 – 10-8 M). Inhibition of nitric oxide (NO) via L-NAME and vascular endothelial growth factor (VEGF) via an anti-VEGF antibody (i.e., Avastin) were used to determine the signaling pathways involved. **RESULTS:** Vasodilation peaked at 63% of maximum dilation to cumulative doses of PTH 1-84. Inhibition of VEGF reduced vasodilation by 38% (PTH, n=5: 63 7%; PTH + anti-VEGF, n=5: 39% relaxation). Inhibition of NO nearly abolished vasodilation in the femoral PNA (PTH: 63 7%; PTH + L-NAME, n=3: 94% relaxation). **DISCUSSION:** To our knowledge, these are the first data to demonstrate vasodilation to PTH in the bone vasculature. Moreover, these data demonstrate two pathways related to PTH that result in NO-mediated signaling; whereby blockade of VEGF receptor binding and NO production reduced vasodilation by 38% and 90%, respectively. This indicates that PTH-stimulated release of VEGF serves to augment endothelial NO independent of a second signaling mechanism which also enhanced NO production. The role of PTH in bone accrual may involve the influence of the bone vascular system and its ability to increase bone perfusion in response to bone metabolism. Further work will elucidate the mechanisms of PTH-mediated bone vasodilation (i.e., signaling related to PKA and PKC in the vascular endothelium) including the role, if any, of the vascular smooth muscle cells.

Supported by University of Texas Arlington Research Enhancement Program.

Disclosures: Rhonda Prishby, None.

MO0411

Effects of One Year Daily Teriparatide Treatment on Trabecular Bone Material Properties in Postmenopausal Osteoporotic Women Previously Treated with Alendronate or Risedronate. Sonja Gamsjaeger¹, Birgit Buchinger¹, Roger Phipps², Klaus Klaushofer¹, Eleftherios Paschalis^{*1}. ¹Ludwig Boltzmann Institute of Osteology at the Hanusch Hospital of WGKK & AUVA Trauma Centre Meidling, 1st Medical Department, Hanusch Hospital, Austria, ²Husson University School of Pharmacy, USA

Many osteoporotic patients treated with teriparatide (TPTD) are likely to have been treated previously with a bisphosphonate (BP). Questions remain about whether BP treatment affects the efficacy of subsequent TPTD therapy.

The purpose of the present study was to investigate TPTD effects on bone material properties after BP treatment. The properties measured were: 1. mineral to matrix ratio, corresponding to ash weight measurements; 2. mineral crystallite maturity / crystallinity, having a direct bearing on crystallite shape and size; 3. relative proteoglycan content, regulating mineralization commencement; 4. pyridinoline to divalent collagen cross-links ratio, two of the major enzymatic collagen cross-links, independent of bone turnover. To do this we used Fourier Transform Infrared Imaging (FTIRI) and Raman spectroscopy to examine thirty two paired iliac crest biopsies (before and after one year TPTD) from sixteen osteoporotic women during

the OPTAMISE clinical trial. Prior to TPTD treatment, these women had previously been treated with either alendronate (ALN, 10mg/day or 70mg/week) or risedronate (RIS, 5mg/day or 30-35mg/week) for at least 24 months (mean duration of therapy 37.2 months for ALN and 38.0 months RIS). The patients stopped their BP therapy and were then treated with TPTD (20µg/day subcutaneously) for 12 months. In addition, we compared the two BPs groups at baseline. Analysis was focused on actively bone forming sites, specifically between fluorescent double labels, thus the results are independent of bone turnover.

TPTD produced significant changes in mineral / matrix ratio, mineral maturity / crystallinity and collagen cross-link ratio, while changes in relative proteoglycan content were observed only in the prior-RIS group. Collagen cross-link ratio was also significantly different between the two BPs groups at baseline, the ALN group of patients having a significantly higher one.

The results show a response to TPTD treatment in newly forming bone material properties. There was a significant difference at baseline in the collagen cross-link ratio between ALN- and RIS-treated patients, suggesting potentially differential effects of BPs on bone material properties. On the other hand, there were no significant differences between the prior-ALN and prior-RIS groups in any of the outcomes after 12 mo TPTD treatment, suggesting that the TPTD effect on the monitored bone material properties is independent of prior BP used.

Disclosures: Eleftherios Paschalis, None.
This study received funding from: P&G Pharmaceuticals

MO0412

Postmenopausal Women Treated with Combination Parathyroid Hormone and Ibandronate Experience Different Cortical Bone Microstructural Changes at the Radius and Tibia: The PICS Study. Anne Schafer^{*1}, Andrew Burghardt², Lisa Palermo², Deborah Sellmeyer³, Sharmila Majumdar², Dennis Black². ¹University of California, San Francisco & the San Francisco VA Medical Center, USA, ²University of California, San Francisco, USA, ³The Johns Hopkins Bayview Medical Center, USA

Parathyroid hormone (PTH) therapy and bisphosphonates are proven to decrease fracture risk in postmenopausal osteoporosis, but their effects on bone microstructure and strength remain insufficiently characterized. While increasing spinal trabecular bone mineral density (BMD) substantially, PTH therapy may decrease cortical BMD, possibly by stimulating intracortical remodeling. We evaluated bone microarchitecture and biomechanics at the radius and tibia in women receiving PTH(1-84) and ibandronate over 1 year. Postmenopausal women with low bone mass (n=43) were treated with either 3 or 6 months of PTH(1-84) (100 µg/day) and either 9 or 12 months of ibandronate (150mg/month) over 1 year. Participants underwent high-resolution peripheral quantitative computed tomography (HR-pQCT) imaging at baseline and after 6 and 12 months of therapy. HR-pQCT evaluation included BMD and microarchitectural assessment, cortical porosity quantification, and micro-finite element analysis including estimation of stiffness and failure load. Cortical thickness and cortical BMD decreased at the radius over 12 months (p<0.01 for each), consistent with changes in dual-energy X-ray absorptiometry at the radius, while these parameters did not change at the tibia (p<0.01 for difference between radius and tibia). In contrast, cortical porosity and cortical pore volume increased at the tibia (p=0.02 and 0.01, respectively) but not at the radius. The percentage of stiffness and failure load deficits at the tibia that were due to cortical porosity increased over time. Meanwhile, there was a differential change in trabecular BMD at the 2 sites, with an increase in trabecular BMD over 12 months at the tibia but a decrease over 6 months at the radius (p=0.04 and <0.01 for difference between radius and tibia over 6 and 12 months, respectively). Overall, stiffness and failure load decreased at the radius, while there were no changes in these measures at the tibia. In summary, our study suggests that changes in response to PTH/ibandronate therapy are different at the radius versus the tibia. At the radius, the decreased cortical thickness and cortical BMD, with no change in trabecular BMD, contributed to decreased estimated bone strength. In contrast, at the tibia, while cortical porosity increased, cortical thickness did not change and trabecular BMD increased, maintaining bone strength. Our results suggest the possibility that weight bearing may optimize the effect of anabolic therapy.

TABLE. Mean 1-year percentage changes in microstructural and biomechanical measures

Parameter	Radius (% change)	Tibia (% change)	p-value for difference (radius vs. tibia)
Cortical thickness	-1.86 ± 2.40*	-0.24 ± 2.10	<0.01
Cortical BMD	-0.55 ± 1.63	0.04 ± 2.03	<0.01
Cortical porosity (CtPo)	1.27 ± 17.83	5.12 ± 12.38	0.28
Cortical pore volume	-0.38 ± 18.03	4.70 ± 12.83	0.16
Trabecular BMD	-0.10 ± 2.56	1.36 ± 2.55*	<0.01
Stiffness	-1.42 ± 2.34*	0.29 ± 2.33	<0.01
Stiffness deficit due to CtPo	2.36 ± 27.62	7.41 ± 19.83	0.28
Failure load	-1.43 ± 2.28*	0.20 ± 2.10	<0.01
Failure load deficit due to CtPo	7.03 ± 32.25	7.41 ± 19.55	0.82

Values in bold are significant changes at p<0.05; *, significant changes at p<0.01

Table

Disclosures: Anne Schafer, None.
This study received funding from: Genentech, Inc., a Member of the Roche Group

MO0413

Teriparatide Treatment for 24 months in Postmenopausal Women with Osteoporosis Differentially Impacts Cortical and Trabecular Bone at the Tibia Assessed by HRpQCT. Jeri Nieves¹, Felicia Cosman¹, Stephanie Boutroy², Nancy Barbuto¹, Marsha Zion¹, Elizabeth Shane³, David Dempster², Robert Lindsay¹. ¹Helen Hayes Hospital, USA, ²Columbia University, USA, ³Columbia University College of Physicians & Surgeons, USA

Teriparatide (TPTD) clearly increases bone mass by BMD and there is histomorphometric evidence of increased bone formation rate at the iliac crest. There are relatively few reports of the longitudinal effects of TPTD on bone structure utilizing High Resolution Peripheral Quantitative Computed Tomography (HRpQCT, Scanco Medical AG). We analyzed scans from 40 women with osteoporosis who were either treatment naive (n=17) or who had been previously treated with alendronate (n=23) and were then randomized to receive daily teriparatide (20 mcg continuously) or cyclic TPTD (20 mcg daily for cycles of 3 months on and 3 months off) for a total treatment period of 24 months. Alendronate treatment was continued (70 mg/week) in the alendronate group. The cyclic and daily TPTD results were not different and were therefore combined. HRpQCT of the tibia was performed at baseline and 2 years. Analysis was limited to those scans with image quality above 3 on the manufacturer's suggested 5 grade scale, those with overlap of 70 % or greater and scans without any artifact. At the tibia, in those on prior alendronate therapy, there were no significant changes in trabecular density or trabecular number, but trabecular thickness increased (3.3%, p<0.05). Furthermore, there were significant reductions in cortical bone density (-2.4%, p<0.005), but no change in cortical thickness. In the treatment naive women, results were similar. There was no change in trabecular density or trabecular number and a significant increase in trabecular thickness (4.7%, p<0.05). In cortical bone, there was no significant change in cortical thickness, but a significant reduction in cortical bone density was seen (-2.3%, p<0.001). In summary, preliminary data indicate that TPTD given for 24 months may improve some aspects of trabecular bone, but a larger sample size may be needed to detect changes in trabecular number and density. There was also a modest decrease in cortical bone density without a decrease in cortical thickness. This contrasts with our prior observations of increased cortical thickness in the iliac crest by histomorphometry. This inconsistency may be due to newly formed bone not yet fully mineralized and/or an increase in cortical porosity. Follow-up HRpQCT measurements of the tibia after antiresorptive treatment alone might provide useful data. Although more patients are needed, HRpQCT may elucidate the effects of TPTD at peripheral skeletal sites

Disclosures: Jeri Nieves, None.

MO0414

Two-Year Effects Of PTH(1-84) On Cortical Bone In Hypoparathyroidism. Stephanie Boutroy¹, Mishaela Rubin², Jim Sliney Jr¹, Rebecca Ives¹, John Bilezikian³. ¹Columbia University Medical Center, USA, ²Columbia University, USA, ³Columbia University College of Physicians & Surgeons, USA

Hypoparathyroidism (HYPOPT), a disorder characterized by hypocalcemia and low PTH levels, is a low turnover disease associated with bone mineral density (BMD) that typically is not reduced. With PTH treatment, cancellous BMD at the lumbar spine increases and cortical BMD at the distal 1/3 radius decreases, yet it is not known to what extent bone microstructure and other aspects of bone quality might be affected. To this end, we studied 30 patients (25 women/5 men, baseline serum calcium 8.61.0 mg/dl and PTH 3.12.3 pg/ml) with HYPOPT who were treated for 2 years with PTH(1-84) [PTH], 100 mcg SC qod. We analyzed volumetric BMD (vBMD) and microstructure by high resolution peripheral quantitative tomography (HRpQCT, Scanco Medical AG) at the distal radius (DR) and tibia (DT) over a 2 year treatment period with PTH. Additional parameters of cortical bone were performed with an advanced algorithm (Burghardt, JBMR 2009 and Nishiyama, JBMR 2009).

At the DR, neither vBMD nor trabecular microarchitecture changed but there was an increase in cortical thickness (+1.2%, p=0.03) as analyzed by advanced segmentation. At the DT, cortical BMD fell (-2.4%, p=0.001) and there was a more heterogeneous distribution of the trabecular network (4.1, p=0.02). Further segmentation of cortical bone confirmed the decrease in cortical vBMD, with an increase cortical pore volume and no change in cortical thickness; thus leading to an increase cortical porosity. The loss in cortical vBMD can not only be explained by this increased cortical porosity but also by the decreased cortical tissue mineral density (TMD, -1.9%, p=0.001).

The results provide new insight into how PTH affects skeletal microstructure when the skeleton is exposed to it de novo. These changes are reminiscent of the skeletal effects of PTH in both primary hyperparathyroidism and PTH treatment of osteoporosis.

Baseline values and percentage changes in cortical parameters at the distal tibia

	Baseline values (mean±SD)	% difference from baseline
Cortical vBMD (mg HA/cm ³)	944 ± 52	-2.5% *
Cortical TMD (mg HA/cm ³)	1006 ± 39	-1.9% *
Cortical thickness (µm)	1325 ± 249	-1.0%
Cortical pore volume (mm ³)	54.1 ± 28.1	11.8% *
Cortical porosity (%)	4.8 ± 1.9	12.2% *

* p<0.05

Baseline values and percentage changes in cortical parameters at the distal tibia

Disclosures: Stephanie Boutroy, None.

MO0415

Antiresorptive Treatment for Spaceflight Induced Bone Atrophy: Preliminary Results. Adrian Leblanc¹, Toshio Matsumoto², Jeff Jones³, Jay Shapiro⁴, Thomas Lang⁵, Linda Shackelford⁶, Scott Smith⁶, Harlan Evans⁷, Elisabeth Spector⁷, Robert Ploutz-Snyder⁸, Jean Sibonga⁶, Toshitaka Nakamura⁹, Kenjiro Kohri¹⁰, Hiroshi Ohshima¹¹. ¹USRABaylor College of Medicine, USA, ²University of Tokushima Graduate School of Medical Sciences, Japan, ³Baylor College of Medicine, USA, ⁴Johns Hopkins, USA, ⁵University of California, San Francisco, USA, ⁶NASA, USA, ⁷Wyle, USA, ⁸USRA, USA, ⁹University of Occupational & Environmental Health, Japan, ¹⁰Nagoya City University, Japan, ¹¹JAXA, Japan

Detailed measurements from the Mir and ISS long duration missions have documented losses in bone mineral density (BMD) from critical skeletal sub-regions. The most important BMD losses are from the femoral hip averaging about -1.6%/mo integral to -2.3%/mo trabecular. Importantly these studies have documented the wide range in individual BMD loss from -0.5 to -5%/mo. Associated elevated urinary Ca increases the risk of renal stone formation during flight, a potential serious impact to mission success. To date, countermeasures to this bone loss have not been satisfactory.

The purpose of this study is to determine if the combined effect of antiresorptive drugs plus the standard in-flight exercise regimen will have a measurable effect on preventing space flight induced bone loss (mass and strength) and reducing renal stone risk. To date, 4 crewmembers have completed the flight portion of the protocol in which crewmembers take a 70-mg alendronate tablet once a week before and during flight, starting 17 days before launch. Compared to previous ISS crewmembers (n=14) not taking alendronate, DXA measurements of the spine, femur neck and total hip were significantly improved from -0.8 0.5%/mo to +1.0 1.1%/mo, -1.1 0.5%/mo to -0.2 0.3%/mo, -1.1 0.5%/mo to +0.04 0.3%/mo respectively. QCT-determined trabecular BMD of the femur neck, trochanter and total hip were significantly improved from -2.7 1.9%/mo to -0.2 0.8%/mo, -2.2 0.9%/mo to -0.3 1.9%/mo and -2.3 1.0%/mo to -0.2 1.8%/mo respectively. Significance was calculated from a one-tailed t test on pre-post difference scores, with corrections for multiple comparisons. Resorption markers were unchanged compared to preflight, in contrast to measurements from previous ISS and MIR crewmembers that showed typical increases of 50-100% above preflight excretion levels. Urinary Ca showed no increase compared to baseline levels, also distinct from the elevated levels of 50% or greater in previous crewmembers.

While these results are encouraging, the current n (4) is small and the SDs are large indicating that while the means are improved there is high variability in individual response. Another confounder is that the exercise protocol has varied over time. Three additional crewmembers have been recruited to participate in this experiment, with expected completion in late 2011.

Disclosures: Adrian Leblanc, None.

MO0416

Atypical Femoral Fractures in Association with Long-term Bisphosphonate Use: Clinical, Radiographic and Bone Biopsy Data from 7 Cases. Aliya Khan¹, Angela Cheung², Sama Thomas¹, Nazir Khan¹, Kenneth Pritzker², Brian Lentle³. ¹McMaster University, Canada, ²University of Toronto, Canada, ³University of British Columbia, Canada

Purpose:

This study describes the patient characteristics and histomorphometric and radiographic features of atypical femoral fractures (AFF) as seen in 7 cases referred for evaluation. Methods: All patients referred for evaluation of AFF were reviewed. Patients meeting the ASBMR criteria for AFF were further evaluated and tetracycline labelled bone biopsies were completed. Radiographs were reviewed by a musculoskeletal radiologist.

Results: All fracture lines were transverse or short oblique with thickened cortices. We report 7 cases of AFF in patients on long term bisphosphonate (BP) therapy. 6 of 7 fractures occurred without a fall or direct trauma to the femur with 1 case occurring after a fall from standing height. All patients were female; average age was 67 yrs (range 54-80 yrs). 2 of the 7 cases were of Chinese descent, 2 were East Indian with 3 being Caucasian. Average BP duration of use was 8.5 years (range 7-14 years). 5 of 7 patients were on alendronate alone, 2 patients were on risendronate. 1 patient had

received 18 months of teriparatide, 3 years prior to the AFF and had received a total of 10 years of BP use prior to teriparatide. Prodromal thigh or groin pain was seen in 5 of the 7 patients for 3 to 12 months prior to fracture. Proton pump inhibitor use was present in 1 patient for the previous 2 years. 1 patient was on prednisone for rheumatoid arthritis.

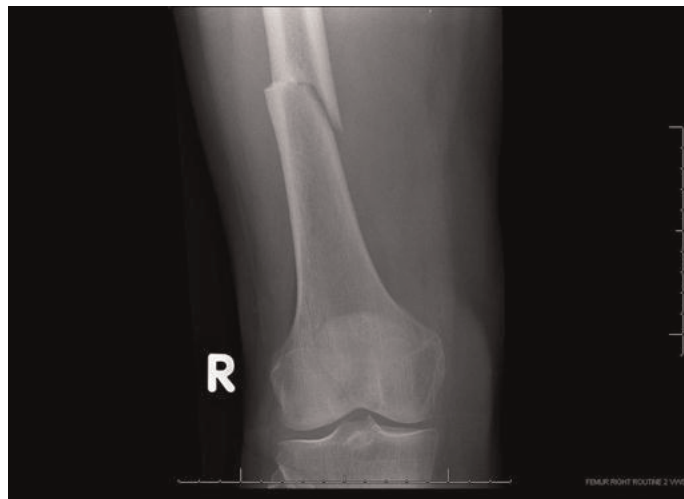
Rheumatoid arthritis was present in 2 cases. Diabetes was not present in any of the 7 cases. Bilaterality occurred in 1 patient with the second AFF occurring 1 month after the first AFF.

Renal function was well preserved with estimated glomerular filtration (eGFR) rates > 60 ml/min in all cases. 25 hydroxy Vitamin D levels were >75 nmol/L in 5 cases. 2 cases had mild Vitamin D insufficiency (>50nmol/L).

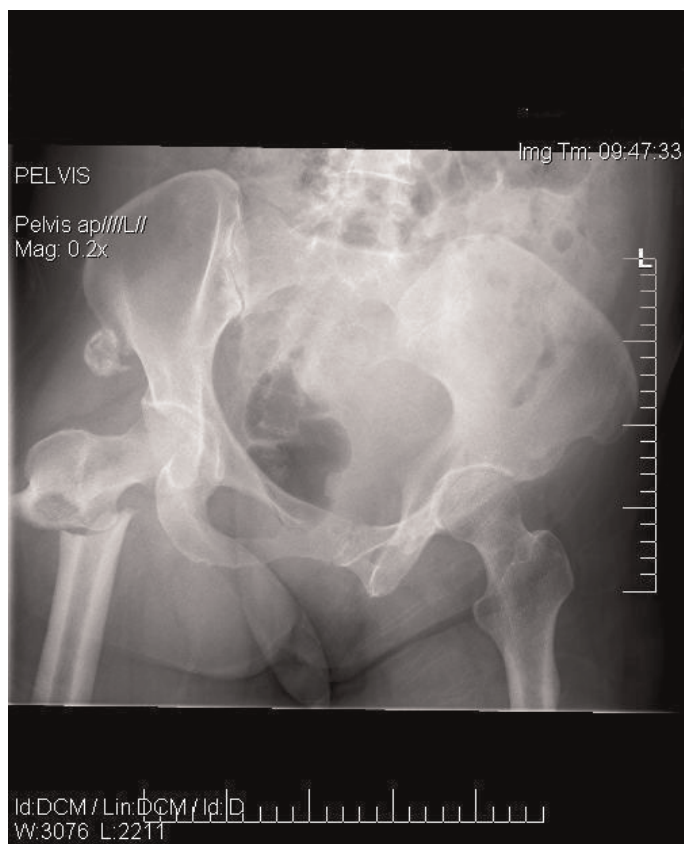
Detailed histomorphometry data will be finalized and presented.

Summary: A large number of the AFF occurred in women of Asian descent, (4 of 7). 6 of the 7 AFF occurred in the absence of a fall. Prodromal pain was commonly seen. Proton pump inhibitors were used in only 1 patient. Histomorphometric features included absence of mineralization abnormalities and decreased bone formation.

Conclusion: AFF in association with long term BP use are being seen in a disproportionately large number of Asian women. Further evaluation of all AFF with identification of predisposing key clinical risk factors is needed. Improved understanding of the pathophysiology may be gained with further histomorphometric data in larger numbers of patients.



Fx.1



Fx.2



Fx.3

Disclosures: Aliya Khan, None.

MO0417

Augmentation of Bisphosphonate Effects Increasing Lumbar Bone Mineral Density and Decreasing Vertebral Deformity by Addition of Active Absorbable Algal Calcium (AAACa). Yoshitomo Itakura¹, Yoshio Fujii², Yasuyuki Takagi³, Takuo Fujita⁴, Mutsumi Ohue⁴, Akimitsu Miyauchi³, Mikio Nakajima⁶. ¹Komatsu Hospital, Japan, ²Calcium Research Institute Kobe Branch, Japan, ³National Hyogo Chuo Hospital, Japan, ⁴Katsuragi Hospital, Japan, ⁵Miyauchi Medical Center, Japan, ⁶Dept of Orthopedic Surgery, Osaka Medical College, Japan

Purpose Bisphosphonates decrease Ca release from bone by suppressing osteoclastic resorption prompting temporary Ca deficiency in other part of the body, fall of serum Ca, increased PTH secretion, rise of cytosolic Ca and disturbance of signal transduction and cell function (Ca Paradox) which may limit the effect of bisphosphonates themselves in return, without adequate Ca supplementation. Effect of addition of active absorbable calcium (AAACa) to bisphosphonates on lumbar bone mineral density (LBMD) and vertebral deformity was therefore studied.

Methods Among 30 subjects with osteoporosis and/or spinal osteoarthritis consented to participate this study, 5 mg / day alendronate was administered in 20 and 2.5 mg/day risendronate in 10 (Treatment 1). AAACa containing 900 mg elementary Ca was then added to the on-going treatment (Treatment 2). At the beginning and throughout the course of both Treatment 1 and 2, LBMD was measured by DXA (DPX, General Electric) in anterior-posterior projection, to calculate mean and SD of L1-L4 and coefficient of variation (CV) as SD/mean (%). Student t-test was applied to test the significance of difference between the 2 groups.

Results Mean LBMD was 0.7930,095 in Treatment 1 and 0.8440,091 in Treatment 2, (P<0.0001) indicating a definite improvement in the latter. Intraindividual CV of L1-L4 was 11.85.9% in the former and 10.46.4% in the latter with a significant fall indicating an alleviation of deformity (p=0.0017). Vertebral deformity due to osteoarthritic changes and other causes was reported to raise CV values from 7.22.9% in subjects younger than 50 years without osteoarthritic changes. No significant differences were noted between alendronate and risendronate in the effect of addition of AAACa on the fall of CV (L1-L4).

Conclusion Increase of LBMD and improvement of vertebral deformity mainly due to osteoarthritic changes in response to bisphosphonate treatment was significantly augmented by addition of AAACa.

Disclosures: Takuo Fujita, None.

MO0418

Biochemical markers and its relation with Bisphosphonate-related Osteonecrosis of the Jaw in Female Osteoporosis patients. Tae-Geon Kwon¹, Je-Yong Choi², So-Young Choi³. ¹Kyungpook National University, School of Dentistry, South Korea, ²Kyungpook National University, School of Medicine, South Korea, ³Kyungpook National University, Republic of Korea

BACKGROUND AND PURPOSE: There had been no agreements that the any biological marker can predict the development and reflect the severity of Bispho-

sphosphate-related osteonecrosis of the jaw (BRONJ). This study intended to determine whether there is any difference in serum biochemical markers of BRONJ patients compared to control patients who were treated with oral bisphosphonates (BP) for osteoporosis but without BRONJ. **PATIENTS AND METHODS:** This retrospective, case-control study analyzed female BRONJ patients (n=55, Age 72.97.3) who was previously treated with oral BP for osteoporosis. Demographic and clinical information were collected with laboratory dates of bone turn-over marker [(C-terminal telopeptide (CTX), Osteocalcin (OCN), bone-specific Alkaline phosphatase (bALP)) and inflammatory activity markers [erythrocyte sedimentation rate (ESR) and C-reactive protein (CRP) level] at the time of the BRONJ diagnosis, 1 and 3 months after the treatment of BRONJ. These were compared to the dates of baseline, 6, 18, 30, and 42 months after the oral BP therapy for female osteoporosis patients without osteonecrosis of the jaw (n=85, Age 71.67.6). **RESULTS:** At the time of diagnosis, BRONJ patients showed significantly higher ESR and CRP than control patients. Compared to serial CTX level after the BP treatment in control patients, measurements of BRONJ patient was not different from any time points. In control patients, bALP level was decreased after the BP treatment and this was level was similar to BRONJ patients. Severity of BRONJ was highly correlated with ESR (r=0.346, p<0.05) and CRP (r=0.312, p<0.05) but not with CTX (r=0.163, p>0.05), OCN (r=-0.043, p>0.05), and bALP (r=0.132, p>0.05). Reduced CTX values were not associated with BRONJ stage, invasiveness of ONJ or sequestrate formation in BRONJ. **CONCLUSION:** Bone turnover marker such as serum CTX level cannot be used for predictor of BRONJ progression or risk assessment of BRONJ.

Disclosures: Tae-Geon Kwon, None.

MO0419

Generic Alendronate Use in Medicare Part D Data. Huifeng Yun^{*1}, Jeffrey Curtis¹, Wilson Smith¹, Robert Matthews¹, Kenneth Saag¹, Nicole Wright¹, Meredith Kilgore², Elizabeth Delzell¹. ¹University of Alabama at Birmingham, USA, ²University of Alabama At Birmingham School of Public Health, USA

Background: Generic alendronate (ALN) was approved in the United States in 2008. Medicare beneficiaries might pay for generic ALN out-of-pocket without submitting claims, resulting in incomplete generic ALN claims in Medicare part D data.

Objectives: To estimate the completeness of identification of generic ALN use in Medicare part D data in 2008; to evaluate characteristics of beneficiaries who switched to generic ALN after being adherent to brand ALN.

Methods: Using 2006-2008 Medicare 5% sample data, we created two cohorts of brand ALN users ('07 and '08) who: used brand ALN during the respective time periods; were not enrolled in a Medicare Advantage plan; had fee-for-services and part D Medicare coverage during 1/1/06-2/6/07 for the '07 cohort or 1/1/07-2/6/08 for the '08 cohort; had a medication possession ratio (MPR) $\geq 80\%$ during that period; and had 11 months of followup (from Feb 6 - Dec 31 in '07 or '08). Medication status at study end was classified as: continued brand product, switched to generic, switched to another bisphosphonate (BP) or presumed discontinued. A higher proportion of discontinuation in the '08 than the '07 cohort would provide evidence of incomplete claims for generic ALN. Cox regression analysis estimated the hazard ratio for discontinuing use in the '08 cohort compared to the '07. Multinomial logistic regression identified factors associated with medication status at the end of follow-up.

Results: Of 9708 ALN users in the '07 cohort; 87.8% continued brand product, 3.3% switched to another BP, and 8.9% discontinued. Of 16720 users in the '08 cohort, 9.6% continued brand ALN, 78.5% switched to generic, 1.4% switched to another BP, and 10.5% discontinued. The adjusted hazard ratio (95% CI) for presumed discontinuation in the '08 cohort compared to '07 cohort was 1.05 (0.97, 1.14). Factors associated with switching to generic were younger age, Asian race, living in rural areas, lower income, higher baseline MPR, and having more comorbidities.

Conclusion: Using a study design that maximized internal validity by evaluating adherent users of ALN, there does not appear to be a substantial amount of missing claims for generic ALN in 2008.

Disclosures: Huifeng Yun, AMGEN, 2
This study received funding from: Amgen

MO0420

Prevention of Postmenopausal Osteoporosis With Two Intermittent Alendronate Regimens: Bone Mineral Density and Bone Markers Changes After 12 months. Yves Boutsen^{*1}, Jacques Jamart², Catherine Vynckier², Thierry Vander Borgh², Jean-Pierre Devogelaer³. ¹Cliniques Universitaires UCL de Mont-Godinne, Belgium, ²Cliniques Universitaires de Mont-Godinne, Belgium, ³St. Luc University Hospital, Belgium

The aim of this prospective study was to compare the efficacy of two regimens of low-dose oral alendronate (ALN) as a prevention of postmenopausal osteoporosis for women who don't want or may not take hormone replacement therapy. Primary end-point was lumbar spine (LS) bone mineral density (BMD) changes after two years.

Secondary end-points included changes in bone markers levels. We present here changes in BMD and C-telopeptide crosslinks of type I collagen (S-CTX) levels after a one-year pre-planned interim analysis.

Patients and methods: A total of 82 postmenopausal women (age range 45-60 years, at least 1 year since menopause) were randomly allocated to receive: ALN 70 mg (Fosamax[®]) every two weeks (group A); a placebo, similar to the ALN tablet, every two weeks (group B) or Fosamax[®] 70 mg once-monthly (group C). All patients were recommended to take supplemental calcium 500mg and vitamin D 400 IU daily. Randomisation was performed by a minimization procedure taking into account baseline BMD and S-CTX values. S-CTX levels were assessed using a one-step ELISA (β -CrossLaps[®]; Roche Diagnostics). Lumbar spine and hip BMD measurement were performed at baseline and after 12 months. Treatment effects were compared between groups by analysis of variance (ANOVA), followed by 2 by 2 comparisons with the method of Least Significant Difference, and studied over time by ANOVA for repeated measurements.

Results: Data were available at 12 months for 76 patients. S-CTX levels (table 1) significantly decreased at 3, 6 and 12 months in both ALN groups (p<0.001 for all comparisons, except p=0.029 for group C at 3 months). Significant difference in S-CTX levels was observed between groups A and B after 3 months (p=0.008), 6 months (p=0.012) and 12 months (p=0.004) and between groups C and B after 6 (p=0.046) and 12 months (p=0.028). Significant LS BMD increase was observed after 12 months in both ALN groups (group A 1.2 %, p < 0.001 ; group C 1.8 %, p=0.005) with a significant difference between groups A and B (p=0.001) and between groups C and B (p=0.01). At the total hip, BMD increase occurred in group A only (0.8%, p=0.039).

Conclusion: One year of intermittent ALN regimen, given 70 mg every two weeks or once-monthly, increased LS BMD with a significant difference as compared to placebo. Both ALN regimens were effective at decreasing rapidly osteoclastic activity in postmenopausal women, the response being slightly delayed with the monthly treatment.

Table 1. S-CTX values expressed as mean \pm SD (pg/ml).

	Baseline	3 months	6 months	12 months
Placebo	526.6 \pm 183.0 n = 27	440.2 \pm 156.5 n = 25	464.9 \pm 261.2 n = 24	444.4 \pm 194.6 n = 22
ALN once-monthly	539.1 \pm 228.0 n = 28	394.5 \pm 221.4 n = 28	343.4 \pm 195.0 n = 28	327.6 \pm 181.6 n = 28
ALN every 2 weeks	522.3 \pm 210.2 n = 28	300.7 \pm 161.9 n = 27	306.1 \pm 187.5 n = 25	285.9 \pm 174.5 n = 26

Table 1

Disclosures: Yves Boutsen, None.

MO0421

Real-Life Effectiveness of Zoledronic Acid in Patients with Osteoporosis. Emmanouil Rampakakis¹, Georges Tsoukas², John S. Sampalis^{*3}. ¹JSS Medical Research, Canada, ²McGill University, Can, ³McGill University & Jewish General Hospital, Canada

Background

The efficacy of zoledronic acid in bone metabolism RA has been demonstrated in several controlled clinical trials. Longitudinal observational studies assessing the real-life effectiveness of therapeutic interventions are essential in order to demonstrate true population based benefits.

Methods

This was a retrospective chart review database analysis with data obtained from 4 clinics on patients initiating treatment with zoledronic acid.

Results

A total of 291 patients were included in this analysis with a mean (SD) age of 64.7 (11.4) years. Among these, 262 (90.0%) patients were female. The mean (SD) T-score at baseline was -2.9 (1.0) and -2.3 (0.8) for the spine and femur, respectively, and the mean (SD) zoledronic acid dose was 4.3 (0.78) mg.

After a single infusion of zoledronic acid, significant improvements were observed in spine bone mass density (BMD) (Mean (SD) = 0.02 (0.05) gm/cm²; P < 0.001), femur BMD (Mean (SD) = 0.01 (0.05) gm/cm²; P < 0.001), alkaline phosphatase (Mean (SD) = -5.5 (18.6) U/l; P < 0.001), and osteocalcin (Mean (SD) = -4.7 (12.7) μ g/ml; P < 0.001).

The changes in these parameters further improved after an additional 2 infusions; mean (SD) changes in spine BMD, femur BMD, alkaline phosphatase, osteocalcin and C-terminal telopeptide of type I collagen were 0.03 (0.06) gm/cm² (P < 0.001), 0.02 (0.06) gm/cm² (P=0.012), -6.9 (23.2) U/l (P=0.046), -4.2 (6.9) μ g/ml (P=0.001), and -0.07 (0.14) (P=0.007), respectively, after 3 infusions.

Conclusions

The results of this real-life study demonstrate that long-term treatment with zoledronic acid is effective in reducing symptom severity and improving bone turnover markers in patients with Osteoporosis.

Disclosures: John S. Sampalis, None.

MO0422

Regional Bone Metabolism at the Lumbar Spine and Hip Following Discontinuation of Alendronate and Risedronate Treatment in Postmenopausal Women. Michelle Frost¹*, Musib Siddique¹, Glen M. Blake¹, Amelia EB. Moore¹, Paul K. Marsden¹, Paul J. Schlever¹, Richard Eastell², Ignac Fogelman³. ¹King's College London, United Kingdom, ²University of Sheffield, United Kingdom, ³Guy's Hospital, United Kingdom

Bisphosphonates such as alendronate (ALN) or risedronate (RIS) have persistent effects on bone following discontinuation of treatment. The aim of this 12-month prospective study was to investigate changes in regional bone metabolism at the lumbar spine and hip following discontinuation of ALN and RIS in postmenopausal women. Positron emission tomography (PET) was used to examine bone metabolism at the spine and hip in 20 postmenopausal women treated with ALN (n=11) or RIS (N=9) for a mean duration of 5 years. Subjects underwent a 1-hour dynamic scan of the lumbar spine and a 10-minute static scan of both hips at baseline and 6 and 12-months following treatment discontinuation. ¹⁸F-fluoride plasma clearance (K_i) at the lumbar spine was calculated using a 3-compartment model. Standardised uptake values (SUV) were calculated for the spine, total hip, femoral neck and femoral shaft. Measurements of K_i and SUV reflect the level of osteoblastic activity in bone and are therefore considered to be a valid measure of bone metabolism. Measurements of BMD at the spine and hip and biochemical markers of bone turnover were also performed. With the exception of a significant decrease in spine BMD in the ALN group BMD remained stable during the 12-month follow-up period. Bone turnover markers increased significantly from baseline by 12 months for both study groups. Measurements of K_i and SUV at the lumbar spine and femoral neck, did not change significantly in either group. In the ALN group SUV at the femoral shaft and total hip increased at 12 months by 33.8% (p = 0.028) and 24.0% (p = 0.013) respectively. No significant changes were observed at any region of the hip following RIS treatment discontinuation. In conclusion, an unexpected decrease in lumbar spine BMD was observed for the ALN group. Bone metabolism at the lumbar spine remained suppressed following treatment discontinuation. A significant increase in SUV at the femoral shaft and total hip after 12 months was observed in the ALN group. The reasons for this differential response at the hip between the ALN and RIS groups are speculative. This study highlights the potential difficulty in identifying meaningful differences between BPs in clinical practice and that it is likely that more than 1 year is required to fully expose these differences.

Disclosures: Michelle Frost, Warner Chilcott, 2
This study received funding from: Warner Chilcott

MO0423

Relationship Between Baseline Serum 25-Hydroxyvitamin D and Response to Risedronate in Postmenopausal Osteoporosis Patients - A Pooled Analysis of Clinical Trials in Japan. Ryo Okazaki¹*, Ryoichi Muraoka². ¹Teikyo University Chiba Medical Center, Japan, ²Ajinomoto Pharmaceuticals Co, Ltd., Japan

Vitamin D deficiency/insufficiency could affect treatment response to bisphosphonates (BPs). However, conflicting results have been reported in this regard. Different cut-off serum 25(OH)D values to define vitamin D status and/or the use or non-use of supplemented vitamin D with BPs may account for this conflict. We performed post-hoc analyses of risedronate (RIS) Phase III trials conducted in Japan to evaluate the influence of basal serum 25(OH)D level on the responses to RIS using various cut-off serum 25(OH)D values. Data from 766 subjects whose serum 25(OH)D were measured prior to RIS administration were analyzed. RIS was administered for 48 weeks without vitamin D supplementation in those trials. With the cutoff level of basal serum 25(OH)D at 20 ng/mL, the lumbar spine BMD increase rates were 5.224.36% in the <20 ng/mL group and 5.884.34% in the ≥20 ng/mL group, which were not significantly different [difference (?) -0.66 (95% CI, -1.51 to 0.18)]. Among bone turnover markers (BTMs) at the baseline, serum bone-type alkaline phosphatase (BAP, U/L) [31.910.2 vs 29.710.1; ? 2.22 (95% CI, 0.42 to 4.03)] and serum CTX (μg/nmol-Cr) [272.3147.7 vs 247.4110.1; ? 25.0 (2.18 to 47.8)] were higher in patients with < 20 ng/mL 25(OH)D, whereas urinary NTX (nmolBCE/ mmol-Cr) [51.023.9 vs 48.921.0; ? 2.08 (-1.10 to 5.28)] were comparable. The differences in BTMs between the groups were gradually disappeared and after 48 weeks of RIS administration all three BTMs were comparable; (BAP: 19.75.9 vs 19.06.2; CTX: 106.667.0 vs 100.269.1; NTX: 29.113.6 vs 28.913.1). In contrast, with the cutoff value of serum 25(OH)D at 15 ng/mL, the BMD increase rates were significantly low in the < 15 ng/mL group compared with > 15 ng/mL at 12, 24, and 48 week. At 48 week BMD increase rates were 3.994.51% in the <15 ng/mL group and 5.844.28% in the ≥15 ng/mL group, respectively (? -1.85, 95% CI, -3.13 to -0.56). Further, when the subjects were stratified into four groups by serum 25(OH)D (<16, 16-20, 20-24 ≥24 ng/mL), BMD increase rates tended to be low, whilst the BTMs tended to be high in the groups with lower serum 25(OH)D. These results suggest that, when using BPs without vitamin D supplementation, serum 25(OH)D level should be adequately increased prior to treatment initiation. Further studies are needed to evaluate whether or not vitamin D status affect BPs response in terms of anti-fracture efficacy.

Disclosures: Ryo Okazaki, None.

MO0424

Relationship of Changes in Total Hip Bone Mineral Density to Vertebral and Non-Vertebral Fracture Risk in Women with Postmenopausal Osteoporosis Treated with Once-Yearly Zoledronic Acid 5 mg (ZOL): the HORIZON-PFT study. Richard Jacques¹, Steven Boonen², Felicia Cosman³, Ian Reid⁴, Douglas Bauer⁵, Dennis Black⁵, Richard Eastell¹. ¹University of Sheffield, United Kingdom, ²Center for Metabolic Bone Disease & Division of Geriatric Medicine, Belgium, ³Helen Hayes Hospital, USA, ⁴University of Auckland, New Zealand, ⁵University of California, San Francisco, USA

Bone mineral density is considered a useful surrogate for fracture risk prediction. However, in some clinical trials the percent change in bone mineral density has not related closely to fracture risk reduction. To examine the reasons for this in more detail, we carried out a year-by-year analysis of the percent of treatment effect (PTE) explained by change in total hip BMD in the HORIZON Pivotal Fracture Trial in which patients received three annual infusions of ZOL 5 mg. We examined the associations between changes in total hip BMD and vertebral and non-vertebral fracture incidence in 7736 women. Altogether 406 women sustained a vertebral fracture (odds ratios were calculated from a logistic model), and 487 women sustained a non-vertebral fracture (hazard ratio was calculated from a Cox model). The table shows the relationship between change in total hip BMD (THBMD) from baseline to 1, 2 and 3 years with vertebral fracture occurring during the same time periods i.e. baseline to 1, 2 and 3 years. We also examined the change from baseline to 3 years and fracture occurring at anytime during the 3 years of the study. PTE was estimated using the Li method (2001).

For non-vertebral fracture, the hazard ratio was not significant on a year-by-year basis, but over the 3 years, the hazard ratio was 0.80 (0.67, 0.95) and the PTE was 59% (23, 152). Thus, change in total hip BMD appears to be a surrogate for fracture risk reduction with zoledronic acid.

	Vertebral fracture risk, odds ratio (95% CI)	PTE by change in THBMD (95% CI)
Year 1	0.40 (0.28, 0.57)	42 (29, 61)
Year 2	0.19 (0.12, 0.31)	39 (28, 54)
Year 3	0.35 (0.25, 0.49)	42 (28, 63)
All 3 years	0.30 (0.24, 0.38)	40 (30, 54)

Table

Disclosures: Richard Eastell, None.
This study received funding from: Novartis Pharmaceuticals

MO0425

The Intra-Venous Zoledronic acid once Yearly (IVORY) observational study: Baseline and one year data. David Kendler^{*}. Osteoporosis Research Centre, Canada

Background: Zoledronic acid (ZOL) is an annual iv bisphosphonate effective for the prevention of vertebral, non vertebral and hip fractures in postmenopausal women, for the treatment in men with osteoporosis (OP) and glucocorticoid-induced OP. IVORY is a 4 year, observational study in a real-life Canadian setting comparing patient adherence and osteoporosis outcomes in patients treated with ZOL and oral bisphosphonate (OBP). Methods: 1504 women with OP over 45 years were recruited in 182 Canadian sites. Patients treated prior to study entry were enrolled in a 2:1 ratio ZOL (n=1029) to OBP (n=475). Through this 1-year data interim analysis we report adherence to therapy, bone mineral density (BMD) changes and SAEs. Results: Baseline demographics were comparable in both groups (Table 1), except in pre-treated patients, where 64.1% (ZOL) and 86.7% (OBP) of patients received an OBP before study entry. The most common fractures prior to study entry were spine (13.5% and 12.6%) and wrist (9.1% and 9.3%) in ZOL and OBP respectively. Mean BMD total hip were 0.76 and 0.78 g/cm² (T-score -1.80 and -1.66) and at lumbar spine were 0.88 and 0.91 g/cm² (T-score -2.33 and -2.12) in Zol and OBP respectively. At one year, lumbar spine BMD remained stable (0.90 g/cm² and 0.91 g/cm²; T-score -2.16 and -2.03 in ZOL and OBP respectively). Both total hip and femoral neck BMD and T-score remained similar in both groups. When stratified, naive patients, mean change BMD at lumbar spine were 0.026 g/cm² and 0.013 g/cm² (3.4% and 1.6%) for Zol and OBP respectively. No difference was observed between ZOL and OBP pre-treated patients from baseline to month 12. No change was observed for the femoral neck and total hip BMD when both ZOL and OBP stratified by naive and pretreated patients were compared. Adherence (patients returning for the one year visit), was 66.8% and 53.1% in the naive patients and 75.1% and 81.9% in the pre-treated group for ZOL and OBP respectively. At one year, SAEs occurred in 4.7% (ZOL) and 3.2% (OBP).

Conclusion: Treatment-naïve ZOL patients were more likely to have a greater increase in BMD compared to OBP. In the pre-treated patients, mean changes in BMD were similar. Annual therapy with ZOL may have a favourable impact on persistence. Longer term follow-up in this real-life setting may show greater BMD and eventually lower fracture incidence with ZOL compared to OBP.

Disclosures: David Kendler, J&J, 2; Pfizer, 2; Merck, 2; Servier, 2; Amgen, 2; GSK, 2; Eli Lilly, 2; Novartis, 2; Boehringer, 2

This study received funding from: Novartis

MO0426

The Use of Screening Radiographs to Detect Incomplete Atypical Femoral Fractures in Asymptomatic Patients on Bisphosphonate Therapy. Renata La Rocca Vieira¹, Zehava Sadka Rosenberg¹, Mary Allison², Shelly Im¹, Valerie Peck¹. ¹NYU Medical Center, USA, ²NYU Langone Medical Center, USA, ³NYU School of Medicine, USA

Objectives: Progression of an incomplete atypical femoral fracture (IF) to a complete fracture in patients on long term bisphosphonate (BISPH) therapy can be catastrophic. Our aims were to determine the frequency and imaging features of IF in asymptomatic patients on long-term BISPH therapy and to identify distinguishing clinical and laboratory markers in the subset of patients who develop these fractures. **Material and methods:** 200 femoral radiographs in 100 asymptomatic patients (93 females, 7 male, age range 57-70, mean 62.8) were prospectively reviewed by 2 radiologists. All patients were on BISPH therapy for at least 3 years and had no history of hip/thigh pain or recent trauma. MRI studies were performed when a fracture was suspected on radiographs. Bone mineral density (BMD), serum calcium, albumin, 25-hydroxy vitamin D, intact parathyroid hormone, serum c telopeptide and urine n telopeptide were obtained in all patients. **Results:** 2 of 100 patients (2%) had 3 IF (bilateral fractures in 1 patient). Both patients, age 50 and 57 respectively, were Caucasian, active and on BISPH therapy for 8 years. The patient with bilateral fractures demonstrated typical features of bisphosphonate-related IF: Bilateral focal, lateral cortical thickening with left incomplete transverse fracture line and no right fracture line. Lumbar spine and femoral neck BMD T-scores were -2.5 and -1.7 respectively. Laboratory data were normal. In the 2nd patient the radiographs were less typical demonstrating linear, intramedullary, subtrochanteric sclerosis. Lumbar spine and right femoral neck BMD T-scores were -1.4 and -2.7 respectively. Laboratory data demonstrated decreased bone turnover. MRI confirmed the radiographic findings in both patients. The 2 patients with IF were significantly younger ($p=0.0286$) than those without IF. There were no significant differences in other clinical or laboratory data ($p>0.15$) between the 2 groups. **Conclusion:** The 2% frequency of IF fractures in asymptomatic patients on long term BISPH therapy is higher than suggested in the literature. Aside from age, there were no significant differences in clinical or laboratory data between the 2 groups. **Clinical relevance:** Early detection of BISPH related IF may require screening radiographs. Larger studies are necessary to validate our findings and identify other discerning clinical and laboratory markers.

Disclosures: Mary Allison, None.

MO0427

Thirteen Cases of Atypical Subtrochanteric and Diaphyseal Femoral Fractures among the 2,238 cases of Femoral Fractures Occurred during 2006 to 2010 in Japan. Yoshitomo Saita¹, Muneaki Ishijima¹, Atsuhiko Mogami², Tomonori Baba³, Masashi Nagao⁴, Kensuke Sakai⁴, Yasuhiro Homma², Rui Kato⁵, Kei Miyagawa⁶, Nana Nagura², Tomoki Wada², Osamu Obavashi², Hogaku Gen⁶, Hajime Kajihara⁵, Masahiko Nozawa⁴, Katsuo Shitoto⁷, Kazuo Kaneko¹. ¹Department of Orthopaedics, Juntendo University School of Medicine, Japan, ²Department of Orthopaedic Surgery, Juntendo Shizuoka Hospital, Japan, ³Department of Orthopaedic Surgery, Juntendo Urayasu Hospital, Japan, ⁴Department of Orthopaedic Surgery, Juntendo Nerima Hospital, Japan, ⁵Department of Orthopaedic Surgery, Koto Hospital, Japan, ⁶Department of Orthopaedic Surgery, Chiba Central Medical Center, Japan, ⁷Department of Orthopaedic Surgery, Juntendo Urayasu Hospital, Japan

The ASBMR task force defined major and minor features of atypical femoral fractures in response to the reports linking long-term use of bisphosphonates (BPs) with these fractures (JBMR, 11, 2267-94, 2010). It recommends that all major features be present to designate as atypical and also developed a case definition so that subsequent studies report on the same condition.

Following this definition, we retrospectively investigated all 2,238 proximal and diaphyseal femoral fractures treated in 6 hospitals related to our university in Japan during 2006-2010.

During this period, 13 cases (9 patients) (0.53%) of atypical fractures were found. All these cases showed major features. While 7 of 13 cases showed subtrochanteric fracture (0.36% of proximal femoral fractures), residual 6 cases were diaphyseal fracture (1.1% of diaphyseal fractures). All the 9 patients were female. While the mean age of 13 cases was 64.5y, that of subtrochanteric fractures (54.0y) were much younger than that of diaphyseal fractures (76.7y) ($p<0.05$). Bilateral fractures were occurred in

4 patients (44%) and in almost same place of their femurs. The majority (88.9%) occurred after oral BPs monotherapy (Alendronate: 6 patients, Risedronate: 2 patients). The duration of BP therapy was; within one year: 1 patient, 1-5 years: 4, over 5 years: 3. The history of glucocorticoids therapy was found in 6 patients (67%). Among them, 4 patients (44%) were long-term glucocorticoid users due to collagen diseases, such as systemic lupus erythematosus and dermatomyositis from their early-life. It should be emphasized that all these glucocorticoid users showed subtrochanteric fractures. The proton pump inhibitors were used in 2 of 9 patients (22%). Twelve of thirteen cases were operated with nail fixation and residual one case with locking plate (due to narrow medullary space). Prophylactic nail fixation was performed in 2 patients, as they complained prodromal pain and radiographic changes were detected in contralateral side. Delayed healing was observed in 4 cases (31%).

If this study is applied to the ASBMR task force evidence hierarchy, this study would be corresponded to have the "acceptable evidence". The atypical femoral fractures were shown to be occurred not only BPs users but also patients who have not been treated with BPs. However, our data suggest that the long-term combination therapy of glucocorticoids and BPs might be one of risk factors for the atypical subtrochanteric fracture.

Disclosures: Yoshitomo Saita, None.

MO0428

Three-monthly i.v. Ibandronate Following Long-term Treatment With Oral Alendronate; Results From a Two-year Prospective Open-labeled Study. Astrid Fahrleitner-Pammer¹, Karlheinz Fenzl², Doris Wagner³, Christian Muschitz⁴, Karin Amrein³, Thomas Pieber⁵, Barbara Obermayer-Pietsch¹, Hans Dimai¹. ¹Medical University Graz, Austria, ²Roche Austria, Austria, ³Medical University of Graz, Austria, ⁴St. Vincent's Hospital, Austria, ⁵Medical University of Graz, Dept of Internal Medicine, Div. of Endocrinology & Metabolism, Austria

Ibandronate (IBN) is a potent third generation bisphosphonate (BP) that is administered intravenously (i.v.) every three months. Therefore, it is widely used as an alternative to oral BPs in patients who are unable to ingest these drugs adequately, or who are prone to, or suffer from gastro-intestinal problems such as chronic gastritis or peptic-ulcer. The aim of the present study was to investigate the effect of IBN i.v. administered three-monthly in postmenopausal women who had previously been on long-term treatment with the oral BP alendronate (ALN).

The present study was carried out at an osteoporosis outpatient facility. 197 consecutive postmenopausal women (mean age 66 + 12 yrs) who had stopped long-term treatment with ALN for GI reasons, were switched to treatment with 3mg IBN three-monthly. The median time of treatment with oral ALN had been 37 + 14 months, and duration of consecutive treatment with IBN was 24 months.

After 2 years of treatment with IBN (following long-term treatment with ALN), serum crosslaps (sCTX) decreased significantly from 2.4 + 1.7 to 0.9 + 0.8 [$p<0.0001$; normal range 1.0 - 3.4nmol/L], and serum osteocalcin levels decreased from 23+14 to 18.2 + 10 [$p<0.0001$; normal range: 1-35 ng/ml]. Bone mineral density (BMD) measurement at the lumbar spine (dual energy X-ray absorptiometry, Hologic QDR 4500) revealed a significant increase of +8% (0.754 + 0.121 versus 0.844 + 0.170g/cm²; $p<0.0001$), and +8% at the femoral neck (0.622 + 0.103 vs 0.685 + 0.124g/cm²; $p<0.0001$). Serum creatinine levels and electrolytes showed no significant change throughout the entire period of observation. Three patients experienced flue-like symptoms after the first IBN injection, but no such side effects were seen after the second injection.

To our knowledge, the present study is the first to assess the effect of 2 years of i.v. IBN treatment following long-term treatment with an oral BP. Our data indicate that patients who have been pre-treated with the potent antiresorptive BP ALN may further benefit from a subsequent treatment with i.v. IBN in terms of increasing BMD, and decreasing bone turnover as assessed by biochemical markers. IBN i.v. 3-monthly appears to be well tolerated with no detrimental effects on renal function.

Disclosures: Astrid Fahrleitner-Pammer, Financial, 5

This study received funding from: Roche Austria

MO0429

Associations Between Osteoporosis (OP) Treatment Change, Adherence, and Incident Fractures Among Members in a Medicare Advantage Prescription Drug (MAPD) Plan. Yihua Xu¹, Melea Ward¹, Hema Viswanathan², John Adams³, Bradley Stolshek², Reginald Clay², John Kallich², Kenneth Saag⁴. ¹Competitive Health Analytics, Inc, USA, ²Amgen Inc., USA, ³RAND Corporation, USA, ⁴University of Alabama at Birmingham, USA

Purpose: High medication adherence (medication possession ratio [MPR] of ≥ 0.8) is known to be associated with better treatment outcomes. Treatment change (i.e. medication switch) patterns in OP and associated impact on MPR and fracture outcomes have not been well characterized. We examined the relationship between OP treatment change, medication adherence, and incident fractures among MAPD members newly initiated on an OP treatment.

Methods: This was a retrospective cohort study of MAPD members, aged ≥ 50 newly initiated on an OP medication between Jan2006 and Dec2008. Treatment change, defined as a change in therapy or dose was examined during the 12 month

MO0431

First Interim Results of the German Non-Interventional Study (NIS) VIVA to Assess the Compliance, Safety, and Effectiveness of Quarterly i.v. Ibandronate (IBN) vs. Weekly Oral Alendronate (ALN) in Patients with Postmenopausal Osteoporosis. Peyman Hadji*. Philipps-University of Marburg, Germany

Purpose: The objectives of this NIS are to evaluate compliance, persistence, safety, and effectiveness of quarterly 3mg i.v. IBN vs. weekly 70mg p.o. ALN in patients with PMO in a real world setting. Here, we present preliminary results from a first interim analysis.

Methods: This NIS was started in MAR-2010 and a total of 6,000 pts have been enrolled until November 2010. Baseline documentation (VB) is available for 5,838 pts; 3,982 pts returned for their 1. interim visit (V1). This interim analysis focused on baseline characteristics and pain reduction from VB at V1; all analyses were purely descriptive. A pre-planned "matched-pairs" analysis was applied in order to enhance the comparability between treatment groups with regard to missing randomization. Criteria for matching included age, BMI, prevalent fractures, prevalent vertebral fractures, pre-treatment with bisphosphonates (BP), concomitant diseases, and start of current treatment in relation to VB date.

Results: As expected, the IBN (N=4,363) and ALN (N=1,475) groups comprised significant differences with regard to baseline characteristics. While median age was 73yrs and median PMO duration was 22yrs in either group, noticeable differences were found for start of current therapy in relation to date of VB (-89,0251 days in the IBN group vs. -205490 days in the ALN group; $p=0.001$), no. of pts with previous fractures (45.7% vs. 40.0%; $p<0.01$) and vertebral fractures (34.3% vs. 27.9%; $p<0.01$), and no. of BP-naïve pts (48.1% vs. 64.9%; $p<0.01$). In addition, differences in the pattern of concomitant diseases were apparent. We performed a matched-pair analysis for 1,778 pts, resulting in 889 pairs of IBN and ALN groups. 3,982 pts had V1 data reported (performed approx. 90 days on median after VB). A reduction in analgesics use from VB to V1 was performed in 39.2% and 34.2% of pts, and the rate of patients with no or mild OSM-related pain had increased from VB to V1 by 16.8 and 12.0%-points (IBN vs. ALN).

Conclusions: The presented data of the first interim analysis suggests that there might be differences with regard to pain reduction between the groups. This needs to be confirmed with the final data in the matched-pair population which are expected to be available in 2012.

Disclosures: Peyman Hadji, None.

This study received funding from: Roche Pharma

MO0432

Optimizing Communication of DXA Results and Fracture Risk to Patients: A Mixed Methods Study. Stephanie Edmonds*¹, Samantha Solimeo¹, Douglas Roblin², Kenneth Saag³, Peter Cram¹. ¹University of Iowa, USA, ²Kaiser Permanente, USA, ³University of Alabama at Birmingham, USA

BACKGROUND: There is growing interest in sharing clinical information with patients to facilitate medical decision making and improve healthcare quality. However, it remains uncertain how to best present this information in a way that patients understand. As part of a multi-center randomized trial, we conducted a mixed-methods study to examine how best to communicate written DXA results and fracture risk information to patients.

METHODS: Our team of clinicians and health communication experts developed three different letters (A, B, and C) and four visual graphic representations of fracture risk (Bar, Stoplight, Arrow, and Faces), designed to be mailed to patients after a DXA appointment. Each letter/graphic combination provided DXA result (T-score), diagnosis (normal, low BMD, osteoporosis) and FRAX fracture risk. We presented the letters and arrays in random order to a convenience sample of adults aged 50 years or older drawn from a large academic medical center. We collected patient demographic information and educational attainment. Participants were asked to identify which letter and graphical representation they preferred as well as ease of understanding and perceived risk of each.

RESULTS: We interviewed 35 subjects (34% female, mean age 65.3 years \pm 8.8, 25.7% completed high school or less). Of the three letters, 36% preferred version A, 33% preferred Letter B, and 31% preferred Letter C. However, Letter B was rated easiest to understand by 33% of respondents while only 25% rated Letter A easiest to understand. Factors that participants felt important in the letters were: a) to give numerical data (e.g., T-score, FRAX) as well as the overall impression; and b) to give patients specific "next steps" to take. Subjects reported that the specific definition of a T-score was confusing, but appreciated a general overview. Of the four graphical arrays, 40% of subjects preferred the "Bar" graph and 17% preferred a "Stoplight" array. Subjects stated the "Bar" image showed their risk category best and was "clean," "clear," and "easy to read."

CONCLUSION: Using a mixed methods approach, we were able to identify a letter and graphical array for effectively conveying DXA results and fracture risk to patients. These templates should be used by others looking to convey DXA results to patients.

(mos) post-index period (date of the first OP medication). Adherence, measured by MPR, was categorized as low (<0.5), partial (0.5 to <0.8), and high (≥ 0.8) at 12 and 24 mos post index. Fractures in the first 12 months post-index were identified based on a validated algorithm. Members who discontinued the index medication and did not restart an OP medication were excluded from the fracture analysis. The relationship between treatment change and incident fracture was evaluated using a pooled logistic regression model which allowed for specification of treatment change to have occurred prior to the fracture using a time varying covariate.

Results: Of 33,823 members identified as having newly initiated OP therapy, 3,573 (10.6%) changed therapy within 12 mos. The proportion of patients with low, partial, and high adherence, respectively, 12 mos post index was 41.4%, 26.7%, and 31.9% in the change cohort, and 51.3%, 17.6%, and 31.1% in the no-change cohort. The proportions at 24 mos post index were 50.1%, 24.3%, and 25.5%, respectively, in the change cohort, and 58.0%, 16.8%, and 25.1%, respectively, in the no-change cohort. The fracture risk analysis included 19,574 members. At 12 and 24 mos, the change cohort had a higher fracture incidence (11.2% and 15.3%, respectively) compared to the no-change cohort (8.2% and 12.7%, respectively). However, fracture incidence was not significantly different between the two cohorts after adjusting for covariates (Odds Ratio=0.98, 95% CI=0.85-1.1, $P=0.77$).

Conclusions: Overall adherence was low in both cohorts. Changing OP therapy was not found to be associated with a decrease in fracture risk. An opportunity to improve fracture outcomes exists given that less than a third of members in each cohort achieved high adherence with currently available therapies.

Disclosures: Bradley Stolshek, *Competitive Health Analytics*, 3

This study received funding from: Amgen Inc

MO0430

Does Medication Adherence Itself Confer Fracture Protection? An Investigation of the Healthy Adherer Effect in Observational Data. Jeffrey Curtis*¹, Jeff Lange², Huifeng Yun¹, Elizabeth Delzell¹. ¹University of Alabama at Birmingham, USA, ²Procter & Gamble, USA

Background

Prior studies have shown a relationship between bisphosphonate (BP) adherence and reduced fractures. One potential concern about the interpretation of this association is the healthy adherer effect, a phenomenon whereby patients who adhere to medications are systematically different than those who do not. The extent to which fracture-adherence analyses might be confounded by the healthy adherer effect in real-world settings is unclear.

Objective

To quantify the association between high adherence with different medications and fracture risk.

Methods

Using Medstat MarketScan from 2000 to 2008, we identified 125,000 women with a new clinical fracture at the hip, spine, humerus, or wrist. We defined three mutually-exclusive cohorts of patients who initiated within 6 months post-fracture: 1) oral BPs; 2) selective serotonin reuptake inhibitors (SSRI); or, 3) ace inhibitor, angiotensin receptor blocker, or calcium channel blocker (ACE/ARB/CCB). These medications were chosen for their expected favorable, unfavorable, and neutral effect on fracture risk. Adherence (medication possession ratio [MPR]) was assessed after 1 year of new use, updated every 90 days. Follow-up time for new fractures began after the MPR measurement and extended up to 4 years. Patients were categorized as highly adherent (MPR $\geq 80\%$) vs. less adherent (MPR $< 50\%$). Cox proportional hazards models evaluated the association between high (vs. low) adherence within each medication group and fracture.

Results

We identified a BP cohort (11,712 patients, mean age=75), SSRI cohort (5,570 patients, mean age=76), and ACE/ARB/CCB cohort (5,731 patients, mean age=77) who initiated these therapies ≤ 6 months after fracture. For these 3 cohorts, 46%, 43%, and 53%, respectively, had MPR $\geq 80\%$ at 12 months.

Crude hazard ratios for hip and non-vertebral fractures (Table) showed that high adherence (vs. lower adherence) with BPs decreased fracture risk; high adherence with SSRIs increased hip fracture risk, and high adherence with ACE/ARB/CCBs was neutral toward fracture risk.

Conclusion

In this observational analysis of women enrolled in a commercial health plan, we did not find evidence of a healthy adherer effect that suggested that medication adherence itself conferred fracture benefit. Based upon this result, observational analyses evaluating the association between osteoporosis medication adherence and fracture risk appear to not be meaningfully confounded by the healthy adherer effect.

Table. Relationship between High (vs. Lower) Adherence to Bisphosphonates, SSRIs, and ACEI/ARB/CCBs

Fracture Type	Bisphosphonates		SSRIs		ACEI/ARB/CCB	
	N, rate per 100py	HR (95% CI)	N, rate per 100py	HR (95% CI)	N, rate per 100py	HR (95% CI)
Hip, adherent	48, 0.5	0.56	47, 1.4	1.42	288, 1.2	1.15
Hip, non-adherent	84, 1.0	0.39-0.80	40, 1.0	0.93-2.17	187, 1.0	0.74-1.77
Nonvertebral, adherent	495, 5.6	0.76	226, 6.7	1.01	54, 6.3	1.05
Nonvertebral, non-adherent	635, 7.3	0.68-0.86	271, 6.6	0.85-1.20	32, 6.0	0.87-1.26

Relationship between High (vs. Lower) Adherence to Bisphosphonates, SSRIs, and ACEI/ARB/CCBs

Disclosures: Jeffrey Curtis, Merck, 2; Eli Lilly, 5; Merck, 5; Novartis, 2; Novartis, 5; Procter and Gamble, 2; Eli Lilly, 2; Amgen, 2; Roche, 2; Amgen, 5; Roche, 5

MO0434

Persistence of Therapy With Zoledronic Acid Infusion For Osteoporosis.Christine Simonelli^{*1}, Julie Morancey¹, Jean Lian², Yoona Kim².
¹HealthEast Osteoporosis Services, USA, ²Novartis, USA

We report the re-infusion rate for zoledronic acid treatment for osteoporosis in our osteoporosis center. To maximize persistence with treatment we developed a simple process to track osteoporosis patients who were treated with annual 5mg zoledronic acid infusion. When patients receive their first infusion a 'tickler' file is created and placed at the month before their next infusion due date. Patients are given a patient education video about osteoporosis and an information brochure on zoledronic acid. Patients are contacted to schedule their clinical appointment the month before their due date if it is not already scheduled. If they miss their appointment an attempt is made to contact them and determine the reason for their failure to comply with prescribed treatment and discuss options. We report one-year follow-up on 74 patients and two-year follow-up on 37 patients who received their first zoledronic acid infusion between August 2008 and January 2010. There were 66 women (89.2%), mean age 71.9 (9.2SD) and 8 men, mean age 71.3 (9.4SD). One prior fracture was noted in 28 patients (37.8%), two prior fractures in 11 (14.9%) and three prior fractures in 7 (9.5%). Twenty-nine patients had prior vertebral fracture (39.2%), 10 prior rib fracture (13.5%), 6 prior hip fracture (8.1%) and 9 prior wrist fracture (12.2%). Sixty-seven patients had prior bisphosphonate use (90.5%); 54 alendronate (73%), 20 oral ibandronate (27%), 11 IV injections of ibandronate (14.9%) and 13 risedronate (17.6%). Thirty-three patients (44.6%) had prior teriparatide use. The most common reasons for choice of zoledronic acid treatment were BMD decline 30 patients (40.5%), GI adverse event on oral bisphosphonate 23 patients (31.1%), known upper GI disease 22 patients (29.7%), completion of teriparatide treatment 22 patients (29.7%). All 74 patients received their first infusion; 57 received their second infusion (76%). Eight patients (13.5%) were greater than one month late for their second infusion; 5 patients (6.8%) changed medication as physician preference, 6 (8.1%) patients lost to follow-up, 2 (2.7%) had BMD improvement and changed to every two year regimen; 2 (2.7%) had serious co-morbidity, 1 (1.4%) had dental work pending and 1 (1.4%) declined second infusion. 20 of 37 patients (54%) had a third infusion. Providing patient education materials and tracking patient appointments allowed for a high 2-year persistence of osteoporosis treatment with zoledronic acid.

Disclosures: Christine Simonelli, Eli Lilly, 5; Amgen, 2; Novartis, 8; Noartis, 2; Amgen, 8; Eli Lilly, 8
This study received funding from: Novartis

MO0435

Persistence, Gaps in Therapy, and Re-initiation of Osteoporosis (OP)

Therapy Among Women in a Commercially Insured US Population. Akhila Balasubramanian^{*1}, Alan Brookhart², Vamshidar Goli³, Cathy Critchlow⁴. ¹Amgen Inc, USA, ²University of North Carolina at Chapel Hill, USA, ³Amgen Inc., USA, ⁴Amgen, USA

Purpose

Long-term persistence is a significant challenge for OP treatment. As such, it is important to understand patterns of utilization, including persistence, discontinuation and re-initiation of OP therapy. This study describes utilization patterns of OP therapy and factors associated with re-initiating therapy following an interruption.

Methods

This study was conducted using 2005-2009 data from a large commercially-insured population. Women aged ≥ 55 yrs who had a new prescription claim for oral OP therapy following a 12 month (baseline) period with no OP therapy claims and ≥ 24 months of follow-up after therapy initiation, were eligible. Discontinuation was defined as the presence of a gap in prescription claims >60 days (30-90 days in sensitivity analyses). Re-initiation was defined as a prescription claim for the same or a different OP therapy following the therapy gap. Kaplan-Meier analysis was used to describe discontinuation and re-initiation patterns within 24 months following therapy initiation. Multivariate Cox regression was used to assess the impact of baseline clinical and demographic factors on re-initiation following the first gap in therapy.

Results

Of the 92,839 subjects, 55%, 42%, and 30% were persistent with therapy at 6, 12, and 24 months following initiation, respectively. Of those who discontinued therapy within 24 months of initiation, 46% re-initiated therapy; the majority (64%) did so within 6 months of discontinuation. Patients were less likely to re-initiate therapy if they were older ($p < 0.0001$), had a history of hospitalization during baseline ($p = 0.0007$), or were on therapy for a shorter (<6 months) period ($p < 0.0001$) prior to therapy interruption. The median time on therapy following re-initiation was 90-197 days across strata of patients categorized by time on and off therapy and with at least 12 months of observation time following discontinuation. Longer allowable gap periods in the definition of discontinuation resulted in slightly lower discontinuation rates, but did not appreciably change the overall findings.

Conclusions

Persistence with OP therapy is low. While approximately half of patients who discontinue treatment return to therapy, their uninterrupted time on therapy upon re-

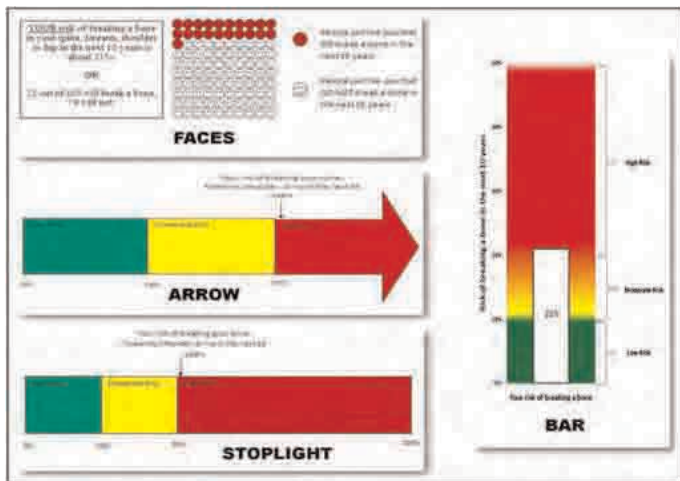


Figure 1: All four graphical arrays depicting a fracture risk of 21% in the next 10 years.

Disclosures: Stephanie Edmonds, None.

MO0433

Osteoporosis Treatment Initiation and Withdrawal: Evidence of Therapeutic Hysteresis in Clinical Practice. William Leslie^{*1}, Suzanne Morin², Lisa Lix³.

¹University of Manitoba, Canada, ²McGill University Health Centre, Canada, ³University of Saskatchewan, Canada

BACKGROUND: BMD testing strongly impacts on physician behavior in terms of osteoporosis therapy (OTX) initiation. Factors leading to OTX withdrawal have not been well studied. **METHODS:** Clinical BMD testing in the Province of Manitoba, Canada, uses an integrated program structure with a BMD database linkable to administrative health databases to identify all OTX dispensations. Prior to Jan 1, 2006, fracture risk reporting was based upon T-scores only; after this date 10-year fracture risk was reported using a FRAX-like model with risk categorized as low ($<10\%$), moderate (10-19%) or high ($>20\%$). Non-HRT OTX use was studied in women age 50+ who underwent BMD testing before (PRE = March 2005-Dec 2005) and after (POST = Jan 2006-Mar 2007) introduction of 10-year fracture risk reporting. We excluded women with any prior non-trauma fracture or with >90 days of steroid use at any time in the preceding 10 years. Two subgroups were defined: women with no OTX use in the year prior to BMD testing ($N=6,581$) and women with moderate to high OTX adherence in the year prior to BMD testing based upon medication possession ratio $>50\%$ ($N=1,352$). We examined the rate of OTX initiation in the untreated women (any OTX dispensation in the year post BMD) and treatment withdrawal in the previously treated women (any OTX dispensation >90 days post BMD). **RESULTS:** The overall rate of OTX initiation in untreated women was 19%, with a significant difference between the periods (PRE 22% vs POST 17%, $P < 0.001$). In contrast, among treated women there was a high rate of OTX persistence with no significant period effect (PRE 88% vs POST 85%, $P=0.074$). Similar results were seen for OTX use >180 days and >365 days post BMD. Although BMD category and risk category strongly affected OTX initiation, there was only a weak effect on OTX withdrawal (POST treatment rates 70% for normal BMD and 76% for low fracture risk). The OTX treatment curves by BMD category or risk category (Figure) for previously untreated and treated women were non superimposable suggesting significant hysteresis (path dependence). **CONCLUSIONS:** OTX withdrawal is infrequent in previously adherent women. BMD results are not a major trigger for treatment withdrawal even when BMD is normal and the estimated fracture risk is low. Factors contributing to treatment withdrawal need to be better defined given concerns regarding adverse effects from long term OTX, particularly among individuals who are not at high fracture risk.

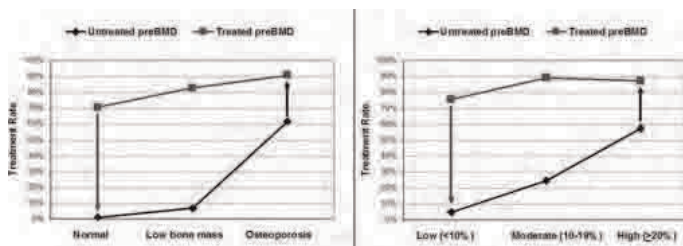


Figure: OTX treatment rates Jan 2006-Mar 2007 according to BMD and 10-year risk category.

Disclosures: William Leslie, None.

initiation remains short. A better understanding of patterns of use of OP medications may inform patient management strategies and design of more effective adherence improvement interventions.

Disclosures: *Akhila Balasubramanian, Amgen Inc, 1; Amgen Inc, 3*
This study received funding from: Amgen Inc

MO0436

The Persistence in the Health District of Cosenza (Calabria, Italy). *Claudia Carbone*¹, Alfonso Reda², Maria Gabriella Bartoletti³, Brunella Piro¹, Luisa Gallo¹.* ¹Servizio Farmaceutico ASP Cosenza, Italy, ²Italy, ³Centro di Riabilitazione Biolife, Italy

The persistence is an important problem in patients treated for the osteoporosis disease. We wanted to see what is the persistence in our referring population. We have considered the patients in the health district of Cosenza in Italy. The treated patients are 11094, all women, above 50 years old, affected by post-menopausal osteoporosis. We have considered two years 2009-2010 and all the patients treated with: teriparatide, parathyroid hormone, raloxifene, alendronate, ibandronate, risedronate. The patients treated by Teriparatide (84) had 6.68 as average prescription for each patient; the patients took the drug less 33% (six months) were 46 (60.7%); between 33 and 66% (between 6-12 months) were 9 (10.7%), till 100% (18 months) were 24 (28.6%). The patients treated by parathyroid hormone (only 2) had 7 as average prescription for each patient. The patients treated by raloxifene (317) had 7.91 as average prescription for each patient; the patients took the drug less 25% (six months) were 178 (56.2%); between 25 and 50% (between 6-12 months) were 38 (11.9%); between 50 and 75% (between 12-18 months) were 60 (18.9%), more 75% were 41 (13%). The patients treated by alendronate (4610) had 7.92 as average prescription for each patient; the patients took the drug less 25% (six months) were 2458 (53.3%); between 25 and 50% (between 6-12 months) were 614 (13.3%); between 50 and 75% (between 12-18 months) were 956 (20.7%), more 75% were 582 (12.7%). The patients treated by ibandronate (1082) had 8.78 as average prescription for each patient; the patients took the drug less 25% (six months) were 539 (49.8%); between 25 and 50% (between 6-12 months) were 143 (13.4%); between 50 and 75% (between 12-18 months) were 228 (21.2%), more 75% were 170 (15.6%). The patients treated by risedronate (2649) had 8.36 as average prescription for each patient; the patients took the drug less 25% (six months) were 1384 (52.2%); between 25 and 50% (between 6-12 months) were 332 (12.6%); between 50 and 75% (between 12-18 months) were 580 (21.9%), more 75% were 353 (13.3%). The patients treated by strontium ranelate (2350) had 4.77 as average prescription for each patient; the patients took the drug less 25% (six months) were 1782 (75.8%); between 25 and 50% (between 6-12 months) were 225 (9.6%); between 50 and 75% (between 12-18 months) were 274 (11.7%), more 75% were 69 (2.9%). Conclusions: Our observation confirms the low persistence at the therapy for osteoporosis.

Disclosures: *Claudia Carbone, None.*

MO0437

Treatment of Osteoporosis with zoledronic acid: what is the Persistence at one year in Clinical Practice?. *Estelle Rose¹, Thierry Lequerre², Chantal Bougneres¹, Pascal Bennet¹, Xavier Le Loet¹, Olivier Vittecoq¹, Alain Daragon*¹.* ¹Rheumatology Department, France, ²Rheumatology Department, France

Purpose: Zoledronic acid 5mg infusion is the only bisphosphonate administered once a year to treat osteoporosis. We could expect to an improved persistence compared to oral forms. Some studies showed a patient preference for a yearly infusion of zoledronic acid compared with oral therapy but no data on adherence or persistence is available. The objective of this study was to assess the proportion of patients who benefit a second infusion of zoledronic acid out of clinic after a first prescription given in the rheumatology department.

Methods: The retrospective study was conducted over 2 years. After searching for patients who received an initial infusion either during hospitalization or following a consultation, between August 2008 and November 2009, we phoned the general practitioners initially to know whether the second infusion was made ?? in the following year. When the general practitioner had no information, we contacted the rheumatologist or sometimes the patients themselves.

Results: Of 52 patients, 7 died within the year after the first infusion and 3 were lost of follow up. Of the 42 evaluable patients, 10 (24%) have not received the second infusion. This overall figure hides a wide disparity between patients who get out of hospitalization (n = 20) and those emerging from the consultation (n = 22). Indeed, after hospitalization 60% of patients received their second infusion against 91% after a consultation. This retrospective study provides disappointing results on the therapeutic persistence of infusions of zoledronic acid. To explain these results, it is possible that patients simply forget the second infusion because of the spacing of one year, or because another disease interfered. Also, the reports of hospitalization for physicians may not highlight enough the need to renew the infusion. Finally, the difference in persistence after hospitalization and after consultation may be explained by the fact that an infusion performed during an hospitalization is less well remembered than an infusion made at home on a given date.

Conclusion: Although the frequency of administration of zoledronic acid is not constraining, persistence seems disappointing with only 76% of second infusion

performed. Improving persistence need a better information for the physician and a systematic specialized consultation at one year could be proposed.

Disclosures: *Alain Daragon, None.*

MO0438

Antioxidant Enzyme Genes' Polymorphisms Influence Raloxifene Therapy Outcome in Postmenopausal Osteoporosis. *Simona Jurkovic Mlakar¹, Andrej Zavratnik², Tomaz Kocjan³, Janez Prezelj⁴, Janja Marc*¹.* ¹Department for Clinical Biochemistry, Faculty of Pharmacy, Slovenia, ²Department of Endocrinology & Diabetes, University Medical Centre Maribor, Slovenia, ³University of Ljubljana Medical Faculty, Slovenia, ⁴Medical faculty, University of Ljubljana, Slovenia

Levels of antioxidative enzymes are decreased in postmenopausal osteoporosis, probably as a consequence of estrogen deficiency. Studies showed that estrogens participate in gene expression of some antioxidant enzymes, for example GPX1. Raloxifene, the selective estrogen receptor modulator, might have even more pronounced antioxidant function than estrogen. For instance, in osteoporotic women on raloxifene the antioxidant enzymes such as catalases and superoxide dismutases, as well as serum concentration of glutathione were found to be increased.

We studied effects of one-year raloxifene treatment on bone mineral density (BMD) and biochemical markers of bone turnover in 52 Slovenian postmenopausal women, aged 60-65 years, in relation to genetic polymorphisms of major antioxidant enzymes involved in the metabolism of glutathione (GPX1, GSR, GSTM3, GSTM1, GSTT1 and GSTP1), thioredoxin system (TXNRD2, TXN) and interceptors of oxygen intermediates (CAT, SOD2 and SOD1).

Bone mineral density (BMD) at lumbar spine (BMD_{ls}), femoral neck (BMD_{fn}) and total hip (BMD_{th}) was measured by DXA and biochemical markers of bone turnover bone alkaline phosphatase (sBALP) and plasma osteocalcin (pOC) were obtained at baseline and after one-year of treatment with raloxifene 60 mg once daily. For genotyping the real-time PCR, triplex-PCR, DHPLC and restriction fragment methods were used.

After treatment there was on average an increase of BMD at lumbar spine and femoral neck of 2.14.5% and 1.65.2%, respectively and a decrease of 0.615.1% at total hip. The increase in BMD_{fn} was significantly greater among individuals with T/T genotype of SOD1 promoter SNP (rs4998557) (p=0.043) and Ile/Ile genotype of GSTM3 gene Val224Ile polymorphism (p=0.022). On the other hand, the same treatment resulted in greater increase of BMD_{ls} in individuals with Ala/Val genotype of GSTP1 gene Ala114Val polymorphism and Ala/Ala genotype of TXNRD2 gene Ala66Ser polymorphism. Interestingly, the significantly greater decrease of plasma osteocalcin concentration was observed among individuals with A/T genotype of 1154-393T>A polymorphism of GSR gene compared to A/A genotype subgroups (p=0.007).

This study shows for the first time a significant influence of SOD1, GSTM3, GSTP1, TXNRD2 and GSR genetic polymorphisms on raloxifene therapy outcome in postmenopausal osteoporosis.

Disclosures: *Janja Marc, None.*

MO0439

Decomposing Health Care Expenditures Relative to Fractures. *Meredith Kilgore*¹, David Becker², Jeffrey Curtis², Kenneth Saag², Elizabeth Delzell², Tarun Arora³, Michael Morrissey².* ¹University of Alabama At Birmingham School of Public Health, USA, ²University of Alabama at Birmingham, USA, ³UAB School of Public Health, USA

Objective: The purpose of this study is to evaluate reasons for health care expenditures both prior to and after the occurrence of fractures among Medicare beneficiaries.

Background: In a previous study we examined health services expenditures immediately prior to and following fractures and used the difference, incremental expenditures, as an estimate of avoidable costs associated with fractures. We also classified expenditures as attributable if they were directly linked to a fracture diagnosis code. Attributable expenditures accounted for only 24-60% of incremental expenditures, depending on the fracture site.

Methods: We examined health care expenditures between 1999 and 2007 among Medicare beneficiaries who experienced fractures (cases) and among beneficiaries who did not experience fractures (controls), matched to cases on age, race and sex. We also examined health care expenditures for cases and controls for 24 months prior to the fracture index date.

Results: When expenditures associated with diagnoses for aftercare, joint pain, and osteoporosis, other musculoskeletal diagnoses, pneumonia and pressure ulcers were included, the fracture of incremental costs directly related to fracture care rises substantially, to between 59% and 71%. We found that expenditures prior to fracture were higher for cases than controls, and that the rate of increase in health care expenditures was much higher among those about to experience hip fractures up to 18 months prior to the event (see figure).

Conclusions: Our findings confirm that the original incremental cost analysis constituted a very reasonable method for estimating avoidable costs associated with fractures and also suggest that patterns of health services utilization may provide a means to improve fracture prediction rules.

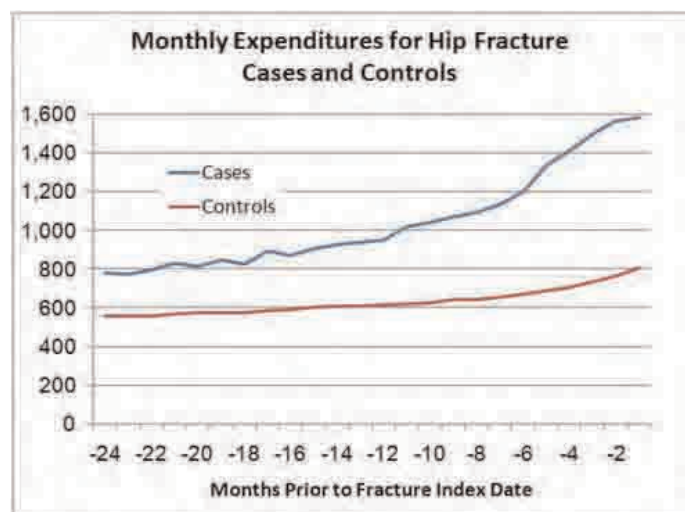


Figure. Expenditure Trends Prior to Hip Fracture

Disclosures: Meredith Kilgore, Amgen, 5; Amgen, 2
This study received funding from: Amgen, Inc.

MO0440

Fracture Liaison Service in a Non-regional Orthopaedic Clinic - A Cost-effective Service. Joe O Beirne¹, John Quinlan¹, Isweri Pillay², Mohamed Ahmed^{*2}. ¹Waterford Regional Hospital, Ireland, ²South Tipperary General Hospital, Ireland

Introduction: Secondary prevention of osteoporotic fracture is widely neglected with only a minority of patients offered investigations and treatment. It is proposed that in Ireland, a dedicated FLS be available in every hospital to which a patient presents, with a fracture. The FLS at South Tipperary General Hospital (STGH) is the first non-regional orthopaedics unit to provide this service in Ireland. The aim of this study was to evaluate the role of a FLS in providing cost-effective secondary fracture prevention.

Methods: All patients attending the orthopaedics service at STGH were screened by the fracture liaison nurse; an existing retrained orthopaedics nurse. Data were entered prospectively on to a standardised proforma. Patients were identified based on age, type of fracture sustained and their risk factors for osteoporosis. Screening consisted of fracture risk estimation, phlebotomy and DXA scanning. Treatment recommendations were based on international guidelines for secondary prevention of osteoporosis and included: Diet and lifestyle modification, calcium and vitamin D supplementation and pharmacotherapy.

Results: A total of 3164 patients attended the fracture clinic between July 2009 and February 2011. 4% (n=124) were identified as having a fragility fracture and fulfilled the criteria for fracture prevention assessment. Of those 80.6% (n=100) were females and 19.4% (n=24) were males. The average age of all patients was 67 years (range 46-94). Nearly 50% of all patients (n=58) had one or more previous fracture. Upper limb fractures accounted for the majority of fragility fractures screened (55.6%), with distal radius fracture being the commonest fracture sustained 23.3% (n=29). 92.7% (n=115) were offered BMD testing and of those 94% (n=108) completed their DXA scan. Two thirds of the patients (n=69) were either osteoporotic or osteopenic. All patients (100%) had blood tests for secondary osteoporosis screening. 90.2% of all patients (n=111) received verbal and written information regarding diet and lifestyle modification, and of those 106 patients (95%) received additional calcium and vitamin D. 48.7% of all patients (N=60) required anti-resorptive therapy.

Conclusion: the FLS at STGH successfully identified those at increased risk of further fragility fractures and effectively delivered an evidence-based standard of care for the secondary prevention of osteoporotic fractures on a Whole Time Equivalent cost-neutral basis.

Table 1: Numbers and distribution of fragility fracture case.

Site of fracture	number	percentage
Distal radius	29	23.3%
Ankle	24	19.3%
Humerus	16	13%
Radius	9	7.2%
Hand	8	6.5%
Foot	8	6.5%
Clavicle	7	5.6%
Scaphoid	7	5.6%
Pelvis	5	4%
Vertebrae	4	3.2%
Hip	3	2.4%
Others	4	3.2%

Table 1

Table 2: Recommendations for (BMD) testing for patients using DXA scan.

Assessments for DXA scan	Total number	Percentage
Patients offered assessment	124	100%
Recommended for DXA	115	92.7%
DXA completed	108	87.1%
Declined or did not attend	7	5.6%
DXA not indicated	9	7.3%

Table 2

Table 3: BMD results for patients with fragility fractures.

T score Category	Normal (T score >1)	Osteopenia (T score -1 to -2.5)	Osteoporosis (T score <-2.5)
DXA result (n=103)	33% (n=34)	37.8% (n=39)	29.1% (n=30)
Female (n=85)	26.2% (n=27)	29.1% (n=30)	27.1% (n=28)
Male (n=18)	6.8% (n=7)	8.7% (n=9)	2% (n=2)

Table 3

Table 4: FLS treatment recommendations.

Outcomes of evaluation	Number	Percentage
Total patients assessed	123	100%
Diet and life style	111	90.2%
Calcium and vit D	106	86.1%
Bisphosphonate	46	37.3%
IV Zoledronic acid	9	7.3%
Teriparatide	4	3.2%
Strontium	1	0.8%
Falls/osteoporosis classes	6	4.9%
Loading dose of vitamin D	21	17%

Table 4

Disclosures: Mohamed Ahmed, None.

MO0441

Healthcare Costs for Males After Closed Fracture in Commercially Insured and Medicare Advantage Populations From a National Health Plan. Susan Brennenman¹, Laura Christensen¹, Nicole Yurgin^{*2}, Ying Fan¹. ¹Innovus, USA, ²Amgen Inc, USA

Purpose: To determine annual total health care costs following hip, vertebral and non-hip/non-vertebral (NHNV) fractures among commercial (COM) and Medicare Advantage Plan (MAP) male enrollees.

Method: Administrative claims from a large, national health plan were analyzed. Men 45 or older were included if they had: at least one medical claim for a new closed fracture (identified through primary ICD-9-CM diagnosis indicating closed hip, vertebral, or NHNV fracture) at a single site between January 1, 2005 and December 31, 2008, were continuously enrolled with the plan for 12 months before and after the fracture, and had at least two fracture-related outpatient visits during the follow-up period. Those with hip, femur, tibia and humerus fractures were required to have

inpatient care associated with the first fracture claim. COM and MAP members were analyzed separately. Costs were calculated and stratified for hip, vertebral, and NHNV fracture patients as paid amounts and were adjusted to 2009 dollars. The difference between the individual patient's 12 month pre-fracture costs and 12 month post fracture costs are reported to estimate the change in costs associated with fracture.

Results: The study identified 18,917 (COM 16,191; MAP 2,726) closed fragility fractures during the study period. The sample mean age was 58 yrs and 74 yrs for COM and MAP, respectively. In the COM group, the proportions of fractures were: 22% vertebral fractures, 4% hip fractures, and 74% NHNV fractures. For the COM members, the difference in healthcare cost 12 months before and after fracture was: \$15,906 for vertebral fractures, \$30,176 for hip fractures and \$8,313 for NHNV fractures. In the MAP group, the proportions of fractures were: 38% vertebral fractures, 9% hip fractures, and 52% NHNV fractures. For the MAP members, the difference in healthcare costs 12 months before and after fracture was: \$7,439 for vertebral fractures, \$25,232 for hip fractures, and \$6,561 for NHNV fractures. In both populations, mean healthcare cost per fracture was highest for hip fracture but hip fracture was the least common type of fracture.

Conclusion: Healthcare costs associated with fragility fractures in men are high. Hip fracture had the highest cost per fracture (~\$30,000 in COM and ~\$25,000 in MAP) but a lower incidence of fracture compared to NHNV and vertebral fractures.

Disclosures: Nicole Yurgin, United Health Group, 3

This study received funding from: Amgen Inc

MO0442

A Phase 3 Study of the Efficacy and Safety of Denosumab in Men With Low Bone Mineral Density: Design of the ADAMO Trial. Eric Orwoll¹, Christence Stubbe Teglbjærg², Bente Langdahl³, Roland Chapurlat⁴, Edward Czerwinski⁵, David L Kendler⁶, Jean-Yves Reginster⁷, Alan Kivitz⁸, E. Michael Lewiecki⁹, Paul Miller¹⁰, Michael A Bolognese¹¹, Henry G Bone¹², Osten Ljunggren¹³, Bo Abrahamsen¹⁴, Yu-Ching Yang¹⁵, Andreas Grauer¹⁵, Cesar Libanati¹⁵, Jesse W Hall¹⁵, Steven Boonen¹⁶.

¹Oregon Health & Science University, USA, ²Centre for Clinical & Basic Research, Denmark, ³Aarhus University Hospital, Denmark, ⁴Hopital Edouard Herriot, France, ⁵Krakow Medical Center, Poland, ⁶University of British Columbia, Canada, ⁷University of Liege, Belgium, ⁸Altoona Center for Clinical Research, USA, ⁹New Mexico Clinical Research & Osteoporosis Center, USA, ¹⁰Colorado Center for Bone Research, USA, ¹¹Bethesda Health Research Center, USA, ¹²Michigan Bone & Mineral Clinic, USA, ¹³Uppsala University, Sweden, ¹⁴University of Southern Denmark & Gentofte Hospital, Denmark, ¹⁵Amgen Inc., USA, ¹⁶Leuven University, Belgium

Purpose: Denosumab increased bone mineral density (BMD) and reduced fractures in both postmenopausal women with osteoporosis (N=7808; Cummings, NEJM, 2009) and in men with prostate cancer on hormone ablation therapy (N=1468; Smith, NEJM, 2009). To evaluate the effects of denosumab in men with osteoporosis, a phase 3, 1-year, double-blind, placebo-controlled study in men with low BMD is currently in progress. Here, we describe the design and participant baseline characteristics of this fully-enrolled, ongoing study.

Methods: ADAMO is a multicenter, randomized, double-blind, placebo-controlled study to compare the efficacy and safety of Denosumab 60 mg every 6 months versus placebo in Males with Osteoporosis. All participants receive daily calcium and vitamin D supplementation throughout the study. Men between 30 to 85 years of age were eligible for enrollment if they had low BMD (T-score ≤ -2.0 and ≥ -3.5 at the lumbar spine or femoral neck) or had experienced a prior major osteoporotic fracture and had a T-score ≤ -1.0 and ≥ -3.5 . The primary efficacy endpoint is the percent change from baseline in lumbar spine BMD. Secondary efficacy endpoints include percent change from baseline in BMD of the total hip, femoral neck, trochanter, and 1/3 radius, and the percent change from baseline in serum C-telopeptide (CTX). Safety endpoints include incidence of adverse events. Following the 1-year, double-blind, placebo-controlled study period, all subjects will receive open-label denosumab for an additional year.

Results: The baseline characteristics of the men who were randomized in the ADAMO study (N=242) were similar to those of men enrolled in other completed male osteoporosis trials. Men in the ADAMO study had a mean age of 65.0 years, 94.2% were white, and 37.2% had a history of fracture (Table 1). Mean T-scores at the lumbar spine and femoral neck were -2.0 and -1.9, respectively. The study results are not available since the trial is ongoing and remains blinded.

Conclusions: In light of the BMD gains and associated fracture reductions reported in the pivotal denosumab fracture trials of postmenopausal women with osteoporosis and of men with prostate cancer on hormone ablation therapy, ADAMO is being performed to confirm the effects of denosumab on BMD and bone turnover markers in men with osteoporosis.

Table 1. Baseline Characteristics of Men Randomized in the ADAMO Study

Characteristic	All Participants N = 242
Age (years)	65.0 \pm 9.8
Age group (years) – %	
< 50	5.8
50 to 59	19.8
60 to 69	38.4
70 to 79	30.6
≥ 80	5.4
Ethnic group – %	
White	94.2
Other	5.8
T-score	
Lumbar spine	-2.0 \pm 1.1
Femoral neck	-1.9 \pm 0.6
Total hip	-1.4 \pm 0.6
History of fracture – %	
Any	37.2
Osteoporotic	22.7
Major osteoporotic*	13.2
Body mass index (kg/m ²)	25.8 \pm 3.6
Serum CTX (ng/mL)	0.41 \pm 0.19
Serum 25 (OH) Vitamin D (ng/mL)	30.15 \pm 9.99
Serum 25 (OH) Vitamin D deficient (< 20 ng/mL) – %	1.7
Total testosterone (ng/dL)	362 \pm 119
Low total testosterone (< 250 ng/dL) – %	14.9
Tobacco use – %	
Never	45.9
Formerly	38.4
Currently	15.7
Alcoholic beverages – %	
None	32.2
≤ 2 per day	58.3
≥ 3 per day	9.5

Data are mean \pm SD unless otherwise noted.

*Includes spine, tail bone, hip, forearm, wrist, and upper arm fractures, and excludes high trauma fractures.

Table 1

Disclosures: Eric Orwoll, Eli Lilly, Amgen, and Merck, 2; Eli Lilly, Merck, Amgen, and Wright Medical Technology, 5

This study received funding from: Amgen Inc.

MO0443

Association Between Polymorphisms In Wnt Antagonist Genes and Bone Response to Hormone Therapy In Postmenopausal Korean Women. Jung-Gu Kim¹, Hoon Kim², Dong Ock Lee³, Seung-Yup Ku³, Seok Hyun Kim³, Young Min Choi³. ¹Seoul National University Hospital, South Korea, ²Department of Obstetrics & Gynecology, Incheon Medical Center, South Korea, ³Department of Obstetrics & Gynecology, College of Medicine, Seoul National University, South Korea

Purpose: The purpose of this study was to investigate the association between polymorphisms in Wnt antagonist genes and bone response to hormone therapy (HT) in postmenopausal Korean women.

Methods: The dickkopf (Dkk) 1 c.318A>G, Dkk2 c.437G>A, Dkk3 c.1003A>G, secreted frizzled related proteins (sFRP) 3 c.970C>G, sFRP4 c.958C>A, and c.1019G>A and sFRP5 c.20G>C polymorphisms were analyzed by polymerase chain reaction-restriction fragment length polymorphism (PCR-REFLP), Taqman assay or direct DNA sequencing in 303 postmenopausal Korean women receiving sequential HT for 1 year. BMD at the lumbar spine and femoral neck was determined by dual energy X-ray absorptiometry.

Results: When a non-responder was defined as a woman who had lost more than 3% of BMD per year after HT, Dkk1 c.318A>G polymorphism and the haplotype genotype of sFRP4 c.958C>A and c.1019G>A polymorphisms among gene polymorphisms studied was associated with the risk of non-response of HT. The GG genotype of Dkk1 c.318A>G polymorphism showed a 2.38-times higher risk of non-response at the lumbar spine and/or femoral neck, as compared with the AA genotype. Among major haplotype genotypes composed of sFRP4 c.958C>A and c.1019G>A polymorphisms, the AA/AG haplotype genotype showed a negative percent changes in BMD at the femoral neck after 1 year of HT. The AG/CG haplotype genotype showed a 2.4 times higher risk of non-response at the lumbar spine and/or femoral neck, compared with the AA/AG haplotype genotype.

Conclusions: The Dkk1 c.318 A>G genotype and haplotype genotype of sFRP4 c.958C>A, and c.1019G>A polymorphisms may be associated with risk of non-response to HT in postmenopausal Korean women.

Funding: This study was supported by a grant (A080012) from the Korea Health technology R&D project, Ministry of Health, Welfare & Family Affairs, Republic of Korea

Disclosures: Jung-Gu Kim, None.

MO0444

Combined Effect of Calcitonin with Risedronate for Osteoporotic Patients with Chronic Back Pain. Michio Hongo^{*1}, Naohisa Miyakoshi², Yuji Kasukawa², Yoshinori Ishikawa³, Yoichi Shimada³. ¹Akita University School of Medicine, Japan, ²Akita University Graduate School of Medicine, Japan, ³Akita University, Japan

Introduction: Calcitonin has been described to reduce acute back pain following vertebral fractures. However, the effect of calcitonin for the osteoporotic patients with chronic back pain is still unclear. The purpose of this study was to evaluate the combined effect of calcitonin with risedronate for osteoporotic patients with chronic back pain. **Methods:** Thirty-seven women with chronic back pain diagnosed as postmenopausal osteoporosis by dual energy absorptiometry of lumbar spine and femoral neck were included in this study, after excluding women with fresh vertebral fractures or severe acute back pain within the last 6 months. The average age was 69 years. Patients were randomly allocated to risedronate group (risedronate alone, n=19) and combined group (risedronate and calcitonin, n=18). Risedronate (17.5 mg) was administered once per week for both groups, and calcitonin (20 unit) was injected for the combined group. Visual analogue scale (VAS) and back extensor strength was assessed at baseline, 1, 3, and 6 months follow up. Bone mineral density, number of fracture by plain lateral radiography, Roland-Morris questionnaire, Short-form-36 (SF-36), and Japanese osteoporosis quality of life score (JOQOL) were evaluated at baseline and 6-months. **Results:** VAS at final follow-up significantly decreased in the combined group compared with baseline (p=0.0008), 1 month (p=0.008), and 3 months (p=0.004). No change was found for VAS in the risedronate group. There was no change for RDQ score in both groups. There were significant improvement in the SF-36 scores for mental health status (p=0.013) and the JOQOL domains for back pain (p=0.04) and general health (p=0.01) in the combined group. Back extensor strength significantly increased in both groups. **Conclusion:** Calcitonin was reported to reduce acute back pain within one month. In contrast, chronic back pain evaluated with visual analogue scale significantly reduced after administration of calcitonin for three months. Risedronate itself has been shown to relief pain, although current results failed to detect the analgesic effect of risedronate alone. The current study suggests that the use of calcitonin combined with risedronate more than three months seems effective for reducing chronic back pain.

Disclosures: Michio Hongo, None.

MO0445

First Experiences with Denosumab in Patients with Painful Disabling Transient Regional Osteoporosis (TRO) of the Hip. Johann D. Ringe^{*}, Parvis Farahmand. Medizinische Klinik 4 (Rheumatology, Osteology) & West German Osteoporosis Center (WOC), Klinikum Leverkusen, University of Cologne, Germany

Introduction: Transient Regional Osteoporosis (TRO; Bone Marrow Edema Syndrome) is an increasingly diagnosed condition characterized by an acute onset of disabling bone pain, which typically occurs at the hips or other localisations of the lower extremities. The subcutaneous injection of Denosumab, a fully human monoclonal antibody to RANKL, is followed by an immediate steep decrease of bone turnover markers, i.e. a rapid and strong decrease of osteoclastic bone resorption. We therefore became interested in studying the efficacy of this new antiresorptive drug in cases with TRO at the hip.

Methods: We enrolled 3 patients with TRO of the hip for this 3-month, open label, case study to investigate the therapeutic efficacy of one subcutaneous injection of 60 mg Denosumab. Additionally all patients received a daily supplementation of 1200 mg calcium and 800 IU vitamin D. Diagnosis of the two men and one woman (mean age 38 years) was based on the typical history of acute pain in one hip, negative findings in x-ray and CT-imaging and finally MRI-finding of bone marrow edema in the affected area. Local pain at the affected hip was measured at onset, after 2 weeks, 1 month, and 3 months, respectively, by a visual analogue scale (VAS 1-10). Walking disability and impairment in quality of life were documented during follow-up. BMD at the lumbar spine and both femoral neck areas was measured at baseline and month 3.

Results: There was a rapid pain reduction from an initial average VAS-score of 9.0 to 3.0, 1.7, and 1.0 at 2 weeks, 1, and 3 months, respectively. The average mobility score (0-3) improved from 2.7 at onset to 0.3 at month 3. DXA measurement had revealed a systemic osteopenia before intervention (average lumbar spine T-Score -2.0) and lower values at the affected hip vs. the unaffected side (average T-Score values -1.7 vs. -0.9). After three months mean increases of +2.3% at the lumbar spine, +7.9% at the affected hip and +0.8 at the unaffected hip were documented. MRI controls at month 3 showed in all cases a significant amelioration. There were no AEs, quality of life increased significantly.

Conclusion: We found that a first injection of Denosumab in patients with TRO of the hip leads to rapid pain relief, improvement of mobility and regression of bone marrow edema. After only 3 months there were highly significant increases in BMD at the involved hip together with a moderate improvement of systemic osteopenia.

Disclosures: Johann D. Ringe, None.

MO0446

Good Vibrations: A Short Term Pilot Study of Low Magnitude Vibration Therapy in Patients with Thalassemia. Catherine Garipey^{*1}, Dru Haines, PNP¹, Ashutosh Lal, MD¹, Ellen Fung². ¹Children's Hospital & Research Center Oakland, USA, ²Children's Hospital & Research Center, Oakland, USA

Approximately 70% of adults with thalassemia (Thal) have low bone mass which can lead to fracture and decreased quality of life. The most effective way to treat low bone mass is through prevention, by building strong, dense bones in childhood. Weight bearing physical activity strengthens bone by increasing mineralization as well as bone size. However, adherence to regular exercise can be difficult for patients with Thal due to low hemoglobin and energy levels or pre-existing cardiomyopathies. Recent advances in the field have shown that low magnitude mechanical stimulation or "vibration therapy", can also strengthen bone. This simple therapy can be conducted in the home without increasing cardiac stress.

A pilot and feasibility trial was conducted to evaluate "vibration therapy" as an anabolic stimulus to bone in 20 patients with Thal (11 Male, 22.1 10.7, range 9-45 yrs). Subjects were asked to stand on the vibrating platform (30 Hz, 0.3g) for 20 min/day, 6 days per week for 6 months. We measured bone parameters by DXA, pQCT and serum markers of bone turnover at baseline, 6 and 12 months post intervention. 13 subjects have completed the protocol to date. Baseline spine and hip Z-scores are -2.41 and -1.708 respectively. Baseline 25OH vitamin D was 2911 ng/mL. As hypothesized, adherence to the intervention is better in the first 3 months (7231%) compared to the second 3 months (5034%, p=0.019). Average length of time on the platform also decreased from 13 to 9 min/day (p=0.003). Two subjects dropped, one adult due to back pain after 1 month and one adolescent due to dizziness after 3 weeks. Thus far, the adult participants are more likely to be adherent to the protocol. Using intention to treat analysis, no differences in aBMD were observed at any site. However, for the most adherent adult participants (>75%), a significant increase in whole body BMC was observed (p=0.02) and a trend towards an increase in hip aBMD (p=0.08). Results for bone markers are pending.

These preliminary findings suggest that vibration therapy may be an effective intervention in subjects with Thal. Similar to previous studies, the intervention was most effective at increasing BMD in those who were adherent to the protocol. Future research should expand upon this study with a larger sample size and include ways to improve adherence in patients burdened by chronic medical conditions.

Disclosures: Catherine Garipey, None.

MO0447

Lycopene Does Not Alter Bone Turnover In a Healthy Population of Men and Women - An Intervention Study. Claire Macdonald^{*1}, David Reid¹, Frank Thies¹, Helen Macdonald². ¹University of Aberdeen, United Kingdom, ²University of Aberdeen Bone & Musculoskeletal Research Programme, United Kingdom

Lycopene, mainly originating from tomatoes, has been associated with lower incidence of osteoporosis and high dietary lycopene intake has been reported to be protective against fracture risk in cross sectional and longitudinal studies. A pilot intervention study showed that high serum lycopene was associated with decreased bone resorption in a population of postmenopausal women. The aim of this investigation was to determine the effects of lycopene intake on percentage change of bone turnover markers amino-terminal procollagen propeptides of type 1 collagen (PINP) and C-terminal telopeptide of type 1 collagen (CTX).

A randomized controlled trial (RCT) was conducted in a healthy population of men and women (N=239) aged 29-69y (mean age [SD] 51.1 [6.8] years). Participants were randomly assigned to 3 groups: 1. high lycopene/tomato diet (minimum 10mg/day), 2. 10mg lycopene supplement and 3. low lycopene/tomato diet. The serum bone formation marker PINP and plasma bone resorption marker bone CTx were measured at baseline (week 4) and at 12 weeks for each of the participants.

Two hundred and twenty seven participants completed the final visit (95%). Serum and plasma was available for 221 participants. One extreme outlier was removed leaving 76 in group 1, 66 in group 2, and 78 in group 3, for analysis.

One-way ANOVA showed no significant difference in percent change in bone turnover between groups (mean [SD]): plasma CTx: +7.7% [27.2%], +6.8% [23.9%] and +5.4% [26.4%] and serum PINP: -1.0% [24.3%], +4.26% [22.0%] and +2.8% [15.4%] in groups 1, 2 and 3 respectively.

These data suggest that an eight-week lycopene supplementation or a diet high in lycopene does not alter bone turnover in a healthy population of men and women. Future research is required to determine whether lycopene effects bone turnover longer term or attenuates bone resorption in groups at high risk of osteoporosis.

Disclosures: Claire Macdonald, None.

MO0448

Oxidative Stress and the Risk of Osteoporosis: the Role of Dietary Polyphenols and Nutritional Supplements in Postmenopausal Women.

Nancy Kang^{*1}, Venketeshwer Rao², Katrine De Asis², Loren Chan³, Leticia Rao¹. ¹University of Toronto, St. Michael's Hospital, Canada, ²University of Toronto, Canada, ³St. Michael's Hospital, Canada

Purpose: Oxidative stress has been shown to be associated with the development of osteoporosis, and antioxidants can be beneficial in counteracting this damaging effect. There is a renewed interest in the use of nutritional supplements which are rich in antioxidants as alternative or complimentary strategies for the prevention and management of osteoporosis because of the reported undesirable side effects of Hormone Replacement Therapy (HRT) and other approved drugs. Nutritional supplements such as greens+TM, a blend of several botanical products, has recently been shown to contain a number of water-soluble antioxidant polyphenols. Another nutritional supplement, greens+bone-builderTM, contains the same formulation as greens+TM, but includes additional antioxidants, vitamins, minerals, trace minerals, and amino acids, all of which have been individually shown to be beneficial to bone. Our laboratory showed that in vitro, greens + and greens+bone-builderTM stimulated bone formation by human osteoblasts. Based on these results, the purpose of our study was to initiate clinical studies to test our hypothesis that greens+bone builder may be effective in reducing oxidative stress, thus potentially reducing the risk of osteoporosis in postmenopausal women.

Methods: Sixty postmenopausal women, 50-60 years old, were recruited for a ten-week clinical trial with the following study design: Week 1, participants recorded their baseline food intake; Week two ('washout' period), they refrained from consuming polyphenol-rich foods and supplements and Weeks 3 to 10, they were randomized to either greens+ bone builderTM (N = 30) or placebo (N = 30), during which they took to take 1 scoop (equivalent of ¼ cup) of their assigned treatment daily. Blood samples collected at week 1, 2, 6, and 10 of supplementation were processed and serum samples assayed for total antioxidant capacity (TAC), lipid, and protein oxidation.

Results: Statistical analysis using two-way ANOVA and t-test showed that greens +bone-builderTM significantly increased total antioxidant capacity (p<0.05) compared to placebo after 10 weeks of treatment. There were no significant differences in lipid and protein oxidation between the placebo and supplemented groups.

Conclusion: Our findings suggest that the daily supplementation of greens+bone-builderTM may be important in reducing the risk of osteoporosis through its antioxidant potential.

Disclosures: Nancy Kang, None.

This study received funding from: Industrial company

MO0449

The Impact of Vitamin K Therapy on Bone Metabolic Markers in Severe Motor and Intellectual Disabilities.

Akiko Kuwabara^{*1}, Akiko Nagae², Naoko Tsugawa³, Mari Kitagawa², Kunihiro Tozawa⁴, Hiroaki Kohno⁵, Masakazu Miura⁶, Toshio Okano³, Masao Kumode², Kiyoshi Tanaka⁷. ¹Osaka Shoin Women's University, Japan, ²Biwako Gakuen Kusatsu Medical & Welfare Center, Japan, ³Kobe Pharmaceutical University, Japan, ⁴EIDIA Co. Ltd., Japan, ⁵Orthopaedics, Japan, ⁶Hokuriku University, Japan, ⁷Kyoto Women's University, Japan

Purpose: Based on our recent finding that vitamin K was deficient both in the liver and bone in subjects with severe motor and intellectual disabilities (SMID) (ASBMR 32nd Annual Meeting), vitamin K therapy to these subjects was studied. Previous studies on vitamin K therapy in subjects with SMID have been scarce, and had limited scope. For example, vitamin K₂ was the only analog employed, and biomarkers reflecting vitamin K status were seldom studied. Then we have aimed to study the effects of vitamin K therapy on biomarkers for vitamin K insufficiency; protein induced by vitamin K absence (PIVKA-II), undercarboxylated osteocalcin (ucOC), and ucOC/OC ratio. PIVKA-II and ucOC are indices for hepatic and skeletal vitamin K insufficiency, respectively. The alteration of bone turnover markers was also studied.

Methods: Forty-one subjects with SMID were assigned to two study groups by their nutritional feeding routes. K₁ group consisted of 24 subjects under enteral feeding. Vitamin K₁ was added in enteral nutrition as a form of RacoTM, ranging from 55 to 219 µg/day (Median; 175 µg/day), with its dose being determined to meet each subject's energy requirement. K₂ group consisted of 17 subjects with oral feeding. They were treated by 15 mg/day of menaquinone-7 (GlakayTM). Study duration was for 3 months. Biomarkers of vitamin K insufficiency and bone turnover markers were measured at baseline and 1-, 3-month after the start of therapy.

Results: Median vitamin K intake in K₂ group was 115.0 µg/day. In K₁ group, it was 66.5 µg/day at baseline and 193.6 µg/day after intervention. At baseline, serum PIVKA-II, ucOC and ucOC/OC ratio were significantly higher in K₁ group than in K₂ group. After 3 months treatment, while K₂ therapy significantly decreased all biomarkers of vitamin K insufficiency, only serum concentrations of PIVKA-II and ucOC/OC ratio significantly decreased in K₁. Serum BAP significantly increased in both therapies. Serum TRACP-5b responded differently to each therapy; significant increase in K₁ therapy, and significant decrease in K₂. Logistic regression analyses revealed that K₂ therapy was a significant factor for changing bone turnover markers beyond minimal significant changes.

Conclusions: The ucOC/OC ratio sensitively responded to K₁ therapy. All biomarkers were sensitive to K₂ therapy. K₂ therapy was more potent than K₁ in changing bone turnover markers such as BAP and TRACP-5b even when adjusted for baseline level of each marker.

Disclosures: Akiko Kuwabara, None.

MO0450

The Potential Effect of Calcitonin in Osteoporotic Patients with Diabetic Peripheral Neuropathy.

Shen Qu^{*1}, Ran Cui², Xiaoyun Cheng³, Peng Yang⁴, Hui Sheng⁵. ¹Tongji University School of Medicine, Peoples Republic of China, ²Tenth People's Hospital of Tongji University, Peoples Republic of China, ³Department of Endocrinology, China, , ⁵Shanghai, Fudan University, Peoples Republic of China

To investigate the effect of calcitonin on osteoporotic patients with painful diabetic neuropathy. Numerous studies report that diabetes is a risk factor for osteoporosis. Osteoporotic patients complicated with diabetes need concurrent treatment of osteoporosis and diabetes. The bone promotion effect and analgesic effect of calcitonin for osteoporotic patients are well known, but this study examines not only the effectiveness of calcitonin for osteoporosis treatment, but also for diabetic neuropathy treatment.

Thirty-nine patients with type 2 diabetes and diabetic neuropathy were recruited for this study. Basic treatment for these patients was comprised of hypoglycemic agents, antihypertensive drugs, and antilepileptic agents. The patients were randomly divided into two groups. Group 1 (G1) patients were given calcitonin injection (20 units, twice weekly) while Group 2 (G2) patients acted as the control. Pain was assessed before start of treatment and then at 2, 4, 8, and 12 weeks of treatment using a visual analogue scale (VAS) and the Wong-Baker Face Scale (FS) method. The patients' subjective assessment of treatment was recorded as "not effective," "effective," or "very effective." Repeated-measures data analysis and a nonparametric test were used to analyze the VAS, FS, and the subjective treatment assessment scores.

Both VAS and FS scores showed that pain was significantly alleviated in G1 (P=0.014 and P=0.014, respectively). With time, the discrepancy between G1 and G2 was more remarkable (P=0.000 and P=0.000, respectively). Patients' subjective assessment of treatment in G1 was not significant at 2 weeks (P=0.760), but it was significant at 4 weeks (P=0.004), 8 weeks (P=0.000), and 12 weeks (P=0.007), which is consistent with the VAS and FS scores.

Calcitonin significantly alleviated pain in osteoporotic patients with painful diabetic neuropathy.

Disclosures: Shen Qu, None.

This study received funding from: Shanghai PJ1408400

MO0451

A Novel Technique for Cement Augmentation of Pedicle Screws Reduces Cement Leakage Rates. A Prospective, Controlled, Clinical Trial in Osteoporotic Bone.

Thomas Blatter^{*}. Orthopaedische Fachklinik Schwarzbach, Deu

Introduction

Cement augmentation techniques have been developed to increase purchase of pedicle screws in osteoporotic bone. Different augmentation techniques are being used based on screw types and surgical methods. For solid screws, vertebral bodies can be pre-filled with cement in a vertebroplasty technique before screws are inserted. In a modification, pre-tapped voids can be filled with cement before screw insertion. As an alternative, fenestrated screws have been developed for in situ injection of cement through the screw itself. Extravertebral, epidural, and endovascular leakage of cement, however, remains a problem in either technique. To reduce leakage rates, a novel augmentation technique was developed.

Methods

Inclusion criteria: fracture type A3 or higher; t-score ? 2.5. **Exclusion criteria:** non-traumatic fractures. Fenestrated screws measuring 6.5mm in diameter were used (CD Horizon Legacy FNS, Medtronic). In the trial group (TG), screw beds were pre-tapped. The tap used has a regular diameter of 5.5mm and can be expanded to 8.0mm after pedicle passage. For the vertebral body, this results in an overtapping of 1.5mm for the screw bed in comparison to the screw itself. After screw insertion, cement augmentation with 1.5cc of PMMA (KyphXHV-RTM, Medtronic) was performed. Leakage rates were evaluated with post op CT scans. In the control group (CG), the screw bed was probed, but not tapped. FU time was 24 months.

Results

In TG, 20 patients with 96 augmented pedicle screws were included. Leakage rate was 8/96 (8.3%). CG consisted of 52 patients with 208 screws. Leakage rate was 41/208 (19.7%). This difference is statistically significant (p<0.005). At 2 years FU, 17/18 patients in TG showed no signs of implant loosening. 1/18 patient suffered from secondary loss of correction with screw cut out. For CG, there were 2/47 cases with implant loosening (p>0.05).

Conclusion

Use of the novel technique described here results in a significant reduction of cement leakage rates if compared to the control group. We found no difference,

however, for the rate of secondary implant loosening. Obviously, the cement leaving the screw is being distributed reliably within the void created around the screw shaft, rather than being directed into unwanted regions of less resistance. On the other hand, implant purchase is not being compromised by this technique.

Disclosures: Thomas Blattert, AOSpine, DePuy, Medtronic, Synthes, 5

MO0452

Methods to Simplify Recruiting for Pragmatic Clinical Trials (PCTs) in Osteoporosis in the Community: iPad vs. Interactive Voice Response (IVRS) Systems. Amy Mudano^{*1}, Lisa Gary¹, Mary Melton¹, Amy Warriner², T. Michael Harrington¹, Meredith Kilgore³, Penelope Jester¹, Nicole Wright¹, Jeffrey Curtis¹, Cora Lewis¹, Elizabeth Delzell¹, Kenneth Saag¹. ¹University of Alabama At Birmingham, USA, ²UAB, USA, ³University of Alabama At Birmingham School of Public Health, USA

Purpose: Osteoporosis PCTs require large numbers of patients and efficient enrollment strategies are needed to conduct such trials in busy physician practices. To facilitate simplified subject recruitment, we developed two screening and enrollment tools using 1) an iPad tablet computer with internet access and 2) an IVRS telephone system accessed via cell phone, and we evaluated patient and physician preference for these tools.

Methods: We recruited community physician offices through the local Practice-Based Research Network. A series of 8 screening questions were developed to determine initial eligibility for a mock PCT of osteoporosis therapeutics. Offices were given 5 days to use the iPad and IVRS technologies for identifying potential study participants. Office staff offered all women age 65 years and older study participation and randomly assigned them to either the iPad or IVRS. Each patient completed the screening questions and a brief survey on preferences for the technologies using a 5-point Likert scale from "strongly agree" to "strongly disagree". Follow-up debriefings were conducted with the office staff to determine the effects of iPad vs. IVRS recruitment on office workflow.

Results:

The iPad and IVRS technology was tested in 7 physician offices. A total of 113 patients (82% of the 138 eligible) participated. All 60 women randomized to the iPad completed the screening questions. Of 53 women randomized to IVRS, only 40 completed all screening questions. The women who tested the iPad were slightly older (average age 75.5 + 7.4) compared to the women who tested the IVRS (average age 73.0 + 6.6) ($p=0.07$). Compared to IVRS, patients who tested the iPad technology found it easier to use and understand and less time-consuming. They were more likely to agree to participate in an osteoporosis clinical trial and would spend extra time in their physician's office to enroll. Office staff reported that recruitment of patients using these technologies was not burdensome and did not interrupt clinic flow. Approximately 30% of patients screened would be potentially eligible to participate in an osteoporosis PCT based on the inclusion criteria.

Conclusion:

Compared to the IVRS phone system, patients preferred use of the iPad technology to complete a short screening survey to determine initial eligibility for an osteoporosis PCT. This process did not put an undue burden on the physician practice and generated a sizable yield of potential study participants.

Disclosures: Amy Mudano, None.

MO0453

How Can We Improve Bone Health in the Long-term Care Setting? Lessons from the ViDOS study. Courtney Kennedy^{*1}, Alexandra Papaioannou², George Ioannidis¹, Lora Giangregorio³, Sharon Marr¹, Suzanne Morin⁴, Lehana Thabane¹, Robert Josse⁵, Richard Crilly⁶, Laura Pickard¹, Susanne King¹, Mary-Lou van der Horst¹, Ruth McCallum¹, Glenda Campbell⁷, Jackie Stroud⁷, Lisa Dolovich¹, Anna Sawka⁸, Lynne Lohfeld¹, Jonathan Adachi⁹. ¹McMaster University, Canada, ²Hamilton Health Sciences, Canada, ³University of Waterloo, Canada, ⁴McGill University Health Centre, Canada, ⁵St. Michael's Hospital, University of Toronto, Canada, ⁶University of Western Ontario, Canada, ⁷Medical Pharmacies Group Limited, Canada, ⁸Toronto General Hospital, Canada, ⁹St. Joseph's Hospital, Canada

The ViDOS study is a Knowledge Translation (KT) Randomized Controlled Trial currently underway in 40 Long-term Care (LTC) homes ($n=20$ intervention, $n=20$ control) across Ontario, Canada. The aim is to implement and evaluate a multi-faceted KT intervention, targeted at interprofessional teams, to increase the uptake of osteoporosis (OP) best practices in the LTC setting using a quality improvement process. Outcomes include prescribing of vitamin D (primary), calcium and pharmacologic therapies; falls and fractures; and organizational-level process/policy changes. The intervention homes take part in three problem based sessions led by an Expert Opinion Leader conducted approximately 6-months apart. The target audience is the Professional Advisory Committee (PAC), an existent committee who meets

quarterly and includes the medical director, director of care, administrator, pharmacist, dietician, and other rehabilitation, nursing, and physician representatives. "Action Planning" for quality improvement is a key component of our multi-faceted study. PAC teams discuss and complete a work-sheet at each session to address barriers and facilitators and identify strategies for improving bone health including specific action items for team members. Ideas generated from initial sessions were used to help guide discussion in subsequent sessions. Currently, 8 intervention homes have completed the action planning process. Common barriers identified include: limited medical history on OP/fractures; lack of assessment of height annually; OP diagnoses often not recorded in electronic system; OP/fractures (and related prescribing) not a specific focus in care plans, falls programs, quarterly reviews; standard admission process does not assess need for vitamin D and pharmacologic therapies; incorrect dispensing of bisphosphonates; cost of vitamin D; lack of information/resources prior to the ViDOS study. PAC teams proposed and/or implemented several strategies for bone health including: incorporating OP/fracture history on admission processes and quarterly reviews; standard admission orders for vitamin D and OP therapies; dietitian review of calcium intakes; quarterly pharmacist review including point of care tools; education of resident/family councils (e.g. DVD on bone health protection). The ViDOS intervention has provided a forum for interprofessional teams to better coordinate efforts and to develop action-oriented policies and procedures that support bone health.

Disclosures: Courtney Kennedy, None.

This study received funding from: sanofi-aventis; Warner Chilcott

MO0454

Serum 25-hydroxyvitamin D in Rural and Urban Postmenopausal Women. Irina Haller^{*1}, Diane Krueger², Jean A Engelke², Neil Binkley³. ¹Essentia Institute of Rural Health, USA, ²University of Wisconsin, Madison, USA, ³University of Wisconsin, USA

Vitamin D status in rural, urban and American Indian (AI) postmenopausal women was compared using data from two phases of a randomized control trial of vitamin D fortified food: an ongoing study focusing on the effect of ethnicity and an earlier phase focused on the effect of age. To date, 41 white and 34 AI women from rural communities in the upper Midwest have been screened for study participation. Eligible women were randomly assigned in 1:1 ratio within each ethnicity cohort to receive a low calorie chocolate disk fortified with 2,500 IU of vitamin D₃ or placebo daily for 4 months. Study activities in the AI cohort are ongoing. Thirty-two rural white women finished the study in January 2011. Additional data included screening results from 34 comparably aged white urban women who completed study by August 2009. AI women were slightly younger than rural and urban women with mean (SE) age of 57.4 (1.1), 62.3 (1.1) and 60.6 (0.6) years, respectively. There were no differences in albumin, creatinine, ALT, or PO₄ between the three groups. Serum calcium was higher ($p<0.01$) in the urban [9.6(0.1) mg/dL] than rural [9.3 (0.1) mg/dL] or AI group [9.3 (0.1) mg/dL]. Mean screening serum 25(OH)D in the AI group [25.3 (1.8) ng/mL] was lower ($p<0.01$) than in rural [34.5 (1.9) ng/mL] or urban group [34.2 (2.2) ng/mL]. Moreover, 37% of rural, 44% of urban and 65% of AI women had low vitamin D status (defined as a 25 (OH)D concentration < 30 ng/mL). Applying a 20 ng/mL cut point, 7% of rural, 12% of urban, and 38% of AI women would be classified as low. On average, among rural white women 25(OH)D increased from 31.2 (1.7) to 48.4 (2.9) ng/mL in the vitamin D group over the 4 months of study, while 25(OH)D was unchanged in the placebo group. There were no changes in serum calcium and urine calcium/creatinine ratio with 4 months of vitamin D supplementation. These preliminary data support previously reported outcomes on safety and efficacy of food fortified with higher dose of vitamin D. Results regarding the effects of ethnicity and rural/urban location on response to vitamin D supplementation by food will be available upon completion of the study in the AI cohort in August 2011. Consistent with our pilot data, AI women had lower vitamin D status compared to white women from rural and urban settings. Further examination of the underlying causes for these differences is warranted.

Disclosures: Irina Haller, None.

MO0455

Solitary Calcium Supplementation in Alendronate Treated Postmenopausal Women with Low Bone Mass Does Not Prevent Secondary Hyperparathyroidism Sufficiently. Oliver Bock^{*1}, Hendrikje Borst¹, Heinz-Jürgen Roth², Martin Runge³, Ze'ev Mazor⁴, Erich Schacht⁵, Peter Martus⁶, Dieter Felsenberg¹. ¹Charité - Campus Benjamin Franklin, Centre for Muscle & Bone Research, Germany, ²Labor Dr. Limbach und Kollegen, Medizinisches Versorgungszentrum, Germany, ³Aerph Kliniken Esslingen-Kennenburg, Germany, ⁴Teva Pharmaceuticals Industries Global Products Division, Israel, ⁵Pharma Consulting, Switzerland, ⁶Charité - Campus Benjamin Franklin, Institute for Biometrics & Clinical Epidemiology, Germany

Objectives: To examine the effect of solitary calcium supplementation on the risk of developing secondary hyperparathyroidism (sHPT) in postmenopausal, alendronate treated women with reduced bone mass and increased risk to fall.

Patients and Methods: This is a post-hoc analysis from the ALFA study, including a total of 279 postmenopausal women (mean age 73.74.7 years), randomized 1:1 into a

placebo-controlled, double-blind study of 3 years (ALFA study) with two treatment arms: daily oral alfacalcidol 1µg or placebo. All patients received alendronate 70mg once weekly and calcium 500mg daily. Biochemical markers of bone turnover, iPTH, 25OH-vitamin D, 1,25(OH)₂-vitamin D and calcium were measured semi-annually (during the first year) and annually (during years 2 and 3).

Results: None of the patients had elevated PTH serum levels before randomization (in accordance with the exclusion criteria of the study). 199 patients completed the study, 193 had all laboratory measurements available at the end of the study. Out of these patients, 36.8% (35/95) of the completers in the control group, but only 6.1% (6/98) in the verum group showed PTH serum levels above 65 ng/l ($p < 0.05$). Serum levels of calcium, 25OH-vitamin D and 1,25(OH)₂-vitamin D did not differ significantly between patients with or without hyperparathyroidism in the control group. Serum calcium levels were, in general, relatively low in both treatment arms with a mean of 2.30(0.09) and 2.32(0.10) mmol/l, respectively. 91.4% (32/35) of cases with elevated PTH in the alendronate/calcium group showed a typical biochemical pattern for sHPT. Contrariwise, three other patients with elevated PTH in this group showed slightly increased serum calcium (2.53, 2.59 and 2.66 mmol/l). This might be considered as an evidence for mild primary hyperparathyroidism as a possible result of autonomous PTH secretion by hyperplastic parathyroid glands in original sHPT.

Conclusions: The results from this post-hoc analysis showed sHPT in a considerable proportion of more than one third in alendronate treated patients who got additional calcium supplementation only. The additional use of alfacalcidol 1 µg daily in the verum arm of this study, however, minimized significantly the risk for sHPT in alendronate/calcium treated patients.

Disclosures: Oliver Bock, Teva Deutschland GmbH, Germany, 8

This study received funding from: Teva Pharmaceutical Industries, Israel; Chugai Pharmaceutical Co.Ltd., Japan

MO0456

The Relationship Between Serum Vitamin D Levels and Bone Histomorphometry In Elderly Patients with Hip Fracture. Abbas Ismail^{*1}, Anthony Freemont², Nicky Makepeace¹, Stockport Bone Group¹. ¹Stockport NHS Trust, United Kingdom, ²University of Manchester, United Kingdom

Background

Vitamin D deficiency is common in elderly people, studies suggesting up to 65% of patients with hip fracture have severe vitamin D deficiency (1). However, routine bone biochemistry is frequently normal despite low or even undetectable serum Vitamin D levels (2). The clinical significance of low serum Vitamin D levels therefore remains uncertain.

Aims

To assess the relationship between serum vitamin D concentration and bone biochemistry with static bone histomorphometry parameters in elderly patients with hip fracture.

Methods

Hip fracture patients were identified prospectively from the Orthopaedic wards in Stockport, UK between July 2009 and July 2010. After obtaining consent, blood samples were taken for serum vitamin D and bone biochemistry prior to surgery. Parathyroid hormone levels were not measured. Serum 25-hydroxy vitamin D levels were measured by mass spectrometry. At the time of surgery for the hip fracture the operating orthopaedic surgeon retained either the femoral head in the case of subcapital fracture or took a small bone biopsy in the case of trochanteric hip fracture. The bone samples underwent histomorphometric analysis at the University of Manchester. Dynamic histomorphometry was not possible because of the clinical setting in which the bone samples were obtained.

Results

18 hip fracture patients were included in the analysis, 12 female and 6 male, mean age 84.2 years (range 70-92 years). There were 15 subcapital fractures and 3 trochanteric hip fractures. 15 patients had low serum Vit D levels of less than 20ng/mL and 5 patients had very low levels of less than 12ng/mL (normal level > 30ng/mL). In all 18 patients, bone histomorphometry showed evidence of osteoporosis with the mean age and sex adjusted Z score for trabecular bone volume being -2.8 and mean Z score compared to peak bone mass being -5.6. However, there was no evidence of mineralization defect or osteomalacia in any of the bone samples. Serum calcium and alkaline phosphatase levels were within normal limits.

Conclusion

In this preliminary study of elderly hip fracture patients, low or very low serum vitamin D levels were not associated with either biochemical nor histological evidence of osteomalacia although osteoporosis was universal. However, treatment with vitamin D may still be of benefit to help reduce falls by improving muscle strength.

1. Segal E et al. Adherence to vitamin D supplementation in elderly patients after hip fracture. J American Ger Soc, 2004;52(3) 474

2. Singh SK et al. Does routine blood bone biochemistry predict vitamin D insufficiency in elderly patients with low velocity fractures? J Orthopaedic Surgery 2004;12(1):31-34

Disclosures: Abbas Ismail, None.

This study received funding from: Shire Pharmaceuticals

MO0457

Effects of Adenosine Triphosphate (ATP) on Bone and Fat Metabolism. Solveig Petersen^{*}, Susanne Syberg, Peter Schwarz, Niklas Jorgensen. Copenhagen University Hospital Glostrup, Denmark

Adenosine triphosphate (ATP) is a molecule of life. Inside the cell it provides energy and participates in other essential processes while outside of the cell it acts as a short-range signal between cells. Extracellular ATP signalling, also known as purinergic signalling, includes a range of P2 receptors, that are important in the regulation of bone turnover, but ATP might also be implicated in fat/energy metabolism. The aim of this study was therefore to investigate the in vivo effects of ATP treatment on bone and fat metabolism in mice.

Female mice were ovariectomized (OVX) or sham operated (SHAM) at the age of 16 weeks. Twelve mice were randomly allocated to each treatment group after 4 weeks. Vehicle (VEH), 40 mg/kg PTH (PTH), 33 mg/kg ATP (ATP) or a combination of ATP and PTH (ATP/PTH) were administered twice daily for 28 days. After sacrifice, bone mineral density (BMD) and body composition (fat % and % lean mass) were assessed on a PIXImus DXA scanner. Serum and bones were collected for analysis of bone markers and fat/energy metabolism including blood glucose (BG).

BMD levels decreased upon OVX from (meanSEM) 0.0505 (0.0008) g/cm² to 0.0485 (0.0010) g/cm². By treating OVX mice with ATP alone BMD was only slightly changed to 0.0480(0.0008) g/cm². PTH alone significantly increased the BMD to 0.0519(0.0012) g/cm². As expected, body weight of the animals increased upon OVX in all treatment groups, but no differences were detected between VEH and the different treatments. More interestingly, fat percent was significantly different between groups ($p < 0.01$). OVX increased fat % (VEH: 17.80.4% vs. SHAM: 15.70.4%), while ATP treatment prevented the OVX-induced increase either or in combination with PTH (ATP: 16.60.5%; ATP/PTH: 15.80.5%). PTH alone did not alter fat %. However, when looking at BG, major differences between groups were detected ($p < 0.001$). Firstly, OVX did not change BG compared to SHAM (VEH: 3.50.1 mM vs. SHAM: 3.60.2 mM), and neither did PTH treatment (PTH: 3.90.2 mM). In contrast, ATP administered alone (ATP: 7.60.5 mM) or in combination with PTH (ATP/PTH: 7.20.5 mM) significantly increased BG levels in the animals.

In conclusion, OVX induced increased body weight and fat % and reduced BMD in the animals. Furthermore, treatment with the nucleotide ATP, induced profound changes in BG and counteracted the OVX-induced increase in fat %. Thus, ATP might therefore act diabetogenic. The exact mechanism is still undetermined.

Disclosures: Solveig Petersen, None.

MO0458

Enhanced Peri-Implant Bone Formation and Fixation by Sclerostin Antibody in a Rat Ovariectomy Model. Amarjit Viridi^{*1}, Kotaro Sena¹, Min Liu², Hua Zhu Ke³, D. Rick Sumner¹. ¹Rush University Medical Center, USA, ²Amgen, USA, ³Amgen, Inc., USA

Effective fixation of orthopedic implants is dependent on the quantity and quality of de novo peri-implant bone formation. This becomes an issue when the host bone stock at the site is depleted as seen in osteoporosis. Sclerostin is a negative regulator of bone formation and treatment of intact and ovariectomized rats with a sclerostin-neutralizing monoclonal antibody has shown marked increase in bone formation. This study sought to determine if sclerostin antibody (Scl-AbIII) treatment enhances peri-implant bone formation and fixation in an ovariectomy rat model (ovx).

Ovx or sham-ovx surgery was performed on 4.5-mo old rats. After 6.5 months, titanium implants were placed bilaterally in the distal femurs. Animals receiving no implants were used as baseline control to reveal bone loss due to ovx. The rats with implants were randomly assigned to receive sclerostin antibody treatment (Scl AbIII [Amgen Inc. and UCB Inc.]; 25mg/kg; twice weekly; subQ) or saline as control. After 4, 8, or 12 weeks (n=12 each), bone surrounding the implant was assessed by micro computed tomography (µCT) while mechanical pull-out testing revealed strength of fixation, stiffness and energy to failure.

µCT confirmed severe osteopenia in ovx with lower BV/TV (-77%), Tb.N (-69%) and Tb.Th (-16%), and higher Tb.Sp (258%, all $p < 0.001$). Scl-AbIII treatment in the sham-ovx group led to increased BV/TV (50 to 106%) and Tb.Th (44 to 131%) at all time points ($p < 0.001$), decreased Tb.Sp (-16 to -26%) at 4 and 8 weeks ($p < 0.05$), but no change in Tb.N. Strength of fixation and energy to failure were increased at 8 (33%) and 12 weeks (97%, $p < 0.01$) and stiffness was increased at 4 weeks (87%, $p < 0.05$). Scl AbIII treatment in the ovx group elevated BV/TV (97 to 177%) and Tb.Th (46% to 74%) at 4 and 12 weeks ($p < 0.05$) as well as strength of fixation (100%) at 12 weeks ($p < 0.05$), stiffness (126%) at 4 weeks ($p < 0.05$) and energy to failure at 8 and 12 weeks (143 to 215%, $p < 0.05$). In general, positive benefits of Scl AbIII treatment in the ovx were delayed compared to the sham-ovx presumably because of the severity of ovx-induced osteopenia. More specifically, the trabecular architecture and mechanical fixation values following Scl AbIII treatment for 12 weeks in the ovx rats were similar in magnitude to those of the 4 week sham-ovx rats. The findings of this study support the utility of inhibiting sclerostin to achieve improved implant fixation in individuals with osteopenia.

Disclosures: Amarjit Viridi, Amgen Inc., 2

This study received funding from: Amgen Inc.

MO0459

Growth Hormone Partly Counteracts Immobilisation-induced Bone and Muscle Loss. Marie-Claire Grubbe¹, Jesper Thomsen², Annemarie Bruel^{1,2}.¹Aarhus University, Denmark, ²University of Aarhus, Denmark

Growth hormone (GH) increase bone mass by stimulating periosteal bone formation through activation of osteoblasts. Furthermore, GH has an anabolic effect on skeletal muscles. The aim of the study was to investigate whether treatment with GH could attenuate the loss of bone and muscle mass during immobilisation in a rat model.

Immobilisation was obtained by injecting 4 IU Botox (BTX) into the muscles of the right hind limb, thereby inducing a loss of bone and muscle. Sixty female Wistar rats, 3-months-old, were divided into the following groups: Baseline, control, BTX, BTX+GH, and control+GH (n=12 in each group). GH was given as s.c. injections at a dosage of 5 mg/kg/d divided into two daily doses. The experiment lasted for 4 weeks. The rectus femoris muscles were weighed and the mean muscle cell diameter was estimated using stereology. The BMC of the entire femora were determined with DEXA. The microstructure of the distal femoral metaphysis was analysed using μ CT. Fracture strength of the femoral mid-diaphysis, femoral neck, and distal femoral metaphysis was determined using a materials testing machine. Dynamic histomorphometry was performed on the femoral mid-diaphysis.

Compared to the controls, BTX reduced rectus femoris muscle mass by 67% ($P < 0.001$), mean muscle cell diameter by 73% ($P < 0.001$), total femoral BMC by 15% ($P < 0.001$), distal femoral metaphysis BV/TV by 24% ($P < 0.05$) and trabecular thickness by 15% ($P < 0.001$), periosteal bone formation rate by 71% ($P < 0.001$), and fracture strength of the femoral mid-diaphysis by 12% ($P < 0.01$), femoral neck by 17% ($P < 0.05$), and distal femoral metaphysis by 25% ($P < 0.01$). Compared to BTX, BTX+GH resulted in significantly higher rectus femoris muscle mass ($P < 0.001$), total femoral BMC ($P < 0.01$), and periosteal bone formation rate ($P < 0.01$). Furthermore, BTX+GH tended to have increased mean muscle cell diameter ($P < 0.065$). In contrast, no significant differences were found between BTX and BTX+GH in any of the microstructural measures at the distal femoral metaphysis. Likewise, the fracture strength at any of the tested sites did not differ between BTX and BTX+GH.

The BTX-induced loss in muscle mass, BMC, and bone formation rate was partly inhibited by treatment with GH. In contrast, treatment with GH did not influence the loss of mechanical strength, which may be due to the relative short treatment period.

Disclosures: Annemarie Bruel, None.

MO0460

Osteogenic Effects of Black Bear PTH (1-84) in a Mouse Model of Duchenne Muscular Dystrophy. Sarah Gray¹, Meghan McGee-Lawrence², Samantha Wojda¹, Seth Donahue³. ¹Michigan Technological University, USA, ²Mayo Clinic, USA, ³Michigan Technological University, USA

Duchenne muscular dystrophy (DMD) is a progressive X-linked disease affecting cardiac and skeletal muscle. By the age of 5, boys with DMD show diminished mobility, and are usually confined to a wheelchair by 12-15 years of age. Decreased mobility, which decreases mechanical stresses on bone, has a deleterious effect on the long bones of the lower limb. In boys with DMD, approximately 20% will experience a long bone fracture by the age of 16 compared to 2-4% in healthy boys. These fractures often result from falls from standing height or falls from a wheelchair.

An anabolic therapy for bone could be beneficial in preventing fractures in DMD patients. During disuse (hibernation), black bears maintain a balance in bone formation and resorption. Human parathyroid hormone (hPTH) has been shown to be anabolic for bone, and black bear PTH (bbPTH) may be even more anabolic to account for the bone maintenance observed during hibernation. The aim of this study was to evaluate black bear PTH's potential to prevent and restore bone losses characteristic of DMD.

Dystrophin-deficient male *mdx* mice (a model of DMD recently shown to have low bone mass) and C57BL/6 wild-type controls were injected daily with 24 nmol/kg bbPTH (1-84) or acidic saline vehicle for six weeks. At the conclusion of the study, animals were euthanized by carbon dioxide asphyxiation and their leg bones were extracted for evaluation.

Micro-computed tomography of distal femoral trabecular bone demonstrated *mdx* mice have lower ($p = 0.0024$) bone volume fraction (BV/TV) than wild-type mice. However, treatment with bbPTH increased BV/TV in *mdx* mice to beyond wild-type levels ($p = 0.0002$). We also found *mdx* mice are more responsive to bbPTH treatment than wild-type mice, with a 7-fold increase in BV/TV in *mdx* mice compared to a 2-fold BV/TV increase in wild type mice. Treatment with bbPTH increased trabecular number ($p < 0.0001$) and trabecular thickness ($p < 0.0001$) in *mdx* mice, but not wild-type mice.

Three-point bend testing of femurs to measure cortical bone strength showed no differences in either ultimate force or energy to failure between *mdx* and wild-type mice ($p > 0.1314$) or between bbPTH and vehicle treatments ($p > 0.1445$).

Increases in trabecular microarchitecture with bbPTH administration indicate an increased level of bone formation. Over time, this increased formation could lead to increased resistance to fracture, improving the quality of life for patients with Duchenne muscular dystrophy.

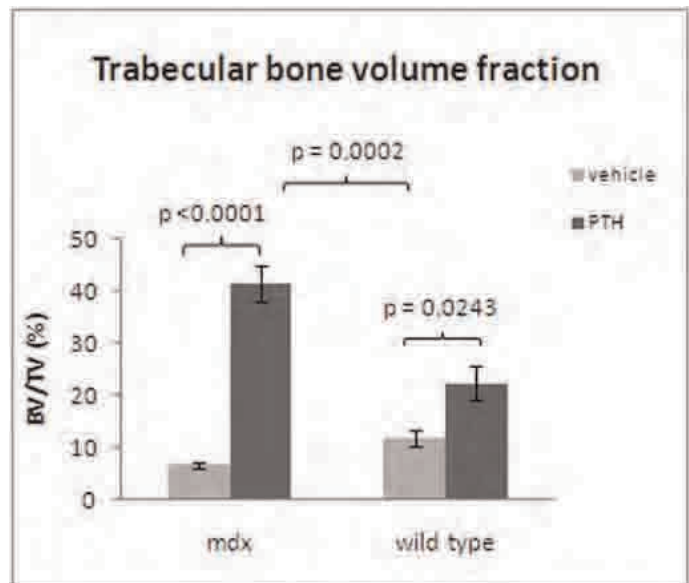


Figure 1 - Bone Volume Fraction

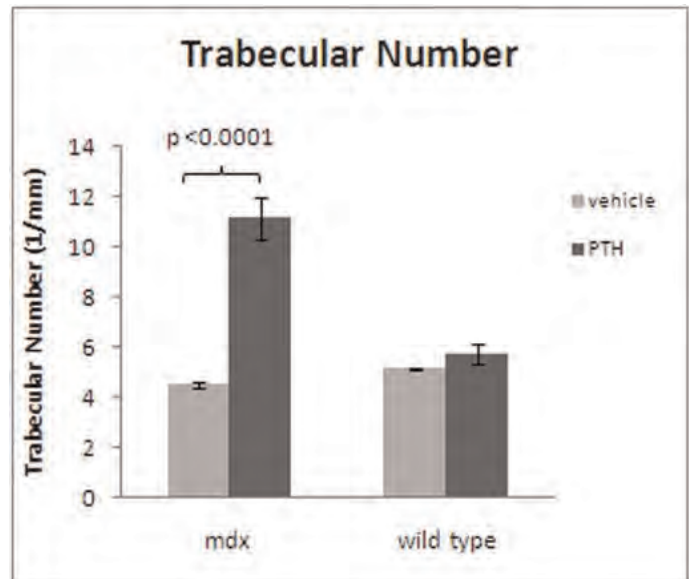


Figure 2 - Trabecular Number

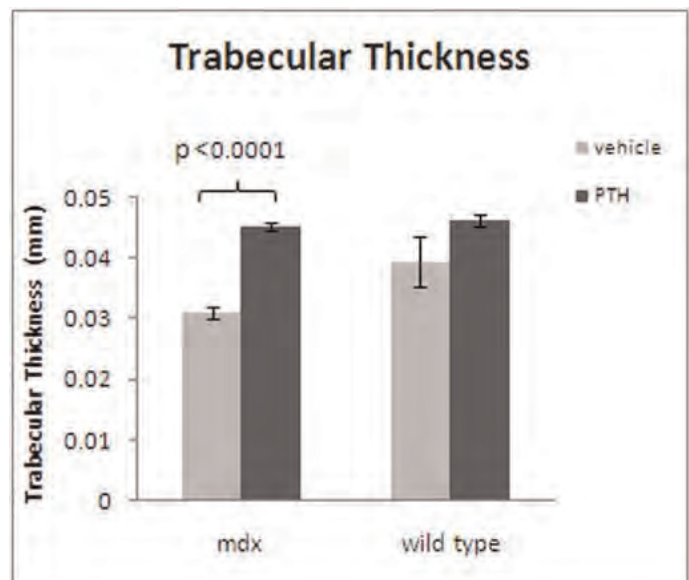


Figure 3 - Trabecular Thickness

MO0462

Sclerostin Antibody Increases Peri-implant Bone Formation in Sham-ovariectomized and Ovariectomized Rats. John Irish^{*1}, Amarjit Viri², Kotaro Sena², Min Liu³, Hua Zhu Ke⁴, D. Rick Sumner². ¹Rush University, USA, ²Rush University Medical Center, USA, ³Amgen, USA, ⁴Amgen, Inc., USA

Improving implant fixation in orthopedics and dentistry is of interest because of growing concerns with implant loosening. Neutralizing sclerostin is a promising approach to enhancing bone volume and use of sclerostin antibody (Scl-Ab) has been shown to enhance implant fixation in rat models. Here, we test the hypothesis that Scl-Ab increases bone formation rate (BFR) at the endocortical and trabecular surfaces and at the marrow-facing and implant-facing surfaces of the rim of bone adjacent to the implant in rats with normal and depressed bone volume. 4.5-month old Sprague-Dawley rats received sham-ovx or ovx followed by bilateral femoral intramedullary titanium rod insertion in the distal femur 6.5 months later. The rats were injected twice-weekly with either saline or Scl-Ab (25mg/kg) throughout the study or with Scl-Ab for the first 2, 4 or 8 weeks, for rats terminated at 4, 8 or 12 weeks, respectively (n = 7-9 per group/time). BFR/BS and BV/TV were determined for a metaphyseal region of interest adjacent to the implant. BFR/BS was elevated in sham-ovx and ovx rats treated with Scl-Ab throughout the duration of the study compared to the saline controls at most of the bone surfaces at all 3 time points (Table 1). BFR/BS remained elevated compared to saline controls in the group receiving 2 weeks of Scl-Ab followed by 2 weeks of no treatment, but in groups in which there was a 4 week period between cessation of Scl-Ab treatment and termination, BFR/BS had returned to control levels with rare exception (Table 1). BV/TV in the treatment cessation groups was not different from the groups with Scl-Ab throughout for all timepoints. Generally, increases in mineralizing surface rather than increases in mineral apposition rate accounted for the elevated BFR/BS. BFR/BS tended to decrease over time in rats in which Scl-Ab was administered throughout the study, but remained elevated compared to the saline-injected controls at 3 of the 4 bone surfaces at 12 weeks (Table 1). Thus, the increase in peri-implant BFR induced by Scl-Ab treatment had similar bone surface- and time-dependence in sham-ovx and ovx rats. These increases were no longer apparent 4 weeks after discontinuation of treatment, but reversion of BFR to control levels was not associated with a decrease in BV/TV. It remains to be determined if elevated BFR during Scl-Ab administration at all 4 of these surfaces contributes equally to the increased mechanical fixation observed in rat models.

		BFR/BS	Trabecular	Endocortical	Marrow-Facing	Implant-Facing
Sham-Ovx	4 week	ThrhgOut	↑	↑	↑	↑
		On/Off	↑	↑	↑	↑
	8 week	ThrhgOut	↑	↑	↑	↑
		On/Off	↔	↔	↔	↔
	12 week	ThrhgOut	↑	↑	↑	↔
		On/Off	↔	↔	↔	↔
Ovx	4 week	ThrhgOut	↑	↑	↑	↔
		On/Off	↑	↑	↑	↔
	8 week	ThrhgOut	↑	↑	↔	↔
		On/Off	↔	↔	↑	↔
	12 week	ThrhgOut	↑	↑	↑	↔
		On/Off	↔	↔	↑	↔

Table 1. BFR/BS compared to the saline controls (↑, p < 0.05; ↔, p > 0.05). ThrhgOut = Scl-Ab given throughout duration of the study. On/Off = Scl-Ab given for first 2 weeks (4 week groups), 4 weeks (8 week groups), or 8 weeks (12 week groups).

Table 1

Disclosures: John Irish, NIH, 2

This study received funding from: Amgen-UCB

MO0463

Smurf Inhibition Does Not Increase Bone Mass. Ina Kramer¹, Janet Dawson-King¹, Rohan Beckwith², Rene Lattmann¹, Nils Ostermann¹, Marcel JJ Blommers¹, Ji-Hu Zhang², Michael Kiffe¹, Alex Shih-Min Huang², Michaela Kneissel¹, Sabine Guth-Gundel^{*1}. ¹Novartis Institutes for BioMedical Research, Switzerland, ²Novartis Institutes for Biomedical Research, USA

It has been previously demonstrated that deletion of the E3 ubiquitin ligase Smurf1 results in increased bone formation and mass in naive animals and in an arthritis model of bone loss. The described increase in bone mineral density was progressive, but relatively modest. A concomitant increase in Smurf2 levels was observed indicating putative functional compensation. We hence aimed at generating a dual Smurf1/2 inhibitor as a potential novel bone anabolic principle for treatment of osteoporosis and arthritis induced bone loss. Through a combination of biochemical, biophysical, and cellular assays we identified a specific low molecular weight Smurf1/2 inhibitor. The compound inhibits Smurf1 and 2 with low nM IC50 in a biochemical auto-ubiquitination assay and stabilizes Smurf1 protein substrates in cellular assays.

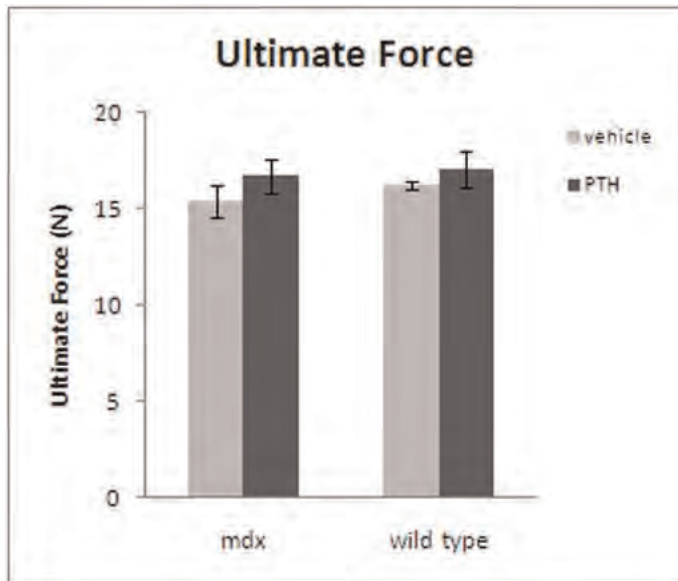


Figure 4 - Femoral Ultimate Force

Disclosures: Sarah Gray, None.

This study received funding from: Auros, Inc.

MO0461

Sclerostin Antibody Enhances Spine Fusion in a Rat Posterolateral Transverse Process Fusion Model: Preliminary Results. Andre Shaffer^{*1}, Owolabi A Shonuga¹, Brandon Hirsch², Matthew E Cunningham³, Jeffrey E Mait⁴, Chaoyang Li⁵, Hua Zhu Ke⁶, Joseph Lane³. ¹Hospital For Special Surgery / Weill Cornell Medical College, USA, ²Hospital for Special Surgery / Yale University School of Medicine, USA, ³Hospital for Special Surgery, USA, ⁴Hospital for Special Surgery / SUNY Downstate Medical Center, USA, ⁵Amgen, Incorporated, USA, ⁶Amgen, Inc., USA

Introduction

Sclerostin is a Wnt-signaling pathway inhibitor specific to bone. Monoclonal antibodies to sclerostin (Scl-Ab) have been shown to enhance bone mass and healing in diaphyseal fracture models in animals[1,2]. Spinal fusion is a commonly performed procedure indicated in a number of conditions including degenerative and traumatic conditions[3]. We hypothesize that lumbar spinal fusion is enhanced by subcutaneous Scl-Ab injections.

Methods

Sixty male 10 wk old Lewis rats underwent posterolateral intertransverse process spine fusion between L4 and L5 with 0.2g of morselized bone graft from a donor rat and randomized prior to surgery into two groups. Rats were started on a twice weekly regimen of saline (n=30) or 0.25 mg/kg Scl-Ab (Amgen, Inc, Thousand Oaks, CA) on post-op day 2 that continued until sacrifice at six wks postoperatively. At sacrifice spines were harvested en-bloc from sacrum to L1 and cleaned of soft tissue. Harvested spines were frozen and underwent microCT (uCT) imaging. Thawed spines (n=30) were evaluated for gross motion by manual palpation by three blinded authors, with fusion defined as no motion and scored by consensus. uCT was evaluated for total bone mass in the spines (n=30) and fusion mass in selected spines from each group (n=6).

Results

Manual palpation revealed no statistically significant differences between the two groups. Scl-Ab and saline, with fusion rates by manual palpation of 61% and 60% respectively (p = 0.92). uCT imaging revealed significantly increased bone volume in the spines of animals treated with Scl-Ab with mean bone volume of 554.7458.71 mg HA/ccm and 362.11134.60 mg HA/ccm in spines treated with Scl-Ab and saline respectively (p < 0.001). Bone volume in the fusion mass was also significantly increased in spines treated with Scl-Ab over saline (BV=255.53040.63 mg HA/ccm [Scl-Ab], BV=137.2618.71 mg HA/ccm in [saline], p < 0.001).

Conclusions

Scl-Ab is an effective adjunct for spinal fusion in a rat model, showing increased bone mineral volume and density in the fusion mass and entire spine. Scl-Ab increased fusion mass and overall bone stock. While greater fusion rate was not seen, bone in Scl-Ab treated animals was denser and fusion mass contained more bone than saline treated animals. Greater bone volume and density may lead to greater clinical benefits, since greater bone density and growth is associated with lower rates of pseudoarthrosis and instrumentation failure in spinal fusion.[4,5,6,7]

Disclosures: Andre Shaffer, None.

This study received funding from: Amgen Inc

Direct binding of the compound to the targets was demonstrated by NMR and other biophysical methods. Since its pharmacokinetic (PK) properties allow for oral in vivo application we tested the impact of 8-week twice daily application of three doses, predicted to be sufficient for Smurf1/2 inhibition in vivo, on bone mass in skeletally mature female rats. Moreover we analyzed the bone phenotype of Smurf1 and Smurf2 KO mice during growth and ageing. Bone mass and density changes were monitored by microCT and pQCT. Serum osteocalcin and TRAP levels were determined at 4 and 8 month of age. In addition we subjected rats treated with the Smurf 1/2 inhibitor and Smurf1 and Smurf2 KO mice to antigen-induced arthritis. Knee swelling and bone changes were monitored. Despite its favorable PK profile the compound had no impact on bone mass, density and biomarkers. Consistent with these results and in partial opposition to published data neither Smurf1 KO nor Smurf2 KO mice displayed increased bone mineral density over the 8 month monitoring period. While the compound did not induce any bone changes in the antigen-induced arthritis model it reduced knee swelling thus demonstrating in vivo efficacy. In line with the latter observation a reduction in knee swelling was also observed in Smurf1 KO and Smurf2 KO mice. Taken together, our data demonstrate the feasibility to develop specific Smurf1/2 inhibitors identifying E3 ubiquitin ligases as novel drug targets. However, they also suggest that inhibition of Smurf1 and Smurf2 does not provide a bone anabolic strategy for restoration of bone mineral density.

Disclosures: Sabine Guth-Gundel, Novartis, 3

MO0464

Comparison of Zoledronic Acid and Teriparatide Effects on Iliac Bone Microarchitecture, Remodeling and Collagen Crosslinks in Ewes. Nathalie R Portero-Muzy¹, Pascale M Chavassieux², Mary L Boussein³, Evelyne Gineyts¹, Roland D Chapurlat¹. ¹INSERM, UMR1033, Universite de Lyon, France, ²INSERM UMR1033, Universite de Lyon, France, ³Orthopedic Biomechanics Laboratory, Beth Israel Deaconess Medical Center & Harvard Medical School, USA

Zoledronic acid and teriparatide have different mechanism of action. Their respective effects on 3D-microarchitecture, collagen crosslink composition and bone remodeling have not been compared. Thus, we conducted an experimental study to distinguish their effect in the iliac bone, in ewes. Three groups of 24 aged ewes received either vehicle (CTRL; 8.4±0.4 yrs, n = 8); single injection of 10 mg of zoledronic acid (ZOL; 8.1±0.4 yrs, n = 8) or daily injection of 20µg/d of teriparatide (TPTD; 8.1±0.4 yrs, n = 8). After double tetracycline labeling, a transiliac bone biopsy was collected after 3 months. 3D-microarchitecture was assessed with Scanco microCT 40 with a 20µm³ isotropic voxel size. The content of both mature enzymatic crosslinks pyridinoline (PYD), deoxypyridinoline (DPD) and the non-enzymatic crosslink pentosidine (PEN) were analyzed by reverse phase-HPLC. Static and dynamic parameters of bone remodeling were measured by 2D-histomorphometry. Three months after a single dose of ZOL, MS/BS, BFR/BS and Acf were significantly decreased by 97.8% (p<0.001), 95.3% and 94.7% (p<0.01) respectively when compared to CTRL. Tb.BV/TV by histomorphometry was 31.3% and 33.6% higher in ZOL than in CTRL and TPTD (p<0.04 and p<0.01 respectively). This was confirmed by 3D-µCT measurements which showed an increase in Tb.BV/TV (19.8%, p<0.04), ConnD (30%, p<0.03) and TbN* (8.3%, p<0.03) vs CTRL. ZOL had, in the cortical bone, lower DPD and a higher PYD/DPD ratio (p=0.05) compared to CTRL. In contrast, after 3 months of TPTD, the bone turnover (ie, MS/BS, BFR/BS and Acf) was significantly higher than in ZOL, but was not significantly different than CTRL. Tb.BV/TV evaluated with 3D-µCT did not differ from CTRL. DPD was decreased and PYR/DPD ratio increased in TPTD when compared to CTRL (p<0.01). In conclusion, in adult ewes ZOL improves bone microarchitecture parameters within 3 months, whereas the effect of TPTD seems to take longer. These observations might depend on skeletal site, and other sites with different proportion of trabecular and cortical bone should be examined.

	CTRL	ZOL	TPTD
MS/BS (%)	11.1±8.3	0.2±0.6	13.5±10.4
BFR/BS (µm ³ /µm ² /d)	0.095±0.073	0.004±0.007	0.112±0.087
Tb.BV/TV (%)	17.2±3.9	20.6±1.8	17.9±2.6
Tb.Th* (mm)	0.15±0.02	0.15±0.01	0.14±0.02
Tb.N* (1/mm)	1.2±0.1	1.3±0.1	1.3±0.2
Ct DPD	28.7±5.1	23±9	19.7±5.7
Ct PYD	242.3±94.7	224.1±76.6	224.5±73.4
Ct PEN	10.7±3.2	12.2±2.8	15.6±11.5

Table

Disclosures: Nathalie R Portero-Muzy, None.

MO0465

Effect of Timing of Post-Exercise Carbohydrate and Protein Ingestion on Markers of Bone Turnover. Julie Greeves^{*1}, Ricardo Costa², Neil Walsh³, Craig Sale⁴, Ruth Hobson⁴, John Dutton⁵, William Fraser⁵. ¹HQ Army Recruiting & Training Division, United Kingdom, ²Coventry University, United Kingdom, ³Bangor University, United Kingdom, ⁴Nottingham Trent University, United Kingdom, ⁵University of Liverpool, United Kingdom

Oral administration of carbohydrate (CHO) and protein (PRO), shown to suppress bone resorption at rest, might also attenuate the marked increase in bone resorption associated with running (Scott et al. 2010, JCEM, 95, 3918-25). CHO-PRO consumption is an established post-exercise feeding strategy, rapidly replenishing energy stores if ingested within 60 min of exercise. CHO-PRO might also modulate bone resorption in a time-dependent manner. This study aimed to examine the influence of immediate or delayed ingestion of CHO-PRO on bone metabolism following prolonged exercise. Eight male runners (age: 29 10 y; height: 1.79 0.08 m; body mass [BM]: 72.7 7.4 kg; VO2max: 61.5 6.1 ml·kg⁻¹·min⁻¹) completed 3 randomised feeding interventions after 2 h of running at 75% VO2max. During control (CON), participants received water (12 ml·kg BM⁻¹) immediately and 1 h post-exercise. During immediate feeding (IF), participants received a CHO-PRO solution equal to 1.2 g CHO·kg BM⁻¹ and 0.4 g PRO·kg BM⁻¹ immediately post-exercise and water 1 h post-exercise. During delayed feeding (DF), participants received water immediately post-exercise and CHO-PRO solution 1 h post-exercise. Venous blood samples were obtained before exercise (BASE), immediately post-exercise (POST), and every 20 min until 140 min post-exercise. Serum/plasma was analysed for Ò-CTX, PINP, OC and PTH. Data were analysed using Linear Mixed Model ANOVA, and post-hoc with Newman-Keuls and Dunnett's test. There was a significant condition x time interaction for Ò-CTX (P<0.001), but not for PINP, OC or PTH. Ò-CTX increased between BASE and 20 (P<0.05), 40 and 60 min post-exercise in all conditions (p<0.005), but decreased below BASE between 100 and 140 min in IF (P<0.05), and 120 and 140 min in DF (P<0.05). Differences between groups are shown in Table 1. Main effects of time were significant for PINP, OC and PTH (P<0.0001). The increase in bone resorption following exhaustive exercise is attenuated with post-exercise feeding of CHO-PRO. These effects are observed earlier with immediate feeding, but are comparable 140 post-exercise. In addition to the widely acknowledged benefit of early post-exercise CHO-PRO ingestion for restoring energy supply, these findings suggest that post-exercise ingestion of CHO-PRO has favourable effects on bone turnover. This work was sponsored by the UK Ministry of Defence (Army)

		BASE	Post	20	40	60	80	100	120	140
Ò-CTX (µg·mL ⁻¹)	CON	0.53	0.56	0.56	0.61	0.59§	0.54§	0.51§	0.48*§	0.46*§
		±0.36	±0.29	±0.29	±0.30	±0.28	±0.26	±0.24	±0.22	±0.22
IF		0.48	0.61	0.60	0.63	0.53	0.46	0.40	0.33	0.28
		±0.32	±0.32	±0.33	±0.37	±0.29	±0.28	±0.24	±0.19	±0.18
DF		0.51	0.59	0.57	0.61	0.61**	0.57	0.48	0.41	0.32
		±0.35	±0.29	±0.31	±0.33	±0.32	±0.31	±0.30	±0.22	±0.18

*diff from DF (P<0.001), §Diff from IF (P<0.001), ** diff to IF (P<0.01)

Table 1: Mean (SD) concentrations of Ò-CTX between post-exercise feeding conditions

Disclosures: Julie Greeves, None.

MO0466

Effects of Dietary Coral Calcium and Zeolite on Ovariectomy Induced Bone Loss. Jameela Banu^{*1}, Erika Varela¹, Ganesh Halade¹, Ali Bahadur¹, Kokichi Hanaoka², Gabriel Fernandes³. ¹University of Texas Health Science Center at San Antonio, USA, ²Bio-REDOX Laboratory Inc, Japan, ³University of Texas Health Science Centre, USA

Patients that have osteoporosis mainly lose calcium from bones making them weaker and easily susceptible to fractures. Supplementation of calcium is one treatment option for such condition. The source of calcium however plays an important role in the amount of calcium that is assimilated into bone. Naturally occurring coral calcium and zeolite are popular nutritional supplements, and probably they can be used to prevent bone loss. We have measured bone loss in ovariectomized (OVX) mice supplemented with coral calcium and Zeolite.

Female C57BL/6 mice, 3 months of age were purchased from Jackson laboratories and divided into the following groups: 1. AIN93 -SHAM (10% CO); 2. AIN93 - OVX (10% CO); 3. AIN93+0.5% calcium - SHAM; 4. AIN93+0.5% calcium - OVX; 5. AIN93+1% Coral powder - SHAM; 6. AIN93+1% Coral powder - OVX; 7. AIN93 +1% Zeolite powder - SHAM; 8. AIN93+1% Zeolite powder - OVX. The mice were either sham-operated (n=10/group) or ovariectomized (OVX; n=10/group). One week after surgery, they were put on the respective diets for the next 6 months and sacrificed. Serum was analyzed for bone biochemical markers. Long bones were analyzed using µCT densitometry and lumbar vertebrae were analyzed using DXA.

There was significant decrease in the trabecular number and increase in trabecular separation in distal femoral metaphysis of control OVX mice, while the calcium, coral

calcium and zeolite fed mice did not show significant differences between sham and OVX mice. Bone mineral density (BMD) of the lumbar vertebrae (L2-L4) was significantly decreased in control OVX mice, when compared to those of control sham mice. BMD of calcium, coral calcium and zeolite fed mice did not change significantly between the treated sham and OVX mice. Bone turnover markers like alkaline phosphatase and osteocalcin increased in OVX mice fed coral calcium significantly.

In conclusion, coral calcium and zeolite protect ovariectomy induced bone loss in mice.

Disclosures: Jameela Banu, None.

MO0467

Soy Isoflavones, Alone or in Combination with Risedronate, Do Not Reduce Bone Resorption in Ovariectomized Rats. Emily Hohman*, George McCabe, Connie Weaver. Purdue University, USA

Bisphosphonates are highly effective in reducing risk for osteoporotic fractures, but have recently been associated with adverse effects following long term use. Combination therapy with other antiresorptive therapies may increase effectiveness of bisphosphonates and allow for reduced doses, possibly reducing risk for adverse effects. Soy isoflavones have been shown to reduce bone resorption in post-menopausal women, making them a potential co-therapy agent. We investigated the effects of dietary soy isoflavones alone and in combination with two doses of risedronate on bone resorption as measured by deep bone label excretion in ovariectomized (OVX) rats. Four-month-old rats were given an intravenous injection of 50 μ Ci 45 Ca following one month of recovery from OVX. After an additional month to allow the 45 Ca clear from soft tissues and label only bone, urine was collected to determine baseline 45 Ca excretion. Twenty rats were then assigned to receive soy isoflavone and risedronate treatments in a semi-randomized, crossover design. The treatments were 1) a soy isoflavone diet (875 mg/kg diet Novasoy added to AIN-93M diet, total isoflavone content = 350 mg/kg diet), 2) low risedronate (0.8 μ g/kg body weight sodium risedronate injected subcutaneously every other day), 3) low risedronate + soy isoflavone diet, 4) high risedronate (1.2 μ g/kg body weight sodium risedronate injected subcutaneously every other day), and 5) high risedronate + soy isoflavone diet. Treatments were given for ten days with ten day recovery periods between treatments. Twenty-four-hour urine pools collected throughout the treatments were analyzed for 45 Ca by liquid scintillation counting. Relative resorption (RR) was calculated as the ratio of 45 Ca excretion during treatment to 45 Ca excretion during the baseline period, adjusted for time and subject. On the soy isoflavone diet (trt 1), RR was 1.18 ($p=0.01$), indicating that bone resorption was not reduced. Risedronate alone significantly reduced bone resorption at both the low (trt 2, RR=0.70, $p<0.0001$) and high (trt 4, RR=0.78, $p<0.0001$) doses. Addition of soy isoflavones to risedronate did not further reduce bone resorption (low risedronate + soy [trt 3], RR=0.76, $p<0.0001$; high risedronate + soy [trt 5], RR=0.76, $p<0.0001$). These results indicate that soy isoflavones may not be effective as a monotherapy or as a co-therapy with risedronate for preventing bone resorption in the OVX rat model of post-menopausal osteoporosis.

Disclosures: Emily Hohman, None.

MO0468

Estradiol Release Kinetics Determine Tissue Response in Ovariectomized Rats and Mice. Ingrid Kantner*¹, Christiane Otto², Reinhard Nubbemeyer², Jenny Schkoldow², Iris Fuchs², Elisabeth Krah², Richardus Vonk², Christiane Schuler¹, Karl-Heinrich Fritzsche², Reinhold Erben¹. ¹University of Veterinary Medicine, Austria, ²Bayer Schering Pharma AG, Germany

Estrogen replacement is an effective therapy of postmenopausal symptoms such as hot flushes, bone loss, and vaginal dryness. Major side effects are the stimulation of uterine and mammary gland epithelial cell proliferation as well as hepatic estrogenicity. In this study in ovariectomized (OVX) rats and mice, we tested the hypothesis that the tissue response to estradiol might be modulated by different release kinetics. Pulsed release kinetics were achieved by intraperitoneal (i.p.) or subcutaneous (s.c.) administration of estradiol dissolved in physiological saline containing 10% ethanol (EtOH/NaCl), whereas continuous release kinetics were achieved by s.c. injection of estradiol dissolved in benzyl benzoate/ricinus oil (B/R, 1:5). Initial 3-day and 3-week experiments in OVX rats and mice showed that pulsed i.p. estradiol had a profoundly reduced stimulatory effect on uterus and mammary gland compared with continuous release kinetics, whereas both release kinetics prevented vaginal atrophy. Based on these results, we compared the effects of pulsed (s.c. in EtOH/NaCl) versus continuous (s.c. in B/R) estradiol release kinetics on bone, uterus, mammary gland, and liver in a 4-month study in 6-month-old OVX rats. We found that both application regimens had comparable ability to protect against ovariectomy-induced bone loss. However, pulsed estradiol resulted in lower uterine weight, reduced induction of hepatic gene expression, and a lower proliferative effect on the mammary gland, relative to continuous estradiol. We conclude that estradiol release kinetics can determine organ responsiveness, a fact which might be exploited to reduce unwanted side effects of estradiol therapy.

Disclosures: Ingrid Kantner, None.

This study received funding from: Bayer Schering Pharma AG

MO0469

Callus Resolution and Fracture Healing is Not Hindered in Cathepsin-K Null Mice. Michael Gentile^{*1}, Do Soung², Gregg Wesolowski¹, Pavithra Ramakrishnan¹, Carlyle Horrell¹, Hicham Drissi², Le Thi Duong³. ¹Merck & Co., Inc., USA, ²University of Connecticut Health Center, USA, ³Merck Research Laboratories, USA

Cathepsin K (CatK) is a cysteine protease expressed predominantly in osteoclasts which degrades demineralized bone matrix. Adult CatK deficient mice have high bone mass in both cortical and cancellous regions as the result of significant reduction in osteoclastic bone resorption as well as enhanced bone formation. Here, a mouse femur fracture model was employed to assess fracture healing in CatK knock-out (KO) versus wild type (WT) mice. Pre-pin stabilized, mid-diaphyseal femoral fractures (Fx) were made with an Einhorn device in 8-11 week old mice. Callus formation and resolution were assessed *in vivo* via a dental x-ray at the time of Fx and at 4, 7, 14, 21, and 28 days. Based on blind scoring of Fx radiographs at 14 days, KO and WT mice were randomized into 3 groups ($n=6-8$ /group) which were sacrificed at for 14, 18 and 28 days post-Fx, respectively. Similar procedures were applied in a separate experiment to assess callus strength at 28 and 42 days. The fractured and intact contra-lateral femora were harvested and the calluses were assessed *ex vivo* by caliper, DEXA, μ CT and histomorphometry. Original cortical bone within the forming callus was manually excluded from μ CT slices allowing assessment of bone formed post fracture. The callus size as assessed by caliper, DEXA-derived area, histomorphometry and μ CT-derived volume was similar in KO vs. WT at 14 days with a strong trend towards smaller callus size in KO at 18 and 28 days post-Fx. The calluses from KO mice had statistically significantly ($p<0.05$, one way ANOVA, Fisher's PLSD) greater overall BMD at each timepoint relative to WT controls as assessed by both DEXA and μ CT. Callus BMC as measured by μ CT demonstrated a higher trend in KO mice at 14 days and gradually declined from 14 to 28 days during callus resolution in both KO vs. WT bones. Histomorphometric analysis of calluses revealed higher bone area/total callus area, % in KO vs. WT at all time points. Cartilage area/total callus area, % was similar in KO vs. WT at all time points. Furthermore, CatK KO calluses had overall higher bone mass at all time points. Biomechanical testing and histomorphometric analyses are ongoing to determine callus turnover and strength during the healing process. We conclude that callus resolution and healing of fracture is not hindered in Cat K deficient mice.

Disclosures: Michael Gentile, None.

MO0470

Cellular and Molecular Mechanisms Of Accelerated Fracture Healing By Cox-2 Gene Therapy. Studies In A Multiple Fracture Mouse Model. Vishal Kothari¹, Xiaobing Zhang², K.H. William Lau³, David Baylink², Amitava Das^{*2}. ¹Loma Linda University School of Medicine, USA, ²Loma Linda University, USA, ³Loma Linda University School of Medicine, USA

Cox-2 gene therapy is highly effective in accelerating bridging of fracture gaps, but the mechanism by which the Cox-2 gene therapy promotes fracture repair is not known. This study sought to determine the cellular and molecular mechanisms of Cox-2 to promote fracture repair using a multiple fractures model, in which 3 fractures were created on the tibia of C57BL/6 mice by 3-point bending. The lenti-Cox-2-GFP or lenti-GFP control vector was injected into fracture site on day 1. Our study indicated that Cox-2 therapy affected the fracture repair at two distinct phases: 1) at an early phase, therapy reduced the callus size, and 2) at a later phase, it promoted remodeling of the cartilaginous callus and bony bridging of the fracture gap. Accordingly, the Cox-2-treated mice formed smaller cartilaginous calluses at day 7-14 ($p<0.001$) and had less cartilage content at day 14-21 ($p<0.001$) than control mice. Two findings of our mechanistic exploration of the reduction in callus size are novel. First, expression of Sox-9 mRNA was 7-fold less in Cox-2-treated calluses than in control calluses (9.2 vs. 67.6-fold, $p<0.04$, $n=3$) at day 14. This decrease corresponds to the reduction in callus size (6.10.9 vs. 9.81.0, $p<0.01$, $n=6$), implying that Cox-2 reduces chondroblastic differentiation of MSCs in the callus. Second, the therapy increased cellular staining of vWF and α -SMA (>2.5 -fold over controls) in the cartilaginous callus at day 14-21, suggesting an increase in angiogenesis. This was associated with 2-fold increase ($p<0.05$) in TRAP+ osteoclasts along the surface of the woven bone. The removal of cartilage was also associated with an earlier and more robust onset of osteogenesis (2-fold increase in osteocalcin+ cells, $p<0.001$), indicating that Cox-2 promotes bony remodeling of callus cartilage. Injection of endostatin (2.5 mg/kg/day for 10 days) into the fracture site at the time of the viral injection to block angiogenesis resulted in a marked increase in staining for hypertrophic chondrocytes with concomitant reduction in TRAP activity ($p<0.01$). Thus, angiogenesis is essential for the Cox-2-mediated remodeling of cartilaginous callus. In conclusion, the mechanism whereby Cox-2 promotes fracture healing involved 2 independent actions: 1) decreased formation of cartilaginous callus at an early phase, and 2) promoted angiogenesis-dependent cartilage remodeling at a later phase which involved a more robust osteogenesis to support bridging and accelerated fracture healing.

Disclosures: Amitava Das, None.

This study received funding from: Department of Defense, USA

MO0471

Combined Effect of Methylprednisolone and Fish Oil ^{RX} Against Bone Mineral Density Loss in Spontaneous Autoimmune Disease Prone MRL-lpr/lpr Mice. Md Rahman*, Paul Williams, Kazi Nishu, Gabriel Fernandes. University of Texas Health Science Centre, USA

MRL-lpr/lpr mice spontaneously develop various manifestations of autoimmunity including an inflammatory arthropathy and immune complex glomerulonephritis. Autoimmune diseases induce bone mineral density (BMD) loss in this mouse. This study examines the combined effect of immunosuppressive drug, methylprednisolone (MP) and anti-inflammatory fish oil RX against bone mineral density loss in MRL-lpr/lpr female mice. At 4 months of age mice were either treated weekly with PBS or 5 mg/kg MP or 20 mg/kg MP and fed AIN93M diet supplemented either with 4% corn oil or 4% fish oil RX daily for 8 weeks. Before starting the drug injection and dietary intervention, mice were scanned with dual energy x-ray absorptiometry (DXA) to determine the baseline BMD values. Mice were again scanned with DXA 8 weeks later just before sacrifice to determine final BMD values. Slight protection of BMD loss in femur, tibia and lumbar regions was observed in MP and FO alone treated groups as compared to PBS and CO treated groups. However BMD loss protection in femur, tibia and lumbar regions was dramatic in combined MP and FO RX treated groups as compared to other groups. Higher protection of BMD loss was correlated with lower number of tartrate resistant acid phosphatase positive area and higher number of alkaline phosphatase positive area in tibial sections. Treatment of mice with MP and FO RX prevented the development of glomerulonephritis and reduced the intensity of inflammatory arthritis in MRL-lpr/lpr mice. These data emphasize the importance of suppressing inflammation by immunosuppressive drug and fish oil RX in mice with active autoimmune diseases to maintain bone health. Grant support: R01AT004259-04 and K01AG034233-02

Disclosures: Md Rahman, None.

MO0472

Comparison of the Efficacy of Odanacatib or Alendronate on Bone Remodeling and Biomechanical Properties of the Lumbar Spine in Estrogen-deficient Rhesus Monkeys. Brenda Pennypacker*, Charles Chen², Ya Zhuo², Maureen Pickarski², Le Thi Duong¹. ¹Merck Research Laboratories, USA, ²Merck & Co., Inc., USA

Cathepsin K (CatK) is a lysosomal cysteine protease highly expressed in osteoclasts that degrades Type I collagen during bone resorption. Odanacatib (ODN) is a selective, potent and reversible CatK inhibitor in development for the treatment of osteoporosis. We previously reported that ODN treatment reduced trabecular bone remodeling, while increasing cortical bone formation in ovariectomized (OVX) rhesus monkeys. Here, direct comparison of the efficacy and bone quality in the lumbar spine of ODN and alendronate (ALN) were compared on BMD, bone turnover, strength and collagen organization in the lumbar vertebrae (LV). OVX rhesus monkeys (age 12-22 yrs; N=16/group) were treated either with vehicle, ODN (2mg/kg/d, po), or ALN (30µg/kg/wk, sc). The ODN dose provided steady state exposure of 11µM•24h as compared to the equivalent clinical 50 mg dose exposure of ~7 µM•24h. A group of age- and BMD-matched intact monkeys (Int, N=12) was included as control. Calcein (8 mg/kg, IM) at 12 mo. and tetracycline (40 mg/kg IV) prior to necropsy were given at 14-d intervals. A significant treatment-related increase in LV4-5 BMD vs. Veh was observed in ODN (6.7%) and ALN groups (6.4%). Compared to Veh, ODN and ALN significantly reduced (p<0.001) trabecular LV2 mineralizing surface (MS/BS, %) and bone formation rate (BFR/BS). Static measurements including osteoblast surface (Ob/BS, %), osteoid surface (OS/BS, %) and thickness (Os.Th, µm), and osteoclast surface (OcS/BS, %) and number (OcN/BS, #/mm) were measured. ODN and ALN both decrease Ob/BS and OS/BS vs Veh. Unlike ALN, ODN increases OcS/BS and OcN/BS. Increases in LV4-5 peak load, apparent strength, yield load, and yield stress were noted for ODN- vs. ALN-treated monkeys, compared to Veh or Intact. From compression testing, peak load from all groups was positively correlated with DXA-derived BMD (R=0.699, p<0.0001) and BMC (R=0.4656, p<0.005), and QCT-derived BMD (R=0.577, p<0.001) and BMC (R=0.670, p<0.0001). LV2 trabecular collagen orientation (ROI 0.8X0.55 mm²) was scored by polarized light microscopy. There was no significant difference in the percentage of non-lamellar vs. lamellar bone over total bone area between groups. Taken together, the present data demonstrates that comparable to ALN, ODN treatment for 20 mo. at an equivalent daily clinical exposure effectively increases BMD, reduces bone remodeling, and maintains normal bone strength and collagen organization in OVX non human primates.

Disclosures: Brenda Pennypacker, None.

MO0473

Effects of Herb Extracts on Osteoclasts, Osteoblasts and Chondrocytes as Novel Drug Candidates for Osteoporosis. Seika Banka¹, Satoru Shintani¹, Kazunaga Yazawa², Kondo Seiji¹, Yoshiki Mukudai³. ¹Department of Oral & Maxillofacial Surgery, School of Dentistry, Showa University, Japan, ²Laboratory of Nutraceuticals & Functional Foods Science, Graduate School Marine Science & Technology, Tokyo University of Marine Science & Technology, Japan, ³Showa University, Japan

[Purpose] In these latter years, the therapy for osteoporosis (OP) is the most required for the quality of life. Bisphosphonate is the most applied for the therapy for osteoporosis, regardless of the serious side effects, such as ?Bisphosphonate Related Osteonecrosis of the Jaw. Therefore, it is suggested that study for finding a novel drug instead of bisphosphonates is a matter of great urgency. In the present study, we sought the herb extracts, which is effective on the therapy for OP *in vitro*, among more than 400 samples.

[Methods] At the first screening, RAW264.7 cells were utilized. The cells were grown at the presence of receptor activator NF-kappa B ligand (RANKL), were derived to osteoclasts, and were cultured for other 3 days in the presence of various herb extracts. Thereafter, the cells were subjected to TRAP staining, and the herb extracts, which effected on suppression and/or apoptosis to the osteoclasts, were subjected to the subsequent experiments. In the next, MC3T3 cells were grown in the differentiation medium, and supplemented with the herb extracts, which were selected from the experiments in RAW264.7 cells, for 3 day. As well, ATDC5 cells were grown in the presence of ITS (Insulin-Transferrin-Sodium selenite), and were driven into the proliferating chondrocytes. These 2 strains were, then, subjected to alkaline phosphatase (ALPase) assay, DNA measurement assay, sulfated glucosaminoglycan measurement assay, calcium measurement assay and osteocalcin ELISA assay, which are the differentiation markers of osteoblasts and chondrocytes. Thereby, further screening was carried out, for effects of proliferation and differentiation on osteoblast and chondrocytes.

[Results] After third screening, 3 herb extracts were found, and all of those increased apoptosis on osteoclasts, whereas, had proliferating and differential effects on both osteoblasts and chondrocytes. In addition, the effective dosage of the herb extracts was from 1 to 1000 mg/ml.

[Conclusions] In the present study, we found the several herb extracts, which might be novel drugs for OP. At present, purifying of the molecules, which are comprised in the herb and are effective for the therapy of OP, and *in vivo* experiments are ongoing. In addition, patents for the herb extracts are under application in Japan.

Disclosures: Yoshiki Mukudai, None.

MO0474

Calcium-Sensing Receptor Mediated Suppression of cAMP by Agonists and Allosteric Modulators. Vimesh Avlani*, Arthur Conigrave². ¹University of Sydney, Aus, ²University of Sydney, Australia

The extracellular calcium-sensing receptor (CaR) is a multimodal chemosensor that belongs to G Protein-Coupled Receptor (GPCR) class C. The CaR couples to the heterotrimeric G-proteins G_{q/11}, G_{i/o} & G_{12/13} resulting in the activation of various signalling pathways. The CaR is also subjected to allosteric modulation by compounds like L-amino acids, glutathione and its analogues including S-methylglutathione (SMG) that bind in the Venus Fly Trap domain and phenylalkylamines including NPS R-467 and Cinacalcet that bind in the heptahelical domains. The majority of CaR signalling studies use the activation of G_{q/11} as measure of CaR activity. However, systematic characterization of CaR mediated activation of other G-proteins such G_{i/o} and G_{12/13} and second messengers such as cAMP and ERK_{1/2} are required for a detailed understanding of CaR signalling and biological activity. In the present study we show that CaR mediated reduction in cellular cAMP levels arises from reduction in its synthesis as well as an increase in its degradation. Real-time measurement of changes in intracellular cAMP levels was achieved using the cAMP biosensor CFPnd-Epac1-cpVenus in a Fluorescence Resonance Energy Transfer (FRET)-based microfluorescence assay. EPac is a guanine nucleotide exchange protein directly activated by cAMP. All allosteric modulators tested, including L-Phenylalanine, SMG, NPS R-467 and cinacalcet enhanced extracellular calcium (Ca²⁺) induced decreases in cAMP levels. Overnight treatment of cells with pertussis toxin, an inhibitor of G_{i/o} G-protein, abolished not only Ca²⁺_o mediated cAMP inhibition but also the effects of the allosteric modulators suggesting a key requirement for G_{i/o} G-proteins. Isobutyl Methyl Xanthine (IBMX), a phosphodiesterase (PDE) inhibitor, also significantly reduced the potency of Ca²⁺_o. The results suggest that CaR mediated reduction in cAMP requires both inactivation of adenylyl cyclase via G_{i/o} and activation of PDE.

Disclosures: Vimesh Avlani, None.

MO0475

Alpha-2-Macroglobulin as a Biomarker for Glucocorticoid-induced Osteonecrosis of the Femoral Head. Alberto Carli¹, Edward J Harvey², Mireille Savegh¹, Bouziane Azeddine^{*1}, Ailian Li³, Ayoub Nahal², Rene Michel², Janet E Henderson³, Chantal Seguin². ¹McGill University, Canada, ²McGill University Health Centre, Canada, ³McGill University Health Centre-Research Institute, Canada

Relevance: Osteonecrosis (ON) of the femoral head is a serious complication of high dose glucocorticoid (GC) therapy in young people with haematologic malignancy. These patients present with end stage osteoarthritis, associated with endothelial dysfunction and loss of vascular integrity, which requires total hip arthroplasty for symptomatic relief. The current study was designed to test the hypothesis that genetic susceptibility predisposes individuals to GC-induced ON and that alpha-2-macroglobulin (A2M) may be a biomarker for the onset of disease.

Methods: Young adult Wistar Kyoto and Fischer rats were randomized to receive the equivalent of a daily dose of 1.5mg/kg/day of prednisone or placebo by slow release pellets implanted subcutaneously and bled each month for serum glucose and A2M before being euthanized at six months. Femoral heads were harvested and scanned at high resolution by micro computed tomography (m CT) before embedding and sectioning for histological analyses.

Results: Serum A2M remained below 10µg/ml in all placebo treated rats and variable increases were seen between two and four months of treatment in GC treated rats. Median levels dropped back to baseline in Fischer rats but remained elevated in Wistar Kyoto rats at six months. Subchondral bone was reduced in both Fischer and Wistar Kyoto rats treated with GC compared with placebo treated control and preliminary histological analyses that are still ongoing revealed some evidence of ON in either strain. However, unlike all Fischer rats most of GC treated Wistar Kyoto rats showed evidence of articular cartilage degradation.

Conclusion: We have shown Wistar Kyoto rats to be susceptible to GC-induced degeneration of the femoral head in association with elevated circulating levels of A2M.

Disclosures: Bouziane Azeddine, None.

MO0476

ROS, FoxOs, and Akt are Critical Mediators of the Actions of both Glucocorticoids and TNFα on Osteoblastic Cells. Maria Almeida^{*}, Li Han, Elena Ambrogini, Shoshana Bartell, Srividhya Iyer, Aaron Warren, Charles O'Brien, Robert Jilka, Robert Weinstein, Stavros Manolagas. Center for Osteoporosis & Metabolic Bone Diseases, Central Arkansas Veterans Healthcare System, University of Arkansas for Medical Sciences, USA

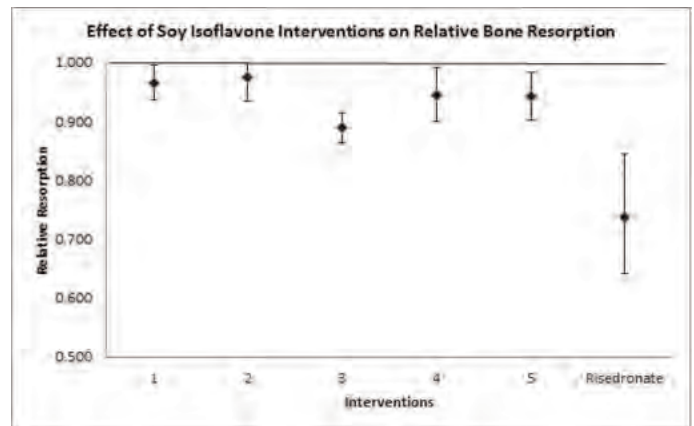
An increase in endogenous glucocorticoids (GC) or inflammatory cytokines are thought to contribute to the age-associated loss of bone mass and strength but the molecular mechanisms responsible for their deleterious effects on bone are unclear. Based on this and evidence that oxidative stress (OS) is a causal mechanism of the insulin resistance produced by these two agents, we tested the hypothesis that their adverse skeletal effects also result from increased OS. We report that dexamethasone (Dex) or TNFα increased reactive oxygen species (ROS), the phosphorylation of p66^{shc}, an amplifier of H₂O₂ generation in mitochondria, and the activity of FoxOs, transcription factors that defend against OS, in several established osteoblast cell models as well as murine calvaria-derived osteoblasts. These effects were abrogated in osteoblasts from p66^{shc} knockout mice or by the addition of Apocinin or LY393351, agents that inhibit activation of PKCβ which is required for ROS-induced phosphorylation of p66^{shc}. The effects of Dex and TNFα were also abrogated by the anti-oxidants NAC and Ebselen. In addition, both, Dex and TNFα induced the apoptosis of osteoblasts and this effect was abrogated in osteoblasts from mice lacking p66shc or wild type osteoblasts treated simultaneously with the anti-oxidants. The pro-apoptotic effect of Dex or TNFα was also abrogated in osteoblasts derived from mice in which FoxO3 has been selectively overexpressed in osteocalcin expressing cells. Further, TNFα or Dex suppressed the Wnt3-induced activation of a TCF-reporter construct, and this effect was attenuated in calvaria cells from FoxO1,3,4 knockout animals, but not by PKCβ inhibitors. The suppressive effects of Dex and TNFα on TCF transcription were prevented by transient transfection of a plasmid expressing Akt, a kinase that is inhibited by Dex and TNFα. In agreement with the in vitro findings, administration of prednisolone for 28 days to 5-month-old C57BL/6 mice increased ROS levels in the bone marrow, as well as p66shc phosphorylation in bone, and these effects were prevented by administration of NAC. We conclude that ROS-induced activation of a PKCβ/p66 signaling cascade is responsible for the pro-apoptotic effects of Dex and TNFα on osteoblastic cells. Moreover, activation of FoxOs and inhibition of Akt by GCs and TNFα are cell-autonomous mechanisms of Wnt/β-catenin antagonism contributing to the adverse effects of GC excess and inflammatory cytokines on bone alike.

Disclosures: Maria Almeida, None.

MO0477

A Moderate Oral Dose of Mixed Isoflavones Was Most Effective at Reducing Bone Resorption in Postmenopausal Women. Jessica Wiersma^{*1}, Berdine Martin¹, George McCabe¹, Linda McCabe¹, George Jackson¹, Munro Peacock², Stephen Barnes³, Connie Weaver¹. ¹Purdue University, USA, ²Indiana University Medical Center, USA, ³University of Alabama, USA

The ability of soy isoflavones to reduce bone loss associated with estrogen deficiency is hypothesized to be dependent on isoflavone composition and dose. The aim of the study was to determine the response of genistein alone and as part of a mixed isoflavone supplement on bone resorption in postmenopausal women. The study was a blinded, randomized, crossover trial in which subjects received 5 soy isoflavone extract interventions; a bisphosphonate (risedronate) as an active control was administered at the end of the study period. The 5 interventions were as follows: purified genistein (>80% pure) as 1) 44 mg genistein and 53 mg total isoflavones and 2) 94 mg genistein and 114 mg total isoflavones, or mixed isoflavones containing various ratios as 3) 46 mg genistein, 44 mg daidzein, and 105 mg total isoflavones, 4) 91 mg genistein, 55 mg daidzein, and 161 mg total isoflavones per day, and 5) 96 mg genistein, 93 mg daidzein, and 220 mg total isoflavones. Subjects were 14 healthy postmenopausal women who received intravenous ⁴⁵Ca to label their skeletons. Treatments were given as 50 day interventions with 50 day washouts. Bone resorption was assessed by multiple measurements of urinary ⁴⁵Ca. Relative resorption (RR) was calculated as the difference between the measured ⁴⁵Ca excretion in the intervention period and the expected value determined from all washout periods. Serum measurements of isoflavones to verify compliance and bioavailability and biochemical markers of bone turnover were taken at the end of each intervention and washout period. All interventions except for 2) were able to reduce bone resorption (RR=0.889 to 0.966, p<0.05). The risedronate RR was 0.737 (p=0.0009). Genistein did not demonstrate an antiresorptive dose response and other isoflavones were neither agonistic nor antagonistic. A moderate level of mixed Isoflavones (intervention 3), Novasoy[®] was most effective at reducing bone resorption.



Effect of Soy Treatments on Bone Resorption

Disclosures: Jessica Wiersma, None.

MO0478

DNA Binding Mutations in ERα Lead to Suppression of Wnt Signaling in Bone. Ulrike Moedder¹, Sundeep Khosla¹, David Monroe^{*2}. ¹College of Medicine, Mayo Clinic, USA, ²Mayo Foundation, USA

Estrogens play vital roles in the function, homeostasis and remodeling of bone. The cellular mechanisms of estrogen receptor (ER) action can broadly be categorized into those involving direct binding to estrogen response elements (classical), or indirect DNA binding (non-classical). The generation of non-classical ER knock-in (NERKI) mice provides a unique opportunity to define these pathways in bone. Previous data from our laboratory have demonstrated that mice expressing only the NERKI receptor exhibit an osteoporotic phenotype; however, the mechanism(s) for this remain unresolved. Gene expression analyses of cortical bone from NERKI mice revealed suppression of lymphoid enhancer factor-1 (Lef1) expression, a classic Wnt-responsive transcription factor that associates with β-catenin. Since Wnt signaling is generally considered bone anabolic, this observation leads to the interesting hypothesis that NERKI-induced suppression of Wnt signaling may contribute to the low bone mass phenotype. To this end, we generated NERKI mice crossed with TOPGAL transgenic mice, a reporter strain that expresses β-galactosidase (β-gal) in response to Lef1-mediated Wnt signaling. Histochemical analysis of β-gal stained bone sections revealed significantly less β-gal in NERKI mice, confirming suppression of Wnt activity in vivo. Adenoviral expression of the NERKI receptor using an in vitro cell system revealed suppression of the Wnt target genes Tcf7, connexin 43 and versican when compared to wildtype ERα, confirming the in vivo findings. Interestingly, expression of NERKI caused induction of axin2, dickkopf homolog (DKK)-3, DKK4, secreted frizzled-related protein-4 and sclerostin, all known

repressors of Wnt signaling. Furthermore, expression of wildtype ER α , but not NERK1, stimulated Wnt activity in a lentiviral-mediated reporter assay. Collectively, these data suggest the osteoporotic phenotype of NERK1 mice may involve the suppression of Lef1-mediated Wnt signaling through both the repression of activators and stimulation of repressors of Wnt signaling. The inability of NERK1 to properly regulate Wnt activity may be due to the elimination of classical ER signaling as well as interference in the known roles of ER α in intracellular trafficking of β -catenin. Experiments are underway to discriminate among these possibilities.

Disclosures: David Monroe, None.

MO0479

Estrogen Protects Against Arthritis and Inflammation-Mediated Bone Loss Via Estrogen Receptor Alpha. Cecilia Engdahl¹, Anna Borjesson², Ulrika Islander², Sara Windahl², Alexandra Stubelius², Annica Andersson², Andree Krust³, Pierre Chambon³, Claes Ohlsson⁴, Hans Carlsten², Marie Lagerquist⁵. ¹Centre for Bone & Arthritis Research, GU, Sahlgrenska Academy, Medicine, Sweden, ²Center for Bone & Arthritis Research, Sahlgrenska Academy, Sweden, ³Institut de Genetique et de Biologie Moleculaire et Cellulaire (CNRS UMR7104; INSERM U596; ULP, College de France), France, ⁴Center for Bone Research At the Sahlgrenska Academy, Sweden, ⁵Sahlgrenska University Hospital, Sweden

Background: Many inflammatory diseases including rheumatoid arthritis leads to bone loss. The female sex hormone estrogen can prevent bone loss, but due to negative side-effects, long-term estrogen treatment is no longer an option.

Objective: The aim of this study is to investigate the mechanism behind the protective effects of estrogen against inflammation-mediated bone loss in order to facilitate the development of new estrogen-like treatment strategies lacking negative side-effects.

Methods: We have used transgenic female mice lacking estrogen receptor alpha (ER α)¹. The mice were ovariectomized and a placebo or estradiol (1.5 μ g/day) pellet was implanted subcutaneously. 10 days after the operation, arthritis (AIA, antigen-induced arthritis) was induced in one knee by injection of methylated BSA (mBSA), while the other knee was used as internal control and injected with saline. At termination, 14 days after the induction of arthritis, knees were harvested for histological examination of bone destruction. T lymphocytes in the spleen were analyzed using flow cytometry and proliferation assay.

Results: We observed that estrogen protects against both synovitis (-22%, $p < 0.05$) and bone erosion (-62%, $p < 0.001$) in wild type (WT) females, while no protective effect of estrogen was detected in females lacking ER α . Both the frequency of T lymphocytes (-29%, $p < 0.01$) and T cell proliferation (-52%, $p < 0.001$) in spleen was decreased after estrogen treatment in WT mice, while no effect of estrogen was seen in mice lacking ER α .

Conclusions: These findings lead us to conclude that ER α is required for the protective effects of estrogen against inflammation-mediated bone loss and that T cells might be involved in the estrogenic anti-arthritis and bone-protective effects.

References: 1. Dupont et al, *Development*, 127(19):4277-91, 2000

Disclosures: Marie Lagerquist, None.

MO0480

Estrogen Response Element Binding Protein is a Multi-Site Regulator in Bone Cells at the Level of Chromatin Remodeling, Transcription and mRNA Handling. Hong Chen^{*1}, Linda Gilbert², Thomas Lisse³, Martin Hewison⁴, Mark Nanes⁵, John Adams⁶. ¹VA / Emory University School of Medicine, USA, ²VA medical Center at Atlanta, USA, ³UCLA/Orthopaedic Hospital Research Center, USA, ⁴UCLA, USA, ⁵VA Medical Center & Emory University, USA, ⁶University of California, Los Angeles, USA

The estrogen response element binding protein (ERE-BP) is a heterogeneous nuclear ribonucleoprotein that competes in a dominant-negative mode with the estradiol (E2)-liganded estrogen receptor-alpha (ER) for occupation of EREs possessing a half-site motif of AGGTCA. ERE-BP stimulates pre-osteoblast (preOB)-like cell RANKL expression by 2-4-fold, antagonizing E2 up-regulation of OPG and enhancing osteoclastogenesis. Although the RANKL promoter (8000bp) in human preOB does not harbor a full ERE, it does possess a consensus half-site to which both the ER and ERE-BP are bound in chromatin immunoprecipitation (ChIP) assays with an affinity for ERE-BP >> E2-liganded ER > unliganded ER. ERE-BP directly stimulates RANKL transcription 2-3 fold. Increased transcription is also observed with the histone deacetylase inhibitor trichostatin A (TSA). Recruitment of HDAC3 to the RANKL promoter was inhibited by ERE-BP over-expression in preOB cells and completely blocked in the presence of TSA. These events were accompanied by a 4-fold increase in acetylated histone 3, suggesting that ERE-BP acts to preserve euchromatin at the RANKL gene locus. Binding in *cis* to DNA in the RANKL promoter is not the only means by which ERE-BP can interact in *trans* with nucleic acid recognition motifs. Compared to vector-alone transfected cells, preOB over-expressing the ERE-BP demonstrated a specific binding of the ERE-BP, but not the ER, to an AGGUCA *cis* element in the 3'UTR instability domain of the RANKL mRNA by RNA immunoprecipitation (RIP) assay. As was previously observed in its ds DNA binding activity, the ERE-BP cycled on and off the AGGUCA ssRNA

element at 45-minute intervals. Finally, ERE-BP over-expression was shown to be capable of regulating mRNA splicing events, presumably through its ss nucleic acid binding actions, in an E2-ER-ERE-driven CD44 minigene expressed in preOB; ERE-BP over-expression increased the ratio of spliced:unspliced minigene present in preOB cells. In sum these data suggest that when abundantly expressed in preOB, ERE-BP can promote the generation of mature RANKL RNA via its ability to interact in *trans* with RNA and DNA, modulating chromatin remodeling, transcription, splicing and 3'UTR-controlled mRNA handling events.

Disclosures: Hong Chen, None.

MO0481

1, 25-dihydroxyvitamin D Inhibits Growth and Induces Apoptosis of Breast Cancer Stem Cells. Jiarong Li^{*1}, Jing Lian¹, Richard Kremer². ¹McGill University, Canada, ²McGill University, Royal Victoria Hospital, Canada

Growth of many types of cancer is sustained by cancer stem cells (CSC's). It is widely believed that tumour recurrence is linked to CSC's survival following standard therapeutic regimen. 1,25-dihydroxyvitamin D (1,25(OH)2D) is a potent growth inhibitor of many cancers including breast cancer. However, its effect against CSC's has never been investigated. In this study we isolated breast cancer cells from polyomavirus middle T transgenic mice. Single-cell suspensions isolated from mouse mammary tumours were suspended at a density of 40,000 cells per millilitre in mamoculture basal medium containing proliferation supplements (Stemcell Technologies, Vancouver, Canada) in 6 well ultra low attachment tissue culture plates. Primary mammospheres were allowed to form in serum free medium containing increasing concentrations of 1, 25(OH)2D or vehicle. At 7 days primary mammospheres were centrifuged, dissociated with trypsin for 5 minutes at 37C and passed through a 23 gauge needle to obtain single cells. Cells were plated at a density of 10,000 cells per millilitre in ultra low attachment tissue culture plates to obtain secondary spheres. At 7 days the process was repeated to obtain tertiary mammospheres. Before each passage spheres were counted manually using Zeiss Axiovision software (Carl Zeiss, Jena, Germany) and isolated cells were also analyzed by immunofluorescence. Breast CSC's were identified by CD44, CD24 and ALDH1 staining. Apoptosis was examined by TUNEL assay and bcl2 expression. Addition of 1, 25(OH)2D resulted in a dose dependent growth inhibition of primary mammosphere cultures with 50% inhibition seen at 10⁻⁷M concentration. This inhibition was sustained in secondary and tertiary mammospheres. There was also a significant reduction in ALDH1 positive cells and a significant increase in apoptotic cell death in 1, 25(OH)2D treated mammospheres.

These data therefore suggest that 1, 25(OH)2D exerts its anti-cancer effect at least in part through inhibition of cell viability and engenderment of apoptosis in the CSC's population.

Disclosures: Jiarong Li, None.

MO0482

25-Hydroxyvitamin D, Parathyroid Hormone and Muscle Relationships in Early Pubertal Adolescents. Jamie Williams¹, Ashley Ferira¹, Emma Laing^{*1}, Dorothy Hausman¹, Connie Weaver², Munro Peacock³, Kathleen Hill⁴, Berdine Martin², Stuart Warden⁵, Norman Pollock⁶, Richard Lewis¹. ¹The University of Georgia, USA, ²Purdue University, USA, ³Indiana University Medical Center, USA, ⁴Indiana University School of Medicine, USA, ⁵Indiana University, USA, ⁶Georgia Health Sciences University, USA

The link between vitamin D status and muscle is an emerging area of interest based on studies in older adults that demonstrate a positive influence of vitamin D on muscle strength and function. Much less is known regarding this relationship in pediatric populations, of which a large number of US children have low circulating 25-hydroxyvitamin D [25(OH)D] concentrations. The objective of this study was to determine associations between serum 25(OH)D and intact parathyroid hormone (PTH) and muscle-related parameters [i.e., radial and tibial muscle cross-sectional area (MCSA) and density by peripheral quantitative computed tomography, forearm muscle strength by handgrip dynamometry, and total body fat-free soft tissue (FFST) by DXA] in early pubertal children (N=126), and if race and sex modify these relationships. Serum 25(OH)D and PTH concentrations were measured using RIA. Black (n=21) and white (n=40) males (aged 10 to 13 years) and black (n=25) and white (n=40) females (aged 9 to 12 years) living at 34N latitude participated in this study. Statistical analyses were performed using bivariate and partial correlations, controlling for race and sex. No significant relationships were found between serum 25(OH)D and MCSA, muscle density, forearm strength or FFST. Serum 25(OH)D was negatively correlated with PTH ($r = -0.36$; $p < 0.01$). PTH was positively related to radial and tibial MCSA ($r > 0.19$; $p < 0.04$) and negatively related to tibial muscle density ($r = -0.22$; $p = 0.02$). Though not statistically significant, PTH was positively related to FFST ($r = 0.16$; $p = 0.08$). After adjusting for differences in race and sex, positive correlations for PTH remained for radial and tibial MCSA, and showed a significant relationship to FFST ($r > 0.21$; $p < 0.03$). This cross-sectional study did not support a relationship between serum 25(OH)D and muscle strength indices in a sample of early pubertal children. However, the results suggest that PTH may be a more relevant marker of muscle function than 25(OH)D in early pubertal children. A vitamin D intervention trial is underway to help elucidate these relationships and

determine if there is an optimal vitamin D status for musculoskeletal strength and development during growth.

Disclosures: Emma Laing, None.

MO0483

Associations between Serum Vitamin D, Cardiometabolic Risk Factors and Visceral Adiposity in Obese Children. Ashley Ferira¹, Norman Pollock², Emma Laing¹, Dorothy Hausman³, Yanbin Dong², Richard Lewis¹, Catherine L. Davis². ¹The University of Georgia, USA, ²Georgia Health Sciences University, USA, ³University of Georgia, USA

Limited data exist on the relationship between circulating vitamin D levels and cardiometabolic risk factors (CMR), particularly in children at risk for cardiovascular disease and diabetes. This study examined whether lower vitamin D levels are associated with CMR in obese (OB) children living in the southeastern United States (latitude: 33N). Associations between vitamin D levels and adiposity distribution were also determined. OB sedentary children (N=222, aged 7-11 years, 58% female, 58% black) were classified into four groups: OB+Healthy (n=43), OB+1CMR (n=94), OB+2CMR (n=59), and metabolic syndrome (OB+≥3CMR, n=26). Serum 25-hydroxyvitamin D (25-OHD) concentrations were assayed by RIA. CMR were measured using standard methods and defined according to pediatric definitions of metabolic syndrome: fasting glucose ≥100 mg/dL, HDL cholesterol ≤40 mg/dL, triglycerides ≥110 mg/dL, systolic or diastolic blood pressure ≥90th percentile for age, sex and height, and waist circumference ≥90th percentile for age and sex. Visceral adipose tissue and subcutaneous adipose tissue were assessed using magnetic resonance imaging. The CMR distributions in the participants were: 19% with fasting glucose ≥100 mg/dL, 18% with triglycerides ≥110 mg/dL, 25% with HDL-cholesterol ≤40 mg/dL, 3% with blood pressure ≥90th percentile for age, sex and height, and 67% with waist circumference ≥90th percentile for age and sex. Using ANCOVA, controlling for age, sex, race and season, 25-OHD levels were examined across participants grouped by number of features of the metabolic syndrome. Serum 25-OHD levels were significantly higher in OB+Healthy and OB+1CMR groups compared to those with metabolic syndrome (both $P < 0.05$, Figure). Multiple linear regression, adjusting for the same covariates, revealed that fasting glucose ($\beta = -0.18$), HDL-cholesterol ($\beta = 0.19$), waist circumference ($\beta = -0.19$), and visceral adipose tissue ($\beta = -0.24$) were associated with 25-OHD concentrations (all $P < 0.04$). No relations were found between 25-OHD and triglyceride level, blood pressure or subcutaneous adipose tissue. In obese children, lower circulating vitamin D levels are associated with multiple measures known to increase cardiometabolic disease risk. In addition, it appears that greater levels of visceral, rather than subcutaneous, adiposity may be an important mediating factor in the correlation between lower vitamin D levels and increasing number of risk factors for cardiovascular disease and diabetes.

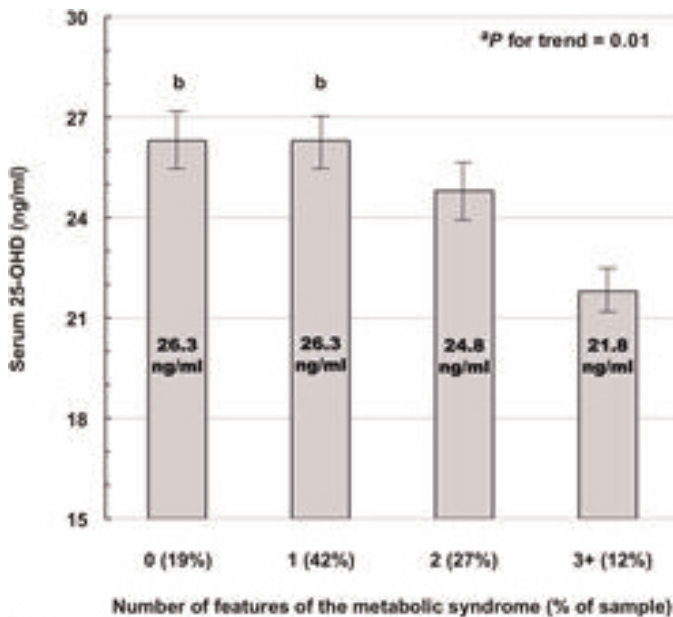


FIGURE. Mean (±SE) serum 25-OHD concentrations by number of features of the metabolic syndrome in 7-11 year old obese children (N=222). * P for trend on the basis of analysis of covariance, adjusted for age, sex, race, and season. $^{\dagger}P < 0.05$, significantly different from metabolic syndrome group (Tukey's honestly significant difference adjustment for multiple comparisons).

Disclosures: Ashley Ferira, None.

MO0484

Co-expression of Human hnRNPC1 and C2 Suppresses Vitamin D Receptor-mediated Transcriptional Responses in Mouse Osteoblastic Cells. Thomas Lisse¹, Rene Chun², John Adams³, Martin Hewison⁴. ¹UCLA/Orthopaedic Hospital Research Center, USA, ²Orthopedic Hospital Research Center UCLA, USA, ³University of California, Los Angeles, USA, ⁴UCLA, USA

Heterogeneous nuclear ribonucleoprotein (hnRNP) C plays a key role in RNA processing but also exerts a dominant negative effect on responses to 1,25-dihydroxyvitamin D (1,25D) by functioning as a vitamin D response element-binding protein (VDRE-BP). While constitutive over-expression of hnRNPC results in a form of hereditary vitamin D-resistant rickets (HVDRR) in both humans and New World Primates (NWP), the actions of hnRNPC have never been directly assessed in mouse bone or bone cells. The physiologically active form of human hnRNP C is a tetramer of hnRNPC1 (huC1) and hnRNPC2 (huC2). As such, oligomerization and organization of subunits is critical to in vivo nucleic acid-binding activity. Studies were therefore carried out to determine whether huC1/C2 proteins expressed in mouse osteoblastic cells promote resistance to 1,25D as observed in higher species. Transient (CMV) over-expression of either huC1 or huC2 alone, or stable lentiviral transfection using a bone-specific mouse type I collagen (2.3kb) promoter-driven huC1 plasmid resulted in no change in 1,25D-induced (10 nM, 6 hrs) Cyp24a1 mRNA expression compared to empty vector control. By contrast, co-over-expression of both huC1 and huC2 or use of a bone-specific polycistronic vector using a "self-cleaving" 2A peptide to co-express huC1/C2 suppressed Cyp24a1 mRNA and another osteoblast target for 1,25D, the mTOR-inhibitor DDIT4, in a 1,25D-dose-dependent manner. In all cases, endogenous levels of mouse hnRNPC mRNA remained constant following transfection with huC1/C2. Structural diversity of hnRNP C between human/NWPs and mouse/rat/rabbit/dog was highlighted by sequence variations at the last helix in the CLZ domain. The predicted loss of distal helical function in hnRNP Cs from lower species provides an explanation for the lack of interaction between huC1/C2 and their mouse counterparts. These data provide new evidence of a role for hnRNP C1/C2 as a dominant-negative-acting inhibitor of 1,25D-driven gene expression in bone, and further suggest that species-specific tetramerization is a crucial determinant of its actions as a regulator of VDR-directed transactivation.

Disclosures: Thomas Lisse, None.

MO0485

Comparison of Two Fully Automated Total 25 Vitamin D Immunoassays. Heather Pham¹, Benny Larsson². ¹Immunodiagnostic Systems, United Kingdom, ²Universitetssjukhuset i Malmö, Sweden

Background: Two fully automated immunoassays for Total 25-OH vitamin D were compared with a validated liquid chromatography-tandem mass spectrometry (LC-MS/MS) method. We assessed the analytical performance of the IDS-iSYS 25-OH vitamin D assay on the IDS-iSYS platform and compared it to a recently commercialized Architect 25-OH vitamin D.

Methods: The IDS-iSYS 25-OH Vitamin D assay is based on chemiluminescence technology for use on the IDS-iSYS platform. This method is traceable to UV quantification. The Architect 25-OH Vitamin D assay is a delayed one-step immunoassay and is referenced against the Liaison Total Vitamin D method. The LC-MS/MS method used protein precipitation of serum with a hexa-deuterated 25-OH vitamin D3 internal standard to correct for recovery. The ionisation source was APCI, and the method was calibrated with Chromsystems calibrator. This calibrator has direct traceability to NIST reference standards for 25-OH vitamin D3 and 25-OH vitamin D2. The Total 25-OH vitamin D level was measured in 88 serum samples using the above described methods. The correlation between the methods was analysed using Passing-Bablok comparison fit; the 25-OH vitamin D levels were classified by vitamin D status.

Results: A comparison of IDS-iSYS 25-OH vitamin D with LC-MS/MS yielded the regression equation: IDS-iSYS = 1.03 x (LC-MS/MS) + 1.50 (average bias: +2.6ng/mL). The corresponding equation with Architect was: IDS-iSYS = 0.69 x (Architect) - 1.24 (average bias: -15.5ng/mL). The comparison between Architect and LC-MS/MS produced an equation: Architect = 1.55 x (LC-MS/MS) + 3.10 (average bias: +17.9ng/mL). Table below summarised number of samples classified vitamin D status by each method.

Conclusions: The IDS-iSYS 25-OH vitamin D concentrations were in good agreement with those determined by the LC-MS/MS. It has proven itself as a sensitive and precise fully automated, co-specific 25-OH vitamin D assay for clinical laboratories. On the contrary, the Architect was not only under-classified insufficient samples; it also classified 5 samples as possible intoxication.

25-OH vitamin D Level (ng/mL)	Number of samples (%)		
	LC-MS/MS	IDS-iSYS	Architect
Insufficient <30	51 (58%)	47 (53%)	29 (33%)
Sufficient 30-100	37 (42%)	41 (47%)	54 (61%)
Possible Intoxication >100	0	0	5 (6%)

Number of samples classified vitamin D status

Disclosures: Heather Pham, Immunodiagnostic System, 3

MO0486

Effect of Growth Factors on Vitamin D Receptor and its Role in Vitamin D-Mediated Growth Suppression in Porcine Coronary Artery Smooth Muscle Cells. Gaurav Gupta¹, Tanupriya Agrawal¹, Devendra Agrawal². ¹Creighton University, USA, ²Creighton University School of Medicine, USA

Purpose: Recent studies have demonstrated that Vitamin D, a steroid hormone precursor, has biological activity in different tissues including cardiomyocytes, cancer cells, cells of immune system, and vascular smooth muscle cells (VSMC). Calcitriol is the bioactive form of vitamin D that binds to vitamin D receptor (VDR) in target cells and triggers downstream signaling to produce phenotypic changes in these cells. These effects suggest potential use of VDR ligands in the management of different diseases including restenosis. VSMC proliferation by platelet derived growth factor (PDGF)-BB and insulin like growth factor (IGF-1) play an important role in development and progression of restenosis. The purpose of this study was to examine the effect of PDGF-BB and IGF-1 stimulation on VDR expression in porcine coronary artery smooth muscle cells (PCASMCs). We also examined the effect of calcitriol on PDGF-BB and IGF-1 induced proliferation in VDR knockdown PCASMCs.

Methods: PCASMCs were isolated and cultured from domestic swine. PCASMCs were stimulated with PDGF-BB and IGF-1 with and without calcitriol and mRNA and protein expression of VDR were analyzed by real-time PCR and Western blot, respectively. PCASMCs were transfected with control siRNA or VDR siRNA and cells proliferation was examined after stimulation with platelet derived growth factor (PDGF)-BB and insulin like growth factor (IGF)-1 with and without calcitriol by analyzing proliferating cell nuclear antigen (PCNA) expression and MTT assay.

Results: Stimulation of PCASMCs with IGF-1 and PDGF-BB significantly downregulated mRNA transcripts and protein expression of VDR in PCASMCs. VDR expression was significantly downregulated by VDR siRNA in PCASMCs. Anti-proliferative effect of calcitriol was abolished in PCASMCs treated with VDR siRNA.

Conclusion: These data suggest that high concentration of PDGF-BB and IGF-1 downregulate VDR expression in PCASMCs. Calcitriol acts through VDR to inhibit PDGF-BB and IGF-1 induced cell proliferation in PCASMCs. Thus, downregulation of VDR in SMCs of post interventional arteries due to high concentration of growth factors could be a potentially contributing factor in neointimal hyperplasia.

Disclosures: Gaurav Gupta, None.

MO0487

Prevalence of Vitamin D Deficiency and Its Relationship with Sun Exposure and Skin Phototype in Elderly Men Living in the Tropics. marcelo cabral¹, carla borges¹, Daniele Fontan², Leonardo Bandeira¹, NARRIANE CHAVES¹, Francisco Bandeira³. ¹doctor(MD), Brazil, ²Brazil, ³UPE, Brazil

Objectives: To determine the prevalence of vitamin D deficiency among men and, its association with sun exposure and skin phototypes in the city of Recife, Brazil (8°S), in 284 men (mean age 69.446.49 years, body mass index(BMI) 25.674.31 Kg/ m2, sun index= hours of sun exposure per week x fraction of body surface area exposed=5.495.05). **Methods:** We evaluated the serum levels of 25 hydroxyvitamin D (25OHD), the sun index and skin phototype according to Fitzpatrick classification. **Results:** The mean serum 25OHD was 27.8713.52 ng/ml. The prevalence of vitamin D deficiency was 31.5% (95% CI 26.236.8) and 66.7% (95% CI 61.372.1) when cutoff of less than 20ng/ml and 30ng/ml were used, respectively. There were no statistically significant differences (p=0.113) between the mean serum 25OHD (23.9814.66 vs 29.8813.78) of the individuals in the lower quartile of the sun index(Q1:1.96), compared with those in the upper quartile(Q4:7.86), nor the prevalence of vitamin D deficiency between lower quartile and upper quartile (33.3% x 27.1%) when a cut point of 30ng/ml for serum 25OHD levels was used. Mean sun index was significantly different between those who had serum 25OHD levels below or above 20ng/ml(4.463.69 vs 6.015.54, p=0.006); however, no differences were seen when the cutoff of 25ng/ml(5.074.31 vs 5.955.69;p=0.149) and 30ng/ml(5.224.43 vs 6.126.14;p=0.160) were used. After adjustment, by linear regression analysis, for potential confounders, the sun index and body mass index were positively and negatively associated with serum 25OHD, respectively. Most subjects (67%) had skin types IV,V or VI. Low calcium intake was observed in 72% of the individuals, and only seven (2.5%) were using vitamin supplements. **Conclusion:** We found a high prevalence of vitamin D deficiency in elderly men, despite a high sun exposure. Sun exposure, had an independent effect on serum 25OHD levels, but this effect had a minimal impact on prevalence rates, suggesting that even large amounts of sun exposure may not be sufficient to achieve serum 25OHD targets of 25-30ng/ml.

Disclosures: Francisco Bandeira, None.

MO0488

Similar Vitamin D₂ and D₃ Pharmacokinetics with a Single and Daily Doses. Silvina Mastaglia¹, Mariana Seijo², Graciela Brito³, Guillermo Keller⁴, Julia Somoza⁵, Roberto Diez⁴, Guillermo Di Girolamo⁴, Beatriz Oliveri⁵. ¹Seccion Osteopatías Medicas, Hospital de Clínicas, Universidad de Buenos Aires. Consejo Nacional de Investigaciones Científicas y Tecnológicas (CONICET), Argentina, ²Seccion Osteopatías Medicas, Hospital de Clínicas, Universidad de Buenos Aires, Argentina, ³Seccion Osteopatías Medicas, Hospital de Clínicas, Universidad de Buenos Aires. Agencia Nacional de Promocion Científica y Tecnológica (ANPCyT), Argentina, ⁴2 Catedra de Farmacología, Facultad de Medicina, Universidad de Buenos Aires, Argentina, ⁵Seccion Osteopatías Medicas, Hospital de Clínicas, Universidad de Buenos Aires. Consejo Nacional de Investigaciones Científicas y Tecnológicas (CONICET), Argentina

Some studies found cholecalciferol (D3) to be superior to ergocalciferol (D2) based on the effect of increasing or maintaining serum 25-hydroxyvitamin-D (25OHD) levels. However, others reported both calciferols to be equivalent. The aim of this study was to clarify and compare the pharmacokinetics of D2 and D3. We carried out a single-blind, placebo-controlled randomized trial during 11 weeks (September to December 2010) in Buenos Aires city (34°S). Thirty-three young healthy volunteers (7M/ 26F) with an age of (meanSD) 33.46 years and BMI 22.62 Kg/m2 were included. The subjects were divided in groups: D2 (n=11); D3 (n=11) and placebo (n=11). In the D groups the subjects received at the start a single dose of 100,000IU and 4,800 IU/day (d) of the vitamin D allocated from 7 to 21 d. No vitamin D was administered from 22 to 77 d. The serum samples were obtained at basal and d: 3, 7, 14, 21, 35, 49, 63 and 77 to measure sCa, sP, iPTH, BAP, 25OHD (RIA-DIASORIN) and 2 hours urinary uCa/uCr ratio. Baseline 25OHD (ng/ml) levels were: D2: 16.37; D3: 24.26 (p<0.01) and placebo: 22.67. No differences were observed in the other biochemical parameters whereas placebo values of 25OHD did not increase over treatment, vitamin D administration augmented serum 25OHD levels in each sampling point, as shown in figure 1. To take into account variability in basal 25OHD serum levels, subtraction of basal values was performed before pharmacokinetic analysis. For D3-treated subjects, AUC was 1107481 ng.d.ml-1 (range 331-1920, 95%CI 823-1391), ke -0.2460.104 day-1 (range: -0.479 to -0.125, 95%CI -0.307 to -0.185) and t_{1/2} 3.2671.274 days (range 1.448-5.545, 95%CI 2.514-4.020). For D2-treated subjects AUC was 1005352 ng.d.ml-1 (range 638-1784, 95%CI 797-1213), ke -0.3210.245 day-1 (range: -0.911 to -0.107, 95%CI -0.466 to -0.176) and t_{1/2} 3.1051.658 days (range 0.761-6.469, 95%CI 2.124-4.085). Under this administration scheme, no pharmacokinetic differences were found between the two treatments. **Conclusion:** under the experimental conditions selected, vitamin D2 was equally effective as vitamin D3 in raising and maintaining 25OHD and levels.

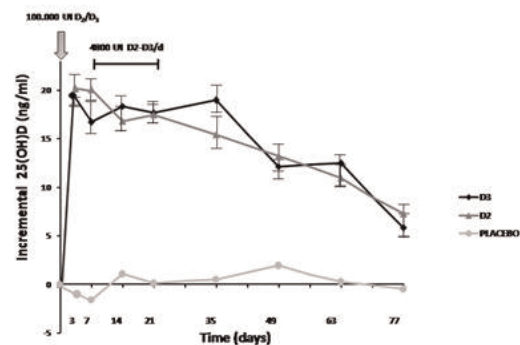


Figure 1: Incremental serum 25(OH)D levels mean ± SE in the time course corresponding to the two calciferol and placebo treatment groups.

Figure 1

Disclosures: Silvina Mastaglia, None.

MO0489

State of the Art of Vitamin D Assays: Latest Generation Assays. Christopher-John Farrell¹, Steven Martain², Isabella Straub³, Paul Williams⁴, Markus Herrmann⁴. ¹PaLMS & Laverty Pathology, Australia, ²Laverty Pathology, Australia, ³University of Sydney, Australia, ⁴Royal Prince Alfred Hospital & University of Sydney, Australia

Background: A number of pre-existing automated vitamin D assays have recently been modified and several new assays have been launched. This study aimed to

compare latest generation automated vitamin D immunoassays with liquid chromatography tandem mass spectrometry (LCMS) measurement.

Methods: 170 randomly selected serum samples were divided into 6 aliquots, stored at -20°C and analysed in batches, with freshly thawed aliquots used for all analyses. Vitamin D was measured by LCMS (2 different methods at independent laboratories), a radioimmunoassay (RIA) from DiaSorin as well as 5 automated chemiluminescent immunoassays from Abbott, DiaSorin, IDS, Roche and Siemens. The Roche assay used was the recent monoclonal vitamin D assay which specifically detected 25-hydroxy vitamin D₃. All other immunoassays detected both 25-hydroxy vitamin D₂ and D₃ and reported a total vitamin D result. The DiaSorin immunoassay was a pre-market assay. To assess intra- and inter-assay variability we measured 5 replicates of a high and of a low serum pool over 5 consecutive days.

Results: The two LCMS methods correlated well with $r = 0.984$ and an average bias of 2.0%. In the cohort tested, all immunoassays correlated well with LCMS with the exception of Roche (table 1). At vitamin D levels between 25-120 nmol/L DiaSorin, Siemens and RIA showed excellent accuracy, while Abbott, IDS and Roche exhibited variable bias (table 1). Vitamin D levels < 20 nmol/L were only measured accurately by DiaSorin, IDS and RIA, while Siemens and Abbott showed substantial bias at these concentrations. Intra- and inter-assay precision differed between assays but was within the acceptable range for all tests.

Conclusion: Latest generation automated vitamin D immunoassays demonstrated significantly improved performance and compared well with LCMS. While most automated assays produced acceptable results across the clinically relevant range Siemens and DiaSorin demonstrated superior accuracy. The assays tested showed variable performance at low vitamin D concentrations and laboratories should adapt their reportable range accordingly.

	Versus avg. of 2 LC Tandem MS methods		
	Correlation coefficient	Avg. bias if vit D > 25 nmol/L	Avg. bias if vit D < 25 nmol/L
Abbott	0.932	25.21%	102.62%
Ulisson (pre)	0.954	-0.40%	32.21%
Siemens	0.941	3.97%	119.30%
Roche	0.678	-17.62%	32.57%
IDS	0.954	13.44%	14.82%
RIA	0.984	-5.38%	10.26%

Table 1

Disclosures: Markus Herrmann, None.

MO0490

Vitamin D Supplementation does not Change Expression of Human Cathelicidin in Neutrophils in Young Healthy Subjects. Silvina Mastaglia¹, Clarisa Marotte^{*2}, Gabriel Bryk³, Julia Somoza¹, Graciela Brito⁴, Mariana Seijo³, MarÚa Fornari⁵, Roberto Diez⁶, Beatriz Oliveri¹. ¹Seccion OsteopatÚas Medicas, Hospital de CIÚnicas, Universidad de Buenos Aires. National Council for Scientific & Technologic Research (CONICET), Argentina, ²Seccion OsteopatÚas Medicas, Hospital de CIÚnicas, Universidad de Buenos Aires. National Council for Scientific & Technologic Research (CONICET), Argentina, ³Seccion OsteopatÚas Medicas, Hospital de CIÚnicas, Universidad de Buenos Aires, Argentina, ⁴Seccion OsteopatÚas Medicas, Hospital de CIÚnicas, Universidad de Buenos Aires. Agencia Nacional de Promocion CientÚfica y Tecnologica (ANPCyT), Argentina, ⁵Laboratorio de Analisis CIÚnicos Fornari Bioalpha SA, Buenos Aires, Argentina, ⁶2 Catedra de FarmacologÚa, Facultad de Medicina, Universidad de Buenos Aires, Argentina

The antimicrobial peptide cathelicidin (hCAP18) is stored in several cell types of the system immune, mainly in the granules of neutrophils (PMN). 1,25 (OH)₂D is a direct inducer of expression of the gene encoding hCAP18. The aim of the present study was to evaluate the expression of leukocytes' cathelicidin in young healthy volunteers supplemented with vitamin D₂ and D₃. Thirty-three young healthy volunteers (7M/ 26F) with an age of (mean SD) 33.4 6 years and BMI of 22.6 2 Kg/m² were included in this randomized placebo controlled trial for 11 weeks (Sep-Dec 2010). Subjects were allocated to the following groups: Vitamin D₂ (n=11); Vitamin D₃ (n=11) and placebo (n=11). At the start of the study a single dose (100,000 IU/day) of vitamin D₂ or D₃ according to the group was administered. Thereafter, from d 7th to 21st of the study, volunteers received 4,800 IU/d of the corresponding vitamin D. No vitamin D was administered from 22 to 77 d. No infection or allergic symptoms were reported during the study. At baseline and d: 7, 21, and 63 blood samples were obtained to measure serum Ca, P, BAP and 25OHD (RIA-DIASORIN). At each sampling point, the expression of hCAP18 in peripheral blood PMN was assessed by flow cytometry with a FACSort® (Becton-Dickinson, San Jose,

CA, USA) and the CellQuest® software (Becton-Dickinson), using the mouse monoclonal antibody OSX12 (Abcam, UK), specific for hCAP18, and a secondary incubation with FITC anti-murine IgG (Abcam). A protocol of permeation used for neutrophil myeloperoxidase was used, and myeloperoxidase labeling was included as control. Region corresponding to PMN was defined by side and forward scattering; PMN expressing a higher level of hCAP18 were identified in the fluorescence histogram of the neutrophils region and defined as M1. Most (>95%) PMN expressed intra-granular cathelicidin, either at the basal sample or after vitamin D or placebo treatment. Only 1% to 2% depicted higher expression (Figure1). No significant differences were observed among groups in the expression hCAP18 in PMN, either as level of expression (mean fluorescence) or as percentage of cells over-expressing hCAP18, in spite of the significant increment of 25OHD levels in both supplemented groups (d7:100%;d21:90% and d63:60% compared to basal levels). Under these experimental conditions, PMNs cathelicidin is not modified by vitamin D supplementation, independently of calciferol used.

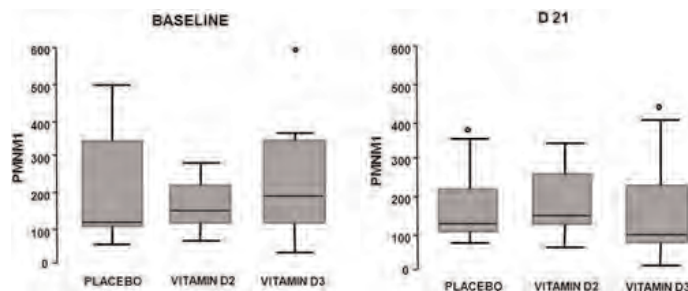


Figure 1: Comparison of hCAP18 expression in PMN-M1 baseline and D21 of the study

Disclosures: Clarisa Marotte, None.

MO0491

TSH and Bone: An Update. Li Sun^{*1}, Ramkumarie Baliram¹, L.L. Zhu¹, R. Latif¹, G. Colaianni¹, T. Yuen¹, G. Zhu¹, J. Berkowitz¹, Y. Peng¹, S. Fritz¹, J. Li¹, J. Iqbal¹, T. F. Davies¹, Mone Zaidi². ¹Mount Sinai School of Medicine, USA, ²Mount Sinai Medical Center, USA

We have shown that TSH receptor (TSHR) deficient mice exhibit bone loss; that TSH inhibits bone resorption by suppressing TNF α ; and that TSH stimulates bone formation to restore post-ovariectomy bone loss. We now extend these observations. We show that murine ES cells can be induced to form mature, mineralizing osteoblasts. TSH stimulates osteoblast differentiation by activating protein kinase C δ and up-regulating the Wnt components Frz (frizzled) and Wnt5a. We suggest that a TSH-induced, fast-forward, short loop permits Wnt5a production in bone marrow, which not only enhances osteoblast differentiation, but also stimulates osteoprotegerin synthesis to inhibit resorption. In separate studies, we provide direct evidence that effects of TSHR deficiency on bone are mediated through TNF α . We generated compound mutants by crossing TSHR^{-/-} with TNF α ^{+/-} mice. Micro-CT confirmed reduced BV/TV as a function of decreasing TSHR levels, accompanied by increased trabecular spacing and reduced trabecular number. The genetic deletion of TNF α completely reversed the bone loss in both TSHR genotypes. Thus, for example BV/TV of TSHR^{+/-}/TNF α ^{+/-} mice was significantly greater than that of TSHR^{+/-}/TNF α ^{+/+} mice. Likewise, the enhanced TRAP-positive osteoclast and CFU-f/CFU-ob seen in TSHR^{-/-} mice was abrogated in compound mutants lacking TNF α . That the genetic removal of TNF α fully rescued osteopenia in TSHR^{-/-} mice proved that TNF α mediates, at least in part, the bone loss of TSHR deficiency. Finally, to determine that TSHR deficiency causes the bone loss in hyperthyroidism, wild type and TSHR^{-/-} mice were first treated with carbimazole, and then, implanted with 0, 1, or 5 mg T4 pellets to render the mice hypothyroid, euthyroid or hyperthyroid, respectively. The hypothesis was that, if TSHR-deficiency caused bone loss independently of high T4 levels, then bone mass (BMD) and bone resorption (serum CTx) would be markedly greater in hyperthyroid-TSHR^{-/-} than in hyperthyroid-TSHR^{+/+} mice. This indeed was the case, establishing that, at least in the setting of experimental hyperthyroidism, TSHR deficiency was permissive to further bone loss. Together, the studies substantiate the osteo-protective action of TSH, establish its mediation through TNF α suppression, and prove that TSH deficiency is an independent trigger for bone loss in hyperthyroidism.

Disclosures: Li Sun, None.

ADULT BONE AND MINERAL WORKING GROUP

WG1

Teriparatide, Vitamin D, and Calcium Healed Bilateral Subtrochanteric Stress Fractures in a Postmenopausal Woman with a 13-Year History of Continuous Alendronate Therapy. Stephen J. Gomberg, Rosanna L. Wustrack, Nicola Napoli, Claude D. Arnaud, and Dennis M. Black; West Oaks Orthopaedic Associates (S.J.G.), Thousand Oaks, California 91361; University of California; San Francisco (R.L.W., C.D.A., D.M.B.), San Francisco, California 94143; and Università Campus Bio-Medico di Roma (N.N.), 00128 Rome, Italy.

Background: Oral bisphosphonates comprise the most widely prescribed class of antiosteoporotic drugs. Recent reports, however, propose a link between prolonged bisphosphonate use and atypical, low-energy, subtrochanteric fractures. **Objectives:** The aim was to describe the clinical course of a patient treated long-term with alendronate who developed subtrochanteric stress fractures and to propose a hypothesis to explain teriparatide's potential contribution in healing the patient's stress fractures. **Results:** Magnetic resonance imaging (MRI) showed classical bilateral stress fractures of the mid-femora. Baseline serum 25-hydroxyvitamin D3 was low; bone-specific alkaline phosphatase was slightly increased; serum carboxyterminal cross-linking telopeptide of bone collagen and urine aminoterminal cross-linking telopeptide of bone collagen were low to normal, as was serum osteocalcin. Dual-energy x-ray absorptiometry showed osteopenic vertebral bone mineral density and osteoporotic hip values. Treatment with large doses of oral vitamin D increased serum 25-hydroxyvitamin D3 to normal within 2 months, after which it remained in the normal range with maintenance doses. High pain, present as an initial symptom, intensified, and the MRI appearance of the fractures worsened. Teriparatide treatment commenced, and 6 months later, repeat MRI showed decreased edema at the fracture sites with faint cortical bridging. High pain and lower limb weakness disappeared over the next year, and complete fracture healing was established (MRI). **Conclusions:** Based upon the chronology of fracture healing in our patient and published evidence that teriparatide heals stress fractures in a rat model, we think that teriparatide was probably primary in this patient's positive response to therapy, with calcium, vitamin D therapy, and alendronate discontinuation playing secondary roles. (J Clin Endocrinol Metab 96: 0000-0000, 2011).

WG2

Familial Fibrogenesis Imperfecta Ossium (FFIO) Bhadada SK*, Bhansali A*, Rao DS** Department of Endocrinology Postgraduate Institute of Medical Education & Research Chandigarh, India*. Bone and Mineral Laboratory, Henry Ford Health System, Detroit, Michigan, USA**.

Introduction: Fibrogenesis imperfecta ossium (FIO) is an uncommon, crippling, relentlessly progressive and ultimately fatal metabolic bone disease. The disease is of adult onset with unknown etiology. Clinically, it is characterized by generalized bone pains, multiple spontaneous fractures in both the axial and appendicular skeleton. The plasma biochemistry is normal except for elevated alkaline phosphatase activity. A distinctive "fishnet appearance" is observed on radiographs in advanced disease. Histopathology consists of abundant osteoblasts and osteoclasts with thick osteoid seams. Tetracycline labeling of decalcified bone tissue confirms the presence of osteomalacia. However, on polarized light microscopy, bone collagen fibrils are not birefringent. We describe a family of FIO, in whom four adult members were affected, suggesting an autosomal dominant inheritance pattern. To the best of our knowledge this is the largest family of FIO in the world literature. **Case Report (Index Case):** A 40-year-old man presented with a 10 year history of generalized bone pains requiring round the clock analgesics. One year before presentation he developed spontaneous pain in the right hip, since then he had required a stick to walk. A worsening of symptoms 3 months before presentation meant that then required the help of somebody to perform the activities of daily life. He had strong family history of similar illness in the mother, maternal uncle and younger brother, with both his mother and maternal uncle having died after prolonged similar illness. He had difficulty in getting up from squatting position and needed a stick to help with walking. The hip joint movements were painful and restricted. The rest of the systemic examination was non-contributory. His laboratory evaluations including TmP/GFR were normal except mild elevation in total alkaline phosphatase (AP). The serum intact PTH level by immunochemiluminometry was 30 pg/ml (reference range: 10-69 pg/ml). Serum 25-hydroxyvitamin D level was 59.9 (reference range 9 – 37 ng/ml). Serum 1,25-hydroxyvitamin D level was 76.6 ng/ml. Arterial blood gases and urine pH were within normal range. Thyroid function tests were normal. Serum tissue transglutaminase antibody (tTG) titre was negative. Urine for Bence Jones protein was negative and serum electrophoresis was normal. Radiographs of the skull and hands were normal. The lumbar spine showed "rugger-jersey" spine with osteopenia. Views of the pelvis showed bilateral coxavara and bilateral femur neck fracture with "fishnet appearance". The chest radiograph showed multiple Looser zones with fractures of several ribs. The lower end of tibia showed "fishnet appearance", tendon calcification and new bone formation. Bone mineral density (BMD) of the hip with a T-score of -2.2 SD. Magnetic resonance imaging of pelvis showed fracture of bilateral neck and hypointense marrow on T1W and T2W sequences. A 99mTc MDP bone scan showed increased radiotracer uptake bilaterally in the shoulders, elbows, wrists, small joints of

hands, multiple sites at bilateral ribs, the entire vertebral column, and lower end of tibia but not the skull. Transiliac bone biopsy showed thickened bony trabeculae with obliteration of marrow spaces and at places, focal areas of exaggerated osteoclastic activity. There was prominent osteoblastic proliferation as well as osteoid like areas were also seen. At places it showed sclerosis, eaten up edges of bone and foci of new calcification (bone formation). With the above mentioned clinical and investigation profile a diagnosis of FIO was considered most likely.

Conclusion: To the best of our knowledge, this is the largest family of FIO and index patient successfully treated with a bone formation and antiresorptive agent with positive outcome.

WG3

Characteristic clinical and radiologic features of Prodromal Bone Deterioration (PBD) in patients on long term bisphosphonate therapy: A case series of seven patients. Manjari Devidi, Shijing Qiu, Saroj Palnitkar, D. Sudhaker Rao. Saint Joseph Hospital, Chicago, IL & Bone & Mineral Research Laboratory, Henry Ford Hospital, Detroit MI.

There has been a great concern about long term use of bisphosphonate (BP) resulting in severe suppression of bone turnover, impaired ability to repair microdamage, and atypical femoral fractures (AFF). We report a case series of 7 patients (all women) with post menopausal osteoporosis on long term BP therapy (duration 3-13 years), who were referred for evaluation and advise for possible BP induced insufficiency fracture of the outer cortex of the femoral mid-shaft with little or no trauma. The mean age was 65.57 years (range 52 to 87 years). Retrospectively six out of these patients had mid thigh pain and characteristic radiographic findings of focal cortical beaking with lucency along the lateral aspect of proximal third of the femur, confirmed by bone scan and/or MRI as insufficiency fracture. A few had bilateral findings even though the pain was unilateral. Bone turnover markers were low to low normal at presentation. Although the incidence of AFF due to BP use is thought to be very rare accounting for about 1% of all femur fractures, the incidence of incomplete femoral outer lateral femoral fractures, which we designated as prodromal bone deterioration (PBD), is likely to be lot higher considering the fact that they can occur without prodromal pain and likely underreported by the physicians. Our retrospective study suggests that prodromal thigh pain is not a prerequisite to PBD and may explain the sudden onset of complete AFFs without trauma; "break & fall" instead of the usual "fall & break" paradigm. Our experience with potential role of bone scan in selected patients to detect impending AFF, prophylactic intra-medullary rod to prevent complete AFF, and anabolic therapy to promote PBD healing will be discussed.

WG4

Vitamin D and Calcium Nutritional Status in Patients with Hip Fractures & Elective Joint Replacement Surgery: Preliminary Results of a Prospective Case Controlled Study. S. Makhoul-Ahwach, S. Ahmadi, J. Miragaya, L. Garcia MD, J. Shah, D. Cadena, N. Shareef, M. Al-Abed, J. Khalil, S. T. Guthrie, M. Laker MD, A. Al-shoha, D. Sudhaker Rao. Bone Mineral Research Laboratory, Henry Ford Hospital, Detroit, MI, USA.

Background: Much has been written about the role of vitamin D in the pathogenesis of hip fractures (HFx), but very little is known about the calcium and vitamin D nutritional (VDN) status in acute HFx patients. **Materials & Methods:** We measured serum 25-OHD levels, the best available index of VDN, and PTH, a reasonable surrogate marker for both calcium and VDN status, in acute HFx and elective joint replacement surgery (JRS) patients. Both groups of patients were recruited during the same time period (2009 – 2010) with a final target of at least 100 patients in each group. This is a preliminary report of the first 66 patients (21 HFx & 45 JRS). The main outcome measures were serum 25-OHD and PTH levels. **Results:** As expected, the HFx patients were older (by 10y) and lighter than the JRS patients, but the proportion of genders was similar in the 2 groups (Table). Interestingly, mean 25-OHD was lower in the HFx, but not significantly, than in JRS patients (Table). However, serum PTH levels were significantly higher in the HFx patients.

Variable	HPF Patients	JRS Patients	p≤
Age (years)	76 9	67 9	<0.001
Men/Women (n)	6/15	12/33	n.s.
BMI (kg/m ²)	25.7 6.1	30.6 7.0	0.008
25-OHD (ng/ml)	19.0 11.2	23.7 11.3	n.s.
PTH (pg/ml)	140 160	118 48	<0.05
Ca (mg/dl)	8.2 0.57	8.4 0.66	n.s.
P (mg/dl)	3.0 0.97	2.64 0.79	n.s.
Mg (mEq/L)	2.00 0.28	2.08 0.35	n.s.

Serum Ca, P, & Mg (Table) were similar in the 2 groups. The proportion of patients with 25-OHD <15 or <20, or <30 ng/ml was significantly higher in the HFx compared to JRS patients. Most disturbing was that only 3 of the 21 HFx patients ever had a bone density. **Conclusions:** Many HFx patients still have lower VDN but much better than reported a decade ago implying some improvement in VDN. However, continued high PTH levels imply that calcium intake is also very poor. Chronic hyperparathyroidism, however initiated, may be more important in the pathogenesis of HFx than VDN as has been long assumed, but further studies are needed either to refute or support this hypothesis.

WG5

Case Report: Severe Renal Osteodystrophy in a 40 Year Old Female with End Stage Renal Disease. Maria Princess M. Landicho, MD, FPCP, Thelma D. Crisostomo, MD, FPCP, FPSEM, FACE, Pauline Camacho, MD, FACE, Section of Endocrinology, Makati Medical Center, Philippines.

For full abstract text, see MO0166.

WG6

Oncogenic Osteomalacia: What we have been missing, what we need to do and what we need to change. Ekram T, Dalal I, Bolton C, van Holsbeeck M, Rao D.

Tumor-induced osteomalacia is a rare paraneoplastic syndrome which results in significant morbidity due to generalized skeletal pain, myalgia, fatigue and fractures. The causative tumor, usually a benign osseous or soft tissue tumor, secretes a substance which causes renal phosphate wasting, impaired vitamin D metabolism and osteomalacia. AIM: The purpose of this exhibit is to: 1) Define the role of the physician including the radiologist in clenching the diagnosis of oncogenic osteomalacia -clinical cases of our four patients including pitfalls 2) Identifying a step wise approach in the diagnosis of oncogenic osteomalacia using musculoskeletal radiology and nuclear medicine modalities along with appropriate laboratory work up. 3) Discuss the emergence and pathophysiology of oncogenic hypophosphatemic-osteomalacia. Case series: We describe four patients in whom hypophosphatemic-osteomalacia for years before proper imaging was obtained. We'll discuss what they perceived on their clinical scenario and how the diagnostic workup was achieved. We'll describe what imaging modality used for localization and timing and frequency of testing if previous study was negative. Patients demonstrated characteristic hypophosphatemia, low calculated renal absorption of phosphate and elevated FGF-23. Diagnosis of this rare paraneoplastic syndrome is often delayed and difficulty isolating the causative tumor causes further delay in definitive treatment. We also suggest an imaging algorithm based on these cases and a literature review. The role of radiology in workup is crucial and has not been comprehensively defined. A vast array of imaging modalities may be used in search for the causative tumor including Tc-99m MDP bone scintigraphy, In-111 pentetreotide scintigraphy (Octreoscan), Tc-99m sestamibi scintigraphy, screening MRI, CT, PET CT and FGF-23 venous sampling. Conclusion:

Our cases represent the unfortunately typical pattern of diagnosis and workup for tumor-induced osteomalacia in that patients suffer long before a diagnosis is made and undergo different imaging before identification of the tumor which allows for definitive treatment. It is hoped that the presented imaging algorithm will expedite identification of the causative tumor and definitive treatment.